Journal of Function Spaces

Recent Advances of Fractional Calculus in Applied Science

Lead Guest Editor: Yusuf Gurefe
Guest Editors: Behrouz Parsa Moghaddam and Luisa Morgado

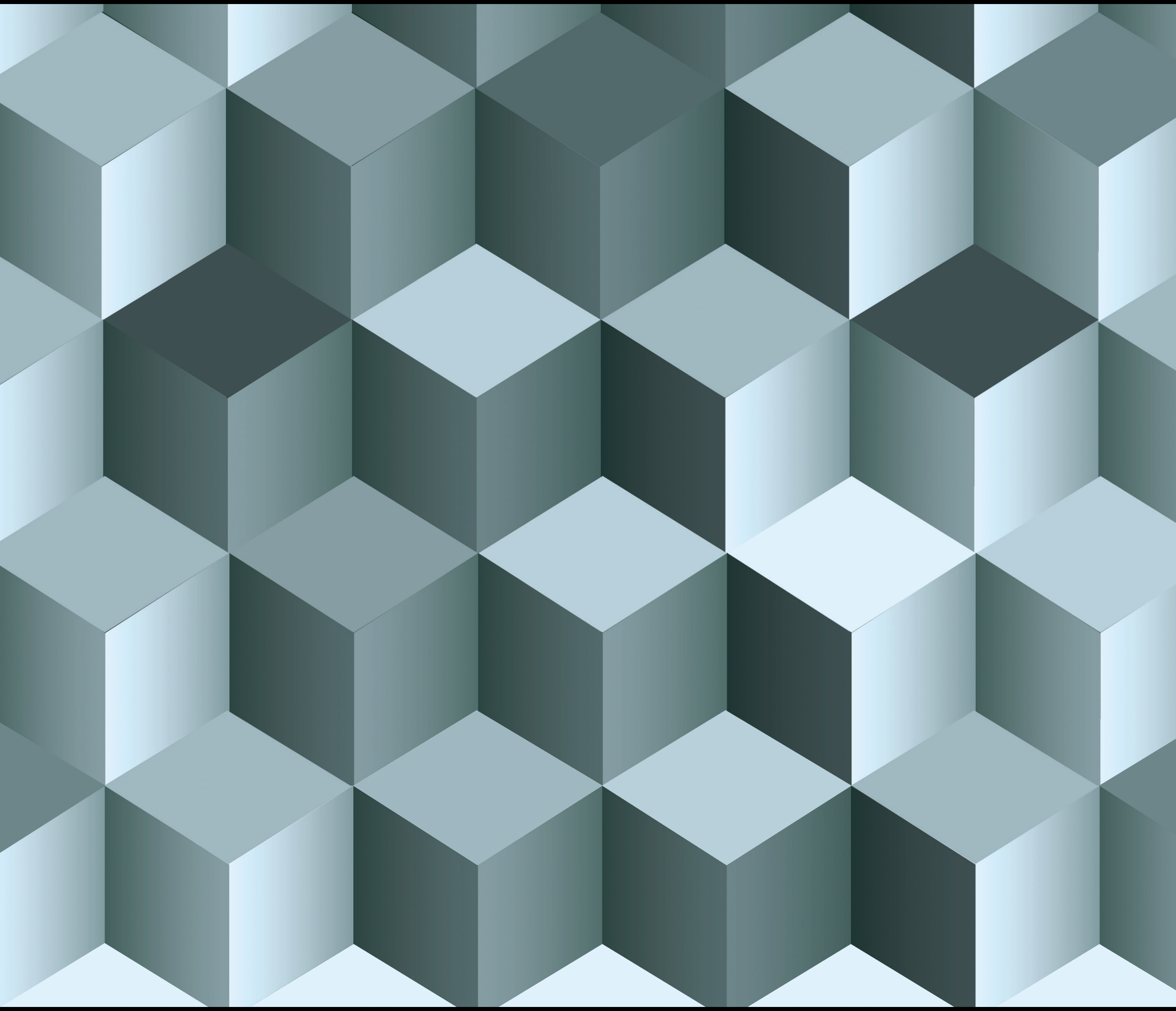

Recent Advances of Fractional Calculus in Applied Science

Journal of Function Spaces

Recent Advances of Fractional Calculus in Applied Science

Lead Guest Editor: Yusuf Gurefe
Guest Editors: Behrouz Parsa Moghaddam and Luisa Morgado

Contents

Contents

Contents

Hindawi
Journal of Function Spaces
Volume 2023, Article ID 8283092, 17 pages
https://doi.org/10.1155/2023/8283092

Research Article

Some Novel Optical Solutions for the Generalized M-Fractional Coupled NLS System

Baojian Hong [1], Jiaxin Zhou [2], Xingchen Zhu [2] and Yiting Wang [3]

[1] *Faculty of Mathematical Physics, Nanjing Institute of Technology, Nanjing 211167, China*
[2] *Faculty of Energy and Power Engineering, Nanjing Institute of Technology, Nanjing 211167, China*
[3] *Faculty of Electric Power Engineering, Nanjing Institute of Technology, Nanjing 211167, China*

Correspondence should be addressed to Baojian Hong; hbj@njit.edu.cn

Received 9 September 2022; Revised 20 November 2022; Accepted 2 June 2023; Published 20 June 2023

Academic Editor: Yusuf Gurefe

In this work, some novel optical solutions for the $(1+1)$-dimensional generalized M-fractional coupled nonlinear Schrödinger system (GMFCNLS) arising in ocean engineering, plasma waves, and nonlinear optics have been investigated. After utilizing a modified $(G'/G, 1/G)$-expansion method and the $G'/(bG'+G+a)$-expansion method, many types of novel optical solutions including the bell-shape soliton solutions, the blow-up solutions, the periodic wave solutions, and the mixed solitary wave solutions are obtained; if we select different values of wave velocity, coefficients, and orders, the dynamic properties and physical structures of these optical solutions are simulated and discussed, which can help us to further understand the inner structure of the system.

1. Introduction

In recent years, due to the wide application of nonlinear partial differential equations (PDE) especially fractional PDE models in engineering and mathematical physics, many topics in these fields have been characterized, including mechanics [1, 2], ecological and economic systems [3], atmospheric space science [4], and optical fiber systems [5–7]. For a better explanation of the complex feature of these phenomena, searching for analytic explicit solutions of these models plays an important and significant role. Up to now, many powerful methods for this subject have been built: the improved F-expansion method [8], the G'/G-expansion method [9], the improved G'/G^2-expansion method [10], the improved $(m+G'/G)$-expansion method [11], the $(G'/G, 1/G)$-expansion method [12], the improved extended Tanh technique [13], the subequation technique [14], the Sine-Gordon expansion method [15], the EXP $(-\varphi(\xi))$ technique [16], the Bäcklund transformation method [17], the Darboux transformation method [18], the Hirota bilinear method [19], the first integral method [20], the Jacobi elliptic function expansion method [21], the Lie symmetry method [22], the new Kudryashov method [23], etc. [24–30].

Some classical definitions about the fractional derivative are discussed and established by many researchers till now, including Riemann-Liouville's fractional derivatives [31], Caputo's fractional derivatives [32], He's fractional derivative [33], Jumarie's fractional derivative [34], Atangana's fractional derivative [35], conformable fractional derivative [36], and the M-fractional derivative [37–39], which will be utilized in this article.

In the present article, we consider the following $(1+1)$-dimensional generalized M-fractional coupled nonlinear Schrödinger equations (GMFCNLS) in the form [40–48]

$$\begin{cases} iD_t^\alpha q_1 + i\rho D_x^\beta q_1 + \sigma D_x^{2\beta} q_1 + \delta\left(|q_1|^2 + \gamma|q_2|^2\right)q_1 = 0, & 0<\alpha\le 1, 0<\beta\le 1, \\ iD_t^\alpha q_2 - i\rho D_x^\beta q_2 + \sigma D_x^{2\beta} q_2 + \delta\left(\gamma|q_1|^2 + |q_2|^2\right)q_2 = 0, \end{cases} \tag{1}$$

where $D_t^\alpha = D_{M,t}^{\gamma_2,\alpha}$, $D_x^\beta = D_{M,x}^{\gamma_1,\beta}$, $D_x^{2\beta} = D_{M,x}^{\gamma_1,\beta}(D_{M,x}^{\gamma_1,\beta})$, $D_x^{3\beta} = D_{M,x}^{\gamma_1,\beta}(D_{M,x}^{\gamma_1,\beta}(D_{M,x}^{\gamma_1,\beta}))$ mean the M-fractional derivative [37]. The coefficients $\rho, \sigma, \delta, \gamma$ are real constants; $q_1 = q_1(x,t)$, and $q_2 = q_2(x,t)$ are two complex valued functions with respect to the time t and the propagation distance x. In fact, Equation (1) occur in many fields, such as nonlinear optics, ocean engineering, and plasma waves. If we select $\rho = 0$, functions q_1, q_2 represent the amplitudes of circularly polarized waves in a nonlinear optical fiber, nonzero constant δ represents self-focusing and self-defocusing nonlinearity, and nonzero constant γ represents cross-phase modulation and self-phase modulation [40]; the authors investigated the analytical solutions of Equation (1) by using the extended trial equation method [41], bifurcation analysis method [42], fractional Riccati method [43], Kudryashov's method [44], etc. [45]. If we select $\alpha = \beta = 1$, $\rho = \lambda/2$, $\sigma = 1/2$, and $\delta = 1$, Equation (1) is focused in ocean engineering; functions q_1, q_2 represent the complex envelope amplitudes of the two modulated weak resonant waves in two polarizations. The quadratic dispersions and cubic terms represent the interactions; furthermore, various interesting phenomena, including nonlinear pulse stabilization, pedestal elimination in compressed pulses, and multicomponent Bose-Einstein condensation, can be described in Equation (1) [46]. The exact solutions of Equation (1) have been found by utilizing the generalized Kudryashov procedure in Ref. [47] and direct Ansatz method in Ref. [48].

Here, let us review some basic definitions and properties about the M-fractional derivative which will be further used in this paper.

Definition 1. For a function $f(t)$: $[0,\infty) \longrightarrow R$, we defined the M-fractional derivative operator $f(t)$ of order α as

$$D_{M,t}^{\gamma,\alpha} f(t) = \lim_{\varepsilon \longrightarrow 0} \frac{f\left(tE_\gamma\left(\varepsilon t^{1-\alpha}\right)\right) - f(t)}{\varepsilon}, \quad \gamma > 0, 0 < \alpha \le 1, \tag{2}$$

where $E_\gamma(t) = \sum_{k=0}^{\infty} t^k/\Gamma(\gamma k + 1)$ is a truncated Mittag-Leffler function of one parameter.

Also, we have the following important properties [37–39]:

(1) $D_{M,t}^{\gamma,\alpha} f(t) = (t^{1-\alpha}/\Gamma(\gamma+1))(df(t)/dt)$

(2) $D_{M,t}^{\gamma,\alpha}(af(t) + bg(t)) = aD_{M,t}^{\gamma,\alpha} f(t) + bD_{M,t}^{\gamma,\alpha} g(t), \forall a, b \in R$

(3) $D_{M,t}^{\gamma,\alpha}(f(t)g(t)) = f(t)D_{M,t}^{\gamma,\alpha} g(t) + g(t)D_{M,t}^{\gamma,\alpha} f(t)$

(4) $D_{M,t}^{\gamma,\alpha}(f(t)/g(t)) = [g(t)D_{M,t}^{\gamma,\alpha} f(t) - f(t)D_{M,t}^{\gamma,\alpha} g(t)]/g^2(t)$

(5) $D_{M,t}^{\gamma,\alpha}(f \circ g)(t) = f'(g(t))D_{M,t}^{\gamma,\alpha} g(t) = (t^{1-\alpha}/\Gamma(\gamma+1))f'(g(t))(dg(t)/dt)$

The paper is organized as follows: In Section 2, we introduce the modified $(G'/G, 1/G)$-expansion method and the $G'/(bG' + G + a)$-expansion method, while in Section 3, some new types of soliton pulse solutions of the GMFCNLS are found and discussed by utilizing the proposed method. Finally, the conclusion is presented in Section 4.

2. Description of the Two Methods

2.1. The Modified $(G'/G, 1/G)$-Expansion Method. The $(G'/G, 1/G)$-expansion method has been proposed by many authors recently [12, 49]; we give some formal modification about this method in order to simplify the solving procedure for Equation (1); a brief description of the technique is presented as follows.

Step 1. Consider the following nonlinear M-fractional partial differential equation:

$$E\left(u, u_t^\alpha, u_x^\beta, uu_x^\beta, \cdots\right) = 0. \tag{3}$$

Step 2. Using a wave transformation,

$$u(x,t) = u(\xi), \xi = \frac{\Gamma(\gamma_1 + 1)}{\beta} kx^\beta + \frac{\Gamma(\gamma_2 + 1)}{\alpha} \omega t^\alpha, \quad \gamma_{1,2} > 0, \tag{4}$$

where constants k and ω are to be determined latter. Equation (3) is converted into a nonlinear ordinary differential equation (ODE):

$$O\left(u, u', u'', uu', \cdots\right) = 0. \tag{5}$$

Step 3. Assume that Equation (3) has the following solution:

$$u = \sum_{i=0}^{N} a_i \psi^i + \sum_{i=1}^{N} b_i \psi^{i-1} \phi, \tag{6}$$

where N is a balance number, $\phi = \phi(\xi) = G'/G$, $\psi = \psi(\xi) = 1/G$, and a_i, b_i and variable function $\xi = \xi(x,t)$ are determined later. And $G = G(\xi)$ is a solution of the following auxiliary ODE:

$$G'' = \varepsilon G - \varepsilon \mu, \tag{7}$$

where $\varepsilon = \pm 1$, μ is an arbitrary real number. We can find the following constrained condition:

$$\begin{cases} \phi' = \varepsilon - \varepsilon\mu\psi - \phi^2, \\ \psi' = -\phi\psi, \\ \phi^2 = \varepsilon - 2\varepsilon\mu\psi - \varepsilon\left(b^2 - \varepsilon c^2 - \mu^2\right)\psi^2, \end{cases} \tag{8}$$

where arbitrary constants μ, b and c satisfied the relation $a^2 + b^2 + \mu^2 \neq 0$. Equation (7) admits the following solutions.

Case 1. When $\varepsilon = 1$, we have $G = b\cosh\xi + c\sinh\xi + \mu$; thus,

$$\begin{aligned}\phi &= \frac{G'}{G} = \frac{b\sinh\xi + c\cosh\xi}{b\cosh\xi + c\sinh\xi + \mu},\\ \psi &= \frac{1}{G} = \frac{1}{b\cosh\xi + c\sinh\xi + \mu}.\end{aligned} \tag{9}$$

Case 2. When $\varepsilon = -1$, we have $G = b\cos\xi + c\sin\xi + \mu$; thus,

$$\begin{aligned}\phi &= \frac{G'}{G} = \frac{-b\sin\xi + c\cos\xi}{b\cos\xi + c\sin\xi + \mu},\\ \psi &= \frac{1}{G} = \frac{1}{b\cos\xi + c\sin\xi + \mu}.\end{aligned} \tag{10}$$

Step 4. Substitute Equations (8) and (6) into Equation (5), and set the coefficients of $\psi^i (i = 0, 1, 2, \cdots, N)$ and $\psi^{i-1}\phi (i = 1, 2, \cdots, N)$ to zero to yield a set of algebraic equations (AEs) for a_i, b_i, b, c, μ, k, and ω. After solving the AEs and substituting each of the solutions $\phi(\xi), \psi(\xi)$ from (9) and (10) along with (4) into Equation (3), we can get the solutions of Equation (3).

Remark 2. It was noticed that Refs. [12, 49] were focused on collecting the coefficients of ϕ^i and $\phi\psi^{i-1}$ to zero, but we are collecting the coefficients of ψ^i and $\psi^{i-1}\phi$ to zero, each of these two ways is correct; the collected direction is decided by the solutions' forms of these target equations.

2.2. The $G'/(bG' + G + a)$-Expansion Method. With the similar steps about the technique 2.1, we give the main steps about this method.

Step 1. Assume that Equation (3) has the following solution:

$$u = \sum_{i=0}^{N} c_i F^i, \tag{11}$$

where $F = F(\xi) = G'/bG' + G + a$ and c_i and variable function $\xi = \xi(x, t)$ are determined later. $b \neq 0, a$ are arbitrary constants, and $G = G(\xi)$ is a solution of the following auxiliary ODE:

$$G'' = -\frac{\lambda}{b}G' - \frac{\mu}{b^2}G - \frac{\mu}{b^2}a, \tag{12}$$

where λ and μ are two arbitrary real numbers. We can find the following constrained condition:

$$F' = (\lambda - \mu - 1)F^2 + \frac{1}{b}(2\mu - \lambda)F - \frac{1}{b^2}\mu. \tag{13}$$

Equation (13) admits the following solutions.

Case 1. When $\Delta = \lambda^2 - 4\mu > 0$, we have $G = -a + p_1 e^{(1/2b)(-\lambda-\sqrt{\Delta})\xi} + p_2 e^{(1/2b)(-\lambda+\sqrt{\Delta})\xi}$; a, p_1, and p_2 are arbitrary constants that satisfy $a^2 + p_1^2 + p_2^2 \neq 0$, so does in Case 2; thus,

$$\begin{aligned}F_1 &= \frac{p_1\left(\lambda + \sqrt{\Delta}\right) + p_2\left(\lambda - \sqrt{\Delta}\right)e^{\sqrt{\Delta}/b\xi}}{bp_1\left(\lambda - 2 + \sqrt{\Delta}\right) + bp_2\left(\lambda - 2 - \sqrt{\Delta}\right)e^{\sqrt{\Delta}/b\xi}} = \frac{\left[\lambda(p_2 - p_1) - \sqrt{\Delta}(p_2 + p_1)\right]\sinh\left(\sqrt{\Delta}/2b\xi\right) + \left[\lambda(p_2 + p_1) - \sqrt{\Delta}(p_2 - p_1)\right]\cosh\left(\sqrt{\Delta}/2b\xi\right)}{b\left[(\lambda - 2)(p_2 - p_1) - \sqrt{\Delta}(p_2 + p_1)\right]\sinh\left(\sqrt{\Delta}/2b\xi\right) + b\left[(\lambda - 2)(p_2 + p_1) - \sqrt{\Delta}(p_2 - p_1)\right]\cosh\left(\sqrt{\Delta}/2b\xi\right)},\\ F_1 &= \begin{cases} F_{1.1} = \dfrac{\lambda - 2\mu}{2b(\lambda - \mu - 1)} - \dfrac{\sqrt{\Delta}}{2b(\lambda - \mu - 1)}\tanh\left(\dfrac{\sqrt{\Delta}}{2b}\xi\right), (\lambda - 2)(p_2 - p_1) - \sqrt{\Delta}(p_2 + p_1) = 0,\\ F_{1.2} = \dfrac{\lambda - 2\mu}{2b(\lambda - \mu - 1)} - \dfrac{\sqrt{\Delta}}{2b(\lambda - \mu - 1)}\coth\left(\dfrac{\sqrt{\Delta}}{2b}\xi\right), (\lambda - 2)(p_2 + p_1) - \sqrt{\Delta}(p_2 - p_1) = 0.\end{cases}\end{aligned} \tag{14}$$

Case 2. When $\Delta = \lambda^2 - 4\mu < 0$, we have

$$\begin{aligned}G &= e^{-\lambda/2b\xi}\left(p_1\cos\left(\frac{\sqrt{-\Delta}}{2b}\xi\right) + p_2\sin\left(\frac{\sqrt{-\Delta}}{2b}\xi\right)\right) - a,\\ F_2 &= \frac{\left(\lambda p_1 - \sqrt{-\Delta}p_2\right)\cos\left(\sqrt{-\Delta}/2b\xi\right) + \left(\lambda p_2 + \sqrt{-\Delta}p_1\right)\sin\left(\sqrt{-\Delta}/2b\xi\right)}{b\left((\lambda - 2)p_1 - \sqrt{-\Delta}p_2\right)\cos\left(\sqrt{-\Delta}/2b\xi\right) + b\left((\lambda - 2)p_2 + \sqrt{-\Delta}p_1\right)\sin\left(\sqrt{-\Delta}/2b\xi\right)},\\ F_2 &= \begin{cases} F_{2.1} = \dfrac{\lambda - 2\mu}{2b(\lambda - \mu - 1)} + \dfrac{\sqrt{-\Delta}}{2b(\lambda - \mu - 1)}\tan\left(\dfrac{\sqrt{-\Delta}}{2b}\xi\right), (\lambda - 2)p_2 + \sqrt{-\Delta}p_1 = 0,\\ F_{2.2} = \dfrac{\lambda - 2\mu}{2b(\lambda - \mu - 1)} - \dfrac{\sqrt{-\Delta}}{2b(\lambda - \mu - 1)}\cot\left(\dfrac{\sqrt{-\Delta}}{2b}\xi\right), (\lambda - 2)p_1 - \sqrt{-\Delta}p_2 = 0.\end{cases}\end{aligned} \tag{15}$$

Step 2. Substitute Equations (11) and (13) into Equation (5), and set the coefficients of F^i to zero to yield a set of AEs for c_i, b, λ, μ, k, and ω. After solving the AEs and substituting each of the solutions F_1, F_2 along with (11) and (4) into Equation (3), we can get the solutions of Equation (3).

In the following, we will use these two methods to solve the GMFCNLS.

3. Exact Solutions to the GMFCNLS

3.1. Exact Solutions. We can give the following function and traveling wave transformation:

$$\begin{aligned}q_1 &= u(\xi)e^{i\eta_1},\\ q_2 &= v(\xi)e^{i\eta_2},\end{aligned} \tag{16}$$

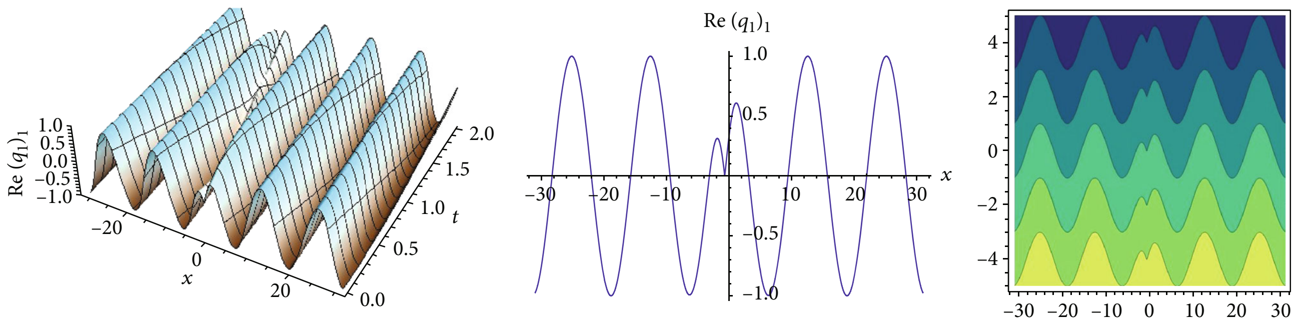

Figure 1: The 3D plot, 2D plot, and contour plot of Re $(q_1)_1$ with $\alpha = 1$, $\beta = 1$, and $\gamma_1 = \gamma_2 = 1$.

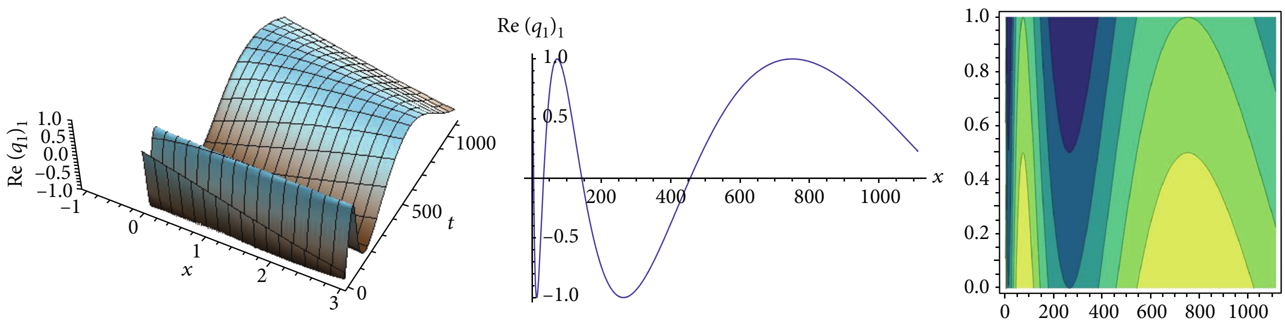

Figure 2: The 3D plot, 2D plot, and contour plot of Re $(q_1)_1$ with $\alpha = 0.18$, $\beta = 0.9$, and $\gamma_1 = \gamma_2 = 1$.

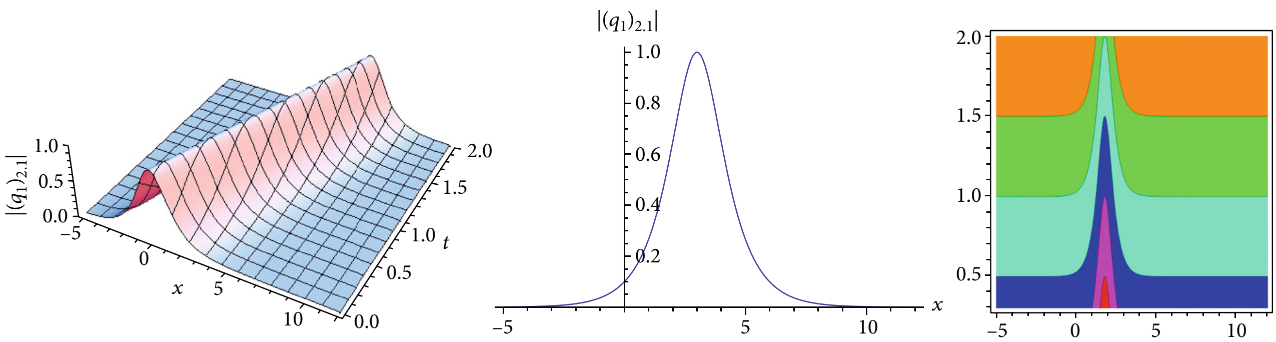

Figure 3: The 3D plot, 2D plot, and contour plot of bell-shape soliton solution $|(q_1)_{2.1}|$.

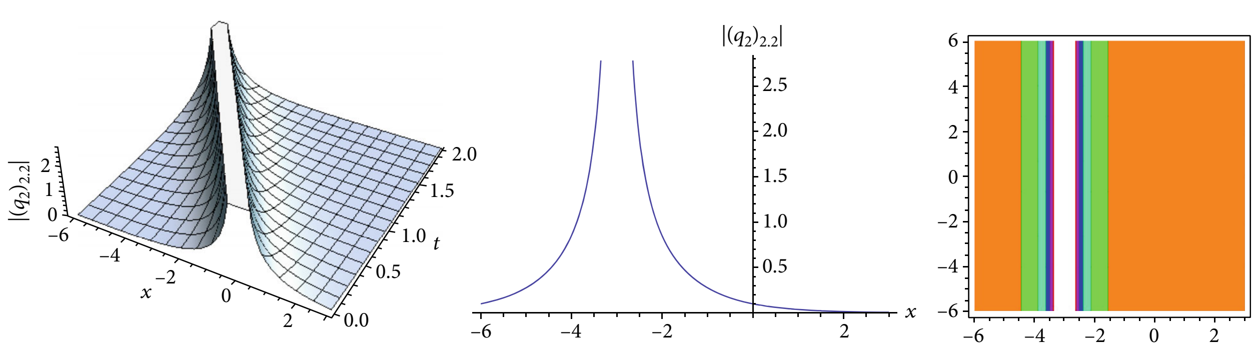

Figure 4: The blow-up pulse solutions' 3D plot, 2D plot, and contour plot of $|(q_2)_{2.2}|$.

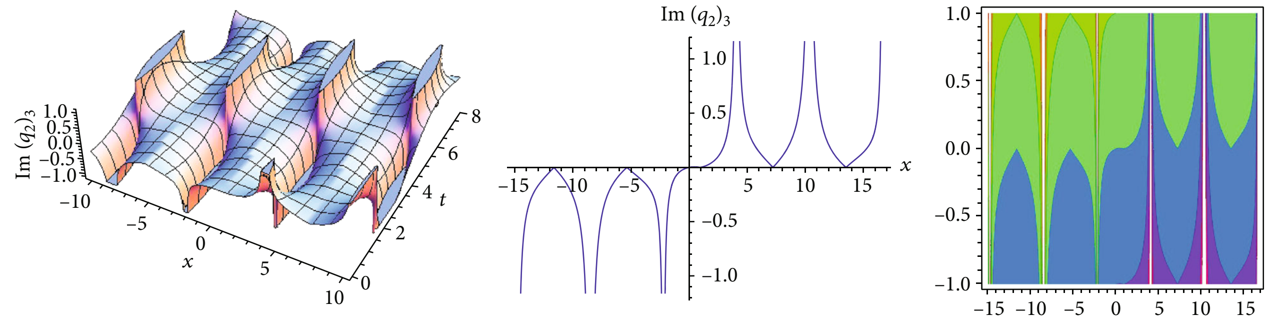

Figure 5: The periodic pulse solutions' 3D plot, 2D plot, and contour plot of Im $(q_2)_3$.

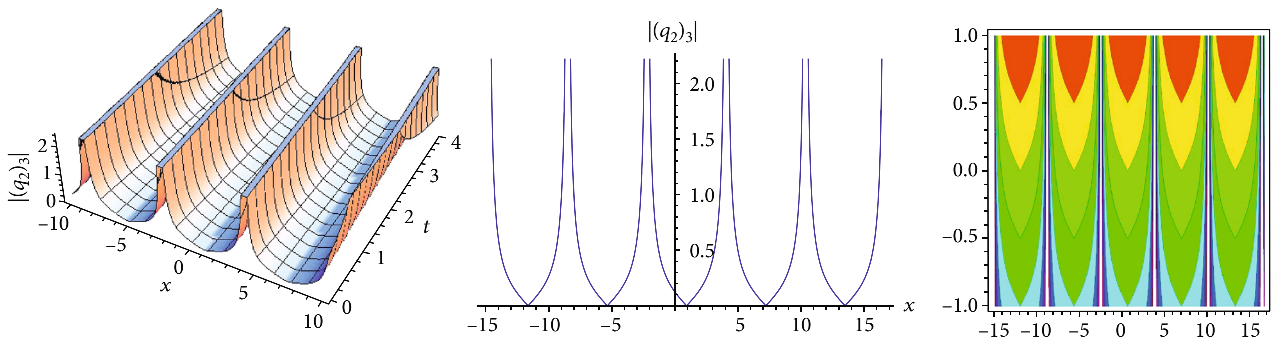

Figure 6: The periodic pulse solutions' 3D plot, 2D plot, and contour plot of $|(q_2)_3|$.

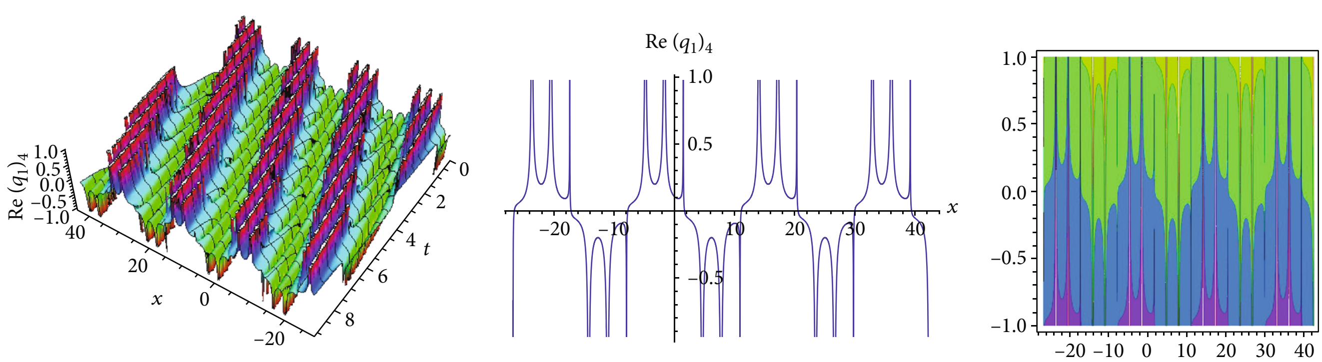

Figure 7: The 3D plot, 2D plot, and contour plot of the periodic wave solution Re $(q_1)_4$.

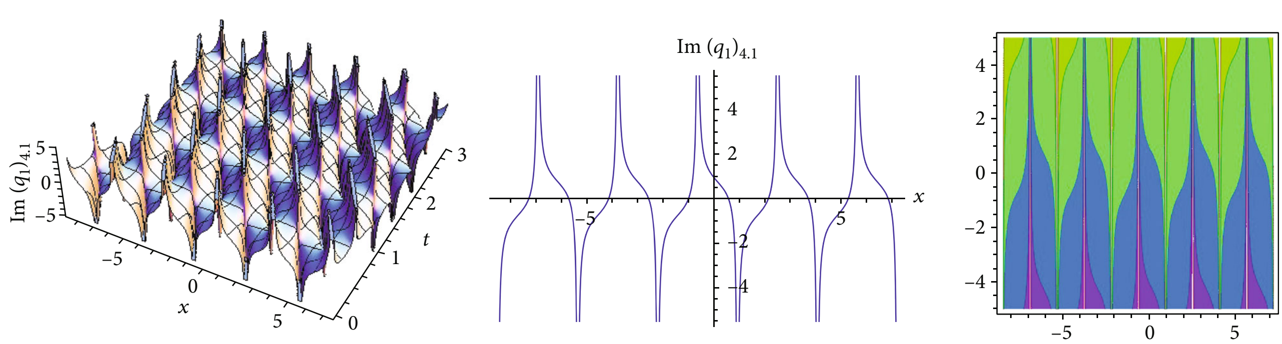

Figure 8: The 3D plot, 2D plot, and contour plot of the periodic wave solution Im $(q_1)_{4.1}$.

$$
\begin{aligned}
\xi &= \frac{\Gamma(\gamma_1+1)}{\beta} kx^{\beta} + \frac{\Gamma(\gamma_2+1)}{\alpha} \omega t^{\alpha},\\
\eta_1 &= \frac{\Gamma(\gamma_1+1)}{\beta} k_1 x^{\beta} + \frac{\Gamma(\gamma_2+1)}{\alpha} c_1 t^{\alpha},\\
\eta_2 &= \frac{\Gamma(\gamma_1+1)}{\beta} k_2 x^{\beta} + \frac{\Gamma(\gamma_2+1)}{\alpha} c_2 t^{\alpha},\\
&\gamma_1, \gamma_2 > 0,
\end{aligned}
\tag{17}
$$

where constants k, k_1, k_2 and ω, c_1, c_2 are to be determined latter.

Substituting Equations (16) and (17) into Equation (1) and separating the real part and the imaginary part, we obtain

$$
\begin{cases}
\sigma k^2 u_{\xi\xi} - \left(k_1^2\sigma + \rho k_1 + c_1\right)u + \delta\left(u^2 + \gamma v^2\right)u = 0,\\
\sigma k^2 v_{\xi\xi} - \left(k_2^2\sigma - \rho k_2 + c_2\right)v + \delta\left(\gamma u^2 + v^2\right)v = 0,\\
(\omega + \rho k + 2\sigma k k_1)u_{\xi} = 0,\\
(\omega - \rho k + 2\sigma k k_2)v_{\xi} = 0.
\end{cases}
\tag{18}
$$

From (18), we obtain

$$
\omega = -\sigma k(k_1 + k_2). \tag{19}
$$

According to the homogeneous balance method, we assume that Equation (18) has the following solutions:

$$
\begin{cases}
u(\xi) = a_0 + a_1\psi + a_2\phi,\\
v(\xi) = b_0 + b_1\psi + b_2\phi.
\end{cases}
\tag{20}
$$

Substitute Equations (20) and (8) into Equation (18), and set the coefficients of ψ^i and $\psi^{i-1}\phi$ to zero to yield a set of AEs for the unknowns a_0, a_1, a_2, b_0, b_1, b_2, k, k_1, k_2, c_1, c_2, and ω.

$$
\begin{aligned}
\psi^0 :& -c1a_0 + \delta a_0^3 + 3\delta\varepsilon a_0 a_2^2 + \gamma\delta a_0 b_0^2 + 2\gamma\delta\varepsilon a_2 b_0 b_2 + \gamma\delta\varepsilon a_0 b_2^2\\
&- \rho a_0 k_1 - \sigma a_0 k_1^2 = 0,\\
\phi :& -c1a_2 + 3\delta a_0^2 a_2 + \delta\varepsilon a_2^3 + \gamma\delta a_2 b_0^2 + 2\gamma\delta a_0 b_0 b_2 + \gamma\delta\varepsilon a_2 b_2^2\\
&- \rho a_2 k_1 - \sigma a_2 k_1^2 = 0,\\
\psi :& -c1a_1 + k^2\varepsilon\sigma a_1 + 3\delta a_0^2 a_1 - 6\delta\varepsilon\mu a_0 a_2^2 + 3\delta\varepsilon a_1 a_2^2 + \gamma\delta a_1 b_0^2\\
&+ 2\gamma\delta a_0 b_0 b_1 - 4\gamma\delta\varepsilon\mu a_2 b_0 b_2 + 2\gamma\delta\varepsilon a_2 b_1 b_2\\
&- 2\gamma\delta\varepsilon\mu a_0 b_2^2 + \gamma\delta\varepsilon a_1 b_2^2 - \rho a_1 k_1 - \sigma a_1 k_1^2 = 0,\\
\phi\psi :& -k^2\varepsilon\mu\sigma a_2 + 6\delta a_0 a_1 a_2 - 2\delta\varepsilon\mu a_2^3 + 2\gamma\delta a_2 b_0 b_1 + 2\gamma\delta a_1 b_0 b_2\\
&+ 2\gamma\delta a_0 b_1 b_2 - 2\gamma\delta\varepsilon\mu a_2 b_2^2 = 0,\\
\psi^2 :& -3k^2\varepsilon\mu\sigma a_1 + 3\delta a_0 a_1^2 - 3b^2\delta\varepsilon a_0 a_2^2 + 3c^2\delta\varepsilon^2 a_0 a_2^2\\
&+ 3\delta\varepsilon\mu^2 a_0 a_2^2 - 6\delta\varepsilon\mu a_1 a_2^2 + 2\gamma\delta a_1 b_0 b_1 + \gamma\delta a_0 b_1^2\\
&- 2b^2\gamma\delta\varepsilon a_2 b_0 b_2 + 2c^2\gamma\delta\varepsilon^2 a_2 b_0 b_2 + 2\gamma\delta\varepsilon\mu^2 a_2 b_0 b_2\\
&- 4\gamma\delta\varepsilon\mu a_2 b_1 b_2 - b^2\gamma\delta\varepsilon a_0 b_2^2 + c^2\gamma\delta\varepsilon^2 a_0 b_2^2\\
&+ \gamma\delta\varepsilon\mu^2 a_0 b_2^2 - 2\gamma\delta\varepsilon\mu a_1 b_2^2 = 0,\\
\phi\psi^2 :& -2b^2\mathrm{k}^2\varepsilon\sigma a_2 + 2c^2 k^2\varepsilon^2\sigma a_2 + 2k^2\varepsilon\mu^2\sigma a_2\\
&+ 3\delta a_1^2 a_2 - b^2\delta\varepsilon a_2^3 + c^2\delta\varepsilon^2 a_2^3 + \delta\varepsilon\mu^2 a_2^3 + \gamma\delta a_2 b_1^2\\
&+ 2\gamma\delta a_1 b_1 b_2 - b^2\gamma\delta\varepsilon a_2 b_2^2 + c^2\gamma\delta\varepsilon^2 a_2 b_2^2\\
&+ \gamma\delta\varepsilon\mu^2 a_2 b_2^2 = 0,\\
\psi^3 :& -2b^2 k^2\varepsilon\sigma a_1 + 2c^2 k^2\varepsilon^2\sigma a_1 + 2k^2\varepsilon\mu^2\sigma a_1\\
&+ \delta a_1^3 - 3b^2\delta\varepsilon a_1 a_2^2 + 3c^2\delta\varepsilon^2 a_1 a_2^2 + 3\delta\varepsilon\mu^2 a_1 a_2^2\\
&+ \gamma\delta a_1 b_1^2 - 2b^2\gamma\delta\varepsilon a_2 b_1 b_2 + 2c^2\gamma\delta\varepsilon^2 a_2 b_1 b_2\\
&+ 2\gamma\delta\varepsilon\mu^2 a_2 b_1 b_2 - b^2\gamma\delta\varepsilon a_1 b_2^2 + c^2\gamma\delta\varepsilon^2 a_1 b_2^2\\
&+ \gamma\delta\varepsilon\mu^2 a_1 b_2^2 = 0,\\
\psi^0 :& -c2b_0 + \gamma\delta a_0^2 b_0 + \gamma\delta\varepsilon a_2^2 b_0 + \delta b_0^3 + 2\gamma\delta\varepsilon a_0 a_2 b_2\\
&+ 3\delta\varepsilon b_0 b_2^2 + \rho b_0 k_2 - \sigma b_0 k_2^2 = 0,\\
\phi :& 2\gamma\delta a_0 a_2 b_0 - c2b_2 + \gamma\delta a_0^2 b_2 + \gamma\delta\varepsilon a_2^2 b_2 + 3\delta b_0^2 b_2\\
&+ \delta\varepsilon b_2^3 + \rho b_2 k_2 - \sigma b_2 k_2^2 = 0,\\
\psi :& 2\gamma\delta a_0 a_1 b_0 - 2\gamma\delta\varepsilon\mu a_2^2 b_0 - c2b_1 + k^2\varepsilon\sigma b_1 + \gamma\delta a_0^2 b_1\\
&+ \gamma\delta\varepsilon a_2^2 b_1 + 3\delta b_0^2 b_1 - 4\gamma\delta\varepsilon\mu a_0 a_2 b_2 + 2\gamma\delta\varepsilon a_1 a_2 b_2\\
&- 6\delta\varepsilon\mu b_0 b_2^2 + 3\delta\varepsilon b_1 b_2^2 + \rho b_1 k_2 - \sigma b_1 k_2^2 = 0,\\
\phi\psi :& 2\gamma\delta a_1 a_2 b_0 + 2\gamma\delta a_0 a_2 b_1 - k^2\varepsilon\mu\sigma b_2 + 2\gamma\delta a_0 a_1 b_2\\
&- 2\gamma\delta\varepsilon\mu a_2^2 b_2 + 6\delta b_0 b_1 b_2 - 2\delta\varepsilon\mu b_2^3 = 0,\\
\psi^2 :& \gamma\delta a_1^2 b_0 - b^2\gamma\delta\varepsilon a_2^2 b_0 + c^2\gamma\delta\varepsilon^2 a_2^2 b_0 + \gamma\delta\varepsilon\mu^2 a_2^2 b_0\\
&- 3k^2\varepsilon\mu\sigma b_1 + 2\gamma\delta a_0 a_1 b_1 - 2\gamma\delta\varepsilon\mu a_2^2 b_1 + 3\delta b_0 b_1^2\\
&- 2b^2\gamma\delta\varepsilon a_0 a_2 b_2 + 2c^2\gamma\delta\varepsilon^2 a_0 a_2 b_2 + 2\gamma\delta\varepsilon\mu^2 a_0 a_2 b_2\\
&- 4\gamma\delta\varepsilon\mu a_1 a_2 b_2 - 3b^2\delta\varepsilon b_0 b_2^2 + 3c^2\delta\varepsilon^2 b_0 b_2^2\\
&+ 3\delta\varepsilon\mu^2 b_0 b_2^2 - 6\delta\varepsilon\mu b_1 b_2^2 = 0,\\
\phi\psi^2 :& 2\gamma\delta a_1 a_2 b_1 - 2b^2 k^2\varepsilon\sigma b_2 + 2c^2 k^2\varepsilon^2\sigma b_2 + 2k^2\varepsilon\mu^2\sigma b_2\\
&+ \gamma\delta a_1^2 b_2 - b^2\gamma\delta\varepsilon a_2^2 b_2 + c^2\gamma\delta\varepsilon^2 a_2^2 b_2 + \gamma\delta\varepsilon\mu^2 a_2^2 b_2\\
&+ 3\delta b_1^2 b_2 - b^2\delta\varepsilon b_2^3 + c^2\delta\varepsilon^2 b_2^3 + \delta\varepsilon\mu^2 b_2^3 = 0,\\
\psi^3 :& -2b^2 k^2\varepsilon\sigma b_1 + 2c^2 k^2\varepsilon^2\sigma b_1 + 2k^2\varepsilon\mu^2\sigma b_1 + \gamma\delta a_1^2 b_1\\
&- b^2\gamma\delta\varepsilon a_2^2 b_1 + c^2\gamma\delta\varepsilon^2 a_2^2 b_1 + \gamma\delta\varepsilon\mu^2 a_2^2 b_1 + \delta b_1^3\\
&- 2b^2\gamma\delta\varepsilon a_1 a_2 b_2 + 2c^2\gamma\delta\varepsilon^2 a_1 a_2 b_2 + 2\gamma\delta\varepsilon\mu^2 a_1 a_2 b_2\\
&- 3b^2\delta\varepsilon b_1 b_2^2 + 3c^2\delta\varepsilon^2 b_1 b_2^2 + 3\delta\varepsilon\mu^2 b_1 b_2^2 = 0.
\end{aligned}
\tag{21}
$$

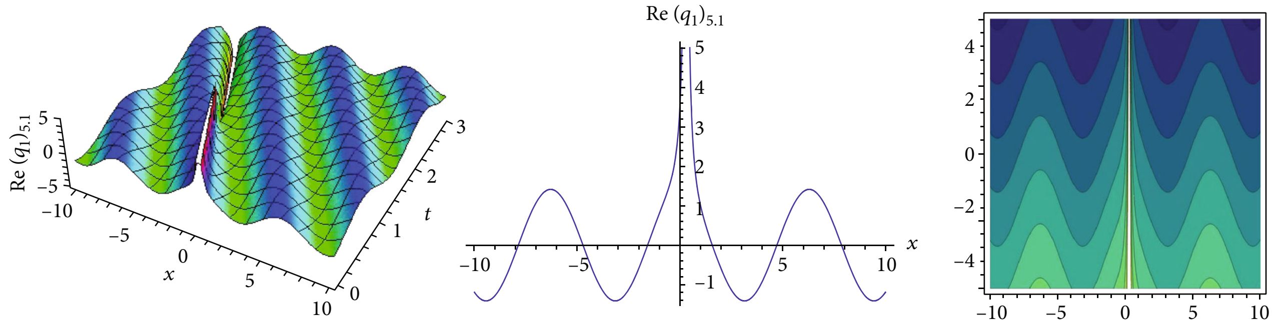

FIGURE 9: The 3D plot, 2D plot, and contour plot of the singular wave pulse Re $(q_1)_{5.1}$.

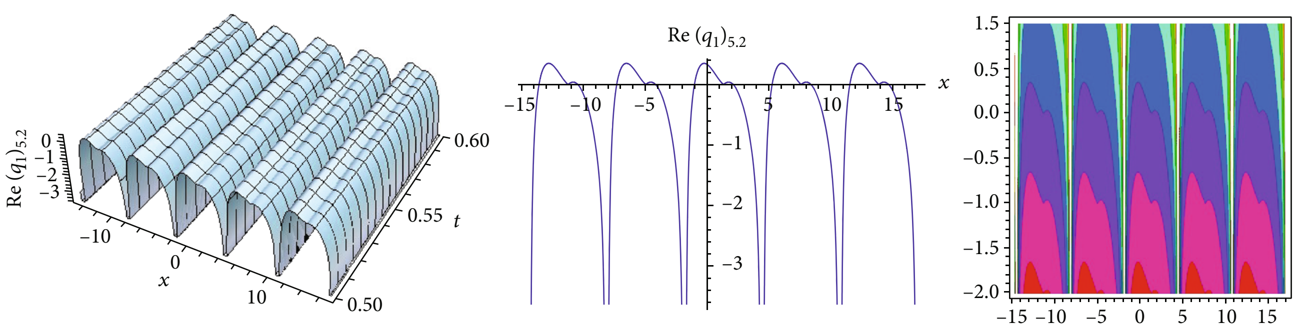

FIGURE 10: The 3D plot, 2D plot, and contour plot of the singular periodic wave pulse Re $(q_1)_{5.2}$.

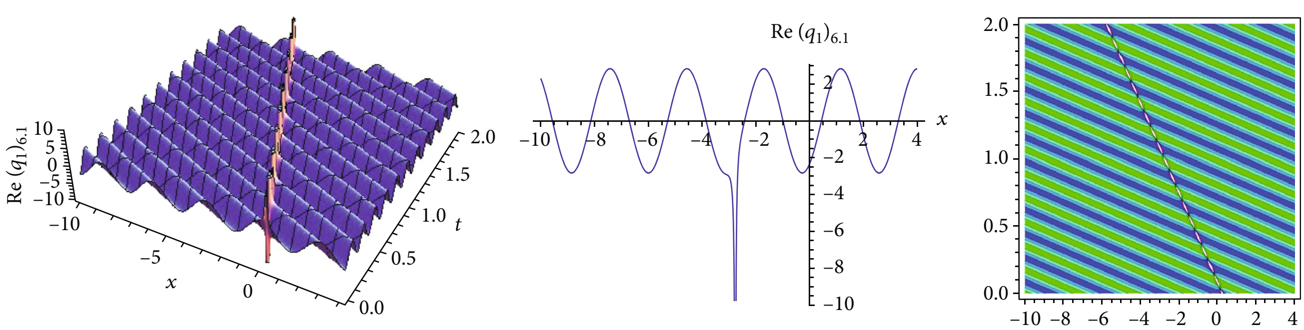

FIGURE 11: The 3D plot, 2D plot, and contour plot of Re $(q_1)_{6.1}$.

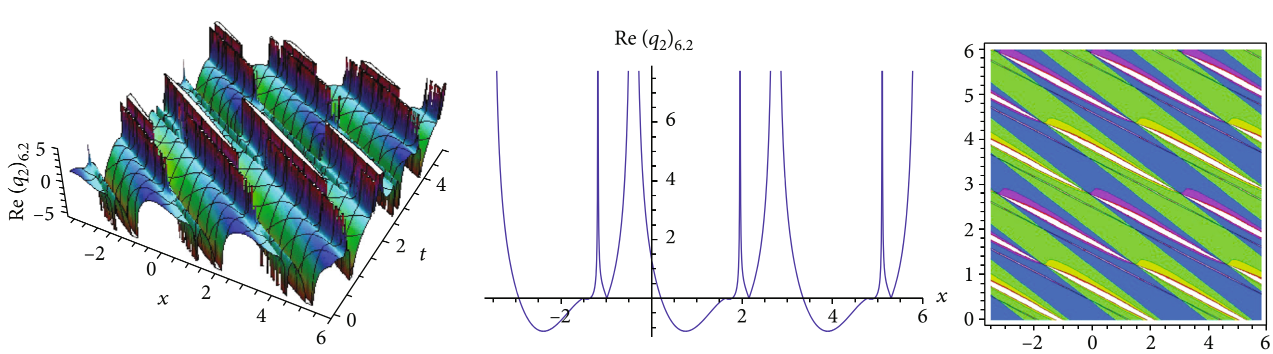

FIGURE 12: The 3D plot, 2D plot, and contour plot of Re $(q_2)_{6.2}$.

Solving the AEs along with (16) and (17) results in the following solutions:

Family 3 ($\varepsilon = 1$). In this situation, we produce the following solutions of the above AEs.

Case 1.

$$\begin{aligned} &a_0 = a_1 = b_0 = b_1 = 0,\\ &a_2 = \pm k\sqrt{\frac{-\sigma}{2\delta(\gamma+1)}},\\ &b_2 = \pm k\sqrt{\frac{-\sigma}{2\delta(\gamma+1)}},\\ &b = \sqrt{c^2+\mu^2},\\ &c_1 = -\frac{1}{2}k^2\sigma - k_1\rho - k_1^2\sigma,\\ &c_2 = -\frac{1}{2}k^2\sigma + k_2\rho - k_2^2\sigma. \end{aligned} \tag{22}$$

From Equations (9), (16), (17), and (20), we deduce the traveling wave solutions of Equation (1) as follows:

$$\begin{aligned} (q_1)_1 &= \pm k\sqrt{\frac{-\sigma}{2\delta(\gamma+1)}}\frac{\sqrt{c^2+\mu^2}\sinh\xi_1 + c\cosh\xi_1}{\sqrt{c^2+\mu^2}\cosh\xi_1 + c\sinh\xi_1 + \mu}e^{i\eta_{1.1}},\\ (q_2)_1 &= \pm k\sqrt{\frac{-\sigma}{2\delta(\gamma+1)}}\frac{\sqrt{c^2+\mu^2}\sinh\xi_1 + c\cosh\xi_1}{\sqrt{c^2+\mu^2}\cosh\xi_1 + c\sinh\xi_1 + \mu}e^{i\eta_{2.1}},\\ \xi_1 &= \frac{k\Gamma(\gamma_1+1)}{\beta}x^\beta - \frac{\sigma k(k_1+k_2)\Gamma(\gamma_2+1)}{\alpha}t^\alpha,\\ \eta_{1.1} &= \frac{k_1\Gamma(\gamma_1+1)}{\beta}x^\beta - \left(\frac{1}{2}k^2\sigma + k_1\rho + k_1^2\sigma\right)\frac{\Gamma(\gamma_2+1)}{\alpha}t^\alpha,\\ \eta_{2.1} &= \frac{k_2\Gamma(\gamma_1+1)}{\beta}x^\beta - \left(\frac{1}{2}k^2\sigma - k_2\rho + k_2^2\sigma\right)\frac{\Gamma(\gamma_2+1)}{\alpha}t^\alpha. \end{aligned} \tag{23}$$

Selecting the following parameters in $(q_1)_1$, we can get some graphical simulation in Figures 1 and 2.

$$\begin{aligned} &k = \alpha = \beta = \gamma = 1,\\ &\sigma = -4,\\ &\delta = 1,\\ &c = 3,\\ &\mu = 4,\\ &b = 5,\\ &k_1 = 0.5,\\ &k_2 = 1.5,\\ &\rho = 4. \end{aligned} \tag{24}$$

Case 2.

$$\begin{aligned} &a_0 = b_0 = a_2 = b_2 = 0,\\ &a_1 = \pm k\sqrt{\frac{2\sigma(b^2-c^2)}{\delta(\gamma+1)}},\\ &b_1 = \pm k\sqrt{\frac{2\sigma(b^2-c^2)(1-\gamma)}{\delta}},\\ &c_1 = k^2\sigma - k_1^2\sigma - k_1\rho,\\ &c_2 = k^2\sigma - k_2^2\sigma + k_2\rho. \end{aligned} \tag{25}$$

From Case 2, we get the following traveling wave solution of Equation (1):

$$\begin{aligned} (q_1)_2 &= \frac{\pm k\sqrt{2\sigma(b^2-c^2)/\delta(\gamma+1)}e^{i\eta_{1.2}}}{b\cosh\xi_2 + c\sinh\xi_2 + \mu},\\ (q_2)_2 &= \frac{\pm k\sqrt{2\sigma(b^2-c^2)(1-\gamma)/\delta}e^{i\eta_{2.2}}}{b\cosh\xi_2 + c\sinh\xi_2 + \mu},\\ \xi_2 &= \frac{k\Gamma(\gamma_1+1)}{\beta}x^\beta - \sigma k(k_1+k_2)\frac{\Gamma(\gamma_2+1)}{\alpha}t^\alpha,\\ \eta_{1.2} &= \frac{k_1\Gamma(\gamma_1+1)}{\beta}x^\beta + \left(k^2\sigma - k_1^2\sigma - k_1\rho\right)\frac{\Gamma(\gamma_2+1)}{\alpha}t^\alpha,\\ \eta_{2.2} &= \frac{k_2\Gamma(\gamma_1+1)}{\beta}x^\beta + \left(k^2\sigma - k_2^2\sigma + k_2\rho\right)\frac{\Gamma(\gamma_2+1)}{\alpha}t^\alpha. \end{aligned} \tag{26}$$

In this result, we can deduce the traveling wave solution of Equation (1) as follows:

$$\begin{aligned} (q_1)_{2.1} &= \pm k\sqrt{\frac{2\sigma}{\delta(\gamma+1)}}\operatorname{sech}\xi_2 e^{i\eta_{1.2}},\\ (q_2)_{2.1} &= \pm k\sqrt{\frac{2\sigma(1-\gamma)}{\delta}}\operatorname{sech}\xi_2 e^{i\eta_{2.2}},\\ \mu &= c = 0,\\ (q_1)_{2.2} &= \pm k\sqrt{\frac{-2\sigma}{\delta(\gamma+1)}}\operatorname{csch}\xi_2 e^{i\eta_{1.2}},\\ (q_2)_{2.2} &= \pm k\sqrt{\frac{-2\sigma(1-\gamma)}{\delta}}\operatorname{csch}\xi_2 e^{i\eta_{2.2}},\\ \mu &= b = 0. \end{aligned} \tag{27}$$

Selecting $k = k_1 = 1$, $k_2 = 2$, $\delta = 1$, $\rho = -1$, $\alpha = \beta = 1$, $\gamma = \gamma_1 = \gamma_2 = 1$, and $\sigma = 1$ in $(q_1)_{2.1}$ and $\sigma = -1$ in $(q_1)_{2.2}$, we obtain the famous bell-shape soliton solutions and blow-up solution which is simulated in Figures 3 and 4.

Remark 4. If we let $\alpha=\beta=1$, $\rho=\lambda/2$, $\sigma=1/2$, and $\delta=1$, the solutions $(q_1)_{2.1}$, $(q_2)_{2.1}$ and $(q_1)_{2.2}$, $(q_2)_{2.2}$ contain solutions (8) and (14) in Refs. [48].

Family 5 ($\varepsilon=-1$). In this situation, we produce the following solutions of the above AEs.

Case 3.

$$\begin{aligned} &a_0=a_1=b_0=b_1=0,\\ &a_2=-k\sqrt{\frac{-\sigma}{2\delta(\gamma+1)}},\\ &b_2=-k\sqrt{\frac{-\sigma}{2\delta(\gamma+1)}},\\ &\mu=\sqrt{c^2+b^2},\\ &c_1=\frac{1}{2}k^2\sigma-k_1\rho-k_1^2\sigma,\\ &c_2=\frac{1}{2}k^2\sigma+k_2\rho-k_2^2\sigma. \end{aligned} \tag{28}$$

From Equations (10), (16), (17), and (20), we can deduce the following periodic solutions of Equation (1):

$$\begin{aligned} (q_1)_3&=\frac{k\sqrt{-\sigma/2\delta(\gamma+1)}(b\sin\xi_3-c\cos\xi_3)e^{i\eta_{1.3}}}{b\cos\xi_3+c\sin\xi_3+\sqrt{c^2+b^2}},\\ (q_2)_3&=\frac{k\sqrt{-\sigma/2\delta(\gamma+1)}(b\sin\xi_3-c\cos\xi_3)e^{i\eta_{2.3}}}{b\cos\xi_3+c\sin\xi_3+\sqrt{c^2+b^2}},\\ \xi_3&=\frac{k\Gamma(\gamma_1+1)}{\beta}x^\beta-\sigma k(k_1+k_2)\frac{\Gamma(\gamma_2+1)}{\alpha}t^\alpha,\\ \eta_{1.3}&=\frac{k_1\Gamma(\gamma_1+1)}{\beta}x^\beta+\left(\frac{1}{2}k^2\sigma-k_1\rho-k_1^2\sigma\right)\frac{\Gamma(\gamma_2+1)}{\alpha}t^\alpha,\\ \eta_{2.3}&=\frac{k_2\Gamma(\gamma_1+1)}{\beta}x^\beta+\left(\frac{1}{2}k^2\sigma+k_2\rho-k_2^2\sigma\right)\frac{\Gamma(\gamma_2+1)}{\alpha}t^\alpha. \end{aligned} \tag{29}$$

If we select the following parameters, the periodic pulse solutions can be simulated in Figures 5 and 6.

$$\begin{aligned} &k=\alpha=\beta=\gamma=\rho=1,\\ &\sigma=-0.5,\\ &\delta=2,\\ &c=4,\\ &\mu=5,\\ &b=3,\\ &k_1=\frac{1}{6},\\ &k_2=\frac{1}{3},\\ &\rho=1. \end{aligned} \tag{30}$$

Case 4.

$$\begin{aligned} &a_0=a_2=b_0=b_2=0,\\ &a_1=\pm k\sqrt{\frac{-2\sigma(b^2+c^2)}{\delta(\gamma+1)}},\\ &b_1=\pm k\sqrt{\frac{-2\sigma(b^2+c^2)}{\delta(\gamma+1)}},\\ &\mu=0,\\ &c_1=-k^2\sigma-k_1^2\sigma-k_1\rho,\\ &c_2=-k^2\sigma-k_2^2\sigma+k_2\rho. \end{aligned} \tag{31}$$

In this result, we have

$$\begin{aligned} (q_1)_4&=\frac{\pm k\sqrt{-2\sigma(b^2+c^2)/\delta(\gamma+1)}}{b\cos\xi_4+c\sin\xi_4}e^{i\eta_{1.4}},\\ (q_2)_4&=\frac{\pm k\sqrt{-2\sigma(b^2+c^2)/\delta(\gamma+1)}}{b\cos\xi_4+c\sin\xi_4}e^{i\eta_{2.4}},\\ \xi_4&=\frac{k\Gamma(\gamma_1+1)}{\beta}x^\beta-\sigma k(k_1+k_2)\frac{\Gamma(\gamma_2+1)}{\alpha}t^\alpha,\\ \eta_{1.4}&=\frac{k_1\Gamma(\gamma_1+1)}{\beta}x^\beta-\left(k^2\sigma+k_1^2\sigma+k_1\rho\right)\frac{\Gamma(\gamma_2+1)}{\alpha}t^\alpha,\\ \eta_{2.4}&=\frac{k_2\Gamma(\gamma_1+1)}{\beta}x^\beta-\left(k^2\sigma+k_2^2\sigma-k_2\rho\right)\frac{\Gamma(\gamma_2+1)}{\alpha}t^\alpha. \end{aligned} \tag{32}$$

Thus,

$$\begin{aligned} &(q_1)_{4.1}=\pm k\sqrt{\frac{-2\sigma}{\delta(\gamma+1)}}\sec\xi_4 e^{i\eta_{1.4}},\\ &(q_2)_{4.1}=\pm k\sqrt{\frac{-2\sigma}{\delta(\gamma+1)}}\sec\xi_4 e^{i\eta_{2.4}},\\ &c=0,\\ &(q_1)_{4.2}=\pm k\sqrt{\frac{-2\sigma}{\delta(\gamma+1)}}\csc\xi_4 e^{i\eta_{1.4}},\\ &(q_2)_{4.2}=\pm k\sqrt{\frac{-2\sigma}{\delta(\gamma+1)}}\csc\xi_4 e^{i\eta_{2.4}},\\ &b=0. \end{aligned} \tag{33}$$

The singular trigonometric function solutions $(q_1)_4$ can be simulated in Figures 7 and 8 by selecting $k=\alpha=\beta=\gamma=\gamma_1=\gamma_2=1$, $\sigma=-1$, $\delta=25$, $c=4$, $b=3$, $k_1=1/3$, $k_2=2/3$, $\rho=1/3$, and $t=1$ in $(q_1)_4$ and $k=1$, $\sigma=-1$, $\delta=1$, $k_1=1$, $k_2=2$, $\rho=1$, $\beta=1$, $\alpha=1$, $\gamma=1$, $\gamma_1=2$, and $\gamma_2=2$ in $(q_1)_{4.1}$.

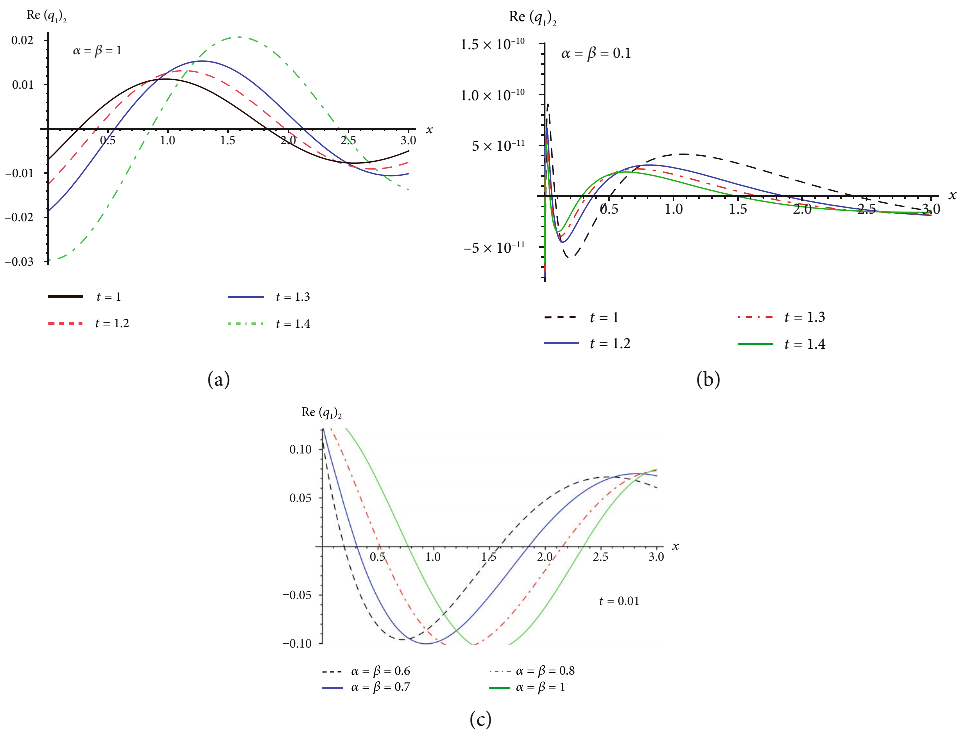

Figure 13: The changes of Re $(q_1)_2$ for the different values of a, β and t.

In the following, let us consider the $G'/bG'+G+a$ method; we assume that Equation (18) has the following solutions:

$$\begin{cases} u(\xi)=a_0+a_1F+a_{-1}F^{-1}=a_0+a_1\dfrac{G'}{bG'+G+a}+a_{-1}\left(\dfrac{G'}{bG'+G+a}\right)^{-1}, \\ v(\xi)=b_0+b_1F+b_{-1}F^{-1}=b_0+b_1\dfrac{G'}{bG'+G+a}+b_{-1}\left(\dfrac{G'}{bG'+G+a}\right)^{-1}. \end{cases} \tag{34}$$

Substituting Equations (34) and (13) into Equation (18), without loss of generality, we chose $b=1$ here, and set the coefficients of F^i to zero to yield the following AEs:

$$\begin{aligned} F^0 :& k^2\lambda\sigma a_{-1}-k^2\lambda^2\sigma a_{-1}-2k^2\mu\sigma a_{-1}+3k^2\lambda\mu\sigma a_{-1} \\ &-2k^2\mu^2\sigma a_{-1}+\delta a_0^3+k^2\lambda\mu\sigma a_1-2k^2\mu^2\sigma a_1+6\delta a_{-1}a_0a_1 \\ &+2\gamma\delta a_1b_{-1}b_0+\gamma\delta a_0b_0^2+2\gamma\delta a_0b_{-1}b_1+2\gamma\delta a_{-1}b_0b_1 \\ &-a_0c_1-\rho a_0k_1-\sigma a_0k_1^2=0, \end{aligned}$$

$$\begin{aligned} F^1 :& k^2\lambda^2\sigma a_1+2k^2\mu\sigma a_1-6k^2\lambda\mu\sigma a_1+6k^2\mu^2\sigma a_1+3\delta a_0^2a_1 \\ &+3\delta a_{-1}a_1^2+\gamma\delta a_1b_0^2+2\gamma\delta a_1b_{-1}b_1+2\gamma\delta a_0b_0b_1 \\ &+\gamma\delta a_{-1}b_1^2-a_1c_1-\rho a_1k_1-\sigma a_1k_1^2=0, \end{aligned}$$

$$\begin{aligned} F^2 :& 3k^2\lambda\sigma a_1-3k^2\lambda^2\sigma a_1-6k^2\mu\sigma a_1+9k^2\lambda\mu\sigma a_1-6k^2\mu^2\sigma a_1 \\ &+3\delta a_0a_1^2+2\gamma\delta a_1b_0b_1+\gamma\delta a_0b_1^2=0, \end{aligned}$$

$$\begin{aligned} F^3 :& 2k^2\sigma a_1-4k^2\lambda\sigma a_1+2k^2\lambda^2\sigma a_1+4k^2\mu\sigma a_1-4k^2\lambda\mu\sigma a_1 \\ &+2k^2\mu^2\sigma a_1+\delta a_1^3+\gamma\delta a_1b_1^2=0, \end{aligned}$$

$$\begin{aligned} F^{-1} :& k^2\lambda^2\sigma a_{-1}+2k^2\mu\sigma a_{-1}-6k^2\lambda\mu\sigma a_{-1}+6k^2\mu^2\sigma a_{-1} \\ &+3\delta a_{-1}a_0^2+3\delta a_{-1}^2a_1+\gamma\delta a_1b_{-1}^2+2\gamma\delta a_0b_{-1}b_0 \\ &+\gamma\delta a_{-1}b_0^2+2\gamma\delta a_{-1}b_{-1}b_1-a_{-1}c_1-\rho a_{-1}k_1-\sigma a_{-1}k_1^2=0, \end{aligned}$$

$$\begin{aligned} F^{-2} :& 3k^2\lambda\mu\sigma a_{-1}-6k^2\mu^2\sigma a_{-1}+3\delta a_{-1}^2a_0+\gamma\delta a_0b_{-1}^2 \\ &+2\gamma\delta a_{-1}b_{-1}b_0=0, \end{aligned}$$

$$F^{-3} : 2k^2\mu^2\sigma a_{-1}+\delta a_{-1}^3+\gamma\delta a_{-1}b_{-1}^2=0,$$

$$\begin{aligned} F^0 :& k^2\lambda\sigma b_{-1}-k^2\lambda^2\sigma b_{-1}-2k^2\mu\sigma b_{-1}+3k^2\lambda\mu\sigma b_{-1} \\ &-2k^2\mu^2\sigma b_{-1}+2\gamma\delta a_0a_1b_{-1}+\gamma\delta a_0^2b_0+2\gamma\delta a_{-1}a_1b_0 \\ &+\delta b_0^3+k^2\lambda\mu\sigma b_1-2k^2\mu^2\sigma b_1+2\gamma\delta a_{-1}a_0b_1+6\delta b_{-1}b_0b_1 \\ &-b_0c_2+\rho b_0k_2-\sigma b_0k_2^2=0, \end{aligned}$$

$$\begin{aligned} F^1 :& \gamma\delta a_1^2b_{-1}+2\gamma\delta a_0a_1b_0+k^2\lambda^2\sigma b_1+2k^2\mu\sigma b_1-6k^2\lambda\mu\sigma b_1 \\ &+6k^2\mu^2\sigma b_1+\gamma\delta a_0^2b_1+2\gamma\delta a_{-1}a_1b_1+3\delta b_0^2b_1+3\delta b_{-1}b_1^2 \\ &-b_1c_2+\rho b_1k_2-\sigma b_1k_2^2=0, \end{aligned}$$

$$\begin{aligned} F^2 :& \gamma\delta a_1^2b_0+3k^2\lambda\sigma b_1-3k^2\lambda^2\sigma b_1-6k^2\mu\sigma b_1+9k^2\lambda\mu\sigma b_1 \\ &-6k^2\mu^2\sigma b_1+2\gamma\delta a_0a_1b_1+3\delta b_0b_1^2=0, \end{aligned}$$

$$F^3: 2k^2\sigma b_1 - 4k^2\lambda\sigma b_1 + 2k^2\lambda^2\sigma b_1 + 4k^2\mu\sigma b_1 - 4k^2\lambda\mu\sigma b_1 + 2k^2\mu^2\sigma b_1 + \gamma\delta a_1^2 b_1 + \delta b_1^3 = 0,$$

$$F^{-1}: k^2\lambda^2\sigma b_{-1} + 2k^2\mu\sigma b_{-1} - 6k^2\lambda\mu\sigma b_{-1} + 6k^2\mu^2\sigma b_{-1} + \gamma\delta a_0^2 b_{-1} + 2\gamma\delta a_{-1}a_1 b_{-1} + 2\gamma\delta a_{-1}a_0 b_0 + 3\delta b_{-1}b_0^2 + \gamma\delta a_{-1}^2 b_1 + 3\delta b_{-1}^2 b_1 - b_{-1}c_2 + \rho b_{-1}k_2 - \sigma b_{-1}k_2^2 = 0,$$

$$F^{-2}: 3k^2\lambda\mu\sigma b_{-1} - 6k^2\mu^2\sigma b_{-1} + 2\gamma\delta a_{-1}a_0 b_{-1} + \gamma\delta a_{-1}^2 b_0 + 3\delta b_{-1}^2 b_0 = 0,$$

$$F^{-3}: 2k^2\mu^2\sigma b_{-1} + \gamma\delta a_{-1}^2 b_{-1} + \delta b_{-1}^3 = 0,$$

$$F^0: k^2\lambda\sigma a_{-1} - k^2\lambda^2\sigma a_{-1} - 2k^2\mu\sigma a_{-1} + 3k^2\lambda\mu\sigma a_{-1} - 2k^2\mu^2\sigma a_{-1} + \delta a_0^3 + k^2\lambda\mu\sigma a_1 - 2k^2\mu^2\sigma a_1 + 6\delta a_{-1}a_0 a_1 + 2\gamma\delta a_1 b_{-1}b_0 + \gamma\delta a_0 b_0^2 + 2\gamma\delta a_0 b_{-1}b_1 + 2\gamma\delta a_{-1}b_0 b_1 - a_0 c_1 - \rho a_0 k_1 - \sigma a_0 k_1^2 = 0,$$

$$F^1: k^2\lambda^2\sigma a_1 + 2k^2\mu\sigma a_1 - 6k^2\lambda\mu\sigma a_1 + 6k^2\mu^2\sigma a_1 + 3\delta a_0^2 a_1 + 3\delta a_{-1}a_1^2 + \gamma\delta a_1 b_0^2 + 2\gamma\delta a_1 b_{-1}b_1 + 2\gamma\delta a_0 b_0 b_1 + \gamma\delta a_{-1}b_1^2 - a_1 c_1 - \rho a_1 k_1 - \sigma a_1 k_1^2 = 0,$$

$$F^2: 3k^2\lambda\sigma a_1 - 3k^2\lambda^2\sigma a_1 - 6k^2\mu\sigma a_1 + 9k^2\lambda\mu\sigma a_1 - 6k^2\mu^2\sigma a_1 + 3\delta a_0 a_1^2 + 2\gamma\delta a_1 b_0 b_1 + \gamma\delta a_0 b_1^2 = 0,$$

$$F^3: 2k^2\sigma a_1 - 4k^2\lambda\sigma a_1 + 2k^2\lambda^2\sigma a_1 + 4k^2\mu\sigma a_1 - 4k^2\lambda\mu\sigma a_1 + 2k^2\mu^2\sigma a_1 + \delta a_1^3 + \gamma\delta a_1 b_1^2 = 0,$$

$$F^{-1}: k^2\lambda^2\sigma a_{-1} + 2k^2\mu\sigma a_{-1} - 6k^2\lambda\mu\sigma a_{-1} + 6k^2\mu^2\sigma a_{-1} + 3\delta a_{-1}a_0^2 + 3\delta a_{-1}^2 a_1 + \gamma\delta a_1 b_{-1}^2 + 2\gamma\delta a_0 b_{-1}b_0 + \gamma\delta a_{-1}b_0^2 + 2\gamma\delta a_{-1}b_{-1}b_1 - a_{-1}c_1 - \rho a_{-1}k_1 - \sigma a_{-1}k_1^2 = 0,$$

$$F^{-2}: 3k^2\lambda\mu\sigma a_{-1} - 6k^2\mu^2\sigma a_{-1} + 3\delta a_{-1}^2 a_0 + \gamma\delta a_0 b_{-1}^2 + 2\gamma\delta a_{-1}b_{-1}b_0 = 0,$$

$$F^{-3}: 2k^2\mu^2\sigma a_{-1} + \delta a_{-1}^3 + \gamma\delta a_{-1}b_{-1}^2 = 0,$$

$$F^0: k^2\lambda\sigma b_{-1} - k^2\lambda^2\sigma b_{-1} - 2k^2\mu\sigma b_{-1} + 3k^2\lambda\mu\sigma b_{-1} - 2k^2\mu^2\sigma b_{-1} + 2\gamma\delta a_0 a_1 b_{-1} + \gamma\delta a_0^2 b_0 + 2\gamma\delta a_{-1}a_1 b_0 + \delta b_0^3 + k^2\lambda\mu\sigma b_1 - 2k^2\mu^2\sigma b_1 + 2\gamma\delta a_{-1}a_0 b_1 + 6\delta b_{-1}b_0 b_1 - b_0 c_2 + \rho b_0 k_2 - \sigma b_0 k_2^2 = 0,$$

$$F^1: \gamma\delta a_1^2 b_{-1} + 2\gamma\delta a_0 a_1 b_0 + k^2\lambda^2\sigma b_1 + 2k^2\mu\sigma b_1 - 6k^2\lambda\mu\sigma b_1 + 6k^2\mu^2\sigma b_1 + \gamma\delta a_0^2 b_1 + 2\gamma\delta a_{-1}a_1 b_1 + 3\delta b_0^2 b_1 + 3\delta b_{-1}b_1^2 - b_1 c_2 + \rho b_1 k_2 - \sigma b_1 k_2^2 = 0,$$

$$F^2: \gamma\delta a_1^2 b_0 + 3k^2\lambda\sigma b_1 - 3k^2\lambda^2\sigma b_1 - 6k^2\mu\sigma b_1 + 9k^2\lambda\mu\sigma b_1 - 6k^2\mu^2\sigma b_1 + 2\gamma\delta a_0 a_1 b_1 + 3\delta b_0 b_1^2 = 0,$$

$$F^3: 2k^2\sigma b_1 - 4k^2\lambda\sigma b_1 + 2k^2\lambda^2\sigma b_1 + 4k^2\mu\sigma b_1 - 4k^2\lambda\mu\sigma b_1 + 2k^2\mu^2\sigma b_1 + \gamma\delta a_1^2 b_1 + \delta b_1^3 = 0,$$

$$F^{-1}: k^2\lambda^2\sigma b_{-1} + 2k^2\mu\sigma b_{-1} - 6k^2\lambda\mu\sigma b_{-1} + 6k^2\mu^2\sigma b_{-1} + \gamma\delta a_0^2 b_{-1} + 2\gamma\delta a_{-1}a_1 b_{-1} + 2\gamma\delta a_{-1}a_0 b_0 + 3\delta b_{-1}b_0^2 + \gamma\delta a_{-1}^2 b_1 + 3\delta b_{-1}^2 b_1 - b_{-1}c_2 + \rho b_{-1}k_2 - \sigma b_{-1}k_2^2 = 0,$$

$$F^{-2}: 3k^2\lambda\mu\sigma b_{-1} - 6k^2\mu^2\sigma b_{-1} + 2\gamma\delta a_{-1}a_0 b_{-1} + \gamma\delta a_{-1}^2 b_0 + 3\delta b_{-1}^2 b_0 = 0,$$

$$F^{-3}: 2k^2\mu^2\sigma b_{-1} + \gamma\delta a_{-1}^2 b_{-1} + \delta b_{-1}^3 = 0,$$

$$F^0: k^2\lambda\sigma a_{-1} - k^2\lambda^2\sigma a_{-1} - 2k^2\mu\sigma a_{-1} + 3k^2\lambda\mu\sigma a_{-1} - 2k^2\mu^2\sigma a_{-1} + \delta a_0^3 + k^2\lambda\mu\sigma a_1 - 2k^2\mu^2\sigma a_1 + 6\delta a_{-1}a_0 a_1 + 2\gamma\delta a_1 b_{-1}b_0 + \gamma\delta a_0 b_0^2 + 2\gamma\delta a_0 b_{-1}b_1 + 2\gamma\delta a_{-1}b_0 b_1 - a_0 c_1 - \rho a_0 k_1 - \sigma a_0 k_1^2 = 0,$$

$$F^1: k^2\lambda^2\sigma a_1 + 2k^2\mu\sigma a_1 - 6k^2\lambda\mu\sigma a_1 + 6k^2\mu^2\sigma a_1 + 3\delta a_0^2 a_1 + 3\delta a_{-1}a_1^2 + \gamma\delta a_1 b_0^2 + 2\gamma\delta a_1 b_{-1}b_1 + 2\gamma\delta a_0 b_0 b_1 + \gamma\delta a_{-1}b_1^2 - a_1 c_1 - \rho a_1 k_1 - \sigma a_1 k_1^2 = 0,$$

$$F^2: 3k^2\lambda\sigma a_1 - 3k^2\lambda^2\sigma a_1 - 6k^2\mu\sigma a_1 + 9k^2\lambda\mu\sigma a_1 - 6k^2\mu^2\sigma a_1 + 3\delta a_0 a_1^2 + 2\gamma\delta a_1 b_0 b_1 + \gamma\delta a_0 b_1^2 = 0,$$

$$F^3: 2k^2\sigma a_1 - 4k^2\lambda\sigma a_1 + 2k^2\lambda^2\sigma a_1 + 4k^2\mu\sigma a_1 - 4k^2\lambda\mu\sigma a_1 + 2k^2\mu^2\sigma a_1 + \delta a_1^3 + \gamma\delta a_1 b_1^2 = 0,$$

$$F^{-1}: k^2\lambda^2\sigma a_{-1} + 2k^2\mu\sigma a_{-1} - 6k^2\lambda\mu\sigma a_{-1} + 6k^2\mu^2\sigma a_{-1} + 3\delta a_{-1}a_0^2 + 3\delta a_{-1}^2 a_1 + \gamma\delta a_1 b_{-1}^2 + 2\gamma\delta a_0 b_{-1}b_0 + \gamma\delta a_{-1}b_0^2 + 2\gamma\delta a_{-1}b_{-1}b_1 - a_{-1}c_1 - \rho a_{-1}k_1 - \sigma a_{-1}k_1^2 = 0,$$

$$F^{-2}: 3k^2\lambda\mu\sigma a_{-1} - 6k^2\mu^2\sigma a_{-1} + 3\delta a_{-1}^2 a_0 + \gamma\delta a_0 b_{-1}^2 + 2\gamma\delta a_{-1}b_{-1}b_0 = 0,$$

$$F^{-3}: 2k^2\mu^2\sigma a_{-1} + \delta a_{-1}^3 + \gamma\delta a_{-1}b_{-1}^2 = 0,$$

$$F^0: k^2\lambda\sigma b_{-1} - k^2\lambda^2\sigma b_{-1} - 2k^2\mu\sigma b_{-1} + 3k^2\lambda\mu\sigma b_{-1} - 2k^2\mu^2\sigma b_{-1} + 2\gamma\delta a_0 a_1 b_{-1} + \gamma\delta a_0^2 b_0 + 2\gamma\delta a_{-1}a_1 b_0 + \delta b_0^3 + k^2\lambda\mu\sigma b_1 - 2k^2\mu^2\sigma b_1 + 2\gamma\delta a_{-1}a_0 b_1 + 6\delta b_{-1}b_0 b_1 - b_0 c_2 + \rho b_0 k_2 - \sigma b_0 k_2^2 = 0,$$

$$F^1: \gamma\delta a_1^2 b_{-1} + 2\gamma\delta a_0 a_1 b_0 + k^2\lambda^2\sigma b_1 + 2k^2\mu\sigma b_1 - 6k^2\lambda\mu\sigma b_1 + 6k^2\mu^2\sigma b_1 + \gamma\delta a_0^2 b_1 + 2\gamma\delta a_{-1}a_1 b_1 + 3\delta b_0^2 b_1 + 3\delta b_{-1} b_1^2 - b_1 c_2 + \rho b_1 k_2 - \sigma b_1 k_2^2 = 0,$$

$$F^2: \gamma\delta a_1^2 b_0 + 3k^2\lambda\sigma b_1 - 3k^2\lambda^2\sigma b_1 - 6k^2\mu\sigma b_1 + 9k^2\lambda\mu\sigma b_1 - 6k^2\mu^2\sigma b_1 + 2\gamma\delta a_0 a_1 b_1 + 3\delta b_0 b_1^2 = 0,$$

$$F^3: 2k^2\sigma b_1 - 4k^2\lambda\sigma b_1 + 2k^2\lambda^2\sigma b_1 + 4k^2\mu\sigma b_1 - 4k^2\lambda\mu\sigma b_1 + 2k^2\mu^2\sigma b_1 + \gamma\delta a_1^2 b_1 + \delta b_1^3 = 0,$$

$$F^{-1}: k^2\lambda^2\sigma b_{-1} + 2k^2\mu\sigma b_{-1} - 6k^2\lambda\mu\sigma b_{-1} + 6k^2\mu^2\sigma b_{-1} + \gamma\delta a_0^2 b_{-1} + 2\gamma\delta a_{-1}a_1 b_{-1} + 2\gamma\delta a_{-1}a_0 b_0 + 3\delta b_{-1} b_0^2 + \gamma\delta a_{-1}^2 b_1 + 3\delta b_{-1}^2 b_1 - b_{-1}c_2 + \rho b_{-1}k_2 - \sigma b_{-1}k_2^2 = 0,$$

$$F^{-2}: 3k^2\lambda\mu\sigma b_{-1} - 6k^2\mu^2\sigma b_{-1} + 2\gamma\delta a_{-1}a_0 b_{-1} + \gamma\delta a_{-1}^2 b_0 + 3\delta b_{-1}^2 b_0 = 0,$$

$$F^{-3}: 2k^2\mu^2\sigma b_{-1} + \gamma\delta a_{-1}^2 b_{-1} + \delta b_{-1}^3 = 0. \quad (35)$$

After solving the above equations, we have the following:

Case 5.

$$\begin{aligned} &a_0 = b_0 = a_{-1} = b_{-1} = 0,\\ &a_1 = \pm k(\mu-1)\sqrt{\frac{-2\sigma}{\delta(\gamma+1)}},\\ &b_1 = \pm k(\mu-1)\sqrt{\frac{-2\sigma}{\delta(\gamma+1)}},\\ &\lambda = 2\mu,\\ &c_1 = -2k^2(\mu-1)\mu\sigma - k_1\rho - k_1^2\sigma,\\ &c_2 = -2k^2(\mu-1)\mu\sigma + k_2\rho - k_2^2\sigma. \end{aligned} \quad (36)$$

From Case 5, we can determine the following solutions:

$$\begin{aligned}
(q_1)_{5.1} &= \frac{\pm k(\mu-1)\sqrt{-2\sigma/\delta(\gamma+1)}\left\{\left[2\mu(p_2-p_1)-\sqrt{\Delta}(p_2+p_1)\right]\sinh\left(\sqrt{\Delta}/2b\xi_5\right)+\left[2\mu(p_2+p_1)-\sqrt{\Delta}(p_2-p_1)\right]\cosh\left(\sqrt{\Delta}/2b\xi_5\right)\right\}}{b\left[2(\mu-1)(p_2-p_1)-\sqrt{\Delta}(p_2+p_1)\right]\sinh\left(\sqrt{\Delta}/2b\xi_5\right)+b\left[2(\mu-1)(p_2+p_1)-\sqrt{\Delta}(p_2-p_1)\right]\cosh\left(\sqrt{\Delta}/2b\xi_5\right)} e^{i\eta_{1.5}},\\
(q_2)_{5.1} &= \frac{\pm k(\mu-1)\sqrt{-2\sigma/\delta(\gamma+1)}\left\{\left[2\mu(p_2-p_1)-\sqrt{\Delta}(p_2+p_1)\right]\sinh\left(\sqrt{\Delta}/2b\xi_5\right)+\left[2\mu(p_2+p_1)-\sqrt{\Delta}(p_2-p_1)\right]\cosh\left(\sqrt{\Delta}/2b\xi_5\right)\right\}}{b\left[2(\mu-1)(p_2-p_1)-\sqrt{\Delta}(p_2+p_1)\right]\sinh\left(\sqrt{\Delta}/2b\xi_5\right)+b\left[2(\mu-1)(p_2+p_1)-\sqrt{\Delta}(p_2-p_1)\right]\cosh\left(\sqrt{\Delta}/2b\xi_5\right)} e^{i\eta_{2.5}},\\
(q_1)_{5.2} &= \frac{\pm k(\mu-1)\sqrt{-2\sigma/\delta(\gamma+1)}\left[\left(2\mu p_1-\sqrt{-\Delta}p_2\right)\cos\left(\sqrt{-\Delta}/2b\xi_5\right)+\left(2\mu p_2+\sqrt{-\Delta}p_1\right)\sin\left(\sqrt{-\Delta}/2b\xi_5\right)\right]}{b\left(2(\mu-1)p_1-\sqrt{-\Delta}p_2\right)\cos\left(\sqrt{-\Delta}/2b\xi_5\right)+b\left(2(\mu-1)p_2+\sqrt{-\Delta}p_1\right)\sin\left(\sqrt{-\Delta}/2b\xi_5\right)} e^{i\eta_{1.5}},\\
(q_2)_{5.2} &= \frac{\pm k(\mu-1)\sqrt{-2\sigma/\delta(\gamma+1)}\left[\left(2\mu p_1-\sqrt{-\Delta}p_2\right)\cos\left(\sqrt{-\Delta}/2b\xi_5\right)+\left(2\mu p_2+\sqrt{-\Delta}p_1\right)\sin\left(\sqrt{-\Delta}/2b\xi_5\right)\right]}{b\left(2(\mu-1)p_1-\sqrt{-\Delta}p_2\right)\cos\left(\sqrt{-\Delta}/2b\xi_5\right)+b\left(2(\mu-1)p_2+\sqrt{-\Delta}p_1\right)\sin\left(\sqrt{-\Delta}/2b\xi_5\right)} e^{i\eta_{2.5}},\\
\xi_5 &= \frac{k\Gamma(\gamma_1+1)}{\beta}x^\beta - \sigma k(k_1+k_2)\frac{\Gamma(\gamma_2+1)}{\alpha}t^\alpha, \quad \Delta = 4\mu^2 - 4\mu,\\
\eta_{1.5} &= \frac{k_1\Gamma(\gamma_1+1)}{\beta}x^\beta - \left(2k^2(\mu-1)\mu\sigma + k_1\rho + k_1^2\sigma\right)\frac{\Gamma(\gamma_2+1)}{\alpha}t^\alpha,\\
\eta_{2.5} &= \frac{k_2\Gamma(\gamma_1+1)}{\beta}x^\beta - \left(2k^2(\mu-1)\mu\sigma - k_2\rho + k_2^2\sigma\right)\frac{\Gamma(\gamma_2+1)}{\alpha}t^\alpha.
\end{aligned} \quad (37)$$

For solutions $(q_1)_{5.1}$, $(q_2)_{5.1}$, we have $\Delta > 0$, $\mu \in (-\infty,0) \cup (1,\infty)$.

For solutions $(q_1)_{5.2}$, $(q_2)_{5.2}$, we have $\Delta < 0$, $\mu \in (0,1)$.

Remark 6. If we select $(\mu - 1 + \sqrt{\mu^2 - \mu})p_1 = (1 - \mu + \sqrt{\mu^2 - \mu})p_2$, $\mu \in (-\infty,0) \cup (1,+\infty)$, and $\mu p_1 = \sqrt{\mu(1-\mu)}\, p_2$, $\mu \in (0,1)$, these solutions $(q_1)_{5.1}$, $(q_2)_{5.1}$, and $(q_1)_{5.2}$, $(q_2)_{5.2}$ contain the following solutions which including the kink and antikink wave solutions.

$$\begin{aligned}
(q_1)_{5.1.1} &= \pm\frac{k}{b}\sqrt{\frac{-2\sigma\mu(\mu-1)}{\delta(\gamma+1)}}\tanh\left(\frac{\sqrt{\mu-\mu^2}}{b}\xi_5\right)e^{i\eta_{1.5}},\\
(q_2)_{5.1.1} &= \pm\frac{k}{b}\sqrt{\frac{-2\sigma\mu(\mu-1)}{\delta(\gamma+1)}}\tanh\left(\frac{\sqrt{\mu-\mu^2}}{b}\xi_5\right)e^{i\eta_{2.5}},\\
(q_1)_{5.1.2} &= \pm\frac{k}{b}\sqrt{\frac{-2\sigma\mu(\mu-1)}{\delta(\gamma+1)}}\coth\left(\frac{\sqrt{\mu-\mu^2}}{b}\xi_5\right)e^{i\eta_{1.5}},\\
(q_2)_{5.1.2} &= \pm\frac{k}{b}\sqrt{\frac{-2\sigma\mu(\mu-1)}{\delta(\gamma+1)}}\coth\left(\frac{\sqrt{\mu-\mu^2}}{b}\xi_5\right)e^{i\eta_{2.5}},\\
(q_1)_{5.2.1} &= \pm\frac{k}{b}\sqrt{\frac{-2\sigma\mu(1-\mu)}{\delta(\gamma+1)}}\cot\left(\frac{\sqrt{\mu-\mu^2}}{b}\xi_5\right)e^{i\eta_{1.5}},\\
(q_2)_{5.2.1} &= \pm\frac{k}{b}\sqrt{\frac{-2\sigma\mu(1-\mu)}{\delta(\gamma+1)}}\cot\left(\frac{\sqrt{\mu-\mu^2}}{b}\xi_5\right)e^{i\eta_{2.5}},\\
(q_1)_{5.2.2} &= \pm\frac{k}{b}\sqrt{\frac{-2\sigma\mu(1-\mu)}{\delta(\gamma+1)}}\tan\left(\frac{\sqrt{\mu-\mu^2}}{b}\xi_5\right)e^{i\eta_{1.5}},\\
(q_2)_{5.2.2} &= \pm\frac{k}{b}\sqrt{\frac{-2\sigma\mu(1-\mu)}{\delta(\gamma+1)}}\tan\left(\frac{\sqrt{\mu-\mu^2}}{b}\xi_5\right)e^{i\eta_{2.5}}.
\end{aligned} \tag{38}$$

Selecting

$$\begin{aligned}
&k = \alpha = \beta = \gamma = b = \rho = \delta = k_1 = 1,\\
&\mu = 2,\\
&\lambda = 4,\\
&\sigma = -1,\\
&k_2 = 2,\\
&\gamma_1 = \gamma_2 = 1,\\
&p_1 = 4,\\
&p_2 = 10,
\end{aligned} \tag{39}$$

we obtain the unbounded solitary wave solution $(q_1)_{5.1}$ which is simulated in Figure 9.

Selecting

$$\begin{aligned}
&k = k_1 = b = c = 1,\\
&\mu = \frac{1}{2},\\
&\lambda = 1,\\
&\sigma = -1,\\
&\delta = 1,\\
&k_2 = 2,\\
&\rho = \frac{3}{2},\\
&\gamma_1 = \gamma_2 = 1,\\
&p_1 = -1,\\
&p_2 = \frac{13}{2},
\end{aligned} \tag{40}$$

we obtain the periodic wave solution $(q_1)_{5.2}$ which is simulated in Figure 10.

Case 6.

$$\begin{aligned}
&a_0 = b_0 = 0,\\
&a_1 = \pm k(\mu - 1)\sqrt{\frac{-2\sigma}{\delta(\gamma+1)}},\\
&b_1 = \pm k(\mu - 1)\sqrt{\frac{-2\sigma}{\delta(\gamma+1)}},\\
&a_{-1} = \pm k\mu\sqrt{\frac{-2\sigma}{\delta(\gamma+1)}},\\
&\lambda = 2\mu,\\
&b_{-1} = \pm k\mu\sqrt{\frac{-2\sigma}{\delta(\gamma+1)}},\\
&c_1 = -k_1\rho - k_1^2\sigma - 8k^2(-1+\mu)\mu\sigma,\\
&c_2 = k_2\rho - k_2^2\sigma - 8k^2(-1+\mu)\mu\sigma.
\end{aligned} \tag{41}$$

From Case 6, we obtain the following solutions:

Clearly, we can find that $F_{6.1}, F_{6.2}$ contain the following

$$
\begin{aligned}
(q_1)_{6.1} &= \left(\pm k(-1+\mu)\sqrt{\frac{-2\sigma}{\delta(\gamma+1)}}F_{6.1} \pm k\mu\sqrt{\frac{-2\sigma}{\delta(\gamma+1)}}F_{6.1}^{-1}\right)e^{i\eta_{1.6}},\\
(q_2)_{6.1} &= \left(\pm k(-1+\mu)\sqrt{\frac{-2\sigma}{\delta(\gamma+1)}}F_{6.1} \pm k\mu\sqrt{\frac{-2\sigma}{\delta(\gamma+1)}}F_{6.1}^{-1}\right)e^{i\eta_{2.6}},\\
F_{6.1} &= \frac{\left[2\mu(p_2-p_1)-\sqrt{\Delta}(p_2+p_1)\right]\sinh\left(\sqrt{\Delta}/2b\xi_6\right)+\left[2\mu(p_2+p_1)-\sqrt{\Delta}(p_2-p_1)\right]\cosh\left(\sqrt{\Delta}/2b\xi_6\right)}{b\left[2(\mu-1)(p_2-p_1)-\sqrt{\Delta}(p_2+p_1)\right]\sinh\left(\sqrt{\Delta}/2b\xi_6\right)+b\left[2(\mu-1)(p_2+p_1)-\sqrt{\Delta}(p_2-p_1)\right]\cosh\left(\sqrt{\Delta}/2b\xi_6\right)}, \quad \mu\in(-\infty,0)\cup(1,\infty),\\
(q_1)_{6.2} &= \left(\pm k(-1+\mu)\sqrt{\frac{-2\sigma}{\delta(\gamma+1)}}F_{6.2} \pm k\mu\sqrt{\frac{-2\sigma}{\delta(\gamma+1)}}F_{6.2}^{-1}\right)e^{i\eta_{1.6}},\\
(q_2)_{6.2} &= \left(\pm k(-1+\mu)\sqrt{\frac{-2\sigma}{\delta(\gamma+1)}}F_{6.2} \pm k\mu\sqrt{\frac{-2\sigma}{\delta(\gamma+1)}}F_{6.2}^{-1}\right)e^{i\eta_{2.6}},\\
F_{6.2} &= \frac{\left(2\mu p_1-\sqrt{-\Delta}p_2\right)\cos\left(\sqrt{-\Delta}/2b\xi_6\right)+\left(2\mu p_2+\sqrt{-\Delta}p_1\right)\sin\left(\sqrt{-\Delta}/2b\xi_6\right)}{b\left(2(\lambda-1)p_1-\sqrt{-\Delta}p_2\right)\cos\left(\sqrt{-\Delta}/2b\xi_6\right)+b\left(2(\lambda-1)p_2+\sqrt{-\Delta}p_1\right)\sin\left(\sqrt{-\Delta}/2b\xi_6\right)}, \mu\in(0,1),\\
\xi_6 &= \frac{k\Gamma(\gamma_1+1)}{\beta}x^\beta - \sigma k(k_1+k_2)\frac{\Gamma(\gamma_2+1)}{\alpha}t^\alpha, \quad \Delta = 4\mu^2-4\mu,\\
\eta_{1.6} &= \frac{k_1\Gamma(\gamma_1+1)}{\beta}x^\beta - \left(8k^2(\mu-1)\mu\sigma + k_1\rho + k_1^2\sigma\right)\frac{\Gamma(\gamma_2+1)}{\alpha}t^\alpha,\\
\eta_{2.6} &= \frac{k_2\Gamma(\gamma_1+1)}{\beta}x^\beta - \left(8k^2(\mu-1)\mu\sigma - k_2\rho + k_2^2\sigma\right)\frac{\Gamma(\gamma_2+1)}{\alpha}t^\alpha.
\end{aligned} \tag{42}
$$

solutions:

$$
\begin{aligned}
F_{6.1.1} &= -\frac{\mu}{b\sqrt{(-1+\mu)\mu}}\tanh\left(\frac{1}{b}\sqrt{\mu^2-\mu}\xi_6\right),\\
p_1 &= \frac{\mu-1-\sqrt{\mu^2-\mu}}{\mu-1+\sqrt{\mu^2-\mu}}p_2,\\
&\mu\in(-\infty,0)\cup(1,\infty),\\
F_{6.1.2} &= -\frac{\mu}{b\sqrt{(-1+\mu)\mu}}\coth\left(\frac{1}{b}\sqrt{\mu^2-\mu}\xi_6\right),\\
p_1 &= \frac{1-\mu+\sqrt{\mu^2-\mu}}{\mu-1+\sqrt{\mu^2-\mu}}p_2,\\
&\mu\in(-\infty,0)\cup(1,\infty),\\
F_{6.2.1} &= \frac{\mu^2}{b(1-3\mu+3\mu^2)} - \frac{(1-\mu)\sqrt{\mu-\mu^2}}{b(1-3\mu+3\mu^2)}\tan\left(\frac{\sqrt{\mu-\mu^2}}{b}\xi_6\right),\\
p_1 &= \frac{1-2\mu}{\sqrt{\mu-\mu^2}}p_2, \mu\in(0,1),\\
F_{6.2.2} &= \frac{\mu^2}{b(1-3\mu+3\mu^2)} + \frac{(1-\mu)\sqrt{\mu-\mu^2}}{b(1-3\mu+3\mu^2)}\cot\left(\frac{\sqrt{\mu-\mu^2}}{b}\xi_6\right),\\
p_1 &= \frac{\sqrt{\mu-\mu^2}}{2\mu-1}p_2, \mu\in(0,1).
\end{aligned} \tag{43}
$$

The mixed solitary wave solutions and trigonometric function solutions are simulated in Figures 11 and 12 after selecting the following parameters for $(q_1)_{6.1}$ and $(q_2)_{6.2}$:

$$
\begin{aligned}
b &= 1,\\
\sigma &= -1,\\
\gamma = \gamma_1 = \gamma_2 = \delta = k &= k_1 = 1,\\
\mu = k_2 &= 2,\\
\rho &= 1,\\
p_1 &= 16,\\
p_2 &= 22,\\
\Delta &= 8,
\end{aligned} \tag{44}
$$

$$\begin{aligned} b &= 0.5, \\ \sigma &= -1, \\ \gamma = \gamma_1 = \gamma_2 = \delta = k &= k_1 = 1, \\ \mu &= 0.5, \\ k_2 &= 2, \\ \rho &= 1, \\ p_1 &= -2, \\ p_2 &= 4, \\ \Delta &= -1. \end{aligned} \tag{45}$$

3.2. Results and Discussion. After utilizing the two methods, we get many types of exact solutions of Equation (1), including the solitary wave solution, the famous bell-shape soliton solution, the kink and antikink solutions, the blow-up pattern solution, and the unbounded solutions and the periodic wave solution. Compared with some other techniques [43, 44, 47], these two methods can be used to obtain some general solutions, including the mixed solitary wave solutions and periodic wave solutions of Equation (1).

Some structures of these solutions are simulated in above Figures 1–12. The visualization can help us to better understanding the dynamic behavior and physical and propagation characteristics of the coupled model. For example, from Figures 1 and 2, if we let $t = 0.1, \alpha = \beta = 1$, we can find that the waveform of Re $(q_1)_1$ is distorted between (−1.6,−1.4) but changes dramatically with the fractional order $\alpha = 0.18, \beta = 0.9, \gamma_1 = \gamma_2 = 1$. The real part of $(q_1)_2$ changes very slowly when the values of time variable t and fractional order factor α, β vary in a small range (see Figure 13), but the values shake rapidly since $t > 1, \alpha, \beta > 0.1$ after comparing Figures 13(a)–13(c), the ranges of Re $(q_1)_2$ vary from $(-5 \times 10^{-11}, 1.5 \times 10^{-10})$ to $(-10^{-1}, 10^{-1})$. We believe that these simulations can help us to further understand the inner structure of this model.

4. Conclusion

In brief, six types of new exact solutions for the GMFCNLS have been found after utilizing the modified $(G'/G, 1/G)$ and $G'/(bG' + G + a)$ methods. Some propagation behavior of these solutions is discussed and simulated, the graphs of which shows that these explicit solutions are propagated through different patterns; the efficient and significant method can be used to many other nonlinear models such as $(2+1)$-dimensional breaking soliton equation, Ginzburg-Landau's equation, Ostrovsky's equation, and Boussinesq-Burgers' equation. Finally, all these solutions obtained in the present article have been checked by the mathematical software.

Data Availability

All the data are available within the article.

Conflicts of Interest

The authors declare that they have no known conflict in this paper.

Acknowledgments

This project was supported by the Jiangsu University Students Practical Innovation Training Program Guidance Project of Jiangsu Province (Grant No. 202211276054Y) and Natural Science Research Projects of Institutions of Higher Learning in Jiangsu Province (Grant No. 18KJB110013).

References

[1] R. F. Zhang and S. Bilige, "Bilinear neural network method to obtain the exact analytical solutions of nonlinear partial differential equations and its application to p-gBKP equation," *Nonlinear Dynamics*, vol. 95, no. 4, pp. 3041–3048, 2019.

[2] M. Omidi, B. Arab, A. H. H. Rasanan, J. A. Rad, and K. Parand, "Learning nonlinear dynamics with behavior ordinary partial system of the differential equations: looking through the lens of orthogonal neural networks," *Engineering with Computers*, vol. 38, no. S2, pp. 1635–1654, 2022.

[3] A. Almutairi, H. El-Metwally, M. A. Sohaly, and I. M. Elbaz, "Lyapunov stability analysis for nonlinear delay systems under random effects and stochastic perturbations with applications in finance and ecology," *Advances in Difference Equations*, vol. 2021, no. 1, Article ID 186, 2021.

[4] P. Korn, "A regularity-aware algorithm for variational data assimilation of an idealized coupled atmosphere–ocean model," *Journal of Scientific Computing*, vol. 79, no. 2, pp. 748–786, 2019.

[5] A. Yokus and H. M. Baskonus, "Dynamics of traveling wave solutions arising in fiber optic communication of some nonlinear models," *Soft Computing*, vol. 26, no. 24, pp. 13605–13614, 2022.

[6] H. G. Abdelwahed, E. K. El-Shewy, M. A. E. Abdelrahman, and A. F. Alsarhana, "On the physical nonlinear (n+1)-dimensional Schrodinger equation applications," *Results in Physics*, vol. 21, article 103798, 2021.

[7] M. E. Samei, L. Karimi, and M. K. A. Kaabar, "To investigate a class of multi-singular pointwise defined fractional q–integro-differential equation with applications," *AIMS Mathematics*, vol. 7, no. 5, pp. 7781–7816, 2022.

[8] M. Ozisik, M. Bayram, A. Secer, M. Cinar, A. Yusuf, and T. A. Sulaiman, "Optical solitons to the (1+2)-dimensional chiral nonlinear Schrödinger equation," *Optical and Quantum Electronics*, vol. 54, no. 9, pp. 1–13, 2022.

[9] S. K. Mohanty, O. V. Kravchenko, and A. N. Dev, "Exact traveling wave solutions of the Schamel Burgers' equation by using generalized-improved and generalized $G'G$ expansion methods," *Results in Physics*, vol. 33, article 105124, 2022.

[10] S. T. Mohyud-Din and S. Bibi, "Exact solutions for nonlinear fractional differential equations using $G'G2$-expansion method," *Alexandria Engineering Journal*, vol. 57, no. 2, pp. 1003–1008, 2018.

[11] H. F. Ismael, H. Bulut, and H. M. Baskonus, "Optical soliton solutions to the Fokas–Lenells equation via sine-Gordon expansion method and $(m + (G'/G))$-expansion method," *Pramana*, vol. 94, no. 1, pp. 1–9, 2020.

[12] A. Yokus, H. Durur, H. Ahmad, P. Thounthong, and Y. F. Zhang, "Construction of exact traveling wave solutions of the Bogoyavlenskii equation by $(G'/G,1/G)$-expansion and $(1/G')$-expansion techniques," *Results in Physics*, vol. 19, article 103409, 2020.

[13] A. M. Elsherbeny, R. El-Barkouky, H. M. Ahmed, R. M. I. El-Hassani, and A. H. Arnous, "Optical solitons and another solutions for Radhakrishnan-Kundu-Laksmannan equation by using improved modified extended tanh-function method," *Optical and Quantum Electronics*, vol. 53, no. 12, pp. 1–15, 2021.

[14] H. Durur, A. Kurt, and O. Tasbozan, "New travelling wave solutions for KdV6 equation using sub equation method," *Applied Mathematics and Nonlinear Sciences*, vol. 5, no. 1, pp. 455–460, 2020.

[15] G. Yel, H. Bulut, and E. İlhan, "A new analytical method to the conformable chiral nonlinear Schrödinger equation in the quantum Hall effect," *Pramana*, vol. 96, no. 1, pp. 1–11, 2022.

[16] J. Fei, Z. Ma, and W. Cao, "Soliton molecules of new (2+1)-dimensional Burgers-type equation," *The European Physical Journal Plus*, vol. 137, no. 1, pp. 1–11, 2022.

[17] D. C. Lu and B. J. Hong, "Bäcklund transformation and n-soliton-like solutions to the combined KdV-Burgers equation with variable coefficients," *International Journal of Nonlinear Science*, vol. 2, no. 1, pp. 3–10, 2006.

[18] V. A. Matveev and M. A. Salle, *Darboux Transformations and Solitons*, Springer Verlag, Berlin, Heidelberg, 1991.

[19] X. B. Hu and W. X. Ma, "Application of Hirota's bilinear formalism to the Toeplitz lattice–some special soliton-like solutions," *Physics Letters A*, vol. 293, no. 3-4, pp. 161–165, 2002.

[20] W. X. Ma, M. S. Osman, S. Arshed, N. Raza, and H. M. Srivastava, "Practical analytical approaches for finding novel optical solitons in the single-mode fibers," *Chinese Journal of Physics*, vol. 72, pp. 475–486, 2021.

[21] B. J. Hong, "New Jacobi elliptic functions solutions for the variable-coefficient mKdV equation," *Applied Mathematics and Computation*, vol. 215, no. 8, pp. 2908–2913, 2009.

[22] A. M. Nass, "Lie symmetry analysis and exact solutions of fractional ordinary differential equations with neutral delay," *Applied Mathematics and Computation*, vol. 347, pp. 370–380, 2019.

[23] S. M. Mirhosseini-Alizamini, N. Ullah, J. Sabi'u, H. Rezazadeh, and M. Inc, "New exact solutions for nonlinear Atangana conformable Boussinesq-like equations by new Kudryashov method," *International Journal of Modern Physics B*, vol. 35, no. 12, article 2150163, 2021.

[24] B. J. Hong, D. C. Lu, and W. Chen, "Exact and approximate solutions for the fractional Schrödinger equation with variable coefficients," *Advances in Difference Equations*, vol. 2019, no. 1, Article ID 370, 2019.

[25] B. J. Hong, "Abundant explicit solutions for the M-fractional coupled nonlinear Schrödinger–KdV equations," *Journal of Low Frequency Noise, Vibration and Active Control*, vol. 41, 2023.

[26] J. H. He, "Fractal calculus and its geometrical explanation," *Results in Physics*, vol. 10, pp. 272–276, 2018.

[27] E. K. Jaradat, O. Alomari, M. Abudayah, and A.'. M. al-Faqih, "An approximate analytical solution of the nonlinear Schrödinger equation with harmonic oscillator using homotopy perturbation method and Laplace-Adomian decomposition method," *Advances in Mathematical Physics*, vol. 2018, Article ID 6765021, 11 pages, 2018.

[28] B. Ghanbari, K. S. Nisar, and M. Aldhaifallah, "Abundant solitary wave solutions to an extended nonlinear Schrödinger's equation with conformable derivative using an efficient integration method," *Advances in Difference Equations*, vol. 2020, no. 1, Article ID 328, 2020.

[29] B. Ghanbari, M. Inc, A. Yusuf, D. Baleanu, and M. Bayram, "Families of exact solutions of Biswas-Milovic equation by an exponential rational function method," *Tbilisi Mathematical Journal*, vol. 13, no. 2, pp. 39–65, 2020.

[30] C. Yue, D. C. Lu, M. M. A. Khater, A.-H. Abdel-Aty, W. Alharbi, and R. A. M. Attia, "On explicit wave solutions of the fractional nonlinear DSW system via the modified Khater method," *Fractals*, vol. 28, no. 8, article 2040034, 2020.

[31] A. Haq, "Partial-approximate controllability of semi-linear systems involving two Riemann-Liouville fractional derivatives," *Chaos, Solitons and Fractals*, vol. 157, article 111923, 2022.

[32] M. Caputo, "Linear models of dissipation whose Q is almost frequency independent–II," *Geophysical Journal International*, vol. 13, no. 5, pp. 529–539, 1967.

[33] J. H. He, "A tutorial review on fractal spacetime and fractional calculus," *International Journal of Theoretical Physics*, vol. 53, no. 11, pp. 3698–3718, 2014.

[34] C. S. Liu, "Counterexamples on Jumarie's three basic fractional calculus formulae for non- differentiable continuous functions," *Chaos, Solitons and Fractals*, vol. 109, pp. 219–222, 2018.

[35] A. Atangana, D. Baleanu, and A. Alsaedi, "Analysis of time-fractional Hunter-Saxton equation: a model of neumatic liquid crystal," *Open Physics*, vol. 14, no. 1, pp. 145–149, 2016.

[36] R. Khalil, M. Al Horani, A. Yousef, and M. Sababheh, "A new definition of fractional derivative," *Journal of Computational and Applied Mathematics*, vol. 264, pp. 65–70, 2014.

[37] I. Siddique, M. M. M. Jaradat, A. Zafar, K. Bukht Mehdi, and M. S. Osman, "Exact traveling wave solutions for two prolific conformable M-fractional differential equations via three diverse approaches," *Results in Physics*, vol. 28, article 104557, 2021.

[38] S. Salahshour, A. Ahmadian, S. Abbasbandy, and D. Baleanu, "*M*-fractional derivative under interval uncertainty: theory, properties and applications," *Chaos, Solitons and Fractals*, vol. 117, pp. 84–93, 2018.

[39] S. W. Yao, R. Manzoor, A. Zafar, M. Inc, S. Abbagari, and A. Houwe, "Exact soliton solutions to the Cahn-Allen equation and predator-prey model with truncated M-fractional derivative," *Results in Physics*, vol. 37, article 105455, 2022.

[40] R. W. Boyd, *Nonlinear Optics*, Academic Press, San Diego, CA, USA, 1992.

[41] M. Lakestani and J. Manafian, "Analytical treatment of nonlinear conformable time-fractional Boussinesq equations by three integration methods," *Optical and Quantum Electronics*, vol. 50, no. 1, pp. 1–33, 2018.

[42] T. Han, Z. Li, and X. Zhang, "Bifurcation and new exact traveling wave solutions to time-space coupled fractional nonlinear Schrodinger equation," *Physics Letters A*, vol. 395, article 127217, 2021.

[43] B. H. Wang, P. H. Lu, C. Q. Dai, and Y. X. Chen, "Vector optical soliton and periodic solutions of a coupled fractional nonlinear Schrodinger equation," *Results in Physics*, vol. 17, article 103036, 2020.

[44] M. Eslami, "Exact traveling wave solutions to the fractional coupled nonlinear Schrodinger equations," *Applied Mathematics and Computation*, vol. 285, pp. 141–148, 2016.

[45] P. F. Dai and Q. B. Wu, "An efficient block Gauss-Seidel iteration method for the space fractional coupled nonlinear

Schrodinger equations," *Applied Mathematics Letters*, vol. 117, article 107116, 2021.

[46] C. R. Menyuk, "Stability of solitons in birefringent optical fibers II arbitrary amplitudes," *Journal of the Optical Society of America B*, vol. 5, no. 2, pp. 392–402, 1988.

[47] J. Gu, A. Akbulut, M. Kaplan, M. K. A. Kaabar, and X. G. Yue, "A novel investigation of exact solutions of the coupled nonlinear Schrodinger equations arising in ocean engineering, plasma waves, and nonlinear optics," *Engineering and Science*, vol. 6, 2022.

[48] A.-M. Wazwaz, W. Albalawi, and S. A. el-Tantawy, "Optical envelope soliton solutions for coupled nonlinear Schrodinger equations applicable to high birefringence fibers," *Optik*, vol. 255, article 168673, 2022.

[49] E. M. E. Zayed and K. A. E. Alurrfi, "The $G'G,1G$-expansion method and its applications to two nonlinear Schrodinger equations describing the propagation of femtosecond pulses in nonlinear optical fibers," *Optik*, vol. 127, no. 4, pp. 1581–1589, 2016.

Hindawi
Journal of Function Spaces
Volume 2023, Article ID 5921425, 12 pages
https://doi.org/10.1155/2023/5921425

Research Article

Numerical Solution for Arbitrary Domain of Fractional Integro-differential Equation via the General Shifted Genocchi Polynomials

Jian Rong Loh,[1] **Chang Phang**,[2] **and Abdulnasir Isah**[3]

[1]*Foundation in Engineering, Faculty of Science and Engineering, University of Nottingham Malaysia, Semenyih, Selangor, Malaysia*
[2]*Department of Mathematics and Statistics, Universiti Tun Hussein Onn Malaysia, Pagoh, Johor, Malaysia*
[3]*Department of Mathematics Education, Tishk International University, Erbil, Iraq*

Correspondence should be addressed to Chang Phang; pchang@uthm.edu.my

Received 21 July 2022; Revised 14 October 2022; Accepted 6 April 2023; Published 24 May 2023

Academic Editor: Yusuf Gurefe

The Genocchi polynomial has been increasingly used as a convenient tool to solve some fractional calculus problems, due to their nice properties. However, like some other members in the Appell polynomials, the nice properties are always limited to the interval defined in $[0, 1]$. In this paper, we extend the Genocchi polynomials to the general shifted Genocchi polynomials, $S_n^{(a,b)}(x)$, which are defined for interval $[a, b]$. New properties for this general shifted Genocchi polynomials will be introduced, including the determinant form. This general shifted Genocchi polynomials can overcome the conventional formula of finding the Genocchi coefficients of a function $f(x)$ that involves $f^{(n-1)}(x)$ which may not be defined at $x = 0, 1$. Hence, we use the general shifted Genocchi polynomials to derive the operational matrix and hence to solve the Fredholm-type fractional integro-differential equations with arbitrary domain $[a, b]$.

1. Introduction

The Genocchi polynomials, $G_n(x)$, is one of the members of the Appell polynomials, $A_n(x)$, satisfying the differential relation $(dA_n(x))/dx = nA_{n-1}(x), n = 1, 2, 3, \cdots$. Besides, many new results are obtained in the field of number theory and combinatory [1–4], the Genocchi polynomials are also applied successfully to solve some kind of fractional calculus problems, and its advantages were described in [5–9] mostly via its operational matrix. However, most of the results are applied over the interval $[0, 1]$. Furthermore, for function approximation by using the Genocchi polynomials, the conventional formula of finding the Genocchi coefficients of a function $f(x)$ involves $f^{(n-1)}(x)$ which may not be defined at $x = 0, 1$. To overcome these drawbacks, we propose the general shifted Genocchi polynomials which are more suitable for larger interval $[a, b]$, where $a, b \geq 0$. Hence, in this paper, with the new general shifted Genocchi polynomials, we derive its operational matrix, and then, we solve the fractional integro-differential equation (FIDE) with arbitrary domain, i.e., not limited to interval $[0, 1]$.

FIDE is an equation which contains a fractional derivative term ${}_0D_x^\alpha f(x)$, where α denotes the fractional order derivative with $\lceil \alpha \rceil = n$, i.e., $(n-1 < \alpha \leq n)$ and an integral kernel operator term $\tilde{K}f(x) = \int K(x, t, f(t))dt$. This paper considers the arbitrary domain FIDE of the 2nd-kind nonhomogeneous Fredholm type of the following special class:

$$\begin{aligned} {}_0D_x^\alpha f(x) &= h(x) + \lambda \int_a^b K(x, t) f(t) dt, \\ f^{(i)}(x_i) &= y_i, i = 1, \cdots, n, \end{aligned} \tag{1}$$

where $f(x)$ is the unknown function to be solved, $K(x, t)$ is the integral kernel, ${}_0D_x^\alpha(x)$ is Caputo's fractional derivative, and $h(x)$ is the nonhomogeneous forced term.

On top of that, solving FIDE is always not an easy task, and reliable numerical methods are needed. Furthermore, for the Fredholm-type problems, the existing numerical methods are mostly applicable for interval $[0,1]$. Some of the early published works which for FIDE in $[0,1]$ are including the collocation method via polynomial spline function [10], the fractional differential transform method [11], and the Taylor expansion method [12]. In this research direction, some researches focus on solving the special class of FIDE, which includes solving fractional partial integro-differential equations by the resolvent kernel method, the Laplace transform [13], and the Laguerre polynomial [14], solving fractional integro-differential equations via the fractional-order Euler polynomials [15] and the Jacobi wavelets [16], solving fourth-order time FIDE with a weakly singular kernel by compact finite difference scheme [17] and nonlinear time-fractional partial integro-differential equation by finite difference scheme [18], and solving nonlinear two-dimensional fractional integro-differential equations via hybrid function [19]. However, the FIDE with the arbitrary domain is relatively less concerned by researchers, and so far, the successful methods applied to this type of problem are limited to the Chebyshev wavelet method [20]. For more methods as well as theories of FIDE/FDE, we refer the readers to some well-known books such as [21, 22].

The rest of the paper is organized as follows: Section 2 is devoted to preliminary results including basic definition, properties and determinant form of the general shifted Genocchi polynomials, $S_n^{(a,b)}(x)$, function approximation by $S_n^{(a,b)}(x)$, and theorem for the analytical expression of the integral of the product of the two general shifted Genocchi polynomials $T_{(n,m)}=\int_a^b S_n^{(a,b)}(x)S_m^{(a,b)}(x)dx$. Section 3 is the main result of this paper, which includes the derivation of a new operational matrix associated with the general shifted Genocchi polynomials. Besides that, the procedure of approximating the integral kernel in terms of the general shifted Genocchi polynomials and analytical expression of the kernel matrix is also explained in this section. Sections 4 and 5 are devoted to the procedure used in this paper and some numerical examples. Section 6 is the conclusion of this paper.

2. Preliminary Results

Here, first, we recall the function approximation by the original Genocchi polynomials. For this purpose, we may approximate a continuous function $f(x)$ in interval $[0,1]$ in terms of the Genocchi polynomials, $G_n(x)$, as the basis [23, 24] as follows:

$$f(x)=\sum_{n=1}^{\infty} c_n G_n(x), \tag{2}$$

where $G_n(x)$ are the Genocchi polynomials and the Genocchi coefficients are denoted by c_n. But normally, this process is done by using the truncated Genocchi series as follows:

$$f(x) \simeq \sum_{n=1}^{N} c_n G_n(x), \tag{3}$$

where in matrix notation,

$$f(x)=\mathbf{C}^T\mathbf{G}(x), \tag{4}$$

where $\mathbf{C}=[c_1,c_2,\cdots,c_N]^T$ is the Genocchi coefficient matrix and $\mathbf{G}(x)=[G_1(x),G_2(x),\cdots,G_N(x)]^T$ is the Genocchi basis matrix. The Genocchi coefficients, c_n, can be calculated as

$$c_n=\frac{1}{2n!}\left(f^{(n-1)}(0)+f^{(n-1)}(1)\right), n=1,2,\cdots N. \tag{5}$$

2.1. General Shifted Genocchi Polynomials: Definitions and Basic Properties. Equation (5) fails to work for functions that are not $(n-1)$-differentiable at the points $x=0$ or $x=1$. An example is given as follows where the coefficient, c_3, is undefined:

Let $N=3, x^{3/2}\approx\sum_{n=1}^{3}c_nG_n(x)=c_1G_1(x)+c_2G_2(x)+c_3G_3(x)$, we obtain

$$\begin{aligned} c_3&=\frac{1}{2(3!)}\left(\left.\frac{d^2}{dx^2}x^{3/2}\right|_{x=0}+\left.\frac{d^2}{dx^2}x^{3/2}\right|_{x=1}\right)\\ &=\frac{1}{2(3!)}\left(\left.\frac{3}{4\sqrt{x}}\right|_{x=0}+\left.\frac{3}{4\sqrt{x}}\right|_{x=1}\right). \end{aligned} \tag{6}$$

To avoid this problem, we define the general shifted Genocchi polynomials by shifting $G_n(x)$ from the interval $[0,1]$ to the interval $[a,b], 0\le a\le b$, i.e., $S_n(x)=G_n((x-a)/(b-a))$, which results in the following definition:

Definition 1. The general shifted Genocchi polynomials $S_n^{(a,b)}(x)$ of order n is defined over the interval $[a,b]$ as

$$S_n^{(a,b)}(x)=G_n\left(\frac{x-a}{b-a}\right)=\sum_{k=0}^{n}\binom{n}{k}g_{n-k}\left(\frac{x-a}{b-a}\right)^k=\sum_{r=0}^{n}\binom{n}{r}s_{n-r}^{(a,b)}x^r, \tag{7}$$

where $s_{n-r}^{(a,b)}=\sum_{k=r}^{n}\left(\left(\left((-a)^{k-r}\right)(g_{n-k})\right)\binom{n}{k}\binom{k}{r}\right)/\left((b-a)^k\binom{n}{r}\right)$ is the general shifted Genocchi number, and let $S_0^{(a,b)}(x)=0$.

The generating function for the general shifted Genocchi polynomials can be expressed as

$$\frac{2t}{e^t+1}e^{((x-a)/(b-a))t}=\sum_{n=0}^{\infty}S_n^{(a,b)}\frac{t^n}{n!}, (|t|<\pi). \tag{8}$$

If we choose $a = 2$, $b = 4$, the first few terms of the general shifted Genocchi polynomials are

$$\begin{aligned} S_1^{(2,4)}(x) &= 1, \\ S_2^{(2,4)}(x) &= x - 3, \\ S_3^{(2,4)}(x) &= \frac{3}{4}x^2 - \frac{9}{2}x + 6, \\ S_4^{(2,4)}(x) &= \frac{1}{2}x^3 - \frac{9}{2}x^2 + 12x - 9, \\ S_5^{(2,4)}(x) &= \frac{5}{16}x^4 - \frac{15}{4}x^3 + 15x^2 - \frac{45}{2}x + 10. \end{aligned} \tag{9}$$

Figures 1 and 2 show the first few original Genocchi polynomials and the general shifted Genocchi polynomials.

Some of the important properties inherited from the classical Genocchi polynomials are

$$\frac{dS_n^{(a,b)}(x)}{dx} = \frac{n}{b-a} S_{n-1}^{(a,b)}(x), n \geq 1, \tag{10}$$

$$\frac{d^k S_n^{(a,b)}(x)}{dx^k} = \begin{cases} 0, & n \leq k, \\ \dfrac{k! \begin{pmatrix} n \\ k \end{pmatrix}}{(b-a)^k} S_{n-k}^{(a,b)}(x), & n > k, \end{cases} \quad k, n \in \mathbb{N} \cup \{0\}, \tag{11}$$

$$S_n^{(a,b)}(a) + S_n^{(a,b)}(b) = G_n(0) + G_n(1) = 0, n > 1. \tag{12}$$

Theorem 2. *Given an arbitrary integrable continuous function $f(x) \in C^{N-1}(R)$, it can be approximated in terms of the general shifted Genocchi polynomials $S_n^{(a,b)}(x)$ up to order N (i.e., polynomial degree = $N - 1$) by*

$$f(x) \approx \sum_{j=1}^{N} c_j S_j^{(a,b)}(x) = \mathbf{C}^T \mathbf{S}(x). \tag{13}$$

Then, the general shifted Genocchi coefficient c_j is given by

$$c_j = \frac{(b-a)^{j-1}}{2(j!)} \left(f^{(j-1)}(a) + f^{(j-1)}(b) \right). \tag{14}$$

Proof. Let $f(x) = \sum_{k=1}^{N} c_k S_k^{(a,b)}(x)$. Using Equations (11) and (12), for $1 \leq j$

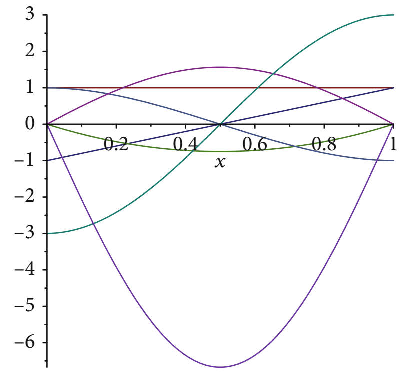

Figure 1: The first few original Genocchi polynomials (in interval [0, 1]).

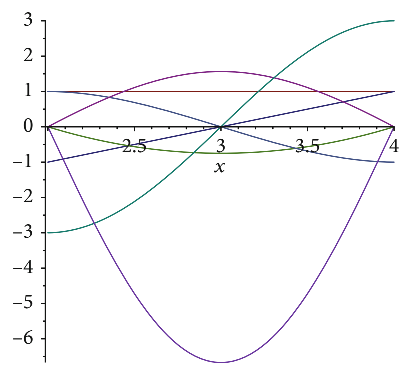

Figure 2: The first few general shifted Genocchi polynomials (in interval [2, 4]).

$$\begin{aligned} & f^{(j-1)}(a) + f^{(j-1)}(b) \\ &= \sum_{k=1}^{N} c_k \frac{d^{j-1}}{dx^{j-1}} \left(S_k^{(a,b)}(a) + S_k^{(a,b)}(b) \right) \\ &= \sum_{k=j}^{N} c_k \frac{(j-1)! \begin{pmatrix} k \\ j-1 \end{pmatrix}}{(b-a)^{j-1}} \left(S_{k-(j-1)}^{(a,b)}(a) + S_{k-(j-1)}^{(a,b)}(b) \right) \\ &= c_j \frac{(j-1)! \begin{pmatrix} j \\ j-1 \end{pmatrix}}{(b-a)^{j-1}} \left(S_1^{(a,b)}(a) + S_1^{(a,b)}(b) \right) \\ &\quad + \sum_{k=j+1}^{N} c_k \frac{(j-1)! \begin{pmatrix} k \\ j-1 \end{pmatrix}}{(b-a)^{j-1}} \left(S_{k-(j-1)}^{(a,b)}(a) + S_{k-(j-1)}^{(a,b)}(b) \right) \\ &= 2c_j \frac{(j!)}{(b-a)^{j-1}}. \end{aligned} \tag{15}$$

Rearrange the above equation, we obtain $c_j = ((b-a)^{j-1} / (2(j!))(f^{(j-1)}(a) + f^{(j-1)}(b))$. □

2.2. Determinant Form of the General Shifted Genocchi Polynomial Sequence. In this subsection, we will explain that this new general shifted Genocchi polynomial sequence can be also expressed in determinant form and recurrence relation, via modifying the work in [25, 26] for the shifted Genocchi polynomial sequence. For this process, we shift the order of the general shifted Genocchi polynomial sequence from n to $n+1$; that is, we have $\mathrm{Sh}_n^{(a,b)}(x) = S_{n+1}^{(a,b)}(x)$, where $\mathrm{Sh}_n^{(a,b)}(x)$ denotes the general shifted Genocchi polynomial sequence.

Lemma 3. *The determinant form of the general shifted Genocchi polynomial sequence, $Sh_n^{(a,b)}(x)$, which n > 0, is given by*

$$\mathrm{Sh}_n^{(a,b)}(x) = \frac{(-1)^n}{\prod_{i=0}^{n} s_{i,i}} \begin{vmatrix} 1 & \dfrac{x}{b-a} & \dfrac{x^2}{(b-a)^2} & \cdots & \dfrac{x^{n-1}}{(b-a)^{(n-1)}} & \dfrac{x^n}{(b-a)^n} \\ s_{0,0} & s_{1,0} & s_{2,0} & \cdots & s_{n-1,0} & s_{n,0} \\ 0 & s_{1,1} & s_{2,0} & \cdots & s_{n-1,1} & s_{n,1} \\ \vdots & \ddots & \ddots & & \vdots & \vdots \\ \vdots & & \ddots & \ddots & \vdots & \vdots \\ 0 & \cdots & & & & \end{vmatrix}, \tag{16}$$

and the recurrence relation of the general shifted Genocchi polynomial sequence, $Sh_n^{(a,b)}(x)$, can be written as

$$Sh_n^{(a,b)}(x) = \frac{1}{s_{n,n}}\left(x^n - \sum_{j=0}^{n-1} s_{n,j} Sh_j^{(a,b)}(x)\right). \tag{17}$$

In order to obtain values for $s_{i,j}$, we follow Costabile et al.'s method [25], which we summarize as follows:

Step 1. From $S_n^{(a,b)}(x) = \sum_{r=0}^{n} \binom{n}{r} s_{n-r}^{(a,b)} x^r$, we obtain the general shifted Genocchi number, $s_i^{(a,b)}$; hence, we calculate the lower triangular Toeplitz matrix, $\mathbf{T}_S$, with entries

$$t_{i,j} = \frac{s_{i+1-j}^{(a,b)}}{(i+1-j)!}. \tag{18}$$

Step 2. Calculate the upper triangular matrix $\mathbf{S}$ via

$$\mathbf{S} = \mathbf{D}_2^{-1}\mathbf{T}_S^{-1}\mathbf{D}_1^{-1}, \tag{19}$$

where $\mathbf{D}_1 = \mathrm{diag}\{(i+1)! | i = 0, 1, \cdots\}$ and $\mathbf{D}_2 = \mathrm{diag}\{1/i! | i = 0, 1, \cdots\}$. The values for $s_{i,j}$ can be obtained using the entries of $\mathbf{S}$.

To show the result of the determinant form of the general shifted Genocchi polynomial sequence, we present that $\mathrm{Sh}_3^{(2,5)}(x)$ $(a=2, b=5, n=3)$ and $\mathrm{Sh}_4^{(2,5)}(x)$ $(a=2, b=5, n=4)$ are given by

$$\mathrm{Sh}_3^{(2,5)}(x) = \frac{(-1)^3}{1/4!} \begin{vmatrix} 1 & \frac{x}{3} & \frac{x^2}{3^2} & \frac{x^3}{3^3} \\ 1 & \frac{7}{6} & \frac{29}{18} & \frac{133}{54} \\ 0 & \frac{1}{2} & \frac{7}{6} & \frac{29}{12} \\ 0 & 0 & \frac{1}{3} & \frac{7}{6} \end{vmatrix},$$
$$\mathrm{Sh}_4^{(2,5)}(x) = \frac{(-1)^4}{1/5!} \begin{vmatrix} 1 & \frac{x}{3} & \frac{x^2}{3^2} & \frac{x^3}{3^3} & \frac{x^4}{3^4} \\ 1 & \frac{7}{6} & \frac{29}{18} & \frac{133}{54} & \frac{641}{162} \\ 0 & \frac{1}{2} & \frac{7}{6} & \frac{29}{12} & \frac{133}{27} \\ 0 & 0 & \frac{1}{3} & \frac{7}{6} & \frac{29}{9} \\ 0 & 0 & 0 & \frac{1}{4} & \frac{7}{6} \end{vmatrix}. \tag{20}$$

Hence, the determinant form of the above general shifted Genocchi polynomial sequence is as follows:

$$S_4^{(2,5)}(x) = \mathrm{Sh}_3^{(2,5)}(x) = \frac{4}{27}x^3 - \frac{14}{9}x^2 + \frac{40}{9}x - \frac{77}{27},$$
$$S_5^{(2,5)}(x) = \mathrm{Sh}_4^{(2,5)}(x) = \frac{5}{81}x^4 - \frac{70}{81}x^3 + \frac{100}{27}x^2 - \frac{385}{81}x + \frac{50}{81}. \tag{21}$$

2.3. Integral of Product of the General Shifted Genocchi Polynomials. In this subsection, we derive the analytical expression for the integral of the product of the two general shifted Genocchi polynomials which will be used frequently in the later parts of the paper. This results in the following theorem:

Theorem 4. *Given any two general shifted Genocchi polynomials $S_n^{(a,b)}(x)$, $S_m^{(a,b)}(x)$, for $0 \le x$*

$$\begin{aligned}\gamma_{n,m}^{(a,b)}(x) &= \int S_n^{(a,b)}(x) S_m^{(a,b)}(x)dx = \int_0^x S_n^{(a,b)}(x) S_m^{(a,b)}(x)dx \\ &= \sum_{r=0}^{n-1} (-1)^r (b-a) \frac{n_{(r)}}{(m+1)^{(r+1)}} \\ &\quad \cdot \left(S_{n-r}^{(a,b)}(x) S_{m+1+r}^{(a,b)}(x) - S_{n-r}^{(a,b)}(0) S_{m+1+r}^{(a,b)}(0) \right),\end{aligned} \tag{22}$$

where $n_{(r)}$ is the falling factorial and $(m+1)^{(r+1)}$ is the rising factorial. For $[a, b]$, $0 \le a \le b$, we have

$$\begin{aligned}\gamma_{n,m}^{(a,b)} &= \gamma_{n,m}^{(a,b)}(b) - \gamma_{n,m}^{(a,b)}(a) = \int_a^b S_n^{(a,b)}(x) S_m^{(a,b)}(x)dx \\ &= \sum_{r=0}^{n-1} (-1)^r (b-a) \frac{n_{(r)}}{(m+1)^{(r+1)}} \\ &\quad \cdot \left(S_{n-r}^{(a,b)}(b) S_{m+1+r}^{(a,b)}(b) - S_{n-r}^{(a,b)}(a) S_{m+1+r}^{(a,b)}(a) \right) \\ &= \sum_{r=0}^{n-1} (-1)^r (b-a) \frac{n_{(r)}}{(m+1)^{(r+1)}} \\ &\quad \cdot \left(S_{n-r}^{(a,b)}(b) S_{m+1+r}^{(a,b)}(b) - g_{n-r} g_{m+1+r} \right),\end{aligned} \tag{23}$$

where $g_k = S_k^{(a,b)}(a) = G_k(0)$.

Proof. In order to prove this theorem, we need the following expression:

$$\begin{aligned}\frac{dS_m^{(a,b)}(x)}{dx} &= \frac{m}{b-a} S_{m-1}^{(a,b)}(x), \\ \int_0^x S_m^{(a,b)}(x)dx &= \frac{b-a}{m+1} \left(S_{m+1}^{(a,b)}(x) - S_{m+1}^{(a,b)}(0) \right).\end{aligned} \tag{24}$$

For

$$\gamma_{n,m}^{(a,b)}(x) = \int_0^x S_n^{(a,b)}(x) S_m^{(a,b)}(x)dx, \tag{25}$$

and hence, using integration by parts, we have

$$\begin{aligned}\gamma_{n,m}^{(a,b)}(x) &= S_n^{(a,b)}(x) \left(\frac{(b-a)\left(S_{m+1}^{(a,b)}(x) - S_{m+1}^{(a,b)}(0) \right)}{m+1} \right) \\ &\quad - \int_0^x \left(\frac{n}{b-a} S_{n-1}^{(a,b)}(x) \right) \frac{(b-a)\left(S_{m+1}^{(a,b)}(x) - S_{m+1}^{(a,b)}(0) \right)}{m+1} dx \\ &= S_n^{(a,b)}(x) \left(\frac{(b-a)\left(S_{m+1}^{(a,b)}(x) - S_{m+1}^{(a,b)}(0) \right)}{m+1} \right) \\ &\quad - \frac{n}{m+1} \int_0^x S_{n-1}^{(a,b)}(x) S_{m+1}^{(a,b)}(x)dx \\ &\quad + \frac{n}{m+1} S_{m+1}^{(a,b)}(0) \int_0^x S_{n-1}^{(a,b)}(x)dx \\ &= \frac{b-a}{m+1} S_n^{(a,b)}(x) \left(S_{m+1}^{(a,b)}(x) - S_{m+1}^{(a,b)}(0) \right) \\ &\quad - \frac{n}{m+1} \int_0^x S_{n-1}^{(a,b)}(x) S_{m+1}^{(a,b)}(x)dx \\ &\quad + \frac{b-a}{m+1} S_{m+1}^{(a,b)}(0) \left(S_n^{(a,b)}(x) - S_n^{(a,b)}(0) \right) \\ &= \frac{b-a}{m+1} \left(S_n^{(a,b)}(x) S_{m+1}^{(a,b)}(x) - S_n^{(a,b)}(0) S_{m+1}^{(a,b)}(0) \right) \\ &\quad - \frac{n}{m+1} \int_0^x S_{n-1}^{(a,b)}(x) S_{m+1}^{(a,b)}(x)dx.\end{aligned} \tag{26}$$

By using Equation (25), we obtain

$$\begin{aligned}\gamma_{n,m}^{(a,b)}(x) &= (b-a) \left(\frac{S_n^{(a,b)}(x) S_{m+1}^{(a,b)}(x) - S_n^{(a,b)}(0) S_{m+1}^{(a,b)}(0)}{m+1} \right) \\ &\quad - \frac{n}{m+1} \gamma_{n-1,m+1}^{(a,b)}(x) \\ &= (b-a) \left(\frac{S_n^{(a,b)}(x) S_{m+1}^{(a,b)}(x) - S_n^{(a,b)}(0) S_{m+1}^{(a,b)}(0)}{m+1} \right) \\ &\quad - \frac{n}{m+1} \left((b-a) \left(\frac{S_{n-1}^{(a,b)}(x) S_{m+2}^{(a,b)}(x) - S_{n-1}^{(a,b)}(0) S_{m+2}^{(a,b)}(0)}{m+2} \right) \right. \\ &\quad \left. - \frac{n-1}{m+2} \gamma_{n-2,m+2}^{(a,b)}(x) \right) \\ &= (b-a) \left(\frac{S_n^{(a,b)}(x) S_{m+1}^{(a,b)}(x) - S_n^{(a,b)}(0) S_{m+1}^{(a,b)}(0)}{m+1} \right) \\ &\quad + \frac{(-1)^1 (b-a) n}{m+1} \left(\frac{S_{n-1}^{(a,b)}(x) S_{m+2}^{(a,b)}(x) - S_{n-1}^{(a,b)}(0) S_{m+2}^{(a,b)}(0)}{m+2} \right. \\ &\quad \left. + \frac{(-1)^2 n(n-1)}{(m+1)(m+2)} \gamma_{n-2,m+2}^{(a,b)}(x) \right) = \cdots.\end{aligned} \tag{27}$$

These processes continue recursively for n times, and then, we will obtain

$$
\begin{aligned}
&= \cdots = \sum_{r=0}^{n-1} (-1)^r (b-a) \frac{n(n-1)\cdots(n-r+1)}{(m+1)\cdots(m+r)} \\
&\quad \cdot \left(S_{n-r}^{(a,b)}(x) S_{m+1+r}^{(a,b)}(x) - S_{n-r}^{(a,b)}(0) S_{m+1+r}^{(a,b)}(0) \right) \\
&= \sum_{r=0}^{n-1} (-1)^r (b-a) \frac{n_{(r)}}{(m+1)^{(r+1)}} \\
&\quad \cdot \left(S_{n-r}^{(a,b)}(x) S_{m+1+r}^{(a,b)}(x) - S_{n-r}^{(a,b)}(0) S_{m+1+r}^{(a,b)}(0) \right).
\end{aligned} \tag{28}
$$

□

3. Main Result

3.1. General Shifted Genocchi Polynomial Operational Matrix of Fractional Derivative. In this section, we will derive the analytical expression of the general shifted Genocchi polynomial operational matrix of fractional derivative in the Caputo sense, which is the $N \times N$ matrix ${}_0\mathbf{P}_S^{\alpha}$, where

$$
{}_0D_x^{\alpha\mathbf{S}(x)} = {}_0\mathbf{P}_S^{\alpha}\mathbf{S}(x),
$$

$$
{}_0D_x^{\alpha} \begin{bmatrix} S_1^{(a,b)} \\ S_2^{(a,b)} \\ \vdots \\ S_N^{(a,b)} \end{bmatrix} = \begin{bmatrix} \rho_{11} & \rho_{12} & \cdots & \rho_{1N} \\ \rho_{21} & \rho_{22} & \cdots & \rho_{2N} \\ \vdots & \cdots & \cdots & \vdots \\ \rho_{N1} & \rho_{N2} & \cdots & \rho_{NN} \end{bmatrix} \begin{bmatrix} S_1^{(a,b)} \\ S_2^{(a,b)} \\ \vdots \\ S_N^{(a,b)} \end{bmatrix}. \tag{29}
$$

To derive the ${}_0\mathbf{P}_S^{\alpha}$, we first prove the following Lemma 5.

Lemma 5. *Caputo's fractional derivative of fractional order α of a general shifted Genocchi polynomial, $S_i^{(a,b)}(x)$, of order i is given by*

$$
{}_0D_x^{\alpha} S_i^{(a,b)}(x) = \begin{cases} \displaystyle\sum_{r=\lceil\alpha\rceil}^{i} \sum_{k=0}^{r-\lceil\alpha\rceil} \frac{(-a)^{r-\lceil\alpha\rceil-k} i! g_{i-r} x^{\lceil\alpha\rceil-\alpha+k}}{(b-a)^r (i-r)!(r-\lceil\alpha\rceil-k)!\Gamma(\lceil\alpha\rceil-\alpha+k+1)}, n-1<\alpha\le n, n\in\mathbb{N}, & i\ge\alpha \\ 0, & i<\alpha. \end{cases} \tag{30}
$$

Proof. For $n-1<\alpha\le n$, $n=\lceil\alpha\rceil$

$$
\begin{aligned}
{}_0D_x^{\alpha} S_i^{(a,b)}(x) &= \frac{1}{\Gamma(n-\alpha)} \int_0^x (x-t)^{n-\alpha-1} \frac{d^n}{dt^n} G_i\left(\frac{t-a}{b-a}\right) dt \\
&= \frac{1}{\Gamma(n-\alpha)} \int_0^x (x-t)^{n-\alpha-1} \frac{d^n}{dt^n} \sum_{r=0}^{i} \binom{i}{r} g_{i-r} \left(\frac{t-a}{b-a}\right)^r dt \\
&= \frac{1}{\Gamma(n-\alpha)} \sum_{r=n}^{i} \frac{\binom{i}{r} g_{i-r}}{(b-a)^r} n! \binom{r}{n} \\
&\quad \cdot \int_0^x (x-t)^{n-\alpha-1} (t-a)^{r-n} dt \\
&= \frac{1}{\Gamma(n-\alpha)} \sum_{r=n}^{i} \frac{\binom{i}{r} g_{i-r}}{(b-a)^r} n! \binom{r}{n} \\
&\quad \cdot \int_0^x (x-t)^{n-\alpha-1} \sum_{k=0}^{r-n} \binom{r-n}{k} t^k (-a)^{r-n-k} dt \\
&= \frac{1}{\Gamma(n-\alpha)} \sum_{r=n}^{i} \sum_{k=0}^{r-n} \frac{(-a)^{r-n-k} \binom{i}{r} \binom{r-n}{k} g_{i-r}}{(b-a)^r} n! \\
&\quad \cdot \binom{r}{n} \int_0^x (x-t)^{n-\alpha-1} t^k dt.
\end{aligned} \tag{31}
$$

Substitute $t = xu$,

$$
\begin{aligned}
{}_0D_x^{\alpha} S_i^{(a,b)}(x) &= \frac{1}{\Gamma(n-\alpha)} \sum_{r=n}^{i} \sum_{k=0}^{r-n} \frac{(-a)^{r-n-k} \binom{i}{r} \binom{r-n}{k} g_{i-r}}{(b-a)^r} n! \\
&\quad \cdot \binom{r}{n} x^{n-\alpha+k} \int_0^1 (1-u)^{n-\alpha-1} u^k du \\
&= \frac{1}{\Gamma(n-\alpha)} \sum_{r=n}^{i} \sum_{k=0}^{r-n} \frac{(-a)^{r-n-k} \binom{i}{r} \binom{r-n}{k} g_{i-r}}{(b-a)^r} n! \\
&\quad \cdot \binom{r}{n} x^{n-\alpha+k} B(k+1, n-\alpha) = \frac{1}{\Gamma(n-\alpha)} \\
&\quad \cdot \sum_{r=n}^{i} \sum_{k=0}^{r-n} \frac{(-a)^{r-n-k} \binom{i}{r} \binom{r-n}{k} g_{i-r}}{(b-a)^r} n! \binom{r}{n} x^{n-\alpha+k} \\
&\quad \cdot \frac{\Gamma(k+1)\Gamma(n-\alpha)}{\Gamma(n-\alpha+k+1)} \\
&= \sum_{r=n}^{i} \sum_{k=0}^{r-n} \frac{(-a)^{r-n-k} i! g_{i-r}}{(b-a)^r (i-r)!(r-n-k)!\Gamma(n-\alpha+k+1)} x^{n-\alpha+k},
\end{aligned} \tag{32}
$$

where $B(x, y)$ is the beta function which can be found using $\int_0^1 u^{x-1}(1-u)^{y-1} du$ for $\text{Re}(x), \text{Re}(y) > 0$. □

Hence, we obtain the theorem for operational matrix ${}_0\mathbf{P}_S^{\alpha}$ as follows:

Theorem 6. *Given a set $S_i^{(a,b)}(x), i = 1, \cdots N$ of the N general shifted Genocchi polynomials, the general shifted Genocchi polynomial operational matrix of fractional derivative in the Caputo sense of order α over the interval $[0, 1]$ is the $N \times N$ matrix ${}_0P_S^{\alpha}$, given by*

$$
{}_0\mathbf{P}_S^{\alpha} = M^{(\alpha)} = \begin{pmatrix} 0 & 0 & \cdots & 0 \\ \vdots & \vdots & \cdots & \vdots \\ 0 & 0 & \cdots & 0 \\ \sum_{k=\lceil\alpha\rceil}^{\lceil\alpha\rceil} \rho_{\lceil\alpha\rceil,1} & \sum_{k=\lceil\alpha\rceil}^{\lceil\alpha\rceil} \rho_{\lceil\alpha\rceil,2} & \cdots & \sum_{k=\lceil\alpha\rceil}^{\lceil\alpha\rceil} \rho_{\lceil\alpha\rceil,N} \\ \vdots & \vdots & \cdots & \vdots \\ \sum_{k=\lceil\alpha\rceil}^{i} \rho_{i,1} & \sum_{k=\lceil\alpha\rceil}^{i} \rho_{i,2} & \cdots & \sum_{k=\lceil\alpha\rceil}^{i} \rho_{i,N} \\ \vdots & \vdots & \cdots & \vdots \\ \sum_{k=\lceil\alpha\rceil}^{N} \rho_{N,1} & \sum_{k=\lceil\alpha\rceil}^{N} \rho_{N,2} & \cdots & \sum_{k=\lceil\alpha\rceil}^{N} \rho_{N,N} \end{pmatrix}, \tag{33}
$$

where $\rho_{i,j}$ is given by

$$
\rho_{i,j} = \frac{(b-a)^{j-1}}{2(j!)} \sum_{r=n}^{i} \sum_{k=0}^{r-n} \frac{(-a)^{r-n-k} i! g_{i-r} \left(a^{n-\alpha+k-j+1} + b^{n-\alpha+k-j+1}\right)}{(b-a)^r (i-r)!(r-n-k)!\Gamma(n-\alpha+k-j+2)}. \tag{34}
$$

Proof. Let ${}_0D_x^{\alpha} S_i^{(a,b)}(x) = \sum_{j=1}^{N} \rho_{ij} S_j^{(a,b)}(x)$. Then, using the function approximation as in Theorem 2 and Caputo's fractional derivative for $S_i^{(a,b)}(x)$ in Lemma 5, we have

$$
\begin{aligned}
\rho_{ij} &= \frac{(b-a)^{j-1}}{2(j!)} \left(\frac{d^{j-1}}{dx^{j-1}} {}_0D_x^{\alpha} S_i^{(a,b)}(x) \Big|_{x=a} + \frac{d^{j-1}}{dx^{j-1}} {}_0D_x^{\alpha} S_i^{(a,b)}(x) \Big|_{x=b} \right) \\
&= \frac{(b-a)^{j-1}}{2(j!)} \left(\frac{d^{j-1}}{dx^{j-1}} \sum_{r=n}^{i} \sum_{k=0}^{r-n} \frac{(-a)^{r-n-k} i! g_{i-r} x^{n-\alpha+k}}{(b-a)^r (i-r)!(r-n-k)!\Gamma(n-\alpha+k+1)} \Bigg|_{x=a} \right. \\
&\qquad \left. + \frac{d^{j-1}}{dx^{j-1}} \sum_{r=n}^{i} \sum_{k=0}^{r-n} \frac{(-a)^{r-n-k} i! g_{i-r} x^{n-\alpha+k}}{(b-a)^r (i-r)!(r-n-k)!\Gamma(n-\alpha+k+1)} \Bigg|_{x=b} \right) \\
&= \frac{(b-a)^{j-1}}{2(j!)} \times \sum_{r=n}^{i} \sum_{k=0}^{r-n} \frac{(-a)^{r-n-k} i! g_{i-r} (j-1)! \binom{n-\alpha+k}{j-1} \left(x^{n-\alpha+k-j+1}\big|_{x=a} + x^{n-\alpha+k-j+1}\big|_{x=b} \right)}{(b-a)^r (i-r)!(r-n-k)!\Gamma(n-\alpha+k+1)} \\
&= \frac{(b-a)^{j-1}}{2(j!)} \sum_{r=n}^{i} \sum_{k=0}^{r-n} \frac{(-a)^{r-n-k} i! g_{i-r} \left(a^{n-\alpha+k-j+1} + b^{n-\alpha+k-j+1}\right)}{(b-a)^r (i-r)!(r-n-k)!\Gamma(n-\alpha+k-j+2)}.
\end{aligned} \tag{35}
$$

□

As the formula given in Theorem 6 may fail to work for $a = 0$, we use the matrix approach to derive the ${}_0\mathbf{P}_S^{\alpha}$ as given in Theorem 8. To prove Theorem 8, we need the following lemma:

Lemma 7. *The matrix Θ_N defined as $\Theta_N = \int_0^1 ({}_0D_x^{\alpha} S(x)) * S^T(x) dx$ is given by*

$$
\Theta_N = [\theta_{ik}]_{N \times N} = \left[\int_0^1 {}_0D_x^{\alpha} G_i(x) G_k(x) dx \right]_{N \times N}, \tag{36}
$$

where

$$
\theta_{ik} = \sum_{r=\lceil\alpha\rceil}^{i} \sum_{p=0}^{k} \frac{i! \binom{k}{p} g_{i-r} g_{k-p}}{(i-r)!(r-\alpha+p+1)\Gamma(r-\alpha+1)}. \tag{37}
$$

Proof. From Caputo's fractional derivative of the Genocchi polynomials [5, 23, 24], we have

$$
\begin{aligned}
{}_0D_x^{\alpha} G_i(x) &= \sum_{r=\lceil\alpha\rceil}^{i} \frac{i! g_{i-r}}{(i-r)!\Gamma(r-\alpha+1)} x^{r-\alpha} \\
{}_0D_x^{\alpha} G_i(x) G_k(x) &= \left(\sum_{r=\lceil\alpha\rceil}^{i} \frac{i! g_{i-r}}{(i-r)!\Gamma(r-\alpha+1)} x^{r-\alpha} \right) \left(\sum_{p=0}^{k} \binom{k}{p} g_{k-p} x^p \right) \\
&= \sum_{r=\lceil\alpha\rceil}^{i} \sum_{p=0}^{k} \frac{i! g_{i-r}}{(i-r)!\Gamma(r-\alpha+1)} \binom{k}{p} g_{k-p} x^{r-\alpha+p}.
\end{aligned} \tag{38}
$$

Integrate both sides, and we obtain

$$
\begin{aligned}
\int_0^1 {}_0D_x^{\alpha} G_i(x) G_k(x) dx &= \sum_{r=}^{i} \sum_{p=0}^{k} \frac{i! g_{i-r}}{(i-r)!\Gamma(r-\alpha+1)} \binom{k}{p} g_{k-p} \int_0^1 x^{r-\alpha+p} dx \\
&= \sum_{r=\lceil\alpha\rceil}^{i} \sum_{p=0}^{k} \frac{i! \binom{k}{p} g_{i-r} g_{k-p}}{(i-r)!(r-\alpha+p+1)\Gamma(r-\alpha+1)}.
\end{aligned} \tag{39}
$$

□

Theorem 8. *Given a set $S_i^{(a,b)}(x), i = 1, \cdots N$ of the N general shifted Genocchi polynomials, the general shifted Genocchi polynomial operational matrix of Caputo's fractional derivative of order α over the interval $[a, b]$ is the $N \times N$ matrix ${}_0P_S^{\alpha}$, given by*

$$
{}_0\mathbf{P}_S^{\alpha} = \Theta_N \mathbf{T}^{(a,b)^{-1}}, \tag{40}
$$

where Θ_N is given in Lemma 7 and $\mathbf{T}^{(a,b)} = [\gamma_{nm}^{(a,b)}]_{N \times N}$ with elements $\gamma_{nm}^{(a,b)}$ is given in Theorem 4.

Proof. From Equation (29),

$$\begin{aligned}{}_0D_x^\alpha \mathbf{S}(x) &= {}_0\mathbf{P}_S^\alpha \mathbf{S}(x),\\ ({}_0D_x^\alpha \mathbf{S}(x))\mathbf{S}^T(x) &= {}_0\mathbf{P}_S^\alpha \mathbf{S}(x)\mathbf{S}^T(x),\\ \int_0^1 ({}_0D_x^\alpha \mathbf{S}(x))\mathbf{S}^T(x)dx &= {}_0\mathbf{P}_S^\alpha \left(\int_0^1 \mathbf{S}(x)\mathbf{S}^T(x)dx\right),\\ \Theta_N &= {}_0\mathbf{P}_S^\alpha \mathbf{T}_0^{(0,1)},\\ \mathbf{P}_S^\alpha &= \Theta_N \mathbf{T}^{(0,1)^{-1}}.\end{aligned} \tag{41}$$

□

3.2. Approximation of Integral Kernel by the General Shifted Genocchi Polynomials. Here, we approximate the integral kernel $K(x,t)$ in terms of the truncated series of the general shifted Genocchi polynomials $S_n^{(a,b)}(x)$:

$$\begin{aligned}K(x,t) &= \sum_{i=1}^{\infty}\sum_{j=1}^{\infty} k_{ij}S_i^{(a,b)}(x)S_j^{(a,b)}(t) \approx \sum_{i=1}^{N}\sum_{j=1}^{N} k_{ij}S_i^{(a,b)}(x)S_j^{(a,b)}(t)\\ &= \mathbf{S}^T(x)\mathbf{K}_S\mathbf{S}(t).\end{aligned} \tag{42}$$

We present two approaches for obtaining the kernel matrix $\mathbf{K}_S$.

3.2.1. Method 1: Conventional Genocchi Coefficient Formula. Using the conventional method of finding the Genocchi coefficients for a single variable function $f(x)$, we can extend the formula to a two-variable function $K(x,t)$ which is continuous and $(N-1)$ differentiable in interval $[0,1]$. This results in the following theorem:

Theorem 9. *Let $K(x,t)$ be a two-variable continuous function in $C^{N-1}([0,1])$. Then, $K(x,t)$ can be approximated in terms of the general shifted Genocchi polynomials up to order N, i.e., $K(x,t) \approx \sum_{i=1}^N\sum_{j=1}^N k_{ij}S_i^{(a,b)}(x)S_j^{(a,b)}(t) = \mathbf{S}^T(x)\mathbf{K}_S\mathbf{S}(t)$, $N \in \mathbb{N}$, where $\mathbf{S}$ is the general shifted Genocchi polynomial basis matrix and $\mathbf{K}_S$ is the $N\times N$ integral kernel matrix in the general shifted Genocchi basis given by*

$$\begin{aligned}\mathbf{K}_S &= [k_{ij}]_{N\times N},\\ k_{ij} &= \frac{(b-a)^{i+j-2}}{4(i!j!)}\left(K_{(x,t)}^{(i-1,j-1)}(a,a) + K_{(x,t)}^{(i-1,j-1)}(a,b)\right.\\ &\quad\left. + K_{(x,t)}^{(i-1,j-1)}(b,a) + K_{(x,t)}^{(i-1,j-1)}(b,b)\right),\end{aligned} \tag{43}$$

where

$$K_{(x,t)}^{(i-1,j-1)}(a,b) = \frac{\partial^{i-1}}{\partial x^{i-1}}\frac{\partial^{j-1}}{\partial t^{j-1}}K(x,t)\bigg|_{x=a,t=b}. \tag{44}$$

Proof. Assume that the kernel $K(x,t)$ is approximated using N number of the general shifted Genocchi polynomials, i.e.,

$$\begin{aligned}K(x,t) \approx &= \sum_{i=1}^{N}\sum_{j=1}^{N} k_{ij}S_i^{(a,b)}(x)S_j^{(a,b)}(t)\\ &= \sum_{j=1}^{N}\left(\sum_{i=1}^{N} k_{ij}S_i^{(a,b)}(x)\right)S_j^{(a,b)}(t).\end{aligned} \tag{45}$$

Set $\phi_j(x) = \sum_{i=1}^N k_{ij}S_i^{(a,b)}(x)$. Hence, $K(x,t) = \sum_{j=1}^N \phi_j(x) S_j^{(a,b)}(t)$. Using the formula of the general shifted Genocchi coefficients for $S_j^{(a,b)}(t)$ (i.e., Theorem 2 with respect to t variable),

$$\phi_j(x) = \frac{(b-a)^{j-1}}{2(j!)}\left(\frac{\partial^{j-1}K(x,t)}{\partial t^{j-1}}\bigg|_{t=a} + \frac{\partial^{j-1}K(x,t)}{\partial t^{j-1}}\bigg|_{t=b}\right). \tag{46}$$

Now using the above expression of $\phi_j(x)$ together with the formula of the general shifted Genocchi coefficients for $S_i^{(a,b)}(x)$ (i.e., with respect to x variable) instead, we obtain

$$\begin{aligned}k_{ij} &= \frac{(b-a)^{i-1}}{2(i!)}\left(\frac{\partial^{i-1}\phi_j(x)}{\partial x^{i-1}}\bigg|_{x=a} + \frac{\partial^{i-1}\phi_j(x)}{\partial x^{i-1}}\bigg|_{x=b}\right)\\ &= \frac{(b-a)^{i-1}}{2(i!)}\left[\frac{\partial^{i-1}}{\partial x^{i-1}}\frac{(b-a)^{j-1}}{2(j!)}\left(\frac{\partial^{j-1}K(x,t)}{\partial t^{j-1}}\bigg|_{t=a} + \frac{\partial^{j-1}K(x,t)}{\partial t^{j-1}}\bigg|_{t=b}\right)\bigg|_{x=a}\right.\\ &\quad\left. + \frac{\partial^{i-1}}{\partial x^{i-1}}\frac{(b-a)^{j-1}}{2(j!)}\left(\frac{\partial^{j-1}K(x,t)}{\partial t^{j-1}}\bigg|_{t=a} + \frac{\partial^{j-1}K(x,t)}{\partial t^{j-1}}\bigg|_{t=b}\right)\bigg|_{x=b}\right]\\ &= \frac{(b-a)^{i-1}(b-a)^{j-1}}{4(i!j!)}\left[\left(\frac{\partial^{i-1}}{\partial x^{i-1}}\frac{\partial^{j-1}K(x,t)}{\partial t^{j-1}}\bigg|_{x=a,t=a}\right.\right.\\ &\quad\left. + \frac{\partial^{i-1}}{\partial x^{i-1}}\frac{\partial^{j-1}K(x,t)}{\partial t^{j-1}}\bigg|_{x=a,t=b}\right) + \left(\frac{\partial^{i-1}}{\partial x^{i-1}}\frac{\partial^{j-1}K(x,t)}{\partial t^{j-1}}\bigg|_{x=b,t=a}\right.\\ &\quad\left.\left. + \frac{\partial^{i-1}}{\partial x^{i-1}}\frac{\partial^{j-1}K(x,t)}{\partial t^{j-1}}\bigg|_{x=b,t=b}\right)\right].\end{aligned} \tag{47}$$

In a similar way, the above approach can be extended to finding the general shifted Genocchi coefficients for the approximation of a multivariable function. □

3.2.2. Method 2: Matrix Method. The classical way will not work for the kernel function not differentiable at $x, t = 0, 1$; then, we can adopt the matrix approach similar to that of finding the general shifted Genocchi coefficients in Theorem 2 to arrive at the following theorem:

Theorem 10. *Let $K(x,t)$ be a two-variable continuous function in $C^{N-1}([a,b])$. Then, $K(x,t)$ can be approximated in terms of the general shifted Genocchi polynomials up to order N, i.e., $K(x,t) \approx \sum_{i=1}^N\sum_{j=1}^N k_{ij}S_i^{(a,b)}(x)S_j^{(a,b)}(t) = S^T(x)K_S S(t)$, $N \in \mathbb{N}$, where S is the general shifted Genocchi polynomial basis matrix and K_S is the $N\times N$ integral kernel matrix in the general shifted Genocchi basis given by*

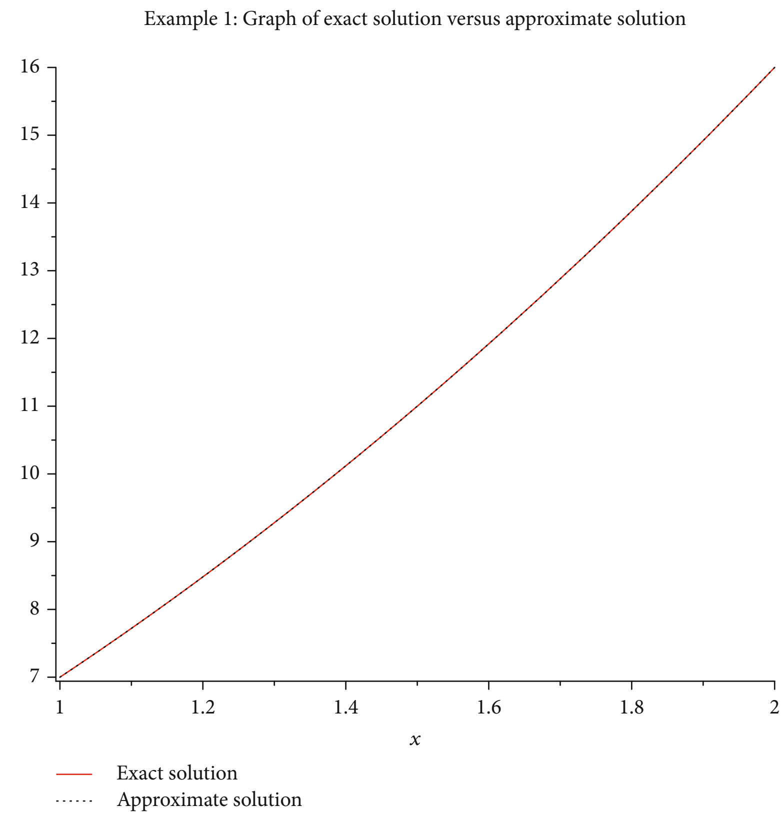

Figure 3: Comparison of exact solution $f(x)$ (red colour) and approximate solution $f^*(x)$ (dot line) of Example 1 for $N = 4$.

$$\mathbf{K}_S = \left(\mathbf{T}^{(\mathbf{a},\mathbf{b})}\right)^{-1} \mathbf{N}_S \left(\mathbf{T}^{(\mathbf{a},\mathbf{b})}\right)^{-1}, \tag{48}$$

where

$$\begin{aligned}
\mathbf{N}_S &= \left[\eta_{pq}\right]_{N\times N} = \left[\int_a^b\int_a^b K(x,t) S_p^{(a,b)}(x) S_q^{(a,b)}(t)\,dx\,dt\right]_{N\times N}, \\
\left(\mathbf{T}^{(\mathbf{a},\mathbf{b})}\right)^{-1} &= \left(\left[\gamma_{n,m}^{(a,b)}\right]_{N\times N}\right)^{-1} \\
&= \left(\left[\sum_{r=0}^{n-1} \frac{(-1)^r (b-a) n_{(r)}}{(m+1)^{(r+1)}} \left(S_{n-r}^{(a,b)}(b) S_{m+1+r}^{(a,b)}(b) - g_{n-r} g_{m+1+r}\right)\right]_{N\times N}\right)^{-1}.
\end{aligned} \tag{49}$$

Proof. From, $K(x,t) \approx \mathbf{S}^T(x)\mathbf{K}_S\mathbf{S}(t)$,

$$\begin{aligned}
\mathbf{S}(x) K(x,t) &= \mathbf{S}(x)\mathbf{S}^T(x)\mathbf{K}_S\mathbf{S}(t), \\
\int_a^b \mathbf{S}(x) K(x,t)\,dx &= \left(\int_a^b \mathbf{S}(x)\mathbf{S}^T(x)\,dx\right)\mathbf{K}_S\mathbf{S}(t) \\
&= \mathbf{T}^{(a,b)}\mathbf{K}_S\mathbf{S}(t), \\
\left(\int_a^b \mathbf{S}(x) K(x,t)\,dx\right)\mathbf{S}^T(t) &= \mathbf{T}^{(a,b)}\mathbf{K}_S\mathbf{S}(t)\mathbf{S}^T(t), \\
\int_a^b\int_a^b K(x,t)\mathbf{S}(x)\mathbf{S}^T(t)\,dx\,dt &= \mathbf{T}^{(a,b)}\mathbf{K}_S\left(\int_a^b \mathbf{S}(t)\mathbf{S}^T(t)\,dt\right),
\end{aligned} \tag{50}$$

Table 1: Comparison of the approximate solution $f^*(x)$ using $N = 4$ with exact solution $f(x) = 2x^2 + 3x + 2$ and absolute errors for Example 1.

t	Exact sol. $f(x)$	Approx. sol. $f^*(x)$	Abs. error $\lvert f(x) - f^*(x)\rvert$
1.0	7.0000000000	7.0000000000	0
1.1	7.7200000000	7.7200000000	0
1.2	8.4800000000	8.4800000000	0
1.3	9.2800000000	9.2800000000	0
1.4	10.1200000000	10.1200000000	0
1.5	11.0000000000	11.0000000000	0
1.6	11.9200000000	11.9200000000	0
1.7	12.8800000000	12.8800000000	0
1.8	13.8800000000	13.8800000000	0
1.9	14.9200000000	14.9200000000	0
2.0	16.0000000000	16.0000000000	0

where $\mathbf{T}^{(a,b)} = \int_a^b \mathbf{S}(x)\mathbf{S}^T(x)\,dx = \int_a^b \mathbf{S}(t)\mathbf{S}^T(t)\,dt$. Define $\mathbf{N}_S = \int_a^b\int_a^b K(x,t)\mathbf{S}(x)\mathbf{S}^T(t)\,dx\,dt$. Thus,

$$\begin{aligned}
\mathbf{N}_S &= \mathbf{T}^{(a,b)}\mathbf{K}_S\mathbf{T}^{(a,b)}, \\
\mathbf{K}_S &= \left(\mathbf{T}^{(a,b)}\right)^{-1}\mathbf{N}_S\left(\mathbf{T}^{(a,b)}\right)^{-1}.
\end{aligned} \tag{51}$$

□

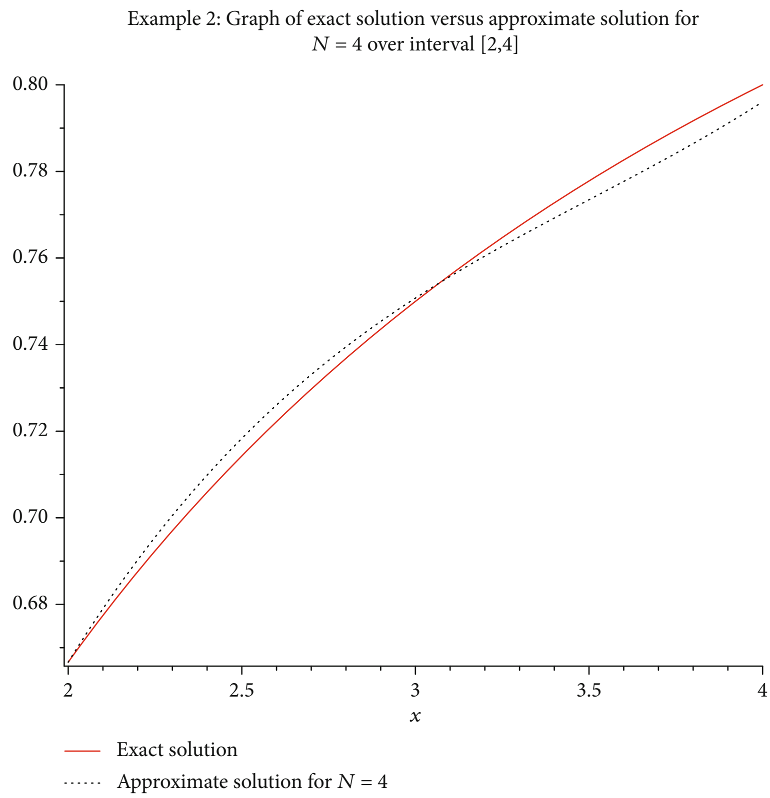

FIGURE 4: Comparison of exact solution $f(x)$ (red colour) and approximate solution $f^*(x)$ (dot line) of Example 2 for $N = 4$.

4. Procedure of Solving Arbitrary Domain Fractional Integro-differential Equation

We will adopt the same approach as the other operational matrix methods for solving FIDE by approximating each term in the equation by the general shifted Genocchi polynomials. From the following class of the 2nd-kind Fredholm FIDE,

$$ {}_0D_x^{\alpha} f(x) = h(x) + \lambda \int_a^b K(x,t) f(t) dt, \tag{52} $$

$$ f^{(i)}(x_i) = y_i, i = 1, \cdots, m. \tag{53} $$

Now, we approximate each term in Equation (52) with the corresponding approximation using the N order of the general shifted Genocchi polynomials,

$$ \begin{aligned} {}_0D_x^{\alpha} f(x) &\approx \mathbf{C}_0^T \mathbf{P}_S^{\alpha} \mathbf{S}(x), \\ h(x) &\approx \mathbf{H}^T \mathbf{S}(x), \\ K(x,t) &\approx \mathbf{S}^T(x) \mathbf{K}_S \mathbf{S}(t). \end{aligned} \tag{54} $$

Hence, FIDE in Equation (52) in matrix form becomes:

$$ \begin{aligned} &\mathbf{S}^T(x)({}_0\mathbf{P}_S^{\alpha})^T \mathbf{C} = \mathbf{S}^T(x)\mathbf{H} + \lambda \int_a^b \mathbf{S}^T(x) \mathbf{K}_S \mathbf{S}(t) \mathbf{S}^T(t) \mathbf{C} dt, \\ &\mathbf{S}^T(x)({}_0\mathbf{P}_S^{\alpha})^T \mathbf{C} = \mathbf{S}^T(x)\mathbf{H} + \lambda \mathbf{S}^T(x) \mathbf{K}_S \left(\int_a^b \mathbf{S}(t) \mathbf{S}^T(t) dt \right) \mathbf{C}, \\ &\mathbf{S}^T(x)\left(({}_0\mathbf{P}_S^{\alpha})^T \mathbf{C} - \mathbf{H} - \lambda \mathbf{K}_S T^{(a,b)} \mathbf{C} \right) = \mathbf{0}, \end{aligned} \tag{55} $$

where $T^{(a,b)} = \int_a^b \mathbf{S}(t)\mathbf{S}^T(t)dt = [\gamma_{nm}^{(a,b)}]_{N\times N}$. Then, we select the N equally spaced points within the interval $[a,b]$, i.e., $v_r = a + ((b-a)(r-1))/(N-1), r = 1, \cdots, N$ as the collocation points and substituting these into Equation (55), and we obtain a system of $N+1$ algebraic equations in terms of the N general shifted Genocchi coefficients $\mathbf{C} = [c_1 \cdots c_N]^T$. Choosing any $N-1$ equations from the above system together with the initial conditions, $f(x_0) = \mathbf{S}^T(x)\mathbf{C} = y_0$, we can solve for the general shifted Genocchi coefficients $\mathbf{C} = [c_1 \cdots c_N]^T$ of the unknown function $f(x)$. The approximate solution $f^*(x) = \mathbf{C}^T\mathbf{S}(x)$ will be compared to the exact solution $f(x)$ over the interval $[a,b]$.

5. Numerical Examples

Here are two examples of FIDE of Equation (1) which are solved using the proposed method via the general shifted Genocchi polynomials and its operational matrix. The computation was done via Maple software.

Example 1. Consider the following FIDE:

$$ {}_0D_x^{(5/3)} f(x) = 6x^{1/3} \frac{\sqrt{3}\Gamma(2/3)}{\pi} - \frac{471}{10} x^2 + \int_1^2 x^2 t^3 f(t) dt. \tag{56} $$

Let $f(1) = 7$, the exact solution is $f(x) = 2x^2 + 3x + 2$. Since $[a,b] = [1,2]$, we use the general shifted Genocchi

Table 2: Comparison of the approximate solution $f^*(x)$ using $N=4$ with exact solution $f(x)=x/(x+1)$ and absolute errors for Example 2.

t	Exact sol. $f(x)$	Approx. sol. $f^*(x)$	Abs. error $\lvert f(x)-f^*(x)\rvert$
2.0	0.6666666667	0.6666666670	$3.00000E-10$
2.1	0.6774193548	0.6790021440	$1.58279E-03$
2.2	0.6875000000	0.6902602348	$2.76023E-03$
2.3	0.6969696970	0.7005176063	$3.54791E-03$
2.4	0.7058823529	0.7098509254	$3.96857E-03$
2.5	0.7142857143	0.7183368566	$4.05114E-03$
2.6	0.7222222222	0.7260520712	$3.82985E-03$
2.7	0.7297297297	0.7330732332	$3.34350E-03$
2.8	0.7368421053	0.7394770103	$2.63490E-03$
2.9	0.7435897436	0.7453400700	$1.75033E-03$
3.0	0.7500000000	0.7507390792	$7.39079E-04$
3.1	0.7560975610	0.7557507047	$3.46856E-04$
3.2	0.7619047619	0.7604516132	$1.45315E-03$
3.3	0.7674418605	0.7649184721	$2.52339E-03$
3.4	0.7727272727	0.7692279476	$3.49933E-03$
3.5	0.7777777778	0.7734567083	$4.32107E-03$
3.6	0.7826086957	0.7776814195	$4.92728E-03$
3.7	0.7872340426	0.7819787491	$5.25529E-03$
3.8	0.7916666667	0.7864253656	$5.24130E-03$
3.9	0.7959183673	0.7910979325	$4.82043E-03$
4.0	0.8000000000	0.7960731198	$3.92688E-03$

polynomials over the interval $[1,2]$, i.e., $S_i^{(1,2)}(x)$ to solve the problem. Let us choose $N=4$ to approximate $f(x)\approx\sum_{i=1}^{4}c_i S_i^{(1,2)}(x)$.

The proposed method gives the general shifted Genocchi coefficients as $c_1=23/2, c_2=9/2, c_3=2/3, c_4=0,$ and therefore, the approximate solution produced is $f^*(x)=c_1 S_1^{(1,2)}(x)+c_2S_2^{(1,2)}(x)+c_3S_3^{(1,2)}(x)+c_4S_4^{(1,2)}(x)=2x^2+3x+2$ which reproduces the exact solution over the interval $[1,2]$. Figure 3 shows both $f(x)$ and $f^*(x)$ over the interval $[1,2]$. The numerical results and absolute errors are shown in Table 1.

Example 2. Consider the following FIDE:

$$ {}_0D_x^{1/2}f(x)=\frac{\sqrt{x}(x+1)^{3/2}+(x+1)\tan\mathrm{h}^{-1}\left(\sqrt{x/(x+1)}\right)}{(x+1)^{5/2}\sqrt{\pi}}+x\left(\ln\left(\frac{3}{5}\right)-4\right)+\int_2^4 xtf(t)dt. \tag{57}$$

Let $f(2)=2/3$, the exact solution is $f(x)=x/(x+1)$. Let us choose orders of $N=4$ of the general shifted Genocchi polynomials over the interval $[a,b]=[2,4]$ to approximate $f(x)$ and compare the graphs and absolute errors between the exact solution and approximate solutions of orders $N=4$. Figure 4 shows both $f(x)$ and $f^*(x)$ of orders $N=4$ over the interval $[2,4]$. The numerical results and absolute errors are shown in Table 2, which shows our method of high accuracy.

6. Conclusion

In this paper, the 2nd-kind nonhomogeneous Fredholm FIDE is solved using the general shifted Genocchi polynomials $S_n^{(a,b)}(x)$. We introduce the general shifted Genocchi polynomials and derive the formula for computing the general shifted Genocchi coefficients. Some new properties for the general shifted Genocchi polynomials were introduced including the determinant form. Also, we derive the analytical expression of the integral of the product of the general shifted Genocchi polynomials, $\mathbf{T}_{(n,m)}$; the integral kernel matrix, $\mathbf{K}_S$; and the general shifted Genocchi polynomial operational matrix of Caputo's fractional derivatives, ${}_0\mathbf{P}_S^{\alpha}$. By approximating each term in the FIDE in terms of the general shifted Genocchi polynomials, the equation is transformed into a system of algebraic equations. With the use of the collocation method over the interval $[a,b]$ and the initial condition given, the arbitrary domain Fredholm FIDE can be solved with very high accuracy with only few terms of the general shifted Genocchi polynomials. For future work, we hope we can extend this approach to other types of Appell polynomials, such as the Bernoulli polynomials which had been used widely such as in [27]. Apart from that, we hope we can use this general shifted Genocchi polynomial approach to solve other kinds of fractional calculus problems, such as those in [28, 29], or inverse fractional calculus problems [30, 31].

Data Availability

No data were used to support this study.

Conflicts of Interest

The authors declare that they have no conflict of interest.

Acknowledgments

This research was supported by Universiti Tun Hussein Onn Malaysia (UTHM) through Tier 1 (vot Q380).

References

[1] T. Kim, D. San Kim, J. Kwon, and H. Y. Kim, "A note on degenerate Genocchi and poly-Genocchi numbers and polynomials," *Journal of Inequalities and Applications*, vol. 2020, no. 1, p. 13, 2020.

[2] D. S. Lee and H. K. Kim, "On the new type of degenerate poly-Genocchi numbers and polynomials," *Advances in Difference Equations*, vol. 2020, no. 1, p. 15, 2020.

[3] W. A. Khan and D. Srivastava, "Certain properties of Apostol-type Hermite based Frobenius-Genocchi polynomials," *Kragujevac Journal of Mathematics*, vol. 45, no. 6, pp. 859–872, 2021.

[4] U. Duran, M. Acikgoz, and S. Araci, "Construction of the type 2 poly-Frobenius-Genocchi polynomials with their certain applications," *Advances in Difference Equations*, vol. 2020, no. 1, p. 14, 2020.

[5] C. Phang, A. Isah, and Y. T. Toh, "Poly-Genocchi polynomials and its applications," *AIMS Mathematics*, vol. 6, no. 8, pp. 8221–8238, 2021.

[6] S. Sadeghi Roshan, H. Jafari, and D. Baleanu, "Solving FDEs with Caputo-Fabrizio derivative by operational matrix based on Genocchi polynomials," *Mathematical Methods in the Applied Sciences*, vol. 41, no. 18, pp. 9134–9141, 2018.

[7] H. Dehestani, Y. Ordokhani, and M. Razzaghi, "The novel operational matrices based on 2D-Genocchi polynomials: solving a general class of variable-order fractional partial integro-differential equations," *Computational and Applied Mathematics*, vol. 39, no. 4, pp. 1–32, 2020.

[8] E. Hashemizadeh, M. A. Ebadi, and S. Noeiaghdam, "Matrix method by Genocchi polynomials for solving nonlinear Volterra integral equations with weakly singular kernels," *Symmetry*, vol. 12, no. 12, p. 2105, 2020.

[9] A. Isah and C. Phang, "A collocation method based on Genocchi operational matrix for solving Emden-Fowler equations," *Journal of Physics: Conference Series*, vol. 1489, article 012022, 2020.

[10] E. Rawashdeh, "Numerical solution of fractional integro-differential equations by collocation method," *Applied Mathematics and Computation*, vol. 176, no. 1, pp. 1–6, 2006.

[11] A. Arikoglu and I. Ozkol, "Solution of fractional integro-differential equations by using fractional differential transform method," *Chaos, Solitons & Fractals*, vol. 40, no. 2, pp. 521–529, 2009.

[12] L. Huang, X.-F. Li, Y. Zhao, and X.-Y. Duan, "Approximate solution of fractional integro-differential equations by Taylor expansion method," *Computers & Mathematics with Applications*, vol. 62, no. 3, pp. 1127–1134, 2011.

[13] J. R. Loh, C. Phang, and K. G. Tay, "New method for solving fractional partial integro-differential equations by combination of Laplace transform and resolvent kernel method," *Chinese Journal of Physics*, vol. 67, pp. 666–680, 2020.

[14] A. Daşcıoğlu and D. Varol, "Laguerre polynomial solutions of linear fractional integro-differential equations," *Mathematical Sciences*, vol. 15, no. 1, pp. 47–54, 2021.

[15] S. Rezabeyk, S. Abbasbandy, and E. Shivanian, "Solving fractional-order delay integro-differential equations using operational matrix based on fractional-order Euler polynomials," *Mathematical Sciences*, vol. 14, no. 2, pp. 97–107, 2020.

[16] L. J. Rong and P. Chang, "Jacobi wavelet operational matrix of fractional integration for solving fractional integro-differential equation," *Journal of Physics: Conference Series*, vol. 693, p. 012002, 2016.

[17] D. Xu, W. Qiu, and J. Guo, "A compact finite difference scheme for the fourth-order time-fractional integro-differential equation with a weakly singular kernel," *Numerical Methods for Partial Differential Equations*, vol. 36, no. 2, pp. 439–458, 2020.

[18] J. Guo, D. Xu, and W. Qiu, "A finite difference scheme for the nonlinear time-fractional partial integro- differential equation," *Mathematical Methods in the Applied Sciences*, vol. 43, no. 6, pp. 3392–3412, 2020.

[19] K. Maleknejad, J. Rashidinia, and T. Eftekhari, "Operational matrices based on hybrid functions for solving general nonlinear two-dimensional fractional integro-differential equations," *Computational and Applied Mathematics*, vol. 39, no. 2, pp. 1–34, 2020.

[20] M. Heydari, M. R. Hooshmandasl, F. M. Maalek Ghaini, and M. Li, "Chebyshev wavelets method for solution of nonlinear fractional integro-differential equations in a large interval," *Advances in Mathematical Physics*, vol. 2013, Article ID 482083, 12 pages, 2013.

[21] K. Diethelm, *The Analysis of Fractional Differential Equations*, vol. 2004 of Lecture Notes in Mathematics, , Springer, 2010.

[22] I. Podlubny, *Fractional Differential Equations, Mathematics in Science and Engineering*, Academic press New York, 1999.

[23] H. Dehestani, Y. Ordokhani, and M. Razzaghi, "On the applicability of Genocchi wavelet method for different kinds of fractional-order differential equations with delay," *Numerical Linear Algebra with Applications*, vol. 26, no. 5, p. 2259, 2019.

[24] J. R. Loh and C. Phang, "A new numerical scheme for solving system of Volterra integro-differential equation," *Alexandria Engineering Journal*, vol. 57, no. 2, pp. 1117–1124, 2018.

[25] F. A. Costabile, M. I. Gualtieri, and A. Napoli, "Recurrence relations and determinant forms for general polynomial sequences. Application to Genocchi polynomials," *Integral Transforms and Special Functions*, vol. 30, no. 2, pp. 112–127, 2019.

[26] F. A. Costabile, "Polynomial sequences: elementary basic methods and application hints. A survey," *Revista de la Real Academia de Ciencias Exactas, Físicas y Naturales. Serie A. Matemáticas*, vol. 113, no. 4, pp. 3829–3862, 2019.

[27] C. Phang, Y. T. Toh, and F. S. Md Nasrudin, "An operational matrix method based on poly-Bernoulli polynomials for solving fractional delay differential equations," *Computation*, vol. 8, no. 3, p. 82, 2020.

[28] A. Faghih and P. Mokhtary, "A novel Petrov-Galerkin method for a class of linear systems of fractional differential equations," *Applied Numerical Mathematics*, vol. 169, pp. 396–414, 2021.

[29] A. Faghih and P. Mokhtary, "Non-linear system of multi-order fractional differential equations: theoretical analysis and a robust fractional Galerkin implementation," *Journal of Scientific Computing*, vol. 91, no. 2, 2022.

[30] A. Taghavi, A. Babaei, and A. Mohammadpour, "A stable numerical scheme for a time fractional inverse parabolic equation," *Inverse Problems in Science and Engineering*, vol. 25, no. 10, pp. 1474–1491, 2017.

[31] A. Babaei and S. Banihashemi, "A stable numerical approach to solve a timefractional inverse heat conduction problem," *Iranian Journal of Science and Technology, Transactions A: Science*, vol. 42, no. 4, pp. 2225–2236, 2018.

Hindawi
Journal of Function Spaces
Volume 2023, Article ID 2726735, 11 pages
https://doi.org/10.1155/2023/2726735

Research Article

Reproducing Kernel Method with Global Derivative

Nourhane Attia,[1] **Ali Akgül**,[2,3,4] **and Abdon Atangana**[5,6]

[1]*National High School for Marine Sciences and Coastal (ENSSMAL), Dely Ibrahim University Campus, Bois des Cars, B.P. 19, 16320, Algiers, Algeria*
[2]*Department of Computer Science and Mathematics, Lebanese American University, Beirut, Lebanon*
[3]*Siirt University, Art and Science Faculty, Department of Mathematics, 56100 Siirt, Turkey*
[4]*Near East University, Mathematics Research Center, Department of Mathematics, Near East Boulevard, PC: 99138, Nicosia/Mersin 10, Turkey*
[5]*Institute for Groundwater Studies, Faculty of Natural and Agricultural Sciences, University of the Free State, South Africa*
[6]*Department of Medical Research, China Medical University Hospital, China Medical University, Taichung, Taiwan*

Correspondence should be addressed to Nourhane Attia; n.attia@enssmal.dz

Received 19 May 2022; Accepted 2 September 2022; Published 19 May 2023

Academic Editor: Yusuf Gurefe

Ordinary differential equations describe several phenomena in different fields of engineering and physics. Our aim is to use the reproducing kernel Hilbert space method (RKHSM) to find a solution to some ordinary differential equations (ODEs) that are described by using the global derivative. In this research, we used the RKHSM to construct new numerical solutions for nonlinear ODEs with global derivative. The used method systematically produces analytic and approximate solutions in the series's form. We tested three applications for showing the performance of the RKHSM.

1. Introduction

In the last decades, the rate of change has been increasingly used for understanding the instantaneous changes that arise in widespread fields. Thinking of the derivative as representing a rate of change is very useful when solving physics problems. The derivative plays a fundamental role in forming the ordinary differential equations (ODEs) that are of great importance because of their ability to describe numerous phenomena in physics, such as electrical networks, oscillating and vibrating systems, satellite orbits, and chemical reactions. Finding the ODEs' solutions is the key to understanding nature, but it is hard and sometimes impossible to get the exact solutions of most real-life ODEs, especially the nonlinear ones. And for such a case, one resorts to numerical methods.

The RKHSM is a widely used numerical method for solving nonlinear ODEs (NODEs). This method which was proposed in 1908 [1] is an effective numerical method for complex nonlinear problems without discretization. Many researchers applied it to solve several types of equations [2–14]. The principal advantages of this method are

(1) the feature that is it is easy to be applied, especially because it is meshfree

(2) its capability to deal with diverse complex differential equations

(3) the uniform convergence between the numerical and exact solutions as well as their derivatives

This research aims to provide a new convenient method using the reproducing kernel (RK) theory for obtaining the solution of some nonlinear ODEs that are described by using the global derivative.

In this paper and for the first time, the RKHSM is used for constructing numerical solutions for the nonlinear ODEs with global derivative.

The next section shows some basic definitions and theorems concerning RK theory and global derivative. The description of the RKHSM and its application to the proposed problem are presented in the third section. The RKHSM's effectiveness and the solutions' accuracy are validated through three applications in the fourth section. Finally, the conclusion is given.

2. Preliminaries

This section covers the theory required to understand the RKHSM we will apply to solve some important nonlinear ODEs with global derivative.

Definition 1. A global derivative of a differentiable function f is [15]

$$D_g f(x) = \lim_{x_1 \longrightarrow x} \frac{f(x_1) - f(x)}{g(x_1) - g(x)}, \tag{1}$$

in which the function g is an increasing nonzero.

Remark 2. If the function g is differentiable then [15]

$$D_g f(x) = \lim_{x_1 \longrightarrow x} \frac{((f(x_1) - f(x))/(x_1 - x))}{((g(x_1) - g(x))/(x_1 - x))} = \frac{f'(x)}{g'(x)}. \tag{2}$$

Remark 3. The global derivative covers the following three cases that we are going to deal with throughout the numerical part:

(1) Case 1: let us choose $g(x) = x$:

$$D_g f(x) = \frac{f'(x)}{g'(x)} = \frac{f'(x)}{(x)'} = \frac{f'(x)}{1} = f'(x). \tag{3}$$

Hence, the classical derivative is a special case of global derivative.

(2) Case 2: let us choose $g(x) = x^\alpha$:

$$D_g f(x) = \frac{f'(x)}{g'(x)} = \frac{f'(x)}{(x^\alpha)'} = \frac{1}{\alpha x^{\alpha-1}} f'(x). \tag{4}$$

Hence, the fractal derivative is a special case of global derivative.

(3) Case 3: let us choose g(x) = sin (x):

$$D_g f(x) = \frac{f'(x)}{g'(x)} = \frac{f'(x)}{(\sin(x))'} = \frac{1}{\cos(x)} f'(x). \tag{5}$$

Definition 4. A function $K : X \times X \longrightarrow \mathbb{C}$ which satisfies

(1) $K(\cdot, x) \in H$ for all $x \in X$

(2) $\langle f, K(\cdot, x)\rangle = f(x)$ for all $f \in H$ and for all $x \in X$

is called a reproducing kernel of H; H is a Hilbert space over $X \neq \varnothing$.

Definition 5. We set [16].

$$W_2^2[0, T] = \left\{ f(x) | \text{The functions } f \text{ and } f' \text{ are absolutely continuous in } [0, T], f'' \in L^2[0, T], \text{ and } f(0) = 0 \right\}. \tag{6}$$

An inner product on $W_2^2[0, T]$ is

$$\langle f, g\rangle_{W_2^2} = \sum_{j=0}^{1} f^{(i)}(0) g^{(i)}(0) + \int_0^T f''(x) g''(x) dx, \tag{7}$$

and its norm is denoted by

$$\|f\|_{W_2^2} = \sqrt{\langle f, f\rangle_{W_2^2}}, \tag{8}$$

for all $f, g \in W_2^2[0, T]$.

Theorem 6. *The function*

$$S_\tau(x) = \begin{cases} x\tau + \dfrac{1}{2}x^2\tau - \dfrac{1}{6}x^3 & , x \le \tau, \\ \tau x + \dfrac{1}{2}\tau^2 x - \dfrac{1}{6}\tau^3 & , x > \tau, \end{cases} \tag{9}$$

is the reproducing kernel function of $W_2^2[0, T]$,

For the proof of this theorem, see [17].

Definition 7. We set [16].

$$W_2^1[0, T] = \left\{ f(x) | f \text{ is absolutely continuous in } [0, T] \text{ and } f' \in L^2[0, T] \right\}. \tag{10}$$

An inner product on $W_2^1[0,T]$ is

$$\langle f,g\rangle_{W_2^1} = f(0)g(0) + \int_0^T f'(x)g'(x)dx, \quad (11)$$

and its norm is denoted by

$$\|f\|_{W_2^1} = \sqrt{\langle f,f\rangle_{W_2^1}}, \quad (12)$$

for all $f, g \in W_2^1[0,T]$.

Theorem 8. *The function*

$$R_\tau(x) = \begin{cases} 1+x & , x \le \tau, \\ 1+\tau & , x > \tau, \end{cases} \quad (13)$$

is the reproducing kernel function of $W_2^1[0,T]$.

For the proof of this theorem, see [17].

3. Solution Methodology

We now consider the 1^{st}-order nonlinear ODE,

$$\begin{cases} D_g f(x) = F(x, f(x)), & x \in [0,T], T \in \mathbb{R}^*, \\ f(0) = \lambda, \end{cases} \quad (14)$$

where D_g is the global derivative, f is the unknown, F is a function of x and $f(x)$, and λ is a constant.

To apply the RKHSM, let us begin with making a change of variable to homogenize the initial condition $f(0) = \lambda$:

$$u(x) = f(x) - \lambda. \quad (15)$$

Replacing $f(x)$ by $u(x) + \lambda$ in (14) gives

$$\begin{cases} D_g u(x) = \bar{F}(x, u(x)), & x \in [0,T], T \in \mathbb{R}^*, \\ u(0) = 0, \end{cases} \quad (16)$$

where $\bar{F}$ is a nonlinear function of x and $u(x)$.

The second step is to define a linear operator $A : W_2^2[0, T] \longrightarrow W_2^1[0,T]$ such that

$$Au(x) = D_g u(x). \quad (17)$$

We use this linear operator to get

$$\begin{cases} Au(x) = \bar{F}(x, u(x)), & x \in [0,T], T \in \mathbb{R}^*, \\ u(0) = 0. \end{cases} \quad (18)$$

The next step is to build an orthogonal function system of $W_2^2[0,T]$. Let

$$\psi_i(x) = A^* \kappa_i(x), \quad (19)$$

where

(i) $\kappa_i(x) = R_{x_i}(x)$; $R_{x_i}(x)$ represents the RK function of $W_2^1[0,T]$

(ii) The set $\{x_i\}_{i=1}^{\infty}$ is dense in $[0,T]$

(iii) A^* is the adjoint of A

Now, to find $\{\bar{\psi}_i\}_{i=1}^{\infty}$, we need to use Gram-Schmidt's process:

$$\bar{\psi}_i(x) = \sum_{k=1}^{i} \varpi_{ik}\psi_k(x), \quad \varpi_{ii} > 0, i = 1, 2, \cdots. \quad (20)$$

where $\{\psi_i\}_{i=1}^{\infty}$ denotes the function system in $W_2^2[0,T]$ obtained by

$$\begin{aligned} \psi_i(x) = A^*\kappa_i(x) &= \langle A^*\kappa_i(\eta), S_x(\eta)\rangle_{W_2^2} = \langle \kappa_i(\eta), AS_x(\eta)\rangle_{W_2^1} \\ &= \left\langle R_{\eta_i}(\eta), AS_x(\eta)\right\rangle_{W_2^1} = A_\eta S_x(\eta)|_{\eta=x_i}. \end{aligned} \quad (21)$$

And the coefficients ϖ_{ik} can be found by

$$\varpi_{ij} = \begin{cases} \dfrac{1}{\|\psi_1\|}, & \text{for} \quad i = j = 1, \\ \dfrac{1}{e_i}, & \text{for} \quad i = j \ne 1, \\ -\dfrac{1}{e_i}\displaystyle\sum_{k=j}^{i-1} C_{ik}\varpi_{kj}, & \text{for} \quad i > j, \end{cases} \quad (22)$$

where $e_i = \left(\|\psi_i\|^2 - \sum_{k=1}^{i-1} C_{ik}^2\right)^{1/2}$, $C_{ik} = \langle \psi_i, \bar{\psi}_k\rangle_{W_2^2}$.

Theorem 9. *Suppose $\{x_i\}_{i=1}^{\infty}$ is dense in $[0,T]$, then $\{\psi_i\}_{i=1}^{\infty}$ is the complete system of $W_2^2[0,T]$.*

Proof. We know that $\psi_i(x) \in W_2^2[0,T]$. So, for each fixed $u(x) \in W_2^2[0,T]$, it follows

$$\langle u(x), \psi_i(x)\rangle_{W_2^2} = 0, \; i = 1, 2, \cdots. \quad (23)$$

Since

$$\begin{aligned} \langle u(x), \psi_i(x)\rangle_{W_2^2} &= \langle u(x), A^*\kappa_i(x)\rangle_{W_2^2} \\ &= \langle Au(x), \kappa_i(x)\rangle_{W_2^1} \\ &= Au(x_i) = 0, \end{aligned} \quad (24)$$

and $\{x_i\}_{i=1}^{\infty}$ is dense on the interval $[0,T]$, we have

$$Au(x) = 0. \quad (25)$$

Then,

$$A^{-1}(Au(x)) = A^{-1}(0), \tag{26}$$

that gives

$$u(x) = 0. \tag{27}$$

□

Lemma 10. *Assume $u \in W_2^2[0,T]$, then*

$$\left\| u^{(\mathfrak{i})}(x) \right\|_C \le \mathfrak{C} \| u(x) \|_{W_2^2}, \quad \mathfrak{i} = 0, 1, \tag{28}$$

where $\mathfrak{C} \ge 0$ and $\| u(x) \|_C = \max_{x \in [0,T]} |u(x)|$.

Proof. $\forall x \in [0, T]$ we have

$$u^{(\mathfrak{i})}(x) = \left\langle u(\cdot), \partial_x^{(\mathfrak{i})} S_x(\cdot) \right\rangle_{W_2^2}, \quad \mathfrak{i} = 0, 1. \tag{29}$$

Using the expression of $\partial_x^{(\mathfrak{i})} S_x(\cdot)$, we can reach

$$\left\| \partial_x^{(\mathfrak{i})} S_x \right\|_{W_2^2} \le \mathfrak{C}_{\mathfrak{i}}, \quad \mathfrak{i} = 0, 1. \tag{30}$$

Consequently,

$$\begin{aligned} \left| u^{(\mathfrak{i})}(x) \right| &= \left| \left\langle u(\cdot), \partial_x^{(\mathfrak{i})} S_x(\cdot) \right\rangle_{W_2^2} \right| \\ &\le \left\| \partial_x^{(\mathfrak{i})} S_x \right\|_{W_2^2} \| u \|_{W_2^2} \\ &\le \mathfrak{C}_{\mathfrak{i}} \| u \|_{W_2^2}, \mathfrak{i} = 0, 1. \end{aligned} \tag{31}$$

where $\mathfrak{C} = \max_{\mathfrak{i}=0,1} \{ \mathfrak{C}_{\mathfrak{i}} \}$. Then Lemma 10 follows from (31). □

Theorem 11. *Assume $\{x_{\mathfrak{i}}\}_{\mathfrak{i}=1}^{\infty}$ is dense in $[0,T]$ and problem (18) has a solution that should be unique on $W_2^2[0,T]$. Therefore, the solution of (18) is*

$$u(x) = \sum_{\mathfrak{i}=1}^{\infty} \sum_{k=1}^{\mathfrak{i}} \varpi_{\mathfrak{i}k} \bar{F}(x_k, u(x_k)) \bar{\psi}_{\mathfrak{i}}(x). \tag{32}$$

While the solution of (14) is

$$f(x) = \sum_{\mathfrak{i}=1}^{\infty} \sum_{k=1}^{\mathfrak{i}} \varpi_{\mathfrak{i}k} \bar{F}(x_k, u(x_k)) \bar{\psi}_{\mathfrak{i}}(x) + \lambda. \tag{33}$$

Proof. Firstly, the fact that $\{\bar{\psi}_{\mathfrak{i}}(x)\}_{\mathfrak{i}=1}^{\infty}$ is a complete orthonormal basis in $W_2^2[0,T]$ allows us to write

$$\begin{aligned} u(x) &= \sum_{\mathfrak{i}=1}^{\infty} \langle u(x), \bar{\psi}_{\mathfrak{i}}(x) \rangle_{W_2^2} \bar{\psi}_{\mathfrak{i}}(x) \\ &= \sum_{\mathfrak{i}=1}^{\infty} \left\langle u(x), \sum_{k=1}^{\mathfrak{i}} \varpi_{\mathfrak{i}k} \psi_k(x) \right\rangle_{W_2^2} \bar{\psi}_{\mathfrak{i}}(x) \\ &= \sum_{\mathfrak{i}=1}^{\infty} \sum_{k=1}^{\mathfrak{i}} \varpi_{\mathfrak{i}k} \langle u(x), \psi_k(x) \rangle_{W_2^2} \bar{\psi}_{\mathfrak{i}}(x) \\ &= \sum_{\mathfrak{i}=1}^{\infty} \sum_{k=1}^{\mathfrak{i}} \varpi_{\mathfrak{i}k} \langle u(x), A^* \kappa_k(x) \rangle_{W_2^2} \bar{\psi}_{\mathfrak{i}}(x) \\ &= \sum_{\mathfrak{i}=1}^{\infty} \sum_{k=1}^{\mathfrak{i}} \varpi_{\mathfrak{i}k} \langle Au(x), \kappa_k(x) \rangle_{W_2^1} \bar{\psi}_{\mathfrak{i}}(x) \\ &= \sum_{\mathfrak{i}=1}^{\infty} \sum_{k=1}^{\mathfrak{i}} \varpi_{\mathfrak{i}k} \langle Au(x), R_x(x_k) \rangle_{W_2^1} \bar{\psi}_{\mathfrak{i}}(x) \\ &= \sum_{\mathfrak{i}=1}^{\infty} \sum_{k=1}^{\mathfrak{i}} \varpi_{\mathfrak{i}k} \bar{\mathrm{F}}(x_k, u(x_k)) \bar{\psi}_{\mathfrak{i}}(x), \end{aligned} \tag{34}$$

with $\bar{\mathrm{F}}(x_k, u(x_k)) = Au(x_k)$.

Secondly, by replacing $g(\varsigma)$ by its formula (32) in the transformation (15), we get

$$u(x) = \sum_{\mathfrak{i}=1}^{\infty} \sum_{k=1}^{\mathfrak{i}} \varpi_{\mathfrak{i}k} \bar{\mathrm{F}}(x_k, u(x_k)) \bar{\psi}_{\mathfrak{i}}(x) + \lambda. \tag{35}$$

We now write the RKHSM's solution $u_n(x)$ as

$$u_n(x) = \sum_{\mathfrak{i}=1}^{n} \sum_{k=1}^{\mathfrak{i}} \varpi_{\mathfrak{i}k} \bar{\mathrm{F}}(x_k, u(x_k)) \bar{\psi}_{\mathfrak{i}}(x). \tag{36}$$

The space $W_2^2[0,T]$ is a Hilbert space, hence

$$\sum_{\mathfrak{i}=1}^{\infty} \sum_{k=1}^{\mathfrak{i}} \varpi_{\mathfrak{i}k} \bar{\mathrm{F}}(x_k, u(x_k)) \bar{\psi}_{\mathfrak{i}}(x) < \infty, \tag{37}$$

which means that $u_n(x)$ converges to $u(x)$ in the norm. □

Theorem 12.

(1) $u_n(x)$ converges uniformly to $u(x)$

(2) $u_n'(x)$ converges uniformly to $u'(x)$

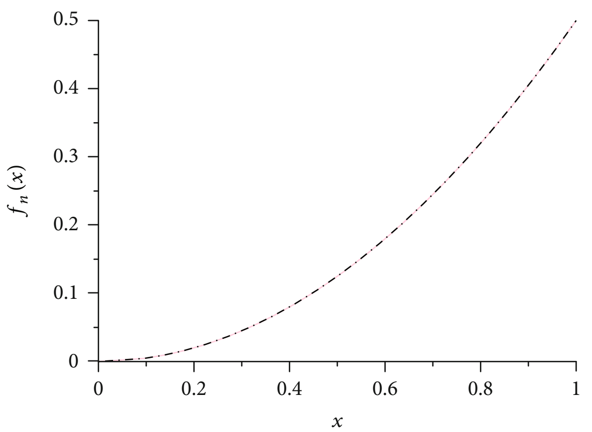

FIGURE 1: Exact and RKHSM's solutions for Example 1 with $g(x) = x$.

Proof. For the first result, we need to estimate the term on the left below:

$$\begin{aligned} &\forall x \in [0, T], \\ &|u_n(x) - u(x)| = \left|\langle u_n(\cdot) - u(\cdot), S_x(\cdot)\rangle_{W_2^2}\right| \\ &\qquad \leq \|S_x\|_{W_2^2}\|u_n - u\|_{W_2^2} \\ &\qquad \leq \mathscr{C}_0\|u_n - u\|_{W_2^2}, \end{aligned} \tag{38}$$

where $\mathscr{C}_0$ is a constant.

Following the same way, we get

$$\left|u_n'(x) - u'(x)\right| \leq \|\partial_x S_x\|_{W_2^2}\left\|u_n' - u'\right\|_{W_2^2}, \tag{39}$$

due to the uniform boundedness of $\partial_x S_x(\cdot)$, we have

$$\|\partial_x S_x\|_{W_2^2} \leq \mathscr{C}_1, \tag{40}$$

where $\mathscr{C}_1$ is a positive constant.

Therefore

$$\left|u_n'(x) - u'(x)\right| \leq \mathscr{C}_1\left\|u_n' - u'\right\|_{W_2^2}. \tag{41}$$

□

4. A Numerical Experiment

This section is the numerical part that assures the efficiency of the proposed method by testing three examples. The rate of convergence of the presented method is as follows [18]:

$$(O_c)_n = \frac{-\ln(E_n/E_{n/2})}{\ln(2)}, \tag{42}$$

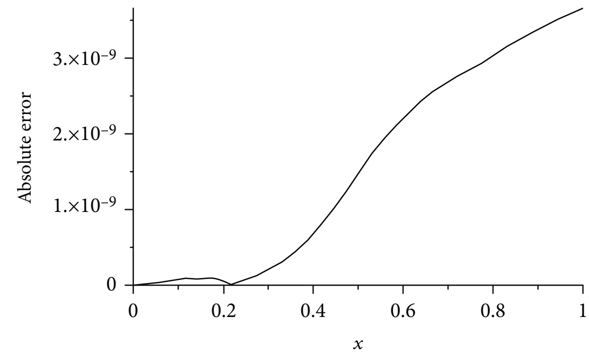

FIGURE 2: Absolute error of the RKHSM for Example 1 with $g(x) = x$.

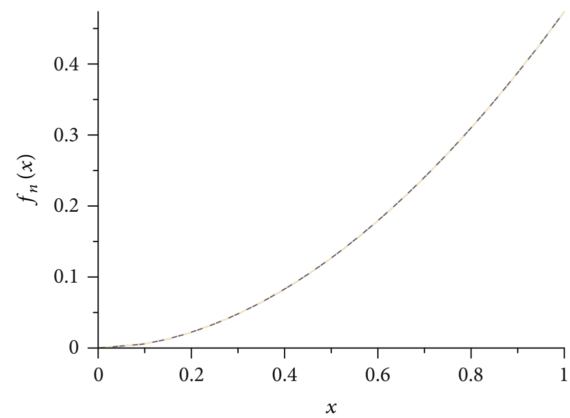

FIGURE 3: Exact and RKHSM's solutions for Example 1 with $g(x) = x^{0.9}$.

where

$$E_n = \max_{x\in[0,1]}|f(x) - f_n(x)|. \tag{43}$$

Now, how to apply the RKHSM can be summarized in the following procedure:

Step 1. Fix n.

Step 2. Set $\psi_i(x_i) = A_\eta S_x(\eta)|_{\eta=x_i}$.

Step 3. Calculate the orthogonalization coefficients ϖ_{ij} using (22).

Step 4. Set $\overline{\psi}_i(x_i) = \sum_{k=1}^{i}\varpi_{ik}\psi_k(x_i)$, $\varpi_{ii} > 0$, $i = 1, 2, \cdots, n$.

Step 5. Choose an initial guess $u_0(x_1)$.

Step 6. Set $i = 1$.

Step 7. Set $\Lambda_i = \sum_{k=1}^{i}\varpi_{ik}\overline{F}(x_k, u(x_k))$.

Step 8. $u_i(x_i) = \sum_{\ell=1}^{i}\Lambda_\ell\overline{\psi}_\ell(x_\ell)$.

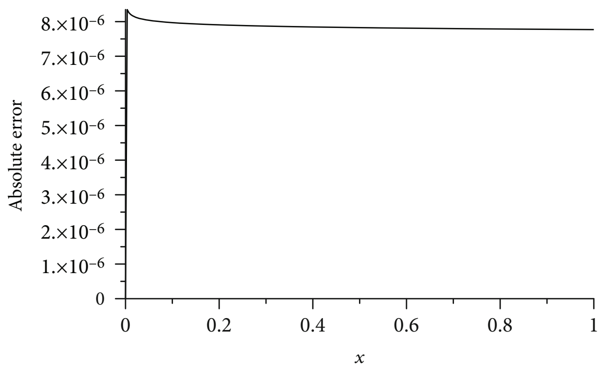

Figure 4: Absolute error of the RKHSM for Example 1 with $g(x) = x^{0.9}$.

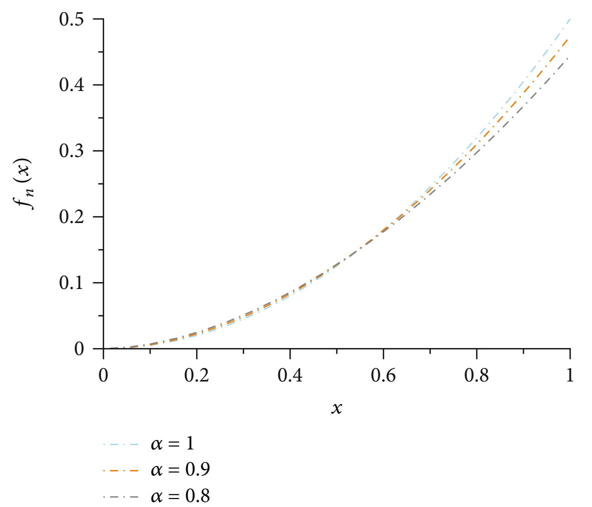

Figure 5: RKHSM's solutions for Example 1 with $g(x) = x^{\alpha}$: $\alpha = 1, \alpha = 0.9$, and $\alpha = 0.8$.

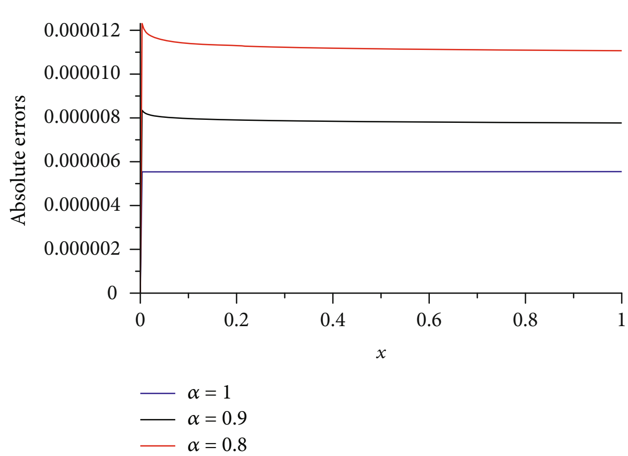

Figure 6: Absolute errors of the RKHSM for Example 1 with $g(x) = x^{\alpha}$ and $\alpha \in \{1\,;0.9\,;0.8\}$.

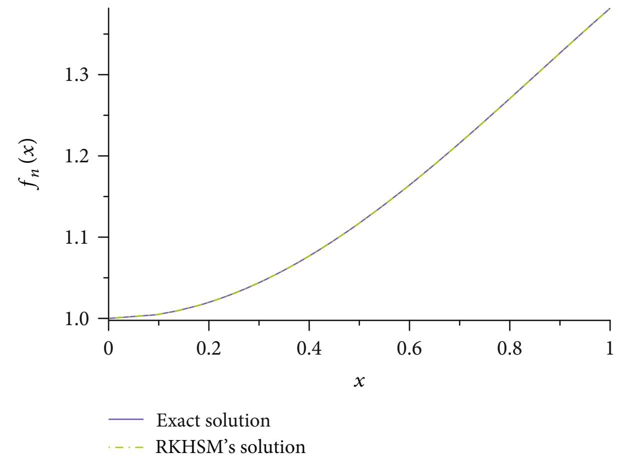

Figure 7: Exact and RKHSM's solutions for Example 1 with $g(x) = \sin(x)$.

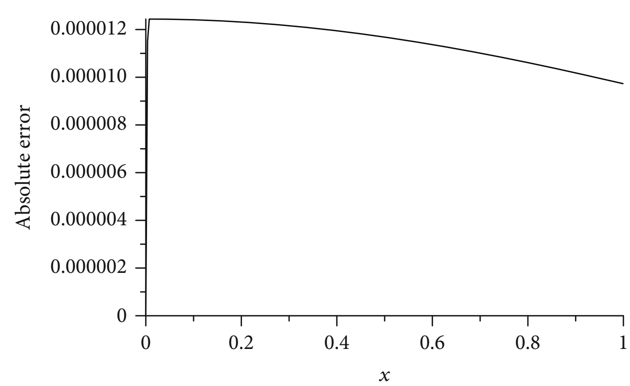

Figure 8: Absolute error of the RKHSM for Example 1 with $g(x) = \sin(x)$.

Table 1: Rate of convergence for Example 1 with $g(x) = x$.

n	Maximum absolute error	$(O_c)_n$
2	0.0833	——
4	0.0250	1.74
8	0.0069	1.85
16	0.0018	1.92
32	0.0005	1.96
64	0.0001	1.98
128	0.0000	1.99

Step 9. If $\mathfrak{i} < n$, set $\mathfrak{i} = \mathfrak{i} + 1$. Go to Step 7. Else stop.

where $x_{\mathfrak{i}} = \mathfrak{i}/n$, $\mathfrak{i} = 1, 2, \cdots, n$ and n is the number of collocation points.

Example 1. Taking the following linear ODE with global derivative:

$$\begin{cases} D_g f(x) = x, & x \in [0, 1], \\ f(0) = 0. \end{cases} \tag{44}$$

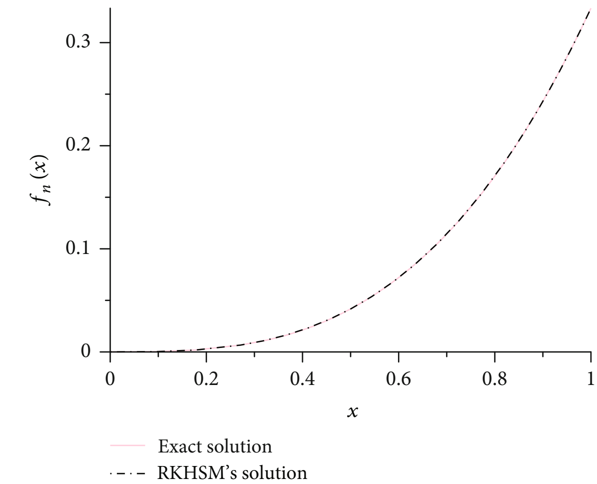

FIGURE 9: Exact and RKHSM's solutions for Example 2 with $g(x) = x$.

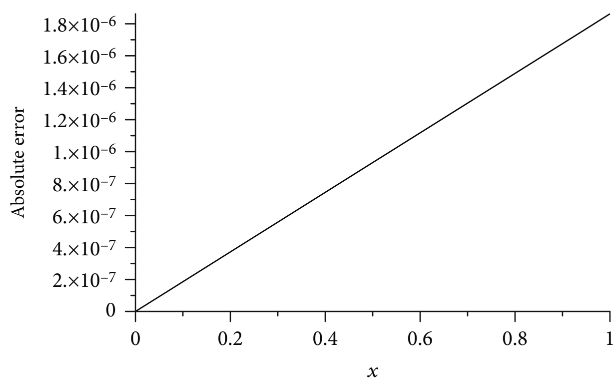

FIGURE 10: Absolute error of the RKHSM for Example 2 with $g(x) = x$.

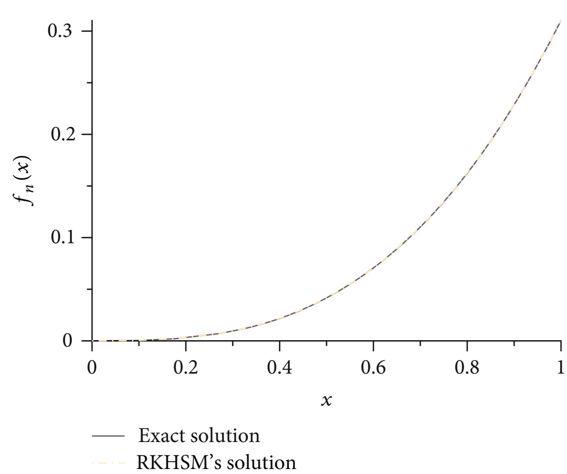

FIGURE 11: Exact and RKHSM's solutions for Example 2 with $g(x) = x^{0.9}$.

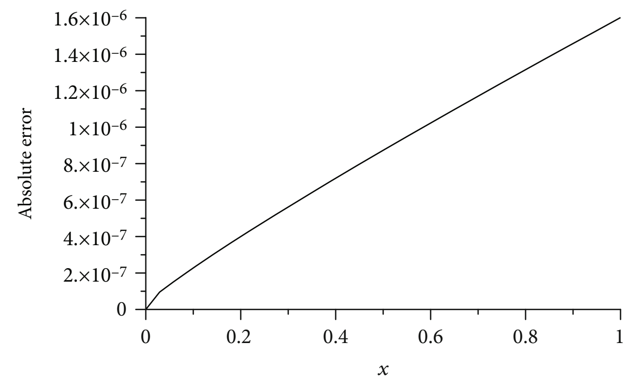

FIGURE 12: Absolute error of the RKHSM for Example 2 with $g(x) = x^{0.9}$.

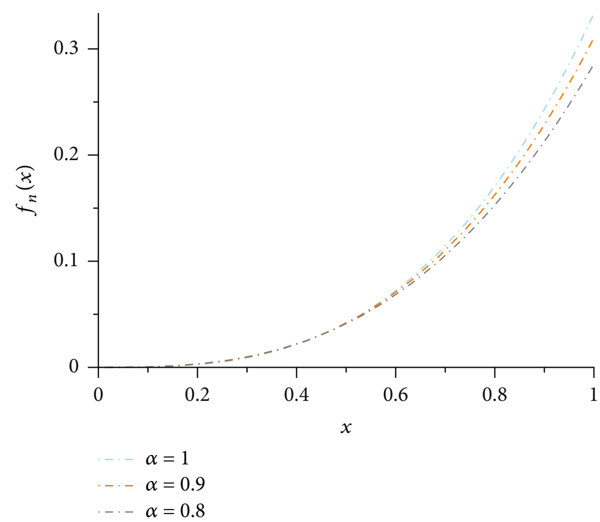

FIGURE 13: RKHSM's solutions for Example 2 with $g(x) = x^{\alpha}$: $\alpha = 1, \alpha = 0.9$, and $\alpha = 0.8$.

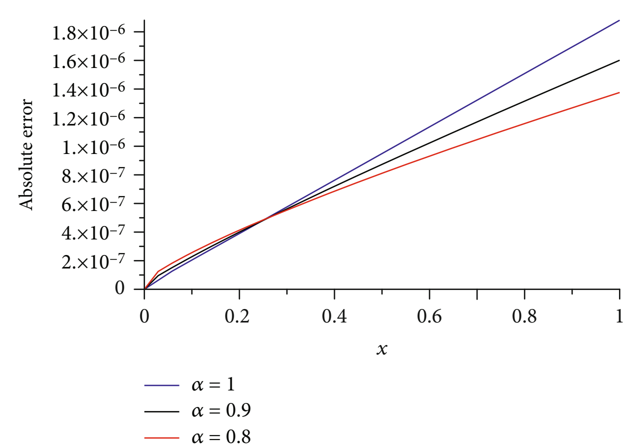

FIGURE 14: Absolute errors of the RKHSM for Example 2 with $g(x) = x^{\alpha}$ and $\alpha \in \{1 ; 0.9 ; 0.8\}$.

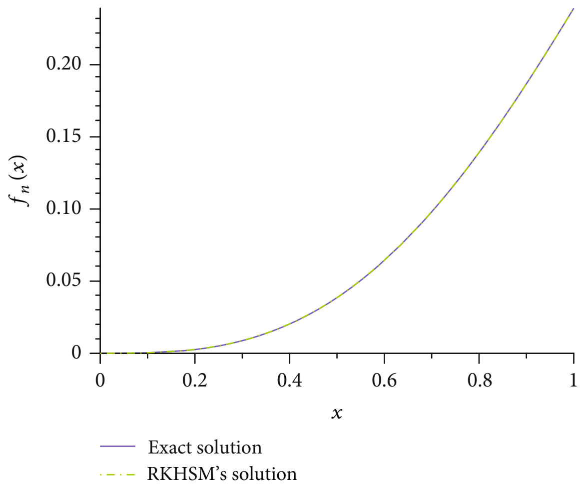

FIGURE 15: Exact and RKHSM's solutions for Example 2 with $g(x) = \sin(x)$.

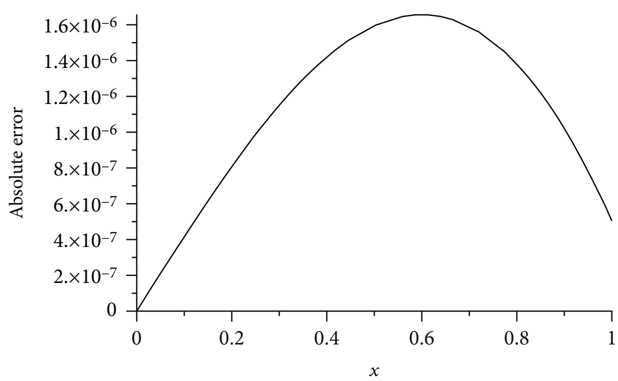

FIGURE 16: Absolute error of the RKHSM for Example 2 with $g(x) = \sin(x)$.

As the initial condition is homogeneous. We can then directly define a bounded linear operator A as

$$\begin{aligned} A : W_2^2[0,1] &\longrightarrow W_2^1[0,1] \\ f(x) &\longrightarrow Af(x) = D_g f(x). \end{aligned} \tag{45}$$

Taking $n = 100$ collocation points in which $x_i = i/n$, $i = 1, 2 \cdots, n$. The approximate solution for Example 1 is found using the RKHSM for different cases of the function $g(x)$ in the global derivative when $g(x)$ equals x, x^α, and $\sin(x)$. For each case, the results are compared with the exact solution. Figure 1 shows the exact solution and the RKHSM's solution with $g(x) = x$. The absolute error of this case is plotted in Figure 2. In Figure 3, we compared the exact solution with the RKHSM's solution when $g(x) = x^\alpha$ with $\alpha = 0.9$, and its absolute error is given in Figure 4, whereas in Figures 5 and 6, we depicted the obtained results for $\alpha = 1, 0.9$, and 0.8 together. Figures 7 and 8 are where the results of the last case of $g(x)$ are given. We can see from these figures that the graphs' behavior is very similar. To highlight more comparisons between the RKHSM and the exact solution, we gave the rate of convergence for $g(x) = x$ in Table 1, and we drew the absolute error for each case through the figures presented. What we can observe here is that the RKHSM's solution is very close to the exact one. And this confirms that the proposed method is effective.

TABLE 2: Rate of convergence for Example 2 with $g(x) = x$.

n	Maximum absolute error	$(O_c)_n$
2	0.0833	——
4	0.0167	2.32
8	0.0035	2.26
16	0.0008	2.18
32	0.0002	2.11
64	0.0000	2.06

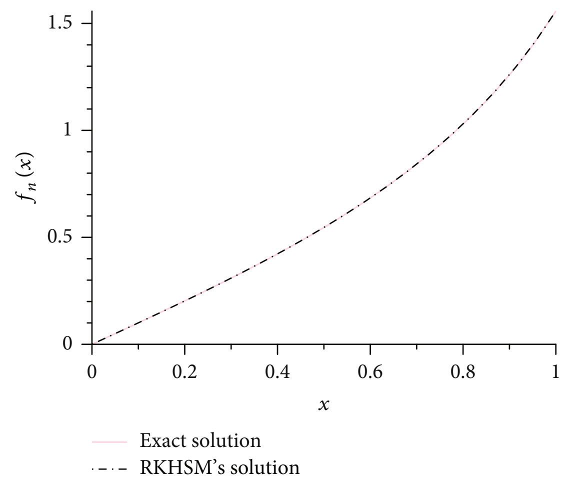

FIGURE 17: Exact and RKHSM's solutions for Example 3 with $g(x) = x$.

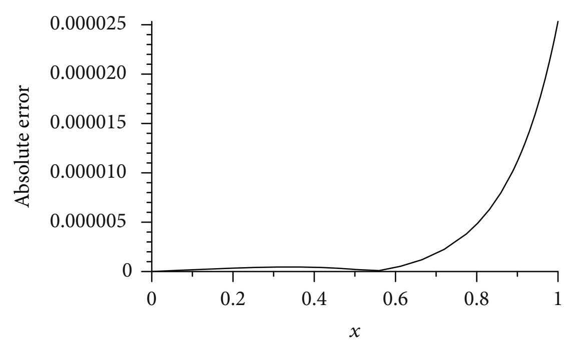

FIGURE 18: Absolute error of the RKHSM for Example 3 with $g(x) = x$.

Example 2. Taking the following linear ODE with global derivative:

$$\begin{cases} D_g f(x) = x^2, & x \in [0,1], \\ f(0) = 0. \end{cases} \tag{46}$$

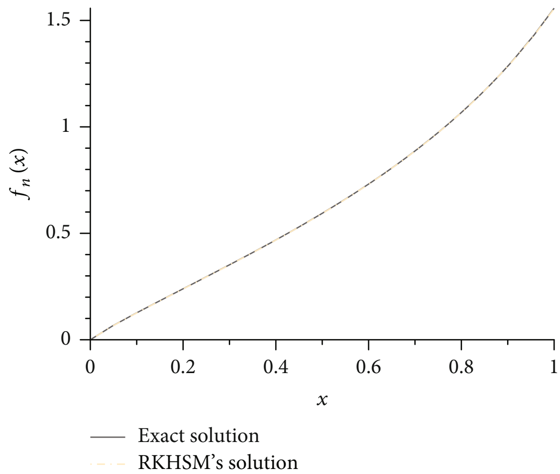

Figure 19: Exact and RKHSM's solutions for Example 3 with $g(x) = x^{0.9}$.

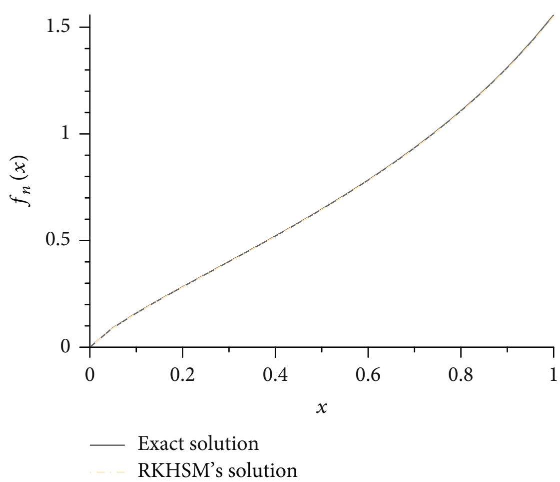

Figure 20: Exact and RKHSM's solutions for Example 3 with $g(x) = x^{0.8}$.

As the initial condition is homogeneous. We can then directly define a bounded linear operator A as

$$\begin{aligned} \mathrm{A} : W_2^2[0,1] &\longrightarrow W_2^1[0,1] \\ f(x) &\longrightarrow Af(x) = D_g f(x). \end{aligned} \tag{47}$$

Taking $n = 100$ collocation points in which $x = \mathfrak{i}/n$, $\mathfrak{i} = 1, 2 \cdots, n$. The approximate solution for Example 2 is found using the RKHSM for different cases of the function $g(x)$ in the global derivative when $g(x)$ equals x,x^α, and sin (x). For each case, the results are compared with the exact solution of each case. Figure 9 shows the exact solution and the RKHSM's solution with $g(x) = x$. The absolute error of this case is plotted in Figure 10. In Figure 11, we compared the exact solution with the RKHSM's solution when $g(x) = x^\alpha$ with $\alpha = 0.9$, and its absolute error is given in Figure 12, whereas in Figures 13 and 14, we depicted the obtained results for $\alpha = 1$,0.9, and 0.8 together. Figures 15 and 16 are where the results of the last case of $g(x)$ are given. We can see from these figures that the graphs' behavior is very similar. To highlight more comparisons between the RKHSM and the exact solution, we gave the rate of convergence for $g(x) = x$ in Table 2, and we drew the absolute error for each case through the figures presented. What we can observe here

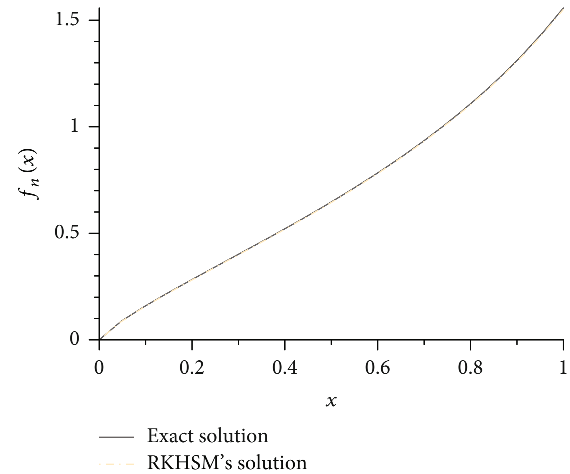

Figure 21: Exact and RKHSM's solutions for Example 3 with $g(x) = x^{0.6}$.

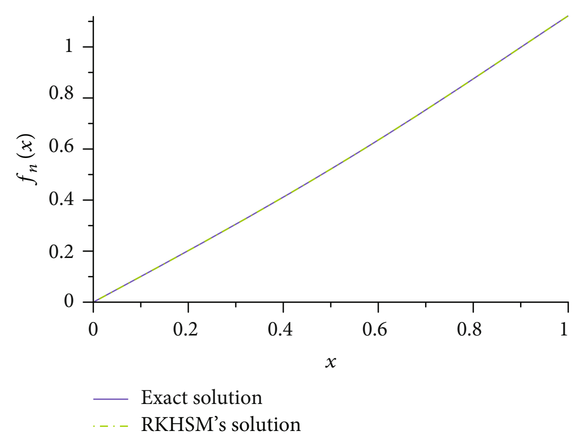

Figure 22: Exact and RKHSM's solutions for Example 3 with $g(x) = \sin(x)$.

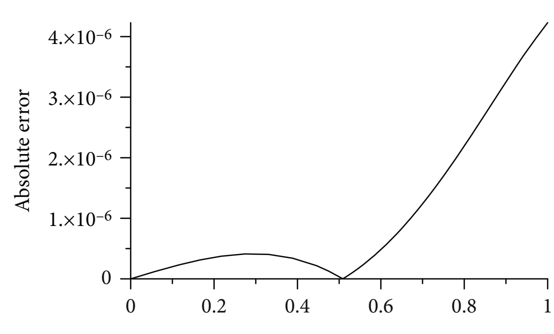

Figure 23: Absolute error of the RKHSM for Example 3 with $g(x) = \sin(x)$.

TABLE 3: Rate of convergence for Example 3 with $g(x) = x$.

n	Maximum absolute error	$(O_c)_n$
2	0.1027	——
4	0.0658	0.64
8	0.0260	1.34
16	0.0078	1.73
32	0.0021	1.89
64	0.0005	1.95

is that the RKHSM's solution is very close to the exact one. And this confirms that the proposed method is effective.

Example 3. Taking the following linear ODE with global derivative:

$$\begin{cases} D_g f(x) = f(x)^2 + 1, & x \in [0, 1], \\ f(0) = 0. \end{cases} \tag{48}$$

As the initial condition is homogeneous. We can then directly define a bounded linear operator A as

$$\begin{aligned} A : W_2^2[0, 1] &\longrightarrow W_2^1[0, 1] \\ f(x) &\longrightarrow Af(x) = D_g f(x). \end{aligned} \tag{49}$$

Taking$n = 100$ collocation points in which $x = \mathfrak{i}/n$, $\mathfrak{i} = 1, 2 \cdots, n$. The approximate solution for Example 3 is found using the RKHSM for different cases of the function $g(x)$ in the global derivative when $g(x)$ equals x,x^α, and sin (x). For each case, the results are compared with the exact solution of each case. Figure 17 shows the exact solution and the RKHSM's solution with $g(x) = x$. The absolute error of this case is plotted in Figure 18. In Figures 19–21, we compared the exact solution with the RKHSM's solution when $g(x) = x^\alpha$ with $\alpha \in \{0.9,0.8,0.6\}$. Figures 22 and 23 are where the results of the last case of $g(x)$ are given. We can see from these figures that the graphs' behavior is very similar. To highlight more comparisons between the RKHSM and the exact solution, we gave the rate of convergence for $g(x) = x$ in Table 3, and we drew the absolute error for each case through the figures presented. What we can observe here is that the RKHSM's solution is very close to the exact one. And this confirms that the proposed method is effective.

5. Conclusion

In this paper, an efficient method, named the reproducing kernel Hilbert space method, is applied successfully for solving nonlinear ODEs described by using the global derivative. The accuracy and applicability of the RKHSM are validated by computing the numerical solutions at many grid points. The results show that the RKHSM is a powerful method to deal with many other nonlinear problems that arise in a large variety of physical problems with different types of derivatives.

Data Availability

All of the necessary data and the implementation details have been included in the manuscript.

Conflicts of Interest

The authors declare that they have no conflicts of interest.

References

[1] S. Zaremba, "Sur le calcul numérique des fonctions demandées dans le problème de Dirichlet et le problème hydrodynamique," *Bulletin International de l'Académie des Sciences de Cracovie*, vol. 68, pp. 125–195, 1908.

[2] O. Abu Arqub, J. Singh, B. Maayah, and M. Alhodaly, "Reproducing kernel approach for numerical solutions of fuzzy fractional initial value problems under the Mittag–Leffler kernel differential operator," *Mathematical Methods in the Applied Sciences*, 2021.

[3] T. Allahviranloo and H. Sahihi, "Reproducing kernel method to solve fractional delay differential equations," *Applied Mathematics and Computation*, vol. 400, article 126095, 2021.

[4] E. Babolian, S. Javadi, and E. Moradi, "RKM for solving Bratu-type differential equations of fractional order," *Mathematical Methods in the Applied Sciences*, vol. 39, no. 6, pp. 1548–1557, 2016.

[5] Y. Chellouf, B. Maayah, S. Momani et al., "Numerical solution of fractional differential equations with temporal two-point BVPs using reproducing kernal Hilbert space method," *AIMS Mathematics*, vol. 6, no. 4, pp. 3465–3485, 2021.

[6] M. Foroutan, A. Ebadian, and H. R. Fazli, "Generalized Jacobi reproducing kernel method in Hilbert spaces for solving the Black-Scholes option pricing problem arising in financial modelling," *Mathematical Modelling and Analysis*, vol. 23, no. 4, pp. 538–553, 2018.

[7] F. Geng and M. Cui, "New method based on the HPM and RKHSM for solving forced Duffing equations with integral boundary conditions," *Journal of Computational and Applied Mathematics*, vol. 233, no. 2, pp. 165–172, 2009.

[8] F. Geng and M. Cui, "A reproducing kernel method for solving nonlocal fractional boundary value problems," *Applied Mathematics Letters*, vol. 25, no. 5, pp. 818–823, 2012.

[9] N. Harrouche, S. Momani, S. Hasan, and M. Al-Smadi, "Computational algorithm for solving drug pharmacokinetic model under uncertainty with nonsingular kernel type Caputo-Fabrizio fractional derivative," *Alexandria Engineering Journal*, vol. 60, no. 5, pp. 4347–4362, 2021.

[10] F. Hemati, M. Ghasemi, and G. R. Khoshsiar, "Numerical solution of the multiterm time-fractional diffusion equation based on reproducing kernel theory," *Numerical Methods for Partial Differential Equations*, vol. 37, pp. 44–68, 2021.

[11] W. Jiang and T. Tian, "Numerical solution of nonlinear Volterra integro-differential equations of fractional order by the reproducing kernel method," *Applied Mathematical Modelling*, vol. 39, no. 16, pp. 4871–4876, 2015.

[12] S. Momani, N. Djeddi, M. Al-Smadi, and S. Al-Omari, "Numerical investigation for Caputo-Fabrizio fractional Riccati and Bernoulli equations using iterative reproducing kernel method," *Applied Numerical Mathematics*, vol. 170, pp. 418–434, 2021.

[13] M. G. Sakar, "Iterative reproducing kernel Hilbert spaces method for Riccati differential equations," *Journal of Computational and Applied Mathematics*, vol. 309, pp. 163–174, 2017.

[14] E. N. Yildirim, A. Akgül, and M. Inc, "Reproducing kernel method for the solutions of non-linear partial differential equations," *Arab Journal of Basic and Applied Sciences*, vol. 28, no. 1, pp. 80–86, 2021.

[15] A. Atangana, "Extension of rate of change concept: from local to nonlocal operators with applications," *Results in Physics*, vol. 19, article 103515, 2020.

[16] M. Cui and Y. Lin, "Nonlinear numerical analysis in the reproducing kernel space," Nova Science Publishers, Inc, New York, 2009.

[17] N. Attia, A. Akgül, D. Seba, and A. Nour, "An efficient numerical technique for a biological population model of fractional order," *Chaos, Solitons and Fractals*, vol. 141, article 110349, 2020.

[18] E. Babolian, S. Javadi, and E. Moradi, "Error analysis of reproducing kernel Hilbert space method for solving functional integral equations," *Journal of Computational and Applied Mathematics*, vol. 300, pp. 300–311, 2016.

Hindawi
Journal of Function Spaces
Volume 2023, Article ID 9077924, 10 pages
https://doi.org/10.1155/2023/9077924

Research Article

An Efficient and Robust Numerical Solver for Impulsive Control of Fractional Chaotic Systems

Zahra Moniri,[1] **Behrouz Parsa Moghaddam**,[2] **and Morteza Zamani Roudbaraki**[3]

[1]*Mathematics Department, University of Mazandaran, Babolsar, Iran*
[2]*Department of Mathematics, Lahijan Branch, Islamic Azad University, Lahijan, Iran*
[3]*Department of Computer, Lahijan Branch, Islamic Azad University, Lahijan, Iran*

Correspondence should be addressed to Behrouz Parsa Moghaddam; parsa@liau.ac.ir

Received 11 August 2022; Revised 20 December 2022; Accepted 13 April 2023; Published 4 May 2023

Academic Editor: Jia-Bao Liu

This paper derives a computationally efficient and fast-running solver for the approximate solution of fractional differential equations with impulsive effects. In this connection, for approximating the fractional-order integral operator, a B-spline version of interpolation by corresponding equal mesh points is adopted. An illustrative example illustrates the accuracy of the new solver results as compared with those of the previous study. The proposed solver's performance is evaluated by the fractional Rössler and susceptible-exposed-infectious impulsive systems. Moreover, the effect of impulsive behaviors is shown for various values of impulsive.

1. Introduction

The impulsive differential equations (IDEs) are mostly investigated systems together with short-time perturbations [1–4]. Impulsive control systems have been studied in many fields such as economics [5], chemostat [6], population ecology [7, 8], engineering [9], and neural networks [10, 11]. Many theoretical and numerical researchers have investigated IDEs in many studies. In [12–15], the existence and uniqueness theorems on IDEs have been analyzed. In addition, analytical and numerical solutions of this kind of equation have been investigated in [16–21] and etc.

Nowadays, one of the most famous branches of mathematical science is the fractional calculus with arbitrary fractional order [22]. The fractional calculus is applied to the model of many phenomena including control [23], mechanics [24], physics [25–27], stock market [28], electronics [29], biology [30], and epidemiology [31, 32]. Recently, fractional impulsive differential equations (FIDEs) are considered in simulations of many systems including chaotic and hyperchaotic systems [33–35], control [36], and neural networks [37]. The existence of the solutions of FIDEs is studied in [38] by using the fixed point method. The existence of solutions for FIDEs with the integral jump and antiperiodic conditions is investigated in [39]. Furthermore, the existence of solutions of these equations is analyzed through a global bifurcation approach in [40]. The existence and stability results are presented in [41].

To the best of the author's knowledge, developing a fast-running solver requires FIDE up to date. This motivates our interest to designate an accurate computational technique for solving the following FIDE:

$$\begin{aligned} &{}^{C}\mathscr{D}^{\beta}_{0,t}u(t) - Q(t, u(t)) = 0, \quad t \in \Upsilon' \coloneqq \Upsilon \setminus \mathscr{T}, \\ &\Delta u(t) = u(t_n^+) - u(t_n) = K_n(u(t_n)), \quad n = 1, 2, \cdots, i, i \in \mathbb{N} \\ &u(0^+) = u_0, \end{aligned} \tag{1}$$

where $0 < \beta < 1$, $Y \coloneqq [0, T]$, $\mathscr{T} \coloneqq \{t_1, t_2, \cdots, t_i\}$, where every t_n satisfies $0 = t_0 < t_1 < \cdots < t_i < t_{i+1} = T$, and plus $Q : Y \times = R \longrightarrow = R$ is jointly continuous function. Moreover, $K_n \coloneqq R \longrightarrow = R$, and $i = [T/\tau]$, where $\tau = t_{i+1} - t_i$ denotes the impulsive interval. Furthermore, $u(t_n^-) = \lim_{\varepsilon \longrightarrow 0^-} u(t_n + \varepsilon)$ and $u(t_n^+) = \lim_{\varepsilon \longrightarrow 0^+} u(t_n + \varepsilon)$ indicate the left and right limits of $u(t)$ at $t = t_n$, respectively.

Throughout this paper, we do choose the Riemann-Liouville fractional integral [42] and fractional derivative in the Caputo sense [43, 44] which are formulated as

$$\begin{aligned} \mathcal{I}_{0,t}^{\beta}u(t) &= \frac{1}{\Gamma(\beta)}\int_0^t u(\varsigma)(t-\varsigma)^{\beta-1}d\varsigma, \\ {}^{C}\mathcal{D}_{0,t}^{\beta}u(t) &= \frac{1}{\Gamma(p-\beta)}\int_0^t \frac{u^{(p)}(\varsigma)}{(t-\varsigma)^{\beta+1-p}}d\varsigma, \quad p \in = N, \end{aligned} \tag{2}$$

where $t,\ \beta, \varsigma \in = R^{+}$ and $p-1<\beta\le p$. In addition, the unknown function, $u(t)$, is continuously differentiable $(p-1)-$ times.

The rest of the paper is arranged as follows. Section 2 suggests an implicit numerical technique, by using base spline interpolation for discretizing the FIDE. Section 3 investigates the performance and accuracy of the new solver by analysing the fractional impulsive Rössler and SEI systems. To sum up, Section 4 proffers the concluding remarks and statements.

2. Theoretical Argument

The proposed benefits of this section are twofold:

(1) It gives a fractional order approximation of the integral nonlocal operators

(2) It provides an accurate and computationally efficient technique for solving FIDE (1)

Thereafter, we consider that $t_m = m\hbar$, $m=\{0,1,\cdots,r\}$, and $\hbar=[T/r]$ means the uniform step size, and $r\in = N$.

Proposition 1. *Assume that $u(t)\in C^2(Y)$ be a function, $\beta>0$ and $\|u^{(2)}(t)\|_{\infty}\le M$, where $M>0$. The approximation of the nonlocal integral, $\mathcal{I}_{0,t_r}^{\beta}[u(t)]$, using the B-spline interpolation can be stated as follows:*

$$\mathcal{I}_{0,t_r}^{\beta}[u(t)] \approx \sum_{m=0}^{r} a_{m,r}u_m \equiv \left(\mathcal{I}_{0,t_r}^{\beta}[u(t)]\right)_{approx}, \tag{3}$$

where

$$a_{m,r} = \frac{\hbar^{\beta}}{\Gamma(\beta+2)} \times \begin{cases} (r-1)^{\beta+1}-(r-\beta-1)(r)^{\beta}, & m=0, \\ (r-m+1)^{\beta+1}+(r-m-1)^{\beta+1}-2(r-m)^{\beta+1}, & 1\le m\le r-1, \\ 1, & m=r. \end{cases} \tag{4}$$

In addition, the truncation error of (3) is

$$\left\| \mathcal{I}_{0,t_r}^{\beta}[u(t)] - \left(\mathcal{I}_{0,t_r}^{\beta}[u(t)]\right)_{approx} \right\|_{\infty} \le \frac{r^{\beta}M}{8\Gamma(\beta+1)}\hbar^{2+\beta}. \tag{5}$$

Proof. The $u(t)-$ approximation function, $S_m(t)$, in $[t_m, t_{m+1}]\subseteq\mathcal{T}$; $m=0,1,\cdots,r-1$, by considering the B-spline interpolation is stated as

$$u_m(t) \approx S_m(t) = \left(\frac{t-t_m}{t_{m+1}-t_m}\right)u(t_{m+1}) + \left(\frac{t-t_{m+1}}{t_m-t_{m+1}}\right)u(t_m). \tag{6}$$

Substituting (6) into (2), we obtain the time discretization form of (2) as follows:

$$\begin{aligned} \mathcal{I}_{0,t_r}^{\beta}[u(t)] &\approx \int_{0+}^{t_r}\frac{1}{\Gamma(\beta)}S_m(\zeta)(t_r-\zeta)^{\beta-1}\mathrm{d}\zeta \\ &= \sum_{m=0}^{r-1}\left(\int_{t_m}^{t_{m+1}}\frac{(t_r-\zeta)^{\beta-1}}{\Gamma(\beta)}\frac{\zeta-t_{m+1}}{t_m-t_{m+1}}\mathrm{d}\zeta\right)u(t_m) \\ &\quad + \sum_{m=0}^{r-1}\left(\int_{t_m}^{t_{m+1}}\frac{(t_r-\zeta)^{\beta-1}}{\Gamma(\beta)}\frac{\zeta-t_m}{t_{m+1}-t_m}\mathrm{d}\zeta\right)u(t_{m+1}). \end{aligned} \tag{7}$$

After rearranging and simplifying the above equation, it leads to (3) where the coefficients $a_{m,r}$ are given by (4).

Subsequently, the B-spline interpolation polynomial $S_m(t)$ satisfies

$$\mathscr{E}_m(t) := u_m(t) - S_m(t) = (t-t_m)(t-t_{m+1})\frac{u''(\eta_m)}{2}, \tag{8}$$

where $\eta_m \in (t_m, t_{m+1})$ and $\mathscr{E}_m(t)$ denote error function. Therefore, we have

$$\begin{aligned} &\left\| \mathcal{I}_{0,t_r}^{\beta}[u(t)] - \left(\mathcal{I}_{0,t_r}^{\beta}[u(t)]\right)_{\text{approx}} \right\|_{\infty} \\ &= \frac{1}{\Gamma(\beta)}\int_0^{t_r}\left\|(t_r-\varsigma)^{\beta-1}\mathscr{E}(\varsigma)\right\|_{\infty}d\varsigma \\ &= \frac{1}{\Gamma(\beta)}\sum_{m=0}^{r-1}\int_{t_m}^{t_{m+1}}(t_r-\varsigma)^{\beta-1}\left\|\frac{u''(\eta_m)}{2}(t-t_m)(t-t_{m+1})\right\|_{\infty}d\varsigma \\ &\le \frac{M}{8\Gamma(\beta)}\hbar^2\sum_{m=0}^{r-1}\int_{t_m}^{t_{m+1}}(t_r-\varsigma)^{\beta-1}d\varsigma = \frac{t_r^{\beta}M}{8\Gamma(\beta+1)}\hbar^2 \\ &= \frac{r^{\beta}M}{8\Gamma(\beta+1)}\hbar^{\beta+2}. \end{aligned} \tag{9}$$

□

In the rest of this section, we designate a fast-running technique for solving FIDE (1) by means of Proposition 1. FIDE (1) is able to state the following two equivalent equations with the same solutions:

$$u(t) = u_0 + \sum_{j=1}^{n}K_j(u_j) + \mathcal{I}_{0,t}^{\beta}Q(t,u(t)), \quad n=1,2,\cdots,i \tag{10}$$

or

$$u(t) = \begin{cases} u_0 + \frac{1}{\Gamma(\beta)} \int_0^t Q(\varsigma, u(\varsigma)) d\varsigma, & t \in [0, t_1], \\ u_0 + K_1(u_1) + \frac{1}{\Gamma(\beta)} \int_0^t Q(\varsigma, u(\varsigma)) d\varsigma, & t \in (t_1, t_2], \\ \vdots & \vdots \\ u_0 + \sum_{j=1}^{i} K_j(u_j) + \frac{1}{\Gamma(\beta)} \int_0^t Q(\varsigma, u(\varsigma)) d\varsigma, & t \in (t_i, T]. \end{cases} \tag{11}$$

By using the presented approximation in Proposition 1, we get the following approximation:

$$\mathcal{F}_{0,t_r}^{\beta} Q(t, u(t)) \approx \sum_{m=0}^{r} a_{m,r} Q(t_m, u_m). \tag{12}$$

Therefore, by replacing (12) with (10) (or (11)), the following equation derives

$$u_r = u_0 + \sum_{j=1}^{i} K_j(u_j) + \sum_{m=0}^{r} a_{m,r} Q(t_m, u_m), \tag{13}$$

where $a_{m,r}$ is given by (4). Due to the nonlinear source term $Q(t, \cdot)$, we have

$$u_r^p = u_0 + \frac{\hbar^\beta}{\Gamma(\beta+1)} \sum_{m=0}^{r-1} b_{m,r} Q(t_m, u_m), \tag{14}$$

where

$$b_{m,r} = (r-m)^\beta - (r-m-1)^\beta, 0 \le m \le r-1. \tag{15}$$

Ultimately, replacing u_r^p in the righthand side of (13) yields

$$u_r = u_0 + \sum_{j=1}^{i} K_j(u_j) + Q(t_r, u_r^p) + \sum_{m=0}^{r-1} a_{m,r} Q(t_m, u_m). \tag{16}$$

3. Numerical Application and Discussion

This section evaluates the accuracy and computational efficiency of the proposed numerical technique. To evaluate the computational impact of this solver, the mean absolute error ($\mathscr{E}_M$),

$$\mathscr{E}_M = \frac{1}{M} \sum_{m=1}^{M} \mathrm{AE}_m, \tag{17}$$

where $\mathrm{AE}_m = |\mathcal{F}_{0,t_m}^{\beta}[u(t)] - (\mathcal{F}_{0,t_m}^{\beta}[u(t)])_{\text{approx}}|$ and M represents the number of interior mesh points, and the convergence order ($\mathscr{C}_{h,M}$)

$$\mathscr{C}_{h,M} = \log_h(\mathscr{E}_M) \tag{18}$$

is considered evaluation criteria. All the computational results are implemented with MATLAB R2019a on an AMD Ryzen 7 5700 U @ 1.80 GHz machine. Furthermore, a comparison is made with the IM algorithm that was formulated and investigated in [45, 46].

Example 2. Let $u(t) = \pi t \sin(\pi t)$. Then, we get

$$\mathcal{F}_{0,t}^{\beta}[u(t)] = \frac{-(\beta+2)}{\pi^{1/2+\beta}\sqrt{t}\Gamma(3+\beta)} \cdot \left((t^2\pi^2 + \beta) S_{3/2+\beta,1/2}(\pi t) + \beta^2\pi^2 t S_{1/2+\beta,3/2}(\pi t) - (\pi t)^{5/2+\beta} \right), \tag{19}$$

where $\beta > 0$ and $S_{\eta,\nu}(t)$ define the Lommel function as

$$S_{\delta,\varrho}(t) = t^{\delta+1} \frac{{}_1F_2([1]; [1/2(\delta-\varrho+3), 1/2(\delta+\varrho+3)]; (-1/4)t^4)}{(\delta+1)^2 - \varrho^2}, \tag{20}$$

where ${}_sF_d(u_1, \cdots, u_s; v_1, \cdots, v_d; t)$ defines the generalized hypergeometric function.

The performance of the presented method is described by $\mathcal{F}_{0,t}^{\beta}[\pi t \sin(\pi t)]$ in Example 2 which is shown in Table 1. Table 1 shows the values of $\mathscr{E}_M$, $\mathscr{C}_{h,M}$, and computational times of Equation (19) with $\hbar = \{0.01, 0.005, 0.002\}$ and $\beta = \{0.4, 0.7, 0.9\}$ in the interval $t \in [0, 1]$. The numerical results display the improved accuracy of the presented scheme compared to the IM scheme [45] in the viewpoint of the $\mathscr{E}_M$, $\mathscr{C}_{h,M}$, and computational times. Figure 1 depicts the curves of Equation (19) for $\beta = \{0.1, 0.2, \cdots, 1\}$ with step size $\hbar = 0.01$. The outcomes in Figure 1 and Table 1 show that the proposed scheme is more accurate and has less computational time than the IM scheme [45].

3.1. Application of the Suggested Solver. In this section, the performance of the suggested solver is investigated for FIDEs.

Application 3. The fractional Rössler system is stated as

$$\begin{aligned} {}^C\mathscr{D}_{0,t}^{\beta_1} x(t) &= -(y(t) + z(t)), \\ {}^C\mathscr{D}_{0,t}^{\beta_2} y(t) &= x(t) + \alpha y(t), \\ {}^C\mathscr{D}_{0,t}^{\beta_3} z(t) &= (x(t) - \theta) z(t) + \chi, \\ x(0) = x_0,\ & y(0) = y_0,\ z(0) = z_0, \end{aligned} \tag{21}$$

where $2 \le \theta \le 11$ and $0 < \beta_1, \beta_2$ and $\beta_3 \le 1$.

In Figure 2, we plot the phase curves of the integer-order and fractional Rössler chaotic system (21) by means of the suggested scheme with initial conditions $x_0 = 0.25$, $y_0 = 0.2$,

Table 1: Comparison of $\mathscr{E}_M$, $\mathscr{C}_{h,M}$, and computational times (sec) of $\mathscr{J}^{\beta}_{0,t}[\pi t \sin(\pi t)]$, for the IM [45] and proposed schemes, when $\beta = \{0.4,0.7,0.9\}$ and step sizes $\hbar = \{0.01,0.005,0.002\}$ in $t \in [0, 1]$.

β	Step size	IM scheme $\mathscr{E}_M$	IM scheme $\mathscr{C}_{h,M}$	IM scheme CPU time	Proposed solver $\mathscr{E}_M$	Proposed solver $\mathscr{C}_{h,M}$	Proposed solver CPU time
0.4	0.01	2.49×10^{-3}	1.30	1.375	7.86×10^{-5}	2.05	0.610
	0.005	9.50×10^{-4}	1.31	4.843	2.00×10^{-5}	2.04	1.906
	0.002	3.62×10^{-4}	1.32	19.468	5.18×10^{-6}	2.03	7.203
0.7	0.01	2.57×10^{-4}	1.79	1.297	5.16×10^{-5}	2.14	0.641
	0.005	8.17×10^{-5}	1.78	4.937	1.29×10^{-5}	2.13	1.922
	0.002	2.58×10^{-5}	1.76	19.109	3.32×10^{-6}	2.11	7.359
0.9	0.01	3.17×10^{-5}	2.25	1.344	3.67×10^{-5}	2.22	0.609
	0.005	9.09×10^{-6}	2.19	4.703	9.10×10^{-6}	2.19	1.859
	0.002	2.59×10^{-6}	2.14	19.641	2.27×10^{-6}	2.17	7.234

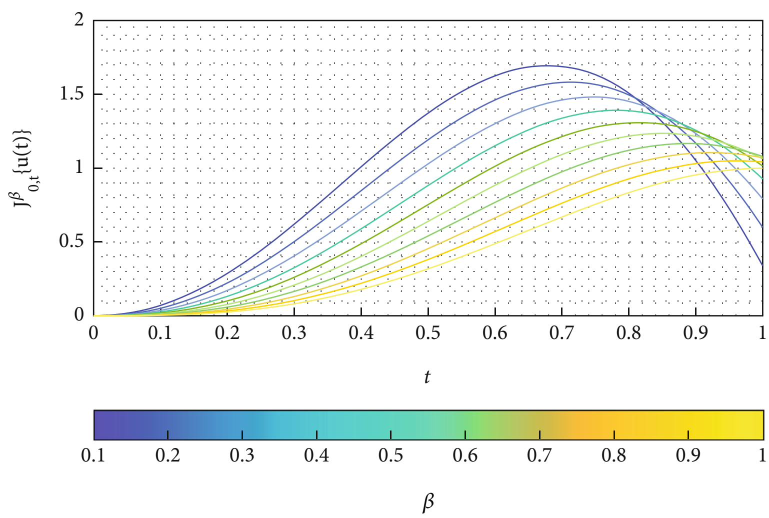

Figure 1: Comparison of the numerical results for Equation (19) applying the proposed scheme for $\beta = \{0.1,0.2,\cdots,1\}$ with step size $\hbar = 0.01$.

and $z_0 = 0.2$ for $\beta_3 = 0.8$ and $\beta_1 = 0.96$, $\beta_2 = 0.9$, and $\theta = 8$ with step size $\hbar = 0.002$ and $T = 100$.

We can rewrite system (21) into the following system:

$$\begin{aligned} {}^{C}\mathscr{D}^{\beta}_{0,t}u(t) &= Au(t) + \Psi(t), \\ u(0) &= u_0, \end{aligned} \tag{22}$$

where $\beta = (\beta_1, \beta_2, \beta_3)$, $u(t) = [x(t), y(t), z(t)]^T$,

$$A = \begin{bmatrix} 0 & -1 & -1 \\ 1 & \alpha & 0 \\ 0 & 0 & \theta \end{bmatrix}, \tag{23}$$

and $\Psi(t) = [0, 0, -x(t)z(t) + \chi]^T$.

Hence, the fractional impulsive control of chaotic system (22) is defined as

$$\begin{aligned} &{}^{C}\mathscr{D}^{\beta}_{0,t}u(t) = Au(t) + \Psi(t), \quad t \in \Upsilon' \coloneqq \Upsilon \setminus \{t_1, t_2, \cdots, t_i\}, \quad \Upsilon \coloneqq [0, T], \\ &\Delta u(t) = u(t_n^+) - u(t_n) = B(u(t_n)), \quad n = 1, 2, \cdots, i, \\ &u(0^+) = u_0, \end{aligned} \tag{24}$$

where $B = \mathrm{diag}\,(-0.58,-0.68,-0.78)$ with initial conditions

$$x(0^+) = 0.25, \quad y(0^+) = 0.2, \quad z(0^+) = 0.2. \tag{25}$$

System (24) with the nonfractional term, i.e., for $\beta = (1, 1, 1)$, and fractional term was studied in [47–49].

In Figure 3, we depict the numerical approximations of system (24) by using the suggested method with the

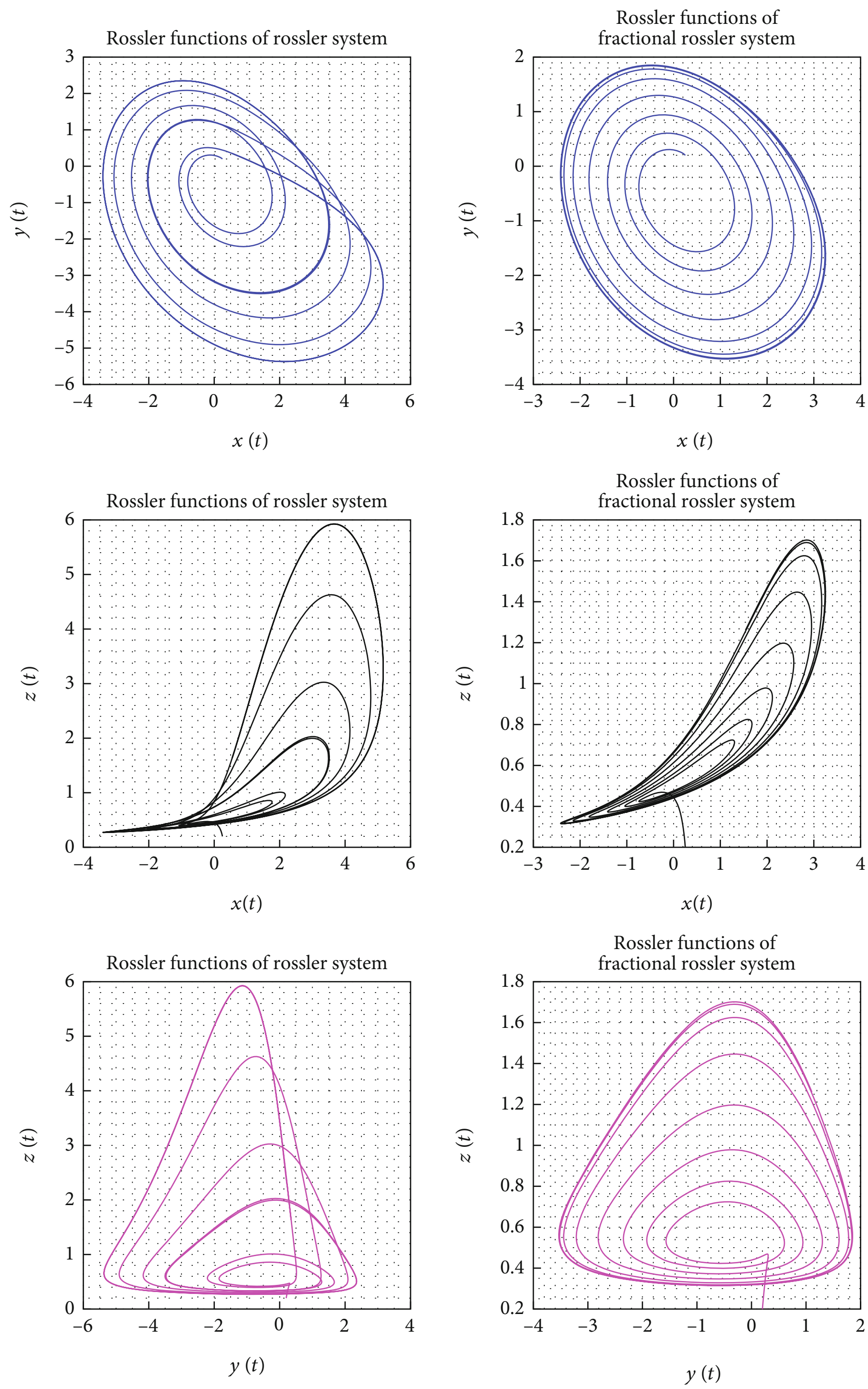

FIGURE 2: Phase curves of the integer-order ($\mathbf{L}: \beta_1 = \beta_2 = \beta_3 = 1$) and fractional ($\mathbf{R}: \beta_1 = 0.96, \beta_2 = 0.9, \beta_3 = 0.8$) Rössler chaotic systems for $\alpha = 0.4$, $\chi = 2$, and $\theta = 8$ with step size $\hbar = 0.02$ and $T = 100$.

impulsive intervals $\tau = 0.01$, in the interval $t \in [0, 10]$ and step size $\hbar = 0.002$ for $\beta_1 = 0.96$, $\beta_2 = 0.9$, and $\beta_3 = 0.8$. We can view the effects of the impulsive behaviors on this system for $\theta = 4$ in these figures.

Application 4. Assume that the functions $S(t)$, $E(t)$, and $I(t)$ denote susceptible, exposed, and infectious pests densities at time t, respectively. Furthermore, the η defines the death rate of exposed and infectious pests. The fractional susceptible-exposed-infectious (SEI) chaotic system is stated as

$$ {}^{C}\mathscr{D}_{0,t}^{\beta_1} S(t) = cS(t)\left(1 - \frac{S(t)}{K}\right) - \frac{lS(t)I(t)}{1 + nS(t)}, $$

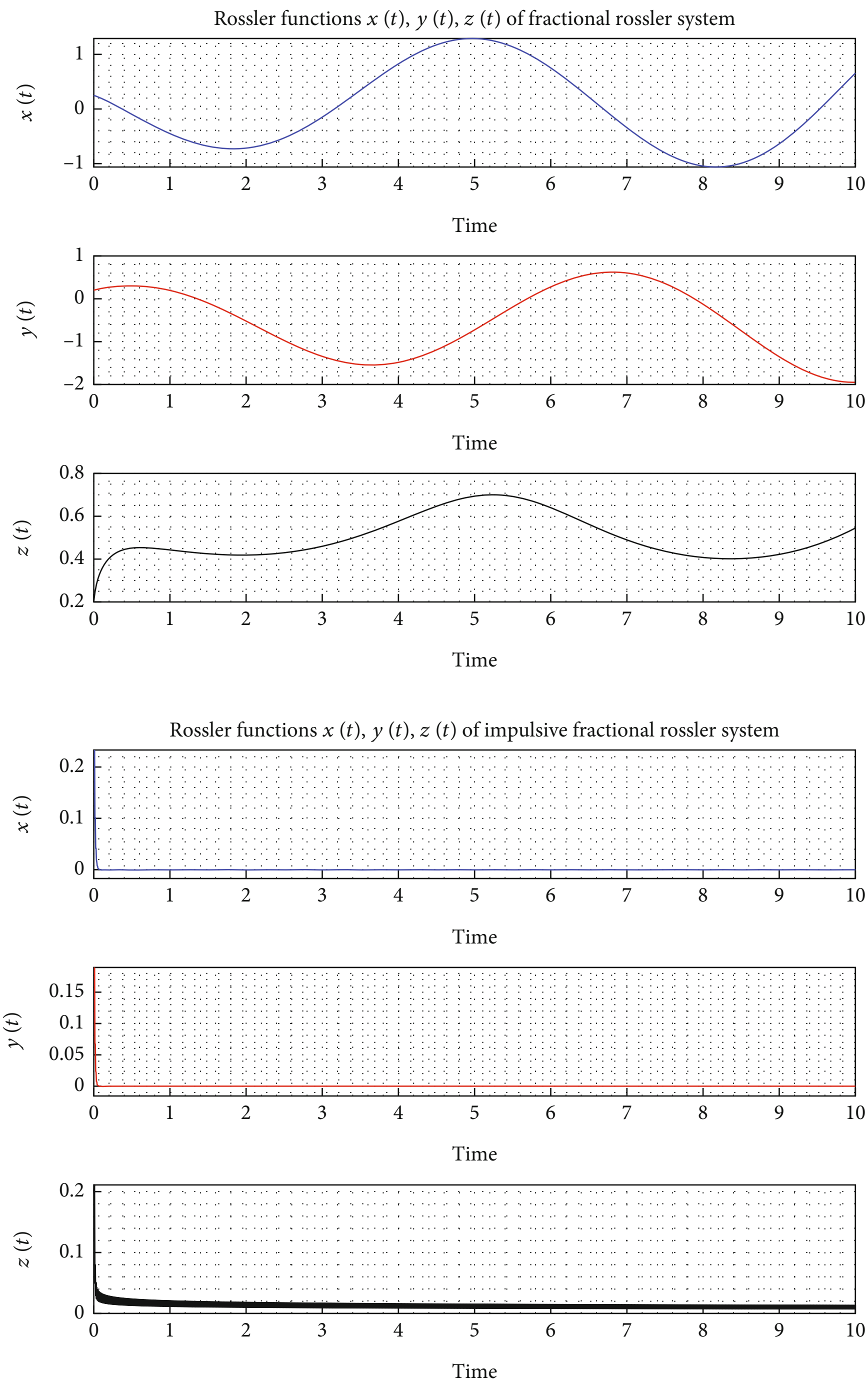

Figure 3: Numerical results of fractional Rössler system without and with, $\tau = 0.01$, impulsive effects for $\alpha = 0.4$, $\chi = 2$, and $\theta = 4$, based on the presented scheme for $\beta_1 = 0.96$, $\beta_2 = 0.92$, and $\beta_3 = 0.80$ with step size $\hbar = 0.005$ and $T = 10$.

$$
\begin{aligned}
{}^{C}\mathscr{D}_{0,t}^{\beta_2}E(t) &= \frac{lS(t)I(t)}{1+nS(t)} - (\phi+\eta)E(t),\\
{}^{C}\mathscr{D}_{0,t}^{\beta_3}I(t) &= \phi E(t) - \eta I(t),\\
S(0) &= S_0, E(0) = E_0, I(0) = I_0,
\end{aligned} \tag{26}
$$

where $0 < \beta_1, \beta_2$ and $\beta_3 \le 1$. Moreover, $S(t)$ grows logistically with a carrying capacity K in the absence of $I(t)$ and with an intrinsic birth rate constant rc.

In Figure 4, we plot the phase curves of the integer-order and fractional SEI system (26) by means of the suggested scheme with initial conditions $x_0 = 0.1$, $y_0 = 0.2$, and $z_0 = 0.3$, plus $c = 1$, $K = 4$, $d = 1.2$, $\phi = 0.8$, $n = 0.2$, and $\eta = 0.2$ for $\beta_1 = 1$, $\beta_2 = 0.9$, and $\beta_3 = 0.9$ with step size $\hbar = 0.005$ and $T = 100$.

We can rewrite system (26) into the following system:

$$
\begin{aligned}
{}^{C}\mathscr{D}_{0,t}^{\beta}u(t) &= Au(t) + \Psi(t),\\
u(0) &= u_0,
\end{aligned} \tag{27}
$$

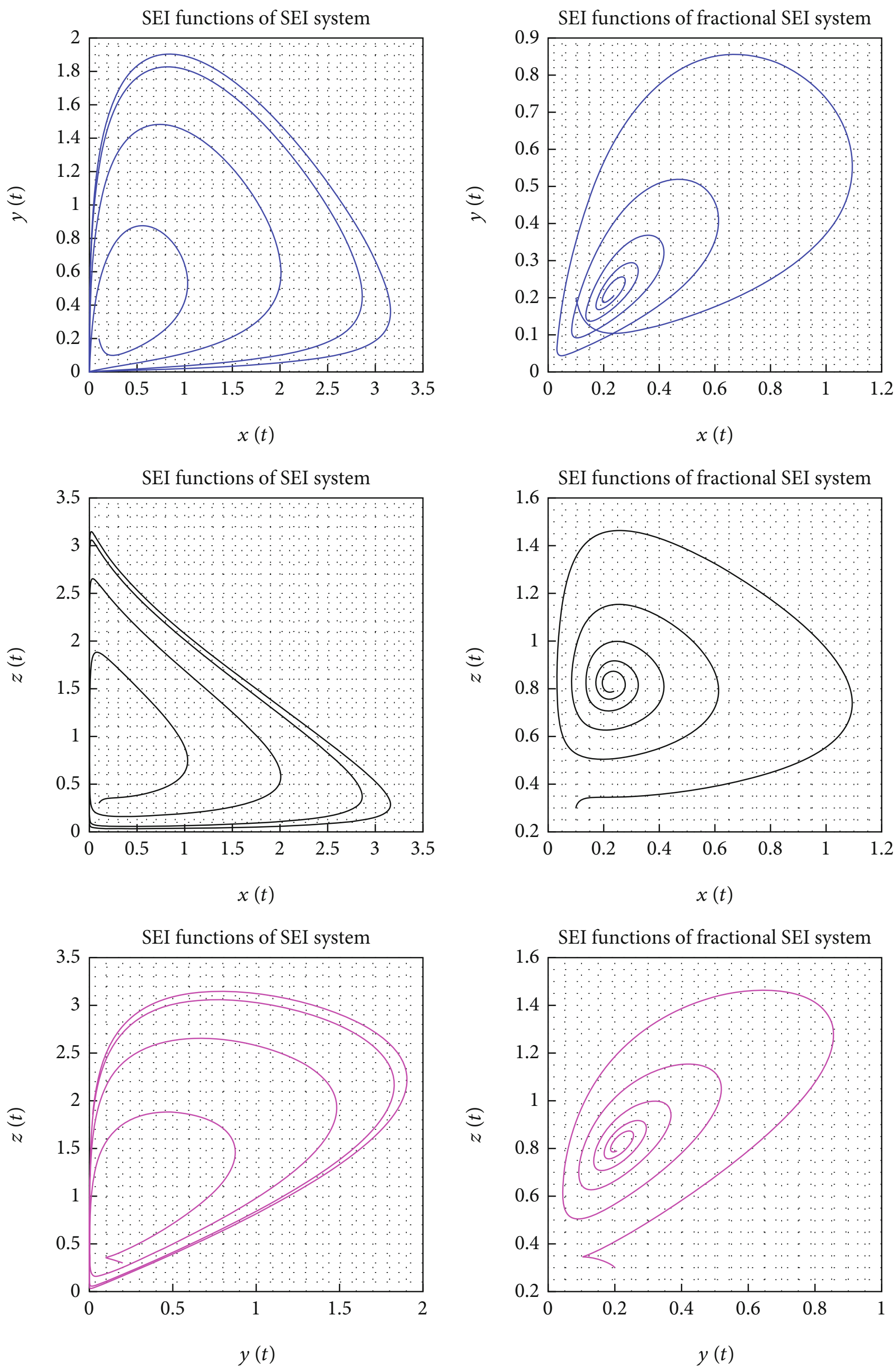

FIGURE 4: Phase curves of the integer-order ($\boldsymbol{L}: \beta_1 = \beta_2 = \beta_3 = 1$) and fractional ($\boldsymbol{R}: \beta_1 = 0.99, \beta_2 = 0.90, \beta_3 = 0.70$) SEI chaotic systems with step size $\hbar = 0.005$ and $T = 100$.

where $\beta = (\beta_1, \beta_2, \beta_3)$, $u(t) = [x(t), y(t), z(t)]^T$,

$$A = \begin{bmatrix} c & 0 & 0 \\ 0 & -(\alpha + \eta) & 0 \\ 0 & \alpha & -\eta \end{bmatrix},$$

$$\Psi(t) = \begin{bmatrix} -\left(\dfrac{c}{K} S(t) - \dfrac{l}{1 + nS(t)} I(t)\right) S(t) \\ \left(\dfrac{l}{1 + nS(t)} I(t)\right) S(t) \\ 0 \end{bmatrix}. \tag{28}$$

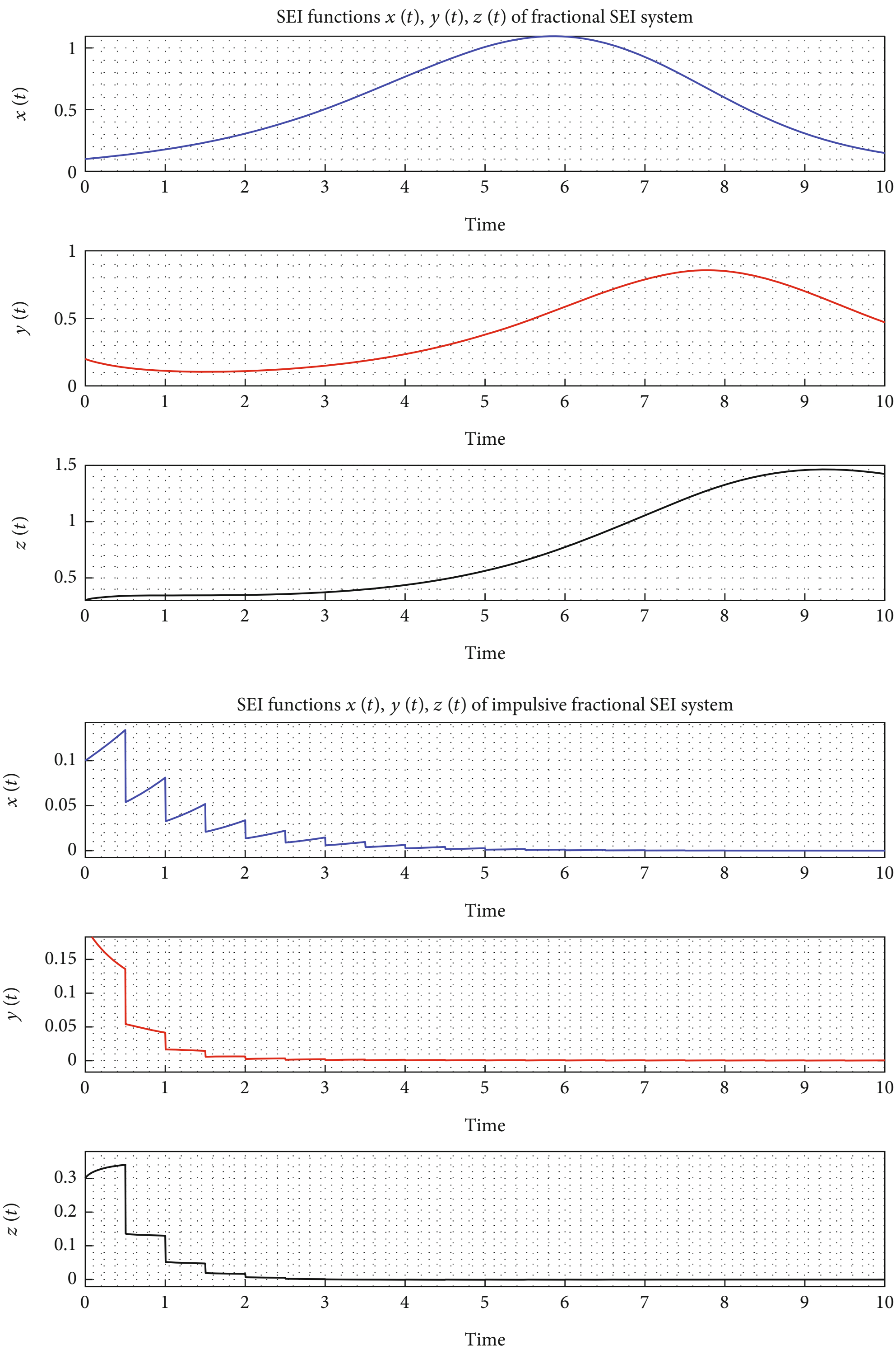

FIGURE 5: Numerical results of the fractional SEI system without and with, $\tau = 0.5$, impulsive effects based on the presented scheme for $\beta_1 = 0.99$, $\beta_2 = 0.90$, and $\beta_3 = 0.70$, with step size $\hbar = 0.005$ and $T = 10$.

Hence, the fractional impulsive control of chaotic system (27) is defined as

$$\begin{aligned} &{}^{C}\mathscr{D}^{\beta}_{0,t}u(t) = Au(t) + \Psi(t), \quad t \in \Upsilon' := \Upsilon \setminus \{t_1, t_2, \cdots, t_i\}, \\ &\Delta u(t) = u(t_n^+) - u(t_n) = B(u(t_n)), \quad n = 1, 2, \cdots, i, \\ &u(0^+) = u_0, \end{aligned} \tag{29}$$

where $\Upsilon := [0, T]$, $B = \text{diag}\,(-0.6, -0.6, -0.6)$ with initial conditions

$$\begin{aligned} x(0^+) &= 0.25, \\ y(0^+) &= 0.2, \\ z(0^+) &= 0.2. \end{aligned} \tag{30}$$

System 24 with the nonfractional term, i.e., for $\beta = (1, 1, 1)$, was studied in [50].

In Figure 5, we depict the numerical approximations of systems (26) and (29) by using the suggested method with the impulsive intervals $\tau = 0.5$, in the interval $t \in [0,100]$ and step size $\hbar = 0.005$ for $\beta_1 = 0.99$, $\beta_2 = 0.90$, and $\beta_3 = 0.70$. We can view the effects of the impulsive behaviors on this system in these figures.

4. Conclusion

In the framework of this study, an implicit numerical algorithm for computing the approximate solutions of fractional impulsive differential equations was presented. This numerical solver relies on the B-spline interpolation to reasonably approximate the nonlocal integral operators. An illustrative example showed the accuracy of the comparison of the results obtained by the IM scheme and proposed numerical technique. The results confirmed the superiority of the presented scheme. Then, the proposed algorithm for solving the fractional chaotic dynamic Rössler and SEI systems was applied, and the results were studied using phase figures. To top it all off, the fractional impulsive systems were approximated by the presented method, and the achievement results of the impulsive behavior were analyzed.

Data Availability

There is no underlying data supporting the results in this study.

Conflicts of Interest

The authors declare that they have no known competing financial interests or personal relationships that could have appeared to influence the work reported in this paper.

References

[1] V. Lakshmikantham and P. S. Simeonov, "Theory of impulsive differential equations," vol. 6, World Scientific, 1989.

[2] M. Benchohra, J. Henderson, and S. Ntouyas, *Impulsive Differential Equations and Inclusions*, vol. 2, Hindawi Publishing Corporation New York, 2006.

[3] G. T. Stamov, *Almost Periodic Solutions of Impulsive Differential Equations*, vol. 2047, Springer Science & Business Media, 2012.

[4] I. Stamova and G. Stamov, "Stability analysis of impulsive functional systems of fractional order," *Communications in Nonlinear Science and Numerical Simulation*, vol. 19, no. 3, pp. 702–709, 2014.

[5] I. Stamova and G. Stamov, *Applied Impulsive Mathematical Models*, Springer International Publishing, 2016.

[6] S. Sun and L. Chen, "Dynamic behaviors of Monod type chemostat model with impulsive perturbation on the nutrient concentration," *Journal of Mathematical Chemistry*, vol. 42, no. 4, pp. 837–847, 2007.

[7] S. Ahmad and G. T. Stamov, "On almost periodic processes in impulsive competitive systems with delay and impulsive perturbations," *Nonlinear Analysis: Real World Applications*, vol. 10, no. 5, pp. 2857–2863, 2009.

[8] J. Yang and Z. Yang, "Stability and permanence of a pest management model with impulsive releasing and harvesting," *Abstract and Applied Analysis*, vol. 2013, Article ID 832701, 18 pages, 2013.

[9] E. Joelianto and H. Y. Sutarto, "Controlled switching dynamical systems using linear impulsive differential equations," in *Intelligent Unmanned Systems: Theory and Applications*, pp. 227–244, Springer, Berlin Heidelberg, 2009.

[10] Y. Zhao, Y. Xia, and W. Ding, "Periodic oscillation for BAM neural networks with impulses," *Journal of Applied Mathematics and Computing*, vol. 28, no. 1-2, pp. 405–423, 2008.

[11] C. Wang, "Piecewise pseudo-almost periodic solution for impulsive non-autonomous high- order Hopfield neural networks with variable delays," *Neurocomputing*, vol. 171, pp. 1291–1301, 2016.

[12] T. Jankowski, "Positive solutions to second order four-point boundary value problems for impulsive differential equations," *Applied Mathematics and Computation*, vol. 202, no. 2, pp. 550–561, 2008.

[13] W. Wang and X. Yang, "Positive periodic solutions for second order differential equations with impulsive effects," *Boundary Value Problems*, vol. 2015, no. 1, 2015.

[14] Q. Wang and M. Wang, "Existence of solution for impulsive differential equations with indefinite linear part," *Applied Mathematics Letters*, vol. 51, pp. 41–47, 2016.

[15] X. Yang, "Existence and multiplicity of weak solutions for a nonlinear impulsive (q,p)-Laplacian dynamical system," *Advances in Difference Equations*, vol. 2017, no. 1, 2017.

[16] H. Chen and J. Sun, "An application of variational method to second-order impulsive differential equation on the half-line," *Applied Mathematics and Computation*, vol. 217, no. 5, pp. 1863–1869, 2010.

[17] H. Hossainzadeh, G. A. Afrouzi, and A. Yazdani, "Application of Adomian decomposition method for solving impulsive differential equations," *Journal of Mathematics and Computer Science*, vol. 2, no. 4, pp. 672–681, 2011.

[18] Z. Yang, "The asymptotic behavior for a class of impulsive delay differential equations," *Abstract and Applied Analysis*, vol. 2013, Article ID 494067, 7 pages, 2013.

[19] Z. Zhang and H. Liang, "Collocation methods for impulsive differential equations," *Applied Mathematics and Computation*, vol. 228, pp. 336–348, 2014.

[20] M. Berenguer, H. Kunze, D. L. Torre, and M. R. Gal'an, "Galerkin method for constrained variational equations and a collage-based approach to related inverse problems," *Journal of Computational and Applied Mathematics*, vol. 292, pp. 67–75, 2016.

[21] L. Mei, H. Sun, and Y. Lin, "Numerical method and convergence order for second-order impulsive differential equations," *Advances in Difference Equations*, vol. 2019, no. 1, 2019.

[22] Y. Zhou, J. Wang, and L. Zhang, *Basic Theory of Fractional Differential Equations*, World Scientific, 2016.

[23] R. Karimi, A. Dabiri, J. Cheng, and E. A. Butcher, "Probabilistic-robust optimal control for uncertain linear time-delay systems by state feedback controllers with memory," in *2018 Annual American Control Conference (ACC)*, pp. 4183–4188, Milwaukee, WI, USA, 2018.

[24] B. P. Moghaddam, A. Dabiri, and J. A. T. Machado, "Application of variableorder fractional calculus in solid mechanics," in

Applications in Engineering, Life and Social Sciences, D. Băleanu and A. M. Lopes, Eds., pp. 207–224, Part A, De Gruyter, 2019.

[25] V. Erturk, E. Godwe, D. Baleanu, P. Kumar, J. Asad, and A. Jajarmi, "Novel fractional-order Lagrangian to describe motion of beam on nanowire," *Acta Physica Polonica A*, vol. 140, no. 3, pp. 265–272, 2021.

[26] A. Jajarmi, D. Baleanu, K. Z. Vahid, H. M. Pirouz, and J. Asad, "A new and general fractional Lagrangian approach: a capacitor microphone case study," *Results in Physics*, vol. 31, article 104950, 2021.

[27] B. P. Moghaddam, M. Pishbin, Z. S. Mostaghim, O. S. Iyiola, A. Galhano, and A. M. Lopes, "A numerical algorithm for solving nonlocal nonlinear stochastic delayed systems with variable-order fractional Brownian noise," *Fractal and Fractional*, vol. 7, no. 4, p. 293, 2023.

[28] Z. S. Mostaghim, B. P. Moghaddam, and H. S. Haghgozar, "Computational technique for simulating variable-order fractional Heston model with application in US stock market," *Mathematical Sciences*, vol. 12, no. 4, pp. 277–283, 2018.

[29] Z. S. Mostaghim, B. P. Moghaddam, and H. S. Haghgozar, "Numerical simulation of fractional-order dynamical systems in noisy environments," *Computational and Applied Mathematics*, vol. 37, no. 5, pp. 6433–6447, 2018.

[30] C. Ionescu, A. Lopes, D. Copot, J. A. T. Machado, and J. H. T. Bates, "The role of fractional calculus in modeling biological phenomena: a review," *Communications in Nonlinear Science and Numerical Simulation*, vol. 51, pp. 141–159, 2017.

[31] D. Baleanu, F. A. Ghassabzade, J. J. Nieto, and A. Jajarmi, "On a new and generalized fractional model for a real cholera outbreak," *Alexandria Engineering Journal*, vol. 61, no. 11, pp. 9175–9186, 2022.

[32] D. Baleanu, M. H. Abadi, A. Jajarmi, K. Z. Vahid, and J. Nieto, "A new comparative study on the general fractional model of COVID-19 with isolation and quarantine effects," *Alexandria Engineering Journal*, vol. 61, no. 6, pp. 4779–4791, 2022.

[33] H. Xi, S. Yu, R. Zhang, and L. Xu, "Adaptive impulsive synchronization for a class of fractional-order chaotic and hyperchaotic systems," *Optik*, vol. 125, no. 9, pp. 2036–2040, 2014.

[34] D. Li, X. P. Zhang, Y. T. Hu, and Y. Y. Yang, "Adaptive impulsive synchronization of fractional order chaotic system with uncertain and unknown parameters," *Neurocomputing*, vol. 167, pp. 165–171, 2015.

[35] X. Zhang, D. Li, and X. Zhang, "Adaptive impulsive synchronization for a class of fractional order complex chaotic systems," *Journal of Vibration and Control*, vol. 25, no. 10, pp. 1614–1628, 2019.

[36] J. Fu, M. Yu, and T.-D. Ma, "Modified impulsive synchronization of fractional order hyperchaotic systems," *Chinese Physics B*, vol. 20, no. 12, article 120508, 2011.

[37] M. S. Ali, G. Narayanan, V. Shekher, A. Alsaedi, and B. Ahmad, "Global Mittag-Leffler stability analysis of impulsive fractional-order complex-valued BAM neural networks with time varying delays," *Communications in Nonlinear Science and Numerical Simulation*, vol. 83, article 105088, 2020.

[38] M. Feckan, Y. Zhou, and J. Wang, "On the concept and existence of solution for impulsive fractional differential equations," *Communications in Nonlinear Science and Numerical Simulation*, vol. 17, no. 7, pp. 3050–3060, 2012.

[39] Y. Qiao and Z. Zhou, "Existence of solutions for a class of fractional differential equations with integral and anti-periodic boundary conditions," *Boundary Value Problems*, vol. 2017, no. 1, 2017.

[40] Y. Guan, Z. Zhao, and X. Lin, "On the existence of solutions for impulsive fractional differential equations," *Advances in Mathematical Physics*, vol. 2017, Article ID 1207456, 12 pages, 2017.

[41] Q. Chen, A. Debbouche, Z. Luo, and J. Wang, "Impulsive fractional differential equations with Riemann-Liouville derivative and iterative learning control," *Chaos, Solitons & Fractals*, vol. 102, pp. 111–118, 2017.

[42] S. G. Samko, A. A. Kilbas, and O. I. Marichev, *Fractional Integrals and Derivatives: Theory and Applications*, Gordon & Breach Science Publishers, 1993.

[43] M. Caputo, "Linear models of dissipation whose Q is almost frequency independent-II," *Geophysical Journal International*, vol. 13, no. 5, pp. 529–539, 1967.

[44] M. Caputo, *Elasticit'a e dissipazione*, Zanichelli, Bologna, Italy, 1969.

[45] F. K. Keshi, B. P. Moghaddam, and A. Aghili, "A numerical approach for solving a class of variable-order fractional functional integral equations," *Computational and Applied Mathematics*, vol. 37, no. 4, pp. 4821–4834, 2018.

[46] B. P. Moghaddam, A. Dabiri, Z. S. Mostaghim, and Z. Moniri, "Numerical solution of fractional dynamical systems with impulsive effects," *International Journal of Modern Physics C*, vol. 34, no. 1, 2023.

[47] J. Sun and Y. Zhang, "Impulsive control of Rossler systems," *Physics Letters A*, vol. 306, no. 5-6, pp. 306–312, 2003.

[48] L. Yang, L. Xiao-Feng, L. Chuan-Dong, and C. Guo, "Impulsive control for synchronization of nonlinear Rössler chaotic systems," *Chinese Physics*, vol. 15, no. 12, pp. 2890–2893, 2006.

[49] A. Razminia, V. J. Majd, and D. Baleanu, "Chaotic incommensurate fractional order Rössler system: active control and synchronization," *Advances in Difference Equations*, vol. 2011, no. 1, 2011.

[50] Z. Xiang, Y. Li, and X. Song, "Dynamic analysis of a pest management SEI model with saturation incidence concerning impulsive control strategy," *Nonlinear Analysis: Real World Applications*, vol. 10, no. 4, pp. 2335–2345, 2009.

Hindawi
Journal of Function Spaces
Volume 2023, Article ID 1980382, 14 pages
https://doi.org/10.1155/2023/1980382

Research Article

A New Version of the Generalized F-Expansion Method for the Fractional Biswas-Arshed Equation and Boussinesq Equation with the Beta-Derivative

Yusuf Pandir [1] and Yusuf Gurefe [2]

[1] *Department of Mathematics, Faculty of Science and Arts, Yozgat Bozok University, Yozgat, Turkey*
[2] *Department of Mathematics, Faculty of Science, Mersin University, Mersin, Turkey*

Correspondence should be addressed to Yusuf Gurefe; ygurefe@gmail.com

Received 20 October 2022; Revised 19 March 2023; Accepted 22 April 2023; Published 2 May 2023

Academic Editor: Calogero Vetro

In this article, a new version of the generalized F-expansion method is proposed enabling to obtain the exact solutions of the Biswas-Arshed equation and Boussinesq equation defined by Atangana's beta-derivative. First, the new version generalized F-expansion method is introduced, and then, the exact solutions of the nonlinear fractional differential equations expressed with Atangana's beta-derivative are given. When the results are examined, it is seen that single, combined, and mixed Jacobi elliptic function solutions are obtained. From the point of view, it is understood that the new version generalized F-expansion method can give significant results in finding the exact solutions of equations containing beta-derivatives.

1. Introduction

In recent years, many articles have been published on obtaining numerical and exact solutions of some physical phenomena that can be mathematically modeled using fractional derivatives [1–4]. Many physical phenomena are usually expressed in nonlinear fractional partial differential equations. These equations have application areas such as biology, engineering, dynamics, control theory, signal processing, chemistry, continuum mechanics, and physics, respectively. There are different types of fractional derivative operators defined in the literature. Examples of these derivative operators are Riemann-Liouville derivative [5], Jumarie's modified Riemann-Liouville derivative [6], Caputo derivative [7], Caputo-Fabrizio [8], and Atangana-Baleanu derivative [9]. It is very substantial to find the exact solutions of the nonlinear fractional differential equations. Different methods aiming to find analytical, numerical, and exact solutions of the nonlinear partial differential equations including these derivative operators have been improved as follows: unified method [10], modified trial equation method [11], extended trial equation method [12], fractional local homotopy perturbation transformation method [13], Fourier spectral method [14], variational iteration method [15], Laplace transforms [16], Chebyshev-Tau method [17], finite difference method [18], finite element method [19], etc.

A new definition of the fractional derivative called as conformable derivative has been given, and the exact solutions of the time-heat differential equation created by using this derivative are obtained [20, 21]. In later years, Atangana et al. [22] gave some new features and definitions about the conformable derivative. By using these definitions and properties, some methods have been applied [23, 24]. In the next year, a new definition of fractional derivative called as beta-derivative was given by Atangana et al. [25]. In that article, they obtained the analytical solution of the Hunter-Saxton equation. Exact solutions of the Hunter-Saxton, Sharma-Tasso-Olver, space-time fractional modified Benjamin-Bona-Mahony, and time fractional Schrödinger equations expressed by Atangana's beta-derivative are obtained by using the first integral method [26]. They applied the fractional subequation method to obtain the exact solutions of the space-time conformable generalized Hirota-Satsuma coupled KdV equation, coupled mKdV equation, and space-time resonance nonlinear Schrodinger equations created with Atangana's beta-derivative [27, 28]. Ghanbari and Gomez-Aguilar attained the exact solutions by applying the generalized exponential rational function method to the Radhakrishnan-Kundu-Lakshmanan equation with Atangana's beta-derivative [29]. Like the problems discussed in this article, it is very difficult to find analytical and numerical solutions for nonlinear partial differential equations involving fractional order derivative, especially problems with complex coefficients and absolute value functions. For this reason, the motivation to research the exact solutions of these problems has occurred. From this point of view, it is considered to apply the new version generalized F-expansion method in order to determine solutions such as rational forms of Jacobi elliptic functions that are not in the literature. The double-period Jacobi elliptic functions and their rational combinations, which cannot be found by every method in the literature, can be reached with a new generalized F-expansion method. This method can be successfully applied to a wide variety of equations.

In this article, for the first time, the new version generalized F-expansion method has been investigated in order to find the exact solutions of the differential equations consisting of Atangana's beta-derivative. With this offered method, it is aimed at finding new and several exact solutions of fractional order differential equations that are not actual in the literature. This method, which has been discussed in some studies in the literature, has been applied to various nonlinear partial differential equations [30–32]. There are different F-expansion methods that allow procuring the elliptic function solutions, which are among these exact solutions [33–36].

Firstly we will investigate the exact solutions of the Biswas-Arshed equation with Atangana's beta-derivative:

$$i{}_0^AD_t^{\beta}\phi + k_1\phi_{xx} + k_2{}_0^AD_t^{\beta}(\phi_x) + i\left(l_1\phi_{xxx} + l_2{}_0^AD_t^{\beta}(\phi_{xx})\right) - i\left(\varepsilon\left(|\phi|^2\phi\right)_x + \mu\phi\left(|\phi|^2\right)_x + \theta|\phi|^2\phi_x\right) = 0, \quad (0 < \beta \le 1), \tag{1}$$

where $\phi = \phi(x, t)$ is a complex function [37–40]; k_1 and k_2 are the parameters of the group velocity dispersion and the spatiotemporal dispersion, respectively; l_1 and l_2 are the parameters of the third-order dispersion and the spatiotemporal third-order dispersion, respectively; ε is the parameter of the self-steepening effect; and μ and θ present the parameters of the nonlinear dispersions. Also, we will research the exact solutions of the Boussinesq equation with the beta-derivative [41]

$${}_0^AD_t^{\beta}\Psi + bD_x^{2\beta}\Psi + cD_x^{2\beta}\left(\Psi^2\right) + \gamma D_x^{4\beta}\Psi = 0, \quad (0 < \beta \le 1), \tag{2}$$

where b, c, and γ are constants. Also, c is the parameter controlling nonlinearity, and γ is the dispersion parameter depending on the rigidity characteristics of the material and compression.

The remaining lines of the article are regulated as follows: in Section 2, Atangana's conformable fractional derivative and its properties are given. In Section 3, the new version generalized F-expansion method is explained in detail. Applications of the method are given in Sections 4 and 5. This article is completed with conclusions in Section 6.

2. The Properties and Definition of Beta-Derivative

There are different definitions of the conformable fractional derivatives in literature. One of them is given by Khalil et al. in the paper [20]. Then, Abdeljawad developed the basic concepts in this conformable fractional calculus [42]. The conformable derivative of the function $g : [0,\infty)$ of the order α from type $t > 0, \alpha \in (0, 1)$ is as follows:

$${}_0D_t^{\alpha}\{g(t)\} = \lim_{\varepsilon \longrightarrow 0} \frac{g\left(t + \varepsilon t^{1-\alpha}\right) - g(t)}{\varepsilon}. \tag{3}$$

When g which is α-differentiable in the interval of $(0, a)$, $a > 0$ and $\lim_{\varepsilon \longrightarrow 0^+} g^{(\alpha)}(t)$ exists, then it can be defined as $g^{(\alpha)}(0) = \lim_{\varepsilon \longrightarrow 0^+} g^{(\alpha)}(t)$.

The other conformable fractional derivative called as the beta-derivative is defined in [22] as

$${}_0^AD_t^{\alpha}\{g(t)\} = \lim_{\varepsilon \longrightarrow 0} \frac{g\left(t + \varepsilon(t + (1/\Gamma(\alpha)))^{1-\alpha}\right) - g(t)}{\varepsilon}. \tag{4}$$

The mathematical model considered in the study that depends on Atangana's conformable fractional derivative is selected because it provides some properties of the basic derivative rules. According to all these cases, the various features of Atangana's conformable fractional derivative are as follows:

(i) If $h \neq 0$ and g functions are differentiable according to beta in the range $\beta \in (0, 1]$, then the equation that the functions f and g can satisfy for all the real numbers q and r is as follows:

$${}_0^AD_x^{\alpha}\{qg(x) + rh(x)\} = q{}_0^AD_x^{\alpha}\{g(x)\} + r{}_0^AD_x^{\alpha}\{h(x)\}. \tag{5}$$

(ii) Let us take any constant p. It can be easily seen that it satisfies the following equality:

$${}_0^AD_x^{\alpha}\{p\} = 0. \tag{6}$$

(iii) ${}_0^AD_x^{\alpha}\{g(x)h(x)\} = h(x){}_0^AD_x^{\alpha}\{g(x)\} + g(x){}_0^AD_x^{\alpha}\{h(x)\}$

(iv) ${}_0^AD_x^{\alpha}\{g(x)/h(x)\} = (h(x){}_0^AD_x^{\alpha}\{g(x)\} - g(x){}_0^AD_x^{\alpha}\{h(x)\})/h^2(x)$

If $\lambda = (x + (1/\Gamma(\alpha)))^{\alpha-1}\nu$ is substituted instead of λ in Equation (4) and $\nu \longrightarrow 0$, when $\lambda \longrightarrow 0$, it is observed as follows:

$$ {}_{0}^{A}D_{x}^{\alpha}\{g(x)\} = \left(x + \frac{1}{\Gamma(\alpha)}\right)^{1-\alpha} \frac{dg(x)}{dx}, \tag{7} $$

with

$$ \eta = \frac{\delta}{\alpha}\left(x + \frac{1}{\Gamma(\alpha)}\right)^{\alpha}, \tag{8} $$

where δ is any constant. Therefore, the relation between Atangana's conformable fractional derivative and the classical derivative is determined as follows:

$$ {}_{0}^{A}D_{x}^{\alpha}\{g(\eta)\} = \delta \frac{dg(\eta)}{d\eta}. \tag{9} $$

3. Definition of the New Version of Generalized F-Expansion Method

In this section, the application steps of the new version of the generalized F-expansion method to obtain the combined and mixed Jacobi elliptic function solutions of differential equations will be given [30–32]. With this new method, different and new results can be acquired from the results obtained from other methods.

Let us consider the partial differential equation with the Atangana (beta) fractional derivative as

$$ \tilde{S}\left(\phi, {}_{0}^{A}D_{t}^{\beta}\phi, {}_{0}^{A}D_{x}^{\beta}\phi, {}_{0}^{A}D_{t}^{2\beta}\phi, {}_{0}^{A}D_{x}^{2\beta}\phi, \cdots,\right) = 0, \quad (0 < \beta \leq 1), \tag{10} $$

where $\phi(x, t, \cdots)$ is an unknown function, $x, t, \cdots$ is the independent variables, and $\tilde{S}$ is a polynomial of ϕ and its fractional derivatives, in which the highest-order derivatives and the nonlinear terms are contained. When we implemented the wave transform to Equation (10),

$$ \begin{aligned} &\phi(x, t) = \phi(\eta), \\ &\eta = \frac{\tau}{\beta}\left(x + \frac{1}{\Gamma(\beta)}\right)^{\beta} + \frac{\lambda}{\beta}\left(t + \frac{1}{\Gamma(\beta)}\right)^{\beta}, \end{aligned} \tag{11} $$

where τ and λ are constants that will be determined later; we can diminish Equation (10) to nonlinear ordinary differential equation

$$ H\left(\phi, \phi', \phi'', \phi''', \cdots\right) = 0, \tag{12} $$

where the prime demonstrates differentiation pursuant to η. Suppose that the solution function of Equation (12) is as follows:

$$ \phi(\eta) = a_0 + \sum_{i=1}^{M}\left(a_i F^i + \frac{b_i}{F^i} + c_i\left(\frac{F'}{F}\right)^i + d_i\left(\frac{F}{F'}\right)^i\right), \tag{13} $$

where $a_0, a_i, b_i, c_i, d_i (i = 1, 2, 3, \cdots, M)$ are constants, $F = F(\eta)$, and $F' = F'(\eta)$. $F(\eta)$ and $F'(\eta)$ functions in Equation (13) provide the following equation:

$$ F'^2(\eta) = PF^4(\eta) + QF^2(\eta) + R, \tag{14} $$

and using Equation (14), the related derivatives are found as follows:

$$ \begin{cases} F''(\xi) = 2PF^3(\xi) + QF(\xi), \\ F'''(\xi) = \left(6PF^2(\xi) + Q\right)F'(\xi), \\ F^{(4)}(\xi) = 24P^2F^5(\xi) + 20PQF^3(\xi) + \left(Q^2 + 12PR\right)F(\xi), \\ F^{(5)}(\xi) = \left(120P^2F^4(\xi) + 60PQF^2(\xi) + Q^2 + 12PR\right)F'(\xi), \\ \cdots \end{cases} \tag{15} $$

where P,Q, and R are all coefficients. To determine the value of M in Equation (13), we use the derivatives in Equation (15). The process of finding the number M is called the balancing process. The number M is a positive number and is determined by balancing the highest-order derivative terms in Equation (12) with the highest-power nonlinear terms. When finding this number in terms of F^M, $1/F^M$, $(F'/F)^M$ and $(F/F')^M$ in the solution function (12) are considered with respect to Equation (14) in conjunction with the degree of derivatives. Therefore, proposed solution function (13) arranged and requisite terms in place of Equation (12) are attached to $(F')^k F^l (k = 0, 1 ; l = 0, \pm 1, \pm 2, \cdots)$ function; then, the polynomial is attained. When this polynomial equation is set to zero, then a system of algebraic equations is attained with the coefficients with respect to zero. When the algebraic equation system is solved according to the specified algorithm, the necessary τ, λ, and $a_0, a_i, b_i, c_i, d_i (i = 1, 2, 3, \cdots, M)$ coefficients for the solution function are found. Thence, the new combined and mixed Jacobi elliptic function solutions are gained. If different values of P,Q, and R are taken, diverse Jacobi elliptic function solutions $F(\eta)$ can be attained from Equation (14).

4. Application of the New Version Method to the Biswas-Arshed Equation

In this section, the new version generalized F-expansion method is implemented to the Biswas-Arshed equation with Atangana's beta-derivative. The Biswas-Arshed equation with Atangana's beta-derivative defines pulse propagation through optical fiber. Optical fibers are the main element of data transmission in telecommunications systems. The main aim of the researchers is to improve the quality of transmitted signals, reduce losses, and increase transmission speed. For this reason, it is important to obtain the solutions of such physical equations.

Hosseini et al. found the exact solutions of Equation (1) via the Jacobi and Kudryashov methods [37]. Akbulut and

Islam implemented modified extended auxiliary equation mapping and improved F-expansion methods to acquire the exact solutions of Eq. (1) in [39]. On the other hand, Han et al. utilized the polynomial full discriminant system method to find the exact solutions of Eq. (1) in [40]. Jacobi elliptic function solutions can be found with the methods in the literature, but it is very difficult to find rational function solutions containing the Jacobi elliptic functions we obtained with the method we used in this article, because the method we used includes not only the F function, which expresses the Jacobi elliptic function solutions obtained from the elliptic differential equation, but also the F'/F and F/F' functions. Thus, the rational function solutions or combined containing Jacobi elliptic functions are reached by this way.

Firstly, we acquaint wave transformation for this complex variable equation:

$$\begin{aligned} \phi(x,t) &= \phi(\eta)e^{i\varphi(x,t)}, \\ \eta &= x - \frac{\rho}{\beta}\left(t + \frac{1}{\Gamma(\beta)}\right)^{\beta}, \\ \varphi(x,t) &= -kx + \frac{\omega}{\beta}\left(t + \frac{1}{\Gamma(\beta)}\right)^{\beta}, \end{aligned} \tag{16}$$

where ρ, κ, and ω are constants which represents the speed of the wave, frequency, and wave number, respectively. By using the wave transformation in Equation (16), Equation (1) reduces the real and imaginary parts as follows:

$$\begin{aligned} &(2\kappa\rho l_2 - 3\kappa l_1 + \omega l_2 + \rho k_2 - k_1)\phi''(\eta) \\ &+ \left(\kappa^3 l_1 - \kappa^2\omega l_2 + \kappa^2 k_1 - \kappa\omega k_2 + \omega\right)\phi(\eta) \\ &+ (\kappa\varepsilon + \kappa\theta)\phi^3(\eta) = 0, \end{aligned} \tag{17}$$

$$\begin{aligned} &(\rho l_2 - l_1)\phi'''(\eta) + \left(-\kappa^2\rho l_2 + 3\kappa^2 l_1 - 2\kappa\omega l_2 - \kappa\rho k_2 \right. \\ &\left. + 2\kappa k_1 - \omega k_2 + \rho\right)\phi'(\eta) + (3\varepsilon + 2\mu + \theta)\phi^2(\eta)\phi'(\eta) = 0. \end{aligned} \tag{18}$$

From Equation (12), the following equations are easily obtained:

$$\begin{aligned} \rho &= \frac{l_1}{l_2}, \\ \varepsilon &= \frac{-2\mu - \theta}{3}, \\ \omega &\frac{2\kappa^2 l_1 l_2 + 2\kappa k_1 l_2 - \kappa k_2 l_1 + l_1}{l_2(2\kappa l_2 + k_2)}. \end{aligned} \tag{19}$$

When these obtained values are substituted in Equation (17), the following second-order nonlinear ordinary differential equation is found:

$$\begin{aligned} &\left(-\kappa l_1 + \frac{2\kappa^2 l_1 l_2 + 2\kappa k_1 l_2 - \kappa k_2 l_1 + l_1}{2\kappa l_2 + k_2} + \frac{l_1 k_2}{l_2} - k_1\right)\phi''(\eta) \\ &+ \left(\kappa^3 l_1 - \frac{\kappa^2\left(2\kappa^2 l_1 l_2 + 2\kappa k_1 l_2 - \kappa k_2 l_1 + l_1\right)}{2\kappa l_2 + k_2}\right. \\ &- \frac{\kappa k_2\left(2\kappa^2 l_1 l_2 + 2\kappa k_1 l_2 - \kappa k_2 l_1 + l_1\right)}{l_2(2\kappa l_2 + k_2)} \\ &\left. + \frac{2\kappa^2 l_1 l_2 + 2\kappa k_1 l_2 - \kappa k_2 l_1 + l_1}{l_2(2\kappa l_2 + k_2)} + \kappa^2 k_1\right)\phi(\eta) \\ &+ \left(\kappa\left(\frac{-2\mu - \theta}{3}\right) + \kappa\theta\right)\phi^3(\eta) = 0. \end{aligned} \tag{20}$$

According to the balance procedure for the functions $\phi''(\eta)$ and $\phi^3(\eta)$ in Equation (20), we can find $M = 1$, so the solution of Equation (1) is assumed that it provides the following equation:

$$\phi(\eta) = a_0 + a_1 F(\eta) + \frac{b_1}{F(\eta)} + c_1\left(\frac{F'(\eta)}{F(\eta)}\right) + d_1\left(\frac{F(\eta)}{F'(\eta)}\right). \tag{21}$$

When the calculated $\phi''(\eta)$ and $\phi^3(\eta)$ expressions from Equation (21) are replaced in Equation (20), a zero polynomial dependent on $F(\eta)$ and $F'(\eta)$ is obtained. When the algebraic equation system, which is found by equating the coefficients of this zero polynomial to zero, is resolved with the help of the Mathematica package program, the a_0, a_1, b_1, c_1, d_1, and κ coefficients are obtained. While applying the method, since the number of variables is more than the number of equations in the solution of the nonlinear algebraic system of equations, some constants in the partial differential equations are taken as arbitrary parameters and the parametric solutions of the system are reached. When the obtained coefficients and the inverse transformation are substituted to the solution function (21), the following exact solutions are obtained, which depends on the elliptic functions of $F(\eta)$ and $F'(\eta)$. If the elliptic function here is specially chosen as $F(\eta) = sn(\eta)$, where $P = m^2$, $Q = -(1 + m^2)$, and $R = 1$, then the new combined and mixed exact solutions are specified in the following cases.

Case 1.

$$\begin{aligned} a_0 &= b_1 = c_1 = d_1 = 0, \\ a_1 &= a_1, \\ l_1 &= \frac{\kappa(\theta - \mu)l_2 a_1^2\left(k_2\left(\kappa^2 + Q\right) - 2\kappa\right)}{3P}, \end{aligned} \tag{22}$$

$$k_1 = \frac{\kappa(\theta - \mu)a_1^2\left(\left(k_2^2 + l_2\right)\left(\kappa^2 + Q\right) - 2\kappa k_2 + 1\right)}{3P}. \tag{23}$$

Substituting Equation (22) into Equation (21), we attain single Jacobi elliptic function solutions of Equation (1).

$$\phi(\eta_1) = A_1 e^{i\varphi_1} sn(\eta_1), \tag{24}$$

where $\eta_1 = x - (\kappa(\theta-\mu)a_1^2(k_2(\kappa^2-1-m^2)-2\kappa)/3m^2\beta)(t+(1/\Gamma(\beta)))^\beta$, $A_1 = a_1$, and $\varphi_1 = -\kappa x - (\kappa(\theta-\mu)a_1^2(1+m^2+\kappa^2+\kappa k_2(1+m^2-\kappa^2))/3m^2\beta)(t+(1/\Gamma(\beta)))^\beta$.

Case 2.

$$\begin{aligned} a_0 &= a_1 = c_1 = d_1 = 0, \\ b_1 &= b_1, \\ l_1 &= \frac{\kappa(\theta-\mu)l_2 b_1^2\left(k_2\left(\kappa^2+Q\right)-2\kappa\right)}{3R}, \end{aligned} \tag{25}$$

$$k_1 = \frac{\kappa(\theta-\mu)b_1^2\left(\left(k_2^2+l_2\right)\left(\kappa^2+Q\right)-2\kappa k_2+1\right)}{3R}. \tag{26}$$

If the obtained coefficients in expression (25) are subrogated in the solution function (21), we find the Jacobi elliptic function solution of Equation (1).

$$\phi(\eta_2) = A_2 e^{i\varphi_2} ns(\eta_2), \tag{27}$$

where $\eta_2 = x - (\kappa(\theta-\mu)b_1^2(k_2(\kappa^2-1-m^2)-2\kappa)/3\beta)(t+(1/\Gamma(\beta)))^\beta$, $A_2 = b_1$, and $\varphi_2 = -\kappa x - (\kappa(\theta-\mu)b_1^2(1+m^2+\kappa^2+\kappa k_2(1+m^2-\kappa^2))/3\beta)(t+(1/\Gamma(\beta)))^\beta$.

Case 3.

$$\begin{aligned} a_0 &= a_1 = b_1 = d_1 = 0, \\ c_1 &= c_1, \\ l_1 &= \frac{\kappa(\theta-\mu)l_2 c_1^2\left(k_2\left(\kappa^2-2Q\right)-2\kappa\right)}{3}, \end{aligned} \tag{28}$$

$$k_1 = \frac{\kappa(\theta-\mu)c_1^2\left(\left(k_2^2+l_2\right)\left(\kappa^2-2Q\right)-2\kappa k_2+1\right)}{3}. \tag{29}$$

When the obtained coefficients in Equation (28) are set into Equation (21), we attain new types of the combined Jacobi elliptic function solution as follows:

$$\phi(\eta_3) = A_3 e^{i\varphi_3} cs(\eta_3) dn(\eta_3), \tag{30}$$

where $\eta_3 = x - (\kappa(\theta-\mu)c_1^2(k_2(\kappa^2+2(1+m^2))-2\kappa)/3\beta)(t+(1/\Gamma(\beta)))^\beta$, $A_3 = c_1$, and $\varphi_3 = -\kappa x + (\kappa(\theta-\mu)c_1^2(2+2m^2-\kappa^2+\kappa k_2(2+2m^2+\kappa^2))/3\beta)(t+(1/\Gamma(\beta)))^\beta$.

Case 4.

$$\begin{aligned} a_0 &= a_1 = b_1 = c_1 = 0, \\ d_1 &= d_1, \\ l_1 &= \frac{\kappa(\theta-\mu)l_2 d_1^2\left(k_2\left(\kappa^2-2Q\right)-2\kappa\right)}{3\left(Q^2-4PR\right)}, \end{aligned} \tag{31}$$

$$k_1 = \frac{\kappa(\theta-\mu)d_1^2\left(\left(k_2^2+l_2\right)\left(\kappa^2-2Q\right)-2\kappa k_2+1\right)}{3\left(Q^2-4PR\right)}. \tag{32}$$

When achieved coefficients in Equation (31) are replaced into Equation (21), we gain new exact solution called as combined Jacobi elliptic function solutions of Equation (1) as follows:

$$\phi(\eta_4) = A_4 e^{i\varphi_4} sc(\eta_4) nd(\eta_4), \tag{33}$$

where $\eta_4 = x - (\kappa(\theta-\mu)d_1^2(k_2(\kappa^2+2(1+m^2))-2\kappa)/3(1-2m^2+m^4)\beta)(t+(1/\Gamma(\beta)))^\beta$, $A_4 = d_1$, and $\varphi_4 = -\kappa x + (\kappa(\theta-\mu)d_1^2(2+2m^2-\kappa^2+\kappa k_2(2+2m^2+\kappa^2))/3(m^2-1)^2\beta)(t+(1/\Gamma(\beta)))^\beta$.

Case 5.

$$\begin{aligned} a_0 &= c_1 = d_1 = 0, \\ a_1 &= a_1, \\ b_1 &= -\sqrt{\frac{R}{P}}a_1, \\ l_1 &= \frac{\kappa(\theta-\mu)l_2 a_1^2\left(k_2\left(\kappa^2+6\sqrt{PR}+Q\right)-2\kappa\right)}{3P}, \end{aligned} \tag{34}$$

$$k_1 = \frac{\kappa(\theta-\mu)a_1^2\left(\left(k_2^2+l_2\right)\left(\kappa^2+6\sqrt{PR}+Q\right)-2\kappa k_2+1\right)}{3P}. \tag{35}$$

Substituting the coefficients in Equation (34) into Equation (21), we get the exact solutions of Equation (1).

$$\phi(\eta_5) = A_5 e^{i\varphi_5} \frac{\left(msn^2(\eta_5)-1\right)}{sn(\eta_5)}, \tag{36}$$

where $\eta_5 = x - (\kappa(\theta-\mu)a_1^2(k_2(\kappa^2-1-m^2+6m)-2\kappa)/3m^2\beta)(t+(1/\Gamma(\beta)))^\beta$, $A_5 = a_1/m$, and $\varphi_5 = -\kappa x - (\kappa(\theta-\mu)a_1^2(1+m^2-6m+\kappa^2+\kappa k_2(1+m^2-6m-\kappa^2))/3m^2\beta)(t+(1/\Gamma(\beta)))^\beta$.

Case 6.

$$a_0 = a_1 = b_1 = 0,$$
$$c_1 = c_1, \quad (37)$$
$$d_1 = -c_1\sqrt{Q^2 - 4PR},$$

$l_1 = \kappa(\theta - \mu)l_2 c_1(6k_2 c_1\sqrt{Q^2 - 4PR} + c_1(k_2(\kappa^2 - 2Q) - 2\kappa))/3$, $k_1 = \kappa(\theta - \mu)c_1(6c_1(k_2^2 + l_2)\sqrt{Q^2 - 4PR} + c_1((k_2^2 + l_2)(\kappa^2 - 2Q) - 2\kappa k_2 + 1))/3$.

When obtained coefficients in Equation (37) are replaced into Equation (21), we get new exact solution named as mixed Jacobi elliptic function solutions of Equation (1) as follows:

$$\phi(\eta_6) = A_3 e^{i\varphi_6}\frac{cn^2(\eta_6)\left(dn^2(\eta_6) - 1\right) + dn^2(\eta_6)}{cn(\eta_6)dn(\eta_6)sn(\eta_6)}, \quad (38)$$

where $\eta_6 = x - (\kappa(\theta - \mu)c_1(6k_2 c_1\sqrt{m^4 - 2m^2 + 1} + c_1(k_2(\kappa^2 + 2 + 2m^2) - 2\kappa))/3\beta)(t + (1/\Gamma(\beta)))^\beta$ and $\varphi_6 = -\kappa x + (\kappa(\theta - \mu)c_1^2(6(m^2 - 1)(1 + \kappa k_2) + 2 + 2m^2 - \kappa^2 + \kappa k_2(2 + 2m^2 + \kappa^2))/3\beta)(t + (1/\Gamma(\beta)))^\beta$.

Case 7.

$$a_0 = d_1 = 0,$$
$$a_1 = -\sqrt{P}c_1 b_1 = -\sqrt{P}c_1,$$
$$c_1 = c_1, \quad (39)$$
$$l_1 = \frac{2\kappa(\theta - \mu)c_1^2 l_2\left(k_2\left(Q + 6\sqrt{PR} - 2\kappa^2\right) - 4\kappa\right)}{3},$$

$$k_1 = \frac{2\kappa(\theta - \mu)c_1^2\left(2 - 4\kappa k_2 - \left(k_2^2 + l_2\right)\left(Q + 6\sqrt{PR} - 2\kappa^2\right)\right)}{3}. \quad (40)$$

When acquired coefficients in Equation (39) are put into Equation (21), we attain new exact combined Jacobi elliptic function solution of Equation (1).

$$\phi(\eta_7) = A_3 e^{i\varphi_7}\frac{\left(cn(\eta_7)dn(\eta_7) - msn^2(\eta_7) - 1\right)}{sn(\eta_7)}, \quad (41)$$

where $\eta_7 = x - (2\kappa(\theta - \mu)c_1^2(k_2(-1 - m^2 + 6m - 2\kappa^2) - 2\kappa)/3\beta)(t + (1/\Gamma(\beta)))^\beta$ and $\varphi_7 = -\kappa x + (2\kappa(\theta - \mu)c_1^2(1 + m^2 - 6m - 2\kappa^2 + \kappa k_2(1 + m^2 - 6m + 2\kappa^2))/3\beta)(t + (1/\Gamma(\beta)))^\beta$.

Remark 1. When the literature review of the obtained results is made, it is seen that all Jacobi elliptic function solutions obtained by the new version generalized F-expansion method of Equation (1) are new and different wave solutions. Besides, two- and three-dimensional graphics of the attained exact solution functions are shown in Figures 1–7 with appropriate coefficient values.

5. Application of the New Version Method to the Boussinesq Equation with Beta-Derivative

In this section, the implementation of the new version of the generalized F-expansion method to Boussinesq equation with beta-derivative is presented. Firstly, we acquaint wave transformation of Equation (2) as follows:

$$\Psi(x, t) = \psi(\vartheta),$$
$$\vartheta = \frac{k}{\beta}\left(x + \frac{1}{\Gamma(\beta)}\right)^\beta - \frac{\sigma}{\beta}\left(t + \frac{1}{\Gamma(\beta)}\right)^\beta, \quad (42)$$

where k and σ are constants. Equation (2) is reduced to a nonlinear 4-order ordinary differential equation in the following form under the transformation (42):

$$\left(\sigma^2 + bk^2\right)\psi'' + ck^2\left(\psi^2\right)'' + \gamma k^4\psi^{(iv)} = 0. \quad (43)$$

If Equation (43) is integrated twice according to ϑ and the integration constant is assumed to be zero, then a nonlinear second-order ordinary differential equation is found as follows:

$$\left(\sigma^2 + bk^2\right)\psi + ck^2\psi^2 + \gamma k^4\psi'' = 0. \quad (44)$$

According to the proposed new version of generalized F-expansion method, before applying the solution function (13) to Equation (44), the balance operation is performed. The balance procedure is applied between the ψ'' term containing the highest-order derivative and the nonlinear ψ^2 terms of the highest order in Equation (44). Accordingly, as a result of the transactions made between the terms providing balancing $M = 1$ is found, thus, the solution function of Equation (2) is as follows:

$$\psi(\vartheta) = a_0 + a_1 F(\vartheta) + a_2 F^2(\vartheta) + \frac{b_1}{F(\vartheta)} + \frac{b_2}{F^2(\vartheta)} + c_1\left(\frac{F'(\vartheta)}{F(\vartheta)}\right) + c_2\left(\frac{F'(\vartheta)}{F(\vartheta)}\right)^2 + d_1\left(\frac{F(\vartheta)}{F'(\vartheta)}\right) + d_2\left(\frac{F(\vartheta)}{F'(\vartheta)}\right)^2. \quad (45)$$

When the computed $\psi''(\vartheta)$ and $\psi^2(\vartheta)$ terms from Equation (45) are substituted in Equation (44), a zero polynomial dependent on $F(\eta)$ and $F'(\eta)$ is attained. When the algebraic equation system is solved with the help of the Mathematica package program, the a_0, a_1, a_2, b_1, b_2, c_1, c_2, d_1, d_2, k, and σ coefficients are acquired. When the obtained coefficients and the inverse transformation are substituted to the solution function (45), the following exact solutions are found, which depends on $F(\eta)$ and $F'(\eta)$. If the elliptic function here is specially chosen as $F(\eta) = sn(\eta)$, where P

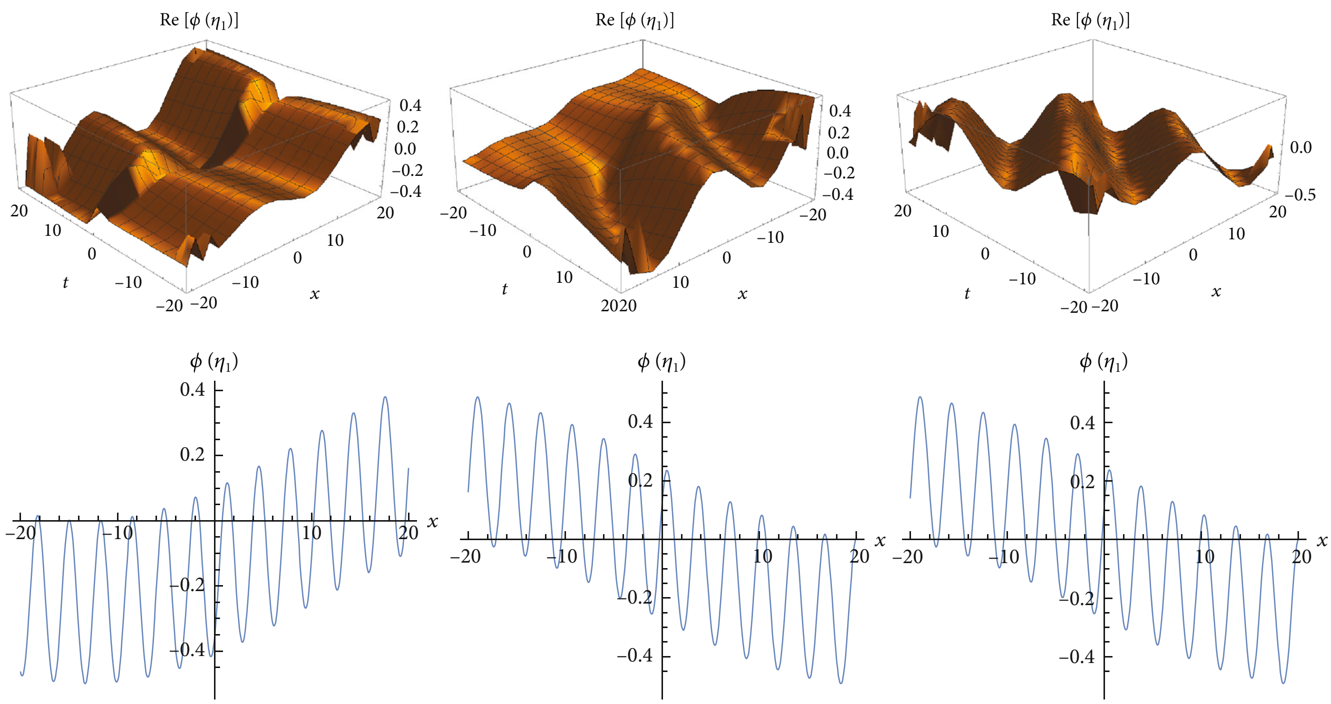

Figure 1: Three- and two-dimensional graphs of the solution $\phi(\eta_1)$ for different $\beta = 0.01, 0.55, 0.98$ corresponding to the values $a_1 = m = 1/2$, $\kappa = -1$, $\theta = 0.3$, $\mu = 0.2$, and $k_2 = 1$.

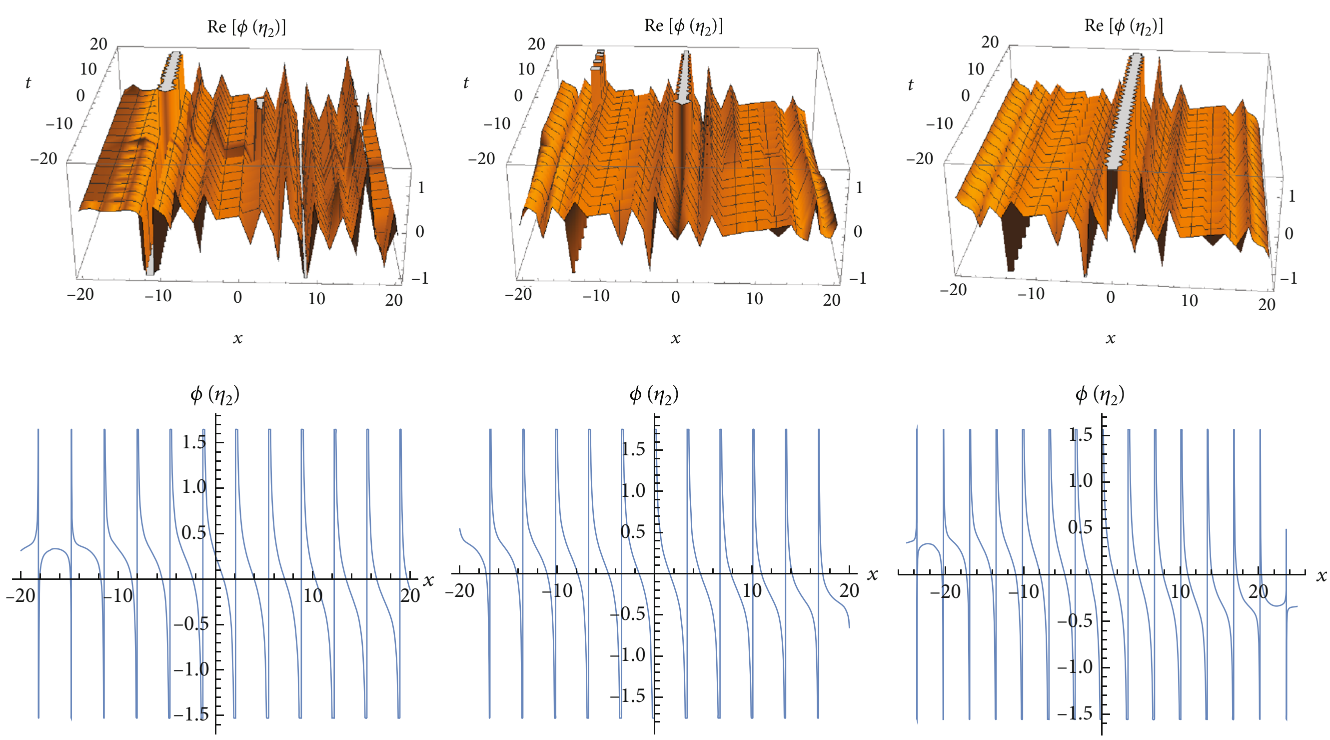

Figure 2: Three-dimensional graphs of the solution $\phi(\eta_2)$ for different $\beta = 0.01, 0.55, 0.98$ corresponding to the values $b_1 = 1/3$, $m = 1/2$, $\kappa = -1$, $\theta = 0.3$, $\mu = 0.2$, and $k_2 = 1$.

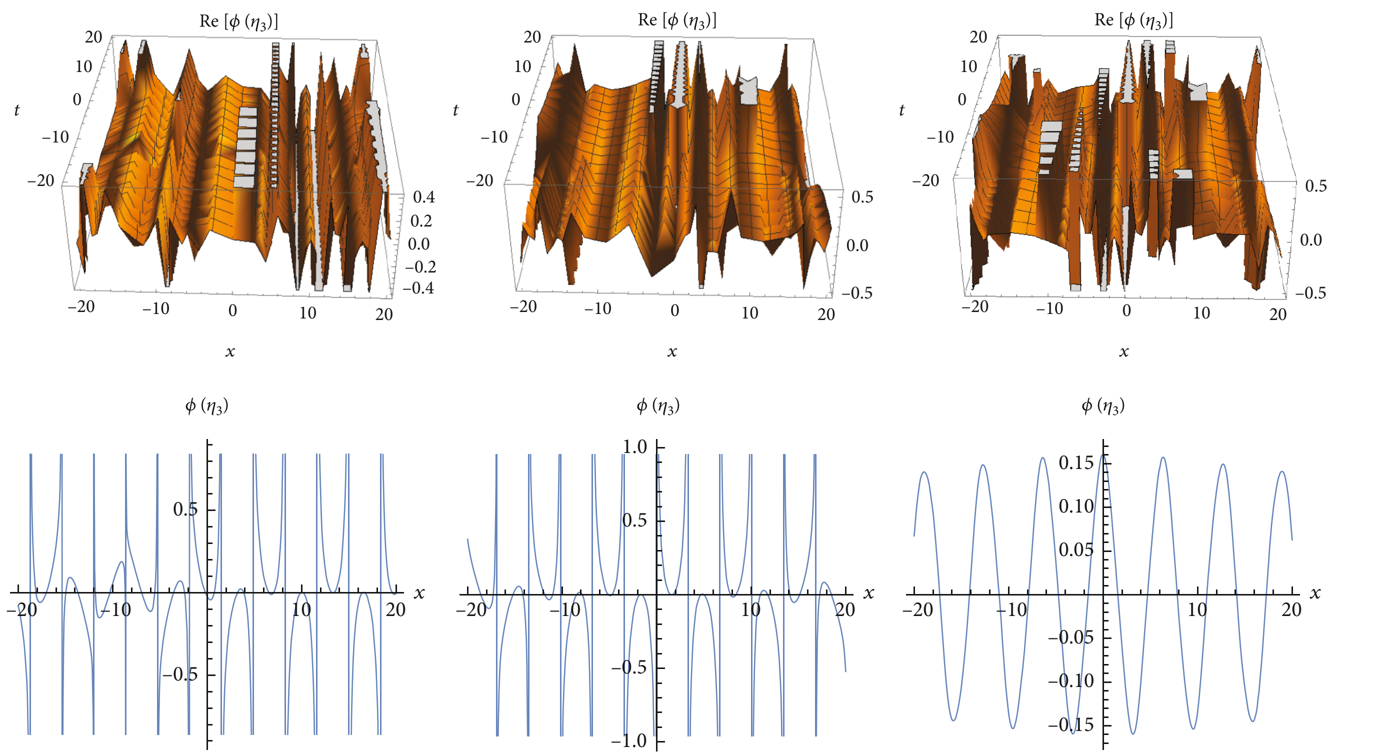

FIGURE 3: Three- and two-dimensional graphs of the solution $\phi(\eta_3)$ for different $\beta = 0.01, 0.55, 0.98$ corresponding to the values $c_1 = 1/4$, $m = 1/2$, $\kappa = -1$, $\theta = 0.3$, $\mu = 0.2$, and $k_2 = 1$.

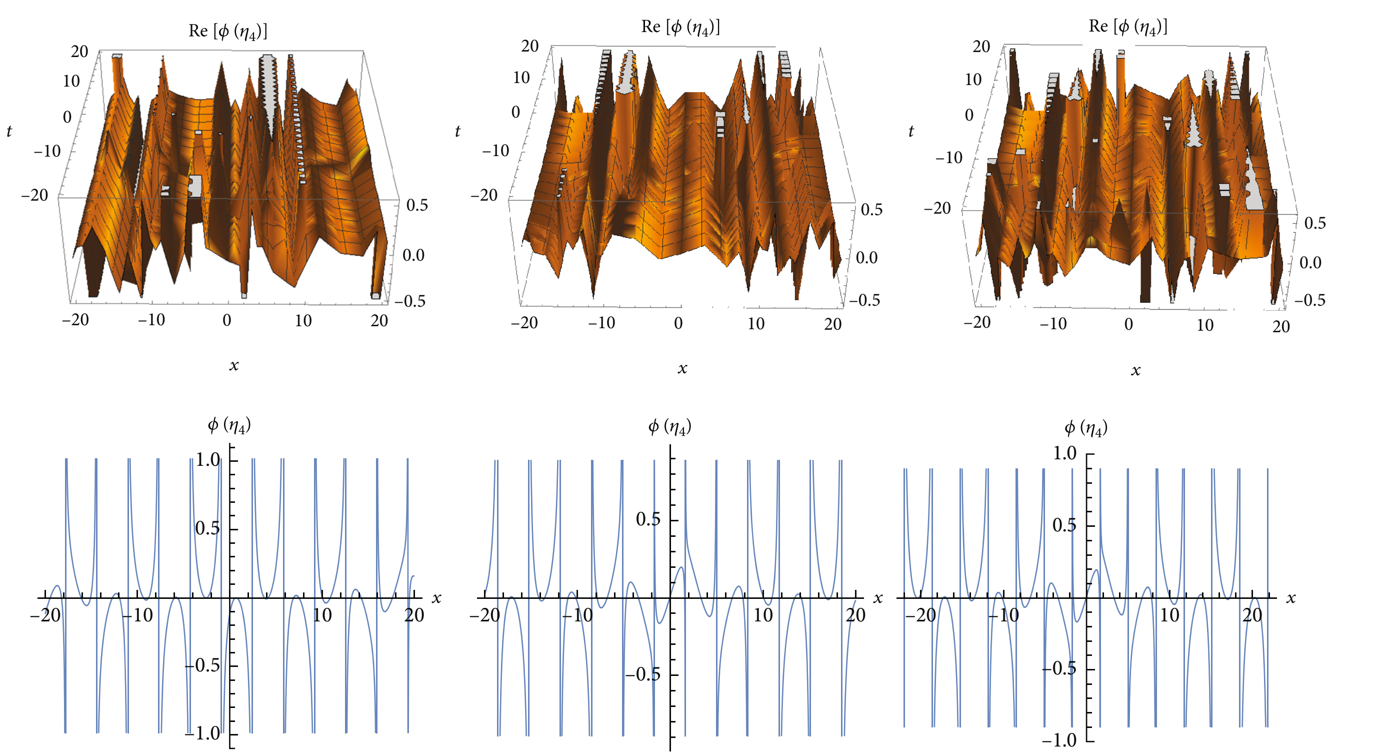

FIGURE 4: Three- and two-dimensional graphs of the solution $\phi(\eta_4)$ for different $\beta = 0.01, 0.55, 0.98$ corresponding to the values $d_1 = 1/5$, $m = 1/2$, $\kappa = -1$, $\theta = 0.3$, $\mu = 0.2$, and $k_2 = 1$.

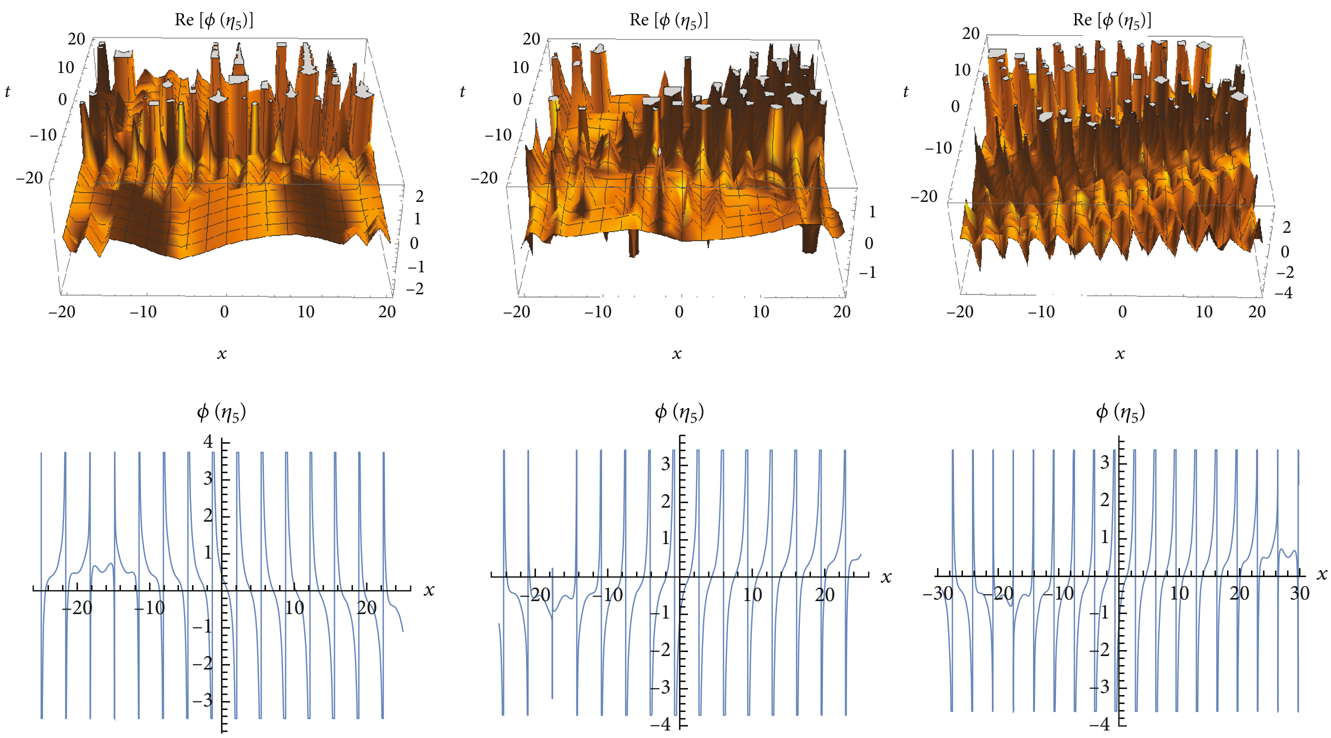

Figure 5: Three- and two-dimensional graphs of the solution $\phi(\eta_5)$ for different $\beta = 0.01, 0.55, 0.98$ corresponding to the values $a_1 = m = 1/2$, $\kappa = -1$, $\theta = 0.3$, $\mu = 0.2$, and $k_2 = 1$.

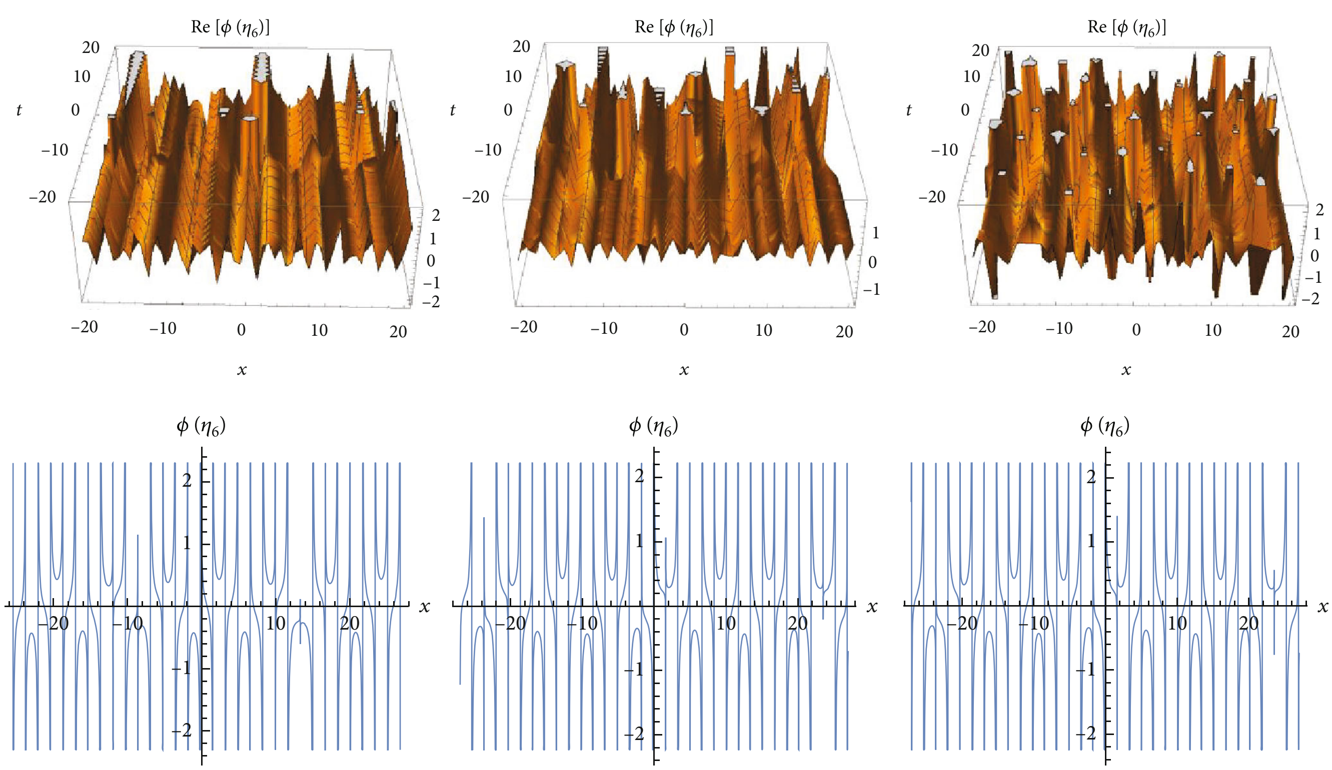

Figure 6: Three- and two-dimensional graphs of the solution $\phi(\eta_6)$ for different $\beta = 0.01, 0.55, 0.98$ corresponding to the values $c_1 = 1/4$, $m = 1/2$, $\kappa = -1$, $\theta = 0.3$, $\mu = 0.2$, and $k_2 = 1$.

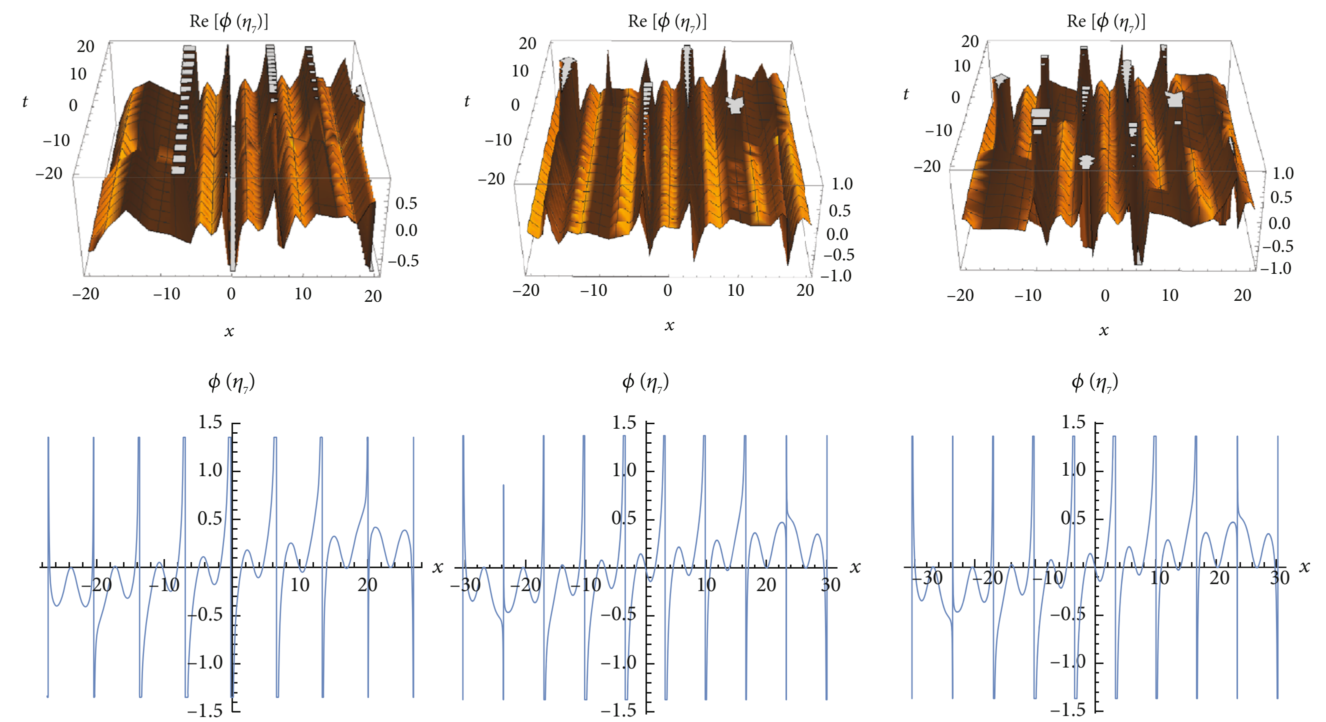

FIGURE 7: Three- and two-dimensional graphs of the solution $\phi(\eta_7)$ for different $\beta = 0.01, 0.55, 0.98$ corresponding to the values $c_1 = 1/4$, $m = 1/2$, $\kappa = -1$, $\theta = 0.3$, $\mu = 0.2$, and $k_2 = 1$.

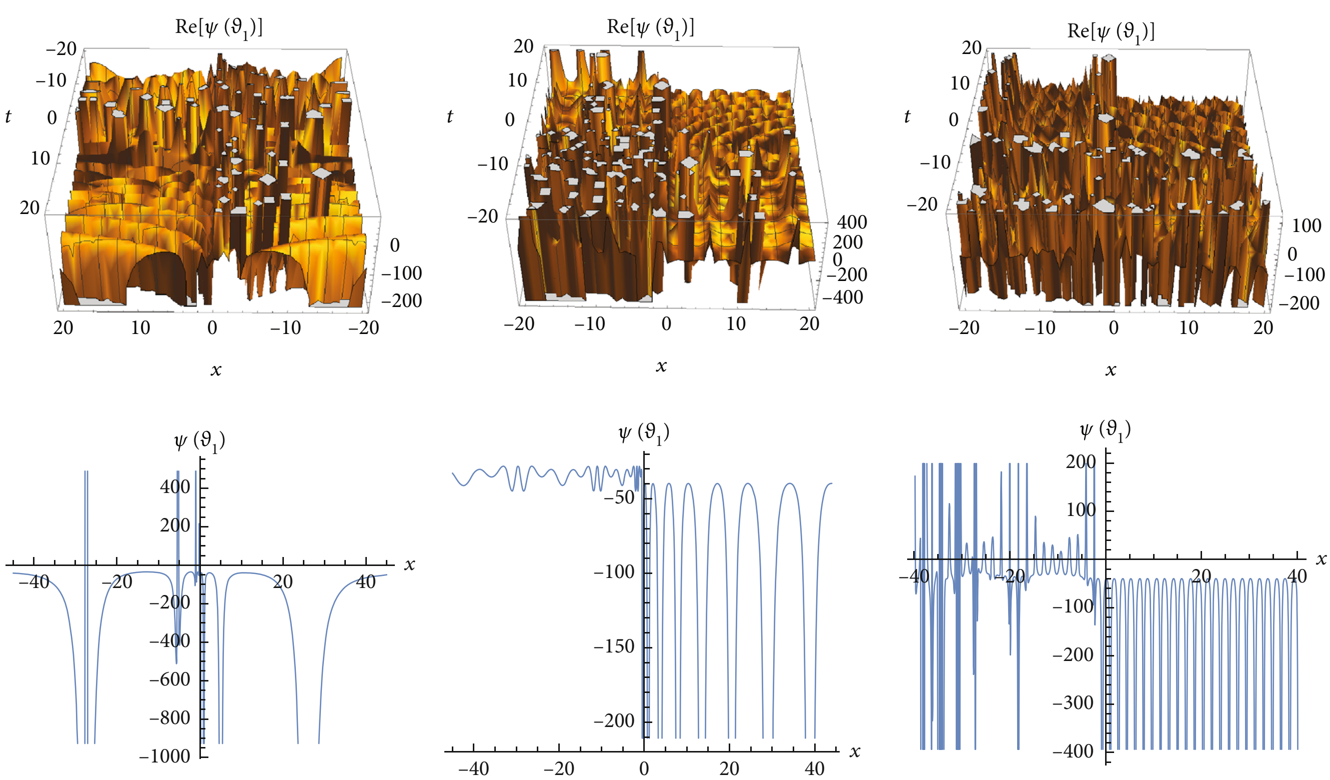

FIGURE 8: Three- and two-dimensional graphs of the solution $\psi(\vartheta_1)$ for different $\beta = 0.01, 0.50, 0.98$ corresponding to the values $c_2 = 1/4$, $m = 1/2$, and $c = k = \gamma = b = 1$.

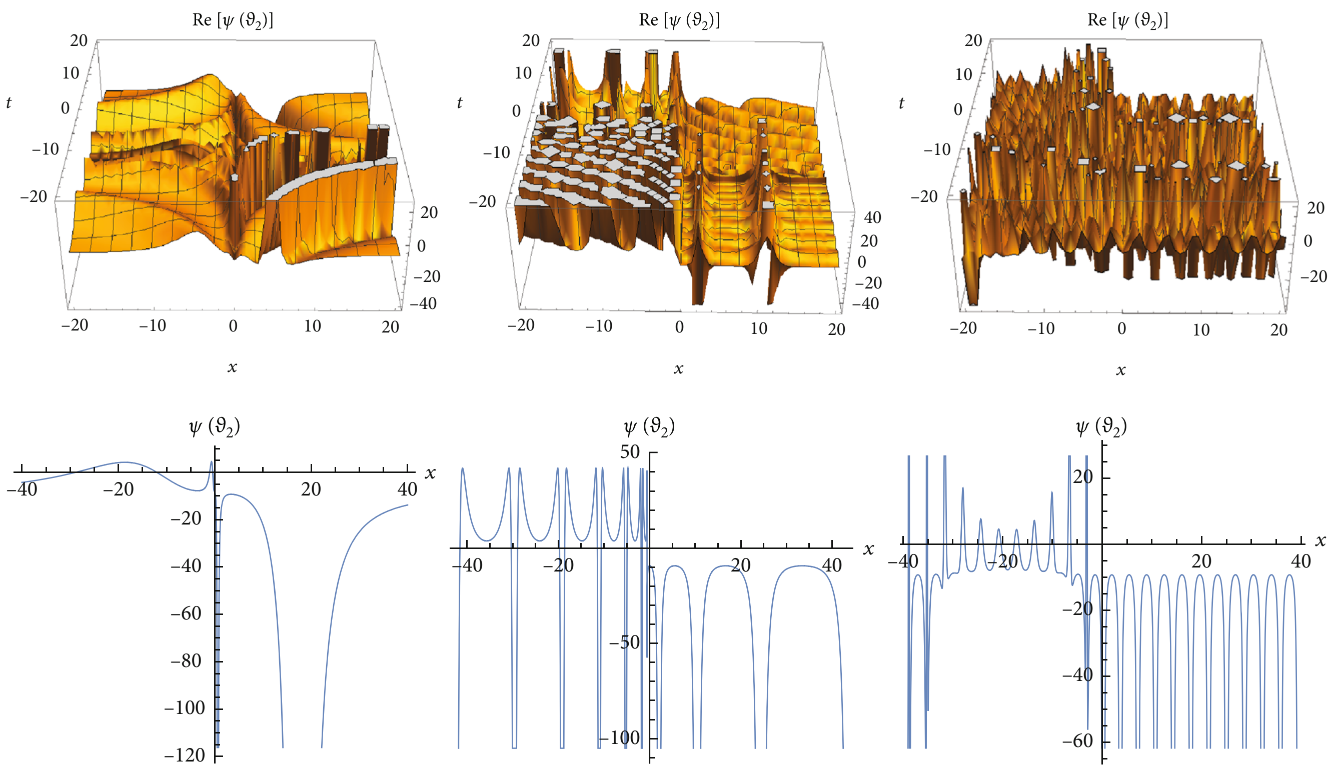

Figure 9: Three- and two-dimensional graphs of the solution $\psi(\vartheta_2)$ for different $\beta = 0.01, 0.50, 0.98$ corresponding to the values $c_2 = 1/4$, $m = 1/2$, and $c = k = \gamma = b = 1$.

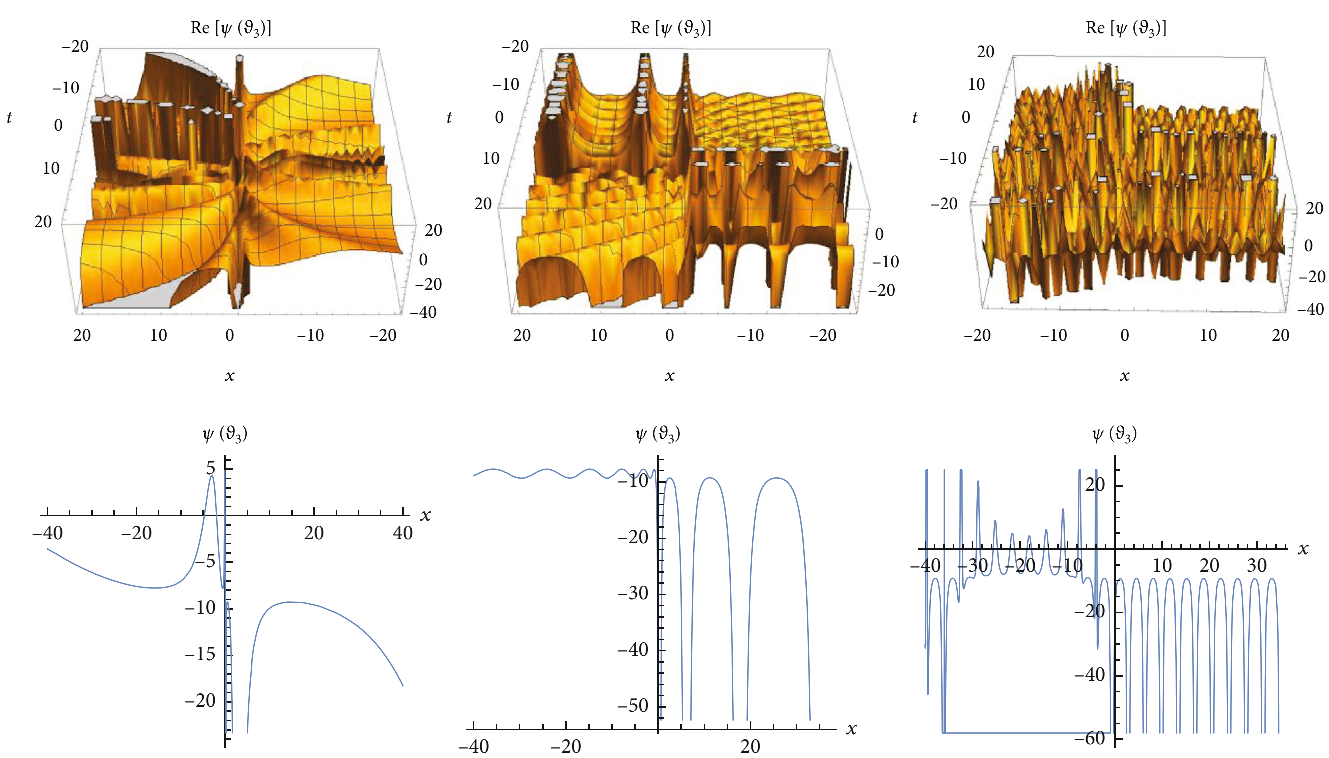

Figure 10: Three- and two-dimensional graphs of the solution $\psi(\vartheta_3)$ for different $\beta = 0.01, 0.50, 0.98$ corresponding to the values $c_2 = 1/4$, $m = 1/2$, and $c = k = \gamma = b = 1$.

$= m^2$, $Q = -(1+m^2)$, and $R = 1$, then the new exact solutions are specified in the following cases.

Case 1.

$$a_0 = \frac{4k^4 Q\gamma - 8k^4\gamma\sqrt{Q^2+12PR}}{ck^2} + 2Qc_2,$$
$$a_1 = b_1 = c_1 = d_1 = 0, \quad (46)$$
$$b_2 = -\frac{\left(Q^2-4PR\right)\left(6k^2\gamma + cc_2\right)}{c},$$

$$a_2 = -\frac{6k^2\gamma - cc_2}{c},$$
$$c_2 = c_2,$$
$$d_2 = \frac{-96k^2PR\gamma}{c}, \quad (47)$$
$$\sigma = -\sqrt{16k^4\gamma\sqrt{Q^2+12PR} - bk^2}.$$

When obtained coefficients in Equation (46) are replaced into Equation (45), we get new exact solution named as mixed Jacobi elliptic function solutions of Equation (2) as follows:

$$\psi(\vartheta_1) = B_1 + B_2\frac{cn^2(\vartheta_1)dn^2(\vartheta_1)}{sn^2(\vartheta_1)} + B_3\frac{sn^2(\vartheta_1)}{cn^2(\vartheta_1)dn^2(\vartheta_1)} + B_4\frac{\left(m^2sn^2(\vartheta_1)cn^2(\vartheta_1) + sn^2(\vartheta_1)dn^2(\vartheta_1) + cn^2(\vartheta_1)dn^2(\vartheta_1)\right)^2}{sn^2(\vartheta_1)cn^2(\vartheta_1)dn^2(\vartheta_1)}$$
$$+ B_5\frac{sn^2(\vartheta_1)cn^2(\vartheta_1)dn^2(\vartheta_1)^2}{\left(m^2sn^2(\vartheta_1)cn^2(\vartheta_1) + sn^2(\vartheta_1)dn^2(\vartheta_1) + cn^2(\vartheta_1)dn^2(\vartheta_1)\right)}, \quad (48)$$

where $B_1 = (4k^2\gamma(-1-m^2) - 8\gamma k^4\sqrt{1+14m^2+m^4} + 2ck^2c_2(-1-m^2)/k^2c)$, $B_2 = (-6k^2\gamma - cc_2)/c$, $B_3 = (-1+2m^2-m^4)(6k^2\gamma + cc_2)/c$, $B_4 = c_2$, $B_5 = -96k^2m^2\gamma/c$, and $\vartheta_1 = (k/\beta)(x + (1/\Gamma(\beta)))^\beta + (\sqrt{16k^4\gamma\sqrt{1+14m^2+m^4} - bk^2}/\beta)(t + (1/\Gamma(\beta)))^\beta$.

Case 2.

$$a_0 = \frac{4k^4 Q\gamma - 2k^4\gamma\sqrt{Q^2+12PR}}{ck^2} + 2Qc_2,$$
$$a_1 = b_1 = c_1 = d_1 = d_2 = 0, \quad (49)$$
$$b_2 = \left(4PR - Q^2\right)c_2,$$

$$a_2 = -\frac{6k^2\gamma - cc_2}{c},$$
$$c_2 = c_2, \quad (50)$$
$$\sigma = -\sqrt{4k^4\gamma\sqrt{Q^2+12PR} - bk^2}.$$

Substituting Equation (49) into Equation (45), we find mixed Jacobi elliptic function solutions of Equation (2).

$$\psi(\vartheta_2) = B_6 + B_7\frac{sn^2(\vartheta_2)dn^2(\vartheta_2) - 1}{sn^2(\vartheta_2)}, \quad (51)$$

where $B_6 = 2k^2\gamma(m^2 - 2 - \sqrt{1+14m^2+m^4})/c$, $B_7 = 6k^2\gamma/c$, and $\vartheta_2 = k/\beta(x + (1/\Gamma(\beta)))^\beta + (\sqrt{4k^4\gamma\sqrt{1+14m^2+m^4} - bk^2}/\beta)(t + (1/\Gamma(\beta)))^\beta$.

Case 3.

$$a_0 = \frac{4k^4 Q\gamma - 2k^4\gamma\sqrt{Q^2+12PR}}{ck^2} + 2Qc_2,$$
$$a_1 = b_1 = c_1 = d_1 = d_2 = 0, \quad (52)$$
$$b_2 = \frac{\left(4PR - Q^2\right)\left(6k^2\gamma + cc_2\right)}{c},$$

$$a_2 = -c_2,$$
$$c_2 = c_2, \quad (53)$$
$$\sigma = \sqrt{4k^4\gamma\sqrt{Q^2+12PR} - bk^2}.$$

Using Equations (45) and (52), we obtain the following mixed Jacobi elliptic functions of Equation (2).

$$\psi(\vartheta_3) = \frac{B_8\left[B_9 + B_{10}dn^2(\vartheta_3) - 2dn^4(\vartheta_3) - cn^2(\vartheta_3)\left((2+B_{11})dn^2(\vartheta_3) - 3\right)\right]}{ccn^2(\vartheta_3)dn^2(\vartheta_3)}, \quad (54)$$

where $B_8 = 2k^2\gamma$, $B_9 = 3 - 3m^2$, $B_{10} = m^2 - 4$, $B_{11} = \sqrt{1 + 14m^2 + m^4}$, and $\vartheta_3 = k/\beta(x + (1/\Gamma(\beta)))^\beta - (\sqrt{4k^4\gamma\sqrt{1 + 14m^2 + m^4} - bk^2}/\beta)(t + (1/\Gamma(\beta)))^\beta$

Remark 2. When the results of Equation (2), which are found using the new version generalized F-expansion method, are examined, the solutions of single, combined, and mixed Jacobi elliptic functions are new. And these solutions are obtained for the first time in the literature. Furthermore, two- and three-dimensional graphics of the attained exact solutions are drawn in Figures 8–10 according to the selected parameter values.

6. Conclusions

In this paper, the new version generalized F-expansion method is applied for the first time to acquire new exact solutions of the Biswas-Arshed and Boussinesq equations defined by Atangana's beta-derivative. This method makes it possible to get dissimilar states of the new Jacobi elliptic function solutions. The new results for the Biswas-Arshed and Boussinesq equations seem to be very diverse and surprising. These exact solutions consist of single, combined, and mixed Jacobi elliptic function solutions. Thus, none of the solution functions obtained by the various methods in Ref. [37–41] articles contain the solutions found by the method used in this article. Owing to the F'/F and F/F' terms contained in the finite series in the applied method, various rational solution combinations of the double-period Jacobi elliptic functions, which have not yet been found in the literature, have been reached. Also, the graphs (Figures 1–10) drawn for these solution functions help us comprehend the complex wave phenomena of the considered physical problems. It is also shown in the Mathematica package program that all exact solutions obtained in this study provide the fractional Biswas-Arshed equation and Boussinesq equation with the beta-derivative. Also, we would like to mention that all codes were written using Mathematica 11 on an HP Z420 workstation, with an Intel (R) Xeon(R) CPU E5-1620 3.8 GHz processor, 32 GB RAM DDR3, and 1 TB storage. As a result, we can say that the new version generalized F-expansion method gives very effective results in obtaining the exact solutions of the nonlinear differential equations defined by Atangana's beta-derivative and contributes to the literature. In our further work, we will implement the new version generalized F-expansion method to other complex fractional systems defined by Atangana's beta-derivative. Also, the method offered in this paper can be generalized in future work for advanced definitions like the paper [43].

Data Availability

No data were used to support this study.

Conflicts of Interest

The authors declare that they have no competing interests.

Authors' Contributions

All authors read and approved the final manuscript.

References

[1] K. M. Owolabi and A. Atangana, "Numerical simulations of chaotic and complex spatiotemporal patterns in fractional reaction diffusion systems," *Computational and Applied Mathematics*, vol. 37, no. 2, pp. 2166–2189, 2018.

[2] J. F. Gomez-Aguilar, "Space-time fractional diffusion equation using a derivative with nonsingular and regular kernel," *Physica A: Statistical Mechanics and its Applications*, vol. 465, pp. 562–572, 2017.

[3] K. M. Owolabi and A. Atangana, "Numerical simulation of noninteger order system in subdiffusive, diffusive, and superdiffusive scenarios," *Journal of Computational and Nonlinear Dynamics*, vol. 12, no. 3, article 031010, pp. 1–7, 2017.

[4] A. H. Bhrawy, "A Jacobi spectral collocation method for solving multi-dimensional nonlinear fractional sub-diffusion equations," *Numerical Algorithms*, vol. 73, no. 1, pp. 91–113, 2016.

[5] R. Metzler and J. Klafter, "The random walk's guide to anomalous diffusion: a fractional dynamics approach," *Physics Reports*, vol. 339, no. 1, pp. 1–77, 2000.

[6] G. Jumarie, "Modified Riemann-Liouville derivative and fractional Taylor series of nondifferentiable functions further results," *Computers & Mathematcs with Applications*, vol. 51, no. 9-10, pp. 1367–1376, 2006.

[7] I. Podlubny, *Fractional Differential Equations*, Academic Press, 1999.

[8] M. Caputo and M. Fabrizio, "Applications of new time and spatial fractional derivatives with exponential kernels," *Progress in Fractional Differentiation & Applications*, vol. 2, no. 1, pp. 1–11, 2016.

[9] A. Atangana and D. Baleanu, "New fractional derivatives with nonlocal and non-singular kernel: theory and application to heat transfer model," *Thermal Science*, vol. 20, no. 2, pp. 763–769, 2016.

[10] A. A. Alderremy, H. I. Abdel-Gawad, K. M. Saad, and S. Aly, "New exact solutions of time conformable fractional Klein Kramer equation," *Optical and Quantum Electronics*, vol. 53, p. 14, 2021.

[11] Y. Pandir, Y. Gurefe, and E. Misirli, "New exact solutions of the time-fractional nonlinear dispersive KdV equation," *International Journal of Modeling and Optimization*, vol. 3, no. 4, pp. 349–352, 2013.

[12] Y. Pandir, Y. Gurefe, and E. Misirli, "The extended trial equation method for some time fractional differential equations," *Discrete Dynamics in Nature and Society*, vol. 2013, Article ID 491359, 13 pages, 2013.

[13] M. Alqhtani, K. M. Saad, R. Shah, W. Weera, and W. M. Hamanah, "Analysis of the fractional-order local Poisson equation in fractal porous media," *Symmetry*, vol. 14, no. 7, p. 1323, 2022.

[14] M. Alqhtani, K. M. Owolabi, K. M. Saad, and E. Pindza, "Efficient numerical techniques for computing the Riesz fractional-

order reaction-diffusion models arising in biology," *Chaos, Solitons & Fractals*, vol. 161, no. 6, article 112394, 2022.

[15] N. Das, R. Singh, A. M. Wazwaz, and J. Kumar, "An algorithm based on the variational iteration technique for the Bratu-type and the Lane-Emden problems," *Journal of Mathematical Chemistry*, vol. 54, no. 2, pp. 527–551, 2016.

[16] H. Jafari and H. K. Jassim, "Numerical solutions of telegraph and Laplace equations on cantor sets using local fractional Laplace decomposition method," *International Journal of Advances in Applied Mathematics and Mechanics*, vol. 2, no. 3, pp. 144–151, 2015.

[17] N. Gurefe, E. G. Kocer, and Y. Gurefe, "Chebyshev-Tau method for the linear Klein-Gordon equation," *International Journal of Physical Sciences*, vol. 7, no. 43, pp. 5723–5728, 2012.

[18] C. Li and F. Zeng, "Finite difference methods for fractional differential equations," *International Journal of Bifurcation and Chaos*, vol. 22, no. 4, article 1230014, pp. 1–28, 2012.

[19] L. B. Feng, P. Zhuang, F. Liu, I. Turner, and Y. T. Gu, "Finite element method for space-time fractional diffusion equation," *Numerical Algorithms*, vol. 72, no. 3, pp. 749–767, 2016.

[20] R. Khalil, M. Al Horani, A. Yousef, and M. Sababheh, "A new definition of fractional derivative," *Journal of Computational and Applied Mathematics*, vol. 264, pp. 65–70, 2014.

[21] Y. Cenesiz and A. Kurt, "The solution of time fractional heat equation with new fractional derivative definition," *8th International Conference on Applied Mathematics, Simulation and Model*, vol. 195, 2014.

[22] A. Atangana, D. Baleanu, and A. Alsaedi, "New properties of conformable derivative," *Open Mathematics*, vol. 13, no. 1, pp. 889–898, 2015.

[23] Y. Çenesiz, D. Baleanu, A. Kurt, and O. Tasbozan, "New exact solutions of Burgers' type equations with conformable derivative," *Waves in Random and complex Media*, vol. 27, no. 1, pp. 103–116, 2017.

[24] W. S. Chung, "Fractional Newton mechanics with conformable fractional derivative," *Journal of Computational and Applied Mathematics*, vol. 290, pp. 150–158, 2015.

[25] A. Atangana, D. Baleanu, and A. Alsaedi, "Analysis of time-fractional Hunter-Saxton equation: a model of neumatic liquid crystal," *Open Physics*, vol. 14, no. 1, pp. 145–149, 2016.

[26] H. Yepez-Martinez, J. F. Gomez-Aguilar, and A. Atangana, "First integral method for non-linear differential equations with conformable derivative," *Mathematical Modelling of Natural Phenomena*, vol. 13, no. 1, pp. 14–14, 2018.

[27] H. Yépez-Martínez and J. F. Gómez-Aguilar, "Fractional sub-equation method for Hirota–Satsuma-coupled KdV equation and coupled mKdV equation using the Atangana's conformable derivative," *Waves in Random and Complex Media*, vol. 29, no. 4, pp. 678–693, 2019.

[28] H. Yepez-Martinez and J. F. Gómez-Aguilar, "Optical solitons solution of resonance nonlinear Schrödinger type equation with Atangana's-conformable derivative using sub-equation method," *Waves in Random and Complex Media*, vol. 31, no. 3, pp. 573–596, 2021.

[29] B. Ghanbari and J. F. Gomez-Aguilar, "The generalized exponential rational function method for Radhakrishnan-Kundu Lakshmanan equation with β-conformable time derivative," *Revista Mexicana de Fisica*, vol. 65, no. 5, pp. 503–518, 2019.

[30] Y. Pandir and N. Turhan, "A new version of the generalized F-expansion method and its applications," *AIP Conference Proceedings*, vol. 1798, no. 1, article 020122, 2017.

[31] Y. Pandir, "A new type of generalized F-expansion method and its application to Sine-Gordon equation," *Celal Bayar University Journal of Science*, vol. 13, no. 3, pp. 647–650, 2017.

[32] Y. Pandir and N. Turhan, "Multiple soliton solutions for nonlinear differential equations with a new version of extended F-expansion method," *Proceedings of the National Academy of Sciences, India Section A: Physical Sciences*, vol. 91, no. 3, pp. 495–501, 2021.

[33] Q. Wang, Y. Chen, and Z. Hongqing, "A new Jacobi elliptic function rational expansion method and its application to (1 + 1)-dimensional dispersive long wave equation," *Chaos, Solitons & Fractals*, vol. 23, no. 2, pp. 477–483, 2005.

[34] X. Yafeng, X. Haili, and Z. Hongqing, "A new extended Jacobi elliptic function expansion method and its application to the generalized shallow water wave equation," *Journal of Applied Mathematics*, vol. 2012, Article ID 896748, 21 pages, 2012.

[35] A. S. Alofi, "Extended Jacobi elliptic function expansion method for nonlinear Benjamin-Bona-Mahony equations," *International Mathematical Forum*, vol. 7, no. 53, pp. 2639–2649, 2012.

[36] I. Enam, "Generalized Jacobi elliptic function method for traveling wave solutions of (2+1)-dimensional breaking soliton equation," *Cankaya University Journal of Science and Engineering*, vol. 7, no. 1, pp. 39–50, 2010.

[37] K. Hosseini, M. Mirzazadeh, M. Ilie, and J. F. Gómez-Aguilar, "Biswas-Arshed equation with the beta time derivative: optical solitons and other solutions," *Optik*, vol. 217, no. 164801, pp. 164801–164807, 2020.

[38] Z. Li, "Bifurcation and traveling wave solution to fractional Biswas-Arshed equation with the beta time derivative," *Chaos, Solitons & Fractals*, vol. 160, article 112249, 2022.

[39] A. Akbulut and S. M. R. Islam, "Study on the Biswas-Arshed equation with the beta time derivative," *International Journal of Applied and Computational Mathematics*, vol. 8, no. 4, pp. 1–13, 2022.

[40] T. Han, Z. Li, and J. Yuan, "Optical solitons and single traveling wave solutions of Biswas-Arshed equation in birefringent fibers with the beta-time derivative," *AIMS Math*, vol. 7, no. 8, pp. 15282–15297, 2022.

[41] H. B. Jebreen, "Some nonlinear fractional PDEs involving β -derivative by using rational $\exp(-\Omega(\eta))$-expansion method," *Complexity*, vol. 2020, Article ID 9179826, 22 pages, 2020.

[42] T. Abdeljawad, "On conformable fractional calculus," *Journal of Computational and Applied Mathematics*, vol. 279, pp. 57–66, 2015.

[43] Y. H. Youssri and A. G. Atta, "Spectral collocation approach via normalized shifted Jacobi polynomials for the nonlinear Lane-Emden equation with fractal-fractional derivative," *Fractal and Fractional*, vol. 7, no. 2, p. 133, 2023.

Hindawi
Journal of Function Spaces
Volume 2023, Article ID 2127600, 10 pages
https://doi.org/10.1155/2023/2127600

Research Article

Qualitative Study on Solutions of Piecewise Nonlocal Implicit Fractional Differential Equations

Mohammed S. Abdo,[1] **Sahar Ahmed Idris**,[2] **Wedad Albalawi**,[3] **Abdel-Haleem Abdel-Aty**,[4] **Mohammed Zakarya**,[5] **and Emad E. Mahmoud**[6]

[1]*Department of Mathematics, Hodeidah University, PO.Box. 3114, Al-Hudaydah, Yemen*
[2]*Department of Industrial Engineering, Faculty of Engineering, King Khalid University, Abha, Saudi Arabia*
[3]*Department of Mathematical Sciences, College of Science, Princess Nourah bint Abdulrahman University, P.O. Box 84428, Riyadh 11671, Saudi Arabia*
[4]*Department of Physics, College of Sciences, University of Bisha, PO. Box 344, Bisha 61922, Saudi Arabia*
[5]*Department of Mathematics, College of Science, King Khalid University, P.O. Box 9004, Abha 61413, Saudi Arabia*
[6]*Department of Mathematics and Statistics, College of Science, Taif University, PO Box 11099, Taif 21944, Saudi Arabia*

Correspondence should be addressed to Mohammed S. Abdo; msabdo@hoduniv.net.ye

Received 29 July 2022; Revised 7 September 2022; Accepted 5 October 2022; Published 28 April 2023

Academic Editor: Yusuf Gurefe

In this paper, we investigate new types of nonlocal implicit problems involving piecewise Caputo fractional operators. The existence and uniqueness results are proved by using some fixed point theorems. Furthermore, we present analogous results involving piecewise Caputo-Fabrizio and Atangana–Baleanu fractional operators. The ensuring of the existence of solutions is shown by Ulam-Hyer's stability. At last, two examples are given to show and approve our outcomes.

1. Introduction

It merits noticing that fractional calculus (FC) has gotten significant thought from scientists and researchers. It is a result of its wide scope of uses in different fields and disciplines. The crucial concepts and definitions of FC have been presented in [1, 2]. In [3, 4], the authors introduced some fundamental history of fractional calculus and its applications to engineering and different areas of science.

Many classes of fractional differential equations (FDEs) have been intensively investigated in the last decades, for instance, theories involving the existence of unique solutions have been notarized [5–7]. Numerical and analytical methods have been evolving with the target to solve such equations [8–10]. These equations have been tracked as useful in modeling some real-world problems with incredible achievement.

The qualitative properties of solutions represent a very important aspect of the theory of FDEs. The formerly aforesaid region has been studied well for classical differential equations. However, for FDEs, there are many aspects that require further studying and reconnoitering. The attention on the existence and uniqueness has been especially focused by applying Riemann-Liouville (R-L), Caputo, Hilfer, and other FDs, see [11–15].

In this regard, Agarwal et al. [16] investigated the existence of solutions of the following Caputo type FDE:

$$\begin{aligned} &{}^{C}\mathbb{D}_{0^+}^{\vartheta}\upsilon(\varkappa) = f(\varkappa, \upsilon(\varkappa)), \varkappa \in [0, T], 0 < \vartheta < 1, \\ &\upsilon(0) + g(\upsilon) = \upsilon_0. \end{aligned} \tag{1}$$

The basic theory of implicit FDEs with Caputo FD has been investigated by Kucche et al. [17]. Wahash et al. [18]

considered the following nonlocal implicit FDEs with ψ-Caputo FD

$$\mathbb{D}_{a^+}^{\vartheta;\psi}\upsilon(\varkappa)=f\left(\varkappa,\upsilon(\varkappa),\mathbb{D}_{a^+}^{\vartheta;\psi}\upsilon(\varkappa)\right),\quad \varkappa\in[a,T],0<\vartheta<1$$
$$\upsilon(a)+g(\upsilon)=\upsilon_a. \tag{2}$$

Problem (2) with $\psi(\varkappa)=\varkappa$ has been studied by Benchohra and Bouriah [19].

Motivated by the above works and inspired by [20], we consider the piecewise Caputo implicit FDE (PC-IFDE) of the type:

$$\begin{aligned}{}^{PC}\mathbb{D}_{0^+}^{\vartheta}\upsilon(\varkappa)&=\Phi\left(\varkappa,\upsilon(\varkappa),{}^{PC}\mathbb{D}_{0^+}^{\vartheta}\upsilon(\varkappa)\right),\\ \upsilon(0)&=\upsilon_0,\end{aligned} \tag{3}$$

and the following piecewise Caputo nonlocal implicit FDE (PC-NIFDE):

$$\begin{aligned}{}^{PC}\mathbb{D}_{0^+}^{\vartheta}\upsilon(\varkappa)&=\Phi\left(\varkappa,\upsilon(\varkappa),{}^{PC}\mathbb{D}_{0^+}^{\vartheta}\upsilon(\varkappa)\right),\\ \upsilon(0)+g(\upsilon)&=\upsilon_0,\end{aligned} \tag{4}$$

where $0<\vartheta\le 1$,$\varkappa\in\mathbb{J}:=[0,b]$,$\upsilon_0\in\mathbb{R}$,$\Phi\in\mathscr{C}(\mathbb{J}\times\mathbb{R},\mathbb{R})$, $g\in\mathscr{C}(\mathbb{J},\mathbb{R})$, and ${}^{PC}\mathbb{D}_{0^+}^{\vartheta}$ represent the piecewise Caputo FD of order ϑ defined by

$${}^{PC}\mathbb{D}_{0^+}^{\vartheta}f(\varkappa)=\begin{cases}\mathbb{D}f(\varkappa)\text{: if }\varkappa\in[0,\varkappa_1],\\ {}^{C}\mathbb{D}_{\varkappa_1}^{\vartheta}f(\varkappa)\text{: if }\varkappa\in[\varkappa_1,b],\end{cases} \tag{5}$$

where $\mathbb{D}f(\varkappa):=(d/d\varkappa)f(\varkappa)$ is a classical derivative on $0\le\varkappa\le\varkappa_1$ and ${}^{C}\mathbb{D}_{\varkappa_1}^{\vartheta}$ is standard Caputo FD on $\varkappa_1\le\varkappa\le b$.

It is essential to note that the utilization of nonlinear condition $\upsilon(0)+g(\upsilon)=\upsilon_0$ in physical issues yields better impact than the initial condition $\upsilon(0)=\upsilon_0$ (see [21]).

We pay attention to the topic of the novel piecewise operators. As far as we could possibly know, no outcomes in the literature are addressing the qualitative aspects of the aforesaid problems by using the piecewise FC. Consequently, by conquering this gap, we will examine the existence, uniqueness, and Ulam-Hyers stability results of piecewise Caputo problems (3) and (4) based on the standard fixed point theorems due to Banach-type and Schauder-type. Furthermore, we present similar results containing piecewise Caputo-Fabrizio (PCF) type and piecewise Atangana-Baleanu (PAB) type. An open problem with respect to another function is suggested.

Remark 1.

(i) If $g(\upsilon)\equiv 0$, then problem (4) reduces to the PC-IFDE (3).

(ii) If ${}^{PC}\mathbb{D}_{0^+}^{\vartheta}\upsilon(\varkappa)={}^{C}\mathbb{D}_{\varkappa_1}^{\vartheta}\upsilon(\varkappa)$, then problem (4) has been studied by Benchohra and Bouriah [19], Haoues et al. [22], and Abdo et al. [11] for $\psi(\varkappa)=\varkappa$.

(iii) Our current results for problem (4) stay available on PC-IFDE (3).

The substance of this paper is coordinated as follows: Section 2 presents a few required outcomes and fundamentals about piecewise FC. Our key outcomes for problem (4) are proved in Section 3. Two examples to make sense of the gained outcomes are built in Section 4. Toward the end, we encapsulate our study in the end section.

2. Primitive Results

In this section, we present some concepts of a piecewise FC. Let

$$\mathscr{C}:=\mathscr{C}(\mathbb{J},\mathbb{R})=\left\{\eta:\mathbb{J}\longrightarrow\mathbb{R};\|\eta\|=\max_{\varkappa\in\mathbb{J}}|\eta(\varkappa)|\right\}. \tag{6}$$

Obviously $\mathscr{C}$ is a Banach space under $\|\eta\|$.

Definition 2 [20]. Let $\vartheta>0$, and $\eta:\mathbb{J}\longrightarrow\mathbb{R}$ be a continuous. Then, the piecewise version of RL integral is given by

$${}^{PRL}\mathbb{I}_{0^+}^{\vartheta}\eta(\varkappa)=\begin{cases}\mathbb{I}\eta(\varkappa),\text{ if }\varkappa\in[0,\varkappa_1],\\ {}^{RL}\mathbb{I}_{\varkappa_1}^{\vartheta}\eta(\varkappa)\text{ if }\varkappa\in[\varkappa_1,b],\end{cases} \tag{7}$$

where $\mathbb{I}\eta(\varkappa) = \int_0^{\varkappa_1}\eta(\varkappa)d\varkappa$ and ${}^{RL}\mathbb{I}_{\varkappa_1}^{\vartheta}\eta(\varkappa) = 1/(\Gamma(\vartheta))\int_{\varkappa_1}^{\varkappa}(\varkappa-t))^{\vartheta-1}\eta(t)dt$.

Definition 3 [20]. Let $0<\vartheta\le 1$, and $\eta:\mathbb{J}\longrightarrow\mathbb{R}$ be a continuous. Then, the piecewise version of Caputo derivative is given by

$${}^{PC}\mathbb{D}_{0^+}^{\vartheta}\eta(\varkappa)=\begin{cases}\mathbb{D}\eta(\varkappa),\text{ if }\varkappa\in[0,\varkappa_1],\\ {}^{C}\mathbb{D}_{\varkappa_1}^{\vartheta}\eta(\varkappa)\text{ if }\varkappa\in[\varkappa_1,b],\end{cases} \tag{8}$$

where $\mathbb{D}\eta(\varkappa)=(d/d\varkappa)\eta(\varkappa)$ and ${}^{C}\mathbb{D}_{\varkappa_1}^{\vartheta}\eta(\varkappa)=1/(\Gamma(1-\vartheta))\int_{\varkappa_1}^{\varkappa}(\varkappa-t))^{-\vartheta}\eta'(t)dt$.

Lemma 4 [20]. *Let $0<\vartheta\le 1$, and $f(0)=0$. Then, the following PC-FDE*

$$\begin{aligned}{}^{PC}\mathbb{D}_{0^+}^{\vartheta}\eta(\varkappa)&=f(\varkappa),\\ \eta(0)&=\varkappa_0,\end{aligned} \tag{9}$$

has the following solution

$$\eta(\varkappa)=\begin{cases}\eta(0)+\int_0^{\varkappa_1}\eta(\varkappa)d\varkappa, \text{ if } \varkappa\in[0,\varkappa_1],\\ \eta(\varkappa_1)+\dfrac{1}{\Gamma(\vartheta)}\int_{\varkappa_1}^{\varkappa}(\varkappa-t)^{\vartheta-1}\eta(t)dt \text{ if } \varkappa\in[\varkappa_1,b].\end{cases} \tag{10}$$

Lemma 5 [20]. *Let $\vartheta\in(0,1]$, and for a given function, $\eta\in\mathscr{C}$. Then,*

$$^{PRL}\mathbb{I}_{0^+}^{\vartheta}\,{}^{PC}\mathbb{D}_{0^+}^{\vartheta}\eta(\varkappa)=\begin{cases}\mathbb{I}\mathbb{D}\eta(\varkappa)=\eta(\varkappa)-\eta(0), \text{ if } \varkappa\in[0,\varkappa_1],\\ {}^{RL}\mathbb{I}_{\varkappa_1}^{\vartheta}\,{}^{C}\mathbb{D}_{\varkappa_1}^{\vartheta}\eta(\varkappa)=\eta(\varkappa)-\eta(\varkappa_1), \text{ if } \varkappa\in[\varkappa_1,b].\end{cases} \tag{11}$$

For our aim, we need the Banach fixed-point theorem [23] and the Schauder fixed-point theorem [24].

3. Main Results

In this section, we give some qualitative analyses of the PC-IFDE and PC-NIFDE.

Lemma 6. *Let $\Phi(\varkappa,\upsilon,\omega)$: $\mathbb{J}\times\mathbb{R}\times\mathbb{R}\longrightarrow\mathbb{R}$ be continuous. Then, PC-NIFDE (4) is equivalent to*

$$\upsilon(\varkappa)=\begin{cases}\upsilon_0-g(\upsilon)+\int_0^{\varkappa_1}\Phi_\upsilon(t)dt \text{ if } \varkappa\in[0,\varkappa_1],\\ \upsilon(\varkappa_1)-g(\upsilon)+\dfrac{1}{\Gamma(\vartheta)}\int_{\varkappa_1}^{\varkappa}(\varkappa-t)^{\vartheta-1}\Phi_\upsilon(t)dt, \text{ if } \varkappa\in[\varkappa_1,b],\end{cases} \tag{12}$$

where $\Phi_\upsilon\in\mathscr{C}$ satisfies the functional equation

$$\Phi_\upsilon(\varkappa)=\begin{cases}\Phi\left(\varkappa,\upsilon_0-g(\upsilon)+\int_0^{\varkappa_1}\Phi_\upsilon(t)dt,\Phi_\upsilon(\varkappa)\right) \text{ if } \varkappa\in[0,\varkappa_1],\\ \Phi\left(\varkappa,\upsilon(\varkappa_1)-g(\upsilon)+\dfrac{1}{\Gamma(\vartheta)}\int_{\varkappa_1}^{\varkappa}(\varkappa-t)^{\vartheta-1}\Phi_\upsilon(t)dt,\Phi_\upsilon(\varkappa)\right), \text{ if } \varkappa\in[\varkappa_1,b].\end{cases} \tag{13}$$

Proof. Let ${}^{PC}\mathbb{D}_{0^+}^{\vartheta}\upsilon(\varkappa)=\Phi_\upsilon(\varkappa)$.

Then, by applying ${}^{PRL}\mathbb{I}_{0^+}^{\vartheta}$, we obtain

$$^{PRL}\mathbb{I}_{0^+}^{\vartheta}\,{}^{PC}\mathbb{D}_{0^+}^{\vartheta}\upsilon(\varkappa)={}^{PRL}\mathbb{I}_{0^+}^{\vartheta}\Phi_\upsilon(\varkappa). \tag{14}$$

□

In view of Lemma 5, we have

Case 1. For $\varkappa\in[0,\varkappa_1]$,

$$\upsilon(\varkappa)=\upsilon(0)+\int_0^{\varkappa_1}\Phi_\upsilon(t)dt. \tag{15}$$

Case 2. For $\varkappa\in[\varkappa_1,b]$,

$$\upsilon(\varkappa)=\upsilon(\varkappa_1)+\frac{1}{\Gamma(\vartheta)}\int_{\varkappa_1}^{\varkappa}(\varkappa-t)^{\vartheta-1}\Phi_\upsilon(t)dt. \tag{16}$$

Using the nonlocal condition in both cases, we obtain

$$\upsilon(\varkappa)=\begin{cases}\upsilon_0-g(\upsilon)+\int_0^{\varkappa_1}\Phi_\upsilon(t)dt, \text{ if } \varkappa\in[0,\varkappa_1],\\ \upsilon(\varkappa_1)-g(\upsilon)+\dfrac{1}{\Gamma(\vartheta)}\int_{\varkappa_1}^{\varkappa}(\varkappa-t)^{\vartheta-1}\Phi_\upsilon(t)dt, \text{ if } \varkappa\in[\varkappa_1,b].\end{cases} \tag{17}$$

So, we get (12). On the other hand, let (13) be satisfied. Set

$$\upsilon(\varkappa)=\begin{cases}\upsilon_0-g(\upsilon)+\int_0^{\varkappa_1}\Phi_\upsilon(t)dt \text{ if } \varkappa\in[0,\varkappa_1],\\ \upsilon(\varkappa_1)-g(\upsilon)+\dfrac{1}{\Gamma(\vartheta)}\int_{\varkappa_1}^{\varkappa}(\varkappa-t)^{\vartheta-1}\Phi_\upsilon(t)dt, \text{ if} \varkappa\in[\varkappa_1,b].\end{cases} \tag{18}$$

This implies that

$$^{PC}\mathbb{D}_{0^+}^{\vartheta}\upsilon(\varkappa)=\begin{cases}\dfrac{d}{d\varkappa}\left(\upsilon_0-g(\upsilon)+\int_0^{\varkappa_1}\Phi_\upsilon(t)dt\right) \text{ if } \varkappa\in[0,\varkappa_1],\\ {}^{C}\mathbb{D}_{\varkappa_1}^{\vartheta}\left(\upsilon(\varkappa_1)-g(\upsilon)+\dfrac{1}{\Gamma(\vartheta)}\int_{\varkappa_1}^{\varkappa}(\varkappa-t)^{\vartheta-1}\Phi_\upsilon(t)dt\right), \text{ if } \varkappa\in[\varkappa_1,b].\end{cases} \tag{19}$$

Since $\mathbb{D}\mathbb{I}\Phi_\upsilon(\varkappa)=(d/d\varkappa)\int_0^{\varkappa_1}\Phi_\upsilon(t)dt=\Phi_\upsilon(\varkappa)$ on $0\le\varkappa\le\varkappa_1$, and ${}^{C}\mathbb{D}_{\varkappa_1}^{\vartheta}\mathbb{I}_{\varkappa_1}^{\vartheta}\Phi_\upsilon(\varkappa)=\Phi_\upsilon(\varkappa)$ on $\varkappa_1\le\varkappa\le b$, we obtain ${}^{PC}\mathbb{D}_{0^+}^{\vartheta}\upsilon(\varkappa)=\Phi_\upsilon(\varkappa)$, and hence

$$^{PC}\mathbb{D}_{0^+}^{\vartheta}\upsilon(\varkappa)=\Phi\left(\varkappa,\upsilon(\varkappa),{}^{PC}\mathbb{D}_{0^+}^{\vartheta}\upsilon(\varkappa)\right), \text{for each } \varkappa\in\mathbb{J}. \tag{20}$$

The next assumptions will be applied in the sequel:

(Assu_1) The functions $\Phi:\mathbb{J}\times\mathbb{R}\times\mathbb{R}\longrightarrow\mathbb{R}$, $\Omega:\mathbb{R}^+\longrightarrow(0,\infty)$, and $\varphi,\psi:\mathbb{J}\longrightarrow\mathbb{R}$ are continuous with Ω that is a nondecreasing such that

$$|\Phi(\varkappa,\upsilon,\omega)|\le\varphi(\varkappa)\Omega(|\upsilon|)+\psi(\varkappa)|\omega|, \text{for each } (\varkappa,\upsilon,\omega)\in\mathbb{J}\times\mathbb{R}\times\mathbb{R}. \tag{21}$$

(Assu_2) $g:\mathscr{C}\longrightarrow\mathbb{R}$ is continuous and compact with $|g(\upsilon)|\le a|\upsilon|+b$, for $\upsilon\in\mathscr{C}$,$a,b>0$.

(Assu_3) There exist $\kappa_1,\kappa_2>0$, such that $0<\kappa_1,\kappa_2<1$, and

$$|\Phi(\varkappa,\upsilon,\omega)-\Phi(\varkappa,\bar{\upsilon},\bar{\omega})|\le\kappa_1|\upsilon-\bar{\upsilon}|+\kappa_2|\omega-\bar{\omega}|, \text{for each } \varkappa\in\mathbb{J},\upsilon,\omega,\bar{\upsilon},\bar{\omega}\in\mathbb{R}. \tag{22}$$

(Assu_4) There exists $\kappa_3 > 0$, such that $0 < \kappa_3 < 1$ and $|g(v) - g(\omega)| \le \kappa_3 |v - \omega|$, for $v, \omega \in \mathscr{C}$.

Now, we shall prove the existence theorem for (4) based on Schauder's theorem.

Theorem 7. *Let (Assu_1) and (Assu_2) hold.*

Then, piecewise Caputo FNIDE (4) has at least one solution on $\mathbb{J}$.

Proof. Consider the operator $Q : \mathscr{C} \longrightarrow \mathscr{C}$, such that $(Qv)(\varkappa) = v(\varkappa)$, i.e.,

$$(Qv)(\varkappa) = \begin{cases} v_0 - g(v) + \int_0^{\varkappa_1} \Phi_v(t)dt, \text{ if } \varkappa \in [0, \varkappa_1], \\ v(\varkappa_1) - g(v) + \frac{1}{\Gamma(\vartheta)} \int_{\varkappa_1}^{\varkappa} (\varkappa - t)^{\vartheta - 1} \Phi_v(t)dt, \text{ if } \varkappa \in [\varkappa_1, b], \end{cases} \tag{23}$$

where $\Phi_v \in \mathscr{C}$, with $\Phi_v(\varkappa) := \Phi(\varkappa, v(\varkappa), \Phi_v(\varkappa))$. Define the ball

$$\mathcal{S}_\beta = \{v \in \mathscr{C} : \|v\|_{\mathscr{C}} \le \beta\}, \tag{24}$$

where

$$\beta \ge \max\left\{ |v_0| + a\beta + b + \frac{\varphi^\star \Omega(\beta)}{1 - \psi^\star} b, |v(\varkappa_1)| + a\beta + b + \frac{\varphi^\star \Omega(\beta)}{1 - \psi^\star} \frac{(b - \varkappa_1)^\vartheta}{\Gamma(\vartheta + 1)} \right\}, \tag{25}$$

$\varphi^\star = \sup |\varphi(\varkappa)|$, and $\psi^\star = \sup |\psi(\varkappa)|$, with $0 < \psi^\star < 1$. □

For any $v \in \mathcal{S}_\beta$, and by (Assu_1), we have

$$\begin{aligned} |\Phi_v(\varkappa)| &= |\Phi(\varkappa, v(\varkappa), \Phi_v(\varkappa))| \\ &\le \varphi(\varkappa)\Omega(\|v\|_{\mathscr{C}}) + \psi(\varkappa)|\Phi_v(\varkappa)| \\ &\le \varphi^\star \Omega(\beta) + \psi^\star \|\Phi_v\|_{\mathscr{C}}. \end{aligned} \tag{26}$$

Since $\psi^\star < 1$, we obtain

$$\|\Phi_v\|_{\mathscr{C}} \le \frac{\varphi^\star \Omega(\beta)}{1 - \psi^\star}. \tag{27}$$

Hence, the proceed is in the following steps:

Step 1. $Q(\mathcal{S}_\beta)$ is bounded.

Case 1. For $\varkappa \in [0, \varkappa_1]$, we have

$$\begin{aligned} |(Qv)(\varkappa)| &\le |v_0| + \sup_{v \in \mathcal{S}_\beta} |g(v)| + \sup_{\varkappa \in 0, \varkappa_1]} \int_0^{\varkappa_1} |\Phi_v(t)|dt \\ &\le |v_0| + a\|v\|_{\mathscr{C}} + b + \frac{\varphi^\star \Omega(\beta)}{1 - \psi^\star} \varkappa_1 \\ &\le |v_0| + a\beta + b + \frac{\varphi^\star \Omega(\beta)}{1 - \psi^\star} \varkappa_1 \le \beta. \end{aligned} \tag{28}$$

Case 2. For $\varkappa \in [\varkappa_1, b]$, we have

$$\begin{aligned} |(Qv)(\varkappa)| &\le \sup_{\varkappa \in \varkappa_1, b]} |v(\varkappa_1)| + \sup_{v \in \mathcal{S}_\beta} |g(v)| \\ &\quad + \frac{1}{\Gamma(\vartheta)} \sup_{\varkappa \in \varkappa_1, b]} \int_{\varkappa_1}^{\varkappa} (\varkappa - t)^{\vartheta - 1} |\Phi_v(t)|dt \\ &\le |v(\varkappa_1)| + a\|v\|_{\mathscr{C}} + b + \frac{\varphi^\star \Omega(\beta)}{1 - \psi^\star} \frac{(b - \varkappa_1)^\vartheta}{\Gamma(\vartheta + 1)} \\ &\le |v(\varkappa_1)| + a\beta + b + \frac{\varphi^\star \Omega(\beta)}{1 - \psi^\star} \frac{(b - \varkappa_1)^\vartheta}{\Gamma(\vartheta + 1)} \le \beta. \end{aligned} \tag{29}$$

From (28) and (29), we conclude that $\|Qv\|_{\mathscr{C}} \le \beta$. Thus, $Q(\mathcal{S}_\beta) \subset \mathcal{S}_\beta$. Since $\mathcal{S}_\beta$ is bounded, then $Q(\mathcal{S}_\beta)$ is bounded.

Step 2. $Q : \mathcal{S}_\beta \longrightarrow \mathcal{S}_\beta$ is continuous. Let a sequence (v_n) such that $v_n \longrightarrow v$ in $\mathcal{S}_\beta$ as $n \longrightarrow \infty$. Then, for $\varkappa \in [0, \varkappa_1]$, we have

$$|(Qv_n)(\varkappa) - (Qv)(\varkappa)| \le |g(v_n) - g(v)| + \int_0^{\varkappa_1} |\Phi_{v_n}(t) - \Phi_v(t)|dt. \tag{30}$$

For $\varkappa \in [\varkappa_1, b]$, we have

$$\begin{aligned} |(Qv_n)(\varkappa) - (Qv)(\varkappa)| &\le |v_n(\varkappa_1) - v(\varkappa_1)| + |g(v_n) - g(v)| \\ &\quad + \frac{1}{\Gamma(\vartheta)} \int_{\varkappa_1}^{\varkappa} (\varkappa - t)^{\vartheta - 1} |\Phi_{v_n}(t) - \Phi_v(t)|dt, \end{aligned} \tag{31}$$

where $\Phi_v, \Phi_{v_n} \in \mathscr{C}$, with $\Phi_{v_n}(\varkappa) := \Phi(\varkappa, v_n(\varkappa), \Phi_{v_n}(\varkappa))$ and $\Phi_v(\varkappa) := \Phi(\varkappa, v(\varkappa), \Phi_v(\varkappa))$. Since $v_n \longrightarrow v$ as $n \longrightarrow \infty$ and Φ_v, Φ_{v_n}, Φ, and g are continuous, the Lebesgue dominated convergence theorem gives that

$$\|Qv_n - Qv\|_{\mathscr{C}} \longrightarrow 0, \text{as } n \longrightarrow \infty. \tag{32}$$

Step 3. $Q(\mathcal{S}_\beta)$ is equicontinuous. Let $\varkappa \in 0, \varkappa_1]$, then $\varkappa_m < \varkappa_n \in 0, \varkappa_1]$, we have

$$\begin{aligned} |(Qv)(\varkappa_n) - (Qv)(\varkappa_m)| &\le |g(v(\varkappa_n)) - g(v(\varkappa_m))| \\ &\quad + (\varkappa_n - \varkappa_m) \frac{\varphi^\star \Omega(\beta)}{1 - \psi^\star}. \end{aligned} \tag{33}$$

Let $\varkappa \in [\varkappa_1, b]$, then $\varkappa_m < \varkappa_n \in [\varkappa_1, b]$, we have

$$\begin{aligned}
&|(Q\upsilon)(\varkappa_n) - (Q\upsilon)(\varkappa_m)| \\
&\quad \le |g(\upsilon(\varkappa_n)) - g(\upsilon(\varkappa_m))| + \left| \frac{1}{\Gamma(\vartheta)} \int_{\varkappa_1}^{\varkappa_n} (\varkappa_n - t)^{\vartheta-1} \Phi_\upsilon(t) dt \right. \\
&\quad \left. - \frac{1}{\Gamma(\vartheta)} \int_{\varkappa_1}^{\varkappa_m} (\varkappa_m - t)^{\vartheta-1} \Phi_\upsilon(t) dt \right| \\
&\quad \le |g(\upsilon(\varkappa_n)) - g(\upsilon(\varkappa_m))| + \frac{1}{\Gamma(\vartheta)} \int_{\varkappa_1}^{\varkappa_n} (\varkappa_n - t)^{\vartheta-1} \\
&\quad - (\varkappa_m - t)^{\vartheta-1} |\Phi_\upsilon(t)| dt + \frac{1}{\Gamma(\vartheta)} \int_{\varkappa_n}^{\varkappa_m} (\varkappa_m - t)^{\vartheta-1} |\Phi_\upsilon(t)| dt \\
&\quad \le |g(\upsilon(\varkappa_n)) - g(\upsilon(\varkappa_m))| + \frac{(\varkappa_n - \varkappa_1)^\vartheta}{\Gamma(\vartheta+1)} \frac{\varphi^\star \Omega(\beta)}{1 - \psi^\star} \\
&\quad + \left(\frac{(\varkappa_m - \varkappa_n)^\vartheta - (\varkappa_m - \varkappa_1)^\vartheta}{\Gamma(\vartheta+1)} + \frac{(\varkappa_m - \varkappa_n)^\vartheta}{\Gamma(\vartheta+1)} \right) \frac{\varphi^\star \Omega(\beta)}{1 - \psi^\star} \\
&\quad \le |g(\upsilon(\varkappa_n)) - g(\upsilon(\varkappa_m))| + \frac{2(\varkappa_m - \varkappa_n)^\vartheta}{\Gamma(\vartheta+1)} \frac{\varphi^\star \Omega(\beta)}{1 - \psi^\star}.
\end{aligned} \tag{34}$$

Since g is continuous and compact, (33) and (34) give

$$|(Q\upsilon)(\varkappa_n) - (Q\upsilon)(\varkappa_m)| \longrightarrow 0, \text{as } \varkappa_m \longrightarrow \varkappa_n. \tag{35}$$

That means Q is relatively compact on $\mathcal{S}_\beta$. So, Q is completely continuous due to the Arzela–Ascolli theorem. Thus, Schauder's theorem shows that problem (4) has at least one solution.

Next, we prove the uniqueness theorem for (4) based on Banach's theorem.

Theorem 8. *Let (Assu$_3$)-(Assu$_4$) hold.*

If $\max_{\varkappa \in \mathbb{J}} \{\zeta_1, \zeta_2\} = \zeta < 1$, *then PC-NIFDE (4) has a unique solution on* $\mathbb{J}$, *where*

$$\begin{aligned}
\zeta_1 &:= \kappa_3 + \frac{\kappa_1}{1 - \kappa_2} \varkappa_1, \\
\zeta_2 &:= \kappa_3 + \frac{\kappa_1}{1 - \kappa_2} \frac{(b - \varkappa_1)^\vartheta}{\Gamma(\vartheta + 1)}.
\end{aligned} \tag{36}$$

Proof. Consider υ and $\bar{\upsilon}$ in $\mathscr{C}$, then

$$\begin{aligned}
&|\Phi_\upsilon(\varkappa) - \Phi_{\bar{\upsilon}}(\varkappa)| \\
&\quad = |\Phi(\varkappa, \upsilon(\varkappa), \Phi_\upsilon(\varkappa)) - \Phi(\varkappa, \bar{\upsilon}(\varkappa), \Phi_{\bar{\upsilon}}(\varkappa))| \\
&\quad \le \kappa_1 |\upsilon(\varkappa) - \bar{\upsilon}(\varkappa)| + \kappa_2 |\Phi_\upsilon(\varkappa) - \Phi_{\bar{\upsilon}}(\varkappa)|,
\end{aligned} \tag{37}$$

which implies that

$$|\Phi_\upsilon(\varkappa) - \Phi_{\bar{\upsilon}}(\varkappa)| \le \frac{\kappa_1}{1 - \kappa_2} |\upsilon(\varkappa) - \bar{\upsilon}(\varkappa)|. \tag{38}$$

□

Hence, we have two cases:

Case 1. For $\varkappa \in [0, \varkappa_1]$,

$$\begin{aligned}
&|(Q\upsilon)(\varkappa) - (Q\bar{\upsilon})(\varkappa)| \\
&\quad \le |g(\upsilon) - g(\bar{\upsilon})| + \int_0^{\varkappa_1} |\Phi_\upsilon(t) - \Phi_{\bar{\upsilon}}(t)| dt \\
&\quad \le \left(\kappa_3 + \frac{\kappa_1 \varkappa_1}{1 - \kappa_2} \right) \|\upsilon - \bar{\upsilon}\|_{\mathscr{C}}.
\end{aligned} \tag{39}$$

Case 2. For $\varkappa \in [\varkappa_1, b]$,

$$\begin{aligned}
&|(Q\upsilon)(\varkappa) - (Q\bar{\upsilon})(\varkappa)| \\
&\quad \le |g(\upsilon) - g(\bar{\upsilon})| + \frac{1}{\Gamma(\vartheta)} \int_{\varkappa_1}^{\varkappa} (\varkappa - t))^{\vartheta-1} |\Phi_\upsilon(t) - \Phi_{\bar{\upsilon}}(t)| dt \\
&\quad \le \left(\kappa_3 + \frac{(b - \varkappa_1)^\vartheta}{\Gamma(\vartheta + 1)} \frac{\kappa_1}{1 - \kappa_2} \right) \|\upsilon - \bar{\upsilon}\|_{\mathscr{C}}.
\end{aligned} \tag{40}$$

Consequently,

$$\|Q\upsilon - Q\bar{\upsilon}\|_{\mathscr{C}} \le \zeta \|\upsilon - \bar{\upsilon}\|_{\mathscr{C}}. \tag{41}$$

Since $\zeta < 1$, Q is a contraction. Thus, Banach's theorem shows that PC-NIFDE (4) has a unique solution that exists on $\mathbb{J}$.

3.1. An Analogous Results

3.1. An Analogous Results. In this part, we show some analogous results according to our preceding outcomes.

3.1.1. Piecewise Caputo-Fabrizio NIFDE (PCF-NIFDE). Consider the following PCF-NIFDE

$$\begin{aligned}
&{}^{PCF}\mathbb{D}_{0^+}^\vartheta \upsilon(\varkappa) = \Phi\left(\varkappa, \upsilon(\varkappa), {}^{PCF}\mathbb{D}_{0^+}^\vartheta \upsilon(\varkappa)\right), \\
&\upsilon(0) + g(\upsilon) = \upsilon 0,
\end{aligned} \tag{42}$$

where ${}^{PCF}\mathbb{D}_{0^+}^\vartheta$ is the piecewise derivative in the Caputo-Fabrizio sense (see [20]) defined by

$${}^{PCF}\mathbb{D}_{0^+}^\vartheta \upsilon(\varkappa) = \begin{cases} \mathbb{D}\upsilon(\varkappa) = \dfrac{d\upsilon}{dx}, \text{if } \varkappa \in [0, \varkappa_1], \\ {}^{CF}\mathbb{D}_{\varkappa_1}^\vartheta \upsilon(\varkappa) = \dfrac{(2 - \vartheta)\aleph(\vartheta)}{2(1 - \vartheta)} \displaystyle\int_{\varkappa_1}^{\varkappa} \exp\left(\lambda(\varkappa - t)\right) \upsilon'(\varkappa) dt \text{ if } \varkappa \in [\varkappa_1, b], \end{cases} \tag{43}$$

where $\aleph(\vartheta) = (2/2 - \vartheta)$,$\lambda = (\vartheta/\vartheta - 1)$, and ${}^{CF}\mathbb{D}_{\varkappa_1}^\vartheta$ are the classical Caputo-Fabrizio FD (see [25]).

Let $\Phi_\upsilon(\varkappa) \coloneqq \Phi(\varkappa, \upsilon(\varkappa), \Phi_\upsilon(\varkappa))$; based on PCF-NIFDE (42), the results in Theorems 7 and 8 can be presented by

$$\upsilon(\varkappa) = \begin{cases} \upsilon_0 - g(\upsilon) + \mathbb{I}_{\Phi_\upsilon(\varkappa)}, \text{ if } \varkappa \in [0, \varkappa_1] \\ \upsilon(\varkappa_1) - g(\upsilon) + {}^{CF}\mathbb{I}^{\vartheta}_{\varkappa_1}\Phi_\upsilon(\varkappa), \text{ if } \varkappa \in [\varkappa_1, b] \end{cases} = \begin{cases} \upsilon_0 - g(\upsilon) + \int_0^{\varkappa_1}\Phi_\upsilon(t)dt, \text{ if } \varkappa \in [0, \varkappa_1], \\ \upsilon(\varkappa_1) - g(\upsilon) + \frac{2(1-\vartheta)}{\aleph(\vartheta)(2-\vartheta)}\Phi_\upsilon(\varkappa) + \frac{2\vartheta}{\aleph(\vartheta)(2-\vartheta)}\int_{\varkappa_1}^{\varkappa}\Phi_\upsilon(t)dt, \text{ if } \varkappa \in [\varkappa_1, b], \end{cases} \tag{44}$$

where $\mathbb{I}_{\Phi_\upsilon(\varkappa)} = \int_0^{\varkappa_1}\Phi_\upsilon(t)dt$ and ${}^{CF}\mathbb{I}^{\vartheta}_{0^+}$ are a Caputo-Fabrizio integral on $\varkappa_1 \le \varkappa \le b$ (see [25]).

3.1.2. Piecewise Atangana-Baleanu NIFDE (PAB-NIFDE). Consider the following PAB-NIFDE

$$\begin{aligned} &{}^{PAB}\mathbb{D}^{\vartheta}_{0^+}\upsilon(\varkappa) = \Phi\left(\varkappa, \upsilon(\varkappa), {}^{PAB}\mathbb{D}^{\vartheta}_{0^+}\upsilon(\varkappa)\right), \\ &\upsilon(0) + g(\upsilon) = \upsilon0, \end{aligned} \tag{45}$$

where ${}^{PAB}\mathbb{D}^{\vartheta}_{0^+}$ is the piecewise derivative in the Atangana-Baleanu sense defined by (see [20])

$${}^{PAB}\mathbb{D}^{\vartheta}_{0^+}\upsilon(\varkappa) = \begin{cases} \mathbb{D}_{\upsilon(\varkappa)} = \frac{d\upsilon}{dx}, \text{ if } \varkappa \in [0, \varkappa_1], \\ {}^{AB}\mathbb{D}^{\vartheta}_{0^+}\upsilon(\varkappa) = \frac{(2-\vartheta)\aleph(\vartheta)}{2(1-\vartheta)}\int_{\varkappa_1}^{\varkappa} \exp\left(\lambda(\varkappa - t)\right)\upsilon'(\varkappa)dt \text{ if } \varkappa \in [\varkappa_1, b], \end{cases} \tag{46}$$

where $\aleph(\vartheta)$ is the normalization function that satisfies $\aleph(1) = \aleph(0) = 1$; $\lambda = (\vartheta/(\vartheta - 1))$, and ${}^{AB}\mathbb{D}^{\vartheta}_{0^+}$ are the classical Atangana-Baleanu FD ([26]).

Based on PAB-NIFDE (45), the results in Theorems 7 and 8 can be presented by

$$\upsilon(\varkappa) = \begin{cases} \upsilon_0 - g(\upsilon) + \mathbb{I}_{\Phi_\upsilon(\varkappa)}, \text{ if } \varkappa \in [0, \varkappa_1] \\ \upsilon(\varkappa_1) - g(\upsilon) + {}^{AB}\mathbb{I}^{\vartheta}_{\varkappa_1}\Phi_\upsilon(\varkappa), \text{ if } \varkappa \in [\varkappa_1, b] \end{cases} = \begin{cases} \upsilon_0 - g(\upsilon) + \int_0^{\varkappa_1}\Phi_\upsilon(t)dt, \text{ if } \varkappa \in [0, \varkappa_1], \\ \upsilon(\varkappa_1) - g(\upsilon) + \frac{1-\vartheta}{\aleph(\vartheta)}\Phi_\upsilon(\varkappa) + \frac{\vartheta}{\aleph(\vartheta)}\frac{1}{\Gamma(\vartheta)}\int_{\varkappa_1}^{\varkappa}(\varkappa - t)^{\vartheta-1}\Phi_\upsilon(t)dt, \text{ if } \varkappa \in \{\varkappa_1, b], \end{cases} \tag{47}$$

where ${}^{AB}\mathbb{I}^{\vartheta}_{0^+}$ is the Atangana-Baleanu integral on $\varkappa_1 \le \varkappa \le b$ (see [26]).

Remark 9. Following the strategy of proof utilized in the previous part, we can get the existence results for nonlinear problems (42) and (45).

3.2. UH Stability Analysis. In this portion, we give the UH Stability of problem (4).

Definition 10. PC-NIFDE (4) is UH stable if there exists a $K_f > 0$, such that for all $\varepsilon > 0$ and each solution $\omega \in \mathscr{C}$ of the inequality.

$$\left|{}^{PC}\mathbb{D}^{\vartheta}_{0^+}\omega(\varkappa) - \Phi_\omega(\varkappa)\right| \le \varepsilon, \varkappa \in \mathbb{J}, \tag{48}$$

there exists a solution $\upsilon \in \mathscr{C}$ of PC-NIFDE (4) that satisfies

$$|\omega(\varkappa) - \upsilon(\varkappa)| \le K_f\varepsilon, \tag{49}$$

where $\Phi_\omega(\varkappa) \coloneqq {}^{PC}\mathbb{D}^{\vartheta}_{0^+}\omega(\varkappa)$ and $\Phi_\omega(\varkappa) = \Phi(\varkappa, \omega(\varkappa), \Phi_\omega(\varkappa))$.

Remark 11. $\omega \in \mathscr{C}$ satisfies inequality (48) if there exist function $\sigma \in \mathscr{C}$ with

(i) $|\sigma(\varkappa)| \le \varepsilon, \varkappa \in \mathbb{J}$

(ii) For all $\varkappa \in \mathbb{J}$

$${}^{PC}\mathbb{D}^{\vartheta}_{0^+}\omega(\varkappa) = \Phi_\omega(\varkappa) + \sigma(\varkappa). \tag{50}$$

Lemma 12. *Let $0 < \vartheta \le 1$, and $\omega \in \mathscr{C}$ is a solution of inequality (48). Then, ω satisfies*

$$\begin{aligned} &\left|\omega(\varkappa) - \mathscr{W}_0 - \int_0^{\varkappa_1}\Phi_\omega(t)dt\right| \le \varkappa_1\varepsilon, \text{ if } \varkappa \in [0, \varkappa_1],. \\ &\left|\omega(\varkappa) - \mathscr{W}_1 - \frac{1}{\Gamma(\vartheta)}\int_{\varkappa_1}^{\varkappa}(\varkappa - t)\right)^{\vartheta-1}\Phi_\omega(t)dt\right| \\ &\quad \le \frac{(b-\varkappa_1)^{\vartheta}}{\Gamma(\vartheta+1)}\varepsilon, \text{ if } \varkappa \in [\varkappa_1, b], \end{aligned} \tag{51}$$

where $\mathscr{W}_0 = \omega_0 - g(\omega)$ and $\mathscr{W}_1 = \omega(\varkappa_1) - g(\omega)$.

Proof. Let ω be a solution of (48).

By part (ii) of Remark 11, we have

$$\begin{aligned} {}^{PC}\mathbb{D}_{0^+}^{\vartheta}\omega(\varkappa) &= \Phi_\omega(\varkappa)+\sigma(\varkappa), \\ \omega(0)+g(\omega) &= \omega_0. \end{aligned} \tag{52}$$

Then, the solution of problem (52) is

$$\omega(\varkappa)=\begin{cases} \mathscr{W}_0+\int_0^{\varkappa_1}[\Phi_\omega(t)+\sigma(t)]dt, \text{ if } \varkappa\in[0,\varkappa_1], \\ \mathscr{W}_1+\dfrac{1}{\Gamma(\vartheta)}\displaystyle\int_{\varkappa_1}^{\varkappa}(\varkappa-t)\Big)^{\vartheta-1}[\Phi_\omega(t)+\sigma(t)]dt, \text{ if } \varkappa\in[\varkappa_1,b]. \end{cases} \tag{53}$$

□

Again by (i) of Remark 11, we obtain

$$\begin{aligned} &\left|\omega(\varkappa)-\mathscr{W}_0-\int_0^{\varkappa_1}\Phi_\omega(t)dt\right| \\ &\quad\le\int_0^{\varkappa_1}|\sigma(t)|dt\le\varepsilon\varkappa_1, \text{ for } \varkappa\in[0,\varkappa_1], \\ &\left|\omega(\varkappa)-\mathscr{W}_1-\frac{1}{\Gamma(\vartheta)}\int_{\varkappa_1}^{\varkappa}(\varkappa-t))^{\vartheta-1}\Phi_\omega(t)dt\right| \\ &\quad\le\frac{1}{\Gamma(\vartheta)}\int_{\varkappa_1}^{\varkappa}(\varkappa-t)^{\vartheta-1}|\sigma(t)|dt \\ &\quad\le\frac{(b-\varkappa_1)^\vartheta}{\Gamma(\vartheta+1)}\varepsilon, \text{ for } \varkappa\in[\varkappa_1,b]. \end{aligned} \tag{54}$$

Theorem 13. *Under the assumptions of Theorem 8. Then, the solution of PC-NIFDE (4) is HU and GHU stable.*

Proof. Let $\omega\in\mathscr{C}$ be a solution of inequality (48), and $\upsilon\in\mathscr{C}$ be a unique solution of the following PC-NIFDE.

$${}^{PC}\mathbb{D}_{0^+}^{\vartheta}\upsilon(\varkappa)=\Phi_\upsilon(\varkappa), \tag{55}$$

□

From Lemma 12, we obtain

$$\upsilon(\varkappa)=\begin{cases} \mathscr{V}_0+\int_0^{\varkappa_1}\Phi_\upsilon(t)dt, \text{ if } \varkappa\in[0,\varkappa_1], \\ \mathscr{V}_1+\dfrac{1}{\Gamma(\vartheta)}\displaystyle\int_{\varkappa_1}^{\varkappa}(\varkappa-t)^{\vartheta-1}\Phi_\upsilon(t)dt, \text{ if } \varkappa\in[\varkappa_1,b], \end{cases} \tag{56}$$

where $\mathscr{V}_0=\upsilon_0-g(\upsilon)$ and $\mathscr{V}_1=\upsilon(\varkappa_1)-g(\upsilon)$. Clearly, if $\upsilon(0)+g(\upsilon)=\omega(0)+g(\omega)$, then $\mathscr{V}_0=\mathscr{W}_0$, and $\mathscr{V}_1=\mathscr{W}_1$. Hence, (56) becomes

$$\upsilon(\varkappa)=\begin{cases} \mathscr{W}_0+\int_0^{\varkappa_1}\Phi_\upsilon(t)dt, \text{ if } \varkappa\in[0,\varkappa_1], \\ \mathscr{W}_1+\dfrac{1}{\Gamma(\vartheta)}\displaystyle\int_{\varkappa_1}^{\varkappa}(\varkappa-t)^{\vartheta-1}\Phi_\upsilon(t)dt, \text{ if } \varkappa\in[\varkappa_1,b]. \end{cases} \tag{57}$$

Using Lemma 12 and (Assu_4) for $\varkappa\in 0,\varkappa_1]$, we have

$$\begin{aligned} |\omega(\varkappa)-\upsilon(\varkappa)| &= \left|\omega(\varkappa)-\mathscr{W}_0-\int_0^{\varkappa_1}\Phi_\upsilon(t)dt\right| \\ &\le\left|\omega(\varkappa)-\mathscr{W}_0-\int_0^{\varkappa_1}\Phi_\omega(t)dt\right| \\ &\quad+\int_0^{\varkappa_1}|\Phi_\omega(t)-\Phi_\upsilon(t)|dt \\ &\le\varepsilon\varkappa_1+\frac{\kappa_1}{1-\kappa_2}\int_0^{\varkappa_1}|\omega(t)-\upsilon(t)|dt. \end{aligned} \tag{58}$$

Using classical Gronwall's Lemma [27], we obtain

$$\begin{aligned} |\omega(\varkappa)-\upsilon(\varkappa)| &\le\varepsilon\varkappa_1\exp\left(\int_0^{\varkappa_1}\frac{\kappa_1}{1-\kappa_2}\right)dt \\ &=\varepsilon\varkappa_1\exp\left(\frac{\kappa_1\varkappa_1}{1-\kappa_2}\right)\coloneqq\varepsilon K_0. \end{aligned} \tag{59}$$

For $\varkappa\in\varkappa_1,b]$, we have

$$\begin{aligned} |\omega(\varkappa)-\upsilon(\varkappa)| &= \left|\omega(\varkappa)-\mathscr{W}_1-\frac{1}{\Gamma(\vartheta)}\int_{\varkappa_1}^{\varkappa}(\varkappa-t)^{\vartheta-1}\Phi_\upsilon(t)dt\right| \\ &\le\left|\omega(\varkappa)-\mathscr{W}_1-\frac{1}{\Gamma(\vartheta)}\int_{\varkappa_1}^{\varkappa}(\varkappa-t)^{\vartheta-1}\Phi_\omega(t)dt\right| \\ &\quad+\frac{1}{\Gamma(\vartheta)}\int_{\varkappa_1}^{\varkappa}(\varkappa-t)^{\vartheta-1}|\Phi_\omega(t)-\Phi_\upsilon(t)|dt \\ &\le\frac{(b-\varkappa_1)^\vartheta}{\Gamma(\vartheta+1)}\varepsilon+\frac{\kappa_1}{1-\kappa_2}\frac{1}{\Gamma(\vartheta)}\int_{\varkappa_1}^{\varkappa}(\varkappa-t)^{\vartheta-1}|\omega(t)-\upsilon(t)|dt. \end{aligned} \tag{60}$$

Using fractional Gronwall's Lemma [27], we obtain

$$\begin{aligned} |\omega(\varkappa)-\upsilon(\varkappa)| &\le\frac{(b-\varkappa_1)^\vartheta}{\Gamma(\vartheta+1)}\varepsilon+\frac{\varepsilon}{\Gamma(\vartheta+1)}\frac{\kappa_1}{1-\kappa_2} \\ &\quad\times\frac{1}{\Gamma(\vartheta)}\int_{\varkappa_1}^{\varkappa}(\varkappa-t)^{\vartheta-1}(b-\varkappa_1)^\vartheta dt \\ &\le\frac{(b-\varkappa_1)^\vartheta}{\Gamma(\vartheta+1)}\varepsilon+\frac{\kappa_1(b-\varkappa_1)^\vartheta}{\Gamma(\vartheta+1)(1-\kappa_2)}\frac{(b-\varkappa_1)^\vartheta}{\Gamma(\vartheta+1)}\varepsilon \\ &=\frac{(b-\varkappa_1)^\vartheta}{\Gamma(\vartheta+1)}\left(\frac{\kappa_1}{(1-\kappa_2)}+\frac{1}{\Gamma(\vartheta+1)}\right)\varepsilon\coloneqq\varepsilon K_{1.} \end{aligned} \tag{61}$$

It follows from (59) and (61) that

$$|\omega(\varkappa) - \upsilon(\varkappa)| \le \begin{cases} K_0\varepsilon, \text{for } \varkappa \in [0, \varkappa_1], \\ K_1\varepsilon, \text{for } \varkappa \in [\varkappa_1, b], \end{cases} \tag{62}$$

where

$$K_0 = \varkappa_1 \exp\left(\frac{\kappa_1\varkappa_1}{1-\kappa_2}\right), \quad K_1 = \frac{(b-\varkappa_1)^\vartheta}{\Gamma(\vartheta+1)}\left(\frac{\kappa_1}{(1-\kappa_2)} + \frac{1}{\Gamma(\vartheta+1)}\right). \tag{63}$$

Hence, PC-NIFDE (4) is UH stable in $\mathscr{C}$. Moreover, if there exists a nondecreasing function, $\varphi : \mathbb{R}^+ \longrightarrow \mathbb{R}^+$, such that $\varphi(\varepsilon) = \varepsilon$. Then, from (62), we have

$$|\omega(\varkappa) - \upsilon(\varkappa)| \le \begin{cases} K_0\varphi(\varepsilon), \text{for } \varkappa \in [0, \varkappa_1], \\ K_1\varphi(\varepsilon), \text{for } \varkappa \in [\varkappa_1, b], \end{cases} \tag{64}$$

with $\varphi(0) = 0$, which proves PC-NIFDE (4) is GUH stable in $\mathscr{C}$.

4. Examples

In this portion, we present two examples to illustrate the reported results.

Example 1. Consider the following PC-NIFDE

$$\begin{aligned} &{}^{PC}\mathbb{D}^{1/3}_{0^+}\upsilon(\varkappa) = \Phi\left(\varkappa, \upsilon(\varkappa), {}^{PC}\mathbb{D}^{1/3}_{0^+}\upsilon(\varkappa)\right), \quad \varkappa[\in 0, 1], \\ &\upsilon(0) + \sum_{i=1}^{n} c_i\upsilon(\varkappa i) = \frac{1}{4}, \end{aligned} \tag{65}$$

or

$$\begin{aligned} &\upsilon'(\varkappa) = \Phi\left(\varkappa, \upsilon(\varkappa), \upsilon'(\varkappa)\right), \varkappa \in \left[0, \frac{1}{2}\right], \\ &{}^{C}\mathbb{D}^{1/3}_{1/2^+}\upsilon(\varkappa) = \Phi\left(\varkappa, \upsilon(\varkappa), {}^{C}\mathbb{D}^{1/3}_{1/2^+}\upsilon(\varkappa)\right), \text{if } \varkappa \in \left[\frac{1}{2}, 1\right], \\ &\upsilon(0) + \sum_{i=1}^{n} c_i\upsilon(\varkappa_i) = \frac{1}{4}, \end{aligned} \tag{66}$$

where $\vartheta = 1/3, \upsilon_0 = 1/4, 0 < \varkappa_1 = 1/2 < \cdots < \varkappa_n < 1 = b$, and c_i are positive constants with $\sum_{i=1}^{n} c_i < 1/5$. Set

$$\begin{aligned} &\Phi(\varkappa, \upsilon, \omega) = \frac{e^{-\varkappa}}{(8+e^{\varkappa})(2+|\upsilon|+|\omega|)}, \varkappa \in [0, 1], \upsilon, \omega \in [0,\infty), \\ &g(\upsilon) = \sum_{i=1}^{n} c_i\upsilon(\varkappa_i), \upsilon \in [0,\infty). \end{aligned} \tag{67}$$

Let $\upsilon, \omega, \bar{\upsilon}, \bar{\omega} \in [0,\infty)$, $\varkappa \in [0, 1]$. Then,

$$\begin{aligned} &|f(\varkappa, \upsilon, \omega) - f(\varkappa, \bar{\upsilon}, \bar{\omega})| \\ &\quad \le \frac{e^{-\varkappa}}{(8+e^{\varkappa})}\left|\frac{|\upsilon-\bar{\upsilon}| + |\omega-\bar{\omega}|}{(2+|\upsilon|+|\omega|)(2+|\bar{\upsilon}|+|\bar{\omega}|)}\right| \\ &\quad \le \frac{1}{9}|\upsilon-\bar{\upsilon}| + \frac{1}{9}|\omega-\bar{\omega}|. \end{aligned} \tag{68}$$

Hence, the condition (Assu_3) holds with $\kappa_1 = \kappa_2 = 1/9$. Also we have

$$\begin{aligned} |g(\upsilon) - g(\omega)| &= \left|\sum_{i=1}^{n} c_i\upsilon(\varkappa_i) - \sum_{i=1}^{n} c_i\omega(\varkappa_i)\right| \\ &\le \sum_{i=1}^{n} c_i|\upsilon-\omega| \le \frac{1}{5}|\upsilon-\omega|. \end{aligned} \tag{69}$$

Hence, the condition (Assu_4) holds with $\kappa_3 = 1/5$. Moreover, the following condition

$$\begin{aligned} \max\{\zeta_1, \zeta_2\} &= \max\left\{\kappa_3 + \frac{\kappa_1}{1-\kappa_2}\varkappa_1, \kappa_3 + \frac{\kappa_1}{1-\kappa_2}\frac{(b-\varkappa_1)^\vartheta}{\Gamma(\vartheta+1)}\right\} \\ &= \max\left\{\frac{21}{80}, \frac{1}{5} + \frac{1}{8\sqrt[3]{2}\Gamma(4/3)}\right\} \\ &= \frac{1}{5} + \frac{1}{8\sqrt[3]{2}\Gamma(4/3)} < 1, \end{aligned} \tag{70}$$

is satisfied with $\varkappa_1 = (1/2)$, and $b = 1$. Thus, with the assistance of Theorem 8, problem (65) has a unique solution $[0, 1]$. Further, since $1 - (\kappa_1\varkappa_1/1-\kappa_2) = (15/16) < 1$, and $1 - ((b-\varkappa_1)^\vartheta/\Gamma(\vartheta+1))(\kappa_1/1-\kappa_2) = 1 - (1/8\sqrt[3]{2}\Gamma(4/3)) < 1$, then

$$K_0 = \varkappa_1 \exp\left(\frac{\kappa_1\varkappa_1}{1-\kappa_2}\right) = \frac{1}{2}e^{1/16} > 0, \tag{71}$$

and

$$\begin{aligned} K_1 &= \frac{(b-\varkappa_1)^\vartheta}{\Gamma(\vartheta+1)}\left(\frac{\kappa_1}{(1-\kappa_2)} + \frac{1}{\Gamma(\vartheta+1)}\right) \\ &= \frac{(1/8) + (1/(\Gamma(4/3)))}{\sqrt[3]{2}\Gamma(4/3)} > 0, \end{aligned} \tag{72}$$

which implies that problem (65) is HU stable.

Example 2. Consider the following PC-NIFDE

$$
\begin{aligned}
&{}^{PC}\mathbb{D}_{1/4^+}^{1/2}\upsilon(\varkappa) = \Phi\left(\varkappa, \upsilon(\varkappa), {}^{PC}\mathbb{D}_{1/4^+}^{1/2}\upsilon(\varkappa)\right), \varkappa \in \left[\frac{1}{4}, 1\right],\\
&\upsilon\left(\frac{1}{4}\right) + \frac{1}{2}\sin\left(\frac{\upsilon(\varkappa)}{3}\right) + \frac{1}{9} = 1,
\end{aligned}
\tag{73}
$$

or

$$
\begin{aligned}
&\upsilon'(\varkappa) = \Phi\left(\varkappa, \upsilon(\varkappa), \upsilon'(\varkappa)\right), \varkappa \in \left[\frac{1}{4}, \frac{1}{2}\right],\\
&{}^{C}\mathbb{D}_{1/2^+}^{1/2}\upsilon(\varkappa) = \Phi\left(\varkappa, \upsilon(\varkappa), {}^{C}\mathbb{D}_{1/2^+}^{1/2}\upsilon(\varkappa)\right), \text{if } \varkappa \in \left[\frac{1}{2}, 1\right],\\
&\upsilon\left(\frac{1}{4}\right) + \frac{1}{2}\sin\left(\frac{\upsilon(\varkappa)}{3}\right) + \frac{1}{9} = 1,
\end{aligned}
\tag{74}
$$

where $\varkappa_1 = (1/2), \vartheta = (1/2), \upsilon_0 = 1$. Set

$$
\Phi(\varkappa, \upsilon(\varkappa), \omega(\varkappa)) = \frac{1}{(10 + \varkappa^2)}\left(\frac{\upsilon(\varkappa) + \omega(\varkappa)}{(1 + |\upsilon(\varkappa)| + |\omega(\varkappa)|)} + \frac{1}{90}\right),
\tag{75}
$$

for $\varkappa \in [(1/4), 1], \upsilon, \omega \in [0,\infty)$, and

$$
g(\upsilon) = \frac{1}{2}\sin\left(\frac{\upsilon}{3}\right) + \frac{1}{9}, \upsilon \in [0,\infty).
\tag{76}
$$

Let $\upsilon, \omega \in [0,\infty)$ and $\varkappa \in [(1/4), 1]$. Then,

$$
\begin{aligned}
|\Phi(\varkappa, \upsilon, \omega)| &= \left|\frac{1}{(10 + \varkappa^2)}\left(\frac{\upsilon + \omega}{(1 + |\upsilon| + |\omega|)} + \frac{1}{90}\right)\right|\\
&\leq \frac{1}{(10 + \varkappa^2)}\left(|\upsilon| + |\omega| + \frac{1}{90}\right).
\end{aligned}
\tag{77}
$$

Putting $\Omega(|\upsilon|) = |\upsilon| + (1/90)$, and $\varphi(\varkappa) = \psi(\varkappa) = (1/(10 + \varkappa^2))$ Then, $|\Phi(\varkappa, \upsilon, \omega)| \leq \varphi(\varkappa)\Omega(|\upsilon|) + \psi(\varkappa)|\omega|$ valid for any $(\varkappa, \upsilon, \omega) \in [(1/4), 1] \times [0,\infty) \times [0,\infty)$, and $\psi^* = (16/161) < 1$. Also, $|g(\upsilon)| \leq (1/6)|\upsilon| + (1/9) = a|\upsilon| + b$. Hence, $(Assu_1)$ and $(Assu_2)$ hold. Thus, all the assumptions of Theorem 7 are satisfied. Hence, problem (73) has a solution on $[(1/4), 1]$.

5. Conclusions

Somewhat recently, numerous methodologies have been proposed to portray behaviors of some complex world problems emerging in numerous scholarly fields. One of these problems is the multistep behavior shown by certain problems. In this regard, Atangana and Araz [20] introduced the concept of piecewise derivative. As an extra contribution to this subject, existence, uniqueness, and UH stability results for PC-NIFDE (4) involving a piecewise Caputo FD have been obtained. Our approach to this work has been based on Banach's and Schaefer's fixed-point theorem and Gronwall's Lemma. In light of our current results, the solution form for analogous problems containing piecewise Caputo-Fabrizio and Atangana–Baleanu operators have been presented. Finally, we have created two examples to validate the results obtained.

As an open problem, it will be very interesting to study the present problems on piecewise fractional operators with another function that is more general; precisely, one has to consider in problem (2) with ${}^{PC}\mathbb{D}_{0^+}^{\vartheta;\psi}$ such that

$$
{}^{PC}\mathbb{D}_{0^+}^{\vartheta;\psi}f(\varkappa) = \begin{cases} \mathbb{D}_\psi : \text{if } \varkappa \in [0, \varkappa_1],\\ {}^{C}\mathbb{D}_{\varkappa_1}^{\vartheta;\psi}f(\varkappa) : \text{if } \varkappa \in [\varkappa_1, b], \end{cases}
\tag{78}
$$

where $\mathbb{D}_\psi \coloneqq ((1/(\psi'(\varkappa)))(d/d\varkappa))$ and ${}^{C}\mathbb{D}_{0^+}^{\vartheta;\psi}$ are ψ-Caputo FD of order ϑ introduced by Almeida [28].

Data Availability

No real data were used to support this study. The data used in this study are hypothetical.

Conflicts of Interest

No conflicts of interest are related to this work.

Acknowledgments

The authors extend their appreciation to the Deanship of Scientific Research at King Khalid University for funding this work through large group research project under grant number R.G.P.2/204/43.

References

[1] K. B. Oldham and J. Spanier, "The fractional calculus: theory and applications of differentiation and integration to arbitrary order," in *Mathematics in Science and Engineering*, Academic Press, New York, 1974.

[2] A. A. Kilbas, H. M. Srivastava, and J. J. Trujillo, "Theory and applications of fractional differential equations," in *North-Holland Mathematics Studies, 204*, Elsevier Science B.V, Amsterdam, 2006.

[3] A. Loverro, *Fractional calculus: History, Definitions and Applications for the Engineer, Rapport Technique*, Univeristy of Notre Dame: Department of Aerospace and Mechanical Engineering, 2004.

[4] R. Hilfer, *Three Fold Introduction to Fractional Derivatives*, Foundations and Applications, Germany, Anomalous Transport, 2008.

[5] F. Jarad, T. Abdeljawad, and Z. Hammouch, "On a class of ordinary differential equations in the frame of Atangana-Baleanu fractional derivative," *Chaos, Solitons and Fractals*, vol. 117, pp. 16–20, 2018.

[6] S. Abbas, M. Benchohra, J. R. Graef, and J. Henderson, "Implicit fractional differential and integral equations," *Implicit Fractional Differential and Integral Equations. de Gruyter*, vol. 26, 2018.

[7] P. Agarwal, M. R. Sidi Ammi, and J. Asad, "Existence and uniqueness results on time scales for fractional nonlocal

thermistor problem in the conformable sense," *Advances in Difference Equations*, vol. 2021, no. 1, 2021.

[8] Z. Odibat and D. Baleanu, "Numerical simulation of initial value problems with generalized Caputo-type fractional derivatives," *Applied Numerical Mathematics*, vol. 156, pp. 94–105, 2020.

[9] A. Atangana and J. F. Gómez-Aguilar, "Numerical approximation of Riemann-Liouville definition of fractional derivative: from Riemann-Liouville to Atangana-Baleanu," *Numerical Methods for Partial Differential Equations*, vol. 34, no. 5, pp. 1502–1523, 2018.

[10] M. Alesemi, N. Iqbal, and M. S. Abdo, "Novel investigation of fractional-order Cauchy-reaction diffusion equation involving Caputo-Fabrizio operator," *Journal of Function Spaces*, vol. 2022, Article ID 4284060, 14 pages, 2022.

[11] M. S. Abdo, A. G. Ibrahim, and S. K. Panchal, "Nonlinear implicit fractional differential equation involving-Caputo fractional derivative," *In Proceedings of the Jangjeon Mathematical Society*, vol. 22, no. 3, pp. 387–400, 2019.

[12] M. Benchohra, S. Bouriah, and J. J. Nieto, "Existence and Ulam stability for nonlinear implicit differential equations with Riemann-Liouville fractional derivative," *Demonstratio Mathematica*, vol. 52, no. 1, pp. 437–450, 2019.

[13] A. Salim, M. Benchohra, J. E. Lazreg, J. J. Nieto, and Y. Zhou, "Nonlocal initial value problem for hybrid generalized Hilfer-type fractional implicit differential equations," *Nonautonomous Dynamical Systems*, vol. 8, no. 1, pp. 87–100, 2021.

[14] Y. Guo, M. Chen, X. B. Shu, and F. Xu, "The existence and Hyers-Ulam stability of solution for almost periodical fractional stochastic differential equation with fBm," *Stochastic Analysis and Applications*, vol. 39, no. 4, pp. 643–666, 2021.

[15] Y. Guo, X. B. Shu, Y. Li, and F. Xu, "The existence and Hyers–Ulam stability of solution for an impulsive RiemannLiouville fractional neutral functional stochastic differential equation with infinite delay of order $1 < \beta < 2$," *Boundary Value Problems*, vol. 2019, 18 pages, 2019.

[16] R. P. Agarwal, M. Benchohra, and S. Hamani, "A survey on existence results for boundary value problems of nonlinear fractional differential equations and inclusions," *Acta Applicandae Mathematicae*, vol. 109, no. 3, pp. 973–1033, 2010.

[17] K. D. Kucche, J. J. Nieto, and V. Venktesh, "Theory of nonlinear implicit fractional differential equations," *Differential Equations Dynamical Systems*, vol. 28, no. 1, pp. 1–17, 2020.

[18] H. A. Wahash, M. S. Abdo, and S. K. Panchal, "Existence and Ulam-Hyers stability of the implicit fractional boundary value problem with ψ-Caputo fractional derivative," *Journal of Applied Mathematics and Computational Mechanics*, vol. 19, no. 1, pp. 89–101, 2020.

[19] M. Benchohra and S. Bouriah, "Existence and stability results for nonlinear boundary value problem for implicit differential equations of fractional order," *Moroccan Journal of Pure and Applied Analysis*, vol. 1, no. 1, pp. 1–16, 2015.

[20] A. Atangana and S. I. Araz, "New concept in calculus: piecewise differential and integral operators," *Chaos, Solitons and Fractals*, vol. 145, article 110638, 2021.

[21] A. Bashir and S. Sivasundaram, "Some existence results for fractional integro-differential equations with nonlocal conditions," *Communications in Applied Analysis*, vol. 12, pp. 107–112, 2008.

[22] M. Haoues, A. Ardjouni, and A. Djoudi, "Existence, interval of existence and uniqueness of solutions for nonlinear implicit Caputo fractional differential equations," *TJMM*, vol. 10, no. 1, pp. 09–13, 2018.

[23] Y. Zhou, *Basic Theory of Fractional Differential Equations*, vol. 6, World Scientific, Singapore, 2014.

[24] A. Granas and J. Dugundji, *Fixed Point Theory*, Springer, New York, 2003.

[25] M. Caputo and M. Fabrizio, "A new definition of fractional derivative without singular kernel," *Progress in Fractional Differentiation & Applications*, vol. 1, no. 2, pp. 73–85, 2015.

[26] A. Atangana and D. Baleanu, "New fractional derivatives with nonlocal and non-singular kernel: theory and application to heat transfer model," *Thermal Science*, vol. 20, no. 2, pp. 763–769, 2016.

[27] H. Ye, J. Gao, and Y. Ding, "A generalized Gronwall inequality and its application to a fractional differential equation," *Journal of Mathematical Analysis and Applications*, vol. 328, no. 2, pp. 1075–1081, 2007.

[28] R. Almeida, "A Caputo fractional derivative of a function with respect to another function," *Communications in Nonlinear Science and Numerical Simulation*, vol. 44, pp. 460–481, 2017.

Hindawi
Journal of Function Spaces
Volume 2023, Article ID 9748605, 10 pages
https://doi.org/10.1155/2023/9748605

Research Article

Method of Particular Solutions for Second-Order Differential Equation with Variable Coefficients via Orthogonal Polynomials

Huantian Xie, Zhaozhong Zhang, Ziwu Jiang, and Jianwei Zhou

School of Mathematics and Statistics, Linyi University, Linyi, 276000 Shandong, China

Correspondence should be addressed to Jianwei Zhou; jwzhou@yahoo.com

Received 12 July 2022; Revised 7 September 2022; Accepted 13 September 2022; Published 26 April 2023

Academic Editor: Yusuf Gurefe

In this paper, with classic Legendre polynomials, a method of particular solutions (MPS, for short) is proposed to solve a kind of second-order differential equations with a variable coefficient on a unit interval. The particular solutions, satisfying the natural Dirichlet boundary conditions, are constructed with orthogonal Legendre polynomials for the variable coefficient case. Meanwhile, we investigate the a-priori error estimates of the MPS approximations. Two a-priori error estimations in H^1- and L^∞-norms are shown to depict the convergence order of numerical approximations, respectively. Some numerical examples and convergence rates are provided to validate the merits of our proposed meshless method.

1. Introduction

In the past decades, various numerical methods are designed for solving kinds of differential equations, such as finite element method [1–3], spectral method [4–6], shifted Legendre approximation [7, 8], and differential transformation method [9, 10]. To avoid the constraints and workload of region divisions, a new family of computational methods has emerged. The so-called meshless or mesh-free methods have been investigated and used by many researchers. The advantage of meshless methods reads that the interpolation accuracy is not significantly affected by the nodal distribution. And hence meshless methods attract great attentions in various disciplines for treating a large variety of engineering problems. In fact, the MPS is originally proposed with the radial basis functions for solving various kinds of differential equations. Recently, the MPS has been continuously employed to solve various interesting models and proven to be an effective method in numerical simulations. For more details about this numerical scheme, please refer to [11–13] and the references cited therein.

To the best of our current knowledge, the meshless schemes, including Kansa method [14], method of fundamental solutions [15], method of particular solutions [16, 17], element-free Galerkin method [18], local point interpolation [19], and boundary knot method [20], are widely used to approximate a large class of partial differential equations in science and engineering fields. As reported in the literatures, the MPS has been applied to solve the Navier-Stokes problem [21], wave propagation problem [22], and time-fractional diffusion problem [23]. Despite the effectiveness of the MPS, there are some disadvantages such as the ill-conditioned collocation matrix, the uncertainty of the shape parameters, and difficulties in deriving the closed-form particular solutions for general differential operators, and for more details, please refer to [12, 17, 24–26] and the references cited therein.

In order to overcome these disadvantages, lots of works have been done on efficient numerical schemes for the MPS. And many basis functions have been designed to discretize partial differential equations. Chebyshev polynomials [11, 27], polynomials basis functions [16, 18, 28], and trigonometric functions [29] were employed with their closed-form particular solutions to approximate kinds of models. However, few results about error estimates of the MPS are illustrated in the current literatures.

In this paper, Legendre polynomials are used to design the particular solutions for the MPS. Specially, boundary conditions are naturally imposed, and the corresponding discretized scheme is constructed in a collocation scheme.

The closed-form particular solutions for given differential operators with variable coefficients are derived via recursive relationships of Legendre polynomials. Compared with the radial basis functions for the MPS, our proposed scheme provides a simple approach to effectively solve a kind of differential equations with variable coefficients.

Meanwhile, with an orthogonal projector and the Aubin-Nitsche duality argument, we provide rigorous studies on two a-priori error estimates for this numerical method. For sufficiently smooth solutions, the a-priori error estimations show that asymptotic super-exponential convergence orders of the MPS approximations are readily achieved in H^1- and L^∞-norms.

The remainder of this paper is organized as follows. Some preliminaries and a brief review of the MPS are presented in Section 2. The numerical procedures of the MPS for solving differential equations with variable coefficients are proposed in Section 3. In Section 4, two a-priori error estimates are given in different norms with rigorous proofs. And three numerical examples are provided with numerical errors and convergence orders to demonstrate the effectiveness of the proposed methods in Section 5. Furthermore, some conclusions and discussions are listed in Section 6. And in the last part, an appendix is given to sketch a rigorous proof for the recalled lemma.

2. Preliminaries

Let us introduce some basic notations which will be used in the sequel. Hereafter, we select a unit interval $I = (-1, 1)$ to show the sketch of the MPS approximations and a-priori error estimates and adopt the standard notation $W^{m,q}(I)$ for Sobolev space on I. Setting $W_0^{m,q}(I) = \{v \in W^{m,q}(I)$: $(d^k v/dx^k)(\pm 1) = 0, 0 \le k \le m-1\}$, we denote $H_0^m(I) = W_0^{m,2}(I)$ and $\|\cdot\|_m = \|\cdot\|_{m,2}$. Specially, $\|\cdot\|_\infty$ and $\|\cdot\|$ denote the norms in $L^\infty(I)$ and $L^2(I)$, respectively. We use C and c to denote different constants in different formulae. For simplicity, we omit subscripts if $m = 0$. Particularly, if $m = 1$, we set

$$H_0^1(I) = \left\{ v \in W^{1,2}(I) \colon v(\pm 1) = 0 \right\}. \tag{1}$$

Thereby, the scalar product in $L^2(I)$ and bilinear form in $H^1(I)$ are defined as

$$(v, w) = \int_I v(x) w(x) dx, \forall v, w \in L^2(I), \tag{2}$$

$$a(v, w) = \int_I \omega(x) v'(x) w'(x) dx, \forall v, w \in H^1(I). \tag{3}$$

We define the following polynomial sets:

$$\begin{aligned} \tilde{P}_N &= \{p_N(x) \colon \text{the degree of } p_N(x) \le N\}, \\ P_N &= \left\{ v \in \tilde{P}_N : v(\pm 1) = 0 \right\}. \end{aligned} \tag{4}$$

2.1. Legendre Polynomials. We denote by $L_i(x)$ the i-th degree Legendre polynomial with $x \in I$. Three-term recurrence relationship for Legendre polynomials reads

$$(i+1) L_{i+1}(x) = (2i+1) x L_i(x) - i L_{i-1}(x), i \ge 1, \tag{5}$$

and $L_0(x) = 1, L_1(x) = x$.

We recall that $\{L_i(x)\}_{i \ge 1}$ satisfy

$$L_i(\pm 1) = (\pm 1)^i, i \ge 1, \tag{6}$$

and hence there holds

$$L_i(x) - L_{i+2}(x) \in P_N(x), 0 \le i \le N-2. \tag{7}$$

Also, there is an orthogonality

$$\left(L_i(x), L_j(x)\right) = \begin{cases} 0, i \ne j, \\ \dfrac{2}{2i+1}, i = j. \end{cases} \tag{8}$$

And for $i \le N$, it is obvious that $L'_i(x) \in \tilde{P}_{N-1}$ and

$$(2i+1) L_i(x) = L'_{i+1}(x) - L'_{i-1}(x), i \ge 1. \tag{9}$$

2.2. The Method of Particular Solutions. In this subsection, we consider the second-order differential equation with homogeneous Dirichlet boundary condition:

$$\begin{cases} \left(\omega(x)(u(x))'\right)' = f(x), x \in I, \\ u(\pm 1) = 0, \end{cases} \tag{10}$$

and the constraint on $\omega(x)$ will be stated in the sequel.

By (3), we obtain the equivalent weak formulation of (10) reads: finding $u \in H_0^1(I)$ such that

$$a(u, v) = -(f, v), \forall v \in H_0^1(I). \tag{11}$$

In view of (9), we design the corresponding particular solutions for (10) as

$$\psi_i(x) = \frac{L_{i+1}(x) - L_{i-1}(x)}{2i+1}, i \ge 1, \tag{12}$$

which guarantee $\psi_i(\pm 1) = 0$.

And then we define $\mathscr{P}_N$ as

$$\mathscr{P}_N = \operatorname{span}\{\psi_1(x), \psi_2(x), \cdots, \psi_{N-1}(x)\}, \tag{13}$$

where $\psi_i(x)$ satisfies the homogeneous Dirichlet boundary conditions in (10). For more details about the completeness of $\mathscr{P}_N$ in (13), please refer to [30].

According to (13), the MPS approximation of $u(x)$ can be stated as

$$u_N(x) = \sum_{j=1}^{N-1} c_j \psi_j(x), \forall x \in I, \tag{14}$$

where $\{c_j\}_{i=1}^{N-1}$ are the coefficients to be determined. For the sake of convenience, we use $\{x_k\}_{k=1}^{M}$ to denote the collocations in the interval. And then the corresponding equivalent collocation scheme for (10) reads: finding $u_N \in \mathscr{P}_N$ such that

$$\left(\left(\omega(x_k)(u_N(x_k))'\right)', v_k\right) = (f(x_k), v_k), k = 1, 2, \cdots, M, \tag{15}$$

where $v_k = \delta(x - x_k)$ denotes the Dirac delta distribution on x_k. For readers interested in the collocation approximations, please refer to [31].

3. The Model Problem and Its Approximation Scheme

3.1. The Model Problem with $\omega(x) = 1 - x^2$. In the following parts, we focus on $\omega(x) = 1 - x^2$. Since there does not exist any positive constant c satisfying $\omega(x) \geq c$ in I, we miss the sufficient conditions for the uniqueness of (10). And hence we have to restate the uniqueness of the solution for (11) with some novel techniques.

Theorem 1. *For $\omega(x) = 1 - x^2$, there exists a unique weak solution $u \in H_0^1(I)$ of (11).*

Proof. For any $v, w \in H^1(I)$, there holds

$$|a(v, w)| \leq \|v\|_1 \|w\|_1, \tag{16}$$

where we used $|\omega(x)| \leq 1$. One directly states the continuation of the bilinear form and also the existence of solutions.

Now we are at the point to investigate the uniqueness of the solution for (10). Obviously, the bilinear form is not elliptic. We have to prove the uniqueness with new techniques. Assuming there exist two solutions u_1 and u_2 satisfying (10), one readily gets that for all $x \in I$, there almost holds

$$\left(\omega(x)u_1'(x)\right)' = \left(\omega(x)u_2'(x)\right)', \tag{17}$$

which means

$$\begin{cases} \left(\left(1 - x^2\right) \mathscr{U}'(x)\right)' = 0, x \in I, \\ \mathscr{U}(\pm 1) = 0, \end{cases} \tag{18}$$

where $\mathscr{U}(x) = u_1(x) - u_2(x)$.

Now, we turn to prove that the solution of boundary value problem (18) is zero. And hence we employ integrations by parts to get the unique solution

$$\mathscr{U}(x) = \frac{c_1}{2} \ln \frac{1 + x}{1 - x} + c_2, a.e. x \in I. \tag{19}$$

Considering the boundary conditions and properties of function $\ln(x)$ at $x = \pm 1$, we easily declare that $c_1 = 0$ and $c_2 = 0$, which means $\mathscr{U}(x) = 0, a.e. x \in I$. Then, we readily depict that $u_1(x) = u_2(x), a.e. x \in I$, which directly verifies the uniqueness of solution of (11). □

3.2. The MPS with Legendre Polynomials. Noticing that, one of the challenges of the MPS is how to derive closed-form particular solutions for given differential operators. Although the particular solutions are not unique, it is always a complicated task to find appropriate particular solutions for given differential operators. In general, finding or designing closed-form particular solutions are nontrivial (for more details on this topic, please refer to [32] and the references therein).

It is well-known that the size of globally dense matrices in the MPS grows with the increase of collocation points and will cause bigger condition numbers of resultant matrices. Hence, the crucial task of the MPS is to choose pertinent $\tilde{P}_N$ such that the basis functions are as simple as possible. According to the recursive relationships of Legendre polynomials, we derive efficient basis functions for corresponding particular solutions bit by bit.

With (9), it is direct to state that

$$\left(\frac{L_{i+1}(x) - L_{i-1}(x)}{2i + 1}\right)' = L_i(x), i \geq 1. \tag{20}$$

And then we have

$$\left(\left(1 - x^2\right)\left(\frac{L_{i+1}(x) - L_{i-1}(x)}{2i + 1}\right)'\right)' = \left(\left(1 - x^2\right)L_i(x)\right)'. \tag{21}$$

Hence, the basis functions for the approximations of the right hand term can be set as

$$\begin{aligned} \phi_i(x) &= \left(\left(1 - x^2\right)L_i(x)\right)' \\ &= \left(1 - x^2\right)L_i'(x) - 2xL_i(x), 1 \leq i \leq N - 1, \end{aligned} \tag{22}$$

which satisfy the following identity

$$\left(\left(1 - x^2\right)\left(\psi_i(x)\right)'\right)' = \phi_i(x), 1 \leq i \leq N - 1. \tag{23}$$

One readily gets that the discretized formulation of (11) reads: finding $u_N \in \mathscr{P}_N$ such that

$$a(u_N, v_N) = -(f, v_N), \forall v_N \in \mathscr{P}_N. \tag{24}$$

The details about the equivalent weak formulation can be found in [31]. Meanwhile, the existence and uniqueness of the numerical solution in $\mathscr{P}_N$ of (24) can be readily proved by the same techniques given in Theorem 1.

4. *The* A-Priori Error Estimates

In this section, we study *a-priori* error estimates of the MPS approximations by an orthogonal projector. For any $w \in H_0^1(I)$, there holds

$$w(x) = \sum_{i=1}^{\infty} \widehat{w}_i \psi_i(x). \tag{25}$$

In view of orthogonal properties of Legendre polynomials and (20), we get the following identities:

$$\psi_i'(x) = L_i(x), i \geq 1. \tag{26}$$

We recall the first derivative orthogonal projector $1\Pi_0^N : H_0^1(I) \mapsto \mathscr{P}_N$ such that

$$\left(\left(w - 1\Pi_0^N w \right)', v'_N \right) = 0, v_N \in \mathscr{P}_N. \tag{27}$$

Here, an error estimate for this first derivative orthogonal projector is shown in the following lemma.

Lemma 2 (see [4, 33]). *For all $v \in H_0^1(I) \cap H^m(I) (m \geq 1)$, there holds*

$$\left\| v - 1\Pi_0^N v \right\|_l \leq cN^{l-m} \|v\|_m, l = 0, 1. \tag{28}$$

4.1. The A-Priori Error Estimate in $\boldsymbol{H}^1$-Norm. The Aubin-Nitsche duality argument is employed to investigate error estimates of the MPS approximations in H^1-norm.

Lemma 3 (See [34, 35]). *For bounded interval I and $F \in H^{-1}(I)$, we set y_F as the unique solution of the following homogeneous boundary value problem*

$$\left(y_F', v' \right) = \langle F, v \rangle, \tag{29}$$

where $\langle \cdot, \cdot \rangle$ stands for the dual product on $H^{-1}(I) \times H_0^1(I)$. Then, $y_F \in H^1(I)$, and there holds

$$\|y_F\|_1 \leq c\|F\|_{-1}. \tag{30}$$

By the above results, we derive the following a-priori error estimate.

Theorem 4. *Let u and u_N be the solutions of (11) and (15), respectively. Then for all $u \in H_0^1(I) \cap H^m(I)$, it holds that*

$$\|u - u_N\|_1 \leq CN^{1-m} \|u\|_m. \tag{31}$$

Proof. It follows that

$$\begin{aligned}
\|u - u_N\|_1 &== \sup_{F \in H^{-1}(I)} \frac{|\langle F, u - u_N \rangle|}{\|F\|_{-1}} \\
&\overset{(4.3)}{=} \sup_{F \in H^{-1}(I)} \frac{\left((u - u_N)', y'_F \right)}{\|F\|_{-1}} \\
&= \sup_{F \in H^{-1}(I)} \frac{\left((u - u_N)', \left(y_F - 1\Pi_0^N y_F \right)' \right)}{\|F\|_{-1}} \\
&= \sup_{F \in H^{-1}(I)} \frac{\left(\left(u - 1\Pi_0^{N-1} u \right)', \left(y_F - 1\Pi_0^N y_F \right)' \right)}{\|F\|_{-1}} \\
&\leq \left\| \left(u - 1\Pi_0^N u \right)' \right\| \cdot \sup_{F \in H^{-1}(I)} \frac{\left\| y_F - 1\Pi_0^N y_F \right\|_1}{\|F\|_{-1}} \\
&\overset{(4.2)(4.4)}{\leq} c \left\| \left(u - 1\Pi_0^N u \right)' \right\| \\
&\overset{(4.2)}{\leq} CN^{1-m} \|u\|_m.
\end{aligned} \tag{32}$$

Then, the a-priori error estimation in (31) is yielded. □

4.2. The A-Priori Error Estimate in $\boldsymbol{L}^\infty$-Norm. In this subsection, we give the corresponding error estimate in L^∞-norm with a rigorous relationship during $L^\infty(I)$ and $H^1(I)$.

Lemma 5. *For all $v \in H^1(I)$, there holds the following estimate*

$$\|v\|_\infty^2 \leq \|v\|^2 + 4\left\| v' \right\|^2. \tag{33}$$

Proof. Since the interval is bounded, one gets that $W^{m,2}(I) \subset W^{m,1}(I)$. By the embedding theorems (refer to Chapter 12 in [36]), we know that $W^{1,1}(I)$ is embedded in $L^\infty(I)$. Furthermore, $H^1(I)$ is a subset of $W^{1,1}(I)$ due to the bounded interval I. Hence, $H^1(I)$ is embedded in $L^\infty(I)$. About the constants within the above estimate, please refer to the Theorem 1.9 in [37] for further details. And a theoretical proof is listed in the appendix, which improves the proof given in [38]. □

Theorem 6. *Let u and u_N be the solutions of (11) and (15), respectively. Then, for all $u \in H_0^1(I) \cap H^m(I)$, there holds*

$$\|u - u_N\|_\infty \leq CN^{1-m} \|u\|_m. \tag{34}$$

Proof. It is clear that $u - u_N \in H^1(I)$. Then,

$$\begin{aligned}
\|u - u_N\|_\infty^2 &\overset{(4.6)}{\leq} \|u - u_N\|^2 + 4\left\| (u - u_N)' \right\|^2 \\
&\leq \left(C_I^2 + 4 \right) \left\| (u - u_N)' \right\|^2 \\
&\overset{(4.5)}{\leq} cN^{2(1-m)} \|u\|_m^2,
\end{aligned} \tag{35}$$

Table 1: Errors of $u-u_N$ and orders of convergence for Example 7.

N	$\|u-u_N\|_\infty$	$\|(u-u_N)'\|_\infty$	$\|u-u_N\|$	$\|(u-u_N)'\|$	Order
2	2.6781e-01	1.6331e-00	1.3512e-00	4.3813e-00	/
4	2.6248e-02	3.6964e-01	1.3282e-01	7.1212e-01	2.6620
8	9.9027e-05	3.9703e-03	4.8942e-04	5.9872e-03	6.9139
16	1.1428e-10	2.0526e-08	5.5757e-10	2.9599e-08	17.6304
32	9.9920e-16	7.9936e-15	3.5289e-15	1.4668e-14	20.9041
64	6.6613e-16	5.5511e-15	2.2505e-15	6.9826e-15	1.0401

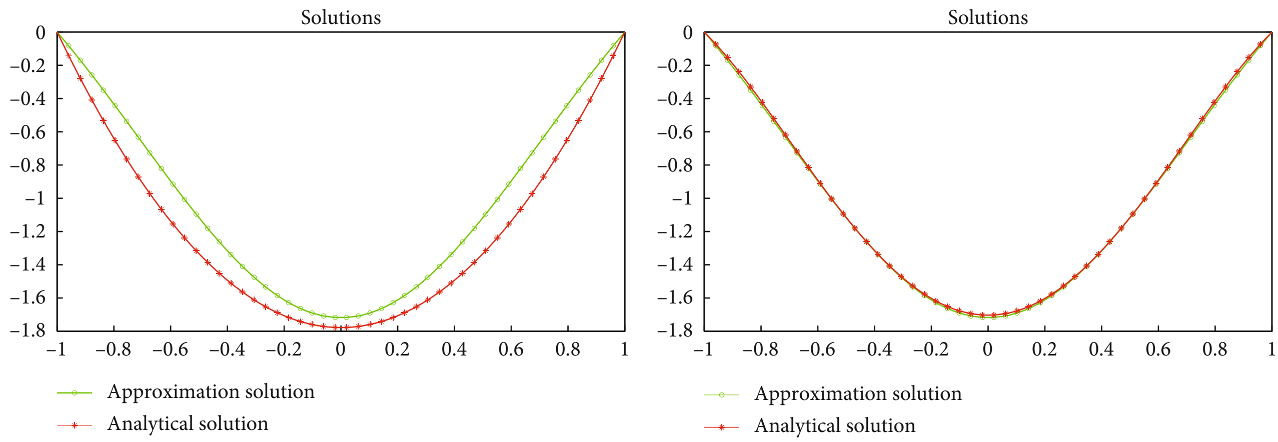

(a) $N=2$ (b) $N=4$

Figure 1: Pointwise curve of u and u_N at two different N.

where C_I denotes the constant within the Poincaré inequality. One readily gets that the desired result listed in (34) holds. □

The above two a-priori error estimations, which are given in H^1- and L^∞- norms, show that an asymptotic super-exponential convergence order for the MPS approximations can be achieved for any sufficiently smooth solution.

5. Numerical Results

In the following different kinds of numerical examples, we show the approximation data in tables and figures, which illustrate the efficiency of the MPS for (10). For simplicity, we evenly select distributed nodes as the collocation points.

Example 7. Setting the boundary value problem (10) with

$$f(x)=\left(4x^4-10x^2+2\right)e^{1-x^2}, \tag{36}$$

we get the analytic solution

$$u(x)=1-e^{1-x^2}. \tag{37}$$

Obviously, this analytic solution is sufficient smooth on I. The numerical data listed in Table 1 show error estimates of numerical approximations and the first derivatives of numerical solutions versus N, respectively. And two a-priori error estimations with L^∞- and L^2-norms verify our theoretical analyses. Hence, by the numerical data in the first five columns, we obtain the high accuracy property of the MPS approximations.

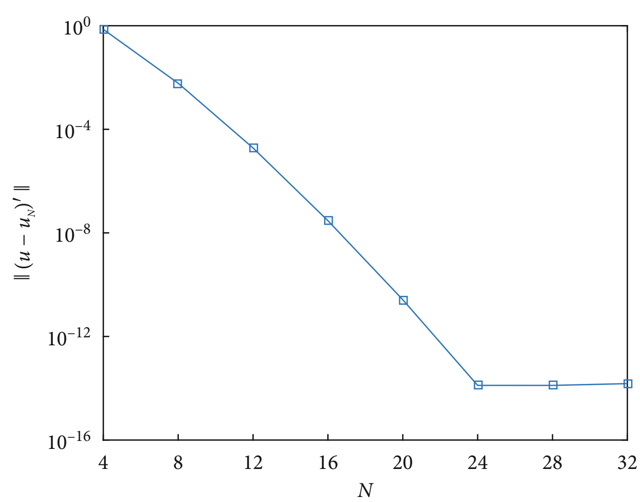

Figure 2: Errors of $\|(u-u_N)'\|$ versus N in the semi-logarithmic scale.

TABLE 2: Errors of $u - u_N$ and orders of convergence for Example 8.

N	$\|u-u_N\|_\infty$	$\|(u-u_N)'\|_\infty$	$\|u-u_N\|$	$\|(u-u_N)'\|$	Order
2	2.2879e-01	2.5276e+00	8.6146e-01	5.7626e+00	/
4	1.7595e-02	3.8416e-01	5.6339e-02	6.8030e-01	3.0934
8	1.5157e-05	8.6969e-04	3.3639e-05	1.3211e-03	9.0126
16	4.1144e-13	2.4593e-11	1.7072e-12	3.8911e-11	25.0161
32	4.4408e-16	1.7763e-15	1.3686e-15	4.3076e-15	13.0729
64	1.1102e-15	4.4408e-15	4.8534e-15	6.9881e-15	0. 9125

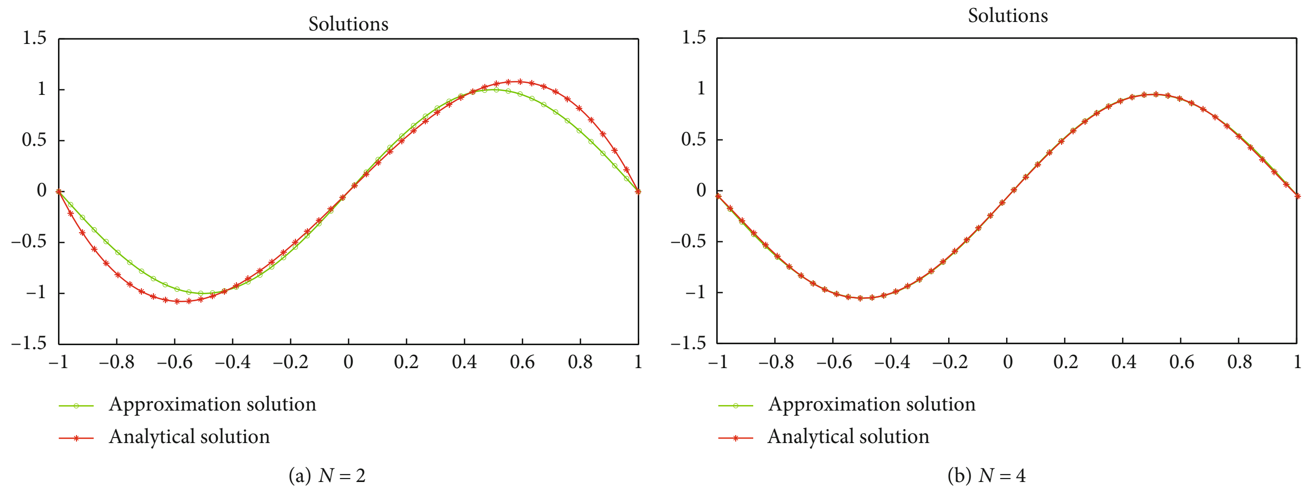

FIGURE 3: u and u_N at two different N.

The last column depicts the convergent orders, which will validate the high efficiency of the MPS. Since the errors arrive at the machine accuracy, the convergence order, 1.0401 in the last column, has no essential significance. Here, the convergence order is calculated by

$$\log_{N_{i+1}/N_i} \frac{error_i}{error_{i+1}}, \tag{38}$$

where the subscripts denote corresponding i-th and $(i+1)$-th information. It is obvious that for any sufficiently smooth analytic solution, the convergence orders of the MPS can be sharply enhanced by the increased N.

For the given right-hand side function f in (36), the analytic solutions and the MPS approximations of $N = 2$ and $N = 4$ are pointwise delineated in Figure 1.

And numerical results of $\|(u-u_N)'\|$ are shown by the semi-logarithmic scale in Figure 2. By the Poincaré inequality, we know that the approximation errors in H^1-norm are naturally consistent with our proposed a-priori error estimates. These figures show the efficiency of the MPS approximations for this example.

Following the above numerical data shown in Table 1 and Figures 1 and 2, it is clear that the numerical errors decrease exponentially with increased N. And hence, the convergence and high accuracy of our proposed numerical scheme are demonstrated.

Example 8. We consider the boundary value problem (10) with

$$f(x) = -2\pi x \cos(\pi x) - \pi^2 (1 - x^2) \sin(\pi x), \tag{39}$$

and the corresponding analytic solution reads

$$u(x) = \sin(\pi x). \tag{40}$$

By our proposed MPS schemes, corresponding numerical errors are listed in Table 2. Also convergence orders are given, which depict the finite algebraic convergence properties. Since numerical data of $N = 32$ and $N = 64$ approach the machine accuracy, which lead to that the last convergence order 0.9125 is unworthy of consideration. And the curves of numerical solution and analytic solution are shown in Figure 3.

Considering the above results and figures, we readily know the sharply approximation properties of the MPS.

Example 9. In this example, we consider the boundary value problem (10) with

$$f(x) = 5(6x^2 - 1)(1 - x^2)^{3/2}, \tag{41}$$

Table 3: Errors of $u - u_N$ and orders of convergence for Example 9.

N	$\|u - u_N\|_\infty$	$\|(u - u_N)'\|_\infty$	$\|u - u_N\|$	$\|(u - u_N)'\|$	Order
2	4.0971e-01	2.2952e-00	2.0526e-00	6.5743e-00	/
4	4.7082e-02	7.9970e-01	2.4208e-01	1.4037e-00	2.2734
8	9.9885e-04	5.8015e-02	4.9670e-03	8.3329e-02	4.0929
16	1.8621e-05	7.0230e-03	7.9775e-05	9.9683e-03	3.0659
32	2.2089e-06	7.4329e-04	1.3539e-05	1.0517e-03	3.2444
64	3.7025e-07	3.2285e-05	2.3867e-06	4.5686e-05	4.5230

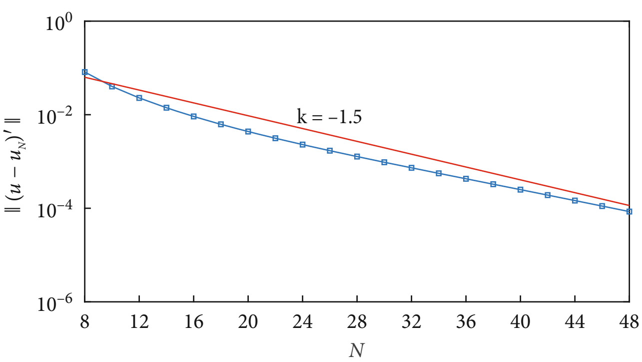

Figure 4: Errors of $\|(u - u_N)'\|$ versus N in semi-logarithmic scale and reference convergence line.

and the corresponding analytic solution

$$u(x) = \left(1 - x^2\right)^{5/2}. \tag{42}$$

Since the third derivative of this solution is singular at the boundary points $x = \pm 1$, the convergence order is not exponential. By the MPS schemes, numerical errors of our proposed approximations are listed in Table 3. And the convergence orders are shown in the last column, which depict the finite algebraic convergence properties.

Furthermore, considering accumulations of round-off errors and convergence orders, we show that the MPS approximations perform well for this kind of second-order differential equations.

Here, we present Figure 4 to show the errors of numerical solutions against various N by semi-logarithmic scale. The error curve of $\|(u - u_N)'\|$ is around the reference line, whose slope reads $\mathrm{k} = -1.5$. This indicates that our error estimates uniformly predict the numerical errors of the MPS, which is consistent with the regularity of the given solution.

In the light of kinds of classical solutions with different smoothness, we demonstrate that our a-priori error estimates uniformly predict the errors of the MPS approximations. Furthermore, considering accumulations of round-off errors, the current section verifies our theoretical results for the model problems with the proposed MPS approximations.

6. Conclusions

The highlight of this work is that we skillfully employed Legendre polynomials to solve second-order differential equations by the MPS. To investigate the efficiency and accuracy of proposed numerical schemes, we study the errors of corresponding numerical approximations. By orthogonal projector and Aubin-Nitsche duality argument, we obtain the a-priori error estimate in H^1-norm with rigorous analyses. Meanwhile, with the help of relationships between L^∞- and H^1-norms on any bounded interval, we readily get corresponding *a-priori* error estimate in L^∞-norm. In the numerical examples, three analytic solutions with different regularity are selected: One is with finite smoothness and others are with infinite regularity. Furthermore, convergence orders and numerical errors are listed to confirm our theoretical results, which also validate the efficiency and high accuracy of the MPS.

The success of dealing with this typical model problem by the MPS will pave the way for solving other more challenging models in science and engineering applications. In our ongoing researches, corresponding further discussions have been listed for the MPS in high dimensional domains, such as how to design the basis functions and corresponding particular solutions based on orthogonal polynomials and how to select collocation points for singular domains. Fortunately, the tensor product of orthogonal polynomials will help us to reformulate the particular solutions and corresponding discretizations. We believe that this method will be applicable for a large amount of partial differential equations and is an efficient numerical scheme in applications.

Appendix

A. The Proof of Lemma 4.3

This appendix follows the proof of both Theorem 7.10 in [39] and (3.9) in [38] and gives a rigorous proof for Lemma 5 on any bounded interval (a, b).

Firstly, we proceed from $\forall v \in C^\infty[a, b]$. By the first mean value theorem of integrals, we know that there exists a $\sigma \in (a, b)$ satisfying

$$\|v\|^2 = \int_a^b |v(x)|^2 dx = |v(\sigma)|^2 (b - a). \tag{A.1}$$

Meanwhile, by the Newton-Leibniz integration formula, we have

$$v(x) = v(\sigma) + \int_\sigma^x v'(t)dt. \tag{A.2}$$

One readily gets

$$\begin{aligned} |v(x)|^2 &= \left| v(\sigma) + \int_\sigma^x v'(t)dt \right|^2 \le 2\left[|v(\sigma)|^2 + \left| \int_\sigma^x v'(t)dt \right|^2 \right] \\ &\le 2\left[|v(\sigma)|^2 + \left| \left(\int_\sigma^x |v'(t)|^2 dt \right)^{1/2} \left(\int_\sigma^x dt \right)^{1/2} \right|^2 \right] \\ &= 2\left[|v(\sigma)|^2 + |x-\sigma| \int_\sigma^x |v'(t)|^2 dt \right] \\ &\overset{(A.1)}{\le} \frac{2}{b-a}\|v\|^2 + 2|b-a|\|v'\|^2. \end{aligned} \tag{A.3}$$

Hence, in view of $C^\infty[a,b]$ is dense in $H^1(a,b)$, then for any $v \in H^1(a,b)$, there exists $\{v_k(x)\} \in C^\infty[a,b]$ satisfying

$$\|v - v_k\|_1 \longrightarrow 0, k \longrightarrow \infty. \tag{A.4}$$

Now it is obvious that

$$v_k - v_l \in C^\infty[a,b], \forall k, l. \tag{A.5}$$

By (A.3), one arrives at

$$|v_k(x) - v_l(x)|^2 \le \frac{2}{b-a}\|v_k - v_l\|^2 + 2|b-a| \cdot \|(v_k - v_l)'\|^2. \tag{A.6}$$

Then for $\forall x \in [a,b]$ and $k, l \longrightarrow \infty$, there holds

$$\begin{aligned} &\max_{x\in[a,b]} |v_k(x) - v_l(x)|^2 \\ &\overset{(A.4)}{\le} \frac{2}{b-a}\|v_k - v_l\|^2 + 2|b-a| \cdot \|(v_k - v_l)'\|^2 \overset{(A.3)}{\longrightarrow} 0, \end{aligned} \tag{A.7}$$

which means that $\{v_k(x)\}$ is a Cauchy sequence in $C[a,b]$.

Meanwhile, in the light of the completeness of $C[a,b]$, we know that there exists $\tilde{v} \in C[a,b]$ such that

$$v_k \overset{C[a,b]}{\longrightarrow} \tilde{v}, k \longrightarrow \infty, \tag{A.8}$$

i.e.,

$$\max_{x\in[a,b]} |v_k(x) - \tilde{v}(x)| \longrightarrow 0, k \longrightarrow \infty. \tag{A.9}$$

Secondly, we identify the relationship between v and $\tilde{v}$. By Minkowski's inequality and Lebesgue integration, we have

$$\begin{aligned} \left(\int_{(a,b)} |v - \tilde{v}|^2 \right)^{1/2} &\le \left(\int_{(a,b)} |v - v_k|^2 \right)^{1/2} \\ &\quad + \left(\int_{(a,b)} |v_k - \tilde{v}|^2 \right)^{1/2}, \end{aligned} \tag{A.10}$$

then for $k \longrightarrow \infty$, there holds

$$\begin{aligned} \left(\int_{(a,b)} |v - \tilde{v}|^2 \right)^{1/2} &\le \lim_{k\longrightarrow\infty} \max_{x\in[a,b]} |\tilde{v}(x) - v_k(x)| (b-a)^{1/2} \\ &\quad + \lim_{k\longrightarrow\infty} \|v_k - \tilde{v}\|_1 \\ &= 0, \end{aligned} \tag{A.11}$$

i.e.,

$$\int_{(a,b)} |v - \tilde{v}|^2 = 0. \tag{A.12}$$

Therefore,

$$v(x) = \tilde{v}(x), a.e. x \in [a,b]. \tag{A.13}$$

Finally, by (A.3), we know that for all v_k, there holds

$$|v_k(x)|^2 \le \frac{2}{b-a}\|v_k\|^2 + 2|b-a| \cdot \|v'_k\|^2. \tag{A.14}$$

Then,

$$\begin{aligned} |\tilde{v}(x)|^2 &\overset{(A.5)}{=} \lim_{k\longrightarrow\infty} |v_k(x)|^2 \\ &\le \frac{2}{b-a} \lim_{k\longrightarrow\infty} \|v_k\|^2 + 2|b-a| \cdot \lim_{k\longrightarrow\infty} \|v'_k\|^2 \\ &\overset{(A.3)}{=} \frac{2}{b-a}\|v\|^2 + 2|b-a| \cdot \|v'\|^2. \end{aligned} \tag{A.15}$$

With the help of (A.13), we directly get

$$|v(x)|^2 \le \frac{2}{b-a}\|v\|^2 + 2|b-a| \cdot \|v'\|^2, a.e. x \in (a,b), \tag{A.16}$$

which means

$$\|v\|_\infty^2 \le \frac{2}{b-a}\|v\|^2 + 2|b-a| \cdot \|v'\|^2. \tag{A.17}$$

This is the desired result in Lemma 5.

Data Availability

Data available on request from the authors.

Conflicts of Interest

The authors declare that they have no conflicts of interest.

Authors' Contributions

The authors contributed equally to this work.

Acknowledgments

This work is partly supported by Natural Science Foundation of China (Nos. 12271233 and 11926355), and Natural Science Foundation of Shandong Province (Nos. ZR2019YQ05, 2019KJI003, and ZR2018LA008).

References

[1] P. G. Ciarlet, *The Finite Element Method for Elliptic Problems*, Society for Industrial and Applied Mathematics, 2002.

[2] H. F. Niu, D. P. Yang, and J. W. Zhou, "Numerical analysis of an optimal control problem governed by the stationary Navier-Stokes equations with global velocity-constrained," *Communications in Computational Physics*, vol. 24, no. 5, pp. 1477–1502, 2018.

[3] Z. J. Zhou and Z. Y. Tan, "Finite element approximation of optimal control problem governed by space fractional equation," *Journal of Scientific Computing*, vol. 78, no. 3, pp. 1840–1861, 2019.

[4] C. Canuto, M. Y. Hussaini, A. Quarteroni, and T. A. Zang, *Spectral Methods in Fluid Dynamics*, Springer, Berlin, 1988.

[5] L. Zhang and Z. J. Zhou, "Spectral Galerkin approximation of optimal control problem governed by Riesz fractional differential equation," *Applied Numerical Mathematics*, vol. 143, pp. 247–262, 2019.

[6] J. W. Zhou, H. Y. Li, and Z. Z. Zhang, "A posteriori error estimates of spectral approximations for second order partial differential equations in spherical geometries," *Journal of Scientific Computing*, vol. 90, no. 1, 2022.

[7] S. Yüzbasi, "A shifted Legendre method for solving a population model and delay linear Volterra integro-differential equations," *International Journal of Biomathematics*, vol. 10, no. 7, article 1750091, 2017.

[8] S. Yüzbasi and M. Sezer, "Shifted Legendre approximation with the residual correction to solve pantograph-delay type differential equations," *Applied Mathematical Modelling*, vol. 39, no. 21, pp. 6529–6542, 2015.

[9] E. Hetmaniok, M. Pleszczyński, and Y. Khan, "Solving the integral-differential equations with delayed argument by using the DTM method," *Sensors*, vol. 22, no. 11, p. 4124, 2022.

[10] Z. M. Odibat, "Differential transform method for solving Volterra integral equation with separable kernels," *Mathematical and Computer Modelling*, vol. 48, no. 7-8, pp. 1144–1149, 2008.

[11] C. S. Chen, M. A. Golberg, and R. Schaback, "Recent developments in the dual reciprocity method using compactly supported radial basis functions," in *Transformation of Domain Effects to the Boundary*, Y. F. Rashed, Ed., WIT Press, 2003.

[12] H. D. Cheng, "Particular solutions of Laplacian, Helmholtz-type, and polyharmonic operators involving higher order radial basis functions," *Engineering Analysis with Boundary Elements*, vol. 24, no. 7-8, pp. 531–538, 2000.

[13] C. Franke and R. Schaback, "Solving partial differential equations by collocation using radial basis functions," *Applied Mathematics & Computation*, vol. 93, no. 1, pp. 73–82, 1998.

[14] E. J. Kansa, "Multiquadrics-a scattered data approximation scheme with applications to computational fluid-dynamics-II solutions to parabolic, hyperbolic and elliptic partial differential equations," *Computers & Mathematics with Applications*, vol. 19, no. 8-9, pp. 147–161, 1990.

[15] G. Fairweather and A. Karageorghis, "The method of fundamental solutions for elliptic boundary value problems," *Advances in Computational Mathematics*, vol. 9, no. 1/2, pp. 69–95, 1998.

[16] C. S. Chen, C. M. Fan, and P. H. Wen, "The method of approximate particular solutions for solving elliptic problems with variable coefficients," *International Journal of Computational Methods*, vol. 8, no. 3, pp. 545–559, 2011.

[17] M. A. Golberg, A. S. Muleshkov, and C. S. Chen, "Particular solutions of Helmholtz-type operators using higher order polyharmonic splines," *Computational Mechanics*, vol. 23, no. 5, pp. 411–419, 1999.

[18] T. Belytschko, Y. Lu, and L. Gu, "Element free Galerkin method," *International Journal for Numerical Methods in Engineering*, vol. 37, no. 2, pp. 229–256, 1994.

[19] G. R. Liu and Y. T. Gu, "Boundary meshfree methods based on the boundary point interpolation methods," *Engineering Analysis with Boundary Elements*, vol. 28, no. 5, pp. 475–487, 2004.

[20] W. Chen, "Symmetric boundary knot method," *Engineering Analysis with Boundary Elements*, vol. 26, no. 6, pp. 489–494, 2002.

[21] X. Zhang, M. Chen, C. S. Chen, and Z. Li, "Localized method of approximate particular solutions for solving unsteady Navier-Stokes problem," *Applied Mathematical Modelling*, vol. 40, no. 3, pp. 2265–2273, 2016.

[22] P. H. Wen and C. S. Chen, "The method of particular solutions for solving scalar wave equations, international journal for numerical methods in biomedical," *Engineering*, vol. 26, no. 12, pp. 1878–1889, 2010.

[23] L. Yan and F. L. Yang, "The method of approximate particular solutions for the time fractional diffusion equation with a nonlocal boundary condition," *Computers & Mathematics with Applications*, vol. 70, no. 3, pp. 254–264, 2015.

[24] M. A. Golberg, A. S. Muleshkov, C. S. Chen, and A. H.-D. Cheng, "Polynomial particular solutions for certain partial differential operators," *Numerical Methods for Partial Differential Equations*, vol. 19, no. 1, pp. 112–133, 2003.

[25] A. S. Muleshkov and M. Golberg, "Particular solutions of the multi-Helmholtz-type equation," *Engineering Analysis with Boundary Elements*, vol. 31, no. 7, pp. 624–630, 2007.

[26] G. Yao, C. S. Chen, and C. C. Tsai, "A revisit on the derivation of the particular solution for the differential operator Δ^2-λ^2," *Advances in Applied Mathematics and Mechanics*, vol. 1, no. 6, pp. 750–768, 2009.

[27] C. S. Chen, S. W. Lee, and C. S. Huang, "Derivation of particular solutions using Chebyshev polynomial based functions," *International Journal of Computational Methods*, vol. 4, no. 1, pp. 15–32, 2007.

[28] K. E. Atkinson, "The numerical evaluation of particular solutions for Poisson's equation," *IMA Journal of Numerical Analysis*, vol. 5, no. 3, pp. 319–338, 1985.

[29] C. S. Chen, M. Ganesh, M. A. Golberg, and A. H.-D. Cheng, "Multilevel compact radial functions based computational schemes for some elliptic problems," *Computers & Mathematics with Application*, vol. 43, no. 3-5, pp. 359–378, 2002.

[30] J. Shen, "Efficient spectral-Galerkin method I," *SIAM Journal on Scientific Computing*, vol. 15, no. 6, pp. 1489–1505, 1994.

[31] Z. Zhang, "Superconvergence of a Chebyshev spectral collocation method," *Journal of Scientific Computing*, vol. 34, no. 3, pp. 237–246, 2008.

[32] F. F. Dou, Y. S. Liu, and C. S. Chen, "The method of particular solutions for solving nonlinear Poisson problems," *Computers & Mathematics with Applications*, vol. 77, no. 2, pp. 501–513, 2019.

[33] J. W. Zhou and D. P. Yang, "An improved a posteriori error estimate for the Galerkin spectral method in one dimension," *Computers & Mathematics with Applications*, vol. 61, no. 2, pp. 334–340, 2011.

[34] I. Babuska, J. Osborn, and J. Pitkäranta, "Analysis of mixed methods using mesh dependent norms," *Mathematics of Computation*, vol. 35, no. 152, pp. 1039–1062, 1980.

[35] A. Charbonneau, K. Dossou, and R. Pierre, "A residual-based a posteriori error estimator for the Ciarlet-Raviart formulation of the first biharmonic problem," *Numerical Methods for Partial Differential Equations*, vol. 13, no. 1, pp. 93–111, 1997.

[36] G. Leoni, *A First Course in Sobolev Spaces*, AMS, Rhode Island, 2009.

[37] X. M. Xiang, *Numerical Analysis of Spectral Method*, Science Press, Beijing, 2000.

[38] B. Y. Guo and Z. Q. Wang, "Legendre-Gauss collocation methods for ordinary differential equations," *Advances in Computational Mathematics*, vol. 30, no. 3, pp. 249–280, 2009.

[39] D. Gilbarg and N. S. Trudinger, *Elliptic Partial Differential Equations of Second Order*, Springer, Berlin, 2001.

Hindawi
Journal of Function Spaces
Volume 2023, Article ID 5322092, 15 pages
https://doi.org/10.1155/2023/5322092

Research Article

Adaptation of the Novel Cubic B-Spline Algorithm for Dealing with Conformable Systems of Differential Boundary Value Problems concerning Two Points and Two Fractional Parameters

Omar Abu Arqub,[1] **Soumia Tayebi**,[2] **Shaher Momani**,[3,4] **and Marwan Abukhaled**[5]

[1]*Department of Mathematics, Faculty of Science, Al-Balqa Applied University, Salt 19117, Jordan*
[2]*Department of Mathematics, University of Ahmed Zabana, Relizane, Algeria*
[3]*Department of Mathematics, Faculty of Science, The University of Jordan, Amman 11942, Jordan*
[4]*Department of Mathematics and Sciences, College of Humanities and Sciences, Ajman University, Ajman, UAE*
[5]*Department of Mathematics and Statistics, American University of Sharjah, Sharjah 26666, UAE*

Correspondence should be addressed to Omar Abu Arqub; o.abuarqub@bau.edu.jo

Received 5 August 2022; Revised 25 November 2022; Accepted 3 April 2023; Published 25 April 2023

Academic Editor: Luisa Morgado

Recently, conformable calculus has appeared in many abstract uses in mathematics and several practical applications in engineering and science. In addition, many methods and numerical algorithms have been adapted to it. In this paper, we will demonstrate, use, and construct the cubic B-spline algorithm to deal with conformable systems of differential boundary value problems concerning two points and two fractional parameters in both regular and singular types. Here, several linear and nonlinear examples will be presented, and a model for the Lane-Emden will be one of the applications presented. Indeed, we will show the complete construction of the used spline through the conformable derivative along with the convergence theory, and the error orders together with other results that we will present in detail in the form of tables and graphs using Mathematica software. Through the results we obtained, it became clear to us that the spline approach is effective and fast, and it requires little compulsive and mathematical burden in solving the problems presented. At the end of the article, we presented a summary that contains the most important findings, what we calculated, and some future suggestions.

1. Introduction

At present, in addition to the past tens of years, the applications of FDPs have expanded to include many physical and engineering applications [1–3]. In one place, we find application for them in kinetics energy [4], anomalous diffusion [5], movement of fluids [6], movement of waves [7], electrical engineering [8], and some of the fields of computer science [9], whilst in another place, we see some abstract uses of theories and definitions, which are originally found to organize the mathematical aspect of fractional derivatives in solving several fractional models like cholera outbreak [10] and partial FDPs [11]. From the definition of Riemann, the fractional differential began, and then different definitions appeared, such as Caputo, Fabrizio, and Atangana [12, 13].

Many of the definitions of fractional derivatives have strong features that make them a target in the modeling of many scientific phenomena, and at the same time, they have weaknesses in some characteristics that made some researchers search for a mathematically appropriate definition that is consistent with many of the laws and theorems found in the classical derivative. Therefore, in this paper, we will use the definition of the CD as a new approach to solving BVPs in their regular and singular states by adopting the CBSA to it. Conformable calculus proposed by [14] and theorized by [15] appears in several fields of applied sciences and abstract analysis as stellar mathematical agents to characterize hereditary behaviors with the memory of many substances. The CD has been successfully exercised in diverse physical and engineering application fields (herein, we try to list it briefly so that we do not prolong the reader and do not increase the size of the paper as much as possible) as in the formulation of fuzzy differential problems [16], in Newton mechanics [17], in Burgers' model [18], in population growth model [19], and in traveling wave field [20].

Systems of BVPs which are a mixture of several FDPs subject to given BCs represent very important issues in solving real-world models. Because of this rise, studying numerical and analytical solutions to these systems is an enticing topic for scientists. These kinds of systems are usually difficult to solve analytically, especially for singular, nonlinear, and nonhomogenous cases. To this end, extensive research has been carried out to obtain numerical schemes and various methods as utilized in the literature as follows: n [21], the authors applied the Adomian decomposition scheme; in [22], the authors described the sinc collocation algorithm; and in [23] the authors utilized the fractional Lagrangian approach.

The spline approach is an ongoing research subject in various diverse and pervasive science areas such as numerical analysis, signal processing, and computational physics [24–26]. It is a crucial method for solving-modeling many FDPs like singular BVPs [27], nonfractional Bratu-type BVPs [28], nonfractional LEP [29], and fractional physiology problem [30] (herein, we try to list it briefly so that we do not prolong the reader and do not increase the size of the paper as much as possible). CBS is the most common BS, which Schoenberg coined the expression BS, and it is an abbreviation of the word "basis spline". In computational mathematics, BS is a spline function with the lowest description interval for a given degree of smoothness and domain decomposition.

Here, we will show the complete construction of the used CBSA through the CD along with the convergence theory and other results that we will present in detail in the form of tables and graphs using the Mathematica software. Anyhow, we will solve the following:

(i) Conformable system of FDPs of regular type:

$$\begin{aligned} &T^{\theta_1}\Psi + a_1(\varsigma)T^{\delta_1}\Psi + a_2(\varsigma)\Psi + T^{\theta_2}\Phi + a_3(\varsigma)T^{\delta_2}\Phi \\ &\quad + a_4(\varsigma)\Phi + N_1(\Psi,\Phi) \\ &\quad = \mathscr{F}_1(\varsigma), \\ &T^{\theta_2}\Phi + b_1(\varsigma)T^{\delta_2}\Phi + b_2(\varsigma)\Phi + T^{\theta_1}\Psi + b_3(\varsigma)T^{\delta_1}\Psi \\ &\quad + b_4(\varsigma)\Psi + N_2(\Psi,\Phi) \\ &\quad = \mathscr{F}_2(\varsigma), \end{aligned} \tag{1}$$

concerning the BC

$$\begin{aligned} \Psi(a) = \alpha_1, \Phi(a) = \alpha_2, \\ \Psi(b) = \beta_1, \Phi(b) = \beta_2. \end{aligned} \tag{2}$$

(ii) Conformable LEP of singular type as

$$\begin{aligned} T^{\theta_1}\Psi + \frac{\eta_1}{\varsigma}T^{\delta_1}\Psi + a_2(\varsigma)\Psi + a_4(\varsigma)\Phi + N_1(\Psi,\Phi) = \mathscr{F}_1(\varsigma), \\ T^{\theta_2}\Phi + \frac{\eta_2}{\varsigma}T^{\delta_2}\Phi + b_2(\varsigma)\Phi + b_4(\varsigma)\Psi + N_2(\Psi,\Phi) = \mathscr{F}_2(\varsigma), \end{aligned} \tag{3}$$

concerning the BC

$$\begin{aligned} \Psi(0) = \rho_1, \Phi(0) = \varepsilon_1, \\ \Psi(1) = \rho_2, \Phi(1) = \varepsilon_2. \end{aligned} \tag{4}$$

Herein, $\Psi = \Psi(\varsigma)$, $\Phi = \Phi(\varsigma)$, $0 < \delta_1, \delta_2 \leq 1$, $1 < \theta_1, \theta_2 \leq 2$, $\alpha_p, \beta_p, \rho_p, \varepsilon_p \in \mathbb{R}$, $\eta_1, \eta_2 \geq 0$, and $T^{\delta_1}, T^{\delta_2}, T^{\theta_1}, T^{\theta_2}$ stands for CDs of order $\delta_1, \delta_2, \theta_1, \theta_2$, respectively; N_1 and N_2 are nonlinear functions in Ψ, Φ, $\mathscr{F}_1(\varsigma)$, and $\mathscr{F}_2(\varsigma)$; and $a_q(\varsigma)$ and $b_q(\varsigma)$ with $q = 1.2.3.4$ are continuous functions. Further, the CD of $T^{\delta}\mathscr{H}(\varsigma)$ is expressed as

$$T^{\omega}\mathscr{H}(\varsigma) = \lim_{\xi \longrightarrow 0} \frac{\mathscr{H}^{(\lceil\omega\rceil-1)}\left(\varsigma + \xi\varsigma^{\lceil\omega\rceil-\omega}\right) - \mathscr{H}^{(\lceil\omega\rceil-1)}(\varsigma)}{\xi}, \tag{5}$$

with $\omega \in (n, n+1]$, $\mathscr{H} : [0,\infty) \longrightarrow \mathbb{R}$ be n-differentiable for all $\varsigma > 0$, and $T^{\delta}\mathscr{H}(\varsigma) = \varsigma^{\lceil\delta\rceil-\delta}\mathscr{H}^{(\lceil\delta\rceil)}(\varsigma)$.

The motivation of our article can be summarized as follows: Often, real solutions to FDPs are not available and cannot be calculated or predicted because most of the problems are of nonlinear or nonhomogeneous type, or their coefficients are variables and not constants. Therefore, dealing with these issues, in this case, requires the utilization of numerical methods and algorithms, and here in our paper, we proposed the CBSA for ease of dealing with it and the ease of writing its computer program and because it is also accurate and does not require combining it with other numerical methods to obtain the required approximation. In addition to its convergence, its error order is guaranteed by the theories and results that we presented in our coming sections.

The basic structure herein was built as next. Section 2 proposes and formulates the CBSA for handling systems of BVPs concerning the CD. Section 3 deals with solving a singular system of conformable LEP by using the CBSA. Section 4 explores and discusses the convergence analysis together with the error order of the utilized CBSA. In Section 5, by using tables and graphs, some treatment examples are examined to offer the accuracy and fineness of the CBSA using Mathematica 11 software. At the end of the article, we presented a summary that contains the most important findings, what we calculated, and some future suggestions.

2. Formulation of the CBSA for Handling Systems of BVPs

In this section, the CBSA is used to construct and obtain approximations of the mentioned systems of conformable FDPs for both regular and singular types. Herein, we will consider two computational cases according to the nature of the shapes functions $N_1(\Psi,\Phi)$ and $N_2(\Psi,\Phi)$.

Assume that $\Pi:\{a=\varsigma_0<\varsigma_1<\cdots<\varsigma_{r-1}<\varsigma_r=b\}$ be a partition of $[a,b]$ with mesh points $\varsigma_k=a+k\hbar$, $k=0,1,\cdots,r$ wherein $\varsigma_0=a$, $\varsigma_r=b$, and $\hbar=(b-a)/r$. By introducing knots $\varsigma_{-2}<\varsigma_{-1}<\varsigma_0$ and $\varsigma_r<\varsigma_{r+1}<\varsigma_{r+2}$, Π becomes

$$\Pi:\{\varsigma_{-2}<\varsigma_{-1}<\varsigma_0=a<\varsigma_1<\cdots<\varsigma_r=b<\varsigma_{r+1}<\varsigma_{r+2}\}. \quad (6)$$

Define $\zeta_3(\Pi)=\{n(\varsigma)\in C^2[a,b]\}$ such that $n(\varsigma)$ is piecewise, 3rd-degree polynomials around Π. Anyhow, the 3rd-degree BSs is

$$B_{k,3}(\varsigma)=\frac{1}{6\hbar^3}\begin{cases}(\varsigma-\varsigma_{k-2})^3, & \varsigma_{k-2}\le\varsigma<\varsigma_{k-1},\\ -3(\varsigma-\varsigma_{k-1})^3+3\hbar(\varsigma-\varsigma_{k-1})^2+3\hbar^2(\varsigma-\varsigma_{k-1})+\hbar^3, & \varsigma_{k-1}\le\varsigma<\varsigma_k,\\ -3(\varsigma_{k+1}-\varsigma)^3+3\hbar(\varsigma_{k+1}-\varsigma)^2+3\hbar^2(\varsigma_{k+1}-\varsigma)+\hbar^3, & \varsigma_k\le\varsigma<\varsigma_{k+1},\\ (\varsigma_{k+2}-\varsigma)^3, & \varsigma_{k+1}\le\varsigma<\varsigma_{k+2},\\ 0, & \text{otherwise}.\end{cases} \quad (7)$$

To solve (1) and (2) together with (3) and (4) numerically, $T^{\delta}B_{k,3}(\varsigma)$ and $T^{\theta}B_{k,3}(\varsigma)$ evaluation is needed, where $0<\delta\le1$ and $1<\theta\le2$. Using the propositions of CD, one has

$$T^{\delta}B_{k,3}(\varsigma)=\frac{\varsigma^{1-\delta}}{2\hbar^3}\begin{cases}(\varsigma-\varsigma_{k-2})^2, & \varsigma_{k-2}\le\varsigma<\varsigma_{k-1},\\ -3(\varsigma-\varsigma_{k-1})^2+2\hbar(\varsigma-\varsigma_{k-1})+\hbar^2, & \varsigma_{k-1}\le\varsigma<\varsigma_k,\\ 3(\varsigma_{k+1}-\varsigma)^2-2\hbar(\varsigma_{k+1}-\varsigma)-\hbar^2, & \varsigma_k\le\varsigma<\varsigma_{k+1},\\ -(\varsigma_{k+2}-\varsigma)^2, & \varsigma_{k+1}\le\varsigma<\varsigma_{k+2},\\ 0, & \text{otherwise}.\end{cases} \quad (8)$$

$$T^{\theta}B_{k,3}(\varsigma)=\frac{\varsigma^{2-\theta}}{\hbar^3}\begin{cases}\varsigma-\varsigma_{k-2}, & \varsigma_{k-2}\le\varsigma<\varsigma_{k-1},\\ \hbar-3(\varsigma-\varsigma_{k-1}), & \varsigma_{k-1}\le\varsigma<\varsigma_k,\\ \hbar-3(\varsigma_{k+1}-\varsigma), & \varsigma_k\le\varsigma<\varsigma_{k+1},\\ (\varsigma_{k+2}-\varsigma), & \varsigma_{k+1}\le\varsigma<\varsigma_{k+2},\\ 0, & \text{otherwise}.\end{cases} \quad (9)$$

To formulate the required approximation using the CBSA, let

$$\begin{aligned}\widehat{\Psi}(\varsigma)&=\sum_{k=-1}^{r+1}\mu_k B_{k,3}(\varsigma),\\ \widehat{\Phi}(\varsigma)&=\sum_{k=-1}^{r+1}\nu_k B_{k,3}(\varsigma),\end{aligned} \quad (10)$$

be a cubic BS interpolating function of $\Psi(\varsigma)$ and $\Phi(\varsigma)$, respectively, with knots Π, where μ_k,ν_k are unknown, and $B_{k,3}(\varsigma)$ are the 3rd-degree BS functions which are defined in (7).

Therefore, from (7), (8), and (9) the value of $\widehat{\Psi}(\varsigma)$, $T^{\delta_1}\widehat{\Psi}(\varsigma)$, $T^{\theta_1}\widehat{\Psi}(\varsigma)$ and $\widehat{\Phi}(\varsigma)$, $T^{\delta_2}\widehat{\Phi}(\varsigma)$, $T^{\theta_2}\widehat{\Phi}(\varsigma)$ at knot ς_k can be simplified as

$$\begin{aligned}\widehat{\Psi}(\varsigma_k)&=\sum_{k=-1}^{r+1}\mu_k B_{k,3}(\varsigma_k)\\ &=\mu_{k-1}B_{k-1,3}(\varsigma_k)+\mu_k B_{k,3}(\varsigma_k)+\mu_{k+1}B_{k+1,3}(\varsigma_k),\\ T^{\delta_1}\widehat{\Psi}(\varsigma_k)&=\sum_{k=-1}^{r+1}\mu_k T^{\delta_1}B_{k,3}(\varsigma_k)\\ &=\mu_{k-1}T^{\delta_1}B_{k-1,3}(\varsigma_k)+\mu_k T^{\delta_1}B_{k,3}(\varsigma_k)\\ &\quad+\mu_{k+1}T^{\delta_1}B_{k+1,3}(\varsigma_k),\\ T^{\theta_1}\widehat{\Psi}(\varsigma_k)&=\sum_{k=-1}^{r+1}\mu_k T^{\theta_1}B_{k,3}(\varsigma_k)\\ &=\mu_{k-1}T^{\theta_1}B_{k-1,3}(\varsigma_k)+\mu_k T^{\theta_1}B_{k,3}(\varsigma_k)\\ &\quad+\mu_{k+1}T^{\theta_1}B_{k+1,3}(\varsigma_k),\end{aligned} \quad (11)$$

where B's, $T^{\delta_1}B$'s, and $T^{\theta_1}B$'s are given, respectively, as

$$\begin{aligned}B_{k-1,3}(\varsigma_k)&=\frac{1}{6},\\ B_{k,3}(\varsigma_k)&=\frac{2}{3},\\ B_{k+1,3}(\varsigma_k)&=\frac{1}{6}.\end{aligned} \quad (12)$$

$$\begin{aligned} T^{\delta_1} B_{\hbar-1,3}(\varsigma_\hbar) &= \frac{1}{2\hbar}\varsigma_\hbar^{1-\delta_1}, \\ T^{\delta_1} B_{\hbar,3}(\varsigma_\hbar) &= 0, \\ T^{\delta_1} B_{\hbar+1,3}(\varsigma_\hbar) &= -\frac{1}{2\hbar}\varsigma_\hbar^{1-\delta_1}. \end{aligned} \tag{13}$$

$$\begin{aligned} T^{\theta_1} B_{\hbar-1,3}(\varsigma_\hbar) &= \frac{1}{\hbar^2}\varsigma_\hbar^{2-\theta_1}, \\ T^{\theta_1} B_{\hbar,3}(\varsigma_\hbar) &= -\frac{2}{\hbar^2}\varsigma_\hbar^{2-\theta_1}, \\ T^{\theta_1} B_{\hbar+1,3}(\varsigma_\hbar) &= \frac{1}{\hbar^2}\varsigma_\hbar^{2-\theta_1}. \end{aligned} \tag{14}$$

Anyhow, one can write

$$\begin{aligned} \widehat{\Psi}(\varsigma_\hbar) &= \frac{1}{6}\mu_{\hbar-1} + \frac{2}{3}\mu_\hbar + \frac{1}{6}\mu_{\hbar+1}, \\ T^{\delta_1}\widehat{\Psi}(\varsigma_\hbar) &= -\frac{1}{2\hbar}\varsigma_\hbar^{1-\delta_1}\mu_{\hbar-1} + \frac{1}{2\hbar}\varsigma_\hbar^{1-\delta_1}\mu_{\hbar+1}, \\ T^{\theta_1}\widehat{\Psi}(\varsigma_\hbar) &= \frac{1}{\hbar^2}\varsigma_\hbar^{2-\theta_1}\mu_{\hbar-1} - \frac{2}{\hbar^2}\varsigma_\hbar^{2-\theta_1}\mu_\hbar + \frac{1}{\hbar^2}\varsigma_\hbar^{2-\theta_1}\mu_{\hbar+1}. \end{aligned} \tag{15}$$

Similarly, one can get the following regarding $\widehat{\Phi}$:

$$\begin{aligned} \widehat{\Phi}(\varsigma_\hbar) &= \frac{1}{6}\nu_{\hbar-1} + \frac{2}{3}\nu_\hbar + \frac{1}{6}\nu_{\hbar+1}, \\ T^{\delta_2}\widehat{\Phi}(\varsigma_\hbar) &= -\frac{1}{2\hbar}\varsigma_\hbar^{1-\delta_2}\nu_{\hbar-1} + \frac{1}{2\hbar}\varsigma_\hbar^{1-\delta_2}\nu_{\hbar+1}, \\ T^{\theta_2}\widehat{\Phi}(\varsigma_\hbar) &= \frac{1}{\hbar^2}\varsigma_\hbar^{2-\theta_2}\nu_{\hbar-1} - \frac{2}{\hbar^2}\varsigma_\hbar^{2-\theta_2}\nu_\hbar + \frac{1}{\hbar^2}\varsigma_\hbar^{2-\theta_2}\nu_{\hbar+1}. \end{aligned} \tag{16}$$

Firstly, we will theorize the linear conformable BVP systems. In this case, $N_1(\Psi,\Phi) = N_2(\Psi,\Phi) = 0$ in (1). Thus, the approximation solutions (10) and their CDs should satisfy the given differential equation at points $\varsigma = \varsigma_\hbar$ when $\hbar = 1, 2, \cdots, r$. This can be done by substituting (10) with (1). Anyhow, the resulting formulas for $\hbar = 1, 2, \cdots, r$ should be

$$\begin{cases} T^{\theta_1}\widehat{\Psi}(\varsigma_\hbar) + a_1(\varsigma_\hbar)T^{\delta_1}\widehat{\Psi}(\varsigma_\hbar) + a_2(\varsigma_\hbar)\widehat{\Psi}(\varsigma_\hbar) + T^{\theta_2}\widehat{\Phi}(\varsigma_\hbar) + a_3(\varsigma_\hbar)T^{\delta_2}\widehat{\Phi}(\varsigma_\hbar) + a_4(\varsigma_\hbar)\widehat{\Phi}(\varsigma_\hbar) = \mathcal{F}_1(\varsigma_\hbar), \\ T^{\theta_2}\widehat{\Phi}(\varsigma_\hbar) + b_1(\varsigma_\hbar)T^{\delta_2}\widehat{\Phi}(\varsigma_\hbar) + b_2(\varsigma_\hbar)\widehat{\Phi}(\varsigma_\hbar) + T^{\theta_1}\widehat{\Psi}(\varsigma_\hbar) + b_3(\varsigma_\hbar)T^{\delta_1}\widehat{\Psi}(\varsigma_\hbar) + b_4(\varsigma_\hbar)\widehat{\Psi}(\varsigma_\hbar) = \mathcal{F}_2(\varsigma_\hbar), \end{cases} \tag{17}$$

with the BCs

$$\begin{aligned} \widehat{\Psi}(\varsigma_\hbar) &= \alpha_1, \text{ for } \hbar = a, \\ \widehat{\Psi}(\varsigma_\hbar) &= \beta_1, \text{ for } \hbar = b, \\ \widehat{\Phi}(\varsigma_\hbar) &= \alpha_2, \text{ for } \hbar = a, \\ \widehat{\Phi}(\varsigma_\hbar) &= \beta_2, \text{ for } \hbar = b. \end{aligned} \tag{18}$$

To proceed more, (15) and (16) are substituted into (17) and (18) and will be resulting in $[G]_{2(r+3)\times 2(r+3)}B = Q$ system of unknowns $\mu_{-1}, \mu_0, \cdots, \mu_{r+1}, \nu_{-1}$, and $\nu_0, \cdots, \nu_{r+1}$ with

$$\begin{aligned} B &= [\mu_{-1}, \mu_0, \cdots, \mu_{r+1}, \nu_{-1}, \nu_0, \cdots, \nu_{r+1}]^T, \\ Q &= 6\left[\alpha_1, \hbar^2\mathcal{F}_1(\varsigma_0), \hbar^2\mathcal{F}_1(\varsigma_1), \cdots, \hbar^2\mathcal{F}_1(\varsigma_r), \beta_1, \alpha_2, \hbar^2\mathcal{F}_2 \cdot (\varsigma_0), \hbar^2\mathcal{F}_2(\varsigma_1), \cdots, \hbar^2\mathcal{F}_2(\varsigma_r), \beta_2\right]. \end{aligned} \tag{19}$$

Herein, $[G]_{2(r+3)\times 2(r+3)}$ and its corresponding elements are provided by

$$G = \begin{bmatrix} G_1 & \cdots & G_2 \\ \vdots & \ddots & \vdots \\ G_3 & \cdots & G_4 \end{bmatrix}. \tag{20}$$

$$G_1 = \begin{bmatrix} 1 & 4 & 1 & 0 & \cdots & 0 & 0 \\ g_1(\varsigma_0) & p_1(\varsigma_0) & q_1(\varsigma_0) & 0 & \cdots & 0 & 0 \\ 0 & g_1(\varsigma_1) & p_1(\varsigma_1) & q_1(\varsigma_1) & 0 & \cdots & 0 \\ \vdots & \vdots & \vdots & \vdots & \vdots & \vdots & \vdots \\ 0 & \cdots & \cdots & 0 & g_1(\varsigma_r) & p_1(\varsigma_r) & q_1(\varsigma_r) \\ 0 & \cdots & \cdots & 0 & 1 & 4 & 1 \end{bmatrix}, \tag{21}$$

$$G_2 = \begin{bmatrix} 0 & 0 & 0 & 0 & \cdots & 0 & 0 \\ g_2(\varsigma_0) & p_2(\varsigma_0) & q_2(\varsigma_0) & 0 & \cdots & 0 & 0 \\ 0 & g_2(\varsigma_1) & p_2(\varsigma_1) & q_2(\varsigma_1) & 0 & \cdots & 0 \\ \vdots & \vdots & \vdots & \vdots & \vdots & \vdots & \vdots \\ 0 & \cdots & \cdots & 0 & g_2(\varsigma_r) & p_2(\varsigma_r) & q_2(\varsigma_r) \\ 0 & \cdots & \cdots & 0 & 0 & 0 & 0 \end{bmatrix}, \tag{22}$$

$$G_3 = \begin{bmatrix} 0 & 0 & 0 & 0 & \cdots & 0 & 0 \\ g_3(\varsigma_0) & p_3(\varsigma_0) & q_3(\varsigma_0) & 0 & \cdots & 0 & 0 \\ 0 & g_3(\varsigma_1) & p_3(\varsigma_1) & q_3(\varsigma_1) & 0 & \cdots & 0 \\ \vdots & \vdots & \vdots & \vdots & \vdots & \vdots & \vdots \\ 0 & \cdots & \cdots & 0 & g_3(\varsigma_r) & p_3(\varsigma_r) & q_3(\varsigma_r) \\ 0 & \cdots & \cdots & 0 & 0 & 0 & 0 \end{bmatrix}, \quad (23)$$

$$G_4 = \begin{bmatrix} 1 & 4 & 1 & 0 & \cdots & 0 & 0 \\ g_4(\varsigma_0) & p_4(\varsigma_0) & q_4(\varsigma_0) & 0 & \cdots & 0 & 0 \\ 0 & g_4(\varsigma_1) & p_4(\varsigma_1) & q_4(\varsigma_1) & 0 & \cdots & 0 \\ \vdots & \vdots & \vdots & \vdots & \vdots & \vdots & \vdots \\ 0 & \cdots & \cdots & 0 & g_4(\varsigma_r) & p_4(\varsigma_r) & q_4(\varsigma_r) \\ 0 & \cdots & \cdots & 0 & 1 & 4 & 1 \end{bmatrix}. \quad (24)$$

Also, the coefficients in the submatrices G_1, G_2, G_3, and G_4 have the form

$$\begin{aligned} g_1(\varsigma_k) &= 6\varsigma_k^{2-\theta_1} - a_1(\varsigma_k)3\hbar\varsigma_k^{1-\delta_1} + \hbar^2 a_2(\varsigma_k), \\ p_1(\varsigma_k) &= -12\varsigma_k^{2-\theta_1} + 4\hbar^2 a_2(\varsigma_k), \\ q_1(\varsigma_k) &= 6\varsigma_k^{2-\theta_1} + a_1(\varsigma_k)3\hbar\varsigma_k^{1-\delta_1} + \hbar^2 a_2(\varsigma_k). \end{aligned} \quad (25)$$

$$\begin{aligned} g_2(\varsigma_k) &= 6\varsigma_k^{2-\theta_2} + a_3(\varsigma_k)3\hbar\varsigma_k^{1-\delta_2} + \hbar^2 a_4(\varsigma_k), \\ p_2(\varsigma_k) &= -12\varsigma_k^{2-\theta_2} + 4\hbar^2 a_4(\varsigma_k), \\ q_2(\varsigma_k) &= 6\varsigma_k^{2-\theta_2} + a_3(\varsigma_k)3\hbar\varsigma_k^{1-\delta_2} + \hbar^2 a_4(\varsigma_k). \end{aligned} \quad (26)$$

$$\begin{aligned} g_3(\varsigma_k) &= 6\varsigma_k^{2-\theta_2} + b_1(\varsigma_k)3\hbar\varsigma_k^{1-\delta_2} + \hbar^2 b_2(\varsigma_k), \\ p_3(\varsigma_k) &= -12\varsigma_k^{2-\theta_2} + 4\hbar^2 b_2(\varsigma_k), \\ q_3(\varsigma_k) &= 6\varsigma_k^{2-\theta_2} + b_1(\varsigma_k)3\hbar\varsigma_k^{1-\delta_2} + \hbar^2 b_2(\varsigma_k). \end{aligned} \quad (27)$$

$$\begin{aligned} g_4(\varsigma_k) &= 6\varsigma_k^{2-\theta_1} + b_3(\varsigma_k)3\hbar\varsigma_k^{2-\delta_1} + \hbar^2 b_4(\varsigma_k), \\ p_4(\varsigma_k) &= -12\varsigma_k^{2-\theta_1} + 4\hbar^2 b_4(\varsigma_k), \\ q_4(\varsigma_k) &= 6\varsigma_k^{2-\theta_1} + b_3(\varsigma_k)3\hbar\varsigma_k^{1-\delta_1} + \hbar^2 b_4(\varsigma_k). \end{aligned} \quad (28)$$

Secondly, we will theorize the nonlinear conformable BVP systems in this case of $N_1(\Psi, \Phi)$ and $N_2(\Psi, \Phi)$ are nonlinear functions of Ψ and Φ differ from zero. Anyhow, the substituting of (10) and its CDs in (1) and (2) at $\varsigma = \varsigma_k$ when $k = 0, 1, \cdots, r$ will gives

$$\begin{aligned} \mathscr{F}_1(\varsigma_k) = &\sum_{k=-1}^{r+1} \mu_k \left[T^{\theta_1} B_{k,3}(\varsigma_k) + a_1(\varsigma_k) T^{\delta_1} B_{k,3}(\varsigma_k) + a_2(\varsigma_k) B_{k,3}(\varsigma_k) \right] \\ &+ \sum_{k=-1}^{r+1} \nu_k \left[T^{\theta_2} B_{k,3}(\varsigma_k) + a_3(\varsigma_k) T^{\delta_2} B_{k,3}(\varsigma_k) + a_4(\varsigma_k) B_{k,3}(\varsigma_k) \right] \\ &+ N_1\left(\sum_{k=-1}^{r+1} \mu_k B_{k,3}(\varsigma_k), \sum_{k=-1}^{r+1} \nu_k B_{k,3}(\varsigma_k) \right). \end{aligned} \quad (29)$$

$$\begin{aligned} \mathscr{F}_2(\varsigma_k) = &\sum_{k=-1}^{r+1} \nu_k \left[T^{\theta_2} B_{k,3}(\varsigma_k) + b_1(\varsigma_k) T^{\delta_2} B_{k,3}(\varsigma_k) + b_2(\varsigma_k) B_{k,3}(\varsigma_k) \right] \\ &+ \sum_{k=-1}^{r+1} \mu_k \left[T^{\theta_1} B_{k,3}(\varsigma_k) + b_3(\varsigma_k) T^{\delta_1} B_{k,3}(\varsigma_k) + b_4(\varsigma_k) B_{k,3}(\varsigma_k) \right] \\ &+ N_2\left(\sum_{k=-1}^{r+1} \mu_k B_{k,3}(\varsigma_k), \sum_{k=-1}^{r+1} \nu_k B_{k,3}(\varsigma_k) \right). \end{aligned} \quad (30)$$

subject to the same BCs (18).

Recalling, the BS functions at $\{\varsigma_k\}_{k=0}^{r}$ are determined by substitution (12), (13), and (14) in (29), (30), and (18).

3. The CBSA for Handling Singular Systems of CDs

Now, we will spend the CBSA to build a numerical solution for the singular conformable LEP. We start by overcoming the singularity at $\varsigma = 0$ and then employing our proposed procedure scheme.

To solve the singular LEP in its CD case, we first write (3) in the standard form as

$$\begin{aligned} T^{\theta_1}\Psi(\varsigma) + \frac{\eta_1}{\varsigma} T^{\delta_1}\Psi(\varsigma) + Q_1(\varsigma, \Psi(\varsigma), \Phi(\varsigma)) = 0, \\ T^{\theta_2}\Phi(\varsigma) + \frac{\eta_2}{\varsigma} T^{\delta_2}\Phi(\varsigma) + Q_2(\varsigma, \Psi(\varsigma), \Phi(\varsigma)) = 0, \end{aligned} \quad (31)$$

concerning the BC

$$\begin{aligned} \Psi(0) = \rho_1, \Phi(0) = \varepsilon_1, \\ \Psi(1) = \rho_2, \Phi(1) = \varepsilon_2, \end{aligned} \quad (32)$$

where the set functions Q_1 and Q_2 are given as

$$\begin{aligned} Q_1(\varsigma, \Psi(\varsigma), \Phi(\varsigma)) = a_2(\varsigma)\Psi(\varsigma) + a_4(\varsigma)\Phi(\varsigma) + N_1(\Psi(\varsigma), \Phi(\varsigma)) - \mathscr{F}_1(\varsigma), \\ Q_2(\varsigma, \Psi(\varsigma), \Phi(\varsigma)) = b_2(\varsigma)\Phi(\varsigma) + b_4(\varsigma)\Psi(\varsigma) + N_2(\Psi(\varsigma), \Phi(\varsigma)) - \mathscr{F}_2(\varsigma). \end{aligned} \quad (33)$$

More focused, to take off the singularity $\varsigma = 0$, one can be employing the following next steps:

Multiplying (31) with ς gives

$$\begin{aligned}&\varsigma T^{\theta_1}\Psi(\varsigma)+\eta_1 T^{\delta_1}\Psi(\varsigma)+\varsigma Q_1(\varsigma,\Psi(\varsigma),\Phi(\varsigma))=0,\\&\varsigma T^{\theta_2}\Phi(\varsigma)+\eta_2 T^{\delta_2}\Phi(\varsigma)+\varsigma Q_2(\varsigma,\Psi(\varsigma),\Phi(\varsigma))=0.\end{aligned}\tag{34}$$

(i) Taking the CD of order δ_1 and δ_2, respectively, from both sides of (34), one has

$$\begin{aligned}&T^{\delta_1}\left(\varsigma T^{\theta_1}\Psi(\varsigma)\right)+\eta_1 T^{\delta_1}T^{\delta_1}\Psi(\varsigma)+T^{\delta_1}(\varsigma Q_1(\varsigma,\Psi(\varsigma),\Phi(\varsigma)))=0,\\&T^{\delta_2}\left(\varsigma T^{\theta_2}\Phi(\varsigma)\right)+\eta_2 T^{\delta_2}T^{\delta_2}\Phi(\varsigma)+T^{\delta_2}(\varsigma Q_2(\varsigma,\Psi(\varsigma),\Phi(\varsigma)))=0.\end{aligned}\tag{35}$$

(ii) Using the properties of the CD, one obtains

$$\begin{aligned}&\varsigma^{1-\delta_1}T^{\theta_1}\Psi(\varsigma)+\varsigma T^{\delta_1}T^{\theta_1}\Psi(\varsigma)+\eta_1 T^{\delta_1}T^{\delta_1}\Psi(\varsigma)\\&\quad+\varsigma^{1-\delta_1}Q_1(\varsigma,\Psi(\varsigma),\Phi(\varsigma))+\varsigma T^{\delta_1}Q_1(\varsigma,\Psi(\varsigma),\Phi(\varsigma))=0,\\&\varsigma^{1-\delta_2}T^{\theta_2}\Phi(\varsigma)+\varsigma T^{\delta_2}T^{\theta_2}\Phi(\varsigma)+\eta_2 T^{\delta_2}T^{\delta_2}\Phi(\varsigma)\\&\quad+\varsigma^{1-\delta_2}Q_2(\varsigma,\Psi(\varsigma),\Phi(\varsigma))+\varsigma T^{\delta_2}Q_2(\varsigma,\Psi(\varsigma),\Phi(\varsigma))=0.\end{aligned}\tag{36}$$

(iii) Substituting $\theta_1=\theta_2=2$ and $\delta_1=\delta_2=1$ in (36) at $\varsigma=0$, one gets

$$\begin{aligned}&(\eta_1+1)\Psi''(0)+Q_1(0,\Psi(\varsigma),\Phi(\varsigma))=0,\\&(\eta_2+1)\Phi''(0)+Q_2(0,\Psi(\varsigma),\Phi(\varsigma))=0.\end{aligned}\tag{37}$$

Putting (10) in (31), (32), and (37) at $\varsigma=\varsigma_\hbar$ it follows that

$$\begin{aligned}&T^{\theta_1}\widehat{\Psi}(\varsigma_\hbar)+\frac{\eta_1}{\varsigma_\hbar}T^{\delta_1}\widehat{\Psi}(\varsigma_\hbar)+Q_1\left(\varsigma_\hbar,\widehat{\Psi}(\varsigma_\hbar),\widehat{\Phi}(\varsigma_\hbar)\right)=0,\text{ for }\hbar=1,\cdots,\nu,\\&(\eta_1+1)\widehat{\Psi}''(0)+Q_1\left(0,\widehat{\Psi}(\varsigma_\hbar),\widehat{\Phi}(\varsigma_\hbar)\right)=0,\text{ for }\hbar=0,\\&T^{\theta_2}\widehat{\Phi}(\varsigma_\hbar)+\frac{\eta_2}{\varsigma_\hbar}T^{\delta_2}\widehat{\Phi}(\varsigma_\hbar)+Q_2\left(\varsigma_\hbar,\widehat{\Psi}(\varsigma_\hbar),\widehat{\Phi}(\varsigma_\hbar)\right)=0,\text{ for }\hbar=1,\cdots,\nu,\\&(\eta_2+1)\widehat{\Phi}''(0)+Q_2\left(0,\widehat{\Psi}(\varsigma_\hbar),\widehat{\Phi}(\varsigma_\hbar)\right)=0,\text{ for }\hbar=0,\\&\widehat{\Psi}(\varsigma_0)=\rho_1,\text{ for }\varsigma_0=0,\\&\widehat{\Psi}(\varsigma_\nu)=\rho_2,\text{ for }\varsigma_\nu=1,\\&\widehat{\Phi}(\varsigma_0)=\varepsilon_1,\text{ for }\varsigma_0=0,\\&\widehat{\Phi}(\varsigma_\nu)=\varepsilon_2,\text{ for }\varsigma_\nu=1.\end{aligned}\tag{38}$$

This drives a system of $2(\nu+3)$ equations with the same number of unknowns which can be treated to obtain the vectors $\mu_\hbar$ and $\nu_\hbar$; consequently an approximation of $\Psi(\varsigma)$ and $\Phi(\varsigma)$.

4. Error and Convergence Analysis

Herein, to guarantee the behavior of the approximate CBSA solutions, we utilized two main analyses: the first one concerning error analysis and the second one concerning convergence analysis.

Using the CBSA approximations (15) and (16), the following relations can be established:

$$\begin{aligned}&\frac{\hbar}{6}\left[\left(\frac{1}{6}\right)\widehat{\Psi}'(\varsigma_{\hbar-1})+\left(\frac{2}{3}\right)\widehat{\Psi}'(\varsigma_\hbar)+\left(\frac{1}{6}\right)\widehat{\Psi}'(\varsigma_{\hbar+1})\right]\\&\quad=\frac{1}{2}\varsigma_\hbar^{1-\delta_1}\left[\widehat{\Psi}(\varsigma_{\hbar+1})+\widehat{\Psi}(\varsigma_{\hbar-1})\right],\end{aligned}\tag{39}$$

$$\begin{aligned}\hbar^2T^{\theta_1}\widehat{\Psi}(\varsigma_\hbar)=\varsigma_\hbar^{2-\theta_1}&\Big[6\left(\widehat{\Psi}(\varsigma_{\hbar+1})+\widehat{\Psi}(\varsigma_\hbar)\right)\\&-2\hbar\left(2\widehat{\Psi}'(\varsigma_\hbar)+\widehat{\Psi}'(\varsigma_{\hbar+1})\right)\Big].\end{aligned}\tag{40}$$

In notation for the operator $E^\epsilon(\widehat{\Psi}(\varsigma_\hbar))=\widehat{\Psi}(\varsigma_{\hbar+\epsilon})$ with $\epsilon\in\mathbb{Z}$, we can write (39) and (40) as

$$\frac{\hbar}{6}\left[\left(\frac{1}{6}\right)E^{-1}+\left(\frac{2}{3}\right)I+\left(\frac{1}{6}\right)E\right]\widehat{\Psi}'(\varsigma_\hbar)=\frac{1}{2}\varsigma_\hbar^{1-\delta_1}\left[E+E^{-1}\right]\Psi(\varsigma_\hbar),\tag{41}$$

$$\hbar^2T^{\theta_1}\widehat{\Psi}(\varsigma_\hbar)=\varsigma_\hbar^{2-\theta_1}\left[6(E+\mathrm{I})\Psi(\varsigma_\hbar)-2\hbar(2\mathrm{I}+E)\Psi'(\varsigma_\hbar)\right].\tag{42}$$

Moreover, if $\Lambda=d/d\varsigma$, we have got

$$\begin{aligned}E\left(\widehat{\Psi}(\varsigma_\hbar)\right)=\widehat{\Psi}(\varsigma_\hbar+\hbar)&=\sum_{\hbar=0}^{\infty}\frac{\hbar^\hbar\widehat{\Psi}^{(\hbar)}(\varsigma_\hbar)}{\hbar!}\\&=\sum_{\hbar=0}^{\infty}\frac{(\hbar\Lambda)^\hbar}{\hbar!}\widehat{\Psi}(\varsigma_\hbar)=e^{(\hbar\Lambda)}\widehat{\Psi}(\varsigma_\hbar).\end{aligned}\tag{43}$$

It implies that $E=e^{\hbar\Lambda}$. Similarly, we have $E^{-1}=e^{-\hbar\Lambda}$ and we can get

$$\begin{aligned}&E+E^{-1}=2\left(1+\frac{(\hbar\Lambda)^2}{2!}+\frac{(\hbar\Lambda)^4}{4!}+\frac{(\hbar\Lambda)^6}{6!}+\cdots\right),\\&E-E^{-1}=2\left(\hbar\Lambda+\frac{(\hbar\Lambda)^3}{3!}+\frac{(\hbar\Lambda)^5}{5!}+\frac{(\hbar\Lambda)^7}{7!}+\cdots\right).\end{aligned}\tag{44}$$

Thus, (39) can be represented serially as

$$\left[1+\frac{1}{3}\left(\frac{(\hbar\Lambda)^2}{2!}+\frac{(\hbar\Lambda)^4}{4!}+\frac{(\hbar\Lambda)^6}{6!}+\cdots\right)\right]\widehat{\Psi}'(\varsigma_\hbar) = \varsigma_\hbar^{1-\delta_1}\left(\Lambda+\frac{\hbar^2\Lambda^3}{3!}+\frac{\hbar^4\Lambda^5}{5!}+\frac{\hbar^6\Lambda^7}{7!}+\cdots\right)\Psi(\varsigma_\hbar), \tag{45}$$

$$\widehat{\Psi}'(\varsigma_\hbar)=\varsigma_\hbar^{1-\delta_1}\left(\Lambda+\frac{\hbar^2\Lambda^3}{3!}+\frac{\hbar^4\Lambda^5}{5!}+\frac{\hbar^6\Lambda^7}{7!}+\cdots\right)\cdot\left[1+\left(\frac{(\hbar\Lambda)^2}{6}+\frac{(\hbar\Lambda)^4}{72}+\frac{(\hbar\Lambda)^6}{2160}+\cdots\right)\right]^{-1}\Psi(\varsigma_\hbar), \tag{46}$$

$$\begin{aligned}\widehat{\Psi}'(\varsigma_\hbar)&=\varsigma_\hbar^{1-\delta_1}\left(\Lambda+\frac{\hbar^2\Lambda^3}{3!}+\frac{\hbar^4\Lambda^5}{5!}+\frac{\hbar^6\Lambda^7}{7!}+\cdots\right)\\&\quad\cdot\left[1-\left(\frac{(\hbar\Lambda)^2}{6}+\frac{(\hbar\Lambda)^4}{72}+\frac{(\hbar\Lambda)^6}{2160}+\cdots\right)+\left(\frac{(\hbar\Lambda)^2}{6}+\frac{(\hbar\Lambda)^4}{72}+\cdots\right)^2+\cdots\right]\Psi(\varsigma_\hbar)\\&=\varsigma_\hbar^{1-\delta_1}\left(\Lambda+\frac{\hbar^2\Lambda^3}{3!}+\frac{\hbar^4\Lambda^5}{5!}+\frac{\hbar^6\Lambda^7}{7!}+\cdots\right)\cdot\left(1-\frac{(\hbar\Lambda)^2}{6}+\frac{(\hbar\Lambda)^4}{72}-\frac{(\hbar\Lambda)^6}{2160}+\cdots\right)\Psi(\varsigma_\hbar)\\&=\varsigma_\hbar^{1-\delta_1}\left(\Lambda-\frac{\hbar^4\Lambda^5}{180}+\frac{\hbar^6\Lambda^7}{1512}-\cdots\right)\Psi(\varsigma_\hbar).\end{aligned} \tag{47}$$

Hence, after ranking, one can write

$$\begin{aligned}T^{\delta_1}\widehat{\Psi}(\varsigma_\hbar)&=\varsigma_\hbar^{1-\delta_1}\Psi'(\varsigma_\hbar)-\frac{\hbar^4}{180}\varsigma_\hbar^{1-\delta_1}\Psi^{(5)}(\varsigma_\hbar)+\cdots\\&=T^{\delta_1}\Psi(\varsigma_\hbar)-\frac{\hbar^4}{180}\varsigma_\hbar^{1-\delta_1}\Psi^{(5)}(\varsigma_\hbar)+\cdots.\end{aligned} \tag{48}$$

By applying the same technique as (40), we may extract

$$\begin{aligned}T^{\theta_1}\widehat{\Psi}(\varsigma_\hbar)&=\varsigma_\hbar^{2-\theta_1}\Psi''(\varsigma_\hbar)-\frac{\hbar^2}{12}\varsigma_\hbar^{2-\theta_1}\Psi^{(4)}(\varsigma_\hbar)+\frac{\hbar^4}{360}\varsigma_\hbar^{2-\theta_1}\Psi^{(6)}(\varsigma_\hbar)+\cdots\\&=T^{\theta_1}\Psi(\varsigma_\hbar)-\frac{\hbar^2}{12}\varsigma_\hbar^{2-\theta_1}\Psi^{(4)}(\varsigma_\hbar)+\frac{\hbar^4}{360}\varsigma_\hbar^{2-\theta_1}\Psi^{(6)}(\varsigma_\hbar)+\cdots.\end{aligned} \tag{49}$$

Let us now describe the expression $e_1(\varsigma)=\Psi(\varsigma)-\widehat{\Psi}(\varsigma)$ for error. Using (48) and (49) in $e(\varsigma_\hbar)$ expansion of the Taylor series, one gets

$$\begin{aligned}e_1(\varsigma_\hbar+\hbar)&=e(\varsigma_\hbar)+\hbar e'(\varsigma_\hbar)+\frac{\hbar^2}{2!}e''(\varsigma_\hbar)+\cdots\\&=\left(\Psi(\varsigma_\hbar)-\widehat{\Psi}(\varsigma_\hbar)\right)+\hbar\left(\Psi'(\varsigma_\hbar)-\widehat{\Psi}'(\varsigma_\hbar)\right)+\frac{\hbar^2}{2!}\left(\Psi''(\varsigma_\hbar)-\widehat{\Psi}''(\varsigma_\hbar)\right)+\cdots\\&=\left(\Psi(\varsigma_\hbar)-\widehat{\Psi}(\varsigma_\hbar)\right)+\hbar\varsigma_\hbar^{\delta_1-1}\left(T^{\delta_1}\widehat{\Psi}(\varsigma_\hbar)-T^{\delta_1}\Psi(\varsigma_\hbar)\right)+\frac{\hbar^2}{2!}\varsigma_\hbar^{\theta_1-2}\left(T^{\theta_1}\widehat{\Psi}(\varsigma_\hbar)-T^{\theta_1}\Psi(\varsigma_\hbar)\right)+\cdots.\end{aligned} \tag{50}$$

Hence,

$$e_1(\varsigma_\hbar+\hbar)=-\frac{\hbar^4}{24}\Psi^{(4)}(\varsigma_\hbar)+\frac{\hbar^5}{180}\Psi^{(5)}(\varsigma_\hbar)+\frac{\hbar^6}{720}\Psi^{(6)}(\varsigma_\hbar)+\cdots. \tag{51}$$

Similarly, we have

$$e_2(\varsigma_\hbar+\hbar)=-\frac{\hbar^4}{24}\Phi^{(4)}(\varsigma_\hbar)+\frac{\hbar^5}{180}\Phi^{(5)}(\varsigma_\hbar)+\frac{\hbar^6}{720}\Phi^{(6)}(\varsigma_\hbar)+\cdots. \tag{52}$$

As a score, it is obvious that our CBSA approximation is $O(\hbar^4)$ accurate.

In the convergence approach, we will prove the convergence of the CBSA for Dirichlet BC. Let $\Psi(\varsigma)$ and $\Phi(\varsigma)$ be the exact solutions of (1) and (2). Also, let $\widehat{\Psi}(\varsigma)$ and $\widehat{\Phi}(\varsigma)$ in (10) be the cubic BS approximations to $\Psi(\varsigma)$ and $\Phi(\varsigma)$, respectively. Due to round-off errors in computations, we will assume that $\mathcal{S}_1(\varsigma)=\sum_{\hbar=-1}^{r+1}\widehat{\mu}_\hbar B_{\hbar,3}(\varsigma)$ and $S_2(\varsigma)=\sum_{\hbar=-1}^{r+1}\widehat{\nu}_\hbar B_{\hbar,3}(\varsigma)$ be the computed BS approximations to $\widehat{\Psi}(\varsigma)$ and $\widehat{\Phi}(\varsigma)$, respectively, where $\widehat{\mu}_\hbar=(\widehat{\mu}_{-1},\widehat{\mu}_0,\cdots,\widehat{\mu}_{r+1})$ and $\widehat{\nu}_\hbar=(\widehat{\nu}_{-1},\widehat{\nu}_0,\cdots,\widehat{\nu}_{r+1})$.

To estimate the errors $\|(\Psi(\varsigma),\Phi(\varsigma))-(\widehat{\Psi}(\varsigma),\widehat{\Phi}(\varsigma))\|_\infty$ we must estimate $\|(\Psi(\varsigma),\Phi(\varsigma))-(\mathcal{S}_1(\varsigma),\mathcal{S}_1(\varsigma))\|_\infty$ and $\|(\mathcal{S}_1(\varsigma),\mathcal{S}_1(\varsigma))-(\widehat{\Psi}(\varsigma),\widehat{\Phi}(\varsigma))\|_\infty$, wherein $\|.\|$ represents the ∞-norm.

Firstly, we will consider the linear cases as follows:

$$\begin{aligned}L_1\left(\widehat{\Psi},\widehat{\Phi}\right)&=\mathcal{F}_1(\varsigma),\\L_2\left(\widehat{\Psi},\widehat{\Phi}\right)&=\mathcal{F}_2(\varsigma),\end{aligned} \tag{53}$$

with the BCs (2) will lead to the linear system $GB=Q$.

$$\begin{aligned}L_1(\mathcal{S}_1,\mathcal{S}_2)&=\mathcal{F}_1^*(\varsigma),\\L_2(\mathcal{S}_1,\mathcal{S}_2)&=\mathcal{F}_2^*(\varsigma),\end{aligned} \tag{54}$$

with the BCs (2) will lead to the linear system $GB^*=Q^*$.

Then it follows that $G(B-B^*)=(Q-Q^*)$, where

$$B-B^*=[(\widehat{\mu}_{-1}-\mu_{-1}),\cdots,(\widehat{\mu}_{r+1}-\mu_{r+1}),(\widehat{\nu}_{-1}-\nu_{-1}),\cdots,(\widehat{\nu}_{r+1}-\nu_{r+1})]^T, \tag{55}$$

$$\begin{aligned}Q-Q^*=6\hbar^2[0,(\mathcal{F}_1(\varsigma_0)-\mathcal{F}_1^*(\varsigma_0)),\cdots,(\mathcal{F}_1(\varsigma_r)\\ -\mathcal{F}_1^*(\varsigma_r)),0,0,(\mathcal{F}_2(\varsigma_0)\\ -\mathcal{F}_2^*(\varsigma_0)),\cdots,(\mathcal{F}_2(\varsigma_r)-\mathcal{F}_2^*(\varsigma_r)),0].\end{aligned} \tag{56}$$

Theorem 1. *Suppose that $\Psi(\varsigma),\Phi(\varsigma)\in C^5[a,b]$ and $\Pi:\{a=\varsigma_0<\varsigma_1<\cdots<\varsigma_{r-1}<\varsigma_r=b\}$ be the equally spaced partition of $[a,b]$ with step size $\hbar$. If $\mathcal{S}$ is the cubic BS function that interpolates the values of the function u at the knots $\varsigma_0,\cdots,\varsigma_r\in\Pi$, then there exist constants γ_q which do not depend on $\hbar$ such that for $\varsigma\in[a,b]$ with $b>a\geq 0$, we have*

$$\begin{aligned}&\|(\Psi(\varsigma),\Phi(\varsigma))-(\mathcal{S}_1(\varsigma),\mathcal{S}_1(\varsigma))\|_\infty\leq\gamma_1\hbar^4,\\ &\left\|T^\delta(\Psi(\varsigma),\Phi(\varsigma))-T^\delta(\mathcal{S}_1(\varsigma),\mathcal{S}_1(\varsigma))\right\|_\infty\leq\gamma_2\hbar^4, 0<\delta\leq 1,\\ &\left\|T^\theta(\Psi(\varsigma),\Phi(\varsigma))-T^\theta(\mathcal{S}_1(\varsigma),\mathcal{S}_1(\varsigma))\right\|_\infty\leq\gamma_3\hbar^2, 1<\theta\leq 2.\end{aligned} \tag{57}$$

Proof. Using the prior results, one can find

$$\begin{aligned}|\mathcal{F}_1(\varsigma_k)-\mathcal{F}_1^*(\varsigma_k)|&=\left|\mathrm{L}_1\left(\widehat{\Psi},\widehat{\Phi}\right)-\mathrm{L}_1(\mathcal{S}_1,\mathcal{S}_2)\right|\\ &\leq\left|T^{\theta_1}\widehat{\Psi}(\varsigma_k)-T^{\theta_1}\mathcal{S}_1(\varsigma_k)\right|\\ &\quad+|a_1(\varsigma_k)|\left|T^{\delta_1}\widehat{\Psi}(\varsigma_k)-T^{\delta_1}\mathcal{S}_1(\varsigma_k)\right|\\ &\quad+|a_2(\varsigma_k)|\left|\widehat{\Psi}(\varsigma_k)-\mathcal{S}_1(\varsigma_k)\right|\\ &\quad+\left|T^{\theta_2}\widehat{\Phi}(\varsigma_k)-T^{\theta_2}\mathcal{S}_2(\varsigma_k)\right|\\ &\quad+|a_3(\varsigma_k)|\left|T^{\delta_2}\widehat{\Phi}(\varsigma_k)-T^{\delta_2}\mathcal{S}_2(\varsigma_k)\right|\\ &\quad+|a_4(\varsigma_k)|\left|\widehat{\Phi}(\varsigma_k)-\mathcal{S}_2(\varsigma_k)\right|.\end{aligned} \tag{58}$$

Again, one can write

$$\begin{aligned}|\mathcal{F}_1(\varsigma_k)-\mathcal{F}_1^*(\varsigma_k)|\leq\gamma_3\hbar^2+\|a_1(\varsigma_k)\|_\infty\gamma_2\hbar^4\\ +\|a_2(\varsigma_k)\|_\infty\gamma_1\hbar^4+\gamma_3'\hbar^2\\ +\|a_3(\varsigma_k)\|_\infty\gamma_2'\hbar^4+\|a_4(\varsigma_k)\|_\infty\gamma_1'\hbar^4.\end{aligned} \tag{59}$$

Since $\hbar\ll 1$, one has

$$\|\mathcal{F}_1(\varsigma_k)-\mathcal{F}_1^*(\varsigma_k)\|\leq M\hbar^2, \tag{60}$$

$$\|\mathcal{F}_2(\varsigma_k)-\mathcal{F}_2^*(\varsigma_k)\|\leq M_1\hbar^2. \tag{61}$$

From (60) and (61), we can find

$$\|Q-Q^*\|_\infty\leq 6\hbar^4 M. \tag{62}$$

The matrix G is monotone and thus nonsingular [31]. Hence, we can write

$$(B-B^*)=G^{-1}(Q-Q^*). \tag{63}$$

Now, we determine row sums $\mathcal{S}_{-1},\mathcal{S}_0,\cdots,\mathcal{S}_{2(r+2)}$ of the matrix G as follows:

$$\begin{gathered}\mathcal{S}_{-1}=6,\\ \mathcal{S}_p=\sum_{q=0}^{r}a_{pq}=6\hbar^2a_2(\varsigma_k)+6\hbar^2a_4(\varsigma_k), p=0,\cdots,r+1,\\ \mathcal{S}_{r+1}=6,\\ \mathcal{S}_{r+2}=6,\\ \mathcal{S}_p'=\sum_{q=r+3}^{2r+3}a_{pq}=6\hbar^2b_2(\varsigma_k)+6\hbar^2b_4(\varsigma_k), p=r+3,\cdots,2r+3,\\ \mathcal{S}_{2r+4}=6.\end{gathered} \tag{64}$$

Thus, if a_{kq} indicates the $(k,q)^{\text{th}}$ element of the matrix G, then we can write

$$\mathcal{S}_k=\sum_{q=-1}^{2r+4}a_{kq}, k=-1,\cdots,2r+4. \tag{65}$$

Let a_{pk}^{-1} indicates the $(k,q)^{\text{th}}$ element of G^{-1}. Then, the matrix norms are defined as

$$\|G^{-1}\|=\max_{-1\leq p\leq 2r+4}\sum_{k=-1}^{2r+4}|a_{pk}^{-1}|. \tag{66}$$

So, we have

$$I=G^{-1}G=\sum_{k=-1}^{2r+4}a_{pk}^{-1}a_{kq}, p=-1,\cdots,2r+4, q=-1,\cdots,2r+4, \tag{67}$$

and $\|G^{-1}G\|=1$ which gives also

$$\begin{gathered}\sum_{q=-1}^{2r+4}\sum_{k=-1}^{2r+4}a_{pk}^{-1}a_{kq}=1, p=-1,\cdots,2r+4,\\ \sum_{k=-1}^{2r+4}a_{pk}^{-1}\left(\sum_{q=-1}^{2r+4}a_{kq}\right)=1, p=-1,\cdots,2r+4,\\ \sum_{k=-1}^{2r+4}a_{pk}^{-1}\mathcal{S}_k=1, p=-1,\cdots,2r+4.\end{gathered} \tag{68}$$

Let $\mathcal{S}_{\hbar}^* = \min \mathcal{S}_{\hbar}$. Then we get

$$\sum_{\hbar=-1}^{2r+4} a_{p\hbar}^{-1} \leq \frac{1}{\mathcal{S}_{\hbar}^*}, \tag{69}$$

where $\mathcal{S}_{\hbar}^* = 6\hbar^2 \min \left(a_2(\varsigma_{\hbar}) + a_4(\varsigma_{\hbar}), b_2(\varsigma_{\hbar}) + b_4(\varsigma_{\hbar})\right) = 6\hbar^2 M$. Thus

$$\|B - B^*\| = \left\|G^{-1}\right\| \|(Q - Q^*\| \leq \hbar^2 \widehat{M}. \tag{70}$$

Using the definition of cubic BS basis functions in (7), one can obtain that

$$\sum_{\hbar=-1}^{r+1} \left|B_{\hbar,3}(\varsigma)\right| \leq \frac{5}{3}, a \leq \varsigma \leq b, \tag{71}$$

$$\begin{aligned} &\left\|\left(\mathcal{S}_1(\varsigma) - \widehat{\Psi}(\varsigma), \mathcal{S}_2(\varsigma) - \widehat{\Phi}(\varsigma)\right)\right\|_\infty \\ &= \left\|\left(\sum_{\hbar=-1}^{r+1} \widehat{\mu}_{\hbar} B_{\hbar,3}(\varsigma) - \sum_{\hbar=-1}^{r+1} \mu_{\hbar} B_{\hbar,3}(\varsigma), \sum_{\hbar=-1}^{r+1} \widehat{\nu}_{\hbar} B_{\hbar,3}(\varsigma) - \sum_{\hbar=-1}^{r+1} \nu_{\hbar} B_{\hbar,3}(\varsigma)\right)\right\| \\ &= \|(\widehat{\mu}_{\hbar} - \mu_{\hbar}, \widehat{\nu}_{\hbar} - \nu_{\hbar})\| \sum_{\hbar=-1}^{r+1} \left|B_{\hbar,3}(\varsigma)\right| \leq \frac{5}{3}\hbar^2 \widehat{M}. \end{aligned} \tag{72}$$

Hence,

$$\begin{aligned} &\left\|(\mathcal{S}_1(\varsigma), \mathcal{S}_1(\varsigma)) - \left(\widehat{\Psi}(\varsigma), \widehat{\Phi}(\varsigma)\right)\right\|_\infty \\ &= \left\|\left(\mathcal{S}_1(\varsigma) - \widehat{\Psi}(\varsigma), \mathcal{S}_2(\varsigma) - \widehat{\Phi}(\varsigma)\right)\right\|_\infty \\ &\leq \frac{5}{3}\hbar^2 \widehat{M}. \end{aligned} \tag{73}$$

Thus, $\|(\Psi(\varsigma), \Phi(\varsigma)) - (\mathcal{S}_1(\varsigma), \mathcal{S}_1(\varsigma))\|_\infty \leq \gamma_1 \hbar^4$ and $\|(\Psi(\varsigma), \Phi(\varsigma)) - (\widehat{\Psi}(\varsigma), \widehat{\Phi}(\varsigma))\|_\infty \leq w\hbar^2$. □

5. Application and Numerical Simulation

To highlight the importance and strength of what we presented in terms of analysis and mathematical construction concerning the CBSA, we need to discuss several practical examples, and this is what we will present in this special part.

Hither, $\widehat{\Psi}(\varsigma_{\hbar}), \widehat{\Phi}(\varsigma_{\hbar})$ will approximate $\Psi(\varsigma_{\hbar}), \Phi(\varsigma_{\hbar})$, respectively. Indeed, $\mathcal{A}_\Psi(\varsigma_{\hbar}) = |\Psi - \widehat{\Psi}|(\varsigma_{\hbar})$ and $\mathcal{A}_\Phi(\varsigma_{\hbar}) = |\Phi - \widehat{\Phi}|(\varsigma_{\hbar})$ denote the absolute errors, whilst $\mathcal{R}_\Psi(\varsigma_{\hbar}) = |\Psi - \widehat{\Psi}||\Psi|^{-1}(\varsigma_{\hbar})$ and $\mathcal{R}_\Phi(\varsigma_{\hbar}) = |\Phi - \widehat{\Phi}||\Phi|^{-1}(\varsigma_{\hbar})$ denote the relative errors.

Example 2. We test the following conformable linear system:

$$\begin{aligned} &T^{4/3}\Psi(\varsigma) - 3\varsigma^3 T^{1/2}\Psi(\varsigma) + T^{5/4}\Phi(\varsigma) \\ &\quad + T^{1/3}\Phi(\varsigma) + (1 + \varsigma)\Phi(\varsigma) = \mathcal{F}_1(\varsigma), \\ &T^{5/4}\Phi(\varsigma) + \cosh(\varsigma) T^{1/3}\Phi(\varsigma) + \frac{\varsigma^3}{\varsigma^2(1-\varsigma)+1}\Phi(\varsigma) + T^{4/3}\Psi(\varsigma) \\ &\quad + T^{1/2}\Psi(\varsigma) + \left(2\varsigma^2 - 3\varsigma\right)\Psi(\varsigma) = \mathcal{F}_2(\varsigma), \end{aligned} \tag{74}$$

$$\begin{aligned} \mathcal{F}_1(\varsigma) &= -2\varsigma^{2/3} - 2\varsigma^{3/4} - 2\varsigma^{5/3} + 6\varsigma^{7/4} \\ &\quad - \varsigma^2 + 3\varsigma^{8/3} - 3\varsigma^{7/2} + \varsigma^4 + 6\varsigma^{9/2}, \\ \mathcal{F}_2(\varsigma) &= (1 - 2\varsigma)\sqrt{\varsigma} - \varsigma^{2/3} + 2\varsigma^{3/4}(-1 + 3\varsigma) \\ &\quad + \varsigma^3\left(3 - 5\varsigma + 2\varsigma^2\right) - \frac{(-1+\varsigma)\varsigma^4}{1 + \varsigma^2 - \varsigma^3} \\ &\quad + \varsigma^{5/3}(-2 + 3\varsigma)\cosh(\varsigma), \end{aligned} \tag{75}$$

concerning the BCs

$$\begin{aligned} &\Psi(0.5) = 0.25, \Phi(0.5) = -0.125, \\ &\Psi(1) = \Phi(1) = 0. \end{aligned} \tag{76}$$

Herein, the exact solutions are

$$\begin{aligned} \Psi(\varsigma) &= \varsigma(1 - \varsigma), \\ \Phi(\varsigma) &= \varsigma^2(\varsigma - 1). \end{aligned} \tag{77}$$

Concerning Example 2 and using CBSA, the related numerical solutions for $r = 10$ are displayed in Table 1. Additionally, the graphics of $\mathcal{A}_\Psi(\varsigma_{\hbar})$ and $\mathcal{A}_\Phi(\varsigma_{\hbar})$ for $r = 10$ are given in Figure 1. Hither, it can be observed from the figure and table that the result data is sufficient accuracy and are firmly connected.

Example 3. We test the following conformable nonlinear system:

$$\begin{aligned} &T^{3/2}\Psi(\varsigma) + T^{1/4}\Psi(\varsigma) + T^{3/2}\Psi(\varsigma)\Psi(\varsigma) \\ &\quad + \exp(\Phi(\varsigma)) + \cos(\varsigma)\Phi(\varsigma) = \mathcal{F}_1(\varsigma), \\ &T^{3/2}\Phi(\varsigma) + T^{1/4}\Phi(\varsigma) + T^{1/2}\Psi(\varsigma) T^{1/4}\Phi(\varsigma) \\ &\quad + \ln(\Psi(\varsigma)) + 2\varsigma\Phi(\varsigma) = \mathcal{F}_2(\varsigma), \end{aligned} \tag{78}$$

$$\begin{aligned} \mathcal{F}_1(\varsigma) &= e^{-2\varsigma^2}\left[e^{2\varsigma^2}\left(\left(1 + \varsigma^2 + \cos(\varsigma)\ln\left(1 + \varsigma^2\right)\right)\right)\right. \\ &\quad \left. + 2\sqrt{\varsigma}\left(-1 + 2\varsigma^2\right) + 2\sqrt{\varsigma}e^{\varsigma^2}\left(-1 - \varsigma^{5/4} + 2\varsigma^2\right.\right], \\ \mathcal{F}_2(\varsigma) &= \frac{1}{1+\varsigma^2}\left(-\frac{2\sqrt{\varsigma}\left(1 - \varsigma^2\right)}{1 + \varsigma^2} + 2\varsigma^{7/4} - 4e^{\varsigma^2}\varsigma^{13/4}\right) \\ &\quad + e^{-2\varsigma^2} + 2\varsigma\ln\left(1 + \varsigma^2\right), \end{aligned} \tag{79}$$

Table 1: Solutions result with $\mathscr{r} = 10$ in Example 2.

ς_k	$\Psi(\varsigma_k)$	$\widehat{\Psi}(\varsigma_k)$	$\mathscr{A}_\Psi(\varsigma_k)$	$\Phi(\varsigma_k)$	$\widehat{\Phi}(\varsigma_k)$	$\mathscr{A}_\Phi(\varsigma_k)$
0.50	0.2500	0.2500	0	-0.125000	-0.125000	0
0.55	0.2475	0.2475	0	-0.136125	-0.136125	1.1102×10^{-16}
0.60	0.2400	0.2400	1.9429×10^{-16}	-0.144000	-0.144000	2.4980×10^{-16}
0.65	0.2275	0.2275	2.7756×10^{-17}	-0.147875	-0.147875	1.3045×10^{-15}
0.70	0.2100	0.2100	9.4369×10^{-16}	-0.147000	-0.147000	3.0531×10^{-16}
0.75	0.1875	0.1875	1.1102×10^{-16}	-0.140625	-0.140625	1.1657×10^{-15}
0.80	0.1600	0.1600	9.4369×10^{-16}	-0.128000	-0.128000	8.3267×10^{-17}
0.85	0.1275	0.1275	2.7756×10^{-17}	-0.108375	-0.108375	1.3739×10^{-15}
0.90	0.0900	0.0900	1.1935×10^{-15}	-0.081000	-0.081000	2.3592×10^{-16}
0.95	0.0475	0.0475	1.2490×10^{-16}	-0.045125	-0.045125	1.2212×10^{-15}
1.00	0	0	0	0	0	0

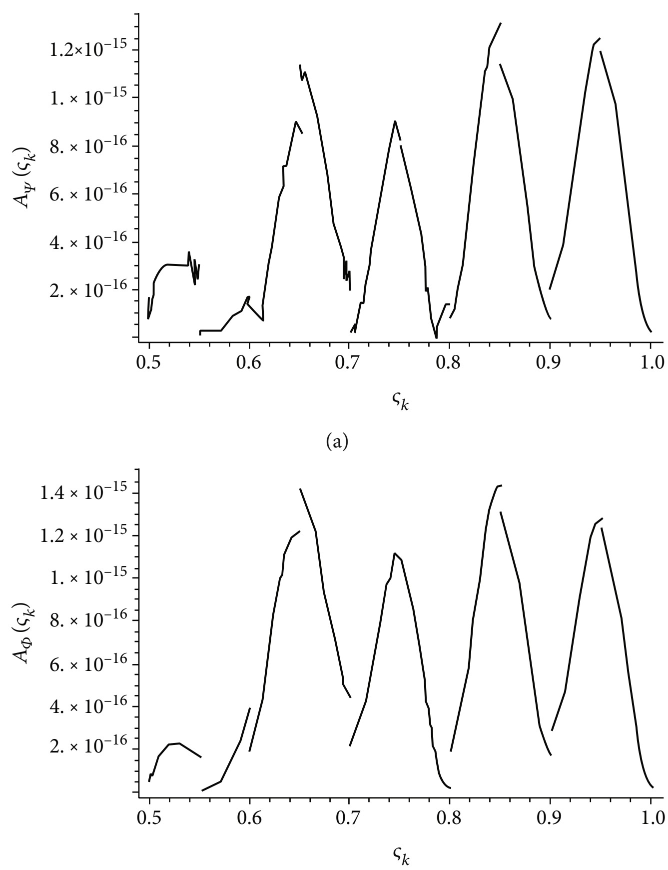

(a)

(b)

Figure 1: Graphical results with $\mathscr{r} = 10$ in Example 2: (a) $\mathscr{A}_\Psi(\varsigma_k)$ and (b) $\mathscr{A}_\Phi(\varsigma_k)$.

concerning the BCs

$$\begin{aligned} &\Psi(1) = e^{-1}, \Phi(1) = \ln(2), \\ &\Psi(2) = e^{-4}, \Phi(2) = \ln(5). \end{aligned} \tag{80}$$

Herein, the exact solutions are

$$\begin{aligned} &\Psi(\varsigma) = e^{-\varsigma^2}, \\ &\Phi(\varsigma) = \ln\left(1 + \varsigma^2\right). \end{aligned} \tag{81}$$

Table 2: Solutions result of $\mathscr{A}_{\Psi}(\varsigma_{\hbar})$ with $\nu = \{10,20,40,80,160\}$ in Example 3.

$\varsigma_{\hbar}$	$\nu = 10$	$\nu = 20$	$\nu = 40$	$\nu = 80$	$\nu = 160$
1	0	0	0	0	0
1.1	1.41417×10^{-4}	3.53949×10^{-5}	8.85131×10^{-6}	2.21299×10^{-6}	5.53257×10^{-7}
1.2	2.17765×10^{-4}	5.44737×10^{-5}	1.36205×10^{-5}	3.40526×10^{-6}	8.51323×10^{-7}
1.3	2.41486×10^{-4}	6.03663×10^{-5}	1.50913×10^{-5}	3.77281×10^{-6}	9.43202×10^{-7}
1.4	2.27054×10^{-4}	5.67117×10^{-5}	1.41747×10^{-5}	3.54349×10^{-6}	8.85859×10^{-7}
1.5	1.88993×10^{-4}	4.71574×10^{-5}	1.17837×10^{-5}	2.94558×10^{-6}	7.36374×10^{-7}
1.6	1.40251×10^{-4}	3.49512×10^{-5}	8.73088×10^{-6}	2.18229×10^{-6}	5.45546×10^{-7}
1.7	9.11547×10^{-5}	2.26784×10^{-5}	5.66277×10^{-6}	1.41527×10^{-6}	3.53789×10^{-7}
1.8	4.89733×10^{-5}	1.21551×10^{-5}	3.03330×10^{-6}	7.57986×10^{-7}	1.89475×10^{-7}
1.9	1.80044×10^{-5}	4.45136×10^{-6}	1.10975×10^{-6}	2.77246×10^{-7}	6.92995×10^{-8}
2	0	0	0	0	0

Concerning Example 3 and to show the compatibility between $(\Psi(\varsigma_{\hbar}), \Phi(\varsigma_{\hbar}))$ and $(\widehat{\Phi}(\varsigma_{\hbar}), \widehat{\Psi}(\varsigma_{\hbar}))$, the values of $\mathscr{A}_{\Psi}(\varsigma_{\hbar})$ and $\mathscr{A}_{\Phi}(\varsigma_{\hbar})$ are summarized in Tables 2 and 3, respectively, for $\nu = \{10,20,40,80,160\}$. Additionally, the graphics of $\mathscr{A}_{\Psi}(\varsigma_{\hbar})$ and $\mathscr{A}_{\Phi}(\varsigma_{\hbar})$ for $\nu = 160$ are given in Figure 2. Whilst, the graphics of $(\Psi(\varsigma_{\hbar}), \widehat{\Psi}(\varsigma_{\hbar}))$ and $(\Phi(\varsigma_{\hbar}), \widehat{\Phi}(\varsigma_{\hbar}))$ for $\nu \in \{20, 40\}$ are given in Figure 3. Again, it can be observed from the figure and table that the result data is sufficient accuracy and firmly connected.

Example 4. We test the following linear conformable LEP system:

$$T^{4/3}\Psi(\varsigma) + \frac{2}{\varsigma} T^{1/2}\Psi(\varsigma) + \varsigma\Phi(\varsigma) + e^{\varsigma}\Psi(\varsigma) = \mathscr{F}_1(\varsigma),$$
$$T^{4/3}\Phi(\varsigma) + \frac{1}{\varsigma} T^{1/2}\Phi(\varsigma) + 2\sin(\varsigma)\Phi(\varsigma) + 2\varsigma\Psi(\varsigma) = \mathscr{F}_2(\varsigma), \tag{82}$$

$$\mathscr{F}_1(\varsigma) = e^{\varsigma} + \varsigma - \varsigma^2 + \varsigma^3 + 2\pi\left(1 + 2\varsigma^{1/6}\right)\cos(\pi\varsigma) + \left(4\sqrt{\varsigma} + 2\varsigma^{2/3} + \varsigma^2 e^{\varsigma} - \pi^2\varsigma^{8/3}\right)\sin(\pi\varsigma),$$
$$\mathscr{F}_2(\varsigma) = 2\varsigma^{5/6} - \varsigma^{-1/4}(1 + 2\varsigma) + 2\left(1 - \varsigma + \varsigma^2\right)\sin(\varsigma) + 2\varsigma\left(1 + \varsigma^2\right)\sin(\pi\varsigma), \tag{83}$$

concerning the BCs

$$\Psi(0) = \Phi(0) = 1,$$
$$\Psi(1) = \Phi(1) = 1. \tag{84}$$

Herein, the exact solutions are

$$\Psi(\varsigma) = \varsigma^2 \sin(\pi\varsigma) + 1,$$
$$\Phi(\varsigma) = \varsigma^2 - \varsigma + 1. \tag{85}$$

Concerning Example 4 and to show the compatibility between $(\Psi(\varsigma_{\hbar}), \Phi(\varsigma_{\hbar}))$ and $(\widehat{\Phi}(\varsigma_{\hbar}), \widehat{\Psi}(\varsigma_{\hbar}))$, the values of $(\mathscr{A}_{\Psi}(\varsigma_{\hbar}), \mathscr{R}_{\Psi}(\varsigma_{\hbar}))$ and $(\mathscr{A}_{\Phi}(\varsigma_{\hbar}), \mathscr{R}_{\Phi}(\varsigma_{\hbar}))$ are summarized together in Table 4 for $\nu = 60$. Whilst the graphics of $(\mathscr{A}_{\Psi}(\varsigma_{\hbar}), \mathscr{R}_{\Psi}(\varsigma_{\hbar}))$ and $(\mathscr{A}_{\Phi}(\varsigma_{\hbar}), \mathscr{R}_{\Phi}(\varsigma_{\hbar}))$ for $\nu = 60$ are given in Figure 4. Indeed, the graphics of $(\Psi(\varsigma_{\hbar}), \widehat{\Psi}(\varsigma_{\hbar}))$ and $(\Phi(\varsigma_{\hbar}), \widehat{\Phi}(\varsigma_{\hbar}))$ for $\nu \in \{60, 80\}$ are given in Figure 5. Hither, it can be observed from the figure and table that the result data is sufficient accuracy and are firmly connected.

Example 5. We test the following nonlinear singular LEP system:

$$T^{5/4}\Psi(\varsigma) + \frac{2}{\varsigma} T^{1/5}\Psi(\varsigma) + \sinh(\varsigma)\Phi^2(\varsigma) + \frac{\Psi(\varsigma)}{\Psi^2(\varsigma) + 1} = \mathscr{F}_1(\varsigma),$$
$$T^{5/4}\Phi(\varsigma) - \frac{1}{\varsigma} T^{1/5}\Phi(\varsigma) + 2\cos(\Psi(\varsigma)) = \mathscr{F}_2(\varsigma), \tag{86}$$

$$\mathscr{F}_1(\varsigma) = \varsigma^{3/4}(-3 + 6\varsigma) + \varsigma^{-1/5}\left(1 - 6\varsigma + 6\varsigma^2\right) + \frac{2 + \varsigma - 3\varsigma^2 + 2\varsigma^3}{2 + 0.5\left(2 + \varsigma - 3\varsigma^2 + 2\varsigma^3\right)^2} + \cos^2(\varsigma)\sinh(\varsigma),$$
$$\mathscr{F}_2(\varsigma) = -\varsigma^{3/4} - \cos\left(0.5\left(2 + \varsigma - 3\varsigma^2 + 2\varsigma^3\right)\right) + \varsigma^{-1/5}\sin(\varsigma), \tag{87}$$

concerning the BCs

$$\Psi(0) = \Phi(0) = 1,$$
$$\Psi(1) = 1, \Phi(1) = \cos(1). \tag{88}$$

Herein, the exact solutions are

$$\Psi(\varsigma) = \varsigma^3 - 1.5\varsigma^2 + 0.5\varsigma + 1,$$
$$\Phi(\varsigma) = \cos(\varsigma). \tag{89}$$

Table 3: Solutions result of $\mathscr{A}_{\Phi}(\varsigma_k)$ with $r = \{10,20,40,80,160\}$ in Example 3.

ς_k	$r = 10$	$r = 20$	$r = 40$	$r = 80$	$r = 160$
1	0	0	0	0	0
1.1	3.76804×10^{-7}	1.68330×10^{-8}	6.23761×10^{-10}	4.57952×10^{-10}	1.33368×10^{-16}
1.2	3.49244×10^{-6}	1.00246×10^{-6}	2.58702×10^{-7}	6.51818×10^{-8}	1.63269×10^{-8}
1.3	9.15243×10^{-6}	2.44919×10^{-6}	6.22382×10^{-7}	1.56226×10^{-7}	3.90960×10^{-8}
1.4	1.47071×10^{-5}	3.85284×10^{-6}	9.74249×10^{-7}	2.44253×10^{-7}	6.11065×10^{-8}
1.5	1.86288×10^{-5}	4.83271×10^{-6}	1.21920×10^{-6}	3.05490×10^{-7}	7.64158×10^{-8}
1.6	1.97846×10^{-5}	5.10561×10^{-6}	1.28643×10^{-6}	3.22237×10^{-7}	8.05984×10^{-8}
1.7	1.76475×10^{-5}	4.54048×10^{-6}	1.14322×10^{-6}	2.86312×10^{-7}	7.16099×10^{-8}
1.8	1.25707×10^{-5}	3.22885×10^{-6}	8.12645×10^{-7}	2.03502×10^{-7}	5.08967×10^{-8}
1.9	5.94475×10^{-6}	1.52547×10^{-6}	3.83849×10^{-7}	9.61176×10^{-8}	2.40391×10^{-8}
2	0	0	0	0	0

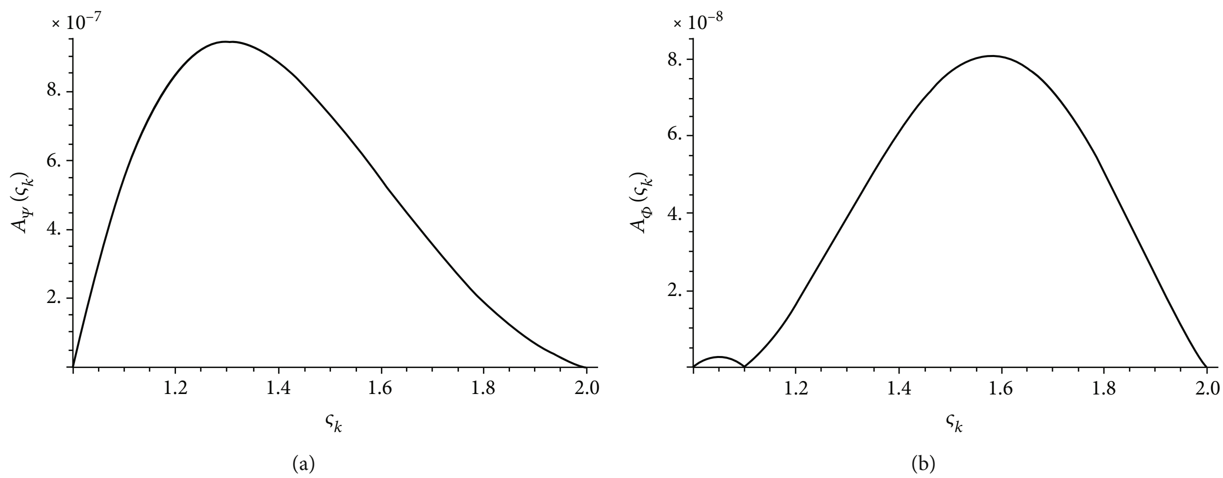

Figure 2: Graphical results with $r = 160$ in Example 3: (a) $\mathscr{A}_{\Psi}(\varsigma_k)$ and (b) $\mathscr{A}_{\Phi}(\varsigma_k)$.

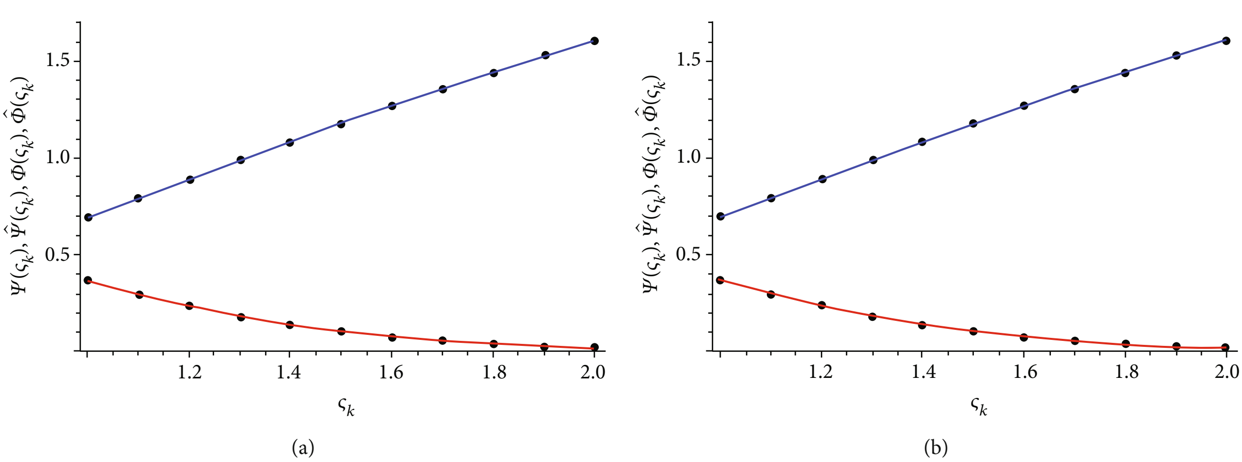

Figure 3: Graphical results of $(\Psi(\varsigma_k), \widehat{\Psi}(\varsigma_k))$ and $(\Phi(\varsigma_k), \widehat{\Phi}(\varsigma_k))$ in Example 3 as red: Ψ, blue: Φ, black stars: $(\widehat{\Psi}, \widehat{\Phi})$: (a) $r = 10$ and (b) $r = 40$.

Table 4: Solutions result with $r = 60$ in Example 4.

ς_k	$\widehat{\Psi}(\varsigma_k)$	$\mathscr{A}_{\Psi}(\varsigma_k)$	$\mathscr{R}_{\Psi}(\varsigma_k)$	$\widehat{\Phi}(\varsigma_k)$	$\mathscr{A}_{\Phi}(\varsigma_k)$	$\mathscr{R}_{\Phi}(\varsigma_k)$
0	0	0	0	0	0	0
0.1	1.00322	1.257708×10^{-4}	1.253833×10^{-4}	0.910011	1.123178×10^{-5}	1.234262×10^{-5}
0.2	1.02363	1.163980×10^{-4}	1.137241×10^{-4}	0.840011	1.091802×10^{-5}	1.299764×10^{-5}
0.3	1.07291	9.657157×10^{-5}	9.001727×10^{-5}	0.790009	9.231926×10^{-6}	1.168598×10^{-5}
0.4	1.15223	6.463408×10^{-5}	5.609774×10^{-5}	0.760007	6.638852×10^{-6}	8.735332×10^{-6}
0.5	1.25002	2.332187×10^{-5}	1.865750×10^{-5}	0.750004	3.618730×10^{-6}	4.824973×10^{-6}
0.6	1.34238	2.035114×10^{-5}	1.516049×10^{-5}	0.760001	7.687164×10^{-7}	1.011469×10^{-6}
0.7	1.39636	5.596469×10^{-5}	4.007731×10^{-5}	0.789999	1.289339×10^{-6}	1.632074×10^{-6}
0.8	1.37611	7.143946×10^{-5}	5.191132×10^{-5}	0.839998	2.083354×10^{-6}	2.480184×10^{-6}
0.9	1.25025	5.543125×10^{-5}	4.433423×10^{-5}	1.25025	1.502923×10^{-6}	1.651564×10^{-6}
1	1	0	0	1	0	0

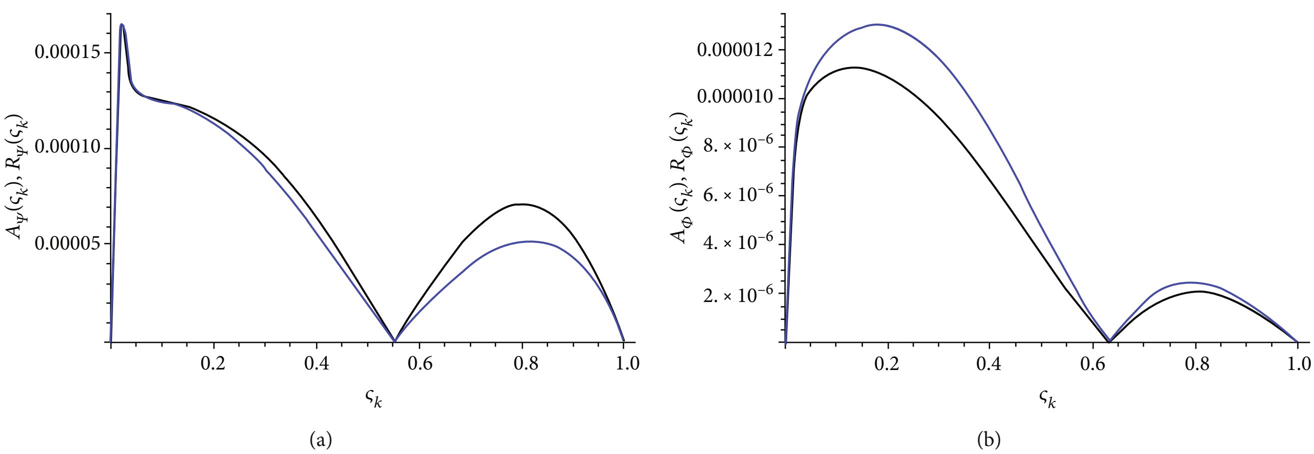

Figure 4: Graphical results with $r = 60$ in Example 4 as black: $\mathscr{A}$ and blue: $\mathscr{R}$: (a) $(\mathscr{A}_{\Psi}(\varsigma_k), \mathscr{R}_{\Psi}(\varsigma_k))$ and (b) $(\mathscr{A}_{\Phi}(\varsigma_k), \mathscr{R}_{\Phi}(\varsigma_k))$.

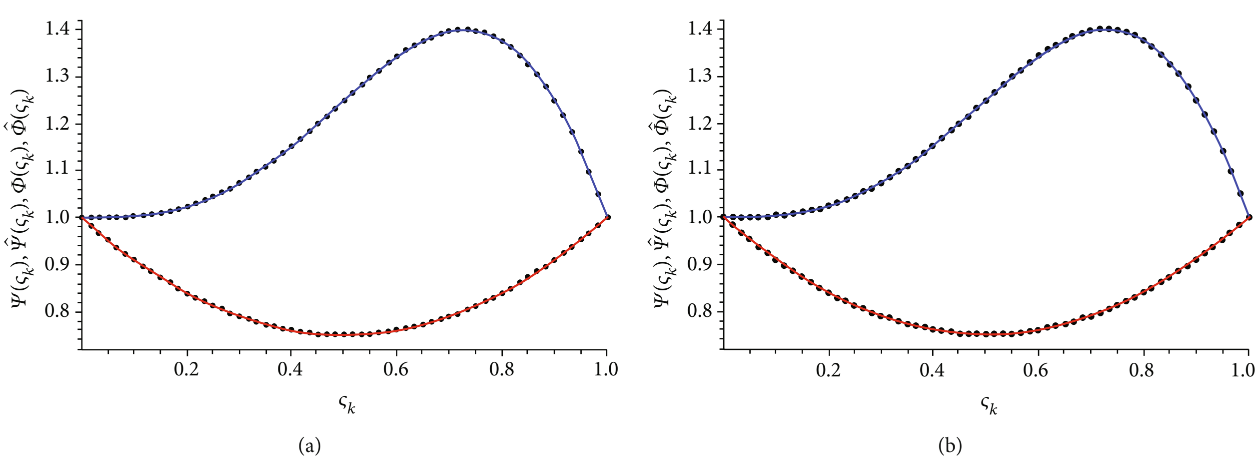

Figure 5: Graphical results of $(\Psi(\varsigma_k), \widehat{\Psi}(\varsigma_k))$ and $(\Phi(\varsigma_k), \widehat{\Phi}(\varsigma_k))$ in Example 4 as blue: Ψ, red: Φ, and black stars: $(\widehat{\Psi}, \widehat{\Phi})$: (a) $r = 60$, and (b) $r = 80$.

Table 5: Solutions result with $\mathscr{r} = 60$ in Example 5.

ς_{k}	$\widehat{\Psi}(\varsigma_{k})$	$\mathscr{A}_{\Psi}(\varsigma_{k})$	$\mathscr{R}_{\Psi}(\varsigma_{k})$	$\widehat{\Phi}(\varsigma_{k})$	$\mathscr{A}_{\Phi}(\varsigma_{k})$	$\mathscr{R}_{\Phi}(\varsigma_{k})$
0	1	0	0	1	0	0
0.1	1.036	4.687946×10^{-7}	4.525045×10^{-7}	0.995004	4.007344×10^{-7}	4.027465×10^{-7}
0.2	1.048	4.781665×10^{-7}	4.562657×10^{-7}	0.980066	1.038737×10^{-6}	1.059864×10^{-7}
0.3	1.042	4.717943×10^{-7}	4.527776×10^{-7}	0.955335	1.677880×10^{-6}	1.756324×10^{-6}
0.4	1.024	4.499979×10^{-7}	4.394512×10^{-7}	0.921059	2.198900×10^{-6}	2.387355×10^{-6}
0.5	1.000	4.099687×10^{-7}	4.099687×10^{-7}	0.877580	2.526306×10^{-6}	2.878711×10^{-6}
0.6	0.976	3.505588×10^{-7}	3.591791×10^{-7}	0.825333	2.609380×10^{-6}	3.161598×10^{-6}
0.7	0.958	2.734979×10^{-7}	2.854884×10^{-7}	0.764840	2.414309×10^{-6}	3.156611×10^{-6}
0.8	0.952	1.837305×10^{-7}	1.929942×10^{-7}	0.696705	1.920084×10^{-6}	2.755944×10^{-6}
0.9	0.964	8.918082×10^{-8}	9.251122×10^{-8}	0.621609	1.116007×10^{-6}	1.795349×10^{-7}
1	1	0	0	0.540302	0	0

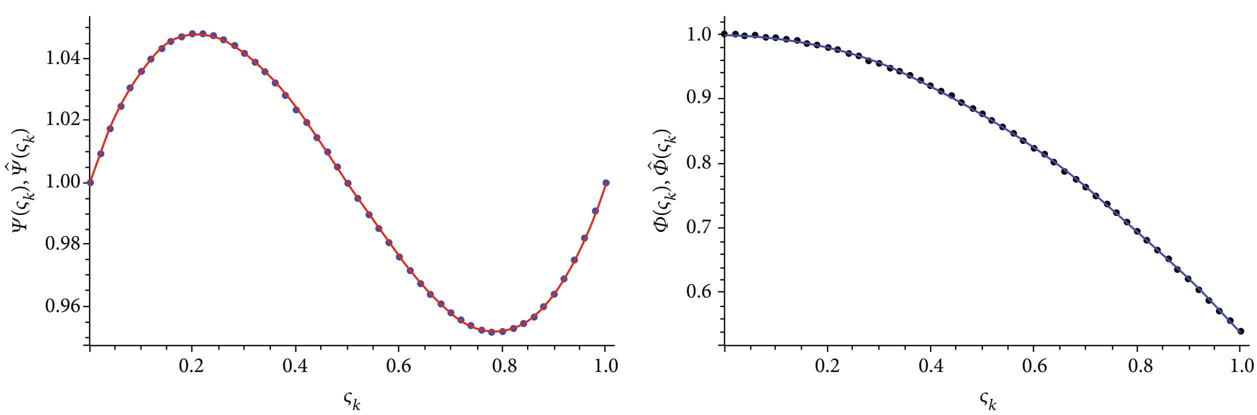

(a) (b)

Figure 6: Graphical results with $\mathscr{r} = 60$ in Example 5 as red: Ψ, blue: Φ, and black stars: $(\widehat{\Psi}, \widehat{\Phi})$: (a) $(\Psi(\varsigma_{k}), \widehat{\Psi}(\varsigma_{k}))$ and (b) $(\Phi(\varsigma_{k}), \widehat{\Phi}(\varsigma_{k}))$.

Concerning Example 5 and to show the compatibility between $(\Psi(\varsigma_{k}), \Phi(\varsigma_{k}))$ and $(\widehat{\Phi}(\varsigma_{k}), \widehat{\Psi}(\varsigma_{k}))$, the values of $(\mathscr{A}_{\Psi}(\varsigma_{k}), \mathscr{R}_{\Psi}(\varsigma_{k}))$ and $(\mathscr{A}_{\Phi}(\varsigma_{k}), \mathscr{R}_{\Phi}(\varsigma_{k}))$ are summarized together in Table 5 for $\mathscr{r} = 60$. Indeed, the graphics of $(\Psi(\varsigma_{k}), \widehat{\Psi}(\varsigma_{k}))$ and $(\Phi(\varsigma_{k}), \widehat{\Phi}(\varsigma_{k}))$ for $\mathscr{r} = 60$ are given in Figure 6. Hither, it can be observed from the figure and table that the result data is sufficient accuracy and are firmly connected.

6. Summary and Future Suggestions

Throughout this study, the CBSA is used to get soft and fineness approximations of BVPs for conformable systems concerning two points and two fractional parameters in both regular and singular types. Several linear and nonlinear examples will be examined, and a model for the Lane-Emden will be one of the applications presented. The complete construction of the used spline through the CD along with the convergence theory, and the error orders together with other results are utilized in detail in the form of tables and graphs using Mathematica 11 software. From the reported results, it can be concluded that CBSA is a very effective scheme that obtains numerical approximations to conformable systems of BVPs. The main characteristics noted here are that the spline approach is effective and fast, and it requires little compulsive and mathematical burden in solving the problems presented. In the coming work, we will apply the CBSA to solve the Lotka-Volterra model despite CD.

Abbreviations

CD: Conformable derivative
BVP: Boundary value problem
CBSA: Cubic B-spline algorithm
FDP: Fractional differential problem
BS: B-spline
LEP: Lane-Emden problem
BC: Boundary condition.

Data Availability

No datasets are associated with this manuscript. The datasets used for generating the plots and results during the current study can be directly obtained from the numerical simulation of the related mathematical equations in the manuscript.

Conflicts of Interest

The authors declare that they have no conflicts of interest.

Acknowledgments

The authors gratefully acknowledge that the work in this paper was partly supported by the Faculty Research grant FRG22-E-S89 from the American University of Sharjah.

References

[1] R. Hilfer, *Applications of Fractional Calculus in Physics*, World Scientific, Singapore, 2000.

[2] K. S. Miller and B. Ross, *An Introduction to the Fractional Calculus and Fractional Differential Equations*, Wiley, USA, 1993.

[3] K. Diethelm, D. Baleanu, and E. Scalas, *Fractional Calculus: Models and Numerical Methods*, World Scientific, Singapore, 2012.

[4] G. M. Zaslavsky, "Chaos, fractional kinetics, and anomalous transport," *Physics Reports*, vol. 371, no. 6, pp. 461–580, 2002.

[5] Z. Chen, P. Qiu, X.-J. Yang, Y. Feng, and J. Liu, "A new fractional derivative model for the anomalous diffusion problem," *Thermal Science*, vol. 23, Supplement 3, pp. 1005–1011, 2019.

[6] A. Atangana and J. F. Gómez-Aguilar, "Decolonisation of fractional calculus rules: breaking commutativity and associativity to capture more natural phenomena," *The European Physical Journal Plus*, vol. 133, no. 4, p. 166, 2018.

[7] A. Atangana, S. T. Demiray, and H. Bulut, "Modelling the nonlinear wave motion within the scope of the fractional calculus," *Abstract and Applied Analysis*, vol. 2014, Article ID 481657, 7 pages, 2014.

[8] G. A. J. Francisco, R. G. Juan, G. C. Manuel, and R. H. J. Roberto, "Fractional RC and LC electrical circuits," *Ingeniería, Investigación y Tecnología*, vol. 15, no. 2, pp. 311–319, 2014.

[9] S. Arora, T. Mathur, S. Agarwal, K. Tiwari, and P. Gupta, "Applications of fractional calculus in computer vision: a survey," *Neurocomputing*, vol. 489, pp. 407–428, 2022.

[10] D. Baleanu, F. A. Ghassabzade, J. J. Nieto, and A. Jajarmi, "On a new and generalized fractional model for a real cholera outbreak," *Alexandria Engineering Journal*, vol. 61, no. 11, pp. 9175–9186, 2022.

[11] M. Sultana, U. Arshad, A. H. Abdel-Aty, A. Akgül, M. Mahmoud, and H. Eleuch, "New numerical approach of solving highly nonlinear fractional partial differential equations via fractional novel analytical method," *Fractal and Fractional*, vol. 6, no. 9, p. 512, 2022.

[12] E. C. de Oliveira and J. A. T. Machado, "A review of definitions for fractional derivatives and integrals," *Mathematical Problems in Engineering*, vol. 2014, Article ID 238459, 6 pages, 2014.

[13] A. Atangana and D. Baleanu, "New fractional derivatives with non-local and non-singular kernel: theory and application to heat transfer model," *Thermal Science*, vol. 20, no. 2, pp. 763–769, 2016.

[14] R. Khalil, M. Al Horani, A. Yousef, and M. Sababheh, "A new definition of fractional derivative," *Journal of Computational and Applied Mathematics*, vol. 264, pp. 65–70, 2014.

[15] T. Abdeljawad, "On conformable fractional calculus," *Journal of Computational and Applied Mathematics*, vol. 279, pp. 57–66, 2015.

[16] O. Abu Arqub and M. Al-Smadi, "Fuzzy conformable fractional differential equations: novel extended approach and new numerical solutions," *Soft Computing*, vol. 24, no. 16, pp. 12501–12522, 2020.

[17] W. S. Chung, "Fractional Newton mechanics with conformable fractional derivative," *Journal of Computational and Applied Mathematics*, vol. 290, pp. 150–158, 2015.

[18] A. Kurt, Y. Çenesiz, and O. Tasbozan, "On the solution of burgers' equation with the new fractional derivative," *Open Physics*, vol. 13, p. 45, 2015.

[19] A. Jajarmi, D. Baleanu, S. S. Sajjadi, and J. J. Nieto, "Analysis and some applications of a regularized Ψ-Hilfer fractional derivative," *Journal of Computational and Applied Mathematics*, vol. 415, article 114476, 2022.

[20] M. Eslami, "Exact traveling wave solutions to the fractional coupled nonlinear Schrodinger equations," *Applied Mathematics and Computation*, vol. 285, pp. 141–148, 2016.

[21] H. Jafari and V. D. Gejji, "Solving a system of nonlinear fractional differential equations using Adomian decomposition," *Journal of Computational and Applied Mathematics*, vol. 196, no. 2, pp. 644–651, 2006.

[22] V. F. Hatipoglu, S. Alkan, and A. Secer, "An efficient scheme for solving a system of fractional differential equations with boundary conditions," *Advances in Difference Equations*, vol. 2017, no. 1, 2017.

[23] A. Jajarmi, D. Baleanu, K. Z. Vahid, H. M. Pirouz, and J. H. Asad, "A new and general fractional Lagrangian approach: a capacitor microphone case study," *Results in Physics*, vol. 31, article 104950, 2021.

[24] C. de Boor, *A Practical Guide to Splines*, Springer, USA, 1978.

[25] D. Salomon, *Curves and Surfaces for Computer Graphics*, Springer, USA, 2006.

[26] B. Heinemann and P. M. Prenter, *Splines and Variational Methods*, Wiley, USA, 1975.

[27] M. Abukhaled, S. A. Khuri, and A. Sayfy, "A numerical approach for solving a class of singular boundary value problems arising in physiology," *International Journal of Numerical Analysis and Modeling*, vol. 8, pp. 353–363, 2011.

[28] M. Abukhaled, S. A. Khuri, and A. Sayfy, "Spline-based numerical treatments of Bratu-type equations," *Palestine Journal of Mathematics*, vol. 1, pp. 63–70, 2012.

[29] M. Lakestani and M. Dehghan, "Four techniques based on the B-spline expansion and the collocation approach for the numerical solution of the Lane–Emden equation," *Mathematical Methods in the Applied Sciences*, vol. 36, no. 16, pp. 2243–2253, 2013.

[30] H. Çağlar, N. Caglar, and M. Ozer, "B-spline solution of non-linear singular boundary value problems arising in physiology," *Chaos, Solitons & Fractals*, vol. 39, no. 3, pp. 1232–1237, 2009.

[31] P. Henrici, *Discrete Variable Methods in Ordinary Differential Equations*, Wiley, USA, 1962.

Hindawi
Journal of Function Spaces
Volume 2023, Article ID 2824703, 11 pages
https://doi.org/10.1155/2023/2824703

Research Article

Couple Stress Sodium Alginate-Based Casson Nanofluid Analysis through Fick's and Fourier's Laws with Inclined Microchannel

Dolat Khan,[1] **Musawa Yahya Almusawa**,[2] **Waleed Hamali**,[2] **and M. Ali Akbar**[3]

[1]*Faculty of Science, King Mongkut's University of Technology Thonburi (KMUTT), 126 Pracha Uthit Rd., Bang Mod, Thung Khru, Bangkok 10140, Thailand*
[2]*Department of Mathematics, Faculty of Science, Jazan University, Saudi Arabia*
[3]*Department of Applied Mathematics, University of Rajshahi, Bangladesh*

Correspondence should be addressed to M. Ali Akbar; ali.akbar@ru.ac.bd

Received 22 October 2022; Revised 3 December 2022; Accepted 24 March 2023; Published 19 April 2023

Academic Editor: Yusuf Gurefe

Casson nanofluid plays a vital role in food industries with sodium alginate nanoparticles. That is why many researchers used Casson nanofluid in their study. Due to this, the main objective of this study is to investigate the inclined microchannel flow of a Casson nanofluid based on sodium alginate (SA) under a few stresses. Because the plate at $y = d$ is stationary and the plate at $y = 0$ is in motion, the fluid flows. Physically existent things utilize partial differential equations as a method of derivation. By using dimensionless variables, the underlying PDEs are dimensionless. Applying Fourier's and Fick's laws to the time-fractional model makes the classical model dimensionally stable by generalization. A generalized fractional model is solved using the Laplace and Fourier integral transformations. In addition, the parametric influence of other physical elements, such as the Casson parameter, coupling velocity, temperature, and stress parameters, is considered (Grashof, Schmidt, and Prandtl numbers). Concentration distributions are shown using graphs and discussed with accompanying text. We compute and describe the Sherwood number, rate of heat transfer, and skin friction. It is concluded that skin friction and Nusselt number can be enhanced by adding nanoparticle. Also, the fractional derivative makes the study more realistic by incorporating Fick's and Fourier's laws as compared to the classical one.

1. Introduction

The term "nanomaterials" means materials that have a size of 100 nanometers or less, while nanotechnology refers to the kind of technology that produces these materials. The structure of nanomaterials as well as their characteristics is taken into consideration when classifying them into one of four groups [1]. Choi [2] was the first researcher to investigate the terminology associated with nanofluids. He came up with the term "nanofluid" to describe the fluids that included particles with diameters of less than 100 nanometers. Karthik et al. explained the rationale behind why nanosized particles are favored over microsized particles in a variety of applications [3]. Significant improvements in thermophysical characteristics have been seen when comparing nanoparticles to microparticles. Nanofluids may be used for a variety of purposes, including the cooling of air conditioning systems, the cooling of power plants, and the improvement of diesel generator efficiency [4]. Normally, water and ethylene glycol are used as the basis fluids in heat transfer systems. The manufacturing of nanoparticles involves the use of a variety of components, which may be generally classified as metallic, such as copper [5], metal oxide, such as iron oxide, and carbon-based, such as graphite. CuO [6], chalcogenide sulfides, selenides, and tellurides, all of which were discussed [7], along with several other particles, such as carbon nanotubes [8]. According to the available research, the average size of a single particle ranges from

20 to 100 nm [9, 10]. A type of nanofluid flow in a porous media with Newtonian heating and magnetohydrodynamic flow of Casson-type fluid is studied by Khan et al. [11].

In 1959, Casson came out with the first Casson fluid model. Oka [12] was the first person to look at fluids from Casson in tubes. Honey, blood, soup, jelly, stuff, slurries, and artificial fluids are all types of Casson fluids. Ahmad et al. [13] wrote about Casson nanofluid that was heated in a Newtonian way. Khan et al. [14] investigated the effects of a magnetic field, a chemical reaction, heat generation, and Newton cooling law, on the flow of Casson fluid over a moving stretched surface in a porous medium. Furthermore, Mackolil and Mahanthesh [15] examined the exact and statistical analysis of Casson nanofluid. Statistical techniques like probable error and regression are used to examine the rate of heat transfer and skin friction. Besides, many studies are reported to investigate the statistical analysis for various nanofluids [16–18]. Recently, Satya Narayana et al. [19] report a 3D flow for Casson-type couple stress nanofluid. It is discovered that the non-Newtonian pair stress fluid's temperature is greater than that of the viscous case. For increased heat transmission, it may be proposed that the matching viscous fluid in industrial applications be switched out for the Casson couple stress nanofluid.

Couple stress fluids (CSF) are different from standard viscous fluids in that they have a specific material constant. These fluids' (CSFs) rheological characteristics have a wide range of applications such as the crude oil extraction process, the solidification of liquid crystals, electrostatic precipitations, aerodynamic heating phenomena, and colloidal and suspension solutions [20]. Stokes [21] developed the idea of CSF theory, where he incorporated CSFs into account in addition to the classical Cauchy stress. It is the most straightforward modification of the theory of the conventional fluid that takes into account polar effects like the presence of CSs and body couples. Stokes provides a thorough explanation of CSF theory in his work *Theories of Fluids with Microstructure* [22], where he also lists a variety of issues that scholars have examined in relation to couple stress theory. The phenomena of pumping fluids, the synthesis of lubricants and biological processes, the solidification of liquid crystals, and the solidification of animal blood are only a few illustrations of the extraordinary applications of CSF models in our everyday life. Researchers have taken the CSF model into consideration for a variety of scientific and physical problems. Many fascinating problems involving CSFs or micropolar fluids may be found in the references [23, 24]. Khan et al. [25] used the time-fractional derivative definitions of Caputo-Fabrizio to find the solutions to the two phase CS fluid channel flow. Ali et al. [26] have looked at the flow of laminar and unstable pair stress fluid between infinite numbers of plates. Using lubricant as the base fluid, Laplace and Fourier transforms were used to find exact solutions. They found that adding nanoparticles to engine oil made the oil 12.8% more effective.

Fractional calculus [27] is the study of the many ways that differentiation and integration can be used to find the power of real and complex numbers. Ross [28] explained how fractional calculus changed from 1695 to 1900. Many physical and natural problems cannot be shown by the classical derivative, so fractional calculus is used to solve these problems. Scientists have been very interested in fractional derivatives for the past 30 years. In response to this interest, many scientists have come up with different ways to explain what a fractional derivative is. Riemann-Liouville [29] was the most typical approach to describing things in the 18th century. Despite the fact that the R-L formulation of the fractional derivative has been shown to perform effectively in many physical contexts, there are two basic approaches to applying this concept. Differentiating the constant term may not result in zero, and certain aspects of the Laplace transform are irrelevant in practice. Caputo fractional derivatives are utilized in physics, chemistry, economics, and other fields of research. They may also be employed in everyday situations. CFD is used to investigate processes such as diffusion, signal processing, material mechanical characteristics, image processing, pharmacokinetics, damping, and bioengineering. CFD [30] is a modified version of fractional calculus that corrects the issues produced by the R-L formulation. However, since the CFD kernel contains a singularity, CFD cannot be utilized to represent certain materials with large differences [31]. It cannot give a good description of what happened. Caputo-Fabrizio [32] suggests a new definition with a kernel that is not singular to get around the singularity problem in CFD. Several researchers [33–37] looked at this new idea as part of their work. CF fractional derivative is used by a number of studies to look at the effect on memory. Akhtar [38] used time-fractional Caputo and CF derivatives to study the flow of couple stress fluids (CSFs) between two parallel plates.

The existing literature does not take into consideration the fact that by utilizing Fick's and Fourier's laws, closed-form solutions for the flow of Casson fluid down a microchannel may be discovered. In terms of pair stress, we focused on the plate's motion at $y = 0$, which generates a flow SA-based Casson nanofluid through an inclined microchannel. The governing partial differential equations are nondimensionalized by employing dimensionless variables, and the energy and mass equations are fractionalized using Fick's and Fourier's laws. Caputo's definition is applied to the fractional model, and the resulting partial differential equations (PDEs) are solved by combining Laplace and Fourier transforms. Tables and figures are used to graphically present the data. It is possible to calculate the effect of various parameters on the skin friction, Nusselt number, and Sherwood number.

2. Mathematical Formulation

Consider the flow of CS SA-based Casson nanofluid along with the inclined microchannel. The flow is considered in the x-direction. Initially $(t \le 0)$, both the fluid and the plates are at rest with the same concentration C_d and temperature T_d. After some time $(t > 0)$, the plate at $y = 0$ is carried with constant velocity $u_0 H(t)$, where u_0 is the characteristic velocity, while the second plate stays static. The moving plate's temperature and concentration rise to T_1 and C_1, respectively, and then remain constant, as illustrated in Figure 1.

The continuity and momentum equation of the CSNF and energy equation are given by

$$
\begin{aligned}
&\nabla \cdot \vec{V} = 0,\\
&\rho_{\mathrm{nf}} \frac{\partial \vec{V}}{\partial t} = -\nabla p - \mu_{\mathrm{nf}} \nabla \times \nabla \times \vec{V} - \lambda \nabla \times \nabla \times \nabla \times \nabla \times \vec{V}\\
&\qquad + g(\rho\beta_T)_{\mathrm{nf}}(T - T_\infty) + \rho_{\mathrm{nf}} \vec{b}_1,\\
&(\rho Cp)_{\mathrm{nf}} \frac{\partial \vec{T}}{\partial t} = k_{\mathrm{nf}} \nabla \times \nabla \times \vec{T},\\
&D_{\mathrm{nf}} \frac{\partial \vec{C}}{\partial t} = k_{\mathrm{nf}} \nabla \times \nabla \times \vec{C}.
\end{aligned} \tag{1}
$$

Since unidirectional flow has been taken into consideration, the provided flow's velocity, temperature, and concentration fields are as follows:

$$
\left.
\begin{aligned}
\vec{V} &= (u(\zeta, t), 0, 0),\\
\vec{T} &= (T(\zeta, t), 0, 0),\\
\vec{C} &= (C(\zeta, t), 0, 0).
\end{aligned}
\right\} \tag{2}
$$

Equation for an incompressible Casson fluid flow

$$
\begin{aligned}
&\tau = \tau_0 + \mu_{\mathrm{nf}} \dot{\gamma},\\
&\tau = \begin{cases} 2\left(\mu_n + \dfrac{P_\lambda}{\sqrt{2\pi}}\right) e_{ab}, \pi > \pi_c, \\[2mm] 2\left(\mu_n + \dfrac{P_\lambda}{\sqrt{2\pi_c}}\right) e_{ab}, \pi < \pi_c. \end{cases}
\end{aligned} \tag{3}
$$

Under these, we get the final problem formulation as follows:

$$
\begin{aligned}
\rho_{\mathrm{nf}} \frac{\partial u(\zeta, t)}{\partial t} &= \mu_{\mathrm{nf}} \left(1 + \frac{1}{\beta}\right) \frac{\partial^2 u(\zeta, t)}{\partial \zeta^2} - \lambda \frac{\partial^4 u(\zeta, t)}{\partial \zeta^4}\\
&\quad + (\rho\beta_T)_{\mathrm{nf}} g \cos(\gamma)(T - T_d)\\
&\quad + (\rho\beta_C)_{\mathrm{nf}} g \cos(\gamma)(C - C_d),
\end{aligned} \tag{4}
$$

$$
\frac{\partial T(\zeta, t)}{\partial t} = -\frac{1}{(\rho C_P)_{\mathrm{nf}}} \frac{\partial q(\zeta, t)}{\partial \zeta}. \tag{5}
$$

Fourier's law:

$$
\frac{1}{k_{\mathrm{nf}}} q(\zeta, t) = -\frac{\partial T(\zeta, t)}{\partial \zeta}. \tag{6}
$$

The thermal balance equation:

$$
\frac{\partial C(\zeta, t)}{\partial t} = -\frac{\partial S(\zeta, t)}{\partial \zeta}. \tag{7}
$$

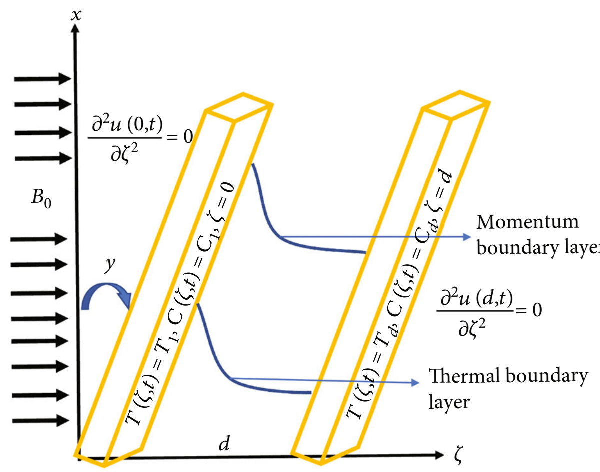

Figure 1: Geometry of the flow.

Fick's law:

$$
\frac{1}{D_{\mathrm{nf}}} S(\zeta, t) = -\frac{\partial C(\zeta, t)}{\partial \zeta}. \tag{8}
$$

These are the physical conditions:

$$
\left.
\begin{aligned}
&u(\zeta, t)|_{t-0} = 0, u(\zeta, t)|_{\zeta=0} = u_0 H(t), u(\zeta, t)|_{\zeta=d} = 0,\\
&T(\zeta, t) = T_d, C(\zeta, t) = C_d, t = 0,\\
&T(\zeta, t) = T_1, C(\zeta, t) = C_1, \zeta = 0,\\
&T(\zeta, t) = T_d, C(\zeta, t) = C_d, \zeta = d,\\
&\frac{\partial^2 u(0, t)}{\partial \zeta^2} = \frac{\partial^2 u(d, t)}{\partial \zeta^2} = 0.
\end{aligned}
\right\} \tag{9}
$$

Terms for $(\rho C_p)_{\mathrm{nf}}, (\rho\beta_T)_{\mathrm{nf}}, (\rho\beta_C)_{\mathrm{nf}}, \mu_{\mathrm{nf}}, \rho_{\mathrm{nf}}, D_{\mathrm{nf}}, k_{\mathrm{nf}}$ are given by Khan et al. [11].

$$
\begin{aligned}
\mu_{\mathrm{nf}} &= \mu_f \frac{1}{(1-\phi)^{2.5}},\\
\rho_{\mathrm{nf}} &= \rho_f (1-\phi) + \rho_s \phi,\\
\rho_{\mathrm{nf}} &= \rho_f (1-\phi) + \rho_s \phi,\\
(\rho C_p)_{\mathrm{nf}} &= (\rho C_p)_f (1-\phi) + (\rho C_p)_s \phi,\\
(\rho\beta_T)_{\mathrm{nf}} &= (\rho\beta_T)_f (1-\phi) + (\rho\beta_T)_s \phi,\\
(\rho\beta_C)_{\mathrm{nf}} &= (\rho\beta_C)_f (1-\phi) + (\rho\beta_C)_s \phi,\\
D_{\mathrm{nf}} &= D_f \frac{1}{1+\phi}.
\end{aligned} \tag{10}
$$

To get a PDE system without dimensions, we define the following variables without dimensions:

$$\begin{aligned} u^* &= \frac{u}{u_0}, \\ \zeta^* &= \frac{\zeta}{d}, \\ T^* &= \frac{T - T_d}{T_1 - T_d}, \\ t^* &= \frac{\upsilon t}{d^2}, \\ C^* &= \frac{C - C_d}{C_1 - C_d}, \\ q^* &= \frac{qd}{k_f(T_1 - T_d)}, \\ S^* &= \frac{Sd}{k_f(C_1 - C_d)}. \end{aligned} \tag{11}$$

By eliminating the $*$ signs and replacing them with these dimensionless variables, Equations (4)–(9) become

$$\begin{aligned} \frac{\partial u(\zeta,t)}{\partial t} = {} & \frac{b_2}{b_1}\beta_1 \frac{\partial^2 u(\zeta,t)}{\partial \zeta^2} - \frac{1}{b_1}\lambda \frac{\partial^4 u(\zeta,t)}{\partial \zeta^4} \\ & + \frac{b_3}{b_1} T(\zeta,t)\mathrm{Gr}\cos(\gamma) \\ & + \frac{b_4}{b_1} C(\zeta,t)\mathrm{Gm}\cos(\gamma), \end{aligned} \tag{12}$$

$$\frac{\partial T(\zeta,t)}{\partial t} = -\frac{b_6}{\mathrm{Pr} b_5}\frac{\partial q(\zeta,t)}{\partial \zeta}, \tag{13}$$

$$q(\zeta,t) = -\frac{\partial T(\zeta,t)}{\partial \zeta}, \tag{14}$$

$$\mathrm{Sc}\frac{\partial C(\zeta,t)}{\partial t} = -\frac{1}{b_7}\frac{\partial S(\zeta,t)}{\partial \zeta}, \tag{15}$$

$$S(\zeta,t) = -\frac{\partial C(\zeta,t)}{\partial \zeta}, \tag{16}$$

$$\left.\begin{aligned} & u(\zeta,t)|_{t-0} = 0, u(\zeta,t)|_{y=0} = 1, u(d,t)|_{\zeta=d} = 0, \\ & T(\zeta,t) = T_d, C(\zeta,t) = 0, t = 0, \\ & T(\zeta,t) = 1, C(\zeta,t) = 1, \zeta = 0, \\ & T(\zeta,t) = 0, C(\zeta,t) = 0, \zeta = d, \\ & \frac{\partial^2 u(0,t)}{\partial \zeta^2} = \frac{\partial^2 u(d,t)}{\partial \zeta^2} = 0, \end{aligned}\right\} \tag{17}$$

$$\begin{aligned} b_1 &= 1 - \phi + \phi\frac{\rho_s}{\rho_f}, \\ b_2 &= \frac{1}{(1-\phi)^{2.5}}, \\ b_3 &= 1 - \phi + \phi\frac{(\rho\beta_T)_s}{(\rho\beta_T)_f}, \\ b_4 &= 1 - \phi + \phi\frac{(\rho\beta_C)_s}{(\rho\beta_C)_f}, \\ b_5 &= 1 - \phi + \phi\frac{(\rho C_p)_s}{(\rho C_p)_f}, \\ b_6 &= \frac{k_s + 2k_f - 2\phi(k_f - k_s)}{k_s + 2k_f + \phi(k_f - k_s)}, \\ b_7 &= \frac{1}{1+\phi}, \\ \beta_1 &= 1 + \frac{1}{\beta}. \end{aligned} \tag{18}$$

The general FAFL are used in the following ways:

$$q(\zeta,t) = -{}^{C}D_t^{1-\alpha}\left(\frac{\partial T(\zeta,t)}{\partial \zeta}\right), \quad 0 < \alpha \le 1, \tag{19}$$

$$S(\zeta,t) = -{}^{C}D_t^{1-\alpha}\left(\frac{\partial C(\zeta,t)}{\partial \zeta}\right), \quad 0 < \alpha \le 1. \tag{20}$$

In this equation, ${}^{C}D_t^{1-\alpha}(.)$ stands for the Caputo time-fractional operator, and its definition is as follows:

$${}^{C}D_t^{\alpha}(K_1(\zeta,t)) = \frac{1}{\Gamma(1-\alpha)}\int_0^t (t-s)^{-\alpha}K_1(\zeta,t)ds = K(\zeta,t) * \xi_\alpha(t). \tag{21}$$

In this case, $\xi_\alpha(t) = t^{-\alpha}/\Gamma(1-\alpha)$ is the singular power law kernel. Moreover,

$$\begin{aligned} L(\xi_\alpha(t)) &= \frac{1}{s^{(1-\alpha)}}, \\ (\xi_{1-\alpha}(t) * \xi_\alpha(t)) &= 1, \\ \xi_0(t) &= L^{-1}\left(\frac{1}{s}\right) = 1, \\ \xi_1(t) &= L^{-1}(1) = \delta(t). \end{aligned} \tag{22}$$

In this instance, $\delta(t)$ is for a Dirac delta function. It is possible to write using Equation (21) and the properties mentioned in (22):

$$\left.\begin{aligned} {}^{C}D_t^{0}(K_1(\zeta,t)) &= K_1(\zeta,t) - K_1(\zeta,0), \\ {}^{C}D_t^{1}(K_1(\zeta,t)) &= \frac{\partial C(\zeta,t)}{\partial t}. \end{aligned}\right\} \tag{23}$$

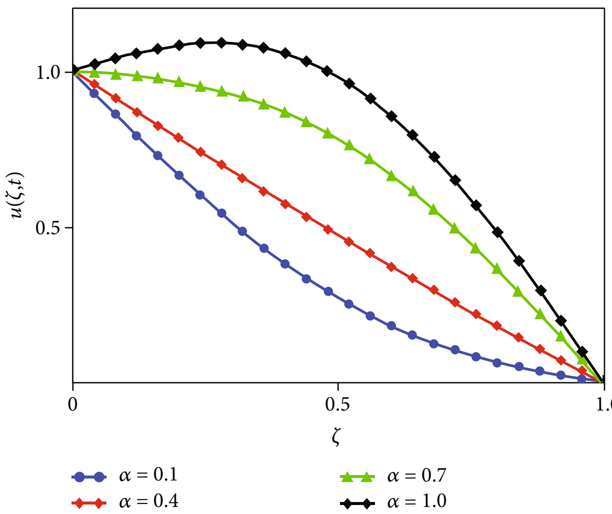

FIGURE 2: Influence of several values of α on velocity profile.

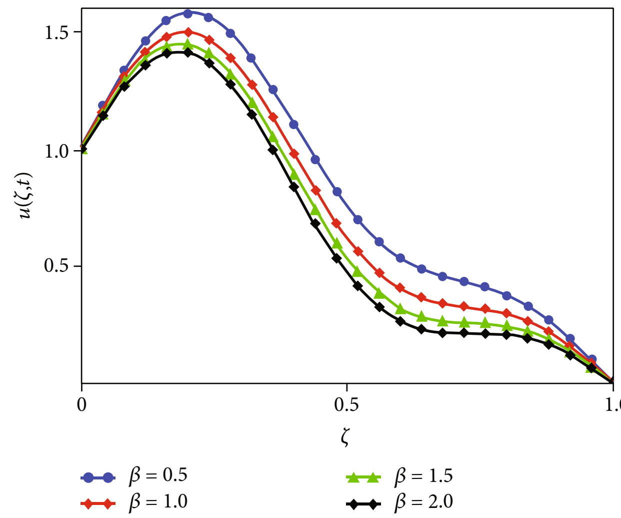

FIGURE 3: Impact of different values of β on velocity profile.

Equations (19) and (20) may be written using the Caputo fractional derivative.

$$\frac{\partial T(\zeta,t)}{\partial t} = \frac{b_6}{b_5 \mathrm{Pr}} {}^{C}D_t^{1-\alpha} \frac{\partial^2 T(\zeta,t)}{\partial \zeta^2}, \tag{24}$$

$$\mathrm{Sc}\frac{\partial C(\zeta,t)}{\partial t} = \frac{1}{b_7} {}^{C}D_t^{1-\alpha}\left(\frac{\partial^2 C(\zeta,t)}{\partial \zeta^2}\right). \tag{25}$$

In order to derive the simplified form of Equations (24) and (25), we consider the time-fractional integral operator:

$$v_t^{\alpha}(K_1(\zeta,t)) = \left(\xi_{1-\alpha}{}^{*}K_1\right)(t) = \frac{1}{\Gamma(\alpha)}\int_0^t (t-s)^{\alpha-1}K_1(\zeta,s)ds. \tag{26}$$

The inverse operator of the fractional derivative ${}^{C}D_t^{\alpha}$ described in Equation (26) is Equation (21). Equations (24) and (25) may be expressed using the properties described in [39] as follows:

$${}^{C}D_t^{\alpha}T(\zeta,t) = \frac{b_6}{b_5 \mathrm{Pr}}\left(\frac{\partial^2 T(\zeta,t)}{\partial \zeta^2}\right), \tag{27}$$

$${}^{C}D_t^{\alpha}C(\zeta,t) = \frac{1}{b_7 \mathrm{Sc}}\left(\frac{\partial^2 C(\zeta,t)}{\partial \zeta^2}\right). \tag{28}$$

3. Solution of the Problem

3.1. Solution of Energy Field. When we apply the LT to Equation (27), we obtain

$$\mathrm{Pr}s^{\alpha}\bar{T}(\zeta,s) = \frac{b_6}{b_5}\left(\frac{d^2\bar{T}(\zeta,s)}{d\zeta^2}\right), \tag{29}$$

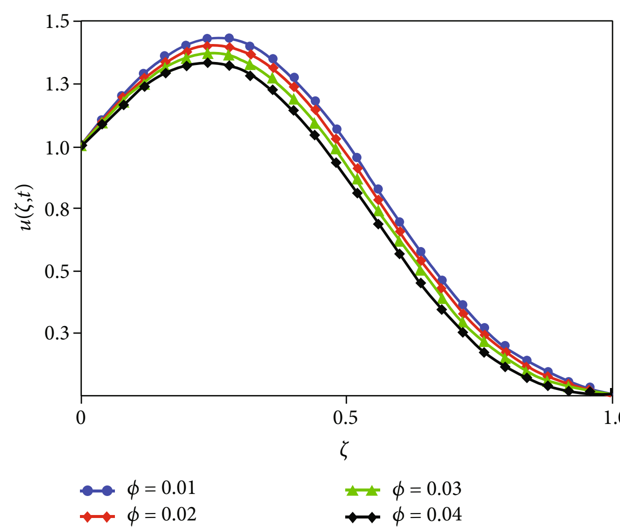

FIGURE 4: Impact of different values of ϕ on velocity profile.

and the transformed ICs and BCs are given by

$$\left.\begin{aligned}&\bar{u}(\zeta,t) = \bar{T}(\zeta,t) = ,\bar{C}(\zeta,0) = 0, t = 0,\\&\bar{u}(\zeta,s) = \bar{T}(\zeta,s) = \bar{C}(\zeta,s) = \frac{1}{s}, \frac{\partial^2\bar{u}(\zeta,s)}{\partial\zeta^2} = 0, \zeta = 0,\\&\bar{T}(\zeta,s) = \bar{C}(\zeta,s) = \bar{u}(\zeta,s) = \frac{\partial^2\bar{u}(\zeta,s)}{\partial\zeta^2} = 0, \zeta = 1.\end{aligned}\right\} \tag{30}$$

Now, using the conditions in Equation (30), we apply the FSFT to Equation (29), and we get

$$\bar{T}(k,s) = \frac{k\pi b_6}{b_5 \mathrm{Pr}}\left(\frac{1}{s(s^{\alpha}+L)}\right), \tag{31}$$

where $L = (k\pi)^2(b_6/\mathrm{Pr}b_5)$.

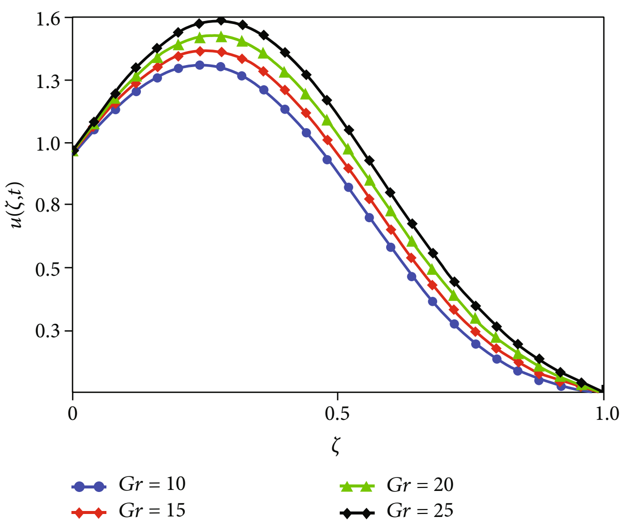

FIGURE 5: Impact of different values of Gr on velocity profile.

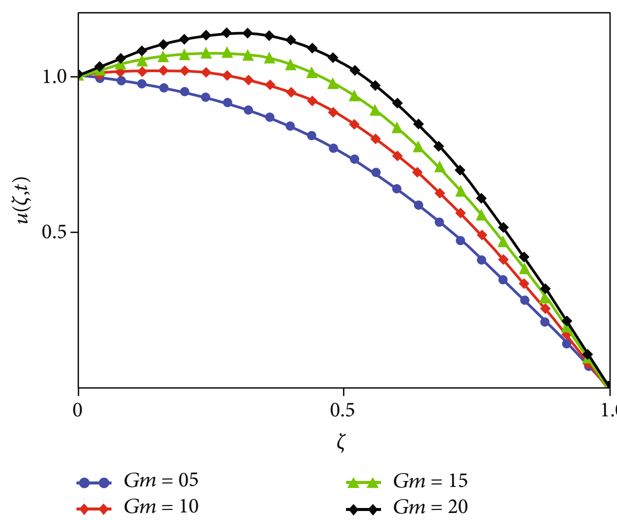

FIGURE 6: Impact of different values of Gm on velocity profile.

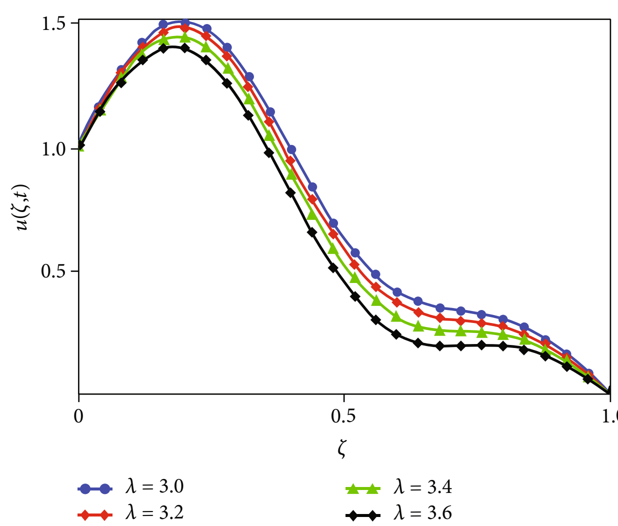

FIGURE 7: Impact of different values of λ on velocity profile.

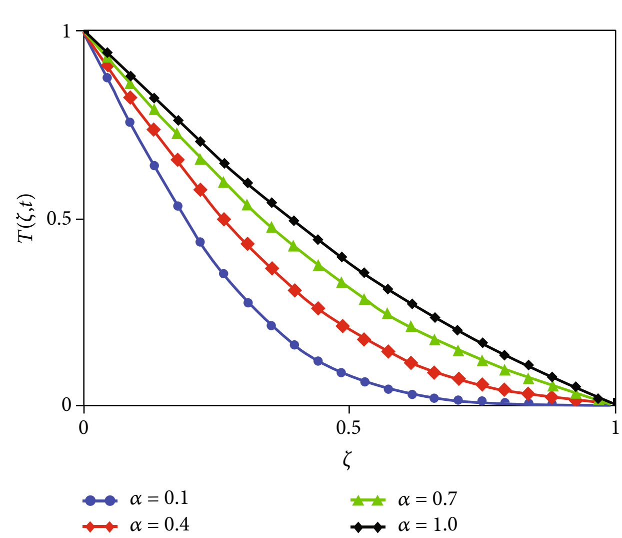

FIGURE 8: Impact of α on temperature distribution.

When inverse transformations are used, Equation (31) looks like this:

$$T(\zeta, t) = (1-\zeta) - 2\sum_{k=1}^{\infty} \frac{1}{k\pi} \cdot E_\alpha \left(\frac{-(k\pi)^2 t^\alpha}{\mathrm{Pr}} \frac{b_6}{b_5} \right) \sin(k\pi\zeta). \quad (32)$$

3.2. Solution of Concentration Field. Applying the LT to Equation (28), we get the following:

$$s^\alpha \bar{C}(\zeta, s) = \frac{1}{\mathrm{Sc} b_7} \left(\frac{d^2 \bar{C}(\zeta, s)}{d\zeta^2} \right). \quad (33)$$

Now, using the conditions in Equation (30), we apply the FSFT to Equation (33), and we get

$$\bar{C}(k, s) = \frac{k\pi}{b_7 \mathrm{Sc}} \left(\frac{1}{s\left(s^\alpha + L'\right)} \right), \quad (34)$$

where $L' = (k\pi)^2/\mathrm{Sc}$.

When inverse LT and FSFT are used, Equation (31) looks like this:

$$C(\zeta, t) = (1-\zeta) - 2\sum_{k=1}^{\infty} \frac{1}{k\pi} \cdot E_\alpha \left(\frac{-(k\pi)^2 t^\alpha}{b_7 \mathrm{Sc}} \right) \sin(k\pi\zeta), \quad (35)$$

when the Mittag-Leffler function $E_\alpha(-\alpha t^\alpha) = \sum_{k=0}^{\infty} (-\alpha t)^k / \Gamma(\alpha k + 1)$ is used.

3.3. Solution of Momentum Equation. LT applied to Equation (12) allows us to write

$$\bar{u}(\zeta,s)=\frac{b_2}{b_1}\left(1+\frac{1}{\beta}\right)\frac{d^2\bar{u}(\zeta,s)}{d\zeta^2}-\frac{\lambda}{b_1}\frac{d^4\bar{u}(\zeta,s)}{d\zeta^4}+\frac{b_4}{b_1}\mathrm{Gm}\cos(\gamma)\bar{C}(\zeta,s)+\frac{1}{b_1}b_3\mathrm{Gr}\cos(\gamma)\bar{T}(\zeta,s). \tag{36}$$

Using Equation (36), the finite Fourier sine transform, and the substitution of Equations (31) and (34), we obtain

$$\begin{aligned}\bar{u}(k,s)=&\frac{R_1}{R_2 s}+\frac{R_1}{R_2(s+R_2)}\\&+\frac{b_6}{b_5}\frac{Grk\pi}{\mathrm{Pr}R_2}\frac{b_3}{b_1}\cos(\gamma)\left(\frac{1}{s(s^\alpha+L)}-\frac{1}{(s+R_2)(s^\alpha+L)}\right)\\&+\frac{\mathrm{Gm}k\pi}{b_7\mathrm{Sc}R_2}\frac{b_4}{b_1}\cos(\gamma)\left(\frac{1}{s\left(s^\alpha+L'\right)}-\frac{1}{(s+R_2)\left(s^\alpha+L'\right)}\right).\end{aligned} \tag{37}$$

Applying the inverse LT, we get the following expression for Equation (37).

$$\begin{aligned}\bar{u}(k,t)=&\frac{R_1}{R_2}\left(1+e^{-R_2t}\right)+\frac{\mathrm{Gr}}{k\pi}\frac{b_3}{b_1}\cos(\gamma)\left(1-E_\alpha\left(\frac{b_6}{b_5}\frac{-(k\pi)^2}{\mathrm{Pr}}t^\alpha\right)\right)\\&+\frac{\mathrm{Gm}}{k\pi}\frac{b_4}{b_1}\cos(\gamma)\left(1-E_\alpha\left(\frac{-(k\pi)^2}{b_7\mathrm{Sc}}t^\alpha\right)\right)\\&-\frac{b_6}{b_5}\frac{\mathrm{Gr}k\pi}{\mathrm{Pr}R_2}\frac{b_3}{b_1}\cos(\alpha)\int_0^\tau t^{\alpha-1}E_{\alpha,\alpha}(-Lt^\alpha)*e^{-R_2(t-\tau)}d\tau\\&-\frac{\mathrm{Gm}k\pi}{\mathrm{Sc}b_7R_2}\frac{b_4}{b_1}\cos(\alpha)\int_0^\tau t^{\alpha-1}E_{\alpha,\alpha}\left(-L't^\alpha\right)*e^{-R_2(t-\tau)}d\tau.\end{aligned} \tag{38}$$

The final accurate solution to Equation (36) is obtained by transforming Equation (36) using inverse FSFT.

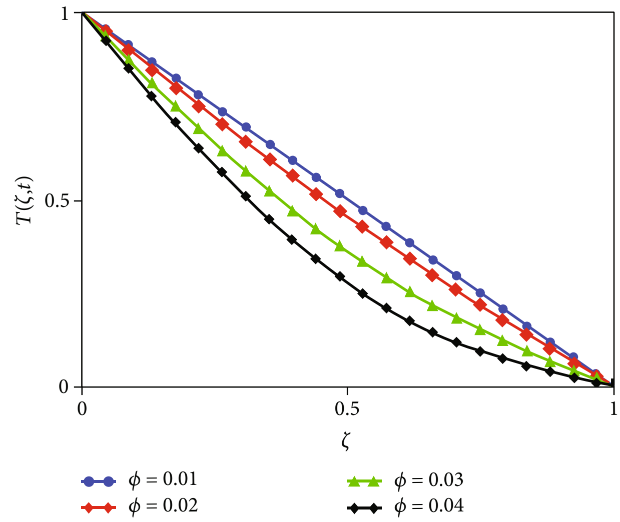

Figure 9: Impact of ϕ on temperature distribution.

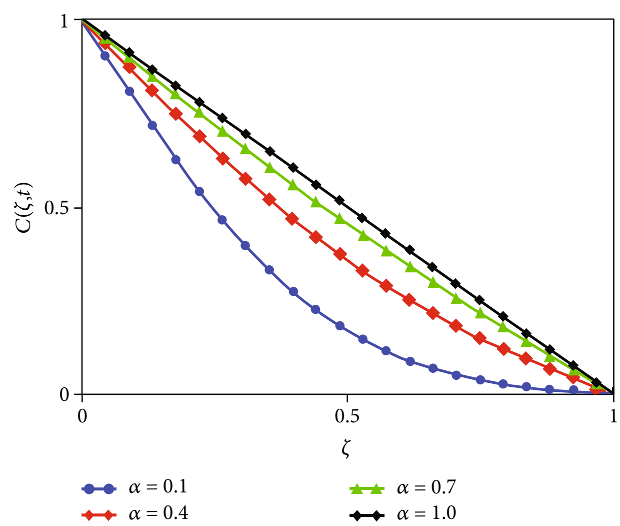

Figure 10: Impact of α on concentration distribution.

$$u(\zeta,t)=\left\{\begin{array}{l}(1-\zeta)+2\sum_{k=1}^{\infty}\frac{1}{k\pi}\exp(-k\pi R_2t)\sin(k\pi\zeta)+2\mathrm{Gr}\frac{b_3}{b_1}\cos(\gamma)\sum_{k=1}^{\infty}\frac{1}{k\pi}\left(1-E_\alpha\left(\frac{b_6}{b_5}\frac{-(k\pi)^2}{\mathrm{Pr}}t^\alpha\right)\right)\sin(k\pi\zeta)\\ +2\mathrm{Gm}\frac{b_4}{b_1}\cos(\gamma)\sum_{k=1}^{\infty}\frac{1}{k\pi}\left(1-E_\alpha\left(\frac{-(k\pi)^2}{b_7\mathrm{Sc}}t^\alpha\right)\right)\sin(k\pi\zeta)-2\frac{b_6}{b_5}\frac{\mathrm{Gr}}{\mathrm{Pr}}\frac{b_3}{b_1}\cos(\gamma)\sum_{k=1}^{\infty}\frac{k\pi}{R_2}\sin(k\pi\zeta)\\ \int_0^\tau t^{\alpha-1}E_{\alpha,\alpha}(-Lt^\alpha)\times e^{-R_2(t-\tau)}d\tau-2\frac{\mathrm{Gm}}{b_7\mathrm{Sc}}\frac{b_4}{b_1}\cos(\gamma)\sum_{k=1}^{\infty}\frac{k\pi}{R_2}\sin(k\pi\zeta)\int_0^\tau t^{\alpha-1}E_{\alpha,\alpha}\left(-L't^\alpha\right)\times e^{-R_2(t-\tau)}d\tau\end{array}\right\}, \tag{39}$$

where $R=(b_2/b_1)(1+(1/\beta)),R_1=R(k\pi)+(\lambda/b_1)(k\pi)^3$, and $R_2=k\pi R_1$.

3.4. Skin Friction and Nusselt Number. The comparative from Ahmad et al. [39] obtains skin friction terms from Equation (39) and Nusselt number expressions from Equation (32).

$$\begin{aligned} \mathrm{Cf} &= \frac{1}{(1-\phi)^{2.5}}\left(1+\frac{1}{\beta}\right)\frac{\partial u(\zeta,t)}{\partial \zeta}\bigg|_{\zeta=0} - \lambda\frac{\partial^3 u(\zeta,t)}{\partial \zeta^3}\bigg|_{\zeta=0}, \\ \mathrm{Nu} &= -b_6\frac{\partial T(\zeta,t)}{\partial \zeta}\bigg|_{\zeta=0}. \end{aligned} \tag{40}$$

4. Result and Discussion

An investigation of the unsteady, unidirectional, and incompressible flow of couple stress SA-based Casson nanofluid through inclined microchannel is worked out in this article. A fractional model is developed by using the laws of Fourier and Fick, respectively. By combining the Laplace and Fourier finite sine transforms, it is possible to find closed-form solutions. After being calculated and put into a table, the skin friction, Sherwood number, and Nusselt number of the boundary layer flow are each given as a number. Figures 2–12 show how the distributions of speed, temperature, and concentration change when different embedded parameters are changed.

Figures 2, 8, and 10 demonstrate how the fractional parameter α impacts the profile of fluid velocity, the distribution of temperatures, and the distribution of concentrations. Different integral velocity profiles are created, which is different from the classical model. The easiest way to fit these many integral profiles might be to use real data or results from experiments.

Figure 3 shows what happens to the speed profile when the Casson parameter β is changed. When the value of the Casson parameter β rises, the flow decelerates, as shown by the graphs. The science behind this is that when the value of β is raised, the viscous forces that provide resistance and slow the flow are also raised.

The effects of volume friction ϕ on velocity profile, temperature distribution, and concentration distribution are depicted in Figures 4, 9, and 11. As a result of sedimentation, the range is between 0 and 0.04 when it reaches 0.08 when it is measured. A rise in the nanoparticle volume friction percentage will, in either scenario, result in a lower temperature, as well as a change in the concentration distribution and the velocity profile.

Figures 5 and 6 show how Gr and Gm influence the velocity of the SA-based Casson nanofluid under CS. These pictures show that a function of these values that rises implies that the velocity goes up. Because they are going up, the buoyancy forces are going up, which causes the viscosity of the fluid to move down, which makes the fluid move faster. There is evidence that this statement is true.

The velocity profile flattens out when the couple stress parameter λ drops, as seen in Figure 7, which shows how λ affects velocity. Physics-wise, this behavior happens because increasing λ also increases the viscosity, which slows the Casson nanofluid based on SA.

The concentration is shown in Figure 12 for various Schmidt number Sc values. As the Schmidt number rises, the concentration boundary layer thickness falls. The Schmidt number decreased both the consecration and the

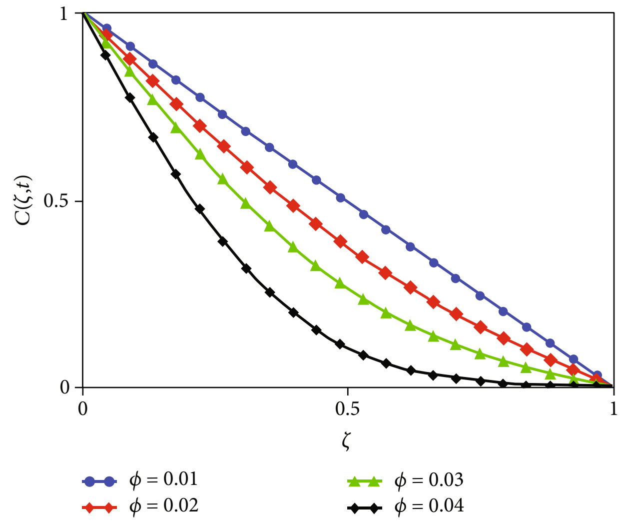

FIGURE 11: Impact of ϕ on concentration distribution.

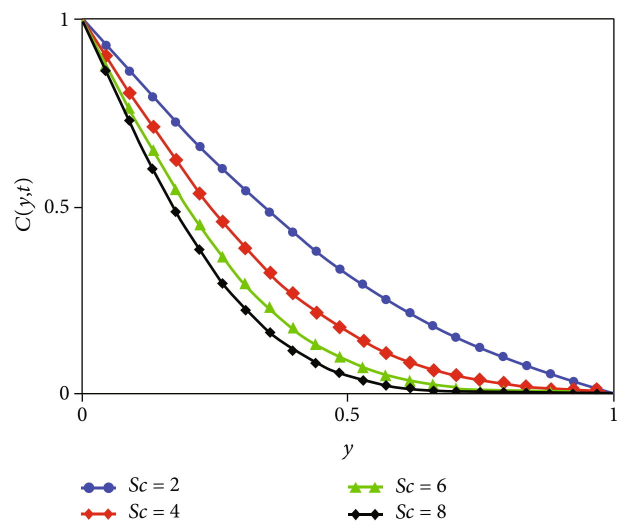

FIGURE 12: Impact of Sc on concentration distribution.

TABLE 1: Thermophysical properties.

Material	Base fluids SA	Nanoparticles Al_2O_3	Cu	TiO_2	Ag
$\rho(\mathrm{kg/m^3})$	989	3970	8933	4250	10500
$c_p(\mathrm{J/kgK})$	4175	765	385	686.2	235
$K(\mathrm{W/mK})$	0.613	40	401	8.9528	429
$\beta \times 10^{-5}(\mathrm{K^{-1}})$	0.99	0.85	1.67	0.9	1.89

Table 2: The effect of different parameters onCf.

t	α	β	λ	ϕ	Gm	Gr	Cf
0.9	0.5	2	2	0.01	5	2	**1.06033**
0.9	**0.6**	2	2	0.01	5	2	**1.00032**
0.9	0.5	**3**	2	0.01	5	2	**4.00632**
0.9	0.5	2	**4**	0.01	5	2	**5.23687**
0.9	0.5	2	2	**0.03**	5	2	**1.71032**
0.9	0.5	2	2	0.01	**10**	2	**0.23124**
0.9	0.5	2	2	0.01	5	**3**	**0.91119**

Table 3: The effect of different parameters on Nu.

t	α	ϕ	Nu
1	0.5	0.01	2.32203
1.5	0.5	0.01	2.92772
1	0.6	0.01	2.00024
1	0.5	0.03	3.94575

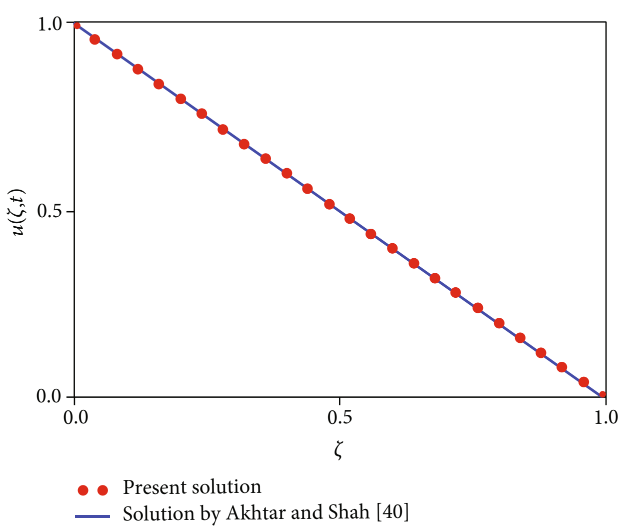

Figure 13: Comparison of the current solution with Akhtar and Shah [40].

velocity profile since it measures the proportion of viscous forces to mass diffusivity. Physically, the velocity of the SA-based Casson nanofluid decreases as viscous forces rise.

Table 1 displays the thermophysical characteristics of nanoparticles for your review. Table 2 displays the variation in skin friction caused by different parameter values. Skin friction is significant in several engineering areas, especially civil engineering. The viscous forces and, consequently, the surface friction increase as β raises. Skin friction is decreased by raising Gr and Gm. By raising Gr and Gm, the buoyancy forces rise, the viscosity drops, and the surface friction goes down as a result. Table 2 clearly illustrates how skin friction reduces as volume friction ϕ increases.

The Nusselt number is shown in Table 3. An increase in momentum diffusivity leads to a decrease in the thickness of the thermal boundary layer, which in turn decreases the Nusselt number since the Prandtl number Pr measures the relationship between momentum and thermal diffusivity. By putting $\alpha = 1, M = 0, \mathrm{Gr} = \mathrm{Gm} = 0, t = 1, \beta \longrightarrow \infty$, and $\phi = 0$, our solution is reduced to the solution of Akhtar and Shah [40], which is presented in Figure 13, which validates our solution.

5. Conclusion

This article describes how the classical model is now turned into a time-fractional model utilizing Fick's and Fourier's equations in line with Caputo's definition. Laplace and Fourier integral transforms are used to get accurate solutions. Visual illustrations and physical descriptions are used to show how different embedded elements affect the distributions of velocity, temperature, and concentration. The present work's main conclusions are as follows:

(1) Using Fick's and Fourier's laws, the time derivative is adapted into a time-fractional model

(2) The fractional models offer a wider range of answers since they are more realistic. Considering the relevant data, these solutions could be the best

(3) In accordance with the concept of skin friction, the impact of different variables on skin friction is completely different from the impact of velocity

(4) By increasing the volume friction, as a result, the temperature profile, concentration profile, and velocity profile decrease

Nomenclature

$\vec{V}$: Velocity vector
k_{nf}: Thermal conductivity of the nanofluid
T_d: Embedded temperature
C_d: Embedded concentration
$\vec{b}_1$: Body force vector
ρ_{nf}: Density of nanofluid
g: Gravitational acceleration
$(\beta_T)_{\mathrm{nf}}$: Coefficient of thermal expansion of nanofluid
$(Cp)_{\mathrm{nf}}$: Heat capacitance of the nanofluid
$\vec{C}$: Concentration vector
$\vec{T}$: Temperature vector
p: Pressure
μ_{nf}: Dynamic viscosity of nanofluid
λ: Couple stress parameter
β: Casson fluid parameter
γ: Inclination angle
$\pi = e_{ab}$: Factor of the deformation rate
μ_n: Plastic dynamic viscosity
P_λ: Yield stress of fluid
Nu: Nusselt number
Cf: Skin friction
Gr: Grashof number
Gm: Mass Grashof number

Pr: Prandtl number
Sc: Schmidt number
ϕ: Volume friction of nanofluid
$C(\zeta, t)$: Concentration
$T(\zeta, t)$: Temperature
$V(\zeta, t)$: Velocity
d: Distance between parallel plates
D_{nf}: Thermal diffusivity of nanofluid.

Data Availability

All the data used is available in the manuscript.

Conflicts of Interest

The authors declare no competing interests.

Authors' Contributions

Dolat Khan was responsible for supervision, methodology, and draft writing; Musawa Yahya Almusawa was the project administrator and responsible for methodology; M. Ali Akbar was responsible for funding and draft writing; Waleed Hamali was responsible for the investigation, methodology, and draft writing.

References

[1] S. K. Das, N. Putra, P. Thiesen, and W. Roetzel, "Temperature dependence of thermal conductivity enhancement for nanofluids," *Journal of Heat Transfer*, vol. 125, no. 4, pp. 567–574, 2003.

[2] S. U. Choi and J. A. Eastman, "Enhancing thermal conductivity of fluids with nanoparticles," (No. ANL/MSD/CP-84938; CONF-951135-29). Argonne National Lab.(ANL), Argonne, IL (United States), 1995.

[3] V. Karthik, S. Sahoo, S. K. Pabi, and S. Ghosh, "On the phononic and electronic contribution to the enhanced thermal conductivity of water-based silver nanofluids," *International Journal of Thermal Sciences*, vol. 64, pp. 53–61, 2013.

[4] J. A. Eastman, S. U. S. Choi, S. Li, W. Yu, and L. J. Thompson, "Anomalously increased effective thermal conductivities of ethylene glycol-based nanofluids containing copper nanoparticles," *Applied Physics Letters*, vol. 78, no. 6, pp. 718–720, 2001.

[5] Q. Li, Y. M. Xuan, J. Jiang, and J. W. Xu, "Experimental investigation on flow and convective heat transfer feature of a nanofluid for aerospace thermal management," *Yuhang Xuebao/ Journal of Astronautics(China)*, vol. 26, no. 4, pp. 391–394, 2005.

[6] S. Z. Heris, S. G. Etemad, and M. N. Esfahany, "Experimental investigation of oxide nanofluids laminar flow convective heat transfer," *International Communications in Heat and Mass Transfer*, vol. 33, no. 4, pp. 529–535, 2006.

[7] S. K. Das, S. U. Choi, W. Yu, and T. Pradeep, *Nanofluids: Science and Technology*, John Wiley & Sons, 2007.

[8] D. J. Faulkner, D. R. Rector, J. J. Davidson, and R. Shekarriz, "Enhanced heat transfer through the use of nanofluids in forced convection," in *ASME International Mechanical Engineering Congress and Exposition (Vol. 4711, pp. 219-224)*, Anaheim, California, USA, 2004.

[9] W. Y. Lai, B. Duculescu, P. E. Phelan, and R. S. Prasher, "Convective heat transfer with nanofluids in a single 1.02-mm tube," in *ASME International Mechanical Engineering Congress and Exposition (Vol. 47861, pp. 337-342)*, Chicago, Illinois, USA, 2006.

[10] Y. Xuan and Q. Li, "Investigation on convective heat transfer and flow features of nanofluids," *Journal of Heat Transfer*, vol. 125, no. 1, pp. 151–155, 2003.

[11] A. Khan, D. Khan, I. Khan, F. Ali, and M. Imran, "MHD flow of sodium alginate-based Casson type nanofluid passing through a porous medium with Newtonian heating," *Scientific Reports*, vol. 8, no. 1, pp. 1–12, 2018.

[12] S. Oka, "An approach to α unified theory of the flow behavior of time-independent non-Newtonian suspensions," *Japanese Journal of Applied Physics*, vol. 10, no. 3, p. 287, 1971.

[13] K. Ahmad, Z. Hanouf, and A. Ishak, "MHD Casson nanofluid flow past a wedge with Newtonian heating," *The European Physical Journal Plus*, vol. 132, no. 2, pp. 1–11, 2017.

[14] D. Khan, A. Khan, I. Khan, F. Ali, and I. Tlili, "Effects of relative magnetic field, chemical reaction, heat generation and Newtonian heating on convection flow of Casson fluid over a moving vertical plate embedded in a porous medium," *Scientific Reports*, vol. 9, no. 1, pp. 1–18, 2019.

[15] J. Mackolil and B. Mahanthesh, "Exact and statistical computations of radiated flow of nano and Casson fluids under heat and mass flux conditions," *Journal of Computational Design and Engineering*, vol. 6, no. 4, pp. 593–605, 2019.

[16] B. Mahanthesh, "Statistical and exact analysis of MHD flow due to hybrid nanoparticles suspended in $C_2H_6O_2$-H_2O hybrid base fluid," in *Mathematical Methods in Engineering and Applied Sciences*, pp. 185–228, CRC Press, 2020.

[17] J. Mackolil and B. Mahanthesh, "Time-dependent nonlinear convective flow and radiative heat transfer of Cu-Al_2O_3-H_2O hybrid nanoliquid with polar particles suspension: a statistical and exact analysis," *BioNanoScience*, vol. 9, no. 4, pp. 937–951, 2019.

[18] B. Mahanthesh, T. S. Ashlin, B. J. Gireesha, S. A. Shehzad, and M. N. Bashir, "Time-dependent flow due to noncoaxial rotation of an infinite vertical surface subjected to an exponential space-dependent heat source: an exact analysis," *Research*, vol. 48, no. 7, pp. 3162–3185, 2019.

[19] P. V. Satya Narayana, N. Tarakaramu, G. Sarojamma, and I. L. Animasaun, "Numerical simulation of nonlinear thermal radiation on the 3D flow of a couple stress Casson nanofluid due to a stretching sheet," *Journal of Thermal Science and Engineering Applications*, vol. 13, no. 2, 2021.

[20] T. D. Dass, S. R. Gunakala, and D. M. Comissiong, "Combined effect of variable-viscosity and surface roughness on the squeeze film characteristics of infinitely wide rectangular plate with couple stress fluid, velocity-slip and ferrofluid lubricant," *Materials Today: Proceedings*, vol. 56, pp. 1717–1725, 2022.

[21] V. K. Stokes, *Theories of Fluids with Microstructure: An Introduction*, Springer Science & Business Media, 2012.

[22] B. Mahanthesh, B. J. Gireesha, N. S. Shashikumar, T. Hayat, and A. Alsaedi, "Marangoni convection in Casson liquid flow due to an infinite disk with exponential space dependent heat source and cross-diffusion effects," *Results in Physics*, vol. 9, pp. 78–85, 2018.

[23] S. O. Adesanya and O. D. Makinde, "Effects of couple stresses on entropy generation rate in a porous channel with convective heating," *Computational and Applied Mathematics*, vol. 34, no. 1, pp. 293–307, 2015.

[24] E. A. Ashmawy, "Unsteady Couette flow of a micropolar fluid with slip," *Meccanica*, vol. 47, no. 1, pp. 85–94, 2012.

[25] D. Khan, G. Ali, P. Kumam, M. Y. Almusawa, and A. M. Galal, "Time fractional model of free convection flow and dusty two-phase couple stress fluid along vertical plates," *ZAMM-Journal of Applied Mathematics and Mechanics/Zeitschrift für Angewandte Mathematik und Mechanik*, article e202200369, 2016.

[26] F. Ali, Z. Ahmad, M. Arif, I. Khan, and K. S. Nisar, "A time fractional model of generalized Couette flow of couple stress nanofluid with heat and mass transfer: applications in engine oil," *IEEE Access*, vol. 8, pp. 146944–146966, 2020.

[27] R. Gorenflo and F. Mainardi, "Fractional calculus," in *Fractals and Fractional Calculus in Continuum Mechanics*, pp. 223–276, Springer, Vienna, 1997.

[28] B. Ross, "The development of fractional calculus 1695-1900," *Historia Mathematica*, vol. 4, no. 1, pp. 75–89, 1977.

[29] T. F. Nonnenmacher and R. Metzler, "On the Riemann-Liouville fractional calculus and some recent applications," *Fractals*, vol. 3, no. 3, pp. 557–566, 1995.

[30] S. Jiang, J. Zhang, Q. Zhang, and Z. Zhang, "Fast evaluation of the Caputo fractional derivative and its applications to fractional diffusion equations," *Communications in Computational Physics*, vol. 21, no. 3, pp. 650–678, 2017.

[31] J. M. Cruz-Duarte, J. Rosales-Garcia, C. R. Correa-Cely, A. Garcia-Perez, and J. G. Avina-Cervantes, "A closed form expression for the Gaussian-based Caputo-Fabrizio fractional derivative for signal processing applications," *Communications in Nonlinear Science and Numerical Simulation*, vol. 61, pp. 138–148, 2018.

[32] Y. Yang, W. Xu, W. Jia, and Q. Han, "Stationary response of nonlinear system with Caputo-type fractional derivative damping under Gaussian white noise excitation," *Nonlinear Dynamics*, vol. 79, no. 1, pp. 139–146, 2015.

[33] M. Caputo, "Linear models of dissipation whose Q is almost frequency independent—II," *Geophysical Journal International*, vol. 13, no. 5, pp. 529–539, 1967.

[34] E. F. D. Goufo, "Application of the Caputo-Fabrizio fractional derivative without singular kernel to Korteweg-de Vries-Burgers equation," *Mathematical Modelling and Analysis*, vol. 21, no. 2, pp. 188–198, 2016.

[35] M. Caputo and M. Fabrizio, "A new definition of fractional derivative without singular kernel," *Progress in Fractional Differentiation & Applications*, vol. 1, no. 2, pp. 1–13, 2015.

[36] P. Kumam and W. Watthayu, "A novel comparative case study of entropy generation for natural convection flow of proportional-Caputo hybrid and Atangana baleanu fractional derivative," *Scientific Reports*, vol. 11, no. 1, pp. 1–11, 2021.

[37] D. Khan, A. ur Rahman, P. Kumam, W. Watthayu, K. Sitthithakerngkiet, and A. M. Galal, "Thermal analysis of different shape nanoparticles on hyperthermia therapy on breast cancer in a porous medium: a fractional model," *Heliyon*, vol. 8, no. 8, article e10170, 2022.

[38] S. Akhtar, "Flows between two parallel plates of couple stress fluids with time-fractional Caputo and Caputo-Fabrizio derivatives," *The European Physical Journal Plus*, vol. 131, no. 11, pp. 1–13, 2016.

[39] S. Ahmad, S. U. Haq, F. Ali, I. Khan, and K. S. Nisar, "Time fractional analysis of channel flow of couple stress Casson fluid using Fick's and Fourier's laws," *Scientific Reports*, vol. 12, no. 1, pp. 1–16, 2022.

[40] S. Akhtar and N. A. Shah, "Exact solutions for some unsteady flows of a couple stress fluid between parallel plates," *Ain Shams Engineering Journal*, vol. 9, no. 4, pp. 985–992, 2018.

Hindawi
Journal of Function Spaces
Volume 2023, Article ID 6704537, 7 pages
https://doi.org/10.1155/2023/6704537

Research Article

Analysis of Fractional Kundu-Eckhaus and Massive Thirring Equations Using a Hybridization Scheme

Muhammad Nadeem [1] **and Hanan A. Wahash** [2]

[1]School of Mathematics and Statistics, Qujing Normal University, Qujing 655011, China
[2]Department of Mathematics, Albaydha University, Albaydha, Yemen

Correspondence should be addressed to Hanan A. Wahash; hawahash@baydaauniv.net

Received 28 September 2022; Revised 24 October 2022; Accepted 13 March 2023; Published 28 March 2023

Academic Editor: Yusuf Gurefe

This paper deals with the study of fractional Kundu-Eckhaus equation (FKEE) and fractional massive Thirring problem (FMTP) that appear in the quantum field theory, weakly nonlinear dispersive water waves, and nonlinear optics. Since the variational iteration method involves integration, the Laplace transform involves convolution theorem in recurrence relation to derive the series solution. To avoid some assumptions and hypothesis, we apply a two-scale approach for such a nonlinear complex model. The fractional differential equation may be transformed into its partner equation using He's fractional complex transform, and then, the nonlinear elements can be readily handled using the homotopy perturbation method (HPM). Numerical results are derived in a rapid converge series form to improve the accuracy of the scheme greatly. Graphical representations and error distribution show that the two-scale approach is a very convenient tool.

1. Introduction

In recent years, fractional calculus (FC) has assumed a greater significance in mathematical theory and widely used in many fields including ecology, physics, astronomy, and economics. Researchers are increasingly realizing that the fractional framework may be compatible with a wide range of phenomena in common applied sciences after the concepts of FC were successfully applied to a variety of different features. Mathematical models of many physical processes are developed using fractional differential equations. They are employed not only in mathematics but also in physics, dynamical systems, power systems, and applied science [1–3]. Kundu and Eckhaus [4, 5] introduced the FKKE which is studied in quantum field theory and many dispersion phenomena.

$$iD_\xi^\alpha \Psi(\varsigma,\xi) + \Psi_{\varsigma\varsigma} + 2\Psi\left(|\Psi|^2\right)_\varsigma + \Psi|\Psi|^4 = 0, \quad 0 < \alpha \leq 1. \quad (1)$$

The FKKE is a combination of Lax couples, higher conserved portion, particular soliton solution, and rogue wave solution. It is very essential to develop a scientific design that acts on behalf of ultrashort light pulses in a glass fiber. This model will be used to demonstrate the propagation of light across an optical cable. The fractional massive Thirring problem (FMTP)

$$\begin{aligned} &i\left(D_\xi^\alpha \Psi + \Psi_\varsigma\right) + \Phi + \Psi|\Phi|^2 = 0 \\ &i\left(D_\xi^\alpha \Phi + \Phi_\varsigma\right) + \Psi + \Phi|\Psi|^2 = 0 \end{aligned} \quad (2)$$

was autonomously introduced in 1958 by Thirring. It is a nonlinear coupled fractional differential equation which appears in the quantum field theory [6, 7]. Feng and Wang [8] discussed the algebraic curve method to obtain the explicit particular solitary solutions for the Kundu equation and the derivative Schrodinger equation. Yi and

Liu [9] employed the bifurcation approach to explore the bifurcations of traveling wave solutions for the Kundu equation. Luo and Nadeem [10] established Mohand transform with HPM to obtain the numerical solution of FKEE and coupled FMTP.

Many authors [11–13] have studied the various features of this equation, its generalities, and relationship with other nonlinear equations. It is classified to a variation of famous integrable equations such as nonlinear Schrodinger equation and also several nonlinear equations through a gauge transformation. Many researchers have studied this equation through various approaches such as gauge transformation [14], Lie symmetry method [15], Bernoulli subequation method [16], Backlund transformation [17], sine-Gordon expansion approach [18], Darboux transformation [19], and rogue wave solutions [20]. A lot of researchers introduced numerous semianalytical and numerical methods to study the fractional derivatives and fractional differential equations. He [21] constructed a technique which is called HPM that does not depend upon a small parameter to estimate the approximate solution of a nonlinear model. Later, Nadeem and Li [22] combined HPM with the Laplace transform to find the approximate solution of nonlinear vibration systems and nonlinear wave equations. It can be seen that HPM is a powerful tool and effective for nonlinear problems [23, 24]. It is however challenging to identify the analytical solutions for the most of the problems, and therefore, these problems can be tended by semianalytical methods. The objective of this paper is to suggest two-scale approach for quantum phenomena in fractal environments. The two-scale approach is the most friendly approach which converts fractional differential equations into its differential partner equations to make it extremely easy for the solution procedure.

The structure of this paper is formed as follows: in Section 2, we briefly explain the concept of HPM for a nonlinear problem. A two-scale approach with a numerical problem has been presented in Sections 3 and 4. In Section 5, we will explain the obtained results and discussion through our suggested approach. Section 6 will be our conclusions.

2. Basic Idea of Homotopy Perturbation Method

We assume the following nonlinear problem to present the concept of HPM [22]:

$$T_1(\Psi) - h(r) = 0, \quad r \in \Omega, \tag{3}$$

with boundary conditions

$$T_2\left(\Psi, \frac{\partial \Psi}{\partial S}\right) = 0, \quad \Psi \in \Gamma, \tag{4}$$

where T_1 is particular operators, T_2 is a boundary operator, $h(r)$ is a known function, and Γ is the boundary of the domain Ω. We can divide operator T_1 into two parts, R and S with considering linear and nonlinear operators, respectively. Thus, Equation (2) may also be stated as

$$R(\Psi) + S(\Psi) - h(r) = 0. \tag{5}$$

According to the homotopy strategy, we develop a homotopy $\rho(r, \theta)$: $\Omega \times [0, 1] \longrightarrow \mathbb{R}$ which satisfies

$$H(\Psi, \theta) = (1-\theta)[R(\Psi) - R(\Psi_0)] + \theta[R(\Psi) - S(\Psi) - h(r)], \tag{6}$$

or

$$H(\Psi, \theta) = R(\Psi) - R(\Psi_0) + pL(\Psi_0) + \theta[S(\Psi) - h(r)] = 0, \tag{7}$$

where $\theta \in [0, 1]$ is termed as homotopy parameter and Ψ_0 is an initial guess of Equation (2) that complies with the boundary conditions. Since the definition of HPM states that θ is estimated as a small parameter, so, we may consider the solution of Equation (5) in terms of a power series of θ such as

$$\Psi = \Psi_0 + \theta\Psi_1 + \theta^2\Psi_2 + \cdots. \tag{8}$$

Choosing $\theta = 1$, the estimated solution of Equation (2) is acquired as

$$\Psi = \lim_{\theta \longrightarrow 1} \Psi = \Psi_0 + \Psi_1 + \Psi_2 + \Psi_3 + \cdots. \tag{9}$$

The nonlinear terms are evaluated as

$$S\Psi(\varsigma, \xi) = \sum_{n=0}^{\infty} \theta^n H_n(\Psi), \tag{10}$$

where polynomials $H_n(\Psi)$ are presented such as

$$H_n(\Psi_0 + \Psi_1 + \cdots + \Psi_n) = \frac{1}{n!}\frac{\partial^n}{\partial \theta^n}\left(S\left(\sum_{i=0}^{\infty} \theta^i \Psi_i\right)\right)_{\theta=0}, \quad n = 0, 1, 2, \cdots. \tag{11}$$

Since the series depends on the nonlinear operator S, therefore, the results obtained in Equation (8) are convergent.

3. Fractional Complex Transform

In this segment, we illustrate the concept of fractional complex transform in such a way that it concerts a fractional problem into its differential parts such as [25–27]

$$\Delta S = \frac{\Delta \xi^{\alpha}}{\Gamma(1+\alpha)}, \tag{12}$$

where ΔS is nominated as a slighter scale. On a slighter scale, FKEE reacts discontinuously, in particular at the top of the solitary wave, whereas the heavier scale forecasts a coherent solitary wave. We use this transformation of Equation (12) in a fractional differential problem to change a fractal space in a lighter scale. Thus, a smooth space refers to a smooth space with a heavier scale, also called as the two-scale transform [28, 29].

4. Numerical Application

Example 1. We may rewrite Equation (1) such as

$$\frac{\partial^{\alpha}\Psi}{\partial\xi^{\alpha}} = i\Psi_{\varsigma\varsigma} + i2\Psi\left(|\Psi|^2\right)_{\varsigma} + i\Psi|\Psi|^4, \tag{13}$$

with the following initial conditions

$$\Psi(\varsigma, 0) = \mu e^{i\varsigma}. \tag{14}$$

Now, we use Equation (12) to convert it in differential parts. So, Equation (13) can be written as

$$\frac{\partial\Psi}{\partial S} = i\Psi_{\varsigma\varsigma} + 2i\Psi\left(|\Psi|^2\right)_{\varsigma} + i\Psi|\Psi|^4. \tag{15}$$

We may write it as follows:

$$\frac{\partial\Psi}{\partial S} = i\Psi_{\varsigma\varsigma} + 2i\left(\Psi\Psi_{\varsigma}\bar{\Psi} + \Psi^2\bar{\Psi}_{\varsigma}\right) + i\Psi^3\bar{\Psi}^2, \tag{16}$$

where $|\Psi|^2 = \Psi\bar{\Psi}$ and $\bar{\Psi}$ is the conjugate of Ψ.

We can select $\Psi(\varsigma, 0) = \mu e^{i\varsigma}$ by using the given initial values. Thus, HPM can be employed to Equation (16) to get the following series:

$$\begin{aligned}
\frac{\partial\Psi_1}{\partial S} &= i\Psi_{0\varsigma\varsigma} + 2i\left(\Psi_0\Psi_{0\varsigma}\bar{\Psi}_0 + \Psi^2{}_0\bar{\Psi}_{0\varsigma}\right) + i\Psi^3{}_0\bar{\Psi}^2{}_0,\\
\frac{\partial\Psi_2}{\partial S} &= i\Psi_{1\varsigma\varsigma} + 2i\Big(\Psi_0\Psi_{0\varsigma}\bar{\Psi}_1 + \Psi_0\Psi_{1\varsigma}\bar{\Psi}_0 + \Psi_1\Psi_{0\varsigma}\bar{\Psi}_0\\
&\quad + \Psi^2{}_0\bar{\Psi}_{1\varsigma} + 2\Psi_0\Psi_{1\varsigma}\bar{\Psi}_{0\varsigma}\\
&\quad + i\left(2\bar{\Psi}_0\bar{\Psi}_1\Psi^3{}_0 + 3\Psi^2{}_0\Psi_1\bar{\Psi}^2{}_0\right)\Big),\\
\frac{\partial\Psi_3}{\partial S} &= i\Psi_{2\varsigma\varsigma} + 2i\Big(\Psi_0\Psi_{0\varsigma}\bar{\Psi}_2 + \Psi_0\Psi_{1\varsigma}\bar{\Psi}_1 + \Psi_0\Psi_{2\varsigma}\bar{\Psi}_0\\
&\quad + \Psi_1\Psi_{0\varsigma}\bar{\Psi}_1 + \Psi_1\Psi_{1\varsigma}\bar{\Psi}_0 + \Psi_2\Psi_{0\varsigma}\bar{\Psi}_0 + \Psi^2{}_0\bar{\Psi}_{2\varsigma}\\
&\quad + 2\Psi_0\Psi_1\bar{\Psi}_{1\varsigma} + \Psi^2{}_1\bar{\Psi}_{0\varsigma}\Big) + i\Big(\bar{\Psi}^2{}_1\Psi^3{}_0 + 2\bar{\Psi}_0\bar{\Psi}_2\Psi^3{}_0\\
&\quad + 6\Psi^2{}_0\Psi_1\bar{\Psi}_0\bar{\Psi}_1 + 3\Psi_0\Psi^2{}_1\bar{\Psi}^2{}_0 + 3\Psi^2{}_0\Psi_2\bar{\Psi}^2{}_0\Big).
\end{aligned} \tag{17}$$

Hence, the derived results are obtained as follows:

$$\begin{aligned}
\Psi_0 &= \mu e^{i\varsigma},\\
\Psi_1 &= i\mu e^{i\varsigma}\left(\mu^4 - 1\right)S,\\
\Psi_2 &= -\mu e^{i\varsigma}\left(\mu^4 - 1\right)^2\frac{S^2}{2},\\
\Psi_3 &= \mu e^{i\varsigma}\left(i + 4\mu^2 - i\mu^4\right)\left(\mu^4 - 1\right)^2\frac{S^3}{6}.
\end{aligned} \tag{18}$$

On continuing this process, we can achieve the following series:

$$\begin{aligned}
\Psi(\varsigma, S) &= \mu e^{i\varsigma} + i\mu e^{i\varsigma}\left(\mu^4 - 1\right)S - \mu e^{i\varsigma}\left(\mu^4 - 1\right)^2\frac{S^2}{2}\\
&\quad + \mu e^{i\varsigma}\left(i + 4\mu^2 - i\mu^4\right)\left(\mu^4 - 1\right)^2\frac{S^3}{6} + \cdots.
\end{aligned} \tag{19}$$

Using Equation (12), we can get

$$\begin{aligned}
\Psi(\varsigma, \xi) &= \mu e^{i\varsigma} + i\mu e^{i\varsigma}\left(\mu^4 - 1\right)\frac{\xi^{\alpha}}{\Gamma(1+\alpha)}\\
&\quad - \frac{\mu e^{i\varsigma}}{2}\left(\mu^4 - 1\right)^2\left(\frac{\xi^{\alpha}}{\Gamma(1+\alpha)}\right)^2\\
&\quad + \frac{\mu e^{i\varsigma}}{6}\left(i + 4\mu^2 - i\mu^4\right)\left(\mu^4 - 1\right)^2\left(\frac{\xi^{\alpha}}{\Gamma(1+\alpha)}\right)^3 + \cdots,
\end{aligned} \tag{20}$$

which can be in closed form of [30, 31] at $\alpha = 1$

$$\Psi(\varsigma, \xi) = \frac{e^{i\varsigma}}{\left[1 + \left(1/\mu^4 - 1\right)e^{4i\xi}\right]^{1/4}}. \tag{21}$$

Example 2. We may rewrite Equation (2) such as

$$\begin{aligned}
&\left(\frac{\partial^{\alpha}\Psi}{\partial\xi^{\alpha}} + \frac{\partial\Psi}{\partial\varsigma}\right) - i\Phi - i\Psi|\Phi|^2 = 0,\\
&\left(\frac{\partial^{\alpha}\Phi}{\partial\xi^{\alpha}} + \frac{\partial\Phi}{\partial\varsigma}\right) - i\Psi - i\Phi|\Psi|^2 = 0,
\end{aligned} \tag{22}$$

with the following initial conditions:

$$\begin{aligned}
\Psi(\varsigma, 0) &= \mu e^{i\varsigma},\\
\Phi(\varsigma, 0) &= \eta e^{i\varsigma}.
\end{aligned} \tag{23}$$

Now, we use Equation (12) to convert it in differential parts. So, the above system of Equation (22) becomes as

$$\begin{aligned} &\frac{\partial \Psi}{\partial S} + \frac{\partial \Psi}{\partial \varsigma} - i\Phi - i\Psi|\Phi|^2 = 0, \\ &\frac{\partial \Phi}{\partial S} + \frac{\partial \Phi}{\partial \varsigma} - i\Psi - i\Phi|\Psi|^2 = 0. \end{aligned} \tag{24}$$

We may write it as follows:

$$\begin{aligned} &\frac{\partial \Psi}{\partial S} + \frac{\partial \Psi}{\partial \varsigma} - i\Phi - i\Psi\Phi\bar{\Phi} = 0, \\ &\frac{\partial \Phi}{\partial S} + \frac{\partial \Phi}{\partial \varsigma} - i\Psi - i\Phi\Psi\bar{\Psi} = 0, \end{aligned} \tag{25}$$

where $|\Psi|^2 = \Psi\bar{\Psi}$ and $|\Phi|^2 = \Phi\bar{\Phi}$ with $\bar{\Psi}$ and $\bar{\Phi}$ are the conjugate of Ψ and Φ, respectively.

We can select $\Psi(\varsigma, 0) = \mu e^{i\varsigma}$ and $\Phi(\varsigma, 0) = \eta e^{i\varsigma}$ by using the given initial values. Thus, HPM can be employed to Equation (25) to get the following series:

$$\begin{aligned} &\frac{\partial \Psi_1}{\partial S} + \frac{\partial \Psi_0}{\partial \varsigma} - i\Phi_0 - i\Psi_0\Phi_0\bar{\Phi}_0 = 0, \quad \Psi_1(\varsigma, 0) = 0, \\ &\frac{\partial \Phi_1}{\partial S} + \frac{\partial \Phi_0}{\partial \varsigma} - i\Psi_0 - i\Phi_0\Psi_0\bar{\Psi}_0 = 0, \quad \Psi_1(\varsigma, 0) = 0, \\ &\frac{\partial \Psi_2}{\partial S} + \frac{\partial \Psi_1}{\partial \varsigma} - i\Phi_1 - i\left(\Psi_0\Phi_0\bar{\Phi}_1 + \Psi_0\Phi_1\bar{\Phi}_0 + \Psi_1\Phi_0\bar{\Phi}_0\right) = 0, \\ &\qquad \Psi_2(\varsigma, 0) = 0, \\ &\frac{\partial \Phi_2}{\partial S} + \frac{\partial \Phi_1}{\partial \varsigma} - i\Psi_1 - i\left(\Phi_0\Psi_0\bar{\Psi}_1 + \Phi_0\Psi_1\bar{\Psi}_0 + \Phi_1\Psi_0\bar{\Psi}_0\right) = 0, \\ &\qquad \Phi_2(\varsigma, 0) = 0, \\ &\frac{\partial \Psi_3}{\partial S} + \frac{\partial \Psi_2}{\partial \varsigma} - i\Phi_2 - i\left(\Psi_0\Phi_0\bar{\Phi}_2 + \Psi_0\Phi_1\bar{\Phi}_2\right. \\ &\qquad \left. + \Psi_0\Phi_2\bar{\Phi}_0 + \Psi_1\Phi_0\bar{\Phi}_1 + \Psi_1\Phi_1\bar{\Phi}_0 + \Psi_2\Phi_0\bar{\Phi}_0\right) = 0, \\ &\qquad \Psi_3(\varsigma, 0) = 0, \\ &\frac{\partial \Phi_3}{\partial S} + \frac{\partial \Phi_2}{\partial \varsigma} - i\Psi_2 - i\left(\Phi_0\Psi_0\bar{\Psi}_2 + \Phi_0\Psi_1\bar{\Psi}_1 + \Phi_0\Psi_2\bar{\Psi}_0\right. \\ &\qquad \left. + \Phi_1\Psi_0\bar{\Psi}_1 + \Phi_1\Psi_1\bar{\Psi}_0 + \Phi_2\Psi_0\bar{\Psi}_0\right) = 0, \quad \Phi_3(\varsigma, 0) = 0. \end{aligned} \tag{26}$$

Hence, the derived results are obtained as follows:

$$\begin{aligned} &\Psi(\varsigma, 0) = \mu e^{i\varsigma}, \\ &\Phi(\varsigma, 0) = \eta e^{i\varsigma}, \\ &\Psi_1(\varsigma, S) = ie^{i\varsigma}\left[\eta - \mu + \eta^2\mu\right]S, \\ &\Phi_1(\varsigma, S) = ie^{i\varsigma}\left[\mu - \eta + \mu^2\eta\right]S, \\ &\Psi_2(\varsigma, S) = i^2e^{i\varsigma}\left[\eta^3 + 2\mu + \eta^4\mu + 2\eta^2\mu\left(-2 + \mu^2\right)\right. \\ &\qquad \left. + \eta\left(-2 + 3\mu^2\right)\right]\frac{S^2}{2}, \\ &\Phi_2(\varsigma, S) = i^2e^{i\varsigma}\left[\mu^3 + 2\eta + \mu^4\eta + 2\mu^2\eta\left(-2 + \eta^2\right)\right. \\ &\qquad \left. + \mu\left(-2 + 3\eta^2\right)\right]\frac{S^2}{2}. \end{aligned} \tag{27}$$

On continuing this process, we can achieve the following series:

$$\begin{aligned} \Psi(\varsigma, S) &= \mu e^{i\varsigma} + ie^{i\varsigma}\left[\eta - \mu + \eta^2\mu\right]S + i^2e^{i\varsigma}\left[\eta^3 + 2\mu + \eta^4\mu\right. \\ &\qquad \left. + 2\eta^2\mu\left(-2 + \mu^2\right) + \eta\left(-2 + 3\mu^2\right)\right]\frac{S^2}{2} + \cdots, \\ \Phi(\varsigma, S) &= \eta e^{i\varsigma} + ie^{i\varsigma}\left[\mu - \eta + \mu^2\eta\right]S + i^2e^{i\varsigma}\left[\mu^3 + 2\eta + \mu^4\eta\right. \\ &\qquad \left. + 2\mu^2\eta\left(-2 + \eta^2\right) + \mu\left(-2 + 3\eta^2\right)\right]\frac{S^2}{2} + \cdots. \end{aligned} \tag{28}$$

Using Equation (12), we can get

$$\begin{aligned} \Psi(\varsigma, \xi) &= \mu e^{i\varsigma} + ie^{i\varsigma}\left[\eta - \mu + \eta^2\mu\right]\eta^\alpha + \frac{i^2}{2}e^{i\varsigma}\left[\eta^3 + 2\mu + \eta^4\mu\right. \\ &\qquad \left. + 2\eta^2\mu\left(-2 + \mu^2\right) + \eta\left(-2 + 3\mu^2\right)\right]\left(\frac{\eta^\alpha}{\Gamma(1+\alpha)}\right)^2 + \cdots, \\ \Phi(\varsigma, \xi) &= \eta e^{i\varsigma} + ie^{i\varsigma}\left[\mu - \eta + \mu^2\eta\right]\eta^\alpha + \frac{i^2}{2}e^{i\varsigma}\left[\mu^3 + 2\eta + \mu^4\eta\right. \\ &\qquad \left. + 2\mu^2\eta\left(-2 + \eta^2\right) + \mu\left(-2 + 3\eta^2\right)\right]\left(\frac{\eta^\alpha}{\Gamma(1+\alpha)}\right)^2 + \cdots. \end{aligned} \tag{29}$$

By solving the above equations and using the approximate solution,

$$\begin{aligned} \Psi(\varsigma, \xi) &= \sum_{i=0}^{N} \Psi_i(\varsigma, \eta)\left(\frac{1}{n}\right)^i, \\ \Phi(\varsigma, \xi) &= \sum_{i=0}^{N} \Phi_i(\varsigma, \eta)\left(\frac{1}{n}\right)^i. \end{aligned} \tag{30}$$

5. Results and Discussion

This segment presents the results and discussion for the analytical solution of the FKKE and FMTP. It is believed that after a small number of repetitions, the predicted results quickly approach the exact solution. Figure 1 have been demonstrated into two parts: (a) the real part of the surface solution and (b) the imaginary part of the surface solution at $-1 \le \varsigma \le 1$ and $0 \le \xi \le 1$ with $\alpha = 1$. Figure 2 provides (a) real part of plot distribution and (b) imaginary part of plot distribution for $\alpha = 0.25, 0.50, 0.75, 1$ at $\xi = 1$. Similarly, Figure 3

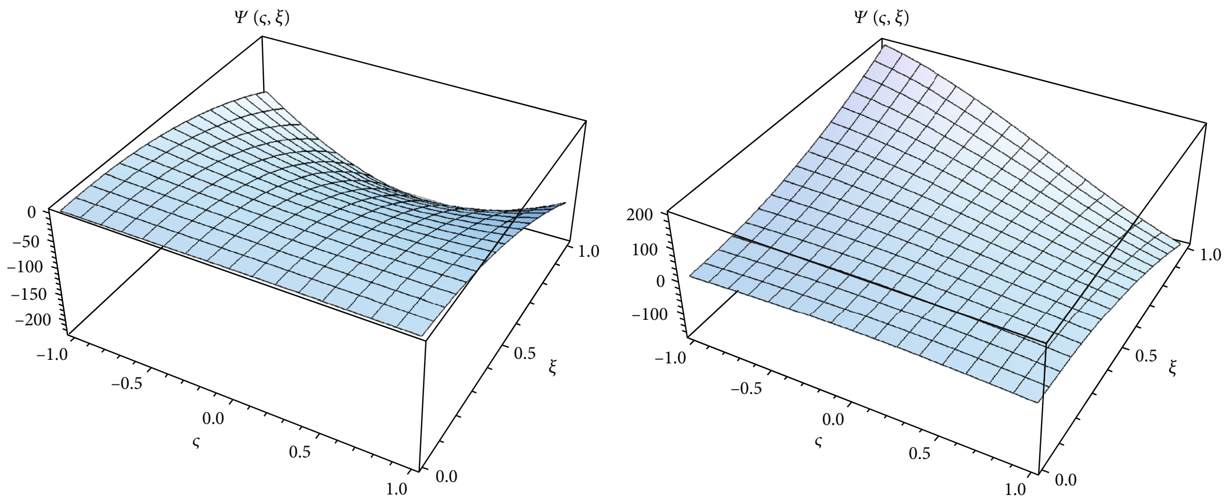

(a) Real part of surface solution

(b) Imaginary part of surface solution

Figure 1: Surface solution of Equation (13) when $\alpha = 1$.

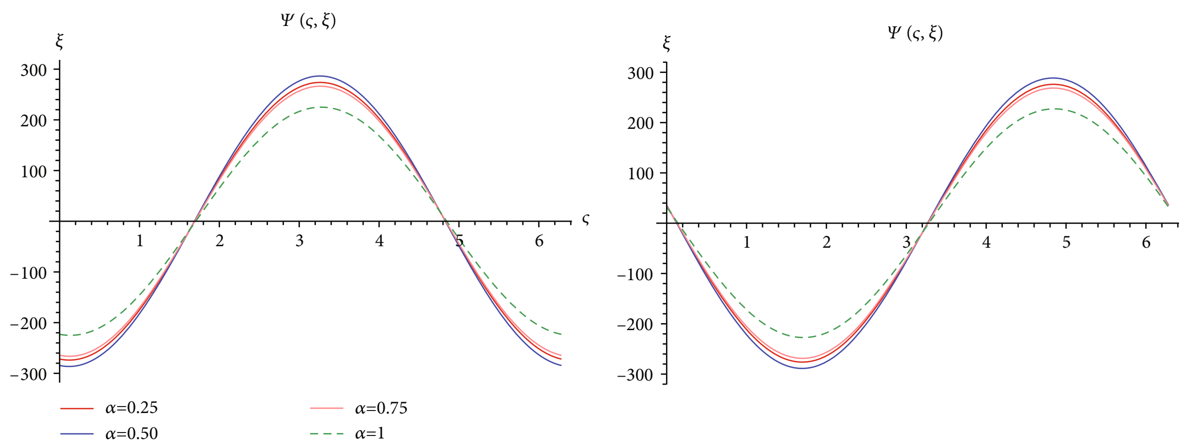

(a) Real part of plot distribution

(b) Imaginary part of plot distribution

Figure 2: Plot distribution for different values of α at $\xi = 1$.

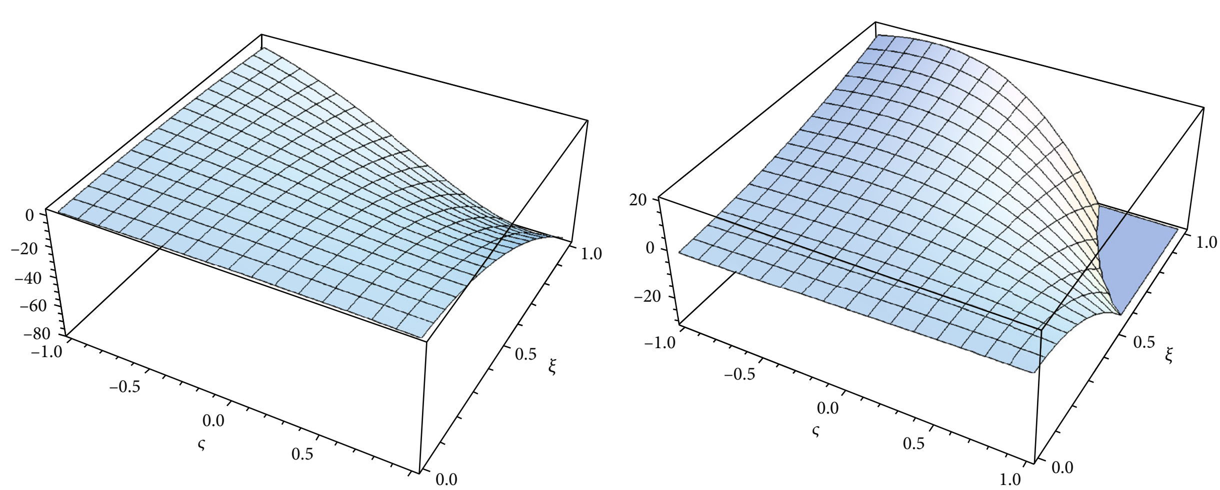

(a) Real part of Ψ and Φ

(b) Imaginary part of Ψ and Φ

Figure 3: Surface solution of Equation (22) when $\alpha = 1$.

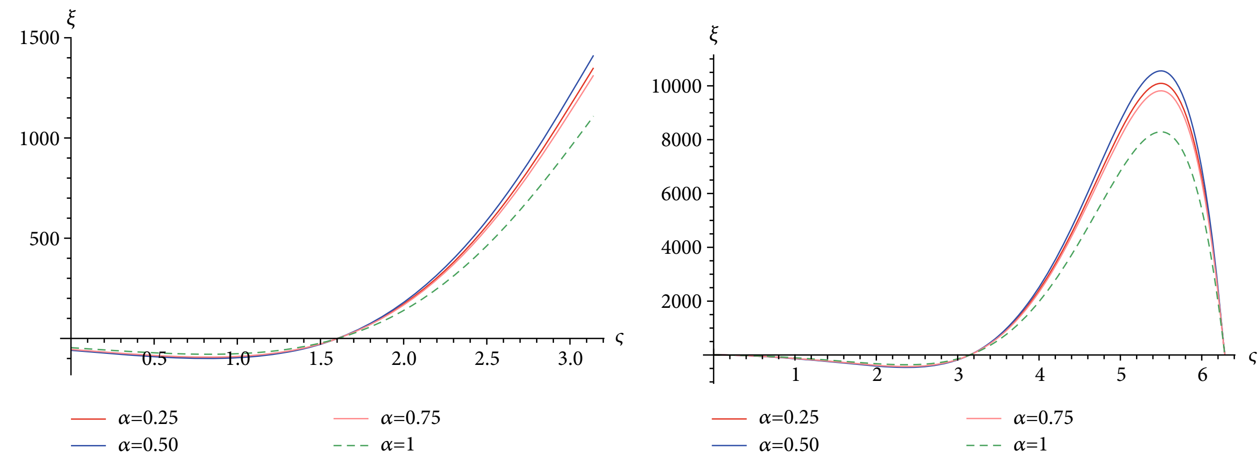

(a) Real part of plot distribution for Ψ and Φ

(b) Imaginary part of plot distribution for Ψ and Φ

Figure 4: Plot distribution for different values of α at $\xi = 1$.

has been divided into two parts: (a) real part of Ψ and Φ and (b) imaginary part of Ψ and Φ at $-1 \leq \varsigma \leq 1$ and $0 \leq \xi \leq 5$ with $\alpha = 1$. Figure 4 provides (a) real part of plot distribution for Ψ and Φ and (b) imaginary part of plot distribution for Ψ and Φ for $\alpha = 0.25, 0.50, 0.75, 1$ at $\xi = 1$. We consider $\mu = \eta = 2$ for the graphical representation in both examples.

6. Conclusion

In the present work, we have successfully applied a two-scale approach for the analytical solution of the FKKE and FMTP that arises in quantum field theory. This two-scale approach is capable to handle the PDES of fractional order without any small perturbation theory. We converted the fractional derivative into classical form and implemented the scheme of HPM. The obtained results declare that the two-scale approach possesses a high level of accuracy. The leading novelty of the suggested approach consists of the following beauty that it can deal promptly without any discretization. We used Mathematica 11 to represent the graphical structures and the iterative results. The graphical representations and plot distributions reveal that this approach has an excellent performance in finding the analytical solution of the FKKE and FMTP. In the future, we believe that the two-scale approach is suitable and feasible for other fractional differential problems arising in science and engineering.

Data Availability

All the data are available within the article.

Conflicts of Interest

The authors claim to have no conflicts of interest.

References

[1] Y. Wang and J.-Y. An, "Amplitude–frequency relationship to a fractional duffing oscillator arising in microphysics and tsunami motion," *Journal of Low Frequency Noise, Vibration and Active Control*, vol. 38, no. 3-4, pp. 1008–1012, 2019.

[2] M. S. Abdo and S. K. Panchal, "Fractional integro-differential equations involving ψ-Hilfer fractional derivative," *Advances in Applied Mathematics and Mechanics*, vol. 11, no. 2, pp. 338–359, 2019.

[3] H. M. Sedighi and F. Daneshmand, "Static and dynamic pull-in instability of multi-walled carbon nanotube probes by Hes iteration perturbation method," *Journal of Mechanical Science and Technology*, vol. 28, no. 9, pp. 3459–3469, 2014.

[4] A. Kundu, "Landau–Lifshitz and higher-order nonlinear systems gauge generated from nonlinear Schrödinger-type equations," *Journal of Mathematical Physics*, vol. 25, no. 12, pp. 3433–3438, 1984.

[5] W. Eckhaus, "The Long-Time Behaviour for Perturbed Wave-Equations and Relatedproblems," in *Trends in Applications of Pure Mathematics to Mechanics*, pp. 168–194, Springer, 1986.

[6] V. E. Korepin, "Direct calculation of the S matrix in the massive Thirring model," *Teoreticheskaya Matematicheskaya Fizika*, vol. 41, no. 2, pp. 953–967, 1979.

[7] W. E. Thirring, "A soluble relativistic field theory," *Annals of Physics*, vol. 3, no. 1, pp. 91–112, 1958.

[8] Z. Feng and X. Wang, "Explicit exact solitary wave solutions for the Kundu equation and the derivative Schrödinger equation," *Physica Scripta*, vol. 64, no. 1, pp. 7–14, 2001.

[9] Y. Yi and Z. Liu, "The bifurcations of traveling wave solutions of the Kundu equation," *Journal of Applied Mathematics*, vol. 2013, Article ID 137475, 9 pages, 2013.

[10] X. Luo and M. Nadeem, "Mohand homotopy transform scheme for the numerical solution of fractional Kundu-Eckhaus and coupled fractional massive Thirring equations," *Scientific Reports*, vol. 13, no. 1, p. 3995, 2023.

[11] H. Zhang, "Various exact travelling wave solutions for Kundu equation with fifth-order nonlinear term," *Reports on Mathematical Physics*, vol. 65, no. 2, pp. 231–239, 2010.

[12] W. Zhang, Y. Qin, Y. Zhao, and B. Guo, "Orbital stability of solitary waves for Kundu equation," *Journal of Differential Equations*, vol. 247, no. 5, pp. 1591–1615, 2009.

[13] C. Liu, J. Liu, P. Zhou, and M. Chen, "Exact solutions with bounded periodic amplitude for Kundu equation

and derivative nonlinear Schrödinger equation," *Journalof Advances in Mathematics and Computer Science*, vol. 16, no. 5, pp. 1–6, 2016.

[14] A. Kundu, "Exact solutions to higher-order nonlinear equations through gauge transformation," *Physica D: Nonlinear Phenomena*, vol. 25, no. 1-3, pp. 399–406, 1987.

[15] M. Toomanian and N. Asadi, "Reductions for Kundu-Eckhaus equation via Lie symmetry analysis," *Mathematical Sciences*, vol. 7, no. 1, p. 50, 2013.

[16] H. M. Baskonus and H. Bulut, "On the complex structures of Kundu-Eckhaus equation via improved Bernoulli sub-equation function method," *Waves in Random and Complex Media*, vol. 25, no. 4, pp. 720–728, 2015.

[17] P. Wang, B. Tian, K. Sun, and F.-H. Qi, "Bright and dark soliton solutions and Bäcklund transformation for the Eckhaus–Kundu equation with the cubic–quintic nonlinearity," *Applied Mathematics and Computation*, vol. 251, pp. 233–242, 2015.

[18] M. Ilie, J. Biazar, and Z. Ayati, "Resonant solitons to the nonlinear Schrodinger equation with different forms of nonlinearities," *Optik*, vol. 164, pp. 201–209, 2018.

[19] D. Qiu, J. He, Y. Zhang, and K. Porsezian, "The Darboux transformation of the Kundu–Eckhaus equation," *Proceedings of the Royal Society A: Mathematical, Physicaland Engineering Sciences*, vol. 471, no. 2180, article 20150236, 2015.

[20] X. Wang, B. Yang, Y. Chen, and Y. Yang, "Higher-order rogue wave solutions of the Kundu–Eckhaus equation," *Physica Scripta*, vol. 89, no. 9, article 095210, 2014.

[21] J.-H. He, "Homotopy perturbation technique," *Computer Methods in Applied Mechanics and Engineering*, vol. 178, no. 3-4, pp. 257–262, 1999.

[22] M. Nadeem and F. Li, "He–Laplace method for nonlinear vibration systems and nonlinear wave equations," *Journal of Low Frequency Noise, Vibration and Active Control*, vol. 38, no. 3-4, pp. 1060–1074, 2019.

[23] J. Biazar, Z. Ayati, and M. R. Yaghouti, "Homotopy perturbation method for homogeneous Smoluchowsk's equation," *Numer. Methods Partial Differential Equation*, vol. 26, no. 5, pp. 1146–1153, 2010.

[24] J. Biazar and H. Ghazvini, "Exact solutions for nonlinear Burgers' equation by homotopy perturbation method," *Numerical Methods for Partial Differential Equation*, vol. 25, no. 4, pp. 833–842, 2009.

[25] J.-H. He, S. Elagan, and Z. Li, "Geometrical explanation of the fractional complex transform and derivative chain rule for fractional calculus," *Physics Letters*, vol. 376, no. 4, pp. 257–259, 2012.

[26] Z.-B. Li and J.-H. He, "Fractional complex transform for fractional differential equations," *Mathematical and Computational Applications*, vol. 15, no. 5, pp. 970–973, 2010.

[27] K.-L. Wang and S.-W. Yao, "He's fractional derivative for the evolution equation," *Thermal Science*, vol. 24, no. 4, pp. 2507–2513, 2020.

[28] Q. T. Ain and J.-H. He, "On two-scale dimension and its applications," *Thermal Science*, vol. 23, no. 3, Part B, pp. 1707–1712, 2019.

[29] J.-H. He and F.-Y. Ji, "Two-scale mathematics and fractional calculus for thermodynamics," *Thermal Science*, vol. 23, no. 4, pp. 2131–2133, 2019.

[30] A. A. Arafa and A. M. S. Hagag, "Q-homotopy analysis transform method applied to fractional Kundu–Eckhaus equation and fractional massive Thirring model arising in quantum field theory," *Asian-European Journal of Mathematics*, vol. 12, no. 3, article 1950045, 2019.

[31] O. González-Gaxiola, "The Laplace-Adomian decomposition method applied to the Kundu-Eckhaus equation," *International Journal of Mathematics And its Applications*, vol. 5, no. 1(A), pp. 1–12, 2017.

Hindawi
Journal of Function Spaces
Volume 2023, Article ID 5484241, 9 pages
https://doi.org/10.1155/2023/5484241

Research Article

Approximate Solutions of Multidimensional Wave Problems Using an Effective Approach

Muhammad Nadeem,[1] **Qura tul Ain**,[2] **and Yahya Alsayaad**[3]

[1]*School of Mathematics and Statistics, Qujing Normal University, 655011 Qujing, China*
[2]*Department of Mathematics, Guizhou University, 550025 Guiyang, China*
[3]*Department of Physics and Mathematics, Al-Hudaydah and Zabid Hodeidan University, Yemen*

Correspondence should be addressed to Muhammad Nadeem; nadeem@mail.qjnu.edu.cn
and Yahya Alsayaad; yahyaalsayyad2022@hoduniv.net.ye

Received 4 October 2022; Revised 2 November 2022; Accepted 24 November 2022; Published 9 February 2023

Academic Editor: Yusuf Gurefe

The main goal of this paper is to introduce a new scheme for the approximate solution of 1D, 2D, and 3D wave equations. The recurrence relation is very important to deal with the approximate solution of differential problems. We construct a scheme with the help of the Laplace-Carson integral transform ($\mathbb{L}_c$IT) and the homotopy perturbation method (HPM), called Laplace-Carson homotopy integral transform method ($\mathbb{L}_c$HITM). $\mathbb{L}_c$IT produces the recurrence relation and destructs the restriction of variables whereas HPM gives the successive iteration of the relation using the initial conditions. The convergence analysis is provided to study the wave equation with multiple dimensions. Some numerical examples are considered to show the efficiency of this scheme. Graphical representation and plot distribution between the approximate and the exact solution predict the high rate of convergence of this approach.

1. Introduction

Numerous physical phenomena in real world are modeled using partial differential equations (PDEs) in a variety of applied science fields including fluid dynamics, mathematical biology, quantum physics, chemical kinetics, and linear optics [1–3]. There are various perturbation approaches that can be used to analytically solve the PDEs. Although the calculations for these strategies are pretty straightforward, their limitations are predicated on the assumption of small parameters. As a result, many researchers are searching for novel methods to get around these restrictions. Various researchers and scientists have studied multiple novel methods for getting the analytical solution that are reasonably close to the precise solutions such as homotopy analysis method [4], modified extended tanh method [5], new Kudryashov's method [6], Chun-Hui He's iteration method [7], subequation method [8], exp-function method [9], modified exponential rational method [10], homotopy asymptotic method [11], modified extended tanh expansion [12], fractal variational iteration transform method [13], Laplace homotopy perturbation transform method [14], residual power series (RPS) method [15], and Adomian decomposition method [16]. In the past, many experts and researchers established the application of the homotopy perturbation method (HPM) [17, 18] in various physical problems, because this approach consistently transforms the challenging issue into a straightforward resolution. The method yields a physical problem, because this approach consistently transforms the challenging issue into a straightforward resolution. The method yields a very rapid convergence of the solution perturbation theory and showed the ability to be a very strong mathematical tool.

The wave equation, which describes the wave propagation phenomenon, is a partial differential equation for a scalar function. It is influenced by time and one or more spatial factors. The wave equations perform an important role in different area of engineering, physics, and scientific applications. Wazwaz [19] studied linear and nonlinear problems in bounded and unbounded domains using the variational iteration method. Ghasemi et al. [20] employed the homotopy perturbation method to derive the numerical solution of two-dimensional nonlinear differential equation. Keskin and Oturanc [21] applied reduced differential transform method to various wave equations. Ullah et al. [22] proposed optimal homotopy asymptotic method to obtain the analytic series solution of wave equations. Adwan et al. [23] presented the numerical solution of multidimensional wave equations and showed the accuracy of proposed techniques. Jleli et al. [24] studied the framework of the homotopy perturbation transform method for analytic treatment of wave equations. Mullen and Belytschko [25] provided the finite element scheme for the examination of two-dimensional wave equation and considered some semidiscretizations. These schemes have many limitations and assumptions in finding the approximate solution of the problems. To overcome these limitations and restriction of variable, we introduce a new iterative strategy for the approximate solution of multidimensional wave problem.

The variational iteration method (VIM), Laplace transform, and homotopy analysis method (HAM) have some limitations such as VIM involves the integration and produces the constant of integration, Laplace transform involves the convolution theorem, and HAM also considered some assumptions. The Laplace-Carson integral transform is very easy to implement to the differential problems. The purpose of this paper is to apply $\mathbb{L}_c$HITM with the combination of the Laplace-Carson integral transform and the HPM for wave problems of different dimensions. Less computations, fast convergence, and significant results make this scheme unique and different than other approaches of literature. This strategy derives the series of solution with fast convergence and yields the approximate solution very close to the precise solution. This approach is more useful and reliable for the solution of these problems. This paper is introduced as follows: in Section 2, we give a brief detail of the Laplace-Carson integral transform. In Section 3, we present the formulation of $\mathbb{L}_c$HITM for solving multidimensional problems. We provide the convergence analysis in Section 4. Some numerical applications are demonstrated to show the effectiveness in Section 5, and eventually, we discuss the conclusion in Section 6.

2. Preliminary Definitions of $\mathbb{L}_c$IT

In this section, we describe a few fundamental characteristics and concepts of $\mathbb{L}_c$IT that are very helpful in the formulation of this scheme.

Definition 1. Let $\vartheta(\phi)$ be a function precise for $\sigma \geq 0$; then,

$$\mathscr{L}\{\vartheta(\phi)\} = F(s) = \int_0^\infty \vartheta(\phi) e^{-\sigma\phi} d\phi \tag{1}$$

is called the Laplace transform.

Definition 2. The $\mathbb{L}_c$IT of a function $\vartheta(\phi)$ is defined as [26]

$$\mathbb{L}_c[\vartheta(\phi)] = R(\sigma) = \sigma \int_0^\infty \vartheta(\phi) e^{-\sigma\phi} d\phi, \phi \geq 0, k_1 \leq \sigma \leq k_2, \tag{2}$$

where $\mathbb{L}_c$ represents the symbol of $\mathbb{L}_c$IT, k_1 and k_2 are constants, and σ is the independent variable of the transformed function ϕ. Conversely, since $R(\sigma)$ is the $\mathbb{L}_c$IT of function $\vartheta(\phi)$, then

$$\mathbb{L}_c^{-1}[R(\sigma)] = \vartheta(\phi). \tag{3}$$

$\mathbb{L}_c^{-1}$ is called inverse $\mathbb{L}_c$IT.

Proposition 3. *Let* $\mathbb{L}_c\{\vartheta_1(\phi)\} = R_1(\sigma)$ *and* $\mathbb{L}_c\{\vartheta_2(\phi)\} = R_2(\sigma)$*; then [27]*

$$\begin{aligned} &\mathbb{L}_c\{au_1(\phi) + bu_2(\phi)\} = aS\{\vartheta_1(\phi)\} + bS\{\vartheta_2(\phi)\}, \\ &\Rightarrow \mathbb{L}_c\{au_1(\phi) + bu_2(\phi)\} = aR_1(\sigma) + bR_2(\sigma). \end{aligned} \tag{4}$$

Proposition 4. *If* $\mathbb{A}\{\vartheta(\phi)\} = R(\sigma)$*, the differential properties are defined as [26, 27]*

$$\begin{aligned} &\mathbb{L}_c\left\{\vartheta'(\phi)\right\} = \sigma R(\sigma) - \sigma\vartheta(0), \\ &\mathbb{L}_c\left\{\vartheta''(\phi)\right\} = \sigma^2 R(\sigma) - \sigma^2\vartheta(0) - \sigma\vartheta'(0), \\ &\mathbb{L}_c\{\vartheta^m(\phi)\} = \sigma^m R(\sigma) - \sigma^m\vartheta(0) - \sigma^{m-1}\vartheta'(0) - \cdots - \sigma\vartheta^{m-1}(0). \end{aligned} \tag{5}$$

3. Formulation of $\mathbb{L}_c$HITM

In this segment, we formulate the strategy of $\mathbb{L}_c$HITM for finding the approximate solutions of 1D, 2D, and 3D wave equation flows. We observe that this strategy is independent of integration and any hypothesis during the formulation of this scheme. We consider a differential problem such that

$$\vartheta''(\varsigma, \phi) = \vartheta(\varsigma, \phi) + g(\vartheta) + g(\varsigma, \phi), \tag{6}$$

with initial condition

$$\begin{aligned} \vartheta(\varsigma, 0) &= a_1, \\ \vartheta_\phi(\varsigma, 0) &= a_2, \end{aligned} \tag{7}$$

where ϑ denotes the function in region of time ϕ, $g(\vartheta)$ is considered as a nonlinear term, and $g(\varsigma, \phi)$ is source term arbitrary constant a. Employing $\mathbb{L}_c$IT on Equation (6), it yields

$$\mathbb{L}_c\left[\vartheta''(\varsigma, \phi)\right] = \mathbb{L}_c[\vartheta(\varsigma, \phi) + g(\vartheta) + g(\varsigma, \phi)]. \tag{8}$$

Using proposition (5) of $\mathbb{L}_c$IT, we obtain

$$\sigma^2 R(\sigma) - \sigma^2 \vartheta(\varsigma, 0) - \sigma \vartheta'(\varsigma, 0) = \mathbb{L}_c[\vartheta(\varsigma, \phi) + g(\vartheta) + g(\varsigma, \phi)]. \tag{9}$$

Hence, $R(\sigma)$ is evaluated such as

$$R[\sigma] = \vartheta(\varsigma, 0) + \frac{\vartheta'(\varsigma, 0)}{\sigma} + \frac{1}{\sigma^2}\mathbb{L}_c[\vartheta(\varsigma, \phi) + g(\vartheta) + g(\varsigma, \phi)]. \tag{10}$$

Operating inverse $\mathbb{L}_c$IT on Equation (10), we get

$$\vartheta(\varsigma, \phi) = \vartheta(\varsigma, 0) + \phi\vartheta'(\varsigma, 0) + \mathbb{L}_c^{-1}\left[\frac{1}{\sigma^2}\mathbb{L}_c\{\vartheta(\varsigma, \phi) + g(\vartheta) + g(\varsigma, \phi)\}\right]. \tag{11}$$

Using initial conditions, we get

$$\vartheta(\varsigma, \phi) = a_1 + \phi a_2 + \mathbb{L}_c^{-1}\left[\frac{1}{\sigma^2}\mathbb{L}_c\{\vartheta(\varsigma, \phi) + g(\vartheta) + g(\varsigma, \phi)\}\right]. \tag{12}$$

Using proposition (4), we obtain

$$\vartheta(\varsigma, \phi) = a_1 + \phi a_2 + \mathbb{L}_c^{-1}\left[\frac{1}{\sigma^2}\mathbb{L}_c\{g(\varsigma, \phi)\}\right] + \mathbb{L}_c^{-1}\left[\frac{1}{\sigma^2}\mathbb{L}_c[\vartheta(\varsigma, \phi) + g(\vartheta)]\right]. \tag{13}$$

This implies that

$$\vartheta(\varsigma, \phi) = G(\varsigma, \phi) + \mathbb{L}_c^{-1}\left[\frac{1}{\sigma^2}\mathbb{L}_c[\vartheta(\varsigma, \phi) + g(\vartheta)]\right]. \tag{14}$$

Equation (14) is called the formulation of $\mathbb{L}_c$HITM of Equation (6) and

$$G(\varsigma, \phi) = a_1 + \phi a_2 + \mathbb{L}_c^{-1}\left[\frac{1}{\sigma^2}\mathbb{L}_c\{g(\varsigma, \phi)\}\right]. \tag{15}$$

We introduce HPM in such a way that

$$\vartheta(\phi) = \sum_{i=0}^{\infty} p^i \vartheta_i(n) = \vartheta_0 + p^1\vartheta_1 + p^2\vartheta_2 + \cdots, \tag{16}$$

and nonlinear terms $g(\vartheta)$ are evaluated by considering an algorithm:

$$g(\vartheta) = \sum_{i=0}^{\infty} p^i H_i(\vartheta) = H_0 + p^1 H_1 + p^2 H_2 + \cdots, \tag{17}$$

where H_n polynomials are derived as

$$H_n(\vartheta_0 + \vartheta_1 + \cdots + \vartheta_n) = \frac{1}{n!}\frac{\partial^n}{\partial p^n}\left(g\left(\sum_{i=0}^{\infty} p^i \vartheta_i\right)\right)_{p=0}, \quad n = 0, 1, 2, \cdots. \tag{18}$$

Use Equations (16)–(18) in Equation (14) to compare the identical power of p such as

$$\begin{aligned}
p^0 &: \vartheta_0(\varsigma, \phi) = G(\varsigma, \phi), \\
p^1 &: \vartheta_1(\varsigma, \phi) = \mathbb{L}_c^{-1}\left[\frac{1}{\sigma^2}\mathbb{L}_c\{\vartheta_0(\varsigma, \phi) + H_0(\vartheta)\}\right], \\
p^2 &: \vartheta_2(\varsigma, \phi) = \mathbb{L}_c^{-1}\left[\frac{1}{\sigma^2}\mathbb{L}_c\{\vartheta_1(\varsigma, \phi) + H_1(\vartheta)\}\right], \\
p^3 &: \vartheta_3(\varsigma, \phi) = \mathbb{L}_c^{-1}\left[\frac{1}{\sigma^2}\mathbb{L}_c\{\vartheta_2(\varsigma, \phi) + H_2(\vartheta)\}\right], \\
&\vdots .
\end{aligned} \tag{19}$$

On proceeding this process, this yields

$$\vartheta(\varsigma, \phi) = \vartheta_0 + \vartheta_1 + \vartheta_2 + \cdots = \sum_{i=0}^{\infty} \vartheta_i. \tag{20}$$

Thus, Equation (20) is the approximate result of the differential problem (6).

4. Convergence Analysis

Let P and Q be Banach spaces where $X : P \longrightarrow Q$ is a nonlinear mapping. If the series produced by HPM is

$$\vartheta_n(P, \varsigma) = X(\vartheta_{n-1}(P, \varsigma)) = \sum_{i=0}^{n-1} \vartheta_i(P, \varsigma), \quad n = 1, 2, 3 \cdots, \tag{21}$$

the following conditions must be true:

(1) $\|\vartheta_n(P, \varsigma) - \vartheta(P, \varsigma)\| \le \varphi^n \|\vartheta(P, \varsigma) - \vartheta(P, \varsigma)\|$

(2) $\vartheta_n(P, \varsigma)$ is forever in the neighbourhood of $\vartheta(P, x)$ meaning $\vartheta_n(P, \varsigma) \in B(\vartheta(P, \varsigma), r) = \{\vartheta^*(P, \varsigma)/\|\vartheta^*(P, \varsigma) - \vartheta(P, \varsigma)\|\}$

(3) $\lim_{n \longrightarrow \infty} \vartheta_n(P, x) = \vartheta(P, \varsigma)$

Proof.

(1) We demonstrate condition (1) by recognition on n, such as $\|\vartheta_1 - \vartheta\| = \|G(\vartheta_0) - \vartheta\|$, and the Banach fixed point theorem states that X has a fixed point ϑ, i.e.,

$X(\vartheta)=\vartheta$; therefore,

$$\begin{aligned}\|\vartheta_1-\vartheta\|&=\|G(\vartheta_0)-\vartheta\|=\|G(\vartheta_0)-G(\vartheta)\|\\&\le\varphi\|\vartheta_0-\vartheta\|=\varphi\|\vartheta(P,\varsigma)-\vartheta\|,\end{aligned}\tag{22}$$

where X is a nonlinear mapping. Consider that $\|\vartheta_{n-1}-\vartheta\|\le\varphi^{n-1}\|\vartheta(P,0)-\vartheta(P,x)\|$ is an induction hypothesis; then,

$$\|\vartheta_n-\vartheta\|=\|G(\vartheta_{n-1})-G(\vartheta)\|\le\varphi\|\vartheta_{n-1}-\vartheta\|\le\varphi\varphi^{n-1}\|\vartheta(P,\varsigma)-\vartheta\|\tag{23}$$

(2) Our initial challenge is to demonstrate the $\vartheta(P,\varsigma)\in B(\vartheta(P,\varsigma),r)$, which is attained by replacing m. Thus, $m=1$, $\|\vartheta(P,\varsigma)-\vartheta(P,\varsigma)\|=\|\vartheta(P,0)-\vartheta(P,\varsigma)\|\le r$ with $\vartheta(P,0)$ as an initial condition. Consider that $\|\vartheta(P,x)-\vartheta(P,\varsigma)\|\le r$ for $m-2$ is an induction theory, so

$$\begin{aligned}\|\vartheta(P,\varsigma)-\vartheta(P,\varsigma)\|&=\vartheta_{m-2}(P,\varsigma)-\left.\frac{f_m(P)}{\Gamma(\delta-m+1)}x^{\delta-m}\right\|\\&\le\|\vartheta_{m-1}(P,\varsigma)-\vartheta(P,\varsigma)\|\\&\quad+\left\|\frac{f_m(P)}{\Gamma(\delta-m+1)}x^{\delta-m}\right\|=r\end{aligned}\tag{24}$$

Now, $\forall n\ge1$, using (1) we get

$$\|\vartheta_n-\vartheta\|\le\varphi^n\|\vartheta(P,\varsigma)-\vartheta\|\le\varphi^n r\le r.\tag{25}$$

(3) Using condition (2) and $\lim_{n\longrightarrow\infty}\varphi^n=0$, it provides that $\lim_{n\longrightarrow\infty}\|\vartheta_n-\vartheta\|=0$; hence,

$$\lim_{n\longrightarrow\infty}\vartheta_n=\vartheta\tag{26}$$

Thus, ϑ converges. □

5. Numerical Applications

We illustrate some numerical applications to check the validity and authenticity of $\mathbb{L}_c$HITM. We observe that this strategy is extremely convenient to utilize and generate the series of convergence much easier than other schemes. We also study the physical behaviors of these surface solutions. The error distribution is obtained graphically to show that the results obtained by $\mathbb{L}_c$HITM are very close to the precise results.

5.1. Example 1. Suppose a one-dimensional wave equation

$$\frac{\partial^2\vartheta}{\partial\phi^2}=\frac{\partial^2\vartheta}{\partial\varsigma^2}-3\vartheta,\tag{27}$$

with the initial condition

$$\begin{aligned}&\vartheta(\varsigma,0)=0,\\&\vartheta_\phi(\varsigma,0)=2\cos(\varsigma),\end{aligned}\tag{28}$$

and boundary condition

$$\begin{aligned}&\vartheta(0,\phi)=\sin(2\phi),\\&\vartheta_\varsigma(\pi,\phi)=-\sin(2\phi).\end{aligned}\tag{29}$$

Using $\mathbb{L}_c$IT on Equation (27), we obtain $R(\sigma)$ such as

$$R[\sigma]=\vartheta(\varsigma,0)+\frac{\vartheta'(\varsigma,0)}{\sigma}+\frac{1}{\sigma^2}\mathbb{A}\left[\frac{\partial^2\vartheta}{\partial\varsigma^2}-3\vartheta\right].\tag{30}$$

Using inverse $\mathbb{L}_c$IT, it yields

$$\vartheta(\varsigma,\phi)=\vartheta(\varsigma,0)+\phi\vartheta_\phi(\varsigma,0)+\mathbb{L}_c^{-1}\left[\frac{1}{\sigma^2}\mathbb{L}_c\left\{\frac{\partial^2\vartheta}{\partial\varsigma^2}-3\vartheta\right\}\right].\tag{31}$$

Now, apply HPM to obtain He's polynomials

$$\sum_{i=0}^{\infty}p^i\vartheta_i(\varsigma,\phi)=2\phi\cos(\varsigma)+\mathbb{L}_c^{-1}\left[\frac{1}{\sigma^2}\mathbb{L}_c\left\{\sum_{i=0}^{\infty}p^i\frac{\partial^2\vartheta_i}{\partial\varsigma^2}-3\sum_{i=0}^{\infty}p^i\vartheta\right\}\right].\tag{32}$$

Evaluating similar components of p, we obtain

$$\begin{aligned}&p^0:\vartheta_0(\varsigma,\phi)=\vartheta(\varsigma,0)=2\phi\cos(\varsigma),\\&p^1:\vartheta_1(\varsigma,\phi)=\mathbb{L}_c^{-1}\left[\frac{1}{\sigma^2}\mathbb{L}_c\left\{\frac{\partial^2\vartheta_0}{\partial\varsigma^2}-3\vartheta_0\right\}\right]=-\frac{(2\phi)^3}{3!}\cos(\varsigma),\\&p^2:\vartheta_2(\varsigma,\phi)=\mathbb{L}_c^{-1}\left[\frac{1}{\sigma^2}\mathbb{L}_c\left\{\frac{\partial^2\vartheta_1}{\partial\varsigma^2}-3\vartheta_1\right\}\right]=\frac{(2\phi)^5}{5!}\cos(\varsigma),\\&p^3:\vartheta_3(\varsigma,\phi)=\mathbb{L}_c^{-1}\left[\frac{1}{\sigma^2}\mathbb{L}_c\left\{\frac{\partial^2\vartheta_2}{\partial\varsigma^2}-3\vartheta_2\right\}\right]=-\frac{(2\phi)^7}{7!}\cos(\varsigma),\\&p^4:\vartheta_4(\varsigma,\phi)=\mathbb{L}_c^{-1}\left[\frac{1}{\sigma^2}\mathbb{L}_c\left\{\frac{\partial^2\vartheta_3}{\partial\varsigma^2}-3\vartheta_3\right\}\right]=\frac{(2\phi)^9}{9!}\cos(\varsigma),\\&\vdots.\end{aligned}\tag{33}$$

In the similar way, we can consider the approximate series such as

$$\vartheta(\varsigma,\phi)=\vartheta_0(\varsigma,\phi)+\vartheta_1(\varsigma,\phi)+\vartheta_2(\varsigma,\phi)+\vartheta_3(\varsigma,\phi)+\vartheta_4(\varsigma,\phi)+\cdots,$$
$$(\varsigma,\phi)=\cos(\varsigma)\left(2\phi-\frac{(2\phi)^3}{3!}+\frac{(2\phi)^5}{5!}-\frac{(2\phi)^7}{7!}+\frac{(2\phi)^9}{9!}\right)+\cdots, \tag{34}$$

which can approach to

$$\vartheta(\varsigma,\phi)=\cos(\varsigma)\sin(2\phi). \tag{35}$$

Figure 1 contains two diagrams: (a) the $\mathbb{L}_c$HITM results of $\vartheta(\varsigma,\phi)$ and (b) the exact results of $\vartheta(\varsigma,\phi)$ at $-2\le\varsigma\le 2$ and $0\le\phi\le 0.5$ for 1D wave problem. Figure 2 represents the graphical error of 1D wave equation between the approximate and the precise solutions at $0\le\varsigma\le 20$ with $\phi=0.5$. We observe that the current approach demonstrates the strong agreement with the precise answer to the problem (5.1) only after a few iterations. The rate of convergence shows that $\mathbb{L}_c$HITM is a relatable approach for $\vartheta(\varsigma,\phi)$. It states that we can effectively model any surface in accordance with the desired physical processes appearing in science and engineering.

5.2. Example 2. Suppose a two-dimensional wave equation

$$\frac{\partial^2\vartheta}{\partial\phi^2}=2\left(\frac{\partial^2\vartheta}{\partial\varsigma^2}+\frac{\partial^2\vartheta}{\partial\xi^2}\right)+6\phi+2\varsigma+4\xi, \tag{36}$$

with the initial condition

$$\begin{aligned}\vartheta(\varsigma,\xi,0)&=0,\\ \vartheta_\phi(\varsigma,\xi,0)&=2\sin(\varsigma)\sin(\xi),\end{aligned} \tag{37}$$

and boundary condition

$$\begin{aligned}\vartheta(0,\xi,\phi)&=\phi^3+2\phi^2\xi,\\ \vartheta_\varsigma(\pi,\xi,\phi)&=\phi^3+\pi\phi^2+2\phi^2\xi,\\ \vartheta(\varsigma,0,\phi)&=\phi^3+\phi^2\varsigma,\\ \vartheta_\varsigma(\varsigma,\pi,\phi)&=\phi^3+2\pi\phi^2+\phi^2\varsigma.\end{aligned} \tag{38}$$

Apply $\mathbb{L}_c$IT on

$$\mathbb{L}_c\left[\frac{\partial^2\vartheta}{\partial\phi^2}\right]=\mathbb{L}_c\left[2\left(\frac{\partial^2\vartheta}{\partial\varsigma^2}+\frac{\partial^2\vartheta}{\partial\xi^2}\right)+6\phi+2\varsigma+4\xi\right]. \tag{39}$$

Using the property functions of $\mathbb{L}_c$IT, we obtain

$$\begin{aligned}\sigma^2R(\sigma)-\vartheta(\varsigma,0)-\frac{\vartheta'(\varsigma,0)}{\sigma}&=\mathbb{L}_c\left[2\left(\frac{\partial^2\vartheta}{\partial\varsigma^2}+\frac{\partial^2\vartheta}{\partial\xi^2}\right)+6\phi+2\varsigma+4\xi\right],\\ \sigma^2R(\sigma)-\vartheta(\varsigma,0)-\frac{\vartheta'(\varsigma,0)}{\sigma}&=\mathbb{L}_c\left[2\left(\frac{\partial^2\vartheta}{\partial\varsigma^2}+\frac{\partial^2\vartheta}{\partial\xi^2}\right)\right]+6\mathbb{L}_c[\phi]+2\varsigma\mathbb{L}_c[1]+4\xi\mathbb{L}_c[1].\end{aligned} \tag{40}$$

Hence, $R(\sigma)$ is evaluated. Using $\mathbb{L}_c$IT on Equation (36), we obtain $R(\sigma)$ such as

$$R[\sigma]=\frac{6}{\sigma^3}+\frac{2\varsigma}{\sigma^2}+\frac{4\xi}{\sigma^2}+\vartheta(\varsigma,0)+\frac{\vartheta'(\varsigma,0)}{\sigma}+\frac{1}{\sigma^2}\mathbb{L}_c\left[2\left(\frac{\partial^2\vartheta}{\partial\varsigma^2}+\frac{\partial^2\vartheta}{\partial\xi^2}\right]\right.. \tag{41}$$

Using inverse $\mathbb{L}_c$IT, it yields

$$\begin{aligned}\vartheta(\varsigma,\xi,\phi)&=\phi^3+\varsigma\phi^2+2\xi\phi^2+\vartheta(\varsigma,0)+\phi\vartheta_\phi(\varsigma,0)\\ &\quad+\mathbb{L}_c^{-1}\left[\frac{1}{\sigma^2}\mathbb{L}_c\left\{2\left(\frac{\partial^2\vartheta}{\partial\varsigma^2}+\frac{\partial^2\vartheta}{\partial\xi^2}\right\}\right]\right..\end{aligned} \tag{42}$$

Now, apply HPM to obtain He's polynomials

$$\begin{aligned}\sum_{i=0}^{\infty}p^i\vartheta_i(\varsigma,\xi,\phi)&=\phi^3+\varsigma\phi^2+2\xi\phi^2+2\phi\sin(\varsigma)\sin(\xi)\\ &\quad+\mathbb{L}_c^{-1}\left[\frac{1}{\sigma^2}\mathbb{L}_c\left\{2\left(\sum_{i=0}^{\infty}p^i\frac{\partial^2\vartheta_i}{\partial\varsigma^2}+\sum_{i=0}^{\infty}p^i\frac{\partial^2\vartheta_i}{\partial\xi^2}\right)\right\}\right].\end{aligned} \tag{43}$$

Evaluating similar components of p, we obtain

$$\begin{aligned}p^0&:\vartheta_0(\varsigma,\xi,\phi)=\vartheta(\varsigma,0)=\phi^3+\varsigma\phi^2+2\xi\phi^2+2\phi\sin(\varsigma)\sin(\xi),\\ p^1&:\vartheta_1(\varsigma,\xi,\phi)=\mathbb{L}_c^{-1}\left[\frac{1}{\sigma^2}\mathbb{L}_c\left\{\frac{\partial^2\vartheta_0}{\partial\varsigma^2}+\frac{\partial^2\vartheta_0}{\partial\xi^2}\right\}\right]=-\frac{(2\phi)^3}{3!}\sin(\varsigma)\sin(\xi),\\ p^2&:\vartheta_2(\varsigma,\xi,\phi)=\mathbb{L}_c^{-1}\left[\frac{1}{\sigma^2}\mathbb{L}_c\left\{\frac{\partial^2\vartheta_1}{\partial\varsigma^2}+\frac{\partial^2\vartheta_1}{\partial\xi^2}\right\}\right]=\frac{(2\phi)^5}{5!}\sin(\varsigma)\sin(\xi),\\ p^3&:\vartheta_3(\varsigma,\xi,\phi)=\mathbb{L}_c^{-1}\left[\frac{1}{\sigma^2}\mathbb{L}_c\left\{\frac{\partial^2\vartheta_2}{\partial\varsigma^2}+\frac{\partial^2\vartheta_2}{\partial\xi^2}\right\}\right]=-\frac{(2\phi)^7}{7!}\sin(\varsigma)\sin(\xi),\\ p^4&:\vartheta_4(\varsigma,\xi,\phi)=\mathbb{L}_c^{-1}\left[\frac{1}{\sigma^2}\mathbb{L}_c\left\{\frac{\partial^2\vartheta_3}{\partial\varsigma^2}+\frac{\partial^2\vartheta_3}{\partial\xi^2}\right\}\right]=\frac{(2\phi)^9}{9!}\sin(\varsigma)\sin(\xi),\\ &\vdots.\end{aligned} \tag{44}$$

In the similar way, we can consider the approximate series such as

$$\begin{aligned}\vartheta(\varsigma,\xi,\phi)&=\vartheta_0(\varsigma,\xi,\phi)+\vartheta_1(\varsigma,\xi,\phi)+\vartheta_2(\varsigma,\xi,\phi)+\vartheta_3(\varsigma,\xi,\phi)\\ &\quad+\vartheta_4(\varsigma,\xi,\phi)+\cdots,\\ \vartheta(\varsigma,\xi,\phi)&=\phi^3+\varsigma\phi^2+2\xi\phi^2+\sin(\varsigma)\sin(\xi)\\ &\quad\cdot\left(2\phi-\frac{(2\phi)^3}{3!}+\frac{(2\phi)^5}{5!}-\frac{(2\phi)^7}{7!}+\frac{(2\phi)^9}{9!}\right)+\cdots,\end{aligned} \tag{45}$$

which can approach to

$$\vartheta(\varsigma,\xi,\phi)=\phi^3+\varsigma\phi^2+2\xi\phi^2+\sin(\varsigma)\sin(\xi)\sin(2\phi). \tag{46}$$

Figure 3 contains two diagrams: (a) the $\mathbb{L}_c$HITM results of $\vartheta(\varsigma,\xi,\phi)$ and (b) the exact results of $\vartheta(\varsigma,\xi,\phi)$ at $-1\le\varsigma\le 1$

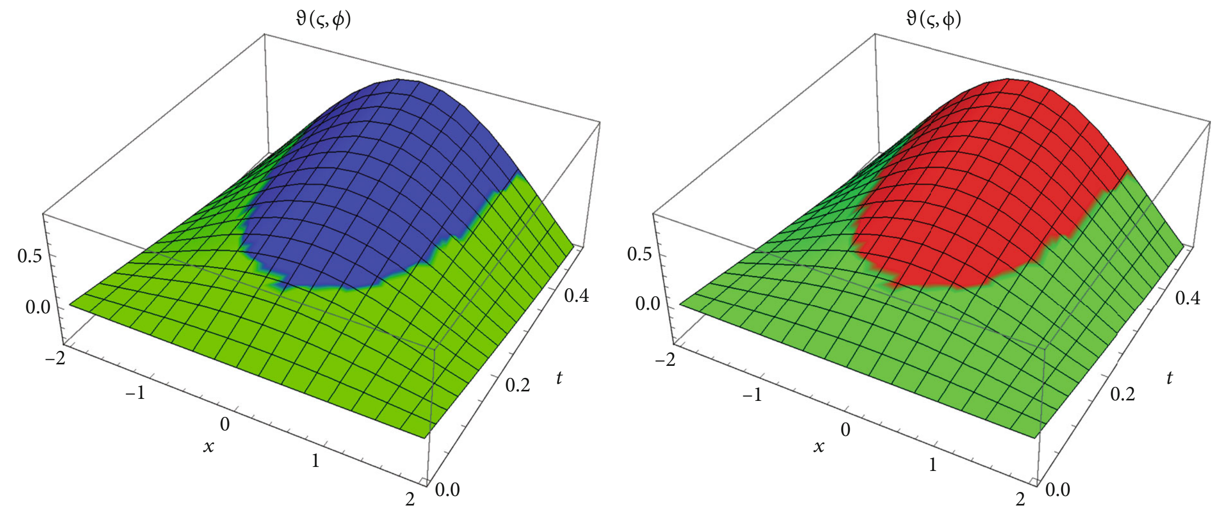

(a) Surface plot for approximate results

(b) Surface plot for precise results

Figure 1: Surface solutions of 1D wave equation.

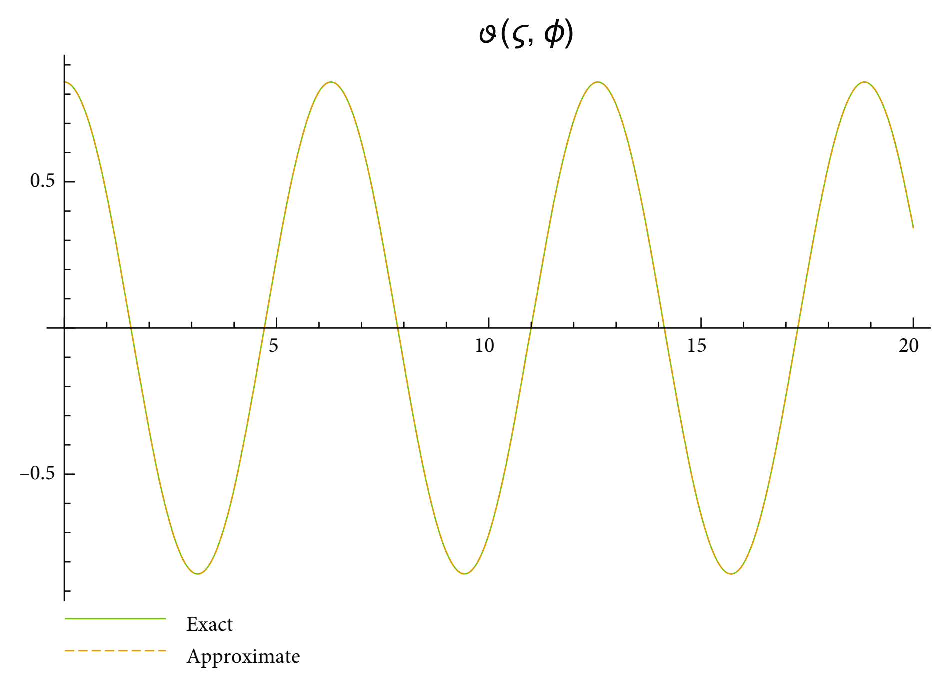

Figure 2: Graphical error between the approximate and the precise results of $\vartheta(\varsigma, \phi)$.

and $0 \le \phi \le 0.1$ with $\xi = 0.5$ for 2D wave problem. Figure 4 represents the graphical error of 2D wave equation between the approximate and the precise solutions at $0 \le \varsigma \le 20$ with $\xi = 0.01$ and $\phi = 0.01$. We observe that current approach demonstrates the strong agreement with the precise answer to the problem (5.2) only after a few iterations. The rate of convergence shows that $\mathbb{L}_c$HITM is a reliable approach for $\vartheta(\varsigma, \xi, \phi)$. It states that we can effectively model any surface in accordance with the desired physical processes appearing in nature.

5.3. *Example 3.* Consider the three-dimensional wave problem

$$\frac{\partial^2 \vartheta}{\partial \phi^2} = \frac{\varsigma^2}{18} \frac{\partial^2 \vartheta}{\partial \varsigma^2} + \frac{\xi^2}{18} \frac{\partial^2 \vartheta}{\partial \xi^2} + \frac{\eta^2}{18} \frac{\partial^2 \vartheta}{\partial \eta^2} - \vartheta, \tag{47}$$

with the initial condition

$$\begin{aligned} \vartheta(\varsigma, \xi, \eta, 0) &= 0, \\ \vartheta_\phi(\varsigma, \xi, \eta, 0) &= \varsigma^4 \xi^4 \eta^4, \end{aligned} \tag{48}$$

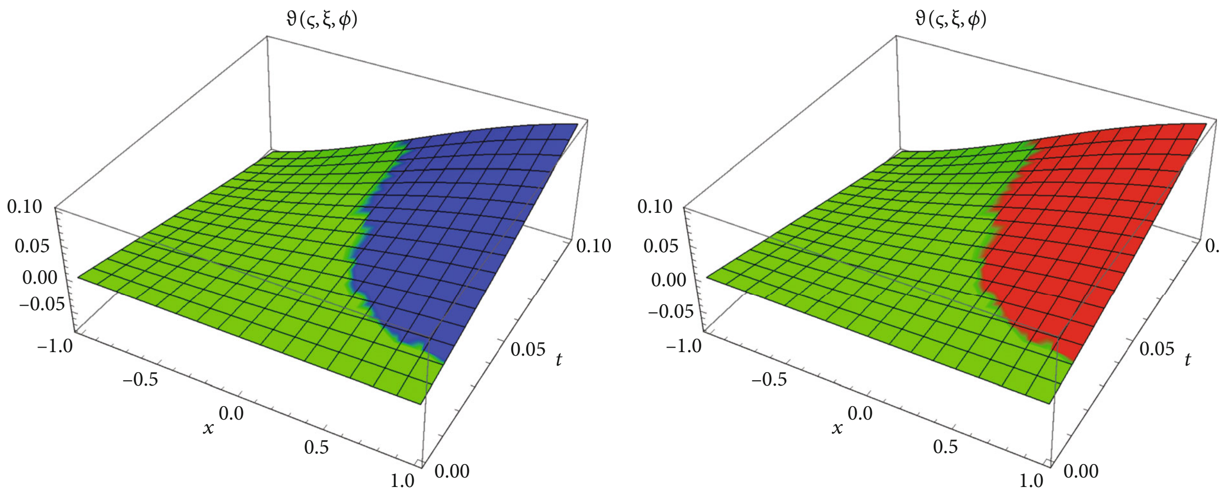

(a) Surface plot for approximate results

(b) Surface plot for precise results

Figure 3: Surface solutions of 2D wave equation.

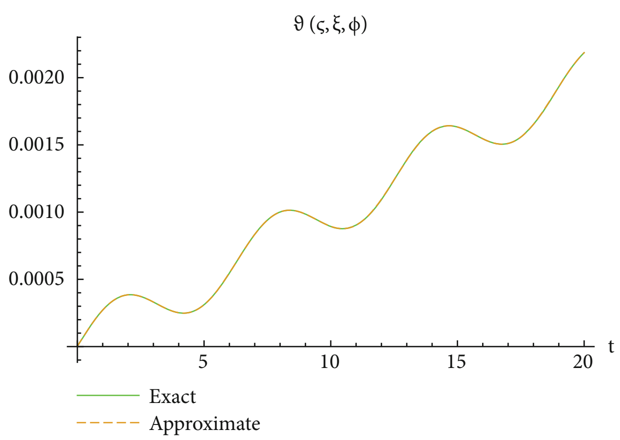

Figure 4: Graphical error between the approximate and the precise results of $\vartheta(\varsigma, \xi, \phi)$.

and boundary condition

$$\begin{aligned} &\vartheta(0, \xi, \eta, \phi) = 0, \\ &\vartheta(1, \xi, \eta, \phi) = \xi^4 \eta^4 \sinh(\phi), \\ &\vartheta(\varsigma, 0, \eta, \phi) = 0, \\ &\vartheta(\varsigma, 1, \eta, \phi) = \varsigma^4 \eta^4 \sinh(\phi), \\ &\vartheta(\varsigma, \xi, 0, \phi) = 0, \\ &\vartheta(\varsigma, \xi, 1, \phi) = \varsigma^4 \xi^4 \sinh(\phi). \end{aligned} \tag{49}$$

Using $\mathbb{L}_c$IT on Equation (47), we obtain $R(\sigma)$ such as

$$R[\sigma] = \vartheta(\varsigma, 0) + \frac{\vartheta'(\varsigma, 0)}{\sigma} + \frac{1}{\sigma^2}\mathbb{L}_c\left[\frac{\varsigma^2}{18}\frac{\partial^2\vartheta}{\partial\varsigma^2} + \frac{\xi^2}{18}\frac{\partial^2\vartheta}{\partial\xi^2} + \frac{\eta^2}{18}\frac{\partial^2\vartheta}{\partial\eta^2} - \vartheta\right]. \tag{50}$$

Using inverse $\mathbb{L}_c$IT, it yields

$$\begin{aligned} \vartheta(\varsigma, \xi, \eta, \phi) &= \vartheta(\varsigma, 0) + \phi\vartheta_\phi(\varsigma, 0) + \mathbb{L}_c^{-1} \\ &\cdot \left[\frac{1}{\sigma^2}\mathbb{L}_c\left\{\frac{\varsigma^2}{18}\frac{\partial^2\vartheta}{\partial\varsigma^2} + \frac{\xi^2}{18}\frac{\partial^2\vartheta}{\partial\xi^2} + \frac{\eta^2}{18}\frac{\partial^2\vartheta}{\partial\eta^2} - \vartheta\right\}\right]. \end{aligned} \tag{51}$$

Now, apply HPM to obtain He's polynomials

$$\begin{aligned} \sum_{i=0}^{\infty} p^i \vartheta(\varsigma, \xi, \eta, \phi) &= \phi\varsigma^4\xi^4\eta^4 + \mathbb{L}_c^{-1}\left[\frac{1}{\sigma^2}\mathbb{L}_c\left\{\sum_{i=0}^{\infty} p^i \frac{\varsigma^2}{18}\frac{\partial^2\vartheta_i}{\partial\varsigma^2}\right.\right. \\ &\left.\left. + \sum_{i=0}^{\infty} p^i \frac{\xi^2}{18}\frac{\partial^2\vartheta_i}{\partial\xi^2} + \sum_{i=0}^{\infty} p^i \frac{\eta^2}{18}\frac{\partial^2\vartheta_i}{\partial\eta^2} - \sum_{i=0}^{\infty} p^i\vartheta\right\}\right]. \end{aligned} \tag{52}$$

Evaluating similar components of p, we obtain

$$\begin{aligned} p^0 &: \vartheta_0(\varsigma, \xi, \eta, \phi) = \vartheta(\varsigma, \xi, \eta, 0) = \phi\varsigma^4\xi^4\eta^4, \\ p^1 &: \vartheta_1(\varsigma, \xi, \phi) = \mathbb{L}_c^{-1}\left[\frac{1}{\sigma^2}\mathbb{L}_c\left\{\frac{\varsigma^2}{18}\frac{\partial^2\vartheta_0}{\partial\varsigma^2} + \frac{\xi^2}{18}\frac{\partial^2\vartheta_0}{\partial\xi^2} + \frac{\eta^2}{18}\frac{\partial^2\vartheta_0}{\partial\eta^2} - \vartheta_0\right\}\right] = \frac{\phi^3}{3!}\varsigma^4\xi^4\eta^4, \\ p^2 &: \vartheta_2(\varsigma, \xi, \phi) = \mathbb{L}_c^{-1}\left[\frac{1}{\sigma^2}\mathbb{L}_c\left\{\frac{\varsigma^2}{18}\frac{\partial^2\vartheta_1}{\partial\varsigma^2} + \frac{\xi^2}{18}\frac{\partial^2\vartheta_1}{\partial\xi^2} + \frac{\eta^2}{18}\frac{\partial^2\vartheta_1}{\partial\eta^2} - \vartheta_1\right\}\right] = \frac{\phi^5}{5!}\varsigma^4\xi^4\eta^4, \\ p^3 &: \vartheta_3(\varsigma, \xi, \phi) = \mathbb{L}_c^{-1}\left[\frac{1}{\sigma^2}\mathbb{L}_c\left\{\frac{\varsigma^2}{18}\frac{\partial^2\vartheta_2}{\partial\varsigma^2} + \frac{\xi^2}{18}\frac{\partial^2\vartheta_2}{\partial\xi^2} + \frac{\eta^2}{18}\frac{\partial^2\vartheta_2}{\partial\eta^2} - \vartheta_2\right\}\right] = \frac{\phi^7}{7!}\varsigma^4\xi^4\eta^4, \\ p^4 &: \vartheta_4(\varsigma, \xi, \phi) = \mathbb{L}_c^{-1}\left[\frac{1}{\sigma^2}\mathbb{L}_c\left\{\frac{\varsigma^2}{18}\frac{\partial^2\vartheta_3}{\partial\varsigma^2} + \frac{\xi^2}{18}\frac{\partial^2\vartheta_3}{\partial\xi^2} + \frac{\eta^2}{18}\frac{\partial^2\vartheta_3}{\partial\eta^2} - \vartheta_3\right\}\right] = \frac{\phi^9}{9!}\varsigma^4\xi^4\eta^4, \\ &\vdots. \end{aligned} \tag{53}$$

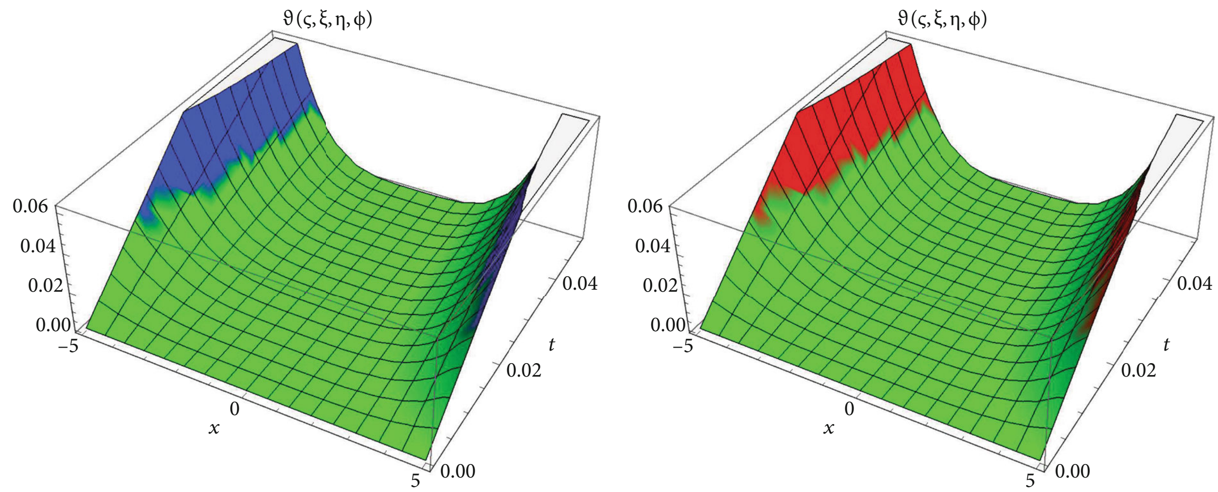

(a) Surface plot for approximate results

(b) Surface plot for precise results

Figure 5: Surface solutions of 3D wave equation.

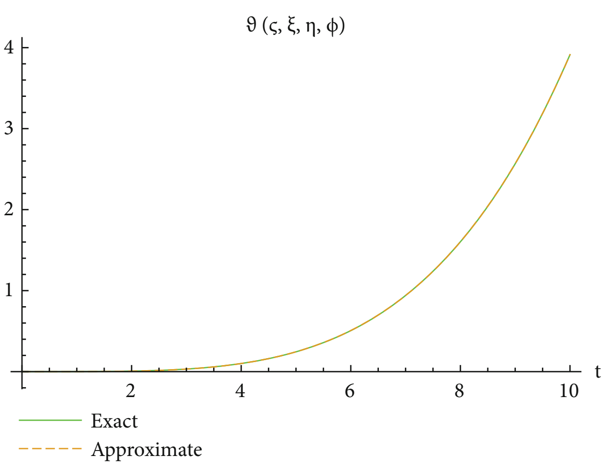

Figure 6: Graphical error between the approximate and the precise results of $\vartheta(\varsigma, \xi, \eta, \phi)$.

In the similar way, we can consider the approximate series such as

$$\vartheta(\varsigma, \xi, \eta, \phi) = \vartheta_0(\varsigma, \xi, \eta, \phi) + \vartheta_1(\varsigma, \xi, \eta, \phi) + \vartheta_2(\varsigma, \xi, \eta, \phi) + \vartheta_3(\varsigma, \xi, \eta, \phi) + \vartheta_4(\varsigma, \xi, \eta, \phi) + \cdots,$$

$$\vartheta(\varsigma, \xi, \eta, \phi) = \varsigma^4 \xi^4 \eta^4 \left(\phi + \frac{\phi^3}{3!} + \frac{\phi^5}{5!} + \frac{\phi^7}{7!} + \frac{\phi^9}{9!} \right) + \cdots, \quad (54)$$

which can approach to

$$\vartheta(\varsigma, \xi, \eta, \phi) = \varsigma^4 \xi^4 \eta^4 \sinh(\phi). \quad (55)$$

Figure 5 contains two diagrams: (a) the $\mathbb{L}_c$HITM results of $\vartheta(\varsigma, \xi, \eta, \phi)$ and (b) the exact results of $\vartheta(\varsigma, \xi, \eta, \phi)$ at $-5 \le \varsigma \le 5$ and $0 \le \phi \le 0.05$ with $\xi = 0.5$ and $\eta = 0.5$ for 3D wave problem. Figure 6 represents the graphical error of 3D wave equation between the approximate and the precise solutions at $0 \le \varsigma \le 10$ with $\xi = 0.5$, $\varsigma = 0.5$, and $\phi = 0.1$. We observe that the current approach demonstrates the strong agreement with the precise answer to the problem (5.3) only after a few iterations. The rate of convergence shows that $\mathbb{L}_c$HITM is a reliable approach for $\vartheta(\varsigma, \xi, \eta, \phi)$. It states that we can effectively model any surface in accordance with the desired physical processes appearing in nature.

6. Conclusion

In this paper, we construct a new scheme known as the Laplace-Carson homotopy integral transform method ($\mathbb{L}_c$HITM) for obtaining the approximate solution of 1D, 2D, and 3D wave equations. The main advantage of $\mathbb{L}_c$IT is that the recurrence relation produces the iteration without any assumption of a small parameter. HPM helps to produce successive iterations in the recurrence relation. The obtained results show that this approach is very simple to utilize and derive the series solution in the convergence form. Some graphical results are demonstrated to show the physical nature of these wave problems. The graphical error of plot distortion shows that $\mathbb{L}_c$HITM has the best agreement with the exact solution. We encourage the readers can extend this scheme for the numerical solution of a nonlinear coupled system of fractional order in science and engineering for their future work.

Data Availability

All the data are available within the article.

Conflicts of Interest

The authors declare that they have no competing of interest.

References

[1] M. Z. Liu, X. Q. Cao, X. Q. Zhu, B. N. Liu, and K. C. Peng, "Variational principles and solitary wave solutions of generalized nonlinear Schr¨odinger equation in the ocean," *Journal of Applied and Computational Mechanics*, vol. 7, no. 3, pp. 1639–1648, 2021.

[2] M. Cakmak and S. Alkan, "A numerical method for solving a class of systems of nonlinear pantograph differential equations," *Alexandria Engineering Journal*, vol. 61, no. 4, pp. 2651–2661, 2022.

[3] S. Momani and Z. Odibat, "Analytical approach to linear fractional partial differential equations arising in fluid mechanics," *Physics Letters A*, vol. 355, no. 4-5, pp. 271–279, 2006.

[4] M. Dehghan, J. Manafian, and A. Saadatmandi, "Key words: nonlinear differential-difference equations; exp-function method; N-soliton solutions," *Zeitschrift für Naturforschung-A*, vol. 65, no. 11, pp. 935–949, 2010.

[5] K. Raslan, K. K. Ali, and M. A. Shallal, "The modified extended tanh method with the Riccati equation for solving the space-time fractional EW and MEW equations," *Chaos, Solitons & Fractals*, vol. 103, pp. 404–409, 2017.

[6] H. Rezazadeh, N. Ullah, L. Akinyemi et al., "Optical soliton solutions of the generalized non-autonomous nonlinear Schrodinger equations by the new Kudryashov's method," *Results in Physics*, vol. 24, article 104179, 2021.

[7] W. A. Khan, "Numerical simulation of Chun-Hui Hes iteration method with applications in engineering," *International Journal of Numerical Methods for Heat & Fluid Flow*, vol. 32, no. 3, pp. 944–955, 2021.

[8] K. A. Gepreel and A. Al-Thobaiti, "Exact solutions of nonlinear partial fractional differential equations using fractional sub-equation method," *Indian Journal of Physics*, vol. 88, no. 3, pp. 293–300, 2014.

[9] S. Zhang, Y. Zhang, and B. Xu, "Exp-function method and reduction transformations for rogue wave solutions of the Davey-Stewartson equations," *Journal of Applied and Computational Mechanics*, vol. 7, no. 1, pp. 102–108, 2021.

[10] A. Althobaiti, S. Althobaiti, K. El-Rashidy, and A. R. Seadawy, "Exact solutions for the nonlinear extended KdV equation in a stratified shear flow using modified exponential rational method," *Results in Physics*, vol. 29, article 104723, 2021.

[11] M. Fiza, H. Ullah, S. Islam, Q. Shah, F. I. Chohan, and M. B. Mamat, "Modifications of the multistep optimal homotopy asymptotic method to some nonlinear KdVequations," *European Journal of Pure and Applied Mathematics*, vol. 11, no. 2, pp. 537–552, 2018.

[12] R. I. Nuruddeen, K. S. Aboodh, and K. K. Ali, "Analytical investigation of soliton solutions to three quantum Zakharov-Kuznetsov equations," *Communications in Theoretical Physics*, vol. 70, no. 4, p. 405, 2018.

[13] K. Wang, "New variational theory for coupled nonlinear fractal Schrödinger system," *International Journal of Numerical Methods for Heat & Fluid Flow*, vol. 32, no. 2, pp. 589–597, 2021.

[14] F. Liu, J. Liu, and M. Nadeem, "A numerical strategy for the approximate solution of the nonlinear time-fractional foam drainage equation," *Fractal and Fractional*, vol. 6, no. 8, p. 452, 2022.

[15] M. Alaroud, M. Al-Smadi, R. Rozita Ahmad, and U. K. Salma Din, "An analytical numerical method for solving fuzzy fractional Volterra integro-differential equations," *Symmetry*, vol. 11, no. 2, p. 205, 2019.

[16] J.-S. Duan, R. Rach, and A.-M. Wazwaz, "Higher order numeric solutions of the Lane–Emden-type equations derived from the multi-stage modified Adomian decomposition method," *International Journal of Computer Mathematics*, vol. 94, no. 1, pp. 197–215, 2017.

[17] J. Biazar and H. Ghazvini, "Convergence of the homotopy perturbation method for partial differential equations," *Nonlinear Analysis: Real World Applications*, vol. 10, no. 5, pp. 2633–2640, 2009.

[18] S. T. Mohyud-Din and M. A. Noor, "Homotopy perturbation method for solving partial differential equations," *Zeitschrift f¨ur Naturforschung A*, vol. 64, no. 3-4, pp. 157–170, 2009.

[19] A.-M. Wazwaz, "The variational iteration method: a reliable analytic tool for solving linear and nonlinear wave equations," *Computers & Mathematics with Applications*, vol. 54, no. 7-8, pp. 926–932, 2007.

[20] M. Ghasemi, M. T. Kajani, and A. Davari, "Numerical solution of two-dimensional nonlinear differential equation by homotopy perturbation method," *Applied Mathematics and Computation*, vol. 189, no. 1, pp. 341–345, 2007.

[21] Y. Keskin and G. Oturanc, "Reduced differential transform method for solving linear and nonlinear wave equations," *Iranian Journal Of Science And Technology Transaction A-Science*, vol. 34, no. 2, p. 133, 2010.

[22] H. Ullah, S. Islam, L. Dennis, T. Abdelhameed, I. Khan, and M. Fiza, "Approximate solution of two-dimensional nonlinear wave equation by optimal homotopy asymptotic method," *Mathematical Problems in Engineering*, vol. 2015, Article ID 380104, 7 pages, 2015.

[23] M. Adwan, M. Al-Jawary, J. Tibaut, and J. Ravnik, "Analytic and numerical solutions for linear and nonlinear multidimensional wave equations," *Arab Journal of Basic and Applied Sciences*, vol. 27, no. 1, pp. 166–182, 2020.

[24] M. Jleli, S. Kumar, R. Kumar, and B. Samet, "Analytical approach for time fractional wave equations in the sense of Yang-Abdel-Aty-Cattani via the homotopy perturbation transform method," *Alexandria Engineering Journal*, vol. 59, no. 5, pp. 2859–2863, 2020.

[25] R. Mullen and T. Belytschko, "Dispersion analysis of finite element semidiscretizations of the two-dimensional wave equation," *International Journal for Numerical Methods in Engineering*, vol. 18, no. 1, pp. 11–29, 1982.

[26] S. Aggarwal, S. D. Sharma, and A. Vyas, "Laplace-Carson transform for the primitive of convolution type Volterra integro-differential equation of first kind," *International Journal of Research and Innovation in Applied Science*, vol. 8, no. 6, pp. 2454–6194, 2020.

[27] P. Kumar and S. Qureshi, "Laplace-Carson integral transform for exact solutions of non-integer order initial value problems with Caputo operator," *Journal of Applied Mathematics and Computational Mechanics*, vol. 19, no. 1, pp. 57–66, 2020.

Hindawi
Journal of Function Spaces
Volume 2023, Article ID 8721106, 8 pages
https://doi.org/10.1155/2023/8721106

Research Article

Impact of Fractional Derivative and Brownian Motion on the Solutions of the Radhakrishnan-Kundu-Lakshmanan Equation

Farah M. Al-Askar

Department of Mathematical Science, Collage of Science, Princess Nourah bint Abdulrahman University, P.O. Box 84428, Riyadh 11671, Saudi Arabia

Correspondence should be addressed to Farah M. Al-Askar; fa.malaskar@gmail.com

Received 8 October 2022; Revised 2 November 2022; Accepted 24 November 2022; Published 30 January 2023

Academic Editor: Yusuf Gurefe

The fractional-stochastic Radhakrishnan-Kundu-Lakshmanan equation (FSRKLE) is considered here. To attain new hyperbolic, elliptic, rational, and trigonometric stochastic-fractional solutions, we use two various methods such as the sine-cosine and the Jacobi elliptic function methods. The solutions acquired are important in understanding some interesting physical phenomena due to the significance of the Radhakrishnan-Kundu-Lakshmanan equation in designing the propagation of solitons through an optical fiber. Furthermore, we graph some of the obtained solutions in 3D to display the influence of fractional derivative and multiplicative noise on these solutions. Finally, we show that when the order of fractional derivative decreases, the surface shrinks, while the multiplicative noise stabilizes the solutions of FSRKLE a round zero.

1. Introduction

Partial differential equations (PDEs) are found in several areas of applied science, including quantum mechanics, plasma physics, nonlinear optics, surface of water waves, hydrodynamics, molecular biology, fluid dynamics, elastic media, and biology. Obtaining solutions of PDEs is crucial for understanding physical phenomena. Therefore, many effective methods, including exp-function method [1], auxiliary equation [2], Darboux transformation [3], sine-cosine [4], Jacobi elliptic function [5], exp $(-\phi(\varsigma))$-expansion [6], sine-Gordon expansion [7], (G'/G)-expansion [8–10], generalized Kudryashov [11], perturbation [12–14], extended trial equation [15, 16], Jacobi elliptic function [17, 18], Riccati equation [19], tanh-coth [20], homotopy perturbation [21], modified decomposition [22], and F-expansion [23], have been constructed to attain exact solutions of PDEs.

Researchers and scientists have focused their attention over the last two decades on fractional differential equations (FDEs) that have been found to be more precise than classical differential equations in explaining complex physical phenomena in the real life. The idea of fractional derivative has been used to define various phenomena including fluid dynamics porous medium, signal processing, viscoelastic materials, ocean wave, electromagnetism, photonic, chaotic systems, wave propagation, optical fiber communication, plasma physics, and nuclear physics. Recently, Atangana and Goufo [24] have suggested the new conformable fractional derivative called beta-derivative. From this point, let us define the Atangana conformable derivative (ACD) for the function $\psi : (0,\infty) \longrightarrow \mathbb{R}$ of order $\beta \in (0, 1]$ as follows:

$$\mathbb{D}_x^{\beta}\psi(x) = \lim_{\varepsilon \longrightarrow 0} \frac{\psi\left(x + \varepsilon(x + (1/\Gamma(\beta)))^{1-\beta}\right) - \psi(x)}{\varepsilon}. \quad (1)$$

The ACD satisfies the following properties for any constant a and b: (1) $\mathbb{D}_x^{\beta}[a\varphi(x) + b\psi(x)] = a\mathbb{D}_x^{\beta}\varphi(x) + b\mathbb{D}_x^{\beta}\psi(x)$, (2) $\mathbb{D}_x^{\beta}[a] = 0$, (3) $\mathbb{D}_x^{\beta}\psi(\theta) = (x + (1/\Gamma(\beta)))^{1-\beta} d\psi/dx$, (4) If $\theta = a/\beta(x + (1/\Gamma(\beta)))^{\beta}$, then $\mathbb{D}_x^{\beta}\psi(\theta) = a d\psi/d\theta$.

Stochastic partial differential equations (SPDEs), on the other hand, have been widely addressed as theoretical equations for spatial-temporal physical, chemical, and biological systems related to random perturbations. The significance of involving stochastic impacts in complex system modeling has been emphasized. For example, there is gaining awareness in using SPDEs to mathematically model complex phenomena in information systems, condensed matter physics, biology, climate systems, electrical and mechanical engineering, materials sciences, and finance.

It is worth noting that two forms widely utilized for stochastic integral are Itô and Stratonovich [25]. Modeling problems primarily determine which form is acceptable; however, once that form is selected, an equivalent equation of the other form can be produced using the same solutions. As a result, the following relationship can be utilized to switch between Itô (written as $\int_0^t \phi dW$) and Stratonovich (written as $\int_0^t \phi \circ dW$):

$$\int_0^t \sigma\phi(s)dW(s) = \int_0^t \sigma\phi(s) \circ dW(s) - \frac{\sigma^2}{2}\int_0^t \phi(s)ds, \tag{2}$$

where $W(t)$ is a Brownian motion (BM).

To satisfy a higher degree of quality agreement, the following stochastic Radhakrishnan-Kundu-Lakshmanan equation (FSRKLE) [26–28] is considered:

$$\begin{aligned} id\varphi + \Big[\gamma_1 \mathbb{D}^\beta_{xx}\varphi - i\gamma_2\mathbb{D}^\beta_x\varphi + \gamma_3|\varphi|^2\varphi - i\gamma_4\varphi\mathbb{D}^\beta_x\left(|\varphi|^2\right) \\ --i\gamma_5\mathbb{D}^\beta_x\left(|\varphi|^2\varphi\right) + i\gamma_6\mathbb{D}^\beta_{xxx}\varphi\Big]dt + i\sigma\varphi \circ dW = 0, \end{aligned} \tag{3}$$

where $\varphi \in \mathbb{C}$, γ_k for $k = 1, 2, 3, 4, 5, 6$ are constants and σ is the noise strength and $\varphi \circ dW$ is multiplicative Brownian motion in the Stratonovich sense. Recently, many investigators have created exact solutions of FSRKLE (3), with $\beta = 0$ and $\sigma = 0$, using different methods such as extended simple equation method [29], first integral method [30], sine-cosine method [31], Lie group analysis [32], and trial equation method [33].

The motivation of this article is to attain the exact solutions for FSRKLE (3). We use two separate approaches, the sine-cosine and the Jacobi elliptic function methods, to provide a wide range of solutions, including hyperbolic, trigonometric, rational, and elliptic functions. The acquired solutions are helpful for understanding several fascinating scientific events because of the significance of the RKL in describing the propagation of solitons through an optical fiber. Also, by creating 3D representations of the obtained FSRKLE (3) solutions, we examine the effect of BM on these solutions.

The article is in the following format: in Section 2, we determine the wave equation of the FSRKLE (3) by applying a suitable wave transformation. To develop the analytical solutions for the FSRKLE in Section 3, we use two different approaches (3). In Section 4, the impact of the BM on the solutions obtained is examined. The final section of the document is the conclusion.

2. Wave Equation for FSRKLE

To obtain the wave equation of the FSRKLE (3), the following transformation is utilized:

$$\begin{aligned} \varphi(x,t) &= \psi(\zeta)e^{\left(iq(x,t)-\sigma W(t)-\sigma^2 t\right)}, \\ \zeta &= \frac{1}{\beta}\left(x + \frac{1}{\Gamma(\beta)}\right)^\beta - \nu t, \\ q(x,t) &= -\frac{k}{\beta}\left(x + \frac{1}{\Gamma(\beta)}\right)^\beta + \omega t, \end{aligned} \tag{4}$$

where the function ψ is deterministic and ν,k, and ω are unknown constants. Putting Equation (4) into Equation (3) and utilizing

$$\begin{aligned} d\varphi &= \left[\left(-\nu\psi' + i\omega\psi + \frac{1}{2}\sigma^2\psi - \sigma^2\psi\right)dt - \sigma\psi dW\right]e^{\left[iq(x,t)-\sigma W(t)-\sigma^2 t\right]}, \\ &= \left[\left(-\nu\psi' + i\omega\psi\right)dt - \sigma\psi \circ dW\right]e^{\left(iq(x,t)-\sigma W(t)-\sigma^2 t\right)}, \end{aligned} \tag{5}$$

where $(1/2)\sigma^2\psi$ is the Itô correction term, and

$$\begin{aligned} \mathbb{D}^\beta_x\varphi &= \left(\psi' - ik\psi\right)e^{\left(iq(x,t)-\sigma W(t)-\sigma^2 t\right)}, \\ \mathbb{D}^\beta_{xx}\varphi &= \left[\psi'' - 2ik\psi' - k^2\psi\right]e^{\left(iq(x,t)-\sigma W(t)-\sigma^2 t\right)}, \\ \mathbb{D}^\beta_{xxx}\varphi &= \left[\psi''' - 3ik\psi'' - 3k^2\psi' + ik^3\psi\right]e^{\left(iq(x,t)-\sigma W(t)-\sigma^2 t\right)} \\ \varphi\mathbb{D}^\beta_x\left(|\varphi|^2\right) &= 2\psi^2\psi' e^{\left(iq(x,t)-3\sigma W(t)-3\sigma^2 t\right)}, \\ \mathbb{D}^\beta_x\left(|\varphi|^2\varphi\right) &= \left(3\psi^2\psi' - ik\psi^3\right)e^{\left(iq(x,t)-3\sigma W(t)-3\sigma^2 t\right)}, \end{aligned} \tag{6}$$

we get for imaginary part

$$\begin{aligned} \gamma_6 k^3\psi''' - \left(3\gamma_6 k^2 + \gamma_2 + 2k\gamma_1 + \nu\right)\psi' \\ - (3\gamma_5 + 2\gamma_4)\psi^2\psi' e^{\left(-2\sigma W(t)-2\sigma^2 t\right)} = 0, \end{aligned} \tag{7}$$

and for real part

$$\begin{aligned} (\gamma_1 + 3k\gamma_6)\psi'' - \left(k^2\gamma_1 + k\gamma_2 - k^3\gamma_6\right)\psi \\ + (\gamma_3 - k\gamma_5)\psi^3 e^{\left(-2\sigma W(t)-2\sigma^2 t\right)} = 0. \end{aligned} \tag{8}$$

Taking expectation $\mathbb{E}(\cdot)$ on both sides for Equations (7) and (8) and using

$$\mathbb{E}\left(e^{\sigma W(t)}\right) = e^{\left(\sigma^2/2\right)t}, \tag{9}$$

we have

$$\gamma_6 k^3 \psi''' - (3\gamma_6 k^2 + \gamma_2 + 2k\gamma_1 + \nu)\psi' - (3\gamma_5 + 2\gamma_4)\psi^2\psi' = 0, \tag{10}$$

$$(\gamma_1 + 3k\gamma_6)\psi'' - (\omega + k^2\gamma_1 + k\gamma_2 + k^3\gamma_6)\psi - (k\gamma_5 - \gamma_3)\psi^3 = 0. \tag{11}$$

Integrating Equation (10), we get

$$\gamma_6 k^3 \psi'' - (3\gamma_6 k^2 + \gamma_2 + 2k\gamma_1 + \nu)\psi - \left(\gamma_5 + \frac{2}{3}\gamma_4\right)\psi^3 = 0. \tag{12}$$

We obtain the next constraint conditions where the same function ψ achieves both Equations (11) and (12):

$$\frac{\gamma_1 + 3k\gamma_6}{\gamma_6} = \frac{\omega + k^2\gamma_1 + k\gamma_2 + k^3\gamma_6}{3\gamma_6 k^2 + \gamma_2 + 2k\gamma_1 + \nu} = \frac{3(k\gamma_5 - \gamma_3)}{3\gamma_5 + 2\gamma_4}, \tag{13}$$

whenever

$$\gamma_3 = -\frac{3\gamma_5\gamma_1 + \gamma_1\gamma_4 + 6k\gamma_6\gamma_5 + 3k\gamma_6\gamma_4}{3\gamma_6}, \tag{14}$$

$$\omega = \frac{8k^3\gamma_6^2 + 8k^2\gamma_1\gamma_6 + 2k\gamma_1^2 + 2k\gamma_2\gamma_6 + \gamma_1\gamma_2 + \nu(3k\gamma_6 + \gamma_1)}{\gamma_6}. \tag{15}$$

Plugging Equation (14) into Equation (11), we have the wave equation as follows:

$$\psi'' - \hbar_1\psi^3 - \hbar_2\psi = 0, \tag{16}$$

where

$$\hbar_1 = \frac{3\gamma_5\gamma_1 + \gamma_1\gamma_4 + 9k\gamma_6\gamma_5 + 3k\gamma_6\gamma_4}{3\gamma_6(\gamma_1 + 3k\gamma_6)}, \tag{17}$$

$$\hbar_2 = \frac{9k^3\gamma_6^2 + 9k^2\gamma_1\gamma_6 + 2k\gamma_1^2 + 3k\gamma_2\gamma_6 + \gamma_1\gamma_2 + \nu(3k\gamma_6 + \gamma_1)}{\gamma_6(\gamma_1 + 3k\gamma_6)}. \tag{18}$$

3. The Exact Solutions of the FSRKLE

We employ two various methods such as the Jacobi elliptic function [18] and sine-cosine [4], to determine the exact solutions to Equation (16). As a consequence, we can obtain the solutions of the FSRKLE (3).

3.1. Jacobi Elliptic Function Method. We suppose the solutions of Equation (16) has the type

$$\psi(\zeta) = a + b\,sn(\theta\zeta), \tag{19}$$

where $sn(\theta\zeta) = sn(\theta\zeta, m)$, for $0 < m < 1$, is Jacobi elliptic sine function and a, b, and θ are undefined constants. Differentiate Equation (19) twice, we get

$$\psi''(\zeta) = -(m^2+1)b\theta^2 sn(\theta\zeta) + 2m^2 b\theta^2 sn^3(\theta\zeta). \tag{20}$$

Putting Equations (19) and (20) into Equation (16), we obtain

$$\begin{aligned}&(2m^2b\theta^2 - \hbar_1 b^3)sn^3(\theta\zeta) - 3\hbar_1 ab^2 sn^2(\theta\zeta)\\ &\quad - \left[(m^2+1)b\theta^2 + 3\hbar_1 a^2 b + \hbar_2 b\right]sn(\theta\zeta)\\ &\quad - (\hbar_1 a^3 + a\hbar_2) = 0.\end{aligned} \tag{21}$$

Equating each coefficient of $[sn(\theta\zeta)]^n$ to zero, we have for $n = 0, 1, 2, 3$,

$$\begin{aligned}\hbar_1 a^3 + a\hbar_2 &= 0,\\ (m^2+1)b\theta^2 + 3\hbar_1 a^2 b + \hbar_2 b &= 0,\\ 3\hbar_1 ab^2 sn^2 &= 0,\\ 2m^2 b\theta^2 - \hbar_1 b^3 &= 0.\end{aligned} \tag{22}$$

The outcomes of solving the previous equations are

$$\begin{aligned}a &= 0,\\ b &= \pm\sqrt{\frac{-2m^2\hbar_2}{(m^2+1)\hbar_1}},\\ \theta^2 &= \frac{-\hbar_2}{(m^2+1)}.\end{aligned} \tag{23}$$

As a result, using (19), the solution of Equation (16) is

$$\psi(\zeta) = \pm\sqrt{\frac{-2m^2\hbar_2}{(m^2+1)\hbar_1}}\,sn\left(\sqrt{\frac{-\hbar_2}{(m^2+1)}}\zeta\right). \tag{24}$$

Hence, the exact solution of the FSRKLE (3) is

$$\varphi(x,t) = \pm\sqrt{\frac{-2m^2\hbar_2}{(m^2+1)\hbar_1}}\,sn\left(\sqrt{\frac{-\hbar_2}{(m^2+1)}}\left(\frac{1}{\beta}\left(x + \frac{1}{\Gamma(\beta)}\right)^\beta - \nu t\right)\right)e^{\left[iq(x,t) - \sigma W(t) - \sigma^2 t\right]}, \tag{25}$$

for $\hbar_2 < 0$ and $\hbar_1 > 0$. If $m \longrightarrow 1$, then solution (25) tends to

$$\varphi(x,t) = \pm\sqrt{\frac{-\hbar_2}{\hbar_1}}\tanh\left(\sqrt{\frac{-\hbar_2}{2}}\left(\frac{1}{\beta}\left(x + \frac{1}{\Gamma(\beta)}\right)^\beta - \nu t\right)\right)e^{\left[iq(x,t) - \sigma W(t) - \sigma^2 t\right]}. \tag{26}$$

Analogously, we can replace sn in (19) with $cn(\xi) = cn(\xi, m)$ and $dn(\xi, m) = dn(\xi, m)$ to obtain the following solutions of Equation (16):

$$\psi(\zeta)=\pm\sqrt{\frac{-2m^2\hbar_2}{(2m^2-1)\hbar_1}}cn\left(\sqrt{\frac{\hbar_2}{(2m^2-1)}}\zeta\right),$$
$$\psi(\zeta)=\pm\sqrt{\frac{-2m^2\hbar_2}{(2-m^2)\hbar_1}}dn\left(\sqrt{\frac{\hbar_2}{(2-m^2)}}\zeta\right). \tag{27}$$

Thus, the exact solutions of the FSRKLE (3) are as follows:

$$\varphi(x,t)=\pm\sqrt{\frac{-2m^2\hbar_2}{(2m^2-1)\hbar_1}}cn\left(\sqrt{\frac{-\hbar_2}{(2m^2-1)}}\left(\frac{1}{\beta}\left(x+\frac{1}{\Gamma(\beta)}\right)^{\beta}-\nu t\right)\right)e^{[iq(x,t)-\sigma W(t)-\sigma^2 t]}, \tag{28}$$

for $\hbar_2/(2m^2-1)>0$, $\hbar_1<0$, and

$$\varphi(x,t)=\pm\sqrt{\frac{-2m^2\hbar_2}{(2-m^2)\hbar_1}}dn\left(\sqrt{\frac{\hbar_2}{(2-m^2)}}\left(\frac{1}{\beta}\left(x+\frac{1}{\Gamma(\beta)}\right)^{\beta}-\nu t\right)\right)e^{[iq(x,t)-\sigma W(t)-\sigma^2 t]}, \tag{29}$$

for $\hbar_2>0$, $\hbar_1<0$, respectively. If $m\longrightarrow 1$, then the Equations (28) and (29) tends to

$$\varphi(x,t)=\pm\sqrt{\frac{-2\hbar_2}{\hbar_1}}\,\text{sech}\left(\sqrt{\hbar_2}\left(\frac{1}{\beta}\left(x+\frac{1}{\Gamma(\beta)}\right)^{\beta}-\nu t\right)\right)e^{(iq(x,t)-\sigma W(t)-\sigma^2 t)}, \tag{30}$$

for $\hbar_2>0$, $\hbar_1<0$.

3.2. Sine-Cosine Method. Suppose the solution ψ of Equation (16) takes the form

$$\psi(\zeta)=A\mathbb{Y}^n, \tag{31}$$

where

$$\mathbb{Y}=\cos(B\zeta)\text{ or }\mathbb{Y}=\sin(B\zeta). \tag{32}$$

Setting Equation (31) into Equation (16), we get

$$-AB^2\left[-n^2\mathbb{Y}^n+n(n-1)\mathbb{Y}^{n-2}\right]-\hbar_1A^3\mathbb{Y}^{3n}-\hbar_2A\mathbb{Y}^n=0, \tag{33}$$

rewriting the above equation

$$\left(\hbar_2A-AB^2n^2\right)\mathbb{Y}^n+n(n-1)AB^2\mathbb{Y}^{n-2}+\hbar_1A^3\mathbb{Y}^{3n}=0. \tag{34}$$

Balancing the term of $\mathbb{Y}$ in Equation (34), we obtain

$$n-2=3n\Rightarrow n=-1. \tag{35}$$

Plugging Equation (35) into Equation (34),

$$\left(\hbar_2A-AB^2\right)\mathbb{Y}^{-1}+\left(\hbar_1A^3+2AB^2\right)\mathbb{Y}^{-3}=0. \tag{36}$$

We get by setting each coefficient of $\mathbb{Y}^{-3}$ and $\mathbb{Y}^{-1}$ equal to zero

$$\hbar_2A-AB^2=0, \tag{37}$$

$$\hbar_1A^3+2AB^2=0. \tag{38}$$

By solving Equations (37) and (38), we get

$$B=\sqrt{\hbar_2}\text{ and }A=\sqrt{\frac{-2\hbar_2}{\hbar_1}}. \tag{39}$$

Hence, the solution of Equation (16) is

$$\psi(\zeta)=A\sec(B\zeta)\text{ or }\psi(\zeta)=A\csc(B\zeta). \tag{40}$$

Depending on the sign of $\hbar_1$ and $\hbar_2$, there are numerous cases:

Case 1. If $\hbar_2>0$ and $\hbar_1<0$, then FSRKLE (3) has the solutions

$$\varphi(x,t)=\sqrt{\frac{-2\hbar_2}{\hbar_1}}\sec\left[\sqrt{\hbar_2}\left(\frac{1}{\beta}\left(x+\frac{1}{\Gamma(\beta)}\right)^{\beta}-\nu t\right)\right]e^{\left(i\left(-(k/\beta)(x+(1/\Gamma(\beta)))^{\beta}+\omega t\right)-\sigma W(t)-\sigma^2 t\right)}, \tag{41}$$

or

$$\varphi(x,t)=\sqrt{\frac{-2\hbar_2}{\hbar_1}}\csc\left[\sqrt{\hbar_2}\left(\frac{1}{\beta}x^{\beta}-\nu t\right)\right]e^{\left(i\left(-(k/\beta)(x+(1/\Gamma(\beta)))^{\beta}+\omega t\right)-\sigma W(t)-\sigma^2 t\right)}. \tag{42}$$

Case 2. If $\hbar_2<0$ and $\hbar_1<0$, then the analytical solutions of FSRKLE (3) have the form

$$\varphi(x,t)=i\sqrt{\frac{2\hbar_2}{\hbar_1}}\sec h\left[\sqrt{-\hbar_2}\left(\frac{1}{\beta}\left(x+\frac{1}{\Gamma(\beta)}\right)^{\beta}-\nu t\right)\right]e^{\left(i\left(-(k/\beta)(x+(1/\Gamma(\beta)))^{\beta}+\omega t\right)-\sigma W(t)-\sigma^2 t\right)}, \tag{43}$$

or

$$\varphi(x,t)=\sqrt{\frac{2\hbar_2}{\hbar_1}}\csc h\left[\sqrt{-\hbar_2}\left(\frac{1}{\beta}\left(x+\frac{1}{\Gamma(\beta)}\right)^{\beta}-\nu t\right)\right]e^{\left(i\left(-(k/\beta)(x+(1/\Gamma(\beta)))^{\beta}+\omega t\right)-\sigma W(t)-\sigma^2 t\right)}. \tag{44}$$

Case 3. If $\hbar_2<0$ and $\hbar_1>0$, then the solutions of FSRKLE (3) are

$$\varphi(x,t)=\sqrt{\frac{-2\hbar_2}{\hbar_1}}\sec h\left[\sqrt{-\hbar_2}\left(\frac{1}{\beta}\left(x+\frac{1}{\Gamma(\beta)}\right)^{\beta}-\nu t\right)\right]e^{\left(i\left(-(k/\beta)(x+(1/\Gamma(\beta)))^{\beta}+\omega t\right)-\sigma W(t)-\sigma^2 t\right)}, \tag{45}$$

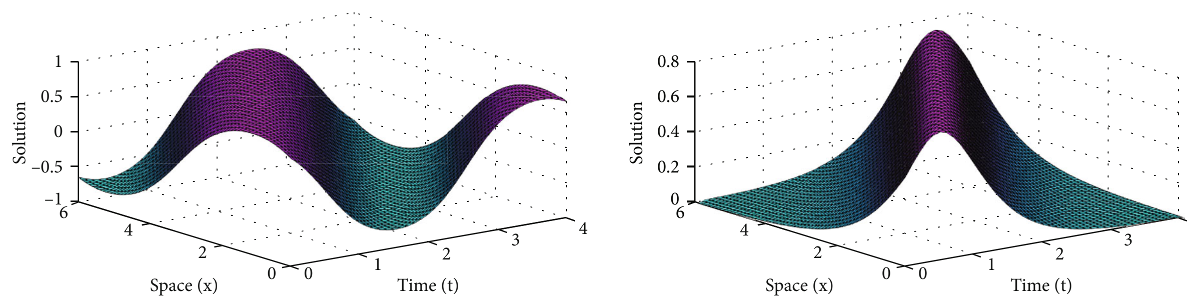

FIGURE 1: 3D diagram of Equations (25) and (45) with $\sigma = 0$.

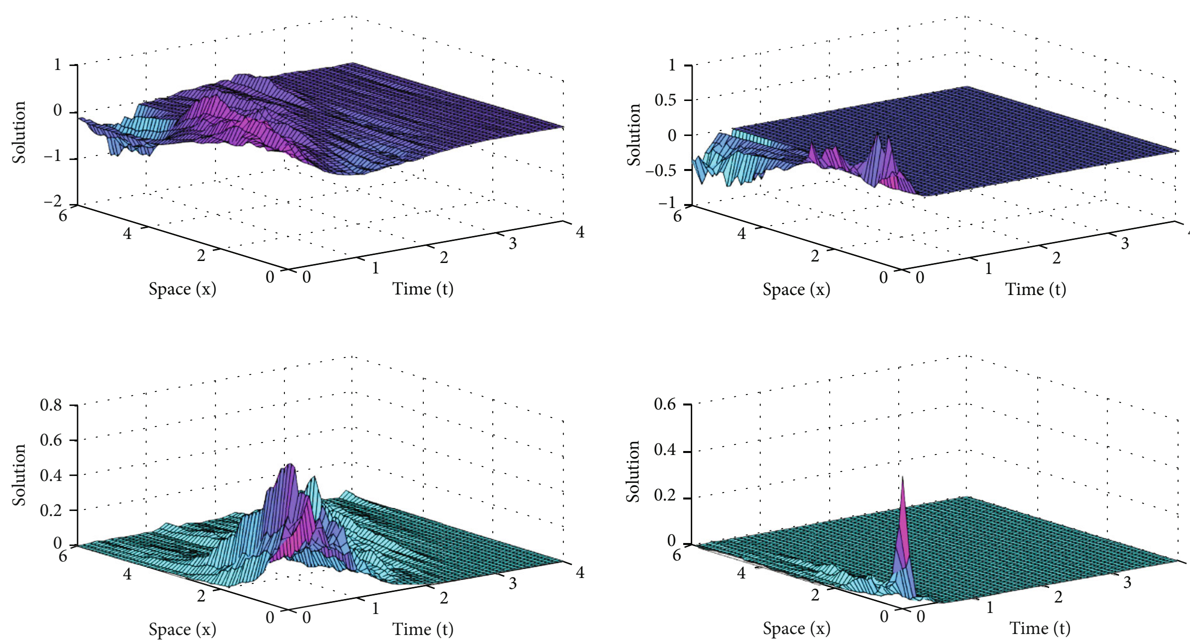

FIGURE 2: 3D diagram of Equations (25) and (45) with $\sigma = 1, 2$.

or

$$\varphi(x,t) = -i\sqrt{\frac{-2\hbar_2}{\hbar_1}} \operatorname{csc} h\left[\sqrt{-\hbar_2}\left(\frac{1}{\beta}\left(x+\frac{1}{\Gamma(\beta)}\right)^{\beta} - \nu t\right)\right] e^{\left(i\left(-(k/\beta)(x+(1/\Gamma(\beta)))^{\beta}+\omega t\right)-\sigma W(t)-\sigma^2 t\right)}. \tag{46}$$

Case 4. If $\hbar_2 > 0$ and $\hbar_1 > 0$, then FSRKLE (3) has the solutions

$$\varphi(x,t) = i\sqrt{\frac{2\hbar_2}{\hbar_1}} \sec\left[\sqrt{\hbar_2}\left(\frac{1}{\beta}\left(x+\frac{1}{\Gamma(\beta)}\right)^{\beta} - \nu t\right)\right] e^{\left(i\left(-(k/\beta)(x+(1/\Gamma(\beta)))^{\beta}+\omega t\right)-\sigma W(t)-\sigma^2 t\right)}, \tag{47}$$

or

$$\varphi(x,t) = i\sqrt{\frac{2\hbar_2}{\hbar_1}} \csc\left[\sqrt{\hbar_2}\left(\frac{1}{\beta}\left(x+\frac{1}{\Gamma(\beta)}\right)^{\beta} - \nu t\right)\right] e^{\left[i\left(-(k/\beta)(x+(1/\Gamma(\beta)))^{\beta}+\omega t\right)-\sigma W(t)-\sigma^2 t\right]}, \tag{48}$$

where $\hbar_1$,$\hbar_2$ are defined in (17).

Remark 1. Setting $\beta = 1$ and $\sigma = 0$ in Equations (41), (42), and (45), we get the identical solutions as asserted in [31].

4. Effect of BM and Fractional Derivative on the Solutions

Here, the impact of BM and the fractional derivative on the exact solutions of the FSRKLE (3) is described. Fix the constants $\gamma_1 = \gamma_2 = \gamma_4 = \gamma_5 = \gamma_6 = 1, k = -1, \nu = 3,$ and $m = 0.5$. Hence, $\gamma_3 = 5/3, \hbar_1 = 4/3$, and $\hbar_2 = -1$. Now, we present some diagrams for various value of σ (intensity of noise) and for $t \in [0, 5]$, $x \in [0, 6]$. We apply the MATLAB to simulate the solutions of Equation (3).

Firstly, the impact of noise: in Figure 1, when $\sigma = 0$, we note that the surface fluctuates.

In Figure 2, if the noise appeared, then after small transit behaviors, the surface gets more planer when the intensity of noise increases as follows:

Secondly, the impact of fractional derivative: in Figures 3 and 4, if $\sigma = 0$, we can observe that as β increases, the surface extends:

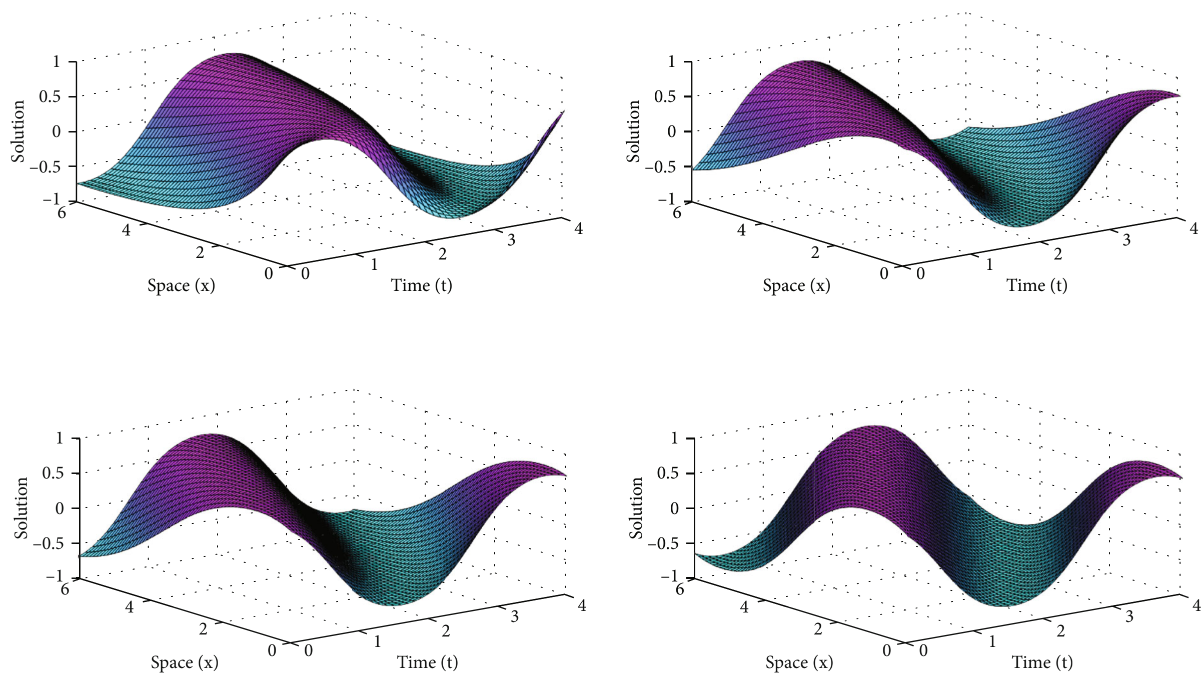

Figure 3: 3D diagram of Equation (25) with $\sigma = 0$ and various β.

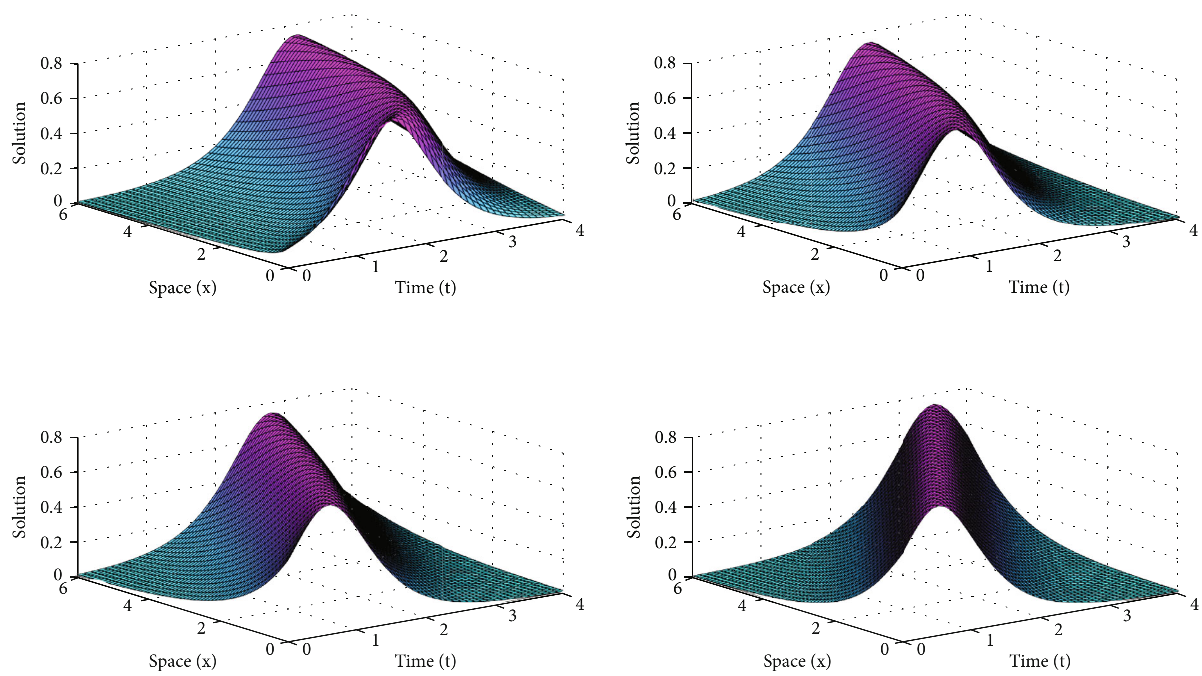

Figure 4: 3D diagram of Equation (45) with $\sigma = 0$ and various β.

5. Conclusions

In this paper, we obtained the exact solutions of the fractional-stochastic Radhakrishnan-Kundu-Lakshmanan Equation (3). To obtain rational, elliptic, trigonometric, and hyperbolic stochastic solutions, we used two different methods: the Jacobi elliptic function and the sine-cosine. Because of the priority of the FSRKLE in fluid dynamics and plasma physics, the results produced are useful for understanding some exciting physical phenomena. Finally, we plotted the obtained solutions using MATLAB tools to provide a number 3D diagram to demonstrate the impact of fractional derivative and multiplicative noise on these solutions. In future work, we can consider the FSRKLE (3) with additive noise.

Data Availability

All data are available in this paper.

Conflicts of Interest

The authors declare that they have no competing interests.

Acknowledgments

This work is supported by the Princess Nourah Bint Abdulrahman University Researchers Supporting Project number (PNURSP2023R273), Princess Nourah bint Abdulrahman University, Riyadh, Saudi Arabia.

References

[1] Y. Gurefe and E. Misirli, "Exp-function method for solving nonlinear evolution equations with higher order nonlinearity," *Computers & Mathematics with Applications*, vol. 61, no. 8, pp. 2025–2030, 2011.

[2] A. Akbulut and M. Kaplan, "Auxiliary equation method for time-fractional differential equations with conformable derivative," *Computers & Mathematcs with Applications*, vol. 75, no. 3, pp. 876–882, 2018.

[3] W. X. Ma and S. Batwa, "A binary darboux transformation for multicomponent NLS equations and their reductions," *Analysis and Mathematical Physics*, vol. 11, no. 2, p. 44, 2021.

[4] A. M. Wazwaz, "A sine-cosine method for handlingnonlinear wave equations," *Mathematical and Computer Modelling*, vol. 40, no. 5-6, pp. 499–508, 2004.

[5] S. Alshammari, W. W. Mohammed, S. K. Samura, and S. Faleh, "The analytical solutions for the stochastic-fractional Broer–Kaup equations," *Mathematical Problems in Engineering*, vol. 2022, Article ID 6895875, 9 pages, 2022.

[6] K. Khan and M. A. Akbar, "The exp(−$\Phi(\xi)$)-expansion method for finding travelling wave solutions of Vakhnenko-Parkes equation," *International Journal of Dynamical Systems and Differential Equations*, vol. 5, no. 1, pp. 72–83, 2014.

[7] H. K. Barman, A. R. Seadawy, M. A. Akbar, and D. Baleanu, "Competent closed form soliton solutions to the Riemann wave equation and the Novikov-Veselov equation," *Results in Physics*, vol. 17, article 103131, 2020.

[8] M. L. Wang, X. Z. Li, and J. L. Zhang, "The (G'G)-expansion method and travelling wave solutions of nonlinear evolution equations in mathematical physics," *Physics Letters A*, vol. 372, no. 4, pp. 417–423, 2008.

[9] H. Zhang, "New application of the (G'/G)-expansion method," *Communications in Nonlinear Science and Numerical Simulation*, vol. 14, no. 8, pp. 3220–3225, 2009.

[10] W. W. Mohammed, M. Alesemi, S. Albosaily, N. Iqbal, and M. El-Morshedy, "The exact solutions of stochastic fractional-space Kuramoto-Sivashinsky equation by using (G'/G)-expansion Method," *Mathematics*, vol. 9, no. 21, p. 2712, 2021.

[11] M. Kaplan, B. Bekir, and A. Akbulut, "A generalized Kudryashov method to some nonlinear evolution equations in mathematical physics," *Nonlinear Dynamics*, vol. 85, no. 4, pp. 2843–2850, 2016.

[12] W. W. Mohammed, "Fast-diffusion limit for reaction–diffusion equations with degenerate multiplicative and additive noise," *Journal of Dynamics and Differential Equations*, vol. 33, no. 1, pp. 577–592, 2021.

[13] W. W. Mohammed and D. Blömker, "Fast-diffusion limit for reaction-diffusion equations with multiplicative noise," *Journal of Mathematical Analysis and Applications*, vol. 496, no. 2, article 124808, 2021.

[14] K. Klepel, D. Blömker, and W. W. Mohammed, "Amplitude equation for the generalized swift Hohenberg equation with noise," *Zeitschrift für Angewandte Mathematik und Physik ZAMP*, vol. 65, no. 6, pp. 1107–1126, 2014.

[15] Y. Gurefe, E. Misirli, A. Sonmezoglu, and M. Ekici, "Extended trial equation method to generalized nonlinear partial differential equations," *Applied Mathematics and Computation*, vol. 219, no. 10, pp. 5253–5260, 2013.

[16] Y. Pandir, Y. Gurefe, and E. Misirli, "The extended trial equation method for some time fractional differential equations," *Discrete Dynamics in Nature and Society*, vol. 2013, Article ID 491359, 13 pages, 2013.

[17] Z. L. Yan, "Abundant families of Jacobi elliptic function solutions of the (2+1)-dimensional integrable Davey-Stewartson-type equation via a new method," *Chaos, Solitons and Fractals*, vol. 18, no. 2, pp. 299–309, 2003.

[18] E. Fan and J. Zhang, "Applications of the Jacobi elliptic function method to special-type nonlinear equations," *Physics Letters A*, vol. 305, no. 6, pp. 383–392, 2002.

[19] F. M. Al-Askar, W. W. Mohammed, and M. Alshammari, "Impact of Brownian motion on the analytical solutions of the space-fractional stochastic approximate long water wave equation," *Symmetry*, vol. 14, no. 4, p. 740, 2022.

[20] W. Malfliet and W. Hereman, "The tanh method. I. Exact solutions of nonlinear evolution and wave equations," *Physica Scripta*, vol. 54, no. 6, pp. 563–568, 1996.

[21] N. Iqbal, A. M. Albalahi, M. S. Abdo, and W. W. Mohammed, "Analytical analysis of fractional-order Newell-Whitehead-Segel equation: a modified homotopy perturbation transform method," *Journal of Function Spaces*, vol. 2022, Article ID 3298472, 10 pages, 2022.

[22] M. Alshammari, N. Iqbal, W. W. Mohammed, and T. Botmart, "The solution of fractional-order system of KdV equations with exponential- decay kernel," *Results in Physics*, vol. 38, article 105615, 2022.

[23] A. Filiz, M. Ekici, and A. Sonmezoglu, "Expansion method and new exact solutions of the Schrödinger-KdV equation," *Scientific World Journal*, vol. 2014, article 534063, 14 pages, 2014.

[24] A. Atangana and E. F. D. Goufo, "Extension of matched asymptotic method to fractional boundary layers problems," *Mathematical Problems in Engineering*, vol. 2014, Article ID 107535, 7 pages, 2014.

[25] P. E. Kloeden and E. Platen, *Numerical Solution of Stochastic Differential Equations*, SpringerVerlag, New York, 1995.

[26] D. D. Ganji, A. Asgari, and Z. Z. Ganji, "Exp-function based solution of nonlinear Radhakrishnan, Kundu and Laskshmanan (RKL) equation," *Acta applicandae mathematicae*, vol. 104, no. 2, article 201209, 2008.

[27] A. Biswas, "1-soliton solution of the generalized Radhakrishnan, Kundu, Lakshmanan equation," *Physics Letters A*, vol. 373, no. 30, pp. 2546–2548, 2009.

[28] B. Sturdevant, D. A. Lott, and A. Biswas, "Topological 1-soliton solution of the generalized Radhakrishnan, Kundu, Lakshmanan equation with nonlinear dispersion," *Modern Physics Letters B*, vol. 24, no. 16, pp. 1825–1831, 2010.

[29] D. Lu, A. R. Seadawy, and M. M. Khater, "Dispersive optical soliton solutions of the generalized Radhakrishnan-Kundu-Lakshmanan dynamical equation with power law nonlinearity and its applications," *Optik*, vol. 164, pp. 54–64, 2018.

[30] S. S. Singh, "Solutions of Kudryashov-Sinelshchikov equation and generalized Radhakrishnan-Kundu-Lakshmanan equation by the first integral method," *International Journal of Physical Research*, vol. 4, no. 2, pp. 37–42, 2016.

[31] J.-L. Zhang and M.-L. Wang, "Various exact solutions for two special type RKL models, chaos," *Solitons Fractals*, vol. 37, no. 1, article 215226, 2008.

[32] A. Bansal, A. Biswas, M. F. Mahmood et al., "Optical soliton perturbation with Radhakrishnan-Kundu-Lakshmanan equation by Lie group analysis," *Optik*, vol. 163, pp. 137–141, 2018.

[33] A. Biswas, Y. Yildirim, E. Yasar et al., "Optical soliton perturbation for Radhakrishnan-Kundu-Lakshmanan equation with a couple of integration schemes," *Optik*, vol. 163, pp. 126–136, 2018.

Hindawi
Journal of Function Spaces
Volume 2022, Article ID 3666348, 22 pages
https://doi.org/10.1155/2022/3666348

Research Article

Numerical and Analytical Simulations of Nonlinear Time Fractional Advection and Burger's Equations

Hassan Khan,[1,2] **Qasim Khan**,[1,3] **Fairouz Tchier**,[4] **Ibrarullah**,[1] **Evren Hincal**,[2] **Gurpreet Singh**,[5] **F. M. O. Tawfiq**,[4] **and Shahbaz Khan**[1]

[1]*Department of Mathematics, Abdul Wali Khan University Mardan, Pakistan*
[2]*Department of Mathematics, Near East University TRNC, Mersin 10, Turkey*
[3]*Department of Mathematics and Information Technology, The Education University of Hong Kong, 10 Lo Ping Road, Tai Po, New Territories, Hong Kong*
[4]*Department of Mathematics, College of Science, King Saud University, P.O. Box 2455, Riyadh 11451, Saudi Arabia*
[5]*School of Mathematical Sciences, Dublin City University, Ireland*

Correspondence should be addressed to Hassan Khan; hassanmath@awkum.edu.pk

Received 15 May 2022; Revised 8 August 2022; Accepted 16 August 2022; Published 6 October 2022

Academic Editor: Yusuf Gurefe

In this paper, the higher nonlinear problems of fractional advection-diffusion equations and systems of nonlinear fractional Burger's equations are solved by using two sophisticated procedures, namely, the q-homotopy analysis transform method and the residual power series method. The proposed methods are implemented with the Caputo operator. The present techniques are utilised in a very comprehensive and effective manner to obtain the solutions to the suggested fractional-order problems. The nonlinearity of the problem was controlled tactfully. The numerical results of a few examples are calculated and analyzed. The tables and graphs are constructed to understand the higher accuracy and applicability of the current method. The obtained results that are in good contact with the actual dynamics of the given problem, which is verified by the graphs and tables. The present techniques require fewer calculations and are associated with a higher degree of accuracy, and therefore can be extended to solve other high nonlinear fractional problems.

1. Introduction

The most powerful tool for researchers to simulate various physical phenomena in applied sciences and nature is known as fractional partial differential equations (FPDEs). The following physical phenomena have been accurately modelled by FPDEs: optics [1], economics [2], fluid traffic [3], electrodynamics [4], hepatitis B virus [5], tuberculosis [6], air foil [7], modelling of earth quack nonlinear oscillation [8], propagation of spherical waves [9], Chaos theory [10], fractional COVID-19 model [11], finance [12], pine wilt disease [13], Zener [14], cancer chemotherapy [15], traffic flow model [16], Poisson-Nernst-Planck diffusion [17], diabetes [18], biomedical and biological [19], and many other numerous applications in various branches of applied mathematics (see [20–22]). Due to these numerous applications, FPDEs and factional calculus have gained more attention from researchers as compared to ordinary calculus.

To obtain the approximate solutions to the above models, researchers use and develop a variety of analytical approaches. The frequently used methods are optimal homotopy asymptotic method (OHAM) [23], Iterative Laplace transform method [24], extended direct algebraic method (EDAM) [25], Adomian decomposition method (ADM) [26], the Finite difference method (FDM) [27], the homotopy perturbation transform technique along with transformation (HPTM) [28], the (G/G')-expansion method [29], the Haar wavelet method (HWM) [30], standard reductive perturbation method [31], the variational iteration procedure with transformation (VITM) [32], and the differential transform method (DTM)

[33]. In this context, Hassan et al. have presented the solutions of some nonlinear FPDEs which can be seen in [34–36]. Some useful methods can be seen in [37–39].

Obtaining the analytical solutions of FPDEs and their systems has been a difficult task for researchers in recent years. In this circumstance, Prakash and Kaur use q-HATM [40] to solve the time-fractional Navier Stokes equation. Similarly, q-HATM was implemented by Kumar et al. and used to obtain the solutions of the fractional long-wave equations in the regularised form [41]. The Schrodinger generalized form of fractional order was solved by Veeresha et al. using q-HATM [42]. The q-HATM convergence was done by El-Tawil and Huseen [43]. The RPSM technique was used by Alquran to solve the drainage equation in [44] and the fractional-order Phi-4 equation in [45]. The Whitham-Broer-Kaup equation of fractional order was analysed by Wang and Chen by using RPSM [46]. RPSM has been used in [47] to find the solution of the fractional Biswas-Milovic equation of multidimensions. Komashynska et al. used the RPSM [48] to solve a system of multipantograph delay differential equations. In [49], RPSM was used to find an approximation solution for the fractional-order Sharma-Tasso-Olever equation. The solutions to the fractional order Schrodinger equations were determined using RPSM in [50]. The RPSM has been used to solve a variety of problems, including the gas dynamic equation [51], the Emden-Fowler equation, Berger-Fisher equation, and the Benney-Lin equation in its fractional format, solved by RPSM in [52]. Similarly, RPSM was used by Al-Smadi [53] to overcome the solutions to initial value problems.

In this paper, the solutions of systems of fractional Berger's equations and nonlinear advection equations were examined by combining two analytical techniques, q-HAM and RPSM. The results are compared to each other as well as the exact solution to the given problems. The current methods are used to compare the solutions methodologies for the analysis of the higher nonlinear problems of fractional advection-diffusion equations and systems of nonlinear fractional Burger's equations in the Caputo sense. The obtained approximate series solutions are fast converging towards the exact solutions of the targeted problems, according to quantitative analysis. It is found that the techniques under discussion are simple and effective for the solutions of FPDE systems. The graphs and tables for the solutions to the targeted problems via RPSM and q-HATM. It is confirmed that the obtained solutions are in good contact with the exact solution to the problems. The fractional order solutions are convergent towards the integer order solutions, which shows the reliability of the fractional solutions. The presented techniques have a wide range of applications and could be used to examine approximate analytical solutions of other nonlinear FPDEs and multidimensional systems of FPDEs in the future.

This paper will be formatted as follows: in the second section, some basic definitions are discussed. In Section 3, the methodology is described, and in Section 4, two separate techniques are used to compare certain numerical results. The conclusion and references are found in the fifth and final section of the paper.

2. Basic Definitions

In this section we will discuss some important definitions

2.1. Definition. The Caputo operator in [54, 55] is given as.

$$\mathfrak{D}_t^{\delta} f(t) = \begin{cases} \dfrac{d^n f(t)}{dt^n}, & \delta = n \in N, \\ \dfrac{1}{\Gamma(n-\delta)} \displaystyle\int_0^t (t-x)^{n-\delta-1} f^{(n)}(x) dx, & n < \delta < n+1, n \in N. \end{cases} \tag{1}$$

2.2. Definition. An expansion of power series (PS) at point $t = t_0$ is known as fractional PS and is given by [56].

$$\sum_{n=0}^{\infty} a_n (t-t_0)^{n\delta} = a_0 + a_1 (t-t_0)^{\delta} + a_2 (t-t_0)^{2\delta} + \cdots,$$

&

$$\sum_{n=0}^{\infty} f_n(x)(t-t_0)^{n\delta} = f_0(x) + f_1(x)(t-t_0)^{\delta} + f_2(x)(t-t_0)^{2\delta} + \cdots, n-1 < \delta \le n, t \ge t_0, \tag{2}$$

note FPS can be expanded at point t_0 is

$$v(x,t) = \sum_{n=0}^{\infty} \frac{\mathfrak{D}_t^{n\delta} v(x,t_0)}{\Gamma(n\delta+1)} (t-t_0)^{n\delta}, 0 \le n-1 < \delta \le m, x \in I, t_0 \le t < t_0 + \mathfrak{R}, \tag{3}$$

which is the Taylor's series expansion form.

2.3. Laplace Transform (LT). The LT for continuous function $\mathfrak{g}(t)$ is defined as [57]

$$G(s) = \mathscr{L}[\mathfrak{g}(t)] = \int_0^{\infty} e^{-st} \mathfrak{g}(t) dt, \tag{4}$$

where $G(s)$ is the LT for the function $\mathfrak{g}(t)$.

2.4. Definition. The LT $\mathscr{L}[v(x,t)]$ of Caputo fractional derivative is given by [57]

$$\mathscr{L}\left[\mathfrak{D}_t^{n\delta} v(x,t)\right] = s^{n\delta} \mathscr{L}[v(x,t)] - \sum_{k=0}^{n-1} s^{n\delta-k-1} v^k(x,0), n-1 < n\delta \le n. \tag{5}$$

2.5. Definition. The LT of two function $k(t) \times \mathfrak{g}(t)$ is defined by [57]

$$\mathscr{L}[k \times \mathfrak{g}] = \mathscr{L}[k(t)] \times \mathscr{L}[\mathfrak{g}(t)], \tag{6}$$

As $k \times \mathfrak{g}$, represent the product between k and $\mathfrak{g}$,

$$(k \times \mathfrak{g})t = \int_0^t k(t) \mathfrak{g}(t-x) dt. \tag{7}$$

2.6. Definition. The LT of fractional derivative is defined as [57]

$$\mathscr{L}\left(\mathfrak{D}_t^{\delta}\mathfrak{g}(x)\right) = s^{\delta}G(s) - \sum_{k=0}^{n-1} s^{\delta-1-k}\mathfrak{g}^{k}(0^{+}), n < \delta \le n+1. \quad (8)$$

where the LT of $\mathfrak{g}(x)$ is denoted by $G(s)$.

2.7. Theorem. Assume that the series solution $\sum_{k=0}^{\infty} u_k(x,t) = \sum_{k=0}^{\infty} u_k(x,t)(1/n)^k$ is convergent to the solution u for a prescribed value of h. If the truncated series

$$\sum_{k=0}^{m} u_k(x,t) = \sum_{k=0}^{m} u_k(x,t)\left(\frac{1}{n}\right) \quad (9)$$

is used as an approximation to the solution $u(x,t)$ of problem, then an upper bound for the error, E_m is estimated as

$$E_m \le \frac{(r/n)^{m+1}}{1-(r/n)} \|u_o(x,t)\| \quad (10)$$

Proof. See [43] □

2.8. Theorem. suppose that $u(t) \in C[t_0, t_0+R]$ and $D_t^{k\alpha}u(t) \in C(t_0, t_0+R) fork = 0, 1, 2, \cdots, n+1$,

where $0 < \alpha \le 1$. Then u could be represented by:

$$u(t) = \sum_{k=0}^{n} \frac{\left(D_{t_0}^{k\alpha u}\right)(t_0)}{\Gamma(k\alpha+1)}(t-t_0)^{k\alpha} + J_{t_0}^{(n+1)\alpha} D_{t_0}^{(n+1)\alpha} u(t), t_0 \le t \le t_0 + R. \quad (11)$$

Proof. See [58]. □

2.9. Theorem. If $|D_{t_0}^{(n+1)\alpha}u(t)| \le M$ on $t_0 \le t \le d$, where $0 < \alpha \le 1$, then the reminder $R_n(t)$ of the generalized Taylor's series will satisfies the inequality:

$$|R_n(t)| \le \frac{M}{\Gamma((n+1)\alpha+1)}(t-t_0)^{(n+1)\alpha}, t_0 \le t \le D. \quad (12)$$

Proof. See [58]. □

2.10. Theorem. Suppose that u has a Fractional power series representation at t_0 of the form

$$u(t) = \sum_{n=0}^{\infty} c_n (t-t_0)^{n\alpha}, 0 \le m-1 < \alpha \le m, t_0 \le t < t_0 + R, \quad (13)$$

where R is the radius of convergence. Then u is analytic in (t_0, t_0+R).

Proof. See [58]. □

3. RPSM and Q-HATM Procedures

To understand main concept of RPSM and q-HATM [59] for system of FPDEs, we consider the following FPDEs system,

$$\begin{cases} \mathfrak{D}_t^{\delta}\upsilon(x,y,z,t) = N(\upsilon(x,y,z,t)) + R(\upsilon(x,y,z,t)), 0 < \delta \le 1, t > 0, \\ \mathfrak{D}_t^{\delta}\vartheta(x,y,z,t) = N(\vartheta(x,y,z,t)) + R(\vartheta(x,y,z,t)), 0 < \delta \le 1, t > 0, \\ \mathfrak{D}_t^{\delta}\varpi(x,y,z,t) = N(\varpi(x,y,z,t)) + R(\varpi(x,y,z,t)), 0 < \delta \le 1, t > 0, \end{cases} \quad (14)$$

with initial condition,

$$\begin{cases} \upsilon(x,y,z,0) = f(x,y,z), \\ \vartheta(x,y,z,0) = g(x,y,z), \\ \varpi(x,y,z,0) = h(x,y,z), \end{cases} \quad (15)$$

where $\mathfrak{D}_t^{\delta}$ the Caputo fractional derivative, R is linear and N is nonlinear operator, respectively, in Eq. (14).

3.1. RPSM Procedure for FPDEs System [60]. Eq. (14) can be simplified as

$$\begin{cases} \upsilon(x,y,z,t) = \sum_{n=0}^{k} f_n(x)\frac{t^{n\delta}}{\Gamma(1+n\delta)}, 0 < \delta \le 1, -\infty < x, y, z < \infty, 0 \le t < R, \\ \vartheta(x,y,z,t) = \sum_{n=0}^{k} g_n(x)\frac{t^{n\delta}}{\Gamma(1+n\delta)}, 0 < \delta \le 1, -\infty < x, y, z < \infty, 0 \le t < R, \\ \varpi(x,y,z,t) = \sum_{n=0}^{k} h_n(x)\frac{t^{n\delta}}{\Gamma(1+n\delta)}, 0 < \delta \le 1, -\infty < x, y, z < \infty, 0 \le t < R, \end{cases} \quad (16)$$

where $\upsilon(x,y,z,t)$, $\vartheta(x,y,z,t)$, and $\varpi(x,y,z,t)$ is the k^{th} truncated series of form

$$\begin{cases} \upsilon_k(x,y,z,t) = \sum_{n=0}^{k} f_n(x,y,z)\frac{t^{n\delta}}{\Gamma(1+n\delta)}, \\ \vartheta_k(x,y,z,t) = \sum_{n=0}^{k} g_n(x,y,z)\frac{t^{n\delta}}{\Gamma(1+n\delta)}, \\ \varpi_k(x,y,z,t) = \sum_{n=0}^{k} h_n(x,y,z)\frac{t^{n\delta}}{\Gamma(1+n\delta)}. \end{cases} \quad (17)$$

In RPSM the $zero^{th}$ approximate solution of $\upsilon(x,y,z,t)$, $\vartheta(x,y,z,t)$, and $\varpi(x,y,z,t)$ is given by

$$\begin{cases} \upsilon_0(x,y,z,t) = \upsilon(x,0) = f(x,y,z), \\ \vartheta_0(x,y,z,t) = \vartheta(x,0) = g(x,y,z), \\ \varpi_0(x,y,z,t) = \varpi(x,0) = h(x,y,z). \end{cases} \quad (18)$$

Eq. (17), implies that,

$$\begin{cases} \upsilon_k(x,y,z,t) = f(x,y,z) + \sum_{n=1}^{k} f_n(x,y,z)\dfrac{t^{n\delta}}{\Gamma(1+n\delta)}, k = 1,2,\cdots, \\ \vartheta_k(x,y,z,t) = g(x,y,z) + \sum_{n=1}^{k} g_n(x,y,z)\dfrac{t^{n\delta}}{\Gamma(1+n\delta)}, k = 1,2,\cdots, \\ \varpi_k(x,y,z,t) = h(x,y,z) + \sum_{n=1}^{k} h_n(x,y,z)\dfrac{t^{n\delta}}{\Gamma(1+n\delta)}, k = 1,2,\cdots, \end{cases} \tag{19}$$

for Eq. (14), the residual function is given by

$$\begin{cases} \operatorname{Re} s_\upsilon(x,y,z,t) = \mathfrak{D}_t^\delta \upsilon(x,y,z,t) - N(\upsilon(x,y,z,t)) - R(\upsilon(x,y,z,t)), \\ \operatorname{Re} s_\vartheta(x,y,z,t) = \mathfrak{D}_t^\delta \vartheta(x,y,z,t) - N(\vartheta(x,y,z,t)) - R(\vartheta(x,y,z,t)), \\ \operatorname{Re} s_\varpi(x,y,z,t) = \mathfrak{D}_t^\delta \varpi(x,y,z,t) - N(\varpi(x,y,z,t)) - R(\varpi(x,y,z,t)), \end{cases} \tag{20}$$

so, the k^{th} residual function becomes

$$\begin{cases} \operatorname{Re} s_{\upsilon,k}(x,y,z,t) = \mathfrak{D}_t^\delta \upsilon_k(x,y,z,t) - N(\upsilon_k(x,y,z,t)) - R(\upsilon_k(x,y,z,t)), \\ \operatorname{Re} s_{\vartheta,k}(x,y,z,t) = \mathfrak{D}_t^\delta \vartheta_k(x,y,z,t) - N(\vartheta_k(x,y,z,t)) - R(\vartheta_k(x,y,z,t)), \\ \operatorname{Re} s_{\varpi,k}(x,y,z,t) = \mathfrak{D}_t^\delta \varpi_k(x,y,z,t) - N(\varpi_k(x,y,z,t)) - R(\varpi_k(x,y,z,t)). \end{cases} \tag{21}$$

As in [61, 62], it is clear that $\operatorname{Re} s(x,y,z,t) = 0$ and $\lim_{nt_o\infty} \operatorname{Re} s_k(x,y,z,t) = \operatorname{Re} s(x,y,z,t)$. Therefore, $\mathfrak{D}_t^{n\delta}$ Re $s_\upsilon(x,y,z,t) = 0$, $\mathfrak{D}_t^{n\delta}$ Re $s_\vartheta(x,y,z,t) = 0$, and $\mathfrak{D}_t^{n\delta}$ Re $s_\varpi(x,y,z,t) = 0$. In the Caputo definition, the constant has zero derivative therefore $\mathfrak{D}_t^{n\delta}$ Re $s(x,y,z,0) = \mathfrak{D}_t^{n\delta}$ Re $s_k(x,y,z,0) = 0$, $k = 0,1,\cdots,n$ which mean that $\mathfrak{D}_t^{n\delta}$ of Re $s_\upsilon(x,y,z,t)$, Re $s_\vartheta(x,y,z,t)$, Re $s_\varpi(x,y,z,t)$, and Re $s_k(x,y,z,t)$ are $t = 0$ matching at $n = 0,1,\cdots,k$; .

To determine $f_1(x,y,z), f_2(x,y,z), f_3(x,y,z), \cdots, g_1(x,y,z), g_2(x,y,z), g_3(x,y,z), \cdots$, and $h_1(x,y,z), h_2(x,y,z), h_3(x,y,z), \cdots$, we substitute $k = 0,1,\cdots$, in Eq. (17), and then the obtained results are put in Eq. (19). In the final step, we apply $\mathfrak{D}_t^{(k)\delta}$ on both sides we obtained the following

$$\begin{cases} \mathfrak{D}_t^{(k)\delta} \operatorname{Re} s_{\upsilon,k}(x,y,z,0) = 0, k = 0,1,\cdots, \\ \mathfrak{D}_t^{(k)\delta} \operatorname{Re} s_{\vartheta,k}(x,y,z,0) = 0, k = 0,1,\cdots, \\ \mathfrak{D}_t^{(k)\delta} \operatorname{Re} s_{\varpi,k}(x,y,z,0) = 0, k = 0,1,\cdots. \end{cases} \tag{22}$$

3.2. Q-HATM Procedure for FPDEs System [63]. Using LT, Eq. (14) can be simplified as

$$\begin{cases} s^\delta \mathscr{L}\{\upsilon(x,y,z,t)\} - \sum_{k=0}^{n-1} s^{\delta-k-1}\upsilon^{(k)}(x,y,z,0) + \mathscr{L}\{R\upsilon(x,y,z,t) + N\upsilon(x,y,z,t)\} = \mathscr{L}\{f(x,y,z,t)\}, \\ s^\delta \mathscr{L}\{\vartheta(x,y,z,t)\} - \sum_{k=0}^{n-1} s^{\delta-k-1}\vartheta^{(k)}(x,y,z,0) + \mathscr{L}\{R\vartheta(x,y,z,t) + N\vartheta(x,y,z,t)\} = \mathscr{L}\{g(x,y,z,t)\}, \\ s^\delta \mathscr{L}\{\varpi(x,y,z,t)\} - \sum_{k=0}^{n-1} s^{\delta-k-1}\varpi^{(k)}(x,y,z,0) + \mathscr{L}\{R\varpi(x,y,z,t) + N\varpi(x,y,z,t)\} = \mathscr{L}\{h(x,y,z,t)\}, \end{cases} \tag{23}$$

so Eq. (23), implies that

$$\begin{cases} \mathscr{L}\{\upsilon(x,y,z,t)\} - \frac{1}{s^{\delta}}\sum_{k=0}^{n-1} s^{\delta-k-1}\upsilon^{(k)}(x,y,z,0) + \frac{1}{s^{\delta}}\mathscr{L}[R\upsilon(x,y,z,t) \\ +N\upsilon(x,y,z,t) - f(x,y,z,t)] = 0, \\ \mathscr{L}\{\vartheta(x,y,z,t)\} - \frac{1}{s^{\delta}}\sum_{k=0}^{n-1} s^{\delta-k-1}\vartheta^{(k)}(x,y,z,0) + \frac{1}{s^{\delta}}\mathscr{L}[R\vartheta(x,y,z,t) \\ +N\vartheta(x,y,z,t) - g(x,y,z,t)] = 0, \\ \mathscr{L}\{\varpi(x,y,z,t)\} - \frac{1}{s^{\delta}}\sum_{k=0}^{n-1} s^{\delta-k-1}\varpi^{(k)}(x,y,z,0) + \frac{1}{s^{\delta}}\mathscr{L}[R\varpi(x,y,z,t) \\ +N\varpi(x,y,z,t) - h(x,y,z,t)] = 0. \end{cases} \tag{24}$$

We define the nonlinear operator is

$$\begin{cases} N[\theta(x,y,z,t;q)] = L\{\theta(x,y,z,t;q)\} - \frac{1}{s^{\delta}}\sum_{k=o}^{n-1} s^{\delta-k-1}\theta^{(k)}(x,y,z,t;q)(0^{+}) \\ +\frac{1}{s^{\delta}}\mathscr{L}[R\upsilon(x,y,z,t) + N\upsilon(x,y,z,t) - f(x,y,z,t)], \\ N[\theta(x,y,z,t;q)] = L\{\theta(x,y,z,t;q)\} - \frac{1}{s^{\delta}}\sum_{k=o}^{n-1} s^{\delta-k-1}\theta^{(k)}(x,t;q)(0^{+}) \\ +\frac{1}{s^{\delta}}\mathscr{L}[R\vartheta(x,y,z,t) + N\vartheta(x,y,z,t) - g(x,y,z,t)], \\ N[\theta(x,y,z,t;q)] = L\{\theta(x,t;q)\} - \frac{1}{s^{\delta}}\sum_{k=o}^{n-1} s^{\delta-k-1}\theta^{(k)}(x,y,z,t;q)(0^{+}) \\ +\frac{1}{s^{\delta}}\mathscr{L}[R\varpi(x,y,z,t) + N\varpi(x,y,z,t) - h(x,y,z,t)], \end{cases} \tag{25}$$

where $q \in [0, (1/n)]$, $\theta(x,y,z,t;q)$ is real function of x, y, z, t, and q.

Homotopy can be constructed as

$$\begin{cases} (1-nq)[\mathscr{L}\{\theta(x,y,z,t;q) - \upsilon_0(x,y,z,t)\}] = \hbar q H(x,y,z,t) N[\theta(x,y,z,t;q)], \\ (1-nq)[\mathscr{L}\{\theta(x,y,z,t;q) - \vartheta_0(x,y,z,t)\}] = \hbar q H(x,y,z,t) N[\theta(x,y,z,t;q)], \\ (1-nq)[\mathscr{L}\{\theta(x,y,z,t;q) - \varpi_0(x,y,z,t)\}] = \hbar q H(x,y,z,t) N[\theta(x,y,z,t;q)]. \end{cases} \tag{26}$$

In Eq. (26), the auxiliary parameter, nonzero auxiliary function and embedding parameter are $h \neq 0$, $H(x,y,z,t)$ and $n \geq 1$, $q \in [0,(1/n)]$, respectively. $\mathscr{L}$ denotes Laplacian operator and υ_0, ϑ_0, and ϖ_0 are the initial conditions. The following results are obtained at $q=0$ and $q=1/n$,

$$\begin{cases} \theta(x,y,z,t;0) = \upsilon_0(x,y,z,t) \text{ and } \theta\left(x,y,z,t;\frac{1}{n}\right) = \upsilon(x,y,z,t), \\ \theta(x,y,z,t;0) = \vartheta_0(x,y,z,t) \text{ and } \theta\left(x,y,z,t;\frac{1}{n}\right) = \vartheta(x,y,z,t), \\ \theta(x,y,z,t;0) = \varpi_0(x,y,z,t) \text{ and } \theta\left(x,y,z,t;\frac{1}{n}\right) = \varpi(x,y,z,t)s. \end{cases} \tag{27}$$

By using Taylor theorem $\theta(x,y,z,t;q)$ can be expressed as

$$\begin{cases} \theta(x,y,z,t;q) = \upsilon_0(x,y,z,t) + \sum_{m=1}^{\infty} \upsilon_m(x,y,z,t)q^m, \\ \theta(x,y,z,t;q) = \vartheta_0(x,y,z,t) + \sum_{m=1}^{\infty} \vartheta_m(x,y,z,t)q^m, \\ \theta(x,y,z,t;q) = \varpi_0(x,y,z,t) + \sum_{m=1}^{\infty} \varpi_m(x,y,z,t)q^m, \end{cases} \tag{28}$$

where

$$\begin{cases} \upsilon_m(x,y,z,t) = \frac{1}{m!}\left[\frac{\partial^m \theta(x,y,z,t;q)}{\partial q^m}\right]\Big|_{q=0}, \\ \vartheta_m(x,y,z,t) = \frac{1}{m!}\left[\frac{\partial^m \theta(x,y,z,t;q)}{\partial q^m}\right]\Big|_{q=0}, \\ \varpi_m(x,y,z,t) = \frac{1}{m!}\left[\frac{\partial^m \theta(x,y,z,t;q)}{\partial q^m}\right]\Big|_{q=0}. \end{cases} \tag{29}$$

After simplification, we have

$$\begin{cases} \upsilon_m(x,y,z,t) = \upsilon_0(x,y,z,t) + \sum_{m=1}^{\infty} \upsilon_m(x,y,z,t)\left(\frac{1}{n}\right)^m, \\ \vartheta_m(x,y,z,t) = \vartheta_0(x,y,z,t) + \sum_{m=1}^{\infty} \vartheta_m(x,y,z,t)\left(\frac{1}{n}\right)^m, \\ \varpi_m(x,y,z,t) = \varpi_0(x,y,z,t) + \sum_{m=1}^{\infty} \varpi_m(x,y,z,t)\left(\frac{1}{n}\right)^m, \end{cases} \tag{30}$$

Taking the m-times derivatives of Eq. (26), put $q=0$, implies the $zero^{th}$ order solution

$$\begin{cases} \mathscr{L}\{\upsilon_m(x,y,z,t) - k_m\upsilon_{m-1}(x,y,z,t)\} = \hbar H(x,y,z,t)\mathfrak{R}_m\left(\overleftarrow{\upsilon}_{m-1}\right), \\ \mathscr{L}\{\vartheta_m(x,y,z,t) - k_m\vartheta_{m-1}(x,y,z,t)\} = \hbar H(x,y,z,t)\mathfrak{R}_m\left(\overleftarrow{\vartheta}_{m-1}\right), \\ \mathscr{L}\{\varpi_m(x,y,z,t) - k_m\varpi_{m-1}(x,y,z,t)\} = \hbar H(x,y,z,t)\mathfrak{R}_m\left(\overleftarrow{\varpi}_{m-1}\right). \end{cases} \tag{31}$$

where the vectors are defined as

$$\begin{cases} \overleftarrow{\upsilon}_m = \{\upsilon_0(x,y,z,t), \upsilon_1(x,y,z,t), \cdots, \upsilon_m(x,y,z,t)\}, \\ \overleftarrow{\vartheta}_m = \{\vartheta_0(x,y,z,t), \vartheta_1(x,y,z,t), \cdots, \vartheta_m(x,y,z,t)\}, \\ \overleftarrow{\varpi}_m = \{\varpi_0(x,y,z,t), \varpi_1(x,y,z,t), \cdots, \varpi_m(x,y,z,t)\}. \end{cases} \tag{32}$$

The following recursive formula is obtained by taking inverse LT of Eq. (31),

$$\begin{cases} \upsilon_m(x,y,z,t) = k_m(x,y,z,t)\upsilon_{m-1}(x,y,z,t) + \hbar\mathscr{L}^{-1}\left\{H(x,y,z,t)\mathfrak{R}_m\left(\overleftarrow{\upsilon}_{m-1}\right)\right\}, \\ \vartheta_m(x,y,z,t) = k_m(x,y,z,t)\vartheta_{m-1}(x,y,z,t) + \hbar\mathscr{L}^{-1}\left\{H(x,y,z,t)\mathfrak{R}_m\left(\overleftarrow{\vartheta}_{m-1}\right)\right\}, \\ \varpi_m(x,y,z,t) = k_m(x,y,z,t)\varpi_{m-1}(x,y,z,t) + \hbar\mathscr{L}^{-1}\left\{H(x,y,z,t)\mathfrak{R}_m\left(\overleftarrow{\varpi}_{m-1}\right)\right\}. \end{cases} \tag{33}$$

Where

$$\begin{cases} \mathfrak{R}_m\left(\overleftarrow{\upsilon}_{m-1}\right) = \dfrac{1}{(m-1)!}\left[\dfrac{\partial^{m-1}N[\theta(x,y,z,t;q)]}{\partial q^{m-1}}\right]\Bigg|_{q=0}, \\ \mathfrak{R}_m\left(\overleftarrow{\vartheta}_{m-1}\right) = \dfrac{1}{(m-1)!}\left[\dfrac{\partial^{m-1}N[\theta(x,y,z,t;q)]}{\partial q^{m-1}}\right]\Bigg|_{q=0}, \\ \mathfrak{R}_m\left(\overleftarrow{\varpi}_{m-1}\right) = \dfrac{1}{(m-1)!}\left[\dfrac{\partial^{m-1}N[\theta(x,y,z,t;q)]}{\partial q^{m-1}}\right]\Bigg|_{q=0}, \end{cases} \tag{34}$$

$$k_m = \begin{cases} 0, & m \le 1, \\ n, & m > 1. \end{cases} \tag{35}$$

Eq. (33) and Eq. (35) are known q-HATM series solutions for the given system.

4. Numerical Results

4.1. Example. Consider nonlinear advection-diffusion equation of the form [64]

$$\frac{\partial^\delta \upsilon}{\partial t^\delta} = -\upsilon\frac{\partial \upsilon}{\partial x} + \upsilon - \upsilon^2, 0 < \delta \le 1, \tag{36}$$

with ICs

$$\upsilon(x,0) = e^{-x}, \tag{37}$$

and exact solution at $\delta = 1$

$$\upsilon(x,t) = e^{t-x}. \tag{38}$$

4.1.1. RPSM-Solution

(1) 1st Iteration. Using RPSM, the k^{th} truncated series of Eq. (36), can obtain

$$\upsilon_k(x,t) = \sum_{n=0}^{k} f_n(x)\frac{t^{n\delta}}{\Gamma(1+n\delta)}, \tag{39}$$

the 1st approximate is given as

$$\upsilon_0(x,t) = \upsilon(x,0) = f(x), \tag{40}$$

Eq. (39) should be written as

$$\upsilon_k(x,t) = f(x) + \sum_{n=1}^{k} f_n(x)\frac{t^{n\delta}}{\Gamma(1+n\delta)}, k = 1, 2, \cdots, \tag{41}$$

put $k = 1$ in Eq. (41), we get

$$\upsilon_1(x,t) = f(x) + f_1(x)\frac{t^\delta}{\Gamma(1+\delta)}, \tag{42}$$

where $\upsilon(x,0) = f(x) = e^{-x}$,

$$\upsilon_1(x,t) = e^{-x} + f_1(x)\frac{t^\delta}{\Gamma(1+\delta)}. \tag{43}$$

The residual function of Eq. (36), is given by

$$Res\upsilon(x,t) = \frac{\partial^\delta \upsilon}{\partial t^\delta} + \upsilon\frac{\partial \upsilon}{\partial x} - \upsilon + \upsilon^2. \tag{44}$$

The k^{th} residual function $\mathrm{Res}\upsilon(x,t)$ is given by,

$$Res\upsilon_k(x,t) = \frac{\partial^\delta \upsilon_k}{\partial t^\delta} + \upsilon_k\frac{\partial \upsilon_k}{\partial x} - \upsilon_k + \upsilon_k^2, \tag{45}$$

put $k = 1$ in the Eq. (45), we obtain

$$Res\upsilon_1(x,t) = \begin{cases} f_1(x) + \left(e^{-x} + f_1(x)\dfrac{t^\delta}{\Gamma(1+\delta)}\right)\left(-e^{-x} + f_1'(x)\dfrac{t^\delta}{\Gamma(1+\delta)}\right) \\ -\left(e^{-x} + f_1(x)\dfrac{t^\delta}{\Gamma(1+\delta)}\right) + \left(e^{-2x} + f_1(x)\dfrac{e^{-x}t^\delta}{\Gamma(1+\delta)} + 2e^{-x}f_1(x)\dfrac{e^{-x}t^\delta}{\Gamma(1+\delta)}\right), \end{cases} \tag{46}$$

we have

$$\mathrm{Res}\upsilon_1(x,0) = 0. \tag{47}$$

Eq. (46), will become

$$f_1(x) = e^{-x}. \tag{48}$$

(2) 2nd Iteration. for $k = 2$ Eq. (41), can be written as

$$\upsilon_2(x,t) = f(x) + f_1(x)\frac{t^\delta}{\Gamma(1+\delta)} + f_2(x)\frac{t^{2\delta}}{\Gamma(1+2\delta)}, \tag{49}$$

where $f(x) = e^{-x}$, and $f_1(x) = e^{-x}$,

$$\upsilon_2(x,t) = e^{-x} + \frac{e^{-x}t^\delta}{\Gamma(1+\delta)} + f_2(x)\frac{t^{2\delta}}{\Gamma(1+2\delta)}, \tag{50}$$

put $k = 2$ in Eq. (45), we obtain

$$\mathrm{Res}v_2(x,t)=\frac{\partial^\delta v_2}{\partial t^\delta}+v_2\frac{\partial v_2}{\partial x}-v_2+v_1^2, \tag{51}$$

$$\begin{aligned}\mathrm{Res}v_2(x,t)&=\left(e^{-x}+f_2(x)\frac{t^\delta}{\Gamma(1+\delta)}\right)+\left(e^{-x}+\frac{e^{-x}t^\delta}{\Gamma(1+\delta)}+f_2(x)\frac{t^{2\delta}}{\Gamma(1+2\delta)}\right)\left(-e^{-x}-\frac{e^{-x}t^\delta}{\Gamma(1+\delta)}+f_2'(x)\frac{t^{2\delta}}{\Gamma(1+2\delta)}\right)\\&\quad-\left(e^{-x}+\frac{e^{-x}t^\delta}{\Gamma(1+\delta)}+f_2(x)\frac{t^{2\delta}}{\Gamma(1+2\delta)}\right)+\left(e^{-x}+\frac{e^{-x}t^\delta}{\Gamma(1+\delta)}+f_2(x)\frac{t^{2\delta}}{\Gamma(1+2\delta)}\right)^2,\end{aligned} \tag{52}$$

as we know that

$$D_t^{(k-1)\delta}\mathrm{Res}v_k(x,t)=0, \tag{53}$$

for $k=2$ Eq. (53), become as

$$D_t^{\delta}\mathrm{Res}v_2(x,t)=0, \tag{54}$$

using D_t^δ on Eq. (52), we get

$$D_t^\delta\mathrm{Res}v_2(x,t)=\begin{cases}f_2(x)+\left(e^{-x}+f_2(x)\frac{t^\delta}{\Gamma(1+\delta)}\right)\left(-e^{-x}+f_2'(x)\frac{t^\delta}{\Gamma(1+\delta)}\right)\\-\left(e^{-x}+f_2(x)\frac{t^\delta}{\Gamma(1+\delta)}\right)+\left(e^{-x}+f_2(x)\frac{t^\delta}{\Gamma(1+\delta)}\right)^2,\end{cases} \tag{55}$$

put $D_t^\delta\mathrm{Res}v_2(x,0)=0$ in Eq. (55), we obtain

$$f_2(x)=e^{-x}. \tag{56}$$

(3) 3rd Iteration. Put $k=3$ in Eq. (41), we obtain

$$v_3(x,t)=f(x)+f_1(x)\frac{t^\delta}{\Gamma(1+\delta)}+f_2(x)\frac{t^{2\delta}}{\Gamma(1+2\delta)}+f_3(x)\frac{t^{3\delta}}{\Gamma(1+3\delta)}, \tag{57}$$

where $f(x)=e^{-x}$, $f_1(x)=e^{-x}$, and $f_2(x)=e^{-x}$,

$$v_3(x,t)=e^{-x}+\frac{e^{-x}t^\delta}{\Gamma(1+\delta)}+\frac{e^{-x}t^{2\delta}}{\Gamma(1+2\delta)}+f_3(x)\frac{t^{3\delta}}{\Gamma(1+3\delta)}, \tag{58}$$

put $k=3$ in Eq. (45) we obtain

$$Resv_3(x,t)=\frac{\partial^\delta v_3}{\partial t^\delta}+v_3\frac{\partial v_3}{\partial x}-v_3+v_3^2, \tag{59}$$

$$Resv_3(x,t)=\begin{cases}\left(e^{-x}+\frac{e^{-x}t^\delta}{\Gamma(1+\delta)}+f_3(x)\frac{t^{2\delta}}{\Gamma(1+2\delta)}\right)+\left(e^{-x}+\frac{e^{-x}t^\delta}{\Gamma(1+\delta)}+\frac{e^{-x}t^{2\delta}}{\Gamma(1+2\delta)}+f_3(x)\frac{t^{3\delta}}{\Gamma(1+3\delta)}\right)\\\left(-e^{-x}-\frac{e^{-x}t^\delta}{\Gamma(1+\delta)}-\frac{e^{-x}t^{2\delta}}{\Gamma(1+2\delta)}+f_3'(x)\frac{t^{3\delta}}{\Gamma(1+3\delta)}\right)-\left(e^{-x}+\frac{e^{-x}t^\delta}{\Gamma(1+\delta)}+\frac{e^{-x}t^{2\delta}}{\Gamma(1+2\delta)}+f_3(x)\frac{t^{3\delta}}{\Gamma(1+3\delta)}\right)\\+\left(e^{-x}+\frac{e^{-x}t^\delta}{\Gamma(1+\delta)}+\frac{e^{-x}t^{2\delta}}{\Gamma(1+2\delta)}+f_3(x)\frac{t^{3\delta}}{\Gamma(1+3\delta)}\right)^2,\end{cases} \tag{60}$$

put $k=3$ in Eq. (53), we obtain

$$D_t^{2\delta}Resv_3(x,t)=0, \tag{61}$$

applying $D_t^{2\delta}$ on both sides of the Eq. (60), we get

$$\begin{aligned}D_t^{2\delta}Resv_2(x,t)&=f_3(x)+\left(e^{-x}+f_3(x)\frac{t^\delta}{\Gamma(1+\delta)}\right)\left(-e^{-x}+f_3'(x)\frac{t^\delta}{\Gamma(1+\delta)}\right)\\&\quad-\left(e^{-x}+f_3(x)\frac{t^\delta}{\Gamma(1+\delta)}\right)+\left(e^{-x}+f_3(x)\frac{t^\delta}{\Gamma(1+\delta)}\right)^2,\end{aligned} \tag{62}$$

put $D_t^\delta Resv_2(x,0)=0$ in Eq. (62), we obtain

$$f_2(x)=e^{-x}. \tag{63}$$

The RPSM solution of Eq. (36), is given as

$$\begin{aligned}v(x,t)&=f(x)+f_1(x)\frac{t^\delta}{\Gamma(1+\delta)}+f_2(x)\frac{t^{2\delta}}{\Gamma(1+2\delta)}+f_3(x)\frac{t^{3\delta}}{\Gamma(1+3\delta)}+\cdots,\\v(x,t)&=e^{-x}+\frac{e^{-x}t^\delta}{\Gamma(1+\delta)}+\frac{e^{-x}t^{2\delta}}{\Gamma(1+2\delta)}+\frac{e^{-x}t^{3\delta}}{\Gamma(1+3\delta)}+\cdots.\end{aligned} \tag{64}$$

4.1.2. Q-HATM Solution

(1) 1st Iteration. Taking LT of Eq. (36), and simplifying

$$s^{\delta}\mathscr{L}[v(x,t)]-\sum_{k=0}^{n-1}s^{\delta-k-1}v_k(x,0)+\mathscr{L}\left(v\frac{\partial v}{\partial x}-v+v^2\right)=0,$$
$$\mathscr{L}[v(x,t)]-\frac{1}{s^{\delta}}s^{\delta-1}v_0(x,0)+\frac{1}{s^{\delta}}\mathscr{L}\left(v\frac{\partial v}{\partial x}-v+v^2\right)=0,$$
$$\mathscr{L}[v(x,t)]-\frac{e^{-x}}{s}+\frac{1}{s^{\delta}}\mathscr{L}\left(v\frac{\partial v}{\partial x}-v+v^2\right)=0. \tag{65}$$

The nonlinear term N is defined as

$$N[\theta(x,t;q)]=\mathscr{L}[\theta(x,t;q)]-\frac{e^{-x}}{s}+\frac{1}{s^{\delta}}\mathscr{L}\left(v\frac{\partial v}{\partial x}-v+v^2\right). \tag{66}$$

Using the procedure of q-HATM

$$v_m(x,t)=k_m v_{m-1}(x,t)+h\mathscr{L}^{-1}[R_m(v_{m-1})], \tag{67}$$

put $m=1$ in the Eq. (67), we obtain

$$v_1(x,t)=k_1 v_0(x,t)+h\mathscr{L}^{-1}[R_1(v_0)], \tag{68}$$

$$R_m(v_{m-1})=\mathscr{L}(v_{m-1})-\left(1-\frac{k_m}{n}\right)\frac{e^{-x}}{s}+\frac{1}{s^{\delta}}\mathscr{L}\left(\sum_{i=0}^{m-1}v_i\frac{\partial v_{m-1-i}}{\partial x}-v_{m-1}+\sum_{i=0}^{m-1}v_i v_{m-1-i}\right), \tag{69}$$

put $m=1$ in Eq. (69), we obtain

$$R_1(v_0)=\mathscr{L}(v_0)-\left(1-\frac{k_1}{n}\right)\frac{e^{-x}}{s}+\frac{1}{s^{\delta}}\mathscr{L}\left(v_0\frac{\partial v_0}{\partial x}-v_0+v_0v_0\right),$$
$$R_1(v_0)=\mathscr{L}(e^{-x})-\left(1-\frac{k_1}{n}\right)\frac{e^{-x}}{s}+\frac{1}{s^{\delta}}\mathscr{L}\left(e^{-x}\frac{\partial}{\partial x}e^{-x}-e^{-x}+e^{-x}e^{-x}\right),$$
$$R_1(v_0)=\frac{e^{-x}}{s}-\frac{e^{-x}}{s}+\frac{1}{s^{\delta}}\mathscr{L}\left(-e^{-2x}-e^{-x}+e^{-2x}\right),$$
$$R_1(v_0)=-\frac{e^{-x}}{s^{\delta+1}}, \tag{70}$$

put in Eq. (68), we obtain

$$v_1(x,t)=h\mathscr{L}^{-1}\left[-\frac{e^{-x}}{s^{\delta+1}}\right],$$
$$v_1(x,t)=-\frac{e^{-x}ht^{\delta}}{\Gamma(1+\delta)}. \tag{71}$$

(2) 2nd Iteration. Put $m=2$ in the Eq. (67), we obtain

$$v_2(x,t)=k_2 v_1(x,t)+h\mathscr{L}^{-1}[R_2(v_1)], \tag{72}$$

put $m=2$ in Eq. (69), we obtain

$$R_2(v_1)=\mathscr{L}(v_1)-\left(1-\frac{k_2}{n}\right)\frac{e^{-x}}{s}+\frac{1}{s^{\delta}}\mathscr{L}\left(v_0\frac{\partial v_1}{\partial x}+v_1\frac{\partial v_0}{\partial x}-v_1+v_1v_0+v_0v_1\right),$$
$$=-\frac{e^{-x}h}{s^{\delta+1}}+\frac{e^{-x}ht}{s^{2\delta+1}}, \tag{73}$$

put in Eq. (72), we obtain

$$v_2(x,t)=-\frac{e^{-x}nht^{\delta}}{\Gamma(1+\delta)}+h\mathscr{L}^{-1}\left[-\frac{e^{-x}h}{s^{\delta+1}}+\frac{e^{-x}ht}{s^{2\delta+1}}\right],$$
$$v_2(x,t)=-\frac{e^{-x}nht^{\delta}}{\Gamma(1+\delta)}-\frac{e^{-x}h^2t^{\delta}}{\Gamma(\delta+1)}+\frac{e^{-x}h^2t^{2\delta}}{\Gamma(2\delta+1)}. \tag{74}$$

(3) 3rd Iteration. Put $m=3$ in the Eq. (67), we obtain

$$v_3(x,t)=k_3 v_2(x,t)+h\mathscr{L}^{-1}[R_3(v_2)], \tag{75}$$

put $m=3$ in Eq. (69), we obtain

$$R_3(v_2)=\mathscr{L}(v_2)-\frac{e^{-x}}{s}+\frac{1}{s^{\delta}}\mathscr{L}\left(v_0\frac{\partial v_2}{\partial x}+v_1\frac{\partial v_1}{\partial x}+v_2\frac{\partial v_0}{\partial x}-v_2+v_0v_2+v_1v_1+v_2v_0\right),$$
$$=-\frac{e^{-x}nh}{s^{\delta+1}}-\frac{e^{-x}h^2}{s^{\delta+1}}+\frac{2e^{-x}h^2}{s^{2\delta+1}}+\frac{e^{-x}nh}{s^{2\delta+1}}-\frac{e^{-x}h^2}{s^{3\delta+1}}, \tag{76}$$

put in Eq. (75), we obtain

$$v_3(x,t)=n\left(-\frac{e^{-x}nht^{\delta}}{\Gamma(1+\delta)}-\frac{e^{-x}h^2t^{\delta}}{\Gamma(\delta+1)}+\frac{e^{-x}h^2t^{2\delta}}{\Gamma(2\delta+1)}\right)+h\mathscr{L}^{-1}\left[-\frac{e^{-x}nh}{s^{\delta+1}}-\frac{e^{-x}h^2}{s^{\delta+1}}+\frac{2e^{-x}h^2}{s^{2\delta+1}}+\frac{e^{-x}nh}{s^{2\delta+1}}-\frac{e^{-x}h^2}{s^{3\delta+1}}\right],$$
$$v_3(x,t)=-\frac{e^{-x}n^2ht^{\delta}}{\Gamma(1+\delta)}-\frac{e^{-x}nh^2t^{\delta}}{\Gamma(\delta+1)}+\frac{e^{-x}nh^2t^{2\delta}}{\Gamma(2\delta+1)}-\frac{e^{-x}nh^2t^{\delta}}{\Gamma(\delta+1)}-\frac{e^{-x}h^3t^{\delta}}{\Gamma(\delta+1)}+\frac{2e^{-x}h^3t^{2\delta}}{\Gamma(2\delta+1)}+\frac{e^{-x}nh^2t^{2\delta}}{\Gamma(2\delta+1)}-\frac{e^{-x}h^3t^{3\delta}}{\Gamma(3\delta+1)}. \tag{77}$$

The q-HATM solution of Eq. (36), is given as

$$
\begin{aligned}
&\upsilon(x,t)=\upsilon_0(x,t)+\upsilon_1(x,t)+\upsilon_2(x,t)+\upsilon_3(x,t)+\cdots,\\
&\upsilon(x,t)=e^{-x}-\frac{e^{-x}ht^{\delta}}{\Gamma(1+\delta)}-\frac{e^{-x}nht^{\delta}}{\Gamma(1+\delta)}-\frac{e^{-x}h^2t^{\delta}}{\Gamma(\delta+1)}+\frac{e^{-x}h^2t^{2\delta}}{\Gamma(2\delta+1)}-\frac{e^{-x}n^2ht^{\delta}}{\Gamma(1+\delta)}-\frac{e^{-x}nh^2t^{\delta}}{\Gamma(\delta+1)}+\frac{e^{-x}nh^2t^{2\delta}}{\Gamma(2\delta+1)}\\
&\quad-\frac{e^{-x}nh^2t^{\delta}}{\Gamma(\delta+1)}-\frac{e^{-x}h^3t^{\delta}}{\Gamma(\delta+1)}+\frac{2e^{-x}h^3t^{2\delta}}{\Gamma(2\delta+1)}+\frac{e^{-x}nh^2t^{2\delta}}{\Gamma(2\delta+1)}-\frac{e^{-x}h^3t^{3\delta}}{\Gamma(3\delta+1)}+\cdots.
\end{aligned}
\tag{78}
$$

4.2. Example. The system of 3D Burgers' equation are [65, 66]

$$
\begin{cases}
\upsilon_t^{\delta}+\upsilon\upsilon_x+\vartheta\upsilon_y+\varpi\upsilon_z-\upsilon_{xx}-\upsilon_{yy}-\upsilon_{zz}=0,\\
\vartheta_t^{\delta}+\upsilon\vartheta_x+\vartheta\vartheta_y+\varpi\vartheta_z-\vartheta_{xx}-\vartheta_{yy}-\vartheta_{zz}=0,\\
\varpi_t^{\delta}+\upsilon\varpi_x+\vartheta\varpi_y+\varpi\varpi_z-\varpi_{xx}-\varpi_{yy}-\varpi_{zz}=0,
\end{cases}
\tag{79}
$$

the initial condition of Eq. (79), are

$$
\begin{aligned}
\upsilon(x,y,z,0)&=-0.5x+y+z,\vartheta(x,y,z,0)\\
&=x-0.5y+z,\varpi(x,y,z,0)=x+y-0.5z.
\end{aligned}
\tag{80}
$$

The exact solution of the Eq. (79) at $\delta=1$, are

$$
\begin{cases}
\upsilon(x,y,z,t)=\dfrac{-0.5x+y+z-2.25xt}{1-2.25t^2},\\
\vartheta(x,y,z,t)=\dfrac{x-0.5y+z-2.25yt}{1-2.25t^2},\\
\varpi(x,y,z,t)=\dfrac{x+y-0.5z-2.25zt}{1-2.25t^2}.
\end{cases}
\tag{81}
$$

4.2.1. RPSM-Solution

(1) 1st Iteration. The k^{th} truncated series of the solution of Eq. (79), using RPSM, we obtain

$$
\begin{cases}
\upsilon_k(x,y,z,t)=\displaystyle\sum_{n=0}^{k}f_n(x,y,z)\frac{t^{n\delta}}{\Gamma(1+n\delta)},\\
\vartheta_k(x,y,z,t)=\displaystyle\sum_{n=0}^{k}g_n(x,y,z)\frac{t^{n\delta}}{\Gamma(1+n\delta)},\\
\varpi_k(x,y,z,t)=\displaystyle\sum_{n=0}^{k}h_n(x,y,z)\frac{t^{n\delta}}{\Gamma(1+n\delta)},
\end{cases}
\tag{82}
$$

the $zero^{th}$ RPSM approximate solution of Eq. (79), is given by

$$
\begin{cases}
\upsilon_0(x,y,z,t)=\upsilon(x,y,z,0)=f(x,y,z),\\
\vartheta_0(x,y,z,t)=\vartheta(x,y,z,0)=g(x,y,z),\\
\varpi_0(x,y,z,t)=\varpi(x,y,z,0)=h(x,y,z),
\end{cases}
\tag{83}
$$

the Eq. (82), should be written as

$$
\begin{cases}
\upsilon_k(x,y,z,t)=f(x,y,z)+\displaystyle\sum_{n=1}^{k}f_n(x,y,z)\frac{t^{n\delta}}{\Gamma(1+n\delta)},k=1,2,\cdots,\\
\vartheta_k(x,y,z,t)=g(x,y,z)+\displaystyle\sum_{n=1}^{k}g_n(x,y,z)\frac{t^{n\delta}}{\Gamma(1+n\delta)},k=1,2,\cdots,\\
\varpi_k(x,y,z,t)=h(x,y,z)+\displaystyle\sum_{n=1}^{k}h_n(x,y,z)\frac{t^{n\delta}}{\Gamma(1+n\delta)},k=1,2,\cdots,
\end{cases}
\tag{84}
$$

put $k=1$ in Eq. (84), we get

$$
\begin{cases}
\upsilon_1(x,y,z,t)=f(x,y,z)+f_1(x,y,z)\dfrac{t^{\delta}}{\Gamma(1+\delta)},\\
\vartheta_1(x,y,z,t)=g(x,y,z)+g_1(x,y,z)\dfrac{t^{\delta}}{\Gamma(1+\delta)},\\
\varpi_1(x,y,z,t)=g(x,y,z)+g_1(x,y,z)\dfrac{t^{\delta}}{\Gamma(1+\delta)},
\end{cases}
\tag{85}
$$

where

$$
\begin{cases}
\upsilon(x,y,z,0)=f(x,y,z)=-0.5x+y+z,\\
\vartheta(x,y,z,0)=g(x,y,z)=x-0.5y+z,\\
\varpi(x,y,z,0)=h(x,y,z)=x+y-0.5z,
\end{cases}
$$

$$
\begin{cases}
\upsilon_1(x,y,z,t)=-0.5x+y+z+f_1(x,y,z)\dfrac{t^{\delta}}{\Gamma(1+\delta)},\\
\vartheta_1(x,y,z,t)=x-0.5y+z+g_1(x,y,z)\dfrac{t^{\delta}}{\Gamma(1+\delta)},\\
\varpi_1(x,y,z,t)=x+y-0.5z+h_1(x,y,z)\dfrac{t^{\delta}}{\Gamma(1+\delta)}.
\end{cases}
\tag{86}
$$

The residual function of Eq. (79), is given by

$$\begin{cases} \mathrm{Res}\upsilon(x,y,z,t)=\dfrac{\partial^{\delta}\upsilon}{\partial t^{\delta}}+\upsilon\dfrac{\partial\upsilon}{\partial x}+\vartheta\dfrac{\partial\upsilon}{\partial y}+\varpi\dfrac{\partial\upsilon}{\partial z}-\dfrac{\partial^{2}\upsilon}{\partial x^{2}}-\dfrac{\partial^{2}\upsilon}{\partial y^{2}}-\dfrac{\partial^{2}\upsilon}{\partial z^{2}}, \\ \mathrm{Res}\vartheta(x,y,z,t)=\dfrac{\partial^{\delta}\vartheta}{\partial t^{\delta}}+\upsilon\dfrac{\partial\vartheta}{\partial x}+\vartheta\dfrac{\partial\vartheta}{\partial y}+\varpi\dfrac{\partial\vartheta}{\partial z}-\dfrac{\partial^{2}\vartheta}{\partial x^{2}}-\dfrac{\partial^{2}\vartheta}{\partial y^{2}}-\dfrac{\partial^{2}\vartheta}{\partial z^{2}}, \\ \mathrm{Res}\varpi(x,y,z,t)=\dfrac{\partial^{\delta}\varpi}{\partial t^{\delta}}+\upsilon\dfrac{\partial\varpi}{\partial x}+\vartheta\dfrac{\partial\varpi}{\partial y}+\varpi\dfrac{\partial\varpi}{\partial z}-\dfrac{\partial^{2}\varpi}{\partial x^{2}}-\dfrac{\partial^{2}\varpi}{\partial y^{2}}-\dfrac{\partial^{2}\varpi}{\partial z^{2}}, \end{cases} \tag{87}$$

where the k^{th} residual function of $Res\upsilon(x,y,t)$, $Res\vartheta(x,y,t)$, and $Res\varpi(x,y,t)$ is given by

$$\begin{cases} \mathrm{Res}\upsilon_k(x,y,z,t)=\dfrac{\partial^{\delta}\upsilon_k}{\partial t^{\delta}}+\upsilon_k\dfrac{\partial\upsilon_k}{\partial x}+\vartheta_k\dfrac{\partial\upsilon_k}{\partial y}+\varpi_k\dfrac{\partial\upsilon_k}{\partial z}-\dfrac{\partial^{2}\upsilon_k}{\partial x^{2}}-\dfrac{\partial^{2}\upsilon_k}{\partial y^{2}}-\dfrac{\partial^{2}\upsilon_k}{\partial z^{2}}, \\ \mathrm{Res}\vartheta_k(x,y,z,t)=\dfrac{\partial^{\delta}\vartheta_k}{\partial t^{\delta}}+\upsilon_k\dfrac{\partial\vartheta_k}{\partial x}+\vartheta_k\dfrac{\partial\vartheta_k}{\partial y}+\varpi_k\dfrac{\partial\vartheta_k}{\partial z}-\dfrac{\partial^{2}\vartheta_k}{\partial x^{2}}-\dfrac{\partial^{2}\vartheta_k}{\partial y^{2}}-\dfrac{\partial^{2}\vartheta_k}{\partial z^{2}}, \\ \mathrm{Res}\varpi_k(x,y,z,t)=\dfrac{\partial^{\delta}\varpi_k}{\partial t^{\delta}}+\upsilon_k\dfrac{\partial\varpi_k}{\partial x}+\vartheta_k\dfrac{\partial\varpi_k}{\partial y}+\varpi_k\dfrac{\partial\varpi_k}{\partial z}-\dfrac{\partial^{2}\varpi_k}{\partial x^{2}}-\dfrac{\partial^{2}\varpi_k}{\partial y^{2}}-\dfrac{\partial^{2}\varpi_k}{\partial z^{2}}, \end{cases} \tag{88}$$

put $k=1$ in the Eq. (88), we obtain

$$\begin{cases} \mathrm{Res}\upsilon_1(x,y,z,t)=\dfrac{\partial^{\delta}\upsilon_1}{\partial t^{\delta}}+\upsilon_1\dfrac{\partial\upsilon_1}{\partial x}+\vartheta_1\dfrac{\partial\upsilon_1}{\partial y}+\varpi_1\dfrac{\partial\upsilon_1}{\partial z}-\dfrac{\partial^{2}\upsilon_1}{\partial x^{2}}-\dfrac{\partial^{2}\upsilon_1}{\partial y^{2}}-\dfrac{\partial^{2}\upsilon_1}{\partial z^{2}}, \\ \mathrm{Res}\vartheta_1(x,y,z,t)=\dfrac{\partial^{\delta}\vartheta_1}{\partial t^{\delta}}+\upsilon_1\dfrac{\partial\vartheta_1}{\partial x}+\vartheta_1\dfrac{\partial\vartheta_1}{\partial y}+\varpi_1\dfrac{\partial\vartheta_1}{\partial z}-\dfrac{\partial^{2}\vartheta_1}{\partial x^{2}}-\dfrac{\partial^{2}\vartheta_1}{\partial y^{2}}-\dfrac{\partial^{2}\vartheta_1}{\partial z^{2}}, \\ \mathrm{Res}\varpi_1(x,y,z,t)=\dfrac{\partial^{\delta}\varpi_1}{\partial t^{\delta}}+\upsilon_1\dfrac{\partial\varpi_1}{\partial x}+\vartheta_1\dfrac{\partial\varpi_1}{\partial y}+\varpi_1\dfrac{\partial\varpi_1}{\partial z}-\dfrac{\partial^{2}\varpi_1}{\partial x^{2}}-\dfrac{\partial^{2}\varpi_1}{\partial y^{2}}-\dfrac{\partial^{2}\varpi_1}{\partial z^{2}}, \end{cases} \tag{89}$$

$$\begin{cases} =f_1(x,y,z)+\left(-0.5x+y+z+f_1(x,y,z)\dfrac{t^{\delta}}{\Gamma(1+\delta)}\right)\left(-0.5+f_1'(x,y,z)\dfrac{t^{\delta}}{\Gamma(1+\delta)}\right) \\ +\left(x-0.5y+z+f_1(x,y,z)\dfrac{t^{\delta}}{\Gamma(1+\delta)}\right)\left(1+f_1'(x,y,z)\dfrac{t^{\delta}}{\Gamma(1+\delta)}\right) \\ +\left(x+y-0.5z+f_1(x,y,z)\dfrac{t^{\delta}}{\Gamma(1+\delta)}\right)\left(1+f_1'(x,y,z)\dfrac{t^{\delta}}{\Gamma(1+\delta)}\right) \\ -\left(f_1''(x,y,z)\dfrac{t^{\delta}}{\Gamma(1+\delta)}\right)-\left(f_1''(x,y,z)\dfrac{t^{\delta}}{\Gamma(1+\delta)}\right)-\left(f_1''(x,y,z)\dfrac{t^{\delta}}{\Gamma(1+\delta)}\right), \\ =g_1(x,y,z)+\left(-0.5x+y+z+g_1(x,y,z)\dfrac{t^{\delta}}{\Gamma(1+\delta)}\right)\left(1+g_1'(x,y,z)\dfrac{t^{\delta}}{\Gamma(1+\delta)}\right) \\ +\left(x-0.5y+z+g_1(x,y,z)\dfrac{t^{\delta}}{\Gamma(1+\delta)}\right)\left(-0.5+g_1'(x,y,z)\dfrac{t^{\delta}}{\Gamma(1+\delta)}\right) \\ +\left(x+y-0.5z+g_1(x,y,z)\dfrac{t^{\delta}}{\Gamma(1+\delta)}\right)\left(1+g_1'(x,y,z)\dfrac{t^{\delta}}{\Gamma(1+\delta)}\right) \\ -\left(g_1''(x,y,z)\dfrac{t^{\delta}}{\Gamma(1+\delta)}\right)-\left(g_1''(x,y,z)\dfrac{t^{\delta}}{\Gamma(1+\delta)}\right)-\left(g_1''(x,y,z)\dfrac{t^{\delta}}{\Gamma(1+\delta)}\right), \\ =h_1(x,y,z)+\left(-0.5x+y+z+h_1(x,y,z)\dfrac{t^{\delta}}{\Gamma(1+\delta)}\right)\left(1+h_1'(x,y,z)\dfrac{t^{\delta}}{\Gamma(1+\delta)}\right) \\ +\left(x-0.5y+z+h_1(x,y,z)\dfrac{t^{\delta}}{\Gamma(1+\delta)}\right)\left(1+h_1'(x,y,z)\dfrac{t^{\delta}}{\Gamma(1+\delta)}\right) \\ +\left(x+y-0.5z+h_1(x,y,z)\dfrac{t^{\delta}}{\Gamma(1+\delta)}\right)\left(-0.5+h_1'(x,y,z)\dfrac{t^{\delta}}{\Gamma(1+\delta)}\right) \\ -\left(h_1''(x,y,z)\dfrac{t^{\delta}}{\Gamma(1+\delta)}\right)-\left(h_1''(x,y,z)\dfrac{t^{\delta}}{\Gamma(1+\delta)}\right)-\left(h_1''(x,y,z)\dfrac{t^{\delta}}{\Gamma(1+\delta)}\right), \end{cases} \tag{90}$$

we know that

$$\begin{cases} \mathrm{Res}\upsilon_1(x,y,z,0)=0, \\ \mathrm{Res}\vartheta_1(x,y,z,0)=0, \\ \mathrm{Res}\varpi_1(x,y,z,0)=0, \end{cases} \tag{91}$$

put in Eq. (90), we obtain

$$\begin{cases} f_1(x,y,z)=-2.25x, \\ g_1(x,y,z)=-2.25y, \\ h_1(x,y,z)=-2.25z. \end{cases} \tag{92}$$

(2) 2nd Iteration. Put $k=2$ in Eq. (84), we obtain

$$\begin{cases} \upsilon_2(x,y,z,t)=f(x,y,z)+f_1(x,y,z)\dfrac{t^{\delta}}{\Gamma(1+\delta)}+f_2(x,y,z)\dfrac{t^{2\delta}}{\Gamma(1+2\delta)}, \\ \vartheta_2(x,y,z,t)=g(x,y,z)+g_1(x,y,z)\dfrac{t^{\delta}}{\Gamma(1+\delta)}+g_2(x,y,z)\dfrac{t^{2\delta}}{\Gamma(1+2\delta)}, \\ \varpi_2(x,y,z,t)=h(x,y,z)+h_1(x,y,z)\dfrac{t^{\delta}}{\Gamma(1+\delta)}+h_2(x,y,z)\dfrac{t^{2\delta}}{\Gamma(1+2\delta)}, \end{cases} \tag{93}$$

where

$$\upsilon(x,y,z,0)=f(x,y,z)=-0.5x+y+z, f_1(x,y,z)=-2.25x$$
$$\vartheta(x,y,z,0)=g(x,y,z)=x-0.5y+z, g_1(x,y,z)=-2.25y,$$
$$\varpi(x,y,z,0)=h(x,y,z)=x+y-0.5z, h_1(x,y,z)=-2.25z,$$
$$\begin{cases} \upsilon_2(x,y,z,t)=-0.5x+y+z-\dfrac{2.25xt^{\delta}}{\Gamma(1+\delta)}+f_2(x,y,z)\dfrac{t^{2\delta}}{\Gamma(1+2\delta)}, \\ \vartheta_2(x,y,z,t)=x-0.5y+z-\dfrac{2.25yt^{\delta}}{\Gamma(1+\delta)}+g_2(x,y,z)\dfrac{t^{2\delta}}{\Gamma(1+2\delta)}, \\ \varpi_2(x,y,z,t)=x+y-0.5z-\dfrac{2.25zt^{\delta}}{\Gamma(1+\delta)}+h_2(x,y,z)\dfrac{t^{2\delta}}{\Gamma(1+2\delta)}, \end{cases} \tag{94}$$

put $k=2$ in the Eq. (88), we obtain

$$\begin{cases} Res\upsilon_2(x,y,z,t)=\dfrac{\partial^{\delta}\upsilon_2}{\partial t^{\delta}}+\upsilon_2\dfrac{\partial\upsilon_2}{\partial x}+\vartheta_2\dfrac{\partial\upsilon_2}{\partial y}+\varpi_2\dfrac{\partial\upsilon_2}{\partial z}-\dfrac{\partial^2\upsilon_2}{\partial x^2}-\dfrac{\partial^2\upsilon_2}{\partial y^2}-\dfrac{\partial^2\upsilon_2}{\partial z^2}, \\ Res\vartheta_2(x,y,z,t)=\dfrac{\partial^{\delta}\vartheta_2}{\partial t^{\delta}}+\upsilon_2\dfrac{\partial\vartheta_2}{\partial x}+\vartheta_2\dfrac{\partial\vartheta_2}{\partial y}+\varpi_2\dfrac{\partial\vartheta_2}{\partial z}-\dfrac{\partial^2\vartheta_2}{\partial x^2}-\dfrac{\partial^2\vartheta_2}{\partial y^2}-\dfrac{\partial^2\vartheta_2}{\partial z^2}, \\ Res\varpi_2(x,y,z,t)=\dfrac{\partial^{\delta}\varpi_2}{\partial t^{\delta}}+\upsilon_2\dfrac{\partial\varpi_2}{\partial x}+\vartheta_2\dfrac{\partial\varpi_2}{\partial y}+\varpi_2\dfrac{\partial\varpi_2}{\partial z}-\dfrac{\partial^2\varpi_2}{\partial x^2}-\dfrac{\partial^2\varpi_2}{\partial y^2}-\dfrac{\partial^2\varpi_2}{\partial z^2}, \end{cases} \tag{95}$$

$$\begin{cases} Res\upsilon_2(x,y,z,t)=-2.25x+f_2(x,y,z)\dfrac{t^{\delta}}{\Gamma(1+\delta)}+\left(-0.5x+y+z-\dfrac{2.25xt^{\delta}}{\Gamma(1+\delta)}+f_2(x,y,z)\dfrac{t^{2\delta}}{\Gamma(1+2\delta)}\right) \\ \left(-0.5-\dfrac{2.25t^{\delta}}{\Gamma(1+\delta)}+f_2'(x,y,z)\dfrac{t^{2\delta}}{\Gamma(1+2\delta)}\right)+\left(x-0.5y+z-\dfrac{2.25yt^{\delta}}{\Gamma(1+\delta)}+f_2(x,y,z)\dfrac{t^{2\delta}}{\Gamma(1+2\delta)}\right) \\ \left(1+f_2'(x,y,z)\dfrac{t^{2\delta}}{\Gamma(1+2\delta)}\right)+\left(x+y-0.5z-\dfrac{2.25zt^{\delta}}{\Gamma(1+\delta)}+f_2(x,y,z)\dfrac{t^{2\delta}}{\Gamma(1+2\delta)}\right) \\ \left(1+f_2'(x,y,z)\dfrac{t^{2\delta}}{\Gamma(1+2\delta)}\right)-f_2''(x,y,z)\dfrac{t^{2\delta}}{\Gamma(1+2\delta)}-f_2''(x,y,z)\dfrac{t^{2\delta}}{\Gamma(1+2\delta)} \\ -f_2''(x,y,z)\dfrac{t^{2\delta}}{\Gamma(1+2\delta)}, \\ Res\vartheta_2(x,y,z,t)=-2.25y+g_2(x,y,z)\dfrac{t^{\delta}}{\Gamma(1+\delta)}+\left(-0.5x+y+z-\dfrac{2.25xt^{\delta}}{\Gamma(1+\delta)}+g_2(x,y,z)\dfrac{t^{2\delta}}{\Gamma(1+2\delta)}\right) \\ \left(1+g_2'(x,y,z)\dfrac{t^{2\delta}}{\Gamma(1+2\delta)}\right)+\left(x-0.5y+z-\dfrac{2.25yt^{\delta}}{\Gamma(1+\delta)}+g_2(x,y,z)\dfrac{t^{2\delta}}{\Gamma(1+2\delta)}\right) \\ \left(-0.5-\dfrac{2.25t^{\delta}}{\Gamma(1+\delta)}+g_2'(x,y,z)\dfrac{t^{2\delta}}{\Gamma(1+2\delta)}\right)+\left(x+y-0.5z-\dfrac{2.25zt^{\delta}}{\Gamma(1+\delta)}+g_2(x,y,z)\dfrac{t^{2\delta}}{\Gamma(1+2\delta)}\right) \\ \left(1+g_2'(x,y,z)\dfrac{t^{2\delta}}{\Gamma(1+2\delta)}\right)-g_2''(x,y,z)\dfrac{t^{2\delta}}{\Gamma(1+2\delta)}-g_2''(x,y,z)\dfrac{t^{2\delta}}{\Gamma(1+2\delta)} \\ \left.-g_2''(x,y,z)\dfrac{t^{2\delta}}{\Gamma(1+2\delta)}\right), \\ Res\varpi_2(x,y,z,t)=-2.25z+h_2(x,y,z)\dfrac{t^{\delta}}{\Gamma(1+\delta)}+\left(-0.5x+y+z-\dfrac{2.25xt^{\delta}}{\Gamma(1+\delta)}+h_2(x,y,z)\dfrac{t^{2\delta}}{\Gamma(1+2\delta)}\right) \\ \left(1+h_2'(x,y,z)\dfrac{t^{2\delta}}{\Gamma(1+2\delta)}\right)+\left(x-0.5y+z-\dfrac{2.25yt^{\delta}}{\Gamma(1+\delta)}+h_2(x,y,z)\dfrac{t^{2\delta}}{\Gamma(1+2\delta)}\right) \\ \left(1+h_2'(x,y,z)\dfrac{t^{2\delta}}{\Gamma(1+2\delta)}\right)+\left(x+y-0.5z-\dfrac{2.25zt^{\delta}}{\Gamma(1+\delta)}+h_2(x,y,z)\dfrac{t^{2\delta}}{\Gamma(1+2\delta)}\right) \\ \left(-0.5-\dfrac{2.25t^{\delta}}{\Gamma(1+\delta)}+h_2'(x,y,z)\dfrac{t^{2\delta}}{\Gamma(1+2\delta)}\right)-h_2''(x,y,z)\dfrac{t^{2\delta}}{\Gamma(1+2\delta)} \\ -h_2''(x,y,z)\dfrac{t^{2\delta}}{\Gamma(1+2\delta)}-h_2''(x,y,z)\dfrac{t^{2\delta}}{\Gamma(1+2\delta)}, \end{cases} \tag{96}$$

we know that

$$\begin{cases} D_t^{(k-1)\delta} Resv_k(x,y,z,t)=0, \\ D_t^{(k-1)\delta} Res\vartheta_k(x,y,z,t)=0, \\ D_t^{(k-1)\delta} Res\varpi_k(x,y,z,t)=0, \end{cases} \tag{97}$$

put $k=2$ in Eq. (97), we obtain

$$\begin{cases} D_t^{\delta} Resv_2(x,y,z,t)=0, \\ D_t^{\delta} Res\vartheta_2(x,y,z,t)=0, \\ D_t^{\delta} Res\varpi_2(x,y,z,t)=0, \end{cases} \tag{98}$$

applying D_t^{δ}, on both sides of the Eq. (96), we get

$$\begin{cases}
D_t^{\delta} Resv_2(x,y,z,t) = \begin{pmatrix} f_2(x,y,z)+\left(-0.5x+y+z-\frac{2.25xt^{\delta}}{\Gamma(1+\delta)}+f_2(x,y,z)\frac{t^{2\delta}}{\Gamma(1+2\delta)}\right) \\ \left(-2.25+f_2'(x,y,z)\frac{t^{\delta}}{\Gamma(1+\delta)}\right)+\left(-2.25x+f_2(x,y,z)\frac{t^{\delta}}{\Gamma(1+\delta)}\right)\left(-0.5-\frac{2.25t^{\delta}}{\Gamma(1+\delta)}\right. \\ \left.+f_2'(x,y,z)\frac{t^{2\delta}}{\Gamma(1+2\delta)}\right)+\left(x-0.5y+z-\frac{2.25yt^{\delta}}{\Gamma(1+\delta)}+f_2(x,y,z)\frac{t^{2\delta}}{\Gamma(1+2\delta)}\right)\left(f_2'(x,y,z)\frac{t^{\delta}}{\Gamma(1+\delta)}\right) \\ +\left(-2.25y+f_2(x,y,z)\frac{t^{\delta}}{\Gamma(1+\delta)}\right)\left(1+f_2'(x,y,z)\frac{t^{2\delta}}{\Gamma(1+2\delta)}\right) \\ +\left(x+y-0.5z-\frac{2.25zt^{\delta}}{\Gamma(1+\delta)}+f_2(x,y,z)\frac{t^{2\delta}}{\Gamma(1+2\delta)}\right)\left(f_2'(x,y,z)\frac{t^{\delta}}{\Gamma(1+\delta)}\right) \\ +\left(-2.25z+f_2(x,y,z)\frac{t^{\delta}}{\Gamma(1+\delta)}\right)\left(1+f_2'(x,y,z)\frac{t^{2\delta}}{\Gamma(1+2\delta)}\right) \\ -\left(f_2''(x,y,z)\frac{t^{\delta}}{\Gamma(1+\delta)}\right)-\left(f_2''(x,y,z)\frac{t^{\delta}}{\Gamma(1+\delta)}\right)-\left(f_2''(x,y,z)\frac{t^{\delta}}{\Gamma(1+\delta)}\right), \end{pmatrix} \\
D_t^{\delta} Res\vartheta_2(x,y,z,t) = \begin{pmatrix} g_2(x,y,z)+\left(-0.5x+y+z-\frac{2.25xt^{\delta}}{\Gamma(1+\delta)}+g_2(x,y,z)\frac{t^{2\delta}}{\Gamma(1+2\delta)}\right) \\ \left(g_2'(x,y,z)\frac{t^{\delta}}{\Gamma(1+\delta)}\right)+\left(-2.25x+g_2(x,y,z)\frac{t^{\delta}}{\Gamma(1+\delta)}\right)\left(1+g_2'(x,y,z)\frac{t^{2\delta}}{\Gamma(1+2\delta)}\right) \\ +\left(x-0.5y+z-\frac{2.25yt^{\delta}}{\Gamma(1+\delta)}+g_2(x,y,z)\frac{t^{2\delta}}{\Gamma(1+2\delta)}\right)\left(-2.25+g_2'(x,y,z)\frac{t^{\delta}}{\Gamma(1+\delta)}\right) \\ +\left(-2.25y+g_2(x,y,z)\frac{t^{\delta}}{\Gamma(1+\delta)}\right)\left(-0.5-\frac{2.25t^{\delta}}{\Gamma(1+\delta)}+g_2'(x,y,z)\frac{t^{2\delta}}{\Gamma(1+2\delta)}\right) \\ +\left(x+y-0.5z-\frac{2.25zt^{\delta}}{\Gamma(1+\delta)}+g_2(x,y,z)\frac{t^{2\delta}}{\Gamma(1+2\delta)}\right)\left(g_2'(x,y,z)\frac{t^{\delta}}{\Gamma(1+\delta)}\right) \\ +\left(-2.25z+g_2(x,y,z)\frac{t^{\delta}}{\Gamma(1+\delta)}\right)\left(1+g_2'(x,y,z)\frac{t^{2\delta}}{\Gamma(1+2\delta)}\right) \\ -g_2''(x,y,z)\frac{t^{\delta}}{\Gamma(1+\delta)}-f_2''(x,y,z)\frac{t^{\delta}}{\Gamma(1+\delta)}-g_2''(x,y,z)\frac{t^{\delta}}{\Gamma(1+\delta)}, \end{pmatrix} \\
D_t^{\delta} Res\varpi_2(x,y,z,t) = \begin{pmatrix} h_2(x,y,z)+\left(-0.5x+y+z-\frac{2.25xt^{\delta}}{\Gamma(1+\delta)}+h_2(x,y,z)\frac{t^{2\delta}}{\Gamma(1+2\delta)}\right) \\ \left(h_2'(x,y,z)\frac{t^{\delta}}{\Gamma(1+\delta)}\right)+\left(-2.25x+h_2(x,y,z)\frac{t^{\delta}}{\Gamma(1+\delta)}\right)\left(1+h_2'(x,y,z)\frac{t^{2\delta}}{\Gamma(1+2\delta)}\right) \\ +\left(x-0.5y+z-\frac{2.25yt^{\delta}}{\Gamma(1+\delta)}+h_2(x,y,z)\frac{t^{2\delta}}{\Gamma(1+2\delta)}\right)\left(h_2'(x,y,z)\frac{t^{\delta}}{\Gamma(1+\delta)}\right) \\ +\left(-2.25y+f_2(x,y,z)\frac{t^{\delta}}{\Gamma(1+\delta)}\right)\left(1+h_2'(x,y,z)\frac{t^{2\delta}}{\Gamma(1+2\delta)}\right) \\ +\left(x+y-0.5z-\frac{2.25zt^{\delta}}{\Gamma(1+\delta)}+h_2(x,y,z)\frac{t^{2\delta}}{\Gamma(1+2\delta)}\right)\left(-2.25+h_2'(x,y,z)\frac{t^{\delta}}{\Gamma(1+\delta)}\right) \\ +\left(-2.25z+h_2(x,y,z)\frac{t^{\delta}}{\Gamma(1+\delta)}\right)\left(-0.5-\frac{2.25t^{\delta}}{\Gamma(1+\delta)}+h_2'(x,y,z)\frac{t^{2\delta}}{\Gamma(1+2\delta)}\right) \\ -h_2''(x,y,z)\frac{t^{\delta}}{\Gamma(1+\delta)}-h_2''(x,y,z)\frac{t^{\delta}}{\Gamma(1+\delta)}-h_2''(x,y,z)\frac{t^{\delta}}{\Gamma(1+\delta)}, \end{pmatrix}
\end{cases} \tag{99}$$

we know that

$$\begin{cases} D_t^{\delta} Res\upsilon_2(x, y, z, 0) = 0, \\ D_t^{\delta} Res\vartheta_2(x, y, z, 0) = 0, \\ D_t^{\delta} Res\varpi_2(x, y, z, 0) = 0, \end{cases} \tag{100}$$

put in Eq. (99), we obtain

$$\begin{cases} f_2(x, y, z) = -2.25x + 4.5y + 4.5z, \\ g_2(x, y, z) = 4.5x - 2.25y + 4.5z, \\ h_2(x, y, z) = 4.5x + 4.5y - 2.25z. \end{cases} \tag{101}$$

The solution of Eq. (79), in term of RPSM is given by

$$\begin{cases} \upsilon(x, y, z, t) = f(x, y, z) + f_1(x, y, z)\dfrac{t^{\delta}}{\Gamma(1+\delta)} + f_2(x, y, z)\dfrac{t^{2\delta}}{\Gamma(1+2\delta)} + \cdots, \\ \vartheta(x, y, z, t) = g(x, y, z) + g_1(x, y, z)\dfrac{t^{\delta}}{\Gamma(1+\delta)} + g_2(x, y, z)\dfrac{t^{2\delta}}{\Gamma(1+2\delta)} + \cdots, \\ \varpi(x, y, z, t) = h(x, y, z) + h_1(x, y, z)\dfrac{t^{\delta}}{\Gamma(1+\delta)} + h_2(x, y, z)\dfrac{t^{2\delta}}{\Gamma(1+2\delta)} + \cdots, \end{cases}$$

$$\begin{cases} \upsilon(x, y, z, t) = -0.5x + y + z - \dfrac{2.25xt^{\delta}}{\Gamma(1+\delta)} + \dfrac{(-2.25x + 4.5y + 4.5z)t^{2\delta}}{\Gamma(1+2\delta)} + \cdots, \\ \vartheta(x, y, z, t) = x - 0.5y + z - \dfrac{2.25yt^{\delta}}{\Gamma(1+\delta)} + \dfrac{(4.5x - 2.25y + 4.5z)t^{2\delta}}{\Gamma(1+2\delta)} + \cdots, \\ \varpi(x, y, z, t) = x + y - 0.5z - \dfrac{2.25zt^{\delta}}{\Gamma(1+\delta)} + \dfrac{(4.5x + 4.5y - 2.25z)t^{2\delta}}{\Gamma(1+2\delta)} + \cdots. \end{cases} \tag{102}$$

4.2.2. Q-HATM Solution

(1) 1st Iteration. Taking LT of Eq. (79), and simplifying we obtain

$$\begin{cases} \mathscr{L}[\upsilon(x, y, z, t)] - \dfrac{(-0.5x + y + z)}{s} + \dfrac{1}{s^{\delta}}\mathscr{L}\left(\upsilon\dfrac{\partial \upsilon}{\partial x} + \vartheta\dfrac{\partial \upsilon}{\partial y} + \varpi\dfrac{\partial \upsilon}{\partial z} - \dfrac{\partial^2 \upsilon}{\partial x^2} - \dfrac{\partial^2 \upsilon}{\partial y^2} - \dfrac{\partial^2 \upsilon}{\partial z^2}\right) = 0, \\ \mathscr{L}[\vartheta(x, y, z, t)] - \dfrac{(x - 0.5y + z)}{s} + \dfrac{1}{s^{\delta}}\mathscr{L}\left(\upsilon\dfrac{\partial \vartheta}{\partial x} + \vartheta\dfrac{\partial \vartheta}{\partial y} + \varpi\dfrac{\partial \vartheta}{\partial z} - \dfrac{\partial^2 \vartheta}{\partial x^2} - \dfrac{\partial^2 \vartheta}{\partial y^2} - \dfrac{\partial^2 \vartheta}{\partial z^2}\right) = 0, \\ \mathscr{L}[\varpi(x, y, z, t)] - \dfrac{(x + y - 0.5z)}{s} + \dfrac{1}{s^{\delta}}\mathscr{L}\left(\upsilon\dfrac{\partial \varpi}{\partial x} + \vartheta\dfrac{\partial \varpi}{\partial y} + \varpi\dfrac{\partial \varpi}{\partial z} - \dfrac{\partial^2 \varpi}{\partial x^2} - \dfrac{\partial^2 \varpi}{\partial y^2} - \dfrac{\partial^2 \varpi}{\partial z^2}\right) = 0. \end{cases} \tag{103}$$

The nonlinear term N is defined as

$$\begin{cases} N[\theta(x, y, z, t; q)] = \mathscr{L}[\theta(x, y, z, t; q)] - \dfrac{(-0.5x + y + z)}{s} + \dfrac{1}{s^{\delta}}\mathscr{L}\left(\upsilon\dfrac{\partial \upsilon}{\partial x} + \vartheta\dfrac{\partial \upsilon}{\partial y} + \varpi\dfrac{\partial \upsilon}{\partial z} - \dfrac{\partial^2 \upsilon}{\partial x^2} \right. \\ \left. - \dfrac{\partial^2 \upsilon}{\partial y^2} - \dfrac{\partial^2 \upsilon}{\partial z^2}\right), \\ N[\theta(x, y, z, t; q)] = \mathscr{L}[\theta(x, y, z, t; q)] - \dfrac{(x - 0.5y + z)}{s} + \dfrac{1}{s^{\delta}}\mathscr{L}\left(\upsilon\dfrac{\partial \vartheta}{\partial x} + \vartheta\dfrac{\partial \vartheta}{\partial y} + \varpi\dfrac{\partial \vartheta}{\partial z} - \dfrac{\partial^2 \vartheta}{\partial x^2} \right. \\ \left. - \dfrac{\partial^2 \vartheta}{\partial y^2} - \dfrac{\partial^2 \vartheta}{\partial z^2}\right), \\ N[\theta(x, y, z, t; q)] = \mathscr{L}[\theta(x, y, z, t; q)] - \dfrac{(x + y - 0.5z)}{s} + \dfrac{1}{s^{\delta}}\mathscr{L}\left(\upsilon\dfrac{\partial \varpi}{\partial x} + \vartheta\dfrac{\partial \varpi}{\partial y} + \varpi\dfrac{\partial \varpi}{\partial z} - \dfrac{\partial^2 \varpi}{\partial x^2} \right. \\ \left. - \dfrac{\partial^2 \varpi}{\partial y^2} - \dfrac{\partial^2 \varpi}{\partial z^2}\right). \end{cases} \tag{104}$$

Use the procedure of q-HATM

$$\begin{cases} \upsilon_m(x,y,z,t) = k_m\upsilon_{m-1}(x,y,z,t) + h\mathscr{L}^{-1}[R_m(\upsilon_{m-1})], \\ \vartheta_m(x,y,z,t) = k_m\vartheta_{m-1}(x,y,z,t) + h\mathscr{L}^{-1}[R_m(\vartheta_{m-1})], \\ \varpi_m(x,y,z,t) = k_m\varpi_{m-1}(x,y,z,t) + h\mathscr{L}^{-1}[R_m(\varpi_{m-1})], \end{cases} \tag{105}$$

put $m = 1$ in the Eq. (105), we obtain

$$\begin{cases} \upsilon_1(x,y,z,t) = k_1\upsilon_0(x,y,z,t) + h\mathscr{L}^{-1}[R_1(\upsilon_0)], \\ \vartheta_1(x,y,z,t) = k_1\vartheta_0(x,y,z,t) + h\mathscr{L}^{-1}[R_1(\vartheta_0)], \\ \varpi_1(x,y,z,t) = k_1\varpi_0(x,y,z,t) + h\mathscr{L}^{-1}[R_1(\varpi_0)], \end{cases} \tag{106}$$

$$\begin{cases} R_m(\upsilon_{m-1}) = \mathscr{L}(\upsilon_{m-1}) - \left(1-\frac{k_m}{n}\right)\left(\frac{(-0.5x+y+z)}{s}\right) + \frac{1}{s^\delta}\mathscr{L}\left(\sum_{i=0}^{m-1}\upsilon_i\frac{\partial\upsilon_{m-1-i}}{\partial x} + \sum_{i=0}^{m-1}\vartheta_i\frac{\partial\upsilon_{m-1-i}}{\partial y}\right. \\ \left. + \sum_{i=0}^{m-1}\varpi_i\frac{\partial\upsilon_{m-1-i}}{\partial z} - \frac{\partial^2\upsilon_{m-1}}{\partial x^2} - \frac{\partial^2\upsilon_{m-1}}{\partial y^2} - \frac{\partial^2\upsilon_{m-1}}{\partial z^2}\right), \\ R_m(\vartheta_{m-1}) = \mathscr{L}(\vartheta_{m-1}) - \left(1-\frac{k_m}{n}\right)\left(\frac{(x-0.5y+z)}{s}\right) + \frac{1}{s^\delta}\mathscr{L}\left(\sum_{i=0}^{m-1}\upsilon_i\frac{\partial\vartheta_{m-1-i}}{\partial x} + \sum_{i=0}^{m-1}\vartheta_i\frac{\partial\vartheta_{m-1-i}}{\partial y}\right. \\ \left. + \sum_{i=0}^{m-1}\varpi_i\frac{\partial\vartheta_{m-1-i}}{\partial z} - \frac{\partial^2\vartheta_{m-1}}{\partial x^2} - \frac{\partial^2\vartheta_{m-1}}{\partial y^2} - \frac{\partial^2\vartheta_{m-1}}{\partial z^2}\right), \\ R_m(\varpi_{m-1}) = \mathscr{L}(\varpi_{m-1}) - \left(1-\frac{k_m}{n}\right)\left(\frac{(x+y-0.5z)}{s}\right) + \frac{1}{s^\delta}\mathscr{L}\left(\sum_{i=0}^{m-1}\upsilon_i\frac{\partial\varpi_{m-1-i}}{\partial x} + \sum_{i=0}^{m-1}\vartheta_i\frac{\partial\varpi_{m-1-i}}{\partial y}\right. \\ \left. + \sum_{i=0}^{m-1}\varpi_i\frac{\partial\varpi_{m-1-i}}{\partial z} - \frac{\partial^2\varpi_{m-1}}{\partial x^2} - \frac{\partial^2\varpi_{m-1}}{\partial y^2} - \frac{\partial^2\varpi_{m-1}}{\partial z^2}\right), \end{cases} \tag{107}$$

put $m = 1$ in Eq. (107), we get

$$\begin{cases} R_1(\upsilon_0) = \mathscr{L}(\upsilon_0) - \left(1-\frac{k_1}{n}\right)\left(\frac{(-0.5x+y+z)}{s}\right) + \frac{1}{s^\delta}\mathscr{L}\left[\upsilon_0\frac{\partial\upsilon_0}{\partial x} + \vartheta_0\frac{\partial\upsilon_0}{\partial y}\right. \\ \left. +\varpi_0\frac{\partial\upsilon_0}{\partial z} - \frac{\partial^2\upsilon_0}{\partial x^2} - \frac{\partial^2\upsilon_0}{\partial y^2} - \frac{\partial^2\upsilon_0}{\partial z^2}\right], \\ R_1(\vartheta_0) = \mathscr{L}(\vartheta_0) - \left(1-\frac{k_1}{n}\right)\left(\frac{(x-0.5y+z)}{s}\right) + \frac{1}{s^\delta}\mathscr{L}\left[\upsilon_0\frac{\partial\vartheta_0}{\partial x} + \vartheta_0\frac{\partial\vartheta_0}{\partial y}\right. \\ \left. +\varpi_0\frac{\partial\vartheta_0}{\partial z} - \frac{\partial^2\vartheta_0}{\partial x^2} - \frac{\partial^2\vartheta_0}{\partial y^2} - \frac{\partial^2\vartheta_0}{\partial z^2}\right], \\ R_1(\varpi_0) = \mathscr{L}(\varpi_0) - \left(1-\frac{k_1}{n}\right)\left(\frac{(x+y-0.5z)}{s}\right) + \frac{1}{s^\delta}\mathscr{L}\left[\upsilon_0\frac{\partial\varpi_0}{\partial x} + \vartheta_0\frac{\partial\varpi_0}{\partial y}\right. \\ \left. +\varpi_0\frac{\partial\varpi_0}{\partial z} - \frac{\partial^2\varpi_0}{\partial x^2} - \frac{\partial^2\varpi_0}{\partial y^2} - \frac{\partial^2\varpi_0}{\partial z^2}\right], \end{cases} \tag{108}$$

$$\begin{cases} = \frac{1}{s^\delta}\mathscr{L}[2.25x] = \frac{2.25x}{s^{\delta+1}}, \\ = \frac{1}{s^\delta}\mathscr{L}[2.25y] = \frac{2.25y}{s^{\delta+1}}, \\ = \frac{1}{s^\delta}\mathscr{L}[2.25z] = \frac{2.25z}{s^{\delta+1}}. \end{cases}$$

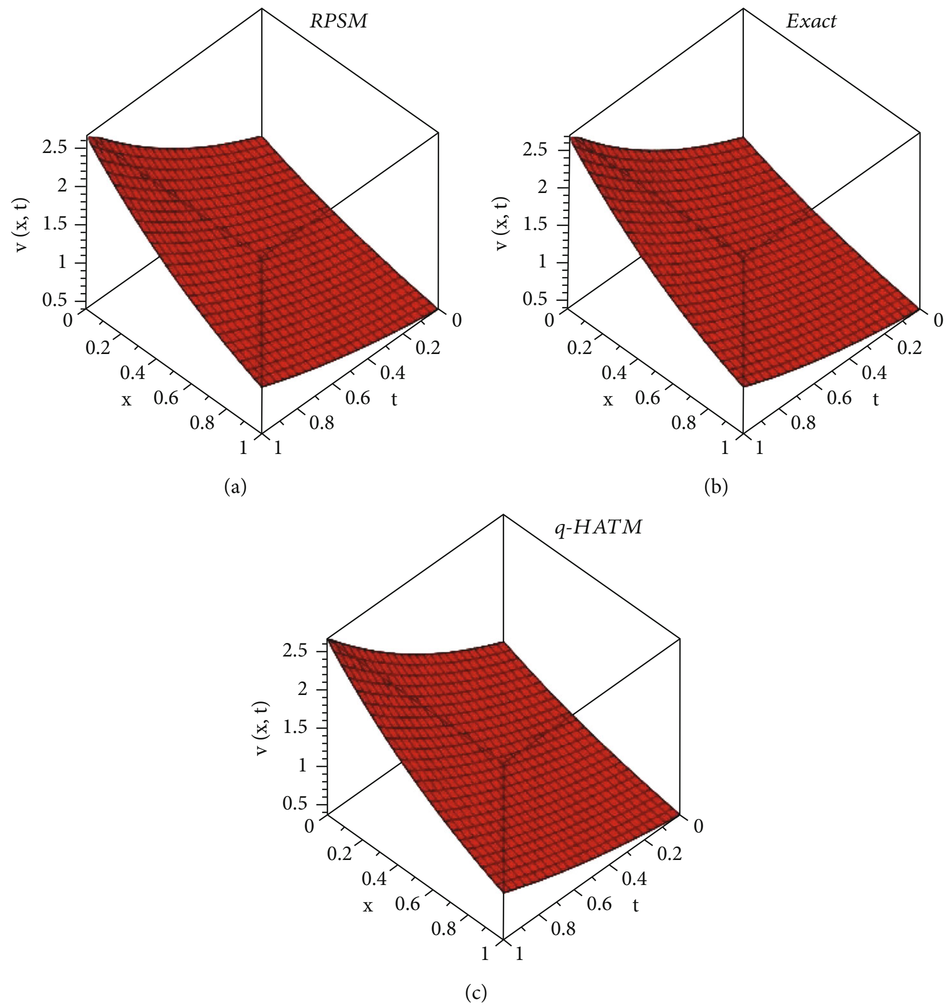

FIGURE 1: 3D plots of (a) RPSM, (b) Exact, and (c) q-HATM $\upsilon-$ solutions at $\delta = 1$ of Example 4.1.

Put in Eq. (106), we obtain

$$\begin{cases} \upsilon_1(x, y, z, t) = \dfrac{2.25hxt^{\delta}}{\Gamma(\delta+1)}, \\ \vartheta_1(x, y, z, t) = \dfrac{2.25hyt^{\delta}}{\Gamma(\delta+1)}, \\ \varpi_1(x, y, z, t) = \dfrac{2.25hzt^{\delta}}{\Gamma(\delta+1)}. \end{cases} \tag{109}$$

(2) 2nd Iteration. Put $m = 2$ in the Eq. (105), we obtain put $m = 2$ in Eq. (107), we obtain

$$\begin{cases} \upsilon_2(x, y, z, t) = k_2\upsilon_1(x, y, z, t) + h\mathscr{L}^{-1}[R_2(\upsilon_1)], \\ \vartheta_2(x, y, z, t) = k_2\vartheta_1(x, y, z, t) + h\mathscr{L}^{-1}[R_2(\vartheta_1)], \\ \varpi_2(x, y, z, t) = k_2\varpi_1(x, y, z, t) + h\mathscr{L}^{-1}[R_2(\varpi_1)], \end{cases} \tag{110}$$

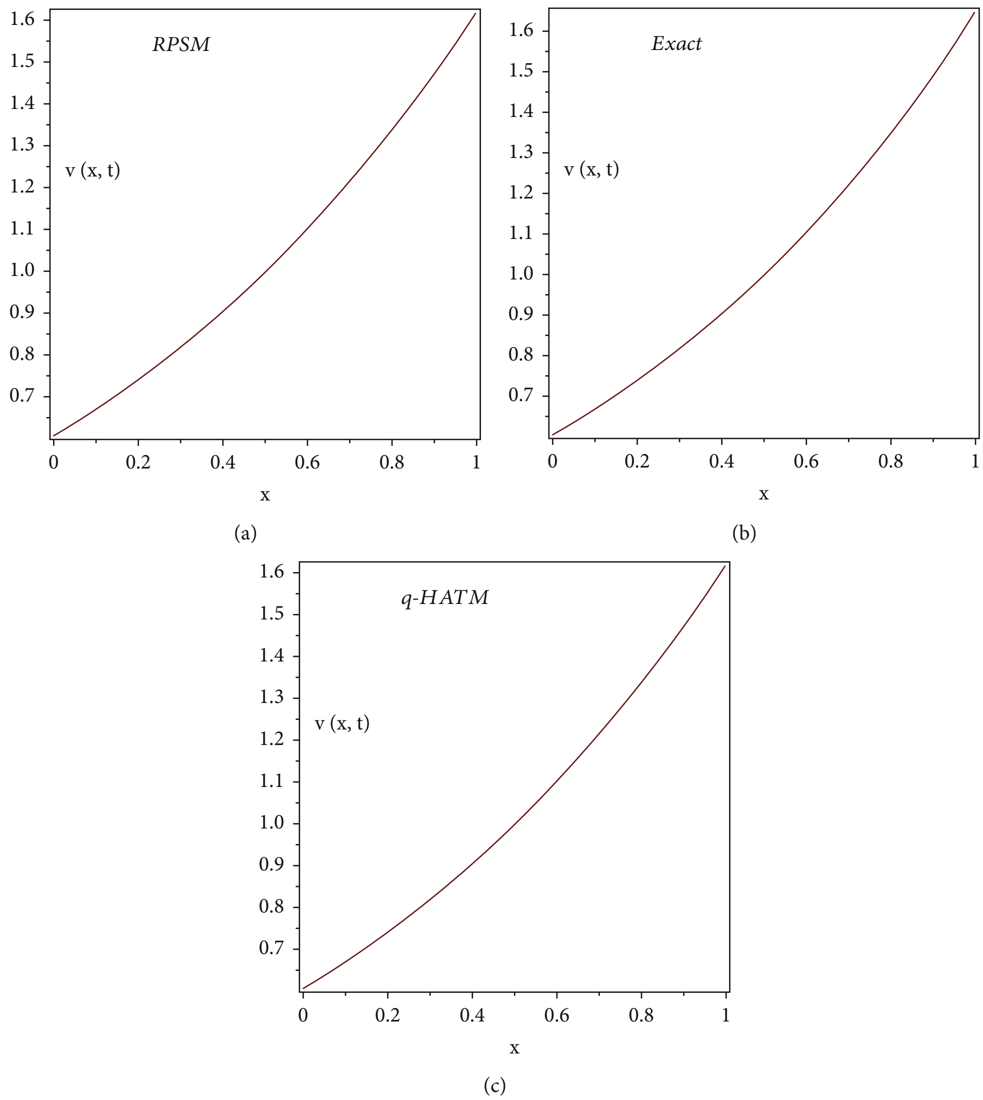

Figure 2: 2D plots of (a) RPSM, (b) Exact, and (c) q-HATM υ – solutions at $\delta = 1$ of Example 4.1.

after simplification we obtain

$$\begin{cases} R_2(\upsilon_1) = \mathscr{L}(\upsilon_1) - \left(1 - \dfrac{k_2}{n}\right)\left(\dfrac{(-0.5x + y + z)}{s}\right) + \dfrac{1}{s^{\delta}}\mathscr{L}\left(\upsilon_0 \dfrac{\partial \upsilon_1}{\partial x} + \upsilon_1 \dfrac{\partial \upsilon_0}{\partial x} + \vartheta_0 \dfrac{\partial \upsilon_1}{\partial y} + \vartheta_1 \dfrac{\partial \upsilon_0}{\partial y}\right. \\ \left. + \varpi_0 \dfrac{\partial \upsilon_1}{\partial z} + \varpi_1 \dfrac{\partial \upsilon_0}{\partial z} - \dfrac{\partial^2 \upsilon_1}{\partial x^2} - \dfrac{\partial^2 \upsilon_1}{\partial y^2} - \dfrac{\partial^2 \upsilon_1}{\partial z^2}\right), \\ R_2(\vartheta_1) = \mathscr{L}(\vartheta_1) - \left(1 - \dfrac{k_2}{n}\right)\left(\dfrac{(x - 0.5y + z)}{s}\right) + \dfrac{1}{s^{\delta}}\mathscr{L}\left(\upsilon_0 \dfrac{\partial \vartheta_1}{\partial x} + \upsilon_1 \dfrac{\partial \vartheta_0}{\partial x} + \vartheta_0 \dfrac{\partial \vartheta_1}{\partial y} + \vartheta_1 \dfrac{\partial \vartheta_0}{\partial y}\right. \\ \left. + \varpi_0 \dfrac{\partial \vartheta_1}{\partial z} + \varpi_1 \dfrac{\partial \vartheta_0}{\partial z} - \dfrac{\partial^2 \vartheta_1}{\partial x^2} - \dfrac{\partial^2 \vartheta_1}{\partial y^2} - \dfrac{\partial^2 \vartheta_1}{\partial z^2}\right), \\ R_2(\varpi_1) = \mathscr{L}(\varpi_1) - \left(1 - \dfrac{k_2}{n}\right)\left(\dfrac{(x + y - 0.5z)}{s}\right) + \dfrac{1}{s^{\delta}}\mathscr{L}\left(\upsilon_0 \dfrac{\partial \varpi_1}{\partial x} + \upsilon_1 \dfrac{\partial \varpi_0}{\partial x} + \vartheta_0 \dfrac{\partial \varpi_1}{\partial y} + \vartheta_1 \dfrac{\partial \varpi_0}{\partial y}\right. \\ \left. + \varpi_0 \dfrac{\partial \varpi_1}{\partial z} + \varpi_1 \dfrac{\partial \varpi_0}{\partial z} - \dfrac{\partial^2 \varpi_1}{\partial x^2} - \dfrac{\partial^2 \varpi_1}{\partial y^2} - \dfrac{\partial^2 \varpi_1}{\partial z^2}\right), \end{cases} \tag{111}$$

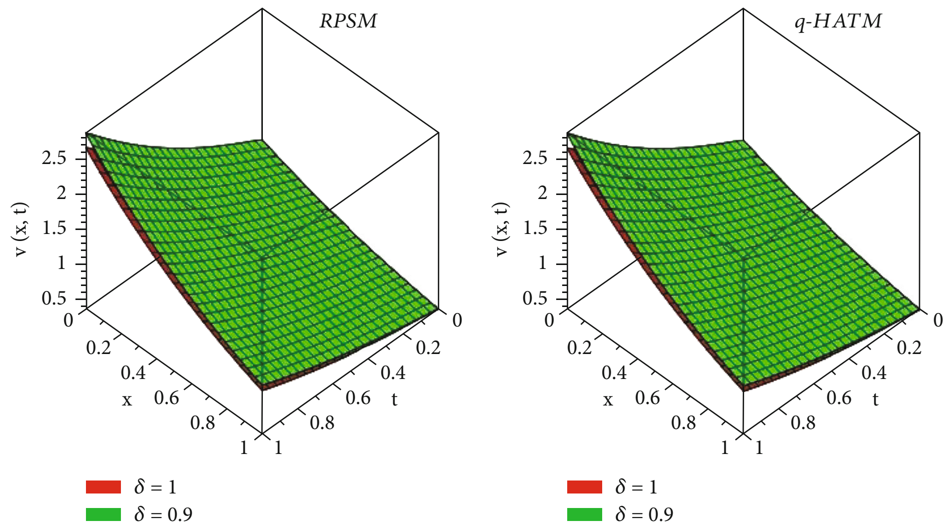

(a) (b)

FIGURE 3: The 3D plots of example 4.1 for fractional order $\delta = 1, 0.9$.

TABLE 1: Solution comparison of RPSM, q-HATM, and Exact with different time and spaces of Example 4.1.

x	t	RPSM $\delta = 0.9$	RPSM $\delta = 1$	q-HATM $\delta = 0.9$	q-HATM $\delta = 1$	Exact $\delta = 1$
0.25	0.001	0.7804183	0.7795799	0.7804183	0.7795799	0.7795799
0.50		0.6077903	0.6071374	0.6077903	0.6071374	0.6071374
0.75		0.4733476	0.4728391	0.4733476	0.4728391	0.4728391
1		0.3686435	0.3682475	0.3686435	0.3682475	0.3682475
0.25	0.005	0.7857118	0.7827045	0.7857118	0.7827045	0.7827045
0.50		0.6119130	0.6095709	0.6119130	0.6095709	0.6095709
0.75		0.4765583	0.4747342	0.4765583	0.4747342	0.4747342
1		0.3711440	0.3697234	0.3711440	0.3697234	0.3697234

Put Eq. (112) in Eq. (110), we obtain

$$\begin{cases} R_2(\upsilon_1) = \dfrac{4.5hy}{s^{\delta+1}} + \dfrac{4.5hz}{s^{\delta+1}}, \\ R_2(\vartheta_1) = \dfrac{4.5hx}{s^{\delta+1}} + \dfrac{4.5hz}{s^{\delta+1}}, \\ R_2(\varpi_1) = \dfrac{4.5hx}{s^{\delta+1}} + \dfrac{4.5hy}{s^{\delta+1}}. \end{cases} \tag{112}$$

The solution of Eq. (79), in term of q-HATM is given by

$$\begin{cases} \upsilon_2(x,y,z,t) = \dfrac{2.25nhxt^{\delta}}{\Gamma(\delta+1)} + \dfrac{4.5h^2yt^{\delta}}{\Gamma(\delta+1)} + \dfrac{4.5h^2zt^{\delta}}{\Gamma(\delta+1)}, \\ \vartheta_2(x,y,z,t) = \dfrac{2.25nhyt^{\delta}}{\Gamma(\delta+1)} + \dfrac{4.5h^2xt^{\delta}}{\Gamma(\delta+1)} + \dfrac{4.5h^2zt^{\delta}}{\Gamma(\delta+1)}, \\ \varpi_2(x,y,z,t) = \dfrac{2.25nhzt^{\delta}}{\Gamma(\delta+1)} + \dfrac{4.5h^2xt^{\delta}}{\Gamma(\delta+1)} + \dfrac{4.5h^2yt^{\delta}}{\Gamma(\delta+1)}. \end{cases} \tag{113}$$

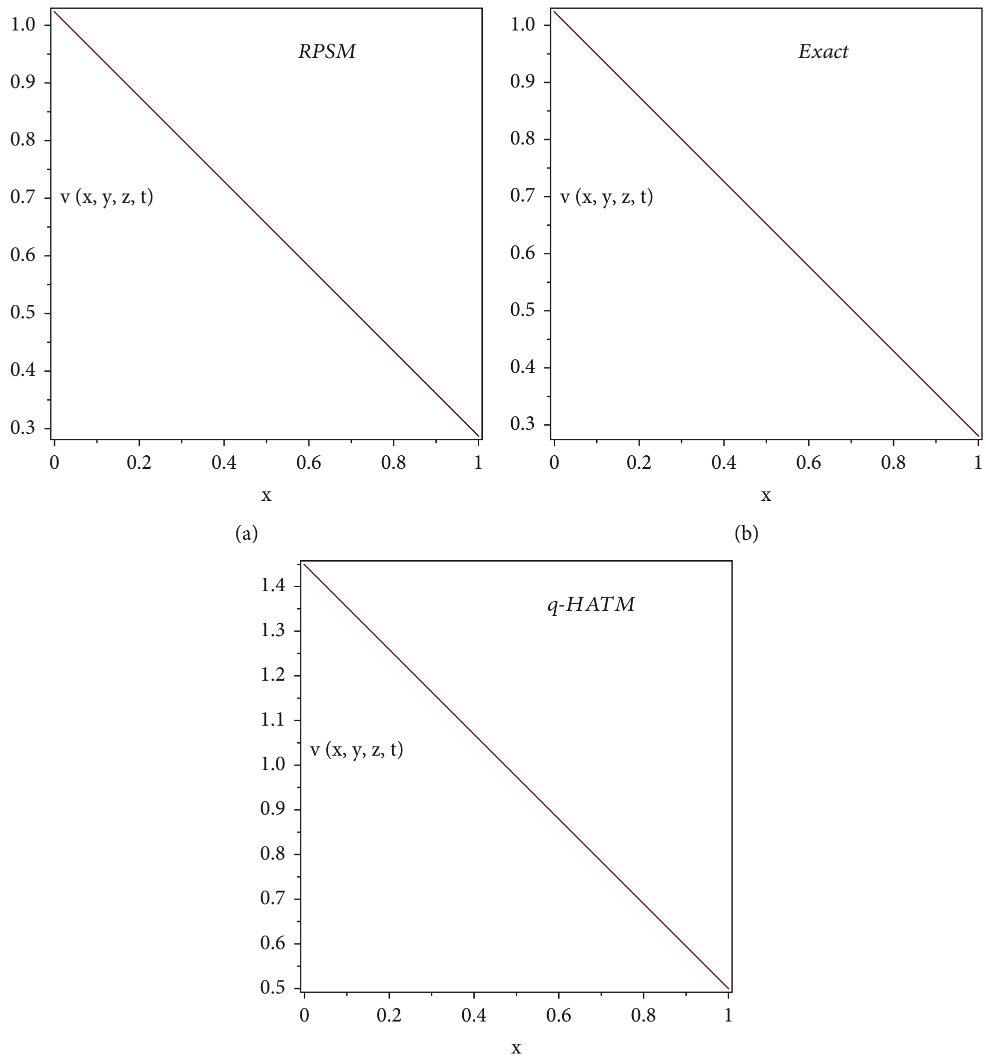

(a) (b) (c)

Figure 4: 2D-solutions plots of (a) RPSM, (b) Exact, and (c) q-HATM, at $\delta = 1$ of Example 4.2.

$$\begin{cases} \upsilon(x,y,z,t) = \upsilon_0(x,y,z,t) + \upsilon_1(x,y,z,t) + \upsilon_2(x,y,z,t), \\ \vartheta(x,y,z,t) = \vartheta_0(x,y,z,t) + \vartheta_1(x,y,z,t) + \vartheta_2(x,y,z,t), \\ \varpi(x,y,z,t) = \varpi_0(x,y,z,t) + \varpi_1(x,y,z,t) + \varpi_2(x,y,z,t), \end{cases}$$

$$\begin{cases} \upsilon(x,y,z,t) = -0.5x + y + z + \dfrac{2.25xt^{\delta}}{\Gamma(1+\delta)} + \dfrac{2.25nhxt^{\delta}}{\Gamma(\delta+1)} + \dfrac{4.5h^2yt^{\delta}}{\Gamma(\delta+1)} + \dfrac{4.5h^2zt^{\delta}}{\Gamma(\delta+1)}, \\ \vartheta(x,y,z,t) = x - 0.5y + z + \dfrac{2.25yt^{\delta}}{\Gamma(1+\delta)} + \dfrac{2.25nhyt^{\delta}}{\Gamma(\delta+1)} + \dfrac{4.5h^2xt^{\delta}}{\Gamma(\delta+1)} + \dfrac{4.5h^2zt^{\delta}}{\Gamma(\delta+1)}, \\ \varpi(x,y,z,t) = x + y - 0.5z + \dfrac{2.25zt^{\delta}}{\Gamma(1+\delta)} + \dfrac{2.25nhzt^{\delta}}{\Gamma(\delta+1)} + \dfrac{4.5h^2xt^{\delta}}{\Gamma(\delta+1)} + \dfrac{4.5h^2yt^{\delta}}{\Gamma(\delta+1)}. \end{cases} \tag{114}$$

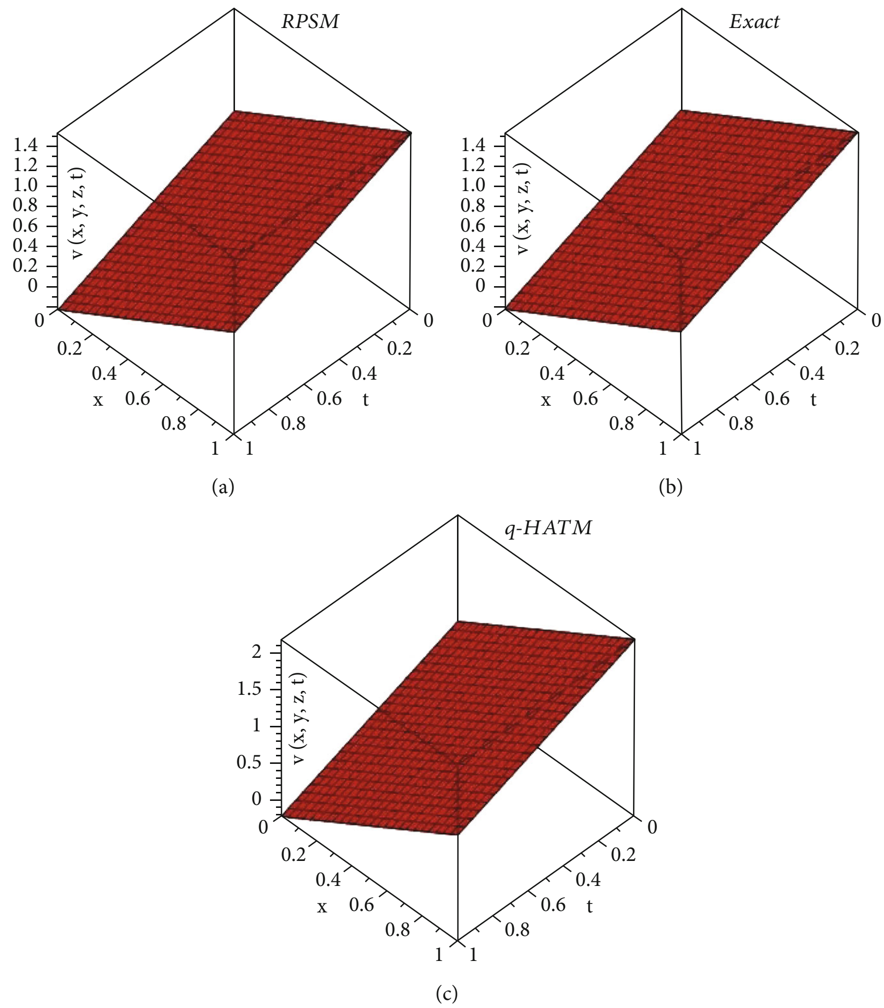

Figure 5: 3D-solutions plots of (a) RPSM, (b) Exact, and (c) q-HATM, at $\delta = 1$ of Example 4.2.

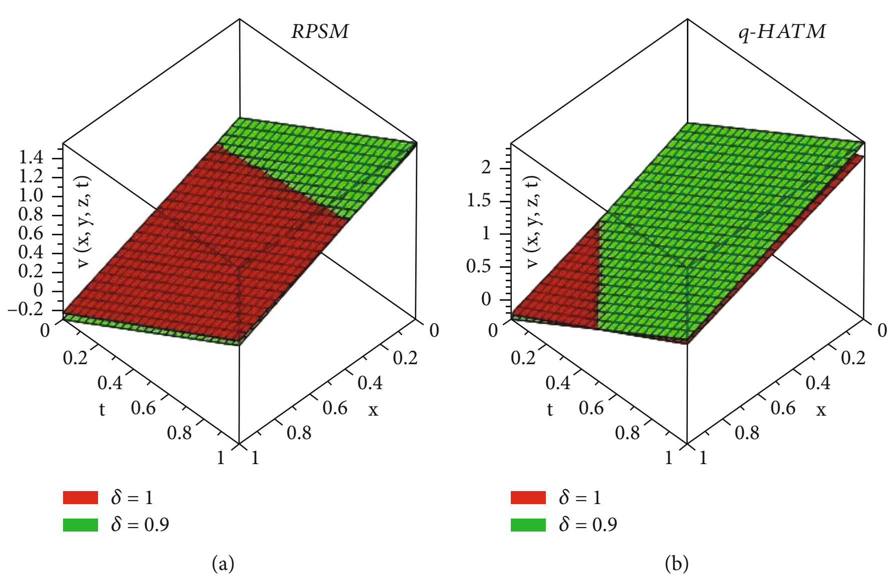

Figure 6: The 3D plots at fractional order δ of Example 4.2.

5. Results and Discussion

Here, we will discuss the numerical solutions. In Figure 1, 3D plots of (a) RPSM, (b) Exact, and (c) q-HATM $\psi-$ solutions at $\delta = 1$ of Example 4.1 are presented. Which are in closed contact with the exact solution of Example 4.1. In Figure 2, 2D plots of (a) RPSM, (b) Exact, and (c) q-HATM $\psi-$ solutions at $\delta = 1$ of Example 4.1 are presented, from which the validity of the proposed methods are confirmed. While in Figure 3, 3D plots of Example 4.1 for fractional order $\delta = 1,0.9$ are plotted. Numerical values of Example 4.1 are presented in Table 1. In Figure 4, 2D-solutions plots and Figure 5 of (a) RPSM, (b) Exact, and (c) q-HATM, at $\delta = 1$ of Example 4.2 are plotted. The RPSM and q-HATM solutions are very closed to the exact solution. The RPSM and q-HATM solutions graphs at different fractional order are plotted in Figure 6.

6. Conclusion

In this paper, the solutions of nonlinear systems of fractional Burger's equations and advection diffusion equation are calculated by using q-HATM and RPSM. The proposed methods provide the results with higher degree of accuracy and using very few terms of their series solutions. The solutions comparison of both techniques are compared with the actual solutions of each problem. The comparison has shown the best compromise between the solutions of the suggested techniques. The fractional-order solutions are calculated successfully and shown to be convergent towards the integer-order solutions. The novelty of this paper is given in the nonlinear fractional solutions which provide the more accurate results as compared to other studies in literature. In the future, the suggested techniques can be utilised easily for the solutions of higher dimensional and nonlinear FPDEs and their systems because of their simple and straightforward implementation.

Data Availability

No data were used to support this study.

Disclosure

This work is performed as part of the employment of the authors.

Conflicts of Interest

No competing interests are declared.

Authors' Contributions

Hassan Khan was responsible for supervision, Qasim khan was responsible for methodology and draft writing, Fairouz Tchier was the project administrator, Ibrar Ullah was responsible for the methodology, Evren Hincal was responsible for funding and draft writing, Gurpreet Singh was responsible for draft writing, F. M. O. Tawfiq was responsible for the investigation, and Shahbaz Khan was responsible for the methodology and draft writing.

Acknowledgments

Researchers Supporting Project (no. RSP-2021/401), King Saud University, Riyadh, Saudi Arabia.

References

[1] S. Longhi, "Fractional Schrödinger equation in optics," *Optics Letters*, vol. 40, no. 6, pp. 1117–1120, 2015.

[2] V. E. Tarasov, "On history of mathematical economics: application of fractional calculus," *Mathematics*, vol. 7, no. 6, p. 509, 2019.

[3] J. H. He, "Homotopy perturbation technique," *Computer Methods in Applied Mechanics and Engineering*, vol. 178, no. 3-4, pp. 257–262, 1999.

[4] H. Nasrolahpour, "A note on fractional electrodynamics," *Communications in Nonlinear Science and Numerical Simulation*, vol. 18, no. 9, pp. 2589–2593, 2013.

[5] S. Ullah, M. A. Khan, and M. Farooq, "A new fractional model for the dynamics of the hepatitis B virus using the Caputo-Fabrizio derivative," *The European Physical Journal Plus*, vol. 133, no. 6, pp. 1–14, 2018.

[6] M. A. Khan, S. Ullah, and M. Farooq, "A new fractional model for tuberculosis with relapse via Atangana-Baleanu derivative," *Chaos, Solitons and Fractals*, vol. 116, pp. 227–238, 2018.

[7] S. Mahmood, R. Shah, and M. Arif, "Laplace adomian decomposition method for multi dimensional time fractional model of Navier-Stokes equation," *Symmetry*, vol. 11, no. 2, p. 149, 2019.

[8] J. H. He, "Nonlinear oscillation with fractional derivative and its applications," *International Conference on Vibrating Engineering*, vol. 98, pp. 288–291, 1998.

[9] Z. E. A. Fellah, M. Fellah, R. Roncen, N. O. Ongwen, E. Ogam, and C. Depollier, "Transient propagation of spherical waves in porous material: application of fractional calculus," *Symmetry*, vol. 14, no. 2, p. 233, 2022.

[10] X. Wu, D. Lai, and H. Lu, "Generalized synchronization of the fractional-order chaos in weighted complex dynamical networks with nonidentical nodes," *Nonlinear Dynamics*, vol. 69, no. 1-2, pp. 667–683, 2012.

[11] A. Din, A. Khan, A. Zeb, M. R. Sidi Ammi, M. Tilioua, and D. F. Torres, "Hybrid method for simulation of a fractional COVID-19 model with real case application," *Axioms*, vol. 10, no. 4, p. 290, 2021.

[12] S. Momani and Z. Odibat, "Analytical solution of a time-fractional Navier-Stokes equation by Adomian decomposition method," *Applied Mathematics and Computation*, vol. 177, no. 2, pp. 488–494, 2006.

[13] M. A. Khan, S. Ullah, K. O. Okosun, and K. Shah, "A fractional order pine wilt disease model with Caputo–Fabrizio derivative," *Advances in Difference Equations*, vol. 2018, no. 1, 2018.

[14] G. A. Birajdar, "Numerical solution of time fractional Navier-stokes equation by discrete Adomian decomposition method," *Nonlinear Engineering*, vol. 3, no. 1, pp. 21–26, 2014.

[15] P. Veeresha, D. G. Prakasha, and H. M. Baskonus, "New numerical surfaces to the mathematical model of cancer chemotherapy effect in Caputo fractional derivatives," *Journal of Nonlinear Science*, vol. 29, no. 1, article 013119, 2019.

[16] Y. Kang, S. Mao, and Y. Zhang, "Fractional time-varying grey traffic flow model based on viscoelastic fluid and its

application," *Transportation Research Part B: Methodological*, vol. 157, pp. 149–174, 2022.

[17] V. B. L. Chaurasia and D. Kumar, "Solution of the time-fractional Navier–Stokes equation," *General Mathematics Notes*, vol. 4, no. 2, pp. 49–59, 2011.

[18] J. Singh, D. Kumar, and D. Baleanu, "On the analysis of fractional diabetes model with exponential law," *Advances in Difference Equations*, vol. 2018, no. 1, pp. 1–15, 2018.

[19] P. Bertsias, S. Kapoulea, C. Psychalinos, and A. S. Elwakil, "A collection of interdisciplinary applications of fractional-order circuits," in *Fractional Order Systems*, pp. 35–69, Academic Press, 2022.

[20] R. Hilfer, Ed., *Applications of Fractional Calculus in Physics*, Orlando, 2000.

[21] A. A. Kilbas, H. M. Srivastava, and J. J. Trujillo, *Theory and applications of fractional differential equations*, vol. 204, Elsevier, 2006.

[22] S. Das, "A note on fractional diffusion equations," *Chaos, Solitons and Fractals*, vol. 42, no. 4, pp. 2074–2079, 2009.

[23] M. Mustahsan, H. M. Younas, S. Iqbal, S. Rathore, K. S. Nisar, and J. Singh, "An efficient analytical technique for time-fractional parabolic partial differential equations," *Frontiers in Physics*, vol. 8, p. 131, 2020.

[24] H. Jafari, M. Nazari, D. Baleanu, and C. M. Khalique, "A new approach for solving a system of fractional partial differential equations," *Computers & Mathematics with Applications*, vol. 66, no. 5, pp. 838–843, 2013.

[25] Z. Korpinar, F. Tchier, and M. Inc, "On optical solitons of the fractional (3+1)-dimensional NLSE with conformable derivatives," *Frontiers in Physics*, vol. 8, p. 87, 2020.

[26] Q. Wang, "Numerical solutions for fractional KdV-Burgers equation by Adomian decomposition method," *Applied Mathematics and Computation*, vol. 182, no. 2, pp. 1048–1055, 2006.

[27] M. Chamekh and T. M. Elzaki, "Explicit solution for some generalized fluids in laminar flow with slip boundary conditions," *The Journal of Mathematics and Computer Science*, vol. 18, no. 3, pp. 272–281, 2018.

[28] Q. Wang, "Homotopy perturbation method for fractional KdV equation," *Applied Mathematics and Computation*, vol. 190, no. 2, pp. 1795–1802, 2007.

[29] K. K. Ali, H. Dutta, R. Yilmazer, and S. Noeiaghdam, "On the new wave behaviors of the Gilson-Pickering equation," *Frontiers in Physics*, vol. 8, p. 54, 2020.

[30] M. ur Rehman and R. A. Khan, "Numerical solutions to initial and boundary value problems for linear fractional partial differential equations," *Applied Mathematical Modelling*, vol. 37, no. 7, pp. 5233–5244, 2013.

[31] M. F. Uddin, M. G. Hafez, I. Hwang, and C. Park, "Effect of Space Fractional Parameter on Nonlinear Ion Acoustic Shock Wave Excitation in an Unmagnetized Relativistic Plasma," *Frontiers in Physics*, vol. 9, p. 766, 2022.

[32] R. Shah, H. Khan, D. Baleanu, P. Kumam, and M. Arif, "A semi-analytical method to solve family of Kuramoto–Sivashinsky equations," *Journal of Taibah University for Science*, vol. 14, no. 1, pp. 402–411, 2020.

[33] A. Secer, M. A. Akinlar, and A. Cevikel, "Similarity solutions for multiterm time-fractional diffusion equation," *Advances in Difference Equations*, vol. 7, 2012.

[34] H. Khan, R. Shah, P. Kumam, D. Baleanu, and M. Arif, "Laplace decomposition for solving nonlinear system of fractional order partial differential equations," *Advances in Difference Equations*, vol. 2020, no. 1, 2020.

[35] A. A. Alderremy, H. Khan, R. Shah, S. Aly, and D. Baleanu, "The analytical analysis of Time-Fractional Fornberg–Whitham equations," *Mathematics*, vol. 8, no. 6, p. 987, 2020.

[36] R. Shah, H. Khan, D. Baleanu, P. Kumam, and M. Arif, "A novel method for the analytical solution of fractional Zakharov–Kuznetsov equations," *Advances in Difference equations*, vol. 2019, no. 1, 2019.

[37] Y. H. Youssri, "Orthonormal ultraspherical operational matrix algorithm for Fractal–Fractional Riccati equation with generalized Caputo derivative," *Fractal and Fractional*, vol. 5, no. 3, p. 100, 2021.

[38] W. M. Abd-Elhameed and Y. H. Youssri, "Spectral tau solution of the linearized time-fractional KdV-type equations," *AIMS Mathematics*, vol. 7, no. 8, pp. 15138–15158, 2022.

[39] R. M. Hafez and Y. H. Youssri, "Shifted Jacobi collocation scheme for multidimensional time-fractional order telegraph equation," *Iranian Journal of Numerical Analysis and Optimization*, vol. 10, no. 1, pp. 195–223, 2020.

[40] A. Prakash and H. Kaur, "Q-homotopy analysis transform method for space and time-fractional KdV-Burger s equation," *Nonlinear Science Letter*, vol. 9, no. 1, pp. 44–61, 2018.

[41] D. Kumar, J. Singh, and D. Baleanu, "A new analysis for fractional model of regularized long-wave equation arising in ion acoustic plasma waves," *Mathematical Methods in the Applied Sciences*, vol. 40, no. 15, pp. 5642–5653, 2017.

[42] P. Veeresha, D. G. Prakasha, and S. Kumar, "A fractional model for propagation of classical optical solitons by using nonsingular derivative," *Mathematical Methods in the Applied Sciences*, 2020.

[43] M. A. El-Tawil and S. N. Huseen, "On convergence of q-homotopy analysis method," *International Journal of Contemporary Mathematical Sciences*, vol. 8, no. 10, pp. 481–497, 2013.

[44] M. Alquran, "Analytical solutions of fractional foam drainage equation by residual power series method," *Mathematical Sciences*, vol. 8, no. 4, pp. 153–160, 2014.

[45] M. Alquran, H. M. Jaradat, and M. I. Syam, "Analytical solution of the time-fractional Phi-4 equation by using modified residual power series method," *Nonlinear Dynamics*, vol. 90, no. 4, pp. 2525–2529, 2017.

[46] L. Wang and X. Chen, "Approximate analytical solutions of time fractional Whitham Broer Kaup equations by a residual power series method," *Entropy*, vol. 17, no. 12, pp. 6519–6533, 2015.

[47] Z. Korpinar and M. Inc, "Numerical simulations for fractional variation of (1 + 1)-dimensional Biswas- Milovic equation," *Optik*, vol. 166, pp. 77–85, 2018.

[48] I. Komashynska, M. Al-Smadi, A. Al-Habahbeh, and A. Ateiwi, "Analytical approximate solutions of systems of multi-pantograph delay differential equations using residual power-series method," *Numerical Analysis*, vol. 8, no. 10, pp. 664–675, 2014.

[49] A. Kumar, S. Kumar, and M. Singh, "RPSM for fractional Sharma-Tasso-Olver equation," *Communications in Numerical Analysis*, vol. 2016, pp. 1–10, 2016.

[50] Y. Zhang, A. Kumar, S. Kumar, D. Baleanu, and X. J. Yang, "Residual power series method for time-fractional Schrödinger equations," *Journal of Nonlinear Sciences and Applications*, vol. 9, no. 11, pp. 5821–5829, 2016.

[51] E. Abuteen and A. Freihet, "Analytical and numerical solution for fractional gas dynamic equations using residual power series method," in *Proceedings of International Conference on Fractional Differentiation and Its Applications (ICFDA)*, Amman, Jordan, 2018.

[52] M. I. Syam, "Analytical solution of the fractional initial Emden fowler equation using the fractional residual power series method," *International Journal of Applied and Computational Mathematics*, vol. 4, no. 4, pp. 1–8, 2018.

[53] A. A. Freihat and M. H. AL-Smadi, "A new reliable algorithm using the generalized differential transform method for the numeric-analytic solution of fractional-order Liu chaotic and hyperchaotic systems," *Pensee*, vol. 75, no. 9, 2013.

[54] M. Caputo, *Elasticita e Dissipazione*, Zanichelli, Bologna, 1969.

[55] M. Caputo, "Linear Models of dissipation whose Q is almost frequency independent–II," *Geophysical Journal of the Royal Astronomical Society*, vol. 13, no. 5, pp. 529–539, 1967.

[56] F. Tchier, M. Inc, Z. S. Korpinar, and D. Baleanu, "Solutions of the time fractional reaction-diffusion equations with residual power series method," *Advances in Mechanical Engineering*, vol. 8, no. 10, 2016.

[57] K. S. Miller and B. Ross, *An Introduction to the Fractional Calculus and Fractional Differential Equations*, Wiley, New York, 1993.

[58] A. El-Ajou, O. Arqub, Z. Zhour, and S. Momani, "New results on fractional power series: theories and applications," *Entropy*, vol. 15, no. 12, pp. 5305–5323, 2013.

[59] H. Khan, Q. Khan, F. Tchier et al., "The Efficient Techniques for Non-Linear Fractional View Analysis of the KdV Equation," *Frontiers in Physics*, vol. 10, p. 614, 2022.

[60] D. G. Prakasha, P. Veeresha, and H. M. Baskonus, "Residual power series method for fractional Swift Hohenberg equation," *Fractal and fractional*, vol. 3, no. 1, p. 9, 2019.

[61] A. Arqub, "Series solution of fuzzy differential equations under strongly generalized differentiability," *Journal of Advanced Research in Applied Mathematics*, vol. 5, no. 1, pp. 31–52, 2013.

[62] O. Abu Arqub, A. El-Ajou, A. S. Bataineh, and I. Hashim, "A representation of the exact solution of generalized Lane-Emden equations using a new analytical method," *Abstract and Applied Analysis*, vol. 2013, Article ID 378593, 10 pages, 2013.

[63] A. Prakash and H. Kaur, "Q-homotopy analysis transform method for space and time-fractional KdV-Burgers equation," *Nonlinear Science Letters*, vol. 9, no. 1, pp. 44–61, 2018.

[64] Y. Patel and J. M. Dhodiya, "Application of differential transform method to solve linear, non-linear reaction convection diffusion and convection diffusion problem," *International Journal of Pure and Apllied Mathematics*, vol. 109, no. 3, pp. 529–538, 2016.

[65] B. K. Singh, P. Kumar, and V. Kumar, "homotopy perturbation method for solving time fractional coupled viscous Burgers' equation in (2+1) and (3+1) dimensions," *International Journal of Applied and Computational Mathematics*, vol. 4, no. 1, pp. 1–25, 2017.

[66] U. Farooq, H. Khan, F. Tchier, E. Hincal, D. Baleanu, and H. Bin Jebreen, "New approximate analytical technique for the solution of time fractional fluid flow models," *Advances in Difference Equations*, vol. 2021, no. 1, 2021.

Hindawi
Journal of Function Spaces
Volume 2022, Article ID 1938290, 8 pages
https://doi.org/10.1155/2022/1938290

Research Article

Remarks on the Initial and Terminal Value Problem for Time and Space Fractional Diffusion Equation

Hoang Luc Nguyen

Division of Applied Mathematics, Thu Dau Mot University, Binh Duong, Vietnam

Correspondence should be addressed to Hoang Luc Nguyen; nguyenhoangluc@tdmu.edu.vn

Received 6 August 2022; Revised 3 September 2022; Accepted 12 September 2022; Published 4 October 2022

Academic Editor: Yusuf Gurefe

The fractional problem for partial differential equation has many applications in science and technology. The main objective of the paper is to investigate the convergence of the mild solution of the diffusion equation with time and space fractional. We consider the problem in two cases which are forward problem and inverse problem. We use new techniques to overcome some of the complex assessments.

1. Introduction

Fractional calculation has been shown to provide many important applications in natural sciences, such as in biological systems, signal processing, fluid mechanics, electrical networks, optical, and viscosity [1–8]. With the development of mathematics, there are now many different definitions of fractional derivatives, for example, Riemann-Liouville, Caputo, Hadamard, and Riesz. Let us refer many various papers on fractional differential equation, for example, Manimaran et al., Tuan et al., Long et al., Long L.D. et al., and Ngoc et al. [9–14]; Adiguzel et al., Li et al., Afshari et al., Alqahtani et al., Karapınar et al., Salim et al., Karapinar et al., and Abdeljawad et al. [15–22]; and Bachir et al., Salim et al., and Baitichea et al. [23–25]. Although most of them have been extensively studied, most mathematicians are interested and studied two derivatives which are Caputo and Riemann-Liouville derivatives.

In this paper, for $\alpha, \beta \in (0,1)$, we are interested to study the following problem:

$$\begin{cases} \partial_t^\alpha u(x,t) + (-\Delta)^\beta u(x,t) = H(x,t), & x,t) \in (0,\pi)\times(0,T), \\ (u(0,t) = u(\pi,t) = 0, & t \in (0,T), \end{cases} \tag{1}$$

with the initial condition

$$u(x,0) = u_0(x), 0 < x < \pi, \tag{2}$$

or the terminal condition

$$u(x,T) = f(x), 0 < x < \pi. \tag{3}$$

There are many results related to the Problem (1) in both aspects: theoretical analysis and numerical analysis. The existence and well-posedness of Problems (1)–(2) and (1)–(3) has been studied in [26]. Jin et al. [27] applied two semidiscrete schemes of Galerkin FEM method in order to approximate the solution of Problems (1) and (2). In [28], the authors investigated a reaction-diffusion equation with a Caputo fractional derivative in time. In [29], the authors established the existence and uniqueness of the weak solution and the regularity of the solution for coupled fractional diffusion system. Mu et al. [30] investigated some initial-boundary value problems for time-fractional diffusion equations. Let us now mention some previous works on terminal value problem Problems (1)–(3). The main current applications of the terminal value problem are hydrodynamic inversion and spoil the image. In [31], the authors used variable total variation to approximate the backward problem for a time-space fractional diffusion equation. Under the interesting paper [32], Ngoc et al. considered the terminal value problem for nonlinear model.

$$\mathbf{D}_{0^+}^{\alpha} u - u_{xx} = F(u). \tag{4}$$

Our main purpose of this paper is to study the convergence of Problem (1) when $\beta \longrightarrow 1^-$. This result gives us the relationship between the solutions of the two Problem (1) with the case $0 < \beta < 1$ and $\beta = 1$. To the best of our knowledge, the research direction on this convergence topic is still limited. The main techniques to solve the our problem is to use Mittag-Leffler evaluations with the combination of the Wright function.

This paper is organized as follows. In Section 2, we focus premilinaries with some background on the definition and evaluations of Mittag-Leffler functions.

2. Premilinaries

Let us consider the Mittag-Leffler function, which is defined by

$$E_{\alpha,\beta}(z) = \sum_{n=0}^{\infty} \frac{z^n}{\Gamma(n\alpha + \beta)}. \tag{5}$$

($z \in \mathbb{C}$), for $\alpha > 0$ and $\beta \in \mathbb{R}$. When $\beta = 1$, it is abbreviated as $E_\alpha(z) = E_{\alpha,1}(z)$.

Lemma 2.1. *The following equality holds (See [33]):*

$$E_{\alpha,1}(-z) = \int_0^\infty \mathbf{\Phi}_\alpha(\theta) e^{-z\theta} d\theta, \quad \text{for } z \in \mathbb{C}, \tag{6}$$

where the Wright function $\mathbf{\Phi}_\alpha(\theta)$ is defined by

$$\mathbf{\Phi}_\alpha(\theta) \coloneqq \sum_{j=0}^{\infty} \frac{\theta^j}{j!\Gamma(-\alpha j + 1 - \alpha)}, \quad 0 < \alpha < 1. \tag{7}$$

In addition, $\mathbf{\Phi}_\alpha(\theta)$ is a probability density function, that is,

$$\mathbf{\Phi}_\alpha(\theta) \geq 0, \quad \text{for } \theta > \text{and} \int_0^\infty \mathbf{\Phi}_\alpha(\theta) = 1. \tag{8}$$

Lemma 2.2. *For $\alpha \in (0,1)$ and $b > -1$, the following properties hold (See [33]):*

$$\int_0^\infty \theta^b \mathbf{\Phi}_\alpha(\theta) d\theta = \frac{\Gamma(b+1)}{\Gamma(b\alpha + 1)}. \tag{9}$$

Let a given positive number $\sigma \geq 0$. Let us also define the Hilbert scale space as follows:

$$\mathbb{H}^\sigma(\Omega) = \left\{ \psi \in L^2(\Omega) \colon \sum_{j=1}^{\infty} j^{2\sigma} \left\langle \psi, \varphi_j \right\rangle^2 < +\infty \right\}, \tag{10}$$

with the following norm $\|\psi\|_{\mathbb{H}^\sigma(\Omega)} = \left(\sum_{j=1}^{\infty} j^{2\sigma} \langle \psi, \varphi_j \rangle^2\right)^{(1/2)}$.

Here we give the following lemma, which will help our proofs later:

Lemma 2.3. *Let $\varepsilon, \varepsilon' > 0$. Then we get the following:*

$$E_{\alpha,1}\left(-j^{2\beta} t^\alpha\right) - E_{\alpha,1}\left(-j^2 t^\alpha\right) \leq C_1(\alpha,\varepsilon) t^{\alpha\varepsilon} (1-\beta)^{\varepsilon\varepsilon'} j^{2\varepsilon + \varepsilon\varepsilon'}. \tag{11}$$

$$E_{\alpha,\alpha}\left(-j^{2\beta} t^\alpha\right) - E_{\alpha,\alpha}\left(-j^2 t^\alpha\right) \leq C_2(\alpha,\varepsilon) t^{\alpha\varepsilon} (1-\beta)^{\varepsilon\varepsilon'} j^{2\varepsilon + \varepsilon\varepsilon'}. \tag{12}$$

Proof. Let us now to study the difference $|E_{\alpha,1}(-j^{2\beta} t^\alpha) - E_{\alpha,1}(-j^2 t^\alpha)|$ for $0 < \beta < 1$. Since the definition of Wright function as in Lemma 2.1, we get that

$$E_{\alpha,1}\left(-j^{2\beta} t^\alpha\right) - E_{\alpha,1}\left(-j^2 t^\alpha\right) = \int_0^\infty \Phi_\alpha(\theta) \exp\left(-j^{2\beta} t^\alpha \theta\right) d\theta - \int_0^\infty \Phi_\alpha(\theta) \exp\left(-j^2 t^\alpha \theta\right) d\theta. \tag{13}$$

Since $j \geq 1$ and $0 < \beta \leq 1$, we know easily that $\exp(-j^{2\beta} t^\alpha \theta) > \exp(-j^2 t^\alpha \theta)$. Hence, we find that

$$\begin{aligned} &\exp\left(-j^{2\beta} t^\alpha \theta\right) - \exp\left(-j^2 t^\alpha \theta\right) \\ &\quad = \exp\left(-j^{2\beta} t^\alpha \theta\right)\left(1 - \exp\left(-\left(j^2 - j^{2\beta}\right) t^\alpha \theta\right)\right). \end{aligned} \tag{14}$$

Using the inequality $1 - e^{-z} \leq C_\varepsilon z^\varepsilon$ for any $\varepsilon > 0$, we find that

$$\exp\left(-j^{2\beta} t^\alpha \theta\right) - \exp\left(-j^2 t^\alpha \theta\right) \leq C_\varepsilon \left(j^2 - j^{2\beta}\right)^\varepsilon t^{\alpha\varepsilon} \theta^\varepsilon. \tag{15}$$

Combining Problems (13) and (15), we derive that

$$\begin{aligned} E_{\alpha,1}\left(-j^{2\beta} t^\alpha\right) - E_{\alpha,1}\left(-j^2 t^\alpha\right) &\leq C_\varepsilon \left(j^2 - j^{2\beta}\right)^\varepsilon t^{\alpha\varepsilon} \left(\int_0^\infty \theta^\varepsilon \Phi_\alpha(\theta) d\theta\right) \\ &= C_\varepsilon \frac{\Gamma(\varepsilon+1)}{\alpha\varepsilon + 1} \left(j^2 - j^{2\beta}\right)^\varepsilon t^{\alpha\varepsilon}. \end{aligned} \tag{16}$$

For any $\varepsilon' > 0$ and noting that $\log(j) \leq j$ for any $j \geq 1$, it is obvious to see that

$$\begin{aligned} j^2 - j^{2\beta} &= j^2(1 - \exp(-(2-2\beta)\log(j))) \\ &\leq j^2 (2 - 2\beta)^{\varepsilon'} |\log(j)|^{\varepsilon'} \\ &\lesssim (1-\beta)^{\varepsilon'} j^{2+\varepsilon'}. \end{aligned} \tag{17}$$

This implies that

$$\left(j^2 - j^{2\beta}\right)^\varepsilon \lesssim (1-\beta)^{\varepsilon\varepsilon'} j^{2\varepsilon + \varepsilon\varepsilon'}. \tag{18}$$

From some above observations, we get that

$$E_{\alpha,1}\left(-j^{2\beta}t^{\alpha}\right) - E_{\alpha,1}\left(-j^{2}t^{\alpha}\right) \le C_1(\alpha,\varepsilon)t^{\alpha\varepsilon}(1-\beta)^{\varepsilon\varepsilon'}j^{2\varepsilon+\varepsilon\varepsilon'}. \tag{19}$$

By a similar argument as above, we also obtain the desired result, Problem (12). □

3. Initial Value Problem

In this section, we focus the following initial value problem under the linear case:

$$\begin{cases} \partial_t^{\alpha} v = -(-\Delta)^{\beta} v(x,t) + H(x,t), & (x,t) \in (0,\pi)\times(0,T), \\ v(0,t) = v(\pi,t) = 0, & t \in (0,T), \\ v(x,0) = v_0(x), & x \in (0,\pi), \end{cases} \tag{20}$$

where v_0 and source function H are defined later.

Theorem 3.1. *Let $v_0 \in \mathbb{H}^p(\Omega)$ and $H \in L^{\infty}(0,T;\mathbb{H}^p(\Omega))$ for any $p>0$. Then we get*

$$\begin{aligned} &\left\| v_\beta(.,t) - v^*(.,t) \right\|_{\mathbb{H}^s(\Omega)} \\ &\quad \lesssim (1-\beta)^{p-s/2}\left[\|v_0\|_{\mathbb{H}^p(\Omega)} + \|H\|_{L^{\infty}(0,T;\mathbb{H}^p(\Omega))}\right] \end{aligned} \tag{21}$$

for any $0 < s < p$.

Proof. The mild solution to Problem (20) with $0<\beta<1$ is defined by

$$\begin{aligned} v_\beta(x,t) = &\sum_{j=1}^{\infty} E_{\alpha,1}\left(-j^{2\beta}t^{\alpha}\right)\left(\int_0^{\pi} v_0(x)\varphi_j(x)dx\right)\varphi_j(x) \\ &+ \sum_{j=1}^{\infty}\left[\int_0^t (t-r)^{\alpha-1}E_{\alpha,\alpha}\left(-j^{2\beta}(t-r)^{\alpha}\right)H_j(r)dr\right]\varphi_j(x), \end{aligned} \tag{22}$$

and the mild solution to Problem (20) with $\beta=1$ is defined by

$$\begin{aligned} v^*(x,t) = &\sum_{j=1}^{\infty} E_{\alpha,1}\left(-j^{2}t^{\alpha}\right)\left(\int_0^{\pi} v_0(x)\varphi_j(x)dx\right)\varphi_j(x) \\ &+ \sum_{j=1}^{\infty}\left[\int_0^t (t-r)^{\alpha-1}E_{\alpha,\alpha}\left(-j^{2}(t-r)^{\alpha}\right)H_j(r)dr\right]\varphi_j(x). \end{aligned} \tag{23}$$

By subtracting both sides of the two expressions above, we get the following difference:

$$\begin{aligned} &v_\beta(x,t) - v^*(x,t) \\ &= \sum_{j=1}^{\infty}\left[E_{\alpha,1}\left(-j^{2\beta}t^{\alpha}\right) - E_{\alpha,1}\left(-j^{2}t^{\alpha}\right)\right]\left(\int_0^{\pi} v_0(x)\varphi_j(x)dx\right)\varphi_j(x) \\ &\quad + \sum_{j=1}^{\infty}\left[\int_0^t (t-r)^{\alpha-1}\left(E_{\alpha,\alpha}\left(-j^{2\beta}(t-r)^{\alpha}\right)\right.\right. \\ &\quad \left.\left. - E_{\alpha,\alpha}\left(-j^{2}(t-r)^{\alpha}\right)\right)H_j(r)dr\right]\varphi_j(x) \\ &= \mathscr{M}_1(x,t) + \mathscr{M}_2(x,t). \end{aligned} \tag{24}$$

Let us first consider the term $\mathscr{M}_1$. By applying Parseval's equality and Lemma 2.3, we find that

$$\begin{aligned} \|\mathscr{M}_1(.,t)\|_{\mathbb{H}^s(\Omega)}^2 &= \sum_{j=1}^{\infty} j^{2s}\left[E_{\alpha,1}\left(-j^{2\beta}t^{\alpha}\right) - E_{\alpha,1}\left(-j^{2}t^{\alpha}\right)\right]^2 \\ &\quad \cdot \left(\int_0^{\pi} v_0(x)\varphi_j(x)dx\right)^2 \\ &\le |C_1(\alpha,\varepsilon,\delta)|^2 t^{2\alpha\varepsilon}(1-\beta)^{2\varepsilon\delta}\sum_{j=1}^{\infty} j^{2s+4\varepsilon+2\varepsilon\delta} \\ &\quad \cdot \left(\int_0^{\pi} v_0(x)\varphi_j(x)dx\right)^2, \end{aligned} \tag{25}$$

where any *delta* >0. Hence, we know that the upper bound

$$\|\mathscr{M}_1(.,t)\|_{\mathbb{H}^s(\Omega)} \lesssim (1-\beta)^{\varepsilon\delta}\|v_0\|_{\mathbb{H}^{s+2\varepsilon+\varepsilon\delta}(\Omega)}. \tag{26}$$

Let us now treat the second term $\mathscr{M}_2$. By using Parseval's equality, we get that

$$\begin{aligned} \|\mathscr{M}_2(.,t)\|_{\mathbb{H}^s(\Omega)}^2 &= \sum_{j=1}^{\infty} j^{2s}\left[\int_0^t (t-r)^{\alpha-1}\left(E_{\alpha,\alpha}\left(-j^{2\beta}(t-r)^{\alpha}\right)\right.\right. \\ &\quad \left.\left. - E_{\alpha,\alpha}\left(-j^{2}r(t-)^{\alpha}\right)\right)H_j(r)dr\right]^2 \\ &\quad \cdot \sum_{j=1}^{\infty} j^{2s}\left[\int_0^t (t-r)^{\alpha-1}\left(E_{\alpha,\alpha}\left(-j^{2\beta}(t-r)^{\alpha}\right)\right.\right. \\ &\quad \left.\left. - E_{\alpha,\alpha}\left(-j^{2}(t-r)^{\alpha}\right)\right)^2 \left|H_j(r)\right|^2 dr\right]. \end{aligned} \tag{27}$$

In view of the second estimate of Lemma 2.3, we derive that

$$\begin{aligned} &\left(E_{\alpha,\alpha}\left(-j^{2\beta}(t-r)^{\alpha}\right) - E_{\alpha,\alpha}\left(-j^{2}(t-r)^{\alpha}\right)\right)^2 \\ &\quad \le \left|C_2\left(\alpha,\varepsilon,\varepsilon'\right)\right|^2 (t-r)^{2\alpha\varepsilon}(1-\beta)^{2\varepsilon\varepsilon'} j^{\left(4\varepsilon+2\varepsilon\varepsilon'\right)} \end{aligned} \tag{28}$$

Combining Problems (27) and (28), we derive that

$$\begin{aligned}\|\mathscr{M}_2(.,t)\|^2_{\mathbb{H}^s(\Omega)} &\le \left|C_2\left(\alpha,\varepsilon,\varepsilon'\right)\right|^2(1-\beta)^{2\varepsilon\varepsilon'}\int_0^t(t-r)^{\alpha-1+2\alpha\varepsilon}\\ &\quad\cdot\left(\sum_{j=1}^{\infty}j^{2s+4\varepsilon+2\varepsilon\varepsilon'}\left|H_j(r)\right|^2\right)dr\\ &= \left|C_2\left(\alpha,\varepsilon,\varepsilon'\right)\right|^2(1-\beta)^{2\varepsilon\varepsilon'}\\ &\quad\cdot\int_0^t(t-r)^{\alpha-1+2\alpha\varepsilon}\|H(r)\|_{\mathbb{H}^{s+2\varepsilon+\varepsilon\varepsilon'}(\Omega)}dr\\ &\le \left|C_2\left(\alpha,\varepsilon,\varepsilon'\right)\right|^2(1-\beta)^{2\varepsilon\varepsilon'}\\ &\quad\cdot\left(\int_0^t(t-r)^{\alpha-1+2\alpha\varepsilon}dr\right)\|H\|^2_{L^\infty\left(0,T;\mathbb{H}^{s+2\varepsilon+\varepsilon\varepsilon'}(\Omega)\right)}.\end{aligned} \tag{29}$$

It is obvious to see that the integral term $\int_0^t(t-r)^{(\alpha-1+2\alpha\varepsilon)}dr$ is convergent. Hence, we obtain that the following estimate:

$$\|\mathscr{M}_2(.,t)\|_{\mathbb{H}^s(\Omega)} \le \left|C_2\left(\alpha,\varepsilon,\varepsilon'\right)\right|(1-\beta)^{\varepsilon\varepsilon'}\|H\|_{L^\infty\left(0,T;\mathbb{H}^{s+2\varepsilon+\varepsilon\varepsilon'}(\Omega)\right)}. \tag{30}$$

Combining Problems (24), (25), and (30), we find that

$$\begin{aligned}&\left\|v_\beta(.,t)-v^*(.,t)\right\|_{\mathbb{H}^s(\Omega)}\\ &\quad\le \|\mathscr{M}_1(.,t)\|_{\mathbb{H}^s(\Omega)}+\|\mathscr{M}_2(.,t)\|_{\mathbb{H}^s(\Omega)}\\ &\quad\lesssim (1-\beta)^{\varepsilon\delta}\|v_0\|_{\mathbb{H}^{s+2\varepsilon+\varepsilon\delta}(\Omega)}+(1-\beta)^{\varepsilon\varepsilon'}\|H\|_{L^\infty\left(0,T;\mathbb{H}^{s+2\varepsilon+\varepsilon\varepsilon'}(\Omega)\right)}.\end{aligned} \tag{31}$$

Since $p>s$, we can choose

$$\varepsilon=\frac{p-s}{4},\ \delta=\varepsilon'=2. \tag{32}$$

This implies that

$$\left\|v_\beta(.,t)-v^*(.,t)\right\|_{\mathbb{H}^s(\Omega)} \lesssim (1-\beta)^{p-s/2}\left[\|v_0\|_{\mathbb{H}^p(\Omega)}+\|H\|_{L^\infty(0,T;\mathbb{H}^p(\Omega))}\right]. \tag{33}$$

□

4. Terminal Value Problem

Theorem 4.1. *Let $f\in\mathbb{H}^b(\Omega)$ and $H\in L^\infty(0,T;\mathbb{H}^b(\Omega))$. Then we get*

$$\begin{aligned}&\left\|u_\beta(.,t)-u_*(.,t)\right\|_{L^m(0,T;\mathbb{H}^s(\Omega))}\\ &\quad\lesssim(1-\beta)^{b-s-2\beta-2/2}\left(\|f\|_{\mathbb{H}^b(\Omega)}+\|H\|_{L^\infty\left(0,T;\mathbb{H}^b(\Omega)\right)}\right)\\ &\qquad+(1-\beta)^{b-s+2\beta+2/2}\|H\|_{L^\infty\left(0,T;\mathbb{H}^b(\Omega)\right)},\end{aligned} \tag{34}$$

for $1<m<1/\alpha$ and $b>s+2\beta+2$.

Proof. The mild solution to terminal value Problem (1) for $0<\beta<1$ is given by

$$\begin{aligned}u_\beta(x,t) &= \sum_{j=1}^{\infty}\frac{E_{\alpha,1}\left(-j^{2\beta}t^\alpha\right)}{E_{\alpha,1}\left(-j^{2\beta}T^\alpha\right)}\left(\int_0^\pi f(x)\varphi_j(x)dx\right)\varphi_j(x)\\ &\quad-\sum_{j=1}^{\infty}\frac{E_{\alpha,1}\left(-j^{2\beta}t^\alpha\right)}{E_{\alpha,1}\left(-j^{2\beta}T^\alpha\right)}\left(\int_0^T(T-r)^{\alpha-1}E_{\alpha,\alpha}\right.\\ &\quad\left.\cdot\left(-j^{2\beta}(T-r)^\alpha\right)H_j(r)dr\right)\varphi_j(x)\\ &\quad+\sum_{j=1}^{\infty}\left[\int_0^t(t-r)^{\alpha-1}E_{\alpha,\alpha}\left(-j^{2\beta}(t-r)^\alpha\right)H_j(r)dr\right]\varphi_j(x),\end{aligned} \tag{35}$$

where

$$H_j(r)=\int_0^\pi H(x,r)\varphi_j(x)dx. \tag{36}$$

The mild solution to terminal value Problem (1) for $\beta=1$ is given by

$$\begin{aligned}u_*(x,t) &= \sum_{j=1}^{\infty}\frac{E_{\alpha,1}\left(-j^2t^\alpha\right)}{E_{\alpha,1}\left(-j^2T^\alpha\right)}\left(\int_0^\pi f(x)\varphi_j(x)dx\right)\varphi_j(x)\\ &\quad-\sum_{j=1}^{\infty}\frac{E_{\alpha,1}\left(-j^2t^\alpha\right)}{E_{\alpha,1}\left(-j^2T^\alpha\right)}\left(\int_0^T(T-r)^{\alpha-1}E_{\alpha,\alpha}\right.\\ &\quad\left.\cdot\left(-j^{2\beta}(T-r)^\alpha\right)H_j(r)dr\right)\varphi_j(x)\\ &\quad+\sum_{j=1}^{\infty}\left[\int_0^t(t-r)^{\alpha-1}E_{\alpha,\alpha}\left(-j^2(t-r)^\alpha\right)H_j(r)dr\right]\varphi_j(x).\end{aligned} \tag{37}$$

Taking the difference of Problems (35) and (37) on both sides, we get the following bound:

$$\begin{aligned}&u_\beta(x,t)-u_*(x,t)\\ &\quad=\sum_{j=1}^{\infty}\left(\frac{E_{\alpha,1}\left(-j^{2\beta}t^\alpha\right)}{E_{\alpha,1}\left(-j^{2\beta}T^\alpha\right)}-\frac{E_{\alpha,1}\left(-j^2t^\alpha\right)}{E_{\alpha,1}\left(-j^2T^\alpha\right)}\right)\left(\int_0^\pi f(x)\varphi_j(x)dx\right)\varphi_j(x)\\ &\quad-\sum_{j=1}^{\infty}\frac{E_{\alpha,1}\left(-j^{2\beta}t^\alpha\right)}{E_{\alpha,1}\left(-j^{2\beta}T^\alpha\right)}\left(\int_0^T(T-r)^{\alpha-1}\left(E_{\alpha,\alpha}\left(-j^{2\beta}(T-r)^\alpha\right)\right.\right.\\ &\quad\left.\left.-E_{\alpha,\alpha}\left(-j^2(T-r)^\alpha\right)\right)H_j(r)dr\right)\varphi_j(x)\\ &\quad+\sum_{j=1}^{\infty}\left(\frac{E_{\alpha,1}\left(-j^{2\beta}t^\alpha\right)}{E_{\alpha,1}\left(-j^{2\beta}T^\alpha\right)}-\frac{E_{\alpha,1}\left(-j^2t^\alpha\right)}{E_{\alpha,1}\left(-j^2T^\alpha\right)}\right)\\ &\quad\cdot\left(\int_0^T(T-r)^{\alpha-1}E_{\alpha,\alpha}\left(-j^2(T-r)^\alpha\right)H_j(r)dr\right)\varphi_j(x)\end{aligned}$$

$$+\sum_{j=1}^{\infty}\left[\int_0^t (t-r)^{\alpha-1}\left(E_{\alpha,\alpha}\left(-j^{2\beta}(t-r)^{\alpha}\right)\right.\right.$$
$$\left.\left.-E_{\alpha,\alpha}\left(-j^2(t-r)^{\alpha}\right)\right)H_j(r)dr\right]\varphi_j(x) \quad (38)$$
$$=J_1(x,t)+J_2(x,t)+J_3(x,t)+J_4(x,t).$$

Step 1. Estimation of the Term J_1.

In order to evaluate J_1, we need to control the component

$$M_1=\frac{E_{\alpha,1}\left(-j^{2\beta}t^{\alpha}\right)}{E_{\alpha,1}\left(-j^{2\beta}T^{\alpha}\right)}-\frac{E_{\alpha,1}\left(-j^{2}t^{\alpha}\right)}{E_{\alpha,1}\left(-j^{2}T^{\alpha}\right)}. \quad (39)$$

It is obvious to compute the above term as follows:

$$M_1=\frac{E_{\alpha,1}\left(-j^{2\beta}t^{\alpha}\right)-E_{\alpha,1}\left(-j^{2}t^{\alpha}\right)}{E_{\alpha,1}\left(-j^{2\beta}T^{\alpha}\right)}-\frac{E_{\alpha,1}\left(-j^{2\beta}T^{\alpha}\right)-E_{\alpha,1}\left(-j^{2}T^{\alpha}\right)}{E_{\alpha,1}\left(-j^{2\beta}T^{\alpha}\right)E_{\alpha,1}\left(-j^{2}T^{\alpha}\right)}. \quad (40)$$

Since the fact that

$$E_{\alpha,1}\left(-j^{2\beta}T^{\alpha}\right)\geq\frac{C_{\alpha}^{-}}{1+j^{2\beta}T^{\alpha}}\leq\frac{C_{\alpha}}{j^{2\beta}(T^{\alpha}+1)}, \quad (41)$$

we know that

$$\frac{E_{\alpha,1}\left(-j^{2\beta}t^{\alpha}\right)-E_{\alpha,1}\left(-j^{2}t^{\alpha}\right)}{E_{\alpha,1}\left(-j^{2\beta}T^{\alpha}\right)}\leq\frac{C_1(\alpha,\varepsilon)(T^{\alpha}+1)}{C_{\alpha}}t^{\alpha\varepsilon}(1-\beta)^{\varepsilon\varepsilon'}j^{2\varepsilon+\varepsilon\varepsilon'+2\beta}. \quad (42)$$

By a similar explanation as above, we find that

$$\frac{E_{\alpha,1}\left(-j^{2\beta}T^{\alpha}\right)-E_{\alpha,1}\left(-j^{2}T^{\alpha}\right)}{E_{\alpha,1}\left(-j^{2\beta}T^{\alpha}\right)E_{\alpha,1}\left(-j^{2}T^{\alpha}\right)}\lesssim T^{\alpha\varepsilon}(1-\beta)^{\varepsilon\varepsilon'}j^{2\varepsilon+\varepsilon\varepsilon'+2\beta+2}, \quad (43)$$

where the hidden constant depends on $\alpha, T, \varepsilon, \varepsilon'$. From two above observation, we find that

$$M_1=\frac{E_{\alpha,1}\left(-j^{2\beta}t^{\alpha}\right)}{E_{\alpha,1}\left(-j^{2\beta}T^{\alpha}\right)}-\frac{E_{\alpha,1}\left(-j^{2}t^{\alpha}\right)}{E_{\alpha,1}\left(-j^{2}T^{\alpha}\right)}\lesssim(1-\beta)^{\varepsilon\varepsilon'}j^{2\varepsilon+\varepsilon\varepsilon'+2\beta+2}, \quad (44)$$

where the hidden constant depends on α, T, ε. Hence, we obtain that

$$\|J_1\|^2_{\mathbb{H}^s(\Omega)}=\sum_{j=1}^{\infty}j^{2s}\left(\frac{E_{\alpha,1}\left(-j^{2\beta}t^{\alpha}\right)}{E_{\alpha,1}\left(-j^{2\beta}T^{\alpha}\right)}-\frac{E_{\alpha,1}\left(-j^{2}t^{\alpha}\right)}{E_{\alpha,1}\left(-j^{2}T^{\alpha}\right)}\right)^2\cdot\left(\int_0^{\pi}f(x)\varphi_j(x)dx\right)^2\lesssim(1-\beta)^{2\varepsilon\varepsilon'}\sum_{j=1}^{\infty}j^{2s+4\varepsilon+2\varepsilon\varepsilon'+4\beta+4}\left(\int_0^{\pi}f(x)\varphi_j(x)dx\right)^2. \quad (45)$$

It implies that the following bound

$$\|J_1\|_{\mathbb{H}^s(\Omega)}\lesssim(1-\beta)^{\varepsilon\varepsilon'}\|f\|_{\mathbb{H}^{s+2\varepsilon+\varepsilon\varepsilon'+2\beta+2}(\Omega)}. \quad (46)$$

Step 2. Estimation of the Term J_3.

By using Parseval's equality and noting that Problem (44), we find that

$$\|J_3\|^2_{\mathbb{H}^s(\Omega)}=\sum_{j=1}^{\infty}j^{2s}\left(\frac{E_{\alpha,1}\left(-j^{2\beta}t^{\alpha}\right)}{E_{\alpha,1}\left(-j^{2\beta}T^{\alpha}\right)}-\frac{E_{\alpha,1}\left(-j^{2}t^{\alpha}\right)}{E_{\alpha,1}\left(-j^{2}T^{\alpha}\right)}\right)^2\cdot\left(\int_0^T(T-r)^{\alpha-1}E_{\alpha,\alpha}\left(-j^2(T-r)^{\alpha}\right)H_j(r)dr\right)^2\lesssim(1-\beta)^{2\varepsilon\varepsilon'}\sum_{j=1}^{\infty}j^{2s+4\varepsilon+2\varepsilon\varepsilon'+4\beta+4}\left(\int_0^T(T-r)^{\alpha-1}dr\right)\cdot\left(\int_0^T(T-r)^{\alpha-1}\left|H_j(r)\right|^2dr\right)^2, \quad (47)$$

where we have used the fact that $E_{\alpha,\alpha}(-j^2(T-r)^{\alpha})\leq C_{\alpha}$. Hence, we find that

$$\|J_3\|^2_{\mathbb{H}^s(\Omega)}\lesssim\frac{T^{\alpha}}{\alpha}(1-\beta)^{2\varepsilon\varepsilon'}\left(\int_0^T(T-r)^{\alpha-1}\|H(r)\|_{\mathbb{H}^{s+2\varepsilon+\varepsilon\varepsilon'+2\beta+2}(\Omega)}dr\right)\lesssim(1-\beta)^{2\varepsilon\varepsilon'}\|H\|^2_{L^{\infty}\left(0,T;\mathbb{H}^{s+2\varepsilon+\varepsilon\varepsilon'+2\beta+2}(\Omega)\right)}. \quad (48)$$

Step 3. Estimation of the Term J_2.

By using Parseval's equality, we derive that

$$\|J_2\|^2_{\mathbb{H}^s(\Omega)}=\sum_{j=1}^{\infty}j^{2s}\left(\frac{E_{\alpha,1}\left(-j^{2\beta}t^{\alpha}\right)}{E_{\alpha,1}\left(-j^{2\beta}T^{\alpha}\right)}\right)^2\left(\int_0^T(T-r)^{\alpha-1}\cdot\left(E_{\alpha,\alpha}\left(-j^{2\beta}(T-r)^{\alpha}\right)-E_{\alpha,\alpha}\left(-j^2(T-r)^{\alpha}\right)\right)H_j(r)dr\right)^2. \quad (49)$$

It is easy to verify that

$$\frac{E_{\alpha,1}\left(-j^{2\beta}t^{\alpha}\right)}{E_{\alpha,1}\left(-j^{2\beta}T^{\alpha}\right)} \lesssim \frac{1+T^{\alpha}j^{2\beta}}{1+t^{\alpha}j^{2\beta}} \leq T^{\alpha}t^{-\alpha}. \tag{50}$$

Using Hölder's inequality, we derive that

$$\begin{aligned}
&\left(\int_0^T (T-r)^{\alpha-1}\left(E_{\alpha,\alpha}\left(-j^{2\beta}(T-r)^{\alpha}\right)-E_{\alpha,\alpha}\left(-j^{2}(T-r)^{\alpha}\right)\right)H_j(r)dr\right)^2 \\
&\quad\leq \left(\int_0^T (T-r)^{\alpha-1}dr\right)\left(\int_0^T (T-r)^{\alpha-1}\left(E_{\alpha,\alpha}\left(-j^{2\beta}(T-r)^{\alpha}\right)\right.\right. \\
&\qquad \left.\left.-E_{\alpha,\alpha}\left(-j^{2}(T-r)^{\alpha}\right)\right)^2\left|H_j(r)\right|^2dr\right) \\
&\quad\lesssim \int_0^T (T-r)^{\alpha-1}\left(E_{\alpha,\alpha}\left(-j^{2\beta}(T-r)^{\alpha}\right)\right. \\
&\qquad \left.-E_{\alpha,\alpha}\left(-j^{2}(T-r)^{\alpha}\right)\right)^2\left|H_j(r)\right|^2dr.
\end{aligned} \tag{51}$$

By a similar explanation, we can get that the following bound:

$$E_{\alpha,\alpha}\left(-j^{2\beta}t^{\alpha}\right)-E_{\alpha,\alpha}\left(-j^{2}t^{\alpha}\right) \leq C_2(\alpha,\varepsilon,\gamma)t^{\alpha\varepsilon}(1-\beta)^{\varepsilon\gamma}j^{2\varepsilon+\varepsilon\gamma}, \tag{52}$$

for any $\gamma>0$. This implies that

$$\begin{aligned}
&\left(E_{\alpha,\alpha}\left(-j^{2\beta}(T-r)^{\alpha}\right)-E_{\alpha,\alpha}\left(-j^{2}(T-r)^{\alpha}\right)\right)^2 \\
&\quad\lesssim (T-r)^{2\alpha\varepsilon}(1-\beta)^{2\varepsilon\gamma}j^{4\varepsilon+2\varepsilon\gamma}.
\end{aligned} \tag{53}$$

Hence, we get that the following bound:

$$\begin{aligned}
&\int_0^T (T-r)^{\alpha-1}\left(E_{\alpha,\alpha}\left(-j^{2\beta}(T-r)^{\alpha}\right)-E_{\alpha,\alpha}\left(-j^{2}(T-r)^{\alpha}\right)\right)^2\left|H_j(r)\right|^2dr \\
&\quad\lesssim (1-\beta)^{2\varepsilon\gamma}\int_0^T (T-r)^{\alpha+2\alpha\varepsilon-1}j^{4\varepsilon+2\varepsilon\gamma}\left|H_j(r)\right|^2dr.
\end{aligned} \tag{54}$$

Combining Problems (49), (50), and (54), we derive that

$$\begin{aligned}
\|J_2\|^2_{\mathbb{H}^s(\Omega)} &\lesssim t^{-2\alpha}(1-\beta)^{2\varepsilon\gamma}\int_0^T (T-r)^{\alpha+2\alpha\varepsilon-1} \\
&\quad\cdot\left(\sum_{j=1}^{\infty} j^{2s+4\varepsilon+2\varepsilon\gamma}\left|H_j(r)\right|^2\right)dr \\
&= t^{-2\alpha}(1-\beta)^{2\varepsilon\gamma}\int_0^T (T-r)^{\alpha+2\alpha\varepsilon-1}\|H(r)\|^2_{\mathbb{H}^{s+2\varepsilon+\varepsilon\gamma}(\Omega)}dr \\
&\leq t^{-2\alpha}(1-\beta)^{2\varepsilon\gamma}\left(\int_0^T (T-r)^{\alpha+2\alpha\varepsilon-1}dr\right) \\
&\quad\cdot\|H\|^2_{L^{\infty}\left(0,T;\mathbb{H}^{s+2\varepsilon+\varepsilon\gamma}(\Omega)\right)}.
\end{aligned} \tag{55}$$

It is obvious to see that

$$\int_0^T (T-r)^{\alpha+2\alpha\varepsilon-1}dr = \frac{T^{\alpha+2\alpha\varepsilon}}{\alpha+2\alpha\varepsilon}. \tag{56}$$

So, we obtain that the following confirmation

$$\|J_2\|_{\mathbb{H}^s(\Omega)} \lesssim (1-\beta)^{\varepsilon\gamma}t^{-\alpha}\|H\|_{L^{\infty}\left(0,T;\mathbb{H}^{s+2\varepsilon+\varepsilon\gamma}(\Omega)\right)}. \tag{57}$$

Step 4. Estimation of the Term J_4.
By using Parseval's equality and Hölder's inequality, we get that

$$\begin{aligned}
\|J_4\|^2_{\mathbb{H}^s(\Omega)} &= \sum_{j=1}^{\infty} j^{2s}\left(\int_0^t (t-r)^{\alpha-1}\left(E_{\alpha,\alpha}\left(-j^{2\beta}(t-r)^{\alpha}\right)\right.\right. \\
&\quad \left.\left.-E_{\alpha,\alpha}\left(-j^{2}(t-r)^{\alpha}\right)\right)H_j(r)dr\right)^2 \\
&\leq \left(\int_0^t (t-r)^{\alpha-1}dr\right)\sum_{j=1}^{\infty} j^{2s} \\
&\quad\cdot\left(\int_0^t (t-r)^{\alpha-1}\left(E_{\alpha,\alpha}\left(-j^{2\beta}(T-r)^{\alpha}\right)\right.\right. \\
&\quad \left.\left.-E_{\alpha,\alpha}\left(-j^{2}(t-r)^{\alpha}\right)\right)^2\left|H_j(r)\right|^2dr\right).
\end{aligned} \tag{58}$$

By a similar techniques as in Probelem (54), we derive that

$$\begin{aligned}
&\int_0^t (t-r)^{\alpha-1}\left(E_{\alpha,\alpha}\left(-j^{2\beta}(t-r)^{\alpha}\right)-E_{\alpha,\alpha}\left(-j^{2}(t-r)^{\alpha}\right)\right)^2\left|H_j(r)\right|^2dr \\
&\quad\lesssim (1-\beta)^{2\varepsilon\gamma}\int_0^t (t-r)^{\alpha+2\alpha\varepsilon-1}j^{4\varepsilon+2\varepsilon\gamma}\left|H_j(r)\right|^2dr.
\end{aligned} \tag{59}$$

By review two latter observations, we can deduce that

$$\begin{aligned}
\|J_4\|^2_{\mathbb{H}^s(\Omega)} &\lesssim (1-\beta)^{2\varepsilon\gamma}\int_0^t (t-r)^{\alpha+2\alpha\varepsilon-1}\left(\sum_{j=1}^{\infty} j^{2s+4\varepsilon+2\varepsilon\gamma}\left|H_j(r)\right|^2\right)dr \\
&= (1-\beta)^{2\varepsilon\gamma}\int_0^t (t-r)^{\alpha+2\alpha\varepsilon-1}\|H(r)\|^2_{\mathbb{H}^{s+2\varepsilon+\varepsilon\gamma}(\Omega)}dr \\
&\leq (1-\beta)^{2\varepsilon\gamma}\left(\int_0^t (t-r)^{\alpha+2\alpha\varepsilon-1}dr\right)\|H\|^2_{L^{\infty}\left(0,T;\mathbb{H}^{s+2\varepsilon+\varepsilon\gamma}(\Omega)\right)}.
\end{aligned} \tag{60}$$

The above inequality implies that the following estimate:

$$\|J_4\|_{\mathbb{H}^s(\Omega)} \lesssim (1-\beta)^{\varepsilon\gamma}\left(\int_0^t (t-r)^{\alpha+2\alpha\varepsilon-1}dr\right)\|H\|_{L^{\infty}\left(0,T;\mathbb{H}^{s+2\varepsilon+\varepsilon\gamma}(\Omega)\right)} \tag{61}$$

By similar computation as above, we deduce that

$$\|J_4\|_{\mathbb{H}^s(\Omega)} \lesssim (1-\beta)^{\varepsilon\gamma}\|H\|_{L^{\infty}\left(0,T;\mathbb{H}^{s+2\varepsilon+\varepsilon\gamma}(\Omega)\right)}. \tag{62}$$

Combining four steps as above, we deduce that

$$\begin{aligned} &\left\|u_\beta(.,t)-u_*(.,t)\right\|_{\mathbb{H}^s(\Omega)} \\ &\quad \leq \|J_1\|_{\mathbb{H}^s(\Omega)} + \|J_2\|_{\mathbb{H}^s(\Omega)} + \|J_3\|_{\mathbb{H}^s(\Omega)} + \|J_4\|_{\mathbb{H}^s(\Omega)} \\ &\quad \lesssim (1-\beta)^{\varepsilon\varepsilon'}\left(\|f\|_{\mathbb{H}^{s+2\varepsilon+\varepsilon\varepsilon'+2\beta+2}(\Omega)} + \|H\|_{L^\infty\left(0,T;\mathbb{H}^{s+2\varepsilon+\varepsilon\varepsilon'+2\beta+2}(\Omega)\right)}\right) \\ &\qquad + (1-\beta)^{\varepsilon\gamma}(t^{-\alpha}+1)\|H\|_{L^\infty\left(0,T;\mathbb{H}^{s+2\varepsilon+\varepsilon\gamma}(\Omega)\right)}. \end{aligned} \tag{63}$$

Let us choose

$$\varepsilon = \frac{b-s-2\beta-2}{4}, \varepsilon' = 2, \gamma = 2\frac{b-s+2\beta+2}{b-s-2\beta-2}. \tag{64}$$

Then from some above observations, we deduce that the following estimate:

$$\begin{aligned} &\left\|u_\beta(.,t)-u_*(.,t)\right\|_{\mathbb{H}^s(\Omega)} \\ &\quad \lesssim (1-\beta)^{b-s-2\beta-2/2}\left(\|f\|_{\mathbb{H}^b(\Omega)} + \|H\|_{L^\infty\left(0,T;\mathbb{H}^b(\Omega)\right)}\right) \\ &\qquad + (1-\beta)^{b-s+2\beta+2/2}(t^{-\alpha}+1)\|H\|_{L^\infty\left(0,T;\mathbb{H}^b(\Omega)\right)}. \end{aligned} \tag{65}$$

This estimate implies that the desired result, Problem (34). □

5. Conclusion

In this work, we consider the fractional problem for partial differential equation. We investigate the convergence of the mild solution of the diffusion equation with time and space fractional. Moreover, we consider the problem in two cases which are forward problem and inverse problem by using new techniques to overcome some of the complex assessments.

Data Availability

No data were used to support this study.

Conflicts of Interest

The author declares that they have no conflicts of interest.

Acknowledgments

This work is supported by Thu Dau Mot University.

References

[1] B. D. Coleman and W. Noll, "Foundations of linear viscoelasticity," *Reviews of Modern Physics*, vol. 33, no. 2, pp. 239–249, 1961.

[2] P. Clement and J. A. Nohel, "Asymptotic behavior of solutions of nonlinear Volterra equations with completely positive kernels," *SIAM Journal on Mathematical Analysis*, vol. 12, no. 4, pp. 514–535, 1981.

[3] B. de Andrade and A. Viana, "Abstract Volterra integrodifferential equations with applications to parabolic models with memory," *Mathematische Annalen*, vol. 369, no. 3-4, pp. 1131–1175, 2017.

[4] O. Khan, S. Araci, and M. Saif, "Fractional calculus formulas for Mathieu-type series and generalized Mittag-Leffler function," *Journal of Mathematics and Computer Science*, vol. 20, no. 2, pp. 122–130, 2020.

[5] R. S. Ali, S. Mubeen, and M. M. Ahmad, "A class of fractional integral operators with multi-index Mittag-Leffler k-function and Bessel k-function of first kind," *Journal of Mathematics and Computer Science*, vol. 22, no. 3, pp. 266–281, 2021.

[6] R. Agarwal, U. P. Sharma, and R. P. Agarwal, "Bicomplex Mittag-Leffler function and associated properties," *Journal of Nonlinear Sciences and Applications (JNSA)*, vol. 15, no. 1, pp. 48–60, 2022.

[7] P. Long, G. Murugusundaramoorthy, H. Tang, and W. Wang, "Subclasses of analytic and bi-univalent functions involving a generalized Mittag-Leffler function based on quasi-subordination," *Journal of Mathematics and Computer Science*, vol. 26, no. 4, pp. 379–394, 2022.

[8] N. H. Tuan, Y. Zhou, T. N. Thach, and N. H. Can, "Initial inverse problem for the nonlinear fractional Rayleigh-Stokes equation with random discrete data," *Communications in Nonlinear Science and Numerical Simulation*, vol. 78, article 104873, 2019.

[9] J. Manimaran, L. Shangerganesh, and A. Debbouche, "Finite element error analysis of a time-fractional nonlocal diffusion equation with the Dirichlet energy," *Computational and Applied Mathematics*, vol. 382, article 113066, 2021.

[10] J. Manimaran, L. Shangerganesh, and A. Debbouche, "A time-fractional competition ecological model with cross-diffusion," *Mathematical Methods in the Applied Sciences*, vol. 43, no. 8, pp. 5197–5211, 2020.

[11] N. H. Tuan, A. Debbouche, and T. B. Ngoc, "Existence and regularity of final value problems for time fractional wave equations," *Computers & Mathematics with Applications*, vol. 78, no. 5, pp. 1396–1414, 2019.

[12] L. D. Long, H. D. Binh, D. Kumar, N. H. Luc, and N. H. Can, "Stability of fractional order of time nonlinear fractional diffusion equation with Riemann–Liouville derivative," *Mathematical Methods in the Applied Sciences*, vol. 45, no. 10, pp. 6194–6216, 2022.

[13] L. D. Long, N. H. Luc, S. Tatar, D. Baleanu, and N. H. Can, "An inverse source problem for pseudo-parabolic equation with Caputo derivative," *Journal of Applied Mathematics and Computing*, vol. 68, no. 2, pp. 739–765, 2022.

[14] T. B. Ngoc, V. V. Tri, Z. Hammouch, and N. H. Can, "Stability of a class of problems for time-space fractional pseudo-parabolic equation with datum measured at terminal time," *Applied Numerical Mathematics*, vol. 167, pp. 308–329, 2021.

[15] R. S. Adiguzel, U. Aksoy, and E. Karapinar, "New anisotropic models from isotropic solutions," *Mathematical Methods in the Applied Sciences*, vol. 29, no. 1, pp. 67–83, 2006.

[16] C. F. Li, X. N. Luo, and Y. Zhou, "Existence of positive solutions of the boundary value problem for nonlinear fractional differential equations," *Computers & Mathematics with Applications*, vol. 59, no. 3, pp. 1363–1375, 2010.

[17] H. Afshari, S. Kalantari, and E. Karapinar, "Solution of fractional differential equations via coupled fixed point," *Electronic*

Journal of Differential Equations, vol. 2015, no. 286, pp. 1–12, 2015.

[18] B. Alqahtani, H. Aydi, E. Karapınar, and V. Rakočević, "A solution for Volterra fractional integral equations by hybrid contractions," *Mathematics*, vol. 7, no. 8, p. 694, 2019.

[19] E. Karapınar, A. Fulga, M. Rashid, L. Shahid, and H. Aydi, "Large contractions on quasi-metric spaces with an application to nonlinear fractional differential equations," *Mathematics*, vol. 7, no. 5, p. 444, 2019.

[20] A. Salim, M. Benchohra, E. Karapınar, and J. E. Lazreg, "Existence and Ulam stability for impulsive generalized Hilfer-type fractional differential equations," *Advances in Difference Equations*, vol. 2020, no. 1, Article ID 601, 21 pages, 2020.

[21] E. Karapinar, T. Abdeljawad, and F. Jarad, "Applying new fixed point theorems on fractional and ordinary differential equations," *Advances in Difference Equations*, vol. 2019, no. 1, Article ID 421, 2019.

[22] A. Abdeljawad, R. P. Agarwal, E. Karapinar, and P. S. Kumari, "Solutions of the nonlinear integral equation and fractional differential equation using the technique of a fixed point with a numerical experiment in extended b-metric space," *Symmetry*, vol. 11, no. 5, p. 686, 2019.

[23] F. S. Bachir, S. Abbas, M. Benbachir, and M. Benchohra, "Hilfer-Hadamard fractional differential equations; existence and attractivity," *Advances in the Theory of Nonlinear Analysis and Its Application*, vol. 5, no. 1, pp. 49–57, 2021.

[24] A. Salim, M. Benchohra, J. Lazreg, and J. Henderson, "Nonlinear implicit generalized Hilfer-type fractional differential equations with non-instantaneous impulses in Banach spaces," *Advances in the Theory of Nonlinear Analysis and Its Application*, vol. 4, no. 4, pp. 332–348, 2020.

[25] Z. Baitichea, C. Derbazia, and M. Benchohrab, "ψ-Caputo fractional differential equations with multi-point boundary conditions by topological degree theory," *Results in Nonlinear Analysis*, vol. 3, no. 4, pp. 167–178, 2020.

[26] K. Sakamoto and M. Yamamoto, "Initial value/boundary value problems for fractional diffusion-wave equations and applications to some inverse problems," *Journal of Mathematical Analysis and Applications*, vol. 382, no. 1, pp. 426–447, 2011.

[27] B. Jin, R. Lazarov, and Z. Zhou, "Error estimates for a semidiscrete finite element method for fractional order parabolic equations," *SIAM Journal on Numerical Analysis*, vol. 51, no. 1, pp. 445–466, 2013.

[28] R. Tapdigoglu and B. Torebek, "Global existence and blow-up of solutions of the time-fractional space-involution reaction-diffusion equation," *Turkish Journal of Mathematics*, vol. 44, no. 3, pp. 960–969, 2020.

[29] L. Li, L. Jin, and S. Fang, "Existence and uniqueness of the solution to a coupled fractional diffusion system," *Advances in Difference Equations*, vol. 2015, no. 1, Article ID 370, 2015.

[30] J. Mu, B. Ahmad, and S. Huang, "Existence and regularity of solutions to time-fractional diffusion equations," *Computers & Mathematics with Applications*, vol. 73, no. 6, pp. 985–996, 2017.

[31] J. Jia, J. Peng, J. Gao, and Y. Li, "Backward problem for a time-space fractional diffusion equation," *Inverse Problems & Imaging*, vol. 12, no. 3, pp. 773–799, 2018.

[32] T. B. Ngoc, Y. Zhou, D. O'Regan, and N. H. Tuan, "On a terminal value problem for pseudoparabolic equations involving Riemann- Liouville fractional derivatives," *Applied Mathematics Letters*, vol. 106, article 106373, 2020.

[33] R. Gorenflo, Y. Luchko, and F. Mainardi, "Analytical properties and applications of the Wright function," *Fractional Calculus and Applied Analysis*, vol. 2, pp. 383–414, 1999.

Hindawi
Journal of Function Spaces
Volume 2022, Article ID 1680560, 10 pages
https://doi.org/10.1155/2022/1680560

Research Article

Diverse Exact Soliton Solutions of the Time Fractional Clannish Random Walker's Parabolic Equation via Dual Novel Techniques

Imran Siddique,[1] **Khush Bukht Mehdi**,[1] **M. Ali Akbar**,[2] **Hamiden Abd El-Wahed Khalifa**,[3,4] **and Asim Zafar**[5]

[1]*Department of Mathematics, University of Management and Technology, Lahore 54770, Pakistan*
[2]*Department of Applied Mathematics, University of Rajshahi, Bangladesh*
[3]*Department of Operations Research, Faculty of Graduate Studies for Statistical Research, Cairo University, Giza 12613, Egypt*
[4]*Department of Mathematics, College of Science and Arts, Qassim University, Al-Badaya 51951, Saudi Arabia*
[5]*Department of Mathematics, COMSATS University Islamabad, Vehari Campus, Pakistan*

Correspondence should be addressed to M. Ali Akbar; ali_math74@yahoo.com

Received 12 July 2022; Revised 2 September 2022; Accepted 15 September 2022; Published 28 September 2022

Academic Editor: Yusuf Gurefe

In this article, we acquire a variety of new exact traveling wave solutions in the form of trigonometric, hyperbolic, and rational functions for the nonlinear time-fractional Clannish Random Walker's Parabolic (CRWP) equation in the sense of beta-derivative by employing the two modified methods, namely, modified $(G'/G^2)-$ expansion method and modified $F-$ expansion method. The obtained solutions are verified for aforesaid equations through symbolic soft computations. To promote the essential propagated features, some investigated solutions are exhibited in the form of 2D and 3D graphics by passing on the precise values to the parameters under the constrain conditions. The obtained solutions show that the presented methods are effective, straight forward, and reliable as compared to other methods. These methods can also be used to extract the novel exact traveling wave solutions for solving any types of integer and fractional differential equations arising in mathematical physics.

1. Introduction

Investigation of the exact traveling wave solutions for fractional nonlinear partial differential equations (PDEs) plays an important role in the study of nonlinear physical phenomena. Fractional equations, both partial and ordinary ones, have been applied in modeling of many physical, engineering, chemistry, biology, etc. in recent years [1]. There are several definitions of fractional derivatives such as Riemann Liouville [2], conformable fractional derivative [3], beta derivative [4], and new truncated M-fractional derivative [5] are available in literature. Many powerful methods for obtaining exact solutions of nonlinear fractional PDEs have been presented as Hirota's bilinear method [6], sine-cosine method [7], tanh-function method [8], exponential rational function method [9], Kudryashov method [10], sine-Gordon expansion method [11], modified (G'/G)-expansion method [12], extended (G'/G)-expansion method [13], (G'/G)-expansion method [14], tanh-coth expansion method [15], Jacobi elliptic function expansion method [16], first integral method [17], sardar-subequation method [18], new subequation method [19], extended direct algebraic method [20], exp $(-\phi(\eta))$ method [21], Exp_a function method [22], $(1/G')$, $(G'/G, 1/G)$, and modified $(G'/G^2)-$ expansion methods [23, 24], Kudryashov method [25], modified expansion function method [26], new auxiliary equation method [27], extended Jacobi's elliptic expansion function method [28], extended sinh-Gordon equation expansion method [29], modified simplest equation method [30], and many more.

The time-fractional Clannish Random Walker's Parabolic (CRWP) equation [31, 32] is a model that can determine the behavior of two species A and B of random walker who execute a concurrent one- dimensional random walk characterized by an intensification of the clannishness of the members of one species A at point x at a time t, $u(x, t)$, can be expressed by the time- fractional CRWP equation as

$$D_t^{\alpha_1} u + s u_x + q u u_x + r u_{xx} = 0, \quad (1)$$

where α_1 is a parameter describing the order of the fractional time derivative and $0 < \alpha_1 \leq 1$..

The major concern of this existing study is to utilize the novel meanings of fractional-order derivative, named beta fractional derivative [4], for time-fractional CRWP equation, and to find the novel comprehensive exact traveling wave solutions in the form of hyperbolic, trigonometric, and rational functions by employ two modified methods, modified $(G'/G^2)-$ expansion method [33] and modified $F-$ expansion method [34]. Beta-derivative has some interesting consequences in diverse areas including fluid mechanics, optical physics, chaos theory, biological models, disease analysis, and circuit analysis. To the best of our knowledge, the obtained solutions are more general and in different form which have never been reported in previously published studies [31, 32]. Our results also enrich the variety of the dynamics of higher-dimensional nonlinear wave field. It is hoped that these results will provide some valuable information in the higher-dimensional nonlinear field.

By using the modified (G'/G^2) – expansion method [33], traveling wave solutions have been found for the nonlinear Schrödinger equation along third-order dispersion. Different types of traveling wave solutions of the Fokas-Lenells equations have been determined in [35] by this method. Alyahdaly found the general exact traveling wave solutions to the nonlinear evolution equations in [36]. Gepreel and Nofal [37] obtained the analytical solutions for nonlinear evolution equations in mathematical physics. Siddique and Mehdi found the exact traveling wave solutions for two prolific conformable M-fractional differential equations in [23]. Exact solutions for nonlinear integral member of Kadomstev-Petviashvili hierarchy differential equations have been determined by Gepreel [38].

A modified F–expansion method is proposed by taking full advantages of F expansion method and Riccati equation in seeking exact solutions of nonlinear PDEs. Darvishi and Najafi [39] used a modified F-expansion method to handle the foam Drainage equation. Aasaraai [40] used this method to construct new solutions of the nonlinear $(1+2)$-dimensional Maccari's system. Aasaraai and Mehrlatifan [41] applied this method to coupled system of equation. Ali et al. [42] derived dispersive analytical soliton solutions of some nonlinear wave's dynamical model with the help of modified F–expansion method. Darvishi et al. [43] found traveling wave solutions for the $(3+1)$-dimensional breaking soliton equation.

This article organized it as follows: in Section 2, we present beta-derivative and its properties. The descriptions of strategies are given in Section 3. In Section 4, we present a mathematical analysis of the models and its solutions via proposed methods. In Section 5, some graphical representations for some analytical solutions are presented. Some conclusions are drawn in the last section.

2. Beta-Derivative and Its Properties

Definition: suppose a function $h(x)$ that is defined $\forall$ non-negative x. Therefore, the beta-derivative of the function $h(x)$ is given as [4]:

$$D^{\beta}(h(x)) = \lim_{\varepsilon \longrightarrow 0} \frac{h\left(x + \varepsilon (x + (1/\Gamma(\beta)))^{1-\beta}\right) - h(x)}{\varepsilon}, 0 < \beta \leq 1. \quad (2)$$

Properties: assuming that a and b are real numbers, $g(x)$ and $h(x)$ are two functions $\beta-$differentiable and $\beta \in (0, 1]$, then, the following relations can be satisfied

$$i. D^{\beta}(a g(x) + b h(x)) = a D^{\beta}(g(x)) + b D^{\beta}(h(x)), \forall a, b \in R. \quad (3)$$

$$ii. D^{\beta}(g(x) h(x)) = h(x) D^{\beta}(g(x)) + g(x) D^{\beta}(h(x)). \quad (4)$$

$$iii. D^{\beta}\left(\frac{g(x)}{h(x)}\right) = \frac{h(x) D^{\beta}(g(x)) + g(x) D^{\beta}(h(x))}{(h(x))^2}. \quad (5)$$

$$iv. D^{\beta}(g(x)) = \frac{dg(x)}{dx}\left(x + \frac{1}{\Gamma(\beta)}\right)^{1-\beta}. \quad (6)$$

3. Description of Strategies

3.1. The Modified (G'/G^2)-Expansion Method. Let us consider the nonlinear PDE is in the form

$$Q(u, u_t, u_x, u_{xx}, u_{xt}, u_{tt}, \cdots) = 0, \quad (7)$$

where $u = u(x, t)$ is an unknown function, and Q is a polynomial depending on $u(x, t)$ and its various partial derivatives.

Step 1. By wave transformation

$$\eta = x - \nu t, \mathrm{u}(x, t) = U(\eta). \quad (8)$$

Here, ν is the speed of traveling wave.

The wave variable permits us to reduce Eq. (8) into a nonlinear ordinary differential equation (ODE) for $U = U(\eta)$:

$$R\left(U, U', U'', U''', \cdots\right) = 0, \quad (9)$$

where R is a polynomial of $U(\eta)$ and its total derivative with respect to η.

Step 2. Extend the solutions of Eq. (9) in the following form

$$U(\eta) = \sum_{i=0}^{m} \alpha_i \left(\frac{G'}{G^2}\right)^i, \quad (10)$$

where $\alpha_i (i = 0, 1, 2, 3, \cdots, m)$ are constants and find to be later. It is important that $\alpha_i \neq 0$. Integer m can be determined by considering the homogenous balance between the governing nonlinear terms and the highest order derivatives in Eq. (9).

The function $G = G(\eta)$ satisfies the following Riccati equation,

$$\left(\frac{G'}{G^2}\right)' = \lambda_1 \left(\frac{G'}{G^2}\right)^2 + \lambda_0, \quad (11)$$

where λ_0 and λ_1 are constants. We gain the below solutions to Eq. (11) due to different conditions of λ_0:

When $\lambda_0\lambda_1 < 0$,

$$\left(\frac{G'}{G^2}\right) = -\frac{\sqrt{|\lambda_0\lambda_1|}}{\lambda_1} + \frac{\sqrt{|\lambda_0\lambda_1|}}{2}\left[\frac{C_1 \sinh\left(\sqrt{\lambda_0\lambda_1}\eta\right) + C_2 \cosh\left(\sqrt{\lambda_0\lambda_1}\eta\right)}{C_1 \cosh\left(\sqrt{\lambda_0\lambda_1}\eta\right) + C_2 \sinh\left(\sqrt{\lambda_0\lambda_1}\eta\right)}\right]. \quad (12)$$

When $\lambda_0\lambda_1 > 0$,

$$\left(\frac{G'}{G^2}\right) = \sqrt{\frac{\lambda_0}{\lambda_1}}\left[\frac{C_1 \cos\left(\sqrt{\lambda_0\lambda_1}\eta\right) + C_2 \sin\left(\sqrt{\lambda_0\lambda_1}\eta\right)}{C_1 \sin\left(\sqrt{\lambda_0\lambda_1}\eta\right) - C_2 \sin\left(\sqrt{\lambda_0\lambda_1}\eta\right)}\right]. \quad (13)$$

When $\lambda_0 = 0$ and $\lambda_1 \neq 0$,

$$\left(\frac{G'}{G^2}\right) = -\frac{C_1}{\lambda_1(C_1\eta + C_2)}. \quad (14)$$

where C_1 and C_2 are arbitrary constant.

Step 3. By substituting Eq. (10) into Eq. (9) along with Eq. (11) and tracing all coefficients of each$\left(G'/G^2\right)^i$ to zero, then solving that algebraic equations generated in the term a_i, $\lambda_0, \lambda_1, C_1, C_2$ and other parameters.

Step 4. By substituting Eq. (10) of which α_i, ν and other parameters that are found in step 3 into Eq. (8), we get the solutions of Eq. (7).

3.2. The Modified F − Expansion Method. Here, we will describe the basic steps of F − expansion method [34].

$$U(\eta) = a_0 + \sum_{i=1}^{m} a_i F^i(\eta) + \sum_{i=1}^{m} b_i F^{-i}(\eta), \quad (15)$$

where a_0,a_i, and b_i are constants to be determined. $F(\eta)$ satisfies the Riccati equation:

$$F'(\eta) = A + BF(\eta) + CF^2(\eta), \quad (16)$$

where A,B, and C are constants to be determined. The prime denotes $d/d\eta$. Integer m can be determined by considering the homogenous balance between the governing nonlinear terms and the highest order derivatives of $U(\eta)$ in Eq. (9). Given different values of A, B, and C, the different Riccati function solution $F(\eta)$ can be obtained from Eq. (16) (see Table 1).

Step 1. Consider Eqs. (7), (8), and (9).

Step 2. Extend the solution of Eq. (9) in the following form

Step 3. Substituting Eq. (15) along with Eq. (16) into Eq. (9) and collect coefficients of $F^i(\eta)$ to zero yields a system of algebraic equations for a_i and b_i.

Step 4. Solve the system of algebraic equations, probably with the aid of Mathematica. a_i and b_i can be expressed by A, B, and C (or the coefficients of Eq. (9)). Substituting these results into (16), we can obtain the general form of traveling wave solutions to Eq. (9).

Step 5. Selecting A, B, C, and $F(\eta)$ from Table 1 and substituting them along with a_i and b_i into Eq. (15), a series of soliton-like solutions, trigonmetric function solutions, and rational solutions to Eq. (7) can be obtained.

The modified F-expansion method is more effective in obtaining the soliton-like solution, trigonometric function solutions, exponential solutions, and rational solutions of the nonlinear partial deferential equations. This method will yield more rich types solutions of the nonlinear partial deferential equations. It shows that the modified F-expansion method is more powerful in constructing exact solutions of nonlinear PDEs.

4. Application

Time-fractional Clannish Random Walker's Parabolic equation:

Let us assume the transformations:

$$u(x, t) = U(\eta), \eta = x - \frac{c}{\beta}\left(t + \frac{1}{\Gamma(\beta)}\right)^\beta, \quad (17)$$

where c is constant. By using Eq. (17) into Eq. (1), we get the following ordinary differential equation.

$$2(s - c)U + qU^2 + 2rU' = 0. \quad (18)$$

In the following subsections, the proposed methods are applied to extract the required solutions:

4.1. Solutions with the Modified (G'/G^2) − Expansion Method. By applying the homogenous balance technique

Table 1: Relations between A, B, C and corresponding $F(\eta)$ in Eq. (16) [34].

A	B	C	$F(\eta)$
0	1	-1	$1/2 + 1/2 \tanh(\eta/2)$
0	-1	1	$1/2 - 1/2 \coth(\eta/2)$
1/2	0	-1/2	$\coth(\eta) \pm \operatorname{csch}(\eta), \tanh(\eta) \pm i \operatorname{sech}(\eta)$
1	0	-1	$\tanh(\eta), \coth(\eta)$
1/2	0	½	$\sec(\eta) + \tan(\eta), \csc(\eta) - \cot(\eta)$
-1/2	0	-1/2	$\sec(\eta) - \tan(\eta), \csc(\eta) + \cot(\eta)$
1(-1)	0	1(-1)	$\tan(\eta), \cot(\eta)$
0	0	$\neq 0$	$-(1/C\eta + m)$($m$is an arbitrary constant)
Arbitrary constant	0	0	$A\eta$
Arbitrary constant	$\neq 0$	0	$(\exp(B) - A)/B$

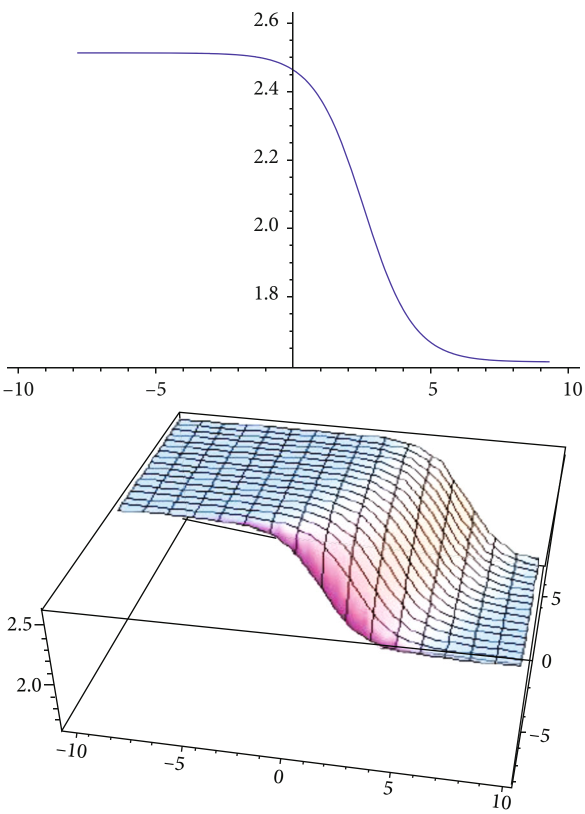

Figure 1: 2D and 3D graphics for hyperbolic traveling wave solution (21) at $\{\beta = 0.5, r = 1, q = 1, \lambda_0 = 0.5, \lambda_1 = 0.5, C_1 = 1, C_2 = 0, c = 1\}$.

between the terms U' and U^2 into Eq. (18), we get $m = 1$. For $m = 1$, Eq. (10) reduces into

$$U(\eta) = a_0 + a_1 \left(\frac{G'}{G^2} \right), \tag{19}$$

where a_0 and a_1 are unknown parameters. By using Eq. (19) along with Eq. (11) into Eq. (18) and summing up all coefficients of same order of (G'/G^2), we get the set of algebraic equations involving a_0, a_1 and other parameters. Solving the obtained set of algebraic equations with Mathematica, we reach the following results:

$$a_0 = \pm \frac{2ir\sqrt{\lambda_0}\sqrt{\lambda_1}}{q}, a_1 = \frac{-2r\lambda_1}{q}, c = s \pm 2ir\sqrt{\lambda_0}\sqrt{\lambda_1}. \tag{20}$$

Now we use the Eqs. (19) and (12)–(14) into Eq. (19) and set the below cases.

if $\lambda_0\lambda_1 < 0$, then

$$u_1(x,t) = \pm \frac{2ir\sqrt{\lambda_0\lambda_1}}{q} + \frac{2r\sqrt{|\lambda_0\lambda_1|}}{q} \left(1 - \frac{\lambda_1}{2} \left[\frac{C_1 \sinh\left(\sqrt{\lambda_0\lambda_1}\eta\right) + C_2 \cosh\left(\sqrt{\lambda_0\lambda_1}\eta\right)}{C_1 \cosh\left(\sqrt{\lambda_0\lambda_1}\eta\right) + C_2 \sinh\left(\sqrt{\lambda_0\lambda_1}\eta\right)} \right] \right). \tag{21}$$

If $\lambda_0\lambda_1 > 0$,then

$$u_2(x,t) = \pm \frac{2ir\sqrt{\lambda_0\lambda_1}}{q} - \frac{2r\lambda_1}{q} \left(\sqrt{\frac{\lambda_0}{\lambda_1}} \left[\frac{C_1 \cos\left(\sqrt{\lambda_0\lambda_1}\eta\right) + C_2 \sin\left(\sqrt{\lambda_0\lambda_1}\eta\right)}{C_1 \sin\left(\sqrt{\lambda_0\lambda_1}\eta\right) - C_2 \cos\left(\sqrt{\lambda_0\lambda_1}\eta\right)} \right] \right), \tag{22}$$

If $\lambda_0 = 0, \lambda_1 \neq 0$,then

$$u_3(x,t) = \frac{2r}{q} \left(\frac{C_1}{C_1\eta + C_2} \right). \tag{23}$$

4.2. Solutions with the Modified F – Expansion Method. By applying the homogenous balance technique between the terms U' and U^2 into Eq. (18), we get $m = 1$. For $m = 1$, Eq. (15) reduces into:

$$U(\eta) = a_0 + a_1 F + \frac{b_1}{F}, \tag{24}$$

where a_0 and a_1 are unknown parameters. By using Eq. (24) along with Eq. (16) into Eq. (18) and summing up all the coefficients of same order of F, we get the set of algebraic equations involving a_0, a_1 and other parameters. Solving the obtained set of algebraic equations with Mathematica, we reach the following results.

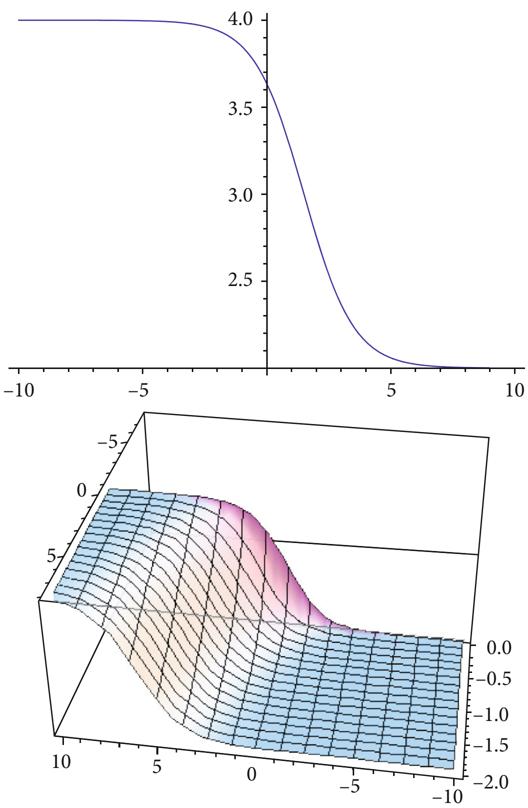

Figure 2: 2D and 3D graphics for hyperbolic traveling wave solution (26) at $\{\beta = 0.5, r = 1, q = 1, c = 1\}$.

Put Eq. (24) into Eq. (18) along with the solution of Eq. (16), we get

For $A = 0$, $B = 1$, and $C = -1$.

$$a_0 = -\frac{2r}{q}, a_1 = \frac{2r}{q}, b_1 = 0, c = s - r. \quad (25)$$

Put Eq. (25) into Eq. (24) along with the solution of Eq. (16), we get

$$u_1(x,t) = -\frac{r}{q}\left(1 - \tanh\left(\frac{\eta}{2}\right)\right). \quad (26)$$

For $A = 0$, $B = -1$, and $C = 1$.

$$a_0 = \frac{2r}{q}, a_1 = -\frac{2r}{q}, b_1 = 0, c = s + r, \quad (27)$$

$$u_2(x,t) = \frac{r}{q}\left(1 + \coth\left(\frac{\eta}{2}\right)\right). \quad (28)$$

For $A = 1/2$, $B = 0$, $C = -1/2$.

Family-I

$$a_0 = -\frac{r}{q}, a_1 = \frac{r}{q}, b_1 = 0, c = s - r, \quad (29)$$

$$u_3(x,t) = -\frac{r}{q}\left(1 - \left(\coth(\eta) + \operatorname{csch}(\eta)\right)\right). \quad (30)$$

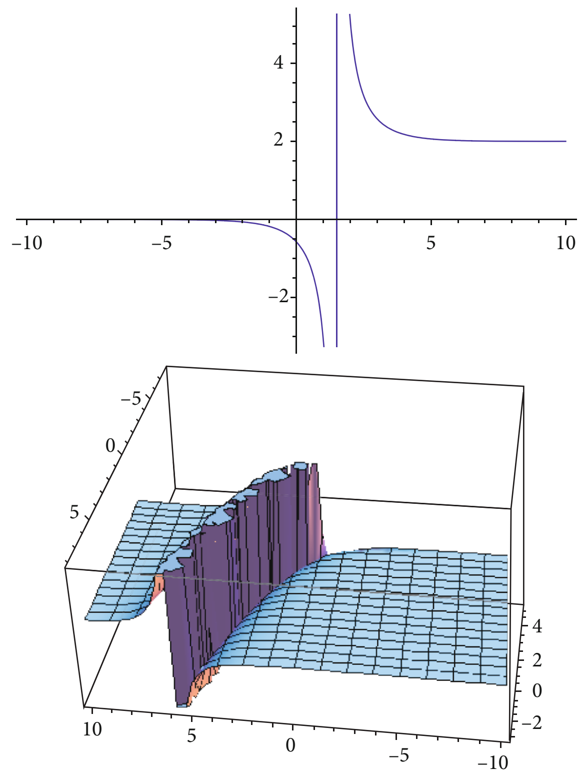

Figure 3: 2D and 3D graphics for hyperbolic traveling wave solution (28) at $\{\beta = 0.5, r = 1, q = 1, c = 1\}$.

Family-II

$$a_0 = -\frac{r}{q}, a_1 = 0, b_1 = \frac{r}{q}, c = s - r, \quad (31)$$

$$u_4(x,t) = -\frac{r}{q}\left(1 - \frac{1}{(\coth(\eta) + \operatorname{csch}(\eta))}\right). \quad (32)$$

Family-III

$$a_0 = \frac{2r}{q}, a_1 = \frac{r}{q}, b_1 = \frac{r}{q}, c = 2r + s, \quad (33)$$

$$u_5(x,t) = \frac{2r}{q}\left(2 + \left((\coth(\eta) + \operatorname{csch}(\eta)) + \frac{1}{(\coth(\eta) + \operatorname{csch}(\eta))}\right)\right). \quad (34)$$

For $A = 1$, $B = 0$, $C = -1$.

Family-I

$$a_0 = -\frac{2r}{q}, a_1 = \frac{2r}{q}, b_1 = \frac{r}{q}, c = s - 2r, \quad (35)$$

$$u_6(x,t) = -\frac{2r}{q}\left(1 - \tanh(\eta)\right). \quad (36)$$

Family-II

$$a_0 = \frac{2r}{q}, a_1 = 0, b_1 = \frac{2r}{q}, c = 2r + s, \quad (37)$$

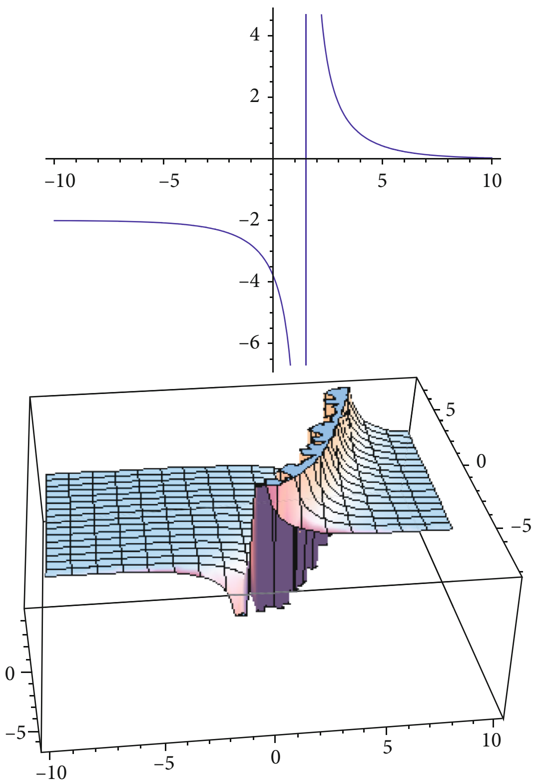

Figure 4: 2D and 3D graphics for hyperbolic traveling wave solution (30) at $\{\beta = 0.5, r = 1, q = 1, c = 1\}$.

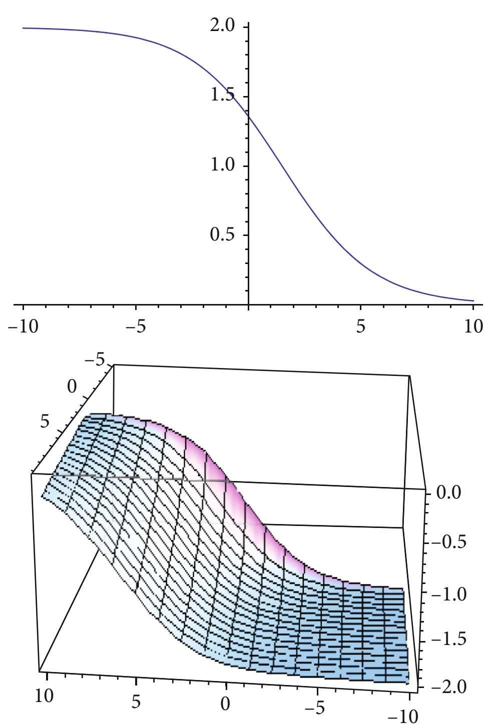

Figure 5: 2D and 3D graphics for hyperbolic traveling wave solution (32) at $\{\beta = 0.5, r = 1, q = 1, c = 1\}$.

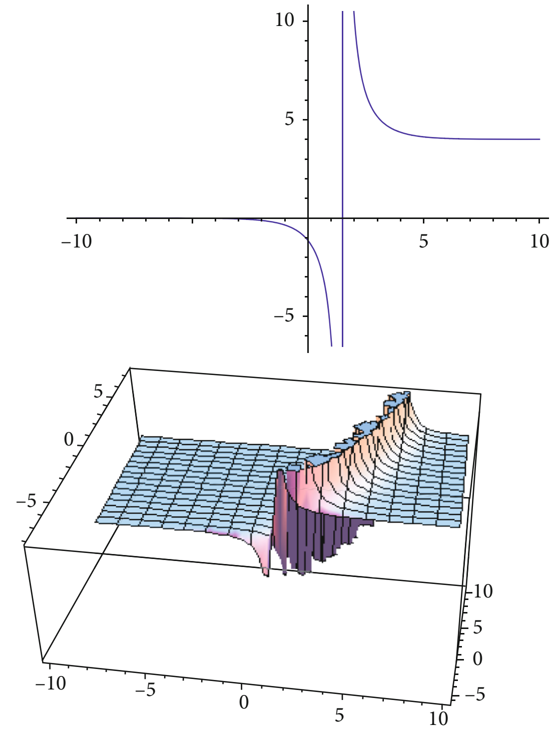

Figure 6: 2D and 3D graphics for hyperbolic traveling wave solution (34) at $\{\beta = 0.5, r = 1, q = 1, c = 1\}$.

$$u_7(x,t) = \frac{2r}{q}\left(1 + \frac{1}{\tanh(\eta)}\right). \tag{38}$$

Family-III

$$a_0 = \frac{4r}{q}, a_1 = \frac{2r}{q}, b_1 = \frac{2r}{q}, c = 4r + s, \tag{39}$$

$$u_8(x,t) = \frac{2r}{q}\left(2 + \left(\tanh(\eta) + \frac{1}{\tanh(\eta)}\right)\right). \tag{40}$$

For $A = C = 1/2$, $B = 0$.
Family-I

$$a_0 = -\frac{ir}{q}, a_1 = -\frac{r}{q}, b_1 = 0, c = s - ir, \tag{41}$$

$$u_9(x,t) = -\frac{r(\tan(\eta) + \sec(\eta))}{q} - \frac{ir}{q}, \tag{42}$$

Family-II

$$a_0 = \frac{ir}{q}, a_1 = 0, b_1 = \frac{ir}{q}, c = s + ir, \tag{43}$$

$$u_{10}(x,t) = \frac{ir}{q(\tan(\eta) + \sec(\eta))} + \frac{ir}{q}. \tag{44}$$

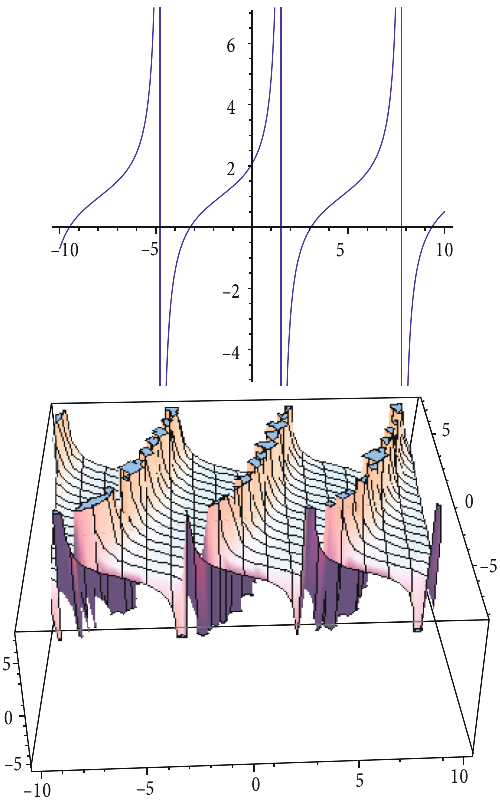

Figure 7: 2D and 3D graphics for trigonometric traveling wave solution (22) at $\{\beta = 0.5, r = 1, q = 1, \lambda_0 = 0.5, \lambda_1 = 0.5, C_1 = 0, C_2 = 1, c = 1\}$.

Family-III

$$a_0 = -\frac{2ir}{q}, a_1 = -\frac{r}{q}, b_1 = \frac{r}{q}, c = s - 2ir, \quad (45)$$

$$u_{11}(x,t) = -\frac{r((\tan(\eta) + \sec(\eta)) - (1/(\tan(\eta) + \sec(\eta))))}{q} - \frac{2ir}{q}. \quad (46)$$

For $A = C = -1/2$, $B = 0$.
Family-I

$$a_0 = \frac{ir}{q}, a_1 = \frac{r}{q}, b_1 = 0, c = s + ir, \quad (47)$$

$$u_{12}(x,t) = -\frac{r(\sec(\eta) - \tan(\eta))}{q} + \frac{ir}{q}. \quad (48)$$

Family-II

$$a_0 = \frac{ir}{q}, a_1 = 0, b_1 = -\frac{r}{q}, c = s + ir, \quad (49)$$

$$u_{13}(x,t) = -\frac{r}{q(\sec(\eta) - \tan(\eta))} + \frac{ir}{q}. \quad (50)$$

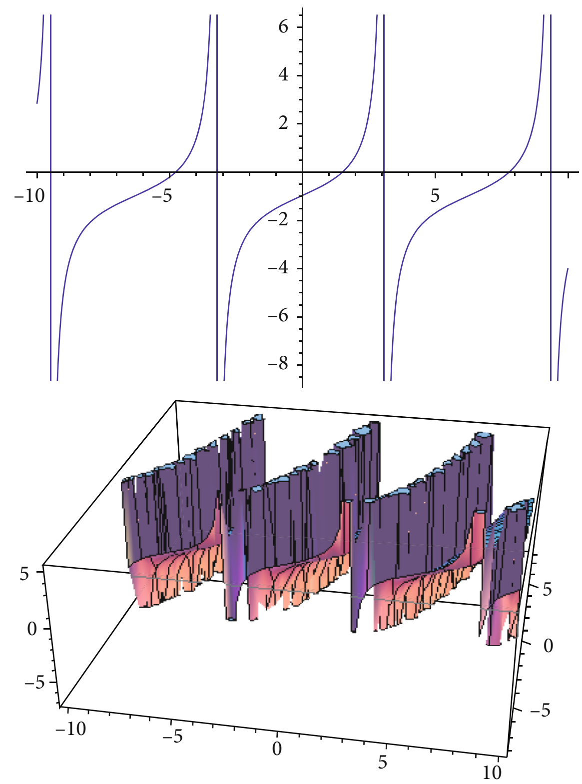

Figure 8: 2D and 3D graphics for trigonometric traveling wave solution (42) at $\{\beta = 0.5, r = 1, q = 1, c = 1\}$.

Family-III

$$a_0 = \frac{2ir}{q}, a_1 = \frac{r}{q}, b_1 = -\frac{r}{q}, c = s + 2ir, \quad (51)$$

$$u_{14}(x,t) = -\frac{r((\sec(\eta) - \tan(\eta)) + (1/(\sec(\eta) - \tan(\eta))))}{q} + \frac{2ir}{q}. \quad (52)$$

For $A = C = -1$, $B = 0$.
Family-I

$$a_0 = -\frac{2ir}{q}, a_1 = \frac{2r}{q}, b_1 = 0, c = s - 2ir, \quad (53)$$

$$u_{15}(x,t) = \frac{2r\cot(\eta)}{q} - \frac{2ir}{q}. \quad (54)$$

Family-II

$$a_0 = \frac{2ir}{q}, a_1 = 0, b_1 = -\frac{2r}{q}, c = s + 2ir, \quad (55)$$

$$u_{16}(x,t) = -\frac{2r}{q\cot(\eta)} + \frac{2ir}{q}. \quad (56)$$

Family-III

$$a_0 = \frac{4ir}{q}, a_1 = \frac{2r}{q}, b_1 = -\frac{2r}{q}, c = s + 4ir, \quad (57)$$

$$u_{17}(x,t)=\frac{2r(\cot(\eta)-(1/\cot(\eta)))}{q}+\frac{4ir}{q}. \tag{58}$$

For $A=0$, $B=0$.

$$a_0=0, a_1=-\frac{2Cr}{q}, b_1=0, c=s, \tag{59}$$

$$u_{18}(x,t)=\frac{2Cr}{q(C\eta+\varepsilon)}. \tag{60}$$

For $B=0$, $C=0$.

$$a_0=0, a_1=0, b_1=\frac{2Ar}{q}, c=s, \tag{61}$$

$$u_{19}(x,t)=\frac{2Ar}{q(A\eta)}. \tag{62}$$

For $C=0$.

$$a_0=\frac{2Br}{q}, a_1=0, b_1=\frac{2Ar}{q}, c=Br+s, \tag{63}$$

$$u_{20}(x,t)=\frac{2Ar}{q(\exp(B\eta)-A)/B}+\frac{2Br}{q}. \tag{64}$$

5. Results and Discussion

In this section, we discuss the graphical interpretation of obtained results. Two powerful analytical methods, namely, modified $(G'/G^2)-$expansion method and modified $F-$expansion method, are used to extract the trigonometric, hyperbolic, and rational wave solutions of the governing model. The physical significance of these solutions is shown by assigning particular values of free parameters. The solutions to Eqs. (22), (42), (44), (46), (48), (50), (52), (54), (56), and (58) present as trigonometric function solutions; the solutions of (21), (26), (28), (30), (32), (34), (36), (38), and (40) present as hyperbolic function solutions; and the solutions of (23), (60), (62), and (64) present as rational function solutions. We explain the dynamic performance of the hyperbolic function answers of Eqs. (21), (26), (28), (30), (32), and (34) which are illustrated in Figures 1–6. In particular, Figures 1–6 demonstrate the 3D shape and 2D graph for different values of the fractional parameter β for the trigonometric function answers of Eqs. (21), (26), (28), (30), (32), and (34). Finally, we explain the dynamic performance of the trigonometric function answers of Eqs. (22) and (34) in Figures 7 and 8, which depict the 3D shape and 2D graph for different values of the fractional parameter β for the trigonometric function answers of Eqs. (22) and (34). The implemented mathematical simulations acknowledge that the answers are of periodic wave shapes and of rational, hyperbolic, and trigonometric categorizations. Furthermore, through observing the construction of the acquired solutions, it could be understood that the parameter β of fractional derivatives has important role in the formulation of all the solutions.

6. Conclusions

In this work, we applied the modified (G'/G^2)-expansion method and modified $F-$expansion method in a satisfactory way to find the novel exact traveling wave solutions of the time-fractional CRWP equation in the sense of beta-derivative. Various obtained solutions are in the form of hyperbolic, trigonometric, and rational forms. To describe the physical phenomena of the time-fractional CRWP model, some solutions are plotted in the form of 2D and 3D by assigning the specific value to the parameters under the constrain conditions. All algebraic computations and graphical representations in this work have been provided for the obtained solutions at various parameters values with the help of Mathematica. It is essential to note that these new solutions of the time-fractional CRWP equation have not been exposed in literature by employed our two analytical modified mathematical methods. Lastly, the studied methods can be potentially applied to solve various nonlinear PDEs that are apparent in many important nonlinear scientific phenomena in physics and engineering.

Data Availability

No data were used to support this study.

Conflicts of Interest

The authors declare that they have no conflicts of interest.

Acknowledgments

The researchers would like to thank the Deanship of Scientific Research, Qassim University for funding the publication of this project.

References

[1] D. Baleanu, K. Diethelm, E. Scalas, and J. J. Trujillo, *Fractional Calculus Models and Numerical Methods. Series on Complexity, Nonlinearity and Chaos*, vol. 5pp. 1–13, World Scientific, Boston, 2nd edition, 2016.

[2] A. Atangana and J. F. Gomez-Aguilar, "Numerical approximation of Riemann-Liouville definition of fractional derivative: from Riemann-Liouville to Atangana-Baleanu," *Numerical Methods for Partial Differential Equations*, vol. 34, no. 5, pp. 1502–1523, 2017.

[3] R. Khalil, M. Al Horani, A. Yousef, and M. Sababheh, "A new definition of fractional derivative," *Journal of Computational and Applied Mathematics*, vol. 264, pp. 65–70, 2014.

[4] B. Ghanbari and J. F. Gomez-Aguilar, "The generalized exponential rational function method for Radhakrishnan-Kundu-Lakshmanan equation with β-conformable time derivative," *Revista Mexicana de Fisica*, vol. 65, no. 5, pp. 503–518, 2019.

[5] J. V. D. C. Sousa and E. C. de Oliveira, "A new truncated M-fractional derivative type unifying some fractional derivative types with classical properties," *International Journal Analysis and Applied*, vol. 16, no. 1, pp. 83–96, 2018.

[6] R. Hirota, "Exact solution of the Korteweg—de Vries equation for multiple collisions of solitons," *Physical Review Letters*, vol. 27, no. 18, pp. 1192–1194, 1971.

[7] C. Yan, "A simple transformation for nonlinear waves," *Physics Letters A*, vol. 224, no. 1-2, pp. 77–84, 1996.

[8] Z. S. Lu and H. Q. Zhang, "On a new modified extended Tanh-function method," *Communications in Theoretical Physics*, vol. 39, no. 4, p. 405, 2003.

[9] B. Ghanbari and J. F. Gómez-Aguilar, "New exact optical soliton solutions for nonlinear Schrödinger equation with second-order spatio-temporal dispersion involving M-derivative," *Modern Physics Letters B*, vol. 33, no. 20, pp. 1950235–1950239, 2019.

[10] I. Jaradat, M. Alquran, S. Qureshi, T. A. Sulaiman, and A. Yusuf, "Convex-rogue, half-kink, cusp-soliton and other bidirectional wave-solutions to the generalized Pochhammer-Chree equation," *Physica Scripta*, vol. 97, no. 5, article 055203, 2022.

[11] H. Bulut, E. N. Aksan, M. Kayhan, and T. A. Sulaıman, "New solitary wave structures to the (3 + 1) dimensional Kadomtsev–Petviashvili and Schrödinger equation," *Journal of Ocean Engineering and Science*, vol. 4, pp. 373–378, 2019.

[12] X. Miao and Z. Zhang, "The modified G'G-expansion method and traveling wave solutions of nonlinear the perturbed nonlinear Schrodinger's equation with Kerr law nonlinearity," *Communications in Nonlinear Science and Numerical Simulation*, vol. 16, no. 11, pp. 4259–4267, 2011.

[13] Z. Zhang, "The extended (G'/G)-expansion method and travelling wave solutions for the perturbed nonlinear Schrödinger's equation with Kerr law nonlinearity," *Pramana*, vol. 82, no. 6, pp. 1011–1029, 2014.

[14] I. Siddique, S. T. R. Rizvi, and F. Batool, "New exact traveling wave solutions of nonlinear evolution equations," *International Journal of Nonlinear Science*, vol. 9, no. 1, pp. 12–18, 2010.

[15] Z. Zhang, "Abundant exact traveling wave solutions for the Klein-Gordon-Zakharov equations via the tanh-coth expansion method and Jacobi elliptic function expansion method," *Romanian Journal of Physics*, vol. 58, no. 7-8, pp. 749–765, 2013.

[16] Z. Zhang, "Jacobi elliptic function expansion method for the mKdVZK and the Hirota equations," *Romanian Journal of Physics*, vol. 60, no. 9, pp. 1384–1394, 2015.

[17] Z. Zhang, "First integral method and exact solutions to nonlinear partial differential equations arising in mathematical physics," *Romanian Reports in Physics*, vol. 65, no. 4, pp. 1155–1169, 2013.

[18] N. Ullah, M. I. Asjad, J. Awrejcewicz et al., "On soliton solutions of fractional-order nonlinear model appears in physical sciences," *AIMS Mathematics*, vol. 7, no. 5, pp. 7421–7440, 2022.

[19] W. Razzaq, A. Zafar, H. M. Ahmed, and W. B. Rabied, "Construction solitons for fractional nonlinear Schrodinger equation with β-time derivative by the new sub-equation method," *Journal of Ocean Engineering and Science*, 2022.

[20] X. Z. Zhang, I. Siddique, K. B. Mehdi, A. A. Elmandouh, and M. Inc, "Novel exact solutions, bifurcation of nonlinear and supernonlinear traveling waves for M-fractional generalized reaction Duffing model and the density dependent M-fractional diffusion reaction equation," *Results in Physics*, vol. 37, article 105485, 2022.

[21] S. Arshed, "New soliton solutions to the perturbed nonlinear Schrodinger equation by $\exp(-\phi(\eta))$expansion method," *Optik*, vol. 220, article 165123, 2020.

[22] K. Hosseini, Z. Ayati, and R. Ansari, "New exact solutions of the Tzitzéica-type equations in non-linear optics using the expafunction method," *Journel of Modern Optics*, vol. 65, no. 7, pp. 847–851, 2018.

[23] I. Siddique and K. B. Mehdi, "Exact traveling wave solutions for two prolific conformable M-Fractional differential equations via three diverse approaches," *Results in Physics*, vol. 28, article 104557, 2021.

[24] I. Siddique, K. B. Mehdi, M. M. M. Jaradat et al., "Bifurcation of some new traveling wave solutions for the time-space M-fractional MEW equation via three altered methods," *Results in Physics*, vol. 41, article 105896, 2022.

[25] K. Hosseini, M. Mirzazadeh, M. Ilie, and S. Radmehr, "Dynamics of optical solitons in the perturbed Gerdjikov-Ivanov equation," *Optik*, vol. 206, article 164350, 2020.

[26] H. Bulut and T. Akturk, "An application of the modified expansion method to nonlinear partial differential equation. Proceedings of international conference on mathematics and mathematics education," *Turkish of Journal Mathematics and Computer Science*, vol. 10, pp. 202–206, 2018.

[27] A. Jhangeer, H. Almusawa, and R. U. Rahman, "Fractional derivative-based performance analysis to Caudrey-Dodd-Gibbon- Sawada-Kotera equation," *Results in Physics*, vol. 36, article 105356, 2022.

[28] A. Zafar, M. Raheel, K. K. Ali, M. Inc, and A. Qaisar, "Optical solitons to the Kundu–Mukherjee–Naskar equation in (2+1)-dimensional form via two analytical techniques," *Journal of Laser Applications*, vol. 34, no. 2, article 022024, 2022.

[29] S. W. Yao, R. Manzoor, A. Zafar, M. Inc, S. Abbagari, and A. Houwe, "Exact soliton solutions to the Cahn-Allen equation and predator-prey model with truncated M-fractional derivative," *Results in Physics*, vol. 37, article 105455, 2022.

[30] M. Raheel, A. Zafar, A. Cevikel, H. Rezazadeh, and A. Bekir, "Exact wave solutions of truncated M-fractional new Hamiltonian amplitude equation through two analytical techniques," *International Journal of Modern Physics B*, 2022.

[31] A. Sivaporn and S. Surattana, "New exact solution for the time fractional clannish random walker's parabolic equation by the improved tan (phi/2)- expansion method. AMM, Chiang Mal University," in *The 22nd Annual Meeting in Mathematics (AMM 2017)*, Department of Mathematics, Faculty of Science Chiang Mai University, Chiang Mai, Thailand, 2017.

[32] O. Guner, A. Bekir, and O. Unsal, "Two reliable methods for solving the time fractional Clannish Random Walker's Parabolic equation," *Optik*, vol. 127, no. 20, pp. 9571–9577, 2016.

[33] Y. Zhang, L. Zhang, and J. Pang, "Application of (G'/G^2) expansion method for solving Schrodinger's equation with three-order dispersion," *Advances in Applied Mathematics*, vol. 6, no. 2, article 212217, 2017.

[34] R. S. Aly and M. H. Raddadi, "Exact and solitary wave solutions of conformable time fractional clannish random walker's parabolic and Ablowitz-Kaup-Newell-Segur equations via modified methods," *Results in Physics*, vol. 26, no. 3, article 104374, 2021.

[35] N. Mahak and G. Akram, "Exact solitary wave solutions of the (1 + 1)-dimensional Fokas-Lenells equation," *Optik*, vol. 208, article 164459, 2020.

[36] H. N. Alyahdaly, "Some applications of the modified (G'/G^2) expansion method in mathematical physics," *Results in Physics*, vol. 13, article 102272, 2019.

[37] K. A. Gepreel and T. A. Nofal, "Analytical solutions for nonlinear evolutions in mathematical physics," *International Journal of Pure and Applied Mathematics*, vol. 106, no. 4, pp. 1003–1016, 2016.

[38] K. A. Gepreel, "Exact solutions for nonlinear integral member of Kadomtsev-Petviashili hierarchy differential equations using the modified (w/g) – expansion method," *Computers and Mathematics with Applications*, vol. 72, pp. 2072–2083, 2016.

[39] M. T. Darvishi, M. Najafi, and M. Najafi, "Traveling wave solutions for foam drainage equation by m*odified* F-expansion method," *Food and Public Health*, vol. 2, no. 1, pp. 6–10, 2012.

[40] A. Aasaraai, "The application of modified F-expansion method solving the Maccari's system," *British Journal of Mathematics and Computer Science*, vol. 11, no. 5, pp. 1–14, 2015.

[41] A. Aasaraai and M. B. Mehrlatifan, "Modified F -expansion method applied to coupled system of equation," *Journal of Sciences, Islamic Republic of Iran*, vol. 24, no. 4, pp. 347–354, 2013.

[42] A. Ali, A. R. Seadawy, and D. Lu, "Dispersive analytical soliton solutions of some nonlinear waves dynamical models via modified mathematical methods," *Advances in Difference Equations*, vol. 2018, no. 1, pp. 1–20, 2018.

[43] M. T. Darvishi, M. Najafi, and M. Najafi, "Traveling wave solutions for the (3+1)dimensional breaking soliton equation by (G'/G) – expansion method and modified F -expansion method," *World Academy of Science, Engineering and Technology*, vol. 5, no. 7, pp. 1100–1105, 2011.

Hindawi
Journal of Function Spaces
Volume 2022, Article ID 4422186, 19 pages
https://doi.org/10.1155/2022/4422186

Research Article

Effective Analytical Computational Technique for Conformable Time-Fractional Nonlinear Gardner Equation and Cahn-Hilliard Equations of Fourth and Sixth Order Emerging in Dispersive Media

Mohammed Al-Smadi,[1,2,3] **Shrideh Al-Omari**,[4] **Yeliz Karaca**,[5] **and Shaher Momani**[2,6]

[1]*Department of Applied Science, Ajloun College, Al-Balqa Applied University, Ajloun 26816, Jordan*
[2]*Nonlinear Dynamics Research Center (NDRC), Ajman University, Ajman 20550, UAE*
[3]*College of Commerce and Business, Lusail University, Lusail, Qatar*
[4]*Faculty of Engineering Technology, Al-Balqa Applied University, Amman 11134, Jordan*
[5]*University of Massachusetts Medical School, Worcester, MA 01655, USA*
[6]*Department of Mathematics, Faculty of Science, The University of Jordan, Amman 11942, Jordan*

Correspondence should be addressed to Shrideh Al-Omari; shridehalomari@bau.edu.jo

Received 8 July 2022; Accepted 8 September 2022; Published 23 September 2022

Academic Editor: Yusuf Gurefe

The aim of this paper is to investigate the approximate solutions of nonlinear temporal fractional models of Gardner and Cahn-Hilliard equations. The fractional models of the Gardner and Cahn-Hilliard equations play an important role in pulse propagation in dispersive media. The time-fractional derivative is observed in the conformable framework. In this orientation, a reliable computationally algorithm is designed and developed by following a residual error and multivariable power series expansion. Basically, the approximate solutions of pulse wave function of the fractional higher-order Gardner and Cahn-Hilliard equations are obtained in the form of a conformable convergent fractional series. Relevant consequences are theoretically and numerically investigated under the conformable sense. Besides, the analysis of the error and convergence of the developed technique are discussed. Some of the unidirectional homogeneous physical applications of the posed models in a finite compact regime are tested to confirm the theoretical aspects, demonstrate different evolutionary dynamics, and highlight the superiority of the novel developed algorithm compared to other existing analytical methods. For this purpose, associated graphs are displayed in two and three dimensions. Growing and decaying modes of the fractional parameters are analyzed for several α values. From a numerical viewpoint, the simulations and results declare that the proposed iterative algorithm is indeed straightforward and appropriate with efficiency for long-wavelength solutions of nonlinear partial differential equations.

1. Introduction

Nonlinear parabolic partial differential equations are superable mathematical tools for describing different evolutionary dynamics, long-wave propagation, growing and decaying modes, and phase separation of many nonlinear physical system [1–4]. Many applications of nonlinear temporal evolution and phase field models may be obtained from various engineering topics, for instance, cosmology, gravity waves, aerodynamics, blood flow, thermodynamics, incompressible, and inviscid fluid [5–9]. On the other aspect as well, the fractional partial systems play out a significance role in modeling several fascinating nonlinear physical complex systems and realizing the interactions of particles, basic physics, phase transition, and the process of dynamic that rule such systems. Indeed, they, in the recent past, have been witnessed by scientists owing to its excellent applications in different fields of sciences, including magneto-acoustic propagation in plasma, electromagnetic, chemical kinetics, control theory, quantum mechanics, dissipative systems, gas-solid flows, granular fluids, and hydrodynamics [10–18]. Nevertheless, different types of fractional operators have been moderated by Riemann-Liouville, Atangana-Baleanu, Erdelyi-Kober, Riesz-Caputo, Hadamard, Grünwald-Letnikov, and local-fractional derivatives and conformable. Although the concept of the nonlocal fractional is more acceptable because of the physical long-term features, a deficiency is there as chain, quotient, and Leibniz rules. In this point, the local fractional operators are based on natural generalization of fractional derivatives to avoid the violation of nonnormal rules, keep the local nature of the derivatives, and explore features of certain convergence [19–23].

So long, many effective techniques have been successfully developed and implemented to deal with various categories of temporal fractional nonlinear evolution equations, such as variational iteration method, differential transform method, homotopy perturbation method, reproducing kernel method, operational matrix method, and Galerkin finite element method, in addition to many traveling wave techniques, including $\tan(\phi(\xi)/2)$-expansion method, generalized Kudryashov method, tanh-coth method, and $\exp(-\phi(\epsilon))$ method [24–31]. Finding exact traveling wave, approximate and soliton solutions of higher order temporal fractional partial differential equations in nonlinear wave situations are an issue for knowing the dynamics system of dispersive waves in the phase fields. In this framework, we plan to build approximate and accurate analytical solution for a class of nonlinear homogeneous time-fractional parabolic partial differential equations of higher order equipped with appropriate initial conditions in terms of conformable sense using a novel analytical-computational algorithm. The main contribution lies in designing a superb iteration algorithm to obtain accurate approximate solutions of the posed models in the form of a rapid convergence series at a lower cost of calculations. This algorithm is free of linearization, perturbation, and any restrictive assumptions for handling dispersive and nonlinear terms. To begin with, we consider the following well-known model for the nonlinear third-order time fractional Gardner equation [13, 14]

$$\partial_t^\alpha u + 6\left(u - \lambda^2 u^2\right) u_x + u_{xxx} = 0,\ 0 < \alpha \le 1, \tag{1}$$

where λ is nontrivial constant parameter, α signifies the order of time-dependent derivatives of fractional order, and $u = u(x, t)$ is wave-profile function scaling spatio-temporal durations of $x \in [a, b]$ and $t \ge 0$. Typically, ∂_t^α represents the variance of u with time and fixed location, and the nonlinear terms uu_x and $u^2 u_x$ refer to wave steepening while the linear dispersive term u_{xxx} refers to wave effects. Therefore, it has a vital role regarding interactions of dispersion and nonlinearity in soliton theory. Hereinafter, ∂_t^α stands to the temporal conformable derivative. The aforementioned phase-field model is widely used in several practical applications, such as phase incompressible and inviscid fluids, quantum field theory, curvature flows, quantum mechanics, and gravitational field. Further, it describes a variety of nonlinear wave propagation phenomena in plasma and solid states [13].

In this investigation as well, we focus on the fourth and sixth order time-fractional Cahn-Hilliard equations [24, 25]:

$$\partial_t^\alpha u = \mu u_x + \left(-u_{xx} - u + u^3\right)_{xx}, 0 < \alpha \le 1, \tag{2}$$

and

$$\partial_t^\alpha u = \mu u u_x + \left(u_{xx} + u - u^3\right)_{xxxx}, 0 < \alpha \le 1, \tag{3}$$

where μ is constant parameter with $\mu \ne 0$. Herein, the nonlinear terms denote the chemical potential of the model, while u_{xxxx} and u_{xxxxxx} denote the dispersive wave effects of the fourth and sixth order system, respectively. This model is profitably used in multiphase incompressible fluid flows, phase ordering dynamics, tumor growth simulation, surface reconstruction, phase separation, image inpainting, spinodal decomposition, and microstructures with elastic inhomogeneity, see [24, 32] for a detailed discussion. Furthermore, the posed models (1)–(3) are involved with initial condition

$$u(x, 0) = f_0(x), x \in [a, b], \tag{4}$$

where $f_0(x)$ is a smooth analytic function of x.

Several types of nonlinear temporal fractional evolution equations have been established in the literature, but several do not assume soliton solutions [33]. Anyhow, the nonlinear time-fractional Gardner and Cahn-Hilliard models are profitably used to describe many nonlinear dispersive wave phenomena arising in nonlinear optics, capillary waves, and plasma physics [34–41]. In [34], nonlocal fourth-order fractional Cahn-Hilliard equation with advection and reaction terms has been considered in the sense of Caputo to investigate the approximate solutions using the homotopy analysis method. Using the new iterative method and q-homotopy analysis method [24], Akinyemi et al. successfully obtained analytical-approximate solutions of the nonlinear fourth and sixth order time-fractional Cahn-Hilliard equations. In [25], homotopy perturbation method has been applied to solve fourth-order Cahn-Hilliard equation with Caputo fractional derivative. Akagi et al. discussed the existence and uniqueness of weak solutions to space-fractional Cahn-Hilliard equation in a bounded domain [35]. Ran and Zhou constructed an implicit difference scheme for the fourth-order time-fractional Cahn-Hilliard equations [36]. In [37], Fourier spectral method has been implemented for time-fractional nonlinear Allen-Cahn and Cahn-Hilliard phase-field models. Prakasha et al. [13] proposed two computational methods for time-fractional Gardner equation and fourth-order Cahn-Hilliard equation in light of Caputo's concept. Arafa and Elmahdy [38] designed residual power series algorithm to solve fractional nonlinear Gardner and Cahn-Hilliard equations under Caputo sense. Hosseini et al. [39] proposed a new technique based on expansion method for finding exact solutions of time-fractional Conformable Cahn-Hilliard equation. Moreover, Jafari et al. [40] developed the fractional subequation method to construct exact-analytical solutions for fractional Cahn-Hilliard model.

By and large, no conventional approach can be found to produce analytical solutions, soliton solutions, or traveling wave solutions of closed-form for such nonlinear fractional-types dispersive PDEs. So, there have been found demand for sophisticated reliable methods to find analytical and approximate solutions to such problems. This paper formulates an iterative computational algorithm for creating analytical-approximate solutions of a class of nonlinear higher-order time-fractional parabolic partial differential equations by utilizing a novel fractional parameter, the conformable derivative. Estimation of errors for the said algorithm is derived as well. Indeed, several numerical examples have been checked in one-dimensional space to verify the great flexibility and efficiency of the novel developed algorithm, among which the third-order homogeneous time-fractional Gardner equation and fourth and sixth-order homogeneous time-fractional Cahn-Hilliard equations. For this purpose, a comparison study is performed between the presented method and other existing methods. Hereinafter, some notations and auxiliary results are retrieved. In Section 3, an analytical algorithm is expanded to solve nonlinear time-fractional parabolic partial differential equations. In Section 4, certain applications are stated to back up the theoretical concept. Further, several numerical techniques and discussions are reported. In Section 5, some concluding remarks are given.

2. Preliminaries and Principal Results

Fractional calculus has been introduced and developed an interesting tool to explain the memory and characteristics of many processes in a variety of fields of pure and applied science. In recent literature, it has been used to formulate many nonlinear partial differential equation systems and exploited to provide a comprehensive and clear explanation of dynamics, dispersion, wave propagation, and evolutionary models in view of spacetime change. In this direction, different fractional derivatives have been suggested to handle such partial equations like Feller, Riemann-Liouville, Caputo-Fabrizio, Riesz, Grünwald, Mittag-Leffler, and conformable concepts [41–44]. Consequently, the conformable operator has been modified as a natural generalization of the standard notation of derivatives [45]. In this portion, the primary concept of conformable fractional derivative and some interesting properties is highlighted. It also briefly illustrates the concept and characteristics of the residual series expansion under the conformable operator to complete the theoretical aspect of this work.

Definition 1 (see [45]). Given a real-valued function $u(t)$ on $[0,\infty)$, the conformable derivative of $u(t)$ at $\alpha \in (0,1)$ is given by

$$\partial_t^\alpha u(t) = \lim_{\varepsilon \longrightarrow 0} \frac{u\left(t+\varepsilon t^{1-\alpha}\right)-u(t)}{\varepsilon}, t>0, \quad (5)$$

where $\partial_t^\alpha u(0)$ is understood to mean $\partial_t^\alpha u(0) = \lim_{t \longrightarrow 0^+} \partial_t^\alpha u(t)$.

Definition 2 (see [46]). Given a real-valued function $u(t)$ on $[s,\infty)$, if $u(t)$ is α-differentiable; then, the α-fractional integral is given by

$$\mathcal{J}_s^\alpha u(t) = \int_s^t \frac{u(\xi)}{\xi^{1-\alpha}} d\xi, t > s \geq 0, \alpha \in (0,1], \quad (6)$$

provided that the integral is Riemann improper.

The following results are some of the basic characteristics gained in terms of $\partial_t^\alpha u(t)$. For additional properties, we refer to [47–50] and the references therein.

Lemma 3. *Let $\alpha \in (0,1]$ and the functions $v(t)$, $u(t)$ be α-differentiable at a point $t \in [0,\infty)$. Then, for all real constants a_1, a_2, a_3, a_4, the following properties hold:*

(i) $\partial_t^\alpha (e_1 v(t) + e_2 u(t)) = e_1 \partial_t^\alpha v(t) + e_2 \partial_t^\alpha u(t)$

(ii) $\partial_t^\alpha [v(t)u(t)] = v(t)\partial_t^\alpha u(t) + u(t)\partial_t^\alpha v(t)$

(iii) $\partial_t^\alpha [v(t)/u(t)] = (u(t)\partial_t^\alpha v(t) - v(t)\partial_t^\alpha u(t))/u^2(t)$, $u(t) \neq 0$

(iv) $\partial_t^\alpha (t^{a_3}) = a_3 t^{a_3-\alpha}$

(v) $\partial_t^\alpha (a_4) = 0$

(vi) *If $u(t)$ is differentiable, then it also holds that* $\partial_t^\alpha u(t) = t^{1-\alpha} du(t)/dt$

Lemma 4 (see [46]). *Given the real-valued functions $u(t)$ and $v(t)$ on $[0,\infty)$, let $\alpha \in (0,1]$, $u(t)$ be first order differentiable and α-differentiable and let $v(t)$ be first order differentiable on the range of $u(t)$. So, the use of the known chain rule yield*

$$\partial_t^\alpha (u \circ v)(t) = t^{1-\alpha} v'(t) u'(v(t)). \quad (7)$$

Definition 5 (see [47]). Given a real-valued function $u(x,t)$ on $[a,b] \times [s,\infty)$, the αth order conformable partial derivative at a point $t \in [0,\infty)$ is defined as

$$\partial_t^\alpha u(x,t) = \lim_{\varepsilon \longrightarrow 0} \frac{u\left(x, t+\varepsilon (t-s)^{1-\alpha}\right) - u(x,t)}{\varepsilon}, \alpha \in (0,1]. \quad (8)$$

Definition 6 (see [47]). Given a real-valued function $u(x,t)$ on $[a,b]\times[s,\infty)$, the αth order conformable integral is defined as

$$\mathcal{I}_s^\alpha u(x,t)=\int_s^t \frac{u(x,\xi)}{(\xi-s)^{1-\alpha}}d\xi, \alpha\in(0,1]. \tag{9}$$

Definition 7 (see [47]). The fractional series expansion at t_0 can be defined as follows

$$\sum_{i=0}^{\infty}\mathcal{C}_i(x)(t-t_0)^{i\alpha}=\mathcal{C}_0(x)+\mathcal{C}_1(x)(t-t_0)^\alpha + \mathcal{C}_2(x)(t-t_0)^{2\alpha}+\cdots, t_0>0, \tag{10}$$

where $\alpha\in(0,1]$, $\mathcal{C}_i(x)$ is the ith unknown coefficient, $t\in[t_0,t_0+\gamma^{1/\alpha})$, $\gamma>0$, and $\gamma^{1/\alpha}$ is the radius of convergence.

Theorem 8 (see [47]). *Given a real-valued function $u(x,t)$ on $[a,b]\times[t_0,t_0+r^{1/\alpha})$, let $u(x,t)$ has many conformable partial derivatives at any point $t\in[0,\infty)$ with the following fractional series expansion at t_0:*

$$u(x,t)=\sum_{i=0}^{\infty}\mathcal{C}_i(x)(t-t_0)^{i\alpha}, \alpha>0, t_0>0. \tag{11}$$

Then, $\mathcal{C}_i(x)$, $i=0,1,2,\cdots$, can be calculated by

$$\mathcal{C}_i(x)=\frac{\partial_{t_0}^{i\alpha}u(x,t_0)}{i!\alpha^i}, \tag{12}$$

in which $\partial_{t_0}^{i\alpha}u(x,t_0)$ is the ith conformable partial derivative of $u(x,t)$ about t_0 so that $\partial_{t_0}^{i\alpha}u(x,t_0)=\partial_{t_0}^{\alpha}.\partial_{t_0}^{\alpha}\cdots\partial_{t_0}^{\alpha}u(x,t_0)$ (i-times).

3. Fundamentals of Conformable Fractional Residual Series Approach

Conformable fractional residual series (CFRS) technique is a semianalytic computational algorithm specifically developed to deal with emerging partial differential equations in various nonlinear dynamical phenomena. This technique is based on extending the generalized arbitrary order Taylor series and minimizing the residual errors to detect the unknown compounds. It possesses many attractive and stimulating features and remarkable ability to deal with nonlinear terms profitably without putting any constraints or transformation of the governing models. Consequently, it has gained wide popularity and has recently become an exciting focus of research and a hot tool used in various applied and computational sciences [41–44]. In this portion, a new algorithm is developed to obtain accurate approximate solutions of the nonlinear homogeneous higher-order time-fractional parabolic partial differential equation involving initial conditions in a limited space time domain. In this context, let us see the nonlinear generalized time fractional sixth order partial differential equation as follows

$$\partial_t^\alpha u(x,t)+\mathcal{N}(u,u^2,u^3,u_x,u_{xx},u_{3x},u_{4x},u_x^2,u_{xx}^2) + u_{6x}(x,t)=0, 0<\alpha\le 1, \tag{13}$$

along with the condition

$$v(x,0)=f_0(x), \tag{14}$$

$x\in[a,b]$, $t\ge 0$, α is the order of conformable time-fractional index, $u_{ix}=\partial^i u(x,t)/\partial x^i$, $i=3,4,5,6$, $f_0(x)$ is a given analytical function, and $u(x,t)$ is an unknown sufficiently differentiable wave-profile function. Herein, $\mathcal{N}$ indicates the nonlinear operator from a Banach space $\mathcal{B}$ to itself in terms of uu_x, uu_{xx}^2, $u_x^2u_{xx}$, uu_xu_{3x}, and u^2u_{4x} over a one-dimensional spatiotemporal domain.

Based on the proposed algorithm, the solution $u(x,t)$ of (13) has following form of fractional series expansion at $t_0=0$:

$$u(x,t)=\sum_{i=0}^{\infty}\mathcal{C}_i(x)\frac{t^{i\alpha}}{i!\alpha^i}, t\ge t_0, \tag{15}$$

provided that $v(x,0)=\mathcal{C}_0(x)=f_0(x)$. So, the n-term truncated series solution $u_n(x,t)$ of $u(x,t)$ in view of the initial condition (14) can be described as

$$u_n(x,t)=\mathcal{C}_0(x)+\sum_{i=1}^{n}\mathcal{C}_i(x)\frac{t^{i\alpha}}{i!\alpha^i}. \tag{16}$$

Basically, the residual error $\mathcal{R}_s(x,t)$ of model (13) is defined as

$$\mathcal{R}_s(x,t)=\partial_t^\alpha u(x,t) + \mathcal{N}(u,u^2,u^3,u_x,u_{xx},u_{3x},u_{4x},u_x^2,u_{xx}^2) + u_{6x}(x,t), \tag{17}$$

and thus the n-term truncated residual of $\mathcal{R}_s(x,t)$ is expressed by

$$\mathcal{R}_s^n(x,t)=\partial_t^\alpha u_n(x,t)+\mathcal{N}(u_n,u_n^2,\cdots,u_{nxx}^2) + u_{n6x}(x,t), \tag{18}$$

where $u_{nkx}=\partial^k u_n(x,t)/\partial_{x^k}$, $\mathcal{R}_s(x,t)=0=\partial_t^{(n-1)\alpha}\mathcal{R}_s(x,t)$, $n=1,2,3,\cdots$, $x\in[a,b]$, $0\le t<\mathcal{T}$, $\mathcal{T}\equiv t_0+r^{1/\alpha}$, and $\partial_t^{(n-1)\alpha}\mathcal{R}_s^n(x,t)_{|t=0}\equiv 0$ for each $n=1,2,3,\cdots$.

To demonstrate the main steps of the residual series algorithm in finding out the values of unknown parameters $\mathcal{C}_i(x)$ of the n-term truncated solution (16), set $n=1$ and equate $\mathcal{R}_s^1(x,t)$ to zero at $t=0$, so that $\mathcal{C}_1(x)$ can be acquired. Thereafter, by applying the operator ∂_t^α on both

Consider the nonlinear generalized time fractional sixth order partial differential equation (13) along with the initial condition (14). Let $u(x,t)$ be a solution of model (13) and (14) that has nth order partial derivatives in conformable sense at any point $t \in [t_0, \mathcal{T})$. Then, to obtain the nth approximation, execute the underlying steps:
Step A. Expand the solution $u(x,t)$ of model (13) about $t_0 = 0$ as follows
$u(x,t) = \sum_{i=0}^{\infty} \mathscr{C}_i(x)(t^{i\alpha}/i!\alpha^i), t \geq t_0$.
Step B. Give a definition of the nth-truncated solution of $u(x,t)$ in view of the initial condition (14) as follows
$u_n(x,t) = \mathscr{C}_0(x) + \sum_{i=1}^{n} \mathscr{C}_i(x)(t^{i\alpha}/i!\alpha^i)$.
Step C. Do truncate the nth residual error of $\mathscr{R}_\jmath(x,t)$ so
$\mathscr{R}_\jmath^n(x,t) = \partial_t^\alpha u_n(x,t) + \mathcal{N}(u_n, u_n^2, \cdots, u_{nxx}^2) + u_{n6x}(x,t)$,
where $u_{nkx} = \partial^k u_n(x,t)/\partial_{x^k}$.
Step D. Invoke the series solution obtained in Step B to the nth-truncated residual error obtained in Step C as follows
$\mathscr{R}_\jmath^n(x,t) = \partial_t^\alpha(\mathscr{C}_0(x) + \sum_{i=1}^{n} \mathscr{C}_i(x)(t^{i\alpha}/i!\alpha^i)) + \mathcal{N}[(\mathscr{C}_0(x) + \sum_{i=1}^{n} \mathscr{C}_i(x)(t^{i\alpha}/i!\alpha^i)), (\mathscr{C}_0(x) + \sum_{i=1}^{n} \mathscr{C}_i(x)(t^{i\alpha}/i!\alpha^i))^2, \cdots,$
$(\mathscr{C}_0(x) + \sum_{i=1}^{n} \mathscr{C}_i(x)(t^{i\alpha}/i!\alpha^i))_{xx}^2] + (\mathscr{C}_0(x) + \sum_{i=1}^{n} \mathscr{C}_i(x)(t^{i\alpha}/i!\alpha^i))_{6x}$.
Step E. Employ $\partial_t^{(n-1)\alpha}$ for every $n = 1, 2, 3, \cdots$ to the obtained equation in Step D to get
$\partial_t^{(n-1)\alpha} \mathscr{R}_\jmath^m(x,t) = \partial_t^{n\alpha}(\mathscr{C}_0(x) + \sum_{i=1}^{n} \mathscr{C}_i(x)(t^{i\alpha}/i!\alpha^i)) + \partial_t^{(n-1)\alpha} \mathcal{N}[(\mathscr{C}_0(x) + \sum_{i=1}^{n} \mathscr{C}_i(x)(t^{i\alpha}/i!\alpha^i)),$
$(\mathscr{C}_0(x) + \sum_{i=1}^{n} \mathscr{C}_i(x)(t^{i\alpha}/i!\alpha^i))^2, \cdots, (\mathscr{C}_0(x) + \sum_{i=1}^{n} \mathscr{C}_i(x)(t^{i\alpha}/i!\alpha^i))_{xx}^2] + \partial_t^{(n-1)\alpha}(\mathscr{C}_0(x) + \sum_{i=1}^{n} \mathscr{C}_i(x)(t^{i\alpha}/i!\alpha^i))_{6x}$.
Step F. To obtain the first few terms for $\mathscr{C}_i(x)$ with the aid of $\partial_t^{(n-1)\alpha} \mathscr{R}_\jmath^n(x,0) = 0$ execute the following subroutine:
F1. In Step E, put n=1, compute $\mathscr{R}_\jmath^1(x,t)$ and find solution for $\mathscr{R}_\jmath^1(x,0) = 0$ to get $\mathscr{C}_1(x)$.
F2. Once again, in Step E, set n=2, compute $\partial_t^\alpha \mathscr{R}_\jmath^2(x,t)$ and find solution for $\partial_t^\alpha \mathscr{R}_\jmath^2(x,0) = 0$ to get $\mathscr{C}_2(x)$.
F3. Once again, n Step E, set $n = 3$, compute $\partial_t^{2\alpha} \mathscr{R}_\jmath^3(x,t)$ and find solution for $\partial_t^{2\alpha} \mathscr{R}_\jmath^3(x,0) = 0$ to get $\mathscr{C}_3(x)$.
F4. Proceed for arbitrary order *k* by setting $n = k$, computing $\partial_t^{(k-1)\alpha} \mathscr{R}_\jmath^k(x,t)$, and establishing the new equation $\partial_t^{(k-1)\alpha} \mathscr{R}_\jmath^k(x,0) = 0$ to get the *k*th coefficients $\mathscr{C}_k(x)$.
Step G. Keep the new components in an infinite series form. In fact, the closed form of the solution can be established in such way, that is, $u(x,t) = \lim_{k \longrightarrow \infty} u_k(x,t)$, if the relation of the pattern is very regular. If it was not the case, the solutions $u_k(x,t)$ can be approximately obtained. Then, Stop.

Algorithm 1

sides of the resulting relevant equation for $n = 2$, and solving $\partial_t^\alpha \mathscr{R}_\jmath^2(x,0) = 0$, the coefficient $\mathscr{C}_2(x)$ can be acquired as well. Continuing likewise, the rest of coefficients $\mathscr{C}_i(x)$ for each $i \geq 3$ of the fractional series expansion (16) can be acquired. To complete the presentation and clarification, the underlying algorithm is dedicated.

Lemma 9. *Let $u(x,t)$ be the solution of PDEs (13) and (14) that has nth order partial derivatives in conformable sense at any point $t \in [t_0, t_0 + r^{1/\alpha})$ and the fractional expansion of equation (15) at $t_0 = 0$. If there exist $\eta(x) > 0$ so that $|\partial_t^{(n+1)\alpha} u(x,\xi)| \leq \eta(x)$ for all $0 < \xi < t$, then, the remainder term holds the underlying inequality*

$$|\mathscr{P}_k(x,t)| \leq \frac{\eta(x)}{(n+1)!\alpha^{n+1}} t^{(n+1)\alpha}, \tag{19}$$

in which $\mathscr{P}_k(x,t) = \sum_{k=n+1}^{\infty} (\partial_t^{k\alpha} u(x,\xi)/\alpha^k k!) t^{k\alpha}$.

Corollary 10. *Let $u(x,t)$ and $u_n(x,t)$ be respectively the analytic and approximate solutions of PDEs (13) and (14). If there exists $\xi \in [0,1]$ so that $\|u_{n+1}(x,t)\| \leq \xi \|u_n(x,t)\|$ for each $(x,t) \in [a,b] \times [t_0, \mathcal{T})$, and $\|f_0(x)\| < \infty$ for $x \in [a,b]$. Then, $u_n(x,t)$ converges to $u(x,t)$ as soon as $n \longrightarrow \infty$.*

Proof. Since $\|u_{n+1}(x,t)\| \leq \xi \|u_n(x,t)\|$ for each $(x,t) \in [a,b] \times [t_0, \mathcal{T})$, then, $\|u_1(x,t)\| \leq \xi \|u_0(x,t)\| = \xi \|f_0(x)\|$, and then, $\|u_2(x,t)\| \leq \xi^2 \|f_0(x)\|$. Subsequently, we have $\|u_n(x,t)\| \leq \xi^n \|f_0(x)\|$. This leads to $\sum_{k=n+1}^{\infty} \|u_k(x,t)\| \leq \|f_0(x)\| \sum_{k=n+1}^{\infty} \lambda^k$. Thus, it can be observed that

$$\begin{aligned} \|u(x,t) - u_n(x,t)\| &= \left\| \sum_{k=n+1}^{\infty} u_k(x,t) \right\| \\ &\leq \sum_{k=n+1}^{\infty} \|u_k(x,t)\| \\ &\leq \sum_{k=n+1}^{\infty} \lambda^k \|f_0(x)\| \\ &= \frac{\lambda^{n+1}}{1-\lambda} \|f_0(x)\| \longrightarrow 0 \text{ for } n \longrightarrow \infty. \end{aligned} \tag{20}$$

□

4. Numerical Experiments and Discussion

Temporal fractional evolution equations are efficient approaches for modeling nonlinear waves and knowing the basic physics, phase separation properties, and evolutionary dynamics that govern these equations. The fractional Gardner and Cahn-Hilliard equations are unidirectional temporal nonlinear parabolic partial differential equations, describe nonlinear wave propagation phenomena, and phase-field separation models [13, 24]. It balances the dispersion and nonlinearity effects of the soliton dynamics. In this portion, the conformable power series algorithm in view of the residual error functions is applied to solve the homogeneous third-order time-fractional Gardner equation as well as the homogeneous fourth and sixth-order time-fractional Cahn-Hilliard equations, which are very common species of higher-order fractional temporal evolution. The simulation of such models is investigated as well. More representative results are introduced with physical interpretations for various fractional parameters to hold up the theoretical framework and produce visualization of wave function behavior. Moreover, different comparisons are produced to justify the effect of our new method. Calculations are performed by Mathematica 12.2 computing system [51].

4.1. Solution of Nonlinear Third-Order Fractional Gardner Equation. The one-dimensional nonlinear third-order fractional Gardner equation (FGE) considered in this portion can be presented in view of the conformable time derivative as follows [13, 14]:

$$\partial_t^\alpha u = -6\left(u - \lambda^2 u^2\right)u_x - u_{xxx}, 0 < \alpha \le 1, \tag{21}$$

along with the underlying initial condition

$$u(x, 0) = \frac{1}{2} + \frac{1}{2}\tanh\left(\frac{x}{2}\right), \tag{22}$$

where λ is constant, $\lambda \neq 0$, $x \in [a, b]$, $t \ge 0$, $u = u(x, t)$ is a sufficiently differentiable function representing the wave-profile scaling spatiotemporal duration of wave propagation in dispersed media. Typically, the nonlinear terms in this model refer to wave steepening, and u_{xxx} refers to wave scattering. The aforementioned equation defines an indispensable model for different nonlinear physical applications in plasma, surface tension, hydrodynamics, etc. [14]. The exact solution of the posed model when $\alpha = 1$ and $\lambda = 1$ is given by

$$u(x, t) = \frac{1}{2} + \frac{1}{2}\tanh\left(\frac{x - t}{2}\right). \tag{23}$$

According the CFRS algorithm, the fractional series solution $u(x, t)$ of the FGE (21) about $t = 0$ can be established as follows

$$u(x, t) = \sum_{i=0}^{\infty} \mathscr{C}_i(x)\frac{t^{i\alpha}}{\alpha^i i!}, \tag{24}$$

provided that $\mathscr{C}_0(x) = u(x, 0) = 1/2(1 + \tanh(x/2))$. Subsequently, the nth fractional series $u_n(x, t)$ in view of the initial condition (22) can be truncated as follows

$$u_n(x, t) = \frac{1}{2} + \frac{1}{2}\tanh\left(\frac{x}{2}\right) + \sum_{i=1}^{n} \mathscr{C}_i(x)\frac{t^{i\alpha}}{\alpha^i i!}, \tag{25}$$

and the residual error function $\mathscr{R}_s(x, t)$ can be expressed as

$$\mathscr{R}_s(x, t) = \partial_t^\alpha u + 6\left(u - \lambda^2 u^2\right)u_x + u_{xxx}, 0 < \alpha \le 1, \tag{26}$$

in which $\mathscr{R}_s(x, t) = 0 = \partial_t^{(n-1)\alpha}\mathscr{R}_s(x, t)$, $n = 1, 2, 3, \cdots$, for each $x \in [a, b]$ and $t \ge 0$.

In this direction as well, the nth truncated error $\mathscr{R}_s^n(x, t)$ of $\mathscr{R}_s(x, t)$ can be expressed as

$$\mathscr{R}_s^n(x, t) = \partial_t^\alpha u_n + 6\left(u_n - \lambda^2 u_n^2\right)u_{nx} + u_{nxxx}, \tag{27}$$

provided that $\mathscr{R}_s^n(x, t) \longrightarrow \mathscr{R}_s(x, t)$ as $n \longrightarrow \infty$, and $\partial_t^{(n-1)\alpha}\mathscr{R}_s^n(x, t)_{|t=0} \equiv 0$ for each $n = 1, 2, 3, \cdots$.

By viewing the representation of the truncated series (25) and minimizing the residual error (27) of the governing equation, the unknown coefficients $\mathscr{C}_i(x)$ can be computed for each value of $i = 1, 2, \cdots, n$ in order to obtain the nth approximate solution $u_n(x, t)$. To begin with, the first fractional series solution at $n = 1$ assumes the form

$$u_1(x, t) = \frac{1}{2} + \frac{1}{2}\tanh\left(\frac{x}{2}\right) + \frac{1}{\alpha}\mathscr{C}_1(x)t^\alpha, \tag{28}$$

as well as the first residual function assumes the form

$$\mathscr{R}_s^1(x, t) = \partial_t^\alpha u_1 + 6\left(u_1 - \lambda^2 u_1^2\right)u_{1x} + u_{1xxx}. \tag{29}$$

Consequently, putting $u_1(x, t)$ into $\mathscr{R}_s^1(x, t)$ to get

$$\begin{aligned} \mathscr{R}_s^1(x, t) = {} & \mathscr{C}_1(x) + \frac{6}{\alpha^3}\left(\alpha\mathscr{C}_0(x) + \mathscr{C}_1(x)t^\alpha\right) \\ & \cdot \left(\alpha\mathscr{C}_0'(x) + \mathscr{C}_1'(x)t^\alpha\right) \\ & \cdot \left(\alpha - \lambda^2\left(\alpha\mathscr{C}_0(x) + \mathscr{C}_1(x)t^\alpha\right)\right) \\ & + \frac{1}{\alpha}\left(\alpha\mathscr{C}_0^{(3)}(x) + \mathscr{C}_1^{(3)}(x)t^\alpha\right). \end{aligned} \tag{30}$$

Herein, with the aid of $\mathscr{R}_s^1(x, t)_{|t=0} = 0$, it yields

$$\mathscr{C}_1(x) + 6\mathscr{C}_0(x)\left(1 - \lambda^2\mathscr{C}_0(x)\right)\mathscr{C}_0'(x) + \mathscr{C}_0^{(3)}(x) = 0, \tag{31}$$

which implies

$$\begin{aligned} \mathscr{C}_1(x) = {} & -\frac{1}{8}\left(1 + \left(4 - 3\lambda^2\right)\cosh(x) + 3\left(1 - \lambda^2\right)\sinh(x)\right) \\ & \cdot \operatorname{sech}^4\left(\frac{x}{2}\right). \end{aligned} \tag{32}$$

Hence, the first series solution $u_1(x,t)$ can be read as

$$u_1(x,t)=\frac{1}{2}+\frac{1}{2}\tanh\left(\frac{x}{2}\right)-\frac{1}{8\alpha}\left(1+\left(4-3\lambda^2\right)\cosh(x)+3\left(1-\lambda^2\right)\sinh(x)\right)\cdot\operatorname{sech}^4\left(\frac{x}{2}\right)t^{\alpha}. \tag{33}$$

Sequentially, the second truncated series $u_2(x,t)$ can be computed for $n=2$ in (27) such that

$$\mathscr{R}_{\jmath}^2(x,t)=\partial_t^{\alpha}u_2+6\left(u_2-\lambda^2u_2^2\right)u_{2x}+u_{2xxx}, \tag{34}$$

where $u_2(x,t)=u_1(x,t)+(1/2\alpha^2)\mathscr{C}_2(x)t^{2\alpha}$. By employing the conformable operator ∂_t^{α} on both sides of equation (34), we get that

$$\partial_t^{\alpha}\mathscr{R}_{\jmath}^2(x,t)=\mathscr{C}_2(x)+6\partial_t^{\alpha}\left(u_2-\lambda^2u_2^2\right)u_{2x}+\frac{1}{\alpha}\left(\mathscr{C}_1^{(3)}(x)+\mathscr{C}_2^{(3)}(x)t^{\alpha}\right). \tag{35}$$

Consequently, solving the term $\partial_t^{\alpha}\mathscr{R}_{\jmath}^2(x,t)_{|t=0}=0$ in the aforementioned equation with the help of Mathematica's symbolic architecture [51] leads to

$$\begin{aligned}\mathscr{C}_2(x)=&-\frac{1}{64}\operatorname{sech}^7\left(\frac{x}{2}\right)\left(24\left(1-\lambda^2\right)\cosh\left(\frac{x}{2}\right)\right.\\&-6\left(22-37\lambda^2+15\lambda^4\right)\cosh\left(\frac{3x}{2}\right)\\&+\left(24-42\lambda^2+18\lambda^4\right)\cosh\left(\frac{5x}{2}\right)\\&+\left(206-204\lambda^2\right)\sinh\left(\frac{x}{2}\right)\\&-\left(129-222\lambda^2+90\lambda^4\right)\sinh\left(\frac{3x}{2}\right)\\&\left.+\left(25-42\lambda^2+18\lambda^4\right)\sinh\left(\frac{5x}{2}\right)\right).\end{aligned} \tag{36}$$

Hence, the solution $u_2(x,t)$ can be given as

$$\begin{aligned}u_2(x,t)=&\frac{1}{2}+\frac{1}{2}\tanh\left(\frac{x}{2}\right)-\frac{1}{8\alpha}\left(1+\left(4-3\lambda^2\right)\cosh(x)\right.\\&\left.+3\left(1-\lambda^2\right)\sinh(x)\right)\operatorname{sech}^4\left(\frac{x}{2}\right)t^{\alpha}\\&-\frac{1}{128\alpha^2}\operatorname{sech}^7\left(\frac{x}{2}\right)\left(24\left(1-\lambda^2\right)\cosh\left(\frac{x}{2}\right)\right.\\&-6\left(22-37\lambda^2+15\lambda^4\right)\cosh\left(\frac{3x}{2}\right)\\&+\left(24-42\lambda^2+18\lambda^4\right)\cosh\left(\frac{5x}{2}\right)\\&+\left(206-204\lambda^2\right)\sinh\left(\frac{x}{2}\right)\\&-\left(129-222\lambda^2+90\lambda^4\right)\sinh\left(\frac{3x}{2}\right)\\&\left.+\left(25-42\lambda^2+18\lambda^4\right)\sinh\left(\frac{5x}{2}\right)\right)t^{2\alpha}.\end{aligned} \tag{37}$$

Continuing in this manner, the truncated series $u_3(x,t)$ of the series expansion (25) may be computed by applying $n=3$ in (27), allowing $\partial_t^{2\alpha}$ to act on both sides of the new relevant equation then establishing $\partial^{2\alpha}\mathscr{R}_{\jmath}^3(x,t)/\partial t^2{}_{|t=0}=0$ with the aid of Mathematica. To finish our process, we can assume that $u_2(x,t)$ is our approximate solution of the FGE (21) along with condition (22). Moreover, the values of $\mathscr{C}_n(x)$ for each $n\geq 3$ may be counted likewise. In what follows, the achieved n terms in the form of an infinite series leads to the solution $u(x,t)$ of the FGEs (21)–(22). Especially, the solution of FGEs (21) and (22) at $\alpha=1$ and $\lambda=1$ can be written in the form

$$\begin{aligned}u(x,t)=&\frac{1}{2}+\frac{1}{2}\tanh\left(\frac{x}{2}\right)-\frac{1}{4}\operatorname{sech}^2\left(\frac{x}{2}\right)t\\&-\operatorname{csch}^3(x)\sinh^4\left(\frac{x}{2}\right)t^2\\&+\frac{1}{48}(2-\cosh(x))\operatorname{sech}^4\left(\frac{x}{2}\right)t^3\\&-\frac{1}{384}\left(\sinh\left(\frac{3x}{2}\right)-11\sinh\left(\frac{x}{2}\right)\right)\\&\cdot\operatorname{sech}^5\left(\frac{x}{2}\right)t^4+\cdots,\end{aligned} \tag{38}$$

which agrees with the analytical solution acquired by q-homotopy analysis transform method (q-HATM), fractional natural decomposition method (FNDM) [13], and q -homotopy analysis method (q-HAM) [14], so that

$$u(x,t)=\frac{1}{2}+\frac{1}{2}\tanh\left(\frac{x-t}{2}\right). \tag{39}$$

In what follows, some graphic representations achieved by the presented algorithm for FGEs (21) and (22) are displayed in Figures 1 and 2. At lease three-dimensional surface plots of the exact solution whereas the fourth approximate solution are depicted in Figure 1 for diverse values of α with $\lambda=1$ over a large enough spatio temporal domain $[-20,20]\times[0,3]$. In Figure 2, the moving and evolutionary dynamics of fractional wave function of FGEs (21) and (22) are provided in 2D graph over $[-10,10]$ versus t at $\lambda=1$ based on different values of α that are given as $\alpha=1$, 0.75, 0.5, and 0.25, respectively. From these graphs, it can be observed the tremendous influence of the fractional parameters α on the solutions' consistency with respect to the time t. By measuring the absolute error $|u-u_3|$, the achieved numerical solutions of FGEs (21) and (22) are given in Table 1 for distinct values of x and fixed $t=0.2$ when $\alpha=1$ and $\lambda=1$ and compared with absolute errors obtained in [13] as well. The efficiency of our method is straightforward from these

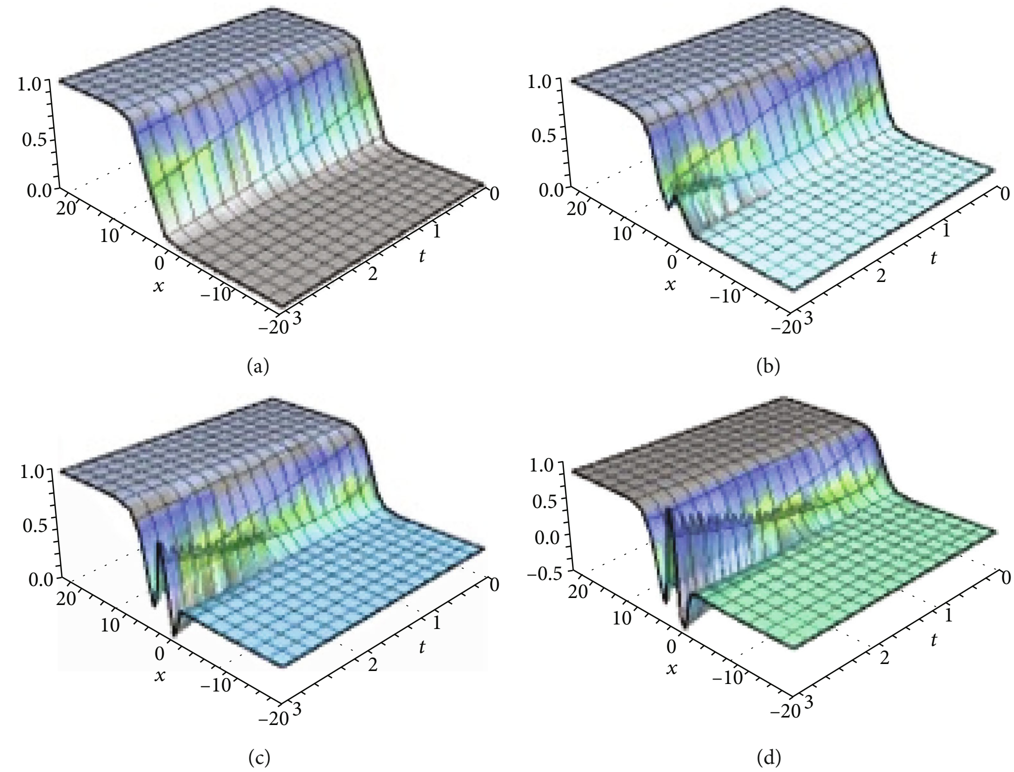

FIGURE 1: Surface wave behavior of $u_4(x,t)$ of FGEs (21) and (22) with $\lambda = 1$ for diverse α: (a) exact, (b) $\alpha = 0.75$, (c) $\alpha = 0.5$, and (d) $\alpha = 0.25$.

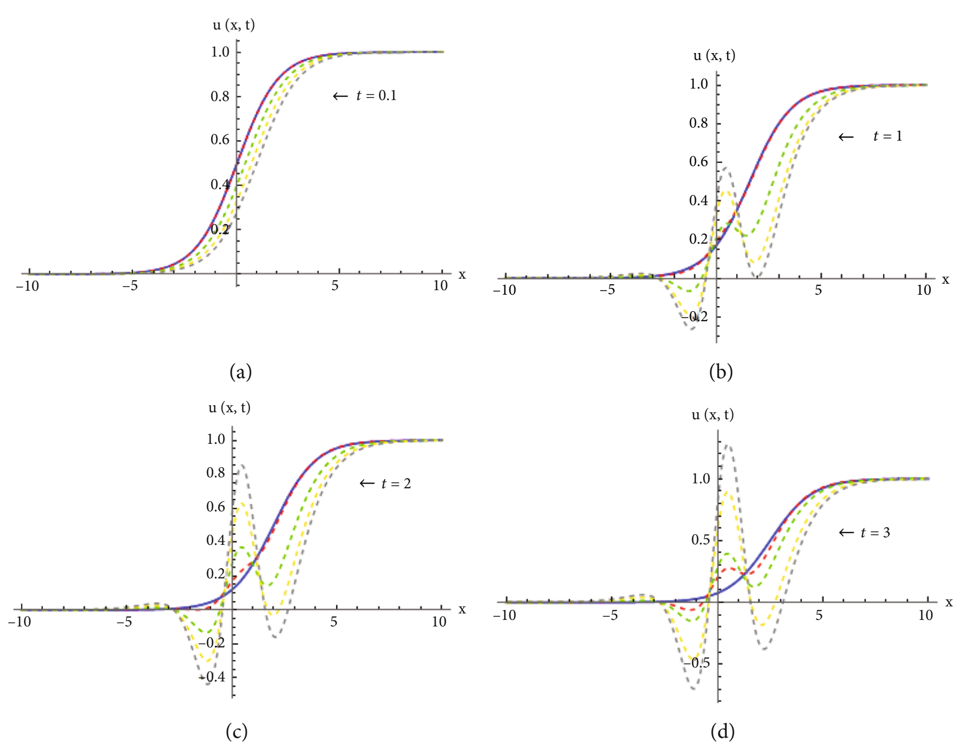

FIGURE 2: Elevation of wave surface of $u_4(x,t)$ of FGEs (21) and (22) with $\lambda = 1$ and fixed t for various values of α, in which exact blue, $\alpha = 1$ red, $\alpha = 0.75$ green, $\alpha = 0.5$ yellow, and $\alpha = 0.25$ gray.

Table 1: Comparison of numerical outcomes for FGEs (21) and (22) with = 0.2,$\alpha = 1$, and $\lambda = 1$.

x_i	$u(x,t)$	$u_3(x,t)$	$\lvert u-u_3\rvert$	$\lvert u-u_3\rvert\lvert u\rvert^{-1}$	FNDM [13]	q-HATM [13]
0.1	0.475021	0.475020	9.95627×10^{-7}	2.09596×10^{-6}	9.95627×10^{-7}	9.95627×10^{-7}
0.2	0.500000	0.499997	2.61331×10^{-6}	5.22661×10^{-6}	2.61331×10^{-6}	2.61331×10^{-6}
0.3	0.524979	0.524975	4.12217×10^{-6}	7.85207×10^{-6}	4.12217×10^{-6}	4.12217×10^{-6}
0.4	0.549834	0.549829	5.46303×10^{-6}	9.93579×10^{-6}	5.46303×10^{-6}	5.46303×10^{-6}
0.5	0.574443	0.574436	6.58827×10^{-6}	1.14690×10^{-5}	6.58827×10^{-6}	6.58827×10^{-6}

Table 2: Absolute errors $\lvert u-u_3\rvert$ for different values of fractional order α at $t=0.2,\lambda=1$ of FGEs (21) and (22).

x_i	$\alpha = 1$	$\alpha = 0.95$	$\alpha = 0.75$	$\alpha = 0.5$	$\alpha = 0.25$
0.1	9.95627×10^{-7}	1.33546×10^{-6}	3.56984×10^{-6}	8.10067×10^{-6}	2.05633×10^{-5}
0.2	2.61331×10^{-6}	3.01435×10^{-6}	5.77678×10^{-6}	3.93725×10^{-5}	1.30242×10^{-4}
0.3	4.12217×10^{-6}	5.86542×10^{-6}	2.67443×10^{-5}	3.11823×10^{-5}	1.65983×10^{-4}
0.4	5.46303×10^{-6}	6.13259×10^{-6}	3.87654×10^{-5}	1.92139×10^{-4}	3.65432×10^{-4}
0.5	6.58827×10^{-6}	8.43010×10^{-6}	1.65438×10^{-5}	1.00045×10^{-4}	3.76543×10^{-4}

results. Moreover, Table 2 provides the absolute errors between the exact solutions and the third approximate solutions of FGEs (21) and(22) for different values of fractional order α such as $\alpha=\{1, 0.95, 0.75, 0.5, 0.25\}$ at $t=0.2$ and $\lambda=1$. These results show good agreement between the solutions when the fractional values differ.

4.2. Solution of Nonlinear Fourth-Order Time-Fractional Cahn-Hilliard Equation. The one-dimensional nonlinear fourth-order fractional Cahn-Hilliard (FCH4) equation considered in this portion can be presented in terms of the conformable time derivative as follows [24, 25]:

$$\partial_t^\alpha u = \mu u_x + 6uu_x^2 + \left(3u^2-1\right)u_{xx} - u_{xxxx}, 0<\alpha\le 1, \tag{40}$$

along with the underlying initial condition

$$u(x,0) = \tanh\left(\frac{x}{\sqrt{2}}\right), \tag{41}$$

where μ is aconstant, $\mu \ne 0$, $x\in[a,b]$, $t\ge 0$, $u=u(x,t)$ is sufficiently differentiable function representing the wave-profile scaling spatiotemporal duration of wave propagation in dispersed media. Herein, the nonlinear terms in this model refer to chemical potential dynamics, and u_{xxxx} refers to wave scattering. This equation has various applications in topology optimization, surface reconstruction, phase separation, phase ordering dynamics, magneto-acoustic propagation in plasma, multiphase incompressible fluid flows, image inpainting, and so forth [25, 32]. The exact solution of the posed model when $\alpha=1$ and $\mu=1$ is given by

$$u(x,t) = \tanh\left(\frac{x+t}{\sqrt{2}}\right). \tag{42}$$

By performing the CFRS algorithm, the fractional series solution $u(x,t)$ of the FCH4 equation (40) about $t=0$ can be constructed as follows

$$u(x,t) = \sum_{i=0}^{\infty} \mathscr{C}_i(x)\frac{t^{i\alpha}}{\alpha^i i!}, \tag{43}$$

provided that $\mathscr{C}_0(x)=u(x,0)=\tanh\left(x/\sqrt{2}\right)$. Subsequently, the nth fractional series $u_n(x,t)$ in view of the initial condition (41) can be truncated by

$$u_n(x,t) = \tanh\left(\frac{x}{\sqrt{2}}\right) + \sum_{i=1}^{n} \mathscr{C}_i(x)\frac{t^{i\alpha}}{\alpha^i i!}, \tag{44}$$

and the error function $\mathscr{R}_s(x,t)$ can be expressed as

$$\begin{aligned}\mathscr{R}_s(x,t) = \partial_t^\alpha u - \mu u_x - 6uu_x^2 - \left(3u^2-1\right)u_{xx}\\ + u_{xxxx}, 0<\alpha\le 1,\end{aligned} \tag{45}$$

in which $\mathscr{R}_s(x,t)=0=\partial_t^{(n-1)\alpha}\mathscr{R}_s(x,t)$, $n=1,2,3,\cdots$, for each $x\in[a,b]$ and $t\ge 0$.

In this orientation as well, the nth truncated error $\mathscr{R}_s^n(x,t)$ of $\mathscr{R}_s(x,t)$ can be expressed as

$$\begin{aligned}\mathscr{R}_s^n(x,t) = \partial_t^\alpha u_n - \mu u_{nx} - 6u_n u_{nx}^2\\ - \left(3u_n^2-1\right)u_{nxx} + u_{nxxxx},\end{aligned} \tag{46}$$

provided that $\mathscr{R}_s^n(x,t)\longrightarrow\mathscr{R}_s(x,t)$ as $n\longrightarrow\infty$, and $\partial_t^{(n-1)\alpha}\mathscr{R}_s^n(x,t)_{|t=0}\equiv 0$ for each $n=1,2,3,\cdots$.

By viewing the representation of the truncated series (44) and minimizing the residual error (46) of the governing equation, the unknown coefficients $\mathscr{C}_i(x)$ can be computed for each value of $i=1,2,\cdots,n$ in order to obtain the nth approximate solution $u_n(x,t)$. To begin with, the first fractional series solution at $n=1$ has the form

$$u_1(x,t)=\tanh\left(\frac{x}{\sqrt{2}}\right)+\frac{1}{\alpha}\mathscr{C}_1(x)t^{\alpha}, \tag{47}$$

as well as the first residual function has the form

$$\begin{aligned}\mathscr{R}_{\jmath}^1(x,t)=\partial_t^{\alpha}u_1-\mu u_{1x}-6u_1u_{1x}^2\\ -\left(3u_1^2-1\right)u_{1xx}+u_{1xxxx}.\end{aligned} \tag{48}$$

Consequently, putting $u_1(x,t)$ into $\mathscr{R}_{\jmath}^1(x,t)$ to get

$$\begin{aligned}\mathscr{R}_{\jmath}^1(x,t)=\mathscr{C}_1(x)-\mu\left(\mathscr{C}_0'(x)+\mathscr{C}_1'(x)\frac{t^{\alpha}}{\alpha}\right)\\ -\frac{3(\alpha\mathscr{C}_0(x)+\mathscr{C}_1(x)t^{\alpha})}{\alpha^3}\\ \cdot\left(2\left(\alpha\mathscr{C}_0'(x)+\mathscr{C}_1'(x)t^{\alpha}\right)^2\right.\\ \left.+(\alpha\mathscr{C}_0(x)+\mathscr{C}_1(x)t^{\alpha})\left(\alpha\mathscr{C}_0''(x)+\mathscr{C}_1''(x)t^{\alpha}\right)\right)\\ +\mathscr{C}_0''(x)+\mathscr{C}_1''(x)\frac{t^{\alpha}}{\alpha}+\left(\mathscr{C}_0^{(4)}(x)+\mathscr{C}_1^{(4)}(x)\frac{t^{\alpha}}{\alpha}\right).\end{aligned} \tag{49}$$

Hence, by using $\mathscr{R}_{\jmath}^1(x,t)_{|t=0}=0$, it yields

$$\begin{aligned}\mathscr{C}_1(x)-\mu\mathscr{C}_0'(x)-6\mathscr{C}_0(x)\mathscr{C}_0'(x)^2+\mathscr{C}_0''(x)\\ -3\mathscr{C}_0''(x)\mathscr{C}_0(x)^2+\mathscr{C}_0^{(4)}(x)=0,\end{aligned} \tag{50}$$

which yields

$$\mathscr{C}_1(x)=\frac{\mu}{\sqrt{2}}\operatorname{sech}^2\left(\frac{x}{\sqrt{2}}\right). \tag{51}$$

Hence, the solution $u_1(x,t)$ is obtained as

$$u_1(x,t)=\tanh\left(\frac{x}{\sqrt{2}}\right)+\frac{\mu}{\sqrt{2}\alpha}\operatorname{sech}^2\left(\frac{x}{\sqrt{2}}\right)t^{\alpha}. \tag{52}$$

Sequentially, we can compute the series $u_2(x,t)$ by assuming $n=2$ in the nth truncated error (46) such that

$$\begin{aligned}\mathscr{R}_{\jmath}^2(x,t)=\partial_t^{\alpha}u_2-\mu u_{2x}-6u_2u_{2x}^2\\ -\left(3u_2^2-1\right)u_{2xx}+u_{2xxxx},\end{aligned} \tag{53}$$

where $u_2(x,t)=\tanh(x/\sqrt{2})+(\mu/\sqrt{2}\alpha)\operatorname{sech}^2(x/\sqrt{2})t^{\alpha}+(1/2\alpha^2)\mathscr{C}_2(x)t^{2\alpha}$. Then, by employing the conformable differential operator ∂_t^{α} on both sides of equation (53), we get that

$$\begin{aligned}\partial_t^{\alpha}\mathscr{R}_{\jmath}^2(x,t)=\mathscr{C}_2(x)-\mu\mathscr{C}_1'(x)-\mu\mathscr{C}_2'(x)\frac{t^{\alpha}}{\alpha}\\ -\partial_t^{\alpha}\left(6u_2u_{2x}^2+\left(3u_2^2-1\right)u_{2xx}\right)\\ +\mathscr{C}_1''(x)+\mathscr{C}_2''(x)\frac{t^{\alpha}}{\alpha}+\mathscr{C}_1^{(4)}(x)+\mathscr{C}_2^{(4)}(x)\frac{t^{\alpha}}{\alpha}.\end{aligned} \tag{54}$$

Now, solving the term $\partial_t^{\alpha}\mathscr{R}_{\jmath}^2(x,t)_{|t=0}=0$ in the above equation with the help of Mathematica's symbolic architecture [51] leads to

$$\mathscr{C}_2(x)=-\mu^2\tanh\left(\frac{x}{\sqrt{2}}\right)\operatorname{sech}^2\left(\frac{x}{\sqrt{2}}\right). \tag{55}$$

Hence, the solution $u_2(x,t)$ can be given by

$$\begin{aligned}u_2(x,t)=\tanh\left(\frac{x}{\sqrt{2}}\right)+\frac{\mu}{\sqrt{2}\alpha}\operatorname{sech}^2\left(\frac{x}{\sqrt{2}}\right)t^{\alpha}\\ -\mu^2\tanh\left(\frac{x}{\sqrt{2}}\right)\operatorname{sech}^2\left(\frac{x}{\sqrt{2}}\right)\frac{t^{2\alpha}}{2\alpha^2}.\end{aligned} \tag{56}$$

Similarly, the truncated series $u_3(x,t)$ of the series expansion (44) can be calculate by assuming $n=3$ in (46), then, by solving the term $\partial^{2\alpha}\mathscr{R}_{\jmath}^3(x,t)/\partial t^2{}_{|t=0}=0$ with the aid of Mathematica's symbolic architecture [51], we get

$$\mathscr{C}_3(x)=\frac{\mu^3}{\sqrt{2}}\left(\operatorname{Cosh}\left(\sqrt{2}x\right)-2\right)\operatorname{sech}^4\left(\frac{x}{\sqrt{2}}\right), \tag{57}$$

which reveals that $u_3(x,t)$ has the form

$$\begin{aligned}u_3(x,t)=\tanh\left(\frac{x}{\sqrt{2}}\right)+\frac{\mu}{\sqrt{2}\alpha}\operatorname{sech}^2\left(\frac{x}{\sqrt{2}}\right)t^{\alpha}\\ -\frac{\mu^2}{2\alpha^2}\tanh\left(\frac{x}{\sqrt{2}}\right)\operatorname{sech}^2\left(\frac{x}{\sqrt{2}}\right)t^{2\alpha}\\ +\frac{\mu^3}{6\sqrt{2}\alpha^3}\left(\operatorname{Cosh}\left(\sqrt{2}x\right)-2\right)\operatorname{sech}^4\left(\frac{x}{\sqrt{2}}\right)t^{3\alpha}.\end{aligned} \tag{58}$$

Proceeding likewise, the solution $u_4(x,t)$ will have the form

$$\begin{aligned}u_4(x,t)=\tanh\left(\frac{x}{\sqrt{2}}\right)+\frac{\mu}{\sqrt{2}\alpha}\operatorname{sech}^2\left(\frac{x}{\sqrt{2}}\right)t^{\alpha}\\ -\frac{\mu^2}{2\alpha^2}\tanh\left(\frac{x}{\sqrt{2}}\right)\operatorname{sech}^2\left(\frac{x}{\sqrt{2}}\right)t^{2\alpha}\\ +\frac{\mu^3}{6\sqrt{2}\alpha^3}\left(\operatorname{Cosh}\left(\sqrt{2}x\right)-2\right)\operatorname{sech}^4\left(\frac{x}{\sqrt{2}}\right)t^{3\alpha}\\ -\frac{\mu^4}{48\alpha^4}\left(\sinh\left(\frac{3x}{\sqrt{2}}\right)-11\sinh\left(\frac{x}{\sqrt{2}}\right)\right)\operatorname{sech}^5\left(\frac{x}{\sqrt{2}}\right)t^{4\alpha}.\end{aligned} \tag{59}$$

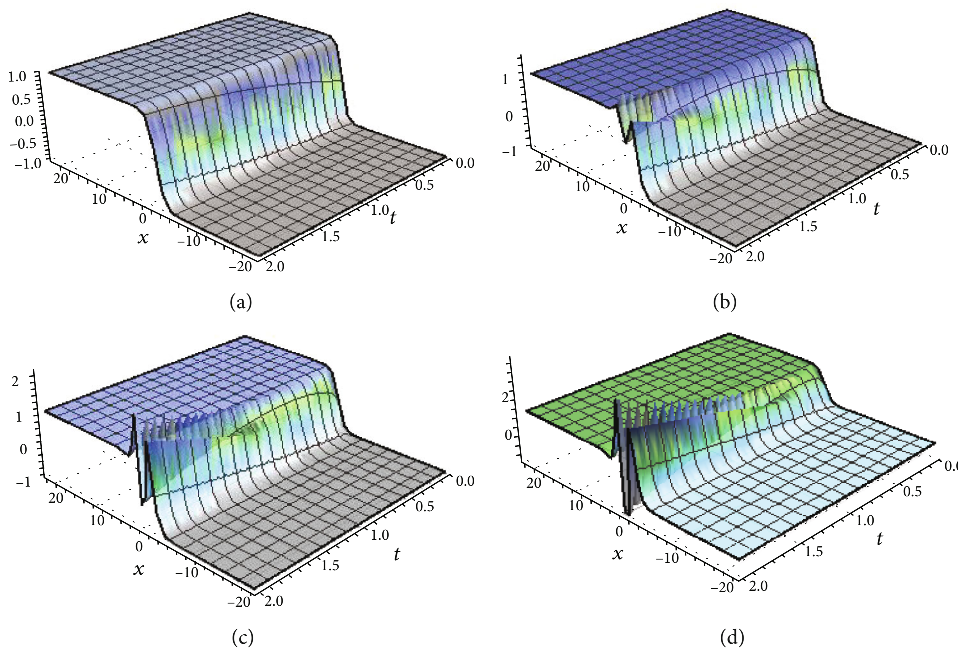

Figure 3: Surface wave behavior of $u_4(x,t)$ of the FCH4 model (40) and (41) with $\mu=1$ for diverse α: (a) exact, (b) $\alpha=0.75$, (c) $\alpha=0.5$, and (d) $\alpha=0.25$.

To close this method, it is assumed that $u_4(x,t)$ is an approximate solution, and $\mathscr{C}_n(x)$, $n\geq 5$ can be followed likewise. Later, by gathering the terms, $u(x,t)$ of the posed model (40) and (41) may be predicted. In particular, the solution of FCH4 equation (40) and (41) at $\alpha=1$ and $\mu=1$ can be written in the form

$$\begin{aligned} u(x,t) &= \tanh\left(\frac{x}{\sqrt{2}}\right)+\frac{1}{\sqrt{2}}\operatorname{sech}^2\left(\frac{x}{\sqrt{2}}\right)t \\ &\quad -\frac{1}{2}\tanh\left(\frac{x}{\sqrt{2}}\right)\operatorname{sech}^2\left(\frac{x}{\sqrt{2}}\right)t^2 \\ &\quad +\frac{1}{6\sqrt{2}}\left(\operatorname{Cosh}\left(\sqrt{2}x\right)-2\right)\operatorname{sech}^4\left(\frac{x}{\sqrt{2}}\right)t^3 \\ &\quad -\frac{1}{48}\left(\sinh\left(\frac{3x}{\sqrt{2}}\right)-11\sinh\left(\frac{x}{\sqrt{2}}\right)\right) \\ &\quad \cdot \operatorname{sech}^5\left(\frac{x}{\sqrt{2}}\right)t^4+\cdots, \end{aligned} \tag{60}$$

which agrees with the analytical solution acquired by homotopy perturbation method (HPM) [25], q-HAM, and new iterative method (NIM) [24], so that

$$u(x,t)=\tanh\left(\frac{x+t}{\sqrt{2}}\right). \tag{61}$$

In the following, 3D graphical simulation of $u_4(x,t)$ of FCH4 model (40) and (41) with respect to different fractional parameter α are shown in Figure 3 for $\mu=1$ over $[-20,20]\times[0,2]$. In Figure 4, 3D surface plots of FCH4 model (40) and (41) are depicted with fix $\alpha=0.75$ versus μ such that $\mu=1$ and $\mu=0.75$ over the spatiotemporal domain $[-6,6]\times[0,3]$. Further, the obtained absolute errors $|u-u_4|$ are reported in Table 3 and compared to those results provided in [24] at $\mu=1$ and $\alpha=1$. The superiority of the present method follows from those results.

(i) Exponential wave solution of FCH4 equation

This segment is an attempt to gain an effective approximate solution to FCH4 equation (40) with the initial condition [24]

$$u(x,0)=e^{\lambda x}, \tag{62}$$

where λ is an arbitrary constant with $\lambda\neq 0$.

According the CFRS algorithm, the nth fractional series solution $u_n(x,t)$ of the FCH4 equation (40) about $t=0$ in view of the initial condition (62) can be expressed as

$$u_n(x,t)=e^{\lambda x}+\sum_{i=1}^{n}\mathscr{C}_i(x)\frac{t^{i\alpha}}{\alpha^i i!}. \tag{63}$$

With the aid of the nth truncated error $\mathscr{R}_{\jmath}^{n}(x,t)$ of (46), the unknown coefficients $\mathscr{C}_i(x)$ of the series expansion (63) can be computed for each value of $i=1,2,\cdots,n$. To achieve this goal, let the first fractional series solution of FCH4 equations (40) and (62) at $n=1$ takes the form

$$u_1(x,t)=e^{\lambda x}+\frac{1}{\alpha}\mathscr{C}_1(x)t^{\alpha}. \tag{64}$$

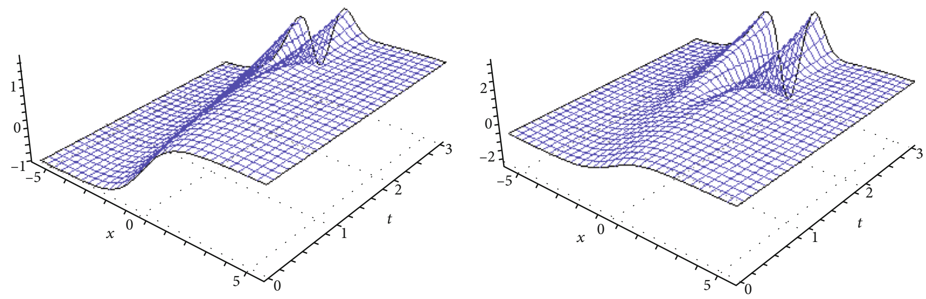

(a) (b)

Figure 4: Surface plots of FCH4 model (40) and (41) with fix $\alpha = 0.75$ versus μ: (a) $\mu = 1$ and (b) $\mu = 0.75$.

Table 3: Comparison of numerical results for FCH4 model (21)-(22) with $\lambda = 1$ and $\alpha = 1$.

t_i	x_i	$u(x,t)$	$u_4(x,t)$	$\lvert u - u_4\rvert$	$\lvert u - u_4\rvert\lvert u\rvert^{-1}$	q-HAM [24]	NIM [24]
0.01	0.0	0.007071	0.007071	2.35697×10^{-12}	3.33332×10^{-10}	2.356975×10^{-12}	1.151971×10^{-7}
	0.1	0.077625	0.077625	2.25475×10^{-12}	2.90466×10^{-11}	2.823765×10^{-10}	1.810671×10^{-7}
	0.2	0.147411	0.147411	1.96920×10^{-12}	1.33586×10^{-11}	5.749512×10^{-11}	6.167394×10^{-8}
	0.3	0.215758	0.215758	1.53980×10^{-12}	7.13667×10^{-12}	3.757261×10^{-11}	1.165205×10^{-9}
0.05	0.0	0.035341	0.035341	7.36197×10^{-9}	2.08315×10^{-7}	7.713501×10^{-8}	4.940148×10^{-5}
	0.1	0.105670	0.105670	7.00209×10^{-9}	6.62637×10^{-8}	1.124520×10^{-6}	8.990891×10^{-5}
	0.2	0.174958	0.174958	6.07535×10^{-9}	3.47246×10^{-8}	2.387229×10^{-7}	3.218897×10^{-5}
	0.3	0.242555	0.242555	4.70990×10^{-9}	1.94178×10^{-8}	1.516340×10^{-7}	4.548965×10^{-7}
0.08	0.0	0.056508	0.056508	7.71350×10^{-8}	1.36502×10^{-6}	7.361971×10^{-9}	1.306675×10^{-5}
	0.1	0.126596	0.126596	7.30464×10^{-8}	5.77003×10^{-7}	1.736922×10^{-7}	2.224480×10^{-5}
	0.2	0.195443	0.195443	6.30668×10^{-8}	3.22687×10^{-7}	3.622408×10^{-8}	7.794449×10^{-6}
	0.3	0.262415	0.262415	4.85727×10^{-8}	1.85099×10^{-7}	2.328496×10^{-8}	1.257660×10^{-7}
0.10	0.0	0.070593	0.070592	2.35226×10^{-7}	3.33214×10^{-6}	2.352262×10^{-7}	9.109940×10^{-5}
	0.1	0.140486	0.140486	2.22113×10^{-7}	1.58103×10^{-6}	2.722916×10^{-6}	1.740220×10^{-4}
	0.2	0.209006	0.209006	1.91136×10^{-7}	9.14497×10^{-7}	5.848640×10^{-7}	6.321236×10^{-5}
	0.3	0.275534	0.275534	1.46559×10^{-7}	5.31908×10^{-7}	3.686350×10^{-7}	8.108096×10^{-7}

Now, substitute $u_1(x,t)$ into $\mathscr{R}_{\jmath}^1(x,t)$ and then solve $\mathscr{R}_{\jmath}^1(x,t)_{|t=0} = 0$ to get

$$\mathscr{C}_1(x) = \lambda\left(\mu - \lambda\left(1 - 9e^{2\lambda x} + \lambda^2\right)\right)e^{\lambda x}. \tag{65}$$

Hence, the solution $u_1(x,t)$ is

$$u_1(x,t) = e^{\lambda x} + \frac{\lambda}{\alpha}\left(\mu - \lambda\left(1 - 9e^{2\lambda x} + \lambda^2\right)\right)e^{\lambda x}t^{\alpha}. \tag{66}$$

Sequentially, substitute $u_2(x,t)$ into the second truncated residual error $\mathscr{R}_{\jmath}^2(x,t)$, apply the conformable operator ∂_t^{α} on both sides of the resulting equation, and solve $\partial_t^{\alpha}\mathscr{R}_{\jmath}^2(x,t)_{|t=0} = 0$ with the aid of Mathematica's symbolic architecture [51] to get

$$\begin{aligned}\mathscr{C}_2(x) = \lambda^2\Big(&675\lambda^2 e^{4\lambda x} + \left(\lambda + \lambda^3 - \mu\right)^2\\ &- 54\lambda\left(2\left(\lambda + 7\lambda^3\right) - \mu\right)e^{2\lambda x}\Big)e^{\lambda x},\end{aligned} \tag{67}$$

which implies that the second series solution is

$$\begin{aligned}u_2(x,t) = e^{\lambda x}\Bigg(&1 + \frac{\lambda}{\alpha}\left(\mu - \lambda\left(1 - 9e^{2\lambda x} + \lambda^2\right)\right)t^{\alpha}\\ &+ \frac{\lambda^2}{2\alpha^2}\Big(675\lambda^2 e^{4\lambda x} + \left(\lambda + \lambda^3 - \mu\right)^2\\ &- 54\lambda\left(2\left(\lambda + 7\lambda^3\right) - \mu\right)e^{2\lambda x}\Big)t^{2\alpha}\Bigg).\end{aligned} \tag{68}$$

In the same fashion, the third and fourth series solutions of FCH4 equations (40) and (62) can be obtained successively as follows

$$\begin{aligned} u_3(x,t) = e^{\lambda x}\Bigg(1 &+ \frac{\lambda}{\alpha}\left(\mu - \lambda\left(1 - 9e^{2\lambda x} + \lambda^2\right)\right)t^{\alpha} \\ &+ \frac{\lambda^2}{2\alpha^2}\Big(675\lambda^2 e^{4\lambda x} + \left(\lambda + \lambda^3 - \mu\right)^2 \\ &- 54\lambda\left(2\left(\lambda + 7\lambda^3\right) - \mu\right)e^{2\lambda x}\Big)t^{2\alpha} \\ &+ \frac{\lambda^3}{6\alpha^3}\Big(123039\lambda^3 e^{6\lambda x} \\ &- 675\lambda^2\left(41\lambda + 713\lambda^3 - 15\mu\right)e^{4\lambda x} \\ &+ \left(\mu - \lambda\left(1 + \lambda^2\right)\right)^3 + 81\lambda\left(3\mu^2 - 12\mu\left(\lambda + 7\lambda^3\right)\right. \\ &\left.+ \lambda^2\left(13 + 194\lambda^2 + 757\lambda^4\right)\right)e^{2\lambda x}\Big)t^{3\alpha}\Bigg), \end{aligned} \tag{69}$$

$$\begin{aligned} u_4(x,t) = u_3(x,t) &+ \frac{\lambda^4}{24\alpha^4}\Big(972\lambda\left(\mu - 2\left(\lambda + 7\lambda^3\right)\right) \\ &\cdot \left(\mu^2 - 4\mu\left(\lambda + 7\lambda^3\right)\right. \\ &\left.+ \lambda^2\left(5 + 82\lambda^2 + 365\lambda^4\right)\right)e^{2\lambda x} \\ &+ 1350\lambda^2\left(75\mu^2 - 10\lambda\mu\left(41 + 713\lambda^2\right)\right. \\ &\left.+ \lambda^2\left(613 + 22898\lambda^2 + 226477\lambda^4\right)\right)e^{4\lambda x} \\ &- 15876\lambda^3\left(732\lambda + 23484\lambda^3 - 217\mu\right)e^{6\lambda x} \\ &+ 39110121\lambda^4 e^{8\lambda x} + \left(\lambda + \lambda^3 - \mu\right)^4\Big)e^{\lambda x}t^{4\alpha}. \end{aligned} \tag{70}$$

To close the process, we assume that $u_4(x,t)$ is the approximate solution. Following the same procedure, the values of $\mathscr{C}_n(x)$, $n \geq 5$ can be also computed. Thus, the expression of the series solution $u(x,t)$ of the FCH4 equation (40) along with condition (62) at $\alpha = 1$ and $\mu = 1$ can be written in the form

$$\begin{aligned} u(x,t) = e^{\lambda x}\Bigg(1 &+ \lambda\left(1 - \lambda\left(1 - 9e^{2\lambda x} + \lambda^2\right)\right)t \\ &+ \frac{\lambda^2}{2!}\Big(\left(\lambda + \lambda^3 - 1\right)^2 - 54\lambda\left(2\left(\lambda + 7\lambda^3\right) - 1\right)e^{2\lambda x} \\ &+ 675\lambda^2 e^{4\lambda x}\Big)t^2 + \frac{\lambda^3}{3!}\Big(123039\lambda^3 e^{6\lambda x} \\ &- 675\lambda^2\left(41\lambda + 713\lambda^3 - 15\right)e^{4\lambda x} \\ &+ \left(1 - \lambda\left(1 + \lambda^2\right)\right)^3 + 81\lambda\Big(3 - 12\left(\lambda + 7\lambda^3\right) \\ &+ \lambda^2\left(13 + 194\lambda^2 + 757\lambda^4\right)\Big)e^{2\lambda x}\Big)t^3 \\ &+ \frac{\lambda^4}{4!}\Big(972\lambda\left(1 - 2\left(\lambda + 7\lambda^3\right)\right)\left(1 - 4\left(\lambda + 7\lambda^3\right)\right. \\ &\left.+ \lambda^2\left(5 + 82\lambda^2 + 365\lambda^4\right)\right)e^{2\lambda x} \\ &+ 1350\lambda^2\left(75 - 10\lambda\left(41 + 713\lambda^2\right)\right. \\ &\left.+ \lambda^2\left(613 + 22898\lambda^2 + 226477\lambda^4\right)\right)e^{4\lambda x} \\ &- 15876\lambda^3\left(732\lambda + 23484\lambda^3 - 217\right)e^{6\lambda x} \\ &+ 39110121\lambda^4 e^{8\lambda x} + \left(\lambda + \lambda^3 - 1\right)^4\Big)t^4 + \cdots\Bigg). \end{aligned} \tag{71}$$

In the following, the 3D behaviors of surface wave function $u_4(x,t)$ of FCH4 model (40) and (62) are displayed in Figure 5 for the parameters $\mu = 1$ and $\lambda = -0.05$ with respect to $\alpha = 1$ and $\alpha = 0.75$ on $[-10, 10] \times [0, 1]$. While the fractional level curves of $u_3(x,t)$ for FCH4 model (40) and (62) are shown in Figure 6 compared to the third approximate solutions obtained in [24] for fix $t = 1$ on $[-15, 15]$ for various α values when $\lambda = -0.05$ and $\lambda = 0.05$. Error estimate for the third approximate solutions of FCH4 model (40) and (62) is provided in Table 4 by computing the absolute errors $|u_3 - u_{q\text{HAM}}|$ and $|u_3 - u_{\text{NIM}}|$ based on the results achieved by q-HAM and NIM [24] for $\alpha = 1$, $\mu = 1$, and $\lambda = 0.01$. From this comparison, it is evident that the results obtained by CFRS are in good agreement with those presented in the literature.

4.3. Solution of Nonlinear Sixth-Order Time-Fractional Cahn-Hilliard Equation. The one-dimensional nonlinear sixth-order fractional Cahn-Hilliard (FCH6) equation considered in this portion can be presented in terms of the conformable time derivative as follows [24]:

$$\begin{aligned} \partial_t^{\alpha} u = \mu u u_x - 18 u u_{xx}^2 - 36 u_x^2 u_{xx} - 24 u u_x u_{xxx} \\ - \left(3u^2 - 1\right)u_{xxxx} + u_{xxxxxx}, \end{aligned} \tag{72}$$

with the condition

$$u(x,0) = \tanh\left(\frac{x}{\sqrt{2}}\right), \tag{73}$$

$0 < \alpha \leq 1$, μ is a constant, $\mu \neq 0$, $x \in [a, b]$, $t \geq 0$, $u = u(x,t)$ is sufficiently differentiable function representing the wave-profile scaling spatiotemporal duration of wave propagation in dispersed media. Herein, the nonlinear terms in this model refer to chemical potential dynamics, and u_{xxxxxx} refers to wave scattering. This equation has applications in topology optimization, surface reconstruction, phase separation, phase ordering dynamics, magneto-acoustic propagation in plasma, multiphase incompressible fluid flows, image inpainting, and so forth [32].

According the CFRS algorithm, the nth fractional series solution $u_n(x,t)$ of the FCH6 equation (72) about $t = 0$ in view of the initial condition (73) can be expressed as

$$u_n(x,t) = \tanh\left(\frac{x}{\sqrt{2}}\right) + \sum_{i=1}^{n} \mathscr{C}_i(x)\frac{t^{i\alpha}}{\alpha^i i!}, \tag{74}$$

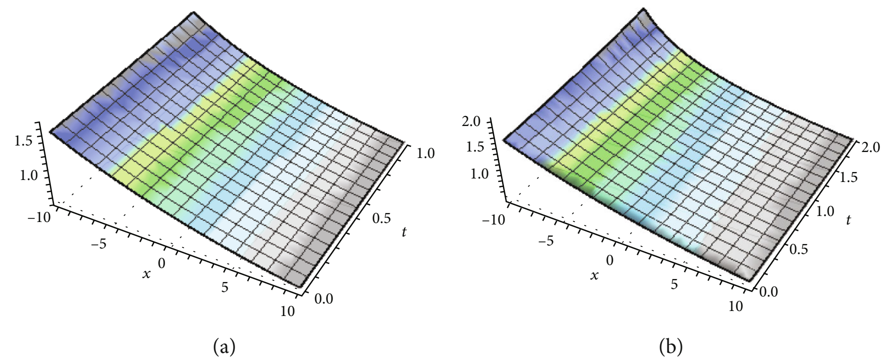

Figure 5: Surface plots of FCH4 model (40)-(62) at $\mu = 1$ and $\lambda = -0.05$ for diverse α: (a) $\alpha = 1$ and (b) $\alpha = 0.75$.

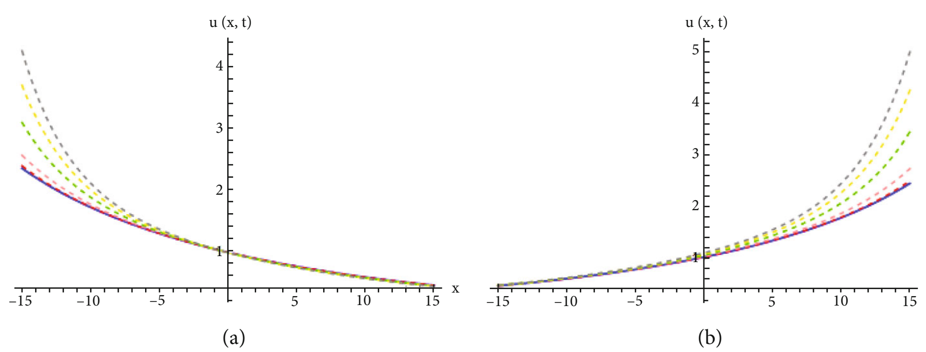

Figure 6: Fractional level curves of $u_3(x, t)$ of FCH4 model (40) and (62) with $t = 1$ and $\mu = 1$: blue for q-HAM [24], red $\alpha = 1$, pink $\alpha = 0.75$, green $\alpha = 0.5$, yellow $\alpha = 0.25$, gray $\alpha = 0.1$; (a) $\lambda = -0.05$ and (b) $\lambda = 0.05$.

Table 4: Comparison of absolute errors of FCH4 model (40) and (62) with = 1,$\mu = 1$, and $\lambda = 0.01$.

t_i	$x = 1$		$x = 5$		$x = 20$	
	$\lvert u_3 - u_{qHAM}\rvert$	$\lvert u_3 - u_{NIM}\rvert$	$\lvert u_3 - u_{qHAM}\rvert$	$\lvert u_3 - u_{NIM}\rvert$	$\lvert u_3 - u_{qHAM}\rvert$	$\lvert u_3 - u_{NIM}\rvert$
0.5	8.8741×10^{-9}	7.7088×10^{-8}	1.0333×10^{-8}	8.7056×10^{-8}	1.8620×10^{-8}	1.4221×10^{-7}
1.0	7.0993×10^{-8}	6.1670×10^{-7}	8.2659×10^{-8}	6.9645×10^{-7}	1.4896×10^{-7}	1.1377×10^{-6}
1.5	2.3960×10^{-7}	2.0814×10^{-6}	2.7898×10^{-7}	2.3505×10^{-6}	5.0274×10^{-7}	3.8396×10^{-6}
2.0	5.6794×10^{-7}	4.9336×10^{-6}	6.6128×10^{-7}	5.5716×10^{-6}	1.1917×10^{-6}	9.1012×10^{-6}
2.5	1.1093×10^{-6}	9.6360×10^{-6}	1.2916×10^{-6}	1.0882×10^{-5}	2.3275×10^{-6}	1.7776×10^{-5}

and the residual error function $\mathscr{R}_{\jmath}(x, t)$ is

$$\mathscr{R}_{\jmath}(x,t) = \partial_t^{\alpha} u - \mu u u_x + 18 u u_{xx}^2 + 36 u_x^2 u_{xx} + 24 u u_x u_{xxx} + \left(3u^2 - 1\right) u_{xxxx} - u_{xxxxxx}. \quad (75)$$

For this purpose, the nth truncated error of $\mathscr{R}_{\jmath}(x, t)$ can be expressed in the form

$$\mathscr{R}_{\jmath}^{n}(x,t) = \partial_t^{\alpha} u_n - \mu u_n u_{nx} + 18 u_n u_{nxx}^2 + 36 u_{nx}^2 u_{nxx} + 24 u_n u_{nx} u_{nxxx} + \left(3u_n^2 - 1\right) u_{nxxxx} - u_{nxxxxxx}. \quad (76)$$

Thus, by minimizing the residual error (76) of the governing equation, the unknown coefficients $\mathscr{C}_i(x)$ of series expansion (74) for each value of $i = 1, 2, \cdots, n$ can be computed. Subsequently, the series solution at $n = 1$ has the form

$$u_1(x,t) = \tanh\left(\frac{x}{\sqrt{2}}\right) + \frac{1}{\alpha}\mathscr{C}_1(x) t^{\alpha}, \quad (77)$$

whereas the first residual function has the form

$$\mathscr{R}_{\jmath}^{1}(x,t) = \partial_t^{\alpha} u_1 - \mu u_1 u_{1x} + 18 u_1 u_{1xx}^2 + 36 u_{1x}^2 u_{1xx} + 24 u_1 u_{1x} u_{1xxx} + \left(3u_1^2 - 1\right) u_{1xxxx} - u_{1xxxxxx}. \quad (78)$$

Now, putting $u_1(x,t)$ into $\mathscr{R}_{\jmath}^1(x,t)$ to get

$$\begin{aligned}\mathscr{R}_{\jmath}^1(x,t) = {} & \mathscr{C}_1(x) - \frac{\mu}{\alpha^2}(\alpha\mathscr{C}_0(x) + \mathscr{C}_1(x)t^\alpha) \\ & \cdot \left(\alpha\mathscr{C}_0'(x) + \mathscr{C}_1'(x)t^\alpha\right) \\ & + \frac{36}{\alpha^3}\left(\alpha\mathscr{C}_0'(x) + \mathscr{C}_1'(x)t^\alpha\right)^2 \\ & \cdot \left(\alpha\mathscr{C}_0''(x) + \mathscr{C}_1''(x)t^\alpha\right) \\ & + \frac{18}{\alpha^3}(\alpha\mathscr{C}_0(x) + \mathscr{C}_1(x)t^\alpha) \\ & \cdot \left(\alpha\mathscr{C}_0''(x) + \mathscr{C}_1''(x)t^\alpha\right)^2 \\ & + \frac{24}{\alpha^3}(\alpha\mathscr{C}_0(x) + \mathscr{C}_1(x)t^\alpha) \\ & \cdot \left(\alpha\mathscr{C}_0'(x) + \mathscr{C}_1'(x)t^\alpha\right) \\ & \cdot \left(\alpha\mathscr{C}_0^{(3)}(x) + \mathscr{C}_1^{(3)}(x)t^\alpha\right) \\ & + \frac{3}{\alpha^3}(\alpha\mathscr{C}_0(x) + \mathscr{C}_1(x)t^\alpha)^2 \\ & \cdot \left(\alpha\mathscr{C}_0^{(4)}(x) + \mathscr{C}_1^{(4)}(x)t^\alpha\right) \\ & - \frac{1}{\alpha}\left(\alpha\mathscr{C}_0^{(4)}(x) + \mathscr{C}_1^{(4)}(x)t^\alpha\right) \\ & - \frac{1}{\alpha}\left(\alpha\mathscr{C}_0^{(6)}(x) + \mathscr{C}_1^{(6)}(x)t^\alpha\right).\end{aligned} \tag{79}$$

By utilizing the fact $\mathscr{R}_{\jmath}^1(x,t)_{|t=0} = 0$, it yields

$$\begin{aligned}& \mathscr{C}_1(x) + 36\mathscr{C}_0'(x)^2\mathscr{C}_0''(x) + \mathscr{C}_0(x) \\ & \cdot \left(18\mathscr{C}_0''(x)^2 - \mathscr{C}_0'(x)\left(\mu - 24\mathscr{C}_0^{(3)}(x)\right)\right) \\ & + 3\mathscr{C}_0(x)^2\mathscr{C}_0^{(4)}(x) - \mathscr{C}_0^{(4)}(x) - \mathscr{C}_0^{(6)}(x) = 0,\end{aligned} \tag{80}$$

which implies that

$$\mathscr{C}_1(x) = \frac{\mu}{\sqrt{2}}\,\operatorname{sech}^2\left(\frac{x}{\sqrt{2}}\right)\tanh\left(\frac{x}{\sqrt{2}}\right). \tag{81}$$

Therefore, the solution $u_1(x,t)$ is

$$u_1(x,t) = \tanh\left(\frac{x}{\sqrt{2}}\right) + \frac{\mu}{\sqrt{2}\alpha}\,\operatorname{sech}^2\left(\frac{x}{\sqrt{2}}\right)\tanh\left(\frac{x}{\sqrt{2}}\right)t^\alpha. \tag{82}$$

Sequentially, the second truncated series $u_2(x,t)$ can be obtained by setting $n = 2$ in (76) such that

$$\begin{aligned}\mathscr{R}_{\jmath}^2(x,t) = {} & \partial_t^\alpha u_2 - \mu u_2 u_{2x} + 18u_2u_{2xx}^2 + 36u_{2x}^2u_{2xx} \\ & + 24u_2u_{2x}u_{2xxx} + \left(3u_2^2 - 1\right)u_{2xxxx} \\ & - u_{2xxxxxx},\end{aligned} \tag{83}$$

where $u_2(x,t) = \tanh(x/\sqrt{2}) + (\mu/\sqrt{2}\alpha)\operatorname{sech}^2(x/\sqrt{2})\tanh(x/\sqrt{2})t^\alpha + (1/2\alpha^2)\mathscr{C}_2(x)t^{2\alpha}$. By employing the operator ∂_t^α on both sides of equation (83), we get

$$\begin{aligned}\partial_t^\alpha\mathscr{R}_{\jmath}^2(x,t) = {} & \mathscr{C}_2(x) - \mu\left(\mathscr{C}_0(x) + \mathscr{C}_1(x)\frac{t^\alpha}{\alpha} + \mathscr{C}_2(x)\frac{t^{2\alpha}}{2\alpha^2}\right) \\ & \cdot \left(\mathscr{C}_0'(x) + \frac{\mathscr{C}_1'(x)t^\alpha}{\alpha} + \frac{\mathscr{C}_2'(x)t^{2\alpha}}{2\alpha^2}\right) \\ & - \partial_t^\alpha\left(18u_2u_{2xx}^2 + 36u_{2x}^2u_{2xx}\right. \\ & \left. + 24u_2u_{2x}u_{2xxx} + \left(3u_2^2 - 1\right)u_{2xxxx}\right) \\ & - \mathscr{C}_0^{(6)}(x) - \frac{\mathscr{C}_1^{(6)}(x)t^\alpha}{\alpha} - \frac{\mathscr{C}_2^{(6)}(x)t^{2\alpha}}{2\alpha^2}.\end{aligned} \tag{84}$$

Solving the term $\partial_t^\alpha\mathscr{R}_{\jmath}^2(x,t)_{|t=0} = 0$ with the aid of Mathematica's symbolic architecture [51] leads to

$$\begin{aligned}& \mathscr{C}_2(x) + 36\mathscr{C}_0'(x)\left(2\mathscr{C}_1'(x)\mathscr{C}_0''(x) + \mathscr{C}_0'(x)\mathscr{C}_1''(x)\right) \\ & + \mathscr{C}_0(x)\left(36\mathscr{C}_0''(x)\mathscr{C}_1''(x) - \mathscr{C}_1'(x)\left(\mu - 24\mathscr{C}_0^{(3)}(x)\right)\right. \\ & \left. + 24\mathscr{C}_0'(x)\mathscr{C}_1^{(3)}(x)\right) - \mathscr{C}_1(x)\left(\mathscr{C}_0'(x)\left(\mu - 24\mathscr{C}_0^{(3)}(x)\right)\right. \\ & \left. + 6\left(3\mathscr{C}_0''(x)^2 + \mathscr{C}_0(x)\mathscr{C}_0^{(4)}(x)\right)\right) \\ & - \mathscr{C}_1^{(4)}(x) + 3\mathscr{C}_0(x)^2\mathscr{C}_1^{(4)}(x) - \mathscr{C}_1^{(6)}(x) = 0,\end{aligned} \tag{85}$$

which implies that

$$\mathscr{C}_2(x) = \frac{\mu}{2}\zeta_1(x)\,\operatorname{sech}^4\left(\frac{x}{\sqrt{2}}\right)\tanh\left(\frac{x}{\sqrt{2}}\right), \tag{86}$$

in which $\zeta_1(x) = \mu(3 - \cosh(\sqrt{2}x)) - 3\sqrt{2}\operatorname{sech}^4(x/\sqrt{2})(249 - 163\cosh(\sqrt{2}x) + 8\cosh(2\sqrt{2}x))$.

Therefore, the series solution $u_2(x,t)$ can be given as

$$\begin{aligned}u_2(x,t) = {} & \tanh\left(\frac{x}{\sqrt{2}}\right) + \frac{\mu}{\sqrt{2}\alpha}\,\operatorname{sech}^2\left(\frac{x}{\sqrt{2}}\right)\tanh\left(\frac{x}{\sqrt{2}}\right)t^\alpha \\ & + \frac{\mu}{4\alpha^2}\zeta_1(x)\,\operatorname{sech}^4\left(\frac{x}{\sqrt{2}}\right)\tanh\left(\frac{x}{\sqrt{2}}\right)t^{2\alpha}.\end{aligned} \tag{87}$$

Following the same procedure, the series $u_3(x,t)$ of (74) can be computed through setting $n = 3$ in (76) and solving the term $\partial^{2\alpha}\mathscr{R}_{\jmath}^3(x,t)/\partial t^2{}_{|t=0} = 0$ to get $\mathscr{C}_3(x)$ as follows

$$\mathscr{C}_3(x) = \frac{\mu}{8}\zeta_2(x)\,\operatorname{sech}^6\left(\frac{x}{\sqrt{2}}\right)\tanh\left(\frac{x}{\sqrt{2}}\right), \tag{88}$$

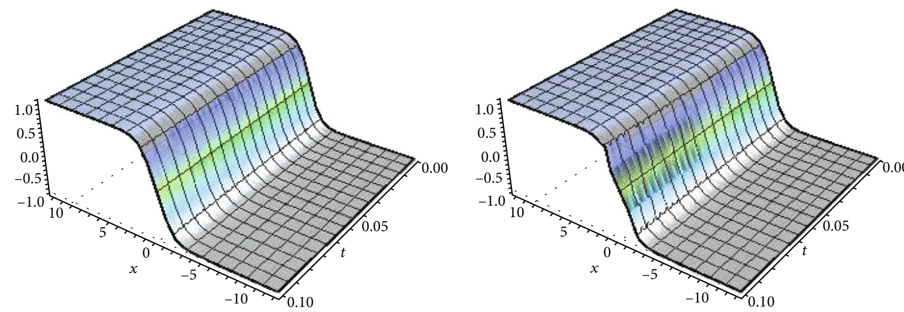

(a)

(b)

FIGURE 7: Surface wave behavior of $u_3(x,t)$ of FCH6 model (72) and (73) with $\mu = 0.01$ for diverse α: (a) $\alpha = 0.75$ and (b) $\alpha = 0.5$.

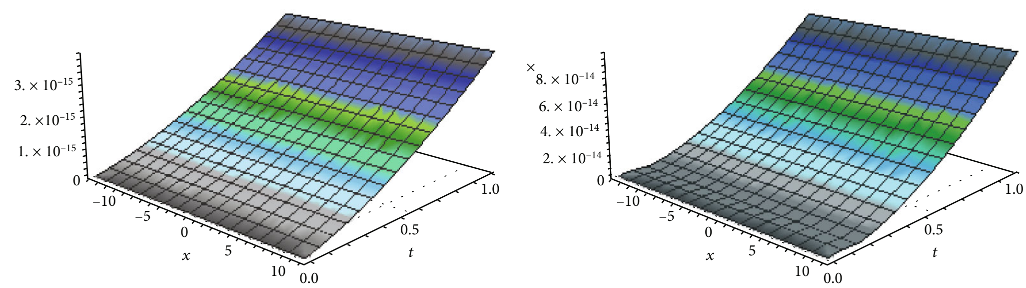

(a)

(b)

FIGURE 8: Surface of absolute error for FCH6 model (72) and (73) at $\mu = 0.01$ and $\alpha = 0.75$: (a) $|u_2 - u_{q\mathrm{HAM}}|$ and (b) $|u_2 - u_{\mathrm{NIM}}|$.

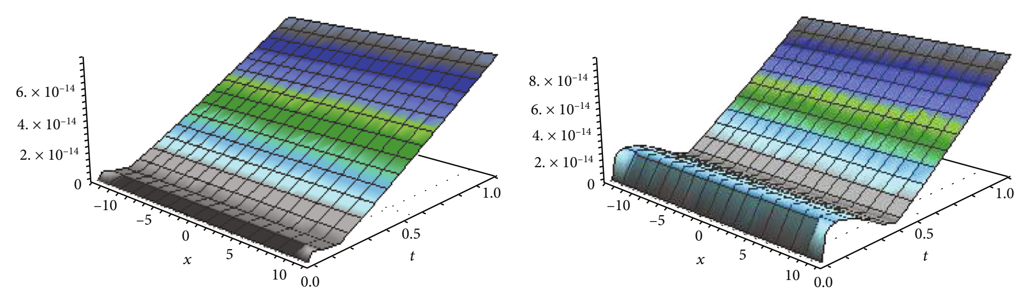

(a)

(b)

FIGURE 9: Surface of absolute error for FCH6 model (72) and (73) at $\mu = 0.01$ and $\alpha = 0.5$: (a) $|u_2 - u_{q\mathrm{HAM}}|$ and (b) $|u_2 - u_{\mathrm{NIM}}|$.

where

$$\begin{aligned}
\zeta_2(x) = {} & \sqrt{2}\mu^2\left(35 - 24\cosh\left(\sqrt{2}x\right) + \cosh\left(2\sqrt{2}x\right)\right) \\
& - 18\sqrt{2}\left(-28600273 + 33907584\cosh\left(\sqrt{2}x\right)\right. \\
& - 7525233\cosh\left(2\sqrt{2}x\right) + 585152\cosh\left(3\sqrt{2}x\right) \\
& \left. - 12286\cosh\left(4\sqrt{2}x\right) + 32\cosh\left(5\sqrt{2}x\right)\right) \\
& \cdot \operatorname{sech}^8\left(\frac{x}{\sqrt{2}}\right) - 48\mu\left(2499 - 96\cosh\left(\sqrt{2}x\right)\right. \\
& \left. - 20\left(-89 + 184\cosh\left(\sqrt{2}x\right)\right)\operatorname{sech}^4\left(\frac{x}{\sqrt{2}}\right)\right),
\end{aligned} \tag{89}$$

which implies that $u_3(x,t)$ has the form

$$\begin{aligned}
u_3(x,t) = {} & \tanh\left(\frac{x}{\sqrt{2}}\right) + \frac{\mu}{\sqrt{2}\alpha}\operatorname{sech}^2\left(\frac{x}{\sqrt{2}}\right)\tanh\left(\frac{x}{\sqrt{2}}\right)t^{\alpha} \\
& + \frac{\mu}{4\alpha^2}\zeta_1(x)\operatorname{sech}^4\left(\frac{x}{\sqrt{2}}\right)\tanh\left(\frac{x}{\sqrt{2}}\right)t^{2\alpha} \\
& + \frac{\mu}{48\alpha^3}\zeta_2(x)\operatorname{sech}^6\left(\frac{x}{\sqrt{2}}\right)\tanh\left(\frac{x}{\sqrt{2}}\right)t^{3\alpha}.
\end{aligned} \tag{90}$$

To close the process, we suppose that $u_3(x,t)$ is the approximate solution. Then, $\mathscr{C}_n(x)$, $n \geq 4$, can be computed similarly. Anyhow, the n-term sequential solution can be written in the form $\mathscr{U}_n(x,t) = \sum_k^n u_k(x,t)$ as well as the solution $u(x,t)$ of the FCH6 equation (72) along with condition (73) can be predicted as $u(x,t)=\lim_{n\longrightarrow\infty}\mathcal{U}_n(x,t)$.

In Figure 7, the behaviors of surface wave function $u_3(x,t)$ for FCH6 model (72) and (73) are presented in 3D with $\mu=0.01$ for diverse α such that $\alpha=0.75$ and $\alpha=0.5$. While the surface plots of absolute error for FCH6 model (72) and (73) based on the results obtained in [24] at $\mu=0.01$ are depicted in Figures 8 and 9 for $\alpha=0.75$ and $\alpha=0.5$, respectively. From these graphs, it is evident that the achieved results are in good agreement with those obtained in [24].

5. Concluding Remarks

In this paper, we have investigated the fractional parabolic partial differential models of Gardner and Cahn-Hilliard equations in conformable sense. Using the fractional residual method, the approximate solution has been successfully acquired of the posed problems without imposing any unsanctified restrictions. Numerical simulation has been carried out to highlight the ability of the suggested method. In this context, it can be concluded that the implemented approximation algorithm is a superior tool for computational purposes, it is computer oriented, it is relatively better compared to the existing numerical methods, and it is a straightforward and simple methodology that needs a few iterations to get accurate solutions. From the graphic representations, it is noticed that the solution behavior is harmonious for different fractional values and consistent with the integer value. In future work, multivariate series expansion based on residual error can be employed for multidimensional fractional evolution models in terms of the conformable derivative.

Data Availability

No data to be declared.

Conflicts of Interest

The authors declare that they have no conflicts of interest.

Authors’ Contributions

All authors contributed equally to this article. They read and approved the final manuscript.

Acknowledgments

This work has been carried out during sabbatical leave granted to the author Mohammed Al-Smadi from Al-Balqa Applied University (BAU) during the academic year 2021/2022.

References

[1] M. Inc, A. Yusuf, A. I. Aliyu, and D. Baleanu, “Soliton solutions and stability analysis for some conformable nonlinear partial differential equations in mathematical physics,” *Optical and Quantum Electronics*, vol. 50, article 190, 2018.

[2] D. Baleanu, M. Inc, A. Yusuf, and A. Aliyu, “Lie symmetry analysis, exact solutions and conservation laws for the time fractional Caudrey-Dodd-Gibbon-Sawada-Kotera equation,” *Communications in Nonlinear Science and Numerical Simulation*, vol. 59, pp. 222–234, 2018.

[3] M. Al-Smadi, N. Djeddi, S. Momani, S. Al-Omari, and S. Araci, “An attractive numerical algorithm for solving nonlinear Caputo–Fabrizio fractional Abel differential equation in a Hilbert space,” *Advances in Difference Equations*, vol. 2021, Article ID 271, 2021.

[4] S. Hasan, M. Al-Smadi, A. Freihet, and S. Momani, “Two computational approaches for solving a fractional obstacle system in Hilbert space,” *Advances in Difference Equations*, vol. 2019, Article ID 55, 2019.

[5] E. Goncalves and D. Zeidan, “Numerical simulation of unsteady cavitation in liquid hydrogen flows,” *Journal of Engineering Systems Modelling and Simulation*, vol. 9, no. 1, pp. 41–51, 2017.

[6] S. Kuila, T. R. Sekhar, and D. Zeidan, “On the Riemann problem simulation for the drift-flux equations of two-phase flows,” *International Journal of Computational Methods*, vol. 13, no. 1, article 1650009, 2016.

[7] Z. Altawallbeh, M. Al-Smadi, I. Komashynska, and A. Ateiwi, “Numerical solutions of fractional systems of two-point BVPs by using the iterative reproducing kernel algorithm,” *Ukrainian Mathematical Journal*, vol. 70, no. 5, pp. 687–701, 2018.

[8] J. Singh, “Analysis of fractional blood alcohol model with composite fractional derivative,” *Chaos, Solitons & Fractals*, vol. 140, article 110127, 2020.

[9] B. Ghanbari, D. Kumar, and J. Singh, “An efficient numerical method for fractional model of allelopathic stimulatory phytoplankton species with Mittag-Leffler law,” *Discrete & Continuous Dynamical Systems-S*, vol. 14, no. 10, pp. 3577–3587, 2021.

[10] O. Abu Arqub and M. Al-Smadi, “An adaptive numerical approach for the solutions of fractional advection- diffusion and dispersion equations in singular case under Riesz's derivative operator,” *Physica A: Statistical Mechanics and its Applications*, vol. 540, article 123257, 2020.

[11] M. Alabedalhadi, M. Al-Smadi, S. Al-Omari, D. Baleanu, and S. Momani, “Structure of optical soliton solution for nonliear resonant space-time Schrödinger equation in conformable sense with full nonlinearity term,” *Physica Scripta*, vol. 95, no. 10, article 105215, 2020.

[12] S. Hasan, M. Al-Smadi, H. Dutta, S. Momani, and S. Hadid, “Multi-step reproducing kernel algorithm for solving Caputo–Fabrizio fractional stiff models arising in electric circuits,” *Soft Computing*, vol. 26, no. 8, pp. 3713–3727, 2022.

[13] D. G. Prakasha, P. Veeresha, and H. M. Baskonus, “Two novel computational techniques for fractional Gardner and Cahn-Hilliard equations,” *Computational and Mathematical Methods*, vol. 1, no. 2, article e1021, 2019.

[14] O. S. Iyiola and O. G. Olayinka, “Analytical solutions of time-fractional models for homogeneous Gardner equation and non-homogeneous differential equations,” *Ain Shams Engineering Journal*, vol. 5, pp. 999–1004, 2014.

[15] A. Atangana and D. Baleanu, “New fractional derivatives with non-local and non-singular kernel: theory and application to heat transfer model,” https://arxiv.org/abs/1602.03408.

[16] B. Bira, T. R. Sekhar, and D. Zeidan, “Exact solutions for some time-fractional evolution equations using Lie group theory,”

Mathematical Methods in the Applied Sciences, vol. 41, no. 16, pp. 6717–6725, 2018.

[17] Z. Korpinar, M. Inc, D. Baleanu, and M. Bayram, "Theory and application for the time fractional Gardner equation with Mittag-Leffler kernel," *Journal of Taibah University for Science*, vol. 13, no. 1, pp. 813–819, 2019.

[18] M. Al-Smadi, S. Momani, N. Djeddi, A. El-Ajou, and Z. Al-Zhour, "Adaptation of reproducing kernel method in solving Atangana–Baleanu fractional Bratu model," *International Journal of Dynamics and Control*, vol. 10, 2022.

[19] D. Baleanu, Y. Ugurlu, M. Inc, and B. Kilic, "Improved (G'/G)-expansion method for the time-fractional biological population model and Cahn-Hilliard equation," *Journal of Computational and Nonlinear Dynamics*, vol. 10, no. 5, pp. 1–8, 2015.

[20] M. Al-Smadi and A. O. Abu, "Computational algorithm for solving Fredholm time-fractional partial integrodifferential equations of Dirichlet functions type with error estimates," *Applied Mathematics and Computation*, vol. 342, pp. 280–294, 2019.

[21] M. Al-Smadi, A. Freihat, H. Khalil, S. Momani, and R. A. Khan, "Numerical multistep approach for solving fractional partial differential equations," *International Journal of Computational Methods*, vol. 14, no. 3, article 1750029, 2017.

[22] H. Günerhan, H. Dutta, M. A. Dokuyucu, and W. Adel, "Analysis of a fractional HIV model with Caputo and constant proportional Caputo operators," *Chaos, Solitons & Fractals*, vol. 139, article 110053, 2020.

[23] M. Al-Smadi, H. Dutta, S. Hasan, and S. Momani, "On numerical approximation of Atangana-Baleanu-Caputo fractional integro-differential equations under uncertainty in Hilbert space," *Mathematical Modelling of Natural Phenomena*, vol. 16, p. 41, 2021.

[24] L. Akinyemi, O. S. Iyiola, and U. Akpan, "Iterative methods for solving fourth- and sixth-order time-fractional Cahn-Hillard equation," *Mathematical Methods in the Applied Sciences*, vol. 43, no. 7, pp. 4050–4074, 2020.

[25] A. Bouhassoun and M. H. Cherif, "Homotopy perturbation method for solving the fractional Cahn-Hilliard equation," *Journal of Interdisciplinary Mathematics*, vol. 18, no. 5, pp. 513–524, 2015.

[26] S. Qureshi, A. Yusuf, A. A. Shaikh, M. Inc, and D. Baleanu, "Fractional modeling of blood ethanol concentration system with real data application," *Chaos: An Interdisciplinary Journal of Nonlinear Science*, vol. 29, no. 1, article 013143, 2019.

[27] P. Veeresha, D. G. Prakasha, and S. Kumar, "A fractional model for propagation of classical optical solitons by using nonsingular derivative," *Mathematical Methods in the Applied Sciences*, vol. 43, 2020.

[28] M. Al-Smadi, "Fractional residual series for conformable time-fractional Sawada–Kotera–Ito, Lax, and Kaup–Kupershmidt equations of seventh order," *Mathematical Methods in the Applied Sciences*, vol. 44, 2021.

[29] H. Singh, A. K. Singh, R. K. Pandey, D. Kumar, and J. Singh, "An efficient computational approach for fractional Bratu's equation arising in electrospinning process," *Mathematical Methods in the Applied Sciences*, vol. 44, no. 13, pp. 10225–10238, 2021.

[30] M. Al-Smadi, O. Abu Arqub, and D. Zeidan, "Fuzzy fractional differential equations under the Mittag-Leffler kernel differential operator of the ABC approach: theorems and applications," *Chaos, Solitons & Fractals*, vol. 146, article 110891, 2021.

[31] A. Akgül, M. S. Hashemi, M. Inc, and S. A. Raheem, "Constructing two powerful methods to solve the Thomas–Fermi equation," *Nonlinear Dynamics*, vol. 87, no. 2, pp. 1435–1444, 2017.

[32] Y. Li, D. Jeong, H. Kim, C. Lee, and J. Kim, "Comparison study on the different dynamics between the Allen-Cahn and the Cahn-Hilliard equations," *Computers & Mathematics with Applications*, vol. 77, no. 2, pp. 311–322, 2019.

[33] M. Inc, "On numerical soliton solution of the Kaup-Kupershmidt equation and convergence analysis of the decomposition method," *Applied Mathematics and Computation*, vol. 172, no. 1, pp. 72–85, 2006.

[34] N. K. Tripathi, S. Das, S. H. Ong, H. Jafari, and M. M. Al Qurashi, "Solution of time-fractional Cahn-Hilliard equation with reaction term using homotopy analysis method," *Advances in Mechanical Engineering*, vol. 9, no. 12, 2017.

[35] G. Akagi, G. Schimperna, and A. Segatti, "Fractional Cahn-Hilliard, Allen-Cahn and porous medium equations," *Journal of Differential Equations*, vol. 261, no. 6, pp. 2935–2985, 2016.

[36] M. Ran and X. Zhou, "An implicit difference scheme for the time-fractional Cahn-Hilliard equations," *Mathematics and Computers in Simulation*, vol. 180, pp. 61–71, 2021.

[37] H. Liu, A. Cheng, H. H. Wang, and J. Zhao, "Time-fractional Allen-Cahn and Cahn-Hilliard phase-field models and their numerical investigation," *Computers & Mathematics with Applications*, vol. 76, no. 8, pp. 1876–1892, 2018.

[38] A. Arafa and G. Elmahdy, "Application of residual power series method to fractional coupled physical equations arising in fluids flow," *International Journal of Differential Equations*, vol. 2018, Article ID 7692849, 10 pages, 2018.

[39] K. Hosseini, A. Bekir, M. Kaplan, and O. Guner, "On a new technique for solving the nonlinear conformable time-fractional differential equations," *Optical and Quantum Electronics*, vol. 49, no. 11, p. 343, 2017.

[40] H. Jafari, H. Tajadodi, N. Kadkhoda, and D. Baleanu, "Fractional subequation method for Cahn-Hilliard and Klein-Gordon equations," *Abstract and Applied Analysis*, vol. 2013, Article ID 587179, 5 pages, 2013.

[41] M. Al-Smadi, O. Abu Arqub, and M. Gaith, "Numerical simulation of telegraph and Cattaneo fractional-type models using adaptive reproducing kernel framework," *Mathematical Methods in the Applied Sciences*, vol. 44, no. 10, pp. 8472–8489, 2021.

[42] M. Al-Smadi, O. Abu Arqub, and S. Momani, "Numerical computations of coupled fractional resonant Schrödinger equations arising in quantum mechanics under conformable fractional derivative sense," *Physica Scripta*, vol. 95, no. 7, article 075218, 2020.

[43] A. Atangana, D. Baleanu, and A. Alsaedi, "New properties of conformable derivative," *Open Mathematics*, vol. 13, no. 1, pp. 889–898, 2015.

[44] M. Al-Smadi, O. Abu Arqub, and S. Hadid, "An attractive analytical technique for coupled system of fractional partial differential equations in shallow water waves with conformable derivative," *Journal of Applied Mathematics and Computing*, vol. 72, no. 8, article 085001, 2020.

[45] R. Khalil, M. Al Horani, A. Yousef, and M. Sababheh, "A new definition of fractional derivative," *Journal of Computational and Applied Mathematics*, vol. 264, pp. 65–70, 2014.

[46] T. Abdeljawad, “On conformable fractional calculus,” *Journal of computational and Applied Mathematics*, vol. 279, pp. 57–66, 2015.

[47] M. Al-Smadi, O. Abu Arqub, and S. Hadid, “Approximate solutions of nonlinear fractional Kundu-Eckhaus and coupled fractional massive Thirring equations emerging in quantum field theory using conformable residual power series method,” *Physica Scripta*, vol. 95, no. 10, article 105205, 2020.

[48] D. R. Anderson and D. J. Ulness, “Newly defined conformable derivatives,” *Advances in Dynamical Systems and Applications*, vol. 10, pp. 109–137, 2015.

[49] C. Chen and Y. Jiang, “Simplest equation method for some time-fractional partial differential equations with conformable derivative,” *Computers & Mathematics with Applications*, vol. 75, no. 8, pp. 2978–2988, 2018.

[50] Q. Feng, “A new approach for seeking coefficient function solutions of conformable fractional partial differential equations based on the Jacobi elliptic equation,” *Chinese Journal of Physics*, vol. 56, no. 6, pp. 2817–2828, 2018.

[51] Wolfram Research, Inc, *Mathematica Edition: Version 12.2*, Wolfram Research, Champaign, IL, 2020.

Hindawi
Journal of Function Spaces
Volume 2022, Article ID 2613133, 21 pages
https://doi.org/10.1155/2022/2613133

Research Article

An Efficient Method for Solving Fractional Black-Scholes Model with Index and Exponential Decay Kernels

Saima Rashid,[1] **Saad Ihsan Butt**,[2] **Zakia Hammouch**,[3,4,5] **and Ebenezer Bonyah**[6]

[1]*Department of Mathematics, Government College University, Faisalabad 38000, Pakistan*
[2]*Department of Mathematics, COMSATS University, Lahore Campus, Islamabad, Pakistan*
[3]*Division of Applied Mathematics, Thu Dau Mot University, Binh Duong Province, Vietnam*
[4]*Department of Mathematics, Ecole Normale Supéerieure de Meknés, Université Moulay Ismail, Meknes 50000, Morocco*
[5]*Department of Medical Research, China Medical University Hospital, Taichung, Taiwan*
[6]*Department of Mathematics Education, University of Education, Winneba, Kumasi Campus, Ghana*

Correspondence should be addressed to Zakia Hammouch; hammouch_zakia@tdmu.edu.vn

Received 16 April 2022; Revised 1 August 2022; Accepted 9 August 2022; Published 21 September 2022

Academic Editor: Alexander Meskhi

The Black-Scholes equation (BSe) is fascinating in the business world for predicting the performance of financial investment valuation systems. The Caputo fractional derivative (CFD) and Caputo-Fabrizio fractional derivative operators are used in this research to analyze the BSe. The Adomian decomposition method (ADM) and the new iterative transform (NIM) approach are combined alongside the Yang transform. In addition, the convergence and uniqueness results for the aforementioned framework have been calculated. The existence and uniqueness results have been established and frequently accompanied innovative aspects of the prospective system in fixed point terminologies. To provide additional insight into such concepts, a variety of illustrations and tabulations are used. Additionally, the provided techniques regulate and modify the obtained analytical results in a really productive fashion, allowing us to modify and regulate the converging domains of the series solution in a pragmatic manner.

1. Introduction

Recently, the investigation of modified derivatives and integrals has grown in prominence in recent decades, owing to its appealing implications in a wide range of disciplines, including Maxwell fluids [1, 2], circuit theory [3], and epidemics [4, 5]. As an outgrowth of conventional integer analysis, fractional calculus (FC) has been exploited to examine the implications and integrals of indefinite powers. Because integer-order derivative and integral operators are being used to simulate all real-world processes, numerous researchers have proposed multiple variations of fractional operators as a modification of the fractional formulations [6–9]. The interaction effect in FC has been utilized to represent numerous processes in thermodynamics, chemical engineering, biomechanics, and other disciplines, despite the fact that the analyzed formulae in FC are typically reluctant to analyze complicated phenomena [10–14]. In addition, fractional differential formulas have a higher granularity than integer differential operators. Illustrations comprise Katugampola, Weyl, Hadamard, Caputo, Riesz, Riemann, and Liouville, Weyl, Jumarie, Caputo and Fabrizio [15], and Grünwald and Letnikov [16]. Likewise, the Liouville-Caputo and Caputo-Fabrizio fractional filtrations are thought to be ideal.

It is imperative to address fractional-order nonlinear partial differential equations (NPDEs) that regulate the foregoing experimental results in order to successfully comprehend such occurrences. There is, however, no universal comprehensive principle that applies to NPDEs in an attempt to obtain a numerical approach. Researchers have determined successful approaches to derive meaningful numerical methods for NPDEs in recent times, including the inverse scattering transform Sin-Cos method (SCM) [17], homotopy perturbation method (HPM) [18], Adomian decomposition method (ADM) [19, 20], new iterative transform method (NITM) [21], variation iteration method

(VIM) [22], G/G' expansion method [23], Lie symmetry analysis (LSA) [24], Haar wavelet method [25], inverse scattering transform [26], simple equation method [27], Bäcklund transformation [28], and henceforth.

In 1973, Fischer Black and Myron Scholes formulated a mathematical formula for passive investment valuation. The pioneering Black-Scholes equation (BSe) is at the core of contemporary financial economics, and it is indeed tough to communicate about mainstream capitalism without mentioning the revolutionary BSe.

The objective of this paper is to leverage the Yang decomposition method (YDM) and the Yang iterative transform method (YITM) to modify the results into a BSe. The fractional interpretation of BSe is characterized in financial services by [29]:

$$\mathbf{D}_{\varrho}^{\delta}\mathcal{U} + \frac{\varpi^2}{2}\mathcal{S}^2\frac{\partial^2\mathcal{U}}{\partial\mathcal{S}^2} + \zeta\mathcal{S}\frac{\partial\mathcal{U}}{\partial\mathcal{S}} - \zeta\mathcal{U} = 0, \tag{1}$$

subject to the playoff mapping

$$\mathcal{U}(\mathcal{S}, \mathcal{T}) = \max(\mathcal{S} - E, 0), \tag{2}$$

where $\mathcal{U}(\mathcal{S}, \varrho)$ denotes the alternative means worth at $\mathcal{S}$ asset prices of the moment, ϱ, and $\mathcal{T}$ indicates the termination term. The symbol E symbolizes share value. The parameter ζ represents the uncertainty of borrowing until it matures. The continual ϖ indicates the unpredictability of a trading asset. The required assumptions are also entailed: a continuous uncertainty risk premium u, no operating charges, the capacity to transact an unrestricted quantity of inventory, and no restrictions on market manipulation. Ultimately, we provide European alternatives. It is also worth mentioning that $\mathcal{U}(0, \varrho) = 0$ and $\mathcal{U}(\mathcal{S}, \mathcal{T}) \approx \mathcal{S}$ as $\mathcal{S} \mapsto \infty$. The parabolic diffusion problem can perhaps be described as the BSe in (1). Inducing the modifications that follow:

$$\begin{aligned} \mathcal{S} &= E\exp(\mathbf{y}_1), \\ \varrho &= \mathcal{T} - \frac{2\tau}{\varpi^2}, \\ \mathcal{U} &= E\mathbf{U}(\mathbf{y}_1, \varrho), \end{aligned} \tag{3}$$

then (1) diminishes to

$$\mathbf{D}_{\varrho}^{\delta}\mathbf{U}(\mathbf{y}_1, \varrho) = \frac{\partial^2\mathbf{U}(\mathbf{y}_1, \varrho)}{\partial\mathbf{y}_1^2} + (\zeta - 1)\frac{\partial\mathbf{U}(\mathbf{y}_1, \varrho)}{\partial\mathbf{y}_1} - \zeta\mathbf{U}(\mathbf{y}_1, \varrho), \tag{4}$$

related initial condition (ICs) are

$$\mathbf{U}(\mathbf{y}_1, 0) = \max(\exp(\mathbf{y}_1) - 1, 0), \tag{5}$$

where ζ designates the threshold when the direct connection involving wage growth and market instability coincides. Cen and Le proposed the generalized fractional BSe in [30]. The BSe is stated as follows:

$$\begin{aligned} \mathbf{D}_{\varrho}^{\delta}\mathbf{U}(\mathbf{y}_1, \varrho) = &-0.08(2 + \sin\mathbf{y}_1)^2\mathbf{y}_1^2\frac{\partial^2\mathbf{U}(\mathbf{y}_1, \varrho)}{\partial\mathbf{y}_1^2} \\ &- 0.06\mathbf{y}_1\frac{\partial\mathbf{U}(\mathbf{y}_1, \varrho)}{\partial\mathbf{y}_1} + 0.06\mathbf{U}(\mathbf{y}_1, \varrho), \end{aligned} \tag{6}$$

supplemented ICs

$$\mathbf{U}(\mathbf{y}_1, 0) = \max(\mathbf{y}_1 - 25\exp(-0.06), 0). \tag{7}$$

The fractional BSe considering a particular resource has been widely explored ([31, 32]). The fractional BSe is a version of the classical BSe that expands its restrictions. The BSe was implemented by Meng and Wang [33] to analyze fractional potential assessment. The fractional BSe was used to determine the insured guarantee valuation for treasury foreign trade in China. Their results indicate that the fractional BSe surpasses the traditional BSe when it pertains to measuring the impact of the pricing system [34]. The Black-Scholes financial theory was calculated using the HPM by Fall et al. [35]. By adopting the Ornstein-Uhlenbeck Procedures, Matadi and Zondi [36] explored the consistent values of BSe. The computational estimation of fractional BSe emerging in the banking system was demonstrated by Kumar et al. [37]. Employing a novel fractional operator, Yavuz and Özdemir [38] suggested a novel strategy for the European efficient market hypothesis.

The ADM introduced a well-known concept during George Adomian's significant surge in 1980. For example, it has been frequently applied to deal with a variety of complex PDEs like the $K(2,2)$ and $K(3,3)$ models [19], biological population model [39], Swift-Hohenberg model [40], and henceforth. The ADM is essential because it overcomes the necessity for a smaller component in the considerations, eliminating the challenges that occur with classic Adomian approaches. The main objective of this research was to leverage the ADM to analyze fractional-order BSe using a recently designed integral transformation known as the "Yang transformation" [41].

Daftardar-Gejji and Jafari [42] proposed NITM in 2006, which is frequently adopted by scholars owing to its usefulness in fractional ODES and PDEs. If a precise result emerges, the iterative method leads to it through repeated estimates. For methodological concerns, a significant fraction of projections can be considered with a satisfactory amount of precision for specific issues. For managing nonlinearity components, the NITM sometimes does not require a restrictive assumption. For instance, researchers exploited NITM to develop analytical results for the fractional Schrödinger equation in [43], and Wang and Liu used NITM to address the fractional Fornberg-Whitham model in [44]. Widatalla and Liu used NITM to develop the Laplace decomposition algorithm in [22].

Due to the aforesaid tendency, we apply the YDM and the YITM to achieve the expressive result of the fractional-order BSe. For renewability algorithmic techniques, the Yang transform efficiently integrates the ADM and NITM. The

Yang transform is a combination of a few different transforms. Both these proposed techniques produce interpretive findings in the sense of a convergent series. The Caputo-Fabrizio fractional derivative operator is used to explain quantitative categorizations of the BSe. The offered methodologies are well demonstrated in modeling and enumeration investigations. The exact-analytical findings are a valuable way to analyze the dynamics of systems that are problematic to computationally analyze, notably for fractional PDEs. Financial and monetary phenomena can be investigated using this approximate expression.

2. Preliminaries

In this part, we address several key ideas, conceptions, and terminologies related to fractional derivative operators involving index and exponential decay as a kernel, as well as the Yang transform's specific repercussions.

Definition 1 (see [9]). The Caputo fractional derivative (CFD) is described as follows:

$$ {}_{0}^{c}\mathbf{D}_{\varrho}^{\delta}\mathbf{U}(\varrho)=\begin{cases}\dfrac{1}{\Gamma(r-\delta)}\displaystyle\int_0^{\varrho}\dfrac{\mathbf{U}^{(r)}(\mathbf{y}_1)}{(\varrho-\mathbf{y}_1)^{\delta+1-r}}d\mathbf{y}_1, r-1<\delta<r,\\ \dfrac{d^r}{d\varrho^r}\mathbf{U}(\varrho), \delta=r.\end{cases} \tag{8}$$

Definition 2 (see [15]). The Caputo fractional derivative operator is described as follows:

$$ {}^{CF}\mathbf{D}_{\varrho}^{\delta}(\mathbf{U}(\varrho))=\frac{(2-\delta)\mathbb{A}(\delta)}{2(1-\delta)}\int_0^{\varrho}\exp\left(-\frac{\delta(\varrho-\mathbf{y}_1)}{1-\delta}\right)\mathbf{U}'(\varrho)d\varrho, \tag{9}$$

where $\mathbf{U}\in\mathbf{H}^1(a_1,a_2)(Sobolev\ space)$, $a_1<a_2$, $\delta\in[0,1]$, and $\mathbb{A}(\delta)$ signifies a normalization function as $\mathbb{A}(\delta)=\mathbb{A}(0)=\mathbb{A}(1)=1$.

Definition 3 (see [15]). The fractional integral of the Caputo-Fabrizio operator is defined as

$$ {}^{CF}\mathcal{I}_{\varrho}^{\delta}(\mathbf{U}(\varrho))=\frac{2(1-\delta)}{(2-\delta)\mathbb{A}(\delta)}\mathbf{U}(\varrho)+\frac{2\delta}{(2-\delta)\mathbb{A}(\delta)}\int_0^{\varrho}\mathbf{U}(\mathbf{y}_1)d\mathbf{y}_1. \tag{10}$$

Definition 4 (see [41]). The Yang transform is described as follows:

$$\mathbf{Y}[\mathbf{U}(\varphi)]=\mathbb{Y}(s_1)=\int_0^{\infty}\mathbf{U}(\varphi)\exp\left(-\frac{\varphi}{s_1}\right)d\varphi, \varphi>0. \tag{11}$$

The Yang transform of a range of vital expressions is as follows:

$$\begin{aligned}\mathbf{Y}[1]&=s_1,\\ \mathbf{Y}[\varphi]&=s_1^2,\\ &\vdots\\ \mathbf{Y}\left[\frac{\varphi^{\delta}}{\Gamma(\delta+1)}\right]&=s_1^{\delta+1}.\end{aligned} \tag{12}$$

Definition 5 (see [41]). The Yang transform of the CFD operator is mentioned as

$$\mathbf{Y}\left\{{}_{0}^{c}\mathbf{D}_{\varrho}^{\delta}(\mathbf{U}(\varrho)),\mathfrak{s}\right\}=\varphi^{-\delta}\mathbf{Q}(\mathfrak{s})-\sum_{\kappa=0}^{\delta-1}\varphi^{1-\delta-\kappa}(\mathfrak{s})\mathbf{U}^{(\kappa)}(0), r-1<\delta<r, \varphi>0. \tag{13}$$

Definition 6 (see [45]). The Yang transform of the Caputo-Fabrizio fractional derivative operator is stated as

$$\mathbf{Y}\left\{{}_{0}^{CF}\mathbf{D}_{\varrho}^{\delta}(\mathbf{U}(\varphi)),s_1\right\}=\frac{\mathbf{Y}[\mathbf{U}(\varphi)-s_1\mathbf{U}(0)]}{1+\delta(s_1-1)}. \tag{14}$$

Definition 7 (see [46]). The Mittag-Leffler function for single parameter is defined as

$$E_{\delta}(z)=\sum_{\kappa=0}^{\infty}\frac{z_1^{\kappa}}{\Gamma(\kappa\delta+1)}, \delta, z_1\in\mathbb{C}, \Re(\delta)\geq 0. \tag{15}$$

3. Algorithmic Configuration for Nonlinear PDEs

Let us surmise the fractional version of nonlinear PDE:

$$\mathbf{D}_{\varrho}^{\delta}\mathbf{U}(\mathbf{y}_1,\varrho)+\mathbf{L}\mathbf{U}(\mathbf{y}_1,\varrho)+\mathbf{N}\mathbf{U}(\mathbf{y}_1,\varrho)=\mathbf{Q}(\mathbf{y}_1,\varrho), \varrho>0, 0<\delta\leq 1 \tag{16}$$

having ICs

$$\mathbf{U}(\mathbf{y}_1,0)=\mathcal{G}(\mathbf{y}_1), \tag{17}$$

where $\mathbf{D}_{\varrho}^{\delta}=\partial^{\delta}\mathbf{U}(\mathbf{y}_1,\varrho)/\partial\varrho^{\delta}$ represents the Caputo-Fabrizio fractional derivative considering the order $\delta\in(0,1]$ whilst $\mathbf{L}$ and $\mathbf{N}$ indicates the linear and nonlinear functionals, respectively. Furthermore, $\mathbf{Q}(\mathbf{y}_1,\varrho)$ indicates the source term.

3.1. Construction of Yang Decomposition Method. Incorporating the Yang transformation to (16), we obtain

$$\mathbf{Y}\left[\mathbf{D}_{\varrho}^{\delta}\mathbf{U}(\mathbf{y}_1,\varrho)+\bar{\mathbf{L}}\mathbf{U}(\mathbf{y}_1,\varrho)+\bar{\mathbf{N}}\mathbf{U}(\mathbf{y}_1,\varrho)\right]=\mathbf{Y}[\mathbf{Q}(\mathbf{y}_1,\varrho)]. \tag{18}$$

Initially, we implement the Yang transform differentiabilty criteria to CFD, and then further implement the Caputo-Fabrizio fractional derivative operator as described in the following:

$$\varphi^{-\delta}\mathscr{U}(\mathbf{y}_1,\varrho)=\sum_{p=0}^{n-1}\varphi^{1-\delta-p}\mathbf{U}^{(p)}(0)+\mathbf{Y}\left[\bar{\mathbf{L}}\mathbf{U}(\mathbf{y}_1,\varrho)+\bar{\mathbf{N}}\mathbf{U}(\mathbf{y}_1,\varrho)\right]+\mathbf{Y}[\mathbf{Q}(\mathbf{y}_1,\varrho)], \tag{19}$$

$$\frac{1}{1+\delta(\varphi-1)}\mathscr{U}(\mathbf{y}_1,\varrho)=\frac{\varphi}{1+\delta(\varphi-1)}\mathbf{U}(0)+\mathbf{Y}\left[\bar{\mathbf{L}}\mathbf{U}(\mathbf{y}_1,\varrho)+\bar{\mathbf{N}}\mathbf{U}(\mathbf{y}_1,\varrho)\right]+\mathbf{Y}[\mathbf{Q}(\mathbf{y}_1,\varrho)]. \tag{20}$$

The inverse Yang transform of (19) and (20), respectively, gives

$$\mathbf{U}(\mathbf{y}_1,\varrho)=\mathbf{Y}^{-1}\left[\sum_{p=0}^{n-1}\varphi^{1-\delta-p}\mathbf{U}^{(p)}(0)+\varphi^{\delta}\mathbf{Y}[\mathbf{Q}(\mathbf{y}_1,\varrho)]\right]-\mathbf{Y}^{-1}\left[\varphi^{\delta}\mathbf{Y}\left[\bar{\mathbf{L}}\mathbf{U}(\mathbf{y}_1,\varrho)+\bar{\mathbf{N}}\mathbf{U}(\mathbf{y}_1,\varrho)\right]\right], \tag{21}$$

$$\mathbf{U}(\mathbf{y}_1,\varrho)=\mathbf{Y}^{-1}[\varphi\mathbf{U}(0)+(1+\delta(\varphi-1))\mathbf{Y}[\mathbf{Q}(\mathbf{y}_1,\varrho)]]-\mathbf{Y}^{-1}\left[(1+\delta(\varphi-1))\mathbf{Y}\left[\bar{\mathbf{L}}\mathbf{U}(\mathbf{y}_1,\varrho)+\bar{\mathbf{N}}\mathbf{U}(\mathbf{y}_1,\varrho)\right]\right]. \tag{22}$$

The infinite series $\mathbf{U}(\mathbf{y}_1,\varrho)$ illustrates the result of the Yang decomposition approach:

$$\mathbf{U}(\mathbf{y}_1,\varrho)=\sum_{p=0}^{\infty}\mathbf{U}_p(\mathbf{y}_1,\varrho). \tag{23}$$

As a consequence, the nonlinear component $\bar{\mathbf{N}}(\mathbf{y}_1,\varrho)$ can be assessed employing the Adomian decomposition approach, as follows:

$$\bar{\mathbf{N}}\mathbf{U}(\mathbf{y}_1,\varrho)=\sum_{p=0}^{\infty}\tilde{A}_p(\mathbf{U}_0,\mathbf{U}_1,\cdots),p=0,1,\cdots, \tag{24}$$

where

$$\tilde{A}_p(\mathbf{U}_0,\mathbf{U}_1,\cdots)=\frac{1}{q!}\left[\frac{d^p}{d\delta^p}\bar{\mathbf{N}}\left(\sum_{j=0}^{\infty}\delta^j\mathbf{U}_j\right)\right]_{\delta=0},q>0. \tag{25}$$

Putting (20) and (24) into (21) and (22), respectively, we attain

$$\sum_{p=0}^{\infty}\mathbf{U}_p(\mathbf{y}_1,\varrho)=\mathscr{G}(\mathbf{y}_1)+\tilde{\mathscr{G}}(\mathbf{y}_1)-\mathbf{Y}^{-1}\left[\varphi^{\delta}\mathbf{Y}\left[\bar{\mathbf{L}}\mathbf{U}(\mathbf{y}_1,\varrho)+\sum_{p=0}^{\infty}\tilde{A}_p\right]\right], \tag{26}$$

$$\sum_{p=0}^{\infty}\mathbf{U}_p(\mathbf{y}_1,\varrho)=\mathscr{G}(\mathbf{y}_1)+\tilde{\mathscr{G}}(\mathbf{y}_1)-\mathbf{Y}^{-1}\left[(1+\delta(\varphi-1))\mathbf{Y}\left[\bar{\mathbf{L}}\mathbf{U}(\mathbf{y}_1,\varrho)+\sum_{p=0}^{\infty}\tilde{A}_p\right]\right]. \tag{27}$$

As a nutshell, the iterative approach for (26) and (27) is as follows:

$$\begin{aligned}\mathbf{U}_0(\mathbf{y}_1,\varrho)&=\mathscr{G}(\mathbf{y}_1)+\tilde{\mathscr{G}}(\mathbf{y}_1),p=0,\\ \mathbf{U}_{q+1}(\mathbf{y}_1,\varrho)&=-\mathbf{Y}^{-1}\left[\varphi^{\delta}\mathbf{Y}\left[\bar{\mathbf{L}}(\mathbf{U}_p(\mathbf{y}_1,\varrho))+\sum_{p=0}^{\infty}\tilde{A}_p\right]\right],q\geq 1,\\ \mathbf{U}_{q+1}(\mathbf{y}_1,\varrho)&=-\mathbf{Y}^{-1}\left[(1+\delta(\varphi-1))\mathbf{Y}\left[\bar{\mathbf{L}}(\mathbf{U}_p(\mathbf{y}_1,\varrho))+\sum_{p=0}^{\infty}\tilde{A}_p\right]\right],q\geq 1.\end{aligned} \tag{28}$$

3.2. Formation of Yang Iterative Transform Method. Implementing the Yang transform to (16) incorporates the ICs (17), ones obtain

$$\mathbf{Y}\left[\mathbf{D}_{\varrho}^{\delta}\mathbf{U}(\mathbf{y}_1,\varrho)+\bar{\mathbf{L}}\mathbf{U}(\mathbf{y}_1,\varrho)+\bar{\mathbf{N}}\mathbf{U}(\mathbf{y}_1,\varrho)\right]=\mathbf{Y}[\mathbf{Q}(\mathbf{y}_1,\varrho)]. \tag{29}$$

First, we apply the differentiation rule of Yang transform for CFD, and then we consider for Caputo-Fabrizio fractional derivative operator, respectively, and we get

$$\mathbf{Y}[\mathbf{U}(\mathbf{y}_1,\varrho)]=\varphi^{\delta}\sum_{p=0}^{n-1}\varphi^{1-\delta-p}(\varrho)\mathbf{U}^{(p)}(\varphi,0)-\varphi^{\delta}\mathbf{Y}\left[\bar{\mathbf{L}}\mathbf{U}(\mathbf{y}_1,\varrho)+\bar{\mathbf{N}}\mathbf{U}(\mathbf{y}_1,\varrho)\right]+\varphi^{\delta}\mathbf{Y}[\mathbf{Q}(\mathbf{y}_1,\varrho)], \tag{30}$$

$$\mathbf{Y}[\mathbf{U}(\mathbf{y}_1,\varrho)]=\varphi^{\delta}\sum_{p=0}^{n-1}\varphi^{1-\delta-p}(\varrho)\mathbf{U}^{(p)}(\varphi,0)-(1+\delta(\varphi-1))\mathbf{Y}\left[\bar{\mathbf{L}}\mathbf{U}(\mathbf{y}_1,\varrho)+\bar{\mathbf{N}}\mathbf{U}(\mathbf{y}_1,\varrho)\right]+(1+\delta(\varphi-1))\mathbf{Y}[\mathbf{Q}(\mathbf{y}_1,\varrho)]. \tag{31}$$

Using the fact of the inverse Yang transform of (30) and (31), respectively, produces

$$\mathbf{U}(\mathbf{y}_1,\varrho)=\mathscr{G}(\varphi)+\mathbf{Y}^{-1}\left\{\varphi^{\delta}\mathbf{Y}[\mathbf{Q}(\mathbf{y}_1,\varrho)]\right\}-\mathbf{Y}^{-1}\left\{\varphi^{\delta}\mathbf{Y}\left[\bar{\mathbf{L}}\mathbf{U}(\mathbf{y}_1,\varrho)+\bar{\mathbf{N}}\mathbf{U}(\mathbf{y}_1,\varrho)\right]\right\}, \tag{32}$$

$$\mathbf{U}(\mathbf{y}_1,\varrho)=\mathscr{G}(\varphi)+\mathbf{Y}^{-1}\{(1+\delta(\varphi-1))\mathbf{Y}[\mathbf{Q}(\mathbf{y}_1,\varrho)]\}-\mathbf{Y}^{-1}\left\{(1+\delta(\varphi-1))\mathbf{Y}\left[\bar{\mathbf{L}}\mathbf{U}(\mathbf{y}_1,\varrho)+\bar{\mathbf{N}}\mathbf{U}(\mathbf{y}_1,\varrho)\right]\right\}. \tag{33}$$

Employing the recursive approach, we determine

$$\mathbf{U}(\mathbf{y}_1, \varrho) = \sum_{p=0}^{\infty} \mathbf{U}_p(\mathbf{y}_1, \varrho). \tag{34}$$

Moreover, utilizing the linearity $\bar{\mathbf{L}}$ of the operator, thus we have

$$\bar{\mathbf{L}}\left(\sum_{p=0}^{\infty} \mathbf{U}_p(\mathbf{y}_1, \varrho)\right) = \sum_{p=0}^{\infty} \bar{\mathbf{L}}\left[\mathbf{U}_p(\mathbf{y}_1, \varrho)\right], \tag{35}$$

and the nonlinearity $\bar{\mathbf{N}}$ handled by (see [42])

$$\begin{aligned} \bar{\mathbf{N}}\left(\sum_{p=0}^{\infty} \mathbf{U}_p(\mathbf{y}_1, \varrho)\right) &= \bar{\mathbf{N}}(\mathbf{U}_0(\mathbf{y}_1, \varrho)) \\ &+ \sum_{q=1}^{\infty}\left[\bar{\mathbf{N}}\left(\sum_{\kappa=0}^{p} \mathbf{U}_p(\mathbf{y}_1, \varrho)\right) - \bar{\mathbf{N}}\left(\sum_{\kappa=0}^{p-1} \mathbf{U}_p(\mathbf{y}_1, \varrho)\right)\right] \\ &= \bar{\mathbf{N}}(\mathbf{U}_0) + \sum_{q=1}^{\infty} D_p, \end{aligned} \tag{36}$$

where $D_p = \bar{\mathbf{N}}(\sum_{\kappa=0}^{p} \mathbf{U}_p) - \bar{\mathbf{N}}(\sum_{\kappa=0}^{p-1} \mathbf{U}_p)$.

Inserting (37), (39), and (36) into (32) and (33), respectively, we observe

$$\begin{aligned} \sum_{p=0}^{\infty} \mathbf{U}_p(\mathbf{y}_1, \varrho) &= \mathscr{G}(\varphi) + \mathbf{Y}^{-1}\left\{\varphi^{\delta}\mathbf{Y}[\mathbf{Q}(\mathbf{y}_1, \varrho)]\right\} \\ &- \mathbf{Y}^{-1}\left\{\varphi^{\delta}\mathbf{Y}\left[\bar{\mathbf{L}}\left(\sum_{\kappa=0}^{p} \mathbf{U}_p(\mathbf{y}_1, \varrho)\right) + \bar{\mathbf{N}}(\mathbf{U}_0) + \sum_{\kappa=1}^{p} D_p\right]\right\}, \end{aligned} \tag{37}$$

$$\begin{aligned} \sum_{p=0}^{\infty} \mathbf{U}_p(\mathbf{y}_1, \varrho) &= \mathscr{G}(\varphi) + \mathbf{Y}^{-1}\{(1+\delta(\varphi-1))\mathbf{Y}[\mathbf{Q}(\mathbf{y}_1, \varrho)]\} \\ &- \mathbf{Y}^{-1}\left\{(1+\delta(\varphi-1))\mathbf{Y}\left[\bar{\mathbf{L}}\left(\sum_{p=0}^{p} \mathbf{U}_p(\mathbf{y}_1, \varrho)\right) + \bar{\mathbf{N}}(\mathbf{U}_0) + \sum_{q=1}^{p} D_p\right]\right\}. \end{aligned} \tag{38}$$

Ultimately, for CFD, we develop appropriate analysis procedure:

$$\begin{aligned} \mathbf{U}_0(\mathbf{y}_1, \varrho) &= \mathscr{G}(\varphi) + \mathbf{Y}^{-1}\left\{\varphi^{\delta}\mathscr{L}[\mathbf{Q}(\mathbf{y}_1, \varrho)]\right\}, \\ \mathbf{U}_1(\mathbf{y}_1, \varrho) &= -\mathbf{Y}^{-1}\left\{\varphi^{\delta}\mathbf{Y}\left[\bar{\mathbf{L}}(\mathbf{U}_0(\mathbf{y}_1, \varrho)) + \bar{\mathbf{N}}(\mathbf{U}_0(\mathbf{y}_1, \varrho))\right]\right\}, \\ &\vdots \\ \mathbf{U}_{q+1}(\mathbf{y}_1, \varrho) &= -\mathbf{Y}^{-1}\left\{\varphi^{\delta}\mathbf{Y}\left[\bar{\mathbf{L}}\left(\mathbf{U}_p(\mathbf{y}_1, \varrho)\right) + D_p\right]\right\}. \end{aligned} \tag{39}$$

The exploratory procedure for the Caputo-Fabrizio fractional derivative operator is shown then:

$$\begin{aligned} \mathbf{U}_0(\mathbf{y}_1, \varrho) &= \mathscr{G}(\varphi) + \mathbf{Y}^{-1}\{(1+\delta(\varphi-1))\mathscr{L}[\mathbf{Q}(\mathbf{y}_1, \varrho)]\}, \\ \mathbf{U}_1(\mathbf{y}_1, \varrho) &= -\mathbf{Y}^{-1}\left\{(1+\delta(\varphi-1))\mathbf{Y}\left[\bar{\mathbf{L}}(\mathbf{U}_0(\mathbf{y}_1, \varrho)) + \bar{\mathbf{N}}(\mathbf{U}_0(\mathbf{y}_1, \varrho))\right]\right\}, \\ &\vdots \\ \mathbf{U}_{q+1}(\mathbf{y}_1, \varrho) &= -\mathbf{Y}^{-1}\left\{(1+\delta(\varphi-1))\mathbf{Y}\left[\bar{\mathbf{L}}\left(\mathbf{U}_p(\mathbf{y}_1, \varrho)\right) + D_p\right]\right\}. \end{aligned} \tag{40}$$

Eventually, the q-term result in series formulation is generated by (37), (39), and (40), and we have

$$\begin{aligned} \mathbf{U}(\mathbf{y}_1, \varrho) \cong\ & \mathbf{U}_0(\mathbf{y}_1, \varrho) + \mathbf{U}_1(\mathbf{y}_1, \varrho) + \mathbf{U}_2(\mathbf{y}_1, \varrho) \\ & + \cdots + \mathbf{U}_p(\mathbf{y}_1, \varrho), q \in \mathbb{N}. \end{aligned} \tag{41}$$

4. Mathematical Formulations of BSM via Caputo-Fabrizio Fractional Derivative Operator

The coming parts will illustrate how well the adequate conditions ensure the formation of a unique solution. Our hypothesis of the existence of solutions in the scenario of YDM is developed by [47].

Theorem 8 (Uniqueness theorem). *For $0 < \varepsilon < 1$, then system (24) has a unique solution, where $\varepsilon = (K_1 + K_2 + K_3)(1 + \delta(\varrho - 1))$.*

Proof. Surmise that there is a set of continuous mappings in the Banach space $\Omega = (\mathbb{C}[\mathscr{I}], \|.\|)$ Considering $\mathscr{I} = [0, \mathscr{T}]$, present the norm $\|.\|$ To continue this, suppose a mapping

$\mathscr{V} : \Omega \mapsto \Omega$ such that

$$\mathbf{U}_{\ell+1}(\mathbf{y}_1, \varrho) = \mathbf{U}(\mathbf{y}_1, \varrho) + \mathbf{Y}^{-1}[(1+\delta(\varphi-1))\mathbf{Y}[\mathbf{L}[\mathbf{U}_\ell(\mathbf{y}_1, \varrho)] + \bar{P}[\mathbf{U}_\ell(\mathbf{y}_1, \varrho)] + \mathbf{N}[\mathbf{U}_\ell(\mathbf{y}_1, \varrho)]]], \ell \geq 0, \quad (42)$$

where $\mathbf{L}[\mathbf{U}(\mathbf{y}_1, \varrho)] \equiv \partial^3 \mathbf{U}(\mathbf{y}_1, \varrho)/\partial \mathbf{y}_1^2$ and $\bar{P}[\mathbf{U}(\mathbf{y}_1, \varrho)] \equiv \partial \mathbf{U}(\mathbf{y}_1, \varrho)/\partial \mathbf{y}_1$. Here, suppose that $\mathbf{L}[\mathbf{U}(\mathbf{y}_1, \varrho)]$ and $\mathbf{N}[\mathbf{U}(\mathbf{y}_1, \varrho)]$ are also Lipschitzian with $|\bar{P}\mathbf{U} - \bar{P}\widehat{\mathbf{U}}| < \mathbf{K}_1|\mathbf{U} - \widehat{\mathbf{U}}|$ and $|\mathbf{L}\mathbf{U} - \mathbf{L}\widehat{\mathbf{U}}| < \mathbf{K}_2|\mathbf{U} - \widehat{\mathbf{U}}|$, where $\mathbf{K}_1$ and $\mathbf{K}_2$ are Lipschitz constant, respectively, and $\mathbf{U}, \widehat{\mathbf{U}}$ are distinct functional values.

$$\begin{aligned}
\|\mathscr{V}\mathbf{U} - \mathscr{V}\widehat{\mathbf{U}}\| &= \max_{\varrho \in \mathscr{J}} |\mathbf{Y}^{-1}[(1+\delta(\varphi-1))\mathbf{Y}[\mathbf{L}[\mathbf{U}(\mathbf{y}_1, \varrho)] \\
&+ \bar{P}[\mathbf{U}(\mathbf{y}_1, \varrho)] + \mathbf{N}[\mathbf{U}(\mathbf{y}_1, \varrho)]]] \\
&- \mathbf{Y}^{-1}[(1+\delta(\varphi-1))\mathbf{Y}[\mathbf{L}[\widehat{\mathbf{U}}(\mathbf{y}_1, \varrho)] \\
&+ \bar{P}[\widehat{\mathbf{U}}(\mathbf{y}_1, \varrho)] + \mathbf{N}[\widehat{\mathbf{U}}(\mathbf{y}_1, \varrho)]]]| \\
&\leq \max_{\varrho \in \mathscr{J}} |\mathbf{Y}^{-1}[(1+\delta(\varphi-1))\mathbf{Y}[\mathbf{L}[\mathbf{U}(\mathbf{y}_1, \varrho)] \\
&- \mathbf{L}[\widehat{\mathbf{U}}(\mathbf{y}_1, \varrho)]]] + \mathbf{Y}^{-1}[(1+\delta(\varphi-1))\mathbf{Y}[\bar{P}[\mathbf{U}(\mathbf{y}_1, \varrho)] \\
&- \bar{P}[\widehat{\mathbf{U}}(\mathbf{y}_1, \varrho)]]] + \mathbf{Y}^{-1}[(1+\delta(\varphi-1))\mathbf{Y}[\mathbf{N}[\mathbf{U}(\mathbf{y}_1, \varrho)] \\
&- \mathbf{N}[\widehat{\mathbf{U}}(\mathbf{y}_1, \varrho)]]]| \leq \max_{\varrho \in \mathscr{J}} [\mathbf{K}_1 \mathbf{Y}^{-1}[(1+\delta(\varphi-1))\mathbf{Y}|\mathbf{U}(\mathbf{y}_1, \varrho) \\
&- \widehat{\mathbf{U}}(\mathbf{y}_1, \varrho)|] + \mathbf{K}_2 \mathbf{Y}^{-1}[(1+\delta(\varphi-1))\mathbf{Y}|\mathbf{U}(\mathbf{y}_1, \varrho) - \widehat{\mathbf{U}}(\mathbf{y}_1, \varrho)|] \\
&+ \mathbf{K}_3 \mathbf{Y}^{-1}[(1+\delta(\varphi-1))\mathbf{Y}|\mathbf{U}(\mathbf{y}_1, \varrho) - \widehat{\mathbf{U}}(\mathbf{y}_1, \varrho)|]] \\
&\leq \max_{\varrho \in \mathscr{J}} (\mathbf{K}_1 + \mathbf{K}_2 + \mathbf{K}_3)\mathbf{Y}^{-1}[(1+\delta(\varphi-1))\mathbf{Y}|\mathbf{U}(\mathbf{y}_1, \varrho) - \widehat{\mathbf{U}}(\mathbf{y}_1, \varrho)|] \\
&\leq (\mathbf{K}_1 + \mathbf{K}_2 + \mathbf{K}_3)\mathbf{Y}^{-1}[(1+\delta(\varphi-1))\mathbf{Y}\|\mathbf{U}(\mathbf{y}_1, \varrho) - \widehat{\mathbf{U}}(\mathbf{y}_1, \varrho)\|] \\
&= (\mathbf{K}_1 + \mathbf{K}_2 + \mathbf{K}_3)\mathbf{Y}^{-1}[(1+\delta(\varphi-1))\varphi\|\mathbf{U}(\mathbf{y}_1, \varrho) - \widehat{\mathbf{U}}(\mathbf{y}_1, \varrho)\|] \\
&= (\mathbf{K}_1 + \mathbf{K}_2 + \mathbf{K}_3)(1+\delta(\varrho-1))\|\mathbf{U}(\mathbf{y}_1, \varrho) - \widehat{\mathbf{U}}(\mathbf{y}_1, \varrho)\|.
\end{aligned} \quad (43)$$

For $0 < \varepsilon < 1$, the functional is contraction. As a result of the Banach contraction fixed point hypothesis, (16) has a fixed value. This produces the intended outcome. □

Theorem 9 (Convergence analysis). *Equation (16) has a generic type solution and will be convergent.*

Proof. Surmise that $\widehat{S}_\ell$ be the *nth* partial sum, that is, $\widehat{S}_\ell = \sum_{m=0}^{\ell} \mathbf{U}_\ell(\mathbf{y}_1, \varrho)$. Further, we exhibit $\{\widehat{S}_\ell\}$ is a Cauchy sequence in Banach space U.

We do it by contemplating a novel kind of Adomian polynomials.

$$\begin{aligned}
\bar{R}(\widehat{S}_\ell) &= \tilde{\mathbf{H}}_\ell + \sum_{p=0}^{\ell-1} \tilde{\mathbf{H}}_p, \\
\mathbf{N}(\widehat{S}_\ell) &= \tilde{\mathbf{H}}_\ell + \sum_{c=0}^{\ell-1} \tilde{\mathbf{H}}_c.
\end{aligned} \quad (44)$$

Now

$$\begin{aligned}
\|\widehat{S}_\ell - \widehat{S}_p\| &= \max_{\varrho \in \mathscr{J}} |\widehat{S}_\ell - \widehat{S}_p| = \max_{\varrho \in \mathscr{J}} \left| \sum_{m=q+1}^{\ell} \widehat{\mathbf{U}}(\mathbf{y}_1, \varrho) \right|, (m = 1, 2, 3, \cdots) \\
&\leq \max_{\varrho \in \mathscr{J}} \left| \mathbf{Y}^{-1}\left[(1+\delta(\varphi-1))\mathbf{Y}\left[\sum_{m=q+1}^{\ell} \mathbf{L}[\mathbf{U}_{\ell-1}(\mathbf{y}_1, \varrho)]\right]\right] \right. \\
&+ \mathbf{Y}^{-1}\left[(1+\delta(\varphi-1))\mathbf{Y}\left[\sum_{m=q+1}^{\ell} \bar{P}[\mathbf{U}_{\ell-1}(\mathbf{y}_1, \varrho)]\right]\right] \\
&\left. + \mathbf{Y}^{-1}\left[(1+\delta(\varphi-1))\mathbf{Y}\left[\sum_{m=q+1}^{\ell} \tilde{\mathbf{H}}_{\ell-1}(\mathbf{y}_1, \varrho)\right]\right] \right| \\
&= \max_{\varrho \in \mathscr{J}} \left| \mathbf{Y}^{-1}\left[(1+\delta(\varphi-1))\mathbf{Y}\left[\sum_{m=q}^{\ell-1} \mathbf{L}[\mathbf{U}_\ell(\mathbf{y}_1, \varrho)]\right]\right] \right. \\
&+ \mathbf{Y}^{-1}\left[(1+\delta(\varphi-1))\mathbf{Y}\left[\sum_{m=q}^{\ell-1} \bar{P}[\mathbf{U}_\ell(\mathbf{y}_1, \varrho)]\right]\right] \\
&\left. + \mathbf{Y}^{-1}\left[(1+\delta(\varphi-1))\mathbf{Y}\left[\sum_{m=q}^{\ell-1} \tilde{\mathbf{H}}_\ell(\mathbf{y}_1, \varrho)\right]\right] \right| \\
&\leq \max_{\varrho \in \mathscr{J}} \left| \mathbf{Y}^{-1}\left[(1+\delta(\varphi-1))\mathbf{Y}\left[\sum_{m=q}^{\ell-1} \mathbf{L}(\widehat{S}_{\ell-1}) - \mathbf{L}(\widehat{S}_{q-1})\right]\right] \right. \\
&+ \mathbf{Y}^{-1}\left[(1+\delta(\varphi-1))\mathbf{Y}\left[\sum_{m=q}^{\ell-1} \bar{P}(\widehat{S}_{\ell-1}) - \bar{P}(\widehat{S}_{q-1})\right]\right] \\
&\left. + \mathbf{Y}^{-1}\left[(1+\delta(\varphi-1))\mathbf{Y}\left[\sum_{m=q}^{\ell-1} \mathbf{N}(\widehat{S}_{\ell-1}) - \mathbf{N}(\widehat{S}_{q-1})\right]\right] \right| \\
&\leq \max_{\varrho \in \mathscr{J}} |\mathbf{Y}^{-1}[(1+\delta(\varphi-1))\mathbf{Y}[\mathbf{L}(\widehat{S}_{\ell-1}) - \mathbf{L}(\widehat{S}_{q-1})]] \\
&+ \mathbf{Y}^{-1}[(1+\delta(\varphi-1))\mathbf{Y}[\bar{P}(\widehat{S}_{\ell-1}) - \bar{P}(\widehat{S}_{q-1})]] \\
&+ \mathbf{Y}^{-1}[(1+\delta(\varphi-1))\mathbf{Y}[\mathbf{N}(\widehat{S}_{\ell-1}) - \mathbf{N}(\widehat{S}_{q-1})]]| \\
&\leq \mathbf{K}_1 \max_{\varrho \in \mathscr{J}} \mathbf{Y}^{-1}|[(1+\delta(\varphi-1))\mathbf{Y}[(\widehat{S}_{\ell-1}) - (\widehat{S}_{q-1})]]| \\
&+ \mathbf{K}_2 \max_{\varrho \in \mathscr{J}} |\mathbf{Y}^{-1}[(1+\delta(\varphi-1))\mathbf{Y}[(\widehat{S}_{\ell-1}) - (\widehat{S}_{q-1})]]| \\
&+ \mathbf{K}_3 \max_{\varrho \in \mathscr{J}} |\mathbf{Y}^{-1}[(1+\delta(\varphi-1))\mathbf{Y}[(\widehat{S}_{\ell-1}) - (\widehat{S}_{q-1})]]| \\
&= (\mathbf{K}_1 + \mathbf{K}_2 + \mathbf{K}_3)\mathbf{Y}^{-1}[(1+\delta(\varphi-1))\varphi\|\widehat{S}_{\ell-1} - \widehat{S}_{q-1}\|. \\
&= (\mathbf{K}_1 + \mathbf{K}_2 + \mathbf{K}_3)(1+\delta(\varrho-1))\|\widehat{S}_{\ell-1} - \widehat{S}_{q-1}\|.
\end{aligned} \quad (45)$$

Assume $n = q + 1$; then

$$\|\widehat{S}_{q+1} - \widehat{S}_p\| \leq \varepsilon\|\widehat{S}_p - \widehat{S}_{q-1}\| \leq \varepsilon^2\|\widehat{S}_{q-1} - \widehat{S}_{q-2}\| \leq \cdots \leq \varepsilon^p\|\widehat{S}_1 - \widehat{S}_0\|, \quad (46)$$

where $\varepsilon = (1 + \delta(\varrho - 1))$. In view of triangular variant, we have

$$\begin{aligned}
\|\widehat{S}_\ell - \widehat{S}_p\| &\leq \|\widehat{S}_{q+1} - \widehat{S}_p\| + \|\widehat{S}_{q+2} - \widehat{S}_{q+1}\| + \cdots + \|\widehat{S}_\ell - \widehat{S}_{\ell-1}\| \\
&\leq [\varepsilon^p + \varepsilon^{q+1} + \cdots + \varepsilon^{\ell-1}]\|\widehat{S}_1 - \widehat{S}_0\| \\
&\leq \varepsilon^p\left(\frac{1 - \varepsilon^{\ell-p}}{\varepsilon}\right)\|\mathbf{U}_1\|,
\end{aligned} \quad (47)$$

since $0 < \varepsilon < 1$, we have $(1 - \varepsilon^{\ell - p}) < 1$, and then

$$\|\widehat{S}_\ell - \widehat{S}_p\| \le \frac{\varepsilon^p}{1-\varepsilon} \max_{\varrho \in \mathcal{J}} \|\mathbf{U}_1\|. \tag{48}$$

Thus, $|\mathbf{U}_1| < \infty$ (since $\mathbf{U}(\mathbf{y}_1, \varrho)$ is bounded). Also, as $q \mapsto \infty$, then $\|\widehat{S}_\ell - \widehat{S}_p\| \mapsto 0$. Therefore, $\{\widehat{S}_1\}$ is a Cauchy sequence in K. Ultimately, $\sum_{n=0}^{\infty} \mathbf{U}_\ell$ is convergent, and the direct result is obtained. □

Theorem 10 (see [47]) (Error estimate). *The absolute inaccuracy of the (16) through (24) sum is determined as*

$$\max_{\varrho \in \mathcal{J}} \left| \mathbf{U}(\mathbf{y}_1, \varrho) - \sum_{\ell=1}^{p} \mathbf{U}_\ell(\mathbf{y}_1, \varrho) \right| \le \frac{\varepsilon^p}{1-\varepsilon} \max_{\varrho \in \mathcal{J}} \|\mathbf{U}_1\|. \tag{49}$$

5. Mathematical Description of BSM Time-Fractional Systems

Here, we construct the estimated analytical solution of BSM considering the CFD and Caputo-Fabrizio fractional derivative operators utilizing the Yang decomposition approach.

5.1. Yang Decomposition Method

Example 1 (see [29]). Surmise the fractional-order BSM (4) supplemented with the (5).

Case 1. To begin, we utilize the Caputo fractional derivative operator employing the Yang decomposition approach to analyze the (4). Implementing the Yang transform on (4), we get

$$\mathbf{Y}\left[\mathbf{D}_\varrho^\delta \mathbf{U}(\mathbf{y}_1, \varrho)\right] = \mathbf{Y}\left[\frac{\partial^2 \mathbf{U}(\mathbf{y}_1, \varrho)}{\partial \mathbf{y}_1^2} + (\zeta - 1)\frac{\partial \mathbf{U}(\mathbf{y}_1, \varrho)}{\partial \mathbf{y}_1} - \zeta \mathbf{U}(\mathbf{y}_1, \varrho)\right]. \tag{50}$$

Utilizing the Yang transform's differentiation criteria gives

$$\begin{aligned} \varphi^{-\delta}(\varrho)\mathbf{Y}[\mathbf{U}(\mathbf{y}_1, \varrho)] &= \phi(\varrho) \sum_{p=0}^{p-1} \varphi^{1-\delta-p} \mathbf{U}^{(p)}(0) \\ &+ \mathbf{Y}\left[\frac{\partial^2 \mathbf{U}(\mathbf{y}_1, \varrho)}{\partial \mathbf{y}_1^2} + (\zeta - 1)\frac{\partial \mathbf{U}(\mathbf{y}_1, \varrho)}{\partial \mathbf{y}_1} - \zeta \mathbf{U}(\mathbf{y}_1, \varrho)\right]. \end{aligned} \tag{51}$$

Utilizing (5), we find

$$\begin{aligned} \mathbf{Y}[\mathbf{U}(\mathbf{y}_1, \varrho)] &= \varphi \max\left(\exp\left(\mathbf{y}_1\right) - 1, 0\right) \\ &+ \varphi^\delta \mathbf{Y}\left[\frac{\partial^2 \mathbf{U}(\mathbf{y}_1, \varrho)}{\partial \mathbf{y}_1^2} + (\zeta - 1)\frac{\partial \mathbf{U}(\mathbf{y}_1, \varrho)}{\partial \mathbf{y}_1} - \zeta \mathbf{U}(\mathbf{y}_1, \varrho)\right]. \end{aligned} \tag{52}$$

Applying the inverse Yang transform produces

$$\begin{aligned} \mathbf{U}(\mathbf{y}_1, \varrho) &= \mathbf{Y}^{-1}[\varphi.\max\left(\exp\left(\mathbf{y}_1\right) - 1, 0\right)] \\ &+ \mathbf{Y}^{-1}\left[\varphi^\delta \mathbf{Y}\left[\frac{\partial^2 \mathbf{U}(\mathbf{y}_1, \varrho)}{\partial \mathbf{y}_1^2} + (\zeta - 1)\frac{\partial \mathbf{U}(\mathbf{y}_1, \varrho)}{\partial \mathbf{y}_1} - \zeta \mathbf{U}(\mathbf{y}_1, \varrho)\right]\right]. \end{aligned} \tag{53}$$

To determine this, apply the Yang decomposition approach as follows:

$$\begin{aligned} \mathbf{U}_0(\mathbf{y}_1, \varrho) &= \mathbf{Y}^{-1}[\varphi.\max\left(\exp\left(\mathbf{y}_1\right) - 1, 0\right)] \\ &= \max\left(\exp\left(\mathbf{y}_1\right) - 1, 0\right). \end{aligned} \tag{54}$$

We predict that the unidentified mapping $\mathbf{U}(\mathbf{y}_1, \varrho)$ may be expressed as an infinite series of the pattern

$$\begin{aligned} \mathbf{U}(\mathbf{y}_1, \varrho) &= \sum_{p=0}^{\infty} \mathbf{U}_p(\mathbf{y}_1, \varrho), \\ \sum_{p=0}^{\infty} \mathbf{U}_{q+1}(\mathbf{y}_1, \varrho) &= \mathbf{Y}^{-1}\left[\varphi^\delta \mathbf{Y}\left[\sum_{p=0}^{\infty} (\mathbf{U}(\mathbf{y}_1, \varrho))_{\mathbf{y}_1\mathbf{y}_1} \right.\right. \\ &\left.\left. + (\zeta - 1)\sum_{p=0}^{\infty} (\mathbf{U}(\mathbf{y}_1, \varrho))_{\mathbf{y}_1} - \zeta \sum_{p=0}^{\infty} (\mathbf{U}(\mathbf{y}_1, \varrho))\right]\right], p = 0, 1, 2, \cdots, \end{aligned} \tag{55}$$

$$\begin{aligned} \mathbf{U}_1(\mathbf{y}_1, \varrho) &= \mathbf{Y}^{-1}\left[\varphi^\delta \mathbf{Y}\left[(\mathbf{U}_0(\mathbf{y}_1, \varrho))_{\mathbf{y}_1\mathbf{y}_1} + (\zeta - 1)(\mathbf{U}_0(\mathbf{y}_1, \varrho))_{\mathbf{y}_1} + \zeta \mathbf{U}_0\right]\right] \\ &= [\zeta \max\left(\exp\left(\mathbf{y}_1\right), 0\right) - \zeta \max\left(\exp\left(\mathbf{y}_1 - 1\right), 0\right)]\mathbf{Y}^{-1}\left[\varphi^{\delta+1}\right] \\ &= [\zeta \max\left(\exp\left(\mathbf{y}_1\right), 0\right) - \zeta \max\left(\exp\left(\mathbf{y}_1 - 1\right), 0\right)]\frac{\varrho^\delta}{\Gamma(\delta + 1)}, \\ \mathbf{U}_2(\mathbf{y}_1, \varrho) &= \mathbf{Y}^{-1}\left[\frac{1}{\varphi^\delta(\varrho)}\mathbf{Y}\left[(\mathbf{U}_1(\mathbf{y}_1, \varrho))_{\mathbf{y}_1\mathbf{y}_1} + (\zeta - 1)(\mathbf{U}_1(\mathbf{y}_1, \varrho))_{\mathbf{y}_1} + \zeta \mathbf{U}_1\right]\right] \\ &= \left[-\zeta^2 \max\left(\exp\left(\mathbf{y}_1\right), 0\right) + \zeta^2 \max\left(\exp\left(\mathbf{y}_1 - 1\right), 0\right)\right]\frac{\varrho^{2\delta}}{\Gamma(2\delta + 1)}, \\ \mathbf{U}_3(\mathbf{y}_1, \varrho) &= \mathbf{Y}^{-1}\left[\frac{1}{\varphi^\delta(\varrho)}\mathbf{Y}\left[(\mathbf{U}_2(\mathbf{y}_1, \varrho))_{\mathbf{y}_1\mathbf{y}_1} + (\zeta - 1)(\mathbf{U}_2(\mathbf{y}_1, \varrho))_{\mathbf{y}_1} + \zeta \mathbf{U}_2\right]\right] \\ &= \left[-\zeta^3 \max\left(\exp\left(\mathbf{y}_1\right), 0\right) + \zeta^3 \max\left(\exp\left(\mathbf{y}_1 - 1\right), 0\right)\right]\frac{\varrho^{3\delta}}{\Gamma(3\delta + 1)}. \\ &\vdots \end{aligned} \tag{56}$$

For Example 1, the series form solution is developed as follows:

$$\begin{aligned}\mathbf{U}(\mathbf{y}_1,\varrho)&=\mathbf{U}_0(\mathbf{y}_1,\varrho)+\mathbf{U}_1(\mathbf{y}_1,\varrho)+\mathbf{U}_2(\mathbf{y}_1,\varrho)+\mathbf{U}_3(\mathbf{y}_1,\varrho)+\cdots\\&=\max\left(\exp\left(\mathbf{y}_1-1\right),0\right)\\&\quad\cdot\left[1-\frac{\zeta\varrho^{\delta}}{\Gamma(\delta+1)}+\frac{\zeta^2\varrho^{2\delta}}{\Gamma(2\delta+1)}-\frac{\zeta^3\varrho^{3\delta}}{\Gamma(3\delta+1)}+\cdots\right]\\&\quad+\max\left(\exp\left(\mathbf{y}_1\right),0\right)\\&\quad\cdot\left[1-1+\frac{\zeta\varrho^{\delta}}{\Gamma(\delta+1)}-\frac{\zeta^2\varrho^{2\delta}}{\Gamma(2\delta+1)}+\frac{\zeta^3\varrho^{3\delta}}{\Gamma(3\delta+1)}+\cdots\right]\\&=\max\left(\exp\left(\mathbf{y}_1-1\right),0\right)E_{\delta}\left(-\zeta(\varrho)^{\delta}\right)\\&\quad+\max\left(\exp\left(\mathbf{y}_1\right),0\right)E_{\delta}\left(1-\zeta(\varrho)^{\delta}\right).\end{aligned}\tag{57}$$

Case 2. The Caputo-Fabrizio fractional derivative operator and the Yang decomposition approach are now used to solve equation (4). Assuming (50) and implementing the Yang transform's differentiation criteria, we obtain

$$\begin{aligned}\frac{1}{1+\delta(1-\varphi)}\mathbf{Y}[\mathbf{U}(\mathbf{y}_1,\varrho)]&=\frac{1}{1+\delta(1-\varphi)}\sum_{p=0}^{p-1}\varphi^{1-\delta-p}(\varrho)\mathbf{U}^{(p)}(0)\\&\quad+\mathbf{Y}\left[\frac{\partial^2\mathbf{U}(\mathbf{y}_1,\varrho)}{\partial\mathbf{y}_1^2}+(\zeta-1)\frac{\partial\mathbf{U}(\mathbf{y}_1,\varrho)}{\partial\mathbf{y}_1}-\zeta\mathbf{U}(\mathbf{y}_1,\varrho)\right].\end{aligned}\tag{58}$$

Utilizing (5), we obtain

$$\begin{aligned}\mathbf{Y}[\mathbf{U}(\mathbf{y}_1,\varrho)]&=\varphi\max\left(\exp\left(\mathbf{y}_1\right)-1,0\right)+(1+\delta(\varphi-1))\mathbf{Y}\\&\quad\cdot\left[\frac{\partial^2\mathbf{U}(\mathbf{y}_1,\varrho)}{\partial\mathbf{y}_1^2}+(\zeta-1)\frac{\partial\mathbf{U}(\mathbf{y}_1,\varrho)}{\partial\mathbf{y}_1}-\zeta\mathbf{U}(\mathbf{y}_1,\varrho)\right],\\\mathbf{U}(\mathbf{y}_1,\varrho)&=\mathbf{Y}^{-1}\left[\varphi.\max\left(\exp\left(\mathbf{y}_1\right)-1,0\right)\right]+\mathbf{Y}^{-1}\\&\quad\cdot\left[(1+\delta(\varphi-1))\mathbf{Y}\left[\frac{\partial^2\mathbf{U}(\mathbf{y}_1,\varrho)}{\partial\mathbf{y}_1^2}+(\zeta-1)\frac{\partial\mathbf{U}(\mathbf{y}_1,\varrho)}{\partial\mathbf{y}_1}-\zeta\mathbf{U}(\mathbf{y}_1,\varrho)\right]\right].\end{aligned}\tag{59}$$

Employing the Yang decomposition approach produces

$$Q_0(\mathbf{y}_1,\varrho)=\mathbf{Y}^{-1}\left[\varphi\max\left(\exp\left(\mathbf{y}_1\right)-1,0\right)\right]=\max\left(\exp\left(\mathbf{y}_1\right)-1,0\right).\tag{60}$$

We predict that the unidentified mapping $\mathbf{U}(\mathbf{y}_1,\varrho)$ may be expressed as an infinite series of the pattern

$$\begin{aligned}&\mathbf{U}(\mathbf{y}_1,\varrho)=\sum_{p=0}^{\infty}\mathbf{U}_p(\mathbf{y}_1,\varrho),\\&\sum_{p=0}^{\infty}\mathbf{U}_{q+1}(\mathbf{y}_1,\varrho)=\mathbf{Y}^{-1}\left[(1+\delta(\varphi-1))\mathbf{Y}\left[\sum_{p=0}^{\infty}(\mathbf{U}(\mathbf{y}_1,\varrho))_{\mathbf{y}_1\mathbf{y}_1}\right.\right.\\&\quad\left.\left.+(\zeta-1)\sum_{p=0}^{\infty}(\mathbf{U}(\mathbf{y}_1,\varrho))_{\mathbf{y}_1}-\zeta\sum_{p=0}^{\infty}(\mathbf{U}(\mathbf{y}_1,\varrho))\right]\right],p=0,1,2,\cdots,\end{aligned}\tag{61}$$

$$\begin{aligned}\mathbf{U}_1(\mathbf{y}_1,\varrho)&=\mathbf{Y}^{-1}\left[(1+\delta(\varphi-1))\mathbf{Y}\left[(\mathbf{U}_0(\mathbf{y}_1,\varrho))_{\mathbf{y}_1\mathbf{y}_1}\right.\right.\\&\quad\left.\left.+(\zeta-1)(\mathbf{U}_0(\mathbf{y}_1,\varrho))_{\mathbf{y}_1}+\zeta\mathbf{U}_0\right]\right]\\&=\left[\zeta\max\left(\exp\left(\mathbf{y}_1\right),0\right)-\zeta\max\left(\exp\left(\mathbf{y}_1-1\right),0\right)\right]\\&\quad\cdot(1+\delta(\varrho-1)),\\\mathbf{U}_2(\mathbf{y}_1,\varrho)&=\mathbf{Y}^{-1}\left[(1+\delta(\varphi-1))\mathbf{Y}\left[(\mathbf{U}_1(\mathbf{y}_1,\varrho))_{\mathbf{y}_1\mathbf{y}_1}\right.\right.\\&\quad\left.\left.+(\zeta-1)(\mathbf{U}_1(\mathbf{y}_1,\varrho))_{\mathbf{y}_1}+\zeta\mathbf{U}_1\right]\right]\\&=-\left[\zeta^2\max\left(\exp\left(\mathbf{y}_1\right),0\right)+\zeta^2\max\left(\exp\left(\mathbf{y}_1-1\right),0\right)\right]\\&\quad\cdot\left((1-\delta)^2+2\varrho\delta(1-\delta)+\frac{\rho^2\delta^2}{2}\right),\\\mathbf{U}_3(\mathbf{y}_1,\varrho)&=\mathbf{Y}^{-1}\left[(1+\delta(\varphi-1))\mathbf{Y}\left[(\mathbf{U}_2(\mathbf{y}_1,\varrho))_{\mathbf{y}_1\mathbf{y}_1}\right.\right.\\&\quad\left.\left.+(\zeta-1)(\mathbf{U}_2(\mathbf{y}_1,\varrho))_{\mathbf{y}_1}+\zeta\mathbf{U}_2\right]\right]\\&=-\frac{\left[\zeta^3\max\left(\exp\left(\mathbf{y}_1\right),0\right)+\zeta^3\max\left(\exp\left(\mathbf{y}_1-1\right),0\right)\right]}{\mathbb{A}^3(\delta)}\\&\quad\times\left((1-\delta)^3+3\varrho^2\delta^2(1-\delta)\frac{\rho^2}{2}+3\varrho\delta(1-\delta)^2+\frac{\varrho^3\delta^3}{3}\right),\vdots\end{aligned}\tag{62}$$

For Example 1, the series form solution is developed as follows:

$$\begin{aligned}\mathbf{U}(\mathbf{y}_1,\varrho)&=\mathbf{U}_0(\mathbf{y}_1,\varrho)+\mathbf{U}_1(\mathbf{y}_1,\varrho)+\mathbf{U}_2(\mathbf{y}_1,\varrho)+\mathbf{U}_3(\mathbf{y}_1,\varrho)\\&\quad+\cdots,=\max\left(\exp\left(\mathbf{y}_1-1\right),0\right)\\&\quad\cdot\left[1-\frac{\zeta\varrho^{\delta}}{\Gamma(\delta+1)}+\frac{\zeta^2\varrho^{2\delta}}{\Gamma(2\delta+1)}-\frac{\zeta^3\varrho^{3\delta}}{\Gamma(3\delta+1)}+\cdots\right]\\&\quad+\max\left(\exp\left(\mathbf{y}_1\right),0\right)\\&\quad\cdot\left[1-1+\frac{\zeta\varrho^{\delta}}{\Gamma(\delta+1)}-\frac{\zeta^2\varrho^{2\delta}}{\Gamma(2\delta+1)}+\frac{\zeta^3\varrho^{3\delta}}{\Gamma(3\delta+1)}+\cdots\right]\\&=\max\left(\exp\left(\mathbf{y}_1-1\right),0\right)E_{\delta}\left(-\zeta(\varrho)^{\delta}\right)\\&\quad+\max\left(\exp\left(\mathbf{y}_1\right),0\right)E_{\delta}\left(1-\zeta(\varrho)^{\delta}\right).\end{aligned}\tag{63}$$

Considering the Taylor series expansion and assigning

$\delta = 1$, the exact findings of Example 1 can be determined as

$$\mathbf{U}(\mathbf{y}_1, \varrho) = \max(\exp(\mathbf{y}_1 - 1), 0)\exp(-\zeta\varrho) + \max(\exp(\mathbf{y}_1), 0)[1 - \exp(-\zeta\varrho)]. \tag{64}$$

Example 2 (see [30]). Surmise the fractional-order BSM (6) supplemented with the (7).

Case 1. To begin, we utilize the Caputo fractional derivative operator, employing the Yang decomposition approach to analyze the (6). Implementing the Yang transform on (6), we get

$$\mathbf{Y}\left[\mathbf{D}_\varrho^\delta \mathbf{U}(\mathbf{y}_1, \varrho)\right] = \mathbf{Y}\left[-0.08(2 + \sin \mathbf{y}_1)^2 \mathbf{y}_1^2 \frac{\partial^2 \mathbf{U}(\mathbf{y}_1, \varrho)}{\partial \mathbf{y}_1^2} - 0.06\mathbf{y}_1 \frac{\partial \mathbf{U}(\mathbf{y}_1, \varrho)}{\partial \mathbf{y}_1} + 0.06\mathbf{U}(\mathbf{y}_1, \varrho)\right]. \tag{65}$$

Utilizing the Yang transform's differentiation criteria, gives

$$\varphi^{-\delta}\mathbf{Y}[\mathbf{U}(\mathbf{y}_1, \varrho)] = \sum_{p=0}^{n-1} \varphi^{1-\delta-p}(\varrho)\mathbf{U}^{(p)}(0) + \mathbf{Y}\left[-0.08(2 + \sin \mathbf{y}_1)^2 \mathbf{y}_1^2 \frac{\partial^2 \mathbf{U}(\mathbf{y}_1, \rho)}{\partial \mathbf{y}_1^2} - 0.06\mathbf{y}_1 \frac{\partial \mathbf{U}(\mathbf{y}_1, \varrho)}{\partial \mathbf{y}_1} + 0.06\mathbf{U}(\mathbf{y}_1, \varrho)\right]. \tag{66}$$

Utilizing (7), we find

$$\mathbf{Y}[\mathbf{U}(\mathbf{y}_1, \varrho)] = \varphi.\max(\mathbf{y}_1 - 25\exp(-0.06), 0) + \varphi^\delta \mathbf{Y}\left[-0.08(2 + \sin \mathbf{y}_1)^2 \mathbf{y}_1^2 \frac{\partial^2 \mathbf{U}(\mathbf{y}_1, \varrho)}{\partial \mathbf{y}_1^2} - 0.06\mathbf{y}_1 \frac{\partial \mathbf{U}(\mathbf{y}_1, \varrho)}{\partial \mathbf{y}_1} + 0.06\mathbf{U}(\mathbf{y}_1, \varrho)\right]. \tag{67}$$

Applying the inverse Yang transform produces

$$\mathbf{U}(\mathbf{y}_1, \varrho) = \mathbf{Y}^{-1}[\varphi.\max(\mathbf{y}_1 - 25\exp(-0.06), 0)] + \mathbf{Y}^{-1}\left[\varphi^\delta \mathbf{Y}\left[-0.08(2 + \sin \mathbf{y}_1)^2 \mathbf{y}_1^2 \frac{\partial^2 \mathbf{U}(\mathbf{y}_1, \varrho)}{\partial \mathbf{y}_1^2} - 0.06\mathbf{y}_1 \frac{\partial \mathbf{U}(\mathbf{y}_1, \varrho)}{\partial \mathbf{y}_1} + 0.06\mathbf{U}(\mathbf{y}_1, \varrho)\right]\right]. \tag{68}$$

To determine this, apply the Yang decomposition approach as follows:

$$Q_0(\mathbf{y}_1, \varrho) = \mathbf{Y}^{-1}[\varphi.\max(\mathbf{y}_1 - 25\exp(-0.06), 0)] = \max(\mathbf{y}_1 - 25\exp(-0.06), 0). \tag{69}$$

We predict that the unidentified mapping $\mathbf{U}(\mathbf{y}_1, \varrho)$ may be expressed as an infinite series of the pattern

$$\mathbf{U}(\mathbf{y}_1, \varrho) = \sum_{p=0}^{\infty} \mathbf{U}_p(\mathbf{y}_1, \varrho),$$
$$\sum_{p=0}^{\infty} \mathbf{U}_{q+1}(\mathbf{y}_1, \varrho) = \mathbf{Y}^{-1}\left[\varphi^\delta \mathbf{Y}\left[\sum_{p=0}^{\infty} (\mathbf{U}(\mathbf{y}_1, \varrho))_{\mathbf{y}_1\mathbf{y}_1} + (\zeta - 1)\sum_{p=0}^{\infty} (\mathbf{U}(\mathbf{y}_1, \varrho))_{\mathbf{y}_1} - \zeta \sum_{p=0}^{\infty} (\mathbf{U}(\mathbf{y}_1, \varrho))\right]\right], p = 0, 1, 2, \cdots, \tag{70}$$

$$\begin{aligned}
\mathbf{U}_1(\mathbf{y}_1, \varrho) &= \mathbf{Y}^{-1}\left[\varphi^\delta \mathbf{Y}\left[(\mathbf{U}_0(\mathbf{y}_1, \varrho))_{\mathbf{y}_1\mathbf{y}_1} + (\zeta - 1)(\mathbf{U}_0(\mathbf{y}_1, \varrho))_{\mathbf{y}_1} + \zeta\mathbf{U}_0\right]\right] \\
&= [\zeta \max(\exp(\mathbf{y}_1), 0) - \zeta \max(\exp(\mathbf{y}_1 - 1), 0)]\mathbf{Y}^{-1}\left[\varphi^{\delta+1}\right] \\
&= [\zeta \max(\exp(\mathbf{y}_1), 0) - \zeta \max(\exp(\mathbf{y}_1 - 1), 0)]\frac{\varrho^\delta}{\Gamma(\delta + 1)}, \\
\mathbf{U}_2(\mathbf{y}_1, \varrho) &= \mathbf{Y}^{-1}\left[\frac{1}{\varphi^\delta(\varrho)}\mathbf{Y}\left[(\mathbf{U}_1(\mathbf{y}_1, \varrho))_{\mathbf{y}_1\mathbf{y}_1} + (\zeta - 1)(\mathbf{U}_1(\mathbf{y}_1, \varrho))_{\mathbf{y}_1} + \zeta\mathbf{U}_1\right]\right] \\
&= \left[-\zeta^2 \max(\exp(\mathbf{y}_1), 0) + \zeta^2 \max(\exp(\mathbf{y}_1 - 1), 0)\right]\frac{\varrho^{2\delta}}{\Gamma(2\delta + 1)}, \\
\mathbf{U}_3(\mathbf{y}_1, \varrho) &= \mathbf{Y}^{-1}\left[\frac{1}{\varphi^\delta(\varrho)}\mathbf{Y}\left[(\mathbf{U}_2(\mathbf{y}_1, \varrho))_{\mathbf{y}_1\mathbf{y}_1} + (\zeta - 1)(\mathbf{U}_2(\mathbf{y}_1, \varrho))_{\mathbf{y}_1} + \zeta\mathbf{U}_2\right]\right] \\
&= \left[-\zeta^3 \max(\exp(\mathbf{y}_1), 0) + \zeta^3 \max(\exp(\mathbf{y}_1 - 1), 0)\right]\frac{\varrho^{3\delta}}{\Gamma(3\delta + 1)}. \\
&\vdots
\end{aligned} \tag{71}$$

For Example 2, the series form solution is developed as follows:

$$\begin{aligned}
\mathbf{U}(\mathbf{y}_1, \varrho) &= \mathbf{U}_0(\mathbf{y}_1, \varrho) + \mathbf{U}_1(\mathbf{y}_1, \varrho) + \mathbf{U}_2(\mathbf{y}_1, \varrho) + \mathbf{U}_3(\mathbf{y}_1, \varrho) + \cdots = \max(\mathbf{y}_1 - 25\exp(-0.06), 0) \\
&\quad + (\mathbf{y}_1 - \max(\mathbf{y}_1 - 25\exp(-0.06)), 0) \times \left[1 - 1 - \frac{0.06\varrho^\delta}{\Gamma(\delta + 1)} - \frac{0.0036\varrho^{2\delta}}{\Gamma(2\delta + 1)} - \frac{0.000216\varrho^{3\delta}}{\Gamma(3\delta + 1)} + \cdots\right] \\
&= \max(\mathbf{y}_1 - 25\exp(-0.06), 0) + (\mathbf{y}_1 - \max(\mathbf{y}_1 - 25\exp(-0.06), 0))\left[1 - E_\delta\left(0.06(\varrho)^\delta\right)\right].
\end{aligned} \tag{72}$$

Case 2. The Caputo-Fabrizio fractional derivative operator and the Yang decomposition approach are now used to solve the (6).

Assuming (65) and implementing the Yang transform's differentiation criteria, we obtain

$$\frac{1}{1+\delta(\varphi-1)}\mathbf{Y}[\mathbf{U}(\mathbf{y}_1,\varrho)]=\frac{1}{1+\delta(\varphi-1)}\sum_{p=0}^{n-1}\varphi^{1-\delta-p}(\varrho)\mathbf{U}^{(p)}(0)+\mathbf{Y}\left[-0.08(2+\sin\mathbf{y}_1)^2\mathbf{y}_1^2\frac{\partial^2\mathbf{U}(\mathbf{y}_1,\varrho)}{\partial\mathbf{y}_1^2}-0.06\mathbf{y}_1\frac{\partial\mathbf{U}(\mathbf{y}_1,\varrho)}{\partial\mathbf{y}_1}+0.06\mathbf{U}(\mathbf{y}_1,\varrho)\right]. \tag{73}$$

Utilizing (7), we obtain

$$\mathbf{Y}[\mathbf{U}(\mathbf{y}_1,\varrho)]=\varphi.\max(\mathbf{y}_1-25\exp(-0.06),0)+(1+\delta(\varphi-1))\mathbf{Y}\left[-0.08(2+\sin\mathbf{y}_1)^2\mathbf{y}_1^2\frac{\partial^2\mathbf{U}(\mathbf{y}_1,\varrho)}{\partial\mathbf{y}_1^2}-0.06\mathbf{y}_1\frac{\partial\mathbf{U}(\mathbf{y}_1,\varrho)}{\partial\mathbf{y}_1}+0.06\mathbf{U}(\mathbf{y}_1,\varrho)\right]. \tag{74}$$

Employing the inverse Yang transform gives

$$\mathbf{U}(\mathbf{y}_1,\varrho)=\mathbf{Y}^{-1}[\varphi.\max(\mathbf{y}_1-25\exp(-0.06),0)]+\mathbf{Y}^{-1}\cdot\left[(1+\delta(\varphi-1))\mathbf{Y}\left[-0.08(2+\sin\mathbf{y}_1)^2\mathbf{y}_1^2\frac{\partial^2\mathbf{U}(\mathbf{y}_1,\varrho)}{\partial\mathbf{y}_1^2}-0.06\mathbf{y}_1\frac{\partial\mathbf{U}(\mathbf{y}_1,\varrho)}{\partial\mathbf{y}_1}+0.06\mathbf{U}(\mathbf{y}_1,\varrho)\right]\right]. \tag{75}$$

Employing the Yang decomposition approach, we obtain

$$\begin{aligned}Q_0(\mathbf{y}_1,\varrho)&=\mathbf{Y}^{-1}[\varphi.\max(\mathbf{y}_1-25\exp(-0.06),0)]\\&=\max(\mathbf{y}_1-25\exp(-0.06),0).\end{aligned} \tag{76}$$

We predict the unidentified mapping $\mathbf{U}(\mathbf{y}_1,\varrho)$ may be expressed as an infinite series of the pattern

$$\mathbf{U}(\mathbf{y}_1,\varrho)=\sum_{p=0}^{\infty}\mathbf{U}_p(\mathbf{y}_1,\varrho),$$

$$\sum_{p=0}^{\infty}\mathbf{U}_{q+1}(\mathbf{y}_1,\varrho)=\mathbf{Y}^{-1}\left[(1+\delta(\varphi-1))\mathbf{Y}\left[-0.08(2+\sin\mathbf{y}_1)^2\mathbf{y}_1^2\sum_{p=0}^{\infty}(\mathbf{U}(\mathbf{y}_1,\varrho))_{\mathbf{y}_1\mathbf{y}_1}-0.06\mathbf{y}_1\sum_{p=0}^{\infty}(\mathbf{U}(\mathbf{y}_1,\varrho))_{\mathbf{y}_1}+0.06\sum_{p=0}^{\infty}(\mathbf{U}(\mathbf{y}_1,\varrho))\right]\right],\ p=0,1,2,\cdots, \tag{77}$$

$$\begin{aligned}\mathbf{U}_1(\mathbf{y}_1,\varrho)&=\mathbf{Y}^{-1}\left[(1+\delta(\varphi-1))\mathbf{Y}\left[-0.08(2+\sin\mathbf{y}_1)^2\mathbf{y}_1^2(\mathbf{U}_0(\mathbf{y}_1,\varrho))_{\mathbf{y}_1\mathbf{y}_1}-0.06\mathbf{y}_1(\mathbf{U}_0(\mathbf{y}_1,\varrho))_{\mathbf{y}_1}-0.06\mathbf{U}_0\right]\right]\\&=[-0.06\mathbf{y}_1+0.06\max(\mathbf{y}_1-25\exp(-0.06),0)](1-\delta(\varrho-1)),\\\mathbf{U}_2(\mathbf{y}_1,\varrho)&=\mathbf{Y}^{-1}\left[(1+\delta(\varphi-1))\mathbf{Y}\left[-0.08(2+\sin\mathbf{y}_1)^2\mathbf{y}_1^2(\mathbf{U}_1(\mathbf{y}_1,\varrho))_{\mathbf{y}_1\mathbf{y}_1}-0.06\mathbf{y}_1(\mathbf{U}_1(\mathbf{y}_1,\varrho))_{\mathbf{y}_1}-0.06\mathbf{U}_1\right]\right]\\&=([-0.0036\mathbf{y}_1+0.0036\max(\mathbf{y}_1-25\exp(-0.06),0)])\left((1-\delta)^2+2\varrho\delta(1-\delta)+\frac{\varrho^2\delta^2}{2}\right),\\\mathbf{U}_3(\mathbf{y}_1,\varrho)&=\mathbf{Y}^{-1}\left[(1+\delta(\varphi-1))\mathbf{Y}\left[-0.08(2+\sin\mathbf{y}_1)^2\mathbf{y}_1^2(\mathbf{U}_2(\mathbf{y}_1,\varrho))_{\mathbf{y}_1\mathbf{y}_1}-0.06\mathbf{y}_1(\mathbf{U}_2(\mathbf{y}_1,\varrho))_{\mathbf{y}_1}-0.06\mathbf{U}_2\right]\right]\\&=-\frac{[-0.000216\mathbf{y}_1+0.00216\max(\mathbf{y}_1-25\exp(-0.06),0)]}{\mathbb{A}^3(\delta)}\\&\quad\times\left((1-\delta)^3+3\varrho^2\delta^2(1-\delta)\frac{\varrho^2}{2}+3\varrho\delta(1-\delta)^2+\frac{\varrho^3\delta^3}{3}\right),\\&\ \ \vdots\end{aligned} \tag{78}$$

For Example 2, the series form solution is developed as follows:

$$\mathbf{U}(\mathbf{y}_1,\varrho)=\mathbf{U}_0(\mathbf{y}_1,\varrho)+\mathbf{U}_1(\mathbf{y}_1,\varrho)+\mathbf{U}_2(\mathbf{y}_1,\varrho)+\mathbf{U}_3(\mathbf{y}_1,\varrho)+\cdots=\max(\mathbf{y}_1-25\exp(-0.06),0)-(0.06\mathbf{y}_1-0.06\max(\mathbf{y}_1-25\exp(-0.06),0))(1-\delta(\varrho-1))-(0.0036\mathbf{y}_1-0.0036\max(\mathbf{y}_1-25\exp(-0.06),0))\cdot\left((1-\delta)^2+2\varrho\delta(1-\delta)+\frac{\varrho^2\delta^2}{2}\right)-.\cdots \tag{79}$$

Considering the Taylor series expansion and assigning $\delta=1$, the exact findings of Example 2 can be determined as

$$\mathbf{U}(\mathbf{y}_1,\varrho)=\max(\mathbf{y}_1-25\exp(-0.06),0)+(\mathbf{y}_1-\max(\mathbf{y}_1-25\exp(-0.06),0))[1-\exp(-0.06\varrho)]. \tag{80}$$

5.2. Yang Iterative Transform Method

Example 3 (see [29]). Surmise the fractional-order BSM (4) supplemented with the (5).

Case 1. To begin, we utilize the Caputo fractional derivative operator, employing the Yang decomposition approach to analyze the (4). Implementing the Yang transform on (4), we get

$$\varphi^{-\delta}\mathbf{Y}[\mathbf{U}(\mathbf{y}_1,\varrho)]=\sum_{p=0}^{n-1}\varphi^{1-\delta-p}(\varrho)\mathbf{U}^{(p)}(0)+\mathbf{Y}\left[\frac{\partial^2\mathbf{U}(\mathbf{y}_1,\varrho)}{\partial\mathbf{y}_1^2}+(\zeta-1)\frac{\partial\mathbf{U}(\mathbf{y}_1,\varrho)}{\partial\mathbf{y}_1}-\zeta\mathbf{U}(\mathbf{y}_1,\varrho)\right]. \tag{81}$$

It follows that

$$\mathbf{Y}[\mathbf{U}(\mathbf{y}_1,\varrho)]=\varphi.\max(\exp(\mathbf{y}_1)-1,0)+\varphi^{\delta}(\varrho)\mathbf{Y}\cdot\left[\frac{\partial^2\mathbf{U}(\mathbf{y}_1,\varrho)}{\partial\mathbf{y}_1^2}+(\zeta-1)\frac{\partial\mathbf{U}(\mathbf{y}_1,\varrho)}{\partial\mathbf{y}_1}-\zeta\mathbf{U}(\mathbf{y}_1,\varrho)\right]. \tag{82}$$

In view of the proposed algorithm in Section 3.2, we find

$$\mathbf{U}_0(\mathbf{y}_1,\varrho)=\mathbf{Y}^{-1}\left[\varphi^{\delta}\max(\exp(\mathbf{y}_1)-1,0)\right]=\max(\exp(\mathbf{y}_1)-1,0),$$

$$\mathbf{U}_1(\mathbf{y}_1,\varrho)=\mathbf{Y}^{-1}\left[\varphi^{\delta}\mathbf{Y}\left[(\mathbf{U}_0(\mathbf{y}_1,\varrho))_{\mathbf{y}_1\mathbf{y}_1}+(\zeta-1)(\mathbf{U}_0(\mathbf{y}_1,\varrho))_{\mathbf{y}_1}+\zeta\mathbf{U}_0\right]\right]=[\zeta\max(\exp(\mathbf{y}_1),0)-\zeta\max(\exp(\mathbf{y}_1-1),0)]\mathbf{Y}^{-1}\left[\frac{\phi(\mathfrak{s})}{\varphi^{\delta+1}(\mathfrak{s})}\right]=[\zeta\max(\exp(\mathbf{y}_1),0)-\zeta\max(\exp(\mathbf{y}_1-1),0)]\frac{\varrho^{\delta}}{\Gamma(\delta+1)},$$

$$\mathbf{U}_2(\mathbf{y}_1,\varrho)=\mathbf{Y}^{-1}\left[\varphi^{\delta}\mathbf{Y}\left[(\mathbf{U}_1(\mathbf{y}_1,\varrho))_{\mathbf{y}_1\mathbf{y}_1}+(\zeta-1)(\mathbf{U}_1(\mathbf{y}_1,\varrho))_{\mathbf{y}_1}+\zeta\mathbf{U}_1\right]\right]=\left[-\zeta^2\max(\exp(\mathbf{y}_1),0)+\zeta^2\max(\exp(\mathbf{y}_1-1),0)\right]\frac{\varrho^{2\delta}}{\Gamma(2\delta+1)},$$

$$\mathbf{U}_3(\mathbf{y}_1,\varrho)=\mathbf{Y}^{-1}\left[\varphi^{\delta}\mathbf{Y}\left[(\mathbf{U}_2(\mathbf{y}_1,\varrho))_{\mathbf{y}_1\mathbf{y}_1}+(\zeta-1)(\mathbf{U}_2(\mathbf{y}_1,\varrho))_{\mathbf{y}_1}+\zeta\mathbf{U}_2\right]\right]=\left[-\zeta^3\max(\exp(\mathbf{y}_1),0)+\zeta^3\max(\exp(\mathbf{y}_1-1),0)\right]\frac{\varrho^{3\delta}}{\Gamma(3\delta+1)}.$$
$$\vdots \tag{83}$$

The result in series representation is

$$\mathbf{U}(\mathbf{y}_1,\varrho)=\mathbf{U}_0(\mathbf{y}_1,\varrho)+\mathbf{U}_1(\mathbf{y}_1,\varrho)+\mathbf{U}_2(\mathbf{y}_1,\varrho)+\mathbf{U}_3(\mathbf{y}_1,\varrho)+.\cdots \tag{84}$$

Eventually, we have

$$\mathbf{U}(\mathbf{y}_1,\varrho)=\mathbf{U}_0(\mathbf{y}_1,\varrho)+\mathbf{U}_1(\mathbf{y}_1,\varrho)+\mathbf{U}_2(\mathbf{y}_1,\varrho)+\mathbf{U}_3(\mathbf{y}_1,\varrho)+\cdots=\max(\exp(\mathbf{y}_1-1),0)\cdot\left[1-\frac{\zeta\varrho^{\delta}}{\Gamma(\delta+1)}+\frac{\zeta^2\varrho^{2\delta}}{\Gamma(2\delta+1)}-\frac{\zeta^3\varrho^{3\delta}}{\Gamma(3\delta+1)}+\cdots\right]+\max(\exp(\mathbf{y}_1),0)\left[1-1+\frac{\zeta\varrho^{\delta}}{\Gamma(\delta+1)}-\frac{\zeta^2\varrho^{2\delta}}{\Gamma(2\delta+1)}+\frac{\zeta^3\varrho^{3\delta}}{\Gamma(3\delta+1)}+\cdots\right]=\max(\exp(\mathbf{y}_1-1),0)E_{\delta}\left(-\zeta(\varrho)^{\delta}\right)+\max(\exp(\mathbf{y}_1),0)E_{\delta}\left(1-\zeta(\varrho)^{\delta}\right). \tag{85}$$

Case 2. The (4) is now addressed utilizing the Caputo-Fabrizio fractional derivative operator and the Yang iterative transform method.

Assuming (4) and implementing the Yang transform's differentiation criteria, we obtain

$$\frac{1}{1+\delta(\varphi-1)}\mathbf{Y}[\mathbf{U}(\mathbf{y}_1,\varrho)]=\frac{1}{1+\delta(\varphi-1)}\sum_{p=0}^{p-1}\varphi^{1-\delta-p}(\varrho)\mathbf{U}^{(p)}(0)+\mathbf{Y}\left[\frac{\partial^2\mathbf{U}(\mathbf{y}_1,\varrho)}{\partial\mathbf{y}_1^2}+(\zeta-1)\frac{\partial\mathbf{U}(\mathbf{y}_1,\varrho)}{\partial\mathbf{y}_1}-\zeta\mathbf{U}(\mathbf{y}_1,\varrho)\right]. \tag{86}$$

It follows that

$$\mathbf{Y}[\mathbf{U}(\mathbf{y}_1,\varrho)]=\varphi.\max(\exp(\mathbf{y}_1)-1,0)+(1+\delta(\varphi-1))\mathbf{Y}\cdot\left[\frac{\partial^2\mathbf{U}(\mathbf{y}_1,\varrho)}{\partial\mathbf{y}_1^2}+(\zeta-1)\frac{\partial\mathbf{U}(\mathbf{y}_1,\varrho)}{\partial\mathbf{y}_1}-\zeta\mathbf{U}(\mathbf{y}_1,\varrho)\right]. \tag{87}$$

In view of the proposed algorithm in Section 3.2, we find

$$\mathbf{U}_0(\mathbf{y}_1,\varrho)=\mathbf{Y}^{-1}[\varphi.\max(\exp(\mathbf{y}_1)-1,0)]=\max(\exp(\mathbf{y}_1)-1,0),$$

$$\mathbf{U}_1(\mathbf{y}_1,\varrho)=\mathbf{Y}^{-1}\Big[(1+\delta(\varphi-1))\mathbf{Y}\Big[(\mathbf{U}_0(\mathbf{y}_1,\varrho))_{\mathbf{y}_1\mathbf{y}_1}+(\zeta-1)(\mathbf{U}_0(\mathbf{y}_1,\varrho))_{\mathbf{y}_1}+\zeta\mathbf{U}_0\Big]\Big]=(\zeta\max(\exp(\mathbf{y}_1),0)-\zeta\max(\exp(\mathbf{y}_1-1),0))(1-\delta(\varrho-1)),$$

$$\mathbf{U}_2(\mathbf{y}_1,\varrho)=\mathbf{Y}^{-1}\Big[(1+\delta(\varphi-1))\mathbf{Y}\Big[(\mathbf{U}_1(\mathbf{y}_1,\varrho))_{\mathbf{y}_1\mathbf{y}_1}+(\zeta-1)(\mathbf{U}_1(\mathbf{y}_1,\varrho))_{\mathbf{y}_1}+\zeta\mathbf{U}_1\Big]\Big]=-\Big(\Big[\zeta^2\max(\exp(\mathbf{y}_1),0)+\zeta^2\max(\exp(\mathbf{y}_1-1),0)\Big]\Big)\cdot\left((1-\delta)^2+2\varrho\delta(1-\delta)+\frac{\varrho^2\delta^2}{2}\right),$$

$$\mathbf{U}_3(\mathbf{y}_1,\varrho)=\mathbf{Y}^{-1}\Big[(1+\delta(\varphi-1))\mathbf{Y}\Big[(\mathbf{U}_2(\mathbf{y}_1,\varrho))_{\mathbf{y}_1\mathbf{y}_1}+(\zeta-1)(\mathbf{U}_2(\mathbf{y}_1,\varrho))_{\mathbf{y}_1}+\zeta\mathbf{U}_2\Big]\Big]=-\Big(\Big[\zeta^3\max(\exp(\mathbf{y}_1),0)+\zeta^3\max(\exp(\mathbf{y}_1-1),0)\Big]\Big)\times\left((1-\delta)^3+3\varrho\delta(1-\delta)^2+3\frac{\varrho^2}{2}\delta^2(1-\delta)+\frac{\varrho^3\delta^3}{3}\right).$$

$$\vdots \tag{88}$$

The result in series representation is

$$\mathbf{U}(\mathbf{y}_1,\varrho)=\mathbf{U}_0(\mathbf{y}_1,\varrho)+\mathbf{U}_1(\mathbf{y}_1,\varrho)+\mathbf{U}_2(\mathbf{y}_1,\varrho)+\mathbf{U}_3(\mathbf{y}_1,\varrho)+.\cdots \tag{89}$$

Eventually, we have

$$\mathbf{U}(\mathbf{y}_1,\varrho)=\mathbf{U}_0(\mathbf{y}_1,\varrho)+\mathbf{U}_1(\mathbf{y}_1,\varrho)+\mathbf{U}_2(\mathbf{y}_1,\varrho)+\mathbf{U}_3(\mathbf{y}_1,\varrho)+\cdots=\max(\exp(\mathbf{y}_1-1),0)\cdot\left[1-\zeta(1+\delta(\varrho-1))-\zeta^2\left((1-\delta)^2+2\varrho\delta(1-\delta)+\frac{\varrho^2\delta^2}{2}\right)-\cdots\right]+\max(\exp(\mathbf{y}_1),0)\Big[-\zeta(1+\delta(\varrho-1))-\zeta^2\cdot\left((1-\delta)^2+2\varrho\delta(1-\delta)+\frac{\varrho^2\delta^2}{2}\right)-\cdots\Big]. \tag{90}$$

Example 4 (see [30]). Surmise the fractional-order BSM (6) supplemented with the (7).

Case 1. To begin, we utilize the Caputo fractional derivative operator employing the Yang iterative transform method to analyze the (6). Implementing the Yang transform on (6), we get

$$\varphi^{-\delta}\mathbf{Y}[\mathbf{U}(\mathbf{y}_1,\varrho)]=\sum_{p=0}^{p-1}\varphi^{1-\delta-p}(\varrho)\mathbf{U}^{(p)}(0)+\mathbf{Y}\cdot\left[-0.08(2+\sin\mathbf{y}_1)^2\mathbf{y}_1^2\frac{\partial^2\mathbf{U}(\mathbf{y}_1,\varrho)}{\partial\mathbf{y}_1^2}-0.06\mathbf{y}_1\frac{\partial\mathbf{U}(\mathbf{y}_1,\varrho)}{\partial\mathbf{y}_1}+0.06\mathbf{U}(\mathbf{y}_1,\varrho)\right]. \tag{91}$$

It follows that

$$\mathbf{Y}[\mathbf{U}(\mathbf{y}_1,\varrho)]=\varphi.\max(\mathbf{y}_1-25\exp(-0.06),0)+\varphi^{\delta}\mathbf{Y}\cdot\left[-0.08(2+\sin\mathbf{y}_1)^2\mathbf{y}_1^2\frac{\partial^2\mathbf{U}(\mathbf{y}_1,\varrho)}{\partial\mathbf{y}_1^2}-0.06\mathbf{y}_1\frac{\partial\mathbf{U}(\mathbf{y}_1,\varrho)}{\partial\mathbf{y}_1}+0.06\mathbf{U}(\mathbf{y}_1,\varrho)\right]. \tag{92}$$

In view of the proposed algorithm in Section 3.2, we have

$$\mathbf{U}_0(\mathbf{y}_1,\varrho)=\mathbf{Y}^{-1}[\varphi.\max(\mathbf{y}_1-25\exp(-0.06),0)]=\max(\mathbf{y}_1-25\exp(-0.06),0),$$

$$\mathbf{U}_1(\mathbf{y}_1,\varrho)=\mathbf{Y}^{-1}\Big[\varphi^{\delta}\mathbf{Y}\Big[-0.08(2+\sin\mathbf{y}_1)^2\mathbf{y}_1^2(\mathbf{U}_0(\mathbf{y}_1,\varrho))_{\mathbf{y}_1\mathbf{y}_1}-0.06\mathbf{y}_1(\mathbf{U}_0(\mathbf{y}_1,\varrho))_{\mathbf{y}_1}-0.06\mathbf{U}_0\Big]\Big]=[-0.06\mathbf{y}_1+0.06\max(\mathbf{y}_1-25\exp(-0.06),0)]\mathbf{Y}^{-1}\cdot\Big[\varphi^{\delta+1}(\mathfrak{s})\Big]=[-0.06\mathbf{y}_1+0.06\max\cdot(\mathbf{y}_1-25\exp(-0.06),0)]\frac{\varrho^{\delta}}{\Gamma(\delta+1)},$$

$$\mathbf{U}_2(\mathbf{y}_1,\varrho)=\mathbf{Y}^{-1}\Big[\varphi^{\delta}\mathbf{Y}\Big[-0.08(2+\sin\mathbf{y}_1)^2\mathbf{y}_1^2(\mathbf{U}_1(\mathbf{y}_1,\varrho))_{\mathbf{y}_1\mathbf{y}_1}-0.06\mathbf{y}_1(\mathbf{U}_1(\mathbf{y}_1,\varrho))_{\mathbf{y}_1}-0.06\mathbf{U}_1\Big]\Big]=[-0.0036\mathbf{y}_1+0.0036\max\cdot(\mathbf{y}_1-25\exp(-0.06),0)]\frac{\varrho^{2\delta}}{\Gamma(2\delta+1)},$$

$$\mathbf{U}_3(\mathbf{y}_1,\varrho)=\mathbf{Y}^{-1}\Big[\varphi^{\delta}\mathbf{Y}\Big[-0.08(2+\sin\mathbf{y}_1)^2\mathbf{y}_1^2(\mathbf{U}_2(\mathbf{y}_1,\varrho))_{\mathbf{y}_1\mathbf{y}_1}-0.06\mathbf{y}_1(\mathbf{U}_2(\mathbf{y}_1,\varrho))_{\mathbf{y}_1}-0.06\mathbf{U}_2\Big]\Big]=[-0.000216\mathbf{y}_1+0.00216\max\cdot(\mathbf{y}_1-25\exp(-0.06),0)]\frac{\varrho^{3\delta}}{\Gamma(3\delta+1)},\vdots \tag{93}$$

The result in series representation is

$$\mathbf{U}(\mathbf{y}_1,\varrho)=\mathbf{U}_0(\mathbf{y}_1,\varrho)+\mathbf{U}_1(\mathbf{y}_1,\varrho)+\mathbf{U}_2(\mathbf{y}_1,\varrho)+\mathbf{U}_3(\mathbf{y}_1,\varrho)+.\cdots \tag{94}$$

Consequently, we have

$$\begin{aligned}\mathbf{U}(\mathbf{y}_1,\varrho) &= \mathbf{U}_0(\mathbf{y}_1,\varrho)+\mathbf{U}_1(\mathbf{y}_1,\varrho)+\mathbf{U}_2(\mathbf{y}_1,\varrho)+\mathbf{U}_3(\mathbf{y}_1,\varrho)\\ &\quad +\cdots, = \max\left(\mathbf{y}_1-25\exp(-0.06),0\right)\\ &\quad +\left(\mathbf{y}_1-\max\left(\mathbf{y}_1-25\exp(-0.06)\right)\right)\\ &\quad \times\left[1-1-\frac{0.06\varrho^{\delta}}{\Gamma(\delta+1)}-\frac{0.0036\varrho^{2\delta}}{\Gamma(2\delta+1)}-\frac{0.000216\varrho^{3\delta}}{\Gamma(3\delta+1)}+\cdots\right]\\ &= \max\left(\mathbf{y}_1-25\exp(-0.06),0\right)\\ &\quad +\left(\mathbf{y}_1-\max\left(\mathbf{y}_1-25\exp(-0.06)\right)\right)\left[1-E_{\delta}\left(0.06(\varrho)^{\delta}\right)\right].\end{aligned} \tag{95}$$

Case 2. The Caputo-Fabrizio fractional derivative operator and the Yang iterative transform method are now used to solve the (6).

Assuming (6) and implementing the Yang transform's differentiation criteria, we obtain

$$\begin{aligned}\frac{1}{1+\delta(\varphi-1)}\mathbf{Y}[\mathbf{U}(\mathbf{y}_1,\varrho)] &= \frac{1}{1+\delta(\varphi-1)}\sum_{p=0}^{n-1}\varphi^{1-\delta-p}(\varrho)\mathbf{U}^{(p)}(0)\\ &\quad +\mathbf{Y}\left[-0.08(2+\sin\mathbf{y}_1)^2\mathbf{y}_1^2\frac{\partial^2\mathbf{U}(\mathbf{y}_1,\varrho)}{\partial\mathbf{y}_1^2}-0.06\mathbf{y}_1\frac{\partial\mathbf{U}(\mathbf{y}_1,\varrho)}{\partial\mathbf{y}_1}+0.06\mathbf{U}(\mathbf{y}_1,\varrho)\right].\end{aligned} \tag{96}$$

It follows that

$$\begin{aligned}\mathbf{Y}[\mathbf{U}(\mathbf{y}_1,\varrho)] &= \varphi.\max\left(\mathbf{y}_1-25\exp(-0.06),0\right)+(1+\delta(\varphi-1))\mathbf{Y}\\ &\quad \cdot\left[-0.08(2+\sin\mathbf{y}_1)^2\mathbf{y}_1^2\frac{\partial^2\mathbf{U}(\mathbf{y}_1,\varrho)}{\partial\mathbf{y}_1^2}-0.06\mathbf{y}_1\frac{\partial\mathbf{U}(\mathbf{y}_1,\varrho)}{\partial\mathbf{y}_1}+0.06\mathbf{U}(\mathbf{y}_1,\varrho)\right].\end{aligned} \tag{97}$$

In view of the proposed algorithm in Section 3.2, we have

$$\begin{aligned}\mathbf{U}_0(\mathbf{y}_1,\varrho) &= \mathbf{Y}^{-1}\left[\varphi.\max\left(\mathbf{y}_1-25\exp(-0.06),0\right)\right]\\ &= \max\left(\mathbf{y}_1-25\exp(-0.06),0\right),\end{aligned}$$

$$\begin{aligned}\mathbf{U}_1(\mathbf{y}_1,\varrho) &= \mathbf{Y}^{-1}\left[(1+\delta(\varphi-1))\mathbf{Y}\left[-0.08(2+\sin\mathbf{y}_1)^2\mathbf{y}_1^2(\mathbf{U}_0(\mathbf{y}_1,\varrho))_{\mathbf{y}_1\mathbf{y}_1}\right.\right.\\ &\quad \left.\left.-0.06\mathbf{y}_1(\mathbf{U}_0(\mathbf{y}_1,\varrho))_{\mathbf{y}_1}-0.06\mathbf{U}_0\right]\right] = (-0.06\mathbf{y}_1+0.06\max\\ &\quad \cdot\left(\mathbf{y}_1-25\exp(-0.06),0\right))(1-\delta(\varrho-1)),\end{aligned}$$

$$\begin{aligned}\mathbf{U}_2(\mathbf{y}_1,\varrho) &= \mathbf{Y}^{-1}\left[(1+\delta(\varphi-1))\mathbf{Y}\left[-0.08(2+\sin\mathbf{y}_1)^2\mathbf{y}_1^2(\mathbf{U}_1(\mathbf{y}_1,\varrho))_{\mathbf{y}_1\mathbf{y}_1}\right.\right.\\ &\quad \left.\left.-0.06\mathbf{y}_1(\mathbf{U}_1(\mathbf{y}_1,\varrho))_{\mathbf{y}_1}-0.06\mathbf{U}_1\right]\right]\\ &= \left(-0.0036\mathbf{y}_1+0.0036\max\left(\mathbf{y}_1-25\exp(-0.06),0\right)\right)\\ &\quad \cdot\left((1-\delta)^2+2\varrho\delta(1-\delta)+\frac{\varrho^2\delta^2}{2}\right),\end{aligned}$$

$$\begin{aligned}\mathbf{U}_3(\mathbf{y}_1,\varrho) &= \mathbf{Y}^{-1}\left[(1+\delta(\varphi-1))\mathbf{Y}\left[-0.08(2+\sin\mathbf{y}_1)^2\mathbf{y}_1^2(\mathbf{U}_2(\mathbf{y}_1,\varrho))_{\mathbf{y}_1\mathbf{y}_1}\right.\right.\\ &\quad \left.\left.-0.06\mathbf{y}_1(\mathbf{U}_2(\mathbf{y}_1,\varrho))_{\mathbf{y}_1}-0.06\mathbf{U}_2\right]\right]\\ &= -\left(\left[-0.000216\mathbf{y}_1+0.00216\max\left(\mathbf{y}_1-25\exp(-0.06),0\right)\right]\right)\\ &\quad \times\left((1-\delta)^3+3\varrho\delta(1-\delta)^2+3\delta^2(1-\delta)\frac{\varrho^2\delta^2}{2}+\frac{\varrho^3\delta^3}{3}\right),\vdots\end{aligned} \tag{98}$$

The result in series representation is

$$\mathbf{U}(\mathbf{y}_1,\varrho) = \mathbf{U}_0(\mathbf{y}_1,\varrho)+\mathbf{U}_1(\mathbf{y}_1,\varrho)+\mathbf{U}_2(\mathbf{y}_1,\varrho)+\mathbf{U}_3(\mathbf{y}_1,\varrho)+.\cdots \tag{99}$$

Consequently, we have

$$\begin{aligned}\mathbf{U}(\mathbf{y}_1,\varrho) &= \mathbf{U}_0(\mathbf{y}_1,\varrho)+\mathbf{U}_1(\mathbf{y}_1,\varrho)+\mathbf{U}_2(\mathbf{y}_1,\varrho)+\mathbf{U}_3(\mathbf{y}_1,\varrho)\\ &\quad +\cdots = \max\left(\mathbf{y}_1-25\exp(-0.06),0\right)\\ &\quad -\left(0.06\mathbf{y}_1-0.06\max\left(\mathbf{y}_1-25\exp(-0.06),0\right)\right)(1+\delta(\varrho-1))\\ &\quad -\left(0.0036\mathbf{y}_1-0.0036\max\left(\mathbf{y}_1-25\exp(-0.06),0\right)\right)\\ &\quad \cdot\left((1-\delta)^2+2\varrho\delta(1-\delta)+\frac{\varrho^2\delta^2}{2}\right)-\cdots.\end{aligned} \tag{100}$$

5.3. Results and Explanation. Throughout this investigation, two distinct methodologies are being employed to assess the precise analytical solutions of fractional-order BSe. For various spatial and temporal parameters, the CFD and Caputo-Fabrizio fractional derivative operators in MATLAB package 21 facilitate appropriate numerical findings for the BSe option revenue frameworks utilizing multiple orders.

We built modeling tests for many Brownian deformations involving different $\mathbf{y}_1$ parameters, and the results are shown in Table 1 for Examples 1 and 3, respectively. Table 2 illustrates a computational evaluation of the HPM [35] and the Yang decomposition technique for (4) in accordance with absolute error, considering both fractional derivative operators into account.

Table 3 illustrates the results of a mathematical model for the BSe used in Examples 2 and 4. Table 4 reports the interpretation of an evaluation of the HPM [35] and predicted approaches. The synthetically produced profiles are significantly better reliable and pragmatic than the old ones, as evidenced by this analysis.

For Example 1, Figure 1 displays the evolution of the Yang decomposition technique's data from $\mathbf{U}(\mathbf{y}_1,\varrho)$. Figures 1(a) and 1(b) exhibit the performance of precise and approximation BSe option pricing findings using the CFD operator, whilst Figures 2(a) and 2(b) presents the profile for different Brownian motion $\delta=0.9$ and $\delta=0.8$, respectively. Figures 3(a) and 3(b) indicate the absolute errors conducted and fractional-order fluctuation of $\mathbf{U}(\mathbf{y}_1,\varrho)$. At $\delta=0.7,0.8,0.9,1.0$. The multiple fractional orders act similarly.

Trying to continue in the analogous trend, Figures 4(a) and 4(b) visually depict the precise-approximate repercussions $\mathbf{U}(\mathbf{y}_1,\varrho)$ for (6) using the Yang decomposition

Table 1: The actual, YDM_{CFD} and YDM_{CF} results of Example 1 for multiple fractional-orders with changing terms of $\mathbf{y}_1$ and ϱ.

$\mathbf{y}_1$	ϱ	$\delta = 0.7$	$\delta = 0.8$	$\delta = 0.9$	$\delta = 1(YDM_{CFD})$	$\delta = 1(YDM_{CF})$	Exact
	0.6	0.4705192388	0.4756690138	0.4741190479	0.4705192388	0.4704162259	0.4705168133
	0.7	0.6142259772	0.5911676480	0.5697105760	0.5502060671	0.5502060671	0.5501940469
0.1	0.8	0.4844025326	0.4904274856	0.4919950943	0.4905118580	0.4902676792	0.4905042402
	0.9	0.6956692898	0.6956692898	0.6576549272	0.6380690943	0.6380690943	0.6378819374
	1.0	0.7281682904	0.7121411619	0.6954314260	0.6777823827	0.6777823827	0.6773315511
	0.6	0.5786689713	0.5809834455	0.5790903128	0.5746934962	0.5745676759	0.5746905335
	0.7	0.5855031178	0.5903021597	0.5902216376	0.5870000028	0.5868002049	0.5869945315
0.3	0.8	0.8043692685	0.7782694482	0.7525069160	0.7275064817	0.7275064817	0.7274331662
	0.9	0.4889649311	0.4971196426	0.5004383409	0.5002728118	0.4999251430	0.5002606476
	1.0	0.4931268549	0.5034252607	0.5085881420	0.5098806767	0.5094037649	0.5098621947
	0.6	0.7067878775	0.7096147828	0.7073025053	0.7019322213	0.7017785440	0.7019286027
	0.7	0.7151351230	0.7209966860	0.7209966860	0.7208983361	0.7169634225	0.7169567397
0.5	0.8	0.7226436619	0.7316318354	0.7339704329	0.7317577044	0.7313934324	0.7317463400
	0.9	0.7294499607	0.7416153606	0.7465662767	0.7463193362	0.7458006755	0.7463011895
	1.0	0.7356588213	0.7510222374	0.7587243512	0.7606525865	0.7599411177	0.7606250146
	0.6	0.8632726629	0.8667254528	0.8639012308	0.8573419511	0.8571542493	0.8573375314
	0.7	0.8734680117	0.8806273409	0.8805072160	0.8757011017	0.8754030381	0.8756929394
0.7	0.8	0.8826389617	0.8936171417	0.8964735111	0.8937708784	0.8933259556	0.8937569979
	0.9	0.8909521937	0.9058110468	0.9118581095	0.9115564957	0.9109230019	0.9115343312
	1.0	0.8985357133	0.9173006321	0.9267080152	0.9290631671	0.9281941771	0.9290294906
	0.6	1.054403612	1.058620859	1.055171346	1.047159824	1.046930564	1.047154426
	0.7	1.066856239	1.075600663	1.075453942	1.069583741	1.069219685	1.069573771
0.9	0.8	1.078057662	1.091466442	1.094955219	1.091654216	1.091110786	1.091637262
	0.9	1.088211467	1.106360111	1.113746010	1.113377618	1.112603867	1.113350546
	1.0	1.097473998	1.120393522	1.131883726	1.134760315	1.133698928	1.134719182

Table 2: For estimated outcomes of $\mathbf{U}(\mathbf{y}_1, \varrho)$ at $\delta = 1$ considering multiple choices of $\mathbf{y}_1$ and ϱ, examine HPM [35], YDM_{CFD}, and YDM_{CF} of Example 1.

$\mathbf{y}_1$	ϱ	$\|\text{Exact} - \text{HPM}\|$	$\|\text{Exact} - YDM_{CFD}\|$	$\|\text{Exact} - YDM_{CF}\|$
	0.6	7.900000×10^{-3}	2.425509×10^{-6}	1.005999×10^{-4}
	0.7	1.099099×10^{-3}	4.479656×10^{-6}	1.591007×10^{-4}
0.1	0.8	4.244800×10^{-2}	7.617867×10^{-6}	2.365698×10^{-4}
	0.9	9.107607×10^{-2}	1.216420×10^{-6}	3.355046×10^{-4}
	1.0	5.478550×10^{-2}	1.848200×10^{-6}	4.584298×10^{-4}
	0.6	9.980000×10^{-4}	2.962700×10^{-6}	1.228576×10^{-4}
	0.7	5.400763×10^{-3}	5.471300×10^{-6}	1.943266×10^{-4}
0.3	0.8	7.800998×10^{-2}	9.304400×10^{-6}	2.889363×10^{-4}
	0.9	3.900567×10^{-3}	1.485740×10^{-6}	4.097862×10^{-4}
	1.0	5.100562×10^{-2}	2.257400×10^{-6}	5.599274×10^{-4}
	0.6	3.009801×10^{-3}	3.618600×10^{-6}	1.500587×10^{-4}
	0.7	6.400789×10^{-3}	6.682800×10^{-6}	2.373511×10^{-4}
0.5	0.8	9.660009×10^{-3}	1.136440×10^{-5}	3.529076×10^{-4}
	0.9	2.934890×10^{-2}	1.814670×10^{-5}	5.005140×10^{-4}
	1.0	6.000989×10^{-3}	2.757190×10^{-5}	6.838969×10^{-4}
	0.6	2.560000×10^{-3}	4.419700×10^{-6}	1.832821×10^{-4}
	0.7	2.200000×10^{-2}	8.162300×10^{-6}	2.899013×10^{-4}
0.7	0.8	1.056900×10^{-3}	1.388050×10^{-5}	4.310423×10^{-4}
	0.9	34.008890×10^{-3}	2.216450×10^{-5}	6.113293×10^{-4}
	1.0	8.000956×10^{-3}	3.367650×10^{-5}	8.353135×10^{-4}
	0.6	7.789435×10^{-2}	5.398000×10^{-6}	2.238620×10^{-6}
	0.7	3.000897×10^{-2}	9.970000×10^{-6}	3.540860×10^{-4}
0.9	0.8	2.788609×10^{-2}	1.695400×10^{-5}	5.264760×10^{-4}
	0.9	6.560000×10^{-3}	2.707200×10^{-5}	7.466790×10^{-4}
	1.0	2.000043×10^{-2}	4.113300×10^{-5}	1.020254×10^{-3}

Table 3: The actual, YDM_{CFD} and YDM_{CF} results of Example 2 for multiple fractional-orders with changing terms of $\mathbf{y}_1$ and ϱ.

$\mathbf{y}_1$	ϱ	$\delta = 0.7$	$\delta = 0.8$	$\delta = 0.9$	$\delta = 1(JDM_{CFD})$	$\delta = 1(JDM_{ABC})$	Exact
	0.6	0.0026121375	0.0020293922	0.0015639815	0.0011964072	0.0011964072	0.001196407
	0.7	0.4793694085	0.4832985317	0.4832326058	0.4805949543	0.4804313735	0.4805904747
0.1	0.8	0.0055797208	0.0048449971	0.0041732529	0.0035677944	0.0035677944	0.003567793
	0.9	0.0067961194	0.0060754949	0.0053880675	0.0047428608	0.0047428608	0.0047428580
	1.0	0.0079145429	0.0072365565	0.0065645469	0.0059109000	0.0059109000	0.0059108933
	0.6	0.0052242750	0.0040587845	0.0031279630	0.0023928144	0.0023928144	0.0023928143
	0.7	0.0084408706	0.0070345154	0.0058151760	0.0047713152	0.0047713152	0.0047713148
0.3	0.8	0.011159441	0.0096899942	0.0083465059	0.0071355888	0.0071355888	0.0071355870
	0.9	0.013592238	0.012150989	0.010776135	0.0094857216	0.0094857216	0.0094857160
	1.0	0.015829085	0.014473113	0.013129093	0.011821800	0.011821800	0.0118217866
	0.6	0.0078364125	0.0060881767	0.0046919445	0.0035892216	0.0035892216	0.0035892215
	0.7	0.012661305	0.010551773	0.0087227641	0.0071569728	0.0071569728	0.0071569722
0.5	0.8	0.016739162	0.014534991	0.012519758	0.010703383	0.010703383	0.0107033805
	0.9	0.020388358	0.018226484	0.016164202	0.014228582	0.014228582	0.0142285741
	1.0	0.023743628	0.021709669	0.019693640	0.017732700	0.017732700	0.0177326799
	0.6	0.010448550	0.0081175690	0.0062559261	0.0047856288	0.0047856288	0.0047856287
	0.7	0.016881741	0.014069030	0.011630352	0.0095426304	0.0095426304	0.0095426296
0.7	0.8	0.022318883	0.019379988	0.016693011	0.016693011	0.016693011	0.0142711740
	0.9	0.027184477	0.024301979	0.021552270	0.018971443	0.018971443	0.0189714321
	1.0	0.031658171	0.028946226	0.026258187	0.023643600	0.023643600	0.0236435732
	0.6	0.013060687	0.010146961	0.0078199076	0.0059820360	0.0059820360	0.005982035
	0.7	0.021102176	0.017586288	0.014537940	0.011928288	0.011928288	0.011928287
0.9	0.8	0.027898604	0.024224985	0.020866264	0.017838972	0.017838972	0.017838967
	0.9	0.033980597	0.030377474	0.026940337	0.023714304	0.023714304	0.023714290
	1.0	0.039572714	0.036182782	0.032822734	0.029554500	0.029554500	0.029554466

Table 4: For estimated outcomes of $\mathbf{U}(\mathbf{y}_1, \varrho)$ at $\delta = 1$ considering multiple choices of $\mathbf{y}_1$ and ϱ, examine HPM [35], YDM_{CFD},and YDM_{CF} of Example 2.

$\mathbf{y}_1$	ϱ	$\|Exact - HPM\|$	$\|Exact - YDM_{CFD}\|$	$\|Exact - YDM_{CF}\|$
0.1	0.6	3.00450×10^{-10}	2.00000×10^{-11}	2.00000×10^{-11}
	0.7	2.00000×10^{-9}	4.4796×10^{-6}	1.80000×10^{-10}
	0.8	9.50000×10^{-9}	8.80000×10^{-10}	8.80000×10^{-10}
	0.9	3.89000×10^{-8}	2.76000×10^{-9}	2.76000×10^{-9}
	1.0	7.70000×10^{-8}	6.70000×10^{-9}	6.70000×10^{-9}
0.3	0.6	5.780000×10^{-10}	4.00000×10^{-11}	4.00000×10^{-11}
	0.7	4.80000×10^{-9}	3.60000×10^{-10}	3.60000×10^{-10}
	0.8	2.98000×10^{-8}	1.76000×10^{-9}	1.76000×10^{-9}
	0.9	6.45000×10^{-8}	5.52000×10^{-9}	5.52000×10^{-9}
	1.0	2.47000×10^{-7}	1.34000×10^{-8}	1.34000×10^{-8}
0.5	0.6	7.96600×10^{-10}	6.00000×10^{-11}	6.00000×10^{-11}
	0.7	6.785000×10^{-9}	5.40000×10^{-10}	5.40000×10^{-10}
	0.8	3.98000×10^{-8}	2.64000×10^{-9}	2.64000×10^{-9}
	0.9	9.31000×10^{-8}	8.28000×10^{-9}	8.28000×10^{-9}
	1.0	3.003000×10^{-7}	2.01000×10^{-8}	2.01000×10^{-8}
0.7	0.6	9.890000×10^{-10}	8.00000×10^{-11}	8.00000×10^{-11}
	0.7	9.80000×10^{-9}	7.20000×10^{-10}	7.20000×10^{-10}
	0.8	4.94000×10^{-8}	3.52000×10^{-9}	3.52000×10^{-9}
	0.9	2.89000×10^{-7}	1.10400×10^{-8}	1.10400×10^{-8}
	1.0	3.60089×10^{-7}	2.68000×10^{-8}	2.68000×10^{-8}
0.9	0.6	2.9900×10^{-9}	1.00000×10^{-10}	1.00000×10^{-10}
	0.7	11.00011×10^{-9}	9.00000×10^{-10}	9.00000×10^{-10}
	0.8	6.40000×10^{-8}	4.40000×10^{-9}	4.40000×10^{-9}
	0.9	2.87000×10^{-7}	1.38000×10^{-8}	1.38000×10^{-8}
	1.0	4.89000×10^{-7}	3.35000×10^{-8}	3.35000×10^{-8}

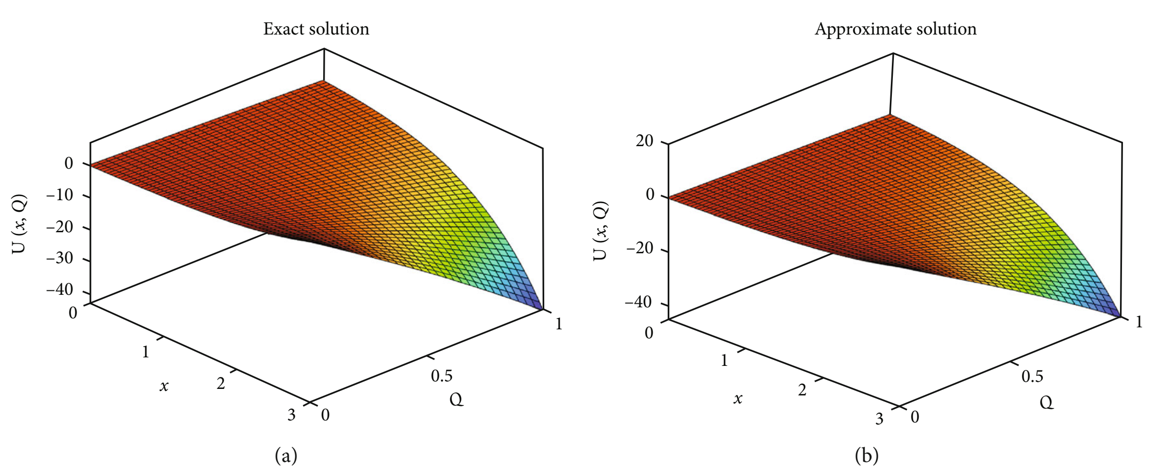

Figure 1: Three-dimensional illustration via CFD of Example 1 when $\delta = 1$. (a) Exact solution. (b) Approximate solution.

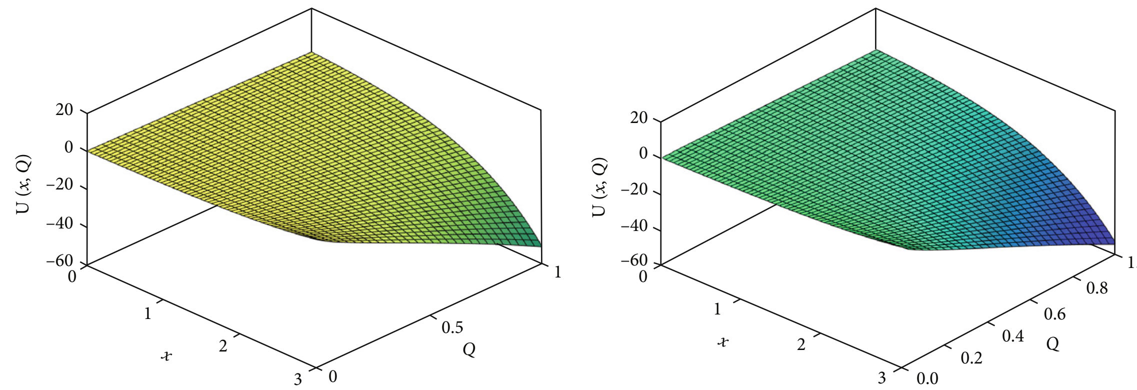

(a) (b)

FIGURE 2: Three-dimensional illustration of the approximate solution via CFD of Example 1 when (a) $\delta = 0.9$ and $\delta = 0.8$.

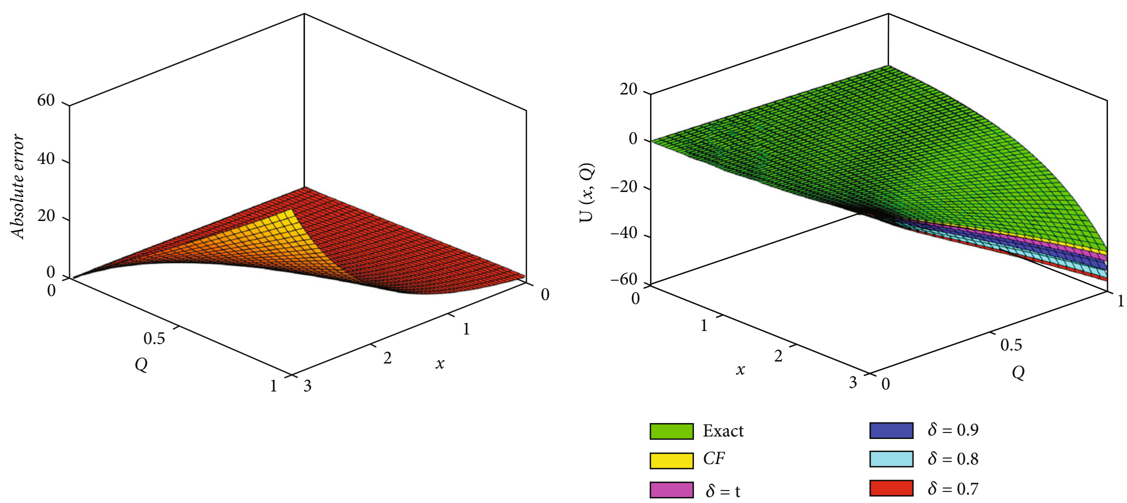

(a) (b)

FIGURE 3: Three-dimensional illustration via the CFD of Example 1. (a) Absolute error. (b) Multiple fractional-order.

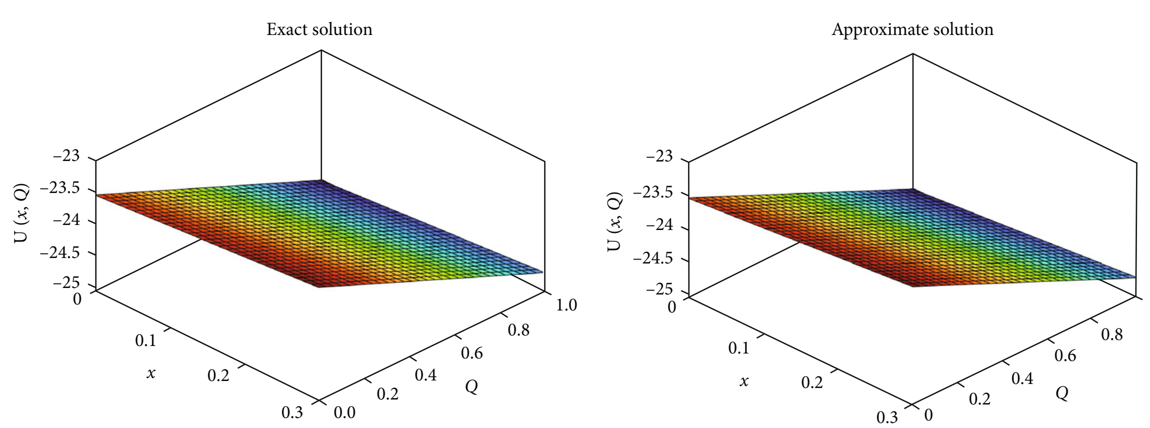

(a) (b)

FIGURE 4: Three-dimensional illustration via CFD of Example 1 when $\delta = 1$. (a) Exact solution. (b) Approximate solution.

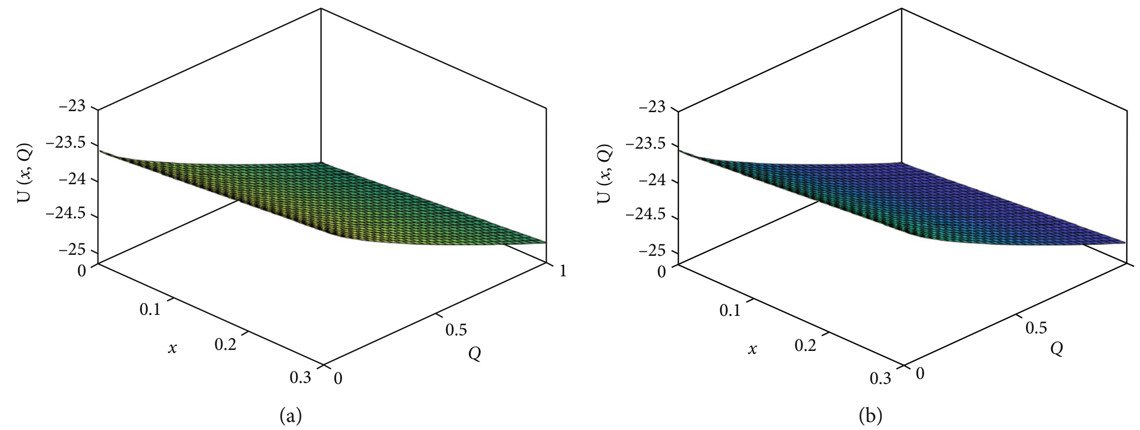

Figure 5: Three-dimensional illustration of the approximate solution via CFD of Example 1 when (a) $\delta = 0.9$ and $\delta = 0.8$.

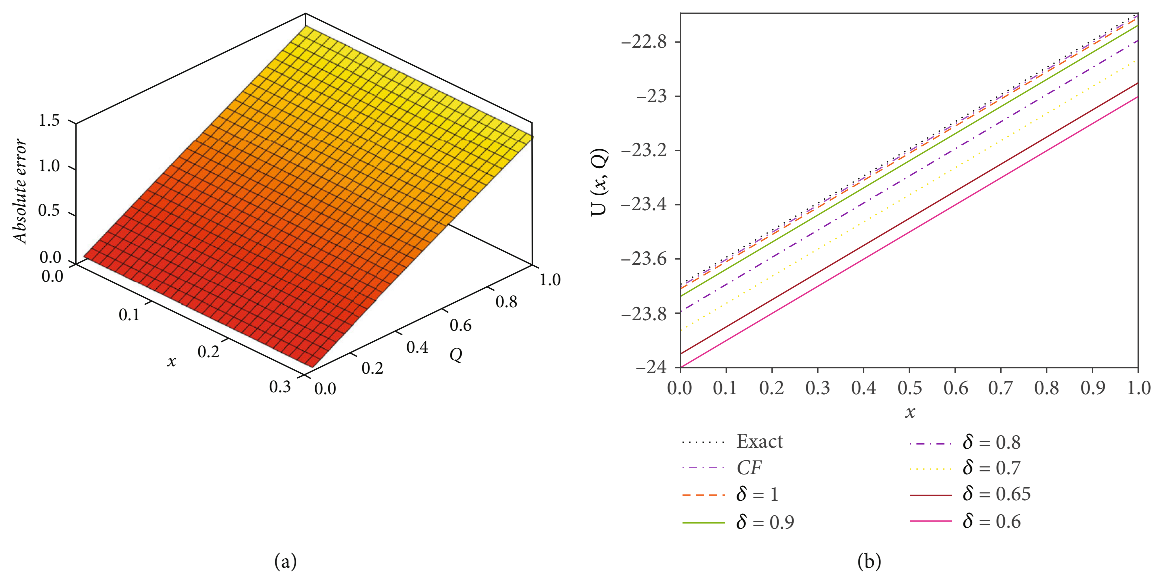

Figure 6: Three-dimensional illustration via the CFD of Example 1. (a) Absolute error. (b) Multiple fractional-order.

approach on the contents of the choices, whilst Figures 5(a) and 5(b) present the profile for Brownian motion $\delta = 0.9$ and $\delta = 0.8$, respectively. The absolute error and sensitivity of gathered information for (6) involving different numerical and Brownian movements of $\delta = 0.7, 0.8, 0.9$ and 1 are illustrated in Figures 6(a) and 6(a). Furthermore, Figure 6(b) refers to the dynamic of the two-dimensional alternatives of the analysis values $\mathbf{U}(\mathbf{y}_1, \varrho)$ for (6). Finally, we deduce that as the amount of the time-dependent component improves, the hierarchy of the feature images tends to rise as well. It is important to remember that the fractional order has a simulatory effect on the diffusion mechanism.

6. Conclusion

The Adomian decomposition approach and the new iterative transform procedure have been leveraged to analyze the Yang transform. To interact effectively with the BSe, the Caputo and Caputo-Fabrizio fractional derivative operators have been constructed. Considering the supposition of fractional order, numerous new outcomes have been presented. To clarify the crucial aspects of the fractional frameworks under evaluation, diverse visualizations were attempted to explicate these results. The suggested scheme identifies the findings without any underlying limitations, deconvolution, or quantization. Our transformation has been described in terms of refinement and inventiveness. When comparing our results to those discovered in existing academic publications, it becomes clear that our approaches in the European Choice Valuation framework are exceptional. The schemes' effective and comprehensive execution is investigated and confirmed in an attempt to display that it may be applicable to other nonlinear evolutionary models that emerge in business and accountancy.

Data Availability

No data were used to support this study.

Conflicts of Interest

The authors declare that they have no competing interests.

Authors' Contributions

All authors read and approved the final manuscript.

References

[1] Y.-M. Chu, S. Bashir, M. Ramzan, and M. Y. Malik, "Model-based comparative study of magnetohydrodynamics unsteady hybrid nanofluid flow between two infinite parallel plates with particle shape effects," *Mathematical Methods in the Applied Sciences*, 2022.

[2] K. Karthikeyan, P. Karthikeyan, H. M. Baskonus, K. Venkatachalam, and Y.-M. Chu, "Almost sectorial operators on Ψ-Hilfer derivative fractional impulsive integro-differential equations," *Mathematical Methods in the Applied Sciences*, vol. 45, no. 13, pp. 8045–8059, 2022.

[3] S. A. Iqbal, M. G. Hafez, Y.-M. Chu, and C. Park, "Dynamical analysis of nonautonomous *RLC* circuit with the absence and presence of Atangana-Baleanu fractional derivative," *Journal of Applied Analysis and Computation*, vol. 12, no. 2, pp. 770–789, 2022.

[4] T.-H. Zhao, O. Castillo, H. Jahanshahi et al., "A fuzzy-based strategy to suppress the novel coronavirus (2019-NCOV) massive outbreak," *Applied and Computational Mathematics*, vol. 20, no. 1, pp. 160–176, 2021.

[5] S. Rashid, F. Jarad, and A. A. G. Ahmad, "A novel fractal-fractional order model for the understanding of an oscillatory and complex behavior of human liver with non-singular kernel," *Results in Physics*, vol. 35, no. 2, article 105292, 2022.

[6] M. Alqhtani, K. M. Owolabi, and K. M. Saad, "Spatiotemporal (target) patterns in sub-diffusive predator-prey system with the Caputo operator," *Chaos, Solitons & Fractals*, vol. 160, article 112267, 2022.

[7] M. Alqhtani and K. M. Saad, "Numerical solutions of space-fractional diffusion equations via the exponential decay kernel," *AIMS Mathematics*, vol. 7, no. 4, pp. 6535–6549, 2022.

[8] S. Aljhani, M. S. Md Noorani, K. M. Saad, and A. K. Alomari, "Numerical solutions of certain new models of the time-fractional Gray-Scott," *Journal of Function Spaces*, vol. 2021, Article ID 2544688, 12 pages, 2021.

[9] I. Podlubny, *Fractional Differential Equations*, Academic Press, San Diego, CA, USA, 1999.

[10] S. Rashid, S. Sultana, Y. Karaca, A. Khalid, and Y.-M. Chu, "Some further extensions considering discrete proportional fractional operators," *Fractals*, vol. 30, no. 1, article 2240026, 2022.

[11] S. Narges Hajiseyedazizi, M. E. Samei, J. Alzabut, and Y.-M. Chu, "On multi-step methods for singular fractional q-integro-differential equations," *Open Mathematics*, vol. 19, no. 1, pp. 1378–1405, 2021.

[12] S. Rashid, E. I. Abouelmagd, A. Khalid, F. B. Farooq, and Y.-M. Chu, "Some recent developments on dynamical $\hbar$-discrete fractional type inequalities in the frame of nonsingular and nonlocal kernels," *Fractals*, vol. 30, no. 2, article 2240110, 2022.

[13] F.-Z. Wang, M. N. Khan, I. Ahmad, H. Ahmad, H. Abu-Zinadah, and Y.-M. Chu, "Numerical solution of traveling waves in chemical kinetics: time-fractional fishers equations," *Fractals*, vol. 30, no. 2, article 2240051, 2022.

[14] S. Rashid, E. I. Abouelmagd, S. Sultana, and Y.-M. Chu, "New developments in weighted n-fold type inequalities via discrete generalized h-proportional fractional operators," *Fractals*, vol. 30, no. 2, article 2240056, 2022.

[15] M. Caputo and M. Fabrizio, "A new definition of fractional derivative without singular kernel," *Progress in Fractional Differentiation & Applications*, vol. 73, pp. 1–13, 2015.

[16] R. Scherer, S. L. Kalla, Y. Tang, and J. Huanget, "The Grunwald-Letnikov method for fractional differential equations," *Computers & Mathematcs with Applications*, vol. 62, no. 3, pp. 902–917, 2011.

[17] S. Bibi and S. T. Mohyud-Din, "Traveling wave solutions of KdVs using sine-cosine method," *Journal of the Association of Arab Universities for Basic and Applied Sciences*, vol. 15, no. 1, pp. 90–93, 2014.

[18] A. H. Zedan and E. El-Adrous, "The application of the homotopy perturbation method and the homotopy analysis method to the generalized Zakharov equations," *Abstract and Applied Analysis*, vol. 2012, Article ID 561252, 19 pages, 2012.

[19] S. Rashid, R. Ashraf, and F. Jarad, "Strong interaction of Jafari decomposition method with nonlinear fractional-order partial differential equations arising in plasma via the singular and nonsingular kernels," *AIMS Mathematics*, vol. 7, no. 5, 2022.

[20] S. Rashid, Z. Hammouch, H. Aydi, A. G. Ahmad, and A. M. Alsharif, "Novel computations of the time-fractional Fisher's model via generalized fractional integral operators by means of the Elzaki transform," *Fractal and Fractional*, vol. 5, no. 3, p. 94, 2021.

[21] S. Widatalla and M. Z. Liu, "New iterative method based on Laplace decomposition algorithm," *Journal of Applied Mathematics*, vol. 2013, Article ID 286529, 7 pages, 2013.

[22] A. -M. Wazwaz, "The variational iteration method: a reliable analytic tool for solving linear and nonlinear wave equations," *Computational and Applied Mathematics*, vol. 54, no. 7-8, pp. 926–932, 2007.

[23] H. O. Roshid, M. A. Akbar, N. Alam, F. Hoque, and N. Rahman, "New extended G/G'-expansion method to solve nonlinear evolution equation: the (3+1)-dimensional potential-YTSF equation," *Springer Plus*, vol. 3, no. 122, 2014http://www.springerplus.com/content/3/1/122.

[24] E. Yasar, Y. Yildirim, and C. M. Khalique, "Lie symmetry analysis, conservation laws and exact solutions of the seventh-order time fractional Sawada-Kotera-Ito equation," *Results in Physics*, vol. 6, pp. 322–328, 2016.

[25] H. A. Zedan and E. Alaidarous, "Haar Wavelet method for the system of integral equations," *Abstract and Applied Analysis*, vol. 2014, Article ID 418909, 9 pages, 2014.

[26] M. J. Ablowitz and P. A. Clarkson, *Solitons, Nonlinear Evolution Equations and Inverse Scattering*, Cambridge University Press, 2010.

[27] N. A. Kudryashov, "Simplest equation method to look for exact solutions of nonlinear differential equations," *Chaos, Solitons & Fractals*, vol. 24, no. 5, pp. 1217–1231, 2005.

[28] C. H. Gu, *Soliton theory and its application*, Zhejiang Science and Technology Press, 1990.

[29] N. Özdemir and M. Yavuz, "Numerical solution of fractional Black-Scholes equation by using the multivariate Padé approximation," *Acta Physica Polonica A*, vol. 132, no. 3-II, pp. 1050–1053, 2017.

[30] Z. Cen and A. Le, "A robust and accurate finite difference method for a generalized Black–Scholes equation," *Journal of Computational and Applied Mathematics*, vol. 235, no. 13, pp. 3728–3733, 2011.

[31] P. Wilmott, J. Dewynne, and S. Howison, *Option Pricing: Mathematical Models and Computation*, Oxford Financial Press, Oxford, 1993.

[32] C. Vazquez, "An upwind numerical approach for an American and European option pricing model," *Applied Mathematics and Computation*, vol. 97, no. 2-3, pp. 273–286, 1998.

[33] L. Meng and M. Wang, "Comparison of Black-Scholes formula with fractional Black-Scholes formula in the foreign exchange option market with changing volatility," *Asia-Pacific Financial Markets*, vol. 17, no. 2, pp. 99–111, 2010.

[34] Q. Fu, K. Wang, and X. Liu, "The foreign exchange option pricing based on the fractional Black-Scholes model and valuation," *Price Monthly*, vol. 369, pp. 68–70, 2008.

[35] A. N. Fall, S. N. Ndiaye, and N. Sene, "Black–Scholes option pricing equations described by the Caputo generalized fractional derivative," *Chaos, Solitons & Fractals*, vol. 125, pp. 108–118, 2019.

[36] M. B. Matadi and P. L. Zondi, "Invariant solutions of Black-Scholes equation with Ornstein-Uhlenbeck process," *Symmetry*, vol. 13, no. 5, p. 847, 2021.

[37] S. Kumar, D. Kumar, and J. Singh, "Numerical computation of fractional Black-Scholes equation arising in financial market," *Egyptian Journal of Basic and Applied Sciences*, vol. 1, no. 3-4, pp. 177–183, 2014.

[38] M. Yavuz and N. Özdemir, "A different approach to the European option pricing model with new fractional operator," *Mathematical Modelling of Natural Phenomena*, vol. 13, no. 1, p. 12, 2018.

[39] S. Rashid, R. Ashraf, and E. Bonyah, "On analytical solution of time-fractional biological population model by means of generalized integral transform with their uniqueness and convergence analysis," *Journal of Function Spaces*, vol. 2022, Article ID 7021288, 29 pages, 2022.

[40] S. Rashid, R. Ashraf, and F. S. Bayones, "A novel treatment of fuzzy fractional Swift–Hohenberg equation for a hybrid transform within the fractional derivative operator," *Fractal and Fractional*, vol. 5, no. 4, p. 209, 2021.

[41] X. -J. Yang, "A new integral transform method for solving steady heat-transfer problem," *Thermal Science*, vol. 20, supplement 3, pp. 639–642, 2016.

[42] V. Daftardar-Gejji and H. Jafari, "An iterative method for solving nonlinear functional equations," *Journal of Mathematical Analysis and Applications*, vol. 316, no. 2, pp. 753–763, 2006.

[43] S. Rashid, R. Ashraf, and M. Tahir, "On novel analytical solution of time-fractional Schrödinger equation within a hybrid transform," *Mathematical Sciences*, pp. 1–19, 2022.

[44] K. Wang and S. Liu, "Application of new iterative transform method and modified fractional homotopy analysis transform method for fractional Fornberg-Whitham equation," *Journal of Nonlinear Sciences and Applications*, vol. 9, no. 5, pp. 2419–2433, 2016.

[45] S. Ahmad, A. Ullah, A. Akgül, and M. De la Sen, "A novel homotopy perturbation method with applications to nonlinear fractional order KdV and Burger equation with exponential-decay kernel," *Journal of Function Spaces*, vol. 2021, Article ID 8770488, 11 pages, 2021.

[46] M. G. Mittag-Leffler, "Sur la nouvelle fonction Ea(x)," *Comptes Rendus. Académie des Sciences*, vol. 2, p. 1003, 1903.

[47] I. El-Kalla, "Convergence of the Adomian method applied to a class of nonlinear integral equations," *Applied Mathematics Letters*, vol. 21, no. 4, pp. 372–376, 2008.

Hindawi
Journal of Function Spaces
Volume 2022, Article ID 5613708, 13 pages
https://doi.org/10.1155/2022/5613708

Research Article

Diverse Precise Traveling Wave Solutions Possessing Beta Derivative of the Fractional Differential Equations Arising in Mathematical Physics

Imran Siddique,[1] **Arshad M. Mirza**,[2] **Kausar Shahzadi**,[1] **M. Ali Akbar**,[3] **and Fahd Jarad**[4,5]

[1]*Department of Mathematics, University of Management and Technology, Lahore 54770, Pakistan*
[2]*Department of Physics, University of Management and Technology, Lahore 54770, Pakistan*
[3]*Department of Applied Mathematics, University of Rajshahi, Bangladesh*
[4]*Department of Mathematics, Cankaya University, Etimesgut, Ankara 06790, Turkey*
[5]*Department of Medical Research, China Medical University Hospital, China Medical University, Taichung 40402, Taiwan*

Correspondence should be addressed to M. Ali Akbar; ali_math74@yahoo.com and Fahd Jarad; fahd@cankaya.edu.tr

Received 30 May 2022; Revised 12 August 2022; Accepted 9 September 2022; Published 19 September 2022

Academic Editor: Yusuf Gurefe

In this paper, we obtain the novel exact traveling wave solutions in the form of trigonometric, hyperbolic and exponential functions for the nonlinear time fractional generalized reaction Duffing model and density dependent fractional diffusion-reaction equation in the sense of beta-derivative by using three fertile methods, namely, Generalized tanh (GT) method, Generalized Bernoulli (GB) sub-ODE method, and Riccati-Bernoulli (RB) sub-ODE method. The derived solutions to the aforementioned equations are validated through symbolic soft computations. To promote the vital propagated features; some investigated solutions are exhibited in the form of 2D and 3D graphics by passing on the specific values to the parameters under the confine conditions. The accomplished solutions show that the presented methods are not only powerful mathematical tools for generating more solutions of nonlinear time fractional partial differential equations but also can be applied to nonlinear space-time fractional partial differential equations.

1. Introduction

Soliton theory has much importance because many equations of mathematical physics have the solution of soliton type. Waves are generated when some disturbance occurs in the phenomena. Soliton interaction takes place when two or more soliton come close to each other. Solitons exhibit particle-like properties because the energy is—at any instant—confined to a limited region of space. The most important technical application of the soliton is that these are used in the optical fibers to carry the digital information. In electromagnetic soliton studies, the transverse electromagnetic wave travels between two strips of super conducting metal.

Fractional calculus has captured the interest of several scholars during the past two centuries. Multiple nonlinear aspects, biological processes, fluid mechanics, chemical processes, etc., are modelled using them. Fractional order partial differential equations (PDEs) serve as the generalization of PDEs in the traditional integer-order. The literature contains several dentitions of fractional derivatives, such as the Hadamard derivative (1892) [1], the Weyl derivative [2], Riesz derivative [3], He's fractional derivative [4], Local derivative [5], Riemann-Liouville [6, 7], Abel-Riemann derivative [8], Caputo [9], Caputo-Fabrizio [10], Atangana-Baleanu derivative in the context of Caputo [11], the conformable fractional derivative [12, 13], and the new truncated M-fractional derivative [14]. Atangana et al. in [15] have recently created the new beta-derivative which satisfies a lot of characteristics that have been considered as limitations for the fractional derivatives. This derivative has some appealing consequences in diverse areas including fluid mechanics, optical physics, chaos theory, biological models, disease analysis, circuit analysis, and others.

Nonlinear fractional differential equations (NLFDEs) occur more frequently in engineering applications and different research areas [16–20]. Then, many real-life problems can be modeled by ordinary or partial differential equations involving the derivatives of fractional order. In order to better understand and apply these physical phenomena in practical scientific research, it is important to find their exact solutions. Finding exact solutions of most of the NLFDEs is not easy, so searching and constructing exact solutions of NLFDEs is a continuing investigation. Recently, many powerful methods for obtaining exact solutions of nonlinear partial differential equations (NLPDEs) have been presented, such as exponential rational function method [21], $\exp_a$ function, and the hyperbolic function methods [22]. (G'/G)-expansion method [23, 24], $(G'/G, 1/G)$-expansion method [25, 26], Sardar-subequation method [27], new subequation method [28], Riccati equation method [29], homotopy perturbation method [30], extended direct algebraic method [31], Kudryashov method [32], Exp-function method [33], the modified extended exp-function method [34], F-expansion method [35], the Backlund transformation method [36], the extended tanh-method [37], Jacobi elliptic function expansion methods [38], extended sinh-Gordon equation expansion method [39], and different other methods [40–43].

The core aim of this work is to establish the exact traveling wave solutions of the fractional generalized reaction doffing model arising in mathematical biology [44, 45] and the density dependent fractional diffusion-reaction equation with the beta-derivative based on three different methods, the Generalized tanh (GT) method [46], Generalized Bernoulli (GB) sub-ODE method [47], and Riccati-Bernoulli (RB) sub-ODE method [48]. These methods are the most direct and effective algebraic methods used for obtaining the exact traveling wave solutions of nonlinear partial differential equations. In [49], Jafari et al. applied the fractional subequation method to construct exact solutions of the fractional generalized reaction Duffing model and in [50], Eslami et al. applied the first integral method to obtain the exact solutions of fractional generalized reaction Duffing model and the exact solutions of fractional diffusion-reaction equation. Uddin et al. [44] obtained the close form solutions of the fractional generalized reaction Duffing model and the density dependent fractional diffusion reaction equation by using the $(G'/G, 1/G)$-expansion method. In [51] Xia et al. applied hyperbolic function to obtain new explicit and exact travelling wave solutions for a class of nonlinear evolution equations. Sonmezoglu [52] applied extended Jacobi elliptic function expansion to construct the exact solutions of these models.

This paper is organized as follows: In Section 2, we present beta derivative and its properties. The descriptions of strategies are given in Section 3. In Sections 4 and 5, we present a mathematical analysis of the models and its solutions via proposed methods. In Section 6, the graphical comparisons of our obtained exact traveling wave solutions are represented in both 2D and 3D plots for various values of parameters. At the end, conclusions are announced in Section 7.

2. Beta Derivative and Its Properties

Definition. The beta-derivative is defined as [15, 53]

$$ {}_0^A D_x^\alpha (f(x)) = \lim_{\varepsilon \longrightarrow 0} \frac{f(x + \epsilon (x + (1/\Gamma(\alpha)))) - f(x)}{\epsilon}, 0 < \alpha \leq 1. \tag{1} $$

Properties of Beta Derivative. Beta derivative has the following properties:

(1)

$$ {}_0^A D_x^\alpha [af(x) + bg(x)] = a {}_o^A D_x^\alpha f(x) + b {}_o^A D_x^\alpha g(x) \tag{2} $$

(2) ${}_0^A D_x^\alpha (c) = 0$, for any constant c

(3)

$$ {}_0^A D_x^\alpha [f(x) . g(x)] = g(x) {}_o^A D_x^\alpha f(x) + f(x) {}_o^A D_x^\alpha g(x) {}_0^A \tag{3} $$

(4)

$$ {}_0^A D_x^\alpha \left[\frac{f(x)}{g(x)} \right] = \frac{g(x) {}_0^a D_x^\alpha f(x) - f(x) {}_0^a D_x^\alpha g(x)}{g^2(x)} \tag{4} $$

Considering $\epsilon = (x + (1/\Gamma(\alpha)))^{\alpha - 1} h$, $h \longrightarrow 0$ when $\epsilon \longrightarrow 0$, therefore we have

$$ {}_0^A D_x^\alpha f(x) = \left(x + \frac{1}{\Gamma(\alpha)} \right)^{1-\alpha} \frac{df(x)}{d(x)}, \tag{5} $$

with $\xi = (l/\alpha)(x + (1/\Gamma(\alpha)))^\alpha$, where l is a constant.

(5)

$$ {}_0^A D_x^\alpha \left[\frac{f(\xi)}{g(x)} \right] = l \frac{df(\xi)}{d(\xi)}. \tag{6} $$

The proofs of the above beta properties were simply presented in [11].

3. Description of Strategies

3.1. Riccati-Bernoulli (RB) Sub-ODE Method. In this section, we represent the basic steps of the RB sub-ODE method [48]. Let us consider the nonlinear partial differential equation of the following form:

$$ F(u, u_x, u_t, u_{xx}, u_{tt}, u_{xt}, \cdots) = 0, \tag{7} $$

where $u = u(x, t)$ is an unknown function and F is a polynomial depending on $u(x, t)$ and its various partial derivatives.

Step 1. By wave transformation

$$u(x, t) = u(\xi), \xi = sx + nt + d. \quad (8)$$

The wave variable permits us to reduce Equation (8) into a nonlinear ordinary differential equation for $u = u(\xi)$:

$$H\left(u, u', u'', \cdots\right) = 0, \quad (9)$$

where H is a polynomial of $u(\xi)$ and its total derivative with respect to ξ.

Step 2. Assume that the solution of Equation (9) can be expressed as:

$$u' = a_1 u^{2-m} + b_1 u + c_1 u^m, \quad (10)$$

where a_1, b_1, c_1 and m are constant to be determined later.

Equation (10) has the solution as follows:

Case 1. When $m = 1$, the solution of Equation (10) is

$$u(\xi) = Ce^{(a_1+b_1+c_1)\xi}. \quad (11)$$

Case 2. When $m \neq 1, b_1 = 0, c_1 = 0$, the solution of Equation (10) is

$$u(\xi) = ((a_1(m-1))((\xi - c_1)))^{(1/(m-1))}. \quad (12)$$

Case 3. When $m \neq 1, b_1 \neq 0, c_1 = 0$, then solution of Equation (10)

$$u(\xi) = \left(-\frac{a_1}{b_1} + Ce^{b_1(m-1)\xi}\right)^{(1/(m-1))}. \quad (13)$$

Case 4. When $m \neq 1, a_1 = 0, b_1{}^2 - 4a_1c_1 < 0$, thus the solution of Equation (10)

$$u(\xi) = \left(-\frac{b_1}{2a_1} + \frac{\sqrt{4a_1c_1 - b_1{}^2}}{2a_1} \cdot \tan\left(\frac{(1-m)\sqrt{4a_1c_1 - b_1{}^2}}{2}(\xi + C)\right)\right)^{(1/(m-1))},$$

$$u(\xi) = \left(-\frac{b_1}{2a_1} + \frac{\sqrt{4a_1c_1 - b_1{}^2}}{2a_1} \cdot \cot\left(\frac{(1-m)\sqrt{4a_1c_1 - b_1{}^2}}{2}(\xi + C)\right)\right)^{(1/(m-1))}. \quad (14)$$

Case 5. When $m \neq 1, a_1 \neq 0, b_1{}^2 - 4a_1c_1 > 0$, the solutions of Equation (10) are

$$u(\xi) = \left(-\frac{b_1}{2a_1} + \frac{\sqrt{b_1{}^2 - 4a_1c_1}}{2a_1} \cdot \cot\left(\frac{(1-m)\sqrt{b_1{}^2 - 4a_1c_1}}{2}(\xi + C)\right)\right)^{(1/(m-1))}, \quad (15)$$

$$u(\xi) = \left(-\frac{b_1}{2a_1} + \frac{\sqrt{b_1{}^2 - 4a_1c_1}}{2a_1} \cdot \tan\left(\frac{(1-m)\sqrt{b_1{}^2 - 4a_1c_1}}{2}(\xi + C)\right)\right)^{(1/(1-m))}. \quad (16)$$

Case 6. When $m \neq 1, a_1 \neq 0, b_1{}^2 - 4a_1c_1 = 0$, the solution of Equation (10) is

$$u(\xi) = \left(\frac{1}{a_1(m-1)(\xi + C)} - \frac{b_1}{2a_1}\right)^{(1/(1-m))}, \quad (17)$$

where C is an arbitrary constant.

4. Mathematical Analyses of the Models and Its Solutions

4.1. For Fractional Generalized Reaction Duffing Model. Here, we consider the fractional generalized reaction Duffing model in the forms in [45].

$$\frac{\partial^{2\alpha}u(x,t)}{\partial t^{2\alpha}} + p\frac{\partial^{2\alpha}u(x,t)}{\partial x^{2\alpha}} + qu(x,t) + ru^2(x,t) + su^3(x,t) = 0, \quad t > 0, 0 < \alpha \leq 1, \quad (18)$$

where p, q, r and s are all constants.

If we take $r = 0$, Equation (18) reduces to the following nonlinear wave equation:

$$\frac{\partial^{2\alpha}u(x,t)}{\partial t^{2\alpha}} + p\frac{\partial^{2\alpha}u(x,t)}{\partial x^{2\alpha}} + qu(x,t) + su^3(x,t) = 0, \quad t > 0, 0 < \alpha \leq 1. \quad (19)$$

Let us assume the transformation:

$$u(x,t) = u(\xi), \xi = \frac{k}{\alpha}\left(x + \frac{1}{\Gamma(\alpha)}\right)^{\alpha} - \frac{c}{\alpha}\left(t + \frac{1}{\Gamma(\alpha)}\right)^{\alpha}, \quad (20)$$

where k and c are constants.

By using Equation (20) into Equation (19), we get the following ODE:

$$c^2u'' + pk^2u'' + qu + su^3 = 0. \quad (21)$$

In the following sections, the proposed methods are applied to extract the required solutions:

4.2. Solutions with GT Method [46]. Considering the homogenous balancing between the terms u'' and u^3 in Equation (21), we get $N = 1$. For $N = 1$, we write the solution of Equation (9) in the following form [46]:

$$u(\xi) = a_0 + a_1\varphi(\xi), \tag{22}$$

where a_0 and a_1 are unknown parameters.

Substituting Equation (22) into Equation (21) and setting each coefficient polynomial to zero gives a set of algebraic equations for a_0 and a_1 as follows:

$$\varphi^3 : 2c^2a_1 + 2k^2pa_1 + sa_1^3 = 0, \tag{23}$$

$$\varphi^2 : 3sa_0{a_1}^2 = 0, \tag{24}$$

$$\varphi^1 : 2c^2Ca_1 + 2Ck^2pa_1 + qa_1 + 3sa_0^2a_1 = 0, \tag{25}$$

$$\varphi^0 : qa_0 + sa_0^3 = 0. \tag{26}$$

Solving the system of algebraic equations in (23) with the help of software MATHEMATICA, we obtain the following solutions:

$$a_0 = 0, a_1 = \pm\frac{\sqrt{q}}{\sqrt{C}\sqrt{s}}, c = \pm\frac{\sqrt{-2Ck^2p - q}}{\sqrt{2}\sqrt{C}}. \tag{27}$$

Case 1. For C <0,

$$u_1(x, t) = \pm\frac{\sqrt{q}}{\sqrt{s}}\left(-i\tanh\sqrt{-C}\xi\right), \tag{28}$$

$$u_2(x, t) = \pm\frac{\sqrt{q}}{\sqrt{s}}\left(-i\coth\sqrt{-C}\xi\right). \tag{29}$$

Case 2. For C >0.

$$u_3(x, t) = \pm\frac{\sqrt{q}}{\sqrt{s}}\left(\tan\left(\sqrt{C}\xi\right)\right). \tag{30}$$

$$u_4(x, t) = \mp\frac{\sqrt{q}}{\sqrt{s}}\left(\cot\left(\sqrt{C}\xi\right)\right). \tag{31}$$

4.3. Solutions with GB Sub-ODE Method [47]. Consider the homogenous balancing in Equation (21), we get $N = 1$. For $N = 1$, we write the solution of Equation (9) in the following form:

$$u(\xi) = a_0 + a_1\varphi(\xi), \tag{32}$$

where a_0 and a_1 are unknown parameters.

Substituting Equation (32) into Equation (21) and setting each coefficient polynomial to zero gives a set of algebraic equations for a_0 and a_1 as follows:

$$\varphi^3 : 2c^2\mu^2a_1 + 2k^2p\mu^2a_1 + s{a_1}^3 = 0, \tag{33}$$

$$\varphi^2 : -3c^2\lambda\mu a_1 - 3k^2p\lambda\mu a_1 + 3sa_0a_1^2 = 0, \tag{34}$$

$$\varphi^1 : qa_1 + c^2\lambda^2a_1 + k^2p\lambda^2a_1 + 3sa_0^2a_1 = 0, \tag{35}$$

$$\varphi^0 : qa_0 + sa_0^3 = 0. \tag{36}$$

Solving the system of algebraic equations in (33) with the help of software MATHEMATICA, we obtain the following solutions:

$$a_0 = \pm i\frac{\sqrt{q}}{\sqrt{s}}, a_1 = \pm\frac{2i\sqrt{q}\mu}{\sqrt{s}\lambda}, c_1 = \pm\frac{\sqrt{2q - k^2p\lambda^2}}{\lambda}. \tag{37}$$

Case 1.

$$u_1(x, t) = \pm i\frac{\sqrt{q}}{\sqrt{s}} \mp \frac{i\sqrt{q}}{\sqrt{s}}\left(\tanh\left(\frac{\lambda}{2}\xi\right) - 1\right). \tag{38}$$

Case 2.

$$u_2(x, t) = \pm i\frac{\sqrt{q}}{\sqrt{s}} \mp \frac{i\sqrt{q}}{\sqrt{s}}\left(\coth\left(\frac{\lambda}{2}\xi\right) - 1\right). \tag{39}$$

4.4. Solutions with RB Sub-ODE Method. Considering the homogenous balancing in Equation (21), we get $N = 1$. For $N = 1$, Equation (9) has the solution:

$$u' = a_1u^{2-m} + b_1u + c_1u^m, \tag{40}$$

where a_1, b_1, c_1, and m are constant to be determined later.

Setting $m = 0$ and each coefficient polynomial to zero gives a set of algebraic equations for a_1, b_1, and c_1 as follows:

$$u^3 : s + 2c^2a_1^2 + 2k^2pa_1^2 = 0, \tag{41}$$

$$u^2 : 3c^2a_1b_1 + 3k^2pa_1b_1 = 0, \tag{42}$$

$$u^1 : q + c^2{b_1}^2 + k^2p{b_1}^2 + 2c^2a_1c_1 + 2k^2pa_1c_1 = 0, \tag{43}$$

$$u^0 : c^2b_1c_1 + k^2pb_1c_1 = 0. \tag{44}$$

Solving the system of algebraic equations in (41) with the help of software MATHEMATICA, we obtain the following solutions:

$$\begin{aligned} a_1 &= -\frac{\sqrt{s}}{\sqrt{2}\sqrt{-c^2 - k^2p}}, \\ b_1 &= 0, \\ c_1 &= -\frac{q}{\sqrt{2}\sqrt{-c^2 - k^2p}\sqrt{s}}. \end{aligned} \tag{45}$$

Case 1. When $m = 1$, we have

$$u(\xi) = Ce^{\left(\left(\left(-\sqrt{s}\right)/\left(\sqrt{2}\sqrt{-c^2-k^2p}\right)\right)-\left(q/\left(\sqrt{2}\sqrt{-c^2-k^2p}\sqrt{s}\right)\right)\right)\xi}. \tag{46}$$

Case 2. When $m \neq 1, a_1 \neq 0$, and $b_1^2 - 4a_1c_1 < 0$, we have

$$u(\xi) = \left(\frac{\sqrt{q}}{\sqrt{s}} \tan \frac{\sqrt{q}}{\sqrt{2}\sqrt{c^2 - k^2 p}} (\xi + C) \right), \quad (47)$$

$$u(\xi) = \left(-\frac{\sqrt{q}}{\sqrt{s}} \cot \frac{\sqrt{q}}{\sqrt{2}\sqrt{c^2 - k^2 p}} (\xi + C) \right). \quad (48)$$

5. Density Dependent Fractional Diffusion Reaction Equation

Density dependent fractional diffusion reaction equation which is widely used in mathematical biology in the form [44, 45]

$$\frac{\partial^\alpha u(x,t)}{\partial t^\alpha} + ku(x,t)\frac{\partial^\alpha u(x,t)}{\partial x^\alpha} = D\frac{\partial^{2\alpha} u(x,t)}{\partial x^{2\alpha}} + au(x,t) - bu^2(x,t), \quad t > 0, 0 < \alpha \leq 1, \quad (49)$$

Let us assume the transformation:

$$u(x,t) = u(\xi), \xi = \frac{p}{\alpha}\left(x + \frac{1}{\Gamma(\alpha)}\right)^\alpha - \frac{c}{\alpha}\left(t + \frac{1}{\Gamma(\alpha)}\right)^\alpha. \quad (50)$$

Here p and c are constants. By using Equation (50) into Equation (49), we get the following ODE:

$$Dp^2 u'' - cu' - kpuu' + au - bu^2 = 0. \quad (51)$$

5.1. Solutions with GT Method [46]. By applying homogenous balancing technique between the terms u'' and uu' into Equation (51), we get $N = 1$. For $N = 1$, we write the solution of Equation (9) in the following form [46]:

$$u(\xi) = a_0 + a_1\varphi(\xi), \quad (52)$$

where a_0 and a_1 are unknown parameters.

Substituting Equation (52) into Equation (51) and setting each coefficient polynomial to zero gives a set of algebraic equations for a_0 and a_1 as follows:

$$\begin{aligned} \varphi^3 &: 2Dp^2 a_1 - kpa_1^2 = 0, \\ \varphi^2 &: ca_1 - kpa_0 a_1 - b{a_1}^2 = 0, \\ \varphi^1 &: aa_1 + 2CDp^2 a_1 - 2ba_0 a_1 - Ckpa_1^2 = 0, \\ \varphi^0 &: aa_0 - ba_0^2 + cCa_1 - Ckpa_0 a_1 = 0. \end{aligned} \quad (53)$$

By using the software MATHEMATICA, we obtain the following solutions:

$$a_0 = \frac{a}{2b}, a_1 = \pm\frac{ia}{2b\sqrt{C}}, c = \pm\frac{ia}{2\sqrt{C}}, p = 0. \quad (54)$$

Case 1. For C <0,

$$u_1(x,t) = \frac{a}{2b} \pm \frac{a}{2b}\left(\tanh \sqrt{-C}\xi\right), \quad (55)$$

$$u_2(x,t) = \frac{a}{2b} \pm \frac{a}{2b}\left(\coth \sqrt{-C}\xi\right). \quad (56)$$

Case 2. For C >0,

$$u_3(x,t) = \frac{a}{2b} \pm \frac{ia}{2b}\left(\tan\left(\sqrt{C}\xi\right)\right), \quad (57)$$

$$u_4(x,t) = \frac{a}{2b} \mp \frac{ia}{2b}\left(\cot\left(\sqrt{C}\xi\right)\right). \quad (58)$$

5.2. Solutions with GB Sub-ODE Method. By applying homogenous balancing technique between the terms into Equation (51), we get $N = 1$. For $N = 1$, we write the solution of Equation (9) in the following form [47]:

$$u(\xi) = a_0 + a_1\varphi(\xi), \quad (59)$$

where a_0 and a_1 are unknown parameters.

Substituting Equation (59) into Equation (51) and setting each coefficient polynomial to zero gives a set of algebraic equations for a_0 and a_1 as follows:

$$\begin{aligned} \varphi^3 &: 2Dp^2\mu^2 a_1 - kp\mu a_1^2 = 0, \\ \varphi^2 &: c\mu a_1 - 3Dp^2\lambda\mu a_1 - kp\mu a_0 a_1 - b{a_1}^2 + kp\lambda{a_1}^2 = 0, \\ \varphi^1 &: aa_1 - c\lambda a_1 + Dp^2\lambda^2 a_1 - 2ba_0 a_1 + kp\lambda a_0 a_1 = 0, \\ \varphi^0 &: aa_0 - ba_0^2 = 0. \end{aligned} \quad (60)$$

By using the software MATHEMATICA, we obtain the following solutions:

$$a_0 = \frac{a}{b}, a_1 = -\frac{a\mu}{b\lambda}, c = -\frac{4ab^2D - a^2k^2}{4b^2D\lambda}, p = -\frac{ak}{2bD\lambda}. \quad (61)$$

Case 1.

$$u_1(x,t) = \frac{a}{b} + \frac{a}{2b}\left(\tanh\left(\frac{\lambda}{2}\xi\right) - 1\right). \quad (62)$$

Case 2.

$$u_2(x,t) = \frac{a}{b} + \frac{a}{2b}\left(\coth\left(\frac{\lambda}{2}\xi\right) - 1\right). \quad (63)$$

5.3. Solutions with RB Sub-ODE Method. By applying homogenous balancing technique, the terms u'' and uu' into Equation (54) we get $N = 1$.

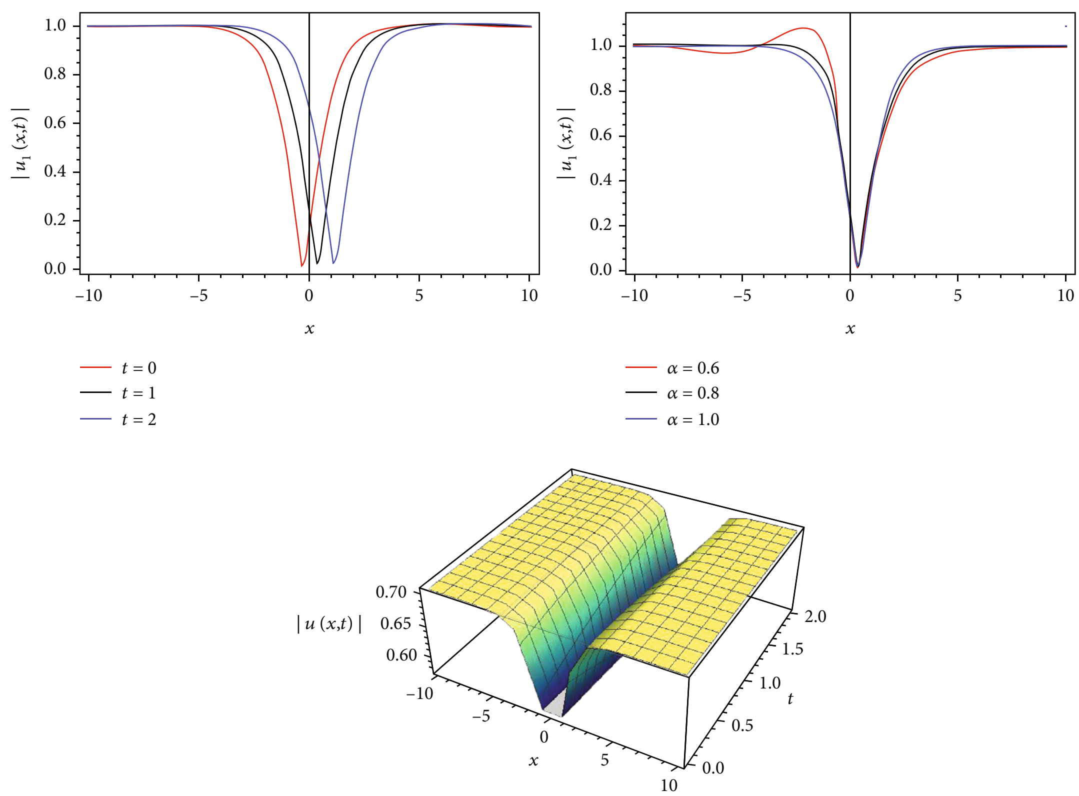

FIGURE 1: 2D and 3D graphics of Case 1 for hyperbolic traveling wave solution (28) at $\{\alpha = 0.6, \mathrm{k} = 0.7, q = 1, s = 1, \mathrm{C} = -1, c = 0.5\}$.

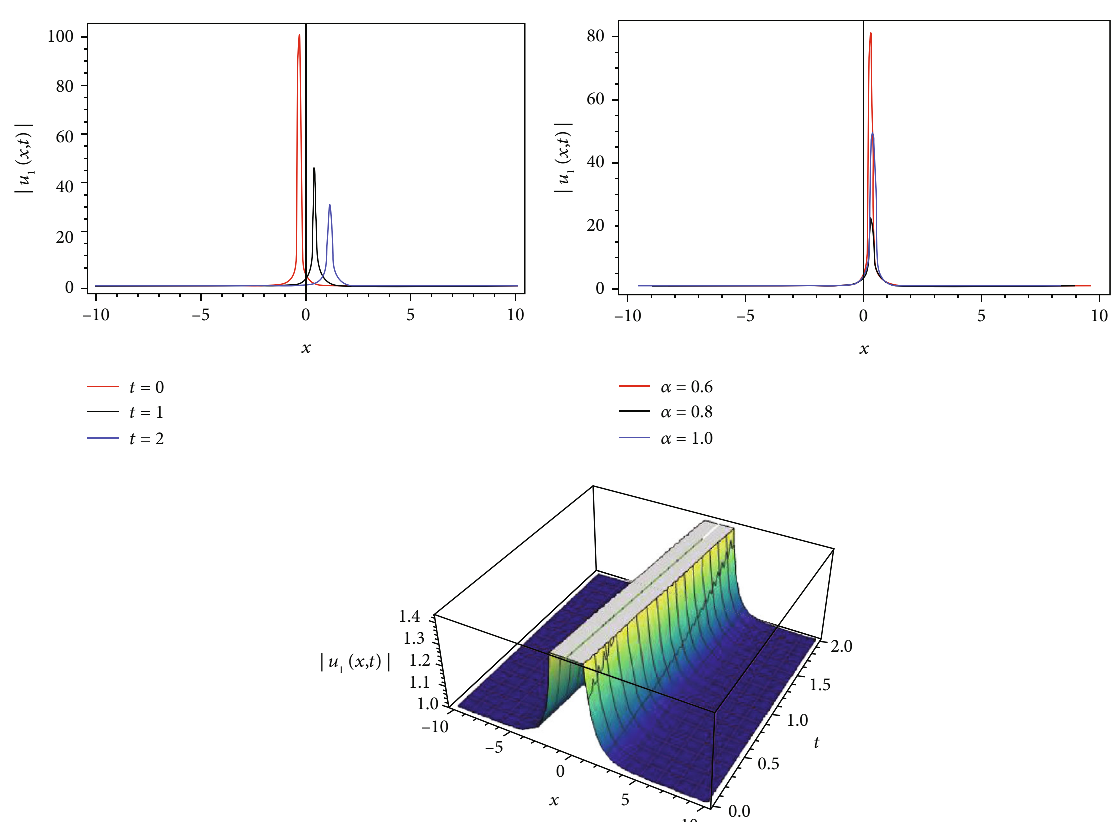

FIGURE 2: 2D and 3D graphics of Case 1 for hyperbolic traveling wave solution (29) at $\{\alpha = 0.6, \mathrm{k} = 0.7, q = 1, s = 1, \mathrm{C} = -1, c = 0.5.\}$.

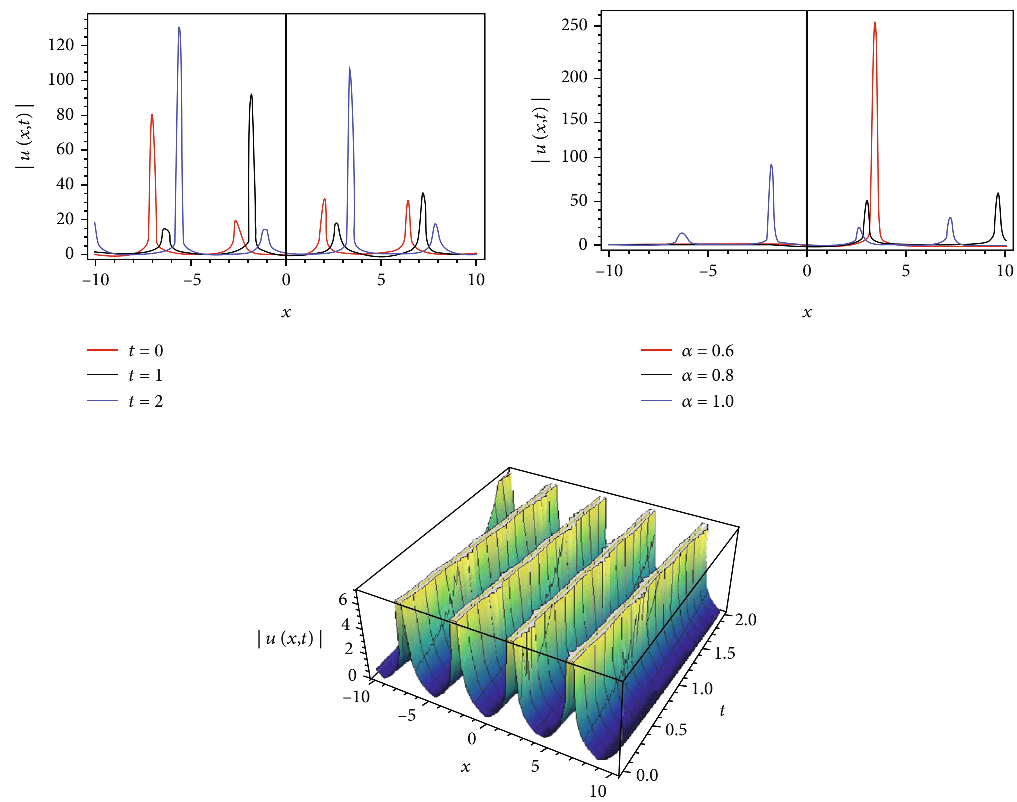

Figure 3: 2D and 3D graphics of Case 2 for trigonometric traveling wave solution (30) at $\{\alpha = 0.6, \mathrm{k} = 0.7, q = 1, s = 1, \mathrm{C} = 1, c = 0.5\}$.

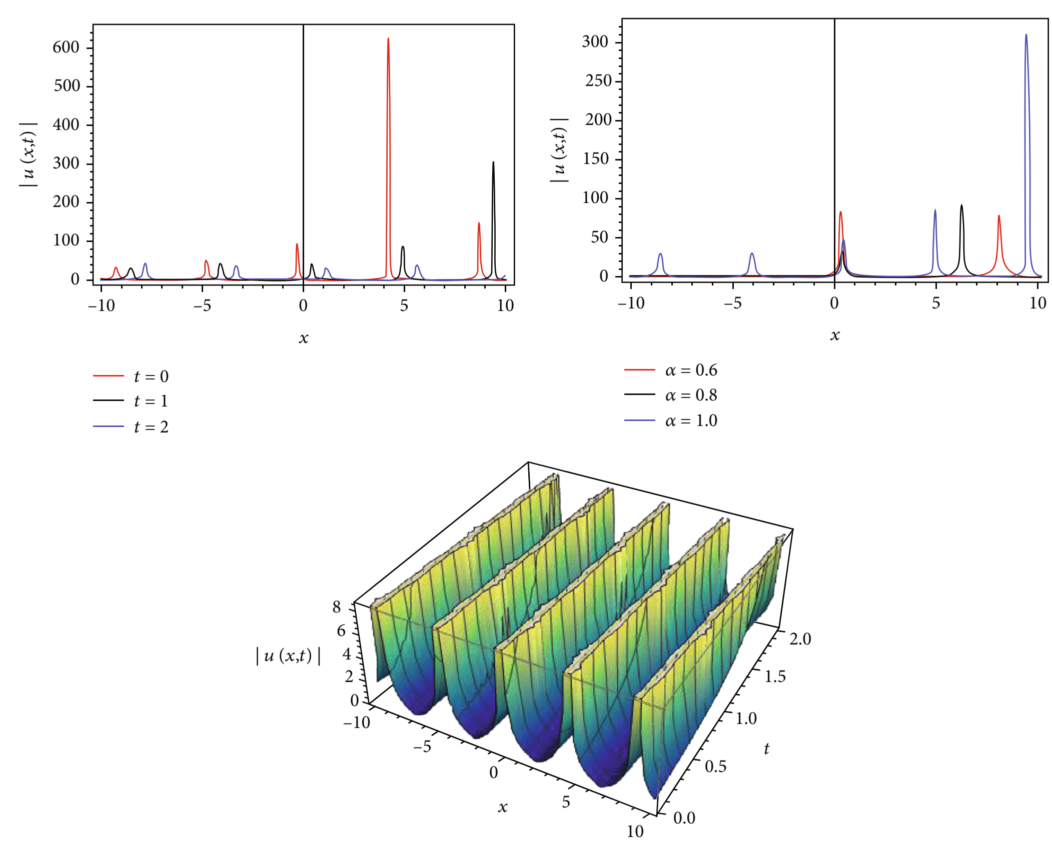

Figure 4: 2D and 3D graphics of Case 2 for trigonometric traveling wave solution (31) at $\{\alpha = 0.6, \mathrm{p} = 0.7, q = 1, s = 1, \mathrm{C} = -1, c = 0.5\}$.

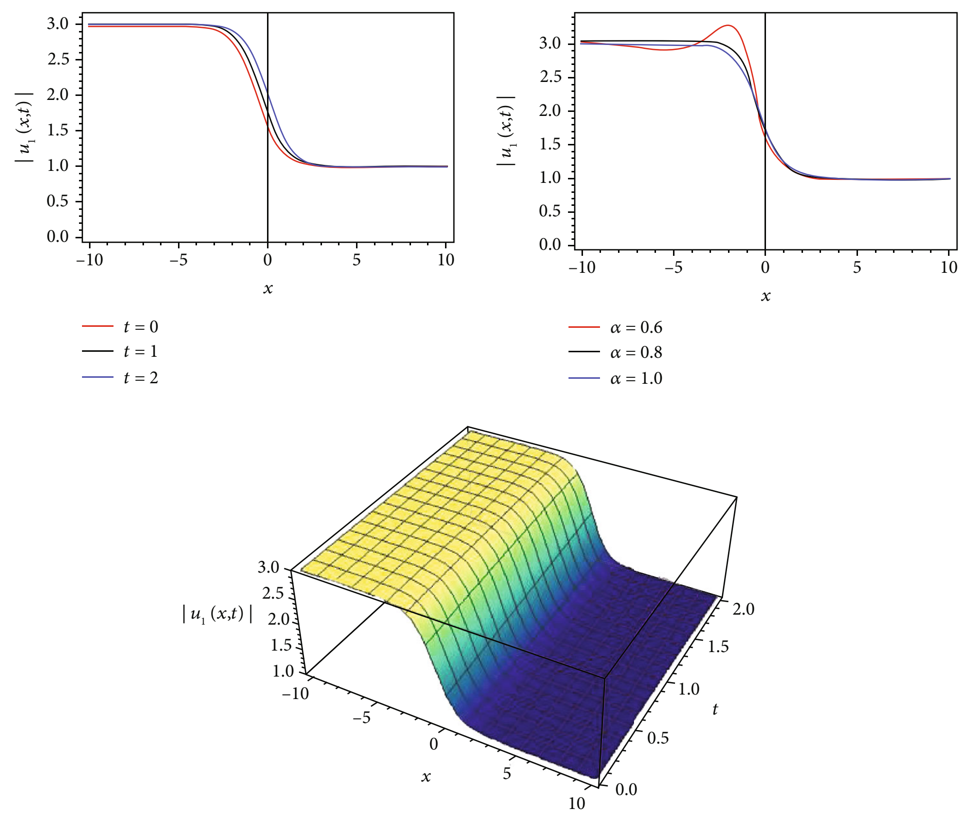

FIGURE 5: 2D and 3D graphics of Case 1 for hyperbolic traveling wave solution (38) at $\{\alpha = 0.6, k = 1.5, q = 1, s = 1, c = 0.5, \lambda = 1\}$.

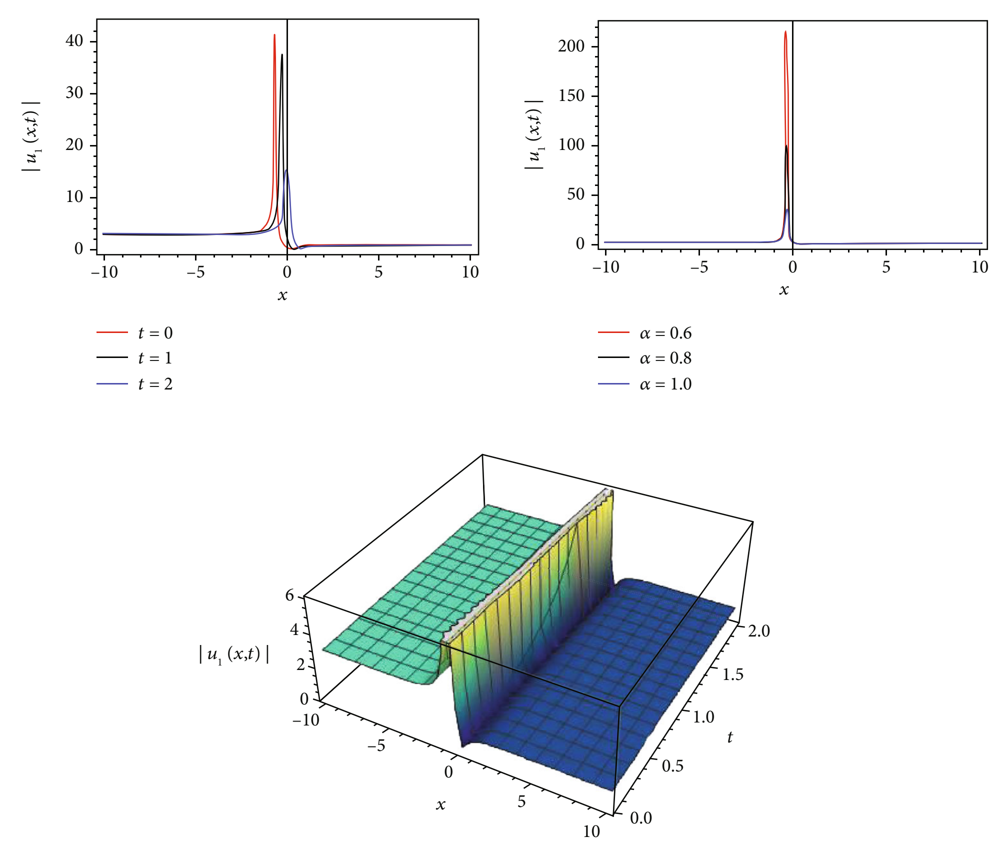

FIGURE 6: 2D and 3D graphics of Case 2 for hyperbolic traveling wave solution (39) at $\{\alpha = 0.6, k = 1.5, q = 1, s = 1, c = 0.5, \lambda = 1\}$.

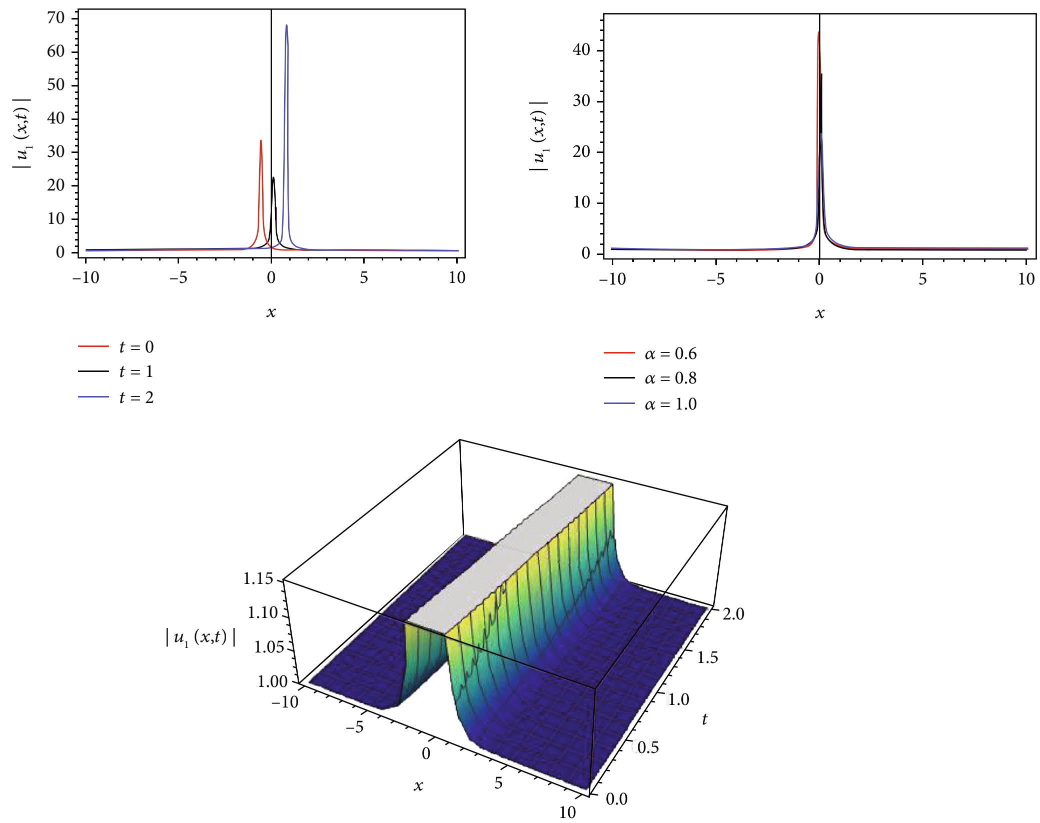

Figure 7: 2D and 3D graphics of Case 1 for hyperbolic traveling wave solution (47) at $\{\alpha = 0.6, \mathrm{k} = 0.7, q = 1, s = 1, \mathrm{C} = -1, c = 0.5\}$

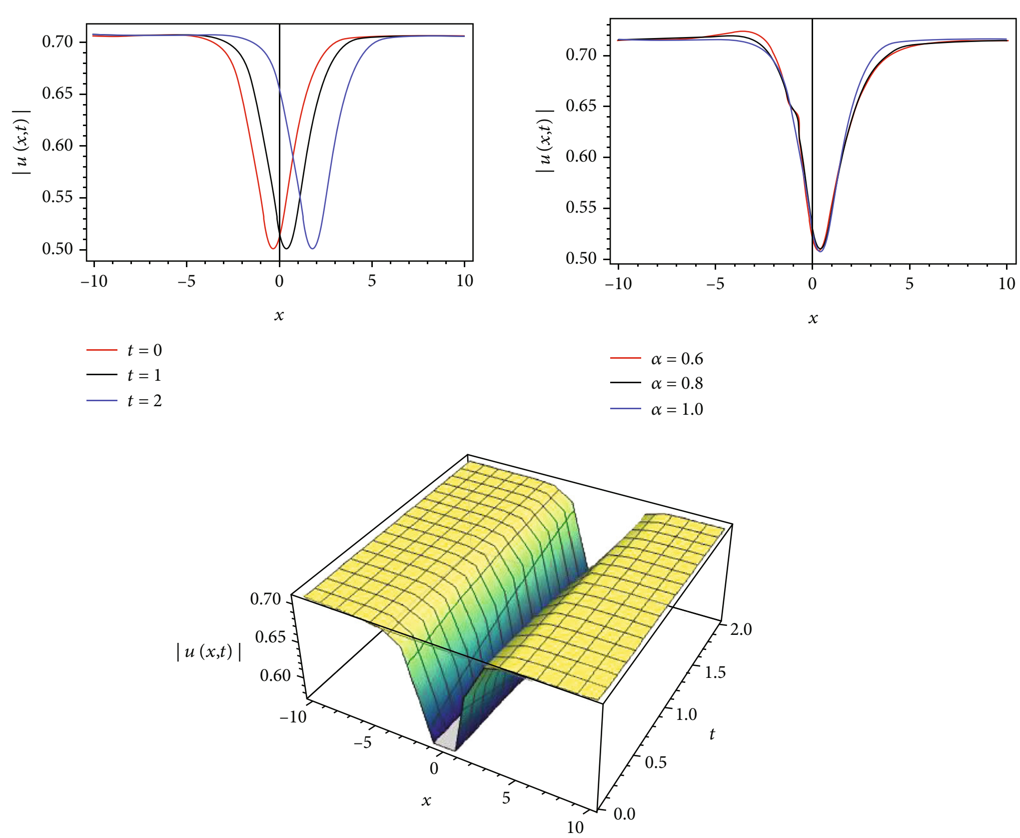

Figure 8: 2D and 3D graphics of Case 1 for hyperbolic traveling wave solution (55) at $\{\alpha = 0.6, \mathrm{k} = 0.7, q = 1, s = 1, \mathrm{C} = -1, c = 0.5\}$

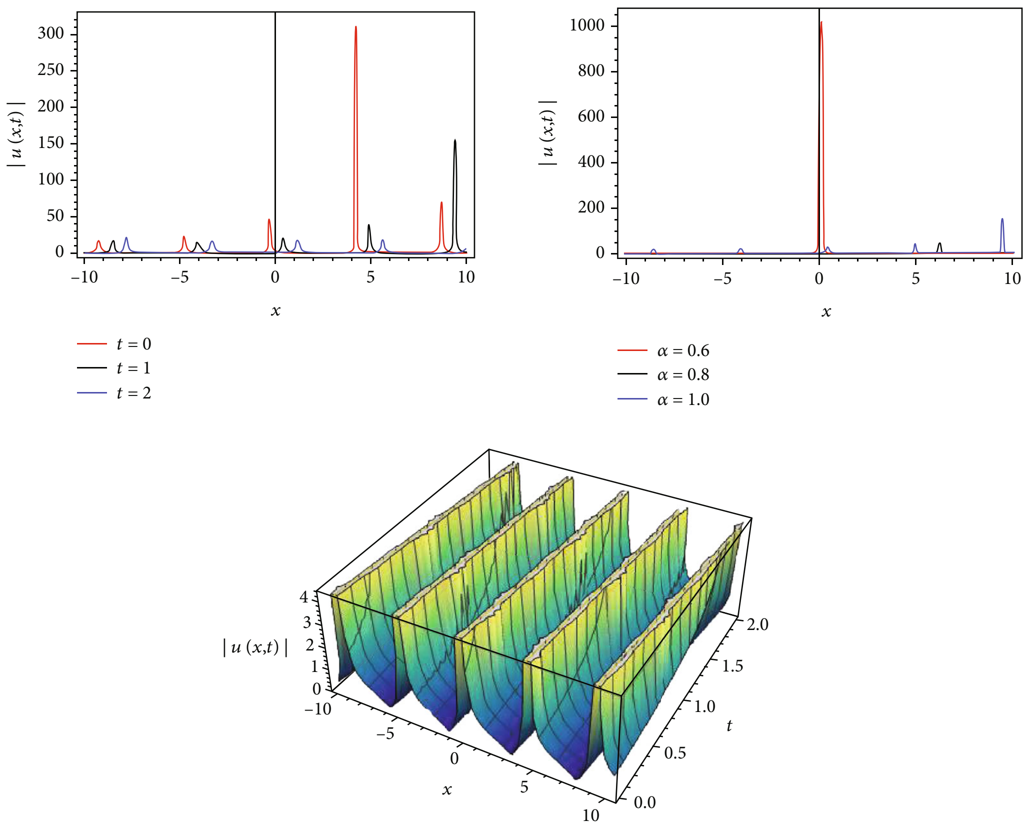

Figure 9: 2D and 3D graphics of Case 2 for trigonometric traveling wave solution (57) at $\{\alpha = 0.6, \mathrm{k} = 0.7, q = 1, s = 1, \mathrm{C} = 1, c = 0.5\}$.

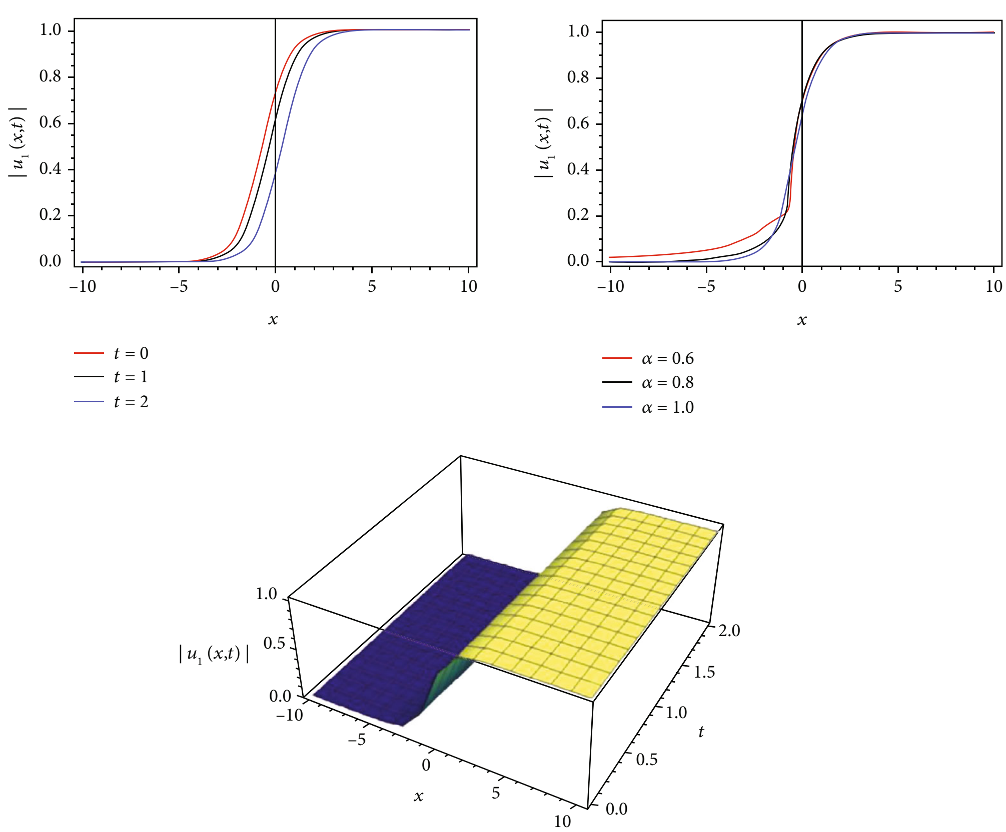

Figure 10: 2D and 3D graphics of Case 1 for hyperbolic traveling wave solution (62) at $\{\alpha = 0.6, \mathrm{k} = 0.7, a = 1, b = 1, \mathrm{c} = 0.5, \lambda = 1\}$.

For $N=1$, Equation (9) has the solution given as:

$$u' = a_1 u^{2-m} + b_1 u + c_1 u^m, \tag{64}$$

where a_1, b_1, c_1 and m are constant to be determined later.

Substituting Equation (64) into Equation (51), setting $m=0$ and each coefficient polynomial to zero gives a set of algebraic equations for a_1, b_1, and c_1 as follows:

$$u^4 : -kpa_1 + 2Dp^2a_1^2 = 0, \tag{65}$$

$$u^3 : -b + ca_1 - kpb_1 + 3Dp^2a_1b_1 = 0, \tag{66}$$

$$u^2 : a + cb_1 + Dp^2{b_1}^2 - kpc_1 + 2Dp^2a_1c_1 = 0, \tag{67}$$

$$u^1 : cc_1 + Dp^2b_1c_1 = 0. \tag{68}$$

By using the software MATHEMATICA, we obtain the following solutions:

$$a_1 = \frac{k}{2Dp}, b_1 = -\frac{ak}{2bDp}, c_1 = 0, c = \frac{\left(4b^2D + ak^2\right)p}{2bk}. \tag{69}$$

Case 1. When $m=1$, we have

$$u(\xi) = Ce^{((k/(2Dp))-(ak/(2bDp)))\xi}. \tag{70}$$

Case 2. When $m \neq 1$, $b_1 \neq 0$, and $c_1 = 0$, we have

$$u(\xi) = \left(-\frac{b}{a} + Ce^{((ak/(2bDp))\xi)}\right)^{-1}. \tag{71}$$

The above obtained solutions to the fractional generalized reaction Duffing model and density dependent fractional diffusion reaction equation are compared with those available in the earlier study and claimed to be recorded in the literature for the first time [25, 45].

6. Results and Discussions

To show the dynamics and behavior of our obtained solutions, various exact traveling wave solutions in Equations (28), (29), (30), (31), (38), (39), (48), (55), (57), and (62) are graphically represented and compared in both 3D and 2D plots in Figures 1–10 for various parameters' values. A 3D plot highlights the amount of variation over a while or compares multiple wave items. The 2D line plots are used to represent very high and low frequency and amplitude. The plots are constructed with unique values of $\alpha \in (0, 1]$ for different values of free parameters. The plots denote many natures, such as the trigonometric, hyperbolic and solitary wave solutions, and other forms of the solution generated by the correct physical description by choosing different free parameters. We can observe from the plotted graphs in Figures 1–10 that the wave's frequency and amplitude change with the change of fractional and time parameters.

7. Conclusions

In this article, three methods GT, GB sub-ODE, and RB sub-ODE have been applied to construct a variety of novel exact traveling wave solutions in the form of exponential, hyperbolic, and trigonometric functions of the generalized reaction Duffing model and density dependent fractional diffusion reaction equation arising in Mathematical biology. We have also depicted some of the obtained solutions graphically (3D surface graphs and 2D line plots) and concluded that the results we obtained are accurate, efficient, and versatile in mathematical physics. It is worth to noticing that compared to previous works [25, 26, 44, 45]; the results obtained in this paper are presented for the first time. Lastly, it can be concluded that our offered methods are more effective, reliable, and powerful, which give bounteous consistent solutions to NLPFDEs arise in different fields of nonlinear sciences.

Data Availability

No data were used to support this study.

Conflicts of Interest

The authors declare that they have no conflicts of interest.

References

[1] J. T. Machado, V. Kiryakova, and F. Mainardi, "Recent history of fractional calculus," *Communication in Nonlinear Science and Numerical Simulation*, vol. 16, no. 3, pp. 1140–1153, 2011.

[2] H. Weyl, "Bemerkungen zum Begriff des differential quotienten gebrochener Ordnung," *Vierteljshr. Naturforsch. Gesellsch. Zürich*, vol. 62, pp. 296–302, 1917.

[3] M. Riesz, "L'intégrale de Riemann-Liouville et le problème de Cauchy pour l'équation des ondes," *Bulletin de la Société Mathématique de France*, vol. 67, pp. 153–170, 1939.

[4] K. L. Wang and S. Y. Liu, "He's fractional derivative and its application for fractional Fornberg-Whitham equation," *Thermal Science*, vol. 1, pp. 54–54, 2016.

[5] Y. Chen, Y. Yan, and K. Zhang, "On the local fractional derivative," *Journal of Mathematical Analysis and Applications*, vol. 362, no. 1, pp. 17–33, 2010.

[6] A. A. Kilbas, H. M. Srivastava, and J. J. Trujillo, *Theory and Applications of Fractional Differential Equations*, Elsevier, Amsterdam, UK, 2006.

[7] J. M. Kimeu, *Fractional Calculus: Definitions and Applications*, Western Kentucky University, 2009.

[8] E. I. Kaikina, "Fractional derivative of Abel type on a half-line," *Transactions of the American Mathematical Society*, vol. 364, no. 10, pp. 5149–5172, 2012.

[9] S. Miller and B. Ross, *An Introduction to the Fractional Calculus and Fractional Differential Equations*, Wiley, New York, NY, USA, 1993.

[10] M. Caputo and M. Fabrizio, "A new definition of fractional differential without singular kernel," *Progress in Fractional Differentiation & Applications*, vol. 1, no. 2, pp. 1–13, 2015.

[11] A. Atangana and D. Baleanu, "New fractional derivatives with non-local and non-singular kernel. Theory and application to

heat transfer model," *Thermal Science*, vol. 20, no. 2, pp. 763–769, 2016.

[12] R. Khalil, M. A. Horani, A. Yousef, and M. Sababheh, "A new definition of fractional derivative," *Jornal of Computational and Applied Mathematics*, vol. 264, pp. 65–70, 2014.

[13] A. Atangana, D. Baleanu, and A. Alsaedi, "New properties of conformable derivative," *Open Mathematics*, vol. 13, no. 1, pp. 889–898, 2015.

[14] J. V. Sousa and E. C. de Oliveira, "A new truncated M-fractional derivative type unifying some fractional derivative types with classical properties," *International Journal of Analysis and Applications*, vol. 16, no. 1, pp. 83–96, 2018.

[15] A. Atangana, D. Baleanu, and A. Alsaedi, "Analysis of time-fractional Hunter-Saxton equation: a model of neumatic liquid crystal," *Open Physics*, vol. 14, no. 1, pp. 145–149, 2016.

[16] I. Podlubny, *Fractional Differential Equation*, Academic Press, San Diego, CA, USA, 1999.

[17] K. J. Wang, G. D. Wang, and H. W. Zhu, "A new perspective on the study of the fractal coupled Boussinesq–Burger equation in shallow water," *Fractals*, vol. 29, no. 5, p. 2150122, 2021.

[18] M. A. E. Abdelrahman, M. A. Sohaly, and Y. F. Alharbi, "Fundamental stochastic solutions for the conformable fractional NLSE with spatiotemporal dispersion via exponential distribution," *Physica Scripta*, vol. 96, no. 12, article 125223, 2021.

[19] M. A. E. Abdelrahman, S. Z. Hassan, R. A. Alomair, and D. M. Alsaleh, "Fundamental solutions for the conformable time fractional Phi-4 and space-time fractional simplified MCH equations," *AIMS Mathematics*, vol. 6, no. 6, pp. 6555–6568, 2021.

[20] M. Alshammari, W. W. Mohammed, and M. Yar, "Novel Analysis of fuzzy fractional Klein-Gordon model via Semianalytical method," *Journal of Function Spaces*, vol. 2022, Article ID 4020269, 9 pages, 2022.

[21] H. Rezazadeh, M. S. Osman, M. Eslami et al., "Hyperbolic rational solutions to a variety of conformable fractional Boussinesq-like equations," *Nonlinear Engineering*, vol. 8, no. 1, pp. 224–230, 2019.

[22] A. Zafar, A. Bekir, M. Raheel, and H. Rezazadeh, "Investigation for optical soliton solutions of two nonlinear Schrödinger equations via two concrete finite series methods," *International Journal of Applied and Computational Mathematics*, vol. 6, no. 3, pp. 1–13, 2020.

[23] I. Siddique, S. T. R. Rizvi, and F. Batool, "New exact traveling wave solutions of nonlinear evolution equations," *International Journal of Nonlinear Science*, vol. 9, no. 1, pp. 12–18, 2010.

[24] Y. Shang, "The Analytical Solutions for Stochastic Fractional-Space Burgers' Equation," *Journal of Mathematics*, vol. 2022, Article ID 9878885, 8 pages, 2022.

[25] I. Siddique, M. M. M. Jaradat, A. Zafar, and M. S. Osman, "Exact traveling wave solutions for two prolific conformable M-fractional differential equations via three diverse approaches," *Results in Physics*, vol. 28, p. 104557, 2021.

[26] X. Z. Zhang, I. Siddique, K. B. Mehdi, A. A. Elmandouh, and M. Inc, "Novel exact solutions, bifurcation of nonlinear and supernonlinear traveling waves for M-fractional generalized reaction Duffing model and the density dependent M-fractional diffusion reaction equation," *Results in Physics*, vol. 37, p. 105485, 2022.

[27] N. Ullah, M. I. Asjad, J. Awrejcewicz, T. Muhammad, and D. Baleanu, "On soliton solutions of fractional-order nonlinear model appears in physical sciences," *AIMS Mathematics*, vol. 7, no. 5, pp. 7421–7440, 2022.

[28] W. Razzaq, A. Zafar, H. M. Ahmed, and W. B. Rabied, "Construction solitons for fractional nonlinear Schrodinger equation with β-time derivative by the new sub-equation method," *Journal of Ocean Engineering and Science*, 2022.

[29] Y. Yıldırım and M. Mirzazadeh, "Optical pulses with Kundu-Mukherjee-Naskar model in fiber communication systems," *Chinese Journal of Physics*, vol. 64, pp. 183–193, 2020.

[30] N. Iqbal, A. M. Albalahi, M. S. Abdo, and W. W. Mohammed, "Analytical analysis of fractional-order Newell-Whitehead-Segel equation: a modified homotopy perturbation transform method," *Journal of Function Spaces*, vol. 2022, Article ID 3298472, 10 pages, 2022.

[31] A. Jhangeer, A. R. Seadawy, F. Ali, and A. Ahmed, "New complex waves of perturbed Shrodinger equation with Kerr law nonlinearity and Kundu-Mukherjee-Naskar equation," *Results in Physics*, vol. 16, p. 102816, 2020.

[32] K. Hosseini, M. Mirzazadeh, M. Ilied, and S. Radmehr, "Dynamics of optical solitons in the perturbed Gerdjikov-Ivanov equation," *Optik*, vol. 206, p. 164350, 2020.

[33] A. Bekir and A. Boz, "Exact solutions for nonlinear evolution equations using Exp-function method," *Physics Letters A*, vol. 372, no. 10, pp. 1619–1625, 2008.

[34] A. Tozar, O. Tasbozan, and A. Kurt, "Analytical solutions of Cahn-Hillard phase-field model for spinodal decomposition of a binary system," *Europhysics Letters*, vol. 130, no. 2, p. 24001, 2020.

[35] M. Wang and X. Li, "Extended F-expansion method and periodic wave solutions for the generalized Zakharov equations," *Physics Letters A*, vol. 343, no. 1-3, pp. 48–54, 2005.

[36] L. Tian and J. Yin, "Stability of multi-compacton solutions and Backlund transformation in K (m, n ,1)," *Chaos, Solitons and Fractals*, vol. 23, no. 1, pp. 159–169, 2005.

[37] A. M. Wazwaz, "The extended tanh method for new compact and noncompact solutions for the KP- BBM and the ZK-BBM equations," *Chaos, Solitons and Fractals*, vol. 38, no. 5, pp. 1505–1516, 2008.

[38] G. T. Liu and T. Y. Fan, "New applications of developed Jacobi elliptic function expansion methods," *Physics Letters A*, vol. 345, no. 1-3, pp. 161–166, 2005.

[39] D. Kumar, J. Manafian, F. Hawlader, and A. Ranjbaran, "New closed form soliton and other solutions of the Kundu-Eckhaus equation via the extended sinh-Gordon equation expansion method," *Optik*, vol. 160, pp. 159–167, 2018.

[40] K. K. Ali, C. Cattani, J. F. Gómez-Aguilar, D. Baleanu, and M. S. Osman, "Analytical and numerical study of the DNA dynamics arising in oscillator-chain of Peyrard-Bishop model," *Chaos, Solitons & Fractals*, vol. 139, p. 110089, 2020.

[41] F. M. Al-Askar, W. W. Mohammed, and M. Alshammari, "Impact of Brownian motion on the analytical solutions of the space-fractional stochastic approximate long water wave equation," *Symmetry*, vol. 14, no. 4, p. 740, 2022.

[42] M. Alshammari, N. Iqbal, W. W. Mohammed, and T. Botmart, "The solution of fractional-order system of KdV equations with exponential- decay kernel," *Results in Physics*, vol. 38, p. 105615, 2022.

[43] M. S. Osman and K. K. Ali, "Optical soliton solutions of perturbing time-fractional nonlinear Schrodinger equations," *Optik*, vol. 209, p. 164589, 2020.

[44] M. Hafiz Uddin, M. A. Akbar, M. Md Ashrafuzzaman, and A. Haque, "Close form solutions of the fractional generalized reaction duffing model and the density dependent fractional diffusion reaction equation," *Applied and Computational Mathematics*, vol. 6, no. 4, pp. 177–184, 2017.

[45] O. Guner and A. Bekir, "Exact solutions of some fractional differential equations arising in mathematical biology," *International Journal of Biomathematics*, vol. 8, no. 1, p. 1550003, 2015.

[46] N. Taghizadeh and M. Najand, "Generalized tanh method with the Riccati equation for solving the sixth-order Ramani equation," *Mathematica Aeterna*, vol. 2, no. 5, pp. 483–487, 2012.

[47] M. A. Salam, M. S. Uddin, and P. Dey, "Generalized Bernoulli sub- ODE method and its application," *Analysis of Pure and Applied Mathematics*, vol. 10, no. 1, pp. 1–6, 2015.

[48] X. F. Yang, Z. C. Deng, and Y. Wei, "A Riccati-Bernoulli sub-ODE method for nonlinear partial differential equations and its application," *Advances in Difference Equations*, vol. 2015, no. 1, p. 17, 2015.

[49] H. Jafari, H. Tajododi, D. Baleanu, A. A. Al-Zahrani, Y. A. Alhamed, and A. H. Zahid, "Fractional sub-equation method for the fractional generalized reaction duffing model and nonlinear fractional Sharma-Tasso-Olver equation," *Central European Journal of Physics*, vol. 11, no. 10, pp. 1482–1486, 2013.

[50] M. Eslami, B. F. Vajargah, M. Mirzazadeh, and A. Biswas, "Application of first integral method to fractional partial differential equations," *Indian Journal of Physics*, vol. 88, no. 2, pp. 177–184, 2014.

[51] T. C. Xia, H. Q. Zhang, and Z. Y. Yan, "New explicit and exact travelling wave solutions for a class of nonlinear evolution equations," *Applied Mathematics and Mechanics*, vol. 22, no. 7, pp. 788–793, 2001.

[52] M. Sonmezoglu, "Exact solutions for some fractional differential equations," *Advances in Mathematical Physics*, vol. 2015, Article ID 567842, 10 pages, 2015.

[53] A. Yusuf, M. Inc, A. I. Aliyu, and D. Baleanu, "Optical solitons possessing beta derivative of the Chen-Lee-Liu equation in optical fibers," *Frontiers in Physics*, vol. 7, p. 34, 2019.

Hindawi
Journal of Function Spaces
Volume 2022, Article ID 1399951, 9 pages
https://doi.org/10.1155/2022/1399951

Research Article

On ψ-Caputo Partial Hyperbolic Differential Equations with a Finite Delay

Mohammed S. Abdo,[1] **Mohammed Zakarya**,[2,3] **Emad E. Mahmoud**,[4] **Saeed M. Ali**,[5] **and Abdel-Haleem Abdel-Aty**[6]

[1]*Department of Mathematics, Hodeidah University, P.O. Box 3114, Al-Hudaydah, Yemen*
[2]*Department of Mathematics, College of Science, King Khalid University, P.O. Box 9004, Abha 61413, Saudi Arabia*
[3]*Department of Mathematics, Faculty of Science, Al-Azhar University, 71524 Assiut, Egypt*
[4]*Department of Mathematics and Statistics, College of Science, Taif University, P.O. Box 11099, Taif 21944, Saudi Arabia*
[5]*Department of Basic Engineering Sciences, College of Engineering, Imam Abdulrahman Bin Faisal University, P.O. Box 1982, Dammam 34151, Saudi Arabia*
[6]*Department of Physics, College of Sciences, University of Bisha, P.O. Box 344 Bisha 61922, Saudi Arabia*

Correspondence should be addressed to Mohammed S. Abdo; msabdo@hoduniv.net.ye

Received 12 June 2022; Accepted 1 September 2022; Published 19 September 2022

Academic Editor: Yusuf Gurefe

In this work, we are concerned with some qualitative analyses of fractional-order partial hyperbolic functional differential equations under the ψ-Caputo type. To be precise, we investigate the existence and uniqueness results based on the nonlinear alternative of the Leray-Schauder type and Banach contraction mapping. Moreover, we present two similar results to nonlocal problems. Then, the guarantee of the existence of solutions is shown by Ulam-Hyer's stability. Two examples will be given to illustrate the abstract results. Eventually, some known results in the literature are extended.

1. Introduction

Since fractional calculus (FC) has a decent global correlation execution to reflect the historical reliance process of the improvement of system functions and can likewise describe the characteristics of the dynamic system itself, it turned into a strong mathematical gadget to describe a few complex developments, unpredictable phenomena, memory highlights, and other aspects. FC theory was vastly utilized by mathematicians as well as scientific experts, engineers, financial analysts, scholars, and physicists (see [1–4]). Riemann, in 1876, suggested the definition of the Riemann-Liouville (RL) fractional derivative (FD). Caputo originally proposed one more definition of FD through a changed RL fractional integral (FI) toward the start of the twentieth century, to be specific, a Caputo FD. One issue in this field is the major and extraordinary number of possible various definitions of FD and FI; settling on the choice of the best operator for every specific framework is a significant issue. One method for conquering this issue is to consider overall definitions, of which the classical ones can be viewed as specific cases [5, 6].

In this regard, Almeida [7] and Sousa and de Oliveira [8] recently introduced ψ-Caputo FD and ψ-Hilfer FD of one variable, respectively, from which it is feasible to obtain a wide class of FDs already well established. Sousa and de Oliveira [9] have very recently expanded ψ-Hilfer FD with two variables. Therefore, one of the aims of this work is to introduce some qualitative analyses of solutions based on ψ-Caputo FD with two variables.

Then again, functional differential equations (FDEs) and fractional FDEs with finite delay show up frequently in applications as models of equations, and consequently, the investigation of these kinds of equations has gotten incredible consideration somewhat recently; see, for instance, [10–14] and the references in those. The literature connected with the existence of solutions of fractional partial FDEs with a finite delay was processed very slowly; see, for instance, [15–19].

The background and survey in the literature relative to classical fractional partial hyperbolic FDEs can be found in the monograph of Abbas et al. [19]. Sousa and de Oliveira [9] discussed the stability of fractional partial hyperbolic DEs without delay under the ψ-Hilfer operator. Baitiche et al. [20] established the existence result of coupled systems of fractional partial hyperbolic DEs without delay.

This work is concerned with the existence, uniqueness, and Ulam-Hyer (HU) stability of the solution to the ψ-Caputo-type fractional partial hyperbolic FDE with finite delay:

$$\begin{gathered} {}^{C}\mathscr{D}_{0+}^{r;\psi}\varkappa(\varkappa,\tau)=\mathfrak{F}\left(\varkappa,\tau,\varkappa_{(\varkappa,\tau)}\right),(\varkappa,\tau)\in J_1:=[0,c]\times[0,d],\\ \varkappa(\varkappa,\tau)=\varphi(\varkappa,\tau),(\varkappa,\tau)\in J_2:=[-\kappa_1,c]\times[-\kappa_2,d]\setminus(0,c]\times(0,d],\\ \varkappa(\varkappa,0)=\phi_1(\varkappa),\varkappa(0,\tau)=\phi_2(\tau),\varkappa\in[0,c],\tau\in[0,d], \end{gathered} \tag{1}$$

and the ψ-Caputo-type fractional nonlocal partial hyperbolic FDE with finite delay:

$$\begin{gathered} {}^{C}\mathscr{D}_{\ell+}^{r;\psi}\varkappa(\varkappa,\tau)=\mathfrak{F}\left(\varkappa,\tau,\varkappa_{(\varkappa,\tau)}\right),(\varkappa,\tau)\in J_1:=[0,c]\times[0,d],\\ \varkappa(\varkappa,\tau)=\varphi(\varkappa,\tau),(\varkappa,\tau)\in J_2:=[-\kappa_1,c]\times[-\kappa_2,d]\setminus(0,c]\times(0,d],\\ \varkappa(\varkappa,0)+h_1(\varkappa)=\phi_1(\tau),\varkappa(0,\tau)+h_1(\varkappa)=\phi_2(\tau),\varkappa\in[0,c],\tau\in[0,d], \end{gathered} \tag{2}$$

where $c, d, \kappa_1, \kappa_2 > 0$,$r=(\mu,\nu)\in(0,1]\times(0,1]$,${}^{C}\mathscr{D}_{\ell^+}^{r;\psi}$ is the ψ-Caputo FD of order r with respect to another function ψ, which is increasing, and $\partial\psi/\partial u, \partial\psi/\partial\tau\neq 0$, for $(\varkappa,\tau)\in J_1$, $\ell=(0,0)$,$\varphi(\cdot,\cdot)\in\mathscr{C}:=\mathscr{C}([-\kappa_1,0]\times[-\kappa_2,0],\mathbb{R})$, $\mathfrak{F}:J_1\times\mathscr{C}\longrightarrow\mathbb{R}$,$\phi_1:[0,c]\longrightarrow\mathbb{R}$,$\phi_2:[0,d]\longrightarrow\mathbb{R}$ are absolutely continuous with $\phi_1(\varkappa)=\varphi(\varkappa,0)$,$\phi_2(\tau)=\varphi(0,\tau)$, $\forall\varkappa\in[0,c]$,$\forall\tau\in[0,d]$, and $h_1,h_2:C(J_1,\mathbb{R})\longrightarrow\mathbb{R}$ are continuous.

This paper is concerned with the qualitative analyses of fractional partial hyperbolic FDEs, which are very new, and the implementation of the ψ-fractional operator makes it more general and novel, unlike the classical fractional operators. To be precise, we are interested in investigating the existence, uniqueness, and Ulam-Hyer's stability results for our problems (1)–(2). These results initiate the investigation of ψ-Caputo fractional partial hyperbolic FDEs with a finite delay, which mainly includes a more general fractional operator based on another function ψ. To be certain, in the analysis of our results, we essentially use fixed point theorems (FPTs) of the Leray-Schauder type and Banach type. Our outcomes can be interpreted as extensions of preceding results that Abbas et al. [19] and Sousa and de Oliveira [9] obtained for classical FHDEs, which can be considered a contribution to the literature.

The rest of the work has been organized as follows. Section 2 is devoted to some essential connotations of ψ-fractional calculus with auxiliary lemmas to problems at hand. The existence, uniqueness, and UH stability results based on fixed point techniques are provided in Section 3. Suitable examples are given in Section 4. In Section 5, we present the conclusions.

2. Preliminary Results

In this section, we give some notations and essential definitions of fractional partial integrals and derivatives (FPIs and FPDs) and some function spaces to simplify the forthcoming analysis. Let $J_1=[0,c]\times 0,d]$, $J_2:=[-\kappa_1,c]\times-\kappa_2,d]\setminus(0,c]\times(0,d]$, where $c,d,\kappa_1,\kappa_2>0$,$\ell=(0,0)$, and $r=(\mu,\nu)\in(0,1]\times(0,1]$. Denote $\mathscr{C}:=\mathscr{C}([-\kappa_1,0]\times-[\kappa_2,0],\mathbb{R})$ the space of continuous functions on $[-\kappa_1,0]\times-\kappa_2,0]$. Note that $\mathscr{C}$ is the Banach space with the norm

$$\|z\|_{\mathscr{C}}=\sup_{(\varkappa,\tau)\in[-\kappa_1,0]\times[-\kappa_2,0]}|z(\varkappa,\tau)|, \tag{3}$$

and let $C(J_1,\mathbb{R})$ be the Banach space with the norm

$$\|z\|_{\infty}=\sup_{(\varkappa,\tau)\in[0,c]\times[0,d]}|z(\varkappa,\tau)|. \tag{4}$$

The space $\mathscr{L}^1(J_1,\mathbb{R})$ is endowed with the norm

$$\|z\|_{\mathscr{L}^1}=\int_0^c\int_0^d|z(\varkappa,\tau)|d\varkappa d\tau. \tag{5}$$

For any $z_{(\varkappa,\tau)}:[-\kappa_1,c]\times-\kappa_2,d]\longrightarrow\mathbb{R}$, where $(\varkappa,\tau)\in J_1$, we have

$$z_{(\varkappa,\tau)}(\theta,\theta)=z(\varkappa+\theta,\tau+\theta),\text{for}(\theta,\theta)\in[-\kappa_1,0]\times[-\kappa_2,0]. \tag{6}$$

Define the space $\mathscr{C}([-\kappa_1,c]\times-\kappa_2,d],\mathbb{R})$ as

$$\mathscr{C}_{(c,d)}=\left\{z:[-\kappa_1,c]\times-\kappa_2,d]\longrightarrow\mathbb{R}:z|_{J_2}=\varphi\in\mathscr{C},z|_{J_1}\in C(J_1,\mathbb{R})\right\}, \tag{7}$$

where $z|_{J_1}$ is the restriction of z to J_1, which is a Banach space with the norm

$$\|z\|_{\mathscr{C}_{(c,d)}}=\sup_{(\varkappa,\tau)\in[-\kappa_1,c]\times[-\kappa_2,d]}|z(\varkappa,\tau)|. \tag{8}$$

In the forthcoming analysis, let us consider $\psi(\cdot)$ to be an increasing and positive monotone function on J_1 with $\psi_\varkappa(\cdot)$, $\psi_\tau(\cdot)\neq 0$ on J_1, where $\psi_\varkappa=\partial\psi/\partial\varkappa$ and $\psi_\tau=\partial\psi/\partial\tau$. On the whole paper, keep in mind $\psi^{\theta-1}(y,m):=(\psi(y)-\psi(m))^{\theta-1}$.

Definition 1 (see [9]). Let $\ell=(0,0)$,$r=(\mu,\nu)$, where $\mu,\nu>0$. Then, the ψ-RL FPI of a function of two variables $z(\varkappa,\tau)\in$

$\mathscr{L}^1(J_1, \mathbb{R})$ of order r is given by

$$\mathscr{I}^{r;\psi}_{\ell^+} z(\varkappa,\tau) = \frac{1}{\Gamma(\mu)\Gamma(\nu)} \int_0^{\varkappa}\int_0^{\tau} \psi_{\varkappa}(\theta)\psi_{\tau}(\zeta)\psi^{\mu-1}(\varkappa,\theta)\psi^{\nu-1}(\tau,\zeta) z(\theta,\zeta) d\theta d\zeta. \tag{9}$$

Also, we have

$$\begin{aligned} \mathscr{I}^{\mu}_{0^+} z(\varkappa,\tau) &= \frac{1}{\Gamma(\mu)} \int_0^{\varkappa} \psi_{\varkappa}(\theta)\psi^{\mu-1}(\varkappa,\theta) z(\theta,\tau) d\theta, \\ \mathscr{I}^{\nu}_{0^+} z(\varkappa,\tau) &= \frac{1}{\Gamma(\nu)} \int_0^{\tau} \psi_{\tau}(\theta)\psi^{\nu-1}(\tau,\theta) z(\varkappa,\theta) d\theta. \end{aligned} \tag{10}$$

Definition 2 (see [9]). Let $\ell = (0,0)$, and $r = (\mu,\nu)$, where $0 < \mu, \nu \leq 1$. Then, the ψ-RL FPD of a function $z(\varkappa,\tau) \in \mathscr{L}^1(J_1, \mathbb{R})$ of order r is defined by

$$\mathscr{D}^{r;\psi}_{\ell^+} z(\varkappa,\tau) = \left(\frac{1}{\psi_{\varkappa}\psi_{\tau}} \frac{\partial^2}{\partial\varkappa\partial\tau}\right) \mathscr{I}^{1-r;\psi}_{\ell^+} z(\varkappa,\tau). \tag{11}$$

Definition 3 (see [9]). Let $\ell = (0,0)$, $r = (\mu,\nu)$, where $0 < \mu, \nu \leq 1$, and $\psi \in C^1(J_1, \mathbb{R})$. Then, the ψ-Caputo FPD of a function $z(\varkappa,\tau) \in C^1(J_1, \mathbb{R})$ of order r is defined by

$${}^{C}\mathscr{D}^{r;\psi}_{\ell^+} z(\varkappa,\tau) = \mathscr{I}^{1-r;\psi}_{\ell^+} \left(\frac{1}{\psi_{\varkappa}\psi_{\tau}} \frac{\partial^2}{\partial\varkappa\partial\tau}\right) z(\varkappa,\tau). \tag{12}$$

Lemma 4 (see [9]). *Let $r = (\mu,\nu) \in (0,\infty) \times (0,\infty)$, and ξ_1, $\xi_2 > -1$. Then,*

$$\mathscr{I}^{r;\psi}_{\ell^+} \psi^{\xi_1-1}(\varkappa,0)\psi^{\xi_2-1}(\tau,0) = \frac{\Gamma(\xi_1)}{\Gamma(\mu+\xi_1)} \frac{\Gamma(\xi_2)}{\Gamma(\nu+\xi_2)} \psi^{\mu+\xi_1-1}(\varkappa,0)\psi^{\nu+\xi_2-1}(\tau,0). \tag{13}$$

Lemma 5 (see [9]). *Let $r = (\mu,\nu) \in (0,1] \times (0,1]$, and $\xi_1, \xi_2 > -1$. Then,*

$$\mathscr{D}^{r;\psi}_{\ell^+} \psi^{\xi_1-1}(\varkappa,0)\psi^{\xi_2-1}(\tau,0) = \frac{\Gamma(\xi_1)}{\Gamma(\mu-\xi_1)} \frac{\Gamma(\xi_2)}{\Gamma(\nu-\xi_2)} \psi^{\mu-\xi_1-1}(\varkappa,0)\psi^{\nu-\xi_2-1}(\tau,0). \tag{14}$$

Lemma 6 (see [7]). *Let $0 < r < 1$, and $h : [c,d] \longrightarrow \mathbb{R}$ is continuous. Then,*

$${}^{C}\mathscr{D}^{r,\psi}_{c^+} \mathscr{I}^{r,\psi}_{c^+} h(\varkappa) = h(\varkappa), \mathscr{I}^{r,\psi}_{c^+} {}^{C}\mathscr{D}^{r,\psi}_{c^+} h(\varkappa) = h(\varkappa) - h(c). \tag{15}$$

Lemma 7. *The following problem*

$$\begin{aligned} &{}^{C}\mathscr{D}^{r;\psi}_{0+} z(\varkappa,\tau) = f(\varkappa,\tau), (\varkappa,\tau) \in [0,c] \times [0,d], \\ &z(\varkappa,0) = \phi_1(\varkappa), z(0,\tau) = \phi_2(\tau), \varkappa \in [0,c], \tau \in [0,d], \end{aligned} \tag{16}$$

with $\phi_1(0) = \phi_2(0)$ which has a solution $z(\varkappa,\tau) \in \mathscr{C}([0,c] \times 0,d], \mathbb{R})$ if and only if $z(\varkappa,\tau)$ satisfies

$$z(\varkappa,\tau) = \eta(\varkappa,\tau) + \mathscr{I}^{r;\psi}_{0^+} f(\varkappa,\tau), (\varkappa,\tau) \in 0,c] \times 0,d], \tag{17}$$

where $\eta(\varkappa,\tau) = \phi_1(\varkappa) + \phi_2(\tau) - \phi_1(0)$.

Proof. The proof is primitive and similar to the proof of Lemma 3.2 given in [21], so it can be omitted. □

Here, we only refer to source [22] of the results of Leray-Schauder and Banach FPT.

3. Main Results

Let us begin by describing what we mean by a solution to problem (1).

Definition 8. A function z is a solution of (1), if $z \in \mathscr{C}_{(c,d)}$ and $(D^2 z_{\varkappa\tau})(\varkappa,\tau)$ exists and is integrable.

Theorem 9. *Let the following assumptions hold:*

(A1) $\mathfrak{F} : J_1 \times \mathscr{C} \longrightarrow \mathbb{R}$ is continuous.

(A2) There exists $L_{\mathfrak{F}} > 0$ such that

$$|\mathfrak{F}(\varkappa,\tau,z) - \mathfrak{F}(\varkappa,\tau,\upsilon)| \leq L_{\mathfrak{F}} \|z-\upsilon\|_{\mathscr{C}}, (\varkappa,\tau) \in J_1, z, \upsilon \in \mathscr{C}. \tag{18}$$

If

$$\sigma \coloneqq \frac{\psi^{\mu}(c,0)\psi^{\nu}(d,0)}{\Gamma(\mu+1)\Gamma(\nu+1)} L_{\mathfrak{F}} < 1, \tag{19}$$

then there exists a unique solution for the ψ-Caputo problem (1) on $[-\kappa_1, c] \times -\kappa_2, d)$.

Proof. Consider the operator $\mathscr{K} : \mathscr{C}_{(c,d)} \longrightarrow \mathscr{C}_{(c,d)}$ defined by $(\mathscr{K}z)(\varkappa,\tau) = z(\varkappa,\tau)$, i.e.,

$$(\mathscr{K}z)(\varkappa,\tau) = \begin{cases} \varphi(\varkappa,\tau), & (\varkappa,\tau) \in J_2, \\ \eta(\varkappa,\tau) + \dfrac{1}{\Gamma(\mu)\Gamma(\nu)} \displaystyle\int_0^{\varkappa}\int_0^{\tau} \psi_{\mathrm{u}}(\theta)\psi^{\mu-1}(\varkappa,\theta)\psi_{\tau}(\zeta)\psi^{\nu-1}(\tau,\zeta) \times \mathfrak{F}\left(\theta,\zeta,z_{(\theta,\zeta)}\right) d\zeta d\theta, & (\varkappa,\tau) \in J_1, \end{cases} \tag{20}$$

where $\eta(\varkappa,\tau) := \phi_1(\varkappa) + \phi_2(\tau) - \phi_1(0)$.

Let $z, \omega \in \mathscr{C}_{(c,d)}$, and $(\varkappa,\tau) \in [-\kappa_1, c] \times [-\kappa_2, d]$. Then,

$$\begin{aligned}
&|(\mathscr{K}z)(\varkappa,\tau) - (\mathscr{K}\omega)(\varkappa,\tau)| \\
&\le \frac{1}{\Gamma(\mu)\Gamma(\nu)} \int_0^\varkappa \int_0^\tau \psi_\varkappa(\theta)\psi^{\mu-1}(\varkappa,\theta)\psi_\tau(\zeta)\psi^{\nu-1}(\tau,\zeta) \\
&\quad \times \left|\mathfrak{F}\left(\theta,\zeta,z_{(\theta,\zeta)}\right) - \mathfrak{F}\left(\theta,\zeta,\omega_{(\theta,\zeta)}\right)\right| d\zeta d\theta \\
&\le \frac{L_{\mathfrak{F}}}{\Gamma(\mu)\Gamma(\nu)} \int_0^\varkappa \int_0^\tau \psi_\varkappa(\theta)\psi^{\mu-1}(\varkappa,\theta)\psi_\tau(\zeta)\psi^{\nu-1}(\tau,\zeta) \\
&\quad \times \left\|z_{(\theta,\zeta)} - \omega_{(\theta,\zeta)}\right\|_{\mathscr{C}} d\zeta d\theta \\
&\le \frac{L_{\mathfrak{F}}}{\Gamma(\mu)\Gamma(\nu)} \|z-\omega\|_{\mathscr{C}_{(c,d)}} \int_0^\varkappa \psi_{\mathrm{u}}(\theta)\psi^{\mu-1}(\varkappa,\theta) \int_0^\tau \psi_\tau(\zeta)\psi^{\nu-1}(\tau,\zeta) d\zeta d\theta \\
&\le \frac{L_{\mathfrak{F}}}{\Gamma(\mu)\Gamma(\nu)} \|z-\omega\|_{\mathscr{C}_{(c,d)}} \frac{\psi^\nu(d,0)}{\nu} \int_0^\varkappa \psi_\varkappa(\theta)\psi^{\mu-1}(\varkappa,\theta) d\theta \\
&\le \frac{L_{\mathfrak{F}}\psi^\mu(c,0)\,\psi^\nu(d,0)}{\Gamma(\mu+1)\Gamma(\nu+1)} \|z-\omega\|_{\mathscr{C}_{(c,d)}}.
\end{aligned} \tag{21}$$

which implies

$$\|(\mathscr{K}z) - (\mathscr{K}\omega)\|_{\mathscr{C}_{(c,d)}} \le \sigma \|z-\omega\|_{\mathscr{C}_{(c,d)}}. \tag{22}$$

Since $\sigma < 1$, the operator $\mathscr{K}$ is a contraction. This means that $\mathscr{K}$ has a unique fixed point by Banach's FPT. □

Theorem 10. *Let (A1) and the following assumption hold:*

(A3) There exist $p, q \in C(J_1, \mathbb{R})$ such that

$$|\mathfrak{F}(\varkappa,\tau,z)| \le p(\varkappa,\tau) + q(\varkappa,\tau)\|z\|_{\mathscr{C}}, (\varkappa,\tau) \in J_1, z \in \mathscr{C}. \tag{23}$$

If $\rho := \|q\|_\infty \psi^\mu(c,0)\psi^\nu(d,0)/\Gamma(\mu+1)\Gamma(\nu+1) < 1$, then there exists at least one solution for the ψ-Caputo problem (1) on $[-\kappa_1, c] \times -\kappa_2, d]$.

Proof. Consider the operator $\mathscr{K} : \mathscr{C}_{(c,d)} \longrightarrow \mathscr{C}_{(c,d)}$ defined by (20); then, we show that $\mathscr{K}$ is completely continuous.

Step 1: $\mathscr{K}$ is continuous. Let $\{z_n\}$ be a sequence such that $z_n \longrightarrow z$ in $\mathscr{C}_{(c,d)}$. Then,

$$\begin{aligned}
&|(\mathscr{K}z_n)(\varkappa,\tau) - (\mathscr{K}z)(\varkappa,\tau)| \\
&\le \frac{1}{\Gamma(\mu)\Gamma(\nu)} \int_0^\varkappa \int_0^\tau \psi_\varkappa(\theta)\psi^{\mu-1}(\varkappa,\theta)\psi_\tau(\zeta)\psi^{\nu-1}(\tau,\zeta) \\
&\quad \times \left|\mathfrak{F}\left(\theta,\zeta,z_{n_{(\theta,\zeta)}}\right) - \mathfrak{F}\left(\theta,\zeta,z_{(\theta,\zeta)}\right)\right| d\zeta d\theta \\
&\le \frac{1}{\Gamma(\mu)\Gamma(\nu)} \int_0^c \int_0^d \psi_\varkappa(\theta)\psi^{\mu-1}(\varkappa,\theta)\psi_\tau(\zeta)\psi^{\nu-1}(\tau,\zeta) \\
&\quad \times \sup_{(\theta,\zeta)\in J_1} \left|\mathfrak{F}\left(\theta,\zeta,z_{n_{(\theta,\zeta)}}\right) - \mathfrak{F}\left(\theta,\zeta,z_{(\theta,\zeta)}\right)\right| d\zeta d\theta \\
&\le \frac{\psi^\mu(c,0)\,\psi^\nu(d,0)}{\Gamma(\mu+1)\Gamma(\nu+1)} \left\|\mathfrak{F}\left(\cdot,\cdot,z_{n_{(\cdot,\cdot)}}\right) - \mathfrak{F}\left(\cdot,\cdot,z_{(\cdot,\cdot)}\right)\right\|_\infty.
\end{aligned} \tag{24}$$

Since $\mathfrak{F}$ is continuous, $\|(\mathscr{K}z_n) - (\mathscr{K}z)\|_{\mathscr{C}_{(c,d)}} \longrightarrow 0$, as $n \longrightarrow \infty$.

Step 2: $\mathscr{K}(B_\xi)$ is bounded in $\mathscr{C}_{(c,d)}$, where $B_\xi = \{z \in \mathscr{C}_{(c,d)} : \|z\|_{\mathscr{C}_{(c,d)}} \le \xi\}$, for any $\xi > 0$.

Set

$$\xi > \max\left\{\|\varphi\|_{\mathscr{C}}, \frac{\lambda}{1-\rho}\right\}, \tag{25}$$

where

$$\lambda := \|\eta\|_\infty + \left(\frac{\|p\|_\infty \psi^\mu(c,0)\,\psi^\nu(d,0)}{\Gamma(\mu+1)\Gamma(\nu+1)}\right). \tag{26}$$

For $(\varkappa,\tau) \in J_2$, we get

$$|(\mathscr{K}z)(\varkappa,\tau)| \le \sup_{(\varkappa,\tau)\in J_2} |\varphi(\varkappa,\tau)| = \|\varphi\|_{\mathscr{C}}. \tag{27}$$

Let $(\varkappa,\tau) \in J_1$, and $z \in B_\xi$. Then,

$$\begin{aligned}
|(\mathscr{K}z)(\varkappa,\tau)| &\le |\eta(\varkappa,\tau)| + \frac{1}{\Gamma(\mu)\Gamma(\nu)} \int_0^\varkappa \int_0^\tau \psi_\varkappa(\theta)\psi^{\mu-1}(\varkappa,\theta)\psi_\tau(\zeta)\psi^{\nu-1}(\tau,\zeta) \\
&\quad \times \left|\mathfrak{F}\left(\theta,\zeta,z_{(\theta,\zeta)}\right)\right| d\zeta d\theta \\
&\le |\eta(\varkappa,\tau)| + \frac{1}{\Gamma(\mu)\Gamma(\nu)} \int_0^\varkappa \int_0^\tau \psi_\varkappa(\theta)\psi^{\mu-1}(\varkappa,\theta)\psi_\tau(\zeta)\psi^{\nu-1}(\tau,\zeta) p(\theta,\zeta) d\zeta d\theta \\
&\quad + \frac{1}{\Gamma(\mu)\Gamma(\nu)} \int_0^\varkappa \int_0^\tau \psi_\varkappa(\theta)\psi^{\mu-1}(\varkappa,\theta)\psi_\tau(\zeta)\psi^{\nu-1}(\tau,\zeta) q(\theta,\zeta) \left\|z_{(\theta,\zeta)}\right\|_{\mathscr{C}} d\zeta d\theta \\
&\le \|\eta\|_\infty + \frac{\|p\|_\infty}{\Gamma(\mu)\Gamma(\nu)} \int_0^\varkappa \int_0^\tau \psi_\varkappa(\theta)\psi^{\mu-1}(\varkappa,\theta)\psi_\tau(\zeta)\psi^{\nu-1}(\tau,\zeta) d\zeta d\theta \\
&\quad + \frac{\|q\|_\infty \|z\|_{\mathscr{C}(c,d)}}{\Gamma(\mu)\Gamma(\nu)} \int_0^\varkappa \int_0^\tau \psi_\varkappa(\theta)\psi^{\mu-1}(\varkappa,\theta)\psi_\tau(\zeta)\psi^{\nu-1}(\tau,\zeta) d\zeta d\theta \\
&\le \|\eta\|_\infty + (\|p\|_\infty + \|q\|_\infty \xi) \frac{\psi^\mu(c,0)\,\psi^\nu(d,0)}{\Gamma(\mu+1)\Gamma(\nu+1)} = \lambda + \rho\xi.
\end{aligned} \tag{28}$$

Due to (25), (27), and (28), $\|(\mathscr{K}z)\|_{\mathscr{C}_{(c,d)}} \le \xi$, or $(\mathscr{K}z) \in B_\xi$, which implies that $\mathscr{K}(B_\xi)$ is bounded in $\mathscr{C}_{(c,d)}$.

Step 3: $\mathscr{K}(B_\xi)$ is equicontinuous in $\mathscr{C}_{(c,d)}$. Let $z \in B_\xi$, and $(\varkappa_1,\tau_1), (\varkappa_2,\tau_2) \in [-\kappa_1, c] \times [-\kappa_2, d]$ with $\varkappa_1 < \varkappa_2, \tau_1 < \tau_2$. If ($\varkappa_1,\tau_1), (\varkappa_2,\tau_2) \in J_1$ and $z \in B_\xi$. Then,

$$\begin{aligned}
&|(\mathscr{K}z)(\varkappa_2,\tau_2) - (\mathscr{K}z)(\varkappa_1,\tau_1)| \\
&\le |\eta(\varkappa_2,\tau_2) - \eta(\varkappa_1,\tau_1)| + \frac{1}{\Gamma(\mu)\Gamma(\nu)} \int_0^{\varkappa_1} \int_0^{\tau_1} \psi_\varkappa(\theta)\psi_\tau(\zeta) \left[\psi^{\mu-1}(\varkappa_2,\theta)\psi^{\nu-1}(\tau_2,\zeta)\right. \\
&\quad \left. - \psi^{\mu-1}(\varkappa_1,\theta)\psi^{\nu-1}(\tau_1,\zeta)\right] \times \left|\mathfrak{F}\left(\theta,\zeta,z_{(\theta,\zeta)}\right)\right| d\zeta d\theta \\
&\quad + \frac{1}{\Gamma(\mu)\Gamma(\nu)} \int_{\varkappa_1}^{\varkappa_2} \int_{\tau_1}^{\tau_2} \psi_\varkappa(\theta)\psi_\tau(\zeta) \left[\psi^{\mu-1}(\varkappa_2,\theta)\psi^{\nu-1}(\tau_2,\zeta)\right] \left|\mathfrak{F}\left(\theta,\zeta,z_{(\theta,\zeta)}\right)\right| d\zeta d\theta \\
&\quad + \frac{1}{\Gamma(\mu)\Gamma(\nu)} \int_0^{\varkappa_1} \int_{\tau_1}^{\tau_2} \psi_\varkappa(\theta)\psi_\tau(\zeta) \left[\psi^{\mu-1}(\varkappa_2,\theta)\psi^{\nu-1}(\tau_2,\zeta)\right] \left|\mathfrak{F}\left(\theta,\zeta,z_{(\theta,\zeta)}\right)\right| d\zeta d\theta \\
&\quad + \frac{1}{\Gamma(\mu)\Gamma(\nu)} \int_{\varkappa_1}^{\varkappa_2} \int_0^{\tau_1} \psi_\varkappa(\theta)\psi_\tau(\zeta) \left[\psi^{\mu-1}(\varkappa_2,\theta)\psi^{\nu-1}(\tau_2,\zeta)\right] \left|\mathfrak{F}\left(\theta,\zeta,z_{(\theta,\zeta)}\right)\right| d\zeta d\theta \\
&\le \|\eta(\varkappa_2,\tau_2) - \eta(\varkappa_1,\tau_1)\|_\infty + \frac{\|p\|_\infty + \|q\|_\infty \xi}{\Gamma(\mu)\Gamma(\nu)} \int_0^{\varkappa_1} \int_0^{\tau_1} \psi_{\mathrm{u}}(\theta)\psi_\tau(\zeta) \left[\psi^{\mu-1}(\varkappa_2,\theta)\psi^{\nu-1}(\tau_2,\zeta)\right. \\
&\quad \left. - \psi^{\mu-1}(\varkappa_1,\theta)\psi^{\nu-1}(\tau_1,\zeta)\right] d\zeta d\theta + \frac{\|p\|_\infty + \|q\|_\infty \xi}{\Gamma(\mu)\Gamma(\nu)} \int_{\varkappa_1}^{\varkappa_2} \int_{\tau_1}^{\tau_2} \psi_\varkappa(\theta)\psi_\tau(\zeta) \\
&\quad \times \left[\psi^{\mu-1}(\varkappa_2,\theta)\psi^{\nu-1}(\tau_2,\zeta)\right] d\zeta d\theta + \frac{\|p\|_\infty + \|q\|_\infty \xi}{\Gamma(\mu)\Gamma(\nu)} \int_0^{\varkappa_1} \int_{\tau_1}^{\tau_2} \psi_\varkappa(\theta)\psi_\tau(\zeta) \\
&\quad \times \left[\psi^{\mu-1}(\varkappa_2,\theta)\psi^{\nu-1}(\tau_2,\zeta)\right] d\zeta d\theta + \frac{\|p\|_\infty + \|q\|_\infty \xi}{\Gamma(\mu)\Gamma(\nu)} \int_{\varkappa_1}^{\varkappa_2} \int_0^{\tau_1} \psi_\varkappa(\theta)\psi_\tau(\zeta) \\
&\quad \times \left[\psi^{\mu-1}(\varkappa_2,\theta)\psi^{\nu-1}(\tau_2,\zeta)\right] d\zeta d\theta \le \|\eta(\varkappa_2,\tau_2) - \eta(\varkappa_1,\tau_1)\|_\infty \\
&\quad + \frac{\|p\|_\infty + \|q\|_\infty \xi}{\Gamma(\mu+1)\Gamma(\nu+1)} \left[2\psi^\nu(\tau_2,0)\psi^\mu(\varkappa_2,\varkappa_1) + 2\psi^\mu(\varkappa_2,0)\psi^\nu(\tau_2,\tau_1)\right. \\
&\quad \left. + \psi^\nu(\tau_1,0)\psi^\mu(\varkappa_1,0) - \psi^\nu(\tau_2,0)\psi^\mu(\varkappa_2,0) - 2\psi^\nu(\tau_2,\tau_1)\psi^\mu(\varkappa_2,\varkappa_1)\right].
\end{aligned} \tag{29}$$

If $-\kappa_1 \le \varkappa_1 \le \varkappa_2 \le 0$, and $-\kappa_2 \le \tau_1 \le \tau_2 \le 0$, then

$$|(\mathscr{K}z)(\varkappa_2, \tau_2) - (\mathscr{K}z)(\varkappa_1, \tau_1)| \le |\varphi(\varkappa_2, \tau_2) - \varphi(\varkappa_1, \tau_1)|. \tag{30}$$

If $-\kappa_1 \le \varkappa_1 < 0 < \varkappa_2 \le c$, and $-\kappa_2 \le \tau_1 < 0 < \tau_2 \le d$, then

$$\begin{aligned} &|(\mathscr{K}z)(\varkappa_2, \tau_2) - (\mathscr{K}z)(\varkappa_1, \tau_1)| \\ &\quad\le |(\mathscr{K}z)(\varkappa_2, \tau_2) - (\mathscr{K}z)(0,0)| + |(\mathscr{K}z)(0,0) - (\mathscr{K}z)(\varkappa_1, \tau_1)| \\ &\quad\le \|\eta(\varkappa_2, \tau_2) - \eta(0,0)\|_\infty + \frac{\|p\|_\infty + \|q\|_\infty \xi}{\Gamma(\mu+1)\Gamma(\nu+1)} [2\psi^\nu(\tau_2, 0)\psi^\mu(\varkappa_2, 0) \\ &\qquad + 2\psi^\mu(\varkappa_2, 0)\psi^\nu(\tau_2, 0) + \psi^\nu(0,0)\psi^\mu(0,0) - \psi^\nu(\tau_2, 0)\psi^\mu(\varkappa_2, 0) \\ &\qquad - 2\psi^\nu(\tau_2, 0)\psi^\mu(\varkappa_2, 0)] + |\varphi(0,0) - \varphi(\varkappa_1, \tau_1)|. \end{aligned} \tag{31}$$

In all previous cases, as $\varkappa_1 \longrightarrow \varkappa_2$, $\tau_1 \longrightarrow \tau_2$, and the uniform continuity of η on J_1 and φ on J_2 implies that for any $\varepsilon > 0$, there exists $\delta > 0$, independent of $\varkappa_1, \varkappa_2$, τ_1, τ_2 and z, such that $|(\mathscr{K}z)(\varkappa_2, \tau_2) - (\mathscr{K}z)(\varkappa_1, \tau_1)| \le \varepsilon$ whenever $|\psi(\varkappa_2) - \psi(\varkappa_1)| \le \delta/2$ and $|\psi(\tau_2) - \psi(\tau_1)| \le \delta/2$. Therefore, $\mathscr{K}(B_\xi)$ is equicontinuous. It follows from the Arzela–Ascoli theorem that $\mathscr{K}$ is compact.

Step 4: $\mathscr{K}(B_\xi)$ a priori bounds. ∃ an open set $\Omega \subseteq \mathscr{C}_{(c,d)}$ with $z \ne \aleph \mathscr{K} z$, for $\aleph \in (0,1)$, and $z \in \partial\Omega$. Let $(\varkappa, \tau) \in [-\kappa_1, c] \times [-\kappa_2, d]$ and $z \in \mathscr{C}_{(c,d)}$ with $z \ne \aleph\mathscr{K}z$, for some $\aleph \in (0,1)$. Then,

$$\begin{aligned} |z(\varkappa, \tau)| &\le \aleph|\eta(\varkappa, \tau)| + \frac{\aleph}{\Gamma(\mu)\Gamma(\nu)} \int_0^\varkappa\int_0^\tau \psi_\varkappa(\theta)\psi^{\mu-1}(\varkappa, \theta)\psi_\tau(\zeta)\psi^{\nu-1}(\tau, \zeta)\left|\mathfrak{F}\left(\theta, \zeta, z_{(\theta,\zeta)}\right)\right| d\zeta d\theta \\ &\le |\eta(\varkappa, \tau)| + \frac{1}{\Gamma(\mu)\Gamma(\nu)} \int_0^\varkappa\int_0^\tau \psi_\varkappa(\theta)\psi^{\mu-1}(\varkappa, \theta)\psi_\tau(\zeta)\psi^{\nu-1}(\tau, \zeta) \\ &\quad \cdot \left[p(\theta, \zeta) + q(\theta, \zeta)\left\|z_{(\theta,\zeta)}\right\|_{\mathscr{C}}\right] d\zeta d\theta \\ &\le \|\eta\|_\infty + \frac{\|p\|_\infty \psi^\mu(c, 0)\,\psi^\nu(d, 0)}{\Gamma(\mu+1)\Gamma(\nu+1)} \\ &\quad + \frac{\|q\|_\infty}{\Gamma(\mu)\Gamma(\nu)} \int_0^\varkappa\int_0^\tau \psi_{\mathrm{u}}(\theta)\psi^{\mu-1}(\varkappa, \theta)\psi_\tau(\zeta)\psi^{\nu-1}(\tau, \zeta)\|z\|_{\mathscr{C}_{(c,d)}} d\zeta d\theta. \end{aligned} \tag{32}$$

If $(\varkappa, \tau) \in J_1$, then (32) becomes

$$\begin{aligned} \|z(\varkappa, \tau)\|_\infty &\le \|\eta\|_\infty + \frac{\|p\|_\infty \psi^\mu(c, 0)\,\psi^\nu(d, 0)}{\Gamma(\mu+1)\Gamma(\nu+1)} \\ &\quad + \frac{\|q\|_\infty}{\Gamma(\mu)\Gamma(\nu)} \int_0^\varkappa\int_0^\tau \psi_\varkappa(\theta)\psi^{\mu-1}(\varkappa, \theta)\psi_\tau(\zeta)\psi^{\nu-1}(\tau, \zeta)\|z(\theta, \zeta)\|_\infty d\zeta d\theta \\ &\le \|\eta\|_\infty + \frac{\|p\|_\infty + \|q\|_\infty\|z(\varkappa, \tau)\|_\infty}{\Gamma(\mu+1)\Gamma(\nu+1)} \psi^\mu(c, 0)\,\psi^\nu(d, 0), \end{aligned} \tag{33}$$

which implies

$$\|z(\varkappa, \tau)\|_\infty \le \frac{\lambda}{1-\rho} \coloneqq M. \tag{34}$$

For $(\varkappa, \tau) \in J_2, \|z(\varkappa, \tau)\|_\infty = \|\varphi\|_{\mathscr{C}}$.
Consequently,

$$\|z\|_\infty = \max\left\{M, \|\varphi\|_{\mathscr{C}}\right\} \coloneqq \xi^*. \tag{35}$$

Set

$$\Omega = \left\{z \in \mathscr{C}_{(c,d)} : \|z\|_\infty < \xi^* + 1\right\}. \tag{36}$$

□

Through our choice Ω, nothing $z \in \partial\Omega$ such that $z = \aleph \mathscr{K}z, 0 < \aleph < 1$.

As conclusion, the Leray-Schauder FPT shows that $\mathscr{K}$ has a fixed point $z \in \Omega \subset \mathscr{C}_{(c,d)}$ such that $z = \mathscr{K}z$ which is a solution to problem.

We now provide two results on the nonlocal problem (2), and their proofs are quite similar to the preceding results. In addition, the results in Theorems 9 and 10 can be presented by

$$(\mathscr{K}z)(\varkappa, \tau) = \begin{cases} \varphi(\varkappa, \tau), & (\varkappa, \tau) \in J_2, \\ \eta(\varkappa, \tau) + h_1(z) + h_2(z) + \dfrac{1}{\Gamma(\mu)\Gamma(\nu)} \times \displaystyle\int_0^\varkappa\int_0^\tau \psi_\varkappa(\theta)\psi^{\mu-1}(\varkappa, \theta)\psi_\tau(\zeta)\psi^{\nu-1}(\tau, \zeta)\mathfrak{F}\left(\theta, \zeta, z_{(\theta,\zeta)}\right) d\zeta d\theta & (\varkappa, \tau) \in J_1. \end{cases} \tag{37}$$

Theorem 11. *Let (A1) and (A2) be satisfied. If there exist* $L_{h_1}, L_{h_2} > 0$ *such that*

$$\begin{aligned} |h_1(z) - h_1(v)| &\le L_{h_1}\|z - v\|_\infty, \quad \text{for } z, v \in \mathscr{C}(J_1, \mathbb{R}), \\ |h_2(z) - h_2(v)| &\le L_{h_2}\|z - v\|_\infty, \quad \text{for } z, v \in \mathscr{C}(J_1, \mathbb{R}), \end{aligned} \tag{38}$$

with $\Lambda \coloneqq L_{h_1} + L_{h_2} + \sigma < 1$, *where* σ *is defined by (19); then, there exists a unique solution for the* ψ*-Caputo problem (2) on* $[-\kappa_1, c] \times -\kappa_2, d]$.

Theorem 12. *Let (A1) and (A3) be satisfied. If there exist* $d_{h_1}, d_{h_2} > 0$ *such that*

$$\begin{aligned} \|h_1(z)\| &\le d_{h_1}\left(1 + \|z\|_\infty\right), \quad \text{for } z \in \mathscr{C}(J_1, \mathbb{R}^n), \\ \|h_2(z)\| &\le d_{h_2}\left(1 + \|z\|_\infty\right), \quad \text{for } z \in \mathscr{C}(J_1, \mathbb{R}^n), \end{aligned} \tag{39}$$

with $\rho < 1$, where ρ is defined by (A3); then, there exists at least one solution for the ψ-Caputo problem (2) on $[-\kappa_1, c] \times [-\kappa_2, d]$.

Now, we provide the UH and GUH stability of the ψ-problem (2).

Definition 13. (see (2)). Problem ((2)) is UH stable if there exists a $\chi_\varphi > 0$ such that $\forall \varepsilon > 0$ and each solution $\omega(\varkappa, \tau) \in \mathscr{C}_{(c,d)}$ of the inequality

$$\begin{aligned} &\left| {}^{C}\mathscr{D}_{\ell^+}^{r;\psi}\omega(\varkappa,\tau) - \mathfrak{F}\left(\varkappa,\tau,\omega_{(\varkappa,\tau)}\right)\right| \le \varepsilon, \quad (\varkappa,\tau) \in J_1, \\ &|\omega(\varkappa,\tau) - \varphi(\varkappa,\tau)| \le \varepsilon, \quad (\varkappa,\tau) \in J_2, \end{aligned} \tag{40}$$

there exists a solution $z(\varkappa, \tau) \in \mathscr{C}_{(c,d)}$ of (2) satisfies

$$\|\omega(\varkappa,\tau) - z(\varkappa,\tau)\|_{\mathscr{C}_{(c,d)}} \le \chi_\varphi \varepsilon. \tag{41}$$

Remark 14. $\omega(\varkappa, \tau) \in \mathscr{C}_{(c,d)}$ satisfies (40) iff there exists $\varsigma(\varkappa, \tau) \in \mathscr{C}_{(c,d)}$ with

(i) $|\varsigma(\varkappa,\tau)| \le \varepsilon, \varkappa \in J_1$

(ii) for all $\varkappa \in J_1$

$$ {}^{C}\mathscr{D}_{\ell^+}^{r;\psi}\omega(\varkappa,\tau) = \mathfrak{F}\left(\varkappa,\tau,\omega_{(\varkappa,\tau)}\right) + \varsigma(\varkappa,\tau). \tag{42}$$

Lemma 15. *Let $r = (\mu, \nu) \in (0, 1] \times (0, 1]$, and $\omega(\varkappa, \tau) \in \mathscr{C}_{(c,d)}$ is a solution of (40). Then, $\omega(\varkappa, \tau)$ satisfies*

$$\begin{aligned} &\left|\omega(\varkappa,\tau) - \omega_0(\varkappa,\tau) - \frac{1}{\Gamma(\mu)\Gamma(\nu)}\int_0^\varkappa \psi_\varkappa(\theta)\psi^{\mu-1}(\varkappa,\theta)\int_0^\tau \psi_\tau(\zeta)\psi^{\nu-1}(\tau,\zeta)\mathfrak{F}\right. \\ &\left.\times\left(\theta,\zeta,\omega_{(\theta,\zeta)}\right)d\zeta d\theta\right| \le \varepsilon\frac{\psi^\nu(d,0)}{\Gamma(\nu+1)}\frac{\psi^\mu(c,0)}{\Gamma(\mu+1)}, \end{aligned} \tag{43}$$

for $(\varkappa, \tau) \in J_1$, where $\omega_0(\varkappa, \tau) = \eta(\varkappa, \tau) + h_1(\omega) + h_2(\omega)$. Moreover, $|\omega(\varkappa, \tau) - \varphi(\varkappa, \tau)| = 0$, for $(\varkappa, \tau) \in J_2$.

Proof. Let $\omega(\varkappa, \tau)$ is a solution of (40). It follows from (ii) of Remark 14that

$$\begin{aligned} &{}^{C}\mathscr{D}_{\ell+}^{r;\psi}\omega_{(\varkappa,\tau)} = \mathfrak{F}\left(\varkappa,\tau,\omega_{(\varkappa,\tau)}\right) + \varsigma(\varkappa,\tau), (\varkappa,\tau) \in J_1, \\ &\omega(\varkappa,\tau) = \varphi(\varkappa,\tau),\ (\varkappa,\tau) \in J_2, \\ &\omega(\varkappa,0) + h_1(\omega) = \phi_1(\varkappa), \omega(0,\tau) + h_2(\omega) = \phi_2(\tau), (\varkappa,\tau) \in J_1. \end{aligned} \tag{44}$$

Then, the solution of problem (44) is

$$\omega(\varkappa,\tau) = \begin{cases} |\varphi(\varkappa,\tau)|, & (\varkappa,\tau) \in J_2, \\ \eta(\varkappa,\tau) + h_1(\omega) + h_2(\omega) + \dfrac{1}{\Gamma(\mu)\Gamma(\nu)} \times \displaystyle\int_0^\varkappa\int_0^\tau \psi_\varkappa(\theta)\psi^{\mu-1}(\varkappa,\theta)\psi_\tau(\zeta)\psi^{\nu-1}(\tau,\zeta)\left[\mathfrak{F}\left(\theta,\zeta,\omega_{(\theta,\zeta)}\right) + \varsigma(\theta,\zeta)\right]d\zeta d\theta, & (\varkappa,\tau) \in J_1. \end{cases} \tag{45}$$

Once more by (i) of Remark 14, we get

$$\begin{aligned} &\left|\omega(\varkappa,\tau) - \omega_0(\varkappa,\tau) - \frac{1}{\Gamma(\mu)\Gamma(\nu)}\int_0^\varkappa \psi_\varkappa(\theta)\psi^{\mu-1}(\varkappa,\theta)\int_0^\tau \psi_\tau(\zeta)\psi^{\nu-1}(\tau,\zeta)\mathfrak{F}\left(\theta,\zeta,\omega_{(\theta,\zeta)}\right)d\zeta d\theta\right| \\ &\le \frac{1}{\Gamma(\mu)\Gamma(\nu)}\int_0^\varkappa\int_0^\tau \psi_\varkappa(\theta)\psi^{\mu-1}(\varkappa,\theta)\psi_\tau(\zeta)\psi^{\nu-1}(\tau,\zeta)|\varsigma(\theta,\zeta)|d\zeta d\theta \\ &\le \frac{\varepsilon}{\Gamma(\mu)\Gamma(\nu)}\int_0^\varkappa \psi_\varkappa(\theta)\psi^{\mu-1}(\varkappa,\theta)\int_0^\tau \psi_\tau(\zeta)\psi^{\nu-1}(\tau,\zeta)d\zeta d\theta \\ &= \varepsilon\frac{\psi^\nu(\tau,0)}{\Gamma(\nu+1)}\frac{1}{\Gamma(\mu)}\int_0^\varkappa \psi_\varkappa(\theta)\psi^{\mu-1}(\varkappa,\theta)d\theta \\ &= \varepsilon\frac{\psi^\nu(\tau,0)}{\Gamma(\nu+1)}\frac{\psi^\mu(\varkappa,0)}{\Gamma(\mu+1)} \le \varepsilon\frac{\psi^\nu(d,0)}{\Gamma(\nu+1)}\frac{\psi^\mu(c,0)}{\Gamma(\mu+1)}, \end{aligned} \tag{46}$$

for $(\varkappa, \tau) \in J_2$. For $(\varkappa, \tau) \in J_2$, we obtain $|\omega(\varkappa, \tau) - \varphi(\varkappa, \tau)| = |\varphi(\varkappa, \tau) - \varphi(\varkappa, \tau)| = 0$. □

Theorem 16. *Under assumptions of Theorem 9, the solution of the problem (2) is HU and GHU stable on $[-\kappa_1, c] \times -\kappa_2, d]$.*

Proof. Let $\omega(\varkappa, \tau) \in \mathscr{C}$ be a solution of (40), and $z(\varkappa, \tau) \in \mathscr{C}_{(c,d)}$ is a unique solution of the following problem:

$$\begin{aligned} &{}^{C}\mathscr{D}_{\ell+}^{r;\psi}z(\varkappa,\tau) = \mathfrak{F}\left(\varkappa,\tau,z_{(\varkappa,\tau)}\right), (\varkappa,\tau) \in J_1, \\ &z(\varkappa,\tau) = \varphi(\varkappa,\tau),\ (\varkappa,\tau) \in J_2, \\ &z(\varkappa,0) + h_1(z) = \omega(\varkappa,0) + h_1(\omega), z(0,\tau) + h_2(z) \\ &\quad = \omega(0,\tau) + h_2(\omega), (\varkappa,\tau) \in J_1. \end{aligned} \tag{47}$$

The previous problem has a solution

$$z(\varkappa,\tau) = \begin{cases} \varphi(\varkappa,\tau), & (\varkappa,\tau) \in J_2, \\ z_0(\varkappa,\tau) + \dfrac{1}{\Gamma(\mu)\Gamma(\nu)}\displaystyle\int_0^\varkappa \psi_\varkappa(\theta)\psi^{\mu-1}(\varkappa,\theta)\int_0^\tau \psi_\tau(\zeta)\psi^{\nu-1}(\tau,\zeta)\mathfrak{F}\left(\theta,\zeta,z_{(\theta,\zeta)}\right)d\zeta d\theta & (\varkappa,\tau) \in J_1, \end{cases} \tag{48}$$

where $z_0(\varkappa,\tau) \coloneqq \eta(\varkappa,\tau)+h_1(z)+h_2(z)$.

Since $z(\varkappa,0)+h_1(z)=\omega(\varkappa,0)+h_1(\omega)$ and $z(0,\tau)+h_2(z)=\omega(0,\tau)+h_2(\omega)$, we have $z_0(\varkappa,\tau)=\omega_0(\varkappa,\tau)$. Indeed,

$$\begin{aligned} z_0(\varkappa,\tau) &= \eta(\varkappa,\tau)+h_1(z)+h_2(z) \\ &= \eta(\varkappa,\tau)-z(\varkappa,0)+\omega(\varkappa,0)+h_1(\omega)-z(0,\tau)+\omega(0,\tau)+h_2(\omega) \\ &= \eta(\varkappa,\tau)-\phi_1(\varkappa)+\phi_1(\varkappa)+h_1(\omega)-\phi_2(\tau)+\phi_2(\tau)+h_2(\omega) \\ &= \eta(\varkappa,\tau)+h_1(\omega)+h_2(\omega)=\omega_0(\varkappa,\tau). \end{aligned} \tag{49}$$

Hence, (48) becomes

$$z(\varkappa,\tau) = \begin{cases} \varphi(\varkappa,\tau), & (\varkappa,\tau)\in J_2, \\ \omega_0(\varkappa,\tau)+\dfrac{1}{\Gamma(\mu)\Gamma(\nu)}\displaystyle\int_0^{\varkappa}\psi_{\varkappa}(\theta)\psi^{\mu-1}(\varkappa,\theta)\int_0^{\tau}\psi_{\tau}(\zeta)\psi^{\nu-1}(\tau,\zeta)\mathfrak{F}\left(\theta,\zeta,z_{(\theta\zeta)}\right)d\zeta d\theta & (\varkappa,\tau)\in J_1. \end{cases} \tag{50}$$

Note that, $|\omega(\varkappa,\tau)-z(\varkappa,\tau)|=0$, for all $(\varkappa,\tau)\in J_2$.

Using Lemma 15 and (A2), for $(\varkappa,\tau)\in J_1$, we have

$$\begin{aligned} |\omega(\varkappa,\tau)-z(\varkappa,\tau)| &= \left|\omega(\varkappa,\tau)-\omega_0(\varkappa,\tau)-\frac{1}{\Gamma(\mu)\Gamma(\nu)}\int_0^{\varkappa}\psi_{\varkappa}(\theta)\psi^{\mu-1}(\varkappa,\theta)\int_0^{\tau}\psi_{\tau}\right. \\ &\quad \left.\times(\zeta)\psi^{\nu-1}(\tau,\zeta)\mathfrak{F}\left(\theta,\zeta,z_{(\theta\zeta)}\right)d\zeta d\theta\right| \\ &\le \left|\omega(\varkappa,\tau)-\omega_0(\varkappa,\tau)-\frac{1}{\Gamma(\mu)\Gamma(\nu)}\int_0^{\varkappa}\psi_{\varkappa}(\theta)\psi^{\mu-1}(\varkappa,\theta)\int_0^{\tau}\psi_{\tau}(\zeta)\psi^{\nu-1}(\tau,\zeta)\mathfrak{F}\right. \\ &\quad \left.\times\left(\theta,\zeta,\omega_{(\theta\zeta)}\right)d\zeta d\theta\right|+\frac{1}{\Gamma(\mu)\Gamma(\nu)}\int_0^{\varkappa}\psi_{\varkappa}(\theta)\psi^{\mu-1}(\varkappa,\theta)\int_0^{\tau}\psi_{\tau}(\zeta)\psi^{\nu-1}(\tau,\zeta)|\mathfrak{F} \\ &\quad \times\left(\theta,\zeta,\omega_{(\theta\zeta)}\right)-\mathfrak{F}\left(\theta,\zeta,z_{(\theta\zeta)}\right)\Big|d\zeta d\theta \\ &\le \varepsilon\frac{\psi^{\nu}(d,0)}{\Gamma(\nu+1)}\frac{\psi^{\mu}(c,0)}{\Gamma(\mu+1)}+L_{\mathfrak{F}}\left\|\omega_{(\theta\zeta)}-z_{(\theta\zeta)}\right\|_{\mathscr{C}}\frac{\psi^{\nu}(d,0)}{\Gamma(\nu+1)}\frac{\psi^{\mu}(c,0)}{\Gamma(\mu+1)}\le\varepsilon\frac{\sigma}{L_{\mathfrak{F}}}+\sigma\|\omega-z\|_{\mathscr{C}(c,d)}, \end{aligned} \tag{51}$$

which implies

$$\|\omega-z\|_{\mathscr{C}(c,d)}\le\frac{\sigma}{L_{\mathfrak{F}}(1-\sigma)}\varepsilon. \tag{52}$$

Taking $\chi_{\varphi}\coloneqq\sigma/L_{\mathfrak{F}}(1-\sigma)$ such that $\sigma<1$, then (51) becomes

$$\|\omega-z\|_{\mathscr{C}(c,d)}\le\chi_{\varphi}\varepsilon. \tag{53}$$

Hence, problem (2) is UH stable. Moreover, if there exists a nondecreasing function $\Psi:[0,\infty)\longrightarrow 0,\infty)$ such that $\Psi(\varepsilon)=\varepsilon$, then we have with $\Psi(0)=0$,

$$\|\omega-z\|_{\mathscr{C}(c,d)}\le\Psi(\varepsilon), \tag{54}$$

which proves that problem (2) is also GUH stable. □

4. Examples

In this portion, we provide two examples of partial hyperbolic FDEs having fractional order and satisfying the obtained results. All computational work will be performed through MATLAB.

Example 1. Consider a ψ-Caputo fractional partial hyperbolic FDE

$$\begin{aligned} {}^{C}\mathscr{D}_{0+}^{r;\psi}\varkappa(\varkappa,\tau) &= \frac{1}{2e^{\varkappa+\tau+2}(1+|\varkappa(\varkappa-1,\tau-2)|)},\ (\varkappa,\tau)\in[0,1]\times[0,1], \\ \varkappa(\varkappa,\tau) &= \varkappa+\tau^2,\ (\varkappa,\tau)\in[-1,1]\times[-2,1]\setminus(0,1]\times(0,1], \\ \varkappa(\varkappa,0) &= \varkappa,\ \varkappa(0,\tau)=\tau^2,\ \varkappa,\tau\in[0,1], \end{aligned} \tag{55}$$

where $r=(\mu,\nu)$, $\mu=1/2$, $\nu=1/3$, $\varphi(\varkappa,\tau)=\varkappa+\tau^2$, $c=d=1$, $\kappa_1=1$, $\kappa_2=2$, $\phi_1(\varkappa)=\varkappa$, $\phi_2(\tau)=\tau^2$. Consider $\mathfrak{F}(\varkappa,\tau,\bar{z})=1/(3e^{\varkappa+\tau+2}(1+\bar{z}(\varkappa-1,\tau-2)))$, for $(\varkappa,\tau,\bar{z})\in 0,1]\times 0,1]\times\mathscr{C}([-1,0]\times -2,0],\mathbb{R})$. Let $z,\upsilon\in\mathscr{C}([-1,0]\times -2,0],\mathbb{R})$, and $(\varkappa,\tau)\in 0,1]\times 0,1]$. Then,

$$\begin{aligned} &\left|\mathfrak{F}\left(\varkappa,\tau,z_{(\varkappa,\tau)}\right)-\mathfrak{F}\left(\varkappa,\tau,\upsilon_{(\varkappa,\tau)}\right)\right| \\ &\quad\le\frac{1}{3e^2}|z(\varkappa-1,\tau-2)-\upsilon(\varkappa-1,\tau-2)|\le\frac{1}{3e^2}\|z-\upsilon\|_{\mathscr{C}}. \end{aligned} \tag{56}$$

So, assumptions (A1) and (A2) are satisfied with $L_{\mathfrak{F}}=1/3e^2$. Moreover, the condition $\sigma=2/(3^{5/6}e^2\sqrt{\pi}\Gamma(1/3))<1$ with $\psi(\varkappa)=\varkappa/3$, $\psi(\tau)=\tau e^{\tau-1}/3$ and $c=d=1$. Hence, Theorem 9 shows that problem (55) has a unique solution defined on $[-1,1]\times[-2,1]$.

Example 2. Consider a ψ-Caputo fractional partial hyperbolic FDE

$$\begin{aligned} {}^{C}\mathscr{D}_{0+}^{r;\psi}\varkappa(\varkappa,\tau) &= \frac{e^{-\varkappa-\tau}}{4+e^{\varkappa+\tau}}\left(1+\frac{|\varkappa(\varkappa-1,\tau-2)|}{(1+|\varkappa(\varkappa-1,\tau-2)|)}\right), \\ &\quad\cdot(\varkappa,\tau)\in\left[0,\frac{1}{3}\right]\times\left[0,\frac{1}{3}\right], \\ \varkappa(\varkappa,\tau) &= \varkappa^2+\tau,\ (\varkappa,\tau)\in\left[-1,\frac{1}{3}\right]\times\left[-2,\frac{1}{3}\right]\setminus\left(0,\frac{1}{3}\right]\times\left(0,\frac{1}{3}\right], \\ \varkappa(\varkappa,0) &= \varkappa^2,\ \varkappa(0,\tau)=\tau,\ \varkappa,\tau\in\left[0,\frac{1}{3}\right], \end{aligned} \tag{57}$$

where $r=(\mu,\nu)$, $\mu=1/2$, $\nu=1/3$, $\varphi(\varkappa,\tau)=\varkappa^2+\tau$, $c=d=1/3$, $\kappa_1=1$, $\kappa_2=2$, $\phi_1(\varkappa)=\varkappa^2$, $\phi_2(\tau)=\tau$. Consider $\mathfrak{F}(\varkappa,\tau,\bar{z})=(e^{-\varkappa-\tau}/(4+e^{\varkappa+\tau}))(1+\bar{z}/(1+\bar{z}))$, for $(\varkappa,\tau,\bar{z})\in[0,1/3]\times[0,1/3]\times\mathscr{C}([-1,0]\times -2,0],\mathbb{R})$. Let $z\in\mathscr{C}([-1,0]\times -2,0],\mathbb{R})$, and $(\varkappa,\tau)\in[0,1/3]\times[0,1/3]$. Then,

$$\begin{aligned} \left|\mathfrak{F}\left(\varkappa,\tau,z_{(\varkappa,\tau)}\right)\right| &\le\frac{e^{-\varkappa-\tau}}{4+e^{\varkappa+\tau}}\left|1+\frac{z_{(\varkappa,\tau)}}{1+z_{(\varkappa,\tau)}}\right|\le\frac{e^{-\varkappa-\tau}}{4+e^{\varkappa+\tau}}+\frac{e^{-\varkappa-\tau}}{4+e^{\varkappa+\tau}}\left|z_{(\varkappa,\tau)}\right| \\ &\le\frac{e^{-\varkappa-\tau}}{4+e^{\varkappa+\tau}}+\frac{e^{-\varkappa-\tau}}{4+e^{\varkappa+\tau}}\|z\|_{\mathscr{C}}. \end{aligned} \tag{58}$$

Thus, (A3) holds with $p(\varkappa,\tau)=q(\varkappa,\tau)=e^{-\varkappa-\tau}/(4+e^{\varkappa+\tau})$, where $\|q\|_{\infty}=1/5$. To verify that $\rho<1$, we select $\psi(\varkappa)=e^{\varkappa/3}$

and $\psi(\tau) = \sqrt{\tau + 1}$, then find that

$$\psi^{\mu}(c, 0) = (\psi(c) - \psi(0))^{\mu} = \left(e^{c/3}\right)^{1/2} = \sqrt{e^{1/9}},$$
$$\psi^{\nu}(d, 0) = (\psi(d) - \psi(0))^{\nu} = \left(\sqrt{d+1}\right)^{1/3} = \left(2\sqrt{\frac{2}{3}}\right)^{1/3}, \quad (59)$$

and $\rho \approx 0.314 < 1$. So, all assumptions of Theorem 10 are satisfied. Hence, Theorem 10 shows that problem (57) has a solution defined on $[-1, 1/3] \times [-2, 1/3]$.

Remark 3. Our current outcomes on problems (1) and (2) can be interpreted as extensions of preceding results of Abbas et al. [19], for $\psi(\varkappa) = \varkappa$.

Remark 4. As special cases, it is possible to obtain other results for similar problems involving various FDs such as Caputo-Katugampola FD (for $(\varkappa) = (\varkappa^{\rho}), \rho > 0$), Caputo-Hadamard FD (for $\psi(\varkappa) = \ln(\varkappa)$), and other FDs, for different choices of $\psi(\cdot)$.

5. Conclusion

Somewhat recently, several fractional definitions have been proposed to describe the behaviors of some complex world problems arising in many scientific fields. In this regard, Sousa and de Oliveira [9] introduced the concept of the multivariate partial fractional derivative with respect to another function. As an additional contribution to this topic, existence and uniqueness results have been obtained for two types of Cauchy and nonlocal fractional partial hyperbolic FDEs (1) and (2) involving ψ-Caputo FD with two variables. We have presented several results based on Banach's and Leray-Schauder's fixed point theorem. In light of our present results, special cases of similar problems containing several partial fractional operators have been presented according to different choices of the ψ function. Moreover, we have provided the stability results in UH and GUH sense. Lastly, two suitable examples that validate the obtained results were given.

It is interesting to approach current problems with infinite delay, and this is what we are thinking of in future research. One can also study the same present problem in terms of the generalized fractional derivative that was recently proposed in [23, 24].

Data Availability

Data are available upon request.

Conflicts of Interest

No conflicts of interest are related to this work.

Acknowledgments

The authors extend their appreciation to the Deanship of Scientific Research at King Khalid University for funding this project under grant number R.G.P. 2/29/43. Taif University Researchers Supporting Project number TURSP-2020/20, Taif University, Taif, Saudi Arabia. The authors are thankful to the Deanship of Scientific Research at University of Bisha, Saudi Arabia, for supporting this work..

References

[1] K. Diethelm, *The Analysis of Fractional Differential Equations: an Application-Oriented Exposition Using Differential Operators of Caputo Type*, Springer, New York, 2010.

[2] M. El-Shahed and A. Salem, "An extension of Wright function and its properties," *Journal of Mathematics*, vol. 2015, Article ID 950728, 11 pages, 2015.

[3] S. Samko, A. Kilbas, and O. Marichev, *Fractional Integrals and Derivatives, Theory and Applications*, Gordon and Breach Science Publishers, Amsterdam, The Netherlands, 1993.

[4] R. Herrmann, *Fractional Calculus: an Introduction for Physicists*, World Scientific, New Jersey, 2014.

[5] I. Podlubny, *Fractional Differential Equations*, Academic Press, San Diego, CA, USA, 1999.

[6] A. A. Kilbas, H. M. Srivastava, and J. J. Trujillo, *Theory and Applications of Fractional Differential Equations*, Elsevier B.V, Amsterdam, The Netherlands, 2006.

[7] R. Almeida, "A Caputo fractional derivative of a function with respect to another function," *Communications in Nonlinear Science and Numerical Simulation*, vol. 44, pp. 460–481, 2017.

[8] J. V. D. Sousa and E. C. de Oliveira, "On the ψ-Hilfer fractional derivative," *Communications in Nonlinear Science and Numerical Simulation*, vol. 60, pp. 72–91, 2018.

[9] J. V. D. Sousa and E. C. de Oliveira, "On the stability of a hyperbolic fractional partial differential equation," *Differential Equations and Dynamical Systems*, pp. 1–22, 2019.

[10] A. V. Kim, "Functional differential equations," in *Functional Differential Equations*, pp. 41–59, Springer, Dordrecht, 1999.

[11] A. Boutiara, M. S. Abdo, and M. Benbachir, "Existence results for ψ-Caputo fractional neutral functional integro-differential equations with finite delay," *Turkish Journal of Mathematics*, vol. 44, no. 6, pp. 2380–2401, 2020.

[12] M. S. Abdo, "Weighted fractional neutral functional differential equations," *Journal of Siberian Federal University. Mathematics Physics*, vol. 11, no. 5, pp. 535–549, 2018.

[13] M. S. Abdo and S. K. Panchal, "Existence and continuous dependence for fractional neutral functional differential equations," *Journal of Mathematical Modeling*, vol. 5, no. 2, pp. 153–170, 2017.

[14] Y. Zhou, *Basic Theory of Fractional Differential Equations*, 6 Singapore World Scientific, 2014.

[15] S. Abbas and M. Benchohra, "Darboux problem for partial functional differential equations with infinite delay and Caputo's fractional derivative," *Advances in Dynamical Systems and Applications*, vol. 5, no. 1, pp. 1–19, 2010.

[16] S. Abbas and M. Benchohra, "Upper and lower solutions method for partial hyperbolic functional differential equations with Caputo's fractional derivative," *Libertas Mathematica*, vol. 31, pp. 103–110, 2011.

[17] S. Abbas, M. Benchohra, and L. Gorniewicz, "Existence theory for impulsive partial hyperbolic functional differential equations involving the Caputo fractional derivative," *Scientiae Mathematicae Japonicae*, vol. 72, no. 1, pp. 49–60, 2010.

[18] S. Abbas, M. Benchohra, and Y. Zhou, "Fractional order partial hyperbolic functional differential equations with state-dependent delay," *International Journal of Dynamical Systems and Differential Equations*, vol. 3, no. 4, pp. 459–490, 2011.

[19] S. Abbas, M. Benchohra, and G. M. N'Guérékata, *Topics in Fractional Differential Equations (vol. 27)*, Springer Science & Business Media, 2012.

[20] Z. Baitiche, C. Derbazi, M. Benchohra, and Y. Zhou, "A new class of coupled systems of nonlinear hyperbolic partial fractional differential equations in generalized Banach spaces involving the ψ-Caputo fractional derivative," *Symmetry*, vol. 13, no. 12, p. 2412, 2021.

[21] S. Abbas and M. Benchohra, "Darboux problem for perturbed partial differential equations of fractional order with finite delay," *Nonlinear Analysis: Hybrid Systems*, vol. 3, no. 4, pp. 597–604, 2009.

[22] A. Granas and J. Dugundji, *In Fixed Point Theory*, Springer, New York, 2003.

[23] M. Abu-Shady and M. K. Kaabar, "A generalized definition of the fractional derivative with applications," *Mathematical Problems in Engineering*, vol. 2021, Article ID 9444803, 9 pages, 2021.

[24] M. Abu-Shady and M. K. Kaabar, "A novel computational tool for the fractional-order special functions arising from modeling scientific phenomena via Abu-ShadyKaabar fractional derivative," *Computational and Mathematical Methods in Medicine*, vol. 2022, Article ID 2138775, 5 pages, 2022.

Hindawi
Journal of Function Spaces
Volume 2022, Article ID 8736030, 12 pages
https://doi.org/10.1155/2022/8736030

Research Article

Analytical Investigation of Nonlinear Fractional Harry Dym and Rosenau-Hyman Equation via a Novel Transform

Saleh Alshammari,[1] **Naveed Iqbal**,[1] **and Mohammad Yar**[2]

[1]*Department of Mathematics, College of Science, University of Ha'il, Ha'il 2440, Saudi Arabia*
[2]*Department of Mathematics, Kabul Polytechnic University, Kabul, Afghanistan*

Correspondence should be addressed to Naveed Iqbal; n.iqbal@uoh.edu.sa and Mohammad Yar; myar@kpu.edu.af

Received 26 July 2022; Accepted 26 August 2022; Published 9 September 2022

Academic Editor: Yusuf Gurefe

We use a new integral transform approach to solve the fractional Harry Dym equation and fractional Rosenau-Hyman equation in this work. The Elzaki transform and the integral transformation are combined in the suggested method (ET). To handle two nonlinear problems, we first construct the Elzaki transforms of the Caputo fractional derivative (CFD) and Atangana-Baleanu fractional derivative (ABFD). The ultimate purpose of this study is to find an error analysis that demonstrates that our final result converges to the exact and approximate result. The convergent series form solution demonstrates the method's efficiency in resolving several types of fractional differential equations. Furthermore, the solutions obtained in this study agree well with the exact solutions; thus, this strategy is powerful and efficient as an alternate way for obtaining approximate solutions to both linear and nonlinear fractional differential equations.

1. Introduction

Fractional calculus FC history dates back 300 years. FC originated with Leibniz's usage of the nth derivative notation in his papers in 1695. L'Hopital raises a query from Leibniz about the result of his nth derivative notation if the order of "n" is 1 /2 [1]. Many phenomena in engineering and other fields can be effectively represented by models based on fractional calculus, that is, the theory of fractional derivatives and integrals of fractional noninteger order. Respectable interest in fractional calculus has been utilised in several studies in recent years, such as regular variation in thermodynamics, biophysics, blood flow phenomena, aerodynamics, viscoelasticity, electrical circuits, electro-analytical chemistry, biology, and control theory [2–5].

Due to their prevalence in a wide range of applications and accurate description of nonlinear processes, researchers are increasingly focusing on fractional order differential equations, particularly fractional partial differential equations (FPDEs). FPDEs are the most common mathematical tools used to simulate diverse physical phenomena in applied sciences such as physics, engineering, and other social sciences. Many applications of science and engineering, including as material sciences, biology, chemistry, fluid dynamics, chemical kinetics, and many other physical processes, use modelling in the form of FPDE systems [6–10]. For the solution of fractional-order PDE problems, different analytical and numerical methodologies have been developed in the literature. The numerical schemes are a finite difference scheme with nonuniform time steps [11–13], a higher order numerical scheme [14], an implicit finite-difference scheme [15], a compact difference scheme [16], Adomian decomposition method [17], homotopy analysis transform method [18], fractional-order reduced differential transform method [19], variational iteration method [20], natural transform decomposition method [21], Elzaki transform decomposition method [22], iterative methods [23–25], and much more [26–30]. The abovementioned techniques have the straight forward implementations to both linear and nonlinear FDEs.

In the present study, we implement the Elzaki transform in connection with the CFD and ABC operators to solve two nonlinear problems. We consider fractional Harry Dym equation and fractional Rosenau-Hyman equation of the form

$$D_\tau^\rho \psi(\upsilon,\tau)=\psi^3(\upsilon,\tau)\psi_{\upsilon\upsilon\upsilon}(\upsilon,\tau), \quad (1)$$

having initial source

$$\psi(\upsilon,0)=\left(a-\frac{3\sqrt{b}}{2}\upsilon\right)^{2/3}, \quad (2)$$

and

$$D_\tau^\rho \psi(\upsilon,\tau)=\psi(\upsilon,\tau)\psi_{\upsilon\upsilon\upsilon}(\upsilon,\tau)+\psi(\upsilon,\tau)\psi_\upsilon(\upsilon,\tau)+3\psi_\upsilon(\upsilon,\tau)\psi_{\upsilon\upsilon}(\upsilon,\tau), \quad (3)$$

having initial source

$$\psi(\upsilon,0)=-\frac{8}{3}c\cos^2\left(\frac{\upsilon}{4}\right). \quad (4)$$

The Harry Dym is a crucial dynamical equation that is used in a variety of physical systems. The Harry Dym equation was initially published in Kruskal and Moser [31] and is credited to Harry Dym in an unpublished study from 1973-1974. It denotes a system in which dispersion and nonlinearity are inextricably linked. Harry Dym is a totally integrable nonlinear evolution equation that obeys an infinite number of conversion rules but lacks the Painleve property. The Harry Dym equation is closely related to the Korteweg-de Vries equation, and this equation has been used to hydrodynamic problems [32]. The Sturm-Liouville operator is linked to the Lax pair of the Harry Dym equation. This operator is spectrally transformed into the Schrodinger operator by the Liouville transformation [33]. Rosenau and Hyman [34] found the Rosenau-Hyman equation, which arises in the creation of patterns in liquid drops with compaction solutions. The Rosenau-Hyman equation compact on investigations is useful in applied sciences and mathematical physics [35–38].

The following is how the rest of the paper is structured: we begin with basic preliminaries and definitions of fractional calculus in Section 2. The proposed method's general methodology is introduced in Section 3. Section 4 focuses on applying the approach to a set of test problems, using graphs and tables to demonstrate the technique's efficiency. The discussion and conclusion of this work were delivered in Section 5.

2. Preliminaries

In this section, we mention the following basic definitions of fractional calculus.

Definition 1. The fractional derivative in Caputo manner (CFD) is given as [39]

$${}_0^C D_\tau^\rho(\kappa(\tau))=\begin{cases}\dfrac{1}{\Gamma(m-\rho)}\displaystyle\int_0^\tau \frac{\kappa^m(\eta)}{(\tau-\eta)^{\rho+1-m}}d\eta, & m-1<\rho<m,\\ \dfrac{d^m}{d\tau^m}\kappa(\tau), & \rho=m.\end{cases} \quad (5)$$

Definition 2. The Atangana-Baleanu Caputo operator (ABC) is defined as [40]

$${}_m^{\mathrm{ABC}}D_\tau^\rho(\kappa(\tau))=\frac{N(\rho)}{1-\rho}\int_m^\tau \kappa'(\eta)E_\rho\left[-\frac{\rho(\tau-\eta)^\rho}{1-\rho}\right]d\eta, \quad (6)$$

where $\kappa\in H^1(\alpha,\beta),\beta>\alpha,\rho\in[0,1]$. A normalisation function equal to 1 when $\rho=0$ and $\rho=1$ is represented by $N(\rho)$ in Eq. (6).

Definition 3. The fractional integral operator in ABC manner is given as [40]

$${}_m^{\mathrm{ABC}}I_\tau^\rho(\kappa(\tau))=\frac{1-\rho}{N(\rho)}\kappa(\tau)+\frac{\rho}{\Gamma(\rho)N(\rho)}\int_m^\tau \kappa(\eta)(\tau-\eta)^{\rho-1}d\eta. \quad (7)$$

Definition 4. For exponential function in set A, the Elzaki transform is given as [41, 42]

$$A=\left\{\kappa(\tau):\ \exists G,p_1,p_2>0,|\kappa(\tau)|<Ge^{|\tau|/p_j},\text{ if }\tau\in(-1)^j\times[0,\infty)\right\}. \quad (8)$$

G is a finite number, but p_1 and p_2 may be finite or infinite for a function selected in the set.

Definition 5. The Elzaki transform of $\kappa(\tau)$ is given as [42]

$$\mathscr{E}\{\kappa(\tau)\}(\mu)=\tilde{U}(\mu)=\mu\int_0^\infty e^{-\tau/\mu}\kappa(\tau)d\tau, \quad (9)$$

where $\tau\geq 0,p_1\leq\mu\leq p_2$.

Theorem 6. *(Elzaki transformation convolution theorem, [43]) The following equality holds:*

$$\mathscr{E}\{\kappa*v\}=\frac{1}{\mu}\mathscr{E}(\kappa)\mathscr{E}(v), \quad (10)$$

where $\mathscr{E}\{.\}$ represents Elzaki transform.

Definition 7. The Elzaki transform of ${}_0^C D_\tau^\rho(\kappa(\tau))$ CFD operator is as [44]

$$\mathscr{E}\left\{{}_0^C D_\tau^\rho(\kappa(\tau))\right\}(\mu)=\mu^{-\rho}\tilde{U}(\mu)-\sum_{k=0}^{m-1}\mu^{2-\rho+k}\kappa^k(0), \quad (11)$$

where $m-1<\rho<m$.

Theorem 8. *The Elzaki transform of ${}_m^{ABC}D_\tau^\rho(\kappa(\tau))$ ABC operator is as*

$$\mathscr{E}\left\{{}_m^{ABC}D_\tau^\rho(\kappa(\tau))\right\}(\mu)=\frac{N(\rho)\mu}{\rho\mu^\rho+1-\rho}\left(\frac{\tilde{U}(\mu)}{\mu}-\mu\kappa(0)\right), \quad (12)$$

where $\mathscr{E}\{\kappa(\tau)\}\mu=\tilde{U}(\mu)$.

Proof. From Definition 2, we get

$$\mathscr{E}\left\{ {}_{m}^{ABC}D_{\tau}^{\rho}(\kappa(\tau)) \right\}(\mu) = \mathscr{E}\left\{ \frac{N(\rho)}{1-\rho} \int_0^{\tau} \kappa'(\eta) E_{\rho}\left[-\frac{\rho(\tau-\eta)^{\rho}}{1-\rho} \right] d\eta \right\}(\mu). \tag{13}$$

Then, from Elzaki transform definition and its convolution, we obtain

$$\begin{aligned} \mathscr{E}\left\{ {}_{m}^{ABC}D_{\tau}^{\rho}(\kappa(\tau)) \right\}(\mu) &= \mathscr{E}\left\{ \frac{N(\rho)}{1-\rho} \int_0^{\tau} \kappa'(\eta) E_{\rho}\left[-\frac{\rho(\tau-\eta)^{\rho}}{1-\rho} \right] d\eta \right\} \\ &= \frac{N(\rho)}{1-\rho} \frac{1}{\mu} \mathscr{E}\left\{ \kappa'(\eta) \right\} \mathscr{E}\left\{ E_{\rho}\left[-\frac{\rho\tau^{\rho}}{1-\rho} \right] d\eta \right\} \\ &= \frac{N(\rho)}{1-\rho} \left[\frac{\tilde{U}(\mu)}{\mu} - \mu\kappa(0) \right] \left[\int_0^{\infty} e^{-1/\mu} E_{\rho}\left[-\frac{\rho\tau^{\rho}}{1-\rho} \right] d\tau \right] \\ &= \frac{N(\rho)\mu}{\rho\mu^{\rho} + 1 - \rho} \left[\frac{\tilde{U}(\mu)}{\mu} - \mu\kappa(0) \right]. \end{aligned} \tag{14}$$

□

3. Description of the Technique via a New Integral Transform

In this part, we presented the general methodology used in this article to solve fractional nonlinear PDE as

$$\begin{gathered} D_{\tau}^{\rho}\psi(\upsilon,\tau) + L(\psi(\upsilon,\tau)) + N(\psi(\upsilon,\tau)) = \theta(\upsilon,\tau), \\ (\upsilon,\tau) \in [0,1] \times [0,T], \kappa - 1 < \rho < \kappa, \end{gathered} \tag{15}$$

with initial source

$$\frac{\partial^z \psi}{\partial \tau^z}(\upsilon, 0) = \kappa_z(\upsilon), z = 0, 1, \cdots, \kappa - 1, \tag{16}$$

and the boundary sources

$$\psi(0,\tau) = \gamma_0(\tau), \psi(\upsilon,\tau) = \gamma_1(\tau), \tau \geq 0, \tag{17}$$

Here, known functions are $\kappa_z, \theta, \gamma_0$, and γ_1. In Eq. (15), $D_{\tau}^{\rho}\psi(\upsilon,\tau)$ represents the Caputo or ABC fractional derivatives whereas $L(.)$ and $N(.)$ are linear and nonlinear terms. (1)-(2) and (3)-(4) represent the problems to be solved. By means of Elzaki transform of CFD in Eq. (11) and ABC in Eq. (12), we take $E\{\psi(\upsilon,\tau)\}(\mu) = \tilde{\zeta}(\upsilon,\mu)$ in Eq. (15). Thus, by means of Caputo fractional derivative, we get

$$\tilde{\zeta}(\upsilon,\mu) = \mu^{\rho}\left(\widetilde{\theta}(\upsilon,\mu) - \mathscr{E}[L(\psi(\upsilon,\tau)) + N(\psi(\upsilon,\tau))] \right) + \mu^2\psi(\upsilon,0). \tag{18}$$

Also by means of ABC derivative, we get

$$\tilde{\zeta}(\upsilon,\mu) = \left(\frac{\rho\mu^{\rho} + 1 - \rho}{N(\rho)} \right) \left(\widetilde{\theta}(\upsilon,\mu) - \mathscr{E}[L(\psi(\upsilon,\tau)) + N(\psi(\upsilon,\tau))] \right) + \mu^2\psi(\upsilon,0). \tag{19}$$

Here, $\mathscr{E}[\theta(\upsilon,\tau)] = \widetilde{\theta}(\upsilon,\mu)$. Now by taking the Elzaki transform of the boundary conditions, we obtain

$$\mathscr{E}[\gamma_0(\tau)] = \tilde{\zeta}(0,\mu), \mathscr{E}[\gamma_1(\tau)] = \tilde{\zeta}(1,\mu), \mu \geq 0. \tag{20}$$

We get the solution of Eqs. (15)-(17) by means of perturbation technique

$$\tilde{\zeta}(\upsilon,\mu) = \sum_{\mathscr{E}=0}^{\infty} \mathscr{X}^{\mathscr{E}} \tilde{\zeta}_{\mathscr{E}}(\upsilon,\mu), \mathscr{E} = 0, 1, 2, \cdots. \tag{21}$$

In Eq. (15), the nonlinear terms are calculated as

$$N[\psi(\upsilon,\tau)] = \sum_{\mathscr{E}=0}^{\infty} \mathscr{X}^{\mathscr{E}} \varphi_{\mathscr{E}}(\upsilon,\tau), \tag{22}$$

and the terms $\upsilon_{\mathscr{E}}(\upsilon,\tau)$ are taken in [45] as

$$\upsilon_{\mathscr{E}}(\psi_0,\psi_1,\cdots,\psi_{\mathscr{E}}) = \frac{1}{\mathscr{E}!} \frac{\partial^{\mathscr{E}}}{\partial \omega^{\mathscr{E}}} \left[N\left(\sum_{i=0}^{\infty} \omega^i \psi_i \right) \right]_{\lambda=0}, \mathscr{E} = 0, 1, 2, \cdots. \tag{23}$$

For Caputo operator, the solution is determined as by putting Eqs. (21) and (22) into Eq. (18),

$$\begin{aligned} \sum_{\mathscr{E}=0}^{\infty} \mathscr{X}^{\mathscr{E}} \tilde{\zeta}(\upsilon,\mu) = -\mathscr{X}\mu^{\rho} \left(\mathscr{E}\left[L\left(\sum_{\mathscr{E}=0}^{\infty} \mathscr{X}^{\mathscr{E}} \psi_{\mathscr{E}}(\upsilon,\tau) \right) + \sum_{\mathscr{E}=0}^{\infty} \mathscr{X}^{\mathscr{E}} \varphi_{\mathscr{E}}(\upsilon,\tau) \right] \right) \\ + \mu^{\rho}\left(\widetilde{\theta}(\upsilon,\mu) \right) + \mu^2\psi(\upsilon,0). \end{aligned} \tag{24}$$

Also for Atangana-Baleanu operator, the solution is determined as by putting Eqs. (21) and (22) into Eq. (19),

$$\begin{aligned} \sum_{\mathscr{E}=0}^{\infty} \mathscr{X}^{\mathscr{E}} \tilde{\zeta}(\upsilon,\mu) = -\mathscr{X} \left(\frac{\rho\mu^{\rho} + 1 - \rho}{N(\rho)} \right) \left(\mathscr{E}\left[L\left(\sum_{\mathscr{E}=0}^{\infty} \mathscr{X}^{\mathscr{E}} \psi_{\mathscr{E}}(\upsilon,\tau) \right) + \sum_{\mathscr{E}=0}^{\infty} \mathscr{X}^{\mathscr{E}} \varphi_{\mathscr{E}}(\upsilon,\tau) \right] \right) \\ + \left(\frac{\rho\mu^{\rho} + 1 - \rho}{N(\rho)} \right) \left(\widetilde{\theta}(\upsilon,\mu) \right) + \mu^2\psi(\upsilon,0). \end{aligned} \tag{25}$$

Then, by solving (24) and (25) in terms of $\mathscr{X}$, the given Caputo homotopies are obtained:

$$\begin{aligned} \mathscr{X}^0 &: \tilde{\zeta}_0(\upsilon,\mu) = \mu^{\rho}\left(\widetilde{\theta}(\upsilon,\mu) \right) + \mu^2\psi(\upsilon,0), \\ \mathscr{X}^1 &: \tilde{\zeta}_1(\upsilon,\mu) = -\mu^{\rho}\mathscr{E}[L(\psi_0(\upsilon,\tau)) + \varphi_0(\upsilon,\tau)], \\ \mathscr{X}^2 &: \tilde{\zeta}_2(\upsilon,\mu) = -\mu^{\rho}\mathscr{E}[L(\psi_1(\upsilon,\tau)) + \varphi_1(\upsilon,\tau)], \\ &\vdots \\ \mathscr{X}^{n+1} &: \tilde{\zeta}_{n+1}(\upsilon,\mu) = -\mu^{\rho}\mathscr{E}[L(\psi_n(\upsilon,\tau)) + \varphi_n(\upsilon,\tau)]. \end{aligned} \tag{26}$$

In addition, the ABC homotopies are obtained as given:

$$\begin{aligned}
\mathcal{X}^0 &: \tilde{\zeta}_0(\upsilon,\mu) = \left(\frac{\rho\mu^\rho + 1 - \rho}{N(\rho)}\right)\tilde{\theta}(\upsilon,\mu) + \mu^2\psi(\upsilon,0),\\
\mathcal{X}^1 &: \tilde{\zeta}_1(\upsilon,\mu) = -\left(\frac{\rho\mu^\rho + 1 - \rho}{N(\rho)}\right)\mathscr{E}[L(\psi_0(\upsilon,\tau)) + \varphi_0(\upsilon,\tau)],\\
\mathcal{X}^2 &: \tilde{\zeta}_2(\upsilon,\mu) = -\left(\frac{\rho\mu^\rho + 1 - \rho}{N(\rho)}\right)\mathscr{E}[L(\psi_1(\upsilon,\tau)) + \varphi_1(\upsilon,\tau)],\\
&\vdots\\
\mathcal{X}^{n+1} &: \tilde{\zeta}_{n+1}(\upsilon,\mu) = -\left(\frac{\rho\mu^\rho + 1 - \rho}{N(\rho)}\right)\mathscr{E}[L(\psi_n(\upsilon,\tau)) + \varphi_n(\upsilon,\tau)].
\end{aligned} \tag{27}$$

When $\mathcal{X} \longrightarrow 1$, we get Eqs. (26) and (27) approximate solution for Eqs. (24) and (25) as

$$\Delta_n(\upsilon,\mu) = \sum_{\sigma=0}^{n} \tilde{\zeta}_\sigma(\upsilon,\mu). \tag{28}$$

Now by taking inverse ET of Eq. (28), we get the approximate solution of Eq. (15)

$$\psi(\upsilon,\mu) \cong \psi_n(\upsilon,\tau) = \mathscr{E}^{-1}|\{\rho_n(\upsilon,\mu)\}. \tag{29}$$

4. Applications

In this part, we will solve problems in Eqs. (1)-(4) by implementing Elzaki transform. First, we implement Elzaki transform technique in combination with Caputo derivative to solve problem (1) having initial source (2). By taking the Elzaki transform, we get

$$\tilde{\zeta}(\upsilon,\mu) = \mu^\rho \mathscr{E}\left[\psi^3(\upsilon,\tau)\psi_{\upsilon\upsilon\upsilon}(\upsilon,\tau)\right] + \mu^2\psi(\upsilon,0). \tag{30}$$

Now applying Elzaki perturbation transform technique in Eq. (30), we obtain

$$\sum_{\mathscr{E}=0}^{\infty} \mathcal{X}^{\mathscr{E}}\tilde{\zeta}_{\mathscr{E}}(\upsilon,\mu) = +\mu^2\psi(\upsilon,0). \tag{31}$$

On taking Elzaki inverse transform of Eq. (31), we get

$$\sum_{\mathscr{E}=0}^{\infty} \mathcal{X}^{\mathscr{E}}\psi_{\mathscr{E}}(\upsilon,\mu) = \mathcal{X}\mathscr{E}^{-1}\left[\mu^\rho\mathscr{E}\left[\left(\sum_{\mathscr{E}=0}^{\infty}\mathcal{X}^{\mathscr{E}}\varphi_{\mathscr{E}}(\upsilon,\tau)\right)\right]\right] + \mathscr{E}^{-1}\left[\mu^2\psi(\upsilon,0)\right]. \tag{32}$$

In Eq. (43), the $\upsilon_{\mathscr{E}}(.)$ denotes the nonlinear terms given in Eq. (24),

$$\begin{aligned}
\varphi_0(\psi) &= \psi_0^3(\psi_0)_{\upsilon\upsilon\upsilon},\\
\varphi_1(\psi) &= \psi_0^3(\psi_1)_{\upsilon\upsilon\upsilon} + 3\psi_0^2\psi_1(\psi_0)_{\upsilon\upsilon\upsilon},\\
&\vdots .
\end{aligned} \tag{33}$$

Thus by considering powers of $\mathcal{X}$, we get Caputo operator solution as

$$\begin{aligned}
\mathcal{X}^0 &: \psi_0(\upsilon,\tau) = \mathscr{E}^{-1}\left[\mu^2\left(a - \frac{3\sqrt{b}}{2}\upsilon\right)^{2/3}\right] = \left(a - \frac{3\sqrt{b}}{2}\upsilon\right)^{2/3},\\
\mathcal{X}^1 &: \psi_1(\upsilon,\tau) = \mathscr{E}^{-1}[\mu^\rho\mathscr{E}[L(\varphi_0(\upsilon,\tau))]] = -b^{3/2}\left(a - \frac{3\sqrt{b}}{2}\upsilon\right)^{-1/3}\frac{\tau^\rho}{\Gamma(\rho+1)},\\
\mathcal{X}^2 &: \psi_2(\upsilon,\tau) = \mathscr{E}^{-1}[\mu^\rho\mathscr{E}[L(\varphi_1(\upsilon,\tau))]] = -\frac{b^3}{2}\left(a - \frac{3\sqrt{b}}{2}\upsilon\right)^{-4/3}\frac{\tau^{2\rho}}{\Gamma(2\rho+1)},\\
&\vdots .
\end{aligned} \tag{34}$$

The series form solution of the problem is given as

$$\psi(\upsilon,\tau) = \left(\left(a - \frac{3\sqrt{b}}{2}\upsilon\right)^{2/3} - b^{3/2}\left(a - \frac{3\sqrt{b}}{2}\upsilon\right)^{-1/3}\frac{\tau^\rho}{\Gamma(\rho+1)} - \frac{b^3}{2}\left(a - \frac{3\sqrt{b}}{2}\upsilon\right)^{-4/3}\frac{\tau^{2\rho}}{\Gamma(2\rho+1)} + \cdots\right), \tag{35}$$

which gives the solution at $(\rho = 1)$ as $\left(a - 3\sqrt{b}/2(\upsilon + b\tau)\right)^{2/3}$.

Now, we implement Elzaki transform technique in combination with Atangana-Baleanu operator to solve same problem. By taking the Elzaki transform, we get

$$\tilde{\zeta}(\upsilon,\mu) = \left(\frac{\rho\mu^\rho + 1 - \rho}{N(\rho)}\right)\mathscr{E}\left[\psi^3(\upsilon,\tau)\psi_{\upsilon\upsilon\upsilon}(\upsilon,\tau)\right] + \mu^2\psi(\upsilon,0). \tag{36}$$

Now applying Elzaki perturbation transform technique to (36), we obtain

$$\sum_{\mathscr{E}=0}^{\infty} \mathcal{X}^{\mathscr{E}}\tilde{\zeta}_{\mathscr{E}}(\upsilon,\mu) = \mathcal{X}\left(\frac{\rho\mu^\rho + 1 - \rho}{N(\rho)}\right)\mathscr{E}\left[\left(\sum_{\mathscr{E}=0}^{\infty}\mathcal{X}^{\mathscr{E}}\varphi_{\mathscr{E}}(\upsilon,\tau)\right)\right] + \mu^2\psi(\upsilon,0). \tag{37}$$

On taking Elzaki inverse transform of Eq. (37), we get

$$\sum_{\mathscr{E}=0}^{\infty} \mathcal{X}^{\mathscr{E}}\psi_{\mathscr{E}}(\upsilon,\tau) = \mathcal{X}\mathscr{E}^{-1}\left[\left(\frac{\rho\mu^\rho + 1 - \rho}{N(\rho)}\right)\mathscr{E}\left[\left(\sum_{\mathscr{E}=0}^{\infty}\mathcal{X}^{\mathscr{E}}\varphi_{\mathscr{E}}(\upsilon,\tau)\right)\right]\right] + \mathscr{E}^{-1}\left[\mu^2\psi(\upsilon,0)\right]. \tag{38}$$

In Eq.(38), $v_{\mathscr{E}}(.)$ denotes the nonlinear terms given in Eq. (23). By repeating the same process for nonlinear terms, we obtain the following terms:

$$\begin{aligned}
\mathscr{X}^0 &: \psi_0(v,\tau) = \mathscr{E}^{-1}\left[\mu^2\left(a-\frac{3\sqrt{b}}{2}v\right)^{2/3}\right] = \left(a-\frac{3\sqrt{b}}{2}v\right)^{2/3},\\
\mathscr{X}^1 &: \psi_1(v,\tau) = \mathscr{E}^{-1}\left[\left(\frac{\rho\mu^\rho+1-\rho}{N(\rho)}\right)\mathscr{E}[\varphi_0(v,\tau)]\right] = \left(\frac{-b^{3/2}\left(a-\left(3\sqrt{b}/2\right)v\right)^{-1/3}}{N(\rho)}\right)\left(\frac{\rho\tau^\rho}{\Gamma(\rho+1)}+1-\rho\right),\\
\mathscr{X}^2 &: \psi_2(v,\tau) = \mathscr{E}^{-1}\left[\left(\frac{\rho\mu^\rho+1-\rho}{N(\rho)}\right)\mathscr{E}[\varphi_1(v,\tau)]\right] = \left(\frac{-b^3/2\left(a-\left(3\sqrt{b}/2\right)v\right)^{-4/3}}{N^2(\rho)}\right)\left(\frac{(\rho\tau^\rho)^2}{\Gamma(2\rho+1)}+\frac{2\rho(1-\rho)\tau^\rho}{\Gamma(\rho+1)}+(1-\rho)^2\right),\\
&\vdots\,.
\end{aligned} \tag{39}$$

Thus, the approximate solution by means of ABC operator is given as

$$\begin{aligned}
\psi(v,\tau) = \sum_{\sigma=0}^{n}\psi_\sigma(v,\tau) &= \left(a-\frac{3\sqrt{b}}{2}v\right)^{2/3} + \left(\frac{-b^{3/2}\left(a-\left(3\sqrt{b}/2\right)v\right)^{-1/3}}{N(\rho)}\right)\left(\frac{\rho\tau^\rho}{\Gamma(\rho+1)}+1-\rho\right)\\
&+ \left(\frac{-b^3/2\left(a-\left(3\sqrt{b}/2\right)v\right)^{-4/3}}{N^2(\rho)}\right)\left(\frac{(\rho\tau^\rho)^2}{\Gamma(2\rho+1)}+\frac{2\rho(1-\rho)\tau^\rho}{\Gamma(\rho+1)}+(1-\rho)^2\right)+\cdots,
\end{aligned} \tag{40}$$

which gives the solution at $(\rho=1)$ as $\left(a-3\sqrt{b}/2(v+b\tau)\right)^{2/3}$.

Second, we implement Elzaki transform technique in combination with Caputo derivative to solve problem (3) having initial source (4). By taking the Elzaki transform, we get

$$\tilde{\zeta}(v,\mu) = \mu^\rho\mathscr{E}[\psi(v,\tau)\psi_{vvv}(v,\tau)+\psi(v,\tau)\psi_v(v,\tau)+3\psi_v(v,\tau)\psi_{vv}(v,\tau)]+\mu^2\psi(v,0). \tag{41}$$

Now applying Elzaki perturbation transform technique in Eq. (41), we obtain

$$\sum_{\mathscr{E}=0}^{\infty}\mathscr{X}^{\mathscr{E}}\tilde{\zeta}_{\mathscr{E}}(v,\mu) = \mathscr{X}\mu^\rho\mathscr{E}\left[\left(\sum_{\mathscr{E}=0}^{\infty}\mathscr{X}^{\mathscr{E}}\varphi_{\mathscr{E}}(v,\tau)\right)\right]+\mu^2\psi(v,0). \tag{42}$$

On taking Elzaki inverse transform of Eq. (42), we get

$$\begin{aligned}
\sum_{\mathscr{E}=0}^{\infty}\mathscr{X}^{\mathscr{E}}\psi_{\mathscr{E}}(v,\mu) &= \mathscr{X}\mathscr{E}^{-1}\left[\mu^\rho\mathscr{E}\left[\left(\sum_{\mathscr{E}=0}^{\infty}\mathscr{X}^{\mathscr{E}}\varphi_{\mathscr{E}}(v,\tau)\right)\right]\right]\\
&+\mathscr{E}^{-1}\left[\mu^2\psi(v,0)\right].
\end{aligned} \tag{43}$$

Table 1: Comparison of absolute errors of proposed method solution at various fractional-orders with $a, b = 1$ for problem 1.

τ	υ	$\rho = 0.4$	$\rho = 0.6$	$\rho = 0.8$	$\rho = 1(\mathrm{ETM}_{\mathrm{CFD}})$	$\rho = 1(\mathrm{ETM}_{\mathrm{ABC}})$
	0.2	3.0035700000E-04	2.0035600000E-04	1.0035400000E-04	3.5300000000E-07	3.5300000000E-07
	0.4	3.0033900000E-04	2.0033800000E-04	1.0033600000E-04	3.3500000000E-07	3.3500000000E-07
0.01	0.6	3.0031800000E-04	2.0031700000E-04	1.0031500000E-04	3.1400000000E-07	3.1400000000E-07
	0.8	3.0029400000E-04	2.0029300000E-04	1.0029100000E-04	2.9000000000E-07	2.9000000000E-07
	1	3.0026800000E-04	2.0026700000E-04	1.0026500000E-04	2.6400000000E-07	2.6400000000E-07
	0.2	3.0071500000E-04	2.0071200000E-04	1.0071000000E-04	7.0700000000E-07	7.0700000000E-07
	0.4	3.0067800000E-04	2.0067500000E-04	1.0067300000E-04	6.7000000000E-07	6.7000000000E-07
0.02	0.6	3.0063600000E-04	2.0063300000E-04	1.0063100000E-04	6.2800000000E-07	6.2800000000E-07
	0.8	3.0058900000E-04	2.0058600000E-04	1.0058400000E-04	5.8100000000E-07	5.8100000000E-07
	1	3.0053500000E-04	2.0053200000E-04	1.0053000000E-04	5.2700000000E-07	5.2700000000E-07
	0.2	3.0107100000E-04	2.0106700000E-04	1.0106400000E-04	1.0600000000E-06	1.0600000000E-06
	0.4	3.0101600000E-04	2.0101200000E-04	1.0100900000E-04	1.0050000000E-06	1.0050000000E-06
0.03	0.6	3.0095300000E-04	2.0094900000E-04	1.0094600000E-04	9.4200000000E-07	9.4200000000E-07
	0.8	3.0088200000E-04	2.0087800000E-04	1.0087500000E-04	8.7100000000E-07	8.7100000000E-07
	1	3.0080100000E-04	2.0079700000E-04	1.0079400000E-04	7.9000000000E-07	7.9000000000E-07
	0.2	3.0142700000E-04	2.0142200000E-04	1.0141800000E-04	1.4130000000E-06	1.4130000000E-06
	0.4	3.0135400000E-04	2.0134900000E-04	1.0134500000E-04	1.3400000000E-06	1.3400000000E-06
0.04	0.6	3.0127000000E-04	2.0126500000E-04	1.0126100000E-04	1.2560000000E-06	1.2560000000E-06
	0.8	3.0117600000E-04	2.0117100000E-04	1.0116700000E-04	1.1620000000E-06	1.1620000000E-06
	1	3.0106700000E-04	2.0106200000E-04	1.0105800000E-04	1.0530000000E-06	1.0530000000E-06
	0.2	3.0178400000E-04	2.0177900000E-04	1.0177300000E-04	1.7670000000E-06	1.7670000000E-06
	0.4	3.0169200000E-04	2.0168700000E-04	1.0168100000E-04	1.6750000000E-06	1.6750000000E-06
0.05	0.6	3.0158700000E-04	2.0158200000E-04	1.0157600000E-04	1.5700000000E-06	1.5700000000E-06
	0.8	3.0146900000E-04	2.0146400000E-04	1.0145800000E-04	1.4520000000E-06	1.4520000000E-06
	1	3.0133300000E-04	2.0132800000E-04	1.0132200000E-04	1.3160000000E-06	1.3160000000E-06

In Eq. (43), $\upsilon_{\mathscr{E}}(.)$ denotes the nonlinear terms given in Eq. (24),

$$\begin{aligned}
\varphi_0(\psi) &= \psi_0(\psi_0)_\upsilon + 3(\psi_0)_\upsilon(\psi_0)_{\upsilon\upsilon} + \psi_0(\psi_0)_{\upsilon\upsilon\upsilon}, \\
\varphi_1(\psi) &= \psi_1(\psi_0)_\upsilon + \psi_0(\psi_1)_\upsilon + 3(\psi_1)_\upsilon(\psi_0)_{\upsilon\upsilon} + 3(\psi_0)_\upsilon(\psi_1)_{\upsilon\upsilon} + \psi_1(\psi_0)_{\upsilon\upsilon\upsilon} + \psi_0(\psi_1)_{\upsilon\upsilon\upsilon}, \\
&\vdots
\end{aligned} \tag{44}$$

Thus by considering powers of $\mathscr{X}$, we get Caputo operator solution as

$$\begin{aligned}
\mathscr{X}^0 &: \psi_0(\upsilon,\tau) = \mathscr{E}^{-1}\left[\mu^2\left(-\frac{8}{3}c\cos^2\left(\frac{\upsilon}{4}\right)\right)\right] = -\frac{8}{3}c\cos^2\left(\frac{\upsilon}{4}\right), \\
\mathscr{X}^1 &: \psi_1(\upsilon,\tau) = \mathscr{E}^{-1}[\mu^\rho\mathscr{E}[L(\varphi_0(\upsilon,\tau))]] = -\frac{2}{3}c^2\sin\left(\frac{\upsilon}{2}\right)\frac{\tau^\rho}{\Gamma(\rho+1)}, \\
\mathscr{X}^2 &: \psi_2(\upsilon,\tau) = \mathscr{E}^{-1}[\mu^\rho\mathscr{E}[L(\varphi_1(\upsilon,\tau))]] + \mathscr{E}^{-1}[\mu^\rho\mathscr{E}[\upsilon_1(\upsilon,\tau)]] = \frac{1}{3}c^3\cos\left(\frac{\upsilon}{2}\right)\frac{\tau^{2\rho}}{\Gamma(2\rho+1)}, \\
&\vdots
\end{aligned} \tag{45}$$

The series form solution of the problem is given as

$$\psi(\upsilon,\tau) = \left(-\frac{8}{3}c\cos^2\left(\frac{\upsilon}{4}\right) - \frac{2}{3}c^2\sin\left(\frac{\upsilon}{2}\right)\frac{\tau^\rho}{\Gamma(\rho+1)} + \frac{1}{3}c^3\cos\left(\frac{\upsilon}{2}\right)\frac{\tau^{2\rho}}{\Gamma(2\rho+1)} + \cdots\right), \tag{46}$$

which gives the solution at $(\rho = 1)$ as, $-8/3c\cos^2(1/4(\upsilon - c\tau))$.

Now, we implement Elzaki transform technique in combination with Atangana-Baleanu operator to solve same problem.

Table 2: Comparison of absolute errors of proposed method solution at various fractional-orders with $c = 0.5$ for problem 2.

τ	υ	$\rho = 0.4$	$\rho = 0.6$	$\rho = 0.8$	$\rho = 1(\mathrm{ETM}_{\mathrm{CFD}})$	$\rho = 1(\mathrm{ETM}_{\mathrm{ABC}})$
	0.2	5.0265200000E-04	3.3503800000E-04	1.6749500000E-04	2.0000000000E-08	2.0000000000E-08
	0.4	1.0002620000E-03	6.6670800000E-04	3.3329700000E-04	2.1000000000E-08	2.1000000000E-08
0.01	0.6	1.4878770000E-03	9.9171600000E-04	4.9576800000E-04	1.9000000000E-08	1.9000000000E-08
	0.8	1.9606260000E-03	1.3068160000E-03	6.5328500000E-04	1.9000000000E-08	1.9000000000E-08
	1	2.4137850000E-03	1.6088580000E-03	8.0427600000E-04	1.8000000000E-08	1.8000000000E-08
	0.2	5.0535100000E-04	3.3681900000E-04	1.6839800000E-04	8.2000000000E-08	8.2000000000E-08
	0.4	1.0055720000E-03	6.7019200000E-04	3.3503200000E-04	8.2000000000E-08	8.2000000000E-08
0.02	0.6	1.4957440000E-03	9.9686700000E-04	4.9831800000E-04	8.0000000000E-08	8.0000000000E-08
	0.8	1.9709720000E-03	1.3135820000E-03	6.5662400000E-04	7.7000000000E-08	7.7000000000E-08
	1	2.4265060000E-03	1.6171720000E-03	8.0837000000E-04	7.4000000000E-08	7.4000000000E-08
	0.2	5.0779200000E-04	3.3845200000E-04	1.6925200000E-04	1.8600000000E-07	1.8600000000E-07
	0.4	1.0103250000E-03	6.7333600000E-04	3.3662600000E-04	1.8400000000E-07	1.8400000000E-07
0.03	0.6	1.5027620000E-03	1.0014910000E-03	5.0063600000E-04	1.7900000000E-07	1.7900000000E-07
	0.8	1.9801840000E-03	1.3196410000E-03	6.5964500000E-04	1.7300000000E-07	1.7300000000E-07
	1	2.4378200000E-03	1.6246040000E-03	8.1206200000E-04	1.6500000000E-07	1.6500000000E-07
	0.2	5.1008200000E-04	3.4000300000E-04	1.7008800000E-04	3.3200000000E-07	3.3200000000E-07
	0.4	1.0147360000E-03	6.7627600000E-04	3.3814400000E-04	3.2700000000E-07	3.2700000000E-07
0.04	0.6	1.5092490000E-03	1.0057910000E-03	5.0282100000E-04	3.1800000000E-07	3.1800000000E-07
	0.8	1.9886830000E-03	1.3252570000E-03	6.6247400000E-04	3.0700000000E-07	3.0700000000E-07
	1	2.4482470000E-03	1.6314820000E-03	8.1550800000E-04	2.9300000000E-07	2.9300000000E-07
	0.2	5.1227100000E-04	3.4150300000E-04	1.7092100000E-04	5.1800000000E-07	5.1800000000E-07
	0.4	1.0189040000E-03	6.7907600000E-04	3.3961600000E-04	5.1100000000E-07	5.1100000000E-07
0.05	0.6	1.5153560000E-03	1.0098610000E-03	5.0491600000E-04	4.9800000000E-07	4.9800000000E-07
	0.8	1.9966670000E-03	1.3305580000E-03	6.6517100000E-04	4.8000000000E-07	4.8000000000E-07
	1	2.4580280000E-03	1.6379590000E-03	8.1877900000E-04	4.5700000000E-07	4.5700000000E-07

By taking the Elzaki transform, we get

$$\tilde{\zeta}(\upsilon,\mu) = \left(\frac{\rho\mu^{\rho}+1-\rho}{N(\rho)}\right)\mathscr{E}[\psi(\upsilon,\tau)\psi_{\upsilon\upsilon\upsilon}(\upsilon,\tau) + \psi(\upsilon,\tau)\psi_{\upsilon}(\upsilon,\tau) + 3\psi_{\upsilon}(\upsilon,\tau)\psi_{\upsilon\upsilon}(\upsilon,\tau)] + \mu^{2}\psi(\upsilon,0). \tag{47}$$

Now applying Elzaki perturbation transform technique to Eq. (47), we obtain

$$\sum_{\mathscr{E}=0}^{\infty}\mathscr{X}^{\mathscr{E}}\tilde{\zeta}_{\mathscr{E}}(\upsilon,\mu) = \mathscr{X}\left(\frac{\rho\mu^{\rho}+1-\rho}{N(\rho)}\right)\mathscr{E}\left[\left(\sum_{\mathscr{E}=0}^{\infty}\mathscr{X}^{\mathscr{E}}\varphi_{\mathscr{E}}(\upsilon,\tau)\right)\right] + \mu^{2}\psi(\upsilon,0). \tag{48}$$

On taking Elzaki inverse transform of Eq. (48), we get

$$\sum_{\mathscr{E}=0}^{\infty}\mathscr{X}^{\mathscr{E}}\psi_{\mathscr{E}}(\upsilon,\tau) = \mathscr{X}\mathscr{E}^{-1}\left[\left(\frac{\rho\mu^{\rho}+1-\rho}{N(\rho)}\right)\mathscr{E}\left[\left(\sum_{\mathscr{E}=0}^{\infty}\mathscr{X}^{\mathscr{E}}\varphi_{\mathscr{E}}(\upsilon,\tau)\right)\right]\right] + \mathscr{E}^{-1}\left[\mu^{2}\psi(\upsilon,0)\right]. \tag{49}$$

In Eq. (38), $\upsilon_{\mathscr{E}}(.)$ denotes the nonlinear terms given in Eq. (23). By repeating the same process for nonlinear terms, we obtain the following terms:

$$\begin{aligned}
\mathscr{X}^{0}&: \psi_{0}(\upsilon,\tau) = \mathscr{E}^{-1}\left[\mu^{2}\left(-\frac{8}{3}c\cos^{2}\left(\frac{\upsilon}{4}\right)\right)\right] = \left(-\frac{8}{3}c\cos^{2}\left(\frac{\upsilon}{4}\right)\right),\\
\mathscr{X}^{1}&: \psi_{1}(\upsilon,\tau) = \mathscr{E}^{-1}\left[\left(\frac{\rho\mu^{\rho}+1-\rho}{N(\rho)}\right)\mathscr{E}[\varphi_{0}(\upsilon,\tau)]\right] = \left(\frac{-2/3c^{2}\sin(\upsilon/2)}{N(\rho)}\right)\left(\frac{\rho\tau^{\rho}}{\Gamma(\rho+1)}+1-\rho\right),\\
\mathscr{X}^{2}&: \psi_{2}(\upsilon,\tau) = \mathscr{E}^{-1}\left[\left(\frac{\rho\mu^{\rho}+1-\rho}{N(\rho)}\right)\mathscr{E}[\varphi_{1}(\upsilon,\tau)]\right] = \left(\frac{1/3c^{3}\cos(\upsilon/2)}{N^{2}(\rho)}\right)\left(\frac{(\rho\tau^{\rho})^{2}}{\Gamma(2\rho+1)}+\frac{2\rho(1-\rho)\tau^{\rho}}{\Gamma(\rho+1)}+(1-\rho)^{2}\right),\\
&\vdots
\end{aligned} \tag{50}$$

Table 3: Comparison of the exact and proposed method solution at various values of ρ with $a, b = 1$ for problem 1.

τ	υ	$\rho = 0.4$	$\rho = 0.6$	$\rho = 0.8$	$\rho = 1$(approx)	$\rho = 1$(exact)
	0.2	2.391919	2.392019	2.392119	2.392219	2.392219
	0.4	2.260796	2.260896	2.260996	2.261096	2.261096
0.01	0.6	2.125753	2.125853	2.125953	2.126053	2.126054
	0.8	1.986275	1.986375	1.986475	1.986575	1.986576
	1	1.841714	1.841814	1.841914	1.842015	1.842014
	0.2	2.391918	2.392018	2.392118	2.392218	2.392218
	0.4	2.260795	2.260895	2.260995	2.261095	2.261096
0.02	0.6	2.125752	2.125852	2.125952	2.126052	2.126053
	0.8	1.986274	1.986374	1.986474	1.986574	1.986575
	1	1.841713	1.841813	1.841913	1.842013	1.842014
	0.2	2.391917	2.392017	2.392117	2.392217	2.392218
	0.4	2.260794	2.260894	2.260994	2.261094	2.261095
0.03	0.6	2.125751	2.125851	2.125951	2.126051	2.126052
	0.8	1.986273	1.986373	1.986473	1.986573	1.986574
	1	1.841712	1.841812	1.841912	1.842012	1.842013
	0.2	2.391916	2.392016	2.392116	2.392216	2.392217
	0.4	2.260793	2.260893	2.260993	2.261093	2.261094
0.04	0.6	2.125750	2.125850	2.125950	2.126051	2.126052
	0.8	1.986272	1.986372	1.986472	1.986572	1.986573
	1	1.841711	1.841811	1.841911	1.842011	1.842012
	0.2	2.391915	2.392015	2.392115	2.392215	2.392216
	0.4	2.260792	2.260892	2.260992	2.261093	2.261094
0.05	0.6	2.125749	2.125849	2.125949	2.126050	2.126051
	0.8	1.986271	1.986371	1.986471	1.986572	1.986573
	1	1.841710	1.841810	1.841910	1.842011	1.842012

Thus, the approximate solution by means of ABC operator is given as

$$\begin{aligned}\psi(\upsilon,\tau) = \sum_{\sigma=0}^{n}\psi_\sigma(\upsilon,\tau) &= \left(-\frac{8}{3}c\cos^2\left(\frac{\upsilon}{4}\right)\right) + \left(\frac{-2/3c^2\sin(\upsilon/2)}{N(\rho)}\right)\left(\frac{\rho\tau^\rho}{\Gamma(\rho+1)}+1-\rho\right)\\ &+\left(\frac{1/3c^3\cos(\upsilon/2)}{N^2(\rho)}\right)\left(\frac{(\rho\tau^\rho)^2}{\Gamma(2\rho+1)}+\frac{2\rho(1-\rho)\tau^\rho}{\Gamma(\rho+1)}+(1-\rho)^2\right)+\cdots,\end{aligned} \tag{51}$$

which gives the solution at $(\rho = 1)$ as, $-8/3c\cos^2(1/4(\upsilon - c\tau))$.

5. Results and Discussion

In this article, a detailed investigation of error analysis between exact and approximate solutions, as stated by Tables 1 and 2, has been conducted with greater accuracy. In table, calculating the absolute error at various fractional-orders demonstrates the simplicity and accuracy of the provided method. The error analysis between the exact and approximate solutions is shown in Tables 1 and 2, indicating that the series solution quickly converges to a small value. Also, in Tables 3 and 4, we show the numerical simulation of the proposed method solution. As a result, we will only use the third order of the series solution throughout the numerical evolution. The correctness of the error analytical result will be increased by inserting more terms of approximation solution. Figures 1 and 2 depict the

Table 4: Comparison of the exact and proposed method solution at various values of ρ with $c = 0.5$ for problem 2.

τ	υ	$\rho = 0.4$	$\rho = 0.6$	$\rho = 0.8$	$\rho = 1$(approx)	$\rho = 1$(exact)
	0.2	-1.330522	-1.330354	-1.330186	-1.330019	-1.330019
	0.4	-1.321077	-1.320744	-1.320410	-1.320077	-1.320077
0.01	0.6	-1.305094	-1.304598	-1.304102	-1.303606	-1.303606
	0.8	-1.282732	-1.282079	-1.281425	-1.280772	-1.280772
	1	-1.254215	-1.253410	-1.252605	-1.251801	-1.251801
	0.2	-1.330541	-1.330372	-1.330204	-1.330036	-1.330035
	0.4	-1.321116	-1.320780	-1.320445	-1.320110	-1.320110
0.02	0.6	-1.305151	-1.304652	-1.304154	-1.303656	-1.303656
	0.8	-1.282808	-1.282150	-1.281493	-1.280837	-1.280837
	1	-1.254307	-1.253498	-1.252689	-1.251881	-1.251881
	0.2	-1.330560	-1.330390	-1.330221	-1.330052	-1.330052
	0.4	-1.321153	-1.320816	-1.320480	-1.320143	-1.320143
0.03	0.6	-1.305208	-1.304706	-1.304205	-1.303705	-1.303705
	0.8	-1.282882	-1.282221	-1.281561	-1.280902	-1.280901
	1	-1.254399	-1.253585	-1.252773	-1.251961	-1.251961
	0.2	-1.330579	-1.330409	-1.330239	-1.330069	-1.330069
	0.4	-1.321191	-1.320852	-1.320514	-1.320176	-1.320176
0.04	0.6	-1.305263	-1.304760	-1.304257	-1.303754	-1.303754
	0.8	-1.282955	-1.282291	-1.281629	-1.280966	-1.280966
	1	-1.254489	-1.253672	-1.252856	-1.252041	-1.252041
	0.2	-1.330597	-1.330426	-1.330256	-1.330085	-1.330085
	0.4	-1.321228	-1.320888	-1.320549	-1.320209	-1.320209
0.05	0.6	-1.305318	-1.304813	-1.304308	-1.303803	-1.303803
	0.8	-1.283028	-1.282361	-1.281696	-1.281031	-1.281031
	1	-1.254578	-1.253758	-1.252939	-1.252121	-1.252120

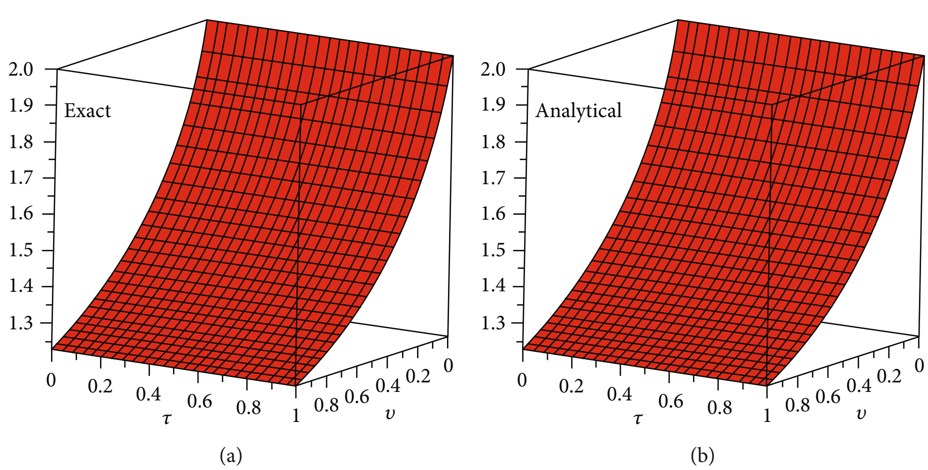

Figure 1: The graphical layout of the exact solution, proposed method solution at $\rho = 1$ and at various fractional orders of $\rho = 1, 0.8, 0.6, 0.4$ with $a, b = 1$ for problem 1.

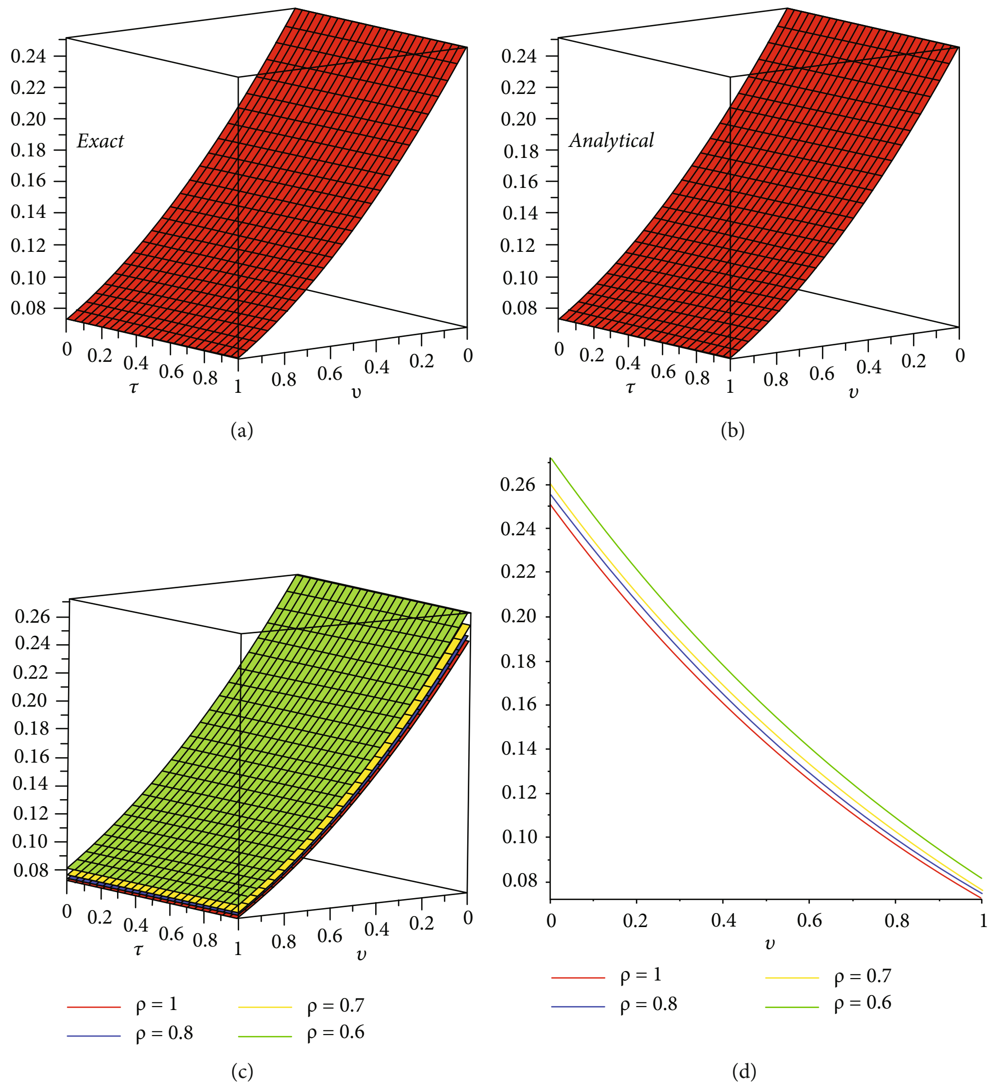

Figure 2: The graphical layout of the exact solution, proposed method solution at $\rho = 1$ and at various fractional orders of $\rho = 1, 0.8, 0.6, 0.4$ with $c = 0.5$ for problem 2.

behaviour of the exact and proposed approach solutions and describe the properties of the approximate solution. We also present the proposed approach solution at different fractional-orders for a better understanding of the problems characteristics. We concluded that the recommended technique solution was in good agreement with the exact solution based on the tables and graphs.

6. Conclusion

The main goal of this study is to use an efficient technique to determine the solution to the fractional Harry Dym equation and fractional Rosenau-Hyman equation. The proposed method is used in addition to two fractional derivatives: Caputo fractional derivative and Atangana-Baleanu fractional derivative. Tables and figures are used to specify the results of the comparative solution. The tables and figures show that the suggested technique solution and the exact result have a better understanding. From the derived results, it shows the reliability of the algorithm, and it is greatly suitable for nonlinear fractional partial differential equation.

Data Availability

The numerical data used to support the findings of this study are included within the article.

Conflicts of Interest

The authors declare that there are no conflicts of interest regarding the publication of this article.

References

[1] A. Loverro, *Fractional Calculus: History, Definitions and Applications for the Engineer*, Rapport technique, Univeristy of Notre Dame: Department of Aerospace and Mechanical Engineering, 2004.

[2] A. A. A. Kilbas, H. M. Srivastava, and J. J. Trujillo, *Theory and Applications of Fractional Differential Equations (Vol. 204)*, Elsevier Science Limited, 2006.

[3] I. Podlubny, *Fractional Differential Equations*, vol. 198, Academic Press, San Diego, California, USA, 1999.

[4] M. Yavuz and T. Abdeljawad, "Nonlinear regularized long-wave models with a new integral transformation applied to the fractional derivative with power and Mittag-Leffler kernel," *Advances in Difference Equations*, vol. 2020, no. 1, Article ID 367, 2020.

[5] S. G. Samko, A. A. Kilbas, and O. I. Marichev, *Fractional Integrals and Derivatives (Vol. 1)*, Gordon and Breach Science Publishers, Yverdon, Yverdon-les-Bains, Switzerland, 1993.

[6] B. Batiha, M. S. M. Noorani, I. Hashim, and K. Batiha, "Numerical simulations of systems of PDEs by variational iteration method," *Physics Letters A*, vol. 372, no. 6, pp. 822–829, 2008.

[7] A. M. Wazwaz, "The variational iteration method for solving linear and nonlinear systems of PDEs," *Computers and Mathematics with Applications*, vol. 54, no. 7-8, pp. 895–902, 2007.

[8] N. A. Shah, E. R. El-Zahar, A. Akgül, A. Khan, and J. Kafle, "Analysis of fractional-order regularized long-wave models via a novel transform," *Journal of Function Spaces*, vol. 2022, Article ID 2754507, 16 pages, 2022.

[9] A. A. Alderremy, S. Aly, R. Fayyaz, A. Khan, R. Shah, and N. Wyal, "The analysis of fractional-order nonlinear systems of third order KdV and burgers equations via a novel transform," *Complexity*, vol. 2022, Article ID 4935809, 24 pages, 2022.

[10] N. Iqbal, T. Botmart, W. W. Mohammed, and A. Ali, "Numerical investigation of fractional-order Kersten-Krasil'shchik coupled KdV-mKdV system with Atangana-Baleanu derivative," *Advances in Continuous and Discrete Models*, vol. 2022, no. 1, article 37, pp. 1–20, 2022.

[11] S. Alshammari, N. Iqbal, and M. Yar, "Fractional-view analysis of space-time fractional Fokker-Planck equations within Caputo operator," *Journal of Function Spaces*, vol. 2022, Article ID 4471757, 12 pages, 2022.

[12] Y. N. Zhang, Z. Z. Sun, and H. L. Liao, "Finite difference methods for the time fractional diffusion equation on non-uniform meshes," *Journal of Computational Physics*, vol. 265, pp. 195–210, 2014.

[13] H. Yasmin and N. Iqbal, "A comparative study of the fractional coupled burgers and Hirota-Satsuma KdV equations via analytical techniques," *Symmetry*, vol. 14, no. 7, p. 1364, 2022.

[14] G. S. Priya, P. Prakash, J. J. Nieto, and Z. Kayar, "Higher-order numerical scheme for the fractional heat equation with Dirichlet and Neumann boundary conditions," *Numerical Heat Transfer, Part B: Fundamentals*, vol. 63, no. 6, pp. 540–559, 2013.

[15] K. Mustapha, "An implicit finite-difference time-stepping method for a sub-diffusion equation, with spatial discretization by finite elements," *IMA Journal of Numerical Analysis*, vol. 31, no. 2, pp. 719–739, 2011.

[16] G. H. Gao and Z. Z. Sun, "A compact finite difference scheme for the fractional sub-diffusion equations," *Journal of Computational Physics*, vol. 230, no. 3, pp. 586–595, 2011.

[17] S. A. El-Wakil, A. Elhanbaly, and M. A. Abdou, "Adomian decomposition method for solving fractional nonlinear differential equations," *Applied Mathematics and Computation*, vol. 182, no. 1, pp. 313–324, 2006.

[18] K. M. Saad and A. A. Al-Shomrani, "An application of homotopy analysis transform method for Riccati differential equation of fractional order," *Journal of Fractional Calculus and Applications*, vol. 7, no. 1, pp. 61–72, 2016.

[19] V. K. Srivastava, M. K. Awasthi, and S. Kumar, "Analytical approximations of two and three dimensional time-fractional telegraphic equation by reduced differential transform method," *Egyptian Journal of Basic and Applied Sciences*, vol. 1, no. 1, pp. 60–66, 2014.

[20] M. Areshi, A. Khan, R. Shah, and K. Nonlaopon, "Analytical investigation of fractional-order Newell-Whitehead-Segel equations via a novel transform," *AIMS Mathematics*, vol. 7, no. 4, pp. 6936–6958, 2022.

[21] N. A. Shah, Y. S. Hamed, K. M. Abualnaja, J. D. Chung, R. Shah, and A. Khan, "A comparative analysis of fractional-order Kaup-Kupershmidt equation within different operators," *Symmetry*, vol. 14, no. 5, p. 986, 2022.

[22] K. Nonlaopon, A. M. Alsharif, A. M. Zidan, A. Khan, Y. S. Hamed, and R. Shah, "Numerical investigation of fractional-order Swift-Hohenberg equations via a novel transform," *Symmetry*, vol. 13, no. 7, p. 1263, 2021.

[23] N. Iqbal, A. M. Albalahi, M. S. Abdo, and W. W. Mohammed, "Analytical analysis of Fractional-Order Newell-Whitehead-Segel equation: A modified homotopy perturbation transform method," *Journal of Function Spaces*, vol. 2022, Article ID 3298472, 2022.

[24] R. Ali, I. Khan, A. Ali, and A. Mohamed, "Two new generalized iteration methods for solving absolute value equations using M-matrix," *AIMS Mathematics*, vol. 7, no. 5, pp. 8176–8187, 2022.

[25] R. Ali, A. Ali, and S. Iqbal, "Iterative methods for solving absolute value equations," *The Journal of Mathematics and Computer Science*, vol. 26, pp. 322–329, 2021.

[26] T. Botmart, R. P. Agarwal, M. Naeem, A. Khan, and R. Shah, "On the solution of fractional modified Boussinesq and approximate long wave equations with non-singular kernel operators," *AIMS Mathematics*, vol. 7, no. 7, pp. 12483–12513, 2022.

[27] M. K. Alaoui, R. Fayyaz, A. Khan, R. Shah, and M. S. Abdo, "Analytical investigation of Noyes–Field model for time-fractional Belousov–Zhabotinsky reaction," *Complexity*, vol. 2021, Article ID 3248376, 21 pages, 2021.

[28] A. Saad Alshehry, M. Imran, A. Khan, R. Shah, and W. Weera, "Fractional view analysis of Kuramoto-Sivashinsky equations with non-singular kernel operators," *Symmetry*, vol. 14, no. 7, p. 1463, 2022.

[29] P. Sunthrayuth, H. A. Alyousef, S. A. El-Tantawy, A. Khan, and N. Wyal, "Solving fractional-order diffusion equations in a plasma and fluids via a novel transform," *Journal of Function Spaces*, vol. 2022, Article ID 1899130, 19 pages, 2022.

[30] R. Ali and K. Pan, "The solution of the absolute value equations using two generalized accelerated overrelaxation methods," *Asian-European Journal of Mathematics*, vol. 15, article 2250154, 2022.

[31] M. D. Kruskal and J. Moser, *Dynamical Systems, Theory and Applications, Lecturer Notes Physics*, Springer, Berlin, Germany, 1975.

[32] G. L. Vasconcelos and L. P. Kadanoff, "Stationary solutions for the Saffman-Taylor problem with surface tension," *Physical Review A*, vol. 44, no. 10, pp. 6490–6495, 1991.

[33] F. Gesztesy and K. Unterkofler, "Isospectral deformations for Strum-Liouville and Dirac-type operators and associated

nonlinear evolution equations," *Reports on Mathematical Physics*, vol. 31, no. 2, pp. 113–137, 1992.

[34] P. Rosenau and J. M. Hyman, "Compactons: solitons with finite wavelength," *Physical Review Letters*, vol. 70, no. 5, pp. 564–567, 1993.

[35] B. Mihaila, A. Cardenas, F. Cooper, and A. Saxena, "Stability and dynamical properties of Rosenau-Hyman compactons using Padé approximants," *Physical Review E*, vol. 81, no. 5, 2010.

[36] D. Bazeia, A. Das, L. Losano, and M. J. Santos, "Traveling wave solutions of nonlinear partial differential equations," *Applied Mathematics Letters*, vol. 23, no. 6, pp. 681–686, 2010.

[37] F. Rus and F. R. Villatoro, "Self-similar radiation from numerical Rosenau-Hyman compactons," *Journal of Computational Physics*, vol. 227, no. 1, pp. 440–454, 2007.

[38] F. Rus and F. R. Villatoro, "Pade numerical method for the Rosenau-Hyman compacton equation," *Mathematics and Computers in Simulation*, vol. 76, no. 1-3, pp. 188–192, 2007.

[39] I. Podlubnv, *Fractional Differential Equations*, vol. 6, Academic Press, San Diego, Boston, 1999.

[40] A. Atangana and D. Baleanu, "New fractional derivatives with nonlocal and non-singular kernel: theory and application to heat transfer model," *Thermal Science*, vol. 20, no. 2, pp. 763–769, 2016.

[41] T. M. Elzaki, "The new integral transform Elzaki transform," *Global Journal of Pure and Applied Mathematics*, vol. 7, pp. 57–64, 2011.

[42] A. A. Alderremy, T. M. Elzaki, and M. Chamekh, "New transform iterative method for solving some Klein-Gordon equations," *Results in Physics*, vol. 10, pp. 655–659, 2018.

[43] H. Kim, "The time shifting theorem and the convolution for Elzaki transform," *International Journal of Pure and Applied Mathematics*, vol. 87, pp. 261–271, 2013.

[44] A. H. Sedeeg, "A coupling Elzaki transform and homotopy perturbation method for solving nonlinear fractional heat-like equations," *American Journal of Mathematical and Computer Modelling*, vol. 1, pp. 15–20, 2016.

[45] A. Ghorbani, "Beyond Adomian polynomials: he polynomials," *Chaos, Solitons and Fractals*, vol. 39, no. 3, pp. 1486–1492, 2009.

Hindawi
Journal of Function Spaces
Volume 2022, Article ID 3777566, 5 pages
https://doi.org/10.1155/2022/3777566

Research Article

Fractional Fourier Transform and Ulam Stability of Fractional Differential Equation with Fractional Caputo-Type Derivative

Arunachalam Selvam,[1] **Sriramulu Sabarinathan**,[1] **Samad Noeiaghdam**,[2,3] **and Vediyappan Govindan**[4]

[1]*Department of Mathematics, SRM Institute of Science & Technology, Kattankulathur, 603 203 Tamil Nadu, India*
[2]*Industrial Mathematics Laboratory, Baikal School of BRICS, Irkutsk National Research Technical University, Irkutsk 664074, Russia*
[3]*Department of Applied Mathematics and Programming, South Ural State University, Lenin Prospect 76, Chelyabinsk 454080, Russia*
[4]*Department of Mathematics, Dmi St John the Baptist University, 800-Central Africa, Malawi*

Correspondence should be addressed to Vediyappan Govindan; govindoviya@gmail.com

Received 5 August 2022; Accepted 23 August 2022; Published 6 September 2022

Academic Editor: Yusuf Gurefe

In this paper, we study the Ulam-Hyers-Mittag-Leffler stability for a linear fractional order differential equation with a fractional Caputo-type derivative using the fractional Fourier transform. Finally, we provide an enumeration of the chemical reactions of the differential equation.

1. Introduction

Fractional differential equations have more attention in the research area of mathematics, and there has been significant progress in this field. However, this idea is not new and as old as differential equations. The differential equations of fractional order have proved to be valuable tools in modeling multiple phenomena in different areas of science and engineering. Indeed, it has many uses in biology, physics, electromagnetics, mechanics, electrochemistry, etc. [1–3]. Fractional calculus was initiated from a question raised by L'Hospital to Leibniz, which related to his generalization of meaning of notation $(d^n y/dx^n)d$ for the derivative of order $n \in \mathcal{N} := 0, 1, 2, \cdots$, when $n = 1/2$?. In his reply, dated September 30, 1695, Leibniz wrote to L'Hospital [4], "This is an apparent paradox from which one-day useful consequences will be drawn." Recently, Ozaktas and Kutay [5] published on this topic, dealing with different characteristics in different ways.

A functional equation is stable if for each approximate answer there is a definite quantity about it. In 1940, the simulation and a hit theory suggested by Ulam [6] prompted the study of stability issues for numerous functional equations. He gave the University of Wisconsin Mathematical Colloquium a long form of talks, presenting a variety of unresolved questions. He raised one of the questions that were connected to the stability of the functional equation: "Give conditions for a linear function near an approximately linear function to exist." The first result concerning the stability of functional equations was presented by Hyers [7] in 1941. The stability of the form is subsequently referred to as Hyers-Ulam stability. In 1978, the generalization associated with the Hyers theorem given by Rassias [8] makes it possible for the Cauchy difference to be unbounded. In 2004, Jung [9] studied the Hyers-Ulam stability of the differential equations $\vartheta(s)p'(s) = p(s)$. Jung [10, 11] continuously published the general setting for Hyers-Ulam stability of first-order linear differential equations. In 2006, Jung [12] concentrated on the Hyers-Ulam stability of an arrangement of differential equations with coefficients through the utilization of a matrix approach. Ponmana Selvan et al. [13] have solved the different types of Ulam stability for the approximate solution of a special type of mth-order linear differential equation with initial and boundary conditions.

Zhang and Li [14] studied the Ulam stabilities of m-dimensional fractional differential systems with order $1 < \alpha < 2$ in 2011, and in the same year, Li and Zhang [15] proved the stability of fractional order derivative for differential equations. In 2013, Ibrahim [16] investigated the Ulam-Hyers stability for iterative Cauchy fractional differential equations and Lane-Emden equations. Kalvandi et al. [17], Liu *et al.* [18], and Vu et al. [19] presented and proved the different types of Hyers-Ulam stability of a linear fractional differential equations.

In 2012, Wang et al. [20] carried out pioneering work on the Hyers-Ulam stability for fractional differential equations with Caputo derivative using a fixed point approach, and in the same year, Wang and Zhou [21] proved the Hyers-Ulam stability of nonlinear impulsive problems for fractional differential equations. Wang et al. [22] investigated the Mittag-Leffler-Ulam-Hyers stability of fractional evolution equations.

In 2020, Unyong *et al.* [23] studied Ulam stabilities of linear fractional order differential equations in Lizorkin space using the fractional Fourier transform, and in the same year, Hammachukiattikul et al. [24] derived some Ulam-Hyers stability outcomes for fractional differential equations. In the next year, Ganesh *et al.* [25] derived some Mittag-Leffler-Hyers-Ulam stability, which makes sure the existence and individuation of an answer for a delay fractional differential equation by using the fractional Fourier transform. In 2022, Ganesh et al. [26] carried out pioneering in the field with the Hyers-Ulam stability for fractional order implicit differential equations with two Caputo derivatives using a fractional Fourier transform.

Motivated and inspired by the above results, in this paper, because of the help of fractional Fourier transform, we would like to investigate the Ulam-Hyers-Mittag-Leffler and Ulam-Hyers-Rassias-Mittag-Leffler stability of linear fractional order differential equations with the fractional Caputo-type derivative of the form:

$$\left({}^{\mathscr{C}}\mathscr{D}_{0+}^{\sigma}p\right)(s) + \eta\, p(s) = q(s), \tag{1}$$

where $q(s)$ is a $m-$times continuously differentiable function and ${}^{\mathscr{C}}\mathscr{D}_{0+}^{\sigma}$ is the fractional Caputo-type derivative of order $\sigma \in (m-1, m)$, $m \in N^{+}$.

2. Preliminaries

The following definitions, theorems, notations, and lemmas will be used to obtain the main objectives of this paper.

Definition 1 (see [27]). The one dimension fractional Fourier transform with rotational angle σ of function $p(s) \in \mathscr{L}'(\mathscr{R})$ is given by

$$\mathscr{F}_{\sigma}[p(s)](\omega) = \widehat{p}_{\sigma}(\omega) = \int_{\mathscr{R}} K_{\sigma}(s,\omega)p(s)ds, \omega \in \mathscr{R}, \tag{2}$$

where the kernel

$$K_{\sigma}(s,\omega) = \begin{cases} \mathscr{C}_{\sigma} e^{\left(\left(i\left(p^2+\omega^2\right)\cot\sigma\right)/2\right)-ip\omega\operatorname{cosec}\sigma}, & \text{if } \sigma \neq m\pi, \\ \dfrac{1}{\sqrt{2\pi}} e^{-ip\omega}, & \text{if } \sigma = \dfrac{\pi}{2}, \end{cases}$$
$$\mathscr{C}_{\sigma} = \sqrt{\frac{1 - i\cot\sigma}{2\pi}}. \tag{3}$$

As such, the inversion formula of fractional Fourier transform is given by

$$p(s) = \frac{1}{2\pi}\int_{\mathscr{R}} K_{\sigma}(s,\omega)\widehat{p}_{\sigma}(\omega)d\omega, s \in \mathscr{R}, \tag{4}$$

where the kernel

$$K_{\sigma}(\bar{s},\omega) = \begin{cases} \mathscr{C}'_{\sigma} e^{\left(\left(-i\left(p^2+\omega^2\right)\cot\sigma\right)/2\right)+ip\omega\operatorname{cosec}\sigma}, & \text{if } \sigma \neq m\pi, \\ \dfrac{1}{\sqrt{2\pi}} e^{ip\omega}, & \text{if } \sigma = \dfrac{\pi}{2}, \end{cases}$$
$$\mathscr{C}'_{\sigma} = \sqrt{2\pi(1 + i\cot\sigma)}. \tag{5}$$

Definition 2. The Mittag-Leffler function is given in the following manner:

$$\mathbb{E}_{\sigma}(s) = \sum_{m=0}^{\infty}\frac{s^m}{\Gamma(\sigma m + 1)}, \quad (\sigma > 0) \text{ (One parameter)},$$
$$\mathbb{E}_{\sigma,\mu}(s) = \sum_{m=0}^{\infty}\frac{s^m}{\Gamma(\sigma m + \mu)}, \quad (\sigma > 0, \mu > 0) \text{ (Two parameters)}. \tag{6}$$

where σ and μ are nonnegative constant.

Definition 3 (see [28]). The fractional integral operator of order $s > 0$ of a function $p \in \mathscr{L}^1(\mathscr{R}^+)$ is written as

$$I_{0+}^{\sigma}p(s) = \frac{1}{\Gamma(\sigma)}\int_0^s (s-u)^{(\sigma-1)}p(u)\,du, s > 0, \tag{7}$$

where $\Gamma(.)$ is the gamma function and $\mathscr{R}e > 0$.

Definition 4 (see [28]). The Riemann-Liouville fractional order derivative of $s > 0$, $m-1 < \sigma < m$, $m \in \mathscr{N}$, is written as

$$\left({}^{\mathscr{RL}}\mathscr{D}_{0+}^{\sigma}p\right)(s) = \frac{1}{\Gamma(m-\sigma)}\left(\frac{d}{ds}\right)^m\int_0^s (s-u)^{(m-\sigma-1)}p(u)du, \tag{8}$$

where the function $p(s)$ is a continuous derivatives upto order $(m-1)$.

Definition 5 (see [28]). The fractional Caputo-type derivative of order $s > 0, m-1 < \sigma < m, m \in \mathcal{N}$, is written as

$$\left({}^{\mathscr{C}}\mathscr{D}_{0+}^{\sigma}p\right)(s) = \frac{1}{\Gamma(m-\sigma)}\int_0^s (s-u)^{(m-\sigma-1)}p^{(n)}(u)du, \quad (9)$$

where the function $p(s)$ is a continuous derivatives up to order $(m-1)$. Then, let $s > 0, \sigma \in \mathscr{R}, m-1 < \sigma < m, m \in \mathcal{N}$. The relation between Caputo and Riemann-Liouville fractional derivative is given by

$$\left({}^{\mathscr{C}}\mathscr{D}_{0+}^{\sigma}p\right)(s) = \left(\mathscr{D}_{0+}^{\sigma}p\right)(s) - \sum_{k=0}^{m-1}\frac{(s-a)^{k-\sigma}}{\Gamma(k-\sigma+1)}p^{(k)}(0). \quad (10)$$

Definition 6. Equation (1) has Ulam-Hyers-Mittag-Leffler stability, if there exist a continuously differentiable function $p(s)$ satisfying the inequality

$$\left|\left({}^{\mathscr{C}}\mathscr{D}_{0+}^{\sigma}p\right)(s) + \eta p(s) - q(s)\right| \le \varepsilon \mathbb{E}_{\sigma}(s), \forall s > 0, \quad (11)$$

for every $\varepsilon > 0$, there exists a solution $p_{\sigma}(s)$ satisfying Equation (1) such that

$$|p(s) - p_{\sigma}(s)| \le \mathscr{H}\varepsilon\mathbb{E}_{\sigma}(s), \quad (12)$$

where $\mathscr{H}$ is a nonnegative and stability constant.

Definition 7. The considered $\phi : (0,\infty) \longrightarrow (0,\infty)$ is a function. Equation (1) has Ulam-Hyers-Rassias-Mittag-Leffler stability, if there exist a continuously differentiable function $p(s)$ satisfying the inequality

$$\left|\left({}^{\mathscr{C}}\mathscr{D}_{0+}^{\sigma}p\right)(s) + \eta p(s) - q(s)\right| \le \varepsilon\phi(s)\mathbb{E}_{\sigma}(s), \forall s > 0, \quad (13)$$

for every $\varepsilon > 0$, there exists a solution $p_{\sigma}(s)$ satisfying Equation (1) such that

$$|p(s) - p_{\sigma}(s)| \le \mathscr{H}\phi(s)\varepsilon\mathbb{E}_{\sigma}(s), \quad (14)$$

where $\mathscr{H}$ is a nonnegative and stability constant.

3. Main Results

In this section, we will investigate to help of fractional Fourier transform to study the Ulam-Hyers-Mittag-Leffler stability of (1).

Theorem 8. *If a function $p(s)$ satisfies the inequality (11) for every $\varepsilon > 0$, there exists a solution $p_{\sigma}(s)$ satisfying Equation (1) such that*

$$|p(s) - p_{\sigma}(s)| \le \mathscr{H}\varepsilon\mathbb{E}_{\sigma}(s). \quad (15)$$

Proof. Let us choose a function $y(s)$ follow as

$$y(s) = \left({}^{\mathscr{C}}\mathscr{D}_{0+}^{\sigma}p\right)(s) + \eta p(s) - q(s). \quad (16)$$

Now,

$$y(s) = (\mathscr{D}^{\sigma}p)(s) - \sum_{k=0}^{m-1}\frac{s^{k-\sigma}}{\Gamma(k-\sigma+1)}p^{(k)}(0) + \eta p(s) - q(s), \forall s > 0. \quad (17)$$

Taking $\mathscr{F}_{\sigma}$ (the fractional Fourier transform oprator) onto both sides of Equation (17), we have

$$\begin{aligned}\mathscr{F}_{\sigma}\{y(s)\} &= \mathscr{F}_{\sigma}\left\{\mathscr{D}^{\sigma}p(s) - \sum_{k=0}^{m-1}\frac{s^{k-\sigma}}{\Gamma(k-\sigma+1)}p^{(k)}(0) + \eta p(s) - q(s)\right\} \\ &= \left(i\omega^{n/\sigma}\right)^{\sigma}\mathscr{F}_{\sigma}\{p(s)\} - e^{i\omega^{n/\sigma}a}\sum_{k=0}^{m-1}a_k\frac{s^{k-\sigma}}{\Gamma(k-\sigma+1)\left(i\omega^{n/\sigma}\right)^{k-\sigma+1}} \\ &\quad + \eta\mathscr{F}_{\sigma}(p(s)) - \widehat{G}_a(\omega),\end{aligned} \quad (18)$$

where $p^{(k)}(0) = a_k$, for $k = 0, 1, \cdots, m-1$ and

$$\begin{aligned}\mathscr{F}_{\sigma}\{p(s)\} &= \frac{\mathscr{F}_{\sigma}\{y(s)\}}{\left(\left(i\omega^{n/\sigma}\right)+\eta\right)} \\ &\quad + \frac{e^{i\omega^{n/\sigma}a}}{\left(\left(i\omega^{n/\sigma}\right)+\eta\right)}\sum_{k=0}^{m-1}\frac{a_k}{\left(\left(i\omega^{n/\sigma}\right)+\eta\right)} + \frac{\widehat{G}_a(\omega)}{\left(\left(i\omega^{n/\sigma}\right)+\eta\right)}.\end{aligned} \quad (19)$$

Setting

$$p_{\sigma}(s) = \sum_{k=n}^{p-1}a_k p_k(0) + \int_0^s (s-\nu)^{\nu-1}\mathbb{E}_{\sigma}\left[\eta(s-\nu)^{\nu-1}\right]q(s)d\nu. \quad (20)$$

By using fractional Fourier transform to (20), we have

$$\mathscr{F}_{\sigma}\{p_{\sigma}(s)\} = \frac{e^{i\omega^{n/\sigma}a}}{\left(\left(i\omega^{n/\sigma}\right)+\eta\right)}\sum_{k=0}^{m-1}\frac{a_k}{\left(\left(i\omega^{n/\sigma}\right)+\eta\right)} + \frac{\widehat{G}_a(\omega)}{\left(\left(i\omega^{n/\sigma}\right)+\eta\right)}. \quad (21)$$

Hence,

$$\begin{aligned}\left({}^{\mathscr{C}}\mathscr{D}_{0+}^{\sigma}p\right)(s) + \eta p(s) &= \left(i\omega^{n/\sigma}\right)^{\sigma}\mathscr{F}_{\sigma}\{p(s)\} \\ &\quad - e^{i\omega^{n/\sigma}a}\sum_{k=0}^{m-1}a_k\frac{s^{k-\sigma}}{\Gamma(k-\sigma+1)\left(i\omega^{n/\sigma}\right)^{k-\sigma+1}} \\ &\quad + \eta\mathscr{F}_{\sigma}(p(s)) - \widehat{G}_a(\omega) \\ &= q(s).\end{aligned} \quad (22)$$

□

Since $\mathcal{F}_\sigma$ is one-to-one operator, $({}^{\mathscr{C}}\mathcal{D}_{0+}^{\sigma}p)(s)+\eta p(s)=q(s)$. Now, its follows form (19) and (21) that

$$\mathcal{F}_\sigma\{p(s)\}-\mathcal{F}_\sigma\{p_\sigma(s)\}=\frac{\mathcal{F}_\sigma\{y(s)\}}{((i\omega^{n/\sigma})+\eta)}. \tag{23}$$

Using the convolution property, we obtain

$$\mathcal{F}_\sigma\{p(s)-p_\sigma(s)\}=\mathcal{F}_\sigma\{y(s)\}*\frac{1}{((i\omega^{n/\sigma})+\eta)}=y(s)*y_\sigma(s), \tag{24}$$

where $y_\sigma(s)=1/((i\omega^{n/\sigma})+\eta)$. In view of (13), we have

$$|y(s)|\le \varepsilon\mathbb{E}_\sigma(s), \forall s>0. \tag{25}$$

Now, applying the modules on both sides of Equation (24), we get

$$\begin{aligned}|p(s)-p_\sigma(s)|&=\left|\int_0^s (s-x)^{\sigma-1}\mathbb{E}_\sigma(\eta(s-\nu)^\sigma)*y(s)d\nu\right|\\&\le |y(s)|\left|\int_0^s (s-\nu)^{\sigma-1}\mathbb{E}_\sigma(\eta(s-\nu)^\sigma)d\nu\right|\\&\le \varepsilon\mathbb{E}_\sigma(s)\left|\int_0^s (s-\nu)^{\sigma-1}\mathbb{E}_\sigma(\eta(s-x)^\sigma)d\nu\right|\\&\le \mathcal{H}\varepsilon\mathbb{E}_\sigma(s).\end{aligned} \tag{26}$$

where $\mathcal{H}=|\int_0^s (s-x)^{\sigma-1}\mathbb{E}_\sigma(\eta(s-x)^\sigma)d\nu|$. Thus Equation (1) has Ulam-Hyers-Mittag-Leffler stability.

Corollary 9. *The considered $\phi:(0,\infty)\longrightarrow(0,\infty)$ is a function. If a function $p(s)$ satisfies the inequality (13), for every $\varepsilon>0$, there exists a solution $p_\sigma(s)$ satisfying Equation (1) such that*

$$|p(s)-p_a(s)|\le \mathcal{H}\phi(s)\varepsilon\mathbb{E}_\sigma(s), \forall s>0. \tag{27}$$

i.e., Equation (1) has Ulam-Hyers-Rassias-Mittag-Leffler stability.

4. Applications

In this section, the standard kinetic equation in the chemical reaction that will be used to analyze this experimental data is revealed by the equation as follows: where $\mathcal{L}=$ xylan; $\mathcal{M}=$ xylose; $\mathcal{N}=$ products of decomposition; $r_1=$ release rate of sugar; $r_2=$ decomposition rate of sugar. The model is presented in Figure 1.

Material balance for components: "$\mathcal{L}$" and "$\mathcal{M}$" for the first-order kinetic equation, we get

$$-\frac{d\mathcal{N}_{\mathcal{L}}(s)}{ds}=r_1\mathcal{N}_{\mathcal{L}}(s), \tag{28}$$

in which the initial concentration at $s=0$ is presented by $\mathcal{N}_{\mathcal{L}}=\mathcal{N}_{\mathcal{L}_0}$. Also, we have the same direction for material $\mathcal{M}$:

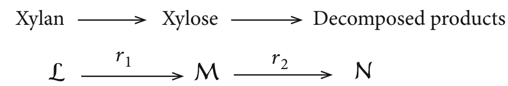

FIGURE 1: The presented model.

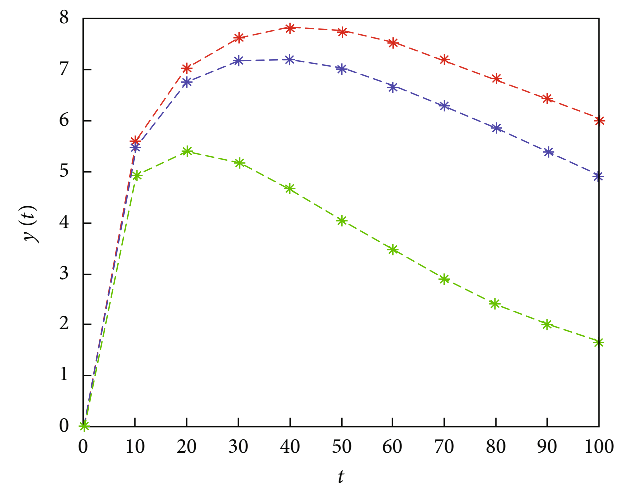

FIGURE 2: Solution of Equation (32) for different values $(r_1=0.012\&r_2=0.005)$, $(r_1=0.014\&r_2=0.005)$, and $(r_1=0.025\&r_2=0.005)$ with $\sigma=1/2$.

$$-\frac{d\mathcal{N}_{\mathcal{M}}(s)}{ds}=r_1\mathcal{N}_{\mathcal{L}}(s)-r_2\mathcal{N}_{\mathcal{M}}(s), \tag{29}$$

in which the initial concentration at $s=0$ is presented by $\mathcal{N}_{\mathcal{M}}=\mathcal{N}_{\mathcal{M}_0}$. Equation (29) can be integrated and, using the provided boundary condition, yields

$$\mathcal{N}_{\mathcal{L}}(s)=\mathcal{N}_{\mathcal{L}_0}\quad \exp(-r_1 s). \tag{30}$$

Substituting (30) for (29) yields

$$\frac{d\mathcal{N}_{\mathcal{M}}(s)}{ds}+r_2\mathcal{N}_{\mathcal{M}}(s)=r_1\mathcal{N}_{\mathcal{L}_0}\quad \exp(-r_1 s). \tag{31}$$

Now, if we take the fractional Caputo derivative in (31) instead of the classical ones, we have

$${}^{\mathscr{C}}\mathcal{D}^{\sigma}\mathcal{N}_{\mathcal{M}}(s)+r_2\mathcal{N}_{\mathcal{M}}(s)=r_1\mathcal{N}_{\mathcal{L}_0}\quad \exp(-r_1 s). \tag{32}$$

Figure 2 shows the solution of Equation (32) for various r_1 and r_2.

5. Conclusions

In this paper, the objective is investigated by using the fractional Fourier transform to study the Ulam-Hyers-Mittag-Leffler stability of linear fractional differential equations. The required outcomes have been achieved by using the fractional Fourier transform. We could reach the suitable approximation value of xylose after a certain period of time, which is crucial for analyzing the kinetic equation in the chemical reaction process.

Data Availability

No data were used to support this study.

Conflicts of Interest

The authors declare that they have no conflicts of interest.

References

[1] P. Agarwal and S. Jain, "Further results on fractional calculus of Srivastava polynomials," *Bulletin of Mathematical Analysis and Applications*, vol. 3, no. 2, pp. 167–174, 2011.

[2] P. Agarwal, S. Jain, S. Agarwal, and M. Nagpal, "On a new class of integrals involving Bessel functions of the first kind," *Communications in Numerical Analysis*, vol. 2014, pp. 1–7, 2014.

[3] P. Agarwal, U. Baltaeva, and Y. Alikulov, "Solvability of the boundary-value problem for a linear loaded integro-differential equation in an infinite three-dimensional domain," *Chaos, Solitons and Fractals*, vol. 140, p. 110108, 2020.

[4] S. F. Lacroix, *Traité du calcul différentiel et du calcul intégral Tome 3, Traité du calcul différentiel et du calcul intégral*, Elsevier, Paris: Courcier, 1819.

[5] H. M. Ozaktas and M. A. Kutay, "The fractional Fourier transform," in *2001 European Control Conference (ECC)*, pp. 1477–1483, 2001.

[6] S. M. Ulam, *Chapter IV, Problem in Modern Mathematics, Science Editors*, Willey, New York, 1960.

[7] D. H. Hyers, "On the stability of the linear functional equation," *Proceedings of the National Academy of Sciences*, vol. 27, no. 4, pp. 222–224, 1941.

[8] T. M. Rassias, "On the stability of the linear mapping in Banach spaces," *Proceedings of the American Mathematical Society*, vol. 72, no. 2, pp. 297–300, 1978.

[9] S. M. Jung, "Hyers-Ulam stability of linear differential equations of first order," *Applied Mathematics Letters*, vol. 17, no. 10, pp. 1135–1140, 2004.

[10] S. M. Jung, "Hyers-Ulam stability of linear differential equations of first order, III," *Journal of Mathematical Analysis and Applications*, vol. 311, no. 1, pp. 139–146, 2005.

[11] S. M. Jung, "Hyers-Ulam stability of linear differential equations of first order, II," *Applied Mathematics Letters*, vol. 19, no. 9, pp. 854–858, 2006.

[12] S. M. Jung, "Hyers-Ulam stability of a system of first order linear differential equations with constant coefficients," *Journal of Mathematical Analysis and Applications*, vol. 320, no. 2, pp. 549–561, 2006.

[13] A. Ponmana Selvan, S. Sabarinathan, and A. Selvam, "Approximate solution of the special type differential equation of higher order using Taylor's series," *Journal of Mathematics and Computer Science*, vol. 27, no. 2, pp. 131–141, 2022.

[14] F. Zhang and C. Li, "Stability analysis of fractional differential systems with order lying in (1, 2)," *Advances in Difference Equations*, vol. 2011, Article ID 213485, 17 pages, 2011.

[15] C. P. Li and F. R. Zhang, "A survey on the stability of fractional differential equations," *The European Physical Journal Special Topics*, vol. 193, no. 1, pp. 27–47, 2011.

[16] R. W. Ibrahim, "Stability of fractional differential equations," *International Journal of Mathematics and Computer Science Engineering*, vol. 7, no. 3, pp. 212–217, 2013.

[17] V. Kalvandi, N. Eghbali, and J. M. Rassia, "Mittag-Leffler-Hyers-Ulam stability of fractional differential equations of second order," *Journal of Mathematical Extension*, vol. 13, pp. 1–15, 2019.

[18] K. Liu, J. Wang, Y. Zhou, and D. O'Regan, "Hyers-Ulam stability and existence of solutions for fractional differential equations with Mittag-Leffler kernel," *Chaos, Solitons & Fractals*, vol. 132, p. 109534, 2020.

[19] H. Vu, T. V. An, and N. V. Hoa, "Ulam-Hyers stability of uncertain functional differential equation in fuzzy setting with Caputo-Hadamard fractional derivative concept," *Journal of Intelligent Fuzzy Systems*, vol. 38, no. 2, pp. 2245–2259, 2020.

[20] J. Wang, L. Lv, and Y. Zhou, "Ulam stability and data dependence for fractional differential equations with Caputo derivative," *Electronic Journal of Qualitative Theory of Differential Equations*, vol. 63, no. 63, pp. 1–10, 2011.

[21] J. R. Wang and Y. Zhou, "Mittag-Leffler-Ulam stabilities of fractional evolution equations," *Applied Mathematics Letters*, vol. 25, no. 4, pp. 723–728, 2012.

[22] J. R. Wang, Y. Zhou, and M. Feckan, "Nonlinear impulsive problems for fractional differential equations and Ulam stability," *Computers & Mathematcs with Applications*, vol. 64, no. 10, pp. 3389–3405, 2012.

[23] B. Unyong, A. Mohanapriya, A. Ganesh et al., "Fractional Fourier transform and stability of fractional differential equation on Lizorkin space," *Advances in Difference Equations*, vol. 2020, no. 1, article 578, 23 pages, 2020.

[24] P. Hammachukiattikul, A. Mohanapriya, A. Ganesh et al., "A study on fractional differential equations using the fractional Fourier transform," *Advances in Difference Equations*, vol. 2020, no. 1, article 691, 22 pages, 2020.

[25] A. Ganesh, V. Govindan, J. R. Lee, A. Mohanapriya, and C. Park, "Mittag-Leffler-Hyers-Ulam stability of delay fractional differential equation via fractional Fourier transform," *Results in Mathematics*, vol. 76, no. 4, pp. 1–7, 2021.

[26] A. Ganesh, S. Deepa, D. Baleanu et al., "Hyers-Ulam-Mittag-Leffler stability of fractional differential equations with two caputo derivative using fractional fourier transform," *AIMS Mathematics*, vol. 7, no. 2, pp. 1791–1810, 2022.

[27] A. I. Zayed, "Fractional Fourier transform of generalized functions," *Integral Transforms and Special Functions*, vol. 7, no. 3-4, pp. 299–312, 1998.

[28] A. A. Kilbas and J. J. Trujillo, "Differential equations of fractional order: methods results and problem—I," *Applicable Analysis*, vol. 78, no. 1-2, pp. 153–192, 2001.

Hindawi
Journal of Function Spaces
Volume 2022, Article ID 4842344, 14 pages
https://doi.org/10.1155/2022/4842344

Research Article

New Fractional Estimates of Simpson-Mercer Type for Twice Differentiable Mappings Pertaining to Mittag-Leffler Kernel

Saad Ihsan Butt,[1] **Saima Rashid**,[2] **Iram Javed**,[1] **Khuram Ali Khan**,[3] **and Rostin Matendo Mabela**[4]

[1] *COMSATS University Islamabad, Lahore Campus, Pakistan*
[2] *Department of Mathematics, Government College University, Faisalabad 38000, Pakistan*
[3] *Department of Mathematics, University of Sargodha, Sargodha 40100, Pakistan*
[4] *Department of Maths and Computer Science, Faculty of Science, University of Kinshasa, Democratic Republic of the Congo*

Correspondence should be addressed to Rostin Matendo Mabela; rostin.mabela@unikin.ac.cd

Received 24 April 2022; Revised 30 June 2022; Accepted 25 July 2022; Published 5 September 2022

Academic Editor: Behrouz Parsa Moghaddam

The main motivation of this study is to introduce a novel auxiliary result of Simpson's formula by employing the Mercer scheme for twice differentiable functions involving the Atangana-Baleanu (AB) fractional integral operator concerned with the Mittag-Leffler as a nonsingular or nonlocal kernel. Thus, by employing Mercer's convexity on twice differentiable mappings along with Hölder's and power-mean inequalities, one can develop a variety of new Simpson's error estimates. Lastly, some applications to q-digamma function and modified Bessel functions are presented. Furthermore, the graphical illustrations described the efficiency and applicability of the proposed technique with success. We make links between our findings and a number of well-known discoveries in the literature. It is hoped that the proposed methodology will provide a new venue in the numerical techniques for calculating the quadrature formulae.

1. Introduction

Convex functions have gained a lot of popularity in recent years. Convex functions are frequently used in various areas of current analysis in a variety of mathematical disciplines. They are magical, especially in optimization theory, because they have so many useful properties. Inequality theory and convex functions have a strong relationship. Convex functions can be used to obtain a variety of important and useful inequalities. Due to wide range of implementations, it is among the most advanced branches of mathematical modeling. Convex functions are the topic of research in a number of disciplines due to their applicability in inequality theory and defined as:

$$\phi(\kappa\varkappa + (1-\kappa)\varkappa_1) \le \kappa\phi(\varkappa) + (1-\kappa)\phi(\varkappa_1), \quad (1)$$

where $\phi : [\zeta_1, \zeta_2] \subseteq \mathfrak{R} \longrightarrow \mathfrak{R}$ is a convex function which holds for all $\varkappa, \varkappa_1 \in [\zeta_1, \zeta_2]$ and $\kappa \in [0, 1]$.

Additional information of different types of convexity and their contribution to inequalities can be found here, see [1, 2]. The improvement and exploration of the integral inequalities referring to convex functions is primarily motivated based on the research and findings presented in these books. Because of their wide range of implementations such as probability theory, information theory, computational problems, and optimization, the Jensen and related inequalities are essential and well-known inequalities for convex functions. See [3, 4] and references there in.

One of the most significant inequality that we may say is the natural extension of convex function is Jensen-Mercer inequality [5] given as:

$$\phi\left(\zeta_1 + \zeta_2 - \sum_{j=1}^{n} \Theta_j \varkappa_j\right) \le \phi(\zeta_1) + \phi(\zeta_2) - \sum_{j=1}^{n} \Theta_j \phi(\varkappa_j), \quad (2)$$

where ϕ on $[\zeta_1, \zeta_2]$ is a convex function $\forall \varkappa_j \in [\zeta_1, \zeta_2]$ and all $\Theta_j \in [0, 1]$ where

$$\sum_{j=1}^{n} \Theta_j = 1. \quad (3)$$

It is the most effective inequality in predicting the estimations of bounds of distance functions in information theory [6].

Many researchers put an effort in this direction to build new results such as fractional variants of Hermite Jensen-Mercer type inequalities along with applications [7], Moradi and Furuichi worked for the improvement and generalization of Jensen-Mercer-type inequalities [8], Kian and Moslehian worked for the improvement of operator Jensen-Mercer inequality [9], Niezgoda worked on generalization of Mercer's result on convex function [10], and Harovath gave some notes on Jensen-Mercer inequality [11]. A lot of work has been done on Jensen-Mercer-type inequality in Yang's Calculus, one can see [12, 13].

An inequality which is notable as Simpson's inequality is as follows.

Theorem 1 (see [14]). *Suppose that $\phi : [\zeta_1, \zeta_2] \longrightarrow \mathbb{R}$ is a four-time continuously differentiable mapping on (ζ_1, ζ_2), and let $\|\phi^{(4)}\|_\infty = \sup_{\varkappa \in (\zeta_1, \zeta_2)} |\phi^{(4)}(\varkappa)| < \infty$, then the following inequality holds:*

$$\left| \frac{1}{3}\left[\frac{\phi(\zeta_1) + \phi(\zeta_2)}{2} + 2\phi\left(\frac{\zeta_1 + \zeta_2}{2}\right)\right] - \frac{1}{\zeta_2 - \zeta_1}\int_{\zeta_1}^{\zeta_2} \phi(\varkappa)d\varkappa \right| \leq \frac{1}{2880}\left\|\phi^{(4)}\right\|_\infty (\zeta_2 - \zeta_1)^4. \quad (4)$$

The results of Simpson type inequalities for convex mappings have been looked by various writers because convex theory is an excellent technique to deal with a sizable number of issues from various mathematical disciplines. Specifically, differentiable functions are utilized to demonstrate some Simpson's type inequalities for s-convex functions [15], and then, the inequality extended to Riemann-Liouville fractional integrals [16]. A lot of work has been done utilizing this inequality for first derivative, one can see [17, 18].

Sarikaya et al. [19] explored numerous Simpson type inequalities for functions whose second derivatives are convex. The first and second outcomes on fractional Simpson inequality for twice differentiable functions were established in [14, 20]. With the help of these articles, the aim of this paper is to extend the results given in [19] for twice differentiable functions to generalized fractional integrals. Nowadays, twice differentiable functions are topic of interest for most of the researchers. We will use Mercer convexity along with twice differentiability for Simpson type inequalities to improve our outcomes and give new bounds.

Here, a lemma that is given in [14] stated as follows.

Lemma 2. *If there is a mapping $\phi : [\zeta_1, \zeta_2] \longrightarrow \mathbb{R}$ that is absolutely continuous on (ζ_1, ζ_2) considering $\phi'' \in L_1([\zeta_1, \zeta_2])$, then the following equality holds:*

$$\begin{aligned} &\frac{1}{6}\left[\phi(\zeta_1) + 4\phi\left(\frac{\zeta_1 + \zeta_2}{2}\right) + \phi(\zeta_2)\right] \\ &\quad - \frac{2^{\varpi - 1}\Gamma(\varpi + 1)}{(\zeta_2 - \zeta_1)^{\varpi}}\left[J^{\varpi}_{\zeta_2 -}\phi\left(\frac{\zeta_1 + \zeta_2}{2}\right) + J^{\varpi}_{\zeta_1 +}\phi\left(\frac{\zeta_1 + \zeta_2}{2}\right)\right] \\ &= \frac{(\zeta_2 - \zeta_1)^2}{8(\varpi + 1)}\int_0^1 \left(\frac{1}{3}\left[1 - 2\varpi(1 - \kappa) + \left(2 - 3\kappa^{\varpi}\right)\kappa\right]\right) \\ &\quad \times \left[\phi''\left(\left(\frac{1 + \kappa}{2}\zeta_2 + \frac{1 - \kappa}{2}\zeta_1\right)\right) + \phi''\left(\left(\frac{1 + \kappa}{2}\zeta_1 + \frac{1 - \kappa}{2}\zeta_2\right)\right)\right] d\kappa. \end{aligned} \quad (5)$$

We will extend this result for a new fractional integral operator along with mercer convexity. It is not easy to deal with double derivative; we have worked on double derivative for a new operator along with Mercer convexity. It is completely new idea, and in this way, the generalized outcomes will increase its worth and captures interest of many scholars toward this field.

The generalization of classical calculus, fractional calculus, is widely used in sciences, particularly engineering. The classical calculus offers an excellent method for modelling and explaining numerous essential dynamic processes in most sections of applied sciences. The hypothesis of fractional calculus was developed to merge and generalise n -fold integration and integer-order differentiation. The field of applied sciences includes fractional analysis. Many results based on fractional models have been published in various fields of science [21].

The fractional operators of integral and derivative helps in improving the relationships between mathematics and other specialisations by providing solutions that are more closely related to real-world problems. Fractional integral and derivative operators have evolved over time [22, 23]. Some fractional numerical simulations can be seen in [24, 25]. In their review article "Fractional calculus in the sky," [26] D. Baleanu and R. P. Agrwal, two esteemed professors, provide the most recent compact review of fractional calculus.

Definition 3 (see [27]). Let $\zeta_2 > \zeta_1$, $\varpi \in [0, 1]$ and $\phi \in H^1(\zeta_1, \zeta_2)$, then the new fractional derivative is:

$$ {}^{ABC}_{\zeta_1}D^{\varpi}_{\kappa}[\phi(\kappa)] = \frac{B(\varpi)}{1 - \varpi}\int_{\zeta_1}^{\kappa} \phi'(\varkappa)E_{\varpi}\left[-\varpi\frac{(\kappa - \varkappa)^{\varpi}}{(1 - \varpi)}\right]d\varkappa. \quad (6)$$

Definition 4 (see [27]). Let $\phi \in H^1(\zeta_1, \zeta_2)$, $\zeta_1 > \zeta_2$, $\varpi \in [0, 1]$, then we have:

$$ {}^{ABR}_{\zeta_1}D^{\varpi}_{\kappa}[\phi(\kappa)] = \frac{B(\varpi)}{1 - \varpi}\frac{d}{d\kappa}\int_{\zeta_1}^{\kappa} \phi(\varkappa)E_{\varpi}\left[-\varpi\frac{(\kappa - \varkappa)^{\varpi}}{(1 - \varpi)}\right]d\varkappa. \quad (7)$$

Definition 5 (see [27]). Let $\phi \in H^1(\zeta_1, \zeta_2)$, then with nonlocal kernel, the fractional integral operator is defined as:

$$ {}^{AB}_{\zeta_1}I^{\varpi}_{\kappa}\{\phi(\kappa)\} = \frac{1-\varpi}{B(\varpi)}\phi(\kappa) + \frac{\varpi}{B(\varpi)\Gamma(\varpi)}\int_{\zeta_1}^{\kappa}\phi(\varkappa_1)(\kappa-\varkappa_1)^{\varpi-1}d\varkappa_1, \tag{8} $$

where $\zeta_2 > \zeta_1, \varpi \in [0, 1]$.

In [28], AB-fractional integral operator's right hand side is:

$$ {}^{AB}_{\zeta_2}I^{\varpi}_{\kappa}\{\phi(\kappa)\} = \frac{1-\varpi}{B(\varpi)}\phi(\kappa) + \frac{\varpi}{B(\varpi)\Gamma(\varpi)}\int_{\kappa}^{\zeta_2}\phi(\varkappa_1)(\varkappa_1-\kappa)^{\varpi-1}d\varkappa_1. \tag{9} $$

Because the normalization function $B(\varpi)$ is positive, any positive function has a positive fractional AB-integral. It is worth noting that the classical integral is obtained when the order is $\varpi \longrightarrow 1$, while the initial function is obtained when the order is $\varpi \longrightarrow 0$. In the theory of integral inequalities involving AB operators, there has been some recent progress. One can see in [29, 30].

The purpose of this analysis is to utilize the AB integral operator to propose novel Mercer type inequalities for convex functions. The utmost objective is to acquire outcomes that create particular Mercer type inequalities by employing AB operators and elaborate the facts more appropriately in terms of the operator's qualities and kernel structure. Inequalities of the classical Mercer type and their different versions are created in the case when we have $\varpi = 1$ in the obtained results. This significant achievement is attributed to the AB fractional integral operator exhibiting the heredity characteristic. The exponential and power law functions are not as good as the generalized Mittag-Leffler function with robust memory entangled in the AB fractional formulation. Furthermore, the Atangana-Baleanu fractional-order derivative is at the same time Liouville-Caputo and Caputo-Fabrizio thus possesses Markovian and non-Markovian properties. Meanwhile, the graphical construction represents the comparison between the error and error estimates clearly with the aid of MATLAB 2021 package. Finally, the obtained outcomes were backed up by diminished outcomes and implementations.

2. Novel Simpson's Atangana-Baleanu Inequalities

Here, we present Mercer type Simpson's inequalities for Atangana-Baleanu integral operator for differentiable functions on (ν_1, ν_2). For this, we give a new Atangana-Baleanu integral operator auxiliary identity that will serve to produce subsequent results for improvements.

Lemma 6. *If there is a mapping $\phi : [\nu_1, \nu_2] \longrightarrow \mathbb{R}$ that is absolutely continuous on (ν_1, ν_2) considering $\phi'' \in L_1([\nu_1, \nu_2])$, where $\zeta_1, \zeta_2 \in [\nu_1, \nu_2]$, then the following equality holds:*

$$ \begin{aligned} &\frac{1}{6}\left[\phi(\nu_1+\nu_2-\zeta_1) + 4\phi\left(\nu_1+\nu_2-\frac{\zeta_1+\zeta_2}{2}\right) + \phi(\nu_1+\nu_2-\zeta_2)\right] \\ &- \frac{2^{\varpi-1}}{(\zeta_2-\zeta_1)^{\varpi}}\left[{}^{AB}_{(\nu_1+\nu_2-\zeta_1)}I^{\varpi}_{(\nu_1+\nu_2-\zeta_1+\zeta_2/2)}\phi\left(\nu_1+\nu_2-\frac{\zeta_1+\zeta_2}{2}\right)\right. \\ &\left. + {}^{AB}_{(\nu_1+\nu_2-\zeta_2)}I^{\varpi}_{\nu_1+\nu_2-\zeta_1+\zeta_2/2}\phi\left(\nu_1+\nu_2-\frac{\zeta_1+\zeta_2}{2}\right)\right] \\ &+ \frac{2(1-\varpi)2^{\varpi-1}}{B(\varpi)(\zeta_2-\zeta_1)^{\varpi}}\phi\left(\nu_1+\nu_2-\frac{\zeta_1+\zeta_2}{2}\right) \\ &= \frac{(\zeta_2-\zeta_1)^2}{8(\varpi+1)}\int_0^1 \frac{1}{B(\varpi)\Gamma(\varpi)}\left(\frac{1}{3}\left[1-2\varpi(1-\kappa) + \left(2-3\kappa^{\varpi}\right)\kappa\right]\right) \\ &\times\left[\phi''\left(\nu_1+\nu_2-\left(\frac{1+\kappa}{2}\zeta_2+\frac{1-\kappa}{2}\zeta_1\right)\right)\right. \\ &\left.+\phi''\left(\nu_1+\nu_2-\left(\frac{1+\kappa}{2}\zeta_1+\frac{1-\kappa}{2}\zeta_2\right)\right)\right]d\kappa. \end{aligned} \tag{10} $$

Proof. We note that

$$ \begin{aligned} I_1 = {}&\frac{1}{B(\varpi)\Gamma(\varpi)}\int_0^1\left(\frac{1}{3}\left[1-2\varpi(1-\kappa)+\left(2-3\kappa^{\varpi}\right)\kappa\right]\right) \\ &\times\left[\phi''\left(\nu_1+\nu_2-\left(\frac{1+\kappa}{2}\zeta_2+\frac{1-\kappa}{2}\zeta_1\right)\right)\right]d\kappa, \end{aligned} \tag{11} $$

using integration by parts; we obtain

$$ \begin{aligned} &= \frac{1}{B(\varpi)\Gamma(\varpi)}\left(\frac{1}{3}\left[1-2\varpi(1-\kappa)+\left(2-3\kappa^{\varpi}\right)\kappa\right]\right) \\ &\quad\cdot\left[\frac{\phi'(\nu_1+\nu_2-(((1+\kappa)/2)\zeta_2+((1-\kappa)/2)\zeta_1))}{(\zeta_1-\zeta_2)/2}\right]\Bigg|_0^1 \\ &\quad- \frac{1}{B(\varpi)\Gamma(\varpi)}\int_0^1\left(\frac{2(\varpi+1)}{3}-(\varpi+1)\kappa^{\varpi}\right) \\ &\quad\cdot\left[\frac{\phi'(\nu_1+\nu_2-(((1+\kappa)/2)\zeta_2+((1-\kappa)/2)\zeta_1))}{(\zeta_1-\zeta_2)/2}\right]d\kappa \\ &= \frac{-2(1-2\varpi)}{3(\zeta_1-\zeta_2)B(\varpi)\Gamma(\varpi)}\phi'\left(\nu_1+\nu_2-\frac{\zeta_1+\zeta_2}{2}\right) \\ &\quad- \frac{2}{(\zeta_1-\zeta_2)B(\varpi)\Gamma(\varpi)}\times\int_0^1\left(\frac{2(\varpi+1)}{3}-(\varpi+1)\kappa^{\varpi}\right) \\ &\quad\cdot\left[\phi'\left(\nu_1+\nu_2-\left(\frac{1+\kappa}{2}\zeta_2+\frac{1-\kappa}{2}\zeta_1\right)\right)\right]d\kappa \\ &= \frac{2(1-2\varpi)}{3(\zeta_2-\zeta_1)B(\varpi)\Gamma(\varpi)}\phi'\left(\nu_1+\nu_2-\frac{\zeta_1+\zeta_2}{2}\right) \\ &\quad+ \frac{4(\varpi+1)}{3(\zeta_2-\zeta_1)^2B(\varpi)\Gamma(\varpi)}\phi(\nu_1+\nu_2-\zeta_2) \\ &\quad+ \frac{8(\varpi+1)}{3(\zeta_2-\zeta_1)^2B(\varpi)\Gamma(\varpi)}\phi\left(\nu_1+\nu_2-\frac{\zeta_1+\zeta_2}{2}\right) \\ &\quad- \frac{4\varpi(\varpi+1)}{(\zeta_2-\zeta_1)^2B(\varpi)\Gamma(\varpi)}\int_0^1\kappa^{\varpi-1}\phi\left(\nu_1+\nu_2-\left(\frac{1+\kappa}{2}\zeta_2+\frac{1-\kappa}{2}\zeta_1\right)\right)d\kappa. \end{aligned} \tag{12} $$

By the change of the variable $\varkappa = \nu_1 + \nu_2 - (((1+\kappa)/2)\zeta_2 + ((1-\kappa)/2)\zeta_1)$ for $\kappa \in [0,1]$, we have

$$\begin{aligned}
&= \frac{2(1-2\varpi)}{3(\zeta_2-\zeta_1)B(\varpi)\Gamma(\varpi)}\phi'\left(\nu_1+\nu_2-\frac{\zeta_1+\zeta_2}{2}\right) \\
&\quad + \frac{4(\varpi+1)}{3(\zeta_2-\zeta_1)^2B(\varpi)\Gamma(\varpi)}\phi(\nu_1+\nu_2-\zeta_2) \\
&\quad + \frac{8(\varpi+1)}{3(\zeta_2-\zeta_1)^2B(\varpi)\Gamma(\varpi)}\phi\left(\nu_1+\nu_2-\frac{\zeta_1+\zeta_2}{2}\right) \\
&\quad - \frac{8\varpi(\varpi+1)2^{\varpi-1}}{B(\varpi)\Gamma(\varpi)(\zeta_2-\zeta_1)^{\varpi+2}}\int_{\nu_1+\nu_2-\zeta_2}^{\nu_1+\nu_2-\zeta_1+\zeta_2/2}\phi(\varkappa) \\
&\quad \cdot\left(\left(\nu_1+\nu_2-\frac{\zeta_1+\zeta_2}{2}\right)-\varkappa\right)^{\varpi-1}d\varkappa.
\end{aligned} \tag{13}$$

Add and subtract $(1-\varpi)/B(\varpi)(8(\varpi+1)2^{\varpi-1})/((\zeta_2-\zeta_1)^{\varpi+2})\phi(\nu_1+\nu_2-((\zeta_1+\zeta_2)/2))$ in Equation (13); we have

$$\begin{aligned}
&= \frac{2(1-2\varpi)}{3(\zeta_2-\zeta_1)B(\varpi)\Gamma(\varpi)}\phi'\left(\nu_1+\nu_2-\frac{\zeta_1+\zeta_2}{2}\right) \\
&\quad + \frac{4(\varpi+1)}{3(\zeta_2-\zeta_1)^2B(\varpi)\Gamma(\varpi)}\phi(\nu_1+\nu_2-\zeta_2) \\
&\quad + \frac{8(\varpi+1)}{3(\zeta_2-\zeta_1)^2B(\varpi)\Gamma(\varpi)}\phi\left(\nu_1+\nu_2-\frac{\zeta_1+\zeta_2}{2}\right) \\
&\quad - \left[\frac{(1-\varpi)}{B(\varpi)}\frac{8(\varpi+1)2^{\varpi-1}}{(\zeta_2-\zeta_1)^{\varpi+2}}\phi\left(\nu_1+\nu_2-\frac{\zeta_1+\zeta_2}{2}\right)\right. \\
&\quad + \frac{8\varpi(\varpi+1)2^{\varpi-1}}{B(\varpi)\Gamma(\varpi)(\zeta_2-\zeta_1)^{\varpi+2}}\int_{\nu_1+\nu_2-\zeta_2}^{\nu_1+\nu_2-\zeta_1+\zeta_2/2}\phi(\varkappa) \\
&\quad \left.\cdot\left(\left(\nu_1+\nu_2-\frac{\zeta_1+\zeta_2}{2}\right)-\mathrm{u}\right)^{\varpi-1}d\varkappa\right] \\
&\quad + \frac{(1-\varpi)}{B(\varpi)}\frac{8(\varpi+1)2^{\varpi-1}}{(\zeta_2-\zeta_1)^{\varpi+2}}\phi\left(\nu_1+\nu_2-\frac{\zeta_1+\zeta_2}{2}\right),
\end{aligned} \tag{14}$$

$$\begin{aligned}
&= \frac{2(1-2\varpi)}{3(\zeta_2-\zeta_1)B(\varpi)\Gamma(\varpi)}\phi'\left(\nu_1+\nu_2-\frac{\zeta_1+\zeta_2}{2}\right) \\
&\quad + \frac{4(\varpi+1)}{3(\zeta_2-\zeta_1)^2B(\varpi)\Gamma(\varpi)}\phi(\nu_1+\nu_2-\zeta_2) \\
&\quad + \frac{8(\varpi+1)}{3(\zeta_2-\zeta_1)^2B(\varpi)\Gamma(\varpi)}\phi\left(\nu_1+\nu_2-\frac{\zeta_1+\zeta_2}{2}\right) - \frac{8(\varpi+1)2^{\varpi-1}}{(\zeta_2-\zeta_1)^{\varpi+2}} \\
&\quad \cdot\left({}^{AB}_{(\nu_1+\nu_2-\zeta_2)}I^{\varpi}_{(\nu_1+\nu_2-((\zeta_1+\zeta_2)/2))}\phi\left(\nu_1+\nu_2-\frac{\zeta_1+\zeta_2}{2}\right)\right) \\
&\quad + \frac{(1-\varpi)}{B(\varpi)}\frac{8(\varpi+1)2^{\varpi-1}}{(\zeta_2-\zeta_1)^{\varpi+2}}\phi\left(\nu_1+\nu_2-\frac{\zeta_1+\zeta_2}{2}\right).
\end{aligned} \tag{15}$$

Similarly, we have

$$\begin{aligned}
I_2 &= \frac{1}{B(\varpi)\Gamma(\varpi)}\int_0^1\left(\frac{1}{3}\left[1-2\varpi(1-\kappa)+\left(2-3\kappa^{\varpi}\right)\kappa\right]\right) \\
&\quad \times\left[\phi''\left(\nu_1+\nu_2-\left(\frac{1+\kappa}{2}\zeta_1+\frac{1-\kappa}{2}\zeta_2\right)\right)\right]d\kappa,
\end{aligned} \tag{16}$$

using integration by parts; we obtain

$$\begin{aligned}
&= \frac{-2(1-2\varpi)}{3(\zeta_2-\zeta_1)B(\varpi)\Gamma(\varpi)}\phi'\left(\nu_1+\nu_2-\frac{\zeta_1+\zeta_2}{2}\right) \\
&\quad + \frac{4(\varpi+1)}{3(\zeta_2-\zeta_1)^2B(\varpi)\Gamma(\varpi)}\phi(\nu_1+\nu_2-\zeta_1) \\
&\quad + \frac{8(\varpi+1)}{3(\zeta_2-\zeta_1)^2B(\varpi)\Gamma(\varpi)}\phi\left(\nu_1+\nu_2-\frac{\zeta_1+\zeta_2}{2}\right) \\
&\quad - \frac{4\varpi(\varpi+1)}{(\zeta_2-\zeta_1)^2B(\varpi)\Gamma(\varpi)}\int_0^1\kappa^{\varpi-1}\phi \\
&\quad \cdot\left(\nu_1+\nu_2-\left(\frac{1+\kappa}{2}\zeta_1+\frac{1-\kappa}{2}\zeta_2\right)\right)d\kappa.
\end{aligned} \tag{17}$$

By the change of the variable $\varkappa = \nu_1 + \nu_2 - (((1+\kappa)/2)\zeta_1 + ((1-\kappa)/2)\zeta_2)$ for $\kappa \in [0,1]$, we have

$$\begin{aligned}
&= \frac{-2(1-2\varpi)}{3(\zeta_2-\zeta_1)B(\varpi)\Gamma(\varpi)}\phi'\left(\nu_1+\nu_2-\frac{\zeta_1+\zeta_2}{2}\right) \\
&\quad + \frac{4(\varpi+1)}{3(\zeta_2-\zeta_1)^2B(\varpi)\Gamma(\varpi)}\phi(\nu_1+\nu_2-\zeta_1) \\
&\quad + \frac{8(\varpi+1)}{3(\zeta_2-\zeta_1)^2B(\varpi)\Gamma(\varpi)}\phi\left(\nu_1+\nu_2-\frac{\zeta_1+\zeta_2}{2}\right),
\end{aligned} \tag{18}$$

$$\begin{aligned}
&-\frac{8\varpi(\varpi+1)2^{\varpi-1}}{B(\varpi)\Gamma(\varpi)(\zeta_2-\zeta_1)^{\varpi+2}}\int_{\nu_1+\nu_2-\zeta_1+\zeta_2/2}^{\nu_1+\nu_2-\zeta_1}\phi(\varkappa) \\
&\cdot\left(\varkappa-\left(\nu_1+\nu_2-\frac{\zeta_1+\zeta_2}{2}\right)\right)^{\varpi-1}d\varkappa.
\end{aligned} \tag{19}$$

Add and subtract $(1-\varpi/B(\varpi))(8(\varpi+1)2^{\varpi-1}/(\zeta_2-\zeta_1)^{\varpi+2})\phi(\nu_1+\nu_2-\zeta_1+\zeta_2/2)$ in Equation (19); we have

$$\begin{aligned}
&= \frac{-2(1-2\varpi)}{3(\zeta_2-\zeta_1)B(\varpi)\Gamma(\varpi)}\phi'\left(\nu_1+\nu_2-\frac{\zeta_1+\zeta_2}{2}\right) \\
&\quad + \frac{4(\varpi+1)}{3(\zeta_2-\zeta_1)^2B(\varpi)\Gamma(\varpi)}\phi(\nu_1+\nu_2-\zeta_1) \\
&\quad + \frac{8(\varpi+1)}{3(\zeta_2-\zeta_1)^2B(\varpi)\Gamma(\varpi)}\phi\left(\nu_1+\nu_2-\frac{\zeta_1+\zeta_2}{2}\right) \\
&\quad - \left[\frac{(1-\varpi)}{B(\varpi)}\frac{8(\varpi+1)2^{\varpi-1}}{(\zeta_2-\zeta_1)^{\varpi+2}}\phi\left(\nu_1+\nu_2-\frac{\zeta_1+\zeta_2}{2}\right)\right.
\end{aligned}$$

$$+\frac{8\varpi(\varpi+1)2^{\varpi-1}}{B(\varpi)\Gamma(\varpi)(\zeta_2-\zeta_1)^{\varpi+2}}\int_{\nu_1+\nu_2-\zeta_1+\zeta_2/2}^{\nu_1+\nu_2-\zeta_1}\phi(\varkappa)\cdot\left(\left(\nu_1+\nu_2-\frac{\zeta_1+\zeta_2}{2}\right)-\varkappa\right)^{\varpi-1}d\varkappa] + \frac{(1-\varpi)}{B(\varpi)}\frac{8(\varpi+1)2^{\varpi-1}}{(\zeta_2-\zeta_1)^{\varpi+2}}\phi\left(\nu_1+\nu_2-\frac{\zeta_1+\zeta_2}{2}\right), \tag{20}$$

$$= \frac{-2(1-2\varpi)}{3(\zeta_2-\zeta_1)B(\varpi)\Gamma(\varpi)}\phi'\left(\nu_1+\nu_2-\frac{\zeta_1+\zeta_2}{2}\right) + \frac{4(\varpi+1)}{3(\zeta_2-\zeta_1)^2B(\varpi)\Gamma(\varpi)}\phi(\nu_1+\nu_2-\zeta_1) + \frac{8(\varpi+1)}{3(\zeta_2-\zeta_1)^2B(\varpi)\Gamma(\varpi)}\phi\left(\nu_1+\nu_2-\frac{\zeta_1+\zeta_2}{2}\right) - \frac{8(\varpi+1)2^{\varpi-1}}{(\zeta_2-\zeta_1)^{\varpi+2}}\cdot\left({}^{AB}_{(\nu_1+\nu_2-\zeta_1)}I^{\varpi}_{(\nu_1+\nu_2-\zeta_1+\zeta_2/2)}\phi\left(\nu_1+\nu_2-\frac{\zeta_1+\zeta_2}{2}\right)\right) + \frac{(1-\varpi)}{B(\varpi)}\frac{8(\varpi+1)2^{\varpi-1}}{(\zeta_2-\zeta_1)^{\varpi+2}}\phi\left(\nu_1+\nu_2-\frac{\zeta_1+\zeta_2}{2}\right). \tag{21}$$

Add Equations (15) and (21), also multiplying both sides by $(\zeta_2-\zeta_1)^2/8(\varpi+1)$, then we get

$$\frac{1}{6}\left[\phi(\nu_1+\nu_2-\zeta_1)+4\phi\left(\nu_1+\nu_2-\frac{\zeta_1+\zeta_2}{2}\right)+\phi(\nu_1+\nu_2-\zeta_2)\right] - \frac{2^{\varpi-1}}{(\zeta_2-\zeta_1)^{\varpi}}\left[{}^{AB}_{(\nu_1+\nu_2-\zeta_1)}I^{\varpi}_{(\nu_1+\nu_2-\zeta_1+\zeta_2/2)}\phi\left(\nu_1+\nu_2-\frac{\zeta_1+\zeta_2}{2}\right) + {}^{AB}_{(\nu_1+\nu_2-\zeta_2)}I^{\varpi}_{\nu_1+\nu_2-\zeta_1+\zeta_2/2}\phi\left(\nu_1+\nu_2-\frac{\zeta_1+\zeta_2}{2}\right)\right] + \frac{2(1-\varpi)2^{\varpi-1}}{B(\varpi)(\zeta_2-\zeta_1)^{\varpi}}\phi\left(\nu_1+\nu_2-\frac{\zeta_1+\zeta_2}{2}\right). \tag{22}$$

This concludes Lemma's proof. □

Remark 7. If we choose $\varpi=1$, $\nu_1=\zeta_1$, and $\nu_2=\zeta_2$ in Lemma 6, then we have

$$\frac{1}{6}\left[\phi(\zeta_1)+4\phi\left(\frac{\zeta_1+\zeta_2}{2}\right)+\phi(\zeta_2)\right]-\frac{1}{\zeta_2-\zeta_1}\int_{\zeta_1}^{\zeta_2}\phi(\varkappa)d\varkappa = \frac{(\zeta_2-\zeta_1)^2}{48}\int_0^1\left[4\kappa-3\kappa^2-1\right]\cdot\left[\phi''\left(\frac{1+\kappa}{2}\zeta_1+\frac{1-\kappa}{2}\zeta_2\right)+\phi''\left(\frac{1+\kappa}{2}\zeta_2+\frac{1-\kappa}{2}\zeta_1\right)\right]d\kappa, \tag{23}$$

which is a new equality in literature.

Remark 8. If we choose $\nu_1=\zeta_1$ and $\nu_2=\zeta_2$ in Lemma 6, then we have

$$\frac{1}{6}\left[\phi(\zeta_1)+4\phi\left(\frac{\zeta_1+\zeta_2}{2}\right)+\phi(\zeta_2)\right]-\frac{2^{\varpi-1}}{(\zeta_2-\zeta_1)^{\varpi}}\cdot\left[{}^{AB}_{\zeta_2}I^{\varpi}_{(\zeta_1+\zeta_2/2)}\phi\left(\frac{\zeta_1+\zeta_2}{2}\right)+{}^{AB}_{\zeta_1}I^{\varpi}_{\zeta_1+\zeta_2/2}\phi\left(\frac{\zeta_1+\zeta_2}{2}\right)\right] + \frac{2(1-\varpi)2^{\varpi-1}}{B(\varpi)(\zeta_2-\zeta_1)^{\varpi}}\phi\left(\frac{\zeta_1+\zeta_2}{2}\right) = \frac{(\zeta_2-\zeta_1)^2}{8(\varpi+1)}\int_0^1\frac{1}{B(\varpi)\Gamma(\varpi)}\left(\frac{1}{3}\left[1-2\varpi(1-\kappa)+\left(2-3\kappa^{\varpi}\right)\kappa\right]\right)\times\left[\phi''\left(\frac{1+\kappa}{2}\zeta_1+\frac{1-\kappa}{2}\zeta_2\right)+\phi''\left(\left(\frac{1+\kappa}{2}\zeta_2+\frac{1-\kappa}{2}\zeta_1\right)\right)\right]d\kappa, \tag{24}$$

which is a new equality via the Atangana-Baleanu in fractional calculus.

Theorem 9. *Let ϕ be defined as in Lemma 6, and if $|\phi''|$ is convex on $[\nu_1,\nu_2]$, then we have the following inequality:*

$$\left|\frac{1}{6}\left[\phi(\nu_1+\nu_2-\zeta_1)+4\phi\left(\nu_1+\nu_2-\frac{\zeta_1+\zeta_2}{2}\right)+\phi(\nu_1+\nu_2-\zeta_2)\right] - \frac{2^{\varpi-1}}{(\zeta_2-\zeta_1)^{\varpi}}\left[{}^{AB}_{(\nu_1+\nu_2-\zeta_1)}I^{\varpi}_{(\nu_1+\nu_2-\zeta_1+\zeta_2/2)}\phi\left(\nu_1+\nu_2-\frac{\zeta_1+\zeta_2}{2}\right) + {}^{AB}_{(\nu_1+\nu_2-\zeta_2)}I^{\varpi}_{\nu_1+\nu_2-\zeta_1+\zeta_2/2}\phi\left(\nu_1+\nu_2-\frac{\zeta_1+\zeta_2}{2}\right)\right] + \frac{2(1-\varpi)2^{\varpi-1}}{B(\varpi)(\zeta_2-\zeta_1)^{\varpi}}\phi\left(\nu_1+\nu_2-\frac{\zeta_1+\zeta_2}{2}\right)\right| \le \frac{(\zeta_2-\zeta_1)^2}{8(\varpi+1)}Y_1(\varpi)\left[2|\phi''(\nu_1)|+2|\phi''(\nu_2)|-\left[|\phi''(\zeta_1)|+|\phi''(\zeta_2)|\right]\right], \tag{25}$$

where $Y_1(\varpi)$ is defined by

$$Y_1(\varpi)=\begin{cases}\dfrac{1}{B(\varpi)\Gamma(\varpi)}\dfrac{(1-\varpi)^2}{3(\varpi+2)}, & \text{if } 0<\varpi\le\dfrac{1}{2},\\[2ex] \dfrac{1}{B(\varpi)\Gamma(\varpi)}\left(2\left(\dfrac{(\kappa_{\varpi})^{\varpi+2}}{(\varpi+2)}-\dfrac{(1-2\varpi)\kappa_{\varpi}+(\varpi+1)(\kappa_{\varpi})^2}{3}\right)+\dfrac{(1-\varpi)^2}{3(\varpi+2)}\right), & \text{if } \varpi>\dfrac{1}{2}.\end{cases} \tag{26}$$

Proof. We will start the proof by looking at modulus in Lemma 6,

$$\begin{aligned}
&\left|\frac{1}{6}\left[\phi(\nu_1+\nu_2-\zeta_1)+4\phi\left(\nu_1+\nu_2-\frac{\zeta_1+\zeta_2}{2}\right)+\phi(\nu_1+\nu_2-\zeta_2)\right]\right.\\
&\quad-\frac{2^{\varpi-1}}{(\zeta_2-\zeta_1)^{\varpi}}\left[{}^{AB}_{(\nu_1+\nu_2-\zeta_1)}I^{\varpi}_{(\nu_1+\nu_2-\zeta_1+\zeta_2/2)}\phi\left(\nu_1+\nu_2-\frac{\zeta_1+\zeta_2}{2}\right)\right.\\
&\quad\left.+{}^{AB}_{(\nu_1+\nu_2-\zeta_2)}I^{\varpi}_{\nu_1+\nu_2-\zeta_1+\zeta_2/2}\phi\left(\nu_1+\nu_2-\frac{\zeta_1+\zeta_2}{2}\right)\right]\\
&\quad\left.+\frac{2(1-\varpi)2^{\varpi-1}}{B(\varpi)(\zeta_2-\zeta_1)^{\varpi}}\phi\left(\nu_1+\nu_2-\frac{\zeta_1+\zeta_2}{2}\right)\right|\\
&\le\frac{(\zeta_2-\zeta_1)^2}{8(\varpi+1)}\frac{1}{B(\varpi)\Gamma(\varpi)}\int_0^1\left|\left(\frac{1}{3}\left[1-2\varpi(1-\kappa)+\left(2-3\kappa^{\varpi}\right)\kappa\right]\right)\right|\\
&\quad\times\left[\left|\phi''\left(\nu_1+\nu_2-\left(\frac{1+\kappa}{2}\zeta_2+\frac{1-\kappa}{2}\zeta_1\right)\right)\right|\right.\\
&\quad\left.+\left|\phi''\left(\nu_1+\nu_2-\left(\frac{1+\kappa}{2}\zeta_1+\frac{1-\kappa}{2}\zeta_2\right)\right)\right|\right]d\kappa.
\end{aligned}\tag{27}$$

By using the convexity of $|\phi''|$ with Jensen-Mercer Inequality, we have

$$\begin{aligned}
&\left|\frac{1}{6}\left[\phi(\nu_1+\nu_2-\zeta_1)+4\phi\left(\nu_1+\nu_2-\frac{\zeta_1+\zeta_2}{2}\right)+\phi(\nu_1+\nu_2-\zeta_2)\right]\right.\\
&\quad-\frac{2^{\varpi-1}}{(\zeta_2-\zeta_1)^{\varpi}}\left[{}^{AB}_{(\nu_1+\nu_2-\zeta_1)}I^{\varpi}_{(\nu_1+\nu_2-\zeta_1+\zeta_2/2)}\phi\left(\nu_1+\nu_2-\frac{\zeta_1+\zeta_2}{2}\right)\right.\\
&\quad\left.+{}^{AB}_{(\nu_1+\nu_2-\zeta_2)}I^{\varpi}_{\nu_1+\nu_2-\zeta_1+\zeta_2/2}\phi\left(\nu_1+\nu_2-\frac{\zeta_1+\zeta_2}{2}\right)\right]\\
&\quad\left.+\frac{2(1-\varpi)2^{\varpi-1}}{B(\varpi)(\zeta_2-\zeta_1)^{\varpi}}\phi\left(\nu_1+\nu_2-\frac{\zeta_1+\zeta_2}{2}\right)\right|\\
&\le\frac{(\zeta_2-\zeta_1)^2}{8(\varpi+1)}\frac{1}{B(\varpi)\Gamma(\varpi)}\int_0^1\left|\left(\frac{1}{3}\left[1-2\varpi(1-\kappa)+\left(2-3\kappa^{\varpi}\right)\kappa\right]\right)\right|\\
&\quad\times\left[|\phi''(\nu_1)|+|\phi''(\nu_2)|-\left(\frac{1+\kappa}{2}|\phi''(\zeta_2)|+\frac{1-\kappa}{2}|\phi''(\zeta_1)\right)\right.\\
&\quad\left.+|\phi''(\nu_1)|+|\phi''(\nu_1)|-\left(\frac{1+\kappa}{2}|\phi''(\zeta_1)|+\frac{1-\kappa}{2}|\phi''(\zeta_2)\right)\right]d\kappa.
\end{aligned}\tag{28}$$

⇒ To evaluate the above integral, assume the mapping $\varsigma:[0,1]\longrightarrow\mathbb{R}$ where

$$\varsigma(\kappa)=\frac{1}{B(\varpi)\Gamma(\varpi)}\left(\frac{1}{3}\left[1-2\varpi(1-\kappa)+\left(2-3\kappa^{\varpi}\right)\kappa\right]\right)\text{ with }\varpi>0.\tag{29}$$

(1) If $0<\varpi\le(1/2)$, then we have

$$\int_0^1|\varsigma(\kappa)|d\kappa=\frac{1}{B(\varpi)\Gamma(\varpi)}\frac{1-\varpi^2}{3(\varpi+2)}.\tag{30}$$

(2) If $\varpi>(1/2)$, then there exists a real number κ_{ϖ} such that $0<\varpi<1$, and we have

$$\int_0^1|\varsigma(\kappa)|d\kappa=\frac{1}{B(\varpi)\Gamma(\varpi)}\left(2\left(\frac{(\kappa_{\varpi})^{\varpi+2}}{\varpi+2}-\frac{(1-2\varpi)\kappa_{\varpi}+(\varpi+1)(\kappa_{\varpi})^2}{3}\right)+\frac{1-\varpi^2}{3(\varpi+2)}\right).\tag{31}$$

Hence, we have

$$\begin{aligned}
&\Rightarrow\left|\frac{1}{6}\left[\phi(\nu_1+\nu_2-\zeta_1)+4\phi\left(\nu_1+\nu_2-\frac{\zeta_1+\zeta_2}{2}\right)+\phi(\nu_1+\nu_2-\zeta_2)\right]\right.\\
&\quad-\frac{2^{\varpi-1}}{(\zeta_2-\zeta_1)^{\varpi}}\left[{}^{AB}_{(\nu_1+\nu_2-\zeta_1)}I^{\varpi}_{(\nu_1+\nu_2-\zeta_1+\zeta_2/2)}\phi\left(\nu_1+\nu_2-\frac{\zeta_1+\zeta_2}{2}\right)\right.\\
&\quad\left.+{}^{AB}_{(\nu_1+\nu_2-\zeta_2)}I^{\varpi}_{\nu_1+\nu_2-\zeta_1+\zeta_2/2}\phi\left(\nu_1+\nu_2-\frac{\zeta_1+\zeta_2}{2}\right)\right]\\
&\quad\left.+\frac{2(1-\varpi)2^{\varpi-1}}{B(\varpi)(\zeta_2-\zeta_1)^{\varpi}}\phi\left(\nu_1+\nu_2-\frac{\zeta_1+\zeta_2}{2}\right)\right|\\
&\le\frac{(\zeta_2-\zeta_1)^2}{8(\varpi+1)}Y_1(\varpi)\left[2|\phi''(\nu_1)|+2|\phi''(\nu_2)|-\left[|\phi''(\zeta_1)|+|\phi''(\zeta_2)|\right]\right].
\end{aligned}\tag{32}$$

This concludes theorem's proof. □

Remark 10. If we choose $\varpi=1$ and $\kappa_{\varpi}=1/3$, in Theorem 9, then we have the inequality

$$\begin{aligned}
&\left|\frac{1}{6}\left[\phi(\nu_1+\nu_2-\zeta_1)+4\phi\left(\nu_1+\nu_2-\frac{\zeta_1+\zeta_2}{2}\right)+\phi(\nu_1+\nu_2-\zeta_2)\right]\right.\\
&\quad\left.-\frac{1}{\zeta_2-\zeta_1}\int_{\nu_1+\nu_2-\zeta_2}^{\nu_1+\nu_2-\zeta_1}\phi(\varkappa)d\varkappa\right|\\
&\quad\le\frac{(\zeta_2-\zeta_1)^2}{162}\left[2|\phi''(\nu_1)|+2|\phi''(\nu_2)|-\left[|\phi''(\zeta_1)|+|\phi''(\zeta_2)|\right]\right],
\end{aligned}\tag{33}$$

which is Mercer variant of an identity proved by Sarikaya et al. in [19].

Remark 11. If we choose $\varpi=1$, $\nu_1=\zeta_1$, and $\nu_2=\zeta_2$ in Theorem 9, then $\kappa_{\varpi}=1/3$, and we have the inequality

$$\begin{aligned}
&\left|\frac{1}{6}\left[\phi(\zeta_1)+4\phi\left(\frac{\zeta_1+\zeta_2}{2}\right)+\phi(\zeta_2)\right]-\frac{1}{\zeta_2-\zeta_1}\int_{\zeta_1}^{\zeta_2}\phi(\varkappa)d\varkappa\right|\\
&\quad\le\frac{(\zeta_2-\zeta_1)^2}{162}\left[|\phi''(\zeta_1)|+|\phi''(\zeta_2)|\right],
\end{aligned}\tag{34}$$

which is proved by Sarikaya et al. in [19].

Remark 12. If we choose $\nu_1 = \zeta_1$ and $\nu_2 = \zeta_2$ in Theorem 9, then we have the inequality

$$\left|\frac{1}{6}\left[\phi(\zeta_1) + 4\phi\left(\frac{\zeta_1+\zeta_2}{2}\right) + \phi(\zeta_2)\right] - \frac{2^{\varpi-1}\Gamma(1+\varpi)}{(\zeta_2-\zeta_1)^{\varpi}}\left[J^{\varpi}_{\zeta_2-}\phi\left(\frac{\zeta_1+\zeta_2}{2}\right) + J^{\varpi}_{\zeta_1+}\phi\left(\frac{\zeta_1+\zeta_2}{2}\right)\right]\right| \leq \frac{(\zeta_2-\zeta_1)^2}{8(\varpi+1)}\Omega_1(\varpi)\left[\left|\phi''(\zeta_1)\right| + \left|\phi''(\zeta_2)\right|\right]\Big|, \tag{35}$$

which is proved by Hezenci et al. in [14].

Remark 13. If we choose $\varpi = 1$ and $\kappa_{\varpi} = 1/3$ in Remark 12 then we have the inequality

$$\left|\frac{1}{6}\left[\phi(\zeta_1) + 4\phi\left(\frac{\zeta_1+\zeta_2}{2}\right) + \phi(\zeta_2)\right] - \frac{1}{\zeta_2-\zeta_1}\int_{\zeta_1}^{\zeta_2}\phi(\varkappa)d\varkappa\right| \leq \frac{(\zeta_2-\zeta_1)^2}{162}\left[\left|\phi''(\zeta_1)\right| + \left|\phi''(\zeta_2)\right|\right], \tag{36}$$

which is proved by Sarikaya et al. in [19].

Theorem 14. *Let ϕ be defined as in Lemma 6, then for $\mathfrak{q} > 1$, there is a mapping $|\phi''|^{\mathfrak{q}}$ that is convex on $[\nu_1, \nu_2]$, then we have identity:*

$$\begin{aligned}&\left|\frac{1}{6}\left[\phi(\nu_1+\nu_2-\zeta_1) + 4\phi\left(\nu_1+\nu_2-\frac{\zeta_1+\zeta_2}{2}\right) + \phi(\nu_1+\nu_2-\zeta_2)\right]\right.\\ &\quad - \frac{2^{\varpi-1}}{(\zeta_2-\zeta_1)^{\varpi}}\left[{}^{AB}_{(\nu_1+\nu_2-\zeta_1)}I^{\varpi}_{(\nu_1+\nu_2-\zeta_1+\zeta_2/2)}\phi\left(\nu_1+\nu_2-\frac{\zeta_1+\zeta_2}{2}\right)\right.\\ &\quad \left. + {}^{AB}_{(\nu_1+\nu_2-\zeta_2)}I^{\varpi}_{\nu_1+\nu_2-\zeta_1+\zeta_2/2}\phi\left(\nu_1+\nu_2-\frac{\zeta_1+\zeta_2}{2}\right)\right]\\ &\quad \left. + \frac{2(1-\varpi)2^{\varpi-1}}{B(\varpi)(\zeta_2-\zeta_1)^{\varpi}}\phi\left(\nu_1+\nu_2-\frac{\zeta_1+\zeta_2}{2}\right)\right|\\ &\leq \frac{(\zeta_2-\zeta_1)^2}{8(\varpi+1)}Y_1(\varpi,p)\left(\frac{1}{B(\varpi)\Gamma(\varpi)}\left[2\left|\phi''(\nu_1)\right|^{\mathfrak{q}} + 2\left|\phi''(\nu_2)\right|^{\mathfrak{q}}\right.\right.\\ &\quad \left.\left. - \left(\left|\phi''(\zeta_2)\right|^{\mathfrak{q}} + \left|\phi''(\zeta_1)\right|^{\mathfrak{q}}\right)\right]\right)^{1/\mathfrak{q}},\end{aligned} \tag{37}$$

where $\mathfrak{p}, \mathfrak{q} > 1$ are conjugate exponents and Y is defined by

$$Y_1(\varpi,\mathfrak{p}) = \left(\frac{1}{B(\varpi)\Gamma(\varpi)}\int_0^1\left|\frac{1}{3}\left[1-2\varpi(1-\kappa) + \left(2-3\kappa^{\varpi}\right)\kappa\right]\right|^{p}d\kappa\right)^{1/\mathfrak{p}}. \tag{38}$$

Proof. Using Hölder's inequality in Lemma 6, we obtain

$$\begin{aligned}&\left|\frac{1}{6}\left[\phi(\nu_1+\nu_2-\zeta_1) + 4\phi\left(\nu_1+\nu_2-\frac{\zeta_1+\zeta_2}{2}\right) + \phi(\nu_1+\nu_2-\zeta_2)\right]\right.\\ &\quad - \frac{2^{\varpi-1}}{(\zeta_2-\zeta_1)^{\varpi}}\left[{}^{AB}_{(\nu_1+\nu_2-\zeta_1)}I^{\varpi}_{(\nu_1+\nu_2-\zeta_1+\zeta_2/2)}\phi\left(\nu_1+\nu_2-\frac{\zeta_1+\zeta_2}{2}\right)\right.\\ &\quad \left. + {}^{AB}_{(\nu_1+\nu_2-\zeta_2)}I^{\varpi}_{\nu_1+\nu_2-\zeta_1+\zeta_2/2}\phi\left(\nu_1+\nu_2-\frac{\zeta_1+\zeta_2}{2}\right)\right]\\ &\quad \left. + \frac{2(1-\varpi)2^{\varpi-1}}{B(\varpi)(\zeta_2-\zeta_1)^{\varpi}}\phi\left(\nu_1+\nu_2-\frac{\zeta_1+\zeta_2}{2}\right)\right|\\ &\leq \frac{(\zeta_2-\zeta_1)^2}{8(\varpi+1)} \times \left\{\left(\frac{1}{B(\varpi)\Gamma(\varpi)}\int_0^1\left|\left(\frac{1}{3}[1-2\varpi(1-\kappa)\right.\right.\right.\right.\\ &\quad \left.\left. + \left(2-3\kappa^{\varpi}\right)\kappa]\right)\Big|^{\mathfrak{p}}d\kappa\right)^{1/\mathfrak{p}}\left(\frac{1}{B(\varpi)\Gamma(\varpi)}\int_0^1\right|\phi''\\ &\quad \cdot\left.\left(\nu_1+\nu_2-\left(\frac{1+\kappa}{2}\zeta_2+\frac{1-\kappa}{2}\zeta_1\right)\right)\right|^{\mathfrak{q}}d\kappa\Bigg)^{1/\mathfrak{q}}\\ &\quad + \left(\frac{1}{B(\varpi)\Gamma(\varpi)}\int_0^1\left|\left(\frac{1}{3}\left[1-2\varpi(1-\kappa) + \left(2-3\kappa^{\varpi}\right)\kappa\right]\right)\right|^{\mathfrak{p}}d\kappa\right)^{1/\mathfrak{p}}\\ &\quad \left.\cdot\left(\frac{1}{B(\varpi)\Gamma(\varpi)}\int_0^1\left|\phi''\left(\nu_1+\nu_2-\left(\frac{1+\kappa}{2}\zeta_1+\frac{1-\kappa}{2}\zeta_2\right)\right)\right|^{\mathfrak{q}}d\kappa\right)^{1/\mathfrak{q}}\right\}.\end{aligned} \tag{39}$$

By using the convexity of $|\phi''|^{\mathfrak{q}}$ with Jensen-Mercer Inequality, we obtain

$$\begin{aligned}&\left|\frac{1}{6}\left[\phi(\nu_1+\nu_2-\zeta_1) + 4\phi\left(\nu_1+\nu_2-\frac{\zeta_1+\zeta_2}{2}\right) + \phi(\nu_1+\nu_2-\zeta_2)\right]\right.\\ &\quad - \frac{2^{\varpi-1}}{(\zeta_2-\zeta_1)^{\varpi}}\left[{}^{AB}_{(\nu_1+\nu_2-\zeta_1)}I^{\varpi}_{(\nu_1+\nu_2-\zeta_1+\zeta_2/2)}\phi\left(\nu_1+\nu_2-\frac{\zeta_1+\zeta_2}{2}\right)\right.\\ &\quad \left. + {}^{AB}_{(\nu_1+\nu_2-\zeta_2)}I^{\varpi}_{\nu_1+\nu_2-\zeta_1+\zeta_2/2}\phi\left(\nu_1+\nu_2-\frac{\zeta_1+\zeta_2}{2}\right)\right]\\ &\quad \left. + \frac{2(1-\varpi)2^{\varpi-1}}{B(\varpi)(\zeta_2-\zeta_1)^{\varpi}}\phi\left(\nu_1+\nu_2-\frac{\zeta_1+\zeta_2}{2}\right)\right|\\ &\leq \frac{(\zeta_2-\zeta_1)^2}{8(\varpi+1)}\left(\frac{1}{B(\varpi)\Gamma(\varpi)}\int_0^1\left|\left(\frac{1}{3}\left[1-2\varpi(1-\kappa) + \left(2-3\kappa^{\varpi}\right)\kappa\right]\right)\right|^{\mathfrak{p}}d\kappa\right)^{1/\mathfrak{p}}\\ &\quad \times\left\{\frac{1}{B(\varpi)\Gamma(\varpi)}\left(\int_0^1\left(\left|\phi''(\nu_1)\right|^q + \left|\phi''(\nu_2)\right|^q\right.\right.\right.\\ &\quad \left.\left. - \left(\frac{1+\kappa}{2}\left|\phi''(\zeta_2)\right|^q + \frac{1-\kappa}{2}\left|\phi''(\zeta_1)\right|^q\right)\right)d\kappa\right)^{1/\mathfrak{q}}\\ &\quad + \left(\frac{1}{B(\varpi)\Gamma(\varpi)}\int_0^1\left(\left|\phi''(\nu_1)\right|^q + \left|\phi''(\nu_2)\right|^q\right.\right.\\ &\quad \left.\left.\left. - \left(\frac{1+\kappa}{2}\left|\phi''(\zeta_2)\right|^q + \frac{1-\kappa}{2}\left|\phi''(\zeta_1)\right|^q\right)\right)d\kappa\right)^{1/\mathfrak{q}}\right\}.\end{aligned} \tag{40}$$

$$\begin{aligned}&\Rightarrow\left|\frac{1}{6}\left[\phi(\nu_1+\nu_2-\zeta_1) + 4\phi\left(\nu_1+\nu_2-\frac{\zeta_1+\zeta_2}{2}\right) + \phi(\nu_1+\nu_2-\zeta_2)\right]\right.\\ &\quad - \frac{2^{\varpi-1}}{(\zeta_2-\zeta_1)^{\varpi}}\left[{}^{AB}_{(\nu_1+\nu_2-\zeta_1)}I^{\varpi}_{(\nu_1+\nu_2-\zeta_1+\zeta_2/2)}\phi\left(\nu_1+\nu_2-\frac{\zeta_1+\zeta_2}{2}\right)\right.\\ &\quad \left. + {}^{AB}_{(\nu_1+\nu_2-\zeta_2)}I^{\varpi}_{\nu_1+\nu_2-\zeta_1+\zeta_2/2}\phi\left(\nu_1+\nu_2-\frac{\zeta_1+\zeta_2}{2}\right)\right]\\ &\quad \left. + \frac{2(1-\varpi)2^{\varpi-1}}{B(\varpi)(\zeta_2-\zeta_1)^{\varpi}}\phi\left(\nu_1+\nu_2-\frac{\zeta_1+\zeta_2}{2}\right)\right|\end{aligned}$$

$$\leq \frac{(\zeta_2-\zeta_1)^2}{8(\varpi+1)}\left(\frac{1}{B(\varpi)\Gamma(\varpi)}\int_0^1\left|\left(\frac{1}{3}\left[1-2\varpi(1-\kappa)+\left(2-3\kappa^{\varpi}\right)\kappa\right]\right)\right|^{\mathfrak{p}}d\kappa\right)^{1/\mathfrak{p}}$$
$$\times\left\{\left(\frac{1}{B(\varpi)\Gamma(\varpi)}\left(\left|\phi''(\nu_1)\right|^{\mathfrak{q}}+\left|\phi''(\nu_2)\right|^{\mathfrak{q}}-\frac{3\left|\phi''(\zeta_2)\right|^{\mathfrak{q}}+\left|f''(\zeta_1)\right|^{\mathfrak{q}}}{4}\right)\right)^{1/\mathfrak{q}}\right.$$
$$\left.+\left(\frac{1}{B(\varpi)\Gamma(\varpi)}\left(\left|\phi''(\nu_1)\right|^{\mathfrak{q}}+\left|\phi''(\nu_2)\right|^{\mathfrak{q}}-\frac{\left|\phi''(\zeta_2)\right|^{\mathfrak{q}}+3\left|\phi''(\zeta_1)\right|^{\mathfrak{q}}}{4}\right)\right)^{1/\mathfrak{q}}\right\}. \tag{41}$$

This concludes theorem's proof. □

Corollary 15. *If we choose $\varpi = 1$, $\nu_1 = \zeta_1$, and $\nu_2 = \zeta_2$ in Theorem 14, then $t_\varpi = 1/3$, and we have the inequality*

$$\left|\frac{1}{6}\left[\phi(\zeta_1)+4\phi\left(\frac{\zeta_1+\zeta_2}{2}\right)+\phi(\zeta_2)\right]-\frac{1}{\zeta_2-\zeta_1}\int_{\zeta_1}^{\zeta_2}\phi(\varkappa)d\varkappa\right|$$
$$\leq \frac{(\zeta_2-\zeta_1)^2}{162}Y(1,\mathfrak{p})\left[\left|\phi''(\zeta_1)\right|^{\mathfrak{q}}+\left|\phi''(\zeta_2)\right|^{\mathfrak{q}}\right]^{1/\mathfrak{q}}, \tag{42}$$

which is given by Hezenci et al. in [14].

Theorem 16. *Let ϕ be defined as in Lemma 6, then for $\mathfrak{q} > 1$, there is a mapping $|\phi''|^{\mathfrak{q}}$ that is convex on $[\nu_1, \nu_2]$, then we have identity:*

$$\left|\frac{1}{6}\left[\phi(\nu_1+\nu_2-\zeta_1)+4\phi\left(\nu_1+\nu_2-\frac{\zeta_1+\zeta_2}{2}\right)+\phi(\nu_1+\nu_2-\zeta_2)\right]\right.$$
$$-\frac{2^{\varpi-1}}{(\zeta_2-\zeta_1)^{\varpi}}\left[{}^{AB}_{(\nu_1+\nu_2-\zeta_1)}I^{\varpi}_{(\nu_1+\nu_2-\zeta_1+\zeta_2/2)}\phi\left(\nu_1+\nu_2-\frac{\zeta_1+\zeta_2}{2}\right)\right.$$
$$\left.+{}^{AB}_{(\nu_1+\nu_2-\zeta_2)}I^{\varpi}_{\nu_1+\nu_2-\zeta_1+\zeta_2/2}\phi\left(\nu_1+\nu_2-\frac{\zeta_1+\zeta_2}{2}\right)\right]$$
$$\left.+\frac{2(1-\varpi)2^{\varpi-1}}{B(\varpi)(\zeta_2-\zeta_1)^{\varpi}}\phi\left(\nu_1+\nu_2-\frac{\zeta_1+\zeta_2}{2}\right)\right|$$
$$\leq\frac{(\zeta_2-\zeta_1)^2}{8(\varpi+1)}Y_1(\varpi)^{1-1/\mathfrak{q}}\left\{\left(Y_1(\varpi)\left[\left|\phi''(\nu_1)\right|^{\mathfrak{q}}+\left|\phi''(\nu_2)\right|^{\mathfrak{q}}\right]\right.\right.$$
$$\left.-\frac{(Y_1(\varpi)+Y_2(\varpi))\left|\phi''(\zeta_2)\right|^{\mathfrak{q}}+(Y_1(\varpi)-Y_2(\varpi))\left|\phi''(\zeta_1)\right|^{\mathfrak{q}}}{2}\right)^{1/\mathfrak{q}}$$
$$+\left(Y_1(\varpi)\left[\left|\phi''(\nu_1)\right|^{\mathfrak{q}}+\left|\phi''(\nu_2)\right|^{\mathfrak{q}}\right]\right.$$
$$\left.\left.-\frac{(Y_1(\varpi)+Y_2(\varpi))\left|\phi''(\zeta_1)\right|^{\mathfrak{q}}+(Y_1(\varpi)-Y_2(\varpi))\left|\phi''(\zeta_2)\right|^{\mathfrak{q}}}{2}\right)^{1/\mathfrak{q}}\right\}, \tag{43}$$

where $Y_1(\varpi)$ is defined in Theorem 9 and $Y_2(\varpi)$ is defined by

$$Y_2(\varpi)=\begin{cases}\dfrac{1}{B(\varpi)\Gamma(\varpi)}\dfrac{\left(3-\varpi-2\varpi^2\right)}{18(\varpi+3)}, & \text{if } 0<\varpi\leq\dfrac{1}{2},\\ \dfrac{1}{B(\varpi)\Gamma(\varpi)}\left(2\left(\dfrac{(\kappa_\varpi)^{\varpi+3}}{(\varpi+3)}-\dfrac{3(1-2\varpi)(\kappa_\varpi)^2+4(\varpi+1)(\kappa_\varpi)^3}{18}\right)+\dfrac{(1-\varpi)^2}{3(\varpi+2)}\right), & \text{if } \varpi>\dfrac{1}{2}.\end{cases} \tag{44}$$

Proof. By applying the power-mean inequality in Lemma 6, we get

$$\left|\frac{1}{6}\left[\phi(\nu_1+\nu_2-\zeta_1)+4\phi\left(\nu_1+\nu_2-\frac{\zeta_1+\zeta_2}{2}\right)+\phi(\nu_1+\nu_2-\zeta_2)\right]\right.$$
$$-\frac{2^{\varpi-1}}{(\zeta_2-\zeta_1)^{\varpi}}\left[{}^{AB}_{(\nu_1+\nu_2-\zeta_1)}I^{\varpi}_{(\nu_1+\nu_2-\zeta_1+\zeta_2/2)}\phi\left(\nu_1+\nu_2-\frac{\zeta_1+\zeta_2}{2}\right)\right.$$
$$\left.+{}^{AB}_{(\nu_1+\nu_2-\zeta_2)}I^{\varpi}_{\nu_1+\nu_2-\zeta_1+\zeta_2/2}\phi\left(\nu_1+\nu_2-\frac{\zeta_1+\zeta_2}{2}\right)\right]$$
$$\left.+\frac{2(1-\varpi)2^{\varpi-1}}{B(\varpi)(\zeta_2-\zeta_1)^{\varpi}}\phi\left(\nu_1+\nu_2-\frac{\zeta_1+\zeta_2}{2}\right)\right|$$
$$\leq\frac{(\zeta_2-\zeta_1)^2}{8(\varpi+1)}\times\left[\frac{1}{B(\varpi)\Gamma(\varpi)}\left(\int_0^1\left|\left(\frac{1}{3}\left[1-2\varpi(1-\kappa)+\left(2-3\kappa^{\varpi}\right)\kappa\right]\right)\right|d\kappa\right)^{1-1/\mathfrak{q}}\right.$$
$$\times\left(\frac{1}{B(\varpi)\Gamma(\varpi)}\int_0^1\left|\left(\frac{1}{3}\left[1-2\varpi(1-\kappa)+\left(2-3\kappa^{\varpi}\right)\kappa\right]\right)\right|\right.$$
$$\left.\times\left|\phi''\left(\nu_1+\nu_2-\left(\frac{1+\kappa}{2}\zeta_2+\frac{1-\kappa}{2}\zeta_1\right)\right)\right|^{\mathfrak{q}}d\kappa\right)^{1/\mathfrak{q}}$$
$$+\left(\frac{1}{B(\varpi)\Gamma(\varpi)}\int_0^1\left|\left(\frac{1}{3}\left[1-2\varpi(1-\kappa)+\left(2-3\kappa^{\varpi}\right)\kappa\right]\right)\right|d\kappa\right)^{1-1/\mathfrak{q}}$$
$$\times\left(\frac{1}{B(\varpi)\Gamma(\varpi)}\int_0^1\left|\left(\frac{1}{3}\left[1-2\varpi(1-\kappa)+\left(2-3\kappa^{\varpi}\right)\kappa\right]\right)\right|\right.$$
$$\left.\left.\times\left|\phi''\left(\nu_1+\nu_2-\left(\frac{1+\kappa}{2}\zeta_1+\frac{1-\kappa}{2}\zeta_2\right)\right)\right|^{\mathfrak{q}}d\kappa\right)^{1/\mathfrak{q}}\right]. \tag{45}$$

⇒ To evaluate the above integral, assume the mapping $\varsigma : [0, 1] \longrightarrow \mathbb{R}$, where

$$\varsigma(\kappa)=\frac{1}{B(\varpi)\Gamma(\varpi)}\left(\frac{1}{3}\left[1-2\varpi(1-\kappa)+\left(2-3\kappa^{\varpi}\right)\kappa\right]\right) \text{ with } \varpi>0. \tag{46}$$

(1) Let us consider $0 < \varpi \leq (1/2)$, then we have

$$\int_0^1 |\varsigma(\kappa)|\kappa d\kappa = \frac{1}{B(\varpi)\Gamma(\varpi)}\left(\frac{3-\varpi-2\varpi^2}{18(\varpi+3)}\right). \tag{47}$$

(2) If $\varpi > (1/2)$, then there exists a real number κ_ϖ such that $0 < \varpi < 1$, and we have

$$\int_0^1 |\varsigma(\kappa)|\kappa d\kappa = \frac{1}{B(\varpi)\Gamma(\varpi)}\left(2\left(\frac{(\kappa_\varpi)^{\varpi+3}}{\varpi+3} - \frac{3(1-2\varpi)(\kappa_\varpi)^2 + 4(\varpi+1)(\kappa_\varpi)^3}{18}\right) + \frac{3+\varpi-2\varpi^2}{18(\varpi+3)}\right). \tag{48}$$

Since $|\phi''|^q$ is convex and taking into account Jensen-Mercer Inequality, we obtain

$$\begin{aligned}
&\frac{1}{B(\varpi)\Gamma(\varpi)}\int_0^1 \left|\left(\frac{1}{3}\left[1-2\varpi(1-\kappa)+\left(2-3\kappa^\varpi\right)\kappa\right]\right)\right| \\
&\quad\cdot\left|\phi''\left(\nu_1+\nu_2-\left(\frac{1+\kappa}{2}\zeta_2+\frac{1-\kappa}{2}\zeta_1\right)\right)\right|^q d\kappa \\
&\le \frac{1}{B(\varpi)\Gamma(\varpi)}\int_0^1 \left|\left(\frac{1}{3}\left[1-2\varpi(1-\kappa)+\left(2-3\kappa^\varpi\right)\kappa\right]\right)\right| \\
&\quad\times\left[\left|\phi''(\nu_1)\right|^q+\left|\phi''(\nu_2)\right|^q\right. \\
&\quad\left.-\left(\frac{1+\kappa}{2}\left|\phi''(\zeta_2)\right|^q+\frac{1-\kappa}{2}\left|\phi''(\zeta_1)\right|^q\right)\right]d\kappa \\
&= Y_1(\varpi)\left[\left|\phi''(\nu_1)\right|^q \middle| + \phi''(\nu_2)\right|^q\Big] \\
&\quad-\frac{(Y_1(\varpi)+Y_2(\varpi))\left|\phi''(\zeta_2)\right|^q+(Y_1(\varpi)-Y_2(\varpi))\left|\phi''(\zeta_1)\right|^q}{2}.
\end{aligned} \tag{49}$$

And similarly,

$$\begin{aligned}
&\frac{1}{B(\varpi)\Gamma(\varpi)}\int_0^1 \left|\left(\frac{1}{3}\left[1-2\varpi(1-\kappa)+\left(2-3\kappa^\varpi\right)\kappa\right]\right)\right| \\
&\quad\cdot\left|\phi''\left(\nu_1+\nu_2-\left(\frac{1+\kappa}{2}\zeta_1+\frac{1-\kappa}{2}\zeta_2\right)\right)\right|^q d\kappa \\
&\le \frac{1}{B(\varpi)\Gamma(\varpi)}\int_0^1 \left|\left(\frac{1}{3}\left[1-2\varpi(1-\kappa)+\left(2-3\kappa^\varpi\right)\kappa\right]\right)\right| \\
&\quad\times\left[\left|\phi''(\nu_1)\right|^q+\left|\phi''(\nu_2)\right|^q\right. \\
&\quad\left.-\left(\frac{1+\kappa}{2}\left|\phi''(\zeta_1)\right|^q+\frac{1-\kappa}{2}\left|\phi''(\zeta_2)\right|^q\right)\right]d\kappa \\
&= Y_1(\varpi)\left[\left|\phi''(\nu_1)\right|^q+\left|\phi''(\nu_2)\right|^q\right] \\
&\quad-\frac{(Y_1(\varpi)+Y_2(\varpi))\left|\phi''(\zeta_1)\right|^q+(Y_1(\varpi)-Y_2(\varpi))\left|\phi''(\zeta_2)\right|^q}{2}.
\end{aligned} \tag{50}$$

Finally, we obtain

$$\begin{aligned}
&\Rightarrow\left|\frac{1}{6}\left[\phi(\nu_1+\nu_2-\zeta_1)+4\phi\left(\nu_1+\nu_2-\frac{\zeta_1+\zeta_2}{2}\right)\right.\right. \\
&\quad+\phi(\nu_1+\nu_2-\zeta_2)\Big]-\frac{2^{\varpi-1}}{(\zeta_2-\zeta_1)^\varpi} \\
&\quad\cdot\Big[{}^{AB}_{(\nu_1+\nu_2-\zeta_1)}I^{\varpi}_{(\nu_1+\nu_2-\zeta_1+\zeta_2/2)}\phi\left(\nu_1+\nu_2-\frac{\zeta_1+\zeta_2}{2}\right) \\
&\quad+{}^{AB}_{(\nu_1+\nu_2-\zeta_2)}I^{\varpi}_{\nu_1+\nu_2-\zeta_1+\zeta_2/2}\phi\left(\nu_1+\nu_2-\frac{\zeta_1+\zeta_2}{2}\right)\Big] \\
&\quad\left.+\frac{2(1-\varpi)2^{\varpi-1}}{B(\varpi)(\zeta_2-\zeta_1)^\varpi}\phi\left(\nu_1+\nu_2-\frac{\zeta_1+\zeta_2}{2}\right)\right| \\
&\le\frac{(\zeta_2-\zeta_1)^2}{8(\varpi+1)}Y_1(\varpi)^{1-1/q}\left\{\left(Y_1(\varpi)\left[\left|\phi''(\nu_1)\right|^q+\left|\phi''(\nu_2)\right|^q\right]\right.\right. \\
&\quad\left.-\frac{(Y_1(\varpi)+Y_2(\varpi))\left|\phi''(\zeta_2)\right|^q+(Y_1(\varpi)-Y_2(\varpi))\left|\phi''(\zeta_1)\right|^q}{2}\right)^{1/q} \\
&\quad+\left(Y_1(\varpi)\left[\left|\phi''(\nu_1)\right|^q+\left|\phi''(\nu_2)\right|^q\right]\right. \\
&\quad\left.\left.-\frac{(Y_1(\varpi)+Y_2(\varpi))\left|\phi''(\zeta_1)\right|^q+(Y_1(\varpi)-Y_2(\varpi))\left|\phi''(\zeta_2)\right|^q}{2}\right)^{1/q}\right\}.
\end{aligned} \tag{51}$$

This completes the proof. □

Remark 17. If we choose $\varpi = 1$ and $\kappa_\varpi = (1/3)$, in Theorem 16, then we have the inequality

$$\begin{aligned}
&\left|\frac{1}{6}\left[\phi(\nu_1+\nu_2-\zeta_1)+4\phi\left(\nu_1+\nu_2-\frac{\zeta_1+\zeta_2}{2}\right)+\phi(\nu_1+\nu_2-\zeta_2)\right]\right. \\
&\quad\left.-\frac{1}{\zeta_2-\zeta_1}\int_{\nu_1+\nu_2-\zeta_2}^{\nu_1+\nu_2-\zeta_1}\phi(\varkappa)d\varkappa\right| \\
&\le(\zeta_2-\zeta_1)^2\left(\frac{1}{162}\right)^{1-1/q}\left[\left(\frac{1}{162}\left|\phi''(\nu_1)\right|^q+\frac{1}{162}\left|\phi''(\nu_2)\right|^q\right.\right. \\
&\quad\left.-\left(\frac{59}{3^5 2^7}\left|\phi''(\zeta_1)\right|^q+\frac{133}{3^5 2^7}\left|\phi''(\zeta_2)\right|^q\right)\right)^{1/q} \\
&\quad+\left(\frac{1}{162}\left|\phi''(\nu_1)\right|^q+\frac{1}{162}\left|\phi''(\nu_2)\right|^q\right. \\
&\quad\left.\left.-\left(\frac{59}{3^5 2^7}\left|\phi''(\zeta_2)\right|^q+\frac{133}{3^5 2^7}\left|\phi''(\zeta_1)\right|^q\right)\right)^{1/q}\right],
\end{aligned} \tag{52}$$

which is Mercer variant of an identity proved by Sarikaya et al. in [19].

Remark 18. If we take $\varpi = 1$, $\nu_1 = \zeta_1$, and $\nu_2 = \zeta_2$ in Theorem 16, then Theorem 16 reduce to

$$\left|\frac{1}{6}\left[\phi(\zeta_1)+4\phi\left(\frac{\zeta_1+\zeta_2}{2}\right)+\phi(\zeta_2)\right]-\frac{1}{\zeta_2-\zeta_1}\int_{\zeta_1}^{\zeta_2}\phi(\varkappa)d\varkappa\right| \le (\zeta_2-\zeta_1)^2\left(\frac{1}{162}\right)^{1-1/\mathfrak{q}}\left[\left(\frac{59}{3^5 2^7}\left|\phi''(\zeta_1)\right|^{\mathfrak{q}}+\frac{133}{3^5 2^7}\left|\phi''(\zeta_2)\right|^{\mathfrak{q}}\right)^{1/\mathfrak{q}} + \left(\frac{59}{3^5 2^7}\left|\phi''(\zeta_2)\right|^{\mathfrak{q}}+\frac{133}{3^5 2^7}\left|\phi''(\zeta_1)\right|^{\mathfrak{q}}\right)^{1/\mathfrak{q}}\right], \tag{53}$$

which is proved by Sarikaya et al. in [19].

Remark 19. If we take $\nu_1=\zeta_1$ and $\nu_2=\zeta_2$ in Theorem 16, then Theorem 16 reduce to

$$\left|\frac{1}{6}\left[\phi(\zeta_1)+4\phi\left(\frac{\zeta_1+\zeta_2}{2}\right)+\phi(\zeta_2)\right]-\frac{2^{\varpi-1}\Gamma(1+\varpi)}{(\zeta_2-\zeta_1)^{\varpi}}\cdot\left[J^{\varpi}_{\zeta_2-}\phi\left(\frac{\zeta_1+\zeta_2}{2}\right)+J^{\varpi}_{\zeta_1+}\phi\left(\frac{\zeta_1+\zeta_2}{2}\right)\right]\right| \le \frac{(\zeta_2-\zeta_1)^2}{8(\varpi+1)}\Omega_1(\varpi)^{1-1/q} \cdot\left\{\left(\frac{(\Omega_1(\varpi)+\Omega_2(\varpi))\left|\phi''(\zeta_2)\right|^{\mathfrak{q}}+(\Omega_1(\varpi)-\Omega_2(\varpi))\left|\phi''(\zeta_1)\right|^{\mathfrak{q}}}{2}\right)^{1/q} + \left(\frac{(\Omega_1(\varpi)+\Omega_2(\varpi))\left|\phi''(\zeta_1)\right|^{\mathfrak{q}}+(\Omega_1(\varpi)-\Omega_2(\varpi))\left|\phi''(\zeta_2)\right|^{\mathfrak{q}}}{2}\right)^{1/q}\right\}, \tag{54}$$

which is proved by Hezenci et al. in [14].

Remark 20. If we take $\varpi=1$ in Remark 19, then we have

$$\left|\frac{1}{6}\left[\phi(\zeta_1)+4\phi\left(\frac{\zeta_1+\zeta_2}{2}\right)+\phi(\zeta_2)\right]-\frac{1}{\zeta_2-\zeta_1}\int_{\zeta_1}^{\zeta_2}\phi(\varkappa)d\varkappa\right| \le (\zeta_2-\zeta_1)^2\left(\frac{1}{162}\right)^{1-1/\mathfrak{q}}\left[\left(\frac{59}{3^5 2^7}\left|\phi''(\zeta_1)\right|^{\mathfrak{q}}+\frac{133}{3^5 2^7}\left|\phi''(\zeta_2)\right|^{\mathfrak{q}}\right)^{1/\mathfrak{q}} + \left(\frac{59}{3^5 2^7}\left|\phi''(\zeta_2)\right|^{\mathfrak{q}}+\frac{133}{3^5 2^7}\left|\phi''(\zeta_1)\right|^{\mathfrak{q}}\right)^{1/\mathfrak{q}}\right], \tag{55}$$

which is proved by Sarikaya et al. in [19].

3. Applications

3.1. Q-Digamma Function. The $\varphi_{\mathbf{q}}$-digamma function, which is described as the logarithmic derivative of the q -gamma function, is an essential function related to the $\mathbf{q}$ -gamma function. A few papers had also additionally been utilized that explore the monotonicity and complete monotonicity characteristics for functions linked with the $\mathbf{q}$ -gamma and $\mathbf{q}$-digamma functions, which tends to result in remarkable inequalities. One can see in [31, 32].

Assume the $\mathbf{q}$-analogue of the digamma function φ for $0<\mathbf{q}<1$ is the $\mathbf{q}$-digamma function $\varphi_{\mathbf{q}}$ and is (see [33, 34]) given as:

$$\varphi_{\mathbf{q}}=-\ln(1-\mathbf{q})+\ln\mathbf{q}\sum_{k=0}^{\infty}\frac{q^{k+\varkappa}}{1-q^{k+\varkappa}}=-\ln(1-\mathbf{q})+\ln\mathbf{q}\sum_{k=0}^{\infty}\frac{q^{k\varkappa}}{1-q^{k\varkappa}}. \tag{56}$$

For $\mathbf{q}\ge 1$ and $\varkappa>0$,$\mathbf{q}$-digamma function $\varphi_{\mathbf{q}}$ can be given as:

$$\begin{aligned}\varphi_{\mathbf{q}}&=-\ln(\mathbf{q}-1)+\ln\mathbf{q}\left[\varkappa-\frac{1}{2}-\sum_{k=0}^{\infty}\frac{\mathbf{q}^{-(k+\varkappa)}}{1-\mathbf{q}^{-(k+\varkappa)}}\right]\\&=-\ln(\mathbf{q}-1)+\ln\mathbf{q}\left[\varkappa-\frac{1}{2}-\sum_{k=0}^{\infty}\frac{\mathbf{q}^{-k\varkappa}}{1-\mathbf{q}^{-k\varkappa}}\right].\end{aligned} \tag{57}$$

Proposition 21. *Assume that $\zeta_1,\zeta_2,\nu_1,\nu_2\in\mathbb{R}$ such that $0<\nu_1<\nu_2$,$q\ge 1$,$0<q<1$, and $q^{-1}=1-p^{-1}$. Then, the following inequality is valid:*

$$\left|\frac{1}{6}\left\{\varphi_q'(\nu_1+\nu_2-\zeta_1)+4\varphi_q'\left(\nu_1+\nu_2-\frac{\zeta_1+\zeta_2}{2}\right)+\varphi_q'(\nu_1+\nu_2-\zeta_2)\right\} - \frac{\varphi_q(\nu_1+\nu_2-\zeta_1)-\varphi_q(\nu_1+\nu_2-\zeta_2)}{\zeta_2-\zeta_1}\right| \le (\zeta_2-\zeta_1)^2\left(\frac{1}{162}\right)^{1-1/q}\left[\left\{\frac{1}{162}\left|\varphi_q^{(3)}(\nu_1)\right|^q + \frac{1}{162}\left|\varphi_q^{(3)}(\nu_2)\right|^q-\left(\frac{59}{3^5 2^7}\left|\varphi_q^{(3)}(\zeta_1)\right|^q + \frac{133}{3^5 2^7}\left|\varphi_q^{(3)}(\zeta_2)\right|^q\right)\right\}^{1/q}+\left\{\frac{1}{162}\left|\varphi_q^{(3)}(\nu_1)\right|^q + \frac{1}{162}\left|\varphi_q^{(3)}(\nu_2)\right|^q-\left(\frac{59}{3^5 2^7}\left|\varphi_q^{(3)}(\zeta_2)\right|^q + \frac{133}{3^5 2^7}\left|\varphi_q^{(3)}(\zeta_1)\right|^q\right)\right\}^{1/q}\right]. \tag{58}$$

Proof. The assertion can be obtained immediately by using Remark 17 with the $\phi(\varkappa)\longrightarrow\varphi_q'(\varkappa)$ for all $\mathbf{q}>0$, and consequently, $\phi''(\varkappa):=\varphi_{\mathbf{q}}^{(3)}(\varkappa)$ is convex on the same interval $(0,\infty)$. □

Proposition 22. *Assume that ζ_1,ζ_2 are the real numbers such that $0<\zeta_1<\zeta_2$,$q\ge 1$,$0<\mathbf{q}<1$, and $q^{-1}=1-p^{-1}$. Then, the following inequality is valid:*

$$\left|\frac{1}{6}\left\{\varphi_q'(\zeta_1)+4\varphi_q'\left(\frac{\zeta_1+\zeta_2}{2}\right)+\varphi_q'(\zeta_2)\right\}-\frac{\varphi_q(\zeta_2)-\varphi_q(\zeta_1)}{\zeta_2-\zeta_1}\right| \le (\zeta_2-\zeta_1)^2\left(\frac{1}{162}\right)^{1-1/q}\left[\left\{\frac{59}{3^5 2^7}\left|\varphi_{\mathbf{q}}^{(3)}(\zeta_1)\right|^q+\frac{133}{3^5 2^7}\left|\varphi_{\mathbf{q}}^{(3)}(\zeta_2)\right|^q\right\}^{1/q} + \left\{\frac{59}{3^5 2^7}\left|\varphi_{\mathbf{q}}^{(3)}(\zeta_2)\right|^q+\frac{133}{3^5 2^7}\left|\varphi_{\mathbf{q}}^{(3)}(\zeta_1)\right|^q\right\}^{1/q}\right]. \tag{59}$$

Proof. The assertion can be obtained immediately by using Remark 18 with the $\phi(\varkappa)\longrightarrow\varphi_{\mathbf{q}}'(\varkappa)$ for all $\mathbf{q}>0$, and consequently, $\phi''(\varkappa):=\varphi_{\mathbf{q}}^{(3)}(\varkappa)$ is convex on the same interval $(0,\infty)$. □

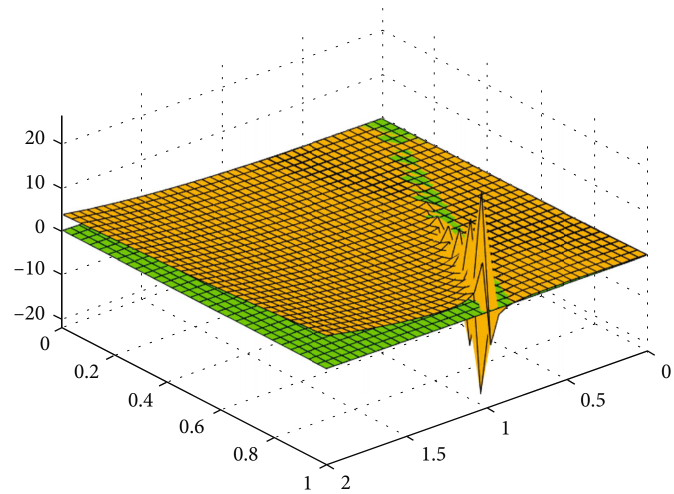

FIGURE 1: Three-dimensional illustration of the error and error bounds for (43).

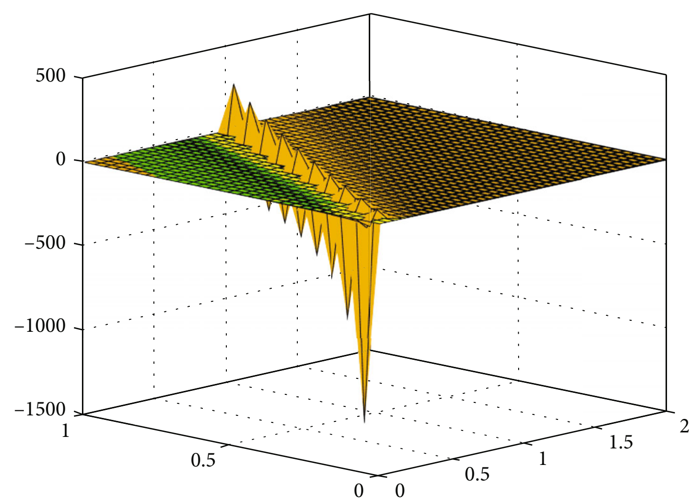

FIGURE 2: Three-dimensional illustration of the error and error bounds for (53).

3.2. Modified Bessel Function. Bessel functions were named after Friedrich Wilhelm Bessel (1784-1846); however, Daniel Bernoulli is generally credited with being the first to introduce the concept of Bessels functions in 1732. Numerous results about Bessel functions have been established by utilizing its generating function (see [35]).

We know the first type of modified Bessel function $\mathfrak{B}\tau_1$, which has the series interpretation (see [33], p.77).

$$\mathfrak{B}_{\tau_1}(\varkappa) = \Sigma_{\mathfrak{n}\geq 0} \frac{(\varkappa/2)^{\tau_1+2\mathfrak{n}}}{\mathfrak{n}!\Gamma(\tau_1+\mathfrak{n}+1)}. \tag{60}$$

where $\varkappa \in \mathfrak{R}$ and $\tau_1 > -1$, while the second type modified Bessel function ϕ_{τ_1} (see [33], p.78) is usually defined as

$$\phi_{\tau_1}(\varkappa) = \frac{\pi}{2} \frac{\mathfrak{B}_{-\tau_1}(\varkappa) - \mathfrak{B}_{\tau_1}(\varkappa)}{\sin \tau_1 \pi}. \tag{61}$$

Consider the function $\Psi_{\tau_1}(\varkappa)$: $\mathfrak{R} \longrightarrow [1,\infty)$ defined by

$$\Psi_{\tau_1}(\varkappa) = 2^{\tau_1}\Gamma(\tau_1+1)\varkappa^{-\tau_1}\phi_{\tau_1}(\varkappa), \tag{62}$$

Here, first, second- and third-order derivative formula of $\Psi_{\tau_1}(\varkappa)$ is given as in [33]:

$$\Psi_{\tau_1}'(\varkappa) = \frac{\varkappa}{2(\tau_1+1)} \Psi_{\tau_1+1}(\varkappa), \tag{63}$$

$$\Psi_{\tau_1}''(\varkappa) = \frac{\varkappa^2}{4(\tau_1+1)(\tau_1+2)} \Psi_{\tau_1+2}(\varkappa) + \frac{1}{2(\tau_1+1)} \Psi_{\tau_1+1}(\varkappa), \tag{64}$$

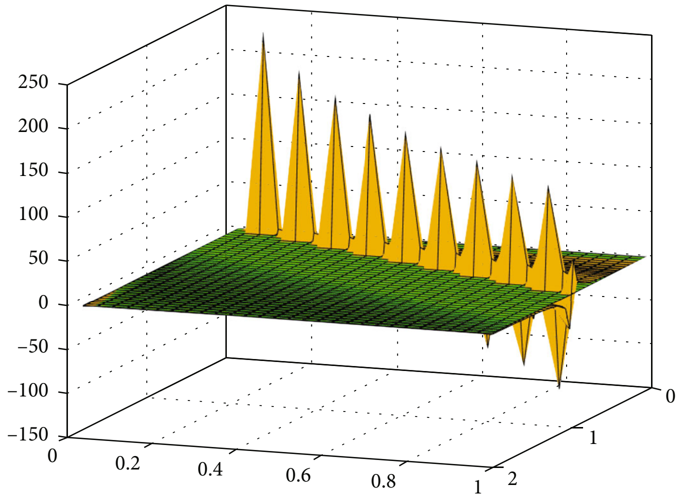

FIGURE 3: Three-dimensional illustration of the error and error bounds for (55).

$$\Psi_{\tau_1}'''(\varkappa) = \frac{\varkappa^3}{4(\tau_1+1)(\tau_1+2)(\tau_1+3)}\Psi_{\tau_1+3}(\varkappa) + \frac{3\varkappa}{4(\tau_1+1)(\tau_1+2)}\Psi_{\tau_1+2}(\varkappa). \tag{65}$$

Proposition 23. *Suppose that $\zeta_1, \zeta_2, \nu_1, \nu_2 \in \mathbb{R}$ such that $0 < \nu_1 < \nu_2$, and $\tau_1 > -1$. Then, we have*

$$\begin{aligned}
&\left|\frac{1}{6}\left\{\frac{(\nu_1+\nu_2-\zeta_1)}{2(\tau_1+1)}\Psi_{\tau_1+1}(\nu_1+\nu_2-\zeta_1) + 4\frac{(\nu_1+\nu_2-((\zeta_1+\zeta_2)/2))}{2(\tau_1+1)}\Psi_{\tau_1+1}\left(\nu_1+\nu_2-\frac{\zeta_1+\zeta_2}{2}\right) + \frac{\nu_1+\nu_2-\zeta_2}{2(\tau_1+1)}\Psi_{\tau_1+1}(\nu_1+\nu_2-\zeta_2)\right\} - \frac{\Psi_m(\nu_1+\nu_2-\zeta_1)-\Psi_m(\nu_1+\nu_2-\zeta_2)}{\zeta_2-\zeta_1}\right| \\
&\le (\zeta_2-\zeta_1)^2\left(\frac{1}{162}\right)^{1-1/q} \times \left[\left\{\frac{1}{162}\left(\frac{\nu_1^3}{4(\tau_1+1)(\tau_1+2)(\tau_1+3)}\Psi_{\tau_1+3}(\nu_1) + \frac{3\nu_1}{4(\tau_1+1)(\tau_1+2)}\Psi_{\tau_1+2}(\nu_1)\right)^q + \frac{1}{162}\left(\frac{\nu_2^3}{4(\tau_1+1)(\tau_1+2)(\tau_1+3)}\Psi_{\tau_1+3}(\nu_2) + \frac{3\nu_2}{4(\tau_1+1)(\tau_1+2)}\Psi_{\tau_1+2}(\nu_2)\right)^q \right.\right. \\
&\quad - \left\{\frac{59}{3^5 2^7}\left(\frac{\zeta_1^3}{4(\tau_1+1)(\tau_1+2)(\tau_1+3)}\Psi_{\tau_1+3}(\zeta_1) + \frac{3\zeta_1}{4(\tau_1+1)(\tau_1+2)}\Psi_{\tau_1+2}(\zeta_1)\right)^q + \frac{133}{3^5 2^7}\left(\frac{\zeta_2^3}{4(\tau_1+1)(\tau_1+2)(\tau_1+3)}\Psi_{\tau_1+3}(\zeta_2) + \frac{3\zeta_2}{4(\tau_1+1)(\tau_1+2)}\Psi_{\tau_1+2}(\zeta_2)\right)^q\right\}\Bigg\}^{1/q} \\
&\quad + \left\{\frac{1}{162}\left(\frac{\nu_1^3}{4(\tau_1+1)(\tau_1+2)(\tau_1+3)}\Psi_{\tau_1+3}(\nu_1) + \frac{3\nu_1}{4(\tau_1+1)(\tau_1+2)}\Psi_{\tau_1+2}(\nu_1)\right)^q + \frac{1}{162}\left(\frac{\nu_2^3}{4(\tau_1+1)(\tau_1+2)(\tau_1+3)}\Psi_{\tau_1+3}(\nu_2) + \frac{3\nu_2}{4(\tau_1+1)(\tau_1+2)}\Psi_{\tau_1+2}(\nu_2)\right)^q \right. \\
&\quad \left.\left. - \left\{\frac{59}{3^5 2^7}\left(\frac{\zeta_2^3}{4(\tau_1+1)(\tau_1+2)(\tau_1+3)}\Psi_{\tau_1+3}(\zeta_2) + \frac{3\zeta_2}{4(\tau_1+1)(\tau_1+2)}\Psi_{\tau_1+2}(\zeta_2)\right)^q + \frac{133}{3^5 2^7}\left(\frac{\zeta_1^3}{4(\tau_1+1)(\tau_1+2)(\tau_1+3)}\Psi_{\tau_1+3}(\zeta_1) + \frac{3\zeta_1}{4(\tau_1+1)(\tau_1+2)}\Psi_{\tau_1+2}(\zeta_1)\right)^q\right\}\right\}^{1/q}\right].
\end{aligned} \tag{66}$$

Proof. The required result follows immediately from Remark 17 utilizing $\phi(\varkappa) = \Psi_{\tau_1}'(\varkappa)$, $\varkappa > 0$, and the identities (66) and (63). □

Proposition 24. *Suppose that $\tau_1 > -1$ and $0 < \zeta_1 < \zeta_2$. Then, we have*

$$\begin{aligned}
&\left|\frac{1}{6}\left\{\frac{\zeta_1}{2(\tau_1+1)}\Psi_{\tau_1+1}(\zeta_1) + 4\frac{\zeta_1+\zeta_2}{4(\tau_1+1)}\Psi_{\tau_1+1}\left(\frac{\zeta_1+\zeta_2}{2}\right) + \frac{\zeta_2}{2(\tau_1+1)}\Psi_{\tau_1+1}(\zeta_2)\right\} - \frac{\Psi_m(\zeta_2)-\Psi_m(\zeta_1)}{\zeta_2-\zeta_1}\right| \\
&\le (\zeta_2-\zeta_1)^2\left(\frac{1}{162}\right)^{1-1/q} \times \left[\left\{\frac{59}{3^5 2^7}\left(\frac{\zeta_1^3}{4(\tau_1+1)(\tau_1+2)(\tau_1+3)}\Psi_{\tau_1+3}(\zeta_1) + \frac{3\zeta_1}{4(\tau_1+1)(\tau_1+2)}\Psi_{\tau_1+2}(\zeta_1)\right)^q + \frac{133}{3^5 2^7}\left(\frac{\zeta_2^3}{4(\tau_1+1)(\tau_1+2)(\tau_1+3)}\Psi_{\tau_1+3}(\zeta_2) + \frac{3\zeta_2}{4(\tau_1+1)(\tau_1+2)}\Psi_{\tau_1+2}(\zeta_2)\right)^q\right\}^{1/q}\right. \\
&\quad \left. + \left\{\frac{59}{3^5 2^7}\left(\frac{\zeta_2^3}{4(\tau_1+1)(\tau_1+2)(\tau_1+3)}\Psi_{\tau_1+3}(\zeta_2) + \frac{3\zeta_2}{4(\tau_1+1)(\tau_1+2)}\Psi_{\tau_1+2}(\zeta_2)\right)^q + \frac{133}{3^5 2^7}\left(\frac{\zeta_1^3}{4(\tau_1+1)(\tau_1+2)(\tau_1+3)}\Psi_{\tau_1+3}(\zeta_1) + \frac{3\zeta_1}{4(\tau_1+1)(\tau_1+2)}\Psi_{\tau_1+2}(\zeta_1)\right)^q\right\}^{1/q}\right].
\end{aligned} \tag{67}$$

Proof. The required result follows immediately from Remark 18 utilizing $\phi(\varkappa) = \Psi_{\tau_1}'(\varkappa), \varkappa > 0$, and the identities (66) and (63). □

4. Conclusion

The study deal with the investigation of Simpson-Mercer type inequalities for twice differentiable functions. Adopting the novel approach, we extended the study of Simpson-Mercer type integral inequalities using Hölder's and power-mean integral inequalities via Atangana-Baleanu (AB) fractional integral operators. It is interesting to extend such findings to the Atangana-Baleanu (AB) operator and also to other convexities. Various representations were used to explain the findings to clarify the important aspects of the fractional inequalities under consideration, such as Figures 1–3, which illustrate the error bounds for the dominant findings. We believe that our newly introduced idea and concept will have very deep research in the captivating field of numerical analysis and inequalities. The strategy's effective and productive execution is investigated and confirmed in order to show that it may be applied to coordinated convex functions that emerge in fractional calculus, especially to fractal and fractional integral operators.

Data Availability

No data were used to support this study.

Conflicts of Interest

The authors declare that they have no competing interests.

Authors' Contributions

S.I. Butt provided the main ideas of the article and is a major contributor in starting the initial draft and conceptualization. S. Rashid dealt with the methodology and investigation. I. Javed contributed to editing of the original draft and handle latex work. K. A. Khan performed the validation, formal analysis, and writing revised version. R. M. Mabela performed review and editing along with the submission of manuscript. All authors read and approved the final manuscript.

References

[1] S. S. Dragomir and C. E. M. Pearce, "Selected topics on Hermite-Hadamard inequalities and applications," in *RGMIA Monographs*, Victoria University, 2000.

[2] P. Agarwal, S. S. Dragomir, M. Jleli, and B. Samet, *Advances in Mathematical Inequalities and Applications*, Springer, Singapore, 2018.

[3] S. I. Butt, M. K. Bakula, D. Pecaric, and J. Pecaric, "Jensen-Grüss inequality and its applications for the Zipf-Mandelbrot law," *Mathematical Methods in the Applied Sciences*, vol. 44, no. 2, pp. 1664–1673, 2021.

[4] S. Khan, M. A. Khan, S. I. Butt, and Y. M. Chu, "A new bound for the Jensen gap pertaining twice differentiable functions with applications," *Advances in Difference Equations*, vol. 2020, no. 1, Article ID 333, 2020.

[5] A. M. Mercer, "A variant of Jensen's inequality," *JIPAM - Journal of Inequalities in Pure and Applied Mathematics*, vol. 4, no. 4, 2003.

[6] M. A. Khan, Z. Husain, and Y. M. Chu, "New estimates for Csiszár divergence and Zipf–Mandelbrot entropy via Jensen–Mercer's inequality," *Complexity*, vol. 2020, Article ID 8928691, 8 pages, 2020.

[7] S. I. Butt, M. Umar, S. Rashid, A. O. Akdemir, and Y. M. Chu, "New Hermite–Jensen–Mercer-type inequalities via K-fractional integrals," *Advances in Difference Equations*, vol. 2020, no. 1, Article ID 635, p. 24, 2020.

[8] H. R. Moradi and S. Furuichi, "Improvement and generalization of some Jensen-Mercer-type inequalities," *Journal of Mathematical Inequalities*, vol. 14, no. 2, pp. 377–383, 2007.

[9] M. Kian and M. Moslehian, "Refinements of the operator Jensen-Mercer inequality," *Algebra*, vol. 26, pp. 742–753, 2013.

[10] M. Niezgoda, "A generalization of Mercer's result on convex functions," *Nonlinear Analysis: Theory, Methods and Applications*, vol. 71, no. 7-8, pp. 2771–2779, 2009.

[11] L. Harovath, "Some notes on Jensen-Mercer's type inequalities; extensions and refinements with applications," *Mathematical Inequalities & Applications*, vol. 24, no. 4, pp. 1093–1111, 1998.

[12] S. I. Butt, S. Yousaf, H. Ahmed, and T. A. Nofal, "Jensen-Mercer inequality and related results in the fractal sense with applications," *Fractals*, vol. 30, no. 1, p. 2240008, 2022.

[13] P. Xu, S. I. Butt, S. Yousaf, A. Aslam, and T. J. Zia, "Generalized Fractal Jensen-Mercer and Hermite-Mercer type inequalities via _h_ -convex functions involving Mittag-Leffler kernel," *Alexandria Engineering Journal*, vol. 61, no. 6, pp. 4837–4846, 2022.

[14] F. Hezenci, H. Budak, and H. Kara, "New version of fractional Simpson type inequalities for twice differentiable functions," *Advances in Difference Equations*, vol. 2021, no. 1, Article ID 460, p. 10, 2021.

[15] M. Z. Sarikaya, E. Set, and M. E. Ozdemir, "On new inequalities of Simpson's type for s-convex functions," *Computers and Mathematics with Applications*, vol. 60, no. 8, pp. 2191–2199, 2010.

[16] M. Iqbal, S. Qaisar, and S. Hussain, "On Simpson's type inequalities utilizing fractional integrals," *Journal of Computational Analysis and Applications*, vol. 23, no. 6, pp. 1137–1145, 2017.

[17] M. E. Ozdemir, A. O. Akdemir, and H. Kavurmaci, "On the Simpson's inequality for convex functions on the co-ordinates," *Turkish journal of analysis and number theory*, vol. 2, no. 5, pp. 165–169, 2014.

[18] T. S. Du, J. G. Liao, and Y. J. Li, "Properties and integral inequalities of Hadamard-Simpson type for the generalized (s, m)-Preinvex functions," *Journal of Nonlinear Sciences and Applications*, vol. 9, no. 5, pp. 3112–3126, 2016.

[19] M. Z. Sarikaya, E. Set, and M. E. Ozdemir, "On new inequalities of Simpson's type for functions whose second derivatives absolute values are convex," *Journal of applied mathematics, statistics and informatics*, vol. 9, no. 1, pp. 37–45, 2013.

[20] X. You, F. Hezenci, H. Budak, and H. Kara, "New Simpson type inequalities for twice differentiable functions via generalized fractional integrals," *AIMS Mathematics*, vol. 7, no. 3, pp. 3959–3971, 2022.

[21] R. Gorenflo, "Fractional calculus," in *Courses and Lectures-International Centre for Mechanical Sciences*, vol. 378, pp. 277–290, Springer, Vienna, 1997.

[22] T. Abdeljawad and D. Baleanu, "On fractional derivatives with exponential kernel and their discrete versions," *Reports on Mathematical Physics*, vol. 80, no. 1, pp. 11–27, 2017.

[23] R. Khalil, M. Al Horani, A. Yousef, and M. Sababheh, "A new definition of fractional derivative," *Journal of Computational and Applied Mathematics*, vol. 264, pp. 65–70, 2014.

[24] Z. S. Mostaghim, B. P. Moghaddam, and H. S. Haghgozar, "Numerical simulation of fractional-order dynamical systems in noisy environments," *Computational and Applied Mathematics*, vol. 37, no. 5, pp. 6433–6447, 2018.

[25] A. M. Vargas, "Finite difference method for solving fractional differential equations at irregular meshes," *Mathematics and Computers in Simulation*, vol. 193, pp. 204–216, 2022.

[26] D. Baleanu and R. P. Agarwal, "Fractional calculus in the sky," *Advances in Difference Equations*, vol. 2021, no. 1, Article ID 117, 2021.

[27] A. Atangana and D. Baleanu, "New fractional derivatives with nonlocal and non-singular kernel: theory and application to

heat transfer model," *Thermal Science*, vol. 20, no. 2, pp. 763–769, 2016.

[28] T. Abdeljawad and D. Baleanu, "Integration by parts and its applications of a new nonlocal fractional derivative with Mittag-Leffler nonsingular kernel," *Journal of Nonlinear Sciences and Applications*, vol. 10, no. 3, pp. 1098–1107, 2017.

[29] E. Set, S. I. Butt, A. O. Akdemir, A. Karaoglan, and T. Abdeljawad, "New integral inequalities for differentiable convex functions via Atangana-Baleanu fractional integral operators," *Chaos, Solitons and Fractals*, vol. 143, article 110554, 2021.

[30] S. I. Butt, S. Yousaf, A. O. Akdemir, and M. A. Dokuyucu, "New Hadamard-type integral inequalities via a general form of fractional integral operators," *Chaos, Solitons and Fractals*, vol. 148, article 111025, 2021.

[31] N. Batir, "Monotonicity properties of q-digamma and q-trigamma functions," *Journal of Approximation Theory*, vol. 192, pp. 336–346, 2015.

[32] A. Salem, "Complete monotonicity properties of functions involving q-gamma and q-digamma functions," *Mathematical Inequalities & Applications*, vol. 17, no. 3, pp. 801–811, 1998.

[33] G. N. Watson, *A Treatise on the Theory of Bessel Functions*, Cambridge university press, 1995.

[34] S. Jain, K. Mehrez, D. Baleanu, and P. Agarwal, "Certain Hermite-Hadamard inequalities for logarithmically convex functions with applications," *Mathematics*, vol. 7, no. 2, p. 163, 2019.

[35] F. Bowman, "Introduction to Bessel functions," *Courier Corporation*, vol. 27, no. 4, 2012.

Hindawi
Journal of Function Spaces
Volume 2022, Article ID 7512754, 14 pages
https://doi.org/10.1155/2022/7512754

Research Article

Local and Global Existence and Uniqueness of Solution for Class of Fuzzy Fractional Functional Evolution Equation

Kinda Abuasbeh,[1] **Ramsha Shafqat**,[2] **Azmat Ullah Khan Niazi**,[2] **and Muath Awadalla**[1]

[1]*Department of Mathematics and Statistics, College of Science, King Faisal University, Hafuf, Al Ahsa 31982, Saudi Arabia*
[2]*Department of Mathematics and Statistics, The University of Lahore, Sargodha 40100, Pakistan*

Correspondence should be addressed to Kinda Abuasbeh; kabuasbeh@kfu.edu.sa and Ramsha Shafqat; ramshawarriach@gmail.com

Received 2 May 2022; Accepted 29 July 2022; Published 5 September 2022

Academic Editor: Luisa Morgado

For fuzzy fractional functional evolution equations, the concept of global and local existence and uniqueness will be presented in this work. We employ the contraction principle and successive approximations for global and local existence and uniqueness, respectively, as given $\begin{cases} {}_0^cD_q^H x(\mathfrak{J}) = f(\mathfrak{J}, x_{\mathfrak{J}}) + \int_0^{\mathfrak{J}} g(\mathfrak{J}, s, x_s)ds, \mathfrak{J} \geq \mathfrak{J}_0, \mathfrak{J} \in [0, T], \\ x(\mathfrak{J}) = \psi(\mathfrak{J} - \mathfrak{J}_0) = \psi_0, \in C_\sigma, \mathfrak{J}_0 \geq \mathfrak{J} \geq \mathfrak{J}_0 - \sigma, \\ x'(\mathfrak{J}) = \psi'(\mathfrak{J}) = \psi_1, \end{cases}$ where C_σ denotes the set of fuzzy continuous mapping defined on $[\mathfrak{J}_0 - \sigma, T]$ and $\sigma > 1$. We also use this method to solve fuzzy fractional functional evolution equations with fuzzy population models and distributed delays using fuzzy fractional functional evolution equations. To explain these results, some theorems are given. Finally, certain fuzzy fractional functional evolution equations are illustrated.

1. Introduction

In reality, to show fractional-order demeanor which can change with time and space in case of a large number of physical processes, fractional calculus authorizes the operations of differentiation and integration of fractional-order. The fractional-order can be applied to both imaginary and real numbers. Because of its wide range of applications in disciplines like mechanics, electrical engineering, signal processing, thermal systems, robotics and control, signal processing, and many others, the theory of fuzzy sets continues to attract academics' attention [1–3]. Therefore, it has been noticed that it is the center of increasing interest of researchers during the past few years.

In real-world systems, delays can be recognized everywhere, and there has been widespread interest in the study of delay differential equations for many years. Fractional differential equations are becoming more important in system models in biology, chemistry, physics, and other sciences. There is a large form of evidence about functional differential equations and their methods. On the other hand, we can seldom be certain that dynamic in a system is perfectly modeled using deterministic ordinary differential equations because the knowledge of dynamical systems is either unclear or incomplete. If the model's underlying structure is based on subjective decisions, one way to incorporate these is to use the fuzziness aspect, which contributes to the consideration of fuzzy fractional functional evolution equations. In the context of fuzzy-valued analysis and set-valued differential equations, fuzzy differential equations were first studied as a separate subject. The analysis of fuzzy differential equations can be expressed in a variety of ways. In biology, chemistry, physics, and other sciences, fractional differential equations are becoming more significant in system models. The reader is referred to the monographs [4, 5], and the references therein, as there is a large quantity of literature dealing with delay differential equations and their applications. As a new branch of fuzzy mathematics, the study of fuzzy delay differential equations is growing in popularity. Over the last few years, both theory and applications have been widely discussed. The study of fuzzy delay fractional functional evolution equations has numerous interpretations in the literature.

Puri and Ralescu defined H-differentiability for fuzzy functions using the Hukuhara derivative of multivalued functions. In the context of fuzzy differential equations in a time-dependent manner, Seikkala and Kaleva proposed and investigated this definition. The fuzzy initial value issue has a unique local solution if f is continuous and satisfies the Lipschitz condition with respect to u, as Kaleva established in [6].

$$U'(\mathfrak{J}) = f(\mathfrak{J}, u), u(0) = u_0 \, on(\mathbf{E^m}, \mathscr{D}). \tag{1}$$

He proved that the Peano theorem is invalid in [6], since metric space $(\mathbf{E^m}, \mathscr{D})$ can be locally compact. Peano's existence theorem for FDEs on $(\mathbf{E^m}, \mathscr{D})$ was proven by Nieto [7] if f is bounded and continuous. Buckley and Feuring [8] gave reasonable general formulation to the fuzzy first-order initial value problem. Citations [9, 10] present the existence of theorems for solutions to the fuzzy initial value problem under a wide range of assumptions. This H-differentiability-based approach has the disadvantage of having an increasing length of support for each solution of FDE. As a result, this method is inappropriate for modeling and fails to describe any of the complex properties of ordinary differential equations, that is, stability, periodicity, bifurcation, and other phenomena [11]. This problem is solved using FDE, which can be read as a family of differential inclusions [12]. We do not have a derivative for fuzzy-number-valued equations, which is a key drawback of differential inclusions.

The above-mentioned method for fuzzy-number-valued functions with highly generalized differentiability was recently solved by Bede and Gal [13]. The derivative is maintained in this case, and the support length of the FDE solution may decrease, but the uniqueness is lost. On fuzzy differential equations, there is a lot of literature. In comparison, FFDEs and their implementations were only briefly mentioned in a few articles. Park and his colleagues' [14] approximate solutions of fuzzy functional integral equations were studied. Park et al. [15] examined the presence of almost periodic and asymptotically almost periodic solutions for FFDEs. For nonlinear fuzzy neutral functional differential equations, Balasubramaniam and Muralisankar [16] investigate local uniqueness and existence theorem. Guo et al. [17] developed existence results for fuzzy impulsive functional differential equations using Hüllermeier's level-wise method [13], which they then applied to fuzzy population models. Abbas et al. [18, 19] worked on a partial differential equation. Niazi et al. [20], Iqbal et al. [21], Shafqat et al. [22], Abuasbeh et al. [23], and Alnahdi et al.'s [24] existence and uniqueness of the FFEE were investigated.

Khastan et al. proved the existence of two fuzzy solutions for fuzzy delay differential equations using the concept of generalized differentiability. Hoa et al. established the global existence and uniqueness results for fuzzy delay differential equations using the concept of generalized differentiability. Moreover, the authors have extended and generalized some comparison theorems and stability theorems for fuzzy delay differential equations with the definition of a new Lyapunov-like function. Besides that, some very important extensions of the fuzzy delay dierential equations were introduced. The author considered the FDE with the initial value

$$X'(\mathfrak{J}) = f(\mathfrak{J}, x(\mathfrak{J})), x(\mathfrak{J}_0) = x_0 \in \mathbf{E^d}, \tag{2}$$

where $f : [0,\infty) \times \mathbf{E^d} \longrightarrow \mathbf{E^d}$ and the symbol $'$ denotes the first type of Hukuhara derivative, that is, the classical Hukuhara derivative. O. Kaleva also discussed the properties of differentiable fuzzy mappings and showed that if f is continuous and $f(\mathfrak{J}, x)$ satisfies the Lipschitz condition concerning to x, then, there exists a unique local solution for the fuzzy initial value problem. V. Lupulescu proved several theorems stating the existence, uniqueness, and boundedness of solutions to fuzzy differential equations with the concept of the inner product on the fuzzy space. Guo et al. [25] and Shu et al. [26] studied the fractional differential equation.

In [27], V. Lupulescu considered the fuzzy functional differential equation

$$\begin{aligned} x'(\mathfrak{J}) &= f(\mathfrak{J}, x_{\mathfrak{J}}), \mathfrak{J} \geq \mathfrak{J}_0, \\ x(\mathfrak{J}) &= \phi(\mathfrak{J} - t_0) \in \mathbf{E^d}, \mathfrak{J}_0 \geq \mathfrak{J} \geq \mathfrak{J}_0 - \sigma, \end{aligned} \tag{3}$$

where $f : [0,\infty) \times C_\sigma \longrightarrow \mathbf{E^d}$ and the symbol $'$ denotes the first type Hukuhara derivative called classical Hukuhara derivative. The author studied the local and global existence and uniqueness results by using the method of successive approximations and contraction principle.

We used Caputo derivative to prove the uniqueness and existence of several uniqueness and existence theorems for fuzzy fractional functional differential equations (FFFDEs) under certain conditions, inspired by the above research:

$$\begin{aligned} {}_0^c D_q^H x(\mathfrak{J}) &= f(\mathfrak{J}, x_{\mathfrak{J}}) + \int_0^{\mathfrak{J}} g(\mathfrak{J}, s, x_s) \mathrm{ds}, \mathfrak{J} \geq \mathfrak{J}_0, \mathfrak{J} \in [0, T], \\ x(\mathfrak{J}) &= \psi(\mathfrak{J} - \mathfrak{J}_0) = \psi_0 \in C_\sigma, \mathfrak{J}_0 \geq \mathfrak{J} \geq \mathfrak{J}_0 - \sigma \\ x'(\mathfrak{J}) &= \psi'(\mathfrak{J}) = \psi_1, \end{aligned} \tag{4}$$

where C_σ denotes the set of fuzzy continuous mapping defined on $[\mathfrak{J}_0 - \sigma, T]$ and $\sigma > 1$. $x_{\mathfrak{J}}$ denotes the fuzzy mapping $x(\mathfrak{J}_s)$, $\mathfrak{J}_0 - \sigma \leq s \leq T$; that is, $x_{\mathfrak{J}} \in C_\sigma$. The goal of this study is to use the method of contraction principle and consecutive approximations to show local and global uniqueness and existence theorems for the fuzzy fractional functional differential Equation (4) under certain conditions.

The following is a description of the paper's structure. As a warm-up, we will make some basic observations on fuzzy sets and the differentiability and integrability features of fuzzy functions. In Section 3, we show the local uniqueness and existence theorem for the solution to the initial value problem for FFFDEs using the successive approximation method. Section 4 proves the global uniqueness and existence theorem for the initial value solution. A problem involving fuzzy fractional functional differential equations is solved using contraction theory. Finally, we apply what we have learned about FDEs to two different forms of fuzzy differential equations: FFFDEs with fuzzy population and distributed delays models.

2. Preliminaries

The set of all nonempty, compact convex subsets of $\mathbf{R^m}$ is denoted by $\mathscr{K}_c(\mathbf{R^m})$. The Hausdorff distance between sets $A, B \in \mathscr{K}_c(\mathbf{R^m})$ is defined as

$$d_H(A, B) = \max\left\{\sup_{a\in A}\inf_{b\in B}||a-b||, \sup_{b\in B}\inf_{a\in A}||a-b||\right\}. \quad (5)$$

Denote $\{\mathbf{E^m} = x : \mathbf{R^m} \longrightarrow 0, 1|\,; x \text{ satisfies (a)} - \text{(d) below}\}$.

In the above equation,

(a) x is normal due to the exists of $\mathbf{R^m}$, $x(u_0) = 1$

(b) x is fuzzy convex, for $\mathbf{R^m}$, $0 \le \lambda \le 1$, $x(\lambda u + (1-\lambda)v) \ge \min\{x(u), x(v)\}$

(c) x is upper semicontinuous function on $\mathbf{R^m}$

(d) $[x]^0 = cl\{s \in \mathbf{R^m}/x(\mathfrak{I}) > 0\}$ is compact

$1 < \beta \le 2$, represent $[x]^\beta = \{u \in \mathbf{R^m}/x(\mathfrak{I}) \ge \beta\}$. Then, from (a) to (b), it shows, β-level set $[x]^\beta \mathfrak{I} \in \mathscr{K}_c(\mathbf{R^m}) \forall 1 \le \beta \le 2$. We define $\tilde{0} \in \mathbf{E^m}$ as $\tilde{0}(u) = 1$ if $u = 0$ and $\tilde{0}(u) = 0$ if $u \ne 0$ for later purposes.

Using Zadeh's extension theorem, we can have scalar multiplication and addition in fuzzy number space $\mathbf{E^m}$ as shown in

$$[x \oplus y]^\beta = [x]^\beta \oplus [y]^\beta, [kx]^\beta = k[x]^\beta, \quad (6)$$

where $x, y \in \mathbf{E^m}, k \in \mathbf{R^m}$ and $1 \le \beta \le 2$.

Define $\mathscr{D} : \mathbf{E^m} \times \mathbf{E^m} \longrightarrow \mathbf{R}^+$ by notation

$$\mathscr{D}(x, y) = \sup_{1\le\beta\le2} d_H\left\{[x]^\beta, [y]^\beta\right\}. \quad (7)$$

where $\mathscr{D}$ is Hausdorff a metric for nonempty compact sets in $\mathbf{R^m}$ and $(\mathbf{E^m}, \mathscr{D})$ is a complete metric space [28].

It is very simple to notice that $\mathscr{D}$ is a metric in $\mathbf{E^m}$. By using the properties of $\mathscr{D}(x, y)$:

(a) $(\mathbf{E^m}, \mathscr{D})$ is a complete metric space

(b) $\mathscr{D}(x \oplus z, y \oplus z) = \mathscr{D}(x, y)$ and $\mathscr{D}(x, y) = \mathscr{D}(x, y) \forall x, y, z \in \mathbf{E^m}$

(c) $\mathscr{D}(\lambda x, \lambda y) = |\lambda|\mathscr{D}(x, y) \forall x, y \in \mathbf{E^m}$ and $\lambda \in \mathbf{R^m}$

(d) $\mathscr{D}(x, y) \le \mathscr{D}(x, z) + \mathscr{D}(z, y)$

If we denote $\|x\|_{\mathfrak{G}} = \mathscr{D}(x, \tilde{0}), x \in \mathbf{E^m}$, then, $\|x\|_{\mathfrak{G}}$ has properties of an usual norm on$\mathbf{E^m}$ [29]:

(i) $\|x\|_{\mathfrak{G}} = 0$ if $x = \tilde{0}$

(ii) $\|\lambda x\|_{\mathfrak{G}} = |\lambda|\|x\|_{\mathfrak{G}} \forall x, y \in \mathbf{E^m}$

(iii) $\|x + y\|_{\mathfrak{G}} \le \|x\|_{\mathfrak{G}} + \|y\|_{\mathfrak{G}} \forall x, y \in \mathbf{E^m}$

(iv) $\mathscr{D}(\beta x, \gamma x) \le |\beta - \gamma| D(x, \tilde{0}), \forall \beta, \gamma \ge 1$ or $\beta, \gamma \le 1, x \in \mathbf{E^m}$

On $\mathbf{E^m}$, we can describe subtraction !, also known as H -difference [30], as follows: $s \ominus v$ has significance if $\omega \in \mathbf{E^m}$, $x = y + z$ exists.

Suppose $a, b \in \mathbf{R^m}, f \in \mathscr{C}(I, \mathbf{E^m})$, if we represent $\|f\| = H(f, \tilde{0})$, then, $\|f\|$ has properties of an usual norm on $\mathbf{E^m}$ [29],

(i) $\|f\| = 0$ if $f = \tilde{0}$

(ii) $\|\lambda f\| = |\lambda|\|f\| \forall f \in \mathbb{C}(I, \mathbf{E^m}), \lambda \in \mathbf{R^m}$

(iii) $\|f \oplus h\| \le \|f\| \oplus \|h\| \forall f, h \in (I, \mathbf{E^m})$

(iv) $H(\beta f, \gamma f) \le |\beta - \gamma| H(f, \tilde{0}), \forall \beta, \gamma \ge 0$ or $\beta, \gamma \le 0$, $f \in \mathbb{C}(I, \mathbf{E^m})$

Definition 1. The mapping $\mathscr{F} : \mathrm{I} \longrightarrow \mathbf{E^m}$ is Hukuhara differentiable at $\mathfrak{I} \in I$ if exists $\mathscr{G}'(\mathfrak{I}) \in \mathbf{E^m}$ similar to the limits:

$$\lim_{h\longrightarrow0^+}\frac{\mathscr{G}(\mathfrak{I}_0 + h) \ominus \mathscr{G}(\mathfrak{I}_0)}{h} \text{ and } \lim_{h\longrightarrow0^+}\frac{\mathscr{G}(\mathfrak{I}_0) \ominus \mathscr{G}(\mathfrak{I}_0 - h)}{h}, \quad (8)$$

and is equal and exists to $\mathscr{G}'(\mathfrak{I})$.

We can remember some properties of integrability and measurability for fuzzy set-valued mappings [28].

Definition 2. If $\mathscr{G} : \mathrm{I} \longrightarrow \mathbf{E^m}$ is fuzzy function, that is

$$[\mathscr{G}(\mathfrak{I})]^\beta = \left[\mathscr{G}_1^\beta(\mathfrak{I}), \mathscr{G}_2^\beta(\mathfrak{I})\right], \beta \in [1, 2], \quad (9)$$

and there exists $\mathscr{G}'(\mathfrak{I}_0)$ for some $\mathfrak{I}_0 \in I$, and now

$$\left[\mathscr{G}'(\mathfrak{I}_0)\right]^\beta = \left[\left(\mathscr{G}_1^\beta\right)'(\mathfrak{I}_0), \left(\mathscr{G}_2^\beta\right)'(\mathfrak{I}_0)\right], \beta \in [1, 2]. \quad (10)$$

Definition 3. The mapping $\mathscr{G} : I \in \mathbf{E^m}$ is strongly measurable if for all $\beta \in [1, 2]$, then, the set-valued function $\mathscr{G}_\beta : \mathrm{I} \longrightarrow \mathrm{M_j}\mathbf{R^m}$define by $\mathscr{G}_\beta(\mathfrak{I}) = [\mathscr{G}(\mathfrak{I})]^\beta$ is Lebesgue measurable.

The mapping $\mathscr{G} : I \in \mathbf{E^m}$ is known as integrably bounded if there exists an integrable function j like

$$||x|| \leq J(\mathfrak{J}) \forall x \in \mathscr{G}_0(\mathfrak{J}). \quad (11)$$

Definition 4. Suppose $\mathscr{G}$: I $\in \mathbf{E^m}$. Then, the equation defines integral of $\mathscr{G}$ over I, which is expressed by $\int_I \mathscr{G}(\mathfrak{J})\mathrm{dt}$, $[\int_I \mathscr{G}(\mathfrak{J})\mathrm{dt}]^\beta = \int_I \mathscr{G}_\beta(\mathfrak{J})d\mathfrak{J} = \{\int_I \mathscr{G}(\mathfrak{J})d\mathfrak{J}/f : I \longrightarrow \mathbf{R^m}$ is measurable selection for $\mathscr{G}_\beta\} \forall \beta \in [1, 2]$.

Also, strongly measurable and integrably bounded mapping $\mathscr{G} : I \longrightarrow \mathbf{E^m}$ is said to be integrable over I if and only if

$$\int_I \mathscr{G}(\mathfrak{J})d\mathfrak{J} \in \mathbf{E^m}. \quad (12)$$

Proposition 5 (Aumann [31]). *$\mathscr{G}$ is integrable if $\mathscr{G} : I \in \mathbf{E^m}$ is integrably bounded and strongly measurable.*

Proposition 6 (Kaleve [28]). *It is integrable over I if $\mathscr{G} : I \longrightarrow \mathbf{E^m}$ is continuous. Furthermore, function $\mathscr{F}(\mathfrak{J}) = \int_{\mathfrak{J}_0}^{\mathfrak{J}} \mathscr{G}(s)ds$, $\mathfrak{J}_0, \mathfrak{J} \in I$ is differentiable in this case, and $\mathscr{F}'(\mathfrak{J}) = \mathscr{G}(\mathfrak{J})$.*

Proposition 7 (Kaleve [28]). *Suppose $\mathscr{G}, H : I \in \mathbf{E^m}$ be integrable and $\lambda \in \mathbf{R^m}$. Now*

(i) $\int_I (\mathscr{G}(\mathfrak{J}) \oplus H(\mathfrak{J}))d\mathfrak{J} = \int_I \mathscr{G}(\mathfrak{J})d\mathfrak{J} \oplus \int_I H(\mathfrak{J})d\mathfrak{J}$

(ii) $\int_I \lambda \mathscr{G}(\mathfrak{J})d\mathfrak{J} = \lambda \int_I \mathscr{F}(\mathfrak{J})d\mathfrak{J}$

(iii) $\mathscr{D}(\mathscr{G}, H)$ *is integrable*

(iv) $\mathscr{D}(\int_I \mathscr{G}(\mathfrak{J})d\mathfrak{J}, \int_I H(\mathfrak{J})d\mathfrak{J}) \int_I \mathscr{D}(\mathscr{G}, H)(\mathfrak{J})d\mathfrak{J}$

(v) $\int_{\mathfrak{J}_0}^{\mathfrak{J}_2} \mathscr{G}(\mathfrak{J})d\mathfrak{J} = \int_{\mathfrak{J}_0}^{\mathfrak{J}_1} \mathscr{G}(\mathfrak{J})d\mathfrak{J} + \int_{\mathfrak{J}_1}^{\mathfrak{J}_2} \mathscr{G}(\mathfrak{J})d\mathfrak{J}$, *for* $\mathfrak{J}_0, \mathfrak{J}_1, \mathfrak{J}_2 \in I$

If I is compact interval of $\mathbf{R^m}$, then represent $\mathbb{C}(I, \mathbf{E^m}) = \{f : I \longrightarrow \mathbf{E^m}$; f is continuous functions on $I\}$, equipped with metric

$$\mathscr{D}(x, y) = \sup_{\mathfrak{J} \in I} \mathscr{D}(x(\mathfrak{J}), y(\mathfrak{J})). \quad (13)$$

Now, $(\mathbb{C}, H)$ is a complete metric space.

We call C_σ space $C([-\sigma, 0], \mathbf{E^m})$ for positive numbers σ. Represent it as well:

$$\mathscr{D}_\sigma(x, y) = \sup_{\mathfrak{J} \in [-\sigma, 0]} \mathscr{D}(x(\mathfrak{J}), y(\mathfrak{J})), \quad (14)$$

metric on space C_σ. For a given constant $\rho > 0$, put $B_\rho := \{\varphi \in C_\sigma ; \mathscr{D}_\sigma(\varphi, 0) \leq \rho\}$.

Suppose $x(.) \in C([-\sigma, \infty), \mathbf{E^m})$. Now, for all $\mathfrak{J} \in [0, \infty)$, denoted by x_1 element of C_σ defined by $x_1(s) = x(\mathfrak{J} + s)$, $s \in [-\sigma, 0]$.

Definition 8 (Fuzzy Strongly Continuous Semigroups) [30, 31]. A family $\{\mathrm{T}(\mathfrak{J}), \mathfrak{J} \geq 0\}$ is fuzzy strongly continuous semigroup of operators from $\mathbf{E^m}$ into itself if

(i) $T(0) = k$ identity mapping on $\mathbf{E^m}$

(ii) $T(\mathfrak{J} \oplus m) = T(\mathfrak{J})T(m) \forall \mathfrak{J}, m \geq 0$

(iii) function $h : [0, \infty[\longrightarrow \mathbf{E^m}$, defined by $h(\mathfrak{J}) = T(\mathfrak{J})x$ at $\mathfrak{J} = 0 \forall x \in \mathbf{E^m}$ is continuous

$$\lim_{\mathfrak{J} \longrightarrow 0^+} T(\mathfrak{J})x = x. \quad (15)$$

(iv) There are two constants $R > 0$ and ω like

$$\mathscr{D}(T(\mathfrak{J})x, T(\mathfrak{J})y) \leq Re^\omega D(x, y), \text{for} \mathfrak{J} \geq 0, x, y \in \mathbf{E^m}. \quad (16)$$

Specially, if $\omega = 0$ and $\mathbf{R^m} = 1$, $\{T(\mathfrak{J}), \mathfrak{J} \geq 0\}$ is a contraction fuzzy semigroup.

Lemma 9. *If $\mathscr{G} : [0, \infty) \times C_\sigma \longrightarrow \mathbf{E^m}$ is jointly continuous function and $x : [-\sigma, \infty) \longrightarrow \mathbf{E^m}$ is continuous function, now, function $\mathfrak{J} \mapsto \mathscr{G}(\mathfrak{J}, x_\mathfrak{J})$: $[0, \infty) \longrightarrow \mathbf{E^m}$ is also continuous.*

Proof. Assume that fixed $(\tau, \varphi) \times C_\sigma$ and $\varepsilon > 0$. $\mathscr{G} : [0, \infty) \times C_\sigma \longrightarrow \mathbf{E^m}$ are jointly continuous, there exists $\delta_1 > 0$ that is for all $(\mathfrak{J}, \psi) \in [0, \infty) \times C_\sigma$ with $|\mathfrak{J} - \tau| + \mathscr{D}_\sigma(\varphi, \psi) < \delta_1$, $\mathscr{D}[\mathscr{G}(\mathfrak{J}, \psi), \mathscr{G}(\tau, \varphi)] < \varepsilon$. On the other way, $x : [-\sigma, \infty) \longrightarrow \mathbf{E^m}$ is continuous; now, it is uniformly continuous on compact interval $I_1 = [\max\{-\sigma, \tau - \sigma - \delta_1\}, \tau + \delta_1]$. There exists $\delta_2 > 0$; for all $\mathfrak{J}_1, \mathfrak{J}_2 \in I_1$ with $|\mathfrak{J}_1 - \mathfrak{J}_2| < \delta_2$, we have $\mathscr{D}[x(\mathfrak{J}_1), x(\mathfrak{J}_2)] < \delta_1/2$. After, for all $s \in [-\sigma, 0]$, $\tau + s \in I_1$, and $\mathfrak{J} + \mathrm{s} \in I_1$ if $|\mathfrak{J} - \tau| < \delta_1/2$, now, $|(\mathfrak{J} + \mathrm{s}) - (\tau + \mathrm{s})| < \delta_2$, and it shows that

$$\begin{aligned} \mathscr{D}_\sigma(x_\mathfrak{J}, x_\tau) &= \sup_{-\sigma \leq s \leq 0} \mathscr{D}[x_\mathfrak{J}(\mathrm{s}), x_\tau(\mathrm{s})] \\ &= \sup_{-\sigma \leq s \leq 0} \mathscr{D}[x(\mathfrak{J} + \mathrm{s}), x(\tau + \mathrm{s})] \leq \delta_1/2. \end{aligned} \quad (17)$$

Therefore, $|\mathfrak{J} - \tau| + \mathscr{D}_\sigma(x_\mathfrak{J}, x_\tau) < \delta_1$, since $\mathscr{G}$ is jointly continuous, $\mathscr{D}[\mathscr{G}(\mathfrak{J}, x_\mathfrak{J}), \mathscr{G}(\tau, x_\tau)] < \varepsilon$. This implies that function $\mathfrak{J} \mapsto \mathscr{G}(\mathfrak{J}, x_\mathfrak{J})$: $[0, \infty) \longrightarrow \mathbf{E^m}$ is continuous. □

Remark 10. If $\mathscr{G} : [0, \infty) \times C_\sigma \longrightarrow \mathbf{E^m}$ is jointly continuous function and $x : [-\sigma, \infty) \longrightarrow \mathbf{E^m}$ is continuous function, then, function $\mathfrak{J} \mapsto \mathscr{G}(\mathfrak{J}, x_1)$: $[0, \infty) \longrightarrow \mathbf{E^m}$ on each compact interval $[\tau, T]$ is integrable. Furthermore, function $\mathscr{F}(\mathfrak{J}) = \int_\tau^\mathfrak{J} \mathscr{G}(s, x_s)\mathrm{ds}$, $\mathfrak{J} \in [\tau, T]$ is differentiable in this case, and $\mathscr{F}'(\mathfrak{J}) = \mathscr{G}(\mathfrak{J}, x_\mathfrak{J})$.

Remark 11. If $\mathscr{G} : [0, \infty) \times C_\sigma \longrightarrow \mathbf{E^m}$ is jointly continuous function and $x : [-\sigma, \infty) \longrightarrow \mathbf{E^m}$ is continuous function, then, function $\mathfrak{J} \mapsto \mathscr{G}(\mathfrak{J}, x_1)$: $[0, \infty) \longrightarrow \mathbf{E^m}$ on each compact interval $[\tau, T]$ is bounded. On each compact interval $[0, T]$, function $\mathfrak{J} \mapsto \mathcal{G}(\mathfrak{J}, 0): [0,\infty) \longrightarrow \mathbf{E^m}$ is also bounded.

Definition 12. We say that $\mathcal{G} : [0,\infty) \times C_\sigma \longrightarrow \mathbf{E^m}$ is locally Lipschitz if $a, b \in [0,\infty)$ and $\rho > 0$, and there exists $L > 0$,

$$\mathcal{D}[\mathcal{G}(\mathfrak{J}, \varphi), \mathcal{G}(\mathfrak{J}, \psi) \le L\mathcal{D}_\sigma(\varphi, \psi), a \le \mathfrak{J} \le b, \varphi, \psi \in B_\rho. \tag{18}$$

Lemma 13. *Assume that $\mathcal{G} : [0,\infty) \times C_\sigma \longrightarrow \mathbf{E^m}$ is locally Lipschitz and continuous. Now, for all compact interval $J \subset [0,\infty)$ and $\rho > 0$, there exists $\mathcal{K} > 0$,*

$$\mathcal{D}\left[\mathcal{G}(\mathfrak{J}, \varphi), \tilde{0}\right] \le \mathcal{K}, \mathfrak{J} \in J, \varphi \in B_\rho. \tag{19}$$

Proof. $\mathfrak{J} \in J$, then

$$\begin{aligned}\mathcal{D}\left[\mathcal{G}(\mathfrak{J}, \varphi), \tilde{0}\right] &\le \mathcal{D}[\mathcal{G}(\mathfrak{J}, \varphi), \mathcal{G}(\mathfrak{J}, 0)] + \mathcal{D}\left[\mathcal{G}(\mathfrak{J}, 0), \tilde{0}\right] \\ &\le L\mathcal{D}_\sigma(\varphi, 0) + \mathcal{D}\left[\mathcal{G}(\mathfrak{J}, 0), \tilde{0}\right] \le \rho L + \eta,\end{aligned} \tag{20}$$

where $\eta := \sup_{\mathfrak{J}\in J} D[\mathcal{G}(\mathfrak{J}, 0), \tilde{0}]$. □

Definition 14 (see [32]). The RL fractional derivative is defined as

$${}_a\mathcal{D}^p_{\mathfrak{J}} f(\mathfrak{J}) = \left(\frac{d}{d\mathfrak{J}}\right)^{n+1} \int_a^{\mathfrak{J}} (\mathfrak{J} - \tau)^{n-p} f(\tau) d\tau, n \le p \le n + 1. \tag{21}$$

Definition 15 (see [32]). The Caputo fractional derivatives ${}^c_a\mathcal{D}^\alpha_{\mathfrak{J}} f(\mathfrak{J})$ of order $\alpha \in \mathbf{E}^+$ are defined by

$${}^c_a\mathcal{D}^\alpha_{\mathfrak{J}} f(\mathfrak{J}) = {}_a\mathcal{D}^\alpha_{\mathfrak{J}} \left(f(\mathfrak{J}) - \sum_{k=0}^{n-1} \frac{f^{(k)}(a)}{k!} (\mathfrak{J} - a)^k \right), \tag{22}$$

respectively, where $n = [\alpha] + 1$ for $\alpha \notin N_0$; $n = \alpha$ for $\alpha \in N_0$.

We investigate the Caputo fractional derivative of order $1 < \alpha \le 2$ in this study; e.g.,

$${}^c_a\mathcal{D}^{3/2}_{\mathfrak{J}} f(\mathfrak{J}) = {}_aD^{3/2}_{\mathfrak{J}} \left(f(\mathfrak{J}) - \sum_{k=0}^{n-1} \frac{f^{(k)}(a)}{k!} (\mathfrak{J} - a)^k \right). \tag{23}$$

Definition 16 (see [33]). The Wright function ψ_α is defined by

$$\begin{aligned}\psi_\alpha(\theta) &= \sum_{n=0}^{\infty} \frac{(-\theta)^n}{n!\Gamma(-\alpha n + 1 - \alpha)} \\ &= \frac{1}{\pi} \sum_{n=1}^{\infty} \frac{(-\theta)^n}{(n-1)!} \Gamma(n\alpha) \sin(n\pi\alpha),\end{aligned} \tag{24}$$

where $\theta \in \mathbb{C}$ with $0 < \alpha < 1$.

Lemma 17 (see [33]). *Let $\{C(\mathfrak{J})\}\mathfrak{J} \in \mathbf{Rm}$ be a strongly continuous cosine family in X satisfying $\|C(\mathfrak{J})\|_{L_b(X)} \le Me^{\omega|\mathfrak{J}|}$, $\mathfrak{J} \in \mathbf{R^m}$, and let A be the infinitesimal generator of $\{C(\mathfrak{J})\}$ $\mathfrak{J} \in \mathbf{Rm}$. Then, for $\operatorname{Re} \lambda > \omega, \lambda^2 \in \rho(A)$*

$$\begin{aligned}\lambda R\left(\lambda^2 ; A\right)x &= \int_0^\infty e^{-\lambda\mathfrak{J}} C(\mathfrak{J})x d\mathfrak{J}, R\left(\lambda^2 ; A\right)x \\ &= \int_0^\infty e^{-\lambda\mathfrak{J}} S(\mathfrak{J})x d\mathfrak{J}, \textit{for } x \in X.\end{aligned} \tag{25}$$

Lemma 18. *For $x(\mathfrak{J}) = \psi_0$, if $u_{\mathfrak{J}}$ is the solution of Equation (4), then, the solution $u_{\mathfrak{J}}$ is given by*

$$\begin{aligned}x_{\mathfrak{J}} &= C_q(\mathfrak{J})\psi_0 + \mathcal{K}_q(\mathfrak{J})\psi_1 + \int_0^{\mathfrak{J}} (\mathfrak{J} - s)^{q-1} P_q(\mathfrak{J} - s) \\ &\cdot \left[f(s, x_s) + \int_0^{\mathfrak{J}} g(\mathfrak{J}, s, x_s) ds \right] ds, \mathfrak{J} \in [0, T],\end{aligned} \tag{26}$$

such that

$$\begin{aligned}C_q(\mathfrak{J}) &= \int_0^\infty M_q C(\mathfrak{J}^q\zeta) d\zeta, \mathcal{K}_q(\mathfrak{J}) = \int_0^{\mathfrak{J}} C_q(s) ds, P_q(\mathfrak{J}) \\ &= \int_0^\infty q\zeta M_q C(\mathfrak{J}^q\zeta) d\zeta,\end{aligned} \tag{27}$$

where $C_q(\mathfrak{J})$ and $\mathcal{K}_q(\mathfrak{J})$ are continuous with $C(0) = I$ and $\mathcal{K}(0) = I$, $|C_q(\mathfrak{J})| \le c, c > 1$ and $|\mathcal{K}_q(\mathfrak{J})| \le c, c > 1, \forall \mathfrak{J} \in [0, T]$.

3. Local Uniqueness and Existence

For $\mathcal{G} : [0,\infty) \times C_\sigma \longrightarrow \mathbf{E^m}$, we assume the fuzzy Caputo functional equation:

$$\begin{aligned}{}^C_0D^q_H x(\mathfrak{J}) &= f(\mathfrak{J}, x_{\mathfrak{J}}) + \int_0^{\mathfrak{J}} g(\mathfrak{J}, s, x_s) ds, \mathfrak{J} \ge \mathfrak{J}_0, \mathfrak{J} \in [0, T], \\ x(\mathfrak{J}) &= \psi(\mathfrak{J} - \mathfrak{J}_0) = \psi_0 \in C_\sigma, \mathfrak{J}_0 \ge \mathfrak{J} \ge \mathfrak{J}_0 - \sigma, \\ u'(\mathfrak{J}) &= \psi'(\mathfrak{J}) = \psi_1.\end{aligned} \tag{28}$$

According to the solution of FFFDE (4) on interval $[\mathfrak{J}_0, b]$, we mean continuous function $x : [\mathfrak{J}_0 - \sigma, b) \longrightarrow \mathbf{E^m}$; that is, $x(\mathfrak{J}) = \varphi(\mathfrak{J} - \mathfrak{J}_0)$ for $\mathfrak{J} \in [\mathfrak{J}_0 - \sigma, b]$ for $\mathfrak{J} \in [0, T]$ and x is differentiable on $(\mathfrak{J}_0, b]$ and ${}^c_0\mathcal{D}^q_H x(\mathfrak{J}) = f(\mathfrak{J}, x_{\mathfrak{J}}) + \int_0^{\mathfrak{J}} g(\mathfrak{J}, s, x_s) ds, \mathfrak{J} \in [0, T]$.

Theorem 19. *Suppose set $\mathcal{G} : [0,\infty) \times C_\sigma \longrightarrow \mathbf{E^m}$ is locally Lipschitz and continuous. Now, for all $(\mathfrak{J}_0, \varphi) \in [0,\infty) \times C_\sigma$, there exists $\mathfrak{J} > \mathfrak{J}_0$; that is, FFFDE (4) has unique solution $x : [\mathfrak{J}_0 - \sigma, \mathfrak{J}] \longrightarrow \mathbf{E^m}$.*

Proof. Any positive number will satisfy as $\rho > 0$. Then, there exists $L > 0$; that is, $\mathscr{G}$ is Lipschitz locally.

$$\mathscr{D}[\mathscr{G}(\mathfrak{J}, \varphi), \mathscr{G}(\mathfrak{J}, \psi)] \le L\mathscr{D}_\sigma(\varphi, \psi), \mathfrak{J}_0 \le \mathfrak{J} \le h, \varphi, \psi \in B_{2\rho}, \tag{29}$$

for some $h > \mathfrak{J}_0$. According to Lemma 13, there exists $\mathscr{K} > 0$, $\mathscr{D}[\mathscr{F}(\mathfrak{J}, \varphi), \tilde{0}] \le \mathscr{K}$ for $(\mathfrak{J}, \varphi) \in [\mathfrak{J}_0, h] \times B_{2\rho}$. Suppose $T \coloneqq \min \{h, \rho/\mathscr{K}\}$. We assume set $\mathbf{E^m}$ of all functions $x \in C([\mathfrak{J}_0 - \sigma, T], \mathbf{E^m})$; then, $x(\mathfrak{J}) = \varphi(\mathfrak{J} - \mathfrak{J}_0)$ on $[\mathfrak{J}_0 - \sigma, \mathfrak{J}_0]$ and $\mathscr{D}[x(\mathfrak{J}), \tilde{0}] \le 2\rho$ on $[\mathfrak{J}_0, T]$. If $y \in \mathbf{E^m}$, we define continuous function $\omega : [\mathfrak{J}_0 - \sigma, T] \longrightarrow \mathbf{E^m}$ by

$$w(\mathfrak{J}) \coloneqq \begin{cases} f(\mathfrak{J}, x_\mathfrak{J}) + \int_0^\mathfrak{J} g(\mathfrak{J}, \mathrm{s}, x_\mathrm{s})\mathrm{ds}, \mathfrak{J} \ge \mathfrak{J}_0, \mathrm{t}_0 \ge \mathfrak{J} \ge \mathfrak{J}_0 - \sigma, \\ \varphi(0) + C_q(\mathfrak{J})\psi_0 + \mathscr{K}_q(\mathfrak{J})\psi_1 + \int_0^\mathfrak{J} (\mathfrak{J} - \mathrm{s})^{q-1} P_q(\mathfrak{J} - \mathrm{s}) \left[f(\mathrm{s}, y_\mathrm{s}) + \int_0^\mathfrak{J} g(\mathfrak{J}, \mathrm{s}, y_\mathrm{s}) ds \right] \mathrm{ds} \in [0, T]. \end{cases} \tag{30}$$

Now, for $\mathfrak{J} \in [0, T]$

$$\mathscr{D}\left[w(\mathfrak{J}), \tilde{0}\right] \ge \mathscr{D}\left[\left[\int_0^\mathfrak{J} f(\mathrm{s}, y_\mathrm{s}), \tilde{0}\right)\mathrm{ds}\right] + \int_0^\mathfrak{J} \mathscr{D}\left[\left[\int_0^\mathfrak{J} \left(g(\mathfrak{J}, \mathrm{s}, y_\mathrm{s}), \tilde{0}\right)\mathrm{ds}\right]\mathrm{ds} \ge 2\rho T, \tag{31}$$

and so $\omega \in \mathbf{E^m}$. We will use method of successive approximations to solve (4) by constructing series of continuous functions. $x^m : [\mathfrak{J}_0 - \sigma, T] \longrightarrow \mathbf{E^m}$ beginning with initial continuous function

$$x^0(\mathfrak{J}) \coloneqq \begin{cases} f(\mathfrak{J}, x_\mathfrak{J}) + \int_0^\mathfrak{J} g(\mathfrak{J}, \mathrm{s}, x_\mathrm{s})\mathrm{ds}, \mathfrak{J} \ge \mathfrak{J}_0, \mathfrak{J}_0 \ge \mathfrak{J} \ge \mathfrak{J}_0 - \sigma, \\ \varphi(0) + C_q(\mathfrak{J})\psi_0 + \mathscr{K}_q(\mathfrak{J})\psi_1 \mathfrak{J} \in [0, T]. \end{cases} \tag{32}$$

Clearly, $\mathscr{D}[{}_0^c\mathscr{D}_H^q x^0(\mathfrak{J}), \tilde{0}] \le \rho$ on $[0, T]$. Further, define

$$x^{m+1}(\mathfrak{J}) \coloneqq \begin{cases} f(\mathfrak{J}, x_\mathfrak{J}) + \int_0^\mathfrak{J} g(\mathfrak{J}, \mathrm{s}, x_\mathrm{s}) d\mathrm{s}, \mathfrak{J} \ge \mathfrak{J}_0, \mathfrak{J}_0 \ge \mathfrak{J} \ge \mathfrak{J}_0 - \sigma, \\ \varphi(0) + C_q(\mathfrak{J})\psi_0 + \mathscr{K}_q(\mathfrak{J})\psi_1 + \int_0^\mathfrak{J} (\mathfrak{J} - \mathrm{s})^{q-1} P_q(\mathfrak{J} - \mathrm{s}) \left[f(\mathrm{s}, x_\mathrm{s}^m) + \int_0^\mathfrak{J} g(\mathfrak{J}, \mathrm{s}, x_\mathrm{s}^m) d\mathrm{s} \right] d\mathrm{s}, \mathfrak{J} \in [0, T], \end{cases} \tag{33}$$

if $= 0, 1, \cdots$. Then, for $\mathfrak{J} \in [0, T]$, now

$$\begin{aligned} \mathscr{D}\left[x^1(\mathfrak{J}), u^0(\mathfrak{J})\right] &\le \mathscr{D}\left(\int_0^\mathfrak{J} (\mathfrak{J} - \mathrm{s})^{q-1} P_q(\mathfrak{J} - \mathrm{s}) \cdot \left[f\left(\mathrm{s}, x_\mathrm{s}^0\right) + \int_0^\mathfrak{J} g\left(\mathfrak{J}, \mathrm{s}, x_\mathrm{s}^0\right) ds\right] \mathrm{ds}, \tilde{0}\right) \\ &\le \mathscr{K}(T - 0). \end{aligned} \tag{34}$$

By Equations (29) and (33), we find

$$\begin{aligned} \mathscr{D}\left[x^{m+1}(\mathfrak{J}), x^m(\mathfrak{J})\right] &\le \mathscr{D}\left(\int_0^\mathfrak{J} (\mathfrak{J} - \mathrm{s})^{q-1} P_q(\mathfrak{J} - \mathrm{s}) \cdot \left[f\left(\mathrm{s}, x_\mathrm{s}^m\right) + \int_0^\mathfrak{J} g\left(\mathfrak{J}, \mathrm{s}, x_\mathrm{s}^m\right) ds\right] \mathrm{ds}, \right. \\ &\qquad \left. \int_0^\mathfrak{J} (\mathfrak{J} - \mathrm{s})^{q-1} P_q(\mathfrak{J} - \mathrm{s}) \cdot \left[f\left(\mathrm{s}, x_\mathrm{s}^{m-1}\right) + \int_0^\mathfrak{J} g\left(\mathfrak{J}, \mathrm{s}, x_\mathrm{s}^{m-1}\right) ds\right] \mathrm{ds}\right) \\ &\le \int_0^\mathfrak{J} L^2 \mathscr{D}_\sigma\left(\left[x_\mathrm{s}^m + \int_0^\mathfrak{J} g\left(\mathfrak{J}, \mathrm{s}, x_\mathrm{s}^m\right)\right], \left[x_\mathrm{s}^{m-1} + \int_0^\mathfrak{J} g\left(\mathfrak{J}, \mathrm{s}, x_\mathrm{s}^{m-1}\right) ds\right]\right) \mathrm{ds} \\ &\le \int_0^\mathfrak{J} L^2 \sup_{\theta \in [s-T, s]} D\left(\left[x^m(\theta) + \int_0^\mathfrak{J} g(\mathfrak{J}, \mathrm{s}, x^m(\theta)) ds\right], \left[x^{m-1}(\theta) + \int_0^\mathfrak{J} g\left(\mathfrak{J}, \mathrm{s}, x^{m-1}(\theta)\right) ds\right]\right) \mathrm{ds}, \mathfrak{J} \in [0, T]. \end{aligned} \tag{35}$$

In particular,

$$\mathscr{D}\left[x^2(\mathfrak{J}), x^1(\mathfrak{J})\right] = \frac{\mathscr{K}}{L^2} \frac{\left[L^2(\mathfrak{J} - T)\right]^2}{2!}, \mathfrak{J} \in [0, T]. \tag{36}$$

If we suppose

$$\mathscr{D}\left[x^m(\mathfrak{J}), x^{m-1}(\mathfrak{J})\right] \le \frac{\mathscr{K}}{L^2} \frac{\left[L^2(\mathfrak{J} - T)\right]^m}{m!}, \mathfrak{J} \in [0, T], \tag{37}$$

now

$$\mathscr{D}\left[x^{m+1}(\mathfrak{J}), x^m(\mathfrak{J})\right] = \frac{\mathscr{K}}{L^2} \frac{\left[L^2(\mathfrak{J} - T)\right]^{m+1}}{(m+1)!}, \mathfrak{J} \in [0, T]. \tag{38}$$

(37) holds for any $m \ge 2$, according to mathematical induction. As a result, the sequence $\sum_{m=2}^\infty \mathscr{D}[x^m(\mathfrak{J}), x^{m-1}(\mathfrak{J})]$ is a sequence $\{x^m\}_{m\ge 0}$ that is uniformly convergent on $[0, T]$. As a result, there is a continuous function $x : [0, T] \longrightarrow \mathbf{E^m}$,

which is $\sup_{0\le\mathfrak{I}\le T} \mathscr{D}[x^m(\mathfrak{I}), x(\mathfrak{I})] \longrightarrow 0$ as $m \longrightarrow \infty$. Since then

$$\begin{aligned}&\mathscr{D}\left(\left[f(\mathrm{s}, x_{\mathrm{s}}^m) + \int_0^{\mathfrak{I}} g(\mathfrak{I}, \mathrm{s}, x_{\mathrm{s}}^m)ds\right], \left[f\left(\mathrm{s}, x_{\mathrm{s}}^{m-1}\right) + \int_0^{\mathfrak{I}} g\left(\mathfrak{I}, \mathrm{s}, x_{\mathrm{s}}^{m-1}\right)ds\right]\right)\\ &\quad\le L^2\mathscr{D}_\sigma\left(\left[x_{\mathrm{s}}^m + \int_0^{\mathfrak{I}} g(\mathfrak{I}, \mathrm{s}, x_{\mathrm{s}}^m)ds\right], \left[x_{\mathrm{s}} + \int_0^{\mathfrak{I}} g(\mathfrak{I}, \mathrm{s}, x_{\mathrm{s}})ds\right]\right)\mathrm{ds}\\ &\quad\le \sup_{0\le\mathfrak{I}\le T} \mathscr{D}[x^m(\mathfrak{I}), x(\mathfrak{I})].\end{aligned} \tag{39}$$

We have deduced

$$\begin{aligned}&\mathscr{D}\left(\left[f(\mathrm{s}, x_{\mathrm{s}}^m) + \int_0^{\mathfrak{I}} g(\mathfrak{I}, \mathrm{s}, x_{\mathrm{s}}^m)ds\right]\mathrm{ds},\right.\\ &\qquad\left.\left[f\left(\mathrm{s}, x_{\mathrm{s}}^{m-1}\right) + \int_0^{\mathfrak{I}} g\left(\mathfrak{I}, \mathrm{s}, x_{\mathrm{s}}^{m-1}\right)ds\right]\mathrm{ds}\right) \longrightarrow 0,\end{aligned} \tag{40}$$

uniformly on $[0, T]$ as $m \longrightarrow \infty$. Therefore,

$$\begin{aligned}&\mathscr{D}\left(\int_0^{\mathfrak{I}}\left[f(\mathrm{s}, x_{\mathrm{s}}^m) + \int_0^{\mathfrak{I}} g(\mathfrak{I}, \mathrm{s}, x_{\mathrm{s}}^m)ds\right]\mathrm{ds},\right.\\ &\qquad\left.\int_0^{\mathfrak{I}}\left[f\left(s, x_{\mathrm{s}}^{m-1}\right) + \int_0^{\mathfrak{I}} g\left(t, s, x_{\mathrm{s}}^{m-1}\right)ds\right]\mathrm{ds}\right)\\ &\quad\le \int_0^{\mathfrak{I}}\mathscr{D}\left(\left[f(\mathrm{s}, x_{\mathrm{s}}^m) + \int_0^{\mathfrak{I}} g(\mathfrak{I}, \mathrm{s}, x_{\mathrm{s}}^m)ds\right]\mathrm{ds},\right.\\ &\qquad\left.\left[f\left(\mathrm{s}, x_{\mathrm{s}}^{m-1}\right) + \int_0^{\mathfrak{I}} g\left(\mathfrak{I}, \mathrm{s}, x_{\mathrm{s}}^{m-1}\right)ds\right]\mathrm{ds}\right)\mathrm{ds}.\end{aligned} \tag{41}$$

It follows that

$$\begin{aligned}&\lim_{m\longrightarrow\infty}\int_0^{\mathfrak{I}}\left[f(\mathrm{s}, x_{\mathrm{s}}^m) + \int_0^{\mathfrak{I}} g(\mathfrak{I}, \mathrm{s}, x_{\mathrm{s}}^m)ds\right]\mathrm{ds}\\ &\quad= \int_0^{\mathfrak{I}}\left[f\left(\mathrm{s}, x_{\mathrm{s}}^{m-1}\right) + \int_0^{\mathfrak{I}} g\left(\mathfrak{I}, \mathrm{s}, x_{\mathrm{s}}^{m-1}\right)ds\right]\mathrm{ds}, \mathfrak{I} \in [0, T].\end{aligned} \tag{42}$$

Extending x to $[\mathfrak{I}_0 - \sigma, \mathfrak{I}_0]$ in usual way by $x(\mathfrak{I}) = f(\mathfrak{I}, x_{\mathfrak{I}}) + \int_0^{\mathfrak{I}} g(\mathfrak{I}, \mathrm{s}, x_{\mathrm{s}})ds$ for $\mathfrak{I} \in [0, T]$, then, by (33), we obtain that

$$x(\mathfrak{I}) = \begin{cases} f(\mathfrak{I}, x_{\mathfrak{I}}) + \int_0^{\mathfrak{I}} g(\mathfrak{I}, \mathrm{s}, x_{\mathrm{s}})\mathrm{ds}, \mathfrak{I} \ge \mathfrak{I}_0, \mathfrak{I}_0 \ge \mathfrak{I} \ge \mathfrak{I}_0 - \sigma,\\ \varphi(0) + C_q(\mathfrak{I})\psi_0 + \mathscr{K}_q(\mathfrak{I})\psi_1 + \int_0^{\mathfrak{I}}(\mathfrak{I} - \mathrm{s})^{q-1}P_q(\mathfrak{I} - \mathrm{s})\left[f(\mathrm{s}, x_{\mathrm{s}}) + \int_0^{\mathfrak{I}} g(\mathfrak{I}, \mathrm{s}, x_{\mathrm{s}})\right]\mathrm{ds}, \in [0, T], \end{cases} \tag{43}$$

and x is the solution for Equation (4). To prove uniqueness, suppose $y : [\mathfrak{I}_0 - \sigma, T] \longrightarrow \mathbf{E^m}$ be second solution for (4). For all $\mathfrak{I} \in [0, T]$,

$$\begin{aligned}\mathscr{D}[x(\mathfrak{I}), y(\mathfrak{I})] &= \mathscr{D}\left(\int_0^{\mathfrak{I}}(\mathfrak{I} - \mathrm{s})^{q-1}P_q(\mathfrak{I} - \mathrm{s})[f(\mathrm{s}, x_{\mathrm{s}})\right.\\ &\quad\left.+ \int_0^{\mathfrak{I}} g(\mathfrak{I}, \mathrm{s}, x_{\mathrm{s}})ds\right]\mathrm{ds}, \int_0^{\mathfrak{I}}(\mathfrak{I} - \mathrm{s})^{q-1}P_q(\mathfrak{I} - \mathrm{s})\\ &\quad\left.\cdot\left[f(\mathrm{s}, y_{\mathrm{s}}) + \int_0^{\mathfrak{I}} g(\mathfrak{I}, \mathrm{s}, y_{\mathrm{s}})ds\right]\mathrm{ds}\right) \le \mathscr{D}_\sigma(x_{\mathrm{s}}, y_{\mathrm{s}})\\ &\le L^2\int_0^{\mathfrak{I}}\sup_{\theta\in[\mathrm{s}-\sigma,\mathrm{s}]}\mathscr{D}[x(\theta), y(\theta)]\mathrm{ds}.\end{aligned} \tag{44}$$

If we assume $\xi(\mathrm{s}) \coloneqq \sup_{r\in[\mathrm{s}-\sigma,\mathrm{s}]}\mathscr{D}[x(r), y(r)]$, $\mathrm{s} \in [0, T]$, now

$$\xi(\mathfrak{I}) \le L^2\int_0^{\mathfrak{I}}\xi(s)\mathrm{ds}, \tag{45}$$

and by Gronwall's lemma, we obtained $\xi(\mathfrak{I}) = 0$ on $[0, T]$. This establishes uniqueness solutions for (4). □

Remark 20. The contraction principle can be used to prove local uniqueness and existence theorem for initial value problems (28). Suppose $P : \mathbf{E^m} \longrightarrow \mathbf{E^m}$ be defined as

$$(Px)(\mathfrak{I}) = \begin{cases} f(\mathfrak{I}, x_{\mathfrak{I}}) + \int_0^{\mathfrak{I}} g(\mathfrak{I}, \mathrm{s}, x_{\mathrm{s}})d\mathrm{s}, \mathfrak{I} \ge \mathfrak{I}_0, \mathfrak{I}_0 \ge \mathfrak{I} \ge \mathfrak{I}_0 - \sigma,\\ \varphi(0) + C_q(\mathfrak{I})\psi_0 + \mathscr{K}_q(\mathfrak{I})\psi_1 + \int_0^{\mathfrak{I}}(\mathfrak{I} - \mathrm{s})^{q-1}P_q(\mathfrak{I} - \mathrm{s})\left[f(\mathrm{s}, x_{\mathrm{s}}) + \int_0^{\mathfrak{I}} g(\mathfrak{I}, \mathrm{s}, x_{\mathrm{s}})d\mathrm{s}\right]d\mathrm{s}, \mathfrak{I} \in [0, T], \end{cases} \tag{46}$$

For $\mathfrak{I} \in [0, T]$,

$$\begin{aligned}\mathscr{D}[(Px)(\mathfrak{I}), (Py)(\mathfrak{I})] &= \mathscr{D}\left(\int_0^{\mathfrak{I}}(\mathfrak{I} - \mathrm{s})^{q-1}P_q(\mathfrak{I} - \mathrm{s})[f(\mathrm{s}, x_{\mathrm{s}})\right.\\ &\quad+ \int_0^{\mathfrak{I}} g(\mathfrak{I}, \mathrm{s}, x_{\mathrm{s}})ds\Big]\mathrm{ds}, \int_0^{\mathfrak{I}}(\mathfrak{I} - \mathrm{s})^{q-1}\\ &\quad\left.\cdot P_q(\mathfrak{I} - \mathrm{s})\left[f(\mathrm{s}, y_{\mathrm{s}}) + \int_0^{\mathfrak{I}} g(\mathfrak{I}, \mathrm{s}, y_{\mathrm{s}})ds\right]\mathrm{ds}\right)\\ &\le L^2\mathscr{D}_\sigma(x_{\mathrm{s}}, y_{\mathrm{s}}) \le L^2\int_0^{\mathfrak{I}}\sup_{\theta\in[\mathrm{s}-\sigma,\mathrm{s}]}\mathscr{D}[x(\theta), y(\theta)]\mathrm{ds}\\ &\le L^2\mathfrak{I}\mathscr{D}(x, y).\end{aligned} \tag{47}$$

Hence

$$\mathscr{D}(Px, Py) \le L^2\mathfrak{I}\mathscr{D}(x, y)\forall x, y \in \mathbf{E^m}, \tag{48}$$

where $P : \mathbf{E^m} \longrightarrow \mathbf{E^m}$ is contraction only if $L\mathfrak{I} < 2$. However, if we deal with successive approximations indirectly (33), we can show that iterations converge, and initial value problem (28) has unique solution on interval $[0, T]$ under merely the assumption $\mathscr{K}T < \rho$, without constraint $L\mathfrak{I} < 2$. The discrepancy is resolved by noting that all functions $x \in C([\mathfrak{I}_0 - \sigma, T], \mathbf{E^m})$, $x(\mathfrak{I}) = \varphi(\mathfrak{I} - \mathfrak{I}_0)$ on $[0, T]$ have several equivalent metrics on space $\mathbf{E}^{\mathbf{m}}$. In fact, metric

$$\mathscr{D}_\sigma(x, y) = \sup_{\mathfrak{I}_0-\sigma\leq\mathfrak{I}\leq T} \mathscr{D}[x(\mathfrak{I}), y(\mathfrak{I})]e^{-a\mathfrak{I}}, a > 0, \tag{49}$$

is equivalent to metric $\mathscr{D}(x, y)$. Then

$$\mathscr{D}(x, y)e^{-aT} \leq \mathscr{D}_\sigma(x, y) \leq \mathscr{D}(x, y)\forall x, y \in \mathbf{E}^{\mathbf{m}}. \tag{50}$$

Using metric (49) and function $\mathscr{G} : [0,\infty) \times C_\sigma \longrightarrow \mathbf{E}^{\mathbf{m}}$ is continuous and satisfies the global Lipschitz condition:

$$\mathscr{D}[\mathscr{G}(\mathfrak{I}, \varphi), \mathscr{G}(\mathfrak{I}, \psi)] \leq L^2\mathscr{D}_\sigma(\varphi, \psi), 0 \leq \mathfrak{I} \leq T, \varphi, \psi \in C_\sigma. \tag{51}$$

In [34], uniqueness and existence of solution for (28) on interval $[0, T]$ were illustrated.

Theorem 21. *Let function $\mathscr{G} : [0,\infty) \times C_\sigma \longrightarrow \mathbf{E}^{\mathbf{m}}$ be locally Lipschitz and continuous. If $(\mathfrak{I}_0, \varphi), (\mathfrak{I}_0, \psi) \in [0,\infty) \times C_\sigma$ and $x(\varphi)$: $[\mathfrak{I}_0 - \sigma, \omega_1) \longrightarrow \mathbf{E}^{\mathbf{m}}$ and $x(\psi)$: $[\mathfrak{I}_0 - \sigma, \omega_2) \longrightarrow \mathbf{E}^{\mathbf{m}}$ are unique solutions of (28) with $x(\mathfrak{I}) = f(\mathfrak{I}, x_\mathfrak{I}) + \int_0^\mathfrak{I} g(\mathfrak{I}, s, x_s)ds$ on $[\mathfrak{I}_0 - \sigma, \mathfrak{I}_0]$, now*

$$\mathscr{D}[x(\varphi)(\mathfrak{I}), x(\psi)(\mathfrak{I})] \leq \mathscr{D}_\sigma(\varphi, \psi)e^{L^2(\mathfrak{I}-0)}\forall\mathfrak{I} \in [\mathfrak{I}_0, \omega), \tag{52}$$

where $\omega = \min \{\omega_1, \omega_2\}$.

Proof. On $[\mathfrak{I}_0, \omega)$ solution, $x(\varphi)$ satisfies relation

$$x(\mathfrak{I}) = \begin{cases} f(\mathfrak{I}, x_\mathfrak{I}) + \int_0^\mathfrak{I} g(\mathfrak{I}, s, x_s)ds, \mathfrak{I} \geq \mathfrak{I}_0, \mathfrak{I}_0 \geq \mathfrak{I} \geq \mathfrak{I}_0 - \sigma, \\ \varphi(0) + C_q(\mathfrak{I})\psi_0 + \mathscr{K}_q(\mathfrak{I})\psi_1 + \int_0^\mathfrak{I} (\mathfrak{I} - \mathrm{s})^{q-1}P_q(\mathfrak{I} - \mathrm{s})\left[f(\mathrm{s}, x_\mathrm{s}) + \int_0^\mathfrak{I} g(\mathfrak{I}, \mathrm{s}, x_\mathrm{s})ds\right]ds, \mathfrak{I} \in [0, \omega], \end{cases} \tag{53}$$

and $x(\psi)$ satisfies the same relation as φ, but with ψ instead of φ. Then, for $\mathfrak{I} \in [\mathfrak{I}_0, \omega)$,

$$\begin{aligned} \mathscr{D}[x(\varphi)(\mathfrak{I}), x(\psi)(\mathfrak{I})] &\leq \mathscr{D}[\varphi(0), \psi(0)] + \mathscr{D}\left[C_q(\mathfrak{I})\varphi_0, C_q(\mathfrak{I})\psi_0\right] \\ &+ \mathscr{D}\left[\mathscr{K}_q(\mathfrak{I})\varphi_1, \mathscr{K}_q(\mathfrak{I})\psi_1\right] + \int_0^\mathfrak{I} \mathscr{D}\left[(\mathfrak{I} - \mathrm{s})^{q-1}P_q(\mathfrak{I} - \mathrm{s})\right. \\ &\cdot \left[f(\mathrm{s}, x_\mathrm{s}) + \int_0^\mathfrak{I} g(\mathfrak{I}, \mathrm{s}, x_\mathrm{s})ds\right]\mathrm{ds}, (\mathfrak{I} - \mathrm{s})^{q-1}P_q(\mathfrak{I} - \mathrm{s}) \\ &\cdot \left.\left[f(\mathrm{s}, y_\mathrm{s}) + \int_0^\mathfrak{I} g(\mathfrak{I}, \mathrm{s}, y_\mathrm{s})ds\right]\mathrm{ds}\right] \leq \mathscr{D}_\sigma(\varphi, \psi) \\ &+ \mathscr{D}_\sigma(\varphi_0, \psi_0) + \mathscr{D}_\sigma(\varphi_1, \psi_1) \\ &+ L^2\int_0^\mathfrak{I} \sup_{r\in[\mathfrak{I}_0-\sigma,\mathrm{s}]} \mathscr{D}_\sigma[x(\varphi)(r), x(\psi)(r)]\mathrm{ds}. \end{aligned} \tag{54}$$

If suppose $\omega(\mathrm{s}) = \sup_{r\in[\mathfrak{I}_0-\sigma,\mathrm{s}]} \mathscr{D}_\sigma[x(\varphi)(r), x(\psi)(r)], \mathfrak{I}_0 \leq \mathrm{s} \leq \mathfrak{I}$, then

$$\omega(\mathfrak{I}) \leq \mathscr{D}_\sigma(\varphi, \psi)e^{L\mathfrak{I}}, \mathfrak{I}_0 \leq \mathfrak{I} < \omega, \tag{55}$$

implying that (52) holds. □

4. Global Existence and Uniqueness

For a given constant $a > 0$, consider set $\mathbf{E}_\mathbf{a}^\mathbf{m}$ of all functions $x \in C([\mathfrak{I}_0 - \sigma,\infty), \mathbf{E}^{\mathbf{m}})$; that is, $x(\mathfrak{I}) = f(\mathfrak{I}, x_\mathfrak{I}) + \int_0^\mathfrak{I} g(\mathfrak{I}, \mathrm{s}, x_\mathrm{s})\mathrm{ds}$ on $[\mathfrak{I}_0 - \sigma, \mathfrak{I}_0]$ and $\sup_{\mathfrak{I}\geq\mathfrak{I}_0-\sigma} \mathscr{D}[x(\mathfrak{I}), \tilde{0}]e^{-a\mathfrak{I}} < \infty$. On $\mathbf{E}_\mathbf{a}^\mathbf{m}$, define the following metric:

$$\mathscr{D}_\sigma(x, y) = \sup_{\mathfrak{I}\mathfrak{I}_0-\sigma} \mathscr{D}[x(\mathfrak{I}), y(\mathfrak{I})]e^{-a\mathfrak{I}}. \tag{56}$$

Lemma 22. *$(\mathbf{E}_\mathbf{a}^\mathbf{m}, \mathscr{D}_a)$ is complete metric space.*

Proof. Suppose $\{x_m\}_{m\geq2}$ be Cauchy sequence in $\mathbf{E}_\mathbf{a}^\mathbf{m}$. Now, for each $\varepsilon > 0$, there exists $m_\varepsilon \in \mathbb{N}\forall m, p \geq m_\varepsilon$, and we obtain $\mathscr{D}_\sigma(x_m, y_p) < \varepsilon$. Hence

$$\mathscr{D}\left[x_m(\mathfrak{I}), y_p(\mathfrak{I})\right] \leq \mathscr{D}_\sigma\left(x_m, y_p\right)e^{a\mathfrak{I}} \leq \varepsilon e^\mathfrak{I}, \tag{57}$$

and so

$$\mathscr{D}\left[x_m(\mathfrak{I}), x_p(\mathfrak{I})\right] \leq \varepsilon e^{a\mathfrak{I}}\forall m, p \geq m_\varepsilon \text{ and } \mathfrak{I} \geq \mathfrak{I}_0 - \sigma. \tag{58}$$

For each $\mathfrak{I} \geq \mathfrak{I}_0 - \sigma$, $\{x_m(\mathfrak{I})\}_{m\geq2}$ is Cauchy sequence in $\mathbf{E}^{\mathbf{m}}$. $(\mathbf{E}^{\mathbf{m}}, \mathscr{D})$ is a complete metric space, and there exists $x(\mathfrak{I}) = \lim_{m\longrightarrow\infty} x_m(\mathfrak{I})$ for $\mathfrak{I} \geq \mathfrak{I}_0 - \sigma$. Now, $x \in \mathbf{E}_\sigma$. Evidently, $x(\mathfrak{I}) = f(\mathfrak{I}, x_\mathfrak{I}) + \int_0^\mathfrak{I} g(\mathfrak{I}, \mathrm{s}, x_\mathrm{s})\mathrm{ds}$ on $[\mathfrak{I}_0 - \sigma, \mathfrak{I}_0]$. From (58), we get $\lim_{p\longrightarrow\infty} \mathscr{D}[x_m(\mathfrak{I}), x(\mathfrak{I})] \leq \varepsilon e^{a\mathfrak{I}}, \forall m \geq m_\varepsilon$ and $\mathfrak{I} \geq \mathfrak{I}_0$. Now, x is continuous function on $[\mathfrak{I}_0, \infty)$. Suppose $\varepsilon > 0$ and $\mathrm{s} \geq \mathfrak{I}_0$. Then, there exists $m = m'_\varepsilon \in \mathbb{N}$, $\mathscr{D}[x_m(\mathfrak{I}), x(\mathfrak{I})](\varepsilon/6)e^{a(\mathfrak{I}-\mathrm{s})}, \forall\mathfrak{I} \geq \mathfrak{I}_0$. Since x_m is continuous function, now, there exists $\delta_\varepsilon^1 > 1$, $\mathscr{D}[x_m(\mathfrak{I}), x_m(\mathrm{s})] \leq (\varepsilon/3)$ for $\mathfrak{I} \geq \mathfrak{I}_0$. Since$x_m$ is continuous function, then, there exists $\delta_\varepsilon^1 > 1$ that is $\mathscr{D}[x_m(\mathfrak{I}), x_m(\mathrm{s})] \leq (\varepsilon/3)$ for $\mathfrak{I} \geq \mathfrak{I}_0$ with $|\mathfrak{I} - \mathrm{s}| \leq \delta_\varepsilon^1$. There exists $\delta_\varepsilon^2 > 1$; that is, $e^{a(\mathfrak{I}-\mathrm{s})} \leq 2$ for $\mathfrak{I} \geq \mathfrak{I}_0$ with $|\mathfrak{I} - \mathrm{s}| \leq \delta_\varepsilon^2$. Assume $\delta_\varepsilon = \min \{\delta_\varepsilon^1, \delta_\varepsilon^2\}$. Now, for every $\mathfrak{I} \geq \mathfrak{I}_0$ with $|\mathfrak{I} - \mathrm{s}| \leq \delta_\varepsilon$,

$$\begin{aligned} \mathscr{D}[x(\mathfrak{I}), x(\mathrm{s})] &\leq \mathscr{D}[x(\mathfrak{I}), x_m(\mathfrak{I})] + \mathscr{D}[x_m(\mathfrak{I}), x_m(\mathrm{s})] \\ &+ \mathscr{D}[x_m(\mathrm{s}), x(\mathrm{s})] \leq \left(\frac{\varepsilon}{6}\right)e^{a(\mathfrak{I}-\mathrm{s})} + \frac{\varepsilon}{3} + \frac{\varepsilon}{6} \leq \varepsilon, \end{aligned} \tag{59}$$

where x is continuous function on $[\mathfrak{I}_0, \infty)$. Now

$$\sup_{\mathfrak{I}\geq\mathfrak{I}_0-\sigma} \mathscr{D}\left[x(\mathfrak{I}), \tilde{0}\right]e^{-a\mathfrak{I}} < \infty. \tag{60}$$

Since

$$\mathscr{D}\left[x(\mathfrak{J}),\tilde{0}\right] \le \mathscr{D}[x(\mathfrak{J}),x_m(\mathfrak{J})] + \mathscr{D}\left[x_m(\mathfrak{J}),\tilde{0}\right] \forall \mathfrak{J} \ge \mathfrak{J}_0 - \sigma \text{ and } m \ge 1. \tag{61}$$

Now

$$\begin{aligned}\sup_{\mathfrak{J}\ge\mathfrak{J}_0-\sigma} \mathscr{D}\left[x(\mathfrak{J}),\tilde{0}\right]e^{-a\mathfrak{J}} &\le \sup_{\mathfrak{J}\ge\mathfrak{J}_0-\sigma} \mathscr{D}[x(\mathfrak{J}),x_m(\mathfrak{J})]e^{-a\mathfrak{J}} \\ &\quad + \sup_{\mathfrak{J}\ge\mathfrak{J}_0-\sigma} \mathscr{D}\left[x_m(\mathfrak{J}),\tilde{0}\right]e^{-a\mathfrak{J}} \\ &= \mathscr{D}_\sigma(x,x_m) + \sup_{\mathfrak{J}\ge\mathfrak{J}_0-\sigma} \mathscr{D}\left[x_m(\mathfrak{J}),\tilde{0}\right]e^{-a\mathfrak{J}},\end{aligned} \tag{62}$$

$\lim_{m\longrightarrow\infty} \mathscr{D}_\sigma(x,x_m) = 1$ and $x_m \in \mathbf{E}^{\mathbf{m}}_{\mathbf{a}} \forall m \ge 2$, we get

$$\sup_{\mathfrak{J}\ge\mathfrak{J}_0-\sigma} \mathscr{D}\left[x(\mathfrak{J}),\tilde{0}\right]e^{-a\mathfrak{J}} < \infty. \tag{63}$$

Moreover, $x \in \mathbf{E}^{\mathbf{m}}_{\mathbf{a}}$. So, $(\mathbf{E}^{\mathbf{m}}_{\mathbf{a}}, \mathscr{D}_a)$ is complete metric space. The fuzzy differential Equation (28) is then considered under the following conditions:

$(\mathbf{J_1})$ There exist $L > 0$; that is

$$\mathscr{D}[\mathscr{G}(\mathfrak{J},\varphi),\mathscr{G}(\mathfrak{J},\psi)] < L^2 D_\sigma(\varphi,\psi) \forall \varphi,\psi \in C_\sigma \text{ and } \mathfrak{J} \ge 1. \tag{64}$$

$(\mathbf{J_2})$ $\mathscr{G} : [0,\infty) \times C_\sigma \longrightarrow \mathbf{E}^{\mathbf{m}}$ is jointly continuous.

$(\mathbf{J_3})$ There exists $M > 0$ and $b > 0$,

$$\mathscr{D}\left[\mathscr{G}(\mathfrak{J},0),\tilde{0}\right] \le Me^{b\mathfrak{J}} \forall \mathfrak{J} \ge 1. \tag{65}$$

Suppose $P : C([-\sigma,\infty),\mathbf{E}^{\mathbf{m}}) \longrightarrow C([-\sigma,\infty),\mathbf{E}^{\mathbf{m}})$, defined as

$$(Px)(\mathfrak{J}) = \begin{cases} f(\mathfrak{J},x_{\mathfrak{J}}) + \int_0^{\mathfrak{J}} g(\mathfrak{J},\mathrm{s},x_\mathrm{s})ds, \ \mathfrak{J} \ge \mathfrak{J}_0, \mathfrak{J}_0 \ge \mathfrak{J} \ge \mathfrak{J}_0 - \sigma, \\ \mathscr{D}_\sigma(\varphi,\psi) + C_q(\mathfrak{J})\psi_0 + \mathscr{K}_q(\mathfrak{J})\psi_1 + \int_0^{\mathfrak{J}} (\mathfrak{J}-\mathrm{s})^{q-1} P_q(\mathfrak{J}-\mathrm{s}) \left[f(\mathrm{s},x_\mathrm{s}) + \int_0^{\mathfrak{J}} g(\mathfrak{J},\mathrm{s},x_\mathrm{s})\right] ds, \ \mathfrak{J} \in [0,T]. \end{cases} \tag{66}$$

□

Lemma 23. *If $\mathscr{G} : [0,\infty) \times C_\sigma \longrightarrow \mathbf{E}^{\mathbf{m}}$ satisfies assumptions $(\mathbf{J}_1) - (\mathbf{J}_2)$ and $a > b$, then, $P(\mathbf{E}^{\mathbf{m}}_{\mathbf{a}}) \subset \mathbf{E}^{\mathbf{m}}_{\mathbf{a}}$.*

Proof. Suppose $x \in \mathbf{E}^{\mathbf{m}}_{\mathbf{a}}$. For each $\mathfrak{J} \ge \mathfrak{J}_0$,

$$\begin{aligned}\mathscr{D}\left[(Px)(\mathfrak{J}),\tilde{0}\right] &= \mathscr{D}\left[\varphi(0) + C_q(\mathfrak{J})\psi_0 + \mathscr{K}_q(\mathfrak{J})\psi_1 + \int_0^{\mathfrak{J}} (\mathfrak{J}-\mathrm{s})^{q-1} \right. \\ &\quad \left. \cdot P_q(\mathfrak{J}-\mathrm{s}) \left[f(\mathrm{s},x_\mathrm{s}) + \int_0^{\mathfrak{J}} g(\mathfrak{J},\mathrm{s},x_\mathrm{s})\mathrm{ds}\right]\mathrm{ds},\tilde{0}\right] \\ &\le \mathscr{D}\left[\varphi(0),\tilde{0}\right] + \mathscr{D}\left[C_q(\mathfrak{J})\psi_0,\tilde{0}\right] + \mathscr{D}\left[\mathscr{K}_q(\mathfrak{J})\psi_1,\tilde{0}\right] \\ &\quad + \mathscr{D}\left[\left[\int_0^{\mathfrak{J}} (\mathfrak{J}-\mathrm{s})^{q-1} P_q(\mathfrak{J}-\mathrm{s})[f(\mathrm{s},x_\mathrm{s}) \right.\right. \\ &\quad \left.\left. + \int_0^{\mathfrak{J}} g(\mathfrak{J},\mathrm{s},x_\mathrm{s})\mathrm{ds}\right]\mathrm{ds},\tilde{0}\right] \le \mathscr{D}\left[\varphi(0),\tilde{0}\right] \\ &\quad + \mathscr{D}\left[C_q(\mathfrak{J})\psi_0,\tilde{0}\right] + \mathscr{D}\left[\mathscr{K}_q(\mathfrak{J})\psi_1,\tilde{0}\right] \\ &\quad + \int_0^{\mathfrak{J}} \left(L^2 D_\sigma\left(x_\mathrm{s},\tilde{0}\right) + Me^{\mathrm{bs}}\right)\mathrm{ds} \le \mathscr{D}\left[\varphi(0),\tilde{0}\right] \\ &\quad + \mathscr{D}\left[C_q(\mathfrak{J})\psi_0,\tilde{0}\right] + \mathscr{D}\left[\mathscr{K}_q(\mathfrak{J})\psi_1,\tilde{0}\right] \\ &\quad + L^2 \int_0^{\mathfrak{J}} \left(D_\sigma\left(x_\mathrm{s},\tilde{0}\right)\right)\mathrm{ds} + \frac{M}{b}e^{b\mathfrak{J}}.\end{aligned} \tag{67}$$

Since $x \in \mathbf{E}^{\mathbf{m}}_{\mathbf{a}}$, there exists $\rho > 1$, $\mathscr{D}[x(\mathfrak{J}),\tilde{0}] \le \rho e^{a\mathfrak{J}} \forall \mathfrak{J} \ge \mathfrak{J}_0 - \sigma$,

$$\sup_{\theta\in[-\sigma,0]} D\left[x(\mathfrak{J}+0),\tilde{0}\right] \le \mathscr{D}\left[\varphi(0),\tilde{0}\right] \le \rho e^{a\mathfrak{J}} \forall \mathfrak{J} \ge \mathfrak{J}_0,$$

$$\begin{aligned}\mathscr{D}\left[(Px)(\mathfrak{J}),\tilde{0}\right] &\le \mathscr{D}\left[\varphi(0),\tilde{0}\right] + \mathscr{D}\left[C_q(\mathfrak{J})\psi_0,\tilde{0}\right] + \mathscr{D}\left[\mathscr{K}_q(\mathfrak{J})\psi_1,\tilde{0}\right] \\ &\quad + L^2 \int_0^{\mathfrak{J}} \sup_{\theta\in[-\sigma,0]} \mathscr{D}\left[x(\mathfrak{J}+0),\tilde{0}\right]ds + \frac{M}{b}e^{b\mathfrak{J}} \\ &\le \mathscr{D}\left[\varphi(0),\tilde{0}\right] + \mathscr{D}\left[C_q(\mathfrak{J})\psi_0,\tilde{0}\right] + \mathscr{D}\left[\mathscr{K}_q(\mathfrak{J})\psi_1,\tilde{0}\right] \\ &\quad + \frac{\rho L^2}{a}e^{a\mathfrak{J}_0} + \frac{M}{b}e^{b\mathfrak{J}}.\end{aligned} \tag{68}$$

Thus

$$\begin{aligned}\sup_{t\ge\mathfrak{J}_0} \mathscr{D}\left[(Px)(\mathfrak{J}),\tilde{0}\right]e^{-a\mathfrak{J}} &\le \sup_{\mathfrak{J}\ge\mathfrak{J}_0}\left(\mathscr{D}\left[\varphi(0),\tilde{0}\right] + \mathscr{D}\left[C_q(\mathfrak{J})\psi_0,\tilde{0}\right] \right. \\ &\quad \left. + \mathscr{D}\left[\mathscr{K}_q(\mathfrak{J})\psi_1,\tilde{0}\right] + \frac{\rho L^2}{a}e^{a\mathfrak{J}_0} + \frac{M}{b}e^{b\mathfrak{J}}\right)e^{-a\mathfrak{J}} \\ &\le \mathscr{D}\left[\varphi(0),\tilde{0}\right] + \mathscr{D}\left[C_q(\mathfrak{J})\psi_0,\tilde{0}\right] + \mathscr{D}\left[\mathscr{K}_q(\mathfrak{J})\psi_1,\tilde{0}\right] \\ &\quad + \frac{1}{b}\left(\rho L^2 + M\right).\end{aligned} \tag{69}$$

Let

$$3\mathscr{K} = \sup_{\theta\in[\mathfrak{I}_0-\sigma,\mathfrak{I}_0]} \mathscr{D}\left[\varphi(0),\tilde{0}\right] + \mathscr{D}\left[C_q(\mathfrak{I})\psi_0,\tilde{0}\right] + \mathscr{D}\left[\mathscr{K}_q(\mathfrak{I})\psi_1,\tilde{0}\right]. \tag{70}$$

Now

$$\sup_{\mathfrak{I}\geq\mathfrak{I}_0} \mathscr{D}\left[(Px)(\mathfrak{I}),\tilde{0}\right]e^{-a\mathfrak{I}} \leq 3\mathscr{K} + \frac{1}{b}\left(\rho L^2 + M\right) < \infty, \tag{71}$$

and $Px \in \mathbf{E}_{\mathbf{a}}^{\mathbf{m}}$. □

Lemma 24. *If $\mathscr{F} : [0,\infty) \times C_\sigma \longrightarrow \mathbf{E}^{\mathbf{m}}$ satisfies $(\mathbf{J}_1) - (\mathbf{J}_3)$ and $L < a$, then, P is contraction on $\mathbf{E}_{\mathbf{a}}^{\mathbf{m}}$.*

Proof. Suppose $x, y \in \mathbf{E}_{\mathbf{a}}^{\mathbf{m}}$. Now, for each $\mathfrak{I} \geq \mathfrak{I}_0$

$$\begin{aligned}\mathscr{D}[(Px)(\mathfrak{I}),(Py)(\mathfrak{I})] &= \mathscr{D}\left[\int_0^{\mathfrak{I}} (\mathfrak{I}-\mathrm{s})^{q-1}P_q(\mathfrak{I}-\mathrm{s}) \cdot \left[f(\mathrm{s},x_{\mathrm{s}}) + \int_0^{\mathfrak{I}} g(\mathfrak{I},\mathrm{s},x_{\mathrm{s}})d\mathrm{s}\right]d\mathrm{s}, \int_0^{\mathfrak{I}} (\mathfrak{I}-\mathrm{s})^{q-1}P_q(\mathfrak{I}-\mathrm{s}) \cdot \left[f(\mathrm{s},y_{\mathrm{s}}) + \int_0^{\mathfrak{I}} g(\mathfrak{I},\mathrm{s},y_{\mathrm{s}})d\mathrm{s}\right]d\mathrm{s}\right] \leq \int_0^{\mathfrak{I}} L^2\mathscr{D}_\sigma(x_{\mathrm{s}},y_{\mathrm{s}})d\mathrm{s}\\ &= L^2\int_0^{\mathfrak{I}} \sup_{r\in[-\sigma,0]} \mathscr{D}[x(r+\mathrm{s}),y(r+\mathrm{s})]ds\\ &= L^2\int_0^{\mathfrak{I}} \sup_{\theta\in[\mathrm{s}-\sigma,\mathrm{s}]} \mathscr{D}[x(\theta),y(\theta)]d\mathrm{s}.\end{aligned} \tag{72}$$

From (29), $\mathfrak{D}[x(\mathfrak{I}),y(\mathfrak{I})] \leq \mathscr{D}_\sigma(x,y)e^{a\mathfrak{I}}\forall\mathfrak{I} \geq \mathfrak{I}_0 - \sigma$. So

$$\sup_{r\in[-\sigma,0]} \mathscr{D}[x(r),y(r)] \leq \mathscr{D}_\sigma(x,y)e^{\mathfrak{I}}\forall\mathfrak{I} \geq \mathfrak{I}_0. \tag{73}$$

For every $\mathfrak{I} \geq \mathfrak{I}_0$,

$$\begin{aligned}\mathscr{D}[(Px)(\mathfrak{I}),(Py)(\mathfrak{I})] &\leq L^2 \sup_{r\in[-\sigma,0]} \mathscr{D}[x(r),y(r)]ds\\ &= \frac{L^2}{a}\mathscr{D}_a(x,y)e^{a\mathfrak{I}_0}\left[e^{a(\mathfrak{I}-\mathfrak{I}_0)} - 1\right],\end{aligned} \tag{74}$$

and so

$$\begin{aligned}\mathscr{D}_\sigma(Px,Py) &= \sup_{\mathfrak{I}\geq\mathfrak{I}_0-\sigma} \mathscr{D}[(Px)(\mathfrak{I}),(Py)(\mathfrak{I})]e^{-a\mathfrak{I}}\\ &\leq \frac{L^2}{a}\mathscr{D}_a(x,y) \leq \mathscr{D}_a(x,y).\end{aligned} \tag{75}$$

Hence

$$\frac{L^2}{a} < 1. \tag{76}$$

Therefore, P is contraction on $\mathbf{E}_{\mathbf{a}}^{\mathbf{m}}$. □

Theorem 25. *Let function $\mathscr{G} : [0,\infty) \times C_\sigma \longrightarrow \mathbf{E}^{\mathbf{m}}$ satisfies assumptions $(\mathbf{J}_1) - (\mathbf{J}_3)$. Then, for each $(\mathfrak{I}_0,\varphi) \in C_\sigma$, FFDE (28) has unique solution on $[\mathfrak{I}_0,\infty)$.*

Proof. Assume

$$a > \max\left\{b, L^2\right\}. \tag{77}$$

We can deduce that the operator $P : \mathbf{E}_{\mathbf{a}} \longrightarrow \mathbf{E}_{\mathbf{a}}$ is contraction using Lemmas 23 and 24. As a result, there is only one $x \in \mathbf{E}_{\mathbf{a}}^{\mathbf{m}}$, which is $Px = x$. x is continuous function,

$$x(\mathfrak{I}) = f(\mathfrak{I},x_{\mathfrak{I}}) + \int_0^{\mathfrak{I}} g(\mathfrak{I},\mathrm{s},x_{\mathrm{s}})d\mathrm{s}, \tag{78}$$

on $[\mathfrak{I}_0 - \sigma, T]$. Moreover,

$$x(\mathfrak{I}) = C_q(\mathfrak{I})\psi_0 + \mathscr{K}_q(\mathfrak{I})\psi_1 + \int_0^{\mathfrak{I}} (\mathfrak{I}-\mathrm{s})^{q-1}P_q(\mathfrak{I}-\mathrm{s}) \cdot \left[f(\mathrm{s},x_{\mathrm{s}}) + \int_0^{\mathfrak{I}} g(\mathfrak{I},\mathrm{s},x_{\mathrm{s}})\right]d\mathrm{s}, \tag{79}$$

for every $T \geq \mathfrak{I}_0$. Since x is continuous and $\mathscr{G}$ satisfies $(\mathbf{J_2})$, by Lemma 9 and Remark 10,

$$\mathrm{s} \mapsto f(\mathrm{s},x_{\mathrm{s}}) + \int_0^{\mathfrak{I}} g(\mathfrak{I},\mathrm{s},x_{\mathrm{s}})d\mathrm{s}, \tag{80}$$

is an integrable function on $[\mathfrak{I}_0, T]$. By Remark 10, x is differentiable function and

$${}_0^c\mathscr{D}_q^H x(\mathfrak{I}) = f(\mathfrak{I},x_{\mathfrak{I}}) + \int_0^{\mathfrak{I}} g(\mathfrak{I},\mathrm{s},x_{\mathrm{s}})d\mathrm{s}, \tag{81}$$

for every $\mathfrak{I}_0 \geq T$. Theorem 25 is proved. □

5. Applications

5.1. Fuzzy Fractional Functional Evolution Equations with Distributed Delay. In below sections, we will look at class of delay fuzzy fractional functional evolution equations with distributed delay. Consider following delay fuzzy fractional functional differential equations with $m \in \mathbb{N}$ and $0 < \sigma_1 < \sigma_2 < \sigma_m < \sigma$ delay times:

$$
\begin{aligned}
{}_0^cD_q^H x(\mathfrak{I}) &= \int_{-\sigma}^{\mathfrak{I}} \left(\mathcal{G}_0(s, x_{\mathfrak{I}}(\mathfrak{I}+s)) + \int_0^{\mathfrak{I}} g(\mathfrak{I}, s, x_s)ds\right)ds + \sum_{i=1}^{m} \mathcal{G}_i(\mathfrak{I}, x_{\mathfrak{I}}(\mathfrak{I}-\sigma_i)),\\
x(\mathfrak{I}) &= \psi(\mathfrak{I}-\mathfrak{I}_0) = \psi_0 \in C_\sigma,\\
x'(\mathfrak{I}) &= \psi'(\mathfrak{I}) = \psi_1,
\end{aligned} \tag{82}
$$

where $\mathcal{G}_i : [0,\infty) \times \mathbf{E}^\mathbf{m} \longrightarrow \mathbf{E}^\mathbf{m}, i = 0, 1, \cdots, m,$ are some functions. Let, function $\mathcal{G}_i : [0,\infty) \times C_\sigma \longrightarrow \mathbf{E}^\mathbf{m}$ satisfies the following assumptions:

$(\mathbf{J_1}')$ There exist $L_i > 0$,

$$
\mathcal{D}[\mathcal{G}_i(\mathfrak{I}, x), \mathcal{G}_i(\mathfrak{I}, y)] \le L_i[x, y] \forall x, y \in \mathbf{E}^\mathbf{m} \text{ and } \mathfrak{I} \ge 0. \tag{83}
$$

$(\mathbf{J_2}')\mathcal{G}_i : [0,\infty) \times \mathbf{E}^\mathbf{m} \longrightarrow \mathbf{E}^\mathbf{m}$ is jointly continuous.

$(\mathbf{J_3}')$ There exist $M_i > 0$ and $b_i > 0$ that is

$$
\mathcal{D}\left[\mathcal{G}_i(\mathfrak{I}, 0), \tilde{0}\right] \le M_i e^{b_i \mathfrak{I}} \forall \mathfrak{I} \ge 0. \tag{84}
$$

Then, function $\mathcal{G} : [0,\infty) \times C_\sigma \longrightarrow \mathbf{E}^\mathbf{m}$ is defined as

$$
\begin{aligned}
\mathcal{G}(\mathfrak{I}, \varphi) = &\int_{-\sigma}^{\mathfrak{I}} \left(\mathcal{G}_0(\mathfrak{I}_0, \varphi(\mathfrak{I}_0)) + \int_0^{\mathfrak{I}} g(\mathfrak{I}_0, \mathrm{s}, x_{\mathrm{s}})ds\right)ds\\
&+ \sum_{i=1}^{m} \mathcal{G}_i(\mathfrak{I}, \varphi(\mathfrak{I}-\sigma_i)),
\end{aligned} \tag{85}
$$

and satisfies also assumptions $(\mathbf{J_1}) - (\mathbf{J_2})$. $\mathcal{F}$ is jointly continuous. For all $i = 0, 1, \cdots, m$. For function $\mathcal{G}_i$, suppose L_i be Lipschitz constant. Now

$$
\begin{aligned}
&\mathcal{D}[\mathcal{G}(\mathfrak{I}, \varphi), \mathcal{G}(\mathfrak{I}, \varphi)]\\
&\quad \le \int_{-\sigma}^{\mathfrak{I}} \mathcal{D}[\mathcal{F}_0(\mathfrak{I}_0, \varphi(\mathfrak{I}_0)), \mathcal{F}_0(\mathfrak{I}_0, \psi(\mathfrak{I}_0))]d\mathfrak{I}_0\\
&\qquad + \sum_{i=1}^{m} \mathcal{D}[\mathcal{F}_i(\mathfrak{I}, \varphi(-\sigma_i), \psi(-\sigma_i))]\\
&\quad \le \left(\sigma L_0 + \sum_{i=1}^{m} L_i\right) \mathcal{D}_\sigma(\varphi, \psi),
\end{aligned} \tag{86}
$$

and $\mathcal{G}$ satisfies $(\mathbf{J_1})$. We obtain

$$
\begin{aligned}
\mathcal{D}\left[\mathcal{G}(\mathfrak{I}, 0), \tilde{0}\right] \le \mathcal{D}\left[a, \tilde{0}\right] &+ \int_{-\sigma}^{\mathfrak{I}} \mathcal{D}\left[\mathcal{F}_0(\mathfrak{I}_0, 0), \tilde{0}\right] d\mathfrak{I}_0\\
&+ \sum_{i=1}^{m} \mathcal{D}\left[\mathcal{G}_i(\mathfrak{I}_0, 0), \tilde{0}\right] = \mathcal{D}\left[a, \tilde{0}\right]\\
&+ \frac{M_0}{b_0}\left(1 - e^{b_0 \sigma}\right) + \sum_{i=1}^{m} M_i e^{b_i \mathfrak{I}}.
\end{aligned} \tag{87}
$$

Now, we find $M_{m+1} > 1$ and $b_{m+1} > 1$,

$$
\mathcal{D}\left[a, \tilde{0}\right] + \left(\frac{M_0}{b_0}\right)\left(1 - e^{b_0 \sigma}\right) \le M_{m+1} e^{b_{m+1} \mathfrak{I}} \forall \mathfrak{I} \ge 0, \tag{88}
$$

and we get

$$
\mathcal{D}\left[\mathcal{G}(\mathfrak{I}, \varphi), \tilde{0}\right] \le M e^{b \mathfrak{I}_0} \forall \mathfrak{I} \ge 0, \tag{89}
$$

where $M \coloneqq \max\{M_i\, ; i = 1, 2, \cdots, m+1\}$ and $b = \max\{b_i\, ; i = 1, 2, \cdots, m+1\}$. As a result, $\mathcal{G}$ satisfies $(\mathbf{J_3})$.

As a result, we get below result.

5.2. Fuzzy Population Models. First, we demonstrate how to use the following method to explain the initial problem for fuzzy fractional functional delay differential equation:

$$
\begin{aligned}
{}_0^cD_q^H x(\mathfrak{I}) = f(\mathfrak{I}, x_{\mathfrak{I}}) &+ \int_0^{\mathfrak{I}} g(\mathfrak{I}, s, x_s)ds, \mathfrak{I} \ge \mathfrak{I}_0, \mathfrak{I} \in [0, T],\\
x(\mathfrak{I}) &= \psi(\mathfrak{I}-\mathfrak{I}_0) = \psi_0 \in C_\sigma, \mathfrak{I}_0 \ge \mathfrak{I} \ge \mathfrak{I}_0 - \sigma,\\
x'(\mathfrak{I}) &= \psi'(\mathfrak{I}) = \psi_1,
\end{aligned} \tag{90}
$$

where $\mathcal{G} : [0,\infty) \times \mathbf{E}^\mathbf{m} \longrightarrow \mathbf{E}^\mathbf{m}$ is derived from the continuous function $F : [0,\infty) \times \mathbf{R}^\mathbf{m} \longrightarrow \mathbf{R}^\mathbf{m}$ using Zadeh's extension concept. Since $[\mathcal{G}(\mathfrak{I}, x_{\mathfrak{I}})]^\beta = f(\mathfrak{I}, [x_{\mathfrak{I}}]^\beta) \forall \beta \in [1, 2]$ and $x \in \mathbf{E}^\mathbf{m}$, then, Kaleva [10] denotes

$$
\begin{aligned}
&[x(\mathfrak{I})]^\beta = \left[x_1^\beta(\mathfrak{I}), x_2^\beta(\mathfrak{I})\right], \left[x'(\mathfrak{I})\right]^\beta = \left[\left(x_1^\beta\right)'(\mathfrak{I}), \left(x_2^\beta\right)'(\mathfrak{I})\right], [\varphi(\mathfrak{I})]^\beta = \left[\varphi_1^\beta(\mathfrak{I}), \varphi_2^\beta(\mathfrak{I})\right],\\
&[\mathcal{G}(\mathfrak{I}, x(\mathfrak{I}-\sigma))]^\beta = \left[\mathcal{G}_1^\beta\left(\mathfrak{I}, x_1^\beta(\mathfrak{I}-\sigma), x_2^\beta(\mathfrak{I}-\sigma)\right), \mathcal{G}_2^\beta\left(\mathfrak{I}, x_1^\beta(\mathfrak{I}-\sigma), x_2^\beta(\mathfrak{I}-\sigma)\right)\right],\\
&\mathcal{G}_1^\beta\left(\mathfrak{I}, x_1^\beta(\mathfrak{I}-\sigma), x_2^\beta(\mathfrak{I}-\sigma)\right) = \min\left\{F(\mathfrak{I}, u)\, ; u \in \left[x_1^\beta(\mathfrak{I}-\sigma), x_2^\beta(\mathfrak{I}-\sigma)\right]\right\},\\
&\mathcal{G}_2^\beta\left(\mathfrak{I}, x_1^\beta(\mathfrak{I}-\sigma), x_2^\beta(\mathfrak{I}-\sigma)\right) = \max\left\{F(\mathfrak{I}, u)\, ; u \in \left[x_1^\beta(\mathfrak{I}-\sigma), x_2^\beta(\mathfrak{I}-\sigma)\right]\right\}.
\end{aligned} \tag{91}
$$

Problem (90) is now transformed into the following parameterized delay differential model using these notations:

$$
\begin{aligned}
\left(x_1^\beta\right)'(\mathfrak{I}) &= \mathcal{G}_1^\beta\left(\mathfrak{I}, x_1^\beta(\mathfrak{I}-\sigma), x_2^\beta(\mathfrak{I}-\sigma)\right), \mathfrak{I} \ge 0,\\
\left(x_2^\beta\right)'(\mathfrak{I}) &= \mathcal{G}_2^\beta\left(\mathfrak{I}, x_1^\beta(\mathfrak{I}-\sigma), x_2^\beta(\mathfrak{I}-\sigma)\right), \mathfrak{I} \ge 0,
\end{aligned} \tag{92}
$$

with initial conditions

$$
\begin{aligned}
\left(x_1^\beta\right)(\mathfrak{I}) &= \varphi_1^\beta, -\sigma \le \mathfrak{I} \le \mathfrak{I}_0,\\
\left(x_2^\beta\right)'(\mathfrak{I}) &= \varphi_2^\beta, -\sigma \le \mathfrak{I} \le \mathfrak{I}_0.
\end{aligned} \tag{93}
$$

We can solve the methods (92) and (93). If (x_1^β, x_2^β) is the solution (92) and (93), we can establish a fuzzy solution $x(\mathfrak{I})$ for Equation (90) using representation theorem of Negoita-Ralescu [35]:

$$
[x(\mathfrak{I})]^\beta = \left[x_1^\beta, x_2^\beta\right] \forall \beta \in [1, 2]. \tag{94}
$$

5.2.1. Fuzzy Fractional Functional Time-Delay Malthusian Model. Suppose the initial value problem for a Malthusian model with a fuzzy fractional functional time delay in the example:

$$\begin{aligned} \mathcal{N}'(\mathfrak{J}) &= r\mathcal{N}(\mathfrak{J}-1), \mathfrak{J} \geq 0, \\ \mathcal{N}(\mathfrak{J}) &= \mathcal{N}_0, -1 \leq \mathfrak{J} \leq 0, \end{aligned} \tag{95}$$

$$[\mathcal{N}_0]^\beta = (1-\beta)[-1,1], \beta \in [1,2] \text{ and } r > 1. \tag{96}$$

Zadeh's extension concept is used to obtain function $\mathcal{G} : \mathbf{E^m} \longrightarrow \mathbf{E^m}$ described by $\mathcal{G}(\mathcal{N}(\mathfrak{J}-1)) = r\mathcal{N}(\mathfrak{J}-1)$ from function $f(u) = ru, u \in \mathbf{R^m}$.

If $[\mathcal{N}(\mathfrak{J})]^\beta = [\mathcal{N}_1(\mathfrak{J}), \mathcal{N}_2(\mathfrak{J})]$, then

$$\begin{aligned} \left[\mathcal{N}'(\mathfrak{J})\right]^\beta &= \left[\mathcal{N}_1'(\mathfrak{J}), \mathcal{N}_2'(\mathfrak{J})\right], [r\mathcal{N}(\mathfrak{J}-1)]^\beta \\ &= [r\mathcal{N}_1(\mathfrak{J}-1), r\mathcal{N}_2(\mathfrak{J}-1)]. \end{aligned} \tag{97}$$

As a result, we solve fractional functional differential equations:

$$\begin{aligned} \mathcal{N}_1'(\mathfrak{J}) &= r\mathcal{N}_1(\mathfrak{J}-1), \mathfrak{J} \geq 0, \\ \mathcal{N}_2(\mathfrak{J}) &= -\alpha, -1 \leq \mathfrak{J} \leq 0, \end{aligned} \tag{98}$$

$$\begin{aligned} \mathcal{N}_2'(\mathfrak{J}) &= r\mathcal{N}_2(\mathfrak{J}-1), \mathfrak{J} \geq 0, \\ \mathcal{N}_1(\mathfrak{J}) &= \alpha, -1 \leq \mathfrak{J} \leq 0, \end{aligned} \tag{99}$$

where $\alpha = 1 - \alpha$. The system of steps is used to solve Equation (98). For $0 \leq \mathfrak{J} \leq 1$, we get

$$\begin{cases} -r\alpha, \\ \mathcal{N}_1(0) = -\alpha, \end{cases} \tag{100}$$

with solution $\mathcal{N}_1(\mathfrak{J}) = -\alpha - r\alpha\mathfrak{J}$ for $0 \leq \mathfrak{J} \leq 1$. For $1 \leq \mathfrak{J} \leq 2$, we get

$$\begin{cases} -r\alpha - r^2\alpha(\mathfrak{J}-1), \\ \mathcal{N}_1(1) = -\alpha - r\alpha, \end{cases} \tag{101}$$

with the solution $\mathcal{N}_1(\mathfrak{J}) = -\alpha - r\alpha - r\alpha\mathfrak{J} - (1/2)r^2\alpha(\mathfrak{J}-1)^2$ for $1 \leq \mathfrak{J} \leq 2$. For each $n \in \mathbb{N}$, the solution of (98) has polynomial form $\mathcal{N}_1(\mathfrak{J}) = \sum_{p=1}^{n+1} a_p \mathfrak{J}^p$ on $[n, n+1]$. Also, the solution of (99) has polynomial form when $\mathcal{N} - 2(\mathfrak{J}) = \sum_{p=1}^{n+1} b_p \mathfrak{J}^p$ on $[n, n+1]$. According to Negoita-Ralescu representation theorem [35], the solution of (95) has form on $[n, n+1]$:

$$[\mathcal{N}(\mathfrak{J})]^\beta = \left[\sum_{p=1}^{n+1} a_p \mathfrak{J}^p, \sum_{p=1}^{n+1} b_p \mathfrak{J}^p\right], \tag{102}$$

for every $\beta \in [1,2]$ and $n \in \mathbb{N}$.

Example 1. One of the deficiency of population models in time-delay Malthusian model is that in every case, when population change instantly, birth rate is supposed to change. Moreover, when members of the population hit a certain age before giving birth, we should assume time delay in the model [34].

$$\mathcal{N}'(\mathfrak{J}) = r\mathcal{N}(\mathfrak{J}-\sigma), \tag{103}$$

where population growth rate at time $\mathfrak{J}$ is determined by population at time $\mathfrak{J} - \sigma$.

Also, assume, for time-delay Malthusian model, a more realistic approach should take into account both effect of a time delay and changing of environment. Therefore, it is interesting and necessary to study the general delay-distributed equation:

$$\mathcal{N}'(\mathfrak{J}) = \sum_{p=1}^{n} r_p \mathcal{N}\left(\mathfrak{J} - \sigma_p\right) + \int_{-\sigma}^{\mathfrak{J}} r\mathcal{N}(\mathfrak{J} + s) ds. \tag{104}$$

5.2.2. Fuzzy Fractional Functional Ehrlich Ascites Tumor Model. To explain tumor model of fuzzy fractional function Ehrlich Ascites, consider fuzzy delay equation:

$$\begin{aligned} \mathcal{N}'(\mathfrak{J}) &= r\mathcal{N}(\mathfrak{J}-1)(1-\mathcal{N}(\mathfrak{J}-1)), \mathfrak{J} \geq 0, \\ \mathcal{N}(\mathfrak{J}) &= \mathcal{N}_0, -1 \leq \mathfrak{J} \leq 0, \end{aligned} \tag{105}$$

where $[\mathcal{N}_0]^\beta = \alpha[-1,1], \alpha = ((1-\beta)/2), \beta \in [0,1]$. Assume that $r \in (0,2]$. The function $\mathcal{G} : \mathbf{E^m} \longrightarrow \mathbf{E^m}$, defined by $\mathcal{G}(\mathcal{N}(\mathfrak{J}-1)) = r\mathcal{N}(\mathfrak{J}-1)(1-\mathcal{N}(\mathfrak{J}-1))$, is obtained from function $f(u) = ru(1-u), u \in \mathbf{R^m}$, using Zadeh's extension principle. We get

$$\left[\mathcal{N}'(\mathfrak{J})\right]^\beta = [r\mathcal{N}(\mathfrak{J}-1)(1-\mathcal{N}(\mathfrak{J}-1))]^\beta, \beta \in [0,1]. \tag{106}$$

We remark, function $f(u) = ru(1-u)$ is increasing on $(-\infty, 1/2)$ and decreasing on $(1/2, \infty)$, and $\max_{u \in \mathfrak{R}} f(u) = r/4$. Using the procedure of steps [36] and Negoita-Ralescu representation theorem [35], we can obtain the solution to (105). If $0 \leq \mathfrak{J} \leq 1$, now, we have

$$\begin{aligned} \mathcal{N}'(\mathfrak{J}) &= r\mathcal{N}_0(2-\mathcal{N}_0), \mathfrak{J} \geq 0, \\ \mathcal{N}(0) &= \alpha, -1 \leq \mathfrak{J} \leq 1. \end{aligned} \tag{107}$$

Since $\alpha \leq 1/2$, then, for $0 \leq \mathfrak{J} \leq 1$,

$$\begin{aligned} \left[\mathcal{N}'(\mathfrak{J})\right]^\beta &= [r\mathcal{N}_0(1-\mathcal{N}_0)]^\beta = \left[\min_{-\alpha \leq u \leq \alpha} f(u), \max_{-\alpha \leq u \leq \alpha} f(u)\right] \\ &= [-r\alpha(1+\alpha), r\alpha(1-\alpha)]. \end{aligned} \tag{108}$$

As a result, we solve differential equations on $[0,1]$

$$\left[\mathcal{N}'(\mathfrak{J})\right]^\beta = [-r\alpha(1+\alpha), r\alpha(1-\alpha)], \tag{109}$$

with initial condition

$$[\mathcal{N}(0)]^{\beta} = [-\alpha, \alpha]. \tag{110}$$

Further, for (52) on [0,1], the solution

$$[\mathcal{N}(\mathfrak{J})]^{\beta} = [\mathcal{N}_{11}(\mathfrak{J}), \mathcal{N}_{21}(\mathfrak{J})], \mathfrak{J} \in [0, 1], \tag{111}$$

where

$$\begin{aligned}\mathcal{N}_{11}(\mathfrak{J}) = -\alpha - r\alpha(1+\alpha)\mathfrak{J}, \mathcal{N}_{21}(\mathfrak{J}) \\ = \alpha + r\alpha(1-\alpha)\mathfrak{J}, \beta \in [0, 1].\end{aligned} \tag{112}$$

Moreover, $\mathcal{N}_{11}(\mathfrak{J}) \leq 0$ and $1/2 \leq \mathcal{N}_{21}(\mathfrak{J}) \leq 1$ on $[0, 1]$, for $1 \leq \mathfrak{J} \leq 2$,

$$\begin{aligned}\left[\mathcal{N}'(\mathfrak{J})\right]^{\beta} &= [r\mathcal{N}(\mathfrak{J}-1)(1-\mathcal{N}(\mathfrak{J}-1))]^{\beta} \\ &= \left[\min_{\mathcal{N}_{11}(\mathfrak{J}-1)\leq u\leq \mathcal{N}_{21}(\mathfrak{J}-1)} f(u), \max_{\mathcal{N}_{11}(\mathfrak{J}-1)\leq u\leq \mathcal{N}_{21}(\mathfrak{J}-1)} f(u)\right] \\ &= \left[-r\alpha + r\alpha(1+\alpha)(\mathfrak{J}-1)(1+\alpha+r\alpha(1+\alpha)(\mathfrak{J}-1)), \frac{r^2}{4}\left(1-\frac{r}{4}\right)\right].\end{aligned} \tag{113}$$

As it follows, we solve the differential equation on [1 , 2]:

$$\left[\mathcal{N}'(\mathfrak{J})\right]^{\beta} = \left[-r\alpha + r\alpha(1+\alpha)(\mathfrak{J}-1)(1+\alpha+r\alpha(1+\alpha)(\mathfrak{J}-1)), \frac{r^2}{4}\left(1-\frac{r}{4}\right)\right]. \tag{114}$$

As a result, we get (105) on $[1, 2]$, as follows:

$$[\mathcal{N}(\mathfrak{J})]^{\beta} = [\mathcal{N}_{12}(\mathfrak{J}), \mathcal{N}_{22}(\mathfrak{J})], \beta \in [1, 2], \tag{115}$$

where

$$\begin{aligned}\mathcal{N}_{12}(\mathfrak{J}) &= -\alpha - 2r\alpha(1+\alpha) - r\alpha(1+\alpha)(\mathfrak{J}-1) \\ &\quad - r^2\alpha(1+\alpha)(2+\alpha)\frac{(\mathfrak{J}-1)^2}{2} - r^3\alpha^2\frac{(\mathfrak{J}-1)^3}{3}, \\ \mathcal{N}_{22}(\mathfrak{J}) &= \alpha + r\alpha(1-\alpha) + \frac{r^2}{4}\left(1-\frac{r}{4}\right)\mathfrak{J}, \mathfrak{J} \in [0, 1].\end{aligned} \tag{116}$$

This procedure can be continued on [21, 37].

Example 2. To explain the Ehrlich ascities tumor, the following logistic equation was suggested in [9]:

$$\mathcal{N}'(\mathfrak{J}) = r\mathcal{N}(\mathfrak{J}-\sigma)\left(1-\frac{\mathcal{N}(\mathfrak{J}-\sigma)}{\mathcal{K}}\right). \tag{117}$$

The delay associated cell cycle [37] is represented by σ, where r is net tumor replication and $\mathcal{K}$ is caring capacity. This equation differs from the traditional Verhulst-Hutchinson equation [38], which has only one delay expression.

Many independent characteristics of state variables can affect population dynamics: natural and social resources, medical care, job environment, and crime, habitations. Classically, the exact value of these attributes cannot always be calculated and evaluated since they are unknown and can only be conjectured. As a result, the Ehrlich ascities tumor model should be a more realistic solution.

6. Conclusion

The solution to fuzzy fractional functional differential equations possesses global uniqueness and existence, as shown in this paper. We have used the successive approximation method to prove a local uniqueness and existence result. Future research on fuzzy neutral fractional functional differential equations could benefit from the findings of this study. Other alternative research approaches include a fuzzy fractional functional differential equation approach based on other fuzzy differentiability concepts (see [8, 11]).

Data Availability

No new data were created this study.

Conflicts of Interest

The authors declare that they have no known competing financial interests or personal relationships that could have appeared to influence the work reported in this paper.

Authors' Contributions

All authors contributed equally to the writing of this paper. All authors read and approved the final manuscript.

Acknowledgments

This work was supported by the Deanship of Scientific Research, Vice Presidency for Graduate Studies and Scientific Research, King Faisal University, Saudi Arabia [Project No. GRANT560], King Faisal University (KFU), Ahsa, Saudi Arabia. The authors, therefore, acknowledge technical and financial support of DSR at KFU.

References

[1] B. Ahmad and J. J. Nieto, "Existence results for a coupled system of nonlinear fractional differential equations with three-point boundary conditions," *Computers & Mathematics with Applications*, vol. 58, no. 9, pp. 1838–1843, 2009.

[2] B. Ahmad, S. K. Ntouyas, R. P. Agarwal, and A. Alsaedi, "On fractional differential equations and inclusions with nonlocal and average-valued (integral) boundary conditions," *Advances in Difference Equations*, vol. 2016, 18 pages, 2016.

[3] S. S. Mansouri, M. Gachpazan, and O. S. Fard, "Existence, uniqueness and stability of fuzzy fractional differential equations with local Lipschitz and linear growth conditions," *Advances in Difference Equations*, vol. 2017, 13 pages, 2017.

[4] S. S. Chang and L. A. Zadeh, "On fuzzy mapping and control," *Fuzzy sets, fuzzy logic, and fuzzy systems: selected papers by Lotfi a Zadeh*, pp. 180–184, 1996.

[5] M. Chen and C. Han, "Some topological properties of solutions to fuzzy differential systems," *Information Sciences*, vol. 197, pp. 207–214, 2012.

[6] O. Kaleva, "The Cauchy problem for fuzzy differential equations," *Fuzzy Sets and Systems*, vol. 35, no. 3, pp. 389–396, 1990.

[7] J. J. Nieto, "The Cauchy problem for continuous fuzzy differential equations," *Fuzzy Sets and Systems*, vol. 102, no. 2, pp. 259–262, 1999.

[8] J. J. Buckley and T. Feuring, "Fuzzy differential equations," *Fuzzy Sets and Systems*, vol. 110, no. 1, pp. 43–54, 2000.

[9] S. Song and C. Wu, "Existence and uniqueness of solutions to Cauchy problem of fuzzy differential equations," *Fuzzy Sets and Systems*, vol. 110, no. 1, pp. 55–67, 2000.

[10] X. Xiaoping and F. Yongqiang, "On the structure of solutions for fuzzy initial value problem," *Fuzzy Sets and Systems*, vol. 157, no. 2, pp. 212–229, 2006.

[11] P. Diamond, "Stability and periodicity in fuzzy differential equations," *IEEE Transactions on Fuzzy Systems*, vol. 8, no. 5, pp. 583–590, 2000.

[12] E. Hüllermeier, "An approach to modelling and simulation of uncertain dynamical systems," *International Journal of Uncertainty, Fuzziness and Knowledge-Based Systems*, vol. 5, no. 2, pp. 117–137, 1997.

[13] B. Bede and S. G. Gal, "Generalizations of the differentiability of fuzzy-number-valued functions with applications to fuzzy differential equations," *Fuzzy Sets and Systems*, vol. 151, no. 3, pp. 581–599, 2005.

[14] J. Y. Park, S. Y. Lee, and J. U. Jeong, "The approximate solutions of fuzzy functional integral equations," *Fuzzy Sets and Systems*, vol. 110, no. 1, pp. 79–90, 2000.

[15] J. Y. Park, I. H. Jung, and M. J. Lee, "Almost periodic solutions of fuzzy systems," *Fuzzy Sets and Systems*, vol. 119, no. 3, pp. 367–373, 2001.

[16] P. Balasubramaniam and S. Muralisankar, "Existence and uniqueness of fuzzy solution for the nonlinear fuzzy integro-differential equations," *Applied Mathematics Letters*, vol. 14, no. 4, pp. 455–462, 2001.

[17] M. Guo, X. Xue, and R. Li, "Impulsive functional differential inclusions and fuzzy population models," *Fuzzy Sets and Systems*, vol. 138, no. 3, pp. 601–615, 2003.

[18] A. Abbas, R. Shafqat, M. B. Jeelani, and N. H. Alharthi, "Significance of chemical reaction and Lorentz force on third-grade fluid flow and heat transfer with Darcy–Forchheimer law over an inclined exponentially stretching sheet embedded in a porous medium," *Symmetry*, vol. 14, no. 4, p. 779, 2022.

[19] A. Abbas, R. Shafqat, M. B. Jeelani, and N. H. Alharthi, "Convective heat and mass transfer in third-grade fluid with Darcy–Forchheimer Relation in the presence of thermal-diffusion and diffusion-thermo effects over an exponentially inclined stretching sheet surrounded by a porous medium: a CFD study," *Processes*, vol. 10, no. 4, p. 776, 2022.

[20] A. U. K. Niazi, J. He, R. Shafqat, and B. Ahmed, "Existence, uniqueness, and Eq–Ulam-type stability of fuzzy fractional differential equation," *Fractal and Fractional*, vol. 5, no. 3, p. 66, 2021.

[21] N. Iqbal, A. U. K. Niazi, R. Shafqat, and S. Zaland, "Existence and uniqueness of mild solution for fractional-order controlled fuzzy evolution equation," *Journal of Function Spaces*, vol. 2021, Article ID 5795065, 8 pages, 2021.

[22] R. Shafqat, A. U. K. Niazi, M. B. Jeelani, and N. H. Alharthi, "Existence and uniqueness of mild solution where $\alpha \in (1,2)$ for fuzzy fractional evolution equations with uncertainty," *Fractal and Fractional*, vol. 6, no. 2, p. 65, 2022.

[23] K. Abuasbeh, R. Shafqat, A. U. K. Niazi, and M. Awadalla, "Local and global existence and uniqueness of solution for time-fractional fuzzy Navier–Stokes equations," *Fractal and Fractional*, vol. 6, no. 6, p. 330, 2022.

[24] A. S. Alnahdi, R. Shafqat, A. U. K. Niazi, and M. B. Jeelani, "Pattern formation induced by fuzzy fractional-order model of COVID-19," *Axioms*, vol. 11, no. 7, p. 313, 2022.

[25] Y. Guo, M. Chen, X. B. Shu, and F. Xu, "The existence and Hyers-Ulam stability of solution for almost periodical fractional stochastic differential equation with fBm," *Stochastic Analysis and Applications*, vol. 39, no. 4, pp. 643–666, 2021.

[26] Y. Shi, "A study on the mild solution of impulsive fractional evolution equations," *Applied Mathematics and Computation*, vol. 273, pp. 465–476, 2016.

[27] V. Lupulescu, "On a class of fuzzy functional differential equations," *Fuzzy Sets and Systems*, vol. 160, no. 11, pp. 1547–1562, 2009.

[28] O. Kaleva, "Fuzzy differential equations," *Fuzzy Sets and Systems*, vol. 24, no. 3, pp. 301–317, 1987.

[29] C. G. Gal and S. G. Gal, "Semigroups of operators on spaces of fuzzy-number-valued functions with applications to fuzzy differential equations," 2013, https://arxiv.org/abs/1306.3928.

[30] D. Otrocol and V. Ilea, "Ulam stability for a delay differential equation," *Open Mathematics*, vol. 11, no. 7, pp. 1296–1303, 2013.

[31] R. J. Aumann, "Integrals of set-valued functions," *Journal of Mathematical Analysis and Applications*, vol. 12, no. 1, pp. 1–12, 1965.

[32] I. Podlubny, *Fractional differential equations*, Academic Press, 1999.

[33] J. J. Nieto and R. R. López, "Applications of contractive-like mapping principles to fuzzy equations," *Revista Matemática Complutense*, vol. 19, no. 2, pp. 361–383, 2006.

[34] C. C. Travis and G. F. Webb, "Cosine families and abstract nonlinear second order differential equations," *Acta Mathematica Hungarica*, vol. 32, no. 1-2, pp. 75–96, 1978.

[35] C. V. Negoiţă and D. A. Ralescu, *Applications of Fuzzy Sets to Systems Analysis*, Birkhäuser, Basel, Switzerland, 1975.

[36] Y. Kuang, *Delay Differential Equations: With Applications in Population Dynamics*, Academic press, 1993.

[37] K. H. Jack, "Theory of functional differential equations," *Applied Mathematical Sciences*, vol. 3, 1981.

[38] R. Schuster and H. Schuster, "Reconstruction models for the Ehrlich ascites tumor of the mouse," *Mathematical population dynamics*, vol. 2, pp. 335–348, 1995.

Hindawi
Journal of Function Spaces
Volume 2022, Article ID 6261970, 10 pages
https://doi.org/10.1155/2022/6261970

Research Article

Some New Generalized Fractional Newton's Type Inequalities for Convex Functions

Jarunee Soontharanon,[1] Muhammad Aamir Ali,[2] Hüseyin Budak,[3] Pinar Kösem,[3] Kamsing Nonlaopon,[4] and Thanin Sitthiwirattham[5]

[1]*Department of Mathematics, Faculty of Applied Science, King Mongkut's University of Technology North Bangkok, Bangkok 10800, Thailand*
[2]*Jiangsu Key Laboratory for NSLSCS, School of Mathematical Sciences, Nanjing Normal University, Nanjing, China*
[3]*Department of Mathematics, Faculty of Science and Arts, Düzce University, Düzce, Turkey*
[4]*Department of Mathematics, Faculty of Science, Khon Kaen University, Khon Kaen 40002, Thailand*
[5]*Mathematics Department, Faculty of Science and Technology, Suan Dusit University, Bangkok 10300, Thailand*

Correspondence should be addressed to Kamsing Nonlaopon; nkamsi@kku.ac.th

Received 21 April 2022; Revised 1 July 2022; Accepted 1 August 2022; Published 2 September 2022

Academic Editor: Behrouz Parsa Moghaddam

In this paper, we establish some new Newton's type inequalities for differentiable convex functions using the generalized Riemann-Liouville fractional integrals. The main edge of the newly established inequalities is that these can be turned into several new and existing inequalities for different fractional integrals like Riemann-Liouville fractional integrals, *k*-fractional integrals, Katugampola fractional operators, conformable fractional operators, Hadamard fractional operators, and fractional operators with the exponential kernel without proving one by one. It is also shown that the newly established inequalities are the refinements of the previously established inequalities inside the literature.

1. Introduction

The fascinating idea of inequalities has long been a topic of discussion in various mathematical disciplines. Fractional calculus, quantum calculus, operator theory, numerical analysis, operator equations, network theory, and quantum information theory are just a few fascinating applications. This is a very active study topic right now, and the interplay between different areas has enriched it. Numerical integration and definite integral estimation are important aspects of applied sciences. Among the numerical techniques, Simpson's rules are crucial that can be stated as follows:

(1) Simpson's 1/3 rule:

$$\int_{\theta_1}^{\theta_2} \mathfrak{G}(\varkappa)d\varkappa \approx \frac{\theta_2-\theta_1}{6}\left[\mathfrak{G}(\theta_1)+\mathfrak{G}\left(\frac{\theta_1+\theta_2}{2}\right)+\mathfrak{G}(\theta_2)\right] \tag{1}$$

(2) Simpson's 3/8 rule (Newton rule):

$$\int_{\theta_1}^{\theta_2} \mathfrak{G}(\varkappa)d\varkappa \approx \frac{\theta_2-\theta_1}{8}\left[\mathfrak{G}(\theta_1)+3\mathfrak{G}\left(\frac{\theta_1+2\theta_2}{3}\right)+3\mathfrak{G}\left(\frac{2\theta_1+\theta_2}{3}\right)+\mathfrak{G}(\theta_2)\right] \tag{2}$$

Researchers have used fractional calculus to develop different fractional integral inequalities that are beneficial in approximation theory due to their importance. Inequalities like Hermite-Hadamard, Simpson's, midpoint, Ostrowski's, and trapezoidal inequalities are examples of inequalities that may be used to find the boundaries of numerical integration formulas. The bounds of trapezoidal formula and inequality of Hermite-Hadamard type using the Riemann-Liouville fractional integrals were established in [1]. Set [2] used differentiable convexity and established fractional Ostrowski's type inequalities. İscan and Wu [3] proved some bounds of numerical integration and inequality of the Hermite-Hadamard type for reciprocal convex functions via Riemann-Liouville fractional integrals. The bounds of midpoint and a new version of fractional inequality of Hermite-Hadamard type were established by Sarikaya and Yildrim in [4]. The bounds for Simpson's 1/3 formula were obtained by Sarikaya et al. [5] using the general convexity and Riemann-Liouville fractional integral operators. In [6], the authors found some new bounds for Simpson's 1/3 formula using the Riemann-Liouville fractional integrals. The authors of [7] used s-convexity and found some bounds for Simpson's 1/3 formula. In 2020, Sarikaya and Ertugral [8] gave a new class of fractional integrals called generalized fractional integrals and established Hermite-Hadamard-type inequalities connected to the newly defined class of integrals. The main advantage of the newly defined class of fractional integral operators is that it can be converted into the classical integral, Riemann-Liouville fractional integrals, k-fractional integrals, Hadamard fractional integrals, etc. In [9], Zhao et al. obtained some bounds for a trapezoidal formula using the reciprocal convex functions and generalized fractional integral operators. Budak et al. [10] established some bounds for Simpson's 1/3 formula for differentiable convex functions using the generalized fractional integrals. Some bounds for the q-Simpson's and Newton's type inequalities were proved by Budak et al. in [11]. Siricharuanun et al. proved some inequalities of Simpson and Newton type by using quantum numbers in [12]. Until recent years, Newton-type inequalities for fractional integrals had not been proven. Recently, Sitthiwirattham et al. [13] used the Riemann-Liouville fractional integrals operators and obtained some bounds for Newton formula.

Motivated by the ongoing studies, we obtain some new bounds/inequalities for Newton formula using the convexity and generalized fractional integrals. The main edge of newly established inequalities is that these can be converted into classical Newton inequalities, Riemann-Liouville fractional Newton inequalities and new Newton inequalities for k-fractional integrals without establishing one by one. These results can be helpful in finding the error bounds of Newton formulas in fractional calculus, which is the main motivation of this paper. Moreover, the main difference between the results proved in [11–13] and the results of this paper is that while the papers [11, 12] are derived on Newton type inequalities for quantum integrals and the paper [13] focus on Newton type inequalities for Riemann-Liouville fractional integrals operators, we prove some inequalities of Newton type by using the generalized fractional integrals. These inequalities generalize the results of the paper [13] and give some new inequalities for k-fractional integrals, Hadamard fractional integrals, conformable fractional integrals, etc.

On the other hand, there are many other papers related to our topic. One can consult [14–25] and references therein for more inequalities via fractional integrals. Moreover, several papers focused on the functions of bounded variation to prove some important inequalities such as the Ostrowski type [26], Simpson type [27, 28], trapezoid type [29, 30], and midpoint type [31]. For more applications of fractional calculus in other areas of mathematical sciences, one can consult [32–41].

A description of the paper is as follows: In Section 2, the fundamentals of fractional calculus, as well as other pertinent research in this field, are briefly discussed. In Section 3, we develop an essential identity that is vital in identifying the key outcomes of the paper. In Section 4, we use generalized fractional integrals to derive some new Newton's type inequalities for differentiable convex functions. For functions of bounded variation, Section 5 contains certain fractional Newton-type inequalities. Section 6 concludes with some future study ideas.

2. Fractional Integrals and Related Inequalities

Several fundamental fractional integral notations and concepts are reviewed in this section. Different fractional integrals are also used to recall various inequalities.

Definition 1. A function $\mathfrak{G} : I \longrightarrow \mathbb{R}$, where I is an interval in $\mathbb{R}$, is called convex, if it satisfies the inequality

$$\mathfrak{G}(t\varkappa + (1-t)y) \le t\mathfrak{G}(\varkappa) + (1-t)\mathfrak{G}(y), \tag{3}$$

where $\varkappa, y \in I$ and $t \in [0, 1]$.

Definition 2 ([42, 43]). Let $\mathfrak{G} \in L_1[\theta_1, \theta_2]$. The Riemann-Liouville fractional integrals (RLFIs) $J^{\alpha}_{\theta_1+}\mathfrak{G}$ and $J^{\alpha}_{\theta_2-}\mathfrak{G}$ of order $\alpha > 0$ with $\theta_1 \ge 0$ are defined as follows:

$$\begin{aligned} J^{\alpha}_{\theta_1+}\mathfrak{G}(\varkappa) &= \frac{1}{\Gamma(\theta_1)}\int_{\theta_1}^{\varkappa} (\varkappa - t)^{\alpha-1}\mathfrak{G}(t)dt, \varkappa > \theta_1, \\ J^{\alpha}_{\theta_2-}\mathfrak{G}(\varkappa) &= \frac{1}{\Gamma(\alpha)}\int_{\varkappa}^{\theta_2} (t - \varkappa)^{\alpha-1}\mathfrak{G}(t)dt, \varkappa < \theta_2, \end{aligned} \tag{4}$$

respectively, where the well-known Gamma function is represented by Γ.

Definition 3 ([44]). Let $\mathfrak{G} \in L_1[\theta_1, \theta_2]$. The k-Riemann-Liouville fractional integrals (KRLFIs) $\mathcal{J}^{\alpha,k}_{\theta_1+}\mathfrak{G}$ and $\mathcal{J}^{\alpha,k}_{\theta_2-,k}\mathfrak{G}$ of order $\alpha, k > 0$ with $\theta_1 \ge 0$ are defined as follows:

$$\begin{aligned} \mathcal{J}^{\alpha,k}_{\theta_1+}\mathfrak{G}(\varkappa) &= \frac{1}{k\Gamma_k(\alpha)}\int_{\theta_1}^{\varkappa} (\varkappa - t)^{(\alpha/k)-1}\mathfrak{G}(t)dt, \varkappa > \theta_1, \\ \mathcal{J}^{\alpha,k}_{\theta_2-,k}\mathfrak{G}(\varkappa) &= \frac{1}{k\Gamma_k(\alpha)}\int_{\varkappa}^{\theta_2} (t - \varkappa)^{(\alpha/k)-1}\mathfrak{G}(t)dt, \varkappa < \theta_2, \end{aligned} \tag{5}$$

respectively, where Γ_k is the well-known k-Gamma function.

Definition 4 ([8]). Let $\mathfrak{G} \in L_1[\theta_1, \theta_2]$. The generalized fractional integrals (GRLFIs) ${}_{\theta_1+}I_{\varphi}\mathfrak{G}$ and ${}_{\theta_2-}I_{\varphi}\mathfrak{G}$ with $\theta_1 \ge 0$ are defined as follows:

$$\begin{aligned} {}_{\theta_1+}I_{\varphi}\mathfrak{G}(\varkappa) &= \int_{\theta_1}^{\varkappa} \frac{\varphi(\varkappa - t)}{\varkappa - t}\mathfrak{G}(t)dt, \varkappa > \theta_1, \\ {}_{\theta_2-}I_{\varphi}\mathfrak{G}(\varkappa) &= \int_{\varkappa}^{\theta_2} \frac{\varphi(t - \varkappa)}{t - \varkappa}\mathfrak{G}(t)dt, \varkappa < \theta_2, \end{aligned} \tag{6}$$

respectively, where the mapping is $\varphi : [0,\infty) \longrightarrow [0,\infty)$. One can consult [8] for further information of function φ.

Remark 5. The GRLFIs are significant because they can be converted into classical Riemann integrals, RLFIs, and KFIs for $\varphi(\lambda) = \lambda$, $\varphi(\lambda) = \lambda^{\alpha}/\Gamma(\alpha)$ and $\varphi(\lambda) = \lambda^{\alpha/k}/k\Gamma_k(\alpha)$, respectively. For more choices of the function φ, one can recapture the different fractional integrals like Katugampola fractional operators, conformable fractional integrals, Hadamard fractional operators, and fractional operators with the exponential kernel (see [8]).

In [45], Ertuğral and Sarikaya used GRLFIs and proved the following Simpson's type inequalities for differentiable convex functions.

Theorem 6. *Let $\mathfrak{G} : I \subset \mathbb{R} \longrightarrow \mathbb{R}$ be a differentiable function over I° and $\mathfrak{G}' \in L_1[\theta_1, \theta_2]$. If $|\mathfrak{G}'|$ is convex over $[\theta_1, \theta_2]$, then the following inequality holds:*

$$\begin{aligned}&\left|\frac{1}{6}\left[\mathfrak{G}(\theta_1) + 4\mathfrak{G}\left(\frac{\theta_1+\theta_2}{2}\right) + \mathfrak{G}(\theta_2)\right]\right.\\&\left.\quad - \frac{1}{2\Theta(1)}\left[{}_{\theta_1+}I_{\varphi}\mathfrak{G}\left(\frac{\theta_1+\theta_2}{2}\right) + {}_{\theta_2-}I_{\varphi}\mathfrak{G}\left(\frac{\theta_1+\theta_2}{2}\right)\right]\right|\\&\le \frac{\theta_2-\theta_1}{2\Theta(1)}\Omega(t)\left[|\mathfrak{G}'(\theta_1)| + |\mathfrak{G}'(\theta_2)|\right],\end{aligned} \tag{7}$$

where

$$\begin{aligned}\Omega(t) &= \int_0^1 \left|\frac{\Theta(t)}{2} - \frac{\Theta(1)}{3}\right| dt,\\ \Theta(\varkappa) &= \int_0^{\varkappa} \frac{\varphi((\theta_2-\theta_1)/2t)}{t} dt.\end{aligned} \tag{8}$$

It is worth mentioning here that the inequality (7) can be turned into classical Simpson's inequality, RLFIs Simpson's inequality, and KRLFIs inequality as follows:

(i) For $\varphi(t) = t$, the following Simpson's inequality for classical Riemann-integral holds (see [5]):

$$\begin{aligned}&\left|\frac{1}{6}\left[\mathfrak{G}(\theta_1) + 4\mathfrak{G}\left(\frac{\theta_1+\theta_2}{2}\right) + \mathfrak{G}(\theta_2)\right] - \frac{1}{\theta_2-\theta_1}\int_{\theta_1}^{\theta_2}\mathfrak{G}(\varkappa)d\varkappa\right|\\&\le \frac{5(\theta_2-\theta_1)}{72}\left[|\mathfrak{G}'(\theta_1)| + |\mathfrak{G}'(\theta_2)|\right]\end{aligned} \tag{9}$$

(ii) For $\varphi(t) = t^{\alpha}/\Gamma(\alpha)$, the following Simpson's inequality for RLFIs holds (see [45]):

$$\begin{aligned}&\left|\frac{1}{6}\left[\mathfrak{G}(\theta_1) + 4\mathfrak{G}\left(\frac{\theta_1+\theta_2}{2}\right) + \mathfrak{G}(\theta_2)\right]\right.\\&\left.\quad - \frac{\Gamma(\alpha+1)}{2^{1-\alpha}(\theta_2-\theta_1)^{\alpha}}\left[J^{\alpha}_{\theta_1+}\mathfrak{G}\left(\frac{\theta_1+\theta_2}{2}\right) + J^{\alpha}_{\theta_2-}\mathfrak{G}\left(\frac{\theta_1+\theta_2}{2}\right)\right]\right|\\&\le \frac{\theta_2-\theta_1}{2}F(\alpha)\left[|\mathfrak{G}'(\theta_1)| + |\mathfrak{G}'(\theta_2)|\right],\end{aligned} \tag{10}$$

where

$$F(\alpha) = \left(\frac{2}{3}\right)^{(1/\alpha)+1}\left(\frac{\alpha}{\alpha+1}\right) + \frac{1}{2(\alpha+1)} - \frac{1}{3} \tag{11}$$

(iii) For $\varphi(t) = t^{\alpha/k}/k\Gamma_k(\alpha)$, the following Simpson's inequality for KRLFIs holds (see [45]):

$$\begin{aligned}&\left|\frac{1}{6}\left[\mathfrak{G}(\theta_1) + 4\mathfrak{G}\left(\frac{\theta_1+\theta_2}{2}\right) + \mathfrak{G}(\theta_2)\right]\right.\\&\left.\quad - \frac{\Gamma_k(\alpha+k)}{2^{1-\alpha/k}(\theta_2-\theta_1)^{\alpha/k}}\left[\mathcal{J}^{\alpha,k}_{\theta_1+}\mathfrak{G}\left(\frac{\theta_1+\theta_2}{2}\right) + \mathcal{J}^{\alpha,k}_{\theta_2-}\mathfrak{G}\left(\frac{\theta_1+\theta_2}{2}\right)\right]\right|\\&\le \frac{\theta_2-\theta_1}{2}F(\alpha,k)\left[|\mathfrak{G}'(\theta_1)| + |\mathfrak{G}'(\theta_2)|\right],\end{aligned} \tag{12}$$

where

$$F(\alpha,k) = \left(\frac{2}{3}\right)^{k/\alpha+1}\left(\frac{\alpha}{\alpha+k}\right) + \frac{k}{2(\alpha+k)} - \frac{1}{3} \tag{13}$$

Remark 7. If we set $\alpha = k = 1$ in (10) and (12), then we obtain the classical Simpson's inequality (9).

3. An Identity

In this section, we prove an integral equality in order to demonstrate the primary findings of the paper. For brevity, we shall use the following notation throughout the paper:

$$Y(\varkappa) = \int_0^{\varkappa} \frac{\varphi(((\theta_2-\theta_1)/3)u)}{u} du < +\infty. \tag{14}$$

Lemma 8. *If $\mathfrak{G} : I \subset \mathbb{R} \longrightarrow \mathbb{R}$ is a function such that $\mathfrak{G}$ is differentiable over I° and $\mathfrak{G}' \in L_1[\theta_1, \theta_2]$, then the following identity holds for GRLFIs:*

$$\begin{aligned}&\frac{1}{3Y(1)}\left[{}_{\theta_1+}I_{\varphi}\mathfrak{G}\left(\frac{2\theta_1+\theta_2}{3}\right) + {}_{(2\theta1+\theta2)/3+}I_{\varphi}\mathfrak{G}\left(\frac{\theta_1+2\theta_2}{3}\right)\right.\\&\left.\quad + {}_{(\theta1+2\theta2)/3+}I_{\varphi}\mathfrak{G}(\theta_2)\right] - \frac{1}{8}\left[\mathfrak{G}(\theta_1) + 3\mathfrak{G}\left(\frac{2\theta_1+\theta_2}{3}\right)\right.\\&\left.\quad + 3\mathfrak{G}\left(\frac{\theta_1+2\theta_2}{3}\right) + \mathfrak{G}(\theta_2)\right] = \frac{\theta_2-\theta_1}{9Y(1)}[I_1 + I_2 + I_3],\end{aligned} \tag{15}$$

where

$$\begin{aligned}I_1 &= \int_0^1 \left(Y(t) - \frac{5Y(1)}{8}\right)\mathfrak{G}'\left(t\theta_1 + (1-t)\frac{2\theta_1+\theta_2}{3}\right)dt,\\ I_2 &= \int_0^1 \left(Y(t) - \frac{Y(1)}{2}\right)\mathfrak{G}'\left(t\frac{2\theta_1+\theta_2}{3} + (1-t)\frac{\theta_1+2\theta_2}{3}\right)dt,\end{aligned}$$

$$I_3=\int_0^1\left(Y(t)-\frac{3Y(1)}{8}\right)\mathfrak{G}'\left(t\frac{\theta_1+2\theta_2}{3}+(1-t)\theta_2\right)dt. \tag{16}$$

Proof. Using the laws of integration by parts and variables change, we have

$$\begin{aligned}I_1&=\int_0^1\left(Y(t)-\frac{5Y(1)}{8}\right)\mathfrak{G}'\left(t\theta_1+(1-t)\frac{2\theta_1+\theta_2}{3}\right)dt\\&=\frac{3}{(\theta_2-\theta_1)}\int_0^1\frac{\varphi(((\theta_2-\theta_1)/3)t)}{t}\mathfrak{G}\left(t\theta_1+(1-t)\frac{2\theta_1+\theta_2}{3}\right)dt\\&\quad-\frac{Y(1)}{\theta_2-\theta_1}\left[\frac{15}{8}\mathfrak{G}\left(\frac{2\theta_1+\theta_2}{3}\right)+\frac{9}{8}\mathfrak{G}(\theta_1)\right]\\&=\frac{3}{\theta_2-\theta_1}{}_{\theta_1+}I_{\varphi}\mathfrak{G}\left(\frac{2\theta_1+\theta_2}{3}\right)-\frac{Y(1)}{\theta_2-\theta_1}\left[\frac{15}{8}\mathfrak{G}\left(\frac{2\theta_1+\theta_2}{3}\right)+\frac{9}{8}\mathfrak{G}(\theta_1)\right].\end{aligned} \tag{17}$$

Also, we have

$$\begin{aligned}I_2&=\int_0^1\left(Y(t)-\frac{Y(1)}{2}\right)\mathfrak{G}'\left(t\frac{2\theta_1+\theta_2}{3}+(1-t)\frac{\theta_1+2\theta_2}{3}\right)dt\\&=\frac{3}{\theta_2-\theta_1}{}_{(2\theta_1+\theta_2)/3+}I_{\varphi}\mathfrak{G}\left(\frac{\theta_1+2\theta_2}{3}\right)\\&\quad-\frac{Y(1)}{\theta_2-\theta_1}\left[\frac{3}{2}\mathfrak{G}\left(\frac{\theta_1+2\theta_2}{3}\right)+\frac{3}{2}\mathfrak{G}\left(\frac{2\theta_1+\theta_2}{3}\right)\right],\end{aligned} \tag{18}$$

$$\begin{aligned}I_3&=\int_0^1\left(Y(t)-\frac{3Y(1)}{8}\right)\mathfrak{G}'\left(t\frac{\theta_1+2\theta_2}{3}+(1-t)\theta_2\right)dt\\&=\frac{3}{\theta_2-\theta_1}{}_{(\theta_1+2\theta_2)/3+}I_{\varphi}\mathfrak{G}(\theta_2)-\frac{Y(1)}{\theta_2-\theta_1}\left[\frac{9}{8}\mathfrak{G}(\theta_2)\right.\\&\quad\left.+\frac{15}{8}\mathfrak{G}\left(\frac{\theta_1+2\theta_2}{3}\right)\right].\end{aligned} \tag{19}$$

As a consequence, we may get the resultant equality by adding (17)–(19) and multiplying the resultant one by $(\theta_2-\theta_1)/9Y(1)$. □

4. Newton's Inequalities for Convex Functions

We will utilize GRLFIs to demonstrate some new Newton's inequalities for differentiable convex functions in this section. We use the following notations for sake of brevity:

$$\begin{aligned}A_1(\alpha)&=\int_0^1 t\left|Y(t)-\frac{3Y(1)}{8}\right|dt,\\A_2(\alpha)&=\int_0^1\left|Y(t)-\frac{3Y(1)}{8}\right|dt,\\A_3(\alpha)&=\int_0^1 t\left|Y(t)-\frac{Y(1)}{2}\right|dt,\\A_4(\alpha)&=\int_0^1\left|Y(t)-\frac{Y(1)}{2}\right|dt,\\A_5(\alpha)&=\int_0^1 t\left|Y(t)-\frac{5Y(1)}{8}\right|dt,\\A_6(\alpha)&=\int_0^1\left|Y(t)-\frac{5Y(1)}{8}\right|dt.\end{aligned} \tag{20}$$

Theorem 9. *If $|\mathfrak{G}'|$ is a convex function and assumptions of Lemma 8 hold, then we obtain the following Newton's type inequality:*

$$\begin{aligned}&\left|\frac{1}{3Y(1)}\left[{}_{\theta_1+}I_{\varphi}\mathfrak{G}\left(\frac{2\theta_1+\theta_2}{3}\right)+{}_{(2\theta_1+\theta_2)/3+}I_{\varphi}\mathfrak{G}\left(\frac{\theta_1+2\theta_2}{3}\right)\right.\right.\\&\quad\left.+{}_{(\theta_1+2\theta_2)/3+}I_{\varphi}\mathfrak{G}(\theta_2)\right]-\frac{1}{8}\left[\mathfrak{G}(\theta_1)+3\mathfrak{G}\left(\frac{2\theta_1+\theta_2}{3}\right)\right.\\&\quad\left.\left.+3\mathfrak{G}\left(\frac{\theta_1+2\theta_2}{3}\right)+\mathfrak{G}(\theta_2)\right]\right|\\&\le\frac{\theta_2-\theta_1}{27Y(1)}\left[\left|\mathfrak{G}'(\theta_2)\right|(3A_2(\alpha)-A_1(\alpha)+2A_4(\alpha)\right.\\&\quad-A_3(\alpha)+A_6(\alpha)-A_5(\alpha))+\left|\mathfrak{G}'(\theta_1)\right|(A_1(\alpha)\\&\quad\left.+A_4(\alpha)+A_3(\alpha)+2A_6(\alpha)+A_5(\alpha))\right].\end{aligned} \tag{21}$$

Proof. Using the convexity of $|\mathfrak{G}'|$ and the modulus in (15), we get

$$\begin{aligned}&\left|\frac{1}{3Y(1)}\left[{}_{\theta_1+}I_{\varphi}\mathfrak{G}\left(\frac{2\theta_1+\theta_2}{3}\right)+{}_{(2\theta_1+\theta_2)/3+}I_{\varphi}\mathfrak{G}\left(\frac{\theta_1+2\theta_2}{3}\right)\right.\right.\\&\quad\left.+{}_{(\theta_1+2\theta_2)/3+}I_{\varphi}\mathfrak{G}(\theta_2)\right]-\frac{1}{8}\left[\mathfrak{G}(\theta_1)+3\mathfrak{G}\left(\frac{2\theta_1+\theta_2}{3}\right)\right.\\&\quad\left.\left.+3\mathfrak{G}\left(\frac{\theta_1+2\theta_2}{3}\right)+\mathfrak{G}(\theta_2)\right]\right|\\&\le\frac{\theta_2-\theta_1}{9}\left[\int_0^1\left|Y(t)-\frac{3Y(1)}{8}\right|\left|\mathfrak{G}'\left(t\frac{\theta_1+2\theta_2}{3}+(1-t)\theta_2\right)\right|dt\right.\\&\quad+\int_0^1\left|Y(t)-\frac{Y(1)}{2}\right|\left|\mathfrak{G}'\left(t\frac{2\theta_1+\theta_2}{3}+(1-t)\frac{\theta_1+2\theta_2}{3}\right)\right|dt\\&\quad\left.+\int_0^1\left|Y(t)-\frac{5Y(1)}{8}\right|\left|\mathfrak{G}'\left(t\theta_1+(1-t)\frac{2\theta_1+\theta_2}{3}\right)\right|dt\right]\\&=\frac{\theta_2-\theta_1}{9}\left[\int_0^1\left|Y(t)-\frac{3Y(1)}{8}\right|\left|\mathfrak{G}'\left(\frac{3-t}{3}\theta_2+\frac{t}{3}\theta_1\right)\right|dt\right.\\&\quad+\int_0^1\left|Y(t)-\frac{Y(1)}{2}\right|\left|\mathfrak{G}'\left(\frac{2-t}{3}\theta_2+\frac{1+t}{3}\theta_1\right)\right|dt\\&\quad\left.+\int_0^1\left|Y(t)-\frac{5Y(1)}{8}\right|\left|\mathfrak{G}'\left(\frac{1-t}{3}\theta_2+\frac{2+t}{3}\theta_1\right)\right|dt\right]\\&\le\frac{\theta_2-\theta_1}{9}\left[\left|\mathfrak{G}'(\theta_2)\right|\int_0^1\frac{3-t}{3}\left|Y(t)-\frac{3Y(1)}{8}\right|dt\right.\\&\quad+\left|\mathfrak{G}'(\theta_1)\right|\int_0^1\frac{t}{3}\left|Y(t)-\frac{3Y(1)}{8}\right|dt+\left|\mathfrak{G}'(\theta_2)\right|\int_0^1\frac{2-t}{3}\left|Y(t)\right.\end{aligned}$$

$$
\begin{aligned}
&- \frac{Y(1)}{2}|dt + |\mathfrak{G}'(\theta_1)|\int_0^1 \frac{1+t}{3}\left|Y(t) - \frac{Y(1)}{2}\right|dt \\
&+ |\mathfrak{G}'(\theta_2)|\int_0^1 \frac{1-t}{3}\left|Y(t) - \frac{5Y(1)}{8}\right|dt \\
&+ |\mathfrak{G}'(\theta_1)|\int_0^1 \frac{2+t}{3}\left|Y(t) - \frac{5Y(1)}{8}\right|dt] \qquad (22)\\
&= \frac{\theta_2-\theta_1}{27Y(1)}\left[|\mathfrak{G}'(\theta_2)|(3A_2(\alpha) - A_1(\alpha) + 2A_4(\alpha)\right. \\
&- A_3(\alpha) + A_6(\alpha) - A_5(\alpha)) + |\mathfrak{G}'(\theta_1)|(A_1(\alpha) \\
&+ A_4(\alpha) + A_3(\alpha) + 2A_6(\alpha) + A_5(\alpha))].
\end{aligned}
$$

The proof is now completed. □

Remark 10. In Theorem 9, we have the following:

(i) By setting $\varphi(t) = t$, we reclaim the inequality established in ([13], Remark 3)

(ii) By setting $\varphi(t) = t^\alpha/\Gamma(\alpha)$, we reclaim the inequality established in ([13], Theorem 4)

Corollary 11. *By setting $\varphi(t) = t^{\alpha/k}/k\Gamma_k(\alpha)$ in Theorem 9, we get the following new Newton's inequality for KRLFIs:*

$$
\begin{aligned}
&\left|\frac{3^{\alpha/k-1}\Gamma_k(\alpha+1)}{(\theta_2-\theta_1)^{\alpha/k}}\left[\mathcal{J}^{\alpha,k}_{\theta_1+}\mathfrak{G}\left(\frac{2\theta_1+\theta_2}{3}\right) + \mathcal{J}^{\alpha,k}_{(2\theta_1+\theta_2)/3+}\mathfrak{G}\left(\frac{\theta_1+2\theta_2}{3}\right)\right.\right. \\
&\left. + \mathcal{J}^{\alpha,k}_{(\theta_1+2\theta_2)/3+}\mathfrak{G}(\theta_2)\right] - \frac{1}{8}\left[\mathfrak{G}(\theta_1) + 3\mathfrak{G}\left(\frac{2\theta_1+\theta_2}{3}\right)\right. \\
&\left.\left. + 3\mathfrak{G}\left(\frac{\theta_1+2\theta_2}{3}\right) + \mathfrak{G}(\theta_2)\right]\right| \\
&\le \frac{\theta_2-\theta_1}{27}\left[|\mathfrak{G}'(\theta_2)|(3A_2(\alpha,k) - A_1(\alpha,k) + 2A_4(\alpha,k)\right. \\
&- A_3(\alpha,k) + A_6(\alpha,k) - A_5(\alpha,k)) + |\mathfrak{G}'(\theta_1)|(A_1(\alpha,k) \\
&+ A_4(\alpha,k) + A_3(\alpha,k) + 2A_6(\alpha,k) + A_5(\alpha,k))],
\end{aligned} \qquad (23)
$$

where

$$
\begin{aligned}
A_1(\alpha,k) &= \int_0^1 t\left|t^{\alpha/k} - \frac{3}{8}\right|dt = \frac{\alpha}{\alpha+2k}\left(\frac{3}{8}\right)^{(\alpha+2k)/\alpha} + \frac{k}{\alpha+2k} - \frac{3}{16}, \\
A_2(\alpha,k) &= \int_0^1 \left|t^{\alpha/k} - \frac{3}{8}\right|dt = \frac{2\alpha}{\alpha+k}\left(\frac{3}{8}\right)^{(\alpha+k)/\alpha} + \frac{k}{\alpha+k} - \frac{3}{8}, \\
A_3(\alpha,k) &= \int_0^1 t\left|t^{\alpha/k} - \frac{1}{2}\right|dt = \frac{\alpha}{\alpha+2k}\left(\frac{1}{2}\right)^{(\alpha+2k)/\alpha} + \frac{k}{\alpha+2k} - \frac{1}{4}, \\
A_4(\alpha,k) &= \int_0^1 \left|t^{\alpha/k} - \frac{1}{2}\right|dt = \frac{2\alpha}{\alpha+k}\left(\frac{1}{2}\right)^{(\alpha+k)/\alpha} + \frac{1}{\alpha+k} - \frac{1}{2}, \\
A_5(\alpha,k) &= \int_0^1 t\left|t^{\alpha/k} - \frac{5}{8}\right|dt = \frac{\alpha}{\alpha+2k}\left(\frac{5}{8}\right)^{(\alpha+2k)/a} + \frac{k}{\alpha+2k} - \frac{5}{16}, \\
A_6(\alpha,k) &= \int_0^1 \left|t^{\alpha/k} - \frac{5}{8}\right|dt = \frac{2\alpha}{\alpha+k}\left(\frac{5}{8}\right)^{(\alpha+k)/a} + \frac{k}{\alpha+k} - \frac{5}{8}.
\end{aligned} \qquad (24)
$$

Theorem 12. *If $|\mathfrak{G}'|^q$, $q \ge 1$ is a convex function and assumptions of Lemma 8 hold, then we get the following Newton's type inequality:*

$$
\begin{aligned}
&\left|\frac{1}{3Y(1)}\left[{}_{\theta_1+}I_\varphi\mathfrak{G}\left(\frac{2\theta_1+\theta_2}{3}\right) + {}_{(2\theta1+\theta2)/3+}I_\varphi\mathfrak{G}\left(\frac{\theta_1+2\theta_2}{3}\right)\right.\right. \\
&\left. + {}_{(\theta1+2\theta2)/3+}I_\varphi\mathfrak{G}(\theta_2)\right] - \frac{1}{8}\left[\mathfrak{G}(\theta_1) + 3\mathfrak{G}\left(\frac{2\theta_1+\theta_2}{3}\right)\right. \\
&\left.\left. + 3\mathfrak{G}\left(\frac{\theta_1+2\theta_2}{3}\right) + \mathfrak{G}(\theta_2)\right]\right| \\
&\le \frac{\theta_2-\theta_1}{9Y(1)}\left[A_2^{1-(1/q)}(\alpha)\left(|\mathfrak{G}'(\theta_2)|^q\frac{3A_2(\alpha)-A_1(\alpha)}{3}\right.\right. \\
&\left. + |\mathfrak{G}'(\theta_1)|^q\frac{A_1(\alpha)}{3}\right)^{1/q} + A_4^{1-(1/q)}(\alpha) \\
&\cdot\left(|\mathfrak{G}'(\theta_2)|^q\frac{2A_4(\alpha)-A_3(\alpha)}{3} + |\mathfrak{G}'(\theta_1)|^q\frac{A_4(\alpha)+A_3(\alpha)}{3}\right)^{1/q} \\
&+ A_6^{1-(1/q)}(\alpha)\left(|\mathfrak{G}'(\theta_2)|\frac{A_6(\alpha)-A_5(\alpha)}{3}\right. \\
&\left.\left. + |\mathfrak{G}'(\theta_1)|^q\frac{2A_6(\alpha)+A_5(\alpha)}{3}\right)^{1/q}\right].
\end{aligned} \qquad (25)
$$

Proof. Applying power mean inequality in (15) after taking the modulus, we have

$$
\begin{aligned}
&\left|\frac{1}{3Y(1)}\left[{}_{\theta_1+}I_\varphi\mathfrak{G}\left(\frac{2\theta_1+\theta_2}{3}\right) + {}_{(2\theta1+\theta2)/3+}I_\varphi\mathfrak{G}\left(\frac{\theta_1+2\theta_2}{3}\right)\right.\right. \\
&\left. + {}_{(\theta1+2\theta2)+}I_\varphi\mathfrak{G}(\theta_2)\right] - \frac{1}{8}\left[\mathfrak{G}(\theta_1) + 3\mathfrak{G}\left(\frac{2\theta_1+\theta_2}{3}\right)\right. \\
&\left.\left. + 3\mathfrak{G}\left(\frac{\theta_1+2\theta_2}{3}\right) + \mathfrak{G}(\theta_2)\right]\right| \frac{\theta_2-\theta_1}{9Y(1)}\left[\int_0^1\left|Y(t) - \frac{3Y(1)}{8}\right||\mathfrak{G}' \right. \\
&\cdot\left(\frac{3-t}{3}\theta_2 + \frac{t}{3}\theta_1\right)\Big|dt + \int_0^1\left|Y(t) - \frac{Y(1)}{2}\right||\mathfrak{G}' \\
&\cdot\left(\frac{2-t}{3}\theta_2 + \frac{1+t}{3}\theta_1\right)\Big|dt + \int_0^1\left|Y(t) - \frac{5Y(1)}{8}\right||\mathfrak{G}' \\
&\left.\cdot\left(\frac{1-t}{3}\theta_2 + \frac{2+t}{3}\theta_1\right)\Big|dt\right] \\
&\le \frac{\theta_2-\theta_1}{9Y(1)}\left[\left(\int_0^1\left|Y(t) - \frac{3Y(1)}{8}\right|dt\right)^{1-(1/q)}\left(\int_0^1\left|Y(t) - \frac{3Y(1)}{8}\right||\mathfrak{G}'\right.\right. \\
&\left.\cdot\left(\frac{3-t}{3}\theta_2 + \frac{t}{3}\theta_1\right)\Big|^q dt\right)^{(1/q)} + \left(\int_0^1\left|Y(t) - \frac{Y(1)}{2}\right|dt\right)^{1-(1/q)} \\
&\cdot\left(\int_0^1\left|Y(t) - \frac{Y(1)}{2}\right||\mathfrak{G}'\left(\frac{2-t}{3}\theta_2 + \frac{1+t}{3}\theta_1\right)\Big|^q dt\right)^{(1/q)} \\
&+ \left(\int_0^1\left|Y(t) - \frac{5Y(1)}{8}\right|dt\right)^{1-(1/q)}\left(\int_0^1\left|Y(t) - \frac{5Y(1)}{8}\right||\mathfrak{G}'\right. \\
&\left.\left.\cdot\left(\frac{1-t}{3}\theta_2 + \frac{2+t}{3}\theta_1\right)\Big|^q dt\right)^{1/q}\right].
\end{aligned} \qquad (26)
$$

Using the convexity of $|\mathfrak{G}'|^q$, we have

$$\begin{aligned}
&\left|\frac{\theta_2-\theta_1}{3Y(1)}\left[{}_{\theta_1+}I_{\varphi}\mathfrak{G}\left(\frac{2\theta_1+\theta_2}{3}\right)+{}_{(2\theta_1+\theta_2)/3+}I_{\varphi}\mathfrak{G}\left(\frac{\theta_1+2\theta_2}{3}\right)\right.\right.\\
&\quad\left.+{}_{(\theta_1+2\theta_2)/3+}I_{\varphi}\mathfrak{G}(\theta_2)\right]-\frac{1}{8}\left[\mathfrak{G}(\theta_1)+3\mathfrak{G}\left(\frac{2\theta_1+\theta_2}{3}\right)\right.\\
&\quad\left.\left.+3\mathfrak{G}\left(\frac{\theta_1+2\theta_2}{3}\right)+\mathfrak{G}(\theta_2)\right]\right|\\
&\leq\frac{\theta_2-\theta_1}{9Y(1)}\left[\left(\int_0^1\left|Y(t)-\frac{3Y(1)}{8}\right|dt\right)^{1-(1/q)}\right.\\
&\quad\times\left(\left|\mathfrak{G}'(\theta_2)\right|^q\int_0^1\frac{3-t}{3}\left|Y(t)-\frac{3Y(1)}{8}\right|dt+\left|\mathfrak{G}'(\theta_1)\right|^q\right.\\
&\quad\left.\cdot\int_0^1\frac{t}{3}\left|Y(t)-\frac{3Y(1)}{8}\right|dt\right)^{(1/q)}+\left(\int_0^1\left|Y(t)-\frac{Y(1)}{2}\right|dt\right)^{1-(1/q)}\\
&\quad\times\left(\left|\mathfrak{G}'(\theta_2)\right|^q\int_0^1\frac{2-t}{3}\left|Y(t)-\frac{Y(1)}{2}\right|dt+\left|\mathfrak{G}'(\theta_1)\right|^q\right.\\
&\quad\left.\cdot\int_0^1\frac{1+t}{3}\left|Y(t)-\frac{Y(1)}{2}\right|dt\right)^{(1/q)}+\left(\int_0^1\left|Y(t)-\frac{5Y(1)}{8}\right|dt\right)^{1-(1/q)}\\
&\quad\times\left(\left|\mathfrak{G}'(\theta_2)\right|^q\int_0^1\frac{1-t}{3}\left|Y(t)-\frac{5Y(1)}{8}\right|dt\right.\\
&\quad\left.\left.+\left|\mathfrak{G}'(\theta_1)\right|^q\int_0^1\frac{2+t}{3}\left|Y(t)-\frac{5Y(1)}{8}\right|dt\right)^{(1/q)}\right]\\
&=\frac{\theta_2-\theta_1}{9Y(1)}\left[A_2^{1-(1/q)}(\alpha)\left(\left|\mathfrak{G}'(\theta_2)\right|^q\frac{3A_2(\alpha)-A_1(\alpha)}{3}\right.\right.\\
&\quad\left.+\left|\mathfrak{G}'(\theta_1)\right|^q\frac{A_1(\alpha)}{3}\right)^{(1/q)}+A_4^{1-(1/q)}(\alpha)\\
&\left(\left|\mathfrak{G}'(\theta_2)\right|^q\frac{2A_4(\alpha)-A_3(\alpha)}{3}+\left|\mathfrak{G}'(\theta_1)\right|^q\frac{A_4(\alpha)+A_3(\alpha)}{3}\right)^{1/q}\\
&\quad+A_6^{1-(1/q)}(\alpha)\left(\left|\mathfrak{G}'(\theta_2)\right|\frac{A_6(\alpha)-A_5(\alpha)}{3}\right.\\
&\quad\left.\left.+\left|\mathfrak{G}'(\theta_1)\right|^q\frac{2A_6(\alpha)+A_5(\alpha)}{3}\right)^{(1/q)}\right].
\end{aligned}\tag{27}$$

Thus, the proof is completed. □

Remark 13. In Theorem 12, we have the following:

(i) By setting $\varphi(t)=t$, we reclaim the inequality established in ([13], Remark 4)

(ii) By setting $\varphi(t)=t^{\alpha}/\Gamma(\alpha)$, we reclaim the inequality established in ([13], Theorem 5)

Corollary 14. *By setting $\varphi(t)=t^{\alpha/k}/k\Gamma_k(\alpha)$ in Theorem 12, we obtain the following new Newton's inequality for KRLFIs:*

$$\begin{aligned}
&\left|\frac{3^{(\alpha/k)-1}\Gamma_k(\alpha+1)}{(\theta_2-\theta_1)^{\alpha/k}}\left[\mathcal{J}^{\alpha,k}_{\theta_1+}\mathfrak{G}\left(\frac{2\theta_1+\theta_2}{3}\right)+\mathcal{J}^{\alpha,k}_{(2\theta_1+\theta_2)/3+}\mathfrak{G}\left(\frac{\theta_1+2\theta_2}{3}\right)\right.\right.\\
&\quad\left.+\mathcal{J}^{\alpha,k}_{(\theta_1+2\theta_2)/3+}\mathfrak{G}(\theta_2)\right]-\frac{1}{8}[\mathfrak{G}(\theta_1)\\
&\quad\left.+3\mathfrak{G}\left(\frac{2\theta_1+\theta_2}{3}\right)+3\mathfrak{G}\left(\frac{\theta_1+2\theta_2}{3}\right)+\mathfrak{G}(\theta_2)]\right|\\
&\leq\frac{\theta_2-\theta_1}{9}\left[A_2^{1-(1/q)}(\alpha,k)\left(\left|\mathfrak{G}'(\theta_2)\right|^q\frac{3A_2(\alpha,k)-A_1(\alpha,k)}{3}\right.\right.\\
&\quad\left.+\left|\mathfrak{G}'(\theta_1)\right|^q\frac{A_1(\alpha,k)}{3}\right)^{(1/q)}+A_4^{1-(1/q)}(\alpha,k)\\
&\quad\cdot\left(\left|\mathfrak{G}'(\theta_2)\right|^q\frac{2A_4(\alpha,k)-A_3(\alpha,k)}{3}+\left|\mathfrak{G}'(\theta_1)\right|^q\frac{A_4(\alpha,k)+A_3(\alpha,k)}{3}\right)^{(1/q)}\\
&\quad+A_6^{1-(1/q)}(\alpha,k)\left(\left|\mathfrak{G}'(\theta_2)\right|\frac{A_6(\alpha,k)-A_5(\alpha,k)}{3}\right.\\
&\quad\left.\left.+\left|\mathfrak{G}'(\theta_1)\right|^q\frac{2A_6(\alpha,k)+A_5(\alpha,k)}{3}\right)^{(1/q)}\right].
\end{aligned}\tag{28}$$

Theorem 15. *If $|\mathfrak{G}'|^q$, $q>1$ is a convex function and assumptions of Lemma 8 hold, then we have the following Newton's type inequality:*

$$\begin{aligned}
&\left|\frac{1}{3Y(1)}\left[{}_{\theta_1+}I_{\varphi}\mathfrak{G}\left(\frac{2\theta_1+\theta_2}{3}\right)+{}_{(2\theta_1+\theta_2)/3+}I_{\varphi}\mathfrak{G}\left(\frac{\theta_1+2\theta_2}{3}\right)\right.\right.\\
&\quad\left.+{}_{(\theta_1+2\theta_2)/3+}I_{\varphi}\mathfrak{G}(\theta_2)\right]-\frac{1}{8}[\mathfrak{G}(\theta_1)\\
&\quad\left.+3\mathfrak{G}\left(\frac{2\theta_1+\theta_2}{3}\right)+3\mathfrak{G}\left(\frac{\theta_1+2\theta_2}{3}\right)+\mathfrak{G}(\theta_2)]\right|\\
&\leq\frac{\theta_2-\theta_1}{9Y(1)}\left[A_7^{(1/p)}(\alpha,p)\left(\frac{5\left|\mathfrak{G}'(\theta_2)\right|^q+\left|\mathfrak{G}'(\theta_1)\right|^q}{6}\right)^{(1/q)}\right.\\
&\quad+A_8^{(1/p)}(\alpha,p)\left(\frac{\left|\mathfrak{G}'(\theta_2)\right|^q+\left|\mathfrak{G}'(\theta_1)\right|^q}{2}\right)^{(1/q)}\\
&\quad\left.+A_9^{(1/p)}(\alpha,p)\left(\frac{\left|\mathfrak{G}'(\theta_2)\right|^q+5\left|\mathfrak{G}'(\theta_1)\right|^q}{6}\right)^{(1/q)}\right],
\end{aligned}\tag{29}$$

where $q^{-1}+p^{-1}=1$ and

$$\begin{aligned}
A_7(\alpha,p)&=\int_0^1\left|Y(t)-\frac{3Y(1)}{8}\right|^p dt,\\
A_8(\alpha,p)&=\int_0^1\left|Y(t)-\frac{Y(1)}{2}\right|^p dt,\\
A_9(\alpha,p)&=\int_0^1\left|Y(t)-\frac{5Y(1)}{8}\right|^p dt.
\end{aligned}\tag{30}$$

Proof. Applying Hölder's inequality in (15) after taking the modulus, we have

$$\begin{aligned}
&\left|\frac{1}{3Y(1)}\left[{}_{\theta_1+}I_{\varphi}\mathfrak{G}\left(\frac{2\theta_1+\theta_2}{3}\right)+{}_{(2\theta_1+\theta_2)/3+}I_{\varphi}\mathfrak{G}\left(\frac{\theta_1+2\theta_2}{3}\right)\right.\right.\\
&\quad\left.+{}_{(\theta_1+2\theta_2)/3+}I_{\varphi}\mathfrak{G}(\theta_2)\right]-\frac{1}{8}\left[\mathfrak{G}(\theta_1)+3\mathfrak{G}\left(\frac{2\theta_1+\theta_2}{3}\right)\right.\\
&\quad\left.+3\mathfrak{G}\left(\frac{\theta_1+2\theta_2}{3}\right)+\mathfrak{G}(\theta_2)]\right|\\
&=\frac{\theta_2-\theta_1}{9Y(1)}\left[\int_0^1\left|Y(t)-\frac{3Y(1)}{8}\right|\left|\mathfrak{G}'\left(\frac{3-t}{3}\theta_2+\frac{t}{3}\theta_1\right)\right|dt\right.\\
&\quad+\int_0^1\left|Y(t)-\frac{Y(1)}{2}\right|\left|\mathfrak{G}'\left(\frac{2-t}{3}\theta_2+\frac{1+t}{3}\theta_1\right)\right|dt\\
&\quad\left.+\int_0^1\left|Y(t)-\frac{5Y(1)}{8}\right|\left|\mathfrak{G}'\left(\frac{1-t}{3}\theta_2+\frac{2+t}{3}\theta_1\right)\right|dt\right]\\
&\leq\frac{\theta_2-\theta_1}{9Y(1)}\left[\left(\int_0^1\left|Y(t)-\frac{3Y(1)}{8}\right|^p dt\right)^{(1/p)}\right.\\
&\quad\cdot\left(\int_0^1\left|\mathfrak{G}'\left(\frac{3-t}{3}\theta_2+\frac{t}{3}\theta_1\right)\right|^q dt\right)^{(1/q)}+\left(\int_0^1\left|Y(t)-\frac{Y(1)}{2}\right|^p dt\right)^{(1/p)}\\
&\quad\cdot\left(\int_0^1\left|\mathfrak{G}'\left(\frac{2-t}{3}\theta_2+\frac{1+t}{3}\theta_1\right)\right|^q dt\right)^{(1/q)}+\left(\int_0^1\left|Y(t)-\frac{5Y(1)}{8}\right|^p dt\right)^{(1/p)}\\
&\quad\left.\cdot\left(\int_0^1\left|\mathfrak{G}'\left(\frac{1-t}{3}\theta_2+\frac{2+t}{3}\theta_1\right)\right|^q dt\right)^{(1/q)}\right].
\end{aligned}\tag{31}$$

From convexity of $|\mathfrak{G}'|^q$, $q>1$, we obtain

$$\left|\frac{\theta_2-\theta_1}{3Y(1)}\left[{}_{\theta_1+}I_\varphi\mathfrak{G}\left(\frac{2\theta_1+\theta_2}{3}\right)+{}_{(2\theta_1+\theta_2)/3+}I_\varphi\mathfrak{G}\left(\frac{\theta_1+2\theta_2}{3}\right)+{}_{(\theta_1+2\theta_2)/3+}I_\varphi\mathfrak{G}(\theta_2)\right]-\frac{1}{8}\left[\mathfrak{G}(\theta_1)+3\mathfrak{G}\left(\frac{2\theta_1+\theta_2}{3}\right)+3\mathfrak{G}\left(\frac{\theta_1+2\theta_2}{3}\right)+\mathfrak{G}(\theta_2)\right]\right|$$
$$\leq\frac{\theta_2-\theta_1}{9Y(1)}\left[\left(\int_0^1\left|Y(t)-\frac{3Y(1)}{8}\right|^p dt\right)^{(1/p)}\cdot\left(\left|\mathfrak{G}'(\theta_2)\right|^q\int_0^1\frac{3-t}{3}dt+\left|\mathfrak{G}'(\theta_1)\right|^q\int_0^1\frac{t}{3}dt\right)^{(1/q)}+\left(\int_0^1\left|Y(t)-\frac{Y(1)}{2}\right|^p dt\right)^{(1/p)}\left(\left|\mathfrak{G}'(\theta_2)\right|^q\int_0^1\frac{2-t}{3}dt+\left|\mathfrak{G}'(\theta_1)\right|^q\int_0^1\frac{1+t}{3}dt\right)^{(1/q)}+\left(\int_0^1\left|Y(t)-\frac{5Y(1)}{8}\right|^p dt\right)^{(1/p)}\cdot\left(\left|\mathfrak{G}'(\theta_2)\right|^q\int_0^1\frac{1-t}{3}dt+\left|\mathfrak{G}'(\theta_1)\right|^q\int_0^1\frac{2+t}{3}dt\right)^{(1/q)}\right]$$
$$=\frac{\theta_2-\theta_1}{9Y(1)}\left[A_7^{(1/p)}(\alpha,p)\left(\frac{5\left|\mathfrak{G}'(\theta_2)\right|^q+\left|\mathfrak{G}'(\theta_1)\right|^q}{6}\right)^{(1/q)}+A_8^{(1/p)}(\alpha,p)\left(\frac{\left|\mathfrak{G}'(\theta_2)\right|^q+\left|\mathfrak{G}'(\theta_1)\right|^q}{2}\right)^{(1/q)}+A_9^{(1/p)}(\alpha,p)\left(\frac{\left|\mathfrak{G}'(\theta_2)\right|^q+5\left|\mathfrak{G}'(\theta_1)\right|^q}{6}\right)^{(1/q)}\right]. \tag{32}$$

Thus, the proof is completed. □

Remark 16. In Theorem 15, we have the following:

(i) By setting $\varphi(t)=t$, we reclaim the inequality established in ([13], Remark 5)

(ii) By setting $\varphi(t)=t^\alpha/\Gamma(\alpha)$, we reclaim the inequality established in ([13], Theorem 6)

Corollary 17. *By setting $\varphi(t)=t^{\alpha/k}k\Gamma_k(\alpha)$ in Theorem 15, we obtain the following new Newton's inequality for KRLFIs:*

$$\left|\frac{3^{(\alpha/k)-1}\Gamma_k(\alpha+1)}{(\theta_2-\theta_1)^{\alpha/k}}\left[\mathcal{J}^{\alpha,k}_{\theta_1+}\mathfrak{G}\left(\frac{2\theta_1+\theta_2}{3}\right)+\mathcal{J}^{\alpha,k}_{(2\theta_1+\theta_2)/3+}\mathfrak{G}\left(\frac{\theta_1+2\theta_2}{3}\right)+\mathcal{J}^{\alpha,k}_{(\theta_1+2\theta_2)/3+}\mathfrak{G}(\theta_2)\right]-\frac{1}{8}\left[\mathfrak{G}(\theta_1)+3\mathfrak{G}\left(\frac{2\theta_1+\theta_2}{3}\right)+3\mathfrak{G}\left(\frac{\theta_1+2\theta_2}{3}\right)+\mathfrak{G}(\theta_2)\right]\right|\leq\frac{\theta_2-\theta_1}{9}$$
$$\cdot\left[A_7^{(1/p)}(\alpha,p,k)\left(\frac{5\left|\mathfrak{G}'(\theta_2)\right|^q+\left|\mathfrak{G}'(\theta_1)\right|^q}{6}\right)^{(1/q)}+A_8^{(1/p)}(\alpha,k,p)\left(\frac{\left|\mathfrak{G}'(\theta_2)\right|^q+\left|\mathfrak{G}'(\theta_1)\right|^q}{2}\right)^{(1/q)}+A_9^{(1/p)}(\alpha,k,p)\left(\frac{\left|\mathfrak{G}'(\theta_2)\right|^q+5\left|\mathfrak{G}'(\theta_1)\right|^q}{6}\right)^{(1/q)}\right], \tag{33}$$

where $q^{-1}+p^{-1}=1$ and

$$A_7(\alpha,k,p)=\int_0^1\left|t^{\alpha/k}-\frac{3}{8}\right|^p dt,$$
$$A_8(\alpha,k,p)=\int_0^1\left|t^{\alpha/k}-\frac{1}{2}\right|^p dt, \tag{34}$$
$$A_9(\alpha,k,p)=\int_0^1\left|t^{\alpha/k}-\frac{5}{8}\right|^p dt.$$

5. Fractional Newton-Type Inequality for Functions of Bounded Variation

In this section, we prove a Newton-type inequality for function of bounded variation via generalized fractional integrals.

Theorem 18. *Let $\mathfrak{G}:[\theta_1,\theta_2]\longrightarrow\mathbb{R}$ be a function of bounded variation on $[\theta_1,\theta_2]$. Then we have the following Newton-type inequality for generalized fractional integrals:*

$$\left|\frac{1}{3Y(1)}\left[{}_{\theta_1+}I_\varphi\mathfrak{G}\left(\frac{2\theta_1+\theta_2}{3}\right)+{}_{(2\theta_1+\theta_2)/3+}I_\varphi\mathfrak{G}\left(\frac{\theta_1+2\theta_2}{3}\right)+{}_{(\theta_1+2\theta_2)/3+}I_\varphi\mathfrak{G}(\theta_2)\right]-\frac{1}{8}\left[\mathfrak{G}(\theta_1)+3\mathfrak{G}\left(\frac{2\theta_1+\theta_2}{3}\right)+3\mathfrak{G}\left(\frac{\theta_1+2\theta_2}{3}\right)+\mathfrak{G}(\theta_2)\right]\right|\leq\frac{5}{24}\bigvee_{\theta_1}^{\theta_2}(\mathfrak{G}), \tag{35}$$

where $\bigvee_c^d(\mathfrak{G})$ denotes the total variation of $\mathfrak{G}$ on $[c,d]$.

Proof. Define the mapping $\Psi_\varphi(\varkappa)$ by

$$\Psi_\varphi(\varkappa)=\begin{cases} Y\left(\dfrac{3}{\theta_2-\theta_1}\left(\dfrac{2\theta_1+\theta_2}{3}-\varkappa\right)\right)-\dfrac{5Y(1)}{8}, & \text{for } \theta_1\leq\varkappa\leq\dfrac{2\theta_1+\theta_2}{3};\\ Y\left(\dfrac{3}{\theta_2-\theta_1}\left(\dfrac{\theta_1+2\theta_2}{3}-\varkappa\right)\right)-\dfrac{Y(1)}{2}, & \text{for } \dfrac{2\theta_1+\theta_2}{3}<\varkappa\leq\dfrac{\theta_1+2\theta_2}{3};\\ Y\left(\dfrac{3}{\theta_2-\theta_1}(\theta_2-\varkappa)\right)-\dfrac{3Y(1)}{8}, & \text{for } \dfrac{\theta_1+2\theta_2}{3}<\varkappa\leq\theta_2. \end{cases} \tag{36}$$

It follows from that

$$\int_{\theta_1}^{\theta_2}\Psi_{\varphi}(\varkappa)d\mathfrak{G}(\varkappa)=\int_{\theta_1}^{(2\theta_1+\theta_2)/3}\left(Y\left(\frac{3}{\theta_2-\theta_1}\left(\frac{2\theta_1+\theta_2}{3}-\varkappa\right)\right)-\frac{5Y(1)}{8}\right)d\mathfrak{G}(\varkappa)+\int_{(2\theta_1+\theta_2)/3}^{(\theta_1+2\theta_2)/3}\left(Y\left(\frac{3}{\theta_2-\theta_1}\left(\frac{\theta_1+2\theta_2}{3}-\varkappa\right)\right)-\frac{Y(1)}{2}\right)d\mathfrak{G}(\varkappa)+\int_{(\theta_1 2+\theta_2)/3}^{\theta_2}\left(Y\left(\frac{3}{\theta_2-\theta_1}(\theta_2-\varkappa)\right)-\frac{3Y(1)}{8}\right)d\mathfrak{G}(\varkappa). \tag{37}$$

Integrating by parts, we get

$$\begin{aligned}\int_{\theta_1}^{(2\theta_1+\theta_2)/3}&\left(Y\left(\frac{3}{\theta_2-\theta_1}\left(\frac{2\theta_1+\theta_2}{3}-\varkappa\right)\right)-\frac{5Y(1)}{8}\right)d\mathfrak{G}(\varkappa)\\&=\left(Y\left(\frac{3}{\theta_2-\theta_1}\left(\frac{2\theta_1+\theta_2}{3}-\varkappa\right)\right)-\frac{5Y(1)}{8}\right)\mathfrak{G}(\varkappa)\Big|_{\theta_1}^{(2\theta_1+\theta_2)/3}+\int_{\theta_1}^{(2\theta_1+\theta_2)/3}\frac{\varphi(((2\theta_1+\theta_2)/3)-\varkappa)}{((2\theta_1+\theta_2)/3)-\varkappa}\mathfrak{G}(\varkappa)d\varkappa\\&=-\frac{5Y(1)}{8}\mathfrak{G}\left(\frac{2\theta_1+\theta_2}{2}\right)-\frac{3Y(1)}{8}\mathfrak{G}(\theta_1)+{}_{\theta_1+}I_{\varphi}\mathfrak{G}\left(\frac{2\theta_1+\theta_2}{3}\right).\end{aligned} \tag{38}$$

Similarly, we have

$$\begin{aligned}\int_{(2\theta_1+\theta_2)/3}^{(\theta_1+2\theta_2)/3}&\left(Y\left(\frac{3}{\theta_2-\theta_1}\left(\frac{\theta_1+2\theta_2}{3}-\varkappa\right)\right)-\frac{Y(1)}{2}\right)d\mathfrak{G}(\varkappa)\\&=-\frac{Y(1)}{2}\mathfrak{G}\left(\frac{\theta_1+2\theta_2}{2}\right)-\frac{Y(1)}{2}\mathfrak{G}\left(\frac{2\theta_1+\theta_2}{2}\right)+\frac{2\theta_1+\theta_2}{3}+I_{\varphi}\mathfrak{G}\left(\frac{2\theta_1+\theta_2}{3}\right),\end{aligned} \tag{39}$$

$$\begin{aligned}\int_{(\theta_1+2\theta_2)/3}^{\theta_2}&\left(Y\left(\frac{3}{\theta_2-\theta_1}(\theta_2-\varkappa)\right)-\frac{3Y(1)}{8}\right)d\mathfrak{G}(\varkappa)\\&=-\frac{3Y(1)}{8}\mathfrak{G}(\theta_2)-\frac{5Y(1)}{8}\mathfrak{G}\left(\frac{\theta_1+2\theta_2}{2}\right)+\frac{\theta_1+2\theta_2}{3}+I_{\varphi}\mathfrak{G}(\theta_2).\end{aligned} \tag{40}$$

By putting the equalities (38)–(40) in (37), we have

$$\begin{aligned}&\Bigg|\frac{1}{3Y(1)}\left[{}_{\theta_1+}I_{\varphi}\mathfrak{G}\left(\frac{2\theta_1+\theta_2}{3}\right)+\frac{2\theta_1+\theta_2}{3}+I_{\varphi}\mathfrak{G}\left(\frac{\theta_1+2\theta_2}{3}\right)+\frac{\theta_1+2\theta_2}{3}+I_{\varphi}\mathfrak{G}(\theta_2)\right]-\frac{1}{8}\left[\mathfrak{G}(\theta_1)+3\mathfrak{G}\left(\frac{2\theta_1+\theta_2}{3}\right)\right.\\&\left.+3\mathfrak{G}\left(\frac{\theta_1+2\theta_2}{3}\right)+\mathfrak{G}(\theta_2)\right]\Bigg|=\int_{\theta_1}^{\theta_2}\Psi_{\varphi}(\varkappa)d\mathfrak{G}(\varkappa).\end{aligned} \tag{41}$$

It is well known that if $g,\mathfrak{G}:[\theta_1,\theta_2]\longrightarrow\mathbb{R}$ are such that g is continuous on $[\theta_1,\theta_2]$ and $\mathfrak{G}$ is of bounded variation on $[\theta_1,\theta_2]$, then $\int_{\theta_1}^{\theta_2}g(t)d\mathfrak{G}(t)$ exist and

$$\left|\int_{\theta_1}^{\theta_2}g(t)d\mathfrak{G}(t)\right|\le\sup_{t\in[\theta_1,\theta_2]}|g(t)|\bigvee_{\theta_1}^{\theta_2}(\mathfrak{G}). \tag{42}$$

On the other hand, using (42), we get

$$\begin{aligned}&\Bigg|\frac{1}{3Y(1)}\left[{}_{\theta_1+}I_{\varphi}\mathfrak{G}\left(\frac{2\theta_1+\theta_2}{3}\right)+\frac{2\theta_1+\theta_2}{3}+I_{\varphi}\mathfrak{G}\left(\frac{\theta_1+2\theta_2}{3}\right)+\frac{\theta_1+2\theta_2}{3}+I_{\varphi}\mathfrak{G}(\theta_2)\right]-\frac{1}{8}\left[\mathfrak{G}(\theta_1)+3\mathfrak{G}\left(\frac{2\theta_1+\theta_2}{3}\right)\right.\\&\left.+3\mathfrak{G}\left(\frac{\theta_1+2\theta_2}{3}\right)+\mathfrak{G}(\theta_2)\right]\Bigg|=\frac{1}{3Y(1)}\left|\int_{\theta_1}^{\theta_2}\Psi_{\varphi}(\varkappa)d\mathfrak{G}(\varkappa)\right|\\&\le\frac{1}{3Y(1)}\Bigg[\Bigg|\int_{\theta_1}^{(2\theta_1+\theta_2)/3}\left(Y\left(\frac{3}{\theta_2-\theta_1}\left(\frac{2\theta_1+\theta_2}{3}-\varkappa\right)\right)-\frac{5Y(1)}{8}\right)d\mathfrak{G}(\varkappa)\Bigg|+\Bigg|\int_{(2\theta_1+\theta_2)/3}^{(\theta_1+2\theta_2)/3}\cdot\left(Y\left(\frac{3}{\theta_2-\theta_1}\left(\frac{\theta_1+2\theta_2}{3}-\varkappa\right)\right)-\frac{Y(1)}{2}\right)d\mathfrak{G}(\varkappa)\Bigg|\\&+\Bigg|\int_{(\theta_1+2\theta_2)/3}^{\theta_2}\left(Y\left(\frac{3}{\theta_2-\theta_1}(\theta_2-\varkappa)\right)-\frac{3Y(1)}{8}\right)d\mathfrak{G}(\varkappa)\Bigg|\Bigg]\\&\le\frac{1}{3Y(1)}\Bigg[\sup_{\varkappa\in[\theta_1,(2\theta_1+\theta_2)/3]}\left|Y\left(\frac{3}{\theta_2-\theta_1}\left(\frac{2\theta_1+\theta_2}{3}-\varkappa\right)\right)-\frac{5Y(1)}{8}\right|\bigvee_{\theta_1}^{(2\theta_1+\theta_2)/3}(\mathfrak{G})+\sup_{\varkappa\in[(2\theta_1+\theta_2)/3,(\theta_1+2\theta_2)/3]}\left|Y\cdot\left(\frac{3}{\theta_2-\theta_1}\left(\frac{\theta_1+2\theta_2}{3}-\varkappa\right)\right)-\frac{Y(1)}{2}\right|\bigvee_{(2\theta_1+\theta_2)/3}^{(\theta_1+2\theta_2)/3}(\mathfrak{G})\\&+\sup_{\varkappa\in[(\theta_1+2\theta_2)/3,\theta_2]}\left|Y\left(\frac{3}{\theta_2-\theta_1}(\theta_2-\varkappa)\right)-\frac{3Y(1)}{8}\right|\bigvee_{(\theta_1+2\theta_2)/3}^{\theta_2}(\mathfrak{G})\Bigg]=\frac{1}{3Y(1)}\left[\frac{5Y(1)}{8}\bigvee_{\theta_1}^{(2\theta_1+\theta_2)/3}(\mathfrak{G})+\frac{Y(1)}{2}\bigvee_{(2\theta_1+2\theta_2)/3}^{(\theta_1+2\theta_2)/3}(\mathfrak{G})+\frac{5Y(1)}{8}\bigvee_{(\theta_1+2\theta_2)/3}^{\theta_2}(\mathfrak{G})\right]\le\frac{5}{24}\bigvee_{\theta_1}^{\theta_2}(\mathfrak{G}).\end{aligned} \tag{43}$$

This completes the proof. □

Remark 19. In Theorem 18, we have the following:

(i) If we take $\varphi(t)=t$, then we recapture the inequality proved in ([46], Corollary 3)

(ii) If we set $\varphi(t)=t^{\alpha}/\Gamma(\alpha)$, then we recapture the inequality established in ([13], Theorem 7)

Corollary 20. *If we choose* $\varphi(t) = (t^{(\alpha/k)}/k\Gamma_k(\alpha))$, *then we obtain the following new Newton's inequality for KRLFIs:*

$$\begin{aligned}&\left|\frac{3^{(\alpha/k)-1}\Gamma_k(\alpha+1)}{(\theta_2-\theta_1)^{\alpha/k}}\left[\mathcal{J}^{\alpha,k}_{\theta_1}+\mathfrak{G}\left(\frac{2\theta_1+\theta_2}{3}\right)+\mathcal{J}^{\alpha,k}_{(2\theta_1+\theta_2)/3}\right.\right.\\&\left.+\mathfrak{G}\left(\frac{\theta_1+2\theta_2}{3}\right)+\mathcal{J}^{\alpha,k}_{(\theta_1+2\theta_2)/3}+\mathfrak{G}(\theta_2)\right]\\&-\frac{1}{8}\left[\mathfrak{G}(\theta_1)+3\mathfrak{G}\left(\frac{2\theta_1+\theta_2}{3}\right)\right.\\&\left.\left.+3\mathfrak{G}\left(\frac{\theta_1+2\theta_2}{3}\right)+\mathfrak{G}(\theta_2)\right]\right|\leq\frac{5}{24}\bigvee_{\theta_1}^{\theta_2}(\mathfrak{G}).\end{aligned} \tag{44}$$

6. Conclusion

We demonstrated some new Simpson's second-type inequalities for differentiable convex functions using Riemann-Liouville fractional integrals. Furthermore, we established fractional Newton-type inequalities for bounded variation functions. It is also shown that the newly established inequalities are an extension of the previously obtained inequalities. It is worth to mentioning here that we can obtain similar inequalities via Katugampola fractional operators, conformable fractional operators, Hadamard fractional operators, and fractional operators with the exponential kernel for different choices of the function φ. In their future work, future researchers can get similar inequalities for various types of convexity and coordinated convexity on fractals, which is an exciting and new problem.

Data Availability

Data sharing is not applicable to this paper as no data sets were generated or analyzed during the current study.

Conflicts of Interest

The authors declare that they have no competing interests.

Acknowledgments

This research was funded by the National Science, Research and Innovation Fund (NSRF) and King Mongkut's University of Technology North Bangkok with contract no. KMUTNB-FF-65-49.

References

[1] M. Z. Sarikaya, E. Set, H. Yaldiz, and N. Başak, "Hermite-Hadamard's inequalities for fractional integrals and related fractional inequalities," *Mathematical and Computer Modelling*, vol. 57, no. 9-10, pp. 2403–2407, 2013.

[2] E. Set, "New inequalities of Ostrowski type for mappings whose derivatives are *s*-convex in the second sense via fractional integrals," *Computers & Mathematics with Applications*, vol. 63, no. 7, pp. 1147–1154, 2012.

[3] İ. İşcan and S. Wu, "Hermite-Hadamard type inequalities for harmonically convex functions via fractional integrals," *Applied Mathematics and Computation*, vol. 238, pp. 237–244, 2014.

[4] M. Z. Sarikaya and H. Yildrim, "On Hermite-Hadamard type inequalities for Riemann-Liouville fractional integrals," *Miskolc Mathematical Notes*, vol. 17, no. 2, pp. 1049–1059, 2016.

[5] M. Z. Sarikaya, E. Set, and M. E. Özdemir, "On new inequalities of Simpson's type for *s*-convex functions," *Computers & Mathematics with Applications*, vol. 60, no. 8, pp. 2191–2199, 2010.

[6] C. Peng, C. Zhou, and T. S. Du, "Riemann-Liouville fractional Simpson's inequalities through generalized (m, h_1, h_2)-preinvexity," *Italian Journal of Pure and Applied Mathematics*, vol. 38, pp. 345–367, 2017.

[7] J. Chen and X. Huang, "Some new inequalities of Simpson's type for *s*-convex functions via fractional integrals," *Filomat*, vol. 31, no. 15, pp. 4989–4997, 2017.

[8] M. Z. Sarikaya and F. Ertugral, "On the generalized Hermite-Hadamard inequalities," *Annals of the University of Craiova-Mathematics and Computer Science Series*, vol. 47, pp. 193–213, 2020.

[9] D. Zhao, M. A. Ali, A. Kashuri, and H. Budak, "Generalized fractional integral inequalities of Hermite–Hadamard type for harmonically convex functions," *Advances in Difference Equations*, vol. 2020, no. 1, Article ID 137, 2020.

[10] H. Budak, F. Hezenci, and H. Kara, "On parameterized inequalities of Ostrowski and Simpson type for convex functions via generalized fractional integrals," *Mathematical Methods in the Applied Sciences*, vol. 44, no. 17, pp. 12522–12536, 2021.

[11] H. Budak, S. Erden, and M. A. Ali, "Simpson and Newton type inequalities for convex functions via newly defined quantum integrals," *Mathematical Methods in the Applied Sciences*, vol. 44, no. 1, pp. 378–390, 2021.

[12] P. Siricharuanun, S. Erden, M. A. Ali, H. Budak, S. Chasreechai, and T. Sitthiwirattham, "Some new Simpson's and Newton's formulas type inequalities for convex functions in quantum calculus," *Mathematics*, vol. 9, article 1992, 2021.

[13] T. Sitthiwirattham, K. Nonlaopon, M. A. Ali, and H. Budak, "Riemann-Liouville fractional Newton's type inequalities for differentiable convex functions," *Fractal and Fractional*, vol. 6, no. 3, p. 175, 2022.

[14] M. U. Awan, S. Talib, Y.-M. Chu, M. A. Noor, and K. I. Noor, "Some new refinements of Hermite–Hadamard-type inequalities involving -Riemann–Liouville fractional integrals and applications," *Mathematical Problems in Engineering*, vol. 2020, Article ID 3051920, 10 pages, 2020.

[15] A. Kashuri and R. Liko, "Generalized trapezoidal type integral inequalities and their applications," *Journal of Analysis*, vol. 28, no. 4, pp. 1023–1043, 2020.

[16] M. A. Khan, A. Iqbal, M. Suleman, and Y.-M. Chu, "Hermite–Hadamard type inequalities for fractional integrals via Green's function," *Journal of Inequalities and Applications*, vol. 2018, no. 1, Article ID 161, 2018.

[17] M. A. Khan, T. Ali, S. S. Dragomir, and M. Z. Sarikaya, "Hermite–Hadamard type inequalities for conformable fractional integrals," *Revista de la Real Academia de Ciencias Exactas, Físicas y Naturales. Serie A. Matemáticas*, vol. 112, no. 4, pp. 1033–1048, 2018.

[18] E. Set, J. Choi, and A. Gözpinar, "Hermite-Hadamard type inequalities for the generalized *k*-fractional integral operators," *Journal of Inequalities and Applications*, vol. 2017, no. 1, Article ID 206, 2017.

[19] M. Tunç, "On new inequalities for h-convex functions via Riemann-Liouville fractional integration," *Univerzitet u Nišu*, vol. 27, no. 4, pp. 559–565, 2013.

[20] M. Vivas-Cortez, M. A. Ali, A. Kashuri, and H. Budak, "Generalizations of fractional Hermite-Hadamard-Mercer like inequalities for convex functions," *AIMS Mathematics*, vol. 6, no. 9, pp. 9397–9421, 2021.

[21] D. Zhao, M. A. Ali, A. Kashuri, H. Budak, and M. Z. Sarikaya, "Hermite–Hadamard-type inequalities for the interval-valued approximately h-convex functions via generalized fractional integrals," *Journal of Inequalities and Applications*, vol. 2020, no. 1, Article ID 222, 2020.

[22] D. Zhao, M. A. Ali, C. Promsakon, and T. Sitthiwirattham, "Some generalized fractional integral inequalities for convex functions with applications," *Fractal and Fractional*, vol. 6, no. 2, p. 94, 2022.

[23] S. K. Sahoo, M. Tariq, H. Ahmad, J. Nasir, H. Aydi, and A. Mukheimer, "New Ostrowski-type fractional integral inequalities via generalized exponential-type convex functions and applications," *Symmetry*, vol. 13, no. 8, p. 1429, 2021.

[24] S. K. Sahoo, H. Ahmad, M. Tariq, B. Kodamasingh, H. Aydi, and M. De la Sen, "Hermite–Hadamard type inequalities involving k-fractional operator for (h, m)-convex functions," *Symmetry*, vol. 13, no. 9, article 1686, 2021.

[25] M. Tariq, S. K. Sahoo, J. Nasir, H. Aydi, and H. Alsamir, "Some Ostrowski type inequalities via n-polynomial exponentially s -convex functions and their applications," *AIMS Mathematics*, vol. 6, no. 12, pp. 13272–13290, 2021.

[26] S. S. Dragomir, "On the Ostrowskis integral inequality for mappings with bounded variation and applications," *Mathematical Inequalities & Applications*, vol. 4, no. 1, pp. 59–66, 2001.

[27] S. S. Dragomir, R. P. Agarwal, and P. Cerone, "On Simpson's inequality and applications," *Journal of Inequalities and Applications*, vol. 5, 579 pages, 2000.

[28] S. S. Dragomir, "On Simpson's quadrature formula for mappings of bounded variation and applications," *Tamkang Journal of Mathematics*, vol. 30, no. 1, pp. 53–58, 1999.

[29] M. W. Alomari, "A companion of the generalized trapezoid inequality and applications," *Journal of Mathematics and Applications*, vol. 36, pp. 5–15, 2013.

[30] S. S. Dragomir, "On trapezoid quadrature formula and applications," *Kragujevac Journal of Mathematics*, vol. 23, pp. 25–36, 2001.

[31] S. S. Dragomir, "On the midpoint quadrature formula for mappings with bounded variation and applications," *Kragujevac Journal of Mathematics*, vol. 22, pp. 13–19, 2000.

[32] S. Rashid, R. Ashraf, and E. Bonyah, "On analytical solution of time-fractional biological population model by means of generalized integral transform with their uniqueness and convergence analysis," *Journal of Function Spaces*, vol. 2022, Article ID 7021288, 29 pages, 2022.

[33] S. Rashid, R. Ashraf, and F. Jarad, "Strong interaction of Jafari decomposition method with nonlinear fractional-order partial differential equations arising in plasma via the singular and nonsingular kernels," *AIMS Mathematics*, vol. 7, no. 5, pp. 7936–7963, 2022.

[34] S. Rashid, F. Jarad, A. G. Ahmad, and K. M. Abualnaja, "New numerical dynamics of the heroin epidemic model using a fractional derivative with Mittag-Leffler kernel and consequences for control mechanisms," *Results in Physics*, vol. 35, article 105304, 2022.

[35] S. Rashid, F. Jarad, and A. G. Ahmad, "A novel fractal-fractional order model for the understanding of an oscillatory and complex behavior of human liver with non-singular kernel," *Results in Physics*, vol. 35, article 105292, 2022.

[36] S. Rashid, M. K. A. Kaabar, A. Althobaiti, and M. S. Alqurashi, "Constructing analytical estimates of the fuzzy fractional-order Boussinesq model and their application in oceanography," *Journal of Ocean Engineering and Science*, 2022.

[37] B. P. Moghaddam and Z. S. Mostaghim, "Modified finite difference method for solving fractional delay differential equations," *Boletim da Sociedade Paranaense de Matemática*, vol. 35, no. 2, pp. 49–58, 2017.

[38] B. P. Moghaddam and Z. S. Mostaghim, "A novel matrix approach to fractional finite difference for solving models based on nonlinear fractional delay differential equations," *Ain Shams Engineering Journal*, vol. 5, no. 2, pp. 585–594, 2014.

[39] B. P. Moghaddam, A. Dabiri, and J. A. T. Machado, "Application of variable-order fractional calculus in solid mechanics," in *Applications in Engineering. Life and Social Sciences, Part A*, vol. 7, pp. 207–224, 2019.

[40] B. P. Moghaddam, A. M. Lopes, J. A. T. Machado, and Z. S. Mostaghim, "Computational scheme for solving nonlinear fractional stochastic differential equations with delay," *Stochastic Analysis and Applications*, vol. 37, no. 6, pp. 893–908, 2019.

[41] B. P. Moghaddam, Z. S. Mostaghim, A. A. Pantelous, and J. A. T. Machado, "An integro quadratic spline-based scheme for solving nonlinear fractional stochastic differential equations with constant time delay," *Communications in Nonlinear Science and Numerical Simulation*, vol. 92, article 105475, 2021.

[42] R. Gorenflo and F. Mainardi, *Fractional Calculus: Integral and Differential Equations of Fractional Order*, Springer Verlag, Wien, 1997.

[43] A. A. Kilbas, H. M. Srivastava, and J. J. Trujillo, *Theory and Applications of Fractional Differential Equations*, Elsevier, Amsterdam, 2006.

[44] S. Mubeen and G. M. Habibullah, "k-fractional integrals and application," *International Journal of Contemporary Mathematical Sciences*, vol. 7, pp. 89–94, 2012.

[45] F. Ertuğral and M. Z. Sarikaya, "Simpson type integral inequalities for generalized fractional integral," *Revista de la Real Academia de Ciencias Exactas, Físicas y Naturales. Serie A. Matemáticas*, vol. 113, no. 4, pp. 3115–3124, 2019.

[46] M. W. Alomari, "A companion of Dragomir's generalization of the Ostrowski inequality and applications to numerical integration," *Ukrainian Mathematical Journal*, vol. 64, no. 4, pp. 491–510, 2012.

Hindawi
Journal of Function Spaces
Volume 2022, Article ID 2388557, 33 pages
https://doi.org/10.1155/2022/2388557

Research Article

A Study on the Fractal-Fractional Epidemic Probability-Based Model of SARS-CoV-2 Virus along with the Taylor Operational Matrix Method for Its Caputo Version

Shahram Rezapour,[1,2] **Sina Etemad**,[1] **İbrahim Avcı**,[3] **Hijaz Ahmad**,[4] **and Azhar Hussain**[5]

[1]*Department of Mathematics, Azarbaijan Shahid Madani University, Tabriz, Iran*
[2]*Department of Medical Research, China Medical University Hospital, China Medical University, Taichung, Taiwan*
[3]*Department of Computer Engineering, Faculty of Engineering, Final International University, Kyrenia, Northern Cyprus Mersin 10, Turkey*
[4]*Section of Mathematics, International Telematic University Uninettuno, Corso Vittorio Emanuele II, 00186 Rome, Italy*
[5]*Department of Mathematics, University of Chakwal, Chakwal 48800, Pakistan*

Correspondence should be addressed to Sina Etemad; sina.etemad@azaruniv.ac.ir

Received 4 May 2022; Revised 20 July 2022; Accepted 29 July 2022; Published 1 September 2022

Academic Editor: Yusuf Gurefe

SARS-CoV-2 is a strain of the large coronavirus family that has led to COVID-19 disease. The virus has been one of the deadliest known viruses in the world to date. Rapid mutations and the creation of new strains cause researchers to focus on the dynamic behaviors of the virus and to analyze it accurately through clinical research and mathematical models. In this paper, from the point of view of mathematical modeling, we intend to focus on the dynamic behavior of the system and examine its analytical and numerical aspects in two different structures. In other words, by recalling newly formulated hybrid fractional-fractal operators, we present a fractal-fractional probability-based model of SARS-CoV-2 virus for the first time and extract its equivalent compact fractal-fractional IVP to investigate its existence and stability criteria. A type of special admissible contractions will help us in this regard. Moreover, based on the source data, we simulate our system according to algorithms derived by Adams-Bashforth method and explain the effects of variation of the dimension of fractal and fractional order on dynamics of solutions. Finally, we transform our fractal-fractional model into a Caputo probability-based model of SARS-CoV-2 to derive solutions via the operational matrix method under Taylor's basis. The numerical simulations show close behaviors for both of models.

1. Introduction

From birth to death, humans are always at risk for a variety of diseases; the source of these infectious diseases is mainly microorganisms such as parasites, fungi, viruses, and bacteria. Over the centuries, various epidemics have killed millions of people everywhere on the planet and caused great loss of life and property to families and governments. Recently, in late 2019, the international community contracted a new type of viral respiratory disease that was reported to have originated in Wuhan, China. For the sake of rapid spread of this unknown disease in Wuhan, scientists have used a variety of terms to describe the viral cause of the disease. According to the standard classifications in virology and considering its geographical location, it was first temporarily named Wuhan coronavirus and then the new coronavirus 2019 (2019-nCov). Finally, in 2020, an international committee from the World Health Organization (WHO), which works to classify viruses, used the official title SARS-CoV-2, which interprets the severe acute respiratory syndrome of coronavirus 2 [1]; and later, in order not to be confused with the SARS virus, the committee used the abbreviated title COVID-19 [2].

Extensive medical research was conducted worldwide to identify the nature and spread of the virus, and on January 20, human-to-human transmission of the virus was proved [3]. The virus has also been shown to be transmitted via respiratory droplets such as coughing and sneezing and even talking indoors without ventilation [4, 5]. In addition, subsequent studies have shown that the best site for infection is the nasal cavity, through which it gradually and immediately enters the lungs and infects it [6]. However, other studies have shown that some wild animals, such as bats, mice, rabbits, and mink, can also transmit the SARS-CoV-2 virus to humans [7]. In these two years, no part of the human environments has been spared from the virus, even the most remote islands. As of March 10, 2022, more than 450 million people have been infected with COVID-19, of which more than six million have died, based on the approved reports of the World Health Organization [8]. In some cases, people with the SARS-CoV-2 virus have severe clinical symptoms and are hospitalized, but in most cases, patients with the SARS-CoV-2 virus do not need to be admitted to treatment centers and are treated with antiviral drugs such as remdesivir [9].

Due to the high rate of transmission of the virus and the development of its various strains, there was a need for definitive treatment to control the epidemic. Therefore, knowledge of the pathobiology of the SARS-CoV-2 virus was essential. Because vaccines are always an important tool in the fight against all epidemics, we have also seen extensive efforts to produce safe and effective vaccines for the SARS-CoV-2 virus by large pharmaceutical companies. Of course, it should be noted that in addition to mass vaccination to eradicate the virus completely, it is necessary for human societies to continue to maintain social distance and use masks indoors. It is still unknown whether the vaccines are effective in killing the disease.

In this regard, to accurately analyze the prevalence of the SARS-CoV-2 virus worldwide and predict its upward or downward trends, researchers turned to simulating the dynamics of the virus by mathematical models. Of course, it should be noted that in recent decades, mathematical models have always been helpful in studying the dynamics of various types of diseases and engineering processes, and through various modeling, scientists and researchers have been able to achieve their study goals. In this direction, fractional mathematical models are among the most widely used methods in the field of accurate analysis and evaluation of data. Known fractional operators such as Caputo, Atangana-Baleanu, and Caputo-Fabrizio fractional derivatives are efficient mathematical tools for defining and designing mathematical systems, so that their role can be clearly observed in newly published papers, for example, the modelling of anthrax in animals [10], genetic regulatory networks [11], mumps virus [12], Zika virus [13], mosaic disease [14], computer viruses [15], thermostat control [16], pantograph equation [17], Q-fever [18], hybrid equation of p-Laplacian operators [19], geographical models [20, 21], codynamics of COVID-19 and diabetes [22], chemical compounds such as methylpropane [23], and immunogenic tumor [24]. Also, due to difficulties of solving fractional differential equations analytically, developing efficient numerical methods with different fractional operators for such equations becomes an important focus for researchers; for example, in [25], fractional derivative generalized Atangana-Baleanu differentiability has been implemented to solve fuzzy fractional differential equations. Also, in 2021, Erturk et al. [26] used fractional calculus theory to investigate the motion of a beam on an internally bent nanowire. In [27], Jajarmi et al. presented a new and general fractional formulation to investigate the complex behaviors of a capacitor microphone dynamical system. Alqhtani et al. [28] presented that two important physical examples that are of current and recurring interests are considered, in which the classical time derivative was modeled with the Caputo fractional derivative leading the system of equations to subdiffusive fractional reaction-diffusion models of predator-prey type, together with some numerical experiments. In [29], Aljhani et al. discuss a one-dimensional time-fractional Gray-Scott model with Liouville-Caputo, Caputo-Fabrizio-Caputo, and Atangana-Baleanu-Caputo fractional derivatives. They also utilize the fractional homotopy analysis transformation method to obtain approximate solutions.

Numerous articles about SARS-CoV-2 or COVID-19 have recently been published in scientific journals around the world, including a few examples: DarAssi et al. [30] presented a model of SARS-CoV-2 with hospitalization in the form of a variable-order fractional model of Caputo's differential equations, in which they studied the asymptotic stability of the system. In the same direction, Gu et al. [31] also designed the comprehensive Caputo model of SARS-CoV-2 virus in the framework of the constant-order operator and analyzed the stable solutions of the system w.r.t. the index R_0 (reproduction number). Under a five-compartmental SEIRD model, and using real data from Italian medical authorities, Rajagopal et al. [32] conducted a case study of the disease and analyzed system behavior in both classical and fractional modes. In another case research of the prevalence of SARS-CoV-2 in France and Colombia, Quintero and Gutiérrez-Carvajal [33] examined the evolution of the disease under the bound optimization method. In 2021, Zamir et al. [34] formulated a model of COVID-19 in nine subclasses and focused the elimination and control of the infection caused by COVID-19. Jain et al. [35] presented a prediction model of COVID-19 by using numerous machine learning models, such as SVM, Naïve Bayes, K-nearest neighbors, AdaBoost, gradient boosting, XGBoost, random forest, ensembles, and neural networks. Baleanu et al. [36] introduced a generalized version of fractional models for the COVID-19 pandemic, including the effects of isolation and quarantine. In [37], Ali et al. investigate the transmission dynamics of a fractional-order mathematical model of COVID-19 under five subclasses, susceptible, exposed, asymptomatic infected, symptomatic infected, and recovered, using the Caputo fractional derivative. In 2022, Ozkose et al. [38] developed a new model of the Omicron strain of SARS-CoV-2 virus and, based on data collected across the United Kingdom, studied the relationship between this strain and heart attack. They also analyzed the sensitivity of the system and fitting of the parameters using the LCM method.

In addition to these articles, many other researchers have published articles on COVID-19 dynamics and evaluated a variety of models under different conditions and assumptions. For instances, we can mention stochastic models of COVID-19 [39], or even various case studies of COVID-19 from all over the world like [40–44]. Most researchers simultaneously studied the models of COVID-19 analytically and numerically and evaluated the types of dynamic behaviors of the solutions under singular and nonsingular systems that can be mentioned like [45, 46]. In the theoretical study of all these mentioned models, the theoretical results are among the basic parts of the analysis of mathematical models, because the existence of a solution for a system allows us to continue to study other properties such as stable solutions, equilibrium solutions, numerical solutions, and their simulations. Usually, fixed point theory is effective in this field, and its role can be observed in boundary and initial value problems [47].

By defining mathematical models and the refinement of numerical approaches, there is a need to use new mathematical operators with high computational capabilities to model processes. As a result, Atangana [48] used fractal derivatives to introduce a new type of hybrid operators and introduced fractional-fractal derivatives into the world of modeling in 2017. In fact, to define these advanced operators, he used two arguments to represent the order of the operator and the dimension of the operator, which he called the fractional order and the fractional dimension of the fractional-fractional derivatives, respectively [48]. Atangana then divided these derivatives into three different categories and, with the help of different integral kernels, extracted the numerical algorithms associated with them. Then, in the last year, these numerical techniques were used in some new studies in which researchers simulated the approximate solutions of fractional-fractal models of new infectious diseases. In 2021, Arfan et al. [49] designed a prey-predation structure for the four-compartmental fractal-fractional model of syn-ecosymbiosis and examined some conditions for species survival in an ecological system. Abdulwasaa et al. [50] conducted a case study with these fractal-fractional operators in which they examined the dynamics of new cases and the number of deaths from the COVID-19 epidemic over a specific period of time in India. Shah et al. [51] conducted the same study on a new model in Pakistan. Khan et al. [52] simulated and evaluated models of smoking at the incidence rate under the Caputo fractal-fractional derivative operator. Arif et al. [53] utilized the same fractal-fractional operators in engineering to analyze MHD stress fluid in a single channel. Alqhtani et al. [54] studied three models of fractal-fractional Michaelis-Menten enzymatic reaction (FFMMER) and presented these models based on three different kernels, namely, power law, exponential decay, and Mittag-Leffler kernels.

In this work, considering the importance of symptomatic and asymptomatic populations in spreading of virus, we present the new fractal-fractional probability-based model of SARS-CoV-2 virus by dividing the total population into four subclasses such as susceptible, asymptomatic, symptomatic, and recovered individuals. In [55], the authors designed a five-compartmental Caputo fractional epidemic model for the novel coronavirus in which the impact of environmental transmission is considered in the final result. This model motivates us to study an extended model of transmission of SARS-CoV-2 virus via advanced hybrid operators. In this paper, we get help from these newly extended hybrid fractal-fractional operators and discuss a new hybrid model of transmission of SARS-CoV-2 virus analytically and numerically. If we want to focus on the novelty and contribution of this manuscript, it is notable that for the first time, our system is a fractal-fractional probability-based model of SARS-CoV-2 virus in which we apply new hybrid fractal-fractional derivatives for modeling of the power law type kernel. Also, in this model, a probability-based structure of transmission of virus is considered. In other words, if p is the probability that both categories susceptible and infected interact and this leads to the asymptomatic category, in that case, $(1-p)$ stands for the portion of the infected persons that may automatically belong to the symptomatic category. On the other hand, it should be kept in mind that when people become infected with the SARS-CoV-2 virus, they may not have any symptoms, but at the same time, some people may experience severe complications and show specific symptoms. Therefore, the feature of our model is that we have divided the group of people infected with the virus into two categories: symptomatic and asymptomatic. Also, from mathematical point of view, a specific approach of fixed point methods is applied via ϕ-admissible ϕ-ψ-contractions to discuss the existence criterion, in which it shows the applicability of new fixed point techniques in the applied problems. Also, another novelty of this study is that in addition to fractal-fractional analysis of the SARS-CoV-2 model, we extend its Caputo-type version to compare our previous results with solutions of the fractional model under the Taylor operational matrix method. Also, note that in this paper, we consider both fractional and fractal-fractional derivatives as the full memory. We can study similar models by using the short memory. In this direction, refer to [56, 57].

In this study, from a numerical point of view, we present two numerical techniques for the approximate solution of the considered model of SARS-CoV-2 virus under two different fractional operator derivative. The first technique is the Adams-Bashforth technique which is applied to probability-based model of SARS-CoV-2 under fractal-fractional operator in this study. The ABM is a very stable technique and allows us explicitly to determine the numerical solution at an instant time from the solutions in the previous instants. Using the higher-order Adams-Bashforth method actually becomes more unstable as the timestep is reduced. So that, the corrector step need to be added to avoid much of this instability. This can be mentioned as a disadvantage of AB technique. The second method is a collocation type of the well-known spectral methods; fractional Taylor operational matrix method is applied to solve probability-based model of SARS-CoV-2 under Caputo operator first time in this paper. The main advantage of spectral methods is that they are easy to apply for both finite and infinite intervals and when the solution of a given problem is smooth, spectral methods have very good error properties, namely, the so-called "exponential convergence." Thanks to these advantages, for solving many different types of integral and differential equations numerically, spectral methods received considerable interest in recent years. When the solution is not smooth enough, the stability and accuracy of these methods are decreasing, which is an important disadvantage because of limiting the applicability. In this work, we compare our results obtained from FTOMM with the Adams-Bashforth simulations.

The structure of the manuscript is arranged as follows: some definitions of ϕ-admissible ϕ-ψ-contractions and fractal-fractional derivatives are presented in the next section. We describe our main fractal-fractional model in Section 3 along with the meanings of parameters. Under two different fixed point methods, we guarantee the existence property for solutions of the system in Section 4. Section 5 deals with the Lipschitz and uniqueness properties. Then, in Section 6, we discuss UHR-stable solutions for each four state functions separately. To predict the future of state functions and their analysis numerically, we simulate them via the Adams-Bashforth method in two subsections of Section 7. In the next step, in Section 8, we give the Caputo-type of transmission of the SARS-CoV-2 virus, and in several subsections, we describe our method via the Taylor operational matrix technique, and after some simulations, we compare our numerical results in both fractal-fractional and fractional systems in the context of some graphs and tables. The conclusions and further study suggestions are presented in Section 9.

2. Basic Concepts

Some basic notions on the fractal-fractional operators and fixed point theory are assembled.

Let Ψ display a subclass of nondecreasing operators like $\psi : [0,\infty) \longrightarrow [0,\infty)$ s.t.

$$\sum_{j=1}^{\infty} \psi^j(\mathfrak{t}) < \infty, \psi(\mathfrak{t}) < \mathfrak{t}, \forall \mathfrak{t} > 0. \tag{1}$$

Definition 1 (see [58]). Let $\mathbb{X}$ be a normed space and $\mathcal{F} : \mathbb{X} \longrightarrow \mathbb{X}$ and $\phi : \mathbb{X}^2 \longrightarrow \mathbb{R}_{\geq 0}$.

$(p)\mathcal{F}$ is ϕ-ψ-contraction if for $u_1, u_2 \in \mathbb{X}$,

$$\phi(u_1, u_2)\mathbf{d}(\mathcal{F}u_1, \mathcal{F}u_2) \leq \psi(d(u_1, u_2)). \tag{2}$$

(q) $\mathcal{F}$ is ϕ-admissible if $\phi(u_1, u_2) \geq 1$ yields $\phi(\mathcal{F}u_1, \mathcal{F}u_2) \geq 1$.

Definition 2 (see [48]). Let $\mathcal{F}$ be fractal differentiable on (a, b) of order ν. The fractional-fractal ω^{th}-derivative of the function $\mathcal{F}$ via the power law type kernel in the Riemann-Liouville sense is defined by

$$\begin{gathered} {}^{\mathbf{FFP}}\mathfrak{D}_{a,\mathfrak{t}}^{\omega,\nu}\mathcal{F}(\mathfrak{t}) = \frac{1}{\Gamma(n-\omega)} \frac{\mathrm{d}}{\mathrm{d}\mathfrak{t}^{\nu}} \int_a^{\mathfrak{t}} (\mathfrak{t} - \mathfrak{m})^{n-\omega-1} \mathcal{F}(\mathfrak{m})\, \mathrm{d}\mathfrak{m}, \\ \cdot (n - 1 < \omega, \nu \leq n \in \mathbb{N}), \end{gathered} \tag{3}$$

where $d\mathcal{F}(\mathfrak{m})/\mathrm{d}\mathfrak{m}^{\nu} = \lim_{\mathfrak{t}\longrightarrow\mathfrak{m}}((\mathcal{F}(\mathfrak{t}) - \mathcal{F}(\mathfrak{m}))/(\mathfrak{t}^{\nu} - \mathfrak{m}^{\nu}))$ is the fractal derivative.

It is known that if $\nu = 1$, then the fractal-fractional derivative ${}^{\mathbf{FFP}}\mathfrak{D}_{a,\mathfrak{t}}^{\omega,\nu}$ is reduced to the standard derivative ${}^{\mathbf{RL}}\mathfrak{D}_{a,\mathfrak{t}}^{\omega}$ of order ω.

Definition 3 (see [48]). Let $\mathcal{F}$ be continuous on (a, b). The fractional-fractal integral of the function $\mathcal{F}$ with fractional order ω and fractal order ν is

$${}^{\mathbf{FFP}}\mathfrak{J}_{a,\mathfrak{t}}^{\omega,\nu}\mathcal{F}(\mathfrak{t}) = \frac{\nu}{\Gamma(\omega)} \int_a^{\mathfrak{t}} \mathfrak{m}^{\nu-1} (\mathfrak{t} - \mathfrak{m})^{\omega-1} \mathcal{F}(\mathfrak{m})\, \mathrm{d}\mathfrak{m}. \tag{4}$$

3. Description of the Model for SARS-CoV-2 Virus

Khan et al. [59, 60] modeled a mathematical structure of dynamics of SARS-CoV-2 virus in the form of four initial value problems equipped with four state functions $\mathcal{S}$, $\mathcal{P}_1$, $\mathcal{P}_2$, and $\mathcal{R}$, which are a part of total population. This model is

$$\begin{cases} \dfrac{\mathrm{d}\mathcal{S}(\mathfrak{t})}{\mathrm{d}\mathfrak{t}} = \Theta - r\mathcal{P}_1(\mathfrak{t})\mathcal{S}(\mathfrak{t}) - rs\mathcal{P}_2(\mathfrak{t})\mathcal{S}(\mathfrak{t}) - (b + b_1)\mathcal{S}(\mathfrak{t}), \\ \dfrac{\mathrm{d}\mathcal{P}_1(\mathfrak{t})}{\mathrm{d}\mathfrak{t}} = p[r\mathcal{P}_1(\mathfrak{t})\mathcal{S}(\mathfrak{t}) + rs\mathcal{P}_2(\mathfrak{t})\mathcal{S}(\mathfrak{t})] - (b_1 + b_2 + r_1)\mathcal{P}_1(\mathfrak{t}), \\ \dfrac{\mathrm{d}\mathcal{P}_2(\mathfrak{t})}{\mathrm{d}\mathfrak{t}} = (1 - p)[r\mathcal{P}_1(\mathfrak{t})\mathcal{S}(\mathfrak{t}) + rs\mathcal{P}_2(\mathfrak{t})\mathcal{S}(\mathfrak{t})] + qr_1\mathcal{P}_1(\mathfrak{t}) - (b_1 + b_3 + r_2)\mathcal{P}_2(\mathfrak{t}), \\ \dfrac{\mathrm{d}\mathcal{R}(\mathfrak{t})}{\mathrm{d}\mathfrak{t}} = r_1(1 - q)\mathcal{P}_1(\mathfrak{t}) + r_2\mathcal{P}_2(\mathfrak{t}) + b\mathcal{S}(\mathfrak{t}) - b_1\mathcal{R}(\mathfrak{t}), \end{cases} \tag{5}$$

where $\mathcal{S}(\mathfrak{t})$ stands for the people belonging to the susceptible category, $\mathcal{P}_1(\mathfrak{t})$ is the people belonging to the asymptomatic category, $\mathcal{P}_2(\mathfrak{t})$ is the people belonging to the symptomatic category, and $\mathcal{R}(\mathfrak{t})$ stands for the people belonging to the recovered category at the time $\mathfrak{t} \in \mathbb{J} \coloneqq [0, T]$, $(T > 0)$. Based on these assumptions, the infected categories are taken to be symptomatic class and asymptomatic class, because asymptomatic persons are considered as the main factor of transmission of disease. It is to be noted that the variables, constants, and parameters are nonnegative.

Inspired by the aforesaid standard epidemic model, we here consider the fractal-fractional epidemic probability-based model of the SARS-CoV-2 virus in the following structure:

$$\begin{cases} {}^{\mathbf{FFP}}\mathfrak{D}_{0,\mathfrak{t}}^{\omega,\nu}\mathcal{S}(\mathfrak{t}) = \Theta - r\mathcal{P}_1(\mathfrak{t})\mathcal{S}(\mathfrak{t}) - rs\mathcal{P}_2(\mathfrak{t})\mathcal{S}(\mathfrak{t}) - (b + b_1)\mathcal{S}(\mathfrak{t}), \\ {}^{\mathbf{FFP}}\mathfrak{D}_{0,\mathfrak{t}}^{\omega,\nu}\mathcal{P}_1(\mathfrak{t}) = p[r\mathcal{P}_1(\mathfrak{t})\mathcal{S}(\mathfrak{t}) + rs\mathcal{P}_2(\mathfrak{t})\mathcal{S}(\mathfrak{t})] - (b_1 + b_2 + r_1)\mathcal{P}_1(\mathfrak{t}), \\ {}^{\mathbf{FFP}}\mathfrak{D}_{0,\mathfrak{t}}^{\omega,\nu}\mathcal{P}_2(\mathfrak{t}) = (1-p)[r\mathcal{P}_1(\mathfrak{t})\mathcal{S}(\mathfrak{t}) + rs\mathcal{P}_2(\mathfrak{t})\mathcal{S}(\mathfrak{t})] + qr_1\mathcal{P}_1(\mathfrak{t}) - (b_1 + b_3 + r_2)\mathcal{P}_2(\mathfrak{t}), \\ {}^{\mathbf{FFP}}\mathfrak{D}_{0,\mathfrak{t}}^{\omega,\nu}\mathcal{R}(\mathfrak{t}) = r_1(1-q)\mathcal{P}_1(\mathfrak{t}) + r_2\mathcal{P}_2(\mathfrak{t}) + b\mathcal{S}(\mathfrak{t}) - b_1\mathcal{R}(\mathfrak{t}), \end{cases} \tag{6}$$

subject to

$$\begin{aligned} \mathcal{S}(0) &= \mathcal{S}_0 > 0, \\ \mathcal{P}_1(0) &= \mathcal{P}_{1,0} \geq 0, \\ \mathcal{P}_2(0) &= \mathcal{P}_{2,0} \geq 0, \\ \mathcal{R}(0) &= \mathcal{R}_0 \geq 0, \end{aligned} \tag{7}$$

where ${}^{\mathbf{FFP}}\mathfrak{D}_{0,\mathfrak{t}}^{\omega,\nu}$ is the fractional-fractal derivative of the fractional order $\omega \in (0, 1]$ and the fractal order $\nu \in (0, 1]$ via the power law type kernel. We have

$$\mathcal{N}(\mathfrak{t}) = \mathcal{S}(\mathfrak{t}) + \mathcal{P}_1(\mathfrak{t}) + \mathcal{P}_2(\mathfrak{t}) + \mathcal{R}(\mathfrak{t}), \tag{8}$$

in which as we said above, $\mathcal{N}(\mathfrak{t})$ means the total population at the time $\mathfrak{t} \in \mathbb{J} \coloneqq [0, T]$, $(T > 0)$.

About parameters, the total natural death rate along with the rate of disease-related death for both infected groups is specified by the symbols b_1, b_2, and b_3, respectively. We show the rate of transmission of disease by r, and its reduced rate is denoted by the symbol s. The vaccination rate is given by b, and Θ stands for the newborn rate. The probability of the asymptomatic persons is illustrated by p, and the probability of these persons that recover in the symptomatic step is specified by q. Moreover, r_2 is the recovery rate in relation to asymptomatic persons and accordingly, and r_1 is the recovery rate in relation to the symptomatic persons.

4. Existence of Solutions

In this position, we shall get help fixed point theory to the suggested fractal-fractional IVP (6). For the qualitative analysis, we define the Banach space $\mathbb{X} = \mathbb{Y}^4$, where $\mathbb{Y} = C(\mathbb{J}, \mathbb{R})$, as

$$\begin{aligned} \|\mathcal{X}\|_{\mathbb{X}} &= \|(\mathcal{S}, \mathcal{P}_1, \mathcal{P}_2, \mathcal{R})\|_{\mathbb{X}} \\ &= \max\{|\mathcal{S}(\mathfrak{t})| + |\mathcal{P}_1(\mathfrak{t})| + |\mathcal{P}_2(\mathfrak{t})| + |\mathcal{R}(\mathfrak{t})| : \mathfrak{t} \in \mathbb{J}\}. \end{aligned} \tag{9}$$

We write the R.H.S. of model (6) by

$$\begin{cases} \mathcal{F}_1(\mathfrak{t}, \mathcal{S}(\mathfrak{t}), \mathcal{P}_1(\mathfrak{t}), \mathcal{P}_2(\mathfrak{t}), \mathcal{R}(\mathfrak{t})) = \Theta - r\mathcal{P}_1(\mathfrak{t})\mathcal{S}(\mathfrak{t}) - rs\mathcal{P}_2(\mathfrak{t})\mathcal{S}(\mathfrak{t}) - (b + b_1)\mathcal{S}(\mathfrak{t}), \\ \mathcal{F}_2(\mathfrak{t}, \mathcal{S}(\mathfrak{t}), \mathcal{P}_1(\mathfrak{t}), \mathcal{P}_2(\mathfrak{t}), \mathcal{R}(\mathfrak{t})) = p[r\mathcal{P}_1(\mathfrak{t})\mathcal{S}(\mathfrak{t}) + rs\mathcal{P}_2(\mathfrak{t})\mathcal{S}(\mathfrak{t})] - (b_1 + b_2 + r_1)\mathcal{P}_1(\mathfrak{t}), \\ \mathcal{F}_3(\mathfrak{t}, \mathcal{S}(\mathfrak{t}), \mathcal{P}_1(\mathfrak{t}), \mathcal{P}_2(\mathfrak{t}), \mathcal{R}(\mathfrak{t})) = (1-p)[r\mathcal{P}_1(\mathfrak{t})\mathcal{S}(\mathfrak{t}) + rs\mathcal{P}_2(\mathfrak{t})\mathcal{S}(\mathfrak{t})] + qr_1\mathcal{P}_1(\mathfrak{t}) - (b_1 + b_3 + r_2)\mathcal{P}_2(\mathfrak{t}), \\ \mathcal{F}_4(\mathfrak{t}, \mathcal{S}(\mathfrak{t}), \mathcal{P}_1(\mathfrak{t}), \mathcal{P}_2(\mathfrak{t}), \mathcal{R}(\mathfrak{t})) = r_1(1-q)\mathcal{P}_1(\mathfrak{t}) + r_2\mathcal{P}_2(\mathfrak{t}) + b\mathcal{S}(\mathfrak{t}) - b_1\mathcal{R}(\mathfrak{t}). \end{cases} \tag{10}$$

Hence,

$$\begin{cases} {}^{\mathbf{RL}}\mathfrak{D}_{0,\mathfrak{t}}^{\omega}\mathcal{S}(\mathfrak{t}) = \nu\mathfrak{t}^{\nu-1}\mathcal{F}_1(\mathfrak{t}, \mathcal{S}(\mathfrak{t}), \mathcal{P}_1(\mathfrak{t}), \mathcal{P}_2(\mathfrak{t}), \mathcal{R}(\mathfrak{t})), \\ {}^{\mathbf{RL}}\mathfrak{D}_{0,\mathfrak{t}}^{\omega}\mathcal{P}_1(\mathfrak{t}) = \nu\mathfrak{t}^{\nu-1}\mathcal{F}_2(\mathfrak{t}, \mathcal{S}(\mathfrak{t}), \mathcal{P}_1(\mathfrak{t}), \mathcal{P}_2(\mathfrak{t}), \mathcal{R}(\mathfrak{t})), \\ {}^{\mathbf{RL}}\mathfrak{D}_{0,\mathfrak{t}}^{\omega}\mathcal{P}_2(\mathfrak{t}) = \nu\mathfrak{t}^{\nu-1}\mathcal{F}_3(\mathfrak{t}, \mathcal{S}(\mathfrak{t}), \mathcal{P}_1(\mathfrak{t}), \mathcal{P}_2(\mathfrak{t}), \mathcal{R}(\mathfrak{t})), \\ {}^{\mathbf{RL}}\mathfrak{D}_{0,\mathfrak{t}}^{\omega}\mathcal{R}(\mathfrak{t}) = \nu\mathfrak{t}^{\nu-1}\mathcal{F}_4(\mathfrak{t}, \mathcal{S}(\mathfrak{t}), \mathcal{P}_1(\mathfrak{t}), \mathcal{P}_2(\mathfrak{t}), \mathcal{R}(\mathfrak{t})). \end{cases} \tag{11}$$

By (11), we derive the following IVP:

$$\begin{cases} {}^{\mathbf{RL}}\mathfrak{D}^{\omega}_{0,\mathfrak{t}}\mathcal{X}(\mathfrak{t}) = \nu\mathfrak{t}^{\nu-1}\mathcal{F}(\mathfrak{t},\mathcal{X}(\mathfrak{t})), \omega,\nu \in (0,1], \\ \mathcal{X}(0) = \mathcal{X}_0, \end{cases} \tag{12}$$

where

$$\begin{aligned} \mathcal{X}(\mathfrak{t}) &= (\mathcal{S}(\mathfrak{t}), \mathcal{P}_1(\mathfrak{t}), \mathcal{P}_2(\mathfrak{t}), \mathcal{R}(\mathfrak{t}))^T, \\ \mathcal{X}_0 &= (\mathcal{S}_0, \mathcal{P}_{1,0}, \mathcal{P}_{2,0}, \mathcal{R}_0)^T, \\ \mathcal{F}(\mathfrak{t},\mathcal{X}(\mathfrak{t})) &= \begin{cases} \mathcal{F}_1(\mathfrak{t},\mathcal{S}(\mathfrak{t}),\mathcal{P}_1(\mathfrak{t}),\mathcal{P}_2(\mathfrak{t}),\mathcal{R}(\mathfrak{t})), \\ \mathcal{F}_2(\mathfrak{t},\mathcal{S}(\mathfrak{t}),\mathcal{P}_1(\mathfrak{t}),\mathcal{P}_2(\mathfrak{t}),\mathcal{R}(\mathfrak{t})), \\ \mathcal{F}_3(\mathfrak{t},\mathcal{S}(\mathfrak{t}),\mathcal{P}_1(\mathfrak{t}),\mathcal{P}_2(\mathfrak{t}),\mathcal{R}(\mathfrak{t})), \\ \mathcal{F}_4(\mathfrak{t},\mathcal{S}(\mathfrak{t}),\mathcal{P}_1(\mathfrak{t}),\mathcal{P}_2(\mathfrak{t}),\mathcal{R}(\mathfrak{t})). \end{cases} \end{aligned} \tag{13}$$

Now, the fractional-fractal integral acts on (12), and it becomes

$$\mathcal{X}(\mathfrak{t}) = \mathcal{X}(0) + \frac{\nu}{\Gamma(\omega)}\int_0^{\mathfrak{t}} \mathfrak{m}^{\nu-1}(\mathfrak{t}-\mathfrak{m})^{\omega-1}\mathcal{F}(\mathfrak{m},\mathcal{X}(\mathfrak{m}))\,d\mathfrak{m}. \tag{14}$$

In other words, the extended form of the above fractal-fractional integral is represented as

$$\begin{cases} \mathcal{S}(\mathfrak{t}) = \mathcal{S}_0 + \frac{\nu}{\Gamma(\omega)}\int_0^{\mathfrak{t}} \mathfrak{m}^{\nu-1}(\mathfrak{t}-\mathfrak{m})^{\omega-1}\mathcal{F}_1(\mathfrak{m},\mathcal{S}(\mathfrak{m}),\mathcal{P}_1(\mathfrak{m}),\mathcal{P}_2(\mathfrak{m}),\mathcal{R}(\mathfrak{m}))\,d\mathfrak{m}, \\ \mathcal{P}_1(\mathfrak{t}) = \mathcal{P}_{1,0} + \frac{\nu}{\Gamma(\omega)}\int_0^{\mathfrak{t}} \mathfrak{m}^{\nu-1}(\mathfrak{t}-\mathfrak{m})^{\omega-1}\mathcal{F}_2(\mathfrak{m},\mathcal{S}(\mathfrak{m}),\mathcal{P}_1(\mathfrak{m}),\mathcal{P}_2(\mathfrak{m}),\mathcal{R}(\mathfrak{m}))\,d\mathfrak{m}, \\ \mathcal{P}_2(\mathfrak{t}) = \mathcal{P}_{2,0} + \frac{\nu}{\Gamma(\omega)}\int_0^{\mathfrak{t}} \mathfrak{m}^{\nu-1}(\mathfrak{t}-\mathfrak{m})^{\omega-1}\mathcal{F}_3(\mathfrak{m},\mathcal{S}(\mathfrak{m}),\mathcal{P}_1(\mathfrak{m}),\mathcal{P}_2(\mathfrak{m}),\mathcal{R}(\mathfrak{m}))\,d\mathfrak{m}, \\ \mathcal{R}(\mathfrak{t}) = \mathcal{R}_0 + \frac{\nu}{\Gamma(\omega)}\int_0^{\mathfrak{t}} \mathfrak{m}^{\nu-1}(\mathfrak{t}-\mathfrak{m})^{\omega-1}\mathcal{F}_4(\mathfrak{m},\mathcal{S}(\mathfrak{m}),\mathcal{P}_1(\mathfrak{m}),\mathcal{P}_2(\mathfrak{m}),\mathcal{R}(\mathfrak{m}))\,d\mathfrak{m}. \end{cases} \tag{15}$$

Consider the operator $G:\mathbb{X}\longrightarrow\mathbb{X}$ as

$$G(\mathcal{X}(\mathfrak{t})) = \mathcal{X}(0) + \frac{\nu}{\Gamma(\omega)}\int_0^{\mathfrak{t}} \mathfrak{m}^{\nu-1}(\mathfrak{t}-\mathfrak{m})^{\omega-1}\mathcal{F}(\mathfrak{m},\mathcal{X}(\mathfrak{m}))d\mathfrak{m}. \tag{16}$$

In the preceding, we recall the required fixed point theorem in connection with our aim for proving the existence results.

Theorem 4 (see [58]). *Assume* $(\mathbb{X},\mathbf{d})$ *as a Banach space,* $\phi:\mathbb{X}\times\mathbb{X}\longrightarrow\mathbb{R}$, $\psi\in\Psi$, *and* $\mathcal{F}:\mathbb{X}\longrightarrow\mathbb{X}$ *as an* ϕ-ψ-*contraction s.t.*

(1) $\mathcal{F}$ *is* ϕ-*admissible*

(2) $\exists u_0\in\mathbb{X}, s.t.\phi(u_0,\mathcal{F}u_0)\geq 1$

(3) *for any sequence* $\{u_n\}$ *in* $\mathbb{X}$ *with* $u_n\longrightarrow u$ *and* $\phi(u_n, u_{n+1})\geq 1$ *for all* $n\geq 1$, *we have* $\phi(u_n,u)\geq 1,\forall n\in\mathbb{N}$

Then, $\exists u*$ *s.t.* $\mathcal{F}(u*)=u*$.

Now, the first existence result is proved here under some special operators.

Theorem 5. *Let* $\exists\mathfrak{T}:\mathbb{R}\times\mathbb{R}\longrightarrow\mathbb{R}$, $\exists$ *a continuous map* $\mathcal{F}:\mathbb{J}\times\mathbb{X}\longrightarrow\mathbb{X}$, *and* $\exists$ *a nondecreasing map* $\psi\in\Psi$. *Let* $(\mathfrak{B}_1)\forall\mathcal{X}_1,\mathcal{X}_2\in\mathbb{X}$, *and* $\mathfrak{t}\in\mathbb{J}$,

$$|\mathcal{F}(\mathfrak{t},\mathcal{X}_1(\mathfrak{t}))-\mathcal{F}(\mathfrak{t},\mathcal{X}_2(\mathfrak{t}))|\leq\tilde{\ell}\,\psi(|\mathcal{X}_1(\mathfrak{t})-\mathcal{X}_2(\mathfrak{t}|), \tag{17}$$

with $\mathfrak{T}(\mathcal{X}_1(\mathfrak{t}),\mathcal{X}_2(\mathfrak{t}))\geq 0$, *where* $\tilde{\ell}=(\Gamma(\nu+\omega))/(\nu T^{\nu+\omega-1}\Gamma(\nu))$.

$(\mathfrak{B}_2)$ $\mathcal{X}_0\in\mathbb{X}$ *exists so that* $\forall\mathfrak{t}\in\mathbb{J}$,

$$\mathfrak{T}(\mathcal{X}_0(\mathfrak{t}),G(\mathcal{X}_0(\mathfrak{t})))\geq 0, \tag{18}$$

and also, the inequality

$$\mathfrak{T}(\mathcal{X}_1(\mathfrak{t}),\mathcal{X}_2(\mathfrak{t}))\geq 0, \tag{19}$$

gives

$$\mathfrak{T}(G(\mathcal{X}_1(\mathfrak{t})),G(\mathcal{X}_2(\mathfrak{t})))\geq 0, \tag{20}$$

for any $\mathcal{X}_1,\mathcal{X}_2\in\mathbb{X}$ *and* $\mathfrak{t}\in\mathbb{J}$.

$(\mathfrak{B}_3)\forall\{\mathcal{X}_n\}_{n\geq 1}$ *belonging to* $\mathbb{X}$ *with* $\mathcal{X}_n\longrightarrow\mathcal{X}$ *and*

$$\mathfrak{T}(\mathcal{X}_n(\mathfrak{t}),\mathcal{X}_{n+1}(\mathfrak{t}))\geq 0, \tag{21}$$

for each n *and* $\mathfrak{t}\in\mathbb{J}$, *we get*

$$\mathfrak{T}(\mathscr{X}_n(\mathbf{t}), \mathscr{X}(\mathbf{t})) \geq 0. \tag{22}$$

In such a case, ∃ is a solution for the fractal-fractional problem (12), and so there exists a solution for the given fractal-fractional epidemic model of SARS-CoV-2 virus (6).

Proof. Let $\mathscr{X}_1$ and $\mathscr{X}_2$ be two members belonging to $\mathbb{X}$ with

$$\mathfrak{T}(\mathscr{X}_1(\mathbf{t}), \mathscr{X}_2(\mathbf{t})) \geq 0, \tag{23}$$

for each $\mathbf{t} \in \mathbb{J}$. Then, by definition of the Beta function, we may write

$$\begin{aligned} &|G(\mathscr{X}_1(\mathbf{t})) - G(\mathscr{X}_2(\mathbf{t}))| \\ &\quad \leq \frac{\nu}{\Gamma(\omega)} \int_0^{\mathbf{t}} \mathbf{m}^{\nu-1}(\mathbf{t}-\mathbf{m})^{\omega-1} |\mathscr{F}(\mathbf{m}, \mathscr{X}_1(\mathbf{m})) - \mathscr{F}(\mathbf{m}, \mathscr{X}_2(\mathbf{m}))| \, d\mathbf{m} \\ &\quad \leq \frac{\nu}{\Gamma(\omega)} \int_0^{\mathbf{t}} \mathbf{m}^{\nu-1}(\mathbf{t}-\mathbf{m})^{\omega-1} \tilde{\ell} \psi(\mathscr{X}_1(\mathbf{m}) - \mathscr{X}_2(\mathbf{m}|) d\mathbf{m} \\ &\quad \leq \frac{\nu \tilde{\ell} T^{\nu+\omega-1} \mathbb{B}(\nu, \omega)}{\Gamma(\omega)} \psi(\|\mathscr{X}_1 - \mathscr{X}_2\|_{\mathbb{X}}) \\ &\quad = \frac{\nu T^{\nu+\omega-1} \Gamma(\nu)}{\Gamma(\nu+\omega)} \tilde{\ell} \psi(\|\mathscr{X}_1 - \mathscr{X}_2\|_{\mathbb{X}}). \end{aligned} \tag{24}$$

Consequently, we have

$$\begin{aligned} \|G(\mathscr{X}_1) - G(\mathscr{X}_2)\|_{\mathbb{X}} &\leq \frac{\nu T^{\nu+\omega-1} \Gamma(\nu)}{\Gamma(\nu+\omega)} \tilde{\ell} \psi(\|\mathscr{X}_1 - \mathscr{X}_2\|_{\mathbb{X}}) \\ &= \psi(\|\mathscr{X}_1 - \mathscr{X}_2\|_{\mathbb{X}}). \end{aligned} \tag{25}$$

Now, $\phi : \mathbb{X} \times \mathbb{X} \longrightarrow [0,\infty)$ is introduced by the this rule:

$$\phi(\mathscr{X}_1, \mathscr{X}_2) = \begin{cases} 1 \text{ if } \mathfrak{T}(\mathscr{X}_1(\mathbf{t}), \mathscr{X}_2(\mathbf{t})) \geq 0, \\ 0 \text{ otherwise.} \end{cases} \tag{26}$$

Then, for every $\mathscr{X}_1, \mathscr{X}_2 \in \mathbb{X}$, we will get

$$\phi(\mathscr{X}_1, \mathscr{X}_2) \mathbf{d}(G(\mathscr{X}_1), G(\mathscr{X}_2)) \leq \psi(\mathbf{d}(\mathscr{X}_1, \mathscr{X}_2)). \tag{27}$$

Thus, G is found as an ϕ-ψ-contraction. To verify that G is ϕ-admissible, let $\mathscr{X}_1, \mathscr{X}_2 \in \mathbb{X}$ be arbitrary and $\phi(\mathscr{X}_1, \mathscr{X}_2) \geq 1$. By definition of ϕ, we have

$$\mathfrak{T}(\mathscr{X}_1(\mathbf{t}), \mathscr{X}_2(\mathbf{t})) \geq 0. \tag{28}$$

Then, by $(\mathfrak{P}_2)$, $\mathfrak{T}(G(\mathscr{X}_1(\mathbf{t})), G(\mathscr{X}_2(\mathbf{t}))) \geq 0$ is satisfied. Again, the definition of ϕ gives $\phi(G(\mathscr{X}_1), G(\mathscr{X}_2)) \geq 1$. Thus, G is ϕ-admissible.

On the other hand, the condition $(\mathfrak{P}_2)$ guarantees the existence of $\mathscr{X}_0 \in \mathbb{X}$. In this case, for each $\mathbf{t} \in \mathbb{J}$, $\mathfrak{T}(\mathscr{X}_0(\mathbf{t}), G(\mathscr{X}_0(\mathbf{t}))) \geq 0$ holds. Clearly, we get $\phi(\mathscr{X}_0, G(\mathscr{X}_0)) \geq 1$. These show that the conditions (1) and (2) of Theorem 4 are fulfilled.

Now, we assume that $\{\mathscr{X}_n\}_{n\geq 1}$ is a sequence in $\mathbb{X}$ s.t. $\mathscr{X}_n \longrightarrow \mathscr{X}$, and for all n, $\phi(\mathscr{X}_n, \mathscr{X}_{n+1}) \geq 1$. By virtue of definition of ϕ,

$$\mathfrak{T}(\mathscr{X}_n(\mathbf{t}), \mathscr{X}_{n+1}(\mathbf{t})) \geq 0. \tag{29}$$

Therefore, in the light of hypothesis $(\mathfrak{P}_3)$, we obtain

$$\mathfrak{T}(\mathscr{X}_n(\mathbf{t}), \mathscr{X}(\mathbf{t})) \geq 0. \tag{30}$$

This indicates that $\phi(\mathscr{X}_n, \mathscr{X}) \geq 1$ for every n. This guarantees the condition (3) of Theorem 4. Ultimately, by utilizing Theorem 4, we conclude that it found a fixed point for G like $\mathscr{X}^* \in \mathbb{X}$. This implies that $\mathscr{X}^* = (\mathscr{S}^*, \mathscr{P}_1^*, \mathscr{P}_2^*, \mathscr{R}^*)^T$ is interpreted as a solution of the fractal-fractional model of SARS-CoV-2 (6) and the argument is finally completed. □

In the sequel, we use the Leray-Schauder criterion to prove the existence result.

Theorem 6 (see [61]). *Regard $\mathbb{X}$ as a Banach space, $\mathbb{E}$ as a bounded closed set in $\mathbb{X}$ with the convexity property, and an open set $\mathbb{O} \subseteq \mathbb{E}$ with $0 \in \mathbb{O}$. The compact continuous map $G : \bar{\mathbb{O}} \longrightarrow \mathbb{E}$, either*

(i) G possesses fixed point in $\bar{\mathbb{O}}$ or

(ii) ∃∈$\partial\mathbb{O}$ and $\mu \in (0, 1)$ s.t. $\varkappa = \mu G(\varkappa)$.

Theorem 7. *Assume $\mathscr{F} \in C(\mathbb{J} \times \mathbb{X}, \mathbb{X})$ along with the following:*

(C1): $\varphi \in L^1(\mathbb{J}, \mathbb{R}^+)$ and an increasing map $B \in C([0,\infty), (0,\infty))$ exist provided that

$$|\mathscr{F}(\mathbf{t}, \mathscr{X}(\mathbf{t}))| \leq \varphi(\mathbf{t}) B(|\mathscr{X}(\mathbf{t})|) \tag{31}$$

(C2): There exist $\gamma > 0$ with

$$\frac{\gamma}{\Lambda + \Delta \varphi_0^* B(\gamma)} > 1, \tag{32}$$

in which $\varphi_0^* = \sup_{\mathbf{t}\in\mathbb{J}} |\varphi((t))|$ and Λ, Δ are given in () and ()

Then, a solution exists for fractal-fractional problem (12), and so a solution exists for the given fractal-fractional model of SARS-CoV-2 virus (6) on $\mathbb{J}$.

Proof. We define a map $G : \mathbb{X} \longrightarrow \mathbb{X}$ as in (15) and the ball

$$V_\varepsilon = \{\mathscr{X} \in \mathbb{X} : \|\mathscr{X}\|_{\mathbb{X}} \leq \varepsilon\}, \tag{33}$$

for some $\varepsilon > 0$. From the continuity of $\mathscr{F}$, we yield the continuity of operator G. (C1) gives

$$
\begin{aligned}
|G(\mathscr{X}(\mathbf{t}))| &\le |\mathscr{X}(0)| + \frac{\nu}{\Gamma(\omega)}\int_0^t m^{\nu-1}(\mathbf{t}-\mathbf{m})^{\omega}|\mathscr{F}(\mathbf{m},\mathscr{X}(\mathbf{m})))|\mathbf{dm} \\
&\le \mathscr{X}_0 + \frac{\nu}{\Gamma(\omega)}\int_0^t m^{\nu-1}(\mathbf{t}-\mathbf{m})^{\omega}\varphi(\mathbf{m})B(\mathscr{X}(\mathbf{m}))\mathbf{dm} \\
&\le \mathscr{X}_0 + \frac{\nu T^{\nu+\omega-1}\mathbb{B}(\nu,\omega)}{\Gamma(\omega)}\varphi_0^* B(\|\mathscr{X}\|_{\mathbb{X}}) \\
&\le \mathscr{X}_0 + \frac{\nu T^{\nu+\omega-1}\Gamma(\nu)}{\Gamma(\nu+\omega)}\varphi_0^* B(\varepsilon),
\end{aligned} \tag{34}
$$

for $\mathscr{X} \in V_\varepsilon$. Consequently, we obtain

$$
\|G(\mathscr{X}(\mathbf{t}))\| \le \mathscr{X}_0 + \frac{\nu T^{\nu+\omega-1}\Gamma(\nu)}{\Gamma(\nu+\omega)}\varphi_0^* B(\varepsilon) < \infty. \tag{35}
$$

This gives the uniformally boundedness of the operator G on $\mathbb{X}$. We now verify the equicontinuity of operator G. For the purpose, arbitrarily, take $\mathbf{t}, \mathbf{t}' \in [0, T]$ such that $\mathbf{t} < \mathbf{t}'$ and $\mathscr{X} \in V_\varepsilon$. Assuming

$$
\sup_{\mathbf{t},\mathscr{X}\in\mathbb{J}\times\mathbb{V}_\varepsilon} |\mathscr{F}(\mathbf{t},\mathscr{X}(\mathbf{t}))| = \mathscr{F}^* < \infty, \tag{36}
$$

estimate

$$
\begin{aligned}
&\left|G\left(\mathscr{X}\left(\mathbf{t}'\right)\right) - G(\mathscr{X}(\mathbf{t}))\right| \\
&= \left|\frac{\nu}{\Gamma(\omega)}\int_0^{\mathbf{t}'} m^{\nu-1}\left(\mathbf{t}'-\mathbf{m}\right)^{\omega-1}|\mathscr{F}(\mathbf{m},\mathscr{X}(\mathbf{m}))|\mathbf{dm} - \frac{\nu}{\Gamma(\omega)}\int_0^{\mathbf{t}} m^{\nu-1}(\mathbf{t}-\mathbf{m})^{\omega-1}|\mathscr{F}(\mathbf{m},\mathscr{X}(\mathbf{m}))|\mathbf{dm}\right| \\
&\le \frac{\nu\mathscr{F}^*}{\Gamma(\omega)}\left(\int_0^{\mathbf{t}'} m^{\nu-1}\left(\mathbf{t}'-\mathbf{m}\right)^{\omega-1}\mathbf{dm} - \int_0^{\mathbf{t}} m^{\nu-1}(\mathbf{t}-\mathbf{m})^{\omega}\mathbf{dm}\right) \\
&\le \frac{\nu\mathscr{F}^*\mathbb{B}(\nu,\omega)}{\Gamma(\omega)}\left[\mathbf{t}'^{\nu+\omega-1} - \mathbf{t}^{\nu+\omega-1}\right] \\
&= \frac{\nu\mathscr{F}^*\Gamma(\nu)}{\Gamma(\nu+\omega)}\left[\mathbf{t}'^{\nu+\omega-1} - \mathbf{t}^{\nu+\omega-1}\right],
\end{aligned} \tag{37}
$$

which is independent of $\mathscr{X}$, as $\mathbf{t}' \longrightarrow \mathbf{t}$, the R.H.S. of above, tends to 0. It implies that

$$
\left\|G\left(\mathscr{X}\left(\mathbf{t}'\right)\right) - G(\mathscr{X}(\mathbf{t}))\right\|_{\mathbb{X}} \longrightarrow 0. \tag{38}
$$

This confirms the equicontinuity of G. Arzelà-Ascoli's theorem implies the compactness of operator G on V_ε. The hypothesis of Theorem 6 on the operator G has now been verified. Utilizing (C2), we construct

$$
\mathbb{P} = \left\{\mathscr{X} \in \mathbb{X} : \|\mathscr{X}\|_{\mathbb{X}} < \gamma\right\}, \tag{39}
$$

for some $\gamma > 0$ via

$$
\mathscr{X}_0 + \frac{\nu T^{\nu+\omega-1}\Gamma(\nu)}{\Gamma(\nu+\omega)}\varphi_0^* B(\gamma) < \gamma. \tag{40}
$$

Utilizing (C1) and by (35), we write

$$
\|G\mathscr{X}\|_{\mathbb{X}} \le \mathscr{X}_0 + \frac{\nu T^{\nu+\omega-1}\Gamma(\nu)}{\Gamma(\nu+\omega)}\varphi_0^* B(\mathscr{X}). \tag{41}
$$

Now, we assume the existence of $\mathscr{X} \in \partial\mathbb{P}$ and $\alpha \in (0,1)$ subject to $\mathscr{X} = \alpha G(\mathscr{X})$. For such α and $\mathscr{X}$, by (41), one may write that

$$
\begin{aligned}
\gamma = \|\mathscr{X}\|_{\mathbb{X}} &= \alpha\|G\mathscr{X}\|_{\mathbb{X}} \\
&< \mathscr{X}_0 + \frac{\nu T^{\nu+\omega-1}\Gamma(\nu)}{\Gamma(\nu+\omega)}\varphi_0^* B(\|\mathscr{X}\|_{\mathbb{X}}) \\
&< \mathscr{X}_0 + \frac{\nu T^{\nu+\omega-1}\Gamma(\nu)}{\Gamma(\nu+\omega)}\varphi_0^* B(\gamma) < \gamma,
\end{aligned} \tag{42}
$$

which is impossible. Therefore, (ii) is not valid, and by Theorem 6, G possesses a fixed point in $\overline{\mathbb{P}}$. Therefore, the fractal-fractional model of SARS-CoV-2 virus (6) admits a solution and so proof is complete. □

5. Uniqueness Result

Lemma 8. *Assume* $\mathscr{S}, \mathscr{P}_1, \mathscr{P}_2, \mathscr{R}, \mathscr{S}^*, \mathscr{P}_1^*, \mathscr{P}_2^*, \mathscr{R}^* \in \mathbb{Y} = C(\mathbb{J}, \mathbb{R})$. *Let (H1)* $\|\mathscr{S}\| \le \lambda_1$, $\|\mathscr{P}_1\| \le \lambda_2$, $\|\mathscr{P}_1\| \le \lambda_3$, *and* $\|\mathscr{R}\| \le \lambda_4$ *for some* $\lambda_1, \lambda_2, \lambda_3, \lambda_4 > 0$.

Then, the kernels $\mathscr{F}_1$, $\mathscr{F}_2$, $\mathscr{F}_3$, *and* $\mathscr{F}_4$ *given in (10) satisfied the Lipschitz property w.r.t. the corresponding components if* $\varpi_1, \varpi_2, \varpi_3, \varpi_4 < 1$, *where*

$$
\begin{aligned}
\varpi_1 &= q\lambda_1 + r, \\
\varpi_2 &= r + s, \\
\varpi_3 &= r + b, \\
\varpi_4 &= r.
\end{aligned} \tag{43}
$$

Proof. Starting from the kernel $\mathscr{F}_1$, for each $\mathscr{S}, \mathscr{S}^* \in \mathbb{Y}$, we estimate

$$
\begin{aligned}
&\|\mathscr{F}_1(\mathbf{t},\mathscr{S}(\mathbf{t}),\mathscr{P}_1(\mathbf{t}),\mathscr{P}_2(\mathbf{t}),\mathscr{R}(\mathbf{t})) - \mathscr{F}_1(\mathbf{t},\mathscr{S}^*(\mathbf{t}),\mathscr{P}_1(\mathbf{t}),\mathscr{P}_2(\mathbf{t}),\mathscr{R}(\mathbf{t}))\| \\
&= \|(p - q\mathscr{S}(\mathbf{t})\mathscr{P}_2(\mathbf{t}) - r\mathscr{S}(\mathbf{t})) - (p - q\mathscr{S}^*(\mathbf{t})\mathscr{P}_2(\mathbf{t}) - r\mathscr{S}^*(\mathbf{t}))\| \\
&\le [q\|\mathscr{P}_2(\mathbf{t})\| + r]\|\mathscr{S}(\mathbf{t}) - \mathscr{S}^*(\mathbf{t})\| \\
&\le [q\lambda_3 + r]\|\mathscr{S}(\mathbf{t}) - \mathscr{S}^*(\mathbf{t})\| \\
&= \varpi_1\|\mathscr{S}(\mathbf{t}) - \mathscr{S}^*(\mathbf{t})\|.
\end{aligned} \tag{44}
$$

This shows that the kernel $\mathscr{F}_1$ is Lipschitz w.r.t. $\mathscr{S}$ with constant $\varpi_1 < 1$. Regarding the kernel function $\mathscr{F}_2$, for each $\mathscr{P}_1, \mathscr{P}_1^* \in \mathbb{Y} \coloneqq C(\mathbb{J}, \mathbb{R})$, we estimate

$$\begin{aligned}&\|\mathscr{F}_2(\mathbf{t},\mathscr{S}(\mathbf{t}),\mathscr{P}_1(\mathbf{t}),\mathscr{P}_2(\mathbf{t}),\mathscr{R}(\mathbf{t}))\\&\quad-\mathscr{F}_2(\mathbf{t},\mathscr{S}(\mathbf{t}),\mathscr{P}_1^*(\mathbf{t}),\mathscr{P}_2(\mathbf{t}),\mathscr{R}(\mathbf{t}))\|\\&=\|(q\mathscr{S}(\mathbf{t})\mathscr{P}_2(\mathbf{t})-(r+s)\mathscr{P}_1(\mathbf{t}))\\&\quad-(q\mathscr{S}^*(\mathbf{t})\mathscr{P}_2(\mathbf{t})-(r+s)\mathscr{P}_1^*(\mathbf{t}))\|\\&\le[r+s]\|\mathscr{P}_1(\mathbf{t})-\mathscr{P}_1^*(\mathbf{t})\|\\&=\varpi_2\|\mathscr{P}_1(\mathbf{t})-\mathscr{P}_1^*(\mathbf{t})\|.\end{aligned}\tag{45}$$

This leads that $\mathscr{F}_2$ is Lipschitz w.r.t. $\mathscr{P}_1$ with constant $\varpi_2<1$. Now for each $\mathscr{P}_2,\mathscr{P}_2^*\in\mathbb{Y}$, we have

$$\begin{aligned}&\|\mathscr{F}_3(\mathbf{t},\mathscr{S}(\mathbf{t}),\mathscr{P}_1(\mathbf{t}),\mathscr{P}_2(\mathbf{t}),\mathscr{R}(\mathbf{t}))\\&\quad-\mathscr{F}_3(\mathbf{t},\mathscr{S}(\mathbf{t}),\mathscr{P}_1(\mathbf{t}),\mathscr{P}_2^*(\mathbf{t}),\mathscr{R}(\mathbf{t}))\|\\&=\|(s\mathscr{P}_1(\mathbf{t})-(r+b)\mathscr{P}_2(\mathbf{t}))\\&\quad-(s\mathscr{P}_1(\mathbf{t})-(r+b)\mathscr{P}_2^*(\mathbf{t}))\|\\&\le[r+b]\|\mathscr{P}_2(\mathbf{t})-\mathscr{P}_2^*(\mathbf{t})\|\\&=\varpi_3\|\mathscr{P}_2(\mathbf{t})-\mathscr{P}_2^*(\mathbf{t})\|.\end{aligned}\tag{46}$$

This shows that $\mathscr{F}_3$ is Lipschitz w.r.t. $\mathscr{P}_2$ with constant $\varpi_3<1$. Now for each $\mathscr{R},\mathscr{R}^*\in\mathbb{Y}$, we have

$$\begin{aligned}&\|\mathscr{F}_4(\mathbf{t},\mathscr{S}(\mathbf{t}),\mathscr{P}_1(\mathbf{t}),\mathscr{P}_2(\mathbf{t}),\mathscr{R}(\mathbf{t}))\\&\quad-\mathscr{F}_4(\mathbf{t},\mathscr{S}(\mathbf{t}),\mathscr{P}_1(\mathbf{t}),\mathscr{P}_2(\mathbf{t}),\mathscr{R}^*(\mathbf{t}))\|\\&=\|(b\mathscr{P}_2(\mathbf{t})-r\mathscr{R}(\mathbf{t}))-(b\mathscr{P}_2(\mathbf{t})-r\mathscr{R}^*(\mathbf{t}))\|\\&\le[r]\|\mathscr{R}(\mathbf{t})-\mathscr{R}^*(\mathbf{t})\|=\varpi_4\|\mathscr{R}(\mathbf{t})-\mathscr{R}^*(\mathbf{t})\|.\end{aligned}\tag{47}$$

This shows that $\mathscr{F}_4$ is Lipschitz w.r.t. $\mathscr{R}$ with constant $\varpi_4<1$. From the above, we conclude that the kernels $\mathscr{F}_i, i=1,2,3,4$, are Lipschitzian w.r.t. the corresponding component with constants $\varpi_i, i=1,2,3,4$, respectively. □

We study the uniqueness result for solution to the presumed fractal-fractional model (6) based on the conclusions gained in Lemma 8.

Theorem 9. *Assume (H1), then the given fractal-fractional model of SARS-CoV-2 virus (6) has a unique solution if*

$$\frac{\nu T^{\nu+\omega-1}\Gamma(\nu)}{\Gamma(\nu+\omega)}\varpi_i<1,\ i\in 1,2,3,4.\tag{48}$$

Proof. The outcome of the theorem is assumed to be invalid. That is to say, there is another solution for the given fractional-fractal model of SARS-CoV-2 virus (6). Assume that $(\mathscr{S}^*(t),\mathscr{P}_1^*(t),\mathscr{P}_2^*(t),\mathscr{R}^*(t))$ is another solution with $(\mathscr{S}_0,,\mathscr{P}_{1,0},\mathscr{P}_{2,0},\mathscr{R})$ such that by (16), we have

$$\begin{aligned}\mathscr{S}^*(\mathbf{t})&=\mathscr{S}_0+\frac{\nu}{\Gamma(\omega)}\int_0^{\mathbf{t}}\mathbf{m}^{\nu-1}(\mathbf{t}-\mathbf{m})^{\omega-1}\mathscr{F}_1(\mathbf{m},\mathscr{S}^*(\mathbf{m})),\mathscr{P}_1^*(\mathbf{m}),\mathscr{P}_2^*(\mathbf{m}),\mathscr{R}^*(\mathbf{m})\mathbf{dm},\\\mathscr{P}_1^*(\mathbf{t})&=\mathscr{P}_{1,0}+\frac{\nu}{\Gamma(\omega)}\int_0^{\mathbf{t}}\mathbf{m}^{\nu-1}(\mathbf{t}-\mathbf{m})^{\omega-1}\mathscr{F}_2(\mathbf{m},\mathscr{S}^*(\mathbf{m})),\mathscr{P}_1^*(\mathbf{m}),\mathscr{P}_2^*(\mathbf{m}),\mathscr{R}^*(\mathbf{m})\mathbf{dm},\\\mathscr{P}_2^*(\mathbf{t})&=\mathscr{P}_{2,0}+\frac{\nu}{\Gamma(\omega)}\int_0^{\mathbf{t}}\mathbf{m}^{\nu-1}(\mathbf{t}-\mathbf{m})^{\omega-1}\mathscr{F}_3(\mathbf{m},\mathscr{S}^*(\mathbf{m})),\mathscr{P}_1^*(\mathbf{m}),\mathscr{P}_2^*(\mathbf{m}),\mathscr{R}^*(\mathbf{m})\mathbf{dm},\\\mathscr{R}^*(\mathbf{t})&=\mathscr{R}_0+\frac{\nu}{\Gamma(\omega)}\int_0^{\mathbf{t}}\mathbf{m}^{\nu-1}(\mathbf{t}-\mathbf{m})^{\omega-1}\mathscr{F}_4(\mathbf{m},\mathscr{S}^*(\mathbf{m})),\mathscr{P}_1^*(\mathbf{m}),\mathscr{P}_2^*(\mathbf{m}),\mathscr{R}^*(\mathbf{m})\mathbf{dm}.\end{aligned}\tag{49}$$

Now, we can estimate

$$\begin{aligned}|\mathscr{S}(t)-\mathscr{S}^*(t)|&\le\frac{\nu}{\Gamma(\omega)}\int_0^{\mathbf{t}}\mathbf{m}^{\nu-1}(\mathbf{t}-\mathbf{m})^{\omega-1}\\&\quad\times|\mathscr{F}_1(\mathbf{m},\mathscr{S}(\mathbf{m}),\mathscr{P}_1(\mathbf{m}),\mathscr{P}_2(\mathbf{m}),\mathscr{R}(\mathbf{m}))\\&\quad-\mathscr{F}_1(\mathbf{m},\mathscr{S}^*(\mathbf{m}),\mathscr{P}_1^*(\mathbf{m}),\mathscr{P}_2^*(\mathbf{m}),\mathscr{R}^*(\mathbf{m}))|\mathbf{dm}\\&\le\frac{\nu}{\Gamma(\omega)}\int_0^{\mathbf{t}}\mathbf{m}^{\nu-1}(\mathbf{t}-\mathbf{m})^{\omega-1}\varpi_1\|\mathscr{S}-\mathscr{S}^*\|\mathbf{dm}\\&\le\frac{\nu T^{\nu+\omega-1}\Gamma(\nu)}{\Gamma(\nu+\omega)}\varpi_1\|\mathscr{S}-\mathscr{S}^*\|,\end{aligned}\tag{50}$$

and so

$$\left[1-\frac{\nu T^{\nu+\omega-1}\Gamma(\nu)}{\Gamma(\nu+\omega)}\varpi_1\right]\|\mathscr{S}-\mathscr{S}^*\|\le 0.\tag{51}$$

It is true if $\|\mathscr{S}-\mathscr{S}^*\|=0$, and accordingly, $\mathscr{S}=\mathscr{S}^*$. Next, from

$$\|\mathscr{P}_1-\mathscr{P}_1^*\|\le\left[1-\frac{\nu T^{\nu+\omega-1}\Gamma(\nu)}{\Gamma(\nu+\omega)}\varpi_2\right]\|\mathscr{P}_1-\mathscr{P}_1^*\|,\tag{52}$$

we get

$$\left[1-\frac{\nu T^{\nu+\omega-1}\Gamma(\nu)}{\Gamma(\nu+\omega)}\varpi_2\right]\|\mathscr{P}_1-\mathscr{P}_1^*\|\leq 0. \tag{53}$$

This implies that $\|\mathscr{P}_1-\mathscr{P}_1^*\|=0$ and so $\mathscr{P}_1=\mathscr{P}_1^*$. Also, we have

$$\|\mathscr{P}_2-\mathscr{P}_2^*\|\leq\left[1-\frac{\nu T^{\nu+\omega-1}\Gamma(\nu)}{\Gamma(\nu+\omega)}\varpi_3\right]\|\mathscr{P}_2-\mathscr{P}_2^*\|. \tag{54}$$

This gives

$$\left[1-\frac{\nu T^{\nu+\omega-1}\Gamma(\nu)}{\Gamma(\nu+\omega)}\varpi_3\right]\|\mathscr{P}_2-\mathscr{P}_2^*\|\leq 0. \tag{55}$$

This implies that $\|\mathscr{P}_2-\mathscr{P}_2^*\|=0$ and so $\mathscr{P}_2=\mathscr{P}_2^*$. Finally, from

$$\|\mathscr{R}-\mathscr{R}^*\|\leq\left[1-\frac{\nu T^{\nu+\omega-1}\Gamma(\nu)}{\Gamma(\nu+\omega)}\varpi_4\right]\|\mathscr{R}-\mathscr{R}^*\|, \tag{56}$$

we get

$$\left[1-\frac{\nu T^{\nu+\omega-1}\Gamma(\nu)}{\Gamma(\nu+\omega)}\varpi_4\right]\|\mathscr{R}-\mathscr{R}^*\|\leq 0. \tag{57}$$

This implies that $\|\mathscr{R}-\mathscr{R}^*\|=0$ and so $\mathscr{R}=\mathscr{R}^*$. Consequently, we get

$$(\mathscr{S}(\mathfrak{t}),\mathscr{P}_1(\mathfrak{t}),\mathscr{P}_2(\mathfrak{t}),\mathscr{R}(\mathfrak{t}))=(\mathscr{S}^*(\mathfrak{t}),\mathscr{P}_1^*(\mathfrak{t}),\mathscr{P}_2^*(\mathfrak{t}),\mathscr{R}^*(\mathfrak{t})). \tag{58}$$

This shows that the fractal-fractional model of SARS-CoV-2 virus (6) has exactly one solution. □

6. UH and UHR Stability Criterion

We now proceed to review stable solutions in the context of the Ulam-Hyers (UH) and Ulam-Hyers-Rassias (UHR) to the given fractal-fractional model of SARS-CoV-2 virus (6).

Definition 10. The fractal-fractional model of SARS-CoV-2 virus (6) is UH-stable if $\exists 0<\mathrm{M}_{\mathscr{F}_i}\in\mathbb{R}$, $i=1,2,3,4$ s.t. $\forall\varepsilon_i>0$ and $\forall$, $(\mathscr{S}^*,\mathscr{P}_1^*,\mathscr{P}_2^*,\mathscr{R}^*)\in\mathbb{X}$ fulfilling

$$\begin{cases}\left|{}^{\mathbf{FFP}}\mathfrak{D}_{0,\mathfrak{t}}^{\omega,\nu}\mathscr{S}^*(\mathfrak{t})-\mathscr{F}_1(\mathfrak{t},\mathscr{S}^*(\mathfrak{t}),\mathscr{P}_1^*(\mathfrak{t}),\mathscr{P}_2^*(\mathfrak{t}),\mathscr{R}^*(\mathfrak{t}))\right|<\varepsilon_1,\\ \left|{}^{\mathbf{FFP}}\mathfrak{D}_{0,\mathfrak{t}}^{\omega,\nu}\mathscr{P}_1^*(\mathfrak{t})-\mathscr{F}_2(\mathfrak{t},\mathscr{S}^*(\mathfrak{t}),\mathscr{P}_1^*(\mathfrak{t}),\mathscr{P}_2^*(\mathfrak{t}),\mathscr{R}^*(\mathfrak{t}))\right|<\varepsilon_2,\\ \left|{}^{\mathbf{FFP}}\mathfrak{D}_{0,\mathfrak{t}}^{\omega,\nu}\mathscr{P}_2^*(\mathfrak{t})-\mathscr{F}_3(\mathfrak{t},\mathscr{S}^*(\mathfrak{t}),\mathscr{P}_1^*(\mathfrak{t}),\mathscr{P}_2^*(\mathfrak{t}),\mathscr{R}^*(\mathfrak{t}))\right|<\varepsilon_3,\\ \left|{}^{\mathbf{FFP}}\mathfrak{D}_{0,\mathfrak{t}}^{\omega,\nu}\mathscr{R}^*(\mathfrak{t})-\mathscr{F}_4(\mathfrak{t},\mathscr{S}^*(\mathfrak{t}),\mathscr{P}_1^*(\mathfrak{t}),\mathscr{P}_2^*(\mathfrak{t}),\mathscr{R}^*(\mathfrak{t}))\right|<\varepsilon_4.\end{cases} \tag{59}$$

There exist $(\mathscr{S},\mathscr{P}_1,\mathscr{P}_2,\mathscr{R})\in\mathbb{X}$ satisfying the given fractal-fractional model of SARS-CoV-2 virus (6) with

$$\begin{cases}|\mathscr{S}^*(\mathfrak{t})-\mathscr{S}(\mathfrak{t}))|\leq M_{\mathscr{F}_1}\varepsilon_1,\forall\mathfrak{t}\in\mathbb{J},\\ |\mathscr{P}_1^*(\mathfrak{t})-\mathscr{P}_1(\mathfrak{t}))|\leq M_{\mathscr{F}_2}\varepsilon_2,\forall\mathfrak{t}\in\mathbb{J},\\ |\mathscr{P}_2^*(\mathfrak{t})-\mathscr{P}_2(\mathfrak{t}))|\leq M_{\mathscr{F}_3}\varepsilon_3,\forall\mathfrak{t}\in\mathbb{J},\\ |\mathscr{R}^*(\mathfrak{t})-\mathscr{R}(\mathfrak{t}))|\leq M_{\mathscr{F}_4}\varepsilon_4,\forall\mathfrak{t}\in\mathbb{J}.\end{cases} \tag{60}$$

Definition 11. The given fractal-fractional model of SARS-CoV-2 virus (6) is generalized UH-stable if $\exists\mathrm{M}_{\mathscr{F}_i}\in C(\mathbb{R}^+,\mathbb{R}^+)$, $i=1,2,3,4$ with $\mathrm{M}_{\mathscr{F}_i}(0)=0$ s.t. $\forall\varepsilon_i>0$ and $\forall(\mathscr{S}^*,\mathscr{P}_1^*,\mathscr{P}_2^*,\mathscr{R}^*)\in\mathbb{X}$ fulfilling

$$\begin{cases}\left|{}^{\mathbf{FFP}}\mathfrak{D}_{0,\mathfrak{t}}^{\omega,\nu}\mathscr{S}^*(\mathfrak{t})-\mathscr{F}_1(\mathfrak{t},\mathscr{S}^*(\mathfrak{t}),\mathscr{P}_1^*(\mathfrak{t}),\mathscr{P}_2^*(\mathfrak{t}),\mathscr{R}^*(\mathfrak{t}))\right|<\varepsilon_1,\\ \left|{}^{\mathbf{FFP}}\mathfrak{D}_{0,\mathfrak{t}}^{\omega,\nu}\mathscr{P}_1^*(\mathfrak{t})-\mathscr{F}_2(\mathfrak{t},\mathscr{S}^*(\mathfrak{t}),\mathscr{P}_1^*(\mathfrak{t}),\mathscr{P}_2^*(\mathfrak{t}),\mathscr{R}^*(\mathfrak{t}))\right|<\varepsilon_2,\\ \left|{}^{\mathbf{FFP}}\mathfrak{D}_{0,\mathfrak{t}}^{\omega,\nu}\mathscr{P}_2^*(\mathfrak{t})-\mathscr{F}_3(\mathfrak{t},\mathscr{S}^*(\mathfrak{t}),\mathscr{P}_1^*(\mathfrak{t}),\mathscr{P}_2^*(\mathfrak{t}),\mathscr{R}^*(\mathfrak{t}))\right|<\varepsilon_3,\\ \left|{}^{\mathbf{FFP}}\mathfrak{D}_{0,\mathfrak{t}}^{\omega,\nu}\mathscr{R}^*(\mathfrak{t})-\mathscr{F}_4(\mathfrak{t},\mathscr{S}^*(\mathfrak{t}),\mathscr{P}_1^*(\mathfrak{t}),\mathscr{P}_2^*(\mathfrak{t}),\mathscr{R}^*(\mathfrak{t}))\right|<\varepsilon_4.\end{cases} \tag{61}$$

There exist a solution $(\mathscr{S},\mathscr{P}_1,\mathscr{P}_2,\mathscr{R})\in\mathbb{X}$ of the given fractal-fractional model of SARS-CoV-2 virus (6) with

$$\begin{cases}|\mathscr{S}^*(\mathfrak{t})-\mathscr{S}(\mathfrak{t}))|\leq M_{\mathscr{F}_1}\varepsilon_1,\forall\mathfrak{t}\in\mathbb{J},\\ |\mathscr{P}_1^*(\mathfrak{t})-\mathscr{P}_1(\mathfrak{t}))|\leq M_{\mathscr{F}_2}\varepsilon_2,\forall\mathfrak{t}\in\mathbb{J},\\ |\mathscr{P}_2^*(\mathfrak{t})-\mathscr{P}_2(\mathfrak{t}))|\leq M_{\mathscr{F}_3}\varepsilon_3,\forall\mathfrak{t}\in\mathbb{J},\\ |\mathscr{R}^*(\mathfrak{t})-\mathscr{R}(\mathfrak{t}))|\leq M_{\mathscr{F}_4}\varepsilon_4,\forall\mathfrak{t}\in\mathbb{J}.\end{cases} \tag{62}$$

Remark 12. Note that $(\mathscr{S}^*,\mathscr{P}_1^*,\mathscr{P}_2^*,\mathscr{R}^*)\in\mathbb{X}$ is a solution of (59) iff $\exists\eta_1,\eta_2,\eta_3,\eta_4\in C([0,T],\mathbb{R})$ (depending upon $\mathscr{S}^*$, $\mathscr{P}_1^*$, $\mathscr{P}_2^*$, $\mathscr{R}^*$, respectively) so that for all $\mathfrak{t}\in\mathbb{J}$,

(i) $|\eta_i(\mathfrak{t})|<\varepsilon_i$, $(i=1,2,3,4)$

(ii) We have

$$\begin{cases}\left|{}^{\mathbf{FFP}}\mathfrak{D}_{0,\mathfrak{t}}^{\omega,\nu}\mathscr{S}^*(\mathrm{t})-\mathscr{F}_1(\mathfrak{t},\mathscr{S}^*(\mathrm{t}),\mathscr{P}_1^*(\mathrm{t}),\mathscr{P}_2^*(\mathrm{t}),\mathscr{R}^*(\mathrm{t}))\right|+\eta_1(\mathrm{t}),\\ \left|{}^{\mathbf{FFP}}\mathfrak{D}_{0,\mathfrak{t}}^{\omega,\nu}\mathscr{P}_1^*(\mathrm{t})-\mathscr{F}_2(\mathfrak{t},\mathscr{S}^*(\mathrm{t}),\mathscr{P}_1^*(\mathrm{t}),\mathscr{P}_2^*(\mathrm{t}),\mathscr{R}^*(\mathrm{t}))\right|+\eta_2(\mathrm{t}),\\ \left|{}^{\mathbf{FFP}}\mathfrak{D}_{0,\mathfrak{t}}^{\omega,\nu}\mathscr{P}_2^*(\mathrm{t})-\mathscr{F}_3(\mathfrak{t},\mathscr{S}^*(\mathrm{t}),\mathscr{P}_1^*(\mathrm{t}),\mathscr{P}_2^*(\mathrm{t}),\mathscr{R}^*(\mathrm{t}))\right|\eta_3(\mathrm{t}),\\ \left|{}^{\mathbf{FFP}}\mathfrak{D}_{0,\mathfrak{t}}^{\omega,\nu}\mathscr{R}^*(\mathrm{t})-\mathscr{F}_4(\mathfrak{t},\mathscr{S}^*(\mathrm{t}),\mathscr{P}_1^*(\mathrm{t}),\mathscr{P}_2^*(\mathrm{t}),\mathscr{R}^*(\mathrm{t}))\right|\eta_4(\mathrm{t})\end{cases} \tag{63}$$

Definition 13. The fractal-fractional model of SARS-CoV-2 virus (6) is UHR-stable w.r.t. functions Ψ_i, $i=1,2,3,4$, if $\exists$ $0<\mathrm{M}_{\mathscr{F}_i,\Psi_i}\in\mathbb{R}$, $i=1,2,3,4$ s.t. $\forall\varepsilon_i>0$ and $\forall(\mathscr{S}^*,\mathscr{P}_1^*,\mathscr{P}_2^*,\mathscr{R}^*)\in\mathbb{X}$ fulfilling

$$\begin{cases} \left|{}^{FFP}\mathfrak{D}_{0,t}^{\omega,\nu}\mathcal{S}^*(t) - \mathcal{F}_1(t, \mathcal{S}^*(t), \mathcal{P}_1^*(t), \mathcal{P}_2^*(t), \mathcal{R}^*(t))\right| < \varepsilon_2\Psi_2(t). \\ \left|{}^{FFP}\mathfrak{D}_{0,t}^{\omega,\nu}\mathcal{P}_1^*(t) - \mathcal{F}_2(t, \mathcal{S}^*(t), \mathcal{P}_1^*(t), \mathcal{P}_2^*(t), \mathcal{R}^*(t))\right| < \varepsilon_2\Psi_2(t), \\ \left|{}^{FFP}\mathfrak{D}_{0,t}^{\omega,\nu}\mathcal{P}_2^*(t) - \mathcal{F}_3(t, \mathcal{S}^*(t), \mathcal{P}_1^*(t), \mathcal{P}_2^*(t), \mathcal{R}^*(t))\right| < \varepsilon_3\Psi_3(t), \\ \left|{}^{FFP}\mathfrak{D}_{0,t}^{\omega,\nu}\mathcal{R}^*(t) - \mathcal{F}_4(t, \mathcal{S}^*(t), \mathcal{P}_1^*(t), \mathcal{P}_2^*(t), \mathcal{R}^*(t))\right| < \varepsilon_4\Psi_4(t). \end{cases} \tag{64}$$

There exist $(\mathcal{S}, \mathcal{P}_1, \mathcal{P}_2, \mathcal{R}) \in \mathbb{X}$ satisfying the given fractal-fractional model of SARS-CoV-2 virus (6) with

$$\begin{cases} |\mathcal{S}^*(t) - \mathcal{S}(t))| \le M_{\mathcal{F}_1,\Psi_1}\varepsilon_1\Psi_1(t), \forall t \in \mathbb{J}, \\ |\mathcal{P}_1^*(t) - \mathcal{P}_1(t))| \le M_{\mathcal{F}_2,\Psi_1}\varepsilon_2\Psi_2(t), \forall t \in \mathbb{J}, \\ |\mathcal{P}_2^*(t) - \mathcal{P}_2(t))| \le M_{\mathcal{F}_3,\Psi_3}\varepsilon_3\Psi_3(t), \forall t \in \mathbb{J}, \\ |\mathcal{R}^*(t) - \mathcal{R}(t))| \le M_{\mathcal{F}_4,\Psi_1}\varepsilon_4\Psi_4(t), \forall t \in \mathbb{J}. \end{cases} \tag{65}$$

Definition 14. The given fractal-fractional model of SARS-CoV-2 virus (6) is generalized UHR-stable w.r.t. Ψ_i, i = 1, 2, 3, 4, if $\exists M_{\mathcal{F}_i,\Psi_i} \in \mathbb{R}$, i = 1, 2, 3, 4 with $M_{\mathcal{F}_i}(0) = 0$ s.t. $\forall \varepsilon_i > 0$ and $\forall(\mathcal{S}^*, \mathcal{P}_1^*, \mathcal{P}_2^*, \mathcal{R}^*) \in \mathbb{X}$ fulfilling

$$\begin{cases} \left|{}^{FFP}\mathfrak{D}_{0,t}^{\omega,\nu}\mathcal{S}^*(t) - \mathcal{F}_1(t, \mathcal{S}^*(t), \mathcal{P}_1^*(t), \mathcal{P}_2^*(t), \mathcal{R}^*(t))\right| < \Psi_1(t), \\ \left|{}^{FFP}\mathfrak{D}_{0,t}^{\omega,\nu}\mathcal{P}_1^*(t) - \mathcal{F}_2(t, \mathcal{S}^*(t), \mathcal{P}_1^*(t), \mathcal{P}_2^*(t), \mathcal{R}^*(t))\right| < \Psi_2(t), \\ \left|{}^{FFP}\mathfrak{D}_{0,t}^{\omega,\nu}\mathcal{P}_2^*(t) - \mathcal{F}_3(t, \mathcal{S}^*(t), \mathcal{P}_1^*(t), \mathcal{P}_2^*(t), \mathcal{R}^*(t))\right| < \Psi_3(t), \\ \left|{}^{FFP}\mathfrak{D}_{0,t}^{\omega,\nu}\mathcal{R}^*(t) - \mathcal{F}_4(t, \mathcal{S}^*(t), \mathcal{P}_1^*(t), \mathcal{P}_2^*(t), \mathcal{R}^*(t))\right| < \Psi_4(t). \end{cases} \tag{66}$$

There exist a solution $(\mathcal{S}, \mathcal{P}_1, \mathcal{P}_2, \mathcal{R}) \in \mathbb{X}$ of the given fractal-fractional model of SARS-CoV-2 virus (6) with

$$\begin{cases} |\mathcal{S}^*(t) - \mathcal{S}(t))| \le M_{\mathcal{F}_1,\Psi_1}\Psi_1(t), \forall t \in \mathbb{J}, \\ |\mathcal{P}_1^*(t) - \mathcal{P}_1(t))| \le M_{\mathcal{F}_2,\Psi_2}\Psi_2(t), \forall t \in \mathbb{J}, \\ |\mathcal{P}_2^*(t) - \mathcal{P}_2(t))| \le M_{\mathcal{F}_3,\Psi_3}\Psi_3(t), \forall t \in \mathbb{J}, \\ |\mathcal{R}^*(t) - \mathcal{R}(t))| \le M_{\mathcal{F}_4,\Psi_4}\Psi_4(t), \forall t \in \mathbb{J}. \end{cases} \tag{67}$$

Remark 15. Note that $(\mathcal{S}^*, \mathcal{P}_1^*, \mathcal{P}_2^*, \mathcal{R}^*) \in \mathbb{X}$ is a solution of (64) iff there exists $\eta_1, \eta_2, \eta_3, \eta_4 \in C([0, T], \mathbb{R})$ (depending upon $\mathcal{S}^*, \mathcal{P}_1^*, \mathcal{P}_2^*, \mathcal{R}^*$, respectively) so that for all $t \in \mathbb{J}$,

(i) $|\eta_i(t)| < \Psi_i(\mathfrak{T})\varepsilon_i$, $(i = 1, 2, 3, 4)$

(ii) We have

$$\begin{cases} {}^{FFP}\mathfrak{D}_{0,t}^{\omega,\nu}\mathcal{S}^*(t) = \mathcal{F}_1(t, \mathcal{S}^*(t), \mathcal{P}_1^*(t), \mathcal{P}_2^*(t), \mathcal{R}^*(t)) + \eta_1(t), \\ {}^{FFP}\mathfrak{D}_{0,t}^{\omega,\nu}\mathcal{P}_1^*(t) = \mathcal{F}_2(t, \mathcal{S}^*(t), \mathcal{P}_1^*(t), \mathcal{P}_2^*(t), \mathcal{R}^*(t)) + \eta_2(t). \\ {}^{FFP}\mathfrak{D}_{0,t}^{\omega,\nu}\mathcal{P}_2^*(t) = \mathcal{F}_3(t, \mathcal{S}^*(t), \mathcal{P}_1^*(t), \mathcal{P}_2^*(t), \mathcal{R}^*(t)) + \eta_3(t), \\ {}^{FFP}\mathfrak{D}_{0,t}^{\omega,\nu}\mathcal{R}^*(t) = \mathcal{F}_4(t, \mathcal{S}^*(t), \mathcal{P}_1^*(t), \mathcal{P}_2^*(t), \mathcal{R}^*(t)) + \eta_4(t) \end{cases} \tag{68}$$

Theorem 16. *The given fractal-fractional model of SARS-CoV-2 virus (6) is UH-stable on $\mathbb{J} := [0, T]$, and it is generalized UH-stable such that*

$$\frac{\nu T^{\nu+\omega-1}\Gamma(\nu)}{\Gamma(\nu+\omega)}\varpi_i < 1, i \in \{1, 2, 3, 4\}, \tag{69}$$

where ϖ_i are given by () provided that the assumption (H1) is valid.

Proof. Let $\varepsilon_1 > 0$ and $\mathcal{S}^* \in \mathbb{Y}$ be arbitrary so that

$$\left| {}^{FFP}\mathfrak{D}_{0,t}^{\omega,\nu}\mathcal{S}^*(t) - \mathcal{F}_1(t, \mathcal{S}^*(t), \mathcal{P}_1^*(t), \mathcal{P}_2^*(t), \mathcal{R}^*(t))\right| < \varepsilon_1. \tag{70}$$

Then, in view of Remark 12, we can find a function $\eta_1(t)$ satisfying

$${}^{FFP}\mathfrak{D}_{0,t}^{\omega,\nu}\mathcal{S}^{ast}(t) = \mathcal{F}_1\left(t, \mathcal{S}^{ast}(t), \mathcal{P}_1^{ast}(t), \mathcal{P}_2^{ast}(t), \mathcal{R}^*(t)\right) + \eta_1(t), \tag{71}$$

with $|\eta_1(t)| \le \varepsilon_1$. So

$$\begin{aligned} \mathcal{S}^*(t) = \mathcal{S}_0 + \frac{\nu}{\Gamma(\omega)}\int_0^t \mathfrak{m}^{\nu-1}(t-\mathfrak{m})^{\omega-1}\mathcal{F}_1(\mathfrak{m}, \mathcal{S}^*(\mathfrak{m}), \mathcal{P}_1^* \\ \cdot (\mathfrak{m}), \mathcal{P}_2^*(\mathfrak{m}), \mathcal{R}^*(\mathfrak{m}))d\mathfrak{m} \\ + \frac{\nu}{\Gamma(\omega)}\int_0^t \mathfrak{m}^{\nu-1}(t-\mathfrak{m})^{\omega-1}\eta_1(\mathfrak{m})d\mathfrak{m}. \end{aligned} \tag{72}$$

By Theorem 9, let $\mathcal{S} \in \mathbb{Y}$ be the unique solution of the given fractal-fractional model of NOV-COV-2 virus (). Then, $\mathcal{S}(t)$ is given by

$$\begin{aligned} \mathcal{S}(t) = \mathcal{S}_0 + \frac{\nu}{\Gamma(\omega)}\int_0^t \mathfrak{m}^{\nu-1}(t-\mathfrak{m})^{\omega-1}\mathcal{F}_1 \\ \cdot (\mathfrak{m}, \mathcal{S}(\mathfrak{m}), \mathcal{P}_1(\mathfrak{m}), \mathcal{P}_2(\mathfrak{m}), \mathcal{R}(\mathfrak{m}))d\mathfrak{m}. \end{aligned} \tag{73}$$

Then,

$$|\mathcal{S}^*(\mathfrak{t})-\mathcal{S}(\mathfrak{t})| \leq \frac{\nu}{\Gamma(\omega)}\int_0^{\mathfrak{t}} \mathfrak{m}^{\nu-1}(\mathfrak{t}-\mathfrak{m})^{\omega-1}|\eta_1(\mathfrak{m})|\mathbf{d}\mathfrak{m} + \frac{\nu}{\Gamma(\omega)}\int_0^{\mathfrak{t}} \mathfrak{m}^{\nu-1}(\mathfrak{t}-\mathfrak{m})^{\omega-1} \times |\mathcal{F}_1(\mathfrak{m},\mathcal{S}^*(\mathfrak{m}),\mathcal{P}_1^*(\mathfrak{m}),\mathcal{P}_2^*(\mathfrak{m}),\mathcal{R}^*(\mathfrak{m})) - \mathcal{F}_1(\mathfrak{m},\mathcal{S}(\mathfrak{m}),\mathcal{P}_1(\mathfrak{m}),\mathcal{P}_2(\mathfrak{m}),\mathcal{R}(\mathfrak{m}))|\mathbf{d}\mathfrak{m},$$

$$\leq \frac{\nu T^{\nu+\omega-1}\Gamma(\nu)}{\Gamma(\nu+\omega)}\varepsilon_1 + \frac{\nu T^{\nu+\omega-1}\Gamma(\nu)}{\Gamma(\nu+\omega)}\varpi_1\|\mathcal{S}^*-\mathcal{S}\|. \tag{74}$$

Hence, we get

$$\|\mathcal{S}^*-\mathcal{S}\| \leq \frac{\left(\left(\nu T^{\nu+\omega-1}\Gamma(\nu)\right)/(\Gamma(\nu+\omega))\right)\varepsilon_1}{1-\left(\left(\nu T^{\nu+\omega-1}\Gamma(\nu)\right)/(\Gamma(\nu+\omega))\right)\varpi_1}. \tag{75}$$

If we let $M_{\mathcal{F}_1} = ((\nu T^{\nu+\omega-1}\Gamma(\nu))/(\Gamma(\nu+\omega)))/(1-((\nu T^{\nu+\omega-1}\Gamma(\nu))/(\Gamma(\nu+\omega)))\varpi_1)$, then $\|\mathcal{S}^*-\mathcal{S}\| \leq M_{\mathcal{F}_1}\varepsilon_1$. Similarly, we have

$$\|\mathcal{P}_1^*-\mathcal{P}_1\| \leq M_{\mathcal{F}_2}\varepsilon_2, \|\mathcal{P}_2^*-\mathcal{P}_2\| \leq M_{\mathcal{F}_3}\varepsilon_3, \|\mathcal{R}^*-\mathcal{R}\| \leq M_{\mathcal{F}_4}\varepsilon_4, \tag{76}$$

where

$$M_{\mathcal{F}_i} = \frac{\left(\nu T^{\nu+\omega-1}\Gamma(\nu)\right)/(\Gamma(\nu+\omega))}{1-\left(\left(\nu T^{\nu+\omega-1}\Gamma(\nu)\right)/(\Gamma(\nu+\omega))\right)\varpi_i}, (i \in \{2,3,4\}). \tag{77}$$

Hence, the UH stability of the given fractal-fractional model (6) is fulfilled. Next, by assuming

$$M_{\mathcal{F}_i}(\varepsilon_i) = \frac{\left(\left(\nu T^{\nu+\omega-1}\Gamma(\nu)\right)/(\Gamma(\nu+\omega))\right)\varepsilon_i}{1-\left(\left(\nu T^{\nu+\omega-1}\Gamma(\nu)\right)/(\Gamma(\nu+\omega))\right)\varpi_i}, (i \in \{1,2,3,4\}), \tag{78}$$

with $M_{\mathcal{F}_i}(0)=0$, the generalized UH stability of the given fractional-fractal model (6) is fulfilled. □

In the next result, UHR stability for the given fractal-fractional model of SARS-CoV-2 (6) is studied:

Theorem 17. *The condition $(H1)$ is assumed to be held:*

(H'): ∃ increasing mappings $\Psi_i \in C([0,T],\mathbb{R}^+)$, $(i \in \{1,2,3,4\}$ and $\exists \Lambda_{\Psi_i} > 0$ such that $\forall \mathfrak{t} \in \mathbb{J}$,

$$^{\mathbf{FFP}}\mathcal{J}_{0,\mathfrak{t}}^{\omega,\nu}\Psi_i(\mathfrak{t}) < \Lambda_{\Psi_i}\Psi_i(\mathfrak{t}), (i \in \{1,2,3,4\}. \tag{79}$$

Then, the given fractal-fractional model of SARS-CoV-2 virus (6) is UHR and generalized UHR-stable.

Proof. For every $\varepsilon_1 > 0$ and $\forall \mathcal{S}^* \in \mathbb{Y}$ satisfying

$$\left|{}^{\mathbf{FFP}}\mathcal{D}_{0,\mathfrak{t}}^{\omega,\nu}\mathcal{S}^*(\mathfrak{t}) - \mathcal{F}_1(\mathfrak{t},\mathcal{S}^*(\mathfrak{t}),\mathcal{P}_1^*(\mathfrak{t}),\mathcal{P}_2^*(\mathfrak{t}),\mathcal{R}^*(\mathfrak{t}))\right| < \varepsilon_1\Psi_1(\mathfrak{t}), \quad \exists \eta(\mathfrak{t}) \text{ s.t. } {}^{\mathbf{FFP}}\mathcal{D}_{0,\mathfrak{t}}^{\omega,\nu}\mathcal{S}^*(\mathfrak{t}) = \mathcal{F}_1(\mathfrak{t},\mathcal{S}^*(\mathfrak{t}),\mathcal{P}_1^*(\mathfrak{t}),\mathcal{P}_2^*(\mathfrak{t}),\mathcal{R}^*(\mathfrak{t})) + \eta_1(\mathfrak{t}), \tag{80}$$

with $\eta_1(\mathfrak{t}) \leq \varepsilon_1\Psi_1(\mathfrak{t})$. It follows that

$$\mathcal{S}^*(\mathfrak{t}) = \mathcal{S}_0 + \frac{\nu}{\Gamma(\omega)}\int_0^{\mathfrak{t}} \mathfrak{t}^{\nu-1}(\mathfrak{t}-\mathfrak{t})^{\omega-1}\mathcal{F}_1(\mathfrak{t},\mathcal{S}^*(\mathfrak{t}),\mathcal{P}_1^*(\mathfrak{t}),\mathcal{P}_2^*(\mathfrak{t}),\mathcal{R}^*(\mathfrak{t}))\mathbf{d}\mathfrak{t} + \frac{\nu}{\Gamma(\omega)}\int_0^{\mathfrak{t}} \mathfrak{t}^{\nu-1}(\mathfrak{t}-\mathfrak{t})^{\omega-1}\eta_1(\mathfrak{t})\mathbf{d}\mathfrak{t}. \tag{81}$$

By Theorem 9, let $\mathcal{S} \in \mathbb{Y}$ be the unique solution of the given fractal-fractional model of SARS-CoV-2 virus (6). Then, $\mathcal{S}(\mathfrak{t})$ is given by

$$\mathcal{S}(\mathfrak{t}) = \mathcal{S}_0 + \frac{\nu}{\Gamma(\omega)}\int_0^{\mathfrak{t}} \mathfrak{t}^{\nu-1}(\mathfrak{t}-\mathfrak{t})^{\omega-1}\mathcal{F}_1(\mathfrak{t},\mathcal{S}(\mathfrak{t}),\mathcal{P}_1(\mathfrak{t}),\mathcal{P}_2(\mathfrak{t}),\mathcal{R}(\mathfrak{t}))\mathbf{d}\mathfrak{t}. \tag{82}$$

Then, by (61),

$$|\mathcal{S}^*(\mathfrak{t})-\mathcal{S}(\mathfrak{t})| \leq \frac{\nu}{\Gamma(\omega)}\int_0^{t} m^{\nu-1}(\mathfrak{t}-\mathfrak{m})^{\omega-1}|h_1(\mathfrak{m})|\mathbf{d}\mathfrak{m} + \frac{\nu}{\Gamma(\omega)}\int_0^{\mathfrak{t}} \mathfrak{m}^{\nu-1}(\mathfrak{t}-\mathfrak{m})^{\omega-1} \times |\mathcal{F}_1(\mathfrak{m},\mathcal{S}^*(\mathfrak{m}),\mathcal{P}_1^*(\mathfrak{m}),\mathcal{P}_2^*(\mathfrak{m}),\mathcal{R}^*(\mathfrak{m})) - \mathcal{F}_1(\mathfrak{m},\mathcal{S}(\mathfrak{m}),\mathcal{P}_1(\mathfrak{m}),\mathcal{P}_2(\mathfrak{m}),\mathcal{R}(\mathfrak{m}))\mathbf{d}\mathfrak{m}| \leq \frac{\varepsilon_1\nu}{\Gamma(\omega)}\int_0^{\mathfrak{t}} \mathfrak{m}^{\nu-1}(\mathfrak{t}-\mathfrak{m})^{\omega-1}\Psi_1(\mathfrak{m})\mathbf{d}\mathfrak{m} + \frac{\nu T^{\nu+\omega-1}\Gamma(\nu)}{\Gamma(\nu+\omega)}\varpi_1\|\mathcal{S}^*-\mathcal{S}\| \leq \varepsilon_1\Lambda_{\Psi_1}\Psi_1 + \frac{\nu T^{\nu+\omega-1}\Gamma(\nu)}{\Gamma(\nu+\omega)}\varpi_1\|\mathcal{S}^*-\mathcal{S}\|. \tag{83}$$

Accordingly, it gives

$$\|\mathcal{S}^*-\mathcal{S}\| \leq \frac{\varepsilon_1\Lambda_{\Psi_1}\Psi_1}{1-\left(\left(\nu T^{\nu+\omega-1}\Gamma(\nu)\right)/(\Gamma(\nu+\omega))\right)\varpi_1}. \tag{84}$$

If we let

$$M_{(\mathcal{F}_1,\Psi_1)} = \frac{\Lambda_{\Psi_1}}{1-\left(\left(\nu T^{\nu+\omega-1}\Gamma(\nu)\right)/(\Gamma(\nu+\omega))\right)\varpi_1}, \tag{85}$$

then $\|\mathcal{S}^* - \mathcal{S}\| \le \varepsilon_1 M_{(\mathcal{F}_1,\Psi_1)} \Psi_1$. Similarly, we have

$$\begin{aligned}\|\mathcal{P}_1^* - \mathcal{P}_1\| &\le \varepsilon_2 M_{(\mathcal{F}_2,\Psi_2)} \Psi_2, \|\mathcal{P}_2^* - \mathcal{P}_2\| \\ &\le \varepsilon_3 M_{(\mathcal{F}_3,\Psi_3)} \Psi_3, \|\mathcal{R}^* - \mathcal{R}\| \\ &\le \varepsilon_4 M_{(\mathcal{F}_4,\Psi_4)} \Psi_4,\end{aligned} \tag{86}$$

where

$$M_{(\mathcal{F}_i,\Psi_i)} = \frac{\Lambda_{\Psi_i}}{1 - \left(\left(\nu T^{\nu+\omega-1} \Gamma(\nu) \right) / \left(\Gamma(\nu+\omega) \right) \right) \varpi_i}, (i \in \{1,2,3,4\}). \tag{87}$$

Hence, the given fractal-fractional model of SARS-CoV-2 virus (6) is stable in the sense of UHR. Along with this, by setting $\varepsilon_i = 1\,; (i \in \{1,2,3,4\})$, the mentioned fractal-fractional model of SARS-CoV-2 virus (6) is generalized UHR-stable. □

7. Numerical Algorithms and Simulations

7.1. Numerical Adams-Bashforth Method. In this section, we describe the numerical scheme in relation to the fractal-fractional model of SARS-CoV-2 virus (6). For this, we have taken help from the technique regarding two-step Lagrange polynomials called fractional Adams-Bashforth method (ABM). To begin this process, we follow the numerical method of fractal-fractional integral equations (15) using a new approach at $\mathbf{t}_{n+1}$. In other words, we discretize the mentioned equation (15) for $\mathbf{t} = \mathbf{t}_{n+1}$, and we have

$$\begin{cases} \mathcal{S}(\mathbf{t}_{n+1}) = \mathcal{S}_0 + \dfrac{\nu}{\Gamma(\omega)} \displaystyle\int_0^{\mathbf{t}_{n+1}} (\mathbf{t}_{n+1} - \mathbf{m})^{\omega-1} \mathcal{H}_1(\mathbf{m})\, d\mathbf{m}, \\ \mathcal{P}_1(\mathbf{t}_{n+1}) = \mathcal{P}_{1,0} + \dfrac{\nu}{\Gamma(\omega)} \displaystyle\int_0^{\mathbf{t}_{n+1}} (\mathbf{t}_{n+1} - \mathbf{m})^{\omega-1} \mathcal{H}_2(\mathbf{m})\, d\mathbf{m}, \\ \mathcal{P}_2(\mathbf{t}_{n+1}) = \mathcal{P}_{2,0} + \dfrac{\nu}{\Gamma(\omega)} \displaystyle\int_0^{\mathbf{t}_{n+1}} (\mathbf{t}_{n+1} - \mathbf{m})^{\omega-1} \mathcal{H}_3(\mathbf{m})\, d\mathbf{m}, \\ \mathcal{R}(\mathbf{t}_{n+1}) = \mathcal{R}_0 + \dfrac{\nu}{\Gamma(\omega)} \displaystyle\int_0^{\mathbf{t}_{n+1}} (\mathbf{t}_{n+1} - \mathbf{m})^{\omega-1} \mathcal{H}_4(\mathbf{m})\, d\mathbf{m}, \end{cases} \tag{88}$$

where

$$\begin{cases} \mathcal{H}_1(\mathbf{m}) = \mathbf{m}^{\nu-1} \mathcal{F}_1(\mathbf{m}, \mathcal{S}(\mathbf{m}), \mathcal{P}_1(\mathbf{m}), \mathcal{P}_2(\mathbf{m}), \mathcal{R}(\mathbf{m})), \\ \mathcal{H}_2(\mathbf{m}) = \mathbf{m}^{\nu-1} \mathcal{F}_2(\mathbf{m}, \mathcal{S}(\mathbf{m}), \mathcal{P}_1(\mathbf{m}), \mathcal{P}_2(\mathbf{m}), \mathcal{R}(\mathbf{m})), \\ \mathcal{H}_3(\mathbf{m}) = \mathbf{m}^{\nu-1} \mathcal{F}_3(\mathbf{m}, \mathcal{S}(\mathbf{m}), \mathcal{P}_1(\mathbf{m}), \mathcal{P}_2(\mathbf{m}), \mathcal{R}(\mathbf{m})), \\ \mathcal{H}_4(\mathbf{m}) = \mathbf{m}^{\nu-1} \mathcal{F}_4(\mathbf{m}, \mathcal{S}(\mathbf{m}), \mathcal{P}_1(\mathbf{m}), \mathcal{P}_2(\mathbf{m}), \mathcal{R}(\mathbf{m})). \end{cases} \tag{89}$$

By approximating above integrals, we get

$$\begin{cases} \mathcal{S}(\mathbf{t}_{n+1}) = \mathcal{S}_0 + \dfrac{\nu}{\Gamma(\omega)} \displaystyle\sum_{l=0}^{n} \int_{\mathbf{t}_l}^{\mathbf{t}_{l+1}} (\mathbf{t}_{n+1} - \mathbf{m})^{\omega-1} \mathcal{H}_1(\mathbf{m}) d\mathbf{m}, \\ \mathcal{P}_1(\mathbf{t}_{n+1}) = \mathcal{P}_{1,0} + \dfrac{\nu}{\Gamma(\omega)} \displaystyle\sum_{l=0}^{n} \int_{\mathbf{t}_l}^{\mathbf{t}_{l+1}} (\mathbf{t}_{n+1} - \mathbf{m})^{\omega-1} \mathcal{H}_2(\mathbf{m}) d\mathbf{m}, \\ \mathcal{P}_2(\mathbf{t}_{n+1}) = \mathcal{P}_{2,0} + \dfrac{\nu}{\Gamma(\omega)} \displaystyle\sum_{l=0}^{n} \int_{\mathbf{t}_l}^{\mathbf{t}_{l+1}} (\mathbf{t}_{n+1} - \mathbf{m})^{\omega-1} \mathcal{H}_3(\mathbf{m}) d\mathbf{m}, \\ \mathcal{R}(\mathbf{t}_{n+1}) = \mathcal{R}_0 + \dfrac{\nu}{\Gamma(\omega)} \displaystyle\sum_{l=0}^{n} \int_{\mathbf{t}_l}^{\mathbf{t}_{l+1}} (\mathbf{t}_{n+1} - \mathbf{m})^{\omega-1} \mathcal{H}_4(\mathbf{m}) d\mathbf{m}. \end{cases} \tag{90}$$

In the sequel, we approximate the functions $\mathcal{H}_1, \mathcal{H}_2, \mathcal{H}_3$, and $\mathcal{H}_4$, introduced by (89), on the interval $[\mathbf{t}_l, \mathbf{t}_{l+1}]$ via two-step Lagrange interpolation polynomials with the step size $\mathbf{h} = \mathbf{t}_l - \mathbf{t}_{l-1}$ as

$$\begin{aligned} \mathcal{H}_{1,l}^*(\mathbf{m}) &\simeq \frac{\mathbf{m} - \mathbf{t}_{l-1}}{\mathbf{h}} \mathbf{t}_l^{\nu-1} \mathcal{F}_1(\mathbf{m}_l, \mathcal{S}_l, \mathcal{P}_{1,l}, \mathcal{P}_{2,l}, \mathcal{R}_l) \\ &\quad - \frac{\mathbf{m} - \mathbf{t}_l}{\mathbf{h}} \mathbf{t}_{l-1}^{\nu-1} \mathcal{F}_1(\mathbf{m}_{l-1}, \mathcal{S}_{l-1}, \mathcal{P}_{1,l-1}, \mathcal{P}_{2,l-1}, \mathcal{R}_{l-1}), \\ \mathcal{H}_{2,l}^*(\mathbf{m}) &\simeq \frac{\mathbf{m} - \mathbf{t}_{l-1}}{\mathbf{h}} \mathbf{t}_l^{\nu-1} \mathcal{F}_2(\mathbf{m}_l, \mathcal{S}_l, \mathcal{P}_{1,l}, \mathcal{P}_{2,l}, \mathcal{R}_l) \\ &\quad - \frac{\mathbf{m} - \mathbf{t}_l}{\mathbf{h}} \mathbf{t}_{l-1}^{\nu-1} \mathcal{F}_2(\mathbf{m}_{l-1}, \mathcal{S}_{l-1}, \mathcal{P}_{1,l-1}, \mathcal{P}_{2,l-1}, \mathcal{R}_{l-1}), \\ \mathcal{H}_{3,l}^*(\mathbf{m}) &\simeq \frac{\mathbf{m} - \mathbf{t}_{l-1}}{\mathbf{h}} \mathbf{t}_l^{\nu-1} \mathcal{F}_3(\mathbf{m}_l, \mathcal{S}_l, \mathcal{P}_{1,l}, \mathcal{P}_{2,l}, \mathcal{R}_l) \\ &\quad - \frac{\mathbf{m} - \mathbf{t}_l}{\mathbf{h}} \mathbf{t}_{l-1}^{\nu-1} \mathcal{F}_3(\mathbf{m}_{l-1}, \mathcal{S}_{l-1}, \mathcal{P}_{1,l-1}, \mathcal{P}_{2,l-1}, \mathcal{R}_{l-1}), \\ \mathcal{H}_{4,l}^*(\mathbf{m}) &\simeq \frac{\mathbf{m} - \mathbf{t}_{l-1}}{\mathbf{h}} \mathbf{t}_l^{\nu-1} \mathcal{F}_4(\mathbf{m}_l, \mathcal{S}_l, \mathcal{P}_{1,l}, \mathcal{P}_{2,l}, \mathcal{R}_l) \\ &\quad - \frac{\mathbf{m} - \mathbf{t}_l}{\mathbf{h}} \mathbf{t}_{l-1}^{\nu-1} \mathcal{F}_4(\mathbf{m}_{l-1}, \mathcal{S}_{l-1}, \mathcal{P}_{1,l-1}, \mathcal{P}_{2,l-1}, \mathcal{R}_{l-1}). \end{aligned} \tag{91}$$

Then, we have

$$\begin{cases} \mathcal{S}(\mathbf{t}_{n+1}) = \mathcal{S}_0 + \dfrac{\nu}{\Gamma(\omega)} \displaystyle\sum_{l=0}^{n} \int_{\mathbf{t}_l}^{\mathbf{t}_{l+1}} (\mathbf{t}_{n+1} - \mathbf{m})^{\omega-1} \mathcal{H}_{1,l}^*(\mathbf{m}) d\mathbf{m}, \\ \mathcal{P}_1(\mathbf{t}_{n+1}) = \mathcal{P}_{1,0} + \dfrac{\nu}{\Gamma(\omega)} \displaystyle\sum_{l=0}^{n} \int_{\mathbf{t}_l}^{\mathbf{t}_{l+1}} (\mathbf{t}_{n+1} - \mathbf{m})^{\omega-1} \mathcal{H}_{2,l}^*(\mathbf{m}) d\mathbf{m}, \\ \mathcal{P}_2(\mathbf{t}_{n+1}) = \mathcal{P}_{2,0} + \dfrac{\nu}{\Gamma(\omega)} \displaystyle\sum_{l=0}^{n} \int_{\mathbf{t}_l}^{\mathbf{t}_{l+1}} (\mathbf{t}_{n+1} - \mathbf{m})^{\omega-1} \mathcal{H}_{3,l}^*(\mathbf{m}) d\mathbf{m}, \\ \mathcal{R}(\mathbf{t}_{n+1}) = \mathcal{R}_0 + \dfrac{\nu}{\Gamma(\omega)} \displaystyle\sum_{l=0}^{n} \int_{\mathbf{t}_l}^{\mathbf{t}_{l+1}} (\mathbf{t}_{n+1} - \mathbf{m})^{\omega-1} \mathcal{H}_{4,l}^*(\mathbf{m}) d\mathbf{m}. \end{cases} \tag{92}$$

By evaluating above integrals directly, the approximate solutions of the given fractional-fractal model of SARS-CoV-2 virus (6) are given by

$$\begin{aligned}
\mathcal{S}_{n+1} &= \mathcal{S}_0 + \frac{\nu \mathbf{h}^{\omega}}{\Gamma(\omega+2)} \sum_{l=0}^{n} \Big[\mathbf{t}_l^{\nu-1} \mathcal{F}_1(\mathbf{t}_l, \mathcal{S}_l, \mathcal{P}_{1,l}, \mathcal{P}_{2,l}, \mathcal{R}_l) Y_{(n,l)} \\
&\quad - \mathbf{t}_{l-1}^{\nu-1} \mathcal{F}_1(\mathbf{t}_{l-1}, \mathcal{S}_{l-1}, \mathcal{P}_{1,l-1}, \mathcal{P}_{2,l-1}, \mathcal{R}_{l-1}) \widehat{Y}_{(n,l)} \Big], \\
\mathcal{P}_{1,n+1} &= \mathcal{P}_{1,0} + \frac{\nu \mathbf{h}^{\omega}}{\Gamma(\omega+2)} \sum_{l=0}^{n} \Big[\mathbf{t}_l^{\nu-1} \mathcal{F}_2(\mathbf{t}_l, \mathcal{S}_l, \mathcal{P}_{1,l}, \mathcal{P}_{2,l}, \mathcal{R}_l) Y_{(n,l)} \\
&\quad - \mathbf{t}_{l-1}^{\nu-1} \mathcal{F}_2(\mathbf{t}_{l-1}, \mathcal{S}_{l-1}, \mathcal{P}_{1,l-1}, \mathcal{P}_{2,l-1}, \mathcal{R}_{l-1}) \widehat{Y}_{(n,l)} \Big], \\
\mathcal{P}_{2,n+1} &= \mathcal{P}_{2,0} + \frac{\nu \mathbf{h}^{\omega}}{\Gamma(\omega+2)} \sum_{l=0}^{n} \Big[\mathbf{t}_l^{\nu-1} \mathcal{F}_3(\mathbf{t}_l, \mathcal{S}_l, \mathcal{P}_{1,l}, \mathcal{P}_{2,l}, \mathcal{R}_l) Y_{(n,l)} \\
&\quad - \mathbf{t}_{l-1}^{\nu-1} \mathcal{F}_3(\mathbf{t}_{l-1}, \mathcal{S}_{l-1}, \mathcal{P}_{1,l-1}, \mathcal{P}_{2,l-1}, \mathcal{R}_{l-1}) \widehat{Y}_{(n,l)} \Big], \\
\mathcal{R}_{n+1} &= \mathcal{R}_0 + \frac{\nu \mathbf{h}^{\omega}}{\Gamma(\omega+2)} \sum_{l=0}^{n} \Big[\mathbf{t}_l^{\nu-1} \mathcal{F}_4(\mathbf{t}_l, \mathcal{S}_l, \mathcal{P}_{1,l}, \mathcal{P}_{2,l}, \mathcal{R}_l) Y_{(n,l)} \\
&\quad - \mathbf{t}_{l-1}^{\nu-1} \mathcal{F}_4(\mathbf{t}_{l-1}, \mathcal{S}_{l-1}, \mathcal{P}_{1,l-1}, \mathcal{P}_{2,l-1}, \mathcal{R}_{l-1}) \widehat{Y}_{(n,l)} \Big],
\end{aligned} \tag{93}$$

where

$$\begin{aligned}
Y_{(n,l)} &= (n+1-l)^{\omega}(n-l+2+\omega) - (n-l)^{\omega}(n-l+2+2\omega), \\
\widehat{Y}_{(n,l)} &= (n+1-l)^{\omega+1} - (n-l)^{\omega}(n-l+1+\omega),
\end{aligned} \tag{94}$$

where ω is the fractional order of the given fractal-fractional system (6).

7.2. Simulations Based on Adams-Bashforth Method. In this section, using the AB method for fractal-fractional, we present approximate solutions for the fractal-fractional probability-based model of SARS-CoV-2 virus (6). We demonstrate simulations to observe the behavior of four subclasses of SARS-CoV-2, which are $\mathcal{S}$, $\mathcal{P}_1$, $\mathcal{P}_2$, and $\mathcal{R}$ under the different set of parameters.

To provide a numerical simulation, we start by determining the value of the parameters by using reported cases in Turkey from 01 January 2021 to 03 July 2021. The birth rate for the Turkey in 2021 is 15.408 births per 1000 people, and the death rate is $b_1 = 5.5$ per 1000 people. The Turkey's population on 1st of January was $\mathcal{N} = 84339067$. Since we use the day as time limit, we can calculate the newborn rate as $\Theta = (84339067 \times 15.408)/(1000 \times 365)$. To estimate the remaining parameters, we use the curve fitting technique with the data reported for SARS-CoV-2. Using this method, we determine the parameters as follows: $p = 0.4$, $r = 0.003$, $s = 0.05$, $b = 0.05$, $r_1 = 0.05$, and $r_2 = 0.6$, and we assume $q = 0.2$, $b_2 = 0.04$, and $b_3 = 0.6$. Also, the stepsize for the time interval is choosen as $h = 10^{-3}$. As a first visualization, in Figure 1, we demonstrate the real data versus present model simulation. Then, behaviors of four subclasses are presented

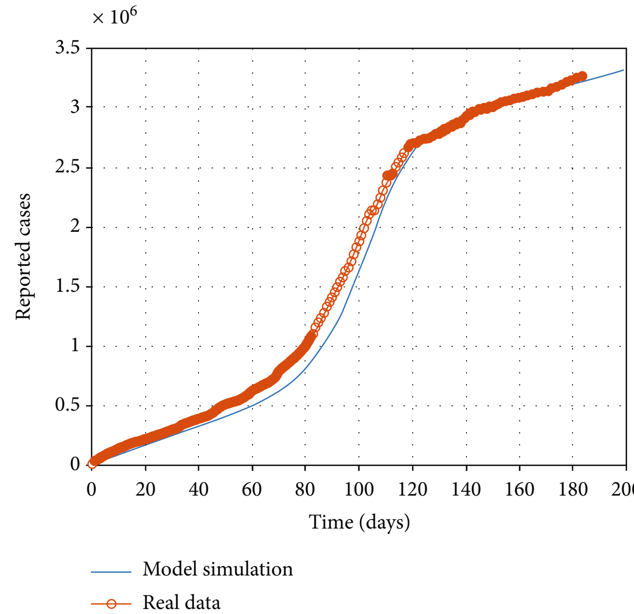

FIGURE 1: Simulated data vs. Real data for the SARS-CoV-2 cases in Turkey from 01 January 2021 to 03 July 2021.

in Figures 2(a)–2(d) with the chosen initial values $\mathcal{S} = 100$, $\mathcal{P}_1 = 90$, $\mathcal{P}_2 = 80$, and $\mathcal{R} = 70$, respectively, and under various fractal-fractional orders ω and ν.

Now, we simulate and discuss the dynamics of the model based on the parameters provided by [60]. Based on this source, we assume $\Theta = 30$, $r = 0.003$, $s = 0.05$, $b = 0.05$, $b_1 = 0.05$, $p = 0.4$, $b_2 = 0.04$, $r_1 = 0.05$, $q = 0.2$, $b_3 = 0.6$, and $r_2 = 0.6$. Finally, the initial values for state functions are $\mathcal{S}(0) = 0.5$, $\mathcal{P}_1(0) = 0.3$, $\mathcal{P}_2(0) = 0.2$, and $\mathcal{R}(0) = 0.1$. In different figures, we will show the behaviors of four state functions $\mathcal{S}$, $\mathcal{P}_1$, $\mathcal{P}_2$, and $\mathcal{R}$ by assuming different values for fractal and fractional orders $\omega = \nu = 1.00, 0.99, 0.98, 0.97, 0.96, 0.95$.

In Figures 3(a) and 3(b), we illustrate the obtained dynamics of all four state functions $\mathcal{S}$, $\mathcal{P}_1$, $\mathcal{P}_2$, and $\mathcal{R}$ by the use of ABM with the vaccination rate (a) $b = 0.05$ and (b) $b = 0.1$, respectively. The great impact of the vaccine can be clearly observed from these illustrations as increasing the vaccination rate decreases the infected population and increases the recovered population.

In Figure 4, the susceptible subclass $\mathcal{S}(t)$ is demonstrated with the initial value $\mathcal{S}(0) = 0.5$. From this illustration, we observed that the graphs of this category of people converge quickly to a stable case at higher fractal-fractional orders and slowly to such a stable case at lower fractal-fractional orders. Also, we can see that by increasing the fractal-fractional orders, the density of $\mathcal{S}(t)$ also increases.

In Figure 5, the asymptomatic subclass $\mathcal{P}_1(t)$ is demonstrated with the initial value $\mathcal{P}_1(t) = 0.3$. From this illustration, we observed that the graphs of this category of people converge quickly to a stable case at higher fractal-fractional orders and slowly to such a stable case at lower fractal-fractional orders. Also, we can see that by increasing the fractal-fractional orders, the density of asymptomatic category $\mathcal{P}_1(t)$ also increases.

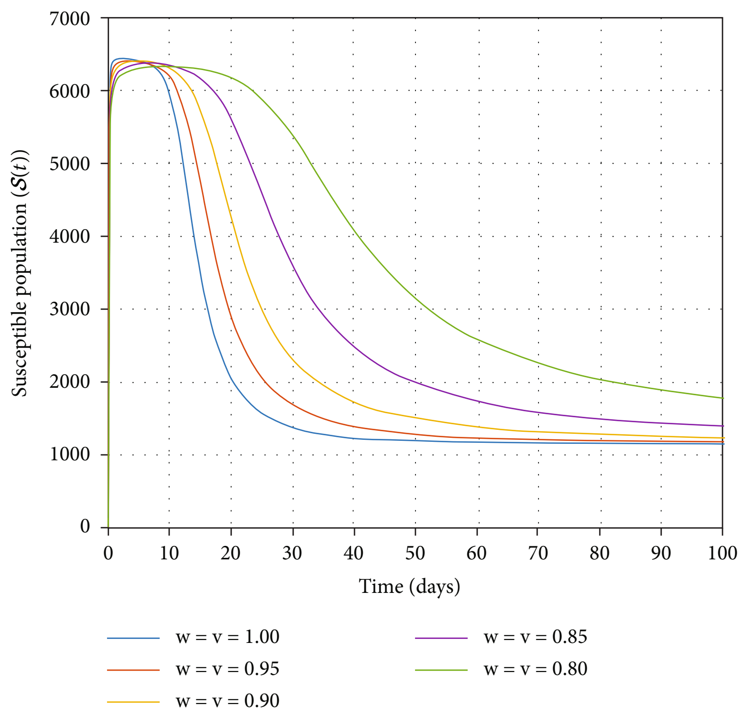

(a)

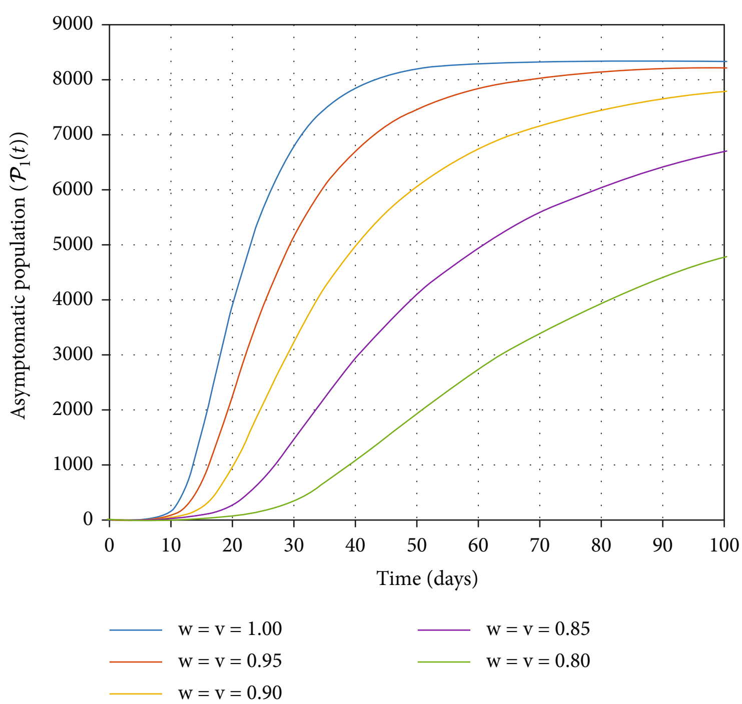

(b)

FIGURE 2: Continued.

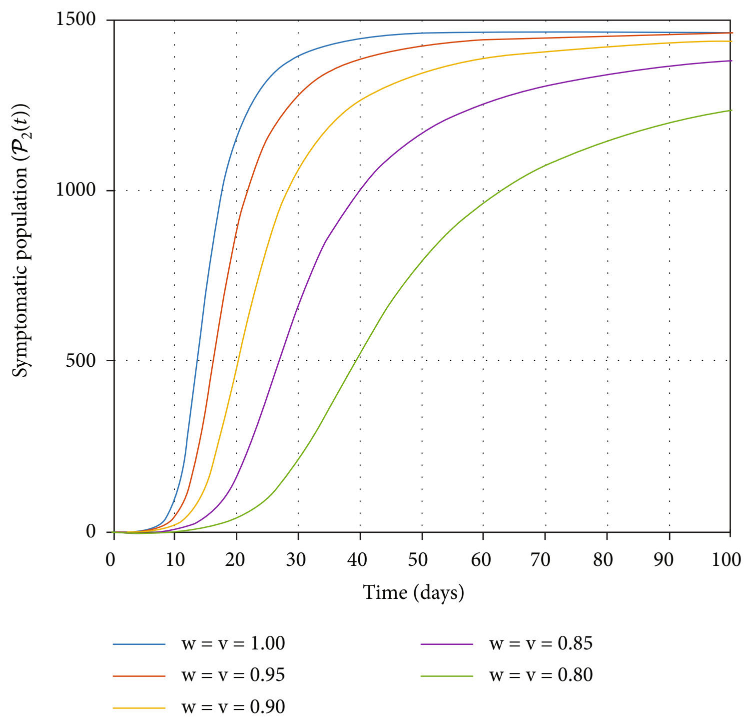

(c)

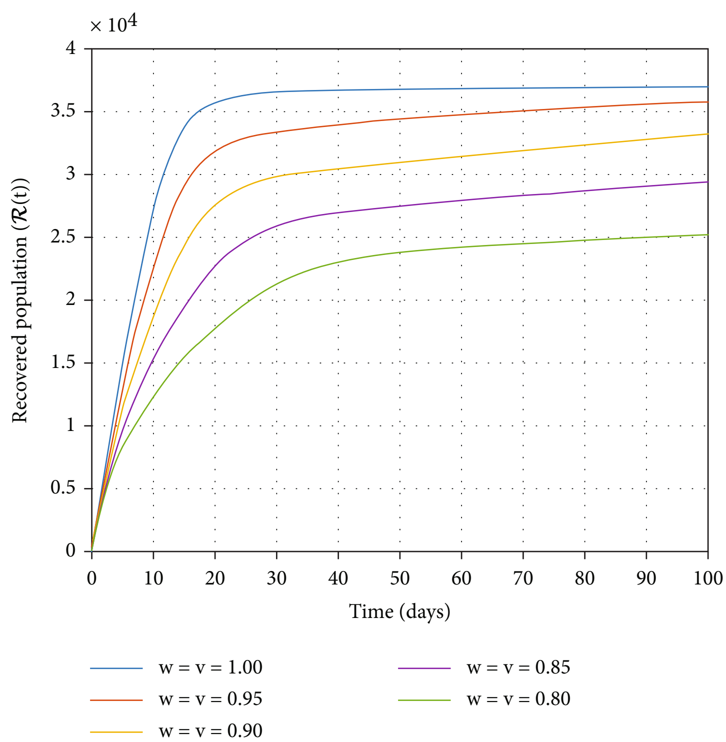

(d)

Figure 2: Behaviors of each compartments: (a) $\mathcal{S}(t)$, (b) $\mathcal{P}_1(t)$, (c) $\mathcal{P}_2(t)$, and (d) $\mathcal{R}(t)$ under various fractal-fractional orders $\omega = \nu = 1, 0.95, 0.90, 0.85, 0.80$ with the estimated parameters from the reported data.

In Figure 6, the symptomatic subclass $\mathcal{P}_2(t)$ is presented with the initial value $\mathcal{P}_2(t) = 0.2$. From this illustration, we can see that the graphs of this category of people converge quickly to a stable case at higher fractal-fractional orders and slowly to such a stable case at lower fractal-fractional orders. Also, we can see that by increasing the fractal-fractional orders, the density of symptomatic category $\mathcal{P}_2(t)$ also increases.

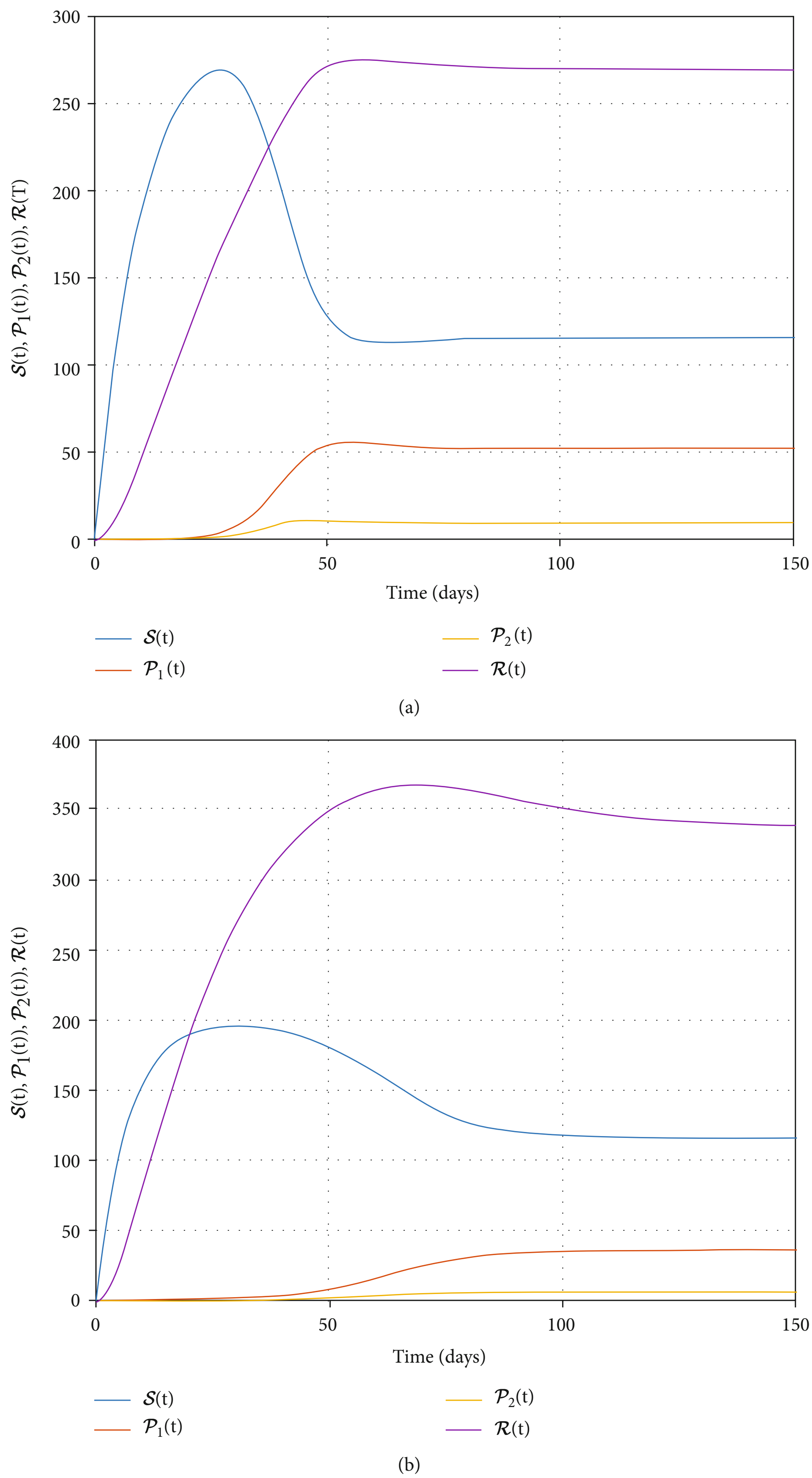

(b)

Figure 3: Behaviors of four trajectories for (a) vaccination rate $b = 0.05$ and (b) vaccination rate $b = 0.1$, under fractal-fractional order $\omega = \nu = 1$.

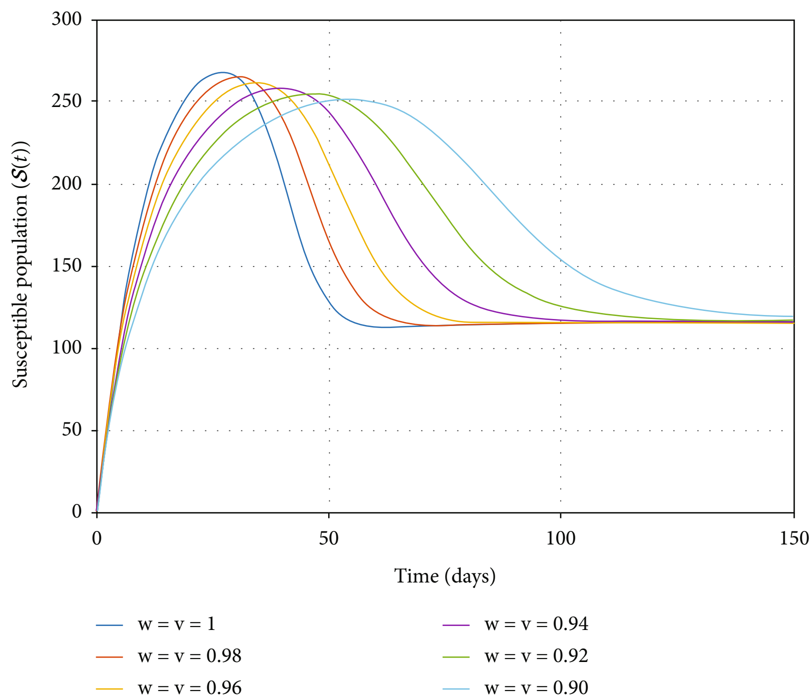

Figure 4: Behavior of $\mathcal{S}(t)$ by changing fractal-fractional order ω and v.

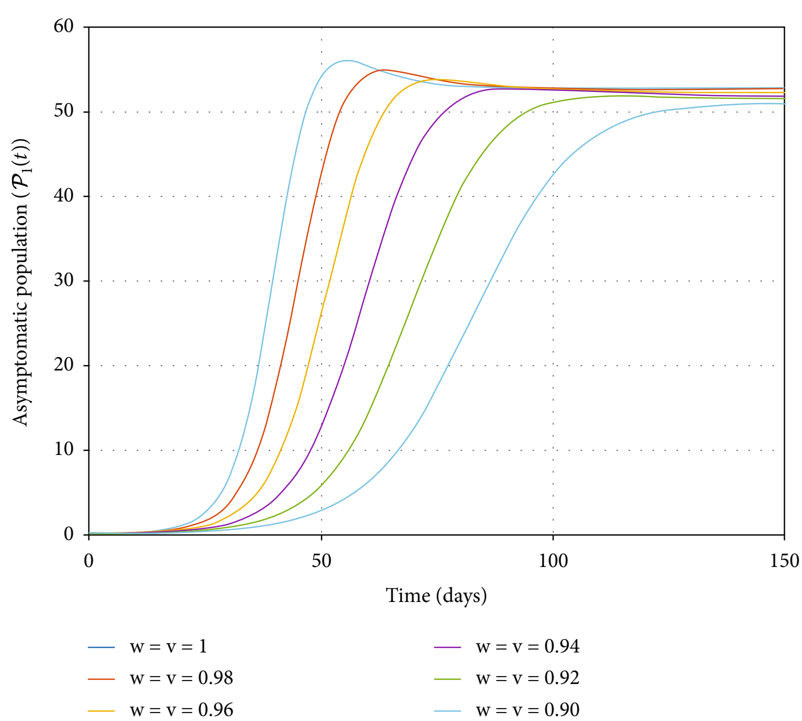

Figure 5: Behavior of $\mathcal{P}_1(t)$ by changing fractal-fractional order ω and v.

In Figure 7, the recovered category $\mathcal{R}(t)$ is demonstrated with the initial value $\mathcal{R}(t) = 0.1$. From this illustration, we observed that the graphs of this category of people converge quickly to a stable case at higher fractal-fractional orders and slowly to such a stable case at lower fractal-fractional orders. Also, we can see that by increasing the fractal-fractional orders, the density of recovered population $\mathcal{R}(t)$ also increases.

It is seen that the graphs of all four category of people have the similar behaviors regarding to different values of

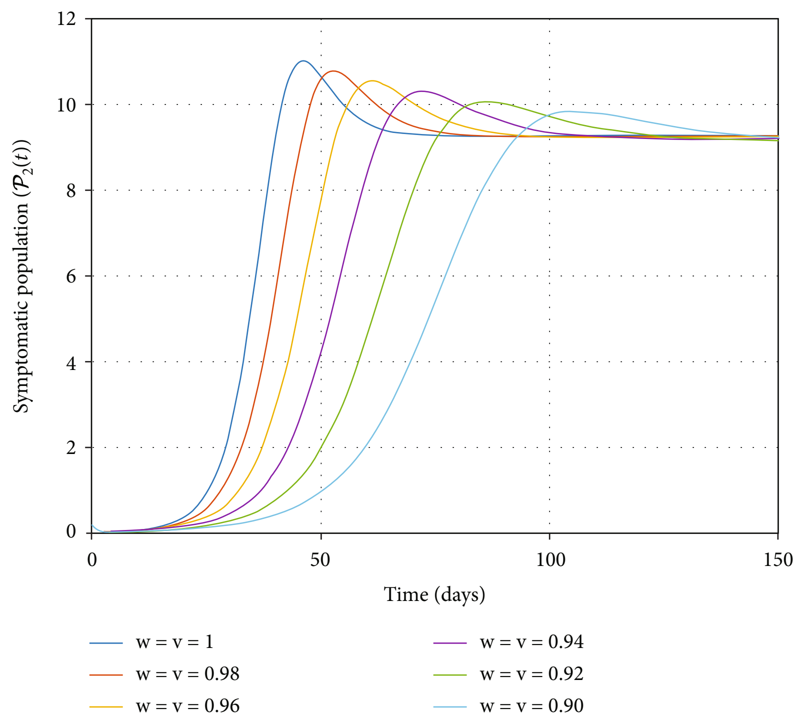

FIGURE 6: Behavior of $\mathscr{P}_2(t)$ by changing fractal-fractional order ω and v.

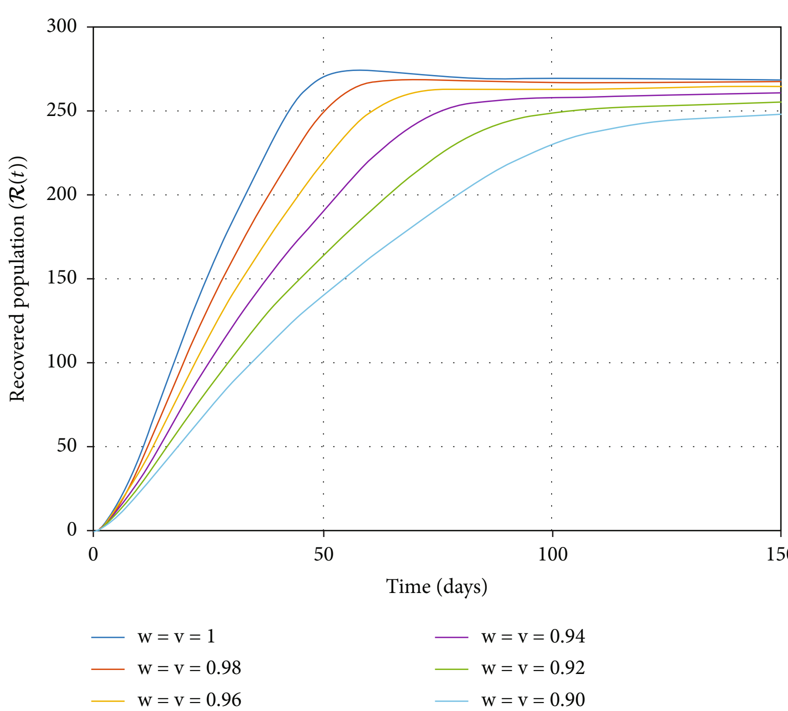

FIGURE 7: Behavior of $\mathscr{R}(t)$ by changing fractal-fractional order ω and v.

fractal-fractional orders, and they converge quickly to a stable case at higher fractal-fractional orders and slowly to such a stable case at lower fractal-fractional orders. Also, the densities of all four group of population are increasing as the fractal-fractional order increases.

8. Model Dynamics in the Caputo Sense

In this section, we convert the presented fractal-fractional epidemic probability-based model of SARS-CoV-2 virus (6) into a Caputo-type model. The main motivation of this replacement is to compare the proposed model in two different type and capture the memory effects on the given model by using different fractional-order dynamics. The new formulation of the proposed model is as follows:

$$\begin{cases} {}^{C}\mathfrak{D}_{0,t}^{\omega}\mathcal{S}(t) = \Theta - r\mathcal{P}_1(t)\mathcal{S}(t) - rs\mathcal{P}_2(t)\mathcal{S}(t) - (b + b_1)\mathcal{S}(t), \\ {}^{C}\mathfrak{D}_{0,t}^{\omega}\mathcal{P}_1(t) = p[r\mathcal{P}_1(t)\mathcal{S}(t) + rs\mathcal{P}_2(t)\mathcal{S}(t)] - (b_1 + b_2 + r_1)\mathcal{P}_1(t), \\ {}^{C}\mathfrak{D}_{0,t}^{\omega}\mathcal{P}_2(t) = (1-p)[r\mathcal{P}_1(t)\mathcal{S}(t) + rs\mathcal{P}_2(t)\mathcal{S}(t)] + qr_1\mathcal{P}_1(t) - (b_1 + b_3 + r_2)\mathcal{P}_2(t), \\ {}^{C}\mathfrak{D}_{0,t}^{\omega}\mathcal{R}(t) = r_1(1-q)\mathcal{P}_1(t) + r_2\mathcal{P}_2(t) + b\mathcal{S}(t) - b_1\mathcal{R}(t), \end{cases} \quad (95)$$

where

$${}^{\mathbf{C}}\mathfrak{D}_{0,t}^{\omega}u(t) = {}^{\mathbf{RL}}\mathfrak{I}_{0,t}^{\eta-\omega}\left(\frac{d^{\eta}}{dt^{\eta}}u(t)\right), \eta - 1 < \omega \le \eta, \eta \in \mathbb{N}. \quad (96)$$

The Caputo fractional derivative satisfies the Newton–Leibniz formula for every $0 < \omega < 1$, that is,

$${}^{\mathbf{RL}}\mathfrak{I}_{0,t}^{\omega}\left({}^{\mathbf{C}}\mathfrak{D}_{0,t}^{\omega}u(t)\right) = u(t) - \sum_{j=0}^{\lceil\omega\rceil-1} u^{(j)}(0)\frac{t^j}{j!}. \quad (97)$$

In recent years, many researchers have developed a number of numerical methods to solve different types of fractional-order models. In this section, our aim is to use a new method called the FTOMM (see ref. [62, 63]) method (fractional Taylor operational matrix method), to solve the probability-based model of the SARS-CoV-2 virus (95) in the Caputo settings.

8.1. Function Approximation and Operational Matrix. The Taylor vector of the fractional order is given as [64]

$$T_{n\kappa} = \left[1, t^{\kappa}, t^{2\kappa}, \cdots, t^{n\kappa}\right], \quad (98)$$

where $n \in \mathbb{N}$ and $\kappa > 0$. Let $T_{n\kappa} \subset S$ where $S \in L^2[0, 1]$. For any $\varphi \in M$, since $M = \text{span}\{1, t^{\kappa}, t^{2\kappa}, \cdots, t^{n\kappa}\}$ is a vector space of finite dimension in S, thus φ possesses a unique best apporoximation φ_*, that is,

$$\forall\widehat{\varphi} \in M, \|\varphi - \varphi_*\| \le \|\varphi - \widehat{\varphi}\|. \quad (99)$$

Then, the function φ is approximated by the fractional-order Taylor vector by

$$\varphi \simeq \varphi_* = \sum_{j=0}^{n} g_j t^{j\kappa} = G^T T_{n\kappa}, \quad (100)$$

where $G^T = [g_0, g_1, \cdots, g_m]$ are the unique coefficients.

Consider $F_{(t,\omega)}$ as an operational matrix of ω^{th}-integration with $(m+1)^2$ dimension. Then, the ω^{th}-R-L-integration of the Taylor vector defined in equation (98) is

$${}^{\mathbf{RL}}\mathfrak{I}_{0,t}^{\omega}T_{n\kappa}(t) = F_{(t,\omega)}T_{nk}(t). \quad (101)$$

By applying the ω^{th}-R-L integral for $T_{n\kappa}$, it becomes

$${}^{\mathbf{RL}}\mathfrak{I}_{0,t}^{\omega}(T_{n\kappa}(t)) = \left[\frac{1}{\Gamma(\omega+1)}t^{\omega}, \frac{\Gamma(\kappa+1)}{\Gamma(\kappa+\omega+1)}t^{\kappa+\omega}, \cdots, \frac{\Gamma(n\kappa+1)}{\Gamma(n\kappa+\omega+1)}t^{n\kappa+\omega}\right]. \quad (102)$$

Thus, (102) can be reformulated as

$${}^{\mathbf{RL}}\mathfrak{I}_{0,t}^{\omega}(T_{n\kappa}(t)) = t^{\omega}S_{\omega}T_{n\kappa}(t), \quad (103)$$

where

$$S_{\omega} = \text{diag}\left[\frac{1}{\Gamma(\omega+1)}, \frac{\Gamma(\kappa+1)}{\Gamma(\kappa+\omega+1)}, \frac{\Gamma(2\kappa+1)}{\Gamma(2\kappa+\omega+1)}, \cdots, \frac{\Gamma(n\kappa+1)}{\Gamma(n\kappa+\omega+1)}\right]. \quad (104)$$

Set $\Phi_{(t,\omega)} = t^{\omega}S_{\omega}$. In this case, the fractional Taylor operational matrix of integration is reformulated by

$$F_{(t,\omega)} = \text{diag}\left[\Phi_{(t,\omega)}, \Phi_{(t,\omega)}, \cdots, \Phi_{(t,\omega)}\right]. \quad (105)$$

The product of two Taylor basis vectors is

$${}^{\mathbf{RL}}\mathfrak{I}_{0,t}^{\omega}\left(T_{n\kappa}(t)T_{n\kappa}^T(t)\right) = t^{\omega}P_{\omega} * \left(T_{n\kappa}(t)T_{n\kappa}^T(t)\right), \quad (106)$$

where

$$P_\omega = \begin{bmatrix} \frac{1}{\Gamma(\omega+1)} & \frac{\Gamma(\kappa+1)}{\Gamma(\kappa+\omega+1)} & \cdots & \frac{\Gamma(n\kappa+1)}{\Gamma(n\kappa+\omega+1)} \\ \frac{\Gamma(\kappa+1)}{\Gamma(\kappa+\omega+1)} & \frac{\Gamma(2\kappa+1)}{\Gamma(2\kappa+\omega+1)} & \cdots & \frac{\Gamma((n+1)\kappa+1)}{\Gamma((n+1)\kappa+\omega+1)} \\ \vdots & \vdots & \vdots & \vdots \\ \frac{\Gamma(n\kappa+1)}{\Gamma(\kappa+\omega+1)} & \frac{\Gamma((n+1)\kappa+1)}{\Gamma((n+1)\kappa+\omega+1)} & \cdots & \frac{\Gamma(2n\kappa+1)}{\Gamma(2n\kappa+\omega+1)} \end{bmatrix}, \tag{107}$$

$$T_{n\kappa}(\mathbf{t})T_{n\kappa}^T(\mathbf{t}) = \begin{bmatrix} 1 & \mathbf{t}^{\omega} & \mathbf{t}^{2\omega} & \cdots & \mathbf{t}^{n\omega} \\ \mathbf{t}^{\omega} & \mathbf{t}^{2\omega} & \mathbf{t}^{3\omega} & \cdots & \mathbf{t}^{(n+1)\omega} \\ \mathbf{t}^{2\omega} & \mathbf{t}^{3\omega} & \mathbf{t}^{4\omega} & \cdots & \mathbf{t}^{(n+2)\omega} \\ \vdots & \vdots & \vdots & \vdots & \vdots \\ \mathbf{t}^{n\omega} & \mathbf{t}^{(n+1)\omega} & \mathbf{t}^{(n+2)\omega} & \cdots & \mathbf{t}^{2n\omega} \end{bmatrix}. \tag{108}$$

Again, by utilizing ${}^{\mathbf{RL}}\mathfrak{J}_{0,\mathbf{t}}^{\omega}$ on the matrix (108), we get

$${}^{\mathbf{RL}}\mathfrak{J}_{0,\mathbf{t}}^{\omega}\left(T_{n\kappa}(\mathbf{t})T_{n\kappa}^T(\mathbf{t})\right) = \begin{bmatrix} \frac{1}{\Gamma(\omega+1)} & \frac{\Gamma(\kappa+1)}{\Gamma(\kappa+\omega+1)}\mathbf{t}^{\omega} & \cdots & \frac{\Gamma(n\kappa+1)}{\Gamma(n\kappa+\omega+1)}\mathbf{t}^{n\omega} \\ \frac{\Gamma(\kappa+1)}{\Gamma(\kappa+\omega+1)}\mathbf{t}^{\omega} & \frac{\Gamma(2\kappa+1)}{\Gamma(2\kappa+\omega+1)}\mathbf{t}^{2\omega} & \cdots & \frac{\Gamma((n+1)\kappa+1)}{\Gamma((n+1)\kappa+\omega+1)}\mathbf{t}^{(n+1)\omega} \\ \vdots & \vdots & \vdots & \vdots \\ \frac{\Gamma(n\kappa+1)}{\Gamma(\kappa+\omega+1)}\mathbf{t}^{n\omega} & \frac{\Gamma((n+1)\kappa+1)}{\Gamma((n+1)\kappa+\omega+1)}\mathbf{t}^{(n+1)\omega} & \cdots & \frac{\Gamma(2n\kappa+1)}{\Gamma(2n\kappa+\omega+1)}\mathbf{t}^{2n\omega} \end{bmatrix}. \tag{109}$$

8.2. Application of FTOMM on the SARS-CoV-2 Model. In this part, the suggested FTOMM method is utilized to the model of SARS-CoV-2 virus given in (95).

We start by expanding ${}^{\mathbf{C}}\mathfrak{D}_{0,\mathbf{t}}^{\omega}\mathcal{S}(\mathbf{t})$, ${}^{\mathbf{C}}\mathfrak{D}_{0,\mathbf{t}}^{\omega}\mathcal{P}_1(\mathbf{t})$, ${}^{\mathbf{C}}\mathfrak{D}_{0,\mathbf{t}}^{\omega}\mathcal{P}_2(\mathbf{t})$, and ${}^{\mathbf{C}}\mathfrak{D}_{0,\mathbf{t}}^{\omega}\mathcal{R}(\mathbf{t})$ with the help of a fractional Taylor basis vector as following:

$$\begin{cases} {}^{\mathbf{C}}\mathfrak{D}_{0,\mathbf{t}}^{\omega}\mathcal{S}(\mathbf{t}) \approx C^T T_{n\kappa}(\mathbf{t}), \\ {}^{\mathbf{C}}\mathfrak{D}_{0,\mathbf{t}}^{\omega}\mathcal{P}_1(\mathbf{t}) \approx K^T T_{n\kappa}(\mathbf{t}), \\ {}^{\mathbf{C}}\mathfrak{D}_{0,\mathbf{t}}^{\omega}\mathcal{P}_2(\mathbf{t}) \approx L^T T_{n\kappa}(\mathbf{t}), \\ {}^{\mathbf{C}}\mathfrak{D}_{0,\mathbf{t}}^{\omega}\mathcal{R}(\mathbf{t}) \approx N^T T_{n\kappa}(\mathbf{t}). \end{cases} \tag{110}$$

Next, operating the ω^{th}-R-L integral on above equations and using initial values $\mathcal{S}(0)$,$\mathcal{P}_1(0)$,$\mathcal{P}_2(0)$, and $\mathcal{R}(0)$, we get

$$\begin{cases} \mathcal{S}(\mathbf{t}) \approx C^T F_{(\mathbf{t},\omega)} T_{n\kappa}(\mathbf{t}) + \mathcal{S}(0), \\ \mathcal{P}_1(\mathbf{t}) \approx K^T F_{(\mathbf{t},\omega)} T_{n\kappa}(\mathbf{t}) + \mathcal{P}_1(0), \\ \mathcal{P}_2(\mathbf{t}) \approx L^T F_{(\mathbf{t},\omega)} T_{n\kappa}(\mathbf{t}) + \mathcal{P}_2(0), \\ \mathcal{R}(\mathbf{t}) \approx N^T F_{(\mathbf{t},\omega)} T_{n\kappa}(\mathbf{t}) + \mathcal{R}(0). \end{cases} \tag{111}$$

Substituting (110) and (111) into SARS-CoV-2 model (95), we get

$$\begin{aligned} C^T T_{n\kappa}(\mathbf{t}) = \Theta - r&\left[\left(K^T F_{(\mathbf{t},\omega)} T_{n\kappa}(\mathbf{t}) + \mathcal{S}_1(0)\right)\left(C^T F_{(\mathbf{t},\omega)} T_{n\kappa}(\mathbf{t}) + \mathcal{S}(0)\right)\right] \\ &- rs\left[\left(K^T F_{(\mathbf{t},\omega)} T_{n\kappa}(\mathbf{t}) + \mathcal{P}_1(0)\right)\left(C^T F_{(\mathbf{t},\omega)} T_{n\kappa}(\mathbf{t}) + \mathcal{S}(0)\right)\right] \\ &- (b+b_1)\left(C^T F_{(\mathbf{t},\omega)} T_{n\kappa}(\mathbf{t}) + \mathcal{S}(0)\right), \end{aligned}$$

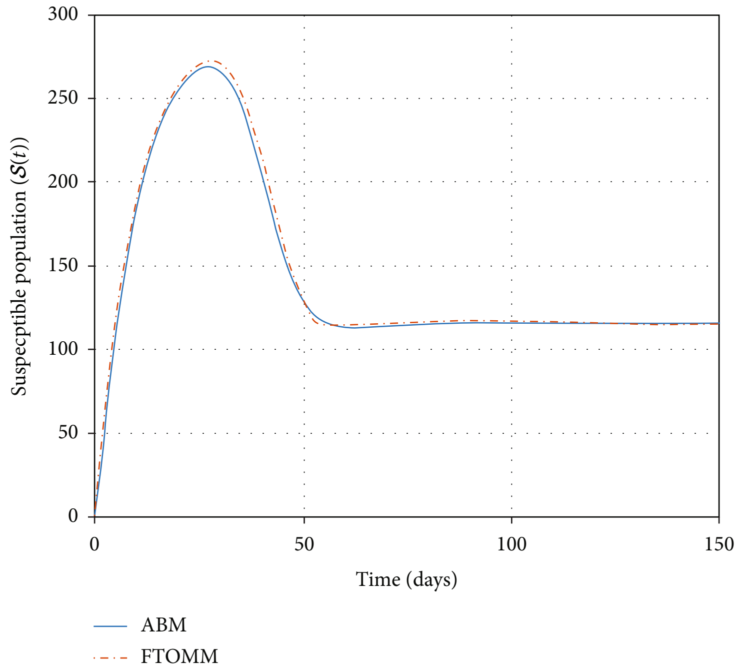

(a)

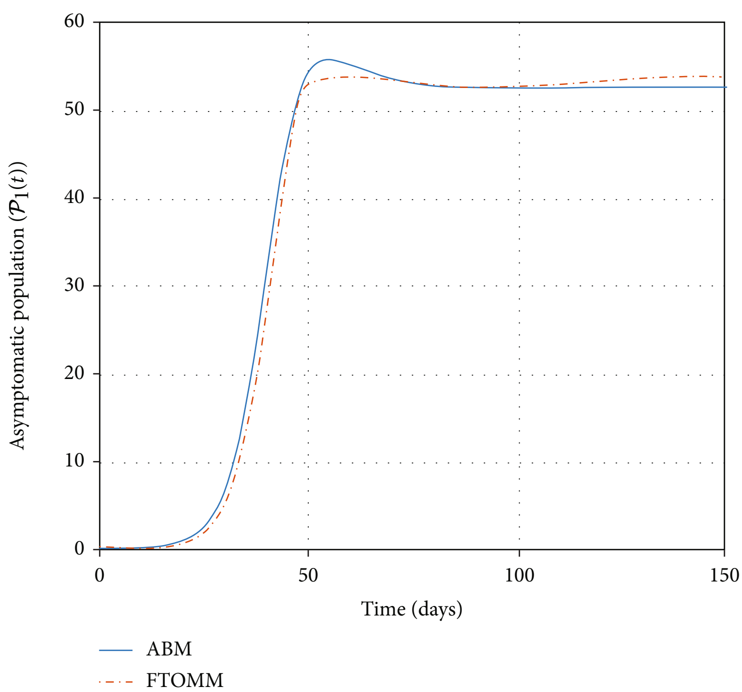

(b)

Figure 8: Continued.

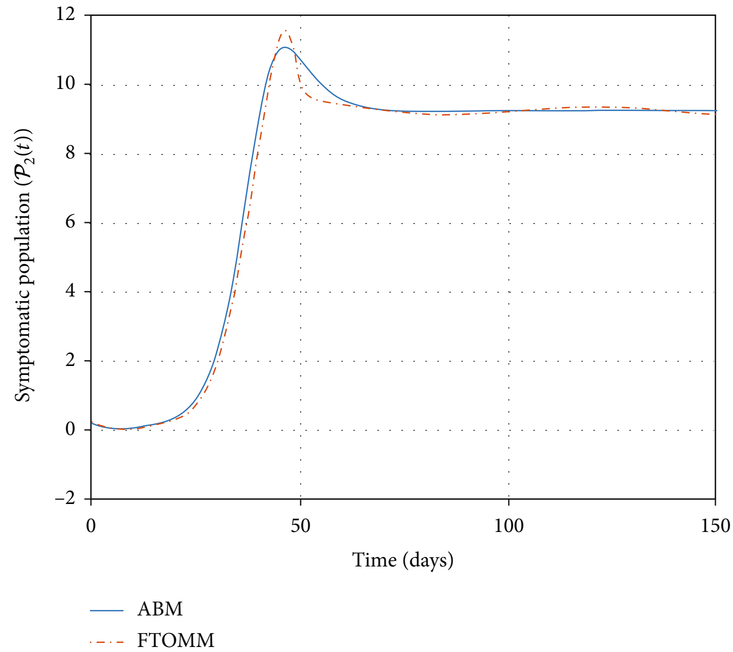

(c)

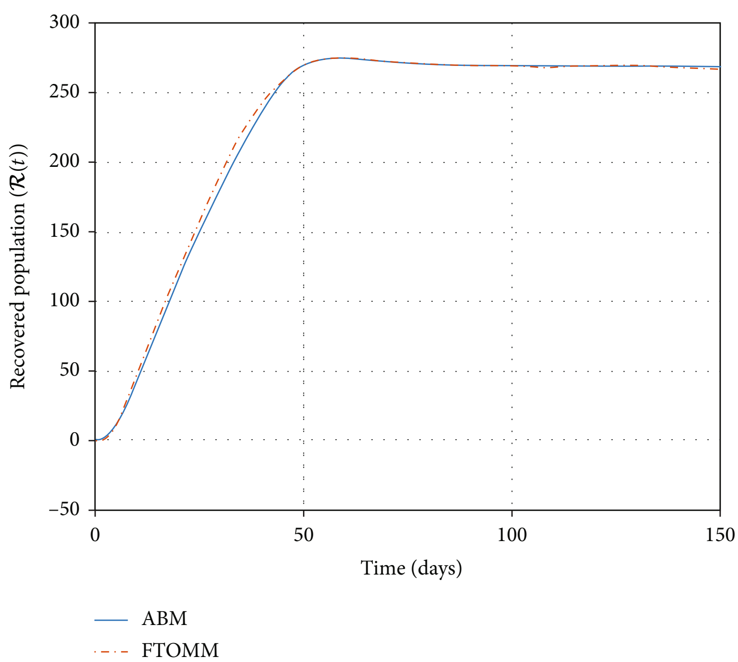

(d)

Figure 8: Comparisons between the ABM and FTOMM for the parametric values.

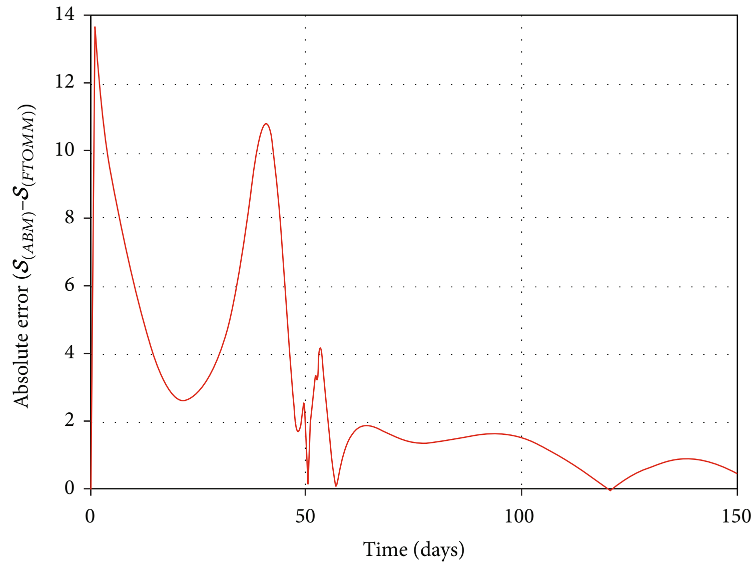

(a)

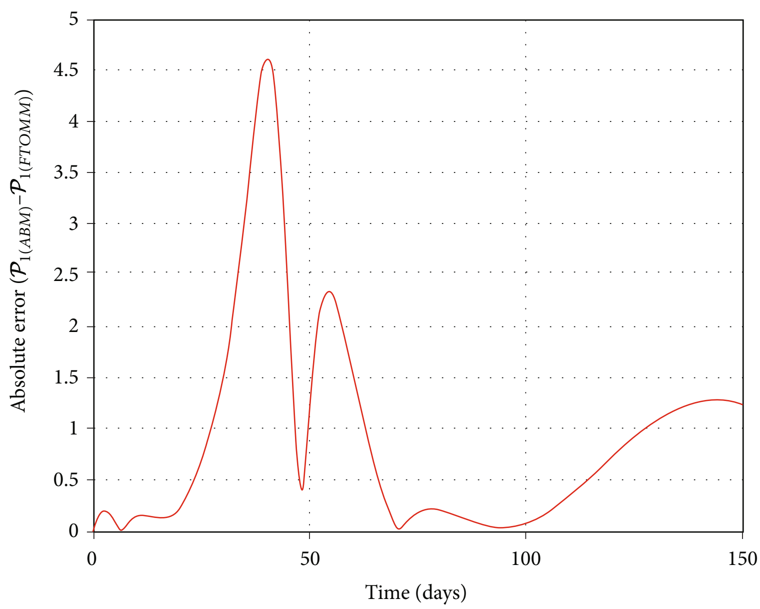

(b)

Figure 9: Continued.

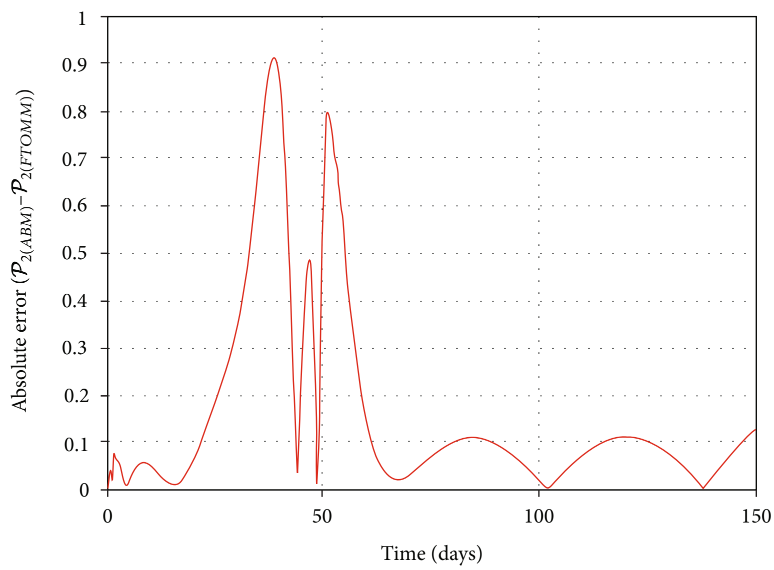

(c)

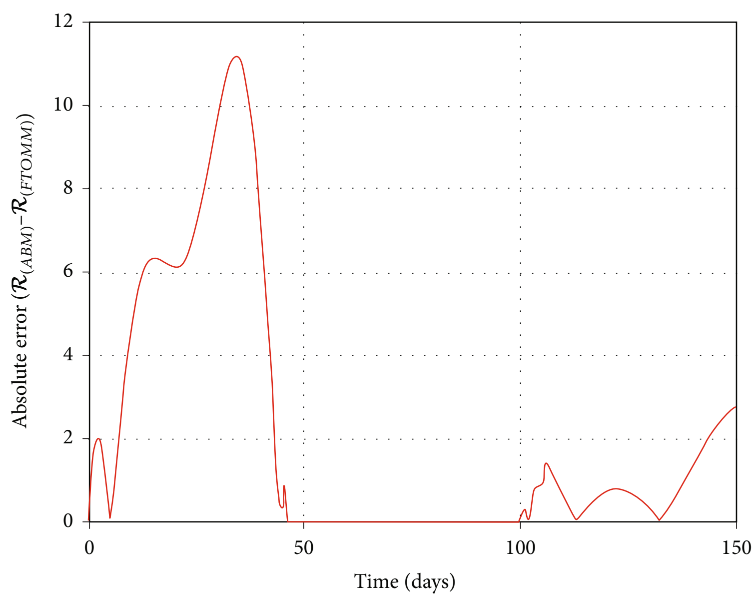

(d)

FIGURE 9: Absolute error comparisons between the ABM and FTOMM for the parametric values.

$$
\begin{aligned}
K^T T_{n\kappa}(\mathfrak{t}) &= \mathrm{pr}\left[\left(K^T F_{(\mathfrak{t},\omega)} T_{n\kappa}(\mathfrak{t}) + \mathscr{P}_1(0)\right)\left(C^T F_{(\mathfrak{t},\omega)} T_{n\kappa}(\mathfrak{t}) + \mathscr{S}(0)\right)\right] \\
&\quad + \mathrm{prs}\left[\left(K^T F_{(\mathfrak{t},\omega)} T_{n\kappa}(\mathfrak{t}) + \mathscr{P}_1(0)\right)\left(C^T F_{(\mathfrak{t},\omega)} T_{n\kappa}(\mathfrak{t}) + \mathscr{S}(0)\right)\right] \\
&\quad - (b_1 + b_2 + r_1)\left(K^T F_{(\mathfrak{t},\omega)} T_{n\kappa}(\mathfrak{t}) + \mathscr{P}_1(0)\right), \\
L^T T_{n\kappa}(\mathfrak{t}) &= (1-p)r\left[\left(K^T F_{(\mathfrak{t},\omega)} T_{n\kappa}(\mathfrak{t}) + \mathscr{P}_1(0)\right)\right. \\
&\quad \left.\cdot \left(C^T F_{(\mathfrak{t},\omega)} T_{n\kappa}(\mathfrak{t}) + \mathscr{S}(0)\right)\right] \\
&\quad + (1-p)rs\left[\left(K^T F_{(\mathfrak{t},\omega)} T_{n\kappa}(\mathfrak{t}) + \mathscr{P}_1(0)\right)\right. \\
&\quad \left.\cdot \left(C^T F_{(\mathfrak{t},\omega)} T_{n\kappa}(\mathfrak{t}) + \mathscr{S}(0)\right)\right] \\
&\quad + (qr_1)\left(K^T F_{(\mathfrak{t},\omega)} T_{n\kappa}(\mathfrak{t}) + \mathscr{P}_1(0)\right) \\
&\quad - (b_1 + b_3 + r_2)\left(L^T F_{(\mathfrak{t},\omega)} T_{n\kappa}(\mathfrak{t}) + \mathscr{P}_2(0)\right), \\
N^T T_{n\kappa}(\mathfrak{t}) &= r_1(1-q)\left(K^T F_{(\mathfrak{t},\omega)} T_{n\kappa}(\mathfrak{t}) + \mathscr{P}_1(0)\right) \\
&\quad + r_2\left(L^T F_{(\mathfrak{t},\omega)} T_{n\kappa}(\mathfrak{t}) + \mathscr{P}_2(0)\right) \\
&\quad + b\left(C^T F_{(\mathfrak{t},\omega)} T_{n\kappa}(\mathfrak{t}) + \mathscr{S}(0)\right) \\
&\quad - b_1\left(N^T F_{(\mathfrak{t},\omega)} T_{n\kappa}(\mathfrak{t}) + \mathscr{R}(0)\right).
\end{aligned}
\tag{112}
$$

Now, by using above equations and collocation points $\mathfrak{t}_j = j/n$, where $j = 0, 1, \cdots n$, we derive a system of $4n+4$ algebraic nonlinear equations with $4n+4$ unknown coefficients. This system is solved efficiently for the unknown coefficient vectors C^T, K^T, L^T, and N^T by using the Newton method in MATLAB software.

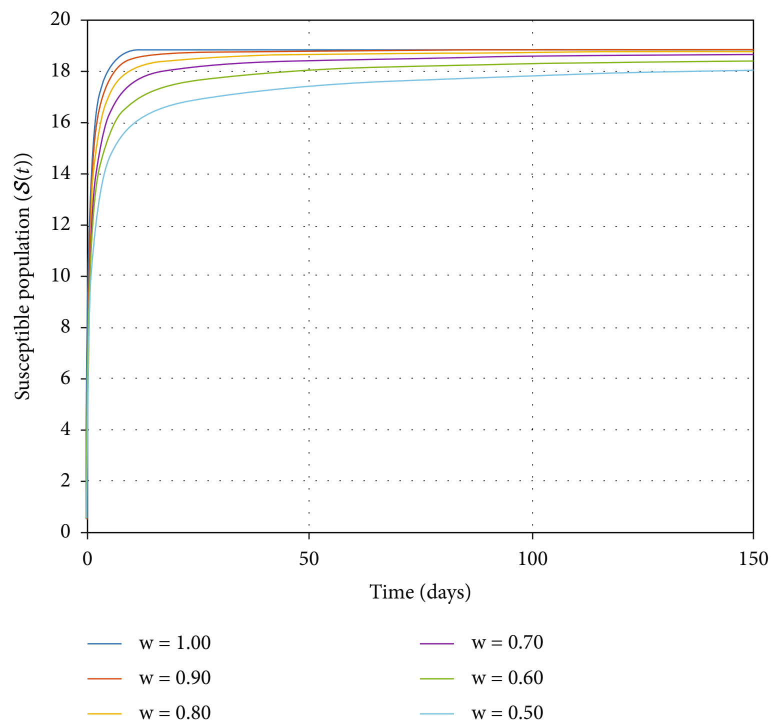

FIGURE 10: $\mathcal{S}(\mathfrak{t})$ by changing ω where $m = 7$.

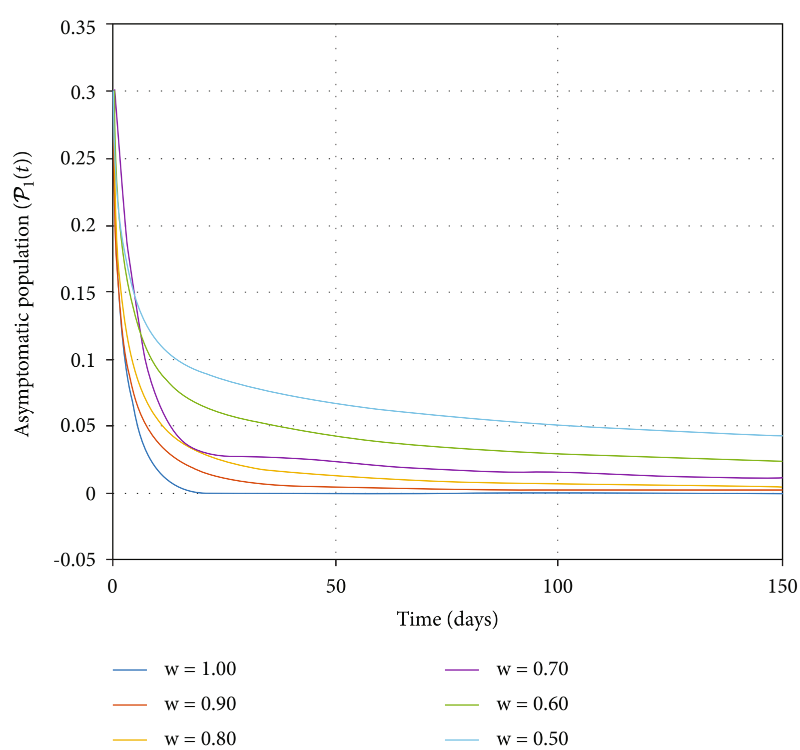

FIGURE 11: $\mathcal{P}_1(\mathfrak{t})$ by changing ω where $m = 7$.

As a final step, substituting the vectors of coefficients C^T, K^T, L^T, and N^T into (111), we obtain for $\mathcal{S}(\mathfrak{t})$, $\mathcal{P}_1(\mathfrak{t})$, $\mathcal{P}_2(\mathfrak{t})$, and $\mathcal{R}(\mathfrak{t})$ approximately.

8.3. Simulations Based on FTOMM Method and Comparison with Adams-Bashforth Method. In this section, all graphical results of the fractional SARS-CoV-2 model (95) by using

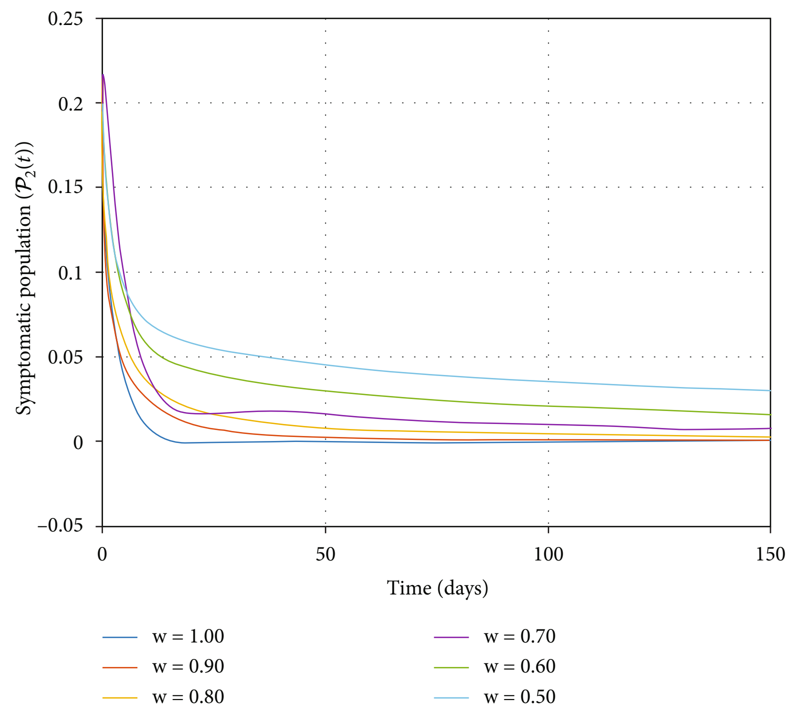

FIGURE 12: $\mathscr{P}_2(\mathfrak{t})$ by changing ω where $m = 7$.

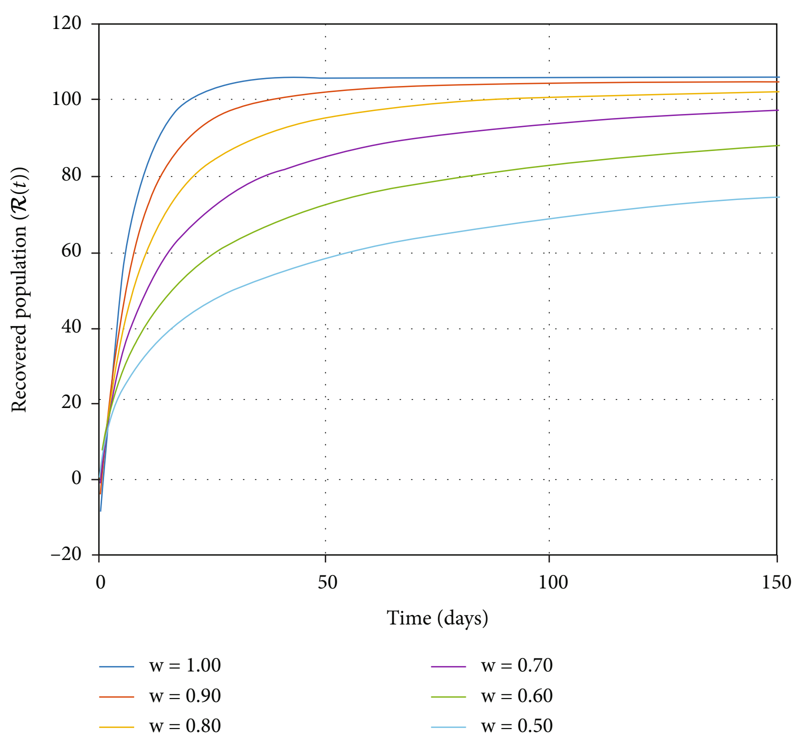

FIGURE 13: $\mathscr{R}(\mathfrak{t})$ by changing ω where $m = 7$.

FTOMM and their comparison between ABM are illustrated through Figures 8–14. To see the correctness and having a comparison, we illustrate the graphical representation of the presented model at several values of ω.

In Figure 8, we present a comparison of obtained solutions by use of the ABM and FTOMM for the parametric values assumed in subsection 7.2. From Figures 8(a)–8(d), we can clearly conclude that the both acquired numerical

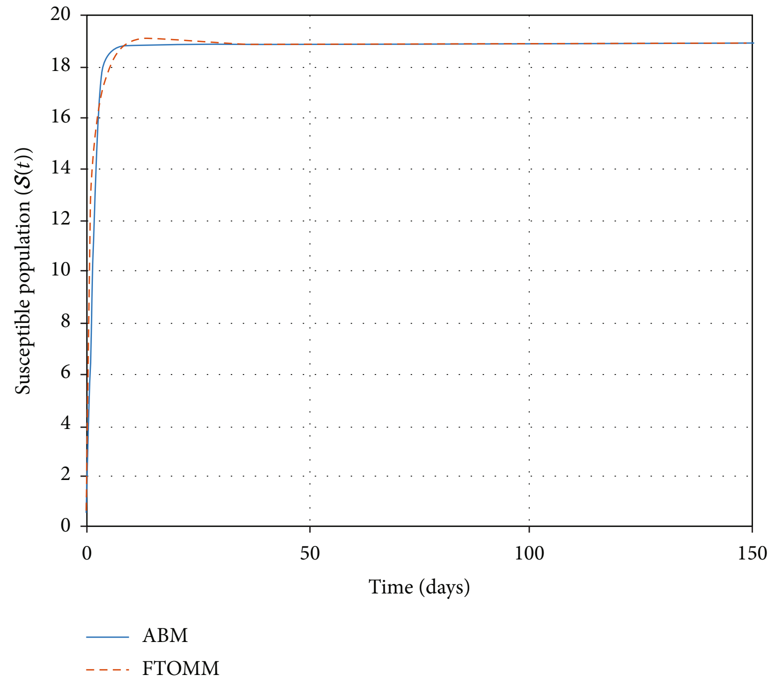

(a)

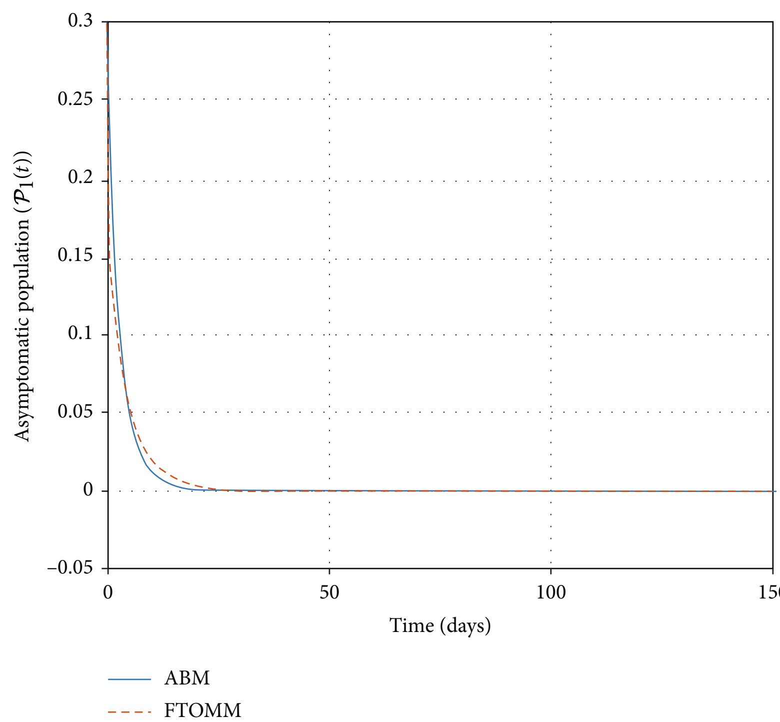

(b)

FIGURE 14: Continued.

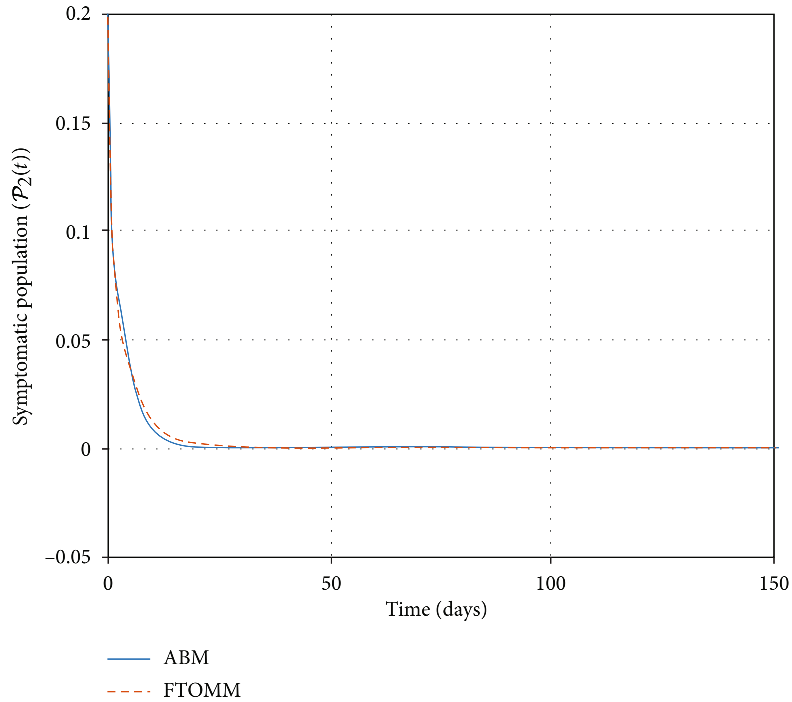

(c)

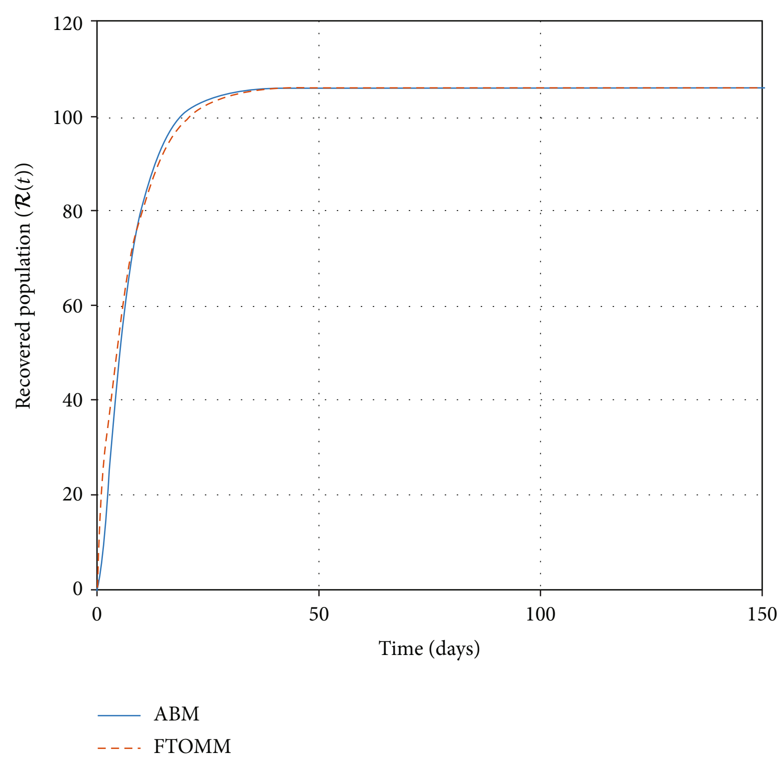

(d)

Figure 14: Comparisons between the ABM and FTOMM for the parametric values of S_2.

solutions of four state functions $\mathcal{S}(\mathbf{t})$, $\mathcal{P}_1(\mathbf{t})$, $\mathcal{P}_2(\mathbf{t})$, and $\mathcal{R}(\mathbf{t})$ by use of ABM and FTOMM are identical.

In Table 1, we present the solutions of four subclasses $\mathcal{S}(t)$, $\mathcal{P}_1(t)$, $\mathcal{P}_2(t)$, and $\mathcal{R}(t)$ obtained by use of the Adams-Bashforth and fractional Taylor operational matrix methods.

In Figure 9, we give the graphical illustration of the absolute errors of four subclasses $\mathcal{S}(\mathbf{t})$, $\mathcal{P}_1(\mathbf{t})$, $\mathcal{P}_2(\mathbf{t})$, and $\mathcal{R}(\mathbf{t})$

Table 1: Compared approximate results of four state functions obtained by ABM and FTOMM. (a) $\mathcal{S}$, (b) $\mathcal{P}_1$, (c) $\mathcal{P}_2$, and (d) $\mathcal{R}$).

(a)

t	$\mathcal{S}_{(\text{ABM})}$	$\mathcal{S}_{(\text{FTOMM})}$
0	0.50	0.50
25	266.9033	269.7917
50	129.1402	130.4819
75	114.4625	115.8542
100	115.6538	117.1644
125	115.6506	115.2917
150	115.6489	115.1839

(b)

t	$\mathcal{P}_{1(\text{ABM})}$	$\mathcal{P}_{1(\text{FTOMM})}$
0	0.30	0.30
25	2.6859	1.9753
50	54.1815	52.9918
75	53.1316	53.3214
100	52.6601	52.7443
125	52.6713	53.5863
150	52.6717	53.9160

(c)

t	$\mathcal{P}_{2(\text{ABM})}$	$\mathcal{P}_{2(\text{FTOMM})}$
0	0.20	0.20
25	1.9753	0.8732
50	10.7542	10.1061
75	9.2629	9.1954
100	9.2682	9.2501
125	9.2702	9.3729
150	9.2702	9.1423

(d)

t	$\mathcal{R}_{(\text{ABM})}$	$\mathcal{R}_{(\text{FTOMM})}$
0	0.10	0.10
25	150.9550	158.0875
50	270.5701	270.5721
75	271.7889	271.7783
100	269.6428	269.7108
125	269.2052	269.9315
150	269.0798	266.3295

obtained by the Adams-Bashforth and fractional Taylor operational matrix methods.

In this part, by using FTOMM, we simulate and discuss the behavior of the model based on the parametric values of the set S_2 provided by [60]. From this source, we assume the new parametric values to be $\Theta = 20$, $r = 0.079$, $s = 0.0001$, $b = 0.9$, $b_1 = 0.16$, $p = 0.29$, $b_2 = 0.11$, $r_1 = 0.45$, $q = 0.2$, $b_3 = 0.8$, and $r_2 = 0.9$. Finally, the initial values for state functions are the following:

$$\begin{aligned} \mathcal{S}(0) &= 0.5, \\ \mathcal{P}_1(0) &= 0.3, \\ \mathcal{P}_2(0) &= 0.2, \\ \mathcal{R}(0) &= 0.1. \end{aligned} \tag{113}$$

In Figures 10–13, we present the behaviors of solutions of four state functions $\mathcal{S}(\mathbf{t})$, $\mathcal{P}_1(\mathbf{t})$, $\mathcal{P}_2(\mathbf{t})$, and $\mathcal{R}(\mathbf{t})$, respectively, which are obtained by using FTOMM for some values of $\omega = 1.00, 0.90, 0.80, 0.70, 0.60, 0.50$ where $\mathbf{t} \in [0,150]$.

From Figure 10, we can see the illustration of $\mathcal{S}(\mathbf{t})$ with initial value $S(0) = 0.5$ for several values of ω. It can be observed from this graph that the order of fractional derivative has an effect on convergence of people of susceptible category to stable case. Namely, at higher fractional orders, it converges slowly to a stable case, while at lower fractional order, this process is more quickly. About the density of $\mathcal{S}(\mathbf{t})$, we can observe that by increasing the fractional order, the density also increases. Also, we can clearly see that the fractional orders are highly consistent with integer order when using FTOMM.

From Figures 11–13, we can see the illustration of $\mathcal{P}_1(\mathbf{t})$, $\mathcal{P}_2(\mathbf{t})$, and $\mathcal{R}(\mathbf{t})$ with $\mathcal{P}_1(0) = 0.3$, $\mathcal{P}_2(0) = 0.2$, and $\mathcal{R}(0) = 0.1$, respectively, for some values of ω. It can be observed from these graphs that at higher fractional orders, people of asymptomatic, symptomatic, and recovered categories converge slowly to a stable case, while at lower fractional order, it is more quickly. Also, we observe that by increasing the fractional orders, the densities of $\mathcal{S}(\mathbf{t})$, $\mathcal{P}_1(\mathbf{t})$, $\mathcal{P}_2(\mathbf{t})$, and $\mathcal{R}(\mathbf{t})$ increases too.

In Figure 14, we present the comparison of the obtained solutions by use of the ABM and FTOMM for the parametric values of set S_2. From Figures 14(a)–14(d), we can clearly see that the both obtained approximate solutions of four state functions $\mathcal{S}(\mathbf{t})$, $\mathcal{P}_1(\mathbf{t})$, $\mathcal{P}_2(\mathbf{t})$, and $\mathcal{R}(\mathbf{t})$ by use of ABM and FTOMM are behaving identical.

It is clear from all figures that both obtained solutions by fractional Taylor operational matrix method and Adams-Bashforth method are identical. We can conclude that fractional Taylor operational matrix method gives almost the same results as the results acquired by Adams-Bashforth technique. Also, more accurate results can be obtained by enhancing the value of m and κ. Due to the simplicity of FTOMM, it is effective and has advantages for mathematical modelling of dynamics of SARS-CoV-2 virus.

9. Conclusions

In this manuscript, a fractal-fractional epidemic probability-based model of the SARS-CoV-2 virus with four compartments including susceptible, asymptomatic, symptomatic, and recovered was designed. By recalling a special group of contractions, named ϕ-admissible ϕ-ψ-contractionas, we proved the existence property for fixed points of a fractal-fractional operator which is the same soultion of the mentioned system. Furthermore, other theoretical properties like stable solutions and their uniqueness for each compartments of the fractal-fractional model were established. We derived numerical solutions via the Adams-Bashforth and simulated them from several aspects such as variations of fractal-fractional dimension orders. Further, we formulated a Caputo type of the fractional model and compared its solutions obtained by the FTOMM method, with the previous ones of the fractal-fractional model. All simulations showed similar and close outcomes. From all illustrations presented in this work, we observed that the population of infected people converge quickly to a stable case at higher fractal-fractional orders and slowly to such a stable case at lower fractal-fractional orders. Also, we can see that by increasing the fractal-fractional orders, the density of susceptible population also increases. Also, from Figure 3, we can see that the probability of disease extinction increases with vaccination rate. All the numerical results and calculations are obtained with the help of MATLAB version R2019A. In the future, we aim to compare the results of our methods in the framework of other types of nonsingular kernels. Also, as a future study, the techniques introduced in this study can be modified to apply to other diseases and new variants of SARS-CoV-2 for different compartments.

Data Availability

Data sharing is not applicable to this article as no datasets were generated or analyzed during the current study.

Conflicts of Interest

The authors declare that they have no competing interests.

Authors' Contributions

The authors declare that the study was realized in collaboration with equal responsibility. All authors read and approved the final manuscript.

Acknowledgments

The first and second authors would like to thank the Azarbaijan Shahid Madani University.

References

[1] D. Fox, "What you need to know about the novel coronavirus," *Nature cell biology*, 2020.

[2] M. Hoffmann, H. Kleine-Weber, S. Schroeder et al., "SARS-CoV-2 cell entry depends on ACE2 and TMPRSS2 and is blocked by a clinically proven protease inhibitor," *Cell*, vol. 181, no. 2, pp. 271–280.e8, 2020.

[3] J. F. Chan, S. Yuan, K. H. Kok et al., "A familial cluster of pneumonia associated with the 2019 novel coronavirus indicating person-to-person transmission: a study of a family cluster," *Lancet*, vol. 395, no. 10223, pp. 514–523, 2020.

[4] M. Klompas, M. A. Baker, and C. Rhee, "Airborne transmission of SARS-CoV-2," *Journal of the American Medical Association*, vol. 324, no. 5, pp. 441-442, 2020.

[5] P. Anfinrud, C. E. Bax, and A. Bax, "Visualizing speech-generated oral fluid droplets with laser light scattering," *New England Journal of Medicine*, vol. 382, pp. 2061–2063, 2020.

[6] Y. J. Hou, K. Okuda, C. E. Edwards et al., "SARS-CoV-2 reverse genetics reveals a variable infection gradient in the respiratory tract," *Cell*, vol. 182, no. 2, pp. 429–446.e14, 2020.

[7] A. Banerjee, K. Mossman, and M. L. Baker, "Zooanthroponotic potential of SARS-CoV-2 and implications of reintroduction into human populations," *Cell Host & Microbe*, vol. 29, no. 2, pp. 160–164, 2021.

[8] http://www.covid19.who.int/, Accessed March 10, 2022.

[9] E. Mahase, "Covid-19: what treatments are being investigated?," *BMJ*, vol. 368, p. m1252, 2020.

[10] S. Rezapour, S. Etemad, and H. Mohammadi, "A mathematical analysis of a system of Caputo-Fabrizio fractional differential equations for the anthrax disease model in animals," *Advances in Difference Equations*, vol. 2020, no. 1, Article ID 481, 2020.

[11] A. Pratap, R. Raja, R. P. Agarwal, J. Alzabut, M. Niezabitowski, and E. Hincal, "Further results on asymptotic and finite-time stability analysis of fractional-order time-delayed genetic regulatory networks," *Neurocomputing*, vol. 475, pp. 26–37, 2022.

[12] H. Mohammadi, S. Kumar, S. Rezapour, and S. Etemad, "A theoretical study of the Caputo-Fabrizio fractional modeling for hearing loss due to mumps virus with optimal control," *Chaos, Solitons & Fractals*, vol. 144, article 110668, 2021.

[13] A. Ali, Q. Iqbal, J. K. K. Asamoah, and S. Islam, "Mathematical modeling for the transmission potential of Zika virus with optimal control strategies," *The European Physical Journal Plus*, vol. 137, no. 1, p. 146, 2022.

[14] P. Kumar, V. S. Erturk, and H. Almusawa, "Mathematical structure of mosaic disease using microbial biostimulants via Caputo and Atangana-Baleanu derivatives," *Results in Physics*, vol. 24, p. 104186, 2021.

[15] R. Zarin, H. Khaliq, A. Khan, D. Khan, A. Akgul, and U. W. Humphries, "Deterministic and fractional modeling of a computer virus propagation," *Results in Physics*, vol. 33, p. 105130, 2022.

[16] D. Baleanu, S. Etemad, and S. Rezapour, "A hybrid Caputo fractional modeling for thermostat with hybrid boundary value conditions," *Boundary Value Problems*, vol. 2020, no. 1, Article ID 64, 2020.

[17] J. Alzabut, G. M. Selvam, R. A. El-Nabulsi, D. Vignesh, and M. E. Samei, "Asymptotic stability of nonlinear discrete fractional pantograph equations with non-local initial conditions," *Symmetry*, vol. 13, no. 3, p. 473, 2021.

[18] J. K. K. Asamoah, E. Okyere, E. Yankson et al., "Non-fractional and fractional mathematical analysis and simulations for Q fever," *Chaos, Solitons & Fractals*, vol. 156, article 111821, 2022.

[19] H. Khan, C. Tunc, W. Chen, and A. Khan, "Existence theorems and Hyers-Ulam stability for a class of hybrid fractional differential equations with p -Laplacian operator," *Journal of Applied Analysis and Computation*, vol. 8, no. 4, pp. 1211–1226, 2018.

[20] Y. Rahmani, M. M. Alizadeh, H. Schuh, J. Wickert, and L. C. Tsai, “Probing vertical coupling effects of thunderstorms on lower ionosphere using GNSS data,” *Advances in Space Research*, vol. 66, no. 8, pp. 1967–1976, 2020.

[21] Y. Rahmani and M. M. Alizadeh, “Irregularities in electron density above mesoscale thunderstorms using global navigation satellite systems measurements,” in *7th Workshop on Vertical Coupling in Atmosphere-Ionosphere Systems*, GFZ, Potsdam, Germany, 2018.

[22] A. Omame, U. K. Nwajeri, M. Abbas, and C. P. Onyenegecha, “A fractional order control model for diabetes and COVID-19 co-dynamics with Mittag-Leffler function,” *Alexandria Engineering Journal*, vol. 61, no. 10, pp. 7619–7635, 2022.

[23] S. Rezapour, C. T. Deressa, A. Hussain, S. Etemad, R. George, and B. Ahmad, “A theoretical analysis of a fractional multi-dimensional system of boundary value problems on the methylpropane graph via fixed point technique,” *Mathematics*, vol. 10, no. 4, p. 568, 2022.

[24] A. Jajarmi, D. Baleanu, K. Zarghami Vahid, and S. Mobayen, “A general fractional formulation and tracking control for immunogenic tumor dynamics,” *Mathematical Methods in the Applied Sciences*, vol. 45, no. 2, pp. 667–680, 2022.

[25] S. Salahshour, A. Ahmadian, B. A. Pansera, and M. Ferrara, “Uncertain inverse problem for fractional dynamical systems using perturbed collage theorem,” *Communications in Nonlinear Science and Numerical Simulation*, vol. 94, no. 94, article 105553, 2021.

[26] V. S. Erturk, E. Godwe, D. Baleanu, P. Kumar, J. Asad, and A. Jajarmi, “Novel fractional-order Lagrangian to describe motion of beam on nanowire,” *Acta Physica Polonica A*, vol. 140, no. 3, pp. 265–272, 2021.

[27] A. Jajarmi, D. Baleanu, K. Z. Vahid, H. M. Pirouz, and J. H. Asad, “A new and general fractional Lagrangian approach: a capacitor microphone case study,” *Results in Physics*, vol. 31, p. 104950, 2021.

[28] M. Alqhtani, K. M. Owolabi, and K. M. Saad, “Spatiotemporal (target) patterns in sub-diffusive predator-prey system with the Caputo operator,” *Chaos, Solitons & Fractals*, vol. 160, article 112267, 2022.

[29] S. Aljhani, M. S. Noorani, K. M. Saad, and A. K. Alomari, “Numerical solutions of certain new models of the time-fractional Gray-Scott,” *Journal of Function Spaces*, vol. 2021, Article ID 2544688, 12 pages, 2021.

[30] M. H. DarAssi, M. A. Safi, M. A. Khan, A. Beigi, A. A. Aly, and M. Y. Alshahrani, “A mathematical model for SARS-CoV-2 in variable-order fractional derivative,” *The European Physical Journal Special Topics*, vol. 231, no. 10, pp. 1905–1914, 2022.

[31] Y. Gu, M. A. Khan, Y. S. Hamed, and B. F. Felemban, “A comprehensive mathematical model for SARS-CoV-2 in Caputo derivative,” *Fractal and Fractional*, vol. 5, no. 4, p. 271, 2021.

[32] K. Rajagopal, N. Hasanzadeh, F. Parastesh, I. I. Hamarash, S. Jafari, and I. Hussain, “A fractional-order model for the novel coronavirus (COVID-19) outbreak,” *Nonlinear Dynamics*, vol. 101, no. 1, pp. 711–718, 2020.

[33] A. S. Quintero and R. E. Gutiérrez-Carvajal, “Modeling the evolution of SARS-CoV-2 using a fractional-order SIR approach,” *TecnoLógicas*, vol. 24, no. 51, article e1866, 2021.

[34] M. Zamir, K. Shah, F. Nadeem et al., “Threshold conditions for global stability of disease free state of COVID-19,” *Results in Physics*, vol. 21, no. 21, article 103784, 2021.

[35] N. Jain, S. Jhunthra, H. Garg et al., “Prediction modelling of COVID using machine learning methods from B-cell dataset,” *Results in physics*, vol. 21, no. 21, article 103813, 2021.

[36] D. Baleanu, M. H. Abadi, A. Jajarmi, K. Z. Vahid, and J. J. Nieto, “A new comparative study on the general fractional model of COVID-19 with isolation and quarantine effects,” *Alexandria Engineering Journal*, vol. 61, no. 6, pp. 4779–4791, 2022.

[37] Z. Ali, F. Rabiei, M. M. Rashidi, and T. Khodadadi, “A fractional-order mathematical model for COVID-19 outbreak with the effect of symptomatic and asymptomatic transmissions,” *The European Physical Journal Plus*, vol. 137, no. 3, pp. 1–20, 2022.

[38] F. Ozkose, M. Yavuz, M. T. Senel, and R. Habbireeh, “Fractional order modelling of omicron SARS-CoV-2 variant containing heart attack effect using real data from the United Kingdom,” *Chaos, Solitons & Fractals*, vol. 157, article 111954, 2022.

[39] A. Khan, H. Ullah, M. Zahri et al., “Stationary distribution and extinction of stochastic coronavirus (COVID-19) epidemic model,” *Fractals*, vol. 30, no. 1, article 2240050, 2022.

[40] P. A. Naik, M. Yavuz, S. Qureshi, J. Zu, and S. Townley, “Modeling and analysis of COVID-19 epidemics with treatment in fractional derivatives using real data from Pakistan,” *The European Physical Journal Plus*, vol. 135, no. 10, p. 795, 2020.

[41] M. L. Holshue, C. DeBolt, S. Lindquist et al., “First case of 2019 novel coronavirus in the United States,” *New England Journal of Medicine*, vol. 382, no. 10, pp. 929–936, 2020.

[42] Z. Ali, F. Rabiei, K. Shah, and T. Khodadadi, “Qualitative analysis of fractal-fractional order COVID-19 mathematical model with case study of Wuhan,” *Alexandria Engineering Journal*, vol. 60, no. 1, pp. 477–489, 2021.

[43] Z. Ali, F. Rabiei, K. Shah, and T. Khodadadi, “Modeling and analysis of novel COVID-19 under fractal-fractional derivative with case study of Malaysia,” *Fractals*, vol. 29, no. 1, p. 2150020, 2021.

[44] Z. Ali, F. Rabiei, K. Shah, and Z. A. Majid, “Dynamics of SIR mathematical model for COVID-19 outbreak in Pakistan under fractal-fractional derivative,” *Fractals*, vol. 29, no. 5, article 2150120, 2021.

[45] A. Din, A. Khan, A. Zeb, M. R. S. Ammi, M. Tilioua, and D. F. M. Torres, “Hybrid method for simulation of a fractional COVID-19 model with real case application,” *Axioms.*, vol. 10, no. 4, p. 290, 2021.

[46] M. Rahman, S. Ahmad, R. T. Matoog, N. A. Alshehri, and T. Khan, “Study on the mathematical modelling of COVID-19 with Caputo-Fabrizio operator,” *Chaos, Solitons & Fractals*, vol. 150, article 111121, 2021.

[47] M. I. Abbas and M. A. Ragusa, “Solvability of Langevin equations with two Hadamard fractional derivatives via Mittag–Leffler functions,” *Applicable Analysis*, vol. 101, no. 9, pp. 3231–3245, 2022.

[48] A. Atangana, “Fractal-fractional differentiation and integration: connecting fractal calculus and fractional calculus to predict complex system,” *Chaos, Solitons & Fractals*, vol. 102, pp. 396–406, 2017.

[49] M. Arfan, K. Shah, and A. Ullah, “Fractal-fractional mathematical model of four species comprising of prey-predation,” *Physica Scripta*, vol. 96, no. 12, p. 124053, 2021.

[50] M. Abdulwasaa, M. S. Abdo, K. Shah et al., "Fractal-fractional mathematical modeling and forecasting of new cases and deaths of COVID-19 epidemic outbreaks in India," *Results in Physics*, vol. 20, article 103702, 2021.

[51] K. Shah, M. Arfan, I. Mahariq, A. Ahmadian, S. Salahshour, and M. Ferrara, "Fractal-fractional mathematical model addressing the situation of corona virus in Pakistan," *Results in Physics*, vol. 19, article 103560, 2020.

[52] Z. A. Khan, M. Ur Rahman, and K. Shah, "Study of a fractal-fractional smoking models with relapse and harmonic mean type incidence rate," *Journal of Function Spaces*, vol. 2021, Article ID 6344079, 11 pages, 2021.

[53] M. Arif, P. Kumam, W. Kumam, A. Akgul, and T. Sutthibutpong, "Analysis of newly developed fractal-fractional derivative with power law kernel for MHD couple stress fluid in channel embedded in a porous medium," *Scientific Reports*, vol. 11, no. 1, p. 20858, 2021.

[54] M. Alqhtani and K. M. Saad, "Fractal–fractional Michaelis–Menten enzymatic reaction model via different kernels," *Fractal and Fractional*, vol. 6, no. 1, p. 13, 2022.

[55] A. A. Khan, R. Amin, S. Ullah, W. Sumelka, and M. Altanji, "Numerical simulation of a Caputo fractional epidemic model for the novel coronavirus with the impact of environmental transmission," *Alexandria Engineering Journal*, vol. 61, no. 7, pp. 5083–5095, 2022.

[56] Y. Zhou and Y. Zhang, "Noether symmetries for fractional generalized Birkhoffian systems in terms of classical and combined Caputo derivatives," *Acta Mechanica*, vol. 231, no. 7, pp. 3017–3029, 2020.

[57] W. Sumelka, B. Luczak, T. Gajewski, and G. Z. Voyiadjis, "Modelling of AAA in the framework of time-fractional damage hyperelasticity," *International Journal of Solids and Structures*, vol. 206, pp. 30–42, 2020.

[58] B. Samet, C. Vetro, and P. Vetro, "Fixed point theorems for -ψ -contractive type mappings," *Nonlinear analysis: theory, methods & applications*, vol. 75, no. 4, pp. 2154–2165, 2012.

[59] T. Khan, R. Ullah, G. Zaman, and J. Alzabut, "A mathematical model for the dynamics of SARS-CoV-2 virus using the Caputo-Fabrizio operator," *Mathematical Biosciences and Engineering*, vol. 18, no. 5, pp. 6095–6116, 2021.

[60] T. Khan, R. Ullah, G. Zaman, and Y. El Khatib, "Modeling the dynamics of the SARS-CoV-2 virus in a population with asymptomatic and symptomatic infected individuals and vaccination," *Physica Scripta*, vol. 96, no. 10, article 104009, 2021.

[61] A. Granas and J. Dugundji, *Fixed Point Theory*, Springer-Verlag, New York, 2003.

[62] I. Avci, "Numerical simulation of fractional delay differential equations using the operational matrix of fractional integration for fractional-order Taylor basis," *Fractal and Fractional*, vol. 6, no. 1, p. 10, 2022.

[63] I. Avci and N. I. Mahmudov, "Numerical solutions for multi-term fractional order differential equations with fractional Taylor operational matrix of fractional integration," *Mathematics*, vol. 8, no. 1, p. 96, 2020.

[64] V. S. Krishnasamy, S. Mashayekhi, and M. Razzaghi, "Numerical solutions of fractional differential equations by using fractional Taylor basis," *IEEE/CAA Journal of Automatica Sinica*, vol. 4, no. 1, pp. 98–106, 2017.

Hindawi
Journal of Function Spaces
Volume 2022, Article ID 2297866, 16 pages
https://doi.org/10.1155/2022/2297866

Research Article

New Fractal Soliton Solutions and Sensitivity Visualization for Double-Chain DNA Model

Zara Hassan,[1] Nauman Raza,[1] Abdel-Haleem Abdel-Aty,[2,3] Mohammed Zakarya,[4] Riaz Ur Rahman,[5] Adeela Yasmeen,[1] Abdisalam Hassan Muse,[6] and Emad E. Mahmoud[7]

[1]*Department of Mathematics, University of the Punjab, Quaid-e-Azam Campus, Lahore, Pakistan*
[2]*Department of Physics, College of Sciences, University of Bisha, PO Box 344, Bisha 61922, Saudi Arabia*
[3]*Physics Department, Faculty of Science, Al-Azhar University, Assiut 71524, Egypt*
[4]*Department of Mathematics, College of Science, King Khalid University, P.O. Box 9004, Abha 61413, Saudi Arabia*
[5]*Department of Mathematics, University of Management and Technology, 54770 Lahore, Pakistan*
[6]*Department of Mathematics (Statistics Option) Program, Pan African University, Institute of Basic Science, Technology and Innovation (PAUSTI), Nairobi 6200-00200, Kenya*
[7]*Department of Mathematics and Statistics, College of Science, Taif University, PO Box 11099, Taif 21944, Saudi Arabia*

Correspondence should be addressed to Abdel-Haleem Abdel-Aty; amabdelaty@ub.edu.sa and Abdisalam Hassan Muse; muse.abdisalam@students.jkuat.ac.ke

Received 13 June 2022; Revised 8 July 2022; Accepted 26 July 2022; Published 25 August 2022

Academic Editor: Yusuf Gurefe

This article discusses dynamics of the fractal double-chain deoxyribonucleic acid model. This structure contains two long elastic homogeneous strands that serve as two polynucleotide chains of deoxyribonucleic acid molecules, bounded by an elastic membrane indicating hydrogen bonds between the base pairs of two chains. The semi-inverse variational principle and auxiliary equation method are employed to extricate soliton solutions. The collection of retrieved exact solutions includes bright, dark, periodic, and other solitons. The constraint conditions emerge naturally which ensure the presence of these solutions. Additionally, 2D and 3D graphs showing the impact of fractals on solutions are included. These plots use appropriate parameter values. Furthermore, sensitivity analysis of the considered model is also acknowledged. The outcomes reveal that these techniques are reliable, effective, and applicable to various biological systems.

1. Introduction

Deoxyribonucleic acid (DNA) is an interesting nonlinear model of biological sciences [1, 2]. Since it is needed for protein-coding, inheritance, and genetic instruction manual for life, it contains instructions for cell growth, reproduction, and death of a human. DNA molecules are the foundation of life so their dynamics are one of the interesting problems in biophysics. Researchers have been studying this structure during the last decades [3, 4]. The study of DNA mechanism predicts the presence of significant nonlinear structures. It has been established that localized waves are caused by nonlinearity and these waves are fascinating because they can transmit power without causing power loss [5–7].

Nonlinear partial differential equations (NLPDEs) have been considered for studying several nonlinear physical phenomena. Many physicists and mathematicians have worked hard to develop further precise alternatives to NLPDEs for a better understanding of these processes. Therefore, exact solutions of NLPDEs are essential for exploring physical explanations and qualitative aspects of different mechanisms [8–18]. These solutions demonstrate the dynamics of several nonlinear complex models symbolically and physically. Numerous methods were implemented to attain exact and wave solutions of the nonlinear governing model [19–26].

This paper introduces the fractal double-chain DNA model to scrutinize the double-helix structure. Fractal calculus has been a flourishing subject of biology, mathematics, and physics because it deals with the modeling of distinct nonlinear procedures [27–34]. Since the fractal model covers many powerful properties, which the traditional system fails to explain. The field of biophysics greatly benefits from a unique class of solitary wave solutions referred to as solitons of proposed problems [3]. Wave packets known as solitons propagate at a constant pace and maintain their shape despite nonlinearities and dispersion [35–43]. Semi-inverse scheme and auxiliary equation method (AEM) are two effective techniques implemented to derive a set of solitons in this manuscript.

The Ritz-like approach linked with the variational principle termed as He's semi-inverse variational method [44] is applied to attain the bright solitons of fractal DNA model which may aid biologists to comprehend its physical significance. An effective and straightforward algebraic method for finding soliton solutions is the semi-inverse scheme [45]. Many authors contributed to develop this technique to analyze fractal models in distinct scientific fields [33, 46, 47]. Another method adopted here is AEM that retrieves dark, periodic, bright, and other shaped solitons. This reliable strategy is employed to obtain dual-mode solutions of various equations found in literature [48, 49]. It is the generalization of many existing techniques. By using various values of the parameters and fractal dimension, the nonlinear dynamics of DNA strands can be addressed. The sensitivity analysis assesses how different uncertainties affect the overall level of uncertainty in a mathematical model. Specific boundaries that are dependent on one or more parameters have been applied using this technique.

The rest of the article is organize as follows: The governing model is included in Section 2. In section 3, soliton solutions are extracted along with geometrical analysis by employing semi-inverse method. Section 4 comprises solitons obtained via AEM with graphs. Section 5 of the report discusses the findings. Section 6 provides a sensitivity analysis of the suggested system. The article's conclusion is provided in Section 7.

2. Governing System

Consider the following two general nonlinear dynamical equations which describe double-chain model of DNA:

$$u_{\tau\tau} - \beta_1^2 u_{xx} = \sigma_1 u + \xi_1 uv + \eta_1 u^3 + \alpha_1 uv^2, \tag{1}$$

$$v_{\tau\tau} - \beta_2^2 v_{xx} = \sigma_2 v + \xi_2 u^2 + \eta_2 u^2 v + \alpha_2 v^3 + a, \tag{2}$$

where u is the difference between the top and bottom strands' longitudinal displacements, i.e., the deviations of the bases from their equilibrium positions along the direction of the phosphodiester bridge, which joins the two bases of the same strands, v is the difference between the bottom and top strands' transverse displacements, i.e., the bases displacement from its equilibrium point with the pathway of hydrogen bond which joins two bases of base pair where

$$\beta_1 = \pm\frac{G}{\nu}, \beta_2 = \pm\frac{H}{\nu}, \sigma_1 = -\frac{2\eta}{\nu bh}(h - m_o), \sigma_2 = -\frac{2\eta}{\nu b}, \xi_1 = 2\xi_2 = \frac{2\sqrt{2}\eta m_o}{\nu bh^2},$$
$$\eta_1 = \eta_2 = -\frac{2\eta m_o}{\nu bh^3}, \alpha_1 = \alpha_2 = \frac{4\eta m_o}{\nu bh^3}, a = \frac{\sqrt{2}\eta}{\nu b}(h - m_o), \tag{3}$$

where H, b, G, and ν represent the tension density, cross-sectional area, Young's modulus, and the mass density of each strand, h is the distance between the strands, while η is the stiffness and m_o is the membrane height in positive equilibrium. The difference between the longitudinal displacements of the bottom and top strands is u in equation (1), as opposed to v, which represents the difference between the transverse displacements of the lower and higher strands.

Noq using a transformation:

$$v = eu + f, \tag{4}$$

where e and f are constants, to simplify Equation (1) into the system of equations as follows:

$$u_{\tau\tau} - \beta_1^2 u_{xx} = u^3(\eta_1 + \alpha_1 e^2) + u^2(2\alpha_1 ef + \xi_1 e) + u(\sigma_1 + f\xi_1 + \alpha_1 f^2), \tag{5}$$

$$u_{\tau\tau} - \beta_2^2 u_{xx} = u^3(\eta_2 + \alpha_2 e^2) + u^2\left(3\alpha_2 ef + \frac{\xi_2}{e} + \frac{\eta_2 f}{e}\right) + u(\sigma_2 + 3\alpha_2 f^2) + \frac{\sigma_2 f}{e} + \frac{\alpha_2 f^3}{e} + \frac{a}{e}. \tag{6}$$

Comparing Equations (4) and (5), we infer that $f = h/\sqrt{2}$ and $H = G$. So, Equation (5) can be written as

$$u_{\tau\tau} - \beta_1^2 u_{xx} = Su^3 + Tu^2 + Vu, \tag{7}$$

where

$$S = \frac{\zeta}{h^3}(-2 + 4e^2),$$
$$T = \frac{6\sqrt{2}e\zeta}{h^2},$$
$$V = \left(\frac{-2\zeta}{m_o} + \frac{6\zeta}{h}\right),$$
$$\zeta = \frac{\eta m_o}{\nu b},$$
$$\beta_1 = \frac{G}{\nu}. \tag{8}$$

3. Mathematical Analysis

The wave transformation $u(x, \tau) = u(\delta), \delta = lx + \kappa\tau$ reduces Equation (7) to the following ODE:

$$(\kappa^2 - l^2\beta_1^2)u'' - Su^3 - Tu^2 - Vu = 0, \text{where } \kappa^2 - l^2\beta_1^2 \neq 0. \tag{9}$$

According to [50, 51], a fractal DNA model can be written as

$$\left(\kappa^2 - l^2\beta_1^2\right)\frac{d}{d\delta^\gamma}\left(\frac{du}{d\delta^\gamma}\right) - Su^3 - Tu^2 - Vu = 0, \quad (10)$$

where γ and $du/d\delta^\gamma$ are the fractal dimensional value and derivative, respectively, stated as

$$\frac{du}{d\delta^\gamma} = \Gamma(1+\kappa)\lim_{\delta-\delta_o\longrightarrow\Delta\delta}\frac{u(\delta)-u(\delta_o)}{(\delta-\delta_o)^\kappa}, \quad \Delta\delta \neq 0. \quad (11)$$

The variational principle [44] can be used to produce the following trial-functional:

$$J = \int L d\delta = \int (K - E) d\delta. \quad (12)$$

The variational formulation of Equation (10) is given as

$$J = \int_0^\infty \left[\left(\kappa^2 - l^2\beta_1^2\right)\left(\frac{du}{d\delta^\gamma}\right)^2 + Su^3 + Tu^2 + Vu\right] d\delta^\gamma, \quad (13)$$

where $K = (\kappa^2 - l^2\beta_1^2)[du/d\delta^\gamma]^2$ is the kinetic energy and $E = -Su^3 - Tu^2 - Vu$ is the potential energy.

$$L = \left(\kappa^2 - l^2\beta_1^2\right)\left(\frac{du}{d\delta^\gamma}\right)^2 + Su^3 + Tu^2 + Vu,$$
$$H = \left(\kappa^2 - l^2\beta_1^2\right)\left(\frac{du}{d\delta^\gamma}\right)^2 - Su^3 - Tu^2 - Vu. \quad (14)$$

The above equations are the Lagrangian and Hamiltonian. Using the two scale transformation,

$$A = \delta^\gamma. \quad (15)$$

Equation. (13) can be written as

$$J = \int_0^\infty \left[\left(\kappa^2 - l^2\beta_1^2\right)\left(\frac{du}{dA}\right)^2 + Su^3 + Tu^2 + Vu\right] dA. \quad (16)$$

3.1. Soliton Solutions of Fractal Model. Using Ritz technique, one can construct the solitary wave solution as

$$u = C \sec h(DA), \quad (17)$$

where C and D are constants to be further calculated. Putting Equation (17) into Equation (16), we have

$$J = \frac{C^2}{12D}\left(\pi CT + 6V + 2SC^2\right) + \frac{C^2 D}{6}\left(\kappa^2 - l^2\beta_1^2\right). \quad (18)$$

Setting J stationary with respect to C and D, it results,

$$\frac{\partial J}{\partial C} = \frac{C}{12D}\left(3\pi CT + 12V + 8SC^2\right) + \frac{CD}{3}\left(\kappa^2 - l^2\beta_1^2\right), \quad (19)$$

$$\frac{\partial J}{\partial D} = -\frac{C^2}{12D^2}\left(\pi CT + 6V + 2SC^2\right) + \frac{C^2}{6}\left(\kappa^2 - l^2\beta_1^2\right). \quad (20)$$

From Equations (19) and (20), we have

$$C = \pm\frac{\left(-5\pi T + \sqrt{25\pi^2T^2 - 1152SV}\right)}{24S},$$
$$D = \pm\sqrt{\frac{\left(5\pi T - \sqrt{25\pi^2T^2 - 1152SV}\right)\pi T - 288SV}{288\left(l^2\beta_1^2 - \kappa^2\right)S}}. \quad (21)$$

Now, Equation (17) can be described as

$$u(x,\tau) = \pm\frac{\left(-5\pi T + \sqrt{25\pi^2T^2 - 1152SV}\right)}{24S} \sec h\left[\pm\sqrt{\frac{\left(5\pi T - \sqrt{25\pi^2T^2 - 1152SV}\right)\pi T - 288SV}{288\left(l^2\beta_1^2 - \kappa^2\right)S}} A\right]. \quad (22)$$

Inserting the value of u in Equation (4), then, we have

$$v(x,\tau) = \pm e\frac{\left(-5\pi T + \sqrt{25\pi^2T^2 - 1152SV}\right)}{24S} \sec h\left[\pm\sqrt{\frac{\left(5\pi T - \sqrt{25\pi^2T^2 - 1152SV}\right)\pi T - 288SV}{288\left(l^2\beta_1^2 - \kappa^2\right)S}} A\right] + f, \quad (23)$$

where $A = (lx + \kappa\tau)^\gamma$.

Additionally, we look another soliton solution in the form:

$$u = P \sec h^4(QA), \quad (24)$$

where P and Q are constants to be further calculated. Substituting Equation (24) in Equation (16), we have

$$J = \frac{P^2}{135135Q}\left(16640PT + 30888V + 10752SP^2\right) + \frac{128P^2Q}{315}\left(\kappa^2 - l^2\beta_1^2\right). \quad (25)$$

When we keep J stationary with respect to P and Q, it gives

$$\frac{\partial J}{\partial P} = \frac{P}{45045Q}\left(16640PT + 20592V + 14336SP^2\right) + \frac{256PQ}{315}\left(\kappa^2 - l^2\beta_1^2\right), \quad (26)$$

$$\frac{\partial J}{\partial Q} = -\frac{P^2}{135135Q^2}\left(16640PT + 30888V + 10752SP^2\right) + \frac{128P^2}{315}\left(\kappa^2 - l^2\beta_1^2\right). \quad (27)$$

From Equations (26) and (27), we have

$$P = \pm \frac{\left(-325T + \sqrt{105625T^2 - 486486SV}\right)}{504S},$$
$$Q = \pm \sqrt{\frac{10T\left(325T - \sqrt{105625T^2 - 486486SV}\right) - 18711SV}{99792\left(l^2\beta_1^2 - \kappa^2\right)S}}. \tag{28}$$

Equation (24) becomes

$$u(x,\tau) = \pm \frac{\left(-325T + \sqrt{105625T^2 - 486486SV}\right)}{504S} \sec h^4\left[\pm\sqrt{\frac{10T\left(325T - \sqrt{105625T^2 - 486486SV}\right) - 18711SV}{99792\left(l^2\beta_1^2 - \kappa^2\right)S}}A\right]. \tag{29}$$

Plugging the value of u in Equation (4), we have

$$v(x,\tau) = \pm e \frac{\left(-325T + \sqrt{105625T^2 - 486486SV}\right)}{504S} \sec h^4\left[\pm\sqrt{\frac{10T\left(325T - \sqrt{105625T^2 - 486486SV}\right) - 18711SV}{99792\left(l^2\beta_1^2 - \kappa^2\right)S}}A\right] + f \tag{30}$$

where $A = (lx + \kappa\tau)^\gamma$.

4. Illustration of the AEM

The following statement illustrates the general NLPDE structure:

$$Q(u, u_t, u_x, uu_t, u_t u_{xx}, uu_{tt}, \cdots) = 0, \tag{31}$$

where Q is polynomial function of u and its derivatives in relation to two independent variables t and x. Use the single variable conversion $\delta = lx - \kappa t$ to reduce Equation (31) into ODE of the form:

$$R\left(u, u', u'', uu'', \cdots\right) = 0. \tag{32}$$

Here, R is a polynomial function with both linear and nonlinear terms and the superscripts of u show its ordinary derivative with respect to δ. The algorithm of AEM suggests the initial solution of Equation (32) as

$$u(\delta) = \sum_{i=0}^{M} d_i \beta^{i\phi(\delta)}, \tag{33}$$

satisfying the auxiliary equation

$$\phi'(\delta) = \frac{1}{\ln(\beta)}\left(a\beta^{-\phi(\delta)} + c + b\beta^{\phi(\delta)}\right), \tag{34}$$

where $d_0, d_1, d_2, \ldots, d_M$ are coefficients to be evaluated such that $d_M \neq 0$. The value of M is determined by balancing the highest order derivative and nonlinear term involved in Equation (9).

Now, putting Equation (33) into Equation (9) and performing few steps of algebra yields a system of algebraic equations in $\beta^{\phi(\delta)}$.

The family of solutions of Equation (34) can be obtained as follows:

Family 1. When $c^2 - 4ab < 0$ and $b \neq 0$,

$$\beta^{\phi(\delta)} = \frac{-c}{2b} + \frac{\sqrt{4ab - c^2}}{2b}\tan\left(\frac{\sqrt{4ab - c^2}}{2}\delta\right),$$
$$\beta^{\phi(\delta)} = \frac{-c}{2b} - \frac{\sqrt{4ab - c^2}}{2b}\cot\left(\frac{\sqrt{4ab - c^2}}{2}\delta\right). \tag{35}$$

Family 2. When $c^2 - 4ab > 0$ and $b \neq 0$,

$$\beta^{\phi(\delta)} = \frac{-c}{2b} - \frac{\sqrt{c^2 - 4ab}}{2b}\tan h\left(\frac{\sqrt{c^2 - 4ab}}{2}\delta\right),$$
$$\beta^{\phi(\delta)} = \frac{-c}{2b} - \frac{\sqrt{c^2 - 4ab}}{2b}\cot h\left(\frac{\sqrt{c^2 - 4ab}}{2}\delta\right). \tag{36}$$

Family 3. When $c^2 + 4a^2 < 0$ and $b \neq 0$ and $b = -a$,

$$\beta^{\phi(\delta)} = \frac{c}{2a} - \frac{\sqrt{-4a^2 - c^2}}{2a}\tan\left(\frac{\sqrt{-4a^2 - c^2}}{2}\delta\right),$$
$$\beta^{\phi(\delta)} = \frac{c}{2a} + \frac{\sqrt{-4a^2 - c^2}}{2a}\cot\left(\frac{\sqrt{-4a^2 - c^2}}{2}\delta\right). \tag{37}$$

Family 4. When $c^2 + 4a^2 < 0$ and $b \neq 0$ and $b = -a$,

$$\beta^{\phi(\delta)} = \frac{c}{2a} + \frac{\sqrt{4a^2 + c^2}}{2a}\tan h\left(\frac{\sqrt{4a^2 + c^2}}{2}\delta\right),$$
$$\beta^{\phi(\delta)} = \frac{c}{2a} + \frac{\sqrt{4a^2 + c^2}}{2a}\cot h\left(\frac{\sqrt{4a^2 + c^2}}{2}\delta\right). \tag{38}$$

Family 5. When $c^2 - 4a^2 < 0$ and $b = a$,

$$\beta^{\phi(\delta)} = \frac{-c}{2a} + \frac{\sqrt{4a^2 - c^2}}{2a}\tan\left(\frac{\sqrt{4a^2 - c^2}}{2}\delta\right),$$
$$\beta^{\phi(\delta)} = \frac{-c}{2a} - \frac{\sqrt{4a^2 - c^2}}{2a}\cot\left(\frac{\sqrt{4a^2 - c^2}}{2}\delta\right). \tag{39}$$

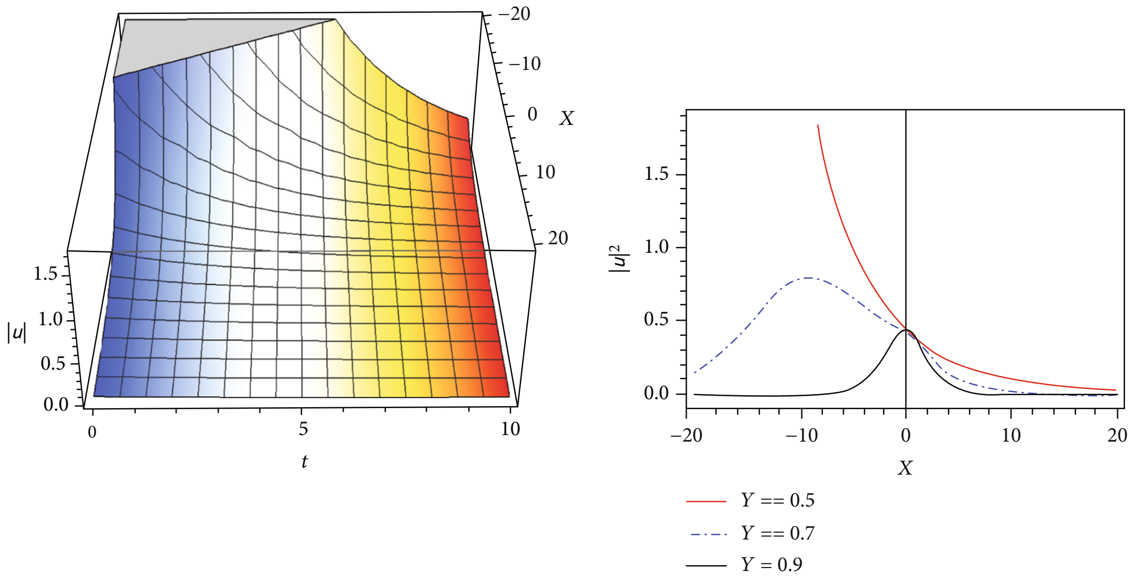

(a) (b)

FIGURE 1: We consider $\kappa = 2$, $l = 1$, $\beta_1 = 1$, $S = -1$, $T = 2$, $V = 1$, and $\gamma = 0.5, 0.7, 0.9$ for the solution described by Equation (22). (a) The 3D sketch of $|u|^2$ taking $\gamma = 0.5$. (b) 2D-plot of $|u|^2$ with three distinct γ values.

Family 6. When $c^2 - 4a^2 > 0$ and $b = a$,

$$\beta^{\phi(\delta)} = \frac{-c}{2a} - \frac{\sqrt{-4a^2 + c^2}}{2a} \tan h \frac{\sqrt{-4a^2 + c^2}}{2} \delta \Bigg),$$
$$\beta^{\phi(\delta)} = \frac{-c}{2a} - \frac{\sqrt{-4a^2 + c^2}}{2a} \cot h \left(\frac{\sqrt{-4a^2 + c^2}}{2} \delta \right). \quad (40)$$

Family 7. When $c^2 = 4ab$,

$$\beta^{\phi(\delta)} = -\frac{2 + c\delta}{2b\delta}. \quad (41)$$

Family 8. When $ab < 0$, $c = 0$ and $b \neq 0$,

$$\beta^{\phi(\delta)} = -\sqrt{\frac{-a}{b}} \tan h \left(\sqrt{-ba}\delta \right),$$
$$\beta^{\phi(\delta)} = -\sqrt{\frac{-a}{b}} \cot h \left(\sqrt{-ba}\delta \right). \quad (42)$$

Family 9. When $c = 0$ and $a = -b$,

$$\beta^{\phi(\delta)} = \frac{1 + e^{-2b\delta}}{-1 + e^{-2b\delta}}. \quad (43)$$

Family 10. When $a = b = 0$,

$$\beta^{\phi(\delta)} = \cos h(c\delta) + \sin h(c\delta). \quad (44)$$

Family 11. When $a = c = K$ and $b = 0$,

$$\beta^{\phi(\delta)} = e^{K\delta} - 1. \quad (45)$$

Family 12. When $b = c = K$ and $a = 0$,

$$\beta^{\phi(\delta)} = \frac{e^{K\delta}}{1 - e^{K\delta}}. \quad (46)$$

Family 13. When $c = a + b$,

$$\beta^{\phi(\delta)} = -\frac{1 - ae^{(a-b)\delta}}{1 - be^{(a-b)\delta}}. \quad (47)$$

Family 14. When $c = -(a + b)$,

$$\beta^{\phi(\delta)} = \frac{a - e^{(a-b)\delta}}{b - e^{(a-b)\delta}}. \quad (48)$$

Family 15. When $a = 0$,

$$\beta^{\phi(\delta)} = \frac{ce^{c\delta}}{1 - be^{c\delta}}. \quad (49)$$

Family 16. When $c = a = b \neq 0$,

$$\beta^{\phi(\delta)} = \frac{1}{2} \left[\sqrt{3} \tan \left(\frac{\sqrt{3}}{2} a\delta \right) - 1 \right]. \quad (50)$$

Family 17. When $a = b$ and $c = 0$,

$$\beta^{\phi(\delta)} = \tan (a\delta). \quad (51)$$

Family 18. When $b = 0$,

$$\beta^{\phi(\delta)} = e^{c\delta} - \frac{m}{n}. \quad (52)$$

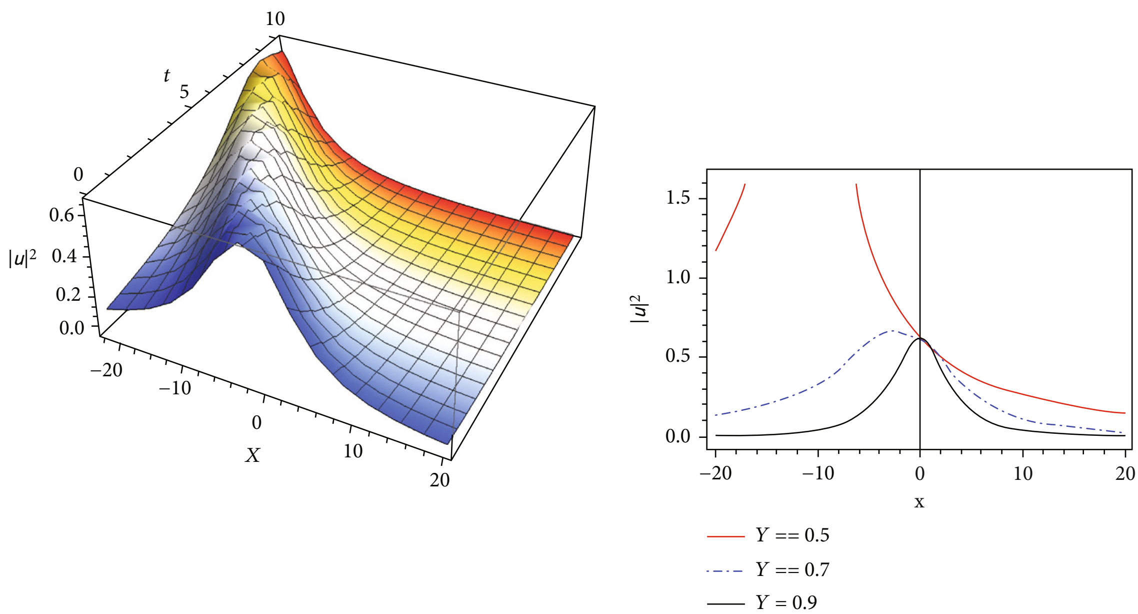

(a) (b)

Figure 2: We suggest $\kappa = 2$, $l = 1$, $\beta_1 = 1$, $S = -1$, $T = 2$, $V = 1$, and $\gamma = 0.5, 0.7, 0.9$ for the solution obtained in Equation (29). (a) The 3D-plot of $|u|^2$ with $\gamma = 0.7$. (b) The 2D-plot of $|u|^2$ with distinct values of γ.

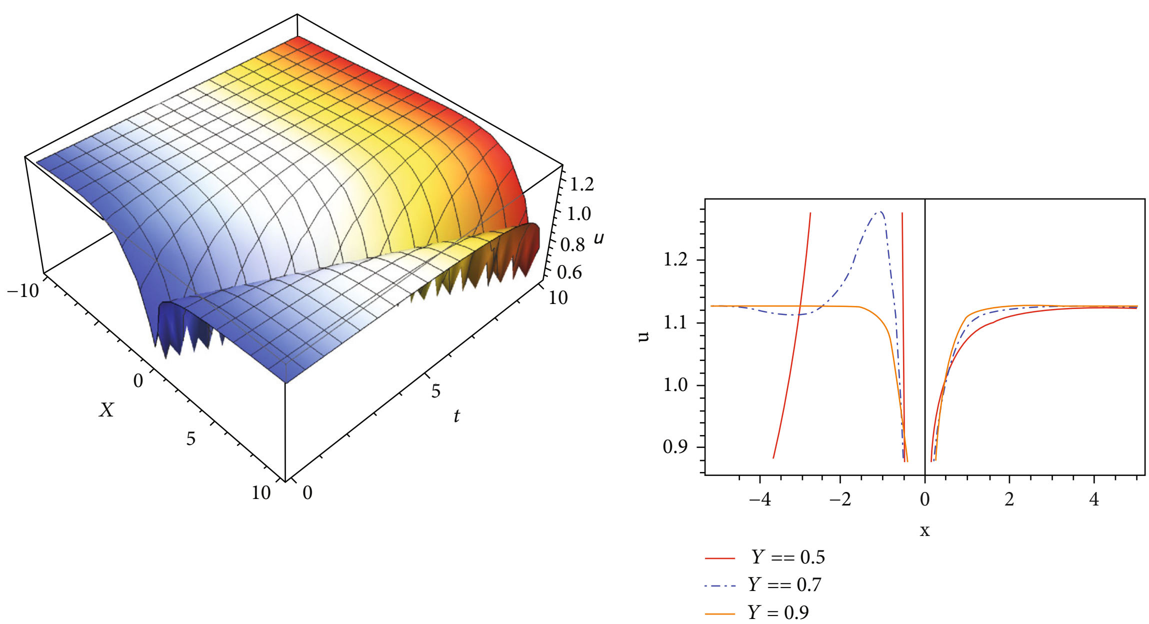

(a) (b)

Figure 3: We suggest $\kappa = -1$, $\beta_1 = 1$, $T = 2$, $V = 1$, $c = 3$, $a = 1$, $b = 1$, and $\gamma = 0.5, 0.7, 0.9$. for the solution $u_{1,1}$. (a) The 3D graph of $u_{1,1}(x, t)$ with $\gamma = 0.3$. (b) The 2D graph of $u_{1,1}(x, t)$ with distinct values of γ.

4.1. Application of AEM. The balancing principle employed to Equation (9) yields the value of index $M = 1$. Hence, Equation (33) takes the form:

$$u(\delta) = d_0 + d_1 \beta^{\phi(\delta)}. \tag{53}$$

Now, invoking Equation (53) into Equation (9) gives a system of equations which is further evaluated via Maple, it generates

$$d_0 = \frac{3V(q\Theta - 1)}{2T}, d_1 = \frac{3bV\Theta}{T}, S = \frac{2T^2}{9V}, l = \frac{-\sqrt{(4ab\kappa^2 - c^2\kappa^2)/\Theta} - V}{\beta_1}, \tag{54}$$

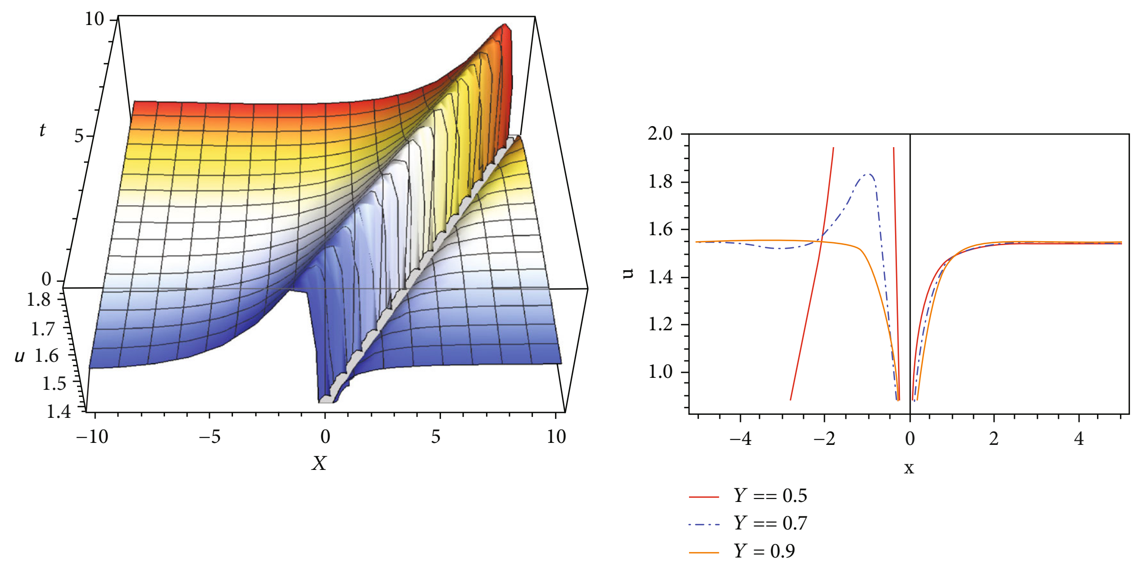

(a) (b)

Figure 4: We take $\kappa=-1$, $\beta_1=1$, $T=2$, $V=1$, $c=3$, $a=1$, $b=1$, and $\gamma=0.5, 0.7, 0.9$. for the solution $|u_{3,1}|$. (a) The 3D graph of $u_{3,1}(x,t)$ with $\gamma=0.3$. (b) The 2D graph of $u_{3,1}(x,t)$ with distinct values of γ.

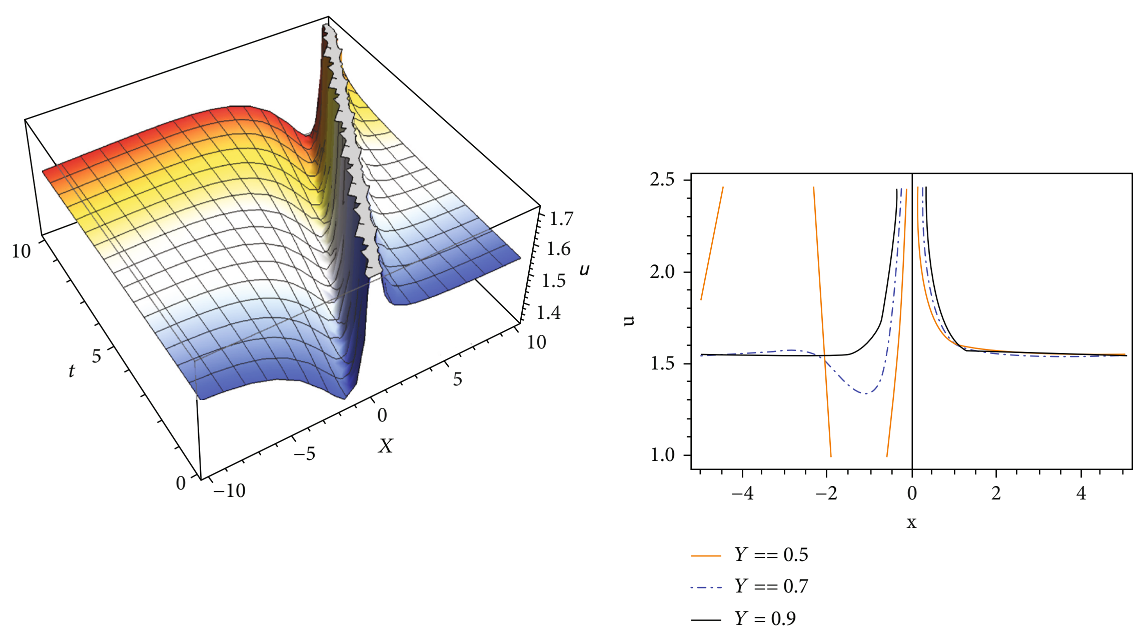

(a) (b)

Figure 5: We take $\kappa=-1$, $\beta_1=1$, $T=2$, $V=1$, $c=3$, $a=1$, $b=1$, and $\gamma=0.5, 0.7, 0.9$ for the solution $|u_{3,2}|$. (a) The 3D graph of $u_{3,2}(x,t)$ with $\gamma=0.3$. (b) The 2D graph of $u_{3,2}(x,t)$ with distinct values of γ.

where

$$\Theta=\sqrt{\frac{-1}{4ab-c^2}}. \tag{55}$$

Insertion of Equation (54) into Equation (53) results to

$$u(\delta)=\frac{3V(c\Theta-1)}{2T}+\frac{3bV\Theta}{T}\beta^{\phi(\delta)}. \tag{56}$$

By substituting the solutions specified by Equation (34) into Equation (58), the solutions retrieved are

For Family 1, when $c^2-4ab<0$ and $b\neq 0$,

$$u_{1,1}(x,t)=\frac{3V(c\Theta-1)}{2T}+\frac{3V\Theta}{T}\left[\frac{-c}{2}+\sqrt{4ab-c^2}\tan\left(\frac{\sqrt{4ab-c^2}}{2}\delta^{\gamma}\right)\right], \tag{57}$$

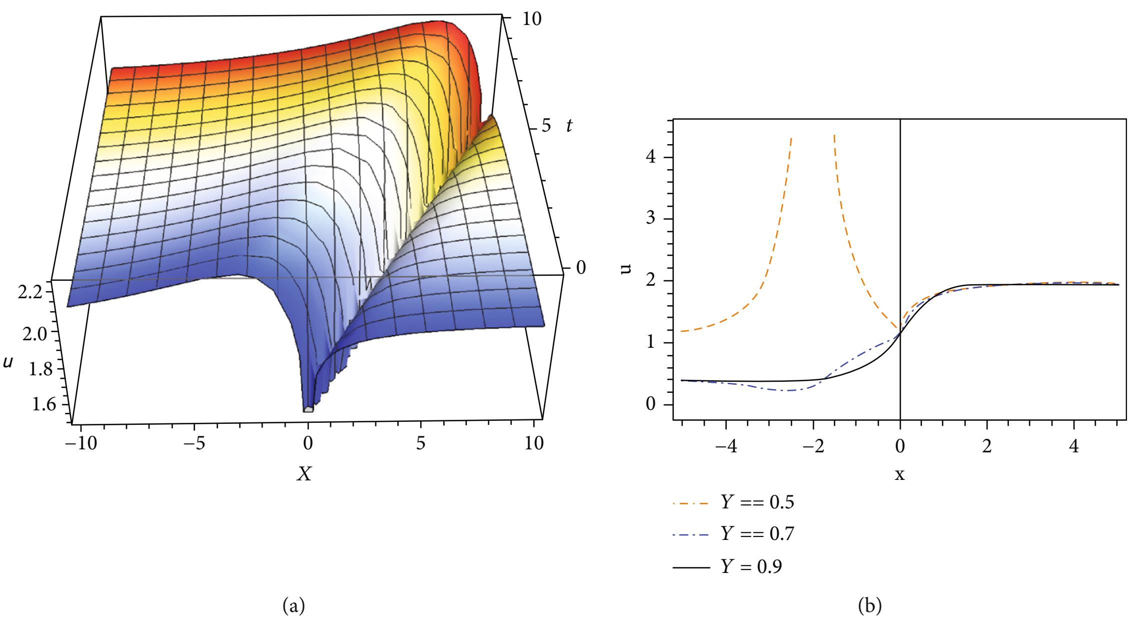

Figure 6: We take $\kappa=-1$, $\beta_1=1$, $T=2$, $V=1$, $c=3$, $a=1$, $b=1$, and $\gamma=0.5, 0.7, 0.9$ for the solution $|u_{5,1}|$. (a) The 3D graph of $u_{5,1}(x,t)$ with $\gamma=0.3$. (b) The 2D graph of $u_{5,1}(x,t)$ with distinct values of γ.

$$u_{1,2}(x,t)=\frac{3V(c\Theta-1)}{2T}+\frac{3V\Theta}{T}\left[\frac{-c}{2}-\sqrt{4ab-c^2}\cot\left(\frac{\sqrt{4ab-c^2}}{2}\delta^\gamma\right)\right], \tag{58}$$

$$v_{1,1}(x,t)=\frac{3eV(c\Theta-1)}{2T}+\frac{3eV\Theta}{T}\left[\frac{-c}{2}+\sqrt{4ab-c^2}\tan\left(\frac{\sqrt{4ab-c^2}}{2}\delta^\gamma\right)\right]+f, \tag{59}$$

$$v_{1,2}(x,t)=\frac{3eV(c\Theta-1)}{2T}+\frac{3eV\Theta}{T}\left[\frac{-c}{2}-\sqrt{4ab-c^2}\cot\left(\frac{\sqrt{4ab-c^2}}{2}\delta^\gamma\right)\right]+f. \tag{60}$$

For Family 2, when $c^2-4ab>0$ and $b\neq 0$,

$$\begin{aligned}
u_{2,1}(x,t)&=\frac{3V(c\Theta-1)}{2T}+\frac{3V\Theta}{T}\left[\frac{-c}{2}-\sqrt{c^2-4ab}\tan h\left(\frac{\sqrt{c^2-4ab}}{2}\delta^\gamma\right)\right],\\
u_{2,2}(x,t)&=\frac{3V(c\Theta-1)}{2T}+\frac{3V\Theta}{T}\left[\frac{-c}{2}-\sqrt{c^2-4ab}\cot h\left(\frac{\sqrt{c^2-4ab}}{2}\delta^\gamma\right)\right],\\
v_{2,1}(x,t)&=\frac{3eV(c\Theta-1)}{2T}+\frac{3eV\Theta}{T}\left[\frac{-c}{2}-\sqrt{c^2-4ab}\tan h\left(\frac{\sqrt{c^2-4ab}}{2}\delta^\gamma\right)\right]+f,\\
v_{2,2}(x,t)&=\frac{3eV(c\Theta-1)}{2T}+\frac{3eV\Theta}{T}\left[\frac{-c}{2}-\sqrt{c^2-4ab}\cot h\left(\frac{\sqrt{c^2-4ab}}{2}\delta^\gamma\right)\right]+f.
\end{aligned} \tag{61}$$

For Family 3, when $c^2+4ab<0$, $b\neq 0$ and $b=-a$,

$$\begin{aligned}
u_{3,1}(x,t)&=\frac{3V(c\Theta-1)}{2T}-\frac{3V\Theta}{T}\left[\frac{c}{2}-\sqrt{4a^2-c^2}\tan\left(\frac{\sqrt{4a^2-c^2}}{2}\delta^\gamma\right)\right],\\
u_{3,2}(x,t)&=\frac{3V(c\Theta-1)}{2T}-\frac{3V\Theta}{T}\left[\frac{c}{2}+\sqrt{4a^2-c^2}\cot\left(\frac{\sqrt{4a^2-c^2}}{2}\delta^\gamma\right)\right],\\
v_{3,1}(x,t)&=\frac{3eV(c\Theta-1)}{2T}-\frac{3eV\Theta}{T}\left[\frac{c}{2}-\sqrt{4a^2-c^2}\tan\left(\frac{\sqrt{4a^2-c^2}}{2}\delta^\gamma\right)\right]+f,\\
v_{3,2}(x,t)&=\frac{3eV(c\Theta-1)}{2T}-\frac{3eV\Theta}{T}\left[\frac{c}{2}+\sqrt{4a^2-c^2}\cot\left(\frac{\sqrt{4a^2-c^2}}{2}\delta^\gamma\right)\right]+f.
\end{aligned} \tag{62}$$

For Family 4, when $c^2+4a^2>0$, $b\neq 0$ and $b=-a$,

$$\begin{aligned}
u_{4,1}(x,t)&=\frac{3V(c\Theta-1)}{2T}-\frac{3V\Theta}{T}\left[\frac{c}{2}+\sqrt{4a^2+c^2}\tan h\left(\frac{\sqrt{4a^2+c^2}}{2}\delta^\gamma\right)\right],\\
u_{4,2}(x,t)&=\frac{3V(c\Theta-1)}{2T}-\frac{3V\Theta}{T}\left[\frac{c}{2}+\sqrt{4a^2+c^2}\cot h\left(\frac{\sqrt{4a^2+c^2}}{2}\delta^\gamma\right)\right],\\
v_{4,1}(x,t)&=\frac{3eV(c\Theta-1)}{2T}-\frac{3eV\Theta}{T}\left[\frac{c}{2}+\sqrt{4a^2+c^2}\tan h\left(\frac{\sqrt{4a^2+c^2}}{2}\delta^\gamma\right)\right]+f,\\
v_{4,2}(x,t)&=\frac{3eV(c\Theta-1)}{2T}-\frac{3eV\Theta}{T}\left[\frac{c}{2}+\sqrt{4a^2+c^2}\cot h\left(\frac{\sqrt{4a^2+c^2}}{2}\delta^\gamma\right)\right]+f.
\end{aligned} \tag{63}$$

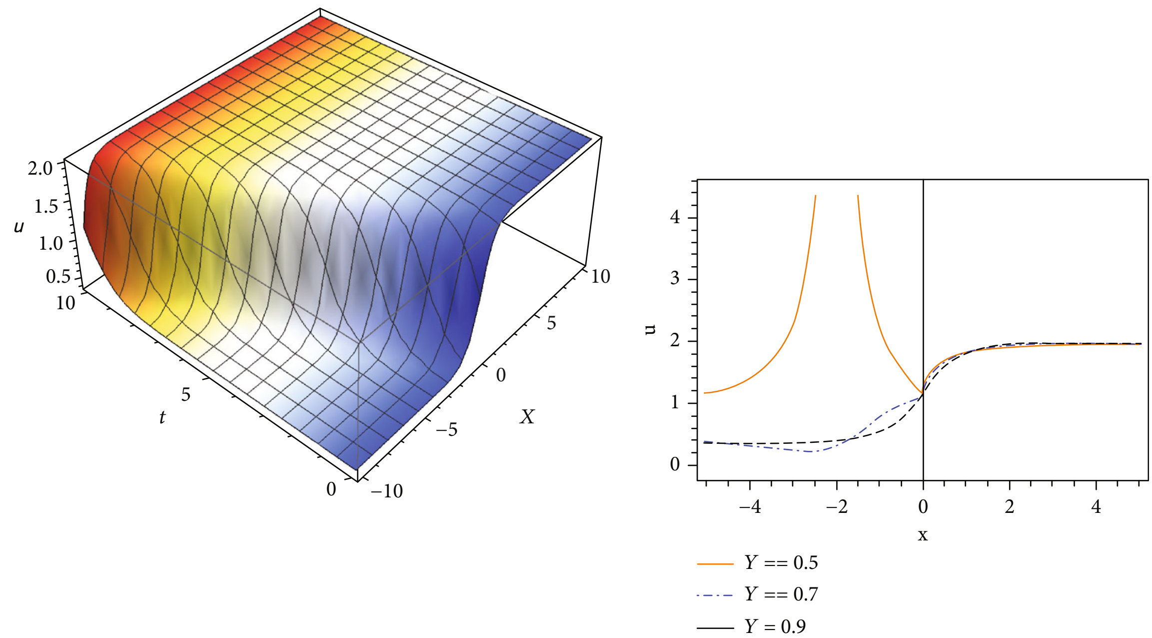

(a) (b)

Figure 7: We consider $\kappa = -1$, $\beta_1 = 1$, $T = 2$, $V = 1$, $c = 3$, $a = 1$, $b = 1$, and $\gamma = 0.5, 0.7, 0.9$ for the solution $|u_{6,1}|$. (a) The 3D graph of $u_{6,1}(x, t)$ with $\gamma = 0.8$. (b) The 2D graph of $u_{6,1}(x, t)$ with distinct values of γ.

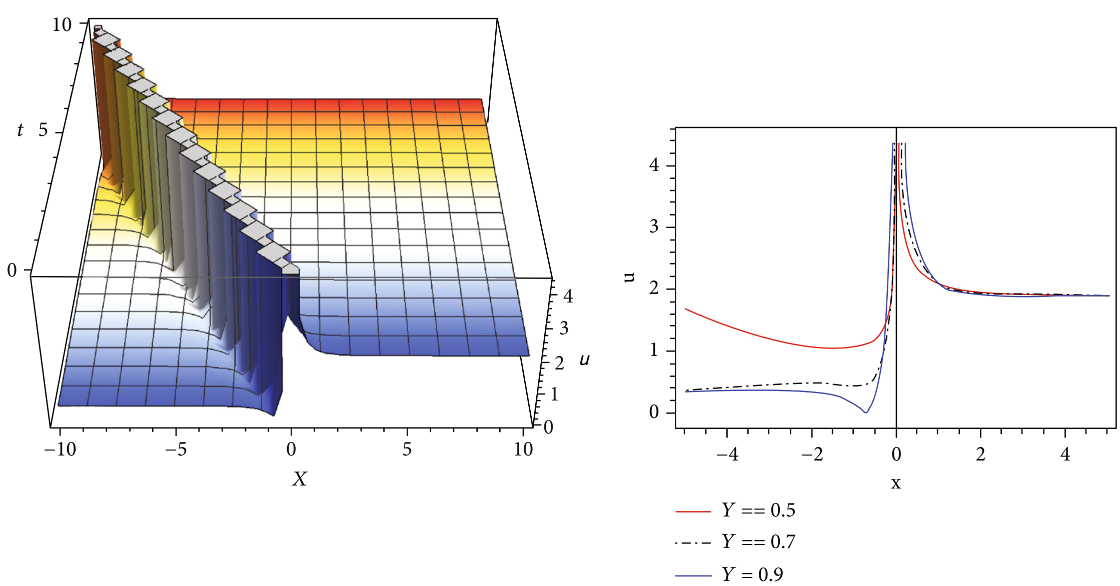

(a) (b)

Figure 8: We suggest $\kappa = -1$, $\beta_1 = 1$, $T = 2$, $V = 1$, $c = 3$, $a = 1$, $b = 1$, and $\gamma = 0.5, 0.7, 0.9$ for the solution $|u_{6,2}|$. (a) The 3D graph of $u_{6,2}(x, t)$ with $\gamma = 0.3$. (b) The 2D graph of $u_{6,2}(x, t)$ with distinct values of γ.

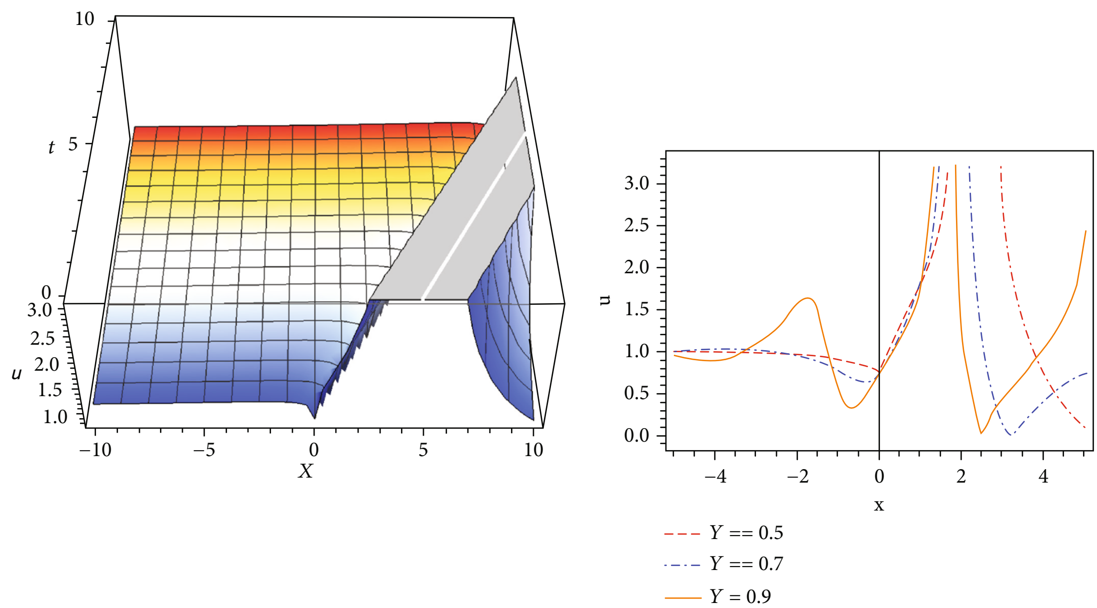

(a) (b)

FIGURE 9: We take $\kappa = -1$, $\beta_1 = 1$, $T = 2$, $V = 1$, $c = 3$, $a = 1$, $b = 1$, and $\gamma = 0.5, 0.7, 0.9$ for the solution $|u_{8,1}|$. (a) The 3D graph of $u_{8,1}(x, t)$ with $\gamma = 0.3$. (b) The 2D graph of $u_{8,1}(x, t)$ with distinct values of γ.

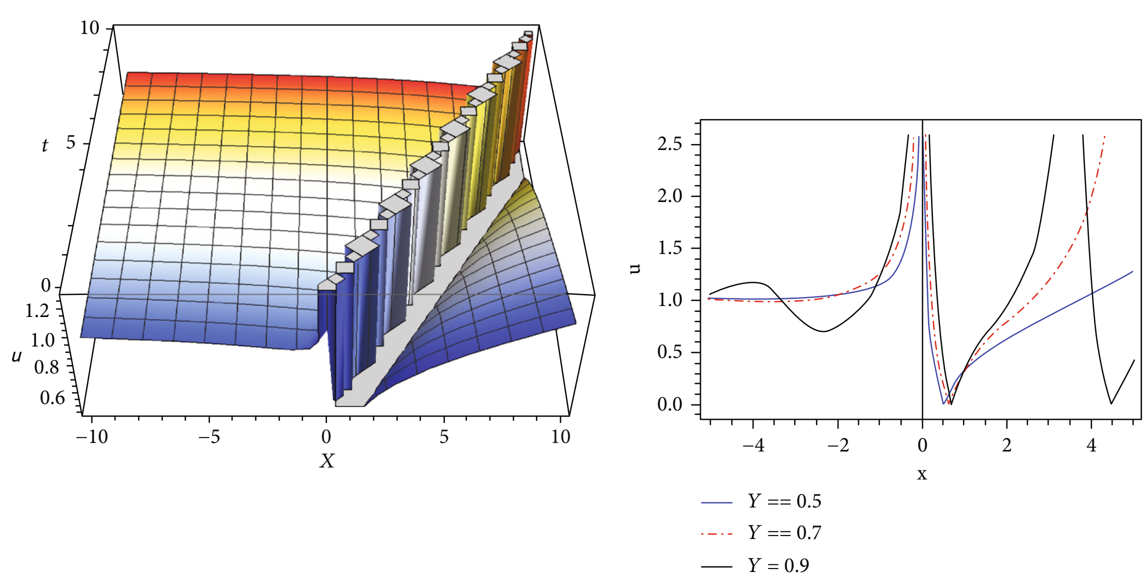

(a) (b)

FIGURE 10: We take $\kappa = -1$, $\beta_1 = 1$, $T = 2$, $V = 1$, $c = 3$, $a = 1$, $b = 1$, and $\gamma = 0.5, 0.7, 0.9$ for the solution $|u_{8,2}|$. (a) The 3D graph of $u_{8,2}(x, t)$ with $\gamma = 0.3$. (b) The 2D graph of $u_{8,2}(x, t)$ with distinct values of γ.

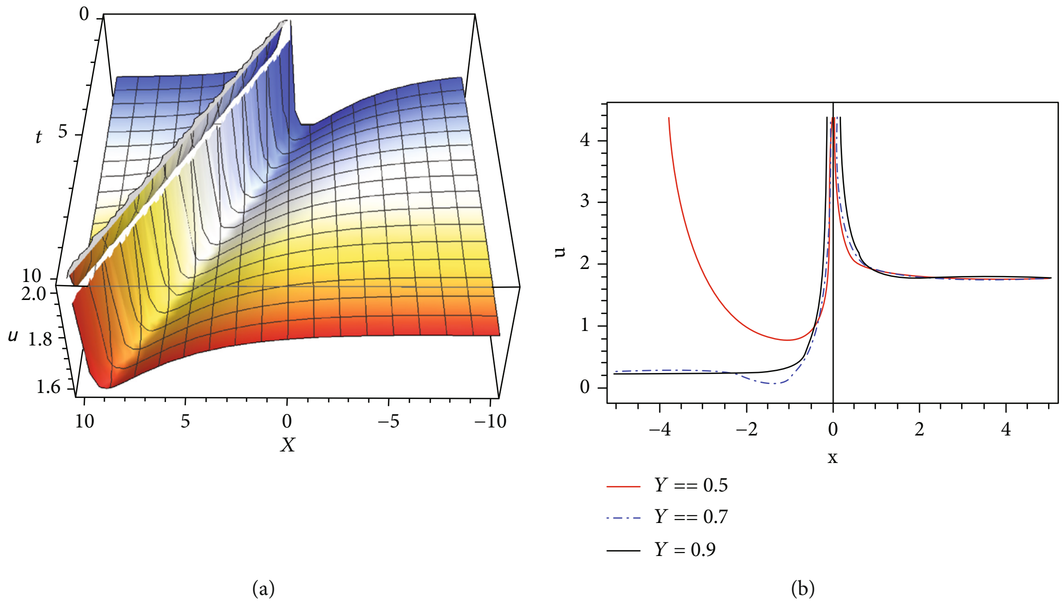

FIGURE 11: In this figure, we take $\kappa = -1$, $\beta_1 = 1$, $T = 2$, $V = 1$, $c = 3$, $a = 1$, $b = 1$, and $\gamma = 0.5, 0.7, 0.9$ for the solution $|u_{15}|$. (a) The 3D graph of $u_{15}(x, t)$ with $\gamma = 0.3$. (b) The 2D graph of $u_{15}(x, t)$ with distinct values of γ.

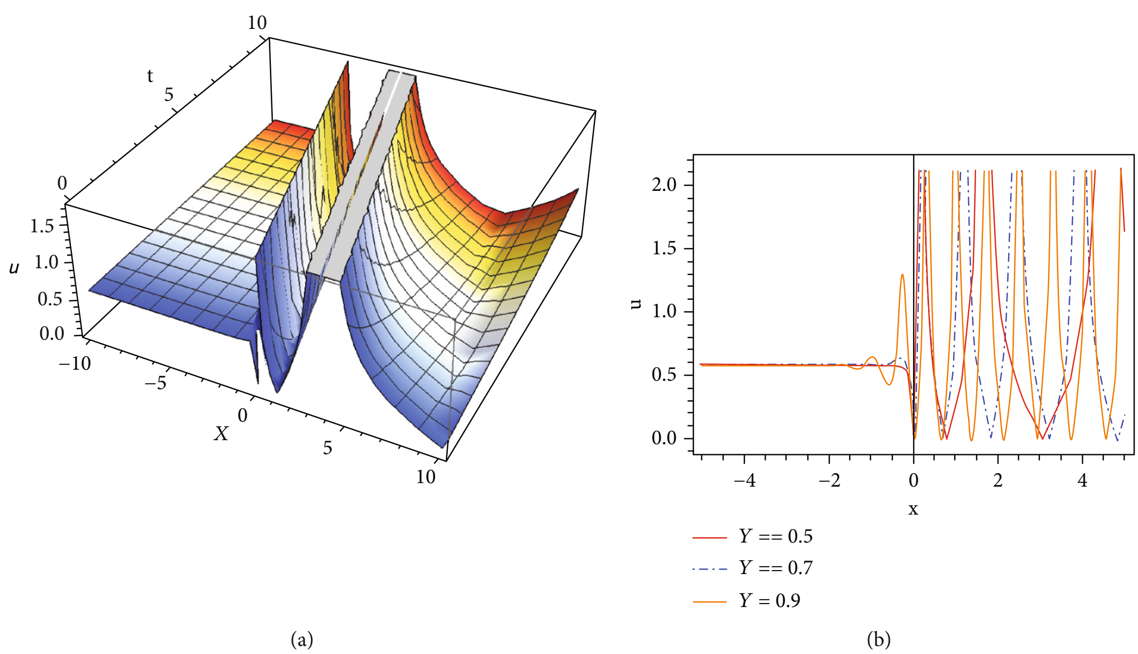

FIGURE 12: In this figure, we take $\kappa = -1$, $\beta_1 = 1$, $T = 2$, $V = 1$, $c = 3$, $a = 1$, $b = 1$, and $\gamma = 0.5, 0.7, 0.9$ for the solution $|u_{16}|$. (a) The 3D graph of $u_{16}(x, t)$ with $\gamma = 0.3$. (b) The 2D graph of $u_{16}(x, t)$ with distinct values of γ.

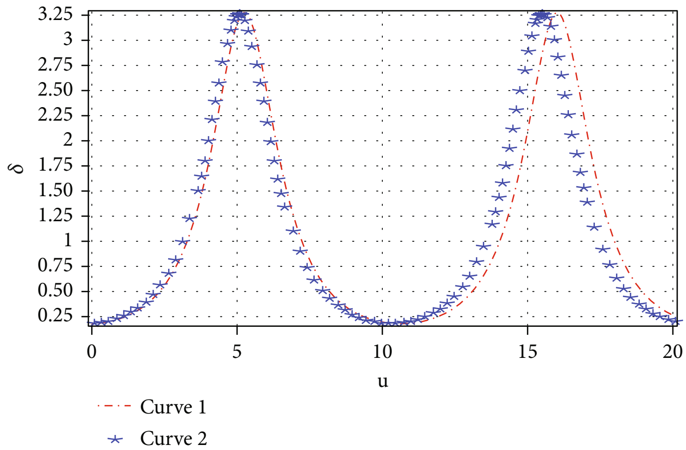

FIGURE 13: Sensitivity of model for initial conditions $(u, \delta) = (0.18, 0.01)$ and $(u, \delta) = (0.2, 0.02)$ with free parameters $S = -1$, $T = 2$, $V = 1$, $\kappa = 2$, $l = 1$, and $\beta_1 = 1$ while both conditions represent the curves in red and blue colors, respectively.

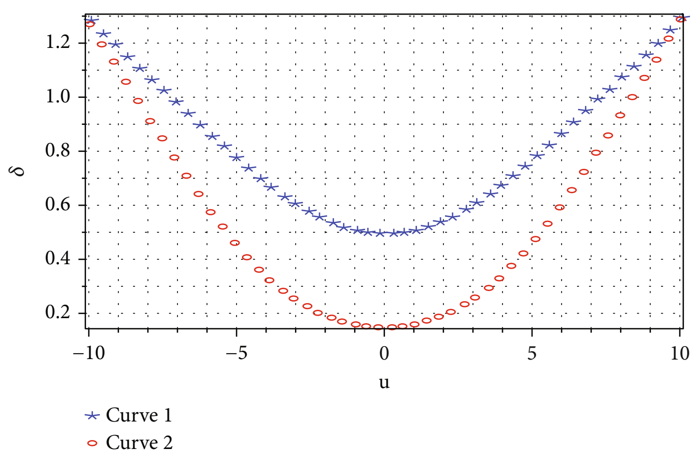

FIGURE 14: Sensitivity of model for initial conditions $(u, \delta) = (0.5, 0.001)$ and $(u, \delta) = (0.15, 0.001)$ with free parameters $S = 1$, $T = -2$, $V = 1$, $\kappa = 2$, $l = 1$, and $\beta_1 = 1$ while both conditions represent the curves in red and blue, respectively.

For Family 5, when $c^2 - 4a^2 < 0$ and $b = a$,

$$\begin{aligned}
u_{5,1}(x,t) &= \frac{3V(c\Theta-1)}{2T} + \frac{3V\Theta}{T}\left[\frac{-c}{2} + \sqrt{4a^2-c^2}\tan\left(\frac{\sqrt{4a^2-c^2}}{2}\delta^{\gamma}\right)\right],\\
u_{5,2}(x,t) &= \frac{3V(c\Theta-1)}{2T} + \frac{3V\Theta}{T}\left[\frac{-c}{2} - \sqrt{4a^2-c^2}\cot\left(\frac{\sqrt{4a^2-c^2}}{2}\delta^{\gamma}\right)\right],\\
v_{5,1}(x,t) &= \frac{3eV(c\Theta-1)}{2T} + \frac{3eV\Theta}{T}\left[\frac{-c}{2} + \sqrt{4a^2-c^2}\tan\left(\frac{\sqrt{4a^2-c^2}}{2}\delta^{\gamma}\right)\right] + f,\\
v_{5,2}(x,t) &= \frac{3eV(c\Theta-1)}{2T} + \frac{3eV\Theta}{T}\left[\frac{-c}{2} - \sqrt{4a^2-c^2}\cot\left(\frac{\sqrt{4a^2-c^2}}{2}\delta^{\gamma}\right)\right] + f.
\end{aligned} \tag{64}$$

For Family 6, when $c^2 - 4a^2 > 0$ and $b = a$,

$$\begin{aligned}
u_{6,1}(x,t) &= \frac{3V(c\Theta-1)}{2T} + \frac{3V\Theta}{T}\left[\frac{-c}{2} - \sqrt{-4a^2+c^2}\tan h\left(\frac{\sqrt{-4a^2+c^2}}{2}\delta^{\gamma}\right)\right],\\
u_{6,2}(x,t) &= \frac{3V(c\Theta-1)}{2T} + \frac{3V\Theta}{T}\left[\frac{-c}{2} - \sqrt{-4a^2+c^2}\cot h\left(\frac{\sqrt{-4a^2+c^2}}{2}\delta^{\gamma}\right)\right],\\
v_{6,1}(x,t) &= \frac{3eV(c\Theta-1)}{2T} + \frac{3eV\Theta}{T}\left[\frac{-c}{2} - \sqrt{-4a^2+c^2}\tan h\left(\frac{\sqrt{-4a^2+c^2}}{2}\delta^{\gamma}\right)\right] + f,\\
v_{6,2}(x,t) &= \frac{3eV(c\Theta-1)}{2T} + \frac{3eV\Theta}{T}\left[\frac{-c}{2} - \sqrt{-4a^2+c^2}\cot h\left(\frac{\sqrt{-4a^2+c^2}}{2}\delta^{\gamma}\right)\right] + f.
\end{aligned} \tag{65}$$

For Family 7, when $c^2 = 4ab$,

$$u_7(x,t) = \frac{3V(c\Theta - 1)}{2T} + \frac{3V\Theta}{T}\left[\frac{-2 + c\delta^\gamma}{2\delta^\gamma}\right],$$
$$v_7(x,t) = \frac{3eV(c\Theta - 1)}{2T} + \frac{3eV\Theta}{T}\left[\frac{-2 + c\delta^\gamma}{2\delta^\gamma}\right] + f. \tag{66}$$

For Family 8, when $ab < 0$, $c = 0$ and $b \neq 0$,

$$u_{8,1}(x,t) = \frac{-3V}{2T} - \frac{3bV\Theta}{T}\left[\sqrt{\frac{-a}{b}}\tan h\left(\sqrt{-ab}\delta^\gamma\right)\right],$$
$$u_{8,2}(x,t) = \frac{-3V}{2T} - \frac{3bV\Theta}{T}\left[\sqrt{\frac{-a}{b}}\cot h\left(\sqrt{-ab}\delta^\gamma\right)\right],$$
$$v_{8,1}(x,t) = \frac{-3eV}{2T} - \frac{3abV\Theta}{T}\left[\sqrt{\frac{-a}{b}}\tan h\left(\sqrt{-ab}\delta^\gamma\right)\right] + f,$$
$$v_{8,2}(x,t) = \frac{-3eV}{2T} - \frac{3abV\Theta}{T}\left[\sqrt{\frac{-a}{b}}\cot h\left(\sqrt{-ab}\delta^\gamma\right)\right] + f. \tag{67}$$

For Family 9, when $c = 0$ and $a = -b$,

$$u_9(x,t) = \frac{-3V}{2T} + \frac{3bV\Theta}{T}\left[\frac{1 + e^{-2b\delta^\gamma}}{-1 + e^{-2b\delta^\gamma}}\right],$$
$$v_9(x,t) = \frac{-3eV}{2T} + \frac{3ebV\Theta}{T}\left[\frac{1 + e^{-2b\delta^\gamma}}{-1 + e^{-2b\delta^\gamma}}\right] + f. \tag{68}$$

For Family 12, when $b = c = K$ and $a = 0$,

$$u_{12}(x,t) = \frac{3V(K\Theta - 1)}{2T} + \frac{3KV\Theta}{T}\left[\frac{e^{K\delta^\gamma}}{1 - e^{K\delta^\gamma}}\right],$$
$$v_{12}(x,t) = \frac{3eV(K\Theta - 1)}{2T} + \frac{3eKV\Theta}{T}\left[\frac{e^{K\delta^\gamma}}{1 - e^{K\delta^\gamma}}\right] + f. \tag{69}$$

For Family 13, when $c = a + b$,

$$u_{13}(x,t) = \frac{3V((a+b)\Theta - 1)}{2T} - \frac{3bV\Theta}{T}\left[\frac{1 - ae^{(a-b)\delta^\gamma}}{1 - be^{(a-b)\delta^\gamma}}\right],$$
$$v_{13}(x,t) = \frac{3eV((a+b)\Theta - 1)}{2T} - \frac{3ebV\Theta}{T}\left[\frac{1 - ae^{(a-b)\delta^\gamma}}{1 - be^{(a-b)\delta^\gamma}}\right] + f. \tag{70}$$

For Family 14, when $c = -(a+b)$,

$$u_{14}(x,t) = \frac{-3V((a+b)\Theta - 1)}{2T} + \frac{3bV\Theta}{T}\left[\frac{a - e^{(a-b)\delta^\gamma}}{b - e^{(a-b)\delta^\gamma}}\right],$$
$$v_{14}(x,t) = \frac{-3eV((a+b)\Theta - 1)}{2T} + \frac{3ebV\Theta}{T}\left[\frac{a - e^{(a-b)\delta^\gamma}}{b - e^{(a-b)\delta^\gamma}}\right] + f. \tag{71}$$

For Family 15, when $a = 0$,

$$u_{15}(x,t) = \frac{3V(c\Theta - 1)}{2T} + \frac{3bV\Theta}{T}\left[\frac{ce^{c\delta^\gamma}}{1 - be^{c\delta^\gamma}}\right],$$
$$v_{15}(x,t) = \frac{3eV(c\Theta - 1)}{2T} + \frac{3ebV\Theta}{T}\left[\frac{ce^{c\delta^\gamma}}{1 - be^{c\delta^\gamma}}\right] + f. \tag{72}$$

For Family 16, when $c = a = b \neq 0$,

$$u_{16}(x,t) = \frac{3V(c\Theta - 1)}{2T} + \frac{3bV\Theta}{2T}\left\{\sqrt{3}\tan\left(\frac{\sqrt{3}}{2}a\delta^\gamma\right) - 1\right\}\Bigg],$$
$$v_{16}(x,t) = \frac{3eV(c\Theta - 1)}{2T} + \frac{3ebV\Theta}{2T}\left\{\sqrt{3}\tan\left(\frac{\sqrt{3}}{2}a\delta^\gamma\right) - 1\right\}\Bigg] + f. \tag{73}$$

For Family 18, when $c = a = 0$,

$$u_{18}(x,t) = \frac{-3V}{2T} - \frac{3V\Theta}{T}\left[\frac{1}{\delta^\gamma}\right],$$
$$v_{18}(x,t) = \frac{-3eV}{2T} - \frac{3eV\Theta}{T}\left[\frac{1}{\delta^\gamma}\right] + f. \tag{74}$$

For Family 17, when $a = b$ and $c = 0$,

$$u_{19}(x,t) = \frac{-3V}{2T} + \frac{3bV\Theta}{T}[\tan(b\delta^\gamma)],$$
$$v_{19}(x,t) = \frac{-3eV}{2T} + \frac{3ebV\Theta}{T}[\tan(b\delta^\gamma)] + f. \tag{75}$$

5. Results and Discussion

This section covers the graphical interpretation of the results and the impact of the fractal parameter on them. Two powerful integration approaches, namely, semi-inverse scheme and AEM are used to extract soliton solutions of governing model. It has been established that the approaches currently provided for the double-chain DNA model, which were utilized to create closed-form exact results, are novel and distinct from those currently in use. The innovative solitonic solution structure and the new equations that yielded distinct types of solutions are the observable characteristics for finding solutions from the method outlined. Graphics that elaborate the various novel exact solitons in the forms of dynamics and nonlinear waves are presented for a physical description of the solutions that have been achieved. The semi-inverse principle offers bright soliton solutions Equations (22), (23), (29), and (30) of the aforesaid system. The physical significance of these solitons is shown in terms of modulus of $u(x, t)$ by assigning particular values of free parameters. Equations (23) and (30) show the same graphical behavior with just translation given in Equation (4) as in the figures. In Figures 1 and 2, these solitons in the form of 3D plots for fractal dimension value $\gamma = 0.8$ and 2D graphs for $\gamma = 0.5,0.7,0.9$ are provided. Dual-wave periodic, dark, bright solitons are raised by executing AEM. The dynamics of DNA strands $u(x, t)$ and $v(x, t)$ are presented in Figures 3–12. 3D sketches for fractal value $\gamma = 0.3$ and 2D graphics for $\gamma = 0.5,0.7,0.9$ are provided. The fractal impact is displayed by the irregularity in the curves of solutions. A few representative solutions are graphically illustrated to consider the appropriate connotation of dual-wave behaviors of the DNA system. The propagation of solitons and collisions of dual-mode pulses are examined using graphs. It is important to note that the proposed schemes may be used to generate soliton solutions for any NLPDE.

6. Sensitivity Analysis

The sensitive analysis of the formulated soliton solutions is demonstrated in this section. There are several research publications on the methods and applications of sensitivity analysis of parameter uncertainty to mathematical problems. The goal of the study is to identify and classify the different types of uncertainty that can affect how well a mathematical equation or framework performs in relation to its inputs. Results are presented based on various parametric values, and sensitivity is investigated by taking into account how a little change in input can significantly alter output. A detailed analysis of Equation (9) is introduced in Figures 13 and 14.

7. Conclusion

In this manuscript, semi-inverse method and AEM have been successfully applied to the double-chain DNA model that is one of the interesting models of current biophysics since it is related to an organism's life. It is likely that the well-known cubic nonlinear Klein-Gordon equation is the linearly reduced model to (1). The fractal DNA system has a high influence because it is used to describe the nonlinear dynamics of DNA molecules. The dark, periodic, bright, and other soliton solutions are derived which may help biologists for physical simulation of suggested equations. It should be highlighted that our results are novel and different from those of earlier investigations [3, 9]. The semi-inverse scheme is a fascinating integration tool to deduce variational principles for various differential models, whereas AEM is compelling to derive a family of dual-wave solitons of any NLPDE. The relevant choices of parameters enable us to discuss fractal behavior of the system. Also, the nature of attained solutions is reviewed by their 3D and 2D graphics. By using various initial conditions, the system is subjected to sensitivity analysis, which is then visualized using graphs. The acquired effects might help spark original suggestions for future biological applications.

Data Availability

Data is available on request.

Conflicts of Interest

The authors have no conflict of interest regarding the publication of this paper.

Authors' Contributions

All authors have equal contribution on this paper.

Acknowledgments

The authors extend their appreciation to the Deanship of Scientific Research at King Khalid University, for funding this project under grant number R.G.P. 2/29/43. Emad E. Mahmoud acknowledges the Taif University Researchers Supporting Project number TURSP-2020/20, Taif University, Taif, Saudi Arabia.

References

[1] M. Aguero, M. Najera, and M. Carrillo, "Nonclassic solitonic structures in DNA's vibrational dynamics," *International Journal of Modern Physics B*, vol. 22, no. 16, pp. 2571–2582, 2008.

[2] G. Gaeta, "Results and limitations of the soliton theory of DNA transcription," *Journal of Biological Physics*, vol. 24, no. 2-4, pp. 81–96, 1999.

[3] A. R. Seadawy, M. Bilal, M. Younis, S. T. R. Rizvi, S. Althobaiti, and M. M. Makhlouf, "Analytical mathematical approaches for the double-chain model of DNA by a novel computational technique," *Chaos, Solitons and Fractals*, vol. 144, article 110669, 2021.

[4] Q. Xian-Min and L. Sen-Yue, "Exact solutions of nonlinear dynamics equation in a new double-chain model of DNA," *Communications in Theoretical Physics*, vol. 39, no. 4, pp. 501–505, 2003.

[5] L. V. Yakushevich, "Nonlinear DNA dynamics: a new model," *Physics Letters A*, vol. 136, no. 7-8, pp. 413–417, 1989.

[6] G. Gaeta, C. Reiss, M. Peyrard, and T. Dauxois, "Simple models of non-linearDNA dynamics," *Rivista del Nuovo cimento*, vol. 17, no. 4, pp. 1–48, 1994.

[7] M. Peyrard and A. R. Bishop, "Statistical mechanics of a nonlinear model for DNA denaturation," *Physical Review Letters*, vol. 62, pp. 2755–2758, 1989.

[8] S. M. Mabrouk, "Explicit solutions of double-chain DNA dynamical system in (2+1)- dimensions," *International Journal of Current Engineering and Technology*, vol. 9, 2019.

[9] Y. L. Ma and B. Q. Li, "Kraenkel-Manna-Merle saturated ferromagnetic system: Darboux transformation and loop-like soliton excitations," *Chaos Solitons And Fractals*, vol. 159, article 112179, 2022.

[10] S. Kumar and M. Niwas, "Exact closed-form solutions and dynamics of solitons for a (2+1)-dimensional universal hierarchy equation via Lie approach," *Pramana*, vol. 95, no. 4, p. 195, 2021.

[11] S. Kumar and A. Kumar, "Dynamical behaviors and abundant optical soliton solutions of the cold bosonic atoms in a zig-zag

optical lattice model using two integral schemes," *Mathematics and Computers in Simulation*, vol. 201, pp. 254–274, 2022.

[12] N. Raza, Z. Hassan, A. R. Butt, R. U. Rahman, A. H. Abdel-Aty, and M. Mahmoud, "New and more dual-mode solitary wave solutions for the Kraenkel–Manna–Merle system incorporating fractal effects," *Mathematical Methods in the Applied Sciences*, vol. 45, no. 5, pp. 2964–2983, 2022.

[13] Y. L. Ma and B. Q. Li, "Bifurcation solitons and breathers for the nonlocal Boussinesq equations," *Applied Mathematics Letters*, vol. 124, article 107677, 2022.

[14] L. Ouahid, M. A. Abdou, and S. Kumar, "Analytical soliton solutions for cold bosonic atoms (CBA) in a zigzag optical lattice model employing efficient methods," *Modern Physics Letters B*, vol. 36, no. 7, article 2150603, 2022.

[15] Y. L. Ma, A. M. Wazwaz, and B. Q. Li, "Two new types of nonlocal Boussinesq equations in water waves: bright and dark soliton solutions," *Chinese Journal of Physics*, vol. 77, p. 1782, 2022.

[16] A. A. Hendi, L. Ouahid, S. Kumar, S. Owyed, and M. A. Abdou, "Dynamical behaviors of various optical soliton solutions for the Fokas–Lenells equation," *Modern Physics Letters B*, vol. 35, no. 34, 2021.

[17] Y. L. Ma, A. M. Wazwaz, and B. Q. Li, "Novel bifurcation solitons for an extended Kadomtsev-Petviashvili equation in fluids," *Physics Letters A*, vol. 413, no. 3-4, article 127585, 2021.

[18] S. Arshed, N. Raza, N. Rahman, A. R. RU Butt, and W. H. Huang, "Sensitive behavior and optical solitons of complex fractional Ginzburg-Landau equation: a comparative paradigm," *Results in Physics*, vol. 28, article 104533, 2021.

[19] B. Q. Li, "New breather and multiple-wave soliton dynamics for generalized Vakhnenko–Parkes equation with variable coefficients," *Journal of Computational and Nonlinear Dynamics*, vol. 16, no. 9, article 091006, 2021.

[20] L. Ouahid, M. A. Abdou, S. Kumar, S. Owyed, and S. S. Ray, "A plentiful supply of soliton solutions for DNA Peyrard–Bishop equation by means of a new auxiliary equation strategy," *International Journal of Modern Physics B*, vol. 35, no. 26, article 2150265, 2021.

[21] Y. L. Ma, A. M. Wazwaz, and B. Q. Li, "A new (3+1)-dimensional Kadomtsev-Petviashvili equation and its integrability, multiple-solitons, breathers and lump waves," *Mathematics and Computers in Simulation*, vol. 187, pp. 505–519, 2021.

[22] S. Kumar and S. K. Dhiman, "Lie symmetry analysis, optimal system, exact solutions and dynamics of solitons of a ($$3+1$$)-dimensional generalised BKP-Boussinesq equation," *Pramana*, vol. 96, no. 1, 2022.

[23] Y. L. Ma, A. M. Wazwaz, and B. Q. Li, "New extended Kadomtsev–Petviashvili equation: multiple soliton solutions, breather, lump and interaction solutions," *Nonlinear Dynamics*, vol. 104, no. 2, pp. 1581–1594, 2021.

[24] S. Kumar and S. Rani, "Lie symmetry reductions and dynamics of soliton solutions of (2+1)-dimensional Pavlov equation," *Pramana*, vol. 94, no. 1, p. 328, 2020.

[25] B. Q. Li and Y. L. Ma, "Interaction dynamics of hybrid solitons and breathers for extended generalization of Vakhnenko equation," *Nonlinear Dynamics*, vol. 102, no. 3, pp. 1787–1799, 2020.

[26] S. Kumar, S. K. Dhiman, and A. Chauhan, "Symmetry reductions, generalized solutions and dynamics of wave profiles for the (2+1)-dimensional system of Broer-Kaup-Kupershmidt (BKK) equations," *Mathematics and Computers in Simulation*, vol. 196, pp. 319–335, 2022.

[27] B. Q. Li and Y. L. Ma, "Extended generalized Darboux transformation to hybrid rogue wave and breather solutions for a nonlinear Schrodinger equation," *Applied Mathematics and Computation*, vol. 386, article 125469, 2020.

[28] S. Kumar, M. Kumar, and D. Kumar, "Computational soliton solutions to (2+1)-dimensional Pavlov equation using lie symmetry approach," *Pramana*, vol. 94, no. 1, p. 28, 2020.

[29] N. Raza, A. Jhangeer, R. U. Rahman, A. R. Butt, and Y. M. Chu, "Sensitive visualization of the fractional Wazwaz-Benjamin-Bona-Mahony equation with fractional derivatives: a comparative analysis," *Results in Physics*, vol. 25, article 104171, 2021.

[30] A. Jhangeer, W. A. Faridi, M. I. Asjad, and A. Akgül, "Analytical study of soliton solutions for an improved perturbed Schrodinger equation with Kerr law non-linearity in non-linear optics by an expansion algorithm," *Partial Differential Equations in Applied Mathematics*, vol. 4, article 100102, 2021.

[31] J. Rao, D. Mihalache, J. He, and Y. Cheng, "Dynamics of general higher-order rogue waves in the two-component nonlinear Schrodinger equation coupled to the Boussinesq equation," *Communications in Nonlinear Science and Numerical Simulation*, vol. 110, article 106382, 2022.

[32] A. Bekir and E. H. M. Zahran, "Painlevé approach and its applications to get new exact solutions of three biological models instead of its numerical solutions," *International Journal of Modern Physics B*, vol. 34, no. 29, article 2050270, 2020.

[33] Y. Khan, "Fractal modification of complex Ginzburg-Landau model arising in the oscillating phenomena," *Results in Physics*, vol. 18, article 103324, 2020.

[34] C. H. He, Y. Shen, F. Y. Ji, and J. H. He, "Taylor series solution for fractal Bratu-Type equation arising in electrospinning process," *Fractals*, vol. 28, no. 1, article 2050011, 2020.

[35] N. Raza and A. Javid, "Generalization of optical solitons with dual dispersion in the presence of Kerr and quadratic-cubic law nonlinearities," *Modern Physics Letters B*, vol. 33, no. 1, article 1850427, 2019.

[36] Z. Hassan, N. Raza, and J. F. Gomez-Aguilar, "Novel optical solitons to the perturbed Gerdjikov–Ivanov equation via collective variables," *Optical and Quantum Electronics*, vol. 53, no. 8, pp. 1–19, 2021.

[37] K. K. Ali, M. S. Osman, and M. Abdel-Aty, "New optical solitary wave solutions of Fokas-Lenells equation in optical fiber via Sine-Gordon expansion method," *Alexandria Engineering Journal*, vol. 59, no. 3, pp. 1191–1196, 2020.

[38] N. Raza, M. Abdullah, A. R. Butt, I. G. Murtaza, and S. Sial, "New exact periodic elliptic wave solutions for extended quantum Zakharov-Kuznetsov equation," *Optical and Quantum Electronics*, vol. 50, no. 4, 2018.

[39] M. S. Osman, "Multi-soliton rational solutions for some nonlinear evolution equations," *Physics*, vol. 14, no. 1, pp. 26–36, 2016.

[40] A. R. Seadawy, M. Iqbal, and D. Lu, "Propagation of kink and anti-kink wave solitons for the nonlinear damped modified Korteweg-de Vries equation arising in ion-acoustic wave in an unmagnetized collisional dusty plasma," *Physica A*, vol. 544, article 123560, 2020.

[41] A. Jhangeer, H. Almusawa, and R. U. Rahman, "Fractional derivative-based performance analysis to Caudrey-Dodd-Gibbon- Sawada-Kotera equation," *Results in Physics*, vol. 36, article 105356, 2022.

[42] N. Raza, A. Jhangeer, H. Rezazadeh, and A. Bekir, "Explicit solutions of the (2 + 1)-dimensional Hirota–Maccari system

arising in nonlinear optics," *International Journal of Modern Physics B*, vol. 33, no. 30, article 1950360, 2019.

[43] M. I. Asjad, W. A. Faridi, A. Jhangeer, H. Ahmad, S. Abdel-Khalek, and N. Alshehri, "Propagation of some new traveling wave patterns of the double dispersive equation," *Open Physics*, vol. 20, no. 1, pp. 130–141, 2022.

[44] J. H. He, "Variational principles for some nonlinear partial differential equations with variable coefficients," *Chaos, Solitons and Fractals*, vol. 19, no. 4, pp. 847–851, 2004.

[45] J. H. He, "Some asymptotic methods for strongly nonlinear equations," *International Journal of Modern Physics B*, vol. 20, no. 10, pp. 1141–1199, 2006.

[46] A. Biswas, D. Milovic, M. Savescu, M. F. Mahmood, and K. R. Khan, "Optical soliton perturbation in nanofibers with improved nonlinear Schrödinger's equation by semi-inverse variational principle," *Journal of Nonlinear Optical Physics and Materials*, vol. 21, no. 4, article 1250054, 2012.

[47] J. Zhang, "Variational approach to solitary wave solution of the generalized Zakharov equation," *Computers and Mathematics with Applications*, vol. 54, no. 7-8, pp. 1043–1046, 2007.

[48] D. Kumar, C. Park, N. Tamanna, G. C. Paul, and M. S. Osman, "Dynamics of two-mode Sawada-Kotera equation: mathematical and graphical analysis of its dual-wave solutions," *Results in Physics*, vol. 19, article 103581, 2020.

[49] H. Rezazadeh, A. Korkmaz, M. Eslami, and S. M. Mirhosseini-Alizamini, "A large family of optical solutions to Kundu–Eckhaus model by a new auxiliary equation method," *Optical and Quantum Electronics*, vol. 51, no. 3, 2019.

[50] J. H. He, "A fractal variational theory for one-dimensional compressible flow in a microgravity space," *Fractals*, vol. 28, no. 2, article 2050024, 2020.

[51] J. H. He, "Fractal calculus and its geometrical explanation," *Results in Physics*, vol. 10, pp. 272–276, 2018.

Hindawi
Journal of Function Spaces
Volume 2022, Article ID 9527666, 7 pages
https://doi.org/10.1155/2022/9527666

Research Article

Oscillation Criteria of Fourth-Order Differential Equations with Delay Terms

Shoura Ahmed Balatta,[1,2] **Ishak Hashim**,[2] **Ahmad Sami Bataineh**,[3] **and Eddie Shahril Ismail**[2]

[1]*Department of Mathematics, Faculty of Education, Seiyun University, Hadhramout, Yemen*
[2]*Department of Mathematical Sciences, Faculty of Science & Technology, Universiti Kebangsaan Malaysia, 43600 Bangi, Selangor, Malaysia*
[3]*Department of Mathematics, Faculty of Science, Al-Balqa Applied University, 19117 Al Salt, Jordan*

Correspondence should be addressed to Shoura Ahmed Balatta; sab74722@gmail.com

Received 23 June 2022; Revised 29 July 2022; Accepted 1 August 2022; Published 24 August 2022

Academic Editor: Yusuf Gurefe

The aim of this paper is to derive oscillation criteria of the following fourth-order differential equation with delay term $(r(x)(z'''(x))^{\gamma})' + \sum_{i=1}^{n} q_i(x) f(z(\eta_i(x))) = 0$, under the assumption $\int_{x_0}^{\infty} r^{-1/\gamma}(s)\mathrm{d}s = \infty$. The results are based on comparison with the oscillatory behaviour of second-order delay equations and the generalised Riccati transformation. Not only do the provided theorems provide an entirely new technique but also they vastly improve on a number of previously published conclusions. We give three examples to illustrate our findings.

1. Introduction

Higher-order neutral differential equations have recently been recognized as being sufficient to describe a variety of real applications [1–4]. As a result, many researchers have studied the qualitative behaviour of solutions of these equations (see [5–8]). The research of oscillation and oscillatory behaviour of these equations, which has been investigated using multiple approaches and techniques, has received special attention (see [9–11]). The attempt to improve the work and obtain a generalised platform that covers all special cases inspires the investigation of fourth- and higher-order equations.

In this work, we are concerned with oscillation of fourth-order delay differential equations of the form

$$\left(r(x)\left(z'''(x)\right)^{\gamma}\right)' + \sum_{i=1}^{n} q_i(x) f(z(\eta_i(x))) = 0, \tag{1}$$

where $x \geq x_0$. Throughout this work, we suppose the following:

(i) $r \in C^1([x_0,\infty), R)$ and γ is a quotient of odd positive integers

(ii) The following condition holds:

$$\int_{x_0}^{\infty} \frac{1}{r^{1/\gamma}(s)} ds = \infty, \tag{2}$$

for $r(x) > 0$, $r'(x) > 0$, and

(iii) $q_i, \eta_i \in C([x_0,\infty), R)$, $q_i(x) \geq 0$, $\eta_i(x) \leq x$, $\lim_{x \longrightarrow \infty} \eta_i(x) = \infty$ $(i = 1, 2, \cdots)$, and $f \in C(R, R)$ such that

$$\frac{f(x)}{x^{\gamma}} \geq \ell > 0, \quad \text{for } x \neq 0. \tag{3}$$

By a solution of (1), we mean a function $z \in C^3[x_z,\infty)$, $x_z \geq x_0$, that has the property $r(x)(z'''(x))^{\gamma} \in C^1[x_z,\infty)$ and fulfills (1) on $[x_z, \infty)$. If a solution of (1) has arbitrarily large zeros on $[x_z, \infty)$, then it is considered oscillatory; otherwise, it is called nonoscillatory. Equation (1) is said to be oscillatory if all its solutions are oscillatory.

Next, we give some previous findings in the literature that are relevant to the present work. Grace [12] has studied the equation

$$\left(r(x)z^{(n-\nu)}(x)\right)^{(\nu)}+q(x)f(z[g(x)])=0, \quad (4)$$

in addition to Agarwal et al. [13] and Xu and Xia [14] who have studied the equation

$$\left(z^{(n-1)}(x)\left|z^{(n-1)}(x)\right|^{\gamma-1}\right)'+f(x,z(\eta(x)))=0, \quad (5)$$

subject to condition (2). Zhang et al. [15] obtained oscillatory criteria of the equation

$$\left(r(x)\left(z'''(x)\right)^{\gamma}\right)'+q(x)z^{\gamma}(\eta(x))=0, \quad (6)$$

with the condition

$$\int_{x_0}^{\infty}\frac{1}{r^{1/\gamma}(u)}\,\mathrm{d}u<\infty. \quad (7)$$

Baculikova et al. [16] used the comparison theory to prove that if

$$y'(x)+q(x)f\left(\frac{\delta\eta^{n-1}(x)}{(n-1)!r^{1/\gamma}(\eta(x))}\right)f\left(y^{1/\gamma}(\eta(x))\right)=0 \quad (8)$$

is oscillatory, then

$$\left(r(x)\left(z^{(n-1)}(x)\right)^{\gamma}\right)'+q(x)f(z(\eta(x)))=0 \quad (9)$$

is oscillatory for even n. Grace et al. [7] presented oscillation criteria for fourth-order delay differential equations of the form

$$\left(r_3\left(r_2\left(r_1z'\right)'\right)'\right)'(x)+q(x)z(\eta(x))=0, \quad (10)$$

under the assumption

$$\int_{x_0}^{\infty}\frac{dt}{r_i(x)}<\infty,\quad i=1,2,3. \quad (11)$$

Using the Riccati transformation, an oscillation criterion for fourth-order neutral delay differential equation of the form

$$\left[r(x)\left([z(x)+p(x)z((\eta(x)))]'''\right)^{\alpha}\right]'+\int_a^b q(x,\xi)f(z(g(x,\xi)))\,d\xi=0 \quad (12)$$

was obtained by Chatzarakis et al. [17]. By using the technique of the Riccati transformation and the theory of comparison with first-order delay equations, Bazighifan and Abdeljawad [18] established some new oscillation criteria for fourth-order advanced differential equations with p-Laplacian-like operator of the form

$$\left(b(x)\left|z'''(x)\right|^{p-2}z'''(x)\right)'+\sum_{i=1}^{j}q_i(x)g(z(\eta_i(x)))=0. \quad (13)$$

Very recently, Bazighifan et al. [19] established new criteria for the oscillatory behaviour of the following fourth-order differential equations with middle term

$$\left(r(x)\left|z'''(x)\right|^{p_1-2}z'''(x)\right)'+\sigma(x)\left|z'''(x)\right|^{p_1-2}z'''(x)+q(x)|z(\tau(x))|^{p_2-2}z(\tau(x))=0, \quad (14)$$

by the comparison technique and employing the Riccati transformation under the condition

$$\int_{x_0}^{\infty}\left[\frac{1}{r(s)}\exp\left(-\int_{x_0}^{s}\frac{\sigma(\eta)}{r(\eta)}\mathrm{d}\eta\right)\right]^{1/p_1-1}ds=\infty. \quad (15)$$

For convenience, in the present work, we denote

$$\begin{aligned}\delta(x)&=\int_x^{\infty}\frac{1}{r^{1/\gamma}(s)}ds,\\ \psi(x)&=\pi(x)\left(\sum_{i=1}^{n}\ell q_i(x)\left(\frac{\eta_i^3(x)}{x^3}\right)^{\gamma}+\frac{\mu x^2-2\gamma}{2r^{1/\gamma}(x)\delta^{\gamma+1}(x)}\right),\\ \varphi(x)&=\frac{\pi'(x)}{\pi(x)}+\frac{(\gamma+1)\mu x^2}{2r^{1/\gamma}(x)\delta(x)},\\ \varphi^*(x)&=\frac{\tau'(x)}{\tau(x)}+\frac{2}{\delta(x)},\\ \psi^*&=\tau(x)\left(\int_x^{\infty}\left(\frac{\ell}{r(x)}\int_x^{\infty}\sum_{i=1}^{n}q_i(s)\frac{\eta_i^{\gamma}(s)}{s^{\gamma}}\mathrm{d}s\right)^{1/\gamma}\mathrm{d}x+\frac{1-r^{-1/\gamma}(x)}{\delta^2(x)}\right),\end{aligned} \quad (16)$$

where $\pi,\tau\in C^1((x_0,\infty),(0,\infty))$. The generalised Riccati transformation is defined as

$$\omega(x)\coloneqq\pi(x)\left(\frac{r(x)\left(z'''\right)^{\gamma}(x)}{z^{\gamma}(x)}+\frac{1}{\delta^{\gamma}(x)}\right), \quad (17)$$

$$\vartheta(x)\coloneqq\tau(x)\left(\frac{z'(x)}{z(x)}+\frac{1}{\delta(x)}\right). \quad (18)$$

We remark that in the study of the asymptotic behaviour of the positive solutions of (1), there are only two cases:

Case 1. $z^{(j)}(x)>0$ for $j=1,2,3$,

Case 2. $z^{(j)}(x)>0$ for $j=1,3$ and $z''(x)<0$.

In this work, using the Riccati approach and a comparison with a second-order equation, we shall obtain oscillation criteria for (1).

2. Some Significant Auxiliary Lemmas

The following lemmas serve as a basis for our findings.

Lemma 1 (see [20]). *Let α be a ratio of two odd numbers; $H>0$ and K are constants. Then,*

$$P^{(\alpha+1)/\alpha}-(P-Q)^{(\alpha+1)/\alpha}\le \frac{P}{\alpha}Q^{1/\alpha}+Q^{1/\alpha}P-\frac{1}{\alpha}Q^{(1+\alpha)/\alpha},\quad PQ\ge 0,\alpha\ge 1,$$
$$\frac{\alpha^{\alpha}}{(\alpha+1)^{\alpha+1}}\frac{K^{\alpha+1}}{H^{\alpha}}\ge Km-Hm^{(\alpha+1)/\alpha},\quad H>0. \tag{19}$$

Lemma 2 (see [17]). *Let $f^{(j)})>0$ and $f^{(n+1)}<0$ for all $j=0,1,\cdots,n$. Then,*

$$\frac{n!}{x^n}f(x)\ge\frac{(n-1)!}{x^{n-1}}\frac{d}{dx}f(x). \tag{20}$$

Lemma 3 (see [21]). *The equation*

$$\left(a(x)\left(m'(x)^{\gamma}\right)\right)'+q(x)m^{\gamma}(x)=0, \tag{21}$$

where $a\in C[x_0,\infty)$, $a(x)>0$, and $q(x)>0$, is nonoscillatory if and only if there exist $x\ge x_0$ and $\sigma\in C^1[x,\infty)$ such that

$$\sigma'(x)+\frac{\gamma}{r^{1/\gamma}(x)}\sigma^{1+1/\gamma}(x)+q(x)\le 0, \tag{22}$$

for $x\ge x_0$.

Lemma 4 (see [22]). *Suppose that $h\in C^n([x_0,\infty),(0,\infty))$; then,*

$$h^{(n-1)}(x)h^{(n)}(x)\le 0, \tag{23}$$

for every $\lambda\in(0,1)$ and $x\ge x_\lambda$.

3. Oscillation Criteria

In this section, we shall obtain some oscillation criteria for equation (1).

Lemma 5. *Suppose that z is a solution of (1) such that $z>0$ and $z^{(j)}>0$ for all $j=1,2,3$. If we have the function $\omega\in C^1[x,\infty)$ defined in (17), where $\pi\in C^1([x_0,\infty),(0,\infty))$, then*

$$\omega'(x)\le-\psi(x)+\varphi(x)\omega(x)-\frac{\gamma\mu x^2}{2(r(x)\pi(x))^{1/\gamma}}\omega^{(\gamma+1)/\gamma}(x), \tag{24}$$

for all $x>x_1$, where x_1 is large enough.

Proof. Let z be a solution of (1) where $z>0$ and $z^{(j)}(x)>0$ for all $j=1,2,3$. Thus, from Lemma 4, we get

$$z'(x)\ge\frac{\mu}{2}x^2z'''(x), \tag{25}$$

for all $\mu\in(0,1)$ and for every large x. From (17), we have that $\omega(x)>0$ for $x\ge x_1$, and

$$\omega'(x)=\pi'(x)\left(\frac{r(x)\left(z'''(x)\right)^{\gamma}(x)}{z^{\gamma}(x)}+\frac{1}{\delta^{\gamma}(x)}\right)+\pi(x)\frac{\left(r(x)\left(z'''(x)\right)^{\gamma}\right)'}{z^{\gamma}(x)}$$
$$-\gamma\pi(x)\frac{z^{\gamma-1}(x)z'(x)r(x)\left(z'''(x)\right)^{\gamma}}{z^{2\gamma}(x)}+\frac{\gamma\pi(x)}{r^{1/\gamma}(x)\delta^{\gamma+1}(x)}. \tag{26}$$

Using (25) and (17), we acquire

$$\omega'(x)\le\frac{\pi'(x)}{\pi(x)}\omega(x)+\pi(x)\frac{\left(r(x)\left(z'''(x)\right)^{\gamma}\right)'}{z^{\gamma}(x)}$$
$$-\gamma\pi(x)\frac{\mu}{2}x^2\frac{r(x)\left(z'''(x)\right)^{\gamma+1}}{z^{\gamma+1}(x)}+\frac{\gamma\pi(x)}{r^{1/\gamma}(x)\delta^{\gamma+1}(x)}$$
$$\le\frac{\pi'(x)}{\pi(x)}\omega(x)+\pi(x)\frac{\left(r(x)\left(z'''(x)\right)^{\gamma}\right)'}{z^{\gamma}(x)}$$
$$-\gamma\pi(x)\frac{\mu}{2}x^2r(x)\left(\frac{\omega(x)}{\pi(x)r(x)}-\frac{1}{r(x)\delta^{\gamma}(x)}\right)^{(\gamma+1)/\gamma}+\frac{\gamma\pi(x)}{r^{1/\gamma}(x)\delta^{\gamma+1}(x)}. \tag{27}$$

Letting $P=\omega(x)/(\pi(x)r(x))$, $Q=1/(r(x)\delta^{\gamma}(x))$, and $\alpha=\gamma$ and by using Lemma 1, we get

$$\left(\frac{\omega(x)}{\pi(x)r(x)}-\frac{1}{r(x)\delta^{\gamma}(x)}\right)^{(\gamma+1)/\gamma}$$
$$\ge\left(\frac{\omega(x)}{\pi(x)r(x)}\right)^{(\gamma+1)/\gamma}$$
$$-\frac{1}{\gamma r^{1/\gamma}(x)\delta(x)}\left((\gamma+1)\frac{\omega(x)}{\pi(x)r(x)}-\frac{1}{r(x)\delta^{\gamma}(x)}\right). \tag{28}$$

From Lemma 2, we obtain $z(x)\ge(x/3)z'(x)$, and hence,

$$\frac{z(\eta_i(x))}{z(x)}\ge\frac{\eta_i^3(x)}{x^3}. \tag{29}$$

From (1), (27), and (28), we obtain

$$\omega'(x)\le\frac{\pi'(x)}{\pi(x)}\omega(x)-\ell\pi(x)\sum_{i=1}^{n}q_i(x)\left(\frac{\eta_i^3(x)}{x^3}\right)^{\gamma}$$
$$-\gamma\pi(x)\frac{\mu}{2}x^2r(x)\left(\frac{\omega(x)}{\pi(x)r(x)}\right)^{(\gamma+1)/\gamma}$$
$$-\gamma\pi(x)\frac{\mu}{2}x^2r(x)\left(\frac{-1}{\gamma r^{1/\gamma}(x)\delta(x)}\left((\gamma+1)\frac{\omega(x)}{\pi(x)r(x)}-\frac{1}{r(x)\delta^{\gamma}(x)}\right)\right)$$
$$+\frac{\gamma\pi(x)}{r^{1/\gamma}(x)\delta^{\gamma+1}(x)}. \tag{30}$$

This implies that

$$\omega'(x) \le \left(\frac{\pi'(x)}{\pi(x)} + \frac{(\gamma+1)\mu x^2}{2r^{1/\gamma}(x)\delta(x)}\right)\omega(x) - \frac{\gamma\mu x^2}{2r^{1/\gamma}(x)\pi^{1/\gamma}(x)}\omega^{(\gamma+1)/\gamma}(x) - \pi(x)\left(\sum_{i=1}^{n}\ell q_i(x)\left(\frac{\eta_i^3(x)}{x^3}\right)^{\gamma} + \frac{\mu x^2 - 2\gamma}{2r^{1/\gamma}(x)\delta^{\gamma+1}(x)}\right). \tag{31}$$

Thus,

$$\omega'(x) \le -\psi(x) + \varphi(x)\omega(x) - \frac{\gamma\mu x^2}{2(r(x)\pi(x))^{1/\gamma}}\omega^{(\gamma+1)/\gamma}(x). \tag{32}$$

The proof is completed. □

Lemma 6. *Let z be a solution of (1) such that $z > 0$ and $z^{(j)}(x) > 0$ for $j = 1, 3$ and $z''(x) < 0$. If the function $\vartheta \in C^1[x,\infty)$ is defined in (18) such that $\tau \in C^1((x_0,\infty),(0,\infty))$, then*

$$\vartheta'(x) \le \varphi^*(x)\vartheta(x) - \psi^*(x) - \frac{1}{\tau(x)}\vartheta^2(x), \tag{33}$$

for all $x > x_1$, where x_1 is large enough.

Proof. Let z be a solution of (1) where $z > 0$ and $z^{(j)}(x) > 0$ for $j = 1, 3$ and $z''(x) < 0$. From Lemma 2, we have that $z(x) \ge xz'(x)$. Integrating this inequality from $\eta(x)$ to x, we obtain

$$z(\eta_i(x)) \ge \frac{\eta_i(x)}{x}z(x). \tag{34}$$

Hence, from (3) we have

$$f(z(\eta_i(x))) \ge \ell\frac{\eta_i^{\gamma}(x)}{x^{\gamma}}z^{\gamma}(x). \tag{35}$$

By integrating (1) from x to u and since $z'(x) > 0$, we get

$$r(u)\left(z'''(u)\right)^{\gamma} - r(x)\left(z'''(x)\right)^{\gamma} = -\int_x^u \sum_{i=1}^{n} q_i(s)f(z(\eta_i(s)))ds \le -\ell z^{\gamma}(x)\int_x^u \sum_{i=1}^{n} q_i(s)\frac{\eta_i^{\gamma}(s)}{s^{\gamma}}ds. \tag{36}$$

Now letting $u \longrightarrow \infty$ yields

$$r(x)\left(z'''(x)\right)^{\gamma} \ge \ell z^{\gamma}(x)\int_x^{\infty}\sum_{i=1}^{n} q_i(s)\frac{\eta_i^{\gamma}(s)}{s^{\gamma}}\mathrm{d}s, \tag{37}$$

and so

$$z'''(x) \ge z(x)\left(\frac{\ell}{r(x)}\int_x^{\infty}\sum_{i=1}^{n} q_i(s)\frac{\eta_i^{\gamma}(s)}{s^{\gamma}}ds\right)^{1/\gamma}. \tag{38}$$

Integrating this from x to ∞ gives

$$z''(x) \le -z(x)\int_x^{\infty}\left(\frac{\ell}{r(x)}\int_x^{\infty}\sum_{i=1}^{n} q_i(s)\frac{\eta_i^{\gamma}(s)}{s^{\gamma}}\mathrm{d}s\right)^{1/\gamma}dx. \tag{39}$$

From (18), we have that $\vartheta(x) > 0$ for $x \ge x_1$ and by differentiating, we get

$$\vartheta'(x) = \frac{\tau'(x)}{\tau(x)}\vartheta(x) + \tau(x)\frac{z''(x)}{z(x)} - \tau(x)\left(\frac{\vartheta(x)}{\tau(x)} - \frac{1}{\delta(x)}\right)^2 + \frac{\tau(x)}{r^{1/r}(x)\delta^2(x)}. \tag{40}$$

Now, using Lemma 1 with $P = \vartheta(x)/\tau(x)$, $Q = 1/\delta(x)$, and $\alpha = 1$ yields

$$\left(\frac{\theta(x)}{\tau(x)} - \frac{1}{\delta(x)}\right)^2 \ge \left(\frac{\theta(x)}{\tau(x)}\right)^2 - \frac{1}{\delta(x)}\left(\frac{2\vartheta(x)}{\tau(x)} - \frac{1}{\delta(x)}\right). \tag{41}$$

From (1), (40), and (41), we have the following:

$$\vartheta'(x) \le \frac{\tau'(x)}{\tau(x)}\vartheta(x) - \tau(x)\int_x^{\infty}\left(\frac{\ell}{r(x)}\int_x^{\infty}\sum_{i=1}^{n} q_i(s)\frac{\eta_i^{\gamma}(s)}{s^{\gamma}}\mathrm{d}s\right)^{1/\gamma}dx - \tau(x)\left(\left(\frac{\vartheta(x)}{\tau(x)}\right)^2 - \frac{1}{\delta(x)}\left(\frac{2\vartheta(x)}{\tau(x)} - \frac{1}{\delta(x)}\right)\right) + \frac{\tau(x)}{r^{1/\gamma}(x)\delta^2(x)}. \tag{42}$$

This implies that

$$\vartheta'(x) \le \left(\frac{\tau'(x)}{\tau(x)} + \frac{2}{\delta(x)}\right)\vartheta(x) - \frac{1}{\tau(x)}\vartheta^2(x) - \tau(x)\left(\int_x^{\infty}\left(\frac{\ell}{r(x)}\int_x^{\infty}\sum_{i=1}^{n} q_i(s)\frac{\eta_i^{\gamma}(s)}{s^{\gamma}}\mathrm{d}s\right)^{1/\gamma}dx + \frac{1 - r^{-1/\gamma}(x)}{\delta^2(x)}\right). \tag{43}$$

Thus,

$$\vartheta'(x) \le \varphi^*(x)\vartheta(x) - \psi^*(x) - \frac{1}{\tau(x)}\vartheta^2(x). \tag{44}$$

The proof is completed. □

Lemma 7. *Let z be a solution of (1) with $z > 0$. If $\pi \in C(x_0,\infty)$ such that*

$$\int_{x_0}^{\infty}\left(\psi(s)-\left(\frac{2}{\mu s^2}\right)^{\gamma}\frac{r(s)\pi(s)(\varphi(s))^{\gamma+1}}{(\gamma+1)^{\gamma+1}}\right)ds=\infty, \tag{45}$$

for some $\mu \in (0,1)$, then z does not fulfill Case 1.

Proof. Let z be a solution of (1) such that $z > 0$. From Lemma 5, we obtain that (24) holds. Using Lemma 1 with

$$K=\varphi(x), H=\frac{\gamma\mu x^2}{\left(2(r(x)\pi(x))^{1/\gamma}\right)}, \tag{46}$$

and $m=\omega$, we get

$$\omega'(x)\le -\psi(x)+\left(\frac{2}{\mu x^2}\right)^{\gamma}\frac{r(x)\pi(x)(\varphi(x))^{\gamma+1}}{(\gamma+1)^{\gamma+1}}. \tag{47}$$

Now, integrating from x_1 to x yields

$$\int_{x_1}^{\infty}\left(\psi(s)-\left(\frac{2}{\mu s^2}\right)^{\gamma}\frac{r(s)\pi(s)(\varphi(s))^{\gamma+1}}{(\gamma+1)^{\gamma+1}}\right)ds\le\omega(x_1), \tag{48}$$

which contradicts (45). So, the proof is complete. □

Lemma 8. *Let z be a solution of (1) with $z > 0$ and $z^{(j)}(x) > 0$ for $j = 1, 3$ and $z''(x) < 0$. If $\tau \in C([x_0,\infty))$ such that*

$$\int_{x_0}^{\infty}\left(\psi^*(s)-\frac{1}{4}\tau(s)(\varphi^*(s))^2\right)ds=\infty, \tag{49}$$

then z does not fulfill Case 2.

Proof. Let z be a solution of (1) such that $z > 0$. From Lemma 6, we get that (33) holds. Using Lemma 1 with

$$H=\varphi^*(x), K=\frac{1}{\tau(x)}, \gamma=1, m=\vartheta, \tag{50}$$

we obtain

$$\omega'(x)\le-\psi^*(x)+\frac{1}{4}\tau(x)(\varphi^*(x))^2. \tag{51}$$

Integrating from x_1 to x gives

$$\int_{x_1}^{\infty}\left(\psi^*(s)-\frac{1}{4}\tau(s)(\varphi^*(s))^2\right)ds\le\omega(x_1), \tag{52}$$

which contradicts (49). This completes the proof. □

Theorem 9. *Let $\pi, \tau \in C[x_0,\infty)$ such that (45) and (49) hold for some $\mu \in (0,1)$. Then, equation (1) is oscillatory.*

Proof. The proof is very similar to the proofs of Lemmas 7 and 8.

Now, by using the comparison method, we develop additional oscillation results for (1) in the following theorem: □

Theorem 10. *Let (2) hold and assume that*

$$\left[\frac{r(x)}{x^{2\gamma}}\left(z'(x)\right)^{\gamma}\right]'+\psi(x)z^{\gamma}(x)=0, \tag{53}$$

$$z''(x)+z(x)\int_{x}^{\infty}\left(\frac{\ell}{r(x)}\int_{x}^{\infty}\sum_{i=1}^{n}q_i(s)\frac{\eta_i^{\gamma}(s)}{s^{\gamma}}\,ds\right)^{1/\gamma}dx=0, \tag{54}$$

are both oscillatory; then, (1) is oscillatory.

Proof. Assume the contrary that (1) has a positive solution z, and by virtue of Lemma 3 and if we set $\pi(x) = 1$ in (24), then we get

$$\omega'(x)+\frac{\gamma\mu x^2}{2r^{1/\gamma}(x)}\omega^{(\gamma+1)/\gamma}+\psi(x)\le 0. \tag{55}$$

Hence, we have that (53) is nonoscillatory, which is a contradiction. If we set $\tau(x) = 1$ in (33), then we obtain

$$\vartheta'(x)+\psi^*(x)+\vartheta^2(x)\le 0. \tag{56}$$

Thus, equation (54) is nonoscillatory, which is a contradiction. The proof is now complete. □

It is well known (see Řehák [23])) that if

$$\int_{x_0}^{\infty}\frac{1}{r(x)}\,\mathrm{d}x=\infty, \lim_{x\longrightarrow\infty}\inf\left(\int_{x_0}^{x}\frac{1}{r(s)}\,\mathrm{d}s\right)\int_{x}^{\infty}q(s)\mathrm{d}s>\frac{1}{4}, \tag{57}$$

then equation (21) with $\gamma = 1$ is oscillatory.

Theorem 11. *Let (2) hold. Assume that*

$$\int_{x_0}^{\infty}\frac{x^2}{r(x)}dx=\infty, \tag{58}$$

and

$$\lim_{x\longrightarrow\infty}\inf\left(\int_{x_0}^{x}\frac{s^2}{r(s)}ds\right)\int_{x}^{\infty}\psi(s)ds>\frac{1}{2\lambda_1}, \tag{59}$$

for some constant $\lambda_1 \in (0,1)$ *and*

$$\lim_{x\longrightarrow\infty} \inf \int_x^\infty \left(\int_x^\infty \left(\frac{\ell}{r(x)} \int_x^\infty \sum_{i=1}^n q_i(s) \frac{\eta_i^\gamma(s)}{s^\gamma} ds \right) dx \right) ds > \frac{1}{4}, \tag{60}$$

then every solution of (1) is oscillatory.

The proof is obvious.

4. Examples

In this section, we provide some examples to prove that the results of Section 3 are valid.

Example 1. Consider

$$z^{(4)}(x) + \left(\frac{q_0 - x^2}{x^4} + \frac{1}{x^2} \right) z(x) = 0, \quad x \geq 1, \tag{61}$$

where $q_0 > 0$.

Let $\gamma = 1$, $r(x) = 1$, $q(x) = ((q_0 - x^2)/x^4 + (1/x^2)) = q_0/x$, and $\eta(x) = x$.

Hence, we have

$$\delta(x_0) = \infty, \psi(x) = \frac{q_0}{x}, \varphi(x) = \frac{3}{x}, \varphi^*(x) = \frac{1}{x}, \psi^*(x) = \frac{q_0}{6x}. \tag{62}$$

If we set $\pi(x) = x^3$, $\tau(x) = x$, and $\ell = 1$, then condition (45) becomes

$$\begin{aligned} &\int_{x_0}^\infty \left(\psi(s) - \left(\frac{2}{\mu s^2} \right)^\gamma \frac{r(s)\pi(s)(\varphi(s))^{\gamma+1}}{(\gamma+1)^{\gamma+1}} \right) ds \\ &= \int_{x_0}^\infty \left(\frac{q_0}{s} - \frac{9}{2\mu s} \right) ds = \left(q_0 - \frac{9}{2\mu} \right) \int_{x_0}^\infty \frac{1}{s} ds \\ &= \infty, \quad \text{if } q_0 > \frac{9}{2\mu}. \end{aligned} \tag{63}$$

Therefore, from Lemma 7, if $q_0 > 9/2\mu$, then (61) has no positive solution z satisfying $z''(x) > 0$. Also, condition (49) becomes

$$\int_{x_0}^\infty \left(\psi^*(s) - \frac{1}{4}\tau(s)(\varphi^*(s))^2 \right) ds = \int_{x_0}^\infty \left(\frac{q_0}{6s} - \frac{1}{4s} \right) ds = \infty, \quad \text{if } q_0 > \frac{3}{2}. \tag{64}$$

From Lemma 8, if $q_0 > 3/2$, then (61) has no positive solution z satisfying $z''(x) < 0$. Thus, from Theorem 9 every solution of (61) is oscillatory if $q_0 > \max\{9/2\mu, 3/2\}$.

Example 2. Consider the following differential equation representing equation (1),

$$\left(x^3 \left(z'''(x) \right)^3 \right)' + \left(\frac{c - x^4}{x^7} + \frac{1}{x^3} \right) z^3(\varepsilon x) = 0, \quad x \geq 1, \tag{65}$$

where $c > 0$ and $0 < \varepsilon < 1$ are constants.

Here, $\gamma = 3$, $r(x) = x^3$, $q(x) = ((c - x^4)/x^7) + (1/x^3) = c/x^7$, and $\eta(x) = \varepsilon x$. Hence,

$$\delta(x) = \infty, \psi(x) = \frac{c\varepsilon^9}{x}, \varphi(x) = \frac{6}{x}, \varphi^*(x) = \frac{1}{x}, \psi^*(x) = \left(\frac{c\varepsilon^3}{48} \right)^{1/3} \frac{1}{x}. \tag{66}$$

If we set $\pi(x) = x^6$, $\tau(x) = x$, and $\ell = 1$, then condition (45) yields

$$\begin{aligned} &\int_{x_0}^\infty \left(\psi(s) - \left(\frac{2}{\mu s^2} \right)^\gamma \frac{r(s)\pi(s)(\varphi(s))^{\gamma+1}}{(\gamma+1)^{\gamma+1}} \right) \mathrm{d}s \\ &= \int_{x_0}^\infty \left(\frac{c\varepsilon^9}{s} - \frac{81}{2\mu^3 s} \right) \mathrm{d}s = \left(c\varepsilon^9 - \frac{81}{2\mu^3} \right) \int_{x_0}^\infty \frac{1}{s} ds. \end{aligned} \tag{67}$$

Therefore, from Lemma 7, if $c > 3/4\varepsilon^3$, then (65) has a solution $z > 0$ satisfying $z''(x) > 0$. Also, from condition (49) we have

$$\begin{aligned} &\int_{x_0}^\infty \left(\psi^*(s) - \frac{1}{4}\tau(s)(\varphi^*(s))^2 \right) \mathrm{d}s \\ &= \int_{x_0}^\infty \left(\left(\frac{c\varepsilon^3}{48} \right)^{1/3} \frac{1}{s} - \frac{1}{4s} \right) ds = \left(\left(\frac{c\varepsilon^3}{48} \right)^{1/3} - \frac{1}{4} \right) \int_{x_0}^\infty \frac{1}{s} ds. \end{aligned} \tag{68}$$

Thus, from Theorem 9, every solution of (65) is oscillatory if

$$c > \max\left\{ \frac{3}{4\varepsilon^3}, \frac{81}{2\varepsilon^9\mu^3} \right\}. \tag{69}$$

Example 3. Consider

$$z^{(4)}(x) + \left(\frac{q_0 x - x^2}{x^5} + \frac{1}{x^3} \right) z\left(\frac{x}{2} \right) = 0, \quad x \geq 1, \tag{70}$$

where $q_0 > 0$.

Let $\gamma = 1$, $r(x) = 1$, $q(x) = (((q_0 x - x^2)/x^5) + (1/x^3)) = q_0/x^4$, and $\eta(x) = x/2$. When $\ell = 1$ is used, condition (59) becomes

$$\lim_{x\longrightarrow\infty}\inf\left(\int_{x_0}^{x}\frac{s^2}{r(s)}\,ds\right)\int_x^\infty\frac{q_0}{s^4}ds = \lim_{x\longrightarrow\infty}\inf\left(\frac{x^3}{3}\right)\int_x^\infty\frac{q_0}{s^4}\mathrm{d}s=\frac{q_0}{9}>\frac{1}{4}, \tag{71}$$

and condition (60) gives

$$\lim_{x\longrightarrow\infty}\inf\int_x^\infty\left(\int_x^\infty\left(\frac{\ell}{r(x)}\int_x^\infty q(s)\frac{\eta^\gamma(s)}{s^\gamma}ds\right)dx\right)ds = \lim_{x\longrightarrow\infty}\inf\int_x^\infty\left(\int_x^\infty\left(\int_x^\infty\frac{q_0}{2s^4}ds\right)dx\right)ds=\frac{q_0}{6}>\frac{1}{4}. \tag{72}$$

Therefore, from Theorem 11, all solutions of (70) are oscillatory if $q_0 > 2.25$.

5. Conclusion

In this paper, we have established some new sufficient criteria which ensure that every solution of the fourth-order differential equations (1) is oscillatory. The approach we used was based on comparisons with the oscillatory behaviour of second-order delay equations and the Riccati transformation. Several illustrative examples have also been presented.

Data Availability

No data were used to support this study.

Disclosure

This work is part of UKM's research # DIP-2021-018.

Conflicts of Interest

All authors have declared they do not have any competing interests.

References

[1] M. Bartusek, M. Cecchi, Z. Dosla, and M. Marini, "Fourth-order differential equation with deviating argument," *Abstract & Applied Analysis*, vol. 2012, article 185242, 17 pages, 2012.

[2] O. Bazighifan, "An approach for studying asymptotic properties of solutions of neutral differential equations," *Symmetry*, vol. 120, no. 4, p. 555, 2020.

[3] O. Bazighifan, H. Alotaibi, and A. Mousa, "Neutral delay differential equations: oscillation conditions for the solutions," *Symmetry*, vol. 13, no. 1, p. 101, 2021.

[4] J. K. Hale, "Retarded functional differential equations: basic theory," in *Theory of Functional Differential Equations*, pp. 36–56, Springer, 1977.

[5] R. Agarwal, S. Grace, and D. O'Regan, *Oscillation Theory for Difference and Functional Differential Equations*, Springer Science & Business Media, 2013.

[6] C. Cesarano, S. Pinelas, F. Al-Showaikh, and O. Bazighifan, "Asymptotic properties of solutions of fourth-order delay differential equations," *Symmetry*, vol. 11, no. 5, p. 628, 2019.

[7] S. Grace, J. Džurina, I. Jadlovská, and T. Li, "On the oscillation of fourth-order delay differential equations," *Advances in Difference Equations*, vol. 2019, no. 118, 2019.

[8] T. Li, B. Baculková, J. Džurina, and C. Zhang, "Oscillation of fourth-order neutral differential equations with p-Laplacian like operators," *Boundary Value Problems*, vol. 2014, no. 1, 2014.

[9] O. Bazighifan and P. Kumam, "Oscillation theorems for advanced differential equations with p-Laplacian like operators," *Mathematics*, vol. 8, no. 5, p. 821, 2020.

[10] O. Bazighifan, T. Abdeljawad, and Q. Al-Mdallal, "Differential equations of even-order with p-Laplacian like operators: qualitative properties of the solutions," *Advances in Difference Equations*, vol. 2021, no. 1, 2021.

[11] C. Zhang, R. Agarwal, M. Bohner, and T. Li, "New results for oscillatory behavior of even-order half-linear delay differential equations," *Applied Mathematics Letters*, vol. 26, no. 2, pp. 179–183, 2013.

[12] S. Grace, "Oscillation theorems for nth-order differential equations with deviating arguments," *Journal of Mathematical Analysis & Applications*, vol. 101, no. 1, pp. 268–296, 1984.

[13] R. Agarwal, S. Grace, and D. O'Regan, "Oscillation criteria for certain nth order differential equations with deviating arguments," *Journal of Mathematical Analysis & Applications*, vol. 262, no. 2, pp. 601–622, 2001.

[14] Z. Xu and Y. Xia, "Integral averaging technique and oscillation of certain even order delay differential equations," *Journal of Mathematical Analysis & Applications*, vol. 292, no. 1, pp. 238–246, 2004.

[15] C. Zhang, T. Li, and S. Saker, "Oscillation of fourth-order delay differential equations," *Journal of Mathematical Sciences*, vol. 201, no. 3, pp. 296–309, 2014.

[16] B. Baculikova, J. Dzurina, and J. Graef, "On the oscillation of higher order delay differential equations," *Journal of Mathematical Sciences*, vol. 187, pp. 387–400, 2012.

[17] G. Chatzarakis, E. Elabbasy, and O. Bazighifan, "An oscillation criterion in 4th-order neutral differential equations with a continuously distributed delay," *Advances in Difference Equations*, vol. 2019, no. 336, 2019.

[18] O. Bazighifan and T. Abdeljawad, "Improved approach for studying oscillatory properties of fourth-order advanced differential equations with p-Laplacian like operator," *Mathematics*, vol. 8, no. 5, p. 656, 2020.

[19] O. Bazighifan, K. Al-Ghafri, M. Al-Kandari, F. Ghanim, and F. Mofarreh, "Half-linear differential equations of fourth order: oscillation criteria of solutions," *Advances in Continuous & Discrete Models*, vol. 2022, no. 1, pp. 1–12, 2022.

[20] R. Agarwal, C. Zhang, and T. Li, "Some remarks on oscillation of second order neutral differential equations," *Applied Mathematics & Computation*, vol. 274, pp. 178–181, 2016.

[21] C. Philos, "On the existence of nonoscillatory solutions tending to zero at ∞ for differential equations with positive delays," *Archiv der Mathematik*, vol. 36, no. 1, pp. 168–178, 1981.

[22] C. Zhang, T. Li, B. Sun, and E. Thandapani, "On the oscillation of higher-order half-linear delay differential equations," *Applied Mathematics Letters*, vol. 24, no. 9, pp. 1618–1621, 2011.

[23] P. Řehák, "How the constants in Hille-Nehari theorems depend on time scales," *Advances in Difference Equations*, vol. 2006, Article ID 64534, 16 pages, 2006.

Hindawi
Journal of Function Spaces
Volume 2022, Article ID 7133824, 9 pages
https://doi.org/10.1155/2022/7133824

Research Article

The Exact Solutions for Fractional-Stochastic Drinfel'd–Sokolov–Wilson Equations Using a Conformable Operator

Farah M. Al-Askar,[1] **Wael W. Mohammed**,[2,3] **Sallieu K. Samura**,[4] **and M. El-Morshedy**[5,6]

[1]*Department of Mathematical Science, College of Science, Princess Nourah Bint Abdulrahman University, P.O. Box 84428, Riyadh 11671, Saudi Arabia*
[2]*Department of Mathematics, Faculty of Science, University of Ha'il, Ha'il 2440, Saudi Arabia*
[3]*Department of Mathematics, Faculty of Science, Mansoura University, Mansoura 35516, Egypt*
[4]*Department of Mathematics and Statistics, Fourah Bay College, University of Sierra Leone, Sierra Leone*
[5]*Department of Mathematics, College of Science and Humanities in Al-Kharj, Prince Sattam Bin Abdulaziz University, Al-Kharj 11942, Saudi Arabia*
[6]*Department of Statistics and Computer Science, Faculty of Science, Mansoura University, Mansoura 35516, Egypt*

Correspondence should be addressed to Wael W. Mohammed; wael.mohammed@mans.edu.eg

Received 20 June 2022; Accepted 2 August 2022; Published 20 August 2022

Academic Editor: Yusuf Gurefe

The fractional-stochastic Drinfel'd–Sokolov–Wilson equations (FSDSWEs) perturbed by the multiplicative Wiener process are studied. The mapping method is used to obtain rational, hyperbolic, and elliptic stochastic solutions for FSDSWEs. Due to the importance of FSDSWEs in describing the propagation of shallow water waves, the derived solutions are significantly more useful and effective in understanding various important challenging physical phenomena. In addition, we use the MATLAB Package to generate 3D graphs for specific FSDSWE solutions in order to discuss the impact of fractional order and the Wiener process on the solutions of FSDSWEs.

1. Introduction

Partial differential equations (PDEs) have grown in popularity because of their broad spectrum of applications in nonlinear science including engineering [1], civil engineering [2], quantum mechanics [3], soil mechanics [4], statistical mechanics [5], population ecology [6], economics [7], and biology [8, 9]. Therefore, finding exact solutions is critical for a better understanding of nonlinear phenomena. To acquire exact solutions to these equations, a variety of methods such as Darboux transformation [10], Hirota's function [11], sine-cosine [12, 13], (G'/G)-expansion [14–16], perturbation [17, 18], Riccati-Bernoulli sub-ODE [19], $\exp(-\phi(\varsigma))$-expansion [20, 21], tanh-sech [22, 23], Jacobi elliptic function [24, 25], and Riccati equation method [26] have been used.

Recently, fractional derivatives are used to characterize a wide range of physical phenomena in mathematical biology, engineering disciplines, electromagnetic theory, signal processing, and other scientific research. These new fractional-order models are better than the previously used integer-order models because fractional-order derivatives and integrals allow for the modeling of distinct substances' memory and hereditary capabilities.

The conformable fractional derivative (CFD) helps us to develop an idea of how physical phenomena act. The CFD is very useful for modelling a variety of physical issues since differential equations with CFD are simpler to solve numerically than those with Caputo fractional derivative or the Riemann-Liouville. Currently, authors are focusing on fractional calculus and creating new operators such the Caputo

Fabrizio, Caputo, Riemann Liouville, and Atangana Baleanu derivatives. The conformable fractional operator [27–30] eliminates some of the restrictions of current fractional operators and provides standard calculus properties such as the derivative of the quotient of two functions, the product of two functions, Rolle's theorem, the chain rule, and the mean value theorem. Here, we use CFD stated in [29]. Therefore, let us state the definition of CFD and its properties as follows [29]:

The CFD of $\varphi : \mathbb{R}^+ \longrightarrow \mathbb{R}$ of order α is defined as

$$\mathbb{D}_y^\alpha \varphi(x) = \lim_{\varepsilon \longrightarrow 0} \frac{\varphi\left(y + \varepsilon y^{1-\alpha}\right) - \varphi(y)}{\varepsilon}. \tag{1}$$

The CFD satisfies

(1) $\mathbb{D}_y^\alpha[a\varphi(y) + b\psi(y)] = a\mathbb{D}_x^\alpha\varphi(y) + b\mathbb{D}_x^\alpha\psi(y),\ a, b \in \mathbb{R}$

(2) $\mathbb{D}_y^\alpha[C] = 0$, C is a constant

(3) $\mathbb{D}_y^\alpha(\varphi \circ \psi)(y) = x^{1-\alpha}\psi'(y)\varphi(\psi(y))$

(4) $\mathbb{D}_y^\alpha[x^y] = yy^{y-\alpha}, y \in \mathbb{R}$

(5) $\mathbb{D}_y^\alpha\psi(y) = y^{1-\alpha}(d\psi/dy)$

On the other hand, in the practically physical system, random perturbations emerge from a variety of natural sources. They cannot be avoided, because noise can cause statistical properties and significant phenomena. Consequently, stochastic differential equations emerged and they started to play a major role in modeling phenomena in oceanography, physics, biology, chemistry, atmosphere, fluid mechanics, and other fields.

Therefore, we consider in this paper the following fractional-stochastic Drinfel'd–Sokolov–Wilson equations (FSDSWEs):

$$d\Psi + [\gamma_1 \Phi \mathbb{D}_x^\alpha \Phi]dt = \sigma\Psi d\beta, \tag{2}$$

$$d\Phi + [\gamma_2 \mathbb{D}_{xxx}^\alpha \Phi + \gamma_3 \Psi \mathbb{D}_x^\alpha \Phi + \gamma_4 \Phi \mathbb{D}_x^\alpha \Psi]dt = \sigma\Phi d\beta, \tag{3}$$

where γ_k for $k = 1, 2, 3, 4$ are nonzero parameters. $\mathbb{D}^\alpha$, for $0 < \alpha \leq 1$, is CFD [29]. $\beta(t)$ is a standard Wiener process (SWP), and σ is the noise strength.

The Drinfel'd–Sokolov–Wilson equations (DSWEs) ((2) and (3)), with $\alpha = 1$ and $\sigma = 0$, evolved from shallow water wave models initially given by Drinfel'd and Sokolov [31, 32] and later refined by Wilson [33]. Due to the importance of DSWEs, several authors have created analytical solutions for this system using a variety of methods, including exp-function method [34], truncated Painlevè method [35], F – expansion method [36], Bäcklund transformation of Riccati equation [37], homotopy analysis method [38], and tanh and extended tanh methods [39]. Furthermore, a few authors obtained exact solutions for fractional DSW using various methods such as Jacobi elliptical function method [40] and complete discrimination system for polynomial method [41], while the analytical fractional-stochastic solutions of FSDSWEs ((2) and (3)) have never been obtained before.

Our aim of this paper is to attain a wide range of solutions including rational, hyperbolic, and elliptic functions for FSDSWEs ((2) and (3)) by using the mapping method. This is the first study to obtain exact solutions to FSDSWEs with combination of a stochastic term and fractional derivative. Also, we utilize MATLAB to generate 3D diagrams for a number of the FSDSWEs ((2) and (3)) developed in this study to demonstrate how the SWP affects these solutions.

This paper will be formatted as follows. In Section 2, the mapping method is used to generate analytic solutions for FSDSWEs ((2) and (3)). In Section 3, we investigate the effect of the SWP and fractional order on the derived solutions. Section 4 presents the paper's conclusion.

2. Analytical Solutions of FSDSWEs

First, let us derive the wave equation of FSDSWEs as follows.

2.1. Wave Equation for FSDSWEs. Let us apply the following wave transformation

$$\begin{aligned}\Psi(x,t) &= \psi(\mu)e^{\left(\sigma\beta(t)-(1/2)\sigma^2 t\right)}, \Phi(x,t)\\ &= \varphi(\mu)e^{\left(\sigma\beta(t)-(1/2)\sigma^2 t\right)},\ \mu\\ &= \frac{1}{\alpha}x^\alpha + \omega t,\end{aligned} \tag{4}$$

to attain the wave equation of FSDSWEs ((2) and (3)), where ψ and φ are real deterministic functions and ω is a constant. Putting Equation (4) into Equations (2) and (3) and using

$$\begin{aligned}d\Psi &= \left[\omega\psi' dt + \sigma\psi d\beta\right]e^{\left(\sigma\beta(t)-(1/2)\sigma^2 t\right)},\\ d\Phi &= \left[\omega\varphi' dt + \sigma\varphi d\beta\right]e^{\left(\sigma\beta(t)-(1/2)\sigma^2 t\right)},\\ \mathbb{D}_x^\alpha\Phi &= \varphi' e^{\left(\sigma\beta(t)-(1/2)\sigma^2 t\right)},\\ \mathbb{D}_x^\alpha\Psi &= \psi' e^{\left(\sigma\beta(t)-(1/2)\sigma^2 t\right)},\\ \mathbb{D}_{xxx}^\alpha\Phi &= \varphi''' e^{\left(\sigma\beta(t)-(1/2)\sigma^2 t\right)},\end{aligned} \tag{5}$$

we attain

$$\omega\psi' + \gamma_1\varphi\varphi' e^{\left(\sigma\beta(t)-(1/2)\sigma^2 t\right)} = 0, \tag{6}$$

$$\omega\varphi' + \gamma_2\varphi''' + \gamma_3\psi\varphi' e^{\left(\sigma\beta(t)-(1/2)\sigma^2 t\right)} + \gamma_4\varphi\psi' e^{\left(\sigma\beta(t)-(1/2)\sigma^2 t\right)} = 0. \tag{7}$$

Taking expectation $\mathbb{E}(\cdot)$ for Equations (6) and (7), we get

$$\omega\psi' + \gamma_1\varphi\varphi' e^{-(1/2)\sigma^2 t}\mathbb{E}\left(e^{\sigma\beta(t)}\right) = 0, \tag{8}$$

$$\omega\varphi' + \gamma_2\varphi''' + \left[\gamma_3\psi\varphi' + \gamma_4\varphi\psi'\right]e^{-(1/2)\sigma^2 t}\mathbb{E}\left(e^{\sigma\beta(t)}\right) = 0. \tag{9}$$

Since $\beta(t)$ is a normal distribution, then $\mathbb{E}(e^{\sigma\beta(t)}) = e^{(\sigma^2/2)t}$. Now, Equations (8) and (9) take the type

$$\omega\psi' + \gamma_1\varphi\varphi' = 0, \tag{10}$$

$$\omega\varphi' + \gamma_2\varphi''' + \gamma_3\psi\varphi' + \gamma_4\varphi\psi' = 0. \tag{11}$$

Integrating Equation (10) and putting the constants of integration equal zero, we get

$$\psi = -\frac{\gamma_1}{\omega}\varphi^2 + C, \tag{12}$$

where C is the integral constant. Plugging Equation (12) into (11) and using Equation (10), we have

$$\gamma_2\varphi''' - \left[\frac{\gamma_1\gamma_3}{2\omega} + \frac{\gamma_1\gamma_4}{\omega}\right]\varphi^2\varphi' + [\omega + C\gamma_3]\varphi' = 0. \tag{13}$$

Integrating Equation (13), we obtain

$$\varphi'' - \ell_1\varphi^3 + \ell_2\varphi = 0, \tag{14}$$

where

$$\begin{aligned} \ell_1 &= \frac{\gamma_1\gamma_3}{6\gamma_2\omega} + \frac{\gamma_1\gamma_4}{3\gamma_2\omega}, \\ \ell_2 &= \frac{\omega}{\gamma_2} + \frac{C\gamma_3}{\gamma_2}. \end{aligned} \tag{15}$$

2.2. The Mapping Method Description. Here, let us describe the mapping method stated in [42]. Assuming the solutions of Equation (14) have the form

$$\varphi(\mu) = \sum_{i=0}^{N} a_i\chi^i, \tag{16}$$

where N is fixed by balancing the linear term of the highest order derivative φ'' with nonlinear term φ^3, a_i, for $i = 1, 2, \cdots a_N$, are constants to be calculated and χ satisfies the first kind of elliptic equation

$$\chi' = \sqrt{\frac{1}{2}p\chi^4 + q\chi^2 + r}, \tag{17}$$

where p, q, and r are real parameters.

We notice that Equation (17) has a variety of solutions depending on p, q, and r as follows (Table 1).

$sn(\mu) = sn(\mu, m)$, $cn(\mu) = cn(\mu, m)$, $dn(\mu, m) = dn(\mu, m)$ are the Jacobi elliptic functions (JEFs) for $0 < m < 1$. When $m \longrightarrow 1$, the JEFs are converted into the hyperbolic functions shown below:

$$\begin{aligned} &cn(\mu) \longrightarrow \operatorname{sech}(\mu), \; sn(\mu) \longrightarrow \tanh(\mu), \; cs(\mu) \longrightarrow \operatorname{csch}(\mu), \\ &ds \longrightarrow \operatorname{csch}(\mu), \qquad dn(\mu) \longrightarrow \operatorname{sech}(\mu). \end{aligned} \tag{18}$$

2.3. Solutions of FSDSWEs. Now, let us determine the parameter N by balancing φ'' with φ^3 in Equation (14) as

$$N + 2 = 3N \Longrightarrow N = 1. \tag{19}$$

Rewriting Equation (17) with $N = 1$ as

$$\varphi = a_0 + a_1\chi. \tag{20}$$

Differentiating Equation (20) twice, we have, by using (17),

$$\varphi'' = a_1q\chi + a_1p\chi^3. \tag{21}$$

Substituting Equations (20) and (21) into Equation (14), we obtain

$$\left(a_1p - \ell_1a_1^3\right)\chi^3 - 3a_0a_1^2\ell_1\chi^2 + \left(a_1q - 3\ell_1a_0^2a_1 + \ell_2a_1\right)\chi - \left(\ell_1a_0^3 - \ell_2a_0\right) = 0. \tag{22}$$

Putting each coefficient of χ^k for $k = 0, 1, 2, 3$ equal zero, we get

$$\begin{aligned} a_1p - \ell_1a_1^3 &= 0, \\ 3a_0a_1^2\ell_1 &= 0, \\ a_1q - 3\ell_1a_0^2a_1 + \ell_2a_1 &= 0, \\ \ell_1a_0^3 - \ell_2a_0 &= 0. \end{aligned} \tag{23}$$

Solving these equations, we obtain

$$a_0 = 0, a_1$$

$$= \pm\sqrt{\frac{p}{\ell_1}}, q = -\ell_2. \tag{24}$$

Table 1: All possible solutions for Equation (17) for different values of p, q, and r.

Case	p	q	r	$\chi(\mu)$
1	$2\mathrm{m}^2$	$-(1+\mathrm{m}^2)$	1	$sn(\mu)$
2	2	$2\mathrm{m}^2-1$	$-\mathrm{m}^2(1-\mathrm{m}^2)$	$ds(\mu)$
3	2	$2-\mathrm{m}^2$	$(1-\mathrm{m}^2)$	$cs(\mu)$
4	$-2\mathrm{m}^2$	$2\mathrm{m}^2-1$	$(1-\mathrm{m}^2)$	$cn(\mu)$
5	-2	$2-\mathrm{m}^2$	(m^2-1)	$dn(\mu)$
6	$\frac{\mathrm{m}^2}{2}$	$\frac{(\mathrm{m}^2-2)}{2}$	$\frac{1}{4}$	$\frac{sn(\mu)}{1\pm dn(\mu)}$
7	$\frac{\mathrm{m}^2}{2}$	$\frac{(\mathrm{m}^2-2)}{2}$	$\frac{\mathrm{m}^2}{4}$	$\frac{sn(\mu)}{1\pm dn(\mu)}$
8	$\frac{-1}{2}$	$\frac{(\mathrm{m}^2+1)}{2}$	$\frac{-(1-\mathrm{m}^2)^2}{4}$	$mcn(\mu)\pm dn(\mu)$
9	$\frac{m^2-1}{2}$	$\frac{(m^2+1)}{2}$	$\frac{(m^2-1)}{4}$	$\frac{dn(\mu)}{1\pm sn(\mu)}$
10	$\frac{1-m^2}{2}$	$\frac{(1-m^2)}{2}$	$\frac{(1-m^2)}{4}$	$\frac{cn(\mu)}{1\pm sn(\mu)}$
11	$\frac{(1-m^2)^2}{2}$	$\frac{(1-m^2)^2}{2}$	$\frac{1}{4}$	$\frac{sn(\mu)}{dn\pm cn(\mu)}$
12	2	0	0	$\frac{c}{\mu}$
13	0	1	0	ce^{μ}

Table 2: All possible solutions for wave Equation (14) when $p > 0$.

Case	p	q	r	$\chi(\mu)$	$\varphi(\mu)$
1	$2m^2$	$-(1+m^2)$	1	$sn(\mu)$	$\pm\sqrt{\frac{p}{\ell_1}}sn(\mu)$
2	2	$2m^2-1$	$-m^2(1-m^2)$	$ds(\mu)$	$\pm\sqrt{\frac{p}{\ell_1}}ds(\mu)$
3	2	$2-m^2$	$(1-m^2)$	$cs(\mu)$	$\pm\sqrt{\frac{p}{\ell_1}}cs(\mu)$
4	$\frac{m^2}{2}$	$\frac{(m^2-2)}{2}$	$1/4$ or $m^2/4$	$\frac{sn(\mu)}{1\pm dn(\mu)}$	$\pm\sqrt{\frac{p}{\ell_1}}\frac{sn(\mu)}{1\pm dn(\mu)}$
5	$\frac{1-m^2}{2}$	$\frac{(1-m^2)}{2}$	$\frac{(1-m^2)}{4}$	$\frac{cn(\mu)}{1\pm sn(\mu)}$	$\pm\sqrt{\frac{p}{\ell_1}}\frac{cn(\mu)}{1\pm sn(\mu)}$
6	$\frac{(1-m^2)^2}{2}$	$\frac{(1-m^2)^2}{2}$	$\frac{1}{4}$	$\frac{sn(\mu)}{dn\pm cn(\mu)}$	$\pm\sqrt{\frac{p}{\ell_1}}\frac{sn(\mu)}{dn\pm cn(\mu)}$
7	2	0	0	$\frac{c}{\mu}$	$\pm\sqrt{\frac{p}{\ell_1}}\frac{c}{\mu}$

Hence, the solution of Equation (14) is

$$\varphi(\mu) = \pm\sqrt{\frac{p}{\ell_1}}\chi(\mu), \tag{25}$$

for $p/\ell_1 > 0$. There are two sets depending only on p and ℓ_1 as follows.

First set: if $p > 0$ and $\ell_1 > 0$, then the solutions $\varphi(\mu)$, from Table 1, of wave Equation (14) are as follows (Table 2).

If $m \longrightarrow 1$, then Table 2 degenerates to Table 3.

Now, using Table 2 (or Table 3 when $m \longrightarrow 1$) and Equations (25) and (12), we get the solutions of FSDSWEs ((2) and (3)), for $p/\ell_1 > 0$, as follows:

$$\Phi(x, t) = \varphi(\mu)e^{\left(\sigma\beta(t)-(1/2)\sigma^2 t\right)}, \tag{26}$$

Table 3: All possible solutions for wave Equation (14) when $p > 0$ and $m \longrightarrow 1$.

Case	p	q	r	$\chi(\mu)$	$\varphi(\mu)$
1	2	-2	1	$\tanh(\mu)$	$\pm\sqrt{\frac{p}{\ell_1}}\tanh(\mu)$
2	2	1	0	$\operatorname{sech}(\mu)$	$\pm\sqrt{p/\ell_1}\operatorname{sech}(\mu)$
3	2	1	0	$\operatorname{csch}(\mu)$	$\pm\sqrt{p/\ell_1}\operatorname{csch}(\mu)$
4	$\frac{1}{2}$	$\frac{-1}{2}$	$\frac{1}{4}$	$\frac{\tanh(\mu)}{1\pm\operatorname{sech}(\mu)}$	$\pm\sqrt{\frac{p}{\ell_1}}\frac{\tanh(\mu)}{1\pm\operatorname{sech}(\mu)}$
5	2	0	0	$\frac{c}{\mu}$	$\pm\sqrt{\frac{p}{\ell_1}}\frac{c}{\mu}$

Table 4: All possible solutions for wave Equation (14) when $p < 0$ and $m \longrightarrow 1$.

Case	p	q	r	$\chi(\mu)$	$\varphi(\mu)$
1	-2	1	0	$\operatorname{sech}(\mu)$	$\pm\sqrt{\frac{p}{\ell_1}}\operatorname{sech}(\mu)$
2	$\frac{-1}{2}$	2	0	$2\operatorname{sech}(\mu)$	$\pm 2\sqrt{\frac{p}{\ell_1}}\operatorname{sech}(\mu)$

Table 5: All possible solutions for wave Equation (14) when $p < 0$.

Case	p	q	r	$\chi(\mu)$	$\varphi(\mu)$
1	$-2m^2$	$2m^2-1$	$(1-m^2)$	$cn(\mu)$	$\pm\sqrt{\frac{p}{\ell_1}}cn(\mu)$
2	-2	$2-m^2$	(m^2-1)	$dn(\mu)$	$\pm\sqrt{\frac{p}{\ell_1}}dn(\mu)$
3	$\frac{-1}{2}$	$\frac{(m^2+1)}{2}$	$\frac{-(1-m^2)^2}{4}$	$mcn(\mu)\pm dn(\mu)$	$\pm\sqrt{\frac{p}{\ell_1}}[mcn(\mu)\pm dn(\mu)]$
4	$\frac{m^2-1}{2}$	$\frac{(m^2+1)}{2}$	$\frac{(m^2-1)}{4}$	$\frac{dn(\mu)}{1\pm sn(\mu)}$	$\pm\sqrt{\frac{p}{\ell_1}}\frac{dn(\mu)}{1\pm sn(\mu)}$

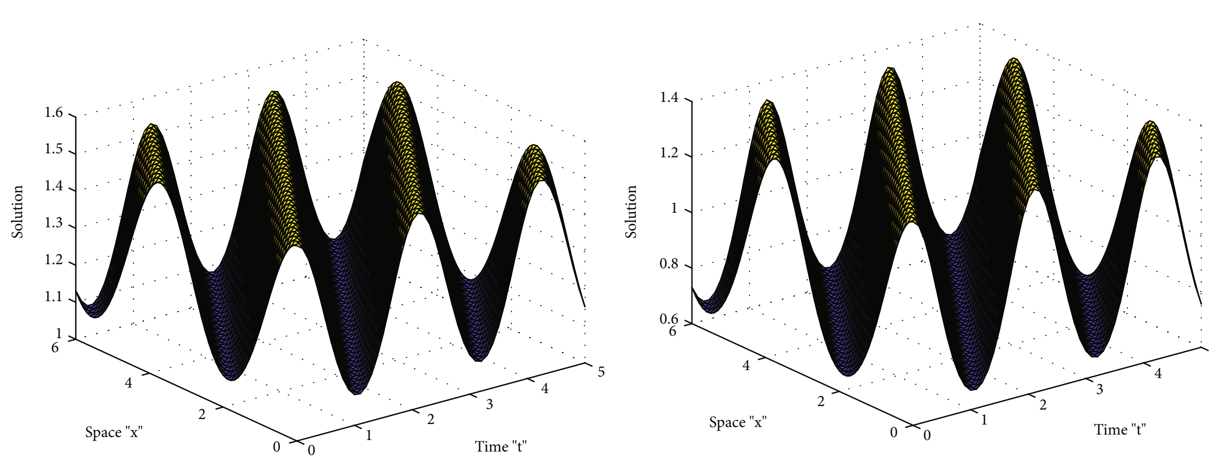

Figure 1: 3D plot of Equations (28) and (29) with $\sigma = 0$ and $\alpha = 1$.

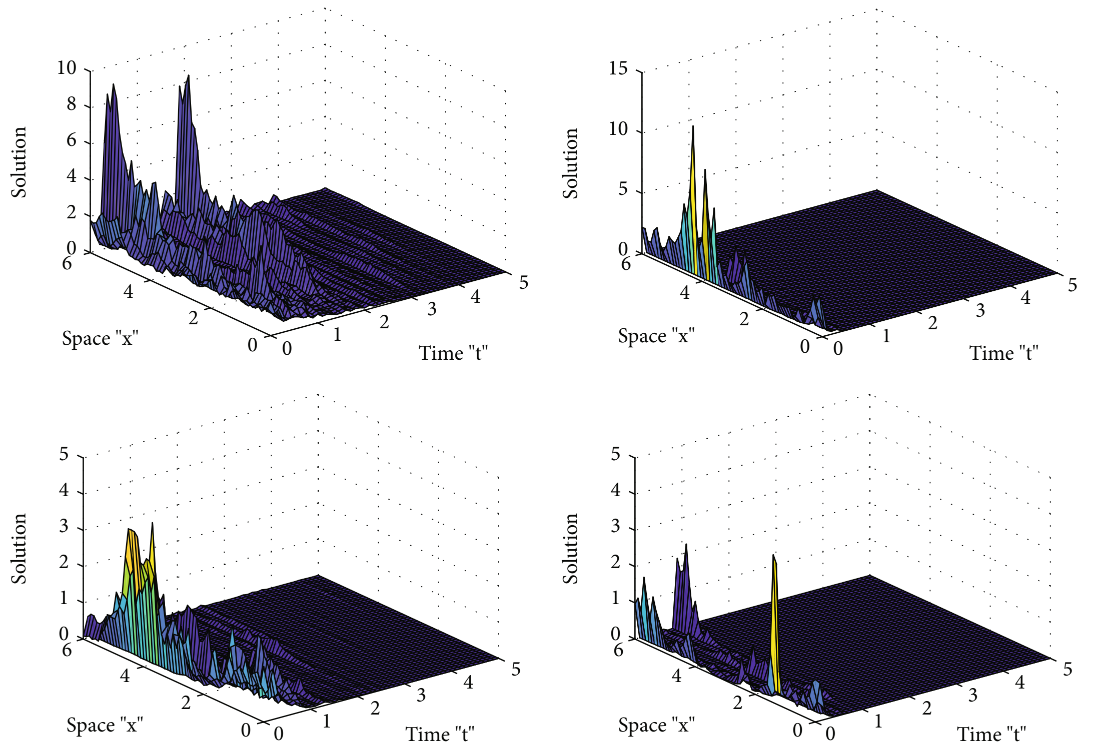

FIGURE 2: 3D plot of Equations (28) and (29) with $\sigma = 1, 2$ and $\alpha = 1$.

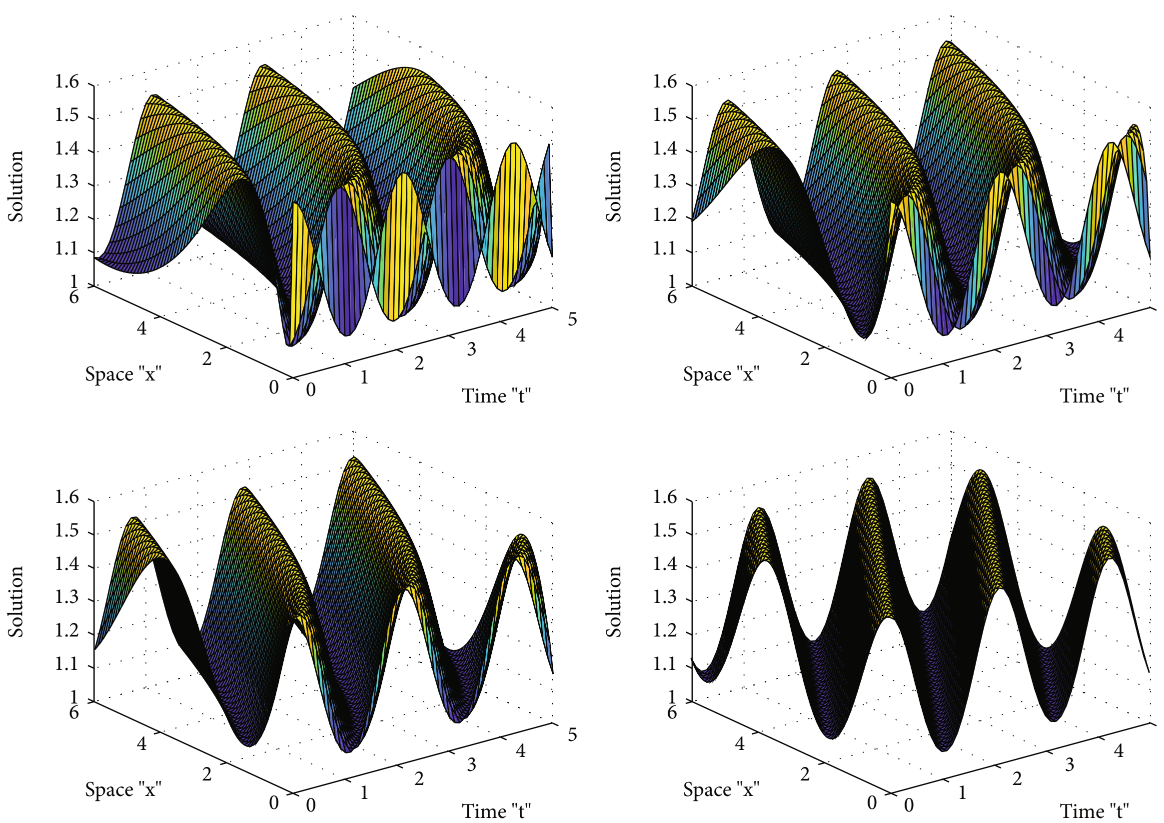

FIGURE 3: 3D plot of Equation (28) with $\sigma = 0$ and different α.

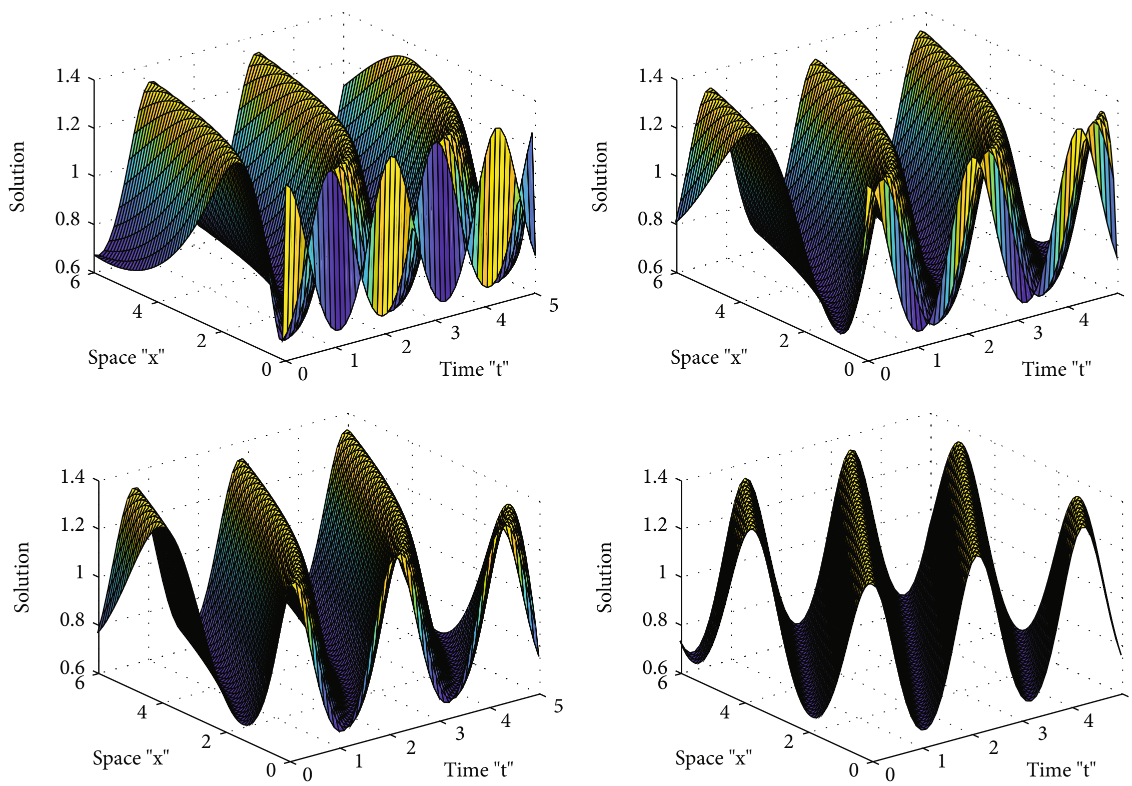

Figure 4: 3D plot of Equation (29) with $\sigma = 0$ and different α.

$$\Psi(x,t) = \left[-\frac{\gamma_1}{\omega}\varphi^2(\mu) + C\right]e^{\left(\sigma\beta(t)-(1/2)\sigma^2 t\right)}, \tag{27}$$

where $\mu = (x^\alpha/\alpha) + \omega t$.

Second set: if $p < 0$ and $\ell_1 < 0$, then the solutions $\varphi(\mu)$, from Table 1, of wave Equation (14) are as follows.

If $m \longrightarrow 1$, then Table 3 degenerates to Table 4.

In this case, using Table 5 (or Table 4 when $m \longrightarrow 1$), we can get the analytical solutions of FSDSWEs ((2) and (3)) as stated in Equations (26) and (27).

3. The Impact of Noise and Fractional Order on the Solutions

The impact of the noise and fractional order on the acquired solutions of FSDSWEs ((2) and (3)) is addressed. MATLAB tools are used to generate graphs for the following solutions:

$$\Phi(x,t) = \sqrt{\frac{p}{\ell_1}}cn\left(\frac{x^\alpha}{\alpha} + \omega t\right)e^{\left(\sigma\beta(t)-(1/2)\sigma^2 t\right)}, \tag{28}$$

$$\Psi(x,t) = \left[-\frac{\gamma_1 p}{\omega \ell_1}cn^2\left(\frac{x^\alpha}{\alpha} + \omega t\right)\right]e^{\left(\sigma\beta(t)-(1/2)\sigma^2 t\right)}, \tag{29}$$

with $C = 0$, $p = -2m^2$, $\gamma_1 = \gamma_2 = 1$, $\gamma_3 = \gamma_4 = 3$, $p = -2$, $q = 2 - m^2$, and $m = 0.5$. Then, $\ell_1 = -6/7$ and $\omega = 7/4$.

Firstly the impact of noise: in the absence of the noise, the surface is periodic (not flat) as we see in Figure 1.

While in Figure 2, if the noise is introduced and its strength σ is raised, the surface becomes substantially flatter as follows.

Secondly the impact of fractional order: in Figures 3 and 4, if $\sigma = 0$, we can see that the surface expands when α is increasing.

From the previous simulations, we may examine the nature of the solution as a double-periodic wave in physical form. We may conclude that it is critical to incorporate some fluctuation when modelling any phenomenon since the ignored terms may have an influence on the solutions.

4. Conclusions

In this paper, we considered the fractional-stochastic Drinfel'd–Sokolov–Wilson equations. This equation is well known in mathematical physics, population dynamics, surface physics, plasma physics, and applied sciences. The analytical solutions to FSDSWEs ((2) and (3)) were successfully attained by utilizing the mapping method. Due to the importance of FSDSWEs, these established solutions are significantly more useful and effective in understanding a variety of critical physical processes. In addition, we utilized the MATLAB software to demonstrate how multiplicative noise and fractional order affected the solutions of FSDSWEs. We may employ additive noise to address the FSDSWEs ((2) and (3)) in future study.

Data Availability

All data are available in this paper.

Conflicts of Interest

The authors declare that they have no competing interests.

Authors' Contributions

All authors contributed equally to the writing of this paper. All authors read and approved the final manuscript.

Acknowledgments

The study was supported by the Princess Nourah Bint Abdulrahman University Researchers Supporting Project number PNURSP2022R273, Princess Nourah Bint Abdulrahman University, Riyadh, Saudi Arabia.

References

[1] J. Sabatier, O. P. Agrawal, and J. A. T. Machado, *Advances in fractional calculus*, vol. 4, Springer, Dordrecht, 2007.

[2] L. Baudouin, A. Rondepierre, and S. Neild, "Robust control of a cable from a hyperbolic partial differential equation model," *IEEE Transactions on Control Systems Technology*, vol. 27, no. 3, pp. 1343–1351, 2019.

[3] N. Laskin, "Nonlocal quantum mechanics: fractional calculus approach," *Applied Physics*, pp. 207–236, 2019.

[4] L. Shao, X. Guo, S. Liu, and G. Zheng, *Effective Stress and Equilibrium Equation for Soil Mechanics*, CRC Press, Boca Raton, FL, USA, 2017.

[5] E. Barkai, R. Metzler, and J. Klafter, "From continuous time random walks to the fractional Fokker-Planck equation," *Physical Review E*, vol. 61, no. 1, pp. 132–138, 2000.

[6] Y. Lin and J. Gao, "Research on diffusion effect of ecological population model based on delay differential equation," *Caribbean Journal of Science*, vol. 52, pp. 333–335, 2019.

[7] E. Scalas, R. Gorenflo, and F. Mainardi, "Fractional calculus and continuous-time finance," *Physica A*, vol. 284, no. 1-4, pp. 376–384, 2000.

[8] M. Barfield, M. Martcheva, N. Tuncer, and R. D. Holt, "Backward bifurcation and oscillations in a nested immuno-eco-epidemiological model," *Journal of Biological Dynamics*, vol. 12, no. 1, pp. 51–88, 2018.

[9] W. W. Mohammed, E. S. Aly, A. E. Matouk, S. Albosaily, and E. M. Elabbasy, "An analytical study of the dynamic behavior of Lotka-Volterra based models of COVID-19," *Results in Physics*, vol. 26, article 104432, 2021.

[10] M. Wen-Xiu and B. Sumayah, "A binary Darboux transformation for multicomponent NLS equations and their reductions," *Analysis and Mathematical Physics*, vol. 11, no. 2, p. 44, 2021.

[11] R. Hirota, "Exact solution of the Korteweg-de Vries equation for multiple collisions of solitons," *Physical Review Letters*, vol. 27, no. 18, pp. 1192–1194, 1971.

[12] A. M. Wazwaz, "A sine-cosine method for handlingnonlinear wave equations," *Mathematical and Computer Modelling*, vol. 40, no. 5-6, pp. 499–508, 2004.

[13] C. Yan, "A simple transformation for nonlinear waves," *Physics Letters A*, vol. 224, no. 1-2, pp. 77–84, 1996.

[14] M. L. Wang, X. Z. Li, and J. L. Zhang, "The (G'/G)-expansion method and travelling wave solutions of nonlinear evolution equations in mathematical physics," *Physics Letters A*, vol. 372, pp. 417–423, 2008.

[15] H. Zhang, "New application of the (G'/G)-expansion method," *Communications in Nonlinear Science and Numerical Simulation*, vol. 14, pp. 3220–3225, 2009.

[16] W. W. Mohammed, M. Alesemi, S. Albosaily, N. Iqbal, and M. El-Morshedy, "The exact solutions of stochastic fractional-space Kuramoto-Sivashinsky equation by using (G'/G)-expansion method," *Mathematics*, vol. 9, article 2712, 2021.

[17] W. W. Mohammed, "Amplitude equation with quintic nonlinearities for the generalized Swift-Hohenberg equation with additive degenerate noise," *Advances in Difference Equations*, vol. 2016, no. 1, Article ID 84, 2016.

[18] W. W. Mohammed, N. Iqbal, and T. Botmart, "Additive noise effects on the stabilization of fractional-space diffusion equation solutions," *Mathematics*, vol. 10, no. 1, p. 130, 2022.

[19] X. F. Yang, Z. C. Deng, and Y. Wei, "A Riccati-Bernoulli sub-ODE method for nonlinear partial differential equations and its application," *Advances in Difference Equations*, vol. 1, 133 pages, 2015.

[20] K. Khan and M. A. Akbar, "The $\exp(-\phi(\varsigma))$-expansion method for finding travelling wave solutions of Vakhnenko-Parkes equation," *International Journal of Dynamical Systems and Differential Equations*, vol. 5, no. 1, pp. 72–83, 2014.

[21] F. M. Al-Askar, W. W. Mohammed, A. M. Albalahi, and M. El-Morshedy, "The influence of noise on the solutions of fractional stochastic Bogoyavlenskii equation," *Fractal and Fractional.*, vol. 6, no. 3, p. 156, 2022.

[22] F. M. Al-Askar, W. W. Mohammed, A. M. Albalahi, and M. El-Morshedy, "The impact of the Wiener process on the analytical solutions of the stochastic $(2+1)$-dimensional breaking soliton equation by using tanh–coth method," *Mathematics*, vol. 10, no. 5, p. 817, 2022.

[23] W. Malfliet and W. Hereman, "The tanh method. I. Exact solutions of nonlinear evolution and wave equations," *Physica Scripta*, vol. 54, no. 6, pp. 563–568, 1996.

[24] Z. L. Yan, "Abundant families of Jacobi elliptic function solutions of the $(2+1)$-dimensional integrable Davey-Stewartson-type equation via a new method," *Chaos, Solitons and Fractals*, vol. 18, no. 2, pp. 299–309, 2003.

[25] E. Fan and J. Zhang, "Applications of the Jacobi elliptic function method to special-type nonlinear equations," *Physics Letters A*, vol. 305, no. 6, pp. 383–392, 2002.

[26] W. W. Mohammed, O. Bazighifan, M. M. Al-Sawalha, A. O. Almatroud, and E. S. Aly, "The influence of noise on the exact solutions of the stochastic fractional-space chiral nonlinear Schrödinger equation," *Fractal and Fractional*, vol. 5, no. 4, p. 262, 2021.

[27] A. A. Kilbas, H. M. Srivastava, and J. J. Trujillo, *Theory and Applications of Fractional Differential Equations*, Elsevier, Amsterdam, 2006.

[28] L. Debnath, "Recent applications of fractional calculus to science and engineering," *International Journal of Mathematics and Mathematical Sciences*, vol. 2003, no. 54, p. 3442, 2003.

[29] R. Khalil, M. Al Horani, A. Yousef, and M. Sababheh, "A new definition of fractional derivative," *Journal of Computational and Applied Mathematics*, vol. 264, pp. 65–70, 2014.

[30] A. Atangana and D. Baleanu, "New fractional derivatives with nonlocal and non-singular kernel: theory and application to heat transfer model," *Thermal Science*, vol. 20, no. 2, pp. 763–769, 2016.

[31] V. G. Drinfeld and V. V. Sokolov, "Equations of Korteweg–de Vries type, and simple Lie algebras," *Doklady Akademii Nauk*, vol. 258, no. 1, pp. 11–16, 1981.

[32] V. G. Drinfel'd and V. V. Sokolov, "Lie algebras and equations of Korteweg-de Vries type," *Journal of Soviet mathematics*, vol. 30, no. 2, pp. 1975–2036, 1985.

[33] G. Wilson, "The affine lie algebra C(1)2 and an equation of Hirota and Satsuma," *Physics Letters A*, vol. 89, no. 7, pp. 332–334, 1982.

[34] E. Misirli and Y. Gurefe, "Exp-function method for solving nonlinear evolution equations," *Mathematical and Computational Applications*, vol. 16, pp. 258–266, 2011.

[35] B. Ren, Z. M. Lou, Z. F. Liang, and X. Y. Tang, "Nonlocal symmetry and explicit solutions for Drinfel'd-Sokolov-Wilson system," *The European Physical Journal Plus*, vol. 131, no. 12, p. 441, 2016.

[36] X. Q. Zhao and H. Y. Zhi, "An improved F-expansion method and its application to coupled Drinfel'd-Sokolov-Wilson equation," *Communications in Theoretical Physics*, vol. 50, pp. 309–314, 2008.

[37] A. H. Arnous, M. Mirzazadeh, and M. Eslami, "Exact solutions of the Drinfel'd–Sokolov–Wilson equation using Bäcklund transformation of Riccati equation and trial function approach," *Pramana-Journal of Physics*, vol. 86, no. 6, pp. 1153–1160, 2016.

[38] R. Arora and A. Kumar, "Solution of the coupled Drinfeld's–Sokolov–Wilson (DSW) system by homotopy analysis method," *Advanced Science, Engineering and Medicine*, vol. 5, no. 10, pp. 1105–1111, 2013.

[39] S. Bibi and S. T. Mohyud-Din, "New traveling wave solutions of Drinefel'd–Sokolov–Wilson equation using tanh and extended tanh methods," *Journal of the Egyptian Mathematical Society*, vol. 22, no. 3, pp. 517–523, 2014.

[40] S. Sahoo and S. S. Ray, "New double-periodic solutions of fractional Drinfeld-Sokolov-Wilson equation in shallow water waves," *Nonlinear Dynamics*, vol. 88, no. 3, pp. 1869–1882, 2017.

[41] S. Chen, Y. Liu, L. Wei, and B. Guan, "Exact solutions to fractional Drinfel'd–Sokolov–Wilson equations," *Chinese Journal of Physics*, vol. 56, no. 2, pp. 708–720, 2018.

[42] Y. Z. Peng, "Exact solutions for some nonlinear partial differential equations," *Physics Letters A*, vol. 314, no. 5-6, pp. 401–408, 2003.

Hindawi
Journal of Function Spaces
Volume 2022, Article ID 3309674, 9 pages
https://doi.org/10.1155/2022/3309674

Research Article

A Numerical Approach for the Analytical Solution of the Fourth-Order Parabolic Partial Differential Equations

Fenglian Liu,[1] **Muhammad Nadeem**,[2] **Ibrahim Mahariq**,[3] **and Suliman Dawood**[4]

[1]*Institute of Land & Resources and Sustainable Development, Yunnan University of Finance and Economics, Kunming 650221, China*
[2]*School of Mathematics and Statistics, Qujing Normal University, Qujing 655011, China*
[3]*College of Engineering and Technology, American University of the Middle East, Kuwait*
[4]*Department of Mathematics, Sheba Region University, Marib, Yemen*

Correspondence should be addressed to Fenglian Liu; zz2105@ynufe.edu.cn and Suliman Dawood; sulimanseddek@gmail.com

Received 1 July 2022; Revised 22 July 2022; Accepted 25 July 2022; Published 16 August 2022

Academic Editor: Yusuf Gurefe

In this study, we propose a new iterative scheme (NIS) to investigate the approximate solution of the fourth-order parabolic partial differential equations (PDEs) that arises in transverse vibration problems. We introduce the Mohand transform as a new operator that is very easy to implement coupled with the homotopy perturbation method. This NIS is capable of reducing the linearization, perturbation, and restrictive assumptions that ruin the nature of the numerical problems. Some numerical examples are demonstrated to legitimate the accuracy and authenticity of this NIS. The computational results are obtained in the shape of a series that converges only after a few iterations. The comparison of the graphical representations shows that NIS is a very simple but also an effective approach for other numerical problems involving complex variables.

1. Introduction

Many physical phenomena of differential equations in complex variables play an important role in science and engineering such as physics, chemical energy, biology, medicine, and engineering [1–3]. These physical phenomena are of great interest in this modern era and are introduced by parabolic PDEs. It is still very difficult to investigate the exact solution of the PDEs in most numerical problems. Therefore, most of the researchers introduced numerous analytical and numerical approaches to provide the approximate solution for these PDEs such as the quintic B-spline collocation method [4], q-HATM [5], quintic B-spline [6], Legendre wavelet method [7], homotopy perturbation transform method [8], and so on [9–11].

Consider the fourth-order parabolic PDEs with variable coefficients [12, 13]

$$\frac{\partial^2 \Psi}{\partial \eta^2} + \alpha(\xi, \S, \theta)\frac{\partial^4 \Psi}{\partial \xi^4} + \frac{1}{\S}\beta(\xi, \S, \theta)\frac{\partial^4 \Psi}{\partial \S^4} + \frac{1}{\theta}\gamma(\xi, \S, \theta)\frac{\partial^4 \Psi}{\partial \theta^4} = g(\xi, \S, \theta, \eta), \tag{1}$$

where $\alpha, \beta, \gamma > 0$, subjected to the following initial conditions

$$\begin{aligned}\Psi(\xi, \S, \theta, 0) &= f_1(\xi, \S, \theta),\\ \frac{\partial \Psi}{\partial \eta}(\xi, \S, \theta, 0) &= f_2(\xi, \S, \theta),\end{aligned} \tag{2}$$

and boundary conditions

$$\begin{aligned}\Psi(a, \S, \theta, \eta) &= g_0(\S, \theta, \eta),\\ \Psi(b, \S, \theta, \eta) &= g_1(\S, \theta, \eta),\\ \Psi(\xi, a, \theta, \eta) &= k_0(\xi, \theta, \eta),\\ \Psi(\xi, b, \theta, \eta) &= k_1(\xi, \theta, \eta),\\ \Psi(\xi, \S, a, \eta) &= h_0(\xi, \S, \eta),\\ \Psi(\xi, \S, b, \eta) &= h_1(\xi, \S, \eta),\end{aligned}$$

$$\frac{\partial^2\Psi}{\partial\xi^2}(a, \S, \theta, \eta) = \bar{g}_0(\S, \theta, \eta),$$
$$\frac{\partial^2\Psi}{\partial\xi^2}(b, \S, \theta, \eta) = \bar{g}_1(\S, \theta, \eta),$$
$$\frac{\partial^2\Psi}{\partial\S^2}(\xi, a, \theta, \eta) = \bar{k}_0(\xi, \theta, \eta),$$
$$\frac{\partial^2\Psi}{\partial\S^2}(\xi, b, \theta, \eta) = \bar{k}_1(\xi, \theta, \eta),$$
$$\frac{\partial^2\Psi}{\partial\theta^2}(\xi, \S, a, \eta) = \bar{h}_0(\xi, \S, \eta),$$
$$\frac{\partial^2\Psi}{\partial\theta^2}(\xi, \S, b, \eta) = \bar{h}_1(\xi, \S, \eta), \quad (3)$$

where f_j, g_j, h_j, k_j, $\bar{g}_j$, $\bar{h}_j$, and $\bar{k}_j$ are continuous functions and j varies from 0 to 1.

Wazwaz [14] used the Adomian decomposition method to examine the analytical solution of transverse vibrations of a uniform flexible beam. Aziz et al. [15] studied the fourth-order nonhomogeneous parabolic partial differential equations that govern the behavior of a vibrating beam by using a new three-level method based on the parametric quintic spline in space and finite difference discretization in time. Biazar and Ghazvini [16] used the variational iteration method for the analytical solution of the fourth-order parabolic equations. Dehghan and Manafian [17] applied HPM for the solution of the fourth-order parabolic PDEs. El-Gamel [18] used the sinc-Galerkin method to examine the fourth-order PDEs in one space variable coefficient. Rashidinia and Mohammadi [19] reported new three-level implicit methods for the numerical solution of the fourth-order nonhomogeneous parabolic PDEs with variable coefficients. Mittal and Jain [20] applied the quintic B-spline method, and Birol [21] used the reduced differential transformation method for the fourth-order nonhomogeneous parabolic partial differential equation. Khan and Sultana [22] used the parametric septic spline for the numerical solution of the fourth-order parabolic PDEs.

The homotopy perturbation method (HPM) was developed by He [23, 24]. HPM gives the solution in the form of a rapid and consecutive series toward the exact solution. Dehghan and Manafian [17] used HPM to obtain the numerical results for the linear and nonlinear boundary value problems. The convergence rate of HPM can be studied through [25]. Nadeem et al. [13] applied the Laplace transform coupled with the homotopy perturbation method to solve the fourth-order parabolic PDEs with variable coefficients. Luo et al. [26] introduced a combined form of the Mohand transform and the homotopy perturbation method to provide the analytical solution of the delay differential equations. Recently, many integral transformations have been introduced to find the approximate solution of ordinary and partial differential equations such as the Elzaki transform [27, 28], Sumudu transform [29], Aboodh transformation [30], Mohand transform [31], and homotopy perturbation method [24].

In this paper, we construct the idea of NIS with the help of the Mohand transform and the homotopy perturbation method for obtaining the approximate solution of partial differential equations. This NIS provides the results in the form of a series that converges to the exact solution very rapidly. This scheme does not require any linearization, variation, and limiting expectations. In particular, this study is organized as follows. In Section (2), we recall some basic definitions of the Mohand transform. In Sections (3) and (4), first, we present the basic idea of HPM and then formulate the idea of NIS for finding the approximate solution of PDEs. We illustrate three examples to present the accuracy and validity of NIS in Section (5). We give a brief discussion of the obtained results in Section (6), and finally, the conclusion is presented in Section (7).

2. Fundamental Concepts of the Mohand Transform

In this section, we introduce some basic definitions and preliminary concepts of the Mohand transform, which reveals the idea of its implementations to functions.

Definition 1. Mohand and Mahgoub [31] presented a new scheme Mohand transform $M(.)$ in order to gain the results of ordinary differential equations, which is defined as

$$\mathbf{M}\{\Psi(\eta)\} = R(w) = w^2\int_0^\infty \Psi(\eta)e^{-w\eta}d\eta, \quad k_1 \le w \le k_2. \quad (4)$$

On the other hand, if $R(w)$ is the Mohand transform of a function $\Psi(\eta)$, then $\Psi(\eta)$ is the inverse of $R(w)$such that

$$\mathbf{M}^{-1}\{R(w)\} = \Psi(\eta), \quad \mathbf{M}^{-1} \text{ is the inverse Mohand operator}. \quad (5)$$

Definition 2. If $\Psi(\eta) = \eta^n$,

$$R(w) = \frac{n!}{w^{n-1}}. \quad (6)$$

Definition 3. If $\mathbf{M}\{\Psi(\eta)\} = R(w)$, then it has the following differential properties:

(i) $\mathbf{M}\{\Psi'(\eta)\} = wR(w) - w^2F(0)$

(ii) $\mathbf{M}\{\Psi''(\eta)\} = w^2R(w) - w^3F(0) - w^2F'(0)$

(iii) $\mathbf{M}\{Fu^n(\eta)\} = w^nR(w) - w^{n+1}F(0) - w^nF'(0) - \cdots - w^nF^{n-1}(0)$

3. Basic Idea of HPM

In this segment, we illustrate a nonlinear functional equation to explain the basic view of HPM [32, 33]. Consider

$$T(\Psi) - g(h) = 0, \quad h \in \Omega, \tag{7}$$

with conditions

$$S\left(\Psi, \frac{\partial \Psi}{\partial n}\right) = 0, \quad h \in \Gamma, \tag{8}$$

where T and S are known as the general functional operator and boundary operator, respectively, and $g(h)$ is a known function with Γ as an interval of the domain Ω. We now divide T into two units such thatT_1 represents a linear and T_2 a nonlinear operator. As a result, we can express Equation (8) such that

$$T_1(\Psi) + T_2(\Psi) - g(h) = 0. \tag{9}$$

Assume a homotopy $\vartheta(h, p): \Omega \times [0, 1] \longrightarrow \mathbb{H}$ in such a way that it is appropriate for

$$H(\vartheta, p) = (1 - p)[T_1(\vartheta) - T_1(\Psi_0)] + p[T_1(\vartheta) - T_2(\vartheta) - g(h)], \tag{10}$$

or

$$H(\vartheta, p) = T_1(\vartheta) - T_1(\Psi_0) + qL(\Psi_0) + p[T_2(\vartheta) - g(h)] = 0, \tag{11}$$

where $p \in [0, 1]$ is the embedding parameter and Ψ_0 is an initial guess of Equation (7), which is suitable for the boundary conditions. The theory of HPM states that p is considered a slight variable, and the solution of Equation (7) in the resulting form of $p$is

$$\vartheta = \vartheta_0 + p\vartheta_1 + p^2\vartheta_2 + p^3\vartheta_3 + \cdots = \sum_{i=0}^{\infty} p^i \vartheta_i. \tag{12}$$

Let $p = 1$, and then the particular solution of Equation (8) is written as

$$\Psi = \lim_{p \longrightarrow 1} \vartheta = \vartheta_0 + \vartheta_1 + \vartheta_2 + \vartheta_3 + \cdots = \sum_{i=0}^{\infty} \vartheta_i. \tag{13}$$

The nonlinear terms can be calculated as

$$T_2\Psi(x, t) = \sum_{n=0}^{\infty} p^n H_n(\Psi). \tag{14}$$

Then, He's polynomials $H_n(\Psi)$ can be obtained using the following expression:

$$H_n(\Psi_0 + \Psi_1 + \cdots + \Psi_n) = \frac{1}{n!}\frac{\partial^n}{\partial p^n}\left(T_2\left(\sum_{i=0}^{\infty} p^i \Psi_i\right)\right)_{p=0}, \quad n = 0, 1, 2, \cdots. \tag{15}$$

The series solution in Equation (14) is mostly convergent due to the convergence rate of the series depending on the nonlinear operator T_2.

4. Formulation of NIS

This segment presents the formulation of a new iterative scheme (NIS) for obtaining the approximate solution of the fourth-order parabolic PDEs. Let us consider a second-order differential equation of the form

$$\Psi''(\xi, \eta) + \Psi(\xi, \eta) + g(\Psi) = g(\xi, \eta), \tag{16}$$

with the following conditions:

$$\begin{aligned} \Psi(\xi, 0) &= a, \\ \Psi'(\xi, 0) &= b, \end{aligned} \tag{17}$$

where Ψ is a function in time domain η, $g(\Psi)$ represents a nonlinear term, and $g(\eta)$ is a source term, whereas a and b are constants. Rewrite Equation (16) again as

$$\Psi''(\xi, \eta) = -\Psi(\xi, \eta) - g(\Psi) + g(\xi, \eta). \tag{18}$$

Now, taking MT on both sides of Equation (18), we obtain

$$\mathbf{M}\left[\Psi''(\xi, \eta)\right] = \mathbf{M}[-\Psi(\xi, \eta) - g(\Psi) + g(\xi, \eta)]. \tag{19}$$

Applying the differential properties of MT, we get

$$w^2 R[w] - w^3\Psi(\xi, 0) - w^2\Psi'(\xi, 0) = \mathbf{M}[-\Psi(\xi, \eta) - g(\Psi) + g(\xi, \eta)]. \tag{20}$$

Thus, $R(w)$ can be obtained from Equation (20) such that

$$R[w] = wu(\xi, 0) + \Psi'(\xi, 0) - \frac{1}{w^2}\mathbf{M}[\Psi(\xi, \eta) + g(\Psi) - g(\xi, \eta)]. \tag{21}$$

Operating the inverse Mohand transform on Equation (21), we get

$$\Psi(\xi, \eta) = G(\xi, \eta) - \mathbf{M}^{-1}\left[\frac{1}{w^2}\mathbf{M}[\Psi(\xi, \eta) + g(\Psi)]\right], \tag{22}$$

where Equation (22) is called the NIS and

$$G(\xi, \eta) = \mathbf{M}^{-1}\left[wu(0) + \Psi'(0) + \frac{1}{w^2} g(\xi, \eta)\right]. \tag{23}$$

Now, we apply HPM on Equation (22). Let

$$\Psi(\eta) = \sum_{i=0}^{\infty} p^i \Psi_i(n) = \Psi_0 + p^1\Psi_1 + p^2\Psi_2 + \cdots, \quad (24)$$

and nonlinear terms $g(\Psi)$ can be calculated by using the following formula:

$$g(\Psi) = \sum_{i=0}^{\infty} p^i H_i(\Psi) = H_0 + p^1 H_1 + p^2 H_2 + \cdots, \quad (25)$$

where $H_n{}'s$ is He's polynomial, which may be computed using the following procedure:

$$H_n(\Psi_0 + \Psi_1 + \cdots + \Psi_n) = \frac{1}{n!}\frac{\partial^n}{\partial p^n}\left(g\left(\sum_{i=0}^{\infty} p^i \Psi_i\right)\right)_{p=0}, \quad n = 0, 1, 2, \cdots. \quad (26)$$

Put Equations (24)–(26) in Equation (22), and comparing the similar factors of p, we get the following consecutive elements:

$$\begin{aligned} p^0 &: \Psi_0(\xi, \eta) = G(\xi, \eta), \\ p^1 &: \Psi_1(\xi, \eta) = -\mathbf{M}^{-1}\left[\frac{1}{w^2}\mathbf{M}\{\Psi_0(\xi, \eta) + H_0(\Psi)\}\right], \\ p^2 &: \Psi_2(\xi, \eta) = -\mathbf{M}^{-1}\left[\frac{1}{w^2}\mathbf{M}\{\Psi_1(\xi, \eta) + H_1(\Psi)\}\right], \\ p^3 &: \Psi_3(\xi, \eta) = -\mathbf{M}^{-1}\left[\frac{1}{w^2}\mathbf{M}\{\Psi_2(\xi, \eta) + H_2(\Psi)\}\right], \\ &\vdots . \end{aligned} \quad (27)$$

In continuing the similar process, we can summarize this series to get the approximate solution such that

$$\Psi(\xi, \eta) = \Psi_0 + \Psi_1 + \Psi_2 + \cdots = \sum_{i=0}^{\infty} \Psi_i. \quad (28)$$

Thus, Equation (28) is to be considered an approximate solution of differential equations of Equation (16).

5. Numerical Examples

In this part, we consider three numerical problems to check the authenticity and validity of NIS. We also demonstrate the solution surface of the illustrated problems for the behavior and a better understanding of this strategy where we see that the solution graphs of the approximate solution and the particular solution coincide with each other only after a few iterations.

5.1. Example 1. Consider the one-dimensional fourth-order parabolic PDEs

$$\frac{\partial^2 \Psi}{\partial \eta^2} + \left(\frac{1}{\xi} + \frac{\xi^4}{120}\right)\frac{\partial^4 \Psi}{\partial \xi^4} = 0, \quad (29)$$

with the initial conditions

$$\begin{aligned} \Psi(\xi, 0) &= 0, \\ \Psi_\eta(\xi, 0) &= 1 + \frac{\xi^5}{120}. \end{aligned} \quad (30)$$

Applying MT on Equation (29) together with the differential property as defined in Equation (6), we get

$$w^2 R(w) - w^3 \Psi(\xi, 0) - w^2 \Psi_\eta(\xi, 0) = -\mathbf{M}\left[\left(\frac{1}{\xi} + \frac{\xi^4}{120}\right)\frac{\partial^4 \Psi}{\partial \xi^4}\right]. \quad (31)$$

Thus, $R(w)$ yields

$$R(w) = w\Psi(\xi, 0) - \Psi_\eta(\xi, 0) - \frac{1}{w^2}\mathbf{M}\left[\left(\frac{1}{\xi} + \frac{\xi^4}{120}\right)\frac{\partial^4 \Psi}{\partial \xi^4}\right]. \quad (32)$$

Using the inverse Mohand transform, we get

$$\Psi(\xi, \eta) = \Psi(\xi, 0) - \eta\Psi_\eta(\xi, 0) - \mathbf{M}^{-1}\left[\frac{1}{w^2}\mathbf{M}\left\{\left(\frac{1}{\xi} + \frac{\xi^4}{120}\right)\frac{\partial^4 \Psi}{\partial \xi^4}\right\}\right]. \quad (33)$$

Applying MHPTM to get He's polynomials, we get

$$\sum_{i=0}^{\infty} p^i \Psi_i(n) = \Psi(\xi, 0) - \eta\Psi_\eta(\xi, 0) - \mathbf{M}^{-1}\left[\frac{1}{w^2}\mathbf{M}\left\{\left(\frac{1}{\xi} + \frac{\xi^4}{120}\right)\sum_{i=0}^{\infty} p^i \frac{\partial^4 \Psi_i}{\partial \xi^4}\right\}\right]. \quad (34)$$

Observing the similar powers of p, we get

$$\begin{aligned} p^0 &: \Psi_0(\xi, \eta) = \left(\frac{1}{\xi} + \frac{\xi^4}{120}\right)\eta, \\ p^1 &: \Psi_1(\xi, \eta) = -\mathbf{M}^{-1}\left[\frac{1}{w^2}\mathbf{M}\left\{\left(\frac{1}{\xi} + \frac{\xi^4}{120}\right)\frac{\partial^4 \Psi_0}{\partial \xi^4}\right\}\right] = -\left(\frac{1}{\xi} + \frac{\xi^4}{120}\right)\frac{\eta^3}{3!}, \\ p^2 &: \Psi_2(\xi, \eta) = -\mathbf{M}^{-1}\left[\frac{1}{w^2}\mathbf{M}\left\{\left(\frac{1}{\xi} + \frac{\xi^4}{120}\right)\frac{\partial^4 \Psi_1}{\partial \xi^4}\right\}\right] = \left(\frac{1}{\xi} + \frac{\xi^4}{120}\right)\frac{\eta^5}{5!}, \\ p^3 &: \Psi_3(\xi, \eta) = -\mathbf{M}^{-1}\left[\frac{1}{w^2}\mathbf{M}\left\{\left(\frac{1}{\xi} + \frac{\xi^4}{120}\right)\frac{\partial^4 \Psi_2}{\partial \xi^4}\right\}\right] = -\left(\frac{1}{\xi} + \frac{\xi^4}{120}\right)\frac{\eta^7}{7!}, \\ p^4 &: \Psi_4(\xi, \eta) = -\mathbf{M}^{-1}\left[\frac{1}{w^2}\mathbf{M}\left\{\left(\frac{1}{\xi} + \frac{\xi^4}{120}\right)\frac{\partial^4 \Psi_3}{\partial \xi^4}\right\}\right] = \left(\frac{1}{\xi} + \frac{\xi^4}{120}\right)\frac{\eta^9}{9!}, \\ &\vdots . \end{aligned} \quad (35)$$

In continuing this process, the approximate solution results can be summarized as

$$\Psi(\xi,\eta)=\Psi_0(\xi,\eta)+\Psi_1(\xi,\eta)+\Psi_2(\xi,\eta)+\Psi_3(\xi,\eta)+\Psi_4(\xi,\eta)+\cdots = \left(1+\frac{\xi^5}{120}\right)\left(\eta-\frac{\eta^3}{3!}+\frac{\eta^5}{5!}-\frac{\eta^7}{7!}+\frac{\eta^9}{9!}\right)+\cdots. \quad (36)$$

This series converges to the particular solution

$$\Psi(\xi,\eta)=\left(1+\frac{\xi^5}{120}\right)\sin\eta. \quad (37)$$

5.2. Example 2. Consider the two-dimensional fourth-order parabolic PDEs

$$\frac{\partial^2\Psi}{\partial\eta^2}+2\left(\frac{1}{\xi^2}+\frac{\xi^4}{6!}\right)\frac{\partial^4\Psi}{\partial\xi^4}+2\left(\frac{1}{\S^2}+\frac{\S^4}{6!}\right)\frac{\partial^4\Psi}{\partial\S^4}=0, \quad (38)$$

with the initial conditions

$$\Psi(\xi,\S,0)=0,\quad \Psi_\eta(\xi,\S,0)=2+\frac{\xi^6}{6!}+\frac{\S^6}{6!}. \quad (39)$$

Applying NIM, we get

$$\Psi(\xi,\S,\eta)=\Psi(\xi,\S,0)-\eta\Psi_\eta(\xi,\S,0)-\mathbf{M}^{-1}\cdot\left[\frac{1}{w^2}\mathbf{M}\left\{2\left(\frac{1}{\xi^2}+\frac{\xi^4}{6!}\right)\frac{\partial^4\Psi}{\partial\xi^4}+2\left(\frac{1}{\S^2}+\frac{\S^4}{6!}\right)\frac{\partial^4\Psi}{\partial\S^4}\right\}\right]. \quad (40)$$

This equation provides He's polynomials

$$\sum_{i=0}^{\infty}p^i\Psi_i(n)=\Psi(\xi,\S,0)-\eta\Psi_\eta(\xi,\S,0)-\mathbf{M}^{-1}\cdot\left[\frac{1}{w^2}\mathbf{M}\left\{2\left(\frac{1}{\xi^2}+\frac{\xi^4}{6!}\right)\sum_{i=0}^{\infty}p^i\frac{\partial^4\Psi_i}{\partial\xi^4}+2\left(\frac{1}{\S^2}+\frac{\S^4}{6!}\right)\sum_{i=0}^{\infty}p^i\frac{\partial^4\Psi_i}{\partial\S^4}\right\}\right]. \quad (41)$$

Observing the similar powers of p, we get

$$p^0:\Psi_0(\xi,\S,\eta)=\left(2+\frac{\xi^6}{6!}+\frac{\S^6}{6!}\right)\eta,$$

$$p^1:\Psi_1(\xi,\S,\eta)=-\mathbf{M}^{-1}\left[\frac{1}{w^2}\mathbf{M}\left\{2\left(\frac{1}{\xi^2}+\frac{\xi^4}{6!}\right)\frac{\partial^4\Psi}{\partial\xi^4}+2\left(\frac{1}{\S^2}+\frac{\S^4}{6!}\right)\frac{\partial^4\Psi}{\partial\S^4}\right\}\right]=-\left(2+\frac{\xi^6}{6!}+\frac{\S^6}{6!}\right)\frac{\eta^3}{3!},$$

$$p^2:\Psi_2(\xi,\S,\eta)=-\mathbf{M}^{-1}\left[\frac{1}{w^2}\mathbf{M}\left\{2\left(\frac{1}{\xi^2}+\frac{\xi^4}{6!}\right)\frac{\partial^4\Psi}{\partial\xi^4}+2\left(\frac{1}{\S^2}+\frac{\S^4}{6!}\right)\frac{\partial^4\Psi}{\partial\S^4}\right\}\right]=\left(2+\frac{\xi^6}{6!}+\frac{\S^6}{6!}\right)\frac{\eta^5}{5!},$$

$$p^3:\Psi_3(\xi,\S,\eta)=-\mathbf{M}^{-1}\left[\frac{1}{w^2}\mathbf{M}\left\{2\left(\frac{1}{\xi^2}+\frac{\xi^4}{6!}\right)\frac{\partial^4\Psi}{\partial\xi^4}+2\left(\frac{1}{\S^2}+\frac{\S^4}{6!}\right)\frac{\partial^4\Psi}{\partial\S^4}\right\}\right]=-\left(2+\frac{\xi^6}{6!}+\frac{\S^6}{6!}\right)\frac{\eta^7}{7!},$$

$$p^4:\Psi_4(\xi,\S,\eta)=-\mathbf{M}^{-1}\left[\frac{1}{w^2}\mathbf{M}\left\{2\left(\frac{1}{\xi^2}+\frac{\xi^4}{6!}\right)\frac{\partial^4\Psi}{\partial\xi^4}+2\left(\frac{1}{\S^2}+\frac{\S^4}{6!}\right)\frac{\partial^4\Psi}{\partial\S^4}\right\}\right]=\left(2+\frac{\xi^6}{6!}+\frac{\S^6}{6!}\right)\frac{\eta^9}{9!},$$

$$\vdots. \quad (42)$$

In continuing this process, the approximate solution results can be summarized as

$$\Psi(\xi,\S,\eta)=\Psi_0(\xi,\S,\eta)+\Psi_1(\xi,\S,\eta)+\Psi_2(\xi,\S,\eta)+\Psi_3(\xi,\S,\eta)+\Psi_4(\xi,\S,\eta)+\cdots=\left(2+\frac{\xi^6}{6!}+\frac{\S^6}{6!}\right)\left(\eta-\frac{\eta^3}{3!}+\frac{\eta^5}{5!}-\frac{\eta^7}{7!}+\frac{\eta^9}{9!}\right)+\cdots. \quad (43)$$

This series converges to the particular solution

$$\Psi(\xi,\S,\eta)=\left(2+\frac{\xi^6}{6!}+\frac{\S^6}{6!}\right)\sin\eta. \quad (44)$$

5.3. Example 3. Consider the three-dimensional fourth-order parabolic PDEs

$$\frac{\partial^2\Psi}{\partial\eta^2}+\left(2\frac{\S+\theta}{\cos(\xi)}-1\right)\frac{\partial^4\Psi}{\partial\xi^4}+\left(\frac{\xi+\theta}{2\cos(\S)}-1\right)\frac{\partial^4\Psi}{\partial\S^4}+\left(\frac{\S+\xi}{2\cos(\theta)}-1\right)\frac{\partial^4\Psi}{\partial\theta^4}=0, \quad (45)$$

with the initial conditions

$$\Psi(\xi,\S,\theta,0)=\xi+\S+\theta-(\cos(\xi)+\cos(\S)+\cos(\theta)),$$
$$\Psi(\xi,\S,\theta,0)=(\cos(\xi)+\cos(\S)+\cos(\theta))-(\xi+\S+\theta). \quad (46)$$

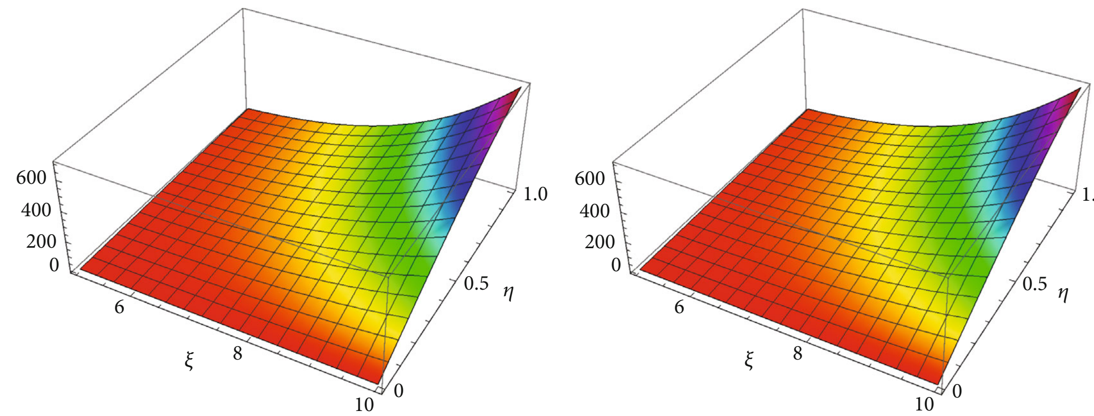

(a) Approximate solution of $\Psi(\xi, \eta)$ for Equation (29)

(b) Particular solution of $\Psi(\xi, \eta)$ for Equation (29)

Figure 1: Surface solutions for the one-dimensional parabolic differential equation.

Applying NIM, we get

$$\Psi(\xi, \S, \theta, \eta) = \Psi(\xi, \S, 0) - \eta\Psi_\eta(\xi, \S, 0) - \mathbf{M}^{-1} \cdot \left[\frac{1}{w^2}\mathbf{M}\left\{\left(2\frac{\S+\theta}{\cos(\xi)} - 1\right)\frac{\partial^4\Psi}{\partial\xi^4} + \left(\frac{\xi+\theta}{2\cos(\S)} - 1\right)\frac{\partial^4\Psi}{\partial\S^4} + \left(\frac{\S+\xi}{2\cos(\theta)} - 1\right)\frac{\partial^4\Psi}{\partial\theta^4}\right\}\right]. \quad (47)$$

This equation provides He's polynomials

$$p^0 : \Psi_0(\xi, \S, \theta, \eta) = w\Psi(\xi, \S, 0) - \Psi_\eta(\xi, \S, 0)(1-\eta),$$

$$p^1 : \Psi_1(\xi, \S, \theta, \eta) = -\mathbf{M}^{-1}\left[\frac{1}{w^2}\mathbf{M}\left\{\left(2\frac{\S+\theta}{\cos(\xi)} - 1\right)\frac{\partial^4\Psi}{\partial\xi^4} + \left(\frac{\xi+\theta}{2\cos(\S)} - 1\right)\frac{\partial^4\Psi}{\partial\S^4} + \left(\frac{\S+\xi}{2\cos(\theta)} - 1\right)\frac{\partial^4\Psi}{\partial\theta^4}\right\}\right],$$

$$p^2 : \Psi_2(\xi, \S, \theta, \eta) = -\mathbf{M}^{-1}\left[\frac{1}{w^2}\mathbf{M}\left\{\left(2\frac{\S+\theta}{\cos(\xi)} - 1\right)\frac{\partial^4\Psi}{\partial\xi^4} + \left(\frac{\xi+\theta}{2\cos(\S)} - 1\right)\frac{\partial^4\Psi}{\partial\S^4} + \left(\frac{\S+\xi}{2\cos(\theta)} - 1\right)\frac{\partial^4\Psi}{\partial\theta^4}\right\}\right],$$

$$p^3 : \Psi_3(\xi, \S, \theta, \eta) = -\mathbf{M}^{-1}\left[\frac{1}{w^2}\mathbf{M}\left\{\left(2\frac{\S+\theta}{\cos(\xi)} - 1\right)\frac{\partial^4\Psi}{\partial\xi^4} + \left(\frac{\xi+\theta}{2\cos(\S)} - 1\right)\frac{\partial^4\Psi}{\partial\S^4} + \left(\frac{\S+\xi}{2\cos(\theta)} - 1\right)\frac{\partial^4\Psi}{\partial\theta^4}\right\}\right],$$

$$p^4 : \Psi_4(\xi, \S, \theta, \eta) = -\mathbf{M}^{-1}\left[\frac{1}{w^2}\mathbf{M}\left\{\left(2\frac{\S+\theta}{\cos(\xi)} - 1\right)\frac{\partial^4\Psi}{\partial\xi^4} + \left(\frac{\xi+\theta}{2\cos(\S)} - 1\right)\frac{\partial^4\Psi}{\partial\S^4} + \left(\frac{\S+\xi}{2\cos(\theta)} - 1\right)\frac{\partial^4\Psi}{\partial\theta^4}\right\}\right], \quad (48)$$

which gives

$$\begin{aligned}
\Psi_0(\xi, \S, \eta) &= (\xi + \S + \theta - \cos(\xi) - \cos(\S) - \cos(\theta))(1-\eta),\\
\Psi_1(\xi, \S, \eta) &= (\xi + \S + \theta - \cos(\xi) - \cos(\S) - \cos(\theta))\left(\frac{\eta^2}{2!} - \frac{\eta^3}{3!}\right),\\
\Psi_2(\xi, \S, \eta) &= \left(\xi + \S + \theta - (\cos(\xi) - \cos(\S) - \cos(\theta)\right)\left(\frac{\eta^4}{4!} - \frac{\eta^5}{5!}\right),\\
\Psi_3(\xi, \S, \eta) &= (\xi + \S + \theta - \cos(\xi) - \cos(\S) - \cos(\theta))\left(\frac{\eta^6}{6!} - \frac{\eta^7}{7!}\right),\\
\Psi_4(\xi, \S, \eta) &= (\xi + \S + \theta - \cos(\xi) - \cos(\S) - \cos(\theta))\left(\frac{\eta^8}{8!} - \frac{\eta^9}{9!}\right),\\
&\vdots .
\end{aligned} \quad (49)$$

In continuing this process, the approximate solution results can be summarized as

$$\begin{aligned}
\Psi(\xi, \eta) &= \Psi_0(\xi, \eta) + \Psi_1(\xi, \eta) + \Psi_2(\xi, \eta) + \Psi_3(\xi, \eta) + \Psi_4(\xi, \eta) + \cdots\\
&= (\xi + \S + \theta - \cos(\xi) - \cos(\S) - \cos(\theta))\\
&\quad \cdot \left(1 - \eta + \frac{\eta^2}{2!} - \frac{\eta^3}{3!} + \frac{\eta^4}{4!} - \frac{\eta^5}{5!} + \frac{\eta^6}{6!} - \frac{\eta^7}{7!} + \frac{\eta^8}{8!} - \frac{\eta^9}{9!} + \cdots\right).
\end{aligned} \quad (50)$$

This series converges to the particular solution

$$\Psi(\xi, \eta) = (\xi + \S + \theta - \cos(\xi) - \cos(\S) - \cos(\theta))e^{-\eta}. \quad (51)$$

6. Results and Discussion

In this segment, we present the discussion of some graphical representations in Figures 1–3. It can be seen that the formulated series converges to the particular solution only after a few iterations very rapidly. Figures 1(a) and 1(b) represent the comparison between the approximate solution and the exact solution of Equations (36) and (37) at $0 \le \eta \le 1$ and $0 \le \xi \le 10$, respectively. Figures 2(a) and 2(b) show the comparison between the approximate solution and the particular

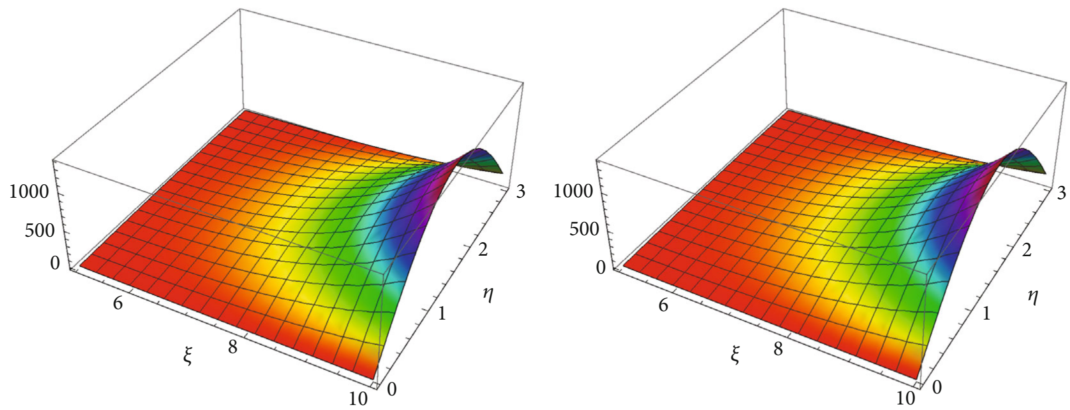

(a) Approximate solution of $\Psi(\xi, \S, \eta)$ for Equation (38) (b) Particular solution of $\Psi(\xi, \S, \eta)$ for Equation (38)

FIGURE 2: Surface solutions for the two-dimensional parabolic differential equation.

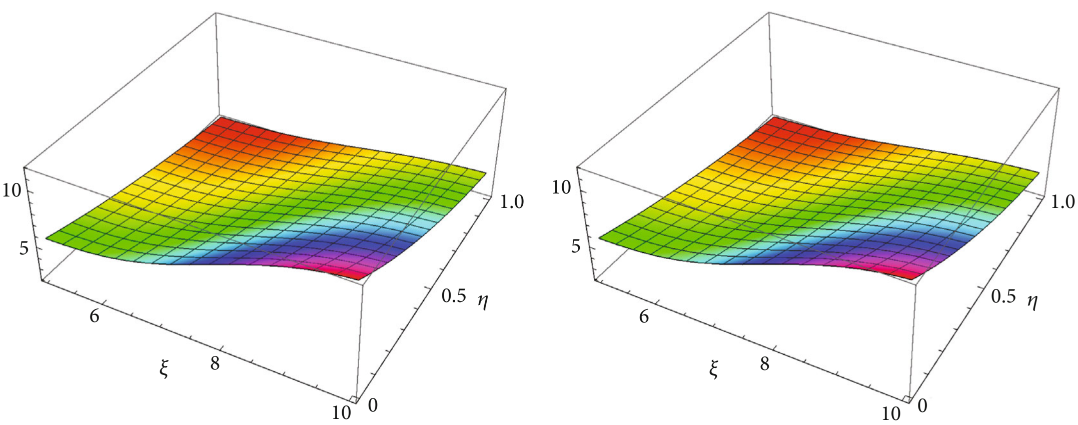

(a) Approximate solution of $\Psi(\xi, \S, \theta, \eta)$ for Equation (45) (b) Particular solution of $\Psi(\xi, \S, \theta, \eta)$ for Equation (45)

FIGURE 3: Surface solutions for the three-dimensional parabolic differential equation.

solution of Equations (43) and (44) at $0 \leq \eta \leq 3$ and $0 \leq \xi \leq 10$, respectively, and similarly, Figures 3(a) and 3(b) represent the comparison between the approximate solution and the particular solution of Equations (50) and (51) at $0 \leq \eta \leq 1$ and $0 \leq \xi \leq 10$, respectively. This comparison shows that NIS is easy to implement and does not require any heavy calculation for the computation of the approximate solution of the fourth-order parabolic PDEs with variable coefficients.

7. Conclusion and Future Work

In this analysis, we successfully employed the NIS to examine the approximate solution of the fourth-order parabolic partial differential equations with variable coefficients. The Mohand transform coupled with HPM has been used to construct the idea of this scheme. This NIS approach is applicable for both the linear and nonlinear partial differential equations. This approach does not require the recurrence relation for the assumption of a variable. This NIS formulates the obtained results of the illustrated problems in the form of a series that converges to the particular solution very rapidly. This approach has an advantage of direct implementation to the numerical problems and confirms the accuracy with full agreement. This NIS is also applicable for the other partial differential equations with fractional derivatives in science and engineering.

Data Availability

All the data are available within the article.

Conflicts of Interest

The authors declare that they have no conflicts of interest.

Authors' Contributions

Fenglian Liu worked on the investigation, methodology, and writing (original draft) of the manuscript. Muhammad Nadeem did work in validation, editing, and improvement of the English language during the revision of the manuscript. Ibrahim Mahariq implemented the software programming to provide the graphical results, whereas Suliman Dawood supervised and approved the manuscript for submission.

References

[1] H. Khan, S.-J. Liao, R. Mohapatra, and K. Vajravelu, "An analytical solution for a nonlinear time-delay model in biology," *Communications in Nonlinear Science and Numerical Simulation*, vol. 14, no. 7, pp. 3141–3148, 2009.

[2] Y. Gu, W. Liao, and J. Zhu, "An efficient high-order algorithm for solving systems of 3-D reaction- diffusion equations," *Journal of Computational and Applied Mathematics*, vol. 155, no. 1, pp. 1–17, 2003.

[3] Q. Zhu, S. Deng, and Y. Chen, "Periodical pressure-driven electrokinetic flow of power-law fluids through a rectangular microchannel," *Journal of Non-Newtonian Fluid Mechanics*, vol. 203, pp. 38–50, 2014.

[4] H. Zhang, X. Han, and X. Yang, "Quintic B-spline collocation method for fourth order partial integro- differential equations with a weakly singular kernel," *Applied Mathematics and Computation*, vol. 219, no. 12, pp. 6565–6575, 2013.

[5] P. Veeresha, D. Prakasha, N. Magesh, A. J. Christopher, and D. U. Sarwe, "Solution for fractional potential KdV and Benjamin equations using the novel technique," *Journal of Ocean Engineering and Science*, vol. 6, no. 3, pp. 265–275, 2021.

[6] S. S. Siddiqi and S. Arshed, "Quintic B-spline for the numerical solution of fourthorder parabolic partial differential equations," *World Applied Sciences Journal*, vol. 23, no. 12, pp. 115–122, 2013.

[7] X. Xu and D. Xu, "A semi-discrete scheme for solving fourth-order partial integro-differential equation with a weakly singular kernel using Legendre wavelets method," *Computational and Applied Mathematics*, vol. 37, no. 4, pp. 4145–4168, 2018.

[8] Y. Khan and Q. Wu, "Homotopy perturbation transform method for nonlinear equations using He's polynomials," *Computers & Mathematics with Applications*, vol. 61, no. 8, pp. 1963–1967, 2011.

[9] G. Hariharan and K. Kannan, "Review of wavelet methods for the solution of reaction-diffusion problems in science and engineering," *Applied Mathematical Modelling*, vol. 38, no. 3, pp. 799–813, 2014.

[10] J. Li, Y. Chen, and G. Liu, "High-order compact ADI methods for parabolic equations," *Computers & Mathematics with Applications*, vol. 52, no. 8-9, pp. 1343–1356, 2006.

[11] G. Sutmann and B. Steffen, "High-order compact solvers for the three-dimensional Poisson equation," *Journal of Computational and Applied Mathematics*, vol. 187, no. 2, pp. 142–170, 2006.

[12] M. AL-Jawary, "Analytic solutions for solving fourth-order parabolic partial differential equations with variable coeffcients," *International Journal of Advanced Scientific and Technical Research*, vol. 3, no. 5, pp. 531–545, 2015.

[13] M. Nadeem, F. Li, and H. Ahmad, "Modified Laplace variational iteration method for solving fourth-order parabolic partial differential equation with variable coefficients," *Computers & Mathematics with Applications*, vol. 78, no. 6, pp. 2052–2062, 2019.

[14] A.-M. Wazwaz, "Analytic treatment for variable coefficient fourth-order parabolic partial differential equations," *Applied Mathematics and Computation*, vol. 123, no. 2, pp. 219–227, 2001.

[15] T. Aziz, A. Khan, and J. Rashidinia, "Spline methods for the solution of fourth-order parabolic partial differential equations," *Applied Mathematics and Computation*, vol. 167, no. 1, pp. 153–166, 2005.

[16] J. Biazar and H. Ghazvini, "He's variational iteration method for fourth-order parabolic equations," *Computers & Mathematics with Applications*, vol. 54, no. 7-8, pp. 1047–1054, 2007.

[17] M. Dehghan and J. Manafian, "The solution of the variable coefficients fourth-order parabolic partial differential equations by the homotopy perturbation method," *Zeitschrift f¨ur Naturforschung A*, vol. 64, no. 7-8, pp. 420–430, 2009.

[18] M. El-Gamel, "A note on solving the fourth-order parabolic equation by the sinc-Galerkin method," *Calcolo*, vol. 52, no. 3, pp. 327–342, 2015.

[19] J. Rashidinia and R. Mohammadi, "Sextic spline solution of variable coefficient fourth-order parabolic equations," *International Journal of Computer Mathematics*, vol. 87, no. 15, pp. 3443–3454, 2010.

[20] R. Mittal and R. Jain, "B-splines methods with redefined basis functions for solving fourth order parabolic partial differential equations," *Applied Mathematics and Computation*, vol. 217, no. 23, pp. 9741–9755, 2011.

[21] I. Birol, "Application of reduced differential transformation method for solving fourth-order parabolic partial differential equations," *The Journal of Mathematics and Computer Science*, vol. 12, no. 2, pp. 124–131, 2014.

[22] A. Khan and T. Sultana, "Numerical solution of fourth order parabolic partial differential equation using parametric septic splines," *Hacettepe Journal of Mathematics and Statistics*, vol. 4, no. 45, pp. 1067–1082, 2016.

[23] J.-H. He, "Addendum: new interpretation of homotopy perturbation method," *International Journal of Modern Physics B*, vol. 20, no. 18, pp. 2561–2568, 2006.

[24] J.-H. He, "Homotopy perturbation method: a new nonlinear analytical technique," *Applied Mathematics and Computation*, vol. 135, no. 1, pp. 73–79, 2003.

[25] J. Biazar and H. Ghazvini, "Convergence of the homotopy perturbation method for partial differential equations," *Nonlinear Analysis: Real World Applications*, vol. 10, no. 5, pp. 2633–2640, 2009.

[26] X. Luo, M. Habib, S. Karim, and H. A. Wahash, "Semianalytical approach for the approximate solution of delay differential equations," *Complexity*, vol. 2022, 6 pages, 2022.

[27] T. M. Elzaki, "The new integral transform Elzaki transform," *Global Journal of Pure and Applied Mathematics*, vol. 7, no. 1, pp. 57–64, 2011.

[28] N. Anjum, M. Suleman, D. Lu, J.-H. He, and M. Ramzan, "Numerical iteration for nonlinear oscillators by Elzaki transform," *Journal of Low Frequency Noise, Vibration and Active Control*, vol. 39, no. 4, pp. 879–884, 2020.

[29] M. Rana, A. Siddiqui, Q. Ghori, and R. Qamar, "Application of He's homotopy perturbation method to Sumudu transform," *International Journal of Nonlinear Sciences and Numerical Simulation*, vol. 8, no. 2, pp. 185–190, 2007.

[30] K. Aboodh, R. Farah, I. Almardy, and A. Osman, "Solving delay differential equations by Aboodh transformation method," *International Journal of Applied Mathematics & Statistical Sciences*, vol. 7, no. 2, pp. 55–64, 2018.

[31] M. Mohand and A. Mahgoub, "The new integral transform Mohand transform," *Applied Mathematical Sciences*, vol. 12, no. 2, pp. 113–120, 2017.

[32] M. A. Noor and S. T. Mohyud-Din, "Variational homotopy perturbation method for solving higher dimensional initial boundary value problems," *Mathematical Problems in Engineering*, vol. 2008, 11 pages, 2008.

[33] T. Allahviranloo, A. Armand, and S. Pirmohammadi, "Variational homotopy perturbation method an efficient scheme for solving partial differential equations in fluid mechanics," *The Journal of Mathematics and Computer Science*, vol. 9, no. 4, pp. 362–369, 2014.

Hindawi
Journal of Function Spaces
Volume 2022, Article ID 8304107, 7 pages
https://doi.org/10.1155/2022/8304107

Research Article

A New Strategy for the Approximate Solution of Hyperbolic Telegraph Equations in Nonlinear Vibration System

Jiao Zeng[1], **Asma Idrees**[2] **and Mohammed S. Abdo**[3]

[1]*Faculty of Science, Yibin University, Yibin 644000, China*
[2]*Department of Mathematics, Riphah International University, Faisalabad 44000, Pakistan*
[3]*Department of Mathematics, Hodeidah University, Al-Hudaydah, Yemen*

Correspondence should be addressed to Mohammed S. Abdo; msabdo@hoduniv.net.ye

Received 10 June 2022; Revised 1 July 2022; Accepted 26 July 2022; Published 10 August 2022

Academic Editor: Yusuf Gurefe

This study examines a new approach for the approximate solution of hyperbolic telegraph equations emerging in magnetic fields and electrical impulse transmissions. We introduce a Laplace-Carson transform coupled with the homotopy perturbation method which is called the Laplace-Carson homotopy perturbation method ($\mathscr{L}_c$-HPM). The most significant feature of this approach is that we do not require any restriction of variables and hypotheses to find the results of nonlinear problems. Further, HPM using He's is applied to reduce the number of computations in nonlinear terms. We demonstrate some graphical results to show that $\mathscr{L}_c$-HPM is a simple and suitable approach for linear and nonlinear problems.

1. Introduction

Most of the nonlinear vibration phenomena are described by unsteady reactions, chaos, splitting processes, and some other multiple norms of motion. This vibration study starts from a large number of components such as high elastic deflection, electrical charge force, and complex absorption [1]. In this manner, a more proper comprehensive knowledge of the nonlinear vibration phenomena is important for the investigation of vibratory incidents. Recently, numerous researchers have paid much attention for the study of the applications of hyperbolic equations. Azab and Gamel [2] constructed a new approach built on a numerical strategy for the study of telegraph equations. Pandit et al. [3] applied a finite difference scheme to find the results of the hyperbolic telegraph problem. Evans and Bulut [4] proposed a new approach to determine the precise results of the telegraph problems in explicit form. Srinivasa and Rezazadeh [5] obtained the numerical solution of the one-dimensional telegraph equation via the wavelet technique. Ding et al. [6] used a nonpolynomial cubic spline approach in space direction for the study of the telegraph equation. Saadatmandi and Dehghan [7] used the Chebyshev tau method to achieve the numerical solution of the hyperbolic telegraph equation. Lakestani and Saray [8] applied scaling functions for the solution of the telegraph equation. Later, Sharifi and Rashidinia [9] applied extended cubic B-spline for the solution of the hyperbolic telegraph equation and also showed the convergence and stability of the method. Khater and Lu [10] investigated the stable analytical solutions of the nonlinear fractional nonlinear time–space telegraph equation by applying the trigonometric-quantic-B-spline method. Das and Gupta [11] used the homotopy analysis method to find the explicit solutions of the telegraph equations. A broad study of hyperbolic telegraph equation can be studied in [12–15].

The basic concept of the homotopy perturbation method (HPM) was suggested by He [16–18] to obtain the solution of some differential equations. Later, many researchers [19, 20] constructed a scheme coupled with Laplace transform and HPM to examine the solution of differential equations. Recently, Aggarwal et al. [21] used Laplace-Carson transform for the first kind of Volterra integrodifferential equation. Later, Kumar and Qureshi [22] obtained the exact solutions of non-integer-order initial value problems with the Caputo operator and confirmed the accuracy of this approach. Thange and Gade [23] introduced some properties of the Laplace-Carson transform with fractional order with the help of convolution theorem. In this paper, we introduce a new approach Laplace-Carson homotopy perturbation method ($\mathscr{L}_c$-HPM) built on Laplace-Carson transform and HPM for the study of hyperbolic telegraph equation. We observe that this strategy is simple to handle and produces the results in the form of series only after a few iterations. This article is arranged as follows: in Section 2, we define the Laplace-Carson transform and its basic properties. In Section 3, we introduce the basic idea of HPM to decompose the nonlinear terms. In Section 4, we illustrate some applications to indicate the competence of $\mathscr{L}_c$-PTM, and at last, some results are discussed with conclusion in Sections 5 and 6, respectively.

2. Fundamental Concepts of Laplace-Carson Transform

Definition 1. Let $f(t)$ be a function precise for $t \geq 0$; then,

$$\mathscr{L}\{f(t)\} = F(s) = \theta \int_0^\infty f(t) e^{-st} dt \tag{1}$$

is called the Laplace transform and s is the independent variable of the transformed function t.

Definition 2. Aggarwal et al. [21] introduced Laplace-Carson transform for the solution of first kind of Volterra integro-differential problem; then,

$$\mathscr{L}_c\{g(t)\} = R(\theta) = \theta \int_0^\infty g(t) e^{-\theta t} dt, \quad k_1 \leq \theta \leq k_2, \tag{2}$$

where $\mathscr{L}_c$ is denoted as Laplace-Carson transform and θ is the independent variable of the transformed function t. On the other hand, let $R(\theta)$ be the Laplace-Carson transform of a function $g(t)$; then, $g(t)$ is the inverse of $R(\theta)$ so that

$$\mathscr{L}_c^{-1}\{R(\theta)\} = g(t), \tag{3}$$

where $\mathscr{L}_c^{-1}$ is called inverse Laplace-Carson transform.

Definition 3. If $g(t) = t^m$, then the Laplace-Carson transform is applied as

$$\mathscr{L}_c\{g(t)\} = R(\theta) = \frac{m!}{\theta^m}. \tag{4}$$

Properties 4. If $\mathscr{L}_c\{g(t)\} = R(\theta)$, then it has the following differential properties [21, 23]:

(a) $\mathscr{L}_c\{g'(t)\} = \theta R(\theta) - \theta G(0)$

(b) $\mathscr{L}_c\{g''(t)\} = \theta^2 R(\theta) - \theta^2 G(0) - \theta G'(0)$

(c) $\mathscr{L}_c\{g^m(t)\} = \theta^m R(\theta) - \theta^m G(0) - \theta^{m-1} G'(0) - \cdots - \theta G^{m-1}(0)$

3. Basic Idea of HPM

In this segment, we illustrate a nonlinear functional equation to explain the basic view HPM [24, 25]. Consider

$$T(u) - g(h) = 0, \quad h \in \Omega, \tag{5}$$

with conditions

$$S\left(u, \frac{\partial u}{\partial n}\right) = 0, \quad h \in \Gamma, \tag{6}$$

where T and S are known as general functional operator and boundary operator, respectively, and $g(h)$ is known function with Γ as a interval of the domain Ω. We now divide T into two units such as T_1 which represents a linear and T_2 a nonlinear operator. As a result, we can express Equation (6) such as

$$T_1(u) + T_2(u) - g(h) = 0. \tag{7}$$

Assume a homotopy $v(h, \theta): \Omega \times [0, 1] \longrightarrow \mathbb{H}$ in such a way that it is appropriate for

$$H(v, \theta) = (1 - \theta)[T_1(v) - T_1(u_0)] + \theta[T_1(v) - T_2(v) - g(h)] \tag{8}$$

or

$$H(v, \theta) = T_1(v) - T_1(u_0) + qL(u_0) + \theta[T_2(v) - g(h)] = 0, \tag{9}$$

where $\theta \in [0, 1]$ is embedding parameter and u_0 is an initial guess of Equation (5), which is suitable for the boundary conditions. The theory of HPM states that θ is considered as a slight variable and the solution of Equation (5) in the resulting form of θ.

$$v = v_0 + \theta v_1 + \theta^2 v_2 + \theta^3 v_3 + \cdots = \sum_{i=0}^{\infty} \theta^i v_i. \tag{10}$$

Let $\theta = 1$; then, the particular of Equation (6) is written as

$$u = \lim_{\theta \longrightarrow 1} v = v_0 + v_1 + v_2 + v_3 + \cdots = \sum_{i=0}^{\infty} v_i. \tag{11}$$

The nonlinear terms can be calculated as

$$T_2 u(x, t) = \sum_{n=0}^{\infty} \theta^n H_n(u). \tag{12}$$

Then, He's polynomials $H_n(u)$ can be obtained using the following expression:

$$H_n(u_0+u_1+\cdots+u_n) = \frac{1}{n!}\frac{\partial^n}{\partial\theta^n}\left(T_2\left(\sum_{i=0}^{\infty}\theta^i u_i\right)\right)_{\theta=0}, \quad n=0,1,2,\cdots. \tag{13}$$

The series solution in Equation (12) is mostly convergent due to and the convergence rate of the series depending on the nonlinear operator T_2.

4. Numerical Applications

In this section, we incorporate the concept of $\mathscr{L}_c$-PTM for obtaining the approximate solution of linear and nonlinear telegraph equations. We observe that only after iteration, this scheme produces excellent accuracy. Mathematical Software 11.0.1 is used to perform the calculations. We present some 2D and 3D graphs for better understanding the behavior of this scheme.

4.1. Example 1. Consider one-dimensional linear hyperbolic telegraph equation

$$\frac{\partial^2 u}{\partial x^2} = \frac{\partial^2 u}{\partial t^2} + \frac{\partial u}{\partial t} + u, \tag{14}$$

with conditions

$$\begin{aligned} u(x,0) &= e^x, \\ u_t(x,0) &= -e^x, \\ u(0,t) &= e^{-t}, \\ u_x(0,t) &= e^{-t}. \end{aligned} \tag{15}$$

Applying Laplace-Carson transform to Equation (14), we get

$$\mathscr{L}_c\left[\frac{\partial^2 u}{\partial x^2}\right] = \mathscr{L}_c\left[\frac{\partial^2 u}{\partial t^2} + \frac{\partial u}{\partial t} + u\right]. \tag{16}$$

Using the properties of Laplace-Carson transform, we get

$$\theta^2 u(\theta,t) - \theta^2 u(0,t) - \theta u'(0,t) = \mathscr{L}_c\left[\frac{\partial^2 u}{\partial t^2} + \frac{\partial u}{\partial t} + u\right], \tag{17}$$

which may be solved further as

$$u(\theta,t) = u(0,t) + \frac{1}{\theta}u'(0,t) + \frac{1}{\theta^2}\mathscr{L}_c\left\{\frac{\partial^2 u}{\partial t^2} + \frac{\partial u}{\partial t} + u\right\}. \tag{18}$$

Applying inverse Laplace-Carson transform, we get

$$u(x,t) = u(0,t) + xu'(0,t) + \mathscr{L}_c^{-1}\left[\frac{1}{\theta^2}\mathscr{L}_c\left\{\frac{\partial^2 u}{\partial t^2} + \frac{\partial u}{\partial t} + u\right\}\right]. \tag{19}$$

Now, we introduce HPM on Equation (38); we get

$$\sum_{n=0}^{\infty}\theta^n u_n(x,t) = u(0,t) + xu'(0,t) + \theta\mathscr{L}_c^{-1} \cdot \left[\frac{1}{\theta^2}\mathscr{L}\left\{\frac{\partial^2}{\partial t^2}\sum_{n=0}^{\infty}\theta^n u_n(x,t) + \frac{\partial}{\partial t}\sum_{n=0}^{\infty}\theta^n u_n(x,t) + \sum_{n=0}^{\infty}\theta^n u_n(x,t)\right\}\right]. \tag{20}$$

On comparing, the following iterations can be obtained:

$$\begin{aligned} \theta^0 &: u_0(x,t) = e^{-t} + xe^{-t}, \\ \theta^1 &: u_1(x,t) = \mathscr{L}_c^{-1}\left[\frac{1}{\theta^2}\mathscr{L}_c\left\{\frac{\partial^2 u_0}{\partial t^2} + \frac{\partial u_0}{\partial t} + u_0\right\}\right] \\ &= e^{-t}\frac{x^2}{2!} + e^{-t}\frac{x^3}{3!}, \\ \theta^2 &: u_2(x,t) = \mathscr{L}_c^{-1}\left[\frac{1}{\theta^2}\mathscr{L}_c\left\{\frac{\partial^2 u_1}{\partial t^2} + \frac{\partial u_1}{\partial t} + u_1\right\}\right] \\ &= e^{-t}\frac{x^4}{4!} + e^{-t}\frac{x^5}{5!}, \\ \theta^3 &: u_3(x,t) = \mathscr{L}_c^{-1}\left[\frac{1}{\theta^2}\mathscr{L}_c\left\{\frac{\partial^2 u_2}{\partial t^2} + \frac{\partial u_2}{\partial t} + u_2\right\}\right] \\ &= e^{-t}\frac{x^6}{6!} + e^{-t}\frac{x^7}{7!}. \\ &\vdots \end{aligned} \tag{21}$$

Hence, the solution can be expressed as

$$\begin{aligned} u(x,t) &== u_1(x,t) + u_2(x,t) + u_3(x,t) + \cdots, \\ u(x,t) &== e^{-t} + xe^{-t} + \frac{x^2}{2!}e^{-t} + \frac{x^3}{3!}e^{-t} + \frac{x^4}{4!}e^{-t} \\ &\quad + \frac{x^5}{5!}e^{-t} + \frac{x^6}{6!}e^{-t} + \frac{x^7}{7!}e^{-t} + \cdots, \\ u(x,t) &= e^{x-t}. \end{aligned} \tag{22}$$

4.2. Example 2. Consider another linear hyperbolic telegraph equation

$$\frac{\partial^2 u}{\partial x^2} = \frac{\partial^2 u}{\partial t^2} + 4\frac{\partial u}{\partial t} + 4u, \tag{23}$$

with initial conditions

$$\begin{aligned} u(x,0) &= 1 + e^{2x}, \\ u_t(x,0) &= -2, \\ u(0,t) &= 1 + e^{-2t}, \\ u_x(0,t) &= 2. \end{aligned} \tag{24}$$

Applying Laplace-Carson transform to Equation (23), we get

$$\mathscr{L}_c\left[\frac{\partial^2 u}{\partial x^2}\right] = \mathscr{L}_c\left[\frac{\partial^2 u}{\partial t^2} + 4\frac{\partial u}{\partial t} + 4u\right]. \tag{25}$$

Using the properties of Laplace-Carson transform, we get

$$\theta^2 u(\theta,t) - \theta^2 u(0,t) - \theta u'(0,t) = \mathscr{L}_c\left[\frac{\partial^2 u}{\partial t^2} + 4\frac{\partial u}{\partial t} + 4u\right], \tag{26}$$

which may be solved further as

$$u(\theta,t) = u(0,t) + \frac{1}{\theta}u'(0,t) + \frac{1}{\theta^2}\mathscr{L}_c\left\{\frac{\partial^2 u}{\partial t^2} + 4\frac{\partial u}{\partial t} + 4u\right\}. \tag{27}$$

Applying inverse Laplace-Carson transform, we get

$$\begin{aligned} u(x,t) = u(0,t) + xu'(0,t) + \mathscr{L}_c^{-1} \\ \cdot \left[\frac{1}{\theta^2}\mathscr{L}_c\left\{\frac{\partial^2 u}{\partial t^2} + 4\frac{\partial u}{\partial t} + 4u\right\}\right]. \end{aligned} \tag{28}$$

Now, we introduce HPM on Equation (28); we get

$$\begin{aligned} \sum_{n=0}^{\infty}\theta^n u_n(x,t) &= u(0,t) + xu'(0,t) + \theta\mathscr{L}_c^{-1} \\ &\cdot \left[\frac{1}{\theta^2}\mathscr{L}\left\{\frac{\partial^2}{\partial t^2}\sum_{n=0}^{\infty}\theta^n u_n(x,t)\right.\right. \\ &\left.\left. + 4\frac{\partial}{\partial t}\sum_{n=0}^{\infty}\theta^n u_n(x,t) + 4\sum_{n=0}^{\infty}\theta^n u_n(x,t)\right\}\right]. \end{aligned} \tag{29}$$

On comparing, the following iterations can be obtained:

$$\begin{aligned} \theta^0 &: u_0(x,t) = 1 + e^{-2t} + 2x, \\ \theta^1 &: u_1(x,t) = \mathscr{L}_c^{-1}\left[\frac{1}{\theta^2}\mathscr{L}_c\left\{\frac{\partial^2 u_0}{\partial t^2} + 4\frac{\partial u_0}{\partial t} + 4u_0\right\}\right] \\ &= 4\frac{x^2}{2!} + 8\frac{x^3}{3!}, \\ \theta^2 &: u_2(x,t) = \mathscr{L}_c^{-1}\left[\frac{1}{\theta^2}\mathscr{L}_c\left\{\frac{\partial^2 u_1}{\partial t^2} + 4\frac{\partial u_1}{\partial t}4 + u_1\right\}\right] \\ &= 16\frac{x^4}{4!} + 32\frac{x^5}{5!}, \\ \theta^3 &: u_3(x,t) = \mathscr{L}_c^{-1}\left[\frac{1}{\theta^2}\mathscr{L}_c\left\{\frac{\partial^2 u_2}{\partial t^2} + 4\frac{\partial u_2}{\partial t} + 4u_2\right\}\right] \\ &= 64\frac{x^6}{6!} + 128\frac{x^7}{7!}. \\ &\vdots \end{aligned} \tag{30}$$

Hence, the solution can be expressed as

$$\begin{aligned} u(x,t) &= u_1(x,t) + u_2(x,t) + u_3(x,t) + \cdots, \\ u(x,t) &= 1 + e^{-2t} + 2x + 4\frac{x^2}{2!} + 8\frac{x^3}{3!} + 16\frac{x^4}{4!} \\ &\quad + 32\frac{x^5}{5!} + 64\frac{x^6}{6!} + 128\frac{x^7}{7!}, \\ u(x,t) &= e^{2x} + e^{-2t}. \end{aligned} \tag{31}$$

4.3. Example 3. Consider nonlinear hyperbolic telegraph equation

$$\frac{\partial^2 u}{\partial t^2} + 2\frac{\partial u}{\partial t} = \frac{\partial^2 u}{\partial x^2} + u^3 - u, \tag{32}$$

with conditions

$$\begin{aligned} u(x,0) &= \frac{1}{2} + \frac{1}{2}\tanh\left(\frac{x}{8} + 5\right), \\ u_t(x,0) &= \frac{3}{16}\operatorname{sec\,h}^2\left(\frac{x}{8} + 5\right), \\ u(0,t) &= \frac{1}{2} + \frac{1}{2}\tanh\left(\frac{3t}{8} + 5\right), \\ u_x(0,t) &= \frac{1}{16}\operatorname{sec\,h}^2\left(\frac{3t}{8} + 5\right). \end{aligned} \tag{33}$$

Applying Laplace-Carson transform on Equation (32), we get

$$\mathscr{L}_c\left[\frac{\partial^2 u}{\partial x^2}\right] = \mathscr{L}_c\left[\frac{\partial^2 u}{\partial t^2} + 2\frac{\partial u}{\partial t} - u^3 + u\right]. \tag{34}$$

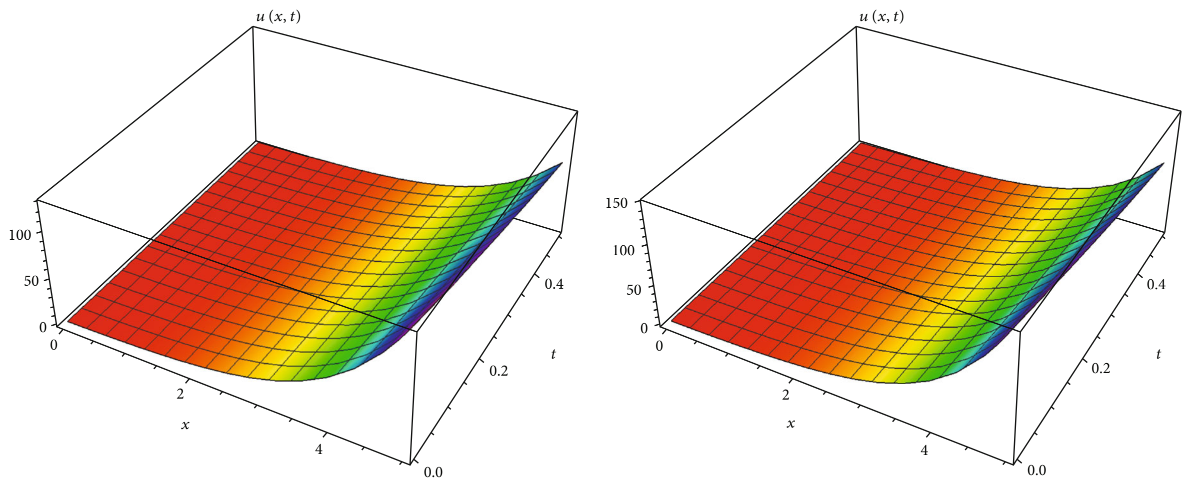

(a) Analytical solution of $u(x,t)$ for Equation (14)

(b) Particular solution of $u(x,t)$ for Equation (14)

Figure 1: Surface solutions for nonlinear hyperbolic telegraph equation.

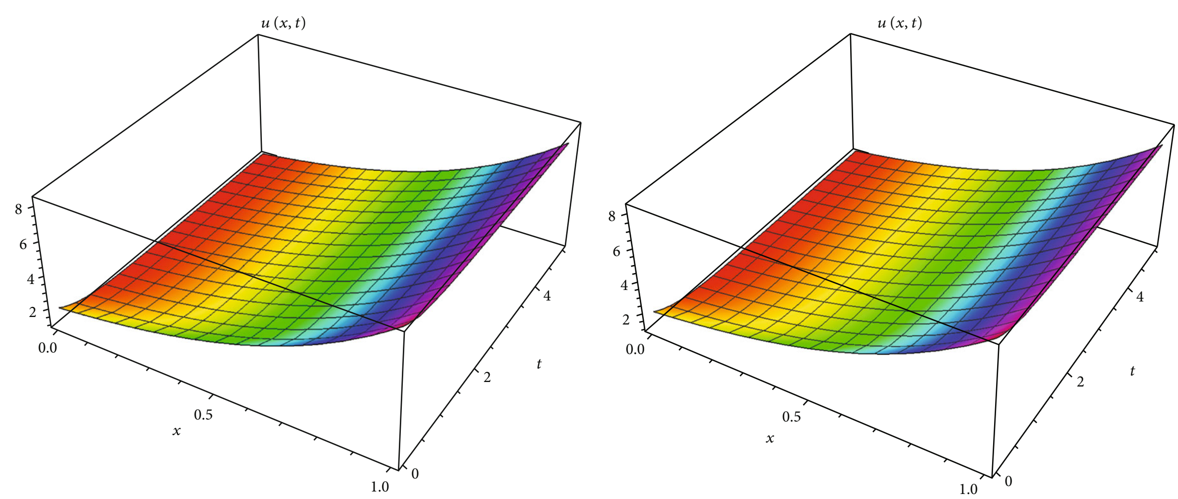

(a) Analytical solution of $u(x,t)$ for Equation (23)

(b) Particular solution of $u(x,t)$ for Equation (23)

Figure 2: Surface solutions for linear hyperbolic telegraph equation.

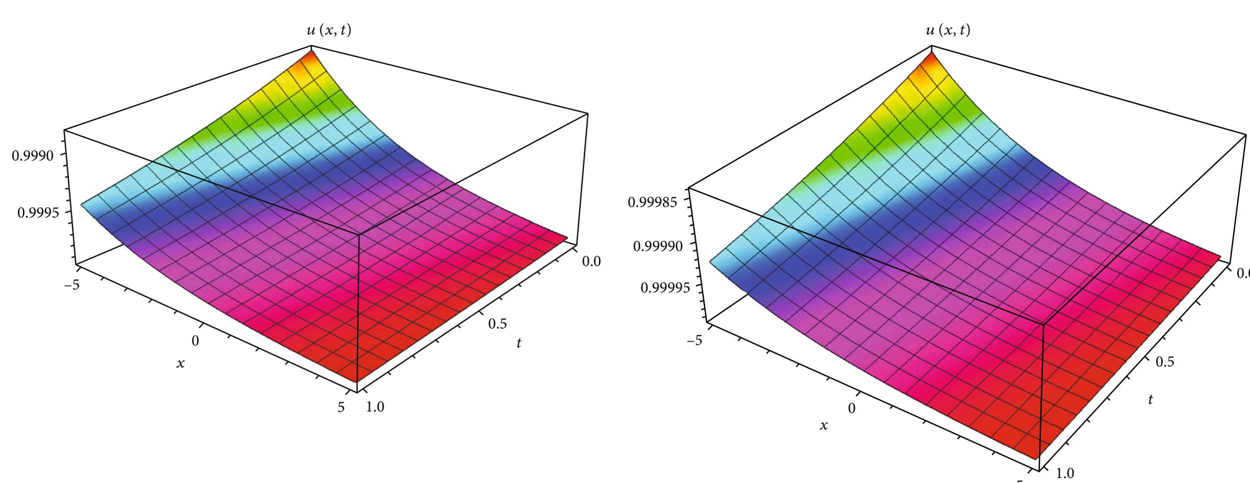

(a) Analytical solution of $u(x,t)$ for Equation (32)

(b) Particular solution of $u(x,t)$ for Equation (32)

Figure 3: Surface solutions for nonlinear hyperbolic telegraph equation.

Using the properties of Laplace-Carson transform, we get

$$\theta^2 u(\theta, t) - \theta^2 u(0, t) - \theta u'(0, t) = \mathscr{L}_c\left[\frac{\partial^2 u}{\partial t^2} + 2\frac{\partial u}{\partial t} - u^3 + u\right], \tag{35}$$

which may be solved further as,

$$u(\theta, t) = u(0, t) + \frac{1}{\theta}u'(0, t) + \frac{1}{\theta^2}\mathscr{L}_c\left\{\frac{\partial^2 u}{\partial t^2} + 2\frac{\partial u}{\partial t} - u^3 + u\right\}. \tag{36}$$

Applying inverse Laplace-Carson transform,

$$u(x, t) = u(0, t) + xu'(0, t) + \mathscr{L}_c^{-1} \cdot \left[\frac{1}{\theta^2}\mathscr{L}_c\left\{\frac{\partial^2 u}{\partial t^2} + 2\frac{\partial u}{\partial t} - u^3 + u\right\}\right]. \tag{37}$$

Now, we introduce HPM on Equation (32); we get

$$\sum_{n=0}^{\infty}\theta^n u_n(x, t) = u(0, t) + xu'(0, t) + \theta\mathscr{L}_c^{-1} \cdot \left[\frac{1}{\theta^2}\mathscr{L}\left\{\frac{\partial^2}{\partial t^2}\sum_{n=0}^{\infty}\theta^n u_n(x, t) + 2\frac{\partial}{\partial t}\sum_{n=0}^{\infty}\theta^n u_n \cdot (x, t) - \sum_{n=0}^{\infty}\theta^n u_n^3(x, t) + \sum_{n=0}^{\infty}\theta^n u_n(x, t)\right.\right]. \tag{38}$$

On comparing, the following iterations can be obtained:

$$\begin{aligned}
\theta^0 &: u_0(x, t) = \frac{1}{2} + \frac{1}{2}\tanh\left(\frac{3t}{8} + 5\right) + x\frac{1}{2}\sec\text{h}^2\left(\frac{3t}{8} + 5\right),\\
\theta^1 &: u_1(x, t) = \mathscr{L}_c^{-1}\left[\frac{1}{\theta^2}\mathscr{L}_c\left\{\frac{\partial^2 u_0}{\partial t^2} + 2\frac{\partial u_0}{\partial t} - u_0^3 + u_0\right\}\right],\\
\theta^2 &: u_2(x, t) = \mathscr{L}_c^{-1}\left[\frac{1}{\theta^2}\mathscr{L}_c\left\{\frac{\partial^2 u_1}{\partial t^2} + \frac{\partial u_1}{\partial t} + u_1 - 3u_0^2 u_1\right\}\right],\\
\theta^3 &: u_3(x, t) = \mathscr{L}_c^{-1}\left[\frac{1}{\theta^2}\mathscr{L}_c\left\{\frac{\partial^2 u_2}{\partial t^2} + \frac{\partial u_2}{\partial t} + u_2 - 3u_0 u_1^2 - 3u_0^2 u_2\right\}\right].\\
&\vdots
\end{aligned} \tag{39}$$

The other iterations are computed with the help of Wolfram Mathematica to obtain $u_1, u_2, u_3, \cdots$, which turns to the particular solution such as

$$u(x, t) = \frac{1}{2} + \frac{1}{2}\tanh\left(\frac{x}{8} + \frac{3t}{8} + 5\right). \tag{40}$$

5. Results and Discussion

This segment presents the discussion of the solution behaviors for the hyperbolic telegraph equations. Figure 1 represents the physical behavior at $0 \le x \le 5$ and $0 \le t \le 0.5$, whereas Figure 2 shows the physical behavior at $0 \le x \le 1$ and $0 \le t \le 5$ for the linear telegraph equations. We observe that the solution graphs turn to the particular solution very rapidly only after a few computations of iterations. Figure 3 represents the solution behavior of nonlinear hyperbolic telegraph equation at $0 \le x \le 5$ and $0 \le t \le 0.5$. The solution graph of the approximate solution is computed only for one iteration which coincides with the exact solation. Graphical representation and physical behavior of the linear and nonlinear hyperbolic telegraph equations demonstrate that the results obtained by $\mathscr{L}_c$-HPM are accurate and agreed with the results of exact solutions which confirm the authenticity of this approach.

6. Conclusion

In this article, we successfully conducted $\mathscr{L}_c$-HPM for finding the approximate solution of hyperbolic telegraph equations. We provided the results in the form of series without any discretization, linearization, or assumptions. The proposed strategy predicts the following fruitful remarks:

(i) $\mathscr{L}_c$-HPM is a direct approach to find the approximate solution of the problems

(ii) This scheme has less computational work, and there is no restriction of variables to obtain the solution

(iii) $\mathscr{L}_c$-HPM is applicable for both linear and nonlinear problems that provides the series solution only after a few iterations

(iv) We made all calculations with the help of Mathematica Software 11.0.1

(v) This approach is also applicable for other nonlinear fractional partial differential equations in science and engineering for future problems

Data Availability

We have provided all the data within the article.

Conflicts of Interest

The authors report that they have no conflicts of interest.

Authors' Contributions

Jiao Zeng worked in investigation, methodology, software, and writing original draft of the manuscript. Asma Idrees did work in validation, editing, and improvement of the English language during the revision of the manuscript.

Mohammed S. Abdo supervised and approved the manuscript during the initial and final submission.

References

[1] Q. Gong, C. Liu, Y. Xu et al., "Nonlinear vibration control with nanocapacitive sensor for electrostatically actuated nanobeam," *Journal of Low Frequency Noise, Vibration and Active Control*, vol. 37, no. 2, pp. 235–252, 2018.

[2] M. El-Azab and M. El-Gamel, "A numerical algorithm for the solution of telegraph equations," *Applied Mathematics and Computation*, vol. 190, no. 1, pp. 757–764, 2007.

[3] S. Pandit, M. Kumar, and S. Tiwari, "Numerical simulation of second-order hyperbolic telegraph type equations with variable coefficients," *Computer Physics Communications*, vol. 187, pp. 83–90, 2015.

[4] D. J. Evans and H. Bulut, "The numerical solution of the telegraph equation by the alternating group explicit (age) method," *International Journal of Computer Mathematics*, vol. 80, no. 10, pp. 1289–1297, 2003.

[5] K. Srinivasa and H. Rezazadeh, "Numerical solution for the fractional-order one-dimensional telegraph equation via wavelet technique," *Simulation*, vol. 22, no. 6, pp. 767–780, 2021.

[6] H.-F. Ding, Y.-X. Zhang, J.-X. Cao, and J.-H. Tian, "A class of difference scheme for solving telegraph equation by new non-polynomial spline methods," *Applied Mathematics and Computation*, vol. 218, no. 9, pp. 4671–4683, 2012.

[7] A. Saadatmandi and M. Dehghan, "Numerical solution of hyperbolic telegraph equa110 tion using the Chebyshev tau method, Numerical Methods for Partial Di_erential Equations: An," *International Journal*, vol. 26, no. 1, pp. 239–252, 2010.

[8] M. Lakestani and B. N. Saray, "Numerical solution of telegraph equation using interpolating scaling functions," *Computers & Mathematics with Applications*, vol. 60, no. 7, pp. 1964–1972, 2010.

[9] S. Sharifi and J. Rashidinia, "Numerical solution of hyperbolic telegraph equation by cubic b-spline collocation method," *Applied Mathematics and Computation*, vol. 281, pp. 28–38, 2016.

[10] M. M. Khater and D. Lu, "Analytical versus numerical solutions of the nonlinear fractional time–space telegraph equation," *Modern Physics Letters B*, vol. 35, no. 19, article 2150324, 2021.

[11] S. Das and P. Gupta, "Homotopy analysis method for solving fractional hyperbolic partial differential equations," *International Journal of Computer Mathematics*, vol. 88, no. 3, pp. 578–588, 2011.

[12] S. Yousefi, "Legendre multiwavelet Galerkin method for solving the hyperbolic 125 telegraph equation, Numerical Methods for Partial Di_erential Equations: An," *International Journal*, vol. 26, no. 3, pp. 535–543, 2010.

[13] M. Hashmi, U. Aslam, J. Singh, and K. S. Nisar, "An efficient numerical scheme for fractional model of telegraph equation," *Alexandria Engineering Journal*, vol. 61, no. 8, pp. 6383–6393, 2022.

[14] M. Dehghan and A. Mohebbi, "High order implicit collocation method for the solution of two-dimensional linear hyperbolic equation, Numerical Methods for Partial Di_erential Equations: An," *International Journal*, vol. 25, no. 1, pp. 232–243, 2009.

[15] B. Bülbül and M. Sezer, "Taylor polynomial solution of hyperbolic type partial differential equations with constant coefficients," *International journal of computer*, vol. 88, no. 3, pp. 533–544, 2011.

[16] J.-H. He, "Homotopy perturbation method: a new nonlinear analytical technique," *Applied Mathematics and Computation*, vol. 135, no. 1, pp. 73–79, 2003.

[17] J.-H. He, "Addendum: new interpretation of homotopy perturbation method," *International Journal of Modern Physics B*, vol. 20, no. 18, pp. 2561–2568, 2006.

[18] J.-H. He, "Recent development of the homotopy perturbation method," *Topological Methods in Nonlinear Analysis*, vol. 31, no. 2, pp. 205–209, 2008.

[19] S. Gupta, D. Kumar, and J. Singh, "Analytical solutions of convection-diffusion problems by combining Laplace transform method and homotopy perturbation method," *Alexandria Engineering Journal*, vol. 54, no. 3, pp. 645–651, 2015.

[20] S. A. Khuri and A. Sayfy, "A Laplace variational iteration strategy for the solution of differential equations," *Applied Mathematics Letters*, vol. 25, no. 12, pp. 2298–2305, 2012.

[21] S. Aggarwal and K. Sanjay, "Laplace-Carson transform for the primitive of convolution type Volterra integro-differential equation of first kind," *International Journal of Research and Innovation in Applied Science*, vol. 8, no. 6, pp. 2454–6194.150, 2020.

[22] P. Kumar and S. Qureshi, "Laplace-Carson integral transform for exact solutions of non-integer order initial value problems with Caputo operator," *Journal of Applied Mathematics and Computational Mechanics*, vol. 19, no. 1, pp. 55–66, 2020.

[23] T. Thange and A. Gade, "Laplace-Carson transform of fractional order,," *Malaya Journal of Matematik (MJM)*, vol. 8, pp. 2253–2258.155, 2021.

[24] K. Wang, "He's frequency formulation for fractal nonlinear oscillator arising in a microgravity space," *Numerical Methods for Partial Differential Equations*, vol. 37, no. 2, pp. 1374–1384, 2021.

[25] M. Nadeem and F. Li, "He–Laplace method for nonlinear vibration systems and nonlinear wave equations," *Journal of Low Frequency Noise, Vibration and Active Control*, vol. 38, pp. 1060–1074, 2019.

Hindawi
Journal of Function Spaces
Volume 2022, Article ID 8008838, 9 pages
https://doi.org/10.1155/2022/8008838

Research Article

Regularization of Inverse Initial Problem for Conformable Pseudo-Parabolic Equation with Inhomogeneous Term

L. D. Long [1,2] and Reza Saadati [3]

[1]Division of Applied Mathematics, Science and Technology Advanced Institute, Van Lang University, Ho Chi Minh City, Vietnam
[2]Faculty of Applied Technology, School of Engineering and Technology, Van Lang University, Ho Chi Minh City, Vietnam
[3]School of Mathematics, Iran University of Science and Technology, Narmak, Tehran, Iran

Correspondence should be addressed to Reza Saadati; rsaadati@eml.cc

Received 1 June 2022; Accepted 15 July 2022; Published 8 August 2022

Academic Editor: Yusuf Gurefe

The main goal of the paper is to approximate two types of inverse problems for conformable heat equation (or called parabolic equation with conformable operator); as follows, we considered two cases: the right hand side of equation such that $F(x, t)$ and $F(x, t) = \varphi(t)f(x)$. Up to now, there are very few surveys working on the results of regularization in $\mathscr{L}^p$ spaces. Our paper is the first work to investigate the inverse problem for conformable parabolic equations in such spaces. For the inverse source problem and the backward problem, use the Fourier truncation method to approximate the problem. The error between the regularized solution and the exact solution is obtained in $\mathscr{L}^p$ under some suitable assumptions on the Cauchy data.

1. Introduction

Partial differential equations (PDEs) have applications in many branches of science and engineering; see for example [1–8]. In this paper, for $s > 1$, we consider the initial value problem for the conformable heat equation (or called parabolic equation with conformable operator)

$$\begin{cases} \frac{{}^{\mathscr{C}}\partial^\beta}{\partial t^\beta}(y(x,t) - k\Delta y(x,t)) + (-\Delta)^s y(x,t) = F(x,t), & x \in \mathscr{D}, t \in (0,T) \\ y(x,t) = 0, & x \in \partial\mathscr{D}, t \in (0,T) \\ y(x,T) = y_T(x), & x \in \mathscr{D} \end{cases}. \tag{1}$$

Here, $\mathscr{D} \subset \mathbb{R}^N$ $(N \geq 1)$ is a bounded domain with the smooth boundary $\partial\mathscr{D}$, and $T > 0$ is a given positive number. Here, ${}^{\mathscr{C}}\partial^\beta/\partial t^\beta$ is called the conformable time derivative with order $\beta \in (0,1)$ (Khalil et al. [9]) for a given function $f : [0, \infty) \longrightarrow \mathbb{R}$; the ${}^{\mathscr{C}}\partial^\beta/\partial t^\beta$ of order $\beta \in (0,1]$ is defined by

$$\frac{{}^{\mathscr{C}}\partial^\beta}{\partial t^\beta} f(t) = \lim_{\epsilon \longrightarrow 0} \frac{f\left(t + \epsilon t^{1-\beta}\right) - f(t)}{\epsilon}, \tag{2}$$

for all $t > 0$. For some $(0, t_0)$, $t_0 > 0$ and the $\lim_{t \longrightarrow t_0^+} ({}^{\mathscr{C}}\partial^\beta/\partial t^\beta) f(t)$ exist, then $({}^{\mathscr{C}}\partial^\beta/\partial t^\beta)f(t_0) = \lim_{t \longrightarrow t_0^+} ({}^{\mathscr{C}}\partial^\beta/\partial t^\beta)f(t)$. Some properties of ${}^{\mathscr{C}}\partial^\beta/\partial t^\beta$ can be found in more detail in [10, 11]. ${}^{\mathscr{C}}\partial^\beta/\partial t^\beta$ is a natural extension of usual derivative, it preserves basic properties of the classical derivative [10, 11], and it is a local and limit-based operator. In [10, 12, 13], we saw some applications. For the convenience of the reader, we will consider two models related to Problem (1) that most mathematicians often study.

(i) The first part of the paper deals with the final value problem for Problem (1) with a linear source function. The new feature of this part is the appearance of observed data, namely, $(y_{T,\delta}, F_\delta) \in \mathscr{L}^p(\mathscr{D}) \times L^\infty(0, T; \mathscr{L}^p(\mathscr{D}))$. This result is well described in Theorem 3. We investigated the problem of restoring the temperature function $y(x,t)$, in the fact that the couple (y_T, F) are noised by the measurement data $(y_{T,\delta}, F_\delta)$ such that:

$$\begin{cases} \|y_{T,\delta}-y_T\|_{\mathscr{L}^p(\mathscr{D})} \le \delta \\ \|F_\delta - F\|_{\mathscr{L}^\infty(0,T;\mathscr{L}^p(\mathscr{D}))} \le \delta \end{cases}. \tag{3}$$

(ii) The second part of the paper deals with the final value problem for Problem (1) with F is a linear source function as follows: $F(x,t)=\Phi(t)f(x)$, where both functions (Φ, f, g) are perturbed by $(\Phi_\delta, f_\delta, g_\delta)$ in $\mathscr{L}^p(0,T)\times\mathscr{L}^p(\mathscr{D})\times\mathscr{L}^p(\mathscr{D})$, respectively

$$\begin{cases} \|\Phi_\delta-\Phi\|_{\mathscr{L}^p(0,T)} \le \delta \\ \|y_{T,\delta}-y_T\|_{\mathscr{L}^p(0,\mathscr{D}} \le \delta \\ \|f_\delta - f\|_{\mathscr{L}^p(\mathscr{D})} \le \delta \end{cases}. \tag{4}$$

The main contributions and novelties of this paper are stated as follows. As we know, two inverse problems are ill-posed in the sense of Hadamard. The well-posed problem satisfies three conditions above: the solution is existence, the solution is uniqueness, and the solution continues on data The problem that violates one of the above three conditions is an ill-posed problem. We need to regularize this problem, to give a good approximation. The number of works on the regularized problem with input data in $\mathscr{L}^2$ is quite abundant. The results of this study can be found in the following documents, attached to the regularization methods: the Tikhonov method, see [14, 15], the Fractional Tikhonov method, see [16], the fractional Landweber method, see [17, 18], the Quasi Boundary method, see [19], the truncation method, see [20], and their references.

However, for $p\neq 2$, results for regularized problem in $\mathscr{L}^p$ are quite rare. We confirm that our paper is the first result for the inverse problem for the conformable parabolic equation when the observed data is in the $\mathscr{L}^p$ space with $p\neq 2$. If the data is not in $\mathscr{L}^2$, the use of Parseval equality is not feasible. In this case, we used the embedding between $\mathscr{L}^p$ and Hilbert scales spaces $\mathbb{X}^s(\mathscr{D})$. These results are well described in Theorem 3 and Theorem 5. The main analytical technique in our paper is to use some embeddings and some analysis estimators related to Hölder inequality. To do this, we learn many interesting techniques from N.H. Tuan [21].

This paper is organized as follows. In Section 2, we state some function spaces and embeddings. In Section 3, we deal with the regularized solution for the inverse source problem for (1). Section 4 gives the mild solution of backward problem in case $F=0$. After that, we solve two problems in the case of observed data in $\mathscr{L}^p$ space.

2. Preliminary Results

Let us recall that the spectral problem

$$\begin{cases} (-\Delta)^s e_m(x) = \lambda_m^s e_m(x), & x\in\mathscr{D} \\ e_m(x)=0, & x\in\partial D \end{cases} \tag{5}$$

admits the eigenvalues $0<\lambda_1\le\lambda_2\le\cdots\le\lambda_m\le\cdots$ with $\lambda_m \longrightarrow \infty$ as $m\longrightarrow\infty$. The corresponding eigenfunctions are $e_m\in H_0^1(\mathscr{D})$.

Definition 1 (Hilbert scale space). We recall the Hilbert scale space, which is given as follows:

$$\mathscr{X}^n(\mathscr{D}) = \left\{ f\in\mathscr{L}^2(\mathscr{D}),\ \sum_{m=1}^{\infty}\lambda_m^{2n}\left(\int_{\mathscr{D}} f(x)e_m(x)dx\right)^2 < \infty \right\}, \tag{6}$$

for any $n\ge 0$. It is well-known that $\mathbb{X}^n(\mathscr{D})$ is a Hilbert space corresponding to the norm

$$\|f\|_{\mathscr{X}^n(\mathscr{D})} = \left(\sum_{m=1}^{\infty}\lambda_m^{2n}\left(\int_{\mathscr{D}} f(x)e_m(x)dx\right)^2\right)^{1/2}, f\in\mathscr{X}^n(\mathscr{D}). \tag{7}$$

Lemma 2 (See [22]). *The following statement is true:*

$$\left.\begin{array}{l} L^p(\mathscr{D})\hookrightarrow\mathscr{X}^\mu(\mathscr{D}),\ if\ -\dfrac{N}{4}<\mu\le 0, p\ge\dfrac{2N}{N-4\mu} \\ \mathscr{X}^\mu(\mathscr{D})\hookrightarrow L^p(\mathscr{D}),\ if\ 0\le\mu<\dfrac{N}{4}, p\le\dfrac{2N}{N-4\mu} \end{array}\right\}. \tag{8}$$

3. Regularization of Backward Problem

In order to find a precise formulation for solutions, we consider the mild solution in Fourier series $y(x,t)=\sum_{m=1}^\infty y_m(t) e_m(x)$, with $y_m(t)=\int_{\mathscr{D}} y(x,t)e_m(x)dx$. Taking the inner product of the equations of Problem (1) with e_m gives

$$\begin{cases} \dfrac{{}^{\mathscr{C}}\partial^\beta}{\partial t^\beta}\langle y(.,t), e_m\rangle + k\lambda_m \dfrac{{}^{\mathscr{C}}\partial^\beta}{\partial t^\beta}\langle y(.,t), e_m\rangle - \lambda_m^s\langle y(.,t), e_m\rangle = \langle F(.,t), e_m\rangle, t\in(0,T) \\ \langle y(.,0), e_m\rangle = \langle y_0, e_m\rangle \end{cases}. \tag{9}$$

The first equation of (9) is a differential equation with a conformable derivative as follows:

$$\frac{{}^{\mathscr{C}}\partial^\beta}{\partial t^\beta} y_m(t) - \lambda_m^s (1 + k\lambda_m)^{-1} y_m(t) = (1 + k\lambda_m)^{-1} F_n(t). \quad (10)$$

Because of the result in [23], the solution of Problem (1) is

$$\begin{aligned}\langle y(.,t), e_m\rangle &= \exp\left(-\frac{\lambda_m^s}{1+k\lambda_m}\frac{t^\beta}{\beta}\right)\langle y(0), e_m\rangle \\ &\quad + \frac{1}{1+k\lambda_m}\int_0^t \theta^{\beta-1}\exp\left(\frac{\lambda_m^s}{1+k\lambda_m}\frac{\theta^\beta - t^\beta}{\beta}\right)\langle F(.,\theta), e_m\rangle d\theta.\end{aligned} \quad (11)$$

Letting $t = T$, we follow from (11) that

$$\begin{aligned}\left(\int_{\mathscr{D}} y_T(x)e_m(x)dx\right) &= \exp\left(-\frac{\lambda_m^s}{1+k\lambda_m}\frac{T^\beta}{\beta}\right)\left(\int_{\mathscr{D}} y_0(x)e_m(x)dx\right) \\ &\quad + \frac{1}{1+k\lambda_m}\int_0^T \theta^{\beta-1}\exp\left(\frac{\lambda_m^s}{1+k\lambda_m}\frac{\theta^\beta - T^\beta}{\beta}\right) \\ &\quad \cdot \left(\int_{\mathscr{D}} F(.,\theta)e_m(x)dx\right)d\theta.\end{aligned} \quad (12)$$

From (12), we have

$$\begin{aligned}\left(\int_{\mathscr{D}} y_0(x)e_m(x)dx\right) &= \left(\exp\left(-\frac{\lambda_m^s}{1+k\lambda_m}\frac{T^\beta}{\beta}\right)\right)^{-1}\left[\left(\int_{\mathscr{D}} y_T(x)e_m(x)dx\right)\right. \\ &\quad - \frac{1}{1+k\lambda_m}\int_0^T \theta^{\beta-1}\exp\left(\frac{\lambda_m^s}{1+k\lambda_m}\frac{\theta^\beta - T^\beta}{\beta}\right) \\ &\quad \left.\cdot \left(\int_{\mathscr{D}} F(x,\theta)e_m(x)dx\right)d\theta\right].\end{aligned} \quad (13)$$

Substituting (13) into (12), we obtain

$$\begin{aligned}\langle y(.,t), e_m\rangle &= \exp\left(\frac{\lambda_m^s}{1+k\lambda_m}\frac{T^\beta - t^\beta}{\beta}\right)\int_{\mathscr{D}} y_T(x)e_m(x)dx \\ &\quad - \frac{1}{1+k\lambda_m}\int_t^T \theta^{\beta-1}\exp\left(\frac{\lambda_m^s}{1+k\lambda_m}\frac{\theta^\beta - t^\beta}{\beta}\right) \\ &\quad \cdot \left(\int_{\mathscr{D}} F(x,\theta)e_m(x)dx\right)d\theta\end{aligned} \quad (14)$$

This leads to

$$\begin{aligned}y(x,t) &= \sum_{m=1}^{+\infty}\exp\left(\frac{\lambda_m^s}{1+k\lambda_m}\frac{T^\beta - t^\beta}{\beta}\right)\left(\int_{\mathscr{D}} y_T(x)e_m(x)dx\right)e_m(x) \\ &\quad - \sum_{m=1}^{+\infty}\frac{1}{1+k\lambda_m}\left(\int_t^T \theta^{\beta-1}\exp\left(\frac{\lambda_m^s}{1+k\lambda_m}\frac{\theta^\beta - t^\beta}{\beta}\right)\right. \\ &\quad \left.\cdot \left(\int_{\mathscr{D}} F(x,\theta)e_m(x)dx\right)d\theta\right)e_m(x).\end{aligned} \quad (15)$$

4. The Mild Solution of Backward Problem in Case $F = 0$

In this section, we investigate the existence and regularity of mild solutions of Problem (1). Firstly, we consider the following initial value problem

$$\begin{cases}\frac{{}^{\mathscr{C}}\partial^\beta}{\partial t^\beta}(y(x,t) - k\Delta y(x,t)) + (-\Delta)^s y(x,t) = 0, & x \in \mathscr{D}, t \in (0,T) \\ y(x,t) = 0, & x \in \partial\mathscr{D}, t \in (0,T) \\ y(x,T) = y_T(x), & x \in \mathscr{D}, t \in (0,T)\end{cases}. \quad (16)$$

According to (15), in this case, we have

$$y(x,t) = \sum_{m=1}^{+\infty}\exp\left(\frac{\lambda_m^s}{1+k\lambda_m}\frac{T^\beta - t^\beta}{\beta}\right)\left(\int_{\mathscr{D}} y_T(x)e_m(x)dx\right)e_m(x). \quad (17)$$

4.1. The Ill-Posedness of Problem (1). In order to prove that the solution to the backward problem is unstable at $F(x,t) = 0$, let us take the perturbed final data $y_{T,j}(x) \in \mathscr{L}^2(\mathscr{D})$, by choosing $y_{T,j}(x) = e_j(x)\lambda_j^{-1/2}$. For $s > 3/2$, let us choose input final data $y_T(x) = 0$; we know that an error in $L^2(\mathscr{D})$ norm between two input final data as follows:

$$\begin{aligned}\left\|y_{T,j} - y_T\right\|_{\mathscr{L}^2(\mathscr{D})} &= \left\|e_j\lambda_j^{-1/2}\right\|_{\mathscr{L}^2(\mathscr{D})} \\ &= \lambda_j^{-1/2} \text{ this leads to } \lim_{j\longrightarrow\infty}\left\|y_{T,j} - y_T\right\|_{\mathscr{L}^2(\mathscr{D})} \\ &= \lim_{j\longrightarrow\infty}\lambda_j^{-1/2} = 0.\end{aligned} \quad (18)$$

Therefore, we obtain

$$y_j(x,t) = \exp\left(\frac{\lambda_j^s}{1+k\lambda_j}\frac{T^\beta - t^\beta}{\beta}\right)y_{T,j}(x). \quad (19)$$

First of all, we have $\lambda_j^s/(1+k\lambda_j) = (\lambda_j^{s-1})/((1/\lambda_j)+k) \geq (\lambda_j^{s-1})/((1/\lambda_j)+k)$, and $((T^\beta - t^\beta)/\beta) \geq 0$; this implies that

$$\exp\left(\frac{\lambda^s}{1+k\lambda_j}\frac{T^\beta - t^\beta}{\beta}\right) \geq \exp\left(\frac{\lambda_j^{s-1}}{\lambda_1^{-1}+k}\frac{T^\beta - t^\beta}{\beta}\right). \quad (20)$$

Next, using the inequality $\exp(x) \geq x$, for $x > 0$, this leads to:

$$\begin{aligned}\left\|y_j(\cdot,t)\right\|_{\mathscr{L}^2(\mathscr{D})} &\geq \left\|\exp\left(\frac{\lambda_j^{s-1}}{\lambda_1^{-1}+k}\frac{T^\beta - t^\beta}{\beta}\right)\frac{1}{\lambda_j^{1/2}}\right\|_{\mathscr{L}^2(\mathscr{D})} \\ &\geq \frac{\lambda_j^{s-3/2}}{\lambda_1^{-1}+k}\frac{T^\beta - t^\beta}{\beta}.\end{aligned} \quad (21)$$

For $s > 3/2$, and from (21), we get

$$\lim_{j\longrightarrow\infty}\left\|y_j(.,t)\right\|_{\mathscr{L}^2(\mathscr{D})} \geq \lim_{j\longrightarrow\infty}\frac{\lambda_j^{s-3/2}}{\lambda_1^{-1}+k}\frac{T^\beta - t^\beta}{\beta} \longrightarrow +\infty. \quad (22)$$

Thus, Problem (1), in general, ill-posed in the Hadamard sense in $\mathscr{L}^2(\mathscr{D})$-norm.

4.2. Regularization of inverse Problem (1) in $\mathscr{L}^p(\mathscr{D})$ space. From (15), we know that the explicit formula of the mild solution

$$\begin{aligned}y(x,t) = &\sum_{m=1}^{+\infty}\exp\left(\frac{\lambda_m^s}{1+k\lambda_m}\frac{T^\beta - t^\beta}{\beta}\right)\left(\int_{\mathscr{D}} y_T(x)e_m(x)dx\right)e_m(x) \\ &- \sum_{m=1}^{+\infty}\frac{1}{1+k\lambda_m}\left(\int_t^T \theta^{\beta-1}\exp\left(\frac{\lambda_m^s}{1+k\lambda_m}\frac{\theta^\beta - t^\beta}{\beta}\right)\right. \\ &\left.\cdot\left(\int_{\mathscr{D}} F(x,\theta)e_m(x)dx\right)d\theta\right)e_m(x).\end{aligned} \quad (23)$$

By applying the Fourier truncation method, we have its approximation

$$\begin{aligned}y_\delta(x,t) = &\sum_{m\leq\mathscr{M}_\delta}\exp\left(\frac{\lambda_m^s}{1+k\lambda_m}\frac{T^\beta - t^\beta}{\beta}\right)\left(\int_{\mathscr{D}} y_{T,\delta}(x)e_m(x)dx\right)e_m(x) \\ &- \sum_{m\leq\mathscr{M}_\delta}\frac{1}{1+k\lambda_m}\left(\int_t^T \theta^{\beta-1}\exp\left(\frac{\lambda_m^s}{1+k\lambda_m}\frac{\theta^\beta - t^\beta}{\beta}\right)\right. \\ &\left.\cdot\left(\int_{\mathscr{D}} F_\delta(x,\theta)e_m(x)dx\right)d\theta\right)e_m(x).\end{aligned} \quad (24)$$

Here, $\mathscr{M}_\delta$ is parameter regularization which is defined later.

Theorem 3. *For $s > 1$, taking $(y_T, F) \in \mathscr{L}^p(0,T)\times\mathscr{L}^\infty(0,T;\mathscr{L}^p(\mathscr{D}))$ for any $0 \leq t \leq T$ for any $1/\beta < p < 2$, assume that (y_T, F) is observed by the couple $(y_{T,\delta}, F_\delta)$ such that*

$$\left\|y_{T,\delta} - y_T\right\|_{\mathscr{L}^p(\mathscr{D})} + \|F - F_\delta\|_{\mathscr{L}^\infty(0,T;\mathscr{L}^p(\mathscr{D}))} \leq \delta, \delta > 0. \quad (25)$$

Let us assume that $u \in \mathscr{L}^\infty(0,T;\mathscr{X}^{n+\sigma})$ for $\sigma > 0$ and $0 < n < N/4$. With $\mathscr{M}_\delta$ such that

$$\lim_{\delta\longrightarrow 0}\mathscr{M}_\delta = +\infty, \lim_{\delta\longrightarrow 0}|\mathscr{M}_\delta|^{n+N/2p-N/4}\exp\left(\frac{T^\beta}{\beta}\mathscr{M}_\delta^{s-1}k^{-1}\right)\delta = 0. \quad (26)$$

Then, the error estimate

$$\|y_\delta - y\|_{\mathscr{L}^{2N/N-4n}(\mathscr{D})} \text{ is of order } \max\cdot\left\{|\mathscr{M}_\delta|^{n+N/2p-N/4}\exp\left((\mathscr{M}_\delta)^{s-1}k^{-1}\frac{T^\beta}{\beta}\right)\delta, |\mathscr{M}_\delta|^{-\sigma}\right\}. \quad (27)$$

Remark 4. One choice for $\mathscr{M}_\delta$ such that

$$\mathscr{M}_\delta = \left(T^{-\beta}\beta(1-\alpha)k\right)^{1/s-1}\left[\log\left(\frac{1}{\delta}\right)\right]^{1/s-1}, \text{for } 0 < \alpha < 1. \quad (28)$$

then $\|y_\delta - y\|_{\mathscr{L}^{2N/(N-4n)}(\mathscr{D})}$ is of order $\max\{\delta^\alpha[\log(1/\delta)]^{(n+N/2p-N/4)/(s-1)}, [\log(1/\delta)]^{-\sigma/(s-1)}\}$.

Proof. Let

$$\begin{aligned}\mathscr{V}_\delta(x,t) = &\sum_{m\leq\mathscr{N}_\delta}\exp\left(\frac{\lambda_m^s}{1+k\lambda_m}\frac{T^\beta - t^\beta}{\beta}\right)\left(\int_{\mathscr{D}} y_T(x)e_m(x)dx\right)e_m(x) \\ &- \sum_{m\leq\mathscr{M}_\delta}\frac{1}{1+k\lambda_m}\left(\int_t^T \theta^{\beta-1}\exp\left(\frac{\lambda_m^s}{1+k\lambda_m}\frac{\theta^\beta - t^\beta}{\beta}\right)\right. \\ &\left.\cdot\left(\int_{\mathscr{D}} F(x,\theta)e_m(x)dx\right)d\theta\right)e_m(x).\end{aligned} \quad (29)$$

It is clear that

$$\begin{aligned}\|y_\delta(\cdot,t) - y(\cdot,t)\|_{\mathscr{X}^n(\mathscr{D})} \leq &\|y_\delta(\cdot,t) - \mathscr{V}_\delta(\cdot,t)\|_{\mathscr{X}^n(\mathscr{D})} \\ &+ \|\mathscr{V}_\delta(\cdot,t) - y(\cdot,t)\|_{\mathscr{X}^n(\mathscr{D})}.\end{aligned} \quad (30)$$

We continue to consider the two components of the right hand side.

Step 1:

$$
\begin{aligned}
y_\delta(x,t) - \mathscr{V}_\delta(x,t) &= \sum_{\lambda_m \le \mathscr{M}_\delta} \exp\left(\frac{\lambda_m^s}{1+k\lambda_m}\frac{T^\beta - t^\beta}{\beta}\right) \cdot \left(\int_{\mathscr{D}} \left(y_{T,\delta}(x) - y_T(x)\right) e_m(x)dx\right) e_m(x) \\
&\quad - \sum_{\lambda_m \le \mathscr{M}_\delta} \frac{1}{1+k\lambda_m}\left(\int_t^T \theta^{\beta-1} \exp\left(\frac{\lambda_m^s}{1+k\lambda_m}\frac{\theta^\beta - t^\beta}{\beta}\right) \cdot \left(\int_{\mathscr{D}} (F_\delta(x,\theta) - F(x,\theta)) e_m(x)dx\right) d\theta\right)) e_m(x) \\
&= \mathscr{H}_1(x,t) - \mathscr{H}_2(x,t).
\end{aligned} \tag{31}
$$

For $s > 1$, it is easy to see that $\lambda_m^s (1+k\lambda_m)^{-1} \le \lambda_m^{s-1} (\lambda_m^{-1} + k)^{-1} \le \lambda_m^{s-1} k^{-1}$. The first term $\mathscr{H}_1(x,t)$ on $\mathscr{X}^n(\mathscr{D})$ is bounded by

$$
\begin{aligned}
\|\mathscr{H}_1(.,t)\|^2_{\mathscr{X}^n(\mathscr{D})} &= \sum_{\lambda_m \le \mathscr{M}_\delta} \lambda_m^{2n} \exp\left(\frac{2\lambda_m^s}{1+k\lambda_m}\frac{T^\beta - t^\beta}{\beta}\right) \cdot \left(\int_{\mathscr{D}} \left(y_{T,\delta}(x) - y_T(x)\right) e_m(x)dx\right)^2 \\
&= \sum_{\lambda_m \le \mathscr{M}_\delta} \lambda_m^{2n+N/p-N/2} \lambda_m^{Np-2N/2p} \exp \cdot \left(2\lambda_m^{s-1} k^{-1} \frac{T^\beta}{\beta}\right) \left(\int_{\mathscr{D}} \left(y_{T,\delta}(x) - y_T(x)\right) e_m(x)dx\right)^2 \\
&\le |\mathscr{M}_\delta|^{2n+N/p-N/2} \exp\left(\frac{2|\mathscr{M}_\delta|^{s-1} k^{-1} T^\beta}{\beta}\right) \sum_{\lambda_m \le \mathscr{M}_\delta} \lambda_m^{Np-2N/2p} \cdot \left(\int_{\mathscr{D}} \left(y_{T,\delta}(x) - y_T(x)\right) e_m(x)dx\right)^2 \\
&\le |\mathscr{M}_\delta|^{2n+N/p-N/2} \exp\left(\frac{2|\mathscr{M}_\delta|^{s-1} k^{-1} T^\beta}{\beta}\right) \left\| y_{T,\delta} - y_T \right\|_{\mathscr{X}^{Np-2N/4p}}.
\end{aligned} \tag{32}
$$

Since the Sobolev space embedding $\mathscr{L}^p(\mathscr{D}) \longrightarrow \mathscr{X}^{(Np-2N)/4p}(\mathscr{D})$, we have

$$
\left\| y_{T,\delta} - y_T \right\|_{\mathscr{X}^{Np-2N/4p(\mathscr{D})}} \le C_1(N,p) \left\| y_{T,\delta} - y_T \right\|_{\mathscr{L}^p(\mathscr{D})}. \tag{33}
$$

This follows from (32) that

$$
\|\mathscr{H}_1(.,t)\|_{\mathscr{X}^n(\mathscr{D})} \le (\mathscr{M}_\delta)^{n+N/2p-N/4} \exp\left(\frac{(\mathscr{M}_\delta)^{s-1} k^{-1} T^\beta}{\beta}\right) C_1(N,p)\delta. \tag{34}
$$

The second term $\mathscr{H}_2(x,t)$ is estimated as follows:

$$
\|\mathscr{H}_2(.,t)\|^2_{\mathscr{X}^n(\mathscr{D})} = \sum_{\lambda_m \le \mathscr{M}_\delta} \frac{\lambda_m^{2n}}{1+k\lambda_m} \left(\int_t^T \theta^{\beta-1} \exp\left(\frac{\lambda_m^s}{1+k\lambda_m}\frac{\theta^\beta - t^\beta}{\beta}\right) \cdot \left(\int_{\mathscr{D}} (F(x,\theta) - F_\delta(x,\theta)) e_m(x)dx\right) d\theta\right))^2 \tag{35}
$$

By the same arguments as above, we find that

$$
\begin{aligned}
\|\mathscr{H}_2(\cdot,t)\|^2_{\mathscr{X}^n(\mathscr{D})} &\le \sum_{\lambda_m \le \mathscr{M}_\delta} \lambda_m^{2n} \left(\int_t^T \theta^{\beta-1} \exp\left(\lambda_m^{s-1} k^{-1} \frac{\theta^\beta - t^\beta}{\beta}\right) \cdot \left(\int_{\mathscr{D}} (F(x,\theta) - F_\delta(x,\theta)) e_m(x)dx\right) d\theta\right)^2 \\
&\le \exp\left(2(\mathscr{M}_\delta)^{s-1} k^{-1} \frac{T^\beta}{\beta}\right) \sum_{\lambda_m \le \mathscr{M}_\delta} \lambda_m^{2n} \cdot \left(\int_t^T \theta^{\beta-1} \left(\int_{\mathscr{D}} (F(x,\theta) - F_\delta(x,\theta)) e_m(x)dx\right) d\theta\right)^2
\end{aligned} \tag{36}
$$

We can see that $\lambda_m^{2n+N/p-N/2} \le |\mathscr{M}_\delta|^{2n+N/p-N/2}$ and $\int_t^T \theta^{\beta-1} d\theta \le (T^\beta - t^\beta)/\beta \le T^\beta/\beta$. From (36), using Holder's inequality, we get

$$
\begin{aligned}
&\sum_{\lambda_m \le \mathscr{M}_\delta} \lambda_m^{2n} \left(\int_t^T \theta^{\beta-1} \left(\int_{\mathscr{D}} (F(x,\theta) - F_\delta(x,\theta)) e_m(x)dx\right) d\theta\right)^2 \\
&\le \sum_{\lambda_m \le \mathscr{M}_\delta} \lambda_m^{2n+N/p-N/2} \lambda_m^{Np-2N/2p} \left(\int_t^T \theta^{\beta-1} d\theta\right) \cdot \left(\int_t^T \theta^{\beta-1} \left(\int_{\mathscr{D}} (F(x,\theta) - F_\delta(x,\theta)) e_m(x)dx\right)^2 d\theta\right) \\
&\le \beta^{-1} T^\beta |\mathscr{M}_\delta|^{2n+N/p-N/2} \left(\int_t^T \theta^{\beta-1} \sum_{\lambda_m \le \mathscr{M}_\delta} \lambda_m^{2n+N/p-N/2} \cdot \left(\int_{\mathscr{D}} (F(x,\theta) - F_\delta(x,\theta)) e_m(x)dx\right)^2 d\theta\right) \\
&\le \beta^{-1} T^\beta |\mathscr{M}_\delta|^{2n+N/p-N/2} \left(\int_t^T \theta^{\beta-1} \|F_\delta(\cdot,t) - F(\cdot,t)\|^2_{\mathscr{X}^{Np-2N/4p}} d\theta\right).
\end{aligned} \tag{37}
$$

This latter inequality together with Sobolev embedding $\mathscr{L}^p(\mathscr{D}) \longrightarrow \mathscr{X}^{(Np-2N)/4p}(\mathscr{D})$ gives us

$$
\begin{aligned}
&\sum_{\lambda_m \le \mathscr{M}_\delta} \lambda_m^{2n} \left(\int_t^T \theta^{\beta-1} \left(\int_{\mathscr{D}} (F(x,\theta) - F_\delta(x,\theta)) e_m(x)dx\right) d\theta\right)^2 \\
&\le \beta^{-1} |C_2(N,p)|^2 T^\beta (\mathscr{M}_\delta)^{2n+N/p-N/2} \cdot \left(\int_t^T \theta^{\beta-1} \|F(x,\theta) - F_\delta(x,\theta)\|^2_{\mathscr{L}^p(\mathscr{D})} d\theta\right) \\
&\le \beta^{-2} |C_2(N,p)|^2 T^{2\beta} |\mathscr{M}_\delta|^{2n+N/p-N/2} \|F - F_\delta\|_{\mathscr{L}^\infty(0,T;\mathscr{L}^p(\mathscr{D}))} \\
&\le \beta^{-2} |C_2(N,p)|^2 T^{2\beta} |\mathscr{M}_\delta|^{2n+N/p-N/2} \delta^2.
\end{aligned} \tag{38}
$$

Combining (36) and (38), we get

$$\|\mathscr{H}_2(\cdot,t)\|^2_{\mathscr{X}^n(\mathscr{D})} \le \exp\left(2(\mathscr{M}_\delta)^{s-1}k^{-1}\frac{T^\beta}{\beta}\right) \cdot |C_2(N,p)|^2 T^{2\beta}|\mathscr{M}_\delta|^{2n+N/p-N/2}\beta^{-2}\delta^2. \quad (39)$$

Taking the square root on the both sides, we have

$$\|\mathscr{H}_2(\cdot,t)\|_{\mathscr{X}^n(\mathscr{D})} \le \exp\left((\mathscr{M}_\delta)^{s-1}k^{-1}\frac{T^\beta}{\beta}\right) \cdot |C_2(N,p)|T^\beta|\mathscr{M}_\delta|^{n+N/2p-N/4}\beta^{-1}\delta. \quad (40)$$

From (34) and (40), we deduce that

$$\begin{aligned}\|y_\delta(\cdot,t)-\mathscr{V}_\delta(\cdot,t)\|_{\mathscr{X}^n(\mathscr{D})} &\le \|\mathscr{H}_1(\cdot,t)\|_{\mathscr{X}^n(\mathscr{D})}+\|\mathscr{H}_2(\cdot,t)\|_{\mathscr{X}^n(\mathscr{D})}\\ &\le |\mathscr{M}_\delta|^{n+N/2p-N/4}\exp\left(\frac{(\mathscr{M}_\delta)^{s-1}k^{-1}T^\beta}{\beta}\right)C_1(N,p)\delta+\exp\\ &\cdot\left((\mathscr{M}_\delta)^{s-1}k^{-1}\frac{T^\beta}{\beta}\right)|C_2(N,p)|T^\beta|\mathscr{M}_\delta|^{n+N/2p-N/4}\beta^{-1}\delta\\ &\le |\mathscr{M}_\delta|^{n+N/2p-N/4}\exp\left((\mathscr{M}_\delta)^{s-1}k^{-1}\frac{T^\beta}{\beta}\right)\delta\\ &\cdot\left(C_1(N,p)+|C_2(N,p)|T^\beta\beta^{-1}\right).\end{aligned} \quad (41)$$

Step 2: Estimate of $\|u(\cdot,t)-\mathscr{V}_\delta(\cdot,t)\|_{\mathscr{X}^n(\mathscr{D})}$.
From the definition (23) and (29), we have

$$\begin{aligned}\|y(\cdot,t)-\mathscr{V}_\delta(\cdot,t)\|^2_{\mathscr{X}^n(\mathscr{D})} &= \sum_{\lambda_m>\mathscr{M}_\delta}\lambda_m^{2n}\left(\int_{\mathscr{D}}u(\cdot,t)e_m(x)dx\right)^2\\ &= \sum_{\lambda_m>\mathscr{M}_\delta}\lambda_m^{-2\sigma}\lambda_m^{2n+2\sigma}\left(\int_{\mathscr{D}}u(\cdot,t)e_m(x)dx\right)^2\\ &\le |\mathscr{M}_\delta|^{-2\sigma}\|u\|^2_{\mathscr{L}^\infty(0,T;\mathscr{X}^{n+\sigma}(\mathscr{D}))}.\end{aligned} \quad (42)$$

Therefore, we get

$$\|y(\cdot,t)-\mathscr{V}_\delta(\cdot,t)\|_{\mathscr{X}^n(\mathscr{D})} \le |\mathscr{M}_\delta|^{-\sigma}\|u\|_{L^\infty(0,T;\mathscr{X}^{n+\sigma}(\mathscr{D})}. \quad (43)$$

Combining two steps and noting that $\mathscr{X}^n(\mathscr{D})\hookrightarrow \mathscr{L}^{2N/(N-4n)}$, $(0<n<N/4)$, we deduce that

$$\begin{aligned}\|y_\delta(\cdot,t)-y(\cdot,t)\|_{\mathscr{L}(\mathscr{D})} &\le C_3(N,n)\|y_\delta(\cdot,t)-\mathscr{V}_\delta(\cdot,t)\|_{\mathscr{X}^n(\mathscr{D})}\\ &\quad + C_3(N,n)\|\mathscr{V}_\delta(\cdot,t)-y(\cdot,t)\|_{\mathscr{X}^n(\mathscr{D})}\\ &\le C_3(N,n)|\mathscr{M}_\delta|^{n+N/2p-N/4}\exp\\ &\cdot\left((\mathscr{M}_\delta)^{s-1}k^{-1}\frac{T^\beta}{\beta}\right)\delta\left(C_1(N,p)+|C_2(N,p)|T^\beta\beta^{-1}\right)\\ &\quad + C_3(N,n)|\mathscr{M}_\delta|^{-\sigma}\|u\|_{\mathscr{L}^\infty(0,T;\mathscr{X}^{n+\sigma}(\mathscr{D})}.\end{aligned} \quad (44)$$

The proof of Theorem 3 is completed. In the following theorem, we give a regularization result in the case that F has a split form $F(x,t)=\Phi(t)f(x)$. □

Theorem 5. *For $s>1$, let us assume that the input data Φ_δ, g_δ, f_δ such that*

$$\|\Phi_\delta-\Phi\|_{\mathscr{L}^p(0,T)}+\left\|y_{T,\delta}-y_T\right\|_{\mathscr{L}^p(\mathscr{D})}+\|f_\delta-f\|_{\mathscr{L}^p(\mathscr{D})}\le\delta. \quad (45)$$

Assume that $u\in\mathscr{L}^\infty(0,T;\mathscr{X}^{n+\sigma}(\mathscr{D}))$ for any $\sigma>0$, then we construct a regularized solution defined by

$$\begin{aligned}\mathscr{W}_\delta(x,t) &= \sum_{m\le\mathscr{B}_\delta}\exp\left(\frac{\lambda_m^s}{1+k\lambda_m}\frac{T^\beta-t^\beta}{\beta}\right)\left(\int_{\mathscr{D}}y_{T,\delta}(x)e_m(x)dx\right)e_m(x)\\ &-\sum_{m\le\mathscr{B}_\delta}\frac{1}{1+k\lambda_m}\left(\int_t^T\theta^{\beta-1}\exp\left(\frac{\lambda_m^s}{1+k\lambda_m}\frac{\theta^\beta-t^\beta}{\beta}\right)\right.\\ &\left.\cdot\left(\int_{\mathscr{D}}f(x)e_m(x)dx\right)\Phi_\delta(\theta)d\theta\right)e_m(x).\end{aligned} \quad (46)$$

Then, the error $\|\mathscr{W}_\delta(.,t)-y(.,t)\|_{\mathscr{L}^{2N/(N-4n)}(\mathscr{D})}$ is of order $\max\{\delta|\mathscr{B}_\delta|^{-\sigma},|\mathscr{B}_\delta|^{n+(N/2p)-(N/4)}\exp((\mathscr{B}_\delta^{s-1}k^{-1}T^\beta)/\beta)\delta\}$.

Remark 6. $\mathscr{B}_\delta=(T^{-\beta}\beta k)^{1/(s-1)}(1-\alpha)^{1/(s-1)}\log(1/\delta)^{1/(s-1)}$, then the error

$$\|\mathscr{W}_\delta(.,t)-y(.,t)\|_{\mathscr{L}^{2N/N-4n}(\mathscr{D})}\text{ is of order }\max\cdot\left\{\delta\left|\log\left(\frac{1}{\delta}\right)\right|^{-\sigma/s-1}\left|\log\left(\frac{1}{\delta}\right)\right|^{n+N/2p-N/4/s-1}\delta^\alpha\right\}. \quad (47)$$

Proof. Since $F(x,t)=\Phi(t)f(x)$, we know that

$$\begin{aligned}\mathscr{Z}_\delta(x,t) &= \sum_{m\le\mathscr{B}_\delta}\exp\left(\frac{\lambda_m^s}{1+k\lambda_m}\frac{T^\beta-t^\beta}{\beta}\right)\left(\int_{\mathscr{D}}y_T(x)e_m(x)dx\right)e_m(x)\\ &-\sum_{m\le\mathscr{B}_\delta}\frac{1}{1+k\lambda_m}\left(\int_t^T\theta^{\beta-1}\exp\left(\frac{\lambda_m^s}{1+k\lambda_m}\frac{\theta^\beta-t^\beta}{\beta}\right)\right.\\ &\left.\cdot\left(\int_{\mathscr{D}}f(x)e_m(x)dx\right)\Phi(\theta)d\theta\right)e_m(x).\end{aligned} \quad (48)$$

The triangle inequality allows us to obtain that

$$\|\mathscr{W}_\delta(\cdot,t)-y(\cdot,t)\|_{\mathscr{X}^n(\mathscr{D})} \le \|\mathscr{W}_\delta(\cdot,t)-\mathscr{Z}_\delta(\cdot,t)\|_{\mathscr{X}^n(\mathscr{D})} + \|\mathscr{Z}_\delta(\cdot,t)-y(\cdot,t)\|_{\mathscr{X}^n(\mathscr{D})}. \tag{49}$$

Next, we will evaluate the right side of (49), by the same way as demonstrated in (42),

$$\|y(\cdot,t)-\mathscr{Z}_\delta(\cdot,t)\|^2_{\mathscr{X}^n(\mathscr{D})} \le |\mathscr{B}_\delta|^{-2\sigma}\|u\|^2_{\mathscr{L}^\infty(0,T;\mathscr{X}^{n+\sigma}(\mathscr{D}))}. \tag{50}$$

It is easy to see that

$$\mathscr{W}_\delta(x,t)-\mathscr{Z}_\delta(x,t)=\mathscr{J}_1(x,t)+\mathscr{J}_2(x,t)+\mathscr{J}_3(x,t). \tag{51}$$

whereby

$$\begin{aligned}
\mathscr{J}_1(x,t) &= \sum_{\lambda_m\le\mathscr{B}_\delta} \exp\left(\frac{\lambda_m^s}{1+k\lambda_m}\frac{T^\beta-t^\beta}{\beta}\right) \cdot \left(\int_{\mathscr{D}}(y_{T,\delta}(x)-y_T(x))e_m(x)dx\right)e_m(x),\\
\mathscr{J}_2(x,t) &= -\sum_{\lambda_m\le\mathscr{B}_\delta}\left[\int_t^T\theta^{\beta-1}\exp\left(\frac{\lambda_m^s}{1+k\lambda_m}\frac{\theta^\beta-t^\beta}{\beta}\right)\Phi_\delta(\theta)d\theta\right] \cdot \left(\int_{\mathscr{D}}(f_\delta(x)-f(x))e_m(x)\right)e_m(x),\\
\mathscr{J}_3(x,t) &= \sum_{\lambda_m\le\mathscr{B}_\delta}\left[\int_t^T\theta^{\beta-1}\exp\left(\frac{\lambda_m^s}{1+k\lambda_m}\frac{\theta^\beta-t^\beta}{\beta}\right)(\Phi(\theta)-\Phi_\delta(\theta))d\theta\right] \cdot \left(\int_{\mathscr{D}}f(x)e_m(x)dx\right)e_m(x).
\end{aligned} \tag{52}$$

We will divide this review into several steps as follows:

Step 1: Estimate of $\|\mathscr{J}_1(\cdot,t)\|_{\mathscr{X}^n(\mathscr{D})}$, we obtain that

$$\|\mathscr{J}_1(\cdot,t)\|_{\mathscr{X}^n(\mathscr{D})} \le C_4(N,p)|\mathscr{B}_\delta|^{n+N/2p-N/4}\exp\left(\mathscr{B}_\delta^{s-1}k^{-1}\frac{T^\beta}{\beta}\right)\delta. \tag{53}$$

Step 2: Due to Parseval's equality, the term $\|\mathscr{J}_2(\cdot,t)\|_{\mathscr{X}^n(\mathscr{D})}$ can be bounded as follows:

$$\|\mathscr{J}_2(\cdot,t)\|_{\mathscr{X}^n(\mathscr{D})} = \sum_{\lambda_m\le\mathscr{B}_\delta}\lambda_m^{2n}\left[\int_t^T\theta^{\beta-1}\exp\left(\frac{\lambda_m^s}{1+k\lambda_m}\frac{\theta^\beta-t^\beta}{\beta}\right)\Phi_\delta(\theta)d\theta\right]^2 \cdot \left(\int_{\mathscr{D}}(f_\delta(x)-f(x))e_m(x)dx\right)^2. \tag{54}$$

Thank to Holder's inequality, we derive that for $p>1$ and $p^*=1+(1/(p-1))$, one has

$$\begin{aligned}
&\left|\int_t^T\theta^{\beta-1}\exp\left(\frac{\lambda_m^s}{1+k\lambda_m}\frac{\theta^\beta-t^\beta}{\beta}\right)\Phi_\delta(\theta)d\theta\right|\\
&\le\left(\int_0^T|\Phi_\delta|^pd\theta\right)^{1/p}\left(\int_t^T\theta^{p^*(\beta-1)}\exp\left(p^*\frac{\lambda_m^s}{1+k\lambda_m}\frac{\theta^\beta-t^\beta}{\beta}\right)d\theta\right)^{1/p^*}\\
&\le\exp\left(\lambda_m^{s-1}k^{-1}\frac{T^\beta}{\beta}\right)\|\Phi_\delta\|_{\mathscr{L}^{p^*}(0,T)}\left(\int_0^T\theta^{p^*(\beta-1)}d\theta\right)^{1/p^*}\\
&\le\left(\frac{p-1}{p\beta-1}\right)^{p-1/p}T^{p\beta-1/p}\exp\left(\lambda_m^{s-1}k^{-1}\frac{T^\beta}{\beta}\right)\|\Phi_\delta\|_{\mathscr{L}^p(0,T)}.
\end{aligned} \tag{55}$$

The latter inequality leads to

$$\begin{aligned}
&\|\mathscr{J}_2(.,t)\|^2_{\mathscr{X}^n(\mathscr{D})}\\
&=\sum_{\lambda_m\le\mathscr{B}_\delta}\lambda_m^{2n}\left[\int_t^T\theta^{\beta-1}\exp\left(\frac{\lambda_m^s}{1+k\lambda_m}\frac{\theta^\beta-t^\beta}{\beta}\right)\Phi_\delta(\theta)d\theta\right]^2 \cdot\left(\int_{\mathscr{D}}(f_\delta(x)-f(x))e_m(x)dx\right)^2\\
&\le\left(\frac{p-1}{p\beta-1}\right)^{2p-2/p}T^{2p\beta-2/p}\|\Phi_\delta(\theta)\|^2_{\mathscr{L}^p(0,T)} \times\sum_{\lambda_m\le\mathscr{B}_\delta}\lambda_m^{2n+N/p-N/2}\lambda_m^{Np-2N/2p}\exp \cdot\left(\frac{2T^\beta\lambda_m^{s-1}k^{-1}}{\beta}\right)\left(\int_{\mathscr{D}}(f_\delta(x)-f(x))e_m(x)dx\right)^2\\
&\le\left(\frac{p-1}{p\beta-1}\right)^{2p-2/p}T^{2p\beta-2/p}\|\Phi_\delta(\theta)\|^2_{\mathscr{L}^p(0,T)}|\mathscr{B}_\delta|^{2n+N/p-N/2}\exp \cdot\left(\frac{2T^\beta|\mathscr{B}_\delta|^{s-1}k^{-1}}{\beta}\right)\times\sum_{\lambda_m\le\mathscr{B}_\delta}\lambda_m^{2n+N/p-N/2}\left(\int_{\mathscr{D}}(f_\delta(x)-f(x))e_m(x)dx\right)^2\\
&\le\left(\frac{p-1}{p\beta-1}\right)^{2p-2/p}T^{2p\beta-2/p}\|\Phi_\delta(\theta)\|^2_{\mathscr{L}^p(0,T)}|\mathscr{B}_\delta|^{2n+N/p-N/2} \times\exp\left(\frac{2T^\beta|\mathscr{B}_\delta|^{s-1}k^{-1}}{\beta}\right)\|f_\delta-f\|_{\mathscr{X}^{Np-2N/4p}(\Omega)}.
\end{aligned} \tag{56}$$

where $s>1/\beta$. In view of Sobolev embedding $\mathscr{L}^p(\mathscr{D})^\circ\mathscr{X}^{(Np-2N)/4p}(\mathscr{D})$, we derive that the following estimate

$$\|\mathscr{J}_2(.,t)\|_{\mathscr{X}^n(\mathscr{D})}\le C_6(p,\beta,T,N)\|\Phi_\delta\|_{\mathscr{L}^p(0,T)}|\mathscr{B}_\delta|^{n+N/2p-N/4}\exp \cdot\left(\frac{T^\beta|\mathscr{B}_\delta|^{s-1}k^{-1}}{\beta}\right)\delta, \tag{57}$$

where

$$C_6(p,\beta,T,N)=\left(\frac{p-1}{p\beta-1}\right)^{p-1/p}T^{p\beta-1/p}C_5(N,p). \tag{58}$$

Step 3: Let us now to consider the term $\|\mathcal{J}_3(.,t)\|_{\mathcal{X}^n(\mathcal{D})}$. By applying Hölder's inequality, we get that for $p>1$ and $p^*=1/(p-1)\cdot$

$$\begin{aligned}&\left|\int_t^T \theta^{\beta-1}\exp\left(\frac{\lambda_m^s}{1+k\lambda_m}\frac{\nu^\beta-t^\beta}{\beta}\right)(\Phi(\theta)-\Phi_\delta(\theta))d\theta\right|\\&\le\left(\int_0^T|\Phi(\theta)-\Phi_\delta(\theta)|^s d\nu\right)^{1/p}\\&\quad\cdot\left(\int_t^T\theta^{p^*(\beta-1)}\exp\left(p^*\frac{\lambda_m^s}{1+k\lambda_m}\frac{\theta^\beta-t^\beta}{\beta}\right)d\nu\right)^{1/p^*}\\&\le\exp\left(\frac{\lambda_m^{s-1}k^{-1}T^\beta}{\beta}\right)\|\Phi_\delta-\Phi\|_{\mathcal{L}^p(0,T)}\left(\int_t^T\nu^{s^*(\beta-1)}d\nu\right)^{1/p^*}\\&\le\left(\frac{p-1}{p\beta-1}\right)^{p-1/p}T^{p\beta-1/p}\exp\left(\frac{T^\beta\lambda_m^{s-1}k^{-1}}{\beta}\right)\|\Phi-\Phi_\delta\|_{\mathcal{L}^p(0,T)}\\&\le\left(\frac{p-1}{p\beta-1}\right)^{p-1/p}T^{p\beta-1/p}\exp\left(\frac{T^\beta\lambda_m^{s-1}k^{-1}}{\beta}\right)\delta.\end{aligned}\tag{59}$$

This inequality together with Parseval's equality allows us to derive that

$$\begin{aligned}&\|\mathcal{J}_3(.,t)\|^2_{\mathcal{X}^n(\mathcal{D})}\\&=\sum_{\lambda_m\le\mathcal{B}_\delta}\lambda_m^{2n}\left(\int_t^T\theta^{\beta-1}\exp\left(\frac{\lambda_m^s}{1+k\lambda_m}\frac{\theta^\beta-t^\beta}{\beta}\right)(\Phi(\theta)-\Phi_\delta(\theta))d\theta\right)^2\\&\quad\cdot\left(\int_{\mathcal{D}}f(x)e_m(x)dx\right)^2\\&\le\left(\frac{p-1}{p\beta-1}\right)^{2p-2/p}T^{2p\beta-2/p}\delta^2\sum_{\lambda_m\le\mathcal{B}_\delta}\lambda_m^{2n+N/p-N/2}\lambda_m^{Np-2N/2p}\exp\\&\quad\cdot\left(\frac{2\lambda_m^{s-1}k^{-1}T^\beta}{\beta}\right)\left(\int_{\mathcal{D}}f(x)e_m(x)dx\right)^2\\&\le\left(\frac{p-1}{p\beta-1}\right)^{2p-2/p}T^{2p\beta-2/p}\delta^2|\mathcal{B}_\delta|^{2n+N/p-N/2}\exp\\&\quad\cdot\left(\frac{2T^\beta|\mathcal{B}_\delta|^{s-1}k^{-1}}{\beta}\right)\|f\|_{\mathcal{X}^{Np-2N/4p}(\Omega)}.\end{aligned}\tag{60}$$

By the fact that $\mathcal{L}^p(\mathcal{D})^\circ\mathcal{X}^{(Np-2N)/4p}(\mathcal{D})$, we deduce that

$$\begin{aligned}\|\mathcal{J}_3(.,t)\|_{\mathcal{X}^n(\mathcal{D})}&\le C_6(p,\beta,T,N)\|f\|_{\mathcal{L}^p(D)}|\mathcal{B}_\delta|^{n+N/2p-N/4}\exp\\&\quad\cdot\left(\frac{T^\beta|\mathcal{B}_\delta|^{s-1}k^{-1}}{\beta}\right)\delta.\end{aligned}\tag{61}$$

Combining Step 1 to Step 3, we get

$$\begin{aligned}&\|\mathcal{J}_1(.,t)\|_{\mathcal{X}^n(\mathcal{D})}+\|\mathcal{J}_2(.,t)\|_{\mathcal{X}^n(\mathcal{D})}+\|\mathcal{J}_3(.,t)\|_{\mathcal{X}^n(\mathcal{D})}\\&\quad\le C_4(N,p)|\mathcal{B}_\delta|^{n+N/2p-N/4}\exp\left(\frac{|\mathcal{B}_\delta|^{s-1}k^{-1}T^\beta}{\beta}\right)\delta\\&\qquad+C_6(p,\beta,T,N)|\mathcal{B}_\delta|^{n+N/2p-N/4}\exp\left(\frac{T^\beta|\mathcal{B}_\delta|^{s-1}k^{-1}}{\beta}\right)\delta\\&\qquad\cdot\left(\|\Phi_\delta\|_{\mathcal{L}^p(0,T)}+\|f\|_{\mathcal{L}^p(D)}\right).\end{aligned}\tag{62}$$

Finally, combining the reviews from above, we conclude that

$$\begin{aligned}&\|\mathcal{W}_\delta(\cdot,t)-y(\cdot,t)\|_{\mathcal{X}^n(\mathcal{D})}\\&\quad\le\delta|\mathcal{B}_\delta|^{-\sigma}\|u\|_{\mathcal{L}^\infty(0,T;\mathcal{X}^{n+\sigma}(\mathcal{D}))}\\&\qquad+C_4(N,p)|\mathcal{B}_\delta|^{n+N/2p-N/4}\exp\left(\mathcal{B}_\delta^{s-1}k^{-1}\frac{T^\beta}{\beta}\right)\delta\\&\qquad+C_6(p,\beta,T,N)|\mathcal{B}_\delta|^{n+N/2p-N/4}\exp\\&\qquad\cdot\left(\frac{T^\beta|\mathcal{B}_\delta|^{s-1}k^{-1}}{\beta}\right)\delta\left(\|\Phi_\delta\|_{\mathcal{L}^p(0,T)}+\|f\|_{\mathcal{L}^p(D)}\right).\end{aligned}\tag{63}$$

□

Data Availability

No data were used to support this study.

Conflicts of Interest

The authors declare that they have no competing interests. The corresponding author is a full-time member of the School of Mathematics, Iran University of Science and Technology, Narmak, Tehran, Iran

Authors' Contributions

All authors conceived of the study, participated in its design and coordination, drafted the manuscript, participated in the sequence alignment, and read and approved the final manuscript.

Acknowledgments

The author Le Dinh Long is supported by Van Lang University.

References

[1] F. M. Alharbia, D. Baleanu, and A. Ebaid, "Physical properties of the projectile motion using the conformable derivative," *Chinese Journal of Physics*, vol. 58, pp. 18–28, 2019.

[2] A. A. Kilbas, O. I. Marichev, and S. G. Samko, *Fractional Integrals and Derivatives (Theory and Applications)*, 1993.

[3] N. H. Tuan, Y. E. Aghdam, H. Jafari, and H. Mesgarani, "A novel numerical manner for two-dimensional space fractional diffusion equation arising in transport phenomena,"

Numerical Methods for Partial Differential Equations, vol. 37, no. 2, pp. 1397–1406, 2021.

[4] E. Karapinar, H. D. Binh, N. H. Luc, and N. H. Can, "On continuity of the fractional derivative of the time-fractional semilinear pseudo-parabolic systems," *Adv. Difference Equ.*, vol. 2021, no. 1, article 70, 2021.

[5] R. S. Adigüzel, Ü. Aksoy, E. Karapinar, and İ. M. Erhan, "On the solution of a boundary value problem associated with a fractional differential equation," *Mathematical Methods in the Applied Sciences*, 2020.

[6] R. Sevinik-Adıgüzel, Ü. Aksoy, E. Karapınar, and İ. M. Erhan, "Uniqueness of solution for higher-order nonlinear fractional differential equations with multi-point and integral boundary conditions," *Revista de la Real Academia de Ciencias Exactas, Físicas y Naturales. Serie A. Matemáticas*, vol. 115, no. 3, article 155, 2021.

[7] R. S. Adiguzel, U. Aksoy, E. Karapinar, and I. M. Erhan, "On the solutions of fractional differential equations via Geraghty type hybrid contractions," *Applied and Computational Mathematics*, vol. 20, no. 2, pp. 313–333, 2021.

[8] N. D. Phuong, "Note on a Allen-Cahn equation with Caputo-Fabrizio derivative," *Results in Nonlinear Analysis*, vol. 4, no. 3, pp. 179–185, 2021.

[9] R. Khalil, M. Al Horani, A. Yousef, and M. Sababheh, "A new definition of fractional derivative," *Journal of Computational and Applied Mathematics*, vol. 264, pp. 65–70, 2014.

[10] T. Abdeljawad, "On conformable fractional calculus," *Journal of Computational and Applied Mathematics*, vol. 279, pp. 57–66, 2015.

[11] A. Jaiswal and D. Bahuguna, "Semilinear conformable fractional differential equations in Banach spaces," *Differential Equations and Dynamical Systems*, vol. 27, no. 1-3, pp. 313–325, 2019.

[12] O. Acan, M. M. Al Qurashi, and D. Baleanu, "New exact solution of generalized biological population model," *The Journal of Nonlinear Sciences and Applications*, vol. 10, no. 7, pp. 3916–3929, 2017.

[13] M. Bouaouid, K. Hilal, and S. Melliani, "Nonlocal telegraph equation in frame of the conformable time-fractional derivative," *Advances in Mathematical Physics*, vol. 2019, Article ID 7528937, 7 pages, 2019.

[14] H. T. Nguyen, D. L. Le, and V. T. Nguyen, "Regularized solution of an inverse source problem for a time fractional diffusion equation," *Applied Mathematical Modelling*, vol. 40, no. 19-20, pp. 8244–8264, 2016.

[15] A. Qian and Y. Li, "Optimal error bound and generalized Tikhonov regularization for identifying an unknown source in the heat equation," *Journal of Mathematical Chemistry*, vol. 49, no. 3, pp. 765–775, 2011.

[16] S. Yang, X. Xiong, and Y. Nie, "Iterated fractional Tikhonov regularization method for solving the spherically symmetric backward time-fractional diffusion equation," *Applied Numerical Mathematics*, vol. 160, pp. 217–241, 2021.

[17] F. Yang, J.-L. Fu, P. Fan, and X.-X. Li, "Fractional Landweber iterative regularization method for identifying the unknown source of the time-fractional diffusion problem," *Acta Applicandae Mathematicae*, vol. 175, no. 1, p. 13, 2021.

[18] N. D. Phuong, N. H. Luc, and L. D. Long, "Modified quasi boundary value method for inverse source problem of the biparabolic equation," *Advances in Theory of Nonlinear Analysis and its Applications*, vol. 4, no. 3, pp. 132–142, 2020.

[19] T. Wei and J. Wang, "A modified quasi-boundary value method for an inverse source problem of the time-fractional diffusion equation," *Applied Numerical Mathematics*, vol. 78, pp. 95–111, 2014.

[20] F. Yang, P. Zhang, and X.-X. Li, "The truncation method for the Cauchy problem of the inhomogeneous Helmholtz equation," *Applicable Analysis*, vol. 98, no. 5, pp. 991–1004, 2019.

[21] N. H. Tuan, "On some inverse problem for bi-parabolic equation with observed data in L^p spaces," *Opuscula Mathematica*, vol. 42, no. 2, pp. 305–335, 2022.

[22] N. H. Tuan and T. Caraballo, "On initial and terminal value problems for fractional nonclassical diffusion equations," *Proceedings of the American Mathematical Society*, vol. 149, no. 1, pp. 143–161, 2021.

[23] N. H. Tuan, T. B. Ngoc, D. Baleanu, and D. O'Regan, "On well-posedness of the sub-diffusion equation with conformable derivative model," *Communications in Nonlinear Science and Numerical Simulation*, vol. 89, article 105332, 2020.

Hindawi
Journal of Function Spaces
Volume 2022, Article ID 6890517, 12 pages
https://doi.org/10.1155/2022/6890517

Research Article

A New Modified Technique of Adomian Decomposition Method for Fractional Diffusion Equations with Initial-Boundary Conditions

Saadia Masood,[1] **Hajira**,[2] **Hassan Khan**,[2,3] **Rasool Shah**,[2] **Saima Mustafa**,[1] **Qasim Khan**,[2,4] **Muhammad Arif**,[2] **Fairouz Tchier**,[5] **and Gurpreet Singh**[6]

[1]*Department of Mathematics, Pir Mehr Ali Shah Arid Agriculture University, Rawalpindi, Pakistan 46000*
[2]*Department of Mathematics, Abdul Wali Khan University Mardan, Pakistan*
[3]*Department of Mathematics, Near East University TRNC, Mersin 10, Turkey*
[4]*Department of Mathematics and Information Technology, The Education University of Hong Kong, 10 Lo Ping Road, Tai Po, New Territories, Hong Kong*
[5]*Department of Mathematics, College of Science, King Saud University, P.O. Box 2455, Riyadh 11451, Saudi Arabia*
[6]*School of Mathematical Sciences, Dublin City University, Ireland*

Correspondence should be addressed to Hassan Khan; hassanmath@awkum.edu.pk
and Qasim Khan; qasim.khan@awkum.edu.pk

Received 7 April 2022; Accepted 25 May 2022; Published 5 August 2022

Academic Editor: Yusuf Gurefe

In general, solving fractional partial differential equations either numerically or analytically is a difficult task. However, mathematicians have tried their best to make the task easy and promoted various techniques for their solutions. In this regard, a very prominent and accurate technique, which is known as the new technique of the Adomian decomposition method, is developed and presented for the solution of the initial-boundary value problem of the diffusion equation with fractional view analysis. The suggested model is an important mathematical model to study the behavior of degrees of memory in diffusing materials. Some important results for the given model at different fractional orders of the derivatives are achieved. Graphs show the obtained results to confirm the accuracy and validity of the suggested technique. These results are in good contact with the physical dynamics of the targeted problems. The obtained results for both fractional and integer orders problems are explained through graphs and tables. Tables and graphs support the physical behavior of each problem and the best of physical analysis. From the results, it is concluded that as the fractional order derivative is changed, the graphs or paths of dynamics are also changed. Therefore, we now choose the best solution or dynamic of the problem at a particular derivative order. It is analyzed that the present technique is one of the best techniques to handle the solutions of fractional partial differential equations having initial and boundary conditions (BCs), which are very rare in literature. Furthermore, a small number of calculations are done to achieve a very high rate of convergence, which is the novelty of the present research work. The proposed method provides the series solution with twice recursive formulae to increase the desired accuracy and is preferred among the best techniques to find the solution of fractional partial differential equations with mixed initials and BCs.

1. Introduction

Fractional Calculus (FC) is the study of derivatives and integration of fractional orders. The idea was first initiated by L'Hospital, who wrote a letter to Leibniz about the noninteger order of derivatives in 1665. After that, the devoted work done by Euler, Lagrange, Abel, and Liouville gives more extension to the field, which is very popular nowadays because of its essential applications in the areas of biology, physics, fluid mechanics, and other sciences [1–3].

Fractional-order differential equations (FPDEs) have a great contribution in the modeling of a variety of complex natural and nonlinear phenomena. FPDEs have made a significant contribution to various scientific research fields, including a diverse range of processes and systems, memories, and various branches of mathematics. The modeling of FPDEs, whether they are with respect to time or space, is more convergent, and many natural phenomena are accurately described by them. The researchers in the fields of anomalous diffusion, dielectric polarization, control theory, and other problems of physical phenomena are interested in FPDEs [4–10]. Since the fractional order of the derivative works more accurately than integer order in describing the properties related to hereditary and where the future state is influenced by the past state, FPDEs give the highest contribution to explaining such types of systems. Psychology, biology, acoustics, chemistry [11], physics, colored noises [12], and continuum mechanics [13] are some of the scientific phenomena and problems that FPDEs are used to model. Special applications of FPDEs can be found in various branches of physics and hydrology, including [14–22]. FPDEs have grown in popularity because, by definition, the fractional derivative is global, whereas the integer order derivative is local [23–25].

In recent years, the development of numerical and analytical methodologies for the solution of FPDEs is a hot topic among the researchers. Obtaining numerical or analytical solutions to FPDEs is never a simple task for mathematicians. Many researchers, on the other hand, have devised a number of novel techniques for dealing with FPDE solutions. Some of the important techniques include the Haar wavelet method (HWM) [26], the Laplace transform method [27], the Elzaki transform decomposition method (ETDM) [28], the Adomian decomposition method (ADM) [29], the finite difference technique [30, 31], the natural transform decomposition approach [32], the Legendre base method [33], the homotopy analysis method [34], the differential transform method [35], the variational iteration approach [36], and the Bernstein polynomial [37].

Many researchers have studied the time-fractional diffusion equations (TFDEs) because of their various applications in science and engineering and other branches of applied sciences. TFDEs are broadly found in physical, biological, and engineering processes [38–41]. The TFDEs are used by Nigmatulin [39] to describe diffusion in media with spectral geometry. The TFDEs are being investigated by many researchers, both analytically and numerically [42, 43]. The solution method of the Laplace transform and a similar method is used to obtain the invariant solution of TFDEs by Gorenlfo et al. [44, 45], and Lin and Zu applied a finite difference scheme in the Legendre spectral method and in space for TFDEs [46]. Dhaigude and Nikam [13] and Schneider and Wyss [43] worked on TFDEs and wave equations to obtain the solution. Moreover, the existence and uniqueness of the targeted problems are shown in [47]. Here, the researchers either used only one from initial boundary conditions (IBCs) to solve the problems. In the current research article, a modified method of ADM is implemented to solve TFDEs with both IBCs suggested by Ali in [48]. The same procedure is applied to the problems of having both initial and BCs in [49] with the homotopy perturbation method, and the results are excellent. Ali applied this new technique in [50] with a variational iteration method to initial-boundary value problems. The procedure becomes accurate because there is a new initial approximate solution with each new iteration. For justification, some examples are discussed in this paper.

ADM was first introduced by Adomian [51] in the 1980s, and it was observed that the technique is beneficial for nonlinear equations. Wazwaz [52] applied the same method to solve different kinds of differential equations. Niu and Wang [53] used the decomposition method to find the solution of fractional heat-like and wave-like equations. Niu and Wang [53] applied this method to boundary value problems to calculate a one-step optimal homotopy analysis method. Pandir and Yildirim used the homotopy perturbation method and ADM in conformable sense [54]. The mathematicians have made several modifications to ADM which have improved the accuracy of the technique, and some of them are [55–57]. Here, a modified technique is implemented to solve the initial and boundary value problems (IBVPs) of TFDEs. In the literature, various authors have used numerical and analytical techniques for the solution of the initial value problems of FPDEs and their systems. However, only a few attempts were made to solve IBVPs of FPDEs and their systems. In this regard, Elaf Jaafar Ali has made a contribution and developed a new technique to solve FPDEs. He modified the existing techniques of ADM to solve IBVPs of FPDEs.

In this paper, we will work on the solution of TFDEs by using a new technique of the Adomian decomposition method (ADM). In literature, some important numerical and analytical techniques have been used for the solutions of time and space fractional diffusion equations [25, 54]. In this article, the work of Elaf Jafaar Ali is further extended to solve IBVPs of TFDEs. The general description of the proposed method is implemented to solve some examples of the suggested problems. The analytical solutions of FPDEs with initial and boundary conditions are very difficult to investigate. In the current work, the analytical solutions of TFDEs are obtained in a very simple and straightforward procedure and provide the closed-form solutions. The less computational work and simplicity are the uniqueness of the present modified technique. The obtained results are displayed through graphs. The graphical representations have shown that there is a close contact between the exact and the approximate solutions of the problems. The solutions are obtained for various fractional-order problems. The fractional order solutions provide useful information about the dynamics of the suggested problems. It is observed that the proposed technique has a very effective procedure for solving FPDEs and their systems with IBCs. However, some limitations are observed while using the present technique, that is, if the FPDEs or their systems have a higher number of IBCs, then the proposed method required a large number of calculations to achieve the results. Mostly, the suggested methods have smaller accuracy at a greater time value and their accuracy increased at a smaller time value. For higher nonlinear problems, the solution components are not easy to compute, so very few terms are calculated to achieve the required solution.

2. Preliminaries

Some definitions that are related to our study are considered in this section.

2.1. Definition. The integral operator of Reimann-Liouville having order δ is given by [40]

$$\left(I_{\sigma}^{\delta}h\right)(\sigma)=\begin{cases}\dfrac{1}{\Gamma(\delta)}\displaystyle\int_0^{\tau}(\sigma-\nu)^{\delta-1}d\nu, & \delta>0,\\ h(\sigma), & \delta=0,\end{cases} \tag{1}$$

where Γ is the gamma function and can be written as

$$\Gamma(\omega)=\int_0^{\infty}e^{-\sigma}\sigma^{\omega-1}d\tau, \quad \omega\in\mathbb{C}. \tag{2}$$

2.2. Definition. The expression for Caputo for fractional order δ is as follows:

$$\left(D^{\delta}h\right)(\sigma)=\frac{\partial^{\delta}h(\sigma)}{\partial\tau^{\delta}}=\begin{cases}I^{m-\delta}\left[\dfrac{\partial^{\delta}h(\sigma)}{\partial\tau^{\delta}}\right], & m-1<\delta\le m, m\in\mathbb{N},\\ \dfrac{\partial^{\delta}h(\sigma)}{\partial\tau^{\delta}}, & \end{cases} \tag{3}$$

where $m\in\mathbb{N}$, $\sigma>0$, $g\in\mathbb{C}_{\tau}$, and $\tau\ge1$.

2.3. Lemma. For $j-1<\delta\le j$ with $j\in\mathbb{N}$ and $h\in\mathbb{C}_{\tau}$ with $\tau\ge-1$, then [58]

$$\begin{cases}I^{\delta}I^{b}=I^{\delta+b}h(\sigma), & b,\delta\ge0,\\ I^{\delta}\sigma^{\lambda}=\dfrac{\Gamma(\lambda+1)}{\Gamma(\delta+\lambda+1)}\sigma^{\delta+\lambda}, & \delta>0,\lambda>-1,\sigma>0,\\ I^{\delta}D^{\delta}h(\sigma)=h(\sigma)-\displaystyle\sum_{k=0}^{j-1}h^{k}(0^{+})\frac{\sigma^{k}}{k!}, & \end{cases} \tag{4}$$

where $\sigma>0$, $j-1<\delta\le j$.

2.4. Definition. The Mittag-Leffler function $E_{\delta}(\rho)$ for $\delta>0$ is

$$E_{\delta}(\rho)=\sum_{m=0}^{\infty}\left(\frac{\rho^{m}}{\Gamma(m\delta+1)}\right), \quad \delta>0,\rho\in\mathbb{C}. \tag{5}$$

3. Adomian Decomposition Method

This method was discovered by Adomian in 1994 for the solution of linear and nonlinear differential and integrodifferential equations [29]. To understand the method, let us consider an equation of the following form:

$$F(\vartheta(\sigma))=g(\sigma), \tag{6}$$

where F is a nonlinear differential operator and g is the known function. We will split the linear term in $F(\vartheta(\sigma))$ into the form $\mathscr{L}\vartheta+R\vartheta$, where $\mathscr{L}$ is the invertible operator, chosen as the highest order derivative, R represents the linear operator, and then, Equation (6) has the representation as follows:

$$\mathfrak{R}\vartheta+R\vartheta+N\vartheta=g, \tag{7}$$

where $N\vartheta$ is the nonlinear term of $F(\vartheta(\sigma))$. Apply $\mathfrak{R}^{-1}$ to Equation (7) on both sides.

$$\vartheta=\varphi+\mathfrak{R}^{-1}(g)-\mathfrak{R}^{-1}(R\vartheta)-\mathfrak{R}^{-1}(N\vartheta), \tag{8}$$

where the constant of integration is φ, and $\mathfrak{R}\varphi=0$.

The following infinite series shows the solution of ADM as

$$\vartheta=\sum_{n=0}^{\infty}\zeta_n. \tag{9}$$

The $N\vartheta$ is a nonlinear term represented by A_n, defined as follows:

$$N\vartheta=\sum_{n=0}^{\infty}A_n. \tag{10}$$

Using the following to calculate A_n,

$$A_n=\frac{1}{n!}\frac{d^n}{d\psi^n}N\left(\sum_{k=0}^{\infty}\left(\psi^k\upsilon_k\right)\right), \quad n=0,1,\cdots. \tag{11}$$

Equation (6) has a solution in the form of a series as follows:

$$\begin{cases}\vartheta_0=\varphi+\mathfrak{R}^{-1}(g), & n=0,\\ \vartheta_{n+1}=\mathfrak{R}^{-1}(R\vartheta_n)-\mathfrak{R}^{-1}(A_n), & n\ge0.\end{cases} \tag{12}$$

4. Modification of ADM

To understand the main idea of the proposed technique, we will take the following one-dimensional equation [48]:

$$D_{\tau}^{\delta}(\vartheta(\sigma,\tau))=\frac{\partial^2\vartheta(\sigma,\tau)}{\partial\sigma^2}+w(\sigma,\tau), \quad 0<\sigma<1,\tau>0,0<\delta<1, \tag{13}$$

having the IBCs as follows:

$$\begin{cases}\vartheta(\sigma,\tau)=\ell_0(\sigma), & \dfrac{\partial\vartheta(\sigma,0)}{\partial\tau}=\ell_1(\sigma), \quad 0\le\sigma\le1,\\ \vartheta(0,\tau)=\hbar_0(\tau), & \vartheta(1,\tau)=\hbar_1(\tau), \quad \tau>0.\end{cases} \tag{14}$$

The source term is represented by $w(\sigma,\tau)$.

The new initial solution (ϑ_n^*) calculated for Equation (13) can be written in operator form as

$$\vartheta_n^* = \vartheta_n(\sigma,\tau) + (1-\sigma)[\hbar_0(\tau) - \vartheta_n(0,\tau)] + \sigma[\hbar_1(\tau) - \vartheta_n(1,\tau)]. \tag{15}$$

In operator form, Equation (13) can be written as

$$\mathfrak{R}\vartheta = \frac{\partial^2\vartheta(\sigma,\tau)}{\partial\sigma^2} + w(\sigma,\tau). \tag{16}$$

$\mathfrak{R}$ is

$$\mathfrak{R} = \frac{\partial^\delta}{\partial\tau^\delta}, \tag{17}$$

so $\mathfrak{R}^{-1}$ is

$$\mathfrak{R}^{-1}(.) = I^\delta(.)d\tau. \tag{18}$$

Applying $\mathfrak{R}^{-1}$ to Equation (16), we obtained

$$\vartheta(\sigma,\tau) = \vartheta(\sigma,0) + \mathfrak{R}^{-1}\left(\frac{\partial^2\vartheta(\sigma,\tau)}{\partial\sigma^2} + w(\sigma,\tau)\right), \tag{19}$$

where $n = 0, 1, \cdots$.

The initial approximation can be written as

$$\vartheta_0(\sigma,\tau) = \vartheta(\sigma,0) + \mathfrak{R}^{-1}(w(\sigma,\tau)), \tag{20}$$

and hence, the iteration formula is

$$\vartheta_{n+1}(\sigma,\tau) = \mathfrak{R}^{-1}\left(\frac{\partial^2\vartheta_*(\sigma,\tau)}{\partial\sigma^2}\right). \tag{21}$$

The initial solutions u_n^* of Equation (13) satisfied both the IBCs, as given in the following:

$$\begin{aligned} at \quad \tau = 0, \quad & \vartheta_n^*(\sigma,0) = \vartheta_n(\sigma,0), \\ \sigma = 0, \quad & \vartheta_n^*(0,\tau) = \hbar_0(\tau), \\ \sigma = 1, \quad & \vartheta_n^*(1,\tau) = \hbar_1(\tau). \end{aligned} \tag{22}$$

The proposed technique works effectively for two-dimensional problems.

5. Numerical Results

In this section, some illustrative examples are solved by the new technique of ADM.

5.1. Example. Consider TFDE of the following form [59]:

$$\begin{aligned} \frac{\partial^\delta\vartheta(\sigma,\tau)}{\partial\tau^\delta} = \frac{\partial^2\vartheta(\sigma,\tau)}{\partial\sigma^2} + \frac{\Gamma(4+\delta)}{6}\sigma^4(2-\sigma)\tau^3 \\ - 4\sigma^2(6-5\sigma)\tau^{3+\sigma}, \quad 0 \le \sigma \le 2, 0 < \delta \le 1, \end{aligned} \tag{23}$$

having the IBCs as follows:

$$\begin{aligned} \vartheta(\sigma,0) = 0, \\ \vartheta(0,\tau) = \vartheta(2,\tau) = 0. \end{aligned} \tag{24}$$

The problem has the analytical solution at $\delta = 1$ as follows:

$$\vartheta(\sigma,\tau) = \sigma^4(2-\sigma)\tau^{3+\delta}. \tag{25}$$

Applying the suggested method of ADM to Equation (23), we have

$$\vartheta_n^*(\sigma,\tau) = \vartheta_n(\sigma,\tau) + (1-\sigma)[0 - \vartheta_n(0,\tau)] + \sigma[0 - \vartheta_n(2,\tau)], \tag{26}$$

where $n = 0, 1, \cdots$.

Applying $\mathfrak{R}$ to Equation (23), we have

$$\mathfrak{R}\vartheta = \frac{\partial^2\vartheta(\sigma,\tau)}{\partial\sigma^2} + \frac{\Gamma(4+\delta)}{6}\sigma^4(2-\sigma)\tau^3 - 4\sigma^2(6-5\sigma)\tau^{3+\sigma}, \tag{27}$$

where $\mathfrak{R} = \partial^\delta/\partial\tau^\delta$ and $\mathfrak{R}^{-1}$ is

$$\mathfrak{R}^{-1}(.) = I^\delta(.)d\tau. \tag{28}$$

Operating Equation (23) by mathcal$\mathfrak{R}^{-1}$, we have

$$\begin{aligned} \vartheta(\sigma,\tau) = u(\sigma,0) + \mathfrak{R}^{-1} \\ \cdot\left(\frac{\partial^2\vartheta(\sigma,\tau)}{\partial\sigma^2} + \frac{\Gamma(4+\delta)}{6}\sigma^4(2-\sigma)\tau^3 - 4\sigma^2(6-5\sigma)\tau^{3+\sigma}\right). \end{aligned} \tag{29}$$

Using ADM solution, the initial approximation becomes

$$\begin{aligned} \vartheta_0(\sigma,\tau) &= \vartheta(\sigma,0) + \mathfrak{R}^{-1}\left(\frac{\Gamma(4+\delta)}{6}\sigma^4(2-\sigma)\tau^3 - 4\sigma^2(6-5\sigma)\tau^{3+\sigma}\right) \\ &= 0 + \frac{\Gamma(4+\delta)\Gamma(4)\sigma^4(2-\sigma)\tau^{3+\delta}}{6\Gamma(4+\delta)} - \frac{4\sigma^2(6-5\sigma)\Gamma(4+\delta)\tau^{3+2\delta}}{\Gamma(4+2\delta)} \\ &= \sigma^4(2-\sigma)\tau^{3+\delta} - \frac{(24\sigma^2+20\sigma^3)\Gamma(4+\delta)\tau^{3+2\delta}}{\Gamma(4+2\delta)}, \end{aligned}$$

$$\vartheta_0(\sigma,\tau) = \sigma^4(2-\sigma)\tau^{3+\delta} - \frac{24\sigma^2\Gamma(4+\delta)\tau^{3+2\delta}}{\Gamma(4+2\delta)} + \frac{20\sigma^3\Gamma(4+\delta)\tau^{3+2\delta}}{\Gamma(4+2\delta)}. \tag{30}$$

With the help of initial approximation ϑ_n^*, the formula for iterations is

$$\vartheta_{n+1}(\sigma,\tau)=\mathfrak{R}^{-1}\left(\frac{\partial^2\vartheta_n^*}{\partial\sigma^2}\right). \tag{31}$$

Use the IBCs in Equation (26), for $n=0$:

$$\begin{aligned}\vartheta_0^*(\sigma,\tau)&=\vartheta_0(\sigma,\tau)+(1-\sigma)[0-\vartheta_0(0,\tau)]+\sigma[0-\vartheta_0(2,\tau)]\\&=\sigma^4(2-\sigma)\tau^{3+\delta}-\frac{24\sigma^2\Gamma(4+\delta)\tau^{3+2\delta}}{\Gamma(4+2\delta)}+\frac{20\sigma^3\Gamma(4+\delta)\tau^{3+2\delta}}{\Gamma(4+2\delta)}\\&=\sigma^4(2-\sigma)\tau^{3+\delta}-\frac{\left(24\sigma^2+20\sigma^3\right)\Gamma(4+\delta)\tau^{3+2\delta}}{\Gamma(4+2\delta)}\\&\quad+(1-\sigma)[0-0]+\sigma\left[0-\left(0-\frac{-16\Gamma(4+\delta)\tau^{3+2\delta}}{\Gamma(4+2\delta)}\right)\right],\end{aligned}$$

$$\begin{aligned}\vartheta_0^*(\sigma,\tau)&=\sigma^4(2-\sigma)\tau^{3+\delta}-\frac{24\sigma^2\Gamma(4+\delta)\tau^{3+2\delta}}{\Gamma(4+2\delta)}\\&\quad+\frac{20\sigma^3\Gamma(4+\delta)\tau^{3+2\delta}}{\Gamma(4+2\delta)}-\frac{16\sigma\Gamma(4+\delta)\tau^{3+2\delta}}{\Gamma(4+2\delta)}.\end{aligned} \tag{32}$$

From Equation (31), we have

$$\begin{aligned}\vartheta_1(\sigma,\tau)&=\mathfrak{R}^{-1}\left(\frac{\partial_\vartheta^2 0^*}{\partial\sigma^2}\right)\\&=\mathfrak{R}^{-1}\left(\left(24\sigma^2-20\sigma^3\right)\tau^{3+\delta}-\frac{48-120\sigma\Gamma(4+\delta)\tau^{3+2\delta}}{\Gamma(4+2\delta)}\right),\end{aligned}$$

$$\begin{aligned}\vartheta_1(\sigma,\tau)&=\frac{24\sigma^2\Gamma(4+\delta)\tau^{3+2\delta}}{\Gamma(4+2\delta)}-\frac{20\sigma^3\Gamma(4+\delta)\tau^{3+2\delta}}{\Gamma(4+2\delta)}\\&\quad-\frac{48\Gamma(4+\delta)\tau^{3+3\delta}}{\Gamma(4+3\delta)}+\frac{120\sigma\Gamma(4+\delta)\tau^{3+3\delta}}{\Gamma(4+3\delta)}.\end{aligned} \tag{33}$$

For $n=1$, Equation (26) becomes

$$\begin{aligned}\vartheta_1^*(\sigma,\tau)&=\vartheta_1(\sigma,\tau)+(1-\sigma)[0-\vartheta_1(0,\tau)]+\sigma[0-\vartheta_1(2,\tau)]\\&=\frac{24\sigma^2\Gamma(4+\delta)\tau^{3+2\delta}}{\Gamma(4+2\delta)}-\frac{20\sigma^3\Gamma(4+\delta)\tau^{3+2\delta}}{\Gamma(4+2\delta)}\\&\quad-\frac{48\Gamma(4+\delta)\tau^{3+3\delta}}{\Gamma(4+3\delta)}+\frac{120\sigma\Gamma(4+\delta)\tau^{3+3\delta}}{\Gamma(4+3\delta)}(1-\sigma)\\&\quad\cdot\left[0+\frac{48\Gamma(4+\delta)\tau^{3+3\delta}}{\Gamma(4+3\delta)}\right]\\&\quad+\sigma\left[0+\frac{64\Gamma(4+\delta)\tau^{3+2\delta}}{\Gamma(4+3\delta)}-\frac{192\Gamma(4+\delta)\tau^{3+3\delta}}{\Gamma(4+3\delta)}\right],\end{aligned}$$

$$\begin{aligned}\vartheta_1^*(\sigma,\tau)&=\frac{24\sigma^2\Gamma(4+\delta)\tau^{3+2\delta}}{\Gamma(4+2\delta)}-\frac{20\sigma^3\Gamma(4+\delta)\tau^{3+2\delta}}{\Gamma(4+2\delta)}\\&\quad-\frac{120\sigma\Gamma(4+\delta)\tau^{3+3\delta}}{\Gamma(4+3\delta)}+\frac{64\sigma\Gamma(4+\delta)\tau^{3+2\delta}}{\Gamma(4+2\delta)}.\end{aligned} \tag{34}$$

From Equation (31), we have

$$\begin{aligned}\vartheta_2(\sigma,\tau)&=L^{-1}\left(\frac{\partial^2\vartheta_1^*}{\partial\sigma^2}\right)\\&=L^{-1}\left(\frac{48\Gamma(4+\delta)tau^{3+2\delta}}{\Gamma(4+2\delta)}-\frac{120\sigma\Gamma(4+\delta)\tau^{3+2\delta}}{\Gamma(4+2\delta)}\right),\end{aligned}$$

$$\vartheta_2(\sigma,\tau)=\frac{48\Gamma(4+\delta)\tau^{3+3\delta}}{\Gamma(4+3\delta)}-\frac{120\sigma\Gamma(4+\delta)\tau^{3+3\delta}}{\Gamma(4+3\delta)}. \tag{35}$$

For $n=2$, Equation (26) becomes

$$\begin{aligned}\vartheta_2^*(\sigma,\tau)&=\vartheta_2(\sigma,\tau)+(1-\sigma)[0-\vartheta_2(0,\tau)]+\sigma[0-\vartheta_2(2,\tau)]\\&=\frac{(48-120\sigma)\Gamma(4+\delta)\tau^{3+3\delta}}{\Gamma(4+3\delta)}\\&\quad+(1-\sigma)[0-\vartheta_2(0,\tau)]+\sigma[0-\vartheta_2(2,\tau)],\\&=\frac{(48-120\sigma)\Gamma(4+\delta)\tau^{3+3\delta}}{\Gamma(4+3\delta)}\\&\quad+(1-\sigma)\left[0-\frac{48\Gamma(4+\delta)\tau^{3+3\delta}}{\Gamma(4+3\delta)}\right]\\&\quad+\sigma\left[0+\frac{192\Gamma(4+\delta)\tau^{3+3\delta}}{\Gamma(4+3\delta)}\right]\\&=\frac{-120\sigma\Gamma(4+\delta)\tau^{3+3\delta}}{\Gamma(4+3\delta)}+\frac{48\sigma\Gamma(4+\delta)\tau^{3+3\delta}}{\Gamma(4+3\delta)}\\&\quad+\frac{192\sigma\Gamma(4+\delta)\tau^{3+3\delta}}{\Gamma(4+3\delta)},\end{aligned}$$

$$\vartheta_2^*(\sigma,\tau)=\frac{120\sigma\Gamma(4+\delta)\tau^{3+3\delta}}{\Gamma(4+3\delta)}. \tag{36}$$

From Equation (31), we have

$$\begin{aligned}\vartheta_3(\sigma,\tau)&=L^{-1}\left(\frac{\partial^2\vartheta_2^*}{\partial\sigma^2}\right),\\&=\mathfrak{R}^{-1}(0)=0.\\&\vdots\end{aligned} \tag{37}$$

Thus, the series form of ADM solution is

$$\begin{aligned}\vartheta(\sigma,\tau)&=\vartheta_0(\sigma,\tau)+\vartheta_1(\sigma,\tau)+\vartheta_2(\sigma,\tau)+\vartheta_3(\sigma,\tau)+\cdots\\&=\sigma^4(2-\sigma)\tau^{3+\delta}-\frac{24\sigma^2\Gamma(4+\delta)\tau^{3+2\delta}}{\Gamma(4+2\delta)}\\&\quad+\frac{20\sigma^3\Gamma(4+\delta)\tau^{3+2\delta}}{\Gamma(4+2\delta)}+\frac{24\sigma^2\Gamma(4+\delta)\tau^{3+2\delta}}{\Gamma(4+2\delta)}\\&\quad-\frac{20\sigma^3\Gamma(4+\delta)\tau^{3+2\delta}}{\Gamma(4+2\delta)}-\frac{48\Gamma(4+\delta)\tau^{3+3\delta}}{\Gamma(4+3\delta)}\\&\quad+\frac{120\sigma\Gamma(4+\delta)\tau^{3+3\delta}}{\Gamma(4+3\delta)}+\frac{48\Gamma(4+\delta)\tau^{3+3\delta}}{\Gamma(4+3\delta)}\\&\quad-\frac{120\sigma\Gamma(4+\delta)\tau^{3+3\delta}}{\Gamma(4+3\delta)}+0+\cdots,\end{aligned}$$

$$\vartheta(\sigma,\tau)=\sigma^4(2-\sigma)\tau^{3+\delta}. \tag{38}$$

5.2. Example. Consider the TFDE of the following form [59]:

$$\frac{\partial^\delta \vartheta(\sigma,\tau)}{\partial \tau^\delta} = \frac{\partial^2 \vartheta(\sigma,\tau)}{\partial \sigma^2} + 3\frac{\Gamma(1/2)}{4}\tau\sigma^4(\sigma-1) - 4\sigma^2(5\sigma-3)\tau^{3/2}, \quad 0 \le \sigma \le 1, 0 < \delta \le 1, \tag{39}$$

having the IBCs as follows:

$$\vartheta(\sigma,0) = 0, \quad \vartheta(0,\tau) = \vartheta(1,\tau) = 0. \tag{40}$$

With analytical solution at $\delta = 1/2$ as follows:

$$\vartheta(\sigma,\tau) = \sigma^4(\sigma-1)\tau^{3/2}. \tag{41}$$

Apply the suggested method of ADM to Equation (39), we have

$$\vartheta_n^*(\sigma,\tau) = \vartheta_n(\sigma,\tau) + (1-\sigma)[0 - \vartheta_n(0,\tau)] + \sigma[0 - \vartheta_n(1,\tau)], \tag{42}$$

where $n = 0, 1, \cdots$.

Applying $\mathfrak{R}$ to Equation (39), we have

$$\mathfrak{R}\vartheta = \frac{\partial^2 \vartheta(\sigma,\tau)}{\partial \sigma^2} + \Gamma\left(\frac{1}{2}\right)4\tau\sigma^4(\sigma-1) - 4\sigma^2(5\sigma-3)\tau^{3/2}, \tag{43}$$

where $\mathfrak{R} = \partial^\delta/\partial\tau^\delta$ and $\mathfrak{R}^{-1}$ is defined as

$$\mathfrak{R}^{-1}(.) = I^\delta(.)d\tau. \tag{44}$$

Operating Equation (39) by $\mathfrak{R}^{-1}$, we have

$$\vartheta(\sigma,\tau) = \vartheta(\sigma,0) + \mathfrak{R}^{-1}\left(3\frac{\Gamma(1/2)}{4}\tau\sigma^4(\sigma-1) - 4\sigma^2(5\sigma-3)\tau^{3/2}\right). \tag{45}$$

Using ADM solution, the initial approximation becomes

$$\vartheta_0(\sigma,\tau) = \vartheta(\sigma,0) + \mathfrak{R}^{-1}\left(3\frac{\Gamma(1/2)}{4}\tau\sigma^4(\sigma-1) - 4\sigma^2(5\sigma-3)\tau^{3/2}\right) = 0 + \frac{3\Gamma(1/2)\Gamma(2)\tau^{\delta+1}\sigma^4(\sigma-1)}{4\Gamma(\delta+2)} - \frac{4\sigma^2(5\sigma-3)\Gamma(5/2)\tau^{3/2+\delta}}{\Gamma(5/2+\delta)},$$

$$\vartheta_0(\sigma,\tau) = \frac{3\Gamma(1/2)\Gamma(2)\tau^{\delta+1}\sigma^4(\sigma-1)}{4\Gamma(\delta+2)} - \frac{20\sigma^3\Gamma(5/2)\tau^{3/2+\delta}}{\Gamma(5/2+\delta)} + \frac{12\sigma^2\Gamma(5/2)\tau^{3/2+\delta}}{\Gamma(5/2+\delta)}. \tag{46}$$

With the help of initial approximation u_n^*, the formula for iterations is

$$\vartheta_{n+1}(\sigma,\tau) = \mathfrak{R}^{-1}\left(\frac{\partial^2 \vartheta_n^*}{\partial \sigma^2}\right). \tag{47}$$

For $n = 0$, put the IBCs into Equation (42).

$$\vartheta_0^*(\sigma,\tau) = \vartheta_0(\sigma,\tau) + (1-\sigma)[0 - \vartheta_0(0,\tau)] + \sigma[0 - \vartheta_0(1,\tau)] = \frac{3\Gamma(1/2)\Gamma(2)\tau^{\delta+1}\sigma^4(\sigma-1)}{4\Gamma(\delta+2)} - \frac{20\sigma^3\Gamma(5/2)\tau^{3/2+\delta}}{\Gamma(5/2+\delta)} + \frac{12\sigma^2\Gamma(5/2)\tau^{3/2+\delta}}{\Gamma(5/2+\delta)} + (1-\sigma)[0-0] + \sigma \cdot \left[\frac{0 + 8\Gamma(5/2)\tau^{3/2+\delta}}{\Gamma(5/2+\delta)}\right],$$

$$\vartheta_0^*(\sigma,\tau) = \frac{3\Gamma(1/2)\Gamma(2)\tau^{\delta+1}\sigma^4(\sigma-1)}{4\Gamma(\delta+2)} - \frac{20\sigma^3\Gamma(5/2)\tau^{3/2+\delta}}{\Gamma(5/2+\delta)} + \frac{12\sigma^2\Gamma(5/2)\tau^{3/2+\delta}}{\Gamma(5/2+\delta)} + \frac{8\sigma\Gamma(5/2)\tau^{3/2+\delta}}{\Gamma(5/2+\delta)}. \tag{48}$$

From Equation (47), we have

$$\vartheta_1(\sigma,\tau) = \mathfrak{R}^{-1}\left(\frac{\partial^2 \vartheta_0^*}{\partial \sigma^2}\right) = \mathfrak{R}^{-1}\left(\frac{3\Gamma(1/2)\Gamma(2)\tau^{\delta+1}\left(20\sigma^3 - 12\sigma^2\right)}{4\Gamma(\delta+2)} - \frac{4(30\sigma-6)\Gamma(5/2)\tau^{3/2+\delta}}{\Gamma(5/2+\delta)}\right),$$

$$\vartheta_1(\sigma,\tau) = \frac{3\Gamma(1/2)\Gamma(2)\tau^{2\delta+1}\left(20\sigma^3 - 12\sigma^2\right)}{4\Gamma(2\delta+2)} - \frac{120\sigma\Gamma(5/2)\tau^{3/2+2\delta}}{\Gamma(5/2+2\delta)} + \frac{24\Gamma(5/2)\tau^{3/2+2\delta}}{\Gamma(5/2+2\delta)}. \tag{49}$$

For $n = 1$ Equation (42), we get

$$\vartheta_1^*(\sigma,\tau) = \vartheta_1(\sigma,\tau) + (1-\sigma)[0 - \vartheta_1(0,\tau)] + \sigma[0 - \vartheta_1(1,\tau)] = \frac{3\Gamma(1/2)\Gamma(2)\tau^{2\delta+1}\left(20\sigma^3 - 12\sigma^2\right)}{4\Gamma(2\delta+2)} - \frac{120\sigma\Gamma(5/2)\tau^{3/2+2\delta}}{\Gamma(5/2+2\delta)} + \frac{24\Gamma(5/2)\tau^{3/2+2\delta}}{\Gamma(5/2+2\delta)} + (1-\sigma)\left(0 - \frac{24\Gamma(5/2)\tau^{3/2+2\delta}}{\Gamma(5/2+2\delta)}\right) + \sigma\left(0 - \frac{24\Gamma(1/2)\Gamma(2)\tau^{2\delta+1}}{4\Gamma(2\delta+2)} + \frac{96\Gamma(5/2)\tau^{3/2+2\delta}}{\Gamma(5/2+2\delta)}\right),$$

$$\vartheta_1^*(\sigma,\tau) = \frac{3\Gamma(1/2)\Gamma(2)\tau^{2\delta+1}\left(20\sigma^3 - 12\sigma^2\right)}{4\Gamma(2\delta+2)} - \frac{24\Gamma(1/2)\Gamma(2)\tau^{2\delta+1}}{4\Gamma(2\delta+2)}. \tag{50}$$

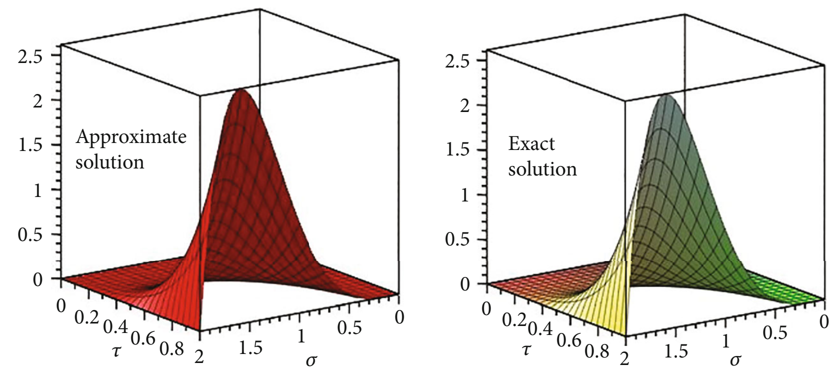

FIGURE 1: 3D plots of the exact and approximate solution for $\delta = 1$ of Example 5.1.

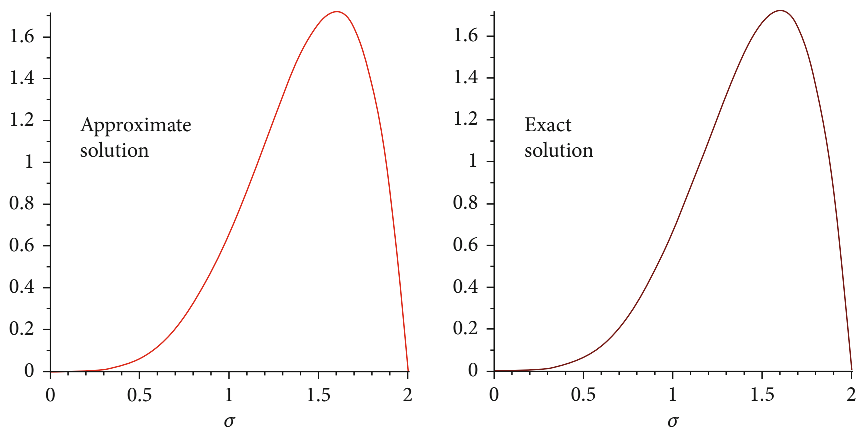

FIGURE 2: 2D plots of the exact and approximate solution for $\delta = 1$ of Example 5.1.

From Equation (47), we have

$$\vartheta_2(\sigma,\tau) = \mathfrak{R}^{-1}\left(\frac{\partial^2 \vartheta_1^*}{\partial \sigma^2}\right) = \mathfrak{R}^{-1}\left(\frac{3(120\sigma - 24)\Gamma(1/2)\tau^{2\delta+1}}{4\Gamma(2\delta+2)}\right),$$
$$\vartheta_2(\sigma,\tau) = \frac{3(120\sigma - 24)\Gamma(1/2)\tau^{3\delta+1}}{4\Gamma(3\delta+2)}. \tag{51}$$

Equation (42), for $n = 2$, is

$$\vartheta_2^*(\sigma,\tau) = \vartheta_2(\sigma,\tau) + (1-\sigma)[0 - \vartheta_2(0,\tau)] + \sigma[0 - \vartheta_2(1,\tau)]$$
$$= \frac{3(120\sigma - 24)\Gamma(1/2)\tau^{3\delta+1}}{4\Gamma(3\delta+2)} + (1-\sigma) \cdot \left[0 - \frac{72\Gamma(1/2)\tau^{3\delta+1}}{\Gamma(3\delta+2)}\right] + \sigma\left[0 - \frac{288\Gamma(1/2)\tau^{3\delta+1}}{\Gamma(3\delta+2)}\right],$$

$$\vartheta_2^*(\sigma,\tau) = \frac{144\sigma\Gamma(1/2)\Gamma(2)\tau^{3\delta+1}}{4\Gamma(3\delta+2)} - \frac{144\Gamma(1/2)\Gamma(2)\tau^{3\delta+1}}{4\Gamma(3\delta+2)}. \tag{52}$$

From Equation (47), we get

$$\vartheta_3(\sigma,\tau) = \mathfrak{R}^{-1}\left(\frac{\partial^2 \vartheta_2^*}{\partial \sigma^2}\right),$$
$$= \mathfrak{R}^{-1}(0) = 0. \tag{53}$$
$$\vdots$$

The series form of ADM solution is

$$\vartheta(\sigma,\tau) = \vartheta_0(\sigma,\tau) + \vartheta_1(\sigma,\tau) + \vartheta_2(\sigma,\tau) + \vartheta_3(\sigma,\tau) + \cdots \frac{3\Gamma(1/2)\Gamma(2)\tau^{2\delta+1}(20\sigma^3 - 12\sigma^2)}{4\Gamma(2\delta+2)} - \frac{4(30\sigma-6)\Gamma(5/2)\tau^{3/2+2\delta}}{\Gamma(5/2+2\delta)} \frac{3(120\sigma-24)\Gamma(1/2)\tau^{3\delta+1}}{4\Gamma(3\delta+2)} + 0 + \cdots. \tag{54}$$

6. Results and Discussion

In Figure 1, the 3D graph of exact and approximate solutions to Example 5.1 is presented. The comparison showed that the graphs of exact and obtained solutions are in good agreement and confirms the validity of the proposed method. In Figure 2, the 2D plot of the exact and approximate solution is constructed and again confirms the validity of the

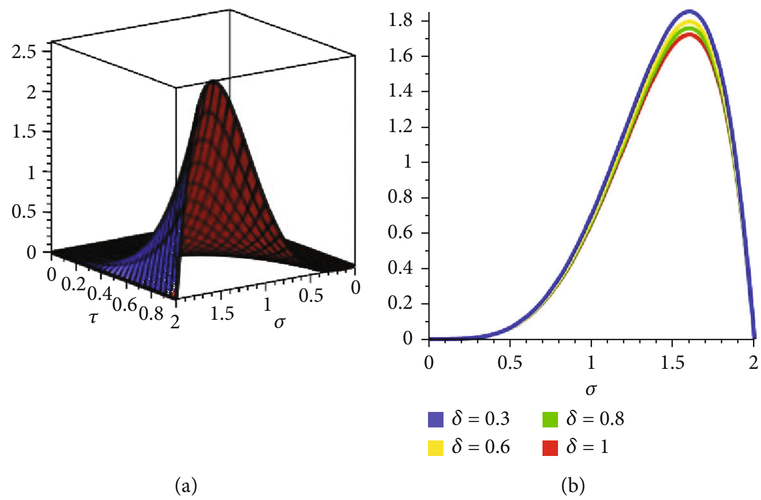

Figure 3: (a) 3D and (b) 2D plots for different fractional value of δ for Example 5.1.

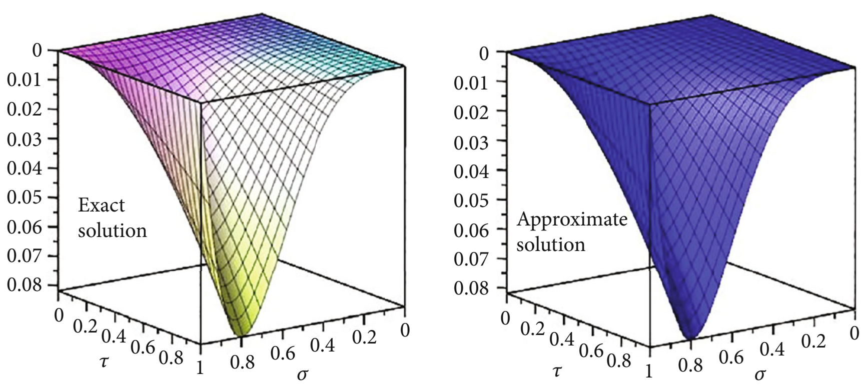

Figure 4: 3D plots of the exact and approximate solution for $\delta = 1$ of Example 5.2.

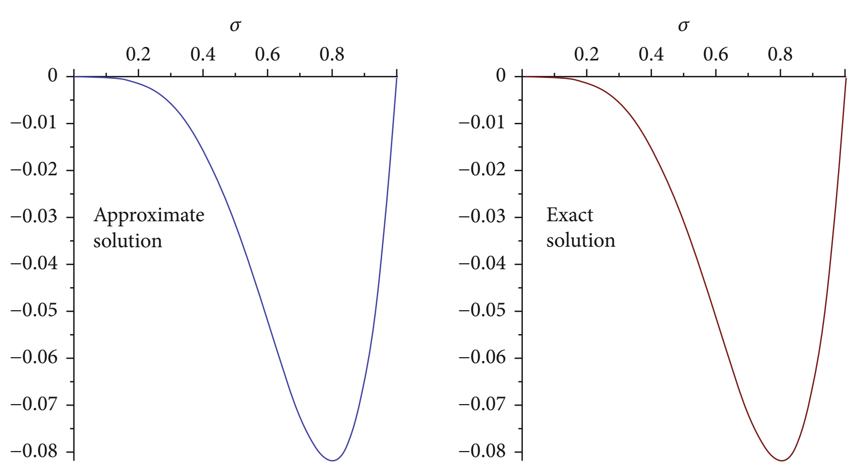

Figure 5: 2D plots of the exact and approximate solution for $\delta = 1$ of Example 5.2.

suggested technique. Figure 3 represents the fractional order solutions of Example 5.1 at $\delta = 0.3, 0.6, 0.8, 1$. The solutions at different fractional orders of the derivative provide the useful information about the dynamics of Example5.1. In Figures 4 and 5, 3D and 2D graphs of exact and obtained solutions are highlighted. From both the presentations, greater accuracy has been observed and the graphs of the derived results are found to be identical to the exact solution of Example 5.2. In Figure 6, the solution of Example 5.2 at different time levels is calculated and obtained useful dynamics for

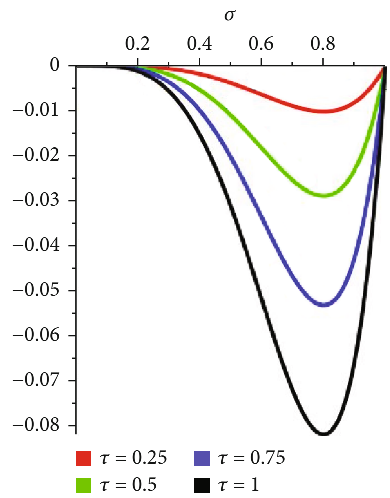

Figure 6: 2D plots for approximate solution of Example 5.2 at $\tau = 0.25, 0.5, 0.75, 1$.

Table 1: Absolute error of Example 5.1 at $\tau = 0.8$.

σ	$\lvert \text{Exact} - \text{ADM} \rvert$ $\delta = 0.3$	$\lvert \text{Exact} - \text{ADM} \rvert$ $\delta = 0.5$	$\lvert \text{Exact} - \text{ADM} \rvert$ $\delta = 0.7$
0.2	6.26×10^{-11}	4.41×10^{-10}	1.58×10^{-10}
0.4	5.3×10^{-10}	1.2×10^{-10}	6.0×10^{-11}
0.6	7.0×10^{-11}	8.0×10^{-10}	2.8×10^{-10}
0.8	4.3×10^{-9}	3.3×10^{-9}	1.0×10^{-10}
1	4.7×10^{-9}	2.0×10^{-10}	2.0×10^{-10}
1.2	1.9×10^{-9}	5.1×10^{-9}	2.5×10^{-9}
1.4	1.6×10^{-8}	5.0×10^{-9}	2.0×10^{-9}
1.6	2.0×10^{-9}	6.0×10^{-9}	1.0×10^{-9}
1.8	2.6×10^{-8}	8.6×10^{-9}	5.0×10^{-10}
2	2.0×10^{-8}	1.0×10^{-8}	2.0×10^{-9}

Table 2: Absolute error of Example 5.2 at $\delta = 1/2$.

σ	$\lvert \text{Exact} - \text{ADM} \rvert$ $\tau = 0.3$	$\lvert \text{Exact} - \text{ADM} \rvert$ $\tau = 0.5$	$\lvert \text{Exact} - \text{ADM} \rvert$ $\tau = 0.7$
0.1	8.748×10^{-21}	3.6348×10^{-20}	5.8352×10^{-20}
0.2	1.5×10^{-22}	2.1×10^{-22}	3.9×10^{-22}
0.3	1.67×10^{-22}	3.20×10^{-20}	4.59×10^{-20}
0.4	1.60×10^{-20}	6.1×10^{-21}	1.443×10^{-19}
0.5	1.30×10^{-22}	1.3×10^{-20}	3.00×10^{-19}
0.6	1.27×10^{-20}	2.1×10^{-20}	1.11×10^{-19}
0.7	4.2×10^{-20}	7.0×10^{-21}	4.40×10^{-19}
0.8	1.5×10^{-20}	1.98×10^{-19}	1.17×10^{-19}
0.9	3.9×10^{-20}	0.000	3.55×10^{-19}
1	0.000	1.722×10^{-19}	0.000

Example 5.2. Table 1 shows the solutions at fractional orders $\delta = 0.3$, 0.5, and 0.7 of Example 5.1. For this purpose, the modified approach of ADM is applied to obtain the solutions. The results are listed in the table, which has confirmed that the suggested method gives the solutions that are in close contact with the analytical solution of the problem. The absolute errors are given for the given analytical and ADM solutions in the table. According to the table, the proposed techniques have the desired degree of accuracy in terms of exact problem solution. In Table 2, the solutions of Example 5.2 are given at different time levels, that is, $\tau = 0.3, 0.5, 0.7$. It is verified from Table 2 that the method provides excellent results at different time levels.

7. Conclusion

In this article, the Adomian decomposition method is implemented along with some new modifications to solve fractional partial differential equation boundary value problems. The proposed technique was found to be very efficient in handling the solution of fractional-order boundary value problems. In particular, the suggested procedure is used to solve some illustrative examples of time-fractional diffusion equations. The solutions are calculated for both fractional and integer order problems, and the present method is observed to be very simple and useful for the solutions to such problems. A comparison between exact and analytical solutions is made with the help of plots and tables. The graphical representation is presented to confirm the validity of the present technique. The solution graphs have confirmed that the derived results are in close contact with the problem's actual solution. Figures 1 and 4 represent 3D solution plots of Example 5.1 and 5.2, respectively, at $\delta = 1$. Both the graphs displayed a very convincing contact between the exact and approximate solutions. In Figures 2 and 5, 2D solution plots are also constructed to confirm the validity of the proposed method. The fractional-order solutions of Example 5.1 and 5.2 are represented in Figures 3 and 6. From the graphical representation of fractional-order problems, it is confirmed that very accurate and useful information is obtained as compared to the integer order of the problems. It is concluded that the solutions at fractional-order derivatives are very useful to analyze the dynamics of the targeted problems of IBVPs. The dual use of initial conditions has made the procedure suitable for using both IBCs simultaneously, which was not the case in the earlier related literature. The solution obtained at each fractional order is found to be converging to the integer order of the targeted problems. Moreover, the proposed method is more accurate and competent to find the solution of nonlinear fractional partial differential equations and, in the future, can be modified for other important fractional nonlinear partial differential equations with higher dimensions.

Data Availability

No data were used to support this study.

Conflicts of Interest

No competing interests are declared.

Authors' Contributions

Saadia Masood performed the investigation, Hajira and Qasim Khan performed the methodology, Hassan Khan performed the supervision, Professor Fairouz Tchier is the project administrator, Rasool Shah has written the original manuscript draft, Saima Mustafa and Gurpreet Singh performed draft writing, and Muhammad Arif contributed to the funding.

Acknowledgments

The authors thank the collaborators of this manuscript. This study is supported by the researchers' supporting project number RSP-2021/401, King Saud University, Riyadh, Saudi Arabia.

References

[1] K. Oldham and J. Spanier, *The Fractional Calculus Theory and Applications of Differentiation and Integration to Arbitrary Order*, Elsevier, 1974.

[2] S. Kumar, "A numerical study for the solution of time fractional nonlinear shallow water equation in oceans," *Zeitschrift fur Naturforschung A*, vol. 68, no. 8-9, pp. 547–553, 2013.

[3] J. J. Yao, A. Kumar, and S. Kumar, "A fractional model to describe the Brownian motion of particles and its analytical solution," *Advances in Mechanical Engineering*, vol. 7, no. 12, Article ID 168781401561887, 2015.

[4] V. F. Morales-Delgado, J. F. Gomez-Aguilar, H. Yepez-Martinez, D. Baleanu, R. F. Escobar-Jimenez, and V. H. Olivares-Peregrino, "Laplace homotopy analysis method for solving linear partial differential equations using a fractional derivative with and without kernel singular," *Advances in Difference Equations*, vol. 2016, no. 1, p. 17, 2016.

[5] J. F. Gomez-Aguilar, H. Yepez-Martinez, J. Torres-Jimenez, T. Cordova-Fraga, R. F. Escobar-Jimenez, and V. H. Olivares-Peregrino, "Homotopy perturbation transform method for nonlinear differential equations involving to fractional operator with exponential kernel," *Advances in Difference Equations*, vol. 2017, no. 1, p. 18, 2017.

[6] A. Atangana and J. F. Gomez Aguilar, "Numerical approximation of Riemann-Liouville definition of fractional derivative: from Riemann-Liouville to Atangana-Baleanu," *Numerical Methods for Partial Differential Equations*, vol. 34, no. 5, pp. 1502–1523, 2018.

[7] S. Qureshi and A. Yusuf, "A new third order convergent numerical solver for continuous dynamical systems," *Journal of King Saud University-Science*, vol. 32, no. 2, pp. 1409–1416, 2020.

[8] S. Qureshi, A. Yusuf, and S. Aziz, "On the use of Mohand integral transform for solving fractional-order classical Caputo differential equations," *Journal of Applied Mathematics and Computational Mechanics*, vol. 19, no. 3, pp. 99–109, 2020.

[9] S. Kirtphaiboon, U. Humphries, A. Khan, and A. Yusuf, "Model of rice blast disease under tropical climate conditions," *Chaos, Solitons & Fractals*, vol. 143, article 110530, 2021.

[10] B. Acay, A. Khan, and A. Yusuf, "Fractional methicillin-resistant Staphylococcus aureus infection model under Caputo operator," *Journal of Applied Mathematics and Computing*, vol. 67, no. 1-2, pp. 755–783, 2021.

[11] W. M. Ahmad and R. El-Khazali, "Fractional-order dynamical models of love," *Chaos, Solitons & Fractals*, vol. 33, no. 4, pp. 1367–1375, 2007.

[12] H. H. Sun, A. Abdelwahab, and B. Onaral, "Linear approximation of transfer function with a pole of fractional power," *IEEE Transactions on Automatic Control*, vol. 29, no. 5, pp. 441–444, 1984.

[13] C. Dhaigude and V. Nikam, "Solution of fractional partial differential equations using iterative method," *Fractional Calculus and Applied Analysis*, vol. 15, no. 4, pp. 684–699, 2012.

[14] H. Khan, R. Shah, P. Kumam, D. Baleanu, and M. Arif, "Laplace decomposition for solving nonlinear system of fractional order partial differential equations," *Advances in Difference Equations*, vol. 2020, no. 1, p. 18, 2020.

[15] I. Podlubny, "An introduction to fractional derivatives, fractional differential equations, to methods of their solution and some of their applications," *Mathematics in Science and Engineering*, vol. 198, 1999.

[16] H. Liu, H. Khan, R. Shah, A. A. Alderremy, S. Aly, and D. Baleanu, "On the fractional view analysis of Keller–Segel equations with sensitivity functions," *Complexity*, vol. 2020, 15 pages, 2020.

[17] A. A. Alderremy, H. Khan, R. Shah, S. Aly, and D. Baleanu, "The analytical analysis of time-fractional Fornberg-Whitham equations," *Mathematics*, vol. 8, no. 6, p. 987, 2020.

[18] B. Baeumer, D. A. Benson, M. M. Meerschaert, and S. W. Wheatcraft, "Subordinated advection-dispersion equation for contaminant transport," *Water Resources Research*, vol. 37, no. 6, pp. 1543–1550, 2001.

[19] D. A. Benson, S. W. Wheatcraft, and M. M. Meerschaert, "Application of a fractional advection-dispersion equation," *Water Resources Research*, vol. 36, no. 6, pp. 1403–1412, 2000.

[20] J. Singh, B. Ganbari, D. Kumar, and D. Baleanu, "Analysis of fractional model of guava for biological pest control with memory effect," *Journal of Advanced Research*, vol. 32, pp. 99–108, 2021.

[21] E. Bonyah, A. K. Sagoe, D. Kumar, and S. Deniz, "Fractional optimal control dynamics of coronavirus model with Mittag-Leffler law," *Ecological Complexity*, vol. 45, article 100880, 2021.

[22] O. Abu Arqub, J. Singh, B. Maayah, and M. Alhodaly, "Reproducing kernel approach for numerical solutions of fuzzy fractional initial value problems under the Mittag–Leffler kernel differential operator," *Mathematical Methods in the Applied Sciences*, 2021.

[23] M. Yavuz, "European option pricing models described by fractional operators with classical and generalized Mittag-Leffler kernels," *Numerical Methods for Partial Differential Equations*, vol. 38, no. 3, pp. 434–456, 2022.

[24] M. Yavuz and N. Sene, "Approximate solutions of the model describing fluid flow using generalized ρ-Laplace transform method and heat balance integral method," *Axioms*, vol. 9, no. 4, p. 123, 2020.

[25] D. A. Koç and M. Gülsu, "Numerical approach for solving time fractional diffusion equation," *An International Journal of Optimization and Control: Theories & Applications (IJOCTA)*, vol. 7, no. 3, pp. 281–287, 2017.

[26] L. Wang, Y. Ma, and Z. Meng, "Haar wavelet method for solving fractional partial differential equations numerically," *Applied Mathematics and Computation*, vol. 227, pp. 66–76, 2014.

[27] H. Jafari, M. Nazari, D. Baleanu, and C. M. Khalique, "A new approach for solving a system of fractional partial differential equations," *Computers & Mathematics with Applications*, vol. 66, no. 5, pp. 838–843, 2013.

[28] R. I. Nuruddeen, "Elzaki decomposition method and its applications in solving linear and nonlinear Schrodinger equations," *Sohag Journal of Mathematics*, vol. 4, no. 2, pp. 31–35, 2017.

[29] H. Jafari and V. Daftardar-Gejji, "Solving linear and nonlinear fractional diffusion and wave equations by Adomian decomposition," *Applied Mathematics and Computation*, vol. 180, no. 2, pp. 488–497, 2006.

[30] M. Hajipour, A. Jajarmi, and D. Baleanu, "On the accurate discretization of a highly nonlinear boundary value problem," *Numerical Algorithms*, vol. 79, no. 3, pp. 679–695, 2018.

[31] M. Hajipour, A. Jajarmi, A. Malek, and D. Baleanu, "Positivity-preserving sixth-order implicit finite difference weighted essentially non-oscillatory scheme for the nonlinear heat equation," *Applied Mathematics and Computation*, vol. 325, pp. 146–158, 2018.

[32] H. Khan, R. Shah, P. Kumam, and M. Arif, "Analytical solutions of fractional-order heat and wave equations by the natural transform decomposition method," *Entropy*, vol. 21, no. 6, p. 597, 2019.

[33] Y. Chen, Y. Sun, and L. Liu, "Numerical solution of fractional partial differential equations with variable coefficients using generalized fractional-order Legendre functions," *Applied Mathematics and Computation*, vol. 244, pp. 847–858, 2014.

[34] H. Jafari and S. Seifi, "Solving a system of nonlinear fractional partial differential equations using homotopy analysis method," *Communications in Nonlinear Science and Numerical Simulation*, vol. 14, no. 5, pp. 1962–1969, 2009.

[35] D. Nazari and S. Shahmorad, "Application of the fractional differential transform method to fractional- order integro-differential equations with nonlocal boundary conditions," *Journal of Computational and Applied Mathematics*, vol. 234, no. 3, pp. 883–891, 2010.

[36] Z. Odibat and S. Momani, "The variational iteration method: an efficient scheme for handling fractional partial differential equations in fluid mechanics," *Computers & Mathematics with Applications*, vol. 58, no. 11-12, pp. 2199–2208, 2009.

[37] A. Baseri, E. Babolian, and S. Abbasbandy, "Normalized Bernstein polynomials in solving space-time fractional diffusion equation," *Advances in Difference Equations*, vol. 2017, no. 1, 2017.

[38] F. Mainardi, "The time fractional diffusion-wave equation," *Radiophysics and Quantum Electronics*, vol. 38, no. 1-2, pp. 13–24, 1996.

[39] R. R. Nigmatullin, "The realization of the generalized transfer equation in a medium with fractal geometry," *Physica status solidi (b)*, vol. 133, no. 1, pp. 425–430, 1986.

[40] J. M. Angulo, M. D. Ruiz-Medina, V. V. Anh, and W. Grecksch, "Fractional diffusion and fractional heat equation," *Advances in Applied Probability*, vol. 32, no. 4, pp. 1077–1099, 2000.

[41] D. A. Murio, "Implicit finite difference approximation for time fractional diffusion equations," *Computers and Mathematics with Applications*, vol. 56, no. 4, pp. 1138–1145, 2008.

[42] W. Wyss, “The fractional diffusion equation,” *Journal of Mathematical Physics*, vol. 27, no. 11, pp. 2782–2785, 1986.

[43] W. R. Schneider and W. Wyss, “Fractional diffusion and wave equations,” *Journal of Mathematical Physics*, vol. 30, no. 1, pp. 134–144, 1989.

[44] R. Gorenflo, Y. Luchko, and F. Mainardi, “Wright functions as scale-invariant solutions of the diffusion-wave equation,” *Journal of Computational and Applied Mathematics*, vol. 118, no. 1-2, pp. 175–191, 2000.

[45] R. Gorenflo, F. Mainardi, D. Moretti, and P. Paradisi, “Time fractional diffusion: a discrete random walk approach,” *Nonlinear Dynamics*, vol. 29, no. 1/4, pp. 129–143, 2002.

[46] Y. Lin and C. Xu, “Finite difference/spectral approximations for the time-fractional diffusion equation,” *Journal of Computational Physics*, vol. 225, no. 2, pp. 1533–1552, 2007.

[47] Y. Luchko and M. Yamamoto, “General time-fractional diffusion equation: some uniqueness and existence results for the initial-boundary-value problems,” *Fractional Calculus and Applied Analysis*, vol. 19, no. 3, pp. 676–695, 2016.

[48] E. J. Ali, “A new technique of initial boundary value problems using Adomian decomposition method,” *International mathematical forum*, vol. 7, no. 17, pp. 799–814, 2012.

[49] H. Jafari and S. Momani, “Solving fractional diffusion and wave equations by modified homotopy perturbation method,” *Physics Letters A*, vol. 370, no. 5-6, pp. 388–396, 2007.

[50] E. J. Ali, “Modified treatment of initial boundary value problems for one dimensional heat-like and wave-like equations using Adomian decomposition method,” *Basrah journal of science*, vol. 30, no. 2A english, pp. 86–105, 2012.

[51] G. Adomian, “Solving frontier problems of physics: the decomposition method; with a preface by Yves Cherruault,” in *Fundamental Theories of Physics*, vol. 60, Springer Science & Business Media, 1994.

[52] A. M. Wazwaz, “The decomposition method applied to systems of partial differential equations and to the reaction-diffusion Brusselator model,” *Applied Mathematics and Computation*, vol. 110, no. 2-3, pp. 251–264, 2000.

[53] Z. Niu and C. Wang, “A one-step optimal homotopy analysis method for nonlinear differential equations,” *Communications in Nonlinear Science and Numerical Simulation*, vol. 15, no. 8, pp. 2026–2036, 2010.

[54] Y. Pandir and A. Yildirim, “Analytical approach for the fractional differential equations by using the extended tanh method,” *Waves in Random and Complex Media*, vol. 28, no. 3, pp. 399–410, 2018.

[55] P. Pue-On and N. Viriyapong, “Modified Adomian decomposition method for solving particular third-order ordinary differential equations,” *Applied Mathematical Sciences*, vol. 6, no. 30, pp. 1463–1469, 2012.

[56] Y. Q. Hasan and L. M. Zhu, “Modified Adomian decomposition method for singular initial value problems in the second-order ordinary differential equations,” *Surveys in Mathematics and its Applications*, vol. 3, pp. 183–193, 2008.

[57] H. Jafari and V. Daftardar-Gejji, “Revised Adomian decomposition method for solving systems of ordinary and fractional differential equations,” *Applied Mathematics and Computation*, vol. 181, no. 1, pp. 598–608, 2006.

[58] R. Shah, H. Khan, D. Baleanu, P. Kumam, and M. Arif, “A novel method for the analytical solution of fractional Zakharov–Kuznetsov equations,” *Advances in Difference Equations*, vol. 2019, no. 1, p. 14, 2019.

[59] L. L. Ferrás, N. J. Ford, M. L. Morgado, and M. Rebelo, “A numerical method for the solution of the time-fractional diffusion equation,” in *International Conference on Computational Science and Its Applications*, pp. 117–131, Cham, 2014.

Hindawi
Journal of Function Spaces
Volume 2022, Article ID 5493056, 9 pages
https://doi.org/10.1155/2022/5493056

Research Article

Approximation Properties of a New Type of Gamma Operator Defined with the Help of k-Gamma Function

Gurhan Icoz [1] **and Seda Demir** [2]

[1] *Department of Mathematics, Faculty of Science, Gazi University, Ankara, Turkey*
[2] *Graduate School of Natural and Applied Sciences, Gazi University, Ankara, Turkey*

Correspondence should be addressed to Gurhan Icoz; gurhanicoz@gazi.edu.tr

Received 13 May 2022; Accepted 27 June 2022; Published 2 August 2022

Academic Editor: Yusuf Gurefe

With the help of the k-Gamma function, a new form of Gamma operator is given in this article. Voronovskaya type theorem, weighted approximation, rates of convergence, and pointwise estimates have been found for approximation features of the newly described operator. Finally, numerical examples have been provided to demonstrate that the operator is approaching the function.

1. Introduction

One of the most important topics in mathematical analysis is approximation theory. The theory is studied in almost every subject, including engineering and physics. Many mathematicians have made investigation in this area. In 1885 [1], Weierstrass claimed that polynomials can approximate every function in the closed interval $[a, b]$. Besides, theorems about this subject are prepared by Korovkin around 1950 [2]. The Korovkin approximation theorem is one of the well-known theorems in mathematics. Their theorems indicate that a series of positive linear operators can converge to the identity operator under specific condition [2]. As a result using these theorems, some studies on linear and positive linear operators have been added to the literature. For example, King [3] introduced the Bernstein operator to preserve the function $a_2(h) = h^2$ in 2003. Then, King constructed a new set of operators with respect to the test functions $\{1, h, h^2\}$ and obtained their linear combinations. On the other hand, one of these operators is the Gamma operator which is constructed by Lupas and Müller [4]. The classical Gamma operator in [4] is expressed as follows:

$$K_m(\varphi ; y) = \frac{y^{m+1}}{\Gamma(m+1)} \int_0^{\infty} e^{-yv} v^m \varphi\left(\frac{m}{v}\right) dv, \forall y \in (0,\infty), m \in \mathbb{N}. \tag{1}$$

Then, in the literature, some researchers introduced the generalizations of Gamma and beta functions and also the extensions of Gamma-type operators and their extensions [5–14]. One of the studies of this topic was by Daz and Pariguan [15]; they introduced and researched k-Gamma function when they were assessing Feynman integrals. k-Gamma function has been showed up various effects on mathematics and applications. One of these effects has been working the Schrodinger equation for harmonium and related models in view of important operations in quantum chemistry [16]. The others have used k-Gamma function for combinatorial analysis in statistic.

According to these studies, the k-Gamma function was defined by Daz and Pariguan as follows:

$$\Gamma_k(z) = \int_0^\infty t^{z-1} e^{-t^k/k} dt, (k \in \mathbb{R}, \operatorname{Re}(z) > 0). \quad (2)$$

As can be seen from the definition, Γ_k is a one parameter deformation of the classical Gamma function such that $\Gamma_k \longrightarrow \Gamma$ as $k \longrightarrow 1$. For $k = 2$, it reduces to an integral of Gaussian functions [17]. When we get $u = -t^k/k$ in equation (2), we find the expression $\Gamma_k(z) = k^{(z/k)-1}\Gamma(z/k)$, and all properties of the classic Gamma operator can be generalized into k-Gamma function. It also led to a few new conclusions for k-Gamma function. A few of them are given that

$$\begin{aligned} \Gamma_k(k) &= 1, \\ \Gamma_k(z+k) &= z\Gamma_k(z), \\ (z)_{n,k} &= \frac{\Gamma_k(z+nk)}{\Gamma_k(z)}, \end{aligned} \quad (3)$$

in [15]. For more such properties of k-Gamma and related functions, we can refer to the article [11, 15, 17].

The primary goal of this research is to give the k-Gamma operator given by (4) and its approximation properties. For the operator in (4), in Section 2, we will use Korovkin theorem in [18]. Then, in Section 3, we will consider the Voronovskaya type theorem. In Section 4, we will examine the weighted approximation. Later, we will give the rates of convergence with Peetre's $\mathscr{K}$-functional and Lipschitz class in Section 5. Moreover, in Section 6, we will obtain pointwise estimates, and finally, in Section 7, we will show the numerical examples for the operators in (4).

2. A New Modification of Gamma Operators Defined with the Help of k-Gamma Function

We shall see a new type of Gamma operators defined with the help of the k-Gamma function in this section, and some findings will be presented in the rest of the article. In this paper, we will use the expressions $a_z(h) = h^z$ and $\psi_{y,z} = (h-y)^z$, $y \in (0,\infty)$ as polynomial functions. The modified representation of the classical Gamma operator is shown as follows:

$$K_m^*(\varphi; y) = \frac{y^{m+1+(1/k)}}{\Gamma_k(mk+k+1)} \int_0^\infty e^{-yv} (vk)^{m+(1/k)} \varphi\left(\frac{m}{v}\right) dv, \forall y \in (0,\infty), k > 0, m \in \mathbb{N}, \quad (4)$$

where for $v > 0$, $\varphi \in C_\gamma(0,\infty) = \{\varphi \in C(0,\infty): \varphi(u) = O(u^\gamma)$, as $u \longrightarrow \infty\}$ for $m > \gamma$. Here $C(0,\infty)$ is the set of continuous functions on $(0,\infty)$. This modified operator is clearly positive and linear in this case. Furthermore, the new Gamma operator defined with the help of the k-Gamma function is directly preserved constant, and test functions are provided in case of limit.

We note that for special case of $k = (1/p)(p \in \mathbb{N})$ in (4), we have Schurer variant of Gamma operators in (1).

The following lemma will be presented without proof and used in fundamental theorems for the rest of the paper.

Lemma 1. *Let $y \in (0,\infty)$. The following are the moment values:*

$$\begin{aligned} K_m^*(a_0(h); y) &= a_0(y), \\ K_m^*(a_1(h); y) &= \frac{mk}{mk+1} a_1(y), \\ K_m^*(a_2(h); y) &= \frac{(mk)^2}{(mk+1)(mk-k+1)} a_2(y), \\ K_m^*(a_3(h); y) &= \frac{(mk)^3}{(mk+1)(mk-k+1)(mk-2k+1)} a_3(y), \\ K_m^*(a_4(h); y) &= \frac{(mk)^4}{(mk+1)(mk-k+1)(mk-2k+1)(mk-3k+1)} a_4(y). \end{aligned} \quad (5)$$

By generalizing the moment values, we have the following lemma.

Lemma 2. *Let $y \in (0,\infty)$ and $z \in \mathbb{N}$, $K_m^*(a_0(h); y) = a_0(y)$. Then, the general formula for the following moment values is obtained*

$$K_m^*(a_z(h); y) = \frac{(mk)^z}{\prod_{i=0}^{z-1}(mk-ki+1)} a_z(y), z = 1, 2, \cdots. \quad (6)$$

Lemma 3. *Let $y \in (0,\infty)$. Using the equations in Lemma 1, the following are obtained:*

$$\begin{aligned} K_m^*\left(\psi_{y,0}(h); y\right) &= 1, \\ K_m^*\left(\psi_{y,1}(h); y\right) &= \frac{-1}{mk+1} a_1(y), \\ K_m^*\left(\psi_{y,2}(h); y\right) &= \frac{mk^2-k+1}{(mk+1)(mk-k+1)} a_2(y), \\ K_m^*\left(\psi_{y,3}(h); y\right) &= \left(\frac{m^3k^3}{(mk+1)(mk-k+1)(mk-2k+1)} - \frac{3m^2k^2}{(mk+1)(mk-k+1)} + \frac{3mk}{mk+1} - 1\right) a_3(y), \\ K_m^*\left(\psi_{y,4}(h); y\right) &= \left(\frac{m^4k^4}{(mk+1)(mk-k+1)(mk-2k+1)(mk-3k+1)} - 4\frac{m^3k^3}{(mk+1)(mk-k+1)(mk-2k+1)} + 6\frac{m^2k^2}{(mk+1)(mk-k+1)} - 4\frac{mk}{mk+1} + 1\right) a_4(y). \end{aligned} \quad (7)$$

As a result of our research, the Schurer variant of Gamma operators have not been defined or used. Also, if it is realized that $k \in \mathbb{R}^+$, it is obtained that our operators are a generalization of the Schurer type operators.

Throughout this paper, we use the norm $\|\varphi\| = \sup\{\varphi(y): y \in (0,\infty)\}$ for $\varphi \in C(0,\infty)$.

Lemma 4. *Let $\varphi \in C_B(0,\infty)$. Then, we get*

$$\|K_m^*(\varphi\,;y)\| \le \|\varphi\|. \tag{8}$$

Proof. By using the result of Lemma 1, we have

$$\begin{aligned}\|K_m^*(\varphi)\| &\le \frac{y^{m+1+(1/k)}}{\Gamma_k(mk+k+1)}\int_0^\infty e^{-yv}(vk)^{m+(1/k)}\left|\varphi\left(\frac{m}{v}\right)\right|dv\\ &\le \|\varphi\|\frac{y^{m+1+(1/k)}}{\Gamma_k(mk+k+1)}\int_0^\infty e^{-yv}(vk)^{m+(1/k)}dv\\ &= \|\varphi\|K_m^*(a_0(h)\,;y) = \|\varphi\|.\end{aligned} \tag{9}$$

Thus, we obtain the desired result. Because the moments are conserved in the limit state of the Korovkin test functions, K_m^* is an approximation process on any compact $T \subset (0,\infty)$, according to the Korovkin theorem in [18]. □

Theorem 5. *Let $\varphi \in C(0,\infty) \cap E$, where $E = \{\varphi : \lim_{y\longrightarrow\infty}(\varphi/1 + y^2) = k\,constant\}$. Then, consistently in each compact subset of $(0,\infty)$, we have*

$$\lim_{m\longrightarrow\infty} K_m^*(\varphi\,;y) = \varphi(y). \tag{10}$$

Proof. By using Lemma 1, when $z = 0, 1, 2$, we get

$$\lim_{m\longrightarrow\infty} K_m^*(a_z(h)\,;y) = a_z(y) \tag{11}$$

for uniformly each compact subset of $(0,\infty)$. Then, using the Korovkin theorem in [18], we give $\lim_{m\longrightarrow\infty} K_m^*(\varphi\,;y) = \varphi(y)$ for uniformly each compact subset of $(0,\infty)$. □

3. Voronovskaya Type Theorem

By establishing Voronovskaya's theorem below, we will illustrate the asymptotic behavior of $(K_m^*)_{m\ge1}$ operators in this section.

Theorem 6. *Let $\varphi \in C(0,\infty) \cap E$ such that $\varphi', \varphi'' \in C(0,\infty) \cap E$. The following limit is valid:*

$$\lim_{m\longrightarrow\infty} m[K_m^*(\varphi\,;y) - \varphi(y)] = -\frac{1}{k}y\varphi'(y) + \frac{1}{2}y^2\varphi''(y). \tag{12}$$

Proof. From the definition of Taylor formula

$$\varphi(h) = \varphi(y) + \varphi'(y)(h-y) + \frac{1}{2}\varphi''(y)(h-y)^2 + \Omega(h,y)(h-y)^2, \tag{13}$$

where

$$\Omega(h,y) = \frac{\varphi''(\delta) - \varphi''(y)}{2}, \tag{14}$$

such that δ lying between y and h and

$$\lim_{h\longrightarrow y}\Omega(h,y) = 0. \tag{15}$$

When the $(K_m^*)_{m\ge1}$ operator is applied to (13), we get

$$\begin{aligned}K_m^*(\varphi\,;y) &= \varphi(y) + \varphi'(y)K_m^*((h-y)\,;y) + \frac{1}{2}\varphi''(y)K_m^*\left((h-y)^2\,;y\right)\\ &\quad + K_m^*\left(\Omega(h,y)(h-y)^2\,;y\right).\end{aligned} \tag{16}$$

To get the formula

$$\begin{aligned}m[K_m^*(\varphi\,;y) - \varphi(y)] &= \varphi'(y)mK_m^*((h-y)\,;y)\\ &\quad + \frac{1}{2}\varphi''(y)mK_m^*\left((h-y)^2\,;y\right)\\ &\quad + mK_m^*\left(\Omega(h,y)(h-y)^2\,;y\right),\end{aligned} \tag{17}$$

multiply both sides of the last inequality by m. In the limit case, this equation is

$$\begin{aligned}\lim_{m\longrightarrow\infty} m[K_m^*(\varphi\,;y) - \varphi(y)] &= \varphi'(y)\lim_{m\longrightarrow\infty} mK_m^*((h-y)\,;y)\\ &\quad + \frac{1}{2}\varphi''(y)\lim_{m\longrightarrow\infty} mK_m^*\left((h-y)^2\,;y\right)\\ &\quad + \lim_{m\longrightarrow\infty} mK_m^*\left(\Omega(h,y)(h-y)^2\,;y\right).\end{aligned} \tag{18}$$

We know the values

$$\begin{aligned}\lim_{m\longrightarrow\infty} mK_m^*((h-y)\,;y) &= \lim_{m\longrightarrow\infty} m\left[\frac{-1}{mk+1}\right]y = \frac{-1}{k}y,\\ \lim_{m\longrightarrow\infty} mK_m^*\left((h-y)^2\,;y\right) &= \lim_{m\longrightarrow\infty} m\left[\frac{mk^2-k+1}{(mk+1)(mk-k+1)}\right]y^2 = y^2,\end{aligned} \tag{19}$$

using Lemma 3. So, we have

$$\begin{aligned}\lim_{m\longrightarrow\infty} m[K_m^*(\varphi\,;y) - \varphi(y)] &= \frac{-1}{k}y\varphi'(y) + \frac{1}{2}\varphi''(y)y^2\\ &\quad + \lim_{m\longrightarrow\infty} mK_m^*\left(\Omega(h,y)\psi_{y,2}(h)\,;y\right).\end{aligned} \tag{20}$$

We show that the limit to the right of the equation in (20) is equal to zero. It can easily be said from the Cauchy-

Schwarz inequality that

$$mK_m^*\Omega(h,y)\psi_{y,2}(h);y\Big) \le \sqrt{K_m^*(\Omega^2(h,y);y)}\sqrt{m^2K_m^*\Big(\psi_{y,4}(h);y\Big)}. \tag{21}$$

Then, using Korovkin theorem, we have

$$\lim_{m\longrightarrow\infty} K_m^*\left(\Omega^2(h;y),y\right) = \Omega^2(y,y) = 0, \tag{22}$$

since $\Omega^2(y,y)=0$ and $\Omega(.,y)\in C(0,\infty)\cap E$ and bounded as $h\longrightarrow\infty$ and in view of fact that

$$K_m^*\Big(\psi_{y,4}(h);y\Big) = O\left(\frac{1}{m^2}\right), \tag{23}$$

where $K_m^*(\psi_{y,4}(h);y) = (3m^2k^4 + m(18k^4 - 22k^3 + 6k^2) - 6k^3 + 11k^2 - 6k + 1)/((mk+1)(mk-k+1)(mk-2k+1)(mk-3k+1))$. The proof is completed when equations (21) and (22) are written in (13). □

4. Weighted Approximation

The Korovkin theorem for weighted approximation of the operators in (4) is given in this section. To demonstrate this, we will follow the theorems given by Gadjiev [19].

Consider $\vartheta(y)=1+y^2$ as continuous weighted function on $\mathbb{R}$, with $\lim_{|y|\longrightarrow\infty}\vartheta(y)=\infty$, $\vartheta(y)\ge 1$ for all $y\in[0,\infty)$. Let us have a look at the weighted spaces below. The property $|\varphi(y)|\le N_\varphi\vartheta(y)$ represents the weighted space of real-valued functions φ on $\mathbb{R}$. This subspace is denoted by

$$B_\vartheta[0,\infty) = \left\{\varphi : [0,\infty)\longrightarrow[0,\infty) : |\varphi(y)|\le N_\varphi\vartheta(y), y\in[0,\infty)\right\}. \tag{24}$$

N_φ is a constant depending on the functions φ.

Since, the weighted subspaces of $B_\vartheta[0,\infty)$ is given by

$$C_\vartheta[0,\infty) = \{\varphi\in B_\vartheta[0,\infty) : \varphi \text{ is continous on } \mathbb{R}\} = C[0,\infty)\cap B_\vartheta[0,\infty). \tag{25}$$

Eventually, additional subspace for all $\varphi\in C_\vartheta[0,\infty)$ for which $\lim_{|y|\longrightarrow\infty}\varphi(y)/\vartheta(y)$ exists finitely defined as

$$C_\vartheta^\kappa[0,\infty) = \left\{\varphi\in C_\vartheta[0,\infty) : \lim_{|y|\longrightarrow\infty}\frac{\varphi(y)}{\vartheta(y)} = \kappa_\varphi \text{ exists and it is finite}\right\}. \tag{26}$$

This κ_φ is a constant dependent on the φ functions. All three mapping spaces above are normed spaces endowed with

$$\|\varphi\|_\vartheta = \sup_{y\in(0,\infty)}\frac{|\varphi(y)|}{\vartheta(y)}. \tag{27}$$

Lemma 7. *Let $\varphi\in C_\vartheta(0,\infty)$. Then, for the modified operator $K_m^*(\varphi)$, we have*

$$\|K_m^*(\varphi)\|_\vartheta \le C\|\varphi\|_\vartheta, \tag{28}$$

which imply that the sequence of the modified operators $K_m^*(\varphi)$ is an approximation process from $C_\vartheta(0,\infty)$ to $B_\vartheta(0,\infty)$.

Proof. The desired result of this lemma is easily obtained from properties of the modified Gamma operator and Lemma 1. □

Gadjiev proposed a weighted approach to linear positive operator sequences for unbounded intervals in [19]. The following theorem is similar to the Gadjiev theorem.

Theorem 8. *Let $\varphi\in C_\vartheta^\kappa(0,\infty)$. For the modified Gamma operator, the following equality holds:*

$$\lim_{m\longrightarrow\infty}\|K_m^*(\varphi;y)-\varphi(y)\|_\vartheta = 0. \tag{29}$$

Proof. It will be enough to show that equivalence is attained for $\lim_{m\longrightarrow\infty}\|K_m^*(a_z;y)-a_z\|_\vartheta = 0, z=0,1,2$ using the theorem in [19]. For $z=0$, we have $\|K_m^*(a_0;y)-a_0\|_\vartheta=0$. Now, let us examine the cases $z=1,2$. When the necessary results for these situations are used,

$$\begin{aligned}\|K_m^*(a_1;y)-a_1\|_\vartheta &= \sup_{y\in(0,\infty)}\frac{|K_m^*(a_1;y)-a_1|}{1+y^2}\\ &= \sup_{y\in(0,\infty)}\frac{|(mk/mk+1)y-y|}{1+y^2}\\ &\le \left|\frac{mk}{mk+1}-1\right|\sup_{y\in(0,\infty)}\frac{y}{1+y^2}.\le\left|\frac{1}{mk+1}\right|\end{aligned} \tag{30}$$

is obtained. If we take the limit of this expression, it becomes

$$\lim_{m\longrightarrow\infty}\frac{1}{mk+1} = 0. \tag{31}$$

Then, we have

$$\begin{aligned}\|K_m^*(a_2;y)-a_2\|_\vartheta &= \sup_{y\in(0,\infty)}\frac{|K_m^*(a_2;y)-a_2|}{1+y^2}\\ &= \sup_{y\in(0,\infty)}\frac{\left|m^2k^2/((mk+1)(mk-k+1))y^2-y^2\right|}{1+y^2}\\ &\le\left|\frac{m^2k^2}{(mk+1)(mk-k+1)}-1\right|\sup_{y\in(0,\infty)}\frac{y^2}{1+y^2}\\ &\le\left|\frac{mk^2-2mk+k-1}{(mk+1)(mk-k+1)}\right|.\end{aligned} \tag{32}$$

If we take the limit of this expression, it becomes

$$\lim_{m\longrightarrow\infty}\frac{mk^2-2mk+k-1}{(mk+1)(mk-k+1)}=0. \tag{33}$$

As a result of the equations obtained above, the evidence is finished. □

5. The Rates of Convergence

Now, we can concentrate on the rates of convergence the modified Gamma operator in terms of the modulus continuity. We shall now show that $K_m^*(\varphi)$ outperforms the classical operator in terms of error estimation. Let us define the following in light of this goal.

The modulus of continuity of w is denoted by $\omega_{y_0}(\varphi,\delta)$ for interval $(0,y_0]$, $y_0\ge 0$ and can be described as follows:

$$\omega_{y_0}(\varphi,\delta)=\sup_{|h-y|\le\delta;y,h\in(0,y_0]}|\varphi(h)-\varphi(y)|. \tag{34}$$

The modulus of continuity $\omega_{y_0}(\varphi,\delta)\longrightarrow 0$ is easily understood as $\delta\longrightarrow 0$ for the function $\varphi\in C_B(0,\infty)$, where $C_B(0,\infty)$ is defined as space of all continuous and bounded functions on the interval $(0,\infty)$. Now, let us look at the rates of convergence theorem for $(K_m^*)_{m\ge1}$.

Theorem 9. *For $y_0>0$ and $\varphi\in C_B(0,\infty)$, let $\omega_{y_0+1}(\varphi,\delta)$ be the modulus of continuity on the finite interval $(0,y_0+1]\subset(0,\infty)$. Then, the following inequality exists:*

$$\begin{aligned}|K_m^*(\varphi;y)-\varphi(y)|\le{}&3N_\varphi\left(\frac{mk^2-k+1}{(mk+1)(mk-k+1)}\right)y_0^2(1+y_0)^2\\&+2\omega_{y_0+1}\left(\varphi,\sqrt{\frac{mk^2-k+1}{(mk+1)(mk-k+1)}y_0^2}\right),\end{aligned} \tag{35}$$

where N_φ is a constant only according as φ.

Proof. Now, let $\varphi\in C_B(0,\infty)$,$0<y\le y_0$, and $h>y_0+1$.Then, we can conclude that

$$|\varphi(h)-\varphi(y)|\le|\varphi(h)|+|\varphi(y)|\le 3N_\varphi(h-y)^2(1+y_0)^2 \tag{36}$$

for $h-y>1$. Then, again let $\varphi\in C_B(0,\infty)$, $0<y\le y_0$. So, the following inequality holds

$$|\varphi(h)-\varphi(y)|\le\omega_{y_0+1}(\varphi,|h-y|)\le\omega_{y_0+1}(\varphi,\delta)\left(1+\frac{1}{\delta}|h-y|\right) \tag{37}$$

for $h\le y_0+1$. As a result, from the above inequalitiy, we deduce that

$$|\varphi(h)-\varphi(y)|\le 3N_\varphi(h-y)^2(1+y_0)^2+\omega_{y_0+1}(\varphi,\delta)\left(1+\frac{1}{\delta}|h-y|\right) \tag{38}$$

for $0<y\le y_0$ and $0<h<\infty$. Applying K_m^* and Cauchy-Schwarz inequality to (38), we obtain

$$\begin{aligned}|K_m^*(\varphi;y)-\varphi(y)|&\le 3N_\varphi K_m^*\left((h-y)^2;y\right)(1+y_0)^2\\&\quad+\omega_{y_0+1}(\varphi,\delta)\left(1+\frac{1}{\delta}\sqrt{K_m^*\left((h-y)^2;y\right)}\right)\\&\le 3N_\varphi\left(\frac{mk^2-k+1}{(mk+1)(mk-k+1)}\right)(1+y_0)^2\\&\quad+2\omega_{y_0+1}\left(\varphi,\sqrt{\left(\frac{mk^2-k+1}{(mk+1)(mk-k+1)}\right)y_0^2}\right).\end{aligned} \tag{39}$$

By choosing $\delta=\sqrt{((mk^2-k+1)/((mk+1)(mk-k+1)))y_0^2}$, we can conclude the proof. □

Let

$$C_B^2(0,\infty)=\left\{\varphi\in C_B(0,\infty)\colon \varphi',\varphi''\in C_B(0,\infty)\right\}, \tag{40}$$

with the norm

$$\|\varphi\|_{C_B^2(0,\infty)}=\|\varphi\|_{C_B(0,\infty)}+\|\varphi'\|_{C_B(0,\infty)}+\|\varphi''\|_{C_B(0,\infty)} \tag{41}$$

also

$$\|\varphi\|_{C_B(0,\infty)}=\sup_{y\in(0,\infty)}|\varphi(y)| \tag{42}$$

in [20].

Theorem 10. *Let K_m^* be the operator defined in (4). Then, for any $\varphi\in C_B^2(0,\infty)$, we have*

$$|K_m^*(\varphi;y)-\varphi(y)|\le\frac{1}{2}\sqrt{\tau}\left(2+\sqrt{\tau}\right)\|\varphi\|_{C_B^2(0,\infty)}, \tag{43}$$

where τ is $K_m^*(\psi_{y,2};y)$ in Lemma 3.

Proof. Let $\varphi\in C_B^2(0,\infty)$. When referring to the Taylor series, obtain

$$\varphi(h)=\varphi(y)+\varphi'(y)(h-y)+\frac{1}{2}\varphi''(\xi)(h-y)^2, \tag{44}$$

where ξ between y and h, from which it follows:

$$|\varphi(h)-\varphi(y)|\le N_1|h-y|+\frac{1}{2}N_2(h-y)^2, \tag{45}$$

where

$$N_1 = \sup_{y\in(0,\infty)} \left|\varphi'(y)\right| = \left\|\varphi'\right\|_{C_B(0,\infty)} \le \|\varphi\|_{C_B^2(0,\infty)},$$
$$N_2 = \sup_{y\in(0,\infty)} \left|\varphi''(y)\right| = \left\|\varphi''\right\|_{C_B(0,\infty)} \le \|\varphi\|_{C_B^2(0,\infty)}, \quad (46)$$

because of (41). Thus, we have

$$|\varphi(h)-\varphi(y)| \le \left(|h-y| + \frac{1}{2}(h-y)^2\right)\|\varphi\|_{C_B^2(0,\infty)}. \quad (47)$$

Since

$$|K_m^*(\varphi;y)-\varphi(y)| = |K_m^*(\varphi(h)-\varphi(y);y)| \le K_m^*(|\varphi(h)-\varphi(y)|;y), \quad (48)$$

and $K_m^*(|h-y|;y) \le K_m^*((h-y)^2;y)^{1/2} = \sqrt{\tau}$, we get

$$|K_m^*(\varphi;y)-\varphi(y)| \le \left(K_m^*(|h-y|;y) + \frac{1}{2}K_m^*((h-y)^2;y)\right)\|\varphi\|_{C_B^2(0,\infty)}$$
$$\le \frac{1}{2}\sqrt{\tau}(2+\sqrt{\tau})\|\varphi\|_{C_B^2;(0,\infty)}. \quad (49)$$

The desired result is obtained. □

The Peetre's $\mathscr{K}$-functional is expressed by

$$K_2^*(\varphi,\delta) = \inf_{C_B^2(0,\infty)}\left\{\|\varphi-\mathrm{u}\|_{C_B(0,\infty)} + \delta\|\mathrm{u}\|_{C_B^2(0,\infty)} : \mathrm{u}\in C_B^2(0,\infty)\right\}. \quad (50)$$

The second-order modulus of continuity is defined by

$$\omega_2(\varphi,\delta) = \sup_{0<\mathrm{u}<\delta}\sup_{y\in(0,\infty)} |\varphi(y+2\mathrm{u}) - 2\varphi(y+\mathrm{u}) + \varphi(\mathrm{u})| \quad (51)$$

in [20]. The relation ω_2 and K_2^* is as follows:

$$K_2^*(\varphi,\delta) \le N\left\{\omega_2(\varphi;\delta) + \min(1,\delta)\|\varphi\|_{C_B(0,\infty)}\right\} \quad (52)$$

in [21].

Theorem 11. *Let $K_m^*(.;.)$ be the operator defined in (4). Then, for any $\varphi \in C_B(0,\infty)$, we have*

$$|K_m^*(\varphi;y)-\varphi(y)| \le 2N\left\{\omega_2\left(\varphi;\sqrt{\Delta_{m,y}}\right) + \min(1,\Delta_{m,y})\|\varphi\|_{C_B(0,\infty)}\right\}, \quad (53)$$

where N is a positive constant and $\Delta_{m,y} = \sqrt{\tau}(2+\sqrt{\tau})/2$ and $\tau = K_m^*(\psi_{y,2};y)$.

Proof. We prove this by using Theorem 10. Let $\mathrm{u}\in C_B^2(0,\infty)$. Since

$$|K_m^*(\varphi;y)-\varphi(y)| \le |K_m^*(\varphi-\mathrm{u};y)| + |K_m^*(\varphi;y)-\mathrm{u}(y)| + |\varphi(y)-\mathrm{u}(y)|$$
$$\le 2\|\varphi-\mathrm{u}\|_{C_B(0,\infty)} + \frac{1}{2}\sqrt{\tau}(2+\sqrt{\tau})\|\mathrm{u}\|_{C_B^2(0,\infty)}$$
$$\le 2\left(\|\varphi-\mathrm{u}\|_{C_B(0,\infty)} + \frac{1}{4}\sqrt{\tau}(2+\sqrt{\tau})\|\mathrm{u}\|_{C_B^2(0,\infty)}\right). \quad (54)$$

By taking infimum over all $\mathrm{u}\in C_B^2(0,\infty)$ on the right side of the last inequality and by using (50), we get

$$|K_m^*(\varphi;y)-\varphi(y)| \le 2K_2^*\left(\varphi;\frac{\sqrt{\tau}(2+\sqrt{\tau})}{4}\right). \quad (55)$$

This completes the proof, by using equation (52). □

6. Pointwise Estimates

Let us look at some pointwise estimates of rates of convergence of $K_m^*(\varphi;y)$. At first, the relationship between the local approximation and the local smoothness of the function is given. In this direction, let us give the following definitions. Let $s\in(0,1]$ and $\widehat{\mathrm{I}}\subset(0,\infty)$. In this case, a function $\varphi\in C_B(0,\infty)$ can be called $\mathrm{Lip}_{N_\varphi}(s)$ on $\widehat{I}$ if the following condition holds:

$$|\varphi(v)-\varphi(y)| \le N_{\varphi,s}|v-y|^s,\ v\in(0,\infty) \text{and}\ y\in\widehat{\mathrm{I}}, \quad (56)$$

where $N_{\varphi,s}$ is a constant that relies on φ and s mentioned above.

Theorem 12. *Let $\varphi\in C_B(0,\infty)\cap Lip_{N_\varphi}(s)$ such that s and $\widehat{I}$ given as above. In the circumstances, we give*

$$|K_m^*(\varphi;y)-\varphi(y)| \le N_{\varphi,s}\left[\left(\frac{mk^2-k+1}{(mk+1)(mk-k+1)}a_2(y)\right)^{s/2} + 2\left(d\left(y,\widehat{I}\right)\right)^s\right],\ y\in(0,\infty), \quad (57)$$

where $N_{\varphi,s}$ given above and $d(y,\widehat{I})$ is the distance between y and $\widehat{I}$. This distance is described as:

$$d\left(y,\widehat{I}\right) = \inf\left\{|v-y|, v\in\widehat{I}\right\} \quad (58)$$

Proof. Let us define the closure of the set $\widehat{I}$ as $\ddot{I}$. Then, one can argue that at least one point $v_0\in\ddot{\mathrm{I}}$ occurs where

$$d\left(y,\widehat{\mathrm{I}}\right) = |y-v_0|. \quad (59)$$

Then, due to the monotonicity properties of $(K_m^*)_{m\ge1}$, we

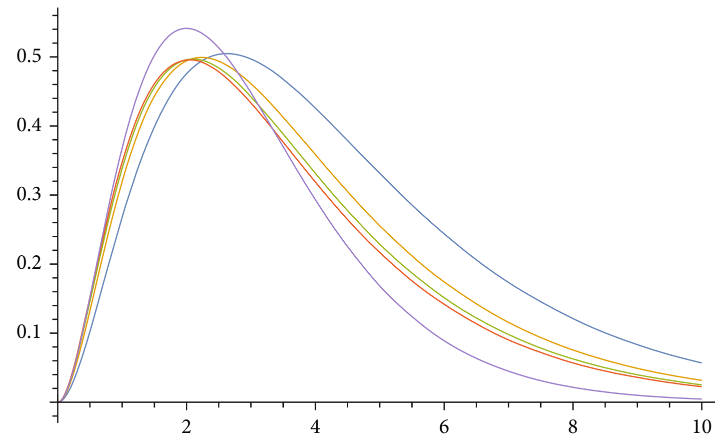

FIGURE 1: Graphics of the K_m^* operator for $k = 1/3, 1, 3, 30$, respectively, and $m = 10$ is fixed (blue for $k = 1/3$, orange for $k = 1$, green for $k = 3$, red for $k = 30$, and purple for $\varphi(y)$).

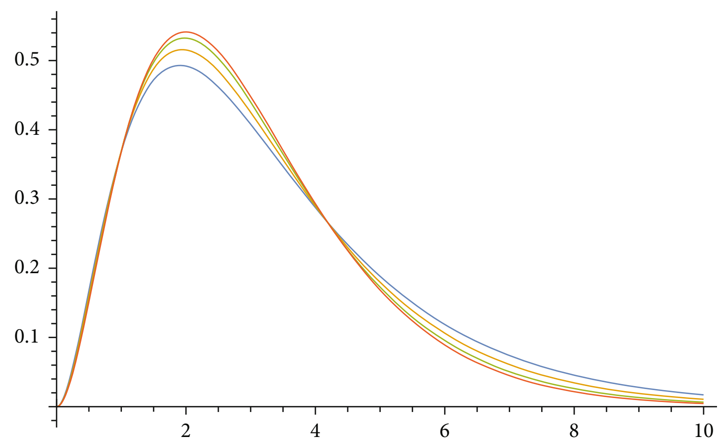

FIGURE 2: Graphics of the K_m^* operator for $m = 10,20,60$, respectively, and $k = 3$ is fixed (blue for $m = 10$, orange for $m = 20$, green for $m = 60$, and red for $\varphi(y)$).

deduce that

$$\begin{aligned}|K_m^*(\varphi;y)-\varphi(y)| &\le K_m^*(|\varphi(v)-\varphi(v_0)|;y)+K_m^*(|\varphi(y)-\varphi(v_0)|;y)\\ &\le N_{\varphi,s}[K_m^*(|v-v_0|^s;y)+|y-v_0|^s]\\ &\le N_{\varphi,s}[K_m^*(|v-y|^s;y)+2|y-v_0|^s].\end{aligned} \tag{60}$$

Then, from the definition of Hölder's inequality, we have

$$\begin{aligned}|K_m^*(\varphi;y)-\varphi(y)| &\le N_{\varphi,s}\left[K_m^*\left(|v-y|^2;y\right)^{S/2}+2\left(d\left(y,\hat{\Gamma}\right)\right)^s\right]\\ &= N_{\varphi,s}\left[\left(\frac{mk^2-k+1}{(mk+1)(mk-k+1)}a_2(y)\right)^{S/2}+2\left(d\left(y,\hat{\Gamma}\right)\right)^s\right],\end{aligned} \tag{61}$$

which concludes the theorem. □

Now, let us try to determine the local direct approximation of the new Gamma operator modification. Let us start with the Lipschitz type maximum function of order s presented in [22] for this goal, that is,

$$\tilde{\omega}_s(\varphi,y)=\sup_{0<v<\infty,\,v\neq y}\frac{|\varphi(v)-\varphi(y)|}{|v-y|^s}, \tag{62}$$

where $s\in(0,1]$ and $y\in(0,\infty)$.

Theorem 13. *For $\varphi\in C_B(0,\infty)$ and $\omega\tilde{}_s\in(0,1]$, the following inequality holds:*

$$|K_m^*(\varphi;y)-\varphi(y)|\le\tilde{\omega}_s(\varphi,y)K_m^*\left(\frac{mk^2-k+1}{(mk+1)(mk-k+1)}a_2(y)\right)^{s/2} \tag{63}$$

for $y\in(0,\infty)$.

Proof. Thanks to the definition of $\omega\tilde{}_s(\phi, y)$ given above and well-known Hölder inequality, we deduce that

$$\begin{aligned}|K_m^*(\varphi;y)-\varphi(y)| &\le K_m^*(|\varphi(v)-\varphi(y)|;y)\le \tilde{\omega}_s(\varphi,y)K_m^*(|v-y|^s;y)\\ &\le \tilde{\omega}_s(\varphi,y)K_m^*(|v-y|^2;y)^{s/2}\\ &\le \tilde{\omega}_s(\varphi,y)K_m^*\left(\frac{mk^2-k+1}{(mk+1)(mk-k+1)}a_2(y)\right)^{s/2}.\end{aligned} \tag{64}$$

As a result, the desired outcome is achieved. □

Now, finally, let us consider the following Lipschitz type space with two parameters, $c, d > 0$, such that

$$\mathrm{Lip}_N^{c,d}(s)=\left(\varphi\in C(0,\infty)\colon |\varphi(v)-\varphi(y)|\le N\frac{|v-y|^s}{(cy^2+dy+v)^{s/2}};y,v\in(0,\infty)\right) \tag{65}$$

introduced in [23] where $s \in (0, 1]$ and N is a positive constant.

Theorem 14. *For $\varphi \in Lip_N^{c,d}(s)$ and $y \in (0,\infty)$, then, we have*

$$|K_m^*(\varphi;y)-\varphi(y)|\le N\left[\frac{[(mk^2-k+1)/((mk+1)(mk-k+1))]a_2(y)}{cy^2+dy}\right], \tag{66}$$

where $c, d > 0$.

Proof. The proof is divided into two parts. For the first, we use $s = 1$, which means

$$\begin{aligned}|K_m^*(\varphi;y)-\varphi(y)| &\le K_m^*(|\varphi(v)-\varphi(y)|;y),\\ &\le NK_m^*\left(\frac{|v-y|}{\sqrt{cy^2+dy+1};y}\right),\\ &\le \frac{N}{\sqrt{cy^2+dy}}K_m^*(|v-y|;y),\end{aligned} \tag{67}$$

for $\varphi \in Lip_N^{c,d}(s)$ and $y \in (0,\infty)$. We conclude that

$$\begin{aligned}|K_m^*(\varphi;y)-\varphi(y)| &\le \frac{N}{\sqrt{cy^2+dy}}\left[K_m^*(|v-y|^2;y)\right]^{1/2}\\ &\le N\left[\frac{[(mk^2-k+1)/((mk+1)(mk-k+1))]a_2(y)}{cy^2+dy}\right]^{1/2},\end{aligned} \tag{68}$$

by using the well-known Cauchy-Schwarz inequality, which validates the theory for $s = 1$. Then, let us consider $s \in (0, 1)$. For $\varphi \in \mathrm{Lip}_N^{c,d}(s)$ and $y \in (0,\infty)$, we obtain that

$$|K_m^*(\varphi;y)-\varphi(y)|\le \frac{N}{(cy^2+dy)^{s/2}}K_m^*(|v-y|^s;y). \tag{69}$$

We derive that

$$\begin{aligned}|K_m^*(\varphi;y)-\varphi(y)| &\le \frac{N}{(cy^2+dy)^{s/2}}K_m^*(|v-y|^s;y)\\ &\le \frac{N}{(cy^2+dy)^{s/2}}(K_m^*(|v-y|;y))^s\end{aligned} \tag{70}$$

with the help of the well-known Hölder inequality. Finally, we have

$$\begin{aligned}|K_m^*(\varphi;y)-\varphi(y)| &\le \frac{N}{(cy^2+dy)^{s/2}}(K_m^*(|v-y|^2;y))^{s/2}\\ &\le N\left[\frac{[(mk^2-k+1)/((mk+1)(mk-k+1))]a_2(y)}{cy^2+dy}\right]^{s/2},\end{aligned} \tag{71}$$

which completes the proof by applying the well-known Cauchy-Schwarz inequality. □

For the case of $c = 1$ and $d = 0$, we have the following corollary.

Corollary 15. *The local estimate in parametric Lipschitz space is obtained for special fixed parameters $c = 1$ and $d = 0$.*

$$|K_m^*(\varphi;y)-\varphi(y)|\le N\left(\frac{mk^2-k+1}{(mk+1)(mk-k+1)}\right) \tag{72}$$

for $\varphi \in Lip_N^{1,0}(s)$ and $y \in (0,\infty)$.

7. Numerical Example

In this section of the article, we provide some numerical examples to verify the rates of convergence of $K_m^*(\varphi;y)$ in two dimensions ($m = 10$ is fixed for Figure 1 and $k = 3$ is fixed for Figure 2). In our first example, we compare the operator $K_m^*(\varphi;y)$ with the classical Gamma operator.

In this example, $K_m^*(\varphi;y)$ and $\varphi(y) = y^2e^{-y}$ applied for $\varphi : [0, 10] \longrightarrow [0,\infty)$.

In Figure 1, it is seen that the operator puts closer to the function as the value of k gets larger ($m = 10$ is fixed). In Figure 2, it is seen that the operator puts closer to the function as the value of m gets larger ($k = 3$ is fixed).

8. Concluding Remarks

We have defined a new form of Gamma operator by considering k-Gamma function. With the operator defined, the conditions of the Korovkin theorem are completed. Later, Voronovskaya type theorem, weighted approximation, the rates of convergence, and pointwise estimates are obtained. Finally, we give numerical example to confirm its approximation.

Data Availability

Data sharing is not applicable to this article as no datasets were generated or analyzed during the current study.

Conflicts of Interest

The authors declare that they have no conflicts of interest.

Acknowledgments

I would like to thank the Scientific and Technological Research Council of Turkey (TUBİTAK) for the graduate scholarship that supported the second author.

References

[1] G. K. Weierstrass, "Uber Die Analytische Darstellbarkeit Sogenannter Willkürlicher Funktionen Einer Reellen Veränderlichen," *Sitzungsberichte der Königlich Preußischen Akademie der Wissenschaften zu Berlin*, vol. 2, pp. 633–639, 1885.

[2] P. P. Korovkin, "On convergence of linear operators in the space of continuous functions," *Doklady Akademii Nauk*, vol. 90, no. 953, pp. 961–964, 1953.

[3] J. King, "Positive linear operators which preserve x^2," *Acta Mathematica Hungarica*, vol. 99, pp. 203–208, 2003.

[4] A. Lupas and M. Müller, "Approximationseigenschaften der Gammaoperatoren," *Mathematische Zeitschrift*, vol. 98, pp. 208–226, 1967.

[5] R. Askey, "The q-Gamma and q-Beta functions," *Applicable Analysis*, vol. 8, no. 2, pp. 125–141, 1978.

[6] W. Cheng and Q. B. Cai, "Generalized (p, q)-Gamma-type operators," *Journal of Function Spaces*, vol. 2020, Article ID 8978121, 10 pages, 2020.

[7] Ö. Betüs and F. Usta, "Approximation of functions by a new type of Gamma operators," *Numerical Methods for Partial Differential Equations*, pp. 1–12, 2020.

[8] Q. B. Cai, B. Cekim, and G. Icoz, "Gamma Generalization Operators Involving Analytic Functions," *Mathematics*, vol. 9, pp. 1547-1548, 2021.

[9] H. Karsli, "Rate of convergence of new Gamma type operators for functions with derivatives of bounded variation," *Mathematical and Computer Modelling*, vol. 45, no. 5-6, pp. 617–624, 2007.

[10] R. Ozaselik, E. E. Kara, F. Usta, and J. K. Ansari, "Approximation properties of a new family of Gamma operators and their applications," *Advances in Difference Equations*, vol. 1, 13 pages, 2021.

[11] C. G. Kokologiannaki and V. Krasniqi, "Some properties of the k-Gamma function," *Le Matematiche*, vol. 68, pp. 13–22, 2013.

[12] K. J. Singh, N. P. Agrawal, and A. Kajla, "Approximation by modified q-Gamma type operators via A-statistical convergence and power series method," *Linear and Multilinear Algebra*, pp. 1–21, 2021.

[13] H. M. Srivastava, G. Icöz, and B. Çekim, "Approximation properties of an extended family of the Szász-Mirakjan beta-type operators," *Axioms*, vol. 8, no. 4, pp. 1–13, 2019.

[14] F. Usta and Ö. Betüs, "New modification of Gamma operators with a better error estimation," *Linear Multilinear Algebra*, vol. 70, no. 11, pp. 1–12, 2020.

[15] R. Daz and E. Pariguan, "On hypergeometric functions and k-Pochhammer symbol," *Divulgaciones Matematicas*, vol. 15, pp. 179–192, 2007.

[16] J. Karwowski and A. H. Witek, "Biconfluent Heun equation in quantum chemistry: harmonium and related systems," *Theoretical Chemistry Accounts*, vol. 1494, no. 133, pp. 1–11, 2014.

[17] A. Tassaddiq, "A new representation of the k-Gamma functions," *Mathematics*, vol. 7, no. 2, pp. 1–3, 2019.

[18] F. Altomare and M. Campiti, *Korovkin-Type Approximation Theory and Its Applications. de Gruyter Studies in Mathematics*, Walter de Gruyter & Co, Berlin, 1994.

[19] A. Gadjiev, "Theorems of Korovkin type," *Mathematical Notes of the Academy of Sciences of the USSR*, vol. 20, no. 5, pp. 995–998, 1976.

[20] R. A. DeVore, G. G. Lorentz, R. A. DeVore, and G. G. Lorentz, *Bernstein Polynomials*, Springer-Verlag, 1993.

[21] A. Ciupa, "A class of integral Favard-Szász type operators," *Studia Universitatis Babes-Bolyai Chemia*, vol. 40, no. 1, pp. 39–47, 1995.

[22] B. Lenze, "On Lipschitz-type maximal functions and their smoothness spaces," *Indagationes Mathematicae (Proceedings)*, vol. 91, no. 1, pp. 53–63, 1988.

[23] M. A. Özarslan and H. AktuÄŸlu, "Local approximation properties for certain King type operators," *Univerzitet u Nišu*, vol. 27, no. 1, pp. 173–181, 2013.

Hindawi
Journal of Function Spaces
Volume 2022, Article ID 9637098, 9 pages
https://doi.org/10.1155/2022/9637098

Research Article

Fractional Complex Transform and Homotopy Perturbation Method for the Approximate Solution of Keller-Segel Model

Xiankang Luo[1] **Muhammad Nadeem**[1] **Mustafa Inc**[2,3,4] **and Suliman Dawood**[5]

[1]*Faculty of Science, Yibin University, 644000 Yibin, China*
[2]*Department of Computer Engineering, Biruni University, Istanbul, Turkey*
[3]*Science Faculty, Department of Mathematics, Firat University, 23119 Elazig, Turkey*
[4]*Department of Medical Research, China Medical University, Taichung, Taiwan*
[5]*Department of Mathematics, Sheba Region University, Marib, Yemen*

Correspondence should be addressed to Muhammad Nadeem; nadeem@yibinu.edu.cn
and Suliman Dawood; sulimanseddek@usr.ac

Received 17 June 2022; Revised 28 June 2022; Accepted 14 July 2022; Published 28 July 2022

Academic Editor: Yusuf Gurefe

In this paper, we propose an innovative approach to determine the approximate solution of the coupled time-fractional Keller-Segel (K-S) model. We use the fractional complex transform (FCT) to switch the model into its differential partner, and then, the homotopy perturbation method (HPM) is introduced to tackle its nonlinear elements using He's polynomials. This two-scale theory helps to define the physical meaning of the FCT for the solution of the K-S model. Some examples are illustrated to show that the proposed scheme presents the significant results. The considerable findings show that this strategy does not require any assumptions and also reduces the massive computations without imposing any constraints. This technique is also suitable in functional studies of fractal calculus due to its powerful and robust support for nonlinear problems.

1. Introduction

Fractional differential equations (FDEs) are the generalizations of classical differential equations with integer orders. It is worth reporting that some mathematical models of integer-order derivatives particularly nonlinear models do not work adequately for most of the cases [1–3]. This is because integer order derivatives are limited operators and are inappropriate for infinite variance whereas fractional order derivatives are worldwide to take account of the domination of the neighborhood. In recent years, nonlinear FDEs in mathematical physics are competing against a principal role in miscellaneous domains, such as biological science, applied science, signal processing, control theory, finance, and fractal dynamics [4–7].

In 1970, Keller and Segel introduced a hypothesis to express the combination system of cellular slime mold by chemical fascination. The K-S model has broadly been practiced for chemotaxis terms due to its competency to capture the key facts and its impulsive nature. The significance of chemotaxis has achieved much attraction due to its crucial function in a broad variety of biological occurrences [8, 9]. In this article, we examine the coupled time-fractional K-S model of the form

$$\begin{aligned}\frac{\partial^\delta \eta}{\partial \wp^\delta} &= a\frac{\partial^2 \eta}{\partial \mathfrak{I}^2} - \frac{\partial}{\partial \mathfrak{I}}\left(\eta \frac{\partial}{\partial \mathfrak{I}}\chi(\varsigma)\right),\\ \frac{\partial^\delta \varsigma}{\partial \wp^\delta} &= b\frac{\partial^2 \varsigma}{\partial \mathfrak{I}^2} + cu - dv,\end{aligned} \tag{1}$$

subject to the initial solutions, we get

$$\begin{aligned}\eta(\mathfrak{I},0) &= \eta_0(\mathfrak{I}),\\ \varsigma(\mathfrak{I},0) &= \varsigma_0(\mathfrak{I}),\end{aligned} \tag{2}$$

where $\eta(\Im, \wp)$ and $\varsigma(\Im, \wp)$ represent the bacterial density and the concentration of chemical substance as a function of $\Im$ and $\wp$, respectively, and $D_{\Im}(\eta(\Im,\wp)D_{\Im}\chi(\varsigma))$ denotes the chemotactic term and shows that the cells are sensitive to the chemicals and are attracted by them [10]. The sensitivity function $\chi(\varsigma)$ is a smooth function which describes the cell's perception and response to the chemical stimulus ς while $a, b, c,$ and d are positive constants. If $\delta = 1$, the time-fractional K-S model (1) leads to a simple nonlinear differential equation that has been studied extensively whereas $D_{\wp}^{\delta}$ taken as Caputo's sense [11] and $D_{\wp}^{\delta} = \partial^{\delta}/\partial\wp^{\delta}$ is He's fractional derivative defined [12, 13]

$$\frac{\partial^{\delta}\eta}{\partial\wp^{\delta}} = \frac{1}{\Gamma(n-\delta)}\frac{d^n}{dt^n}\int (s-\wp)^{n-\delta-1}[\eta_0(s) - \eta(s)]ds. \quad (3)$$

Many actions in physics and engineering can be precisely characterized by utilizing differential equations with various sorts of fractional derivatives. The finding of the approximate and exact solution of FDEs is a very crucial challenge. There have been a lot of developments to solve FDEs in nonlinear dynamics. FDEs are used extensively because they do not have exact solutions, and thus, approximate and numerical solutions are needed. The homotopy perturbation method (HPM) [14] is one of the most famous approaches to achieve the series solutions of linear and nonlinear differential equations of arbitrary orders. Later, various methods have been developed to show that HPM a is very efficient and powerful tool for finding the approximate solution to FDEs [15–18]. In order to get the solution of the K-S model, many powerful and efficient techniques have been suggested to obtain the analytical solutions such as Laplace homotopy perturbation method [19], iterative method [20], homotopy perturbation Sumudu transform [21], and natural homotopy transform method [22] with a logic sensitivity function and small diffusivity. Some partial differential equations with fractional order are not easy to solve, and then, their approximate solution can be evaluated. The two-scale approach converts the fractional order to a simple partial differential equation which is now easy to solve by the homotopy perturbation method.

This study presents the idea of a two-scale method to obtain the solution of the fractional K-S model in Caputo sense. The FCT converts the model into its differential partner, and then, HPM is introduced to bring down the nonlinear terms in algebraic series. The quality of the current method is appropriate to provide the analytical results to the given examples. This study is summarized as follows: In Section (2), we recall some basic definitions of fractional calculus. We present the idea of the homotopy perturbation method and the two-scale approach in Sections (3) and (4), respectively. Some numerical examples are provided to demonstrate the performance of this approach in Section (5) and the discussion of results in Section (6). The conclusion is given in Section (7).

2. Preliminary Concepts

Definition 1. The Riemann-Liouville fractional integral operator of order $\delta > 0$ of a function $f(t) \in C_{\mu}$, $\mu \geq -1$, is defined as [23]

$$J^{\delta}f(\wp) = \frac{1}{\Gamma(1+\delta)}\int_0^{\wp}(\wp-\tau)f(\tau)d\tau, \quad J^0 f(\wp) = f(\wp). \quad (4)$$

Definition 2. The Caputo fractional derivative of $f(\wp)$ in the Caputo sense is given [23]

$$D^{\gamma}w(\Im,\wp) = \begin{cases} \dfrac{1}{\Gamma(\gamma-\delta)}\displaystyle\int_0^{\wp}(\wp-\tau)^{\gamma-\delta-1}\frac{\partial^{\gamma}w(\Im,\wp)}{\partial\tau^{\gamma}}d\tau, & \gamma-1<\delta<\gamma, \\ \dfrac{\partial w(\Im,\wp)}{\partial\wp^{\gamma}}, & \delta=\gamma\in\mathbb{N}. \end{cases} \quad (5)$$

Lemma 3. *If $\gamma - 1 < \delta \leq \gamma$, $\gamma \in \mathbb{N}$, $\wp>0$, $w \in C_{-1}^{\gamma}$, then*

$$D^{\delta}J^{\delta}w(\wp) = w(\wp),$$
$$D^{\delta}J^{\delta}w(\wp) = w(\wp) - \sum_{k=0}^{\gamma-1} w^k(0^+)\frac{\wp^k}{k!}, \quad \wp > 0. \quad (6)$$

The fractional derivatives are considered in Caputo sense which allows the conditions to deal with the expression of the problems.

3. Basic Idea of the Homotopy Perturbation Method

In this segment, we explain the fundamental concept of HPM. Let the following nonlinear equation [24]

$$L(\eta) - f(\varrho) = 0, \varrho \in \Upsilon, \quad (7)$$

with boundary conditions

$$B\left(\eta, \frac{\partial\eta}{\partial n}\right) = 0, \quad \varrho \in \Theta, \quad (8)$$

where L is a general function with boundary operator $B, f(\varrho)$ is analytic function, and Θ is the boundary of the domain Υ. The operator L can normally be separated into two operators with M as a linear and N being a nonlinear operator. Thus, Equation (7) can be accompanied as follows:

$$M(\eta) + N(\eta) - f(\varrho) = 0. \quad (9)$$

Let us consider $\varsigma(r, p): \Upsilon \times [0, 1] \longrightarrow \mathbb{R}$ that confirms or

$$H(\varsigma, q) = (1-q)[L(\varsigma) - M(\eta_0)] + q[L(\varsigma) - N(\varsigma) - f(\varrho)], \quad (10)$$

$$H(\varsigma, q) = L(\varsigma) - M(\eta_0) + qM(\eta_0) + q[N(\varsigma) - f(\varrho)] = 0, \tag{11}$$

where $q \in [0, 1]$ is said to be a homotopy parameter and η_0 is an initial approximation of Equation (7). According to HPM, we can take q as a small element, and suppose that the solution of Equation (11) can be written as a power series of q:

$$\varsigma = \varsigma_0 + qv_1 + q^2\varsigma_2 + \cdots. \tag{12}$$

Considering $q = 1$, the approximate solution of Equation (7) is obtained as follows:

$$\eta = \lim_{q \longrightarrow 1} \varsigma = \varsigma_0 + \varsigma_1 + \varsigma_2 + \varsigma_3 + \cdots. \tag{13}$$

Using Equations (11) and (12), we can identify the similar powers of q to obtain the following series solution form:

$$\begin{aligned} q^0 &: \varsigma_0 - f(\mathfrak{I}) = 0, \\ q^1 &: \varsigma_1 - H(\varsigma_0) = 0, \\ q^2 &: \varsigma_2 - H(\varsigma_0, \varsigma_1) = 0, \\ q^3 &: \varsigma_3 - H(\varsigma_0, \varsigma_1, \varsigma_2) = 0, \\ &\vdots, \end{aligned} \tag{14}$$

where $H(\varsigma_0, \varsigma_1, \varsigma_2, \cdots, \varsigma_j)$ depending upon $\varsigma_0, \varsigma_1, \varsigma_2, \cdots, \varsigma_j$ called He's polynomials can be computed by adopting the following rule:

$$H(\varsigma_0, \varsigma_1, \varsigma_2, \cdots, \varsigma_j) = \frac{1}{j!} \frac{\partial^j}{\partial q^j} N\left(\sum_{i=0}^{j} \varsigma_i q^i \right) \Bigg|_{q=0}. \tag{15}$$

The system of nonlinear equations in (14) is evidently simple to calculate, and thus, the components $\varsigma_i, i \geq 0$ of HPM can be identified easily which leads to the series solutions very rapidly.

4. Fractional Complex Transform

The dimension and scale are highly important elements due to its impressive outcomes and properties of the configuration through the modeling of a problem. FCT is a systematic technique that turns FDEs into its differential parts in a steady period and is described as [25–27]

$$\Delta S = \frac{\Delta \wp^\delta}{\Gamma(1 + \delta)}, \tag{16}$$

where ΔS is the slighter scale and $\Delta \wp$ is the greater scale. The time fractional K-S model reacts discontinuously on a slighter scale, particularly at the highest point whereas it anticipates a plane solitary wave on the greater scale. Thus, Equation (11) is considered two-scale transform [28–30]. The outcomes of any study problem depend on the scale. For an observable scale, the fluid is consistent; therefore, Newton's laws can be applied; however, they are illegitimate at the molecular scale. If the motion is free of time, then Newton's law is acceptable; otherwise, it can be revoked.

4.1. Convergence Theorem. Let P and Q be the Banach spaces and $\varsigma : P \longrightarrow Q$ be a contraction nonlinear mapping. If the sequence generated by HPM such as

$$\eta_n(P, \wp) = \varsigma(\eta_{n-1}(P, \wp)) = \sum_{i=0}^{n-1} \eta_i(P, \wp), \quad n = 1,2,3, \cdots, \tag{17}$$

then the following conditions must be true:

(1) $\|\eta_n(P, \wp) - \eta(P, \wp)\| \leq \varphi^n \|\psi(P, \wp) - \eta(P, \wp)\|$

(2) $\eta_n(P, \wp)$ is always in the neighborhood of $\eta(P, \wp)$ meaning $\eta_n(P, \wp) \in B(\eta(P, \wp), r) = \{\eta^*(P, \wp) / \|\eta^*(P, \wp) - \eta(P, \wp)\|\}$

(3) $\lim_{n \longrightarrow \infty} \eta_n(P, \wp) = \eta(P, \wp)$

Proof.

(1) We prove condition (1) by induction on n, $\|\eta_1 - \eta\| = \|G(\eta_0) - \eta\|$, and according to the Banach fixed point theorem, ς has a fixed point η meaning $\varsigma(\eta) = \eta$; therefore,

$$\|\eta_1 - \eta\| = \|G(\eta_0) - \eta\| = \|G(\eta_0) - G(\eta)\| \leq \varphi \|\eta_0 - \eta\| = \varphi \|\psi(P, \wp) - \eta\|, \tag{18}$$

since ς is a contraction mapping. Assume that $\|\eta_{n-1} - \eta\| \leq \varphi^{n-1} \|\psi(P, 0) - \eta(P, \wp)\|$ is an induction hypothesis, then

$$\|\eta_n - \eta\| = \|G(\eta_{n-1}) - G(\eta)\| \leq \varphi \|\eta_{n-1} - \eta\| \leq \varphi \varphi^{n-1} \|\psi(P, \wp) - \eta\| \tag{19}$$

(2) The first concern is to demonstrate that $\psi(P, \wp) \in B(\eta(P, \wp), r)$, and this is achieved by induction on m. So, for $m = 1$, $\|\psi(P, \wp) - \eta(P, \wp)\| = \|\eta(P, 0) - \eta(P, \wp)\| \leq r$ with $\eta(P, 0)$ the initial condition. Assume that $\|\psi(P, \wp) - \eta(P, \wp)\| \leq r$ for $m - 2$ is an induction hypothesis, then

$$\begin{aligned} \|\psi(P, \wp) - \eta(P, \wp)\| &= \psi_{m-2}(P, \wp) - \frac{f_m(P)}{\Gamma(\delta - m + 1)} \wp^{\delta - m} \Bigg\| \\ &\leq \|\psi_{m-1}(P, \wp) - \eta(P, \wp)\| + \left\| \frac{f_m(P)}{\Gamma(\delta - m + 1)} \wp^{\delta - m} \right\| = r. \end{aligned} \tag{20}$$

Now, for all $n \geq 1$, using condition (1), we have

$$\|\eta_n - \eta\| \leq \varphi^n \|\psi(P,\wp) - \eta\| \leq \varphi^n r \leq r. \quad (21)$$

(3) Using condition (2) and the fact that $\lim_{n\longrightarrow\infty}\phi^n = 0$ yields that $\lim_{n\longrightarrow\infty}\|\eta_n - \eta\| = 0$; therefore,

$$\lim_{n\longrightarrow\infty} \eta_n = \eta. \quad (22)$$

Thus, η converges. □

5. Numerical Examples

In this segment, we implement a two-scale method to achieve the approximate solution of the K-S model in one dimension. Results disclose that this approach is an extremely efficient and powerful aid for solving FDEs.

5.1. Example 1. Consider the K-S model in one dimension given as

$$\frac{\partial^\delta \eta}{\partial \wp^\delta} = a\frac{\partial^2 \eta}{\partial \mathfrak{I}^2} - \frac{\partial}{\partial \mathfrak{I}}\left(\eta \frac{\partial}{\partial \mathfrak{I}}\chi(\varsigma)\right), \quad \frac{\partial^\delta \varsigma}{\partial \wp^\delta} = b\frac{\partial^2 \varsigma}{\partial \mathfrak{I}^2} + c\eta - d\varsigma, \quad (23)$$

with the initial conditions

$$\eta(\mathfrak{I},0) = me^{-\mathfrak{I}^2}, \quad \varsigma(\mathfrak{I},0) = ne^{-\mathfrak{I}^2}. \quad (24)$$

Considering that the sensitivity function $\chi(\varsigma) = 0$; thus, the chemotactic term is zero, i.e., $\partial/\partial\mathfrak{I}(\eta\,\partial/\partial\mathfrak{I}\chi(\varsigma)) = 0$ and using

$$S = \frac{\wp^\delta}{\Gamma(1+\delta)}. \quad (25)$$

Thus, the coupled K-S model of Equation (23) becomes

$$\frac{\partial \eta}{\partial S} = \frac{\partial \eta}{\partial S}, \quad \frac{\partial \varsigma}{\partial S} = b\frac{\partial^2 \varsigma}{\partial \mathfrak{I}^2} + c\eta - d\varsigma. \quad (26)$$

We can use HPM with He's polynomials on the system of Equation (26), and we get

$$\frac{\partial \eta_1}{\partial S} = a\frac{\partial^2 \eta_0}{\partial \mathfrak{I}^2}, \quad \eta_1(\mathfrak{I},0), \quad (27)$$

$$\frac{\partial \varsigma_1}{\partial S} = b\frac{\partial^2 \varsigma_0}{\partial \mathfrak{I}^2} + c\eta_0 - d\varsigma_0, \quad \varsigma_1(\mathfrak{I},0), \quad (28)$$

$$\frac{\partial \eta_2}{\partial S} = a\frac{\partial^2 \eta_1}{\partial \mathfrak{I}^2}, \quad \eta_2(\mathfrak{I},0), \quad (29)$$

$$\frac{\partial \varsigma_2}{\partial S} = b\frac{\partial^2 \varsigma_1}{\partial \mathfrak{I}^2} + c\eta_1 - d\varsigma_1, \quad \varsigma_2(\mathfrak{I},0), \quad (30)$$

$$\frac{\partial \eta_3}{\partial S} = a\frac{\partial^2 \eta_2}{\partial \mathfrak{I}^2}, \quad \eta_3(\mathfrak{I},0), \quad (31)$$

$$\frac{\partial \varsigma_3}{\partial S} = b\frac{\partial^2 \varsigma_2}{\partial \mathfrak{I}^2} + c\eta_2 - d\varsigma_2, \quad \varsigma_3(\mathfrak{I},0). \quad (32)$$

With the help of Equation (24), we can get the following iterations:

$$\eta(\mathfrak{I},0) = me^{-\mathfrak{I}^2}, \quad (33)$$

$$\varsigma(\mathfrak{I},0) = ne^{-\mathfrak{I}^2}, \quad (34)$$

$$\eta_1(\mathfrak{I},S) = 2am\left[-1 + 2\mathfrak{I}^2\right]e^{-\mathfrak{I}^2}S, \quad (35)$$

$$\varsigma_1(\mathfrak{I},S) = \left[2bn\left(2\mathfrak{I}^2 - 1\right) + (cm - dn)\right]e^{-\mathfrak{I}^2}S, \quad (36)$$

$$\eta_2(\mathfrak{I},S) = 4a^2m\left[3 - 12\mathfrak{I}^2 + 4\mathfrak{I}^4\right]e^{-\mathfrak{I}^2}\frac{S^2}{2}, \quad (37)$$

$$\begin{aligned}\varsigma_2(\mathfrak{I},S) = \Big[&d(-cm + dn) + 2acm\left(-1 + 2\mathfrak{I}^2\right) \\ &+ 2b\left(-1 + 2\mathfrak{I}^2\right)(cm - 2dn) \\ &+ 4b^2\left(3 - 12\mathfrak{I}^2 + 4\mathfrak{I}^4\right)\Big]e^{-\mathfrak{I}^2}\frac{S^2}{2},\end{aligned} \quad (38)$$

$$\eta_3(\mathfrak{I},S) = 8a^3m\left[-15 + 90\mathfrak{I}^2 - 60\mathfrak{I}^4 + 8\mathfrak{I}^6\right]e^{-\mathfrak{I}^2}\frac{S^3}{6}, \quad (39)$$

$$\begin{aligned}\varsigma_3(\mathfrak{I},S) = \Big[&d^2(cm - dn) + 2bd(-2cm + 3dn)\left(-1 + 2\mathfrak{I}^2\right) \\ &+ 4a^2cm\left(3 - 12\mathfrak{I}^2 + 4\mathfrak{I}^4\right) \\ &+ 4b^2(cm - 3dn)\left(3 - 12\mathfrak{I}^2 + 4\mathfrak{I}^4\right) \\ &+ 8b^3n\left(-15 + 90\mathfrak{I}^2 - 60\mathfrak{I}^4 + 8\mathfrak{I}^6\right) \\ &+ 2acm\left\{d - 2dx^2 + b\left(6 - 24\mathfrak{I}^2 + 8\mathfrak{I}^4\right)\right\}\Big]e^{-\mathfrak{I}^2}\frac{S^3}{6}.\end{aligned} \quad (40)$$

In the same way, other of the elements can be identified. So, the series solution of Equation (23) with the help of Equation (25) is as follows:

$$\begin{aligned}\eta(\mathfrak{I},\wp) = me^{-\mathfrak{I}^2} &+ 2ame^{-\mathfrak{I}^2}\left[-1 + 2\mathfrak{I}^2\right]\left(\frac{\wp^\delta}{\Gamma(1+\delta)}\right) \\ &+ 2a^2me^{-\mathfrak{I}^2}\left[3 - 12\mathfrak{I}^2 + 4\mathfrak{I}^4\right]\left(\frac{\wp^\delta}{\Gamma(1+\delta)}\right)^2 \\ &+ \frac{4}{3}a^3me^{-\mathfrak{I}^2}\left[-15 + 90\mathfrak{I}^2 - 60\mathfrak{I}^4 + 8\mathfrak{I}^6\right]\left(\frac{\wp^\delta}{\Gamma(1+\delta)}\right)^3,\end{aligned} \quad (41)$$

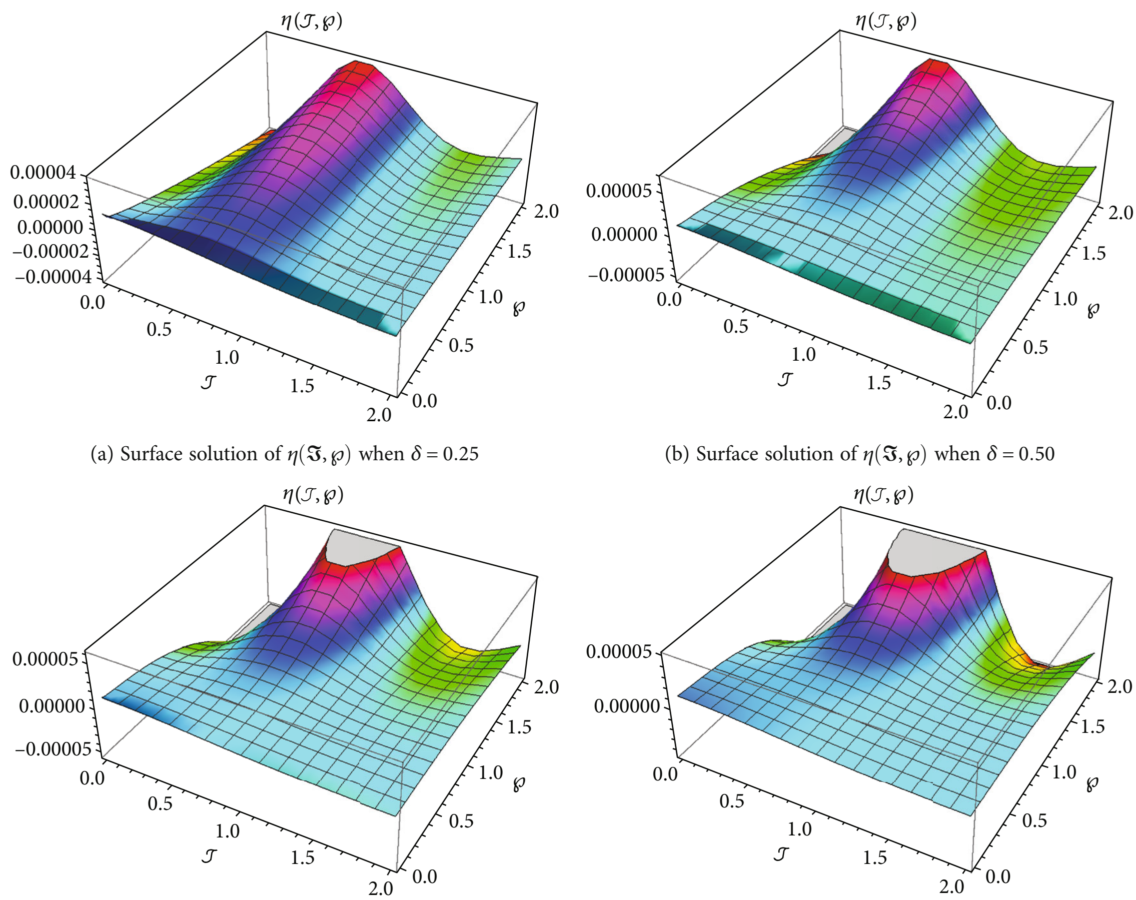

(a) Surface solution of $\eta(\mathfrak{I},\wp)$ when $\delta = 0.25$

(b) Surface solution of $\eta(\mathfrak{I},\wp)$ when $\delta = 0.50$

(c) Surface solution of $\eta(\mathfrak{I},\wp)$ when $\delta = 0.75$

(d) Surface solution of $\eta(\mathfrak{I},\wp)$ when $\delta = 1$

Figure 1: The surface solution of $\eta(\mathfrak{I},\wp)$ for distinct values of δ.

$$\begin{aligned}
\varsigma(\mathfrak{I},\wp) = {} & ne^{-\mathfrak{I}^2} + \left[2bn\left(2\mathfrak{I}^2-1\right)+(cm-dn)\right]e^{-\mathfrak{I}^2}\left(\frac{\wp^\delta}{\Gamma(1+\delta)}\right)\\
& + \frac{1}{2}\left[d(-cm+dn)+2acm\left(-1+2\mathfrak{I}^2\right)\right.\\
& + 2b\left(-1+2\mathfrak{I}^2\right)(cm-2dn)\\
& \left.+ 4b^2\left(3-12\mathfrak{I}^2+4\mathfrak{I}^4\right)\right]e^{-\mathfrak{I}^2}\left(\frac{\wp^\delta}{\Gamma(1+\delta)}\right)^2\\
& + \frac{1}{6}\left[12b^2cm+4bcdm-120b^3n-36b^2dn\right.\\
& - 6bd^2n-d^3n-48b^2cmx^2-8bcdmx^2\\
& + 72b^3nx^2 144b^2dnx^2+12bd^2nx^2+16b^2cmx^4\\
& - 48b^3nx^4-48b^2dnx^4+64b^3nx^6+4a^2cm\left(3-12\mathfrak{I}^2+4\mathfrak{I}^4\right)\\
& \left.+ 2amc\left(d-2dx^2+b\left(6-24\mathfrak{I}^2+8\mathfrak{I}^4\right)\right)\right]e^{-\mathfrak{I}^2}\left(\frac{\wp^\delta}{\Gamma(1+\delta)}\right)^3.
\end{aligned} \tag{42}$$

Only some of terms are evaluated while the other terms can be obtained using the iterative formula. As a result, the solution of the system of Equation (23) is as follows:

$$\begin{aligned}
\eta(\mathfrak{I},\wp) &= \eta(\mathfrak{I},0)+\eta_1(\mathfrak{I},0)+\eta_2(\mathfrak{I},0)+\eta_3(\mathfrak{I},0)+\cdots,\\
\varsigma(\mathfrak{I},\wp) &= \varsigma(\mathfrak{I},0)+\varsigma_1(\mathfrak{I},0)+\varsigma_2(\mathfrak{I},0)+\varsigma_3(\mathfrak{I},0)+\cdots.
\end{aligned} \tag{43}$$

5.2. Example 2.

$$\begin{aligned}
\frac{\partial^\delta \eta}{\partial \wp^\delta} &= a\frac{\partial^2\eta}{\partial \mathfrak{I}^2} - \frac{\partial}{\partial \mathfrak{I}}\left(\eta\frac{\partial}{\partial \mathfrak{I}}\chi(\varsigma)\right),\\
\frac{\partial^\delta \varsigma}{\partial \wp^\delta} &= b\frac{\partial^2\varsigma}{\partial \mathfrak{I}^2} + c\eta - d\varsigma,
\end{aligned} \tag{44}$$

with the initial conditions

$$\begin{aligned}
\eta(\mathfrak{I},0) &= me^{-\mathfrak{I}^2},\\
\varsigma(\mathfrak{I},0) &= ne^{-\mathfrak{I}^2}.
\end{aligned} \tag{45}$$

Considering that the sensitivity function $\chi(\varsigma)=\varsigma$; thus, the chemotactic term becomes $\partial/\partial\mathfrak{I}(\eta\partial/\partial\mathfrak{I}\chi(h)) = \partial\eta/\partial\mathfrak{I}\,\partial h/\partial\mathfrak{I} + \eta\partial^2 h/\partial\mathfrak{I}^2$ and using

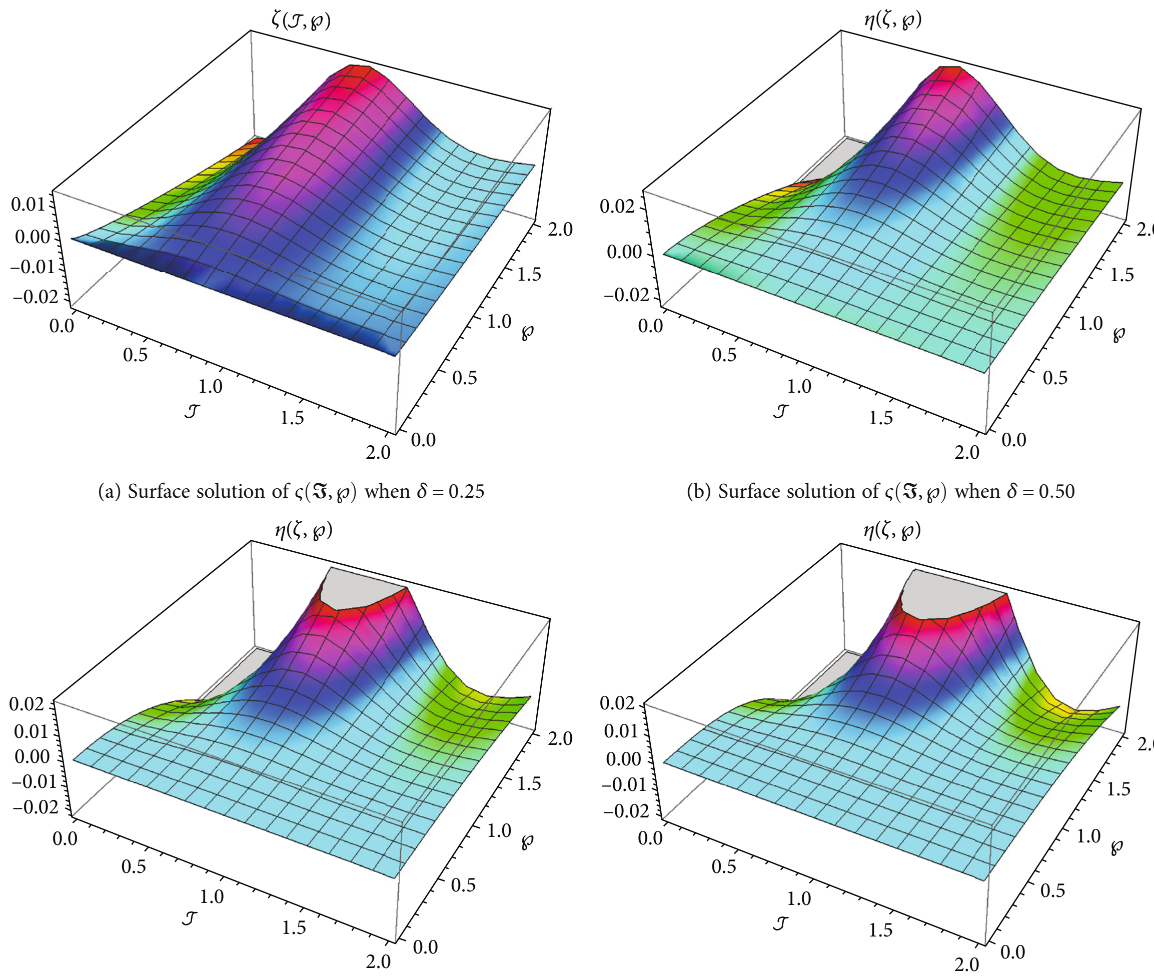

(a) Surface solution of $\varsigma(\mathfrak{J},\wp)$ when $\delta=0.25$

(b) Surface solution of $\varsigma(\mathfrak{J},\wp)$ when $\delta=0.50$

(c) Surface solution of $\varsigma(\mathfrak{J},\wp)$ when $\delta=0.75$

(d) Surface solution of $\varsigma(\mathfrak{J},\wp)$ when $\delta=1$

FIGURE 2: The surface solution of $\varsigma(\mathfrak{J},\wp)$ for distinct values of δ.

$$S=\frac{\wp^{\delta}}{\Gamma(1+\delta)}. \tag{46}$$

Thus, the coupled K-S model of Equation (44) becomes

$$\frac{\partial\eta}{\partial S}=a\frac{\partial^2\eta}{\partial\mathfrak{J}^2}-\frac{\partial\eta}{\partial\mathfrak{J}}\frac{\partial h}{\partial\mathfrak{J}}-\eta\frac{\partial^2 h}{\partial\mathfrak{J}^2}, \tag{47}$$

$$\frac{\partial\varsigma}{\partial S}=b\frac{\partial^2\varsigma}{\partial\mathfrak{J}^2}+c\eta-d\varsigma. \tag{48}$$

Now, using the two-scale approach, with the help of Equation (45), we can get the following iterations directly

$$\eta(\mathfrak{J},0)=me^{-\mathfrak{J}^2}, \tag{49}$$

$$\varsigma(\mathfrak{J},0)=ne^{-\mathfrak{J}^2}, \tag{50}$$

$$\eta_1(\mathfrak{J},S)=2m\left[a\left(2\mathfrak{J}^2-1\right)-ne^{-\mathfrak{J}^2}\left(4\mathfrak{J}^2-1\right)\right]S, \tag{51}$$

$$\varsigma_1(\mathfrak{J},S)=\left[2bn\left(2\mathfrak{J}^2-1\right)+(cm-dn)\right]e^{-\mathfrak{J}^2}S, \tag{52}$$

$$\begin{aligned}\eta_2(\mathfrak{J},S)=2me^{-3\mathfrak{J}^2}\Big[&-cme^{\mathfrak{J}^2}\left(-1+4\mathfrak{J}^2\right)\\&+2a^2e^{2\mathfrak{J}^2}\left(3-12\mathfrak{J}^2+4\mathfrak{J}^4\right)\\&-2ane^{\mathfrak{J}^2}\left(7-58\mathfrak{J}^2+40\mathfrak{J}^4\right)\\&+n\Big\{de^{\mathfrak{J}^2}\left(-1+4\mathfrak{J}^2\right)-2be^{\mathfrak{J}^2}\left(3-18\mathfrak{J}^2+8\mathfrak{J}^4\right)\\&+2n\left(1-18\mathfrak{J}^2+24\mathfrak{J}^4\right)\Big\}\Big]\frac{S^2}{2},\end{aligned} \tag{53}$$

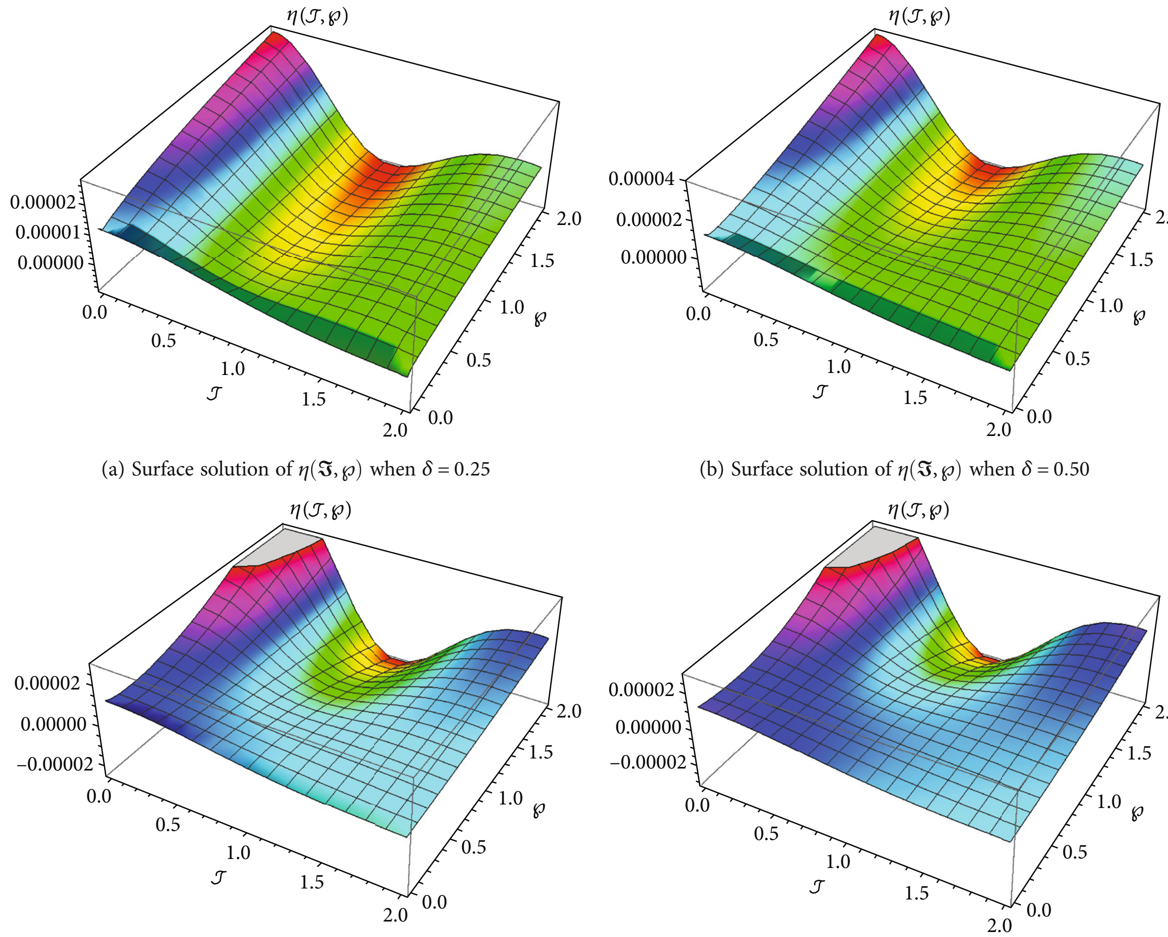

(a) Surface solution of $\eta(\mathfrak{I},\wp)$ when $\delta = 0.25$

(b) Surface solution of $\eta(\mathfrak{I},\wp)$ when $\delta = 0.50$

(c) Surface solution of $\eta(\mathfrak{I},\wp)$ when $\delta = 0.75$

(d) Surface solution of $\eta(\mathfrak{I},\wp)$ when $\delta = 1$

Figure 3: The surface solution of $\eta(\mathfrak{I},\wp)$ for distinct values of δ.

$$\begin{aligned}\varsigma_2(\mathfrak{I},S) = 2e^{-2\mathfrak{I}^2}\Big[&2b^2e^{\mathfrak{I}^2}n\left(3-12\mathfrak{I}^2+4\mathfrak{I}^4\right)\\ &+be^{\mathfrak{I}^2}\left(cm\left(-1+2\mathfrak{I}^2\right)+dn\left(1-6\mathfrak{I}-2\mathfrak{I}^2+4\mathfrak{I}^3\right)\right)\\ &+\mathfrak{I}\Big(-d^2e^{\mathfrak{I}^2}n-2ace^{\mathfrak{I}^2}m\left(-3+2\mathfrak{I}^2\right)\\ &+cm\left(de^{\mathfrak{I}^2}+4n\left(-3+4\mathfrak{I}^2\right)\right)\Big)\Big]\frac{S^2}{2}.\end{aligned} \tag{54}$$

In the same way, other of the elements can be identified. So, the series solution of Equation (44) with the help of Equation (46) is as follows:

$$\begin{aligned}\eta(\mathfrak{I},S) = {}& me^{-\mathfrak{I}^2}+2m\left[a\left(2\mathfrak{I}^2-1\right)-ne^{-\mathfrak{I}^2}\left(4\mathfrak{I}^2-1\right)\right]\left(\frac{\wp^\delta}{\Gamma(1+\delta)}\right)\\ &+me^{-3\mathfrak{I}^2}\Big[-cme^{\mathfrak{I}^2}\left(-1+4\mathfrak{I}^2\right)+2a^2e^{2\mathfrak{I}^2}\left(3-12\mathfrak{I}^2+4\mathfrak{I}^4\right)\\ &-2ane^{\mathfrak{I}^2}\left(7-58\mathfrak{I}^2+40\mathfrak{I}^4\right)+n\Big\{de^{\mathfrak{I}^2}\left(-1+4\mathfrak{I}^2\right)\\ &-2be^{\mathfrak{I}^2}\left(3-18\mathfrak{I}^2+8\mathfrak{I}^4\right)+2n\left(1-18\mathfrak{I}^2+24\mathfrak{I}^4\right)\Big\}\Big]\left(\frac{\wp^\delta}{\Gamma(1+\delta)}\right)^2,\end{aligned} \tag{55}$$

$$\begin{aligned}\varsigma(\mathfrak{I},S) = {}& ne^{-\mathfrak{I}^2}+e^{-\mathfrak{I}^2}\left[2bn\left(2\mathfrak{I}^2-1\right)+(cm-dn)\right]\left(\frac{\wp^\delta}{\Gamma(1+\delta)}\right)\\ &+e^{-2\mathfrak{I}^2}\Big[2b^2e^{\mathfrak{I}^2}n\left(3-12\mathfrak{I}^2+4\mathfrak{I}^4\right)+be^{\mathfrak{I}^2}\left(cm\left(-1+2\mathfrak{I}^2\right)\right.\\ &\left.+dn\left(1-6\mathfrak{I}-2\mathfrak{I}^2+4\mathfrak{I}^3\right)\right)+\mathfrak{I}\Big(-d^2e^{\mathfrak{I}^2}n-2ace^{\mathfrak{I}^2}m\left(-3+2\mathfrak{I}^2\right)\\ &+cm\left(de^{\mathfrak{I}^2}+4n\left(-3+4\mathfrak{I}^2\right)\right)\Big)\Big]\left(\frac{\wp^\delta}{\Gamma(1+\delta)}\right)^2.\end{aligned} \tag{56}$$

6. Results and Discussion

In this segment, we demonstrate the validity and the accuracy of the two-scale approach through the 3D graphical representations. We also present the graphical models and physical behaviors of the time-fractional K-S model. Mathematica program 11.0.1. is used to calculate the iterations and the graphical representations. Figures 1–4 show the surface graphs of the K-S model for $\eta(\mathfrak{I},\wp)$ and $\varsigma(\mathfrak{I},\wp)$, respectively, at different values of δ with $0 \le \mathfrak{I} \le 2$ and $0 \le \wp \le 2$. On behalf of graphical illustrations, we adopt $m = 0.000012$, $n = 0.000016$, $a = 0.5$, $b = 3$, $c = 1$, $d = 2$. The graphical illustrations have validated the convergence of fractional-order

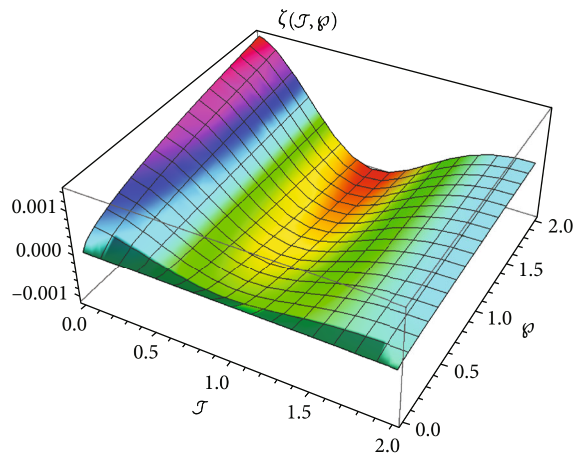

(a) Surface solution of $\varsigma(\mathfrak{I}, \wp)$ when $\delta = 0.25$

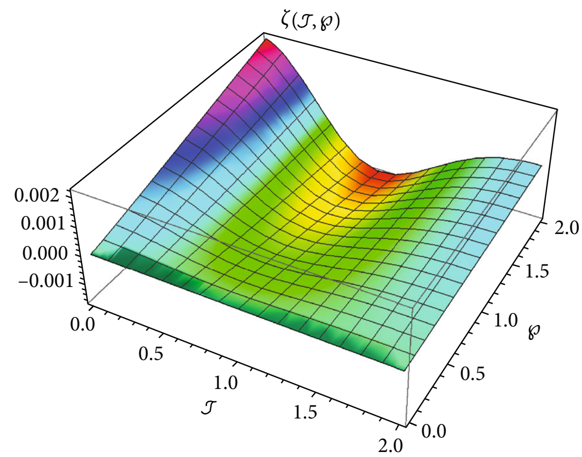

(b) Surface solution of $\varsigma(\mathfrak{I}, \wp)$ when $\delta = 0.50$

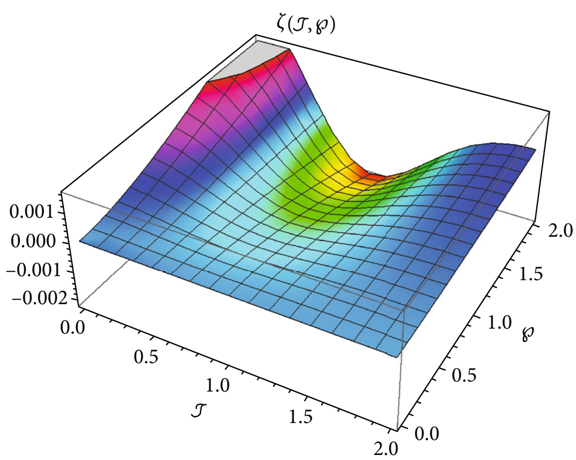

(c) Surface solution of $\varsigma(\mathfrak{I}, \wp)$ when $\delta = 0.75$

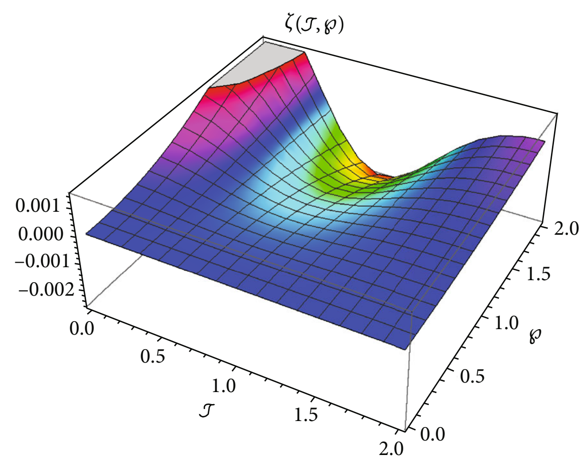

(d) Surface solution of $\varsigma(\mathfrak{I}, \wp)$ when $\delta = 1$

Figure 4: The surface solution of $\varsigma(\mathfrak{I}, \wp)$ for distinct values of δ.

solutions in the direction of integer-order solutions. We calculate the iteration only up to 3 terms, and the series of the solution converges to the exact solution very rapidly. Some more iterations can be evaluated for more accuracy of the approximate solutions. It is noted that the obtained solutions are similar which legitimize the reliability of the proposed strategies:

7. Conclusion

In this study, we have successfully applied a hybrid strategy where FCT has coupled with HPM to investigate the approximate solution of the nonlinear time fractional K-S model. The current association is not just helpful for fractional-order differential equations but also other differential equations with some variants. The main advantage of FCT is that it deals with the nonlinear problems straightforward to customize FDEs into their differential parts. We performed two numerical illustrations of the fractional K-S model to examine the reliability of the suggested approach. The results indicate that the two-scale approach is a more effective and powerful strategy in determining the analytical solutions of nonlinear differential equations. Thus, we conclude that our proposed scheme is suitable and can be considered for the other nonlinear fractional partial differential equations with fractal derivatives in future study.

Data Availability

All the data are available within the article.

Conflicts of Interest

The authors declare that they have no conflicts of interest.

Acknowledgments

This work was supported by the Foundation of Yibin University, China (Grant no. 2019QD07).

References

[1] D. Baleanu, J. A. T. Machado, and A. C. Luo, *Fractional dynamics and control*, Springer Science & Business Media, 2011.

[2] K. S. Miller and B. Ross, *An introduction to the fractional calculus and fractional differential equations*, Wiley, 1993.

[3] I. Podlubny, *Fractional differential equations: an introduction to fractional derivatives, fractional differential equations, to methods of their solution and some of their applications*, Elsevier, 1998.

[4] A. Atangana, "Numerical solution of space-time fractional derivative of groundwater flow equation," *Proceedings of the International Conference of Algebra and Applied Analysis*, vol. 2, p. 20, 2012.

[5] K. M. Owolabi, A. Atangana, and A. Akgul, "Modelling and analysis of fractal-fractional partial differential equations: application to reaction-diffusion model," *Alexandria Engineering Journal*, vol. 59, no. 4, pp. 2477–2490, 2020.

[6] G. W. Wang and T. Z. Xu, "The improved fractional subequation method and its applications to nonlinear fractional partial differential equations," *Romanian Reports in Physics*, vol. 66, no. 3, pp. 595–602, 2014.

[7] L. Debnath, "Recent applications of fractional calculus to science and engineering," *International Journal of Mathematics and Mathematical Sciences*, vol. 2003, 3442 pages, 2003.

[8] F. Haq, K. Shah, Q. M. Al-Mdallal, and F. Jarad, "Application of a hybrid method for systems of fractional order partial differential equations arising in the model of the one-dimensional Keller-Segel equation," *The European Physical Journal Plus*, vol. 134, no. 9, pp. 1–11, 2019.

[9] N. Bournaveas and V. Calvez, "The one-dimensional Keller–Segel model with fractional diffusion of cells," *Nonlinearity*, vol. 23, no. 4, pp. 923–935, 2010.

[10] I. R. Lapidus and R. Schiller, "A mathematical model for bacterial chemotaxis," *Biophysical Journal*, vol. 14, no. 11, pp. 825–834, 1974.

[11] H. Zhang, M. Nadeem, A. Rauf, and Z. G. Hui, "A novel approach for the analytical solution of nonlinear time-fractional di_erential equations," *International Journal of Numerical Methods for Heat & Fluid Flow*, vol. 31, no. 4, pp. 1069–1084, 2020.

[12] K.-L. Wang and S.-W. Yao, "He's fractional derivative for the evolution equation," *Thermal Science*, vol. 24, no. 4, pp. 2507–2513, 2020.

[13] J.-H. He and Z.-B. Li, "Converting fractional differential equations into partial differential equations," *Thermal Science*, vol. 16, no. 2, pp. 331–334, 2012.

[14] J.-H. He, "Homotopy perturbation technique," *Computer Methods in Applied Mechanics and Engineering*, vol. 178, no. 3-4, pp. 257–262, 1999.

[15] J. Biazar and H. Ghazvini, "Exact solutions for nonlinear Burgers' equation by homotopy perturbation method," *Numerical Methods for Partial Differential Equations*, vol. 25, no. 4, pp. 833–842, 2009.

[16] N. Anjum and J. H. He, "Homotopy perturbation method for N/MEMS oscillators," *Mathematical Methods in the Applied Sciences*, 2020.

[17] J. H. He and Y. O. El Dib, "Homotopy perturbation method for Fangzhu oscillator," *Journal of Mathematical Chemistry*, vol. 58, no. 10, pp. 2245–2253, 2020.

[18] H. M. Sedighi and F. Daneshmand, "Static and dynamic pull-in instability of multiwalled carbon nanotube probes by Hes iteration perturbation method," *Journal of Mechanical Science and Technology*, vol. 28, no. 9, pp. 3459–3469, 2014.

[19] V. F. Morales-Delgado, J. F. Gómez-Aguilar, S. Kumar, and M. A. Taneco-Hernández, "Analytical solutions of the Keller-Segel chemotaxis model involving fractional operators without singular kernel," *The European Physical Journal Plus*, vol. 133, no. 5, p. 200, 2018.

[20] A. Atangana, "Extension of the Sumudu homotopy perturbation method to an attractor for one- dimensional Keller-Segel equations," *Applied Mathematical Modelling*, vol. 39, no. 10-11, pp. 2909–2916, 2015.

[21] D. Sharma, G. S. Samra, and P. Singh, "Approximate solution for fractional attractor one-dimensional Keller-Segel equations using homotopy perturbation Sumudu transform method," *Nonlinear Engineering*, vol. 9, no. 1, pp. 370–381, 2020.

[22] H. Liu, H. Khan, R. Shah, A. A. Alderremy, S. Aly, and D. Baleanu, "On the fractional view analysis of Keller–Segel equations with sensitivity functions," *Complexity*, vol. 2020, 15 pages, 2020.

[23] S. Kumar, A. Kumar, and I. K. Argyros, "A new analysis for the Keller-Segel model of fractional order," *Numerical Algorithms*, vol. 75, no. 1, pp. 213–228, 2017.

[24] F. Li and M. Nadeem, "He–Laplace method for nonlinear vibration in shallow water waves," *Journal of Low Frequency Noise, Vibration and Active Control*, vol. 38, no. 3-4, pp. 1305–1313, 2019.

[25] R. W. Ibrahim, "Fractional complex transforms for fractional differential equations," *Advances in Difference Equations*, vol. 2012, no. 1, p. 192, 2012.

[26] J.-H. He, S. Elagan, and Z. Li, "Geometrical explanation of the fractional complex transform and derivative chain rule for fractional calculus," *Physics Letters A*, vol. 376, no. 4, pp. 257–259, 2012.

[27] Z.-B. Li and J.-H. He, "Fractional complex transform for fractional differential equations," *Mathematical and Computational Applications*, vol. 15, no. 5, pp. 970–973, 2010.

[28] Q. T. Ain and J.-H. He, "On two-scale dimension and its applications," *Thermal Science*, vol. 23, no. 3 Part B, pp. 1707–1712, 2019.

[29] J.-H. He, "Fractal calculus and its geometrical explanation," *Results in Physics*, vol. 10, pp. 272–276, 2018.

[30] Q. T. Ain, J.-H. He, N. Anjum, and M. Ali, "The fractional complex transform: a novel approach to the time-fractional Schrödinger equation," *Fractals*, vol. 28, no. 7, article 2050141, 2020.

Hindawi
Journal of Function Spaces
Volume 2022, Article ID 2935740, 10 pages
https://doi.org/10.1155/2022/2935740

Research Article

Fractional Version of Hermite-Hadamard and Fejér Type Inequalities for a Generalized Class of Convex Functions

Lei Geng,[1] **Muhammad Shoaib Saleem**,[2] **Kiran Naseem Aslam**,[2] **and Rahat Bano**[2]

[1]*School of Science, Henan Institute of Technology, Xinxiang 453003, China*
[2]*Department of Mathematics, University of Okara, Okara, Pakistan*

Correspondence should be addressed to Lei Geng; genglei@hait.edu.cn

Received 1 April 2022; Revised 23 May 2022; Accepted 10 June 2022; Published 22 July 2022

Academic Editor: Yusuf Gurefe

In the present paper, we deal with some fractional integral inequalities for strongly reciprocally (p, h)-convex functions. We established fractional version of Hermite-Hadamard and Fejér type inequalities for strongly reciprocally (p, h)-convex functions. Our results extend and generalize many exiting results of literate.

1. Introduction

The convex functions nowadays are widely used in many branches of mathematics like optimization theory, functional analysis, and modeling theory [1, 2]. The interesting geometry of convex functions makes its study distinct from other functions. From geometric point of view, a function $\psi(x)$ is convex provided that the line segment connecting any two points of its graph lies on or above the graph of function. The new inequalities in analysis are always appreciable [3, 4].

Since the classical convexity is not enough to attain certain goals in applied mathematics, so the classical convexity has been generalized in many directions. For recent generalizations, one can see [5, 6].

For the class of convex functions, various inequalities have been developed [7, 8], but the most famous inequality is Hermite-Hadamard's inequality. It is stated as follows:

Let $\psi : M \subseteq \mathbb{R} \longrightarrow \mathbb{R}$ be a convex function, and let d_1, $d_2 \in M$ with $d_1 d_2$; then, the following double inequality holds:

$$\psi\left(\frac{d_1 + d_2}{2}\right) \le \frac{1}{d_2 - d_1}\int_{d_1}^{d_2} \psi(x)dx \le \frac{\psi(d_1) + \psi(d_2)}{2}. \quad (1)$$

In [9], Fejér gave the weighted version of Hermite-Hadamard inequality (1) as follows:

Let $\psi : [d_1, d_2] \subseteq \mathbb{R} \longrightarrow \mathbb{R}$ be a convex function and $w : [d_1, d_2] \longrightarrow \mathbb{R}$ a non-negative, integrable, and symmetric function about $(d_1 + d_2)/2$; then, the following inequality holds:

$$\psi\left(\frac{d_1 + d_2}{2}\right)\int_{d_1}^{d_2} w(x)dx \le \int_{d_1}^{d_2} \psi(x)w(x)dx \le \frac{\psi(d_1) + \psi(d_2)}{2}\int_{d_1}^{d_2} w(x)dx. \quad (2)$$

The aim of present paper is to establish fractional version of Hermite-Hadamard and Fejér type inequalities for a more generalized class of functions. The present paper is organized as follows: The §2 is concerned with some preliminary material. In Section 3, we give some basic results for strongly reciprocally (p,h)-convex functions, and in Sections 4 and 5, we develop Hermite-Hadamard and Fejér type inequalities, respectively, for strongly reciprocally (p,h)-convex function. Moreover, the last section is devoted for fractional integral inequalities.

2. Preliminaries

In this section, we give a brief review of some preliminaries.

Definition 1 (p-convex set see [10, 11]). A set $M=[d_1,d_2]\subseteq\mathbb{R}\setminus\{0\}$ is p -convex set, if

$$\left[\left(jx^p+(1-j)y^p\right)^{1/p}\right]\in M, \tag{3}$$

for all $x,y\in M$, $j\in[0,1]$, where $p=2u+1$ or $p=a/b$, $a=2v+1$, $b=2w+1$ and $u,v,w\in N$.

Definition 2 (p-convex function see [10]). Let $M=[d_1,d_2]\subseteq\mathbb{R}\setminus\{0\}$ be a p -convex set. A function $\psi:M=[d_1,d_2]\longrightarrow\mathbb{R}$ is called p-convex function, if

$$\psi\left[\left(jx^p+(1-j)y^p\right)^{1/p}\right]\le j\psi(x)+(1-j)\psi(y)\in M, \tag{4}$$

holds for all $x,y\in M$ and $j\in[0,1]$.

Definition 3 (Strongly convex function see [4]). A function $\psi:M=[d_1,d_2]\longrightarrow\mathbb{R}$ is called strongly convex function with modulus μ on M, where $\mu\ge0$, if

$$\psi(jx+(1-j)y)\le j\psi(x)+(1-j)\psi(y)-\mu j(1-j)(y-x)^2, \tag{5}$$

holds for all $x,y\in M$ and $j\in[0,1]$.

Definition 4 (Strongly p-convex function see [12]). A function $\psi:M=[d_1,d_2]\longrightarrow\mathbb{R}$ is called strongly p-convex function, if

$$\psi\left[\left(jx^p+(1-j)y^p\right)^{1/p}\right]\le j\psi(x)+(1-j)\psi(y)-\mu j(1-j)(y^p-x^p)^2, \tag{6}$$

holds for all $x,y\in M$ and $j\in[0,1]$.

Definition 5 (Harmonic convex set see [11, 13]). A set $M=[d_1,d_2]\subseteq\mathbb{R}\setminus\{0\}$ is said to be harmonic convex set, if

$$\frac{xy}{jx+(1-j)y}\in M, \tag{7}$$

for all $x,y\in M$ and $j\in[0,1]$.

Definition 6 (Harmonic convex function see [11, 14]). Let $M=[d_1,d_2]\subseteq\mathbb{R}\setminus\{0\}$ be the harmonic convex set. A function $\psi:M=[d_1,d_2]\subseteq\mathbb{R}\setminus\{0\}\longrightarrow\mathbb{R}$ is harmonic convex function, if

$$\psi\left(\frac{xy}{jx+(1-j)y}\right)(1-j)\psi(x)+j\psi(y), \tag{8}$$

holds for all $x,y\in M$ and $j\in[0,1]$.

Definition 7 (p-harmonic convex set see [11, 15]). A set $M=[d_1,d_2]\subseteq\mathbb{R}\setminus\{0\}$ is p -harmonic convex set, if

$$\left[\left(\frac{x^py^p}{jx^p+(1-j)y^p}\right)^{1/p}\right]\in M, \tag{9}$$

for all $x,y\in M$ and $j\in[0,1]$.

Definition 8 (p-harmonic convex function see [11, 15]). Let $M=[d_1,d_2]\subseteq\mathbb{R}\setminus\{0\}$ be p-harmonic convex set. A function $\psi:M=[d_1,d_2]\subseteq\mathbb{R}\setminus\{0\}\longrightarrow\mathbb{R}$ is p-harmonic convex, if

$$\psi\left[\left(\frac{x^py^p}{jx^p+(1-j)y^p}\right)^{1/p}\right]\le(1-j)\psi(x)+j\psi(y), \tag{10}$$

holds for all $x,y\in M$ and $j\in[0,1]$.

Definition 9 (Strongly reciprocally convex function see [16]). Let M be an interval and let $\mu\in(0,\infty)$. A function $\psi:M=[d_1,d_2]\subseteq\mathbb{R}\setminus\{0\}\longrightarrow\mathbb{R}$ is said to be strongly reciprocally convex function with modulus μ on M, if

$$\psi\left(\frac{xy}{jx+(1-j)y}\right)\le(1-j)\psi(x)+j\psi(y)-\mu j(1-j)\left(\frac{1}{x}-\frac{1}{y}\right)^2, \tag{11}$$

holds for all $x,y\in M$ and $j\in[0,1]$.

Definition 10 (Strongly reciprocally p-convex function see [17]). Let M be a p -harmonic convex set and let $\mu\in(0,\infty)$. A function $\psi:M=[d_1,d_2]\subseteq\mathbb{R}\setminus\{0\}\longrightarrow\mathbb{R}$ is said to be strongly reciprocally p-convex function with modulus μ on M, if

$$\psi\left[\left(\frac{x^py^p}{jx^p+(1-j)y^p}\right)^{1/p}\right]\le(1-j)\psi(x)+j\psi(y)-\mu j(1-j)\left(\frac{1}{x^p}-\frac{1}{y^p}\right)^2, \tag{12}$$

holds for all $x,y\in M$ and $j\in[0,1]$.

Definition 11 (h-convex function see [18]). Choose the functions $\psi,h:M=[d_1,d_2]\longrightarrow\mathbb{R}$ that are non-negative; then, ψ is called h-convex function, if

$$\psi(jx+(1-j)y)\le h(j)\psi(x)+h(1-j)\psi(y), \tag{13}$$

for all $x,y\in M$ and $j\in[0,1]$.

Now, we are ready to introduce a new class of convex functions by generalizing the concept of strongly reciprocally p-convex functions, which we will call strongly reciprocally (p,h)-convex functions.

Definition 12 (Strongly reciprocally (p,h)-convex function). Let M be a p-harmonic convex set and let $\mu\in(0,\infty)$. A function $\psi:M=[d_1,d_2]\subseteq\mathbb{R}\setminus\{0\}\longrightarrow\mathbb{R}$ is said to be strongly reciprocally (p, h)-convex function with modulus μ on M, if

$$\psi\left[\left(\frac{x^p y^p}{jx^p + (1-j)y^p}\right)^{1/p}\right] \le h(1-j)\psi(x) + h(j)\psi(y) - \mu j(1-j)\left(\frac{1}{x^p} - \frac{1}{y^p}\right)^2, \quad (14)$$

hold for all $x, y \in M$ and $j \in [0, 1]$.

Throughout the paper, for convenience, we represent the class of strongly reciprocally (p, h) convex functions by $SR(p, h)$.

Remark 13. Inserting $h(j) = j$ in Definition 12, we obtain Definition 10, and inserting $h(j) = j$ and $p = 1$, Definition 12 reduces to Definition 9.

Similarly, from Definition 12, Definitions 6 and 8 can be obtained by inserting $h(j) = j$, $\mu = 0$, $p = 1$, and $h(j) = j$ with $\mu = 0$, respectively.

3. Basic Results

This section collects some basic and straight forward facts based on algebraic operations.

The following proposition is concerned about the addition of two functions from $SR(p, h)$.

Proposition 14. *Let $\psi, \sigma : M \longrightarrow \mathbb{R}$ be two strongly reciprocally (p,h)-convex functions with modulus μ on M; then, $\psi + \sigma : M \longrightarrow \mathbb{R}$ is also strongly reciprocally (p,h)-convex function with modulus μ^* on M, where $\mu^* = 2\mu$.*

Proof. We will start by definition of strongly reciprocally (p,h)-convexity of ψ and σ:

$$\begin{aligned}(\psi+\sigma)\left(\frac{x^p y^p}{jx^p + (1-j)y^p}\right)^{1/p} &= \psi\left[\left(\frac{x^p y^p}{jx^p + (1-j)y^p}\right)^{1/p}\right] + \sigma\left[\left(\frac{x^p y^p}{jx^p + (1-j)y^p}\right)^{1/p}\right] \\ &\le h(j)\psi(x) + h(1-j)\psi(y) - \mu j(1-j)\left(\frac{1}{y^p} - \frac{1}{x^p}\right)^2 \\ &\quad + h(j)\sigma(x) + h(1-j)\sigma(y) - \mu j(1-j)\left(\frac{1}{y^p} - \frac{1}{x^p}\right)^2,\end{aligned} \quad (15)$$

which in turns implies that

$$\begin{aligned}(\psi+\sigma)\left(\frac{x^p y^p}{jx^p + (1-j)y^p}\right)^{1/p} &\le h(j)(\psi+\sigma)(x) + h(1-j)(\psi+\sigma)(y) - 2\mu j(1-j)\left(\frac{1}{y^p} - \frac{1}{x^p}\right)^2 \\ &= h(j)(\psi+\sigma)(x) + h(1-j)(\psi+\sigma)(y) - \mu^* j(1-j)\left(\frac{1}{y^p} - \frac{1}{x^p}\right)^2,\end{aligned} \quad (16)$$

where $\mu^* = 2\mu$ and $\mu \ge 0$. This completes the proof. □

Our next result is concerned with the scalar multiplication of strongly reciprocally (p,h)-convex function.

Proposition 15. *Let $\psi : M \longrightarrow \mathbb{R}$ be a strongly reciprocally (p,h)-convex function; then, for any $\lambda \ge 0$, $\lambda\psi : M \longrightarrow \mathbb{R}$ is also strongly reciprocally (p,h)-convex function with modulus ν^* on M, where $\nu^* = \lambda\mu$.*

Proof. Let $\lambda \ge 0$, $\psi \in SR(p, h)$, we obtain

$$\begin{aligned}\lambda\psi\left[\left(\frac{x^p y^p}{jx^p + (1-j)y^p}\right)^{1/p}\right] + \lambda\left[\psi\left[\left(\frac{x^p y^p}{jx^p + (1-j)y^p}\right)^{1/p}\right]\right] &\le \lambda\left[h(j)\psi(x) + h(1-j)\psi(y) - \mu j(1-j)\left(\frac{1}{y^p} - \frac{1}{x^p}\right)^2\right] \\ &= h(j)\lambda\psi(x) + h(1-j)\lambda\psi(y) - \lambda\mu j(1-j)\left(\frac{1}{y^p} - \frac{1}{x^p}\right)^2 \\ &= h(j)\lambda\psi(x) + h(1-j)\lambda\psi(y) - \nu^* j(1-j)\left(\frac{1}{y^p} - \frac{1}{x^p}\right)^2,\end{aligned} \quad (17)$$

where $\nu^* = \lambda\mu$ and $\mu \ge 0$. This completes the proof. □

Proposition 16. *Let $\psi_i : M \longrightarrow \mathbb{R}$, where $1 \le i \le n$ be in SR (p, h) with modulus μ; then, for $\lambda_i \ge 0$ where $1 \le i \le n$, the function $\psi : M \longrightarrow \mathbb{R}$, where $\psi = \sum_{i=1}^n \lambda_i \psi_i$ is also in $SR(p, h)$ with modulus $\gamma \ge 0$, where $\gamma = \sum_{i=1}^n \lambda_i \mu$.*

Proof. Let M is a p-harmonic convex set. Then, $\forall x, y \in M$ and $j \in [0, 1]$, we have

$$\begin{aligned}\psi\left[\left(\frac{x^p y^p}{jx^p + (1-j)y^p}\right)^{1/p}\right] &= \sum_{i=1}^n \lambda_i \psi_i\left[\left(\frac{x^p y^p}{jx^p + (1-j)y^p}\right)^{1/p}\right] \\ &\le \sum_{i=1}^n \lambda_i\left[h(j)\psi_i(x) + h(1-j)\psi_i(y) - \mu j(1-j)\left(\frac{1}{y^p} - \frac{1}{x^p}\right)^2\right] \\ &= h(j)\sum_{i=1}^n \lambda_i\psi_i(x) + h(1-j)\sum_{i=1}^n \lambda_i\psi_i(y) \\ &\quad - \sum_{i=1}^n \lambda_i\left[\mu j(1-j)\left(\frac{1}{y^p} - \frac{1}{x^p}\right)^2\right] \\ &= h(j)f(x) + h(1-j)\psi(y) - \gamma j(1-j)\left(\frac{1}{y^p} - \frac{1}{x^p}\right)^2,\end{aligned} \quad (18)$$

where $\gamma = \sum_{i=1}^n \lambda_i \mu$. This completes the proof. □

Proposition 17. *Let $\psi_i : M \longrightarrow \mathbb{R}$, where $1 \le i \le n$ be strongly reciprocally (p,h)-convex functions with modulus μ; then $\psi = \max\{\psi_i, i = 1, 2, \cdots, n\}$, is also strongly reciprocally (p,h)-convex functions with modulus μ.*

Proof. Let M is p-harmonic convex set. Then $\forall x, y \in M$ and $j \in [0, 1]$, we have

$$\begin{aligned}\psi\left[\left(\frac{x^p y^p}{jx^p + (1-j)y^p}\right)^{1/p}\right] &= \max\left\{\psi_i\left[\left(\frac{x^p y^p}{jx^p + (1-j)y^p}\right)^{1/p}\right], i = 1, 2, 3, \cdots, n\right\} \\ &= \psi_c\left[\left(\frac{x^p y^p}{jx^p + (1-j)y^p}\right)^{1/p}\right] \\ &\le h(j)\psi_c(x) + h(1-j)\psi_c(y) - \mu j(1-j)\left(\frac{1}{y^p} - \frac{1}{x^p}\right)^2 \\ &= h(j)\max\{\psi_i(x)\} + h(1-j)\max\{\psi_i(y)\} \\ &\quad - \mu j(1-j)\left(\frac{1}{y^p} - \frac{1}{x^p}\right)^2 \\ &= h(j)\psi(x) + h(1-j)\psi(y) - \mu j(1-j)\left(\frac{1}{y^p} - \frac{1}{x^p}\right)^2.\end{aligned} \quad (19)$$

This completes the proof. □

Our next intension is to develop Hermite-Hadamard's inequality for this generalization.

4. Hermite-Hadamard Type Inequality

Theorem 18. *Let $M \subset \mathbb{R} \setminus \{0\}$ be an interval. If $\psi : M \longrightarrow \mathbb{R}$ be a strongly reciprocally (p,h)-convex function with modulus $\mu \geq 0$ and $\psi \in L[d_1, d_2]$, then for $h(1/2) \neq 0$, we have*

$$\frac{1}{2h(1/2)}\left[\psi\left(\frac{2d_1^p d_2^p}{d_1^p + d_2^p}\right)^{1/p} + \frac{\mu}{12}\left(\frac{d_2^p - d_1^p}{d_1^p d_2^p}\right)^2\right] \leq \frac{p\left(d_1^p d_2^p\right)}{d_2^p - d_1^p}\int_{d_1}^{d_2}\frac{\psi(x)}{x^{1+p}}dx \leq \int_0^1 [h(1-j)\psi(d_1) + h(j)\psi(d_2)]\,dj - \frac{\mu}{6}\left(\frac{d_2^p - d_1^p}{d_1^p d_2^p}\right)^2. \tag{20}$$

Proof. Since, $\psi \in SR(p, h)$, and allowing $j = 1/2$ yields

$$\psi\left[\left(\frac{2x^p y^p}{x^p + y^p}\right)^{1/p}\right] \leq h\left(\frac{1}{2}\right)\psi(x) + h\left(\frac{1}{2}\right)\psi(y) - \mu\left(\frac{1}{2}\right)\left(\frac{1}{2}\right)\left(\frac{1}{x^p} - \frac{1}{y^p}\right)^2. \tag{21}$$

Let $x = [((d_1^p d_2^p)/(jd_1^p + (1-j)d_2^p))^{1/p}]$ and $y = [((d_1^p d_2^p)/(jd_2^p + (1-j)d_1^p))^{1/p}]$ and integrating (21) w.r.t j over $[0, 1]$, we obtain

$$\begin{aligned}\psi\left[\left(\frac{2d_1^p d_2^p}{d_1^p + d_2^p}\right)^{1/p}\right] &\leq h\left(\frac{1}{2}\right)\psi\left[\left(\frac{d_1^p d_2^p}{jd_1^p + (1-j)d_2^p}\right)^{1/p}\right] + h\left(\frac{1}{2}\right)\psi\left[\left(\frac{d_1^p d_2^p}{jd_2^p + (1-j)d_1^p}\right)^{1/p}\right] \\ &\quad - \frac{\mu}{4}\left(\frac{d_2^p - d_1^p}{d_1^p d_2^p}\right)^2 (1-2j)^2 \int_0^1 \psi\left[\left(\frac{2d_1^p d_2^p}{d_1^p + d_2^p}\right)^{1/p}\right] dj \\ &\leq \int_0^1 h\left(\frac{1}{2}\right)\psi\left[\left(\frac{d_1^p d_2^p}{jd_1^p + (1-j)d_2^p}\right)^{1/p}\right] dj + \int_0^1 h\left(\frac{1}{2}\right)\psi\left[\left(\frac{d_1^p d_2^p}{jd_2^p + (1-j)d_1^p}\right)^{1/p}\right] dj \\ &\quad - \frac{\mu}{4}\left(\frac{d_2^p - d_1^p}{d_1^p d_2^p}\right)^2 \int_0^1 (1-2j)^2 dj\, \psi\left[\left(\frac{2d_1^p d_2^p}{d_1^p + d_2^p}\right)^{1/p}\right] \\ &\leq 2h\left(\frac{1}{2}\right)\frac{p\left(d_1^p d_2^p\right)}{d_2^p - d_1^p}\int_{d_1}^{d_2}\frac{\psi(x)}{x^{1+p}}dx - \frac{\mu}{12}\left(\frac{d_2^p - d_1^p}{d_1^p d_2^p}\right)^2,\end{aligned} \tag{22}$$

and

$$\begin{aligned}&\psi\left[\left(\frac{2d_1^p d_2^p}{d_1^p + d_2^p}\right)^{1/p}\right] + \frac{\mu}{12}\left(\frac{d_2^p - d_1^p}{d_1^p d_2^p}\right)^2 \\ &\leq 2h\left(\frac{1}{2}\right)\frac{p\left(d_1^p d_2^p\right)}{d_2^p - d_1^p}\int_{d_1}^{d_2}\frac{\psi(x)}{x^{1+p}}dx\,\frac{1}{2h(1/2)} \\ &\quad\times\left[\psi\left[\left(\frac{2d_1^p d_2^p}{d_1^p + d_2^p}\right)^{1/p}\right] + \frac{\mu}{12}\left(\frac{d_2^p - d_1^p}{d_1^p d_2^p}\right)^2\right] \\ &\leq \frac{p\left(d_1^p d_1^p\right)}{d_2^p - d_1^p}\int_{d_1}^{d_2}\frac{\psi(x)}{x^{1+p}}dx,\end{aligned} \tag{23}$$

which gives one side of (20).

For the right side of (20), since $\psi \in SR(p, h)$, so by setting $x = d_1$ and $y = d_2$, we obtain the following result:

$$\psi\left[\left(\frac{d_1^p d_2^p}{jd_1^p + (1-j)d_2^p}\right)^{1/p}\right] \leq h(1-j)\psi(d_1) + h(j)\psi(d_2) - \mu j(1-j)\left(\frac{1}{d_1^p} - \frac{1}{d_2^p}\right)^2. \tag{24}$$

Integrating (24) w.r.t j over $[0, 1]$, we obtain

$$\int_0^1 \psi\left[\left(\frac{d_1^p d_2^p}{jd_1^p + (1-j)d_2^p}\right)^{1/p}\right] dj \leq \int_0^1 h(1-j)\psi(d_1)dj + \int_0^1 h(j)\psi(d_2)dj - \mu\left(\frac{d_2^p - d_1^p}{d_1^p d_2^p}\right)^2 \int_0^1 j(1-j)dj, \tag{25}$$

and

$$\frac{p\left(d_1^p d_2^p\right)}{d_2^p - d_1^p}\int_{d_1}^{d_2}\frac{\psi(x)}{x^{1+p}}dx \leq \int_0^1 [h(1-j)\psi(d_1) + h(j)\psi(d_2)]dj - \frac{\mu}{6}\left(\frac{d_2^p - d_1^p}{d_1^p d_2^p}\right)^2, \tag{26}$$

which is right side of (20), which completes the proof. □

Remark 19.

(1) Inserting $h(j) = j$ and $p = 1$ in Theorem 18, we obtained Hermite-Hadamard inequality for strongly reciprocally convex function [16] (Theorem 3.1)

(2) Insertion $h(j) = j$, $p = 1$, and $\mu = 0$ in Theorem 18 yields Hermite-Hadamard inequality for harmonic convex functions [14] (Theorem 2.4)

Now, we develop Fejér type inequality for this new class of convex functions.

5. Fejér Type Inequality

Theorem 20. *Let $M \subset \mathbb{R} \setminus \{0\}$ be an interval. If $\psi : M \longrightarrow \mathbb{R}$ be a strongly reciprocally (p,h)-convex function with modulus*

$\mu \geq 0$, then for $h(1/2) \neq 0$, we have

$$\frac{1}{2h(1/2)}\left[\psi\left[\left(\frac{2d_1^pd_2^p}{d_1^p+d_2^p}\right)^{1/p}\right]\int_{d_1}^{d_2}\frac{w(x)}{x^{1+p}}dx+\frac{\mu}{(2d_1^pd_2^p)^2}\int_{d_1}^{d_2}\frac{(2d_1^pd_2^p-(d_1^p+d_2^p)x^p)^2w(x)}{x^{1+3p}}dx\right]$$
$$\leq \int_{d_1}^{d_2}\frac{\psi(x)w(x)}{x^{1+p}}dx \leq [\psi(d_1)+\psi(d_2)]\int_{d_1}^{d_2}h\left(\frac{d_1^p(d_2^p-x^p)}{x^p(d_2^p-d_1^p)}\right)\frac{w(x)}{x^{1+p}}dx$$
$$-\frac{\mu}{d_1^pd_2^p}\int_{d_1}^{d_2}\frac{(x^p-d_1^p)(d_2^p-x^p)w(x)}{x^{1+3p}}dx, \tag{27}$$

holds for $d_1, d_2 \in M$ with $d_1 \leq d_2$ and $\psi \in L[d_1, d_2]$, where $w : M \longrightarrow \mathbb{R}$ is a non-negative integrable function that satisfies

$$w\left(\frac{d_1^pd_2^p}{x^p}\right)^{1/p} = w\left[\left(\frac{d_1^pd_2^p}{d_1^p+d_2^p-x^p}\right)^{1/p}\right]. \tag{28}$$

Proof. Since $\psi \in SR(p,h)$, and allowing $j = 1/2$ yields

$$\psi\left[\left(\frac{2x^py^p}{x^p+y^p}\right)^{1/p}\right] \leq h\left(\frac{1}{2}\right)\psi(x)+h\left(\frac{1}{2}\right)\psi(y)-\mu\left(\frac{1}{2}\right)\left(\frac{1}{2}\right)\left(\frac{1}{x^p}-\frac{1}{y^p}\right)^2. \tag{29}$$

Inserting $x = [(d_1^pd_2^p/jd_1^p+(1-j)d_2^p)^{1/p}]$ and $y = [(d_1^pd_2^p/jd_2^p+(1-jd_1^p)^{1/p}]$ in (29), we obtain

$$\psi\left[\left(\frac{2d_1^pd_2^p}{d_1^p+d_2^p}\right)^{1/p}\right] \leq h\left(\frac{1}{2}\right)\psi\left[\left(\frac{d_1^pd_2^p}{jd_1^p+(1-j)d_2^p}\right)^{1/p}\right]+h\left(\frac{1}{2}\right)\psi\left[\left(\frac{d_1^pd_2^p}{jd_2^p+(1-j)d_1^p}\right)^{1/p}\right]$$
$$-\frac{\mu}{4}\left(\frac{jd_1^p+(1-j)d_2^p}{d_1^pd_2^p}-\frac{jd_2^p+(1-j)d_1^p}{d_1^pd_2^p}\right)^2. \tag{30}$$

Since, w is a non-negative symmetric and integrable function, so

$$\psi\left[\left(\frac{2d_1^pd_2^p}{d_1^p+d_2^p}\right)^{1/p}\right]w\left[\left(\frac{d_1^pd_2^p}{jd_1^p+(1-j)d_2^p}\right)^{1/p}\right]$$
$$\leq h\left(\frac{1}{2}\right)\psi\left[\left(\frac{d_1^pd_2^p}{jd_1^p+(1-j)d_2^p}\right)^{1/p}\right]w\left[\left(\frac{d_1^pd_2^p}{jd_1^p+(1-j)d_2^p}\right)^{1/p}\right]$$
$$+h\left(\frac{1}{2}\right)\psi\left[\left(\frac{d_1^pd_2^p}{jd_2^p+(1-j)d_1^p}\right)^{1/p}\right]w\left[\left(\frac{d_1^pd_2^p}{jd_1^p+(1-j)d_2^p}\right)^{1/p}\right]$$
$$-\frac{\mu}{4}\left(\frac{jd_1^p+(1-j)d_2^p}{d_1^pd_2^p}-\frac{jd_2^p+(1-j)d_1^p}{d_1^pd_2^p}\right)^2w\left[\left(\frac{d_1^pd_2^p}{jd_1^p+(1-j)d_2^p}\right)^{1/p}\right]. \tag{31}$$

Integrating inequality (31) w.r.t j over $[0,1]$, we obtain

$$\int_0^1\psi\left[\left(\frac{2d_1^pd_2^p}{d_1^p+d_2^p}\right)^{1/p}\right]w\left[\left(\frac{d_1^pd_2^p}{jd_1^p+(1-j)d_2^p}\right)^{1/p}\right]dj$$
$$\leq \int_0^1h\left(\frac{1}{2}\right)\psi\left[\left(\frac{d_1^pd_2^p}{jd_1^p+(1-j)d_2^p}\right)^{1/p}\right]w\left[\left(\frac{d_1^pd_2^p}{jd_1^p+(1-j)d_2^p}\right)^{1/p}\right]dj$$
$$+\int_0^1h\left(\frac{1}{2}\right)\psi\left[\left(\frac{d_1^pd_2^p}{jd_2^p+(1-j)d_1^p}\right)^{1/p}\right]w\left[\left(\frac{d_1^pd_2^p}{jd_1^p+(1-j)d_2^p}\right)^{1/p}\right]dj$$
$$-\frac{\mu}{4}\int_0^1\left(\frac{jd_1^p+(1-j)d_2^p}{d_1^pd_2^p}-\frac{jd_2^p+(1-j)d_1^p}{d_1^pd_2^p}\right)^2w\left[\left(\frac{d_1^pd_2^p}{jd_1^p+(1-j)d_2^p}\right)^{1/p}\right]dj, \tag{32}$$

and

$$\psi\left[\left(\frac{2d_1^pd_2^p}{d_1^p+d_2^p}\right)^{1/p}\right]\int_{a_1}^{b_1}\frac{w(x)}{x^{1+p}}dx+\frac{\mu}{(2d_1^pd_2^p)^2}\int_{d_1}^{d_2}$$
$$\times\frac{(2d_1^pd_2^p-(d_1^p+d_2^p)x^p)^2w(x)}{x^{1+3p}}dx$$
$$\leq 2h\left(\frac{1}{2}\right)\int_{a_1}^{b_1}\frac{\psi(x)w(x)}{x^{1+p}}dx, \tag{33}$$

so,

$$\frac{1}{2h(1/2)}\left[\psi\left[\left(\frac{2d_1^pd_2^p}{d_1^p+d_2^p}\right)^{1/p}\right]\int_{d_1}^{d_2}\frac{w(x)}{x^{1+p}}dx+\frac{\mu}{(2d_1^pd_2^p)^2}\int_{d_1}^{d_2}\frac{(2d_1^pd_2^p-(d_1^p+d_2^p)x^p)^2w(x)}{x^{1+3p}}dx\right]$$
$$\leq \int_{d_1}^{d_2}\frac{\psi(x)w(x)}{x^{1+p}}dx, \tag{34}$$

which is left side of (27). □

Finally, for the right side of (27), since $\psi \in SR(p,h)$ and by setting $x = d_1$ and $y = d_2$, we obtain the following result:

$$\psi\left[\left(\frac{d_1^pd_2^p}{jd_1^p+(1-j)d_2^p}\right)^{1/p}\right] \leq h(1-j)\psi(d_1)+h(j)\psi(d_2)-\mu j(1-j)\left(\frac{1}{d_1^p}-\frac{1}{d_2^p}\right)^2. \tag{35}$$

Since w is a non-negative symmetric and integrable function, so

$$\psi\left[\left(\frac{d_1^pd_2^p}{jd_1^p+(1-j)d_2^p}\right)^{1/p}\right]w\left[\left(\frac{d_1^pd_2^p}{jd_1^p+(1-j)d_2^p}\right)^{1/p}\right]$$
$$\leq h(1-j)\psi(d_1)w\left[\left(\frac{d_1^pd_2^p}{jd_1^p+(1-j)d_2^p}\right)^{1/p}\right]$$
$$+h(j)\psi(d_2)w\left[\left(\frac{d_1^pd_2^p}{jd_1^p+(1-j)d_2^p}\right)^{1/p}\right]$$
$$-\mu j(1-j)\left(\frac{1}{d_1^p}-\frac{1}{d_2^p}\right)^2w\left[\left(\frac{d_1^pd_2^p}{jd_1^p+(1-j)d_2^p}\right)^{1/p}\right]. \tag{36}$$

Integrating inequality (36) w.r.t j over $[0, 1]$, we obtain

$$\begin{aligned}\int_0^1 \psi\left[\left(\frac{d_1^p d_2^p}{jd_1^p + (1-j)d_2^p}\right)^{1/p}\right] w\left[\left(\frac{d_1^p d_2^p}{jd_1^p + (1-j)d_2^p}\right)^{1/p}\right] dj \\ \le \int_0^1 h(1-j)\psi(d_1) w\left[\left(\frac{d_1^p d_2^p}{jd_1^p + (1-j)d_2^p}\right)^{1/p}\right] dj \\ + \int_0^1 h(j)\psi(d_2) w\left[\left(\frac{d_1^p d_2^p}{jd_1^p + (1-j)d_2^p}\right)^{1/p}\right] dj \\ - \mu\int_0^1 j(1-j)\left(\frac{1}{d_1^p} - \frac{1}{d_2^p}\right)^2 w\left[\left(\frac{d_1^p d_2^p}{jd_1^p + (1-j)d_2^p}\right)^{1/p}\right] dj,\end{aligned} \tag{37}$$

and

$$\begin{aligned}\int_{d_1}^{d_2} \frac{\psi(x)w(x)}{x^{1+p}} dx \le [\psi(d_1) + \psi(d_2)] \int_{a_1}^{b_1} h\left(\frac{d_1^p\left(d_2^p - x^p\right)}{x^p\left(d_2^p - d_1^p\right)}\right) \frac{w(x)}{x^{1+p}} dx \\ - \frac{\mu}{d_1^p d_2^p} \int_{d_1}^{d_2} \frac{\left(x^p - d_1^p\right)\left(d_2^p - x^p\right) w(x)}{x^{1+3p}} dx,\end{aligned} \tag{38}$$

which is the right side of inequality (27); this completes the proof.

Remark 21.

(1) Inserting $h(j) = j$ and $p = 1$ in Theorem 20, we obtained Fejér type inequality for strongly reciprocally convex function [16] (Theorem 3.7)

(2) Insertion $h(j) = j$, in Theorem 20, yields Fejér type inequality for strongly reciprocally p-convex functions [17] (Theorem 3.5)

6. Fractional Integral Inequalities

Fractional integral inequalities are important to study means [19–22]. This section is devoted for some fractional integral inequalities for functions whose derivatives are in $SR(p, h)$. A source for results of the desired type is the following lemma.

Lemma 22 see ([23], Lemma 2.1). *Let $\psi : M = [d_1, d_2] \subseteq \mathbb{R}$ is differentiable defined on the interior M of M. If $\psi' \in L[d_1, d_2]$ and $\lambda \in [0, 1]$, then*

$$\begin{aligned}(1-\lambda)\psi\left[\left(\frac{2d_1^p d_2^p}{d_1^p + d_2^p}\right)^{1/p}\right] + \lambda\left(\frac{\psi(d_1) + \psi(d_2)}{2}\right) - \frac{p\left(d_1^p d_2^p\right)}{d_2^p - d_1^p} \int_{d_1}^{d_2} \frac{\psi(x)}{x^{1+p}} dx \\ = \frac{\left(d_2^p - d_1^p\right)}{2p\left(d_1^p d_2^p\right)} \left[\int_0^{1/2} (2j - \lambda)\left(\frac{d_1^p d_2^p}{jd_1^p + (1-j)d_2^p}\right)^{1+(1/p)} \psi'\left[\left(\frac{a_1^p b_1^p}{ja_1^p + (1-j)b_1^p}\right)^{1/p}\right] dj \right. \\ \left. + \int_{1/2}^1 (2j - 2 + \lambda)\left(\frac{d_1^p d_2^p}{jd_1^p + (1-j)d_2^p}\right)^{1+(1/p)} \psi'\left[\left(\frac{d_1^p d_2^p}{jd_1^p + (1-j)d_2^p}\right)^{1/p}\right] dj\right].\end{aligned} \tag{39}$$

As a first application of Lemma 22, we prove the following result.

Theorem 23. *Let $M = [d_1, d_2] \subset \mathbb{R} \setminus \{0\}$ be a p-harmonic convex set, and let $\psi : M = [d_1, d_2] \subseteq \mathbb{R} \setminus \{0\} \longrightarrow \mathbb{R}$ be differentiable defined on the interior M of M. If $M' \in L[d_1, d_2]$ and $|\psi'|^q$ is strongly reciprocally (p,h)-convex function on M, $q \ge 1$, and $\lambda \in [0, 1]$, then*

$$\begin{aligned}\left|(1-\lambda)\psi\left[\left(\frac{2d_1^p d_2^p}{d_1^p + d_2^p}\right)^{1/p}\right] + \lambda\left(\frac{\psi(d_1) + \psi(d_2)}{2}\right) - \frac{p\left(d_1^p d_2^p\right)}{d_2^p - d_1^p} \int_{d_1}^{d_2} \frac{\psi(x)}{x^{1+p}} dx\right| \\ \le \frac{\left(d_2^p - d_1^p\right)}{2p\left(d_1^p d_2^p\right)} \left[k_1(p, d_1, d_2)^{1-(1/q)} \left[k_{15}(p, d_1, d_2)\left|\psi'(d_1)\right|^q + k_{17}(p, d_1, d_2)\left|\psi'(d_2)\right|^q \right.\right. \\ \left. + k_7(p, d_1, d_2)\mu\right]^{1/q} + k_2(p, d_2, d_1)^{1-(1/q)} \left[k_{18}(p, d_2, d_1)\left|\psi'(d_1)\right|^q \right. \\ \left.\left. + k_{16}(p, d_2, d_1)\left|\psi'(d_2)\right|^q + k_8(p, d_2, d_1)\mu\right]^{1/q}\right],\end{aligned} \tag{40}$$

where

$$k_1(p, d_1, d_2) = \int_0^{1/2} |2j - \lambda| \left(\frac{d_1^p d_2^p}{jd_1^p + (1-j)d_2^p}\right)^{1+(1/p)} dj, \tag{41}$$

$$k_2(p, d_2, d_1) = \int_{1/2}^1 |2j - 2 + \lambda| \left(\frac{d_1^p d_2^p}{jd_1^p + (1-j)d_2^p}\right)^{1+(1/p)} dj, \tag{42}$$

$$k_{15}(p, d_1, d_2) = \int_0^{1/2} h(1-j)|2j - \lambda| \left(\frac{d_1^p d_2^p}{jd_1^p + (1-j)d_2^p}\right)^{1+(1/p)} dj, \tag{43}$$

$$k_{16}(p, d_2, d_1) = \int_{1/2}^1 h(j)|2j - 2 + \lambda| \left(\frac{d_1^p d_2^p}{jd_1^p + (1-j)d_2^p}\right)^{1+(1/p)} dj, \tag{44}$$

$$k_{17}(p, d_1, d_2) = \int_0^{1/2} h(j)|2j - \lambda| \left(\frac{d_1^p d_2^p}{jd_1^p + (1-j)d_2^p}\right)^{1+(1/p)} dj, \tag{45}$$

$$k_{18}(p, d_2, d_1) = \int_{1/2}^1 h(1-j)|2j - 2 + \lambda| \left(\frac{d_1^p d_2^p}{jd_1^p + (1-j)d_2^p}\right)^{1+(1/p)} dj, \tag{46}$$

$$k_7(p, d_1, d_2) = \int_0^{1/2} j(j-1)|2j - \lambda| \left(\frac{d_1^p d_2^p}{jd_1^p + (1-j)d_2^p}\right)^{1+(1/p)} \left(\frac{1}{d_2^p} - \frac{1}{d_1^p}\right)^2 dj, \tag{47}$$

$$k_8(p, d_2, d_1) = \int_{1/2}^1 j(j-1)|2j - 2 + \lambda| \left(\frac{d_1^p d_2^p}{jd_1^p + (1-j)d_2^p}\right)^{1+(1/p)} \left(\frac{1}{d_2^p} - \frac{1}{d_1^p}\right)^2 dj. \tag{48}$$

Proof. Using Lemma 22 and power mean inequality, we have

$$\begin{aligned}&\left|(1-\lambda)\psi\left[\left(\frac{2d_1^pd_2^p}{d_1^p+d_2^p}\right)^{1/p}\right]+\lambda\left(\frac{\psi(d_1)+\psi(d_2)}{2}\right)-\frac{p(d_1^pd_2^p)}{d_2^p-d_1^p}\int_{d_1}^{d_2}\frac{\psi(x)}{x^{1+p}}dx\right|\\
&\le\frac{(d_2^p-d_1^p)}{2p(d_1^pd_2^p)}\left[\int_0^{1/2}\left|(2j-\lambda)\left(\frac{d_1^pd_2^p}{jd_1^p+(1-j)d_2^p}\right)^{1+(1/p)}\right|\times\left|\psi'\left[\left(\frac{d_1^pd_2^p}{jd_1^p+(1-j)d_2^p}\right)^{1/p}\right]\right|dj\right.\\
&\left.+\int_{1/2}^1\left|(2j-2+\lambda)\left(\frac{d_1^pd_2^p}{jd_1^p+(1-j)d_2^p}\right)^{1+(1/p)}\right|\times\left|\psi'\left[\left(\frac{d_1^pd_2^p}{jd_1^p+(1-j)d_2^p}\right)^{1/p}\right]\right|dj\right].\\
&\le\frac{(d_2^p-d_1^p)}{2p(d_1^pd_2^p)}\left[\left(\int_0^{1/2}|(2j-\lambda)|\left(\frac{d_1^pd_2^p}{jd_1^p+(1-j)d_2^p}\right)^{1+(1/p)}dj\right)^{1-(1/q)}\right.\\
&\times\left(\int_0^{1/2}|(2j-\lambda)|\left(\frac{d_1^pd_2^p}{jd_1^p+(1-j)d_2^p}\right)^{1+(1/p)}\times\left|\psi'\left[\left(\frac{d_1^pd_2^p}{jd_1^p+(1-j)d_2^p}\right)^{1/p}\right]\right|^q dj\right)^{1/q}\\
&+\left(\int_{1/2}^1|(2j-2+\lambda)|\left(\frac{d_1^pd_2^p}{jd_1^p+(1-j)d_2^p}\right)^{1+(1/p)}dt\right)^{1-(1/q)}\\
&\times\left(\int_{1/2}^1|(2j-2+\lambda)|\left(\frac{d_1^pd_2^p}{jd_1^p+(1-j)d_2^p}\right)^{1+(1/p)}\right)\\
&\left.\times\left|\psi'\left[\left(\frac{d_1^pd_2^p}{jd_1^p+(1-j)d_2^p}\right)^{1/p}\right]\right|^q dj\right)^{1/q}\right].\end{aligned}\tag{49}$$

Since $|\psi'(x)|^q\in SR(p,h)$, so

$$\begin{aligned}&\left|(1-\lambda)\psi\left[\left(\frac{2d_1^pd_2^p}{d_1^p+d_2^p}\right)^{1/p}\right]+\lambda\left(\frac{\psi(d_1)+\psi(d_2)}{2}\right)-\frac{p(d_1^pd_2^p)}{d_2^p-d_1^p}\int_{d_1}^{d_2}\frac{\psi(x)}{x^{1+p}}dx\right|\\
&\le\frac{(d_2^p-d_1^p)}{2p(d_1^pd_2^p)}\left[\left(\int_0^{1/2}|(2j-\lambda)|\left(\frac{d_1^pd_2^p}{jd_1^p+(1-j)d_2^p}\right)^{1+(1/p)}dj\right)^{1-(1/q)}\right.\\
&\times\left(\int_0^{1/2}|(2j-\lambda)|\left(\frac{d_1^pd_2^p}{jd_1^p+(1-j)d_2^p}\right)^{1+(1/p)}\right.\\
&\left.\times\left[h(1-j)|\psi'(d_1)|^q+h(j)|\psi'(d_2)|^q-\mu j(1-j)\left(\frac{1}{d_2^p}-\frac{1}{d_1^p}\right)^2\right]dj\right)^{1/q}\\
&+\left(\int_{1/2}^1|(2j-2+\lambda)|\left(\frac{d_1^pd_2^p}{jd_1^p+(1-j)d_2^p}\right)^{1+(1/p)}dj\right)^{1-(1/q)}\\
&\times\left(\int_{1/2}^1|(2j-2+\lambda)|\left(\frac{d_1^pd_2^p}{jd_1^p+(1-j)d_2^p}\right)^{1+(1/p)}\right.\\
&\left.\left.\times\left[h(1-j)|\psi'(d_1)|^q+h(j)|\psi'(d_2)|^q-\mu j(1-j)\left(\frac{1}{d_2^p}-\frac{1}{d_1^p}\right)^2\right]dj\right)^{1/q}\right]\\
&=\frac{(d_2^p-d_1^p)}{2p(d_1^pd_2^p)}\left[k_1(p,d_1,d_2)^{1-(1/q)}\left[k_{15}(p,d_1,d_2)|\psi'(d_1)|^q\right.\right.\\
&\left.+k_{17}(p,d_1,d_2)|\psi'(d_2)|^q+k_7(p,d_1,d_2)\mu\right]^{1/q}\\
&+k_2(p,d_2,d_1)^{1-(1/q)}\left[k_{18}(p,d_2,d_1)|\psi'(d_1)|^q+k_{16}(p,d_2,d_1)|\psi'(d_2)|^q\right.\\
&\left.\left.+k_8(p,d_2,d_1)\mu\right]^{1/q}\right].\end{aligned}\tag{50}$$

This completes the proof. □

Remark 24. Inserting $\mu=0$ and $h(j)=j$ in Theorem 23, we obtained [23] Theorem 2.2.

For $q=1$, Theorem 23 reduces to the following result.

Corollary 25. *Let $M=[d_1,d_2]\subset\mathbb{R}\setminus\{0\}$ be a p-harmonic convex set, and let $\psi:M=[d_1,d_2]\subseteq\mathbb{R}\setminus\{0\}\longrightarrow\mathbb{R}$ be differentiable defined on the interior M of M. If $\psi'\in L[d_1,d_2]$ and $|\psi'|^q$ is in $SR(p,h)$ on M and $\lambda\in[0,1]$, then*

$$\begin{aligned}&\left|(1-\lambda)\psi\left[\left(\frac{2d_1^pd_2^p}{d_1^p+d_2^p}\right)^{1/p}\right]+\lambda\left(\frac{\psi(d_1)+\psi(d_2)}{2}\right)-\frac{p(d_1^pd_2^p)}{d_2^p-d_1^p}\int_{d_1}^{d_2}\frac{\psi(x)}{x^{1+p}}dx\right|\\
&\le\frac{(d_2^p-d_1^p)}{2p(d_1^pd_2^p)}\left[(k_{15}(p,d_1,d_2)+k_{18}(p,d_2,d_1))|\psi'(d_1)|\right.\\
&+(k_{16}(p,d_2,d_1)+k_{17}(p,d_1,d_2))|\psi'(d_2)|+(k_7(p,d_1,d_2)\\
&\left.+k_8(p,d_2,d_1))\mu\right],\end{aligned}\tag{51}$$

where $k_{15},k_{16},k_{17},k_{18},k_7$, and k_8 are given by (43) to (48).

Remark 26. Inserting $h(j)=j$ and $\mu=0$ in Corollary 25, we obtained [23] Corollary 2.3.

Using Lemma 22, we can prove the following result.

Theorem 27. *Let $M=[d_1,d_2]\subset\mathbb{R}\setminus\{0\}$ be a p-harmonic convex set, and let $\psi:M=[d_1,d_2]\subseteq\mathbb{R}\setminus\{0\}\longrightarrow\mathbb{R}$ be differentiable defined on the interior M of M. If $M'\in L[d_1,d_2]$ and $|\psi'|^q$ is in $SR(p,h)$ on M, $r,q>1$, $(1/r)+(1/q)=1$ and $\lambda\in[0,1]$, then*

$$\begin{aligned}&\left|(1-\lambda)\psi\left[\left(\frac{2d_1^pd_2^p}{d_1^p+d_2^p}\right)^{1/p}\right]+\lambda\left(\frac{\psi(d_1)+\psi(d_2)}{2}\right)-\frac{p(d_1^pd_2^p)}{d_2^p-d_1^p}\int_{d_1}^{d_2}\frac{\psi(x)}{x^{1+p}}dx\right|\\
&\le\frac{(d_2^p-d_1^p)}{2p(d_1^pd_2^p)}\times\left(\frac{\lambda^{r+1}+(1-\lambda)^{r+1}}{2(r+1)}\right)^{1/r}\\
&\times\left[\left(k_{19}(q,p;d_1,d_2)|\psi'(d_1)|^q+k_{21}(q,p;d_1,d_2)|\psi'(d_2)|^q+k_{13}(q,p;d_1,d_2)\mu\right)^{1/q}\right.\\
&\left.+\left(k_{22}(q,p;d_2,d_1)|\psi'(d_1)|^q+k_{20}(q,p;d_2,d_1)|\psi'(d_2)|^q+k_{14}(q,p;d_2,d_1)\mu\right)^{1/q}\right],\end{aligned}\tag{52}$$

where

$$k_{19}(q,p;d_1,d_2)=\int_0^{1/2}h(1-j)\left(\frac{d_1^pd_2^p}{jd_1^p+(1-j)d_2^p}\right)^{q+(q/p)}dj,\tag{53}$$

$$k_{20}(q,p;d_2,d_1)=\int_{1/2}^1h(j)\left(\frac{d_1^pd_2^p}{jd_1^p+(1-j)d_2^p}\right)^{q+(q/p)}dj,\tag{54}$$

$$k_{21}(q,p;d_1,d_2)=\int_0^{1/2}h(j)\left(\frac{d_1^pd_2^p}{jd_1^p+(1-j)d_2^p}\right)^{q+(q/p)}dj,\tag{55}$$

$$k_{22}(q,p;d_2,d_1)=\int_{1/2}^1h(1-j)\left(\frac{d_1^pd_2^p}{jd_1^p+(1-j)d_2^p}\right)^{q+(q/p)}dj,\tag{56}$$

$$k_{13}(q,p;d_1,d_2)=\int_0^{1/2} j(j-1)\left(\frac{d_1^p d_2^p}{jd_1^p+(1-j)d_2^p}\right)^{q+(q/p)}\left(\frac{1}{b_1^p}-\frac{1}{a_1^p}\right)^2 dj, \tag{57}$$

$$k_{14}(q,p;d_2,d_1)=\int_{1/2}^{1} j(j-1)2j-2+\lambda\left(\frac{d_1^p d_2^p}{jd_1^p+(1-j)d_2^p}\right)^{q+(q/p)}\left(\frac{1}{d_2^p}-\frac{1}{d_1^p}\right)^2 dj. \tag{58}$$

Proof. Using Lemma 22, we have

$$\begin{aligned}&\left|(1-\lambda)\psi\left[\left(\frac{2d_1^p d_2^p}{d_1^p+d_2^p}\right)^{1/p}\right]+\lambda\left(\frac{\psi(d_1)+\psi(d_2)}{2}\right)-\frac{p(d_1^p d_2^p)}{d_2^p-d_1^p}\int_{d_1}^{d_2}\frac{\psi(x)}{x^{1+p}}dx\right|\\&\le\frac{(d_2^p-d_1^p)}{2p(d_1^p d_2^p)}\left[\int_0^{1/2}\left|(2j-\lambda)\left(\frac{d_1^p d_2^p}{jd_1^p+(1-j)d_2^p}\right)^{1+(1/p)}\right|\times\left|\psi'\left[\left(\frac{d_1^p d_2^p}{jd_1^p+(1-j)d_2^p}\right)^{1/p}\right]\right|dj\right.\\&\left.+\int_{1/2}^{1}\left|(2j-2+\lambda)\left(\frac{d_1^p d_2^p}{jd_1^p+(1-j)d_2^p}\right)^{1+(1/p)}\right|\times\left|\psi'\left[\left(\frac{d_1^p d_2^p}{jd_1^p+(1-j)d_2^p}\right)^{1/p}\right]\right|dj\right].\end{aligned} \tag{59}$$

Applying Holder's integral inequality,

$$\begin{aligned}&\left|(1-\lambda)\psi\left[\left(\frac{2d_1^p d_2^p}{d_1^p+d_2^p}\right)^{1/p}\right]+\lambda\left(\frac{\psi(d_1)+\psi(d_2)}{2}\right)-\frac{p(d_1^p d_2^p)}{d_2^p-d_1^p}\int_{d_1}^{d_2}\frac{\psi(x)}{x^{1+p}}dx\right|\\&\le\frac{(d_2^p-d_1^p)}{2p(d_1^p d_2^p)}\left[\left(\int_0^{1/2}|(2j-\lambda)|^r dj\right)^{1/r}\left(\int_0^{1/2}\left|\left(\frac{d_1^p d_2^p}{jd_1^p+(1-j)d_2^p}\right)^{1+(1/p)}\right.\right.\right.\\&\left.\left.\times\psi'\left[\left(\frac{d_1^p d_2^p}{jd_1^p+(1-j)d_2^p}\right)^{1/p}\right]\right|^q dj\right)^{1/q}\\&+\left(\int_{1/2}^{1}|(2j-2+\lambda)|^r dj\right)^{1/r}\left(\int_{1/2}^{1}\left|\left(\frac{d_1^p d_2^p}{jd_1^p+(1-j)d_2^p}\right)^{1+(1/p)}\right.\right.\\&\left.\left.\left.\times\psi'\left[\left(\frac{d_1^p d_2^p}{jd_1^p+(1-j)d_2^p}\right)^{1/p}\right]\right|^q dj\right)^{1/q}\right]\\&=\frac{(d_2^p-d_1^p)}{2p(d_1^p d_2^p)}\left[\left(\int_0^{1/2}|(2j-\lambda)|^r dj\right)^{1/r}\left(\int_0^{1/2}\left(\frac{d_1^p d_2^p}{jd_1^p+(1-j)d_2^p}\right)^{q+(q/p)}\right.\right.\\&\left.\times\left|\psi'\left[\left(\frac{d_1^p d_2^p}{jd_1^p+(1-j)d_2^p}\right)^{1/p}\right]\right|^q dj\right)^{1/q}\\&+\left(\int_{1/2}^{1}|(2j-2+\lambda)|^r dj\right)^{1/r}\\&\left.\times\left(\int_{1/2}^{1}\left(\frac{d_1^p d_2^p}{jd_1^p+(1-j)d_2^p}\right)^{q+(q/p)}\left|\times\psi'\left[\left(\frac{d_1^p d_2^p}{jd_1^p+(1-j)d_2^p}\right)^{1/p}\right]\right|^q dj\right)^{1/q}\right].\end{aligned} \tag{60}$$

Since $|\psi'(x)|^q\in SR(p,h)$, so

$$\begin{aligned}&\left|(1-\lambda)\psi\left[\left(\frac{2d_1^p d_2^p}{d_1^p+d_2^p}\right)^{1/p}\right]+\lambda\left(\frac{\psi(d_1)+\psi(d_2)}{2}\right)-\frac{p(d_1^p d_2^p)}{d_2^p-d_1^p}\int_{d_1}^{d_2}\frac{\psi(x)}{x^{1+p}}dx\right|\\&\le\frac{(d_2^p-d_1^p)}{2p(d_1^p d_2^p)}\left[\left(\int_0^{1/2}|(2j-\lambda)|^r dj\right)^{1/r}\times\left(\int_0^{1/2}\left(\frac{d_1^p d_2^p}{jd_1^p+(1-j)d_2^p}\right)^{q+(q/p)}\right.\right.\\&\left.\times\left[h(1-j)|\psi'(d_1)|^q+h(j)|\psi'(d_2)|^q-\mu j(1-j)\left(\frac{1}{d_2^p}-\frac{1}{d_1^p}\right)^2\right]dj\right)^{1/q}\\&+\left(\int_{1/2}^{1}|(2j-2+\lambda)|^r dj\right)^{1/r}\left(\int_{1/2}^{1}\left(\frac{d_1^p d_2^p}{jd_1^p+(1-j)d_2^p}\right)^{q+(q/p)}\right.\\&\left.\left.\times\left[h(1-j)|\psi'(d_1)|^q+h(j)|\psi'(d_2)|^q-\mu j(1-j)\left(\frac{1}{d_2^p}-\frac{1}{d_1^p}\right)^2\right]dj\right)^{1/q}\right]\\&\le\frac{(d_2^p-d_1^p)}{2p(d_1^p d_2^p)}\left[\left(\int_0^{1/2}|(2j-\lambda)|^r dj\right)^{1/r}\right.\\&\times\left(k_{19}(q,p;d_1,d_2)|\psi'(d_1)|^q+k_{21}(q,p;d_1,d_2)|\psi'(d_2)|^q\right.\\&\left.\times+k_{13}(q,p;d_1,d_2)\mu\right)^{1/q}+\left(\int_0^{1/2}|(2j-2+\lambda)|^r dj\right)^{1/r}\\&\times\left(k_{22}(q,p;d_2,d_1)|\psi'(d_1)|^q+k_{20}(q,p;d_2,d_1)|\psi'(d_2)|^q\right.\\&\left.\left.+k_{14}(q,p;d_2,d_1)\mu\right)^{1/q}\right]\\&\le\frac{(d_2^p-d_1^p)}{2p(d_1^p d_2^p)}\times\left(\frac{\lambda^{r+1}+(1-\lambda)^{r+1}}{2(r+1)}\right)^{1/r}\times\left[\left(\left(k_{19}(q,p;d_1,d_2)|\psi'(d_1)|^q\right.\right.\right.\\&\left.+k_{21}(q,p;d_1,d_2)|\psi'(d_2)|^q+k_{13}(q,p;d_1,d_2)\mu\right)^{1/q}\\&+\left(k_{22}(q,p;d_2,d_1)|\psi'(d_1)|^q+k_{20}(q,p;d_2,d_1)|\psi'(d_2)|^q\right.\\&\left.\left.+k_{14}(q,p;d_2,d_1)\mu\right)^{1/q}\right)\Big].\end{aligned} \tag{61}$$

Which is the required result. □

Remark 28. Inserting $h(j)=j$ and $\mu=0$ in Theorem 27, we obtained [23] Theorem 2.5.

For $\lambda=0$, Theorem 27 reduces to the following result.

Corollary 29. *Let $M=[d_1,d_2]\subset\mathbb{R}\setminus\{0\}$ be a p-harmonic convex set, and let $\psi: M=[d_1,d_2]\subseteq\mathbb{R}\setminus\{0\}\longrightarrow\mathbb{R}$ be differentiable defined on the interior M of M. If $\psi'\in L[d_1,d_2]$ and $|\psi'|^q$ is in $SR(p,h)$ on M, $r,q>1$, $(1/r)+(1/q)=1$ and $\lambda\in[0,1]$, then*

$$\begin{aligned}&\left|\psi\left[\left(\frac{2d_1^p d_2^p}{d_1^p+d_2^p}\right)^{1/p}\right]-\frac{p(d_1^p d_2^p)}{d_2^p-d_1^p}\int_{d_1}^{d_2}\frac{\psi(x)}{x^{1+p}}dx\right|\\&\le\frac{(d_2^p-d_1^p)}{2p(d_1^p d_2^p)}\times\left(\frac{1}{2(r+1)}\right)^{1/r}\left[\left(k_{19}(q,p;d_1,d_2)|\psi'(d_1)|^q\right.\right.\\&\left.+k_{21}(q,p;d_1,d_2)|\psi'(d_2)|^q+k_{13}(q,p;d_1,d_2)\mu\right)^{1/q}\\&+\left(k_{22}(q,p;d_2,d_1)|\psi'(d_1)|^q+k_{20}(q,p;d_2,d_1)|\psi'(d_2)|^q\right.\\&\left.\left.+k_{14}(q,p;d_2,d_1)\mu\right)^{1/q}\right],\end{aligned} \tag{62}$$

where k_{19}, k_{20}, k_{21}, k_{22}, k_{13}, and k_{14} are given by (53)-(58).

Remark 30. Inserting $h(j) = j$ and $\mu = 0$ in Corollary 29, we obtained [23] Corollary 3.5.

For $\lambda = 1$, Theorem 27 reduces to the following result.

Corollary 31. *Let $M = [d_1, d_2] \subset \mathbb{R} \setminus \{0\}$ be a p -harmonic convex set, and let $\psi : M = [d_1, d_2] \subseteq \mathbb{R} \setminus \{0\} \longrightarrow \mathbb{R}$ be differentiable defined on the interior M of M. If $M' \in L[a_1, b_1]$ and $|f'|^q$ is in $SR(p, h)$ on M, $r, q > 1$, $(1/r) + (1/q) = 1$ and $\lambda \in [0, 1]$ then,*

$$\left|\frac{\psi(d_1)+\psi(d_2)}{2} - \frac{p\left(d_1^p d_2^p\right)}{d_2^p - d_1^p}\int_{d_1}^{d_2}\frac{\psi(x)}{x^{1+p}}dx\right| \leq \frac{\left(d_2^p - d_1^p\right)}{2p\left(d_1^p d_2^p\right)} \times \left(\frac{1}{2(r+1)}\right)^{1/r}\left[\left(k_{19}(q,p;d_1,d_2)\left|\psi'(d_1)\right|^q + k_{21}(q,p;d_1,d_2)\left|\psi'(d_2)\right|^q + k_{13}(q,p;d_1,d_2)\mu\right)^{1/q} + \left(k_{22}(q,p;d_2,d_1)\left|\psi'(d_1)\right|^q + k_{20}(q,p;d_2,d_1)\left|\psi'(d_2)\right|^q + k_{14}(q,p;d_2,d_1)\mu\right)^{1/q}\right], \tag{63}$$

where $k_{19}, k_{20}, k_{21}, k_{22}, k_{13}$, and k_{14} are given by (53)-(58).

Remark 32. Inserting $h(j) = j$ and $\mu = 0$ in Corollary 31, we obtained [23] Corollary 3.6.

For $\lambda = 1/3$, Theorem 27 reduces to the following result.

Corollary 33. *Let $M = [d_1, d_2] \subset \mathbb{R} \setminus \{0\}$ be a p-harmonic convex set, and let $\psi : M = [d_1, d_2] \subseteq \mathbb{R} \setminus \{0\} \longrightarrow \mathbb{R}$ be differentiable defined on the interior M of M. If $\psi' \in L[d_1, d_2]$ and $|\psi'|^q$ is in $SR(p, h)$ on M, $r, q > 1$, $(1/r) + (1/q) = 1$ and $\lambda \in [0, 1]$ then,*

$$\left|\frac{1}{6}\left[\psi(d_1) + 4\psi\left[\left(\frac{2d_1^p d_2^p}{d_1^p + d_2^p}\right)^{1/p}\right] + \psi(d_2)\right] - \frac{p\left(d_1^p d_2^p\right)}{d_2^p - d_1^p}\int_{d_1}^{d_2}\frac{\psi(x)}{x^{1+p}}dx\right| \leq \frac{\left(d_2^p - d_1^p\right)}{2p\left(d_1^p d_2^p\right)} \times \left(\frac{1+2^{r+1}}{6.3^r(r+1)}\right)^{1/r}\left[\left(k_{19}(q,p;d_1,d_2)\left|\psi'(d_1)\right|^q + k_{21}(q,p;d_1,d_2)\left|\psi'(d_1)\right|^q + k_{13}(q,p;d_1,d_2)\mu\right)^{1/q} + \left(k_{22}(q,p;d_2,d_1)\left|\psi'(d_1)\right|^q + k_{20}(q,p;d_2,d_1)\left|\psi'(d_2)\right|^q + k_{14}(q,p;d_2,d_1)\mu\right)^{1/q}\right], \tag{64}$$

where $k_{19}, k_{20}, k_{21}, k_{22}, k_{13}$, and k_{14} are given by (53)-(58).

Remark 34. Inserting $h(j) = j$ and $\mu = 0$ in Corollary 33, we obtained [23] Corollary 3.7.

For $\lambda = 1/2$, Theorem 27) reduces to the following result.

Corollary 35. *Let $M = [d_1, d_2] \subset \mathbb{R} \setminus \{0\}$ be a p-harmonic convex set, and let $\psi : M = [d_1, d_2] \subseteq \mathbb{R} \setminus \{0\} \longrightarrow \mathbb{R}$ be differentiable defined on the interior M of M. If $\psi' \in L[d_1, d_2]$ and $|\psi'|^q$ is in $SR(p, h)$ on M, $r, q > 1$, $(1/r) + (1/q) = 1$ and $\lambda \in [0, 1]$ then,*

$$\left|\frac{1}{4}\left[\psi(d_1) + 2\psi\left[\left(\frac{2d_1^p d_2^p}{d_1^p + d_2^p}\right)^{1/p}\right] + \psi(d_2)\right] - \frac{p\left(d_1^p d_2^p\right)}{d_2^p - d_1^p}\int_{d_1}^{d_2}\frac{\psi(x)}{x^{1+p}}dx\right| \leq \frac{\left(d_2^p - d_1^p\right)}{2p\left(d_1^p d_2^p\right)} \times \left(\frac{2}{4.2^r(r+1)}\right)^{1/r}\left[\left(\left(k_{19}(q,p;d_1,d_2)\left|\psi'(d_1)\right|^q + k_{21}(q,p;d_1,d_2)\left|\psi'(d_2)\right|^q + k_{13}(q,p;d_1,d_2)\mu\right)^{1/q} + \left(k_{22}(q,p;d_2,d_1)\left|\psi'(d_1)\right|^q + k_{20}(q,p;d_2,d_1)\left|\psi'(d_2)\right|^q + k_{14}(q,p;d_2,d_1)\mu\right)^{1/q}\right] \tag{65}$$

where $k_{19}, k_{20}, k_{21}, k_{22}, k_{13}$, and k_{14} are given by (53)–(58).

Remark 36. Inserting $h(j) = j$ and $\mu = 0$ in Corollary 35, we obtained [23] Corollary 3.8.

7. Conclusion

Convexity plays very important role in pure and applied mathematics. In many problems, the classical definition of convexity is not enough, so the definition of convex functions is generalized in various directions. In this paper, we developed a new generalization called strongly reciprocally (*p*,*h*)-convex function. We have also developed Hermite-Hadamard and Fejér type inequality for this generalization. Moreover, we conclude that the results proved in this article are the generalization of results in [14, 16, 17, 23].

Data Availability

All data is included within this paper.

Conflicts of Interest

The authors have no conflict of interests.

Authors' Contributions

The authors contributed equally in this paper.

Acknowledgments

This research is supported by Department of Mathematics, University of Okara, Okara Pakistan.

References

[1] B. De Finetti, "Sulle stratificazioni convesse," *Annali di Matematica Pura ed Applicata*, vol. 30, no. 1, pp. 173–183, 1949.

[2] O. L. Manasarian, "Pseudo-convex functions," *SIAM Journal on Control*, vol. 3, pp. 281–290, 1965.

[3] J. E. Peajcariaac and Y. L. Tong, *Convex Functions, Partial Orderings, and Statistical Applications*, Academic Press, 1992.

[4] B. T. Polyak, "Existence theorems and convergence of minimizing sequences for extremal problems with constraints," in *Doklady Akademii Nauk (Vol. 166, no. 2, pp. 287-290)*, Russian Academy of Sciences, 1966.

[5] H. Zhou, M. S. Saleem, W. Nazeer, and A. F. Shah, "Hermite-Hadamard type inequalities for interval-valued exponential type pre-invex functions via Riemann-Liouville fractional integrals," *AIMS Mathematics*, vol. 7, no. 2, pp. 2602–2617, 2022.

[6] Y. Yue, G. Farid, A. K. Demirel, W. Nazeer, and Y. Zhao, "Hadamard and Fejér–Hadamard inequalities for generalized k-fractional integrals involving further extension of Mittag-Leffler function," *AIMS Mathematics*, vol. 7, no. 1, pp. 681–703, 2021.

[7] L. Chen, W. Nazeer, F. Ali, T. Botmart, and S. Mehfooz, "Some midpoint inequalities for η-convex function via weighted fractional integrals," *Journal of Function Spaces*, vol. 2022, 12 pages, 2022.

[8] G. Farid, A. Bibi, and W. Nazeer, "Opial-type inequalities for superquadratic functions," *Univerzitet u Nišu*, vol. 36, no. 1, pp. 89–98, 2022.

[9] L. Fejér, "Uber die Fourierreihen, II," *Math. Naturwiss Anz. Ungar. Akad. Wiss*, vol. 24, pp. 369–390, 1906, See the first reference of the paper https://www.hindawi.com/journals/jam/2014/386806/.

[10] K. S. Zhang and J. P. Wan, "p-Convex functions and their properties," *Pure and Applied Mathematics*, vol. 23, no. 1, pp. 130–133, 2007.

[11] M. A. Noor, K. I. Noor, and S. Iftikhar, "Inequalities via strongly (p,h)-harmonic convex functions," *TWMS Journal of Applied and Engineering Mathematics*, vol. 10, no. 1, pp. 81–94, 2019.

[12] S. Maden, S. Turhan, and Í. Íscan, "Hermite-Hadamard inequality for strongly p-convex function," *Turkish Journal of Mathematics and Computer Science*, vol. 10, pp. 184–189, 2018.

[13] H. N. Shi and J. Zhang, "Some new judgement theorems of Schur geometric and Schur harmonic convexities for a class of symmetric functions," *Journal of Inequalities and Applications*, vol. 2013, 9 pages, 2013.

[14] I. Iscan, "Hermite-Hadamard type inequalities for harmonically convex functions," *Hacettepe Journal of Mathematics and Statistics*, vol. 43, pp. 935–942, 2014.

[15] M. A. Noor, K. I. Noor, and S. Iftikhar, "Hermite-Hadamard inequalities for harmonic nonconvex functions," *MAGNT Research Report*, vol. 4, no. 1, pp. 24–40, 2016.

[16] M. Bracamonte, J. Medina, and M. Vivas, "On some inequalities for strongly reciprocally convex functions," *Extracta Mathematicae*, vol. 33, no. 1, pp. 109–126, 2018.

[17] H. Li, M. S. Saleem, I. Hussain, and M. Imran, "Strongly reciprocally-convex functions and some inequalities," *Journal of Mathematics*, vol. 2020, Article ID 4957141, 9 pages, 2020.

[18] S. Varosanec, "On h-convexity," *Journal of Mathematical Analysis and Applications*, vol. 326, no. 1, pp. 303–311, 2007.

[19] G. Farid and B. Tariq, "Some integral inequalities for m-convex functions via fractional integrals," *Journal Of Inequalities And Special Functions*, vol. 8, no. 1, pp. 170–185, 2017.

[20] G. Farid and G. Abbas, "Generalizations of some Hermite-Hadamard-Fejer type inequalities for p-convex functions via generalized fractional integrals," *Journal of Fractional Calculus and Applications*, vol. 9, no. 2, pp. 56–76, 2018.

[21] I. Iscan, "Hermite-Hadamard and Fejer type inequalities for convex functions via fractional integrals," *Studia Universitatis Babes-Bolyai Mathematica*, vol. 60, no. 3, pp. 355–366, 2015.

[22] B. Y. Xi and F. Qi, "Some integral inequalities of Hermite-Hadamard type for convex functions with applications to means," *Journal of Function Spaces and Applications*, vol. 2012, article 980438, pp. 1–14, 2012.

[23] M. A. Noor and K. I. Noor, "Integral inequalities for differentiable p-harmonic convex functions," *Faculty of Sciences and Mathematics*, vol. 31, no. 20, pp. 6575–6584, 2014.

Hindawi
Journal of Function Spaces
Volume 2022, Article ID 1257104, 9 pages
https://doi.org/10.1155/2022/1257104

Research Article

Some Inequalities of Hermite–Hadamard Type for MT-h-Convex Functions via Classical and Generalized Fractional Integrals

Hengxiao Qi,[1,2] **Waqas Nazeer**,[3] **Fatima Abbas**,[4] **and Wenbo Liao**[5]

[1]*Party School of Shandong Provincial Committee of the Communist Party of China (Shandong Administration College), Jinan 250014, China*
[2]*The Research Center of Theoretical System of Socialism with Chinese Characteristics in Shandong Province, Jinan 250014, China*
[3]*Department of Mathematics, Government College University, Lahore, Pakistan*
[4]*Department of Mathematics, University of Okara, Okara, Pakistan*
[5]*Department of Construction Management and Real Estate, Chongqing Jianzhu College, 400072, Pakistan*

Correspondence should be addressed to Hengxiao Qi; qihengxiao@sina.com and Waqas Nazeer; nazeer.waqas@gmail.com

Received 14 April 2022; Revised 24 May 2022; Accepted 15 June 2022; Published 16 July 2022

Academic Editor: Behrouz Parsa Moghaddam

Convexity plays a vital role in pure and applied mathematics specially in optimization theory, but the classical convexity is not enough to fulfil the needs of modern mathematics; hence, it is important to study generalized notion of convexity. Fraction integral operators also become an important tool for solving problems of model physical and engineering processes that are found to be best described by fractional differential equations. The aim of this paper is to study MT-h-convex functions via fractional integral operators. We establish several Hermite–Hadamard-type inequalities for MT-h-convex function via classical and generalized fractional integrals. We also obtain special means related to our results and present some error estimates for the trapezoidal formulas.

1. Introduction

One of the most important notions in mathematics is convex functions which are very important for both pure and applied mathematicians. Convex functions are helpful in solving problems of optimization theory and many other problems of applied nature.

Definition 1. Let $J \subseteq \mathfrak{R}$ and J^o be interior of J, a mapping $\psi : J \longrightarrow \mathfrak{R}$ said to be convex on J, if the following inequality holds for all $c, d \in J$ and $\lambda \in [0, 1]$,

$$\psi(\lambda c + (1 - \lambda d)) \leq \lambda \psi(c) + (1 - \lambda)\psi(d). \tag{1}$$

The mapping ψ is said to be concave if $-\psi$ is convex.

The theory of inequalities got the attention of many researchers, and the new inequalities are always appreciable not only in real analysis but also the researchers working in applied sciences use inequalities as a very effective tool for analyzing different practical problems and to study various properties of solution of different equations [1]. Jensen-type inequalities, Hardy-type inequalities [2], Gagliardo-Nirenberg-type inequalities [3], Grüss-type inequalities [4], Ostrowski-type inequality [5, 6], etc. are extensively studied in the literature. The most famous inequality in literature is known as Hermite–Hadamard inequality, which has fundamental role in convex analysis. The Hermite–Hadamard-type inequalities for different classes of convex function can be found in [7, 8] and references therein.

Let $\psi : J \subseteq \mathfrak{R} \longrightarrow \mathfrak{R}$ be a convex mapping defined on the interval J of real numbers and $c, d \in J$. Then, the Hermite–Hadamard inequality is as follows:

$$\psi\left(\frac{c+d}{2}\right) \leq \frac{1}{c-d}\int_c^d \psi(\lambda) d\lambda \leq \frac{\psi(c) + \psi(d)}{2}, \tag{2}$$

with $c < d$ and $c, d \in J$. If ψ is concave, then both the inequalities reverse their direction.

Hermite–Hadamard inequality is the most important inequality so far in inequality theory, and several extensions of this inequality are given by researchers in recent years [9]. Our motivation is to establish a generalized version of Hermite–Hadamard-type inequality for MT-h-convex functions. It is worthy to mention here that several results of literature can be obtained from our established results as a particular case by taking suitable values of involved parameters.

Since classical notion of convexity is not enough for solving today's problems, so this notion has been generalized by several researchers to meet the needs of modern mathematics. Now, we present some generalized notions of convexity.

Definition 2 (see [10]). Let $h : I \longrightarrow \mathfrak{R}$ be a nonnegative mapping, $h \neq 0$. The mapping $\psi : J \longrightarrow \mathfrak{R}$ is said to be h-convex, if ψ is nonnegative and for all $c, d \in J$, $\lambda \in (0, 1)$, the following inequality holds:

$$\psi(\lambda c + (1-\lambda)d) \leq h(\lambda)\psi(c) + h(1-\lambda)\psi(d). \tag{3}$$

The mapping is said to be h-concave if inequality (3) is reversed.

Definition 3 (see [11, 12]). A mapping $\psi : J \subseteq \mathfrak{R} \longrightarrow \mathfrak{R}$ is said to be MT-convex on J if it is nonnegative and satisfies the following inequality:

$$\psi(\lambda c + (1-\lambda)d) \leq \frac{\sqrt{\lambda}}{2\sqrt{1-\lambda}}\psi(c) + \frac{\sqrt{1-\lambda}}{2\sqrt{\lambda}}\psi(d). \tag{4}$$

Motivated by the above two notions, we introduce the following notion of MT-h-convex function.

Definition 4. A mapping $\psi : J \subseteq \mathfrak{R} \longrightarrow \mathfrak{R}$ is said to be MT-h-convex on J, if for all $c, d \in J$ and $h(\lambda) \in (0, 1)$, it is nonnegative and satisfies the following inequality:

$$\psi(\lambda c + (1-\lambda)d) \leq \frac{\sqrt{h(\lambda)}}{2\sqrt{h(1-\lambda)}}\psi(c) + \frac{\sqrt{h(1-\lambda)}}{2\sqrt{h(\lambda)}}. \tag{5}$$

Fraction integral operators also become an important tool for solving problems of model physical and engineering processes that are found to be best described by fractional differential equations. Fractional calculus creates a diversity in inequality theory of convex analysis [13, 14].

The following generalized fractional integral operators were introduced by Ertugral and Sariaya [15] as follows:

Let $\rho : [0,\infty) \longrightarrow [0,\infty)$ be such that

$$\int_0^1 \frac{\rho(\lambda)}{\lambda} d\lambda < \infty, \tag{6}$$

then the left-hand-sided and right-hand-sided generalized fractional integral operators are defined as:

$${}_{c}^{+}J_{\rho}\psi(\nu) = \int_c^{\nu} \frac{\rho(\nu-\lambda)}{\nu-\lambda}\psi(\lambda), \nu > c, \tag{7}$$

$${}_{d}^{-}J_{\rho}\psi(\nu) = \int_{\nu}^{d} \frac{\rho(\lambda-\nu)}{\lambda-\nu}\psi(\lambda), \nu < d, \tag{8}$$

respectively.

The following remark justifies the generality of the above fractional integral operators.

Remark 5. (1) If $\rho(\lambda) = \lambda$, then (7) and (8) convert to usual Riemann fractional integral, respectively

$$\begin{aligned} J_c^{+}\psi(\nu) &= \int_c^{\nu} \psi(\lambda)d\lambda, \nu > c, \\ J_d^{-}\psi(\nu) &= \int_{\nu}^{d} \psi(\lambda)d\lambda, \nu < d. \end{aligned} \tag{9}$$

(2) If $\rho(\lambda) = \lambda^{\eta}/\Gamma(\eta)$, then (7) and (8) reduce to the Riemann-Liouville integral [14, 16]

$$\begin{aligned} J_{c^+}^{\eta}\psi(\nu) &= \frac{1}{\Gamma(\eta)}\int_c^{\nu} (\nu-\lambda)^{\eta-1}\psi(\lambda)d\lambda, \nu > c, \\ J_{d^-}^{\eta}\psi(\nu) &= \frac{1}{\Gamma(\eta)}\int_{\nu}^{d} (\lambda-\nu)^{\eta-1}\psi(\lambda)d\lambda, \nu < d. \end{aligned} \tag{10}$$

Here, $\Gamma(\eta) = \int_0^{\infty} t^{-m} m^{\eta-1} dm$ and $J_{c^+}^{0}\psi(\nu) = J_{d^-}^{0}\psi(\nu) = \psi(\nu)$.

Note that, for $\eta = 1$, the Riemann-Liouville integral converts to the classical integrals. For the other interesting special cases of (7) and (8), we refer to the readers [17, 18].

The aim of this paper is to establish Hermite–Hadamard-type inequalities for the proposed notion of MT-h-convex function in the setting of classical and generalized fractional integral operators. As applications of our results, we present special means related with our results. We also establish some error estimates for the trapezoidal formula.

2. Hermite–Hadamard-Type Inequalities via Classical Fractional Integral

First, we present the following identity that has been obtained in [19] which will play a crucial role in the proof of our main results.

Lemma 6. *Let $\psi : J \subset \mathfrak{R} \longrightarrow \mathfrak{R}$ be a differentiable function on J^o and $c, d \in J$ with $c < d$. If $\psi' \in L_1[c, d]$, then the* *following inequality holds:*

$$\frac{(d-\nu)\psi(d)+(\nu-c)\psi(c)}{d-c}-\frac{1}{d-c}\int_c^d\psi(s)ds = \frac{(\nu-c)^2}{d-c}\int_0^1(1-\lambda)\psi'(\lambda\nu+(1-\lambda)c)d\lambda + \frac{(d-\nu)^2}{d-c}\int_0^1(1-\lambda)\psi'(\lambda\nu+(1-\lambda)d)d\lambda, \quad (11)$$

for each $\nu\in[c,d]$.

Theorem 7. *Let* $\psi: J\subset\Re^+\longrightarrow\Re$ *be a differentiable function on* J^o *such that* $\psi'\in L_1[c,d]$ *where* $c,d\in J$. *If* $|\psi'|$ *is MT-h-convex function on* $[c,d]$ *and* $|\psi'|\leq Q$ *where* $\nu\in[c,d]$ *, then we have*

$$\left|\frac{(d-\nu)\psi(d)+(\nu-c)\psi(c)}{d-c}-\frac{1}{d-c}\int_c^d\psi(s)ds\right| \leq Q\frac{(\nu-c)^2+(d-\nu)^2}{d-c}\times\left(\frac{1}{2}(S_1+S_2)\right), \quad (12)$$

where

$$S_1=\int_0^1(1-\lambda)\frac{\sqrt{h(\lambda)}}{\sqrt{h(1-\lambda)}}d\lambda, S_2=\int_0^1(1-\lambda)\frac{\sqrt{h(1-\lambda)}}{\sqrt{h(\lambda)}}d\lambda, \quad (13)$$

with $h(\lambda)/h(1-\lambda)<\infty$ *is finite.*

Proof. From Lemma 6, we have

$$\frac{(d-\nu)\psi(d)+(\nu-c)\psi(c)}{d-c}-\frac{1}{d-c}\int_c^d\psi(s)ds = \frac{(\nu-c)^2}{d-c}\int_0^1(1-\lambda)\psi'(\lambda\nu+(1-\lambda)c)d\lambda + \frac{(d-\nu)^2}{d-c}\int_0^1(1-\lambda)\psi'(\lambda\nu+(1-\lambda)d)d\lambda. \quad (14)$$

Applying mode on both sides,

$$\left|\frac{(d-\nu)\psi(d)+(\nu-c)\psi(c)}{d-c}-\frac{1}{d-c}\int_c^d\psi(s)ds\right| \leq \frac{(\nu-c)^2}{d-c}\int_0^1(1-\lambda)\left|\psi'(\lambda\nu+(1-\lambda)c)\right|d\lambda + \frac{(d-\nu)^2}{d-c}\int_0^1(1-\lambda)\left|\psi'(\lambda\nu+(1-\lambda)d)\right|d\lambda. \quad (15)$$

Employing MT-h-convexity of $|\psi'|$, we have

$$\leq\frac{(\nu-c)^2}{d-c}\int_0^1(1-\lambda)\left[\frac{\sqrt{h(\lambda)}}{2\sqrt{h(1-\lambda)}}\left|\psi'(\nu)\right| + \frac{\sqrt{h(1-\lambda)}}{2\sqrt{h(\lambda)}}\left|\psi'(c)\right|\right]d\lambda + \frac{(d-\nu)^2}{d-c}\int_0^1(1-\lambda) \cdot\left[\frac{\sqrt{h(\lambda)}}{2\sqrt{h(1-\lambda)}}\left|\psi'(\nu)\right|+\frac{\sqrt{h(1-\lambda)}}{2\sqrt{h(\lambda)}}\left|\psi'(d)\right|\right]d\lambda. \quad (16)$$

Since $|\psi'(\nu)|\leq Q$, so

$$\begin{aligned}&\leq Q\frac{(\nu-c)^2}{d-c}\left[\int_0^1(1-\lambda)\frac{\sqrt{h(\lambda)}}{2\sqrt{h(1-\lambda)}}d\lambda + \int_0^1(1-\lambda)\frac{\sqrt{h(1-\lambda)}}{2\sqrt{h(\lambda)}}d\lambda\right]+Q\frac{(d-\nu)^2}{d-c}\\ &\cdot\left[\int_0^1(1-\lambda)\frac{\sqrt{h(\lambda)}}{2\sqrt{h(1-\lambda)}}d\lambda+\int_0^1(1-\lambda)\frac{\sqrt{h(1-\lambda)}}{2\sqrt{h(\lambda)}}d\lambda\right]\\ &\leq Q\frac{(\nu-c)^2}{d-c}\left(\frac{1}{2}(S_1+S_2)\right)+Q\frac{(d-\nu)^2}{d-c}\left(\frac{1}{2}(S_1+S_2)\right)\\ &\leq Q\frac{(\nu-c)^2+(d-\nu)^2}{d-c}\times\left(\frac{1}{2}(S_1+S_2)\right).\end{aligned} \quad (17)$$

The proof is completed. □

Corollary 8. *In Theorem 7, if we substitute* $h(\lambda)=\lambda$, *we get [20] Theorem 7.*

Remark 9. If we take $\nu=(c+d)/2$ in Theorem 7, then we obtain

$$\left|\frac{(d-\nu)\psi(d)+(\nu-c)\psi(c)}{d-c}-\frac{1}{d-c}\int_c^d\psi(s)ds\right| \leq\frac{1}{4}(d-c)Q\times(S_1+S_2). \quad (18)$$

Theorem 10. *Let* $\psi: J\subset\Re^+\longrightarrow\Re$ *be a differentiable function on* J^o *such that* $\psi'\in L_1[c,d]$ *where* $c,d\in J$. *If* $|\psi'|^q$ *is MT-h-convex mapping on* $[c,d]$ *and* $q>1$, $(1/p)+(1/q)=1$ *also* $|\psi'|\leq Q$ *and* $\nu\in[c,d]$, *then we have*

$$\frac{(d-\nu)\psi(d)+(\nu-c)\psi(c)}{d-c}-\frac{1}{d-c}\int_c^d\psi(s)ds \leq\frac{(\nu-c)^2+(d-\nu)^2}{d-c}\times\left(\frac{1}{p+1}\right)^{1/p} \times\left(Q^q\int_0^1\frac{\sqrt{h(\lambda)}}{\sqrt{h(1-\lambda)}}d\lambda\right)^{1/q}. \quad (19)$$

Proof. Assume that $p > 1$ and using Lemma 6, we have

$$\begin{aligned}&\left|\frac{(d-\nu)\psi(d)+(\nu-c)\psi(c)}{d-c}-\frac{1}{d-c}\int_c^d\psi(s)ds\right|\\&\quad\leq\frac{(\nu-c)^2}{d-c}\int_0^1(1-\lambda)\left|\psi'(\lambda\nu+(1-\lambda)c)\right|d\lambda\\&\quad+\frac{(d-\nu)^2}{d-c}\int_0^1(1-\lambda)\left|\psi'(\lambda\nu+(1-\lambda)d)\right|d\lambda.\end{aligned}\tag{20}$$

Using Hölder inequality,

$$\begin{aligned}&\leq\frac{(\nu-c)^2}{d-c}\left(\int_0^1(1-\lambda)^p d\lambda\right)^{1/p}\left(\int_0^1\left|\psi'(\lambda\nu+(1-\lambda)c)\right|^q d\lambda\right)^{1/q}\\&\quad+\frac{(d-\nu)^2}{d-c}\left(\int_0^1(1-\lambda)^p d\lambda\right)^{1/p}\left(\int_0^1\left|\psi'(\lambda\nu+(1-\lambda)d)\right|^q d\lambda\right)^{1/q}.\end{aligned}\tag{21}$$

Since $|\psi'|^q$ is MT-h-convex mapping and $|\psi(\nu)| \leq Q$, so we have

$$\begin{aligned}&\leq\frac{(\nu-c)^2}{d-c}\times\left(\frac{1}{p+1}\right)^{1/p}\times\left(\int_0^1\left[\frac{\sqrt{h(\lambda)}}{2\sqrt{h(1-\lambda)}}\left|\psi'(\nu)\right|^q\right.\right.\\&\quad\left.\left.+\frac{\sqrt{h(1-\lambda)}}{2\sqrt{h(\lambda)}}+\left|\psi'(c)\right|^q\right]\right)^{1/q}+\frac{(d-\nu)^2}{d-c}\\&\quad\times\left(\frac{1}{p+1}\right)^{1/p}\times\left(\int_0^1\left[\frac{\sqrt{h(\lambda)}}{2\sqrt{h(1-\lambda)}}\left|\psi'(\nu)\right|^q\right.\right.\\&\quad\left.\left.+\frac{\sqrt{h(1-\lambda)}}{2\sqrt{h(\lambda)}}+\left|\psi'(d)\right|^q\right]\right)\frac{1}{q}.\end{aligned}\tag{22}$$

Some small calculations yield that

$$\int_0^1\frac{\sqrt{h(\lambda)}}{h(1-\lambda)}d\lambda=\int_0^1\frac{\sqrt{h(1-\lambda)}}{h(\lambda)}d\lambda.\tag{23}$$

This implies that

$$\begin{aligned}&\leq\frac{(\nu-c)^2}{d-c}\times\left(\frac{1}{p+1}\right)^{1/p}\times\left(Q^q\int_0^1\frac{\sqrt{h(\lambda)}}{\sqrt{h(1-\lambda)}}d\lambda\right)^{1/q}\\&\quad+\frac{(d-\nu)^2}{d-c}\times\left(\frac{1}{p+1}\right)^{1/p}\times\left(Q^q\int_0^1\frac{\sqrt{h(\lambda)}}{\sqrt{h(1-\lambda)}}d\lambda\right)^{1/q}\\&=\frac{(\nu-c)^2+(d-\nu)^2}{d-c}\times\left(\frac{1}{p+1}\right)^{1/p}\times\left(Q^q\int_0^1\frac{\sqrt{h(\lambda)}}{\sqrt{h(1-\lambda)}}d\lambda\right)^{1/q}.\end{aligned}\tag{24}$$

The proof is completed. □

Corollary 11. *In Theorem 10, if we substitute $h(\lambda) = \lambda$, we get [20] Theorem 2.4.*

Remark 12. If we take $\nu = (c + d)/2$ in Theorem 10, then we obtain

$$\begin{aligned}&\left|\frac{(d-\nu)\psi(d)+(\nu-c)\psi(c)}{d-c}-\frac{1}{d-c}\int_c^d\psi(s)ds\right|\\&\quad\leq\left(\frac{(d-c)}{2}\right)\times\left(\frac{1}{p+1}\right)^{1/p}\times\left(Q^q\int_0^1\frac{\sqrt{h(\lambda)}}{\sqrt{h(1-\lambda)}}d\lambda\right)^{1/q}.\end{aligned}\tag{25}$$

Theorem 13. *Let $\psi : J \subset \Re^+ \longrightarrow \Re$ be a differentiable function on J^o such that $\psi' \in L_1[c, d]$ with $c < d$ where $c, d \in J$. If $|\psi'|^q$ is MT-h-convex function on $[c, d]$ with $q > 1$ and $|\psi'(\nu)| \leq Q$ where $\nu \in [c, d]$, then we have*

$$\begin{aligned}&\left|\frac{(d-\nu)\psi(d)+(\nu-c)\psi(c)}{d-c}-\frac{1}{d-c}\int_c^d\psi(s)ds\right|\\&\quad\leq\frac{(\nu-c)^2+(d-\nu)^2}{d-c}\times\left(\frac{1}{2}\right)^{1-(1/q)}\left(\frac{1}{2}Q^qS_1+\frac{1}{2}Q^qS_2\right)^{1/q},\end{aligned}\tag{26}$$

where

$$\begin{aligned}S_1&=\int_0^1(1-\lambda)\frac{\sqrt{h(\lambda)}}{\sqrt{h(1-\lambda)}}d\lambda,\\S_2&=\int_0^1(1-\lambda)\frac{\sqrt{h(1-\lambda)}}{\sqrt{h(\lambda)}}d\lambda,\end{aligned}\tag{27}$$

with $h(\lambda)/h(1-\lambda) < \infty$ is finite.

Proof. Using Lemma 6, Hölder inequality, and MT-h-convexity of $|\psi'|^q$, we have

$$\begin{aligned}&\left|\frac{(d-\nu)\psi(d)+(\nu-c)\psi(c)}{d-c}-\frac{1}{d-c}\int_c^d\psi(s)ds\right|\\&\quad\leq\frac{(\nu-c)^2}{d-c}\int_0^1(1-\lambda)\left|\psi'(\lambda\nu+(1-\lambda)c)\right|d\lambda\\&\quad+\frac{(d-\nu)^2}{d-c}\int_0^1(1-\lambda)\left|\psi'(\lambda\nu+(1-\lambda)d)\right|d\lambda\\&\quad\leq\frac{(\nu-c)^2}{d-c}\left(\int_0^1(1-\lambda)d\lambda\right)^{1-(1/q)}\\&\quad\cdot\left(\int_0^1(1-\lambda)\left|\psi'(\lambda\nu+(1-\lambda)c)\right|^q d\lambda\right)^{1/q}\\&\quad+\frac{(d-\nu)^2}{d-c}\left(\int_0^1(1-\lambda)d\lambda\right)^{1-(1/q)}\\&\quad\cdot\left(\int_0^1(1-\lambda)\left|\psi'(\lambda\nu+(1-\lambda)d)\right|^q d\lambda\right)^{1/q}\end{aligned}$$

$$\leq \frac{(v-c)^2}{d-c} \times \left(\frac{1}{2}\right)^{1-(1/q)} \left(\int_0^1 (1-\lambda)\frac{\sqrt{h(\lambda)}}{2\sqrt{h(1-\lambda)}}\left|\psi'(v)\right|^q \cdot d\lambda + \int_0^1 (1-\lambda)\frac{\sqrt{h(\lambda)}}{2\sqrt{h(1-\lambda)}}\left|\psi'(c)\right|^q d\lambda\right)^{1/q} + \frac{(d-v)^2}{d-c} \times \left(\frac{1}{2}\right)^{1-(1/q)} \times \left(\int_0^1 (1-\lambda)\frac{\sqrt{h(\lambda)}}{2\sqrt{h(1-\lambda)}} \cdot \left|\psi'(v)\right|^q d\lambda + \int_0^1 (1-\lambda)\frac{\sqrt{h(\lambda)}}{2\sqrt{h(1-\lambda)}}\left|\psi'(c)\right|^q d\lambda\right)^{1/q}$$
$$\leq \frac{(v-c)^2}{d-c} \times \left(\frac{1}{2}\right)^{1-(1/q)} \left(\frac{1}{2}Q^q S_1 + \frac{1}{Q^q} S_2\right)^{1/q} + \frac{(d-v)^2}{d-c} \times \left(\frac{1}{2}\right)^{1-(1/q)} \left(\frac{1}{2}Q^q S_1 + \frac{1}{Q^q} S_2\right)^{1/q}$$
$$\leq \frac{(v-c)^2+(d-v)^2}{d-c} \times \left(\frac{1}{2}\right)^{1-(1/q)} \left(\frac{1}{2}Q^q S_1 + \frac{1}{2}Q^q S_2\right)^{1/q}. \quad (28)$$

The proof is completed. □

Corollary 14. *In Theorem 13, if we substitute $h(\lambda)=\lambda$, we get [20] Theorem 2.6.*

Remark 15. If we take $v=(c+d)/2$ in Theorem 13, then we obtain

$$\left|\frac{(d-v)\psi(d)+(v-c)\psi(c)}{d-c} - \frac{1}{d-c}\int_c^d \psi(s)ds\right| \leq \frac{(d-c)}{2} \times \left(\frac{1}{2}\right)^{1-(1/q)} \left(\frac{1}{2}Q^q S_1 + \frac{1}{2}Q^q S_2\right)^{1/q}. \quad (29)$$

3. Hermite–Hadamard-Type Inequalities via Generalized Fractional Operators

To establish Hermite–Hadamard-type inequalities via generalized fractional operators for MT-h-convex function, we need the following identity [21].

Lemma 16. *Let $\psi : [c,d] \longrightarrow \Re$ be differentiable function on (c,d) with $c<d$ such that $\psi \in L^1[c,d]$. Then, for each $t \in (0,1)$, we have*

$$\frac{(1-t)^\eta \Omega(1) + t^\eta \nabla(1)}{d-c}\psi(v) - \frac{1}{d-c}\left[(1-t)^\eta\left(w^- I_\rho \psi(c)\right) + t^\eta\left(v^+ I_\rho \psi(d)\right)\right] = (1-t)^{\eta+1}\int_0^1 \Omega(\lambda)\psi'(\lambda v + (1-\lambda)c)d\lambda - t^{\eta+1}\int_0^1 \nabla(\lambda)\psi'(\lambda v + (1-\lambda)d)d\lambda, \quad (30)$$

where $v = tc + (1-t)d$, and

$$\Omega(\lambda) = \int_0^\lambda \frac{\rho((v-c)s)}{s}ds < \infty, \quad \nabla(\lambda) = \int_0^\lambda \frac{\rho((d-v)s)}{s}ds < \infty. \quad (31)$$

Theorem 17. *Let $\psi : [c,d] \longrightarrow \Re$ be a differentiable function on (c,d) and $\psi' \in L^1[c,d]$ with $0 \leq c < d$ and $\eta > 0$. Then, the following inequality holds for each $t \in (0,1)$. If $|\psi'|$ is MT-h-convex on $[c,d]$,*

$$\left|\frac{(1-t)^\eta \Omega(1) + t^\eta \nabla(1)}{d-c}\psi(v) - \frac{1}{d-c}\left[(1-t)^\eta\left(v^- I_\rho \psi(c)\right) + t^\eta\left(v^+ I_\rho \psi(d)\right)\right]\right| \leq \frac{(1-t)^{\eta+1}}{2}\left[M_1|\psi'(v)| + N_1|\psi'(c)|\right] + \frac{t^{\eta+1}}{2}\left[M_1|\psi'(v)| + N_1|\psi'(d)|\right], \quad (32)$$

where the constants M_1, M_2, N_1, and N_2 are

$$M_1 = \int_0^1 \sqrt{\frac{h(\lambda)}{h(1-\lambda)}}|\Omega(\lambda)|d\lambda, \quad M_2 = \int_0^1 \sqrt{\frac{h(\lambda)}{h(1-\lambda)}}|\nabla(\lambda)|d\lambda, \quad N_1 = \int_0^1 \sqrt{\frac{h(1-\lambda)}{h(\lambda)}}|\Omega(\lambda)|d\lambda, \quad N_2 = \int_0^1 \sqrt{\frac{h(1-\lambda)}{h(\lambda)}}|\nabla(\lambda)|d\lambda. \quad (33)$$

Proof. From Lemma 16, we have

$$\frac{(1-t)^\eta \Omega(1) + t^\eta \nabla(1)}{d-c}\psi(v) - \frac{1}{d-c}\left[(1-t)^\eta\left(v^- I_\rho \psi(c)\right) + t^\eta\left(v^+ I_\rho \psi(d)\right)\right] = (1-t)^{\eta+1}\int_0^1 \Omega(\lambda)\psi'(\lambda v + (1-\lambda)c)d\lambda - t^{\eta+1}\int_0^1 \nabla(\lambda)\psi'(\lambda v + (1-\lambda)d)d\lambda. \quad (34)$$

Using mode property on both sides, we obtain

$$\begin{aligned}&\left|\frac{(1-t)^{\eta}\Omega(1)+t^{\eta}\nabla(1)}{d-c}\psi(\nu)\right.\\&\quad\left.-\frac{1}{d-c}\left[(1-t)^{\eta}\left(\nu^{-}I_{\rho}\psi(c)\right)+t^{\eta}\left(\nu^{+}I_{\rho}\psi(d)\right)\right]\right|\\&\le(1-t)^{\eta+1}\int_0^1|\Omega(\lambda)|\left|\psi'(\lambda\nu+(1-\lambda)c)\right|d\lambda\\&\quad+t^{\eta+1}\int_0^1|\nabla(\lambda)|\left|\psi'(\lambda\nu+(1-\lambda)d)\right|d\lambda.\end{aligned}\tag{35}$$

Since$|\psi'|$ is MT-h-convex, so we have

$$\begin{aligned}&\le(1-t)^{\eta+1}\int_0^1|\Omega(\lambda)|\left[\frac{\sqrt{h(\lambda)}}{2\sqrt{h(1-\lambda)}}\left|\psi'(\nu)\right|\frac{\sqrt{h(1-\lambda)}}{2\sqrt{h(\lambda)}}\left|\psi'(c)\right|\right]\\&\quad+t^{\eta+1}\int_0^1|\nabla(\lambda)|\left[\frac{\sqrt{h(\lambda)}}{2\sqrt{h(1-\lambda)}}\left|\psi'(\nu)\right|+\frac{\sqrt{h(1-\lambda)}}{2\sqrt{h(\lambda)}}\left|\psi'(d)\right|\right]d\lambda.\end{aligned}\tag{36}$$

After simplification, we obtain desired result

$$\begin{aligned}&=\frac{(1-t)^{\eta+1}}{2}\left[M_1\left|\psi'(\nu)\right|+N_1\left|\psi'(c)\right|\right]\\&\quad+\frac{t^{\eta+1}}{2}\left[M_1\left|\psi'(\nu)\right|+N_1\left|\psi'(d)\right|\right].\end{aligned}\tag{37}$$

□

Corollary 18. *In Theorem 17, if we substitute $h(\lambda)=\lambda$, we get [21] Theorem 2.1.*

Theorem 19. *Let $\psi:[c,d]\longrightarrow\mathfrak{R}$ be a differentiable function over (c,d) and $\psi'\varepsilon L^1[c,d]$ with $0\le c<d$ and $\eta>0$. If $|\psi'|^q$ is MT-h-convex with $q>1$. Then for each $t\in(0,1)$, the following inequality holds:*

$$\begin{aligned}&\left|\frac{(1-t)^{\eta}\Omega(1)+t^{\eta}\nabla(1)}{d-c}\psi(\nu)\right.\\&\quad\left.-\frac{1}{d-c}\left[(1-t)^{\eta}\left(\nu^{-}I_{\rho}\psi(c)\right)+t^{\eta}\left(\nu^{+}I_{\rho}\psi(d)\right)\right]\right|\\&\le(1-t)^{\eta+1}\left(\int_0^1\left|\Omega(\lambda)^p d\lambda\right.\right)^{1/p}\\&\quad\cdot\left(\frac{1}{2}\left(\left|\psi'(\nu)\right|^q+\left|\psi'(c)\right|^q\right)\int_0^1\frac{\sqrt{h(\lambda)}}{\sqrt{h(1-\lambda)}}d\lambda\right)^{1/q}\\&\quad+t^{\eta+1}\left(\int_0^1\left|\Omega(\lambda)^p d\lambda\right.\right)^{1/p}\\&\quad\cdot\left(\frac{1}{2}\left(\left|\psi'(\nu)\right|^q+\left|\psi'(d)\right|^q\right)\int_0^1\frac{\sqrt{h(\lambda)}}{\sqrt{h(1-\lambda)}}d\lambda\right)^{1/q},\end{aligned}\tag{38}$$

where $(1/p)+(1/q)=1$ and $p>1$.

Proof. By using Lemma 16, Hölder's inequality, and MT-h-convexity of $|\psi'|^q$, we get

$$\begin{aligned}&\left|\frac{(1-t)^{\eta}\Omega(1)+t^{\eta}\nabla(1)}{d-c}\psi(\nu)-\frac{1}{d-c}\right|\\&\quad\cdot\left[(1-t)^{\eta}\left(\nu^{-}I_{\rho}\psi(c)\right)+t^{\eta}\left(\nu^{+}I_{\rho}\psi(d)\right)\right]\\&\le(1-t)^{\eta+1}\int_0^1|\Omega(\lambda)|\left|\psi'(\lambda\nu+(1-\lambda)c)\right|d\lambda\\&\quad+t^{\eta+1}\int_0^1|\nabla(\lambda)|\left|\psi'(\lambda\nu+(1-\lambda)d)\right|d\lambda\\&\le(1-t)^{\eta+1}\left(\int_0^1\left|\Omega(\lambda)^p d\lambda\right.\right)^{1/p}\left(\int_0^1\left|\psi'(\lambda\nu+(1-\lambda)c)\right|^q d\lambda\right)^{1/q}\\&\quad+t^{\eta+1}\left(\int_0^1|\nabla(\lambda)|^p d\lambda\right)^{1/p}\left(\int_0^1\left|\psi'(\lambda\nu+(1-\lambda)d)\right|^q d\lambda\right)^{1/q}\\&\le(1-t)^{\eta+1}\left(\int_0^1\left|\Omega(\lambda)^p d\lambda\right.\right)^{1/p}\left(\int_0^1\left[\frac{\sqrt{h(\lambda)}}{2\sqrt{h(1-\lambda)}}\left|\psi'(\nu)\right|^q\right.\right.\\&\quad\left.\left.+\frac{\sqrt{h(1-\lambda)}}{2\sqrt{h(\lambda)}}\left|\psi'(c)\right|^q\right]d\lambda\right)^{1/q}+t^{\eta+1}\left(\int_0^1\left|\nabla(\lambda)^p d\lambda\right.\right)^{1/p}\\&\quad\cdot\left(\int_0^1\left[\frac{\sqrt{h(\lambda)}}{2\sqrt{h(1-\lambda)}}\left|\psi'(\nu)\right|^q+\frac{\sqrt{h(1-\lambda)}}{2\sqrt{h(\lambda)}}\left|\psi'(d)\right|^q\right]d\lambda\right)^{1/q}.\end{aligned}\tag{39}$$

Since,

$$\int_0^1\frac{\sqrt{h(\lambda)}}{\sqrt{h(1-\lambda)}}d\lambda=\int_0^1\frac{\sqrt{h(1-\lambda)}}{\sqrt{h(\lambda)}}d\lambda,\tag{40}$$

this implies that

$$\begin{aligned}&\le(1-t)^{\eta+1}\left(\int_0^1\left|\Omega(\lambda)^p d\lambda\right.\right)^{1/p}\left(\frac{1}{2}\left(\left|\psi'(\nu)\right|^q+\left|\psi'(c)\right|^q\right)\right.\\&\quad\left.\cdot\int_0^1\frac{\sqrt{h(\lambda)}}{\sqrt{h(1-\lambda)}}d\lambda\right)^{1/q}+t^{\eta+1}\left(\int_0^1\left|\Omega(\lambda)^p d\lambda\right.\right)^{1/p}\\&\quad\cdot\left(\frac{1}{2}\left(\left|\psi'(\nu)\right|^q+\left|\psi'(d)\right|^q\right)\int_0^1\frac{\sqrt{h(\lambda)}}{\sqrt{h(1-\lambda)}}d\lambda\right)^{1/q}.\end{aligned}\tag{41}$$

The proof is completed. □

Corollary 20. *If we substitute $h(\lambda)=\lambda$ in Theorem 19, we obtain [21] Theorem 7.*

Theorem 21. *Let $\psi:[c,d]\longrightarrow\mathfrak{R}$ be a differentiable function on (c,d) and $\psi'\in L^1[c,d]$ with $0\le c<d$ and $\eta>0$. If function*

$|\psi'|^q$ *is MT-h-convex on* $[c, d]$ *for* $q > 1$, *then for each* $t\varepsilon(0, 1)$, *we have*

$$\begin{aligned}&\left|\frac{(1-t)^{\eta}\Omega(1)+t^{\mu}\nabla(1)}{d-c}\psi(\nu)\right.\\&\left.-\frac{1}{d-c}\left[(1-t)^{\eta}\left(\nu^{-}I_{\rho}\psi(c)\right)+t^{\eta}\left(\nu^{+}I_{\rho}\psi(\eta)\right)\right]\right|\\&\le\left(\frac{1}{2}\right)^{1/q}(1-t)^{\eta+1}\left[\int_0^1|\Omega(\lambda)|d\lambda\right]^{1-(1/q)}\\&\cdot\left(M_1|\psi'(\nu)|^q+N_1|\psi'(c)|^q\right)^{1/q}\\&+\left(\frac{1}{2}\right)^{1/q}t^{\eta+1}\left[\int_0^1|\nabla(\lambda)|d\lambda\right]^{1-(1/q)}\\&\cdot\left(M_2|\psi'(\nu)|^q+N_2|\psi'(d)|^q\right)^{1/q}.\end{aligned}\tag{42}$$

Proof. By using Lemma 16, power mean integral inequality, and MT-h-convexity of $|\psi'|^q$, we have

$$\begin{aligned}&\left|\frac{(1-t)^{\eta}\Omega(1)+t^{\mu}\nabla(1)}{d-c}\psi(\nu)\right.\\&\left.-\frac{1}{d-c}\left[(1-t)^{\eta}\left(\nu^{-}I_{\rho}\psi(c)\right)+t^{\eta}\left(\nu^{+}I_{\rho}\psi(\eta)\right)\right]\right|\\&\le(1-t)^{\eta+1}\int_0^1|\Omega(\lambda)||\psi'(\lambda\nu+(1-\lambda)c)|d\lambda\\&+t^{\eta+1}\int_0^1|\nabla(\lambda)||\psi'(\lambda\nu+(1-\lambda)d)|d\lambda\\&\le(1-t)^{\eta+1}\left(\int_0^1|\Omega(\lambda)|d\lambda\right)^{1-(1/q)}\left(\int_0^1|\Omega(\lambda)||\psi'(\lambda\nu+(1-\lambda)c|^q d\lambda\right)^{1/q}\\&+t^{\eta+1}\left(\int_0^1\nabla(\lambda)d\lambda\right)^{1-(1/q)}\left(\int_0^1|\nabla(\lambda)||\psi'(\lambda\nu+(1-\lambda)d|^q d\lambda\right)^{1/q}\\&\le(1-t)^{\eta+1}\left(\int_0^1|\Omega(\lambda)|d\lambda\right)^{1-(1/q)}\left(\int_0^1|\Omega(\lambda)|\left[\frac{\sqrt{h(\lambda)}}{2\sqrt{h(1-\lambda)}}|\psi'(\nu)|^q\right.\right.\\&\left.\left.+\frac{\sqrt{h(1-\lambda)}}{2\sqrt{h(\lambda)}}|\psi'(\nu)|^q\right]d\lambda\right)^{1/q}+t^{\eta+1}\left(\int_0^1|\nabla(\lambda)|d\lambda\right)^{1-(1/q)}\\&\times\left(\int_0^1|\nabla(\lambda)|\left[\frac{\sqrt{h(\lambda)}}{2\sqrt{h(1-\lambda)}}|\psi'(\nu)|^q+\frac{\sqrt{h(1-\lambda)}}{2\sqrt{h(\lambda)}}|\psi'(d)|^q\right]d\lambda\right)^{1/q}\\&\le\left(\frac{1}{2}\right)^{1/q}(1-t)^{\eta+1}\left[\int_0^1|\Omega(\lambda)|d\lambda\right]^{1-(1/q)}\left(M_1|\psi'(\nu)|^q+N_1|\psi'(c)|^q\right)^{1/q}\\&+\left(\frac{1}{2}\right)^{1/q}t^{\eta+1}\left[\int_0^1|\nabla(\lambda)|d\lambda\right]^{1-(1/q)}\left(M_2|\psi'(\nu)|^q+N_2|\psi'(d)|^q\right)^{1/q}.\end{aligned}\tag{43}$$

The proof is completed. □

Corollary 22. *If we substitute identity function* $h(\lambda)=\lambda$ *in Theorem 21, we obtain [21] Theorem 2.3.*

4. Application to Special Means

In this section, we present applications of our results in special means. Firstly, we give definitions of special means.

(1) The arithmetic mean

$$A=A(c,d)=\frac{c+d}{2};\ \mathrm{c},\mathrm{d}\in\mathfrak{R}.\tag{44}$$

(2) The logarithmic mean

$$L(c,d)=\frac{d-c}{\ln|d|-\ln|c|};\ |c|\neq|d|,cd\neq0,\mathrm{c},\mathrm{d}\in\mathfrak{R}.\tag{45}$$

(3) The generalized logarithmic mean

$$L_n(c,d)=\left[\frac{d^{n+1}-c^{n+1}}{(d-c)(n+1)}\right]^{1/n};\ n\in\mathbb{Z}-1,0,c,d\in\mathfrak{R},c\neq d.\tag{46}$$

Now, using the results of §2, we give some applications to special means of real numbers.

Proposition 23. *Assume that* $c, d\in\mathfrak{R}$, $0<c<d$ *and* $n\in\mathbb{Z}$, $|n|\geq 2$. *Then,* $\forall\ q\geq 1$ *following inequality holds:*

$$\begin{aligned}&|A(c^n,d^n)-L_n^n(c,d)|\\&\le\left(\frac{d-c}{2}\right)\times\left(\frac{1}{p+1}\right)^{1/p}\times\left(Q^q\int_0^1\frac{\sqrt{h(\lambda)}}{\sqrt{h(1-\lambda)}}d\lambda\right)^{1/q}\\&|A(c^n,d^n)-L_n^n(c,d)|\\&\le\frac{(d-c)}{2}\times\left(\frac{1}{2}\right)^{1-(1/q)}\left(\frac{1}{2}Q^qS_1+\frac{1}{2}Q^qS_2\right)^{1/q}.\end{aligned}\tag{47}$$

Proof. For $\psi(\nu)=\nu^n$ the statement follows by Remark 12 and 15 where $\nu\in\mathfrak{R}$, $n\in\mathbb{Z}$, $|n|\geq 2$. □

Proposition 24. *Assume that* $c, d\in\mathfrak{R}$, $0<a<d$. *Then,* $\forall\ q\geq 1$, *we have*

$$\begin{aligned}&\left|A\left(c^{-1},d^{-1}\right)-L^{-1}(c,d)\right|\\&\le\left(\frac{d-c}{2}\right)\times\left(\frac{1}{p+1}\right)^{1/p}\times\left(Q^q\int_0^1\frac{\sqrt{h(\lambda)}}{\sqrt{h(1-\lambda)}}d\lambda\right)^{1/q}\\&\left|A\left(c^{-1},d^{-1}\right)-L^{-1}(c,d)\right|\\&\le\frac{(d-c)}{2}\times\left(\frac{1}{2}\right)^{1-(1/q)}\left(\frac{1}{2}Q^qS_1+\frac{1}{2}Q^qS_2\right)^{1/q}.\end{aligned}\tag{48}$$

Proof. The statement follows by Remark 12 and 15 for $\psi(\nu)=1/\nu$. □

5. Estimates of Error for Trapezoidal Formula

Assume that f is a division $c = v_0 < v_1 < \cdots < v_{n-1} < v_n = d$ of interval $[c, d]$ and consider the quadrature formula

$$\int_0^1 \psi(v) d(v) = T_r(\psi, f) + E_r(\psi, f), \tag{49}$$

where

$$T_r(\psi, f) = \sum_{k=0}^{n-1} \frac{\psi(v_k)\psi(v_{k+1})}{2}(v_{k+1} - v_k), \tag{50}$$

for the trapezoidal version $E_r(\psi, f)$ donates the associated approximation error.

Proposition 25. *Let $\psi : J \subseteq \Re \longrightarrow \Re$ be a differentiable function on J^o such that $\psi' \in L_1[c, d]$, where $c, d \in J$ with $c < d$ and $|\psi'|^q$ is MT-h-convex on $[c, d]$. Then, in 24, for every division f of $[c, d]$ and $|\psi'(v)| \le Q$, $v \in [c, d]$, the trapezoidal error estimate satisfies*

$$|E_r(\psi, f)| \le \left(\frac{1}{2}\right) \times \left(\frac{1}{p+1}\right)^{1/p} \times \left(Q^q \int_0^1 \frac{\sqrt{h(\lambda)}}{\sqrt{h(1-\lambda)}} d\lambda\right)^{1/q} \sum_{k=0}^{n-1} (v_{k+1} - v_k)^2, \tag{51}$$

where $p > 1$, $(1/p) + (1/q) = 1$.

Proof. On applying Remark 12 on the subinterval $[v_k, v_{k+1}]$ $(k = 0, 1, 2, \cdots, n-1)$ of the division, we have

$$\begin{aligned} \left| \int_c^d \psi(v) dv - T_r(\psi, f) \right| &= \left| \sum_{k=0}^{n-1} \left\{ \int_{v_k}^{v_k+1} \psi(v) dv - \frac{\psi(v_k) + \psi(v_{k+1})}{2}(v_{k+1} - v_k) \right\} \right| \\ &\le \sum_{k=0}^{n-1} \left| \int_{v_k}^{v_k+1} \psi(v) dv - \frac{\psi(v_k) + \psi(v_{k+1})}{2}(v_{k+1} - v_k) \right| \\ &\le \left(\frac{1}{2}\right) \times \left(\frac{1}{p+1}\right)^{1/p} \times \left(Q^q \int_0^1 \frac{\sqrt{h(\lambda)}}{\sqrt{h(1-\lambda)}} d\lambda\right)^{1/q} \\ &\quad \cdot \sum_{k=0}^{n-1} (v_{k+1} - v_k)^2. \end{aligned} \tag{52}$$

With this, the proof is completed. □

Proposition 26. *Let $\psi : J \subseteq \Re \longrightarrow \Re$ be a differentiable function on J^o such that $\psi' \in L_1[c, d]$, where $c, d \in J$ with $c < d$ and $|\psi'|^q$ is MT-h-convex on $[c, d]$ where $q \ge 1$, for every division f of $[c, d]$ and $|\psi'(v)| \le Q$, $v \in [c, d]$, the trapezoidal error estimate satisfies*

$$|E_r(\psi, f)| \le \left(\frac{1}{2}\right)^{2-(1/q)} \left(\frac{1}{2} Q^q S_1 + \frac{1}{2} Q^q S_2\right)^{1/q} \sum_{k=0}^{n-1} (v_{k+1} - v_k)^2. \tag{53}$$

Proof. By using Remark 15, the proof comes the same as Proposition 25. □

6. Conclusion

Convexity and fractional integral operators are the most important notions to deal with the problems of today's world. In the present paper, we introduced a more general notion of convexity, called as MT-h-convexity. The classical and generalized fractional integral operators are used to establish the most famous and most studied Hermite–Hadamard-type inequalities for the proposed class of convex functions. Applications of presented results to special means are also given. Corollaries and remarks presented in this paper justify the generality of our results. It is interesting to establish Hermite–Hadamard-type inequalities for the other variants of fractional integral operators, like Caputo fractional integral operators and Atangana fractional integral operators.

Data Availability

All data required for this research is included within this paper.

Conflicts of Interest

The authors do not have any conflict of interests.

Authors' Contributions

Hengxiao Qi designed the paper and proved the main results of this paper; Waqas Nazeer analyzed the results, wrote the final version of the paper, and relate this paper with the existing results to justify that the results of this paper are more generalized; Fatima Abbas proposed the problem and supervised this work; and Wenbo Liao wrote the first version of this paper.

Acknowledgments

This work was sponsored by the innovative engineering scientific research supportive project of the Communist Party School of the Shandong Provincial CCP Committee (Shandong Administration College) (2021cx035) and the innovative project of the Shandong Administrative College.

References

[1] B. P. Moghaddam, Z. S. Mostaghim, A. A. Pantelous, and J. T. Machado, "An integro quadratic spline-based scheme for solving nonlinear fractional stochastic differential equations with

constant time delay," *Communications in Nonlinear Science and Numerical Simulation*, vol. 92, article 105475, 2021.

[2] P. Ciatti, M. Cowling, and F. Ricci, "Hardy and uncertainty inequalities on stratified Lie groups," *Advances in Mathematics*, vol. 277, pp. 365–387, 2015.

[3] Y. Sawano and H. Wadade, "*On the Gagliardo-Nirenberg type inequality in the critical Sobolev-Morrey space*," *Journal of Fourier Analysis and Applications*, vol. 19, no. 1, pp. 20–47, 2013.

[4] Z. Dahmani, L. Tabharit, and S. Taf, "New generalizations of Gruss inequality using Riemann-Liouville fractional integrals," *Bulletin of Mathematical Analysis and Applications*, vol. 2, pp. 93–99, 2010.

[5] B. Gavrea and I. Gavrea, "On some Ostrowski type inequalities," *General Mathematics*, vol. 18, pp. 33–44, 2010.

[6] W. J. Lin, "Some Ostrowski type inequalities via Riemann-Liouville fractional integrals for h-convex functions," *Journal of Computational Analysis and Applications*, vol. 16, pp. 998–1004.1, 2014.

[7] M. Z. Sarikaya and H. Yildrim, "On Hermite-Hadamard type inequalities for Riemann-Liouville fractional integrals," *Miskolc Mathematical Notes*, vol. 17, no. 2, pp. 1049–1059, 2016.

[8] P. O. Mohammed, "Inequalities of type Hermite-Hadamard for fractional integrals via differentiable convex functions," *Turkish Journal of Analysis and Number Theory*, vol. 4, no. 5, pp. 135–139, 2016.

[9] Y. Wu, H. P. Yin, and B. N. Guo, "Generalizations of Hermite–Hadamard type integral inequalities for convex functions," *Axioms*, vol. 10, no. 3, p. 136, 2021.

[10] S. Varošanec, "On h-convexity," *Journal of Mathematical Analysis and Applications*, vol. 326, pp. 303–311, 2007.

[11] Y. M. Chu, M. A. Khan, T. U. Khan, and T. Ali, "Generalizations of Hermite–Hadamard type inequalities for MT-convex functions," *Journal of Nonlinear Sciences and Applications*, vol. 9, no. 6, pp. 4305–4316, 2016.

[12] M. Tung and H. Yildirimon, "MT-convexity," 2012, https://arxiv.org/pdf/1205.5453.

[13] A. Fernandez and P. Mohammed, "Hermite-Hadamard inequalities in fractional calculus defined using Mittag-Leffler kernels," *Mathematical Methods in the Applied Sciences*, vol. 44, pp. 8414–8431, 2020.

[14] I. Podlubny, *Fractional Differential Equations*, Academic Press, Inc., San Diego, CA, 1999.

[15] M. Z. Sarikaya and F. Ertugral, *On the Generalized Hermite-Hadamard Inequalities*2017, http://www.researchgate.net/publication/321760443.

[16] S. G. Samko, A. A. Kilbas, and O. I. Marichev, *Fractional Integral and DerivativesTheory and Application*, Gordon and Breach, Yverdon, Switzerland, 1993.

[17] S. Mubeen and G. M. Habibullah, "*k -fractional integrals and application*," *International Journal of Contemporary Mathematical Sciences*, vol. 7, no. 2, pp. 89–94, 2012.

[18] U. N. Katugampola, "New approach to a generalized fractional integral," *Applied Mathematics and Computation*, vol. 218, no. 3, pp. 860–865, 2011.

[19] H. Kavurmaci, M. Avci, and M. E. Özdemir, "New inequalities of Hermite-Hadamard type for convex functions with applications," *Journal of Inequalities and Applications*, vol. 2011, no. 1, p. 11, 2011.

[20] W. Liu, W. Wen, and J. Park, "Hermite-Hadamard type inequalities for MT-convex functions via classical integrals and fractional integrals," *Journal of Nonlinear Sciences and Applications*, vol. 9, no. 3, pp. 766–777, 2016.

[21] J. Han, P. O. Mohammed, and H. Zeng, "Generalized fractional integral inequalities of Hermite-Hadamard-type for a convex function," *Open Mathematics*, vol. 18, pp. 794–806, 2020.

Hindawi
Journal of Function Spaces
Volume 2022, Article ID 4856002, 11 pages
https://doi.org/10.1155/2022/4856002

Research Article

A Comparative Analysis of Fractional Space-Time Advection-Dispersion Equation via Semi-Analytical Methods

Noufe H. Aljahdaly,[1] Rasool Shah,[2] Muhammed Naeem,[3] and Mohammad Asif Arefin[4]

[1]*Mathematics Department, Faculty of Sciences and Arts, King Abdulaziz University, Rabigh, Saudi Arabia*
[2]*Department of Mathematics, Abdul Wali Khan University Mardan 23200, Pakistan*
[3]*Deanship of Joint First Year Umm Al-Qura University Makkah, P.O. Box 715, Saudi Arabia*
[4]*Jashore University of Science and Technology, Jashore 7408, Bangladesh*

Correspondence should be addressed to Muhammed Naeem; mfaridoon@uqu.edu.sa and Mohammad Asif Arefin; asif.math@just.edu.bd

Received 29 April 2022; Revised 9 June 2022; Accepted 29 June 2022; Published 13 July 2022

Academic Editor: Yusuf Gurefe

The approximate solutions of the time fractional advection-dispersion equation are presented in this article. The nonlocal nature of solute movement and the nonuniformity of fluid flow velocity in the advection-dispersion process lead to the formation of a heterogeneous system, which can be modeled using a fractional advection-dispersion equation, which generalizes the classical advection-dispersion equation and replaces the time derivative with the fractional Caputo derivative. Researchers use a variety of numerical techniques to study such fractional models, but the nonlocality of the derivative having fractional order leads to high computation complexity and complex calculations, so the task is to find an efficient technique that requires less computation and provides greater accuracy when numerically solving such models. A innovative techniques, homotopy perturbation method and new iteration method, are used in connection with the Elzaki transform to solve the "fractional advection-dispersion equation" which provides the solution in the convergent series form. When the homotopy perturbation method is used with the Elzaki transform, fast convergent series solutions can be obtained with less computation. By solving some cases of time-fractional advection-dispersion equation with varied initial conditions with the help of new iterative transform method and homotopy perturbation transform method demonstrates the usefulness of the proposed methods.

1. Introduction

For the past 300 years, fractional calculus has been used to generalize the integration and differentiation of integer order to arbitrary order. Due to its nonlocal nature, fractional differential equations are well adapted to explain diverse phenomena in engineering and science, and the researchers' growing interest in this field has led to solving real-world problems in type of fractional differential equations. In addition, fractional derivatives can be used for description in a variety of phenomena that have memory and hereditary properties by mathematical way [1–5]. Fractional order differential equations have been shown to be a valuable tool for revealing hidden characteristics in a variety of real-world processes, including physical sciences, signal processing, electromagnetics, earthquakes, traffic flow, and the study of viscoelastic material properties and many more processes [6–11]. The historical and nonlocal distributed effects are considered via fractional differential coefficients; an outstanding literature on this topic may be found in numerous monographs [12–15]. For this reason, many authors are attracted to knowing the properties of fractional differential equations and vast applications in modeling and engineering fields [16–19].

The ADE is used in the study of solute transport or Brownian motion of particles in a fluid that occurs when advection and particle dispersion occur at the same time [20, 21]. The fractional advection-dispersion equation better represents the phenomenon of anomalous particle diffusion in the transport process; in anomalous diffusion, solute transport is faster or faster than the time's inferred square root given by Baeumer et al. [22]. The equation is used to investigate groundwater pollution, smoke or dust pollution of the atmosphere, and the spread of chemical solutes and pollutant discharges [23]. As a result, FADE has caught the interest of numerous researchers. As a result, the researchers are interested in solving the FADE to determine the solute concentration at a specific time and location [24, 25]. Jaiswal et al. [26] discovered an analytical solution for one-dimensional ADE. Huang et al. [27] developed finite element solutions to the one-dimensional fractional flux ADE. El-Sayed et al. [28] investigated the intermediate fractional ADE. Momani and Odibat [23] used the ADM and variational iteration approach to solve the space-time fractional ADE. In this aspect, Yildirim and Kocak [29] use the homotopy perturbation methodology in Caputo sense to solve the space-time fractional ADE, whereas Hikal and Abu Ibrahim [30] use the Adomian decomposition method. Using the generalized finite rate chemistry model, Alliche and Chikh [31] investigated the nonpremixed chaotic fire of the hydrogen-air downward injector system. Liu et al. [32] investigated various advection-dispersion models using numerical methods. For solar cosmic-ray transport, Rocca et al. [33] established the fractional diffusion-advection equation general solution. Ramani et al. [34] proposed the fractional reduced differential transform method for revisiting the time-fractional Rosenau-Hyman problem's analytical-approximate formulation.

We apply both the novel iterative method presented by Gejji and Jafari [35] and the homotopy perturbation transform method proposed by Madani et al. [36] and Khan and Wu in the current paper [37]. The first technique has been shown to be effective in solving a wide range of nonlinear equations, including algebraic equations, integral equations, ordinary and partial differential equations of integer and fractional order, and systems of equations. The new iterative method is straightforward to explain and use with computer packages, and it produces superior results than the previous Adomain decomposition [38], homotopy perturbation [39], and variational iteration methods [40]. The second technique combines the Elzaki transformation, the homotopy perturbation method, and He's polynomials in a simple manner. The suggested algorithm generates a solution in a rapid convergent series, which could lead to a closed solution. This method has the advantage of being able to combine two powerful methods for finding exact solutions to linear and nonlinear partial differential equations.

2. Basic Definitions

2.1. Definition. The fractional operator D^{σ} having order σ in Abel-Riemann manner is calculated as [41–43]

$$D^{\sigma}\nu(\varphi)=\begin{cases}\dfrac{d^{\jmath}}{d\varphi^{\jmath}}\nu(\varphi), & \sigma=\jmath,\\[2mm] \dfrac{1}{\Gamma(\jmath-\sigma)}\dfrac{d}{d\varphi^{\jmath}}\displaystyle\int_0^{\varphi}\dfrac{\nu(\varphi)}{(\varphi-\mu)^{\sigma-\jmath+1}}d\mu, & \jmath-1<\sigma<\jmath,\end{cases} \tag{1}$$

where $\jmath\in Z^{+}$, $\sigma\in R^{+}$, and

$$D^{-\sigma}\nu(\varphi)=\frac{1}{\Gamma(\sigma)}\int_0^{\varphi}(\varphi-\mu)^{\sigma-1}\nu(\mu)d\mu,\ 0<\sigma\le 1. \tag{2}$$

2.2. Definition. The Abel-Riemann integration operator $\jmath^{\mu}$ having fractional order is given as [35–37]

$$\jmath^{\sigma}\nu(\varphi)=\frac{1}{\Gamma(\sigma)}\int_0^{\varphi}(\varphi-\mu)^{\sigma-1}\nu(\varphi)d\varphi,\quad \varphi>0,\quad \sigma>0. \tag{3}$$

With basic properties:

$$\begin{aligned}\jmath^{\sigma}\varphi^{\jmath}&=\frac{\Gamma(\jmath+1)}{\Gamma(\jmath+\sigma+1)}\varphi^{\jmath+\mu},\\ D^{\sigma}\varphi^{\jmath}&=\frac{\Gamma(\jmath+1)}{\Gamma(\jmath-\sigma+1)}\varphi^{\jmath-\mu}.\end{aligned} \tag{4}$$

2.3. Definition. The fractional Caputo operator D^{σ} having order σ is calculated as [41–43]

$${}^{C}D^{\sigma}\nu(\varphi)=\begin{cases}\dfrac{1}{\Gamma(\jmath-\sigma)}\displaystyle\int_0^{\varphi}\dfrac{\nu^{\jmath}(\mu)}{(\varphi-\mu)^{\sigma-\jmath+1}}d\mu, & \jmath-1<\sigma<\jmath,\\[2mm] \dfrac{d^{\jmath}}{d\varphi^{\jmath}}\nu(\varphi), & \jmath=\sigma.\end{cases} \tag{5}$$

with the following properties:

$$\begin{aligned}&\jmath_{\varphi}^{\sigma}D_{\varphi}^{\sigma}g(\varphi)=g(\varphi)-\sum_{k=0}^{m}g^{k}(0^{+})\frac{\varphi^{k}}{k!},\quad \text{for}\ \varphi>0,\quad \text{and}\ \jmath-1<\sigma\le\jmath,\jmath\in N,\\ &D_{\varphi}^{\sigma}\jmath_{\varphi}^{\sigma}g(\varphi)=g(\varphi).\end{aligned} \tag{6}$$

2.4. Definition. The Elzaki transform of Caputo operator is calculated as [41, 42]

$$E\left[D_{\varphi}^{\sigma}g(\varphi)\right]=s^{-\sigma}E[g(\varphi)]-\sum_{k=0}^{\jmath-1}s^{2-\sigma+k}g^{(k)}(0),\quad \text{where}\quad \jmath-1<\sigma<\jmath. \tag{7}$$

3. Idea of New Iterative Transform Method (NITM)

Let us consider the partial differential equation having fractional order in the form of

$$D_{\rho}^{\sigma}\zeta(\mu,\rho)+N\zeta(\mu,\rho)+M\zeta(\mu,\rho)=h(\mu,\rho),\quad n\in N,\quad n-1<\sigma\le n, \tag{8}$$

having initial condition

$$\zeta^k(\mu, 0) = g_k(\mu), \quad k = 0, 1, 2, \cdots, n-1, \tag{9}$$

where N and M are linear and nonlinear components.

By taking the Elzaki transform of Equation (8), we have

$$E\left[D_\rho^\sigma \zeta(\mu, \rho)\right] + E[N\zeta(\mu, \rho) + M\zeta(\mu, \rho)] = E[h(\mu, \rho)]. \tag{10}$$

By using Elzaki differentiation property

$$\begin{aligned} E[\zeta(\mu, \rho)] = & \sum_{k=0}^{m} s^{2-\sigma+k} u^{(k)}(\mu, 0) + s^\sigma E[h(\mu, \rho)] \\ & - s^\sigma E[N\zeta(\mu, \rho) + M\zeta(\mu, \rho)]. \end{aligned} \tag{11}$$

On taking Elzaki inverse transform of Equation (11),

$$\begin{aligned} \zeta(\mu, \rho) = & E^{-1}\left[\left\{\sum_{k=0}^{m} s^{2-\sigma+k} u^k(\mu, 0) + s^\sigma E[h(\mu, \rho)]\right\}\right] \\ & - E^{-1}[s^\sigma E[N\zeta(\mu, \rho) + M\zeta(\mu, \rho)]]. \end{aligned} \tag{12}$$

Now by using iterative technique, we get

$$\zeta(\mu, \rho) = \sum_{m=0}^{\infty} \zeta_m(\mu, \rho), \tag{13}$$

$$N\left(\sum_{m=0}^{\infty} \zeta_m(\mu, \rho)\right) = \sum_{m=0}^{\infty} N[\zeta_m(\mu, \rho)]. \tag{14}$$

The nonlinear term N is recognized as

$$\begin{aligned} N\left(\sum_{m=0}^{\infty} \zeta_m(\mu, \rho)\right) = & \zeta_0(\mu, \rho) + N\left(\sum_{k=0}^{m} \zeta_k(\mu, \rho)\right) \\ & - M\left(\sum_{k=0}^{m} \zeta_k(\mu, \rho)\right). \end{aligned} \tag{15}$$

By substituting Equations (13), (14), and (15) in Equation (12), we get

$$\begin{aligned} \sum_{m=0}^{\infty} \zeta_m(\mu, \rho) = & E^{-1}\left[s^\sigma\left(\sum_{k=0}^{m} s^{2-\mu+k} u^k(\mu, 0) + E[h(\mu, \rho)]\right)\right] \\ & - E^{-1}\left[s^\sigma E\left[N\left(\sum_{k=0}^{m} \zeta_k(\mu, \rho)\right) - M\left(\sum_{k=0}^{m} \zeta_k(\mu, \rho)\right)\right]\right]. \end{aligned} \tag{16}$$

Thus, the iterative formula is given as

$$\begin{aligned} \zeta_0(\mu, \rho) &= E^{-1}\left[s^\sigma\left(\sum_{k=0}^{m} s^{2-\mu+k} u^k(\mu, 0) + s^\sigma E(g(\mu, \rho))\right)\right], \\ \zeta_1(\mu, \rho) &= -E^{-1}[s^\sigma E[N[\zeta_0(\mu, \rho)] + M[\zeta_0(\mu, \rho)]], \\ \zeta_{m+1}(\mu, \rho) &= -E^{-1}\left[s^\sigma E\left[-N\left(\sum_{k=0}^{m} \zeta_k(\mu, \rho)\right) - M\left(\sum_{k=0}^{m} \zeta_k(\mu, \rho)\right)\right]\right]. \end{aligned} \tag{17}$$

Lastly, Equations (8) and (9) give series form result for m-term as

$$\zeta(\mu, \rho) \cong \zeta_0(\mu, \rho) + \zeta_1(\mu, \rho) + \zeta_2(\mu, \rho) + \cdots + \zeta_m(\mu, \rho), \quad m = 1, 2, \cdots. \tag{18}$$

4. Idea of Homotopy Perturbation Transform Method (HPTM)

Let us consider the fractional partial differential equation having general form.

$$\begin{aligned} D_\rho^\sigma \zeta(\mu, \rho) + M\zeta(\mu, \rho) + N\zeta(\mu, \rho) = h(\mu, \rho), \quad & \rho > 0, \quad 0 < \sigma \le 1, \\ \zeta(\mu, 0) = g(\mu), \quad & \nu \in \Re. \end{aligned} \tag{19}$$

By taking the Elzaki transform of Equation (19)

$$\begin{aligned} E\left[D_\rho^\sigma \zeta(\mu, \rho) + M\zeta(\mu, \rho) + N\zeta(\mu, \rho)\right] &= E[h(\mu, \rho)], \rho > 0, 0 < \sigma \le 1, \\ \zeta(\mu, \rho) &= s^2 g(\mu) + s^\sigma E[h(\mu, \rho)] - s^\sigma E[M\zeta(\mu, \rho) + N\zeta(\mu, \rho)]. \end{aligned} \tag{20}$$

On taking Elzaki inverse transform, we have

$$\zeta(\mu, \rho) = F(x, \rho) - E^{-1}[s^\sigma E\{M\zeta(\mu, \rho) + N\zeta(\mu, \rho)\}], \tag{21}$$

where

$$\begin{aligned} (\mu, \rho) &= E^{-1}\left[s^2 g(\mu) + s^\sigma E[h(\mu, \rho)]\right] \\ &= g(\nu) + E^{-1}[s^\sigma E[h(\mu, \rho)]]. \end{aligned} \tag{22}$$

The perturbation technique of parameter p is given as

$$\zeta(\mu, \rho) = \sum_{k=0}^{\infty} p^k \zeta_k(\mu, \rho), \tag{23}$$

where perturbation parameter is denoted by p and $p \in [0, 1]$.

The nonlinear terms can be calculated as

$$N\zeta(\mu, \rho) = \sum_{k=0}^{\infty} p^k H_k(\zeta_k), \tag{24}$$

where H_n represents He's polynomials in terms of $\zeta_0, \zeta_1, \zeta_2, \cdots, \zeta_n$, and can be expressed as

$$H_n(\zeta_0, \zeta_1, \cdots, \zeta_n) = \frac{1}{\sigma(n+1)} D_p^k \left[N\left(\sum_{k=0}^{\infty} p^k \zeta_k \right) \right]_{p=0}, \quad (25)$$

where $D_p^k = \partial^k / \partial p^k$.

Substituting Equations (24) and (25) in Equation (21), we have

$$\sum_{k=0}^{\infty} p^k \zeta_k(\mu, \rho) = F(\mu, \rho) - p \times \left[E^{-1} \left\{ s^\sigma E \left\{ M \sum_{k=0}^{\infty} p^k \zeta_k(\mu, \rho) + \sum_{k=0}^{\infty} p^k H_k(\zeta_k) \right\} \right\} \right]. \quad (26)$$

On comparison of both sides coefficient of p, we get

$$\begin{aligned} p^0 &: \zeta_0(\mu, \rho) = F(\mu, \rho), \\ p^1 &: \zeta_1(\mu, \rho) = E^{-1}[s^\sigma E(M\zeta_0(\mu, \rho) + H_0(\zeta))], \\ p^2 &: \zeta_2(\mu, \rho) = E^{-1}[s^\sigma E(M\zeta_1(\mu, \rho) + H_1(\zeta))], \\ &\vdots \\ p^k &: \zeta_k(\mu, \rho) = E^{-1}[s^\sigma E(M\zeta_{k-1}(\mu, \rho) + H_{k-1}(\zeta))], k > 0, k \in N. \end{aligned} \quad (27)$$

The $\zeta_k(\mu, \rho)$ term can be calculated easily resulting convergent series. By taking $p \longrightarrow 1$,

$$\zeta(\mu, \rho) = \lim_{M \longrightarrow \infty} \sum_{k=1}^{M} \zeta_k(\mu, \rho). \quad (28)$$

4.1. Example. Consider the time-fractional ADE

$$D_\rho^\sigma \zeta(\mu, \rho) = \ell D_\mu^2 \zeta(\mu, \rho) - D_\mu \zeta(\mu, \rho), \quad (29)$$

with initial condition

$$\zeta(\mu, 0) = e^{-\mu}, \quad (30)$$

where ℓ is the ratio of constant diffusivity and the drift velocity. The exact solution is

$$\zeta(\mu, \phi, \rho) = e^{(1+\ell)\rho - \mu}. \quad (31)$$

By taking the Elzaki transform of Eq. (29), we get

$$E[\nu(\mu, \phi, \rho)] = s^2(e^{-\mu}) + s^\sigma E\left[\ell D_\mu^2 \zeta(\mu, \rho) - D_\mu \zeta(\mu, \rho)\right]. \quad (32)$$

On taking Elzaki inverse transform, we have

$$\nu(\mu, \phi, \rho) = e^{-\mu} + E^{-1}\left(s^\sigma E\left[\ell D_\mu^2 \zeta(\mu, \rho) - D_\mu \zeta(\mu, \rho)\right]\right). \quad (33)$$

Thus by using NITM, we have

$$\begin{aligned} \zeta_0(\mu, \rho) &= e^{-\mu}, \\ \zeta_1(\mu, \rho) &= E^{-1}\left[s^\sigma E\left\{\ell D_\mu^2 \zeta_0(\mu, \rho) - D_\mu \zeta_0(\mu, \rho)\right\}\right] \\ &= e^{-\mu} \frac{(\ell+1)\rho^\sigma}{\Gamma(\sigma+1)}, \\ \zeta_2(\mu, \rho) &= E^{-1}\left[s^\sigma E\left\{\ell D_\mu^2 \zeta_1(\mu, \rho) - D_\mu \zeta_1(\mu, \rho)\right\}\right] \\ &= e^{-\mu} \frac{(\ell+1)^2(\rho^\sigma)^2}{\Gamma(2\sigma+1)}, \\ \zeta_3(\mu, \rho) &= E^{-1}\left[s^\sigma E\left\{\ell D_\mu^2 \zeta_2(\mu, \rho) - D_\mu \zeta_2(\mu, \rho)\right\}\right] \\ &= e^{-\mu} \frac{(\ell+1)^3(\rho^\sigma)^3}{\Gamma(3\sigma+1)}, \\ &\vdots \\ \zeta_n(\mu, \rho) &= E^{-1}\left[s^\sigma E\left\{\ell D_\mu^2 \zeta_n(\mu, \rho) - D_\mu \zeta_n(\mu, \rho)\right\}\right] \\ &= e^{-\mu} \frac{(\ell+1)^n(\rho^\sigma)^n}{\Gamma(n\sigma+1)}, n \geq 0. \end{aligned} \quad (34)$$

The series form solution is given as

$$\zeta(\mu, \rho) = \zeta_0(\mu, \rho) + \zeta_1(\mu, \rho) + \zeta_2(\mu, \rho) + \zeta_3(\mu, \rho) + \cdots \zeta_n(\mu, \rho). \quad (35)$$

Thus, we have

$$\zeta(\mu, \rho) = e^{-\mu}\left\{1 + \frac{(\ell+1)\rho^\sigma}{\Gamma(\sigma+1)} + \frac{(\ell+1)^2\rho^{2\sigma}}{\Gamma(2\sigma+1)} + \frac{(\ell+1)^3\rho^{3\sigma}}{\Gamma(3\sigma+1)} + \cdots + \frac{(\ell+1)^n(\rho^\sigma)^n}{\Gamma(n\sigma+1)}\right\}. \quad (36)$$

Now by using the HPTM, we have

$$\sum_{n=0}^{\infty} p^n w_n(\mu, \rho) = (e^{-\mu}) + p\left\{E^{-1}\left(s^\sigma E\left[\sum_{n=0}^{\infty} p^n H_n(w)\right]\right)\right\}. \quad (37)$$

By Comparing coefficient of p on both sides, we get:

$$\begin{aligned}
p^0 &: w_0(\mu,\rho) = e^{-\mu},\\
p^1 &: w_1(\mu,\rho) = \left[E^{-1}\{s^\sigma E(H_0(w))\}\right] = e^{-\mu}\frac{(\ell+1)\rho^\sigma}{\Gamma(\sigma+1)},\\
p^2 &: w_2(\mu,\rho) = \left[E^{-1}\{s^\sigma E(H_1(w))\}\right] = e^{-\mu}\frac{(\ell+1)^2(\rho^\sigma)^2}{\Gamma(2\sigma+1)},\\
p^3 &: w_3(\mu,\rho) = \left[E^{-1}\{s^\sigma E(H_2(w))\}\right] = e^{-\mu}\frac{(\ell+1)^3(\rho^\sigma)^3}{\Gamma(3\sigma+1)},\\
&\vdots\\
p^n &: w_n(\mu,\rho) = \left[E^{-1}\{s^\sigma E(H_{n-1}(w))\}\right] = e^{-\mu}\frac{(\ell+1)^n(\rho^\sigma)^n}{\Gamma(n\sigma+1)}.
\end{aligned} \tag{38}$$

The solution in series form by means of HPM is given as

$$\zeta(\mu,\rho) = \sum_{n=0}^{\infty} p^n w_n(\mu,\rho). \tag{39}$$

Thus, we have

$$\zeta(\mu,\rho) = e^{-\mu}\left\{1+\frac{(\ell+1)\rho^\sigma}{\Gamma(\sigma+1)}+\frac{(\ell+1)^2\rho^{2\sigma}}{\Gamma(2\sigma+1)} + \frac{(\ell+1)^3\rho^{3\sigma}}{\Gamma(3\sigma+1)}+\cdots+\frac{(\ell+1)^n(\rho^\sigma)^n}{\Gamma(n\sigma+1)}\right\}. \tag{40}$$

4.2. Example. Consider the time-fractional ADE

$$D_\rho^\sigma \zeta(\mu,\rho) = \ell D_\mu^2\zeta(\mu,\rho) - D_\mu\zeta(\mu,\rho), \tag{41}$$

with initial conditions

$$\zeta(\mu,0) = \mu^3-\mu^2. \tag{42}$$

By taking the Elzaki transform of Equation (29), we get

$$E[\nu(\mu,\phi,\rho)] = s^2\left(\mu^3-\mu^2\right) + s^\sigma E\left[\ell D_\mu^2\zeta(\mu,\rho) - D_\mu\zeta(\mu,\rho)\right]. \tag{43}$$

On taking Elzaki inverse transform, we have

$$\nu(\mu,\phi,\rho) = \left(\mu^3-\mu^2\right) + E^{-1}\left(s^\sigma E\left[\ell D_\mu^2\zeta(\mu,\rho) - D_\mu\zeta(\mu,\rho)\right]\right). \tag{44}$$

Thus by using NITM, we have

$$\begin{aligned}
\zeta_0(\mu,\rho) &= \mu^3-\mu^2,\\
\zeta_1(\mu,\rho) &= E^{-1}\left[s^\sigma E\left\{\ell D_\mu^2\zeta_0(\mu,\rho) - D_\mu\zeta_0(\mu,\rho)\right\}\right]\\
&= \left\{-3\mu^2+2\mu(1+3\ell)-2\ell\right\}\frac{\rho^\sigma}{\Gamma(\sigma+1)},\\
\zeta_2(\mu,\rho) &= E^{-1}\left[s^\sigma E\left\{\ell D_\mu^2\zeta_1(\mu,\rho) - D_\mu\zeta_1(\mu,\rho)\right\}\right]\\
&= \{6\mu-2-12\ell\}\frac{(\rho^\sigma)^2}{\Gamma(2\sigma+1)},\\
\zeta_3(\mu,\rho) &= E^{-1}\left[s^\sigma E\left\{\ell D_\mu^2\zeta_2(\mu,\rho) - D_\mu\zeta_2(\mu,\rho)\right\}\right]\\
&= -6\frac{(\rho^\sigma)^3}{\Gamma(3\sigma+1)}.\\
&\vdots
\end{aligned} \tag{45}$$

The series form solution is given as

$$\zeta(\mu,\rho) = \zeta_0(\mu,\rho)+\zeta_1(\mu,\rho)+\zeta_2(\mu,\rho)+\zeta_3(\mu,\rho)+\cdots\zeta_n(\mu,\rho). \tag{46}$$

Thus, we have

$$\zeta(\mu,\rho) = \left(\mu^3-\mu^2\right) + \left\{-3\mu^2+2\mu(1+3\ell)-2\ell\right\}\frac{\rho^\sigma}{\Gamma(\sigma+1)} + \{6\mu-2-12\ell\}\frac{(\rho^\sigma)^2}{\Gamma(2\sigma+1)} - 6\frac{(\rho^\sigma)^3}{\Gamma(3\sigma+1)}+\cdots. \tag{47}$$

Now by applying the HPTM, we have

$$\sum_{n=0}^{\infty} p^n w_n(\mu,\rho) = \left(e^{-\mu}\right) + p\left\{E^{-1}\left(s^\sigma E\left[\sum_{n=0}^{\infty} p^n H_n(w)\right]\right)\right\}. \tag{48}$$

By comparing coefficient of p on both sides, we get

$$\begin{aligned}
p^0 &: w_0(\mu,\rho) = \mu^3 - \mu^2,\\
p^1 &: w_1(\mu,\rho) = \left[E^{-1}\{s^\sigma E(H_0(w))\}\right]\\
&\quad = \left\{-3\mu^2 + 2\mu(1+3\ell) - 2\ell\right\}\frac{\rho^\sigma}{\Gamma(\sigma+1)},\\
p^2 &: w_2(\mu,\rho) = \left[E^{-1}\{s^\sigma E(H_1(w))\}\right]\\
&\quad = \{6\mu - 2 - 12\ell\}\frac{(\rho^\sigma)^2}{\Gamma(2\sigma+1)},\\
p^3 &: w_3(\mu,\rho) = \left[E^{-1}\{s^\sigma E(H_2(w))\}\right] = -6\frac{(\rho^\sigma)^3}{\Gamma(3\sigma+1)}.\\
&\vdots
\end{aligned} \tag{49}$$

The solution in series form by means of HPM is given as

$$\zeta(\mu,\rho) = \sum_{n=0}^{\infty} p^n w_n(\mu,\rho). \tag{50}$$

Thus, we have

$$\begin{aligned}
\zeta(\mu,\rho) &= \left(\mu^3 - \mu^2\right) + \left\{-3\mu^2 + 2\mu(1+3\ell) - 2\ell\right\}\frac{\rho^\sigma}{\Gamma(\sigma+1)}\\
&\quad + \{6\mu - 2 - 12\ell\}\frac{(\rho^\sigma)^2}{\Gamma(2\sigma+1)} - 6\frac{(\rho^\sigma)^3}{\Gamma(3\sigma+1)} + \cdots.
\end{aligned} \tag{51}$$

4.3. Example. Consider the time-fractional ADE

$$D_\rho^\sigma \zeta(\mu,\rho) = \ell D_\mu^2 \zeta(\mu,\rho) - D_\mu \zeta(\mu,\rho), \tag{52}$$

with initial conditions

$$\zeta(\mu,0) = \cos(\mu). \tag{53}$$

By taking the Elzaki transform of Equation (29), we get

$$E[\nu(\mu,\phi,\rho)] = s^2(\cos(\mu)) + s^\sigma E\left[\ell D_\mu^2 \zeta(\mu,\rho) - D_\mu \zeta(\mu,\rho)\right]. \tag{54}$$

On taking Elzaki inverse transform, we have

$$\nu(\mu,\phi,\rho) = \cos(\mu) + E^{-1}\left(s^\sigma E\left[\ell D_\mu^2 \zeta(\mu,\rho) - D_\mu \zeta(\mu,\rho)\right]\right). \tag{55}$$

Thus by using NITM, we have

$$\begin{aligned}
\zeta_0(\mu,\rho) &= \cos(\mu),\\
\zeta_1(\mu,\rho) &= E^{-1}\left[s^\sigma E\left\{\ell D_\mu^2 \zeta_0(\mu,\rho) - D_\mu \zeta_0(\mu,\rho)\right\}\right]\\
&= (\sin(\mu) - \ell\cos(\mu))\frac{\rho^\sigma}{\Gamma(\sigma+1)},\\
\zeta_2(\mu,\rho) &= E^{-1}\left[s^\sigma E\left\{\ell D_\mu^2 \zeta_1(\mu,\rho) - D_\mu \zeta_1(\mu,\rho)\right\}\right]\\
&= \left(-\cos(\mu) - 2\ell\sin(\mu) + \ell^2\cos(\mu)\right)\frac{(\rho^\sigma)^2}{\Gamma(2\sigma+1)},\\
\zeta_3(\mu,\rho) &= E^{-1}\left[s^\sigma E\left\{\ell D_\mu^2 \zeta_2(\mu,\rho) - D_\mu \zeta_2(\mu,\rho)\right\}\right]\\
&= \left(-\sin(\mu) + 3\ell\cos(\mu) + 3\ell^2\sin(\mu) - \ell^3\cos(\mu)\right)\\
&\quad \cdot \frac{(\rho^\sigma)^3}{\Gamma(3\sigma+1)}.\\
&\vdots
\end{aligned} \tag{56}$$

The series form solution is given as

$$\zeta(\mu,\rho) = \zeta_0(\mu,\rho) + \zeta_1(\mu,\rho) + \zeta_2(\mu,\rho) + \zeta_3(\mu,\rho) + \cdots \zeta_n(\mu,\rho). \tag{57}$$

Thus, we have

$$\begin{aligned}
\zeta(\mu,\rho) &= \cos(\mu) + (\sin(\mu) - \ell\cos(\mu))\frac{\rho^\sigma}{\Gamma(\sigma+1)}\\
&\quad + \left(-\cos(\mu) - 2\ell\sin(\mu) + \ell^2\cos(\mu)\right)\frac{(\rho^\sigma)^2}{\Gamma(2\sigma+1)}\\
&\quad + \left(-\sin(\mu) + 3\ell\cos(\mu) + 3\ell^2\sin(\mu) - \ell^3\cos(\mu)\right)\\
&\quad \cdot \frac{(\rho^\sigma)^3}{\Gamma(3\sigma+1)}.
\end{aligned} \tag{58}$$

Now by applying the HPTM, we have

$$\sum_{n=0}^{\infty} p^n w_n(\mu,\rho) = \left(e^{-\mu}\right) + p\left\{E^{-1}\left(s^\sigma E\left[\sum_{n=0}^{\infty} p^n H_n(w)\right]\right)\right\}. \tag{59}$$

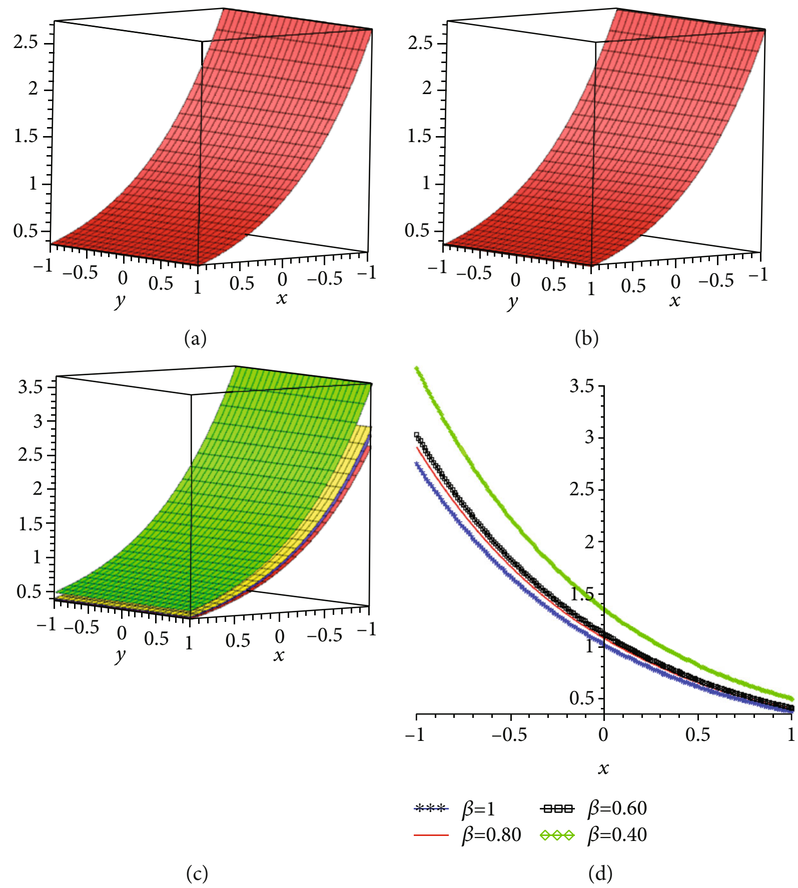

Figure 1: Nature of the exact and proposed technique results of example 1.

By Comparing coefficient of p on both sides, we get:

$$
\begin{aligned}
p^0 &: w_0(\mu,\rho) = \cos(\mu),\\
p^1 &: w_1(\mu,\rho) = \left[E^{-1}\{s^{\sigma}E(H_0(w))\}\right]\\
&\qquad = (\sin(\mu) - \ell\cos(\mu))\frac{\rho^{\sigma}}{\Gamma(\sigma+1)},\\
p^2 &: w_2(\mu,\rho) = \left[E^{-1}\{s^{\sigma}E(H_1(w))\}\right]\\
&\qquad = \left(-\cos(\mu) - 2\ell\sin(\mu) + \ell^2\cos(\mu)\right)\\
&\qquad \cdot\frac{(\rho^{\sigma})^2}{\Gamma(2\sigma+1)},\\
p^3 &: w_3(\mu,\rho) = \left[E^{-1}\{s^{\sigma}E(H_2(w))\}\right]\\
&\qquad = \left(-\sin(\mu) + 3\ell\cos(\mu) + 3\ell^2\sin(\mu)\right.\\
&\qquad \left.- \ell^3\cos(\mu)\right)\frac{(\rho^{\sigma})^3}{\Gamma(3\sigma+1)}.\\
&\qquad \vdots
\end{aligned} \tag{60}
$$

The solution in series form by means of HPM is given as

$$\zeta(\mu,\rho) = \sum_{n=0}^{\infty} p^n w_n(\mu,\rho). \tag{61}$$

Thus, we have

$$
\begin{aligned}
\zeta(\mu,\rho) &= \cos(\mu) + (\sin(\mu) - \ell\cos(\mu))\frac{\rho^{\sigma}}{\Gamma(\sigma+1)}\\
&\quad + \left(-\cos(\mu) - 2\ell\sin(\mu) + \ell^2\cos(\mu)\right)\frac{(\rho^{\sigma})^2}{\Gamma(2\sigma+1)}\\
&\quad + \left(-\sin(\mu) + 3\ell\cos(\mu) + 3\ell^2\sin(\mu) - \ell^3\cos(\mu)\right)\\
&\quad \cdot\frac{(\rho^{\sigma})^3}{\Gamma(3\sigma+1)}.
\end{aligned} \tag{62}
$$

5. Results and Discussion

We implemented NITM and HPTM for finding the approximate solutions of time-fractional ADE. The analytical solution and exact solution are shown in Figures 1(a) and 1(b) at $\sigma = 1$, whereas Figures 1(c) and 1(d) show the absolute error and the solution at various fractional order. Figures 2 and 3 show the behavior of the proposed method solution at various fractional orders. Table 1 shows the comparison of the exact and suggested methods solution in addition with the absolute error at various fractional order. Finally, the figures and table show that the suggested techniques have higher degree of accuracy and rapid convergence towards the exact results.

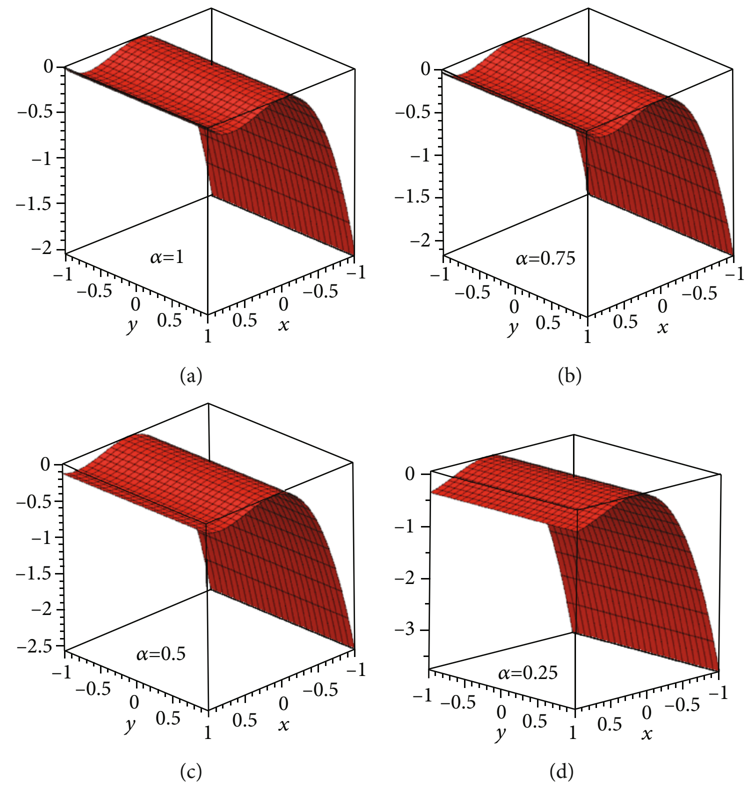

FIGURE 2: Nature of the proposed method solutions at different fractional orders for problem 2.

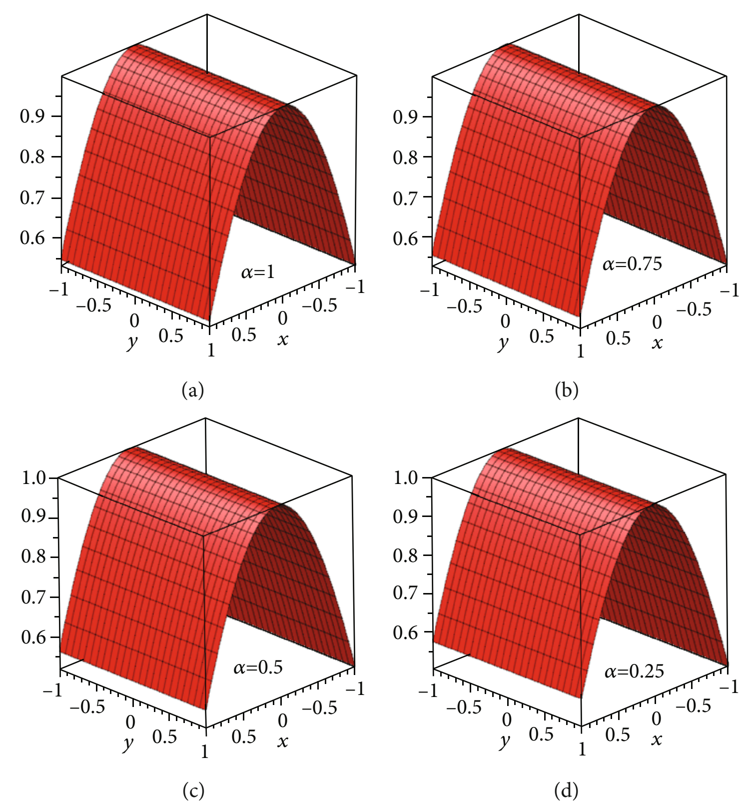

FIGURE 3: Nature of the proposed method solutions at different fractional orders for problem 3.

Table 1: Analysis of the approximate solution by NITM and HPTM for problem 1.

η	ξ	$\lvert Exact - NITM\rvert$ $\sigma = 0.5$	$\lvert Exact - NITM\rvert$ $\sigma = 1$	$\lvert Exact - HPTM\rvert$ $\sigma = 0.7$	$\lvert Exact - HPTM\rvert$ $\sigma = 1$
0.1	0.5	$7.65212627 \times 10^{-02}$	$3.0000000 \times 10^{-10}$	$2.34826106 \times 10^{-02}$	$3.0000000 \times 10^{-10}$
	1	$4.64124920 \times 10^{-02}$	$2.0000000 \times 10^{-10}$	$1.42429233 \times 10^{-02}$	$2.0000000 \times 10^{-10}$
	1.5	$2.81505993 \times 10^{-02}$	$1.0000000 \times 10^{-10}$	$8.63876960 \times 10^{-03}$	$1.0000000 \times 10^{-10}$
	2	$1.70742016 \times 10^{-02}$	$1.0000000 \times 10^{-10}$	$5.23967870 \times 10^{-03}$	$1.0000000 \times 10^{-10}$
	2.5	$1.03560267 \times 10^{-02}$	$4.0000000 \times 10^{-11}$	$3.17802575 \times 10^{-03}$	$4.0000000 \times 10^{-11}$
	3	$6.28124775 \times 10^{-03}$	$2.0000000 \times 10^{-11}$	$1.92757006 \times 10^{-03}$	$2.0000000 \times 10^{-11}$
	3.5	$3.80976934 \times 10^{-03}$	$2.0000000 \times 10^{-11}$	$1.16913033 \times 10^{-03}$	$2.0000000 \times 10^{-11}$
	4	$2.31074191 \times 10^{-03}$	$1.0000000 \times 10^{-11}$	$7.09113390 \times 10^{-04}$	$1.0000000 \times 10^{-11}$
	4.5	$1.40153581 \times 10^{-03}$	$1.0000000 \times 10^{-11}$	$4.30099010 \times 10^{-04}$	$1.0000000 \times 10^{-11}$
	5	$8.50074443 \times 10^{-04}$	$3.0000000 \times 10^{-12}$	$2.60868239 \times 10^{-04}$	$3.0000000 \times 10^{-12}$
0.2	0.5	$1.09371292 \times 10^{-01}$	$5.8000000 \times 10^{-09}$	$3.65660312 \times 10^{-02}$	$5.8000000 \times 10^{-09}$
	1	$6.63370423 \times 10^{-02}$	$3.5000000 \times 10^{-09}$	$2.21784191 \times 10^{-02}$	$3.5000000 \times 10^{-09}$
	1.5	$4.02354500 \times 10^{-02}$	$2.1000000 \times 10^{-09}$	$1.34518911 \times 10^{-02}$	$2.1000000 \times 10^{-09}$
	2	$2.44040340 \times 10^{-02}$	$1.3000000 \times 10^{-09}$	$8.15898440 \times 10^{-03}$	$1.3000000 \times 10^{-09}$
	2.5	$1.48017948 \times 10^{-02}$	$7.8000000 \times 10^{-10}$	$4.94867420 \times 10^{-03}$	$7.8000000 \times 10^{-10}$
	3	$8.97774240 \times 10^{-03}$	$4.7000000 \times 10^{-10}$	$3.00152262 \times 10^{-03}$	$4.7000000 \times 10^{-10}$
	3.5	$5.44527602 \times 10^{-03}$	$2.9000000 \times 10^{-10}$	$1.82051550 \times 10^{-03}$	$2.9000000 \times 10^{-10}$
0.3	4	$3.30272686 \times 10^{-03}$	$1.7000000 \times 10^{-10}$	$1.10419847 \times 10^{-03}$	$1.7000000 \times 10^{-10}$
	4.5	$2.00320511 \times 10^{-03}$	$1.0000000 \times 10^{-10}$	$6.69730230 \times 10^{-04}$	$1.0000000 \times 10^{-10}$
	5	$1.21500531 \times 10^{-03}$	$6.4000000 \times 10^{-11}$	$4.06211915 \times 10^{-04}$	$6.4000000 \times 10^{-11}$
	0.5	$1.35218250 \times 10^{-01}$	$2.9900000 \times 10^{-08}$	$4.73151582 \times 10^{-02}$	$2.9900000 \times 10^{-08}$
	1	$8.20140147 \times 10^{-02}$	$1.8100000 \times 10^{-08}$	$2.86980942 \times 10^{-02}$	$1.8100000 \times 10^{-08}$
	1.5	$4.97440144 \times 10^{-02}$	$1.1000000 \times 10^{-08}$	$1.74062739 \times 10^{-02}$	$1.1000000 \times 10^{-08}$
	2	$3.01712698 \times 10^{-02}$	$6.7000000 \times 10^{-09}$	$1.05574388 \times 10^{-02}$	$6.7000000 \times 10^{-09}$
	2.5	$1.82998002 \times 10^{-02}$	$4.0400000 \times 10^{-09}$	$6.40341033 \times 10^{-03}$	$4.0400000 \times 10^{-09}$
	3	$1.10993899 \times 10^{-02}$	$2.4500000 \times 10^{-09}$	$3.88386470 \times 10^{-03}$	$2.4500000 \times 10^{-09}$
	3.5	$6.73212028 \times 10^{-03}$	$1.4900000 \times 10^{-09}$	$2.35568301 \times 10^{-03}$	$1.4900000 \times 10^{-09}$
	4	$4.08323736 \times 10^{-03}$	$9.0000000 \times 10^{-10}$	$1.42879398 \times 10^{-03}$	$9.0000000 \times 10^{-10}$
	4.5	$2.47660865 \times 10^{-03}$	$5.4000000 \times 10^{-10}$	$8.66607360 \times 10^{-04}$	$5.4000000 \times 10^{-10}$
	5	$1.50213907 \times 10^{-03}$	$3.3200000 \times 10^{-10}$	$5.25623929 \times 10^{-04}$	$3.32000000 \times 10^{-10}$

6. Conclusion

The solutions for time-fractional ADE are successfully obtained using NITM and HPTM in this paper. The study reveals that the derivative having fractional order, as well as the location and time factors, has an impact on solute concentration. For varying values of the fractional parameter σ, solutions are plotted with spatial and time coordinates for three cases. We compare actual and analytical results with the use of graphs and tables, which are in strong agreement with one another, to demonstrate the effectiveness of the proposed methods. Also, the results achieved by implementing the suggested approaches are compared at various fractional orders, confirming that the result comes closer to the exact solution as the value moves from fractional to integer order. The methods should be extended to solve space-time fractional ADE in two or three dimensions. As a result, the NITM and HPTM are effective methods in finding exact and approximate solutions for nonlinear differential equations arising in science and engineering.

Data Availability

The numerical data used to support the findings of this study are included within the article.

Conflicts of Interest

The authors declare that they have no conflicts of interest.

Acknowledgments

The authors would like to thank the Deanship of Scientific Research at Umm Al-Qura University for supporting this work (grant code: 22UQU4310396DSR16).

References

[1] I. Podlubny, *Fractional Differential Equations*, Academic Press, San Diego, 1999.

[2] K. B. Oldham and J. Spanier, *The Fractional Calculus*, Academic Press, New York, 1974.

[3] Y. Qin, A. Khan, I. Ali et al., "An efficient analytical approach for the solution of certain fractional-order dynamical systems," *Energies*, vol. 13, no. 11, article 2725, 2020.

[4] P. Ramani, A. M. Khan, D. L. Suthar, and D. Kumar, "Approximate analytical solution for non-linear Fitzhugh-Nagumo equation of time fractional order through fractional reduced differential transform method," *International Journal of Applied and Computational Mathematics*, vol. 8, no. 2, pp. 1–12, 2022.

[5] N. H. Aljahdaly, A. Akgul, I. Mahariq, and J. Kafle, "A comparative analysis of the fractional-order coupled Korteweg-De Vries equations with the Mittag-Leffler law," *Journal of Mathematics*, vol. 2022, 30 pages, 2022.

[6] J. H. He, "Approximate analytical solution for seepage flow with fractional derivatives in porous media," *Computer Methods in Applied Mechanics and Engineering*, vol. 167, no. 1-2, pp. 57–68, 1998.

[7] P. Sunthrayuth, H. A. Alyousef, S. A. El-Tantawy, A. Khan, and N. Wyal, "Solving fractional-order diffusion equations in a plasma and fluids via a novel transform," *Journal of Function Spaces*, vol. 2022, 19 pages, 2022.

[8] M. K. Alaoui, R. Fayyaz, A. Khan, R. Shah, and M. S. Abdo, "Analytical investigation of Noyes–Field model for time-fractional Belousov–Zhabotinsky reaction," *Complexity*, vol. 2021, 21 pages, 2021.

[9] M. Areshi, A. Khan, R. Shah, and K. Nonlaopon, "Analytical investigation of fractional-order Newell-Whitehead-Segel equations via a novel transform," *AIMS Mathematics*, vol. 7, no. 4, pp. 6936–6958, 2022.

[10] M. Lakestani, M. Dehghan, and S. Irandoust-pakchin, "The construction of operational matrix of fractional derivatives using B-spline functions," *Communications in Nonlinear Science and Numerical Simulation*, vol. 17, no. 3, pp. 1149–1162, 2012.

[11] K. Nonlaopon, M. Naeem, A. M. Zidan, A. Alsanad, and A. Gumaei, "Numerical investigation of the time-fractional Whitham–Broer–Kaup equation involving without singular kernel operators," *Complexity*, vol. 2021, Article ID 7979365, 21 pages, 2021.

[12] M. Alqhtani, K. M. Saad, R. Shah, W. Weera, and W. M. Hamanah, "Analysis of the fractional-order local poisson equation in fractal porous media," *Symmetry*, vol. 14, no. 7, p. 1323, 2022.

[13] K. S. Miller and B. Ross, *An Introduction to the Fractional Calculus and Fractional Differential Equations*, Willey, New York, NY,USA, 1993.

[14] S. G. Samko, A. A. Kilbas, and O. I. Marichev, *Freactional Integral and Derivatives: Theory and Applications*, Gordon & Breach, Switzerland, 1993.

[15] N. A. Shah, H. A. Alyousef, S. A. El-Tantawy, and J. D. Chung, "Analytical investigation of fractional-order Korteweg-De-Vries-type equations under Atangana-Baleanu-Caputo operator: modeling nonlinear waves in a plasma and fluid," *Symmetry*, vol. 14, no. 4, p. 739, 2022.

[16] L. K. Yadav, G. Agarwal, D. L. Suthar, and S. D. Purohit, "Time-fractional partial differential equations: a novel technique for analytical and numerical solutions," *Arab Journal of Basic and Applied Sciences*, vol. 29, no. 1, pp. 86–98, 2022.

[17] N. Abeye, M. Ayalew, D. L. Suthar, S. D. Purohit, and K. Jangid, "Numerical solution of unsteady state fractional advection-dispersion equation," *Arab Journal of Basic and Applied Sciences*, vol. 29, no. 1, pp. 77–85, 2022.

[18] H. Habenom and D. L. Suthar, "Numerical solution for the time-fractional Fokker-Planck equation via shifted Chebyshev polynomials of the fourth kind," *Advances in Difference Equations*, vol. 2020, no. 1, Article ID 315, 2020.

[19] P. Sunthrayuth, R. Ullah, A. Khan, J. Kafle, I. Mahariq, and F. Jarad, "Numerical analysis of the fractional-order nonlinear system of Volterra integro-differential equations," *Journal of Function Spaces*, vol. 2021, Article ID 1537958, 10 pages, 2021.

[20] M. M. Al-Sawalha, R. P. Agarwal, O. Y. Ababneh, and W. Weera, "A reliable way to deal with fractional-order equations that describe the unsteady flow of a polytropic gas," *Mathematics*, vol. 10, no. 13, p. 2293, 2022.

[21] N. Sene, "Fractional advection-dispersion equation described by the Caputo left generalized fractional derivative," *Palestine J. Math*, vol. 10, no. 2, pp. 562–579, 2021.

[22] B. Baeumer, D. A. Benson, and M. M. Meerschaert, "Advection and dispersion in time and space," *Physica A: Statistical Mechanics and its Applications*, vol. 350, no. 2-4, pp. 245–262, 2005.

[23] S. Momani and Z. Odibat, "Numerical solutions of the space-time fractional advection-dispersion equation," *Numerical Methods for Partial Differential Equations*, vol. 25, no. 5, pp. 1238–1259, 2008.

[24] N. Iqbal, A. Akgul, A. Bariq, M. Mossa Al-Sawalha, and A. Ali, "On solutions of fractional-order gas dynamics equation by effective techniques," *Journal of Function Spaces*, vol. 2022, Article ID 3341754, 14 pages, 2022.

[25] H. Khan, U. Farooq, D. Baleanu, P. Kumam, and M. Arif, "Analytical solutions of (2+time fractional order) dimensional physical models, using modified decomposition method," *Applied Sciences*, vol. 10, no. 1, p. 122, 2020.

[26] D. K. Jaiswal, A. Kumar, and R. R. Yadav, "Analytical solution to the one-dimensional advection-diffusion equation with temporally dependent coefficients," *Journal of Water Resource and Protection*, vol. 3, no. 1, pp. 76–84, 2011.

[27] Q. Huang, G. Huang, and H. Zhan, "A finite element solution for the fractional advection-dispersion equation," *Advances in Water Resources*, vol. 31, no. 12, pp. 1578–1589, 2008.

[28] A. M. A. El-Sayed, S. H. Behiry, and W. E. Raslan, "Adomian's decomposition method for solving an intermediate fractional advection-dispersion equation," *Computer and Mathematics with Applications*, vol. 59, no. 5, pp. 1759–1765, 2010.

[29] A. Yildirim and H. Kocak, "Homotopy perturbation method for solving the space-time fractional advection- dispersion equation," *Advances in Water Resources*, vol. 32, no. 12, pp. 1711–1716, 2009.

[30] M. M. Hikal and M. A. Abu Ibrahim, "On Adomian's decomposition method for solving a fractional advection-dispersion equation," *International Journal of Pure and Applied Mathematics*, vol. 104, no. 1, pp. 43–56, 2015.

[31] M. Alliche and S. Chikh, "Study of non-premixed turbulent flame of hydrogen/air downstream co-current injector," *International Journal of Hydrogen Energy*, vol. 43, no. 6, pp. 3577–3585, 2018.

[32] F. Liu, P. Zhuang, and K. Burrage, "Numerical methods and analysis for a class of fractional advection-dispersion models," *Computers & Mathematcs with Applications*, vol. 64, no. 10, pp. 2990–3007, 2012.

[33] M. C. Rocca, A. R. Plastino, A. Plastino, and A. L. De Paoli, "General solution of a fractional diffusion-advection equation for solar cosmic-ray transport," *Physica A: Statistical Mechanics and its Applications*, vol. 447, pp. 402–410, 2016.

[34] P. Ramani, A. M. Khan, and D. L. Suthar, "Revisiting analytical-approximate solution of time fractional Rosenau-Hyman equation via fractional reduced differential transform method," *International Journal on Emerging Technologies*, vol. 10, no. 2, pp. 403–409, 2019.

[35] V. Daftardar-Gejji and H. Jafari, "An iterative method for solving nonlinear functional equations," *Journal of Mathematical Analysis and Applications.*, vol. 316, no. 2, pp. 753–763, 2006.

[36] S. Bhalekar and V. Daftardar-Gejji, "New iterative method: application to partial differential equations," *Applied Mathematics and Computation.*, vol. 203, no. 2, pp. 778–783, 2008.

[37] V. S. Daftardar-Gejji Bhalekar, "Solving fractional boundary value problems with Dirichlet boundary conditions using a new iterative method," *Computers & Mathematics with Applications*, vol. 59, no. 5, pp. 1801–1809, 2010.

[38] G. Adomian, "Solution of physical problems by decomposition," *Computers and Mathematics with Applications.*, vol. 27, no. 9-10, pp. 145–154, 1994.

[39] J. H. He, "Homotopy perturbation technique," *Computer Methods in Applied Mechanics and Engineering.*, vol. 178, no. 3-4, pp. 257–262, 1999.

[40] J. H. He, "Variational iteration method for autonomous ordinary differential systems," *Applied Mathematics and Computation.*, vol. 114, no. 2-3, pp. 115–123, 2000.

[41] K. Nonlaopon, A. M. Alsharif, A. M. Zidan, A. Khan, Y. S. Hamed, and R. Shah, "Numerical investigation of fractional-order Swift-Hohenberg equations via a novel transform," *Symmetry*, vol. 13, no. 7, article 1263, 2021.

[42] H. Khan, A. Khan, P. Kumam, D. Baleanu, and M. Arif, "An approximate analytical solution of the Navier-Stokes equations within Caputo operator and Elzaki transform decomposition method," *Advances in Difference Equations*, vol. 2020, no. 1, Article ID 622, 2020.

[43] H. Khan, A. Khan, M. Al-Qurashi, R. Shah, and D. Baleanu, "Modified modelling for heat like equations within Caputo operator," *Energies*, vol. 13, no. 8, p. 2002, 2020.

Hindawi
Journal of Function Spaces
Volume 2022, Article ID 6333084, 21 pages
https://doi.org/10.1155/2022/6333084

Research Article

A Novel Numerical Technique for Fractional Ordinary Differential Equations with Proportional Delay

Muhammad Imran Liaqat,[1] **Adnan Khan**,[1] **Ali Akgül**,[2] **and Md. Shajib Ali**[3]

[1]*Department of Mathematics, National College of Business Administration & Economics, Lahore, Pakistan*
[2]*Department of Mathematics, Art and Science Faculty, Siirt University, Siirt 56100, Turkey*
[3]*Department of Mathematics, Islamic University, Kushtia 7003, Bangladesh*

Correspondence should be addressed to Md. Shajib Ali; shajib_301@yahoo.co.in

Received 15 April 2022; Accepted 21 June 2022; Published 7 July 2022

Academic Editor: Yusuf Gurefe

Some researchers have combined two powerful techniques to establish a new method for solving fractional-order differential equations. In this study, we used a new combined technique, known as the Elzaki residual power series method (ERPSM), to offer approximate and exact solutions for fractional multipantograph systems (FMPS) and pantograph differential equations (PDEs). In Caputo logic, the fractional-order derivative operator is measured. The Elzaki transform method and the residual power series method (RPSM) are combined in this novel technique. The suggested technique is based on a new version of Taylor's series that generates a convergent series as a solution. Establishing the coefficients for a series, like the RPSM, necessitates computing the fractional derivatives each time. As ERPSM just requires the concept of a zero limit, we simply need a few computations to get the coefficients. The novel technique solves nonlinear problems without the need for He's and Adomian polynomials, which is an advantage over the other combined methods based on homotopy perturbation and Adomian decomposition methods. The relative, recurrence, and absolute errors of the problems are analyzed to evaluate the efficiency and consistency of the presented method. Graphical significances are also identified for various values of fractional-order derivatives. As a result, the procedure is quick, precise, and easy to implement, and it yields outstanding results.

1. Introduction

Many differential equations (DEs) that arise in applications are sufficiently complicated that closed-form solutions are not always feasible. Numerical methods offered a powerful substitute means for solving the DEs under the given initial conditions. Numerous methods have been developed in recent years to solve fractional-order differential equations (FODEs), including the homotopy perturbation method [1], the differential transform method [2], the operational matrix method [3], the conformable Shehu transform decomposition method [4], the variational iteration method [5], the Jacobi collocation method [6], the conformable Shehu transform iterative method [7], the spectral tau method [8], the Legendre wavelet method [9], the fractional natural decomposition method [10], the power series method with the conformable operator [11], and the Chebyshev polynomial method [12].

Integral equations (IEs), DEs, and delay differential equations (DDEs) are all solved by employing integral transforms [13–17], which are among the most valuable techniques in mathematics. The conversion of DEs and IEs into terms of a simple algebraic equation is enabled by the appropriate selection of integral transform. The origins of integral transforms can be traced back to Laplace's work in the 1780s and Fourier's work in 1822 [18]. In the beginning, ordinary and partial DEs were solved using the Laplace transform and the Fourier transform, which are two well-known transforms. These transforms were then applied to FODEs [19–24]. In recent years, researchers have proposed lots of new different transformations to solve a variety of mathematical problems. FODEs are solved using the

Aboodh transform [25], fractional complex transform [26], travelling wave transform [27], Sumudu transform [28], and ZZ transform [29]. These transformations are paired with additional analytical, numerical, or homotopy-based techniques to handle FODEs [30–35]. Numerous mathematicians have recently become interested in a transformation known as the Elzaki transform (ET) [36–41]. The ET was introduced by Elzaki to facilitate the process of solving ordinary and partial DEs in the time domain [42]. The ET is derived from the classical Fourier integral transform.

We examine the functions in set H, which are described as

$$H = \left\{ \Theta(\tau) | \exists M, \Upsilon_1, \Upsilon_2 > 0, |\Theta(\tau) < M e^{|\tau|/\Upsilon_j} \quad \text{if } \tau \in (-1)^j \times [0, \infty) \right\}. \tag{1}$$

The formula for E-T is as follows:

$$E[\Theta(\tau)] = \wp(\upsilon) = \upsilon \int_0^\infty \Theta(\tau) e^{-(\tau/\upsilon)} d\tau, \quad \Upsilon_1 \le \upsilon \le \Upsilon_2. \tag{2}$$

The following are the key advantages of the ET [36–45]:

(i) The ET can easily be applied to the initial value problems with less computational work

(ii) The ET has unit-preserving properties and may be used to solve problems without resorting to the frequency domain

(iii) Numerous nonlinear DEs with variable coefficients, namely, the time-fractional wavelike equations, can be solved with it

(iv) It may handle a variety of difficult problems in engineering, physics, fluid mechanics, chemistry, and dynamics, such as Maxwell's equations and fluid flow problems

The Jordanian mathematician, Arqub, created the RPSM in 2013 [46]. The RPSM is a semianalytical method; it is a combination of Taylor's series and the residual error function. It provides series solutions of linear and nonlinear DEs in the form of convergence series. In 2013, RPSM was implemented for the first time to find solutions to fuzzy DEs. Furthermore, this method has been successfully used to solve a wide range of FODEs, including time-fractional KdV-Burgers equations [47], time-fractional Schrödinger equations [48], the SIR epidemic model of fractional order [49], conformable-type Coudrey–Dodd–Gibbon–Sawada–Kotera [50], time-fractional Swift–Hohenberg problems [51], time-fractional Phi-4 equation [52], and the Zakharov–Kuznetsov equation [53].

Researchers combined two powerful methods to develop a new method for solving FODEs. Some of these groups are described as a combination of the Adomian decomposition method and the Sumudu transform [54], as well as the homotopy analysis method and the natural transform [55] and the Laplace transformation with homotopy perturbation approach [56]. In this study, we applied the novel combined technique, known as the ERPSM, to provide approximate and exact solutions for FMPS and PDEs. To assess the efficiency and consistency of the proposed method, the relative, recurrence, and absolute errors of the problems are examined. Graphical significance is also found for various values of fractional-order derivatives. As a result, the technique is rapid, precise, and simple to use, and it produces excellent results. The set of rules for this new technique depends on transforming the given equation into the ET space, in the second step; establishing a series solution by using the new form of the Taylor series; and then acquiring the solution in the real space of the equation by applying the inverse ET.

This novel technique can be used to construct power series expansion solutions for linear and nonlinear FODEs without perturbation, linearization, or discretization. Unlike the classical power series method, this method does not need to match the coefficients of the corresponding terms, and a recursion relation is not needed. The new method handles nonlinear problems without the need for He's and Adomian polynomials, which is an advantage over existing combination methods based on homotopy perturbation and Adomian decomposition methods. This technique finds the coefficients of the series, relying on the limit concept but not the fractional derivatives as in the RPSM. Thus, only a few calculations are required to determine the coefficients related to RPSM. The closed-form and approximate solutions can be obtained by the proposed method through a quick convergence series.

A PDE is a special kind of delay differential equation (DDE) with a proportional delay. In 1851, the first-time device named "pantograph" was used in the construction of an electric locomotive, which is where this name originated from that time. British Railways decided to make a new kind of electric locomotive in 1960. The target was to construct a new kind of electric locomotive that moves trains faster. The pantograph was a prominent part of the new fast-speed electric locomotive. Pantographs take current from an overhead wire, which is necessary for the locomotive to move. Therefore, Ockendon and Taylor observed the mechanism of the pantograph. As a result, they built a special kind of DDE form:

$$\frac{d\Theta}{d\tau} = \Omega\,\Theta(\tau) + \sigma\,\Theta(\lambda\tau), \quad \tau \ge 0, \tag{3}$$

where Ω, σ are real constants and $0 < k < 1$, $\lambda \in R$. This article was first published in 1971 [57]. Then, such a type of DDE was named PDE. Various studies on PDEs have recently been published in the scientific literature [58–60]. PDEs are widely used in probability theory, nonlinear dynamical systems, astrophysics, quantum mechanics, electrodynamics, and cell growth [61–64]. In this study, we consider the following FMPS:

$$D_\tau^\omega \Theta_1(\tau) = \Omega_1 \Theta_1(\tau) + \Lambda_1(\tau, \Theta_1(\tau), \Theta_2(\tau), \Theta_1(\varpi_1\tau), \Theta_2(\varpi_2\tau)), \tag{4}$$

$$D_\tau^\omega \Theta_2(\tau) = \Omega_2\Theta_2(\tau) + \Lambda_2(\tau, \Theta_1(\tau), \Theta_2(\tau), \Theta_1(\varpi_1\tau), \Theta_2(\varpi_2\tau)), \tag{5}$$

subject to the initial conditions

$$\begin{aligned} \Theta_1(0) &= \mathfrak{I}_1, \\ \Theta_2(0) &= \mathfrak{I}_2, \end{aligned} \tag{6}$$

where $0 < \varpi_1, \varpi_2 \leq 1, \mathfrak{I}_1, \mathfrak{I}_2$ are finite constants; Λ_1, Λ_2 are analytical functions; and D_τ^ω is the Caputo fractional derivative (CFD). The FMPS is a type of DDE that arises in a number of physics and engineering applications, including quantum mechanics, dynamical systems, electronic systems, and population dynamics [65, 66].

The following linear PDE is given as

$$D_\tau^\omega \Theta(\tau) = l\Theta(\tau) + \sum_{j=1}^{s} m_j \Theta\left(u_j\tau\right) + \sum_{j=1}^{t} p_j D_\tau^\omega \Theta\left(q_j\tau\right) + g(\tau), \tag{7}$$

where $0 < \omega \leq 1$, $\tau \geq 0$, $l, m_j, p_j \in R$, $0 < \omega \leq 1$, $u_j > 0$, and $q_j < 1$. D_τ^ω is the CFD of order ω, with the following initial condition:

$$\Theta(0) = \phi. \tag{8}$$

The nonlinear PDE is as follows:

$$D_\tau^\omega \Theta(\tau) = \xi(\tau^\omega, \Theta(\tau), \Theta(\lambda\tau), D_\tau^\omega \Theta(\lambda\tau)), \tag{9}$$

with the initial condition

$$\Theta(0) = \mathfrak{I}. \tag{10}$$

Definition 1 (see [67]) (a novel fractional Taylor series formula in E-T). Assume that $\Theta(\tau)$ is a piecewise continuous and exponential order and that the E-T of $\Theta(\tau)$, $E[\Phi(\tau)] = \wp(\upsilon)$ is provided by a fractional Taylor series.

$$\wp(\upsilon) = \sum_{\nu=0}^{\infty} \hbar_\nu \upsilon^{\nu\omega+2}, \tag{11}$$

where $\hbar_\nu$ is the νth coefficient of the novel fractional Taylor series formula in E-T.

Lemma 2. *Assume that $\Theta_1(\tau)$ and $\Theta_2(\tau)$ are piecewise continuous and of exponential-order functions, and $E[\Theta_1(\tau)] = \wp_1(\upsilon)$, $E[\Theta_2(\tau)] = \wp_2(\upsilon)$, and λ_1, λ_2 are constants. Then, the following axioms hold [67]:*

(i) $\lim_{\upsilon \longrightarrow 0} (1/\upsilon^2)\wp(\upsilon) = \hbar_0$

(ii) $E[D_\tau^\omega \Theta(\tau)] = (\wp(\upsilon)/\upsilon^\omega) - \sum_{r=0}^{\nu-1} \upsilon^{r-\omega+2}\Theta^{(r)}(0)$, $\nu - 1 < \omega \leq \nu$

(iii) $E[D_\tau^{\nu\omega} \Theta(\tau)] = \wp(\upsilon)/\upsilon^{\nu\omega} - \sum_{r=0}^{\nu-1} \upsilon^{(r-\nu)\omega+2}\Theta^{(r)}(0)$, $0 < \omega \leq 1$

The framework of this study is as follows. The fundamental recommendation beyond the ERPSM with convergence and absolute error analysis for FMPS is demonstrated in Section 2. We also demonstrated numerical examples of FMPS to exemplify the competency, potential, and straightforwardness of the new combined technique. The linear and nonlinear PDEs are discussed in Sections 3 and 4, respectively. Finally, our findings are summarized in Section 5.

2. The ERPSM to Demonstrate the FMPS

In this section, we use ERPSM to construct the solutions of the FMPS as in Equations (4) and (5). The main algorithm of this method for solving the FMPS can be summarized by the following steps: applies the E-T to Equation (4). As a result, we get an algebraic form in E-T space. In the second step, using the novel fractional Taylor's series formula in E-T, we represent the solution in the E-T space of the algebraic equation obtained in the first step. The coefficients of this expansion are determined with the help of residual function and limit concept. As a result, we have found a solution to the problem in its original space by taking the inverse E-T.

In the next subsection, we derive the main algorithms of the ERPSM for the FMPS.

2.1. The Algorithm of ERPSM for Solving FMPS. We use the following algorithm to create the solution with the help of ERPSM for the FMPS as shown in Equations (4) and (5):

Step 1. Rewrite Equations (4) and (5). We have

$$D_\tau^\omega \Theta_1(\tau) - \Omega_1\Theta_1(\tau) - \Lambda_1(\tau, \Theta_1(\tau), \Theta_2(\tau), \Theta_1(\varpi_1\tau), \Theta_2(\varpi_2\tau)) = 0, \tag{12}$$

$$D_\tau^\omega \Theta_2(\tau) - \Omega_2\Theta_2(\tau) - \Lambda_2(\tau, \Theta_1(\tau), \Theta_2(\tau), \Theta_1(\varpi_1\tau), \Theta_2(\varpi_2\tau)) = 0. \tag{13}$$

Step 2. We get the following result by implementing the E-T on both sides of Equations (12) and (13).

$$\begin{aligned} &E[D_\tau^\omega \Theta_1(\tau)] - E[\Omega_1\Theta_1(\tau)] \\ &\quad - E[\Lambda_1(\tau, \Theta_1(\tau), \Theta_2(\tau), \Theta_1(\varpi_1\tau), \Theta_2(\varpi_2\tau))] = 0, \end{aligned} \tag{14}$$

$$\begin{aligned} &E[D_\tau^\omega \Theta_2(\tau)] - E[\Omega_2\Theta_2(\tau)] \\ &\quad - E[\Lambda_2(\tau, \Theta_1(\tau), \Theta_2(\tau), \Theta_1(\varpi_1\tau), \Theta_2(\varpi_2\tau))] = 0. \end{aligned} \tag{15}$$

By utilizing the second part of Lemma 2, Equations (14) and (15) become as follows:

$$\wp_1(\upsilon) = \upsilon^2\Theta(0) + \upsilon^\omega \Omega_1 \wp_1(\upsilon) + \upsilon^\omega \Lambda_1^l(\upsilon), \tag{16}$$

$$\wp_2(\upsilon) = \upsilon^2\Theta(0) + \upsilon^\omega \Omega_2 \wp_2(\upsilon) + \upsilon^\omega \Lambda_2^l(\upsilon), \tag{17}$$

where

$$E[\Lambda_1(\tau,\Theta_1(\tau),\Theta_2(\tau),\Theta_1(\varpi_1\tau),\Theta_2(\varpi_2\tau))]=\Lambda_1^l(\upsilon),$$
$$E[\Lambda_2(\tau,\Theta_1(\tau),\Theta_2(\tau),\Theta_1(\varpi_1\tau),\Theta_2(\varpi_2\tau))]=\Lambda_2^l(\upsilon),$$
$$E[\Theta_1(\tau)]=\wp_1(\upsilon),$$
$$E[\Theta_2(\tau)]=\wp_2(\upsilon). \quad (18)$$

Step 3. Assume that algebraic equations (16) and (17) have the solution in the expansion form as

$$\wp_1(\upsilon)=\sum_{\nu=0}^{\infty}\hbar_{1\nu}\upsilon^{\nu\omega+2},$$
$$\wp_2(\upsilon)=\sum_{\nu=0}^{\infty}\hbar_{2\nu}\upsilon^{\nu\omega+2}. \quad (19)$$

The κth-truncated series of $\wp_1(\upsilon)$ and $\wp_2(\upsilon)$ are as

$$\wp_{1\kappa}(\upsilon)=\sum_{\nu=0}^{\kappa}\hbar_{1\nu}\upsilon^{\nu\omega+2},$$
$$\wp_{2\kappa}(\upsilon)=\sum_{\nu=0}^{\kappa}\hbar_{2\nu}\upsilon^{\nu\omega+2}. \quad (20)$$

Step 4. By utilizing the following lemma,

$$\hbar_{1,0}=\lim_{\upsilon\longrightarrow 0}\frac{1}{\upsilon^2}\Theta_1(\tau)=\Theta_1(0),$$
$$\hbar_{2,0}=\lim_{\upsilon\longrightarrow 0}\frac{1}{\upsilon^2}\Theta_2(\tau)=\Theta_2(0). \quad (21)$$

The κth-truncated series becomes

$$\wp_{\kappa,1}(\upsilon)=\Theta_1(0)\upsilon^2+\sum_{\nu=1}^{\kappa}\hbar_{1\nu}\upsilon^{\nu\omega+2}, \quad (22)$$

$$\wp_{\kappa,2}(\upsilon)=\Theta_2(0)\upsilon^2+\sum_{\nu=1}^{\kappa}\hbar_{2,\nu}\upsilon^{\nu\omega+2}. \quad (23)$$

Step 5. Consider the Elzaki residual function (ERF) of Equations (22) and (23) separately, as well as the κth-truncated Elzaki residual functions (ERFs), so that

$$E\mathrm{Res}_1(\upsilon)=\wp_1(\upsilon)-\upsilon^2\Theta(0)-\upsilon^{\omega}\Omega_1\wp_1(\upsilon)-\upsilon^{\omega}\Lambda_1^l(\upsilon), \quad (24)$$

$$E\mathrm{Res}_2(\upsilon)=\wp_2(\upsilon)-\upsilon^2\Theta(0)-\upsilon^{\omega}\Omega_2\wp_2(\upsilon)-\upsilon^{\omega}\Lambda_2^l(\upsilon), \quad (25)$$

$$E\mathrm{Res}_{1,\kappa}(\upsilon)=\wp_{1,\kappa}(\upsilon)-\upsilon^2\Theta(0)-\upsilon^{\omega}\Omega_1\wp_{1,\kappa}(\upsilon)-\upsilon^{\omega}\Lambda_1^l(\upsilon), \quad (26)$$

$$E\mathrm{Res}_{2,\kappa}(\upsilon)=\wp_{2,\kappa}(\upsilon)-\upsilon^2\Theta(0)-\upsilon^{\omega}\Omega_2\wp_{2,\kappa}(\upsilon)-\upsilon^{\omega}\Lambda_2^l(\upsilon). \quad (27)$$

Step 6. Replace the succession arrangement of $\wp_{1,\kappa}(\upsilon)$ and $\wp_{2,\kappa}(\upsilon)$ in Equations (26) and (27).

Step 7. To highlight important facts, we extend some features that arise in the RPSM [67–69].

That is obvious.

$$E\ \mathrm{Re}\ s(\upsilon)=0. \quad (28)$$

Therefore,

$$\lim_{\kappa\longrightarrow\infty}E\mathrm{Res}_k(\upsilon)=E\mathrm{Res}(\upsilon). \quad (29)$$

Since, $\lim_{\upsilon\longrightarrow 0}(1/\upsilon^2)E\ \mathrm{Re}\ s(\upsilon)=0$. It is clear that $\lim_{\upsilon\longrightarrow 0}(1/\upsilon^2)$ $E\mathrm{Res}_k(\upsilon)=0$. As a result, we get the following:

$$\lim_{\upsilon\longrightarrow 0}\left(\frac{1}{\upsilon^{k\omega+2}}E\mathrm{Res}_1(\upsilon)\right)=\lim_{\upsilon\longrightarrow 0}\left(\frac{1}{\upsilon^{k\omega+2}}E\mathrm{Res}_{1,\kappa}(\upsilon)\right)=0,\quad k=1,2,3,\cdots,$$
$$\lim_{\upsilon\longrightarrow 0}\left(\frac{1}{\upsilon^{k\omega+2}}E\mathrm{Res}_2(\upsilon)\right)=\lim_{\upsilon\longrightarrow 0}\left(\frac{1}{\upsilon^{k\omega+2}}E\mathrm{Res}_{2,\kappa}(\upsilon)\right)=0,\quad k=1,2,3,\cdots. \quad (30)$$

Step 8. Replace the κth attained values of $\hbar_{1,\kappa}$ and $\hbar_{2,\kappa}$ into the κth-truncated series of $\wp_{1,\kappa}(\upsilon)$ and $\wp_{2,\kappa}(\upsilon)$ to become the κth-approximate explanation of Equations (16) and (17).

Step 9. Use the inverse E-T on $\wp_{1,\kappa}(\upsilon)$ and $\wp_{2,\kappa}(\upsilon)$ to obtain the κth-approximate solution $\Theta_{1,\kappa}(\tau)$ and $\Theta_{2,\kappa}(\tau)$ in the original space.

The next theorem clarifies and establishes the conditions for the series solutions to converge.

Theorem 3. *Let Z be a Banach space denoted with a suitable norm $\|.\|$ over which the sequence of partial sums $\sum_{\kappa=0}^{\infty}\wp_\kappa(\upsilon)$ is defined. Assume that the initial guess $\wp_0$ remains inside the ball $B_r(\wp)$ of the solution $\wp(\upsilon)$. Then, the series solution $\sum_{\kappa=0}^{\infty}\wp_\kappa(\upsilon)$ converges if $\exists\theta>0$ such that $\|\wp_{\nu+1}(\upsilon)\|\le\theta\|\wp_\nu(\upsilon)\|$.*

Proof. A sequence of partial sums is defined as

$$Y_0=\wp_0(\upsilon),$$
$$Y_1=\wp_0(\upsilon)+\wp_1(\upsilon),$$
$$Y_2=\wp_0(\upsilon)+\wp_1(\upsilon)+\wp_2(\upsilon),$$
$$Y_3=\wp_0(\upsilon)+\wp_1(\upsilon)+\wp_2(\upsilon)+\wp_3(\upsilon),$$
$$\vdots\ \vdots\ \vdots$$
$$Y_\nu=\wp_0(\upsilon)+\wp_1(\upsilon)+\wp_2(\upsilon)+\wp_3(\upsilon)+\cdots+\wp_\nu(\upsilon). \quad (31)$$

Next is that we would have to show that $\{Y_\nu\}_{\nu=0}^{\infty}$ is a Cauchy sequence in Z. To demonstrate this, consider the following relationship:

$$\|Y_{\nu+1}-Y_{\nu}\|=\|\wp_{\nu+1}(\upsilon)\|\le\theta\|\wp_{\nu}(\upsilon)\|\le\theta^2\|\wp_{\nu-1}(\upsilon)\|\\ \le\theta^3\|\wp_{\nu-2}(\upsilon)\|\le\theta^4\|\wp_{\nu-3}(\upsilon)\|\cdots\le\theta^{\nu+1}\|\wp_0(\upsilon)\|, \tag{32}$$

where $\nu=0,1,2,\cdots$.

For every $\nu,\kappa\in N$, $\nu\ge\kappa$, we have

$$\|Y_\nu-Y_\kappa\|=\|(Y_\nu-Y_{\nu-1})+(Y_{\nu-1}-Y_{\nu-2})+(Y_{\nu-2}-Y_{\nu-3})\\ +(Y_{\nu-3}-Y_{\nu-4})\cdots(Y_{\kappa+1}-Y_\kappa)\|. \tag{33}$$

From triangle inequality, we have

$$\|(Y_\nu-Y_{\nu-1})+(Y_{\nu-1}-Y_{\nu-2})+(Y_{\nu-2}-Y_{\nu-3})\\ +(Y_{\nu-3}-Y_{\nu-4})+\cdots(Y_{\kappa+1}-Y_\kappa)\|\le\|(Y_\nu-Y_{\nu-1})\|\\ +\|(Y_{\nu-1}-Y_{\nu-2})\|+\|(Y_{\nu-2}-Y_{\nu-3})\|+\|(Y_{\nu-3}-Y_{\nu-4})\|\\ +\cdots+\|(Y_{\kappa+1}-Y_\kappa)\|, \tag{34}$$

and

$$\|(Y_\nu-Y_{\nu-1})\|+\|(Y_{\nu-1}-Y_{\nu-2})\|+\|(Y_{\nu-2}-Y_{\nu-3})\|\\ +\|(Y_{\nu-3}-Y_{\nu-4})\|+\cdots+\|(Y_{\kappa+1}-Y_\kappa)\|\le\theta^\nu\|\wp_0(\upsilon)\|\\ +\theta^{\nu-1}\|\wp_0(\upsilon)\|+\theta^{\nu-2}\|\wp_0(\upsilon)\|+\cdots+\theta^{\kappa+1}\|\wp_0(\upsilon)\|\\ =\frac{1-\theta^{\nu-\kappa}}{1-\theta}\theta^{\kappa+1}\|\wp_0(\upsilon)\|. \tag{35}$$

Therefore,

$$\|Y_\nu-Y_\kappa\|=\frac{1-\theta^{\nu-\kappa}}{1-\theta}\theta^{\kappa+1}\|\wp_0(\upsilon)\|. \tag{36}$$

Showing that the sequence is bounded, we can obtain for $0<\theta<1$ that

$$\lim_{\nu,\kappa\longrightarrow\infty}\|Y_\nu-Y_\kappa\|=0. \tag{37}$$

□

This proves that the sequence of partial sums generated by ERPSM is Cauchy and hence convergent.

In the next theorem, we determine the maximum truncation error.

Theorem 4. *Let $\wp(\upsilon)$ be the approximate solution of the truncated finite series $\sum_{\nu=0}^{\infty}\wp_\nu(\upsilon)$. Assume it is attainable to acquire a real number $\theta\in(0,1)$, in order that $\|\wp_{\nu+1}(\upsilon)\|\le\theta\|\wp_\nu(\upsilon)\|,\forall\nu\in N$; furthermore, the utmost absolute error is*

$$\left\|\wp(\upsilon)-\sum_{\nu=0}^{\kappa}\wp_\nu(\upsilon)\right\|\le\frac{\theta^{\kappa+1}}{1-\kappa}\|\wp_0(\upsilon)\|. \tag{38}$$

Proof. Let the series $\sum_{\nu=0}^{\kappa}\wp_\nu(\upsilon)$ be finite, then

$$\left\|\wp(\upsilon)-\sum_{\nu=0}^{\kappa}\wp_\nu(\upsilon)\right\|=\left\|\sum_{\kappa+1}^{\infty}\wp_\nu(\upsilon)\right\|,\le\sum_{\kappa+1}^{\infty}\|\wp_\nu(\upsilon)\|,\\ \le\sum_{\kappa+1}^{\infty}\theta^\kappa\|\wp_0(\upsilon)\|,\\ \le\theta^{\kappa+1}\left(1+\theta+\theta^2+\theta^3+\cdots\right)\|\wp_0(\upsilon)\|,\\ \le\left(\frac{\theta^{\kappa+1}}{1-\theta}\right)\|\wp_0(\upsilon)\|. \tag{39}$$

This proof is complete. □

In the next subsection, two problems of FMPS are established to illustrate the performance and appropriateness of the proposed method.

2.2. Numerical Examples. To demonstrate the execution and capability of ERPSM, we investigated two interesting and important problems for FMPS:

Problem 5. Consider the following FMPS:

$$D_\tau^\omega\Theta_1(\tau)-\Theta_1(\tau)+\Theta_2(\tau)-\Theta_1\left(\frac{\tau}{2}\right)+e^{\tau^\omega/2}-e^{-\tau^\omega}=0, \tag{40}$$

$$D_\tau^\omega\Theta_2(\tau)+\Theta_1(\tau)+\Theta_2(\tau)+\Theta_2\left(\frac{\tau}{2}\right)-e^{-(\tau^\omega/2)}-e^{\tau^\omega}=0, \tag{41}$$

with the initial conditions $\Theta_1(0)=1$ and $\Theta_2(0)=1$.

Applying the E-T to Equations (40) and (41), we get

$$E\left[D_\tau^\omega\Theta_1(\tau)-\Theta_1(\tau)+\Theta_2(\tau)-\Theta_1\left(\frac{\tau}{2}\right)+e^{\tau^\omega/2}-e^{-\tau^\omega}\right]=0, \tag{42}$$

$$E\left[D_\tau^\omega\Theta_2(\tau)+\Theta_1(\tau)+\Theta_2(\tau)+\Theta_2\left(\frac{\tau}{2}\right)-e^{-(\tau^\omega/2)}-e^{\tau^\omega}\right]=0. \tag{43}$$

We have the following results from Equations (42) and (43) using the procedure mentioned in Subsection 2.1:

$$\wp_1(\upsilon)=\upsilon^2\Theta_1(0)+\upsilon^\omega\wp_1(\upsilon)-\upsilon^\omega\wp_2(\upsilon)+4\upsilon^\omega\wp_1\left(\frac{\upsilon}{2}\right)\\ -2\frac{\upsilon^{\omega+2}}{2-\upsilon}+\frac{\upsilon^{\omega+2}}{1+\upsilon}, \tag{44}$$

$$\wp_2(\upsilon)=\upsilon^2\Theta_2(0)-\upsilon^\omega\wp_1(\upsilon)-4\upsilon^\omega\wp_2\left(\frac{\upsilon}{2}\right)+2\frac{\upsilon^{\omega+2}}{2+\upsilon}+\frac{\upsilon^{\omega+2}}{1-\upsilon}. \tag{45}$$

Assume that Equations (44) and (45) have a series solution in the following form:

$$\wp_1(\upsilon) = \sum_{\nu=0}^{\infty} \hbar_{1,\nu}\upsilon^{\nu\omega+2},$$
$$\wp_2(\upsilon) = \sum_{\nu=0}^{\infty} \hbar_{2,\nu}\upsilon^{\nu\omega+2}. \tag{46}$$

The κth-truncated expansion is as follows:

$$\wp_{1,\kappa}(\upsilon) = \sum_{\nu=0}^{\kappa} \hbar_{1,\nu}\upsilon^{\nu\omega+2},$$
$$\wp_{2,\kappa}(\upsilon) = \sum_{\nu=0}^{\kappa} \hbar_{2,\nu}\upsilon^{\nu\omega+2}. \tag{47}$$

By using the first part of Lemma 2, the κth-truncated series becomes

$$\wp_{1,\kappa}(\upsilon) = \upsilon^2 + \sum_{\nu=1}^{\kappa} \hbar_{1,\nu}\upsilon^{\nu\omega+2},$$
$$\wp_{2,\kappa}(\upsilon) = \upsilon^2 + \sum_{\nu=1}^{\kappa} \hbar_{2,\nu}\upsilon^{\nu\omega+2}. \tag{48}$$

The ERFs are formulated as

$$E\mathrm{Res}_1(\upsilon) = \wp_1(\upsilon) - \upsilon^2\Theta_1(0) - \upsilon^{\omega}\wp_1(\upsilon) + \upsilon^{\omega}\wp_2(\upsilon) - 4\upsilon^{\omega}\wp_1\left(\frac{\upsilon}{2}\right) + 2\frac{\upsilon^{\omega+2}}{2-\upsilon} - \frac{\upsilon^{\omega+2}}{1+\upsilon},$$

$$E\mathrm{Res}_2(\upsilon) = \wp_2(\upsilon) - \upsilon^2\Theta_2(0) + \upsilon^{\omega}\wp_1(\upsilon) + 4\upsilon^{\omega}\wp_2\left(\frac{\upsilon}{2}\right) - 2\frac{\upsilon^{\omega+2}}{2+\upsilon} - \frac{\upsilon^{\omega+2}}{1-\upsilon}. \tag{49}$$

The κth-truncated ERF takes the following form:

$$E\mathrm{Res}_{1,\kappa}(\upsilon) = \wp_{1,\kappa}(\upsilon) - \upsilon^2\Theta_1(0) - \upsilon^{\omega}\wp_{1,\kappa}(\upsilon) + \upsilon^{\omega}\wp_{2,\kappa}(\upsilon) - 4\upsilon^{\omega}\wp_{1,\kappa}\left(\frac{\upsilon}{2}\right) + 2\frac{\upsilon^{\omega+2}}{2-\upsilon} - \frac{\upsilon^{\omega+2}}{1+\upsilon},$$

$$E\mathrm{Res}_{2,\kappa}(\upsilon) = \wp_{2,\kappa}(\upsilon) - \upsilon^2\Theta_2(0) + \upsilon^{\omega}\wp_{1,\kappa}(\upsilon) + 4\upsilon^{\omega}\wp_{2,\kappa}\left(\frac{\upsilon}{2}\right) - 2\frac{\upsilon^{\omega+2}}{2+\upsilon} - \frac{\upsilon^{\omega+2}}{1-\upsilon}. \tag{50}$$

Substitute $\kappa = 1, 2, 3, 4, 5$ into Equations (65) and (66) and solve the following expression to find the unknown coefficients.

$$\lim_{\upsilon\longrightarrow 0}\left(\frac{1}{\upsilon^{k\omega+2}}E\mathrm{Res}_{1,\kappa}(\upsilon)\right) = 0,$$
$$\lim_{\upsilon\longrightarrow 0}\left(\frac{1}{\upsilon^{k\omega+2}}E\mathrm{Res}_{2,\kappa}(\upsilon)\right) = 0. \tag{51}$$

Thus, we have

$$\hbar_{1,1} = 1,$$
$$\hbar_{2,1} = -1,$$
$$\hbar_{1,2} = 2 + \frac{1}{(2)^{\omega}} - \frac{3\Gamma(\omega+1)}{2},$$
$$\hbar_{2,2} = \frac{1}{(2)^{\omega}} + \frac{\Gamma(\omega+1)}{2},$$
$$\hbar_{1,3} = \frac{1}{8^{1+\omega}}\left(8 + 2^{\omega+4} + 2^{3\omega+4} - 2^{\omega+2}\left(3 + 4^{\omega+1}\right)(\Gamma(\omega+1) + 38^{\omega}\Gamma(2\omega+1)\right)),$$
$$\hbar_{2,3} = -2 - 2^{1-\omega} - 2^{-3\omega} + \left(1 - 2^{-2\omega-1}\right)\Gamma(\omega+1) + \frac{5}{8}\Gamma(2\omega+1),$$
$$\hbar_{1,4} = -\frac{1}{4^{3\omega+2}}\left(-16 - 2^{\omega+5} - 2^{4\omega+5} - 2^{3\omega+6} - 2^{5\omega+5} - 2^{6\omega+6} + 2^{\omega+3}\left(3 + 2^{3\omega+1} + 3(2)^{5\omega+1} + 2^{2\omega+2}\right) \times \Gamma(\omega+1) + 2^{3\omega+1}\left(2^{3\omega+1} - 3\right)\Gamma(2\omega+1) + 3(2)^{6\omega}\Gamma(3\omega+1)\right),$$
$$\hbar_{2,4} = \frac{1}{4^{3\omega+2}}\left(16 + 2^{2\omega+5} + 2^{3\omega+5} - 2^{4\omega+5} + 2^{5\omega+5} + 2^{\omega+3} \cdot \left(1 - 2^{2\omega+1} + 2^{3\omega+2} + 2^{5\omega+1}\right)\Gamma(\omega+1) - 2^{3\omega+1}\left(8^{\omega+1} + 5\right) \cdot \Gamma(2\omega+1) + \frac{7}{3}\Gamma(3\omega+1)2^{6\omega}\right),$$
$$\begin{aligned}\hbar_{1,5} = {}& 4 + 2^{-9\omega+1} + 2^{-7\omega+2} + 2^{-6\omega+1} + 2^{-5\omega+2} + 2^{-4\omega+1} + 2^{-3\omega+1} \\ & + 4^{-\omega+1} + 2^{-10\omega} - \frac{1}{3}\Gamma(3\omega+1) - 3\times 2^{-4(\omega+1)}\Gamma(3\omega+1) \\ & + 5\times 2^{7}\Gamma(4\omega+1) - 4\Gamma(\omega+1) - \frac{1}{3}\Gamma(3\omega+1) \\ & - 3\times 2^{-4(\omega+1)}\Gamma(3\omega+1) + 5\times 2^{7}\Gamma(4\omega+1) - 4\Gamma(\omega+1) \\ & - (3)(2)^{-9\omega-1}\Gamma(\omega+1) - 2^{-7\omega+1}\Gamma(\omega+1) \\ & - 2^{-5\omega+1}\Gamma(\omega+1) - 2^{-6\omega}\Gamma(\omega+1) - (3)(2)^{-4\omega}\Gamma(\omega+1) \\ & - (3)(4)^{-\omega}\Gamma(\omega+1) - (8)^{-\omega}\Gamma(\omega+1) + \frac{3}{4}\Gamma(2\omega+1) \\ & +-(32)^{-4\omega}\Gamma(\omega+1) - (34)^{-\omega}\Gamma(\omega+1) - (8)^{-\omega}\Gamma(\omega+1),\end{aligned}$$
$$\begin{aligned}\hbar_{2,5} = {}& -4 - 2^{-8\omega+1} - 2^{-7\omega+1} - 2^{-5\omega+2} - 2^{-4\omega+1} - 3\times 2^{-3\omega+1} \\ & - 2^{-\omega+2} - 2^{-10\omega} + \frac{(4^{\omega}+1)\Gamma(\omega+1)}{2^{7\omega}} - \frac{7\Gamma(3\omega+1)}{3\times 2^{(4\omega+4)}} \\ & + 2\Gamma(\omega+1) - \frac{\Gamma(\omega+1)}{2^{9\omega+1}} - \frac{\Gamma(\omega+1)}{2^{6\omega-1}} - 2^{-4\omega}\Gamma(\omega+1) \\ & - 4^{-\omega}\Gamma(\omega+1) + (3)(8)^{-\omega}\Gamma(\omega+1) + \frac{5}{4}\Gamma(2\omega+1) \\ & + 5\times\frac{\Gamma(2\omega+1)}{2^{7\omega+3}} + \frac{\Gamma(2\omega+1)}{2^{4\omega}} + \frac{\Gamma(3\omega+1)}{24} \\ & + \frac{17\Gamma(4\omega+1)}{384}.\end{aligned} \tag{52}$$

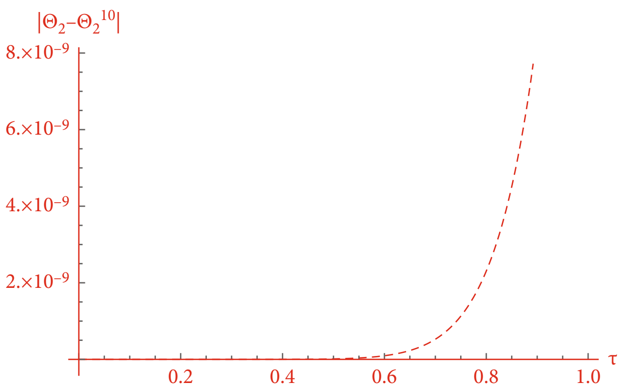

FIGURE 1

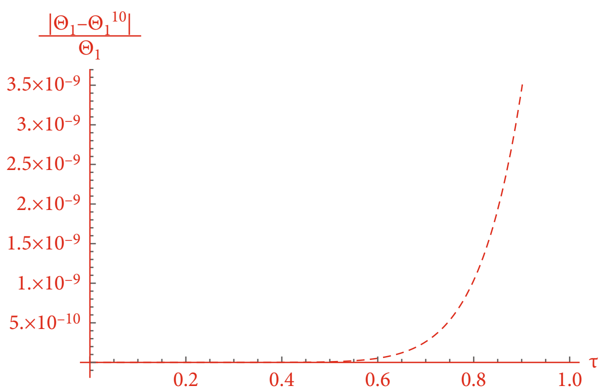

FIGURE 2

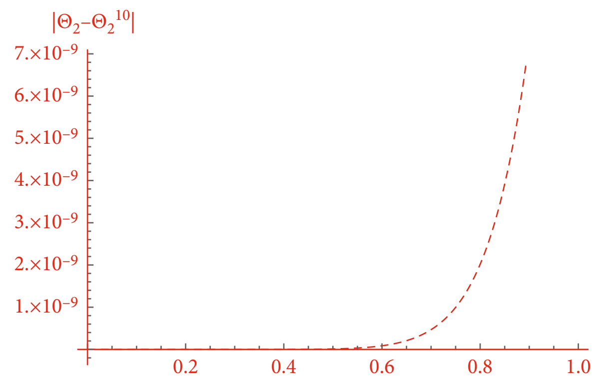

FIGURE 3

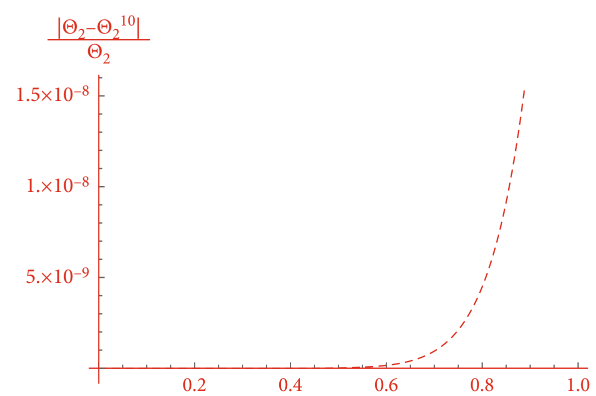

FIGURE 4

We have the following 5th-order approximate solution in the original space for Equations (40) and (41) when $\omega = 1$ uses the procedure mentioned in Subsection 2.1:

$$\Theta_{1,5}(\tau) = 1 + \tau + \frac{\tau^2}{2!} + \frac{\tau^3}{3!} + \frac{\tau^4}{4!} + \frac{\tau^5}{5!}, \tag{53}$$

$$\Theta_{2,5}(\tau) = 1 - \tau + \frac{\tau^2}{2!} - \frac{\tau^3}{3!} + \frac{\tau^4}{4!} - \frac{\tau^5}{5!}. \tag{54}$$

Equations (53) and (54) represent the first five terms of e^{τ} and $e^{-\tau}$, respectively, and therefore the exact solutions of Equations (40) and (41).

The following 2-D graphs show the absolute and relative error for Example 1.

Figures 1 and 2 demonstrate the 2-D graphs of absolute and relative errors in the intervals $\tau \in [0, 1]$ over the ten-step approximate and exact solutions of Equation (40) at $\omega = 1$, respectively. According to the figures, the approximate solution is extremely close to the precise solution. Figures 3 and 4 are graphs of absolute and relative errors in the intervals $\tau \in [0, 1]$ over the ten-step approximate and exact solutions of Equation (41) at $\omega = 1$, respectively. One can perceive the equivalent verdicts depicted for Equation (40).

Error functions are presented to observe the exactness and capability of the numerical method. To prove the exactness and capability of ERPSM, we selected three kinds of error functions, such as absolute, residual, and error functions.

Table 1 shows the absolute and relative errors at reasonable nominated grid points in the interval $\tau \in [0, 1]$ among the five-step approximate and exact solutions of Equations (40) and (41) at $\omega = 1$ attained using ERPSM. Table 1 shows that the approximate and exact solutions are quite close to each other, confirming the effectiveness of the recommended strategy.

Problem 6. Consider the following FMPS:

$$D_{\tau}^{\omega}\Theta_1(\tau) + \Theta_1(\tau) + e^{-\tau^{\omega}} \cos\left(\frac{\tau^{\omega}}{2}\right)\Theta_2\left(\frac{\tau}{2}\right) + 2e^{-(3/4)\tau^{\omega}} \cos \cdot \left(\frac{\tau^{\omega}}{2}\right) \sin\left(\frac{\tau^{\omega}}{4}\right)\Theta_1\left(\frac{\tau}{4}\right) = 0, \tag{55}$$

$$D_{\tau}^{\omega}\Theta_2(\tau) - e^{\tau^{\omega}}\Theta_1^2\left(\frac{\tau}{2}\right) + \Theta_2^2\left(\frac{\tau}{2}\right) = 0, \tag{56}$$

with the initial conditions $\Theta_1(0) = 1, \Theta_2(0) = 0$.

Table 1: The absolute and relative error of Example 1.

τ	Θ_1 Abs.error	Θ_1 Rel.error	Θ_2 Abs.error	Θ_2 Rel.error
0.2	$9.149350321813188\times10^{-8}$	$7.490854479152386\times10^{-8}$	$8.641131510334077\times10^{-8}$	$1.055430186034679\times10^{-7}$
0.4	$6.030974603721262\times10^{-6}$	$4.042683174006208\times10^{-6}$	$5.379368972713294\times10^{-6}$	$8.025075491218842\times10^{-6}$
0.6	$7.080039050877396\times10^{-5}$	$3.885607815121622\times10^{-5}$	$5.963609402637182\times10^{-5}$	$1.086640481073082\times10^{-4}$
0.8	$4.102618258010615\times10^{-4}$	$1.843425212040309\times10^{-4}$	$3.262974505549021\times10^{-4}$	$7.261883310726820\times10^{-4}$
1.0	$1.615161333333059\times10^{-3}$	$5.941846488086295\times10^{-4}$	$1.212774566900720\times10^{-3}$	$3.296663066666799\times10^{-3}$

Applying the E-T to Equations (55) and (56), we get

$$E\left[D_\tau^\omega\Theta_1(\tau)+\Theta_1(\tau)+e^{-\tau^\omega}\cos\left(\frac{\tau^\omega}{2}\right)\Theta_2\left(\frac{\tau}{2}\right)+2e^{-(3/4)\tau^\omega}\cos\cdot\left(\frac{\tau^\omega}{2}\right)\sin\left(\frac{\tau^\omega}{4}\right)\Theta_1\left(\frac{\tau}{4}\right)\right]=0, \tag{57}$$

$$E\left[D_\tau^\omega\Theta_2(\tau)-e^{\tau^\omega}\Theta_1^2\left(\frac{\tau}{2}\right)+\Theta_2^2\left(\frac{\tau}{2}\right)\right]=0. \tag{58}$$

Using the approach mentioned in Subsection 2.1, we obtain the following results from Equations (57) and (58) as

$$\begin{aligned}\wp_1(\upsilon)={}&\upsilon^2\Theta_1(0)-\upsilon^\omega\wp_1(\upsilon)\\&-\upsilon^\omega E\left[E^{-1}\left[\frac{\upsilon^2}{1+\upsilon}\right]E^{-1}\left[\frac{4\upsilon^2}{4+\upsilon^2}\right]E^{-1}\left[4\wp_2\left(\frac{\upsilon}{2}\right)\right]\right]\\&-2\upsilon^\omega E\left[E^{-1}\left[\frac{4\upsilon^2}{4+3\upsilon}\right]E^{-1}\left[\frac{4\upsilon^2}{4+\upsilon^2}\right]E^{-1}\left[\frac{4\upsilon^3}{16+\upsilon^2}\right]\cdot E^{-1}\left[16\wp_1\left(\frac{\upsilon}{4}\right)\right]\right],\end{aligned} \tag{59}$$

$$\begin{aligned}\wp_2(\upsilon)={}&\upsilon^2\Theta_2(0)+\upsilon^\omega E\left[E^{-1}\left[\frac{\upsilon^2}{1-\upsilon}\right]\left(E^{-1}\left[4\wp_1\left(\frac{\upsilon}{2}\right)\right]\right)^2\right.\\&\left.-\left(E^{-1}\left[4\wp_2\left(\frac{\upsilon}{2}\right)\right]\right)^2\right].\end{aligned} \tag{60}$$

Assume that Equations (59) and (60) have the series solution in the following form:

$$\begin{aligned}\wp_1(\upsilon)&=\sum_{\nu=0}^{\infty}\hbar_{1,\nu}\upsilon^{\nu\omega+2},\\\wp_2(\upsilon)&=\sum_{\nu=0}^{\infty}\hbar_{2,\nu}\upsilon^{\nu\omega+2}.\end{aligned} \tag{61}$$

The κth-truncated expansions are as

$$\begin{aligned}\wp_{1,\kappa}(\upsilon)&=\sum_{\nu=0}^{\kappa}\hbar_{1,\nu}\upsilon^{\nu\omega+2},\\\wp_{2,\kappa}(\upsilon)&=\sum_{\nu=0}^{\kappa}\hbar_{2,\nu}\upsilon^{\nu\omega+2}.\end{aligned} \tag{62}$$

By using the first part of Lemma 2, the κth-truncated expansions become

$$\begin{aligned}\wp_{1,\kappa}(\upsilon)&=\upsilon^2+\sum_{\nu=1}^{\kappa}\hbar_{1,\nu}\upsilon^{\nu\omega+2},\\\wp_{2,\kappa}(\upsilon)&=\upsilon^2+\sum_{\nu=1}^{\kappa}\hbar_{2,\nu}\upsilon^{\nu\omega+2}.\end{aligned} \tag{63}$$

The ERFs are formulated as

$$\begin{aligned}E\mathrm{Res}_1(\upsilon)={}&\wp_1(\upsilon)-\upsilon^2+\upsilon^\omega\wp_1(\upsilon)\\&+\upsilon^\omega E\left[E^{-1}\left[\frac{\upsilon^2}{1+\upsilon}\right]E^{-1}\left[\frac{4\upsilon^2}{4+\upsilon^2}E^{-1}\left[4\wp_2\left(\frac{\upsilon}{2}\right)\right]\right]\right.\\&+2\upsilon^\omega E\left[E^{-1}\left[\frac{4\upsilon^2}{4+3\upsilon}\right]E^{-1}\left[\frac{4\upsilon^2}{4+\upsilon^2}\right]E^{-1}\left[\frac{4\upsilon^3}{16+\upsilon^2}\right]\cdot E^{-1}\left[16\wp_1\left(\frac{\upsilon}{4}\right)\right]\right],\\E\mathrm{Res}_2(\upsilon)={}&\wp_2(\upsilon)-\upsilon^\omega E\left[E^{-1}\left[\frac{\upsilon^2}{1-\upsilon}\right]\left(E^{-1}\left[4\wp_1\left(\frac{\upsilon}{2}\right)\right]\right)^2\right.\\&\left.+\left(E^{-1}\left[4\wp_2\left(\frac{\upsilon}{2}\right)\right]\right)^2\right].\end{aligned} \tag{64}$$

The κth-truncated ERF takes the following form:

$$\begin{aligned}E\mathrm{Res}_{1,\kappa}(\upsilon)={}&\wp_{1,\kappa}(\upsilon)-\upsilon^2+\upsilon^\omega\wp_{1,\kappa}(\upsilon)\\&+\upsilon^\omega E\left[E^{-1}\left[\frac{\upsilon^2}{1+\upsilon}\right]E^{-1}\left[\frac{4\upsilon^2}{4+\upsilon^2}\right]E^{-1}\left[4\wp_{2,\kappa}\left(\frac{\upsilon}{2}\right)\right]\right]\\&+2\upsilon^\omega E\left[E^{-1}\left[\frac{4\upsilon^2}{4+3\upsilon}\right]E^{-1}\left[\frac{4\upsilon^2}{4+\upsilon^2}\right]E^{-1}\left[\frac{4\upsilon^3}{16+\upsilon^2}\right]\cdot E^{-1}\left[16\wp_{1,\kappa}\left(\frac{\upsilon}{4}\right)\right]\right],\end{aligned} \tag{65}$$

$$E\mathrm{Res}_{2,\kappa}(\upsilon) = \wp_2, \kappa(\upsilon) - \upsilon^{\omega} E\left[\mathrm{E}^{-1}\left[\frac{\upsilon^2}{1-\upsilon}\right]\left(E^{-1}\left[4\wp_{1,\kappa}\left(\frac{\upsilon}{2}\right)\right]\right)^2\right] + \left(E^{-1}\left[4\wp_{2,\kappa}\left(\frac{\upsilon}{2}\right)\right]\right)^2. \quad (66)$$

Substitute $\kappa = 1, 2, 3, 4, 5$ into Equations (65) and (66) and solve the following expression to find the unknown coefficients.

$$\lim_{\upsilon \longrightarrow 0}\left(\frac{1}{\upsilon^{k\omega+2}} E \,\mathrm{Re}\, s_{1,\kappa}(\upsilon)\right) = 0, \quad \lim_{\upsilon \longrightarrow 0}\left(\frac{1}{\upsilon^{k\omega+2}} E \,\mathrm{Re}\, s_{2,\kappa}(\upsilon)\right) = 0. \quad (67)$$

Thus, we have

$$\hbar_{1,1} = -1,$$

$$\hbar_{2,1} = 1,$$

$$\hbar_{1,2} = 1 - \frac{1}{(2)^{\omega}} - \frac{\Gamma(\omega+1)}{2},$$

$$\hbar_{2,2} = -\frac{1}{(2)^{\omega-1}} + \Gamma(\omega+1),$$

$$\hbar_{1,3} = \frac{3}{8}\Gamma(2\omega+1) + \frac{2^{-1}\left(2^{\omega+1}+1\right)\Gamma((1/2)+\omega)}{\sqrt{\pi}} + \Gamma(\omega+1)\left(\frac{1}{2} - \frac{1}{2^{2\omega}}\right) - 1 + 2^{1-3\omega} + 2^{-\omega},$$

$$\hbar_{2,3} = \frac{1}{8^{\omega}}\left(-2 + 2^{\omega+1} - \frac{2^{4\omega+1}\Gamma((1/2)+\omega)}{\sqrt{\pi}} - 2^{\omega}\Gamma(\omega+1)\right) + \frac{1}{2}\Gamma(2\omega+1),$$

$$\begin{aligned}\hbar_{1,4} = {} & 1 + 2^{-6\omega+1} - 2^{-5\omega+1} - 2^{-3\omega+1} - 2^{-\omega} - \frac{1}{2}\Gamma(\omega+1) - \frac{1}{2\times 8^{\omega}}\Gamma(2\omega+1) \\ & - \frac{2^{-2\omega-1}\left(4^{\omega} + 2^{3\omega+1} - 4\right)\Gamma((1/2)+\omega)}{\sqrt{\pi}} - \frac{3}{8}\Gamma(2\omega+1) - \frac{7}{96}\Gamma(3\omega+1) + \frac{\sqrt{\pi}\Gamma(3\omega+1)}{4^{3\omega+1}\Gamma(1/2+\omega)} \\ & - \frac{3\Gamma(3\omega+1)(2^{\omega}+1)}{2^{2\omega+3}\Gamma(\omega+1)} - \frac{\Gamma(3\omega+1)\left(4^{\omega+1}+2^{\omega}-1\right)}{2^{5\omega+1}\Gamma(2\omega+1)} + \frac{\Gamma(\omega+1)((8^{\omega}+1)\Gamma(2\omega+1) + 8^{\omega}\Gamma(3\omega+1))}{2^{5\omega}\Gamma(2\omega+1)},\end{aligned}$$

$$\begin{aligned}\hbar_{2,4} = {} & -\frac{\Gamma(3\omega+1)(2^{\omega}-3)}{2^{4\omega-1}\Gamma(2\omega+1)\Gamma(\omega+1)} - \frac{\Gamma(3\omega+1)\left(-2^{\omega+1}+3+2^{\omega}\Gamma(\omega+1)\right)}{8^{\omega}\Gamma(2\omega+1)} \\ & + \frac{\Gamma(3\omega+1)}{4^{\omega}\Gamma(\omega+1)\Gamma(\omega+1)} + \frac{\Gamma(3\omega+1)}{6} + \frac{3\Gamma(2\omega+1)}{2^{3\omega+2}} + \frac{\Gamma(\omega+1)}{8^{\omega}} - \frac{\Gamma(3\omega+1)}{2^{\omega}\Gamma(\omega+1)} + \frac{\left(2^{\omega+1}+1\right)\Gamma((1/2)+\omega)}{8^{\omega}\sqrt{\pi}} \\ & - \frac{\Gamma(\omega+1)}{2^{5\omega-1}} + \frac{\left(2+4^{\omega}-8^{\omega}\right)}{2^{6\omega-1}}.\end{aligned} \quad (68)$$

We have the following 5th-order approximate solution in the original space for Equations (55) and (56) when $\omega = 1$ using the procedure mentioned in Subsection 2.1:

$$\Theta_{1,5}(\tau) = 1 - \tau + \frac{\tau^3}{3} - \frac{\tau^4}{6} + \frac{\tau^5}{30}, \quad (69)$$

$$\Theta_{2,5}(\tau) = \tau - \frac{\tau^3}{6} + \frac{\tau^5}{120}. \quad (70)$$

Equations (69) and (70) represent the first five terms of $e^{-\tau}\cos\tau$ and $\sin\tau$, respectively, and therefore the exact solutions of Equations (55) and (56).

In the next section, we will use our new ERPSM to find approximate and exact solutions to linear PDE.

3. The ERPSM to Demonstrate the Linear PDE

In this section, we use our new ERPSM to construct the solutions of the linear PDE as in Equation (7). In the next subsection, we derive the main algorithms of the ERPSM for the linear PDE.

3.1. The Algorithm of ERPSM for Solving Linear PDE. In this subsection, we exploit ERPSM to create the solution to the linear PDE. We start by taking E-T on Equation (7). We get the following:

$$E[D_{\tau}^{\omega}\Theta(\tau)] = lE[\Theta(\tau)] + \sum_{j=1}^{s} m_j E\left[\Theta\left(u_j\tau\right)\right] + \sum_{j=1}^{t} p_j E\left[D_{\tau}^{\omega}\Theta\left(q_j\tau\right)\right] + E[g(\tau)]. \quad (71)$$

By using the second part of Lemma 2, Equation (71) becomes

$$\wp(\upsilon) = \upsilon^2\phi + \upsilon^{\omega} l\wp(\upsilon) + \upsilon^{\omega}\sum_{j=1}^{s} m_i \frac{\wp\left(u_j\upsilon\right)}{{u_i}^2} + \sum_{j=1}^{t} p_j\left(\frac{\wp\left(q_j\upsilon\right)}{{q_j}^2} - \upsilon^2\phi\right) + \upsilon^{\omega} G(\upsilon). \quad (72)$$

Assuming that algebraic equation (72) has the solution in the expansion form as

$$\wp(\upsilon) = \sum_{\nu=0}^{\infty} \hbar_\nu \upsilon^{\nu\omega+2}. \tag{73}$$

The κth-truncated series of $\wp(\upsilon)$ is as follows:

$$\wp_\kappa(\upsilon) = \sum_{\nu=0}^{\kappa} \hbar_\nu \upsilon^{\nu\omega+2}. \tag{74}$$

By using the first part of Lemma 2, we have the following:

$$\hbar_0 = \phi. \tag{75}$$

The κth-truncated series becomes

$$\wp_k(\upsilon) = \phi\upsilon^2 + \sum_{\nu=1}^{k} \hbar_\nu \upsilon^{\nu\omega+2}. \tag{76}$$

Now, define the ERF in the following form:

$$\begin{aligned} E\mathrm{Res}(\upsilon) &= \wp(\upsilon) - \upsilon^2\phi - \upsilon^\omega l\wp(\upsilon) - \upsilon^\omega \sum_{j=1}^{s} m_j \frac{\wp(u_j\upsilon)}{u_j^{\,2}} \\ &\quad - \sum_{j=1}^{t} p_j \left(\frac{\wp\left(q_j\upsilon\right)}{q_j^{\,2}} - \upsilon^2\phi \right) - \upsilon^{\varpi} G(\upsilon). \end{aligned} \tag{77}$$

The κth-ERF is as follows:

$$\begin{aligned} E\mathrm{Res}_k(\upsilon) &= \wp_k(\upsilon) - \upsilon^2\phi - \upsilon^\varpi l\wp_k(\upsilon) - \upsilon^\varpi \sum_{j=1}^{s} m_i \frac{\wp_k(u_j\upsilon)}{u_j^{\,2}} \\ &\quad - \sum_{j=1}^{t} p_j \left(\frac{\wp_k\left(q_j\upsilon\right)}{q_j^{\,2}} - \upsilon^2\phi \right) - \upsilon^{\varpi} G(\upsilon). \end{aligned} \tag{78}$$

To highlight basic points, we generalize certain features that arise in the RPSM [67–69].

It is understandable that

$$E\mathrm{Res}(\upsilon) = 0. \tag{79}$$

Therefore,

$$\lim_{\kappa \longrightarrow \infty} E\mathrm{Res}_k(\upsilon) = E\ \mathrm{Re}\ s(\upsilon). \tag{80}$$

Since, $\lim_{\upsilon \longrightarrow 0} (1/\upsilon^2) E\mathrm{Res}(\upsilon) = 0$. It is obvious that $\lim_{\upsilon \longrightarrow 0} (1/\upsilon^2) E\mathrm{Res}_k(\upsilon) = 0$. As a result, we get the following:

$$\begin{aligned} &\lim_{\upsilon \longrightarrow 0} \left(\frac{1}{\upsilon^{k\omega+2}} E\ \mathrm{Re}\ s(\upsilon) \right) \\ &\quad = \lim_{\upsilon \longrightarrow 0} \left(\frac{1}{\upsilon^{k\omega+2}} E\ \mathrm{Re}\ s_k(\upsilon) \right) = 0, \quad k = 1, 2, 3, \cdots. \end{aligned} \tag{81}$$

To determine the first undefined coefficient $\hbar_1$, substitute $k = 1$, in Equations (76) and (78). As a result, we obtain as following:

$$\begin{aligned} E\mathrm{Res}_1(\upsilon) &= \wp_1(\upsilon) - \upsilon^2\phi - \upsilon^\omega l\wp_1(\upsilon) - \upsilon^\omega \sum_{j=1}^{s} m_j \frac{\wp_1\left(u_j\upsilon\right)}{u_j^{\,2}} \\ &\quad - \sum_{j=1}^{s} p_j \left(\frac{\wp_1\left(q_j\upsilon\right)}{q_j^{\,2}} - \upsilon^2\phi \right) - \upsilon^{\omega} G(\upsilon), \end{aligned} \tag{82}$$

$$\wp_1(\upsilon) = \phi\upsilon^2 + \hbar_1 \upsilon^{2+\omega}, \tag{83}$$

$$\wp_1\left(u_j\upsilon\right) = \phi u_j^2 \upsilon^2 + \hbar_1 u_j^{\,\omega+2} \upsilon^{\omega+2}, \tag{84}$$

$$\wp_1\left(q_j\upsilon\right) = \phi q_j^2 \upsilon^2 + \hbar_1 q_j^{\,\omega+2} \upsilon^{\omega+2}. \tag{85}$$

Using Equations (83), (84), and (85) in (82), we get the following:

$$\begin{aligned} E\ \mathrm{Re}\ s_1(\upsilon) &= \left(\phi\upsilon^2 + \hbar_1\upsilon^{\omega+2}\right) - \upsilon^2\phi - \upsilon^\omega l\left(\phi\upsilon^2 + \hbar_1\upsilon^{\omega+2}\right) \\ &\quad - \upsilon^\omega \sum_{j=1}^{s} m_i \frac{\phi u_j^2\upsilon^2 + \hbar_1 u_j^{\,\omega+2}\upsilon^{\omega+2}}{u_j^{\,2}} \\ &\quad - \sum_{j=1}^{t} p_j \left(\frac{\phi q_j^2\upsilon^2 + \hbar_1 q_j^{\,\omega+2}\upsilon^{\omega+2}}{q_j^{\,2}} - \upsilon^2\phi \right) \\ &\quad - \upsilon^\omega G(\upsilon), \end{aligned} \tag{86}$$

$$\begin{aligned} E\mathrm{Res}_1(\upsilon) &= \hbar_1\upsilon^{\omega+2} - \upsilon^\omega l\left(\phi\upsilon^2 + \hbar_1\upsilon^{\omega+2}\right) \\ &\quad - \upsilon^\omega \sum_{j=1}^{s} m_j\left(\phi\upsilon^2 + \hbar_1 u_j^{\,\omega}\upsilon^{\omega+2}\right) \\ &\quad - \sum_{j=1}^{t} p_j\left(\hbar_1 q_j^{\,\omega}\upsilon^{\omega+2}\right) - \upsilon^\omega G(\upsilon). \end{aligned} \tag{87}$$

Dividing $\upsilon^{2+\omega}$ by Equation (87), we get

$$\begin{aligned} \frac{1}{\upsilon^{2+\omega}} E\mathrm{Res}_1(\upsilon) &= \hbar_1 \frac{1}{\upsilon^{2+\omega}} \upsilon^{\omega+2} - \frac{1}{\upsilon^{2+\omega}} \upsilon^\omega l\left(\phi\upsilon^2 + \hbar_1\upsilon^{\omega+2}\right) \\ &\quad - \frac{1}{\upsilon^{2+\omega}} \upsilon^\omega \sum_{j=1}^{s} m_j\left(\phi\upsilon^2 + \hbar_1 u_j^{\,\omega}\upsilon^{\omega+2}\right) \\ &\quad - \frac{1}{\upsilon^{2+\omega}} \sum_{j=1}^{t} p_j\left(\hbar_1 q_j^{\,\omega}\upsilon^{\omega+2}\right) - \frac{1}{\upsilon^{2+\omega}} \upsilon^\omega G(\upsilon). \end{aligned} \tag{88}$$

By using $\lim_{\upsilon \longrightarrow 0}$ to the Equation (88), we get

$$\lim_{\upsilon \longrightarrow 0} \frac{1}{\upsilon^{2+\omega}} E\text{Res}_1(\upsilon) = \hbar_1 - l\left(\phi + \hbar_1 \lim_{\upsilon \longrightarrow 0} \upsilon^2\right) - \sum_{j=1}^{s} m_j \left(\phi + \hbar_1 u_j^{\ \omega} \lim_{\upsilon \longrightarrow 0} \upsilon^2\right) - \sum_{j=1}^{t} p_j \left(\hbar_1 q_j^{\ \omega}\right) - \lim_{\upsilon \longrightarrow 0} \frac{1}{\upsilon^2} G(\upsilon). \tag{89}$$

When we put $\lim_{\upsilon \longrightarrow 0}((1/\upsilon^{2+\omega})E\text{Res}_1(\upsilon)) = 0$ into Equation (89), we get

$$\hbar_1 = \frac{l\phi + \sum_{j=1}^{s} m_j \phi + g(0)}{1 - \sum_{j=1}^{t} p_j q_j^{\ \omega}}. \tag{90}$$

In the same manner, to determine the second undefined coefficient, put $k = 2$ in Equations (76) and (78); we get the following:

$$\wp_k(\upsilon) = \phi \upsilon^2 + \hbar_1 \upsilon^{\omega+2} + \hbar_2 \upsilon^{2\omega+2}, \tag{91}$$

$$\wp_k\left(u_j \upsilon\right) = \phi u_j^2 \upsilon^2 + \hbar_1 u_j^{\omega+2} \upsilon^{\omega+2} + \hbar_2 u_j^{2\omega+2} \upsilon^{2\omega+2}, \tag{92}$$

$$\wp_k\left(q_j \upsilon\right) = \phi q_j^2 \upsilon^2 + \hbar_1 q_j^{\omega+2} \upsilon^{\omega+2} + \hbar_2 q_j^{2\omega+2} \upsilon^{2\omega+2}, \tag{93}$$

$$E\text{Res}_2(\upsilon) = \wp_2(\upsilon) - \upsilon^2 \phi - \upsilon^{\varpi} l \wp_2(\upsilon) - \upsilon^{\varpi} \sum_{j=1}^{s} m_i \frac{\wp_2\left(u_j \upsilon\right)}{u_j^{\ 2}} - \sum_{j=1}^{t} p_j \left(\frac{\wp_2\left(q_j \upsilon\right)}{q_j^{\ 2}} - \upsilon^2 \phi\right) - \upsilon^{\varpi} G(\upsilon). \tag{94}$$

Using Equations (91), (92), and (93) in (94), we get the following:

$$E\text{Res}_2(\upsilon) = \hbar_1 \upsilon^{\omega+2} + \hbar_2 \upsilon^{2\omega+2} - \left(l\phi \upsilon^{2+\omega} + l\hbar_1 \upsilon^{2\omega+2} + l\hbar_2 \upsilon^{3\omega+2}\right) - \upsilon^{\omega} \sum_{j=1}^{s} m_j \frac{\phi u_j^{\ 2} \upsilon^2 + \hbar_1 u_j^{\varpi+2} \upsilon^{\varpi+2} + \hbar_2 u_j^{\ 2\omega+2} \upsilon^{2\omega+2}}{\rho_i^{\ 2}} - \sum_{j=1}^{t} p_j \left(\frac{\hbar_1 q_j^{\ \omega+2} \upsilon^{\omega+2} + \hbar_2 q_j^{\ 2\omega+2} \upsilon^{2\omega+2}}{q_j^{\ 2}}\right) - \upsilon^{\omega} G(\upsilon). \tag{95}$$

Dividing $\upsilon^{2+2\omega}$ on Eq. (95), we have the following results:

$$\frac{1}{\upsilon^{2\omega+2}} E\text{Res}_2(\upsilon) = \hbar_2 - l\hbar_1 - l\hbar_2 \upsilon^{\omega} + \sum_{j=1}^{s} m_j \omega_1 u_j^{\ \omega} + \sum_{j=1}^{s} m_j \hbar_2 u_j^{\ 2\omega} \upsilon^{\omega} + \sum_{j=1}^{t} p_j \hbar_2 q_j^{\ 2\omega} - \frac{1}{\upsilon^2}\left(\frac{1}{\upsilon^{\omega}} G(\upsilon) - g(0)\right). \tag{96}$$

Apply $\lim_{\upsilon \longrightarrow 0}$ to Equation (96), we get

$$\lim_{\upsilon \longrightarrow 0} \frac{1}{\upsilon^{2\omega+2}} E\text{Res}_2(\upsilon) = \hbar_2 - l\hbar_1 - l\hbar_2 \upsilon^{\omega} + \sum_{j=1}^{s} m_j \hbar_1 u_j^{\ \omega} + \sum_{j=1}^{s} m_j \phi \hbar_2 u_j^{\ 2\omega} \lim_{\upsilon \longrightarrow 0} \upsilon^{\omega} + \sum_{j=1}^{t} p_j \hbar_2 q_j^{\ 2\omega} - \lim_{\upsilon \longrightarrow 0} \frac{1}{\upsilon^2} E[D_{\tau}^{\omega} g(\tau)]. \tag{97}$$

By using the second part of Lemma 2, we have

$$\frac{1}{\upsilon^{\omega}} G(\upsilon) - g(0) = E[D_{\tau}^{\omega} g(\tau)]. \tag{98}$$

Put $\lim_{\upsilon \longrightarrow 0} (1/\upsilon^{2\omega+2})E\text{Res}_2(\upsilon) = 0$ in Equation (97), and we have the second coefficient in the following form:

$$\hbar_2 = \frac{l\hbar_1 + \sum_{j=1}^{s} m_j \hbar_1 u_j^{\ \omega} + (D_{\tau}^{\omega} g(\tau))(0)}{1 - \sum_{j=1}^{t} p_j q_j^{\ 2\omega}}. \tag{99}$$

Now, to define the third coefficient, put $k = 3$ in Equations (76) and (78), and repeat the same steps. We get the following:

$$E\text{Res}_3(\upsilon) = \hbar_1 \upsilon^{\omega+2}\left(1 - \sum_{j=1}^{t} p_j q_j^{\ \omega}\right) + \hbar_2 \upsilon^{2\omega+2}\left(1 - \sum_{j=1}^{t} r_j q_j^{\ 2\omega}\right) + \hbar_3 \upsilon^{3\omega+2} - l\phi \upsilon^{2+\omega} - l\hbar_1 \upsilon^{2\omega+2} - l\hbar_2 \upsilon^{3\omega+2} - l\hbar_3 \upsilon^{4\omega+2} - \phi \upsilon^{\omega+2} \sum_{j=1}^{s} m_j - \hbar_1 \upsilon^{2\omega+2} \sum_{j=1}^{s} m_j u_j^{\ \omega} - \hbar_2 \upsilon^{3\omega+2} \sum_{j=1}^{s} m_j u_j^{\ 2\omega} - \hbar_3 \upsilon^{4\omega+2} \sum_{j=1}^{s} m_j u_j^{\ 3\omega} - \hbar_3 \upsilon^{3\omega+2} \sum_{j=1}^{t} p_j q_j^{\ 3\omega} - \upsilon^{\omega} G(\upsilon). \tag{100}$$

Divide $\upsilon^{2+3\omega}$ by Equation (100).

$$\frac{1}{\upsilon^{3\omega+2}} \mathrm{ERes}_3(\upsilon) = \hbar_3 - l\hbar_2 - l\hbar_3 \upsilon^{\omega} - \hbar_2 \sum_{j=1}^{s} m_j u_j^{2\omega} - \hbar_3 \upsilon^{\omega} \sum_{j=1}^{s} m_j u_j^{3\omega} - \hbar_3 \sum_{j=1}^{t} p_j q_j^{3\omega} - \frac{1}{\upsilon^2} \cdot \left(\frac{1}{\upsilon^{2\omega}} G(\upsilon) - \frac{1}{\upsilon^{2\omega-2}} g(0) - \frac{1}{\upsilon^{\omega-2}} (D_\tau^{\omega} g(\tau))(0) \right), \tag{101}$$

By using $\lim_{\upsilon \longrightarrow 0}$ to Equation (101), we get the third part of Lemma 2 in the following form:

$$(D_\tau^{2\omega} g(\tau))(0) = \lim_{\upsilon \longrightarrow 0} \frac{1}{\upsilon^2} \left(\frac{1}{\upsilon^{2\omega}} G(\upsilon) - \frac{1}{\upsilon^{2\omega-2}} g(0) - \frac{1}{\upsilon^{\omega-2}} (D_\tau^{\omega} g(\tau))(0) \right). \tag{102}$$

Put $\lim_{\upsilon \longrightarrow 0} (1/\upsilon^{3\omega+2}) ERes_3(\upsilon) = 0$, in Equation (101); as a result, we get

$$\hbar_3 = \frac{l\hbar_{(\nu-1)} + \sum_{j=1}^{s} \hbar_{(\nu-1)} m_j u_j^{(\nu-1)\omega} + \left(D_\tau^{(\nu-1)\omega} g(\tau) \right)(0)}{\left(1 - \sum_{j=1}^{t} p_j q_j^{\nu\omega} \right)}. \tag{103}$$

As a consequence of the generalization, we acquire the following:

$$\hbar_\nu = \begin{cases} \hbar_0, & \nu = 0, \\ \dfrac{l\hbar_{(\nu-1)} + \sum_{i=1}^{l} \hbar_{(\nu-1)} m_j u_j^{(\nu-1)\omega} + \left(D_\Upsilon^{(\nu-1)\omega} g(\tau) \right)(0)}{\left(1 - \sum_{j=1}^{t} p_j q_j^{\nu\omega} \right)}, & \nu = 1, 2, 3, \cdots. \end{cases} \tag{104}$$

The κth-approximate solution of Equation (72) is as follows:

$$\wp_k(\upsilon) = \hbar_0 \upsilon^2 + \left(\frac{l\phi + \sum_{j=1}^{s} \beta m_j \phi + g(0)}{1 - \sum_{j=1}^{t} p_j q_j^{\omega}} \right) \upsilon^{2+\omega} + \left(\frac{l\hbar_1 + \sum_{j=1}^{s} m_j \hbar_1 u_j^{\omega} + (D_\tau^{\omega} g(\tau))(0)}{1 - \sum_{j=1}^{t} p_j q_j^{2\omega}} \right) \upsilon^{2+2\omega} + \left(\frac{l\hbar_2 + \sum_{j=1}^{s} \hbar_2 m_j u_j^{2\omega} + \left(D_\tau^{2\omega} g(\tau) \right)(0)}{\left(1 - \sum_{j=1}^{t} p_j q_j^{3\omega} \right)} \right) \upsilon^{2+3\omega} + \cdots + \frac{l\hbar_{(\kappa-1)} + \sum_{i=1}^{l} \hbar_{(\kappa-1)} m_j u_j^{(\kappa-1)\omega} + \left(D_\tau^{(\kappa-1)\omega} g(\tau) \right)(0)}{\left(1 - \sum_{j=1}^{t} p_j q_j^{\kappa\omega} \right)} \upsilon^{2+\kappa\omega}. \tag{105}$$

By taking inverse E-T on Equation (105), we get the κth-step approximate solution in the original space of Equation (7).

$$\Theta_\kappa(\tau) = \hbar_0 + \left(\frac{l\phi + \sum_{j=1}^{s} m_j \phi + g(0)}{1 - \sum_{j=1}^{t} p_j q_j^{\omega}} \right) \frac{\tau^{\omega}}{\Gamma(\omega+1)} + \left(\frac{l\hbar_1 + \sum_{j=1}^{s} m_j \hbar_1 u_j^{\omega} + (D_\tau^{\omega} g(\tau))(0)}{1 - \sum_{j=1}^{t} p_j q_j^{2\omega}} \right) \frac{\tau^{2\omega}}{\Gamma(2\omega+1)} + \left(\frac{\alpha\hbar_2 + \sum_{j=1}^{s} \hbar_2 m_j u_j^{2\omega} + \left(D_\tau^{2\omega} g(\tau) \right)(0)}{\left(1 - \sum_{j=1}^{t} p_j q_j^{3\omega} \right)} \right) \frac{\tau^{3\omega}}{\Gamma(3\omega+1)} + \cdots + \frac{l\hbar_{(\kappa-1)} + \sum_{i=1}^{l} \hbar_{(\kappa-1)} m_j u_j^{(\kappa-1)\omega} + \left(D_\tau^{(\kappa-1)\omega} g(\tau) \right)(0)}{\left(1 - \sum_{j=1}^{t} p_j q_j^{\kappa\omega} \right)} \frac{\tau^{\kappa\omega}}{\Gamma(\kappa\omega+1)}. \tag{106}$$

In the next subsection, one PDE problem is established to illustrate the performance and appropriateness of the suggested method.

3.2. Numerical Example. In this subsection, we provided a problem to validate the performance and effectiveness of ERPSM for linear PDE.

Example 1. Consider the following linear PDE:

$$D_\tau^{\omega} \Theta(\tau) = -\Theta(\tau) + \frac{1}{10} \Theta\left(\frac{4}{5} \tau \right) + \frac{1}{2} \left(\frac{5}{4} \right)^{\omega} D_\tau^{\omega} \Theta\left(\frac{4\tau}{5} \right) + \left(\frac{8\tau^{\omega}}{25} - \frac{1}{2} \right) e^{(-(4\tau^{\omega}/5))} + e^{-\tau^{\omega}}, \quad 0 < \omega \le 1, \tag{107}$$

subject to the initial condition

$$\Theta(0) = 0. \tag{108}$$

By comparing Equation (107) with (7), we get

$$\begin{gathered} \hbar_0 = 0, \\ l = -1, \\ g(\tau) = \left(\frac{8\tau^{\omega}}{25} - \frac{1}{2} \right) e^{(-(4\tau^{\omega}/5))} + e^{-\tau^{\omega}}, \\ t = s = 1, \\ m_1 = 0.1, \\ u_1 = q_1 = 0.8, \\ p_1 = \frac{1}{2} \left(\frac{5}{4} \right)^{\omega}. \end{gathered} \tag{109}$$

The recurrence relation that defines the values of the series coefficients as a result of Equation (104) is

$$\hbar_\nu = \begin{cases} 0, & \nu = 0, \\ \dfrac{\left((1/10)(4/5)^{(\nu-1)\omega} - 1 \right) \hbar_{(\nu-1)} + \left(D_\tau^{(\nu-1)\omega} g \right)(0)}{1 - (1/2)(5/4)^{\omega} (4/5)^{\nu\omega}}, & \nu = 1, 2, 3, \cdots. \end{cases} \tag{110}$$

First of all, we will compute a few of the terms of $(D_{\tau}^{(\nu-1)\omega} g)(0)$.

Expand the following form in a few terms to accomplish this:

$$g(\tau) = \left(\frac{8\tau^{\omega}}{25} - \frac{1}{2}\right) e^{(-(4\tau^{\omega}/5))} + e^{-\tau^{\omega}},$$

$$g(\tau) = \frac{1}{2} - \frac{7\tau^{\omega}}{25} + \frac{21\tau^{2\omega}}{250} - \frac{27\tau^{3\omega}}{1250} + \frac{437\tau^{4\omega}}{75000} - \frac{113\tau^{5\omega}}{75000},$$

$$D_{\tau}^{\omega}[g(\tau)] = -\frac{7\Gamma(\omega+1)}{25} + \frac{21\tau^{\omega}\Gamma(2\omega+1)}{250\Gamma(\omega+1)} - \frac{27\tau^{2\omega}\Gamma(3\omega+1)}{1250\Gamma(2\omega+1)} + \frac{437\tau^{3\omega}\Gamma(4\omega+1)}{75000\Gamma(3\omega+1)} - \frac{113\tau^{4\omega}\Gamma(5\omega+1)}{75000\Gamma(4\omega+1)},$$

$$D_{\tau}^{2\omega}[g(\tau)] = \frac{21\Gamma(2\omega+1)}{250} - \frac{27\tau^{\omega}\Gamma(3\omega+1)}{1250\Gamma(\omega+1)} + \frac{437\tau^{2\omega}\Gamma(4\omega+1)}{75000\Gamma(2\omega+1)} - \frac{113\tau^{3\omega}\Gamma(5\omega+1)}{75000\Gamma(3\omega+1)},$$

$$D_{\tau}^{3\omega}[g(\tau)] = -\frac{27\Gamma(3\omega+1)}{1250} + \frac{437\tau^{\omega}\Gamma(4\omega+1)}{75000\Gamma(\omega+1)} - \frac{113\tau^{2\omega}\Gamma(5\omega+1)}{75000\Gamma(2\omega+1)},$$

$$D_{\tau}^{4\omega}[g(\tau)] = \frac{437\Gamma(4\omega+1)}{75000} - \frac{113\tau^{\omega}\Gamma(5\omega+1)}{75000\Gamma(\omega+1)},$$

$$D_{\tau}^{5\omega}[g(\tau)] = -\frac{113\Gamma(5\omega+1)}{75000}. \tag{111}$$

Returning to Equation (110), we can easily find the values of $\hbar_{\nu}$, for $\nu = 1, 2, 3, 4, 5$, respectively, as

$$\hbar_0 = 0,$$

$$\hbar_1 = 1,$$

$$\hbar_2 = \frac{2(5)^{\omega}(25 + 7\Gamma(\omega+1)) - 5(4)^{\omega}}{25(4^{\omega} - 2(5)^{\omega})},$$

$$\hbar_3 = \frac{(16 - 2(5)^{1+2\omega})(2(5)^{\omega}(5(4)^{\omega} - 2(5)^{\omega}(25 + 7\Gamma(\omega+1)))}{125(4^{\omega} - 2(5)^{\omega})(16^{\omega} - 2(25)^{\omega})} + \frac{21\Gamma(2\omega+1)}{250 - 5^{3-2\omega}16^{\omega}},$$

$$\hbar_4 = \frac{27\Gamma(3\omega+1)}{625(64)^{\omega}(125)^{-\omega} - 1250} - \frac{(64^{\omega} - 10(125)^{\omega})}{5(64)^{\omega} - 10(125)^{\omega}} \times \left(\frac{((64)^{\varpi} - 10(100)^{\varpi})(-5(4)^{\varpi}(5)^{-\varpi} + 50 + 14\Gamma(\varpi+1))}{125(2 - 4^{\varpi}(5)^{-\varpi})(64^{\varpi} - 2(100)^{\varpi}} + \frac{21\Gamma(2\varpi+1)}{250 - 5^{3-2\varpi}16^{\varpi}}\right),$$

$$\hbar_5 = \frac{-437\Gamma(4\omega+1)}{37500(256)^{\omega}(625)^{-\omega} - 75000} - \left(\frac{(256)^{\omega} - 10(625)^{\omega}}{5(256)^{\omega} - 10(625)^{\omega}}\right) \times \left(\frac{27\Gamma(3\omega+1)}{625(64)^{\omega}(125)^{-\omega} - 1250} - \frac{(64^{\omega} - 10(125)^{\omega})}{5(64)^{\omega} - 10(125)^{\omega}} \times \left(\frac{((64)^{\omega} - 10(100)^{\omega})(-5(4)^{\omega}(5)^{-\omega} + 50 + 14\Gamma(\omega+1))}{125(2 - 4^{\omega}(5)^{-\omega})(64^{\omega} - 2(100)^{\omega}} + \frac{21\Gamma(2\omega+1)}{250 - 5^{3-2\omega}16^{\omega}}\right)\right). \tag{112}$$

For $\omega = 1$, we have the following:

$$\begin{aligned} \hbar_0 &= 0, \\ \hbar_1 &= 1, \\ \hbar_2 &= -2, \\ \hbar_3 &= 3, \\ \hbar_4 &= -4, \\ \hbar_5 &= 5. \end{aligned} \tag{113}$$

The 5th-term approximate solution is as follows:

$$\wp_5(\upsilon) = \upsilon^{2+1} - 2\upsilon^{2+2} + 3\upsilon^{2+3} - 4\upsilon^{2+4} + 5\upsilon^{2+5}. \tag{114}$$

By taking inverse E-T on both sides of Equation (114),

$$\Theta_5(\tau) = \tau - \tau^2 + \frac{\tau^3}{2} - \frac{\tau^4}{6} + \frac{\tau^5}{24}. \tag{115}$$

Equation (115) represents first five terms of $\tau e^{-\tau}$; therefore, the exact solution of Equation (107) is $\tau e^{-\tau}$ at $\omega = 1$.

The following 2-D graphs show the absolute and relative errors for Example 1.

Figures 5 and 6 demonstrate the 2-D graphs of absolute and relative errors in the intervals $\tau \in [0, 1]$ over the ten-step approximate and exact solutions of Equation (107) at $\omega = 1$, respectively. According to the figures, the approximate solution is extremely close to the exact solution.

Table 2 shows the absolute and relative errors at reasonable nominated grid points in the interval $\tau \in [0, 1]$ among the five-step approximate and exact solutions of Equation (107) at $\omega = 1$ attained using ERPSM. From Table 2, it can be perceived that the approximate solution is in eminent contract with the exact solution, and this sanctions the efficiency of the recommended method. The convergence of the approximate solution to the exact solution for Equation (107) has been shown numerically as in Table 3. From the obtained results, it is evident that the present technique is an effective and convenient algorithm to solve certain classes of fractional-order DEs with fewer calculations and iteration steps.

In the next section, we will use our new ERPSM to find approximate and exact solutions to nonlinear PDE.

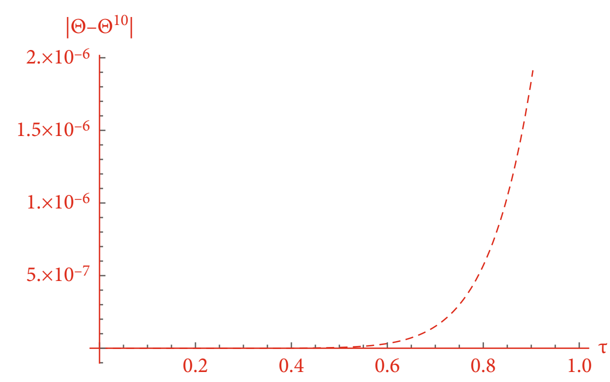

FIGURE 5

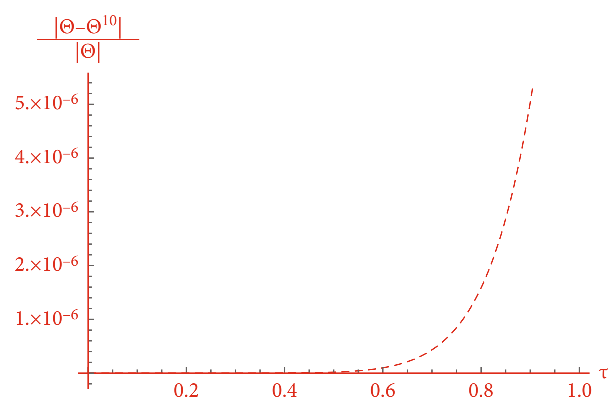

FIGURE 6

TABLE 2: The absolute and relative errors of Example 1.

τ	Abs.error	Rel.error
0.2	$5.1605107029284450 \times 10^{-7}$	$3.1515310030359390 \times 10^{-6}$
0.4	$3.1981585744245145 \times 10^{-5}$	$1.1927729870749216 \times 10^{-4}$
0.6	$3.5301834358408835 \times 10^{-4}$	$1.0720689345454725 \times 10^{-3}$
0.8	$1.9234953728893833 \times 10^{-3}$	$5.3510220976640050 \times 10^{-3}$
1.0	$7.1205587664326390 \times 10^{-3}$	$1.9355685668873270 \times 10^{-2}$

4. The ERPSM to Demonstrate the Nonlinear PDE

In this section, we use our new ERPSM to construct the solutions of the nonlinear PDE as in Equation (9). In the next subsection, we derive the main algorithms of the ERPSM for the nonlinear PDE.

4.1. The Algorithm of ERPSM for Solving Nonlinear PDE. We summarized the method of finding the ERPS solution for the nonlinear PDE with the following algorithm:

Step 1. Rewriting Equation (9), we have

$$D_\tau^\omega \Theta(\tau) - \xi(\tau^\omega, \Theta(\tau), \Theta(\lambda\tau), D_\tau^\omega \Theta(\lambda\tau)) = 0. \quad (116)$$

Step 2. E-T is used on both sides of Equation (116).

$$E[D_\tau^\omega \Theta(\tau)] - E[\xi(\tau^\omega, \Theta(\tau), \Theta(\lambda\tau), D_\tau^\omega \Theta(\lambda\tau))] = 0. \quad (117)$$

By using the second part of Lemma 2, we get the following:

$$\wp(\upsilon) - \upsilon^2 \hbar - \upsilon^\omega \wp(\upsilon) = 0, \quad (118)$$

where $E[\Theta(\tau)] = \wp(\upsilon)$ and $E[\xi(\tau^\omega, \Theta(\tau), \Theta(\lambda\tau), D_\tau^\omega \Theta(\lambda\tau))] = \wp(\upsilon)$.

Step 3. Assume that the solution to Equation (118) has the following extension:

$$\wp(\upsilon) = \sum_{\nu=0}^{\infty} \hbar_\nu \upsilon^{\nu\omega+2}. \quad (119)$$

Introduce the κth-truncated series in the following form:

$$\wp_k(\upsilon) = \sum_{\nu=0}^{k} \hbar_\nu \upsilon^{\nu\omega+2}. \quad (120)$$

Step 4. By using the first part of Lemma 2, we have

$$\hbar_0 = \Theta(0) = \mathfrak{I}. \quad (121)$$

Step 5. The κth-truncated series of $\wp(\upsilon)$ becomes as follows:

$$\wp_k(\upsilon) = \mathfrak{I}\upsilon^2 + \sum_{\nu=1}^{k} \hbar_\nu \upsilon^{\nu\omega+2}. \quad (122)$$

Step 6. Describe the ERF and the κth-ERF of Equation (118), respectively, as follows:

$$E\mathrm{Res}(\upsilon) = \wp(\upsilon) - \upsilon^2 \mathfrak{I} - \upsilon^\omega \wp(\upsilon), \quad (123)$$

$$E\mathrm{Res}_\kappa(\upsilon) = \wp_\kappa(\upsilon) - \upsilon^2 \mathfrak{I} - \upsilon^\omega \wp_\kappa(\upsilon). \quad (124)$$

Step 7. Replace the succession arrangement of $\wp_k(\upsilon)$ as in Equation (120) with (124).

Step 8. Solve the succeeding expression for $\nu = 1, 2, 3, \cdots, \kappa$ step by step to obtain the unknown coefficients

$$\lim_{\upsilon \longrightarrow 0} \left(\frac{1}{\upsilon^{\kappa\omega+2}} E[\mathrm{Res}_\kappa(\upsilon)] \right) = 0, \quad \kappa = 1, 2, 3, \cdots. \quad (125)$$

Step 9. Replace the attained values of $\hbar_\nu$ into the κth-truncated series of $\wp_\kappa(\upsilon)$ to obtain the κth-approximate solution of Equation (118).

Step 10. Use the inverse E-T on $\wp_k(\upsilon)$ to obtain the κth-approximate solution $\Theta_\kappa(\tau)$ in the original space.

In the next subsection, we determine the appropriateness of the recommended method for nonlinear PDFs.

Table 3: The recurrence errors $|\Theta^5(\tau) - \Theta^4(\tau)|$ of the five-step approximate solution with different values of ω for Example 1.

τ	$\omega = 0.7$	$\omega = 0.8$	$\omega = 0.9$	$\omega = 1.0$
0.2	$5.5251129381940380 \times 10^{-7}$	$3.557469322866979 \times 10^{-8}$	$2.210719076023441 \times 10^{-9}$	$1.337989787908603 \times 10^{-10}$
0.4	$6.2509517206696540 \times 10^{-6}$	$5.691950916587166 \times 10^{-7}$	$5.002286239854830 \times 10^{-8}$	$4.281567321307531 \times 10^{-9}$
0.6	$2.5838396081572233 \times 10^{-5}$	$2.881550151522252 \times 10^{-6}$	$3.101552986356802 \times 10^{-7}$	$3.251315184617906 \times 10^{-8}$
0.8	$7.0721445608883680 \times 10^{-5}$	$9.107121466539466 \times 10^{-6}$	$1.131888166924002 \times 10^{-7}$	$1.370101542818409 \times 10^{-7}$
1.0	$1.5443160141456830 \times 10^{-4}$	$2.223418326791861 \times 10^{-5}$	$3.089573833214964 \times 10^{-6}$	$4.181218087214387 \times 10^{-7}$

4.2. Numerical Examples. In this subsection, we will provide two problems with nonlinear PDEs to validate the performance and effectiveness of ERPSM.

Example 2. Examine the following nonlinear fractional pantograph differential equation:

$$D_\tau^\omega[\Theta(\tau] = 1 - 2\Theta^2\left(\frac{\tau}{2}\right), \quad 1 < \omega \le 2, 0 \le \tau \le 1, \tag{126}$$

subject to the initial condition

$$\Theta(0) = 1. \tag{127}$$

By employing E-T on Equation (126),

$$\wp(\upsilon) - \upsilon^2 - \upsilon^{2+\omega} + 2\upsilon^\omega E\left[\left(E^{-1}[4\wp(2\upsilon)]\right)^2\right] = 0. \tag{128}$$

Assume that algebraic equation (128) has the solution in the expansion form as

$$\wp(\upsilon) = \sum_{\nu=0}^{\infty} \hbar_\nu \upsilon^{\nu\omega+2}. \tag{129}$$

The κth-truncated series of Equation (128) is as follows:

$$\wp_k(\upsilon) = \sum_{\nu=0}^{k} \hbar_\nu \upsilon^{\nu\omega+2}. \tag{130}$$

By using the first part of Lemma 2, we get

$$\hbar_0 = \Theta(0) = 1. \tag{131}$$

The κth-truncated series becomes as follows:

$$\wp_k(\upsilon) = \upsilon^2 + \sum_{\nu=1}^{k} \hbar_\nu \upsilon^{\nu\omega+2}. \tag{132}$$

Now, define the ERF in the following form:

$$E[\mathrm{Res}(\upsilon)] = \wp(\upsilon) - \upsilon^2 - \upsilon^{2+\omega} + 2\upsilon^\omega E\left[\left(E^{-1}[4\wp(2\upsilon)]\right)^2\right]. \tag{133}$$

The κth-ERF is as follows:

$$E[\mathrm{Res}_\kappa(\upsilon)] = \wp_\kappa(\upsilon) - \upsilon^2 - \upsilon^{2+\omega} + 2\upsilon^\omega E\left[\left(E^{-1}[4\wp_\kappa(2\upsilon)]\right)^2\right]. \tag{134}$$

Therefore,

$$\lim_{\upsilon \longrightarrow 0} \frac{1}{\upsilon^{\kappa\omega+2}} E[\mathrm{Res}_\kappa(\upsilon)] = 0. \tag{135}$$

To determine the undefined coefficients $\hbar_\nu$, substitute $\kappa = 1, 2, 3, 4, 5,$ in Equations (132) and (134) and then utilize (135); thus, we have

$$\begin{aligned}
\hbar_1 &= -1,\\
\hbar_2 &= 4(2)^{-\omega},\\
\hbar_3 &= -\frac{2\Gamma((1/2)+\omega)}{\sqrt{\pi}\Gamma(1+\omega)} - \frac{16}{(8)^\omega},\\
\hbar_4 &= \frac{8\sqrt{3}(27)^\omega \Gamma((2/3)+\omega)\Gamma((1/3)+\omega)}{(64)^\omega\sqrt{\pi}\Gamma(1+\omega)\Gamma((1/2)+\omega)} + \frac{64}{(64)^\omega} + \frac{8\Gamma((1/2)+\omega)}{(8)^\omega\sqrt{\pi}\Gamma(1+\omega)},\\
\hbar_5 &= -\frac{128\sqrt{3}\Gamma((1/2)+\omega)\Gamma(1/2+2\omega)}{3(54)^\omega\Gamma((1/3)+\omega)\Gamma((2/3)+\omega)\Gamma(1+\omega)} - \frac{32\Gamma((1/2)+2\omega)}{(16)^\omega\Gamma((1/2)+\omega)\Gamma(1+\omega)}\\
&\quad - \frac{16\sqrt{3}(4)^\omega\Gamma((1/2)+\omega)^2\Gamma((1/2)+2\omega)}{3\sqrt{\pi}(27)^\omega\Gamma((1/3)+\omega)\Gamma((2/3)+\omega)\Gamma(1+\omega)^2} - \frac{256}{(1024)^\omega} - \frac{32\sqrt{3}(27)^\omega\Gamma((1/3)+\omega)\Gamma((2/3)+\omega)}{\sqrt{\pi}(1024)^\omega\Gamma((1/2)+\omega)\Gamma(1+\omega)}\\
&\quad - \frac{32\Gamma((1/2)+\omega)}{(128)^\omega\sqrt{\pi}\Gamma(1+\omega)}.
\end{aligned} \tag{136}$$

The five-step approximate solution of Equation (128) is as follows:

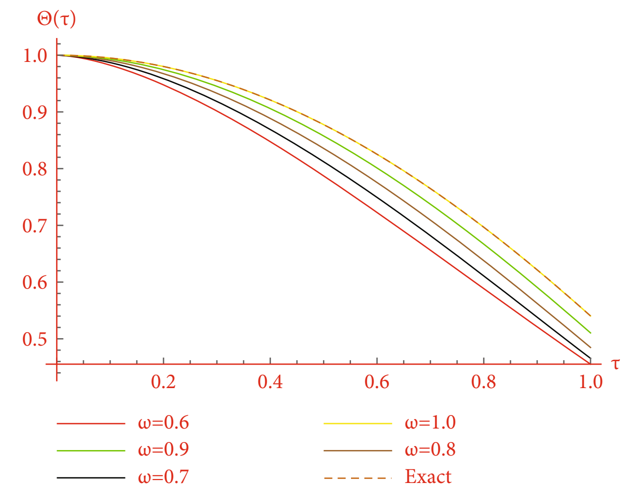

Figure 7

$$\wp_5(\upsilon) = \upsilon^2 - \upsilon^{2+\omega} + 4(2)^{-\omega}\upsilon^{2+2\omega} + \hbar_3\upsilon^{2+3\omega} + \hbar_4\upsilon^{2+4\omega} + \hbar_5\upsilon^{2+5\omega}. \tag{137}$$

By taking inverse E-T at both sides of Equation (137),

$$\Theta_5(\tau) = 1 - \frac{\tau^{\omega}}{\Gamma(1+\omega)} + 4(2)^{-\omega}\frac{\Upsilon^{2\omega}}{\Gamma(1+2\omega)} + \hbar_3\frac{\tau^{3\omega}}{\Gamma(1+3\omega)} + \hbar_4\frac{\tau^{4\omega}}{\Gamma(1+4\omega)} + \hbar_5\frac{\tau^{5\omega}}{\Gamma(1+5\omega)}. \tag{138}$$

For $\omega = 2$, Equation (138) becomes

$$\Theta_5(\tau) = 1 - \frac{\tau^2}{2!} + \frac{\tau^4}{4!} - \frac{\tau^6}{6!} + \frac{\tau^8}{8!} - \frac{\tau^{10}}{10!}. \tag{139}$$

Equation (139) represents the first six terms of $\cos\tau$; therefore, the exact solution of Equation (126) is $\cos\tau$ at $\omega = 2$.

The following 2-D graphs show the behavior of approximate and exact solutions to Example 2.

Figure 7 shows the performance of the five-step approximate solution of Equation (126) for various values of ω and exact solution at $\omega = 2$. Clearly, the findings for various fractional ω values converge to the result in the case of $\omega = 2$. Furthermore, the approximate solution does overlap with the exact solution, which indicates the accuracy and effectiveness of the suggested method.

The following 2-D graphs show the absolute and relative errors for Example 2.

Figures 8 and 9 demonstrate the 2-D graphs of absolute and relative errors in the intervals $\tau \in [0, 1]$ over the five-step approximate and exact solutions of Equation (126) at $\omega = 1$, respectively. The approximate solution is extremely close to the exact solution, as seen in the figures.

Table 4 shows the absolute and relative errors at reasonable nominated grid points in the interval $\tau \in [0, 1]$ among the five-step approximate and exact solutions of Equation (126) at $\omega = 1$ attained using ERPSM. From Table 4, it can be perceived that the approximate and exact solutions are in very good agreement, and this sanctions the efficiency of the recommended method. The convergence of the approximate solution to the exact solution for Equation (126) has been shown numerically as in Table 5. From the obtained results, it is evident that the present technique is an effective and convenient algorithm to solve certain classes of fractional-order DEs with fewer calculations and iteration steps.

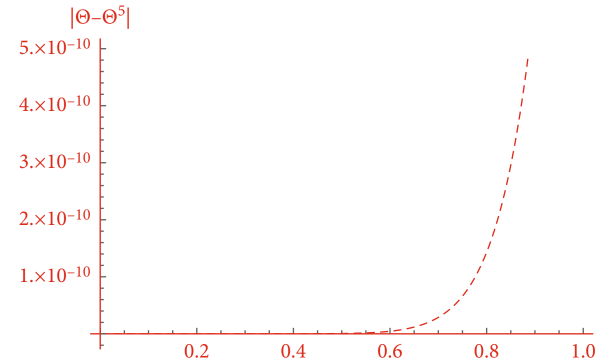

Figure 8

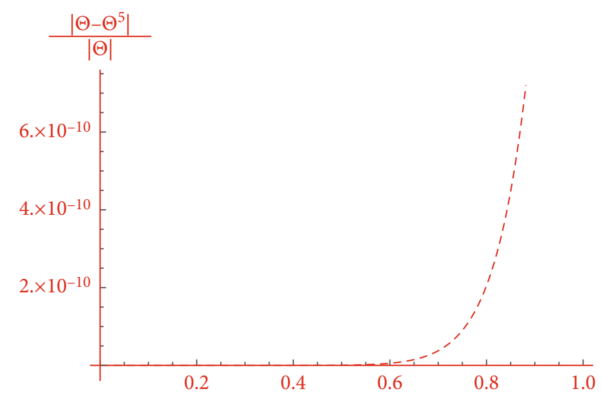

Figure 9

Table 4: The absolute and relative errors of Example 2.

τ	Abs.error	Rel.error
0.2	0.0	0.0
0.4	$3.508304757815494 \times 10^{-14}$	$3.808982011678268 \times 10^{-14}$
0.6	$4.535483100198689 \times 10^{-12}$	$5.495319744192834 \times 10^{-12}$
0.8	$1.429608653680247 \times 10^{-10}$	$2.051951896683681 \times 10^{-10}$
1.0	$7.120558766432639 \times 10^{-9}$	$2.051765518966810 \times 10^{-9}$

Example 3. Consider the following nonlinear PDE:

$$D_\tau^\omega\Theta(\tau) = \frac{1}{2}\Theta(\tau) + \frac{1}{2^{1-\omega}}\Theta\left(\frac{\tau}{2}\right)D_\tau^\omega\Theta\left(\frac{\tau}{2}\right), \quad \tau \geq 0, 0 < \omega \leq 1, \tag{140}$$

TABLE 5: The recurrence errors $|\Theta^5(\tau) - \Theta^4(\tau)|$ of the five-step approximate solution with different values of ω for Example 2.

τ	$\omega = 0.7$	$\omega = 0.8$	$\omega = 0.9$	$\omega = 1.0$
0.2	$6.296560270772086 \times 10^{-20}$	$1.969389500244771 \times 10^{-21}$	$5.554963006701661 \times 10^{-22}$	$2.821869488536155 \times 10^{-24}$
0.4	$2.279598318393725 \times 10^{-17}$	$1.008327424125322 \times 10^{-18}$	$4.022222859549857 \times 10^{-19}$	$2.889594356261023 \times 10^{-21}$
0.6	$7.155401866274551 \times 10^{-16}$	$3.876349353331781 \times 10^{-17}$	$1.893795546581747 \times 10^{-17}$	$1.666285714285714 \times 10^{-19}$
0.8	$8.253027478106390 \times 10^{-15}$	$5.162636411521651 \times 10^{-16}$	$2.912400444857598 \times 10^{-16}$	$2.958944620811287 \times 10^{-18}$
1.0	$5.499819058543307 \times 10^{-14}$	$3.846463867665569 \times 10^{-15}$	$2.426030253023737 \times 10^{-15}$	$2.755731922398591 \times 10^{-17}$

subject to the initial condition

$$\Theta(0) = 1. \tag{141}$$

By employing the E-T on Equation (140),

$$\wp(\upsilon) = \upsilon^2 + \frac{\upsilon^\omega}{2}\wp(\upsilon) + \frac{\upsilon^\omega}{2^{1-\omega}} E\left[E^{-1}\left[4\wp\left(\frac{\upsilon}{2}\right)\right]E^{-1}\left[\frac{4\wp(\upsilon/2)}{\upsilon^\omega} - \upsilon^{2-\omega}\right]\right]. \tag{142}$$

Assume that algebraic equation (142) has the solution in the expansion form as

$$\wp(\upsilon) = \sum_{\nu=0}^{\infty} \hbar_\nu \upsilon^{\nu\omega+2}. \tag{143}$$

The κth-truncated series of Equation (142) is as follows:

$$\wp_k(\upsilon) = \sum_{\nu=0}^{k} \hbar_\nu \upsilon^{\nu\omega+2}. \tag{144}$$

By employing the first part of Lemma 2, we get

$$\hbar_0 = \Theta(0) = 1. \tag{145}$$

The κth-truncated series of Equation (142) becomes as follows:

$$\wp_k(\upsilon) = \upsilon^2 + \sum_{\nu=1}^{k} \hbar_\nu \upsilon^{\nu\omega+2}. \tag{146}$$

Now, define the ERF in the following form:

$$E\,\mathrm{Re}\,s(\upsilon) = \wp(\upsilon) - \upsilon^2 - \frac{\upsilon^\omega}{2}\wp(\upsilon) - \frac{\upsilon^\omega}{2^{1-\omega}} \cdot E\left[E^{-1}\left[4\wp\left(\frac{\upsilon}{2}\right)\right]E^{-1}\left[\frac{4\wp(\upsilon/2)}{\upsilon^\omega} - \upsilon^{2-\omega}\right]\right]. \tag{147}$$

The κth-ERF is as follows:

$$E\mathrm{Res}_\kappa(\upsilon) = \wp_\kappa(\upsilon) - \upsilon^2 - \frac{\upsilon^\omega}{2}\wp_\kappa(\upsilon) - \frac{\upsilon^\omega}{2^{1-\omega}} \cdot E\left[E^{-1}\left[4\wp_\kappa\left(\frac{\upsilon}{2}\right)\right]E^{-1}\left[\frac{4\wp_\kappa(\upsilon/2)}{\upsilon^\omega} - \upsilon^{2-\omega}\right]\right]. \tag{148}$$

To determine the undefined coefficients $\hbar_\nu$, substitute $\kappa = 1, 2, 3, 4$ in Equations (146) and (148) and then solve the equation $\lim_{\upsilon\longrightarrow 0}(1/\upsilon^{\kappa\omega+2})E[\mathrm{Re}\,s_\kappa(\upsilon)] = 0$. By utilizing this algorithm, we get the following first four coefficients of the series Equation (146):

$$\hbar_1 = 1,$$

$$\hbar_2 = \frac{1 + 2^\omega}{-1 + 2^{\omega+1}},$$

$$\hbar_3 = -\frac{(8^\omega - 16^\omega - 2(32)^\omega)\Gamma((1/2) + \omega) + \sqrt{\pi}(2^\omega - 4^\omega - 8^\omega - 16^\omega - 2(32)^\omega)\Gamma(1 + \omega)}{\sqrt{\pi}\Gamma(1 + \omega)\left(8(32)^\omega + 2^{2\omega+2} - 2(8^\omega) - 8(16^\omega) - 2^\omega\right)},$$

$$\begin{aligned}\hbar_4 = {} & \frac{\sqrt{\pi}\left(2 - 2^{-\omega} - 2(4)^\omega + 4(2)^{2\omega} + 5(2)^\omega\right)\Gamma(1 + 3\omega)}{(2(2)^\omega - 1)^2(2(8)^\omega - 1)(2(4)^\omega - 1)\Gamma((1/2) + \omega)\Gamma(1 + \omega)^2} \\ & + \frac{4^\omega(16^\omega + 8^\omega + 2^\omega + 1)\Gamma((1/2) + \omega)}{\sqrt{\pi}(2(2)^\omega - 1)(2(8)^\omega - 1)(2(4)^\omega - 1)\Gamma(1 + \omega)} \\ & + \frac{(1 + 2(8)^\omega + 4^\omega + 3(2)^\omega + (64)^\omega + (16)^\omega + (2)^\omega))}{(2(2)^\omega - 1)(2(8)^\omega - 1)(2(4)^\omega - 1)} \\ & + \frac{(3 + 3(2)^\omega)\Gamma(3\omega)}{(2(2)^\omega - 1)(2(8)^\omega - 1)(2(4)^\omega - 1)\Gamma(1 + \omega)^3}.\end{aligned} \tag{149}$$

The four-step approximate solution of Equation (142) is as follows:

$$\wp_4(\upsilon) = \upsilon^2 + \upsilon^{2+\omega} + \left(\frac{1 + 2^\omega}{1 - 2^{\omega+1}}\right)\upsilon^{2+2\omega} + \hbar_3\upsilon^{2+3\omega} + \hbar_4\upsilon^{2+4\omega}. \tag{150}$$

By employing inverse E-T on both sides of Equation (150),

Table 6: The absolute and relative errors of Example 3.

τ	Abs.error	Rel.error
0.2	$9.149350321813188 \times 10^{-8}$	$7.490854479152386 \times 10^{-8}$
0.4	$6.030974603721262 \times 10^{-6}$	$4.042683174006208 \times 10^{-6}$
0.6	$7.080039050877396 \times 10^{-5}$	$3.885607815121622 \times 10^{-5}$
0.8	$4.102618258010615 \times 10^{-4}$	$1.843425212040309 \times 10^{-4}$
1.0	$1.615161333333059 \times 10^{-3}$	$5.941846488086295 \times 10^{-4}$

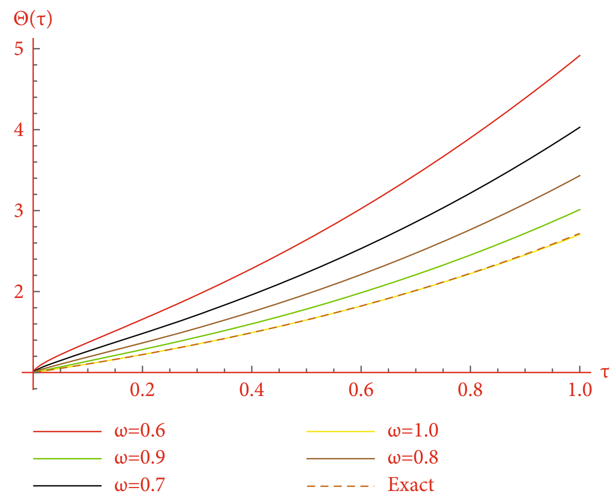

Figure 10

$$\Theta_4(\tau) = 1 + \frac{\tau^{\omega}}{\Gamma(1+\omega)} + \left(\frac{1+2^{\omega}}{1-2^{\omega+1}}\right)\frac{\tau^{2\omega}}{\Gamma(1+2\omega)} + \hbar_3 \frac{\tau^{3\omega}}{\Gamma(1+3\omega)} + \hbar_4 \frac{\tau^{4\omega}}{\Gamma(1+4\omega)}. \quad (151)$$

For$\omega = 1$in Equation (151), it becomes

$$\Theta_4(\tau) = 1 + \tau + \frac{\tau^2}{2!} + \frac{\tau^3}{3!} + \frac{\tau^4}{4!}. \quad (152)$$

Equation (152) represents the first five terms of e^{τ}; therefore, the exact solution of Equation (140) is e^{τ} at $\omega = 1$.

Table 6 shows the absolute and relative errors of the five-step approximate solution of the nonlinear PDE of Example 3 at $\omega = 1$ on various chosen grid points in the interval $\tau \in [0, 1]$. The numerical findings in Table 6 prove that the approximate solution converges to the exact solution quickly. This indicates the accuracy and effectiveness of the suggested scheme.

The following 2-D graphs show the behavior of approximate and exact solutions to Example 3.

Figure 10 exemplifies the performance of the five-step approximate solutions of Equation (140) for some values of ω and exact solution at $\omega = 1$. Apparently, results in cases of fractional values of ω converging result in the case of $\omega = 1$. Furthermore, the approximate result overlaps with the precise result at $\omega = 1$, and this once more agrees with the efficiency and precision of the recommended scheme.

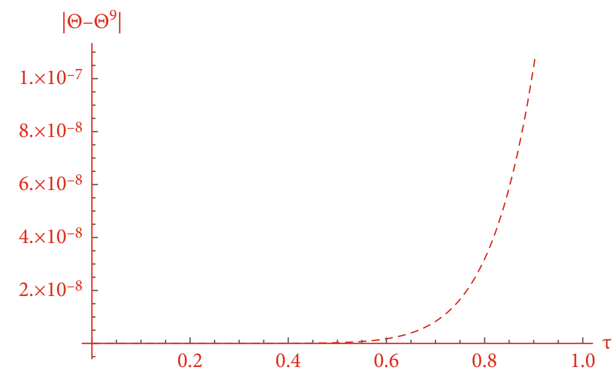

Figure 11

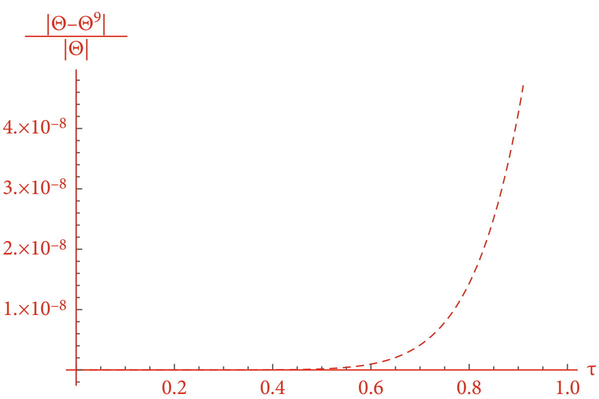

Figure 12

The following 2-D graphs show the absolute and relative errors for Example 3.

Figures 11 and 12 demonstrate the 2-D graphs of absolute and relative errors in the intervals $\tau \in [0, 1]$ over the nine-step approximate and exact solutions of Equation (140) at $\omega = 1$, respectively. The approximate solution is extremely close to the exact solution, as seen in the figures.

5. Conclusion

In this paper, we describe a novel method for solving FMPS and PDEs that combines the RPSM with the E-T. To assess the effectiveness and reliability of ERPSM for FMPS and PDEs, the absolute, relative, and recurrence errors of linear and nonlinear problems are studied graphically and numerically. The interpretation of the 2-D plots and tables for different values of fractional order also validates that the approximate solution is rapidly convergent to the exact solution. The numerical and graphical consequences confirm that the ERPSM is extremely effective and precise.

The ERPSM stands apart from other numerical methods in four major ways. This method has the advantage of requiring no minor or major physical parameter assumptions in the problem. As a result, it applies to both weakly and strongly nonlinear problems, overcoming some of the inherent limits of traditional perturbation approaches. Second, while addressing nonlinear problems, the ERPSM does not require He's polynomials or Adomian polynomials. To solve nonlinear DEs, only a very small number of calculations are needed. As a consequence, it outperforms homotopy analysis and Adomian decomposition methods significantly. Third, the ERPSM provided a simple and rapid way to observe the coefficients of the recommended series as a solution to the problem. In contrast to the traditional RPSM, establishing the coefficients for a series requires computing the fractional derivative every time, while the ERPSM only requires the concept of the limit at zero in establishing the coefficients for the series. Finally, unlike conventional analytic approximation techniques, the ERPSM can create expansion solutions for linear and nonlinear FODEs without the need for perturbation, linearization, or discretization.

Therefore, we conclude that our novel technique is simple to apply, accurate, adaptive, and efficient according to the results. It is significant to consider that implementing the ERPSM to solve other kinds of ordinary and partial DEs of noninteger order is actively attainable. For example, fractional KdV equations, fractional phi-4 equations, and fractional Schrodinger equations.

Data Availability

The numerical data used to support the findings of this study is included within the article.

Conflicts of Interest

The authors declare that they have no competing interests.

Authors' Contributions

The authors declare that the study was realized in collaboration with equal responsibility. All authors read and approved the final manuscript.

References

[1] D.-N. Yu, J.-H. He, and A. G. Garcıa, "Homotopy perturbation method with an auxiliary parameter for nonlinear oscillators," *Journal of Low Frequency Noise, Vibration and Active Control*, vol. 38, no. 3-4, pp. 1540–1554, 2019.

[2] S. Rezapour, B. Tellab, C. T. Deressa, S. Etemad, and K. Nonlaopon, "H-U-type stability and numerical solutions for a nonlinear model of the coupled systems of Navier BVPs via the generalized differential transform method," *Fractal and Fractional*, vol. 5, no. 4, p. 166, 2021.

[3] S. Saha Ray, "A new approach by two-dimensional wavelets operational matrix method for solving variable-order fractional partial integro-differential equations," *Numerical Methods for Partial Differential Equations*, vol. 37, no. 1, pp. 341–359, 2021.

[4] M. I. Liaqat, A. Khan, M. Alam, M. K. Pandit, S. Etemad, and S. Rezapour, "Approximate and closed-form solutions of Newell-Whitehead-Segel equations via modified conformable Shehu transform decomposition method," *Mathematical Problems in Engineering*, vol. 2022, Article ID 6752455, 14 pages, 2022.

[5] N. Anjum and J. H. He, "Laplace transform: making the variational iteration method easier," *Applied Mathematics Letters*, vol. 92, pp. 134–138, 2019.

[6] H. Singh, "Jacobi collocation method for the fractional advection-dispersion equation arising in porous media," *Numerical Methods for Partial Differential Equations*, vol. 38, no. 3, pp. 636–653, 2022.

[7] S. Rezapour, M. I. Liaqat, and S. Etemad, "An effective new iterative method to solve conformable cauchy reaction- diffusion equation via the Shehu transform," *Journal of Mathematics*, vol. 2022, Article ID 4172218, 12 pages, 2022.

[8] M. A. Zaky and J. T. Machado, "Multi-dimensional spectral tau methods for distributed-order fractional diffusion equations," *Computers & Mathematics with Applications*, vol. 79, no. 2, pp. 476–488, 2020.

[9] B. Yuttanan, M. Razzaghi, and T. N. Vo, "Legendre wavelet method for fractional delay differential equations," *Applied Numerical Mathematics*, vol. 168, pp. 127–142, 2021.

[10] P. Veeresha, D. G. Prakasha, and J. Singh, "Solution for fractional forced KdV equation using fractional natural decomposition method," *AIMS Mathematics*, vol. 5, no. 2, pp. 798–810, 2020.

[11] M. I. Liaqat, A. Khan, and A. Akgül, "Adaptation on power series method with conformable operator for solving fractional order systems of nonlinear partial differential equations," *Chaos, Solitons & Fractals*, vol. 157, article 111984, 2022.

[12] A. A. Salih and S. Shihab, "New operational matrices approach for optimal control based on modified Chebyshev polynomials," *Samarra Journal of Pure and Applied Science*, vol. 2, no. 2, pp. 68–78, 2020.

[13] R. Chauhan and S. Aggarwal, "Laplace transform for convolution type linear Volterra integral equation of second kind," *Journal of Advanced Research in Applied Mathematics and Statistics*, vol. 4, no. 3-4, pp. 1–7, 2019.

[14] D. Rani and V. Mishra, "Modification of Laplace Adomian decomposition method for solving nonlinear Volterra integral and integro-differential equations based on Newton Raphson formula," *European Journal of Pure and Applied Mathematics*, vol. 11, no. 1, pp. 202–214, 2018.

[15] S. Aggarwal, A. R. Gupta, and S. D. Sharma, "A new application of Shehu transform for handling Volterra integral equations of first kind," *International Journal of Research in Advent Technology*, vol. 7, no. 4, pp. 438–445, 2019.

[16] S. Vilu, R. R. Ahmad, and U. K. S. Din, "Variational iteration method and Sumudu transform for solving delay differential equation," *International Journal of Differential Equations*, vol. 2019, Article ID 6306120, 6 pages, 2019.

[17] R. M. Jena and S. Chakraverty, "Analytical solution of Bagley-Torvik equations using Sumudu transformation method," *SN Applied Sciences*, vol. 1, no. 3, article 246, 2019.

[18] J. J. Gu, C. An, C. Levi, and J. Su, "Prediction of vortex-induced vibration of long flexible cylinders modeled by a coupled nonlinear oscillator: integral transform solution," *Journal of Hydrodynamics*, vol. 24, no. 6, pp. 888–898, 2012.

[19] V. Namias, "The fractional order Fourier transform and its application to quantum mechanics," *IMA Journal of Applied Mathematics*, vol. 25, no. 3, pp. 241–265, 1980.

[20] P. Hammachukiattikul, A. Mohanapriya, A. Ganesh et al., "A study on fractional differential equations using the fractional Fourier transform," *Advances in Difference Equations*, vol. 2020, no. 1, Article ID 691, 2020.

[21] Y. F. Luchko, H. Martinez, and J. J. Trujillo, "Fractional Fourier transform and some of its applications," *Fractional Calculus and Applied Analysis*, vol. 11, no. 4, pp. 457–470, 2008.

[22] S. Kumar, R. Saxena, and K. Singh, "Fractional Fourier transform and fractional-order calculus-based image edge detection," *Circuits, Systems, and Signal Processing*, vol. 36, no. 4, pp. 1493–1513, 2017.

[23] S. Kazem, "Exact solution of some linear fractional differential equations by Laplace transform," *International Journal of Nonlinear Science*, vol. 16, no. 1, pp. 3–11, 2013.

[24] L. Kexue and P. Jigen, "Laplace transform and fractional differential equations," *Applied Mathematics Letters*, vol. 24, no. 12, pp. 2019–2023, 2011.

[25] M. I. Liaqat, A. Khan, M. Alam, and M. K. Pandit, "A highly accurate technique to obtain exact solutions to time-fractional quantum mechanics problems with zero and non-zero trapping potential," *Journal of Mathematics*, vol. 2022, Article ID 9999070, 20 pages, 2022.

[26] Z. B. Li and J. H. He, "Fractional complex transform for fractional differential equations," *Mathematical and Computational Applications*, vol. 15, no. 5, pp. 970–973, 2010.

[27] J. Liang, S. Elangovan, and J. B. X. Devotta, "Application of wavelet transform in travelling wave protection," *International Journal of Electrical Power & Energy Systems*, vol. 22, no. 8, pp. 537–542, 2000.

[28] H. Z. Mjthap and S. N. Al-Azzawi, "Mixing Sumudu transform and Adomain decomposition method for solving Riccati equation of variable fractional order," *Journal of Interdisciplinary Mathematics*, vol. 22, no. 8, pp. 1559–1563, 2019.

[29] L. Riabi, K. Belghaba, M. H. Cherif, and D. Ziane, "Homotopy perturbation method combined with ZZ transform to solve some nonlinear fractional differential equations," *International Journal of Analysis and Applications*, vol. 17, no. 3, pp. 406–419, 2019.

[30] S. Abbasbandy, "A numerical solution of Blasius equation by Adomian's decomposition method and comparison with homotopy perturbation method," *Chaos, Solitons & Fractals*, vol. 31, no. 1, pp. 257–260, 2007.

[31] S. Rathore, D. Kumar, J. Singh, and S. Gupta, "Homotopy analysis Sumudu transform method for nonlinear equations," *International Journal of Industrial Mathematics*, vol. 4, no. 4, pp. 301–314, 2012.

[32] G. O. Ojo and N. I. Mahmudov, "Aboodh transform iterative method for spatial diffusion of a biological population with fractional-order," *Mathematics*, vol. 9, no. 2, p. 155, 2021.

[33] N. B. Manjare and H. T. Dinde, "Sumudu decomposition method for solving fractional Bratu-type differential equations," *Journal of Scientific Research*, vol. 12, no. 4, pp. 585–605, 2020.

[34] M. S. Alrawashdeh, S. A. Migdady, and I. K. Argyros, "An efficient mechanism to solve fractional differential equations using fractional decomposition method," *Symmetry*, vol. 13, no. 6, p. 984, 2021.

[35] N. G. N'Gbo and Y. Xia, "Traveling wave solution of bad and good modified Boussinesq equations with conformable fractional-order derivative," *Qualitative Theory of Dynamical Systems*, vol. 21, no. 1, pp. 1–21, 2022.

[36] R. M. Jena and S. Chakraverty, "Solving time-fractional Navier–Stokes equations using homotopy perturbation Elzaki transform," *SN Applied Sciences*, vol. 1, no. 1, pp. 1–13, 2019.

[37] W. He, N. Chen, I. Dassios, N. A. Shah, and J. D. Chung, "Fractional system of Korteweg-De Vries equations via Elzaki transform," *Mathematics*, vol. 9, no. 6, p. 673, 2021.

[38] M. Khalid, M. Sultana, F. Zaidi, and U. Arshad, "Application of Elzaki transform method on some fractional differential equations," *Mathematical Theory and Modeling*, vol. 5, no. 1, pp. 89–96, 2015.

[39] N. A. Shah, I. Dassios, and J. D. Chung, "A decomposition method for a fractional-order multi-dimensional telegraph equation via the Elzaki transform," *Symmetry*, vol. 13, no. 1, p. 8, 2021.

[40] A. Salah, "The new combination of semi-analytical iterative method and Elzaki transform for solving some Korteweg-de Vries equations," *Al-Qadisiyah Journal of Pure Science*, vol. 25, no. 1, pp. 23–26, 2020.

[41] S. Rashid, K. T. Kubra, and K. M. Abualnaja, "Fractional view of heat-like equations via the Elzaki transform in the settings of the Mittag–Leffler function," *Mathematical Methods in the Applied Sciences*, 2021.

[42] T. M. Elzaki, "The new integral transform Elzaki transform," *Global Journal of Pure and Applied Mathematics*, vol. 7, no. 1, pp. 57–64, 2011.

[43] S. Rashid, Z. Hammouch, H. Aydi, A. G. Ahmad, and A. M. Alsharif, "Novel computations of the time-fractional Fisher's model via generalized fractional integral operators by means of the Elzaki transform," *Fractal and Fractional*, vol. 5, no. 3, p. 94, 2021.

[44] T. M. Elzaki, "Application of new transform "Elzaki transform" to partial differential equations," *Global Journal of Pure and Applied Mathematics*, vol. 7, no. 1, pp. 65–70, 2011.

[45] T. M. Elzaki, "On the new integral transform "Elzaki transform" fundamental properties investigations and applications," *Global Journal of Mathematical Sciences: Theory and Practical*, vol. 4, no. 1, pp. 1–13, 2012.

[46] L. Wang and X. Chen, "Approximate analytical solutions of time fractional Whitham–Broer–Kaup equations by a residual power series method," *Entropy*, vol. 17, no. 12, pp. 6519–6533, 2015.

[47] M. Alquran, "Analytical solution of time-fractional two-component evolutionary system of order 2 by residual power series method," *Journal of Applied Analysis & Computation*, vol. 5, no. 4, pp. 589–599, 2015.

[48] Y. Zhang, A. Kumar, S. Kumar, D. Baleanu, and X. J. Yang, "Residual power series method for time-fractional Schrödinger equations," *Journal of Nonlinear Sciences and Applications*, vol. 9, no. 11, pp. 5821–5829, 2016.

[49] S. Hasan, A. Al-Zoubi, A. Freihet, M. Al-Smadi, and S. Momani, "Solution of fractional SIR epidemic model using residual power series method," *Applied Mathematics and Information Sciences*, vol. 13, no. 2, pp. 153–161, 2019.

[50] M. Senol, L. Akinyemi, A. Ata, and O. S. Iyiola, "Approximate and generalized solutions of conformable type Coudrey–Dodd–Gibbon–Sawada–Kotera equation," *International Journal of Modern Physics B*, vol. 35, no. 2, p. 2150021, 2021.

[51] D. G. Prakasha, P. Veeresha, and H. M. Baskonus, "Residual power series method for fractional Swift–Hohenberg equation," *Fractal and Fractional*, vol. 3, no. 1, p. 9, 2019.

[52] M. Alquran, H. M. Jaradat, and M. I. Syam, "Analytical solution of the time-fractional Phi-4 equation by using modified residual power series method," *Nonlinear Dynamics*, vol. 90, no. 4, pp. 2525–2529, 2017.

[53] M. Şenol, M. Alquran, and H. D. Kasmaei, "On the comparison of perturbation-iteration algorithm and residual power series method to solve fractional Zakharov-Kuznetsov equation," *Results in Physics*, vol. 9, pp. 321–327, 2018.

[54] A. M. Al-Rozbayani and A. H. Ali, "Applied Sumudu transform with Adomian decomposition method to the coupled Drinfeld–Sokolov–Wilson system," *AL-Rafidain Journal of Computer Sciences and Mathematics*, vol. 15, no. 2, pp. 139–147, 2021.

[55] K. Shah, H. Khalil, and R. A. Khan, "Analytical solutions of fractional order diffusion equations by natural transform method," *Iranian Journal of Science and Technology, Transactions A: Science*, vol. 42, no. 3, pp. 1479–1490, 2018.

[56] M. Madani, M. Fathizadeh, Y. Khan, and A. Yildirim, "On the coupling of the homotopy perturbation method and Laplace transformation," *Mathematical and Computer Modelling*, vol. 53, no. 9-10, pp. 1937–1945, 2011.

[57] J. R. Ockendon and A. B. Tayler, "The dynamics of a current collection system for an electric locomotive," *Proceedings of the Royal Society of London. A. Mathematical and Physical Sciences*, vol. 322, no. 1551, pp. 447–468, 1971.

[58] K. Rabiei and Y. Ordokhani, "Solving fractional pantograph delay differential equations via fractional-order Boubaker polynomials," *Engineering with Computers*, vol. 35, no. 4, pp. 1431–1441, 2019.

[59] M. Usman, M. Hamid, T. Zubair, R. U. Haq, W. Wang, and M. B. Liu, "Novel operational matrices-based method for solving fractional-order delay differential equations via shifted Gegenbauer polynomials," *Applied Mathematics and Computation*, vol. 372, article 124985, 2020.

[60] K. K. Ali, M. A. A. El Salam, and E. M. Mohamed, "Chebyshev operational matrix for solving fractional order delay-differential equations using spectral collocation method," *Arab Journal of Basic and Applied Sciences*, vol. 26, no. 1, pp. 342–353, 2019.

[61] R. Kumar, R. Koundal, K. Srivastava, and D. Baleanu, "Normalized Lucas wavelets: an application to Lane–Emden and pantograph differential equations," *The European Physical Journal Plus*, vol. 135, no. 11, pp. 1–24, 2020.

[62] M. Izadi, Ş. Yüzbaşı, and K. J. Ansari, "Application of Vieta–Lucas series to solve a class of multi-pantograph delay differential equations with singularity," *Symmetry*, vol. 13, no. 12, p. 2370, 2021.

[63] P. Vichitkunakorn, T. N. Vo, and M. Razzaghi, "A numerical method for fractional pantograph differential equations based on Taylor wavelets," *Transactions of the Institute of Measurement and Control*, vol. 42, no. 7, pp. 1334–1344, 2020.

[64] Z. Sabir, D. Baleanu, M. A. Z. Raja, and J. L. Guirao, "Design of neuro-swarming heuristic solver for multi-pantograph singular delay differential equation," *Fractals*, vol. 29, no. 5, article 2140022, 2021.

[65] A. Mosavi, M. Shokri, Z. Mansor, S. N. Qasem, S. S. Band, and A. Mohammadzadeh, "Machine learning for modeling the singular multi-pantograph equations," *Entropy*, vol. 22, no. 9, p. 1041, 2020.

[66] N. R. Anakira, A. Jameel, A. K. Alomari, A. Saaban, M. Almahameed, and I. Hashim, "Approximate solutions of multi-pantograph type delay differential equations using multistage optimal homotopy asymptotic method," *Journal of Mathematical and Fundamental Sciences*, vol. 50, no. 3, pp. 221–232, 2018.

[67] A. Khan, M. I. Liaqat, M. Younis, and A. Alam, "Approximate and exact solutions to fractional order Cauchy reaction-diffusion equations by new combine techniques," *Journal of Mathematics*, vol. 2021, Article ID 5337255, 12 pages, 2021.

[68] R. M. Jena and S. Chakraverty, "Residual power series method for solving time-fractional model of vibration equation of large membranes," *Journal of Applied and Computational Mechanics*, vol. 5, no. 4, pp. 603–615, 2019.

[69] M. I. Syam, "Analytical solution of the fractional initial Emden–Fowler equation using the fractional residual power series method," *International Journal of Applied and Computational Mathematics*, vol. 4, no. 4, pp. 1–8, 2018.

Hindawi
Journal of Function Spaces
Volume 2022, Article ID 4471757, 12 pages
https://doi.org/10.1155/2022/4471757

Research Article

Fractional-View Analysis of Space-Time Fractional Fokker-Planck Equations within Caputo Operator

Saleh Alshammari[1] **Naveed Iqbal**[1] **and Mohammad Yar**[2]

[1]*Department of Mathematics, College of Science, University of Ha'il, Ha'il 2440, Saudi Arabia*
[2]*Department of Mathematics, Polytechnic University in Kabul, Kabul, Afghanistan*

Correspondence should be addressed to Naveed Iqbal; n.iqbal@uoh.edu.sa and Mohammad Yar; myar@kpu.edu.af

Received 16 May 2022; Accepted 13 June 2022; Published 4 July 2022

Academic Editor: Yusuf Gurefe

In this article, we investigate the fractional-order Fokker-Planck equations with the help of the Yang transform decomposition method (YTDM). The YTDM combines Yang transform, Adomian decomposition method, and Adomian polynomials into one method. In the Caputo sense, fractional derivatives of space and time are studied. The convergent series form solution demonstrates the method's efficiency in resolving several types of fractional differential equations. Compared to other methods of finding approximate and exact solutions for nonlinear partial differential equations, this technique is more efficient and time-consuming.

1. Introduction

Fractional calculus, which can be thought of as a generalization of integer-order differentiation and integration, has received much attention in recent decades. Many definitions have been proposed for fractional derivatives, including Riesz, Grunwald-Letnikov, Caputo, Riemann-Liouville, and conformable fractional definitions [1–4]. Noninteger order integral and differential operators contain all historical conditions of the function in a weighted form known as the memory effect. In any case, fractional differential equations (FDEs), specifically fractional partial differential equations, are used to analyze a broad range of physical systems (FPDEs). FPDEs have gained attention due to their widespread application in electrical circuits, electrochemistry, quantum physics, and theoretical biology [5–8]. Furthermore, the nonlocal property of FPDEs is the most important feature for using them in such and other applications, whereas the differential operator having order integer is local. In this light, the next state of a fractional system is determined by both its current and historical states. This ensures that the mathematical model components in physical processes and dynamic systems are highly consistent. However, it is not easy to solve those FDEs, particularly for numerical calculations [9–11]. To handle partial differential equations (PDEs), having order fraction is of physical importance, and effective, trustworthy, and appropriate numerical methods are required [12–14]. Several major strategies have been utilized in this regard, including the fractional operational matrix method (FOMM) [15], Elzaki transform decomposition method (ETDM) [16, 17], homotopy analysis method (HAM) [18], homotopy perturbation method (HPM) [19, 20], iterative Laplace transform method [21], and variational iteration method (FVIM) [22].

The Fokker-Planck equation is a well-known statistical physics equation that Fokker and Planck first proposed to describe a particle's Brownian motion and the change in probability of a random function in time and space [23]. An uncontrolled, second-order truncation of the Kramers-Moyal expansion of the chemical master equation can also be used to obtain the chemical Fokker-Planck equation. This equation proves to be more accurate than the chemical master equation's linear-noise approximation. The Fokker-Planck equation appears in many natural science phenomena, such as probability flux, polymer dynamics, electron relaxation, solid-state systems, quantum optics, and other practical and theoretical models [24].

We have studied Fokker-Planck equations of fractional-order having general form as

$$\varphi^{\gamma}_{\mathfrak{J}}(\mu, \mathfrak{J}) = L\left(\varphi_{\mu}(\mu, \mathfrak{J}) + \varphi_{\mu\mu}(\mu, \mathfrak{J})\right) + N\varphi_{\mu\mu}(\mu, \mathfrak{J}), \mu, \mathfrak{J} > 0, \ \gamma \in (0, 1], \tag{1}$$

with the initial condition

$$\varphi(\mu, 0) = \zeta(\mu). \tag{2}$$

In biological molecules, chemical physics, energy consumption, and engineering, the fractional Fokker-Planck equation (F-FPE) has been successfully applied. Indeed, fractional diffusion, a special kind of F-FPE, has also been used in numerous scenarios such as frequency-dependent damping behaviour of materials, viscoelasticity, and diffusion processes [17]. Unfortunately, finding an accurate solution for FDEs, in general, is difficult. To approximate these solutions, various numerical and analytical techniques are used. Some of the advanced numerical and approximate methods used for F-FPEs include the Laplace transform method [18], the multistep reduced differential transform method [25], the predictor-corrector approach [26], the Adomian decomposition method (ADM) [27], and the variational iteration method (VIM) [28].

In this research, we used the Yang transform decomposition method (YTDM) to solve time-fractional F-FPEs. The Yang transform was proposed by Xiao-Jun Yang and can be utilized to solve a variety of differential equations with constant coefficients. The Adomian decomposition method [29] is a well-known methodology to solve linear and nonlinear differential and partial differential equations and integrodifferential and FDEs that yield accurate solutions in a concurrent series form. The results of the suggested strategy are convincing and offering specific solutions to the problems at work. The fractional problem results obtained through the given approach are also used to analyze the problems fractionally. It has been confirmed that the proposed technique can be implemented to solve various fractional PDEs and related systems.

2. Preliminaries

We covered several fundamental definitions of fractional calculus as well as Yang transform theory features in this part.

Definition 1. The fractional Caputo derivative is defined as

$$D^{\gamma}_{\varphi}\varphi(\mu, \mathfrak{J}) = \frac{1}{\Gamma(k-\gamma)}\int_0^{\mathfrak{J}} (\mathfrak{J} - \vartheta)^{k-\gamma-1}\varphi^{(k)}(\mu, \vartheta)d\vartheta, k-1 < \gamma \le k, k \in N. \tag{3}$$

Definition 2. Xiao-Jun Yang introduced the Yang Laplace transform in 2018. $\varphi(\mathfrak{J})$ or $M(u)$ determines the Yang transform for a function $\varphi(\mathfrak{J})$ and is provided as

$$\mathbf{Y}\{\varphi(\mathfrak{J})\} = M(u) = \int_0^{\infty} e^{-\mathfrak{J}/u}\varphi(\mathfrak{J})d\mathfrak{J}, \mathfrak{J} > 0, u \in (-\mathfrak{J}_1, \mathfrak{J}_2). \tag{4}$$

The inverse Yang transform is given as

$$\mathbf{Y}^{-1}\{M(u)\} = \varphi(\mathfrak{J}). \tag{5}$$

Definition 3. For nth derivatives, the Yang transform is given as

$$\mathbf{Y}\{\varphi^{n}(\mathfrak{J})\} = \frac{M(u)}{u^n} - \sum_{k=0}^{n-1}\frac{\varphi^k(0)}{u^{n-k-1}}, \forall n = 1, 2, 3, \cdots. \tag{6}$$

Definition 4. For derivative having fractional order, the Yang transform is

$$\mathbf{Y}\{\varphi^{\gamma}(\mathfrak{J})\} = \frac{M(u)}{u^{\gamma}} - \sum_{k=0}^{n-1}\frac{\varphi^k(0)}{u^{\gamma-(k+1)}}, 0 < \gamma \le n. \tag{7}$$

3. Idea of YTDM

The general methodology for solving fractional partial differential equations is given as

$$D^{\gamma}_{\mathfrak{J}}\varphi(\mu, \mathfrak{J}) = \mathscr{P}_1(\mu, \mathfrak{J}) + \mathscr{Q}_1(\mu, \mathfrak{J}), 0 < \gamma \le 1, \tag{8}$$

with initial sources

$$\varphi(\mu, 0) = \varphi(\mu), \quad \frac{\partial}{\partial \mathfrak{J}}\varphi(\mu, 0) = \zeta(\mu), \tag{9}$$

where Caputo fractional derivative having order γ is represented by $D^{\gamma}_{\mathfrak{J}} = \partial^{\gamma}/\partial\mathfrak{J}^{\gamma}$; $\mathscr{P}_1$ and $\mathscr{Q}_1$ are linear and nonlinear functions, respectively.

On employing Yang transform, we get

$$\mathbf{Y}\left[D^{\gamma}_{\mathfrak{J}}\varphi(\mu, \mathfrak{J})\right] = \mathbf{Y}[\mathscr{P}_1(\mu, \mathfrak{J}) + \mathscr{Q}_1(\mu, \mathfrak{J})]. \tag{10}$$

By using Yang differentiation property, we have

$$\frac{1}{u^{\gamma}}\left\{M(u) - u\varphi(0) - u^2\varphi'(0)\right\} = \mathbf{Y}[\mathscr{P}_1(\mu, \mathfrak{J}) + \mathscr{Q}_1(\mu, \mathfrak{J})]. \tag{11}$$

From above equation

$$M(\varphi) = u\varphi(0) + u^2\varphi'(0) + u^{\gamma}\mathbf{Y}[\mathscr{P}_1(\mu, \mathfrak{J}) + \mathscr{Q}_1(\mu, \mathfrak{J})]. \tag{12}$$

On applying inverse Yang transform, we have

$$\varphi(\mu,\mathfrak{T})=\varphi(0)+\varphi'(0)+\mathbf{Y}^{-1}[u^\gamma\mathbf{Y}[\mathscr{P}_1(\mu,\mathfrak{T})+\mathscr{Q}_1(\mu,\mathfrak{T})]. \tag{13}$$

The solution in terms of infinite sequence $\varphi(\mu,\mathfrak{T})$ by means of YTDM is

$$\varphi(\mu,\mathfrak{T})=\sum_{m=0}^{\infty}\varphi_m(\mu,\mathfrak{T}). \tag{14}$$

Now, the nonlinear terms by means of Adomian polynomials are decomposed as

$$\mathscr{Q}_1(\mu,\mathfrak{T})=\sum_{m=0}^{\infty}\mathscr{A}_m. \tag{15}$$

The Adomian polynomials all forms of nonlinearity are given as

$$\mathscr{A}_m=\frac{1}{m!}\left[\frac{\partial^m}{\partial\ell^m}\left\{\mathscr{Q}_1\left(\sum_{k=0}^{\infty}\ell^k\mu_k,\sum_{k=0}^{\infty}\ell^k\mathfrak{T}_k\right)\right\}\right]_{\ell=0}. \tag{16}$$

By substituting Equation (35) and Equation (38) into (34), we have

$$\sum_{m=0}^{\infty}\varphi_m(\mu,\mathfrak{T})=\varphi(0)+\varphi'(0)+\mathbf{Y}^{-1}u^\gamma\cdot\left[\mathbf{Y}\left\{\mathscr{P}_1\left(\sum_{m=0}^{\infty}\mu_m,\sum_{m=0}^{\infty}\mathfrak{T}_m\right)+\sum_{m=0}^{\infty}\mathscr{A}_m\right\}\right]. \tag{17}$$

The below terms are derived.

$$\begin{aligned}\varphi_0(\mu,\mathfrak{T})&=\varphi(0)+\mathfrak{T}\varphi'(0),\\ \varphi_1(\mu,\mathfrak{T})&=\mathbf{Y}^{-1}[u^\gamma\mathbf{Y}^+\{\mathscr{P}_1(\mu_0,\mathfrak{T}_0)+\mathscr{A}_0\}],\end{aligned} \tag{18}$$

thus for $m\geq 1$, the general term is given as

$$\varphi_{m+1}(\mu,\mathfrak{T})=\mathbf{Y}^{-1}[u^\gamma\mathbf{Y}^+\{\mathscr{P}_1(\mu_m,\mathfrak{T}_m)+\mathscr{A}_m\}]. \tag{19}$$

Theorem 5. *Here, we will study the convergence analysis as same manner in [30] of the YTDM applied to the fractional order partial differential equation. Let us consider the Hilbert space H which may define by $H=L^2((\alpha,\beta)X[0,T])$ the set of applications:*

$$u:(\alpha,\beta)X[0,T]\longrightarrow with\int_{(\alpha,\beta)X[0,T]}u^2(x,s)dsd\theta<+\infty. \tag{20}$$

Now, we consider the fractional partial differential equation in the above assumptions and let us denote

$$\mathbf{Y}(u)=\frac{\partial^\gamma u}{\partial\mathfrak{T}^\gamma}, \tag{21}$$

then the fractional partial differential equation becomes in an operator form

$$\mathbf{Y}(u)=-\varphi\frac{\partial v(x,\mathfrak{T})}{\partial x}-w\frac{\partial^3 v(x,\mathfrak{T})}{\partial x^3}. \tag{22}$$

The YTDM is convergence if the following two hypotheses are satisfied:

H1: $(\mathbf{Y}(u)-\mathbf{Y}(v),u-v)\geq k\|u-v\|^2$; $k>0,\forall u,v\varepsilon H$

H2: whatever may be $M>0$, there exist a constant $C(M)>0$ such that for $u,v\varepsilon H$ with $\|u\|\leq M$ and $\|v\|\leq M$ we have $(\mathbf{Y}(u)-\mathbf{Y}(v),u-v)\leq C(M)\|u-v\|\|w\|$ for every $w\varepsilon H$

4. Applications

Here, in this part, we implemented YTDM for solving various time-fractional Fokker-Planck equation.

Example 1. Consider F-FPEs of the form

$$\frac{\partial^\gamma}{\partial\mathfrak{T}^\gamma}(\varphi(\mu,\mathfrak{T}))+\frac{\partial}{\partial\mu}\left(\frac{\mu}{6}\varphi(\mu,\mathfrak{T})\right)-\frac{\partial^2}{\partial\mu^2}\left(\frac{\mu^2}{12}\varphi(\mu,\mathfrak{T})\right)=0,\ \mu,\mathfrak{T}>0,\ \gamma\in(0,1], \tag{23}$$

with the initial condition

$$\varphi(\mu,0)=\mu^2. \tag{24}$$

On employing Yang transform, we get

$$\mathbf{Y}\left\{\frac{\partial^\gamma\varphi}{\partial\mathfrak{T}^\gamma}\right\}=\mathbf{Y}\left[-\frac{\partial}{\partial\mu}\left(\frac{\mu}{6}\varphi(\mu,\mathfrak{T})\right)+\frac{\partial^2}{\partial\mu^2}\left(\frac{\mu^2}{12}\varphi(\mu,\mathfrak{T})\right)\right]. \tag{25}$$

By using Yang differentiation property, we have

$$\begin{aligned}\frac{1}{u^\gamma}\{M(u)-u\varphi(0)\}&=\mathbf{Y}\left[-\frac{\partial}{\partial\mu}\left(\frac{\mu}{6}\varphi(\mu,\mathfrak{T})\right)+\frac{\partial^2}{\partial\mu^2}\left(\frac{\mu^2}{12}\varphi(\mu,\mathfrak{T})\right)\right],\\ M(u)&=u\varphi(0)+u^\gamma\mathbf{Y}\left[-\frac{\partial}{\partial\mu}\left(\frac{\mu}{6}\varphi(\mu,\mathfrak{T})\right)+\frac{\partial^2}{\partial\mu^2}\left(\frac{\mu^2}{12}\varphi(\mu,\mathfrak{T})\right)\right].\end{aligned} \tag{26}$$

On applying inverse Yang transform, we have

$$\varphi(\mu,\mathfrak{I})=\varphi(0)+\mathbf{Y}^{-1}\left[u^{\gamma}\left\{\mathbf{Y}\left(-\frac{\partial}{\partial\mu}\left(\frac{\mu}{6}\varphi(\mu,\mathfrak{I})\right)+\frac{\partial^2}{\partial\mu^2}\left(\frac{\mu^2}{12}\varphi(\mu,\mathfrak{I})\right)\right)\right\}\right],$$
$$\varphi(\mu,\mathfrak{I})=\mu^2+\mathbf{Y}^{-1}\left[u^{\gamma}\left\{\mathbf{Y}\left(-\frac{\partial}{\partial\mu}\left(\frac{\mu}{6}\varphi(\mu,\mathfrak{I})\right)+\frac{\partial^2}{\partial\mu^2}\left(\frac{\mu^2}{12}\varphi(\mu,\mathfrak{I})\right)\right)\right\}\right]. \tag{27}$$

The solution in terms of infinite sequence $\varphi(\mu,\mathfrak{I})$ by means of YTDM is

$$\varphi(\mu,\mathfrak{I})=\sum_{m=0}^{\infty}\varphi_m(\mu,\mathfrak{I}),$$
$$\sum_{m=0}^{\infty}\varphi_m(\mu,\mathfrak{I})=\mu^2+\mathbf{Y}^{-1}\left[u^{\gamma}\mathbf{Y}\left[-\frac{\partial}{\partial\mu}\left(\frac{\mu}{6}\varphi(\mu,\mathfrak{I})\right)+\frac{\partial^2}{\partial\mu^2}\left(\frac{\mu^2}{12}\varphi(\mu,\mathfrak{I})\right)\right]\right]. \tag{28}$$

By comparing Equation (28) both sides, we get

$$\varphi_0(\mu,\mathfrak{I})=\mu^2. \tag{29}$$

On $m=0$,

$$\varphi_1(\mu,\mathfrak{I})=\mu^2\frac{\mathfrak{I}^{\gamma}}{2\Gamma(\gamma+1)}. \tag{30}$$

On $m=1$,

$$\varphi_2(\mu,\mathfrak{I})=\mu^2\frac{\mathfrak{I}^{2\gamma}}{8\Gamma(2\gamma+1)}. \tag{31}$$

On $m=2$,

$$\varphi_3(\mu,\mathfrak{I})=\mu^2\frac{\mathfrak{I}^{3\gamma}}{24\Gamma(3\gamma+1)}. \tag{32}$$

The YTDM solution remaining components φ_m for $(m\geq 3)$ are calculated easily. Thus, we define the series form solution as

$$\varphi(\mu,\mathfrak{I})=\sum_{m=0}^{\infty}\varphi_m(\mu,\mathfrak{I})=\varphi_0(\mu,\mathfrak{I})+\varphi_1(\mu,\mathfrak{I})+\varphi_2(\mu,\mathfrak{I})+\varphi_3(\mu,\mathfrak{I})+\cdots,$$
$$\varphi(\mu,\mathfrak{I})=\mu^2+\mu^2\frac{\mathfrak{I}^{\gamma}}{2\Gamma(\gamma+1)}+\mu^2\frac{\mathfrak{I}^{2\gamma}}{8\Gamma(2\gamma+1)}+\mu^2\frac{\mathfrak{I}^{3\gamma}}{24\Gamma(3\gamma+1)}+\cdots. \tag{33}$$

The YTDM solution at $\gamma=1$ is

$$\varphi(\mu,\mathfrak{I})=\mu^2\exp^{\mathfrak{I}/2}. \tag{34}$$

In Figure 1, the first graph shows the exact and second the analytical solution graph, which shows the close contact with each other. In Figure 1, the third and fourth graphs are the three- and two-dimensional graphs concerning different fractional order of problem 1. The figures show that the suggested technique agrees with the actual solution for the given problem. As fractional order approaches integer order, fractional-order solution surfaces converge to the integer-order surface, as depicted by graphs. It means that we may physically model any surface based on the physical events observed in nature.

Example 2. Consider F-FPEs of the form

$$\frac{\partial}{\partial\mathfrak{I}^{\gamma}}(\varphi(\mu,\mathfrak{I}))+\frac{\partial}{\partial\mu}(\mu\varphi(\mu,\mathfrak{I}))-\frac{\partial^2}{\partial\mu^2}\left(\frac{\mu^2}{2}\varphi(\mu,\mathfrak{I})\right)=0,\ \mu,\mathfrak{I}>0,\ \gamma\in(0,1], \tag{35}$$

with the initial condition

$$\varphi(\mu,0)=\mu. \tag{36}$$

On employing Yang transform, we get

$$\mathbf{Y}\left\{\frac{\partial^{\gamma}\varphi}{\partial\mathfrak{I}^{\gamma}}\right\}=\mathbf{Y}\left[-\frac{\partial}{\partial\mu}(\mu\varphi(\mu,\mathfrak{I}))+\frac{\partial^2}{\partial\mu^2}\left(\frac{\mu^2}{2}\varphi(\mu,\mathfrak{I})\right)\right]. \tag{37}$$

By using Yang differentiation property, we have

$$\frac{1}{u^{\gamma}}\{M(u)-u\varphi(0)\}=\mathbf{Y}\left[-\frac{\partial}{\partial\mu}(\mu\varphi(\mu,\mathfrak{I}))+\frac{\partial^2}{\partial\mu^2}\left(\frac{\mu^2}{2}\varphi(\mu,\mathfrak{I})\right)\right], \tag{38}$$

$$M(u) = u\varphi(0) + u^{\gamma}\mathbf{Y}\left[-\frac{\partial}{\partial\mu}(\mu\varphi(\mu,\mathfrak{I})) + \frac{\partial^2}{\partial\mu^2}\left(\frac{\mu^2}{2}\varphi(\mu,\mathfrak{I})\right)\right]. \tag{39}$$

On applying inverse Yang transform, we have

$$\begin{aligned}\varphi(\mu,\mathfrak{I}) &= \varphi(0) + \mathbf{Y}^{-1}\left[u^{\gamma}\left\{\mathbf{Y}\left(-\frac{\partial}{\partial\mu}(\mu\varphi(\mu,\mathfrak{I})) + \frac{\partial^2}{\partial\mu^2}\left(\frac{\mu^2}{2}\varphi(\mu,\mathfrak{I})\right)\right)\right\}\right],\\ \varphi(\mu,\mathfrak{I}) &= \mu + \mathbf{Y}^{-1}\left[u^{\gamma}\left\{\mathbf{Y}\left(-\frac{\partial}{\partial\mu}(\mu\varphi(\mu,\mathfrak{I})) + \frac{\partial^2}{\partial\mu^2}\left(\frac{\mu^2}{2}\varphi(\mu,\mathfrak{I})\right)\right)\right\}\right].\end{aligned} \tag{40}$$

The solution in terms of infinite sequence $\varphi(\mu,\mathfrak{I})$ by means of YTDM is

$$\begin{aligned}\varphi(\mu,\mathfrak{I}) &= \sum_{m=0}^{\infty}\varphi_m(\mu,\mathfrak{I}),\\ \sum_{m=0}^{\infty}\varphi_m(\mu,\mathfrak{I}) &= \mu + \mathbf{Y}^{-1}\left[u^{\gamma}\mathbf{Y}\left[-\frac{\partial}{\partial\mu}(\mu\varphi(\mu,\mathfrak{I})) + \frac{\partial^2}{\partial\mu^2}\left(\frac{\mu^2}{2}\varphi(\mu,\mathfrak{I})\right)\right]\right].\end{aligned} \tag{41}$$

By comparing Equation (41) both sides, we get

$$\varphi_0(\mu,\mathfrak{I}) = \mu. \tag{42}$$

On $m = 0$,

$$\varphi_1(\mu,\mathfrak{I}) = \mu\frac{\mathfrak{I}^{\gamma}}{\Gamma(\gamma+1)}. \tag{43}$$

On $m = 1$,

$$\varphi_2(\mu,\mathfrak{I}) = \mu\frac{\mathfrak{I}^{2\gamma}}{\Gamma(2\gamma+1)}. \tag{44}$$

On $m = 2$,

$$\varphi_3(\mu,\mathfrak{I}) = \mu\frac{\mathfrak{I}^{3\gamma}}{\Gamma(3\gamma+1)}. \tag{45}$$

The YTDM solution remaining components φ_m with ($m \geq 3$) are calculated easily. Thus, we define the series form solution as

$$\begin{aligned}\varphi(\mu,\mathfrak{I}) &= \sum_{m=0}^{\infty}\varphi_m(\mu,\mathfrak{I}) = \varphi_0(\mu,\mathfrak{I}) + \varphi_1(\mu,\mathfrak{I}) + \varphi_2(\mu,\mathfrak{I}) + \varphi_3(\mu,\mathfrak{I}) + \cdots,\\ \varphi(\mu,\mathfrak{I}) &= \mu + \mu\frac{\mathfrak{I}^{\gamma}}{\Gamma(\gamma+1)} + \mu\frac{\mathfrak{I}^{2\gamma}}{\Gamma(2\gamma+1)} + \mu\frac{\mathfrak{I}^{3\gamma}}{\Gamma(3\gamma+1)} + \cdots.\end{aligned} \tag{46}$$

The YTDM solution at $\gamma = 1$ is

$$\varphi(\mu,\mathfrak{I}) = \mu\exp^{\mathfrak{I}}. \tag{47}$$

In Figure 2, the first graph shows the exact and second the analytical solution graph, which shows the close contact with each other. In Figure 2, the third and fourth graphs are the three- and two-dimensional graphs concerning different fractional order of problem 2. The figures show that the suggested technique agrees with the actual solution for the given problem. As fractional order approaches integer order, fractional-order solution surfaces converge to the integer-order surface, as depicted by graphs. It means that we may physically model any surface based on the physical events observed in nature.

Example 3. Consider F-FPEs of the form

$$\frac{\partial}{\partial\mathfrak{I}^{\gamma}}(\varphi(\mu,\mathfrak{I})) + \frac{\partial}{\partial\mu}\left(\frac{4}{\mu}\varphi^2(\mu,\mathfrak{I})\right) - \frac{\partial}{\partial\mu}\left(\frac{\mu}{3}\varphi(\mu,\mathfrak{I})\right) - \frac{\partial^2}{\partial\mu^2}\left(\varphi^2(\mu,\mathfrak{I})\right) = 0, \mu, \mathfrak{I} > 0, \gamma \in (0, 1], \tag{48}$$

with the initial condition

$$\varphi(\mu, 0) = \mu^2. \tag{49}$$

On employing Yang transform, we get

$$\mathbf{Y}\left\{\frac{\partial^{\gamma}\varphi}{\partial\mathfrak{I}^{\gamma}}\right\} = \mathbf{Y}\left[\frac{\partial}{\partial\mu}\left(\frac{\mu}{3}\varphi(\mu,\mathfrak{I})\right) + \frac{\partial^2}{\partial\mu^2}\left(\varphi^2(\mu,\mathfrak{I})\right) - \frac{\partial}{\partial\mu}\left(\frac{4}{\mu}\varphi^2(\mu,\mathfrak{I})\right)\right]. \tag{50}$$

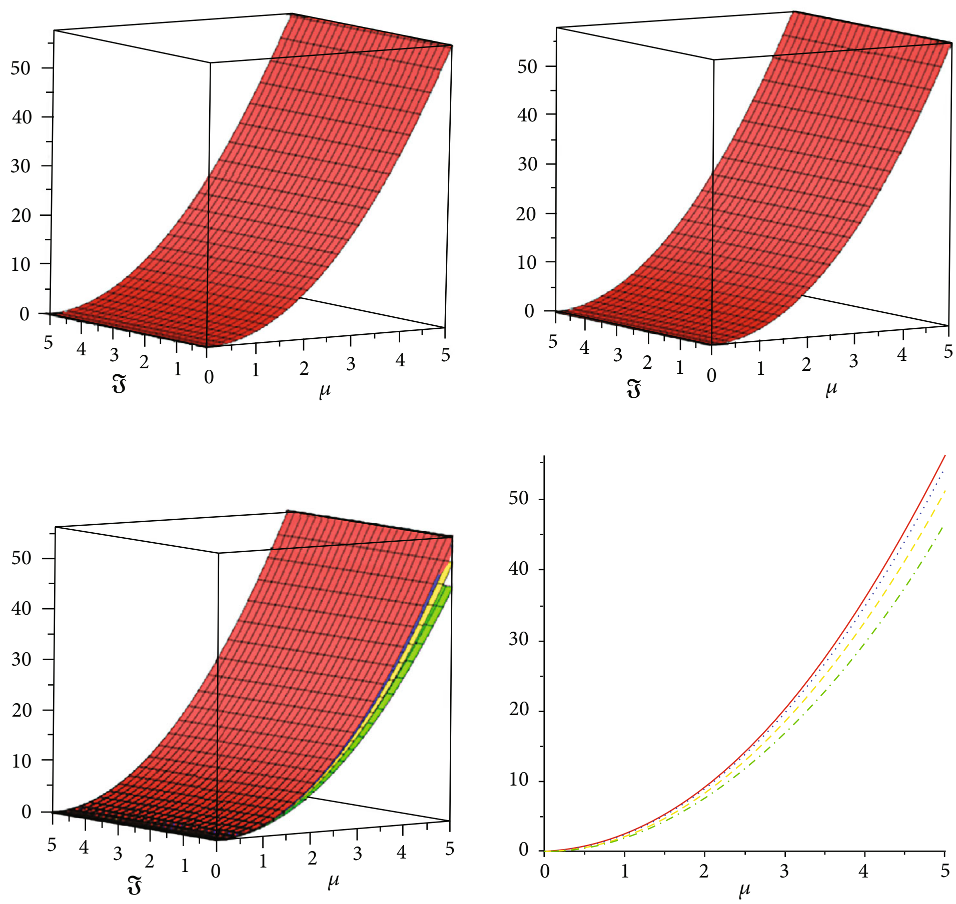

Figure 1: Nature of the exact solution, analytical solution, and solution at various fractional orders of problem 1.

By using Yang differentiation property, we have

$$\frac{1}{u^{\gamma}}\{M(u)-u\varphi(0)\}=\mathbf{Y}\left[\frac{\partial}{\partial\mu}\left(\frac{\mu}{3}\varphi(\mu,\mathfrak{J})\right)+\frac{\partial^2}{\partial\mu^2}\left(\varphi^2(\mu,\mathfrak{J})\right)-\frac{\partial}{\partial\mu}\left(\frac{4}{\mu}\varphi^2(\mu,\mathfrak{J})\right)\right],$$
$$M(u)=u\varphi(0)+u^{\gamma}\mathbf{Y}\left[\frac{\partial}{\partial\mu}\left(\frac{\mu}{3}\varphi(\mu,\mathfrak{J})\right)+\frac{\partial^2}{\partial\mu^2}\left(\varphi^2(\mu,\mathfrak{J})\right)-\frac{\partial}{\partial\mu}\left(\frac{4}{\mu}\varphi^2(\mu,\mathfrak{J})\right)\right]. \quad (51)$$

On applying inverse Yang transform, we have

$$\varphi(\mu,\mathfrak{J})=\varphi(0)+\mathbf{Y}^{-1}\left[u^{\gamma}\left\{\mathbf{Y}\left(\frac{\partial}{\partial\mu}\left(\frac{\mu}{3}\varphi(\mu,\mathfrak{J})\right)+\frac{\partial^2}{\partial\mu^2}\left(\varphi^2(\mu,\mathfrak{J})\right)-\frac{\partial}{\partial\mu}\left(\frac{4}{\mu}\varphi^2(\mu,\mathfrak{J})\right)\right)\right\}\right],$$
$$\varphi(\mu,\mathfrak{J})=\mu^2+\mathbf{Y}^{-1}\left[u^{\gamma}\left\{\mathbf{Y}\left(\frac{\partial}{\partial\mu}\left(\frac{\mu}{3}\varphi(\mu,\mathfrak{J})\right)+\frac{\partial^2}{\partial\mu^2}\left(\varphi^2(\mu,\mathfrak{J})\right)-\frac{\partial}{\partial\mu}\left(\frac{4}{\mu}\varphi^2(\mu,\mathfrak{J})\right)\right)\right\}\right]. \quad (52)$$

Now, by assuming that the infinite series form the function $\varphi(\mu,\mathfrak{J})$ which is unknown, it has the solution as

$$\varphi(\mu,\mathfrak{J})=\sum_{m=0}^{\infty}\varphi_m(\mu,\mathfrak{J}). \quad (53)$$

Thus, the nonlinear terms are defined by the Adomian polynomial $\varphi^2=\sum_{m=0}^{\infty}\mathscr{A}_m$. Using specific concepts, Equation (52) can be rewritten in the form

$$\sum_{m=0}^{\infty}\varphi_m(\mu,\mathfrak{J})=\varphi(\mu,0)+\mathbf{Y}^{-1}\left[u^{\gamma}\mathbf{Y}\left[\frac{\partial}{\partial\mu}\left(\frac{\mu}{3}\varphi(\mu,\mathfrak{J})\right)+\sum_{m=0}^{\infty}\mathscr{A}_m\right]\right],$$
$$\sum_{m=0}^{\infty}\varphi_m(\mu,\mathfrak{J})=\mu^2+\mathbf{Y}^{-1}\left[u^{\gamma}\mathbf{Y}\left[\frac{\partial}{\partial\mu}\left(\frac{\mu}{3}\varphi(\mu,\mathfrak{J})\right)+\sum_{m=0}^{\infty}\mathscr{A}_m\right]\right]. \quad (54)$$

Now, by Adomian polynomial $\mathscr{Q}_1$, the nonlinear terms

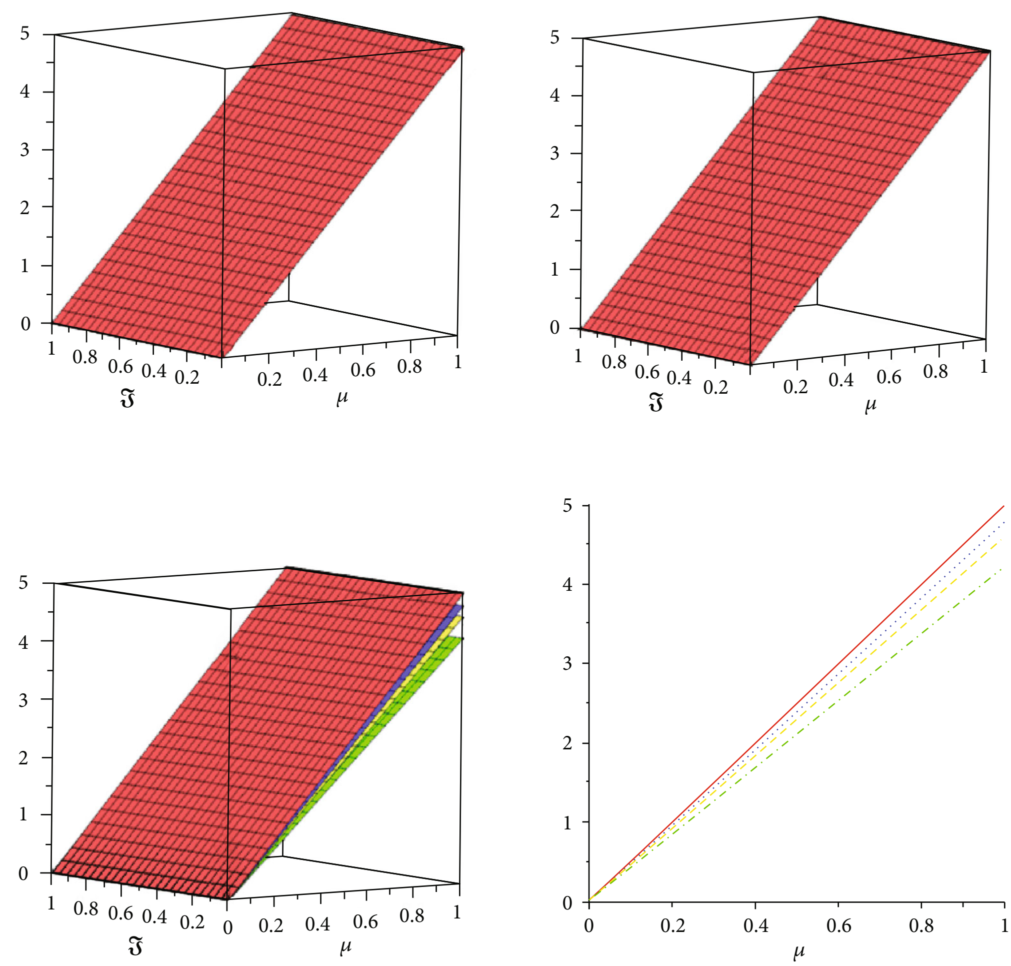

Figure 2: Nature of the exact solution, analytical solution, and solution at various fractional orders of problem 2.

are decomposed according to Equation (38),

$$\begin{aligned}\mathscr{A}_0 &= \varphi_0^2,\\ \mathscr{A}_1 &= 2\varphi_0\varphi_1,\\ \mathscr{A}_2 &= 2\varphi_0\varphi_2 + (\varphi_2)^2.\end{aligned} \tag{55}$$

By comparing Equation (54) both sides, we get

$$\varphi_0(\mu, \mathfrak{I}) = \mu^2. \tag{56}$$

On $m = 0$,

$$\varphi_1(\mu, \mathfrak{I}) = \mu^2 \frac{\mathfrak{I}^{\gamma}}{\Gamma(\gamma + 1)}. \tag{57}$$

On $m = 1$,

$$\varphi_2(\mu, \mathfrak{I}) = \mu^2 \frac{\mathfrak{I}^{2\gamma}}{\Gamma(2\gamma + 1)}. \tag{58}$$

On $m = 2$,

$$\varphi_3(\mu, \mathfrak{I}) = \mu^2 \frac{\mathfrak{I}^{3\gamma}}{\Gamma(3\gamma + 1)}. \tag{59}$$

The YTDM solution remaining components φ_m with ($m \geq 3$) are calculated easily. Thus, we define the series form solution as

$$\begin{aligned}\varphi(\mu, \mathfrak{I}) &= \sum_{m=0}^{\infty} \varphi_m(\mu, \mathfrak{I}) = \varphi_0(\mu, \mathfrak{I}) + \varphi_1(\mu, \mathfrak{I}) + \varphi_2(\mu, \mathfrak{I}) + \varphi_3(\mu, \mathfrak{I}) + \cdots,\\ \varphi(\mu, \mathfrak{I}) &= \mu^2 + \mu^2 \frac{\mathfrak{I}^{\gamma}}{\Gamma(\gamma + 1)} + \mu^2 \frac{\mathfrak{I}^{2\gamma}}{\Gamma(2\gamma + 1)} + \mu^2 \frac{\mathfrak{I}^{3\gamma}}{\Gamma(3\gamma + 1)} + \cdots.\end{aligned} \tag{60}$$

The YTDM solution at $\gamma = 1$ is

$$\varphi(\mu, \mathfrak{I}) = \mu^2 \exp^{\mathfrak{I}}. \tag{61}$$

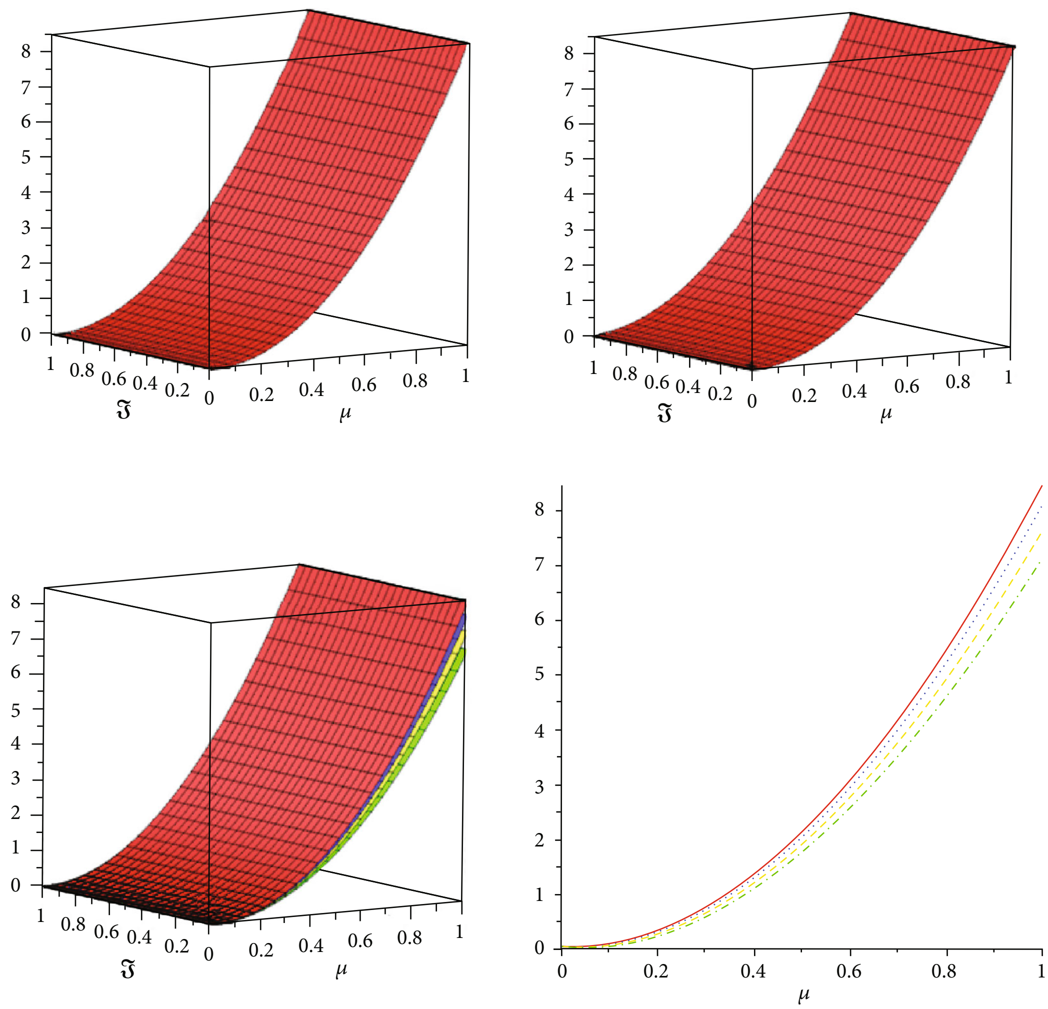

Figure 3: Nature of the exact solution, analytical solution, and solution at various fractional orders of problem 3.

In Figure 3, the first graph shows the exact and second the analytical solution graph, which shows the close contact with each other. In Figure 3, the third and fourth graphs are the three- and two-dimensional graphs concerning different fractional order of problem 3. The figures show that the suggested technique agrees with the actual solution for the given problem. As fractional order approaches integer order, fractional-order solution surfaces converge to the integer-order surface, as depicted by graphs. It means that we may physically model any surface based on the physical events observed in nature.

Example 4. Consider F-FPEs of the form

$$\frac{\partial}{\partial \mathfrak{I}^{\gamma}}(\varphi(\mu,\mathfrak{I})) - \frac{\partial}{\partial \mu}\varphi(\mu,\mathfrak{I}) - \frac{\partial^2}{\partial \mu^2}\varphi(\mu,\mathfrak{I}) = 0,\ \mathfrak{I} > 0,\ \gamma \in (0,1], \tag{62}$$

with the initial condition

$$\varphi(\mu,0) = \mu. \tag{63}$$

On employing Yang transform, we get

$$\mathbf{Y}\left\{\frac{\partial^{\gamma}\varphi}{\partial \mathfrak{I}^{\gamma}}\right\} = \mathbf{Y}\left[\frac{\partial}{\partial \mu}\varphi(\mu,\mathfrak{I}) + \frac{\partial^2}{\partial \mu^2}\varphi(\mu,\mathfrak{I})\right]. \tag{64}$$

By using Yang differentiation property, we have

$$\frac{1}{u^{\gamma}}\{M(u) - u\varphi(0)\} = \mathbf{Y}\left[\frac{\partial}{\partial \mu}\varphi(\mu,\mathfrak{I}) + \frac{\partial^2}{\partial \mu^2}\varphi(\mu,\mathfrak{I})\right],$$
$$M(u) = u\varphi(0) + u^{\gamma}\mathbf{Y}\left[\frac{\partial}{\partial \mu}\varphi(\mu,\mathfrak{I}) + \frac{\partial^2}{\partial \mu^2}\varphi(\mu,\mathfrak{I})\right]. \tag{65}$$

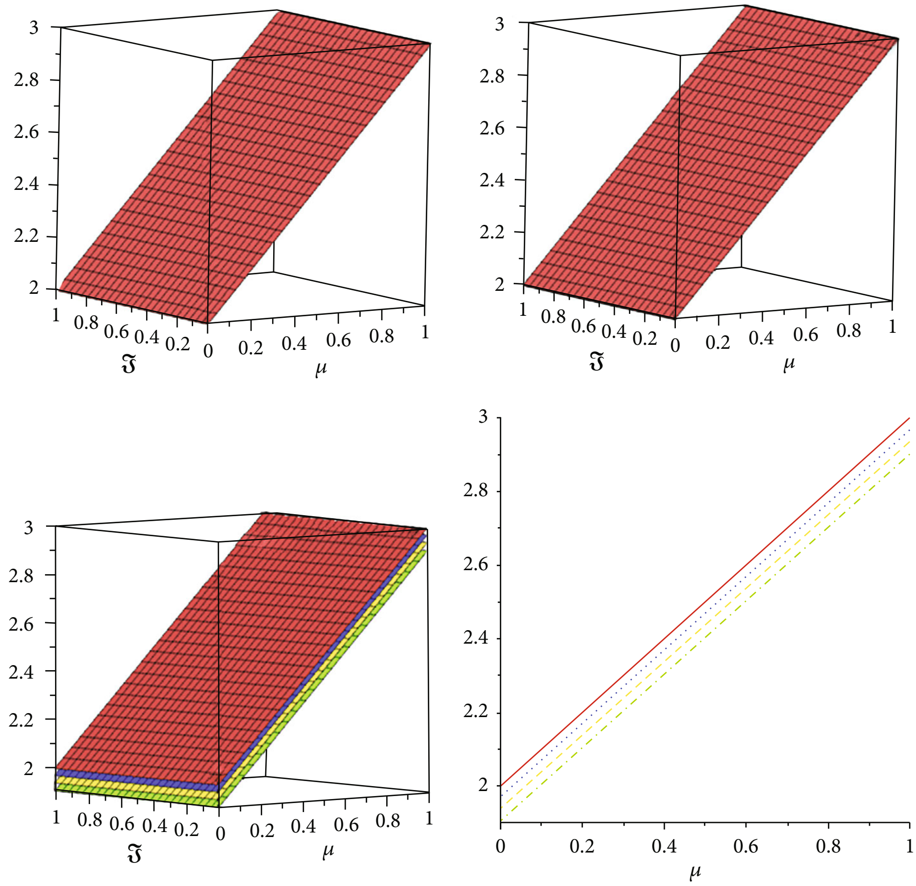

Figure 4: Nature of the exact solution, analytical solution, and solution at various fractional orders of problem 4.

On applying inverse Yang transform, we have

$$\varphi(\mu,\mathfrak{J})=\varphi(0)+\mathbf{Y}^{-1}\left[u^{\gamma}\left\{\mathbf{Y}\left(\frac{\partial}{\partial\mu}\varphi(\mu,\mathfrak{J})+\frac{\partial^2}{\partial\mu^2}\varphi(\mu,\mathfrak{J})\right)\right\}\right],$$
$$\varphi(\mu,\mathfrak{J})=\mu+\mathbf{Y}^{-1}\left[u^{\gamma}\left\{\mathbf{Y}\left(\frac{\partial}{\partial\mu}\varphi(\mu,\mathfrak{J})+\frac{\partial^2}{\partial\mu^2}\varphi(\mu,\mathfrak{J})\right)\right\}\right]. \tag{66}$$

The solution in terms of infinite sequence $\varphi(\mu,\mathfrak{J})$ by means of YTDM is

$$\varphi(\mu,\mathfrak{J})=\sum_{m=0}^{\infty}\varphi_m(\mu,\mathfrak{J}),$$
$$\sum_{m=0}^{\infty}\varphi_m(\mu,\mathfrak{J})=\mu+\mathbf{Y}^{-1}\left[u^{\gamma}\mathbf{Y}\left[\frac{\partial}{\partial\mu}\varphi(\mu,\mathfrak{J})+\frac{\partial^2}{\partial\mu^2}\varphi(\mu,\mathfrak{J})\right]\right]. \tag{67}$$

By comparing Equation (67) both sides, we get

$$\varphi_0(\mu,\mathfrak{J})=\mu. \tag{68}$$

On $m=0$,

$$\varphi_1(\mu,\mathfrak{J})=\frac{\mathfrak{J}^{\gamma}}{\Gamma(\gamma+1)}. \tag{69}$$

On $m=1$,

$$\varphi_2(\mu,\mathfrak{J})=0. \tag{70}$$

On $m=2$,

$$\varphi_3(\mu,\mathfrak{J})=0. \tag{71}$$

The YTDM solution remaining components φ_m with ($m\geq 3$) are calculated easily. Thus, we define the series form solution as

$$\varphi(\mu,\mathfrak{J})=\sum_{m=0}^{\infty}\varphi_m(\mu,\mathfrak{J})=\varphi_0(\mu,\mathfrak{J})+\varphi_1(\mu,\mathfrak{J})+\varphi_2(\mu,\mathfrak{J})+\varphi_3(\mu,\mathfrak{J})+\cdots, \tag{72}$$
$$\varphi(\mu,\mathfrak{J})=\mu+\frac{\mathfrak{J}^{\gamma}}{\Gamma(\gamma+1)}+0+0+\cdots.$$

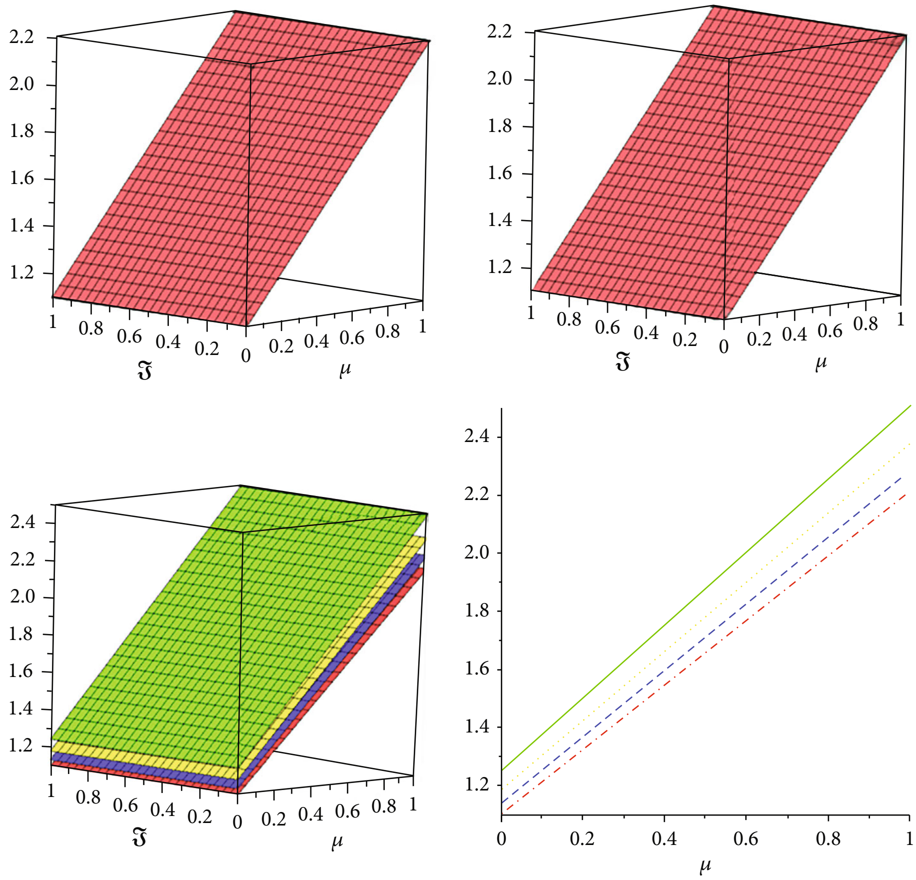

Figure 5: Nature of the exact solution, analytical solution, and solution at various fractional orders of problem 5.

The YTDM solution at $\gamma = 1$ is

$$\varphi(\mu, \mathfrak{T}) = \mu + \mathfrak{T}. \tag{73}$$

In Figure 4, the first graph shows the exact and second the analytical solution graph, which shows the close contact with each other. In Figure 4, the third and fourth graphs are the three- and two-dimensional graphs concerning different fractional order of problem 4. The figures show that the suggested technique agrees with the actual solution for the given problem. As fractional order approaches integer order, fractional-order solution surfaces converge to the integer-order surface, as depicted by graphs. It means that we may physically model any surface based on the physical events observed in nature.

Example 5. Consider F-FPEs of the form

$$\frac{\partial^\gamma}{\partial \mathfrak{T}^\gamma}(\varphi(\mu, \mathfrak{T})) - (1-\mu)\frac{\partial}{\partial \mu}\varphi(\mu, \mathfrak{T}) - \left(e^{\mathfrak{T}}\mu^2\right)\frac{\partial^2}{\partial \mu^2}\varphi(\mu, \mathfrak{T}) = 0, \mathfrak{T} > 0, \ \gamma \in (0, 1], \tag{74}$$

with the initial condition

$$\varphi(\mu, 0) = 1 + \mu. \tag{75}$$

On employing Yang transform, we get

$$\mathbf{Y}\left\{\frac{\partial^\gamma \varphi}{\partial \mathfrak{T}^\gamma}\right\} = \mathbf{Y}\left[(1-\mu)\frac{\partial}{\partial \mu}\varphi(\mu, \mathfrak{T}) + \left(e^{\mathfrak{T}}\mu^2\right)\frac{\partial^2}{\partial \mu^2}\varphi(\mu, \mathfrak{T})\right]. \tag{76}$$

By using Yang differentiation property, we have

$$\begin{aligned}\frac{1}{u^\gamma}\{M(u) - u\varphi(0)\} &= \mathbf{Y}\left[(1-\mu)\frac{\partial}{\partial \mu}\varphi(\mu, \mathfrak{T}) + \left(e^{\mathfrak{T}}\mu^2\right)\frac{\partial^2}{\partial \mu^2}\varphi(\mu, \mathfrak{T})\right], \\ M(u) &= u\varphi(0) + u^\gamma \mathbf{Y}\left[(1-\mu)\frac{\partial}{\partial \mu}\varphi(\mu, \mathfrak{T}) + \left(e^{\mathfrak{T}}\mu^2\right)\frac{\partial^2}{\partial \mu^2}\varphi(\mu, \mathfrak{T})\right].\end{aligned} \tag{77}$$

On applying inverse Yang transform, we have

$$\varphi(\mu,\mathfrak{T})=\varphi(0)+\mathbf{Y}^{-1}\left[u^{\gamma}\left\{\mathbf{Y}\left((1-\mu)\frac{\partial}{\partial\mu}\varphi(\mu,\mathfrak{T})+\left(e^{\mathfrak{T}}\mu^{2}\right)\frac{\partial^{2}}{\partial\mu^{2}}\varphi(\mu,\mathfrak{T})\right)\right\}\right],$$

$$\varphi(\mu,\mathfrak{T})=(1+\mu)+\mathbf{Y}^{-1}\left[u^{\gamma}\left\{\mathbf{Y}\left((1-\mu)\frac{\partial}{\partial\mu}\varphi(\mu,\mathfrak{T})+\left(e^{\mathfrak{T}}\mu^{2}\right)\frac{\partial^{2}}{\partial\mu^{2}}\varphi(\mu,\mathfrak{T})\right)\right\}\right]. \tag{78}$$

The solution in terms of infinite sequence $\varphi(\mu,\mathfrak{T})$ by means of YTDM is

$$\varphi(\mu,\mathfrak{T})=\sum_{m=0}^{\infty}\varphi_m(\mu,\mathfrak{T}), \tag{79}$$

$$\sum_{m=0}^{\infty}\varphi_m(\mu,\mathfrak{T})=(1+\mu)+\mathbf{Y}^{-1}\left[u^{\gamma}\mathbf{Y}\left[(1-\mu)\frac{\partial}{\partial\mu}\varphi(\mu,\mathfrak{T})+\left(e^{\mathfrak{T}}\mu^{2}\right)\frac{\partial^{2}}{\partial\mu^{2}}\varphi(\mu,\mathfrak{T})\right]\right]. \tag{80}$$

By comparing Equation (80) both sides, we get

$$\varphi_0(\mu,\mathfrak{T})=1+\mu. \tag{81}$$

On $m=0$,

$$\varphi_1(\mu,\mathfrak{T})=(1+\mu)\frac{\mathfrak{T}^{\gamma}}{\Gamma(\gamma+1)}. \tag{82}$$

On $m=1$,

$$\varphi_2(\mu,\mathfrak{T})=(1+\mu)\frac{\mathfrak{T}^{2\gamma}}{\Gamma(2\gamma+1)}. \tag{83}$$

On $m=2$,

$$\varphi_3(\mu,\mathfrak{T})=(1+\mu)\frac{\mathfrak{T}^{3\gamma}}{\Gamma(3\gamma+1)}. \tag{84}$$

The YTDM solution remaining components φ_m with ($m\geq 3$) are calculated easily. Thus, we define the series form solution as

$$\varphi(\mu,\mathfrak{T})=\sum_{m=0}^{\infty}\varphi_m(\mu,\mathfrak{T})=\varphi_0(\mu,\mathfrak{T})+\varphi_1(\mu,\mathfrak{T})+\varphi_2(\mu,\mathfrak{T})+\varphi_3(\mu,\mathfrak{T})+\cdots,$$

$$\varphi(\mu,\mathfrak{T})=(1+\mu)+(1+\mu)\frac{\mathfrak{T}^{\gamma}}{\Gamma(\gamma+1)}+(1+\mu)\frac{\mathfrak{T}^{2\gamma}}{\Gamma(2\gamma+1)}+(1+\mu)\frac{\mathfrak{T}^{3\gamma}}{\Gamma(3\gamma+1)}+\cdots. \tag{85}$$

The YTDM solution at $\gamma=1$ is

$$\varphi(\mu,\mathfrak{T})=\exp^{\mathfrak{T}}(1+\mu). \tag{86}$$

In Figure 5, the first graph shows the exact and second the analytical solution graph, which shows the close contact with each other. In Figure 5, the third and fourth graphs are the three- and two-dimensional graphs concerning different fractional order of problem 5. The figures show that the suggested technique agrees with the actual solution for the given problem. As fractional order approaches integer order, fractional-order solution surfaces converge to the integer-order surface, as depicted by graphs. It means that we may physically model any surface based on the physical events observed in nature.

5. Conclusion

The Adomian decomposition approach was expanded in this paper to find explicit and numerical solutions to the F-FPEs. The proposed method is an effective and powerful strategy for solving the proposed equations. The plotted graphs confirm the strong relationship between the exact and analytical results. The approaches provide series form solutions with a higher convergence rate to exact results. While providing quantitatively accurate results, the Adomian decomposition method requires less computational work than existing approaches.

Data Availability

The numerical data used to support the findings of this study are included within the article.

Conflicts of Interest

The authors declare that there are no conflicts of interest regarding the publication of this article.

References

[1] I. Podlubny, *Fractional Differential Equations*, Academic Press, San Diego, CA, 1999.

[2] K. S. Millar and B. Ross, *An Introduction to the Fractional Calculus and Fractional Differential Equations*, Wiley, New York, 1993.

[3] M. Caputo, "Linear models of dissipation whose Q is almost frequency independent–II," *Geophysical Journal International*, vol. 13, no. 5, pp. 529–539, 1967.

[4] M. Al-Smadi, "Simplified iterative reproducing kernel method for handling time-fractional BVPs with error estimation," *Ain Shams Engineering Journal*, vol. 9, no. 4, pp. 2517–2525, 2018.

[5] M. Al-Smadi, "Solving fractional system of partial differential equations with parameters derivative by combining the GDTM and RDTM," *Nonlinear Studies*, vol. 26, pp. 587–601, 2019.

[6] M. Al-Smadi and A. O. Abu, "Computational algorithm for solving Fredholm time-fractional partial integrodifferential equations of Dirichlet functions type with error estimates," *Applied Mathematics and Computation*, vol. 342, pp. 280–294, 2019.

[7] K. Moaddy, A. Freihat, M. Al-Smadi, E. Abuteen, and I. Hashim, "Numerical investigation for handling fractional-order Rabinovich–Fabrikant model using the multistep approach," *Soft Computing*, vol. 22, no. 3, pp. 773–782, 2018.

[8] N. A. Shah, H. A. Alyousef, S. A. El-Tantawy, and J. D. Chung, "Analytical investigation of fractional-order Korteweg-De-Vries-type equations under Atangana-Baleanu-Caputo operator: modeling nonlinear waves in a plasma and fluid," *Symmetry*, vol. 14, no. 4, p. 739, 2022.

[9] N. Iqbal, A. Akgul, A. Bariq, M. Mossa Al-Sawalha, and A. Ali, "On solutions of fractional-order gas dynamics equation by effective techniques," *Journal of Function Spaces*, vol. 2022, Article ID 3341754, 14 pages, 2022.

[10] A. U. K. Niazi, N. Iqbal, F. Wannalookkhee, and K. Nonlaopon, "Controllability for fuzzy fractional evolution equations in credibility space," *Fractal and Fractional*, vol. 5, no. 3, p. 112, 2021.

[11] M. Alesemi, N. Iqbal, and A. A. Hamoud, "The analysis of fractional-order proportional delay physical models via a novel transform," *Complexity*, vol. 2022, Article ID 2431533, 13 pages, 2022.

[12] R. Ali, K. Pan, and A. Ali, "Two new iteration methods with optimal parameters for solving absolute value equations," *International Journal of Applied and Computational Mathematics*, vol. 8, no. 3, article 123, 2022.

[13] N. Iqbal, A. M. Albalahi, M. S. Abdo, and W. W. Mohammed, "Analytical analysis of fractional-order newell-whitehead-segel equation: a modified homotopy perturbation transform method," *Journal of Function Spaces*, vol. 2022, article 3298472, p. 10, 2022.

[14] M. Alshammari, N. Iqbal, W. W. Mohammed, and T. Botmart, "The solution of fractional-order system of KdV equations with exponential-decay kernel," *Results in Physics*, vol. 38, article 105615, p. 14, 2022.

[15] C. S. Singh, H. Singh, V. K. Singh, and O. P. Singh, "Fractional order operational matrix methods for fractional singular integro- differential equation," *Applied Mathematical Modelling*, vol. 40, no. 23-24, pp. 10705–10718, 2016.

[16] S. Mukhtar, R. Shah, and S. Noor, "The numerical investigation of a fractional-order multi-dimensional model of Navier-Stokes equation via novel techniques," *Symmetry*, vol. 14, no. 6, p. 1102, 2022.

[17] K. Nonlaopon, A. M. Alsharif, A. M. Zidan, A. Khan, Y. S. Hamed, and R. Shah, "Numerical investigation of fractional-order Swift-Hohenberg equations via a novel transform," *Symmetry*, vol. 13, no. 7, p. 1263, 2021.

[18] M. Dehghan, J. Manafian, and A. Saadatmandi, "The solution of the linear fractional partial differential equations using the homotopy analysis method," *Zeitschrift für Naturforschung-A*, vol. 65, no. 11, p. 935, 2010.

[19] Y. Qin, A. Khan, I. Ali et al., "An efficient analytical approach for the solution of certain fractional-order dynamical systems," *Energies*, vol. 13, no. 11, p. 2725, 2020.

[20] M. K. Alaoui, R. Fayyaz, A. Khan, R. Shah, and M. S. Abdo, "Analytical investigation of Noyes–Field model for time-fractional Belousov–Zhabotinsky reaction," *Complexity*, vol. 2021, Article ID 3248376, 21 pages, 2021.

[21] H. Khan, A. Khan, M. Al-Qurashi, R. Shah, and D. Baleanu, "Modified modelling for heat like equations within Caputo operator," *Energies*, vol. 13, no. 8, p. 2002, 2020.

[22] M. Areshi, A. Khan, R. Shah, and K. Nonlaopon, "Analytical investigation of fractional-order Newell-Whitehead-Segel equations via a novel transform," *AIMS Mathematics*, vol. 7, no. 4, pp. 6936–6958, 2022.

[23] M. A. Firoozjaee, S. A. Yousefi, and H. Jafari, "A numerical approach to Fokker-Planck equation with space- and time-fractional and non fractional derivatives," *Match-Communications in Mathematical and in Computer Chemistry*, vol. 74, pp. 449–464, 2015.

[24] N. H. Aljahdaly, A. Akgul, I. Mahariq, and J. Kafle, "A comparative analysis of the fractional-order coupled Korteweg–De Vries equations with the Mittag–Leffler law," *Journal of Mathematics*, vol. 2022, Article ID 8876149, 30 pages, 2022.

[25] S. Momani, O. Abu Arqub, A. Freihat, and M. Al-Smadi, "Analytical approximations for Fokker-Planck equations of fractional order in multistep schemes," *Applied and Computational Mathematics*, vol. 15, pp. 319–330, 2016.

[26] W. Deng, "Numerical algorithm for the time fractional Fokker-Planck equation," *Journal of Computational Physics*, vol. 227, no. 2, pp. 1510–1522, 2007.

[27] Z. Odibat and S. Momani, "Numerical solution of Fokker-Planck equation with space- and time-fractional derivatives," *Physics Letters A*, vol. 369, no. 5-6, pp. 349–358, 2007.

[28] G. Adomian, "Solution of physical problems by decomposition," *Computers & Mathematics with Applications*, vol. 27, no. 9-10, pp. 145–154, 1994.

[29] G. Adomian, "A review of the decomposition method in applied mathematics," *Journal of Mathematical Analysis and Applications*, vol. 135, pp. 501–544, 1988.

[30] R. Shah, H. Khan, M. Arif, and P. Kumam, "Application of Laplace-Adomian decomposition method for the analytical solution of third-order dispersive fractional partial differential equations," *Entropy*, vol. 21, no. 4, p. 335, 2019.

Hindawi
Journal of Function Spaces
Volume 2022, Article ID 1561375, 9 pages
https://doi.org/10.1155/2022/1561375

Research Article

On Solutions of Hybrid–Sturm-Liouville–Langevin Equations with Generalized Versions of Caputo Fractional Derivatives

Abdellatif Boutiara[1] **Hanan A. Wahash**[2] **Heba Y. Zahran**[3,4,5] **Emad E. Mahmoud**[6] **Abdel-Haleem Abdel-Aty**[7] **and El Sayed Yousef**[3,4]

[1]*Laboratory of Mathematics and Applied Sciences, University of Ghardaia, 47000, Algeria*
[2]*Department of Mathematics, Albaydaa University, Al Bayda, Yemen*
[3]*Laboratory of Nano-Smart Materials for Science and Technology (LNSMST), Department of Physics, Faculty of Science, King Khalid University, P.O. Box 9004, Abha 61413, Saudi Arabia*
[4]*Research Center for Advanced Materials Science (RCAMS), King Khalid University, P.O. Box 9004, Abha 61413, Saudi Arabia*
[5]*Nanoscience Laboratory for Environmental and Biomedical Applications (NLEBA), Semiconductor Lab., Department of Physics, Faculty of Education, Ain Shams University, Roxy, Cairo 11757, Egypt*
[6]*Department of Mathematics and Statistics, College of Science, Taif University, P.O. Box 11099, Taif 21944, Saudi Arabia*
[7]*Department of Physics, College of Sciences, University of Bisha, P.O. Box 344, Bisha 61922, Saudi Arabia*

Correspondence should be addressed to Hanan A. Wahash; hawahash86@gmail.com

Received 14 April 2022; Accepted 31 May 2022; Published 25 June 2022

Academic Editor: Yusuf Gurefe

The main intention of this research article is to introduce a new class of generalized fractional differential equations that fall into the categories of Sturm-Liouville's, Langevin's, and hybrid's problems involving Y-Caputo fractional derivatives. The existence of the solutions of the proposed equations is discussed by using the technique of the measure of noncompactness related to the fixed point theorem, which is a generalization of Darbo's fixed point theorem. Additionally, pertinent examples are provided along with the different values of the function Y to confirm the validity of the reported results.

1. Introduction

Fractional differential equations (FDEs) with their various branches such as Hybrid Equation (HE), Langevin Equation (LE), and Sturm-Liouville Equation (SLE) are currently well established, due to the number of papers and books edited worldwide. These types of equations have been applied in many applications in different fields, such as engineering and science. Since in recent years, it has achieved a great deal of development and interest by many researchers, for some of these developments in the theory of fractional differential equations, one can look at the monographs of Kilbas et al. [1] and Podlubny [2], where they presented some properties and applications appropriate for various types of fractional operators. Dhage and Lakshmikantham [3] and Dhage et al. [4] made excellent results on hybrid problems, as did Zhao et al. [5] and Ahmad and Ntouyas [6]. The LE [7] is formulated to be a powerful tool for describing the evolution of physical phenomena in volatile environments. Some of recent Langevin's problem is studied through [8–10]. However, SLE has many applications in distinct areas of technical knowledge and engineering [11, 12]. The mix of both fractional SLE and fractional LE might give an adequate description of the dynamic processes described in a fractal medium where fractal and memory properties are inserted with a scattered memory kernel. Recently, the authors in [13] suggested an approach to the fractional model of the SLE and LE. Indeed, they discussed the existence of solutions to the considered systems through fixed point techniques and mathematical inequalities. Muensawat et al. [14] studied antiperiodic BVPs for fractional systems of generalized SL and LE. Boutiara et al. [15] considered fractional LE under Caputo function-dependent kernel fractional derivatives. Existence theorem for psi-fractional HEs has been proven by Suwan et al. [16]. Some qualitative analyses for multiterm LEs with generalized Caputo FDs and diffusion FDE with ABC operators can be found in [17, 18]. The authors in [19] considered a hybrid LE involving Caputo FD and Riemann-Liouville (RL) fractional integral (FI) as follows:

$$\begin{cases} c\mathscr{D}^{\zeta}\left[{}^{c}\mathscr{D}^{\xi}\left[\dfrac{\vartheta(\sigma)}{\mathscr{M}(\sigma,\vartheta(\nu(\sigma)))}\right]-\lambda\vartheta(\sigma)\right]=\mathscr{N}(\sigma,\vartheta(\mu(\sigma)),\mathscr{I}^{\gamma}\vartheta(\mu(\sigma)),\ \sigma\in 0,1], \\ \vartheta(0)=0,\ c\mathscr{D}\xi\left[\dfrac{\vartheta(\sigma)}{\mathscr{M}(\sigma,\vartheta(\nu(\sigma)))}\right]_{\sigma=0}=0,\ \vartheta(1)=\zeta\vartheta(\kappa),\quad 0<\kappa<1,\zeta,\lambda\in\mathbb{R}. \end{cases} \tag{1}$$

Motivated by the above works aforesaid and inspired by [19, 21], in this paper, we deal with the existence of solutions for the following BVP to the nonlinear fractional hybrid–Sturm-Liouville–Langevin differential equation:

$$\begin{cases} c\mathscr{D}^{\zeta,Y}\left[p(\sigma)^{c}\mathscr{D}^{\xi,Y}\left[\dfrac{\vartheta(\sigma)}{\mathscr{M}(\sigma,\vartheta(\nu(\sigma)))}\right]-q(\sigma)\vartheta(\sigma)\right]=\mathscr{N}(\sigma,\vartheta(\mu(\sigma))),\quad \sigma\in\Pi=[a,b], \\ \vartheta(a)=0,\ p(b)^{c}\mathscr{D}^{\xi,Y}\left[\dfrac{\vartheta(\sigma)}{\mathscr{M}(\sigma,\vartheta(\nu(\sigma)))}\right]_{\sigma=b}+q(b)\vartheta(b)=0, \end{cases} \tag{2}$$

where ${}^{c}\mathscr{D}^{r,Y}$ denotes the Y-Caputo FD of order $r\in\{\zeta,\xi\}$, $0<\zeta,\xi\le 1$. Here, $\mathscr{M}\in C(\Pi\times\mathbb{R},\mathbb{R}\setminus\{0\})$, $\mathscr{N}\in C(\Pi\times\mathbb{R},\mathbb{R})$,$\nu,\mu:\Pi\longrightarrow\Pi$ are given functions, $p\in C(\Pi,\mathbb{R}\setminus\{0\})$, and $q\in C(\Pi,\mathbb{R})$. As in Banach spaces, a closed and bounded set is not generally a compact set; just continuity of the function $\mathscr{M}$ does not ensure the existence of a solution to differential equations. Our arguments are principally founded on Darbo's fixed point technique mixed with the technique of measures of noncompactness to set up the existence of solutions for (2). In particular, problem (2) is formed as an overarching structure comprising both fractional SLE, LE, and HE, subjected to boundary conditions involving Y-Caputo FDs. In fact, choosing $q(\sigma)\equiv 0$ on the one hand and $p(\sigma)\equiv 1$, $q(\sigma)=\lambda$, and $\lambda\in\mathbb{R}$, on the other hand, reduces the problem (2) into the fractional Sturm-Liouville problem and the fractional Langevin problem, respectively. Besides, if we set $p(\sigma)\equiv 1$ and $q(\sigma)\equiv 0$, the problem (2) reduces to the fractional sequential hybrid problem.

Observe also that the current results are consistent with some of the literature results when $Y(\sigma)=\sigma$, and they are new even for the special case: $Y(\sigma)=\log\sigma$ and $Y(\sigma)=\sigma^{\rho}$.

Here is a brief outline of the paper. In Section 2, we provide some preliminary facts. Sections 3 and 4 handle the formulation of solutions and the existence of solutions for (2) by using the generalized Darbo's fixed point theorem (D'sFPT) along with the approach of measures of noncompactness in the Banach algebras. Lastly, we give pertinent examples.

2. Preliminaries

Let us start this section with some auxiliary results used in the forthcoming analysis.

Definition 1 (see [1]). The Y-RL FI of order $\zeta>0$ for an integrable function $\vartheta:\Pi\longrightarrow\mathbb{R}$ is given by

$$\mathscr{I}_{a^{+}}^{\zeta;Y}\vartheta(\sigma)=\frac{1}{\Gamma(\zeta)}\int_{a}^{\sigma}Y'(\varsigma)(Y(\sigma)-Y(\varsigma))^{\zeta-1}\vartheta(\varsigma)d\varsigma, \tag{3}$$

where Γ is the gamma function. One can deduce that

$$D_{\sigma}\left(\mathscr{I}_{a^{+}}^{\zeta;Y}\vartheta(\sigma)\right)=Y'(\sigma)\mathscr{I}_{a^{+}}^{\zeta-1;Y}\vartheta(\sigma),\zeta>1, \tag{4}$$

where $D_{\sigma}=d/dt$.

Definition 2 (see [20]). For $n-1<\zeta<n(n\in\mathbb{N})$ and $\vartheta,Y\in C^{n}(\Pi,\mathbb{R})$, the Y-Caputo FD of a function ϑ of order ζ is given by

$${}^{c}\mathscr{D}_{a^{+}}^{\zeta;Y}\vartheta(\sigma)=\mathscr{I}_{a^{+}}^{n-\zeta;Y}\left(\frac{D_{\sigma}}{Y'(\sigma)}\right)^{n}\vartheta(\sigma), \tag{5}$$

where $n=[\zeta]+1$ for $\zeta\notin\mathbb{N}$ and $n=\zeta$ for $\zeta\in\mathbb{N}$.

Also, we can express Y-Caputo FD by

$$ {}^{c}\mathscr{D}_{a^+}^{\zeta;Y}\vartheta(\sigma)=\begin{cases}\displaystyle\int_a^\sigma \frac{Y'(\varsigma)(Y(\sigma)-Y(\varsigma))^{n-\zeta-1}}{\Gamma(n-\zeta)}\left(\frac{D_\sigma}{Y'(\varsigma)}\right)^n\vartheta(\varsigma)d\varsigma, & \text{if } \zeta\notin\mathbb{N},\\ \displaystyle\left(\frac{D_\sigma}{Y'(\sigma)}\right)^n\vartheta(\sigma), & \text{if } \zeta\in\mathbb{N}.\end{cases} \tag{6} $$

Lemma 3 (see [1, 20]). *Let $\zeta,\xi>0$ and $\vartheta\in L^1(\Pi,\mathbb{R})$. Then,*

$$ \mathscr{I}_{a^+}^{\zeta;Y}\mathscr{I}_{a^+}^{\xi;Y}\vartheta(\sigma)=\mathscr{I}_{a^+}^{\zeta+\xi;Y}\vartheta(\sigma), a.e.\sigma\in\Pi. \tag{7} $$

In particular, if $\vartheta\in C(\Pi,\mathbb{R})$, then $\mathscr{I}_{a^+}^{\zeta;Y}\mathscr{I}_{a^+}^{\xi;Y}\vartheta(\sigma)=\mathscr{I}_{a^+}^{\zeta+\xi;Y}\vartheta(\sigma)$, $\sigma\in\Pi$.

Lemma 4 (see [20]). *Let $\zeta>0$. Then, the following holds:*
If $\vartheta\in C(\Pi,\mathbb{R})$, then

$$ {}^{c}\mathscr{D}_{a^+}^{\zeta;Y}\mathscr{I}_{a^+}^{\zeta;Y}\vartheta(\sigma)=\vartheta(\sigma), \quad \sigma\in\Pi. \tag{8} $$

If $\in C^n(\Pi,\mathbb{R})$,$n-1<\zeta<n$. Then,

$$ \mathscr{I}_{a^+}^{\zeta;Y\,c}\mathscr{D}_{a^+}^{\zeta;Y}\vartheta(\sigma)=\vartheta(\sigma)-\sum_{k=0}^{n-1}\frac{\vartheta_Y^{[k]}(a)}{k!}[Y(\sigma)-Y(a)]^k, \quad \sigma\in\Pi. \tag{9} $$

Lemma 5 (see [1, 20]). *Let $\sigma>a,\zeta\geq0$, and $\xi>0$. Then,*

(i) $\mathscr{I}_{a^+}^{\zeta;Y}(Y(\sigma)-Y(a))^{\xi-1}=(\Gamma(\xi)/\Gamma(\xi+\zeta))(Y(\sigma)-Y(a))^{\xi+\zeta-1}$

(ii) ${}^{c}\mathscr{D}_{a^+}^{\zeta;Y}(Y(\sigma)-Y(a))^{\xi-1}=(\Gamma(\xi)/\Gamma(\xi-\zeta))(Y(\sigma)-Y(a))^{\xi-\zeta-1}$

(iii) ${}^{c}\mathscr{D}_{a^+}^{\zeta;Y}(Y(\sigma)-Y(a))^{k}=0$*, for $k<n,n\in\mathbb{N}$*

Let $B(\upsilon,\tilde{r})$ be the closed ball in the Banach space $\mathbb{E}$; if $\upsilon=0$, then $B_r\equiv B(0,\tilde{r})$. Let $\tilde{\mathbb{X}}\subset\mathbb{E}$, such that $\tilde{\mathbb{X}}$ and Conv $\tilde{\mathbb{X}}$ are a closure and a convex closure of $\tilde{\mathbb{X}}$, respectively. And let $M_{\mathbb{E}}$ be the family of the nonempty and bounded subsets of $\mathbb{E}$, while $P_{\mathbb{E}}$ denotes the subfamily of all relatively compact subsets of $M_{\mathbb{E}}$.

Definition 6 (see [22]). We say that $\tilde{\chi}:M_{\mathbb{E}}\longrightarrow 0,\infty)$ is a noncompactness measure in $\mathbb{E}$ if all the assumptions below hold:

(i) $\ker\tilde{\chi}=\{\tilde{\mathbb{X}}\in\mathfrak{M}_{\mathbb{E}}:\tilde{\chi}(\tilde{\mathbb{X}})=0\}$ is nonempty and $\ker\tilde{\chi}\subset P_{\mathbb{E}}$

(ii) $\tilde{\mathbb{Y}}\subset\tilde{\mathbb{X}}$, then $\tilde{\chi}(\tilde{\mathbb{Y}})\leq\tilde{\chi}(\tilde{\mathbb{X}})$

(iii) $\tilde{\chi}(\tilde{\mathbb{Y}})=\tilde{\chi}(\tilde{\mathbb{Y}})=\tilde{\chi}(\mathrm{Conv}\tilde{\mathbb{Y}})$

(iv) $\tilde{\chi}(\lambda_1\tilde{\mathbb{Y}}+\lambda_2\tilde{\mathbb{X}})\leq\lambda_1\tilde{\chi}(\tilde{\mathbb{Y}})+\lambda_2\tilde{\chi}(\tilde{\mathbb{X}}),\lambda_1+\lambda_2=1$

(v) In the case of $(\tilde{\mathbb{Y}}_n)$ being a sequence of closed subsets of $M_{\mathbb{E}}$ with $\tilde{\mathbb{Y}}_{n+1}\subset\tilde{\mathbb{Y}}_n(n\geq1)$ and $\lim_{n\longrightarrow\infty}\tilde{\chi}(\tilde{\mathbb{Y}}_n)=0$, then $\cap_{n=1}^{\infty}\tilde{\mathbb{Y}}_n\neq\varnothing$

Definition 7 (see [22]). Let $\tilde{\mathbb{Y}}$ be a nonempty bounded set and $\subset\tilde{\mathscr{C}}$ be a Banach space. We say that $\mathscr{M}\in\tilde{\mathbb{Y}}$ is a modulus of continuous function, denoted by $\omega(\mathscr{M},\varepsilon)$; if $\forall\mathscr{M}\in\tilde{\mathbb{Y}}$ and $\forall e>0$, we have

$$ \omega(\mathscr{M},\varepsilon)=\sup\{|\mathscr{M}(\sigma)-\mathscr{M}(\varsigma)|:\sigma,\varsigma\in\Pi,|\sigma-\varsigma|\leq\varepsilon\}. \tag{10} $$

Moreover,

$$ \begin{aligned}\omega\left(\tilde{\mathbb{Y}},\varepsilon\right)&=\sup\left\{\omega(\mathscr{M},\varepsilon):\mathscr{M}\in\tilde{\mathbb{Y}}\right\},\\ \omega_0\left(\tilde{\mathbb{Y}}\right)&=\lim_{\varepsilon\longrightarrow0}\omega\left(\tilde{\mathbb{Y}},e\right).\end{aligned} \tag{11} $$

Definition 8 (see [23]). A noncompactness measure $\tilde{\chi}$ in $\tilde{\mathscr{C}}$ satisfies the condition (m) if

$$ \tilde{\chi}(\mathscr{M}\mathscr{N})\leq\|\mathscr{M}\|\tilde{\chi}(\mathscr{N})+\|\mathscr{N}\|\tilde{\chi}(\mathscr{M}), \tag{12} $$

for all $\mathscr{M},\mathscr{N}\in M_{C(\Pi)}$, where $\tilde{\mathscr{C}}:=C(\Pi)$ is the Banach algebra.

Lemma 9 (see [24]). *The condition (m) may be grasped by the noncompactness measure ϑ_0 on $\tilde{\mathscr{C}}$.*
Set

$$ \begin{aligned}S=\Big\{Y:(0,\infty)\longrightarrow(b,\infty):\forall(\upsilon_n)\subset(0,\infty),\lim_{n\longrightarrow\infty}Y(\upsilon_n)\\ =b\Longleftrightarrow\lim_{n\longrightarrow\infty}\upsilon_n=0\Big\}.\end{aligned} \tag{13} $$

Now, we present D'sFPT and generalized D'sFPT to prove that there exists at least one fixed point.

Theorem 10 (see [25, 26]). *Let $\tilde{\mathscr{C}}$ be a Banach space and $\Xi\subset\tilde{\mathscr{C}}$ be a nonempty, bounded, convex, and closed set. Let $\mathscr{K}:\Xi\longrightarrow\Xi$ be continuous. Assume that there is $0\leq$*

$\theta < 1$ *with* υ *as a noncompactness measure in* $\tilde{\mathscr{C}}$ *meeting the following requirements:*

$$\upsilon\left(\mathscr{K}\tilde{\mathbb{Y}}\right) \le \theta\tilde{\chi}\left(\tilde{\mathbb{Y}}\right), \Theta \ne \tilde{\mathbb{Y}} \subseteq \Xi. \tag{14}$$

Then, $\mathscr{K}$ *has a fixed point in* Ξ.

Theorem 11 (see [26]). *Let* $\tilde{\mathscr{C}}$ *be a Banach space and* $V \subset \tilde{\mathscr{C}}$ *be a nonempty, bounded, convex, and closed set, and let* $\mathscr{K} : V \longrightarrow V$ *be continuous. Assume there exist* $\Theta \in S$ *and* $0 \le \theta < 1$ *such that for each nonempty subset* D *of* V *with* $\tilde{\chi}(KD) > 0$,

$$\Theta(\tilde{\chi}(\mathscr{K}\mathscr{D})) \le (\Theta(\tilde{\chi}(\mathscr{D})))^{\theta}, \tag{15}$$

where $\tilde{\chi}$ *is a noncompactness measure in* $\tilde{\mathscr{C}}$. *Then,* $\mathscr{K}$ *has a fixed point in* V.

3. Solution Formulation

This section presents a formulation of the solution to problem (2) along with the assumptions required in the forthcoming analysis. Foremost, we denote by $(\tilde{\mathscr{C}}, \|.\|)$ the space of real valued continuous functions defined on a unit interval Π. It is clearly the Banach space with the norm:

$$\|\vartheta\| = \sup_{\sigma\in\Pi}|\vartheta(\sigma)|, \text{for } \vartheta \in \tilde{\mathscr{C}}. \tag{16}$$

Multiplication is defined as the usual product of real functions.

To prove the existence of solutions to (2), we need the following lemma:

Lemma 12. *The problem (2) is equivalent to the following fractional integral equation:*

$$\begin{aligned}\vartheta(\sigma) = \mathscr{M}(\sigma, \vartheta(\nu(\sigma)))\Bigg\{&\mathscr{I}^{\xi,Y}\left(\frac{1}{p}\mathscr{I}^{\zeta,Y}\mathscr{N}\right)(\sigma, \vartheta(\mu(\sigma))) \\ &- \mathscr{I}^{\xi,Y}\left(\frac{q}{p}\vartheta\right)(\sigma) - \frac{(Y(\sigma) - Y(a))^{\xi}}{p(\sigma)\Gamma(\xi + 1)}\mathscr{I}^{\zeta,Y}\mathscr{N}(b, \vartheta(\mu(b)))\Bigg\}.\end{aligned} \tag{17}$$

Proof. Applying the ζ^{th}-Y-RL integral on (2), we obtain

$${}^{c}\mathscr{D}^{\xi,Y}\left[\frac{\vartheta(\sigma)}{\mathscr{M}(\sigma, \vartheta(\nu(\sigma)))}\right] = \frac{\mathscr{I}^{\zeta,Y}\mathscr{N}(\sigma, \vartheta(\mu(\sigma))) - q(\sigma)\vartheta(\sigma) + k_1}{p(\sigma)}, \tag{18}$$

where $k_1 \in \mathbb{R}$. From the BCs of (2), we get

$$k_1 = -\mathscr{I}^{\zeta,Y}\mathscr{N}(b, \vartheta(\mu(b))). \tag{19}$$

Taking the ξ^{th}-Y-RL integral of (18), one has

$$\begin{aligned}\left[\frac{\vartheta(\sigma)}{\mathscr{M}(\sigma, \vartheta(\nu(\sigma)))}\right] &= \Bigg\{\mathscr{I}^{\xi,Y}\left(\frac{1}{p}\mathscr{I}^{\zeta,Y}\mathscr{N}\right)(\sigma, \vartheta(\mu(\sigma))) - \mathscr{I}^{\xi,Y}\left(\frac{q}{p}\vartheta\right)(\sigma) \\ &\quad - \frac{(Y(\sigma) - Y(a))^{\xi}}{p(\sigma)\Gamma(\xi + 1)}\mathscr{I}^{\zeta,Y}\mathscr{N}(b, \vartheta(\mu(b)))\Bigg\} + k_2,\end{aligned} \tag{20}$$

where $k_2 \in \mathbb{R}$. The BCs of (2) give $k_2 = 0$. In this regard, if we apply the ξ^{th}-Y-Caputo FD and ζ^{th}-Y-Caputo FD to both sides of (17) and use Lemma 5, then the problem (2) immediately is established. □

Before giving the essential result, we shall investigate formula (17) under the following assumptions:

(i) (AS1) Both functions $\nu, \mu : \Pi \longrightarrow \Pi$ are continuous

(ii) (AS2) $\mathscr{M} \in C(\Pi \times \mathbb{R}, \mathbb{R} \setminus \{0\})$, and $\mathscr{N} \in C(\Pi \times \mathbb{R}^2, \mathbb{R})$

(iii) (AS3) There exists a real number $\rho \in (a, b)$ with

$$\begin{aligned}&|\mathscr{M}(\sigma, \nu) - \mathscr{M}(\sigma, \vartheta)| \\ &\quad\le (|\nu - \vartheta| + d)^{\rho} - d^{\rho}, \quad \forall\sigma \in \Pi, \vartheta, \nu \in \mathbb{R}, d \in \mathbb{R}^{+}.\end{aligned} \tag{21}$$

(iv) (AS4) There exists a continuous nondecreasing function $\varphi : \mathbb{R}^{+} \longrightarrow \mathbb{R}^{+}$ with $\varphi(0) = 0$ such that

$$|\mathscr{N}(\sigma, \vartheta)| \le \varphi(\|\vartheta\|), \quad \sigma \in \Pi, \vartheta \in \mathbb{R}. \tag{22}$$

(v) (AS5) There exists $r_0 > 0$ such that

$$\begin{aligned}[(r_0 + d)^{\rho} - d^{\rho} + N]\Bigg\{&\frac{\varphi(r_0)}{\tilde{p}}\frac{(Y(b) - Y(a))^{\zeta+\xi}}{\Gamma(\zeta + \xi + 1)} \\ &+ \frac{\tilde{q}}{\tilde{p}}\frac{r_0(Y(b) - Y(a))^{\zeta}}{\Gamma(\zeta + 1)} \\ &+ \frac{1}{\tilde{p}}\frac{\varphi(r_0)(Y(b) - Y(a))^{\zeta+\xi}}{\Gamma(\zeta + 1)\Gamma(\xi + 1)}\Bigg\} \le r_0,\end{aligned}$$

where

$$\begin{aligned}\Lambda &:= \Bigg\{\frac{\varphi(r_0)}{\tilde{p}}\frac{(Y(b) - Y(a))^{\zeta+\xi}}{\Gamma(\zeta + \xi + 1)} + \frac{\tilde{q}}{\tilde{p}}\frac{r_0(Y(b) - Y(a))^{\zeta}}{\Gamma(\zeta + 1)} \\ &\quad + \frac{1}{\tilde{p}}\frac{\varphi(r_0)(Y(b) - Y(a))^{\zeta+\xi}}{\Gamma(\zeta + 1)\Gamma(\xi + 1)}\Bigg\} \le 1, \\ N &= \sup\{|\mathscr{M}(\sigma, 0)| : \sigma \in \Pi\}, \\ \tilde{p} &= \sup_{\sigma\in\Pi}p(\sigma), \tilde{q} = \sup_{\sigma\in\Pi}q(\sigma).\end{aligned} \tag{24}$$

4. Existence Result

The aim of this section is to discuss the existence of solutions to the problem (2). For this end, we apply Theorems 10 and 11.

Theorem 13 Under hypotheses (AS1)–(AS5). *Then, the problem (2) has a least one solution in the Banach algebra* $\tilde{\mathscr{C}}$.

Proof. Consider the operator $\mathscr{K}:\tilde{\mathscr{C}}\longrightarrow\tilde{\mathscr{C}}$ on the Banach algebra $\tilde{\mathscr{C}}$ as

$$(\mathscr{K}\vartheta)(\sigma)=(\mathscr{F}\vartheta)(\sigma)(\mathscr{G}\vartheta)(\sigma), \tag{25}$$

where

$$\begin{aligned}
(\mathscr{F}\vartheta)(\sigma)&=\mathscr{M}(\sigma,\vartheta(\nu(\sigma))),\\
(\mathscr{G}\vartheta)(\sigma)&=\mathscr{I}^{\xi,Y}\left(\frac{1}{p}\mathscr{I}^{\zeta,Y}\mathscr{N}\right)(\sigma,\vartheta(\mu(\sigma)))\\
&\quad-\mathscr{I}^{\xi,Y}\left(\frac{q}{p}\vartheta\right)(\sigma)-\frac{(Y(\sigma)-Y(a))^{\xi}}{p(\sigma)\Gamma(\xi+1)}G(\mathscr{N}),\\
G(\mathscr{N})&=\mathscr{I}^{\zeta,Y}\mathscr{N}(b,\vartheta(\mu(b))).
\end{aligned} \tag{26}$$

From (AS4), we have

$$\|G(\mathscr{N})\|\le\frac{(Y(b)-Y(a))^{\zeta}}{\Gamma(\zeta+1)}Y(\|\vartheta\|). \tag{27}$$

For the sake of simplicity, we put

$$\mathscr{Q}_Y^{\chi}(\sigma,\varsigma)=\frac{Y'(\varsigma)(Y(\sigma)-Y(\varsigma))^{\chi-1}}{\Gamma(\chi)},\quad \chi>0. \tag{28}$$

□

Now, we divide the proof into several steps.

Step 1. $\mathscr{K}$ transforms $\tilde{\mathscr{C}}$ into itself.

At first, we show that $\forall\vartheta\in\tilde{\mathscr{C}}$ implies that $(\mathscr{K}\vartheta)\in\tilde{\mathscr{C}}$, i.e., $(\mathscr{F}\vartheta)(\mathscr{G}\vartheta)\in\tilde{\mathscr{C}}$ for all $\vartheta\in\tilde{\mathscr{C}}$. Certainly, (AS1) and (AS2) guarantee that if $\vartheta\in\tilde{\mathscr{C}}$, then $(\mathscr{F}\vartheta)\in\tilde{\mathscr{C}}$. It remains to prove if $\vartheta\in\tilde{\mathscr{C}}$, then $(\mathscr{G}\vartheta)\in\tilde{\mathscr{C}}$. Let $\vartheta\in\tilde{\mathscr{C}}$ and $\sigma_2,\sigma_1\in\Pi$ with $\sigma_2>\sigma_1$. By hypothesis (AS4), we get

$$\begin{aligned}
&|\mathscr{G}\vartheta(\sigma_1)-\mathscr{G}\vartheta(\sigma_2)|\\
&\quad=\frac{1}{\tilde{\tilde{p}}}\left|\int_a^{\sigma_1}\mathscr{Q}_Y^{\zeta+\xi}(\sigma_1,\varsigma)\mathscr{M}(\varsigma,\vartheta(\varsigma))d\varsigma\right.\\
&\qquad\left.-\int_a^{\sigma_2}\mathscr{Q}_Y^{\zeta+\xi}(\sigma_2,\varsigma)\mathscr{M}(\varsigma,\vartheta(\varsigma))d\varsigma\right|\\
&\qquad+\frac{\tilde{q}}{\tilde{\tilde{p}}}\left|\int_a^{\sigma_1}\mathscr{Q}_Y^{\zeta}(\sigma_1,\varsigma)\vartheta(\varsigma)d\varsigma-\int_a^{\sigma_2}\mathscr{Q}_Y^{\zeta+\xi}(\sigma_2,\varsigma)\vartheta(\varsigma)d\varsigma\right|\\
&\qquad+\frac{1}{\tilde{\tilde{p}}}\frac{|G(\mathscr{N})|}{\Gamma(\xi+1)}\left((Y(\sigma_2)-Y(a))^{\xi}-(Y(\sigma_1)-Y(a))^{\xi}\right)\\
&\quad\le\frac{1}{\tilde{\tilde{p}}}\left|\int_a^{\sigma_2}\left[\mathscr{Q}_Y^{\zeta+\xi}(\sigma_1,\varsigma)-\mathscr{Q}_Y^{\zeta+\xi}(\sigma_2,\varsigma)\right]\mathscr{M}(\varsigma,\vartheta(\varsigma))d\varsigma\right|\\
&\qquad+\frac{1}{\tilde{\tilde{p}}}\left|\int_{\sigma_2}^{\sigma_1}\mathscr{Q}_Y^{\zeta+\xi}(\sigma_1,\varsigma)\mathscr{M}(\varsigma,\vartheta(\varsigma))d\varsigma\right|\\
&\qquad+\frac{\tilde{q}}{\tilde{\tilde{p}}}\left|\int_a^{\sigma_2}\left[\mathscr{Q}_Y^{\zeta}(\sigma_1,\varsigma)-\mathscr{Q}_Y^{\zeta}(\sigma_2,\varsigma)\right]\mathscr{M}(\varsigma,\vartheta(\varsigma))d\varsigma\right|\\
&\qquad+\frac{\tilde{q}}{\tilde{\tilde{p}}}\left|\int_{\sigma_2}^{\sigma_1}\mathscr{Q}_Y^{\zeta}(\sigma_1,\varsigma)\mathscr{M}(\varsigma,\vartheta(\varsigma))d\varsigma\right|\\
&\qquad+\frac{1}{\tilde{\tilde{p}}}\frac{|G(\mathscr{N})|}{\Gamma(\xi+1)}\left((Y(\sigma_2)-Y(a))^{\xi}-(Y(\sigma_1)-Y(a))^{\xi}\right)\\
&\quad\le\frac{1}{\tilde{\tilde{p}}}\frac{\varphi(\|\vartheta\|)}{\Gamma(\zeta+\xi+1)}\left[\left|(Y(\sigma_1)-Y(a))^{\zeta+\xi}\right.\right.\\
&\qquad\left.-(Y(\sigma_2)-Y(a))^{\zeta+\xi}-(Y(\sigma_1)-Y(\sigma_2))^{\zeta+\xi}\right|\\
&\qquad\left.+(Y(\sigma_1)-Y(\sigma_2))^{\zeta+\xi}\right]\\
&\qquad+\frac{\tilde{q}}{\tilde{\tilde{p}}}\frac{\|\vartheta\|}{\Gamma(\zeta+1)}\left[\left|(Y(\sigma_1)-Y(a))^{\zeta}-(Y(\sigma_2)-Y(a))^{\zeta}\right.\right.\\
&\qquad\left.\left.-(Y(\sigma_1)-Y(\sigma_2))^{\zeta}\right|+(Y(\sigma_1)-Y(\sigma_2))^{\zeta}\right]\\
&\qquad+\frac{1}{\tilde{\tilde{p}}}\frac{\varphi(\|\vartheta\|)(Y(b)-Y(a))^{\zeta}}{\Gamma(\zeta+1)\Gamma(\xi+1)}\\
&\qquad\cdot\left((Y(\sigma_2)-Y(a))^{\xi}-(Y(\sigma_1)-Y(a))^{\xi}\right),
\end{aligned} \tag{29}$$

which tends to be zero uniformly once $\sigma_2\longrightarrow\sigma_1$. It is clear that $\mathscr{G}\vartheta\in\tilde{\mathscr{C}}$ for all $\vartheta\in\tilde{\mathscr{C}}$.

Step 2. An estimate of $\|\mathscr{K}\vartheta\|$ for $\vartheta\in\tilde{\mathscr{C}}$.

Let $\vartheta\in\tilde{\mathscr{C}}$ and $\sigma\in\Pi$. Then, by using our hypothesis, we have

$$\begin{aligned}
|(\mathscr{K}\vartheta)(\sigma)|&=|(\mathscr{F}\vartheta)(\sigma)(\mathscr{G}\vartheta)(\sigma)|\\
&\le(|\mathscr{M}(\sigma,\vartheta(\nu(\sigma)))-\mathscr{M}(\sigma,0)|+|\mathscr{M}(\sigma,0)|)\\
&\quad\times\left\{\frac{1}{\tilde{\tilde{p}}}\int_a^{\sigma}\mathscr{Q}_Y^{\zeta+\xi}(\sigma,\varsigma)|\mathscr{N}(\varsigma,\vartheta(\mu(\varsigma)))|d\varsigma\right.\\
&\quad\left.+\frac{\tilde{q}}{\tilde{\tilde{p}}}\int_a^{\sigma}\mathscr{Q}_Y^{\zeta}(\sigma,\varsigma)|\vartheta(\varsigma)|d\varsigma+\frac{1}{\tilde{\tilde{p}}}\frac{|G(\mathscr{N})|}{\Gamma(\xi+1)}(Y(\sigma)-Y(a))^{\xi}\right\}\\
&\le[(\|\vartheta\|+d)^{\rho}-d^{\rho}+N]\\
&\quad\cdot\left\{\frac{1}{\tilde{\tilde{p}}}\int_a^{\sigma}\mathscr{Q}_Y^{\zeta+\xi}(\sigma,\varsigma)Y(\|\vartheta\|)d\varsigma+\frac{\tilde{q}}{\tilde{\tilde{p}}}\int_a^{\sigma}\mathscr{Q}_Y^{\zeta}(\sigma,\varsigma)\|\vartheta\|d\varsigma\right.\\
&\quad\left.+\frac{1}{\tilde{\tilde{p}}}\frac{\varphi(\|\vartheta\|)(Y(b)-Y(a))^{\zeta+\xi}}{\Gamma(\zeta+1)\Gamma(\xi+1)}\right\}.
\end{aligned} \tag{30}$$

Therefore,

$$\|\mathcal{K}\vartheta\| \leq [(\|\vartheta\| + d)^{\rho} - d^{\rho} + N]\left\{\frac{\varphi(\|\vartheta\|)}{\tilde{p}}\frac{(Y(b) - Y(\varsigma))^{\zeta+\xi}}{\Gamma(\zeta+\xi+1)} + \frac{\tilde{q}}{\tilde{p}}\frac{\|\vartheta\|(Y(b) - Y(\varsigma))^{\zeta}}{\Gamma(\zeta+1)} + \frac{1}{\tilde{p}}\frac{\varphi(\|\vartheta\|)(Y(b) - Y(a))^{\zeta+\xi}}{\Gamma(\zeta+1)\Gamma(\xi+1)}\right\}. \tag{31}$$

Step 3. The operator $\mathcal{K}$ is continuous on $\mathcal{B}_{r_0}$. Here, $\mathcal{B}_{r_0}$ is a subset of $\tilde{\mathcal{C}}$ defined by

$$\mathcal{B}_{r_0} = \left\{\vartheta(\sigma) \in \tilde{\mathcal{C}} : \|\vartheta\| \leq r_0 : \sigma \in \Pi\right\}, \tag{32}$$

with a fixed radius r_0, which satisfies the inequality (AS5).

We shall need to show the continuity of $\mathcal{F}$ and $\mathcal{G}$ on $\mathcal{B}_{r_0}$, separately. For any $\varepsilon > 0$ and $\vartheta, \nu \in \mathcal{B}_{r_0}$, there exists $0 < \delta < (\varepsilon + d^{\rho})^{1/\rho} - d, \ni \|\vartheta - \nu\| \leq \delta$; it follows for $\sigma \in \Pi$ that

$$\begin{aligned}|\mathcal{F}\vartheta(\sigma) - \mathcal{F}\nu(\sigma)| &= |\mathcal{M}(\sigma, \vartheta(\nu(\sigma))) - \mathcal{M}(\sigma, \nu(\nu(\sigma)))| \\ &\leq (|\vartheta(\nu(\sigma)) - (\nu(\sigma))| + d)^{\rho} - d^{\rho} \\ &\leq (\|\vartheta - \nu\| + d)^{\rho} - d^{\rho} \leq (\delta + d)^{\rho} - d^{\rho} < \varepsilon.\end{aligned} \tag{33}$$

Therefore, $\mathcal{F}$ is continuous on $\mathcal{B}_{r_0}$. The continuity of the operator $\mathcal{G}$ is obtained by Lebesgue dominated convergence (LDC) theorem. Indeed, let (ϑ_n) be a sequence such that $\vartheta_n \longrightarrow \vartheta$ in $\mathcal{B}_{r_0}$ with $\|\vartheta_n - \vartheta\| \longrightarrow 0$ as $n \longrightarrow 0$. As $\mu : \Pi \longrightarrow \Pi$ is continuous, we obtain

$$|\vartheta_n(\mu(\sigma))| \leq r_0, \quad \forall n \in \mathbb{N}, \forall \sigma \in \Pi. \tag{34}$$

Since $\mathcal{N}$ is continuous on $\Pi \times [-r_0, r_0]$, it is uniformly continuous on $\Pi \times [-r_0, r_0]$. Now, we set

$$G_0 = \max_{(\sigma,\vartheta)\in\Pi\times[-r_0,r_0]} |(\mathcal{G}\vartheta)(\sigma)|, \tag{35}$$

$$\kappa_0 = \frac{G_0(Y(b) - Y(a))^{\zeta}}{\Gamma(\zeta+1)}. \tag{36}$$

Applying the LDC theorem, we get

$$\begin{aligned}\lim_{n\longrightarrow\infty}(\mathcal{G}\vartheta_n)(\sigma) &= \lim_{n\longrightarrow\infty}\left\{\frac{1}{\tilde{p}}\int_a^{\sigma}\mathcal{Q}_Y^{\zeta+\xi}(\sigma,\varsigma)|\mathcal{N}(\varsigma,\vartheta_n(\mu(\varsigma)))|d\varsigma + \frac{\tilde{q}}{\tilde{p}}\int_a^{\sigma}\mathcal{Q}_Y^{\zeta}(\sigma,\varsigma)|\vartheta_n(\varsigma)|d\varsigma + \frac{|G(\vartheta_n)|}{\Gamma(\xi+1)}(Y(\sigma) - Y(a))^{\xi}\right\} \\ &= \left\{\frac{1}{\tilde{p}}\int_a^{\sigma}\mathcal{Q}_Y^{\zeta+\xi}(\sigma,\varsigma)|\mathcal{N}(\varsigma,\vartheta(\mu(\varsigma)))|d\varsigma + \frac{\tilde{q}}{\tilde{p}}\int_a^{\sigma}\mathcal{Q}_Y^{\zeta}(\sigma,\varsigma)|\vartheta(\varsigma)|d\varsigma + \frac{1}{\tilde{p}}\frac{|G(\vartheta)|}{\Gamma(\xi+1)}(Y(\sigma) - Y(a))^{\xi}\right\} = (\mathcal{G}\vartheta)(\sigma).\end{aligned} \tag{37}$$

Thus, $\mathcal{G}$ is continuous in $\mathcal{B}_{r_0}$.

Due to the continuity of $\mathcal{F}$ and $\mathcal{G}$, the operator $\mathcal{K}$ is continuous in $\mathcal{B}_{r_0}$.

Step 4. We estimate $\vartheta_0(\mathcal{F}\Xi)$ and $\vartheta_0(\mathcal{G}\Xi)$ for $\emptyset \neq \Xi \subset \mathcal{B}_{r_0}$.

At first, we estimate $\vartheta_0(\mathcal{F}\Xi)$. Since $\nu : \Pi \longrightarrow \Pi$ is uniformly continuous, we obtain for any $\varepsilon > 0, \exists\delta > 0$ with $(\delta < \varepsilon), \forall\sigma_1, \sigma_2 \in \Pi$ with $|\sigma_2 - \sigma_1| < \delta$, which implies $|\nu(\sigma_2) - \nu(\sigma_1)| < \varepsilon$. Taking $\vartheta \in \Xi$ and $\sigma_1, \sigma_2 \in \Pi$ with $|\sigma_2 - \sigma_1| < \delta$, under hypothesis (AS5), we get

$$\begin{aligned}|(\mathcal{F}\vartheta)(\sigma_2) - (\mathcal{F}\vartheta)(\sigma_1)| &= |\mathcal{M}(\sigma_2, \vartheta(\nu(\sigma_2))) - \mathcal{M}(\sigma_1, \vartheta(\nu(\sigma_1)))| \\ &\leq |\mathcal{M}(\sigma_2, \vartheta(\nu(\sigma_2))) - \mathcal{M}(\sigma_2, \vartheta(\nu(\sigma_1)))| + |\mathcal{M}(\sigma_2, \vartheta(\nu(\sigma_1))) - \mathcal{M}(\sigma_1, \vartheta(\nu(\sigma_1)))| \\ &\leq [(|\vartheta(\nu(\sigma_2)) - \vartheta(\nu(\sigma_1))| + d)^{\rho} - d^{\rho}] + \omega(\mathcal{M}, \varepsilon) \\ &\leq [(\omega(\Xi, \varepsilon) + d)^{\rho} - d^{\rho}] + \omega(\mathcal{M}, \varepsilon).\end{aligned} \tag{38}$$

Considering

$$\omega(\mathcal{M}, \varepsilon) = \sup\{|\mathcal{M}(\sigma_2, \vartheta) - \mathcal{M}(\sigma_1, \vartheta)| : \sigma_1, \sigma_2 \in \Pi, |\sigma_2 - \sigma_1| < \varepsilon, \vartheta \in [-r_0, r_0]\}, \tag{39}$$

then we can write (38) as

$$\omega(\mathcal{F}\Xi, \varepsilon) \leq \left[(\omega(\Xi, \varepsilon) + b)^{\rho} - b^{\rho}\right] + \omega(\mathcal{M}, \varepsilon). \tag{40}$$

Obviously, $\mathcal{M}(\sigma, \vartheta)$ is uniformly continuous on $\Pi \times [-r_0, r_0]$, and $\omega(M, \varepsilon) \longrightarrow 0$ once $\varepsilon \longrightarrow 0$. Hence, (40) becomes as follows:

$$\omega_0(\mathcal{F}\Xi) \leq (\omega_0(\Xi) + b)^{\rho} - b^{\rho}. \tag{41}$$

Next, since $\mu : \Pi \longrightarrow \Pi$ is uniformly continuous, we have $\forall\varepsilon > 0$, $\exists\delta > 0$ with $(\delta = \delta(\varepsilon))$, $\forall\sigma_1, \sigma_2 \in \Pi$ with $|\sigma_2 - \sigma_1| < \delta$, which implies $|\mu(\sigma_2) - \mu(\sigma_1)| < \varepsilon$. Take into account equations (32), (35), and (36) for each $\varepsilon > 0$. Set

$$\delta = \min\left\{\frac{1}{2}, \frac{\Gamma(\xi+1)\varepsilon}{\kappa_0}, \frac{p^*\Gamma(\zeta+1)\varepsilon}{q^* r_0}, \frac{p^*\Gamma(\zeta+\xi+1)\varepsilon}{4G_0}\right\}. \tag{42}$$

Choosing $\vartheta \in \Xi$ and $\sigma_1, \sigma_2 \in \Pi$ with $|\sigma_2 - \sigma_1| \leq \delta$ yields

$$
\begin{aligned}
|\mathscr{G}\vartheta(\sigma_1)-\mathscr{G}\vartheta(\sigma_2)| &= \frac{1}{\tilde{p}}\left|\int_a^{\sigma_1}\mathcal{Q}_Y^{\zeta+\xi}(\sigma_1,\varsigma)\mathscr{M}(\sigma,\vartheta(\varsigma))d\varsigma-\int_a^{\sigma_2}\mathcal{Q}_Y^{\zeta+\xi}(\sigma_2,\varsigma)\mathscr{M}(\varsigma,\vartheta(\varsigma))d\varsigma\right|+\frac{\tilde{q}}{\tilde{p}}\left|\int_a^{\sigma_1}\mathcal{Q}_Y^{\zeta}(\sigma_1,\varsigma)\vartheta(\varsigma)d\varsigma-\int_a^{\sigma_2}\mathcal{Q}_Y^{\zeta}(\sigma_2,\varsigma)\vartheta(\varsigma)d\varsigma\right| \\
&\quad+\frac{1}{\tilde{p}}\frac{|G(\mathscr{N})|}{\Gamma(\xi+1)}\left((Y(\sigma_2)-Y(a))^{\xi}-(Y(\sigma_1)-Y(a))^{\xi}\right) \\
&\le \frac{1}{\tilde{p}}\frac{G_0}{\Gamma(\zeta+\xi+1)}\left[\left|(Y(\sigma_1)-Y(a))^{\zeta+\xi}-(Y(\sigma_2)-Y(a))^{\zeta+\xi}-(Y(\sigma_1)-Y(\sigma_2))^{\zeta+\xi}\right|+(Y(\sigma_1)-Y(\sigma_2))^{\zeta+\xi}\right] \\
&\quad+\frac{\tilde{q}}{\tilde{p}}\frac{r_0}{\Gamma(\zeta+1)}\left[\left|(Y(\sigma_1)-Y(a))^{\zeta}-(Y(\sigma_2)-Y(a))^{\zeta}-(Y(\sigma_1)-Y(\sigma_2))^{\zeta}\right|\right. \\
&\quad\left.+(Y(\sigma_1)-Y(\sigma_2))^{\zeta}\right]+\frac{1}{\tilde{p}}\frac{\kappa_0}{\Gamma(\xi+1)}\left((Y(\sigma_2)-Y(a))^{\xi}-(Y(\sigma_1)-Y(a))^{\xi}\right).
\end{aligned} \tag{43}
$$

For simplicity's sake, we set

$$\mathscr{H}_Y^{\chi}(\sigma)=(Y(\sigma)-Y(a))^{\chi},\quad \chi>0. \tag{44}$$

The factors $\mathscr{H}_Y^{\zeta}(\sigma_2)-\mathscr{H}_Y^{\zeta}(\sigma_1)$, $\mathscr{H}_Y^{\xi}(\sigma_2)-\mathscr{H}_Y^{\xi}(\sigma_1)$, and $\mathscr{H}_Y^{\zeta+\xi}(\sigma_2)-\mathscr{H}_Y^{\zeta+\xi}(\sigma_1)$ can be estimated as in the following cases:

Case 1. If $0\le\mathscr{H}_Y(\sigma_1)<\delta,\mathscr{H}_Y(\sigma_2)\le 2\delta$, then

$$
\begin{aligned}
\mathscr{H}_Y^{\zeta}(\sigma_2)-\mathscr{H}_Y^{\zeta}(\sigma_1)&\le\mathscr{H}_Y^{\zeta}(\sigma_2)<(2\delta)^{\zeta}\le 2^{\zeta}\delta\le 2\delta, \\
\mathscr{H}_Y^{\xi}(\sigma_2)-\mathscr{H}_Y^{\xi}(\sigma_1)&\le\mathscr{H}_Y^{\xi}(\sigma_2)<(2\delta)^{\xi}\le 2^{\xi}\delta\le 2\delta, \\
\mathscr{H}_Y^{\zeta+\xi}(\sigma_2)-\mathscr{H}_Y^{\zeta+\xi}(\sigma_1)&\le\mathscr{H}_Y^{\zeta+\xi}(\sigma_2)<(2\delta)^{\zeta+\xi}\le 2^{\zeta+\xi}\delta\le 4\delta.
\end{aligned} \tag{45}
$$

Case 2. If $0<\mathscr{H}_Y(\sigma_1)<\mathscr{H}_Y(\sigma_2)\le\delta$, then

$$
\begin{aligned}
\mathscr{H}_Y^{\zeta}(\sigma_2)-\mathscr{H}_Y^{\zeta}(\sigma_1)&\le\mathscr{H}_Y^{\zeta}(\sigma_2)<\delta^{\zeta}\le\zeta\delta<2\delta, \\
\mathscr{H}_Y^{\xi}(\sigma_2)-\mathscr{H}_Y^{\xi}(\sigma_1)&\le\mathscr{H}_Y^{\xi}(\sigma_2)<\delta^{\xi}\le\xi\delta<2\delta, \\
\mathscr{H}_Y^{\zeta+\xi}(\sigma_2)-\mathscr{H}_Y^{\zeta+\xi}(\sigma_1)&\le\mathscr{H}_Y^{\zeta+\xi}(\sigma_2)<\delta^{\zeta+\xi}\le(\zeta+\xi)\delta<4\delta.
\end{aligned} \tag{46}
$$

Case 3. If $\delta\le\mathscr{H}_Y(\sigma_1)<\mathscr{H}_Y(\sigma_2)\le 1$, then

$$
\begin{aligned}
&\mathscr{H}_Y^{\zeta}(\sigma_2)-\mathscr{H}_Y^{\zeta}(\sigma_1)<\zeta\delta<2\delta, \\
&\mathscr{H}_Y^{\xi}(\sigma_2)-\mathscr{H}_Y^{\xi}(\sigma_1)<\xi\delta<2\delta \text{ and } \sigma_2^{a+\xi}-\sigma_1^{a+\xi}<(\zeta+\xi)\delta<4\delta.
\end{aligned} \tag{47}
$$

Accordingly, we obtain $|\mathscr{G}\vartheta(\sigma_2)-\mathscr{G}\vartheta(\sigma_1)|\le\varepsilon$, which implies that $\omega(\mathscr{G}\vartheta,\varepsilon)\le\varepsilon$.

Let $\varepsilon\longrightarrow 0$. Then,

$$\omega_0(\mathscr{G}\Xi)=0. \tag{48}$$

Step 5. We estimate $\omega_0(\mathscr{K}\Xi)$ for $\varnothing=\Xi\in\mathscr{B}_{r_0}$.

By Lemma 9 and equations (32), (41), and (48), we obtain

$$
\begin{aligned}
\omega_0(\mathscr{K}\Xi)&=\omega_0(\mathscr{F}\Xi.\mathscr{G}\Xi)\|\mathscr{F}\Xi\|\omega_0(\mathscr{G}\Xi)+\|\mathscr{G}\Xi\|\omega_0(\mathscr{F}\Xi) \\
&\le\left\|\mathscr{F}\left(\mathscr{B}_{r_0}\right)\right\|\omega_0(\mathscr{G}\Xi)+\left\|\mathscr{G}\left(\mathscr{B}_{r_0}\right)\right\|\omega_0(\mathscr{F}\Xi) \\
&\le[(\omega_0(\Xi)+d)^{\rho}-d^{\rho}]\left\{\frac{\varphi(r_0)}{\tilde{p}}\frac{(Y(\sigma)-Y(\varsigma))^{\zeta+\xi}}{\Gamma(\zeta+\xi+1)}\right. \\
&\quad\left.+\frac{\tilde{q}}{\tilde{p}}\frac{r_0(Y(\sigma)-Y(\varsigma))^{\zeta}}{\Gamma(\zeta+1)}+\frac{1}{\tilde{p}}\frac{\varphi(r_0)(Y(b)-Y(a))^{\zeta+\xi}}{\Gamma(\zeta+1)\Gamma(\xi+1)}\right\} \\
&=[(\omega_0(\Xi)+d)^{\rho}-d^{\rho}]\Lambda.
\end{aligned} \tag{49}
$$

Since $\Lambda\le 1$, the assumption (AS5) gives

$$\omega_0(\mathscr{K}\Xi)+d^{\rho}\le(\omega_0(\Xi)+d)^{\rho}. \tag{50}$$

Thanks to Theorem 10, the contractive condition is fulfilled with $\varphi(\vartheta)=\vartheta+b$, where $\varphi\in S$. By applying Theorem 11, $\mathscr{K}$ has at least fixed point in $\mathscr{B}_{r_0}$. Hence, the problem (2) has at least one solution in $\mathscr{B}_{r_0}$.

5. Examples

Here, we provide two examples to illustrate previous results.

Example 14. Consider the problem (2) with following specific data:

$$p(\sigma)=1,q(\sigma)=\lambda=\frac{1}{100},Y(\sigma)=\sigma. \tag{51}$$

Then, the problem (2) reduces to

Table 1: Examples with some special cases of the Y function.

$Y(\sigma)$	$[a,b]$	ζ	ξ	$\tilde{p}$	$\tilde{q}$	r_0	Λ
σ	$[0,1]$	$\frac{1}{4}$	$\frac{1}{2}$	1	$\frac{1}{100}$	$0 < r_0 \le 1.7924$	$0.5445 < 1$
e^{σ}	$[0,1]$	$\frac{1}{3}$	$\frac{3}{4}$	2	$\frac{2}{25}$	$0 < r_0 \le 0.385$	$0.1613 < 1$
$\ln(\sigma)$	$[1,e]$	$\frac{2}{3}$	$\frac{1}{3}$	$\frac{3}{5}$	$\frac{1}{25}$	$0 < r_0 \le 1.2603$	$0.3034 < 1$
2^{σ}	$[1,2]$	$\frac{1}{2}$	$\frac{1}{2}$	$\frac{3}{2}$	$\frac{1}{35}$	$0 < r_0 \le 0.1807$	$0.0449 < 1$

$$\begin{cases} {}^{c}\mathscr{D}^{1/4}\left[{}^{c}\mathscr{D}^{1/2}\dfrac{3}{\sqrt{\vartheta\left(e^{(\sigma-1)}/2\right)+4^2}}\right]-\dfrac{1}{100}\vartheta(\sigma)\right]=\dfrac{\sigma}{10}\left[\sin\vartheta\left(\sqrt{\sigma}\right)\right], \quad \sigma\in\Pi=[0,1], \\ \vartheta(0)=0,\ \dfrac{2}{2}\left[\dfrac{\vartheta(\sigma)}{\sqrt{\vartheta\left(e^{(\sigma-1)}/2\right)+4^2}}\right]_{\sigma=1}+\dfrac{1}{100}\vartheta(1)=0, \end{cases} \tag{52}$$

where

$$a=0, b=1, \zeta=\frac{1}{4}, \xi=\frac{1}{2}, \lambda=\frac{1}{100}, \nu(\sigma)=\frac{e^{(\sigma-1)}}{2}, \mu(\sigma)=\sqrt{\sigma}. \tag{53}$$

$\mathscr{M}(\sigma,\vartheta)=\sqrt{|\vartheta|+4^2}$,$\mathscr{N}(\sigma,\vartheta)=(1/10)\sin(\vartheta)$, $d=16$, and $N=\sup_{\sigma\in 0,1]}|\mathscr{M}(\sigma,0)|=4$. Thus, (AS1) and (AS2) hold. For (AS3), we obtain $\rho=1/2$. Furthermore, let $z(\vartheta)=\sqrt{|\vartheta|+4^2}-2^2$. Then, $z(0)=0$, and it is a concave function. Since $z(\sigma)$ is concave. As a result, the subadditive property of the concave function allows us to conclude

$$|\mathscr{M}(\sigma,\vartheta_2)-\mathscr{M}(\sigma,\vartheta_1)|=|z(\vartheta_2)-z(\vartheta_1)| \le z(\vartheta_2-\vartheta_1)=\sqrt{|\vartheta_2-\vartheta_1|+4^2}-2^2. \tag{54}$$

Thus, (AS3) holds, with $\rho=1/2$. Moreover, for every $\sigma\in\Pi$ and $\vartheta\in\mathbb{R}$, we obtain

$$|\mathscr{N}(\sigma,\vartheta)|=\left|\frac{\sigma}{10}[\sin\vartheta(\sigma)]\right|\le\frac{1}{10}|\vartheta(\sigma)|, \quad \forall\sigma\in\Pi. \tag{55}$$

Hence, (AS4) holds with $\varphi(\|\vartheta\|)=(1/10)\vartheta$. Finally, (AS5) permitted to provide us the range of r_0 which is obviously

$$0<r_0\le 1.7924. \tag{56}$$

Accordingly, (AS5) confirms that the illustrated example (52) has a solution in $\tilde{\mathscr{C}}$ due to

$$\Lambda=0.544529299<1. \tag{57}$$

Example 15. Depending on the previous example, we present some special cases of Y with different values for some parameters as in Table 1.

6. Conclusions

In this work, we have successfully studied some qualitative properties of the solution to a fractional problem that integrates three different types of BVP; more precisely, we have investigated the existence of the solutions of the Sturm-Liouville–Langevin–hybrid-type FDEs. Our analysis has been based on the technique of the measure of noncompactness along with the generalized Darbo's fixed point theorem. The results were consistent with some of the literature results when $Y(\sigma)=\sigma$, and they are new even for the special case: $Y(\sigma)=\log\sigma$ and $Y(\sigma)=\sigma^{\rho}$.

The problem studied can be extended to a more general problem containing Y-Hilfer FD, and this is what we are considering in future research.

Data Availability

No real data were used to support this study.

Conflicts of Interest

No conflicts of interest are related to this work.

Acknowledgments

The authors thank the Research Center for Advanced Materials Science (RCAMS) at King Khalid University, Saudi Arabia, for funding this work under the grant number RCAMS/KKU/013/20. Emad E. Mahmoud acknowledges Taif University Researchers Supporting Project number TURSP-2020/20, Taif University, Taif, Saudi Arabia.

References

[1] A. A. Kilbas, H. M. Srivastava, and J. J. Trujillo, *Theory and Applications of Fractional Differential Equations*, Elsevier Science B.V., Amsterdam, The Netherlands, 2006, vol. 204 of North-Holland Mathematics Studies.

[2] I. Podlubny, *Fractional Differential Equations*, Academic Press, San Diego, CA, USA, 1999.

[3] B. C. Dhage and V. Lakshmikantham, "Basic results on hybrid differential equations," *Nonlinear Analysis: Hybrid Systems*, vol. 4, no. 3, pp. 414–424, 2010.

[4] B. C. Dhage, G. T. Khurpe, A. Y. Shete, and J. N. Salunke, "Existence and approximate solutions for nonlinear hybrid fractional integro-differential equations," *International Journal of Analysis and Applications*, vol. 11, no. 2, pp. 157–167, 2016.

[5] Y. Zhao, S. Sun, Z. Han, and Q. Li, "Theory of fractional hybrid differential equations," *Computers & Mathematcs with Applications*, vol. 62, no. 3, pp. 1312–1324, 2011.

[6] B. Ahmad and S. K. Ntouyas, "Nonlocal boundary value problems for hybrid fractional differential equations and inclusions of Hadamard type," *Fractional Differential Calculus*, vol. 5, no. 2, pp. 107–123, 2012.

[7] P. Langevin, "Sur la theorie du mouvement brownien," *Comptes Rendus*, vol. 146, pp. 530–533, 1908.

[8] S. C. Lim, M. Li, and L. P. Teo, "Langevin equation with two fractional orders," *Physics Letters A*, vol. 372, no. 42, pp. 6309–6320, 2008.

[9] O. Baghani, "On fractional Langevin equation involving two fractional orders," *Communications in Nonlinear Science and Numerical Simulation*, vol. 42, pp. 675–681, 2017.

[10] A. Chen and Y. Chen, "Existence of solutions to nonlinear Langevin equation involving two fractional orders with boundary value conditions," *Boundary Value Problems*, vol. 2011, 17 pages, 2011.

[11] Q. M. Al-Mdallal, "On the numerical solution of fractional Sturm-Liouville problems," *International Journal of Computer Mathematics*, vol. 87, no. 12, pp. 2837–2845, 2010.

[12] Q. M. Al-Mdallal, "An efficient method for solving fractional Sturm-Liouville problems," *Chaos, Solitons and Fractals*, vol. 40, no. 1, pp. 183–189, 2009.

[13] C. Kiataramkul, K. N. Sotiris, J. Tariboon, and A. Kijjathanakorn, "Generalized Sturm-Liouville and Langevin equations via Hadamard fractional derivatives with anti-periodic boundary conditions," *Boundary Value Problems*, vol. 2016, 13 pages, 2016.

[14] T. Muensawat, K. N. Sotiris, and J. Tariboon, "Systems of generalized Sturm-Liouville and Langevin fractional differential equations," *Advances in Difference Equations*, vol. 2017, Article ID 63, 2017.

[15] A. Boutiara, M. S. Abdo, M. A. Alqudah, and T. Abdeljawad, "On a class of Langevin equations in the frame of Caputo function-dependent-kernel fractional derivatives with antiperiodic boundary conditions," *AIMS Mathematics*, vol. 6, no. 6, pp. 5518–5534, 2021.

[16] I. Suwan, M. S. Abdo, T. Abdeljawad, M. Mater, A. Boutiara, and M. Almalahi, "Existence theorems for ψ-fractional hybrid systems with periodic boundary conditions," *AIMS Mathematics*, vol. 7, no. 1, pp. 171–186, 2021.

[17] S. M. Ali and M. S. Abdo, "Qualitative analysis for multiterm Langevin systems with generalized Caputo fractional operators of different orders," *Mathematical Problems in Engineering*, vol. 2022, Article ID 1879152, 12 pages, 2022.

[18] S. Djennadi, N. Shawagfeh, M. Inc, M. S. Osman, J. F. Gómez-Aguilar, and O. A. Arqub, "The Tikhonov regularization method for the inverse source problem of time fractional heat equation in the view of ABC-fractional technique," *Physica Scripta*, vol. 96, no. 9, article 094006, 2021.

[19] A. Salem and M. Alnegga, "Measure of noncompactness for hybrid Langevin fractional differential equations," *Axioms*, vol. 9, no. 2, p. 59, 2020.

[20] R. Almeida, "A Caputo fractional derivative of a function with respect to another function," *Communications in Nonlinear Science and Numerical Simulation*, vol. 44, pp. 460–481, 2017.

[21] R. Almeida, A. B. Malinowska, and M. T. T. Monteiro, "Fractional differential equations with a Caputo derivative with respect to a kernel function and their applications," *Mathematical Methods in the Applied Sciences*, vol. 41, no. 1, pp. 336–352, 2018.

[22] J. Banas and K. Goebel, *Measures of Noncompactness in Banach Spaces*, Lecture Notes in Pure and Applied Mathematics, Marcel Dekker, New York, NY, USA, 1980.

[23] J. Banas and K. Goebel, "On a class of measures of noncompactness in banach algebras and their application to nonlinear integral equations," *Journal of Analytical and Applied Pyrolysis*, vol. 28, pp. 475–498, 2009.

[24] B. Zidane, G. Kaddour, B. Mouffak, and Z. Yong, "Boundary value problems for hybrid caputo fractional differential equations," *Mathematics*, vol. 7, no. 3, p. 282, 2019.

[25] G. Darbo, "Punti uniti in transformazioni a codominio noncompatton," *Rendiconti del Seminario matematico della Università di Padova*, vol. 24, pp. 84–92, 1955.

[26] M. Jleli, E. Karapnar, D. O'Regan, and B. Samet, "Some generalizations of Darbo's theorem and applications to fractional integral equations," *Fixed Point Theory and Applications*, vol. 2016, 17 pages, 2016.

Hindawi
Journal of Function Spaces
Volume 2022, Article ID 5365810, 9 pages
https://doi.org/10.1155/2022/5365810

Research Article

A New Iterative Method for the Approximate Solution of Klein-Gordon and Sine-Gordon Equations

Jiahua Fang,[1] **Muhammad Nadeem**,[2] **Mustafa Habib**,[3] **Shazia Karim**,[4] and **Hanan A. Wahash**[5]

[1]*Yibin University, Yibin 644000, China*
[2]*Faculty of Science, Yibin University, Yibin 644000, China*
[3]*Department of Mathematics, University of Engineering and Technology, Lahore 54890, Pakistan*
[4]*Department of Basic Sciences, UET Lahore, FSD Campus 54800, Pakistan*
[5]*Department of Mathematics, Albaydaa University, Yemen*

Correspondence should be addressed to Muhammad Nadeem; nadeem@yibinu.edu.cn and Hanan A. Wahash; hawahash@baydaauniv.net

Received 23 May 2022; Accepted 9 June 2022; Published 21 June 2022

Academic Editor: Yusuf Gurefe

This article presents a new iterative method (NIM) for the investigation of the approximate solution of the Klein-Gordon and sine-Gordon equations. This approach is formulated on the combination of the Mohand transform and the homotopy perturbation method. Mohand transform (MT) is capable to handle the linear terms only, thus we introduce homotopy perturbation method (HPM) to tackle the nonlinear terms. This NIM derives the results in the form of a series solution. The proposed method emphasizes the stability of the derived solutions without any linearization, discretization, or hypothesis. Graphical representation and absolute error demonstrate the efficiency and authenticity of this scheme. Some numerical models are illustrated to show the compactness and reliability of this strategy.

1. Introduction

Many linear and nonlinear phenomena appear in several areas of scientific fields like physics, chemistry and biology can be modeled by different type of partial differential equation [1–4]. A broad class of analytical methods and numerical methods have been introduced such as (G'/G)-expansion method [5], Exp-function method [6], Homotopy perturbation method [7], Homotopy analysis method [8], Laplace transform [9], Residual power series [10], Quasi wavelet method [11], Fourier series [12], Chebyshev-Tau method [13], Haar wavelets method [14], trial equation method [15] and Two scale approach [16] to handle these linear and nonlinear PDEs but to reach exact solutions is not an easy way. In past few decades, The Klein-Gordon and sine-Gordon equations are a type of hyperbolic partial differential equation which are often used to describe and simulate the physical phenomena in a variety of fields of engineering and science, i.e., physics, fluid dynamics, mathematical biology and quantum mechanics. Let us consider the Klein-Gordon and sine-Gordon [17],

$$\mathfrak{I}_{\eta\eta}(\xi,\eta) - \mathfrak{I}_{\xi\xi}(\xi,\eta) + c_1\mathfrak{I}(\xi,\eta) + c_2 G(\mathfrak{I}(\xi,\eta)) = f_1(\xi,\eta), \tag{1}$$

$$\mathfrak{I}_{\eta\eta}(\xi,\eta) - \mathfrak{I}_{\xi\xi}(\xi,\eta) + c_3 \sin(\mathfrak{I}(\xi,\eta)) = f_2(\xi,\eta), \tag{2}$$

where $\mathfrak{I}$ is a function of ξ and η; G is a nonlinear function, f_1 and f_2 are known analytic functions whereas c_1, c_2 and c_3 are constants.

In recent years, The Klein-Gordon and sine-Gordon equations have attracted more attention from the scientists due to its applications in plasma, nonlinear wave equations, studying the solutions and condensed matter physics and relativistic physics as a model of dispersive phenomena. Yousif and Mahmood [18] used variational iteration method coupled with homotopy perturbation method to investigate the approximate solution of Klein-Gordon an sine-Gordon equations. Nadeem and Li [17] applied the He-Laplace method to obtain the analytical solution of Klein-Gordon an sine-Gordon equations. Liu.et al. [19] employed Yang transformation for the approximate solution of Klein-Gordon an sine-Gordon equations. Agom and Ogunfiditimi [20] utilized modified Adomian decomposition method for nonlinear Klein-Gordon equations with quadratic nonlinearity. Ikram et. al [21] obtained the approximate solution of linear Klein-Gordon equations using Haar wavelet approach. Lotfi and Alipanah [22] used Legendre spectral element method for solving sine-Gordon equation. Lu [23] applied modified homotopy perturbation method for the solution of sine-Gordon equation. Many authors applied various approaches to investigate the approximate solution of the Klein-Gordon and sine-Gordon equations [24–26].

The homotopy perturbation method (HPM) was first developed by a Chinese mathematician He [27, 28] to present the analytical solution of linear and nonlinear partial differential equation. Later, Nadeem and Li [29] combined HPM with Laplace transform for solving nonlinear vibration systems and nonlinear wave equations to show the accuracy and validity of HPM. Khan and Qingbiao [30] used HPM using He's polynomials for the solution of nonlinear equations. Many authors have performed the accuracy of HPM for different system of PDEs. [31–34].

The main purpose of this paper is to develop a new iterative method (NIM) where Mohand transform is combined with homotopy perturbation method for obtaining the approximate solution of Klein-Gordon and sine-Gordon equations. This scheme derive the results in aspect of series without any linearization, variation and limiting expectations. In addition, this study is organized as follow: In Section 2, we present some basic definitions of Mohand transform. In Section 3, we formulate the idea of new iterative method (NIM) for obtaining the solution of illustrated problems. In Section 4, we executed NIM for finding the approximate solution of the problems to show the accuracy and validity of this approach. Finally, we present some results and discussion in Section 5 and conclusion in Section 6.

2. Fundamentals Concepts of Mohand Transform

In this section, we introduce some basic definitions and preliminaries concepts of Mohand transform which reveals the idea of its implementations to functions.

Definition 1. Let $\mathfrak{I}(\eta)$ be a function precise for $\eta \geq 0$ [17], then

$$\mathscr{L}[\mathfrak{I}(\eta)] = V(\theta) = \int_0^\infty \mathfrak{I}(\eta) e^{-\theta\eta} d\eta, \tag{3}$$

is said to be Laplace transform, where η is function (i.e. a function of time domain), defined on $[0, \infty)$ to a function of θ (i.e. of frequency domain).

Definition 2. If $V(\theta)$ symbolizes the Laplace transform of $\mathfrak{I}(\eta)$, then

$$\mathfrak{I}(\eta) = \mathscr{L}^{-1} V(\theta), \tag{4}$$

is termed as inverse Laplace transform of $V(\theta)$.

Definition 3. Mohand and Mahgoub [35] presented a new scheme Mohand transform $M(.)$ in order to gain the results of ordinary differential equations and is defined as

$$M\{\mathfrak{I}(\eta)\} = R(\theta) = \theta^2 \int_0^\infty \mathfrak{I}(\eta) e^{-\theta\eta} dt, k_1 \leq \theta \leq k_2. \tag{5}$$

On the other hand, if $R(\theta)$ is the Mohand transform of a function $\mathfrak{I}(\eta)$, then $\mathfrak{I}(\eta)$ is the inverse of $R(\theta)$ such as

$$M^{-1}\{R(\theta)\} = \mathfrak{I}(\eta), M^{-1} \text{ is inverse Mohand operator.} \tag{6}$$

Definition 4. If $\mathfrak{I}(\eta) = \eta^m$,

$$R(\theta) = \frac{m!}{\theta^{m-1}}. \tag{7}$$

Definition 5. If $M\{\mathfrak{I}(\eta)\} = R(\theta)$ *,then* it has the following differential properties [36]

(i) $M\{\mathfrak{I}'(\eta)\} = \theta R(\theta) - \theta^2 \mathfrak{I}(0)$

(ii) $M\{\mathfrak{I}''(\eta)\} = \theta^2 R(\theta) - \theta^3 F(0) - \theta^2 \mathfrak{I}'(0)$

(iii) $M\{\mathfrak{I}^m(\eta)\} = \theta^m R(\theta) - \theta^{m+1}\mathfrak{I}(0) - \theta^m \mathfrak{I}'(0) - \cdots - \theta^m \mathfrak{I}^{m-1}(0)$

3. Formulation of New Iterative Method (NIM)

This segment presents the construction of new iterative method (NIM) for obtaining the approximate solution of Klein-Gordon and sine-Gordon equations. Let us consider a nonlinear second order differential equation of the form,

$$\mathfrak{I}_{\eta\eta}(\xi, \eta) + \mathfrak{I}_\eta(\xi, \eta) + \mathfrak{I}(\xi, \eta) + g(\mathfrak{I}) = g(\xi, \eta), \tag{8}$$

with the following conditions

$$\mathfrak{I}(\xi, 0) = a_1, \mathfrak{I}_\eta(\xi, 0) = a_2, \tag{9}$$

where $\mathfrak{I}$ is a function in time domain η, $g(\mathfrak{I})$ represents nonlinear term, $g(\eta)$ is a source term whereas a_1 and a_2 are constants. Rewrite Eq. (8) again

$$\mathfrak{I}_{\eta\eta}(\xi, \eta) + \mathfrak{I}_\eta(\xi, \eta) = -\mathfrak{I}(\xi, \eta) - g(\mathfrak{I}) + g(\xi, \eta). \tag{10}$$

Now, taking MT on both sides of Eq. (10), we obtain

$$M\left[\mathfrak{I}_{\eta\eta}(\xi, \eta) + \mathfrak{I}_\eta(\xi, \eta)\right] = M[-\mathfrak{I}(\eta) - g(\mathfrak{I}) + g(\eta)]. \tag{11}$$

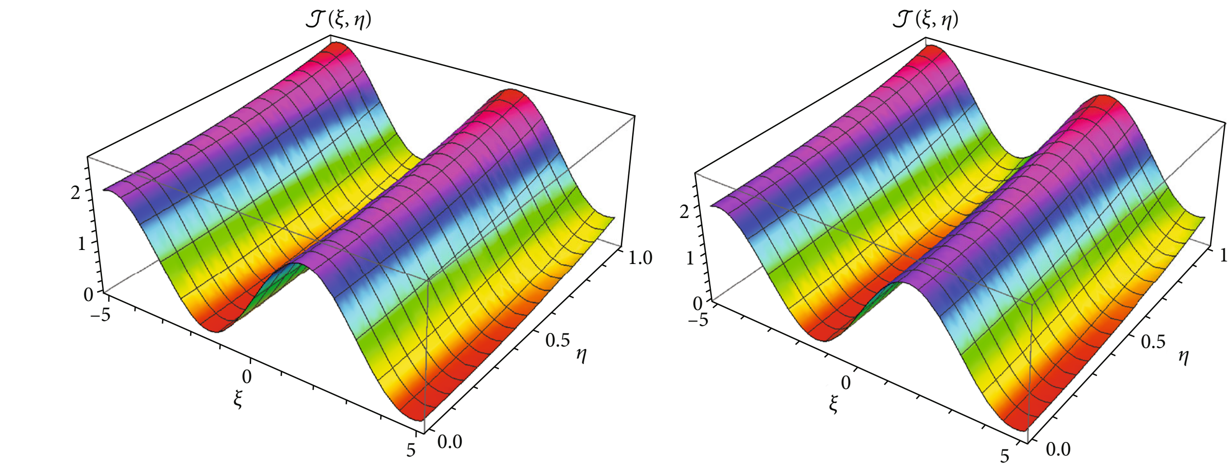

(a) Surface plot for exact solution

(b) Surface plot for approximate solution

Figure 1: Surfaces plots for the linear Klein-Gordon equation.

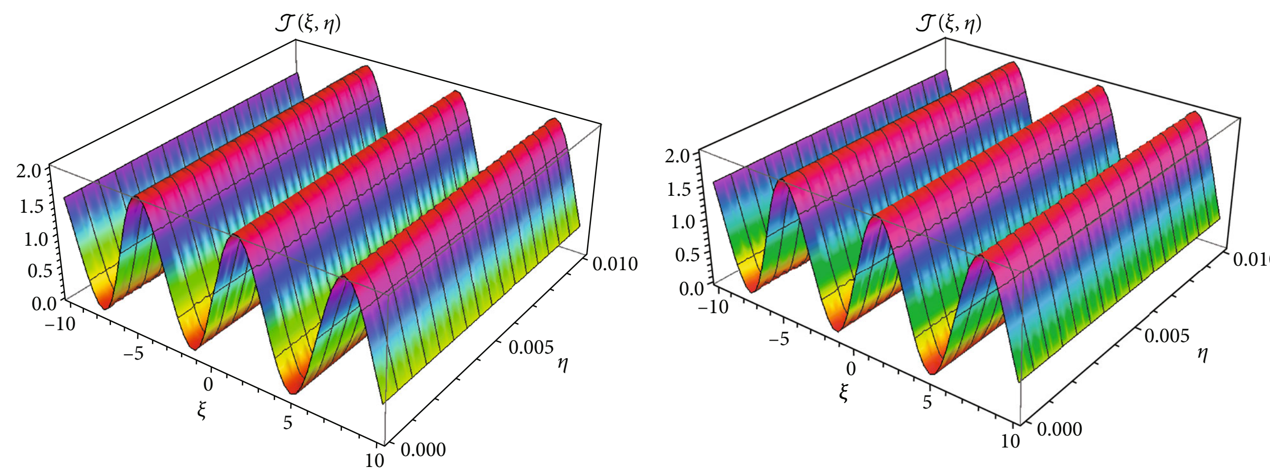

(a) urface plot for exact solution

(b) Surface plot for approximate solution

Figure 2: Surfaces plots for the nonlinear Klein-Gordon equation.

Table 1: The absolute error of $\mathfrak{I}(\xi,\eta)$ for different values of ξ at $\eta = 0.01$.

ξ	Exact solution	Approximate solution	Absolute error
0.5	1.47948	1.47948	0.0000
1	1.84152	1.84152	0.0000
1.5	1.99754	1.99754	0.0000
2	1.90935	1.90935	0.0000
2.5	1.59852	1.59852	0.0000
3	1.14117	1.14117	0.0000
3.5	0.649267	0.649267	0.0000
4	0.243248	0.243248	0.0000
4.5	0.0225199	0.0225199	0.0000
5	0.0411257	0.0411257	0.0000

Table 2: The absolute error of $\mathfrak{I}(\xi,\eta)$ for different values of ξ at $\eta = 0.01$.

ξ	Exact solution	Approximate solution	Absolute error
0.5	1.47929	1.47951	0.00022
1	1.84126	1.8416	0.00034
1.5	1.99725	1.99764	0.00039
2	1.90907	1.90943	0.00036
2.5	1.59831	1.59857	0.00026
3	1.14105	1.14118	0.00013
3.5	0.649213	0.649255	0.000042
4	0.243232	0.243238	6×10^{-6}
4.5	0.0225187	0.0225188	1×10^{-7}
5	0.0411236	0.0411238	2×10^{-7}

Table 3: The absolute error of $\mathfrak{I}(\xi, \eta)$ for different values of η.

η	Exact solution	Approximate solution	Absolute error
0.1	1.57580	1.57582	0.00022
0.2	1.5908	1.59088	0.00034
0.3	1.61579	1.61595	0.00039
0.4	1.65078	1.65094	0.00036
0.5	1.69573	1.69569	0.00026
0.6	1.7506	1.74993	0.00067
0.7	1.81531	1.81327	0.00204
0.8	1.88971	1.88515	0.00456
0.9	1.9736	1.96485	0.00875
1.0	2.06668	2.05142	0.00875

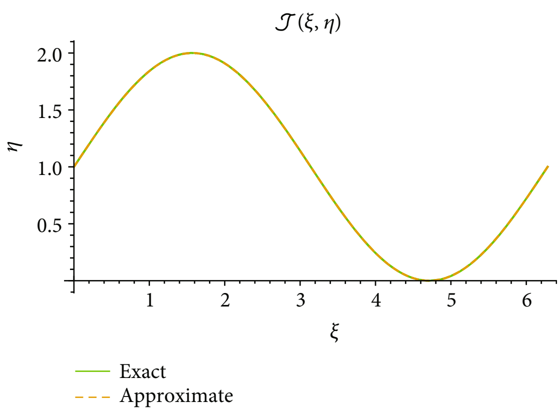

Figure 3: 2D Plot for $\mathfrak{I}(\eta)$ with various parameter of η.

Applying the differential properties of MT, we get

$$\theta^2 R[\theta] - \theta^3 \mathfrak{I}(\xi, 0) - \theta^2 \mathfrak{I}_\eta(\xi, 0) + \theta R[\theta] - \theta^2 \mathfrak{I}(\xi, 0) = M[-\mathfrak{I}(\xi, \eta) - g(\mathfrak{I}) + g(\xi, \eta)]. \quad (12)$$

Thus $R(\theta)$ can be obtained from Eq. (12) such as

$$R[\theta] = \frac{\theta^2 a_1 + \theta^2 a_2 + \theta^3 a_1}{(\theta + \theta^2)} - \frac{M[\mathfrak{I}(\xi, \eta) + g(\mathfrak{I}) - g(\xi, \eta)]}{(\theta + \theta^2)}. \quad (13)$$

Operating inverse Mohand transform, on Eq. (13), we get

$$\mathfrak{I}(\xi, \eta) = G(\xi, \eta) - M^{-1}\left[\frac{M[\mathfrak{I}]}{(\theta + \theta^2)} + \frac{M[g(\mathfrak{I})]}{(\theta + \theta^2)}\right], \quad (14)$$

where

$$G(\xi, \eta) = M^{-1}\left[\frac{\theta^2 a_1 + \theta^2 a_2 + \theta^3 a_1}{(\theta + \theta^2)} + M\left[\frac{g(\xi, \eta)}{(\theta + \theta^2)}\right]\right]. \quad (15)$$

Now, we apply HPM on Eq. (14). Let

$$\mathfrak{I}(\xi, \eta) = \sum_{i=0}^{\infty} p^i \mathfrak{I}_i(m) = \mathfrak{I}_0 + p^1 \mathfrak{I}_1 + p^2 \mathfrak{I}_2 + \cdots, \quad (16)$$

and nonlinear terms $g(\mathfrak{I})$ can be calculated by using formula,

$$g(\mathfrak{I}) = \sum_{i=0}^{\infty} p^i H_i(\mathfrak{I}) = H_0 + p^1 H_1 + p^2 H_2 + \cdots, \quad (17)$$

where $Hm's$ is the He's polynomial, which may be computed using the following procedure.

$$H_m(\mathfrak{I}_0 + \mathfrak{I}_1 + \cdots + \mathfrak{I}_m) = \frac{1}{m!}\frac{\partial^m}{\partial p^m}\left(g\left(\sum_{i=0}^{\infty} p^i \mathfrak{I}_i\right)\right)_{p=0}, m = 0, 1, 2, \cdots \quad (18)$$

Put Eqs. (16), (17) and (18) in Eq. (14) and comparing the similar factors of p, we get the following consecutive elements

$$\begin{aligned}
p^0 &: \mathfrak{I}_0(\xi, \eta) = G(\xi, \eta), \\
p^1 &: \mathfrak{I}_1(\xi, \eta) = -M^{-1}\left[\frac{1}{(\theta + \theta^2)} M\{\mathfrak{I} + H_0(\mathfrak{I})\}\right], \\
p^2 &: \mathfrak{I}_1(\xi, \eta) = -M^{-1}\left[\frac{1}{(\theta + \theta^2)} M\{\mathfrak{I} + H_1(\mathfrak{I})\}\right], \\
p^3 &: \mathfrak{I}_1(\xi, \eta) = -M^{-1}\left[\frac{1}{(\theta + \theta^2)} M\{\mathfrak{I} + H_2(\mathfrak{I})\}\right], \\
&\vdots
\end{aligned} \quad (19)$$

on continuing the similar process, we can summarize this series to get the approximate solution such as

$$\mathfrak{I}(\xi, \eta) = \mathfrak{I}_0(\xi, \eta) + p^1 \mathfrak{I}_1(\xi, \eta) + p^2 \mathfrak{I}_2(\xi, \eta) + + p^3 \mathfrak{I}_3(\xi, \eta) + \cdots. \quad (20)$$

Let $p = 1$ in above equation, thus the analytical solution of Eq. (8) is as follows

$$\mathfrak{I}(\xi, \eta) = \mathfrak{I}_0 + \mathfrak{I}_1 + \mathfrak{I}_2 + \cdots = \sum_{i=0}^{\infty} \mathfrak{I}_i. \quad (21)$$

Thus, Eq. (21) is considered as an approximate solution of nonlinear differential equation (8).

4. Numerical Examples

In this part, we test two examples for the authenticity and validity of MHPTM. We also demonstrate 2D plots for a better understanding of this strategy where we see that the solution graphs of the approximate solution and the exact solution coincide with each other only after a few iterations.

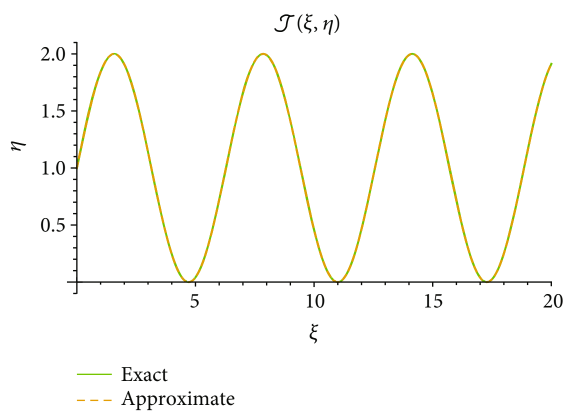

FIGURE 4: 2D Plot for $\mathfrak{I}(\eta)$ with various parameter of η.

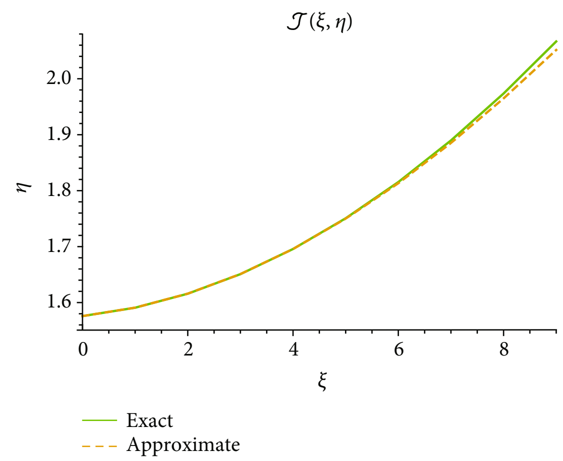

FIGURE 5: 2D Plot for $\mathfrak{I}(\eta)$ with various parameter of η.

4.1. Example 1. Consider a linear Klein-Gordon equation

$$\frac{\partial^2 \mathfrak{I}}{\partial \eta^2} - \frac{\partial^2 \mathfrak{I}}{\partial \xi^2} = \mathfrak{I}, \tag{22}$$

with the initial condition

$$\mathfrak{I}(\xi, 0) = 1 + \sin(\xi), \mathfrak{I}_\eta(\xi, 0) = 0, \tag{23}$$

Applying MT on Eq. (22) together with the differential property as defined in Eq. (7), we get

$$\theta^2 R(\theta) - \theta^3 \mathfrak{I}(0) - \theta^2 \mathfrak{I}'(0) = M\left[\mathfrak{I} + \frac{\partial^2 \mathfrak{I}}{\partial \eta^2}\right]. \tag{24}$$

Using Eq. (23) into Eq. (24) for solving $R(\theta)$, it yields

$$R(\theta) = \theta(1 + \sin(\xi)) + M\left[\mathfrak{I} + \frac{\partial^2 \mathfrak{I}}{\partial \eta^2}\right]. \tag{25}$$

Using inverse Mohand transform on Eq. (25), we get

$$\mathfrak{I}(\xi, \eta) = 1 + \sin(\xi) + M^{-1}\left[\frac{1}{\theta^2} M\left\{\mathfrak{I} + \frac{\partial^2 \mathfrak{I}}{\partial \eta^2}\right\}\right] \tag{26}$$

Applying MHPTM to get the He's polynomials

$$\sum_{i=0}^{\infty} p^i \mathfrak{I}_i(m) = 1 + \sin(\xi) + M^{-1}\left[\frac{1}{\theta^2} M\left\{\sum_{i=0}^{\infty} p^i \mathfrak{I}_i + \sum_{i=0}^{\infty} p^i \left(\frac{\partial^2 \mathfrak{I}}{\partial \eta^2}\right)\right\}\right]. \tag{27}$$

Observing the similar powers of p, we get

$$\begin{aligned}
p^0 &: \mathfrak{I}_0(\xi, \eta) = 1 + \sin(\xi),\\
p^1 &: \mathfrak{I}_1(\eta) = M^{-1}\left[\frac{1}{\theta^2} M\left\{\mathfrak{I}_0 + \frac{\partial^2 \mathfrak{I}_0}{\partial \eta^2}\right\}\right] = \frac{\eta^2}{2},\\
p^2 &: \mathfrak{I}_2(\xi, \eta) = M^{-1}\left[\frac{1}{\theta^2} M\left\{\mathfrak{I}_0 + \frac{\partial^2 \mathfrak{I}_0}{\partial \eta^2}\right\}\right] = 2\frac{\eta^4}{4!},\\
p^3 &: \mathfrak{I}_3(\xi, \eta) = M^{-1}\left[\frac{1}{\theta^2} M\left\{\mathfrak{I}_0 + \frac{\partial^2 \mathfrak{I}_0}{\partial \eta^2}\right\}\right] = 2\frac{\eta^6}{6!},\\
p^4 &: \mathfrak{I}_4(\xi, \eta) = M^{-1}\left[\frac{1}{\theta^2} M\left\{\mathfrak{I}_0 + \frac{\partial^2 \mathfrak{I}_0}{\partial \eta^2}\right\}\right] = 2\frac{\eta^8}{8!},\\
&\vdots .
\end{aligned} \tag{28}$$

On continuing this process, the results of obtained series cab be summarized as,

$$\begin{aligned}
\mathfrak{I}(\xi, \eta) &= \mathfrak{I}_0(\xi, \eta) + \mathfrak{I}_1(\xi, \eta) + \mathfrak{I}_2(\xi, \eta) + \mathfrak{I}_3(\xi, \eta) + \mathfrak{I}_4(\xi, \eta) + \cdots,\\
&= 1 + \sin(\xi) + \frac{\eta^2}{2} + 2\frac{\eta^4}{4!} + 2\frac{\eta^6}{6!} + 2\frac{\eta^8}{8!} + \cdots.
\end{aligned} \tag{29}$$

This series converges to the exact solution

$$\mathfrak{I}(\xi, \eta) = \sin(\xi) + \cosh(\eta). \tag{30}$$

4.2. Example 2. Consider a nonlinear Klein-Gordon equation

$$\frac{\partial^2 \mathfrak{I}}{\partial \eta^2} - \frac{\partial^2 \mathfrak{I}}{\partial \xi^2} = \mathfrak{I}^2, \tag{31}$$

with the initial condition

$$\mathfrak{I}(\xi, 0) = 1 + \sin(\xi), \mathfrak{I}_\eta(\xi, 0) = 0. \tag{32}$$

Applying MT on Eq. (18) together with the differential property as defined in Eq. (2), we get

$$\theta^2 R(\theta) - \theta^3 \mathfrak{I}(0) - \theta^2 \mathfrak{I}'(0) = M\left[\mathfrak{I}^2 + \frac{\partial^2 \mathfrak{I}}{\partial \eta^2}\right]. \tag{33}$$

Using Eq. (21) into Eq. (22) for solving $R(\theta)$, it yields

$$R(\theta) = \theta(1 + \sin(\xi)) + M\left[\mathfrak{I}^2 + \frac{\partial^2 \mathfrak{I}}{\partial \eta^2}\right]. \tag{34}$$

Using inverse Mohand transform on Eq. (18), we get

$$\mathfrak{I}(\xi, \eta) = 1 + \sin(\xi) + M^{-1}\left[\frac{1}{\theta^2} M\left\{\mathfrak{I}^2 + \frac{\partial^2 \mathfrak{I}}{\partial \eta^2}\right\}\right]. \tag{35}$$

Applying MHPTM to get the He's polynomials

$$\sum_{i=0}^{\infty} p^i \mathfrak{I}_i(m) = 1 + \sin(\xi) + M^{-1}\left[\frac{1}{\theta^2} M\left\{\sum_{i=0}^{\infty} p^i \mathfrak{I}_i^2 + \sum_{i=0}^{\infty} p^i \frac{\partial^2 \mathfrak{I}}{\partial \eta^2}\right)\right\}\right]. \tag{36}$$

Observing the similar powers of p, we get

$$\begin{gathered}
p^0 : \mathfrak{I}_0(\xi, \eta) = 1 + \sin(\xi), \\
p^1 : \mathfrak{I}_1(\eta) = M^{-1}\left[\frac{1}{\theta^2} M\left\{\mathfrak{I}_0^2 + \frac{\partial^2 \mathfrak{I}_0}{\partial \eta^2}\right\}\right] = \frac{\eta^2}{2}, \\
p^2 : \mathfrak{I}_2(\xi, \eta) = M^{-1}\left[\frac{1}{\theta^2} M\left\{2\mathfrak{I}_0\mathfrak{I}_1 + \frac{\partial^2 \mathfrak{I}_1}{\partial \eta^2}\right\}\right] = 2\frac{\eta^4}{4!}, \\
p^3 : \mathfrak{I}_3(\xi, \eta) = M^{-1}\left[\frac{1}{\theta^2} M\left\{\mathfrak{I}_1^2 + 2\mathfrak{I}_0\mathfrak{I}_2 + \frac{\partial^2 \mathfrak{I}_2}{\partial \eta^2}\right\}\right] = 2\frac{\eta^6}{6!}, \\
p^4 : \mathfrak{I}_4(\xi, \eta) = M^{-1}\left[\frac{1}{\theta^2} M\left\{2\mathfrak{I}_1\mathfrak{I}_2 + 2\mathfrak{I}_0\mathfrak{I}_3 + \frac{\partial^2 \mathfrak{I}_3}{\partial \eta^2}\right\}\right] = 2\frac{\eta^8}{8!}, \\
\vdots . \\
\mathfrak{I}_0(\xi, \eta) = 1 + \sin(\xi), \\
\mathfrak{I}_1(\xi, \eta) = \left(1 + \sin(\xi) + \sin^2(\xi)\right)\frac{\eta^2}{2}, \\
\mathfrak{I}_2(\xi, \eta) = -(-8 - 9\sin(\xi) + \sin(3\xi))\frac{\eta^4}{48}, \\
\mathfrak{I}_3(\xi, \eta) = (119 - 68\cos(2\xi) + 5\cos(4\xi) + 134\sin(\xi) + 2\sin(3\xi))\frac{\eta^6}{2880}, \\
\mathfrak{I}_4(\xi, \eta) = (681 - 67\cos(\xi) - 404\cos(2\xi) - 27\cos(3\xi) + 19\cos(4\xi) + 1007\sin(\xi) - 272\sin(2\xi) - 147\sin(3\xi) + 160\sin(4\xi) + 10\sin(5\xi))\frac{\eta^8}{80640}, \\
\vdots .
\end{gathered} \tag{37}$$

On continuing this process, the approximate solution cab be summarized as,

$$\mathfrak{I}(\xi, \eta) = \mathfrak{I}_0(\xi, \eta) + \mathfrak{I}_1(\xi, \eta) + \mathfrak{I}_2(\xi, \eta) + \mathfrak{I}_3(\xi, \eta) + \mathfrak{I}_4(\xi, \eta) + \cdots, \tag{38}$$

which is in full agreement with [17, 18].

4.3. Example 3. Consider a nonlinear sine-Gordon equation

$$\frac{\partial^2 \mathfrak{I}}{\partial \eta^2} - \frac{\partial^2 \mathfrak{I}}{\partial \xi^2} = \sin(\mathfrak{I}), \tag{39}$$

with the initial condition

$$\mathfrak{I}(\xi, 0) = \frac{\pi}{2}, \mathfrak{I}_\eta(\xi, 0) = 0. \tag{40}$$

Let $\sin(\mathfrak{I}) = \mathfrak{I} - (\mathfrak{I}^3/6) + (\mathfrak{I}^5/120)$, Thus above equation becomes as

$$\frac{\partial^2 \mathfrak{I}}{\partial \eta^2} - \frac{\partial^2 \mathfrak{I}}{\partial \xi^2} = \mathfrak{I} - \frac{\mathfrak{I}^3}{6} + \frac{\mathfrak{I}^5}{120}. \tag{41}$$

Applying MT on Eq. (41) together with the differential property as defined in Eq. (7), we get

$$\theta^2 R(\theta) - \theta^3 \mathfrak{I}(0) - \theta^2 \mathfrak{I}'(0) = M\left[\frac{\partial^2 \mathfrak{I}}{\partial \xi^2} + \mathfrak{I} - \frac{\mathfrak{I}^3}{6} + \frac{\mathfrak{I}^5}{120}\right]. \tag{42}$$

Using Eq. (40) into Eq. (42) for solving $R(\theta)$, it yields

$$R(\theta) = \theta\left(\frac{\pi}{2}\right) + M\left[\frac{\partial^2 \mathfrak{I}}{\partial \xi^2} + \mathfrak{I} - \frac{\mathfrak{I}^3}{6} + \frac{\mathfrak{I}^5}{120}\right]. \tag{43}$$

Using inverse Mohand transform on Eq. (43), we get

$$\mathfrak{I}(\xi, \eta) = \frac{\pi}{2} + M^{-1}\left[\frac{1}{\theta^2} M\left\{\frac{\partial^2 \mathfrak{I}}{\partial \xi^2} + \mathfrak{I} - \frac{\mathfrak{I}^3}{6} + \frac{\mathfrak{I}^5}{120}\right\}\right]. \tag{44}$$

Applying MHPTM to get the He's polynomials

$$\sum_{i=0}^{\infty} p^i \mathfrak{I}_i(m) = \frac{\pi}{2} + M^{-1}\left[\frac{1}{\theta^2} M\left\{\sum_{i=0}^{\infty} p^i \frac{\partial^2 \mathfrak{I}_i}{\partial \xi^2} + \sum_{i=0}^{\infty} p^i \mathfrak{I}_i - \sum_{i=0}^{\infty} p^i \frac{\mathfrak{I}_i^3}{6} + \left(\sum_{i=0}^{\infty} p^i \frac{\mathfrak{I}_i^5}{120}\right)\right\}\right]. \tag{45}$$

Observing the similar powers of p, we get

$$\begin{aligned}
p^0 &: \mathfrak{I}_0(\xi, \eta) = \frac{\pi}{2}, \\
p^1 &: \mathfrak{I}_1(\eta) = M^{-1}\left[\frac{1}{\theta^2} M\left\{\frac{\partial^2 \mathfrak{I}_0}{\partial \eta^2} + \mathfrak{I}_0 - \frac{\mathfrak{I}_0^3}{6} + \frac{\mathfrak{I}_0^5}{120}\right\}\right], \\
p^2 &: \mathfrak{I}_2(\xi, \eta) = M^{-1}\left[\frac{1}{\theta^2} M\left\{\frac{\partial^2 \mathfrak{I}_1}{\partial \eta^2} + \mathfrak{I}_1 - \frac{1}{2}\mathfrak{I}_0^2 \mathfrak{I}_1 + \frac{1}{24}\mathfrak{I}_0^4 \mathfrak{I}_1\right\}\right], \\
p^3 &: \mathfrak{I}_3(\xi, \eta) = M^{-1}\left[\frac{1}{\theta^2} M\left\{\frac{\partial^2 \mathfrak{I}_2}{\partial \eta^2} + \frac{1}{2}\mathfrak{I}_0 \mathfrak{I}_1^2 + \frac{1}{12}\mathfrak{I}_0^3 \mathfrak{I}_1^2 + \mathfrak{I}_2 - \frac{1}{2}\mathfrak{I}_0^2 \mathfrak{I}_2 + \frac{1}{24}\mathfrak{I}_0^4 \mathfrak{I}_2\right\}\right], \\
&\vdots .
\end{aligned} \tag{46}$$

$$\begin{aligned}
\mathfrak{I}_0(\xi, \eta) &= \frac{\pi}{2}, \\
\mathfrak{I}_1(\xi, \eta) &= \left(\frac{\pi}{2} - \frac{\pi^3}{48} + \frac{\pi^5}{3840}\right)\frac{\eta^2}{2}, \\
\mathfrak{I}_2(\xi, \eta) &= \left(\frac{\pi}{2} - \frac{\pi^3}{12} + \frac{\pi^5}{240} - \frac{\pi^7}{11520} + \frac{\pi^9}{1474560}\right)\frac{\eta^5}{5!}, \\
\mathfrak{I}_3(\xi, \eta) &= -\left(\frac{3\pi^3}{8} - \frac{3\pi^5}{64} + \frac{3\pi^7}{1280} - \frac{11\pi^9}{184320} + \frac{23\pi^{11}}{707788800} - \frac{\pi^{13}}{235929600}\right)\frac{\eta^5}{5!} + \left(\frac{\pi}{2} - \frac{7\pi^3}{48} + \frac{61\pi^5}{3840} - \frac{19\pi^7}{23040} + \frac{6451\pi^9}{2264833200} - \frac{23347\pi^{11}}{21742387200} + \frac{\pi^{13}}{56620800}\right)\frac{\eta^6}{6!}, \\
&\vdots .
\end{aligned} \tag{47}$$

On continuing this process, the approximate solution cab be summarized as,

$$\mathfrak{I}(\xi, \eta) = \mathfrak{I}_0(\xi, \eta) + \mathfrak{I}_1(\xi, \eta) + \mathfrak{I}_2(\xi, \eta) + \mathfrak{I}_3(\xi, \eta) + \mathfrak{I}_4(\xi, \eta) + \cdots, \tag{48}$$

which is in full agreement with [17, 18].

5. Results and Discussion

In this segment, we demonstrate the validity and the accuracy of NIM though the graphical representations. Figure 1 shows the surface solution of linear Klein-Gordon equation for $-5 \leq \xi \leq 5$ at $\eta = 1$ and Figure 2 shows the surface solution of nonlinear Klein-Gordon equation for $-10 \leq \xi \leq 10$ at $\eta = 0.01$. The absolute errors in Tables 1–3 show the comparison between other approaches and the approximate solution obtained by NIM. We also compare the NIM results in Figures 3, 4 and 5 to show the accuracy of the present approach at $\xi = \pi$ and $\xi = 20$ with different values of η. These results show the high accuracy and validity of this approach. All the computations and graphical representations are made with wolfram Mathematica software. These plot distribution and absolute error show that NIM is powerful, straight forward and easy to implement for such kind of linear and nonlinear partial differential equations. We observe that the approximate of sine-Gordon Eq. (39) is independent of ξ variable due to its independent of initial condition in Eq. (40). Thus, it appropriate solution obtained by NIM is also independent of ξ variable.

6. Conclusion

In this study, we have successfully employed the new iterative method (NIM) to obtain the approximate solution of Klein-Gordon and sine-Gordon equations. The obtained results are derived in the form of series and all are in full agreement which shows that NIM is a very simple and straightforward approach for linear and nonlinear problems. The Mohand transform has been used directly without any perturbation theory and recurrence relation which ruins the physical nature of the problem. We also demonstrate the absolute error and 2D plot distribution with various time parameters. The solution graphs and absolute errors have confirmed the validity and reliability of NIM toward the solutions of other nonlinear partial differential equations in science and engineering.

Data Availability

All the data are available within the article.

Conflicts of Interest

The authors declare that they have no competing interests.

Funding

There is no funding to support this article for publication.

References

[1] A. E. Abouelregal, H. Mohammad-Sedighi, S. A. Faghidian, and A. H. Shirazi, "Temperature-dependent physical characteristics of the rotating nonlocal nanobeams subject to a varying heat source and a dynamic LOAD," *Mechanical Engineering*, vol. 19, no. 4, pp. 633–656, 2021.

[2] S. Aggarwal and R. Chaudhary, "A comparative study of Mohand and Laplace transforms," *Journal of Emerging Technologies and Innovative Research*, vol. 6, no. 2, pp. 230–240, 2019.

[3] E. U. Agom and F. O. Ogunfiditimi, "Exact solution of nonlinear Klein-Gordon equations with quadratic nonlinearity by modified adomian decomposition method," *The Journal of Mathematics and Computer Science*, vol. 8, no. 4, pp. 484–493, 2018.

[4] M. N. Alam, "Exact solutions to the foam drainage equation by using the new generalized (G'/G)-expansion method," *Results in Physics*, vol. 5, pp. 168–177, 2015.

[5] Y. Al-qudah, M. Alaroud, H. Qoqazeh, A. Jaradat, S. E. Alhazmi, and S. Al-Omari, "Approximate analytic–numeric fuzzy solutions of fuzzy fractional equations using a residual power series approach," *Symmetry*, vol. 14, no. 4, p. 804, 2022.

[6] S. Arbabi, A. Nazari, and M. T. Darvishi, "A semi-analytical solution of foam drainage equation by Haar wavelets method," *Optik*, vol. 127, no. 13, pp. 5443–5447, 2016.

[7] M. Dehghan, M. Abbaszadeh, and A. Mohebbi, "An implicit RBF meshless approach for solving the time fractional nonlinear sine-Gordon and Klein-Gordon equations," *Engineering Analysis with Boundary Elements*, vol. 50, pp. 412–434, 2015.

[8] Y. O. El-Dib and R. Matoog, "The rank upgrading technique for a harmonic restoring forceâ€Ž of nonlinear oscillators," *Journal of Applied and Computational Mechanics*, vol. 7, no. 2, pp. 782–789, 2021.

[9] H. Gul, S. Ali, K. Shah, S. Muhammad, T. Sitthiwirattham, and S. Chasreechai, "Application of asymptotic homotopy perturbation method to fractional order partial differential equation," *Symmetry*, vol. 13, no. 11, p. 2215, 2021.

[10] N. Gurefe, E. G. Kocer, and Y. Gurefe, "Chebyshev-tau method for the linear klein-Gordon equation," *International Journal of Physical Sciences*, vol. 7, no. 43, pp. 5723–5728, 2012.

[11] Y. Gurefe and E. Misirli, "Exp-function method for solving nonlinear evolution equations with higher order nonlinearity," *Computers & Mathematics with Applications*, vol. 61, no. 8, pp. 2025–2030, 2011.

[12] Y. Gurefe, A. Sonmezoglu, and E. Misirli, "Application of the trial equation method for solving some nonlinear evolution equations arising in mathematical physics," *Pramana*, vol. 77, no. 6, pp. 1023–1029, 2011.

[13] S. Habib, A. Islam, A. Batool, M. U. Sohail, and M. Nadeem, "Numerical solutions of the fractal foam drainage equation," *GEM-International Journal on Geomathematics*, vol. 12, no. 1, pp. 1–10, 2021.

[14] J.-H. He, "Homotopy perturbation method: a new nonlinear analytical technique," *Applied Mathematics and Computation*, vol. 135, no. 1, pp. 73–79, 2003.

[15] J.-H. He, "Recent development of the homotopy perturbation method," *Topological Methods in Nonlinear Analysis*, vol. 31, no. 2, pp. 205–209, 2008.

[16] S. Ikram, S. Saleem, and M. Z. Hussain, "Approximations to linear Klein–Gordon Equations using Haar wavelet," *Ain Shams Engineering Journal*, vol. 12, no. 4, pp. 3987–3995, 2021.

[17] S. K. Jena, S. Chakraverty, M. Malikan, and H. Mohammad-Sedighi, "Hygro-magnetic vibration of the single-walled carbon nanotube with nonlinear temperature distribution based on a modified beam theory and nonlocal strain gradient model," *International Journal of Applied Mechanics*, vol. 12, no. 5, p. 2050054, 2020.

[18] Y. Khan and W. Qingbiao, "Homotopy perturbation transform method for nonlinear equations using He's polynomials," *Computers & Mathematics with Applications*, vol. 61, no. 8, pp. 1963–1967, 2011.

[19] S. Kumar and J. F. Gómez-Aguilar, "Numerical solution of caputo-fabrizio time fractional distributed order reaction-diffusion equation via quasi wavelet based numerical method," *Journal of Applied and Computational Mechanics*, vol. 6, no. 4, pp. 848–861, 2020.

[20] S. Kumar, "A new analytical modelling for fractional telegraph equation via Laplace transform," *Applied Mathematical Modelling*, vol. 38, no. 13, pp. 3154–3163, 2014.

[21] S. Kumbinarasaiah, "A new approach for the numerical solution for nonlinear Klein–Gordon equation," *SeMA Journal*, vol. 77, no. 4, pp. 435–456, 2020.

[22] J. Liu, M. Nadeem, M. Habib, and A. Akgül, "Approximate solution of nonlinear time-fractional klein-Gordon equations using yang transform," *Symmetry*, vol. 14, no. 5, p. 907, 2022.

[23] X. Li, S. Zhang, Y. Wang, and H. Chen, "Analysis and application of the element-free galerkin method for nonlinear sine-Gordon and generalized sinh-Gordon equations," *Computers & Mathematics with Applications*, vol. 71, no. 8, pp. 1655–1678, 2016.

[24] M. Lotfi and A. Alipanah, "Legendre spectral element method for solving sine-Gordon equation," *Advances in Difference Equations*, vol. 2019, no. 1, 2019.

[25] L. Junfeng, "An analytical approach to the sine-Gordon equation using the modified homotopy perturbation method," *Computers & Mathematics with Applications*, vol. 58, no. 11-12, pp. 2313–2319, 2009.

[26] G. M. Moatimid, F. M. F. Elsabaa, and M. H. Zekry, "Approximate solutions of coupled nonlinear oscillations: Stability Analysis," *Journal of Applied and Computational Mechanics*, vol. 7, no. 2, pp. 382–395, 2021.

[27] M. Mohand and A. Mahgoub, "The new integral transform Mohand transform," *Applied Mathematical Sciences*, vol. 12, no. 2, pp. 113–120, 2017.

[28] M. Nadeem and F. Li, "He–Laplace method for nonlinear vibration systems and nonlinear wave equations," *Journal of Low Frequency Noise, Vibration and Active Control*, vol. 38, no. 3-4, pp. 1060–1074, 2019.

[29] M. Nadeem and F. Li, "Modified Laplace Variational Iteration Method for Analytical Approach of Klein–Gordon and Sine–Gordon Equations," *Iranian Journal of Science and Technology, Transactions A: Science*, vol. 43, no. 4, pp. 1933–1940, 2019.

[30] P. Amit Prakash, D. G. P. Veeresha, and M. Goyal, "A homotopy technique for a fractional order multi-dimensional telegraph equation via the Laplace transform," *The European Physical Journal Plus*, vol. 134, no. 1, pp. 1–18, 2019.

[31] H. M. Sedighi, K. H. Shirazi, and J. Zare, "An analytic solution of transversal oscillation of quintic non-linear beam with homotopy analysis method," *International Journal of Non-Linear Mechanics*, vol. 47, no. 7, pp. 777–784, 2012.

[32] K.-L. Wang, "Novel approach for fractal nonlinear oscillators with discontinuities by Fourier series," *Fractals*, vol. 30, no. 1, pp. 2250009–2255787, 2022.

[33] K.-L. Wang, "Fractal solitary wave solutions for fractal nonlinear dispersive Boussinesq-like models," *Fractals*, vol. 30, no. 4, 2022.

[34] A. Yldrm, "He's homotopy perturbation method for solving the space- and time-fractional telegraph equations," *International Journal of Computer Mathematics*, vol. 87, no. 13, pp. 2998–3006, 2010.

[35] A. Majeed, "Approximate solutions for solving the Klein–Gordon and sine-Gordon equations," *Journal of the Association of Arab Universities for Basic and Applied Sciences*, vol. 22, no. 1, pp. 83–90, 2017.

[36] H. Zhang, M. Nadeem, A. Rauf, and Z. G. Hui, "A novel approach for the analytical solution of nonlinear time-fractional differential equations," *International Journal of Numerical Methods for Heat & Fluid Flow*, vol. 31, no. 4, pp. 1069–1084, 2021.

Hindawi
Journal of Function Spaces
Volume 2022, Article ID 6306220, 8 pages
https://doi.org/10.1155/2022/6306220

Research Article

Fractional-Stochastic Solutions for the Generalized $(2+1)$-Dimensional Nonlinear Conformable Fractional Schrödinger System Forced by Multiplicative Brownian Motion

Sahar Albosaily,[1] **Wael W. Mohammed**,[1,2] **Ekram E. Ali**,[1] **R. Sidaoui**,[1] **E. S. Aly**,[3] **and M. El-Morshedy**[4,5]

[1]*Department of Mathematics, Faculty of Science, University of Ha'il, Ha'il 2440, Saudi Arabia*
[2]*Department of Mathematics, Faculty of Science, Mansoura University, Mansoura 35516, Egypt*
[3]*Mathematics Department, Faculty of Science, Jazan University, Jazan 45142, Saudi Arabia*
[4]*Department of Mathematics, College of Science and Humanities in Al-Kharj, Prince Sattam bin Abdulaziz University, Al-Kharj 11942, Saudi Arabia*
[5]*Department of Statistics and Computer Science, Faculty of Science, Mansoura University, Mansoura 35516, Egypt*

Correspondence should be addressed to Wael W. Mohammed; wael.mohammed@mans.edu.eg

Received 13 May 2022; Revised 31 May 2022; Accepted 6 June 2022; Published 19 June 2022

Academic Editor: Yusuf Gurefe

In this paper, the $(2+1)$-dimensional nonlinear conformable fractional stochastic Schrödinger system (NCFSSS) generated by the multiplicative Brownian motion is treated. To get new rational, trigonometric, hyperbolic, and elliptic stochastic solutions, we use two different methods: the sine-cosine and the Jacobi elliptic function methods. Moreover, we use the MATLAB tools to plot our figures to introduce a variety of 2D and 3D graphs to highlight the effect of the multiplicative noise on the exact solutions of the NCFSSS. Finally, we illustrate that the multiplicative Brownian motion stabilizes the solutions of NCFSSS a round zero.

1. Introduction

Stochastic partial differential equations (SPDEs) can be used to represent a wide range of complicated nonlinear physical processes. These kinds of equations appear in a variety of areas including physics, finance, climate dynamics, chemistry, biology, geophysical, engineering, and other fields [1–3].

On the other side, fractional partial differential equations (FPDEs) have gotten a lot of interest because they may illustrate the fundamental components underlying real-world issues. They have been seen in a number of physical phenomena, such as viscoelastic materials with relaxation and creeping functions, the motion of a heavy meager surface in a Newtonian fluid, and relapse subordinate dissipative occupancy of components. As a result, FPDEs are employed in a range of fields, including predicting, describing, and modeling the mechanisms engaged in finance, polymeric materials, a kinematic model of neutron points, engineering, electrical circuits, solid-state physics, optical fibers, chemical kinematics, biogenetics, plasma physics, physics of condensed matter, meteorology, electromagnetic, elasticity, and oceanic spectacles [4–9].

The exact solutions of PDEs are important in nonlinear science. As a result, various analytical techniques, such as tanh-sech [10, 11], Darboux transformation [12], sine-cosine [13, 14], extended simple equation [15], extended sinh-Gordon equation expansion [16], F-expansion [17], Kudryashov technique [18], generalized Kudryashov [19–21], $\exp(-\phi(\varsigma))$-expansion [22], (G'/G)-expansion [23–25], Hirota's function [26], perturbation [5, 27], the Jacobi elliptic function [28, 29], and Riccati-Bernoulli sub-ODE [30], have been created to deal with these types of equations.

To reach a better level of qualitative agreement, the following (2 + 1)-dimensional nonlinear conformable fractional stochastic Schrödinger system (NCFSSS) is addressed:

$$idu + \left[\gamma_1 \mathbb{D}^{\alpha}_{xy} u + \gamma_2 uv\right] dt + i\sigma u d\mathbb{B} = 0, \quad (1)$$

$$\gamma_3 \mathbb{D}^{\alpha}_{x} v + \gamma_4 \mathbb{D}^{\alpha}_{y}\left(|u|^2\right) = 0, \quad (2)$$

where $v \in \mathbb{R}$ while $u \in \mathbb{C}$. $\mathbb{D}^{\alpha}$ is the conformable derivative (CD) [31], and γ_i are arbitrary constants for $i = 1, .., 4$. $\mathbb{B}(t)$ is a Brownian motion (BM), and $ud\mathbb{B}$ is multiplicative noise in the Itô sense.

The NCFSSS ((1) and (2)) is crucial in atomic physics, and the functions v and u have diverse physical meanings in various disciplines of physics such as plasma physics [32] and fluid dynamics [33]. In the hydrodynamic context, v is the induced mean flow, and u is the envelope of the wave packet [33], while, in the context of water waves, v is the velocity potential of the mean flow interacting with the surface waves and u is the amplitude of a surface wave packet [34]. The multiplicative noise $i\sigma u d\mathbb{B}$ plays an important role in the theory of measurements continuous in time in open quantum systems. For more physical interpretations, we refer to [35, 36] and the references therein.

Recently, many authors have established exact solutions of NCFSSS ((1) and (2)) with $\sigma = 0$ and $\alpha = 1$ by employing various techniques, such as applied Kudryashov approach [37], direct approach [38], and the extended modified auxiliary equation [39]. Moreover, Bilal and Ahmad [40] applied three methods such as generalized Kudryashov, modified direct algebraic, and (G'/G^2)-expansion function to attain diverse forms of optical solutions of the NCFSSS ((1) and (2)) with $\sigma = 0$, while the exact solutions of the NCFSSS ((1) and (2)) has not yet been studied.

The motivations of this work are to obtain the exact fractional stochastic solutions of NCFSSS ((1) and (2)). This is the first investigation to acquire the exact solutions of NCFSSS ((1) and (2)) in the presence of stochastic term and fractional-space derivatives. To accomplish a wide variety of solutions, such as trigonometric, hyperbolic, elliptic, and rational functions, we apply two different methods such as the Jacobi elliptic function and the sine-cosine methods. Also, we study the effect of BM on the obtained solutions of NCFSSS ((1) and (2)) by using MATLAB to create 3D and 2D diagrams for some of the obtained solutions here.

The document is laid out as follows: we define and state some features of the CD and BM in Section 2. We employ an appropriate wave transformation in Section 3 to derive the wave equation of NCFSSS ((1) and (2)). While in Section 4, we utilize two methods to create the analytic solutions of the NCFSSS ((1) and (2)). In Section 5, the influence of the BM on the obtained solutions is investigated. The conclusion of the document is displayed last.

2. Preliminaries

Here, we define and state some features of the CD and BM.

Definition 1 (see [31]). Let $\phi : (0,\infty) \longrightarrow \mathbb{R}$, then the CD of ϕ of order $\alpha \in (0, 1]$ is defined as

$$\mathbb{D}^{\alpha}_{x}\phi(x) = \lim_{\kappa \longrightarrow 0} \frac{\phi\left(x + \kappa x^{1-\alpha}\right) - \phi(x)}{\kappa}. \quad (3)$$

Theorem 2. *Let $\phi, H : (0,\infty) \longrightarrow \mathbb{R}$ be differentiable and also α be differentiable functions, then*

$$\mathbb{D}^{\alpha}_{x}(\phi \circ H)(x) = x^{1-\alpha} H'(x)\phi'(H(x)). \quad (4)$$

Let us state some properties of the CD. If a and b are constant, then

(1) $\mathbb{D}^{\alpha}_{x}[a\phi(x) + bH(x)] = a\mathbb{D}^{\alpha}_{x}\phi(x) + b\mathbb{D}^{\alpha}_{x}H(x)$

(2) $\mathbb{D}^{\alpha}_{x}[a] = 0$

(3) $\mathbb{D}^{\alpha}_{x}[x^b] = bx^{b-\alpha}$

(4) $\mathbb{D}^{\alpha}_{x}H(x) = x^{1-\alpha}(dH/dx)$

In next definition, we define Brownian motion $\mathbb{B}(t)$.

Definition 3. Stochastic process $\{\mathbb{B}(t)\}_{t\geq 0}$ is said a Brownian motion if it satisfies:

(1) $\mathbb{B}(0) = 0$

(2) $\mathbb{B}(t)$ is continuous function of $t \geq 0$

(3) $\mathbb{B}(t_2) - \mathbb{B}(t_1)$ is independent for $t_1 < t_2$

(4) $\mathbb{B}(t_2) - \mathbb{B}(t_1)$ has a normal distribution $\aleph(0, t_2 - t_1)$

3. Wave Equation for NCFSSS

The next wave transformation is used to get the wave equation of the NCFSSS ((1) and (2)):

$$\begin{aligned} u(x, y, t) &= \varphi(\zeta)e^{\left(i\hbar - \sigma\mathbb{B}(t) - (1/2)\sigma^2 t\right)}, \\ v(x, y, t) &= \psi(\zeta)e^{\left(-\sigma\mathbb{B}(t) - (1/2)\sigma^2 t\right)}, \end{aligned} \quad (5)$$

with

$$\begin{aligned} \zeta &= \frac{\zeta_1}{\alpha}x^{\alpha} + \frac{\zeta_2}{\alpha}y^{\alpha} - \zeta_3 t, \\ h &= \frac{h_1}{\alpha}x^{\alpha} + \frac{h_2}{\alpha}y^{\alpha} - h_3 t, \end{aligned} \quad (6)$$

where φ and ψ are deterministic functions and ζ_k and $\hbar_k$ for $k = 1, 2, 3$, are nonzero constants. Plugging Equation (5) into

Equations (1) and (2) and using

$$du = \left[\left(-\zeta_3\varphi' + i\hbar_3\varphi\right)dt - \sigma\varphi d\mathbb{B}\right]e^{\left(i\hbar-\sigma\mathbb{B}(t)-(1/2)\sigma^2 t\right)},$$
$$\mathbb{D}_{xy}^{\alpha}u = \left[\zeta_1\zeta_2\varphi'' + i(\hbar_2\zeta_1 + \hbar_1\zeta_2)\varphi' - \hbar_1\hbar_2\varphi\right]e^{\left(i\hbar-\sigma\mathbb{B}(t)-(1/2)\sigma^2 t\right)},$$
$$\mathbb{D}_{y}^{\alpha}\left(|u|^2\right) = 2\zeta_2\varphi\varphi' e^{\left(-\sigma\mathbb{B}(t)-(1/2)\sigma^2 t\right)}, \mathbb{D}_{x}^{\alpha}v = \zeta_1\psi' e^{\left(-\sigma\mathbb{B}(t)-(1/2)\sigma^2 t\right)}, \tag{7}$$

we get for imaginary part

$$\zeta_3 = \hbar_2\zeta_1 + \hbar_1\zeta_2, \tag{8}$$

and for real part

$$\zeta_1\zeta_2\varphi'' - (\hbar_3 + \gamma_1\hbar_1\hbar_2)\varphi + \gamma_2\varphi\psi e^{\left(-\sigma\mathbb{B}(t)-(1/2)\sigma^2 t\right)} = 0, \tag{9}$$

$$\gamma_3\zeta_1\psi' + 2\gamma_4\zeta_2\varphi\varphi' e^{\left(-\sigma\mathbb{B}(t)-(1/2)\sigma^2 t\right)} = 0. \tag{10}$$

Taking expectation $\mathbb{E}(\cdot)$ on both sides for Equations (9) and (10), we have

$$\zeta_1\zeta_2\varphi'' - (\hbar_3 + \gamma_1\hbar_1\hbar_2)\varphi + \gamma_2\varphi\psi e^{-(1/2)\sigma^2 t}\mathbb{E}\left(e^{-\sigma\mathbb{B}(t)}\right) = 0, \tag{11}$$

$$\gamma_3\zeta_1\psi' + 2\gamma_4\zeta_2\varphi\varphi' e^{-(1/2)\sigma^2 t}\mathbb{E}\left(e^{-\sigma\mathbb{B}(t)}\right) = 0. \tag{12}$$

Since $\mathbb{B}(t)$ is standard Gaussian process, hence $\mathbb{E}(e^{-\sigma\mathbb{B}(t)}) = e^{(\sigma^2/2)t}$. Now Equations (11) and (12) have the form

$$\zeta_1\zeta_2\varphi'' - (\hbar_3 + \gamma_1\hbar_1\hbar_2)\varphi + \gamma_2\varphi\psi = 0, \tag{13}$$

$$\gamma_3\zeta_1\psi' + 2\gamma_4\zeta_2\varphi\varphi' = 0. \tag{14}$$

Integrating Equation (14) once and setting the integral constant equal zero yields

$$\psi = -\frac{\gamma_4\zeta_2}{\gamma_3\zeta_1}\varphi^2. \tag{15}$$

Plugging Equation (15) into Equation (13), we get the following wave equation

$$\varphi'' - \Lambda_1\varphi^3 - \Lambda_2\varphi = 0, \tag{16}$$

where

$$\Lambda_1 = \frac{\gamma_2\gamma_4}{\gamma_3\zeta_1^2}, \quad \Lambda_2 = \frac{(\hbar_3 + \gamma_1\hbar_1\hbar_2)}{\zeta_1\zeta_2}. \tag{17}$$

4. The Exact Solutions of the NCFSSS

To find the exact solutions of Equation (16), we use two different methods such as sine-cosine [13, 14] and the Jacobi elliptic function [29] methods. As a result, we are able to obtain the exact solutions of the NCFSSS ((1) and (2)).

4.1. Sine-Cosine Method. Assume the solution φ of Equation (16) has the form

$$\varphi(\zeta) = A\mathbb{Y}^n, \tag{18}$$

where

$$\mathbb{Y} = \cos(B\zeta) \text{ or } \mathbb{Y} = \sin(B\zeta). \tag{19}$$

Setting Equation (18) into Equation (16) we get

$$-AB^2\left[-n^2\mathbb{Y}^n + n(n-1)\mathbb{Y}^{n-2}\right] - \Lambda_1A^3\mathbb{Y}^{3n} - \Lambda_2A\mathbb{Y}^n = 0, \tag{20}$$

rewriting the above equation

$$\left(\Lambda_2A - AB^2n^2\right)\mathbb{Y}^n + n(n-1)AB^2\mathbb{Y}^{n-2} + \Lambda_1A^3\mathbb{Y}^{3n} = 0. \tag{21}$$

Equalizing the term of $\mathbb{Y}$ in Equation (21), we attain

$$n - 2 = 3n \Rightarrow n = -1. \tag{22}$$

Substituting Equation (22) into Equation (21)

$$\left(\Lambda_2A - AB^2\right)\mathbb{Y}^{-1} + \left(\Lambda_1A^3 + 2AB^2\right)\mathbb{Y}^{-3} = 0. \tag{23}$$

Equating each coefficient of $\mathbb{Y}^{-3}$ and $\mathbb{Y}^{-1}$ to zero, we have

$$\Lambda_2A - AB^2 = 0, \quad \Lambda_1A^3 + 2AB^2 = 0. \tag{24}$$

By solving these equations, we get

$$B = \sqrt{\Lambda_2}, \quad A = \sqrt{\frac{-2\Lambda_2}{\Lambda_1}}. \tag{25}$$

Hence, the solution of Equation (16) is

$$\varphi(\zeta) = A\sec(B\zeta) \text{ or } \varphi(\zeta) = A\csc(B\zeta). \tag{26}$$

There are many cases depending on the sign of Λ_1 and Λ_2.

Case 1. If $\Lambda_2 > 0$ and $\Lambda_1 < 0$, then the exact solutions of the NCFSSS ((1) and (2)) are

$$u(x,y,t) = \sqrt{\frac{-2\Lambda_2}{\Lambda_1}} \sec\left[\sqrt{\Lambda_2}\zeta\right] e^{\left(i\hbar - \sigma\mathbb{B}(t) - (1/2)\sigma^2 t\right)},$$
$$v(x,y,t) = \frac{2\Lambda_2\gamma_4\zeta_2}{\Lambda_1\gamma_3\zeta_1} \sec^2\left[\sqrt{\Lambda_2}\zeta\right] e^{\left(-\sigma\mathbb{B}(t) - (1/2)\sigma^2 t\right)}, \quad (27)$$

or

$$u(x,y,t) = \sqrt{\frac{-2\Lambda_2}{\Lambda_1}} \csc\left[\sqrt{\Lambda_2}\zeta\right] e^{\left(i\hbar - \sigma\mathbb{B}(t) - (1/2)\sigma^2 t\right)},$$
$$v(x,y,t) = \frac{2\Lambda_2\gamma_4\zeta_2}{\Lambda_1\gamma_3\zeta_1} \csc^2\left[\sqrt{\Lambda_2}\zeta\right] e^{\left(-\sigma\mathbb{B}(t) - (1/2)\sigma^2 t\right)}. \quad (28)$$

Case 2. If $\Lambda_2 < 0$ and $\Lambda_1 < 0$, then the exact solutions of the NCFSSS ((1) and (2)) are

$$u(x,y,t) = i\sqrt{\frac{2\Lambda_2}{\Lambda_1}} \operatorname{sech}\left[\sqrt{-\Lambda_2}\zeta\right] e^{\left(i\hbar - \sigma\mathbb{B}(t) - (1/2)\sigma^2 t\right)},$$
$$v(x,y,t) = \frac{2\Lambda_2\gamma_4\zeta_2}{\Lambda_1\gamma_3\zeta_1} \sec\mathrm{h}^2\left[\sqrt{-\Lambda_2}\zeta\right] e^{\left(-\sigma\mathbb{B}(t) - (1/2)\sigma^2 t\right)}, \quad (29)$$

or

$$u(x,y,t) = \sqrt{\frac{2\Lambda_2}{\Lambda_1}} \operatorname{csch}\left[\sqrt{-\Lambda_2}\zeta\right] e^{\left(i\hbar - \sigma\mathbb{B}(t) - (1/2)\sigma^2 t\right)},$$
$$v(x,y,t) = \frac{-2\Lambda_2\gamma_4\zeta_2}{\Lambda_1\gamma_3\zeta_1} \csc\mathrm{h}^2\left[\sqrt{-\Lambda_2}\zeta\right] e^{\left(-\sigma\mathbb{B}(t) - (1/2)\sigma^2 t\right)}. \quad (30)$$

Case 3. If $\Lambda_2 < 0$ and $\Lambda_1 > 0$, then the exact solutions of the NCFSSS ((1) and (2)) are

$$u(x,y,t) = \sqrt{\frac{-2\Lambda_2}{\Lambda_1}} \operatorname{sech}\left[\sqrt{-\Lambda_2}\zeta\right] e^{\left(i\hbar - \sigma\mathbb{B}(t) - (1/2)\sigma^2 t\right)},$$
$$v(x,y,t) = \frac{2\Lambda_2\gamma_4\zeta_2}{\Lambda_1\gamma_3\zeta_1} \sec\mathrm{h}^2\left[\sqrt{-\Lambda_2}\zeta\right] e^{\left(-\sigma\mathbb{B}(t) - (1/2)\sigma^2 t\right)}, \quad (31)$$

or

$$u(x,y,t) = -i\sqrt{\frac{-2\Lambda_2}{\Lambda_1}} \operatorname{csch}\left[\sqrt{-\Lambda_2}\zeta\right] e^{\left(i\hbar - \sigma\mathbb{B}(t) - (1/2)\sigma^2 t\right)},$$
$$v(x,y,t) = \frac{-2\Lambda_2\gamma_4\zeta_2}{\Lambda_1\gamma_3\zeta_1} \csc\mathrm{h}^2\left[\sqrt{-\Lambda_2}\zeta\right] e^{\left(-\sigma\mathbb{B}(t) - (1/2)\sigma^2 t\right)}. \quad (32)$$

Case 4. If $\Lambda_2 > 0$ and $\Lambda_1 > 0$, then the exact solution of the NCFSSS ((1) and (2)) are

$$u(x,y,t) = i\sqrt{\frac{2\Lambda_2}{\Lambda_1}} \sec\left[\sqrt{\Lambda_2}\zeta\right] e^{\left(i\hbar - \sigma\mathbb{B}(t) - (1/2)\sigma^2 t\right)},$$
$$v(x,y,t) = \frac{2\Lambda_2\gamma_4\zeta_2}{\Lambda_1\gamma_3\zeta_1} \sec^2\left[\sqrt{\Lambda_2}\zeta\right] e^{\left(-\sigma\mathbb{B}(t) - (1/2)\sigma^2 t\right)}, \quad (33)$$

or

$$u(x,y,t) = i\sqrt{\frac{2\Lambda_2}{\Lambda_1}} \csc\left[\sqrt{\Lambda_2}\zeta\right] e^{\left(i\hbar - \sigma\mathbb{B}(t) - (1/2)\sigma^2 t\right)},$$
$$v(x,y,t) = \frac{2\Lambda_2\gamma_4\zeta_2}{\Lambda_1\gamma_3\zeta_1} \csc^2\left[\sqrt{\Lambda_2}\zeta\right] e^{\left(-\sigma\mathbb{B}(t) - (1/2)\sigma^2 t\right)}, \quad (34)$$

where Λ_1 and Λ_2 are defined in (17) and $\zeta = (\zeta_1/\alpha)x^\alpha + (\zeta_2/\alpha)y^\alpha - \zeta_3 t$ and $\hbar = (h_1/\alpha)x^\alpha + (h_2/\alpha)y^\alpha + h_3 t$.

4.2. The Jacobi Elliptic Function Method. We suppose that the solution to Equation (16) has the type

$$\varphi(\zeta) = a + bsn(\rho\zeta), \quad (35)$$

where a, b, and ρ are undefined constants and $sn(\rho\zeta) = sn(\rho\zeta, m)$ is the Jacobi elliptic sine function (Latin: sinus amplitudinis) for $0 < m < 1$. Differentiate Equation (35) two times, we have

$$\varphi''(\zeta) = -\left(m^2+1\right)b\rho^2 sn(\rho\zeta) + 2m^2 b\rho^2 sn^3(\rho\zeta). \quad (36)$$

Plugging Equations (35) and (36) into Equation (16), we attain

$$\begin{aligned}&\left(2m^2 b\rho^2 - \Lambda_1 b^3\right)sn^3(\rho\zeta) - 3\Lambda_1 ab^2 sn^2(\rho\zeta)\\ &\quad - \left[\left(m^2+1\right)b\rho^2 + 3\Lambda_1 a^2 b + \Lambda_2 b\right]sn(\rho\zeta)\\ &\quad - \left(\Lambda_1 a^3 + a\Lambda_2\right) = 0.\end{aligned} \quad (37)$$

Putting each coefficient of $[sn(\rho\zeta)]^n$ to be zero for $n = 0, 1, 2, 3$, we have

$$\begin{aligned}\Lambda_1 a^3 + a\Lambda_2 &= 0,\\ \left(m^2+1\right)b\rho^2 + 3\Lambda_1 a^2 b + \Lambda_2 b &= 0,\\ 3\Lambda_1 ab^2 sn^2 &= 0,\\ 2m^2 b\rho^2 - \Lambda_1 b^3 &= 0.\end{aligned} \quad (38)$$

When we solve the previous equations, we get

$$\begin{aligned} a &= 0, \\ b &= \pm\sqrt{\frac{-2m^2\Lambda_2}{(m^2+1)\Lambda_1}}, \\ \rho^2 &= \frac{-\Lambda_2}{(m^2+1)}. \end{aligned} \tag{39}$$

As a result, using (35), the solution of Equation (16) is

$$\varphi(\zeta) = \pm\sqrt{\frac{-2m^2\Lambda_2}{(m^2+1)\Lambda_1}}sn\left(\sqrt{\frac{-\Lambda_2}{(m^2+1)}}\zeta\right). \tag{40}$$

Therefore, the exact solution of the NCFSSS ((1) and (2)) is

$$u(x,y,t) = \pm\sqrt{\frac{-2m^2\Lambda_2}{(m^2+1)\Lambda_1}}sn\left(\sqrt{\frac{-\Lambda_2}{(m^2+1)}}\zeta\right)e^{\left(i\hbar-\sigma\mathbb{B}(t)-(1/2)\sigma^2 t\right)}, \tag{41}$$

$$v(x,y,t) = \frac{\gamma_4\zeta_2 m^2\Lambda_2}{(m^2+1)\gamma_3\zeta_1\Lambda_1}sn^2\left(\sqrt{\frac{-\Lambda_2}{(m^2+1)}}\zeta\right)e^{\left(-\sigma\mathbb{B}(t)-(1/2)\sigma^2 t\right)}, \tag{42}$$

for $\Lambda_2 < 0$ and $\Lambda_1 > 0$. If $m \longrightarrow 1$, then the solutions (41) and (42) turn to:

$$\begin{aligned} u(x,y,t) &= \pm\sqrt{\frac{-\Lambda_2}{\Lambda_1}}\tanh\left(\sqrt{\frac{-\Lambda_2}{2}}\zeta\right)e^{\left(i\hbar-\sigma\mathbb{B}(t)-(1/2)\sigma^2 t\right)}, \\ v(x,y,t) &= \frac{\gamma_4\zeta_2\Lambda_2}{2\gamma_3\zeta_1\Lambda_1}\tanh^2\left(\sqrt{\frac{-\Lambda_2}{2}}\zeta\right)e^{\left(-\sigma\mathbb{B}(t)-(1/2)\sigma^2 t\right)}. \end{aligned} \tag{43}$$

In the same way, we can substitute sn in (35) with $cn(\xi) = cn(\xi, m)$ (where$cn$is the elliptic cosine (Latin: cosinus amplitudinis)) and $dn(\xi, m) = dn(\xi, m)$ (where dn is the delta amplitude (Latin: delta amplitudinis)) to derive the solutions of Equation (16) as follows:

$$\begin{aligned} \varphi(\zeta) &= \pm\sqrt{\frac{-2m^2\Lambda_2}{(2m^2-1)\Lambda_1}}cn\left(\sqrt{\frac{-\Lambda_2}{(2m^2-1)}}\zeta\right), \\ \varphi(\zeta) &= \pm\sqrt{\frac{2m^2\Lambda_2}{(2-m^2)\Lambda_1}}dn\left(\sqrt{\frac{-\Lambda_2}{(2-m^2)}}\zeta\right). \end{aligned} \tag{44}$$

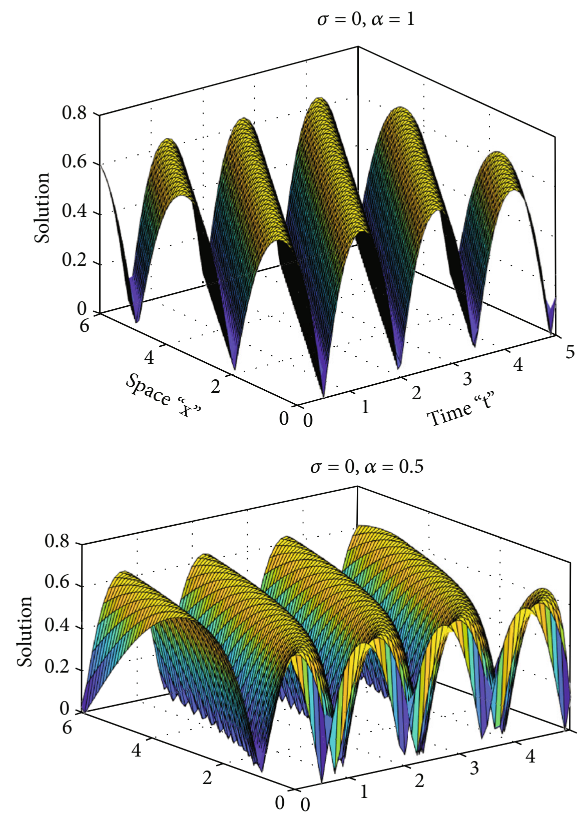

Figure 1: 3D diagrams of Equation (41).

Therefore, the solutions of the NCFSSS ((1) and (2)) are as follows:

$$u(x,y,t) = \pm\sqrt{\frac{-2m^2\Lambda_2}{(2m^2-1)\Lambda_1}}cn\left(\sqrt{\frac{-\Lambda_2}{(2m^2-1)}}\zeta\right)e^{\left(i\hbar-\sigma\mathbb{B}(t)-(1/2)\sigma^2 t\right)}, \tag{45}$$

$$v(x,y,t) = \frac{2\gamma_4\zeta_2 m^2\Lambda_2}{\gamma_3\zeta_1\Lambda_1(2m^2-1)}cn^2\left(\sqrt{\frac{-\Lambda_2}{(2m^2-1)}}\zeta\right)e^{\left(-\sigma\mathbb{B}(t)-(1/2)\sigma^2 t\right)}, \tag{46}$$

for $(\Lambda_2/(2m^2-1)) < 0$, $\Lambda_1 > 0$, and

$$u(x,y,t) = \pm\sqrt{\frac{-2m^2\Lambda_2}{(2m^2-1)\Lambda_1}}dn\left(\sqrt{\frac{-\Lambda_2}{(2m^2-1)}}\zeta\right)e^{\left(i\hbar-\sigma\mathbb{B}(t)-(1/2)\sigma^2 t\right)}, \tag{47}$$

$$v(x,y,t) = \frac{2\gamma_4\zeta_2 m^2\Lambda_2}{\gamma_3\zeta_1\Lambda_1(2-m^2)}dn^2\left(\sqrt{\frac{-\Lambda_2}{(2-m^2)}}\zeta\right)e^{\left(-\sigma\mathbb{B}(t)-(1/2)\sigma^2 t\right)}, \tag{48}$$

for $\Lambda_2 < 0$ and $\Lambda_1 > 0$, respectively. If $m \longrightarrow 1$, then the

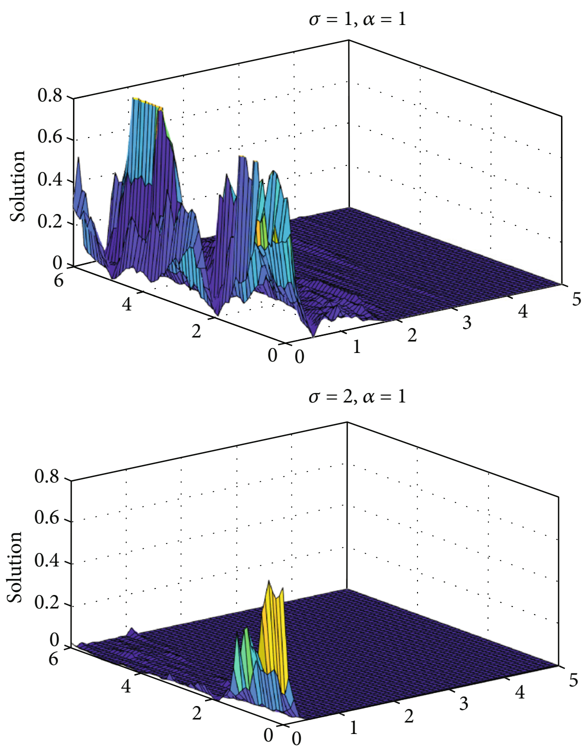

Figure 2: 3D diagrams of Equation (41) with $\alpha = 1$.

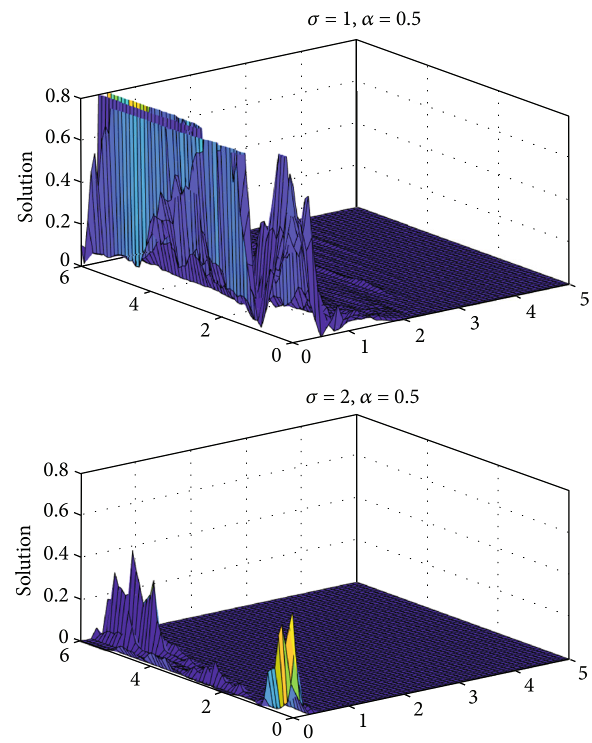

Figure 3: 3D diagrams of Equation (41) with $\alpha = 0.5$.

solutions (45) and (46) and (47) and (48) turn to:

$$u(x, y, t) = \pm\sqrt{\frac{-2\Lambda_2}{\Lambda_1}}\,\text{sech}\left(\sqrt{-\Lambda_2}\zeta\right)e^{\left(i\hbar-\sigma\mathbb{B}(t)-(1/2)\sigma^2 t\right)},$$
$$v(x, y, t) = k^2 m^2 \Lambda_2\,\sec\text{h}^2\left(\sqrt{-\Lambda_2}\zeta\right)e^{\left(-\sigma\mathbb{B}(t)-(1/2)\sigma^2 t\right)}, \quad (49)$$

for $\Lambda_2 < 0$ and $\Lambda_1 > 0$.

5. The Effect of BM on NCFSSS Solutions

The effect of BM on the exact solutions of the NCFSSS ((1) and (2)) is discussed here. Fix the parameters $\gamma_1 = \gamma_2 = -1$, $\gamma_3 = 1, \gamma_4 = -2, \hbar_1 = \hbar_2 = \zeta_1 = \zeta_2 = 1, \hbar_3 = -1$, and $m = 0.5$. Hence, $\zeta_3 = -2, \Lambda_1 = 2$, and $\Lambda_2 = -2$. Now, for various values of α (the fractional derivative order) and σ (noise intensity), we provide a number of graphs for $t \in [0, 5]$ and $x \in [0, 6]$. To draw these graphs, we use the MATLAB tools. In the following Figure 1, if $\sigma = 0$, we can observe how the surface fluctuates as the value of α changes:

While in Figures 2 and 3, we can observe that after small transit patterns, the surface smooths significantly when noise is incorporated, and its intensity increases $\sigma = 1, 2$ for different value of α.

Figure 4 shows 2D graphs of Equation (41) with $\sigma = 0, 0.5, 1, 2$ and with $\alpha = 1$, which highlight the above results.

We may infer from Figures 1–4 the following:

(1) As fractional-order α decreases, the surface shrinks

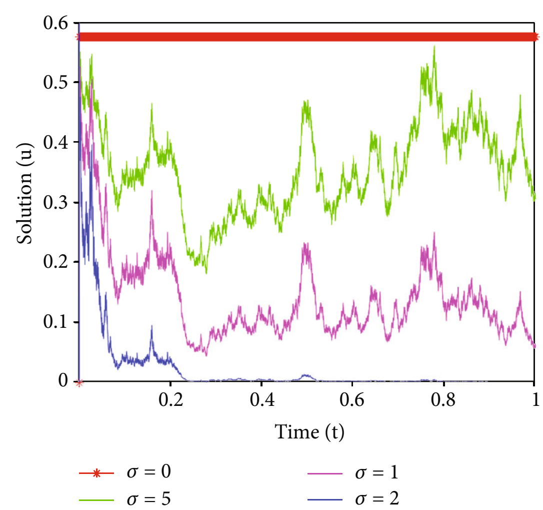

Figure 4: 2D diagrams of Equation (41).

(2) The solutions of NCFSSS are stabilized by BM around zero

6. Conclusions

In this paper, we considered the (2 + 1)-dimensional nonlinear conformable fractional stochastic Schrödinger system ((1) and (2)) which has never been examined before with stochastic term and fractional space at the same time. We employed two different methods such as the sine-cosine and the Jacobi elliptic function methods to get elliptic, trigonometric, rational, and hyperbolic fractional stochastic solutions. These obtained solutions are useful in describing some of interesting physical phenomena due to the importance of the NCFSSS in plasma physics and fluid dynamics. Finally, the effect of BM on the exact solution of the NCFSSS ((1) and (2)) is demonstrated by introducing 3D and 2D graphs for some analytical fractional stochastic solutions. In future study, we can address the NCFSSS ((1) and (2)) with multidimensional multiplicative noise.

Data Availability

All data are available in this paper.

Conflicts of Interest

The authors declare that they have no competing interests.

Authors' Contributions

All authors contributed equally to the writing of this paper. All authors read and approved the final manuscript.

Acknowledgments

This research has been funded by the Scientific Research Deanship at University of Hail, Saudi Arabia, through project number RG-21046.

References

[1] L. Arnold, *Random Dynamical Systems*, Springer-Verlag, 1998.

[2] P. Imkeller and A. H. Monahan, "Conceptual stochastic climate models," *Stochastics and Dynamics*, vol. 2, no. 3, pp. 311–326, 2002.

[3] W. W. Mohammed, "Fast-diffusion limit for reaction–diffusion equations with degenerate multiplicative and additive noise," *Journal of Dynamics and Differential Equations*, vol. 33, no. 1, pp. 577–592, 2021.

[4] S. B. Yuste, L. Acedo, and K. Lindenberg, "Reaction front in an $A + \vec{B}C$ reaction-subdiffusion process," *Physical Review E*, vol. 69, no. 3, article 036126, 2004.

[5] W. W. Mohammed and N. Iqbal, "Impact of the same degenerate additive noise on a coupled system of fractional space diffusion equations," *Fractals*, vol. 30, no. 1, article 2240033, 2022.

[6] D. A. Benson, S. W. Wheatcraft, and M. M. Meerschaert, "The fractional-order governing equation of Lévy motion," *Water Resources Research*, vol. 36, no. 6, pp. 1413–1423, 2000.

[7] S. B. Yuste and K. Lindenberg, "Subdiffusion-limited $A + A$ reactions," *Physical Review Letters*, vol. 87, no. 11, article 118301, 2001.

[8] F. M. Al-Askar, W. W. Mohammed, and M. Alshammari, "Impact of Brownian motion on the analytical solutions of the space-fractional stochastic approximate long water wave equation," *Symmetry*, vol. 14, no. 4, p. 740, 2022.

[9] E. Barkai, R. Metzler, and J. Klafter, "From continuous time random walks to the fractional Fokker-Planck equation," *Physical Review*, vol. 61, no. 1, pp. 132–138, 2000.

[10] A. M. Wazwaz, "The tanh method: exact solutions of the sine-Gordon and the sinh-Gordon equations," *Applied Mathematics and Computation*, vol. 167, no. 2, pp. 1196–1210, 2005.

[11] W. Malfliet and W. Hereman, "The tanh method. I. Exact solutions of nonlinear evolution and wave equations," *Physica Scripta*, vol. 54, no. 6, pp. 563–568, 1996.

[12] M. Wen-Xiu and B. Sumayah, "A binary Darboux transformation for multicomponent NLS equations and their reductions," *Analysis and Mathematical Physics*, vol. 11, no. 2, p. 44, 2021.

[13] A. M. Wazwaz, "A sine-cosine method for handlingnonlinear wave equations," *Mathematical and Computer Modelling*, vol. 40, no. 5-6, pp. 499–508, 2004.

[14] C. Yan, "A simple transformation for nonlinear waves," *Physics Letters A*, vol. 224, no. 1-2, pp. 77–84, 1996.

[15] A. R. Seadawy, A. Ali, and W. A. Albarakati, "Analytical wave solutions of the (2 + 1)-dimensional first integro- differential Kadomtsev-Petviashivili hierarchy equation by using modified mathematical methods," *Results in Physics*, vol. 15, article 102775, 2019.

[16] A. R. Seadawy, D. Kumar, and A. K. Chakrabarty, "Dispersive optical soliton solutions for the hyperbolic and cubic-quintic nonlinear Schrödinger equations via the extended sinh-Gordon equation expansion method," *The European Physical Journal Plus*, vol. 133, no. 5, p. 182, 2018.

[17] N. Celika, A. R. Seadawy, Y. S. Özkan, and E. Yasar, "A model of solitary waves in a nonlinear elastic circular rod: abundant different type exact solutions and conservation laws," *Chaos, Solitons & Fractals*, vol. 143, article 110486, 2021.

[18] A. R. Alharbi, M. B. Almatrafi, and A. R. Seadawy, "Construction of the numerical and analytical wave solutions of the Joseph–Egri dynamical equation for the long waves in nonlinear dispersive systems," *International Journal of Modern Physics B*, vol. 34, no. 30, article 2050289, 2020.

[19] S. T. Demiray and U. Bayrakci, "Soliton solutions for space-time fractional Heisenberg ferromagnetic spin chain equation by generalized Kudryashov method and modified exp -expansion function method," *Revista mexicana de física*, vol. 67, no. 3 May-Jun, pp. 393–402, 2021.

[20] S. T. Demiray, "New soliton solutions of optical pulse envelope $E(Z, \tau)$ with beta time derivative," *Optik*, vol. 223, article 165453, 2020.

[21] S. T. Demiray, "New solutions of Biswas-Arshed equation with beta time derivative," *Optik*, vol. 222, article 165405, 2020.

[22] K. Khan and M. A. Akbar, "The exp $(-\varphi(\varsigma))$-expansion method for finding travelling wave solutions of Vakhnenko-Parkes equation," *International Journal of Dynamical Systems and Differential Equations*, vol. 5, pp. 72–83, 2014.

[23] M. L. Wang, X. Z. Li, and J. L. Zhang, "The (G'/G)-expansion method and travelling wave solutions of nonlinear evolution equations in mathematical physics," *Physics Letters A*, vol. 372, pp. 417–423, 2008.

[24] H. Zhang, "New application of the (G'/G)-expansion method," *Communications in Nonlinear Science and Numerical Simulation*, vol. 14, pp. 3220–3225, 2009.

[25] W. W. Mohammed, M. Alesemi, S. Albosaily, N. Iqbal, and M. El-Morshedy, "The exact solutions of stochastic fractional-space Kuramoto-Sivashinsky equation by using (G'/G)-expansion method," *Mathematics*, vol. 9, p. 2712, 2021.

[26] R. Hirota, "Exact solution of the Korteweg-de Vries equation for multiple collisions of solitons," *Physical Review Letters*, vol. 27, no. 18, pp. 1192–1194, 1971.

[27] W. W. Mohammed, N. Iqbal, and T. Botmart, “Additive noise effects on the stabilization of fractional-space diffusion equation solutions,” *Mathematics*, vol. 10, no. 1, p. 130, 2022.

[28] Z. L. Yan, “Abundant families of Jacobi elliptic function solutions of the (2+1)-dimensional integrable Davey-Stewartson-type equation via a new method,” *Chaos, Solitons and Fractals*, vol. 18, no. 2, pp. 299–309, 2003.

[29] E. Fan and J. Zhang, “Applications of the Jacobi elliptic function method to special-type nonlinear equations,” *Physics Letters A*, vol. 305, no. 6, pp. 383–392, 2002.

[30] X. F. Yang, Z. C. Deng, and Y. Wei, “A Riccati-Bernoulli sub-ODE method for nonlinear partial differential equations and its application,” *Advances in Difference equations*, vol. 2015, no. 1, p. 133, 2015.

[31] R. Khalil, M. Al Horani, A. Yousef, and M. Sababheh, “A new definition of fractional derivative,” *Journal of Computational and Applied Mathematics*, vol. 264, pp. 65–70, 2014.

[32] K. Nishinari, K. Abe, and J. Satsuma, “A new-type of soliton behavior in a two dimensional plasma system,” *Journal of the Physical Society of Japan*, vol. 62, no. 6, pp. 2021–2029, 1993.

[33] M. J. Ablowitz and H. Segur, *Solitons and the Inverse Scattering Transform*, SIAM, Philadelphia, 1981.

[34] A. Davey and K. Stewartson, “On three-dimensional packets of surface waves,” *Proceedings of the Royal Society of London. A. Mathematical and Physical Sciences*, vol. 338, pp. 101–110, 1974.

[35] V. Barbu, M. Röckner, and D. Zhang, “Stochastic nonlinear Schrödinger equations with linear multiplicative noise: rescaling approach,” *Journal of Nonlinear Science*, vol. 24, no. 3, pp. 383–409, 2014.

[36] V. Barbu, M. Röckner, and D. Zhang, “Stochastic nonlinear Schrodinger equations,” *Nonlinear Analysis*, vol. 136, pp. 168–194, 2016.

[37] K. Hosseini, K. Sadri, M. Mirzazadeh, and S. Salahshour, “An integrable (2+1)-dimensional nonlinear Schrodinger system and its optical soliton solutions,” *Optik*, vol. 229, article 166247, 2021.

[38] R. Radha and M. Lakshmanan, “Singularity structure analysis and bilinear form of a (2+1) dimensional non-linear Schrodinger (NLS) equation,” *Inverse Problems*, vol. 10, no. 4, pp. L29–L33, 1994.

[39] A. R. Seadawy, N. Cheemaa, and A. Biswas, “Optical dromions and domain walls in (2+1)-dimensional coupled system,” *Optik*, vol. 227, article 165669, 2021.

[40] M. Bilal and J. Ahmad, “A variety of exact optical soliton solutions to the generalized (2+1)-dimensional dynamical conformable fractional Schrodinger model,” *Results in Physics*, vol. 33, article 105198, 2022.

Hindawi
Journal of Function Spaces
Volume 2022, Article ID 3723867, 12 pages
https://doi.org/10.1155/2022/3723867

Research Article

Some Generalized Formulas of Hadamard-Type Fractional Integral Inequalities

Xiujun Zhang,[1] **Ghulam Farid**,[2] **Hafsa Yasmeen**,[2] **and Kamsing Nonlaopon**[3]

[1]*School of Computer Science, Chengdu University, Chengdu, China*
[2]*Department of Mathematics, COMSATS University Islamabad, Attock Campus, Pakistan*
[3]*Department of Mathematics, Faculty of Science, Khon Kaen University, Khon Kaen 40002, Thailand*

Correspondence should be addressed to Kamsing Nonlaopon; nkamsi@kku.ac.th

Received 26 March 2022; Accepted 12 May 2022; Published 8 June 2022

Academic Editor: Yusuf Gurefe

This paper is aimed at establishing the generalized forms of Riemann-Liouville fractional inequalities of the Hadamard type for a class of functions known as strongly exponentially $(\alpha, h-m)$-p-convex functions. These inequalities provide some general formulas from which one can get associated inequalities for various types of exponentially convex and strongly convex functions. Refinements of well-known inequalities are also deducible from the established theorems.

1. Introduction

The notion of convexity is utilized significantly for finding solutions of essential mathematical problems in subjects of science and engineering. Leading with major developments in several branches of mathematics, convexity made its way in statistics, geometric function theory, graph theory, and economics. In recent decades, classes of functions related to convex functions are frequently used in proving new fractional integral inequalities in the form of numerous refinements and generalizations of classical inequalities.

Let I be an interval of real numbers. A function $f : I \longrightarrow \mathbb{R}$ satisfying $f(xt + (1-t)y) \leq tf(x) + (1-t)f(y)$, for all $x, y \in I$ and $t \in [0, 1]$, is called convex function.

A convex function satisfies the well-known Hadamard inequality:

$$f\left(\frac{x+y}{2}\right) \leq \frac{1}{y-x}\int_x^y f(\xi)d\xi \leq \frac{f(x)+f(y)}{2}. \tag{1}$$

If f is concave function, then, (1) holds in a reverse order. The inequality (1) had/has been studied by many researchers and consequently obtained a lot of its variants by introducing new classes of functions. For example, in [1], it is studied for s-convex functions; in [2], it is studied for $(p-h)$-convex functions; in [3, 4], it is studied for harmonically convex functions; in [5], it is studied for strongly harmonically convex and strongly p-convex functions. Our goal in this paper is to study the inequality (1) for strongly exponentially $(\alpha, h-m)$-p-convex functions.

Definition 1 (see [6]). A function $f : (0, b] \longrightarrow \mathbb{R}$ is called strongly exponentially $(\alpha,\ h\text{-}m)$-p-convex with modulus c ≥ 0, if f is nonnegative and

$$f\left(\left(tx^p + m(1-t)y^p\right)^{1/p}\right) \leq h(t^\alpha)\frac{f(x)}{e^{\eta x}} + mh(1-t^\alpha)\frac{f(y)}{e^{\eta y}} - cmh(t^\alpha)h(1-t^\alpha)\frac{|y^p - x^p|^2}{e^{\eta(x^p+y^p)}}, \tag{2}$$

holds, while $J \subseteq \mathbb{R}$ is an interval containing $(0, 1)$ and $h : J \longrightarrow \mathbb{R}$ is a nonnegative function along with $x, y, m^{-1}y,$

$(tx^p + m(1-t)y^p)^{1/p} \in (0, b]$, $t \in (0,1)$, $p \in \mathbb{R} \setminus \{0\}$, and $(\alpha, m) \in [0,1]^2$.

By using (2), one can find various classes of functions closely related with the convex function and strongly convex functions already defined by different authors. Strongly convex functions provide the refinements of convex functions.

In [2], Theorem 5, if we take $I \subset (0,\infty)$, $p \in \mathbb{R} \setminus \{0\}$, and $h(t) = t$, then, we have the following theorem.

Theorem 2. *Let $f : [a,b] \subset (0,\infty) \longrightarrow \mathbb{R}$ be a positive function such that $f \in L_1[a,b]$. If f is a p-convex function on $[a,b]$, $p \in \mathbb{R} \setminus \{0\}$. Then, the following integral inequality holds:*

$$f\left(\left(\frac{a^p + b^p}{2}\right)^{1/p}\right) \leq \frac{p}{b^p - a^p}\int_a^b \frac{f(t)}{t^{1-p}}dt \leq \frac{f(a)+f(b)}{2}. \quad (3)$$

Our aim in this paper is the derivation of compact forms of Hadamard-type inequalities for strongly exponentially $(\alpha, h-m)$-p-convex functions via Riemann-Liouville fractional integrals involving monotone functions. The established formulas will generate Hadamard-type inequalities for fractional Riemann-Liouville integrals which have been published by various authors in the recent past (see Remarks 11 & 23). Also, Hadamard-type inequalities are deducible for some new classes of functions (see Corollaries 12–32). In the following, we give the definition of Riemann-Liouville fractional integrals:

Definition 3. Let $f \in L_1[a,b]$. Then, Riemann-Liouville fractional integral operators of order μ for a function f, where $\Re(\mu) > 0$, are given by

$$\begin{aligned} I^{\mu}_{a^+}f(x) &= \frac{1}{\Gamma(\mu)}\int_a^x (x-t)^{\mu-1}f(t)dt, \quad x > a, \\ I^{\mu}_{b^-}f(x) &= \frac{1}{\Gamma(\mu)}\int_x^b (t-x)^{\mu-1}f(t)dt, \quad x < b. \end{aligned} \quad (4)$$

Next, we give Hadamard-type inequalities via Riemann-Liouville fractional integrals of convex functions as follows:

Theorem 4 (see [7]). *Let $f : [a,b] \longrightarrow \mathbb{R}$ be a positive function with $0 \leq a < b$ and $f \in L_1[a,b]$. If f is a convex function on $[a,b]$, then, the following fractional integral inequality holds:*

$$f\left(\frac{a+b}{2}\right) \leq \frac{\Gamma(\mu+1)}{2(b-a)^{\mu}}\left[I^{\mu}_{a^+}f(b) + I^{\mu}_{b^-}f(a)\right] \leq \frac{f(a)+f(b)}{2}, \quad (5)$$

with $\mu > 0$.

Theorem 5 (see [8]). *With the assumptions given in Theorem 4, one can have the fractional integral inequality as follows:*

$$\begin{aligned} f\left(\frac{a+b}{2}\right) &\leq \frac{2^{\mu-1}\Gamma(\mu+1)}{(b-a)^{\mu}}\left[I^{\mu}_{((a+b)/2)^+}f(b) + I^{\mu}_{((a+b)/2)^-}f(a)\right] \\ &\leq \frac{f(a)+f(b)}{2}, \end{aligned} \quad (6)$$

with $\mu > 0$.

Theorem 6 (see [7]). *Let $f : [a,b] \longrightarrow \mathbb{R}$ be a differentiable mapping on (a,b) with $a < b$. If $|f'|$ is convex on $[a,b]$, then, the following fractional integral inequality holds:*

$$\begin{aligned} &\left|\frac{f(a)+f(b)}{2} - \frac{\Gamma(\mu+1)}{2(b-a)^{\mu}}\left[I^{\mu}_{a^+}f(b) + I^{\mu}_{b^-}f(a)\right]\right| \\ &\leq \frac{b-a}{2(\mu+1)}\left(1 - \frac{1}{2^{\mu}}\right)\left[\left|f'(a)\right| + \left|f'(b)\right|\right]. \end{aligned} \quad (7)$$

The definition of k-fractional Riemann-Liouville integral operators is given as follows:

Definition 7 (see [9]). Let $f \in L_1[a,b]$, $k > 0$. Then, k-fractional Riemann-Liouville integrals for a function f of order μ where $\Re(\mu) > 0$ are given by

$$\begin{aligned} {}_kI^{\mu}_{a^+}f(x) &= \frac{1}{k\Gamma_k(\mu)}\int_a^x (x-t)^{(\mu/k)-1}f(t)dt, \quad x > a, \\ {}_kI^{\mu}_{b^-}f(x) &= \frac{1}{k\Gamma_k(\mu)}\int_x^b (t-x)^{(\mu/k)-1}f(t)dt, \quad x < b, \end{aligned} \quad (8)$$

where $\Gamma_k(.)$ is defined as follows:

$$\Gamma_k(\mu) = \int_0^{\infty} t^{\mu-1}e^{-\left(t^k/k\right)}dt, \quad \Re(\mu) > 0. \quad (9)$$

The generalized form of Riemann-Liouville fractional integrals is given in the following definition:

Definition 8 (see [10]). Let $f \in L_1[a,b]$. Also, let ψ be an increasing and positive monotone function on $(a,b]$, having a continuous derivative ψ' on (a,b). The left-sided and right-sided fractional integrals of a function f with respect to another function ψ on $[a,b]$ of order μ where $\Re(\mu) > 0$ are given by

$$\begin{aligned} I^{\mu,\psi}_{a^+}f(x) &= \frac{1}{\Gamma(\mu)}\int_a^x \psi'(t)(\psi(x)-\psi(t))^{\mu-1}f(t)dt, \quad x > a, \\ I^{\mu,\psi}_{b^-}f(x) &= \frac{1}{\Gamma(\mu)}\int_x^b \psi'(t)(\psi(t)-\psi(x))^{\mu-1}f(t)dt, \quad x < b. \end{aligned} \quad (10)$$

The definition of the k-analogue of the abovementioned definition is given as follows:

Definition 9 (see [11]). Let f, ψ, μ be the same as in the abovementioned definition. Then, for $k > 0$, the k-analogue of (10) and is given by

$$
\begin{aligned}
{}_kI_{a^+}^{\mu,\psi} f(x) &= \frac{1}{k\Gamma_k(\mu)} \int_a^x \psi'(t)(\psi(x)-\psi(t))^{(\mu/k)-1} f(t)dt, \quad x > a, \\
{}_kI_{b^-}^{\mu,\psi} f(x) &= \frac{1}{k\Gamma_k(\mu)} \int_x^b \psi'(t)(\psi(t)-\psi(x))^{(\mu/k)-1} f(t)dt, \quad x < b.
\end{aligned} \tag{11}
$$

Using the fact that $\Gamma_k(\mu) = k^{(\mu/k)-1}\Gamma(\mu/k)$ in (10) after replacing μ by μ/k, we get

$$
\begin{aligned}
k^{-\mu/k} I_{a^+}^{\mu,\psi} f(x) &= {}_kI_{a^+}^{\mu,\psi} f(x), \\
k^{-\mu/k} I_{b^-}^{\mu,\psi} f(x) &= {}_kI_{b^-}^{\mu,\psi} f(x).
\end{aligned} \tag{12}
$$

For further detailed study on fractional integrals, we refer the readers to [12, 13]. In the next section, we formulate the Hadamard-type inequalities for strongly exponentially $(\alpha, h-m)$-p-convex function via integrals (10) which are compact forms of a plenty of well-known Hadamard-type inequalities holding for classes of convex, strongly convex, and exponentially convex functions. Specifically, one can have refinements of the inequalities proved in recent decades. Several special case inequalities in the form of corollaries are also given.

2. Main Results

We will use the following notations for terms which will appear frequently in the results of this section

$$
\begin{aligned}
c_{\mu,m}(\psi^p(a), \psi^p(b)) = cm\Big[&\mu(\mu+1)(\psi^p(b)-\psi^p(a))^2 + 2 \\
&\cdot \left(\frac{\psi^p(a)}{m} - m\psi^p(b)\right)^2 + 2\mu(\psi^p(b)-\psi^p(a)) \\
&\cdot \left(\frac{\psi^p(a)}{m} - m\psi^p(b)\right)\Big],
\end{aligned}
$$

$$
\begin{aligned}
R_{\alpha,\mu,m,\eta}^{h,H}(\psi^p(a), \psi^p(b)) = cm\mu\Bigg[&g_2(\eta)h\left(\frac{1}{2^\alpha}\right)\frac{(\psi^p(b)-\psi^p(a))^2}{e^{\eta(\psi^p(a)+\psi^p(b))}} \\
&+ mg_3(\eta)H\left(\frac{1}{2}\right)\frac{\left(\psi^p(b)-\left(\psi^p(a)/m^2\right)\right)^2}{e^{\eta((\psi^p(a)/m^2)+\psi^p(b))}}\Bigg] \\
&\int_0^1 h(t^\alpha)H(t)t^{\mu-1}dt,
\end{aligned}
$$

$$
\begin{aligned}
F_{\mu,m}(\psi^p(a), \psi^p(b)) = cm\Big[&\mu(\mu+1)(\psi^p(b)-\psi^p(a))^2 + (\mu^2+5\mu+8) \\
&\cdot \left(\frac{\psi^p(a)}{m} - m\psi^p(b)\right)^2 + 2\mu(\mu+3)\times(\psi^p(b)-\psi^p(a)) \\
&\cdot \left(\frac{\psi^p(a)}{m} - m\psi^p(b)\right)\Big],
\end{aligned}
$$

$$
\begin{aligned}
A_{\alpha,\mu,m,\eta}^{h,H}(f(\psi(a)), f(\psi(b))) = \mu\Bigg[&g_2(\eta)h\left(\frac{1}{2^\alpha}\right)\frac{f(\psi(a))}{e^{\eta\psi(a)}} \\
&+ mg_3(\eta)H\left(\frac{1}{2}\right)\frac{f(\psi(b))}{e^{\eta\psi(b)}}\Bigg]\int_0^1 h(t^\alpha)t^{\mu-1}dt,
\end{aligned}
$$

$$
\begin{aligned}
B_{\alpha,\mu,m,\eta}^{h,H}(f(\psi(a)), f(\psi(b))) = m\mu\Bigg[&g_2(\eta)h\left(\frac{1}{2^\alpha}\right)\frac{f(\psi(b))}{e^{\eta\psi(b)}} \\
&+ mg_3(\eta)H\left(\frac{1}{2}\right)\frac{f(\psi^p(a)/m^2)}{e^{(\eta\psi(a)/m^2)}}\Bigg]\int_0^1 H(t)t^{\mu-1}dt.
\end{aligned} \tag{13}
$$

Theorem 10. *Let $f, \psi : [a^p, mb^p] \subset (0,\infty) \longrightarrow \mathbb{R}$, range $(\psi) \subset [a^p, mb^p]$ be the positive functions such that $f \in L_1[a^p, mb^p]$, and ψ be a differentiable and strictly increasing. If f is strongly exponentially $(\alpha, h-m)$-p-convex function on $[a^p, mb^p]$ such that $p, \eta \in \mathbb{R}$ and $p \neq 0$, then, for $(\alpha, m) \in (0,1]^2$, the following fractional integral inequalities hold:*

(i) If $p > 0$,

$$
\begin{aligned}
&f\left(\left(\frac{\psi^p(a)+m\psi^p(b)}{2}\right)^{1/p}\right) + \frac{c_{\mu,m}(\psi^p(a), \psi^p(b))g_1(\eta)h(1/2^\alpha)H(1/2)}{(\mu+1)(\mu+2)} \\
&\le \frac{\Gamma(\mu+1)}{(m\psi^p(b)-\psi^p(a))^\mu}\left[g_2(\eta)h\left(\frac{1}{2^\alpha}\right)\times I_{\psi^{-1}(\psi^p(a))^+}^{\mu,\psi}(f\circ\phi)\left(\psi^{-1}(m\psi^p(b))\right)\right. \\
&\left.+ m^{\mu+1}g_3(\eta)H\left(\frac{1}{2}\right)I_{\psi^{-1}(\psi^p(b))^-}^{\mu,\psi}(f\circ\phi)\left(\psi^{-1}\left(\frac{\psi^p(a)}{m}\right)\right)\right] \\
&\le A_{\alpha,\mu,m,\eta}^{h,H}(f(\psi(a)), f(\psi(b))) + B_{\alpha,\mu,m,\eta}^{h,H}(f(\psi(a)), f(\psi(b))) \\
&- R_{\alpha,\mu,m,\eta}^{h,H}(\psi^p(a), \psi^p(b)),
\end{aligned} \tag{14}
$$

with $\mu > 0$, $H(t) = h(1-t^\alpha)$, $\phi(t) = \psi^{1/p}(t)$ for all $t \in [a^p, mb^p]$ and

$$
\begin{aligned}
g_1(\eta) &= \begin{cases} e^{-\eta(\psi^p(a)+\psi^p(b))}, & \text{if } \eta > 0, \\ e^{-\eta(m\psi^p(b)+(\psi^p(a)/m))}, & \text{if } \eta < 0, \end{cases} \\
g_2(\eta) &= \begin{cases} e^{-\eta(m\psi^p(b))^{1/p}}, & \text{if } \eta < 0, \\ e^{-\eta\psi(a)}, & \text{if } \eta > 0, \end{cases} \\
g_3(\eta) &= \begin{cases} e^{-\eta\psi(b)}, & \text{if } \eta < 0, \\ e^{-\eta(\psi^p(a)/m)^{1/p}}, & \text{if } \eta > 0 \end{cases}
\end{aligned} \tag{15}
$$

(ii) For $p < 0$, one can have

$$f\left(\left(\frac{\psi^p(a)+m\psi^p(b)}{2}\right)^{1/p}\right)+\frac{c_{\mu,m}(\psi^p(a),\psi^p(b))g_1(\eta)h(1/2^\alpha)H(1/2)}{(\mu+1)(\mu+2)}$$
$$\leq\frac{\Gamma(\mu+1)}{(m\psi^p(b)-\psi^p(a))^\mu}\left[g_2(\eta)h\left(\frac{1}{2^\alpha}\right)\times I^{\mu,\psi}_{\psi^{-1}(\psi^p(a))^-}(f\circ\phi)(\psi^{-1}(m\psi^p(b)))\right.$$
$$\left.+m^{\mu+1}g_3(\eta)H\left(\frac{1}{2}\right)I^{\mu,\psi}_{\psi^{-1}(\psi^p(b))^+}(f\circ\phi)\left(\psi^{-1}\left(\frac{\psi^p(a)}{m}\right)\right)\right]$$
$$\leq A^{h,H}_{\alpha,\mu,m,\eta}(f(\psi(a)),f(\psi(b)))+B^{h,H}_{\alpha,\mu,m,\eta}(f(\psi(a)),f(\psi(b)))$$
$$-R^{h,H}_{\alpha,\mu,m,\eta}(\psi^p(a),\psi^p(b)), \tag{16}$$

with $\mu>0$, $H(t)=h(1-t^\alpha)$, $\phi(t)=\psi^{1/p}(t)$ *for all* $t\in[mb^p, a^p]$ *and*

$$g_1(\eta)=\begin{cases}e^{-\eta(\psi^p(a)+\psi^p(b))}, & \text{if } \eta<0,\\ e^{-\eta(m\psi^p(b)+(\psi^p(a)/m))}, & \text{if } \eta>0,\end{cases}$$
$$g_2(\eta)=\begin{cases}e^{-\eta(m\psi^p(b)1/p}, & \text{if } \eta>0,\\ e^{-\eta\psi(a)}, & \text{if } \eta<0,\end{cases}\tag{17}$$
$$g_3(\eta)=\begin{cases}e^{-\eta\psi(b)}, & \text{if } \eta>0,\\ e^{-\eta(\psi^p(a)/m)^{1/p}}, & \text{if } \eta<0\end{cases}$$

Proof. (i) The following inequality holds for a strongly exponentially $(\alpha,h-m)$-p-convex function

$$f\left(\left(\frac{\psi^p(x)+m\psi^p(y)}{2}\right)^{1/p}\right)\leq h\left(\frac{1}{2^\alpha}\right)\frac{f(\psi(x))}{e^{\eta\psi(x)}}$$
$$+mH\left(\frac{1}{2}\right)\frac{f(\psi(y))}{e^{\eta\psi(y)}}-\frac{cmh(1/2^\alpha)H(1/2)(\psi^p(y)-\psi^p(x))^2}{e^{\eta(\psi^p(x)+\psi^p(y))}}.\tag{18}$$

By setting $\psi(x)=(\psi^p(a)t+m(1-t)\psi^p(b))^{1/p}$, $\psi(y)=((\psi^p(a)/m)(1-t)+\psi^p(b)t)^{1/p}$ in (18) and then integrating on $[0,1]$ after multiplying with $t^{\mu-1}$, one can get

$$\frac{1}{\mu}f\left(\left(\frac{\psi^p(a)+m\psi^p(b)}{2}\right)^{1/p}\right)\leq h\left(\frac{1}{2^\alpha}\right)$$
$$\int_0^1\frac{f((\psi^p(a)t+m(1-t)\psi^p(b)))^{1/p})}{e^{\eta(\psi^p(a)t+m(1-t)\psi^p(b))^{1/p}}}t^{\mu-1}dt+mH\left(\frac{1}{2}\right)$$
$$\times\int_0^1\frac{f\left(((\psi^p(a)/m)(1-t)+\psi^p(b))t)^{1/p}\right)}{e^{\eta((\psi^p(a)/m)(1-t)+\psi^p(b))t)^{1/p}}}t^{\mu-1}dt-cmh\left(\frac{1}{2^\alpha}\right)H\left(\frac{1}{2}\right)$$
$$\int_0^1\frac{((1-t)((\psi^p(a)/m)-m\psi^p(b))+t(\psi^p(b)-\psi^p(a)))^2}{e^{\eta((1-t)((\psi^p(a)/m)+m\psi^p(b))+t(\psi^p(b)+\psi^p(a)))^{1/p}}}t^{\mu-1}dt.\tag{19}$$

Setting $\psi(u)=\psi^p(a)t+m(1-t)\psi^p(b)$ and $\psi(v)=(\psi^p(a)/m)(1-t)+\psi^p(b)t$ in (19) and multiplying by μ, after applying Definition 3, the following inequality can be obtained:

$$f\left(\left(\frac{\psi^p(a)+m\psi^p(b)}{2}\right)^{1/p}\right)\leq\frac{\Gamma(\mu+1)}{(m\psi^p(b)-\psi^p(a))^\mu}$$
$$\cdot\left[g_2(\eta)h\left(\frac{1}{2^\alpha}\right)I^{\mu}_{(\psi^p(a))^+}(f\circ\phi)(m\psi^p(b))+m^{\mu+1}g_3(\eta)H\right.$$
$$\left.\cdot\left(\frac{1}{2}\right)\times I^{\mu}_{(\psi^p(b))^-}(f\circ\phi)\left(\frac{\psi^p(a)}{m}\right)\right]$$
$$-\frac{c_{\mu,m}(\psi^p(a),\psi^p(b))g_1(\eta)h(1/2^\alpha)H(1/2)}{(\mu+1)(\mu+2)}.\tag{20}$$

Now, by using definition of strongly exponentially $(\alpha,h-m)$-p-convex function for f and then integrating the resulting inequality on $[0,1]$ after multiplying with $t^{\mu-1}$, one can get

$$g_2(\eta)h\left(\frac{1}{2^\alpha}\right)\int_0^1 f\left((\psi^p(a)t+m(1-t)\psi^p(b))^{1/p}\right)t^{\mu-1}dt+mg_3$$
$$\cdot(\eta)H\left(\frac{1}{2}\right)\int_0^1 f\left((\psi^p(a)t+m(1-t)\psi^p(b))^{1/p}\right)t^{\mu-1}dt$$
$$\leq\frac{A^{h,H}_{\alpha,\mu,m,\eta}(f(\psi(a)),f(\psi(b)))}{\mu}+\frac{B^{h,H}_{\alpha,\mu,m,\eta}(f(\psi(a)),f(\psi(b)))}{\mu}$$
$$-\frac{R^{h,H}_{\alpha,\mu,m,\eta}(\psi^p(a),\psi^p(b))}{\mu}.\tag{21}$$

Again, using substitution as considered in (20) leads to the second inequality of (14)

(ii) The proof is followed on same lines as the proof of (i) □

Remark 11. The aforementioned version of the Hadamard inequalities gives (i) [4], Theorem 4 for $p=-1$, $m=\alpha=1$, $h=\psi=I$, and $c=\eta=0$; (ii) [3], Theorem 2.4 for $p=-1$, $m=\alpha=\mu=1$, $h=\psi=I$, and $c=\eta=0$; (iii) [14], Theorem 3.10 for $h=\psi=I$ and $c=\eta=0$; (iv) [15], Corollary 2.2 for $\alpha=p=1$, $\psi=I$, and $c=\eta=0$; (v) Theorem 2 for $\alpha=m=p=1$, $h=\psi=I$, and $c=\eta=0$; (vi) [16], Theorem 2.1 for $\alpha=p=1$, $h=\psi=I$, and $c=\eta=0$; (vii) [14], Theorem 2.2 for $\psi=I$ and $c=\eta=0$; (viii) Theorem 1 for $\alpha=\mu=m=1$, $h=\psi=I$, and $c=\eta=0$; (ix) [17], Theorem 2.1 for $\alpha=\mu=m=1$, $p=-1$, $h(t)=t^s$, $\psi=I$, and $c=\eta=0$; (x) [1], Theorem 2.1 for $\alpha=\mu=m=p=1$, $h(t)=t^s$, $\psi=I$, and $c=\eta=0$; and (xi) [6], Theorem 3 for $\psi=I$. Moreover, the refinements of all the deduced results will occur for c > 0.

Corollary 12. *(i) For $p>0$, one can have for the strongly $(\alpha,h-m)$-p-convex function the following fractional integral inequality:*

$$f\left(\left(\frac{\psi^p(a)+m\psi^p(b)}{2}\right)^{1/p}\right)+\frac{c_{\mu,m}(\psi^p(a),\psi^p(b))h(1/2^\alpha)H(1/2)}{(\mu+1)(\mu+2)}$$
$$\leq\frac{\Gamma(\mu+1)}{(m\psi^p(b)-\psi^p(a))^\mu}\left[h\left(\frac{1}{2^\alpha}\right)\times I^{\mu,\psi}_{\psi^{-1}(\psi^p(a))^+}(f\circ\phi)(\psi^{-1}(m\psi^p(b)))\right.$$
$$\left.+m^{\mu+1}H\left(\frac{1}{2}\right)I^{\mu,\psi}_{\psi^{-1}(\psi^p(b))^-}(f\circ\phi)\left(\psi^{-1}\left(\frac{\psi^p(a)}{m}\right)\right)\right]$$
$$\leq A^{h,H}_{\alpha,\mu,m,0}(f(\psi(a)),f(\psi(b)))+B^{h,H}_{\alpha,\mu,m,0}(f(\psi(a)),f(\psi(b)))$$
$$-R^{h,H}_{\alpha,\mu,m,0}(\psi^p(a),\psi^p(b)) \tag{22}$$

Proof. The abovementioned inequality can be deduced by setting $\eta=0$ in (14).

(ii) For $p<0$, one can have for the strongly $(\alpha,h-m)$-p-convex function the following fractional integral inequality:

$$f\left(\left(\frac{\psi^p(a)+m\psi^p(b)}{2}\right)^{1/p}\right)+\frac{c_{\mu,m}(\psi^p(a),\psi^p(b))h(1/2^\alpha)H(1/2)}{(\mu+1)(\mu+2)}$$
$$\leq\frac{\Gamma(\mu+1)}{(m\psi^p(b)-\psi^p(a))^\mu}\left[h\left(\frac{1}{2^\alpha}\right)\times I^{\mu,\psi}_{\psi^{-1}(\psi^p(a))^-}(f\circ\phi)(\psi^{-1}(m\psi^p(b)))\right.$$
$$\left.+m^{\mu+1}H\left(\frac{1}{2}\right)I^{\mu,\psi}_{\psi^{-1}(\psi^p(b))^+}(f\circ\phi)\left(\psi^{-1}\left(\frac{\psi^p(a)}{m}\right)\right)\right]$$
$$\leq A^{h,H}_{\alpha,\mu,m,0}(f(\psi(a)),f(\psi(b)))+B^{h,H}_{\alpha,\mu,m,0}(f(\psi(a)),f(\psi(b)))$$
$$-R^{h,H}_{\alpha,\mu,m,0}(\psi^p(a),\psi^p(b)) \tag{23}$$

□

Proof. The abovementioned inequality can be deduced by setting $\eta=0$ in (16). □

Corollary 13. (*i*) *For $p>0$, one can have for the strongly exponentially $(h-m)$-p-convex function the following fractional integral inequality:*

$$f\left(\left(\frac{\psi^p(a)+m\psi^p(b)}{2}\right)^{1/p}\right)+\frac{c_{\mu,m}(\psi^p(a),\psi^p(b))g_1(\eta)h^2(1/2)}{(\mu+1)(\mu+2)}$$
$$\leq\frac{h(1/2)\Gamma(\mu+1)}{(m\psi^p(b)-\psi^p(a))^\mu}\left[g_2(\eta)\times I^{\mu,\psi}_{\psi^{-1}(\psi^p(a))^+}(f\circ\phi)(\psi^{-1}(m\psi^p(b)))\right.$$
$$\left.+m^{\mu+1}g_3(\eta)H\left(\frac{1}{2}\right)I^{\mu,\psi}_{\psi^{-1}(\psi^p(b))^-}(f\circ\phi)\left(\psi^{-1}\left(\frac{\psi^p(a)}{m}\right)\right)\right]$$
$$\leq A^{h,H}_{1,\mu,m,\eta}(f(\psi(a)),f(\psi(b)))+B^{h,H}_{1,\mu,m,\eta}(f(\psi(a)),f(\psi(b)))$$
$$-R^{h,H}_{1,\mu,m,\eta}(\psi^p(a),\psi^p(b)) \tag{24}$$

Proof. The abovementioned inequality can be deduced by setting $\alpha=1$ in (14).

(ii) For $p<0$, one can have for the strongly exponentially $(h-m)$-p-convex function the following fractional integral inequality:

$$f\left(\left(\frac{\psi^p(a)+m\psi^p(b)}{2}\right)^{1/p}\right)+\frac{c_{\mu,m}(\psi^p(a),\psi^p(b))g_1(\eta)h^2(1/2)}{(\mu+1)(\mu+2)}$$
$$\leq\frac{h(1/2)\Gamma(\mu+1)}{(m\psi^p(b)-\psi^p(a))^\mu}\left[g_2(\eta)\times I^{\mu,\psi}_{\psi^{-1}(\psi^p(a))^-}(f\circ\phi)(\psi^{-1}(m\psi^p(b)))\right.$$
$$\left.+m^{\mu+1}g_3(\eta)H\left(\frac{1}{2}\right)I^{\mu,\psi}_{\psi^{-1}(\psi^p(b))^+}(f\circ\phi)\left(\psi^{-1}\left(\frac{\psi^p(a)}{m}\right)\right)\right]$$
$$\leq A^{h,H}_{1,\mu,m,\eta}(f(\psi(a)),f(\psi(b)))+B^{h,H}_{1,\mu,m,\eta}(f(\psi(a)),f(\psi(b)))$$
$$-R^{h,H}_{1,\mu,m,\eta}(\psi^p(a),\psi^p(b)) \tag{25}$$

□

Proof. The abovementioned inequality can bed deduced by setting $\alpha=1$ in (16). □

Corollary 14. (*i*) *For $p>0$, one can have for the strongly exponentially (s,m)-p-Godunova-Levin function the following fractional integral inequality:*

$$f\left(\left(\frac{\psi^p(a)+m\psi^p(b)}{2}\right)^{1/p}\right)+\frac{c_{\mu,m}(\psi^p(a),\psi^p(b))g_1(\eta)2^{2s}}{(\mu+1)(\mu+2)}$$
$$\leq\frac{\Gamma(\mu+1)}{2^s(m\psi^p(b)-\psi^p(a))^\mu}\left[g_2(\eta)I^{\mu,\psi}_{(\psi^p(a))^+}(f\circ\phi)(\psi^{-1}(m\psi^p(b)))\right.$$
$$\left.+m^{\mu+1}g_3(\eta)I^{\mu,\psi}_{(\psi^p(b))^-}(f\circ\phi)\left(\psi^{-1}\left(\frac{\psi^p(a)}{m}\right)\right)\right]$$
$$\leq A^{t^{-s},(1-t)^{-s}}_{\alpha,\mu,m,\eta}(f(\psi(a)),f(\psi(b)))+B^{t^{-s},(1-t)^{-s}}_{\alpha,\mu,m,\eta}(f(\psi(a)),f(\psi(b)))$$
$$-R^{t^{-s},(1-t)^{-s}}_{\alpha,\mu,m,\eta}(\psi^p(a),\psi^p(b)) \tag{26}$$

Proof. The abovementioned inequality can be deduced by setting $\alpha=1$ and $h(t)=t^{-s}$ in (2.1).

(ii) For $p<0$, one can have for the strongly exponentially (s,m)-p-Godunova-Levin function the following fractional integral inequality:

$$f\left(\left(\frac{\psi^p(a)+m\psi^p(b)}{2}\right)^{1/p}\right)+\frac{c_{\mu,m}(\psi^p(a),\psi^p(b))g_1(\eta)2^{2s}}{(\mu+1)(\mu+2)}$$
$$\leq\frac{\Gamma(\mu+1)}{2^s(m\psi^p(b)-\psi^p(a))^\mu}\left[g_2(\eta)I^{\mu,\psi}_{(\psi^p(a))^-}(f\circ\phi)(\psi^{-1}(m\psi^p(b)))\right.$$
$$\left.+m^{\mu+1}g_3(\eta)I^{\mu,\psi}_{(\psi^p(b))^+}(f\circ\phi)\left(\psi^{-1}\left(\frac{\psi^p(a)}{m}\right)\right)\right]$$
$$\leq A^{t^{-s},(1-t)^{-s}}_{\alpha,\mu,m,\eta}(f(\psi(a)),f(\psi(b)))+B^{t^{-s},(1-t)^{-s}}_{\alpha,\mu,m,\eta}(f(\psi(a)),f(\psi(b)))$$
$$-R^{t^{-s},(1-t)^{-s}}_{\alpha,\mu,m,\eta}(\psi^p(a),\psi^p(b)) \tag{27}$$

□

Proof. The abovementioned inequality can be deduced by setting $\alpha=1$ and $h(t)=t^{-s}$ in (16). □

Corollary 15. (*i*) *For $p>0$, one can have for the strongly exponentially (s,m)-p-convex function in the third sense the following fractional integral inequality:*

$$f\left(\left(\frac{\psi^p(a)+m\psi^p(b)}{2}\right)^{1/p}\right)+\frac{c_{\mu,m}(\psi^p(a),\psi^p(b))g_1(\eta)}{2^{2s}(\mu+1)(\mu+2)}$$
$$\leq\frac{\Gamma(\mu+1)}{(m\psi^p(b)-\psi^p(a))^\mu}\left[g_2(\eta)I^{\mu,\psi}_{(\psi^p(a))^+}(f\circ\phi)\left(\psi^{-1}(m\psi^p(b))\right)\right.$$
$$\left.+m^{\mu+1}g_3(\eta)I^{\mu}_{(\psi^p(b))^-}(f\circ\phi)\left(\psi^{-1}\left(\frac{\psi^p(a)}{m}\right)\right)\right]$$
$$\leq A^{t^s,(1-t)^s}_{\alpha,\mu,m,\eta}(f(\psi(a)),f(\psi(b)))+B^{t^s,(1-t)^s}_{\alpha,\mu,m,\eta}(f(\psi(a)),f(\psi(b)))$$
$$-R^{t^s,(1-t)^s}_{\alpha,\mu,m,\eta}(\psi^p(a),\psi^p(b)) \tag{28}$$

Proof. The abovementioned inequality can be deduced by setting $\alpha=1$ and $h(t)=t^s$ in (14).

(ii) For $p<0$, one can have for the strongly exponentially (s,m)-p-convex function in third sense the following fractional integral inequality:

$$f\left(\left(\frac{\psi^p(a)+m\psi^p(b)}{2}\right)^{1/p}\right)+\frac{c_{\mu,m}(\psi^p(a),\psi^p(b))g_1(\eta)}{2^{2s}(\mu+1)(\mu+2)}$$
$$\leq\frac{\Gamma(\mu+1)}{(m\psi^p(b)-\psi^p(a))^\mu}\left[g_2(\eta)I^{\mu,\psi}_{(\psi^p(a))^-}(f\circ\phi)\left(\psi^{-1}(m\psi^p(b))\right)\right.$$
$$\left.+m^{\mu+1}g_3(\eta)I^{\mu}_{(\psi^p(b))^+}(f\circ\phi)\left(\psi^{-1}\left(\frac{\psi^p(a)}{m}\right)\right)\right]$$
$$\leq A^{t^s,(1-t)^s}_{\alpha,\mu,m,\eta}(f(\psi(a)),f(\psi(b)))+B^{t^s,(1-t)^s}_{\alpha,\mu,m,\eta}(f(\psi(a)),f(\psi(b)))$$
$$-R^{t^s,(1-t)^s}_{\alpha,\mu,m,\eta}(\psi^p(a),\psi^p(b)) \tag{29}$$

□

Proof. The abovementioned inequality can be deduced by setting $\alpha=1$ and $h(t)=t^s$ in (16). □

Corollary 16. (*i*) *For $p>0$, one can have for the strongly exponentially (α,m)-p-convex function the following fractional integral inequality:*

$$f\left(\left(\frac{\psi^p(a)+m\psi^p(b)}{2}\right)^{1/p}\right)+\frac{c_{\mu,m}(\psi^p(a),\psi^p(b))g_1(\eta)(2^\alpha-1)}{2^{2\alpha}(\mu+1)(\mu+2)}$$
$$\leq\frac{\Gamma(\mu+1)}{(m\psi^p(b)-\psi^p(a))^\mu}\left[g_2(\eta)I^{\mu,\psi}_{\psi^{-1}(\psi^p(a))^+}(f\circ\phi)\left(\psi^{-1}(m\psi^p(b))\right)\right.$$
$$\left.+m^{\mu+1}g_3(\eta)(2^\alpha-1)I^{\mu,\psi}_{\psi^{-1}(\psi^p(b))^-}(f\circ\phi)\left(\frac{\psi^p(a)}{m}\right)\right]$$
$$\leq A^{t^\alpha,(1-t^\alpha)}_{\alpha,\mu,m,\eta}(f(\psi(a)),f(\psi(b)))+B^{t^\alpha,(1-t)^\alpha}_{\alpha,\mu,m,\eta}(f(\psi(a)),f(\psi(b)))$$
$$-R^{t^\alpha,(1-t^\alpha)}_{\alpha,\mu,m,\eta}(\psi^p(a),\psi^p(b)) \tag{30}$$

Proof. The abovementioned inequality can be deduced by setting $h(t)=t$ in (14).

(ii) For $p<0$, one can have for the strongly exponentially (α,m)-p-convex function the following fractional integral inequality:

$$f\left(\left(\frac{\psi^p(a)+m\psi^p(b)}{2}\right)^{1/p}\right)+\frac{c_{\mu,m}(\psi^p(a),\psi^p(b))g_1(\eta)(2^\alpha-1)}{2^{2\alpha}(\mu+1)(\mu+2)}$$
$$\leq\frac{\Gamma(\mu+1)}{(m\psi^p(b)-\psi^p(a))^\mu}\left[g_2(\eta)I^{\mu,\psi}_{\psi^{-1}(\psi^p(a))^-}(f\circ\phi)\left(\psi^{-1}(m\psi^p(b))\right)\right.$$
$$\left.+m^{\mu+1}g_3(\eta)(2^\alpha-1)I^{\mu,\psi}_{\psi^{-1}(\psi^p(b))^+}(f\circ\phi)\left(\frac{\psi^p(a)}{m}\right)\right]$$
$$\leq A^{t^\alpha,(1-t^\alpha)}_{\alpha,\mu,m,\eta}(f(\psi(a)),f(\psi(b)))+B^{t^\alpha,(1-t)^\alpha}_{\alpha,\mu,m,\eta}(f(\psi(a)),f(\psi(b)))$$
$$-R^{t^\alpha,(1-t^\alpha)}_{\alpha,\mu,m,\eta}(\psi^p(a),\psi^p(b)) \tag{31}$$

□

Proof. The abovementioned inequality can be deduced by setting $h(t)=t$ in (16). □

Corollary 17. (*i*) *For $p>0$, one can have for the strongly exponentially p-convex function the following fractional integral inequality:*

$$f\left(\left(\frac{\psi^p(a)+\psi^p(b)}{2}\right)^{1/p}\right)+\frac{cg_1(\eta)\left(\mu^2-\mu+2\right)(\psi^p(b)-\psi^p(a))^2}{4(\mu+1)(\mu+2)}$$
$$\leq\frac{\Gamma(\mu+1)}{(\psi^p(b)-\psi^p(a))^\mu}\left[g_2(\eta)I^{\mu,\psi}_{\psi^{-1}(\psi^p(a))^+}(f\circ\phi)\left(\psi^{-1}(\psi^p(b))\right)\right.$$
$$\left.+g_3(\eta)I^{\mu,\psi}_{\psi^{-1}(\psi^p(b))^-}(f\circ\phi)\left(\psi^{-1}(\psi^p(a))\right)\right]$$
$$\leq A^{t,(1-t)}_{1,\mu,m,\eta}(f(\psi(a)),f(\psi(b)))+B^{t,(1-t)}_{1,\mu,m,\eta}(f(\psi(a)),f(\psi(b)))$$
$$-R^{t,(1-t)}_{1,\mu,m,\eta}(\psi^p(a),\psi^p(b)) \tag{32}$$

Proof. The abovementioned inequality can be deduced by setting $\alpha=m=1$ and $h(t)=t$ in (14).

(ii) For $p<0$, one can have for strongly exponentially p-convex function the following fractional integral inequality

$$f\left(\left(\frac{\psi^p(a)+\psi^p(b)}{2}\right)^{1/p}\right)+\frac{cg_1(\eta)\left(\mu^2-\mu+2\right)(\psi^p(b)-\psi^p(a))^2}{4(\mu+1)(\mu+2)}$$
$$\leq\frac{\Gamma(\mu+1)}{(\psi^p(b)-\psi^p(a))^\mu}\left[g_2(\eta)I^{\mu,\psi}_{\psi^{-1}(\psi^p(a))^-}(f\circ\phi)\left(\psi^{-1}(\psi^p(b))\right)\right.$$
$$\left.+g_3(\eta)I^{\mu,\psi}_{\psi^{-1}(\psi^p(b))^+}(f\circ\phi)\left(\psi^{-1}(\psi^p(a))\right)\right]$$
$$\leq A^{t,(1-t)}_{1,\mu,m,\eta}(f(\psi(a)),f(\psi(b)))+B^{t,(1-t)}_{1,\mu,m,\eta}(f(\psi(a)),f(\psi(b)))$$
$$-R^{t,(1-t)}_{1,\mu,m,\eta}(\psi^p(a),\psi^p(b)) \tag{33}$$

□

Proof. The abovementioned inequality can be deduced by setting $\alpha=m=1$ and $h(t)=t$ in (16). □

Corollary 18. *For the strongly exponentially $(\alpha, h-m)$-HA-convex function, the following inequality holds:*

$$\begin{aligned}
&f\left(\frac{2\psi(a)\psi(b)}{\psi(b)+m\psi(a)}\right)+\frac{cmh(1/2^{\alpha})H(1/2)}{(\mu+1)(\mu+2)}\left[\mu(\mu+1)\left(\frac{1}{\psi(b)}-\frac{1}{\psi(a)}\right)^{2}\right.\\
&\left.+2\left(\frac{1}{m\psi(a)}-\frac{m}{\psi(b)}\right)^{2}+2\mu\left(\frac{1}{\psi(b)}-\frac{1}{\psi(a)}\right)\times\left(\frac{1}{m\psi(a)}-\frac{m}{\psi(b)}\right)\right]\\
&\leq\frac{\Gamma(\mu+1)(\psi(a)\psi(b))^{\mu}}{(\psi(b)-m\psi(a))^{\mu}}\left[h\left(\frac{1}{2^{\alpha}}\right)I^{\mu,\psi}_{\psi^{-1}(1/\psi(a))^{-}}(f\circ\phi)\left(\psi^{-1}\left(\frac{m}{\psi(b)}\right)\right)\right.\\
&\left.+m^{\mu+1}H\left(\frac{1}{2}\right)\times I^{\mu,\psi}_{\psi^{-1}(1/\psi(b))^{+}}(f\circ\phi)\left(\psi^{-1}\left(\frac{1}{m\psi(a)}\right)\right)\right]\\
&\leq A^{h,H}_{\alpha,\mu,m,\eta}(f(\psi(a)),f(\psi(b)))+B^{h,H}_{\alpha,\mu,m,\eta}(f(\psi(a)),f(\psi(b)))\\
&-R^{h,H}_{\alpha,\mu,m,\eta}\left(\frac{1}{\psi(a)},\frac{1}{\psi(b)}\right).
\end{aligned}\tag{34}$$

Proof. The abovementioned inequality can be deduced by setting $p=-1$ in (16). □

Corollary 19. *For the strongly exponentially (α, m)-HA-convex function, the following inequality holds:*

$$\begin{aligned}
&f\left(\frac{2\psi(a)\psi(b)}{\psi(b)+\psi(a)m}\right)+\frac{cmg_1(\eta)(2^{\alpha}-1)}{2^{2\alpha}(\mu+1)(\mu+2)}\left[\mu(\mu+1)\left(\frac{\psi(b)-\psi(a)}{\psi(a)\psi(b)}\right)^{2}\right.\\
&\left.+2\left(\frac{\psi(b)-\psi(a)m^{2}}{\psi(a)\psi(b)m}\right)^{2}+\frac{2\mu(\psi(a)-\psi(b))(\psi(b)-\psi(a)m^{2})}{m(\psi(a)\psi(b))^{2}}\right]\\
&\leq\frac{\Gamma(\mu+1)(\psi(a)\psi(b))^{\mu}}{2^{\alpha}(\psi(b)-m\psi(a))^{\mu}}\left[g_2(\eta)I^{\mu,\psi}_{\psi^{-1}(1/\psi(a))^{-}}(f\circ\phi)\left(\psi^{-1}\left(\frac{m}{\psi(b)}\right)\right)\right.\\
&\left.+m^{\mu+1}g_3(\eta)(2^{\alpha}-1)I^{\mu,\psi}_{\psi^{-1}(1/b)^{+}}(f\circ\phi)\left(\psi^{-1}\left(\frac{1}{m\psi(a)}\right)\right)\right]\\
&\leq A^{t^{\alpha},(1-t^{\alpha})}_{\alpha,\mu,m,\eta}(f(\psi(a)),f(\psi(b)))+B^{t^{\alpha},(1-t^{\alpha})}_{\alpha,\mu,m,\eta}(f(\psi(a)),f(\psi(b)))\\
&-R^{t^{\alpha},(1-t^{\alpha})}_{\alpha,\mu,m,\eta}(\psi^{p}(a),\psi^{p}(b)).
\end{aligned}\tag{35}$$

Proof. The abovementioned inequality can be deduced by setting $p=-1$ and $h(t)=t$ in (16). □

Corollary 20. *For the strongly exponentially (s, m)-HA-convex function, the following inequality holds:*

$$\begin{aligned}
&f\left(\frac{2\psi(a)\psi(b)}{\psi(a)m+\psi(b)}\right)+\frac{cmg_1(\eta)}{2^{2s}(\mu+1)(\mu+2)}\left[\mu(\mu+1)\left(\frac{\psi(b)-\psi(a)}{\psi(a)\psi(b)}\right)^{2}\right.\\
&\left.+2\left(\frac{\psi(b)-\psi(a)m^{2}}{\psi(a)\psi(b)m}\right)^{2}+\frac{2\mu(\psi(a)-\psi(b))(\psi(b)\psi(a)m^{2})}{m(\psi(a)\psi(b))^{2}}\right]\\
&\leq\frac{\Gamma(\mu+1)(\psi(a)\psi(b))^{\mu}}{(\psi(b)\psi(a)m)^{\mu}}\left[g_2(\eta)I^{\mu,\psi}_{(1/\psi(a))^{-}}(f\circ\phi)\left(\psi^{-1}\left(\frac{m}{b}\right)\right)\right.\\
&\left.+m^{\mu+1}g_3(\eta)I^{\mu,\psi}_{\psi^{-1}(1/\psi(b))^{+}}(f\circ\phi)\left(\psi^{-1}\left(\frac{1}{m\psi(a)}\right)\right)\right]\\
&\leq A^{t^{s},(1-t)^{s}}_{1,\mu,m,\eta}(f(\psi(a)),f(\psi(b)))+B^{t^{s},(1-t)^{s}}_{1,\mu,m,\eta}(f(\psi(a)),f(\psi(b)))\\
&-R^{t^{s},(1-t)^{s}}_{1,\mu,m,\eta}(\psi^{p}(a),\psi^{p}(b)).
\end{aligned}\tag{36}$$

Proof. The abovementioned inequality can be deduced by setting $p=-1$, $\alpha=1$, and $h(t)=t^{s}$ in (16). □

Corollary 21. *For the Godunova-Levin type of strongly exponentially (s, m)-HA-convex function, the following inequality holds:*

$$\begin{aligned}
&f\left(\frac{2\psi(a)\psi(b)}{\psi(b)+m\psi(a)}\right)+\frac{2^{2s}g_1(\eta)cm}{(\mu+1)(\mu+2)}\left[\mu(\mu+1)\left(\frac{1}{\psi(b)}-\frac{1}{\psi(a)}\right)^{2}\right.\\
&\left.+2\left(\frac{1}{m\psi(a)}-\frac{m}{\psi(b)}\right)^{2}+2\mu\left(\frac{1}{\psi(b)}-\frac{1}{\psi(a)}\right)\times\left(\frac{1}{m\psi(a)}-\frac{m}{\psi(b)}\right)\right]\\
&\leq\frac{2^{s}\Gamma(\mu+1)(\psi(a)\psi(b))^{\mu}}{(\psi(b)-m\psi(a))^{\mu}}\left[g_2(\eta)I^{\mu,\psi}_{\psi^{-1}(1/\psi(a))^{-}}(f\circ\phi)\left(\psi^{-1}\left(\frac{m}{\psi(b)}\right)\right)\right.\\
&\left.+m^{\mu+1}g_3(\eta)\times I^{\mu,\psi}_{\psi^{-1}(1/\psi(b))^{+}}(f\circ\phi)\left(\psi^{-1}\left(\frac{1}{m\psi(a)}\right)\right)\right]\\
&\leq A^{t^{-s},(1-t)^{-s}}_{1,\mu,m,\eta}(f(\psi(a)),f(\psi(b)))+B^{t^{-s},(1-t)^{-s}}_{1,\mu,m,\eta}(f(\psi(a)),f(\psi(b)))\\
&-R^{t^{-s},(1-t)^{-s}}_{1,\mu,m,\eta}(\psi^{p}(a),\psi^{p}(b)).
\end{aligned}\tag{37}$$

Proof. The abovementioned inequality can be deduced by setting $p=-1$, $\alpha=1$, and $h(t)=t^{-s}$ in (2.2). □

The second variant of Hadamard inequality for strongly exponentially $(\alpha, h-m)$-p-convex function is proved as follows.

Theorem 22. *Under the assumption of Theorem 10, the following fractional integral inequalities hold:*

(i) For $p>0$, one can have

$$\begin{aligned}
&f\left(\left(\frac{\psi^{p}(a)+m\psi^{p}(b)}{2}\right)^{1/p}\right)+\frac{F_{\mu,m}(\psi^{p}(a),\psi^{p}(b))g_1(\eta)h(1/2^{\alpha})H(1/2)}{4(\mu+1)(\mu+2)}\\
&\leq\frac{2^{\mu}\Gamma(\mu+1)}{(m\psi^{p}(b)-\psi^{p}(a))^{\mu}}\left[g_2(\eta)h\left(\frac{1}{2^{\alpha}}\right)\times I_{\psi^{-1}((\psi^{p}(a)+m\psi^{p}(b))/2)}\right.\\
&+^{\mu,\psi}(f\circ\phi)(\psi^{-1}(m\psi^{p}(b)))+m^{\mu+1}H\left(\frac{1}{2}\right)g_3(\eta)I_{\psi^{-1}((\psi^{p}(a)}\\
&\left.+m\psi^{p}(b))/2m)^{-}\mu,\psi(f\circ\phi)\left(\psi^{-1}\left(\frac{\psi^{p}(a)}{m}\right)\right)\right]\\
&\leq A^{h,H}_{\alpha,\mu,m,\eta}(f(\psi(a)),f(\psi(b)))+B^{h,H}_{\alpha,\mu,m,\eta}(f(\psi(a)),f(\psi(b)))\\
&-R^{h,H}_{\alpha,\mu,m,\eta}(\psi^{p}(a),\psi^{p}(b)),
\end{aligned}\tag{38}$$

with $\mu>0$, $H(t)=h(1-t^{\alpha})$, $\phi(z)=z^{1/p}$ for all $z\in[a^{p}, mb^{p}]$ and

$$g_1(\eta)=\begin{cases} e^{-\eta(\psi^p(a)+\psi^p(b))}, & \text{if } \eta>0,\\ e^{-\eta(m\psi^p(b)+(\psi^p(a)/m))}, & \text{if } \eta<0,\end{cases}$$
$$g_2(\eta)=\begin{cases} e^{-\eta(m\psi^p(b))^{1/p}}, & \text{if } \eta<0,\\ e^{-\eta\psi(a)}, & \text{if } \eta>0,\end{cases} \tag{39}$$
$$g_3(\eta)=\begin{cases} e^{-\eta\psi(b)}, & \text{if } \eta<0,\\ e^{-\eta(\psi^p(a)/m)^{1/p}}, & \text{if } \eta>0\end{cases}$$

(ii) For $p<0$, one can have

$$\begin{aligned} &f\left(\left(\frac{\psi^p(a)+m\psi^p(b)}{2}\right)^{1/p}\right)+\frac{F_{\mu,m}(\psi^p(a),\psi^p(b))g_1(\eta)h(1/2^\alpha)H(1/2)}{4(\mu+1)(\mu+2)}\\ &\le \frac{2^\mu\Gamma(\mu+1)}{(m\psi^p(b)-\psi^p(a))^\mu}\left[g_2(\eta)h\left(\frac{1}{2^\alpha}\right)\right.\\ &\times I^{\mu,\psi}_{\psi^{-1}((\psi^p(a)+m\psi^p(b))/2)^-}(f\circ\phi)(\psi^{-1}(m\psi^p(b)))\\ &\left.+m^{\mu+1}H\left(\frac{1}{2}\right)g_3(\eta)I^{\mu,\psi}_{\psi^{-1}((\psi^p(a)+m\psi^p(b))/2m)^+}(f\circ\phi)\left(\psi^{-1}\left(\frac{\psi^p(a)}{m}\right)\right)\right]\\ &\le A^{h,H}_{\alpha,\mu,m,\eta}(f(\psi(a)),f(\psi(b)))+B^{h,H}_{\alpha,\mu,m,\eta}(f(\psi(a)),f(\psi(b)))\\ &-R^{h,H}_{\alpha,\mu,m,\eta}(\psi^p(a),\psi^p(b)),\end{aligned} \tag{40}$$

with $\mu>0$, $\phi(z)=z^{1/p}$ for all $z\in[mb^p,a^p]$ and

$$g_1(\eta)=\begin{cases} e^{-\eta(\psi^p(a)+\psi^p(b))}, & \text{if } \eta<0,\\ e^{-\eta(m\psi^p(b)+(\psi^p(a)/m))}, & \text{if } \eta>0,\end{cases}$$
$$g_2(\eta)=\begin{cases} e^{-\eta(m\psi^p(b))^{1/p}}, & \text{if } \eta>0,\\ e^{-\eta\psi(a)}, & \text{if } \eta<0,\end{cases} \tag{41}$$
$$g_3(\eta)=\begin{cases} e^{-\eta\psi(b)}, & \text{if } \eta>0,\\ e^{-\eta(\psi^p(a)/m)^{1/p}}, & \text{if } \eta<0\end{cases}$$

Proof. (i) Let $\psi(x)=(((\psi^p(a)t)/2)+m((2-t)/2)\psi^p(b))^{1/p}$, $\psi(y)=((\psi^p(a)/m)((2-t)/2)+((\psi^p(b)t)/2))^{1/p}$ in (18) and integrating the resulting inequality over the interval $[0,1]$ after multiplying with $t^{\mu-1}$, we get

$$\begin{aligned} &\frac{1}{\mu}f\left(\left(\frac{\psi^p(a)+m\psi^p(b)}{2}\right)^{1/p}\right)\\ &\le h\left(\frac{1}{2^\alpha}\right)\int_0^1\frac{f\left((((\psi^p(b)t)/2)+m((2-t)/2)\psi^p(b))^{1/p}\right)}{e^{\eta(((\psi^p(b)t)/2)+m((2-t)/2)\psi^p(b))^{1/p}}}t^{\mu-1}dt\\ &+mH\left(\frac{1}{2}\right)\int_0^1\frac{f\left(((\psi^p(a)/m)((2-t)/2)+((\psi^p(b)t)/2))^{1/p}\right)}{e^{\eta((\psi^p(a)/m)((2-t)/2)+((\psi^p(b)t)/2))^{1/p}}}t^{\mu-1}dt\\ &-cmh\left(\frac{1}{2^\alpha}\right)H\left(\frac{1}{2}\right)\\ &\int_0^1\frac{((t/2)(\psi^p(b)-\psi^p(a))+((2-t)/2)((\psi^p(a)/m)-m\psi^p(b)))^2}{e^{\eta(((2-t)/2)((\psi^p(a)/m)+m\psi^p(b))+(t/2)(\psi^p(b)+\psi^p(a)))^{1/p}}}t^{\mu-1}dt.\end{aligned} \tag{42}$$

Setting $\psi(u)=((\psi^p(b)t)/2)+m((2-t)/2)\psi^p(b)$ and $\psi(v)=(\psi^p(a)/m)((2-t)/2)+((\psi^p(b)t)/2)$ in (42), then, by applying Definition 3, we get the following inequality:

$$\begin{aligned} &f\left(\left(\frac{\psi^p(a)+m\psi^p(b)}{2}\right)^{1/p}\right)\le\frac{2^\mu\Gamma(\mu+1)}{(m\psi^p(b)-\psi^p(a))^\mu}\\ &\cdot\left[h\left(\frac{1}{2^\alpha}\right)g_2(\eta)I^{\mu,\psi}_{\psi^{-1}((\psi^p(a)+m\psi^p(b))/2)^+}(f\circ\phi)(\psi^{-1}(m\psi^p(b)))\right.\\ &\left.+m^{\mu+1}g_3(\eta)H\left(\frac{1}{2}\right)\times I^{\mu}_{\psi^{-1}((\psi^p(a)+m\psi^p(b))/2m)^-}(f\circ\phi)\left(\psi^{-1}\left(\frac{\psi^p(a)}{m}\right)\right)\right]\\ &-\frac{F_{\mu,m}(\psi^p(a),\psi^p(b))g_1(\eta)h(1/2^\alpha)H(1/2)}{4(\mu+1)(\mu+2)}.\end{aligned} \tag{43}$$

Now, again, using strongly exponentially $(\alpha,h-m)$-p-convexity of f and integrating the resulting inequality over $[0,1]$ after multiplying with $t^{\mu-1}$, we get

$$\begin{aligned} &g_2(\eta)h\left(\frac{1}{2^\alpha}\right)\int_0^1 f\left(\left(\frac{\psi^p(a)t}{2}+m\left(\frac{2-t}{2}\right)\psi^p(b)\right)\right)^{1/p}t^{\mu-1}dt\\ &+mg_3(\eta)H\left(\frac{1}{2}\right)\int_0^1 f\left(\left(\frac{\psi^p(a)t}{2}+m\left(\frac{2-t}{2}\right)\psi^p(b)\right)^{1/p}\right)t^{\mu-1}dt\\ &\le\frac{A^{h,H}_{\alpha,\mu,m,\eta}(f(\psi(a)),f(\psi(b)))}{\mu}+\frac{B^{h,H}_{\alpha,\mu,m,\eta}(f(\psi(a)),f(\psi(b)))}{\mu}\\ &-\frac{R^{h,H}_{\alpha,\mu,m,\eta}(\psi^p(a),\psi^p(b))}{\mu}.\end{aligned} \tag{44}$$

Again, using substitution as considered in (42) leads to the second inequality of (38)

(ii) The proof is followed on the same lines as the proof of (i) □

Remark 23. The aforementioned version of the Hadamard inequalities give (i) [18], Theorem 2.4 for $c=0$ and $\psi=I$; (ii) [14], Theorem 2.4 for $c=\eta=0$ and $\psi=I$; (iii) [19], Theorem 7 for $\alpha=m=1$, $c=\eta=0$, and $h(t)=t$; (iv) [19], Theorem 7 for $\alpha=m=1$, $c=\eta=0$, and $h=\psi=I$; (v) Theorem 3 for $\alpha=m=p=1$, $c=\eta=0$, and $h=\psi=I$; (vi) [20], Theorem 2.1 for $\alpha=1=p$, $c=\eta=0$, and $h=\psi=I$; (vii) [21], Theorem 4 for $\alpha=m=1$, $p=-1$, $c=\eta=0$, and $h=\psi=I$; (viii) [3], Theorem 2.4 for $p=-1$, $\alpha=\mu=m=1$, $c=\eta=0$, and $h=\psi=I$; (ix) [22], Theorem 7 for $\alpha=\mu=m=p=1$, $c=\eta=0$, $h(t)=t^{-s}$, and $\psi=I$; (x) [23], Theorem 3.1 for $\alpha=\mu=m=1$, $p=-1$, $c=\eta=0$, $h(t)=t^{-s}$, and $\psi=I$; (xi) Theorem 1 for $\alpha=\mu=m=1$, $c=\eta=0$, and $h=\psi=I$; (xii) [24], Theorem 2.3 for $\alpha=\mu=m=1$, $\eta=0$, and $h=\psi=I$; (xiii) [25], Theorem 6 for $\alpha=\mu=m=p=1$, $\eta=0$, and $h=\psi=I$; (xiv) [17], Theorem 2.1 for $\alpha=\mu=m=1$, $p=-1$, $c=\eta=0$, $h(t)=t^s$, and $\psi=I$; (xv) [1], Theorem 2.1 for $\alpha=\mu=p=m=1$, $c=\eta=0$, $h(t)=t^s$, and $\psi=I$; and (xvi) [5], Theorem 2.1 for $\alpha=\mu=m=1$, $p=-1$, $\eta=0$, and $h=\psi=I$. Moreover, the refinements of all the deduced results will occur for $c>0$.

Corollary 24. (i) *For $p > 0$, one can have for the strongly $(\alpha, h-m)$-p-convex function the following fractional integral inequality:*

$$\begin{aligned}
&f\left(\left(\frac{\psi^p(a)+m\psi^p(b)}{2}\right)^{1/p}\right)+\frac{c_{\mu,m}(\psi^p(a),\psi^p(b))h(1/2^\alpha)H(1/2)}{(\mu+1)(\mu+2)}\\
&\le \frac{\Gamma(\mu+1)}{(m\psi^p(b)-\psi^p(a))^\mu}\left[h\left(\frac{1}{2^\alpha}\right)\times I^{\mu,\psi}_{\psi^{-1}(\psi^p(a))^+}(f\circ\phi)\left(\psi^{-1}(m\psi^p(b))\right)\right.\\
&\left.+m^{\mu+1}H\left(\frac{1}{2}\right)I^{\mu,\psi}_{\psi^{-1}(\psi^p(b))^-}(f\circ\phi)\left(\psi^{-1}\left(\frac{\psi^p(a)}{m}\right)\right)\right]\\
&\le A^{h,H}_{\alpha,\mu,m,0}(f(\psi(a)),f(\psi(b)))+B^{h,H}_{\alpha,\mu,m,0}(f(\psi(a)),f(\psi(b)))\\
&-R^{h,H}_{\alpha,\mu,m,0}(\psi^p(a),\psi^p(b))
\end{aligned} \tag{45}$$

Proof. The abovementioned inequality can be deduced by setting $\eta = 0$ in (14).

(ii) For $p < 0$, one can have for the strongly $(\alpha, h-m)$-p-convex function the following fractional integral inequality:

$$\begin{aligned}
&f\left(\left(\frac{\psi^p(a)+m\psi^p(b)}{2}\right)^{1/p}\right)+\frac{c_{\mu,m}(\psi^p(a),\psi^p(b))h(1/2^\alpha)H(1/2)}{(\mu+1)(\mu+2)}\\
&\le \frac{\Gamma(\mu+1)}{(m\psi^p(b)-\psi^p(a))^\mu}\left[h\left(\frac{1}{2^\alpha}\right)\times I^{\mu,\psi}_{\psi^{-1}(\psi^p(a))^-}(f\circ\phi)\left(\psi^{-1}(m\psi^p(b))\right)\right.\\
&\left.+m^{\mu+1}H\left(\frac{1}{2}\right)I^{\mu,\psi}_{\psi^{-1}(\psi^p(b))^+}(f\circ\phi)\left(\psi^{-1}\left(\frac{\psi^p(a)}{m}\right)\right)\right]\\
&\le A^{h,H}_{\alpha,\mu,m,0}(f(\psi(a)),f(\psi(b)))+B^{h,H}_{\alpha,\mu,m,0}(f(\psi(a)),f(\psi(b)))\\
&-R^{h,H}_{\alpha,\mu,m,0}(\psi^p(a),\psi^p(b))
\end{aligned} \tag{46}$$

□

Proof. The abovementioned inequality can be deduced by setting $\eta = 0$ in (14); then, one can obtain the required inequality. □

Corollary 25. (i) *For $p > 0$, one can have for the strongly exponentially $(h-m)$-p-convex function the following fractional integral inequality:*

$$\begin{aligned}
&f\left(\left(\frac{\psi^p(a)+m\psi^p(b)}{2}\right)^{1/p}\right)+\frac{F_{\mu,m}(\psi^p(a),\psi^p(b))g_1(\eta)h^2(1/2)}{4(\mu+1)(\mu+2)}\\
&\le \frac{2^\mu h(1/2)\Gamma(\mu+1)}{(m\psi^p(b)-\psi^p(a))^\mu}\left[g_2(\eta)\times I^{\mu,\psi}_{\psi^{-1}((\psi^p(a)+m\psi^p(b))/2)^+}(f\circ\phi)\left(\psi^{-1}(m\psi^p(b))\right)\right.\\
&\left.+m^{\mu+1}g_3(\eta)I^{\mu,\psi}_{\psi^{-1}((\psi^p(a)+m\psi^p(b))/2m)^-}(f\circ\phi)\left(\psi^{-1}\left(\frac{\psi^p(a)}{m}\right)\right)\right]\\
&\le A^{t,(1-t)}_{1,\mu,m,\eta}(f(\psi(a)),f(\psi(b)))+B^{t,(1-t)}_{1,\mu,m,\eta}(f(\psi(a)),f(\psi(b)))\\
&-R^{t,(1-t)}_{1,\mu,m,\eta}(\psi^p(a),\psi^p(b))
\end{aligned} \tag{47}$$

Proof. If $\alpha = 1$ in (38), then, the abovementioned inequality is obtained.

(ii) For $p < 0$, one can have for the strongly exponentially $(h-m)$-p-convex function the following fractional integral inequality:

$$\begin{aligned}
&f\left(\left(\frac{\psi^p(a)+m\psi^p(b)}{2}\right)^{1/p}\right)+\frac{F_{\mu,m}(\psi^p(a),\psi^p(b))g_1(\eta)h^2(1/2)}{4(\mu+1)(\mu+2)}\\
&\le \frac{2^\mu h(1/2)\Gamma(\mu+1)}{(m\psi^p(b)-\psi^p(a))^\mu}\left[g_2(\eta)\times I^{\mu,\psi}_{\psi^{-1}((\psi^p(a)+m\psi^p(b))/2)^-}(f\circ\phi)\left(\psi^{-1}(m\psi^p(b))\right)\right.\\
&\left.+m^{\mu+1}g_3(\eta)I^{\mu,\psi}_{\psi^{-1}((\psi^p(a)+m\psi^p(b))/2m)^+}(f\circ\phi)\left(\psi^{-1}\left(\frac{\psi^p(a)}{m}\right)\right)\right]\\
&\le A^{t,(1-t)}_{1,\mu,m,\eta}(f(\psi(a)),f(\psi(b)))+B^{t,(1-t)}_{1,\mu,m,\eta}(f(\psi(a)),f(\psi(b)))\\
&-R^{t,(1-t)}_{1,\mu,m,\eta}(\psi^p(a),\psi^p(b))
\end{aligned} \tag{48}$$

□

Proof. The abovementioned inequality can be deduced by setting $\alpha = 1$ in (40). □

Corollary 26. (i) *For $p > 0$, one can have for the strongly exponentially (s,m)-p-convex function the following fractional integral inequality:*

$$\begin{aligned}
&f\left(\left(\frac{\psi^p(a)+m\psi^p(b)}{2}\right)^{1/p}\right)+\frac{F_{\mu,m}(\psi^p(a),\psi^p(b))g_1(\eta)}{2^{2s+2}(\mu+1)(\mu+2)}\\
&\le \frac{2^{\mu-s}\Gamma(\mu+1)}{(m\psi^p(b)-\psi^p(a))^\mu}\left[g_1(\eta)I^{\mu,\psi}_{((\psi^p(a)+m\psi^p(b))/2)^+}(f\circ\phi)\left(\psi^{-1}(mb)\right)\right.\\
&\left.+m^{\mu+1}I^{\mu}_{\psi^{-1}((\psi^p(a)+m\psi^p(b))/2m)^-}(f\circ\phi)\left(\psi^{-1}\left(\frac{\psi^p(a)}{m}\right)\right)\right]\\
&\le A^{t^s,(1-t)^s}_{1,\mu,m,\eta}(f(\psi(a)),f(\psi(b)))+B^{t^s,(1-t)^s}_{1,\mu,m,\eta}(f(\psi(a)),f(\psi(b)))\\
&-R^{t^s,(1-t)^s}_{1,\mu,m,\eta}(\psi^p(a),\psi^p(b))
\end{aligned} \tag{49}$$

Proof. The abovementioned inequality can be deduced by setting $\alpha = 1$ and $h(t) = t^s$ in (38).

(ii) For $p < 0$, one can have for the strongly exponentially (s,m)-p-convex function the following fractional integral inequality

$$\begin{aligned}
&f\left(\left(\frac{\psi^p(a)+m\psi^p(b)}{2}\right)^{1/p}\right)+\frac{F_{\mu,m}(\psi^p(a),\psi^p(b))g_1(\eta)}{2^{2s+2}(\mu+1)(\mu+2)}\\
&\le \frac{2^{\mu-s}\Gamma(\mu+1)}{(m\psi^p(b)-\psi^p(a))^\mu}\left[g_1(\eta)I^{\mu,\psi}_{((\psi^p(a)+m\psi^p(b))/2)^-}(f\circ\phi)\left(\psi^{-1}(mb)\right)\right.\\
&\left.+m^{\mu+1}I^{\mu}_{\psi^{-1}((\psi^p(a)+m\psi^p(b))/2m)^+}(f\circ\phi)\left(\psi^{-1}\left(\frac{\psi^p(a)}{m}\right)\right)\right]\\
&\le A^{t^s,(1-t)^s}_{1,\mu,m,\eta}(f(\psi(a)),f(\psi(b)))+B^{t^s,(1-t)^s}_{1,\mu,m,\eta}(f(\psi(a)),f(\psi(b)))\\
&-R^{t^s,(1-t)^s}_{1,\mu,m,\eta}(\psi^p(a),\psi^p(b))
\end{aligned} \tag{50}$$

□

Proof. The abovementioned inequality can be deduced by setting $\alpha = 1$ and $h(t) = t^s$ in (40). □

Corollary 27. (i) *For $p > 0$, one can have for the strongly exponentially Godunova-Levin type of (s,m)-p-convex function the following fractional integral inequality:*

$$f\left(\left(\frac{\psi^p(a)+m\psi^p(b)}{2}\right)^{1/p}\right)+\frac{2^{2s}F_{\mu,m}(\psi^p(a),\psi^p(b))g_1(\eta)}{4(\mu+1)(\mu+2)}$$
$$\leq \frac{2^{\mu+s}\Gamma(\mu+1)}{(m\psi^p(b)-\psi^p(a))^\mu}\left[g_2(\eta)I^{\mu,\psi}_{\psi^{-1}((\psi^p(a)+m\psi^p(b))/2)^+}(f\circ\phi)\left(\psi^{-1}(m\psi^p(b))\right)\right.$$
$$\left.+m^{\mu+1}g_3(\eta)I^{\mu,\psi}_{\psi^{-1}((\psi^p(a)+m\psi^p(b))/2m)^-}(f\circ\phi)\left(\psi^{-1}\left(\frac{\psi^p(a)}{m}\right)\right)\right]$$
$$\leq A^{t^{-s},(1-t)^{-s}}_{1,\mu,m,\eta}(f(\psi(a)),f(\psi(b)))+B^{t^{-s},(1-t)^{-s}}_{1,\mu,m,\eta}(f(\psi(a)),f(\psi(b)))$$
$$-R^{t^{-s},(1-t)^{-s}}_{1,\mu,m,\eta}(\psi^p(a),\psi^p(b)) \tag{51}$$

Proof. The abovementioned inequality can be deduced by setting $\alpha=1$ and $h(t)=t^{-s}$ in (38).

(ii) For $p<0$, one can have for the strongly exponentially Godunova-Levin type of (s,m)-p-convex function the following fractional integral inequality:

$$f\left(\left(\frac{\psi^p(a)+m\psi^p(b)}{2}\right)^{1/p}\right)+\frac{2^{2s}F_{\mu,m}(\psi^p(a),\psi^p(b))g_1(\eta)}{4(\mu+1)(\mu+2)}$$
$$\leq \frac{2^{\mu+s}\Gamma(\mu+1)}{(m\psi^p(b)-\psi^p(a))^\mu}\left[g_2(\eta)I^{\mu,\psi}_{\psi^{-1}((\psi^p(a)+m\psi^p(b))/2)^-}(f\circ\phi)\left(\psi^{-1}(m\psi^p(b))\right)\right.$$
$$\left.+m^{\mu+1}g_3(\eta)I^{\mu,\psi}_{\psi^{-1}((\psi^p(a)+m\psi^p(b))/2m)^+}(f\circ\phi)\left(\psi^{-1}\left(\frac{\psi^p(a)}{m}\right)\right)\right]$$
$$\leq A^{t^{-s},(1-t)^{-s}}_{1,\mu,m,\eta}(f(\psi(a)),f(\psi(b)))+B^{t^{-s},(1-t)^{-s}}_{1,\mu,m,\eta}(f(\psi(a)),f(\psi(b)))$$
$$-R^{t^{-s},(1-t)^{-s}}_{1,\mu,m,\eta}(\psi^p(a),\psi^p(b)) \tag{52}$$

□

Proof. The abovementioned inequality can be deduced by setting $\alpha=1$ and $h(t)=t^{-s}$ in (40). □

Corollary 28. (*i*) *For $p>0$, one can have for the strongly exponentially (α,m)-p-convex function the following fractional integral inequality:*

$$f\left(\left(\frac{\psi^p(a)+m\psi^p(b)}{2}\right)^{1/p}\right)+\frac{(2^\alpha-1)F_{\mu,m}(\psi^p(a),\psi^p(b))g_1(\eta)}{2^{2\alpha+2}(\mu+1)(\mu+2)}$$
$$\leq \frac{2^{\mu-\alpha}\Gamma(\mu+1)}{(m\psi^p(b)-\psi^p(a))^\mu}\left[g_2(\eta)I^{\mu,\psi}_{\psi^{-1}((\psi^p(a)+m\psi^p(b))/2)^+}(f\circ\phi)\psi^{-1}((m\psi^p(b))\right.$$
$$\left.+m^{\mu+1}g_3(\eta)(2^\alpha-1)I^{\mu,\psi}_{\psi^{-1}((\psi^p(a)+m\psi^p(b))/2m)^-}(f\circ\phi)\left(\psi^{-1}\left(\frac{\psi^p(a)}{m}\right)\right)\right]$$
$$\leq A^{t^\alpha,(1-t^\alpha)}_{1,\mu,m,\eta}(f(\psi(a)),f(\psi(b)))+B^{t^\alpha,(1-t)^\alpha}_{1,\mu,m,\eta}(f(\psi(a)),f(\psi(b)))$$
$$-R^{t^\alpha,(1-t)^\alpha}_{1,\mu,m,\eta}(\psi^p(a),\psi^p(b)) \tag{53}$$

Proof. The abovementioned inequality can be deduced by setting $h(t)=t$ in (38).

(ii) For $p<0$, one can have for the strongly exponentially (α,m)-p-convex function the following fractional integral inequality:

$$f\left(\left(\frac{\psi^p(a)+m\psi^p(b)}{2}\right)^{1/p}\right)+\frac{(2^\alpha-1)F_{\mu,m}(\psi^p(a),\psi^p(b))g_1(\eta)}{2^{2\alpha+2}(\mu+1)(\mu+2)}$$
$$\leq \frac{2^{\mu-\alpha}\Gamma(\mu+1)}{(m\psi^p(b)-\psi^p(a))^\mu}\left[g_2(\eta)I^{\mu,\psi}_{\psi^{-1}((\psi^p(a)+m\psi^p(b))/2)^-}(f\circ\phi)\psi^{-1}((m\psi^p(b))\right.$$
$$\left.+m^{\mu+1}g_3(\eta)(2^\alpha-1)I^{\mu,\psi}_{\psi^{-1}((\psi^p(a)+m\psi^p(b))/2m)^+}(f\circ\phi)\left(\psi^{-1}\left(\frac{\psi^p(a)}{m}\right)\right)\right]$$
$$\leq A^{t^\alpha,(1-t^\alpha)}_{1,\mu,m,\eta}(f(\psi(a)),f(\psi(b)))+B^{t^\alpha,(1-t)^\alpha}_{1,\mu,m,\eta}(f(\psi(a)),f(\psi(b)))$$
$$-R^{t^\alpha,(1-t)^\alpha}_{1,\mu,m,\eta}(\psi^p(a),\psi^p(b)) \tag{54}$$

□

Proof. The abovementioned inequality can be deduced by setting $h(t)=t$ in (40). □

Corollary 29. (*i*) *For $p>0$, one can have for strongly exponentially p-convex function the following fractional integral inequality:*

$$f\left(\left(\frac{\psi^p(a)+\psi^p(b)}{2}\right)^{1/p}\right)+\frac{cg_1(\eta)\left((\psi^p(b)-\psi^p(a))^2\right)}{2(\mu+1)(\mu+2)}$$
$$\leq \frac{2^{\mu-1}\Gamma(\mu+1)}{(\psi^p(b)-\psi^p(a))^\mu}\left[g_2(\eta)I^{\mu,\psi}_{\psi^{-1}((\psi^p(a)+m\psi^p(b))/2)^+}(f\circ\phi)\left(\psi^{-1}(\psi^p(b))\right)\right.$$
$$\left.+g_3(\eta)I^{\mu,\psi}_{\psi^{-1}((\psi^p(a)+\psi^p(b))/2)^-}(f\circ\phi)\left(\psi^{-1}(\psi^p(a))\right)\right]$$
$$\leq A^{t^\alpha,(1-t^\alpha)}_{1,\mu,1,\eta}(f(\psi(a)),f(\psi(b)))+B^{t^\alpha,(1-t)^\alpha}_{1,\mu,1,\eta}(f(\psi(a)),f(\psi(b)))$$
$$-R^{t^\alpha,(1-t)^\alpha}_{1,\mu,1,\eta}(\psi^p(a),\psi^p(b)) \tag{55}$$

Proof. The abovementioned inequality can be deduced by setting $\alpha=m=1$ and $h(t)=t$ in (38).

(ii) For $p<0$, one can have for the strongly exponentially p-convex function the following fractional integral inequality:

$$f\left(\left(\frac{\psi^p(a)+\psi^p(b)}{2}\right)^{1/p}\right)+\frac{cg_1(\eta)\left((\psi^p(b)-\psi^p(a))^2\right)}{2(\mu+1)(\mu+2)}$$
$$\leq \frac{2^{\mu-1}\Gamma(\mu+1)}{(\psi^p(b)-\psi^p(a))^\mu}\left[g_2(\eta)I^{\mu,\psi}_{\psi^{-1}((\psi^p(a)+m\psi^p(b))/2)^-}(f\circ\phi)\left(\psi^{-1}(\psi^p(b))\right)\right.$$
$$\left.+g_3(\eta)I^{\mu,\psi}_{\psi^{-1}((\psi^p(a)+m\psi^p(b))/2)^+}(f\circ\phi)\left(\psi^{-1}(\psi^p(a))\right)\right]$$
$$\leq A^{t^\alpha,(1-t^\alpha)}_{1,\mu,1,\eta}(f(\psi(a)),f(\psi(b)))+B^{t^\alpha,(1-t)^\alpha}_{1,\mu,1,\eta}(f(\psi(a)),f(\psi(b)))$$
$$-R^{t^\alpha,(1-t)^\alpha}_{1,\mu,1,\eta}(\psi^p(a),\psi^p(b)) \tag{56}$$

□

Proof. The abovementioned inequality can be deduced by setting $\alpha=m=1$ and $h(t)=t$ in (40). □

Corollary 30. *For the strongly exponentially* (α, m)*-HA-convex function, the following inequality holds:*

$$\begin{aligned}
&f\left(\frac{2\psi(a)\psi(b)}{\psi(a)+m\psi(b)}\right)+\frac{(2^{\alpha}-1)cmg_1(\eta)}{2^{2\alpha+2}(\mu+1)(\mu+2)}\left[\mu(\mu+1)\left(\frac{\psi(b)-\psi(a)}{\psi(a)\psi(b)}\right)^2\right.\\
&\quad\left.+\left(\mu^2+5\mu+8\right)\left(\frac{\psi(b)-\psi(a)m^2}{\psi(a)\psi(b)m}\right)^2+\frac{2\mu(\mu+3)(\psi(a)-\psi(b))}{m(\psi(a)\psi(b))^2}\right]\\
&\quad\le\frac{2^{\mu-\alpha}\Gamma(\mu+1)(\psi(a)\psi(b))^{\mu}}{(\psi(b)-\psi(a)m)^{\mu}}\left[g_2(\eta)I^{\mu,\psi}_{((\psi(b)+m\psi(a))/2)^-}(f\circ\phi)\right.\\
&\quad\cdot\left(\psi^{-1}\left(\frac{m}{\psi(b)}\right)\right)+m^{\mu+1}g_3(\eta)\times(2^{\alpha}-1)I^{\mu}_{((\psi(a)+m\psi(b))/(2\psi(a)\psi(b)m))^+}(f\circ\phi)\\
&\quad\left.\cdot\left(\psi^{-1}\left(\frac{1}{\psi(a)m}\right)\right)\right]\le A^{t^{\alpha},(1-t^{\alpha})}_{1,\mu,m,\eta}(f(\psi(a)),f(\psi(b)))\\
&\quad+B^{t^{\alpha},(1-t)^{\alpha}}_{1,\mu,m,\eta}(f(\psi(a)),f(\psi(b)))-R^{t^{\alpha},(1-t)^{\alpha}}_{1,\mu,m,\eta}\left(\frac{1}{\psi(a)},\frac{1}{\psi(b)}\right).
\end{aligned}\tag{57}$$

Proof. The abovementioned inequality can be deduced by setting $p=-1$ and $h(t)=t$ in (40). □

Corollary 31. *For the strongly exponentially* (s, m)*-HA-convex function, the following inequality holds:*

$$\begin{aligned}
&f\left(\frac{2\psi(a)\psi(b)}{\psi(a)+m\psi(b)}\right)+\frac{cmg_1(\eta)}{2^{2s+2}(\mu+1)(\mu+2)}\left[\mu(\mu+1)\left(\frac{\psi(b)-\psi(a)}{\psi(a)\psi(b)}\right)^2\right.\\
&\quad\left.+\left(\mu^2+5\mu+8\right)\left(\frac{\psi(b)-\psi(a)m^2}{\psi(a)\psi(b)m}\right)^2+\left(\frac{2\mu(\mu+3)(\psi(a)-\psi(b))}{m(\psi(a)\psi(b))^2}\right)\right]\\
&\quad\le\frac{2^{\mu-s}\Gamma(\mu+1)(\psi(a)\psi(b))^{\mu}}{(\psi(b)-\psi(a)m)^{\mu}}\left[g_2(\eta)I^{\mu,\psi}_{((\psi(b)+m\psi(a))/2)^-}(f\circ\phi)\left(\psi^{-1}\left(\frac{m}{\psi(b)}\right)\right)\right.\\
&\quad\left.+m^{\mu+1}g_3(\eta)\times I^{\mu,\psi}_{((\psi(a)+m\psi(b))/(2\psi(a)\psi(b)m))^+}(f\circ\phi)\left(\psi^{-1}\left(\frac{1}{am}\right)\right)\right]\\
&\quad\le A^{t^{s},(1-t)^{s}}_{1,\mu,m,\eta}(f(\psi(a)),f(\psi(b)))+B^{t^{s},(1-t)^{s}}_{1,\mu,m,\eta}(f(\psi(a)),f(\psi(b)))\\
&\quad-R^{t^{s},(1-t)^{s}}_{1,\mu,m,\eta}\left(\frac{1}{\psi(a)},\frac{1}{\psi(b)}\right).
\end{aligned}\tag{58}$$

Proof. The abovementioned inequality can be deduced by setting $p=-1$, $\alpha=1$, and $h(t)=t^s$ in (40). □

Corollary 32. *For the Godunova-Levin type of the strongly exponentially* (s, m)*-HA-convex function, the following inequality holds:*

$$\begin{aligned}
&f\left(\frac{2\psi(a)\psi(b)}{\psi(a)+m\psi(b)}\right)+\frac{cmg_1(\eta)}{2^{2s+2}(\mu+1)(\mu+2)}\left[\mu(\mu+1)\left(\frac{\psi(b)-\psi(a)}{\psi(a)\psi(b)}\right)^2\right.\\
&\quad\left.+\left(\mu^2+5\mu+8\right)\left(\frac{\psi(b)-\psi(a)m^2}{\psi(a)\psi(b)m}\right)^2+\left(\frac{2\mu(\mu+3)(\psi(a)-\psi(b))}{m(\psi(a)\psi(b))^2}\right)\right]\\
&\quad\le\frac{2^{\mu+s}\Gamma(\mu+1)(\psi(a)\psi(b))^{\mu}}{(\psi(b)-\psi(a)m)^{\mu}}\left[g_2(\eta)I^{\mu,\psi}_{((\psi(b)+m\psi(a))/2)^-}(f\circ\phi)\right.\\
&\quad\cdot\left(\psi^{-1}\left(\frac{m}{\psi(b)}\right)\right)+m^{\mu+1}g_3(\eta)I^{\mu}_{((\psi(a)+m\psi(b))/(2\psi(a)\psi(b)m))^+}(f\circ\phi)\\
&\quad\left.\cdot\left(\psi^{-1}\left(\frac{1}{\psi(a)m}\right)\right)\right]\le A^{t^{-s},(1-t)^{-s}}_{1,\mu,m,\eta}(f(\psi(a)),f(\psi(b)))\\
&\quad+B^{t^{-s},(1-t)^{-s}}_{1,\mu,m,\eta}(f(\psi(a)),f(\psi(b)))-R^{t^{-s},(1-t)^{-s}}_{1,\mu,m,\eta}\left(\frac{1}{\psi(a)},\frac{1}{\psi(b)}\right).
\end{aligned}\tag{59}$$

Proof. The abovementioned inequality can be deduced by setting $p=-1$, $\alpha=1$, and $h(t)=t^{-s}$ in (40). □

Remark 33. Using (12) with replacement of μ by μ/k in all the abovementioned inequalities, the k-fractional versions of all the abovementioned results can be obtained.

3. Conclusion

Some inequalities of the Hadamard type for the strongly exponentially $(\alpha, h-m)$-p-convex functions using generalized Riemann-Liouville fractional integrals have been proved. These inequalities give refinements of different Hadamard-type inequalities related to various types of convexities. The outcomes of this paper can also provide the k-fractional versions of established inequalities via parametric substitution along with constant multiplier.

Data Availability

There is no external data required.

Conflicts of Interest

The authors declare that they have no conflicts of interest.

Acknowledgments

The authors thank the National Key Research and Development Program under Grant 2018YFB0904205, Science & Technology Bureau of ChengDu (2020-YF09-00005-SN), Sichuan Science and Technology program (2021YFH0107), and Erasmus + SHYFTE Project (598649-EPP-1-2018-1-FR-EPPKA2-CBHE-JP).

References

[1] S. S. Dragomir and S. Fitzpatrick, "The Hadamard inequalities for s-convex functions in the second sense," *Demonstratio Mathematica*, vol. 32, no. 4, pp. 687–696, 1999.

[2] Z. B. Fang and R. Shi, "On the (p , h) -convex function and some integral inequalities," *Journal of Inequalities and Applications*, vol. 2014, no. 1, 2014.

[3] İ. İşscan, "Hermite-Hadamard type inequalities for harmonically convex functions," *Hacettepe Journal of Mathematics and Statistics*, vol. 6, no. 1014, pp. 935–942, 2014.

[4] İ. İşcan and S. Wu, "Hermite-Hadamard type inequalities for harmonically convex functions via fractional integrals," *Applied Mathematics and Computation*, vol. 238, pp. 237–244, 2014.

[5] M. A. Noor, K. I. Noor, and S. Iftikhar, "Hermite-Hadamard inequalities for strongly harmonic convex functions," *Journal of Inequalities and Special Functions*, vol. 7, no. 3, pp. 99–113, 2016.

[6] G. Farid and H. Yasmeen, "Some fractional integral inequalities for strongly exponentially (α,h-m)-p-convex functions, submitted".

[7] M. Z. Sarikaya, E. Set, H. Yaldiz, and N. Basak, "Hermite-Hadamard's inequalities for fractional integrals and related fractional inequalities," *Mathematical and Computer Modelling*, vol. 57, no. 9-10, pp. 2403–2407, 2013.

[8] M. Z. Sarikaya and H. Yildirim, "On Hermite-Hadamard type inequalities for Riemann-Liouville fractional integrals," *Miskolc Mathematical Notes*, vol. 17, no. 2, pp. 1049–1059, 2017.

[9] S. Mubeen and G. M. Habibullah, "k-Fractional integrals and applications," *International Journal of Contemporary Mathematical Sciences*, vol. 7, pp. 89–94, 2012.

[10] A. A. Kilbas, H. M. Srivastava, and J. J. Trujillo, *Theory and Applications of Fractional Differential Equations*, North-Holland Math. Stud, Elsevier, New York-London, 2006.

[11] A. Akkurt, M. E. Yildirim, and H. Yildirim, "On some integral inequalities for (k,h)-Riemann-Liouville fractional integral," *New Trends in Mathematical Sciences*, vol. 4, no. 2, pp. 138–146, 2016.

[12] K. Miller and B. Ross, *An Introduction to the Fractional Calculus and Fractional Differential Equations*, John Wiley and Sons, Inc., New York, 1993.

[13] S. G. Samko, A. A. Kilbas, and O. I. Marichev, *Fractional Integrals and Derivatives: Theory and Applications, Gordon and Breach, Yverdon*, 1993.

[14] W. Jia, M. Yussouf, G. Farid, and K. A. Khan, "Hadamard and Fejér–Hadamard inequalities forα,h−m−p-convex functions via Riemann–Liouville fractional integrals," *Mathematical Problems in Engineering*, vol. 2021, Article ID 9945114, 12 pages, 2021.

[15] G. Farid, A. U. Rehman, and Q. U. Ain, "Generalized fractional integral inequalities of Hermite–Hadamard type for harmonically convex functions," *Computational Methods for Differential Equations*, vol. 2020, no. 1, pp. 119–140, 2020.

[16] G. Farid, A. U. Rehman, B. Tariq, and A. Waheed, "On Hadamard type inequalities for m-convex functions via fractional integrals," *Journal of Inequalities and Special Functions*, vol. 7, no. 4, pp. 150–167, 2016.

[17] İ. İşscan, "Ostrowski type inequalities for harmonically s -convex functions," *Konuralp Journal of Mathematics*, vol. 3, no. 1, pp. 63–74, 2015.

[18] K. Nonlaopon, G. Farid, M. Yussouf, and E. Bonyah, "New generalized Riemann-Liouville fractional integral versions of Hadamard and Fejér-Hadamard inequalities," *Journal of Mathematics*, vol. 2022, Article ID 8173785, 17 pages, 2022.

[19] M. Kunt and İ. İşscan, "Hermite-Hadamard type inequalities for p-convex functions via fractional integrals," *Moroccan Journal of Pure and Applied Analysis*, vol. 3, no. 1, pp. 22–35, 2017.

[20] G. Farid, A. U. Rehman, and B. Tariq, "On Hadamard-type inequalities for m-convex functions via Riemann-Liouville fractional integrals," *Studia Universitatis Babeş-Bolyai Mathematica*, vol. 62, no. 2, pp. 141–150, 2017.

[21] M. Kunt, İ. İşscan, N. Yazici, and U. Gözütok, "On new inequalities of Hermite-Hadamard-Fejér type for harmonically convex functions via fractional integrals," *Springerplus*, vol. 5, p. 635, 2016.

[22] M. E. Özdemir, "Some inequalities for the s-Godunova–Levin type functions," *The Mathematical Scientist*, vol. 9, no. 1, pp. 27–32, 2015.

[23] M. A. Noor, K. I. Noor, and M. U. Awan, "Integral inequalities for harmonically s-Godunova-Levin functions," *Facta Universitatis. Series: Mathematics and Informatics*, vol. 29, no. 4, pp. 415–424, 2014.

[24] S. Turhan, A. K. Demirel, S. Maden, and İ. İşscan, "Hermite-Hadamard type integral inequalities for trongly p-convex functions," *Turkish Journal of Mathematics and Computer Science*, vol. 10, pp. 184–189, 2018.

[25] N. Merentes and K. Nikodem, "Remarks on strongly convex functions," *Aequationes Math.*, vol. 80, no. 1-2, pp. 193–199, 2010.

Hindawi
Journal of Function Spaces
Volume 2022, Article ID 2754507, 16 pages
https://doi.org/10.1155/2022/2754507

Research Article

Analysis of Fractional-Order Regularized Long-Wave Models via a Novel Transform

Nehad Ali Shah,[1] Essam R. El-Zahar,[2,3] Ali Akgül,[4] Adnan Khan,[5] and Jeevan Kafle[6]

[1]*Department of Mechanical Engineering, Sejong University, Seoul 05006, Republic of Korea*
[2]*Department of Mathematics, College of Science and Humanities in Al-Kharj, Prince Sattam Bin Abdulaziz University, P.O. Box 83, Al-Kharj 11942, Saudi Arabia*
[3]*Department of Basic Engineering Science, Faculty of Engineering, Menoufia University, Shebin El-Kom 32511, Egypt*
[4]*Department of Mathematics, Art and Science Faculty, Siirt University, Siirt 56100, Turkey*
[5]*Department of Mathematics, Abdul Wali Khan University, Mardan 23200, Pakistan*
[6]*Central Department of Mathematics, Tribhuvan University Kritipur, Kathmandu, Nepal*

Correspondence should be addressed to Jeevan Kafle; jeevan.kafle@cdmath.tu.edu.np

Received 8 April 2022; Revised 12 May 2022; Accepted 24 May 2022; Published 6 June 2022

Academic Editor: Yusuf Gurefe

A new integral transform method for regularized long-wave (RLW) models having fractional-order is presented in this study. Although analytical approaches are challenging to apply to such models, semianalytical or numerical techniques have received much attention in the literature. We propose a new technique combining integral transformation, the Elzaki transform (ET), and apply it to regularized long-wave equations in this study. The RLW equations describe ion-acoustic waves in plasma and shallow water waves in seas. The results obtained are extremely important and necessary for describing various physical phenomena. This work considers an up-to-date approach and fractional operators in this context to obtain satisfactory approximate solutions to the proposed problems. We first define the Elzaki transforms of the Caputo fractional derivative (CFD) and Atangana-Baleanu fractional derivative (ABFD) and implement them for solving RLW equations. We can readily obtain numerical results that provide us with improved approximations after only a few iterations. The derived solutions were found to be in close contact with the exact solutions. Furthermore, the suggested procedure has attained the best level of accuracy. In fact, when compared to other analytical techniques for solving nonlinear fractional partial differential equations, the present method might be considered one of the finest.

1. Introduction

Fractional calculus (FC) is a model discipline of mathematics that focuses entirely on fractional-order derivatives and integration. Fractional derivatives and fractional integrations are noninteger-order derivatives and integration that can model various phenomena in engineering and science. FC began in 1695 when L'Hospital asked Leibniz, "What would be the physical meaning of fractional derivative?" This question inspired many great scientists in the eighteenth and nineteenth centuries to focus on fractional calculus, which has a wide range of applications in applied science and technology. Many researchers have demonstrated that fractional generalizations of integer-order models efficiently represent natural phenomena [1–5]. The classical derivatives are local. In contrast, the Caputo fractional derivative is nonlocal, i.e., we can study changes in the neighborhood of a point using classical derivatives. Still, we may analyze changes in an interval using Caputo fractional derivatives. Because of this quality, the Caputo fractional derivative can be used to model a wider range of physical phenomena, including solid mechanics [6, 7], diffusion procedures [8], continuum and statistical mechanics [9], electromagnetism [10], viscoelastic materials [11], fluid mechanics [12], propagation of spherical flames [13], viscoelastic materials [14], and so on [15–17].

Fractional differential equations have been studied for decades due to their widespread application in science and engineering. Fractional partial differential equations are used to describe various phenomena in acoustics, electromagnetics, material science, viscoelasticity, electrochemistry, and plasma physics. Fractional differential equations have numerical solutions that are of great interest. For fractional differential equations, no method provides an accurate solution. Only series solution methods or linearization can generate approximate solutions [18–21]. Nonlinear phenomena can be found in various engineering and science domains, including chemical kinetics, nonlinear spectroscopy, solid state physics, fluid physics, computational biology, quantum mechanics, and thermodynamics. Different higher-order nonlinear partial differential equations (PDEs) define the idea of nonlinearity. Nonlinear models for all physical systems describe basic phenomena. The literature has presented integrative transform approaches for solving fractional differential equations. Elzaki transform (ET) is an integral transform [22] in this context. Several scholars [23–30] have looked at some essential solution approaches for real-world issues, as well as numerical simulations obtained using the novel integral transformation.

In this article, three alternative fractional homogeneous RLW equations are studied; the RLW equations, according to some scientists, are the best equations than the classical Korteweg-de Vries (KdV) equation [31]. We use the Elzaki transform combined with the CFD and ABC operator [32] to solve three special RLW problems. The approximate solutions are then obtained, and the numerical simulations of the solutions are analyzed [33, 34] and provided the nonlinear RLW equations.

$$D^{\delta}_{\mathfrak{I}}\varphi(\psi,\mathfrak{I}) - \varphi_{\psi\psi\mathfrak{I}}(\psi,\mathfrak{I}) + \varphi_{\psi}(\psi,\mathfrak{I}) + \varphi(\psi,\mathfrak{I})\varphi_{\psi}(\psi,\mathfrak{I}) = 0, \tag{1}$$

having initial source

$$\varphi(\psi,0) = 3\alpha \sec h^2(\delta\zeta), \tag{2}$$

$$\mathrm{D}^{\delta}_{\mathfrak{I}}\varphi(\psi,\mathfrak{I}) - 2\varphi_{\psi\psi\mathfrak{I}}(\psi,\mathfrak{I}) + \varphi_{\psi}(\psi,\mathfrak{I}) = 0, \tag{3}$$

having initial source

$$\varphi(\psi,0) = \mathrm{e}^{-\psi}, \tag{4}$$

$$\mathrm{D}^{\delta}_{\mathfrak{I}}\varphi(\psi,\mathfrak{I}) + \varphi_{\psi\psi\psi\psi}(\psi,\mathfrak{I}) = 0, \tag{5}$$

having initial source

$$\varphi(\psi,0) = \sin\psi. \tag{6}$$

Equation (1) is known as a general regularized long-wave equation (GRLWE) having fractional-order, whereas Equations (3) and (5) represents fractional regularized long-wave equations (RLWEs).

Magnetohydrodynamic waves in plasma, ion-acoustic waves in plasma, stress waves in compressed gas bubble mixes, rotating tube flow, and longitudinal dispersive waves in elastic rods are just some of the applications of the RLW equations. The RLW equations are suitable models for many significant physical structures in applied physics and engineering. They also work on a variety of liquid flow phenomena where diffusion is essential, such as in viscous or shock situations. It can be used to simulate any nonlinear wave diffusion problem, including dissipation. Depending on the problem modeling [35], this dissipation could result in heat conduction, viscosity, thermal radiation, chemical reaction, mass diffusion, or other sources. Many necessary ocean research and engineering phenomena, such as minor frequency shallow-water waves and long-waves, are defined by fractional RLW equations. Several experts in ocean shallow liquid waves are interested in nonlinear waves described using the RLW equations having fractional-order. The fractional RLW equations were used to represent nonlinear waves in the ocean. Indeed, the tsunami's massive surface waves are defined by fractional RLW equations. Huge internal waves in the ocean's interior caused by temperature differences that can destroy marine ships could be defined as fractional RLW equations in the existing, exceedingly complex framework.

The article is given as follows: In Section 2, some basic definitions are essential for the formulation of the problem. The method is described in Section 3, using a novel integral transformation. Section 4 presents the main results, numerical simulations, and graphical representations. Finally, Section 5 presents all of the research study's significant findings.

2. Preliminaries

The fundamental concepts with and without a singular kernel of fractional derivatives, fractional integrals, and their Elzaki transform are presented in this section.

Definition 1. The Caputo fractional derivative (CFD) is defined as [1]

$$^{C}D^{\delta}_{\mathfrak{I}}(\mu(\mathfrak{I})) = \begin{cases} \dfrac{1}{\Gamma(m-\delta)}\displaystyle\int_0^{\mathfrak{I}} \dfrac{\mu^m(\eta)}{(\mathfrak{I}-\eta)^{\delta+1-m}}d\eta, m-1<\delta<m, \\ \dfrac{d^m}{d\mathfrak{I}^m}\mu(\mathfrak{I}), \delta = m. \end{cases} \tag{7}$$

Definition 2. The Atangana-Baleanu derivative having fractional-order in the Caputo manner (ABC) is defined as [36]

$$^{ABC}\mathrm{D}^{\delta}_{\mathfrak{I}}(\mu(\mathfrak{I})) = \frac{\mathrm{N}(\delta)}{1-\delta}\int_{\mathrm{m}}^{\mathfrak{I}}\mu'(\eta)\mathrm{E}_{\delta}\left[-\frac{\delta(\mathfrak{I}-\eta)^{\delta}}{1-\delta}\right]d\eta, \tag{8}$$

where $\mu \in H^1(\alpha,\beta), \beta>\alpha, \delta\in[0,1]$. A normalization function equal to 1 when $\delta=0$ and $\delta=1$ is represented by $N(\delta)$ in Equation (8).

Definition 3. The ABC operator fractional integral is given by [36].

$$I_{\mathfrak{J}}^{\delta}(\mu(\mathfrak{J})) = \frac{1-\delta}{N(\delta)}\mu(\mathfrak{J}) + \frac{\delta}{\Gamma(\delta)N(\delta)}\int_{m}^{\mathfrak{J}}\mu(\eta)(\mathfrak{J}-\eta)^{\delta-1}d\eta. \quad (9)$$

Definition 4. In set A, the exponential function Elzaki transform is defined as [37, 38]

$$A = \left\{\mu(\mathfrak{J}): \exists G, p_1, p_2 > 0, |\mu(\mathfrak{J})| < Ge^{|\mathfrak{J}|/p_j}, \text{if} \quad \mathfrak{J} \in (-1)^j \times [0,\infty)\right\}. \quad (10)$$

G is a finite number for a specific function in the set, but p_1, p_2 can be finite or infinite.

Definition 5. The Elzaki transformation of a function $\mu(\mathfrak{J})$ is given by [38].

$$\mathscr{E}\{\mu(\mathfrak{J})\}(\varpi) = \tilde{U}(\varpi) = \varpi\int_{0}^{\infty}e^{-\mathfrak{J}/\varpi}\mu(\mathfrak{J})d\mathfrak{J}, \quad (11)$$

where $\mathfrak{J} \geq 0, \mathrm{p}_1 \leq \varpi \leq \mathrm{p}_2$.

Theorem 6 (Elzaki transformation convolution theorem, [39]). *The following equality holds:*

$$\mathscr{E}\{\mu * \nu\} = \frac{1}{\varpi}\mathscr{E}(\mu)\mathscr{E}(\nu), \quad (12)$$

where Elzaki transform is represented by $\mathscr{E}\{.\}$.

Definition 7. The Elzaki transform of the CFD operator $D_{\mathfrak{J}}^{\delta}(\mu(\mathfrak{J}))$ is given by [40].

$$\mathscr{E}\left\{{}^{C}D_{\mathfrak{J}}^{\delta}(\mu(\mathfrak{J}))\right\}(\varpi) = \varpi^{-\delta}\tilde{U}(\varpi) - \sum_{k=0}^{m-1}\varpi^{2-\delta+k}\mu^{k}(0), \quad (13)$$

where $m-1 < \delta < m$.

Theorem 8. *The ABC fractional derivative* $D_{\mathfrak{J}}^{\delta}(\mu(\mathfrak{J}))$ *Elzaki transform is defined as [32].*

$$\mathscr{E}\left\{{}^{ABC}D_{\mathfrak{J}}^{\delta}(\mu(\mathfrak{J}))\right\}(\varpi) = \frac{N(\delta)\varpi}{\delta\varpi^{\delta}+1-\delta}\left(\frac{\tilde{U}(\varpi)}{\varpi} - \varpi\mu(0)\right), \quad (14)$$

where $\mathscr{E}\{\mu(\mathfrak{J})\}\varpi = \tilde{U}(\varpi)$.

Proof. From Definition 2, we have

$$\mathscr{E}\left\{{}^{ABC}D_{\mathfrak{J}}^{\delta}(\mu(\mathfrak{J}))\right\}(\varpi) = \mathscr{E}\left\{\frac{N(\delta)}{1-\delta}\int_{0}^{\mathfrak{J}}\mu'(\eta)E_{\delta}\left[-\frac{\delta(\mathfrak{J}-\eta)^{\delta}}{1-\delta}\right]d\eta\right\}(\varpi). \quad (15)$$

Then, taking into account the Elzaki transform's definition and convolution, we get

$$\begin{aligned}\mathscr{E}\left\{{}^{ABC}D_{\mathfrak{J}}^{\delta}(\mu(\mathfrak{J}))\right\}(\varpi) &= \mathscr{E}\left\{\frac{N(\delta)}{1-\delta}\int_{0}^{\mathfrak{J}}\mu'(\eta)E_{\delta}\left[-\frac{\delta(\mathfrak{J}-\eta)^{\delta}}{1-\delta}\right]d\eta\right\} \\ &= \frac{N(\delta)}{1-\delta}\frac{1}{\varpi}\mathscr{E}\left\{\mu'(\eta)\right\}\mathscr{E}\left\{E_{\delta}\left[-\frac{\delta\mathfrak{J}^{\delta}}{1-\delta}\right]d\eta\right\} \\ &= \frac{N(\delta)}{1-\delta}\left[\frac{\tilde{U}(\varpi)}{\varpi} - \varpi\mu(0)\right] \\ &\quad \cdot \left[\int_{0}^{\infty}e^{-1/\varpi}E_{\delta}\left[-\frac{\delta\mathfrak{J}^{\delta}}{1-\delta}\right]d\mathfrak{J}\right] \\ &= \frac{N(\delta)\varpi}{\delta\varpi^{\delta}+1-\delta}\left[\frac{\tilde{U}(\varpi)}{\varpi} - \varpi\mu(0)\right].\end{aligned} \quad (16)$$

□

3. Description of the Technique via a New Integral Transform

The essential technique that was employed in this research will be presented in this section of the study. We use the following fractional nonlinear PDE general form to study this methodology:

$$\begin{gathered} D_{\mathfrak{J}}^{\delta}\varphi(\psi,\mathfrak{J}) + L(\varphi(\psi,\mathfrak{J})) + N(\varphi(\psi,\mathfrak{J})) = \theta(\psi,\mathfrak{J}), \\ (\psi,\mathfrak{J}) \in [0,1]\times[0,T], \quad \kappa-1 < \delta < \kappa, \end{gathered} \quad (17)$$

having initial source

$$\frac{\partial^{z}\varphi}{\partial\mathfrak{J}^{z}}(\psi,0) = \mu_{z}(\psi), \quad z = 0, 1, \cdots, \kappa-1, \quad (18)$$

and the boundary sources

$$\begin{aligned}\varphi(0,\mathfrak{J}) &= \gamma_0(\mathfrak{J}), \\ \varphi(1,\mathfrak{J}) &= \gamma_1(\mathfrak{J}), \\ \mathfrak{J} &\geq 0,\end{aligned} \quad (19)$$

where known functions are μ_z, θ, γ_0, and γ_1. In Equation (17), $D_{\mathfrak{J}}^{\delta}\varphi(\psi,\mathfrak{J})$ represents the Caputo or ABC fractional derivatives, $L(.)$ and $N(.)$ denote the linear and nonlinear terms. The recursive steps for handling the specified problems are described (1)-(2), (3)-(4), and (5)-(6). We investigate $E\{\varphi(\psi,\mathfrak{J})\}(\varpi) = \tilde{\zeta}(\psi,\varpi)$ for Equation (17) by taking the Elzaki transform with the aid of CFD in Equation (13) and ABC in Equation (14). The modified functions for the Caputo fractional derivative can then be obtained.

$$\tilde{\zeta}(\psi,\varpi)=\varpi^{\delta}\left(\widetilde{\theta}(\varpi,\mathfrak{I})-\mathscr{E}[L(\varphi(\psi,\mathfrak{I}))+N(\varphi(\psi,\mathfrak{I}))]\right)+\varpi^{2}\varphi(\psi,0). \tag{20}$$

We also get the modified functions for the ABC derivative, which are as follows.

$$\tilde{\zeta}(\psi,\varpi)=\left(\frac{\delta\varpi^{\delta}+1-\delta}{N(\delta)}\right)\left(\widetilde{\theta}(\psi,\varpi)-\mathscr{E}[L(\varphi(\psi,\mathfrak{I}))+N(\varphi(\psi,\mathfrak{I}))]\right)+\varpi^{2}\varphi(\psi,0), \tag{21}$$

where $\mathscr{E}[\theta(\psi,\mathfrak{I})]=\widetilde{\theta}(\psi,\varpi)$. We also get when we consider the Elzaki transforms of the boundary conditions

$$\begin{aligned}\mathscr{E}[\gamma_0(\mathfrak{I})]&=\tilde{\zeta}(0,\varpi),\\ \mathscr{E}[\gamma_1(\mathfrak{I})]&=\tilde{\zeta}(1,\varpi),\\ \varpi&\geq 0.\end{aligned} \tag{22}$$

The solution to Equations (17)–(19) is then obtained by using the perturbation method as

$$\tilde{\zeta}(\psi,\varpi)=\sum_{\mathscr{E}=0}^{\infty}\mathscr{X}^{\mathscr{E}}\tilde{\zeta}_{\mathscr{E}}(\psi,\varpi),\ \mathscr{E}=0,1,2,\cdots. \tag{23}$$

The nonlinear component in Equation (17) can be calculated as

$$N[\varphi(\psi,\mathfrak{I})]=\sum_{\mathscr{E}=0}^{\infty}\mathscr{X}^{\mathscr{E}}\Psi_{\mathscr{E}}(\psi,\mathfrak{I}), \tag{24}$$

and the parts $\Psi_{\mathscr{E}}(\psi,\mathfrak{I})$ are define in as

$$\Psi_{\mathscr{E}}(\varphi_0,\varphi_1,\cdots,\varphi_{\mathscr{E}})=\frac{1}{\mathscr{E}!}\frac{\partial^{\mathscr{E}}}{\partial\nu^{\mathscr{E}}}\left[N\left(\sum_{i=0}^{\infty}\nu^{i}\varphi_i\right)\right]_{\lambda=0},\ \mathscr{E}=0,1,2,\cdots. \tag{25}$$

By putting Equations (23) and (24) into Equation (20), we obtain the components of the Caputo operator's solution:

$$\begin{aligned}\sum_{\mathscr{E}=0}^{\infty}\mathscr{X}^{\mathscr{E}}\tilde{\zeta}(\psi,\varpi)=&-\mathscr{X}\varpi^{\delta}\left(\mathscr{E}\left[L\left(\sum_{\mathscr{E}=0}^{\infty}\mathscr{X}^{\mathscr{E}}\varphi_{\mathscr{E}}(\psi,\mathfrak{I})\right)+\sum_{\mathscr{E}=0}^{\infty}\mathscr{X}^{\mathscr{E}}\Psi_{\mathscr{E}}(\psi,\mathfrak{I})\right]\right)\\&+\varpi^{\delta}\left(\widetilde{\theta}(\psi,\varpi)\right)+\varpi^{2}\varphi(\psi,0).\end{aligned} \tag{26}$$

and by putting Equations (23) and (24) into Equation (21), we have the recursive relation that provides the Atangana-Baleanu operator's solution:

$$\begin{aligned}\sum_{\mathscr{E}=0}^{\infty}\mathscr{X}^{\mathscr{E}}\tilde{\zeta}(\psi,\varpi)=&-\mathscr{X}\left(\frac{\delta\varpi^{\delta}+1-\delta}{N(\delta)}\right)\left(\mathscr{E}\left[L\left(\sum_{\mathscr{E}=0}^{\infty}\mathscr{X}^{\mathscr{E}}\varphi_{\mathscr{E}}(\psi,\mathfrak{I})\right)+\sum_{\mathscr{E}=0}^{\infty}\mathscr{X}^{\mathscr{E}}\Psi_{\mathscr{E}}(\psi,\mathfrak{I})\right]\right)\\&+\left(\frac{\delta\varpi^{\delta}+1-\delta}{N(\delta)}\right)\left(\widetilde{\theta}(\psi,\varpi)\right)+\varpi^{2}\varphi(\psi,0).\end{aligned} \tag{27}$$

Thus, on solving Equations (26) and (27) with respect to $\mathscr{X}$, the given Caputo homotopies are identified:

$$\begin{aligned}\mathscr{X}^{0}&:\tilde{\zeta}_0(\psi,\varpi)=\varpi^{\delta}\left(\widetilde{\theta}(\psi,\varpi)\right)+\varpi^{2}\varphi(\psi,0),\\ \mathscr{X}^{1}&:\tilde{\zeta}_1(\psi,\varpi)=-\varpi^{\delta}\mathscr{E}[L(\varphi_0(\psi,\mathfrak{I}))+\Psi_0(\psi,\mathfrak{I})],\\ \mathscr{X}^{2}&:\tilde{\zeta}_2(\psi,\varpi)=-\varpi^{\delta}\mathscr{E}[L(\varphi_1(\psi,\mathfrak{I}))+\Psi_1(\psi,\mathfrak{I})],\\ &\vdots\\ \mathscr{X}^{n+1}&:\tilde{\zeta}_{n+1}(\psi,\varpi)=-\varpi^{\delta}\mathscr{E}[L(\varphi_n(\psi,\mathfrak{I}))+\Psi_n(\psi,\mathfrak{I})].\end{aligned} \tag{28}$$

Furthermore, we determine the ABC homotopies as follows:

$$\begin{aligned}\mathscr{X}^{0}&:\tilde{\zeta}_0(\psi,\varpi)=\left(\frac{\delta\varpi^{\delta}+1-\delta}{N(\delta)}\right)\widetilde{\theta}(\psi,\varpi)+\varpi^{2}\varphi(\psi,0),\\ \mathscr{X}^{1}&:\tilde{\zeta}_1(\psi,\varpi)=-\left(\frac{\delta\varpi^{\delta}+1-\delta}{N(\delta)}\right)\mathscr{E}[L(\varphi_0(\psi,\mathfrak{I}))+\Psi_0(\psi,\mathfrak{I})],\\ \mathscr{X}^{2}&:\tilde{\zeta}_2(\psi,\varpi)=-\left(\frac{\delta\varpi^{\delta}+1-\delta}{N(\delta)}\right)\mathscr{E}[L(\varphi_1(\psi,\mathfrak{I}))+\Psi_1(\psi,\mathfrak{I})],\\ &\vdots\\ \mathscr{X}^{n+1}&:\tilde{\zeta}_{n+1}(\psi,\varpi)=-\left(\frac{\delta\varpi^{\delta}+1-\delta}{N(\delta)}\right)\mathscr{E}[L(\varphi_n(\psi,\mathfrak{I}))+\Psi_n(\psi,\mathfrak{I})].\end{aligned} \tag{29}$$

When $\mathscr{X}\longrightarrow 1$, we can assume that Equations (28) and (29) represent the approximate solution to Equations (26) and (27); thus, the result is determined by

$$\Delta_n(\psi,\varpi)=\sum_{\sigma=0}^{n}\tilde{\zeta}_{\sigma}(\psi,\varpi). \tag{30}$$

We get the approximate solution of Equation (17), by taking the inverse ET to Equation (30).

$$\varphi(\psi,\varpi)\cong\varphi_n(\psi,\mathfrak{I})=\mathscr{E}^{-1}\left|\{\Delta_n(\psi,\varpi)\}\right.. \tag{31}$$

4. Applications

In this part, we will examine the problems in Equations (1)–(6) by means of Elzaki transform. First, we implement the Elzaki transform technique with the aid of Caputo derivative to solve problem (1) having initial source (2). By taking the Elzaki transform, we get

$$\tilde{\zeta}(\psi, \varpi) = \varpi^{\delta}\mathscr{E}\left[\varphi_{\psi\psi\mathfrak{J}}(\psi, \mathfrak{J}) - \varphi_{\psi}(\psi, \mathfrak{J}) - \varphi(\psi, \mathfrak{J})\varphi_{\psi}(\psi, \mathfrak{J})\right] + \varpi^2\varphi(\psi, 0). \tag{32}$$

We use the Elzaki perturbation transform approach to solve Equation (32) and obtain

$$\begin{aligned}\sum_{\mathscr{E}=0}^{\infty}\mathscr{X}^{\mathscr{E}}\tilde{\zeta}_{\mathscr{E}}(\psi, \varpi) = \mathscr{X}\varpi^{\delta}\mathscr{E}&\left[\left(\sum_{\mathscr{E}=0}^{\infty}\mathscr{X}^{\mathscr{E}}\varphi_{\mathscr{E}}(\psi, \mathfrak{J})\right)_{\psi\psi\mathfrak{J}}\right.\\ &\left.-\left(\sum_{\mathscr{E}=0}^{\infty}\mathscr{X}^{\mathscr{E}}\varphi_{\mathscr{E}}(\psi, \mathfrak{J})\right)_{\psi}\right]\\ &-\mathscr{X}\varpi^{\delta}\mathscr{E}\left[\left(\sum_{\mathscr{E}=0}^{\infty}\mathscr{X}^{\mathscr{E}}\Psi_{\mathscr{E}}(\psi, \mathfrak{J})\right)\right] + \varpi^2\varphi(\psi, 0).\end{aligned} \tag{33}$$

We now have by taking the Elzaki inverse transform to Equation (33),

$$\begin{aligned}\sum_{\mathscr{E}=0}^{\infty}\mathscr{X}^{\mathscr{E}}\varphi_{\mathscr{E}}(\psi, \varpi) = \mathscr{X}\mathscr{E}^{-1}&\left[\varpi^{\delta}\mathscr{E}\left[\left(\sum_{\mathscr{E}=0}^{\infty}\mathscr{X}^{\mathscr{E}}\varphi_{\mathscr{E}}(\psi, \mathfrak{J})\right)_{\psi\psi\mathfrak{J}}\right.\right.\\ &\left.\left.-\left(\sum_{\mathscr{E}=0}^{\infty}\mathscr{X}^{\mathscr{E}}\varphi_{\mathscr{E}}(\psi, \mathfrak{J})\right)_{\psi}\right]\right]\\ &-\mathscr{X}\mathscr{E}^{-1}\left[\varpi^{\delta}\mathscr{E}\left[\left(\sum_{\mathscr{E}=0}^{\infty}\mathscr{X}^{\mathscr{E}}\Psi_{\mathscr{E}}(\psi, \mathfrak{J})\right)\right]\right]\\ &+\mathscr{E}^{-1}\left[\varpi^2\varphi(\psi, 0)\right].\end{aligned} \tag{34}$$

The $\Psi_{\mathscr{E}}(.)$ values in Equation (34) are functions that indicate the nonlinear terms assumed in Equation (26) and are analyzed as follows:

$$\begin{aligned}\Psi_0(\varphi) &= \varphi_0(\varphi_0)_{\psi},\\ \Psi_1(\varphi) &= \varphi_0(\varphi_1)_{\psi} + \varphi_1(\varphi_0)_{\psi},\\ \Psi_2(\varphi) &= \varphi_0(\varphi_2)_{\psi} + \varphi_1(\varphi_1)_{\psi} + \varphi_2(\varphi_0)_{\psi},\\ &\vdots\end{aligned} \tag{35}$$

Then, by examining the associated powers of $\mathscr{X}$, we obtain the terms of the Caputo operator solution:

$$\mathscr{X}^0 : \tilde{\zeta}_0(\psi, \mathfrak{J}) = \mathscr{E}^{-1}\left[\varpi^2 3\alpha \sec h^2(\delta\psi)\right] = 3\alpha \sec h^2(\delta\psi),$$

$$\begin{aligned}\mathscr{X}^1 : \tilde{\zeta}_1(\psi, \mathfrak{J}) &= \mathscr{E}^{-1}\left[\varpi^{\delta}\mathscr{E}[\mathrm{L}(\varphi_0(\psi, \mathfrak{J}))]\right] - \mathscr{E}^{-1}\left[\varpi^{\delta}\mathscr{E}[\Psi_0(\psi, \mathfrak{J})]\right]\\ &= 3\alpha\delta\{1 + 6\alpha\delta + \cos h(2\delta\psi)\} \sec h^4(\delta\psi) \tan h(\delta\psi)\frac{\mathfrak{J}^{\delta}}{\Gamma(\delta+1)},\end{aligned}$$

$$\begin{aligned}\mathscr{X}^2 : \tilde{\zeta}_2(\psi, \mathfrak{J}) &= \mathscr{E}^{-1}\left[\varpi^{\delta}\mathscr{E}[L(\varphi_1(\psi, \mathfrak{J}))]\right] - \mathscr{E}^{-1}\left[\varpi^{\delta}\mathscr{E}[\Psi_1(\psi, \mathfrak{J})]\right]\\ &= -\frac{3}{32}\alpha\delta^2\{-8 - 96\alpha - 576\alpha^2\\ &\quad + 3(-3 - 16\alpha + 144\alpha^2) \cos h(2\delta\psi)\\ &\quad + 48\alpha \cos h(4\delta\psi)\\ &\quad + \cos h(6\delta\psi)\} \sec h^8(\delta\psi)\frac{\mathfrak{J}^{2\delta}}{\Gamma(2\delta+1)},\\ &\vdots\end{aligned} \tag{36}$$

As a result, the approximate solution to the problem is

$$\begin{aligned}\varphi(\psi, \mathfrak{J}) = \Bigg(&3\alpha \sec \mathrm{h}^2(\delta\psi) + 3\alpha\delta\{1 + 6\alpha\delta\\ &+ \cos h(2\delta\psi)\} \sec \mathrm{h}^4(\delta\psi) \tan h(\delta\psi)\frac{\mathfrak{J}^{\delta}}{\Gamma(\delta+1)}\\ &- \frac{3}{32}\alpha\delta^2\{-8 - 96\alpha - 576\alpha^2 + 3(-3 - 16\alpha + 144\alpha^2) \cosh(2\delta\psi)\\ &+ 48\alpha \cosh(4\delta\psi) + \cosh(6\delta\psi)\} \sec \mathrm{h}^8(\delta\psi)\frac{\mathfrak{J}^{2\delta}}{\Gamma(2\delta+1)}, +\cdots\Bigg),\end{aligned} \tag{37}$$

providing the problem's integer-order $(\delta = 1)$ solution, $\varphi(\psi, \mathfrak{J}) = 3\alpha \sec \mathrm{h}^2(\delta(\psi - (1+\alpha)\mathfrak{J}))$.

On the other hand, we use the Elzaki transform in combination with the Atangana-Baleanu operator to solve the problem. First, we use the Elzaki transform to solve the problem:

$$\begin{aligned}\tilde{\zeta}(\psi, \varpi) = &\left(\frac{\delta\varpi^{\delta} + 1 - \delta}{N(\delta)}\right)\mathscr{E}\left[\varphi_{\psi\psi\mathfrak{J}}(\psi, \mathfrak{J}) - \varphi_{\psi}(\psi, \mathfrak{J}) - \varphi(\psi, \mathfrak{J})\varphi_{\psi}(\psi, \mathfrak{J})\right]\\ &+ \varpi^2\varphi(\psi, 0).\end{aligned} \tag{38}$$

To Equation (38), we use the Elzaki perturbation transform approach and get

$$\begin{aligned}\sum_{\mathscr{E}=0}^{\infty}\mathscr{X}^{\mathscr{E}}\tilde{\zeta}_{\mathscr{E}}(\psi, \varpi) = \mathscr{X}&\left(\frac{\delta\varpi^{\delta} + 1 - \delta}{N(\delta)}\right)\mathscr{E}\\ &\cdot\left[\left(\sum_{\mathscr{E}=0}^{\infty}\mathscr{X}^{\mathscr{E}}\varphi_{\mathscr{E}}(\psi, \mathfrak{J})\right)_{\psi\psi\mathfrak{J}} - \left(\sum_{\mathscr{E}=0}^{\infty}\mathscr{X}^{\mathscr{E}}\varphi_{\mathscr{E}}(\psi, \mathfrak{J})\right)_{\psi}\right]\\ &-\mathscr{X}\left(\frac{\delta\varpi^{\delta} + 1 - \delta}{N(\delta)}\right)\mathscr{E}\left[\left(\sum_{\mathscr{E}=0}^{\infty}\mathscr{X}^{\mathscr{E}}\Psi_{\mathscr{E}}(\psi, \mathfrak{J})\right)\right] + \varpi^2\varphi(\psi, 0).\end{aligned} \tag{39}$$

By taking the inverse ET of Equation (39), we get

$$\sum_{\mathscr{E}=0}^{\infty} \mathscr{X}^{\mathscr{E}} \varphi_{\mathscr{E}}(\psi, \mathfrak{J}) = \mathscr{X}\mathscr{E}^{-1}\left[\left(\frac{\delta\varpi^{\delta}+1-\delta}{N(\delta)}\right)\mathscr{E}\left[\left(\sum_{\mathscr{E}=0}^{\infty} \mathscr{X}^{\mathscr{E}} \varphi_{\mathscr{E}}(\psi, \mathfrak{J})\right)_{\psi\psi\mathfrak{J}} - \left(\sum_{\mathscr{E}=0}^{\infty} \mathscr{X}^{\mathscr{E}} \varphi_{\mathscr{E}}(\psi, \mathfrak{J})\right)_{\psi}\right]\right] - \mathscr{X}\mathscr{E}^{-1}\left[\left(\frac{\delta\varpi^{\delta}+1-\delta}{N(\delta)}\right)\mathscr{E}\left[\left(\sum_{\mathscr{E}=0}^{\infty} \mathscr{X}^{\mathscr{E}} \Psi_{\mathscr{E}}(\psi, \mathfrak{J})\right)\right]\right] + \mathscr{E}^{-1}\left[\varpi^{2}\varphi(\psi, 0)\right]. \tag{40}$$

The $\Psi_{\mathscr{E}}(.)$ terms in Equation (40) are nonlinear polynomials that were described in Equation (25). We derive the following results by repeating the methods for nonlinear polynomials:

$$\mathscr{X}^{0} : \varphi_{0}(\psi, \mathfrak{J}) = \mathscr{E}^{-1}\left[\varpi^{2} 3\alpha \sec\text{h}^{2}(\delta\psi)\right] = 3\alpha \sec\text{h}^{2}(\delta\psi),$$

$$\mathscr{X}^{1} : \varphi_{1}(\psi, \mathfrak{J}) = \mathscr{E}^{-1}\left[\left(\frac{\delta\varpi^{\delta}+1-\delta}{N(\delta)}\right)\mathscr{E}[\varphi_{0}(\psi, \mathfrak{J})]\right] - \mathscr{E}^{-1}\left[\left(\frac{\delta\varpi^{\delta}+1-\delta}{N(\delta)}\right)\mathscr{E}[\Psi_{0}(\psi, \mathfrak{J})]\right] = -\frac{3\alpha\delta\{1+6\alpha\delta+\cosh(2\delta\psi)\}\sec\text{h}^{4}(\delta\psi)\tanh(\delta\psi)}{N(\delta)}\left(\frac{\delta\mathfrak{J}^{\delta}}{\Gamma(\delta+1)}+1-\delta\right), \tag{41}$$

$$\mathscr{X}^{2} : \varphi_{2}(\psi, \mathfrak{J}) = \mathscr{E}^{-1}\left[\left(\frac{\delta\varpi^{\delta}+1-\delta}{N(\delta)}\right)\mathscr{E}[\varphi_{1}(\psi, \mathfrak{J})]\right] - \mathscr{E}^{-1}\left[\left(\frac{\delta\varpi^{\delta}+1-\delta}{N(\delta)}\right)\mathscr{E}[\Psi_{1}(\psi, \mathfrak{J})]\right] = -\frac{-3/32\alpha\delta^{2}\left\{-8-96\alpha-576\alpha^{2}+3\left(-3-16\alpha+144\alpha^{2}\right)\cosh(2\delta\psi)+48\alpha\cosh(4\delta\psi)+\cosh(6\delta\psi)\right\}\sec\text{h}^{8}(\delta\psi)}{(N(\delta))^{2}} \cdot \left(\frac{\left(\delta\mathfrak{J}^{\delta}\right)^{2}}{\Gamma(2\delta+1)}+\frac{2\delta(1-\delta)\mathfrak{J}^{\delta}}{\Gamma(\delta+1)}+(1-\delta)^{2}\right), \quad \vdots \tag{42}$$

As a result, based on the ABC operator, the approximate solution is as follows:

$$\varphi(\psi, \mathfrak{J}) = \sum_{\sigma=0}^{n} \varphi_{\sigma}(\psi, \mathfrak{J}) = 3\alpha\sec\text{h}^{2}(\delta\psi) - \frac{3\alpha\delta\{1+6\alpha\delta+\cosh(2\delta\psi)\}\sec\text{h}^{4}(\delta\psi)\tanh(\delta\psi)}{N(\delta)}\left(\frac{\delta\mathfrak{J}^{\delta}}{\Gamma(\delta+1)}+1-\delta\right) - \frac{-3/32\alpha\delta^{2}\left\{-8-96\alpha-576\alpha^{2}+3\left(-3-16\alpha+144\alpha^{2}\right)\cosh(2\delta\psi)+48\alpha\cosh(4\delta\psi)+\cosh(6\delta\psi)\right\}\sec\text{h}^{8}(\delta\psi)^{2}}{(N(\delta))^{2}} \cdot \left(\frac{\left(\delta\mathfrak{J}^{\delta}\right)^{2}}{\Gamma(2\delta+1)}+\frac{2\delta(1-\delta)\mathfrak{J}^{\delta}}{\Gamma(\delta+1)}+(1-\delta)^{2}\right)+\cdots, \tag{43}$$

providing the problem's integer-order ($\delta = 1$) solution, $\varphi(\psi, \mathfrak{T}) = 3\alpha \sec h^2(\delta(\psi - (1+\alpha)\mathfrak{T}))$.

Secondly, we implement the Elzaki transform technique with the aid of Caputo derivative to solve problem (3) having initial source (4). By taking the Elzaki transform, we get

$$\tilde{\zeta}(\psi, \varpi) = \varpi^\delta \mathscr{E}\left[2\varphi_{\psi\psi\mathfrak{T}}(\psi, \mathfrak{T}) - \varphi_\psi(\psi, \mathfrak{T})\right] + \varpi^2 \varphi(\psi, 0). \tag{44}$$

We use the Elzaki perturbation transform approach to solve Equation (44) and obtain

$$\sum_{\mathscr{E}=0}^{\infty} \mathscr{X}^{\mathscr{E}} \tilde{\zeta}_{\mathscr{E}}(\psi, \varpi) = \mathscr{X}\varpi^\delta \mathscr{E}\left[\left(\sum_{\mathscr{E}=0}^{\infty} \mathscr{X}^{\mathscr{E}} \varphi_{\mathscr{E}}(\psi, \mathfrak{T})\right)_{\psi\psi\mathfrak{T}} - \left(\sum_{\mathscr{E}=0}^{\infty} \mathscr{X}^{\mathscr{E}} \varphi_{\mathscr{E}}(\psi, \mathfrak{T})\right)_{\psi}\right] + \varpi^2 \varphi(\psi, 0). \tag{45}$$

We now have by taking the Elzaki inverse transform to Equation (45),

$$\sum_{\mathscr{E}=0}^{\infty} \mathscr{X}^{\mathscr{E}} \tilde{\zeta}_{\mathscr{E}}(\psi, \mathfrak{T}) = \mathscr{X}\mathscr{E}^{-1}\left[\varpi^\delta \mathscr{E}\left[\left(\sum_{\mathscr{E}=0}^{\infty} \mathscr{X}^{\mathscr{E}} \varphi_{\mathscr{E}}(\psi, \mathfrak{T})\right)\right]\right] + \mathscr{E}^{-1}\left[\varpi^2 \varphi(\psi, 0)\right]. \tag{46}$$

Then, by examining the associated powers of $\mathscr{X}$, we obtain the terms of the Caputo operator solution:

$$\begin{aligned}
\mathscr{X}^0 &: \varphi_0(\psi, \mathfrak{T}) = \mathscr{E}^{-1}\left[\varpi^2 e^{-\psi}\right] = e^{-\psi}, \\
\mathscr{X}^1 &: \varphi_1(\psi, \mathfrak{T}) = \mathscr{E}^{-1}\left[\varpi^\delta \mathscr{E}[L(\varphi_0(\psi, \mathfrak{T}))]\right], \\
&= e^{-\psi} \frac{\mathfrak{T}^\delta}{\Gamma(\delta+1)}, \\
\mathscr{X}^2 &: \varphi_1(\psi, \mathfrak{T}) = \mathscr{E}^{-1}\left[\varpi^\delta \mathscr{E}[L(\varphi_1(\psi, \mathfrak{T}))]\right], \\
&= e^{-\psi} \frac{\mathfrak{T}^{2\delta}}{\Gamma(2\delta+1)}, \\
&\vdots
\end{aligned} \tag{47}$$

As a result, the approximate solution to the problem is

$$\varphi(\psi, \mathfrak{T}) = e^{-\psi} + e^{-\psi} \frac{\mathfrak{T}^\delta}{\Gamma(\delta+1)} + e^{-\psi} \frac{\mathfrak{T}^{2\delta}}{\Gamma(2\delta+1)} + \cdots, \tag{48}$$

providing the problem's integer-order ($\delta = 1$) solution $\varphi(\psi, \mathfrak{T}) = e^{(\mathfrak{T}-\psi)}$.

On the other hand, we use the Elzaki transform in combination with the Atangana-Baleanu operator to solve the problem. First, we use the Elzaki transform to solve the problem:

$$\tilde{\zeta}(\psi, \varpi) = \left(\frac{\delta\varpi^\delta + 1 - \delta}{N(\delta)}\right)\left(\mathscr{E}\left[\varphi_{\psi\psi\mathfrak{T}}(\psi, \mathfrak{T}) - \varphi_\psi(\psi, \mathfrak{T})\right]\right) + \varpi^2 \varphi(\psi, 0). \tag{49}$$

To Equation (49), we use the Elzaki perturbation transform approach and get

$$\sum_{\mathscr{E}=0}^{\infty} \mathscr{X}^{\mathscr{E}} \tilde{\zeta}_{\mathscr{E}}(\psi, \varpi) = \left(\frac{\delta\varpi^\delta + 1 - \delta}{N(\delta)}\right) \cdot \left(\mathscr{E}\left[\left(\sum_{\mathscr{E}=0}^{\infty} \mathscr{X}^{\mathscr{E}} \varphi_{\mathscr{E}}(\psi, \mathfrak{T})\right)_{\psi\psi\mathfrak{T}} - \left(\sum_{\mathscr{E}=0}^{\infty} \mathscr{X}^{\mathscr{E}} \varphi_{\mathscr{E}}(\psi, \mathfrak{T})\right)_{\psi}\right]\right) + \varpi^2 \varphi(\psi, 0). \tag{50}$$

By taking the inverse ET of the last equation, we get

$$\sum_{\mathscr{E}=0}^{\infty} \mathscr{X}^{\mathscr{E}} \tilde{\zeta}_{\mathscr{E}}(\psi, \mathfrak{T}) = \mathscr{X}\mathscr{E}^{-1} \cdot \left[\left(\frac{\delta\varpi^\delta + 1 - \delta}{N(\delta)}\right)\mathscr{E}\left[\left(\sum_{\mathscr{E}=0}^{\infty} \mathscr{X}^{\mathscr{E}} \varphi_{\mathscr{E}}(\psi, \mathfrak{T})\right)\right]\right] + \mathscr{E}^{-1}\left[\varpi^2 \varphi(\psi, 0)\right]. \tag{51}$$

Thus, on comparing both sides

$$\begin{aligned}
\mathscr{X}^0 &: \varphi_0(\psi, \mathfrak{T}) = \mathscr{E}^{-1}\left[\varpi^2 e^{-\psi}\right] = e^{-\psi}, \\
\mathscr{X}^1 &: \varphi_1(\psi, \mathfrak{T}) = \mathscr{E}^{-1}\left[\left(\frac{\delta\varpi^\delta + 1 - \delta}{N(\delta)}\right)\mathscr{E}\left[(\varphi_0)_{\psi\psi\mathfrak{T}} - (\varphi_0)_\psi\right]\right] \\
&= \frac{e^{-\psi}}{N(\delta)}\left(\frac{\mathfrak{T}^\delta}{\Gamma(\delta)} + 1 - \delta\right), \\
\mathscr{X}^2 &: \varphi_2(\psi, \mathfrak{T}) = \mathscr{E}^{-1}\left[\left(\frac{\delta\varpi^\delta + 1 - \delta}{N(\delta)}\right)\mathscr{E}\left[(\varphi_1)_{\psi\psi\mathfrak{T}} - (\varphi_1)_\psi\right]\right] \\
&= \frac{e^{-\psi}}{(N(\delta))^2}\left(\frac{\delta^2 \mathfrak{T}^{2\delta}}{\Gamma(2\delta+1)} + \frac{(1-\delta)\delta\mathfrak{T}^{2\delta}}{\Gamma(\delta+1)} + (1-\delta)^2\right)
\end{aligned} \tag{52}$$

As a result, based on the ABC operator, the approximate solution is as follows:

$$\varphi(\psi,\mathfrak{J})=e^{-\psi}+\frac{e^{-\psi}}{N(\delta)}\left(\frac{\mathfrak{J}^{\delta}}{\Gamma(\delta)}+1-\delta\right)+\frac{e^{-\psi}}{(N(\delta))^2}\left(\frac{\delta^2\mathfrak{J}^{2\delta}}{\Gamma(2\delta+1)}+\frac{(1-\delta)\delta\mathfrak{J}^{2\delta}}{\Gamma(\delta+1)}+(1-\delta)^2\right)+\cdots, \tag{53}$$

providing the problem's integer-order $(\delta=1)$ solution, $\varphi(\psi,\mathfrak{J})=e^{(\mathfrak{J}-\psi)}$.

Finally, we use the Elzaki transform approach with the aid of Caputo and ABC derivative operators to solve the problem in Equations (5)–(6). To Equations (5)–(6), we first apply the Elzaki transform with the aid of Caputo derivative:

$$\tilde{\zeta}(\psi,\varpi)=\varpi^{\delta}\mathscr{E}\left[\varphi_{\psi\psi\psi\psi}(\psi,\mathfrak{J})\right]+\varpi^2\varphi(\psi,0). \tag{54}$$

We use the Elzaki perturbation transform approach to solve Equation (54) and obtain

$$\sum_{\mathscr{E}=0}^{\infty}\mathscr{X}^{\mathscr{E}}\tilde{\zeta}_{\mathscr{E}}(\psi,\varpi)=\mathscr{X}\varpi^{\delta}\mathscr{E}\left[\left(\sum_{\mathscr{E}=0}^{\infty}\mathscr{X}^{\mathscr{E}}\varphi_{\mathscr{E}}(\psi,\varpi)\right)_{\psi\psi\psi\psi}\right]+\varpi^2\varphi(\psi,0). \tag{55}$$

We now have by taking the Elzaki inverse transform to Equation (55)

$$\sum_{\mathscr{E}=0}^{\infty}\mathscr{X}^{\mathscr{E}}\varphi_{\mathscr{E}}(\psi,\mathfrak{J})=\mathscr{X}\mathscr{E}^{-1}\left[\varpi^{\delta}\mathscr{E}\left[\left(\sum_{\mathscr{E}=0}^{\infty}\mathscr{X}^{\mathscr{E}}\varphi_{\mathscr{E}}(\psi,\mathfrak{J})\right)\right]\right]+\mathscr{E}^{-1}\left[\varpi^2\varphi(\psi,0)\right]. \tag{56}$$

Then, by examining thsse associated powers of $\mathscr{X}$, we obtain the terms of the Caputo operator solution:

$$\begin{aligned}
\mathscr{X}^0 &: \varphi_0(\psi,\mathfrak{J})=\mathscr{E}^{-1}\left[\varpi^2\sin\psi\right]=\sin\psi,\\
\mathscr{X}^1 &: \varphi_1(\psi,\mathfrak{J})=\mathscr{E}^{-1}\left[\varpi^{\delta}\mathscr{E}[L(\varphi_0(\psi,\mathfrak{J}))]\right],\\
&=-\sin\psi\frac{\mathfrak{J}^{\delta}}{\Gamma(\delta+1)},\\
\mathscr{X}^2 &: \varphi_1(\psi,\mathfrak{J})=\mathscr{E}^{-1}\left[\varpi^{\delta}\mathscr{E}[L(\varphi_1(\psi,\mathfrak{J}))]\right],\\
&=\sin\psi\frac{\mathfrak{J}^{2\delta}}{\Gamma(2\delta+1)},\\
&\vdots
\end{aligned} \tag{57}$$

As a result, the approximate solution to the problem is

$$\varphi(\psi,\mathfrak{J})=\sin\psi-\sin\psi\frac{\mathfrak{J}^{\delta}}{\Gamma(\delta+1)}+\sin\psi\frac{\mathfrak{J}^{2\delta}}{\Gamma(2\delta+1)}+\cdots, \tag{58}$$

providing the problems integer-order $(\delta=1)$ solution $\varphi(\psi,\mathfrak{J})=\sin\psi e^{(-\mathfrak{J})}$.

On the other hand, we use the Elzaki transform in combination with the Atangana-Baleanu operator to solve the problem. First, we use the Elzaki transform to solve the problem:

$$\tilde{\zeta}(\psi,\varpi)=\left(\frac{\delta\varpi^{\delta}+1-\delta}{N(\delta)}\right)\left(\mathscr{E}\left[\varphi_{\psi\psi\psi\psi}(\psi,\mathfrak{J})\right]\right)+\varpi^2\varphi(\psi,0). \tag{59}$$

To Equation (59), we use the Elzaki perturbation transform approach and get

$$\sum_{\mathscr{E}=0}^{\infty}\mathscr{X}^{\mathscr{E}}\tilde{\zeta}_{\mathscr{E}}(\psi,\varpi)=\left(\frac{\delta\varpi^{\delta}+1-\delta}{N(\delta)}\right)\cdot\left(\mathscr{E}\left[\left(\sum_{\mathscr{E}=0}^{\infty}\mathscr{X}^{\mathscr{E}}\varphi_{\mathscr{E}}(\psi,\mathfrak{J})\right)_{\psi\psi\psi\psi}\right]\right)+\varpi^2\varphi(\psi,0). \tag{60}$$

By taking the inverse ET of the last equation, we get

$$\sum_{\mathscr{E}=0}^{\infty}\mathscr{X}^{\mathscr{E}}\varphi_{\mathscr{E}}(\psi,\mathfrak{J})=\mathscr{X}\mathscr{E}^{-1}\left[\left(\frac{\delta\varpi^{\delta}+1-\delta}{N(\delta)}\right)\mathscr{E}\left[\left(\sum_{\mathscr{E}=0}^{\infty}\mathscr{X}^{\mathscr{E}}\varphi_{\mathscr{E}}(\psi,\mathfrak{J})\right)\right]\right]+\mathscr{E}^{-1}\left[\varpi^2\varphi(\psi,0)\right]. \tag{61}$$

Thus, on comparing both sides

$$\begin{aligned}
\mathscr{X}^0 &: \varphi_0(\psi,\mathfrak{J})=\mathscr{E}^{-1}\left[\varpi^2\sin\psi\right]=\sin\psi,\\
\mathscr{X}^1 &: \varphi_1(\psi,\mathfrak{J})=\mathscr{E}^{-1}\left[\left(\frac{\delta\varpi^{\delta}+1-\delta}{N(\delta)}\right)\mathscr{E}\left[(\varphi_0)_{\psi\psi\psi\psi}\right]\right]\\
&=\frac{\sin\psi}{\mathrm{N}(\delta)}\left(\frac{\mathfrak{J}^{\delta}}{\Gamma(\delta)}+1-\delta\right),\\
\mathscr{X}^2 &: \varphi_2(\psi,\mathfrak{J})=\mathscr{E}^{-1}\left[\left(\frac{\delta\varpi^{\delta}+1-\delta}{\mathrm{N}(\delta)}\right)\mathscr{E}\left[(\varphi_1)_{\psi\psi\psi\psi}\right]\right]\\
&=\frac{\sin\psi}{(\mathrm{N}(\delta))^2}\left(\frac{\delta^2\mathfrak{J}^{2\delta}}{\Gamma(2\delta+1)}+\frac{(1-\delta)\delta\mathfrak{J}^{2\delta}}{\Gamma(\delta+1)}+(1-\delta)^2\right).
\end{aligned} \tag{62}$$

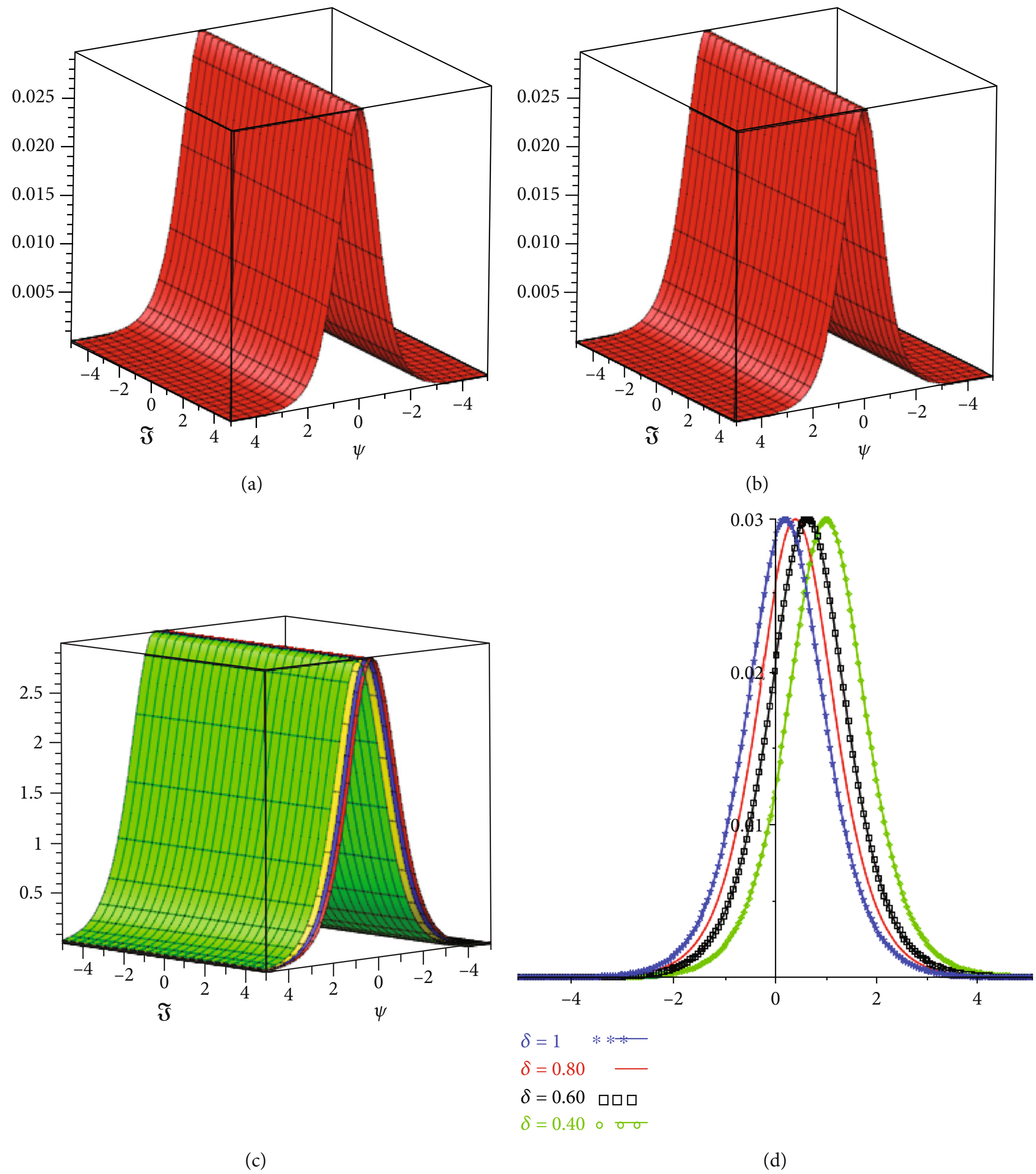

FIGURE 1: Example 1 solution graph (a) exact solution, (b) analytical solution at $\delta = 1$, (c) analytical solution at various fractional-orders of δ, and (d) $\mathfrak{J} = 0.5$.

As a result, based on the ABC operator, the approximate solution is as follows:

$$\varphi(\psi, \mathfrak{J}) = \sin\psi + \frac{\sin\psi}{\mathrm{N}(\delta)}\left(\frac{\mathfrak{J}^{\delta}}{\Gamma(\delta)} + 1 - \delta\right) + \frac{\sin\psi}{(\mathrm{N}(\delta))^2}\left(\frac{\delta^2\mathfrak{J}^{2\delta}}{\Gamma(2\delta+1)} + \frac{(1-\delta)\delta\mathfrak{J}^{2\delta}}{\Gamma(\delta+1)} + (1-\delta)^2\right) + \cdots, \tag{63}$$

providing the problems integer-order $(\delta = 1)$ solution, $\varphi(\psi, \mathfrak{J}) = \sin\psi \exp(-\mathfrak{J})$.

5. Results and Discussion

Figures 1(a) and 1(b) demonstrates the comparison between approximate solution and exact solution, while Figures 1(c) and 1(d) shows the 3D and 2D behavior of proposed methods results at different fractional-orders of the problem given by Equation (1). Figure 1 indicates that approximate solution obtained by the suggested techniques is more close to exact solution. We have shown the exact and approximate solutions in Figures 2(a) and 2(b), and the results to the problem given by Equation (3) with respect to various values of fractional parameter in Caputo and Atangana-Baleanu manner can be seen in Figures 2(c) and 2(d). Figures 3(a) and 3(b) represents the comparison between proposed

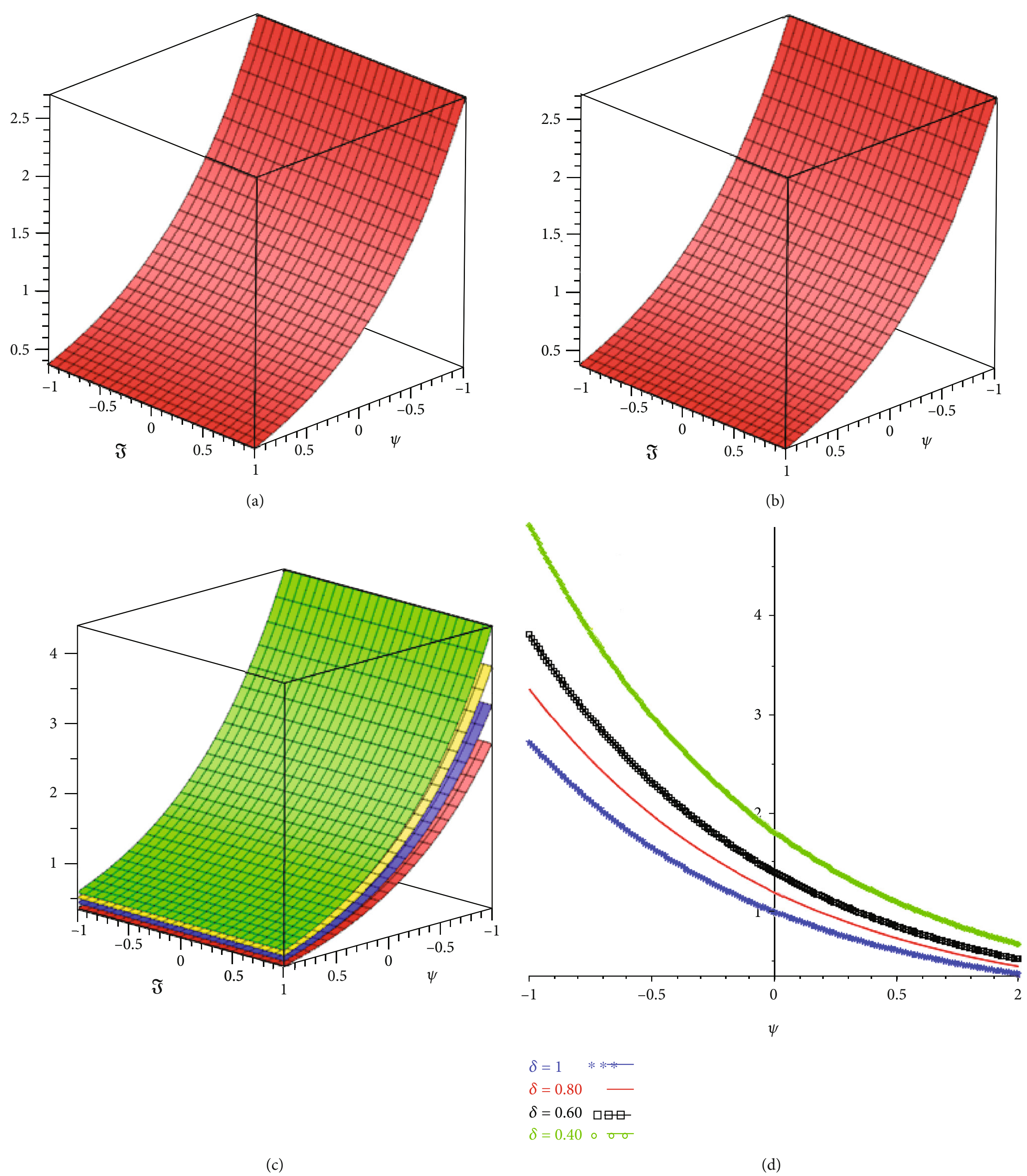

FIGURE 2: Example 2 solution graph (a) exact solution, (b) analytical solution at $\lambda = 1$, (c) analytical solution at various fractional-orders of δ, and (d) $\mathfrak{I} = 0.5$.

method solution and exact solution, whereas Figures 3(c) and 3(d) shows the behavior of the proposed methods as various fractional-orders of the problem given by Equation (5). On the other hand, in Tables 1–3 we presented the absolute error analysis of RLW equation obtained with the help of proposed method at various values of ψ and $\mathfrak{I}$. It is observed from tables that proposed method solution are in good contact with the exact solution and have high level of precisions between results and shows absolute error between results.

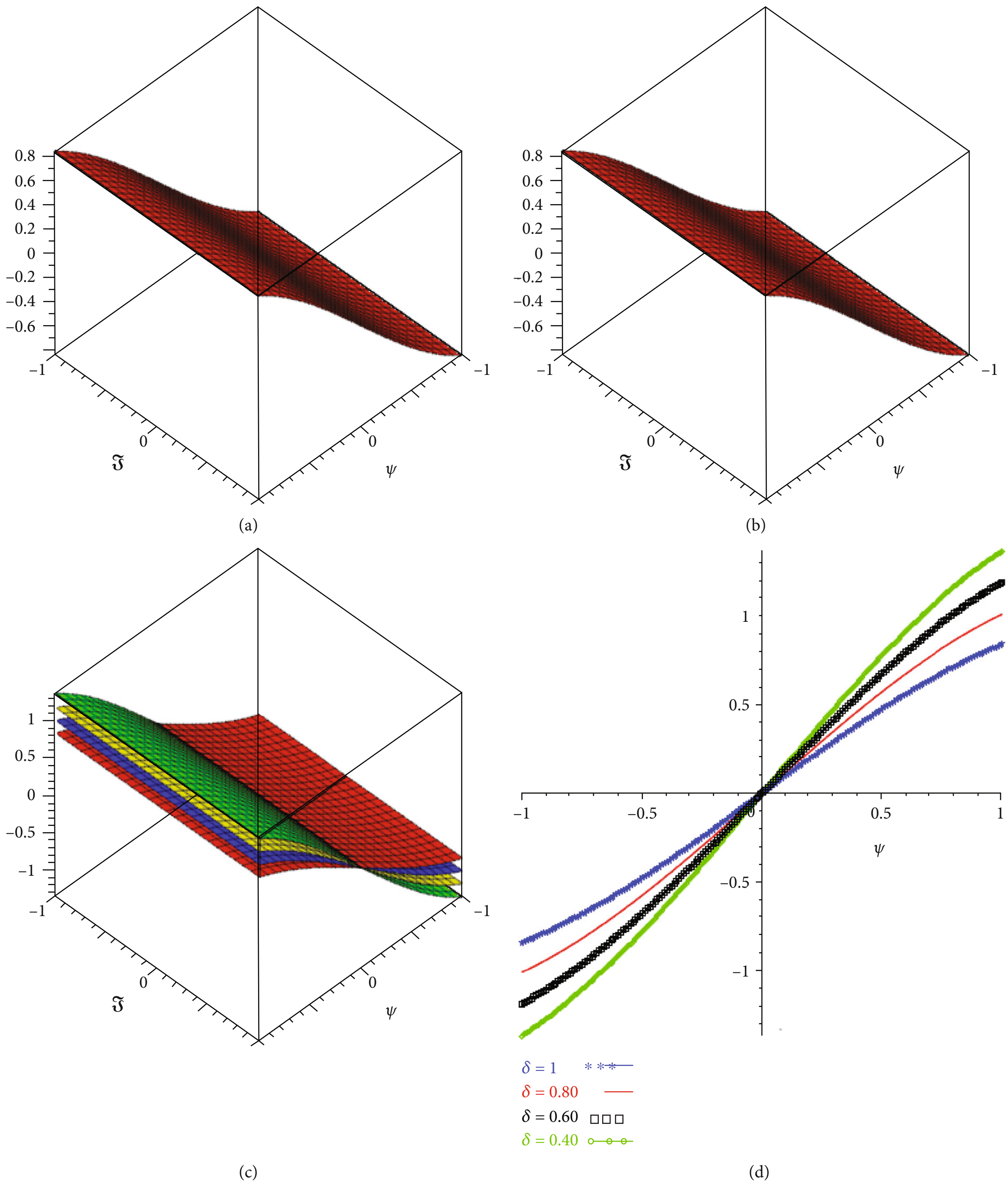

Figure 3: Example 3 solution graph (a) exact solution, (b) analytical solution at $\delta = 1$, (c) analytical solution at various fractional-orders of δ, and (d) $\mathfrak{I} = 0.5$.

Table 1: Comparison at different fractional-order of δ on the basis of error for example 1.

$\mathfrak{I}$	ψ	$\delta = 0.4$	$\delta = 0.6$	$\delta = 0.8$	$\delta = 1(ETM_{CFD})$	$\delta = 1(ETM_{ABC})$
	0.2	3.2544637000E-05	2.2120827000E-05	1.1245160000E-06	4.6950000000E-09	4.6950000000E-09
	0.4	5.6252371000E-05	3.8122367000E-05	1.9326610000E-06	4.5160000000E-09	4.5160000000E-09
1	0.6	6.6977543000E-05	4.5190884000E-05	2.2817165000E-06	2.8920000000E-09	2.8920000000E-09
	0.8	6.6088137000E-05	4.4352512000E-05	2.2282931000E-06	9.6700000000E-10	9.6700000000E-10
	1	5.7917905000E-05	3.8643903000E-05	1.9309485000E-06	4.3500000000E-10	4.3500000000E-10
	0.2	3.2724604000E-05	2.2243772000E-05	1.1309350000E-06	1.4503000000E-08	1.4503000000E-08
	0.4	5.6554664000E-05	3.8325285000E-05	1.9428321000E-06	1.1962000000E-08	1.1962000000E-08
2	0.6	6.7332527000E-05	4.5426381000E-05	2.2932956000E-06	6.3710000000E-09	6.3710000000E-09
	0.8	6.6435085000E-05	4.4580264000E-05	2.2393475000E-06	8.5500000000E-10	8.5500000000E-10
	1	5.8219810000E-05	3.8840174000E-05	1.9403804000E-06	2.7360000000E-09	2.7360000000E-09
	0.2	3.2889983000E-05	2.2359041000E-05	1.1372439000E-06	2.9430000000E-08	2.9430000000E-08
	0.4	5.6826239000E-05	3.8509365000E-05	1.9522428000E-06	2.2347000000E-08	2.2347000000E-08
3	0.6	6.7648218000E-05	4.5636779000E-05	2.3036960000E-06	1.0447000000E-08	1.0447000000E-08
	0.8	6.6741663000E-05	4.4781765000E-05	2.2490874000E-06	3.3000000000E-10	3.3000000000E-10
	1	5.8485407000E-05	3.9012637000E-05	1.9485796000E-06	6.9030000000E-09	6.9030000000E-09
	0.2	3.3047770000E-05	2.2471143000E-05	1.1436601000E-06	4.9484000000E-08	4.9484000000E-08
	0.4	5.7079185000E-05	3.8682371000E-05	1.9612665000E-06	3.5686000000E-08	3.5686000000E-08
4	0.6	6.7939008000E-05	4.5831283000E-05	2.3133582000E-06	1.5130000000E-08	1.5130000000E-08
	0.8	6.7022070000E-05	4.4966048000E-05	2.2579430000E-06	2.5830000000E-09	2.5830000000E-09
	1	5.8727131000E-05	3.9169160000E-05	1.9559187000E-06	1.2932000000E-08	1.2932000000E-08
	0.2	3.3201253000E-05	2.2582205000E-05	1.1502870000E-06	7.4676000000E-08	7.4676000000E-08
	0.4	5.7319182000E-05	3.8847969000E-05	1.9700805000E-06	5.1991000000E-08	5.1991000000E-08
5	0.6	6.8211657000E-05	4.6014233000E-05	2.3224915000E-06	2.0433000000E-08	2.0433000000E-08
	0.8	6.7282969000E-05	4.5137364000E-05	2.2661180000E-06	5.8960000000E-09	5.8960000000E-09
	1	5.8950823000E-05	3.9313444000E-05	1.9625736000E-06	2.0821000000E-08	2.0821000000E-08

Table 2: Comparison at different fractional-order of δ on the basis of error for example 2.

$\mathfrak{I}$	ψ	$\delta = 0.4$	$\delta = 0.6$	$\delta = 0.8$	$\delta = 1(ETM_{CFD})$	$\delta = 1(ETM_{ABC})$
	0.2	2.4586042500E-02	1.6390008900E-02	8.1946786000E-03	4.0000000000E-09	4.0000000000E-09
	0.4	2.0129349000E-02	1.3419004200E-02	6.7092353000E-03	3.4000000000E-09	3.4000000000E-09
1	0.6	1.6480517100E-02	1.0986551500E-02	5.4930573000E-03	2.7000000000E-09	2.7000000000E-09
	0.8	1.3493106100E-02	8.9950275000E-03	4.4973349000E-03	2.3000000000E-09	2.3000000000E-09
	1	1.1047220900E-02	7.3645057000E-03	3.6821064000E-03	1.9000000000E-09	1.9000000000E-09
	0.2	2.4605791800E-02	1.6402716400E-02	8.2008084000E-03	1.6300000000E-08	1.6300000000E-08
	0.4	2.0145518400E-02	1.3429408200E-02	6.7142540000E-03	1.3500000000E-08	1.3500000000E-08
2	0.6	1.6493755500E-02	1.0995069600E-02	5.4971663000E-03	1.1000000000E-08	1.1000000000E-08
	0.8	1.3503944800E-02	9.0020016000E-03	4.5006991000E-03	9.0000000000E-09	9.0000000000E-09
	1	1.1056095000E-02	7.3702156000E-03	3.6848608000E-03	7.3000000000E-09	7.3000000000E-09
	0.2	2.4623948800E-02	1.6414429900E-02	8.2064699000E-03	3.6900000000E-08	3.6900000000E-08
	0.4	2.0160384100E-02	1.3438998600E-02	6.7188893000E-03	3.0200000000E-08	3.0200000000E-08
3	0.6	1.6505926500E-02	1.1002921400E-02	5.5009613000E-03	2.4700000000E-08	2.4700000000E-08
	0.8	1.3513909600E-02	9.0084302000E-03	4.5038062000E-03	2.0200000000E-08	2.0200000000E-08
	1	1.1064253400E-02	7.3754788000E-03	3.6874046000E-03	1.6600000000E-08	1.6600000000E-08
	0.2	2.4641082400E-02	1.6425501600E-02	8.2118269000E-03	6.5500000000E-08	6.5500000000E-08
	0.4	2.0174411900E-02	1.3448063300E-02	6.7232751000E-03	5.3700000000E-08	5.3700000000E-08
4	0.6	1.6517411400E-02	1.1010343000E-02	5.5045521000E-03	4.3900000000E-08	4.3900000000E-08
	0.8	1.3523312700E-02	9.0145064000E-03	4.5067461000E-03	3.6000000000E-08	3.6000000000E-08
	1	1.1071952000E-02	7.3804536000E-03	3.6898117000E-03	2.9400000000E-08	2.9400000000E-08
	0.2	2.4657459500E-02	1.6436096000E-02	8.2169554000E-03	1.0230000000E-07	1.0230000000E-07
	0.4	2.0187820300E-02	1.3456737200E-02	6.7274740000E-03	8.3900000000E-08	8.3900000000E-08
5	0.6	1.6528389400E-02	1.1017444700E-02	5.5079899000E-03	6.8600000000E-08	6.8600000000E-08
	0.8	1.3532300600E-02	9.0203207000E-03	4.5095607000E-03	5.6200000000E-08	5.6200000000E-08
	1	1.1079310700E-02	7.3852140000E-03	3.6921161000E-03	4.6000000000E-08	4.6000000000E-08

Table 3: Comparison at different fractional-order of δ on the basis of error for example 3.

$\mathfrak{I}$	ψ	$\delta = 0.4$	$\delta = 0.6$	$\delta = 0.8$	$\delta = 1(\mathrm{ETM}_{\mathrm{CFD}})$	$\delta = 1(\mathrm{ETM}_{\mathrm{ABC}})$
	0.2	5.9659347000E-03	3.9771240000E-03	1.9884840000E-03	1.0000000000E-09	1.0000000000E-09
	0.4	1.1694026400E-02	7.7956926000E-03	3.8976932000E-03	1.9000000000E-09	1.9000000000E-09
1	0.6	1.6955914200E-02	1.1303471500E-02	5.6515139000E-03	2.8000000000E-09	2.8000000000E-09
	0.8	2.1541823200E-02	1.4360616700E-02	7.1800265000E-03	3.6000000000E-09	3.6000000000E-09
	1	2.5268927700E-02	1.6845249400E-02	8.4222940000E-03	4.2000000000E-09	4.2000000000E-09
	0.2	5.9707330000E-03	3.9802135000E-03	1.9899773000E-03	4.0000000000E-09	4.0000000000E-09
	0.4	1.1703431600E-02	7.8017484000E-03	3.9006205000E-03	7.8000000000E-09	7.8000000000E-09
2	0.6	1.6969551500E-02	1.1312252300E-02	5.6557583000E-03	1.1300000000E-08	1.1300000000E-08
	0.8	2.1559148800E-02	1.4371772300E-02	7.1854188000E-03	1.4300000000E-08	1.4300000000E-08
	1	2.5289250900E-02	1.6858335100E-02	8.4286193000E-03	1.6800000000E-08	1.6800000000E-08
	0.2	5.9751488000E-03	3.9830657000E-03	1.9913610000E-03	8.9000000000E-09	8.9000000000E-09
	0.4	1.1712087200E-02	7.8073393000E-03	3.9033328000E-03	1.7500000000E-08	1.7500000000E-08
3	0.6	1.6982101800E-02	1.1320358900E-02	5.6596910000E-03	2.5400000000E-08	2.5400000000E-08
	0.8	2.1575093500E-02	1.4382071500E-02	7.1904152000E-03	3.2300000000E-08	3.2300000000E-08
	1	2.5307954300E-02	1.6870416200E-02	8.4344802000E-03	3.7900000000E-08	3.7900000000E-08
	0.2	5.9793203000E-03	3.9857663000E-03	1.9926749000E-03	1.5900000000E-08	1.5900000000E-08
	0.4	1.1720263900E-02	7.8126327000E-03	3.9059080000E-03	3.1100000000E-08	3.1100000000E-08
4	0.6	1.6993957600E-02	1.1328034100E-02	5.6634250000E-03	4.5200000000E-08	4.5200000000E-08
	0.8	2.1590155800E-02	1.4391822500E-02	7.1951591000E-03	5.7400000000E-08	5.7400000000E-08
	1	2.5325622600E-02	1.6881854300E-02	8.4400448000E-03	6.7300000000E-08	6.7300000000E-08
	0.2	5.9833121000E-03	3.9883550000E-03	1.9939372000E-03	2.4900000000E-08	2.4900000000E-08
	0.4	1.1728088500E-02	7.8177068000E-03	3.9083824000E-03	4.8700000000E-08	4.8700000000E-08
5	0.6	1.7005302900E-02	1.1335391300E-02	5.6670127000E-03	7.0500000000E-08	7.0500000000E-08
	0.8	2.1604569600E-02	1.4401169600E-02	7.1997171000E-03	8.9600000000E-08	8.9600000000E-08
	1	2.5342530300E-02	1.6892818700E-02	8.4453916000E-03	1.0520000000E-07	1.0520000000E-07

6. Conclusion

The approximate solutions of some particular regularized long-wave equations of fractional-order are determined in this paper using a new integral transform method known as the Elzaki transformation. To begin, we consider the Elzaki transform of the fractional Atangana-Baleanu operator and used it to solve the proposed problems. The used scheme's trustworthiness and efficiency are based on its capacity to provide an appropriate convergence zone for the solution. The excellent accuracy of the findings and the simplicity of the solution approach confirm suggested method supremacy over other numerical methods. Also, we have shown how the Caputo and Atangana-Baleanu fractional operators differ when it comes to finding approximate solutions to the illustrative examples. To ensure the validity of the suggested technique, we showed the results in graphs and tables. The representations of graphs and tables demonstrate that the results obtained by suggested scheme are very accurate. In addition, the behavior of fractional-order results is discussed which confirm that the solution gets closer as the fractional-order tends toward integer-order. Finally, the approximation solution strategy employed is highly efficient and applicable to a wide range of nonlinear equations defining real systems.

Data Availability

The numerical data used to support the findings of this study are included within the article.

Conflicts of Interest

The authors declare that there are no conflicts of interest regarding the publication of this article.

References

[1] I. Podlubny, *Fractional Differential Equations*, Academic Press, New York, 1999.

[2] M. Caputo, *Elasticita e Dissipazione*, Zani-Chelli, Bologna, 1969.

[3] K. S. Miller and B. Ross, *An Introduction to the Fractional Calculus and Fractional Differential Equations*, Wiley, New York, 1993.

[4] D. Baleanu, Z. B. Guvenc, and J. A. Tenreiro Machado, *New Trends in Nanotechnology and Fractional Calculus Applications*, Springer Dordrecht Heidelberg, London New York, 2010.

[5] A. A. Kilbas, H. M. Srivastava, and J. J. Trujillo, *Theory and Applications of Fractional Differential Equations*, vol. 204, Elsevier, Amsterdam, 2006.

[6] Y. A. Rossikhin and M. V. Shitikova, "Application of fractional calculus for dynamic problems of solid mechanics: novel trends and recent results," *Applied Mechanics Reviews*, vol. 63, no. 1, 2010.

[7] Y. A. Rossikhin, "Reflections on two parallel ways in the progress of fractional calculus in mechanics of solids," *Applied Mechanics Reviews*, vol. 63, no. 1, 2010.

[8] Y. Zhang, H. Sun, H. H. Stowell, M. Zayernouri, and S. E. Hansen, "A review of applications of fractional calculus in earth system dynamics," *Chaos, Solitons and Fractals*, vol. 102, pp. 29–46, 2017.

[9] A. Carpinteri, *Fractals and Fractional Calculus in Continuum Mechanics*, F. Mainardi, Ed., vol. 378, Springer, 2014.

[10] N. Engheta, "On fractional calculus and fractional multipoles in electromagnetism," *IEEE Transactions on Antennas and Propagation*, vol. 44, no. 4, pp. 554–566, 1996.

[11] C. Lederman, J. M. Roquejoffre, and N. Wolanski, "Mathematical justification of a nonlinear integro-differential equation for the propagation of spherical flames," *Annali di Matematica Pura ed Applicata*, vol. 183, no. 2, pp. 173–239, 2004.

[12] V. V. Kulish and J. L. Lage, "Application of fractional calculus to fluid mechanics," *Journal of Fluids Engineering*, vol. 124, no. 3, pp. 803–806, 2002.

[13] F. C. Meral, T. J. Royston, and R. Magin, "Fractional calculus in viscoelasticity: an experimental study," *Communications in Nonlinear Science and Numerical Simulation*, vol. 15, no. 4, pp. 939–945, 2010.

[14] R. L. Bagley and P. J. Torvik, "Fractional calculus in the transient analysis of viscoelastically damped structures," *AIAA Journal*, vol. 23, no. 6, pp. 918–925, 1985.

[15] K. Nonlaopon, A. M. Alsharif, A. M. Zidan et al., "Numerical investigation of fractional-order Swift-Hohenberg equations via a novel transform," *Symmetry*, vol. 13, no. 7, p. 1263, 2021.

[16] R. Shah, H. Khan, D. Baleanu, P. Kumam, and M. Arif, "The analytical investigation of time-fractional multi-dimensional Navier-Stokes equation," *Alexandria Engineering Journal*, vol. 59, no. 5, pp. 2941–2956, 2020.

[17] R. Shah, H. Khan, D. Baleanu, P. Kumam, and M. Arif, "A novel method for the analytical solution of fractional Zakharov-Kuznetsov equations," *Advances in Difference Equations*, vol. 2019, no. 1, 14 pages, 2019.

[18] Y. Qin, A. Khan, I. Ali et al., "An efficient analytical approach for the solution of certain fractional-order dynamical systems," *Energies*, vol. 13, no. 11, p. 2725, 2020.

[19] M. K. Alaoui, R. Fayyaz, A. Khan, R. Shah, and M. S. Abdo, "Analytical investigation of Noyes–Field model for time-fractional Belousov–Zhabotinsky reaction," *Complexity*, vol. 2021, Article ID 3248376, 21 pages, 2021.

[20] M. Areshi, A. Khan, R. Shah, and K. Nonlaopon, "Analytical investigation of fractional-order Newell-Whitehead-Segel equations via a novel transform," *AIMS Mathematics*, vol. 7, no. 4, pp. 6936–6958, 2022.

[21] T. Botmart, R. P. Agarwal, M. Naeem, A. Khan, and R. Shah, "On the solution of fractional modified Boussinesq and approximate long wave equations with non-singular kernel operators," *AIMS Mathematics*, vol. 7, no. 7, pp. 12483–12513, 2022.

[22] T. M. Elzaki, "The new integral transform Elzaki transform," *Global Journal of pure and applied mathematics*, vol. 7, no. 1, pp. 57–64, 2011.

[23] H. Khan, A. Khan, M. Al-Qurashi, R. Shah, and D. Baleanu, "Modified modelling for heat like equations within Caputo operator," *Energies*, vol. 13, no. 8, p. 2002, 2020.

[24] T. M. Elzaki and E. M. Hilal, "Homotopy perturbation and Elzaki transform for solving nonlinear partial differential equations," *Mathematical Theory and Modeling*, vol. 2, no. 3, pp. 33–42, 2012.

[25] N. A. Shah, Y. S. Hamed, K. M. Abualnaja, J. D. Chung, R. Shah, and A. Khan, "A comparative analysis of fractional-

order kaup–kupershmidt equation within different operators," *Symmetry*, vol. 14, no. 5, p. 986, 2022.

[26] M. Yavuz, "Characterizations of two different fractional operators without singular kernel," *Mathematical Modelling of Natural Phenomena*, vol. 14, no. 3, p. 302, 2019.

[27] P. Sunthrayuth, F. Ali, A. A. Alderremy, S. Aly, Y. S. Hamed, and J. Katle, "The numerical investigation of fractional-order Zakharov–Kuznetsov equations," *Complexity*, vol. 2021, Article ID 4570605, 13 pages, 2021.

[28] M. Naeem, O. F. Azhar, A. M. Zidan, K. Nonlaopon, and R. Shah, "Numerical analysis of fractional-order parabolic equations via Elzaki transform," *Journal of Function Spaces*, vol. 2021, Article ID 3484482, 10 pages, 2021.

[29] R. Ali and K. Pan, "The solution of the absolute value equations using two generalized accelerated overrelaxation methods," *Asian-European Journal of Mathematics*, no. article 2250154, 2021.

[30] R. Ali, A. Ali, and S. Iqbal, "Iterative methods for solving absolute value equations," *The Journal of Mathematics and Computer Science*, vol. 26, no. 4, pp. 322–329, 2021.

[31] T. B. Benjamin, J. L. Bona, and J. J. Mahony, "Model equations for long waves in nonlinear dispersive systems," *Philosophical Transactions of the Royal Society of London. Series A, Mathematical and Physical Sciences*, vol. 272, no. 1220, pp. 47–78, 1972.

[32] M. Yavuz and T. Abdeljawad, "Nonlinear regularized long-wave models with a new integral transformation applied to the fractional derivative with power and Mittag-Leffler kernel," *Advances in Difference Equations*, vol. 2020, no. 1, 18 pages, 2020.

[33] T. Achouri and K. Omrani, "Numerical solutions for the damped generalized regularized long-wave equation with a variable coefficient by Adomian decomposition method," *Communications in Nonlinear Science and Numerical Simulation*, vol. 14, no. 5, pp. 2025–2033, 2009.

[34] A. Goswami, J. Singh, D. Kumar, S. Gupta, and Sushila, "An efficient analytical technique for fractional partial differential equations occurring in ion acoustic waves in plasma," *Journal of Ocean Engineering and Science*, vol. 4, no. 2, pp. 85–99, 2019.

[35] Y. Khan, R. Taghipour, M. Falahian, and A. Nikkar, "A new approach to modified regularized long wave equation," *Neural Computing and Applications*, vol. 23, no. 5, pp. 1335–1341, 2013.

[36] A. Atangana and D. Baleanu, "New fractional derivatives with nonlocal and non-singular kernel: theory and application to heat transfer model," *Thermal Science*, vol. 20, no. 2, pp. 763–769, 2016.

[37] M. K. Alaoui, K. Nonlaopon, A. M. Zidan, A. Khan, and R. Shah, "Analytical investigation of fractional-order cahn–hilliard and gardner equations using two novel techniques," *Mathematics*, vol. 10, no. 10, p. 1643, 2022.

[38] A. A. Alderremy, T. M. Elzaki, and M. Chamekh, "New transform iterative method for solving some Klein-Gordon equations," *Results in Physics*, vol. 10, pp. 655–659, 2018.

[39] H. Kim, "The time shifting theorem and the convolution for Elzaki transform," *International Journal of Pure and Applied Mathematics*, vol. 87, no. 2, pp. 261–271, 2013.

[40] R. P. Agarwal, F. Mofarreh, W. Luangboon, and K. Nonlaopon, "An analytical technique, based on natural transform to solve fractional-order parabolic equations," *Entropy*, vol. 23, no. 8, p. 1086, 2021.

Hindawi
Journal of Function Spaces
Volume 2022, Article ID 5807120, 8 pages
https://doi.org/10.1155/2022/5807120

Research Article

Applicability of Mönch's Fixed Point Theorem on Existence of a Solution to a System of Mixed Sequential Fractional Differential Equation

Muath Awadalla

Department of Mathematics and Statistics, College of Science, King Faisal University, Hafuf, Al Ahsa 31982, Saudi Arabia

Correspondence should be addressed to Muath Awadalla; mawadalla@kfu.edu.sa

Received 9 April 2022; Accepted 5 May 2022; Published 28 May 2022

Academic Editor: Mohammed S. Abdo

In this paper, we study the existence and uniqueness of the solution for a coupled system of mixed fractional differential equations. The main results are established with the aid of "Mönch's fixed point theorem." In addition, an applied example that supports the theoretical results reached through this study is included.

1. Introduction

Fractional calculus has an extended history, going all the way back to Leibniz's 17th-century explanation of the derivative order in 1965. Mathematicians use fractional calculus to study how derivatives and integrals of noninteger order work and how they change over time. Subsequently, the subject attracted the interest of numerous famous mathematicians, including Fourier, Laplace, Abel, Liouville, Riemann, and Letnikov. For current and wide-ranging analyses of fractional derivatives and their applications, we recommend the monographs [1, 2], and the recently mentioned papers [3, 4].

Many problems in various scientific branches can be successfully studied using partial differential equations, such as theoretical physics, biology, viscosity, electrochemistry, and other physical processes see [5–9]. For example, but not limited, the authors in [10] employed the fractional derivative of the ψ-Caputo type in modeling the logistic population equation, through which they were able to show that the model with the fractional derivative led to a better approximation of the variables than the classical model. In addition, the authors in [11] employed the fractional derivative of the ψ-Caputo type and used the kernel Rayleigh, to improve the model again in modeling the logistic population equation.

The obvious difference between the ordinary differential equation and the fractional differential equation is that the latter is an equation that contains fractional derivatives and also comes in a relationship so that the definition of the fractional derivative is an integral equation on the other side of this equation. Fractional derivatives have drawn the attention of researchers in various fields of research. One of the main goals of solving these equations is to investigate whether these derivatives will help in the future in improving the accuracy of predicting the values of variables in various mathematical models in all sciences, whether in scientific or human aspects.

Before starting this research for solutions to these problems, which are recently considered in the applied sciences, verifying the issue of the existence and uniqueness of such equations is an indispensable thing. To study these conditions, most of the researchers use the most important fixed point theorems in the Banach space, such as the Banach contraction principle and Leray- Schauder theorem see [12–18].

In 2016, Aljoudi et al. [19] published a study investigating the existence results for the following boundary value problem (sequential Hadamard type).

$$\begin{cases} \left({}^{H}D_1^{\nu_1} + \eta^{H}D_1^{\nu_1-1}\right)\xi(\omega) = \varphi_1\left(\omega, \xi(\omega), \zeta(\omega), {}^{H}D_1^{r_1}\zeta(\omega)\right), \\ \left({}^{H}D_1^{\nu_2} + \eta^{H}D_1^{\nu_2-1}\right)\zeta(\omega) = \varphi_2\left(\omega, \xi(\omega), {}^{H}D_1^{r_2}\xi(\omega), \zeta(\omega)\right), \\ \xi(1) = 0,\ \xi(e) = {}^{H}I^{\theta_1}\zeta(\varepsilon_1), \\ \zeta(1) = 0,\ \zeta(e) = {}^{H}I^{\theta_2}\xi(\varepsilon_2), \end{cases} \tag{1}$$

where ${}^{H}D_1^{(.)}, \nu_1, \nu_2 \in (1, 2],\ r_1, r_2 \in (0, 1)$ is the Hadamard fractional derivative, and ${}^{H}I^{\theta_1}$ is the Hadamard fractional integral with order $\theta_1, \theta_2 > 0,\ \varphi_1, \varphi_2 \in C([1, e] \times \mathbb{R}^3, \mathbb{R}), \varepsilon_1, \varepsilon_2 \in [1, e]$.

In 2017, Ahmad and Ntouyas [20] published a study investigating the existence results for the following initial value problem

$$\begin{cases} {}^{CH}D_1^{\nu_1}\left({}^{CH}D_1^{\nu_2}x(t) - f_1(t, x_t)\right) = f_2(t, x_t), & t \in [1, b], \\ x(t) = \varphi(t), & t \in [1-\tau, 1], \\ {}^{CH}D_1^{\nu_2}x(t) = \mu \in \mathbb{R}, \end{cases} \tag{2}$$

where ${}^{CH}D_1^{\nu_i}, \nu_i \in (0, 1), i = 1, 2$ is the Hadamard fractional derivative, $f_i \in [1, b] \times C([-\tau, 0], \mathbb{R}) \longrightarrow \mathbb{R}, \varphi \in C([1-\tau, 1], \mathbb{R}), x_t \in C([-\tau, 0], \mathbb{R})$, where $x_t(\gamma) = x(t+\gamma), \gamma \in [-\tau, 0]$.

Many researchers went deeper in their research beyond the issue of verifying the issue of the existence of a solution to such equations and studied the issue of the stability of these solutions, it can be seen in [21, 22]. Furthermore, many specialists in this field have taken an interest in hybrid partial differential equations see [23–26].

Newly, interest in fractional calculus has increased from a purely mathematical theory and from an applied point of view in various sciences. Focusing on the theory, there are many experts in this field who have studied the existence of solutions for many types' fractional differential equations (FDEs) using the most famous fixed-point theories such as Banach's principle and nonlinear Leary-Schauder alternative. While a few of them tried other theories to examine the existence of solutions to these problems, Derbazi and Baitiche [27] publish one of these scientific papers.

The aim of this paper is to investigate the existence of solutions for the following nonlinear sequential fractional differential equation subject to the Dirichlet boundary conditions.

$$\begin{cases} {}^{C}D^{\alpha_1}\left({}^{CH}D^{\beta_1}\psi(t)\right) = \varsigma(t, \psi(t), \varphi(t)), \\ {}^{C}D^{\alpha_2}\left({}^{CH}D^{\beta_2}\varphi(t)\right) = \xi(t, \psi(t), \varphi(t)), \\ \psi(a) = \psi(T) = 0, \quad \varphi(a) = \varphi(T) = 0, \end{cases} \tag{3}$$

where ${}^{C}D^{\alpha_i}, {}^{CH}D^{\beta_i}$ are the *Caputo* and *Caputo-Hadamard* fractional derivatives of order $0 < \alpha_i, \beta_i \leq 1, i = 1, 2.$ $, a \leq t \leq T$.

In this work, we will try to follow the researchers and specialists in this field, by working to prove the existence of a solution to the problem presented above. In which the work will be presented in this format: Section 2 contains some basic results for fractional calculus. Section 3 shows an important result for the establishment of our main findings, and after that, we present our main findings. In Section 4, an applied example is obtained illustrating what has been obtained in the theoretical aspect of this manuscript. In Section 5, a conclusion and future work section is introduced.

2. Preliminaries

This part is dedicated to presenting some definitions, postulates, and theorems related to the fixed point concept of solutions of differential equations, which will be used to verify the existence of a solution to the system of equations given by Equation (3).

Definition 1 (see [7]). The Hadamard fractional integral of order ν for a continuous function φ is defined as

$$ {}^{H}I^{\nu}\varphi(\omega) = \frac{1}{\Gamma(\nu)}\int_a^{\omega}\left(\ln\frac{\omega}{\tau}\right)^{q-1}\frac{1}{\tau}\varphi(\tau)d\tau, \nu > 0. \tag{4}$$

Definition 2 (see [7]). The Hadamard fractional derivative of order $\nu > 0$ for a continuous function $\varphi : [a, \infty) \longrightarrow \mathbb{R}$ is defined as

$$ {}^{H}D^{\nu}\varphi(\omega) = \delta^n\left({}^{H}I^{\nu}\varphi\right)(\omega), \tag{5}$$

$n-1 < \nu < n, n = [\nu] + 1$, where $\delta = \omega(d/d\omega)$, $[\nu]$ denotes the integer part of the real number ν.

Definition 3 (see [5]). The Caputo-Hadamard fractional derivative of order ν for at least $n-$ times differentiable function $\varphi : [a, \infty) \longrightarrow \mathbb{R}$ is defined as

$$ {}^{CH}D^{\nu}\varphi(\omega) = \frac{1}{\Gamma(n-\nu)}\int_a^{\omega}\left(\ln\frac{\omega}{\tau}\right)^{n-\nu-1}\delta^n\frac{g(\tau)}{\tau}d\tau. \tag{6}$$

Lemma 4 (see [20]). *Let* $u \in C_\delta^n([a, T], \mathbb{R})$, *where* $C_\delta^n[a, T] = \{u : [a, T] \longrightarrow \mathbb{R} : \delta^{(n-1)}u \in C[a, T]\}$, *then* ${}^{H}I^{\nu}({}^{H}D^{\nu}u)(\omega) = u(\omega) - \sum_{k=1}^{n} c_k(\ln(\omega/a))^{\nu-k}$, *and*

$$ {}^{H}I^{\nu}\left({}^{CH}D^{\nu}u\right)(\omega) = u(\omega) - \sum_{k=0}^{n-1} c_k\left(\ln\frac{\omega}{a}\right)^k. \tag{7}$$

Denote the Banach space of all continuous functions z from $[a, T]$ into Q by $C([a, T], Q)$,

accompanied by the norm: $\|z\|_\infty = \sup_{a\leq t\leq T}\{z(t)\}$.

Definition 5 (see [28]). The Kuratowski measure of noncompactness $k(\cdot)$.

Defined on bounded set U of Banach space Q is

$$k(U) := \inf \{r > 0 : U = \cup_{i=1}^{m} U_i \text{ and } \operatorname{diam}(U_i) \le r \text{ for } 1 \le i \le m\}. \tag{8}$$

Lemma 6 (see [28]). *Given the Banach space Q with U, V are two bounded proper subsets of Q, then the following properties hold true*

(I) *If $U \subset V$, then $k(U) \le k(V)$;*

(II) $k(U) = k(\bar{U}) = k(\overline{conv}\, U)$;

(III) *U is relativly compact $\rightleftarrows k(U) = 0$;*

(IV) $k(\delta U) = |\delta| k(U), \delta \in \mathbb{R}$;

(V) $k(U \cup V) = \max \{k(U), k(V)\}$;

(VI) $k(U + V) \le k(U) + k(V), U + V = \{x | x = u + v, u \in U, v \in V\}$;

(VII) $k(U + y) = k(U), \forall y \in Q$.

Lemma 7 (see [29]). *Given an equicontinuous and bounded set $S \subset C([a, T], Q)$, then the function.*

$\omega \mapsto k(S(\omega))$ is continuous on $[a, T]$, $k_C(S) = \max_{\omega \in [a,T]} k(S(\omega))$, and

$$k\left(\int_a^T x(\tau) d\tau\right) \le \left(\int_a^T k(x(\tau)) d\tau\right), S(\tau) = \{x(\tau): x \in S\}. \tag{9}$$

Definition 8 (see [3]). Given the function $\psi : [a, T] \times Q \longrightarrow Q$, ψ satisfy the Carathéodory conditions, if the following conditions applies:

(I) $\psi(\omega, z)$ is measurable in ω for $z \in Q$;

(II) $\psi(\omega, z)$ is continuous in $z \in Q$ for $\omega \in [a, T]$.

Theorem 9 (Mönch's fixed point theorem [4]). *Given a bounded, closed, and convex subset $\Omega \subset Q$, such that $0 \in \Omega$, let also T be a continuous mapping of Ω into itself.*

If $S = \overline{conv}\, T(S)$, or $S = T(S) \cup \{0\}$, then $k(S) = 0$, satisfied $\forall S \subset \Omega$, then T has a fixed point.

3. Existence Results

Let $B = \{(\psi(t), \varphi(t)) | (\psi, \varphi) \in C([a, T], \mathbb{R}) \times C([a, T], \mathbb{R})\}$. Obviously, the defined set B is a Banach space with $\|(\psi, \varphi)\|_B = \|\psi\|_\infty + \|\varphi\|_\infty$.

The measurable functions $(\psi, \varphi) \in C([a, T], \mathbb{R}) \times C([a, T], \mathbb{R})$ are said to be solutions of problem Equation (3) if they satisfy problem (3) associated with the given boundary conditions, our next lemma will introduce the solutions of Equation (3), which indeed needed to investigate the existence results.

Lemma 10. *If $p, q \in C([a, T], \mathbb{R})$, then the solution of*

$$\begin{cases} {}^{C}D^{\alpha_1}\left({}^{CH}D^{\beta_1}\psi(t)\right) = p(t), \\ {}^{C}D^{\alpha_2}\left({}^{CH}D^{\beta_2}\varphi(t)\right) = q(t), \\ \psi(a) = \psi(T) = 0, \varphi(a) = \varphi(T) = 0. \end{cases} \tag{10}$$

With $0 < \alpha_i, \beta_i \le 1$, $i = 1, 2. a \le t \le T$, is given by

$$\begin{aligned} \psi(t) = {} & \frac{1}{\Gamma(\alpha_1)\Gamma(\beta_1)} \int_a^t \int_a^r \left(\ln \frac{t}{r}\right)^{\beta_1 - 1} (r - x)^{\alpha_1 - 1} p(x) dx \frac{dr}{r} \\ & - \left(\frac{\ln (t/a)}{n(T/a)}\right)^{\beta_1} \frac{1}{\Gamma(\alpha_1)\Gamma(\beta_1)} \int_a^T \int_a^r \\ & \cdot \left(\ln \frac{T}{r}\right)^{\beta_1 - 1} (r - x)^{\alpha_1 - 1} p(x) dx \frac{dr}{r}, \end{aligned} \tag{11}$$

$$\begin{aligned} \varphi(t) = {} & \frac{1}{\Gamma(\alpha_2)\Gamma(\beta_2)} \int_a^t \int_a^r \left(\ln \frac{t}{r}\right)^{\beta_2 - 1} (r - x)^{\alpha_2 - 1} q(x) dx \frac{dr}{r} \\ & - \left(\frac{\ln (t/a)}{n(T/a)}\right)^{\beta_2} \frac{1}{\Gamma(\alpha_2)\Gamma(\beta_2)} \int_a^T \int_a^r \\ & \cdot \left(\ln \frac{T}{r}\right)^{\beta_2 - 1} (r - x)^{\alpha_2 - 1} q(x) dx \frac{dr}{r}. \end{aligned} \tag{12}$$

Proof. Apply ${}^{RL}I^{\alpha_i}, i = 1, 2$ to Equation (10), respectively, implies

$${}^{CH}D^{\beta_1}\psi(t) = {}^{RL}I^{\alpha_1} p(t) + c_0, \quad c_0 \in \mathbb{R}, \tag{13}$$

$${}^{CH}D^{\beta_2}\varphi(t) = {}^{RL}I^{\alpha_2} q(t) + d_0, \quad d_0 \in \mathbb{R}. \tag{14}$$

Now, apply ${}^{H}I^{\beta_i}, i = 1, 2$ to Equation (13) and Equation (14), respectively, implies

$$\psi(t) = {}^{H}I^{\beta_1}\left({}^{RL}I^{\alpha_1} p\right)(t) + c_0 \frac{(\ln (t/a))^{\beta_1}}{\Gamma(\beta_1 + 1)} + c_1, c_0, c_1 \in \mathbb{R}, \tag{15}$$

$$\varphi(t) = {}^{H}I^{\beta_2}\left({}^{RL}I^{\alpha_2} q\right)(t) + d_0 \frac{(\ln (t/a))^{\beta_2}}{\Gamma(\beta_2 + 1)} + d_1, d_0, d_1 \in \mathbb{R}. \tag{16}$$

Using the conditions $\psi(a) = 0, \varphi(a) = 0$ in Equation (15) and Equation (16), respectively, yields c_1, d_1 are both zeros. Again the conditions $\psi(T) = 0, \varphi(T) = 0$ in Equation (15) and Equation (16), respectively, give

$$c_0 = -\frac{\Gamma(\beta_1+1)}{(\ln(T/a))^{\beta_1}} {}^H I^{\beta_1}\left({}^{RL}I^{\alpha_1}p\right)(T),$$
$$d_0 = -\frac{\Gamma(\beta_2+1)}{(\ln(T/a))^{\beta_2}} {}^H I^{\beta_2}\left({}^{RL}I^{\alpha_2}q\right)(T). \tag{17}$$

Back substituting $c_i, d_i, i = 1, 2$ obtained above in equations Equation (15) and Equation (16), we get $\psi\ \ (t) = {}^H I^{\beta_1}({}^{RL}I^{\alpha_1}p)(t) - (\ln(t/a)/\ln(T/a))^{\beta_1} {}^H I^{\beta_1}({}^{RL}I^{\alpha_1} p)(T)$, and $\varphi(t) = {}^H I^{\beta_2}({}^{RL}I^{\alpha_2}q)(t) - (\ln(t/a)/\ln(T/a))^{\beta_2} {}^H I^{\beta_2}({}^{RL}I^{\alpha_2}q)(T)$. The proof is completed. □

To begin formulating theoretical results regarding the problem of having a solution to the system of fractional differential equations given by Equation (3). We will force the following conditions to be hold true.

(C1). Assume the functions $\varsigma, \xi : [a, T] \times \mathbb{R}^2 \longrightarrow \mathbb{R}$ satisfy Carathéodory conditions.

(C2). $\exists l_\varsigma, l_\xi \in L^\infty([a, T], \mathbb{R}_+)$, and there exist a nondecreasing continuous function $\vartheta_\varsigma, \vartheta_\xi : \mathbb{R}_+ \longrightarrow \mathbb{R}_+$, such that , $\forall t \in [a, T], \forall(\psi, \varphi) \in B$, we have

$$\|\varsigma(t, \psi, \varphi)\|_\infty \le l_\varsigma(t)\vartheta_\varsigma(\|\psi\|_\infty + \|\varphi\|_\infty),$$
$$\|\xi(t, \psi, \varphi)\|_\infty \le l_\xi(t)\vartheta_\xi(\|\psi\|_\infty + \|\varphi\|_\infty). \tag{18}$$

(C3). Let $S \subset B \times B$, be a bounded set, and $\forall t \in [a, T]$, then

$$\kappa(\varsigma(t, S)) \le l_\varsigma(t)\kappa(S),$$
$$\kappa(\xi(t, S)) \le l_\xi(t)\kappa(S). \tag{19}$$

Also, one can use the fact that $(r-a)^{\alpha_1} \le (T-a)^{\alpha_1}$, to deduce that

$$\begin{aligned}\Xi_1 = \sup_{a\le t\le T}&\left\{\frac{1}{\Gamma(\alpha_1)\Gamma(\beta_1)}\int_a^t\int_a^r\left(\ln\frac{t}{r}\right)^{\beta_1-1}(r-x)^{\alpha_1-1}dx\frac{dr}{r}\right.\\ &\left.+\left(\frac{\ln(t/a)}{\ln(T/a)}\right)^{\beta_1}\frac{1}{\Gamma(\alpha_1)\Gamma(\beta_1)}\int_a^T\int_a^r\left(\ln\frac{T}{r}\right)^{\beta_1-1}(r-x)^{\alpha_1-1}dx\frac{dr}{r}\right\}\\ &\le\frac{2(T-a)^{\alpha_1}(\ln(T/a))^{\alpha_1}}{\Gamma(\alpha_1+1)\Gamma(\beta_1+1)},\\ \Xi_2 = \sup_{a\le t\le T}&\left\{\frac{1}{\Gamma(\alpha_2)\Gamma(\beta_2)}\int_a^t\int_a^r\left(\ln\frac{t}{r}\right)^{\beta_2-1}(r-x)^{\alpha_2-1}dx\frac{dr}{r}\right.\\ &\left.+\left(\frac{\ln(t/a)}{\ln(T/a)}\right)^{\beta_2}\frac{1}{\Gamma(\alpha_2)\Gamma(\beta_2)}\int_a^T\int_a^r\left(\ln\frac{T}{r}\right)^{\beta_2-1}(r-x)^{\alpha_2-1}dx\frac{dr}{r}\right\}\\ &\le\frac{2(T-a)^{\alpha_2}(\ln(T/a))^{\alpha_2}}{\Gamma(\alpha_2+1)\Gamma(\beta_2+1)}.\end{aligned} \tag{20}$$

Theorem 11. *Assume that the conditions (C1), (C2), and (C3) are satisfied. If* $\max\{\Xi_1\bar{l}_\varsigma, \Xi_2\bar{l}_\xi\} < 1$, *then there exist at least one solution for the boundary value problem Equation (3) on* $[a, T]$.

Proof. Beginning with introducing the following continuous operator $\Upsilon : B \longrightarrow B$, as $\Upsilon = (\Upsilon_1(\psi, \varphi)(t), \Upsilon_2(\psi, \varphi)(t))$, where

$$\begin{aligned}\Upsilon_1(\psi,\varphi)(t) = &\frac{1}{\Gamma(\alpha_1)\Gamma(\beta_1)}\int_a^t\int_a^r\left(\ln\frac{t}{r}\right)^{\beta_1-1}(r-x)^{\alpha_1-1}\|\varsigma(x,\psi(x),\varphi(x))\|dx\frac{dr}{r}\\ &-\left(\frac{\ln(t/a)}{\mathrm{n}(T/a)}\right)^{\beta_1}\frac{1}{\Gamma(\alpha_1)\Gamma(\beta_1)}\int_a^T\int_a^r\\ &\cdot\left(\ln\frac{T}{r}\right)^{\beta_1-1}(r-x)^{\alpha_1-1}\|\varsigma(x,\psi(x),\varphi(x))\|dx\frac{dr}{r},\\ \Upsilon_2(\psi,\varphi)(t) = &\frac{1}{\Gamma(\alpha_2)\Gamma(\beta_2)}\int_a^t\int_a^r\left(\ln\frac{t}{r}\right)^{\beta_2-1}(r-x)^{\alpha_2-1}\xi(x,\psi(x),\varphi(x))dx\frac{dr}{r}\\ &-\left(\frac{\ln(t/a)}{\mathrm{n}(T/a)}\right)^{\beta_2}\frac{1}{\Gamma(\alpha_2)\Gamma(\beta_2)}\int_a^T\int_a^r\\ &\cdot\left(\ln\frac{T}{r}\right)^{\beta_2-1}(r-x)^{\alpha_2-1}\xi(x,\psi(x),\varphi(x))dx\frac{dr}{r}.\end{aligned} \tag{21}$$

According to the conditions (C1) and (C2), the operator Υ is well defined. Then, the following operator equation can be an equivalent equation to the fractional equations given by Equation (11) and Equation (12)

$$(\psi, \varphi) = \Upsilon(\psi, \varphi). \tag{22}$$

Subsequently, proving the existence of the solution to Equation (22) is equivalent to proving the existence of a solution to Equation (3).

Let $\Theta_\varepsilon = \{(\psi, \varphi) \in B : \|(\psi, \varphi)\| \le \varepsilon, \varepsilon > 0\}$ be a closed bounded convex ball in B with $\varepsilon \ge \bar{l}_\varsigma \Xi_1 \vartheta_\varsigma(\varepsilon) + \bar{l}_\xi \Xi_2 \vartheta_\xi(\varepsilon)$, where $\bar{l}_\varsigma = \sup_{a\le t\le T} l_\varsigma(t)$,.

For the possibility of applying Mönch's fixed point theorem, we will proceed in the proof in the form of four steps, and thus, we achieve the desired goal by proving the existence of a solution to the equation given in Equation (3).

Firstly, we show that $\Upsilon\Theta_\varepsilon \subset \Theta_\varepsilon$, for this, we let $t \in [a, T]$, and for any $(\psi, \varphi) \in \Theta_\varepsilon$, we have

$$\begin{aligned}\|\Upsilon_1(\psi,\varphi)\|_\infty \le &\frac{1}{\Gamma(\alpha_1)\Gamma(\beta_1)}\int_a^t\int_a^r\\ &\cdot\left(\ln\frac{t}{r}\right)^{\beta_1-1}(r-x)^{\alpha_1-1}\|\varsigma(x,\psi(x),\varphi(x))\|_\infty dx\frac{dr}{r}\\ &+\left(\frac{\ln(t/a)}{\ln(T/a)}\right)^{\beta_1}\frac{1}{\Gamma(\alpha_1)\Gamma(\beta_1)}\int_a^T\int_a^r\\ &\cdot\left(\ln\frac{T}{r}\right)^{\beta_1-1}(r-x)^{\alpha_1-1}\|\varsigma(x,\psi(x),\varphi(x))\|_\infty dx\frac{dr}{r}.\end{aligned} \tag{23}$$

Based on (C2), $\forall t \in [a, T]$, observe that

$$\|\varsigma(t,\psi(t),\varphi(t))\|_\infty \le l_\varsigma(t)\vartheta_\varsigma(\|\psi(t)\|_\infty + \|\varphi(t)\|_\infty) \le \bar{l}_\varsigma\vartheta_\varsigma(\varepsilon), \tag{24}$$

then

$$\begin{aligned}\|\Upsilon_1(\psi,\varphi)\|_\infty &\le \frac{1}{\Gamma(\alpha_1)\Gamma(\beta_1)}\int_a^t\int_a^r\left(\ln\frac{t}{r}\right)^{\beta_1-1}\\ &\cdot (r-x)^{\alpha_1-1} l_\varsigma(t)\vartheta_\varsigma(\|\psi(t)\|_\infty+\|\varphi(t)\|_\infty)dx\frac{dr}{r}\\ &+\left(\frac{\ln(t/a)}{\ln(T/a)}\right)^{\beta_1}\frac{1}{\Gamma(\alpha_1)\Gamma(\beta_1)}\int_a^T\int_a^r\\ &\cdot\left(\ln\frac{T}{r}\right)^{\beta_1-1}(r-x)^{\alpha_1-1}l_\varsigma(t)\vartheta_\varsigma(\|\psi(t)\|_\infty+\|\varphi(t)\|_\infty)dx\frac{dr}{r},\\ &\le \bar{l}_\varsigma\vartheta_\varsigma(\|\psi(t)\|_\infty+\|\varphi(t)\|_\infty)\sup_{a\le t\le T}\\ &\cdot\left\{\frac{1}{\Gamma(\alpha_1)\Gamma(\beta_1)}\int_a^t\int_a^r\left(\ln\frac{t}{r}\right)^{\beta_1-1}(r-x)^{\alpha_1-1}dx\frac{dr}{r}\right.\\ &\left.+\left(\frac{\ln(t/a)}{\ln(T/a)}\right)^{\beta_1}\frac{1}{\Gamma(\alpha_1)\Gamma(\beta_1)}\int_a^T\int_a^r\left(\ln\frac{T}{r}\right)^{\beta_1-1}(r-x)^{\alpha_1-1}dx\frac{dr}{r}\right\}\\ &\le \bar{l}_\varsigma\Xi_1\vartheta_\varsigma(\varepsilon).\end{aligned}\tag{25}$$

Similarly,

$$\begin{aligned}\|\Upsilon_2(\psi,\varphi)\|_\infty &\le \frac{1}{\Gamma(\alpha_2)\Gamma(\beta_2)}\int_a^t\int_a^r\left(\ln\frac{t}{r}\right)^{\beta_2-1}\\ &\cdot (r-x)^{\alpha_2-1} l_\xi(t)\vartheta_\xi(\|\psi(t)\|_\infty+\|\varphi(t)\|_\infty)dx\frac{dr}{r}\\ &+\left(\frac{\ln(t/a)}{\mathrm{n}(T/a)}\right)^{\beta_2}\frac{1}{\Gamma(\alpha_2)\Gamma(\beta_2)}\int_a^T\int_a^r\\ &\cdot\left(\ln\frac{T}{r}\right)^{\beta_2-1}(r-x)^{\alpha_2-1}l_\xi(t)\vartheta_\xi(\|\psi(t)\|_\infty+\|\varphi(t)\|_\infty)dx\frac{dr}{r}\\ &\le \bar{l}_\xi\Xi_2\vartheta_\xi(\varepsilon).\end{aligned}\tag{26}$$

Equation (25) and Equation (26) imply that

$$\|\Upsilon(\psi,\varphi)\|_B=\|\Upsilon_1(\psi,\varphi)\|_\infty+\|\Upsilon_2(\psi,\varphi)\|_\infty\le\bar{l}_\varsigma\Xi_1\vartheta_\varsigma(\varepsilon)+\le\bar{l}_\xi\Xi_2\vartheta_\xi(\varepsilon)\le\varepsilon.\tag{27}$$

This proves that $\Upsilon\Theta_\varepsilon\subset\Theta_\varepsilon$.

Secondly, we need to show the continuity for Υ to see this, we take the sequence $\{u_n=(\psi_n,\varphi_n)\}\in\Theta_\varepsilon$, such that $u_n\longrightarrow u=(\psi,\varphi)$ as $n\longrightarrow\infty$..

Owing to the Carathéodory continuity of ς, it is obvious that

$$\varsigma((\cdot),\psi_n(\cdot),\varphi_n(\cdot))\longrightarrow\varsigma((\cdot),\psi(\cdot),\varphi(\cdot))\text{as } n\longrightarrow\infty.\tag{28}$$

Keeping in mind was given in (C2), one can deduce that

$$\begin{aligned}&\left(\ln\frac{t}{r}\right)^{\beta_1-1}(r-x)^{\alpha_1-1}\|\varsigma((r),\psi_n(r),\varphi_n(r))-\varsigma((r),\psi(r),\varphi(r))\|_\infty\\ &\le\bar{l}_\varsigma\vartheta_\varsigma(\varepsilon)\left(\left(\ln\frac{t}{r}\right)^{\beta_1-1}(r-x)^{\alpha_1-1}\right).\end{aligned}\tag{29}$$

Together with the Lebesgue dominated convergence theorem and the fact that the function $r\mapsto\bar{l}_\varsigma\vartheta_\varsigma(\varepsilon)((\ln(t/r))^{\beta_1-1}(r-x)^{\alpha_1-1})$ is the Lebesgue integrable on $[a,T]$, we have

$$\begin{aligned}&\left(\frac{1}{\Gamma(\alpha_1)\Gamma(\beta_1)}\int_a^t\int_a^r\left(\ln\frac{t}{r}\right)^{\beta_1-1}(r-x)^{\alpha_1-1}\|\varsigma((r),\psi_n(r),\varphi_n(r))-\varsigma((r),\psi(r),\varphi(r))\|_\infty dx\frac{dr}{r}\right.\\ &+\left(\frac{\ln(t/a)}{\ln(T/a)}\right)^{\beta_1}\frac{1}{\Gamma(\alpha_1)\Gamma(\beta_1)}\int_a^T\int_a^r\left(\ln\frac{T}{r}\right)^{\beta_1-1}(r-x)^{\alpha_1-1}\|\varsigma((r),\psi_n(r),\varphi_n(r))\\ &\left.-\varsigma((r),\psi(r),\varphi(r))\|_\infty dx\frac{dr}{r}\right)\longrightarrow 0\text{as } n\longrightarrow\infty.\end{aligned}\tag{30}$$

Yields to $\|\Upsilon_1(\psi_n,\varphi_n)(t)-\Upsilon_1(\psi,\varphi)(t)\|_\infty\longrightarrow 0$ as $n\longrightarrow\infty.\forall t\in[a,T]$, we get

$$\|\Upsilon_1(\psi_n,\varphi_n)-\Upsilon_1(\psi,\varphi)\|_\infty\longrightarrow 0\text{ as } n\longrightarrow\infty,\tag{31}$$

that is the operator Υ_1 is continuous.

In a like manner, we have

$$\|\Upsilon_2(\psi_n,\varphi_n)-\Upsilon_2(\psi,\varphi)\|_\infty\longrightarrow 0\text{ as } n\longrightarrow\infty,\tag{32}$$

Combining (31) and (32), we obtain

$$\|\Upsilon(\psi_n,\varphi_n)-\Upsilon(\psi,\varphi)\|_\infty\longrightarrow 0\text{ as } n\longrightarrow\infty.\tag{33}$$

From equation (33), we conclude that the operator Υ is continuous.

Third, to verify the equicontinuity for the operator Υ, let $t_1,t_2\in[a,T]$, $(t_1<t_2)$, and for any $(\psi,\varphi)\in\Theta_\varepsilon$, then

$$\begin{aligned}&\|\Upsilon_1(\psi,\varphi)(t_2)-\Upsilon_1(\psi,\varphi)(t_1)\|_\infty\\ &\le\frac{1}{\Gamma(\alpha_1)\Gamma(\beta_1)}\int_a^{t_1}\int_a^r\left[\left(\ln\frac{t_2}{r}\right)^{\beta_1-1}-\left(\ln\frac{t_1}{r}\right)^{\beta_1-1}\right]\\ &\times(r-x)^{\alpha_1-1}\|\varsigma(x,\psi(x),\varphi(x))\|_\infty dx\frac{dr}{r}+\frac{1}{\Gamma(\alpha_1)\Gamma(\beta_1)}\int_{t_1}^{t_1}\int_a^r\\ &\times\left(\ln\frac{t_2}{r}\right)^{\beta_1-1}(r-x)^{\alpha_1-1}\|\varsigma(x,\psi(x),\varphi(x))\|_\infty dx\frac{dr}{r}\\ &+\left(\frac{(\ln(t_2/a))^{\beta_1}-(\ln(t_2/a))^{\beta_1}}{\mathrm{l}(\mathrm{n}(T/a))^{\beta_1}\Gamma(\alpha_1)\Gamma(\beta_1)}\right)\int_a^T\int_a^r\left(\ln\frac{T}{r}\right)^{\beta_1-1}\\ &\times(r-x)^{\alpha_1-1}\|\varsigma(x,\psi(x),\varphi(x))\|_\infty dx\frac{dr}{r},\\ &\le(\bar{l}_\varsigma(t)\vartheta_\varsigma(\varepsilon))\times\left(\frac{1}{\Gamma(\alpha_1)\Gamma(\beta_1)}\int_a^{t_1}\int_a^r\left[\left(\ln\frac{t_2}{r}\right)^{\beta_1-1}-\left(\ln\frac{t_1}{r}\right)^{\beta_1-1}\right]\right.\\ &\times(r-x)^{\alpha_1-1}dx\frac{dr}{r}+\frac{1}{\Gamma(\alpha_1)\Gamma(\beta_1)}\int_{t_1}^{t_1}\int_a^r\left(\ln\frac{t_2}{r}\right)^{\beta_1-1}(r-x)^{\alpha_1-1}dx\frac{dr}{r}\\ &\left.+\left[\frac{(\ln(t_2/a))^{\beta_1}-(\ln(t_1/a))^{\beta_1}}{(\ln(T/a))^{\beta_1}\Gamma(\alpha_1)\Gamma(\beta_1)}\right]\int_a^T\int_a^r\left(\ln\frac{T}{r}\right)^{\beta_1-1}(r-x)^{\alpha_1-1}dx\frac{dr}{r}\right)\\ &\longrightarrow 0\ as\ t_1\longrightarrow t_2.\end{aligned}\tag{34}$$

Similarly, we get

$$\begin{aligned}&\|\Upsilon_2(\psi,\varphi)(t_2)-\Upsilon_2(\psi,\varphi)(t_1)\|_\infty\\&\le(\bar{l}_\xi(t)\vartheta_\xi(\varepsilon))\times\left(\frac{1}{\Gamma(\alpha_2)\Gamma(\beta_2)}\int_a^{t_1}\int_a^r\left[\left(\ln\frac{t_2}{r}\right)^{\beta_2-1}-\left(\ln\frac{t_1}{r}\right)^{\beta_2-1}\right](r-x)^{\alpha_2-1}dx\frac{dr}{r}\right.\\&+\frac{1}{\Gamma(\alpha_2)\Gamma(\beta_2)}\int_{t_1}^{t_1}\int_a^r\left(\ln\frac{t_2}{r}\right)^{\beta_2-1}(r-x)^{\alpha_2-1}dx\frac{dr}{r}\\&\left.+\left[\frac{(\ln(t_2/a))^{\beta_2}-(\ln(t_2/a))^{\beta_2}}{\mathrm{l}(\mathrm{n}(T/a))^{\beta_2}\Gamma(\alpha_2)\Gamma(\beta_2)}\right]\int_a^T\int_a^r\left(\ln\frac{T}{r}\right)^{\beta_2-1}(r-x)^{\alpha_2-1}dx\frac{dr}{r}\right)\longrightarrow 0\ as\ t_1\longrightarrow t_2.\end{aligned}\tag{35}$$

Note that the R.H.S's of the above inequalities of Equation (34) and Equation (35) are free of $(\psi,\varphi)\in\Theta_\varepsilon$, which implies that Υ is equicontinuous and bounded.

Fourth and finally, we need to satisfy Mönch's hypothesis, so we let$U=U_1\cap U_2$,.

where $U_1, U_2\subseteq\Theta_\varepsilon$. Moreover, U_1, U_2 are assumed to be bounded and equicontinuous, such that

$$U_1\subset\overline{conv}(\Upsilon_1(U_1)\cup\{0\}),\text{and } U_2\subset\overline{conv}(\Upsilon_2(U_2)\cup\{0\}).\tag{36}$$

Thus, the functions $\mathfrak{I}_1(t)=\kappa(U_1(t)), \mathfrak{I}_2(t)=\kappa(U_2(t))$ are continuous on $[a,T]$.

Based on lemma Equation(10), lemma Equation (11), and (C3), we get

$$\begin{aligned}&\mathfrak{I}_1(t)=\kappa(U_1(t))\le\kappa(\overline{conv}(\Upsilon_1(U_1)(t)\cup\{0\}))\le\kappa(\Upsilon_1(U_1)(t))\\&\le\kappa\left\{\frac{1}{\Gamma(\alpha_1)\Gamma(\beta_1)}\int_a^{t_1}\int_a^r\left[\left(\ln\frac{t_2}{r}\right)^{\beta_1-1}-\left(\ln\frac{t_1}{r}\right)^{\beta_1-1}\right]\right.\\&\cdot(r-x)^{\alpha_1-1}\|\varsigma(x,\psi(x),\varphi(x))\|_\infty dx\frac{dr}{r}+\frac{1}{\Gamma(\alpha_1)\Gamma(\beta_1)}\int_{t_1}^{t_1}\int_a^r\left(\ln\frac{t_2}{r}\right)^{\beta_1-1}\\&\cdot(r-x)^{\alpha_1-1}\|\varsigma(x,\psi(x),\varphi(x))\|_\infty dx\frac{dr}{r}+\left(\frac{(\ln(t_2/a))^{\beta_1}-(\ln(t_2/a))^{\beta_1}}{\ln(T/a)}\right)\\&\left.\cdot\frac{1}{\Gamma(\alpha_1)\Gamma(\beta_1)}\int_a^T\int_a^r\left(\ln\frac{T}{r}\right)^{\beta_1-1}(r-x)^{\alpha_1-1}\|\varsigma(x,\psi(x),\varphi(x))\|_\infty dx\frac{dr}{r}:(\psi,\varphi)\in U_1\right\}\\&\le\frac{1}{\Gamma(\alpha_1)\Gamma(\beta_1)}\int_a^{t_1}\int_a^r\left[\left(\ln\frac{t_2}{r}\right)^{\beta_1-1}-\left(\ln\frac{t_1}{r}\right)^{\beta_1-1}\right](r-x)^{\alpha_1-1}\kappa(\varsigma(x,U_1(x)))dx\frac{dr}{r}\\&+\frac{1}{\Gamma(\alpha_1)\Gamma(\beta_1)}\int_{t_1}^{t_1}\int_a^r\left(\ln\frac{t_2}{r}\right)^{\beta_1-1}(r-x)^{\alpha_1-1}\kappa(\varsigma(x,U_1(x)))dx\frac{dr}{r}\\&+\left(\frac{(\ln(t_2/a))^{\beta_1}-(\ln(t_2/a))^{\beta_1}}{\ln(T/a)}\right)\frac{1}{\Gamma(\alpha_1)\Gamma(\beta_1)}\int_a^T\int_a^r\left(\ln\frac{T}{r}\right)^{\beta_1-1}\\&\cdot(r-x)^{\alpha_1-1}\kappa(\varsigma(x,U_1(x)))dx\frac{dr}{r}\le\frac{1}{\Gamma(\alpha_1)\Gamma(\beta_1)}\int_a^{t_1}\int_a^r\left[\left(\ln\frac{t_2}{r}\right)^{\beta_1-1}-\left(\ln\frac{t_1}{r}\right)^{\beta_1-1}\right]\\&\cdot(r-x)^{\alpha_1-1}l_\varsigma(x)\kappa(U_1(x))dx\frac{dr}{r}+\frac{1}{\Gamma(\alpha_1)\Gamma(\beta_1)}\int_{t_1}^{t_1}\int_a^r\left(\ln\frac{t_2}{r}\right)^{\beta_1-1}\\&\cdot(r-x)^{\alpha_1-1}l_\varsigma(x)\kappa(U_1(x))dx\frac{dr}{r}+\left(\frac{(\ln(t_2/a))^{\beta_1}-(\ln(t_2/a))^{\beta_1}}{\ln(T/a)}\right)\frac{1}{\Gamma(\alpha_1)\Gamma(\beta_1)}\int_a^T\int_a^r\\&\cdot\left(\ln\frac{T}{r}\right)^{\beta_1-1}(r-x)^{\alpha_1-1}l_\varsigma(x)\kappa(U_1(x))dx\frac{dr}{r}\le\Xi_1\bar{l}_\varsigma\|\mathfrak{I}_1\|_\infty.\end{aligned}\tag{37}$$

That is

$\|\mathfrak{I}_1\|\le\Xi_1\bar{l}_\varsigma\|\mathfrak{I}_1\|$, but it is assumed that max $\{\Xi_1\bar{l}_\varsigma,\Xi_2\bar{l}_\xi\}<1$, which implies that $\|\mathfrak{I}_1\|_\infty=0$, i.e.,

$$\mathfrak{I}_1(t)=0,\forall t\in[a,T].\tag{38}$$

In a like manner, we have $\mathfrak{I}_2(t)=0,\forall t\in[a,T]$. So $\kappa(U(t))\le\kappa(U_1(t))=0$ and.

$\kappa(U(t))\le\kappa(U_2(t))=0$, which implies that $U(t)$ is relatively compact in $B\times B$. Now, Arzela-Ascoli is applicable, which means that U is relatively compact in $\Theta_{\varepsilon\cdot,}$ and therefore, using theorem 9, we deduce that the operator Υ has a fixed point (ψ,φ) (solution of the problem Equation (3)) on Θ_ε. And that ends the proof. □

4. Example

In this section, we provide an applied example that supports the theoretical results reached through this study.

Define $\psi_0=\{\psi=(\psi_1,\psi_2,\cdots,\psi_n,\cdots):\lim_{n\longrightarrow\infty}\psi_n=0\}$, it is obvious that z_0 is a Banach space with$\|\psi\|_\infty=\sup_{n\ge1}|\psi_n|$. For this, we consider the following boundary value problem:

$$\begin{cases}{}^{C}D^{0.5}\left({}^{CH}D^{0.75}\psi(t)\right)=\varsigma(t,\psi(t),\varphi(t)), & t\in[1,3],\\{}^{C}D^{0.6}\left({}^{CH}D^{0.9}\varphi(t)\right)=\xi(t,\psi(t),\varphi(t)), & t\in[1,3],\\\psi(1)=\psi(3)=(0,0,0,\cdots,0,\cdots), & \varphi(1)=\varphi(3)=(0,0,0,\cdots,0,\cdots).\end{cases}\tag{39}$$

Here, $\alpha_1=0.5$, $\beta_1=0.75$, $\alpha_2=0.6$, $\beta_2=0.9$, $a=1$, and $T=3$.

Now, let us take for example

$$\begin{aligned}\varsigma(t,\psi(t),\varphi(t))&=\left\{\frac{1}{\ln t+10}\left(\frac{1}{4^n}+\ln(1+|\psi_n|+|\varphi_n|)\right)\right\},n\ge1,\\\xi(t,\psi(t),\varphi(t))&=\left\{\frac{t}{10}\left(\frac{1}{n^4}+\tan^{-1}(1+|\psi_n|+|\varphi_n|)\right)\right\},n\ge1.\end{aligned}\tag{40}$$

$\forall t\in[1,3]$, with$\{\psi_n\}_{n\ge1},\{\varphi_n\}_{n\ge1}\in\psi_0$, assumption (C1) of theorem 11 is satisfied. Furthermore,

$$\begin{aligned}\|\varsigma(t,\psi,\varphi)\|_\infty&\le\left\|\frac{1}{\ln t+10}\left(\frac{1}{4^n}+\ln(1+|\psi_n|+|\varphi_n|)\right)\right\|_\infty\\&\le\frac{1}{\ln t+10}(\|\psi\|+1)=l_\varsigma(t)\vartheta_\varsigma(\|\psi\|).\end{aligned}\tag{41}$$

Similarly,

$$\begin{aligned}\|\xi(t,\psi,\varphi)\|_\infty&\le\left\|\frac{t}{10}\left(\frac{1}{n^4}+\tan^{-1}(1+|\psi_n|+|\varphi_n|)\right)\right\|_\infty\\&\le\frac{t}{10}(\|\psi\|+1)=l_\xi(t)\vartheta_\xi(\|\psi\|).\end{aligned}\tag{42}$$

That is (C2) of theorem 11 is satisfied as well.

Next, if we consider the bounded subset $S \subset \psi_0 \times \psi_0$, we obtain

$$\kappa(\varsigma(t, S)) \leq l_\varsigma(t)\kappa(S),$$
$$\kappa(\xi(t, S)) \leq l_\xi(t)\kappa(S), \quad (43)$$

where in our case, we have $l_\varsigma(t) = 1/\ln t + 9, l_\xi(t) = t/10$; the latter two inequalities show that the condition (C2) of the theorem 11 is satisfied.

Finally, we calculate

$$\bar{l}_\varsigma = \frac{1}{10}, \Xi_1 \leq \frac{2(T-a)^{\alpha_1}(\ln(T/a))^{\alpha_1}}{\Gamma(\alpha_1+1)\Gamma(\beta_1+1)} = 3.6411,$$
$$\bar{l}_\xi = \frac{3}{10}, \Xi_2 \leq \frac{2(T-a)^{\alpha_2}(\ln(T/a))^{\alpha_2}}{\Gamma(\alpha_2+1)\Gamma(\beta_2+1)} = 0.9376. \quad (44)$$

Then, $\max\{\Xi_1\bar{l}_\varsigma, \Xi_2\bar{l}_\xi\} = \max\{0.3611, 0.28128\} = 0.3611 < 1$. So all conditions of theorem 11 satisfied, that is the problem Equation (39) has at least one solution$(\psi, \varphi) \in C([1,3], \psi_0) \times C([1,3], \psi_0)$.

5. Conclusion

In the current paper, we studied the existence and uniqueness of solution for a coupled system of a mixed fractional differential equations. The main results are established by the aid "Mönch's fixed point theorem." In addition, an applied example that supports the theoretical results reached through this study is included. For future work, more investigations can be performed for such a system by applying another type of fractional derivatives to verify the existence and uniqueness issue, stability via Ulam-Hyeres technique is also possible to be verified.

Data Availability

No data sets were used in this study.

Conflicts of Interest

The author declares that he has no conflict of interest.

Acknowledgments

This work was supported through the Annual Funding track by the Deanship of Scientific Research, Vice Presidency for Graduate Studies and Scientific Research, King Faisal University, Saudi Arabia [Project No. GRANT115], King Faisal University (KFU), Ahsa, Saudi Arabia. The author, therefore, acknowledges technical and financial support of DSR at KFU.

References

[1] I. Podlubny, *Fractional Differential Equations: An Introduction to Fractional Derivatives, Fractional Differential Equations, to Methods of their Solution and some of their Applications*, Elsevier, 1998.

[2] A. A. Kilbas, H. M. Srivastava, and J. J. Trujillo, *Theory and Applications of Fractional Differential Equations, Vol. 204*, Elsevier, 2006.

[3] E. Zeidler, *Nonlinear Functional Analysis and Its Applications: Part 2 B: Nonlinear Monotone Operators*, Springer, 1990.

[4] H. Mönch, "Boundary value problems for nonlinear ordinary differential equations of second order in Banach spaces," *Nonlinear Analysis: Theory, Methods & Applications*, vol. 4, no. 5, pp. 985–999, 1980.

[5] J. Wang, W. Wei, and M. Feckan, "Nonlocal Cauchy problems for fractional evolution equations involving Volterra-Fredholm type integral operators," *Miskolc Mathematical Notes*, vol. 13, no. 1, pp. 127–147, 2012.

[6] J. R. Wang, Y. Zhou, and M. Fečkan, "On the nonlocal Cauchy problem for semilinear fractional order evolution equations," *Journal of Mathematics*, vol. 12, no. 6, 922 pages, 2014.

[7] M. Awadalla, Y. Y. N. Yannick, K. A. Asbeh, Y. Y. N. Yannick, and K. A. Asbeh, "Modeling the dependence of barometric pressure with altitude using Caputo and Caputo–Fabrizio fractional derivatives," *Journal of Mathematics*, vol. 2020, Article ID 2417681, 9 pages, 2020.

[8] M. K. A. Kaabar, M. Shabibi, J. Alzabut et al., "Investigation of the fractional strongly singular thermostat model via fixed point techniques," *Mathematics*, vol. 9, no. 18, p. 2298, 2021.

[9] M. M. Matar, M. I. Abbas, J. Alzabut, M. K. A. Kaabar, S. Etemad, and S. Rezapour, "Investigation of the p-Laplacian nonperiodic nonlinear boundary value problem via generalized Caputo fractional derivatives," *Advances in Difference Equations*, vol. 2021, no. 1, 2021.

[10] M. Awadalla, Y. Y. Yameni Noupoue, and K. A. Asbeh, "Psi-Caputo Logistic Population Growth Model," *Journal of Mathematics*, vol. 2021, Article ID 8634280, 9 pages, 2021.

[11] M. Awadalla, Y. Y. Y. Noupoue, and K. Abuasbeh, "Population growth modeling via Rayleigh-Caputo fractional derivative," *Journal of Statistics Applications & Probability*, vol. 10, no. 1, pp. 11–16, 2021.

[12] C. Bai, "Impulsive periodic boundary value problems for fractional differential equation involving Riemann-Liouville sequential fractional derivative," *Journal of Mathematical Analysis and Applications*, vol. 384, no. 2, pp. 211–231, 2011.

[13] B. Ahmad and J. J. Nieto, "Sequential fractional differential equations with three-point boundary conditions," *Computers & Mathematics with Applications*, vol. 64, no. 10, pp. 3046–3052, 2012.

[14] B. Ahmad and J. J. Nieto, "Boundary value problems for a class of sequential integrodifferential equations of fractional order," *Journal of Function Spaces and Applications*, vol. 2013, article 149659, pp. 1–8, 2013.

[15] M. H. Aqlan, A. Alsaedi, B. Ahmad, and J. J. Nieto, "Existence theory for sequential fractional differential equations with anti-periodic type boundary conditions," *Open Mathematics*, vol. 14, no. 1, pp. 723–735, 2016.

[16] M. Klimek, "Sequential fractional differential equations with Hadamard derivative," *Communications in Nonlinear Science and Numerical Simulation*, vol. 16, no. 12, pp. 4689–4697, 2011.

[17] H. Ye and R. Huang, "Initial value problem for nonlinear fractional differential equations with sequential fractional derivative," *Advances in Difference Equations*, vol. 2015, no. 1, 2015.

[18] N. I. Mahmudov and M. Awadalla, "On sequential fractional differential equations with nonlocal integral boundary

conditions," *Journal of Computational Analysis and Applications*, vol. 628, 2019.

[19] S. Aljoudi, B. Ahmad, J. J. Nieto, and A. Alsaedi, "A coupled system of Hadamard type sequential fractional differential equations with coupled strip conditions," *Chaos, Solitons & Fractals*, vol. 91, pp. 39–46, 2016.

[20] B. Ahmad and S. Ntouyas, "Existence and uniqueness of solutions for Caputo-Hadamard sequential fractional order neutral functional differential equations," *Electronic Journal of Differential Equations*, vol. 2017, no. 36, pp. 1–11, 2017.

[21] R. Agarwal, D. O'Regan, and S. Hristova, "Stability of Caputo fractional differential equations by Lyapunov functions," *Applications of Mathematics*, vol. 60, no. 6, pp. 653–676, 2015.

[22] X. Wang, D. Luo, and Q. Zhu, "Ulam-Hyers stability of Caputo type fuzzy fractional differential equations with time-delays," *Chaos, Solitons & Fractals*, vol. 156, article 111822, 2022.

[23] Y. Zhao, S. Sun, Z. Han, and Q. Li, "Theory of fractional hybrid differential equations," *Computers & Mathematics with Applications*, vol. 62, no. 3, pp. 1312–1324, 2011.

[24] S. Sun, Y. Zhao, Z. Han, and Y. Li, "The existence of solutions for boundary value problem of fractional hybrid differential equations," *Communications in Nonlinear Science and Numerical Simulation*, vol. 17, no. 12, pp. 4961–4967, 2012.

[25] B. Ahmad and S. K. Ntouyas, "An existence theorem for fractional hybrid differential inclusions of Hadamard type with Dirichlet boundary conditions," *Abstract and Applied Analysis*, vol. 2014, Article ID 705809, 7 pages, 2014.

[26] B. C. Dhage and S. K. Ntouyas, "Existence results for boundary value problems for fractional hybrid differential inclusions," *Topological Methods in Nonlinear Analysis*, vol. 44, no. 1, pp. 229–238, 2014.

[27] C. Derbazi and Z. Baitiche, "Coupled systems of ψ-Caputo differential equations with initial conditions in Banach spaces," *Mediterranean Journal of Mathematics*, vol. 17, article 169, 2020.

[28] M. Benchohra, J. Henderson, and D. Seba, "Measure of noncompactness and fractional differential equations in Banach spaces," *Communications in Applied Analysis*, vol. 12, no. 4, p. 419, 2008.

[29] D. J. Guo, V. Lakshmikantham, and X. Z. Liu, *Nonlinear Integral Equations in Abstract Spaces*, Kluwer Academic Publishers, Dordrecht, 1996.

Hindawi
Journal of Function Spaces
Volume 2022, Article ID 1035118, 12 pages
https://doi.org/10.1155/2022/1035118

Research Article

Inverse Source Problem for Sobolev Equation with Fractional Laplacian

Nguyen Duc Phuong,[1] Van Tien Nguyen,[2] and Le Dinh Long [3,4]

[1]*Industrial University of Ho Chi Minh City, Ho Chi Minh City, Vietnam*
[2]*Faculty of Math, FPT University HCM, Saigon Hi-Tech Park, Thu Duc City, Ho Chi Minh City, Vietnam*
[3]*Division of Applied Mathematics, Science and Technology Advanced Institute, Van Lang University, Ho Chi Minh City, Vietnam*
[4]*Faculty of Technology, Van Lang University, Ho Chi Minh City, Vietnam*

Correspondence should be addressed to Le Dinh Long; ledinhlong@vlu.edu.vn

Received 25 March 2022; Accepted 4 May 2022; Published 25 May 2022

Academic Editor: Yusuf Gurefe

In this paper, we are interested in the problem of determining the source function for the Sobolev equation with fractional Laplacian. This problem is ill-posed in the sense of Hadamard. In order to edit the instability instability of the solution, we applied the fractional Landweber method. In the theoretical analysis results, we show the error estimate between the exact solution and the regularized solution by using an a priori regularization parameter choice rule and an a posteriori regularization parameter choice rule. Finally, we investigate the convergence of the source function when fractional order $\beta \longrightarrow 1^+$.

1. Introduction

Let Ω be a bounded domain in $\mathbb{R}^N (N \geq 1)$ with sufficiently smooth boundary $\partial\Omega$. In this paper, we are interested to study the following pseudo-parabolic equation

$$\begin{cases} u_t - a\Delta u_t + (-\Delta)^\beta u = F(x,t), & \text{in } \Omega \times (0,T], \\ u|_{\partial\Omega} = 0, & \text{in } \Omega, \end{cases} \tag{1}$$

where $a > 0$ is the diffusion coefficient, F is the source function, and u desribe the distribution of the temperature at position x and time t. The paramater β is the fractional order of Laplacian operator with $\beta \geq 1$.

Pseudo-parabolic equations or called *Sobolev equation* describe describing various important physical phenomena, such as heat conduction involving two temperatures [1], homogeneous liquid permeability in fractured rock [2], unidirectional propagation of long waves in a nonlinearly dispersed medium [3], and its references.

Until now, the results on fractional pseudo-parabolic equations equation are not rich we can mention them in a few some few papers, for example, [1, 4–6]. From the fraction operator $(-\Delta)^\beta$ appearing in the main equation which is nonlocal, many scientists believe that it describes some physical phenomena more accurately than classical integrals differential equation. Properties of fractional operator $(-\Delta)^\beta$ have been described in detail in [1].

For equation (1) we usually divide it into three forms.

(i) The first type is an initial value problem, i.e., determining u when the initial value $u(x,0) = u_0(x)$ and the source function F is known. The results in this category are vibrant and plentiful ([7, 8])

(ii) The second type is terminal value problem, i.e., recovering the function u from the terminal value data $u(x,T) = u_T(x)$ and the source function data F. To the best of our knowledge, there are limited results for the terminal value problem. We can list some recent papers, for example, [9–13]. In general, the terminal value problem is an ill-posed problem; namely, a solution does do not exist, and if a solution exists, it does not depend continuously on the data. The results of the regularized method for this form were recently investigated by [14, 15]

(iii) The last type is inverse source problem, i.e., recovering the source function F if we know the initial value data $u(x,0)=u_0(x)$ and the terminal data $u(x,T)=u_T(x)$

The main purpose of this paper is to determine the source function $F=\psi(t)f(x)$ with the split form when we know that

$$u(x,T)=g(x), \quad u(x,0)=0, x\in\Omega. \tag{2}$$

The question of determining the function f when we know ψ and g will be studied carefully in this paper. It is surprising that the problem of determining the source function for the pseudo-parabolic equation has not been investigated before. We detail the objective of the problem. In practice, the given data$(\psi_\delta, g_\delta)$is noisy by the observed data (ψ, g) by level $\delta>0$ such that

$$\|\psi_\delta-\psi\|_{L^\infty(0,T)}+\|g_\delta-g\|_{L^2(\Omega)}\le\delta. \tag{3}$$

Our main task here is to construct a regularized method which looking for the function f_δ and claims claim that

$$\lim\|f_\delta-f\|=0, \quad \text{when } \delta\longrightarrow 0^+, \tag{4}$$

in the appropriate norm. It can be claimed that our paper was one of the first works on the inverse source problem for the Sobolev equation.

In [7], Tuan-Long-Thinh used the Tikhonov regularization method to regularize regularized an inverse source problem for time fractional diffusion equation. They also introduced two methods, a priori and a posteriori parameter choice rules, to obtain the convergence estimate of the regularized methods. In [16], the authors studied the problem of finding the source distribution for the linear biparabolic equation when we have the final observation. Ma et al. [17] identified the unknown space-dependent source term in a time-fractional diffusion equation by applying the generalized and revised generalized Tikhonov regularization methods. There are many different regularized methods, and in this paper, we choose the fractional Landweber regularization method. The Landweber regularization method was first derived from [18] where the authors applied the filter regularization technique for solving a linear inverse problem. Up to now, the Landweber regularization method has been applied to solve many inverse problems, for example, [19–21] and references therein. This method is beneficial very useful for investigating for the linear ill-posed equation. Recently, Binh et al. [22] studied an inverse source problem for the Rayleigh–Stokes problem using the Tikhonov method.

For the reader's convenience, we would like to outline the main results and novelties of the paper briefly:

(i) The first goal of this paper is to provide the fractional Landweber method to solve this inverse space-dependent source problem for pseudo-parabolic equation. We give the ill-posedness of our inverse source problem and introduce the convergence rate of the fractional Landweber regularized solution. In addition, we obtain the convergence rate by using an apriori parameter choice rule and an a posteriori parameter choice rule. Looking back at the articles [19–21], we realize that the source functions in these papers do not depend on the time function. So, the computation is not complicated. Meanwhile, the source function of the current paper depends on the function ψ which makes the calculation more cumbersome. The presence of (3) makes our problem more clearly complex complex than [19–21]. One point to note is that the method in the article [23] can be applied to our model, but we approach it differently, in a different way.

(ii) The second interesting point in the paper is the investigation of the convergence of the source function when the order of derivative approaches 1. Comparing the difference between the source function of equation (1) with $\beta>1$ and the classical pseudo-parabolic equation $\beta=1$ will help us understand more information about problem (1).

The paper is organized as follows. Section 2 states some preliminary theoretical knowledge. In Section 3, we give the Fourier formula of the source function and also present the ill-posedness of our problem. The conditional stability for the source function source function is also discussed in the same section. Section 4 provides the fractional Landweber regularization method and states a convergence estimate under a priori assumption on the exact solution. The posteriori parameter choice rule is also shown in section 4. Finally, in Section 5, we prove the convergence of the source function in Hilbert scales space with the appropriate assumption of ψ and g.

2. Preliminary Results

Let us consider the operator $\mathscr{A}=-\Delta$ on $\mathbb{V}:=\mathscr{H}_0^1(\Omega)\cap H^2(\Omega)$, and assume that the operator $\mathscr{A}$ has the eigenvalues λ_j such that $0<\lambda_1\le\lambda_2\le\cdots\le\lambda_j\le\cdots$ which approach ∞ as j goes to ∞, The corresponding eigenfunctions are denoted by $e_j\in\mathbb{V}$. Now, let us define fractional powers of $\mathscr{A}$ and its domain. For all $s\ge0$, we define by $\mathscr{A}^s$ the following operator:

$$\mathscr{A}^s v:=\sum_{j=1}^{\infty}\langle v,e_j\rangle\lambda_j^s e_j, v\in D(\mathscr{A}^s)=\left\{v\in L^2(\Omega): \sum_{j=1}^{\infty}\left|\langle v,e_j\rangle\right|^2\lambda_j^{2s}<\infty\right\}. \tag{5}$$

The domain $\mathbb{H}^s(\Omega) = D(\mathcal{A}^s)$ is the Banach space equipped with the norm

$$\|v\|_{D(\mathcal{A}^s)} := \left(\sum_{j=1}^{\infty} \left|\langle v, e_j \rangle\right|^2 \lambda_j^{2s}\right)^{1/2}, \quad v \in D(\mathcal{A}^s). \tag{6}$$

We introduce the following two lemmas, which are useful and helpful in the next proofs.

Lemma 1. *Let $\psi : [0, T] \longrightarrow \mathbb{R}$ such that $\psi_0 \le \psi(t) \le \psi_1$ where ψ_0 and ψ_1 are positive numbers. Let us assume that $\beta \ge 1$. Then, the following estimates are true:*

$$\begin{aligned} &\int_0^T \exp\left(-(T-s)\lambda_j^\beta (1+a\lambda_j)^{-1}\right)\psi(s)ds \le \psi_1 \frac{1+a\lambda_j}{\lambda_j^\beta}, \\ &\frac{1+a\lambda_j}{\lambda_j^\beta}\left[1 - \exp\left(-T\lambda_1^\beta (1+a\lambda_1)^{-1}\right)\right]\psi_0 \\ &\quad \le \int_0^T \exp\left(-(T-s)\lambda_j^\beta (1+a\lambda_j)^{-1}\right)\psi(s)ds. \end{aligned} \tag{7}$$

Proof. Since $\psi(t) \le \psi_1$, we infer that

$$\begin{aligned} &\int_0^T \exp\left(-(T-s)\lambda_j^\beta (1+a\lambda_j)^{-1}\right)\psi(s) \\ &\quad \cdot ds \le \psi_1 \int_0^T \exp\left(-(T-s)\lambda_j^\beta (1+a\lambda_j)^{-1}\right)ds = \psi_1 \frac{1+a\lambda_j}{\lambda_j^\beta}. \end{aligned} \tag{8}$$

□

Since $\psi(t) \ge \psi_0 > 0$, we infer that

$$\begin{aligned} &\int_0^T \exp\left(-(T-s)\lambda_j^\beta (1+a\lambda_j)^{-1}\right)\psi(s) \\ &\quad \cdot ds \ge \psi_0 \int_0^T \exp\left(-(T-s)\lambda_j^\beta (1+a\lambda_j)^{-1}\right) \\ &\quad \cdot ds = \frac{1+a\lambda_j}{\lambda_j^\beta}\left[1 - \exp\left(-T\lambda_j^\beta (1+a\lambda_j)^{-1}\right)\right]\psi_0 \cdot \end{aligned} \tag{9}$$

Let us consider the following function:

$$\Phi(z) = \frac{z^\beta}{1+az}, \quad z > 0. \tag{10}$$

The derivative of it is equal to

$$\Phi'(z) = \frac{a\beta z^{\beta-1} + \beta z^\beta - z^\beta}{(1+az)^2} > 0. \tag{11}$$

This implies that Φ is an increasing function on $(0, +\infty)$. Therefore, we get that

$$\lambda_j^\beta (1+a\lambda_j)^{-1} \ge \lambda_1^\beta (1+a\lambda_1)^{-1}. \tag{12}$$

It follows from (9) that

$$\begin{aligned} &\int_0^T \exp\left(-(T-s)\lambda_j^\beta (1+a\lambda_j)^{-1}\right)\psi(s) \\ &\quad \cdot ds \ge \frac{1+a\lambda_j}{\lambda_j^\beta}\left[1 - \exp\left(-T\lambda_1^\beta (1+a\lambda_1)^{-1}\right)\right]\psi_0. \end{aligned} \tag{13}$$

The proof of the Lemma 1 is completed.

Lemma 2. *Let ψ_0, ψ_1 be positive constants such that $\psi_0 < \psi < \psi_1$. By choosing $\delta \in (0, \psi_1/4)$, and $\mathcal{B}(\psi_0, \psi_1) = \psi_1 + (\psi_0/4)$, we obtain*

$$4^{-1}\psi_0 \le |\psi_\delta(t)| \le \mathcal{B}(\psi_0, \psi_1). \tag{14}$$

Proof. The proof is completed in [26], page 4. □

3. Inverse Source Problem: Explicit Form and Ill-Posedness

Let us first give the explicit of Fourier form of the mild solution to problems (1) and (2). First, taking the inner product of both sides of (1) with $e_j(x)$, we find that

$$\begin{aligned} &\frac{d}{dt}\left(\int_\Omega u(x,t)e_j(x)dx\right) + a\lambda_j\left(\int_\Omega u(x,t)e_j(x)dx\right) \\ &\quad + \lambda_j^\beta\left(\int_\Omega u(x,t)e_j(x)dx\right) = \int_\Omega F(x,t)e_j(x)dx, \end{aligned} \tag{15}$$

and from the initial condition $u(x,0) = 0$, we have that

$$\begin{aligned} \int_\Omega u(x,T)e_j(x)dx = &\int_0^T \exp\left(-(T-s)\lambda_j^\beta (1+a\lambda_j)^{-1}\right) \\ &\cdot \left(\int_\Omega F(x,s)e_j(x)dx\right)ds, \end{aligned} \tag{16}$$

since $F(x,s) = \psi(s)f(x)$; we know that

$$\int_\Omega f(x)e_j(x)dx = \frac{\int_\Omega g(x)e_j(x)dx}{\int_0^T \exp\left(-(T-s)\lambda_j^\beta (1+a\lambda_j)^{-1}\right)\psi(s)ds}. \tag{17}$$

Hence, the source function is defined as follows:

$$f(x) = \sum_{j=1}^{\infty}\left[\frac{\int_\Omega g(x)e_j(x)dx}{\int_0^T \exp\left(-(T-s)\lambda_j^\beta (1+a\lambda_j)^{-1}\right)\psi(s)ds}\right]e_j(x). \tag{18}$$

Let us prove the ill-posedness of inverse source problems

(1) and (2). Logically, we will consider the source function problem as the problem of finding f satisfying (18). From now on, we only treat the source term (18).

Theorem 3. *The problem of determining f that satisfies (18) is ill-posed in the sense of Hadamard.*

Proof. We defined a linear operator $Y : L^2(\Omega) \longrightarrow L^2(\Omega)$ as follows:

$$Yf(x) = \sum_{j=1}^{\infty}\left(\int_0^T \exp\left(-(T-s)\lambda_j^{\beta}\left(1+a\lambda_j\right)^{-1}\right)\psi(s)ds\right) < f, e_j > e_j(x) = \int_\Omega k(x,\xi)f(\xi)d\xi. \tag{19}$$

□

Due to $k(x,\xi) = k(\xi,x)$, we know Y is a self-adjoint operator. Next, its compactness is explained as follows. Let us define the finite rank operators $Y_{\mathcal{N}}$ as follows:

$$Y_N f(x) = \sum_{j=1}^{N}\left(\int_0^T \exp\left(-(T-s)\lambda_j^{\beta}\left(1+a\lambda_j\right)^{-1}\right)\psi(s)ds\right) < f, \quad e_j > e_j(x). \tag{20}$$

By some simple calculations and using Lemma 1, we have

$$\|Y_{\mathcal{N}}f - Yf\|^2_{L^2(\Omega)} \le \underbrace{\psi_1^2\left(\lambda_1^{-1}+a\right)^2}_{\mathcal{A}_1^2} \sum_{j=N+1}^{+\infty} \frac{\left|<f, e_j>\right|^2}{\lambda_j^{2\beta-2}}. \tag{21}$$

From (21), we have

$$\left\| \|Y_N f - Yf\|^2_{L^2(\Omega)} \le \frac{\mathcal{A}_1^2}{\lambda_N^{2\beta-2}} \right\| f\|^2_{L^2(\Omega)} \longrightarrow 0 \text{ in } L\left(L^2(\Omega); L^2(\Omega)\right) \text{ as } N \longrightarrow \infty. \tag{22}$$

Therefore, Y is a compact operator. The SVDs for the linear self-adjoint compact operator Y are

$$Y = \left(\int_0^T \exp\left(-(T-s)\lambda_j^{\beta}\left(1+a\lambda_j\right)^{-1}\right)\psi(s)ds\right), \tag{23}$$

and corresponding eigenvectors are e_j which is an orthonormal basis in $L^2(\Omega)$. Therefore, the inverse source problem we introduced above can be formulated as an operator equation $Yf(x) = g(x)$ where by $g(x)$ is the numerator in formula (18), and by Kirsch, we can conclude that it is ill-posed. The final time data $g_i = \lambda_i e_i$, by (18), the source term corresponding to g_i is

$$\begin{aligned} f_i(x) &= \sum_{j=1}^{\infty}\left(\int_0^T \exp\left(-(T-s)\lambda_j^{\beta}\left(1+a\lambda_j\right)^{-1}\right)\psi(s)ds\right)^{-1} \cdot \left(\int_\Omega g(x)e_j(x)dx\right)e_j(x) \\ &\ge \underbrace{\left(\frac{1}{\lambda_1}+a\right)^{-1}\left[1-\exp\left(-T\lambda_i^{\beta}\left(1+a\lambda_i\right)^{-1}\right)\right]^{-1}\psi_0^{-1}}_{\mathcal{A}_2}\lambda_i^{\beta}, \end{aligned} \tag{24}$$

whereby $\mathcal{A}_1$ is defined in formula (21). The input final data $g = 0$, by (18), the source term corresponding to g is $f = 0$. We have error in $L^2(\Omega)$ norm between g_m and g

$$\lim_{i\longrightarrow+\infty}\|g_i - g\|_{L^2(\Omega)} = \lim_{i\longrightarrow+\infty}\lambda_i^{-1} = 0. \tag{25}$$

Then, the error in L^2 norm between f_i and f is estimated as follows:

$$\|f_i - f\|_{L^2(\Omega)} \ge \frac{\lambda_i}{\mathcal{A}_2} \longrightarrow \lim_{i\longrightarrow+\infty}\|f_i - f\|_{L^2(\Omega)} \ge +\infty. \tag{26}$$

From (25) and (26), we deduce that the solution to problem (1) is unstable in $L^2(\Omega)$.

Next, we consider stability of the inverse source problem.

Theorem 4. *If $f \in \mathcal{D}(\mathcal{A}^s)$ such that*

$$\|f\|_{D(\mathcal{A}^s)} \le \mathcal{E}, s = \frac{k(\beta-1)}{2} \ge 0, \tag{27}$$

then we get

$$\|f\|_{L^2(\Omega)} \le \mathcal{C}_1^{-k/(k+2)}\mathcal{E}^{2/(k+2)}\|g\|^{k/(k+2)}_{L^2(\Omega)}, \tag{28}$$

where $\mathcal{C}_1 = (a[1-\exp(-T\lambda_1^{\beta}(1+a\lambda_1))^{-1}]\psi_0)$.

Proof. From (18) and the Hölder inequality, it gives

$$\begin{aligned} \|f\|^2_{L^2(\Omega)} &= \sum_{j=1}^{\infty}\left[\frac{\int_\Omega g(x)e_j(x)dx}{\int_0^T \exp\left(-(T-s)\lambda_j^{\beta}\left(1+a\lambda_j\right)^{-1}\right)\psi(s)ds}\right]^2 \\ &\le \sum_{j=1}^{\infty}\frac{\left(\int_\Omega g(x)e_j(x)\right)^{2k/(k+2)}}{\left[\int_0^T \exp\left(-(T-s)\lambda_j^{\beta}\left(1+a\lambda_j\right)^{-1}\right)\psi(s)ds\right]^2} \cdot \left(\int_\Omega g(x)e_j(x)dx\right)^{4/k+2} \\ &\le \left(\sum_{j=1}^{\infty}\frac{\left(\int_\Omega f(x)e_j(x)dx\right)^2}{\left(\int_0^T \exp\left(-(T-s)\lambda_j^{\beta}\left(1+a\lambda_j\right)^{-1}\right)\psi(s)ds\right)^k}\right)^{2/k+2} \cdot \left(\sum_{j=1}^{\infty}\left(\int_\Omega g(x)e_j(x)dx\right)^2\right)^{k/k+2}. \end{aligned} \tag{29}$$

Applying Lemma 1 and the priori boundary condition (27), we have

$$\begin{aligned}\sum_{j=1}^{\infty}&\frac{\left(\int_\Omega f(x)e_j(x)dx\right)^2}{\left(\int_0^T \exp\left(-(T-s)\lambda_j^\beta\left(1+a\lambda_j\right)^{-1}\right)\psi(s)ds\right)^k}\\&=\sum_{j=1}^{\infty}\left(\int_\Omega f(x)e_j(x)dx\right)^2\lambda_j^{k(\beta-1)}\\&\quad\cdot\left(a\left[1-\exp\left(-T\lambda_1^\beta(1+a\lambda_1)^{-1}\right)\right]\psi_0\right)^{-k}\le\mathscr{E}^2(\mathscr{C}_1)^{-k}.\end{aligned}\tag{30}$$

Combining (29) to (30), one has

$$\|f\|_{L^2(\Omega)}\le\mathscr{C}_1^{-k/(k+2)}\mathscr{E}^{2/(k+2)}\|g\|_{L^2(\Omega)}^{k/(k+2)},\tag{31}$$

where $\mathscr{C}_1=(a[1-\exp(-T\lambda_1^\beta(1+a\lambda_1)^{-1})]\psi_0)$. The proof of this theorem is completed. □

4. A Fractional Landweber Method and Convergent Rate

In this section, we apply the fractional Landweber regularization method to solve the inverse source problem (1) and give a convergence estimate. The construction of this method and its iterative implementation are clarified in [19]. We denote the fractional Landweber regularization solution with the observed data by

$$\begin{aligned}f_{c(\delta),\delta}(x)=&\sum_{j=1}^{\infty}1-\left[1-b\left(\frac{\lambda_1^{-1}+a}{\lambda_j^{\beta-1}}\right)^2\right]^{c(\delta)}\\&\cdot\frac{\left(\int_\Omega g_\delta(x)e_j(x)dx\right)e_j(x)}{\int_0^T\exp\left(-(T-s)\lambda_j^\beta\left(1+a\lambda_j\right)^{-1}\right)\psi_\delta(s)ds},\end{aligned}\tag{32}$$

$$\begin{aligned}f^d_{c(\delta),\delta}(x)=&\sum_{j=1}^{\infty}\left[1-\left(1-b\left(\frac{\lambda_1^{-1}+a}{\lambda_j^{\beta-1}}\right)^2\right)^{c(\delta)}\right]^d\\&\cdot\frac{\left(\int_\Omega g_\delta(x)e_j(x)dx\right)e_j(x)}{\int_0^T\exp\left(-(T-s)\lambda_j^\beta\left(1+a\lambda_j\right)^{-1}\right)\psi_\delta(s)ds},\end{aligned}\tag{33}$$

$$\begin{aligned}f^d_{c(\delta)}(x)=&\sum_{j=1}^{\infty}\left[1-\left(1-b\left(\frac{\lambda_1^{-1}+a}{\lambda_j^{\beta-1}}\right)^2\right)^{c(\delta)}\right]^d\\&\cdot\frac{\left(\int_\Omega g(x)e_j(x)dx\right)e_j(x)}{\int_0^T\exp\left(-(T-s)\lambda_j^\beta\left(1+a\lambda_j\right)^{-1}\right)\psi(s)ds}.\end{aligned}\tag{34}$$

It is obvious to see that formulas (33) and (34) are more complicated. For simplicity, we put $\mathscr{C}_\beta(a,s,\lambda_j)=\exp(-(T-s)\lambda_j^\beta(1+a\lambda_j)^{-1})$. Expressions (33) and (34) become

$$\begin{aligned}f^d_{c,\delta}(x)=&\sum_{j=1}^{\infty}\left[1-\left(1-b\left(\frac{\lambda_1^{-1}+a}{\lambda_j^{\beta-1}}\right)^2\right)^{c(\delta)}\right]^d\\&\cdot\frac{\left(\int_\Omega g_\delta(x)e_j(x)dx\right)e_j(x)}{\int_0^T\mathscr{C}_\beta\left(a,s,\lambda_j\right)\psi_\delta(s)ds},\ \frac{1}{2}<d<1,\end{aligned}\tag{35}$$

$$\begin{aligned}f^d_{c}(x)=&\sum_{j=1}^{\infty}\left[1-\left(1-b\left(\frac{\lambda_1^{-1}+a}{\lambda_j^{\beta-1}}\right)^2\right)^{c(\delta)}\right]^d\\&\cdot\frac{\left(\int_\Omega g(x)e_j(x)dx\right)e_j(x)}{\int_0^T\mathscr{C}_\beta\left(a,s,\lambda_j\right)\psi(s)ds},\ \frac{1}{2}<d<1,\end{aligned}\tag{36}$$

where $d\in(1/2,1]$ is called the fractional parameter and $c(\delta)\ge1$ is a regularization parameter and $b\in(0,(\lambda_1^{\beta-1}/\lambda_1^{-1}+a)^2)$. If $d=1$, it is the classical Landweber method. Next, we have the following lemmas:

Lemma 5. *For $0<\lambda<1,\tau>0,\ n\in\mathbb{N}$, let $r_n(\lambda):=(1-\lambda)^n$, we get*

$$r_n(\lambda)\lambda^\tau\le\theta_\tau(n+1)^{-\tau},\tag{37}$$

where

$$\theta_\tau=\begin{cases}1, & 0\le\tau\le1,\\ \tau^\tau, & \tau>1.\end{cases}\tag{38}$$

Proof. Please see in [19]. □

Lemma 6. *For $(1/2)<d<1,c(\delta)\ge1$, choosing $b\in(0,(\lambda_1^{\beta-1}/\lambda_1^{-1}+a)^2)$ then $0<b(\lambda_1^{-1}+a/\lambda_1^{\beta-1})^2<1$, by denoting $z=b(\lambda_1^{-1}+a/\lambda_1^{\beta-1})^2$, we have the following estimates:*

$$\begin{aligned}&(a)[1-(1-z)^c]^d\left(\frac{z}{b}\right)^{-1/2}\le b^{1/2}c^{1/2},\\&(b)(1-z)^c\left(\frac{z}{b}\right)^{\varsigma/2}\le\left(\frac{\varsigma}{2b}\right)^{\varsigma/2}c^{-\varsigma/2}.\end{aligned}\tag{39}$$

Proof. The proof can be found in [19]. □

4.1. A Priori Parameter Choice Rule

Theorem 7. *Suppose that f is given by (18) such that $\|f\|_{\mathscr{D}(A^{k(\beta-1)})}\le\mathscr{E}$ for any $\mathscr{E}>0$. Let the data $(\psi,g,\psi_\delta,g_\delta)$ satisfy (3). If we choose $[c(\delta)]=(\mathscr{E}/\delta)^{2/k+1}$, then we obtain*

$$\|f^r_{c(\delta),\delta}-f\|_{L^2(\Omega)}\text{ is of order }\delta^{k/k+1},\tag{40}$$

where $f^d_{c(\delta),\delta}$ is a regularized solution defined in (35).

Proof. By using the triangle inequality, we have

$$\|f^d_{c(\delta),\delta} - f\|_{L^2(\Omega)} \le \|f^d_{c(\delta),\delta} - f^d_{c(\delta)}\|_{L^2(\Omega)} + \|f^d_{c(\delta)} - f\|_{L^2(\Omega)}. \tag{41}$$

□

We receive $\|f^d_{c(\delta),\delta} - f^d_{c(\delta)}\|_{L^2(\Omega)}$ as follows:

$$f^d_{c(\delta),\delta}(x) - f^d_{c(\delta)}(x) = \sum_{j=1}^{\infty}\left[1 - \left(1 - b\left(\frac{\lambda_1^{-1}+a}{\lambda_j^{\beta-1}}\right)^2\right)^{c(\delta)}\right]^d \cdot \left(\frac{\int_\Omega g_\delta(x)e_j(x)dx e_j(x)}{\int_0^T \mathscr{C}_\beta(a,s,\lambda_j)\psi_\delta(s)ds} - \frac{\int_\Omega g(x)e_j(x)dx e_j(x)}{\int_0^T \mathscr{C}_\beta(a,s,\lambda_j)\psi(s)ds}\right). \tag{42}$$

From (42), we get

$$\|f^d_{c(\delta),\delta} - f^d_{c(\delta)}\|_{L^2(\Omega)} = \underbrace{\sum_{j=1}^{\infty}\left[1 - \left(1 - b\left(\frac{\lambda_1^{-1}+a}{\lambda_j^{\beta-1}}\right)^2\right)^{c(\delta)}\right]^d \left(\frac{\int_\Omega (g_\delta(x)-g(x))e_j(x)dx}{\int_0^T \mathscr{C}_\beta(a,s,\lambda_j)\psi_\delta(s)ds}\right)}_{\mathscr{I}_1} + \underbrace{\sum_{j=1}^{\infty}\left[1 - \left(1 - b\left(\frac{\lambda_1^{-1}+a}{\lambda_j^{\beta-1}}\right)^2\right)^{c(\delta)}\right]^d \left(\frac{\int_\Omega g(x)e_j(x)dx}{\int_0^T \mathscr{C}_\beta(a,s,\lambda_j)\psi_\delta(s)ds} - \frac{\int_\Omega g(x)e_j(x)dx}{\int_0^T \mathscr{C}_\beta(a,s,\lambda_j)\psi(s)ds}\right)}_{\mathscr{I}_2}. \tag{43}$$

Using (43), Lemma 6, and Lemma 1 and noting that $|(\lambda_1^{-1}+a)/\lambda_j^{\beta-1}|^{-1}$, we provide the estimation of $\mathscr{I}_1$ as follows:

$$\begin{aligned}\mathscr{I}_1 &\le \sum_{j=1}^{\infty}\left[1 - \left(1 - b\left(\frac{\lambda_1^{-1}+a}{\lambda_j^{\beta-1}}\right)^2\right)^{c(\delta)}\right]^d \left|\frac{\lambda_1^{-1}+a}{\lambda_j^{\beta-1}}\right|^{-1} \\ &\quad\times \left|\frac{\lambda_1^{-1}+a}{\lambda_j^{\beta-1}}\right|\left|\frac{\lambda_j^{\beta-1}}{\lambda_1^{-1}+a}\right|\frac{4}{\psi_0}\left(\frac{\int_\Omega (g_\delta(x)-g(x))e_j(x)dx}{[1-\exp(-T\lambda_1(1+a\lambda_1)^{-1})]]}\right) \\ &\le [c(\delta)]^{1/2}b^{1/2}4\varepsilon\left[\psi_0\left(1-\exp\left(-T\lambda_1(1+a\lambda_1)^{-1}\right)\right)\right]^{-1}.\end{aligned} \tag{44}$$

Next, we have the estimation of $\mathscr{I}_2$

$$\begin{aligned}\mathscr{I}_2 &\le \sum_{j=1}^{\infty}\left|\frac{\int_0^T \mathscr{C}_\beta(a,s,\lambda_j)(\psi(s)-\psi_\delta)ds}{\int_0^T \mathscr{C}_\beta(a,s,\lambda_j)\psi_\delta(s)ds} \times \frac{\int_\Omega g(x)e_j(x)dx e_j(x)}{\int_0^T \mathscr{C}_\beta(a,s,\lambda_j)\psi(s)ds}\right| \\ &\le \frac{4\delta}{\psi_0}\|f\|_{L^2(\Omega)}.\end{aligned} \tag{45}$$

Combining (42) to (45), we derive that

$$\left\|f^d_{c(\delta),\delta} - f^d_{c(\delta)}\right\|_{L^2(\Omega)} \le [c(\delta)]^{1/2}b^{1/2}4\delta \cdot \left[\psi_0\left(1-\exp\left(-T\lambda_1(1+a\lambda_1)^{-1}\right)\right)\right]^{-1} + \frac{4\delta}{\psi_0}\|f\|_{L^2(\Omega)}. \tag{46}$$

Next, we give

$$\begin{aligned}\left\|f^d_{c(\delta)} - f\right\|^2_{L^2(\Omega)} &= \sum_{j=1}^{\infty}\left[1 - \left[1 - \left(1 - b\left(\frac{\lambda_1^{-1}+a}{\lambda_j^{\beta-1}}\right)^2\right)^{c(\delta)}\right]^d\right]^2 \cdot \left|\frac{\int_\Omega g(x)e_j(x)dx}{\int_0^T \mathscr{C}_\beta(a,s,\lambda_j)\psi(s)ds}\right|^2 \\ &\le \sum_{j=1}^{\infty}\left[1 - \left[1 - \left(1 - b\left(\frac{\lambda_1^{-1}+a}{\lambda_j^{\beta-1}}\right)^2\right)^{c(\delta)}\right]^d\right]^2 \\ &\quad\cdot \lambda_j^{-k(\beta-1)}\|f\|^2_{\mathscr{D}(A^{k(\beta-1)})} \le \sum_{j=1}^{\infty}\left[1 - b\left|\frac{\lambda_1^{-1}+a}{\lambda_j^{\beta-1}}\right|^2\right]^{2c(\delta)} \lambda_j^{-k(\beta-1)}\mathscr{C}^2.\end{aligned} \tag{47}$$

From estimate (13) and Lemma 1, we arrive at

$$\begin{aligned}&\int_0^T \exp\left(-(T-s)\lambda_j^\beta(1+a\lambda_j)^{-1}\right) \\ &\quad\cdot ds \ge \frac{1+a\lambda_j}{\lambda_j^\beta}\left[1-\exp\left(-T\lambda_1^\beta(1+a\lambda_1)^{-1}\right)\right] \\ &\ge \frac{a\lambda_j}{\lambda_j^\beta}\left[1-\exp\left(-T\lambda_1^\beta(1+a\lambda_1)^{-1}\right)\right] \ge a\lambda_j^{-(\beta-1)} \\ &\quad\cdot \left[1-\exp\left(-T\lambda_1^\beta(1+a\lambda_1)^{-1}\right)\right].\end{aligned} \tag{48}$$

Hence,

$$\begin{aligned}\lambda_j^{-(\beta-1)} &\le \frac{\int_0^T \exp\left(-(T-s)\lambda_j^\beta(1+a\lambda_j)^{-1}\right)ds}{a\left[1-\exp\left(-T\lambda_1^\beta(1+a\lambda_1)^{-1}\right)\right]} \\ &\le \frac{(\lambda_1^{-1}+a)}{\lambda_j^{\beta-1}a\left[1-\exp\left(-T\lambda_1^\beta(1+a\lambda_1)^{-1}\right)\right]}.\end{aligned} \tag{49}$$

The above estimate (49) implies that

$$\lambda_j^{-k(\beta-1)} \le \frac{(\lambda_1^{-1}+a)^k}{\lambda_j^{k(\beta-1)}a^k\left[1-\exp\left(-T\lambda_1^\beta(1+a\lambda_1)^{-1}\right)\right]^k}. \tag{50}$$

From observation above, using Lemma 6, we conclude that

$$\|f^d_{c(\delta)} - f\|^2_{L^2(\Omega)} \le \sum_{j=1}^{\infty} \left[1 - b\left|\frac{\lambda_1^{-1} + a}{\lambda_j^{\beta-1}}\right|^2\right]^{2c(\delta)} \cdot \left(\frac{(\lambda_1^{-1} + a)}{\lambda_j^{(\beta-1)}}\right)^k \frac{\mathscr{E}^2}{a^k\left[1 - \exp\left(-T\lambda_1^{\beta}(1 + a\lambda_1)^{-1}\right)\right]^k} \le \left(\frac{k}{2b}\right)^k [c(\delta)]^{-k} \frac{\mathscr{E}^2}{a^k\left[1 - \exp\left(-T\lambda_1^{\beta}(1 + a\lambda_1)^{-1}\right)\right]^k}. \tag{51}$$

From (47) and (50), we have

$$\|f^d_{c(\delta)} - f\|_{L^2(\Omega)} \le \left(\frac{k}{2b}\right)^{k/2} [c(\delta)]^{-k/2} \cdot \frac{\mathscr{E}^2}{a^{k/2}\left[1 - \exp\left(-T\lambda_1^{\beta}(1 + a\lambda_1)^{-1}\right)\right]^{k/2}}. \tag{52}$$

Combining (68) to (52), it can be seen

$$\|f^d_{c(\delta)} - f\|_{L^2(\Omega)} \le [c(\delta)]^{1/2} b^{1/2} 4\delta\left[\psi_0\left(1 - \exp\left(-T\lambda_1(1 + a\lambda_1)^{-1}\right)\right)\right]^{-1} + \frac{4\delta}{\psi_0}\|f\|_{L^2(\Omega)} + \left(\frac{k}{2b}\right)^{k/2} \cdot [c(\delta)]^{-k/2} \frac{\mathscr{E}}{a^{k/2}\left[1 - \exp\left(-T\lambda_1^{\beta}(1 + a\lambda_1)^{-1}\right)\right]^{k/2}}. \tag{53}$$

By substituting $c(\delta) = [(\mathscr{E}/\delta)^{2/k+1}]$ in the above expression, we deduce that

$$\|f^d_{c(\delta),\delta} - f\|_{L^2(\Omega)} \le \delta^{k/k+1}\mathscr{E}^{k/k+1}(\mathscr{L}_1 + \mathscr{L}_2), \tag{54}$$

where

$$\mathscr{L}_1 = b^{1/2} 4\left[\psi_0\left(1 - \exp\left(-T\lambda_1(1 + a\lambda_1)^{-1}\right)\right)\right]^{-1} + 4\delta^{k/k+1}\psi_0^{-1}\mathscr{C}_1^{-k/k+2}\|g\|^{k/k+2},$$
$$\mathscr{L}_2 = \left(\frac{k}{2b}\right)^{k/2} \frac{\mathscr{E}}{a^{k/2}\left[1 - \exp\left(-T\lambda_1^{\beta}(1 + a\lambda_1)^{-1}\right)\right]^{k/2}}. \tag{55}$$

The proof of Theorem 7 is completed.

4.2. A Posteriori Parameter Choice Rule. In order to obtain a posteriori convergence error estimate, we apply Morozov's discrepancy principle, which is introduced in [18]. Furthermore, we learn the analysis techniques from previous papers [19–21].

Let us assume that $\sigma > 1$ is a fixed constant. By a similar claim in [19–21], we provide that the general a posteriori rule in the following:

$$\|Yf^d_{c(\delta),\delta} - g_\delta\|_{L^2(\Omega)} \le \sigma\delta. \tag{56}$$

From here on, in this subsection, we need to assume further to further assume that $c(\delta)$ is a natural number that greater than 1. If $\|g_\delta\|_{L^2(\Omega)} \ge \sigma\delta$, then the equation (56) exists in a unique solution.

Lemma 8. *Set $\mathscr{R}(c(\delta)) = \|Yf^\delta_{c(\delta),\delta} - g_\delta\|_{L^2(\Omega)}$ where $0 < \delta < \|g_\delta\|_{L^2(\Omega)}$. Then, we declare that*

(a) *$\mathscr{R}(c(\delta))$ is a continuous function*

(b) *$\mathscr{R}(c(\delta)) \longrightarrow 0$ as $c(\delta) \longrightarrow +\infty$*

(c) *$\mathscr{R}(c(\delta)) \longrightarrow \|g_\delta\|_{L^2(\Omega)}$ as $c(\delta) \longrightarrow 0$*

(d) *$\mathscr{R}(c(\delta))$ is a strictly increasing function for $c(\delta) \in (0, +\infty)$*

Proof. The proof of Lemma 8 is simple and completely similar to that in [19–21]. Hence, we omit it here. □

Lemma 9. *Let us assume that (56) holds. Then, $c(\delta)$ satisfies*

$$c(\delta) \le \left(\frac{2\mathscr{K}^2_\beta(\psi_1, a, T, \lambda_1, \psi_0)}{\sigma^2 - 2}\right)^{1/k+1}\left(\frac{k+1}{2b}\right)\mathscr{E}^{2/k+1}\delta^{-2/k+1}. \tag{57}$$

Proof. From the definition of $c(\delta), d \in (1/2, 1]$, $0 < b|(\lambda_1^{-1} + a)/\lambda_j^{\beta-1}|^2 < 1$, $\|f\|_{\mathscr{D}(\mathscr{A}^{k(\beta-1)})} \le \mathscr{E}$, we have

$$\|Yf^d_{c(\delta),\delta} - g_\delta\|^2_{L^2(\Omega)} = \|\sum_{j=1}^{\infty}\left[1 - \left[1 - \left(1 - b\left|(\lambda_1^{-1} + a)\lambda_j^{1-\beta}\right|^2\right)^{c(\delta)-1}\right]^d\right] \cdot \left(\int_\Omega g_\delta(x)e_j(x)dx\right)\|^2_{L^2(\Omega)}. \tag{58}$$

Using the inequality $(a + b)^2 \le 2(a^2 + b^2)$, we derive that

$$\left\|Yf^d_{c(\delta)-1,\delta} - g_\delta\right\|^2_{L^2(\Omega)} \le \underbrace{2\left\|\sum_{j=1}^{\infty}\left[1 - \left[1 - \left(1 - b\left|(\lambda_1^{-1} + a)\lambda_j^{1-\beta}\right)\right|^2\right)^{c(\delta)-1}\right]^d\right]\left(\int_\Omega(g_\delta(x) - g(x))e_j(x)dx\right)\right\|^2_{L^2(\Omega)}}_{\mathscr{O}_1} + \underbrace{2\left\|\sum_{j=1}^{\infty}\left[1 - \left[1 - \left(1 - b\left|(\lambda_1^{-1} + a)\lambda_j^{1-\beta}\right|^2\right)^{c(\delta)-1}\right]^d\right]\left(\int_\Omega g(x)e_j(x)dx\right)\right\|^2_{L^2(\Omega)}}_{\mathscr{O}_2}. \tag{59}$$

(Step 1) Due to $[1 - [1 - (1 - b|(\lambda_1^{-1} + a)\lambda_j^{1-\beta}|^2)^{c(\delta)-1}]^d] \le 1$ and $\|g_\delta - g\|_{L^2(\Omega)} \le \delta$, from (59), the estimate of $\mathscr{O}_1$ is as follows:

$$\mathcal{O}_1 \le 2\delta^2. \tag{60}$$

(Step 2) $\mathcal{O}_2$ can be bounded as follows:

$$\begin{aligned}\mathcal{O}_2 &\le 2\| \sum_{j=1}^{\infty}\left(1-b\left|\left(\lambda_1^{-1}+a\right)\lambda_j^{1-\beta}\right|^2\right)^{c(\delta)-1}\left|\int_0^T \mathscr{C}_\beta\left(a,s,\lambda_j\right)\psi(s)ds\right| \\ &\cdot\left(\int_\Omega f(x)e_j(x)dx\right)\|_{L^2(\Omega)}^2 \le 2\| \sum_{j=1}^{\infty}\left(1-b\left|\left(\lambda_1^{-1}+a\right)\lambda_j^{1-\beta}\right|^2\right)^{c(\delta)-1} \\ &\cdot\left|\int_0^T \mathscr{C}_\beta\left(a,s,\lambda_j\right)\psi(s)ds\right|^{k+1}\frac{\left(\int_\Omega f(x)e_j(x)dx\right)}{\left|\int_0^T \mathscr{C}_\beta\left(a,s,\lambda_j\right)\psi(s)ds\right|^k}\|_{L^2(\Omega)}^2 \\ &\le 2\| \sum_{j=1}^{\infty}\left(1-b\left|\left(\lambda_1^{-1}+a\right)\lambda_j^{1-\beta}\right|^2\right)^{c(\delta)-1}\left|\left(\lambda_1^{-1}+a\right)\lambda_j^{1-\beta}\right|^{k+1} \\ &\cdot \mathscr{K}_\beta\left(\psi_1,a,T,\lambda_1,\psi_0\right)\mathscr{E}\|_{L^2(\Omega)}^2,\end{aligned} \tag{61}$$

where

$$\mathscr{K}_\beta\left(\psi_1,a,T,\lambda_1,\psi_0\right) = \left|\psi_1\right|^{k+1}\left|a\left[1-\exp\left(-T\lambda_1^\beta\left(1+a\lambda_1\right)^{-1}\right)\right]\psi_0\right|^{-k}. \tag{62}$$

Thanks for the two articles [24, 25], we get the following inequality:

$$(1-\omega)^s\omega^r \le r^r(s+1)^{-r}, \tag{63}$$

for $0<\omega<1, r>0,$ and $s\in\mathbb{N}$. Combining (58) and (63), we deduce that

$$\sigma^2\delta^2 \le 2\delta^2 + 2\left(\frac{k+1}{2b}\right)^{k+1}\left(\frac{1}{c(\delta)}\right)^{k+1}\mathscr{K}_\beta^2\left(\psi_1,a,T,\lambda_1,\psi_0\right)\mathscr{E}^2. \tag{64}$$

This implies that

$$c(\delta) \le \left(\frac{2\mathscr{K}_\beta^2\left(\psi_1,a,T,\lambda_1,\psi_0\right)}{\sigma^2-2}\right)^{1/k+1}\left(\frac{k+1}{2b}\right)\mathscr{E}^{2/k+1}\delta^{-2/k+1}. \tag{65}$$

□

Theorem 10. *Let $f_{c(\delta),\delta}^d$ be the regularized solution which is defined in (33). Suppose that condition (3) is satisfied, and the parameter regularization is chosen by (56). Then we get the following estimate:*

$$\|f_{c(\delta),\delta}^d - f\|_{L^2(\Omega)} \textit{ is of order } \delta^{k/k+1}. \tag{66}$$

Proof. By the triangle inequality, we receive

$$\|f_{c(\delta),\delta}^d - f\|_{L^2(\Omega)} \le \|f_{c(\delta),\delta}^d - f_{c(\delta)}^d\|_{L^2(\Omega)} + \|f_{c(\delta)}^d - f\|_{L^2(\Omega)}. \tag{67}$$

Firstly, we have

$$\begin{aligned}\|f_{c(\delta),\delta}^d - f_{c(\delta)}^d\|_{L^2(\Omega)} &\le \left[c(\delta)\right]^{1/2}b^{1/2}4\delta \\ &\cdot\left[\psi_0\left(1-\exp\left(-T\lambda_1\left(1+a\lambda_1\right)^{-1}\right)\right)\right]^{-1} \\ &+ \frac{4\delta}{\psi_0}\|f\|_{L^2(\Omega)}.\end{aligned} \tag{68}$$

Secondly, we find that

$$\begin{aligned}\left\|f_{c(\delta)}^d - f\right\|_{L^2(\Omega)} &= \left\|\sum_{j=1}^{\infty}\left[1-\left[1-\left(1-b\left|\left(\lambda_1^{-1}+a\right)\lambda_j^{1-\beta}\right|^2\right)^{c(\delta)}\right]^d\right]\right. \\ &\left.\cdot\frac{\left(\int_\Omega g(x)e_j(x)dx\right)e_j(\cdot)}{\left|\int_0^T \mathscr{C}_\beta\left(a,s,\lambda_j\right)\psi(s)ds\right|}\right\|_{L^2(\Omega)}.\end{aligned} \tag{69}$$

In view of Hölder inequality, we follow from (69) that

$$\left\|f_{c(\delta)}^d - f\right\|_{L^2(\Omega)} \le \mathscr{V}_1\mathscr{V}_2, \tag{70}$$

where

$$\begin{aligned}\mathscr{V}_1 &= \left\|\sum_{j=1}^{\infty}\left(1-b\left|\left(\lambda_1^{-1}+a\right)\lambda_j^{1-\beta}\right|^2\right)^{\kappa(\delta)}\left(\int_\Omega f(x)e_j(x)dx\right)e_j(\cdot)\right\|^{1/k+1}, \\ \mathscr{V}_2 &= \left\|\sum_{j=1}^{\infty}\left[1-\left[1-\left(1-b\left|\left(\lambda_1^{-1}+a\right)\lambda_j^{1-\beta}\right|^2\right)^{c(\delta)}\right]^d\right]\frac{\left(\int_\Omega g(x)e_j(x)dx\right)e_j(\cdot)}{\left|\int_0^T \mathscr{C}_\beta\left(a,s,\lambda_j\right)\psi(s)ds\right|}\right\|^{k/k+1}.\end{aligned} \tag{71}$$

□

To continue the proof, we divide it into two steps.

(Step 1) In the estimate of $\mathscr{V}_1$, we have

$$\begin{aligned}\mathscr{V}_1 \le \| &\sum_{j=1}^{\infty}\left(1-b\left|\left(\lambda_1^{-1}+b\right)\lambda_j^{1-\beta}\right|^2\right)^{c(\delta)} \\ &\cdot\lambda_j^{k(\beta-1)}\left(\int_\Omega f(x)e_j(x)dx\right)e_j(\cdot)\|_{L^2(\Omega)}^{1/k+1}.\end{aligned} \tag{72}$$

(Step 2) In the estimate of $\mathscr{V}_2$, we have

$$\mathscr{V}_2 \leq \left(\left\| \sum_{j=1}^{\infty} \left[1 - \left[1 - \left(1 - b \left| \left(\lambda_1^{-1} + a \right) \lambda_j^{1-\beta} \right|^2 \right)^{c(\delta)} \right]^d \right] \cdot \frac{\left(\int_\Omega (g(x) - g_\delta(x)) e_j(x) dx \right) e_j(\cdot)}{\left| \int_0^T \mathscr{C}_\beta (a, s, \lambda_j) \psi(s) ds \right|} \right\|_{L^2(\Omega)} + \left\| \sum_{j=1}^{\infty} \left[1 - \left[1 - \left(1 - b \left| \left(\lambda_1^{-1} + a \right) \lambda_j^{1-\beta} \right|^2 \right)^{c(\delta)} \right]^d \right] \cdot \frac{\left(\int_\Omega g_\delta(x) e_j(x) dx \right) e_j(\cdot)}{\left| \int_0^T \mathscr{C}_\beta (a, s, \lambda_j) \psi(s) ds \right|} \right\|_{L^2(\Omega)} \right)^{k/k+1}. \tag{73}$$

From (73), we have

$$\mathscr{V}_2 \leq \left(\left\| \sum_{j=1}^{\infty} \left(1 - b \left| \left(\lambda_1^{-1} + a \right) \lambda_j^{1-\beta} \right|^2 \right)^{c(\delta)} \right] \frac{\left(\int_\Omega (g(x) - g_\delta(x)) e_j(x) dx \right) e_j(\cdot)}{\left| \int_0^T \mathscr{C}_\beta (a, s, \lambda_j) \psi(s) ds \right|} \right\|_{L^2(\Omega)} + \left\| \sum_{j=1}^{\infty} \left[1 - \left[1 - \left(1 - b \left| \left(\lambda_1^{-1} + a \right) \lambda_j^{1-\beta} \right|^2 \right)^{c(\delta)} \right]^d \right] \frac{\left(\int_\Omega g_\delta(x) e_j(x) dx \right) e_j(\cdot)}{\left| \int_0^T \mathscr{C}_\beta (a, s, \lambda_j) \psi(s) ds \right|} \right\|_{L^2(\Omega)} \right)^{k/k+1} \leq \delta^{k/k+1} (1+\sigma)^{k/k+1} \sup_{\lambda_j > 1} \left[\frac{\lambda_j^{\beta-1}}{\left| \psi_0 \left(\lambda_j^{-1} + a \right) \left[1 - \exp\left(-T\lambda_1 (1 + a\lambda_1)^{-1} \right) \right] \right|} \right]^{k/k+1}. \tag{74}$$

Substituting (73) into (69), it gives

$$\left\| f_{c(\delta)}^d - f \right\|_{L^2(\Omega)} \leq \delta^{k/k+1} \mathscr{E}^{1/k+1} (1+\sigma)^{k/k+1} \left[\frac{1}{\psi_0 a \left[1 - \exp\left(-T\lambda_1 (1 + a\lambda_1)^{-1} \right) \right]} \right]^{k/k+1}. \tag{75}$$

Substituting (65) into (68) and combining estimate (75), we conclude that

$$\left\| f_{c(\delta),\delta}^d - f \right\|_{L^2(\Omega)} \leq \delta^{k/k+1} \mathscr{E}^{1/k+1} (\mathscr{R}_1 + \mathscr{R}_2), \tag{76}$$

where

$$\mathscr{R}_1 = \frac{\left(2\mathscr{K}_\beta^2 (\psi_1, a, T, \lambda_1, \psi_0) \right)^{k/2(k+1)} (k + 1/2b)^{1/2} b^{1/2} 4}{(\sigma^2 - 2)^{-1/2(k+1)} \left[\psi_0 \left(1 - \exp\left(-T\lambda_1 (1 + a\lambda_1)^{-1} \right) \right) \right]} + 4\delta^{k/k+1} \psi_0^{-1} \mathscr{C}_1^{-k/k+2} \|g\|^{k/k+2},$$

$$\mathscr{R}_2 = (1+\sigma)^{k/k+1} \left[\frac{1}{\psi_0 a \left[1 - \exp\left(-T\lambda_1 (1 + a\lambda_1)^{-1} \right) \right]} \right]^{k/k+1}. \tag{77}$$

Theorem 10 is proven.

5. Convergence of the Source Function when $\beta \longrightarrow 1$

In this section, we will first prove the convergence of the source function when $\beta \longrightarrow 1$.

Theorem 11. *Let the Cauchy data $g \in D(\mathscr{A}^{r+2\beta}(\Omega))$ for any $r \geq 0$. Let the function $\psi \in L^\infty(0, T)$. Then, we have the following estimate:*

$$\left\| f^{(\beta)}(x) - f^{(1)}(x) \right\|_{D(\mathscr{A}^r(\Omega))} \lesssim (\beta - 1)^{2-(\beta-1)\varepsilon} \|\psi\|_{L^\infty(0,T)} \|g\|_{D(\mathscr{A}^{r+2\beta}(\Omega))}, \tag{78}$$

where $\varepsilon > 0$ satisfies that $2 - (\beta - 1)\varepsilon > 0$.

Proof. Using the inequality $|e^{-m} - e^{-n}| \leq C_\varepsilon |m - n|^\varepsilon$, we find that for $z > 0$

$$\left| \exp\left(-h\lambda_j^\beta (1 + a\lambda_j)^{-1} \right) - \exp\left(-h\lambda_j (1 + a\lambda_j)^{-1} \right) \right| \leq C_\varepsilon h^\varepsilon \left| \frac{\lambda_j^\beta - \lambda_j}{1 + a\lambda_j} \right|^\varepsilon \leq \frac{C_\varepsilon}{a} h^\varepsilon \lambda_j^{-\varepsilon} \left| \lambda_j^\beta - \lambda_j \right|^\varepsilon. \tag{79}$$

Let us recall Lemma 12 which is proved in [27]. □

Lemma 12. *Assume that $0 \leq a \leq b$ and $0 < z$. For any $\varepsilon > 0$, there always exists $\bar{C}_\varepsilon > 0$ such that*

(a) If $z < 1$ then

$$\left| z^a - z^b \right| \leq \bar{C}_\varepsilon (b - a)^\varepsilon z^{a-\varepsilon} \tag{80}$$

(b) If $z \geq 1$ then

$$\left| z^a - z^b \right| \leq \bar{C}_\varepsilon (b - a)^\varepsilon z^{b+\varepsilon} \tag{81}$$

Let us divide the set of natural number into two sets in the following:

$$\mathbb{N} = \mathbb{N}_1 \cup \mathbb{N}_2, \tag{82}$$

where

$$\mathbb{N}_1 = \left\{ j \in \mathbb{R}, \lambda_j \leq 1 \right\}, \quad \mathbb{N}_2 = \left\{ j \in \mathbb{R}, \lambda_j > 1 \right\}. \tag{83}$$

Let us assume that $j \in \mathbb{N}_1$. Let us recall that the assumption $\beta \geq 1$. By applying Lemma 12, we know that since $\lambda_j \leq 1$ then for any $\theta > 0$

$$\left| \lambda_j^\beta - \lambda_j \right| \leq \bar{C}_{1,\theta} \lambda_j^{1-\theta} (\beta - 1)^\theta. \tag{84}$$

It follows from (79) that

$$\left|\exp\left(-h\lambda_j^{\beta}\left(1+a\lambda_j\right)^{-1}\right)-\exp\left(-h\lambda_j\left(1+a\lambda_j\right)^{-1}\right)\right| \leq \frac{C_\varepsilon \bar{C}_{1,\theta}^{\varepsilon}}{a} h^{\varepsilon}\lambda_j^{-\varepsilon}\lambda_j^{(1-\theta)\varepsilon}(\beta-1)^{\theta\varepsilon} \leq \frac{C_\varepsilon \bar{C}_{1,\theta}^{\varepsilon}}{a} h^{\varepsilon}\lambda_j^{-\theta\varepsilon}(\beta-1)^{\theta\varepsilon}. \quad (85)$$

Let us assume that $j\in\mathbb{N}_2$. By applying Lemma 12, we know that since $\lambda_j>1$, then

$$\left|\lambda_j^{\beta}-\lambda_j\right| \leq \bar{C}_{2,\theta}\lambda_j^{\beta+\theta}(\beta-1)^{\theta}. \quad (86)$$

It follows from (79) that

$$\left|\exp\left(-h\lambda_j^{\beta}\left(1+a\lambda_j\right)^{-1}\right)-\exp\left(-h\lambda_j\left(1+a\lambda_j\right)^{-1}\right)\right| \leq \frac{C_\varepsilon \bar{C}_{1,\theta}^{\varepsilon}}{a} h^{\varepsilon}\lambda_j^{-\varepsilon}\lambda_j^{(\beta+\theta)\varepsilon}(\beta-1)^{\theta\varepsilon} \leq \frac{C_\varepsilon \bar{C}_{1,\theta}^{\varepsilon}}{a} h^{\varepsilon}\lambda_j^{-\varepsilon+\beta\varepsilon+\theta\varepsilon}(\beta-1)^{\theta\varepsilon}. \quad (87)$$

Let us review that

$$f^{(\beta)}(x)=\sum_{j=1}^{\infty}\left[\frac{\int_{\Omega}g(x)e_j(x)dx}{\int_0^T \exp\left(-(T-s)\lambda_j^{\beta}\left(1+a\lambda_j\right)^{-1}\right)\psi(s)ds}\right]e_j(x). \quad (88)$$

By in view of Parseval's equality, we find that

$$f^{(1)}(x)=\sum_{j=1}^{\infty}\left[\frac{\int_{\Omega}g(x)e_j(x)dx}{\int_0^T \exp\left(-(T-s)\lambda_j\left(1+a\lambda_j\right)^{-1}\right)\psi(s)ds}\right]e_j(x). \quad (89)$$

Since two above observations, we derive that

$$\left\|f^{(\beta)}(x)-f^{(1)}(x)\right\|_{D(\mathscr{A}^r(\Omega))}^2 = \sum_{j=1}^{\infty}\left[\frac{\int_{\Omega}g(x)e_j(x)dx}{\int_0^T \exp\left(-(T-s)\lambda_j^{\beta}\left(1+a\lambda_j\right)^{-1}\right)\psi(s)ds} - \frac{\int_{\Omega}g(x)e_j(x)dx}{\int_0^T \exp\left(-(T-s)\lambda_j\left(1+a\lambda_j\right)^{-1}\right)\psi(s)ds}\right]^2\lambda_j^{2r}. \quad (90)$$

First, if $\lambda_j\leq 1$, then using the estimate (85), we get that

$$\left|\int_0^T \exp\left(-(T-s)\lambda_j^{\beta}\left(1+a\lambda_j\right)^{-1}\right)\psi(s)\cdot ds - \int_0^T \exp\left(-(T-s)\lambda_j\left(1+a\lambda_j\right)^{-1}\right)\psi(s)ds\right| \leq \frac{C_\varepsilon \bar{C}_{1,\theta}^{\varepsilon}}{a}\lambda_j^{-\theta\varepsilon}(\beta-1)^{\theta\varepsilon}\left(\int_0^T (T-s)^{\varepsilon}ds\right)\|\psi\|_{L^\infty(0,T)} \leq M_1\|\psi\|_{L^\infty(0,T)}\lambda_j^{-\theta\varepsilon}(\beta-1)^{\theta\varepsilon}, \quad (91)$$

where $M_1=(C_\varepsilon \bar{C}_{1,\theta}^{\varepsilon}/a)(T^{1+\varepsilon}/1+\varepsilon)$. By a similar explanation, if $\lambda_j>1$, then using the estimate (87), we get that

$$\left|\int_0^T \exp\left(-(T-s)\lambda_j^{\beta}\left(1+a\lambda_j\right)^{-1}\right)\psi(s)\cdot ds - \int_0^T \exp\left(-(T-s)\lambda_j\left(1+a\lambda_j\right)^{-1}\right)\psi(s)ds\right| \leq \frac{C_\varepsilon \bar{C}_{1,\theta}^{\varepsilon}}{a}\lambda_j^{-\varepsilon+\beta\varepsilon+\theta\varepsilon}(\beta-1)^{\theta\varepsilon}\left(\int_0^T (T-s)^{\varepsilon}ds\right)\|\psi\|_{L^\infty(0,T)} \leq M_1\|\psi\|_{L^\infty(0,T)}\lambda_j^{-\varepsilon+\beta\varepsilon+\theta\varepsilon}(\beta-1)^{\theta\varepsilon}. \quad (92)$$

By using Lemma 1, we find that

$$\left[\int_0^T \exp\left(-(T-s)\lambda_j^{\beta}\left(1+a\lambda_j\right)^{-1}\right)\psi(s)ds\right]\cdot\left[\int_0^T \exp\left(-(T-s)\lambda_j\left(1+a\lambda_j\right)^{-1}\right)\psi(s)ds\right] \geq \left[1-\exp\left(-T\lambda_1^{\beta}\left(1+a\lambda_1\right)^{-1}\right)\right]^2|\psi_0|^2\left(\frac{1+a\lambda_j}{\lambda_j^{\beta}}\right)^2 = M_2^2\left(\frac{1+a\lambda_j}{\lambda_j^{\beta}}\right)^2 \geq M_2^2a^2\lambda_j^{2-2\beta}, \quad (93)$$

where we denote

$$M_2=\left[1-\exp\left(-T\lambda_1^{\beta}\left(1+a\lambda_1\right)^{-1}\right)\right]|\psi_0|. \quad (94)$$

From some of the above observations, we get that

$$\|f^{(\beta)}(x)-f^{(1)}(x)\|_{D(\mathscr{A}^r(\Omega))}^2 = \sum_{\lambda_j\leq 1}\left[\frac{\int_{\Omega}g(x)e_j(x)dx}{\int_0^T \exp\left(-(T-s)\lambda_j^{\beta}\left(1+a\lambda_j\right)^{-1}\right)\psi(s)ds} - \frac{\int_{\Omega}g(x)e_j(x)dx}{\int_0^T \exp\left(-(T-s)\lambda_j\left(1+a\lambda_j\right)^{-1}\right)\psi(s)ds}\right]^2\lambda_j^{2r}$$

$$+\sum_{\lambda_j>1}\left[\frac{\int_\Omega g(x)e_j(x)dx}{\int_0^T \exp\left(-(T-s)\lambda_j^\beta\left(1+a\lambda_j\right)^{-1}\right)\psi(s)ds}-\frac{\int_\Omega g(x)e_j(x)dx}{\int_0^T \exp\left(-(T-s)\lambda_j\left(1+a\lambda_j\right)^{-1}\right)\psi(s)ds}\right]^2\lambda_j^{2r}$$
$$\leq\left(\frac{M_1}{M_2^2}\right)^2(\beta-1)^{2\theta\varepsilon}\|\psi\|^2_{L^\infty(0,T)}\sum_{\lambda_j\leq 1}\lambda_j^{2\theta\varepsilon-4+4\beta+2r}\cdot\left(\int_\Omega g(x)e_j(x)dx\right)^2+\left(\frac{M_1}{M_2^2}\right)^2(\beta-1)^{2\theta\varepsilon}\|\psi\|^2_{L^\infty(0,T)}\cdot\sum_{\lambda_j>1}\lambda_j^{2\theta\varepsilon-4+4\beta+2r-2\varepsilon+2\beta\varepsilon}\left(\int_\Omega g(x)e_j(x)dx\right)^2. \tag{95}$$

Noting that $\beta \geq 1$, we have that

$$1\leq\left(\frac{\lambda_j}{\lambda_1}\right)^{2\beta\varepsilon-2\varepsilon}. \tag{96}$$

This implies the following estimate:

$$\|f^{(\beta)}(x)-f^{(1)}(x)\|^2_{D(\mathscr{A}^r(\Omega))}\lesssim(\beta-1)^{2\theta\varepsilon}\|\psi\|^2_{L^\infty(0,T)}\cdot\sum_{j=1}^{\infty}\lambda_j^{2\theta\varepsilon-4+4\beta+2r-2\varepsilon+2\beta\varepsilon}\left(\int_\Omega g(x)e_j(x)dx\right)^2. \tag{97}$$

Let us choose θ and ε such that $2\theta\varepsilon+2\beta\varepsilon=4+2\varepsilon$. In order to choose such number θ and ε, we need to choose $\varepsilon>0$ if $\beta=1$ and such that

$$0<\varepsilon<\frac{2}{\beta-1},\quad \beta>1. \tag{98}$$

Let θ be such that $\theta=(2/\varepsilon)+1-\beta$. Then since (()(97)), we deduce that

$$\|f^{(\beta)}(x)-f^{(1)}(x)\|_{D(\mathscr{A}^r(\Omega))}\lesssim(\beta-1)^{\theta\varepsilon}\|\psi\|_{L^\infty(0,T)}\|g\|_{D\left(\mathscr{A}^{r+2\beta}(\Omega)\right)}=(\beta-1)^{2-(\beta-1)\varepsilon}\|\psi\|_{L^\infty(0,T)}\|g\|_{D\left(\mathscr{A}^{r+2\beta}(\Omega)\right)}. \tag{99}$$

Data Availability

No data were used to support this study.

Conflicts of Interest

The authors declare that they have no competing interests.

Authors' Contributions

The authors contributed equally to this the work. The authors read and approved the final manuscript.

Acknowledgments

The author Le Dinh Long is supported by Van Lang University.

References

[1] L. Jin, L. Li, and S. Fang, "The global existence and time-decay for the solutions of the fractional pseudo-parabolic equation," *Computers and Mathematics with Applications*, vol. 73, no. 10, pp. 2221–2232, 2017.

[2] G. I. Barenblatt, I. P. Zheltov, and I. Kochina, "Basic concepts in the theory of seepage of homogeneous liquids in fissured rocks [strata]," *Journal of Applied Mathematics and Mechanics*, vol. 24, no. 5, pp. 1286–1303, 1960.

[3] T. B. Benjamin, J. L. Bona, and J. J. Mahony, ""Model equations for long waves in nonlinear dispersive systems", Philosophical transactions of the Royal Society of London," *Series A, Mathematical and Physical Sciences*, vol. 272, no. 1220, pp. 47–78, 1972.

[4] R. Wang, Y. Li, and B. Wang, "Random dynamics of fractional nonclassical diffusion equations driven by colored noise," *Discrete & Continuous Dynamical Systems*, vol. 39, no. 7, pp. 4091–4126, 2019.

[5] R. Wang, L. Shi, and B. Wang, "Asymptotic behavior of fractional nonclassical diffusion equations driven by nonlinear colored noise on R^N," *Nonlinearity*, vol. 32, no. 11, pp. 4524–4556, 2019.

[6] R. Wang, Y. Li, and B. Wang, "Bi-spatial pullback attractors of fractional nonclassical diffusion equations on unbounded domains with (p, q)-growth nonlinearities," *Applied Mathematics and Optimization*, vol. 84, no. 1, pp. 425–461, 2021.

[7] N. H. Tuan and T. Caraballo, "On initial and terminal value problems for fractional nonclassical diffusion equations," *Proceedings of the American Mathematical Society*, vol. 149, no. 1, pp. 143–161, 2021.

[8] N. H. Tuan, V. V. Au, and R. Xu, "Semilinear Caputo time-fractional pseudo-parabolic equations," *Communications on Pure & Applied Analysis*, vol. 20, no. 2, pp. 583–621, 2021.

[9] M. Warma, H. Antil, and D. Verma, "Optimal control of fractional elliptic PDEs with state constraints and characterization of the dual of fractional-order Sobolev spaces," *Journal of Optimization Theory and Applications*, vol. 186, no. 1, pp. 1–23, 2020.

[10] H. Antil and M. Warma, "Optimal control of fractional semilinear PDEs," *ESAIM*, vol. 26, p. 130, 2020.

[11] H. Antil, D. Verma, and M. Warma, "External optimal control of fractional parabolic PDEs," *ESAIM*, vol. 26, p. 20, 2020.

[12] M. Warma, H. Antil, and R. Khatri, "External optimal control of nonlocal PDEs," *Inverse Problems*, vol. 35, no. 8, p. 084003, 2019.

[13] M. Warma and H. Antil, "Optimal control of the coefficient for fractional and regional fractional p-Laplace equations: approximation and convergence," *Mathematical Control and Related Fields*, vol. 9, pp. 1–38, 2019.

[14] N. H. Luc, L. D. Long, L. T. D. Hang, D. Baleanu, and N. H. Can, "Identifying the initial condition for space-fractional Sobolev equation," *Journal of Applied Analysis & Computation*, vol. 11, no. 5, pp. 2402–2422, 2021.

[15] V. V. Au, J. Hossein, Z. Hammouch, and N. H. Tuan, "On a final value problem for a nonlinear fractional pseudo-

parabolic equation," *Electronic Research Archive*, vol. 29, no. 1, pp. 1709–1734, 2021.

[16] D. H. Q. Nam, D. O'Regan, L. D. Long, T. B. Ngoc, and N. H. Tuan, "Identification of the righthand side in a bi-parabolic equation with final data," *Applicable Analysis*, vol. 101, 2020.

[17] Y. K. Ma, P. Prakash, and A. Deiveegan, "Generalized Tikhonov methods for an inverse source problem of the time- fractional diffusion equation," *Chaos, Solitons and Fractals*, vol. 108, pp. 39–48, 2018.

[18] H. W. Engl, M. Hanke, and A. Neubauer, *Regularization of Inverse Problems*, Kluwer Academic, Boston, 1996.

[19] Y. Han, X. Xiong, and X. Xue, "A fractional Landweber method for solving backward time-fractional diffusion problem," *Computers & Mathematcs with Applications*, vol. 78, no. 1, pp. 81–91, 2019.

[20] Z. S. Jiang and J. Y. Wu, "Recovering space-dependent source for a time-space fractional diffusion wave equation by fractional Landweber method," *Inverse Problems in Science and Engineering*, vol. 29, no. 7, pp. 990–1011, 2021.

[21] F. Yang, L. J. Fu, P. Fan, and X. X. Li, "Fractional Landweber iterative regularization method for identifying the unknown source of the time-fractional diffusion problem," *Acta Applicandae Mathematicae*, vol. 175, no. 1, 2021.

[22] T. T. Binh, H. K. Nashine, D. L. Le, H. L. Nguyen, and N. Can, "Identification of source term for the ill-posed Rayleigh-Stokes problem by Tikhonov regularization method," *Advances in Difference Equations*, vol. 2019, no. 1, 2019.

[23] N. H. Tuan, L. D. Long, and N. V. Thinh, "Regularized solution of an inverse source problem for a time fractional diffusion equation," *Applied Mathematical Modelling*, vol. 40, no. 19-20, pp. 8244–8264, 2016.

[24] A. B. Bakushinsky, M. Y. Kokurin, and A. Smirnova, *Iterative Methods for Ill-Posed Problems*, Inverse and Ill-Posed Problems Series, 2011.

[25] A. K. Louis, *Inverse und Schlecht Gestellte Probleme*, Springer-Verlag, 2013.

[26] N. H. Can, N. H. Luc, D. Baleanu, and Y. Zhou, "Inverse source problem for time fractional diffusion equation with Mittag-Leffler kernel," *Advances in Difference Equations*, vol. 1, 18 pages, 2020.

[27] N. H. Tuan, D. O'regan, and T. B. Ngoc, "Continuity with respect to fractional order of the time fractional diffusion-wave equation," *Evolution Equations & Control Theory*, vol. 9, no. 3, pp. 773–793, 2020.